THE PHYSICAL REVIEW

A JOURNAL OF EXPERIMENTAL AND THEORETICAL PHYSICS

CONDUCTED BY

THE

AMERICAN PHYSICAL SOCIETY

VOLUME 37, SECOND SERIES
JANUARY-JUNE, 1931

THE PHYSICAL REVIEW
MINNEAPOLIS, MINN.

Composed, Printed and Bound by
The Collegiate Press
George Banta Publishing Company
Menasha, Wisconsin

CONTENTS

JANUARY 1, 1931

PROCEEDINGS OF THE AMERICAN PHYSICAL SOCIETY

JANUARY 15, 1931

PROCEEDINGS OF THE AMERICAN PHYSICAL SOCIETY

FEBRUARY 1, 1931

FEBRUARY 15, 1931

PROCEEDINGS OF THE AMERICAN PHYSICAL SOCIETY

MARCH 1, 1931

MARCH 15, 1931

APRIL 1, 1931

APRIL 15, 1931

PROCEEDINGS OF THE AMERICAN PHYSICAL SOCIETY

MAY 1, 1931

MAY 15, 1931

JUNE 1, 1931

JUNE 15, 1931

PROCEEDINGS OF THE AMERICAN PHYSICAL SOCIETY

Second Series *January 1, 1931* *Vol. 37, No. 1*

THE

PHYSICAL REVIEW

ATMOSPHERIC IONIZATION BY COSMIC RADIATION*

By E. O. Hulburt

Naval Research Laboratory

(Received November 22, 1930)

Abstract

From Millikan's measurements of the intensity and the absorption coefficients of cosmic radiation the ionization in the atmosphere is calculated from sea level to 60 km. The electron density is negligibly small in this region. The ion density increases with the height to 3.5×10^3 ion pairs cm^{-3} at about 50 km and is roughly constant above this to 60 or 70 km where the solar ultraviolet light ionization sets in. The 50 km ion bank refracts appreciably radio waves longer than 12 km and being unchanged with the day and night accounts for the propagation of waves longer than 12 km, which are known to show no marked diurnal variations. The agreement with the facts of long radio waves indicates that there exists in the high atmosphere but little cosmic radiation of less penetration than Millikan has already detected.

By considering the effect of the earth's magnetic field on high speed electrons the "run away" electron hypothesis of C. T. R. Wilson to account for cosmic radiation is shown to lead to a distribution most intense at low latitudes and feeble at high latitudes, thereby being in disagreement with Millikan's observation of the constancy of the cosmic radiation with latitude.

1. It is pretty generally accepted, as a result of the work of Hess, Bauer, Swann, Mauchly, Millikan and others,[1] that the ionization in the lower atmosphere is caused primarily by a penetrating radiation of cosmic origin. Over the land in the levels of the atmosphere below about 2 km the radiation from radio-active materials in the earth may cause an appreciable part, as much as a half or more, of the ionization. But from levels above 2 km over the land, and from about sea level upward over the sea, up to the limit of direct observation[2] at about 15 km, the measurements support the view that the ionization is caused by a cosmic radiation coming in from all directions and absorbed exponentially in its passage through the atmosphere.[2,3] In the present paper the ionization due to cosmic radiation is calculated from sea level to about 70 km, where the Kennelly-Heaviside layer begins, and is

* Published with the permission of the Navy Department.

[1] See Hess "The Electrical Conductivity of the Atmosphere and its Causes" (1928), and references cited throughout the present paper.

[2] Millikan and Cameron, Phys. Rev. **31,** 163 (1928).

[3] Millikan and Bowen, Phys. Rev. **22,** 198 (1923); **27,** 353 (1926); Millikan and Otis, Phys. Rev. **27,** 353 and 645 (1926): Millikan and Cameron, Phys. Rev. **28,** 851 (1926); etc.

found to agree with certain facts of the propagation of long wireless waves. A calculation of the ionization by cosmic radiation was made by Benndorf.[4] The more recent observations of cosmic radiation were of course not available to him and he did not consider such actions as the attachment of electrons to oxygen molecules, etc.; the present calculation which includes these factors is thought to be more nearly correct. In section 6 it is shown that the "run away" electron hypothesis of C. T. R. Wilson is inadequate to account for the observed facts of cosmic radiation.

2. The Rate of Productions of Ions in the Atmosphere by Cosmic Radiation

The second column of Table I gives the values of n, the total number of molecules and atoms cm^{-3}, assuming no hydrogen in the atmosphere, for various heights z above sea level. The values of n are from Maris' tables[5] for winter day conditions in temperate latitudes. From $z=0$ to 100 km n is given, within an approximation sufficiently good for the present calculations, by

$$n = n_0 \epsilon^{-pz}, \tag{1}$$

where n_0 is the value of n at sea level and $p=1.38\times10^{-6}$ for z in cm. Since the curve of log n against z is not exactly a straight line p varies a little with z; for z from 100 to 300 km the average value of p is 1.21×10^{-6}, a value used in a former paper.[6] For summer night conditions n is much the same as the values of Table I, for summer day and winter night conditions n is slightly different. We are content, however, to use the winter day values to represent a rough average condition of the atmosphere.

Table I.

1 z	2 n	3 q'	4 q	5 I	6 Temp.	7 α	8 γ
0 km	2.68×10^{19}	1.4	1.4	1.09×10^{-5}	300°K	0.766×10^{-25}	8.25×10^{2}
10	6.77×10^{18}	21.1	5.32	1.51×10^{-4}	260	3.3 "	1.55×10^{3}
20	1.85×10^{18}	54.1	3.72	3.86 "	220	5.4 "	1.92 "
30	4.00×10^{17}		1.08	5.17 "	220	5.4 "	2.22 "
40	8.59×10^{16}		0.24	5.30 "	260	3.3 "	2.91 "
50	2.26×10^{16}		6.26×10^{-2}	5.31 "	300	2.3 "	3.48 "
60	5.58×10^{15}		1.54×10^{-2}	5.31 "	300	2.3 "	3.48 "
70	1.48×10^{15}		4.21×10^{-3}	5.31 "	300	2.3 "	3.48 "
80	3.71×10^{14}		1.02×10^{-3}	5.31 "	300	2.3 "	3.48 "

Millikan, Bowen, Otis and Cameron[2,3], by sending up apparatus in balloons, made direct observations of the ionization due to cosmic radiation up to a height of about 15 km. They calculated[2] the absorption coefficient μ and the values of q' from sea level to 20 km and at the "top" of the at-

[4] Benndorf, Phys. Zeits. **27**, 686 (1926), see also Pederson, "The Propagation of Radio Waves," page 62 (1927).

[5] Maris, Terr. Mag. and Atmos. Elec. **33**, 233 (1928); **34**, 45 (1929).

[6] Hulburt, Phys. Rev. **31**, 1018 (1928).

mosphere, using the Gold[7] tables for the case of radiation entering the atmosphere equally distributed in all directions above the horizontal plane. They found that the radiation became softer, i.e., less penetrating, as z increased, the average absorption coefficient μ per meter of water from $z=0$ to 0.9 km being 0.23 and for z greater than 0.9 km being 0.25. q' is the number cm^{-3} sec^{-1} of ion pairs which would be produced by the cosmic radiation in 1 cm^3 of air at sea level pressure placed at various heights in the atmosphere. The values of q' given in column 3, Table I, are taken from their Table IV, ref. 2.

In dealing with the atmosphere it is more convenient to use q instead of q', where q is the number of ion pairs cm^{-3} sec^{-1} produced in the atmosphere by the cosmic radiation. Then

$$q = q'n/n_0. \tag{2}$$

The values of q calculated from q' for $z=0$ to 20 km are given in column 4, Table I. With $\mu=0.25$ per meter of water the molecular absorption coefficient β of atmospheric molecules, taken to be four parts nitrogen to one part oxygen, is 1.20×10^{-25}, on the assumption that β is proportional to the mass of the absorbing layer. β is defined in the usual way by

$$dI = -I\beta n dz, \tag{3}$$

where dI is the reduction in the intensity of radiation I erg cm^{-2} sec^{-1} in passing through a thickness dz cm of n atmospheric molecules cm^{-3}. Assuming that all of the absorbed energy goes into producing ions,

$$q = I\beta n/w, \tag{4}$$

where w is the work of ionization of the atmospheric particles. For oxygen and nitrogen atoms w is 2.15×10^{-11} and 2.32×10^{-11} erg, corresponding to ionization potentials 13.48 and 14.56 volts, respectively, and a little more for the molecules. With (4) I was calculated directly from the known values of q for $z=0$, 10 and 20 km and was continued into the higher levels by means of the Gold table.[7] The values of I are in column 5, Table I. From I and (4) q was calculated for the levels above 20 km, column 4, Table I. The extrapolation into the high levels assumed that β was constant throughout the region from $z=20$ to 60 km, i.e., that there exists no cosmic radiation of μ greater than 0.25. The evidence from wireless waves, section 5, indicates that this assumption is probably not much in error.

The total rate of production of electrons and positive ions by cosmic radiation in a 1 cm^2 column of the atmosphere from 60 km to interplanetary space is $\int_{60}^{\infty} q dz = 1.54\times10^{-2}/1.21\times10^{-6} = 1.28\times10^4$. This is much less than the production of ionization by the ultraviolet light of the sun, which amounts to 2×10^8 electrons and positive ions sec^{-1} in a 1 cm^2 vertical column above 180 km and many more below this level.[6,8] It is concluded that the

[7] Gold, Proc. Roy. Soc. **82**, 43 (1909).
[8] Hulburt, Phys. Rev. **34**, 1167 (1929).

ionization caused by cosmic radiation in levels above 60 km is inappreciable compared to that produced by solar ultraviolet light in all latitudes at all hours of the day and night.

3. The Ions and Electrons in the Atmosphere Caused by Cosmic Radiation

It is assumed that the cosmic radiation ionizes the air molecules and atoms to produce electrons and positive ions. The electron density y_e, assuming the loss of electrons arises only from recombination with positive ions and attachment to neutral oxygen molecules, is given by the steady state equation

$$q = \alpha_e n y_e^2 + b n' y_e, \tag{5}$$

where α_e is the J. J. Thomson[9] recombination coefficient for electrons and positive ions and b is the coefficient of attachment of electrons to oxygen molecules.[6] n' is the density of oxygen molecules. For $z=0$ $\alpha_e=0.52\times10^{-23}$, $b=8.3\times10^{-14}$ and putting $q=1.4$ into (5) gives $y_e=3\times10^{-6}$. y_e increases with z, but even at $z=60$ km y_e is only of order 10^{-3}. Therefore the electron density in these levels due to the ionizing action of cosmic rays is very small, being much less than 1 electron cm^{-3}. Further, the loss of electrons by attachment to oxygen molecules exceeds by several orders of magnitude the loss by recombination with positive ions. For example at $z=0$ $bn'y_e=1.4$ and $\alpha_e n y_e^2=1.3\times10^{-15}$, and at 60 km are equal to 1.5×10^{-2} and 10^{-13}, respectively. Therefore the electrons do not remain free very long but become attached to oxygen molecules almost as fast as they are formed. We may then take the values of q of column 4, Table I, to be the rates of production of ion pairs and calculate the ion densities which exist in a steady state.

For this case y, the number of ion pairs cm^{-3}, is given by

$$q = \alpha n y^2, \tag{6}$$

where α is the recombination coefficient of positive and negative ions.[9] α is a function of the temperature and the molecular density n for n greater than 10^{18}; the values of the winter day temperatures and of α are given in columns 6 and 7, Table I. The values of y calculated from (6) are given in column 8, Table I, and are plotted as abscissas against z as ordinate in Fig. 1. The values of y for winter night and for summer day and night are the same as those of Fig. 1 within 40%. The ion curve of Fig. 1 was obtained omitting diffusion. This is justifiable, for from Eq. (5), ref. 6, the rate of increase of ions due to diffusion is small compared to q for levels below 80 km. Winds would not be expected to disturb the curve very much. With the values of q of column (4), Table I, it takes roughly 10, 34 and 196 minutes to build up the steady state values of y at $z=0$, 30 and 40 km, respectively. Therefore the air must move upwards or downwards with velocities of the order of kilometers per minute in order to change the ion curve. Such movements seem improbable under ordinary circumstances.

[9] Thomson, Phil. Mag. **47**, 337 (1924); see also ref. 6 and 8 for a discussion of these coefficients.

4. Agreement with Observation

The value 825 ion pairs at sea level of Table I agrees with observation during fine weather, although, to be sure, we can not regard the present calculation, which omits such well-known effects in the lower atmosphere as water vapor, dust, ion clustering, ionization due to the splashing of waves, etc., as being a very complete statement of sea level conditions.

The ion layer of Fig. 1 will not cause appreciable absorption of wireless waves, even for those as long as 100 km. It will, however, refract long waves. The shortest wave, denoted by λ_s, ref. 6, which will be turned back to the earth is 11 km in length, and this only when incident on the layer at as near grazing incidence as possible, in which case the rays leave the earth tangentially (Eq. (26), ref. 6). Waves shorter than 11 km will pierce through the cosmic ion layer at 50 km to be refracted in the higher lying ionization

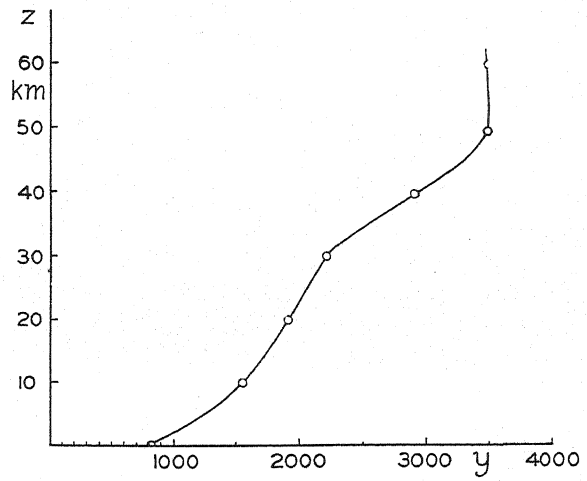

Fig. 1. Density y of ions pairs in the atmosphere caused by cosmic radiation.

above 70 km caused by the solar ultraviolet light. As the wave-length increases beyond 11 km the wave is refracted downward at decreasing angles of incidence on the 50 km layer, until a 90 km wave is returned at normal incidence. All waves longer than this will be returned at all angles of incidence. Thus we should expect low angled rays of wave-length greater than, say, 12 km to be refracted downward by the cosmic ion layer and that the long distance propagation of these wave-lengths should be governed by the layer. Since the cosmic rays are fairly uniformly distributed in direction, their ionization is constant throughout the day and night and therefore communication with waves longer than 12 km should experience no diurnal or seasonal changes. This conclusion is in good accord with observation, it being well known that wireless waves 10 km and less in length exhibit diurnal and seasonal variations and that those of length 15 km and greater show no such variations.

The foregoing agreement with the facts of long wireless waves sets an upper limit to the amount of cosmic radiation of absorption coefficient somewhat greater than $\mu=0.25$ which can be entering the earth's atmosphere. Roughly one may say that the intensity of such radiation can not be as great as 1×10^{-4} cm^{-2} sec^{-1}. For example, suppose that a less penetrating radiation existed for which $I=10^{-4}$ erg cm^{-2} sec^{-1} outside of the atmosphere and $\mu=2.5$ per meter of water or $\beta=1.2\times10^{-24}$. Its ionization in levels below 10 km would be too small to detect, but in levels above 40 km it, together with the ionization of Table I, would give $y=1.2\times10^{4}$. λ_s would be 7 km instead of 12 km, which would be contrary to the observation that λ_s is between 10 and 15 km.

Finally, Hollingsworth[10] interpreted his experiments on interference effects of 15 km radio waves to indicate that the waves reached an effective height of 70 km, although Eckersley[10] thought that the experiments accorded better with a height of about 50 km in agreement with some results of his own.[11] These heights would agree with the curve of Fig. 1 which gives a real height of 40 to 50 km and an effective height of 50 to 70 km, the exact value depending upon the angle of incidence of the wireless ray.

5. The Nature of Cosmic Radiation

The measurements of Millikan in California, Bolivia, Canada, etc., covering magnetic latitudes from about 0 to 78°, showed that the intensity of the cosmic radiation was the same in all these places within 1%, so that at the present time the conclusion is that the intensity is constant over the earth.* Recently Epstein[12] calculated that high speed electrons from an external source impinging on the earth would be diverted by the earth's magnetic field into high latitudes; electrons of 10^9 volt energy could not hit the earth at magnetic latitudes below 58°, and of 2×10^9 volt energy below 50°. He concluded that in order to satisfy Millikan's observation of the uniform intensity of the cosmic rays over the earth the rays might be, (a) electromagnetic rays of cosmic origin, (b) corpuscular rays of higher energy than 10^9 volt, at least 6×10^{10} volt, of cosmic origin, (c) corpuscular rays of terrestrial origin. In later paragraphs we show that (c) is improbable.

We may add a remark about Epstein's conclusions. If the earth were the target of hypothetical high speed electrons of external origin, the earth would accumulate a negative charge. A charge of 7.1×10^5 coulombs would keep 10^9 volt electrons from reaching the earth; if some manner of escape of negative electricity from the earth were postulated the accumulated charge would be less. A negative charge on the earth does not disturb Epstein's analysis. To a fair approximation the electric field due to the charge would merely retard the incoming electrons, so that the 10^9 volt

[10] Hollingsworth, Jr. Inst. Elec. Eng. **64,** 579 (1926).

[11] Round, Eckersley, Tremellen and Lunnon, Jr. Inst. Elec. Eng. **63,** 933 (1925).

* Dr. Epstein kindly told me in a letter of some of Dr. Millikan's latest results at Fort Churchill, Canada.

[12] Epstein, Proc. Nat. Acad. **16,** 658 (1930).

electrons instead of hitting the earth in latitudes above 58° would be restricted to a region of still higher latitude.

According to C. T. R. Wilson,[13] in his experiments and theory of the electric field in thunder clouds, differences of potential of 10^9 volt may exist between the upper and lower portions of a thundercloud, the electric field in the cloud being downward. For a cloud 1 km thick this meant a field of 10^4 volt cm^{-1}. Since the sparking potential of dry air is around 2×10^4 volt cm^{-1}, and since thunder clouds greater than 3 km in thickness are not frequent, it is probable that the total potential difference in thunder clouds would rarely exceed 5×10^9 volt. Electrons accelerated in such a field might soon move so fast that they would experience no collisions and might finally acquire nearly the full energy of the field. They would be "run away" electrons, as he called them, and would constitute a penetrating radiation. Wilson[14] recently has suggested that run away electrons sprayed upward would describe helical paths of large radius around the lines of magnetic force and would enter the lower atmosphere at widely separated parts of the earth. This is case (c) of an earlier paragraph.

In order to examine Wilson's suggestion we use the same equations which Epstein[13] employed in his calculation. The radius of curvature ρ of the path of an electron moving normally to a uniform magnetic field of strength H is

$$\rho = mv/He(1 - v^2/c^2)^{1/2}, \tag{7}$$

where m, e and v are the rest-mass, charge and velocity of the electron, respectively, and c is the velocity of light. All quantities are in c.g.s. electromagnetic units. The energy[15] acquired by the electron in falling through a potential V is

$$Ve = mc^2(1/(1 - v^2/c^2)^{1/2} - 1). \tag{8}$$

Since v is nearly equal to c in the present problem $1/(1-v^2/c^2)^{1/2}$ is very large compared to unity and -1 may be neglected in (8). With this approximation we have from (7) and (8)

$$\rho = V/He. \tag{9}$$

These equations are strictly valid only for slowly varying velocities. However, it may be stated without giving the calculation that the classical radiation term makes a negligible correction and may be omitted.

With $V=5\times10^9$ volts, probably a maximum value, $v=c(1-5.2\times10^{-9})$, and with $H=0.5$ gauss, as at 50° magnetic latitude, ρ is 333 km. At the equator $H=0.3$ gauss, ρ is 520 km and the electron moves westward in approximately a circle of radius 520 km. Thus, keeping in mind the fact that $1/H$ and hence ρ is proportional to r^3, where r is the distance to the center of the earth, in tropical latitudes below $\pm20°$ where H is approximately horizontal the 5×10^9 volt field, mainly vertical, of the thunder cloud sprays

[13] Wilson, see Glazebrook, "Dict. of Applied Physics" **3**, 84 (1923).
[14] Wilson, Jr. Frank. Inst. **208**, 1 (1929).
[15] See Born, "Mechanics of the Atom" (1927).

the run away electrons over a region not greater than about 1000 km square to the westward.

For thunderclouds in high latitudes the electron spray is more spread out. It is difficult to calculate the distribution of the spray exactly, but an approximate idea of the distribution may be obtained. In general a thundercloud in the northern hemisphere can not spray its electrons northward, or one in the southern hemisphere southward. A northern thundercloud can, however, project its electrons southward. The magnetic line of force which touches the earth at magnetic latitude 50° rises to a maximum height of 9100 km above sea level at the magnetic equator. At this height the maximum value of ρ for the 5×10^9 volt electron is about 13,000 km, and by following out the warped helical path of the electron it is found that the electron descends to the earth in latitudes below 50°, swinging always to the westward. Therefore thunder clouds in latitude 50° spray their electrons into areas between the 50° magnetic parallels north and south, those in latitude 40° between the 40° parallels, etc., and the nearer the cloud is to the equator the more local is its run away electron spray.

Electrons ejected by 5×10^9 volt thunder clouds in higher latitudes than 50° start out approximately along the line of magnetic force and, since ρ becomes greater than r, leave the earth never to return; or at least they do so until sufficient positive charge has accumulated on the earth, 3.56×10^6 coulombs, to prevent the escape of any more electrons. After this has happened the high altitude electrons return to the earth mainly in high latitudes but it is difficult to say exactly where they will strike. However, there are relatively few thunderstorms above 50° compared to the number in lower latitudes,[16] and their electron spray will be relatively unimportant. Therefore it is concluded that the run away electron hypothesis would lead to a penetrating radiation which is most intense at low latitudes and which becomes feeble in the high latitudes. This disagrees with Millikan's observations of the constancy of the cosmic radiation with latitude. It would seem that of the various suggestions as to the nature of the cosmic rays only two are left, the rays are electromagnetic rays of cosmic origin or are very high speed electrons of cosmic origin. If the second possibility is considered the question of the charge which would accumulate on the earth must be faced.

[16] Whipple, Roy. Met. Soc. Quarterly Jr. **55**, 1 (1929).

X-RAY DIFFRACTION IN WATER: THE NATURE OF MOLECULAR ASSOCIATION

By G. W. Stewart
Department of Physics, University of Iowa

(Received November 24, 1930)

Abstract

The x-ray diffraction intensity-angle distribution for water and its variation for a temperature of 2° to 98° C, are given. Two important periodicities of 3.24 and 2.11A and a third of 1.13A at 21°C are established in satisfactory agreement with Meyer. The first one *decreases* with increasing temperature and the second *increases*.

It is shown that the conception of molecular complexes explains neither the existence of these periodicities nor their change with temperature. In fact, the description of "association" that involves complexes of two or three or more molecules, should be abandoned in favor of the molecular group conception, (cybotactic condition) emphasized by the author. These groups of molecules containing hundreds and perhaps thousands of molecules in each, have a temporary existence as individuals, have ill-defined boundaries, possess an optimum size and an internal regularity determined by the temperature and molecular forces, and expand anisotropically. The experimental facts are in agreement with this view. A detailed description of the molecular arrangement in water from x-ray data is not at present possible yet it simulates the crystal arrangement in ice. A mathematical treatment of the forces within and between the molecules in such groups can probably be studied with much profit only from the quantum viewpoint.

THE nature of water has received a great deal of attention, not merely because it is the most important liquid, but because its physical properties are unusual. The present paper is not an attempt to discuss the various theories[1] concerning the constitution of water. Its purpose is to give the results of x-ray diffraction studies and to emphasize the conclusions directly toward which these studies, as well as those of other liquids, seem to point.

The examination of crystals by x-rays has shed distinctly new light upon the structure of the solid state. Its method of examination is simple and direct, being based upon both classical and quantum theories, and there seems no doubt but that the space periodicities of concentration obtained by the applications of Braggs' law is correct. During the past few years many liquids have been examined by x-ray diffraction and the conclusion is becoming increasingly strengthened that here, too, the space periodicities may be determined.[2] Indeed, these periodicities, which are clearly made evident by the diffraction experiments, seem to be caused by an approximately orderly space array of molecules in small groups having ill-defined boundaries and temporary individual existence. These groups are not sparsely distributed, but occupy the greater portion of the volume, as can be shown

[1] For a resumé see H. M. Chadwell, Chemical Reviews 4, 375 (1927).
[2] See Stewart, Phys. Rev. 35, 726 (1930).

by a comparison of intensity in the liquid and powdered crystal state.[3] Their magnitude appears to be of the order of hundreds or thousands of molecules, but no exact measurement has been made. The closest approach to such a measurement at present is contained in the experiments of McFarlan[4] which show that an electric field will produce increased orientation of molecules of nitrobenzene to an extent that is far greater than would be expected from the orientation of independent molecules. The effect is so small that computations should perhaps await further data.

Experimental Results

A full description of the apparatus and precautions may be found[5] in an earlier article. The Mo$K\alpha$ doublet radiation was used, being partially isolated by the use of a zirconium oxide filter. In Fig. 1 is shown an x-ray diffraction intensity-angle curve for powdered crystals of triphenylmethane. This shows, because of the comparative isolation of the line at 9°, the small amount of

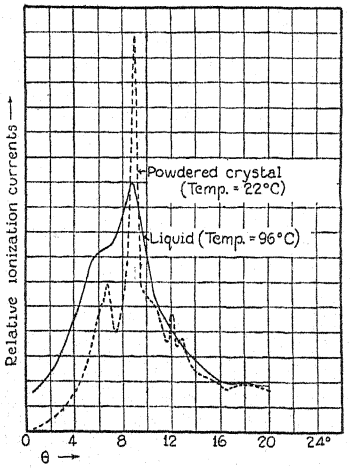

Fig. 1. X-ray diffraction curves for equal masses per unit area of triphenylmethane in liquid and powdered crystal forms.

general Mo$K\alpha$ radiation present. The general radiation is in evidence in the general elevation of the crystal curve. The maximum in the general radiation is about 6°, but the errors caused thereby, as indicated by Fig. 1 are small. A higher voltage would probably increase the general radiation to an undesirable extent. It is also to be borne in mind that the thickness of the specimen of water used was less than 1 cm or less than the optimum thickness. By this second precaution any accentuation of the general radiation by differential absorption is avoided.

[3] For example, see Fig. 1 wherein the same mass of material is used. The integral intensity in the liquid case is comparable to that of the solid.

[4] R. L. McFarlan, Phys. Rev. **35**, 12 (1930).

[5] Stewart and Morrow, Phys. Rev. **30**, 232 (1927).

Fig. 2 shows the uncorrected results of Meyer[6] by the broken line and those of the author by a continuous line. Meyer used a strictly monochromatic radiation obtained by crystal reflection. When the corrections of Meyer are made the alterations occur chiefly at the larger angles. Meyer's method was that of photography while that of the author was the ionization effect. Meyer used a stream of water and the author a thin walled glass tube as a receptacle. His monochromatic radiation gives his curve the greater quantitative weight.

Earlier diffraction experiments with water give the results presented in a foot note.[7] But none had found more than one peak until the careful work of Meyer just cited.[8]

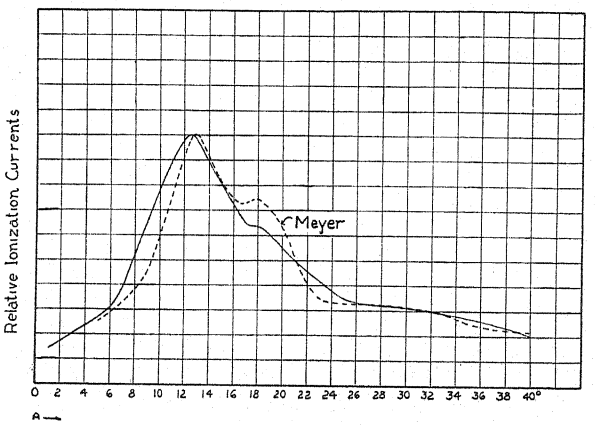

Fig. 2. Diffraction intensity of water, giving comparison of Meyer's uncorrected monochromatic curve with that of the author's. Temperatures 20° and 21°C respectively.

Fig. 3 presents the results for the change in temperature from 2° to 98°C. The tube was heated by hot (and cold) air blasts in such a manner as to prevent the introduction of any scattering material in the path of the x-rays. The temperature as given is correct to within 1.5°C throughout the entire range.

An additional experimental result must be mentioned, though it is not presented in detail because used only as a check experiment on known data. Diffraction curves were obtained with powdered ice, produced by plunging

[6] H. H. Meyer, Ann. d. Physik **5**, 701 (1930).

[7] Sogani, Ind. Jl. Physics I, **IV**, 357 (1927), has one value, 3.27A; Krishnamurti, Ind. Jl. Phys. II, **IV**, 491 (1928) has one value, 3.26A; Keesom in Physica,' p. 118 (1922) and Keesom and de Smedt, Proc. Royal Soc. Amsterdam, **25**, 118 (1922) and **26**, 112 (1923) give the values 3.05A in the first two references and 3.04A in the last. Prins Zeits. f. Physik **56**, 617 (1929) gives one value, 3.1A. He raised the temperature to 80°C with no noticeable alteration.

[8] The author's experimental work preceded the publication of that of Meyer. The former was presented at the April, 1930 meeting of the American Physical Society and described by abstract only in the June 1, 1930 number of the Physical Review. Probably Meyer's article appeared in print a little later, the number of the Annalen reaching the author on July 29th, 1930, but Meyer's work was described in full at that time.

the glass tube receptacle in liquid air. The diffraction curves for two samples were in fair agreement and showed relatively prominent lines at approximately 10.5°, 11.7°, 18° and 19.5°. Dennison[9] used a Mo target and zirconium filter and found the most prominent lines to be at (1) 11.16°, (2) 19.86°, (3) 11.88° and 30.2°, (4) 15.3° and 27.16°, (5) 10.44° and 18.12° and 21.38°, the relative values being 10, 5, 2, 1.5, and 1, respectively. It will now be seen that the liquid peaks at 12.5°, 19° and 31° in Fig. 3 correspond approximately with the most intense lines found by Dennison in an extended in-

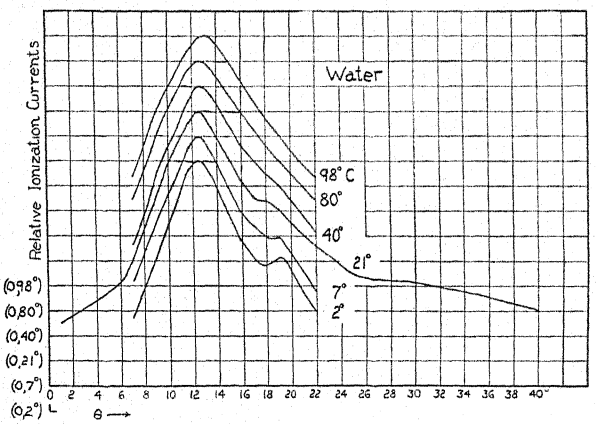

Fig. 3. Displaced diffraction intensity curves of water at different temperatures.

vestigation, and by the author in the brief tests described, in the same apparatus as was used for water. In this approximate correspondence of liquid to solid state H_2O does not differ from other compounds.[10] For example, see the liquid and crystal curves compared in Fig. 1. In case of no substance yet tried do the peaks of a liquid exactly correspond with the lines of the solid, and the difference is not a temperature one. It is evident that such periodicities as are found in the liquid state have strong quantitative similarity to the most important of those in the solid state.

Conclusions

There are several conclusions to be made directly from Fig. 3 and the foregoing assuming that Bragg's diffraction law gives the distances of separation in the periodicities represented by the peaks. Further, it is simplest to assume that these distances, 3.24, 2.11 and 1.13A, corresponding respectively to angles 12.5°, 18.8° and 31.0° of Fig. 2, or, at least the first two, correspond to molecular separations. This assumption is in accord with experiments with other liquids and with the similarity of liquid to solid state. H. H. Meyer gives as his results at 20°C, 3.13, 2.11 and 1.34A. With the assumptions cited, the conclusions are as follows:

[9] Dennison, Phys. Rev. **17**, 20 (1921).

[10] See list of eight liquids given by Krishnamurti, Ind. Jl. Phys. III, **II**, 225 (1928). The present author has tested three additional ones.

1. The distance between molecules (scattering centers) represented by the most prominent peak decreases with temperature, whereas the distance corresponding to the next most important peak seems to increase. H. H. Meyer gives a decrease for the former of 0.0018A per °C, whereas our results show 0.0014A. He obtains a constant position for the second peak.

2. The second peak disappears with increasing temperature. H. H. Meyer showed at 40°C a reduction to two-thirds the value at 3°C.

3. The breadth of the large peak increases with increase in temperature.

4. There is a quantitative similarity between the periodicities found in the liquid and the three most prominent periodicities found in powdered ice.

A few years ago the reader might have concluded at once from Fig. 3 that therein is additional evidence of the complexity of the molecules and of the disappearance of one or more complexes with increasing temperature. But the evidence of to-day would indicate at once the incorrectness of this position. For x-ray diffraction experiments indicate that when two liquids are completely miscible in the proportions used, the marked periodicity found in the solution is not that of either constituent alone, but distinctly of the solution. This has been shown by Krishnamurti[11] with glycerine, ethyl alcohol and lactic acid in an aqueous solution. Meyer[12] used solutions of n-ethyl alcohol and methyl cyclohexane, n-butyl alcohol and orthodimethyl cyclohexane, quinoline and phenol, cyclohexane and tetranitromethane and phenol and water. As an illustration of results, each of the first four mixtures used by Meyer showed but a single periodicity and this was intermediate between the periodicities of the liquids examined separately. These mixtures were totally misicble. The phenol-water mixture showed the same effect when not an emulsion. As an emulsion the two peaks of the constituents were found. The evidence shows that, without exception, two liquids, totally miscible, in solution will show a grouping of molecules (a periodicity) that is not that of either one. It is, therefore, highly probable that, if there were two "complexes" in the water in our present experiment, they would be totally miscible and would not show their individual periodicities. Hence, we may safely conclude that the two peaks in the water diffraction curve correspond to periodicities of *one kind of molecular grouping and one kind only*. The complex molecule interpretation suggested at the beginning of this paragraph is not, therefore, tenable. Moreover, it cannot be claimed that the diffraction peaks with ice indicate several complexes. They correspond to the periodicities in one molecular grouping, one crystal structure. Yet the liquid peaks have a striking similarity that is not explained by the introduction of several complexes but rather, as in ice, by periodicities in one grouping.

Langmuir[13] pointed out a number of years ago that liquids are very much more nearly like solids than like gases. Consider density, compressibility, temperature expansion, specific heats, refractive indices, other

[11] P. Krishnamurti, Ind. Jl. Physics **III**, 331 (1929).

[12] A. W. Meyer, not yet published in full; abstract, Phys. Rev. **35**, 291 (1930).

[13] Langmuir, Jl. Am. Chem. Soc. **39**, 1848 (1917).

optical properties, etc. The only essential difference between liquids and solids is that of fluidity. This one difference has had much to do with the hasty conclusion, held for many years, that the arrangements of molecules in a liquid are as irregular as in a gas. Now we learn from x-ray diffraction experiments that the liquid does have a crude regularity in multitudinous groups, an irregularity of orientation of these groups, and an irregularity of molecules between these temporary groups. With this view it would appear that the simple explanation of molecular association is the association in groups of a relatively large number of molecules and not in complexes consisting of two, three, etc., molecules. The number of molecules in a cybotactic group has not been determined, but one would expect it to be from several hundred to several thousand. Fig. 1 shows that these groups give as much scattering as powdered crystals of the same mass. The groups must therefore be practically everywhere present.

The physical chemist introduced the conception of complexes to account indirectly for the data of vapor pressure, boiling point, latent heat, viscosity, surface tension, etc.[14] But the study of crystals points very clearly to a similarity of crystal forces and internal molecular forces, and gives ample reason to expect that liquid molecules in groups as described must act differently than molecules that are more nearly free as in a gas. Consequently, what formerly has been attributed to forces between molecules in a complex are now seen to be the forces within the groups causing the regularity of arrangement.

Arrangement of molecules in the groups. In order to make the description of "association" more definite, a brief discussion will be given of the present status of the group arrangements.

The arrangement of polarized molecules is not, for example, as suggested illustratively by Debye,[15] the minimum potential configuration of two spheres (molecules) with idealized doublets of infinitesimal length at the centers, thus forming a double molecule with axes of the two doublets in line joining the centers of the spheres. Neither is the arrangement determined solely by the electrical effect of the doublets. With reference to the first point, the experiments in n-alcohols,[16] isomers of n-alcohols,[17] and normal saturated fatty acids,[18] show that when the OH or OOH group is at the end of the chain two groups are adjacent in two molecules having their chain lengths lying in the same straight line. That is, the molecules are arranged head to head (the polarized group) and tail to tail in parallel lines continuing over a group of molecules. The doublets appear at the heads and not centered in the molecule. Moreover, the head to head junction is arranged in an orderly manner with other such junctions in the adjacent parallel lines, so

[14] See Turner "Molecular Association" Longmans, Green and Co., 1915 and Longinescu, Chem. Review **4**, 381 (1929).

[15] Marx Handbook der Radiologie **VI**, 597 (1925).

[16] Stewart and Morrow, Phys. Rev. **30**, 232 (1927).

[17] Stewart and Skinner, Phys. Rev. **31**, 1, (1928).

[18] Morrow, Phys. Rev. **31**, 10 (1928).

that their location forms a definite longitudinal periodicity recognized by x-ray diffraction. The planes associated with these junctions are not normal to the chain lengths. When the polarized OH group is attached not at the end of a chain but removed therefrom by at least one carbon atom,[19] then the double arrangement disappears and the longitudinal periodicity referred to now occurs at a distance corresponding to the length of one molecule and the associated planes are normal to the chain lengths. At the same time the periodicity caused by parallel arrangement of molecules remains. It is to be noticed in the above pictures, we do not have double molecules and the association is that in a group, indeed, similar to the situation in a crystal. The original papers should be consulted for the evidence of the longitudinal grouping and the interpretation of it. So far the grouping (or association) may appear to be regarded as caused primarily by the electrical forces of the doublets. But this is not correct, for it does not account in general for the parallelism of chain molecules. A direct experiment is with n-paraffins.[20] Here the molecules lie parallel and yet they are unpolarized.[21] We are dealing with other intermolecular forces than those due to doublets. In geometric language the "shape" determines the grouping to no small extent. With the paraffins there is no periodicity in the longitudinal direction as with the n-alcohols, etc., and it is evident that this periodicity of the last named may be regarded as caused by the presence of the doublets.

The detailed arrangement of molecules in other than long chain liquid compounds is not ascertained readily by x-ray diffraction, for the lack of approximately perfect regularity in the groups makes the detectable number of periodicities too small. Thus, in the case of water no further conclusion as to detail can be made than already stated. The periodicities are evidently quantitatively similar to the most prominent ones in ice, but this does not, of course, mean like arrangement.

The above discussion states that what was formerly regarded as the peculiar association of two, three or four molecules, as the case may be, now loses its identity in the orderly group formation of molecules. If this be correct, then, since the values formerly computed for the average number of associated molecules change with temperature, there should be evidence for the alteration of the groups with temperature. This proves to be true. Skinner[22] found with a group of liquids that there were changes in the dimension of the periodicity that could not be accounted for by expansion. Similarly, in Fig. 3, it is shown that one such distance increases with temperature while the other decreases. Since neither isotropic nor anisotropic *expansion* accounts for the effect, it may be assumed that there doubtless may occur temperature changes in the molecular forces caused by alterations in molecular "shape," or essentially in the precise arrangement of atomic centers in the molecule. Skinner also showed that in certain cases the in-

[19] Stewart, Phys. Rev. **35,** 726 (1930).
[20] Stewart, Phys. Rev. **31,** 174 (1928).
[21] R. W. Dornte and C. P. Smyth, Jl. Am. Chem. Soc. **52,** 3546 (1930).
[22] Skinner, Phys. Rev. **36,** 11, 1625 (1930).

tensity of the x-ray halo *increased* with increasing temperature. This also suggests alteration in grouping.

The x-ray study is not the only experimental evidence of such internal alteration. We know, for example, that when there are changes in magnetic moment as occurs, for example, in para-azoxyanisol, there must be internal changes in the molecule.

The group conception, as given above, seems to be in harmony with all the facts. On the other hand, there are good reasons for the abandonment of the theory of complexes. Reference to a recent contribution of G. G. Longinescu,[23] who has been an active contributor in this field, will satisfy the reader upon this point. The most important reason for turning from the older conception is that it has proved unprofitable and does not longer serve any useful purpose in stimulating new contributions. Its extended use has increased the inconsistent results and it has ceased to be even empirically satisfactory.

The new conception here proposed seems to be helpful in several respects. First, it suggests that experiments based upon the theory of complexes will not prove profitable and recommends their abandonment. Second, it states that the secret of association lies in an understanding of those forces, call them chemical or physical as one will, which bind atoms together in a molecule and which cause stable configuration in crystals and unstable arrangement in liquids. If, as at present appears, such an "understanding" will only be had through the development of quantum theory, these forces being studied by the energy levels obtained in radiation and absorption spectra of constituent atoms and molecules, then a physical description of the origin of these forces appears improbable. They will appear to exist only because of atomic and molecular energy levels,[24] and the resulting energy changes. They cannot be understood by distributions of electricity and the application of electrical laws. That has proved unsatisfactory even for the simplest atoms. In any event, the cybotactic group conception of association removes the difficulties inherent in molecular complexes and will prove helpful in a study of the nature of the liquid state.

I desire to express appreciation for the experimental skill of Mr. H. A. Zahl, research assistant, who is responsible for the observations involved in this report, and thanks for a supply of conductivity water to Professor J. N. Pearce of this University.

[23] Longinescu, Chemical Review **6**, 381 (1929). See also J. W. Williams, Chemical Review **6**, 589 (1929) and particularly p. 614 *et. seq.*

[24] See Langer, Phys. Rev. **34**, 92 (1929).

ON THE TRANSFORMATION OF LIGHT INTO HEAT IN SOLIDS. I[1]

By. J. Frenkel
Department of Physics, University of Minnesota

(Received November 25, 1930)

Abstract

Starting from the analogy between a crystal and molecule, it is shown that the electronic excitation, forming the first step in the process of light absorption, is not confined to a particular atom, but is diluted between all of them in the form of "excitation waves," similar to sound waves which are used to describe the heat motion in the same crystal. Owing to the interaction between the atoms the excitation state is split up into substates whose number is equal to the number of atoms n (excitation multiplet). By superposing several excitation waves "excitation packets" can be constructed representing the travelling of the excitation state from one atom to another. To each excitation sub-state there corresponds a definite crystal structure (lattice constant, vibration frequencies) slightly different from that of the normal, and giving rise to slightly different vibrational states. This influence of the excitation on the vibrational states provides an indirect coupling between them, which allows the excitation energy to be shared between a few hundred heat-oscillators with practically no direct coupling nor anharmonicity in a radiationless transition which forms the second state of the process of light absorption.

1. Introduction

In A monatomic gas the transformation of the light energy absorbed by an individual atom into heat, that is into the kinetic energy of the translatory motion, is effected, on the quantum theory, through *a collision of the second kind* of the excited atom with some other (usually unexcited) one. If we now look for the corresponding process in a monatomic solid body, where the heat motion is represented by the vibration of a set of "elastic oscillators" (Debye's waves), we at once meet a grave difficulty. This difficulty consists in the apparent inability of the elastic or heat oscillators, so far as they are assumed to be harmonic and uncoupled with each other, to take up the big quantum of energy stored by the excited atom. This quantum is in fact about 100 times larger than the largest energy quantum of the heat oscillators, corresponding to the ratio between the frequency of the absorbed light and the highest frequency of the heat vibrations. In a radiationless discharge of the excitation energy the latter must therefore be either shared between a great many oscillators, which is impossible if they are uncoupled, or be absorbed by a single oscillator jumping at one time over at least 100 energy levels, which is also impossible if the oscillator is harmonic.

The solution of this difficulty seems at first sight to consist simply in taking account of the actually existing coupling between the different oscil-

[1] This paper is an extension of two previous ones on the absorption of light in gases: see J. Frenkel, Zeits. f. Physik **58**, 798 (1929) and **59**, 198 (1930).

lators and their nonharmonic character. It must, however, be rejected for it leads to extremely small probabilities for transitions of the type considered. In fact in order to get a non-vanishing probability for a transition involving N elementary jumps, either by N oscillators making each an elementary jump, or by a single oscillator making an N-fold jump, one must carry out the expansion of the potential energy of the oscillators as a function of their coordinates (or of the displacements of the atoms from their equilibrium positions) up to terms of the N-th order at least.[2] The terms one would get for $N \leqq 100$, even if this was practicable, would be hardly large enough to account for the effect we are considering.

There seems to be a less trivial and more successful solution of the above difficulty, which is suggested *by the analogy between a crystal (representing a solid body) and a molecule.* The usual selection rule for the vibrational quantum number of a molecule (a diatomic molecule, say), restricting its change to unity, holds for such transitions only, for which the electronic state of the molecule remains unaltered. In case however of a combined transition, for instance of a spontaneous transition from an excited state to the normal one with emission of light, the vibrational quantum number can change by any amount (integral, of course) whatever. It may be noted that this "breach" of the selection rule has nothing to do with the possible presence of nonharmonicity, but depends upon the fact that the character of the vibrations in the normal and excited molecule is quite different.

In applying this consideration to a crystal we have only to develop the analogy between an excited crystal and an excited molecule. At the outset we have pictured an excited crystal as differing from the normal one by the presence of one *definite* excited atom. Now in case of a molecule consisting of two identical atoms the excitation cannot be traced to one of them, but has to be considered as a characteristic of the molecule as a whole. The same must be true with respect to a crystal consisting of any number of identical atoms. We thus see that we must first of all revise our conception of an excited crystal by allowing for the identity of all the atoms, and thereafter investigate the influence of the "electronic state" of a crystal on its vibrational states.

2. Excited States of a Crystal; "Excitation-Waves"

We shall assume that the coupling between different—even neighboring—atoms is small compared with the forces holding the electrons within the separate atoms (thus excluding the case of metallic bodies). We shall further suppose that the atoms—or rather the nuclei—are fixed, that is, we shall neglect their vibratory motion, and shall consider only their inner state, characterized by a function of the coordinates of the electrons with respect to the nucleus. Lastly we shall leave out of account the possibility of interchanging the electrons between different atoms and shall consequently assign to a definite atom a definite group of electrons whose coordinates (relative

[2] See below, Section 4.

to the nucleus) will be represented for the sake of brevity by the number of the respective atom $(1, 2, \cdots, n)$.

Then if ψ_{I} and ψ_{II} are the wave functions representing the normal and the excited state of an *isolated* atom, the stationary states of a system of n atoms, of which one is excited and the rest normal, will be represented to a first approximation by a linear aggregate of n factorial functions,

$$\begin{aligned}
\phi_1 &= \psi_{\mathrm{II}}(1)\psi_{\mathrm{I}}(2)\psi_{\mathrm{I}}(3)\cdots\psi_{\mathrm{I}}(n)\\
\phi_2 &= \psi_{\mathrm{I}}(1)\psi_{\mathrm{II}}(2)\psi_{\mathrm{I}}(3)\cdots\psi_{\mathrm{I}}(n)\\
&\cdots\cdots\cdots\cdots\\
\phi_n &= \psi_{\mathrm{I}}(1)\psi_{\mathrm{I}}(2)\psi_{\mathrm{I}}(3)\cdots\psi_{\mathrm{II}}(n)
\end{aligned} \tag{1}$$

with properly chosen coefficients $c_1, c_2, \cdots, c_n$. We have here a particular case of an "exchange degeneracy," which I have already considered previously[3] and which is somewhat similar to the exchange degeneracy met with in the problem of a single electron with n fixed identical nuclei.[4]

There are, as is well known, just n *sets* of coefficients $(c_1, c_2, \cdots, c_n)$, corresponding to the splitting up of the undisturbed state of n isolated atoms with the total energy $W_{\mathrm{II}}+(n-1)W_{\mathrm{I}}$ into n different states, whose energies differ from the preceding value by small amounts W'. These n states will be denoted as the "excitation multiplet" of the crystal. The values of W' for the different components of such a multiplet ("$W'=W_r'$) and the corresponding values of the coefficients $c_l(=c_{rl})$ are determined by the equations

$$\sum_{l=1}^{n} U_{kl}c_l = W'c_k \tag{2}$$

where U_{kl} are the matrix elements of the mutual potential energy of all the atoms U with respect to the functions (1).

Now U must reduce to the form

$$U = \sum_{\alpha<\beta} U(\alpha, \beta; R_{\alpha\beta}) \tag{3}$$

where $U(\alpha, \beta; R_{\alpha\beta})$ is the mutual potential energy of the atoms α and β and $R_{\alpha\beta}=R_{\beta\alpha}$ their distance apart (or rather the distance between the respective nuclei). One has obviously $U(\alpha, \beta; R_{\alpha\beta})=U(\beta, \alpha; R_{\alpha\beta})$. One must not conclude however from this symmetry relation that $U(1, 2, \cdots, n)$ is a symmetrical function of the respective arguments. Interchanging two arguments say 1 and 2—which corresponds eventually to an interchange of the excitation state between the atoms 1 and 2—*we must keep the distances $R_{\alpha\beta}$ fixed*, so that the new energy function obtained by such an interchange is substantially different from the original one.[5]

[3] Zur Theorie der Resonanzverbreiterung von Spektrallinien, Zeits. f. Physik **59, 198** (1930).

[4] This problem is treated in Bloch's theory of metallic conductivity.

[5] The theory can be easily extended to account for the interchanging of the electrons between different atoms. In the simplest case of one electron per atom we have but to replace

Taking into account the orthogonality and normality conditions for the functions ψ_I and ψ_{II},

$$\int \psi_I(\alpha)\psi_{II}^*(\alpha)d\tau_\alpha = 0, \quad \int \psi_I(\alpha)\psi_I^*(\alpha)d\tau_\alpha = \int \psi_{II}(\alpha)\psi_{II}^*(\alpha)d\tau_\alpha = 1,$$

we easily obtain from (3) if $k \neq l$:

$$U_{kl} = \int \cdots \int U\phi_k^*\phi_l \; d\tau_1 \cdots d\tau_n = V_{kl} \tag{4}$$

where V_{kl} is a *function of the distance* R_{kl} *alone* given by

$$V_{kl} = \int\int U(k, l; R_{kl})\psi_{II}^*(k)\psi_I(k)\psi_I^*(l)\psi_{II}(l)d\tau_k d\tau_l \tag{4a}$$

It may be remarked that it is in general complex and therefore different from $V_{lk} = V_{kl}^*$.

For $k = l$ we get

$$U_{kk} \equiv V_{kk} = \sum_{l \neq k} \overline{V}_{kl} \tag{5}$$

where

$$\overline{V}_{kl} = \int\int U(k, l; R_{kl}) \left| \psi_{II}(k) \right|^2 \left| \psi_I(l) \right|^2 d\tau_k d\tau_l \tag{5a}$$

may be defined as the average value of the mutual energy of the atoms k and l when one of them is in the normal and the other in the excited state. This is also of course a function of the distance R_{kl} only; it is moreover symmetrical with respect to k and l.

The equations (2) are very similar to those which determine the normal modes of vibration of a system of coupled classical oscillators with one degree of freedom each; in fact we have but to consider the coefficients c_k as the amplitudes of these oscillators and to replace the energies W' by the square of the classical frequencies (multiplied by a properly chosen proportionality factor). The matrix elements $U_{kl}(k \neq l)$ can be then interpreted as the coupling coefficients (since they actually depend upon the distance of the

---

the functions (1) by the following ones which are antisymmetrical with respect to all the electrons.

$$\phi_1 = \frac{1}{n!^{1/2}} \begin{vmatrix} \psi_{II}(1,1), & \psi_{II}(1,2), & \cdots \psi_{II}(1,n) \\ \psi_I(2,1), & \psi_I(2,2), & \cdots \psi_I(2,n) \\ \cdots & \cdots & \cdots \\ \psi_I(n,1), & \psi_I(n,2) & \cdots \psi_I(n,n) \end{vmatrix}, \quad \phi_2 = \frac{1}{n!^{1/2}} \begin{vmatrix} \psi_I(1,1), & \psi_I(1,2) & \cdots \psi_I(1,n) \\ \psi_{II}(2,1), & \psi_{II}(2,2) & \cdots \psi_{II}(2,n) \\ \cdots & \cdots & \cdots \\ \psi_I(n,1), & \psi_I(n,2) & \cdots \psi_I(n,n) \end{vmatrix}$$

etc. where $\psi_I(k, l)$ and $\psi_{II}(k, l)$ denote the wave functions of the atom formed by the association of the l-th electron to the k-th nucleus, in the normal and excited state respectively. Similar, though somewhat more complicated, results are obtained in the general case of several electrons per atom.

The case of two electrons with all the atoms being in the normal state has been recently treated by E. Hylleraas, Zeits. f. Physik **63**, 771 (1930) in connection with the theory of the cohesive forces in a (non-excited) crystal of sodium hydride.

respective oscillators only), and the U_{kk} as the coefficients of the quasi-elastic forces for the uncoupled oscillators.

Until now the positions of the atoms have remained unspecified. We shall now assume that the nuclei are fixed at the lattice points of the crystal, neglecting the displacements due to the vibratory motion. We shall further assume that the crystal has a rectangular form (or the form of a parallelepiped whose edges are parallel to the crystalline axes). The normal modes of vibration for this case are well known. They do not depend upon the shape of the functions $V_{kl}(R_{kl})$ nor upon the value of the constant $V_0 = V_{kk}$, thus coinciding with respect to the position of the nodal planes with the acoustic or elastic vibrations (for which $V_0 = 0$). These vibrations can be described as *standing waves* with the wave-number components[6]

$$g_1 = \pm r_1/2a_1, \quad g_2 = \pm r_2/2a_2, \quad g_3 = \pm r_3/2a_3 \tag{6}$$

where a_1, a_2, a_3 are the edges of the crystal and r_1, r_2, r_3 numbers specifying the mode of normal vibrations and taking all integral values between 0 and n_1-1, n_2-1, n_3-1, respectively, n_i being the number of atoms along the i-th edged $(n = n_1 n_2 n_3)$.

The triplet $(r_1 r_2 r_3)$ replaces the number r which was introduced to specify the various solutions of the equations (2). The single numbers k and l must be replaced accordingly by triplets $(k_1 k_2 k_3)$, $(l_1 l_2 l_3)$ which may be associated with definite "oscillators," that is definite atoms of the lattice. It may be remarked that the coefficient c_k in (2) refers to that function ϕ_k in (1) which ascribes the excited state to the atom k. The solutions of the equations (2) can now be put in the form

$$c_{r_1,r_2,r_3;k_1,k_2,k_3} = A_{r_1 r_2 r_3} \cos \frac{\pi\delta}{a_1} k_1 r_1 \cos \frac{\pi\delta}{a_2} k_2 r_2 \cos \frac{\pi\delta}{a_3} k_3 r_3 \tag{7}$$

where δ is the lattice constant (for the sake of simplicity the lattice will be pictured as cubical), and $k_1\delta = x_1$, $k_2\delta = x_2$, $k_3\delta = x_3$ the rectangular coordinates of the atom to which the excited state is assigned by the function $\phi_{k_1 k_2 k_3}$. $A_{r_1 r_2 r_3}$ is a normalization coefficient determined by the condition that the integral of the square of the function

$$\chi_{r_1 r_2 r_3}(1, 2, \cdots n) = \sum_{k_1 k_2 k_3} c_{r_1,r_2,r_3;k_1,k_2,k_3} \phi_{k_1 k_2 k_3}(1, 2, \cdots n) \tag{7a}$$

representing the r-th stationary state of the excited crystal (the r_1, r_2, r_3 component of the "excitation multiplet") over the configuration space of all the electrons should be equal to 1.

The energies $W'_{r_1 r_2 r_3}$ of the different states (with respect to the unperturbed energy $W_{II} + (n-1)W_I$) are given directly by substituting in the equations (2) the values (7) of the coefficients c. Since the matrix elements U_{kl} depend only upon the differences $k_1 - l_1$, $k_2 - l_2$, $k_3 - l_3$ one can put $k_1 = k_2 = k_3 = 0$ which gives

$$A_r W_r' = \sum_l U_{0l} c_{rl}$$

[6] The wave number is the reciproal of the wave-length; it is a vector parallel to the direction of the propagation of the waves.

or more fully written

$$W'_{r_1r_2r_3} = \sum_{l_1} \sum_{l_2} \sum_{l_3} U_{000,l_1l_2l_3} \cos \frac{\pi\delta}{a_1} l_1 r_1 \cos \frac{\pi\delta}{a_2} l_2 r_2 \cos \frac{\pi\delta}{a_3} l_3 r_3 \qquad (8)$$

With increasing values of $l_1l_2l_3$, that is with increassing distance $R_{0l} = \delta(l_1^2 + l_2^2 + l_3^2)^{1/2}$, the values of $H'_{000l_1l_2l_3}$ must in general decrease very rapidy. The summation in (8) can be therefore extended practically over all values of the l_i from $-\infty$ to $+\infty$. If the mutual action of neighboring atoms only (with smallest distance apart $R = \delta$) is taken into account, (8) reduces to

$$W'_{r_1r_2r_3} = V_0 + 2V_1\left(\cos\frac{\pi\delta}{a_1} r_1 + \cos\frac{\pi\delta}{a_2} r_2 + \cos\frac{\pi\delta}{a_3} r_3\right) \qquad (8a)$$

where V_1 is the value of (4a) for neighboring atoms and V_0 six times the value of (5a) for the same atoms. The latter value is the average of the mutual potential energy between an excited and an unexcited atom, whereas V_1 has the character of an "exchange energy" which has no classical analogue.

Each stationary state of an excited crystal can be described as a "standing excitation wave" defined by (7) or by

$$c(x_1x_2x_3) = A \cos 2\pi g_1 x_1 \cos 2\pi g_2 x_2 \cos 2\pi g_3 x_3 e^{-2\pi i\nu' t}$$

where $\nu' = W'_r/h$, $x_i = \delta l_i$. Such a standing wave can be obtained by superposing eight "progressive excitation waves" of the type

$$(A/8)e^{2\pi i(g_1x_1 + g_2x_2 + g_3x_3 - \nu' t)}$$

which represent the propagation of the probability for finding the excitation localized in a certain plane of the crystal. By superposing a number of such waves with slightly different values of g_1, g_2, g_3 (that is with slightly different directions of propagation and frequencies $\nu' = w'/h$) it is always possible to construct a wave-packet which will represent the excitation being concentrated in a definite atom or its neighborhood (according to the usual picture). The group velocity of such an "excitation-packet" may be determined by the relations

$$v_i = \partial\nu'/\partial g_i (i = 1, 2, 3). \qquad (9)$$

Putting

$$h\nu' = V_0 + 2V_1(\cos 2\pi g_1\delta + \cos 2\pi g_2\delta + \cos 2\pi g_3\delta)$$

according to (8a) and (6), we get

$$v_i = -\frac{4\pi\delta V_1}{h} \sin 2\pi g_i\delta. \qquad (9a)$$

For small values of g_i that is for long "excitation waves" this expression reduces to

$$v = -\frac{8\pi^2\delta^2 V_1}{h} g \qquad (9b)$$

that is the group velocity is approximately proportional to the wave number. It has in general the same direction so long as the "exchange energy" V_1 is negative. It reaches its maximum value $v \cong 4\pi\delta \,|\, V_1 \,|/h$ for wave-lengths equal approximately to four times the interatomic distance δ. For $\lambda \cong 2\delta$ it falls down to zero and for still shorter wave-lengths becomes opposite to the direction of the wave propagation.[7]

To get a better understanding of the nature of the "excitation waves" it will be well to consider the process corresponding to them in the older quantum theory and in the classical theory. According to the former the exitation energy of an atom can and in fact must be transmitted to one of the other atoms of the same sort either by emission and (resonance) reabsorption, of light or directly in a non-radiative process. The closer the atoms are together, the larger must be the probability of such a non-radiative transmission, that is, the larger the velocity with which the "excited state" will travel from one place to the other. This is expressed by the fact that the group velocity, according to (9a), is proportional to the exchange energy V_1. The ratio $\delta/v_{\max}$ which is of the order of magnitude of h/V_1 can be considered as the shortest time that the excitation remains confined to one definite atom.[8]

From the point of view of the classical theory an atom has to be considered as a harmonic oscillator, whose normal state is that of rest. The energy of the free oscillations, replacing the excitation energy, instead of being concentrated in one single atom (or a small number of them in the general case) has to be distributed here in a more or less uniform manner over all the atoms, each of them possessing accordingly but a very small energy. The excitation waves can be represented in this case by the familiar waves of the electric polarization with exactly the same wave-numbers as has been actually done above in the discussion of the equation (2).[9] It should be noticed however that in the classical theory of the propagation of such waves the interaction between the atoms is considered to be a radiative one, that is proportional to their dipole moment and inversely proportional to the distance, whereas in the wave mechanical theory we are developing this interaction considered as a much more powerful non-radiative (electrostatic) one.[10]

[7] These results are wholly analogous to those implied in Bloch's theory of the electrical conductivity of metals and discussed by R. Peierls.

[8] In case of two atoms h/V_1 is just equal to the time in which the excited state oscillates from one atom to the other.

[9] The situation becomes more complicated if instead of one excited atom we consider the case of two or more excited atoms. cf. J. Frenkel, Zeits. f. Physik 59, 198 (1930) in particular footnote on p. 203.

[10] Cf. G. Breit and E. O. Salant, Phys. Rev. 36, 871 (1930). This paper dealing with the propagation of light in solids contains some results of the present section.

3. The Influence of Excitation on the Geometric and Elastic Properties of a Crystal and its Vibratory Motion

We can now turn to the examination of the influence which an excited state of a crystal (that is a definite component of an excitation multiplet) exerts upon the heretofore neglected vibratory motion of the atoms. The exact way to deal with this question would be to consider simultaneously the "inner" and the "outer" (that is, vibratory) motion of the atoms. But this way is hardly practicable even in the simplest case of a diatomic molecule, and we shall therefore use an approximate method of the same sort which is applied in Debye's theory of specific heats to the determination of the normal vibrations corresponding to the unexcited state.

A normal vibration is described here by a system of standing sound waves of just the same geometrical type as that used in the preceding paragraph to describe the excitation states. It can be thus characterized by specifying the components of the wave-number according to the equations (6) which we shall rewrite in the form

$$g_1' = \pm r_1'/2a_1, \quad g_2' = \pm r_2'/2a_2, \quad g_3' = \pm r_3'/2a_3 \tag{10}$$

the primes serving to distinguish the sound waves from the excitation waves.[11]

The frequency of the vibrations ν' can be determined from the equation

$$\nu' = g'u \tag{11}$$

where u denotes the *velocity of sound*, which is considered as independent of g'. The velocity of sound can be calculated by means of the formula

$$u = (\kappa/\rho)^{1/2}$$

where ρ is the density of the crystal, and κ its elastic modulus, which has different values for the longitudinal and the transverse vibrations.

Now in order to determine κ from atomic data we must consider the vibrationless state of the crystal and compare its energy in the equilibrium state with the energy corresponding to a slightly compressed (or expanded) state in the case of κ_{long} or to a slightly distorted state in the case of κ_{trans}.

Denoting the volume of the crystal with v and its energy—that is the mutual potential energy of all its atoms—in the normal (non-excited) state with W_0 we have, expanding W_0 in a power series with respect to the increment of volume $v-v^0$ ($v^0=v$ in the equilibrium state)

$$W_0 = W_0{}^0 + \frac{1}{2}\left(\frac{\partial^2 W_0}{\partial v^2}\right)^0 (v - v^0)^2.$$

The second term represents the elastic energy

$$\tfrac{1}{2}\,\kappa_0(v-v^0)^2 \cdot v^0$$

[11] We shall drop the primes later on when there will be no danger of confusing the sound waves with the excitation waves.

whence it follows

$$\kappa_0 = v_0{}^0\left(\frac{\partial^2 W_0}{\partial v^2}\right)$$

or putting $v = n\delta^3$

$$\kappa_0 = \frac{\delta_0{}^2}{9}\,\frac{1}{v_0{}^0}\left(\frac{\partial^2 W_0}{\partial \delta^2}\right)^0 = \frac{1}{9n\delta_0}\left(\frac{\partial^2 W_0}{\partial \delta^2}\right)^0. \tag{13}$$

This formula determines the modulus of compressibility for the normal (unexcited) state of the crystal—as denoted by the subscript zero—and hence according to (12) and (11)[12] the frequency of the vibrations associated with this state. It may be remarked that the corresponding equilibrium value of $\delta = \delta_0{}^0 = \delta_0$ is given by the equation $(\partial W_0/\partial v)^0 = 0$ or

$$(\partial W_0/\partial \delta)^0 = 0 \tag{13a}$$

and that δ_0 is related to the density $\rho = \rho_0$ by means of

$$\rho_0 = m/\delta_0{}^3 \tag{13b}$$

m being the mass of an atom.

The above method can now obviously be applied to the determination of the vibrations associated with an excited state of the crystal. To do this we have but to replace in the preceding formulae the energy W_0 by the energy $W_r = W_0 + W'_r$ of one of the components of the excitation multiplet. In this way we shall get for the lattice constant of the crystal δ_r its density ρ_r and its elastic modulus κ_r values depending upon the character of the excitation substate and slightly different from those corresponding to the normal one.

Since the difference $\delta_r - \delta_0 = \Delta\delta_r$ is very small, we have to a first approximation

$$\left(\frac{\partial W_r}{\partial \delta_r}\right)^0 = \left(\frac{\partial W_0}{\partial \delta}\right)_{\delta=\delta_0} + \left(\frac{\partial^2 W_0}{\partial \delta^2}\right)_{\delta=\delta_0} \Delta\delta_r + \left(\frac{\partial W_r'}{\partial \delta}\right)_{\delta=\delta_0} = 0,$$

whence since the first term vanishes (according to 13a)

$$\Delta\delta_r = -\frac{\partial W_r'}{\partial \delta} \Big/ \frac{\partial^2 W_0}{\partial \delta^2} \quad (\delta = \delta_0) \tag{14}$$

The energy W_0 is proportional to the number of atoms n, whereas W'_r according to (8) or (8a) depends upon it in a practically unimportant way. Putting in (8a)

$$a_1 = n_1\delta, \quad a_2 = n_2\delta, \quad a_3 = n_3\delta$$

(where $n_1 n_2 n_3 = n$) we have

$$W_r' = V_0 + 2V_1\left(\cos\frac{\pi r_1}{n_1} + \cos\frac{\pi r_2}{n_2} + \cos\frac{\pi r_3}{n_3}\right) \tag{15}$$

and consequently

$$\Delta\delta_r = -\frac{\partial V_0}{\partial \delta} \Big/ \frac{\partial^2 W_0}{\partial \delta^2} - 2\left(\cos\frac{\pi r_1}{n_1} + \cos\frac{\pi r_2}{n_2} + \cos\frac{\pi r^3}{n_3}\right)\frac{\partial V_1}{\partial \delta} \Big/ \frac{\partial^2 W_0}{\partial \delta^2} \tag{15a}$$

which is of the order of magnitude of $1/n$, since V_1 does not depend upon n.

[12] In the case of longitudinal vibrations.

In the same way we get from (13)

$$\Delta\kappa_r = \kappa_r - \kappa_0 = \frac{2}{9\delta n}\left[\frac{\partial^2 V_0}{\partial\delta^2} + 2\left(\cos\frac{\pi r_1}{n_1} + \cos\frac{\pi r_2}{n_2} + \cos\frac{\pi r_3}{n_3}\right)\right]\frac{\partial^2 V_1}{\partial\delta^2}\cdot \quad (15b)$$

The relative change of $\Delta\kappa_r$ being again of the order of magnitude of $1/n$.

These results seem very natural indeed. We should expect that the change of the geometric and dynamic properties of the crystal lattice, due to the excitation of a few atoms n' depends upon their *relative* number, that is upon the ratio n'/n, which in our case is equal to $1/n$. So long as n' is small compared with n the effects due to the excitation of the separate atoms must obviously behave additively (which would no longer be the case if n' were comparable with n), so that to get the total change of δ or κ we would have but to add the expressions (15a) or (15b) for all the n' excited atoms. It seems however that even with the largest values of n' that can be obtained by illuminating the crystal with intense light of the resonance frequency, the change in the elastic properties will be too minute to be detected by direct measurement.

This change must however manifest itself in an indirect manner by making possible the radiationless transitions of the crystal from an excited state into the normal one with conversion of the excitation energy into that of the vibrational motion, and also of course transitions of the inverse direction, leading to "thermal excitation" of the crystal and corresponding to "inelastic collisions of the first kind" or "activating collisions" in the case of a gas.

4. The Relation between the Variables and Functions describing the Heat Oscillators in the Normal and the Excited Crystal

In order to determine the probability of such transitions we must introduce first of all the "normal coordinates" characterizing the individual heat oscillators, which represent the different modes of vibration (standing elastic waves) of the crystal. Let these coordinates for the unexcited state be denoted by $\xi_1, \xi_2, \cdots \xi_n \cdots \xi_{3n}$ (their number being equal to the number of degrees of freedom); we shall think of the first n as referring to the longitudinal vibrations and the rest to transverse ones.

We have to introduce in the second place the relations between these coordinates and the normal coordinates $\xi_{r1}, \xi_{r2}, \cdots$ which correspond to the r-th excited state. These relations must be derived from the condition that the equilibrium positions of the atoms in the excited state are specified by zero values of the new coordinates ($\xi_{rs}=0$) on the one hand and by definite non-vanishing values $\xi_s = \xi_s^r$ of the old ones on the other.

For the sake of simplicity we shall limit ourselves to the consideration of a *unidimensional* case, that is of a set of n atoms situated on a straight line and capable of moving along this line (that is to perform longitudinal oscillations). Such a set can be conveniently treated as a "bar." In order to allow for the change of length $L=\delta n$ of the bar, due to the excitation of one of its

atoms we shall imagine one of its ends to be fixed and the other free.[13] The normal modes of vibration of such a bar correspond to wave-lengths $\lambda=\lambda_l$ determined by the equation

$$L=\frac{2l+1}{4}\lambda_l=n\delta \tag{16}$$

where $l=0, 1, 2, \cdots n-1$. The displacement Δx_k of an atom whose equilibrium distance from the fixed end is $x_k=k\delta$ can be represented by the sum

$$\Delta x_k=\sum_{l=0}^{n-1}c_{kl}\xi_l \tag{17}$$

where

$$c_{kl}=\gamma\sin\frac{2\pi x_k}{\lambda_l}=\gamma\sin\frac{\pi}{n}\left(l+\frac{1}{2}\right)k \tag{17a}$$

γ being determined by the "normality condition"

$$\sum_{k=0}^{n-1}{}^{2}c_{kl}=1 \tag{17b}$$

and ξ_l denoting the normal coordinate, which characterizes the l-th mode of vibration.

Using the formula

$$\sum_{k=0}^{n-1}e^{i\alpha k}=\sum_{k=0}^{n-1}\cos\alpha k+i\sum_{k=0}^{n-1}\sin\alpha k=\frac{1-e^{i\alpha n}}{1-e^{i\alpha}}$$

which is equivalent to

$$\sum_{k=0}^{n-1}\operatorname{cs}\alpha k=\frac{1+\cos\alpha(n-1)-\operatorname{cs}\alpha n-\operatorname{cs}\alpha}{2(1-\operatorname{cs}\alpha)}=\frac{1}{2}(1-\operatorname{cs}\alpha n)+\frac{\operatorname{sn}\alpha n\operatorname{sn}\alpha}{2(1-\operatorname{cs}\alpha)}$$

$$\sum_{k=0}^{n-1}\operatorname{sn}\alpha k=\frac{\sin\alpha(n-1)-\sin\alpha n+\sin\alpha}{2(1-\operatorname{cs}\alpha)}=-\frac{1}{2}\sin\alpha n+\frac{\operatorname{sn}\alpha(1-\operatorname{cs}\alpha n)}{2(1-\operatorname{cs}\alpha)},$$

we get with the abbreviations $(l+\frac{1}{2})\pi/n=\beta$, $(l'+\frac{1}{2})\pi/n=\beta'$

$$\sum_{k=0}^{n-1}c_{kl}c_{kl'}=\gamma^2\sum_{k=0}^{n-1}\sin\beta k\sin\beta' k=\frac{1}{2}\gamma^2\left[\sum_{k=0}^{n-1}\operatorname{cs}(\beta-\beta')k-\sum_{k=0}^{n-1}\operatorname{cs}(\beta+\beta')k\right]$$

$$=n-1 \text{ if } l'=l \text{ and } (-1)^{l\pm l'+1} \text{ if } l'=l.$$

We thus see that

$$\gamma=(n-1)^{-1/2}$$

and morever that the coordinates ξ_l are *not exactly* orthogonal as they would be in the limiting case $n\to\infty$, $n\delta=L=\text{const.}$

[13] Similar results would be obtained by fixing the middle point of the bar and leaving both ends free and in the opposite phase.

Squaring (17) and summing up with respect to k we have in fact:

$$\sum_{k=0}^{n-1}(\Delta x_k)^2 = \sum_{l=0}^{n-1}\xi_l^2 - \frac{2}{n-1}\sum_{l<l'}(-1)^{l'-l}\xi_l\xi_{l'}.$$

The mutual potential energy of the atoms which in the simplest case is represented by the sum

$$\sum_{k=0}^{n-2}(\Delta x_{k+1} - \Delta x_k)^2$$

also will not be reduced exactly to a sum of squares of the type

$$2\pi^2\sum_{l=0}^{n-1}\nu_l^2\cdot\xi_l^2$$

ν_l being the vibration frequencies, but will contain cross terms vanishing in the limiting case of a continuous bar. The problem of finding the exact normal coordinates that is the exact transformation coefficients c_{kl} in the equations (17) for a given finite value of n is rather complicated and we shall therefore use the "nearly-normal" coordinates defined above.

Since the coefficients c_{kl} do not depend upon the equilibrium spacing between the atoms δ, the same formulae (17) could be used both for the "normal" and for the "excited" bar; it should be remembered however that Δx_k has in both cases a different meaning, the equilibrium position of the k-th atom in the excited state being displaced by $\Delta\delta_r k$ with respect to that corresponding to the normal state. The same position of the atoms which in the normal state is specified by the displacements (17) will be specified from the point of view of the excited state r by the displacements

$$\Delta x_{rk} = \Delta x_k - k\Delta\delta_r = \sum c_{kl}\xi_{rl}$$

whence

$$\sum_{l=0}^{n-1}c_{kl}(\xi_{rl} - \xi_l) = -k\Delta\delta_r.$$

If c_{kl} were the correct transformation coefficients then these equations would be immediately solved by

$$\xi_{rl} - \xi_l = \Delta\xi_{rl} = -\sum_{k=0}^{n-1}c_{kl}k\Delta\delta_r.$$

Introducing here the approximate values

$$c_{kl} = \frac{1}{(n-1)^{1/2}}\sin\frac{\pi}{n}\left(l+\frac{1}{2}\right)k$$

we have

$$\Delta\xi_{rl} = -\frac{\Delta\delta_r}{(n-1)^{1/2}}\sum_{k=0}^{n-1}k\sin\alpha k$$

or

$$\Delta\xi_{rl} \leqq \frac{\Delta\delta_r}{n^{1/2}}\left(\frac{\partial}{\partial\alpha}\sum_{k=0}^{n-1}\cos\alpha k\right)_{\alpha=\pi/n\,(l+1/2)}$$

that is according to the summation formula given above, with $\cos \alpha n = 0$, $\sin \alpha n = (-1)^l$,

$$\Delta\xi_{rl} = (-1)^l \frac{\Delta\delta_r}{2n^{1/2}}\left[n - \frac{1}{1 - \operatorname{cs} \alpha}\right].$$

The second term in the brackets represents probably the error due to the fact that we have been using inexact values for the coefficients c_{kl}. It would have an important influence only in the case of very small values of α corresponding to very long waves.[14]

Dropping it we get finally

$$\Delta\xi_{rl} = (-1)^l \frac{1}{2}\Delta\delta_r n^{1/2} = (-1)^l \frac{1}{2}\frac{\Delta L_r}{n^{1/2}} \tag{18}$$

where $\Delta L_r = n\Delta\delta_r$ denotes the change of length of the whole bar in the r excited state. Since this change is actually due to the presence of one single excited atom, it must be practically independent of the total number of atoms, whence it follows that $\Delta\delta_r$ must be inversely proportional to n, a result which we have derived above from somewhat different considerations for the case of the real three-dimensional crystal. The preceding formula which we can safely extend to this case[15] thus means that the change of the normal coordinates, produced by the excitation of one atom out of n is inversely proportional to the *square root* of n. The coefficient of proportionality $\frac{1}{2}\Delta\delta_r n$ is determined by (15a) and can be shown to be of the order of magnitude of atomic dimensions.

Having established the relation between the normal coordinates of the nonexcited and those of the excited crystal we must now turn to the consideration of the Schrödinger wave functions of the corresponding "heat oscillators." These functions will be denoted by $f_{s,N_s}{}^0(\xi_s)$ for the N_s quantum state of the s-th oscillator in the case of the unexcited crystal and by $f_{s,N_s}{}^r(\xi_{rs})$ in the case of a crystal in the r-th state of an excitation multiplet. The general form of the functions $f_N(\xi)$ is given by the formula

$$f_N(\xi) = [2^N N!(\pi\alpha)^{1/2}]^{-1/2} H_N(\alpha^{1/2}\xi) e^{-1/2\alpha\xi^2} = f_N{}^*(\xi) \tag{19}$$

where H_N is Hermite's polynomial of the N-th degree and α is a constant proportional to the natural frequency of the oscillator ν. If the coordinate ξ is normalized in such a way that the energy of the oscillator is represented by

$$\frac{m}{2}\left[\left(\frac{d\xi}{dt}\right)^2 + 4\pi^2\nu^2\xi^2\right]$$

[14] In this case we should have

$$1 - \cos \alpha \cong \tfrac{1}{2}a^2 = (l + \tfrac{1}{2})^2 \pi/2n^2$$

and

$$c_{kl} \cong (-1)^l \frac{\Delta\delta_r}{n^{1/2}} \frac{n^2}{\pi^2(l + \frac{1}{2})^2}$$

[15] Replacing l by the sum $l_1 + l_2 + l_3$.

then[16]

$$\alpha = 4\pi^2 m\nu/h. \tag{19a}$$

The absolute value of α does not play any role since we can always replace the coordinate ξ by $\eta = \alpha^{1/2}\xi$. If however we have to compare the behavior of the same oscillator for two different values of the frequency parameter $\nu = \nu_0$ and $\nu = \nu_r$ then we must take into account the relative value of α which gives us two different wave functions of the form

$$f_N{}^0(\xi_1) = f_N(\xi_1) \text{ and } f_N{}^{(r)}(\xi_r) = f_N\left[\left(\frac{\nu_{rs}}{\nu_{0s}}\right)^{1/2}\xi_{rs}\right]. \tag{20}$$

The function $f_N(\xi)$ can be defined here and in the sequel by formula (5) with $\alpha = 1$.

5. Determination of the Probability of the Individual Transitions of a Crystal from the Excited to the Normal State (or *vice versa*).

The stationary states of the crystal, including the vibratory motion of the atoms can be described to a first approximation by a wave function Ψ equal to the product of an electronic function $\chi(1, 2 \cdots n)$ specifying the inner states of the atoms and of the functions (20) for all the $3n$ oscillators. We thus get for the r-th excited substate

$$\Psi_r = \chi_r(1, 2, \cdots n) \prod_{s=1}^{3n} f_{N_{rs}}\left[\left(\frac{\nu_{rs}}{\nu_{0s}}\right)^{1/2}\xi_{rs}\right] \tag{21}$$

and for the normal state

$$\Psi_0 = \chi_0(1, 2, \cdots n) \prod f_{N_{0s}}(\xi_s) \tag{22}$$

with

$$\chi_0 = \psi_1(1)\psi_1(2) \cdots \psi_1(n) \tag{22a}$$

which is obviously the same approximation to the electronic function of a number of atoms in the same state, as the functions χ_r defined by (8), are for the case when one of them is excited.

It must be remarked that whereas the factorization of the oscillator functions corresponds to the assumed absence of any direct coupling between them, the multiplication of these functions with the electronic function χ does not mean that there is no coupling between the vibratory and inner motion of the atoms, this coupling being in fact expressed (in an approximate manner of course) by the dependence of the vibration frequencies ν_{rs} upon the electronic state. Through this interaction of the electronic (inner) and the vibratory (outer) motion the different oscillators are actually coupled with each other—in a rather indirect way—and it is just this indirect coupling that enables the simultaneous transition of any number of oscillators

[16] Cf. A. Sommerfeld, Wellenmechanisches Ergänzungsband, p. 18. This normalization corresponds to the condition $\Sigma\xi_s^2 = \Sigma(\Delta\chi)_s^2$ or $\Sigma_i c_{ki}^2 = 1$ used above.

from one state, specified by the quantum numbers N_{01}, $N_{02} \cdots N_{03n}$ to another N_{r1}, $N_{r2} \cdots N_{r3n}$, if this transition is combined with an electronic one, that is with a transition of the crystal from the normal state to an excited one or *vice versa*.

The probability of such a combined transition is determined by the matrix element of the perturbation energy with respect to the functions (21) and (21a). This perturbation energy seems at first sight to be identical with the mutual potential energy of all the atoms U, which has been considered above in connection with its influence on the electronic motion. It will be remembered however, that this influence has been examined on the assumption that the atoms were at rest at the lattice points of the crystal, which corresponds to definite equilibrium values $R_{\alpha\beta}{}^0$ of the interatomic distances $R_{\alpha\beta}$ entering as parameters in the expression (3) for U.

Since we are now concerned with transitions due to the interaction of the electronic and vibratory motion it is necessary to take account of the change of the $R_{\alpha\beta}$'s and consequently of U which are due to the displacements of the atom from their equilibrium positions. This could be done by expanding U in a power series with respect to the differences $R_{\alpha\beta}-R_{\alpha\beta}{}^0$ and expressing the latter through the normal coordinates $\xi_1, \xi_2 \cdots \xi_{3n}$.

The series so obtained would contain next to the equilibrium value of U a sum of squares of the coordinates ξ which must be dropped out, since it represents nothing else but the potential energy of the oscillators (accounted for separately) and further higher powers of the ξ's which should represent a certain degree of anharmonicity and of direct coupling between the oscillators and at the same time a certain alteration of the electronic states as a result of the vibrational motion.

If we did not take into account the indirect coupling (and anharmonicity) expressed by the dependence of the vibration frequencies on the excitation state, we should have to carry out the expansion of U up to terms of the 100-th (or even higher) degree in the ξ's in order to get a nonvanishing probability for transitions involving a 100-fold jump of the oscillators (cf. Introduction). As a matter of fact, however, this is not necessary and we can safely stop at terms of the third order (as is done in the theory of the thermal expansion and thermal conductivity of solids) thus putting

$$U = U^0 + U''' \tag{23}$$

where

$$U''' = \sum_{k,l,m} A_{klm}\xi_k\xi_l\xi_m \tag{23a}$$

the coefficients A_{klm} being certain functions of the electronic (inner) coordinates $1, 2, \cdots n$.

The probability of radiationless transitions from the r-th excited state to the normal one (or *vice versa*) is determined by the matrix element of U with respect to the wave functions (21) and (22)

$$M_r \equiv \int U\psi_0^*\psi_r = \int \cdots \int \cdots \int U\chi_0^*\chi_r d\tau_1 \cdots d\tau_n \cdot \prod_{s=1}^{3n} f_{N_{0s}}(\xi_s) f_{N_{rs}}\left[\left(\frac{\nu_{rs}}{\nu_{0s}}\right)^{1/2}\xi_s\right] d\xi_s.$$

Of course only such states have to be considered which have the same or nearly the same energy (the corresponding transitions are usually denoted as "resonance" ones). The energy of the crystal in the normal state is equal to the sum of the energies of the separate atoms nW_I plus the equilibrium value of their mutual potential energy

$$W_0' = \int \cdots \int U(\chi_0)^2 d\tau_1 \cdots d\tau_n = \sum_{\alpha<\beta} \iint V(\alpha, \beta; R_{\alpha\beta}) \left|\psi_1(\alpha)\right|^2 \left|\psi_1(\beta)\right|^2 d\tau_\alpha d\tau_\beta \tag{25}$$

plus the vibrational energy

$$E_0 = \sum_{s=1}^{3n} h\nu_{0s}(N_{0s} + \tfrac{1}{2}). \tag{25a}$$

The energy of the same crystal in the excited state r is represented similarly by the sum

$$W_{II} + (n-1)W_I + W_r' + E_r$$

where W_r' is given by (8) and

$$E_r = \sum_{s=1}^{3n} h\nu_{rs}(N_{rs} + \tfrac{1}{2}). \tag{25b}$$

The condition for the radiationless transition to be a resonance one is thus expressed by the equation

$$W_{II} - W_I + W_r' - W_0' + \sum_{s=1}^{3n} [h\nu_{rs}(N_{rs} + \tfrac{1}{2}) - h\nu_{0s}(N_{0s} + \tfrac{1}{2})] = 0. \tag{26}$$

This equation can be approximately satisfied for a given r in a number of different ways corresponding to different jumps of the vibrational quantum numbers n_s. The total probability for the crystal to pass from the excited state into the normal one will be proportional to the sum of the squares of the matrix elements (24) (or rather their moduli) for all such "nearly resonance" transitions (see next paragraph).

In computing the matrix elements (24) we must express the normal coordinates of the excited crystal through those of the unexcited one by means of the relation (18). It is however to be kept in mind that these relations hold for the case when the ξ_s's are so normalized that $\Sigma_s \xi_s^2 = \Sigma \Delta x_s^2$, which corresponds to the value (19a) of the parameter α in the functions (19). If we put

$\alpha=1$ in (19), that is replace ξ_s by $\alpha^{1/2}\xi_s$ then in using the relations (18) we must multiply the right hand side by $\alpha^{1/2}$. Putting further $\nu_r/\nu_0=1+\Delta\nu_r/\nu_0$ and noticing that $\Delta\nu_r/\nu_0$ is a small quantity of the order of $1/n$ we can expand $f_N[(\nu_r/\nu_0)^{1/2}\xi_{rs}]=f_N[(\nu_r/\nu_0)^{1/2}(\xi_s+\Delta\xi_{rs})]$ in a series of powers of $1/n^{1/2}$

$$f_N[(\nu_r/\nu_0)^{1/2}\xi_{rs}] = f_N(\xi_s) + \Delta\xi_{rs}f_N'(\xi_s) + O(1/n) \tag{27}$$

$O(1/n)$ denoting the sum of terms of the order of magnitude $1/n$, $1/n^{3/2}$, etc. We shall presently see that all these terms can be dropped, their contribution to the total value of the transition probability (for all the possible individual transitions) decreasing with increase of n (as $1/n$ at least), whereas the contribution of the terms proportional to $\Delta\xi_{rs}$ that is to $1/n^{1/2}$ turns out to be independent of n (see below).

The change of the vibration frequencies connected with the excitation of the crystal is thus immaterial for the transitions we are considering, these transitions being due practically solely to the minute change of the equilibrium distance between the atoms.[17]

We shall first consider that part of M_r which corresponds to U^0 that is

$$M_r^0 = \int\cdots\int U^0\chi_0^*\chi_r d\tau_1\cdots d\tau_n \prod_{i=1}^{3n}\int f_{N_{0s}}(\xi_s)f_{N_{rs}}[(\nu_{rs}/\nu_{0s})^{1/2}\xi_{rs}]d\xi_s. \tag{28}$$

The contribution of each oscillator to M_r^0 is given according to (27) by the factor

$$I_r = \int f_{N_0}(\xi)f_{N_r}(\xi)d\xi + \Delta\xi_r\int f_{N_0}(\xi)f_{N_r}'(\xi)d\xi + O(1/n). \tag{29}$$

If $N_r=N_0$, this factor reduces practically to 1. If $N_r=N_0\pm1$ the first term on the right side vanishes but the second is different from zero, so that $I_r=O(1/n^{1/2})$. If $|N_r-N_0|>1$ the second term vanishes too and I_r turns out to be of the order of $1/n$ or still smaller.

We thus see that *only such transitions have to be taken into account, for which each oscillator either remains in the same state or jumps to the next one.*

From the well-known relation for Hermitian polynomials

$$\frac{d}{d\xi}H_N(\xi) = 2NH_{N-1}(\xi)$$

it follows, according to (19) (with $\alpha=1$):

$$f_N'(\xi) = (2^N N!\pi^{1/2})^{-1/2}2NH_{N-1}(\xi)e^{-\xi^2/2} - \xi f_N(\xi) = (2N)^{1/2}f_{N-1}(\xi) - \xi f_N(\xi)$$

whence for $N_r=N_0\pm1$

$$I_r = -\Delta\xi_r\int f_{N_0}(\xi)f_{N_r}(\xi)\xi d\xi = -\Delta\xi_r\xi_{N_r,N_0}$$

[17] This result applies to some extent to the case of diatomic molecules, where however the frequency shift also plays a marked rôle.

ξ_{N_r,N_0} being the matrix element of ξ. This matrix element is equal to $(N/2)^{1/2}$ where N is the larger of the two numbers N_r and N_0. We thus get for the s-th oscillator ($\Delta\xi_r$ being independent of s)

$$I_{rs} = -\Delta\xi_r(N_s/2)^{1/2} \quad (N_s = N_{0s}, N_{rs} \text{ if } N_{0s} = N_{rs} = \pm 1). \tag{29a}$$

(The same result can be derived directly from the well-known formula for the matrix element of the momentum, that is of the operator $(h/2\pi i)\,\partial/\partial\xi$). Hence it follows that in case of a transition in which p of the $3n$ oscillators jump simultaneously (to one of the next states), while the rest remain in the same state,

$$M_r^0 = \left[-\Delta\xi_r(N/2)^{1/2}\right]^p U_r^0 \tag{30}$$

where N is the geometrical mean of the p numbers N_s and

$$U_r^0 = \int \cdots \int U^0\chi_0\chi_r d\tau_1 \cdots d\tau_n.$$

We shall now briefly examine the second part of M_r, corresponding to U'''' (23a)

$$M_r''' = \sum_{klm} \int \cdots \int A_{klm}\chi_r\chi_0^* d\tau_1 \cdots d\tau_n \phi^r{}_{klm}\Pi'_{klm} \tag{31}$$

where $\phi^r{}_{klm}$ denotes the integral with respect to the coordinates ξ_k, ξ_l, ξ_m containing their product as a factor. This integral is a product of three simple ones with respect to the separate coordinates if the latter are all different, or of two simple ones if $k=l\neq m$; if $k=l=m$, it reduces to an integral with respect to one variable ξ_k containing its cube as a factor. Π'_{klm} denotes the product of factors (29) for all the other normal coordinates ξ. ϕ_{klm} is different from zero in that case only if the corresponding oscillators make together three elementary jumps ($|N_{rk}+N_{rl}+N_{rm}-N_{0k}-N_{0l}-N_{rm}|=3$), one jump each if they are all different, or a double jump and a simple one if $k=l\neq m$, or a single triple-jump if $k=l=m$.

If the total number of jumps performed by all the oscillators in the transition considered is to be equal to p, then in the product Π'_{klm} only $p-3$ factors of the type (29a) must appear, so that M_r''' may be written in the form

$$M_r''' = \sum_{klm} A^r_{klm}\phi^r_{klm}\left[-\Delta\xi_r(N/2)^{1/2}\right]^{p-3} \tag{31a}$$

$A^r{}_{klm}$ being the matrix element of A_{klm} (1, 2, $\cdots$ n) with respect to χ_0 and χ_r. One can say that in the product $\phi^r{}_{klm}\,\Pi'_{klm}$ the first factor refers to jumps which are due to the direct coupling between three or two oscillators (or their anharmonicity) and the second one to the indirect coupling provided by the dependence of the vibrations on the excitation state.

The coefficients A_{klm} can be obviously defined by the formula

$$A_{klm} = \sum_{\alpha\beta\alpha}\left(\frac{\partial^3 U}{\partial x_\alpha \partial x_\beta \partial x_\gamma}\right)_0 \frac{\partial x_\alpha}{\partial \xi_k}\frac{\partial x_\beta}{\partial \xi_m}\frac{\partial x_\gamma}{\partial \xi_n}$$

where $x_\alpha, x_\beta, x_\gamma$ denote the x, y, z coordinates of the atoms ($\alpha, \beta, \gamma = 1, 2 \cdots 3n$), and the differential coefficients $\partial x_\alpha / \partial \xi_k$, etc., are the transformation coefficients which in the unidimensional case considered above were denoted by c_{kl}, equation (17). Since these coefficients are of the order of magnitude of $1/n^{1/2}$, we see that M_r''', so far as its dependence upon n is concerned, is of the order of magnitude $(1/n^{1/2})^3 (1/n^{1/2})^{p-3} = (1/n^{1/2})^p$, that is, of the same order of magnitude as M_r^0 given by (30).

Now M_r^0 contains as factor the matrix element U_r^0 of the mutual potential energy of all the atoms in their normal equilibrium positions with respect to the functions χ_0 and χ_r, and this factor can be easily shown practically to vanish for all excited substates r with the exception of the one $r_1 = r_2 = r_3 = 0$ for which χ_r is symmetrical with respect to the inner coordinates $1, 2 \cdots n$ of all the atoms, that is representing an excitation wave of infinite length (having the same phase throughout the whole crystal). In fact using the expressions (8) for $\chi_r = \chi_{r_1 r_2 r_3}$ and (22a) for $\chi_0 = \phi_0$, we have

$$U_r^0 = \sum_{k_1 k_2 k_3} c_{rk} \int \cdots \int U^0 \phi_0^* \phi_k d\tau_1 \cdots d\tau_n$$

where $\phi_0 = \psi_I(1)\psi_I(2) \cdots \psi_I(n)$, and ϕ_k is obtained from ϕ_0 by replacing the factor $\psi_I(k)$ by $\psi_{II}(k)$. Introducing here the expression (3) for $U = U^0$ we get $\int \cdots \int U^0 \phi_0^* \phi_k d\tau_1 \cdots d\tau_n$ = sum of integrals of the type

$$\int\int U(k, l; R_{kl}) \psi_I^*(k) \psi_{II}(k) \psi_I^*(l) \psi_I(l) d\tau_k d\tau_l$$

with respect to all values of l. Now this sum must obviously be practically independent of k, that is of the location of the atom k within the crystal—so far as *surface effects can be neglected*. Thus the preceding expression for U_r^0 reduces to the product of a constant by the sum $\Sigma_k c_{rk}$ which vanishes (practically, again neglecting surface effects) unless $r_1 = r_2 = r_3 = 0$.

It seems questionable whether the excited substate $r_1 = r_2 = r_3 = 0$ has actually to be taken into account or not. But even if we do not exclude it, we see that the probability of a transition from this state to the normal one, so far as it is determined by U_r^0 need not be much larger than that determined by U_r''' for similar transitions from all the other excited substates, that is transitions involving the same number p of heat oscillators or rather of elementary jumps. The matrix component M_r for such transitions having the order of magnitude $(1/n^{1/2})^p$ the corresponding probability will be proportional to $(1/n)^p$. The coefficient of proportionality cannot be determined accurately unless we restrict ourselves to transitions from the substate $r_1 = r_2 = r_3 = 0$ and neglect U''' with respect to U^0. In this rather fictitious case (which it will however be well to consider for the sake of illustrating that part of the theory which is connected with the dependence of the resulting total probability upon the number of atoms n), the probability of a transition involving the cooperation of p heat oscillators, or rather *the square of the corresponding matrix element*, is given, according to (30) and (18), by

$$M_r^2 = \left| U_r^0 \right|^2 \mu_r^p \tag{32}$$

where

$$\mu_r = \frac{\alpha(\Delta L_r)^2}{8} \frac{N}{n} \tag{32a}$$

L_r being an abbreviation for the product $\Delta\delta_r n$, and α being defined by (19a). α is the reciprocal of the square of a distance which depends upon the frequency ν_s of the corresponding oscillator. For oscillators of the maximum frequency in the acoustical spectrum $\nu_0 \leqq 10^{13}$ this distance $1/\alpha^{1/2}$ is equal to $3\times 10^{-9}/m_H^{1/2}$ cm where m_H is the atomic weight of the crystalline element we are considering with respect to hydrogen. We thus see that the product $\alpha(\Delta L_r)^2$ must be of the order of magnitude 1, at least for the higher frequency oscillators. For oscillators of lower frequencies it must however be smaller, so that these oscillators must be less effective in the transformation of the excitation energy into heat energy not only because their share is smaller, but because they have a smaller probability of getting this share.

In (32a) α and N denote certain (geometrical) mean values for all the p oscillators participating in the transition. Denoting the value of α for oscillators of the highest frequency with α_0, we can put

$$\mu_r = \frac{\alpha_0(\Delta L_r)^2}{8n}\left(\prod_p \frac{\nu_s}{\nu_0} N_s\right)^{1/p} \tag{32b}$$

where $\prod_p$ denotes the product over all the p oscillators we are considering.

6. The Resulting (Statistical) Value of the Probability of Radiationless Transitions

The minimum value of $p = p_0$ is obtained if only oscillators of the highest frequency or next to it are taken into account. This minimum value is given by

$$p_0 = \frac{E_0 - E_r}{h\nu_0} = \frac{W_{II} - W_I + W_r' - W_0'}{h\nu_0} \tag{33}$$

according to (26), and as was mentioned above is of the order of magnitude of 100. Now these oscillators can be picked up from a much larger number Q of oscillators whose frequencies are enclosed within an interval $\nu_0 - \nu = D\nu$ which can be extremely small with respect to ν but at the same time large enough to make Q exceedingly large compared with p. Limiting ourselves to longitudinal waves (which for the same wave-length possess a higher frequency than the transverse ones), we have

$$Q = \frac{4\pi v}{u^3}\nu_0^2 D\nu$$

where v is the volume of the crystal and u the velocity of the longtitudinal waves, or since $v = n\delta^3$ and $(u/\nu_0)^3 = \lambda_0^3 = 4\pi\delta^3/3$

$$Q = 3nD\nu/\nu_0. \tag{33a}$$

It must be emphasized that for a given value of $D\nu$ (or $D\nu/\nu_0$) Q *is proportional to the total number of atoms forming the crystal.* Taking $n \cong 10^{21}$ (which corresponds to a crystal with a volume about 1 cm^3) and $D\nu/\nu_0 = 10^{-13}$, say, we get $Q = 3 \times 10^8$ which is still a million times larger than p_0.

Our p_0 oscillators can be picked up from the set containing Q of them *in a number of different ways*, this number being equal to

$$\binom{Q}{p_0} = \frac{Q(Q-1)\cdots(Q-p_0+1)}{1\cdot 2\cdots p_0} \cong \frac{Q^{p_0}}{p_0!}$$

that is according to (33a) proportional to the p_0-th power of the total number of atoms n.

The total probability of a transition of the crystal from the excited state to the normal one, in which the excitation energy will be shared by *any* p_0 of the Q high frequency oscillators will thus be proportional to the product

$$M_r^2\binom{Q}{p_0} = |U_r^0|^2 \frac{(\mu_r Q)^{p_0}}{p_0!} = \frac{|U_r^0|^2}{p_0!}\left(\frac{3}{8}\alpha(\Delta L_r)^2 N \frac{D\nu}{\nu_0}\right)^{p_0} \tag{34}$$

that is, will be *independent of* n.

The fact that it turns out to be dependent upon the choice of the interval $D\nu$ is naturally explained by our having restricted ourselves to this interval. We can obtain some approximation to the value of the probability of any transition from the excited state to the normal one, or rather to the total value of ΣM_r^2 determining this probability by taking, in the above formula $D\nu/\nu_0 \cong 1/2$ and replacing p_0 by a somewhat larger number $p = 2p_0$ say.

The problem of the determination of the resulting transition probability P_r can be solved exactly by a method which we are presently going to describe. It must be remarked however that in deriving this probability we must not restrict ourselves to the consideration of such transitions only, for which *all* the participating oscillators jump to a higher level. On the contrary we must take account of such transitions (which are under some circumstances by far the more frequent) in which some of the oscillators jump to a higher level and others to the lower one, adding, so to say, their energy to the excitation energy.

Further it must be remembered that the "resonance condition" expressed by the equation (26) or

$$E_0 - E_r = W_{II} - W_I + W_r' - W_0'$$

need not be *exactly* satisfied. In fact we have to consider, theoretically, transitions for which the difference $E_0 - E_r$ has any value whatsoever. Let us denote the sum ΣM_r^2 for all transitions for which the value of $E_0 - E_r$ is enclosed between E and $E+dE$ by $S(E)dE$. Then the transition probability which is actually observed referred to unit time is given by [18]

$$P_r = \frac{4\pi^2}{h} S(E) \tag{35}$$

[18] See, for instance, J. Frenkel, Einführung in die Wellenmechanik p. 211, formula (72a).

E being the resonance value of E_0-E_r, that is, the excitation energy of the crystal, defined by the right hand side of equation (26). E_0-E_r can be expressed as the sum $\Sigma p_s\epsilon_s$ over all the $3n$ oscillators, where $\epsilon_s=h\nu_s$ are the corresponding energy quanta and $p_s=0$, $+1$, or -1 for an oscillator not partaking in the transition, jumping to the next higher level, and the next lower level respectively. The total number of oscillators participating in the transition p is thus equal to $\Sigma|p_s|$, and the excess of oscillators gaining energy over those loosing it Σp_s. It must be remarked that for low temperatures, and in the case of the high frequency oscillators even for room temperatures jumps of the second kind (down) may not be possible, the corresponding oscillators being in the lowest state ($N_{rs}=0$)

We shall first neglect these downward transitions, that is, restrict ourselves to the non-negative values of p_s (0, 1). We shall further, for the sake of simplicity, take the same value of μ_r given by (32a) for all the oscillators (see below).

Our problem then reduces to the determination of the value of the sum

$$\sum{}'\mu_r{}^p = S(\epsilon)d\epsilon/|U_r{}^0|^2$$

for all values of the $p_s(=0, 1)$ satisfying the condition

$$E \leqq \sum p_s\epsilon_s \leqq E+dE \tag{36}$$

p being equal to the sum Σp_i. This problem is quite similar to the familiar problem met with in the Pauli-Fermi statistics of a gas with a given total energy E the p_s representing the possible numbers of particles in the s-th state. From the physical point of view they differ by the fact that instead of calculating the *number of states* of the whole system, that is the sum $\Sigma 1$ under the restriction (36) (the logarithm of $\Sigma 1$ being defined as the entropy), we have to calculate the sum $\Sigma\mu_r{}^p$, and further by the fact that E does not actually represent the energy of the system of oscillators but the change of this energy, the *states* thus being replaced by the *transitions*.

The restriction (36) can be removed by considering instead of the sum $\Sigma'\mu_r{}^p$ the sum $\Sigma\mu_r{}^pe^{-\beta E}$ with suitably adjusted parameter β (corresponding to the reciprocal of the temperature), extended over all possible values of the p_s. The second (unrestricted) sum is of course different from the first (restricted) one, but there exists a simple approximate relation between them. Writing the unrestricted sum in the form

$$\sum\mu_r{}^pe^{-\beta E} = \int_0^\infty S(E)e^{-\beta E}dE$$

(the factor $1/|U_r{}^0|^2$ is dropped for the sake of brevity), we see that the integrand $S(E)e^{-\beta E}$ must have a maximum for some value of E, which by a suitable choice of $\beta(>0)$ can be made to coincide with the given value E_m lying in the interval (36). If this maximum is sharp enough, which is actually the case when E_m is not too small, we can replace the function $S(E)e^{-\beta E}$ by a Gaussian function

$$S(E_m)e^{-\beta E_m}e^{-(E-E_m)^2/\gamma^2}$$

where the parameter γ measures the width (or sharpness) of the maximum.

This gives

$$\sum \mu_r{}^p e^{-\beta E} = S(E_m) e^{-\beta E_m} \int_{-\infty}^{+\infty} e^{-(E-E_m)^2/\gamma^2} d(E - E_m) = S(E_m) e^{-\beta E_m} \gamma \pi^{1/2}$$

or

$$S(E_m) = \frac{e^{\beta E_m}}{\gamma \pi^{1/2}} \sum \mu_r{}^p e^{-\beta E} \tag{37}$$

where the (unrestricted) summation on the right hand side has to be carried out exactly.

The specified value of the parameter β can be easily determined from the condition that the "average" value E for the curve $S(E)e^{-\beta E}$ practically coincides with the extremal value E_m. This gives

$$\overline{E} = \frac{\int ES(E) e^{-\beta E} dE}{\int S(E) e^{-\beta E} dE} = -\frac{\partial}{\partial \beta} \log \int S(E) e^{-\beta} \, dE = E_m$$

or

$$E_m = -\partial \log Z / \partial \beta \tag{37a}$$

where

$$Z = \sum \mu_r{}^p e^{-\beta E} \tag{37b}$$

is the analogue of the "state-sum" (Zustandssumme) of the usual statistical theory. The determination of the parameter γ requires some approximate knowledge of the function $S(E)$ and can be effected after the evaluation of $S(E_m)$ according to (37).

We have

$$Z = \sum_{p_1, p_2 \cdots} \mu^{(p_1+p_2+\cdots)} e^{-\beta(p_1\epsilon_1 + p_2\epsilon_2 + \cdots)} = \prod_s \sum_{ps} \mu_r{}^{p_s} e^{-\beta p_s \epsilon_s}$$
$$= \prod_s (1 + \mu_r e^{-\beta \epsilon_s})$$

whence

$$\log Z = \sum_s \log (1 + \mu_r e^{-\beta \epsilon_s}) = \int_0^{\epsilon_0} \log (1 + \mu_r e^{-\beta \epsilon}) g(\epsilon) d\epsilon \tag{38}$$

$g(\epsilon)d\epsilon$ being the number of oscillators whose energy quanta $\epsilon = h\nu$ lie between ϵ and $\epsilon + d\epsilon$. Restricting ourselves to longitudinal waves we have

$$g(\epsilon)d\epsilon = 3n\epsilon^2 d\epsilon / \epsilon_0{}^3.$$

Now μ_r being a very small number (of the order of $1/n$) we can put with sufficient accuracy

$$\log (1 + \mu_r e^{-\beta\epsilon}) = \mu_r e^{-\beta\epsilon}$$

which gives

$$\log Z = \frac{3n\mu_r}{\epsilon_0{}^3} \int_0^{\epsilon_0} e^{-\beta\epsilon}\epsilon^2 d\epsilon. \tag{38a}$$

This formula shows at once that Z *is actually independent of* n; the same follows from (37) and (37a) for β and for $S(E_m)$, the quantity which determines the probability for which we are looking.

The above results can be easily generalized to allow for the difference of the factor μ_r for different oscillators. Replacing $\mu_r{}^p$ by the product $\Pi\mu_{rs}{}^{p_s}$ we get formulae of the same type as before. In evaluating $\log Z$ according to (38) or (38a) we have to consider μ_r as a function of the index s or of the energy $\epsilon(=\epsilon_s)$.

Denoting the value of μ_{rs} for $\epsilon=\epsilon_0$ and $N_s=1$ with μ_r we have

$$\mu_{rs} = \mu_r \epsilon_s N_s/\epsilon_0$$

so that instead of (38a) we get

$$\log Z = \frac{3n\mu_r}{\epsilon_0{}^4} \int_0^{\epsilon_0} e^{-\beta\epsilon}\epsilon^3 N(\epsilon) d\epsilon. \tag{39}$$

The average value of $N(\epsilon)$ at the temperature T under the assumption of statistical equilibrium is given by Planck's law $N(\epsilon)=1/(e^{\epsilon/kT}-1)$. If we assume this distribution to hold for the initial (excited) state of the crystal then (since $N_{rs}=N_{0s}-1$) the preceding expression has to be increased by 1, the average value of $N(\epsilon)$ thus being

$$N(\epsilon) = 1/(e^{\epsilon/kT} - 1) + 1 = 1/(1 - e^{-\epsilon/kT}). \tag{39a}$$

The above theory can be applied to the estimation of the probability of transitions of the opposite character, that is from the normal state to the excited one, so far as all the participating oscillators jump in the same sense, that is downwards, their energy being converted into the excitation energy. In this case we have to put of course

$$N(\epsilon) = 1/(e^{\epsilon/kT} - 1). \tag{39b}$$

It can be easily shown that our simplified theory, which takes into account jumps of the same sense only, holds for the limiting case that the product $n\mu_r$ (which is independent of n and which is a measure of the change of atomic distance produced by excitation) is very small. The probability of transitions in which p oscillators take part being approximately proportional to $(\mu n)^p/p!$ (cf. equation (34)) a strict economy in the use of the different oscillators will be observed in this case, their number being reduced to the minimum $p_0 = (E_0 - E_r)/h\nu_0 = E_m/\epsilon_0$ and "useless" jumps in the wrong sense practically excluded.

To get a rough idea of what will take place in the opposite case, that is if μn is large, we have to sum up the preceding expression for all values of p starting with $p=p_0$. If $\mu n \ll p_0$ this sum will still practically reduce to the first term. If however $\mu n \gg p_0$ it can be replaced by the sum $\sum_{p=1}^{\infty}(\mu n)^p/p!$ giving $e^{\mu n}$. The same result is obtained by replacing the sum by its maximum term, which corresponds to $p=\mu n$ and putting $p!=(p/e)^p$.

The method applied above for the approximate evaluation of the restricted sum of the products $\mu_{rs}|^{p_s}|$ is no longer applicable when the numbers p_s are allowed to take negative values (-1), for the simple reason that the function $S(E)$ has no tendency to increase in this case with increase of E. To the contrary it has a very flat maximum for $E=0$ and vanishes for $|E|>\Sigma\epsilon_s$. One could get rid of this restriction $E<\Sigma p_s\epsilon_s<E+dE$ in this case by a more general method, involving the use of Dirichlet's disruptive multiplier.[19] It does not seem worth while however to develop this method at a greater length here and we shall satisfy ourselves by making a direct calculation for the simplified case $\epsilon_s=\epsilon=$ const. Our problem can then be stated as follows: The number n is expressed as the sum of three numbers $n'+n''+n'''$, denoting respectively the number of positive, negative and zero values in the sequence $p_1, p_2 \cdots p_n$; to determine the sum $\Sigma'\mu^{n'+n''}$ under the restriction that $n'-n''=p_0=E/\epsilon$.

Since each "partitio" $n=n'+n''+n'''$ can be effected in $n!/n'!n''!n'''!$ different ways (by permuting the numbers p_i) we get

$$\sum{}'\mu^{n'+n''}=\sum_{n''=0}^{n-p}\frac{n!}{n'!n''!n'''!}\mu^{n'+n''}(n'=n''+p_0,\ n'''=n-2n''-p_0).$$

The ratio of the n''-th term of this sum to the preceding one is equal to

$$(n-2n''+p_0+1)(n-2n''+p_0+2)\mu^2/n''(n''+p_0)$$

or approximately so long as n'' is small compared with n

$$(n\mu)^2/n''(n''+p_0).$$

The maximum term is that for which this ratio is equal to 1, the condition $n''\ll n$ being obviously satisfied for $n''(n''+p_0)=(n\mu)^2$. Replacing the sum by its maximum term we have

$$\sum{}'\mu^{n'+n''}\cong(n\mu)^{n'+n''}/n'!n''!$$

This gives if $n''\gg 1$ using Stirling's formula

$$\sum{}'\mu^{n'+n''}=\frac{(n\mu e)^{2n''+p_0-1}}{2\pi n''^{n''}(n''+p_0)^{n''+p_0}} \tag{40}$$

where

$$n''=[(n\mu)^2+(p_0/2)^2]^{1/2}-p_0/2. \tag{40a}$$

[19] That is the integral $\int_0^\infty sn\,ax\cos bx\,dx/x$ which is equal to $\pi/2$ for $a>b$, $-\pi/2$ for $a<b$ and $\pi/4$ for $a=b$.

If $n\mu$ is much larger than p_0 we can put $n''=n\mu$ and reduce the above sum to

$$\sum{}'\mu^{n'+n''} \leqq e^{2n\mu+p_0}/2\pi n\mu.$$

In the opposite case ($n\mu \ll p_0$) we have $n'' \leqq (n\mu)^2/p_0$, the result given by (40) being practically the same as in the case $n''=0$ which corresponds to one-sided jumps, that is

$$\sum{}'\mu^{n'+n''} \leqq (n\mu)^{p_0}/p_0!$$

Which case is usually met with in practice, is difficult to say.

7. Radiative Transitions (Absorption and Emission of Light)

We have considered heretofore only radiationless transitions of the crystal from the excited state to the normal one or vice versa. We must now briefly examine such transitions which are connected with the absorption or emission of light. As has been pointed out in the introduction the excitation of a crystal by incident radiation forms the first stage of the process of light absorption, the second stage being provided by the radiationless transition to the normal state.

The energy levels or spectral terms which have to be considered in this connection are those that have been discussed already in the preceding sections, the energy of one of the excited sub states with respect to the normal state being given by (26). Since there are n-substates, corresponding to one single excitation state of an isolated atom, there must appear in the spectrum of a solid body in general n lines, corresponding to one single line in the spectrum of the gas, so far of course as the initial or the final state is the normal one. The frequencies of these lines, which can be described as forming an "excitation multiplet" are given by

$$\nu_r = (1/h)(W_{II} - W_I - W_0') + W_r'/h \tag{41}$$

if vibrational transitions are not taken into account. Allowing for these transitions we get a still larger number of spectral lines with frequencies differing from the preceding ones by the amounts

$$\Delta\nu_r = \sum[\nu_{rs}(N_{rs}+\tfrac{1}{2}) - \nu_{0s}(N_{0s}+\tfrac{1}{2})]. \tag{41a}$$

The spacing between the main lines (41) is determined approximately by the expression (15) or (8a). It is the smaller, the larger the number of atoms in the crystal. The total width of the multiplet formed by all these lines, is however independent of n and equal approximately to V_0+6V_1, where

$$V_0 = \int\int U(k,l)\,|\psi_{II}(k)|^2\,|\psi_I(l)|^2 d\tau_k d\tau_l \tag{42}$$

and (for the case of a simple cubical lattice)

$$V_1 = 6\int\int U(k,l)\psi_{II}^*(k)\psi_I(k)\psi_I^*(l)\psi_{II}(l)d\tau_k d\tau_l \tag{42a}$$

k and l denoting two neighboring atoms. This width is of the same order of magnitude, or perhaps just a few times larger, than the shift in the spectral levels of two atoms, produced by their combining together into one molecule. The maximum spacing between the lines of such a multiplet is of the order of $2V_1/n$, that is, so small that they should appear in practice as a continuous band even if they had no satellites due to the accompanying vibrational jumps and no natural width, which is measured by the probability of radiationless transitions we have examined before. This natural width (equal to the "mean life" of the corresponding excited substate), being independent of n must be much larger than the spacing between the consecutive lines. We thus see that the resolution of the continuous (band) spectrum of a solid body into single lines, which has been observed by J. Becguerel in the spectra of some rare earths at the temperature of liquid air and recently by W. Obreimow[20] in iodine and other substances at very low temperatures (of liquid hydrogen or helium) cannot be explained without special assumptions about the separation of the lines of an excitation multiplet or their intensities.

It can occur, namely, that for some excitation state II the "exchange energy" (42a) is abnormally small, so that the whole multiplet will appear as a single line, accompanied by satellites due to the vibration jumps. Since the coupling of the electronic states with the vibrational ones is determined partially by the same energy V_1, as the width of the excitation multiplet (see for instance formula (15a) for the change of the crystal lattice δ), these satellites will be rather faint. This may account for the lines observed by Becquerel, which were not very much influenced by the temperature.

Another possible explanation is that only a few of the excited sub-levels can combine with the normal one, these combinations forming a series of more or less widely spaced lines. Now the natural width of these lines due to radiationless transitions will be the smaller the lower the temperature, for as we have seen the coefficients μ_{rs} which determine the probability of such transitions are proportional to the average values of the quantum numbers N_s and must therefore decrease as the temperature decreases. At the same time and in the same measure will the intensity of the satellites decrease due to vibrational jumps. It can thus happen that for sufficiently low temperatures the continuous spectrum of the solid body will be resolved into separate lines, in accordance with Obreimow's observations.

It is however hardly possible to substantiate the above explanation by actual calculation of the intensities of spectral lines, that is of the probabilities of transitions connected with absorption or emission of radiation.

In the simple case of an atom or a molecule these probabilities are determined by the matrix elements of the resulting electric moment of the system. In the case of a molecule consisting of n identical atoms this sum is a symmetrical function of their electronic coordinates $1, 2, \cdots n$. Replacing the molecule by a crystal and considering pure electronic transitions not accompanied by vibrational jumps, we get for the matrix element of this

[20] W. Obreimow and Proc. Amsterdam Acad. de Kaas 31–3, p. 353 (1928).

symmetrical function $P(1, 2, \cdots n)$ with respect to the functions χ_r and χ_0 a value which can be shown to be zero for all the excited substates with the exception of the symmetrical one (by the same argument as in Section 5). It thus seems that, as a matter of fact, the whole multiplet will be reduced to one single line, or there will be no lines whatever if the symmetrical excitation state cannot be realized.

This argument is however fallacious, for in the case of a crystal whose linear dimensions are large or even comparable with the wave-length of the absorbed or emitted light the probability of absorption or emission will be determined not by the resultant electric moment $P(1, 2, \cdots n)$ but by a sum of the moments of the separate atoms $P_k(k)$ multiplied with *certain phase factors, which depend upon the positions of these atoms* R_k. In case of a system of plane electromagnetic waves (of resonance frequency) propagated within the crystals in the direction x, say, with the phase velocity w, these factors would be $e^{i2\pi\nu x_k/w}$, so that the probability of absorption of a single light quantum, that is of the excitation of a single atom, would be measured by the matrix elements with respect to the functions χ_r and χ_0 of the sum $\Sigma P_0(k)e^{i2\pi\nu x_k/w}$. There is no reason why these matrix elements should vanish for most of the substates r, remaining different from zero for a few others.

The computation of the excitation probabilities by the above method can hardly give perfectly correct results, a more consequent quantum-mechanical treatment being necessary in order to obtain them, but it seems fairly certain on the basis of these crude considerations, that nothing like a selection rule for the different terms of an excitation multiplet can be expected to exist.

It is possible that the phenomenon observed by Obreimow is limited to the case of compound substances, which lie outside the scope of this investigation. Preliminary results which I have obtained for such compound crystals, seem to support this conclusion.

BAND SPECTRUM INTENSITIES FOR SYMMETRICAL DIATOMIC MOLECULES. II

By Elmer Hutchisson
University of Pittsburgh
(Received November 10, 1930)

Abstract

In a previous paper the writer derived an approximate expression for intensities in the electronic vibrational bands of symmetrical diatomic molecules, based upon the Franck-Condon theory of transition probabilities. In the present paper the approximation is carried further, by removing the restriction that the oscillations be linear. An extended formula is given making use of the Schrödinger theory of perturbations.

Calculations using this perturbation theory formula are carried out for the hydrogen absorption band spectrum. It is shown that the agreement with experiment is much improved over that obtained on the assumption of harmonic oscillations. Calculations are also made using Morse's potential function in which case the agreement is still further improved, especially for the higher transitions.

I. Introduction

IN A recent[1] paper the writer derived a formula expressing the intensities of the electronic-vibrational bands of symmetrical diatomic molecules as a function of the change in separation of the atoms and the change in the binding force between the atoms caused by the electronic transition. Since the present paper is essentially an extension of the results there obtained, the above paper will be referred to as Part I. The formula developed in Part I was used to calculate the intensities in the absorption spectra of several molecules and approximate agreement with experiment was obtained. Exact agreement was not to be expected due to the fact that the experimental temperatures were unknown and because of the approximations which had to be made in order to carry through the calculations. Three essential assumptions in deriving the intensity formula were: (1) that the complete wave function could be expressed as a product of a function of the electronic coordinates only and a function of the nuclear coordinates only; (2) that the electric moment could be separated into two parts, one of which was constant over the electron integration and the other constant over the nuclear integration and; (3) that the oscillations of the nuclei were simple harmonic. The last assumption was made not because of any theoretical necessity but merely to simplify the algebraic evaluation of the integrals involved. It is the purpose of this second part to extend the formula developed in Part I to the case in which the nuclear oscillations are nonharmonic.

II. Application of the Perturbation Theory

In order to take care of the deviation of the nuclear oscillations from simple harmonic motion, the potential energy between the nuclei may be

[1] E. Hutchisson, Phys. Rev. **36**, 410 (1930).

expressed as a power series in a factor depending upon the displacement of the nuclei from their equilibrium separation r_e*. The Schrödinger equation in this case is:

$$\nabla^2\Psi + 8\pi^2\mu/h^2[W - 2\pi^2\omega_e{}^2I_e\{\xi^2 + c_3\xi^3 + c_4\xi^4 + \cdots\}]\Psi \tag{1}$$

where Ψ = the Schrödinger wave function, W = total energy, μ = the equivalent mass, h = Planck's constant, $\xi = (r - r_e)/r_e$, I_e = moment of inertia at equilibrium separation and ω_e, c_3 and c_4 are constant coefficients in the potential energy. The radial part of the wave equation then has the following form[2]: (letting $\xi = [h^{1/2}/2\pi(\omega_e I_e)]\eta$)

$$F'' + [\{2W/h\omega_e - kK(K+1) - \eta^2\} + k^{1/2}\{2kK(K+1)\eta - c_3\eta^3\} + k\{-3kK(K+1)\eta^2 - c_4\eta^4\}]F = 0 \tag{2}$$

where $k = h/4\pi^2\omega_e I_e$ and K is the rotational quantum number.

The normalized solution of this equation in the first approximation, in which only the first term is considered since k usually has a value less than 0.01, is:

$$F_v{}^0 = (2^v v!\pi^{1/2})^{-1/2}e^{-\eta^2/2}H_v(\eta) \text{ and} \tag{3}$$

$$W_v{}^0 = h\omega_e(v + \tfrac{1}{2}) + (h^2/8\pi^2 I_e)K(K+1) \tag{4}$$

where v is the vibrational quantum number and H is the Hermitian polynominal.

The perturbation terms in the radial waves equation are therefore:

$$V_1 = (k^{1/2}h\omega_e/2)[2kK(K+1)\eta - c_3\eta^3] \tag{5}$$

$$V_2 = (kh\omega_e/2)[-3kK(K+1)\eta^2 - c_4\eta^4]. \tag{6}$$

According to Schrödinger's perturbation theory,[3] we have for the complete wave function:

$$F_v = F_v{}^0 + F_v{}^1 + F_v{}^2 + \cdots = F_v{}^0 + \sum_i A_{vi}F_i{}^0 + \sum_j B_{vj}F_j{}^0 + \cdots \tag{7}$$

where

$$A_{vi} = \int V_1 F_v{}^0 F_i{}^0 d\eta \Big/ (W_v{}^0 - W_i{}^0) \tag{8}$$

and

$$B_{vj} = \frac{\int V_2 F_v{}^0 F_j{}^0 d\eta}{W_v{}^0 - W_j{}^0} + \sum_{e=0}^{\infty} \frac{\int V_1 F_v{}^0 F_e{}^0 d\eta \int V_1 F_e{}^0 F_j{}^0 d\eta}{(W_v{}^0 - W_j{}^0)(W_v{}^0 - W_e{}^0)} - \int V_1 F_v{}^0 F_j{}^0 d\eta \int V_1 F_v{}^0 F_v{}^0 d\eta \Big/ (W_v{}^0 - W_j{}^0)^2 \tag{9}$$

* r_e is used in this part in place of the r_0 of Part I in order that the notation conform with that recommended by band spectroscopists, c.f., R. S. Mullikan, Phys. Rev. **36**, 611 (1930.)

[2] E. Fues, Ann. d. Physik **80**, 367 (1926).

[3] E. U. Condon and P. M. Morse, Quantum Mechanics, pp. 118 ff.

where $v \neq i$ and $v \neq j$ and the limits of integration are taken from $\eta = -\infty$ to $+\infty$ instead of from -1 to $+\infty$ since the addition of the region from -1 to $-\infty$ will not appreciably affect the value of the integral for small quantum numbers. Also we have:

$$A_{vv} = 0 \text{ and } B_{vv} = -\tfrac{1}{2}\sum_i (A_{vi})^2. \tag{10}$$

To evaluate the integrals in the perturbation terms we make use of the recursion formulas

$$\begin{aligned}
\eta F_v^0 &= [(v+1)/2]^{1/2} F_{v+1}^0 + [v/2]^{1/2} F_{v-1}^0 \\
\eta^2 F_v^0 &= [(v+1)(v+2)/2^2]^{1/2} F_{v+2}^0 + [(2v+1)/2] F_v^0 + [v(v-1)/2^2]^{1/2} F_{v-2}^0 \\
\eta^3 F_v^0 &= [(v+1)(v+2)(v+3)/2^3]^{1/2} F_{v+3}^0 + [3^2(v+1)^3/2^3]^{1/2} F_{v+1}^0 \\
&\quad + [3^2 v^3/2^3]^{1/2} F_{v-1}^0 + [v(v-1)(v-2)/2^3]^{1/2} F_{v-3}^0 \\
\eta^4 F_v^0 &= [(v+1)(v+2)(v+3)(v+4)/2^4]^{1/2} F_{v+4}^0 \\
&\quad + [(v+1)(v+2)]^{1/2} [(2v+3)/2] F_{v+2}^0 + 3[(v+1)^2 + v^2]/2^2 F_v^0 \\
&\quad + [v(v-1)]^{1/2} [(2v-1)/2] F_{v-2}^0 + [(v-3)(v-2)(v-1)v/2^4]^{1/2} F_{v-4}^0.
\end{aligned}$$

The values obtained from these recursion formulas are now substituted in the integrals occurring in (8) and (9). The terms in V_1 and V_2 which depend upon the rotational quantum numbers may be neglected if we apply our results to only transitions between the first few rotational quantum states, since for actual molecules k is much smaller than c_3 or c_4. We then obtain the following values for the constants:

$$\begin{aligned}
B_{v,v+4} &= C_{v,v+4} = (1/128)[kc_3^2(4v+7) + 4kc_4][(v+1)(v+2)(v+3)(v+4)]^{1/2} \\
A_{v,v+3} &= C_{v,v+3} = (k^{1/2}c_3/12\cdot 2^{1/2})[(v+1)(v+2)(v+3)]^{1/2} \\
B_{v,v+2} &= C_{v,v+2} = (1/64)[kc_3^2(7v^2+33v+27) + 8kc_4(2v+3)][(v+1)(v+2)]^{1/2} \\
A_{v,v+1} &= C_{v,v+1} = (9k^{1/2}c_3/12\cdot 2^{1/2})[v+1]^{3/2} \\
B_{v,v} &= C_{v,v} = -(kc_3^2/576)[164v^3 + 246v^2 + 256v + 87] \\
A_{v,v-1} &= C_{v,v-1} = -(9k^{1/2}c_3/12\cdot 2^{1/2})[v]^{3/2} \\
B_{v,v-2} &= C_{v,v-2} = (1/64)[kc_3^2(7v^2 - 19v + 1) - 8(2v-1)][v(v-1)]^{1/2} \\
A_{v,v-3} &= C_{v,v-3} = -(k^{1/2}c_3/12\cdot 2^{1/2})[v(v-1)(v-2)]^{1/2} \\
B_{v,v-4} &= C_{v,v-4} = (1/128)[kc_3^2(4v-3) - 4kc_4][v(v-1)(v-2)(v-3)]^{1/2}.
\end{aligned}$$

Since all the A's and B's except those given above are equal to zero we may write the complete wave function in the simple form

$$F_v = \sum_{j=v-4}^{v+4} C_{vj} F_j^0. \tag{11}$$

To obtain a complete expression for the intensity amplitudes it is only necessary to substitute our new wave function into the final expression

(Eq. 11)[4] of Part I. It is hardly worth while to make the substitution explicitly since the resulting expression would take up too much space and would be too cumbersome to use efficiently. However if we have a set of values calculated from the formula of Part I we may immediately obtain the corrected intensity amplitudes from:

$$I_{v'v''} = \sum_{k=v'-4}^{v'+4} \sum_{j=v''-4}^{v''+4} C_{v'k} C_{v''j} I_{kj}^{0}. \tag{12}$$

This expression contains in general 81 terms and therefore requires long calculations to get the required corrected intensities. The expression may be greatly simplified in many cases of absorption since then the lower electronic level is usually in a low state of vibrational excitation and may therefore be quite accurately represented by a harmonic wave function. In this case the expression becomes

$$I_{v'v''} = \sum_{k=v'-4}^{v'+4} C_{v'k} I_{kv''}^{0} \tag{13}$$

which contains only nine terms.

III. Application to Hydrogen Absorption Bands

There are no absorption spectrum measurements which are precise enough to determine how nearly Eq. (12) represents reality for the intensities of vibrational electronic bands. However, to see what changes are introduced by removing the restriction of linear oscillations, computations are carried out for hydrogen. Hydrogen is especially suitable because at room temperatures nearly all of the molecules are in the first vibrational level so that the distribution factor does not enter into the intensity calculations and furthermore Eq. (13) instead of Eq. (12) may be quite accurately applied.

In order to have some comparison between the calculated and observed results the experimentally estimated intensities are given in Table I. They are taken from Schaafsma and Dieke[5] and differ somewhat from those given in Part I. Estimated intensities are given for each rotational transition and show the hopelessness of exact comparisons between theory and experiment. Schaafsma and Dieke especially emphasize the difficulty of making intensity estimates for hydrogen due to the strength of the continuous spectrum in that region.

The constants used in the harmonic oscillator calculations are:

$\omega_e' = 1357.3$	$r_e' = 1.300$	$\alpha = 0.557$
$\omega_e'' = 4376.0$	$r_e'' = 0.750$	$\delta = -0.209$

where α and δ are the constants in Eq. (13) of Part I. These values differ somewhat from the more recent values given by Hyman[6] but small changes in these constants will not change the calculated intensities very much.

[4] The constant term C_3 is given wrong on page 415 of Part I. It should read $[2/\alpha(1+\alpha^2)]^{1/2} e^{-\delta^2/2(1+\alpha^2)}$. This factor is the same for all transitions and therefore has no effect on the value of the relative intensities.

[5] A. Schaafsma and G. H. Dieke, Zeits. f. Physik **55**, 164 (1929).

[6] H. H. Hyman, Phys. Rev. **36**, 187 (1930).

TABLE I. *Intensities in hydrogen absorption.*

A. Experimental (Schaafsma and Dieke)										
Rotational Transition	A_0-B_0	A_0-B_1	A_0-B_2	A_0-B_3	A_0-B_4	A_0-B_5	A_0-B_6	A_0-B_7	A_0-B_8	A_0-B_9
R(0)	0	3	4	2	2	4	1	3	2	3
R(1)	2	3	4	3	2	4	2	3	2	3
R(2)						4	1	3	2	
R(3)				0	0	0	1	1	1	
R(4)								0		
P(1)	2	3	4	5	4	4	2	3	2	3
P(2)	2	2		0	00	0	1	1	1	
P(3)	2	2		0	00	0		0		
B. Calculated										
Harmonic Oscillations	1.00	7.19	22.2	37.7	37.0	19.4	3.58	0.05	1.32	0.03
Perturbation Theory	1.00	6.6	14.1	5.2	4.7	27.4				
Morse's Function	1.00	4.28	10.7	15.5	16.4	12.5	6.96			

The above table gives the estimated relative intensities of many lines in the H_2 absorption bands which have a common initial level A_0. Below are given the corresponding calculated intensities obtained from three different approximations. The occurrence of many gaps in the experimental part of this table is probably due to the intensity of the continuous spectra in this region.

To determine the coefficients in the power series expansion of the potential energy, formulas may be derived if one assumes the relation between the total energy and the quantum numbers as given by Fues.[2] If the potential energy is given by

$$U(\xi) = k(\xi^2 + c_3\xi^3 + c_4\xi^4)$$

we have

$$k = 0.1774 \cdot 10^{-11}\omega_e^2 J_e \text{ ergs}$$
$$c_3 = -(0.2179\alpha'\omega_e J_e^2 + 1)$$
$$c_4 = 1.250c_3^2 - 2.410\omega_e x J_e$$

where α and x are the band spectra constants occurring in the expression for energy as a function of the quantum numbers; (the prime on the α' is used merely to distinguish it from α used in Part I). We then obtain for the potential energy expansions[7]

$$U'(\xi) = 0.459(\xi^2 - 1.560\xi^3 + 2.380\xi^4) \times 10^{-11} \text{ ergs}$$
$$U''(\xi) = 1.587(\xi^2 - 1.561\xi^3 + 1.770\xi^4) \times 10^{-11} \text{ ergs}$$

in which the following constants are used

$$J_e' = 1.404 \times 10^{-40} \text{ gm cm}^2 \qquad \alpha' = 0.96 \text{ cm}^{-1} \qquad \omega_e'x' = 19.54 \text{ cm}^{-1}$$
$$J_e'' = 0.467 \times 10^{-40} \text{ gm cm}^2 \qquad \alpha'' = 2.7 \text{ cm}^{-1} \qquad \omega_e''x'' = 113.5 \text{ cm}^{-1}.$$

[7] These expressions are approximately the same as those given by O. W. Richardson and P. M. Davidson, Proc. Roy. Soc. **A125**, 23 (1929) in which higher powers are included.

From the values of c_3 and c_4 obtained above for U' the coefficients in Eq. (13) are calculated and finally the values given in the table are obtained.

It is desirable to obtain analytical expressions for the intensities calculated by using the wave functions derived from the potential energy given by Morse.[8] The writer has been unable to carry through the necessary integrations in this case. However in order to determine the effect of assuming such a potential function the integrations were carried out graphically and the results are given in Table I. The potential energy function in this case has the form:

$$U(\xi) = D(e^{-2ar_0\xi} - 2e^{-ar_0\xi})$$

where $D = c\omega_e^2 h/4\omega_e x$ and $a = (8\pi^2\mu c\omega_e x/h)^{1/2}$. The same band spectrum constants are used in this case as before. The fundamental constants are taken from Birge.[9]

It is apparent from Table I that the extremely high intensities given by the harmonic oscillator calculations are reduced in both of the more exact calculations in agreement with experiment. The power series calculations are only given as far as the transition $B_5 - A_0$ since even for the last two given the perturbations are so large that scarcely any faith can be placed in the results. When the coefficients c_3 and c_4 in the power series expansion are large as they are in hydrogen, the perturbation theory, even when carried out to two approximations, gives reliable results only for transitions between the lowest vibrational quantum levels.

The calculations based upon Morse's potential energy function are probably more accurate than those using the perturbation theory. This is partly due to the fact that the "A" level as well as the "B" level is corrected for deviations from simple harmonic oscillations. It is probable also that Morse's function approaches reality nearer than a three term power series for the higher transitions. Higher calculations than those given involve small differences between large quantities and are therefore subject to large errors.

These calculations were carried out at the University of Michigan and the writer wishes to express his gratitude to Professor H. M. Randall for the opportunity of spending an extremely interesting and profitable summer in Ann Arbor. The writer wishes also to thank Professor Ruark of the University of Pittsburgh for many helpful suggestions in the preparation of the manuscript.

Note added in proof: J. L. Dunham (Phys. Rev. **36**, 1553 (1930)) has pointed out that since the electric moment does not change nearly as rapidly as the eigenfunctions, the results of Part I and hence Part II, do not need to be restricted to symmetrical molecules for small quantum numbers. The correction given in footnote 4 is noted in his article also.

[8] P. M. Morse, Phys. Rev. **34**, 57 (1929).
[9] R. T. Birge, Reviews of Modern Physics **1**, 1 (1929).

DERIVATION OF HYPERFINE STRUCTURE FORMULAS FOR ONE ELECTRON SPECTRA

By G. Breit
Department of Physics, New York University
(Received November 24, 1930)

Abstract

A short but rigorous derivation is given for the energy level separations caused by a nuclear magnetic moment in a one electron spectrum. Formulas (5) and (7) are general. For weak coupling between the orbital angular momentum and the electron spin formula (6) may be used.

FORMULAS for the hyperfine structure of one electron spectra have been derived by numerous authors.[1] The calculations are in most cases very lengthy and are carried out for special cases. The results may be obtained by the following short and yet rigorous consideration. The interaction energy of a nucleus with an electron of charge $-e$ may be represented by

$$H' = g\mu_0(A\cdot\mathfrak{y}) \tag{1}$$

where $\mathfrak{y}$ is the angular momentum matrix vector of the nucleus in units $h/2\pi$ and $g\mu_0\mathfrak{y}$ is its magnetic moment. μ_0 is the Bohr magneton and g is a numerical factor to be determined by comparison with experiment. Here

$$A = 2\mu_0[r^{-3}L - \mathfrak{d}r^{-3} + 3r(r\mathfrak{d})r^{-5}]/[1 + (eA_0/2mc^2)] + 2\mu_0[\mathfrak{d}r^{-2} - r(r\mathfrak{d})r^{-4}]\frac{d}{dr}[1 + (eA_0/2mc^2)]^{-1} \tag{2}$$

L is the orbital angular momentum in units $h/2\pi$, $2\mathfrak{d}$ is Pauli's spin vector so that $(h/2\pi)\mathfrak{d}$ is the angular momentum of the electron spin, r is the distance from the nucleus and A_0 is the electrostatic potential. Expression (2) may be derived from the Dirac equation by eliminating two wave functions. The first part of (2) is the only important one except for s terms where the second part is responsible for all of the effect. The total angular momentum is

$$F = J + \mathfrak{y} = L + \mathfrak{d} + \mathfrak{y}. \tag{3}$$

The quantum number of F, J, L, $\mathfrak{y}$ we write as f, j, l, i. By well-known theorems about angular momenta we have for the perturbed energy

$$w = g\mu_0(AJ)_j[f(f+1) - i(i+1) - j(j+1)]/[2j(j+1)]. \tag{4}$$

Here $(AJ)_j$ is the value of any diagonal element in the matrix (AJ) in that part of it which belongs to the quantum number j. Substituting $J=L+\mathfrak{d}$ into (AJ) we have except for s terms

[1] J. Hargreaves, Proc. Roy. Soc. **124**, 568 (1929); **127**, 141, 407 (1930). E. Fermi, Zeits.f. Physik **60**, 320 (1930). Unpublished calculations of Casimir quoted in Pauling and Goudsmit's book.

$$(AJ)/2\mu_0 = -\mathfrak{o}^2 r^{-3} + 3(r\mathfrak{o})^2 r^{-5} + 3(rL)(r\mathfrak{o})r^{-5} + r^{-3}L^2.$$

The denominator of the first part of (2) being set here $=1$ since $eA_0/2mc^2$ is in this case small. We note that $rL=0$ and that $3(r\mathfrak{o})^2 - r^2\mathfrak{o}^2 = 0$. We have then

$$w = g\mu_0{}^2(r^{-3}L^2)_j[f(f+1) - i(i+1) - j(j+1)]/[j(j+1)]. \tag{5}$$

This is exact since the coupling to the nucleus is weak. If in addition the coupling of L and $\mathfrak{o}$ is weak we may write $L^2 = l(l+1)$ so that

$$w = g\mu_0{}^2\frac{l(l+1)}{j(j+1)}[f(f+1) - i(i+1) - j(j+1)]\overline{(r^{-3})} \tag{6}$$

For s terms the denominator $1+(eA_0/2mc^2)$ insures the disappearance of the first part of (2) in the approximation of formula (5). In this case

$$(AJ)_j = 2\mu_0\int_0^\infty \psi^2(r)(1/2r^2)\left\{\frac{d}{dr}[1 + (eA_0/2mc^2)]^{-1}\right\}4\pi r^2 dr \doteqdot 4\pi\mu_0\psi^2(0) \tag{6'}$$

in the same approximation as Fermi's.[2] If therefore we add to (6) the statement that for $l=0$

$$[\overline{(r^{-3})}l(l+1)]_{l=0} = 2\pi\psi^2(0) \tag{7}$$

formula (6) becomes complete.

These results in the approximation of equation (6) are in complete agreement with the statements made in Pauling and Goudsmit's book where the calculations of Casimir have been used.

[2] The exact formula for a Coulomb field is found in G. Breit Phys. Rev. **35**, 1447 (1930).

THE DIFFRACTION OF AN ELECTRON-WAVE AT A SINGLE LAYER OF ATOMS

By M. v. Laue*

(Received October 20, 1930)

Abstract

This paper undertakes to estimate the influence of the gradual transition between the field exterior to, and in the interior of a crystal, on the diffraction of electrons. This gradual transition is required by electrostatics. The result is, that this influence may be neglected for electrons whose energy is two hundred volts or more. One can then treat the transition as discontinuous. In the case of slower electrons it seems doubtful, if such a treatment is permissible.

Introduction

THE theory of the diffraction of electrons by a space-lattice has been discussed by Bethe and later, under simplifying assumptions by Morse.[1] These authors integrate the Schrödinger-equation for the internal field in so complete a manner, that little more is to be said. Their treatment of the incidence and reflection at the surface cannot be considered as equally satisfactory. They treat the triply periodic internal field as though it ceases suddenly at a certain plane. This is in complete contradiction to electrostatics, as one may not consider this plane as charged without coming into conflict with the atomistic foundations of the whole theory. The field certainly dies off asymptotically as one proceeds outward. This is doubtless a lack in the theory which, as it seems to us,—might cast doubt on its applicability to the experiments. At least it should be examined to see if and under what circumstances this approximation is justifiable. As a matter of fact it will appear that this is not always the case.

Properly one should treat the atoms as having a finite extension but then the calculations based on the Schrödinger-equation would encounter a difficulty which is only too well known in optics, namely the reflection and refraction at a plane plate with continuously variable refractive index. Of necessity, then, we will treat the atoms as point charges. The order of magnitude of our results will probably not be influenced.

To obtain a comparison let us glance at the theory of Röntgen-interference which is similar to Bethe's in many points. In this treatment one considers the space-lattice of diffracting centers to be bounded by a definite lattice-plane; one can also object to this since the atoms in the boundary planes actually do not occupy exactly the position which they would have if the crystal were continued beyond the boundary. But since a single layer of atoms contributes very little to the resultant intensity of Röntgen-rays this

* Translated from the German by C. Eckart.

[1] H. Bethe, Ann. d. Physik **87**, 55 (1928); P. M. Morse, Phys. Rev. **35**, 1910 (1930).

assumption can have little influence. In the case of electron-diffraction things are essentially different.

Let the primitive periods of the lattice-plane be the vectors $\mathfrak{a}_1$ and $\mathfrak{a}_2$; the reciprocal vectors $\mathfrak{b}_1$, $\mathfrak{b}_2$ which lie in the same plane are defined by the equations

$$(\mathfrak{a}_1\mathfrak{b}_1) = 1,\ (\mathfrak{a}_1\mathfrak{b}_2) = 0,\ (\mathfrak{a}_2\mathfrak{b}_1) = 0,\ (\mathfrak{a}_2\mathfrak{b}_2) = 1. \tag{1}$$

The surface-density of electricity in this plane will be

$$\rho = \sum_1 \rho_m e^{2\pi i(\mathfrak{b}_m \mathfrak{r})} \tag{2}$$

where $\mathfrak{r}$ is the vector drawn from an arbitrary origin in the lattice-plane to the point of consideration, and

$$\mathfrak{b}_m = m_1\mathfrak{b}_1 + m_2\mathfrak{b}_2. \tag{3}$$

The coefficient ρ_0 is zero, since the total charge must vanish. The other coefficients are given by the equation

$$\rho_m = \frac{1}{F}\int \rho e^{-2\pi i(\mathfrak{b}_m \mathfrak{r})} d\sigma,$$

in which F is the area of the parallelogram subtended by $\mathfrak{a}_1$, $\mathfrak{a}_2$, and the integration is to be extended over such a parallelogram. If a positive pole of charge Z lie at $\mathfrak{r}_+ = \delta_1\mathfrak{a}_1 + \delta_2\mathfrak{a}_2$ a negative pole of the same strength at $\mathfrak{r}_- = -(\delta_1\mathfrak{a}_1 + \delta_2\mathfrak{a}_2)$ then according to 1):

$$\rho_m = -\frac{2Z\epsilon}{F} i \sin 2\pi(m_1\delta_1 + m_2\delta_2). \tag{4}$$

We assume that the lattice plane has the equation $z=0$. Then these charges produce the potential

$$\phi = \sum \phi_m e^{2\pi i(\mathfrak{b}_m \mathfrak{r})} e^{-2\pi|\mathfrak{b}_m||z|} \tag{5}$$

in which[2]

$$\phi_m = \frac{\rho_m}{|\mathfrak{b}_m|}. \tag{6}$$

The coefficient ϕ_0 vanishes. It would have to be—because of $\Delta\phi = 0$—a linear function of z and this must vanish because of the boundary conditions at $z = \pm\infty$.

It would be otherwise if we had, e.g., two parallel planes of which the one had a net positive charge, the other an equal negative: then ϕ_0 would be different from zero between the two planes. Also if the atoms were not taken to be point-charges there would be regions in which ϕ_0 did not vanish.

[2] This series is naturally double. The index m represents the pair of indices m_1 and m_2 which occur in (3) explicitly.

The Schrödinger-equation of the free electron

$$\Delta\psi + \frac{8\pi^2\mu}{h^2}E\psi = 0$$

is integrated by the function

$$\psi = e^{2\pi i(K_0 R)}, \quad (K_0) = \frac{1}{h}(2\mu E)^{1/2} \tag{7}$$

in which R is the three-dimensional vector to the point under consideration (Aufpunkt); r is the component of R parallel to the plane $z=0$, μ the mass of electron. We also resolve the vector K_0 into a component k_0 parallel to this plane and one parallel to the z axis—z the magnitude of the latter is $\kappa_0=(K_0^2-k_0^2)^{1/2}$. Then Eq. (7) becomes

$$\psi = \psi_0(z)e^{2\pi i(k_0 r)}, \quad \psi_0(z) = e^{2\pi i\kappa_0 z} \tag{8}$$

We assume that κ_0 is positive; the wave than proceeds from positive to negative z-values.

The Schrödinger-equation of the electron as perturbed by the lattice-plane

$$\Delta\psi + \frac{8\pi^2\mu}{r^2}(E - \epsilon\phi)\psi = 0$$

we attempt to resolve in the form

$$\psi = \sum\psi_m(z)e^{2\pi i(k_0+b_m, r)}.$$

It then reads

$$\Delta\psi = \sum\left(\frac{d^2\psi_m}{dz^2} - 4\pi^2(k_0 + b_m)^2\psi_m\right)e^{2\pi i(k_0+b_m, r)} \tag{9}$$

from which we can cancel the factor $e^{2\pi i k_0 r}$. The remaining equation is then:

$$\sum_m\left(\frac{d^2\psi_m}{dz^2} + 4\pi^2(K_0^2 - (k_0 + b_m)^2)\psi_m\right)e^{2\pi i(b_m r)} = \frac{8\pi^2\epsilon\mu}{h^2}\sum_{p,q}\psi_p(z)\phi_q e^{-2\pi|b_q||z|}e^{2\pi i(b_q+b_q, r)}$$

According to Eq. (3)

$$b_p + b_q = b_{p+q}.$$

Since this equation must be true for every value of the vector r, the separate terms on each side which have the same exponential factor must be identical, i.e.

$$\frac{d^2\psi_m}{dz^2} + 4\pi^2(K_0^2 - (k_0 + b_m)^2)\psi_m = \frac{8\pi^2\epsilon\mu}{h^2}\sum_p\psi_p(z)\phi_{m-p}e^{-2\pi|b_m-p||z|} \tag{10}$$

To solve this system of infinitely many differential-equations with infinitely many unknowns $\psi_m(z)$ we use a method of approximation. As first approximation one will substitute for ψ_0 the value (8) of the wave-function of the unperturbed incident wave, and retain only the term in ψ_0 on the right side of (10). The weaker the intensity of the diffracted waves comes out, the better will be this approximation. Since $\phi_0 = 0$ we then obtain the equation:

$$\frac{d^2\psi_m}{dz^2} + 4\pi^2(K_0^2 - (k_0 + b_m)^2)\psi_m = \frac{8\pi^2\epsilon\mu}{h^2}\psi_0(z)\phi_m e^{-2\pi|b_m||z|} \tag{11}$$

of which the solution satisfies the condition that it must represent *emergent* waves at $z = \pm\infty$ is

$$\begin{aligned}\psi_m(z) = 2\pi i\frac{\epsilon\mu}{h^2}\frac{\phi_m}{\epsilon_m}\Big\{ & e^{2\pi i\epsilon_m z}\int_z^\infty \psi_0(\zeta)e^{-2\pi|b_m||\zeta|}e^{-2\pi i\epsilon_m\zeta}d\zeta \\ & + e^{-2\pi i\epsilon_m z}\int_{-\infty}^z \psi_0(\zeta)e^{-2\pi|b_m||\zeta|}e^{+2\pi i\epsilon_m\zeta}d\zeta\Big\}.\end{aligned} \tag{12}$$

The abbreviation

$$\epsilon_m = (K_0^2 - (k_0 + b_m)^2)^{1/2} \tag{13}$$

has been used. That this is a solution of Eq. (11) will be seen on substitution. For $z = +\infty$ we obtain from (12):

$$\psi_m = 2\pi i\frac{\epsilon\mu}{h^2}\frac{\phi_m}{\epsilon_m}e^{-2\pi i\epsilon_m z}\int_{-\infty}^{+\infty}\psi_0(\zeta)e^{-2\pi|b_m||\zeta|}e^{+2\pi i\epsilon_m\zeta}d\zeta \tag{14}$$

At $z = -\infty$ correspondingly

$$\psi_m = 2\pi i\frac{\epsilon\mu}{h^2}\frac{\phi_m}{\epsilon_m}e^{+2\pi i\epsilon_m z}\int_{-\infty}^{+\infty}\psi_0(\zeta)e^{-2\pi|b_m||\zeta|}e^{-2\pi i\epsilon_m\zeta}d\zeta. \tag{15}$$

These are the emergent waves required by the boundary conditions, at least, if ϵ_m is real and positive.

The latter may always be assumed to be the case, as the sign is not defined by (13). The former is not always true according to (13). In addition to the diffracted homogeneous waves there are also inhomogeneous ones which are propagated along the lattice-plane and die off asymptotically in a direction perpendicular to this plane. For every pair with indices m with real ϵ_m there are always two emergent waves on each side of the lattice-plane.

It will be remarked that Eq. (12) is still valid for such index pairs, m, for which $i\epsilon_m$ is positive and real.[3] If one draws the factor $e^{\pm 2\pi i\epsilon_m z}$ under the integral sign, than the bracket in (13) has the value

$$\int_z^\infty \psi_0(\zeta)e^{-2\pi|b_m||\zeta|}e^{2\pi i\epsilon_m(z-\zeta)}d\zeta + \int_{-\infty}^z \psi_0(\zeta)e^{-2\pi|b_m||\zeta|}e^{-2\pi i\epsilon_m(z-\zeta)}d\zeta$$

[3] Negative real values may be left out of account since the sign of the root in (13) is arbitrary; they must be left out of account, because Eq. (12) is not longer valid when $i\epsilon_m < o$.

in the first of these integrals $z-\zeta$ is negative, in the second positive. They both exist therefore. Only Eqs. (14) and (15) must be changed for this case; but our interest is only for the homogeneous waves, i.e., real values of ϵ_m.

For the justification of this calculation it is essential that Eq. (11) applied to the index pair 0,0 possesses the solution $\psi_0(z)$ as given in Eq. (8). This would not be the case, if ϕ_0 did not vanish. In that case we would encounter the problem of the plane parallel plate as remarked in the introduction and would have to use its solution in evaluating the other ψ_m.

The integrals in (14) and (15) are to be evaluated for real values of ϵ_m and ψ_0 as in (8). They are

$$\int_{-\infty}^{+\infty} e^{2\pi i(\kappa_0 \pm \epsilon_m)\zeta} e^{-2\pi|b_m||\zeta|} d\zeta$$

$$\int_0^{\infty} e^{2\pi i(\kappa_0 \pm \epsilon_m)\zeta} e^{-2\pi|b_m|\zeta} d\zeta + \int_{-\infty}^{0} e^{2\pi i(\kappa_0 \pm \epsilon_m)\zeta} e^{+2\pi|b_m|\zeta} d\zeta$$

$$= 2\int_0^{-\infty} \cos\,(2\pi(\kappa_0 \pm \epsilon_m)\zeta) e^{-2\pi|b_m|\zeta} d\zeta = \frac{1}{\pi} \frac{|b_m|}{(\kappa_0 + \epsilon_m)^2 + b_m^2}$$

If we now use the value of ϕ_m given by (6) and ρ_m given by (4), we obtain

$$\psi_m(z) = \frac{4Z\epsilon^2\mu}{h^2} \frac{\sin 2\pi(m_1\delta_1 + m_2\delta_2)}{F} \frac{e^{\mp 2\pi i\epsilon_m z}}{\epsilon_m[(\kappa_0 \pm \epsilon_m)^2 + b_m^2]} \quad \text{for } z = \pm\infty \quad (16)$$

in which the abbreviations

$$\kappa_0 = (K_0^2 - k_0^2)^{1/2} = |K_0| \cos\theta, \quad |K_0| = \frac{1}{h}(2\mu E)^{1/2}$$

$$\epsilon_m = (K_0^2 - (k_0 + b_m)^2)^{1/2} = (K_0^2 \cos^2\theta - 2(k_0 b_m) - b_m^2)^{1/2}$$

have been used. The angle θ is the angle of incidence of the original electron wave. Only the last of the three fractions in (16) depends on the energy of the electrons, and it diminishes with increasing E approximately as $E.^{-3/2}$ For sufficiently fast electrons the amplitude of every ψ_m-wave is so small, that the diffracting-power of the single atomic layer is insignificant. The neglect of the surface layers is then justified. To obtain an estimate of the lower limit above which this is true we will later evaluate Eq. (16) numerically.

One can best estimate the strength of an inhomogeneous wave if one determines its amplitude in the lattice-plane itself ($z=0$). We designate the real positive quantity $i\epsilon_m$ by η_m. From (12), (6) and (4) it then follows without difficulty that:

$$\psi_m(0) = \frac{4Z\epsilon^2\mu}{h^2} i \sin\ 2\pi(m_1\delta_1 + m_2\delta_2) \frac{|b_m| + \eta_m}{|b_m|(\eta_m)[(b_m + \eta_m)^2 + \kappa_0^2]}.$$

One notices the diminution of the amplitude with increasing indices m_1, m_2.

For numerical purposes we suppose the vectors a_1, a_2 perpendicular the one to another and both of length 4×10^{-8} cm. Then the reciprocal vectors b_1, b_2 will also be perpendicular and of the magnitude 2.5×10^7 cm^{-1}. In each square formed by a_1, a_2 we suppose one positive and one negative charge—each of $Z=1$, but we do not determine their positions more definitely, i.e., the numbers δ_1, δ_2 are thus undetermined. Then the first factor in (16) is

$$\frac{4\epsilon^2\mu}{h^2F} = 1.25\times 10^{22}\ \text{cm}^{-3}.$$

We suppose an electron beam of 150 volts energy to be incident normally on this lattice plane. The de Broglie wave-length is 10^{-8} cm, also $\kappa_0 = |k_0| = 10^8$ cm^{-1}. Then only those homogeneous waves can appear, for which the indices m_1, m_2 are any combination of the numbers ± 1 and 0. This results in 8 emergent beams from each side of the lattice plane. If one index is 0, the other ± 1 Eq. (16) gives

$$\frac{|\psi|^2_{z=+\infty}}{\sin^2(2\pi(m_1\delta_1 + m_2\delta_2))} = 10^{-5}, \quad \frac{|\psi|^2_{z=-\infty}}{\sin^2(2\pi(m_1\delta_1 + m_2\delta_2))} = 4\times 10^{-2}$$

If both indices are ± 1, then one finds

$$\frac{|\psi|^2_{z=+\infty}}{\sin^2(2\pi(m_1\delta_1 + m_2\delta_2))} = 1.5 \times 10^{-5}, \quad \frac{|\psi|^2_{z=-\infty}}{\sin^2(2\pi(m_1\delta_1 + m_2\delta_2))} = 3\times 10^{-3}$$

$\sin^2(\ )$ is the structure factor and obviously depends on the position of the two pointcharges in the elementary parallelogram. Since we set the intensity of the incident wave equal to 1, the foregoing numbers represent the relative intensity of the diffracted rays. As they are small compared with 1, one will conclude firstly, that the present approximation is sufficient, and secondly, that the diffracting-power of the single plane is so small that it is justified to neglect the surface fields as Bethe and Morse have done.

The result is quite different if we consider electrons of energy 37.5 volts, other things remaining the same (wave-length $\lambda = 2\times 10^{-8}$ cm). Then the only possible homogeneous waves are those for which one index is 0, the other ± 1. At $z=+\infty$ the fraction $|\psi|^2/\sin^2(\ )$ has a sufficiently small value, namely 10^{-3}; but for $z=-\infty$ it becomes even greater than 1, which naturally means that the present approximation is useless. In this case it seems that space lattice theories of Bethe and Morse require extension by considerations regarding the surface layers.

In summary we may safely say, despite the fact that the case here considered is far from the real one, that for electrons of 200 or more volts energy

the neglect of the surface action in the space lattice theory of electron diffraction is justified, but that this is not obviously true at smaller velocities.

In the experiments of Stern and his collaboraters on the diffraction of atoms and molecules by crystals, the plane-grating-action of the surface is the only thing observed, no space-lattice effects. The theory of these phenomena one must probably attempt to carry through in a similar manner to the above. The essential difference will be in a different value of the coefficients ϕ_m of the Fourier-series for the potential energy. The form (9) for the wave-function and the approximation introduced in (11) may probably be retained.

SOME PHOTOELECTRIC AND THERMIONIC PROPERTIES OF RHODIUM

By E. H. Dixon
Department of Physics, University of Georgia

(Received November 19, 1930)

Abstract

A thin ribbon of rhodium was subjected to rigorous heat treatment at 950°–1450°C for 1050 hours in a final vacuum of 10^{-8} mm of Hg in order to put it in a stable condition for photoelectric and thermionic measurements. During this period the long wave limit shifted from about 2530A to 3150A and then shifted back to 2509A where it remained during the latter 375 hours of heat treatment.

The photoelectric current was found to increase about 130% as a result of increasing the temperature of the rhodium from 25°C to 950°C. A rather sudden increase took place at about 240°C.

The photoelectric work function at 25°C was determined from the final long wave limit of 2482–2536A to be 4.92 ± 0.06 volts. The long wave limit at 240°C was 2652–2752A which gave a photoelectric work function of 4.57 ± 0.09 volts for this temperature. No further change in long wave limit was observed up to 650°C.

An anomaly was observed at 1100°C where the thermionic current was irregular and where the rate of change of the resistance of the rhodium with temperature changed on increasing the temperature.

The thermionic work function of rhodium, as determined from observations and with Richardson's equation, was 4.58 ± 0.09 volts. This value agrees with the photoelectric work function at 240°C.

Pure hydrogen and oxygen were introduced separately into the experimental tube while the rhodium was in its outgassed equilibrium condition. In the case of hydrogen the wave limit was changed from 2482–2536A to 2378–2482A. In the case of oxygen the wave limit was changed from 2482–2536A to a value so low that it could not be determined by the method used in this work.

AMONG the photoelectric and thermionic studies of metals which have been subjected to rigorous heat treatment, or distillation, there are: DuBridge's[1] extensive study of the thermionic and photoelectric properties of platinum; Cardwell's[2] work with iron and cobalt; Martin's[3] thermionic and photoelectric study of molybdenum; Warner's[4] work with tungsten; the work of Kazda,[5] Dunn,[6] and Hales[7] on mercury; and Goetz's[8] study of tin.

The object of this investigation has been (1) to investigate the photoelectric and thermionic properties of rhodium during and after subjection

[1] DuBridge, Nat. Acad. Sci. **12**, 162 (1926); Phys. Rev. **31**, 236 (1928); Phys. Rev. **32**, 961 (1928).
[2] Cardwell, Nat. Acad. Sci. **14**, 439 (1928); Nat. Acad. Sci. **15**, 544 (1929).
[3] Martin, Phys. Rev. **33**, 991 (1929).
[4] Warner, Nat. Acad. Sci. **13**, 56 (1927); Phys. Rev. **33**, 815 (1929).
[5] Kazda, Phys. Rev. **26**, 643 (1925).
[6] Dunn, Phys. Rev. **29**, 693 (1927).
[7] Hales, Phys. Rev. **32**, 950 (1928).
[8] Goetz, Phys. Rev. **33**, 373 (1929).

to rigorous heat treatment and (2) to introduce known gases in order to determine their effects upon the photoelectric properties of rhodium in the outgassed condition.

Apparatus

The experimental tube was similar to that used by DuBridge[9] with a few exceptions. Charcoal was not used in this work. Potential leads, spot-welded about a quarter of an inch below the ends of the filament, permitted the measurement of the P. D. across the filament. A grounded guard ring was installed between the collecting cylinder lead and all of the other leads of the experimental tube. The fact that Pyrex was sufficiently conducting at 100° C to prevent an accurate measurement of the photoelectric current immediately after cutting off the heating current made this device compulsory. The rhodium, purchased from the American Platinum Works, Newark, N. J. in the purest state that they could furnish, was in the form of ribbons 10 cm long by 0.4 cm wide by 0.004 cm thick. Each ribbon, bent in the form of a loop, was suspended inside a molybdenum collecting cylinder from two fifty mil tungsten leads through which current could be sent to heat the specimen to any desired temperature. All of these devices were enclosed in a Pyrex tube which was connected through two liquid air traps, a mercury cut-off, and a water-cooled mercury diffusion pump to a "Cenco" fore pump. The molybdenum cylinder was provided with two one half inch holes, one for illuminating the specimen and the other for pyrometric measurements of the temperature. A shutter, operated by an external magnet, could cover the opening through which the photo-active light had to pass. A quartz window, attached to the experimental tube by means of a graded quartz-Pyrex seal, served to admit radiation from a Cooper-Hewitt quartz mercury arc which was operated by a current of 3.1 amperes. The vertical arc was enclosed in a metal housing. Pressures lower than 10^{-6} mm of Hg were measured with an ionization manometer which was calibrated by extrapolating from data obtained by means of a McLeod gauge. The extrapolation was based on the work of Dushman and Found.[10] The photoelectric currents due to the full radiation of the mercury arc were measured by means of a Compton[11] electrometer shunted with a resistance of 10^9 ohms, thus permitting the use of the steady deflection method of measuring current. The sensitivity of the electrometer was determined at the time of each observation. The rate of charge method of detecting current was used in getting the long wave limit.

Outgassing Treatment

For 48 hours the molybdenum collecting cylinder was heated by electron bombardment in an auxiliary vacuum system at 800–1000°C before it was introduced into the experimental tube. When the experimental vacuum system was apparently free from leaks and the pressure was as good as could

[9] DuBridge, Phys. Rev. **29**, 451 (1927).
[10] Dushman and Found, Phys. Rev. **23**, 734 (1924).
[11] Compton, Phys. Rev. **14**, 85 (1919).

be read on the McLeod guage (of the order of 10^{-7} mm of Hg), the ionization manometer, the experimental tube, and the second liquid air trap were heated for 94 hours at approximately 400, 500, and 500 degrees C respectively. At the end of this period the pressure was again of the order of 10^{-7} mm of Hg while the tubes were hot. Then, in order to avoid excessive evaporation of the specimen, it was heated by a current at temperatures which were gradually increased from about 900°C to 1250°C and finally to 1450°C. The high vacuum end of the system up to the first liquid air trap was heated with a torch.

Fatigue

In Fig. 1 the photoelectric current due to the full arc is plotted as a function of the time of rest after cutting off the heating current. After fifty hours heating of the specimen there is a marked fatigue which becomes more pronounced until 250 hours of heating. Then it becomes rapidly less marked until

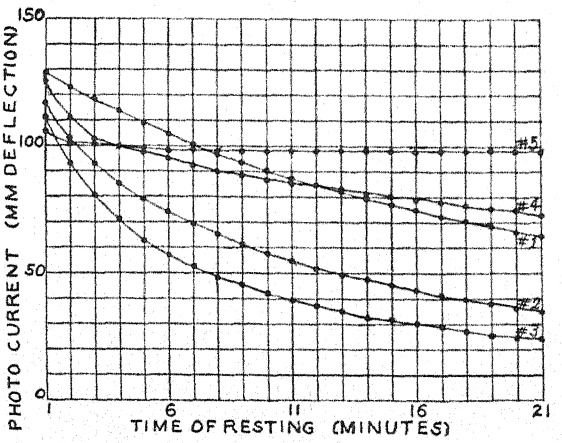

Fig. 1. Decrease of photoelectric sensitivity with time, using full arc.
Curve #1, taken after 50.5 hours of heat treatment.
Curve #2, " " 116.5 " " " "
Curve #3, " " 250.5 " " " "
Curve #4, " " 276.9 " " " "
Curve #5, " " 372.2 " " " "

there is practically no fatigue except for the first four or five minutes after cutting off the heating current. The drop in sensitivity during this short interval can be reasonably attributed to the fact that it required four or five minutes for the filament to cool to approximately room temperature. That this is the probable cause of the rapid initial change was shown by correlating the rate of cooling of the filament, as determined from resistance measurements, with the temperature change of photo-sensitivity. In determining a fatigue curve the first photoelectric observation was taken one minute after the heating current was stopped, and from the above mentioned comparison it was concluded that the filament was at this instant at a temperature of about 240°C. The change in the photo-current during the next

few minutes is associated with a phenomenon discussed in the next paragraph.

Variation of Photoelectric Sensitivity with Temperature

Rhodium, like Pt, Co, W, and Fe in the γ form, has a positive temperature coefficient after it has been subjected to severe outgassing conditions. There is an increase of 130% in the photoelectric current in going from room

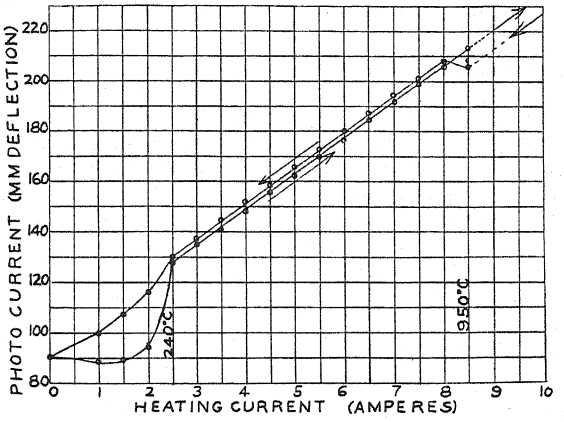

Fig. 2. Total photo-current as a function of heating current.

temperature to a temperature of 950°C. In Fig. 2 the photoelectric current due to the full arc is plotted as a function of the heating current. The temperature was decreased slowly from 1100°C to 950°C and then readings were taken as indicated in Fig. 2. The data for this curve were taken after the filament had been heated for 640 hours at approximately 1250°C. The pressure was 10^{-8} mm of Hg. For each reading five minutes were allowed for

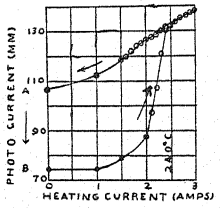

Fig. 3.

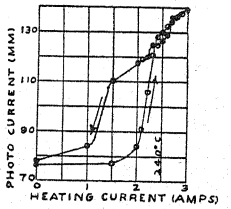

Fig. 4.

attaining temperature equilibrium. The photo-current variation with temperature between 240°C and 950°C can be reproduced without serious difficulty. The difference between the two curves in Fig. 2 between 240°C and 950°C is due to the fact that the specimen was cooled slowly from 1100°C where rhodium exhibits an unusual characteristic. This will be discussed in connection with the thermionic current as a function of temperature. The factors affecting the behavior of rhodium below 240°C are complicated and it

is not always possible to predict in advance the exact type of curve that will result when the temperature is decreased from 240°C to room temperature. The data for the curves in Figs. 3 and 4 were taken under apparently the same conditions, yet the final currents at room temperature are very different. In the case of the curve in Fig. 3—the more frequent type of curve —the final photo-current observed with zero heating current was not stable, but decreased in approximately one hour from the value at *A* to the value at *B*. Under the conditions of Fig. 4 on the other hand a stable condition was reached at once by the same gradual reduction of the heating current to zero. If the heating current was instantly reduced to zero when the filament was at about 1250°C (heating current of 12 amperes) the stable condition represented by *B* would always be reached in about 10 minutes. As mentioned above, almost half of this delay is accounted for by the time required for the filament and its surrounding cylinder to cool to room temperature. The behavior in the range from 240°C down depends also upon the vacuum conditions, a sequence such as that of Fig. 4 occurring only under the best conditions. The complicated situation which these curves suggest will be discussed later.

The Photoelectric Long Wave Limit

During the early stages of outgassing, the long wave limit was obtained by means of Corning glass filters. The final value, however, was located by using various solutions of tartaric acid, acetic acid, and the glass filters. Spectrograms of all filters were made at the same time that they were used. The wave limit was between 2378A and 2482A before any heat treatment. The specimen was heated for five hours at 500°C after which the long wave limit was between 2536A and 2752A. During the baking period of 94 hours it decreased to about 2536A. Then, on heating the rhodium at temperatures

Table I.

Time of heating specimen (hours)	Heating temperature (degrees C)	Long wave limit (angstroms)
25	900	2967
59	1025	2804–2967
81	1025	2804–2967
144	1025	2967–3341
190	1250	2967–3341
213	1250	(2536)–2752
267	1250	(2536)–2752
419	1250	2652–2752
676	1250	2482–2536
1051	1450	2482–2536

varying from 900°C to 1450°C, its long wave limit varied with time of outgassing as indicated in Table I. During the latter 375 hours the long wave limit remained between the 2482A and 2536A lines. Both of these lines are very intense and the limit could be very definitely located between them. If this limit is taken to be characteristic of outgassed rhodium, Einstein's[12] photoelectric equation gives for its photoelectric work function at 25°C

[12] Einstein, Ann. d. Physik **17**, 132 (1905).

$$V = \frac{ch\nu_0}{e} = \frac{c^2h}{e\lambda_0} = \frac{12335}{\lambda_0} = 4.92 \pm 0.06 \text{ volts},$$

where Birge's[13] values for the constants are used and λ_0 is (2482+2536)/2A. The long wave limit for the rhodium at approximately 240°C (corresponding to a heating current of 2.5 amperes) was found to lie between the 2652A and 2752A lines. The average of these values gives for the photoelectric work function at 240°C

$$V = \frac{12335}{2702 \pm 50} = 4.57 \pm 0.09 \text{ volts}.$$

No further change in long wave limit has been observed up to 650°C. Nevertheless, the photo-current continues to increase up to 950°C. An increase in temperature, therefore, appears to increase both the surface work function and the quantum efficiency.

Thermionic Current as a Function of Heating Current

The thermionic current was measured with a Leeds and Northrup galvanometer which had a sensitivity of 1.57×10^{-10} amperes per mm deflection at a scale distance of 1.5 meters. In Fig. 5 the thermionic current is plotted

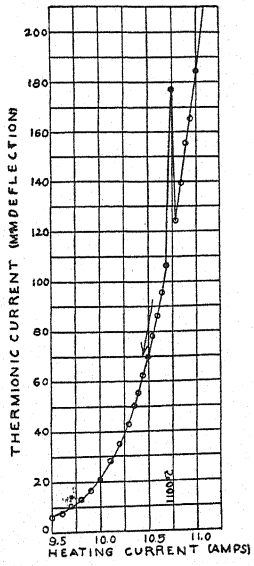

Fig. 5.

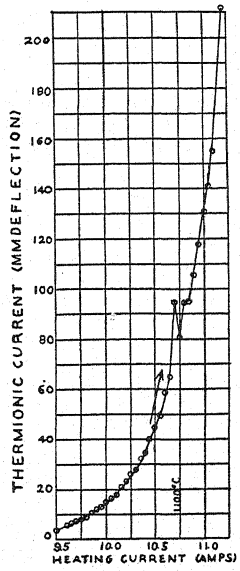

Fig. 6.

as a function of the heating current in amperes. The most interesting part of the curve is at approximately 10.7 amperes (about 1100°C) where the thermionic current is irregular. In the case of gradually decreasing the heating current and observing the thermionic current at short intervals of heating

[13] Birge, Phys. Rev. Supplement 1, 1 (1929).

current, the writer has been able to obtain at about 10.7 amperes of heating current a gradual increase in the thermionic emission (heating current kept constant) until it reached a maximum value corresponding to an increase of temperature of approximately 25°C and then a gradual decrease in emission until equilibrium was reached at a value very close to what it was before the gradual increase began (see Fig. 6). This phenomenon indicates that at about 1100°C a change which liberates heat takes place on cooling rhodium.

Cardwell[14] published a similar thermionic curve for iron in which the thermionic current was irregular at 910°C, where the crystal structure changes from the body centered cubic to the face centered cubic type. One would think that the similar break in the thermionic curve for rhodium is due to the same cause; that is, to a change in the crystal structure. However, it is possible that the break is due to absorption or evolution of gas at this temperature. Nevertheless, it must be remembered that this specimen of rhodium had had more than 600 hours of heat treatment at about 1250°C in a final vacuum of 10^{-8} mm of Hg when the data for this curve were taken, and also that it has been impossible to detect any change in pressure peculiar

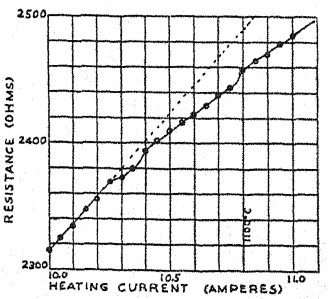

Fig. 7.

to this particular temperature while increasing or decreasing the heating current. The crystal structure of rhodium at various temperatures is now being determined in this laboratory by means of x-rays.

Mendenhall and Ingersoll[15] observed an anomaly at about 1050°C, consisting of an easily reversible change in the radiation of the surface of a small sphere of rhodium heated on a Nernst glower. They reported further that, as the temperature was lowered, the sphere became rather suddenly brighter —the change being seen to spread rapidly over the globule—and that, if the temperature was raised again, the reverse change took place. The fact that these observations were in air at normal pressure, while the present observations were in a very high vacuum, favors the view that the cause is a structure change rather than a gas action.

Resistance as a Function of Heating Current

In Fig. 7 the resistance of the specimen of rhodium is also plotted as a function of the heating current. It is interesting to observe that, at about

[14] Cardwell, Nat. Acad. Sci. **14**, 439 (1928).

[15] Mendenhall and Ingersoll, Phil. Mag. **15**, 205 (1908).

10.3 and 10.7 amperes of heating current, a definite change in slope occurs in the resistance curve. It is reasonable to suppose that the two breaks are due to uneveness of the temperature of the filament, because this curve was taken after the filament had been heated for 575 hours at approximately 1250°C. The fact that the slope of the resistance curve changes abruptly suggests the idea that a change in the structure may be taking place in the rhodium.

The Thermionic Work Function

The black-body temperatures of the rhodium strip were measured with a disappearing filament type of optical pyrometer which had been calibrated at the gold and palladium points and sectored down from the palladium point to the gold point. The readings were corrected for the transmission of the Pyrex window by means of data taken before it was sealed to the experimental tube. Then the true temperatures were computed from the relation

$$1/T - 1/S = \lambda \log \epsilon / c_2 \log e,$$

where T is the true temperature, S the apparent temperature, λ the wavelength used, ϵ the emissivity,[16] c_2 a constant in Wien's equation, and e the

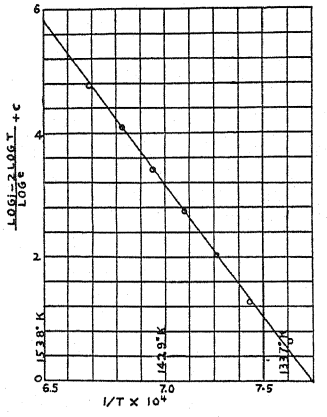

Fig. 8.

Naperian base. Fig. 8 gives the relation between $(\log i - 2 \log T)/(\log e) + C$ and $1/T$. The slope of this curve is the b in Richardson's relation

$$i = AT^2 e^{-b/T},$$

where i is the thermionic current and A is a constant.

$$b = 53{,}100° K.$$

Hence, the thermionic work function is

$$V = \frac{bk}{e} = \frac{53100 \times 1.371 \times 10^{-16} \times 299.8}{4.770 \times 10^{-10}} = 4.58 \text{ volts}.$$

[16] Bulletin of Bureau of Standards **11**, 595 (1914–15).

From other curves it is estimated that the result can be reproduced easily within 2%. Therefore, the thermionic work function is 4.58 ± 0.09 volts. This value agrees with the value given for the photoelectric work function at 2.5 amperes of heating current (approximately 240°C).

The Effect of Pure Hydrogen and Oxygen on Outgassed Rhodium

Extreme care was given to the purification of the hydrogen and oxygen used in this work. Hydrogen, admitted to the experimental tube after 500 hours of heat treatment for the rhodium, changed the long wave limit from the equilibrium value of 2482–2536A (a value characteristic of rhodium after 1000 hours of heat treatment in a final vacuum of 10^{-8} mm of Hg) to 2378–2482A; that is, the limit was changed to approximately the original value characteristic of the specimen before it had received any heat treatment. The photo-current was decreased very quickly from 100 mm deflection to 2 mm. Heating the specimen at 1000°C for one minute in hydrogen at a pressure of one mm of Hg increased the photo-current from 2 mm to 100 mm deflection, but the photo-sensitivity dropped to 3 or 4 mm in 4 minutes after reducing the heating current to zero. Allowing the pumps to remove as much of the hydrogen as possible without heating the rhodium increased the photo-current from 2 mm to 4 mm. Light from the mercury arc increased the photo-current from 2 mm to 4 mm in two hours. The long wave limit characteristic of the rhodium after 1000 hours of heat treatment was attained in 100 hours of heating at 1250°C after this exposure to hydrogen. It is evident that rhodium occludes and adsorbs hydrogen quite well since its photoelectric properties are radically affected by the presence of hydrogen.

Oxygen, admitted to the system after the specimen had regained its stable condition after the introduction of hydrogen, changed the long wave limit from its equilibrium value of 2482–2536A to a value below 2300A. Oxygen was more effective in decreasing the long wave limit than hydrogen. Heating the specimen at 1000°C for one minute in oxygen at a pressure of 1 mm of Hg did not restore the photo-current to its original 100 mm deflection. In order to attain stable conditions again it was necessary to heat the specimen at 1250°C for 100 hours and to heat by means of a torch the high vacuum end of the system several times during this interval.

The following peculiarities of the photoelectric behavior below 240°C require further consideration:

(1) The stable value of the work function at room temperature is 4.92 volts; at 240°C this has changed to 4.57 volts, but no further change is observed from there on up to 650°C.

(2) When the rhodium was cooled as rapidly as possible from 1250°C to room temperature, the stable condition would be reached in 10 minutes after stopping the heating current.

(3) When the temperature was varied slowly from above 240°C, the more usual form of ascending and descending photo-current curve is shown in Fig. 3. Condition *A* is not stable, but changes to *B* in the course of an hour.

(4) Under the best attained vacuum conditions (10^{-8} mm of Hg) a different cycle is observed (Fig. 4) and with the same rate of change of temperature as in Fig. 3, the stable condition (*B*) is reached at once.

(5) It is to be noticed that the better the vacuum (Fig. 4) the more sudden are the changes in photo-current with temperature.

The question is, are these peculiarities caused by changing surface contamination, or do they indicate a structure change in the rhodium occurring at or below 240°C? A simple calculation shows that with a pressure of 10^{-8} mm of Hg and assuming no molecular reflection, it would take from one-half to several hours to form a monomolecular layer on the metal, according to the density one assumes for the gas layer. Hence from (2) above it does not seem likely that condition *B* is due to a gas covered surface, unless the gas layer is stable at high temperatures (1250°C) as well as at room temperature, being perhaps a hydride. Furthermore, in order to account for (1) and (3) this gas layer or hydride must be assumed to be unstable from 240°C up to some higher temperature, the relatively rapid rise in the ascending curve of Fig. 3 being due to the breaking up of the layer. But this does not fit (5), for the sudden drop in the descending branch of Fig. 4 would have to be attributed to the partial formation of the layer, and such rapid formation would be *less* likely to occur under the extremely high vacuum conditions of Fig. 4 than under the somewhat lower vacuum conditions of Fig. 3—which is contrary to fact. The sudden changes so prominent in Fig. 4 strongly suggest that there is an allotropic change at 240°C, and that the structure stable above this temperature can be carried down to lower temperatures in an irregular way, depending upon circumstances. A comparison of Figs. 3 and 4 suggests furthermore that the influence of this change in structure can be easily obscured by changing contamination except under the very best vacuum conditions. This is, however, not a completely satisfactory interpretation of the results.

In conclusion, the writer wishes to express his sincere thanks to Dr. C. E. Mendenhall, under whose direction this work has been done, to Mr. J. B. Davis, the glass-blower, and to Mr. J. P. Foerst, the mechanician.

THE EFFECT OF RESOLVING POWER ON MEASUREMENTS OF THE ABSORPTION COEFFICIENT OF ELECTRONS IN GASES

By R. Ronald Palmer
Department of Physics, University of Minnesota

(Received November 26, 1930)

Abstract

The absorption coefficient of electrons has been studied as a function of the resolving power of the experimental apparatus. An electron beam of 0.4 mm radius was used in a Mayer type of apparatus in which the opening at the end of the scattering chamber was of variable aperture. Values of the absorption coefficient were obtained in helium and in mercury vapor for 20, 40, 80 and 135 volt electrons over an angular aperture range of from 2° to 11° as measured from the end of the electron gun. All curves showed a definite decrease in the absorption coefficient with increase in angular aperture. These curves were corrected for the positive ion current, from the efficiency of ionization data of Bleakney and Smith, to give curves for the total number of electrons collected as a function of the size of the opening. These showed also a definite decrease with increase in aperture, corresponding to a preference for scattered electrons to be deflected through small angles. In helium the curves were steeper the higher the electron velocity, indicating that this preference is more decided for fast electrons than for slower electrons. In mercury vapor the curves were more nearly alike. The results do not indicate as decided a preference for small angle scattering as is indicated by the angular distribution curves of Arnot in mercury vapor. This discrepancy is not explained.

Introduction

EXPERIMENTS [1,2,3,4] designed to determine the angular distribution of electrons after collision with gas molecules indicate a decided preference for small angle scattering. In fact, most of the published curves show a a continued increase in the probability of scattering with decrease in angle, down to as small angles as have been obtained. Such curves for slow incident electrons are not so steep, in general, as are those for faster electrons, but in all cases the scattered electrons show this definite tendency to be concentrated about the forward direction.

The term "absorption coefficient" as applied to electron scattering by gas molecules has concerned itself with a determination of α from the relation $I = I_0 e^{-\alpha x p}$. In such experiments electrons of a definite velocity are caused to move in a beam (whose size and shape depend on the defining electrode system) through a scattering chamber of length x which contains a gas at a known pressure, p. On passing through this scattering chamber certain

[1] E. G. Dymond and E. E. Watson, Proc. Roy. Soc. **A122**, 571 (1929).
[2] G. P. Harnwell, Phys. Rev. **33**, 559; **34**, 661 (1929).
[3] F. L. Arnot, Proc. Roy. Soc. **A125**, 660 (1929).
[4] J. H. McMillen, Phys. Rev. **36**, 1034 (1930).

encounters with gas molecules cause some of the electrons to leave the beam, and so the beam of initial current strength, I_0, is reduced to the value I as given above. Experimentally two general methods have been used to determine α. The path of the electron beam may be a straight one as in a Mayer[5] type of apparatus, or the beam may be focused over a semicircular path by means of a magnetic field as was first done by Ramsauer.[6]

If $I'=I_0-I$ is the current to the scattering chamber, then, for low pressures, from the exponential relation given above, α is proportional to I'/I_0. Thus a determination of α for a particular apparatus is equivalent to measuring the fractional current to the scattering chamber. For low velocity electrons this current is composed merely of those electrons which have been deflected through an angle greater than some average minimum angle, $\bar{\theta}$. This angle is a function of the size of the opening at the end of the scattering chamber and of the length of the path. For electrons with a velocity greater than a certain value there may be ionization at an encounter which will result in at least three charged particles. A certain fraction of these will be collected, depending on the apparatus. If $\Phi_s(\theta)$, $\Phi_e(\theta)$ and $\Phi_i(\theta)$ are the probabilities that the initial electron, the ejected electron and the ion, respectively, will move in the direction θ after such an encounter, and if F^+ is the probability of ionization taking place, then for a Mayer type of apparatus the fractional current to the scattering chamber is

$$I'/I_0 = \int_{\bar{\theta}}^{\pi} (\Phi_s + F^+\Phi_e + F^+\Phi_i)d\theta \qquad (1)$$

where the integral is taken over the possible angles of collection. If it is assumed that the ion has an equal probability of moving in any direction, Φ_i is a constant and the integral of the third term does not change much with a small change in the lower limit of integration, $\bar{\theta}$. The second term, representing the angular distribution function for the ejected electrons has not, to the author's knowledge, been investigated. This distribution may be uniform but it seems more probable that it would be somewhat similar to the distribution for the scattered primary electrons. The first term in the integrand is the probability function, $F(\theta)$, which is measured in angular scattering experiments. As has already been mentioned this function is one which in general increases with decreasing θ, being of particular weight for values of θ near $\bar{\theta}$. Hence one would expect that a small change in the lower limit of integration would produce a large change in the value of Eq. (1). Any distribution of the ejected electrons other than a uniform distribution would enhance this effect. Thus the current collected by the scattering chamber is very decidedly a function of the resolving power of the apparatus. In the Ramsauer type of apparatus the integrals of the second and third terms of Eq. (1) will probably just balance each other. Both the ejected electron and ion will have such energies that their paths will have a smaller radius of curvature than that of

[5] H. F. Mayer, Ann. d. Phys. **64**, 451 (1921).
[6] C. Ramsauer, Ann. d. Phys. **66**, 547 (1921).

the main electron beam, and hence even if initially they were directed along the electron beam they would soon leave it and balance each other at the walls of the scattering chamber. At such an encounter, or any encounter in which the initial electron loses an appreciable amount of energy it too will be removed from the beam regardless of its direction of motion immediately following the encounter. Thus a Ramsauer type of apparatus measures not only the integral of the first term of Eq. (1) but also an additional negative current due to those electrons which lose energy even though they are deflected through angles less than $\bar{\theta}$. On the other hand, in a Mayer type of apparatus the integral of the first term is partially balanced by a part of the positive ion current.

From these considerations one would expect that the magnitude of the absorption coefficient as obtained by various observers using apparatus with different resolutions should exhibit quite a wide range of values. But this does not seem to be the case. Recent measurements by Maxwell,[7] Jones[8] and Brode[9] on the absorption coefficient for electrons in mercury vapor agree much better than would be expected. The author* has also carried out a determination with a Mayer type of apparatus (separate from that used for the work reported in this paper) in which electrons scattered through angles down to 3°, on the average, were counted as having collided. The absorption coefficient was determined for electrons of from 5 to 100 volts velocity and the values agreed within a few percent with those obtained by Brode with a Ramsauer apparatus. These values are but 25 percent greater than those reported by Maxwell. His apparatus defined a collision only if it resulted in a very much larger deflection of the electron. Arnot[3] has obtained an angular scattering curve for electrons in mercury vapor, and a numerical integration of this curve as applied to each individual apparatus indicates that there should be a much greater divergence in the results. Similarly for other gases various observers obtain results more in accord with each other than would be expected.

It was then decided to build a Mayer type of apparatus in which the opening at the end of the scattering chamber could be changed in size, so that the absorption coefficient could be studied in one particular apparatus as a function of the resolving power. Such a study should throw light on the probability of angular scattering, and should enable a check of existing curves Recently Metta Clare Green[10] carried out a similar investigation, but found no consistent variation of the absorption coefficient with opening. Inasmuch as such a result is so definitely in opposition to the results of angular distribution experiments and as the magnitudes of the values obtained for the absorption coefficient differed, in most cases, so radically from accepted values,

[7] L. R. Maxwell, Proc. Nat. Acad. Sci. **12**, 509 (1926).
[8] T. J. Jones, Phys. Rev. **32**, 459 (1928).
[9] R. B. Brode, Proc. Roy. Soc. **A125**, 134 (1929).
* Work not published.
[10] Metta Clare Green, Phys. Rev. **36**, 239 (1930).

such a study should still be fruitful. Measurements were accordingly made in helium and in mercury vapor.

Apparatus

The apparatus used is shown diagrammatically in Fig. 1. It was constructed of copper. Electrons from the tip of the filament, F, were accelerated to a definite velocity between the plates D_1 and D_2, and made to travel in a beam of small cross-section through the scattering chamber, sc, and into the Farady cage, FC. The diameters of the circular openings in the gun, G, were 0.75, 0.50, 0.50 and 0.75 mm for D_1, D_2, D_3 and D_4 respectively. D_5 was about 1.5 mm in diameter, and less than 1 mm from D_4. The distance from D_1 to D_2 was 5.0 mm and from D_1 to the end of the gun, D_4, was 45 mm. The scattering chamber, from D_4 to D_6, was 4.0 cm in length, and the Faraday cage was 16 cm in length. The hairpin filament was a small tungsten wire bent sharply at the opening D_1. It required about 1.5 amperes for satisfactory electron emission. All diaphragms were slightly bevelled, and important surfaces were given a light coat of soot.

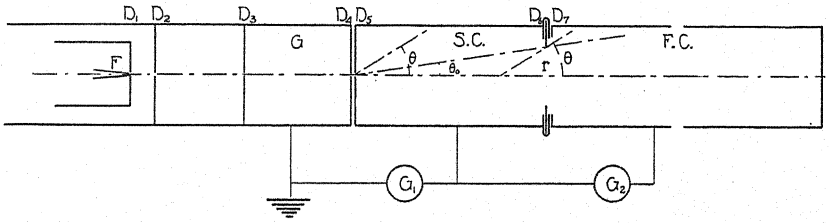

Fig. 1. Diagram of apparatus.

The variable aperture at D_6 was obtained by the use of a 30 cm strip in which were cut a series of holes of different size. The strip could be slid freely back and forth by means of a special magnetic control, which was constructed such that all magnetic material could readily be removed for each reading.

The apparatus was sealed in a Pyrex tube free from wax joints, and vacuum conditions were such that a pressure of less than 10^{-6} mm mercury would build up in 24 hours when the tube was cut off from the pumps. For the measurements in mercury vapor, a trap containing mercury was maintained at a definite temperature, and the calculations were based on the vapor pressure corresponding to that temperature as recorded in the International Critical Tables. Pressures corresponding to various temperatures up to about 20°C were used. The gas pressures for helium were determined from McLeod gauge readings. A side tube containing carbon which had been baked out for several hours at 500°C was used in conjunction with the helium measurements. This tube and the mercury trap were kept at the temperature of liquid air.

A pair of large Helmholtz coils was used to neutralize the earth's field, and the tube was mounted such that the electron beam traveled along the axis of the coils.

METHOD

In a determination of α from the exponential decrease in the intensity of an electron beam a constant, K, must be introduced to account for those electrons which would be collected by the scattering chamber regardless of gas pressure. This constant should depend only on the geometry of the apparatus. The beam of initial strength I_0 is then reduced to $I = KI_0 e^{-\alpha x p}$ after traveling a distance x in a gas at pressure p. The current ratio I/I_0 was measured by the galvanometers, G_2 and G_1 (Fig. 1) for different gas pressures and for different openings at the end of the scattering chamber. From the above equation

$$\log I/I_0 = \log K - \alpha x p/2.3 \tag{2}$$

in which the logarithms are taken to the base 10. If K is a constant, independent of the pressure and electron current for a particular resolution, the log I/I_0 should exhibit linearity when plotted against the pressure. The

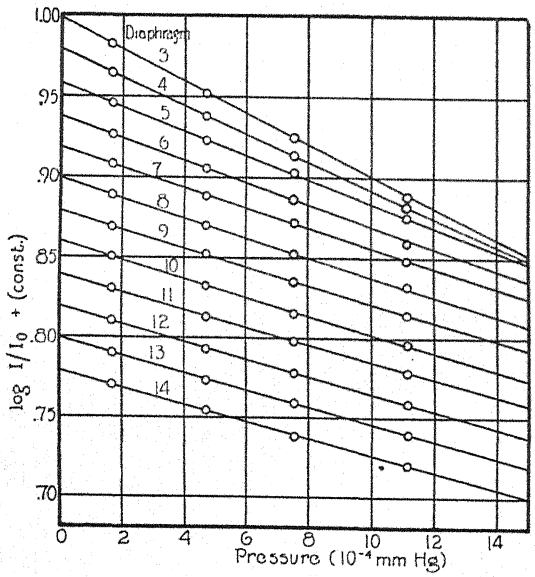

Fig. 2. To show linearity between log I/I_0 and pressure. (80 volt electrons in mercury vapor.)

slope of such a straight line relationship being $\alpha x/2.3$ makes it possible to calculate α. If the pressure used is the observed pressure corrected for thermal diffusion and reduced to the corresponding pressure at 0°C, α is obtained in the usual units, cm²/cm³ per mm pressure at 0°C.

Fig. 2 shows the relation between log I/I_0 (plus an arbitrary constant) and the pressure for 80 volt electrons in mercury vapor; each curve was obtained with a different opening at the end of the scattering chamber. These curves indicate that K was independent of the pressure in each case. The value of log K=log I/I_0 when p=0 shows that K was greater than 0.99 for all openings. Thus at least 99 percent of the original beam was collected by

the Faraday cage when no gas was present. This means that the number of secondary electrons reflected into the scattering chamber from the end of the gun or the end of the Faraday cage was at a satisfactory minimum.

By applying a retarding field between the Faraday cage and the scattering chamber (Fig. 1) the velocity distribution of the electron beam was found to be quite satisfactory. For a 40 volt electron beam, over 95 percent of the electrons had velocities within a few tenths of a volt of the mean. Though this differed from 40 volts by a small amount, the beam will nevertheless be designated as a 40 volt electron beam. The correction will also be disregarded for the other velocities used.

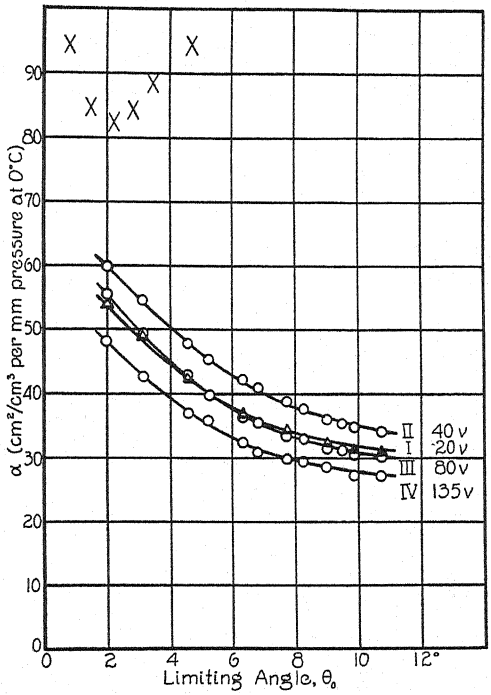

Fig. 3. "Absorption coefficient," α, as a function of the resolving power of the apparatus, in mercury vapor. (X-values given by Metta Clare Green for 37.5 volt electrons.)

The values of α in mercury vapor were for the most part obtained from such curves as those in Fig. 2, which in turn had been determined by four different pressures. Those for helium and some of the mercury values were obtained with but two pressures, one of which was usually zero. The path length value of $x = 4.0$ cm was used for all the calculations.

Results and Discussion

The results of the measurements in mercury vapor are given graphically in Fig. 3, and those for helium in Fig. 4. α is plotted for 20, 40, 80 and 135 volt electrons against the limiting angle, θ_0, giving curves I, II, III and IV respectively. Referring to Fig. 1, this limiting angle is defined as $\theta_0 = \tan^{-1} r/l$

where r is the radius of the opening and l is the length of the scattering chamber. If any electron is deflected through an angle less than this it will not be counted as having collided. The range of values for θ_0 corresponds to a range of diaphragm radii of from 1.4 to 7.6 mm. The experimental points for mercury are averages of two complete sets of readings, differing from each other in most cases by less than 2 percent. The values for helium are averages of

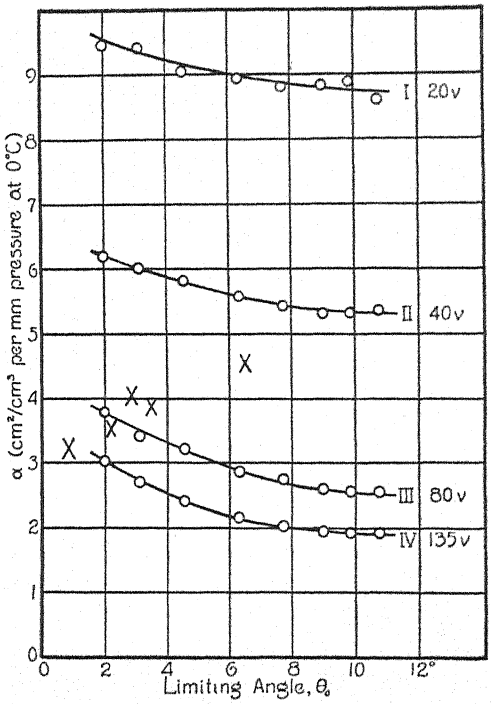

Fig. 4. "Absorption coefficient," α, as a function of the resolving power of the apparatus, in helium. (X-values given by Metta Clare Green for 97 volt electrons.)

four sets of readings with a somewhat larger experimental error. All of the curves show a definite decrease in the absorption coefficient as the size of the opening increases. This, of course, corresponds qualitatively to the tendency for scattering to take place in the forward direction.

If $K=1$, which has been seen to be practically the case, the current to the scattering chamber is $I'=I_0-I=I_0(1-e^{-\alpha xp})$. For low pressures this becomes

$$I'/I_0 = \alpha xp \tag{3}$$

or, α is numerically equal to the negative current to the scattering chamber in terms of a certain number of electrons per primary electron per cm path per mm pressure at 0°C. Thus the curves of Figs. 3 and 4 give the relative negative current collected by the scattering chamber when the size of the opening is changed. As has already been seen, this negative current is the resultant of a positive ion current combined with the scattered and ejected

electron current, the fraction which is due to positive ions depending on the probability of ionization. Hence if these curves are to be discussed with regard to the characteristics of electron scattering they must be corrected for the positive ion current. This correction is made possible by the recent work of Bleakney[11] and of Smith[12] who have determined the efficiency of ionization of electrons in various gases. If F^+ is this efficiency of ionization

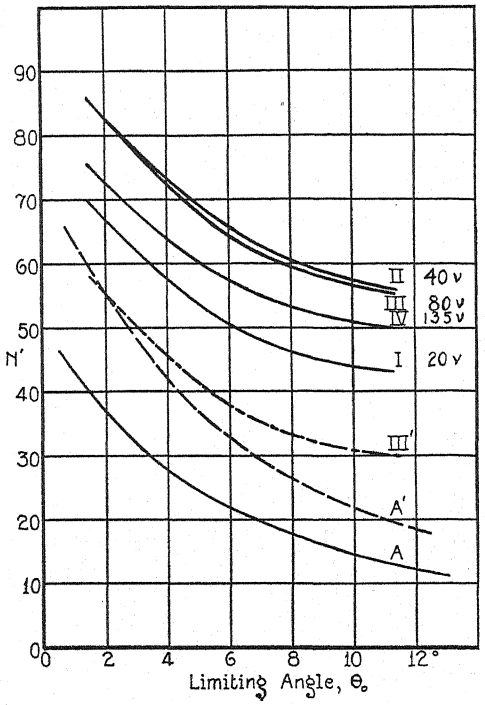

Fig. 5. Number of electrons collected by the scattering chamber, per cm path per primary electron per mm pressure at 0°C, as a function of the resolving power, in mercury vapor. (Curve *A* predicted, as the number of primary electrons scattered, by Arnot's results for 80 volt electrons.)

(given in terms of the number of units of positive charge formed per cm path per primary electron per mm pressure at 0°C) and we assume that the ion has an equal probability of going in any direction,* the positive current to the scattering chamber can be obtained by a simple integration. It is of course a function of θ_0 and is found to vary from $1.10F^+$ at $\theta_0=2°$ to $1.03F^+$ at

[11] Walker Bleakney, Phys. Rev. **35**, 139 (1930).

[12] P. T. Smith, Phys. Rev. **36**, 1293 (1930).

* This assumption seems valid providing the interior of the scattering chamber is a field-free space. A recent investigation by Arnot (Proc. Roy. Soc. **A129**, 361 (1930)) indicated that the positive ions tend to move out perpendicularly to the electron beam. It is doubtful whether his results may be applied here, for they were obtained under different conditions. Intense electron beam currents up to 25 micro-amperes were used, whereas in the work reported here this current did not exceed a tenth of a micro-ampere. However, the results to follow would be substantially the same, even though we accepted Arnot's distribution for the positive ions.

$\theta_0 = 10°$. The values of F^+ given by Bleakney for 20, 40, 80 and 135 volt electrons in mercury vapor are 12.0, 21.2, 25.0 and 22.5 respectively; those given by Smith for the respective voltages in helium are 0.00, 0.63, 1.18 and 1.24. With these values the corrections can be calculated and applied to the curves of Figs. 3 and 4. The corrected curves, representing the total number of electrons collected by the scattering chamber (per primary electron per cm path per mm pressure at 0°C), are given in Figs. 5 and 6, for mercury vapor and helium, respectively. Since these curves deal only with the electrons which are collected they may be used in a comparison of electron scattering.

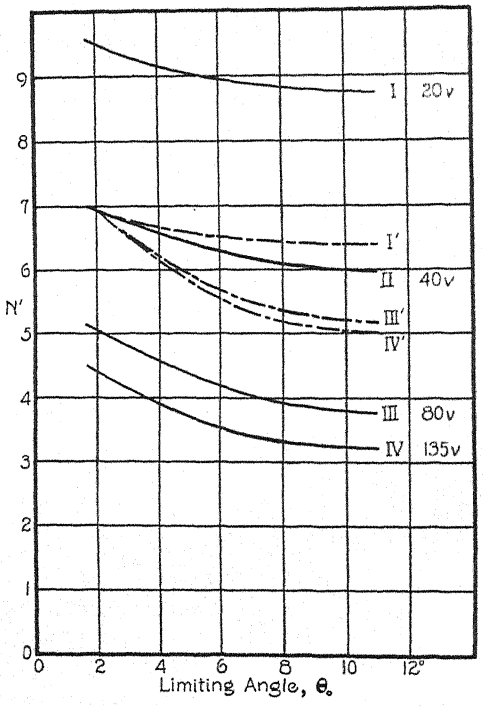

Fig. 6. Number of electrons collected by the scattering chamber, per cm path per primary electron per mm pressure at 0°C, as a function of the resolving power, in helium.

To get a better idea of the relative dependence of this scattering on angular aperture for the different primary velocities, the 20, 80 and 135 volt curves in helium (Fig. 6) have been multiplied by the proper factors to make them coincide with the 40 volt curve at $\theta_0 = 2°$, giving the new curves I′, III′ and IV′ respectively. From this set of curves we notice that as the velocity of the primary electrons becomes greater, the curves become relatively steeper; i.e., a small change in the size of the opening cuts out a relatively greater number of the scattered electrons if the primary electrons have high velocity than if they have a lower velocity. This indicates that scattering of fast electrons is more definitely concentrated in the forward direction than that for slow electrons, and corresponds to the decrease in steepness

of the angular scattering curves with decrease in primary electron velocity, as observed by McMillen.[4] Mercury vapor however, does not exhibit such a marked relative preference. The curves in Fig. 5 show about the same relative change over the range of angles used, being much more alike than are those in helium. This indicates that the angular distribution of scattered electrons in mercury vapor is quite similar over the velocity range of from 20 to 135 volts. This does not imply, however, that the angular distribution for the scattering of primary electrons would be the same over this velocity range. To say anything about this, the distribution of the ejected electrons must be taken into consideration, and it is not likely that this distribution would be the same for primary electrons of different velocities. These relations cannot be checked with existing data for, aside from our lack of knowledge of the behavior of the ejected electron, no investigation has as yet be published in which the angular distribution has been studied as function of electron velocity in mercury vapor.

From the angular scattering curves of Arnot for 80 volt electrons in mercury vapor it is possible to predict the number of primary electrons which should be collected by the scattering chamber for any size opening. He determined the angular distribution for electrons which had not lost energy and also for those which had lost energy. He assumed that these electrons were all primary electrons, even though there is the possibility that an ejected electron may be given sufficient energy such that it will be confused with the group of primary electrons which had lost energy. The calculation for the number of primary electrons collected according to his results can be done in the following way.

Let $F(\theta)d\theta$ be the number of electrons scattered between θ and $\theta+d\theta$ per primary electron per cm path at a definite temperature and pressure. The effective length of path over which electrons deflected through angle θ are collected is $l_e=l-r/\tan\theta$, as can be seen from Fig. 1. Then for N_0 primary electrons the number of electrons deflected between θ and $\theta+d\theta$ which are collected by the scattering chamber is $N_0 p F(\theta) l_e d\theta$ for a gas pressure p which is sufficiently small. The total number collected will then be

$$N' = N_0 p \int_{\theta_0}^{\pi} F(\theta)(l - r/\tan\theta)d\theta. \tag{5}$$

It may be noted that this includes all electrons scattered into the chamber, even those which are deflected through angles greater than 90° giving for them the proper effective path length which is greater than 1. If $F(\theta)$ be known, the function $F(\theta)$ $(l-r/\tan\theta)$ can be plotted against θ for different values of r, and the areas under the resulting curves will represent the relative numbers of primary electrons collected by the scattering chamber for openings of different size. The only assumption which has been made is that the scattering takes place along the axis of the apparatus.

Compton[13] has tabulated Arnot's values for the scattering of 80 volt

[13] K. T. Compton, Rev. Mod. Phys. **2**, 123 (1930).

electrons in mercury vapor in terms of the number of electrons scattered per unit solid angle at angle θ per primary electron per cm path at 20°C and 0.001 mm pressure. $F(\theta)$ is then this function multiplied by $2\pi \sin \theta$. By using these values for $F(\theta)$ and performing the numerical integrations outlined above, $N'/N_0 p$ was obtained for different values of the diaphragm radius. On correcting this result to 0°C and 1 mm pressure (since $F(\theta)$ was given for a temperature of 20°C and a pressure of 0.001 mm) and dividing by the path length, $x = 4.0$ cm, one obtains the predicted values for the number of primary electrons which should be collected by the scattering chamber for various apertures. Curve A of Fig. 5 is the result of this work, plotted in terms of $\theta_0 = \tan^{-1} r/l$. Curve III of the same figure represents the actual number of electrons which were collected experimentally. Assuming the validity of both curves, the difference between their ordinates for a particular value of θ_0 would represent the number of ejected electrons collected by the scattering chamber for that value of θ_0. This difference increases with increasing θ_0 which means that a larger ejected electron current would be collected the larger the diaphragm opening. Such a result can be interpreted only if the ejected electrons obey a distribution which favors scattering in the backward direction, which does not seem reasonable. It is of interest to compare the curves if we assume a uniform distribution for the ejected electrons. The correction to be made to curve III will be practically the same as (but opposite to) the correction which was made for the positive ions, and the resulting curve will be similar to the curve for α. This is given in Fig. 5 as curve III'. To compare this curve with Arnot's the latter has been plotted to a different scale giving curve A'. Both curves, of course, show the preference for small angle scattering, but Arnot's curve makes this preference much more decided. If we had assumed an angular scattering for the ejected electrons favoring scattering in the forward direction, curve III' would have differed much more decidedly from Arnot's predicted curve. It is to be mentioned that Arnot's results were obtained with primary electron currents of several micro-amperes, whereas in the present work no currents greater than a tenth of a micro-ampere were used. As was noted above, the only assumption made in the calculation was that the scattering should take place along the axis. This was approximated quite well, for tests at the end of the scattering chamber indicated that the beam was but 0.8 mm in diameter and hence all of the scattering took place within 0.4 mm of the axis. Thus there remains a definite discrepancy between the two curves which is difficult to explain.

It is of interest to note that the procedure we have just outlined may be reversed, and $F(\theta)$ may be obtained from the experimental curve. Thus, if the experimental curve gives the result

$$f(\theta_0) = \int_{\theta_0=\tan^{-1} r/l}^{\pi} F(\theta) \cdot (l - r/\tan\theta) d\theta \tag{6}$$

then $F(\theta)$ can be determined by differentiating this equation twice. This gives

$$F(\theta_0) = \sin\theta_0/l\left(\cos\theta_0\frac{d^2f(\theta_0)}{d\theta_0{}^2} - 2\sin\theta_0\frac{df(\theta_0)}{d\theta_0}\right). \quad (7)$$

This equation, however, is rather impractical of application for the second derivative bears too much weight. A small error in the experimental determination of $f(\theta_0)$ is amplified in the calculation, which makes $F(\theta)$ very uncertain.

The results of Metta Clare Green[10] which were previously mentioned are given by the crosses in Figs. 3 and 4, for certain electron velocities in mercury vapor and helium. These values are also plotted in terms of $\theta_0 = \tan^{-1}r/l$ where $l = 7.5$ cm in her apparatus. For a given electron velocity she found no definite variation in the absorption coefficient with change in aperture, all the values for a given curve lying within the experimental error of the mean of that group. However such a result is in direct opposition to all angular scattering experiments. In addition, the magnitudes of the values obtained for the absorption coefficient differed in most cases so radically from those obtained by any other observer that it is difficult to place much weight on the results. This may, in part, have been caused by the penetration of electric fields into the scattering chamber at both ends. Such experiments necessitate that the scattering be studied in a field-free space. Otherwise it is difficult to determine the cause of this discrepancy.

This investigation has given further evidence that when electrons are scattered by gas molecules they exhibit a preference for deflection through small angles. It has also been shown that, over the velocity range studied, fast electrons show a greater relative tendency to be deflected through small angles than do slower electrons. This is quite definitely the case for scattering in helium, whereas it is not so marked in mercury vapor. Further, the results in mercury vapor do not indicate as decided a preference for forward scattering as do those of Arnot.

The author wishes to express his gratitude to Professor Tate for his many helpful suggestions and continued interest throughout this work.

HIGH FREQUENCY DISCHARGES IN MERCURY, HELIUM AND NEON*

By Charles J. Brasefield
University of Michigan

(Received November 15, 1930)

Abstract

Measurements were made of the potential drop at the electrodes and the electric force in the positive column of high frequency discharges in mercury, helium and neon for a large number of gas pressures and for frequencies of oscillation between 1.25 and 22.5 megacycles. The results showed that in general, the magnitude of the electric force was too small to produce electrons whose velocity would be sufficient to ionize or excite the gas. It was observed that as the frequency of oscillation increases, the potential drop at the electrodes decreases. Considering the total voltage between electrodes it was found that the high frequency discharge in mercury has its maximum conductivity when operated at a frequency of 17.5 megacycles (17.15 meters) and at a pressure of 0.002 mm; the discharge in helium has its maximum conductivity at 17.5 megacycles and 0.33 mm pressure; the discharge in neon has its maximum conductivity at 7.5 megacycles (40 meters) and 1.0 mm pressure.

Introduction

PREVIOUS work[1] on the conductivity of a high frequency discharge in hydrogen showed that a knowledge of the variation of the total voltage across the discharge with the gas pressure and the frequency of oscillation is not sufficient to determine the mechanism of the discharge, for the potential difference between electrodes consists of two parts. The first is the drop in potential in the body of gas. The second is the drop in potential at the electrodes which includes the dielectric loss in the glass under the electrodes and the drop in potential at the electrodes due to the accumulation of positive space charge, if any. In order to compare experimental results with any theory of the mechanism of the discharge, it is necessary to study the electric field in the positive column of the discharge, in particular, its variation with gas pressure and frequency of oscillation.

The apparatus used and the experimental procedure followed were essentially the same as in the work on hydrogen. Measurements were made of the voltage between electrodes necessary to produce a current of 100 milliamperes in the gas, the distance between electrodes being varied from 40 to 100 cm in 10 cm steps. If the values of the total voltage between electrodes are plotted against the corresponding distances between electrodes, a curve is obtained which, in general, approximates a straight line. Assuming that as the distance between electrodes increases, the drop in potential at the electrodes remains constant, then the slope of the line gives the electric field in

* Publication of the Research Organization of the Grigsby-Grunow Company, Chicago, Illinois.

[1] C. J. Brasefield, Phys. Rev. 35, 1073 (1930).

the positive column which when multiplied by $2^{1/2}$ gives the amplitude of the electric force. Extrapolating the curve to zero distance between electrodes, the potential drop at the electrodes is found. Values of the electric force in the positive column of the discharge as well as the potential drop at the electrodes were in this way obtained for a large number of gas pressures and for ten frequencies of oscillation between 1.25 and 22.5 megacycles.

Results

1. Experiments on mercury. The discharge tube used was 120 cm long, 5.2 cm internal diameter while the electrodes surrounding it were of sheet copper 5 cm wide. Except for a mercury reservoir at one end, the whole tube was surrounded by an electric furnace which kept it at a temperature of about 150°C. To regulate the vapor pressure of the mercury, the reservoir

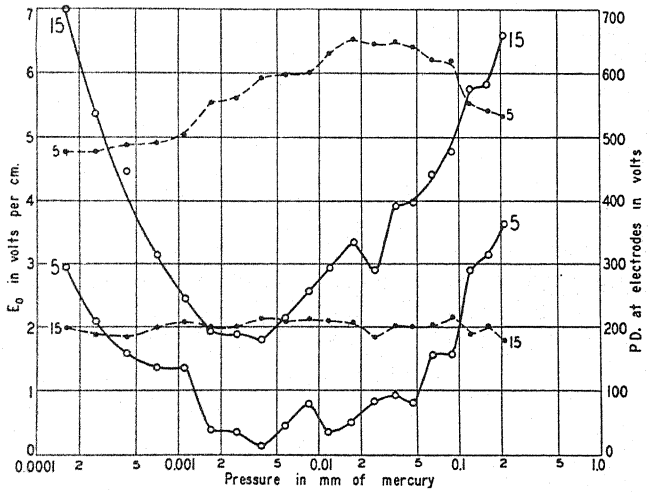

Fig. 1. The variation with pressure of the electric force (solid curves) and the potential drop at electrodes (broken curves) in a high frequency discharge in mercury operated at 5 and 15 megacycles.

was immersed in a water bath which was kept at a constant temperature within 0.2°C during a given run. Measurements were taken at 5° intervals from 0° to 95°C.

Fig. 1 shows, for two typical frequencies of oscillation, the variation with pressure of the electric force and the potential drop at electrodes when a current of 100 milliamperes is passing through the tube. It was observed that as the frequency of oscillation increases, the potential drop at the electrodes decreases from approximately 800 volts at 1.25 megacycles to 200 volts at 15 megacycles. This, without doubt, accounts for the fact that the spark spectrum of mercury was quite pronounced in the region under the electrodes when the discharge was operated at frequencies below 5 megacycles. Considering the total voltage between electrodes, it was found that the discharge

we find $E_{0\min}=0.34\times10^{-6}\times f$ volts per cm. For 25 volt electrons (helium and neon) we find $E_{0\min}=0.53\times10^{-6}\times f$ volts per cm. A glance at Figs. 1, 2, and 3 shows that the majority of the experimental values of E_0 are still less than these minimum values. It appears, therefore, that in the high frequency discharge, electrons whose velocity is sufficient to ionize (or even excite) a gas molecule cannot be produced in the positive column of the discharge.

Of course, it is not necessary that ionization processes in the high frequency discharge be very efficient since the only way ions can disappear is by recombination or diffusion to the walls. The same cannot be said of the excitation processes, however, for the intensity of the light produced in the positive column is quite comparable with the intensity of the light emitted by the positive column of an ordinary Geissler tube carrying the same current. The only source of high velocity electrons imaginable is the region under the electrodes; but it is hard to believe that these electrons should be responsible for all the ionization and excitation in the positive column of the discharge. The writer confesses that he is unable to suggest any reasonable solution of the problem from a consideration of the mechanics of individual electrons; whether or not an explanation of the phenomena can be worked out by considering the volume of ionized gas as a plasma has not as yet been determined.

The writer is indebted to Professor O. S. Duffendack and Professor R. A. Sawyer for advice rendered and also to Mr. J. S. Owens who assisted in the experimental work.

LETTERS TO THE EDITOR

Prompt publication of brief reports of important discoveries in physics may be secured by addressing them to this department. Closing dates for this department are, for the first issue of the month, the twenty-eighth of the preceding month; for the second issue, the thirteenth of the month. The Board of Editors does not hold itself responsible for the opinions expressed by the correspondents.

The Diffraction of Hydrogen Atoms by the Mosaic Structure of Crystals

The de Broglie wave spectra of a beam of hydrogen atoms produced by reflection from a crystal of lithium fluoride have been photographed under conditions of improved technique with the primary features described in abstract No. 2 of the 1930 Chicago Meeting of the American Physical Society. Still more recent plates with higher resolution show another type of spectrum which will be referred to as the secondary spectrum. Although the resolution is still too low in this spectrum to separate the maximum of its wave-length distribution from the specularly reflected zero order beam, it is sufficient to show that the secondary spectrum has four branches lying in the directions corresponding to diffraction by a grating whose lines are parallel to the cleavage planes of the crystal. The fact that the maximum of the wave-length distribution is not resolved permits it to be said that the spacing of the secondary lattice is greater than 50A, and the observations are not in disagreement with a spacing of more than 100A.

These facts are believed to support Zwicky's theory of the mosaic structure of crystals (Helvetica Physica Acta III, 269, 1930). Although the writer is not familiar with any calculations applying to the structure of LiF the spacing of the secondary lattice of these crystals should not differ in order of magnitude from that of rock salt for which Zwicky calculates 110A.

In the experiments the crystals were heated before the exposure was started to the point that the secondary structure of the crystal might well have been developed on the surface by evaporation.

THOMAS H. JOHNSON
The Bartol Research Foundation of the Franklin Institute,
Swarthmore, Pa.,
December 2, 1930.

On Some of the New Ultra-Ionization Potentials of Mercury Vapor

In view of the recent interest in the ultra-ionization potentials of mercury vapor (A. L. Hughes and C. M. Van Atta, Phys. Rev. **36**, 214, 1930, Philip J. Smith, 166th Meeting of the American Physical Society and Curtis R. Haupt, 167th Meeting of the American Physical Society) I would like to call attention to some observations of Mr. R. D. Potter, made at Duke University under my direction and published in the Journal of the Elisha Mitchell Scientific Society, **44**, 31, 1928. Inasmuch as the results of the experiment described in this paper do not seem to have come to the attention of other workers in this field, a brief statement of the results may be of interest.

Electrons from a tungsten filament were projected parallel to the axis of a tube and were collimated by means of a coaxial magnetic field of approximately 250 gauss. Collisions between electrons and mercury atoms occurred in a space midway between two rows of parallel and plane electrodes symmetrically placed with respect to the electron beam. A small electric field between these plates served to draw out positive ions formed in the region of the beam. The electrons after passing between the sets of parallel plates were collected by an electron trap. An accelerating potential of 125 volts inside the electron trap made it a good absorber of electrons. Since the primary electrons were collimated into a beam by the magnetic field they did not strike the edges of the slits in the accelerating plates. This prevented the formation of secondary electrons.

The procedure was to measure the saturated positive ion current and total electron

current for successive values of the accelerating potential, observations being taken at 0.10 volt intervals.

A plot of the ratio of positive ion to total electron current showed a series of abrupt changes in slope which resembled the familiar ones of Franck and Einsporn rather than those reported by J. C. Morris (Phys. Rev. **32**, 447, 1928). Critical potentials were observed at 10.40, 10.66, 11.00, 11.41, 11.72, 12.06, 12.40, 12.80 and 13.25 volts. The values given have been corrected for initial thermal energies, etc., by assuming the potential at which ions were first detectable to be 10.40 volts.

An examination of the results indicates that in the main there is good agreement between the above critical ultra-ionization potentials and those reported in subsequent work mentioned at the beginning of this letter.

WALTER M. NIELSEN
Bartol Research Laboratory of the Franklin Institute,
Swarthmore, Pa.,
December 2, 1930.

Projective Relativity and the Quantum Field

A recent paper[1] by O. Veblen and the present writer showed that the "five-dimensional" relativity theory of Kaluza and O. Klein is to be regarded as a four-dimensional projective theory; a natural generalization of the formalism from this point of view led to a set of field equations which contained not only gravitational and electromagnetic field equations as in the usual relativity theory but also the relativistic Schrödinger equation.

The formalism was based on the symmetric projective tensor $G_{\alpha\beta}$ which may be decomposed as

$$G_{\alpha\beta} = \gamma_{\alpha\beta}\Phi^2 = (\delta_\alpha{}^a\delta_\beta{}^b g_{ab} + \phi_\alpha\phi_\beta)\Phi^2,$$

as explained in P. R.

I have been able to obtain a set of four-dimensional projective field relations which is to the field relations of P. R. what the Dirac wave equation is to the relativistic Schrödinger equation.

The basic quantity of space-time is taken to be a projective vector, H_α, of index N with which is associated one of zero index denoted by h_α. The components of these vectors are not assumed to obey the commutative law of multiplication; they may be regarded as matrices. The restrictions are imposed that

$$H_\alpha H_\beta + H_\beta H_\alpha = 2G_{\alpha\beta} \qquad (1)$$

$$h_\alpha h_\beta + h_\beta h_\alpha = 2\gamma_{\alpha\beta} \qquad (2)$$

where $G_{\alpha\beta}$ and $\gamma_{\alpha\beta}$ commute with everything they multiply. $\gamma_{\alpha\beta}$ are now associated tentatively with the similar quantities of P. R.

Indices of the h's are raised by means of the γ's and the field equations are taken to be

$$h^\alpha\left(\frac{\partial H_\beta}{\partial x^\alpha} - \frac{\partial H_\alpha}{\partial x^\beta}\right) = 0. \qquad (3)$$

A realization of (1) and (2) may be obtained in terms of projective ennuples of vectors in the tangent spaces[2] and a basis consisting of five four-rowed square matrices satisfying[3]

$$E_\sigma E_\tau + E_\tau E_\sigma = 2\delta_{\sigma\tau}1.$$

Denoting the components of the vectors of an ennuple by $h_{\alpha\sigma}$ we set

$$h_\alpha = h_{\alpha\sigma}E_\sigma.$$

Realization of the H's is effected by the introduction of a one-columned four-rowed matrix, Ψ, by

$$H_\alpha = h_\alpha\Psi$$

together with a suitable definition of matrix multiplication.

With the above realization the field Eqs. (3) can be shown to contain Dirac's wave equation for a single electron as a special case (i.e. when gravitation is neglected) of the scalar part of the projective set.

If we inserted the relations

$$G_{\alpha\beta} = \gamma_{\alpha\beta}\Phi^2 \qquad (4)$$

together with (1) and (2) we would be unable to obtain a satisfactory realization on account of the difference between spatial and temporal coordinates. A realization in terms of eight-rowed square matrices for the E's avoids this difficulty but introduces the new difficulty that although the scalar part is still equivalent to Dirac's wave equation the whole set of equations numbers forty and we have merely twenty-eight functions entering them.

The Dirac equation is obtained as a special

[1] O. Veblen and B. Hoffmann, Phys. Rev. **36**, 810 (1930); referred to as P. R.

[2] See the "five-dimensional" formulation due to Zaycoff, Zeits. f. Physik **58**, 833 (1929).

[3] See for example Eddington, Proc. Roy. Soc. **A126**, 696 (1930).

case of part of a system of field relations constructed in close analogy with the system of P. R. There is thus a possibility that the complete system will constitute an improved unification within the relativity theory of the gravitational electromagnetic and quantum aspects of the field.

The complete set of field relations (1), (2) and (3) (and others not mentioned here), can be shown to be invariant under general relativity transformations.

BANESH HOFFMANN
Princeton University,
December 8, 1930.

Thermal Fluctuations of the Surface Potential of a Cathode as Affecting Electron Emission

There are at present two groups of thermionic phenomena in which theory and experiment lie rather far apart. These are (1) the departures of the constant A from the theoretical value, particularly in the case of surface films, and (2) the anomalously large values of the Schottky effect (increase of emission with field) which are also most marked for surface films. The following considerations offer a possible explanation of these difficulties.

Let us select a conductor, one of whose ends is a circular patch of radius r on the surface of the electron emitter, the other end being the surrounding surface. Current may flow from the patch into the underlying material and out again to the surrounding surface. We shall suppose the surface layers of the emitter to have much higher resistance than the underlying material, partly because the surface is a discontinuity, and partly because the surface may be covered purposely with contaminating layers. The resistance of our conductor will then be $R_0=R_s/\pi r^2$ where R_s is the surface resistance per cm² encountered by electrons flowing through the surface. Our conductor is shunted by the capacity C across its end surfaces (infinite for a perfect conductor) which may reasonably be taken as of the form βr. Hence the expression for the effective resistance of our conductor at a frequency ω radians per second is

$$R=\frac{R_0}{1+R_0^2\omega^2C^2}=\frac{R_s}{\pi r^2+\beta^2(\omega^2/\pi)R_s^2}.$$

Johnson[1] has shown that as a result of thermal agitation there will be a mean square e.m.f. across the ends of our conductor given by

$$\bar{V}^2=3.48\times10^{-20}TR(\text{volts})^2$$

where T is the absolute temperature.

We shall take r approximately equal to the critical distance (x_m) which an electron must reach in order to escape from the surface. Hence the fluctuations of the potential of our patch will change appreciably the work function (ϕ) for the escape of electrons from the patch. These fluctuations are equally positive and negative, but since the emission (i) is an exponential function of ϕ, they will give rise to a net increase in emission (a sort of rectification action).

If i_0 is the "normal" electron emission from the patch (including the normal Schottky correction), the relative increase in emission produced by the fluctuations is found to be

$$\frac{i-i_0}{i_0}=2.41\times10^{-12}\frac{R}{T}=\alpha\frac{R}{T}. \qquad (1)$$

The surface may be regarded as made up of a number of such patches, so that the emission from the whole surface will be given by an expression like that above.

For the fluctuation effect to make an appreciable change in emission, the term $\alpha R/T$ must be at least of the order one tenth. If we consider the pure resistance part of R only, and remember that r is of the order 10^{-6} cm, we find that R_s must be of the order 100 ohms/cm². There appears to be no definite experimental evidence against the existence a surface resistance of this order in vacuum. Experiments are projected for measuring this surface resistance and its temperature coefficient. Ionization effects at the surface must modify this resistance in the case of anodes in gas discharges.

The anomalous Schottky effect has been discussed recently by Langmuir.[2] To compare our theory with this effect we form the partial derivative

$$\frac{\partial\ln i}{\partial(F)^{1/2}}=\frac{4.39}{T}+\frac{\alpha}{T+\alpha R}\frac{\partial R}{\partial(F)^{1/2}}. \qquad (2)$$

For weak fields the critical distance is large, r is large, and R approaches zero. Hence

[1] J. B. Johnson, Phys. Rev. **32**, 97 (1928).
[2] I. Langmuir, Reviews of Modern Physics **2**, 150 (1930).

$\partial R/\partial(F)^{1/2}$ is zero, and we have the normal Schottky slope. This is the region in which Nottingham's[3] emission measurements at zero field lie, and also Langmuir and Kingdon's[4] measurements of contact potential. The effect we are considering is absent in this range. As the field is increased, the critical distance decreases, r decreases, R increases, and the increase in $\partial R/\partial(F)^{1/2}$ gives an increased Schottky slope. Finally for very large fields the term involving r in R becomes negligible, and the effective resistance of our conductor becomes independent of the field. Hence $\partial R/\partial(F)^{1/2}$ approaches zero, and the slope approaches the normal Schottky value, as observed.

If we measure the Schottky slopes for ThW at moderately strong fields and for different filament temperatures, we find that the departure from the normal slope is greatest at the lowest temperatures (reference 2, page 156). This is in agreement with the occurrence of the factor $(T+\alpha R)$ in the denominator in Eq. (2).

It is evident that the introduction of a surface resistance, which will vary with temperature, may be made to account for the observed vagaries of the emission constant A by a suitable choice of the temperature coefficient of this resistance. It is hardly profitable to discuss this point without some experimental knowledge of these surface resistances.

In conclusion we may note that these thermal fluctuations of surface potential are perhaps connected with the "flicker" effect.[5] It is evident that such a theory would bear some resemblances to the theory of this effect advanced by Johnson[5] and developed by Schottky,[6] which ascribes the flicker to fluctuations in the composition of the surface. In our case the frequency variation of the effect would be introduced by the variation of R with frequency, the fluctuations of surface potential presumably approaching a maximum value as ω is decreased.

It is hoped to discuss these questions in more detail later, particularly if some experimental evidence can be obtained about the surface resistance and its temperature coefficient.

The writer is indebted to Dr. Langmuir and to Dr. Tonks for discussion of these ideas.

K. H. KINGDON
Research Laboratory,
General Electric Co.,
Schenectady, New York,
December 3, 1930.

[3] Nottingham, Phys. Rev. **36**, 386 (1930).
[4] I. Langmuir and K. H. Kingdon, Phys. Rev. **34**, 129 (1929).
[5] J. B. Johnson, Phys. Rev. **26**, 71 (1925).
[6] W. Schottky, Phys. Rev. **28**, 74 (1926).

Mean Value Theories in Quantum Mechanics

It is known[1] that in some cases there exists a close connection between the equation of classical dynamics and corresponding relations between mean values of quantities in quantum mechanics. Thus, for instance, it has been shown by Ehrenfest that according to Schroedinger's non-relativistic equation the mean momentum $\bar{p}$ is related to the mean position $\bar{q}$ by $\bar{p}=m\dot{\bar{q}}$ and also that the rate of change of the mean momentum $\bar{p}$ is equal to the mean of $-$grad V where V is the potential energy. This theorem has also been generalized to more dimensions by Ruark. While it is satisfactory to see the similarity of classical and quantum relations in such special instances it is nevertheless desirable to bear in mind also a somewhat more general point of view. It is readily seen that according to the transformation theory the reason for the validity of mean value theorems is that the equations of classical theory hold, in the above instance, also in the quantum theory between corresponding matrices. Thus as a consequence of the Hamiltonian form $H=p^2/2m+V(q)$ we have $p=m\dot{q}$, $\dot{p}=-(\partial V/\partial q)$ holding as equations between matrices. If we refer all the matrices to the same reference system e.g. that of q and if we write the probability amplitude as $S(q')$ then we also have

$$\int S^*(q')p(q',q'')S(q')dq'dq'' = m(d/dt)\int S^*(q')q(q'q'')S(q'')dq'dq''$$

or

$$\bar{p} = m\dot{\bar{q}}.$$

We are allowed to use here the equation

$$\frac{d}{dt}\int S^*(q')q(q',q'')S(q'')dq'dq'' = \int S^*(q')\frac{d}{dt}q(q',q'')S(q'')dq'dq''$$

[1] P. Ehrenfest, Zeits. f. Physik **45**, 455 (1927); A. E. Ruark, Phys. Rev. **31**, 533 (1928).

because (1) we may work with $S(q')$ independent of t provided the matrix $q(q', q'')$ involves t as a parameter, (2) the equation is obviously true in the reference system of the energy where $q_{nm}(t) = q_{nm}(0) \exp[(2\pi i/h)(W_n - W_m)t]$ (3) the values of the integrals on the right and left of the above equation are indepedent of the reference system used for matrix representation. In a similar way we have

$$\frac{d\bar{p}}{dt} = \bar{\dot{p}} = -\frac{\overline{\partial V}}{\partial q}.$$

The way in which we use the matrices $q(q', q'')$ is explained very clearly in Schroedinger Sitzungsberichte der preussischen Akademie XXIV p. 417, 1930, and is treated in Weyl's book, chapter II section 15. Remembering that Schroedinger's $\psi(0)$ is our S, it is seen that at any time the averages $\overline{\partial V \partial/q}$ is taken weighing every element of the configuration space in proportion to $\psi^*(t)\psi(t)$ at that point at the particular time i.e. the average is taken in the same way as by Ehrenfest and Ruark. The same can be done for *any other equation which holds between matrix as well as classical quantities*. The only doubtful point of this shorthand proof lies in dealing with singular matrices which must be expressed by means of the δ function. This however, is usually only a formal objection since throwing away the "surface integral" contributions of partial integrations is also a necessary part of the purely wave-mechanical proof such as that of Ehrenfest quoted above.

Although the above statement is simple enough to be called trivial it seems that its physical implication is not always realized. Thus for instance the motion of a non-relativistic spinless electron in a magnetic field is governed by the same equations in quantum and in classical dynamics. The center of mass is therefore moving as the classical center of mass under the action of the mean electromagnetic field in the wave package. This has already been proved a long time ago by Kennard and elucidated by Eckart in connection with a recently suggested explanation of discrepancies between the values of e/m. Similarly with the relativistic Dirac equation the rate of change of the mechanical momentum is known to be given by a formula having the same structure as the classical formula, the classical velocities being replaced by $-c\alpha_i$. Again the mean value theorem holds. The equation which proves this is the one derived by Fock.[2]

$$\frac{d}{dt}(p_1 + eA_1/c) = e\frac{\partial A_0}{\partial x_1} + e\alpha_2\left(\frac{\partial A_2}{\partial x_1} - \frac{\partial A_1}{\partial x_2}\right) - e\alpha_3\left(\frac{\partial A_1}{\partial x_3} - \frac{\partial A_3}{\partial x_1}\right)$$

$$\frac{dx_1}{dt} = -c\alpha_1.$$

Here $p_1 + eA_1/c$ is the momentum in the direction x_1, A_0 is the scalar potential, (A_1, A_2, A_3) is the vector potential and α_1, α_2, α_3, α_4 are Dirac's four-row matrices. The equation proves that the rate of change of the average of $p_1 + eA_1/c$ of a wave package is related to the average force on the wave package by the equation of classical electordynamics

$$F = \rho\{E + [vH]/c\}.$$

G. BREIT

Department of Physics,
New York University,
December 12, 1930.

[2] Fock, Zeits. f. Physik 55, 127 (1929).

Block Structure and Ferromagnetism

In the following a model is proposed for ferromagnetic substance basedson theassumption of the existence of a "block structure" in solids as postulated by Smekal and Zwicky, and some of the properties of this model are pointed out. In a future communication it is hoped to give a more detailed and comprehensive account of the derivations and results indicated below.

A block, according to Zwicky,[1] is a region having the properties of a perfect crystal, surrounded by a surface physically different from the volume. This difference is connected with a local rearrangement of atoms such that along the surface the average interatomic distance is not that prevailing inside of a block. If such blocks exist, it is not unreasonable to assume that each one is spontaneously magnetized as predicted by the Weiss-Heisenberg theory

$$\frac{I_T}{I_0} = \tanh\frac{\mu_B N I_T}{KT}. \qquad (1)$$

[1] F. Zwicky, Helvetica Physica Acta 3, 269 (1930).

In this expression the dependence on H is omitted as it is negligibly small for the field strengths used in most experiments, and its inclusion would add nothing to the following discussion. μ_B is a Bohr magneton. The assumption is now made, and this is the only *new* assumption, that various blocks may be magnetized in various directions, or what amounts to the same thing, any particular block may change the direction in which it is magnetized, and its magnetic moment need not be parallel to those of its neighbors. This is equivalent to saying that the electrons on opposite sides of a block surface are not ferromagnetically coupled to each other. Such a situation is not unthinkable, as such a coupling depends on Heisenberg's resonance integral which is known to be extraordinarily sensitive to variations in inter-atomic spacing, and such variations actually define the surface of a block.

Our model, then, is a group of permanent magnets, having primarily a thermomagnetic interaction. For the present, surface phenomena are neglected. In order to simplify the problem, the blocks are assumed isotropic, so that there are no "directions of easy magnetization." These last two assumptions should be dropped in a more exhaustive discussion. Under these conditions the blocks may be expected to interact in such a way that the magnetization is approximately given by

$$\frac{I}{I_T} = \coth x - \frac{1}{x} \qquad x = \frac{\mu}{KT}(H + LI). \quad (2)$$

Here μ is the block moment and is given by $I_T v$, the saturation intensity at the temperature T multiplied by the volume of a block. L is a factor varying between 0 for long thin blocks whose axis is parallel to H, and 4π for disk shaped blocks. LI represents the internal field. Eqs. (1) and (2) define the behaviour of our model.

The first point of interest is that this model is essentially that of Ewing, with the exception that the elementary magnets, instead of being of atomic dimensions, are somewhat larger. Thus the model is fundamentally capable of describing a magnetization curve and a hysteresis loop, as Ewing demonstrated experimentally. The details are determined by the only two arbitrary constants, appearing in the equations, μ and L. To get an idea of their order of magnitude it is possible to assign values to them which will give observed values for K_0, the initial susceptibility. Using experimental data obtained on iron, nickel and cobalt for K_0 and I_0, and substituting extreme values of L, we find that the block volume contains between 10^2 and 10^5 atoms. An intermediate value of L would give an intermediate block size.

The next point of interest is that this model gives the approach to saturation correctly. In a very thorough investigation Weiss[2] showed that most substances approach saturation according to the formulae

$$I = I_T(1 - a/H) \quad (3)$$

$$I_T = I_0(1 - AT^2). \quad (4)$$

The first of these formulae follows immediately from Eq. (2), and from the constant a it is possible to compute the number of atoms per block. ($a = KT/\mu$; $\mu = vI_T$). With Weiss's data for nickel and iron we get approximately 10^5 atoms per block. Weiss examined the approach to saturation as a function of the temperature between 100°K and 300°K. In this region I_T/I_0 as given by Eq. (1) is very approximately a straight line if plotted as a function of T^2. From the constant A it is possible to compute the molecular field constant N, and the values obtained are quite reasonable. It is true that an extrapolation of (4) for $T=0$ leads to somewhat too high values for I_0, but in general the error so committed will be small.

Further, this model has two Curie-points, a property of most ferromagnetic substances as pointed out by Forrer.[3] θ_p the paramagnetic Curie-point is defined by the modified Curie Equation $x = c/(T-\theta_p)$ for $T > \theta_p$. θ_f, the ferromagnetic Curie-point is in general less than θ_p, and is the temperature at which spontaneous magnetization disappears. θ_p is given in the usual way by Eq. (1). On the other hand Eq. (2) will itself have a Curie-point

$$\theta_f = \frac{\mu L I_T}{3K}.$$

That is, for $T > \theta_f$ the spontaneous magnetization of the whole material[4] will disappear, whereas for $T > \theta_p$ the blocks themselves lose their moments. From this it is evident

[2] P. Weiss, Ann. de Physique **12**, 20 (1929).
[3] R. Forrer, Journ. de Ph. et le Rad. **1**, 49 (1930).

that $\theta_f]_{T=\theta_f} < \theta_p$ as it is actually observed in most substances. A detailed examination shows that $\theta_p - \theta_f =$ approximately 15°C is consistent with blocks containing about 10^5 atoms.

Such an interpretation of θ_f brings with it the necessity of a new explanation of the thermal phenomena at the Curie-point. Such an explanation it is impossible to give until more definite assumptions can be made regarding the surface energies of the blocks, the effect of strains, etc. The fact that acceptance of the proposed model would require the abandonment of our present explanation of thermomagnetic phenomena at the Curie-point, would be a telling argument against such a model, were it not that just here the Weiss Theory is in part not quite satisfactory (in its interpretation of the change in specific heat for $T=\theta$) and in part purely thermodynamic (in the relationship it establishes between the specific heat and the magnetocaloric effect).

In conclusion I wish to point out that blocks containing approximately 10^5 atoms, as here postulated for the explanation of three ferromagnetic phenomena, are of the same order of magnitude as those postulated by Smekal and Zwicky to explain certain mechanical and electrical phenomena.

FRANCIS BITTER
Research Laboratories,
Westinghouse Electric & Manufacturing Co.,
East Pittsburgh, Pa.,
November 19, 1930.

[4] Spontaneous magnetization of the sample need not, of course, include the whole sample. It may be spontaneously magnetized in different directions in different regions. It would be sufficient that large groups of units, in this case larger groups of blocks, should possess a resultant moment in the absence of externally applied fields.

Secondary Electrons from Molybdenum

The writer has continued work begun by Soller (Phys. Rev. **36**, 664, 1930) on the distribution in energy of electrons emitted by a molybdenum target bombarded by a narrow, homogeneous beam of electrons of relatively low energy (20 to 100 volts).

The apparatus was a modification of that of Soller, employing the method of magnetic analysis. The target was heated by electron bombardment for a total of 700 hours. Observations were taken at intervals throughout this outgassing period. With the primary energy held constant, measurements were taken of the number of secondary electrons (N_ϵ) of energy ϵ. By changing the magnetic field, ϵ was made to vary in steps of 0.1 to 0.2 volts from zero up to the primary energy. Curves were plotted for $N_\epsilon/N \times$const. as a function of ϵ where N is the total number of primary electrons.

Curves plotted from the results obtained for a cold target show, in addition to the usual large group of secondary electrons with energy approximately that of the primaries, a low maximum in the region 5 to 15 volts and a second very broad and somewhat higher maximum at an energy approximately one-half that of the primaries. For low primary energies these two groups become merged. In addition there are three well defined maxima corresponding to electrons possessing energies 4.7, 11.2, and 23.2 ($\pm$.4) volts less than the energy of the true reflection maximum. These last maxima are similar to those found by Rudberg (Proc. Roy. Soc. **A127**, 111, 1930) for various metals and indicate the presence of reflected primary electrons which have lost a discrete amount of energy in the process of reflection. The height of these peaks increases as the velocity of the primary electrons decreases. These peaks appeared only after considerable outgassing and became more and more marked with further heating.

In attempting to eliminate the effects due to gas occluded on the surface of a cold target, the following procedure was adopted. With the magnetic field set to correspond to a given value of ϵ the target was heated to a bright yellow for thirty seconds and N_ϵ measured thirty seconds after the bombarding current was cut off. (The target ceased to be visibly red after about 20 seconds.) This procedure was followed through the whole range of values of ϵ. A typical curve obtained from these data was that for a primary energy of 60 volts. Observations taken in this way show a very large group of low velocity secondaries of energy from three to twenty-five volts, and N_ϵ/N now reaches a maximum value at 8 volts which is 27 times as great as the corresponding maximum at 8 volts for a cold target. For higher values of ϵ the values

of N_ϵ/N are more nearly alike for the hot and the cold target, the ratio being 2 at a point just short of the full velocity maximum. The three discrete peaks are greatly enhanced in the case of the freshly heated target.

The large low velocity group disappears rapidly with time, the value of N_ϵ/N at eleven volts changing from 27 to 3 during the first three minutes but there is no such rapid change for higher values of ϵ. After the first three minutes there is no further change for as much as thirty minutes, following which there is a gradual decrease over a period of three or four hours. The gradual decrease after 33 minutes is believed due to the occlusion of gases. The first rapid decrease is of unknown origin but, since it is independent of pressure and occurs in such a short time, it does not seem possible that it can be due to the adsorption of gas. The best vacua were of the order of 10^{-7} mm of Hg.

In addition curves were plotted for the height of the full velocity peak as a function of the primary velocity. These show marked minima at 9.3 and 20.6 volts. The difference between these is 11.3, about the same as the difference between the values of ϵ for the 11.2 and 23.2 volt discrete energy-loss maxima. Corrections for work functions etc., necessary to bring 9.3 and 20.6 into agreement with 11.2 and 23.2 are not unreasonable. The full velocity data were not reliable for primary voltages below 6 volts so that no check was obtained for the 4.7 discrete loss group. It is suggested that these minima in the number of elastically reflected electrons are due to some sort of excitation within the metal, the efficiency of which increases as the energy of the primary electrons approaches that necessary for the excitation. On this assumption the three discrete groups of secondaries are composed of reflected primary electrons which have lost a definite amount of energy in the process of reflection.

LELAND J. HAWORTH
Laboratory of Physics,
University of Wisconsin,
December 20, 1930.

On Collisions of Photons

According to the modern concepts of matter and energy, practically all the properties which are usually attributed to matter, can be associated with radiation. The source of solar and stellar energy can be traced to the "annihilation" of matter. However it is not certain that energy is transformed into matter, but with the help of this hypothesis it is possible to calculate correctly the relative mass of the elementary particles of matter. The identity of matter and energy would thus appear to be almost complete and the principles of the conservation of mass and of energy to be but two aspects of one universal principle.

Following up these considerations one would naturally be led to expect the existence of mutual collisions of photons. Thus the paper "Attempt to Detect Collisions of Photons" by Hughes and Jauncey, which appeared in Physical Review **36**, 773, 1930, is of special interest.

About two years ago this same idea occurred to me and I communicated it to Professor G. Angenheister, Director of the Geophysikalisches Institut, Göttingen, in whose laboratory I was working at the time. But the resources of that institution were not adequate to an experimental verification of the idea. The nature of the effect which I expected was similar to that expected by Hughes and Jauncey. In the calculations regarding the possibility of observing the effect, the faintest star clearly visible by the naked eye, was taken to be of the sixth magnitude, as is usually assumed. Using Zöllner's estimate of the ratio of the magnitude of the sun and Capella (magnitude 0.2) and using Exner's value for the vertical illumination of the sun, the limit of human vision was calculated to be 3 millimicrolux. The sensitivity of the eye is maximum for the frequency 0.58×10^{15}, the quantum of which is 3.8×10^{-12} erg. So the number of quanta received by the eye when receiving the minimum visible light is about 360 per second. This number seemed to be too high to be obtained by the scattering of photons due to the mutual collisions which one would expect at the point of crossing of two beams of light under ordinary conditions. I concluded that the expected effect could not possibly be detected with certainty by an optical method, visual or photographic. (A selenium detector might be better suited for the purpose). My plan, therefore, was to look for the theoretically expected effect with the help of some instrument that would record the elementary effect of single photons and not simply the integrated effect of a multitude. Such

an instrument I recognized in the "Elektronenzählrohr" or even in the so-called "Glimmlampe." For this purpose I wanted to utilize the "Elektronenzählrohren," which I had constructed (with the collaboration of K. Wölcken) primarily for the investigation of gamma and cosmic rays.

Instead of using ordinary light (as Hughes and Jauncey have done) my intention was to use x-rays or gamma-rays, but I could not put my intention into practice for lack of necessary equipments. The negative result of Hughes' and Jauncey's experiment need not necessarily lead to the conclusion that mutual collisions among photons do not occur. Those who have the advantage of a good physical laboratory, may find it worthwhile to try the experiment on the lines indicated above.

In conclusion, I would like to mention that sometime ago I found out that the theoretical possibility of the existence of the nature of the effect in question was pointed out by L. de Broglie as early as 1926 in his book "Ondes es Mouvements" pp. 96–98 (Gauthier-Villars, Paris).

A. K. Das

Alipore Observatory,
Calcutta,
November 11, 1930.

BOOK REVIEWS

Optical Rotatory Power A general discussion held by the Faraday Society. Pp. 198. Aberdeen University Press, 1930. Price 10s 6d.

The contributions to this discussion cover practically all phases of the subject and are grouped under the following headings:

I. The Physical Basis of Optical Rotatory Power (8 papers)
II. Apparatus and Methods (2 papers)
III. The Rotatory Power of Solutions (7 papers)
IV. The Chemical Aspects of Optical Rotatory Power (4 papers).

A considerable portion of the discussion centers about the physical theories of optical activity which are presented in articles by Kuhn, Malleman, Ewald, Temple, and others. The wave mechanics of rotatory polarization is shown to be at present in an unsatisfactory state, the principal short-coming being the lack of a connection between optical activity and structure. Experimental methods especially applicable to the ultra-violet region of the spectrum are reviewed by Descamps. As is shown by Cotton and others, this region of the spectrum is an important one in the study of rotatory dispersion and circular dichroism. Many interesting compounds are discussed in the chemical part of the report.

J. VALASEK

Röntgenographie der Metalle und ihrer Legierungen. M. C. NEUBERGER. Pp. 278, figs. 66. Price RM 25.

This book is a fit companion volume to the author's excellent *Röntgenographie des Eisens und seiner Legierungen*, which appeared about a year ago. Because of this previous work, the author confines himself in the present volume to a treatment of the non-ferrous metals and alloys in the light of x-ray data.

The present work supplies a long-felt want in that it renders available at hand in one volume a mass of x-ray data relating to metals and alloys, which is widely scattered, and which can otherwise be obtained in case of need only by an extensive searching of the literature. These data are critically discussed by the author and, wherever a structure is in dispute, he gives not only the result which he considers as probably correct, but also the conflicting results of other workers. A liberal use of tables of x-ray data and reproductions of original x-ray photographs add to the value of the book.

WILLIAM P. JESSE

Les Applications des Rayons X. J. J. TRILLAT. Pp. 298, figs. 108. Les Presses Universitaires de France, Paris, 1930. Price, 85 francs.

This book, as the title indicates, is written for the benefit of the rapidly growing group who would know something of the recent developments of x-rays as a tool in physics, chemistry and metallurgy. With this practical end in view, the author avoids as much as possible all theoretical aspects of the subject which do not bear directly on the technical uses of x-rays and frequently discusses in detail manipulative methods which may prove valuable to one contemplating work in this field.

The book is divided into two sections. In the first of these, which comprises the first third of the book, the author has an introductory chapter on the elementary principles of crystal structure and of x-ray diffraction. Then follows an extended discussion of various types of x-ray tubes and apparatus and a survey of the different methods of x-ray spectroscopy.

The second part of the book deals with recent advances in the use of x-rays in widely different fields. The first chapter on the metals, while not entirely comprehensive, is probably as complete as the enormous mass of work on the subject will allow in such a limited space. This chapter is followed by a very good account of work on the long chain carbon compounds, the material for which is in a large part taken from the author's own researches. The following chapters deal with cellulose and its derivatives, rubber and resins, the diffraction of x-rays by liquids and a short discussion of colloids. The last section makes a very brief mention of radio-

graphic applications to metals and of chemical analysis by x-rays. A very good bibliography at the end of each chapter is a valuable feature of the book.

The book is clearly written and is by an author who has added something to almost every field discussed. It should prove valuable to anyone interested in the technical uses of x-rays.

WILLIAM P. JESSE

The Principles of Quantum Mechanics. P. A. M. DIRAC at the Clarendon Press, Oxford, 1930. Pp. 257.

A book on quantum mechanics written by Dirac must be of great and in many ways unique interest to physicists. The quantum mechanics of today is not the work of one man; but since the foundation of the theory by Heisenberg and Schroedinger, there have been few cardinal advances which have not been made by Dirac; and in his papers alone one may find the key to the solution of almost any problem which the theory is competent to treat. The fact that a book on quantum mechanics must necessarily be largely an account of Dirac's own work, assures us that his account will be unitary and coherent, and that it will be given in just those terms which have shown themselves most useful to the understanding and the development of the theory.

The title of the book tells us that we shall not find here the detailed solution of many specific problems; what we do find is the development and exposition of the methods by which such problems may most simply be attacked. In this respect Dirac's book is very complete—for so short a book, astonishingly complete. In many cases the methods used by Dirac are considerably simpler and more direct than any to be found elsewhere; this is true of his treatment of angular momentum, of the theory of collisions and of radiation, and of the theory of systems containing similar particles. In this last problem, it is true, Dirac's method does not give Wigner's complet *e* reduction of all matrices; and this renders the application of his method to many problems unnecessarily laborious. A few developments of theoretical significance are not included in the book; of these omissions, possibly the most important are the theory of quantized waves for systems satisfying the exclusion principle, the unitary theory of electromagnetic field and matter, and the theory of the electron in a gravitational field. But these things belong perhaps rather to the quantum mechanics of the future; and their omission will hardly be found to diminish the value of the book.

In some very fundamental respects Dirac's book is like Gibbs' "Elementary Principles of Statistical Mechanics": it is clear, with a clarity dangerous for a beginner, deductive, and in its foundations abstract; its argument is predominantly analytical; the virtual contact with experiment is made quite late in the book. The difficulty which this would present for many readers is largely reduced by Dirac's introductory descriptive chapter, and by conscientious efforts to translate all results into physical terms. But physical ideas are seldom used to advance the argument, and occur chiefly as an aid to exposition. The book remains a difficult book, and one suited only to those who come to it with some familiarity with the theory. It should not be the sole text, nor the first text, in quantum theory, just as that of Gibbs' should not be the first in statistical mechanics. Every part of the theory may be understood from more than one point of view; to see it always and only from one point of view, even if that be the most general, is to understand it only partially.

We must say a few words of Dirac's quasi-postulate-theory foundation of the quantum mechanics. Dirac begins his argument by introducing certain symbols, said for picturesqueness to "represent" states and observable variables of a system, and by laying down axioms for the manipulation of these symbols. These symbols do not represent, as do those more current in mathematical physics, a class of numbers defined by some specific measurement on a system; they represent the class of such classes of numbers, defined by any measurement on the system. Thus Dirac's axioms,—and, in fact, most of his earlier chapters—have an extreme generality; but because the meaning of any equation, in physics, is ultimately to be derived from the numbers given by specific observations, they have also a higher grade of abstractness. This is the price that must be paid for the generality. And Dirac's book will be for many of us so satisfying, that we shall be glad to pay it.

J. R. OPPENHEIMER

PROCEEDINGS OF THE AMERICAN PHYSICAL SOCIETY

MINUTES OF THE CHICAGO MEETING, NOVEMBER 28 AND 29, 1930

The 166th regular meeting of the American Physical Society was held in Chicago, Illinois, at the Ryerson Physical Laboratory and Eckhart Hall of the University of Chicago on Friday and Saturday, November 28 and 29, 1930. The presiding officers were Professor Henry G. Gale, President of the Society, Dr. W. F. G. Swann, Vice-president and Professor O. M. Stewart.

On Friday evening the Physical Society had a dinner at the Hotel Windermere. There were one hundred and ten present. President Gale presided. The after dinner speakers were Dr. A. J. Dempster, Dr. Paul D. Foote, Dr. Herbert E. Ives, Prof. R. Ladenburg, Prof. M. von Laue and Professor R. Scherrer.

At the regular meeting of the Council held on Friday, November 28, 1930 at 10:30 a.m. seventy were elected to membership. *Elected to Membership:* John M. Aitchison, Gerald M. Almy, W. N. Arnquist, John V. Atanasoff, Michael Balas, Willard H. Bennett, J. C. Betz, Paul H. Boots, Robert A. Boyd, James M. Bradford, Maurice J. Brevoort, H. T. Byck, R. W. Carson, Lawrence H. Cook, Winston Cram, C. F. DeVoe, Laurance H. Donnally, J. S. Evans, Robley D. Evans, George Forster, Amelia Frank, Wendell H. Furry, Otto Halpern, R. R. Hancox, Helen Harms, H. Harold Hartzler, Arthur B. Hersey, D. M. Hill, Joseph O. Hirschfelder, Winston L. Hole, Walker Kinkaid, John R. Kerry, William S. Klein, Emeran J. Kolkmeyer, M. R. Krasno, Jules A. Larrivee, Rose LeD. Mooney, Robert Morgan, John M. Nordquist, M. Ostrofsky, Ralph G. Owens, Lyman G. Parratt, R. W. B. Pearse, W. D. Phelps, Lloyd B. Phillips, E. R. Piore, Frank W. Pote, Kurt F. Ritzau, Edward R. Schmid, Frederic A. Scott, Robert Serber, Robert S. Shankland, J. A. Sharpe, J. H. Simons, Albert Smith, Chauncey G. Suits, Shinji Togo, Philander B. Taylor, Melvin C. Terry, Rayen W. Tyler, Oliver G. Vogel, John H. Wanamaker, Mary D. Weber, Donald F. Weekes, George L. Weil, M. F. Weinrich, Lester V. Whitney, Violet Wu, H. M. Zenor and George E. Ziegler.

The regular scientific session consisted of fifty four papers, eight of which —Nos. 17, 18, 20, 26, 32, 33, 43 and 46—were read by title. The abstracts of these papers are given on the following pages. An AUTHOR INDEX will be found at the end.

W. L. SEVERINGHAUS, *Secretary*

1. Measuring the intensity of molecular beams. A. ELLETT AND R. M. ZABEL, *University of Iowa.* A sensitive Pirani gauge has been developed and used to measure the intensity of a molecular beam defined by 0.5 mm circular openings 22 mm apart. The gauge is situated 35 mm from the last opening. A beam of air gives a galvanometer deflection of 1000 cm with a pressure of 1 mm behind the first opening. H_2 produces a deflection of 2000 cm. The galvanometer sensitivity is 11.6 mm per micro-volt. The time lag of the gauge is less than the period of the galvanometer (7 seconds). The limits within which the beam forming system may be expected to give a Maxwellian distribution of velocities are discussed. The final pressure in the gauge due to a given beam depends upon the size of the gauge opening as kinetic theory predicts. The reduction in intensity of beams of air and H_2 by collision with either air or H_2 present in the experimental chamber at various pressures has been measured. The data show that the gauge may be used to measure mean free paths and to obtain more detailed information that has previously been possible as to the probability of scattering through various angles by collision.

2. Diffraction of atomic hydrogen. THOMAS H. JOHNSON, *Bartol Research Foundation, Swarthmore, Pa.* Improvements in the technique of photographing the de Broglie wave diffraction patterns, produced by the reflection of a beam of atomic hydrogen from a cleaved crystal of lithium fluoride, have considerably increased the intensity of these patterns over that of the patterns previously reported. In consequence, new features have been recorded. The patterns obtained by reflection at normal incidence consist (a) of four intense lines radiating from the central specularly reflected spot in directions perpendicular to the two mutually perpendicular sets of rows of similar ions on the surface of the crystal and (b) of four relatively weak, but plainly visible, lines radiating from the same point but perpendicular to the two sets of diagonal rows of alternately dissimilar ions. The gradation of intensity along the "*a*" lines corresponds to the dispersion of the various wave lengths of the Maxwellian velocity distribution by the grating whose lines are the rows of similar ions spaced at intervals of 2.83A. The "*b*" lines have a greater dispersion corresponding to the closer spacing of 2.00A between the rows of alternately dissimilar ions. Similar patterns observed at 45° incidence appear with branches corresponding to the various combinations of the values of 0, -1, $+1$ for m and n in the plane grating formulae $\cos\phi_0-\cos\phi=m\lambda/d$ and $\cos\theta_0-\cos\theta=n\lambda/d$.

3. The value of e/m by deflection experiments. G. E. UHLENBECK AND L. A. YOUNG, *University of Michigan.* To clarify the discussion as to whether or not a quantum mechanical treatment of the motion of electrons in magnetic fields will lead to a formula for e/m, differing from that obtained by classical electrodynamics the following problem was solved. A uniform magnetic field in the z-direction exists in the half-space $x>0$. A plane monochromatic de Broglie wave, travelling in the positive x-direction representing electrons of arbitrary energy, impinges normally on the plane $x=0$. Solutions of the wave equation were found fulfilling appropriate boundary conditions at the plane $x=0$. Currents are calculated quantum mechanically and compared with the corresponding classical expressions. It was found that for electrons possessing energies of the order of magnitude used in deflection experiments, no *observable* deviations from classical results are predicted. Another quantum mechanical effect is diffraction at slits. Simple approximate calculations show that this effect can produce a fractional error in e/m of the order of the de Broglie wave-length divided by the slit width. These results are opposite to the conclusions reached by Page (Phys. Rev. **36**, 444). We may remark that he solved a problem of "stationary states" which does not represent the actual experiments.

4. The diffraction of an electron-wave at a single layer of atoms. M. v. LAUE, Visiting Professor from the University of Berlin. (Introduced by A. H. Compton). This paper undertakes to estimate the influence of the gradual transition between the field exterior to, and in the interior of a crystal, on the diffraction of electrons. This gradual transition is required by electrostatics. The result is that this influence may be neglected for electrons whose energy is two-hundred volts or more. One can then treat the transition as discontinuous. In the case of slower electrons it seems doubtful if such a treatment is permissible.

5. Frequency variations due to the electrodeless discharge. J. T. TYKOCINER AND J. KUNZ, *University of Illinois.* Experiments were carried out to show that an oscillator which excites electrodeless discharges undergoes variations of its frequency due to the reaction of the discharges. These variations were measured by means of a heterodyne method and the results were applied for a study of the intensity and character of the electrodeless discharge currents. The fact was thus disclosed that contrary to a relation calculated on the basis of J. J. Thomson's theory of the ring discharge which demands an increase of frequency, the "ring" discharge causes a decrease of frequency. An extension of the theory was undertaken which takes into account the effect of the capacitance of the excitation coil itself and of the influence of the ionized dielectric in the discharge tube subjected to the action of electrostatic fields. It can thus be shown that due to the electrostatic forces always predominating over the electromagnetic induction, a decrease of frequency must result, whenever the inner conductance of the discharge is small enough to suppress the formation of ring discharges.

6. Interpretation of negative volt ampere characteristics of neon positive column. CLIFTON G. FOUND, *General Electric Co., Schenectady, N.Y.* The voltage gradient in the positive column of a discharge in neon decreases rapidly with increase in current. The decrease in gradient runs parallel to the increase in concentration of metastable atoms and to the increase in light efficiency. Moreover, observations show that the electrons in the positive column have velocities corresponding to a Maxwellian distribution in which electrons with a velocity greater than the resonance potential are absent. This deficiency of electrons with energy sufficient to produce ionization indicates that the positive ions are not formed by a single electronic collision but must be the result of a two stage process such as ionization of metastable atoms by slow electrons. These characteristics indicate that the negative resistance of the positive column is connected with the presence of metastable atoms. This assumption permits an explanation of the inductive impedance of a hot cathode neon tube as measured by W. F. Westendorp by a method which will be described in the near future.

7. The efficiency of ionization of mercury vapor by electron impact near the ionization potential. PHILIP T. SMITH, *University of Minnesota.* Direct measurements of the efficiency of ionization by electron impact, using an electron beam with a very narrow velocity distribution show a series of discontinuous changes in the slope of the efficiency curves as the energy of the impacting electrons is increased. Most of these discontinuities or "ultra-ionization potentials" agree with those previously observed by E. O. Lawrence, (Phys. Rev. **28,** 947 (1926)) and A. L. Hughes and C. M. Van Atta, (Phys. Rev. **36,** 214 (1930)), although several new ones have been observed. Lawrence's values were 10.40, 10.60, 11.29, 11.70, 12.06 volts. Hughes' and Van Atta's 10.40, 10.62, 10.88, 11.28, 11.40, 11.77, 12.16, 12.76. Our values, 10.40, 10.60, 10.76, 10.88, 11.07, 11.27, 11.40, 11.55, 11.70, 11.78, 11.90, 12.06, 12.17, 12.38.

8. Doppler effects in hydrogen with canal rays of uniform velocity. H. F. BATHO AND A. J. DEMPSTER, *University of Chicago.* Positive ions were produced by bombarding hydrogen with low voltage electrons from a hot cathode. The ions formed passed beside the cathode into a strong field where they were accelerated by potentials up to 15,000 volts. The ions then passed into an observation chamber, where the light emitted by the accelerated particles was photographed with a large three-prism spectrograph. With the usual canal-ray tubes broad displacements are obtained as Doppler effects due to the velocity distributions in the ions, maxima are sometimes present suggesting ions of various masses, and the observed displacement is always considerably less than that calculated from the potential difference on the tube. With the present tube sharp displaced lines of the Balmer series are obtained indicating homogeneous velocities, the displacements agree with those calculated from the potential for atomic ions, molecular ions and triatomic molecular ions. These ions break up in the observation chamber giving hydrogen atoms which emit the Balmer series lines with Doppler effects corresponding to the velocities of the ions. At low pressures the displaced line due to the molecule ion becomes the strongest as suggested by previous experiments on the positive-ray analysis of ionization products.

9. A study of the velocities of ions formed in nitrogen by electron impact. W. WALLACE LOZIER, *University of Minnesota.*—In a recent paper (Phys. Rev. **36**, 1285 (1930)) there was described a method which is suitable for a measurement of the velocities of ions formed in molecular gases by electron impact. This method is employed in a study of nitrogen. Above 35 volts electron velocity there are two groups of ions, these being N_2^+ and N^+. The N_2^+ ions possess very little kinetic energy while the majority of the N^+ ions possess about 3.0 equivalent volts velocity, these latter ions resulting from dissociation of molecular ions. The number of N^+ ions increases so rapidly with electron velocity that at about 60 volts electron velocity they actually occur in greater numbers than the N_2^+ ions, a fact which is in striking contrast to the results obtained in hydrogen.

10. The effect of resolving power on the absorption coefficient of electrons in gases. R. RONALD PALMER, *University of Minnesota.*—The absorption coefficient of electrons in helium and in mercury vapor has been studied as a function of the geometry of the experimental apparatus. An electron beam of 0.4 mm radius was used in a Mayer type of apparatus in which the opening at the end of the scattering chamber was of variable aperture. Values of the absorption coefficient were obtained for 20, 40, 80 and 135 volt electrons over an angular aperture range of from 2° to 11° as measured from the end of the electron gun. All curves showed a definite decrease in the absorption coefficient with increase in angular aperture. These curves were corrected for the positive ion current, from the efficiency of ionization data of Bleakney and Smith, to give curves for the total number of electrons collected as a function of the size of the opening. These showed also a definite decrease with increase in aperture, corresponding to a preference for scattering to take place at small angles. In helium the curves were steeper the higher the electron velocity, whereas they were more alike in mercury vapor. From Arnot's angular distribution results it is possible to predict such a curve for 80 volt electrons in mercury vapor. The predicted curve is much steeper, showing a sixty-five per cent decrease as against a thirty-two percent decrease over the same range experimentally. This discrepancy is as yet unexplained.

11. The motion of electrons in argon. H. B. WAHLIN, *University of Wisconsin.*—The mean free path λ of electrons in argon has been determined for the case where the electrons are in thermal equilibrium with the gas, using the alternating potential method for determining mobilities. The value thus found is $\lambda = 0.385$ cm at a pressure of 1 mm. This value is 9.2 times the kinetic theory value $(4(2)^{1/2}$ times the atomic free path). The mobility curves obtained when the current is plotted against the alternating voltage definitely show the influence of the Ramsauer effect.

12. Specific resistances of zinc single crystals. E. P. T. TYNDALL AND A. G. HOYEM. *University of Iowa.*—Measurements made on fourteen single crystals prepared from Kahlbaum's best zinc by the Czochralski-Gomperz method yield values of specific resistance which verify the Voigt-Thomson symmetry relation with considerably more accuracy than has been the case previously. The scattering of results of previous observers (Bridgman, Ware) appears to have been avoided here by more careful attention to experimental conditions, particularly in the determination of cross-sectional area and its variation along the crystal rod, and in temperature control. The increase in resistance due to slight strains found by Bridgman does not exist for these crystals. The specific resistances, perpendicular and parallel to the vertical axis are: $\rho_\perp = 5.88 \times 10^{-6}$, $\rho_\parallel = 6.20 \times 10^{-6}$ ohms/cm³. For a series of 22 crystals prepared from "spectroscopically pure" zinc (from the New Jersey Zinc Co.) the values $\rho_\perp = 5.83 \times 10^{-6}$, $\rho_\parallel = 6.15 \times 10^{-6}$ are obtained. The results, however, are more scattered than for the Kahlbaum crystals, but it is believed that this may be due largely to increased experimental difficulty in handling these much more easily deformable crystals. Thus, the purer zinc shows lower values of specific resistance throughout, but the ratio $\rho_\parallel/\rho_\perp$, is the same for both 1.055.

13. Electromotive force of paraffin membranes. KARL LARK-HOROVITZ AND J. E. FERGUSON, *Purdue University.*—With the method developed by Horovitz some time ago (Proc. Vienna Acad. Sci. **134**, 345(1925)) thin films of paraffin were sealed to glass tubing of known electrode function. These paraffin films are used as one electrode in aqueous solutions of dif-

ferent ionic concentrations. Measuring the change of electro-motive force of the paraffin film as a function of the concentration of ions in the solution by using a binant-electrometer (Dolezalek), the following results were obtained: Paraffin acts as a reversible electrode in respect to cations only. It behaves in solutions of HCl, KCl, NaCl, $AgNO_3$ and NaOH like a reversible electrode in respect to any of the cations contained in the solution after a certain range of concentration has been reached. In solutions of mixtures of electrolytes, paraffin behaves like a mixed electrode, its behavior being in all respects similar to the behavior of glass as described before by Horovitz and collaborators.

14. Contact potential between iron and nickel. G. N. GLASOE, *University of Wisconsin (Introduced by C. E. Mendenhall).*—Specimens of electrolytic iron and electrolytic nickel were outgassed by intensive heat treatment in a high vacuum and the contact potential between them was measured by the Kelvin null method. Photoelectric long wave limits of the specimens were measured by using filters in the path of the light from a quartz mercury arc. The light transmitted by each filter was photographed with a quartz spectrograph immediately after each determination of the photoelectric effect. The results of the measurements made after the Fe and the Ni had been heated for 300 hours were the same as those obtained after some 750 hours of heating. The plates were heated at a temperature of about 900°C at first and then the temperature of the Fe was raised to 1000°C and that of the Ni to 1100°C with no measurable change in the values obtained for the contact potential and long wave limits. The equilibrium value of the contact potential was Fe-Ni+0.20 volt ±0.01 volt. The long wave limit of the Fe was found to be 2646A and that of the Ni to be 2537A. The work functions of the specimens corresponding to these long wave limits are: Fe 4.662 volts, and Ni 4.862 volts. The difference in these values gives the contact potential Fe-Ni+0.20 volt.

15. On the electrical resistance of contacts between solid conductors. J. FRENKEL, *Visiting Professor from Leningrad, University of Minnesota, (Introduced by H. A. Erikson).*—A contact between two solid conducting bodies is visualized as a small gap between them. This gap can be described as a potential hill, over which the electrons, according to the wave mechanical theory, can pass even with insufficient kinetic energy. There must be in general a steady flow of electrons across the gap in both directions, the difference between the two flows being the actually observed current intensity I. The general expression of I as function of the applied potential difference is obtained and discussed for the case of two identical bodies in connection with the resistance of granular structures (thin metallic films, obtained by cathodic pulverisation) and for the case of two different bodies in connection with the rectifying (valve) action.

16. Photoelectric properties of oxide cathodes. W. S. HUXFORD, *Grigsby-Grunow Research Staff, Department of Engineering Research, University of Michigan.*—The effect of applied fields on the photoelectric work function of barium-strontium oxide cathodes has been investigated in the light of recent theories on electron emission from adsorbed metallic films. Photo-currents of the order of 10^{-11} ampere were obtained when the cathodes were illuminated by light from a glass monochromator. The potentials employed were of the order of magnitude of those commonly applied to the electrodes of radio receiving tubes. As the activation of the cathode is carried to a maximum the photoelectric threshold, as measured at room temperatures, moves towards the red end of the spectrum, and the tendency to a condition of non-saturation in the emission increases. The currents due to the electrons emitted under the action of blue light saturate better than those caused by red light. A striking dependence of the photoelectric work-function upon the applied fields has been found. In the case of one cathode, the long wave limit of the photoelectric effect occurred at 9200A with a field of 40 volts per cm and at approximately 10,800A with a field of 8000 volts per cm. A quantitative estimate is made of the modification of the intrinsic surface fields by the impressed fields.

17. Photovoltaic effects in Grignard solutions. II. R. T. DUFFORD, *The University of Missouri.*—New observations are reported which bring out several new facts about the Becquerel effect in Grignard cells. Most important among these are the behavior on closed circuit, and the remarkable effect of certain depolarizers in increasing the current obtainable; and the

evidence that at least two types of response may occur with platinum electrodes. The effect is noted in several compounds not before tested. The work was done at the Research Laboratory, Incandescent Lamp Department of General Electric Co., Cleveland, Ohio.

18. The dielectric polarization of castor oil, linseed oil and tung oil. W. N. STOOPS, *Westinghouse Research Laboratories, East Pittsburgh, Pa. (Introduced by C. F. Hill).*—The dielectric constants and densities of castor oil, linseed oil and tung oil have been measured over the temperature range between 100°C and their freezing points. The dielectric constant and polarization data indicate the presence of polar molecules in the oils. Accordingly the dielectric constants and densities of their dilute solutions in benzene have been measured, and the electric moments calculated by means of the Debye equation. They are 3.7, 3.0 and 2.8×10^{-18} e.s.u. respectively for castor oil, linseed oil and tung oil. From the standpoint of their molecular structure, these oils may be considered as derivatives of the triglyceride of stearic acid. The above values of the electric moment agree well with what would be expected on the basis of the accepted chemical composition of the oils.

19. Orientation of hydrocarbon crystals by an electric field. RALPH D. BENNETT, *University of Chicago.*—Ewing has shown (Phys. Rev. **36**, 378 (1930) that as regards scattering power for x-rays an electret consisting of a mixture of different waxes is anisotropic. The writer has obtained results in agreement with his. Further, paraffin shows a similar anisotropy when allowed to crystallize in an electric field. Müller and his collaborators (Proc. Roy. Soc. **A120,** 437 (1928); Jour. Chem. Soc. **127,** 599 (1925); *et al.*) have shown that the normal hydrocarbon crystals have the form of thin flakes, the long axes of the molecules being perpendicular to the face of largest area. The writer's x-ray measurements indicate that the effect of the electric field is to align these crystals edgewise, i.e. the hydrocarbon chains are perpendicular to the electric field.

20. Change of frequency of x-rays scattered by bound electrons. D. P. MITCHELL AND A. J. O'LEARY, *Columbia University.*—In the Physical Review of June, 1929, one of us (D.P.M.) reported changes in wave-length of the molybdenum $K\alpha_1$ line scattered at 90° from graphite, beryllium and aluminum. These were interpreted as due to the transfer of the binding energy of K and L electrons in the scattering substances. Further investigation of this phenomenon with improved apparatus employing a background compensation method failed to disclose, in addition to the unmodified line, any of the lines previously reported. The line Mo$K\alpha_1$ was scattered from paraffin and graphite at an average angle of 90° and beryllium 154°. The experimental conditions for producing the scattered radiation were as nearly as possible like those of the earlier work. The measurements were made by means of ionization apparatus as before. However, the sensitivity and stability of the new measuring apparatus was sufficient to have disclosed such lines if their intensity exceeded 10 percent of the unmodified Mo$K\alpha_1$ line scattered from paraffin and graphite. The result is in complete accord with similar experimental work already reported by J. A. Bearden and N. S. Gingrich. Unmodified scattering by beryllium was definitely observed although quite weak. No "anti-Stokes" line was observed as previously reported. Such a line should have appeared if its intensity was 50 percent of the unmodified Mo$K\alpha_1$ line.

21. Scattering of x-rays in the neighborhood of 90 degrees. G. E. M. JAUNCEY AND G. G. HARVEY, *Washington University, St. Louis.*—X-rays from a tungsten target tube excited at 90 and 125 kilovolts were scattered by paraffin. The x-rays were filtered through aluminum so as to produce some degree of homogeniety, and the distribution of intensity amongst the wave-lengths still present was determined by an absorption method. The intensity of the x-rays scattered at the above angles by a thin slab of paraffin was calculated for each wave-length present in the primary beam, using the formulas of Dirac and Jauncey. Each wave-length was assumed to be changed on scattering by the Compton value and the proportion of the intensity of each wave-length which was absorbed in the methyl iodide in the ionization chamber was calculated. The total intensity absorbed in the ionization chamber was then found by graphical integration. In the experiment, the ratios of the intensities scattered at

75° and 120° to the intensity scattered at 97°30′ were determined. These ratios were compared with the two theoretical ratios. The agreement is much better with Dirac's than with Jauncey's formula. At the wave-lengths used Dirac's formula is not sufficiently different from the formula of Klein and Nishina for this experiment to discriminate between them.

22. Scattering of x-rays by gases. E. O. WOLLAN, *University of Chicago.*—Measurements of the scattering of x-rays by gases are in progress using a molybdenum target, with Soller slits and matched filters of ZrO_2 and SrO. This arrangement makes possible the use of more homogeneous radiation and more definitely defined scattering angles than have hitherto been reported. The intensity of scattering of hydrogen at 90° has been used as a standard with which the scattering of other gases has been compared. Due to the small intensity of scattering from hydrogen, oxygen was used as a secondary standard, with which direct comparisons of intensity with other gases was made. Measurements of the intensity of scattering from argon at angles from 10° to 90° were obtained, and put on an absolute scale by comparison with oxygen. The scattering per electron for argon was considerably greater than for hydrogen and oxygen over the whole range of angles. This indicates a strong concentration of electrons near the center of the argon atoms.

23. Electron distribution in argon, and the existence of zero point energy. ARTHUR H. COMPTON, *The University of Chicago.*—Data on the scattering of x-rays by argon, reported by Wollan are analyzed by the method recently described by the writer (Phys. Rev. **35**, 925 (1930)) The resulting electron distribution curve (U curve) shows a maximum electron density at about 0.10A from the center of the atom. The data of James and Firth (Proc. Roy. Soc. **A114**, 181 (1927)) on rock salt at 0°K give a maximum electron density of chlorine atoms at about 0.19A from the center, for 900°K at about 0.58A. The difference between the latter two values is due to the thermal motion of the atoms in the crystal. Similarly, the large difference between the radius of maximum electron density in the atoms of argon gas and of chlorine in rock salt at 0°K must mean motion of the chlorine ions in the crystal lattice. The amplitude of this motion is of the order of magnitude predicted on the quantum theory of zero point energy. This confirms the conclusion of James Waller and Hartree, who however based their conclusion on a theoretical rather than an experimental electron distribution for argon and chlorine.

24. Absorption of x-rays in gases. W. W. COLVERT, *University of Chicago.* (*Introduced by A. H. Compton.*)—X-ray spectral lines reflected from a platinum surfaced mirror and by a calcite crystal have been used for absorption measurements with neon, sulphur dioxide, chlorine and argon. The double reflection gives a more nearly homogeneous beam, since the mirror greatly reduces the higher orders of the shorter wave-lengths. The results are summarized in the following table.

Mass absorption coefficients

	0.496A	0.561A	0.631A	0.710A	1.389A	1.539A	2.288A
Ne	.84	1.20	1.69	2.50	16.0	23.4	75.5
Al	1.96	2.71	3.82	5.32	37.3	50.7	149.6
SO_2	1.92	2.67	3.60	5.55	38.5	51.8	162.6
S(Calc)	3.40	4.64	6.89	9.96	66.4	88.4	284.0
Cl	4.14	5.76	8.18	11.52	76.9	102.7	315.0
A	5.06	6.89	9.80	13.0	85.7	114.0	339.4

25. The absorption of the $K\alpha$ line of carbon in various gases. ELMER DERSHEM AND MARCEL SCHEIN, *University of Chicago.*—The mass absorption coefficients of a number of gases for the $K\alpha$ line of carbon ($\lambda = 44.6$A) have been measured with the aid of a specially designed x-ray vacuum spectrograph in which a ruled grating was used to isolate the $K\alpha$ line. A photographic method was used and the densities of the photographic images obtained with and without gas in the chamber were compared by means of a photoelectric photometer. Pre-

liminary values of the mass absorption coefficients (μ/ρ) of the gases used are as follows He 3050; CO_2 4750; N_2 3950; O_2 5800; Ne 11500; SO_2 13000. Work on these and other gases is being continued and the above values may be slightly revised but are believed to be quite accurate.

26. The absorption coefficient of γ-rays from radium C and the effect of the rays on films. CHARLES S. BARRETT AND ROY A. GEZELIUS, *Naval Research Laboratory, Washington, D.C.*—The curve of film density vs. exposure is of the same type for γ-rays as for x-rays. The use of commercial screens of calcium tungstate reduce the exposures required in radiography with γ-rays to about 0.6 those required without screens; lead foil effects a reduction to about 0.75. The rapid increase in effectiveness of calcium tungstate screens with increasing hardness of rays in the x-ray region does not continue into the region of hard γ-rays. Recoil electrons from an aluminum sheet (optimum thickness about 2 mm) placed on the radium side of a film are not as effective for the above purpose as the electrons (chiefly photoelectrons) from lead foil. The linear absorption coefficient μ of γ-rays in iron was determined by densitometer measurements on films exposed under conditions similar to those of radiography, with precautions taken against scattered rays reaching the films from the rear. With blocks 30 cm square and 5–15 cm thick as absorbers and with films directly behind them, placed 45 cm from 250 millicuries of radon, $\mu=0.30$ cm^{-1}. This is in agreement with previous ionization measurements made under conditions where comparable amounts of scattered rays were present. A quantitative technique for γ-ray radiography has been worked out and is being published elsewhere.

27. A simple derivation of the formula for the half-width of the Debye-Scherrer lines. N. RASHEVSKY, *Westinghouse Research Laboratories, East Pittsburgh, Pa.*—In 1918 P. Scherrer published without proof the following expression for the half-width of the Debye-Scherrer lines:

$$h=2(ln2/\pi)^{1/2}\ (\lambda/l\cos\theta)=0.94(\lambda/l\cos\theta)$$

λ being the wave-length of the x-ray beam, l the size of the crystallites and θ the glancing angle. Seljakow and v. Laue independently gave later on rather elaborate analytical derivations of the above formula, their results differing from Scherrer's and from each others only in the value of the numerical factor (Seljakow—0.92; v. Laue—0.9). In the present paper a very simple and short derivation of the above formula is given, showing particularly clearly the physical cause of the broadening of the lines, and giving for the numerical factor the value 0.89.

28. The structure of some groups XO_3. W. H. ZACHARIASEN, *University of Chicago* (Introduced by H. G. Gale).—Through determinations of the crystal lattices of $KBrO_3$, $KClO_3$, $NaClO_3$ and Na_2SO_3 the size and the shape of the groups $(BrO_3)^{-1}$, $(ClO_3)^{-1}$ and $(SO_3)^{-2}$ were examined. These 3 groups show the same type of structure. This special type is also found for the groups $(AsO_3)^{-3}$ and $(SbO_3)^{-3}$ in the crystal lattices of As_2O_3 and Sb_2O_3 as determined by *Bozorth*. The structure type of the above 5 groups is distinctly different from the one of the groups $(BO_3)^{-3}$, $(CO_3)^{-2}$ and $(NO_3)^{-1}$. The cation is displaced an amount Δ out of the plane of the three oxygens, and this displacement can be expressed by: $\Delta=a/12(6)^{1/2}$, where a is the oxygen to oxygen distance in the equilateral triangle. Due to the existing relation between Δ and a, we can describe our type of groups as tetrahedral groups with one tetrahedral corner removed. Common for all groups of this type is that the cation has got only 2 electrons in the outer shell. The asymmetry which characterizes the configuration around the cation may be explained as due to deformation in the outer shell of the cation, where the charge distribution is very diffuse.

29. The building of atoms as related to nuclear abundance and stability. W. D. HARKINS, *University of Chicago.*—Recent investigations emphasize the importance of the rule that the elements of even atomic number are much more abundant than those of odd number. This and other evidence indicate that the most stable nuclei are those whose charge is represented by an even number. An even more important rule is that the most stable nuclei are those which

contain an even number of negative electrons. If the atomic species are divided into four classes according to the evenness or oddness of the number of nuclear electrons and protons, the most stable species are found to belong to Class I, for which these numbers, and the atomic number also, are even. The nuclear spin of all of the species of this class which have been investigated have been found to be zero. The nuclei of complex atoms in general seem to exhibit such relations as to indicate that with the possible exception of the alpha particle, they are built in steps. The particles which seem most likely to take part in increasing the mass of a nucleus are: the alpha-particle, the proton, the electron, the half alpha-particle $(p_2e)^+$, and possibly the neutron, although the last of these may not exist since the ratio of negative to positive electrons in a neutron is unity, which is abnormally high for a complex nucleus. The increase of mass by the addition of an electron may be negative on account of the packing effect.

30. Time lag in the formation of the latent image. LESTER I. ZIMMERMAN, *St. Louis University*. (*Introduced by F. E. Poindexter*).—Series of constant energy exposures were made on Hammer Extra-Fast plates at high and low light intensities by means of flashes of light from a rotating mirror for a range of mirror speeds. The time of illumination of the emulsion grain in each flash varied from 10^{-6} to 5×10^{-8} seconds. It was found that there was a gradual diminution of image density with decreasing time of flash until a critical flash interval was reached, after which the density-flash curve fell rapidly. The breaking point of the graph for high intensities was at a time of flash of approximately 1×10^{-7} seconds while that for the low intensity was 3×10^{-7} seconds. Assuming that the breaking over of the density-flash graphs is real, and not due to some undetermined characteristic of the apparatus, the conclusion is indicated that the formation of the latent image is a resonance process.

31. A study of the latent image at low intensities. FRANKLIN E. POINDEXTER AND LOUIS E. JAMES, *St. Louis University*.—Hammer Extra-Fast plates were exposed to light of very low intensities—the times for normal exposures ranging from thirty to two hundred and forty minutes. Two sources of light were used on each plate. A series of exposures was made with each source separately, a series of each on top of the other and, finally, a series was made when both lights were shining on the plate. It was found that the densities for the simultaneous exposures were in all cases greater than those formed by putting the image due to one source on top of the other. The difference between these densities, however, decreases with increasing intensities of the light sources. The results show that the failure of the reciprocity law is very appreciable even for fast plates at low intensities.

32. The band spectra of scandium-, yttrium-, and lanthanum monoxides. WILLIAM F. MEGGERS AND JOHN A. WHEELER, *Bureau of Standards*.—New data on wave-lengths and relative intensities of band heads in these three molecular spectra have been obtained and have been classified in a number of band systems resulting from transitions between various vibration levels of initial and final electronic states. For ScO 137 band heads are observed; these belong to 5 systems, the 0, 0 transitions of which are at I, 4857.79 and 4858.09A; II, 6017.07A; III, 6036.17A; IV, 6064.31A; V, 6079.30A. The YO spectrum closely resembles that of ScO; 126 band heads were observed; these are assigned to 5 systems with 0, 0 transitions at I, 4817.38 and 4818.20A; II, 5939.08A; III, 5972.04A; IV, 6096.78A; V, 6132.06A. In the LaO spectrum, more than 300 band heads have been measured; they appear to belong to 9 different systems. Our analysis of the LaO bands agrees in the main with that given by Jevons (Proc. Phys. Soc. London **41**, 520 (1929)). All of the bands in these spectra are degraded to red except two groups of LaO which are degraded to violet.

33. Regularities in the second spectrum of xenon. C. J. HUMPHREYS, T. L. DEBRUIN AND W. F. MEGGERS, *Bureau of Standards*.—A new description of the spectrum of ionized xenon (Xe II) has been completed; it gives wave-length and intensity data for about 1600 lines between the limits 2230A and 8716A. The ground doublet ($^2P_{1\,1/2,1/2}$) in this spectrum has been identified among lines observed in the Schumann region by Abbink and Dorgelo (Zeits. f. Physik **47**, 221 (1928)); the levels are separated by 10540 wave-numbers. This spectral term has been connected with others which combine so as to give lines in the visible Xe II spectrum,

and the absolute values of the terms have been fixed by extrapolating series-forming terms to their limits. The ionization potential is found from these spectroscopic data to be 21.1 volts.

34. Hyperfine structure patterns. S. GOUDSMIT AND R. A. FISHER, *University of Michigan.*—Hyperfine structure separations obey the interval rule very accurately. This enables one to construct simple graphs which represent all possible line patterns for given quantum numbers. Such graphs are useful in the interpretation of hyperfine multiplets especially in cases where not all components are resolved. They were successfully applied to preliminary measurements of Bi II hyperfine structure, recently obtained by us. Application to the partly resolved hyperfine multiplets of Mn I (H. E. White and R. Ritschl, Phys. Rev. **35**, 1146 (1930)) gives results which differ considerably from those obtained by White.

35. The transfer of energy between molecules during collisions: quenching of mercury resonance radiation by admixed thallium vapor. O. S. DUFFENDACK, *John Simon Guggenheim Memorial Fellow, University of Michigan.*—The quenching of mercury resonance radiation $\lambda 2537$ by admixed thallium vapor was measured. At 0.8 mm mercury vapor pressure and 750°C the radius of the excited mercury atom has an apparent value 30 times greater than the normal kinetic theory radius. Previous measurements on quenching by permanent gases give a maximum radius 3 times normal. The addition of helium to the Hg-Tl mixture at 750°C permits the measurement of the quenching at 0.001 mm mercury vapor pressure and gives a radius of the excited mercury atom little greater than normal. When N_2 is substituted for He, the radius is somewhat greater. The differences are attributed to differences in the concentration of excited mercury atoms in the $^3P_1$ and $^3P_0$ states. The presence of metastable $^3P_0$ atoms makes the value of the average life of the excited atom uncertain.

The experiments indicate the possibility of isolating the effects of the $^3P_1$ state, in which case a radius very little greater than normal is probable: a result in agreement with estimates made from the quantum-mechanical theory of Kallmann and London (Zeits. f. Phys. Chem. **B2**, 207 (1929)). This investigation was carried out under the direction of Professor J. Franck at Göttingen.

36. The energy of dissociation of mercury molecules. J. G. WINANS, *University of Wisconsin.*—The absorption spectrum and the electrodeless discharge spectrum of mercury vapor between wave-lengths 2200 and 1550 were photographed with a fluorite vacuum spectrograph. In the absorption spectrum, three apparently continuous bands were observed with maxima at 1849, 1807, and 1685. With increasing pressure the 1849 band broadened symmetrically until it over-lapped the 1807 band. With further pressure increase the 1849 band broadened toward longer wave-lengths but retained a sharp short wave limit coinciding with the short wave limit of the 1807 band. In the electrodeless discharge excited by a low voltage Tesla coil, the bands at 1849 and 1685 were emitted, but not the one at 1807. Assuming that this failure of 1807 indicated that molecules which absorb 1807 are dissociated, potential energy curves for Hg_2 can be constructed to explain this. These same curves explain also the peculiar limitation of the 1849 band at the 1807 band. From these curves the energy of dissociation of Hg_2 is found as 0.20 volts. It is necessary to ascribe the 1807 band to an electron transition from a molecular energy level to an atomic energy level. This constitutes a new type of photochemical dissociation. Similar explanations have been made for the band spectra of zinc and cadmium. (Phil. Mag. **7**, 555 (1929).)

37. A spectroscopic study of the decomposition of organic vapors by the electrodeless discharge. DAVID M. GANS AND WILLIAM D. HARKINS, *Department of Chemistry, University of Chicago.*—When subjected to the electrodeless discharge, the vapors of organic compounds at pressures of several tenths of a millimeter of mercury are rapidly decomposed into monatomic and diatomic, neutral and charged fragments, with emission of light. Thus, for benzene, acetylene, and naphthalene, the spectrum reveals the presence of H and C atoms, C^+ ions, and C_2 and CH molecules. With aniline, the spectrum shows, in addition, the violet cyanogen bands, the β bands of NH, and the second positive (N_2) and first negative (N_2^+) groups of nitrogen. The spectrum for phenol contains the water vapor bands, due to OH, and the third

positive group of carbon, due to CO, as well as the decomposition spectrum typical of benzene. These very reactive fragments unite with each other to form brown to black solids of high molecular weight. Sufficiently unsaturated hydrocarbons are completely transformed into insoluble solids as rapidly as vapor enters the flask. Saturated hydrocarbons, like *n*-heptane, form little solid, since hydrogen is liberated, which raises the pressure and tends to extinguish the discharge. Besides dark solids, substituted benzene derivatives generally also give gaseous products, as water for phenol, ammonia or lower amines for aniline, and hydrogen chloride for chlorobenzene. Further work is in progress.

38. A continuous fluorescence emission spectrum which accompanies a change of color and the Raman spectrum. WILLIAM D. HARKINS AND H. E. BOWERS, *University of Chicago.*—In the study of the Raman spectrum of certain liquids a continuous emission spectrum has been found to appear, together with the Raman line spectrum, in each case in which the liquid becomes colored by the action of the radiation from the mercury arc light. The continuous spectrum was always absent when no such change of color occurred. The continuous spectrum was given by eight organic bromine derivatives of the paraffin series and by a solution of ammonia in methyl alcohol. The continuous spectrum is found between 3900 and 5200A, and between 5500 and 5800A.

39. Further study of the absorption of infrared radiation by water vapor. E. K. PLYLER AND W. W. SLEATOR, *University of Michigan.*—By making use of Echelette gratings, a Moll thermal relay and the spectrometer constructed by Meyer and previously described, the authors have re-examined with increased resolution the absorption bands of water vapor whose centers lie near 1.38μ, 1.87μ, 2.66μ, 3.17μ and 6.26μ. The new study has greatly increased the number of measured lines. Especially, near 6.26μ and 3.17μ the number has been more than doubled. The new lines are mostly weak ones, but the work has resulted in better determinations of the wave-lengths of many strong lines which now appear as sharp single effects freed from the former confusion due to overlapping. The center of the harmonic of the great band near 6.26μ is seen to be better placed at 3.168μ than as it was formerly at 3.11μ. It also appears that the band has no absorption at the center, and is of the doublet type like the fundamental.

40. Progressive relationships in the near infrared absorption spectra of the halogen derivatives of benzene. F. S. BRACKETT AND URNER LIDDEL, *Smithsonian Institution and Bureau of Chemistry and Soils, Washington, D.C.*—Automatic records of the near infrared absorption spectra of benzene and its halogen derivatives at an average resolution of 12A to the slit-width are offered. These spectra have been analyzed with respect to the second overtone of that fundamental vibration of benzene occurring in the region of 3.25μ, which probably approximates a linear oscillation of hydrogen with respect to carbon. In the progression benzene 8772 cm^{-1}, iodo-benzene 8780 cm^{-1}, brom-benzene 8787 cm^{-1}, and chlor-benzene 8800 cm^{-1}, a progressive shift to shorter wave-lengths of this second overtone occurring in benzene at the frequency 8772 cm^{-1} is observed. An explanation is offered based on the further reduction of electron density about the carbon centers resulting from the substitution for a single hydrogen of an increasingly electro-negative halogen in each case. Further shifts to shorter wave-lengths were predicted for the higher halogen derivatives. Spectra are offered of the three di-chlor, 1, 2, 4, and 1, 3, 5 tri-chlor, penta-chlor, and para- dibrom-benzenes, which in a general way substantiate these predictions. The general idea of relative decrease in saturation as correlated with increase of frequency is borne out. In the case of benzene, satellites are observed at frequencies occuring at multiples of 162 cm^{-1}. The presence of such a low frequency mode is consistent with the fine structure observed in the visible bands of benzene vapor.

41. Absorption bands of hydrogen halides in the liquid state. E. O. SALANT AND W. WEST, *Washington Square College, New York University.*—The (0, 2) bands of HCl, HBr and HI liquids and the (0, 3) of liquid HI, measured with quartz prism spectrometer, thermopile and galvanometer, show no rotational structure, centers of HCl and HBr bands being displaced to longer waves as compared with corresponding gas bands. The frequencies, with gas-liquid

displacements given in parentheses are, in cm^{-1}: HCl 5543 (125), HBr 4850 (180), HI 4262 and 6262. HI absorption, particularly, is strongly itensified in the liquid. With these values and the Raman lines (Salant and Sandow, Phys. Rev. **32**, 214 (1930)), the vibration frequencies and anharmonic coefficients of the vibrational terms are calculated for the liquefied hydrogen halides (the constants for the gaseous molecules, in parentheses, are from Birge, International Critical Tables, Vol. V):—ω_e: HCl 2800 (2991), HBr 2587 (2647), HI 2262; $x_e\omega_e$: HCl 8.5 (54), HBr 54 (44), HI 44. Differences between spectra of vapors and liquids are discussed. The frequency shifts of the hydrogen halides must be attributed not to a Lorentz-Lorenz force, but to some other, quantum mechanical interactions of the molecules (Breit and Salant, Phys. Rev. **36**, 871 (1930)).

42. Some effects of intense audio-frequency sound. NEWTON GAINES, *University of Texas*—Audible sound of great intensity is produced by magnetostrictive vibration of a nickel tube, two 250-watt radiotron tubes being employed in the apparatus. This sound is used to produce phenomena hitherto obtainable only with piezoelectric crystals vibrating at thirty or forty times the frequency and also entirely new phenomena. The nickel tube itself is vibrated so strongly as to rupture eventually at the middle. A five centimeter mound forms on the surface when the rod oscillates beneath water; this mound is *not* the result of radiation pressure. An air bubble released under water in the neighborhood of the vibrating rod becomes white, and under certain conditions moves against a strong stream of water. Carbon deposited on the sides of the nickel tube goes into colloidal solution when the tube is vibrated under water. The reaction of sonic radiation upon the radiator is demonstrated. Striations in a Kundt tube that are parallel to its axis are produced. Larvae are killed immediately by the sound; colon bacteria are killed, dying off in accordance with a simple logarithmic law. The irradiation of seed by the intense sound changes the rate of growth of the seedlings produced, usually retarding the growth but in certain cases accelerating it as much as 25 percent.

43. Supersonic interferometers. ELIAS KLEIN AND W. D. HERSHBERGER, *Naval Research Laboratory, Bellevue, D.C.*—The methods of applying high frequency sounds to small scale measurements are discussed. An interferometer was constructed and used to measure the velocity of sound in gases, liquids, and solids at frequencies ranging from about 10 to 700 kc. Three types of sources were tried, viz: quartz and rochelle salt crystals and magnetostrictive rods. The determination of the velocity of sound in solids are based upon (1) optimum transmission of sound through a partition whose thickness is an integral number of half wavelengths: (2) relative displacement of the nodal planes in a given liquid due to the immersion of the solid slab in the acoustical path. In the same manner, a small quantity of an unknown liquid is placed in a parallel walled cell and the latter is immersed in a liquid of known acoustic properties. Or, the variation in the velocity of sound with concentration of solution may thus be determined. Reactance and effective resistance of the interferometer (with a liquid medium) as a function of the reflector distance from the sound source were investigated. Approximate values of the impedance, power factor and watts dissipated in the instrument were thus computed. The use of the interferometer as a device for measuring supersonic frequencies is explained.

44. Sound absorption determined by transmission measurements. F. R. WATSON, *University of Illinois.*—A. H. Davis, (Phil. Mag. **50**, 75 (1925); **2**, 543 (1926)) has developed a formula for transmission of sound,—$I'/I = kW/as$, where I is the intensity of the sound incident on a partition, I' is the transmitted intensity, k is the coefficient of transmission, W, the area of the partition and as, the absorption of the surfaces in the receiving room. By suitable measurement of the ratio I'/I, it is thus possible to determine the absorption as. Preliminary tests by means of electrical instruments for the generation and reception of sound have given promising results, thus giving an instrumental substitute for the determination of the time of reverberation by the ear, as required by Sabine's method.

45. The rotating fluid in the relativity theory. EDWARD L. AKELEY, *Purdue University.*—The Einstein equations associated with the quadratic form

$$Adx_0^2+2Cdx_0dx_1+Bdx_1^2+J(du^2+dv^2)$$

where A, B, C and J are functions of u and v only, have been treated by a method which is a generalization of Weyl's theory of the axially symmetric field. The following transformation was used

$$A = e^{d+s}\cos\psi \qquad C = e^{d}\sin\psi$$
$$B = -e^{d-s}\cos\psi \qquad J = -e^{2}.$$

The theory of the rotating fluid was developed in this way. A power series expansion of the type $d = d_0 + d_1\rho + d_2\rho^2$ was used, where $d_2 = d_{20} + (\omega^2/\rho)d_{12}$; $d_3 = d_{30} + d_{22}(\omega^2/\rho) + d_{14}(\omega^4/\rho^2)$. ρ and ω represent respectively the density and the angular velocity of the fluid, and d_{ij} represents the coefficient of $\rho^i\omega^j$ in a double power series expansion in ω and ρ. The first approximation corresponds to the Newtonian theory. It is shown that there is a one to one correspondence between the figures of equilibrium in the two theories, and that the first approximation of the Einstein solution can be obtained from the Newtonian one. The second approximation predicts effects not included in the Newtonian theory. The field corresponding to that of the MacLaurin ellipsoid is developed to a second approximation. The relation of this treatment to the work of others is discussed.

46. Some physical properties of nitrogen. W. Edwards Deming and Lola E. Shupe, *Bureau of Chemistry and Soils, U. S. Department of Agriculture, Washington, D.C.*—The compressibility data on nitrogen obtained by Bartlett and coworkers are extrapolated to cover the range −70 to 600° up to 1200 atmospheres. A sensitive graphical scheme has been devised for obtaining $(dv/dp)_T$, $(dv/dT)_p$, $(d^2v/dT^2)_p$ at any point. It depends on the fact that the derivatives of $\alpha \equiv RT/p - v$ or $\Delta \equiv v(pv/RT - 1)$ enter as correction terms to the derivatives of v, just as α and Δ enter as corrections to v itself. Specific volume, density, coefficients of expansion $(-p/v)(dv/dp)_T$ and $(1/v)(dv/dT)_p$, fugacity, C_p, C_v, $C_p - C_v$, μ are calculated for the various temperatures and pressures. The calculations of C_p agree within 0.2 cal./mole deg. with the experiments of Mackey and Krase (J. Ind. and Eng. Chem. October, 1930) who worked to 700 and 800 atm. from 30 to 150°. The agreement is probably within the experimental error, but the trends of the two sets suggest that a real difference may exist. C_v decreases below 0°C at pressures up to 100 atm.; at higher pressures it increases. Experiment shows that along an isotherm $C_p = C_p^* + bp^2 + cp_3 + \cdots$, the first power of p being absent. It is found that C_p increases fairly uniformly from 10 to 100 atm. along isotherms between 20° and 200°.

47. The specific heat of methane. P. C. Ludolph, *University of Illinois.* (*Introduced by Jakob Kunz.*)—The specific heat of methane has been calculated for the tetrahedral model advanced by Dennison and for the symmetrical pyramid as worked out by Guillemin. The curve for the values obtained from the tetrahedral model has the same shape (linear) as the experimental curve but falls below it (as much as 5 cal./mole at 873°K). The values for the pyramidal model are still lower (9 cal./mole at 873°K). Another curve was obtained for the tetrahedron by redistributing the dimensions of the oscillators so as to get the largest possible values for the specific heat with the given frequencies. This curve is again linear but it still falls below the experimental curve. Some of the discrepancy may be due to an error in the experimental values which would tend to make this curve too high. It may be stated that the specific heat calculations of methane favor the tetrahedral structure.

48. Joule-Thomson effect in helium. J. R. Roebuck and H. Osterberg, *University of Wisconsin.*—After completing the work with air (Proc. Am. Acad. 64, 287 (1930)), the apparatus required extensive modification for use with helium. The effect of small proportions of air as an impurity was measured first, and as this proved very interesting the measurements were extended to the whole range of mixtures, all at the bath temperature 51.68°C, and inlet pressure 201 atm. The isenthalpic curve for pure helium is a straight line of negative slope, rising about 12°C per 200 atm. drop. As small quantities of air are added the curves do not change observably till possibly 10 percent air. With further increase in air the curves shift more and more rapidly over to about 28°C drop for pure air. Simultaneously the straight line for pure helium shifts over to the line, strongly concave toward the pressure axis, for pure air. The surprising result is the very small effect of the first addition of air and the increasing effect

of the equal later additions. Its pleasant aspect is that it effectually removes any worry as to the corruption of the helium data by air impurity. The isenthalpic curves for pure helium have been taken between the temperatures −100°C and +100°C. They are all straight lines of negative slope, and over this range the small erratic variation in the values of the slope exceeds any systematic variation. This value of μ is −0.060°C per atm.

49. A convenient laboratory source of hydrogen. G. W. SARGENT AND WHEELER P. DAVEY, *School of Chemistry and Physics, The Pennsylvania State College.*—Certain lines of research require considerable quantities of a reducing gas at rather infrequent intervals. In such cases the use of tanked or electrolytic hydrogen becomes unduly expensive. We are using a 1 to 3 mixture of nitrogen and hydrogen obtained by cracking NH_3. By slightly raising the outlet end of a 150 pound tank of liquid NH_3, gaseous NH_3 can be boiled off at room temperature, metered through an ordinary dry gas meter and cracked. We find it best to crack the gas in a nickel tube about 1/4 inch in diameter and about 12 feet long, coiled to fit inside an alundum tube which is heated to 1000°C by a nichrome winding. Slight traces of uncracked NH_3 are removed by passing the gas over about six feet of P_2O_5. The gas meter helps determine how much liquid NH_3 is left in the tank. A mercury relief valve by-passes any excess NH_3 into running tap water. A similar valve by-passes any excess H_2 into a pipe leading outdoors. These relief valves prevent dangerous pressures in the hot nickel coil. The apparatus is cheap and compact and gives a large storage capacity of H_2 in the form of liquid NH_3.

50. The deposition of dust on walls. W. J. HOOPER, *Battle Creek College.*—An apparent uncertainty exists in literature dealing with the cause for the peculiar deposition of dust on plaster and lath walls wherein the course of the laths and rafters behind the plaster is outlined in dust, popularly called "lath marks." Conclusive experimental proof of a thermal cause is given which is in agreement with the general theory of the behavior of small particles suspended in an atmosphere in which a temperature gradient exists.

51. Particle size of the disperse phase of nitrocotton solutions. WHEELER P. DAVEY, H. B. DE VORE, *The Pennsylvania State College and E. I. duPont de Nemours and Co.*—It is the purpose of this paper to report measurements made in 1927 on the particle size of nitrocotton in lacquer solutions, using the water-spreading method. (Davey, Science 1926, Eighth Colloid Symposium, 1930). Solutions of a given batch of nitrocotton in a mixture of ethyl acetate and ethyl alcohol would not spread satisfactorily on water at concentrations greater than 0.001 gm per cc. Measurements were taken down to concentrations of 7.8×10^{-6} gm per cc. The corresponding particle diameters were 3.69×10^{-7} cm and 1.54×10^{-7} cm. Over a considerable range the graph of particle diameter against logarithm of concentration is a straight line. Particle diameters at the lowest dilution are equal to about 20 atomic diameters of carbon, i.e. a maximum of about 140 nitrated glucose groups on the assumption of 2/3 complete nitration.

52. On the determination of principal stresses from crossed Nicol observations. R. V. BAUD, *Westinghouse Research Laboratories, East Pittsburgh, Pa.* (*Introduced by N. Rashevsky*).—The information obtained from crossed Nicol observations, combined with the differential equations expressing equilibrium requirements, is sufficient to obtain on basis of a graphical integration, the two principal stresses separately at all points of a "two-dimensional" model. When orthogonal curvilinear coordinates are employed, the differential equations contain the curvatures of the principal stress direction lines. Filon's method consists of expressing the curvatures by certain angles ψ, which he takes from the map of isoclinic lines. The author proposes that an additional map with lines ψ=constant be drawn, which procedure has certain advantages. When the paths of integration have one or more inflections, Filon's method is not entirely satisfactory. As an alternative, it is suggested to express the curvatures by the gradients $\partial\phi/\partial s$, or to measure the curvature by a curvature scale. A new method is suggested further, which consists in the use of polar coordinates. Crossed Nicol observations and "polar integration" combined appear to be the only existing method of studying stress distribution in rotating models. Even for static conditions preference will eventually be given to the "polar integration" in cases where the models have circular contours.

53. The effect of pressures up to 20,000 atmospheres upon some optical properties. THOS. C. POULTER, *Iowa Wesleyan College.*—This is a preliminary report and some of the data are of a qualitative nature. The rotatory power of a water solution of three sugars has been studied as effected by pressure. A rotatory power of ice VI has also been observed. The effect of pressure on the index of refraction of glass and of a paraffin oil has been studied.

54. On the change of the spectral composition of quasi-monochromatic radiation caused by scattering. OTTO HALPERN, *New York University.* (*Introduced by Richard T. Cox.*) It is shown that according to both the classical and quantum theories, there should appear in the scattered light from an ordinary quasi-monochromatic source frequencies corresponding to the proper frequencies of the scattering system and with an intensity of the same order of magnitude as that of the light scattered with unchanged frequency. The effect described affords a method of determining the spectral intensity of a line at an appreciable distance from its center of gravity. Reference is made to certain changes in hardness in the scattering of x-rays.

AUTHOR INDEX

Second Series *January 15, 1931* *Vol. 37, No. 2*

THE
PHYSICAL REVIEW

EFFECTS OF CATHODE-RAY DIFFUSION ON INTENSITIES IN X-RAY SPECTRA

By D. L. Webster, H. Clark, and W. W. Hansen
Stanford University

(Received December 5, 1930)

Abstract

Rediffusion of cathode rays.—The available evidence is reviewed and conclusions formulated on the rediffusion constants and distribution functions needed for the calculation of effects on x-ray emission intensities.

Thin-target x-ray intensities.—A previous paper gave the intensity of the K lines from very thin Ag supported on Be, as a function of voltage, in terms of the intensity at twice the excitation voltage as a standard. In the same terms after correction for two opposing effects, diffusion of cathode rays within the thin target and rediffusion from the beryllium, the corrected values differ from the originals by not over 2 percent. Possible sources of error are reviewed, and it is concluded that none can increase this percentage very greatly. This answers a criticism on the theoretical significance of these data.

Comparison with theories.—Present wave-mechanics theories involve approximations not valid at low voltages, but subject to this qualification Bethe's theory compares very favorably with these data. The best classical-mechanics theory is Thomas's. Empirically, the intensity $=\text{const.}\times U^{-0.8}\log U$, where $U=$(tube voltage)/(excitation voltage).

Thick-target effects.—For line intensities percentage corrections for rediffusion, again taking the intensities at $U=2$ as standard, are more than twice those for thin targets at all voltages in the above range, and are of opposite sign. On continuous spectrum intensities averaged over all directions, these calculations confirm Kramers' suggestion, that most of the non-linear term in the intensity formula is due to rediffusion.

THE effects of diffusion of cathode rays on the intensities in x-ray spectra have become important recently, on account of improvements in research technique. Such improvements, in themselves, do not necessarily increase the effects of diffusion, but as the sources of larger errors of interpretation are eliminated, diffusion comes next in line for treatment. The larger errors, in this case, occur in the study of intensities as functions of cathode-ray energy, and come from two sources. One is the variety of speeds with which the cathode rays strike the atoms, even though they all enter the anode at one speed. The other is the difficulty of separating the parts of the measured radiation coming from atoms ionized by cathode-ray impact and by x-ray absorption. Both these sources of error have now been reduced to negligible

amounts, by the use of targets so thin that the cathode rays penetrate them without serious loss of speed, and that x-rays penetrate them without appreciable absorption. Thus the largest errors remaining may well be those due to cathode-ray diffusion.

In a recent paper[1] on measurements of x-rays from thin targets, we estimated these errors tentatively as "a few percent"; and since the deviations of all the available theories from our data exceeded this amount, the exact calculation of the corrections for these errors was postponed until further data were available. Still more recently, however, Wisshak[2] has questioned our estimate, stating his belief that the correction would prove to be so great as to reverse completely the relations between our data and the leading theories of impact ionization. Evidently the status of these theories depends on the order of magnitude of these corrections. Therefore a calculation of them, at least with sufficient accuracy to make sure of the relation of the data to the theories, becomes imperative.

It is therefore the purpose of this paper to report the results of such a calculation, and incidentally we shall include some by-products, of interest in the interpretation of other data on x-rays and cathode rays.

The Laws of Rediffusion

The effects to be calculated arose from two types of diffusion of the cathode rays, one type occurring within the thin targets themselves, and the other in a block of beryllium used to support the thin targets and to conduct away the heat produced by the cathode rays. Diffusion within a thin target, making the paths of the cathode rays deviate from straight lines normal to the surfaces, causes a slight increase in the number of atoms struck by an average cathode ray. Diffusion in the beryllium must be considered in order to take account of the small percentage of the cathode rays which deviate so far as to be "rediffused," that is to return to the surface of the block and thus to make second impacts on the thin target. The effect of diffusion within the thin target is readily calculated from well-known laws, but to calculate the rediffusion effect we must first examine the available evidence and formulate as well as possible the laws of the phenomena concerned.

The rediffusion constant. First of all, we must find the best value for beryllium, of the "rediffusion constant" p, or fraction of the incident cathode rays that are rediffused. Since none of the data we have found in the literature refer directly to beryllium, we must get the value for it from the data, through the law relating p to the atomic number Z.

To measure p, one must measure the current carried by the rediffused electrons, but not include any of the slow secondary electrons leaving the metal at the same time. The theoretical reason for separating these two classes is that their causes for leaving the metal are different: rediffusion and and ejection by the cathode rays, respectively. The practical reason, for the

[1] D. L. Webster, H. Clark, R. M. Yeatman, and W. W. Hansen, Proc. Nat. Acad. Sci. 14, 679 (1928).

[2] F. Wisshak, Ann. d. Physik 5, 507 (1930).

present purpose, is that the secondary electrons are too slow to produce x-rays as hard as those used in most intensity measurements.

Data on p, for various primary-ray energies, have been obtained by several investigators: Becker,[3] at 35 kv.; Schmidt,[4] with beta rays of about 800 kv.; Schonland,[5] at 10 to 100 kv.; and Stehberger[6] at 2 to 12 kv. The term "rediffusion constant," and its symbol p, do not mean the same quantity in all these papers. In Schonland's it refers to incidence along the normal, in Stehberger's at 50° from it, in Schmidt's and Becker's, at least as recomputed by Lenard[7] and quoted by Stehberger, to incidence "im Normalfall," that is with the cathode rays already completely diffused before they strike the metal. For present purposes, the most important case is that of incidence along the normal, so we shall adopt the definition for that case.

One of the most striking conflicts of values is between those of Becker as recomputed and quoted (Al 0.28, Au 0.68) and those of Schonland (0.13 and 0.50 respectively). A part of this conflict is due to the difference in definition, since Lenard finds for Al along the normal the value 0.23, and this reduces the discrepancy considerably. Another part, however, is probably due to the theory underlying the recomputation, which involved the assumption of sudden absorption of cathode rays by individual atoms. Since this assumption has later been disproved,[8] we may remove this part of the discrepancy by going back to Becker's original values. Thus we obtain Table I.

TABLE I. *Rediffusion constants for incidence along the normal.*

Metal	Al	Cu	"Blattmetall"	Ag	Au
Becker	0.172	—	0.407	0.433	0.496 to 0.56
Schonland	0.13	0.29	—	0.39	0.50

Considering the general improvements in cathode-ray technique between Becker's work in 1905 and Schonland's in 1925, we must indeed congratulate Becker on the smallness of the discrepancy, even though we shall use Schonland's values of p.

A more serious question is presented by Stehberger's data. His values of p at 50° incidence on Al are from 2.5 to 5.5 times Schonland's at normal incidence. This ratio seems far too great. Furthermore, Schonland found p independent of primary voltage, whereas Stehberger found it to decrease rapidly with increasing voltage. To be sure, their ranges of voltage barely overlap; but Schonland gives theoretical reasons for believing that p should be constant, and an important question is, whether Stehberger's data make Schonland's theory unreliable.

[3] A. Becker, Ann. d. Physik **17**, 381 (1905).
[4] H. W. Schmidt, Ann. d. Physik **23**, 671 (1907).
[5] B. F. J. Schonland, Proc. Roy. Soc. **A108**, 187 (1925).
[6] K. H. Stehberger, Ann. d. Physik **86**, 825 (1928).
[7] P. Lenard, "Quantitatives uber Kathodenstrahlen aller Geschwindigkeiten" ed. 1925. p. 226.
[8] W. Bothe "Handbuch der Physik" ed. 1927, Vol. XXIV, Chap. 1, See especially Sec. 25.

The answer to this question appears to us to lie in the method of separation of secondary electrons from rediffused. Both observers found a considerable fraction of the electrons to have energies below 10 or 20 equivalent volts; both adopted a voltage basis for the separation, Stehberger drawing the line at 36 volts and Schonland at 200; and both agreed that any such basis was somewhat arbitrary, and might be incorrect.

On this point, we may use a line of reasoning similar to that of Bothe,[8] about the distribution of velocities among cathode rays transmitted through metal films. Here the Thomson-Whiddington law of retardation makes it impossible for many of the rays to emerge with very small energy, simply because the range of a cathode ray of small energy is so short. For example, if an electron has been retarded until its kinetic energy is only 10 percent of that at incidence, it has only 1 percent of its range still before it, and the chances are very much against that short section of its range intersecting the surface. The same reasoning applies to rediffusion. Many cathode rays rediffuse with half their initial energy or more, so there is no question of any grave difficulty for a cathode ray to return to the surface with a long range still before it, and it is therefore highly improbable that any large fraction of the rediffusion will be in the last 1 percent of the range.

Drawing the line between secondary and rediffused electrons at 36 volts, however, with a primary voltage of 8 or 12 kv., Stehberger found over 30 percent of his "rediffused" electrons to have less than 10 percent of their initial energy. Evidently in view of these considerations of range, there is good ground for belief that these were not rediffused, but secondary.

Furthermore, the distribution of energy among secondary electrons, as calculated by Bothe,[9] should be nearly independent of the primary energy; but their number should decrease rapidly with increasing primary energy, as in fact Stehberger found it did. Thus it may well be that Stehberger's data are not inconsistent, after all, with Schonland's data, or with his theory of the constancy of the rediffusion constant. And so long as we are not concerned with secondary electrons in the x-ray problems at hand, we shall use the values of p obtained at the higher voltages, where secondary electrons were less abundant and the probable error from them was therefore smaller.

Incidentally, if we had adopted the alternative of accepting Stehberger's values of p at low voltages and Schonland's at high, with a graded compromise for the intermediate region, the corrections to the x-ray data would not have been as greatly affected as the values of p, since the influence of the derivative of p with voltage would have largely offset that of the increase in the values of p. The chief difference would have been in the complexity of the problem.

For the thin-target problem, we shall need the rediffusion constant of beryllium, the material of the block supporting the thin targets in some of our own experiments. Since Schonland finds for atomic number $Z=29$, $p=0.29$, and for $Z=13$, $p=0.13$, a reasonable guess for $Z=4$ is $p=0.04$. But for a

[9] W. Bothe, reference 8, Section 42.

more careful estimate, we shall use an equation from Wentzel's[10] theory, which predicts that

$$p = b_1\left(\frac{Z^2\rho}{A\alpha_0}\right) + b_2\left(\frac{Z^2\rho}{A\alpha_0}\right)^2 \tag{1}$$

where b_1 and b_2 are constants, Z and A are atomic number and weight, and α_0/ρ is Lenard's "pure" mass absorption coefficient. Since this theory depends on the hypothesis of absorption, now disproved, this equation must be considered on a semi-empirical basis; but at that, since Lenard found α_0/ρ practically constant for light elements, for which also $A=2Z$, we may extrapolate to low atomic numbers by assuming that

$$p = p_1 Z + p_2 Z^2. \tag{2}$$

This fits all of Schonland's data pretty well, with $p_1=0.011$ and $p_2=-6.0\times10^{-5}$, and for Be it predicts $p=0.043$.

The rediffusion energy distribution. The next problem is to find the best formula for the distribution of the rediffused electrons on a scale of kinetic energy. The data available are far from complete or accurate, but fortunately the answers to the x-ray problems at hand are changed so little by relatively great changes in this distribution function that even a very rough approximation will prove sufficient.

First let us consider some theoretical evidence. Schonland explained the constancy of his rediffusion constants by noting that for cathode rays of all speeds, in any one element, the distance required for a probable deflection of one degree, and the distance required for a loss of kinetic energy of one percent, bear a constant ratio. Thus, although any two cathode rays of different speeds of incidence must have different ranges, the shapes of their paths may be geometrically similar, and the probabilities that they come back to the surface must be the same. Extending this reasoning, their probabilities of coming to the surface with any given fraction of their initial kinetic energy still left, must also be the same. Or in algebraic terms, calling this fraction W, and this probability $pF(W)dW$, with

$$\int_0^1 F(W)dW = 1, \tag{3}$$

$F(W)$ should be independent of V.

Another theoretical point about $F(W)$ is the one discussed above, about the scarcity of electrons of very low energy. Quantitatively, as one may readily prove from the Thomson-Whiddington law, this means that $F(0)=0$, and that its first derivative is finite.

Turning now to the experimental evidence, we have some velocity spectra photographed by Wagner[11] for Al, Cu, Ag and Au at primary voltages from 16 to 40 kv. While an exact translation of the densities in these photographs into

[10] G. Wentzel, Ann. d. Physik **70**, 561 (1923).
[11] P. B. Wagner, Phys. Rev. **35**, 98 (1930).

numbers of electrons is impossible, they do appear to give at least a qualitative confirmation to the theoretical deductions just stated. And without any exact translation, they prove some other points more definitely: first, $F(W)$ is a continuous function, without any sharp peaks; second, there are no electrons rediffused with full primary energy, so that $F(1)=0$; third, reducing W from 1, $F(W)$ rises rapidly to a maximum and then declines, probably more slowly than it rose; and fourth, that the value W_0, where the maximum occurs, is higher for heavy elements than for light. Taking the densities literally, as a rough approximation, W_0 for Al would be about 0.85, for Cu 0.90, and for Ag and Au 0.94.

Confirmatory evidence appears in the spectra of the x-rays produced by the rediffused electrons, investigated by Nicholas[12] with copper and Lorenz[13] with tungsten. While this evidence is not so direct, it indicates the same general sort of preponderance of high energies as Wagner's photographs, and again with no notable change in $F(W)$ with V.

A third line of evidence is on $\overline{W}$, the mean of the values of W for all the rediffused electrons. This may be calculated from measurements by Wisshak[2] on the ratio of the power absorbed by the anode of a gas-filled tube to the whole power input. If it is permissible to neglect the power given to positive ions, this ratio is $(1-p\overline{W})$. According to Wisshak, it is independent of V, from about 3 to 35 kv., having the value 0.8 for Co and Cu, and 0.6 for Mo and Ag. These data, with Schonland's p's, would make $\overline{W}=0.7$ for Co and Cu, and nearly 1 for Mo and Ag. The correction for positive-ion power would reduce these values of $\overline{W}$.

Finally, there is evidence from the total intensity of the x-rays from the back and stem of the target of a Coolidge tube. Assuming the V^2 law of total x-ray intensity, the ratio of this "stem-radiation" to the radiation from the whole target, including the focus, should be $p\overline{W^2}$. Coolidge,[14] with one of his standard tungsten tubes, found this ratio to be 2/11, both with a 2-inch alternative spark gap and with a 10-inch; Ledoux-Lebard and Dauvillier[15] found 20 percent; and Rump,[16] on the basis of this latter figure and some measurements of his own, considered 20 percent correct for any voltage from 43 to 150 kv. at least. For tungsten at normal incidence, equation (2) would make $p=0.48$, so that $\overline{W^2}$ would be about 0.4, and therefore $\overline{W}$ probably about 0.6; but for these 45° targets, p must be somewhat greater and $\overline{W^2}$ correspondingly less. This estimate is lower than those given above, but it agrees in making quantities dependent on p and $F(W)$ independent of V, as required by theory.

All this evidence is still far from a quantitative formula for $F(W)$, but all that is really needed for present purposes is a rough approximation, in a reasonably convenient mathematical form. To satisfy this latter requirement

[12] W. W. Nicholas, Phys. Rev. **29**, 619 (1927).
[13] E. Lorenz, Proc. Nat. Acad. Sci. **14**, 582 (1928).
[14] W. D. Coolidge, G. E. Review **20**, 272 (1917).
[15] P. Ledoux-Lebard and A. Dauvillier, "Physique des Rayons X" p. 45. (quoted by Rump).
[16] W. Rump, Zeits. f. Physik **43**, 254 (1927).

we shall neglect that about the behavior of $F(W)$ at $W=0$, where we shall never need to use it. All other requirements are then satisfied by either of the following formulas:

$$\left.\begin{aligned} F_1(W) &= G(1-W)e^{-g(1-w)}, \\ \text{with } G &= g^2/\{1-(g+1)e^{-g}\}; \end{aligned}\right\} \tag{4}$$

and

$$\left.\begin{aligned} F_2(W) &= Q(1-W)W^q, \\ \text{with } Q &= (q+1)(q+2). \end{aligned}\right\} \tag{5}$$

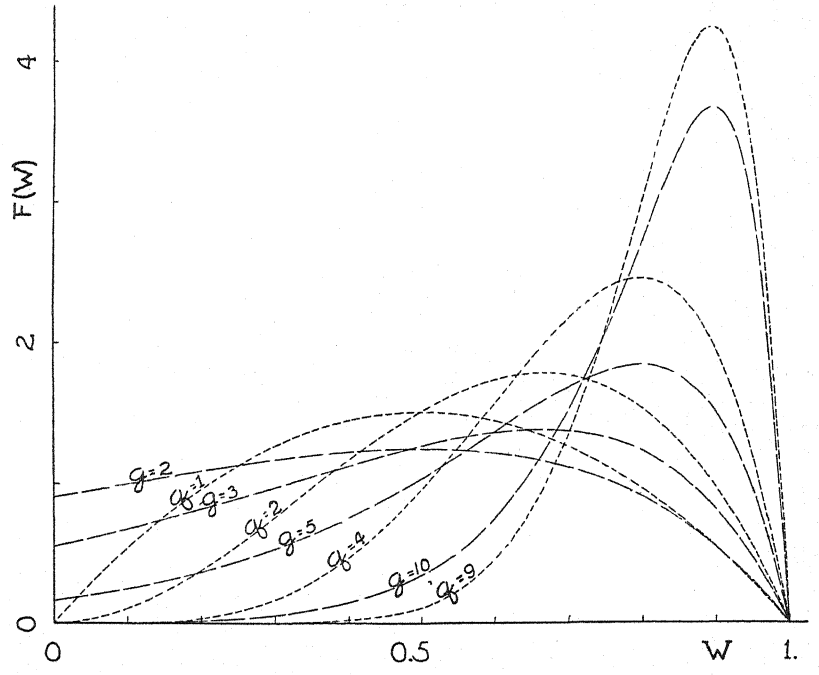

Fig. 1. Graphs of $F_1(W)$ and $F_2(W)$ from equations (4) and (5) respectively.

TABLE II. *Parameters of $F(W)$ in Fig. 1.*

W_0	g	q	$\overline{W}$	$\overline{W^2}$
0.90	10	—	0.800	0.660
0.90	—	9	0.833	0.706
0.80	5	—	0.635	0.454
0.80	—	4	0.714	0.536
0.67	3	—	0.520	0.333
0.67	—	2	0.600	0.400
0.50	2	—	0.455	0.272
0.50	—	1	0.500	0.300

Graphs of these functions, for several values of each parameter, g or q, are shown in Fig. 1; and corresponding values of W_0, $\overline{W}$ and $\overline{W^2}$, for use in selecting the best value of g or q, are listed in Table II.

Briefly, for heavy elements, the evidence on W_0 and $\overline{W}$ seems to favor the higher values listed here for these parameters, and that from $\overline{W^2}$ the lower ones; for light elements, the values must be lower than for heavy. In view of this uncertainty, it is indeed fortunate that the quantities we must calculate for the comparison of x-ray data with theories change so slowly with these parameters that even such rough information as this will suffice to place them within probable limits of experimental error.

The directional distribution of rediffused cathode rays. In the problem of the effect of rediffusion on the intensity of x-rays from a thin target supported on a block of another metal, it is important to know the ratio of the average number of atoms in the thin target, struck by a rediffused ray on its way out, to the number struck by a primary ray on its way in. Since all the corrections for diffusion and rediffusion effects are reasonably small, we shall neglect small quantities of the second order, i.e. in this case, the effect of diffusion within the thin target itself on the ratio of these numbers of atoms. Thus we shall assume that for cathode rays rediffusing at the angle Θ from the normal, this ratio is simply sec Θ. The directional distribution need then be found only with enough accuracy to get a reasonably accurate estimate of the mean value of sec Θ, which we shall call S.

Rediffusion can happen only to cathode rays deflected through more than a right angle, and indeed considerably more unless the paths after deflection through a right angle are much longer than those before. Thus rediffusion comes fairly near to involving complete diffusion, and the assumption of complete diffusion should give a first approximation for S. With this assumption, the probability that any infinitesimal segment of the path of a ray will intersect the surface of the block would be proportional to the sine of the angle this segment makes with the surface, and so the number escaping in a given solid angle $d\Omega$ would be proportional to cos $\Theta d\Omega$. This deduction was indeed verified, for beta rays transmitted through reasonably thick aluminum, by Kovarik and McKeehan.[17] Assuming it to hold for rediffused cathode rays, a simple integration gives $S=2$.

For a better approximation, still with normal incidence, but with incomplete diffusion, we may assume that at any point within the metal, the number of paths in a solid angle $d\Omega$ is a function $f(\Theta)d\Omega$. Then the number emerging in this solid angle will be proportional to $f(\Theta)$ cos $\Theta d\Omega$, and $f(\Theta)$ may be measured directly by catching the emergent rays from an area varying inversely as cos Θ.

It was in this way, but with incidence at 30° from the normal, that Kovarik and McKeehan verified the simple cosine law for transmitted rays. Their rediffused rays, however, showed a minimum in the direction backward toward the source. From a typical graph which they published, it seems prob-

[17] A. F. Kovarik and L. W. McKeehan, Phys. Rev. 6, 426 (1915).

able that if the incidence had been along the normal, the rediffused rays would have been represented well enough for present purposes by the formula

$$f(\Theta) = \text{const.} \times (1 + a\Theta^2), \tag{6}$$

with $1+a(\pi/2)^2=1.4$.

A simple integration then gives

$$S = 2 \cdot \frac{1 + 1.14a}{1 + 0.73a} \cdot \tag{7}$$

If the diffusion had been complete, a would have been zero, making $S=2$, as above; with a as in equation (6), $S=2.11$. For present purposes, the difference is immaterial, and as the foil from which these data were taken was not thick enough for complete diffusion of its transmitted rays, the difference for a thick block may be even less. So in all probability S is somewhere between 2.0 and 2.1.

The Thin-Target Effects

We are now in a position to solve the problem of the effects of diffusion and rediffusion on the intensities of x-rays, and we shall consider first a thin target supported by a thick block. Since targets of this type are useful primarily for line spectra, the intensity will be considered to be that of a line, for example one belonging to a K series, of excitation potential V_K, and we shall write all functions of the tube potential V in terms of the ratio $U=V/V_K$. Letting X_0 stand for the thickness of the target, the intensity of the line, with neither diffusion nor rediffusion, is $X_0 i_0(U)$, where $i_0(U)$ is the intensity per unit length of path. Then with rediffusion, the intensity due to the rediffused rays alone will be called $X_0 r(U)$, and the total intensity will be called $X_0 i(U)$. Now with diffusion within the thin target, the paths of the cathode rays are no longer straight, and the mean length of path of an incident ray within the target is slightly greater than X_0. As it is a function of voltage, we shall call it $X(U)$, and we shall replace X_0 in each of the above expressions by $X(U)$. Strictly speaking, this is not quite accurate for the rediffused rays, but as the error is a small quantity of the second order, we shall neglect it.

Calculation of the effect of rediffusion. With these definitions and the formulas on rediffusion deduced in the preceding section, it is evident that

$$r(U) = pS \int_{1/U}^{1} F(W) i_0(UW) dW. \tag{8}$$

We do not know $i_0(UW)$ accurately, of course, until after $r(U)$ has been calculated. But as will be proved later, we may safely replace it here by either of two functions, used previously in empirical formulas for $i(U)$, and shown graphically in Fig. 2, along with some data. Strictly speaking, these data refer to the function $j(U)=X(U)i(U)/X(2)i(2)$, but X changes very little with U, so this is nearly $i(U)/i(2)$; thus an empirical formula for $j(U)$ will do well enough for $i(U)$, if we can use it with an unknown constant factor. One[1] of the formulas thus obtained is

$$i_1(U) = k_1 \frac{1 - 1/U}{m_1 + U} \text{ if } U > 1, \text{ or } 0 \text{ if } U < 1, \tag{9}$$

with k_1 the unknown constant and m_1 about 3.0. The other[18] is

$$i_2(U) = k_2 U^{-m_2} \log U \text{ if } U > 1, \text{ or } 0 \text{ if } U < 1, \tag{10}$$

with k_2 unknown and m_2 about 0.77.

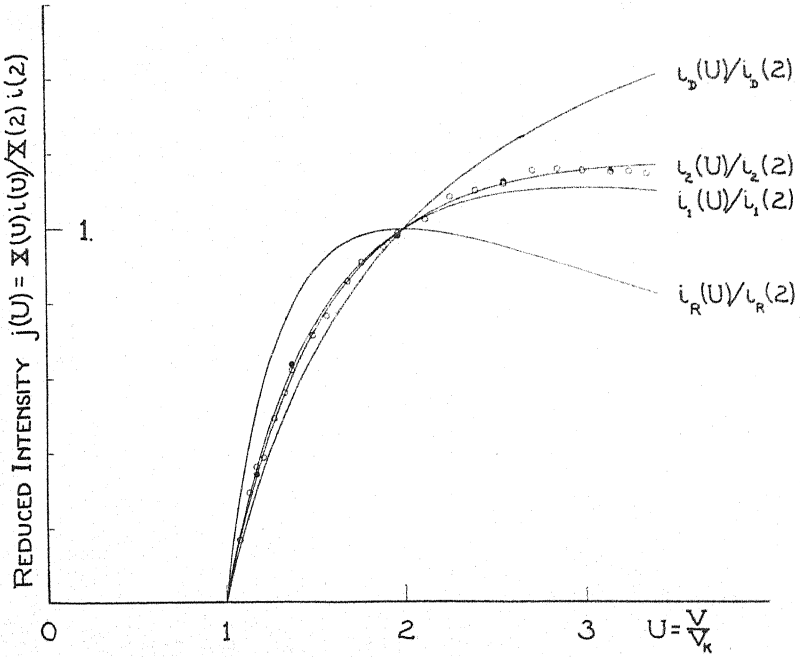

Fig. 2. Uncorrected data and empirical formulas. Black circles, 280A Ag film; white circles, 170A film; black and white circles, data from these films practically coincident.

To see whether the departures of these formulas from i_0 are of any importance here, we have also calculated r with two other functions, departing farther from the corrected graph than either i_1 or i_2, and in opposite directions. One of these functions, suggested by Davis' theory,[19] is

$$i_D(U) = k_D\left(1 - \frac{1}{U}\right); \tag{11}$$

the other, from Rosseland's theory,[20] is

$$i_R(U) = k_R\left(\frac{1}{U} - \frac{1}{U^2}\right). \tag{12}$$

[18] D. L. Webster and W. W. Hansen, Phys. Rev. 33, 535 (1929).
[19] B. Davis, Phys. Rev. 11, 433 (1918).
[20] S. Rosseland, Phil. Mag. 45, 65 (1923).

The resulting values of r agree with those from i_1 and i_2 to better than half of one percent of i, for any value of U in the range covered. So i_1 and i_2 are well within the limits of accuracy needed for this purpose.

For $F(W)$ we may use either of the functions F_1 and F_2 obtained in the preceding section, Eqs. (4) and (5), and tests with the simple intensity functions i_R and i_D show that it makes no notable difference which F is used. For convenience in integration, however, we have used F_1 with i_1, and F_2 with i_2. Thus we obtained two formulas for r, namely

$$\begin{aligned} r_1(U) = pSk_1 \frac{G}{m_1 g U}\big[&(m_1+1)ye^{-y}\{Ei\,y - Ei\,z\} \\ &- ge^{-g}\{Ei\,g - Ei(g/U)\} - m_1\{1 - e^{z-y}\}\big], \end{aligned} \tag{13}$$

where $y = g(m_1+U)/U$ and $z = g(m_1+1)/U$, and

$$\begin{aligned} r_2(U) = pSk_2Q\,U^{-m_2}\Big[&\frac{\log U}{(q+1-m_2)(q+2-m_2)} \\ &- \frac{1 - U^{-q-1+m_2}}{(q+1-m_2)^2} + \frac{1 - U^{-q-2+m_2}}{(q+2-m_2)^2}\Big]. \end{aligned} \tag{14}$$

For comparison of x-ray data with theories, we should like to find the function

$$i_0(U) = i(U) - r(U); \tag{15}$$

but as we have already seen, the data give i, and therefore r also, only with an unknown constant coefficient. To eliminate this coefficient, in our first paper this subject,[1] we plotted the "reduced intensity"

$$j(U) = \frac{X(U)i(U)}{X(2)i(2)} \tag{16}$$

as an empirical function; and now likewise we can compare with theoretical predictions the function

$$j_0(U) = i_0(U)/i_0(2). \tag{17}$$

As an intermediate step, correcting for rediffusion only, we shall make use of the function

$$\begin{aligned} j_r(U) &= \frac{X(U)i_0(U)}{X(2)i_0(2)} = j(U)\cdot\frac{1 - \{r(U)/i(U)\}}{1 - \{r(2)/i(2)\}}, \\ &= j(U)\,\frac{1 + \{r(2)/i_0(2)\}}{1 + \{r(U)/i_0(U)\}}, \end{aligned} \tag{18}$$

and this coefficient of $j(U)$ will be called $c_r(U)$.

To compute c_r we need numerical values of pS and either g or q. It appeared above that p for beryllium was probably about 0.043, and S 2.0 to 2.1.

Thus pS is probably about 0.086 to 0.090, though it may well be outside these limits. So we shall tentatively use the rounder number, 0.090, and if a better value of either p or S is found later, new values for c_r may be found by changing (c_r-1) in proportion to pS.

For g and q, since there is considerable doubt as to the best values to assign to them, we have left room for later improvements in accuracy by making calculations with all the values used in Fig. 1 or Table II. The results are given in Table III.

TABLE III. *Values of 100* (c_r-1).

W_0	g	q	$U=1.0$	1.5	2.0	2.5	3.0	3.5
0.90	10	—	+7.4	+2.2	0	−1.0	−1.6	−2.0
0.90	—	9	+7.9	+2.0	0	−0.8	−1.2	−1.5
0.80	5	—	+4.5	+1.9	0	−1.3	−2.0	−2.9
0.80	—	4	+5.6	+2.5	0	−1.3	−2.2	−2.8
0.67	3	—	+3.1	+1.6	0	−1.2	−2.2	−3.0
0.67	—	2	+3.7	+2.0	0	−1.4	−2.5	−3.3
0.50	2	—	+2.3	+1.4	0	−1.0	−2.0	−2.8
0.50	—	1	+2.5	+1.5	0	−1.3	−2.2	−3.0

The changes actually made in the reduced intensities, by the use of these corrections, are shown in Table IV, for values of U from 1 to 3.3 the limits of the data in Fig. 1. Here, for simplicity, we have averaged the corrections for all of the values of g and q from Table III, that have any reasonable chance of applying to such a light element as beryllium, that is, for $W_0=0.80$, 0.67 and 0.50. And to give a rough indication of the probable error due to the uncertainty in these parameters, we are tabulating with each averaged correction the mean of the deviations from it, given by the six values of g or q.

TABLE IV. *Reduced intensities, corrected for rediffusion.*

U	1.0	1.5	2.0	2.5	3.0	3.3
Average of 100 (c_r-1)	+3.6	+1.8	0	−1.3	−2.2	−2.7
$j(U)$ from empirical graph	0	+0.727	+1	+1.117	+1.148	+1.144
Average of corrections	0	+0.013	0	−0.014	−0.025	−0.031
Mean deviation of corrections	0	0.002	0	0.001	0.002	0.002
Ave. corrected intensity $j_r(U)$	0	+0.740	+1	+1.103	+1.123	+1.113

From this table it is evident that it makes no appreciable difference what value of g or q we use, within the range covered here; and even if the distribution of kinetic energy is not exactly like any of these functions $F(W)$, one could probably represent it pretty accurately by some linear combination of them, and even such a change would make no notable change in the corrections to be applied to $j(U)$.

Calculation of the effect of diffusion within the thin target. To calculate the reduced intensity $j_0(U)$, of Eq. (17), corrected for both rediffusion and

diffusion, we must not only correct the factor $i(U)/i(2)$ in $j(U)$ for rediffusion, but also the factor $X(U)/X(2)$ for diffusion. The basis for this correction is a formula given by Bothe[21] "zum praktischen Gebrauch," namely

$$\lambda = \frac{8.0}{V}\cdot\frac{V+511}{V+1022}\cdot Z\left(\frac{\rho x}{A}\right)^{1/2}. \tag{19}$$

Here λ is the most probable deflection of a cathode ray by multiple scattering in a thickness x of an element of atomic number Z, atomic weight A and density ρ; and λ must be expressed in radians, V in kilovolts, x in microns and ρ in gm/cc.

Letting Θ represent the deflection of any individual cathode ray at the depth x, the contribution of a layer dx to the mean path X will be the mean value for all cathode rays, of sec $\Theta\, dx$. For a thin target, therefore, since sec Θ is nearly enough $(1+\frac{1}{2}\Theta^2)$, and the mean value of Θ^2 is $2\lambda^2$, we have

$$X(U) = \int_0^{X_0}(1+\lambda^2)dx = X_0(1+\tfrac{1}{2}\lambda_0^2), \tag{20}$$

where λ_0 is the value given by equation (19) for λ at $x=X_0$.

The correction factor for diffusion, analogous to $c_r(U)$ for rediffusion, is now obtained from Eqs. (16), (17) and (18), as

$$c_d(U) = X(2)/X(U), \tag{21}$$

so that

$$j_0(U) = j(U)c_r(U)c_d(U). \tag{22}$$

As an illustration, and also for more definite use in the next section, the effect of diffusion in one of our own Ag targets is shown in Table V.

TABLE V. *Effect of diffusion in a 280A Ag target.*

U	=	1.0	1.5	2.0	2.5	3.0	3.5
$X(U)/X_0$	=	1.076	1.034	1.019	1.013	1.009	1.006
$100\ (c_d-1)$	=	−5.2	−1.4	0	+0.6	+1.0	+1.3

Results. Combining the corrections for diffusion and rediffusion, as applied to our data on thin silver, we obtain the reduced intensities in Table VI. Here as in Table IV, the values of $j(U)$, for the round-number values of U used in the computations, were read from the empirical graph in our previous paper, and the values of $j_0(U)$ were computed from them.

TABLE VI. *Reduced intensities, corrected for diffusion and rediffusion.*

U	=	1.0	1.5	2.0	2.5	3.0	3.3
$j(U)$	=	0	0.727	1	1.117	1.148	1.144
$100\ (c_rc_d-1)$	=	−1.8	+0.4	0	−0.7	−1.2	−1.4
$j_0(U)$	=	0	0.730	1	1.109	1.134	1.128

[21] Bothe, reference 8, Section 9.

For the other values of U at which data are given in Fig. 2, we have got the correction factors by interpolation, using Table VI for the 280A target, and a similar table for the 170A, differing only in the smaller correction for diffusion. The results, with the theoretical graphs with which they are to be compared, are shown in Fig. 3.

With regard to the empirical intensity functions, i_1 and i_2 of eqs. (9) and (10) resp., these corrections are so small that they come within the limits of error of i_1, but for i_2 it is best to change m_2 from 0.77 to 0.80.

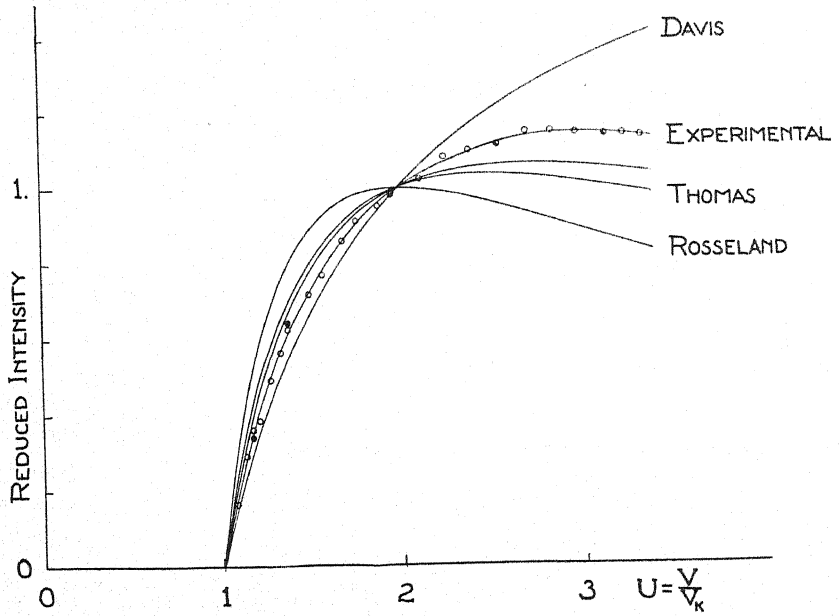

Fig. 3. Corrected data and theoretical graphs.

Reliability of these corrections. In a recent paper on thick-target x-ray measurements, Wisshak[2] reported data differing radically from our thin-target data in their relations to the theories. To compare our data with his he calculated a thick-target intensity function from our thin-target function $i_1(U)$, of Eq. (9), by the same formula that Rosseland had applied to his own theoretical function. The relation between this new thick-target function for Ag and Rosseland's was therefore much like that between the corresponding thin-target functions, shown in Figs. 2 and 3, i.e. the empirical graph was below Rosseland's at low voltages and above at high. Wisshak's empirical graph for the average of Cr and Cu, on the contrary, crossed Rosseland's theoretical graph in the opposite direction, at an angle of the same order of magnitude. Therefore Wisshak concluded, not only that there was a serious discrepancy between Rosseland's theory and his data, but also that the still larger difference between our graph and his must have been due to rediffusion in our target.

The present calculations, however, do not alter the relation between our graph and Wisshak's by anything like the amount indicated by this conclusion. In fact, to bring our graph into agreement with Rosseland's would require the correction, at $U=3$ for example, to be about 10 times as large as our calculations indicate, and for agreement with Wisshak's graph this factor would have to be nearer to 20. This raises the question: Can any of the uncertainties in the quantities or functions we have used be such as to make possible an increase of this order in our corrections?

Any change of g or q, in either direction, would reduce the corrections. Any other change in the energy distribution, keeping within the requirements of the evidence reviewed above, could hardly be such as to render impossible a good approximation by some linear combination of the functions we have used, and this would keep the corrections much as calculated here. A change in the parameter a, of the directional distribution, even to $a=\infty$, which would be so extreme as to make the probability of normal emergence zero, would still introduce only a factor of about 1.5. A change in p, keeping it independent of V, would certainly be limited by the fact that p for Be must be considerably less than for Al, and thus it could not go beyond a factor of 2 or 3. And finally, if p were assumed not independent of V, it could only decrease with increasing V, and this would reduce the correction. Altogether, therefore, any great increase in these corrections appears highly improbable. Evidently we must look elsewhere for the cause of the disagreement between our conclusions and Wisshak's, and in view of the great difficulties in the interpretation of thick-target data, it is our opinion that the cause is probably there.

This conclusion is of especial importance for the major question, which of the theoretical graphs in Fig. 3 is the best; but there is also the question, whether any of them is exact, so it may be well to note here some additional points about the accuracy of these data, not related to these corrections. Three possible sources of systematic error were mentioned in our first paper on these data. One was rediffusion (we had not realized the importance of diffusion within the thin target); another was the presence of some fluorescence radiation, never more than 0.2 percent and therefore negligible; the third was an unexplained darkening of the focal spot during use. This has since been explained, through the kindness of Dauvillier, who pointed out to us by letter an investigation of his,[22] proving such darkening to be due to carbon, which in our case could have come from the carbonization of adsorbed grease vapor by cathode rays (not by heat, because the block was oil-cooled and the power input was low). If this carbon were thick enough to retard the cathode rays appreciably, it might cause serious errors, especially at low voltages. Fortunately, however, after finishing the measurements shown in Fig. 2, we made a very careful study of the intensity function in the first 2 kilovolts above V_K. Here we found effects exactly such as one would predict for a 280A silver target assuming that it retarded the cathode-rays at 25 kv. by about 200

[22] A. Dauvillier, Journ. d. Physique **8**, 1 (1927).

volts, as predicted by the Thomson-Whiddington law, and that an infinitely thin target would give an intensity starting from zero at $U=1$, with a finite derivative. These measurements will be reported in more detail later, along with others with improved apparatus. For the present, the important point is, that if there had been any appreciable retardation in the carbon, it would almost surely have been evident here. So there can hardly have been any serious error from that source.

A similar possibility is that of a deposit of tungsten. But this is ruled out, not only by the above test, but also by the absence of the tungsten K lines at 80 kv.

There may of course be sources of systematic error still unsuspected, and there are the erratic errors, whose magnitude can be judged by the departures of the points from the empirical graph in Fig. 3. But for the present, we shall assume that Fig. 3 is accurate enough to serve as a basis for conclusions about the theories now at hand.

Comparison with Theories

Of the theoretical graphs in Fig. 3, those for Davis and Rosseland are plotted from Eqs. (11) and (12) respectively, and that for Thomas[24] from

$$i_T(U) = k_T \frac{1 - 1/U + (2/3)m_T(1 - 1/U^2)}{1 + U + m_T}, \tag{23}$$

where the parameter m_T is the ratio of the kinetic energy of an atomic electron in a Bohr orbit to its ionization energy.

While these theories based on classical mechanics give definite formulas, the wave mechanics, so far as we know, has been applied only through approximations that become invalid at voltages near the ionization voltage. On this basis Bethe[23] gives a formula, in which the dependence of intensity on U may be expressed by

$$i_B(U) = k_B U^{-1} \log (4U/B) \tag{24}$$

where BeV_K is a quantity of energy, "of the order of magnitude of the ionization energy," eV_K.

Comparing this function with Wisshak's data, which cover about the same range of U as ours, Bethe states that it is probably unsatisfactory for this range, "because the rise of x-ray intensity with increasing excess of the bombardment energy over the ionization energy must be even steeper than in the Thomson [or Rosseland] theory, whereas experimentally it is somewhat more level." Comparing the theories with our experimental graph, however, we should exactly reverse this last clause. In view of the approximations in Bethe's theory, it must of course become invalid as U is reduced toward unity, but in most of this range it apparently agrees with the thin-target data better than with the thick.

[23] H. Bethe, Ann. d. Physik **5**, 325 (1930).
[24] L. H. Thomas, Proc. Camb. Phil. Soc. **23**, 829 (1927).

In the absence of any theoretically calculated value of B, beyond the order-of-magnitude estimate quoted above, we may treat it tentatively as an empirical parameter, and choose a value such as to make the equation fit the data as far down the scale of U as possible. Since i must be zero at $U=1$, this is $B=4$. We have therefore plotted a graph on this basis in Fig. 3, but in view of the arbitrary character of this assumption, we cannot call it exactly a graph for Bethe's theory, and so we are not giving it any name.

A suggestion as to the direction in which a true graph for Bethe's theory might differ from this one is given by his calculation of the effective cross-section of a hydrogen atom for inelastic collisions (including excitation as well as ionization). Here there is a quantity b, analogous to B. At high voltages, b is constant at 0.638; but inspection of the equations from which it is obtained shows that with reduction of voltage it must begin to increase. If B behaves likewise, the true graph for Bethe's theory may run somewhat steeper than the nameless graph of Fig. 3, and thus perhaps agree even better with our experimental graph.

Another interesting aspect of Bethe's equation is its agreement in mathematical form with i_2, at least if m_2 is set equal to 1, as well as B to 4. This function i_2 was suggested first by a study of an empirical relationship between line and continuous spectra; and there some of the data indicated that $m_2=1$. Thus perhaps Bethe's theory may suggest theoretical connections, to match the empirical one between these spectra.

Thick-Target Effects

Effect of rediffusion on line intensities. In a thick target, the effect of rediffusion, removing some of the cathode rays from the target before they have made their quotas of impacts, is to diminish the intensity of the x-rays. Let $I_0(U)$ be the intensity of the rays that would be emitted in a K-series line if there was no such loss, and $I(U)$ the actual intensity. Then the loss,

$$I_0(U) - I(U) = R(U), \tag{25}$$

is equal to the intensity of the rays that the rediffused electrons would emit if they struck another target of the same element and did not rediffuse from it. Thus

$$R(U) = p\int_{1/U}^{1} F(W)I_0(UW)dW. \tag{26}$$

To calculate $R(U)$ we shall proceed much as with the analogous equation, (8), for $r(U)$. The chief difference in the two cases is that the sign of the correction for rediffusion here is opposite to what it was there, because the effect is a loss of impacts rather than a gain.

For I_0 in this integrand, we shall use either of two simple empirical formulas. One[25] of these is

$$I_1(U) = K_1(U-1)^n, \tag{27}$$

[25] D. L. Webster and H. Clark, Proc. Nat. Acad. Sci. 3, 181 (1917); A. Jonsson, Zeits. f. Physik 43, 845 (1927); S. K. Allison, Phys. Rev. 30, 245 (1927).

where n is between 1.3 and 2.1, and K_1 is a constant. The other[26] is

$$I_2(U) = K_2(U^2 - 1), \tag{28}$$

where K_2 also is constant.

Neither of these formulas is very accurate, but in view of other corrections, less definitely known than the one for rediffusion, we shall go no farther with this case than to find the order of magnitude of this correction. And for that, we may use either function, simplifying matters still further by letting $n =$ either 1 or 2, although I_1 with $n = 1$ is very far from correct.

The constants K_1 and K_2 are not so little known as those of the thin-target functions, but there is enough uncertainty here also to make it better for most purposes to use a "reduced intensity," which we shall call

$$J(U) = I(U)/I(2). \tag{29}$$

The corrected reduced intensity is now

$$J_0(U) = J(U)\cdot\frac{1 + \{R(U)/I(U)\}}{1 + \{R(2)/I(2)\}} = J(U)\cdot\frac{1 - \{R(2)/I_0(2)\}}{1 - \{R(U)/I_0(U)\}}, \tag{30}$$

and this correction factor for $J(U)$ will be called $C(U)$.

Values of $C(U)$, corresponding to the $c_r(U)$ of Table III, are shown in Table VII.

TABLE VII. *Values of 100 $(C(U)-1)$ for Ag, $p=0.39$ and $W_0=0.90$.*

$U=$	1.0	1.5	2.0	2.5	3.0	3.5
I_1, n=1, $g=10$	−23.8	−7.2	0.0	+3.3	+5.0	+6.1
I_1, $n=1$, $q=9$	−26.0	−7.4	0.0	+3.0	+4.5	+5.5
I_2, $g=10$	−21.5	−5.9	0.0	+2.3	+3.4	+4.1
I_2, $q=9$	−23.7	−6.1	0.0	+2.2	+3.2	+3.8
I_1, $n=2$, $g=10$	−17.0	−6.0	0.0	+3.1	+4.9	+6.1
I_1, $n=2$, $q=9$	−19.0	−6.6	0.0	+3.2	+5.0	+6.2
Averages	−21.8	−6.5	0.0	+2.8	+4.3	+5.3
100 (c_r-1) from Table 4	3.6	1.8	0.0	−1.3	−2.2	−2.7
$(C-1)/(c_r-1)$	−6.1	−3.6	−2.6	−2.2	−2.0	−2.0

From this table it is evident that the rediffusion correction factors for thick-target line intensities are about 2 to 4 times as far from unity as those for thin. This raises anew the question of the cause of the disagreement between our conclusions and Wisshak's,[2] about the status of the theories of ionization by impact. In Wisshak's interpretation of his data, the allowance for rediffusion consisted in substituting for the measured tube current, the current computed from the voltage and the heat in the target. But as the ratio of these currents was found to be constant, the difference affects only the constant coefficient K, in $I(U)$, and does not affect $J(U)$ at all. So it appears to us that the correction factor $C(U)$ would be useful here. And just as the cor-

[26] Simplified from a formula used by G. Kettmann, Zeits. f. Physik **18**, 359 (1923); and E. C. Unnewehr, Phys. Rev. **22**, 529 (1923).

rection c_r for thin targets shifted our graph toward Wisshak's, this opposite correction C shifts his graph toward ours. Nevertheless, both corrections together move the graphs only about a seventh as far as is necessary to bring them into agreement. Evidently there is some other cause for the difference.

The most obvious suggestion is that there is a real difference between the elements used here by Wisshak and by us, namely between his average of Cr and Cu and our Ag. Another possibility is that the other uncertain factors in the interpretation of thick-target data are responsible for the discrepancy. So it is significant, though ambiguous, that recent data of ours (not yet published) on thick targets of Ag with corrections for target absorption by Kulenkampff's method and for fluorescence radiation by ours,[27] give a far better agreement with the function calculated by Wisshak from our thin-target formula for Ag than do his data on Cr and Cu.

To put this statement into a more quantitative form, we may express all these intensity functions with enough accuracy in terms of the function $I_1(U)$, of Eq. (27), namely $K_1(U-1)^n$. Wisshak's graphs for Cr and Cu make n between 1.3 and 1.4, and his function calculated from our thin Ag makes n about 1.85. Our data on thick Ag make n about 1.65 before correction for rediffusion, and about 1.73 after. The remainder from 1.73 to 1.85 is in the direction one would expect from Kulenkampff's[28] comparison of his continuous-spectrum intensities for thin Al with the intensities calculated from his thick Al by a method the inverse of that which Wisshak used here. So this discrepancy may be ascribed tentatively to the errors in the Thomson-Whiddington law of retardation of the cathode rays, which has been used, for lack of anything more accurate, in all such calculations. The net result, then, is that the apparent discrepancy between the thick and thin-target data may well be no greater than can be expected from the uncertainties in the relations between them.

Details of these comparisons would be beyond the scope of this paper, however, and will therefore be reserved for later consideration, in connection with more data. In the meantime, the values of n given here for thick Ag must be regarded as somewhat provisional, as we are making still further improvements in our apparatus, but they are fairly good up to about 100 kv ($4\ V_K$); and for rays corrected only for target absorption, an exponent 1.6 will serve moderately well up to 180 kv.

Continuous spectra. Turning from the line spectra of thick targets to the continuous, we are rid of the complications of fluorescence, but we run into another complication, arising from the fact that the intensity emitted by a single atom (or a thin target) is not the same in all directions, as proved by Kaye,[29] Duane,[30] Kulenkampff[28] and Nicholas.[31] As it concerns us here, this means that the diffusion of the cathode rays within a thick target will

[27] D. L. Webster, Proc. Nat. Acad. Sci. **14**, 330 (1928).
[28] H. Kulenkampff, Ann. d. Physik **87**, 597 (1928).
[29] G. W. C. Kaye, Proc. Camb. Phil. Soc. **15**, 269 (1909).
[30] W. Duane, Proc. Nat. Acad. Sci. **15**, 805 (1929).
[31] W. W. Nicholas, Bureau of Standards Jour. Res. **2**, 837 (1929).

tend to annul the directional differences that would have occurred without it. This effect has been discussed by Kulenkampff and Nicholas, who have shown that it is practically complete except near the high-frequency limit of the spectrum, and that the directional effects near the high-frequency limit are such as one might expect from the data on thin targets. Having no new contribution to make on this point, we may treat the effect of rediffusion alone by neglecting the directional effects and comparing theoretical predictions, not with intensities in any particular direction, but with the average, so far as it is known, for all directions.

This treatment of the rediffusion effect amounts practically to putting on a somewhat more nearly quantitative basis an idea advanced by Kramers[32] in a paper on his theory of the continuous spectrum. First neglecting rediffusion as well as all directional effects, Kramers found for the thick-target intensity in a range $d\nu$.

$$I_0(V, \nu)d\nu = K_0 Z(\nu_0 - \nu)d\nu = K_0 Z\nu_0 u, \tag{31}$$

where K_0 is a constant, $\nu_0 = eV/h$, and $u = (\nu_0 - \nu)/\nu_0$. Observed intensities are not far from obeying this formula, but they are given more accurately by adding a non-linear term,[33] so that the empirical formula is something like

$$I(V, \nu) = K'Z\nu_0[u + BZ(1 - e^{-Au})], \tag{32}$$

where A is a function of Z, ν and ν_0, and B of ν and ν_0, though perhaps not of Z, and both A and B change only slowly. K' will be defined more explicitly below. Kramers explained the presence of a non-linear term of this general sort, as an effect of rediffusion.

A calculation of I, based on Kramers' theoretical intensity I_0 and the rediffusion formulas used in the first part of this paper, gives, when $F_1(W)$ is used,

$$I_1(V, \nu) = K_0 Z\nu_0[(1 - p)u + p\{(1 - \overline{W})(1 - e^{-\sigma u}) - ue^{-\sigma u}\}], \tag{33}$$

at least if $e^{-\sigma} << 1$, and when $F_2(W)$ is used,

$$I_2(V, \nu) = K_0 Z\nu_0[(1 - p)u + p\{(1 - \overline{W})(1 - v^{q+3}) - uv^{q+2}\}], \tag{34}$$

where $v = 1 - u$.

Each of these functions is much like the empirical function of Eq. (32), in that the larger term, $(1-p)u$, is proportional to u, while the smaller, non-linear, term increases from zero at $u = 0$, more or less like $(1 - e^{-Au})$. Furthermore the ratio of these terms, as a function of Z, contains $p/(1-p)$, which is not far from proportional to Z, like the corresponding ratio in Eq. (32).

With regard to the dependence of the linear term on Z, it is usually said to be simply proportional to Z, with K' in Eq. (32) constant. The best evidence on this point, however, comes from the data of Wagner and Kulen-

[32] H. A. Kramers, Phil. Mag. **46**, 836 (1923).

[33] D. L. Webster, Phys. Rev. **9**, 220 (1917); E. Wagner and H. Kulenkampff, Phys. Zeits. **23**, 503 (1922); D. L. Webster and A. E. Hennings, Phys. Rev. **21**, 312 (1923); W. W. Nicholas, Phys. Rev. **29**, 619 (1927).

kampff,[34] who made an approximate allowance for rediffusion by defining intensity, not as x-ray energy per incident cathode ray, but per unit current as measured by heat in the target. It is in these terms only, that the K' of Eq. (32) is approximately constant. To convert to the intensity definition used here, we must let

$$K' = K(1 - p\overline{W}), \tag{35}$$

with K constant. This new factor $(1-p\overline{W})$, is not far from the $(1-p)$ of Eqs. (33) and (34).

Likewise on integrating to get the total intensity, unresolved, we find

$$E_1 = E_2 = \tfrac{1}{2}K_0 Z\nu_0^2(1 - p\overline{W^2}), \tag{36}$$

and from Eq. (32), neglecting the second term,

$$E = \tfrac{1}{2}K'Z\nu_0^2 = \tfrac{1}{2}KZ\nu_0^2(1 - p\overline{W}), \tag{37}$$

agreeing fairly well with E_1 or E_2.

Thus these formulas describe the main facts of thick-target continuous spectra to a first approximation, confirming Kramers' qualitative predictions. We cannot expect great accuracy here, because the basic formula for $I_0(V, \nu)$ was derived by the Thomson-Whiddington law from a theoretical thin-target formula which agrees only approximately with Kulenkampff's data, and so $I_0(V, \nu)$ itself may be as good as it is, only because of a cancellation of errors. An approximate verification of these thick-target formulas is therefore as much as one can expect.

[34] E. Wagner and H. Kulenkampff, reference 33.

EXPERIMENTAL EVIDENCE FOR ELECTRON VELOCITIES AS THE CAUSE OF COMPTON LINE BREADTH WITH THE MULTICRYSTAL SPECTROGRAPH

By Jesse W. M. DuMond and Harry A. Kirkpatrick
California Institute of Technology, Pasadena

(Received December 1, 1930)

Abstract

The main purpose of this research was to test the correctness of the assumption that the initial velocities of electrons in the scattering body cause the observed breadth of the Compton shifted line. The test consists in observing the natural breadths of the Compton line for different scattering angles and primary wave-lengths and comparing these with the functional dependence of breadth on scattering angle and primary wave-length deduced theoretically on the basis of the assumption under test. It is shown in this paper that if electron velocities are the cause of the breadth then this breadth should increase with the scattering angle according to the approximate formula $\Delta\lambda = K\cos\frac{1}{2}\theta$ where $\Delta\lambda$ is the breadth, θ the scattering angle and K a constant depending on the primary wave-length and the scattering substance. For the same scattering angle and substance the breadth should be proportional to the primary wave-length.

The experimental test was made with the multicrystal spectrograph of fifty units herein briefly described. Three scattering angles were used, $63\frac{1}{2}°$, 90°, 156°, *the inhomogeneity in each case being less than one degree.* The spurious breadth due to this inhomogeneity is negligible compared to the observed breadths. Three very clear cut spectrograms are reproduced representing MoK radiation scattered from graphite together with microphotometer curves taken from them. The increase of shifted line breadth with scattering angle is clearly visible and compares favorably with the theoretical prediction. The increase of line breadth with increasing primary wave-length comparing the breadths of shifted α_1 and shifted β_1 lines seems just detectable. The unshifted lines are very sharp, the α doublet being clearly resolved. Incidentally the cause of the heavy background so frequently observed on Compton effect spectrograms has been found to be non-selective scattering at the crystals and a great reduction of background and improvement in contrast has been effected by the use of baffles to diminish this effect.

The observed shift of the Compton line supports Compton's formula $\delta\lambda = (h/mc)(1-\cos\theta)$ where $h/mc = 24.2$X.U.

The shifted line breadths are greater than those reported by Gingrich and Bearden and possibly Ross but seem to be in general accord with previous breadths obtained at this laboratory and with those of H. M. Sharp and of F. L. Nutting. The reason for these discrepancies is unknown. The possibility of double or higher multiplicities of scattering is being investigated. (See note added in proof at the end of this article.)

Purpose of the Investigation

NEARLY all investigators have observed that the Compton shifted line is broader than either the unshifted line or the primary line. Jauncey,[1] Wentzel[2] and DuMond[3] have each attributed the observed breadth of the

[1] Jauncey, Phys. Rev. **25**, 314–322 (1925); 723–736 (1925).
[2] Wentzel, Zeits. f. Physik **43**, 188 (1927); **43**, 779–787 (1927).
[3] DuMond, Phys. Rev. **33**, 643–658 (1929).

Compton line to the velocities possessed initially by the electrons in the scattering body. DuMond[3], and almost simultaneously, Chandrasekhar[4] have applied the above assumption to the conduction electrons in the interatomic spaces of the crystal lattice in the case of electrically conducting scatterers and the former has shown that the results compared with his observed Compton line structures seem to support favorably the new Fermi, Pauli, Dirac, Sommerfeld statistics for such conduction electrons. It is important to test the correctness of the assumption that the velocities (or more accurately the momenta) of electrons bound in atoms or in the interatomic spaces of the crystal lattice are responsible for Compton line broadening.

We have attempted to test this assumption by observing the dependence of Compton line breadths on the scattering angle in the case of MoK radiation scattered by graphite and comparing this with the theoretical functional dependence to be expected if the assumption be correct that electron velocities cause the breadth. The theoretical considerations will be dealt with first.

PART I. THEORETICAL

GENERAL NON-MATHEMATICAL DISCUSSION

Before passing to the analytical argument we venture to offer a verbal discussion of the cause of Compton line-breadth regarded as a Doppler effect of the random-moving electrons scattering the radiations in order to serve as a guide to the reader through the cold formality of the analysis. The use of the words "Doppler effect" we insist shall not be naïvely interpreted as committing us to any *mechanism* (classical, undulatory or otherwise) to "explain" the wave-length modification associated with scattering of radiation by a moving scattering agent. It is now an old story that the Doppler effect from a moving scatterer can be equally well derived on either the extreme undulatory hypothesis or the extreme corpuscular hypothesis—the latter derivation requiring only the quantum application of the laws of conservation of momentum and energy to the elementary scattering process. *Furthermore the interpretation of the broadening of the Compton line as a Doppler effect of the motion of weakly bound electrons here presented is a perfectly valid first approximation to the quantum mechanical treatment of the effect as given by Wentzel, Gordon and others.* The condition for such validity is that the binding energy of the electron shall be small compared to the energy imparted to the electron in the scattering process. This condition is fulfilled in the present case.

When x-radiation is scattered by the electrons in a scattering body the total effect of the motion of the electrons may be thought of as a superposition of two "Doppler effects"—one caused by the initial motion of the electrons, the other caused by the motion imparted to the electrons by the radiation in the scattering process. The first Doppler effect can in the case of random electron motions have either a positive or a negative sign, depending on whether the electron's initial velocity before scattering has a component directed toward or away from the vector expressing the change in momentum suffered by the

[4] Chandrasekhar, Royal Soc. Proc. **A125,** 231–237 (1929).

radiation in the scattering process. The second Doppler effect can have only one sign (corresponding to an increase in scattered wave-length over incident wave-length) because the momentum imparted to the electron in the scattering process must always be opposite in direction to the vector change in momentum of the radiation. Both Doppler shifts will vanish for zero scattering angle and be a maximum for a scattering angle of 180°.

The first Doppler shift having either positive or negative sign accounts for the broadening of the Compton modified line. The second Doppler shift accounts for the justly famous shift of the Compton line toward longer wave-lengths.

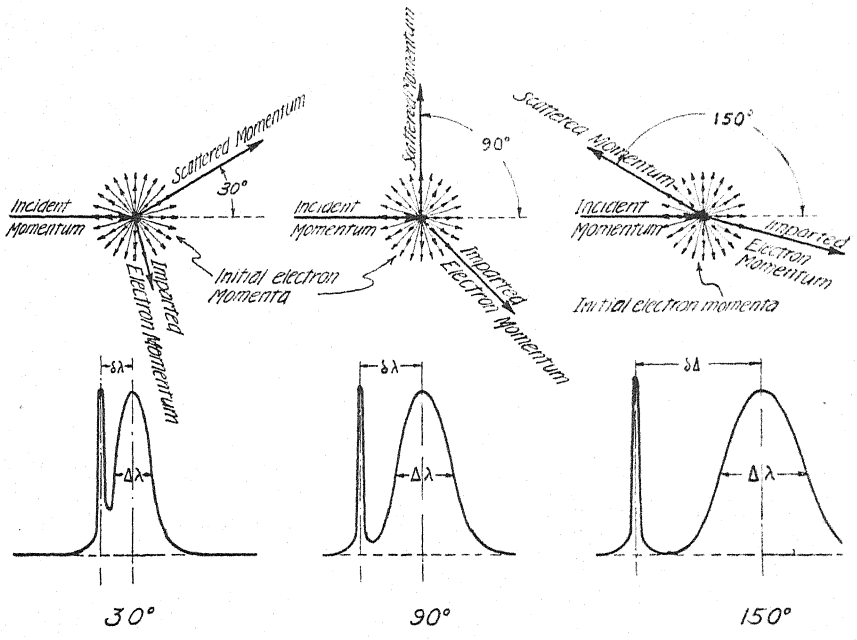

Fig. 1. Schematic illustration of Compton scattering by randomly directed moving electrons for three scattering angles together with idealized spectra of the resulting scattered radiation for each case. The constancy of the initial momentum and the increase in the momentum imparted to the electron with increasing scattering angle is shown. In this diagram the randomly directed initial momenta are *much exaggerated* relative to the imparted momentum.

Let us define the relative breadth $\Delta\lambda_r$ as the breadth at any scattering angle divided by the breadth at 180° scattering angle (maximum breadth). Let us also define the relative shift $\delta\lambda_r$ in an entirely analogous way. The relative breadth and the relative shift will be shown to be given by[5]

[5] It is interesting to note that the relative shift is the *square* of the relative breadth. This is because the *shift* increases with the scattering angle due to *two* causes, (1st because the Doppler effect from *any* moving scatterer increases with the scattering angle, 2nd because the velocity of the moving scatterer itself increases with the scattering angle in the case of the Compton shift) while the *breadth* increases with the scattering angle due to only the first of these causes alone, the velocity of the scattering electron accountable for the breadth being independant of the scattering angle.

$$\text{Breadth } \Delta\lambda_r = \sin \tfrac{1}{2}\theta \text{ approximately}$$
$$\text{Shift } \quad \delta\lambda_r = \sin^2 \tfrac{1}{2}\theta$$

Fig. 1 shows diagrammatically the vectors of light momentum, random initial electron momentum and momentum imparted by the scattering process to the electron for three scattering angles together with an idealized Compton shifted line spectrum for each case. In Fig. 2 the relative breadth and relative

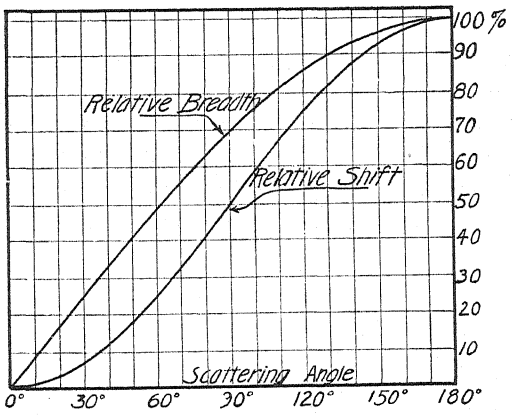

Fig. 2. Relative breadth and relative shift computed for molybdenum K radiation using Eqs. (10) and (8). The relative breadth is the quotient of the breadth at any scattering angle by the maximum breadth which occurs at 180°. The relative shift is similarly defined.

shift are plotted as functions of the scattering angle. In this case the more accurate formula derived below has been used for the computations of relative breadth.

Analytical Solution

Case of one free scattering electron only. The solution of this case in the form of Eq. (5) was obtained by de Broglie in his "Ondes et Mouvements Fasicule" 1. pp. 94–95. The primary radiation is taken as travelling in the positive x-direction. θ is the angle of scattering; ν_1 is the initial frequency; $\beta_1 c$ the speed of the electron before scattering, a_1, b_1, c_1, the direction cosines of its velocity and $a_1 = \cos\theta_1$ so that θ_1 is the angle between the initial electron momentum and the initial light momentum. ν_2 is the frequency of the scattered quantum and its direction of propagation has the direction cosines p, q, r, making angle ϕ with the initial velocity of the electron and angle θ with OX. Fig. 3 shows the relations of the various vectors and angles.
Evidently

$$\cos\phi = a_1 p + b_1 q + c_1 r$$
$$p = \cos\theta.$$

The recoiling electron has a final speed $\beta_2 c$ in the direction defined by the cosines a_2, b_2, c_2.

The following four equations express the conservation of energy and of the

three rectangular components of momentum before and after the scattering process.

$$h\nu_1 + m_0c^2/(1-\beta_1^2)^{1/2} = h\nu_2 + m_0c^2/(1-\beta_2^2)^{1/2} \tag{1}$$

$$h\nu_1/c + (m_0\beta_1 c/(1-\beta_1^2)^{1/2})a_1 = (h\nu_2/c)p + (m_0\beta_2 c/(1-\beta_2^2)^{1/2})a_2 \tag{2}$$

$$(m_0\beta_1 c/(1-\beta_1^2)^{1/2})b_1 = (h\nu_2/c)q + (m_0\beta_2 c/(1-\beta_2^2)^{1/2})b_2 \tag{3}$$

$$(m_0\beta_1 c/(1-\beta_1^2)^{1/2})c_1 = (h\nu_2/c)r + (m_0\beta_2 c/(1-\beta_2^2)^{1/2})c_2 \tag{4}$$

Eliminating a_2, b_2, c_2 and β_2 and letting $\alpha = h\nu_1/m_0c^2$ we obtain on solving for the change in wave-length,

$$\lambda_2 - \lambda_1 = \frac{\beta_1(\cos\theta_1 - \cos\phi)}{1-\beta_1\cos\theta_1}\lambda_1 + \frac{2\alpha\lambda_1 \sin^2\frac{1}{2}\theta}{1-\beta_1\cos\theta_1} \tag{5}$$

where the second term accounts for the simple Compton shift and the first term represents the modification caused by the electron's initial speed β_1.

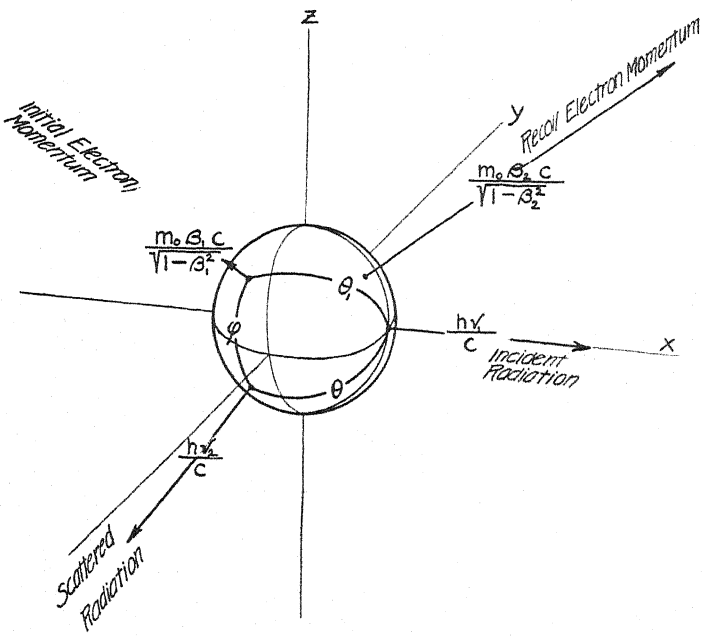

Fig. 3. Illustrating the various angles and vectors involved in Compton scattering by an electron possessing initial momentum. The initial electron momentum is exaggerated. The vectors are shown radiating from a sphere at the origin on which the angles between vectors appear as arcs of great circles. This sphere is shown merely to aid in visualizing the diagram in three dimensions.

As we are particularly interested in the *breadth* of the shifted line we define a wave-length coordinate, $l = \lambda_2 - \lambda_1 - 2\alpha\lambda_1 \sin^2\frac{1}{2}\theta$ so chosen that l has its origin at the "center" of the shifted line (shifted position for scattering by free *initially stationary* electrons) and measures the wave-length deviation given by the first term of the right hand member of Eq. (5). Then

$$l = \frac{\lambda_c \cos\theta_1 - \lambda_1 \cos\phi}{1 - \beta_1 \cos\theta_1}\beta_1 \qquad (6)$$

in which λ_c is the Compton shifted wave-length for the simple case of an initially stationary electron

$$\lambda_c = \lambda_1 + 2\alpha\lambda_1 \sin^2 \tfrac{1}{2}\theta.$$

Equation (6) can be much simplified by describing the direction of the initial electron momentum in terms of a new angle Ψ measured from a reference axis[6] taken in the direction of the change in momentum which the radiation would suffer for the simple Compton case of a stationary electron scattering radiation at the angle θ.

In Fig. 4 let OA be the direction of the incident quantum, OB the direction of the scattered quantum, OC the direction of the electron's initial velocity. Make the vector OA equal in length to λ_c, the vector OB equal in length to

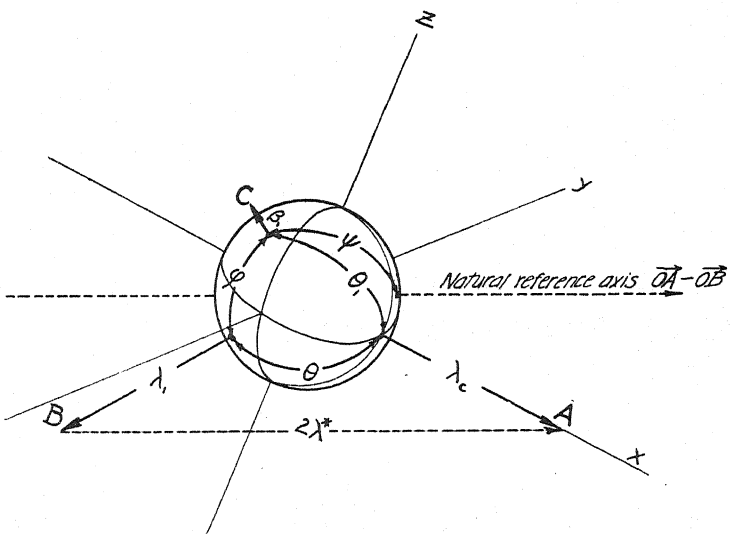

Fig. 4. Illustrating the definition of the "natural" reference axis and of the angle ψ. It should be emphasized that λ_c is the simple Compton shifted wave-length for the case where vector C vanishes ($\beta_1 = 0$) and that therefore λ_c is constant for a given primary wave-length and scattering angle and the direction of the natural reference axis is a constant. Note that λ_c is taken along the *incident* direction and λ_1 along the *scattered* direction. This inversion is caused by the fact that the momenta are inversely as the wave-lengths.

λ_1 and the vector OC equal in length to β_1. We define a new wave-length λ^* represented to the same scale by the distance AB. Now note that the numerator of Eq. (6) can be represented in terms of the vectors of Fig. 4 (designated by their terminii) as the difference of two scalar products

$$\boldsymbol{C} \cdot \boldsymbol{A} - \boldsymbol{C} \cdot \boldsymbol{B}$$

or what is equivalent $\boldsymbol{C} \cdot (\boldsymbol{A} - \boldsymbol{B})$

The vector whose length is λ^* is precisely $(A-B)$ hence if Ψ is the angle between OC and AB we rewrite Eq. (6) as follows

$$l = \frac{\cos\psi}{1-\beta_1\cos\theta_1} 2\beta_1\lambda^* \tag{7}$$

where

$$2\lambda^* = (\lambda_c^2 + \lambda_1^2 - 2\lambda_c\lambda_1\cos\theta)^{1/2}. \tag{8}$$

The denominator is nearly unity in most practical cases. Thus it is evident that the wave-length deviation l from the simple Compton shift caused by a scattering electron having an initial velocity βc (instead of zero velocity) is proportional to the projection $\beta_1\cos\Psi$ of the electron's initial velocity along the direction of the vector representing the change in momentum which the radiation would suffer if scattered by an initially stationary electron through the scattering angle θ.[6]

This latter direction is a stationary axis in space independent of the direction of the electrons' initial motion and the projection on it in question can be either positive or negative, i.e. $\cos\Psi$ may have either sign. Thus the extreme values of l are given (if β^2 is considered negligible compared to unity) by the inequality

$$-2\beta_1\lambda^* + 2\beta_1^2\lambda^*\cos\tfrac{1}{2}(\pi-\theta) \leq l \leq 2\beta_1\lambda^* + 2\beta_1^2\lambda^*\cos\tfrac{1}{2}(\pi-\theta) \tag{9}$$

or if the first power of β be considered negligible compared to unity

$$-\beta_1\lambda^* \leq l \leq 2\beta_1\lambda^* \tag{9.1}$$

In either case therefore l can vary over the wave-length range

$$\Delta\lambda = 4\beta_1\lambda^* \tag{10}$$

for electrons of constant initial speed β_1 and all possible directions of motion.

Case of ensemble of electrons of speed βc and random direction. Since the velocities are uniformly distributed as to direction over the surface of a sphere the probability of scattering by an electron whose velocity makes an angle Ψ to $\Psi+d\Psi$ with the above defined natural reference axis[7] is

$$P(\psi)d\psi = \tfrac{1}{2}\sin\psi d\psi. \tag{11}$$

The probability $P(l)$ of a given deviation l from the Compton shift is then to be obtained from Eqs. (7) (11) and the derivative of (7), by eliminating Ψ and $d\Psi$.[7] This gives

[6] The vector change in light momentum for scattering at angle θ by an *initially stationary electron* constitutes the natural and appropriate reference axis for the problem of scattering at angle θ by moving electrons.

[7] This operation is much simplified if the denominator in Eq. (7) be first set equal to unity. This amounts to neglecting β in comparison to unity. θ_1 is a complicated function of the colatitude ψ and the azimuth ϕ. Taking the above defined natural reference axis as polar axis and the plane of the scattering angle as reference plane we have

$$\cos\theta_1 = \cos\psi\cos\tfrac{1}{2}(\pi-\theta) + \sin\psi\sin\tfrac{1}{2}(\pi-\theta)\cos\varphi$$

$$P(l)dl = (4\beta\lambda^*)^{-1}dl \text{ (approximately)} \qquad (12)$$

The relative error committed in this formula is of the order of β. For $\lambda^* = 740$ X.U. $l = 25$ X.U. the error committed is about 3 percent. For narrower parts of the line structure it is even much less. From Eq. (11), since

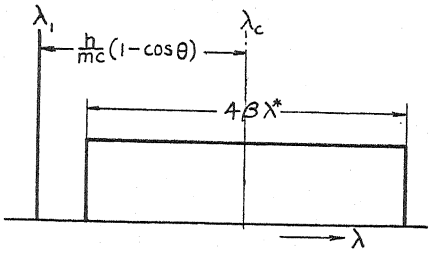

Fig. 5. Spectral distribution curve of originally monochromatic radiation after scattering through angle θ by an ensemble of electrons of initial speeds βc and random directions.

the right hand member is independent of l, it is evident that all deviations l are equally probable within the limits placed by inequality (9). Outside these limits the probability is nihil. Thus (see Fig. 5) a good approximation to the line structure contributed by the randomly directed ensemble of electrons of speeds between β and $\beta+d\beta$ is a rectangular spectral distribution of breadth $4\beta\lambda^*$ and of *area* proportional to the population of the speed class β to $\beta+d\beta$. (This distribution is not quite centered on the Compton shifted position but as can be seen by reference to inequality (9) is displaced toward longer wavelengths by a slight amount $2\beta_1^2\lambda^* \cos\frac{1}{2}(\pi-\theta)$. This shift is wholly inappreciable however for values of β of importance in the experimental case).

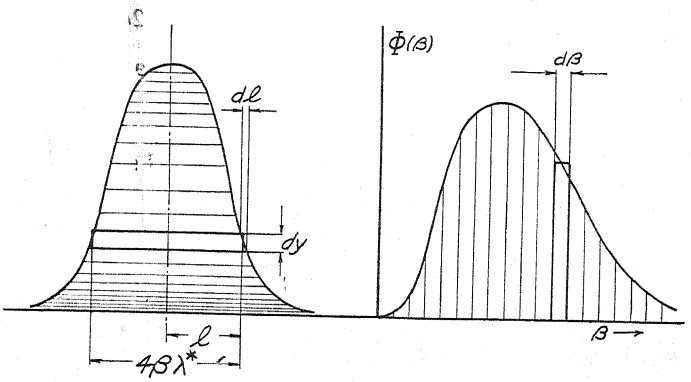

Fig. 6. Illustrating the relation between spectral intensity distribution in the Compton line (left) and population of electron speed states (right). Each elementary rectangle on the left is equal in area to a rectangle on the right while the spectral breadth $4\beta\lambda^*$ of each rectangle on the left is proportional to the abscissa β of the rectangle on the right.

Case of ensemble of electrons with random directions and any speed distribution, $\Phi(\beta)$. The line structure in this case is to be thought of as built up out of an assemblage of rectangles of infinitesimal height each having its

dimensions determined in the same way as the rectangle of Fig. 5. For convenience in adding spectral intensities the rectangles must of course be piled on top of each other in order of decreasing breadth, that is to say decreasing values of β. Referring to Fig. 6 the curve $\Phi(\beta)$ on the right represents the populations of the states or speed ranges β to $\beta+d\beta$ required by the dynamics of the electrons in the solid scattering body while the curve on the left represents the resulting Compton line structure. The elementary rectangular area $2ldy$ in the left hand curve is to be kept proportional to the elementary rectangular area $\Phi(\beta)d\beta$ in the right hand curve. If the constant of proportionality is k we can express the differential equation of the line structure curve in terms of the speed distribution function thus

$$-2ldy = k\Phi(\beta)d\beta \tag{13}$$

since the half breadth of each rectangle is $l=2\beta\lambda^*$ we can replace $d\beta$ by $dl/2\lambda^*$ and β by $l/2\lambda^*$. Dividing Eq. (13) by $-2l$ and integrating from $y=0$, $l=\infty$ to $y=y$, $l=l$ we obtain the equation of the line structure curve for continuous functions which vanish as $l\to\infty$

$$y = -k\int_{l=\infty}^{l=l} l^{-1}\Phi(l/2\lambda^*)dl. \tag{14}$$

Definition of line "breadth." For the purpose of the present investigation we are especially interested in the spectral "breadth" of curves such as shown in Fig. 6 and defined by Eq. (14) and in particular we wish to study the dependence of the breadth on the scattering angle θ. There is no ambiguity

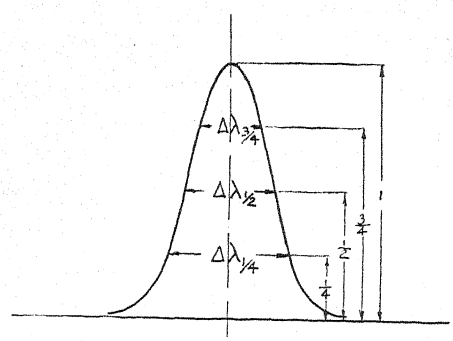

Fig. 7. Illustrating terminology of line breadths.

about the breadth of a rectangular spectral distribution such as is shown in Fig. 5 but real Compton lines resemble more nearly Fig. 6, the scattering electrons being without doubt distributed over a wide range of speeds. We shall speak of the "breadth" $\Delta\lambda_h$ e.g. $\Delta\lambda_{\frac{1}{2}}$, $\Delta\lambda_{\frac{1}{4}}$ meaning the spectral breadth measured across the line structure at a specified proportion of its height. Thus we mean by $\phi\lambda_{\frac{1}{2}}$ the spectral breadth of the line measured at a point half way up from the background to the peak. See Fig. 7.

Dependence of line breadth on scattering angle. Consider what happens

to the Compton line as the scattering angle is varied, keeping the primary wave-length and the material of the scatterer (and therefore $\Phi(\beta)$) always the same. Under these conditions the only quantity that suffers change is λ^* and referring to Fig. 6 it is evident that all the elementary rectangles of breadth $4\beta\lambda^*$ going to make up the line structure will be horizontally extended or contracted in the same proportion. The breadth just defined above, $\Delta\lambda_h$, will always measure the spectral breadth of the rectangle contributed by one and the same class of electrons of speeds between β and $\beta+d\beta$.

Now λ^* defined in Eq. (8) can most easily be visualized graphically. In Fig. 8 we construct triangles for the values of the scattering angle $\theta = 0°$, 22.5°,

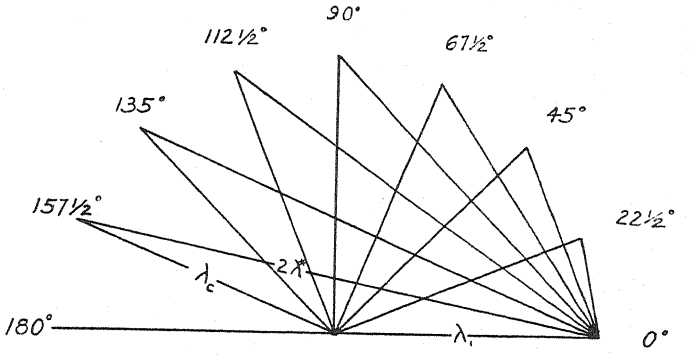

Fig. 8. Graphical construction for λ^*.

45°, 67.5°, 90°, 112.5°, 135°, 157.5°, 180° and make the sides adjacent to θ equal respectively to λ_1 and λ_c where $\lambda_c = \lambda_1 + (h/mc)(1-\cos\theta)$. The third side of this triangle is $2\lambda^*$. Since λ_c and λ_1 are nearly equal an approximation to λ^* is

$$\lambda^* = \lambda_1 \sin \tfrac{1}{2}\theta \text{ (approximately)}$$

Hence it follows that the *relative breadth* $\Delta\lambda_2$ as we have already asserted without proof is

$$\Delta\lambda_r = \frac{\Delta\lambda_h}{\Delta\lambda_{h,\max}} = \frac{4\beta\lambda^*}{4\beta\lambda^*_{\max}} = \sin \tfrac{1}{2}\theta \text{ (approximately)}.$$

The reader is referred to Fig. 2 which shows the dependence of relative breadth on scattering angle along with the relative shift. The accurate formula for λ^*, Equation (8), has been used in plotting this curve.

Recapitulation of Assumptions

The theory here outlined assumes

1. Conservation of momentum and energy in elementary processes.
2. Electron binding energy negligible compared to energy transferred to electron in scattering process.
3. The initial electron velocity small compared to the velocity of light.

4. Probability of scattering by a given class of electrons proportional to population of the class.

Assumption 1 is in accord with quantum as well as classical mechanics.

Assumptions 2 and 3 are most applicable to precisely those cases of interest for the Compton effect from radiation of about the hardness of MoK radiation. Assumption 4 is probably valid for most of the scattering electrons.[8]

Part II. Experimental

Importance of Homogeneity of Scattering Angle

Because the wave-length shift of the Compton modified line depends on the scattering angle the breadth of that line is increased if the scattering angle is not sharply defined in the experimental set up. This spurious breadth due to inhomogeneity of scattering angle was thought by many physicists to be the sole cause of the observed diffuseness of the Compton modified line. At

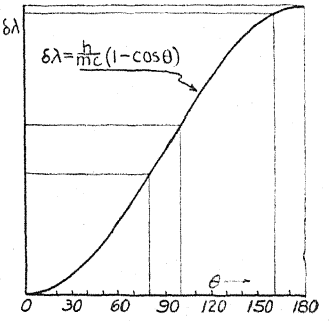

Fig. 9. Illustrating the spurious breadth introduced by a given inhomogeneity of scattering angle at different scattering angles.

only one scattering angle ($\theta = 180°$) a considerable angle inhomogeneity produces very little spurious breadth because the shift has an analytic maximum there. See Fig. 9. Hence several experimenters[9] have studied the breadth of the modified line at large angles of scattering and concluded that a natural breadth exists. There is some disagreement as to its size however.

For our present purpose it is not possible to resort to the convenient device of working at scattering angles near 180° thereby escaping from the necessity of maintaining a very homogeneous scattering angle. Since we are to examine the dependence of modified line breadth on scattering angle it is necessary to work at a number of angles other than 180° and to maintain these angles very homogeneous in each case. As all who have worked in this field are aware, the requirement of homogeneity of scattering angle is antagonistic to the equally pressing requirement of a large solid angle of radiation

[8] See Compton's "X-Rays and Electrons," page 291.

[9] Sharp, Phys. Rev. **26**, 691 (1925); DuMond, Phys. Rev. **33**, 643 (1929), Proc. Nat. Acad. **14**, 875 (1928), Gingrich, Phys. Rev. **36**, 1050 (1930); Nutting, Phys. Rev. **36**, 1267 (1930), Bearden, Phys. Rev. **35**, 1427 (1930).

from the source incident upon the scatterer to give sufficient energy in reasonable exposure times. Unfortunately there are no x-ray lenses to collect x-radiation and render it parallel.

To circumvent these difficulties the authors have constructed the multicrystal spectrograph. This instrument has been described in detail elsewhere[10] and will be touched on but briefly here.

Description of Multicrystal Spectrograph

The instrument consists of fifty small cylindrical units each a Seemann type spectrograph in itself placed vertically on the arc of a horizontal circle of about a half meter radius. Let us call this circle the "major circle" of the instrument. Each unit contains a brass wedge standing at about 0.1 mm

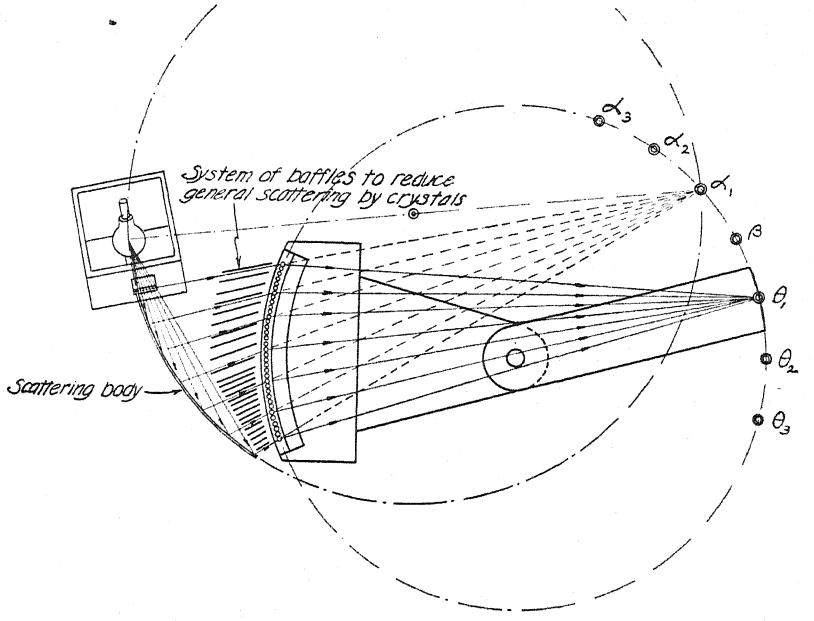

Fig. 10. Geometry of "focussing" and of homogeneity of scattering angle in the multicrystal spectrograph. θ_1, θ_2 and θ_3 show actual positions of $K\alpha$ line in the first second and third orders respectively. The scattering body is shown set to give homogeneous scattering for the first order.

distance from the cleavage face of a small slip of calcite. The units are orientated so that each calcite will reflect the $K\alpha$ doublet of Mo to exactly the same point on a photographic film coinciding with an arc of the major circle on the opposite side from the bank of crystal units. The geometry of the instrument is such that if one such wave-length coincides or focusses at one point on the circularly curved negative all other wave-lengths and orders will

[10] DuMond and Kirkpatrick. Review of Scient. Insts. 1, 88 (1930). The principal improvement made in this instrument since the above article was written consists in the addition of fifty individual adjusting levers for the crystals as well as fifty permanently attached mirrors.

also focus at other points on the negative. In Fig. 10 a wave-length λ_1 is shown focussed from all fifty crystals at the point θ_1. The crystal reflecting planes if produced would all intersect at the point β on the major circle. The incoming radiation, if it were not reflected by the crystals to the point θ_1, would converge in a point α_1 also on the major circle. α_1 and θ_1 are distant from β on opposite sides by an arc 2θ where θ is the Bragg angle for the wave-length in question. We utilize the fact that the directions of incoming rays are concurrent at α_1. A second circle is described so as to pass through both the focal spot of the x-ray tube and through α_1. The scattering body is shaped to coincide with this circle as shown in Fig. 10. Thus the scattering angle is

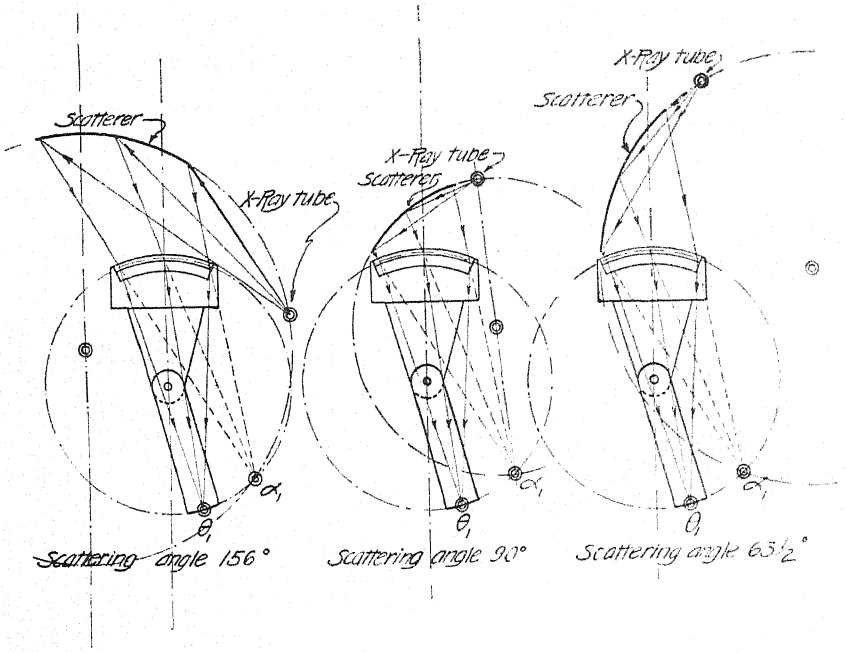

Fig. 11. Geometrical dispositions of x-ray tube, scatterer and spectrograph for the three scattering angles studied.

very nearly homogeneous over all parts of the scatterer. Fig. 11 shows the positions of scatterer, tube and spectrograph for the three angles of scattering which have so far been studied. The principal sources of inhomogeneity of scattering angle are the size of the focal spot of the x-ray tube and the thickness of the scattering body. The use of 50 crystals instead of one permits the tube to be placed much farther away from the scatterer without necessitating unreasonable exposure times and thus permits a great reduction in the inhomogeneity of scattering angle due to the two above mentioned causes.

Precautions as to Planeness of Crystals and Focussing

At first sight the instrument just described seems fantastically difficult to construct and adjust. As a matter of fact however once a set of fifty good

crystals had been obtained and tested for planeness and a satisfactory orientation method was worked out the task of adjusting them to focus accurately took only about two months. We have been pleasantly surprised to find that the crystals have remained in good adjustment for a period up to the present of about three months.

One of the most exacting and difficult requirements was to get good slips of calcite plane over their entire length. *In studying the Compton effect it is absolutely essential that the crystals be plane over the entire length used in reflecting x-rays.* This is because the scattering body constitutes an *extended source* so that the *entire length* of the crystal reflects x-rays to *each point* on the film. Thus a twisted crystal will give blurred diffused spectral lines with an extended source whereas the same crystal would give sharp but inclined or bent lines with a point source. See Fig. 12. Our first care was therefore to insure that all crystals should be "plane." This we tested by means of primary radia-

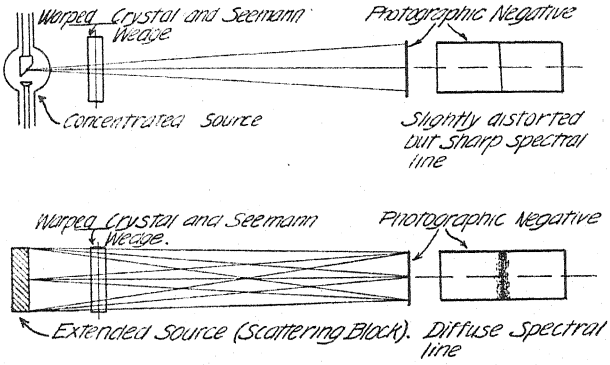

Fig. 12. Illustrating how a warped crystal gives a sharp line with a point source but a blurred line with an extended source.

tion from an x-ray tube placed a short distance from the front of the spectrograph. As the tube was much nearer the crystal than was the negative and had a rather small focal spot only a small portion of the length of the crystal was used in forming the lines on the negative. By moving the x-ray tube up and down parallel to the wedge of the Seemann spectrograph any region in the height of the crystal could be used to reflect spectral lines to the negative. Our practise was to compare in this way the position of lines reflected from four points along the height of the crystal with the lines as reflected from the midpoint of the crystal. Crystals that failed to reflect lines to the same point to within less than half the breadth of a line (or about half an x-unit on our spectrograms) were discarded. The backs of the crystals had to be ground to fit into their holders before such tests had any significance and on account of the numerous discards this constituted one of the most tedious features of the experiment. We take a pardonable pride therefore in calling attention to the great sharpness of the unshifted lines we have obtained. This sharpness bears witness to the planeness and perfection of each and every one of the fifty crystals used as well as to the accuracy with which they are focussed.

The focussing of the crystals was accomplished photographically. After fifty good crystals mounted in the cylindrical Seemann units in the spectrograph had been obtained, one of these near the center was permanently clamped in a predetermined orientation so as to reflect the Mo$K\alpha$ lines in a convenient position on the film. This was called the reference crystal. The other forty-nine units were first roughly orientated by means of a flouroscopic screen so as to reflect their lines at the same point on the film to within a few millimeters. Direct radiation was used, the Mo tube being mounted in a lead box in front of the spectrograph on a large wooden sector turning on a pin directly under the point α_1. Divisions marked on the circular edge of this sector made it possible at a moment's notice to align the tube with any desired crystal. A lead shield was used to isolate all but the crystal under test. The

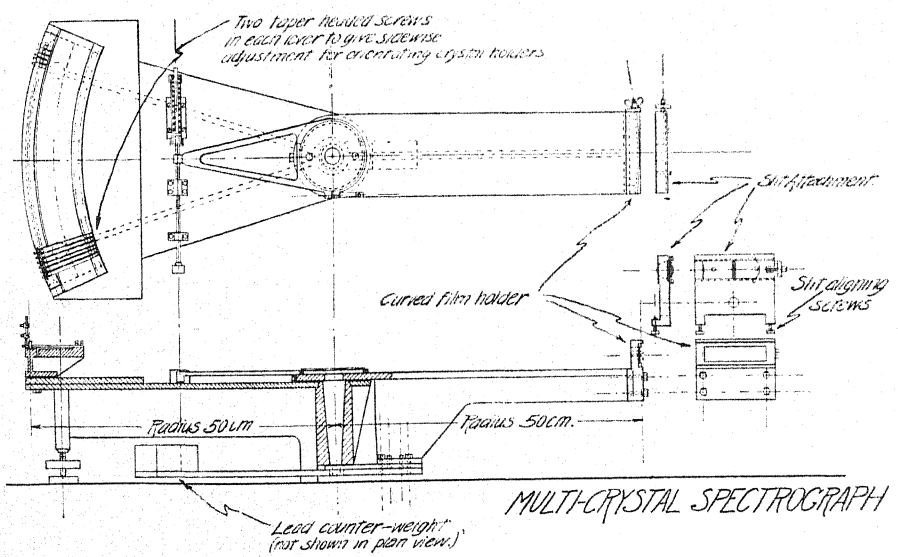

Fig. 13. Plan and elevation of multicrystal spectrograph.

fine adjustment of the crystals by photography consisted in taking a photograph of the $K\alpha$ lines with the reference crystal and then without disturbing the negative taking the $K\alpha$ lines with the crystal to be adjusted. Shields were used in front of the negative so that the reference lines appeared in the middle of the height of the negative while the lines from the crystal under test appeared just above and below. When the focussing of a crystal was acceptable its lines joined those of the reference crystal forming continuous lines across the negative with no perceptible break or jog at the two junction points. Forty-five seconds sufficed to give a good exposure. A complete set of forty-nine such pairs of exposures was made testing the state of adjustment of all crystals against the reference crystal. These exposures appearing on ten pieces of film were all developed, fixed and dried at one time in an especially designed holder, thus economizing enormously on the time over what would be required for separate development. Each crystal was then orientated

through the angle demanded by the error in adjustment indicated in the photographs. This could be done with considerable accuracy, thanks to a small gilded plane mirror permanently mounted on top of each crystal holder. The reflection of a scale 3 meters distant from the mirror was observed with a telescope as a means of measuring the angles through which the crystal must be turned to correct the error indicated on the photographs. After making the indicated orientation adjustments a second set of forty-nine pairs of comparison photographs was taken. A few of the crystals were already found to be in perfectly acceptable focus with respect to the reference lines. These were eliminated from the remainder of the work by dropping small brass covers over their adjusting screws. The cycle was then repeated and each time more and more crystals came into acceptable adjustment until after eleven cycles all had been satisfactorily adjusted.

The fine orientation of the crystals is accomplished by means of a small steel lever, one for each crystal unit, which can be clamped at one end to the projecting shank of the crystal holder. The other end of this lever is given a slight sidewise motion to right or left by two conical headed screws pressing on opposite sides of two conical holes in which they enter loosely. Fig. 13 shows a complete plan and elevation of the entire spectrograph.

Part III. Results

Breadth Not Due to Poor Resolution or Instrumental Defects

The unshifted lines on the Compton effect exposures play the role of a control on the resolution of the spectrograph. Some workers in this field are under the impression that even the unshifted lines in scattered radiation are broader than the primary lines. Such however is not the case as can be plainly seen on our three spectrograms reproduced in Fig. 14. It is quite evident from an inspection of Fig. 14 that the unshifted lines are very much narrower than the broad diffuse distribution of the Compton modified radiation. It therefore cannot be claimed that the observed breadth of the modified line is caused either by poor resolution, poor focussing of crystals, or any other defect in the spectrograph since this latter quite evidently *gives on the same negative very sharp lines.* The $K\alpha$ doublet in the unshifted position is completely resolved.

No intensifying screens have been used in the exposures with the multicrystal spectrograph. This eliminates any possible blurring due to poor contact between the intensifying screen and the negative and any falsification of relative intensity that such screens might cause.

X-Ray Intensities and Exposure Times

An ordinary molybdenum target Coolidge water-cooled x-ray tube placed in a lead housing was used as the source of primary radiation. The radiation passed out of the lead housing through a hole of the right size and shape to give a beam which would just illuminate the whole scatterer with about a centimeter to spare all around. The tube was run at from 20 to 25 m.a. and 50 k.v. continuously 24 hours a day. The exposure times were respectively

360 hours, 223 hours and 897 hours for the scattering angles 63°, 90°, and 156°. The long exposures were necessitated by the great distance from the

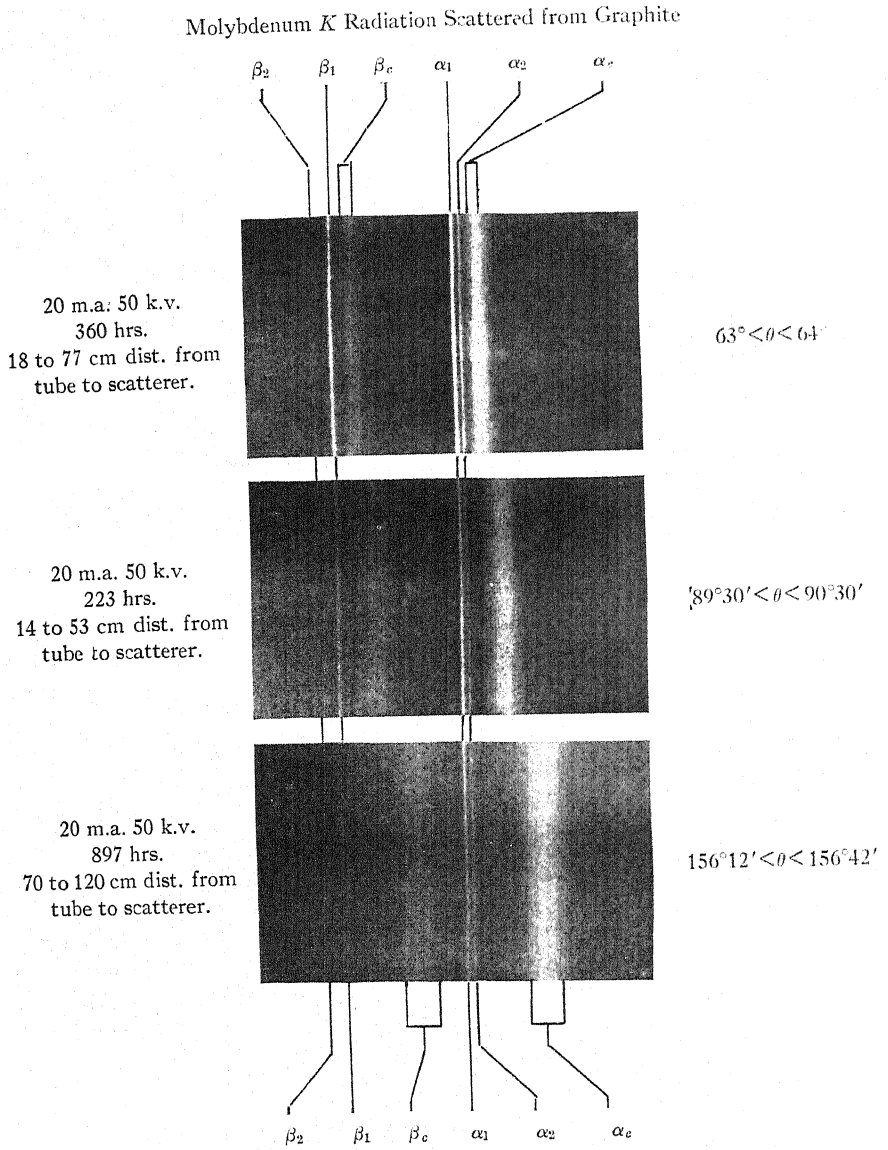

Fig. 14. Spectra of molybdenum K radiation scattered at three very homogeneous scattering angles from graphite, taken with the multicrystal spectrograph. Note sharpness of unshifted lines and increasing breadth of shifted lines as the scattering angle increases.

tube to the scatterer. In the case of the 156° exposure the tube was 120 cm from the far end of the scatterer and 70 cm from the near end. The large distance however gives a huge improvement in homogeneity of scattering angle.

Homogeneity of Scattering Angle

The greatest inhomogeneity of scattering angle in any case is one degree. The inhomogeneities are indicated in Fig. 14. These inhomogeneities could not possibly produce the observed shifted-line breadth but would on the contrary give a breadth of about the same order of magnitude as the width of the narrower unshifted lines.

To insure this homogeneity of the scattering angle the positions of tube and scatterer were accurately located by means of a radius arm capable of describing the circle on which they and the point α_1 must lie. This radius arm carries a plumb-bob at its outer end which can be lowered into close proximity with the curving scatterer and the point α_1. The x-ray focal spot is aligned

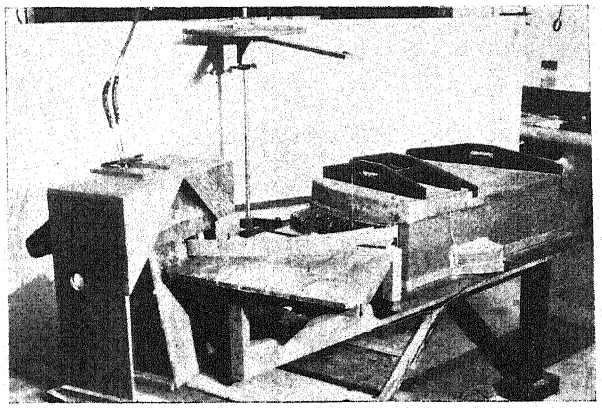

Fig. 15. General view of experimental set-up. Note the radius arm for locating the tube and scatterer, also the baffle plates to reduce background.

with this plumb-bob by sighting from two directions with auxiliary plumb-lines. By measuring the angle through which this radius rod must turn in passing from α_1 to the x-ray focal spot the angle of scattering can be and was measured with more than adequate accuracy. In the general view Fig. 15 of the experimental set-up this radius arm is clearly visible.

Modified Line Breadth Increases With Scattering Angle

Even a cursory glance at the spectra of Fig. 14 shows that the modified line breadth increases with increasing scattering angle. In order to test this quantitatively we have made microphotometric analyses of these spectra. A few of the microphotometer curves are reproduced in Fig. 16, and in Fig. 17 the theoretical curve of relative breadth is plotted for comparison with the points corresponding to observed breadths. The adjustment to the theoretical curve is made for the grand average of the points corresponding to the *largest scattering angle, the other points falling where they will.* The agreement is seen to be as good as the reproducibility of the breadth measurements.

In measuring the breadth of the shifted β_1 line the effect of β_2 is probably

negligible. In the case of the $\alpha_1\alpha_2$ doublet, however, the shifted radiation due to these two components is confounded in one broad band. It is necessary to decompose this into two similar bands 4 X.U. apart and having the relative intensities 2:1 required by the known ratio of intensities of $\alpha_1:\alpha_2$. This decomposition is done by means of the following device: Referring to Fig. 18

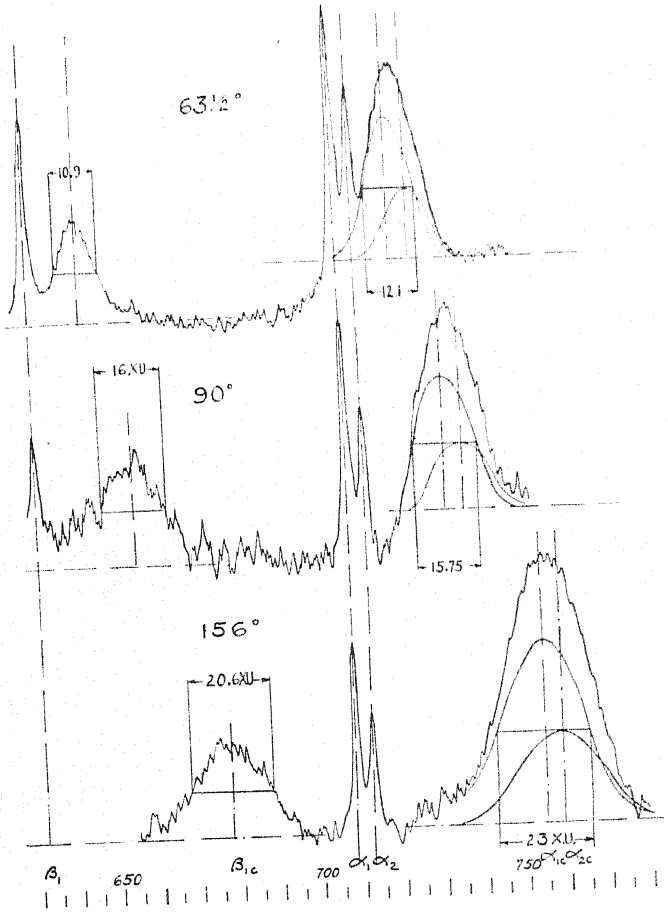

Fig. 16. Microphotometer curves of the spectra shown in Fig. 14. Five such curves (fifteen in all) were obtained for each scattering angle by running the microphotometer slit across the lines in different regions of their height. The three curves here shown are fairly typical of the entire set.

let $F(x)$ be the function representing the observed line structure. Let $f(x)$ be the curve representing the contribution to $F(x)$ made by the α_1 line. Then the contribution made by the α_2 line will evidently be $\frac{1}{2}f(x-\delta)$ where $\delta=4$ X.U., the known wave-length separation of α_1 and α_2. We have then that

$$F(x) = f(x) + \tfrac{1}{2}f(x-\delta)$$

where $F(x)$ is experimentally given and $f(x)$ is to be found. From the experimentally known function $F(x)$ subtract the known function $\frac{1}{2}F(x-\delta)$

$$F(x) - \tfrac{1}{2}F(x-\delta) = f(x) + \tfrac{1}{2}f(x-\delta) - \tfrac{1}{2}f(x-\delta) - \tfrac{1}{4}f(x-2\delta).$$

To this in turn add the known function $\frac{1}{4}F(x-2\delta)$

$$F(x) - \tfrac{1}{2}F(x-\delta) + \tfrac{1}{4}F(x-2\delta) = f(x) - \tfrac{1}{4}f(x-2\delta) + \tfrac{1}{4}f(x-2\delta) + \tfrac{1}{8}f(x-3\delta).$$

Evidently if this process be continued indefinitely we shall have

$$F(x) - \tfrac{1}{2}F(x-\delta) + \tfrac{1}{4}F(x-2\delta) \text{ etc.} = f(x)$$

because the last term neglected will vanish both due to its rapidly decreasing coefficient and due to the diminution in $f(x-n\delta)$ as n becomes large.

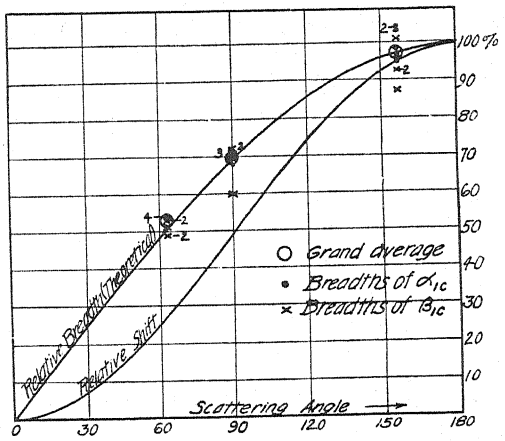

Fig. 17. Measured relative breadths of shifted lines compared with theoretical prediction based on initial electron velocity as the cause of breadth. The full line is the theoretical curve.

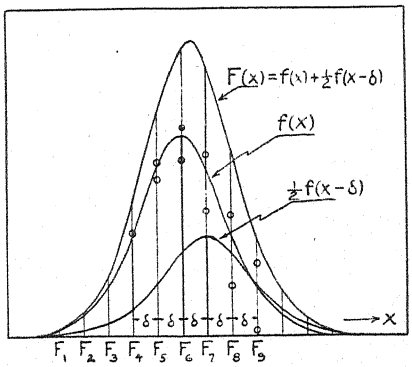

Fig. 18. Illustrating the method of decomposing line structure curves from the $K\alpha$ doublet.

In practise the decomposition can be very rapidly effected graphically by the following procedure. Construct the curve $F(x)$ representing the observed shape of the Compton line to scale and erect equally spaced vertical ordinates

with the spacing δ. The value of the ordinate F_4 say is corrected by subtracting from it half the value of F_3, its first neighbor to the left, then adding a quarter of F_2, subtracting an eighth of F_1, etc., etc., until the amounts to be added to or subtracted from F_4 become negligible. All the ordinates are treated in this same way. By actual trial on curves of the type of the Compton line structure this method has been found to work very well. It is of course an easy matter to check the work by adding the two components obtained in the decomposition process and comparing the sum with the original curve.

In Table I the observed breadths of α_{12c} and β_{1c} at half maximum height are recorded for the three scattering angles studied. Measurements on five microphotometer curves taken across the spectral lines in different regions of their height are recorded for each scattering angle. The tabulated breadths of α_{1c} were obtained graphically by the decomposition method described above.

TABLE I. *Breadths in x-units* $\Delta\lambda_{\frac{1}{2}}$.

$63\frac{1}{2}°$			90°			156°			Microphotometer Run
α_{12c}	α_{1c}	β_{1c}	α_{12c}	α_{1c}	β_{1c}	α_{12c}	α_{1c}	β_{1c}	
13.0	12.1	12.0	16.2	15.6	13.3	22.4	22.8	22.4	1
12.4	11.5	10.9	16.4	15.75	16.0	21.8	21.2	19.4	2
13.0	12.1	11.5	15.75	15.15	15.75	23.0	23.0	20.6	3
13.0	12.1	12.1	16.4	15.75	16.0	23.0	23.0	20.6	4
13.0	12.1	10.9	16.4	15.75	15.2	22.2	21.9	21.5	5
12.9	12.0	11.5	16.2	15.6	15.2	22.5	22.4	20.9	Average
	11.8			15.4			21.6		Grand average of α_{1c} and β_{1c}
	51%			69%			97%		Theoretical relative Breadths

MODIFIED LINE BREADTH INCREASES WITH PRIMARY WAVE-LENGTH

Attention is called to the fact that in Table I the average breadths of α_{1c} are systematically higher than the average breadths of β_{1c}. We do not feel that the precision of our breadth measurements justifies more than a claim to a qualitative agreement with theory in this respect. It is interesting to note however that in each case the longer primary wave-length gives the broader shifted line and that the breadths are in about the same proportion as the wave-length in agreement with the formulae

$$\Delta\lambda = 4\beta\lambda^*$$

$$\lambda^* = (\lambda_1^2 + \lambda_c^2 - 2\lambda_1\lambda_c \cos\theta)^{1/2}$$

$$\lambda_c = \lambda_1 + \frac{h}{mc}(1 - \cos\theta)$$

CAUSE AND ELIMINATION OF HEAVY BACKGROUND

It has been noted by many observers that the background intensity relative to the line intensity in the spectra of scattered radiation is much stronger

than in the case of the primary radiation. Many explanations have been offered for this, all of which probably contributed to the effect in some small measure. We believe that we now have unquestionable evidence however that the great bulk of this enhanced background effect is due to non-selective scattering at the crystals and crystal wedges. General, amorphous, or non-selective x-ray scattering by the crystal in a spectrograph is due to scattering of the modified Compton type. Such scattering is incoherent and hence non-selective as to wave-lengths. It is also non-specular, i.e. the conditions of equality of incidence and reflection angles is not imposed. This means that a given point on the negative can receive radiation of all wave-lengths by this scattering process from all parts of the scattering body. This same point on the negative can by spectrally selective Bragg reflection only receive one wave-length scattered from one very small portion of the scattering body. Hence, though the modified scattering may be small, it is greatly favored by the fact that it is integrated over a wide range of continuous spectrum and over a broad solid angle as large as the scatterer can subtend. With these considerations in mind we have tried the effect of introducing a set of baffle plates in front of the spectrograph in such a way as to greatly limit the solid angle of radiation which can be collected at the crystal and wedge. With these baffles in place each crystal can only "see" a very small segment of the scatterer about three centimeters long at most whereas without the baffles each crystal was exposed to scattered radiation from a large part of the entire 55 cm length of the scatterer. The baffles leave plenty of room for the formation of the entire shifted and unshifted K spectrum however which only covers a range of about three degrees. These baffles can plainly be seen in the general view Fig. 15. See also Fig. 10.

The result of introducing the baffles was most striking. Whereas without the baffles the back-ground fogging of our negatives was so strong as to nearly obscure the unshifted and shifted lines, rendering the negatives quite hopeless for reproduction *this background was entirely suppressed as soon as the baffles were introduced.* We feel certain therefore that the non-specular, non-selective scattering at the crystal faces and wedges is responsible for the heavy background.

Measurements of Shift

As a check on the Compton formula for the shift, $\delta\lambda = (h/mc)\ (1-\cos\theta)$ we have plotted in Fig. 16 the positions predicted for the shifted lines by the above formula assuming $h/mc = 24.2$ X.U. as computed from present accepted values of these constants. The agreement is good and seems to eliminate the possibility of a 9 percent deviation from this value reported recently by other observers.[11]

Critical Discussion of Results

The line breadths which we have observed and reported in this paper are not in accord with the observations of two other observers, namely J. A.

[11] Davis and Mitchell, Phys. Rev. **32**, 331 (1928).

Bearden[12] and N. S. Gingrich[13] both of whom have studied the breadth of the modified line at large scattering angles (to reduce the broadening from angular inhomogeneity) using the double crystal spectrometer. These experimenters obtain lines broader than the unshifted lines but still sufficiently narrow to show partial resolution in the case of the shifted $K\alpha$ doublet. P. A. Ross, using his ingenious balanced filter method, also seems to observe a partial resolution of this doublet. This method however does not give very distinct evidence as to the breadth of the shifted line. Ross' and Bearden's primary wave-lengths were somewhat shorter than those used in the present investigation and Ross' angles of scattering are smaller. Both these conditions would, if the theory presented in this paper is correct, tend to give these observers a somewhat narrower shifted line[14] than that here reported. N. S. Gingrich however reports narrower lines than ours under conditions nearly identical to ours. Indeed his scattering angle is larger and is inhomogenity of scattering angle about twenty times as great as ours. His modified Mo$K\alpha$ radiation observed with the double crystal spectrometer appears as two sharply pointed peaks partially resolved at the base. We are completely at a loss to explain the discrepancy between our results and his. Examination of our photographic spectrograms (here reproduced Fig. 14) shows not the slightest suggestion of resolution of the shifted $K\alpha$ doublet although the resolution of our spectrometer as proved by our well resolved unshifted lines is amply sufficient for this purpose. The principal difference between Gingrich's conditions and ours was the use of the double crystal (high resolution) spectrometer in place of our multicrystal spectrometer, the use of much greater x-ray intensities incident on his scatterer than ours and the presence of much greater inhomogeneity of scattering angle in his case than in ours.

On the other hand however recent photographic results published by F. L. Nutting[15] show a *broad* modified β_1 line in good agreement with our modified line breadths and much too broad to permit of resolution of two lines as close as Mo$K\alpha_{1,2}$. Our present modified line breadths are also in good qualitative agreement with those obtained previously by DuMond[16] for aluminum and beryllium scatterers with a photographic method at large scattering angles. (As the scatterers are different no more than qualitative agreement is to be looked for here). Finally our line breadths agree with those obtained photographically by Sharp[17] under large and homogeneous scattering angles and with primary radiation and scattering substance substantially the same as ours.

We cannot understand why the photographic methods *used with adequate resolution* should yield broader modified lines than the double crystal spectrometer. Perhaps some hitherto unsuspected parameter affects modified line

[12] J. A. Bearden, Phys. Rev. **35**, 1427 (1930).
[13] N. S. Gingrich, Phys. Rev. **36**, 1050 (1930).
[14] J. W. DuMond, Phys. Rev. **36**, 146 (1930).
[15] F. L. Nutting, Phys. Rev. **36**, 1267 (1930).
[16] DuMond, Phys. Rev. **33**, 643 (1929); DuMond, Proc. Natl. Acad. **14**, 875 (1928).
[17] Sharp, Phys. Rev. **26**, 691 (1925).

breadth. Such parameters might be the x-ray intensity incident on the scatterer or the electrical potential of the scatterer. These seem highly unlikely.

We are now carefully investigating the possibility that multiple scattering may exaggerate our line breadths. Our method of doing this is to make an exposure at 156° with a scatterer cut up into small pieces with intervening properly orientated lead baffles which will almost entirely eliminate the possibility of multiple scattering. There are two reasons why we can almost certainly predict a negative result from this control experiment.

First, the scattered radiation from the entire scatterer at a point outside the direct beam but not far distant from the scatterer itself can be faintly seen on a fluorescent screen. At this point it is certainly less than one percent of the intensity of direct radiation incident on the scatterer. It seems then unlikely that the ratio of intensity of scattered radiation from the scatterer incident a second time on the scatterer to primary intensity should be more than one percent and this is too small to account for the discrepancy between our modified line breadth and that of Gingrich.

Second, our present modified line breadths are in agreement with those above mentioned of Sharp, Nutting and DuMond, each of which was obtained under conditions which should give if anything less double and multiple scattering than Gingrich had.

Absolute breadths of shifted lines. Our purpose in this article has been especially to test the *functional dependence* of the natural breadth of the shifted lines on scattering angle and primary wave-length and to compare this with the functional dependence to be expected if the initial velocities of the scattering electrons cause the breadth. We hope to present in the near future a careful study of the electron velocity distributions to be expected from the shapes of our line structure curves. We will state at the present time merely that the breadths of our lines do not seem inconsistent with the velocities to be expected in the carbon atom. A very considerable task of theoretical computation and reduction of our experimentally observed curves remains to be performed before we can definitely draw a favorable or unfavorable comparison between observation and theory on this point. Our observed breadths at half maximum recorded in this paper correspond to a class of electrons the ratio of whose velocities to the velocity of light is $\beta = 0.0076$. This is equivalent to about 15 volts.

In conclusion we wish to express our appreciation of Dr. Millikan's support of this research and of the patience and skill of Julius Pearson, our instrument maker, who developed the technique and did the tedious work of grinding and fitting the small calcite units into their holders.

NOTE ADDED TO PROOF: We have just developed a 900-hour exposure at 156° scattering angle with a graphite scatterer divided into fifty parts by lead baffles so orientated as to permit the entrance of the incident radiation and the exit of the scattered radiation, but arranged to prevent any multiple scattering by exchange of radiation from one unit to another. The units have smaller dimensions than the scatterer used by N. S. Gingrich. We believe therefore that our multiple scattering should be less than his. *The Compton line however on this exposure appears with the same breadth as the one reproduced in this paper.*

REVISED VALUES OF O I TERMS, NEBULAR AND CORONAL LINES OF OXYGEN

By J. J. Hopfield
Department of Physics, University of California
(Received November 14, 1930)

Abstract

The chief triplet of oxygen λ1302 has been measured in the third order of a vacuum grating spectrum having a dispersion of 1.7A per mm.

On the basis of these measurements, the ground triplet term of oxygen $2s^22p^4\,^3P_2$, $^3P_1$, $^3P_0$ has the revised values 109837.1, 109679.17, 109610 .52 giving the *ionization potential of oxygen* as 13.550 volts.

Nebulium lines have been produced in the laboratory for the first time. The two lines λ6300 and λ6364 have been remeasured, and their values, together with the new values of the $^3P_{012}$ term, are used to give more accurate values of the metastable levels of oxygen.

The coronal line λ6374.2 is pointed out as being identical within limits of experimental error with the oxygen line λ6374.29. This would indicate the presence of oxygen in the solar corona.

Introduction

RUNGE and Paschen[1] made the first classification of the spectrum of oxygen. On the basis of their analysis we have known of two types of multiplicity in the terms of this spectrum, namely, those now known as quintet multiplicity and triplet multiplicity. The next extension of our knowledge of this spectrum was the discovery of the ultraviolet triplet series by the author.[2] These series arise from the combinations of a new triplet ground term $2s^22p^4$, $^3P_{012}$ with some of the triplet and quintet terms already known.

At about this time the development of Hund's theory of complex spectra made it manifest that the electron configuration ($2s^22p^4$) of the normal oxygen atom gives rise not only to the $2s^22p^4\,^3P_{012}$ term already found, but also to the $2s^22p^4\,^1D_2$, $2s^22p^4\,^1S_0$ terms as well. These latter terms became as important as the $^3P_{012}$ ground term, since they arise from the same electronic configuration.

The first important discovery in the search for these terms was that due to McLennan[3] and his co-workers, who first reproduced the green auroral line λ5577 in the laboratory and showed that it was due to oxygen. This was confirmed in a quite different manner by the author[4] who found that its wave number was exactly the frequency difference of two strong oxygen lines λ1217 and λ999 which were unclassified at that time.

[1] Runge and Paschen, Ann. d. Physik **61**, 641 (1897); Astrophys. J. **8**, 70 (1898).

[2] J. J. Hopfield, Astrophys. J. **59**, 114 (1924).

[3] J. C. McLennan, J. H. McLeod, and McQuarrie, Proc. Roy. Soc. **A114**, 1 (1927); McLennan, McLeod and R. Ruedy Phil. Mag. **6**, 558 (1928). L. A. Sommer Zeits. f. Physik **51**, 451 (1928).

[4] J. J. Hopfield, Phys. Rev. **29**, 923 (1927).

Bowen's[5] discovery that the prominent nebular lines represent transitions between metastable terms of atoms or their ions suggested at once that the auroral line λ5577 might arise in such a transition in neutral oxygen. This was actually found to be the case by McLennan, Sommer[3] and others by the magnetic splitting of the line showing it to belong to the singlet system, and presumably to the transition $2s^2 2p^4\ {}^1D_2 - 2s^2 2p^4\ {}^1S_0$. The discovery that the two ultraviolet lines λ1217 and λ999[4] involve a new and common term added another to the list of singlet terms. Too few of these terms were as yet known to form a Rydberg series, and no combinations of them with the known oxygen terms had been found.

Frerichs[6] made a most important contribution to our knowledge of these terms when he found a sufficient number of them to form such a series and thus evaluated the limit of the series the $2s^2 2p^4\ {}^1D_2$ metastable term. This fixed the position of the singlet terms with reference to the known scheme of oxygen terms.

His evaluation of the $2s^2 2p^4\ {}^1D_2$ term, however, contains two sources of error, first the rather large error in the measurement of ultraviolet lines, and second, the error of fitting these lines into a none too accurate formula when relatively few lines of the series are known. The experimental errors cannot be obviated but they can be reduced by using more precise instruments. The second error, although it may be large, is an additive one and is of no consequence when one is dealing with lines of the same system. It becomes a serious difficulty when one is dealing with lines forming intersystem combinations when these systems of terms have been independently determined. If, however, such combinations are once identified and measured, this source of error immediately drops out and there is left only the experimental values to be improved. Happily, Paschen[7] has now found such combinations in new lines on plates which I took of the oxygen spectrum while working in his laboratory and Sommer[8] has also found them in the spectrum of the aurora. I have now remeasured these lines, fixing the terms more accurately, and I have also redetermined the value of the $2s^2 2p^4\ {}^3P_{012}$ ground term from new data. These improved values conjointly give a correction of 7.5 cm^{-1} to be added to all the singlet terms. It should be borne in mind that all the singlet terms are not fixed with the same accuracy by this correction. Fortunately, the $2s^2 2p^4\ {}^1D_2$ term is accurately fixed by these corrections, and also the $2s^2 2p^4\ {}^1S_0$ term which is linked to the former by the aurora line. Although the same correction has been added to the remaining singlet terms, they still contain the relatively large error of the original ultraviolet measurements. The remaining terms of the table given by Frerichs are already linked to the Paschen-Runge terms of oxygen and need no correction.

[5] I. S. Bowen, Ast. Soc. of the Pacific Pub. **39**, 295 (1927).
[6] R. Frerichs, Phys. Rev. **36**, 398 (1930); Phys. Rev. **34**, 1239 (1929).
[7] F. Paschen, Die Naturwissenschaften, **34**, 752 (1930).
[8] L. A. Sommer, Die Naturwissenschaften **34**, 752 (1930).

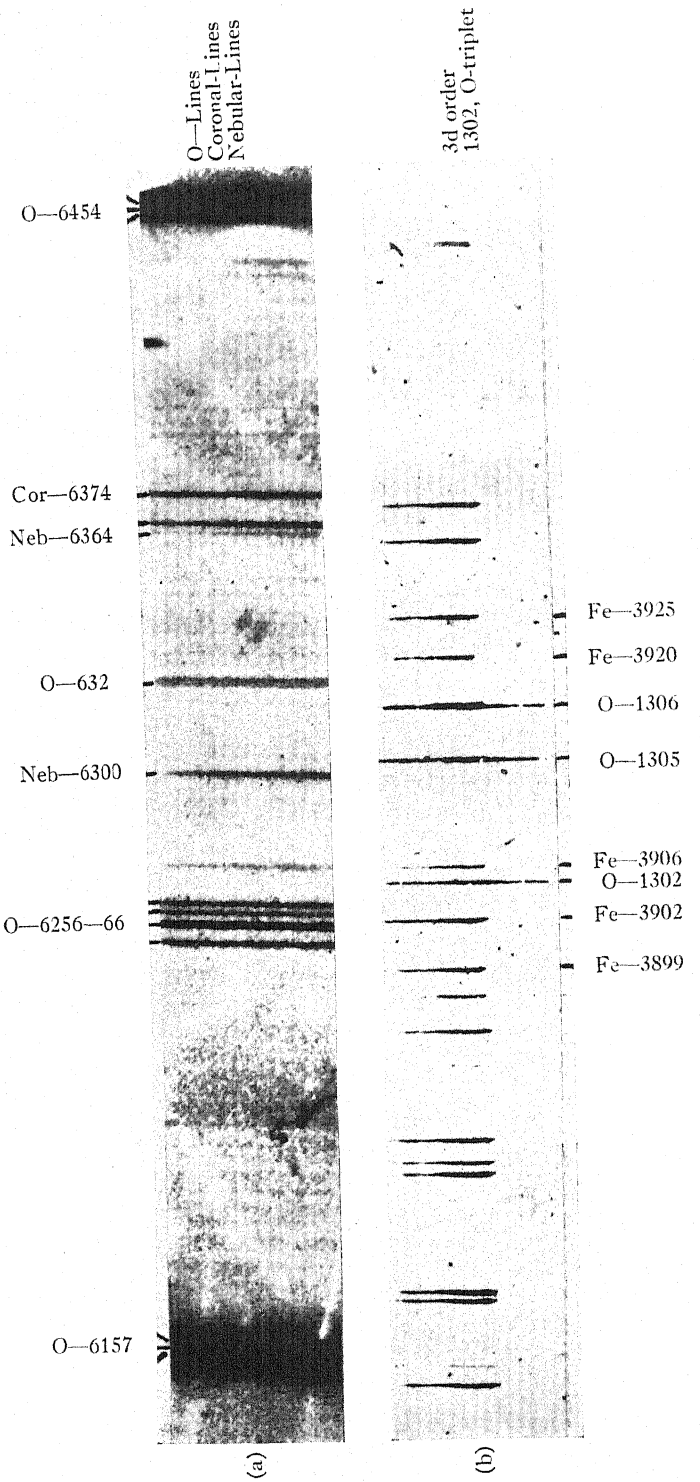

Fig. 1. Oxygen line spectra. (a) Nebular lines and coronal line. (b) Ultraviolet triplet in the third order of spectrum.

Experimental

(a) **Measurements of the λ1302 triplet of oxygen.** The λ1302 triplet of oxygen was photographed in the third order of a 3-meter vacuum grating spectrograph with iron lines of the first order as standards. The spectrograph was designed by the author and built in this laboratory. The dispersion in the third order is 1.7A per mm. Fig. 1b shows these spectra. It is noticed from the figure that the oxygen lines are longer than the iron lines used for comparison. This, of course was due to an adjustable shutter before the plate that limited the comparison spectrum. It was rather fortunate for this purpose that such a shutter had been provided, because two of the lines λλ1305–6 are blended with weak iron lines. λ1302 is quite free from iron lines. The unblended line λ1302 was measured with the iron lines as standards, and a considerable number of iron lines were measured in each direction in order to calibrate the plate. The measurements were obtained from two plates, the one mentioned above and another in which the shutter was not used with the comparison spectrum. The other two lines, λλ1305–6, were measured at the portions showing below the iron spectrum. In this case the plate had not been disturbed from its previous setting in the comparator. λ1302 was used as the reference line and the correction curve already determined for this plate from the iron spectrum was applied.

Since the light from the iron arc was shined through the discharge tube that generated the oxygen spectrum, it is quite certain that the same portion of the grating was illuminated in both cases. Whether the reflecting power of the grating for the regions λ1300 and λ3900 which are here superimposed remained relatively constant for both spectra was of course not determined and would remain as a source of error if the spectra were not exactly focussed. The focus was very sharp, however. The wave-length of these lines, as well as those of the comparison spectrum are given in Table I.

Table I. *Ground triplet term of O I*

λ (vac)	ν (cm^{-1})	Classification	Δν
1302.185	76794.00	$2s^22p^4\ {}^3P_2 - 2s^22p^3s\ {}^3S_1$	
			158.13
1304.872	76635.87	$2s^22p^4\ {}^3P_1 - 2s^22p^3s\ {}^3S_1$	
			68.65
1306.042	76567.22	$2s^22p^4\ {}^3P_0 - 2s^22p^3s\ {}^3S_1$	

Improved values of $^3P_{012}$ ground term.		*Lines used as standards.*	
		λ (I.A.)	λ (I.A.)
$2s^22p^4\ {}^3P_2$	109837.3		
$^3P_1$	109679.17		
$^3P_0$	109610.52	3897.898	3906.484
Ionization potential of O I, 13.550 volts.		3899.713	3920.266
		3902.950	3924.916

(b) **Nebular lines λλ6300, 6364, coronal line λ6374.** Since the two oxygen lines λ6300 and λ6364 are the only "nebulium" lines yet produced in the laboratory, it seems worth while to relate under what laboratory conditions they appeared. The discharge tube was made of quartz. It was Π-shaped, had an

internal diameter of about 8 mm and a total length of about 80 cm. It contained large nickel electrodes in the two legs. The horizontal part of the tube faced the slit of the spectrograph end-on. The whole tube was immersed in a bath of running water for cooling. Pure oxygen was obtained electrolytically. It was dried by passing it over phosphorus pentoxide. The gas was allowed to flow through the discharge tube continuously, being admitted by a torsion capillary valve of glass and pumped out by oil and mercury vapor pumps. The pressure in the discharge tube was not measured but it was estimated to be between 1 and 2 cm. A 5000 volt 5 kilowatt transformer was used without auxiliary inductance or capacity, and the current employed was between 1 and 1.2 amperes being regulated by a flowing water rheostat in series with the discharge tube. After the discharge tube was well cleaned by long running, the spectrum, a part of which is shown in Figure 1a, was photographed. The spectrograph used for making the picture was a Zeiss 3-prism instrument giving a dispersion of 29A per mm at λ6300. Neighboring oxygen lines were used as standards, and the Hartmann interpolation formula with a correction curve was used in measuring the plate. Visual observation of the appearance of the discharge might be of interest. When the tube was viewed end-on through the plane quartz window the discharge formed a red core down the axis of the tube, and this core became gradually more diffuse off the axis. When viewed with the spectroscope the green aurora line was very prominent, being about as strong as the neighboring green triplets. Besides the oxygen lines the only visible lines were Hα. Long exposure photographs also showed traces of the Angstrom CO bands.

The plate used was a panchromatic plate sensitized for infrared as well. The duration of exposure was twelve hours, although two hours' exposure was sufficient to give the "nebulium" oxygen lines.

Table II gives the wave-lengths of the nebular lines and the previously unidentified coronal line λ6374.

TABLE II. *Nebular lines and coronal line of oxygen.*

	λ	I	ν	Classification	$\Delta\nu$
Nebular	6300.23	4	15868.05	$(^4S)2s^22p^4\,{}^3P_2-(^2D)2s^22p^4\,{}^1D_2$	158.70
Nebular	6363.88	1	15709.35	$(^4S)2s^22p^4\,{}^3P_1-(^2D)2s^22p^4\,{}^1D_2$	
Coronal	*6374.292	6	15683.64	Unknown	

Metastable ground terms.

Term	Term values (revised)	Distance from ground level $^3P_2$
$(^2D)2s^22p^4\,{}^1D_2$	93969.5 cm^{-1}	1.957 volts
$(^2P)2s^22p^4\,{}^1S_0$	76044.5	4.168 volts

Oxygen lines used as standards.

λ (I.A.)	
6256.616	6323.283
6264.346	6324.682
6266.692	6366.282

* This value is that obtained from Frerichs' table (loc. cit). The value which I obtain is λ6374.24, and is less accurate than his.

Table III is a list of revised values of the terms of oxygen. The table is copied from Frerichs' work. The corrected terms are indicated by asterisks.

TABLE III. *O I Terms (corrected).*

	$2p$	$^{*3}P_2$: 109837.3 $^{*3}P_1$: 109679.17 $^{*3}P_0$ 109610.52	$^{*1}D_2$: 93969.5	$^{*1}S_0$: 76044.5	
		$2s^22p^3$: ^4S	$2s^22p^3$: ^2D	$2s^22p^3$: ^2P	$2s2p^4$
	$3s$	$^5S_2$: 36069.0 $^3S_1$: 33043.3	$^3D_3$: 8702.9 $^3D_2$: 8690.9 $^3D_1$: 8683.0 $^{*1}D_2$: 7168.5	$^3P_2$: −4072.1 $^3P_1$: −4082.5 $^3P_0$: −4088.8 $^{*1}P_1$: −6083.5	
	$3p$	$^5P_1$: 23211.9 $^5P_2$: 23209.2 $^5P_3$: 23205.8 $^3P_0$: 21207.7 $^3P_1$: 21207.7 $^3P_2$: 21207.2	$^3F_4$: −3876.1 $^3F_3$: −3883.0 $^3F_2$: −3888.7 $^3D_{123}$ $^3P_2$: −3456.4 $^3P_1$: −3459.8 $^1F_3$ $^1D_2$ $^1D_1$	$^3D_3$: −17443.8 $^3D_2$: −17449.5 $^3D_1$: −17452.9 $^3P_{012}$ $^3S_1$ $^1D_2$ $^1P_1$ $^1S_0$	
$2s^22p^3$	$3d$	$^5D_{01234}$: 12417.3 $^3D_{123}$: 12350.0	$^3G_{345}$ $^3F_{234}$ $^3D_{123}$ $^3P_{012}$ $^3S_1$ $^1G_4$ $^{*1}F_3$: −14487.5 $^1D_2$ $^1P_1$ $^1S_0$	$^3F_{234}$ $^3D_{123}$ $^3P_{012}$ $^1F_3$ $^1D_2$ $^1D_1$	
	$4s$	$^5S_2$: 14358.5 $^3D_1$: 13612.5	$^3D_{123}$ $^{*1}D_2$: −12964.5	$^3P_{012}$ $^1P_1$	
	$4p$	$^5P_1$: 10742.5 $^5P_2$: 10743.7 §$^5P_3$: 10744.3 $^3P_{012}$ 10157.5	$^3F_{234}$ $^3D_3$: −15936.6 $^3D_2$: −15944.0 $^3D_1$: −15949.0 $^3P_{012}$ $^1F_3$ $^1D_2$ $^1P_1$	$^3D_{123}$ $^3P_{012}$ $^3S_1$ $^1D_2$ $^1P_1$ $^1S_0$	
	$5s$	$^5S_2$: 7720.8 $^3S_1$: 7425.6	$^3D_{123}$ $^{*1}D_2$: −19295.5	$^3P_{012}$ $^1P_1$	
	$6s$	$^5S_2$: 4817.9 $^3S_1$: 4672.8	$^3D_{123}$ $^{*1}D_2$: −22088.5	$^3P_{012}$ $^1P_1$	
	$7s$	$^5S_2$: 3291.9 $^3S_1$: 3210.2	$^3D_{123}$ $^{*1}D_2$: −23574.5	$^3P_{012}$ $^1P_1$	
$2sp^4$	$2p$				$^3P_2$: −13458.0 $^3P_1$: −13516.9 $^3P_0$: −13548.9

* Altered values of terms: § numerical error corrected.

Tables I and II give excellent agreement of the spacing $2s^22p^4\ ^3P_2$—$2s^22p^4\ ^3P_1$ ground terms. This confirms also the identification of the lines λ6300 and λ6364 with even greater precision than that given by Paschen. The accuracy of the measurement of these two nebular lines as produced in

oxygen together with the more accurate evaluation of the $2s^2 2p^4\ {}^3P_{012}$ ground term justifies the revision of the term values given in Table III.

It is rather remarkable that these nebular lines can be produced in the laboratory when the conditions for their production are extremely low pressures according to Bowen. The pressures in the nebulae are undoubtedly very small, but the pressure in the discharge tube was, as already mentioned, relatively high.

The wave-length of the red coronal line λ6374.2, as given by Campbell and Moore,[9] seems to be identical with the unclassified oxygen line λ6374.29 which is shown as a strong line on the plate, Figure 1a. This line is not entirely new, as Kayser records it in his "Tabelle der Hauptlinien—" as λ6373 and due to oxygen. Frerichs has it in his list of unclassified lines as λ6374.292 This coincidence in the wave-lengths of the oxygen and the coronal line and also the fact that the line occurs in an isolated position in the oxygen spectrum when only lines of O I were present would seem to indicate their identity, and is strong evidence of the presence of oxygen in the sun's corona. Really to prove the identity of these two lines a more accurate determination of the line in the corona is necessary.

Since this line is one of the brightest in the coronal spectrum, being second only to λ5303 of the corona, the terms in oxygen which give rise to it become of great interest. The most promising lead in their identification would be a study of the Zeeman pattern of this line. This, so far as I know, has not yet been made.

This investigation has been greatly assisted by the grant of a fellowship by the John Simon Guggenheim Memorial Foundation that allowed the author the privilege of a year's study in Germany. I am also greatly indebted to Professor F. Paschen, President of the Physikalisch-technische Reichsanstalt, for putting every facility of his excellent spectroscopic laboratory at my disposal.

[9] Campbell and Moore, Publications of the Lick Observatory Bulletin **318**, 8 (1918).

EVIDENCE FOR A Be ISOTOPE OF MASS 8 AND FINE STRUCTURE MEASUREMENTS IN THE BeH BANDS

By William W. Watson and Allan E. Parker
Sloane Physics Laboratory, Yale University

(Received December 2, 1930)

Abstract

An intense spectrogram of the λ4991 BeH band has been obtained in the third order of a 21-foot concave grating with a dispersion of 1.286A per mm. Every P and R line of the (0, 0) band in the strong interval $K''=6$ to 20 is accompanied by a very weak line in the position calculated for Be^8H, except where a strong line of another branch prevents measurement. The relative intensities of the Be^8H and Be^9H lines are about 1:2000. Discussion shows this to be a reliable indication of the presence of a small amount of a beryllium isotope of mass 8.

This BeH band system is composed solely of the $\Delta v=0$ sequence, with the band origins forming a head at the (4, 4) band, thus accounting for band origins on both sides of the (0, 0) origin in this same sequence. The doubling of the branches at the origin is observed, the relative intensities of the components being in complete agreement with those predicted for case b doublet states. The system represents a $^2\Pi\rightarrow{}^2\Sigma$ transition with $A=1.97$ cm^{-1} for the $^2\Pi$ state. Peculiar Λ-type doubling relations and the reverse bending of the branches for high K values are discussed.

Introduction

ALTHOUGH any table showing the α-particle plus proton and electron content of known nuclei[1] leads to the prediction that the nucleus of mass 8 should be found as an isotope of beryllium, the mass spectrograph has failed to reveal it. This has led Atkinson and Houtermans[2] in their theoretical consideration of the possibility of the building-up of the elements in the stars by the penetration of protons into the nuclei to postulate that the Be^8 nucleus is unstable, disintegrating into two α-particles. But it is not certain that nuclei which are integral multiples of α-particle units are necessarily composed solely of α-particles.[3] However, Lord Rayleigh has pointed out[4] specimens of the mineral beryl have been found to contain an unexplained amount of helium. If this helium originated from Be^8, it would indicate that this Be isotope "has existed within geological times, and subsequent to the formation of the mineral." And since nothing is really known about its instability, some Be^8 may very well still exist in Be minerals, as existing temperature conditions would not cause its disintegration. If so, the band spectrum method of isotope study should detect its presence.

Band systems due to the diatomic molecules BeO, BeF, and BeH have

[1] Cf. for example W. D. Harkins, Chem. Reviews **5**, 371 (1928); G. Beck, Zeits. f. Physik **47**, 407 (1928); H. A. Barton, Phys. Rev. **35**, 408 (1930).

[2] R. d'E. Atkinson and F. G. Houtermans, Zeits. f. Physik **54**, 664 (1929).

[3] S. Meyer, Sitz. Akad. Wiss. Wien, **II A**, 138, 431 (1929).

[4] Lord Rayleigh, Nature **123**, 607 (1929).

been obtained in emission from an arc. The arc is not a good source for the detection of faint isotope lines,[5] but the satisfactory production of these spectra in absorption would seem difficult because of the high temperatures necessarily involved. Of the emission spectra that of BeH at λ4991 is the best for this investigation because it can be obtained with very great intensity at high dispersion, and because the bands have the open structure characteristic of hydrides. This band system has been previously examined by one of us,[6] and a preliminary investigation[7] of one of these spectrograms for possible Be^8H lines revealed a number of very weak lines in the calculated positions. It seemed likely that more intense spectrograms at still higher dispersion would give additional and more definite information on the question of the isotopic origin of these faint lines.

Experimental Procedure

The source of radiation was a 110-volt dc arc between beryllium electrodes in a hydrogen atmosphere at about 6 cm pressure. The arc current was held at about 5 amperes. With this reduced hydrogen pressure the Be arc runs much

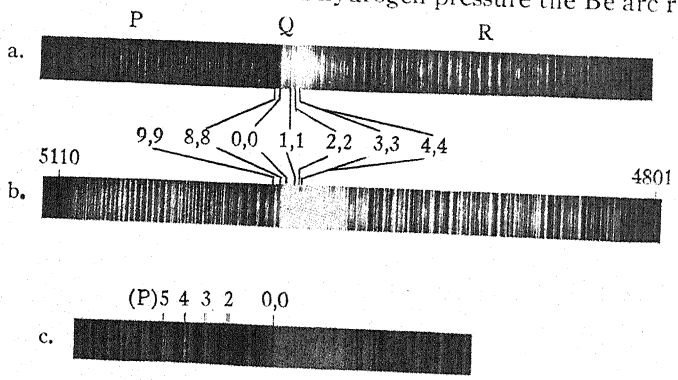

Fig. 1. Reproductions of the λ4991 BeH bands. *a*. Short exposure. Shows the relative arrangement of the *P*, *Q*, and *R* branches and the formation of a vibrational head. *b*. The 10-hour exposure measured for isotope effect. Note the head formed by the *R* branch which near the origin has increasing line spacings towards the violet. *c*. Enlargement of the region of the origins. The doubling of the first *P* branch lines is evident.

steadier and the BeH bands are emitted much stronger than when atmospheric pressure of hydrogen is used. Because of the heat developed, it was found necessary to interrupt the exposure at frequent intervals.

The spectrum was photographed on Eastman panchromatic plates in the third order of a 21-foot concave grating in a stigmatic mounting, the dispersion being 1.286A/mm. For the most intense spectrograms the total elapsed time was 10 hours, but of this we estimate slightly more than 4 hours to be actual exposure time. In Fig. 1b, which is a reproduction of this spectrogram, the great intensity of the principal branches is evident.

[5] A. S. King and R. T. Birge, Astrophys. J. **72**, 19 (1930) discuss this point in detail in connection with their discovery of C^{13} in the spectra of C_2, CO, and CN.
[6] W. W. Watson, Phys. Rev. **32**, 600 (1928).
[7] W. W. Watson, Phys. Rev. **36**, 1019 (1930).

Isotope Effect

In computing the isotope shift of the possible weak lines originating in Be^8H the procedure is as follows. Assuming the masses of the two isotopes to be exactly 9 and 8, and taking the mass of hydrogen as 1, the usual isotopic coefficient $\rho = [(1/8+1)/(1/9+1)]^{\frac{1}{2}} = 1.00625$. If the values of these Be nuclear weights are computed by interpolating between Li and B on the known packing-fraction curve[8] one obtains 9.013 and 8.013. These masses, together with $H = 1.008$, give a value for ρ identical with that just mentioned. We have, then, $\rho - 1 = 0.00625$, $\rho^2 - 1 = 0.01250$, $\rho^3 - 1 = 0.0187$, and $\rho^4 - 1 = 0.0256$.

The vibrational isotope shift is given by

$$\Delta\nu^v = (\rho - 1)[\omega_e'(v' + \tfrac{1}{2}) - \omega_e''(v'' + \tfrac{1}{2})] - (\rho^2 - 1)[\omega_e'x'(v' + \tfrac{1}{2})^2 - \omega_e''x''(v'' + \tfrac{1}{2})^2]$$

which, as we shall concern ourselves only with the P and R branches of the (0,0) band, becomes

$$\tfrac{1}{2}(\rho - 1)(\omega_e' - \omega_e'') - \tfrac{1}{4}(\rho^2 - 1)(\omega_e'x' - \omega_e''x'').$$

Since the bands in this BeH system compose the $\Delta v = 0$ sequence only, the values of the vibration frequencies ω_e' and ω_e'' cannot be exactly determined. However, it is certain that these quantities are almost equal for these bands,[6] and that therefore their difference will be small. Hence the constants $\omega_o' = 2053$ cm^{-1} and $\omega_o'' = 2025$ cm^{-1} computed in the earlier work from the rotational data for the (0, 0) band will suffice in their place. These, together with the $\omega_o'x' - \omega_o''x''$ difference given in reference 6, placed in this vibrational isotope effect equation gives $\Delta\nu^v = +0.11$ cm^{-1}.

The rotational isotope effect has been computed after the accurate manner recommended by Birge,[9] using the coefficients of the rotational energy term from reference 6. Even the sixth powered term in the rotational energy with a mass factor $\rho^6 - 1$ becomes appreciable in this case for $K > 15$, and is equal to 0.05 cm^{-1} at $K = 20$. Since the Be^8 isotope is lighter than the main Be^9, the the rotational istope effect is + (towards higher frequency) in the R branch and − (towards lower frequency) in the P branch. The vibrational contribution of 0.11 cm^{-1} is then to be added to the rotational shift for the R branch lines and subtracted from this shift for the P branch lines.

Calculations of the expected positions of Be^8H lines have thus been made for all of the stronger P- and R-branch lines of the (0, 0) band. Measurement of the plate reveals a very weak line at the calculated point for every P and R line in the interval $K'' = 6$ to 20 except where an overlapping or adjacent strong line of another series makes measurement impossible. Table I gives the comparison of the calculated and observed displacements of these weak lines from the corresponding Be^9H lines. The average discrepancy between the calculated and observed shifts is 0.04 cm^{-1} in the P branch and 0.05 cm^{-1} in

[8] F. W. Aston, Proc. Roy. Soc. **115**, 487 (1927).
[9] R. T. Birge, Trans. Faraday Soc. Dec. 1929.

the R branch, which is of the order of magnitude of the possible electronic isotope shift.

The relative intensities of these weak and main-branch lines are rather difficult to obtain. Fig. 2 is a copy of a microphotometer trace of the $P(17)$, $P(18)$ line region taken with the 40:1 magnification ratio of a Koch-Goos registering microphotometer. Since the deflection for the strongly over-exposed main lines as against that for the background on the plate is no measure of the intensity of these lines, such a trace serves merely to indicate the character and relative positions of these very weak lines among their stronger neighbors. To get some idea of the correct relative intensities of these lines, spectrograms were taken of the bands under identical conditions for various

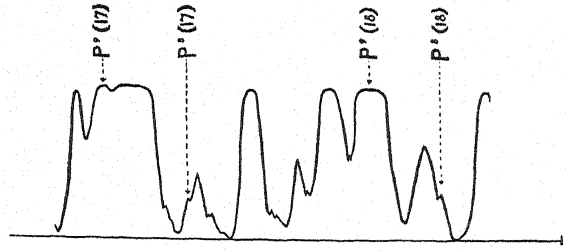

Fig. 2. Copy of microphotometer trace of the region of the BeH bands including the $P(17)$ and $P(18)$ lines showing the very weak lines attributed to Be^8H.

very short times in order to determine the time of exposure which would give the Be^9H lines with the same intensity as noted for the weak Be^8H lines with the long exposure time. An exposure of but 15 seconds, which is approximately 1/1000 that of the 4 hour time for the main exposure, produced the $P(17)$ and $P(18)$ lines with about the same intensity as these Be^8H lines. Comparison of the areas under a microphotometer trace of these 15 second lines and the 4 hour Be^8H lines verified their approximate equality in intensity. Then making allowance for the fact that general background on the plate for the long exposure tends to increase the intensity of very weak lines, the conclusion is reached that the correct relative intensity of the Be^8H and Be^9H lines is more nearly 1:2000.

The Reliability of this Indication of a Be^8 Isotope

The most cogent argument against the conclusion that these measurements indicate that a small amount of a Be isotope of mass 8 really does exist would be that since there are such a large number of lines in this system, the agreements with the computed Be^8H positions may be all just chance coincidences with lines of bands representing transitions between higher vibrational levels. Impurity lines such as H_2 can be ruled out, because there are no indications of them on the portions of our plates beyond the extremes of this band system. Now in the discussion of the fine structure in these bands given below, it is shown that vibrational states as high as (9, 9) are probably present. Since the lines in question are of very low intensity they could belong

only to say the (8, 8) and (9, 9) bands. But the lines of the P-branches of these bands would have in the P-branch region examined a spacing more nearly like that of the (0, 0) band R branch—about 20 cm^{-1} as compared to about 14 cm^{-1} for the (0, 0) band P branch—because of the fact that the (0, 0) band order $B' > B''$ is just reversed. Just the opposite is true of the line spacings in the R branch. The sequence of weak Be^8H lines then could not possibly belong to any one branch of these weaker Be^9H bands. And the probability that if all of these weak lines belong to several different main band

TABLE I. *Comparison of calculated and observed displacements for Be^8H isotope effect in the (0,0) λ4991 BeH band (in cm^{-1} units).*

	νBe^9H obs.	νBe^8H obs.	Obs. shift	Calc. shift
$P(10)$	19844.47	19842.38	−2.09	−2.12
$P(11)$	28.24	25.94	−2.30	−2.32
$P(12)$	12.51	09.88	−2.63	−2.50
$P(16)$	755.15	752.09	−3.06	−3.07
$P(17)$	42.16	9.05	−3.11	−3.17
$P(18)$	29.72	26.47	−3.25	−3.28
$P(19)$	17.97	14.52	−3.45	−3.47
$R(8)$	20223.81	20226.29	+2.48	+2.47
$R(9)$	45.75	48.39	+2.64	+2.73
$R(11)$	89.92	93.19	+3.27	+3.24
$R(12)$	311.91	315.29	+3.38	+3.50
$R(16)$	99.26	403.73	+4.47	+4.45
$R(19)$	462.82	68.00	+5.18	+5.09
$R(20)$	83.61	88.90	+5.29	+5.28

Note: For every line between $K''=6$ and 20 missing in these sequences measurement is impossible because of overlapping stronger lines of other branches.

branches, the totality of agreements indicated in Table I could happen by chance is negligible. It should be emphasized again in this connection that the isotope line has been found for every P and R line of the (0, 0) band for K values from 6 to 20, the interval of maximum intensity, except where a stronger line of some other branch interfered with the measurement.

It would of course be desirable to check these conclusions by the finding of the Be^8, Be^9 isotope effect in some other Be band system. With this in mind we have obtained an intense exposure of the BeO bands at high dispersion. The source was merely a 220-volt d.c. arc between Be metal electrodes in air. A Be^8O^{16} (1, 0) head should lie 10.34A to the violet from the Be^9O^{16} (1, 0) head at λ4427.3, while a Be^9O^{18} (0, 1) head should be found 7.40A to the violet from the Be^9O^{16} (0, 1) head at λ5054.4. These main heads are strongly developed on our plate, but unfortunately the regions on their violet sides are overrun with weak lines representing high rotation levels of the BeO bands in the adjacent sequences due to this form of excitation. Nevertheless the exact points for these calculated weak isotope heads are sufficiently clear, and not a trace of either of them is apparent. In view of the fact that O^{18} is definitely established with an abundance ratio of 1:1075 to O^{16}, our failure here merely means that such an arc is not the proper source for the detection of faint iso-

tope lines. It will apparently be necessary to develop some Be band system either in absorption or in the electric furnace in order to obtain further evidence of the Be^8 isotope.

New Fine Structure Measurements in the BeH Bands

It is the object of this section to present some new details of the BeH system together with their probable interpretation. The earlier work[6] led to the logical assumption that these bands are due to the transition $^2\Pi \rightarrow {}^2\Sigma$ with the $^2\Pi$ state approximately pure case b, because of the apparent lack of observable spin doubling of the lines near the band origins. All of the lines in the bands with the exception of the first R_1 line ($R_1(\frac{1}{2})$) are thus to be considered as the coalescence of the two members of a spin doublet having the same K' and K'' values but differing by one unit in J' and J'' values. In this event the quantum number J has no significance, and the lines are to be designated by their K'' values.

The higher resolution of our third order plates, however, reveals the expected doubling of the lines near the origins. These have only been measured for the P and Q branches of the main $(\frac{1}{2}, \frac{1}{2})$ band, all the first R-branch lines being so close to strong Q-branch lines as to make acurate measurement of

Table II. *Frequencies near the origin in the* λ4991, (0,0) *band of BeH.*

K	R_2(K) $R_1(K)$	$P_2(K)$	$P_1(K)$	$Q_2(K)$	$Q_1(K)$
0	20050.78				
1	72.00			20030.18	20031.97
2	93.27 93.98	19989.55	19991.16	31.26	32.15
3	115.04	70.47	71.40	32.89	33.41d
4	135.97	51.30	51.89	33.41 d	33.76
5	158.11	32.46	32.84	34.82	
6	179.94	13.96	14.25	36.36	
7	201.76	896.08		38.19	

the doublet interval impossible. Table II gives these new data to $K''=7$ which should replace the corresponding part of Table I of ref. 6. This earlier table is then quite correct from $K''=7$ to 45, and is to be supplemented by the additional lines for $K''=45$ to 51 of Table III below. The doubling of the lines $P(2)$, $P(3)$, and $P(4)$ is clearly to be seen in Fig. 1c.

To evaluate the coupling constant A, measuring the interaction energy between L^* and S^*, it is only necessary to substitute our observed doublet intervals in the equation[10]

$$\Delta f(K) = [A\Lambda^2/K(K+1) + \gamma](K + \tfrac{1}{2})$$

given by Mulliken for case b states.[11] The mean value of A so obtained is

[10] R. S. Mulliken, Reviews of Modern Physics **2**, 60 (1930), Eq. (36), p. 108).

[11] As Mulliken has recently pointed out, (Reviews of Modern Physics **2**, 507 (1930)) this equation is only adequate for a very limited range of A/B_v values close to $A=0$. These BeH bands happen to be the one good example of this situation.

1.97 cm^{-1}. Application of the Hill and Van Vleck formula yields practically the same result.[12]

Our observation of the relative intensities of the components in the P-branch doublets gives good confirmation of the assignment $F_1 > F_2$ for the order of the rotational energy levels in this $^2\Pi$ state with an A/B_v lying between 0 and $+4$.[13] The high frequency component is always the stronger, as in the case of the $CH\ ^2\Sigma \rightarrow {}^2\Pi$ bands for the $^2\Pi$ state of which $A/B_v = +2$, whereas for the similar MgH, CaH, etc. bands the high-frequency component is the weaker, in fact much weaker for the lowest rotational levels than is predicted by the theory. For these BeH bands, however, the relative intensities are in very good agreement with the ratios computed with the aid of the intensity equations for case b doublet states developed by Mulliken[14] from the Hönl and London and Sommerfeld and Hönl equations. These intensity ratios for the first three P-branch lines are:

Line	$P_1 : P_2$ (calc.)	(obs.)
$P(2)$	1:0.56	1:0.51
$P(3)$	1:0.70	1:0.83
$P(4)$	1:0.77	1:0.74

The observed intensity ratios were obtained from a comparison of the areas under a microphotometer trace obtained with the Koch-Goos instrument. The larger discrepancy for the $P(3)$ ratios is due to a photographic disturbance produced by an adjacent Fe line of the comparison spectrum.

The comparison of the observed doublet intervals in the first P- and Q-branch lines, together with combination differences, fix definitely the K-values of the lines of the Q-branch, and show that the relative numbering of the lines of the three branches in Table I of the previous work is correct. To evaluate the Λ-type doubling in the $^2\Pi$ state we form the differences

$$\tfrac{1}{2}\{[R(K) - Q(K)] - [Q(K+1) - P(K+1)]\} \cong F_b'(K+\tfrac{1}{2}) - F_a'(K+\tfrac{1}{2}).$$

This doubling starts at $K=1$ with a very small negative value, goes through zero at $K=4$, and increases slowly with K to a value of approximately 10 cm^{-1} at $K=42$. After this it begins to decrease with further increase in the rotational quantum number. For $K'>5$, where the spin doubling becomes negligible, and for $K' \gtrsim 20$ the Λ-type doubling is proportional to $K'(K'+1)$, as predicted by Van Vleck[15] for case b $^2\Pi$ states. The average value of the factor of proportionality is about 0.014. Now Van Vleck shows that with the assumption that the L vector precesses uniformly about the electric axis in the molecule, and for the case $L=1$, this proportionality factor would be of the order of magnitude $4B^2/\nu$. For BeH this quantity is $4(10.16)^2/2\times 10^4 \cong 0.02$. If this same doubling law held for the highest rotational levels, the Λ-type dou-

[12] This value for A should replace the tentative value assigned in Fig. 15 of reference 11. Also the value of $B=7.82$ there given should be 10.16, the value of B_0'' given in reference 7

[13] Cf. R. S. Mulliken, Phys. Rev. **32**, 388 (1928).

[14] R. S. Mulliken, Phys. Rev. **30**, 785 (1927).

[15] J. H. Van Vleck, Phys. Rev. **33**, 467 (1929).

bling would be about 23 cm^{-1} at $K=40$, whereas actually it remains almost constant at 10 cm^{-1} from $K=35$ to 42 and then begins to decrease. This departure from the normal doubling law begins at about $K=20$ where the reversal in the direction of shading of the branches also becomes apparent.[16] Both of these phenomena indicate a marked distortion of the molecule with increase in rotational energy and are evidence for an uncoupling of L from the internuclear axis.

On the long wave-length side of the origin of the (0, 0) band (main Q-branch head) in Fig. 1 two weaker Q-branch heads are to be seen. This may at first seem puzzling, because with the (0, 0) band Q-branch degrading initially toward the violet, successive Q-branches of this $\Delta v=0$ sequence should normally be found on the violet side of the (0, 0) origin. The explanation of this unusual feature lies in the fact that in this band system the vibrational frequencies ω_e' and ω_e'' are almost equal (about 2053 cm^{-1} and 2025 cm^{-1} respectively). Hence the slight differences in the course of the vibrational energy as a function of v in the two states are sufficient to actually produce a change in the sign of the vibrational energy contribution to the radiated energy for $v'=v''\geqq 8$. That is, the successive Q-branch heads rapidly converge to zero separation at the (4, 4) head at about 20064 cm^{-1} as shown in Fig. 1, and then return to lower frequencies. This would make the two weaker Q-branch heads on the red side of the main Q head probably the (8, 8) and (9, 9) Q-branches. The order $B_v'>B_v''$ also reverses at about the (4, 4) band, since these quantities are given approximately by[17]

$$B_v' = 10.45 - 0.325v'; \quad B_v'' = 10.25 - 0.275v''.$$

Therefore the spacing of the lines in the weak R branches of the bands from (4, 4) to (9, 9) should become closer, comparable to that of the P branches in the strong (0, 0) band, thus accounting for the lack of corresponding R-branch heads. Similarly, the weak P-branch for these higher vibrational bands should have a larger spacing more like the (0, 0) R-branch. All of these P and R branches have not been examined in detail, but sufficient measurements have been made to indicate definitely that this is the correct explanation of the rather complex fine structure in this unusual band system.[18]

TABLE III. *Additional frequencies for the* λ4991, (0,0) *BeH band.*

K	$R(K)$	$P(K)$	$Q(K)$
45	20824.26	19581.18	20192.79 d
46	25.32 d	79.08	92.93 d
47	25.32 d	76.51	92.45
48	(24.75)	74.00 d	90.71
49	23.40	70.24	87.83 d
50	21.20	67.36	
51	17.14		

[16] Cf. reference 6 and W. W. Watson, Phys. Rev. **34**, 1013 (1929) for diagrams.

[17] E. Bengtsson, Nature **123**, 529 (1929).

[18] F. A. Jenkins, Phys. Rev. **31**, 539 (1928) has shown that the tail bands in the violet CN system are produced by this same phenomenon; i.e. of the bands in a sequence forming a head and returning into the region beyond the first band head in the sequence.

Finally, it is to be noted in Fig. 1 that the R-branch of the (0, 0) band, the lines of which at the origin start out with increasing spacings, actually forms a head, and several lines of the returning portion are observed on our strongest plate. Corresponding lines in the Q and P branches have also been measured. Table III giving these data supplements Table I of reference 6.

One would expect to find distortions such as those observed in these BeH bands due to large accretions of rotational energy of rather common occurrence in molecular spectra. Actually, however, similar phenomena have been reported only for some He_2 and H_2 levels[19] and for the red CaH bands[20,21]. Possibly the investigation of the rotational structure of molecular spectra lying in the Schumann region and representing predicted higher electronic levels reveal other examples of irregularities of the same nature.

[19] Cf. particularly W. Weizel, Zeits. f. Physik **56**, 727 (1929).
[20] E. Hulthén, Phys. Rev. **29**, 97 (1927).
[21] W. W. Watson and W. Bender, Phys. Rev. **35**, 1513 (1930).

AN APPLICATION OF THE RESONANCE RADIOMETER TO THE REFLECTION SPECTRUM OF QUARTZ

By J. D. Hardy and S. Silverman
Johns Hopkins University

(Received December 1, 1930)

Abstract

The reflection spectrum of quartz has been previously studied by means of both the rock-salt prism spectrometer and the echelette grating spectrometer. Early investigators have shown that for crystalline quartz, with the reflecting surface perpendicular to the optic axis, there is a double reflection maximum, one lying at 8.4μ and the other at 8.9μ; and that fused quartz exhibits a single maximum at 8.8μ. These regions have been studied under high dispersion by the authors using an echelette grating spectrometer. The high resolving power that was obtained was due to the sensitivity of the radiometric device, the resonance radiometer, which was first described by A. H. Pfund.[1] The complete theory of the instrument was developed by one of us.[2] By the use of this large resolving power and dispersion it has been possible to show that these spectra are considerably more complex than were found previously. The usefulness of magnesium oxide as a filter for excluding the higher orders of lower wave-lengths has been tested with gratifying results.

Introduction

PREVIOUS investigators have studied the reflection spectra of quartz with particular attention to crystals cut perpendicular to their optic axes. Among the various investigators Rubens and Nichols,[3] Coblentz,[4] and Gorton[5] employed a prism spectrometer; Wood and Trowbridge[6] used an echelette grating. The results show some agreement as to the wave-lengths of the reflection maxima, which are located at 8.4μ and 8.9μ respectively, but there is an apparent marked difference in the depth of the minimum which separates the maxima. Closer examination of these dissimilar curves shows that they actually represent very approximately the same structure. The work done with the prism spectrometers shows the ratio of the reflecting power of the quartz surfaces to that of a silver surface, while the work done with the grating shows only the energy curve of the source after three reflections from quartz. This makes it difficult to compare directly the results of the grating with those of the prism. Also, it should be pointed out that as very few workers have restricted themselves to similar crystal forms or similar geometrical systems, it is necessary to be cautious in attempting any comparison of the various results. The conditions for observation in the present case are as

[1] A. H. Pfund, Science **69**, 11 (1929).
[2] J. D. Hardy, Rev. Sci. Inst. **1**, 429 (1930).
[3] Rubens and Nichols, Phys. Rev. [1] **4**, 314–324 (1897).
[4] Coblentz, Carnegie Publications, 1906.
[5] Gorton, Phys. Rev. **7**, 66 (1916).
[6] Wood and Trowbridge, Phil. Mag. **20**, 898 (1910).

follows; the angle of incidence was measured to be very close to 30°; the crystal surface was polished smooth and cut perpendicularly to the optic axis; the results are the ratios between the reflecting power of quartz surfaces and that of clean silver. It is thought that if these conditions are approximated it should be possible to use the positions of the reflecton maxima and minimum for calibrating prism spectrometers in the 8μ region.

In the early part of this year, Professor A. H. Pfund made some observations on the reflection from crystalline quartz (not published) and found results differing markedly from those of Coblenz and others. He found, using a very narrow slit, a much lower minimum at 8.6 and some indication of unresolved fine structure. It was decided, therefore, to examine this spectrum with an apparatus whose sensitivity and resolving power would far surpass anything yet applied to this region. The diagram of the spectrometer is shown in Fig. 1.

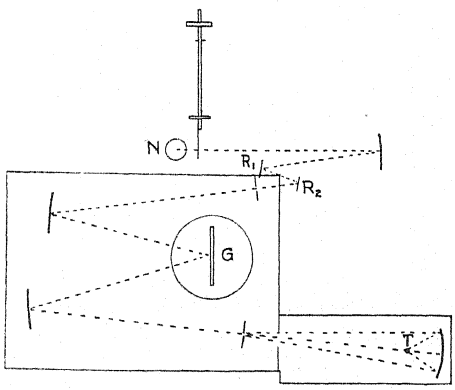

Fig. 1. Spectrometer arrangement for observing the reflection spectra.

Apparatus

The source of light, N_1 was a Nernst glower, run at 0.8 amp. from a storage battery. This light is interrupted periodically by the pendulum of the resonance radiometer; the period of which is adjusted to be equal to twice the optimum period of response of the first thermocouple. The light is then admitted to the spectrometer periodically with the time of admission exactly equal to the time of darkness, and the slit is alternately illuminated and darkened. Light from the Nernst glower is reflected from a concave mirror on to the first quartz plate R_1 which is covered with a layer of MgO. This plate acts as a filter and purifier. The beam is then reflected from a second plate of quartz R_2 to the first slit. This second plate is set in place with a strong spring so that it may be replaced exactly by a silvered surface. The beam then passes through the spectrometer and is focused upon the receiver of the first thermocouple. The grating used was a 5 inch, 1312.5 lines per inch echelette prepared at this University by Professor Wood, and ruled to throw its blaze, or maximum concentration, at 8.5μ. The thermocouple was a Bi-Sb·· Bi-Sn

splashed filament type, with a silver receiver which was covered with bismuth black. It was mounted behind a rock-salt window and evacuated to a non-conducting vacuum. The grating had a dispersion ratio of 570; i.e. at a scale distance of 3.2 meters, 1 mm represented 50A. The calibration was done by means of the higher orders of the 5461 line of the mercury arc, and was accurate to 15A. The slits of the apparatus were 0.07 mm wide, yielding an effective "slit-width" of 15A. This width of slit is the most advantageous in this region both for resolution and intensity giving a resolving power of 80 percent of the theoretical value, or about 4000.

Inasmuch as the resonance radiometer has been recently described in detail, it will be necessary here to outline only its salient points.[2] The first thermocouple is connected to tuned vibration galvanometer 1, which is so constructed that it is highly underdamped with a half-period equal to the time of response of the thermocouple. Galvanometer 2 is identical with 1 except for a device permitting accurate tuning with 1. The two galvanometers and the pendulum are kept in as exact tune as possible. The amplifier light source is a tungsten filament bulb burned at about 3.6 amp. from a storage battery. It lies behind the first grid R_1, and is focused on the concave mirror of galvanometer 1. This mirror then throws an image of R_1 coincident upon a second grid R_2, which is identical with R_1, except that it has a double spacing at the center. Then the beam of light which is transmitted by R_2 is broken into two halves, which are exactly out of phase as regards luminosity. As the mirror of galvanometer 1 rotates, the image of R_1 slides across R_2, darkening one half whilst illuminating the other half. These two beams are then focused by means of a split lens upon a compensating thermocouple T_2, which is in turn connected to the second galvanometer. There will then be two amplifying factors: First, the resonance amplification arising from the periodically interrupted beam falling upon S_1. Secondly, the motion of G_1 causes the image of R_1 to oscillate across R_2, so that the intensity of the light falling upon the junctions of T_2 varies periodically and sets G_2 in turn into a resonance vibration. This second factor may be varied by changing the intensity of S_2. Throughout this experiment the total amplification was kept at about 4000, and deflections which could not be detected on an ordinary high-sensitivity galvanometer ranged as high as 30 centimeters on this instrument.

Method of Procedure

The actual readings were taken as follows: The spectrometer was set for a given wave-length, and the first quartz "purifying" plate was held over a brightly burning ribbon of magnesium. It was coated with a fine, white powder of magnesium oxide. The thickness of the coat was judged sufficient when the whole plate appeared uniform when held against a brilliant back ground. The plate was then placed carefully in its holder, and thereafter left undisturbed. The second quartz plate was put in, and the shutter was removed, allowing the second galvanometer to build up to a maximum. Three or four deflections on each side were noted, with an average deviation, at a scale distance of 1 meter, of about 1 percent. The second quartz plate was

removed, and replaced by a silver surface; the readings were then repeated. The direct ratio of the readings yields the relative reflecting power of quartz and silver. To get the absolute reflecting power, one must correct for the small deviation of the reflection coefficient of silver from that of a perfect reflector. However, this correction is smaller than the experimental error. Inasmuch as direct ratios are taken, it is unnecessary to take any account of water vapor or any other absorbant present in the air path. The magnesium oxide[7] was used with the hope of cutting out the higher orders of lower wave-lengths; an ideal filter would be one which was opaque to 4μ, and perfectly transparent from 7.5 to 9.5μ. As a test for the usefulness of MgO, the first slit was covered by a piece of thin cover-glass, which transmitted fairly well up to 4μ, and which

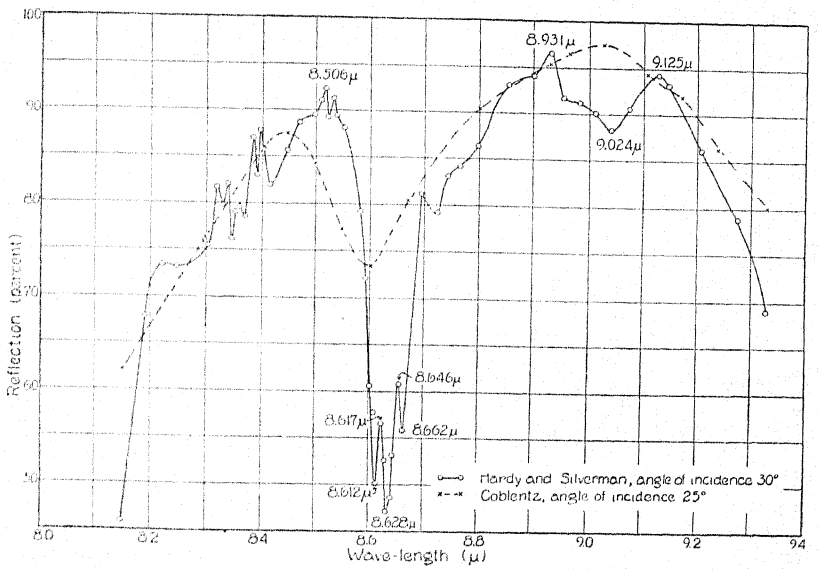

Fig. 2. Reflection spectrum of crystalline quartz. Circles, Hardy and Silverman; crosses, Coblentz.

was opaque to 8μ. With the grating set for 8μ, and with two *silvered* plates in place, one covered with the oxide, no resonance deflection was detected. In passing, it might be noted that even with such a high amplifying factor, the zero unsteadiness was never greater than 2.0 cm in the daytime, and usually around 5 mm at night. Moreover, with an unsteadiness of 2 cm, it was possible to measure deflections of less than four centimeters to an accuracy of a millimeter. In general the deflections were of the order of ten or more centimeters so that the resultant ratios shown on the curves are judged to be accurate to about one percent. The curves shown are the results of several sets of observations which were found to agree among themselves exceedingly well.

[7] A. H. Pfund, Phys. Rev. **36**, 71 (1930).

The position of the grating was checked several times and the wavelengths plotted are accurate to 0.0015μ.

Results

The spectrum of crystal quartz shows a rapidly increasing reflectivity at 8.1μ. Between 8.3 and 8.4 there is considerable fine structure, and a sharp maximum at 8.506μ. The minimum immediately following is triple, showing dips at 8.612, 8.628 and 8.662μ respectively; and peaks at 8.617μ and 8.646μ.

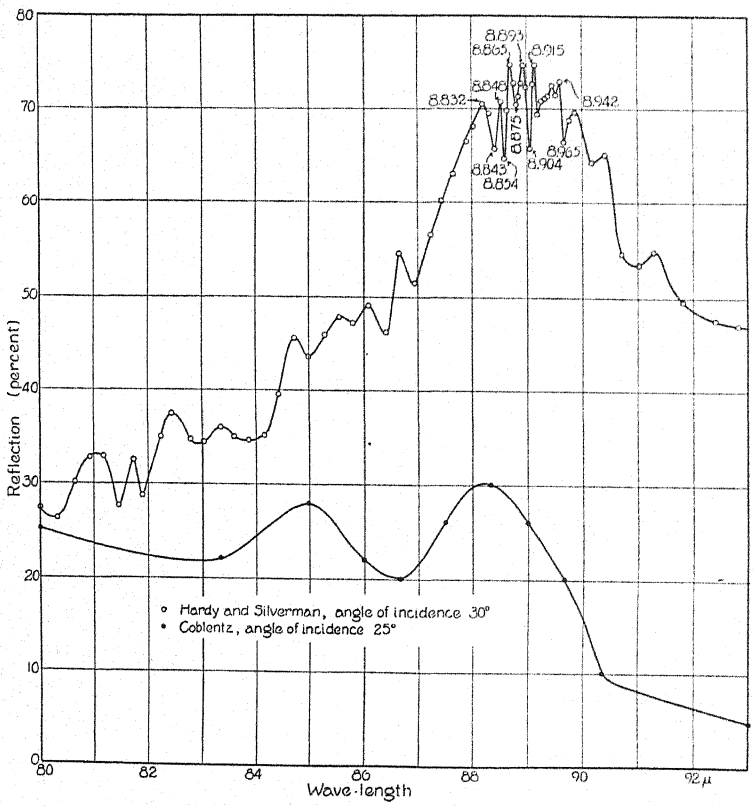

Fig. 3. The reflection spectrum of fused quartz. Circles, Hardy and Silverman, squares, Coblentz.

There is a rise to a maximum at 8.931, a small decline to 9.024 and a shorter rise to 9.125. Following this last maximum the intensity falls off steadily. Dr. A. H. Pfund had previously found indications of the structure at 8.4μ, although he was not able to resolve it, and also of the dip at 8.9μ.

The spectrum of fused quartz is less regular, and nowhere shows any of the regular smoothness attributed to it in the literature.[8,9] It rises from 16 percent

[8] Schaefer and Matossi, "Das Ulrtarote Spektrum," p. 317.
[9] J. Lecompte, "La Spectre Infrarouge," p. 145.

at 7.870μ in a series of staggers to a set of sharp maxima and minima. Maxima appear at 8.832, 8.865, 8.893, 8.913 and 8.942μ. The minimum at 8.904 is particularly sharp. The intensity on the long wave side again falls off in a step-wise fashion.

The resonance radiometer has shown itself to be quite practical in its application to work in infrared spectroscopy. Although it has the disadvantage that in its present form it is not practical to use it as a direct recording instrument, its freedom from unsteadiness and stray disturbances and its reliability in the matter of reproducing readings more than offset its faults.

In conclusion, the authors wish to express their appreciation to Professor A. H. Pfund of this University, whose aid and many suggestions have been invaluable.

RECOMBINATION IN MERCURY VAPOR

By Harold W. Webb* and David Sinclair
Physics Laboratories, Columbia University, New York City

(Received December 6, 1930)

Abstract

The afterglow in ionized mercury vapor was studied as a recombination phenomenon, to determine how its intensity varied with concentration of electrons and of positive ions, vapor pressure and the mean energy of the electrons, the last expressed as a temperature, T. The afterglow was observed in a region outside of the arc to which positive ions and electrons were carried by a stream of vapor, auxiliary electrodes being used to control the electron temperatures. The total number of electrons, N, was assumed closely equal to the number of positive ions. The intensity of the visible part of the afterglow radiation was shown to be closely proportional to the total intensity under the experimental conditions, and was therefore used as a measure of the rate of recombination. This intensity, I, was found to be proportional to the first power instead of to the square of the electron concentration, with possible exceptions at low concentrations and low electron temperatures. I varied with vapor pressure, increasing roughly as the fourth power of the pressure. With increase in electron temperature from 1300° to 5600°K, I decreased by a factor of 2500. From this rapid change in I it is concluded that the afterglow cannot be due to a simple recombination process, since work of other authors with caesium and helium has shown that I should then vary not more rapidly than the reciprocal of the temperature. The results were found to fit either of the following empirical equations: $I=\text{const } N^2/N_0$ or $I=\text{const } N^2/N_1$, where N_0 is the number of fast electrons having energies greater than a determined value and N_1 the number having a definite energy. The values of the critical energies corresponding to these two equations were found to be 1.15 volts and 1.35 volts, respectively.

The results suggest that the recombination in mercury vapor takes place in two stages, of which the second is responsible for the radiation of the series lines, and that the effect of the fast electrons is to reionize from the first stage.

Considerable difficulty was experienced during measurements as the result of changes in the contact potential of the exploring electrodes used for measuring electron temperatures and concentrations. These changes were apparently due to traces of oxygen.

THE recombination of ions and free electrons has been studied in various ways but the nature of the process is still very obscure. The results of these studies have been well summarized in several recent publications,[1] and only a few outstanding points need be reviewed here. Especially have the simple recombination of an ion and an electron accompanied by emission of radiation and the converse process of photoionization been investigated in detail. The most extensive quantitative experiments in this field have been

* The appointment of the senior author as Ernest Kempton Adams Fellow enabled him to secure the collaboration of Mr. Sinclair.

[1] Seeliger Phys. Zeits. **30**, 329 (1929); Mohler, Phys. Rev. Supp. **1**, 216 (1929); Compton and Langmuir, Rev. of Mod. Phys. **2**, 191 (1930).

made by Mohler,[2] who found in caesium vapor and in helium continuous spectra extending from near the series limits to higher frequencies. These spectra are interpreted as due to the recombination of ions with electrons, in which process an electron falls into the lowest energy level of one of the series, the difference in frequency between that of the radiation observed, ν, and that corresponding to the series limit, ν_i, being due to the kinetic energy of the electron before impact, $mv^2/2$. The relation between these frequencies is given by $h\nu = h\nu_i + \frac{1}{2}mv^2$. In these experiments the mean energy of the electrons was about 0.3 volt. Mohler found that the intensity of the radiation varied as a function of the electron velocity, v, and determined the value of the coefficient of recombination; $\alpha = \text{const. } v/(\nu - \nu_i)v^2$, or α is proportional to $1/vv^2$. Theoretical studies[3] of the process give α proportional to $1/v$, $1/vv$, or similar expressions in fair agreement with experiment. It is of particular interest to note that, in these experiments, the rate of recombination of electrons and positive ions was found to vary very slowly with the kinetic energy of the electrons, that is inversely as the first power of the velocity, in marked contrast with results to be described later.

Hayner[4] has shown that the afterglow in mercury vapor is due to some process of the nature of recombination. In her experiments the voltage on a low-voltage arc in mercury vapor was abruptly cut off and the behavior of the radiation which persisted, called the "afterglow," studied in the post-arc period immediately thereafter. The cutting off of the arc voltage extinguished the spectral series lines practically instantaneously, but after a brief transition period of about 10^{-4} sec. the series lines reappeared gradually increasing in intensity, reaching a maximum in about 2×10^{-4} sec. and then gradually decreasing. The behavior of the ionized gas in the experimental tube in the post-arc period gave every evidence that the afterglow was the result of a recombination process involving electrons and positive ions. The dark transition period following the cut-off of the arc voltage was explained as due to the fact that the velocities of the electrons were too great to permit recombination. The subsequent gradual growth of the intensities of the series lines corresponded to the gradual decrease in these velocities due to impacts with neutral atoms, while the decrease following the maximum was the result of the disappearance of ions and electrons due to their recombination and to diffusion to the walls of the tube. The nature of the spectrum of the afterglow furnishes additional evidence that it is produced by a recombination process. In it the ratio of the intensities of the higher members of the spectral series to the intensities of the lower members is very much greater than in spectra resulting from direct impact excitation as are observed in the arc.

Kenty[5] in a similar experiment in argon found like results. The mean energy of the electrons at the time when the afterglow was most intense in the

[2] Mohler, Phys. Rev. **31**, 187 (1928); Mohler and Boeckner, B. S. J. of Res. **2**, 489, **3**, 303 (1929).

[3] Seeliger, reference 1, p. 356.

[4] Hayner, Zeits. f. Physik **35**, 365 (1926).

[5] Kenty, Phys. Rev. **32**, 624 (1928).

post-arc period was determined by the Langmuir probe method as 0.4 volt, confirming the explanation that the recombination in the arc period and in the dark transition period was prevented by the high speed of the electrons and that radiation from recombination only became observable after the electrons had lost most of their energy.

Measurements on gases highly ionized, subject to no impressed field, have in general shown that the distribution of velocities among the electrons is Maxwellian and that a definite "temperature" may be assigned to the distribution. The Langmuir probe method gives a means of determining this temperature and gives also data for computing the concentrations of ions and electrons. The fact that the electrons have such a distribution, or one nearly approaching it, makes it very difficult to reconcile Hayner's results with the theory that the observed afterglow was due to simple recombination of positive ions and electrons, in which the probability of electrons of given velocity recombining with positive ions depends only upon the concentration and velocity of those electrons and the concentration of the ions. For, as we have seen, the most effective electrons in recombination are the slow ones. Now the number of these in a Maxwellian distribution varies with the temperature approximately as $1/T^{3/2}$, the total number being kept constant. Now on liberal estimates the total change in the electron temperature from the transition period, when the intensity of the afterglow was too small to observe to the moment of maximum intensity, was in Hayner's experiment not greater than a ten-fold decrease; on the other hand the change in intensity during this time appears to have been of a different order of magnitude, estimated as at least a thousand-fold increase. The intensity could not therefore have varied as the number of electrons moving slowly enough to have high probability of recombination, unless the velocity distribution was not Maxwellian but one in which the slower electrons were relatively very much scarcer at the higher temperatures. There is every evidence that this was not the case. Considerations of this difficulty in interpreting these results lead to the experiments described in this paper, in which the intensity of the afterglow was studied as a function of electron temperature, concentrations of positive ions and electrons and vapor pressure.

Apparatus and Method

To avoid the difficulties of making precise determinations of electron temperatures and concentrations under the rapidly changing conditions in the "post-arc" period following the cut-off of an arc, the investigations of the afterglow were made in a region outside the arc to which the positive ions and electrons were carried by a stream of vapor. The apparatus used was similar to that described in an earlier paper.[7] The essential parts of the experimental tube, drawn to scale, are shown in Fig. 1. The mercury in the pool below the cathode K, was heated by a furnace, H, and the vapor streamed rapidly past

[6] Rayleigh, Proc. Roy. Soc. **A108**, 262 (1925).
[7] Webb and Wang, Phys. Rev. **33**, 329 (1929).

the cathode and the anode, A, into the branch tube through the gauze, G, past the observation point, P, and was condensed in the region marked C. The cathode was an internally heated nickel cylinder with oxide coating.* The gauze, G, was of nickel wire, 0.03 cm in diameter and 0.6 cm spacing. At P, in the center of the tube, was placed a vertical probe, consisting usually of a platinum wire 0.0025 cm diameter exposed for about 0.5 cm. Opposite the probe was a quartz window 1.2 cm in diameter attached by a graded seal. A side tube 0.7 cm in diameter and 7 cm long closed at the end extended out at right angles near P, and was used in estimating the vapor pressure in the tube at this point. The condenser, C, was cooled by a coil of lead tubing carrying circulating water. This coil could be adjusted as to length and position

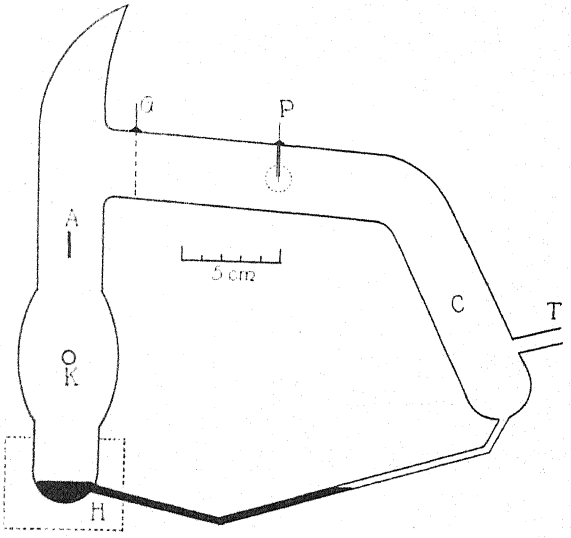

Fig. 1. Diagram of experimental tube.

or replaced by air cooling to control the flow of mercury vapor in the tube. Premature condensation in the tube between the furnace and the condenser was prevented by secondary heaters.

The pumping tube, T, passed first to a McLeod gauge, then to a magnetically operated cut-off and finally to a mercury diffusion pump. During observations this pump was in constant operation.

The arc current was varied up to 10 amperes, with an average potential drop of about 8 volts. From below the anode was emitted the usual low-voltage arc radiation with the higher members of the series relatively weak in intensity, while beginning a little above the anode and extending throughout the branch tube and the condenser was the afterglow in which the higher members of the series were relatively much stronger. The intensity of the

* For this cathode we are indebted to Mr. L. J. Buttolph of the General Electric Vapor Lamp Co.

afterglow at the point P was measured by a specially constructed visual photometer sighted through the quartz window. The radiation thus measured was practically all contributed by the sharp triplet λλ5461, 4358, 4047, and the intensities of these lines were taken as a measure of the total radiation of the afterglow. To justify this assumption spectrograms of the glow at different electron temperatures were made and compared and it was found that at least up to the 11 D and 7 S members the ratios of the intensities of the above triplet to those of the higher members varied only slightly, not sufficiently to introduce serious error. Rayleigh[6] reports considerable variation in these ratios with age of the afterglow, but presumably the conditions in the present investigation were not so widely varied as in his. Furthermore, as will be seen later, small errors resulting from this method of measuring the intensity of the afterglow would not have affected appreciably the nature of the results.

Simultaneously with the intensity measurements observations were taken with the probe to determine the corresponding concentration of the electrons and their temperature. It was assumed that the number of positive ions was practically equal to that of the electrons, which for concentrations of the order observed is probably closely true. The usual logarithm of current to probe vs. probe-voltage plot gave, after deducting the current due to the positive ions, a straight line for voltages below the space potential, the slope of which determined the electron temperature. The concentration of electrons was computed from the space potential, as determined by the break in the curve, and the probe dimensions in the usual way. It should be noted that under the conditions of this experiment the distribution of electron velocities could be followed only up to about 0.7 volt (in a few cases to 1.0 volt) owing to the masking by the positive ions of the electron currents to the probe at greater negative potentials. Therefore the presence of the fast electrons is indicated only by the fact that the Maxwellian distribution holds very closely for the slow electrons and we assume it to hold for higher speeds.

Considerable difficulty was experienced with the probe owing to changes in its contact difference of potential in the course of a measurement. This was evidenced by a gradual shift in the voltage corresponding to a given current to the probe. The curve taken with increasing voltage did not coincide with that for decreasing voltage. The direction and amount of the drift were not always the same but depended upon the material used for the probe, its size and the presence of small amounts of impurities in the tube. In general one to two minutes were required for any phase of the change. When, however, the currents to the probe were large the resultant heating caused more rapid changes. A complete discussion of the many tests made cannot be given here, but it may be noted that similar effects were found with platinum, tungsten, iron and carbon probes; a tungsten probe continuously heated to a temperature of about 1700° C was equally unsteady; a trace of sodium accidentally introduced into the tube resulted in a characteristic fluctuation.

It is probable that this drift was due to traces of oxygen in the tube. To test this an artificial leak was introduced near the cathode, as the result of

which the changes in the contact potential of the probe became very rapid, confirming this conclusion. It was further found that, although all metal parts were pre-outgassed and the tube baked at 500° C for many hours before introducing the mercury, considerable gas was evolved when the arc was running even after many hours of operation. Tests, made by closing the cut-off and measuring the rate of accumulation of gas in the gauge, indicated that there was a gas pressure in the stream of mercury vapor of about 10^{-7} mm at the times when marked drifting occurred. This drifting was never wholly eliminated, but, by continued baking and pumping, conditions were attained under which the drifting was sufficiently small to permit satisfactory measurements.

It is probable that many of the troubles experienced by other observers were due to this cause. The difficulty which Mohler and Boeckner[8] found with a probe in caesium vapor is not surprising, especially the increased unsteadiness when approaching large values of the probe current. It was found also in our work, as in theirs, that a large probe gave less trouble, since it suffered less rise of temperature. Other authors have obtained curves deviating from the expected straight line, or curves which are interpreted as made up of several straight lines indicating several groups of electrons each having a different temperature. Some of these complexities may have been due to effects similar to those described here.

The vapor pressure in the tube at the point of observation depended upon the temperature of the lower furnace and upon the use and position of the cooling coils on the condenser. The magnitude of this pressure was determined approximately by measuring the temperature at which liquid mercury was in equilibrium with the vapor at the end of the small side tube opposite the point of observation.

The electron temperature at the point of observation, though it depended to some extent upon the vapor pressure and the velocity of the vapor streaming from the region of the arc, was usually controlled by the gauze G. A positive potential on G, with respect to the anode, accelerated the electrons in the vapor stream and increased the temperature of those passing through the gauze and down the tube. Temperatures ranging from 1000° to 6000° could be obtained. The application of the positive potential to the gauze also decreased the concentration of the ions and electrons, in some cases as much as 70 percent. The concentration could, however, be brought back to its original value by increasing the arc current.

Results

In determining the relation between the intensity of the afterglow, I, and the electron temperature, T, the vapor pressure was held constant for each series of measurements. It was assumed that the only other variable was the concentration of the electrons, which was equal to that of the ions, and this was kept as nearly constant as possible by adjusting the arc current. As this

[8] Mohler and Boeckner, B. S. J. of Res. 2, 489 (1929).

concentration could be held only approximately constant the relation between intensity and concentration, N, was determined by a series of measurements in which the vapor pressure and electron temperature were kept constant. The results of these determinations are shown in Figure 2, in which the intensity of the afterglow is plotted as a function of the electron concentration. Three typical curves are shown, the differences in the slopes having no significance. These curves show that the intensity is closely proportional to the first power of the electron concentration, and not to the square of this concentration as might be expected if ordinary recombination processes were in question. Therefore, before studying the relation between intensity and

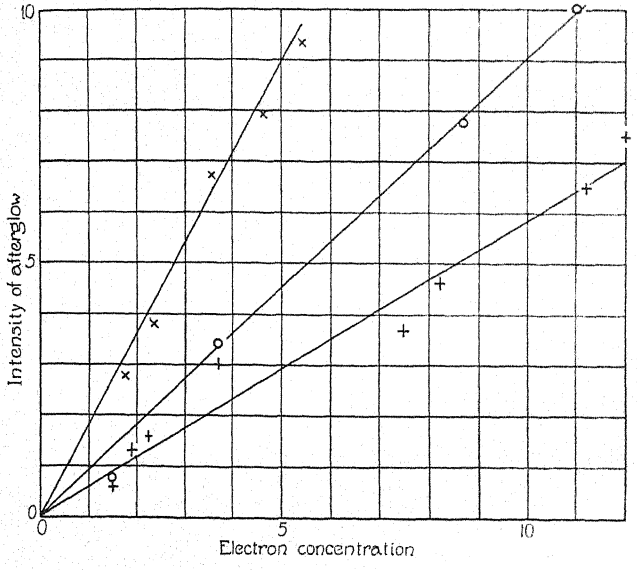

Fig. 2. Intensity of afterglow vs. electron concentration; electron temperature and vapor pressure constant. Scales are arbitrary.

electron temperature the intensities observed were divided by the first power of the corresponding number of electrons. Furthermore throughout any set of measurements of the relation of I to T the variation in N was not large and since the variation of the intensity with electron temperature was very rapid, errors arising from small departures from the first power relation were well within the limits of measurement.

It is interesting to note that Mohler and Boeckner[8] found a similar result with caesium. Contrary to expectation the intensity varied more nearly as the first power than as the square of the concentration of electrons, which was again equal to the number of positive ions. They noted, however, that at low currents the square law held. In the present experiment, also, there was indication that, for small concentrations especially at low electron temperatures, the square law more nearly described the results than the first power law. These results were however, not very dependable.

The relation between the intensity of the afterglow and the vapor pressure, the temperature of the electrons and the number of ions and electrons being held constant, was not precisely determined, owing to experimental difficulties. The results showed, however, a large increase in intensity with increase of vapor pressure. To a rough approximation the intensity varied as the fourth power of the vapor pressure within the limited pressure range observed, 0.06 to 0.10 mm. It is interesting to note that Mohler and Boeckner found in the recombination spectrum of caesium that the intensity increased surprisingly rapidly with vapor pressure, the rate of increase being comparable with that found in the present work.

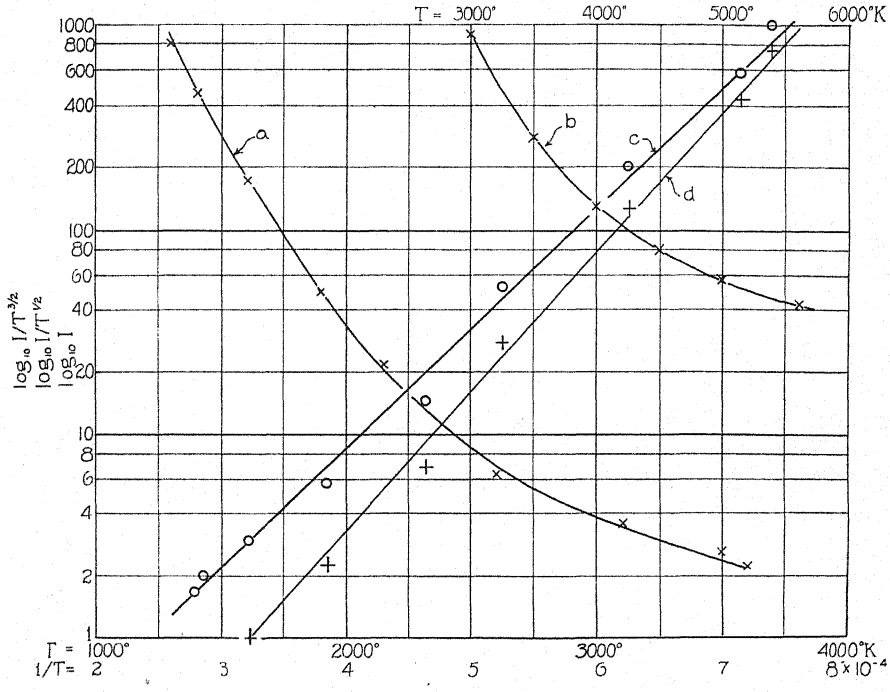

Fig. 3. Intensity of afterglow as a function of electron temperature; vapor pressure and electron concentration constant. Curve a: log I vs. T (lower temperature scale). Curve b: log I vs. T (upper temperature scale). Curve c: log $I/T^{1/2}$ vs. $1/T$. Curve d: log $I/T^{3/2}$ vs. $1/T$.

The experimental results giving the relation between the intensity of the afterglow, I, and the electron temperature are shown in Figure 3. Curve (a) shows the results for a vapor pressure of 0.06 mm. The ordinates are the intensities, corrected for variations in N, plotted for convenience as $\log_{10} I$. The abscissas are electron temperatures in °K. In these measurements N was of the order of 10^{11} per cc.

Curve (b) Figure 3, shows the results for another set of measurements at approximately the same vapor pressure. Owing to the fact that in this case no determinations of N were made, this curve has not been corrected to $N=$

constant. The variation of N over this curve may have been as great as threefold. The intensity scale is furthermore not the same as in Curve (a), owing to the use of a different photometric standard. This curve shows, however, that at higher temperatures the variation of I with T follows roughly the same law as in the lower temperature range. The striking feature of these curves is the very large decrease in I with small relative increase in temperature. Curve (a) shows a decrease in I of about 400 times as T increases from 1300° to 3600°K. Including the data of Curve (b) we see a decrease in I of about 2500 times as T changes from 1300° to 5600°.

Discussion

As pointed out earlier the rapid change of intensity, I, with electron temperature, T, observed in the afterglow cannot be explained by any simple process of recombination in which the decrease in the rate of recombination depends simply upon the increase in the average velocity of all the electrons. For, if the recombination is similar to that observed in caesium, with the coefficient of recombination approximately proportional to $1/v$ (v=electron velocity) and the electrons have a Maxwellian velocity distribution as seems to be the case, to a first approximation I should be proportional to the integral taken over all velocities of the number having a velocity v divided by v. This is equal to const $N^2/T^{\frac{1}{2}}$ where N is the total number of electrons, considered here as held constant. The total change in $1/T^{\frac{1}{2}}$ over the entire range of electron temperatures measured was not greater than 3, while I changed by a factor of nearly 2500, a different order of magnitude. Now, on the other hand, if we consider N_0, the number of electrons having energies greater than some given value, E_0, we see that this can be made to vary with the electron temperature as rapidly as we please, by proper choice of E_0. We have

$$N_0 = N\left[\text{erf}\,(E_0/kT)^{1/2} + (2/\pi^{1/2})(E_0/kT)^{1/2}e^{-E_0/kT}\right]$$

in which expression, if E_0 is not too small, the second term containing the exponential factor is the controlling one. (In the present work neglecting the first term introduces only an inappreciable error.) Now the simplest empirical relation between I and T which fits the results was found to be $I = C_1 T^n e^{C_2/T}$, equation (1), where C_1 and C_2 are constants and n is small. Because of the large value of the exponent the exponential term was found to be the important factor in determining the form of the curve and the precision of the measurements was not sufficient to enable one to differentiate between small values of n. The agreement between experiment and equation (1) can be seen from Curve (c), Figure 3, in which the data of Curve (a) have been replotted, with ordinates $\log_{10}(I/T^{\frac{1}{2}})$ and abscissas $1/T$. The points fall well within the experimental error on the straight line, $\log_{10}(I/T^{\frac{1}{2}}) = \text{const}/T + \log_{10}C_1$. In this plot n was taken as $\frac{1}{2}$ for reasons to be given below. Other series of measurements, taken at vapor pressures ranging from 0.06 mm to 0.10 mm when plotted in the same way gave nearly equally good agreement with the equation.

Now if I be taken proportional to N, as was found to be approximately true, equation (1), after rearranging, becomes:

$$I = \text{const } N^2 \div [N(2/\pi^{1/2})(E_0/kT)^{1/2}e^{-E_0/kT}] = \text{const } N^2 \div N_0 \qquad (2),$$

where k is Boltzmann's constant. Thus we may express our results very well in the simple form, that the intensity of the afterglow varies directly as the square of the total number of electrons and inversely as the number of electrons having energies greater than E_0. If instead of N_0, we consider the number, N_1, of electrons having an energy equal to E_0, we arrive at a similar result. N_1 varies as $(1/T^{3/2})e^{-E_0/kT}$, and if in equation (1) we put $n=3/2$, we obtain the result, $I=\text{const } N^2/N_1$. This results in a linear relation between $\log_{10}(I/T^{3/2})$ and $1/T$, as shown in Curve (*d*) Figure 3, in which the data of Curve (*a*) are expressed in these coordinates. We therefore find that we are in equally good agreement with experiment if in equation (2) we substitute N_1 for N_0, which gives the result that the intensity is inversely proportional to the number of electrons having their energy equal to E_0. The part played by the fast electrons is thus to prevent the afterglow, the effect of electron temperature on the intensity depending primarily upon the change in the number of such electrons. It should be remarked that this general conclusion does not rest solely on the close fit of the results with the relations given above but seems to be a necessary conclusion from the observed rapid change of I with T, so long as we assume that the effect of each electron on the process is a function of its energy and not of the mean energy of the whole group of electrons.

The value of E_0 as determined from the data of Curve (*c*) is 1.15 volt, from Curve (*d*) 1.35 volt. The values found from other series of measurements, when computed as in the case of Curve (*c*), range from 0.95 to 1.20 volt. The lowest value was obtained from a set of measurements covering only the lower temperatures and was probably affected by the fact that the intensities were often found to be less than those corresponding to the above equations when the electron temperature was below 1400°. Considering the precision of the measurements it seems probable that E_0 is a constant, independent of the vapor pressure and other conditions and that the best average of the values determined is 1.15 volt when computed assuming I to depend upon N_0, and 1.35 volt if it depends upon N_1. Furthermore, unless the efficiency of this preventative action of the fast electrons rises very rapidly as their energies approach the value E_0 from below, it seems that we must assume that E_0 is a minimum or a critical value for the energy of an electron which can so function and not an average value.

There has been found no evidence that metastable or excited atoms of the 2^3P states play any major part in the afterglow phenomenon.

Our results suggest that we are dealing with a process more complex than that of a simple recombination in which only a single electron and an ion take part, possibly a recombination process involving two electrons and an ion. The form of equation (2) suggests that this process is of the type illustrated by the following hypothetical picture, suggested by Mr. George Dean.

Assume that under the conditions in question complete recombination is accomplished in two stages, a first stage in which a slow electron falls into an outer level of the positive ion, and a second stage in which the electron makes a transition from this outer level to a lower level with the emission of series line radiation.* The first stage may be assumed to be accompanied by continuous radiation and to be governed by the laws similar to those governing the recombination observed in caesium and helium discussed above. Assume further that fast electrons having energies greater than a certain minimum value E_0 (or electrons having exactly the energy E_0) to be capable of reionizing the atom which has experienced only the first stage of recombination. Let N' be the concentration of such "partially recombined" atoms. The rate of formation of these atoms is $AN^2f(T)$ where $Af(T)$ is the coefficient of recombination, A being constant. The rate at which these atoms would change into normal atoms is given by RN', where R is a transition probability. The rate of reionization of the partially recombined atoms would be $CN'N_0$, where N_0 is, as above, the concentration of electrons having energies in excess of E_0. Now we are observing a steady state in the vapor stream and N' is constant. If we neglect a small term giving the diffusion rate of N' into the space observed, we get

$$AN^2f(T) - RN' - CN'N_0 = 0 \tag{3}$$

or

$$N' = AN^2f(T)/(R + CN_0). \tag{4}$$

Now except for the smaller values of T, R may be neglected with respect to CN_0 in the denominator of equation (4), since for larger values of T, RN' is negligible with respect to $AN^2f(T)$ and therefore with respect to $CN'N_0$. This follows since RN' is proportional to the intensity of the afterglow, I, which decreases very rapidly with increase in temperature while $AN^2f(T)$ varies not faster than $1/T^{3/2}$.

If $f(T)$ is taken equal to a constant we have from (4) $I = \text{const } N^2/N_0$, agreeing with the empirical equation (2) which expresses the experimental results. If $f(T)$ is taken equal to $1/T^{1/2}$, as suggested in the first paragraph of this section, we have $I = \text{const } (1/T^{1/2})(N^2/N_0)$ which gives equally good agreement with experiment. The value of E_0 in this case is about 7 percent lower than in the case of $f(T) = \text{constant}$.

In the above N_1, the number of electrons having exactly the energy E_0, may be substituted for N_0 without further change except that the corresponding values of E_0 would be increased by about 15 percent.

For the smaller values of T at which observations were taken and for small values of N, R may be no longer negligible with respect to CN_0 and we should then find the intensity less than would be expected from equation (2), and would further find for diminishing N that the intensity would vary more

* Compare this with the "initial recombination" postulated by J. Franck (Zeit. f. Physik 47, 509 (1928)): see also L. R. Maxwell (Phys. Rev. **32**, 715 (1928)).

nearly as the second power of N. The experimental results give evidence that this is the case, but are not sufficiently reliable to test this in detail.

It is obvious that the first stage of recombination assumed above may not necessarily involve an electron and a positive ion but may be the formation of some kind of molecular state, which in breaking up leaves the atom with such excitation as is necessary for the radiation of the arc lines. Recent studies by Mohler and Boeckner[9] of the photoionization of caesium indicate that the molecule ion plays a major part in that process and it is therefore probable that it is also an important factor in recombination. The picture given above represents only the type of process which the experimental results seem to indicate as necessary to account for the properties of the afterglow radiation in mercury vapor.

Lawrence[10] and other investigators have found a series of ultra-ionization potentials lying above the normal 10.4 volts ionization potential. The first four of these lie 0.20, 0.89, 1.30 and 1.66 volt, respectively, above 10.4 volts. It is suggested that the critical potential E_0 may be related to one of these ionization potentials.

[9] Boeckner, B. S. J. of Res. 5, 13 (1930); Mohler and Boeckner, B. S. J. of Res. 5, 51, 399, 831 (1930).

[10] Lawrence, Phys. Rev. **28**, 947 (1926); Jarvis, Phys. Rev. **27**, 808 (1926); Hughes and Van Atta, Phys. Rev. **36**, 214 (1930).

ON THE PERSISTENCE OF MOLECULAR ROTATION AND VIBRATION IN COLLISION

By O. Oldenberg
Jefferson Physical Laboratory, Harvard University

(Received December 5, 1930)

Abstract

The present paper attempts to explain some observations on the exchange of vibrational and rotational energy of molecules on the basis of the laws of impact, taking into account the postulate of quantisation. It is pointed out that when one of the bodies involved in the impact is much lighter than the other the exchange of energy becomes improbable. The persistence of rotation of HgH molecules in an excess of nitrogen, suggested by Beutler and Rabinowitsch, is discussed. A related phenomenon is found in some chemical activations produced by H_2 molecules but not by any other molecule. The resonance rule for the probability of impacts of the second kind needs some modification for the exchange of vibrational and rotational energy between molecules. The transfer of vibration and rotation from the excited iodine molecule is discussed. In electron impact, the rotation of the molecule does not change, but the vibration does. This is interpreted on the basis of a hypothesis introduced by Franck and Jordan. Within ordinary gases, N_2 or H_2 or I_2, no persistence of vibration or rotation should be expected.

IN THE present paper, an attempt is made to explain some observations, concerning molecular vibration and rotation from a classical standpoint, taking into account the postulate of quantisation. It should be emphasized, that this treatment of impact is intended to serve only as an approximate picture which may be of value as a starting point for experimental work.

I. Rotation of HgH in N_2

In a recent paper, Beutler and Rabinowitsch[1] offer an interesting interpretation of an experiment carried out several years ago by Wood and Gaviola.[2] These authors investigated the "sensitized fluorescence radiation" of Hg vapor with the addition of very little hydrogen and a considerable amount of nitrogen. Exciting the mercury atoms, they observed in fluorescence the band spectrum of the HgH molecule. It is a strange fact that the intensity distribution within the individual band corresponds approximately to a temperature of 3000°K, although the experiment is carried out at room temperature.

In a thorough discussion, Beutler and Rabinowitsch come to the conclusion that the excited HgH molecules are produced in the following two steps. The first elementary process consists of the exchange reaction $Hg' + H_2 = HgH + H$. In this reaction the 0.62 volt excess atomic energy over the required chemical energy changes partly into rotational energy of the HgH molecule, thus producing a rotation far exceeding the normal value. In a

[1] H. Beutler und E. Rabinowitsch, Zeits. f. Physik. Chem. (B) **8**, 403 (1930).
[2] E. Gaviola and R. W. Wood, Phil. Mag. **6**, 1191 (1928).

later process, this HgH molecule is excited by an impact of the second kind with another excited mercury atom. There are, however, only a very few of these excited mercury atoms. Therefore the authors assume that the anomalous rotation of the molecule HgH, produced in the first process, persists until the HgH collides with an excited Hg atom, in spite of a great many (more than 1000) collisions, most of them with N_2 molecules. It is possible of course, that the HgH molecule is formed with a still higher energy of rotation and gives part of it away. At any rate it is unexpected that the great number of intermediate collisions should fail to reduce the rotational energy to the normal value before the excitation of the molecule takes place. Are we able to understand this apparent persistence of rotational energy by the laws of impact?

An essential feature of the experiment is the heavy molecule HgH, having but a small moment of inertia, colliding with the molecule N_2, which is heavy compared with the H-atom. A reasonable picture of the collision is that the HgH molecule consists of the heavy mercury atom at rest and the H atom revolving about it with highest speed because of its small weight and the ab-

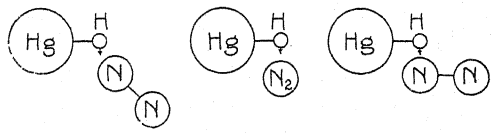

a b c

Fig. 1. Transfer of rotational energy of HgH to N_2

normal rotation produced by the excess energy of the reaction. This system collides with the N_2 molecule, supposed to be comparatively slow and not rotating. This impact is evidently related to the ordinary impact between a light and a heavy particle: the light particle is unable to give away any considerable fraction of its energy on account of the laws of impact.[3] In collision, the rotational energy and the moment of momentum given up by the HgH, split up generally into two parts, one of them going over into *rotation* of the N_2, the other into *translation* of the N_2, knocked away from the heavy system HgH in the direction of the arrow (Fig. 1a).

Since the general discussion of this collision is complicated, it will be sufficient to treat two extreme cases. First, we assume that the fast H atom in its circular orbit collides in a head-on collision (Fig. 1b) with a rigid body, representing the N_2 molecule. Thus from classical mechanics, we come to the result that the H atom is able to give away 1/7.5 of its energy (or less if the collision is not head on).

Let us next consider the other extreme case, in which the rotational energy of the HgH goes over as much as possible into *rotational* energy of the N_2 molecule (Fig. 1c). The fast H atom hits the left N atom, while moving toward its nucleus and perpendicular to the nuclear axis of the N_2 molecule. This col-

[3] Cf. J. Franck, Zeits. f. Physik **25**, 312 (1924) and G. Joos und H. Kulenkampff, Phys. Zeits. **25**, 257 (1924).

lision accelerates the left N atom in a direction, in which it can move an infinitely small distance, without accelerating the right N atom. Therefore, we are allowed to compute the resulting motion of the whole N_2 molecule in two separate steps. In the first step, only the left N atom is accelerated by the fast H atom; and after the collision, in the other step, the kinetic energy of this N atom produces such a translation of the whole N_2 molecule that its center of gravity keeps its velocity constant and in addition the molecule starts its rotation. The result is that the HgH molecule can give away 1/4, or probably less, of its rotational energy. The same reasoning should hold for the persistence of vibrational energy, although no observation of the phenomenon is known.

Since collisions are not head on in general, we understand that the rotational energy of HgH is given away in collision with N_2 molecules only in small steps—or with small probability if only large quanta are available. Thus we understand a persistence over let us say 10 or 20 collisions, but not over many thousand collisions, as suggested by Beutler and Rabinowitsch. This smaller amount of persistence, however, seems to be sufficient, if we assume a slightly different process of excitation. We assume that the metastable atom Hg' excites a HgH molecule with normal rotation, but with considerable vibration. This type of transition is understood by the Franck-Condon rule. When the H atom, vibrating as a part of the HgH molecule, collides with a comparatively heavy body, e.g., the N_2 molecule, its energy may change easily into its own rotational energy. On account of the laws of impact, the heavy N_2 molecule takes away only a small amount of energy. Thus a HgH molecule is produced with strong rotation which may collide, before it radiates, several times with N_2 without losing much of its rotational energy. When in a mixture of molecules containing light and heavy atoms some light atoms have a preferred energy, the general tendency is that equipartition of energy is reached first among the degrees of freedom of the light particles, much later among the degrees of freedom of the heavier particles. When N_2 is replaced by H_2O, we expect a rapid dissipation of the rotational and vibrational energy of HgH on account of the numerous H atoms present.[4] This explanation differs from that of Beutler and Rabinowitsch in that it assumes a persistence of rotation only during the life-time of the excited state, i.e., over a few collisions, but not over the long period between formation and excitation of the HgH molecule.

2. Relation to Activation Energy

In the present theory, the persistence of vibration and rotation is interpreted not as a fundamental quality of these degrees of freedom, but as due to the special interaction of light and heavy bodies in collision. Therefore it

[4] Presumably the peculiar intensity distribution in the HgH bands, observed in the electric discharge by W. Kapuscinski and J. E. Eymers (Zeits f. Physik **54**, 252, 1929) is to be explained by the same phenomenon. However, the process of excitation in the electric discharge is not so well understood as in fluorescence; in the discharge, excitation could take place in the same elementary process as the formation of the molecule HgH, contrary to the fluorescence experiment.

should be expected that this persistence plays a part in chemical activation, because it may happen that some molecules are able to give away activation energy, as far as it is vibration or rotation, not to any partner but only to a selected type of molecule.

Professor G. B. Kistiakowsky has pointed out to me, that possibly this type of selection plays a part in the "mono-molecular" decomposition of some organic compounds. From a thorough experimental and theoretical discussion, Hinshelwood[5] has drawn the conclusion that hydrogen, but no other gas, has a special power to activate the vapors of diethylether, dimethylether, propionic aldehyde and acetaldehyde by thermal impact. These organic molecules contain groups of H atoms. It might be assumed that the energy of activation consists largely of vibration of these H atoms. According to the present argument, their vibration should show a persistence in collision with heavier molecules but not with the lightest molecule H_2. This ability to *give away* vibrational energy should correspond, according to the principle of microscopic reversibility, with the ability to *take up* vibration from a colliding H_2 molecule, but not from heavy molecules.

It remains to explain, however, why helium fails to show the same effect, although it has only two times the weight of H_2. As in the interaction between HgH and N_2, we assume again that the vibration of an H atom, belonging to the organic molecule, is excited by ordinary collision with the H_2 molecule or the He atom. Both of them are somewhat heavier bodies which must have a sufficient excess of energy in order to give the energy of vibration to the bound H atom. From the Raman effect this energy level of vibration of the H atom attached to carbon is known[6] to be approximately 3000 cm^{-1}. According to the laws of impact, the H_2 molecule must have 12.5 percent more energy, whereas the He atom must have 69 percent more energy. Assuming a temperature of 520°C as in Hinshelwoods experiments, we come to the conclusion, that the number of H_2 molecules, able to activate, is ten times larger than the corresponding number of He atoms. This ratio, calculated only from the masses of H_2 and He, seems to be not quite sufficient to explain the observed difference. It should be taken into account, however, that the H_2 molecule with its five or six degrees of freedom contains on the average much more total energy than the He atom with its three degrees of freedom.

3. Probability Rule for Impacts of the Second Kind

On the basis of a group of experiments, Frank and Jordan[7] have established the general rule that in impacts of the second kind most probably the smallest possible amount of energy of *translation* is produced. Kallmann and London[8] derived the same rule from wave mechanics, describing the transfer

[5] C. N. Hinshelwood, Proc. Roy. Soc. **A114,** 84 (1927) and C. N. Hinshelwood and P. I. Askey, Proc. Roy. Soc. **115,** 215 (1927) and **116,** 163 (1927).

[6] D. H. Andrews, Phys. Rev. **36,** 549 (1930).

[7] Cf. J. Franck und P. Jordan, Anregung von Quantensprüngen durch Stösse, Berlin 1926, p. 226.

[8] H. Kallmann und F. London. Zeits. f. physik. Chem. (B) **2,** 207 (1929).

of excitation energy by a resonance phenomenon without introducing the translation in their equations explicitly. Corresponding to this rule, Beutler and Rabinowitsch discussed the persistence of rotation assuming that the rotational energy of HgH should change in collision mainly into *rotational* energy of N_2, only the smallest possible fraction going over into energy of *translation*.

Franck and Jordan based their rule on experiments in which the initial state of the energy is represented by an excited *electronic level*. It is doubtful if this rule applies without modification to the exchange of vibrational and rotational energy between molecules. However, this exchange can be represented to some extent by classical mechanics.[9] The mechanical treatment of exchange of vibrational and rotational energy between two colliding molecules leads necessarily to the formation of a considerable energy of translation, (cf. Fig. 1c) thus violating the rule that no energy fo translation is produced. Hence the rule seems to apply strictly to a limiting very important case i.e. the exchange of energy between electronic levels.[1] For the motion of heavy masses, however, it requires some modification.

4. Rotation and Vibration of I_2 in He

Some related phenomena are known. Beutler and Rabinowitsch refer to the iodine fluorescence radiation, excited by monochromatic light and changed, according to the experiment of Franck and Wood,[11] by the addition of helium. This experiment shows a transfer, although a rather slow one, of rotational energy of the iodine molecule. Some persistence of rotational energy is in this case probably due to the large mass of each iodine atom making impossible the transfer of much energy in a single collision with a light Heatom.

Wood and Loomis[12] describe the transfer of *vibrational* energy from I_2 to He, observed in the same experiment. It takes place very seldom, although from the standpoint of mechanics it could take place as well as the transfer of rotational energy.

We may explain the observation that the vibration is affected less than the rotation by taking into account a general distinction between rotation and vibration. The rotational energy is in any moment kinetic energy, where-

[9] How successful this classical treatment of the nuclear motion is, can be seen in the accomplishments of the theory of intensity distribution in band spectra, based on a mechanical picture by Franck, extended and expressed in wave mechanics by Condon (Proc. Nat. Acad. Sci. **13**, 462 (1927).

[10] If there is kinetic energy of a heavy mass produced—e.g. excitation of Hg going over into vibration of N_2—it should take place indirectly as discussed below, footnote 14.

[11] J. Franck and R. W. Wood, Verh. d. d. phys. Ges. **13**, 78 (1911).

[12] R. W. Wood and F. W. Loomis, Phil. Mag. **6**, 231 (1928). This phenomenon in which the colliding H atom takes up only a small part of the vibrational energy of the heavy I_2 is related to the phenomenon described by Knudsen's "accommodation coefficient" which, in turn, defines the degree to which a reflected gas molecule adjusts its energy to that of the reflecting surface (Ann. d. Physik. **34**, 519 (1911). For Pt and W surfaces this coefficient increases with the molecular weight of the gases.

as in vibration the energy changes continually between the kinetic and potential form. It is available for impact only in the short time interval in which most of it is kinetic and in which the atoms are moving apart. Hence in collisions with a monatomic gas, vibrational energy should show a greater persistence than rotational energy.

In order to explain Wood's and Loomis' observation (the comparatively large persistence of vibration) still another difference between vibration and rotation should be taken into account. Let us consider the inverse process. He atoms of high speed colliding with I_2 molecules, which may be considered to have no appreciable energy. How probable is the transfer of the kinetic energy of the fast He atom into vibration or rotation or translation of the I_2 molecule? For exciting *vibration*, the most favorable direction is along the *line* of the nuclear axis (Fig. 2a). For exciting *rotation*, however,

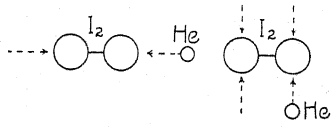

a b

Fig. 2. Excitation of vibration and rotation of the I_2 molecule by the He atom.

the most favorable direction of the He atom is any direction within the two *planes*, represented by dotted lines in Fig. 2b. Finally, for the transfer of energy of *translation* from the He to the I_2, there is no direction preferred within the whole *spherical angle*. Therefore the chance for translation is larger than for rotation, and this again larger than the chance for vibration. We may conclude, that in the inverse process, where the He atom takes up energy, the vibration of the I_2 molecule should be more persistent than the rotation, in agreement with Wood's and Loomis' observation.

5. Excitation of Vibration and Rotation by Electron Impact

Similar considerations may be applied to the excitation of molecular vibration and rotation by electron impact. From his experiments, Harries[13] drew the conclusion, that a 5-volt electron is able to excite *vibration* of the N_2 molecule, but that it cannot excite *rotation* at all. It has been pointed out by Franck and Jordan,[14] that this excitation of vibration cannot be understood by an ordinary elastic collision of the fast electron hitting the molecule head on (Fig. 2a), because the light mass of the electron is not able to give away this large fraction of its energy in elastic collision. The same inability of the electron holds for rotational energy, although the rotational quanta of N_2 are much smaller than the vibrational ones.[15]

[13] W. Harries, Zeits. f. Physik **42**, 26 (1927).

[14] J. Franck and P. Jordan, Anregung von Quantensprüngen durch Stösse, pp. 255 and 244.

[15] W. Rasetti, Phys. Rev. **34**, 367 (1929); the 5-volt electron giving away 1/1400 of its energy to an N atom, cannot excite the rotational quanta of the N_2 molecule. The same result holds in collision with a H_2 molecule.

Instead of the ordinary elastic collision between the 5-volt electron and the N_2 molecule, Franck and Jordan assume that the approaching electron has some influence by its electric field on the law of force keeping the N atoms together. The main difference between both pictures of collision is the following: in the ordinary elastic collision, the impinging electron would transfer part of its energy and impulse directly into translation or vibration or rotation of the molecule. In the hypothesis of Franck and Jordan, however, the electron penetrates the structure of the molecule. Without exciting a higher electronic level of the molecule—the first level requiring 8 volts—the electron modifies by its field the law of force keeping the atoms together. Thus by its mere presence, the electron may shift the equilibrium position of the nuclei, represented by the minimum of the potential curve. The nuclei start the vibration, accelerated not directly by the impact of the electron, but indirectly by the modified law of force. If the passage of the electron across the molecule takes an appreciable time compared with the period of vibration, it may happen, that the electron leaves the molecule in the vibrating state. From our point of view, the main feature of this hypothesis is, that the acceleration of the nuclei is produced indirectly by the modified law of force. This can give rise only to vibration, not to rotation on account of the conservation of moment of momentum. Therefore in collision with 5-volt electrons, we should expect an energy transfer in vibration only, but a strong persistence of rotation. This conclusion is in full agreement with Harries' experiments.[16]

(It would be hard to introduce the corresponding assumption that in the collision between I_2 and He discussed above, the *neutral* He atom, colliding at room temperature with an energy as low as 0.03 volt, causes an appreciable change in the law of force of the I_2 molecule. In this collision between heavy bodies there is no reason to discard the ordinary mechanical picture of the collision.)

6. Exchange of Vibration and Rotation Within Ordinary Gases

In the examples discussed above, some persistence of vibration or rotation is due to the extreme ratio of masses, e.g. of electrons colliding with N_2 molecules. The most important case consists of collisions within the molecules of the same gas, N_2 or H_2 or I_2. No restriction for the energy transfer and therefore no persistence of the same type should be expected.

Concerning these collisions, there are almost no optical data available.[17]

[16] The marked resonance in the transfer of excitation of the Hg atom into vibration of N_2 or CO or H_2O (H. Beutler and E. Rabinowitsch, Zeits. f. physik. Chem. B. **8**, 411 (1930) demonstrates that no appreciable translation is produced. Therefore, this process is very different from a mechanical impact, as should be expected because the initial state of the energy, the excited state of the atom, has no kinetic energy of a heavy mass. It should be described by a similar picture as Franck's and Jordan's, i.e., we assume that the close contact with the excited Hg atom modifies the electronic level and therefore the law of force of the molecule and changes the equilibrium position of the nuclei, thus starting vibration. (Cf. H. Beutler and W. Eisenschimmel, Zeits. f. physik. Chem. **10**, 103, 1930.)

[17] The complicated background in Wood's photographs of the resonance series in I_2 with long exposure (Phil. Mag. **35**, Plate VI, f. 1918) should be due to this process.

Professor A. Eucken called my attention to the fact, that we may draw a conclusion from thermal measurements. It is consistent with our expectation that the ratio of specific heats, measured from the velocity of sound, does not change at the highest frequencies[18] which means that, even for the quickest change of temperature, equipartition is maintained among all degrees of freedom of the diatomic molecule. It should be concluded that vibration and rotation are taking their full share in the exchange of energy. The great experimental difficulty, however, in these experiments should be emphasized.

The classical treatment of impact applied in the present paper is intended to serve only as an approximate picture which may be good as a starting point for experiments. An experimental investigation is under way. A more thorough treatment of these processes on the basis of wave mechanics is being developed by Dr. C. Zener. Some interesting results, published recently by R. Rompe[19] lead to the conclusion that some specific influence of the electronic term takes place. This kind of influence does not lend itself to representation by a classical picture.

Our main conclusion is that the persistence of vibration and rotation can be explained largely by classical ideas. Especially in the complicated interpretation of the HgH fluorescence given by Beutler and Rabinowitsch, the most doubtful detail, i.e., the excitation of abnormally rotating molecules, is understood by a general rule, the equipartition of energy being reached at a rate depending largely on the ratio of the weights of the particles. This result supports the other steps of the interpretation given by Beutler and Rabinowitsch which are of importance in photochemistry.

The author greatly appreciates the criticisms of Professor J. Franck, Professor E. C. Kemble and Dr. C. Zener.

[18] C. D. Reid, Phys. Rev. **35**, 814 (1930) and M. Grabau, to be published in spring 1931.
[19] R. Rompe, Zeits. f. Physik **65**, 425 (1930).

THE INTRAMOLECULAR FIELD AND THE DIELECTRIC CONSTANT

By Frederick G. Keyes and John G. Kirkwood*
Research Laboratory of Physical Chemistry,
Massachusetts Institute of Technology.**

(Received November 28, 1930)

Abstract

A statistical calculation of the average internal field in a dielectric is carried out. The following relation is obtained between the dielectric constant, ϵ, and the molecular polarizability, p_0:

$$\frac{\epsilon-1}{\epsilon+2}V=\frac{4\pi N p_0}{3}\frac{1}{1-\lambda_0\rho}$$

where V is the molal volume, ρ is the density and

$$\lambda_0=\frac{32\pi^2N^2p_0^2}{45B}\left(1+\frac{1}{3}\frac{A}{BRT}\right).$$

Here A and B are the constants of a van der Waal type equation of state. This expression becomes identical with the familiar Clausius-Mosotti relation in the limit of zero density. The formula is applied to dielectric constant measurements on several gases.

Introduction

THE concept of the dielectric constant rests upon a simple empirical basis. Faraday's experiments suggested that the intensity of the field arising from a given distribution of charge was less in a material substance than in free space. There was, moreover, evidence that the field intensity in a non-conducting substance was proportional to the original field intensity in free space. These facts were formulated in the following equation:

$$D=\epsilon E \tag{1}$$

where D, the dielectric displacement, is most simply interpreted as the field intensity existing in free space for the given charge distribution and E is the field intensity arising from the same distribution in a substance of dielectric constant ϵ. In view of the molecular character of the dielectric, it is clear that the measured field E is an average value, for macroscopic measuring systems are incapable of detecting the fluctuations in E occurring in the intervals of space and time associated with the thermal motion of the molecules. The fluctuations in the molecular configuration must, nevertheless, play an important part in determining the average polarization of the moving molecules constituting the dielectric.

Before it is possible to correlate the dielectric constant with the polarizability of the molecules, it is necessary to calculate the average value of the

* National Research Fellow.
** Contribution No. 253.

field effective in polarizing a molecule. Moreover, it is evident that the average internal field, referred to the moving molecule will not be identical with the field E referred to a point fixed relative to the external measuring system.

The Clausius-Mosotti relation is usually accepted as giving the relation between the dielectric constant of a substance and the polarizability of its constituent molecules. The computation of the internal field which leads to this formula purports to be based upon molecular considerations, but in the analysis, use is made of the device of a spherical cavity excised about the molecule. This seems justifiable only when the dielectric material is considered to be a continuum. The empirical success of the resulting formula in no way answers the logical objections to this analysis. For this reason, the use of the Clausius-Mosotti relation except in the case of gases at low density, where it has received adequate empirical confirmation, has been attended by great uncertainty.

There is here presented a statistical calculation of the average internal field leading to a formula which becomes identical with the Clausius-Mosotti relation in the limit of zero density, but which deviates somewhat from it at higher densities.

Limitations of the Case Considered and Derivation of Dielectric Constant Formula

The considerations to follow will be restricted to the relatively simple case of a gas of sufficiently low density so that the probability of molecular encounters involving more than two molecules is insignificantly small; and to temperatures sufficiently high so that an inappreciable fraction of the molecules are in quantized collision states such as may occur in molecular aggregation. Under these conditions the molecules may be regarded as continuously distributed in configuration, and moreover, the potential energy may be expressed as a sum of terms involving the relative coördinates of only two molecules.

It is desired to investigate the effect on the molecules constituting the fluid of an homogeneous external electric field. Take for consideration the region between the parallel plates of a condenser assumed to be filled with a fluid in equilibrium consisting of $n+1$ molecules of identical polarizability. Select for observation a molecule j not in the immediate neighborhood of the boundaries. The instantaneous and total field F_j acting on j may be written,

$$F_j = D + F_j' \tag{2}$$

where, as before, D, the dielectric displacement, is the field arising from the external charge distribution on the condenser plates and F_j' is the field arising from the other molecules of the dielectric. If, however, F_{jk}' is the field arising from an arbitrary molecule k we may write,

$$F_j' = \sum_{k=1}^{n} F_{jk}'. \tag{3}$$

The average value of any F_{jk}' term may be written:

$$\bar{F}_{jk}' = \frac{\int \cdots \int F_{jk}' e^{-u^*/kT} d\tau_1 \cdots d\tau_n}{\int \cdots \int e^{-u^*/kT} d\tau_1 \cdots d\tau_n} \tag{4}$$

where u^* is the total potential energy of the system and $d\tau_1$ is an element of the complete configuration space of a single molecule. The integration is to be extended over all of configuration space available to the molecules.

It will occasionally be convenient to consider F_{jk}' as averaged only over the orientations of the molecules, designated by $\overline{F_{jk}'}$, while the final average of $\overline{F}_{jk}'$ over all configurations of the centers of gravity of the molecule will be denoted by $\bar{\bar{F}}_{jk}'$.

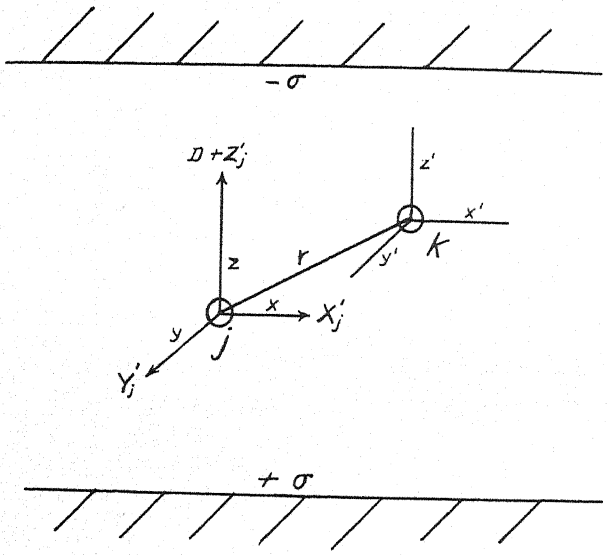

Fig. 1.

We proceed to calculate F_{jk}', the molecular field acting on the molecule j originating in an arbitrary molecule k. Choose a system of rectangular coördinates (x, y, z) whose origin is at the center of gravity of j and z axis parallel to the vector D. Similarly choose a second system (x', y', z'), with origin at the center of gravity of k with axes parallel to (x, y, z) see Fig. 1.

Suppose molecule k to consist of an assembly of charges $e_1 \cdots e_i$ whose average positions in the isolated molecule are given by the coordinates x_{1o}', $y_{1o}', z_{1o}' \cdots x_{io}', y_{io}', z_{io}'$. When a field is present it will be assumed that the perturbed positions, x_i', y_i', z_i' are given by

$$\begin{aligned} x_i' &= x_{i0}' + f_i X_k \\ y_i' &= y_{i0}' + f_i Y_k \\ z_i' &= z_{i0}' + f_i Z_k \end{aligned} \tag{5}$$

where the f_i's are constants and X_k, Y_k, Z_k are the components of the field acting on k. By expanding the potential at the center of j due to all the charges constituting k in a series of powers of x_i', y_i', z_i' there results for the potential ϕ_{jk}'.

$$\begin{aligned}\phi_{jk}' = {} & \sum\frac{e_i}{r} - \frac{1}{r^2}\left[\frac{x}{r}\sum e_i x_i' + \frac{y}{r}\sum e_i y_i' + \frac{z}{r}\sum e_i z_i'\right] \\ & + \frac{1}{2r^3}\left[\left(\frac{3x^2}{r^2}-1\right)\sum e_i x_i'^2 + \left(\frac{3y^2}{r^2}-1\right)\sum e_i y_i'^2\right. \\ & + \left(\frac{3z^2}{r^2}-1\right)\sum e_i z_i'^2 + 6\frac{xy}{r^2}\sum e_i x_i' y_i' + 6\frac{xz}{r^2}\sum e_i x_i' z_i' \\ & \left. + 6\frac{yz}{r^2}\sum e_i y_i' z_i'\right] + \cdots\end{aligned} \tag{6}$$

of which the first term is zero for a neutral molecule. Here x, y, and z represent the coordinates of the center of gravity of k relative to j and r is the separation of the centers. We assume that the field, F_{jk}', defined by this potential may be regarded as homogeneous over the small region occupied by a molecule. For its z component we may write

$$\begin{aligned}Z_{jk}' = -\frac{\partial\phi_{jk}'}{\partial(-z)} = {} & \frac{1}{r^3}\left[\left(\frac{3z^2}{r^2}-1\right)\sum e_i z_i' + \frac{3xz}{r^2}\sum e_i x_i' + \frac{3yz}{r^2}\sum e_i y_i'\right] \\ & - \frac{1}{2r^4}\left[\left(15\frac{z^3}{r^3} - 9\frac{z}{r}\right)\sum e_i z_i'^2 + \left(15\frac{x^2z}{r^3} - 3\frac{z}{r}\right)\sum e_i x_i'^2\right. \\ & + \left(15\frac{y^2z}{r^3} - 3\frac{z}{r}\right)\sum e_i y_i'^2 + \left(30\frac{xz^2}{r^3} - 6\frac{x}{r}\right)\sum e_i x_i' z_i' \\ & \left. + \left(30\frac{yz^2}{r^3} - 6\frac{y}{r}\right)\sum e_i y_i' z_i' - 30\frac{xyz}{r^3}\sum e_i x_i' y_i'\right] + \cdots.\end{aligned} \tag{7}$$

Using this expression for Z_{jk}' in Eq. (4) and integrating over all possible molecular orientations[1] we obtain

$$\bar{\bar{Z}}_{jk}' = \frac{\int\cdots\int \overline{Z_{jk}'} e^{-u/kT} dx_1 dy_1 dz_1 \cdots dx_n dy_n dz_n}{\int\cdots\int e^{-u/kT} dx_1 dy_1 dz_1 \cdots dx_n dy_n dz_n} \tag{8}$$

where u is that part of the potential energy dependent upon the configuration of the centers of gravity of the molecules, $x_1 \cdots z_n$. With the aid of Eq. (4) we may express $\bar{Z}_{jk}'$, the value of Z_{jk}' averaged over all orientations of the molecules with respect to their centers of gravity as

[1] P. Debye, Polar Molecules, 27 (1929).

$$\overline{Z}_{jk}' = \frac{\beta_1}{r^3} + \frac{\beta_2}{r^4} + \cdots = \sum_{m=1}^{\infty} \frac{\beta_m}{r^{m+2}} \tag{9}$$

where

$$\beta_1 = p_0[(3z^2/r^2 - 1)\overline{Z}_k + 3xz\,\overline{X}_k/r^2 + 3yz\overline{Y}_k/r^2]$$
$$\beta_2 = \tfrac{1}{2}k_0[(15z^3/r^3 - 9z/r)\overline{Z_k}^2 + (15x^2z/r^3 - 3z/r)\overline{X_k}^2$$
$$+ (15y^2z/r^3 - 3z/r)\overline{Y_k}^2 + (30xz^2/r^3 - 6x/r)\overline{X_kZ_k}$$
$$+ (30yz^2/r^3 - 6y/r)\overline{Y_kZ_k} - 30xyz\overline{X_kY_k}/r^3]$$

and $p_0=\alpha+\mu^2/3kT$

$$k_0 = \sum e_i f_i^2 + \frac{2\mu}{3kT}\sum e_i r_{i0} f_i + \frac{\mu^2}{15k^2T^2}\sum e_i r_{i0}^2.$$

Here α is the sum of the electronic and atomic polarizabilities, $\sum e_i f_i$, μ is the permanent electric moment of the molecule, r_{i0} the distance of the charge e_i from the center of gravity of the molecule k, k is Boltzmann's constant and T the absolute temperature. $\overline{X}_k$, $\overline{Y}_k$, $\overline{Z}_k$, etc., are the components of the field acting on k, averaged over all molecular orientations.

We shall write Eq. (9) in a slightly different manner:

$$\overline{Z}_{jk}' = \left\{\frac{\beta_1'}{r^3} + \frac{\beta_2'}{r^4} + \cdots\right\} + \left\{\frac{\beta_1''}{r^3} + \frac{\beta_2''}{r^4} + \cdots\right\} \tag{10}$$

where β_1', $\beta_2' \cdots$ are formed by replacing $\overline{Z}_k$, $\overline{X}_k$, $\overline{Y}_k$ etc. in β_1, β_2, by their average values $\overline{\overline{Z}}_k$, $\overline{\overline{X}}_k$, $\overline{\overline{Y}}_k$. Likewise, β_1'', β_2'', are formed by replacing these quantities in β_1, $\beta_2 \cdots$ by the fluctuations from their average values, $\overline{Z}_k - \overline{\overline{Z}}_k$, $\overline{X}_k - \overline{\overline{X}}_k$, $\overline{Y}_k - \overline{\overline{Y}}_k$, etc. It is apparent that the first series on the right hand side of Eq. (10) gives the magnitude which $\overline{Z}_{jk}'$ would have if the molecule k remained rigidly polarized by the average field $\overline{\overline{F}}_k$ throughout all configurations of the centers of gravity of the molecules. The second series gives the contribution to $\overline{Z}_{jk}'$ resulting from the fluctuation of $\overline{F}_k$ from its average value $\overline{\overline{F}}_k$.

From Eqs. (2) and (3) we have

$$Z_j' = \sum_{k=i}^{n} Z_{jk}'$$

and

$$\overline{\overline{Z}}_j' = \sum_{k=1}^{n} \overline{\overline{Z}}_{jk}'. \tag{11}$$

Moreover, it is evident that all of the $\overline{\overline{Z}}_{jk}'$ must be identical, since the molecule k was selected at random from the n molecules surrounding j. Therefore

$$\overline{\overline{Z}}_j' = n\overline{\overline{Z}}_{jk}. \tag{11a}$$

From Eqs. (8), (10) and (11) we obtain

$$\bar{Z}_j = I_1 + I_2$$

where

$$I_1 = n\frac{\int\cdots\int\left(\sum_{m=1}^{\infty}\beta_m'/r^{m+2}\right)e^{-u/kT}dx_1dy_1dz_1\cdots dx_ndy_ndz_n}{\int\cdots\int e^{-u/kT}dx_1dy_1dz_1\cdots dx_ndy_ndz_n}$$

$$I_2 = n\frac{\int\cdots\int\left[\sum_{m=1}^{\infty}\beta_m''/r^{m+2}\right]e^{-u/kT}dx_1\cdots dz_n}{\int\cdots\int e^{-u^0/kT}dx_1\cdots dz_n}.$$

The potential energy of the system may be written

$$u = \tfrac{1}{2}\sum_{j=1}^{n}\sum_{k=1}^{n}(u_{jk}^0 + u_{jk}')$$

where u_{jk}^0 is the normal potential energy of two molecules j and k which has been assumed to depend only upon the relative coordinates of the two, and u'_{jk} is the additional energy when there is an external field present.

It is easily shown that for weak fields, u_{jk}' is always so small relative to kT, that it may be neglected in the evaluation of the integrals of Eq. (10). It will therefore suffice to consider u as given by the normal potential energy u_{jk}^0.[I]

Note I. If $\bar{m}_j$ and $\bar{m}_k$ designate the electric moments of j and k along the z axis, averaged over all molecular orientations, then there may be written approximately, neglecting a term which is constant throughout the region considered.

$$u_{jk}' = -\frac{\bar{m}_j\bar{m}_k}{r^3}\left\{\frac{2z^2}{r^3} + \frac{\alpha}{r^3}\left(\frac{3z^2}{r^2}+1\right)\right\} \qquad \text{(a)}$$

where

$$\bar{m}_j = p_0(D + \bar{F}_j') \qquad \bar{m}_k = p_0(D + \bar{F}_k').$$

We may anticipate the result of the calculation of $\bar{F}_j'$ by assigning to it the approximation $-(8\pi/3)\rho N p_0 D$, where ρ is the density. Also approximately

$$[\overline{(\bar{F}_j' - \bar{\bar{F}}_j')^2}]^{1/2} = \frac{8\pi}{3}Np_0D\left(\frac{3\rho}{4\pi N\sigma^6}\right)^{1/2}$$

where σ is the distance of nearest approach of two molecules. It may therefore be safely assumed that m_j and m_k are in general of the order of magnitude of p_0D. Thus from Eq. (a), the maximum value assignable to $|u_{jk}'|$ is the order of magnitude of

$$|u_{jk}| = (2p_0^2D^2/\sigma^3)(2 + \alpha/\sigma^3).$$

For hydrogen at 300°K we have

$$kT = 4.11 \times 10^{-14} \text{ ergs}$$
$$p_0 = \alpha = 8 \times 10^{-25} \text{ cc}$$
$$\sigma = 2.3 \times 10^{-8} \text{ cm}.$$

For a value of D of 900 volts/cm, there results:

$$|u_{jk}'|/kT \backsim 4 \times 10^{-10}.$$

. . . . . .

Since the series

$$\beta_1'/r^3 + \beta_2'/r^4 + \cdots$$

depends only upon the relative coördinates of j and k, the first integral I_1 becomes

$$I_1 = n \frac{\int\int\int \left(\sum_{m=1}^{\infty} \beta_m'/r^{m+2} \right) e^{-u^0_{jk}/kT} dx_k dy_k dz_k}{\int\int\int e^{-u^0_{jk}/kT} dx_k dy_k dz_k}.$$

In evaluating the latter integral it will be sufficient to employ the van der Waal's or rigid-sphere molecular model. It is assumed then, that the molecules have spherical symmetry relative to the coordinate system fixed in space by the vector D. Lack of spherical symmetry resulting from the orientation of a permanent dipole in the molecule, as well as from the induced deformation of the average configuration of the charges constituting the molecule, will be negligible unless the external field is very large. It will be further assumed that a distance of nearest approach, σ, exists such that

$$u_{jk}^0 = \infty \text{ for } r_{jk} \leqq \sigma$$

When $r_{jk} > \sigma$, $e^{-u_{jk}^0/kT}$ is to be expanded as

$$1 + \sum_{s=1}^{\infty} \frac{1}{S!} \left(-\frac{u_{jk}^0}{KT} \right)^s.$$

The evaluation of I_1 leads to the result

$$I_1 = -\frac{8\pi}{3} n \frac{p_0}{V} \bar{Z}_k.$$

If $I_2 = \lambda \bar{Z}_k$ there results,

$$\bar{Z}_j' = -\bar{Z}_k \left(\frac{8\pi}{3} \frac{n}{V} p_0 - \lambda \right).$$

There is no physical distinction between molecules j and k and accordingly $\bar{Z}_j$ and $\bar{Z}_k$ must be equal.[II]

Note II. First make the approximation

$$\iiint e^{-u^0_{jk}/kT} dx\, dy\, dz$$

where V is the total volume between the plates of the condenser. It will differ from the above integral only by a quantity of the order of magnitude of the volume of a single molecule. After transforming to polar coordinates we obtain:

$$I_1 = \frac{np_0}{V}\int_0^{2\pi}\left[\int_0^{\pi/2}\int_\sigma^{z_1\sec\theta} + \int_{\pi/2}^{\pi}\int_\sigma^{z_2\sec\theta}\right]\left\{\frac{\beta_1'}{r}+\frac{\beta_2'}{r^2}+\cdots\right\}$$
$$\left\{1+\sum_{s=1}^{\infty}\frac{1}{s!}\left(-\frac{u_{jk}^0}{kT}\right)^s\right\}dr\sin\theta d\theta d\phi$$

where z_1 and z_2 are the distances of the molecule j from the two plates of the condenser.

It is possible to expand u_{jk}^0 in powers of $1/r$ of which the dominant term is a/r^6.[2] It is therefore obvious that when the multiplication indicated in the integrand is carried out, all terms except β_1'/r will contain $1/r$ to the second or higher powers. The contribution of these terms to the integral will decrease so rapidly with r that we may safely take the upper limit in the integration over r as ∞. We then may write

$$I_1 = \frac{np_0}{V}\int_0^{2\pi}\left[\int_0^{\pi/2}\int_\sigma^{z_1\sec\theta} + \int_{\pi/2}^{\pi}\int_\sigma^{z_2\sec\theta}\right]\frac{\beta_1'}{r}\sin\theta d\theta dr d\phi + \frac{np_0}{V}\int_\sigma^{\infty}\int_0^{2\pi}\int_0^{\pi}\frac{\beta_1'}{r}\sum_{s=1}^{\infty}\frac{1}{s!}\left(-\frac{u_{jk}^0}{kT}\right)^s$$
$$+\left\{\frac{\beta_2'}{r^2}+\cdots\right\}\left\{1+\sum_{s=1}^{\infty}\frac{1}{s!}\left(-\frac{u_{jk}^0}{kT}\right)^s\right\}\sin\theta d\theta d\phi dr.$$

It is to be remembered that u_{jk}^0 is independent of θ and ϕ, since it has spherical symmetry around j because of the averaging over all mutual orientations of j and k. Moreover, each of the coefficients β_1', β_2', $\cdots$ satisfies the relation

$$\int_0^{2\pi}\int_0^{\pi}\beta_m'\sin\theta d\theta d\phi = 0.$$

It follows that through integration over the angles the second integral vanishes term by term and there remains when we insert the value of β_1'

$$\frac{np_0}{V}\int_0^{2\pi}\left[\int_0^{\pi/2}\int_\sigma^{z_1\sec\theta} + \int_{\pi/2}^{\pi}\int_\sigma^{z_2\sec\theta}\right]\left\{\bar{\bar{Z}}_k(3\cos^2\theta-1)+3\bar{\bar{X}}_k\sin\theta\cos\phi\right.$$
$$\left.+3\bar{\bar{Y}}_k\sin\theta\sin\phi\right\}\sin\theta d\theta\frac{dr}{r}d\phi$$

Integration over r and ϕ yields

$$\frac{2\pi n}{V}p_0\bar{\bar{Z}}_k\left\{-\int_0^{\pi}(3\cos^2\theta-1)\log\cos\theta\sin\theta d\theta+\int_0^{\pi/2}(3\cos^2\theta-1)\log\frac{\sigma}{z_1}\sin\theta d\theta\right.$$
$$\left.+\int_{\pi/2}^{\pi}(3\cos^2\theta-1)\log\frac{\sigma}{z_2}\sin\theta d\theta\right\} = -\frac{8\pi}{3}\frac{np_0}{V}\bar{\bar{Z}}_k.$$

It is to be noted that this quantity is independent both of z_1 and z_2 as well as of σ.

The subscripts may therefore be neglected and the average value of the Z-component of the internal field becomes, if it is remembered that $Z=Z'+D$ (Eq. 4).

$$\bar{\bar{Z}} = \frac{D}{1+\frac{8\pi}{3}\frac{n}{V}p_0-\lambda}. \tag{13}$$

A similar calculation shows that $\bar{\bar{Y}}_j$ and $\bar{\bar{X}}_j$ vanish, and the average value of the resultant internal field F is merely,

$$\bar{\bar{F}} = \frac{D}{1+\frac{8\pi}{3}\frac{n}{V}p_0-\lambda} \tag{14}$$

[2] Eisenschitz and London, Zeits. f. Physik, **60**, 491 (1930).

This equation when combined with the usual classical relations,

$$D = \epsilon E$$
$$D = E + 4\pi P$$
$$P = \frac{n}{V} p_0 \bar{\bar{F}}$$

gives;

$$\frac{\epsilon - 1}{\epsilon + 2} V = \frac{4\pi}{3} N p_0 \frac{1}{1 - \lambda} \tag{15}$$

where v is the molal volume and ϵ is the dielectric constant. Equation (15) reduces to the familiar Clausius-Mosotti relation

$$\frac{\epsilon - 1}{\epsilon + 2} v = \frac{4\pi}{3} N p_0 \tag{16}$$

only if λ is identically zero for all temperatures and pressures. This is not in general true. The quantity λ is a measure of the contribution of the fluctuations in $\bar{F}$. It will be shown that λ is proportional to the density as long as only binary molecular encounters need be considered. For very dense gases, on the other hand, the effect of the fluctuations is less important and λ will be smaller than the formula indicates.

In evaluating the quantity λ it will be sufficient to retain only the dipole term in the $\bar{Z}_{jk}'$ series. It will be conveneint to make use of the identity

$$\bar{Z}_k - \bar{\bar{Z}}_k = \sum_{l=1}^{n-1} (\bar{Z}_{kl}' - \bar{\bar{Z}}_{kl}') + \bar{Z}_{kj}' - \bar{\bar{Z}}_{kj}'$$

λ may then be written

$$\frac{n}{\bar{\bar{Z}}} \frac{\int \cdots \int \psi e^{-u/kT} dx_1 \cdots dz_n}{\int \cdots \int e^{-u/kT} dx_1 \cdots dz_n}$$

where

$$\psi = \frac{p_0}{r^3} \left\{ \left(\frac{3z^2}{r^2} - 1 \right) \left[\sum_{l=1}^{n-1} (\bar{Z}_{kl}' - \bar{\bar{Z}}_{kl}') + (\bar{Z}_{kj}' - \bar{\bar{Z}}_{kj}') \right] + \frac{3xz}{r^2} \left[\sum_{l=1}^{n-1} (\bar{X}_{kl}' - \bar{\bar{X}}_{kl}') + (\bar{X}_{kj}' - \bar{\bar{X}}_{kj}') \right] + \frac{3yz}{r^2} \left[\sum_{l=1}^{n-1} (\bar{Y}_{kl}' - \bar{\bar{Y}}_{kl}') + (\bar{Y}_{kj}' - \bar{\bar{Y}}_{kj}') \right] \right\}.$$

If the integration over the coordinates of all the l molecules is carried out under the assumption that each of the $\bar{Z}_{kl}$ terms is independent of the relative

positions of j and k, there results (consistent with the original postulate of binary encounters)

$$\lambda = \frac{n}{\bar{\bar{Z}}V}\int\int\int\frac{p_0}{r^3}\left[\left(\frac{3z^2}{r^2}-1\right)(\bar{Z}_{kj}'-\bar{\bar{Z}}_{kj}')+\frac{3xz}{r^2}\bar{X}'_{kj}\frac{3yz}{r^2}\bar{Y}'_{kj}\right]e^{-u_{jk}/kT}dxdydz$$

where $\bar{X}_{kj}'$, $\bar{Y}_{kj}'$, $\bar{Z}_{kj}'$ now denote the values of these quantities when the *average field* from the other molecules is acting on both j and k. It is obvious that

$$\bar{Z}_{kj}' = \bar{Z}_{jk}'.$$

Transformation to polar coordinates and integration over the azimuthal angle ϕ yields, since $\bar{X}_{kj}'$ and $\bar{Y}_{kj}'$ are obviously independent of ϕ.

$$\lambda = \frac{2\pi n}{\bar{\bar{Z}}V}\int\int\kappa[\bar{Z}_{kj}'-\bar{\bar{Z}}_{kj}']e^{-u_{jk}^0/kT}r^2\sin\theta dr d\theta$$

and

$$\kappa = \frac{p_0}{r^3}(3\cos^2\theta - 1).$$

It will be seen immediately that the contribution arising from $\bar{\bar{Z}}_{kj}'$ may be ignored since it amounts to

$$-\frac{8\pi n p_0}{V}\frac{\bar{\bar{Z}}_{kj}}{\bar{\bar{Z}}}$$

a quantity of the order of magnitude of $1/n$ since $\bar{\bar{Z}}' = n\bar{\bar{Z}}'_{kj}$. Moreover, it is obvious that after the integration over ϕ

$$\bar{Z}_{kj}' = \kappa\bar{Z}_i = \kappa\left(\sum_{l=1}^{n-1}\bar{\bar{Z}}_{jl} + \bar{Z}_{jk}'\right)$$

$\sum_{l=1}^{n-1}\bar{\bar{Z}}_{jk}$ differs from $\bar{\bar{Z}}$ by a quantity of the order of magnitude of $1/n$. Since $\bar{Z}_{jk}' = \bar{Z}_{kj}'$ the expression for λ becomes, after solving for $\bar{Z}_{kj}$;

$$\lambda = \frac{2\pi n}{V}\int_0^\pi\int_0^\infty\frac{\kappa^2}{1-\kappa}e^{-u_{jk}^0/kT}r^2\sin\theta dr.$$

When $2p_0/\sigma^3$ is small relative to unity and only the first two terms are retained in the expansion of $e^{-u^0_{jk}/kT}$, the above expression is closely approximated by[III]

$$\frac{32\pi^2N^2p_0^2}{45BV}\left(1+\frac{1}{3}\frac{A}{BRT}\right)$$

where A and B are the constants of the van der Waal type of equation of state and v is the molal volume. The condition that $2p_0/\sigma^3$ be small relative to unity is in general fulfilled by non-polar substances. (hydrogen; $2p_0/\sigma^3 = 0.12$). For polar substances where $2p_0/\sigma^3$ often exceeds unity (ammonia; $2p_0/\sigma^3 = 1.6$), it is probable that the above expression is still a fair representation of λ.

Note III. If $\kappa^2/1-\kappa$ is expanded and only the first term of the resulting series retained, the expression for λ becomes

$$\frac{2\pi n}{V}\int_0^\pi \int_\sigma^\infty \frac{p_0^2}{r^4}(3\cos^2\theta - 1)e^{-u_{jk}^0/kT}\sin\theta d\theta dr.$$

If $e^{u_{jk}^0/kT}$ is expanded and only the first two terms

$$1 - \frac{u_{jk}^0}{kT}$$

are retained, and further if it is assumed that

$$u_{jk}^0 = -\frac{a}{r^6} + \cdots$$

one obtains

$$\lambda = \frac{16\pi p_0^2}{15\sigma^3}\frac{n}{V}\left(1 + \frac{Na}{3RT\sigma^3}\right).$$

Since the van der Waal's cohesive pressure constant, A, is given by

$$\frac{\pi N^2}{3}\int_\sigma^\infty e^{-u_{jk}^0/kT}\frac{\partial u_{jk}^0}{\partial r}r^3 dr = \frac{2\pi N^2 a}{3\sigma^3} + \cdots$$

and the volume constant is

$$B = \frac{2\pi}{3}N\sigma^3.$$

It is found approximately that

$$\lambda = \frac{1}{v}\frac{32\pi^2 N^2 p_0^2}{45B}\left(1 + \frac{1}{3}\frac{A}{BRT}\right).$$

If the aggregation effect is ignored and one sets $e^{u_{jk}^0/kT}$ equal to unity, one has

$$\lambda' = \frac{2\pi n}{V}\int_0^\pi \int_\sigma^\infty \frac{p_0^2(3\cos^2\theta - 1)}{r^3 - p_0(3\cos^2\theta - 1)}\sin\theta d\theta\frac{dr}{r}.$$

This integral may be exactly evaluated as

$$\frac{2\pi p_0}{3}\frac{n}{V}\left[4x^2 - \frac{8}{3} + (2x - 2x^3)\ln\frac{x+1}{x-1}\right]$$

where

$$x = \left(\frac{1 + p_0/\sigma^3}{3p_0/\sigma^3}\right)^{1/2}.$$

The quantity remains finite as long as $2p_0/\sigma^3 < 1$. When the logarithm is expanded the first term is

$$\frac{16\pi p_0^2}{15\sigma^3}\frac{n}{V}$$

which agrees with the previous result. Moreover when p_0/σ^3 is in the neighborhood of 0.1, the error introduced by neglecting the remaining terms is found to be less than 3 percent represen-

tation of λ. Even in this case $2p_0/r^3$ remains small until very small values of r are reached. Thus for ammonia $2p_0/r^3<0.2$ when $r>2\sigma$. For smaller values of r, the formulation of the integral ceases to be exact. Here the intensity of the mutual field of j and k becomes so great that an electrical saturation sets in and the electric moments of the two molecules are no longer proportional to the field intensity. If in a very rough manner one replaces p_0 by

$$p_0 + \left\{\frac{1}{\bar{Z}_k} L\left(\frac{\mu \bar{Z}_k}{kT}\right) - \frac{\mu^2}{3kT}\right\}$$

where $L(x)$ is the Langevin function, it is seen that while $1-\kappa$ may differ appreciably from unity, it never becomes extremely small. Moreover, the effect will produce a corresponding diminution in κ^2 so that it should not strongly affect the magnitude of the factor $\kappa^2/(1-\kappa)$ in the integrand.

If one sets $\lambda = \lambda_0 \rho$ where ρ is the density in moles per cc and designates $4\pi N p_0/3$ by P_0, Eq. (15) becomes

$$\frac{\epsilon - 1}{\epsilon + 2} v = \frac{4\pi N p_0}{3} \frac{1}{1 - \lambda_0 \rho} \tag{18}$$

where

$$\lambda_0 = \frac{2P_0^2}{5B}\left(1 + \frac{1}{3}\frac{A}{BRT}\right).$$

Equation (18) becomes identical with the Clausius-Mosotti formula only in the limit of zero density. When ρ is small, they may, however, approximate each other very closely over a considerable range of density. A calculation of λ_0 for air, nitrogen and hydrogen indicates that the factor $1/1-\lambda_0\rho$ gives rise to a deviation of less than .05 percent from the Equation (16) at 100 atm. and 20°C. This is in accord with the experimental results of Tangl[3] who found no measureable deviation from the Clausius-Mosotti law for these substances. Measurements of the dielectric constant of carbon dioxide[4] at high densities indicate that the Clausius-Mosotti function, $(\epsilon-1/\epsilon+2)v$, increases with increasing density as Eq. (18) demands. However, the rate of increase is about twenty times that to be expected from the value of λ_0 calculated from the equation of state constants. It is probable that this gas may not be treated as an assembly of molecules of identical polarizability at the temperatures of the dielectric constant measurements.[IV]

Note IV. [Suppose a mixture of several molecular types corresponding to various vibrational states of the molecule. It is easy to see that if these various states differed in polarizability, a shift in the distribution among them due to a change in density, might well increase the mean molecular polarizability in such a manner as to give rise to the observed effect.]

Measurements of the dielectric constant of ammonia[5] yield values of $(\epsilon-1)$ $v/(\epsilon+2)$ which to 30 to 40 atm. follow Eq. (14), with a value of λ_0 calculated from the equation of state constants. In the higher pressure region the slope of the experimental curve decreases rapidly and a negative deviation from

[3] K. Tangl, Ann. d. Physik **29**, 59 (1908).
[4] F. G. Keyes and J. G. Kirkwood, Phys. Rev. **36**, 754 (1930).
[5] F. G. Keyes and J. G. Kirkwood, Phys. Rev. **36** (1930).

Eq. (14) occurs. This is not surprising since the assumptions underlying the whole of the present analysis are highly simplified.

In the present discussion it has been assumed that the boundaries of the dielectric material consist of two planes perpendicular to the direction of an homogeneous external field. It seems probable that if the boundary surface of the dielectric is of an irregular character, inhomogenity in the average internal field will arise and Eq. (18) will no longer be strictly valid. Such considerations would of course not be of importance at low densities where $\overline{F}$ is small compared to D. Under the latter conditions the simple relation

$$\frac{\epsilon - 1}{3} v = \frac{4\pi}{3} N p_0$$

is valid regardless of the character of the boundary surface.

It is a matter of great interest that the observed deviations from the Clausius-Mosotti relation at high densities are much lower than Eq. (18) predicts. This is not difficult to understand when it is observed that collisions involving more than two molecules will decrease the value of λ, the measure of the contributions of the fluctuations to the average molecular field. In fact, barring effects due to quantized vibrations or rotations, the Clausius-Mosotti function would be expected, on the basis of the present theory, to approach absolute constancy when the molecules were at all instants continuously under one another's mutual influence. The dielectric constant data for liquid carbon dioxide under various pressures proves the supposition tentatively, for the computed Clausius-Mosotti function shows no variation.

SYMBOLS

E	Mean field intensity.
D	Dielectric displacement.
n	Number of molecules.
ϵ	Dielectric constant.
F_j	Total field (sum of molecular and external fields) acting on a molecule j in a dielectric.
F_j'	Molecular field acting on j.
F_{jk}'	The component of F_j' arising from a single molecule k.
$\overline{F}_j'$	Average value of F_j' over all molecular orientations.
$\overline{\overline{F}}_j'$	Average value of F_j' over all configurations of the centers of gravity of the molecules.
$d\tau$	Element of configuration space of a single molecule k.
$[x, y, z]$	Rectangular coordinate system with origin at center of gravity of the molecule j and with z axis parallel to D.
$[x', y', z']$	Rectangular coördinate system with origin at center of molecule k.
$e_1 \cdots e_i$	The charges constituting the molecule k.
$x_{i0}'\ y_{i0}'\ z_{i0}'$	Average coordinates of the charge e_i when there is a perturbing field.
f_i	Elastic constant for linear displacements of e_i from its average position in the molecule.
ϕ_{jk}'	Potential in the interior of the molecule j due to the molecule k.
r	Separation of the centers of gravity of j and k.
X_j, Y_j, Z_j	Components of F_j along the axes of the coördinate system $[x, y, z]$.
X_j', Y_j', Z_j'	Components of F_j' along the axes of the coördinate system $[x, y, z]$.

U^*	Total potential energy of the ensemble of molecules.
U_{jk}^*	Mutual potential energy of the two molecules j and k.
U_{jk}	That part of U_{jk} dependent only upon the configuration of the centers of gravity of j and k.
$U^0{}_{jk}$	The value of U_{jk} when there is no external field.
p_0	Polarizability of a molecule.
α	Sum of electronic and atomic polarizabilities.
μ	Fixed dipole moment of a molecule.
σ	Distance of closest approach of two molecules.
V	Volume of the system.
v	Molal volume.
ρ	Molal density.

LETTERS TO THE EDITOR

Prompt publication of brief reports of important discoveries in physics may be secured by addressing them to this department. Closing dates for this department are, for the first issue of the month, the twenty-eighth of the preceding month; for the second issue, the thirteenth of the month. The Board of Editors does not hold itself responsible for the opinions expressed by the correspondents.

Hyperfine Structure and Polarization of Mercury Resonance Radiation

In a letter to the Editor appearing in the November 15th issue of this Review, S. Mrozowski has described certain experiments on the polarization of the λ2537A resonance radiation of mercury which he finds difficulty in reconciling with the previous work of MacNair and the author.[1] We showed that the low polarization of this resonance line was due to the two outer of its five hyperfine structure components, not the −25.4 m.a. component alone, as Mrozowski appears to assume. He concludes that resonance radiation excited by the −25.4 m.a. component only should show a lower polarization than that excited by the entire pattern. This he finds is not the case. This in itself involves no contradiction, for whether excitation by part of the pattern will produce a polarization different from that due to excitation by the entire pattern depends upon whether the relative population of the upper hyperfine structure levels is changed. For example if all five components originated in a single upper level no change would occur. Other arrangements might lead to the same conclusion, and as the levels are unknown there is no essential contradiction here.

However Olson[2] showed that this resonance radiation excited by an arc run on very low current might be as high as 86 percent polarized instead of the usual 79–80 percent. He supposed this change in the polarization was due to a change in the relative intensities in the h.f.s. pattern, and in fact there appears to be no other possibility. Olson also showed that the product of mean life into Larmor precession frequency did not change. This shows that the polarization is not then independent of *all* relative intensity changes and raises the question why Mrozowski observed no change. The writer has carried out these experiments.

Light from a mercury arc is passed through an absorption cell 8 cm long containing mercury vapor at a pressure of 1.3×10^{-3} mm Hg (20°C) placed in a magnetic field of 2000 gausses intensity. The light passing through this cell polarized with its electric vector parallel to the field was used to excite resonance radiation in Hg vapor. The resonance bulb was placed in a magnetic field of 50 gausses parallel to the electric vector of the exciting light. The resonance radiation so excited showed a polarization very much *less* than 80 percent. This was shown clearly by two photographs of the resonance radiation taken through a Wollaston prism, one of four minutes duration with the absorption cell in place as mentioned above, and one of one minute with no absorption. In the one minute exposure the strong image ($E\|H$) was stronger than the strong image in the four minute exposure, while the weaker image in the four minute exposure was stronger than the weak image in the one minute picture. No attempt was made to measure accurately the polarization of the resonance radiation so excited. It is safe to say that it was not greater than 60 percent.

Precisely similar results were obtained with a magnetic field of 50 gausses parallel to the exciting light beam. Here the excitation is by $E\perp H$. No attempt was made to excite resonance radiation in zero field with this filtered radiation. In order for such results to be significant the stray field of the magnet used on the filter must be very exactly compensated and time for this is not at present available. Spectroscopic stability would lead us to expect the same polarization in zero field as in a field parallel to the electric vector of the exciting light, unless such a field produces a Paschen-Back effect upon the hyperfine structure. If this were the case such a field should also affect the polarization where the excitation is by the entire line, and it is known that this is not the case.

It may be noted further that resonance

[1] Ellett and Mac Nair, Phys. Rev. **31**, 180 (1928).

[2] Olson, Phys. Rev. **32**, 443 (1928).

radiation excited by the unfiltered light from an arc polarized with E parallel to a magnetic field of 1700 gausses shows all five h.f.s. components. This resonance radiation after passing through 7 cm of Hg vapor at 2×10^{-4} mm pressure consists of *both* the outer h.f.s. components and these very little reduced in intensity, while the central three are too weak to appear in the Lummer plate pattern, which seems to require that both outer components are shifted by the field, though MacNair observed a shift of only the short wave-length one.

On this account I think that the excitation in the experiments described above was by both outer components. I have not been able to devise a filter to transmit the -25.4 m.a. component only, as Mrozowski has done, though I have tried fields of various values from 1000–3500 gausses. When -25.2 comes through it is accompanied by $+22.1$.

A. ELLETT

Department of Physics,
University of Iowa,
January 3, 1931.

Application of the Fermi-Thomas Model to Positive Ions

Recently, Baker[1] has attempted to apply the Fermi-Thomas method to the calculation of positive ions. He gives a general discussion of the solutions of Eq. (1) (For notation see Baker's paper) including those which do not satisfy the usual boundary condition $v(\infty)=0$. There are solutions of this equation above and below that given by Fermi and Thomas, and Baker applies the above functions to the physical problem of a positive ion. We believe, however, that these functions have no physical meaning, and that one gets the potential distribution in an ion with the aid of the functions below, which intersect the x-axis. This can be seen from the following argument:

One gets the usual Fermi-Thomas equation by assuming that every cell in phase space for which the energy $p^2/2m-ev$ lies below a given value E_0 contains two electrons and those with higher energy are empty. The value of E_0 is then defined by the total number of electrons. In the case of a neutral atom, the necessary value of E_0 is zero (i.e. equal to the potential at $r=\infty$) and therefore one never introduced it as a parameter. In order to make the number of electrons less than Z, one has to choose a negative value of E_0, so that the number of electrons per unit volume will be given by

$$n=\frac{2^{9/2}\pi m^{3/2}}{3h^3}(ev-E_0)^{3/2} \text{ if } r<r_0$$

and $n=0$, if $r>r_0$

where r_0 is defined by $ev(r_0)=E_0$. The function

$$W(r)=v(r)-\frac{1}{e}E_0$$

then again satisfies Eq. (1) for values $r<r_0$ and

$$\Delta W=0$$

for $r>r_0$. It vanishes at $r=r_0$ and is continuous together with first and second derivatives. The potential distribution of a positive ion can therefore be obtained from one of the curves designated by $\sigma<0$ in Baker's Fig. 1, up to the point where it intersects the x-axis. Beyond this point one simply has a Coulomb field.

EUGEN GUTH
RUDOLF PEIERLS

Physical Institute E.T.H.
Zurich, Switzerland.
December 12, 1930.

[1] E. B. Baker, Phys. Rev. (2) **36**, 630 (1930).

Diffusion of Metallic Vapor in Condensed Spark Discharges

Recently, Beams[1] in a paper on "Spectra in Spark Discharges," referring to the diffusion of metallic vapor into the spark gap during the process of discharging, remarks: "These streamers have been previously observed by several experimenters* but whether they are jets of luminous vapor or pulses of luminosity in the vapor has not yet been completely settled."

The writer[2] begs to submit two shadowgraphs of sparks taken by him at Indiana University in 1926 which suggest at least one mode by which this process takes place, namely, that of vapor pulses. Referring to the accompanying figures, both sparks were photographed under the same circuital conditions with the exception that in the case of Fig. 2 which exhibits a spark somewhat older than that of Fig. 1, the

[1] Beams, Phys. Rev. **35**, 24 (1930).

* E. C. C. Baly, Spectroscopy **2**, 153, Longmans (1927).

[2] Zinszer, Phys. Rev. **29**, 752 (1927); Phil. Mag. **5**, 1098, (1928).

retarding capacity of the illuminating gap was about 1.4 times as great as that under which Fig. 1 was photographed.

A characteristic of the diffusion as noted in Fig. 2, one that is quite general in all of my plates, is the inequality of velocity of positive and negative diffusion. This is proven by the fact that here the diffusion from the negative electrode has almost arrived at the center of the gap space while that from the positive electrode is much less mobile.

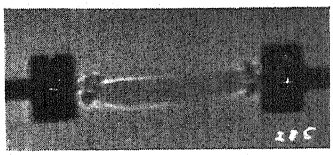

Fig. 1

Fig. 2

Other modes of vapor diffusion as indicated by my collection of negatives show in some cases depending upon the circuital arrangement a discontinuous diffusion, that is, diffusion in the form of small discrete clouds of vapor superimposed on the heated air of the "pilot" spark; also a forced diffusion in the form of tiny globules of vapor corresponding probably to the "jets" mentioned above. A more comprehensive discussion of this matter will follow later.

HARVEY A. ZINSZER
Kansas State Teachers College, Hays, Kans.
December 23, 1930.

Positive Ions Emitted by Iron and Copper

A mass spectrograph study of the positive ion emission from Fe and Cu has shown that at temperature slightly below the melting points of the metals singly charged atoms of Fe and Cu are emitted. In both cases the metals were supported and heated by a tungsten filament. The accompanying curve, Fig. 1, is typical of data obtained from Cu and shows its two isotopes at atomic weights 63 and 65. The Cu used was at least 99.99 percent pure and the gas pressure in the mass spectrograph was kept at or below 10^{-6} cm Hg. The values of the positive ion currents are only relative but the values of the atomic weights are absolute, having been computed from the potentials and magnetic fields used to accelerate and deflect the moving ions, and from the radius of the ion path.

No absolute measurements of the positive ion currents from these metals have yet been made but the mass spectrograph measurements indicate that the currents produced at temperatures very near the respective melting points of these metals are of the order of one one-hundredth of the value of the positive ion currents of potassium which are produced when these metals are first heated.

In an abstract of a paper to be given by H. B. Wahlin at the December meeting of the American Physical Society in Cleveland, there appears a list of metals which it is claimed "give only alkaline ions." Among the metals thus listed are Fe and Cu. The discrepancy between the two reports may be due to a difference of sensitivity in current measurements or to a difference in the temperatures to which the metals were raised.

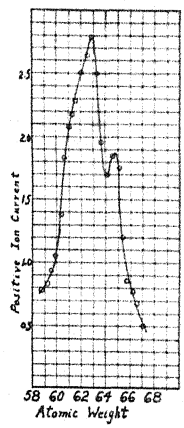

Fig. 1. Positive ion current from Cu.

Preliminary measurements indicate that it is possible to obtain positive ions of nickel by raising its temperature to a value just below its melting point.

LEROY L. BARNES
Cornell University,
December 24, 1930.

Spark Spectrum of Rubidium (Rb II)

The resonance lines of the first spark spectrum of rubidium have been excited in a hollow cathode in helium and photographed with a 1 m vacuum spectrograph. The excitation in helium is only about three volts more than sufficient to excite the resonance lines (Sawyer, Phys. Rev. **36**, 44, 1930) so that all difficulty with higher spectra is avoided and only the resonance lines appear in the vacuum region. The three resonance lines are, λ741.43, ν134875, p_0-s_4; λ711.17, ν140612, p_0-d_5; and λ697.04, ν143464, p_0-s_2 in the Paschen-Meissner notation.

With the separations of the resonance lines as a guide, it has been possible to classify a large number of lines given by Reinheimmer (Reinheimmer, Ann. d. Physik **71**, 162, 1923) and Otsuka (Otsuka, Zeits. f. Physik **36**, 786, 1926) in the rubidium spark spectrum. The energy level scheme given by Reinheimmer is correct but incomplete. It is to be interpreted as transitions from the $4p^5 5p$ levels to the $4p^5 5s$ and $4p^5 4d$ levels. The $4p^5 5s$ levels show hyperfine structure which led to their identification. The $p^5 s$ and $p^5 d$ levels overlap as in K II (Bowen, Phys. Rev. **31**, 494, 1928).

It is interesting to note that the positions of the resonance lines are in good agreement with the excitation potential measurements of Mohler (Mohler, Phys. Rev. **28**, 46, 1926). The calculated resonance potentials are λ741.43, 16.65 volts; λ711.17, 17.36 volts; λ697.04, 17.71 volts, while Mohler gave 16.0 ± 0.5 volts.

GEORGE R. MILLER
OTTO LAPORTE
RALPH A. SAWYER
Department of Physics,
University of Michigan,
December 27, 1930.

The Optical Spectra of Rhenium

Although the discovery of rhenium (75 Re) was announced[1] in 1925, and its characteristic Röntgen spectra were described[2] several years ago, I am not aware that any details concerning its optical spectra have been published. The arc and spark emission spectra of rhenium have recently been photographed in the interval 2300–8000A with the large concave grating at the Bureau of Standards. A sharp division between lines characterizing neutral atoms and those belonging to ionized atoms has been made, and preliminary values of wave-lengths and relative intensities have been obtained. The spectra are of considerable complexity and it appears that the majority of lines have hyperfine structure. A partial list of principal lines of the Re I spectrum is as follows:

Wave-length	Intensity	Wave-number	Combination
3424.6	40 c	29192.2	
3451.9	50 c	28961.3	$a^6S_{2\frac{1}{2}}-b^6P_{1\frac{1}{2}}$
3460.5	200 c	28889.3	$a^6S_{2\frac{1}{2}}-b^6P_{3\frac{1}{2}}$
3464.7	100 c	28854.3	$a^6S_{2\frac{1}{2}}-b^6P_{2\frac{1}{2}}$
4133.4	40 c	24186.4	
4136.46	50	24168.5	
4227.4	100 c	23648.6	
4394.4	40 c	22749.9	
4513.3	200 c	22150.5	
4522.70	50	22104.5	
4791.4	50 c	20864.9	
4889.2	500 c	20447.6	$a^6S_{2\frac{1}{2}}-a^6P_{3\frac{1}{2}}$
4923.92	60	20303.4	
5271.0	100 c	18966.5	$a^6S_{2\frac{1}{2}}-a^6P_{1\frac{1}{2}}$
5275.6	200 c	18946.3	$a^6S_{2\frac{1}{2}}-a^6P_{2\frac{1}{2}}$
5834.31	80	17135.2	
6307.7	40 c	15849.3	$b^6P_{2\frac{1}{2}}-z^6S_{2\frac{1}{2}}$
6321.9	60 c	15813.7	$b^6P_{3\frac{1}{2}}-z^6S_{2\frac{1}{2}}$
6350.7	20 c	15742.0	$b^6P_{1\frac{1}{2}}-z^6S_{2\frac{1}{2}}$

The lines marked *c* are complex and have from 2 to 6 or more components; for such lines the mean wave-length of the group is here rounded off to the nearest 0.1A. The components of the widest lines extend over an interval of about 2 wave-number units; for some

the intervals and intensities diminish toward the red and for others to the violet. The hyperfine structure of many of the lines has been resolved; 4889.2A has 6 components, 3460.5 has 6 also while 3451.9A has 4 and 3464.7A has 5.

The strongest line in the Re spectrum is 4889.2A; it is undoubtedly the *raie ultime* for the spectro-chemical identification of rhenium. This blue line and the green ones at 5271.0 and 5275.6A are the most brilliant lines in the visible spectrum. The ultraviolet lines at 3451.9, 3460.5 and 3464.7A are also very intense and persistent.

An analysis of the spectrum is in progress; it appears that the normal state is represented by a sextet S term, $(5d^5 6s^2)\ {}^6S_{2\frac{1}{2}}$. Both a^6P^0 and b^6P^0 violate the interval rule but the relative intensities and the hyperfine structure of combinations indicate that the levels are correctly identified.

WILLIAM F. MEGGERS

Bureau of Standards,
December 23, 1930.

[1] Noddack and Tacke, Sitzb. Preuss. Akad. Wiss., 1925, 400 (1925).

[2] Berg and Tacke, Sitzb. Preuss. Akad. Wiss., 1925, 405 (1925); Beuthe, Zeits. f. Physik. **46**, 873 (1926); **50**, 762 (1928).

Note on the Heat Capacity of Gases at Low Pressure

In a paper by the writers that appeared in the program for the Chicago meeting on November 28 and 29, 1930, the results of calculations on various physical properties of compressed nitrogen were given. These physical properties are the specific volume, density, fugacity, $-(p/v)\ (dv/dp)_T$, $(1/v)\ (dv/dT)_p$, $C_p - C_v$, C_p, C_v, and μ, all calculated at twelve temperatures and fourteen pressures between $-70°$ and 600°C and between 20 and 1200 atm, mainly from the compressibility data taken by E. P. Bartlett and his collaborators. The calculations were made possible by a sensitive graphical scheme for determining derivatives, which will be described in a complete article that will appear soon. At this time we wish to discuss one of the conclusions that was published in the abstract of the paper, *viz.* the one that says that the power series expressing C_p along an isotherm at pressures not too high must be of the form

$$C_p = C_p^* + bp^2 + cp^3 + \cdots.$$

These calculations of the change in heat capacity with pressure along an isotherm depend on the evaluation of $-T(d^2v/dT^2)_p$ along that isotherm, through the thermodynamic relation $-T(d^2v/dT^2)_p = (dC_p/dp)_T$. Experimental data below 20 atm throughout this temperature range are lacking and it is therefore impossible to decide definitely from them just what course the $-T(d^2v/dT^2)_p$ vs. p isotherms should follow as p approaches zero. At first we thought our determinations of the second derivative indicated that $-T(d^2v/dT^2)_p \to 0$ as $p \to 0$ for at least some of the temperatures. However, Dr. P. H. Emmett of this laboratory, and Professor Beattie of the Massachusetts Institute of Technology, have pointed out to us that our curves do not definitely prove this. We wish to discuss the consequences of the course of these curves in the region of zero pressure.

Since most of the direct calorimetric measurements of C_p have been made at 1 atm, it is necessary that the $-T(d^2v/dT^2)_p$ vs. p isotherms be extended below 20 atm to 1 atm. We have no experimental points in this region, but Professor Beattie has kindly showed us that here an equation of state can perform a great service. This is true if it actually takes account of physical phenomena, for then, by using in it parameters determined by compressibility data from (say) 20 to 100 atm, extrapolation to low pressures can probably be accomplished. It seems likely that the van der Waals' pressure and the tendency toward association should exist clear down to the lowest pressures where they may be identified as A_0/v^2 and c/vT^3 in the Beattie-Bridgeman formula, which gives

$$-T(d^2v/dT^2)_p = 2A_0/RT^2 + 12c/RT^4 \text{ when } p = 0.$$

This does not vanish at finite temperatures unless A_0 and c are both zero, or unless the exponents of v in A_0/v^2 and c/vT^3 are both changed and made greater than 2 and 1 respectively. The van der Waals' and Callendar equations of state, and possibly many others, likewise give expressions for $-T(d^2v/dT^2)_p$ that are not zero.

Accepting the implications of these equations of state, $(dC_p/dp)_T \neq 0$ when $p = 0$, and the first power of p in the above series for C_p would be present; C_p^* would then be the heat capacity at zero pressure. If $(dC_p/dp)_T \to 0$ as

$p \rightarrow 0$, the first power of p would be absent and C_p^* would then be sufficiently defined as the heat capacity at very low pressure, that is, there would exist some low pressure beyond which further expansion is not accompanied by a comparable change in C_p.

The two ideas are different in principle; in the former case there is a property of the gas that is realized only at complete zero pressure; in the latter case the property is realized at some sufficiently low pressure. Apparatus for compressibility or direct calorimetric measurements at low pressures might be devised to settle this matter experimentally.

It should be noted that for the calculations of the physical properties mentioned above, it is not essential to decide between these two points of view, because the area under a $-T(d^2v/dT^2)_p$ vs. p isotherm from $p=1$ to $p=20, 40, 60, \ldots$ atm. is not much affected by its course in the region of a few atmospheres pressure. Our calculations were first made assuming $(dC_p/dp)_T \rightarrow 0$ as $p \rightarrow 0$, and were then repeated using the intercept at most temperatures as given by the Beattie-Bridgeman formula, and the two sets do not differ by more than a few hundredths of a calorie/mole degree, which is well below the probable error of any calorimetric measurement.

The calculations on nitrogen will appear shortly.

W. Edwards Deming
Lola E. Shupe
Bureau of Chemistry and Soils,
U. S. Department of Agriculture,
Washington, D. C.,
December 26, 1930.

The Entropy of Hydrogen

The writer (Proc. Nat. Acad. **15**, 678 (1929)) calculated the exact value for the entropy of hydrogen at 298°K by quantum statistics using the partition function with intercombination of odd and even states. Previous to this, Fowler (Proc. Roy. Soc. **118A**, 52 (1928)) and Giauque and Johnston (J. Am. Chem. Soc. **50**, 3221 (1928)) had discussed the entropy of hydrogen. Fowler neither made himself clear nor, apparently, reached the right conclusion. Giauque and Johnston did not state the exact numerical value to be expected for the entropy of hydrogen, but discussed the method by which the entropy should be calculated. The writer regrets that he misunderstood their proposed method of calculation, and assumed that it would lead to a value differing from the one he had obtained. In a recent note (Phys. Rev. **36**, 1592 (1930)) they have pointed out that it leads to the same result. Since we are in agreement there need be no further discussion on this point.

The writer expects to discuss elsewhere the conditions under which the entropy of matter in a metastable state can be calculated by statistics, but there should be no confusion on this point.

Giauque and Johnston are entirely correct of course in saying that the entropy of hydrogen can be calculated without reference to a possible equilibrium between hydrogen and helium. We can define arbitrarily the entropy of any metastable state of a substance, e.g.; monoclinic sulfur. As soon as we do this the entropy of every other state of the substance which can be reached by a *reversible* transformation is defined. The difficulty with the analogy between a mixture of hydrogen and helium and a mixture of the two kinds of hydrogen is that ortho and para-hydrogen do transform into each other and that the equilibrium will be attained, if the writer is correctly informed, in any ordinary chemical reaction involving hydrogen. The only entropy that can have significance for chemical equilibrium therefore is the entropy of the equilibrium mixture. The non-equilibrium mixture of hydrogen at low temperatures is not a pure substance and yet its entropy must be calculated as a pure substance to have any meaning.

Two other points require brief comment. It is certainly not consistent with the current idea of a molecule in chemistry or physics, to say that there are ten varieties of molecules in hydrogen. There are at most two varieties of molecules. Also the choice of a value of 31.23 E.U. for the entropy of hydrogen seems hard to justify since it is neither a theoretical value nor *as yet* an experimental value. On the other hand it is entirely probable that the value of 33.98 E.U. can be verified experimentally if the heat data are obtained on hydrogen with a suitable catalyst present.

W. H. Rodebush
Chemistry Department,
University of Illinois,
December 26, 1930.

ERRATUM

MAGNETIC SUSCEPTIBILITY OF GASES. PART I, PRESSURE DEPENDENCE

BY FRANCIS BITTER

(Phys. Rev. **36**, 1572, 1930)

On page 1572 of the above mentioned paper a gas mixture is discussed whose composition is given as 89% CO_2+11% O_2. This is obviously an error in transcription, and should read 98.9% CO_2+1.1% O_2. That this is so follows from the fact that, as stated, the concentration of the mixture was calculated from the ratio of the susceptibility of the mixture to that of pure CO_2. This ratio is given as -0.83. If α represents the fraction by volume of O_2 in the mixture, the following relation must be satisfied

$$\frac{(1-\alpha)K_{CO_2}+\alpha K_{O_2}}{K_{CO_2}} = -.83$$

and substituting $K_{CO_2} = -8.3\times10^{-10}$ and $K_{O_2}=0.14\times10^{-6}$ this gives for α 1.1×10^{-2}. In all references to this CO_2-O_2 mixture, the O_2 content should consequently be divided by 10.

The experiment involving this mixture was undertaken to repeat observations made by Glaser, and the intention was to produce a mixture containing about 1% of O_2, as was actually done. I wish to express my indebtedness to H. Buchner[1] for calling my attention to the above error.

FRANCIS BITTER
Westinghouse Research Laboratories
East Pittsburgh, Pa.
January 9.

[1] H. Buchner, Ann. d. Physik. **7**, 728(1930)

BOOK REVIEWS

Sammlung Göschen: Nr. 698, Algemeine und Physikalische Chemie, Zweiter Teil; von PROFESSOR DR. HUGO KAUFFMANN. **Nr. 804, Grundbegriffe der Chemie,** von DR. E. RABINOWITSCH. Published by Walter de Gruyter and Company, Berlin and Leipzig, 1930. Price R.M geb. 1.80 each.

These volumes of the Sammlung Göschen present in a brief but clear manner the fundamental ideas and principles of the subjects which they cover. The volume on "Algemeine und physikalische Chemie" covers the following subjects in 145 pages. (1) Chemical Constitution (2) Thermochemistry (3) Electrochemistry (4) Photochemistry (5) The Properties of Atoms (a) atoms and electrons (b) radioactivity. The little volume on "Grundbegriffe der Chemie" has 148 pages of subject matter divided into two parts. In the first section the elements and chemical compounds are discussed under the headings (a) Constitution, Kind and State of Matter (b) Structure of Matter. Section two is devoted to chemical reactions. Here are discussed reactions and their symbolic representation, heats of reaction and chemical equilibrium. While the consideration of the subject matter must necessarily be brief, the material is correctly and carefully presented. Students in other fields of science should find these volumes especially useful in giving them a brief but clear picture of the field of theoretical chemistry. Students of chemistry wishing to review the subjects will also find these volumes very satisfactory.

L. H. REYERSON

The Theory of The Potential. W. D. MACMILLAN. Pp. xiii+469. Figs. 112. McGraw-Hill Book Co., New York, 1930. Price $5.00.

A short chapter on the calculation of the force of attraction between finite bodies of constant density and simple form is followed by a longer chapter on the Newtonian potential function. Next comes a chapter on vector fields, in which the theorems of Green, Gauss, and Stokes and Poisson's equation are developed. Chapter IV deals with the attraction of surfaces and lines with particular attention to cases where the attraction is not well-defined. This is followed by a chapter on surface distributions of matter in which Green's problem is developed, and one on two-layer surfaces such as are involved in electrostatics and magnetostatics. The last two chapters are on spherical harmonics and ellipsoidal harmonics. A brief bibliography and index close the book. A few problems, more of a mathematical than of a physical nature, are placed at the end of most of the chapters.

Scalar notation is employed throughout, and the potential is taken with the opposite sign to the potential energy in the major part of the text. While this question of sign may not be of much importance in gravitational theory, the confusion necessitated by the change of sign when two-layer surfaces are treated could easily be avoided if the potential were always taken with the same sign as the potential energy, as is the general usage in electrostatics and magnetostatics.

The subject is clearly and logically developed, and only a reasonable amount of mathematical preparation is required of the reader. The book is excellently printed and very free from printer's errors.

LEIGH PAGE

Mechanics for Students of Physics and Engineering. HENRY CREW AND K. K. SMITH. Pp. xvi+371. 215 figures. Macmillan Co., New York, 1930. Price $4.00.

Although an outgrowth of the senior author's "Principles of Mechanics," published a quarter of a century ago and for some time out of print, this text is more than a revision of the earlier work. Not only is the arrangement new, but chapters on statics and wave motion have been added, and the historical setting, which the senior author is so skillful in portraying, has been given a more prominent position than before.

By beginning with statics and its applications, the authors are able to defer the use of the calculus until a quarter of the text has been covered. This makes the book especially suitable for use with elementary students who are starting calculus and mechanics at the same time. The authors point out the value of vector methods at the very beginning, and introduce the vector product as soon as they have occasion to deal with torques. This simplifies the analysis and puts the emphasis where it belongs, that is, on the physical concepts involved instead of upon the auxiliary mathematical methods required for solution.

Statics is followed by kinematics and kinetics, particular emphasis being laid on the parallelism of the dynamics of translation and that of rotation. The concepts of force and mass are analysed more carefully than is customary in elementary texts, a careful distinction being drawn between gravitational and dynamical mass. The applications chosen to illustrate the mechanical principles presented have been most happily chosen, as regards both the stimulation of the reader's interest and the exemplification of the particular point under discussion. Kinetics is followed by chapters on friction, properties of elastic bodies, hydro-mechanics, and wave motion.

The historical rather than the logical method of approach has been followed in the main. While this method of treatment may be subject to criticism in a more advanced text, it doubtless possesses pedagogical advantages in an elementary book. Unquestionably the historical atmosphere which pervades the whole of the treatment is a source of much added interest, particularly to the student who does not intend to specialize in physics.

LEIGH PAGE

PROCEEDINGS

OF THE

AMERICAN PHYSICAL SOCIETY

MINUTES OF THE LOS ANGELES MEETING, DECEMBER 12–13, 1930

The 167th regular meeting of the American Physical Society was held in Rooms 29 and 137 of the Physics-Biology Building of the University of California at Los Angeles, jointly with the Acoustical Society of America, on Friday, December 12th and Saturday, December 13th, 1930. The meeting was called to order by the local secretary of the Pacific Coast at 10:15 on Friday morning. On vote of the members of the Society Professor S. J. Barnett, chairman of the Physics Department, University of California at Los Angeles, presided.

The morning session was devoted to papers on spectroscopy, while the afternoon session consisted of a joint session of the Acoustical Society of America and the American Physical Society dealing with problems of mutual interest. On Saturday morning the program of the Physical Society was continued, dealing largely with topics of general interest exclusive of spectroscopic and mathematical-physical subjects. On Saturday afternoon at four o'clock the meetings resumed for the presentation of papers on mathematical-physical subjects and on x-rays. The meetings adjourned at 5:30.

The members of the Acoustical and Physical Societies attended a joint luncheon on Friday noon in the Y.W.C.A. building of the University of California at Los Angeles. There was a subscription dinner on Friday evening for both societies at the Beverley Hills Hotel. At noon Saturday the members of both societies were entertained at a luncheon given by the members of the Acoustical Society of America resident in Los Angeles, which had been kindly arranged by Professor Vern Knudsen, the luncheon being given at the Hotel Roosevelt.

There were some sixty members of the American Physical Society in attendance, covering representatives from the Pacific Coast as far north as Oregon.

As there were no questions of importance to come before the society at this time the meeting adjourned without holding a business session.

The regular scientific session consisted of thirty-one papers. The abstracts of these papers are given in the following pages. An *Author Index* will be found at the end.

LEONARD B. LOEB
Local Secretary for the Pacific Coast

ABSTRACTS

1. Optical constants of CS_2-gasoline mixtures, at approximately 20°C, over the whole concentration range. L. E. DODD, *University of California at Los Angeles.*—Optical constants, particularly n_D and dispersion values, are obtained with a refractometer of the Abbé type, having heatable prisms. The gasoline used is of the commercial type, and the CS_2 is commercial.

2. Metastable molecules and active nitrogen. JOSEPH KAPLAN. *University of California at Los Angeles.*—Strong uncondensed discharges through mixtures of nitrogen and mercury vapour at pressures of about 5 cm, yielded spectra of the first positive group of nitrogen with intensity distribution remarkably similar to that observed in the nitrogen afterglow. The bands originating on the B_7 and B_9 levels were strongly enhanced whereas in active nitrogen the bands arising on B_6, B_{10}, B_{11} and B_{12} are the unusually intense ones. The difference C_0-A_0 in nitrogen is almost equal to the energy of the mercury atom in the 2^3P_1 level and the difference C_0-A_1 equals the energy of the 2^3P_0 state of mercury. Thus collisions of the second kind between nitrogen molecules in the C_0 or C_1 levels (which are plentiful in the discharge) and Hg atoms, would account for a high concentration of metastable nitrogen molecules in the A_0 and A_1 levels. A second method for producing metastable molecules in these levels arises from the fact that the X_{18} and X_{19} levels of N_2 agree almost exactly with the 2^3P_0 and 2^3P_1 levels of Hg. An accumulation of nitrogen molecules in these levels would yield a large number of metastable N_2 molecules and nitrogen atoms in the electric discharge. The relationship of this experiment to the auroral spectrum is discussed.

3. The ultraviolet band system of sulfur monoxide, a $^3\Sigma\rightarrow{}^3\Sigma$ transition. EMMET V. MARTIN AND F. A. JENKINS, *University of California.*—The SO bands discovered by Henri (Jour. Phys. Rad. **10**, 81, (1929)) in the region λλ2500–3500 have been photographed in the first order of the 15-foot Rowland grating. The source was a quartz discharge tube containing SO_2 at 30 mm pressure, actuated by a condensed discharge with spark gap and inductance. The spectrum appears to be closely analogous to the Schumann-Runge system of O_2 (Holtgreven and Dieke, Ann. d. Physik **3**, 937, (1929)). The characteristic structure found there for a $^3\Sigma\rightarrow{}^3\Sigma$ transition is clearly shown in the SO bands. Thus each band contains only P and R branches, in each of which the lines split into narrow doublets with increasing K. The short-wave component is stronger (in contrast to O_2) and at the highest K values this in turn splits in two, giving clearly resolved triplets. The components of these are of equal intensity and correspond to the triplet levels $J=K+1$, K, and $K-1$. This structure is best shown in the bands with $v'=0$. In the $v'=1$ progression, the P and R branches are usually almost superposed, and irregularities are present which must be ascribed to a number of small perturbations in the rotational levels of the upper state.

4. Zeeman effect of the hyperfine structure in thallium II and III. R. F. BACHER (*National Research Fellow*), *California Institute of Technology.*—The positions and intensities of the Zeeman components of lines which have hyperfine structure can be calculated for intermediate field strengths. This has been done for several of the lines of the first and second spark spectra of thallium which have recently been studied experimentally by McLennan and Durnford. (Roy. Soc. Proc. **A129**, 48, (1930)) The line ($6s7s\ ^3S_1-6s7p\ ^3P_2$) λ5949 of Tl II and the line ($7s\ ^2S_{1/2}-7p\ ^2P_{1\,1/2}$) λ4110 of Tl III have been studied particularly. For field strengths between 20 and 25 kilogauss the former shows an intermediate type of Zeeman effect while the latter shows an incomplete Paschen-Back effect. A comparison shows that there is agreement between the calculated results and experiment, although the observed patterns do not seem to be completely resolved.

5. Preliminary report on an investigation of the spectrum of columbium. ARTHUR S. KING, *Mount Wilson Observatory* AND WILLIAM F. MEGGERS, *Bureau of Standards.*—Analyses of the structures of the very rich spectra of neutral and ionized columbium, although partly successful (Meggers, Jour. Washington Academy of Science **14**, 442, (1924) Meggers and Kiess, J.O.S.A. and R.S.I. **12**, 431, (1926)), could not be extended without new descriptive data and improved

wave-lengths. A comparison of the furnace spectrum with the arc and spark spectra has therefore been made, and has resulted in the temperature classification of 650 of the stronger lines. The wave-lengths of more than 4000 lines have been measured in the arc and spark spectra from λ2640 to λ6900. Tested by "constant differences" between wave-numbers, the average error appears to be less than one part per million, or about 1/10 of the tolerance on values heretofore available. A feature of special interest is the large proportion of columbium lines showing hyperfine structure. Such lines are plentiful in the spectra of both neutral and ionized columbium, and are not confined to groups requiring high excitation. Much variety in width of patterns is found. While some lines are more than one wave-number in width, the components are so closely spaced that high resolution will be required for a study of their structure.

6. New data on the absorption bands of atmospheric oxygen. H. D. BABCOCK AND W. P. HOGE, *Mount Wilson Observatory.*—From numerous new spectrograms and further measurements of earlier plates, revised wave-lengths are derived for 382 oxygen band lines. Significant differences from previous Mount Wilson results occur only for lines most difficult to measure. Principal lines in the *A* band, strong in solar spectrum, were observed with interferometers as fine sharp lines in 30 meters of air. Solar grating spectra of dispersion ranging from 0.8 to 0.12A per mm and resolving power 200,000 to 400,000 were used for other bands. Due to the variety of instrumental equipment available and amount of measurement done, observational errors were reduced to approximately 0.001A for the best material. Improved resolution has thus been obtained and band structure extended to higher rotational states. Accurate wave-lengths are determined for 241 lines in 5 bands of O^{16}–O^{16}, 116 lines in 2 bands of O^{16}–O^{18}, and 25 lines in 1 band of O^{16}–O^{17}. For the *A* band our results differ from those of Badger and Mecke by amounts far exceeding our observational errors. Following a rigorous theoretical study of the isotope effect in band spectra by Birge, a full discussion of the new data will appear in a joint paper giving precise relative masses of O^{16} and O^{18}.

7. Precision determination of atomic mass ratios from band spectra. RAYMOND T. BIRGE, *University of California.*—With sufficiently extensive data available, it is preferable to calculate directly the band constants of two isotopic molecules (such as $O^{16}\cdot O^{16}$ and $O^{18}\cdot O^{16}$), rather than to use the customary method of calculating each line of $O^{18}\cdot O^{16}$ from the observed constants of $O^{16}\cdot O^{16}$. Each pair of constants involves ρ to some power, and $mass_{18}=mass_{16}/(2\rho^2-1)$. Two important relations are $\omega_e{}'=\rho\omega_e$ (vibrational isotope effect), and $B_e{}'=\rho^2 B_e$ (rotational effect). These relations should be theoretically correct to the extent that the electric field is identical for the two molecules (as indicated by the proportional size of the electronic isotope effect). Other relations such as $\alpha_e{}'=\rho^3\alpha_e$, and $x_e{}'=\rho x_e$ should be correct only to the extent that the old mechanics is true (as contrasted with the new mechanics). An independent calculation of $\alpha_e{}'$ (or of α_e) requires data from two bands, and $x_e{}'$ (or x_e) requires three bands. These constants (α_e and x_e) are needed for the extrapolation to B_e and ω_e from the observed B_v and ω_v. A precision method for calculating B_v has been published, and a similar method for obtaining ω_v is now devised. This method is being applied to new data on oxygen obtained by Babcock and Hoge.

8. The rotational Raman effect in carbon dioxide. W. V. HOUSTON AND C. M. LEWIS, *California Institute of Technology.*—By the use of a large, water-cooled mercury arc, and a highly polished reflector, we have been able to reduce the exposure time necessary to secure a spectrum of the light scattered by gases. This has made it possible to use a large spectrograph and to resolve the rotational Raman band of carbon dioxide. The results indicate that, for rotation about an axis perpendicular to the line joining the two oxygen atoms, the spectrum is similar to that of O_2, and indicates a moment of inertia of about 7×10^{-39}. The rotational quantum number jumps by two units, which shows that there are no Q branches in the transitions from the ground state to the upper electronic state which is active in producing the Raman spectrum. Alternate lines are very weak, and it seems probable that they are missing altogether. There is a slight indication of another very much smaller moment of inertia.

9. A determination of e/m from the Zeeman effect. J. S. CAMPBELL AND W. V. HOUSTON, *California Institute of Technology.*—Values of e/m have been obtained from the Zeeman separations of the Cd line λ6439 and the Zn line λ6362. Magnetic fields up to 7500 gauss are produced in a solenoid giving less than 0.1% departure from uniform field strength over a length of 6 cm at the center. The current-field ratio of the solenoid is evaluated by balancing its field against those of single layer standard solenoids. Evaporation of Zn and Cd in the short (6 cm) positive column of a helium discharge at the center of the solenoid gives the desired lines, the Zeeman patterns of which are photographed with a Fabry-Perot interferometer crossed by a prism spectrograph. Measurement of the separations at orders of interference in the neighborhood of 100,000 gives the following values of e/m: Zn λ6362, seven exposures: 1.7577×10^7 e.m. units per gram with a mean deviation of ±0.0005. Cd λ6439, eleven exposures: 1.7573×10^7 with the mean deviation ±0.0015.

10. Emission and absorption spectra of CaF. A. HARVEY (*Commonwealth Fund Fellow*) *University of California.*—High dispersion spectrograms of these bands have been studied for the purpose of (1) searching for possible evidence of the isotopes of Ca, (2) interpreting the appearance of the two visible systems in terms of the known structure types of $^2\Pi\rightarrow{}^2\Sigma$ and $^2\Sigma\rightarrow{}^2\Sigma$ transitions. The observed heads and their intensity distribution have been accounted for in detail in terms of the above transitions, by an approximate evaluation of the molecular constants. Due to the near equality of these constants in the upper and lower states, the heads are in general formed at very high J values. This results in two important modifications in passing from emission to absorption. (1) Certain heads disappear, or are greatly weakened, due to the lower temperature; (2) the intensity maximum in a sequence is shifted toward earlier members. The remarkable appearance of the $^2\Sigma^{(v)}\rightarrow{}^2\Sigma^{(v)}$ sequence in absorption is a natural consequence of these factors, as are also the presence of only one set of heads in the $^2\Pi_{3/2}{}^{(v+1)}\rightarrow{}^2\Sigma^{(v)}$ sequence, and of a new set—shaded toward the red—in $^2\Pi_{1/2}{}^{(v+1)}\rightarrow{}^2\Sigma^{(v)}$, which had previously been thought to be absent. Support for these conclusions has been found in a study of the analogous SrF spectrum.

11. An apparatus for the evaporation of various materials in vacuo. JOHN STRONG AND C. HAWLEY CARTWRIGHT, *California Institute of Technology.*—The evaporation process is much easier and requires less time than sputtering and permits the deposition of many more materials. Moreover, the thickness of the deposited film can be brought under more delicate control. The method is useful for making fine reflecting mirrors of many metals and these can be protected from tarnishing by depositing onto them an extremely thin transparent film of some non-metal such as quartz. Charcoal cooled with liquid air was satisfactory for maintaining the necessary high vacuum. The metallic elements deposited were Al, Sb, Be, Bi, Ca, Cr, Co, Cu, Au, Fe, Pb, Mg, Mn, Ni, Se, Ag, Te, Sn, and Zn. Some alloys may be deposited, such as speculum metal. Some non-metals deposited were quartz, fluorite, the alkali halides, and silver chloride. These materials may be deposited on any surface that is not affected by the high vacuum, such as glass, metal, paper, cloth, rubber, and nitrocellulose.

12. Effects of phase and time shifts on binaural sensation of direction. A. W. NYE AND A. K. STEUNENBERG, *University of Southern California.*—Experiments were made to test the effect of phase and time shifts of pure tones on the binaural sensation of direction. Separately generated tones were led to two ears via independent telephone receivers. Sources consisted of a metal disk rotated by a variable speed motor. Periphery was cut in sine wave and located in front of slits through which light passed to photoelectric cells and associated amplifiers. Two slits were used, one being adjustable so that any desired location with respect to the phase of the sine wave could be obtained. Means for interrupting the two light beams independently were provided. Between 180 dv and 725 dv, 27 observers consistently judged direction as that of the leading phase, with tendency toward greater angle shift at higher frequencies. Interrupted tones gave effect of sound origin on side where sound first arrived. Phase shift exaggerated this if in same direction; if opposed, the temporal ruled first and effect shifted later in favor of phase.

13. On the measurement of galvanometer or radiometer deflections which are ordinarily masked by Brownian movement. SINCLAIR SMITH, *Mount Wilson Observatory.*—Under certain conditions the following technique enables one to measure galvanometer or radiometer deflections which are small compared to the mean amplitude due to Brownian motion. A beam of light from the instrument mirror is brought to a focus on a photographic film and the intensity of the light is reduced to such a value that a relatively long time interval, Δt, is required to record the image on the film. Δt should be several times the average "period" of the Brownian excursions.

When a measurement is made, the instrument is set at the zero position and the recording lamp is turned on for a time Δt. The "effect" is then allowed to act, the photographic film is given a displacement, and when the instrument has had time to reach full deflection, the light is again turned on for a time Δt. The actual deflection is determined later on a comparator. If the damping factor of the instrument, and Δt are properly chosen, and the instrument is free from drift, the photographic image builds up in such a way that it has a sharp maximum making possible excellent comparator settings.

14. Ionization of helium, neon, and argon by alkali positive ions. RICHARD M. SUTTON AND J. CARLISLE MOUZON, *California Institute of Technology.*—A more extensive investigation of the ionizing properties of several positive ions from Kunsman sources has been carried forward by a method previously reported (Phys. Rev. **33**, 364, (1929) and **35**, 694, (1930)). Evidence of ionization of the three lighter noble gases by alkali positive ions from lithium to caesium has been found, setting in at accelerating potentials in the neighborhood of 150 volts and increasing steadily to the highest potential used, 750 volts. Comparison of the relative efficiencies of the process indicates that, for a particular gas, ionization is produced most intensely by that alkali ion which lies closest to the gas in atomic number; i.e., Li^+ ions in helium, Na^+ ions in neon, and K^+ ions in argon. Moreover, the maximum of ionization increases markedly with the atomic weight of gas used, being greatest for argon. Similar results have been determined by Dr. Otto Beeck, (Ann. d. Physik **6**, 1001 (1930)) using a magnetic analysis method well adapted to the purpose. Experiments are now in progress to determine whether mass or electron configuration plays the predominating part in the process. Neither energy nor velocity of the positive ions, or ballistic transfer considerations appear sufficient at present to account for the striking results obtained.

15. Nuclear scattering of high velocity electrons. H. VICTOR NEHER, *California Institute of Technology.*—A homogeneous beam of fast electrons, two millimeters in diameter and equal to a current of 1.5 (10^{-6}) amperes, is allowed to fall normally upon a thin foil. The thickness of the foil is such that single scattering predominates in the angular range through which the scattered electrons are collected. Secondary electrons up to one-fourth the voltage of the primary beam are eliminated by interposing an absorbing foil of known stopping power which allows 98–99% of the electrons scattered by nuclei to pass through. The majority of the secondary electrons from the interposed foil on the collector side are stopped by a retarding potential of 1500 volts. Scattering is obtained as a function of various angles between which the electrons are collected, thickness of foil and voltage of the primary beam. A range of voltage from 45 to 145 K.V. is used. Results show that for aluminum, the absolute value for scattering is from 25 to 50% lower than that obtained by previous workers in this field, and from 20 to 30% higher than the predicted value of wave mechanics with spin and relativity corrections. The large experimental value may be due to radiative effects, which would tend to increase the scattering at larger angles and which have not been incorporated into the theories of scattering to date.

16. The probability law governing ionization by electron impact in mercury vapor. CURTIS R. HAUPT (*Introduced by Ernest O. Lawrence*) *University of California.*—In order to detect any fine structure in the ionization probability function, such as that observed by Lawrence in mercury vapor, it is necessary to employ electron beams of a high degree of homogeneity. The method of magnetic separation, with Faraday cylinder type of ionization chamber used by Lawrence is open to the objection that magnetic orientation of the atoms or

spurious effects arising from electron reflection at the walls of the ionizing chamber might account for the results. With an electron gun type of ionization tube which eliminated the above sources of error, and which permitted realization of a rather high degree of homogeneity in the electron beam, the ultra-ionization potentials discovered by Lawrence were completely checked. In addition, his probability law was verified to within the limits of experimental error and new ionization potentials in the mercury atom were found at 12.3; 12.45; 12.85 and 13.2 volts. On account of striking numerical agreements with spectroscopic data, it is suggested that these new critical potentials are connected with the ionization of metastable mercury atoms. This suggestion is supported by the current-voltage characteristics of the tube itself.

17. Photoelectric properties of atomic layers of potassium on a silver surface. JAMES J. BRADY, *University of California*, (*Introduced by Ernest O. Lawrence*).—In this work atomic layers of potassium were deposited on a silvered glass surface which was maintained at liquid air temperature. By means of a specially designed vacuum tube a well defined beam of potassium atoms could be obtained. The film thickness was determined from the vapor pressure of the heated potassium and the length of time taken for the deposit. The pressure, in turn, was determined from the table given by H. Rowe (Phil. Mag. **3**, 540 (1927)); the temperature of the heated potassium being determined by means of a thermocouple. Spectral distribution curves were taken for various thicknesses of film. The threshold was found to be at a longer wavelength for a monomolecular layer (3×10^{15} atoms per cm^2) than for any other thickness. The maximum emission, however, occurs at about 5 atomic layers. The curves approach the wavelength axis quite steeply for thicknesses of a monomolecular layer or less, in contrast to an asymptotic approach for a greater number of layers. The curves are identical for thicknesses greater than 12 atomic layers.

18. A visual study of the initial stages of spark breakdown in air. FRANK G. DUNNINGTON, *University of California*. (*Introduced by Ernest O. Lawrence*).—With the Kerr cell electro-optical shutter it has been found possible to observe visually the breakdown of a single spark at any stage of its development. This provides a means of determining the initial regions of breakdown (as indicated by their luminosity) and the manner in which the breakdown progresses. At atmospheric pressure in an initially homogeneous field a faint diffuse path first appears connecting the electrodes. A bright spot then develops at the cathode and a conducting filament builds out from it meeting a filament of later origin which has come from the anode. The entire process requires slightly over 10^{-8} sec. for a gap of 6 mm. Initially non-homogeneous fields give various types of breakdown, the initial breakdown region being in the central part of the gap in some cases instead of at the cathode. Space charges that can produce field distortion sufficient to cause localized regions of luminosity can form within 5×10^{-9} sec. In general the effect of moisture in the air increases the field distortion. The low capacity nitrobenzene Kerr cells developed for this study have a time of cut-off less than 10^{-9} sec. Increasing the capacity of the Kerr cell, keeping other factors the same, causes a retardation in cut-off (2.5 times the capacity gave a delay of 2×10^{-9} sec.).

19. The mobility of aged ions in air. N. E. BRADBURY, *University of California*. (*Introduced by L. B. Loeb*).—Investigations by Marshall (Phys. Rev. **34**, 618, (1929)) and Luhr (Phys. Rev. **35**, 1394, (1930)) on the recombination of ions produced by intense x-radiation have shown that the coefficient of recombination decreases continuously as the age of the ions increases after the sharp initial drop due to non-random distribution. An investigation by Luhr and Bradbury (Phys. Rev, **35**, 1398, (1930)) using the same source of ionization and ionization chamber on the mobilities of air ions aged over the same lengths of time using a Langevin method of low resolving power gave negative results. In the present investigations the value of the mobility of air ions produced in pure air by x-rays has been studied for ions between the ages of 0.04 sec and 1 sec. An absolute method devised by Tyndall and Grindley (Proc. Roy. Soc., **110**, 341, (1926)) is used which consists essentially of the application of an intermittent alternating field to parallel plates immersed in a gas. The frequency of the alternations may be varied by means of a commutator system, and at a critical frequency a maximum occurs

in the electometer current-frequency curve from which the mobility may be calculated. For *new* ions of age less than 0.08 sec the average of all determinations gives 2.21 cm/sec/volt/cm for the mobility of the negative ion and 1.59 cm/sec/volt/cm for the positive ion in agreement with absolute values obtained by Loeb and Tyndall and Grindley. By varying the constants of the commutator system the ions could be aged for varying lengths of time. Mobilities measured after ageing show a decrease whose magnitude increases with increasing age until values 10 percent lower than the normal are reached at ages of 1 sec. This effect can be partially correlated with the decrease in the coefficient of recombination.

20. The collision cross-section of thallium atoms for slow electrons. ROBERT B. BRODE, *University of California.*—The average collision cross-section of thallium atoms has been measured by sending a beam of electrons through thallium vapor and observing the decrease in intensity of the beam as a function of the pressure of the vapor. From these data the absorption coefficient, α, i.e. the sum of the collision cross-sections of the atoms in one cubic centimeter of the gas at 1 mm pressure, has been calculated. α plotted as a function of the velocity of the electrons shows a sharp minimum at 1.4 volts, $\alpha=15$, a maximum at 4.5 volts, $\alpha=51$, and then sloping off gradually with $\alpha=31$ at 25 volts and $\alpha=20$ at 100 volts. The thallium atom appears to have about $\frac{1}{2}$ of the effective collision cross-section of a mercury atom for 100 volt electrons. The numerical magnitude of α depends on the density of the thallium vapor which is calculated from the vapor pressure, using the equation, $T \log p = 8890 + 8.55\ T$. However, the data from which this equation was obtained can not be relied upon sufficiently to attach much significance to the difference in size of the Hg and Tl atoms as measured by their effective collision cross-sections. The precision with which the relative values of the absorption coefficients can be observed is independent of this uncertainty of the vapor pressure.

21. The production of high speed mercury ions without the use of high voltages. ERNEST O. LAWRENCE AND DAVID H. SLOAN, *University of California.*—For studies of collision processes involving high speed charged particles we are developing methods for the production of such high speed particles which do not require high voltages. A method for obtaining high speed protons was described at the September meeting of the National Academy of Science (Science **72**, 376, (1930)). For heavier ions we are using a succession of cylinders arranged in line and connected alternately to the inductance of an oscillatory circuit. High frequency voltages of proper amount and frequency accelerate successively ions traveling through the tubes. This method has been demonstrated in principle by R. Wideroe (Ark. F. Elektrot, **21**, 387, (1929)). Our initial experimental arrangement has yielded with little difficulty mercury ions of about 90,000 volt electrons energy using a high frequency exciting voltage of 11,000 volts at a wave-length of 70 meters. A tube capable of much greater voltage amplification is under construction.

22. Polarization of light scattered by H-atoms. BORIS PODOLSKY, *Los Angeles.*—In the solution of the dispersion problem, if the size of the atom is not neglected in comparison with the wave-length of light, the scattered light is found to have a component of the electric vector in the direction of propagation of the incident light. The relative intensity of the two components of scattered light, when observed at right angles to the direction of propagation of the incident light, is computed as a function of the frequency.

23. Selection rules and the angular momentum of light quanta. J. R. OPPENHEIMER, *California Institute of Technology.*—One may deduce the selection rules for angular momentum from the conservation laws for angular momentum by applying these laws to the system atom plus light quantum field. This is done most readily by taking a linear Hamiltonian for light quanta: this gives an angular momentum for the quanta which is in part orbital, and in part a spin momentum which is determined by the polarization of the quanta. In this way one obtains very simply the probability of a violation of the selection rules by the multipole radiation of the atom.

24. On the theory of the scattering of high velocity electrons in hydrogen. HUGH C. WOLFE (*National Research Fellow*), *California Institute of Technology.*—The scattering of

electrons by free protons and by free electrons at rest is investigated, using the Dirac transition probability method. The wave functions used are Darwin's solutions for a free particle of Dirac's linear wave equation. The interaction energy is the perturbation causing transitions. Random distribution of spins is assumed. The relativistic variation of mass with velocity is taken into account. It is found that spin and retardation effects are negligible in the protonic scattering, Mott's formula for nuclear scattering being therefore the best. For the scattering by electrons, three interactions are treated (1) electrostatic, (2) the Gaunt-Eddington form, including spin, (3) the Breit form, including also retardation. The resulting formulae are different from each other and from Mott's non-relativistic formula by terms of order $(v/c)^2$, differing in symmetry as well as in absolute magnitude. These formulae apply to scattering in hydrogen for velocities high enough to treat the proton and electron in the atom as independent but not high enough to require keeping higher powers of (v/c), a good experimental region being from 125,000 to 200,000 volts.

25. Dependence of Compton line breadth on scattering angle with the multicrystal spectrograph. JESSE W. M. DUMOND AND HARRY KIRKPATRICK, *California Institute of Technology.*—Jauncey, Wentzel and DuMond have each attributed the observed breadth of the Compton line to the velocities possessed initially by the electrons in the scattering body. To test the correctness of this assumption the authors have obtained photographic spectrograms of the Compton effect with the multicrystal spectrograph with extremely homogeneous scattering angle for three scattering angles $63\frac{1}{2}°$, 90°, 155° (inhomogenity less than one degree). DuMond has shown (Phys. Rev. **33**, 643, (1929)) that the Compton line breadth for a given scattering material and primary wave-length should increase with the scattering angle if the initial electron velocities cause the breadth. If $\Delta\lambda$ is the line breadth at say half maximum and θ the scattering angle then, according to DuMond's theory

$$\Delta\lambda = K \sin \tfrac{1}{2}\theta \text{ approximately.}$$

The spectrograms and microphotometer curves show an increase in breadth of the Compton shifted line in agreement with this formula. The Compton line breadths however appear to be larger than those observed with the double spectrometer by Bearden and Gingrich and by the balanced filter method of Ross. Further investigations are in progress to determine if possible the cause of this discrepancy.

26. Intensity of monochromatic x-rays reflected from platinum in the neighborhood of the critical angle. HIRAM W. EDWARDS, *University of California at Los Angeles.*—X-radiation from a water-cooled tungsten tube, operated at 50,000 volts, is made monochromatic by reflection from a calcite crystal. The monochromatic ray ($\lambda = 0.69$A) is reflected from a platinum sputtered mirror at various small glancing angles in the region of the critical angle. The intensity of the ray reflected from platinum is measured by an ionization chamber and string electrometer. Experimental values of intensity are found to agree closely with those calculated by the Fresnel classical formula as extended by Thibaud.

27. The natural widths of some x-ray lines in the *L*-spectrum of uranium. JOHN H. WILLIAMS, *University of California.*—The double x-ray spectrometer, with previously examined crystals, has been used to measure the natural widths of the more intense lines in the *L*-spectrum of uranium at 50 kv. Most of the widths are observed in the (1, 1) anti-parallel position. Geometric corrections arising from the vertical spread of the beam have been applied. A broad focus tube has been used in order to insure a true measure of the width. These widths have been found to be greater than those observed for the MoK_α doublet. The half widths at half maximum of the following lines are: UL_{α_1} (in 3 orders), 0.44 *X.U.*; UL_{α_2}, 0.50 *X.U.*; UL_{β_1}, 0.32 *X.U.*; UL_{β_2}, 0.38 *X.U.*; UL_{γ_1}, 0.25 *X.U.* Possible correlations with the transitions involved are suggested.

28. Note on the statistics of nuclei. J. R. OPPENHEIMER, *California Institute of Technology.*—Consider two similar stable configurations, each with p protons and e electrons. It is then possible to give a simple purely analytical proof that the exclusion principle for the electrons and protons requires that the total wave function for the two configurations be

symmetric or antisymmetric in the coordinates of the center of gravity of the two configurations, according to whether p plus e is even or odd. To establish this it is necessary to assume that the configurations are so stably bound that the interaction between the two systems does not appreciably distort their internal motion. This condition, which may be made precise, is necessary and sufficient for the validity of the theorem.

29. Precision determination of the mass ratio of oxygen 18 and 16. H. D. BABCOCK and R. T. BIRGE, *Mount Wilson Observatory and University of California.* The theoretically simple upper level ($^1\Sigma$) of the atmospheric oxygen bands has alone been used in this analysis. Each of the four series (P_1, P_2, R_1, and R_2) gives an independent evaluation of the vibrational interval $\Delta G_{1/2}$ of the A and B bands (similarly for $\Delta G'_{1/2}$ of the A' and B' bands). One thus has an invaluable criterion for the detection of inconsistent data due to blended lines. 54 consistent lines of the A and B bands, and 54 of the A' and B' bands are thus revealed. Using also the results of an analysis of the α and α' bands, we obtain from the *vibrational* isotope effect, mass $O^{18} = 18.0065$ (assuming $O^{16} = 16$ exactly), with an apparent probable error of about one part in a hundred thousand. For the rotational effect only the P_1 and R_1 series are available, and it is more difficult to detect inconsistent data. From the four bands A, A', B and B', mass values varying from 18.002 to 18.016 can be obtained, depending upon the data included. The final results of this *rotational* isotope effect,—as calculated from consistent data by different methods,—are 18.0064 and 18.0074. These are in complete agreement with the vibrational result, when their greater probable error is considered.

30. A tungsten surface with a dual work function. A. H. WARNER, *University of California at Los Angeles.*—In a previous paper (Phys. Rev. **33**, 815 (1929)) the author has attempted to explain certain photoelectric characteristics of a tungsten surface by making the assumption that contaminations occur in patches, which have a different work function than that of the metal. This assumption has been tested by means of a new tube in which one filament of commercial tungsten has been evaporated onto the walls to form a contaminated surface for which the photoelectric properties have been determined. Another filament of the same material has been used to measure the thermionic work functions of the clean and contaminated surface. It also acts as the anode for the photoelectric measurements.

A photo-current first appears at 5800A. The current, though extremely small (about 10^{-14} amps) exhibits maxima and minima corresponding to the illuminating source. It suddenly increases in the vicinity of 2650A, and beyond this point is characteristic of a clean tungsten surface.

It has been possible to activate the filament until it had a work function of 2.29 volts (5400A). It is well known that for pure tungsten the work function is 4.54 volts (2690A). These values are obtained by the use of the equation $i = AT^2e^{-b/t}$.

31. Air resistance of high velocity projectiles. PAUL S. EPSTEIN, *California Institute of Technology.*—The resistance of a rigid body in a current of air is, for high velocities, due almost exclusively to the inertia terms of the hydrodynamic equations. It is, therefore, permissible to neglect viscosity, and then the problem can be solved rigorously, in the two dimensional case, for polygonal contours. The result is that in the limiting case of extremely high velocities v the resistance is given by $\rho v^2 \overline{\cos^2\alpha} S_1$ where ρ is the density of air, S the cross section of the projectile and $\overline{\cos^2\alpha}$ the mean square of the cosine of the angle between v and the normal to the surface of the projectile. For lower velocities the resistance is considerably above this limit.

AUTHOR INDEX

Second Series *February 1, 1931* *Vol. 37, No. 3*

THE

PHYSICAL REVIEW

A MORE ACCURATE AND MORE EXTENDED COSMIC-RAY IONIZATION-DEPTH CURVE, AND THE PRESENT EVIDENCE FOR ATOM-BUILDING

By Robert A. Millikan and G. Harvey Cameron

California Institute

(Received December 9, 1930)

Abstract

The cosmic-ray *ionization-depth curve* has been extended at both its upper and lower ends and made more accurate throughout. The *absorption coefficients* obtained directly from the slope of the curve run from $\mu=0.35$ per m. of water at the top (Pike's Peak) to $\mu=0.028$ at the bottom (80 m. or 262 ft. of water below the top of the atmosphere, thus bringing to light both softer and harder components than the authors had before found. Strong quantitative evidence is presented, on the basis of the Klein-Nishina formula, that the strongest and most absorbable cosmic-ray band arises from the act of formation of helium out of hydrogen. Striking qualitative evidence is found that the three more penetrating bands are due to the formation out of hydrogen of the only other abundant elements oxygen (C, N, O) silicon (Mg, Al, Si, S) and iron (Iron group). Two independent proofs are given that the cosmic-rays enter the earth's atmosphere as photons, namely, (1) they are quite uninfluenced by the earth's magnetic field, and (2) the ionization produced by them in a closed vessel does not increase continually in going to the top of the atmosphere but passes through a maximum. It is shown to follow that the cosmic rays, in coming from their place of origin to the earth have not passed through an amount of matter that is appreciable in comparison with the thickness of the earth's atmosphere and that they must therefore originate in interstellar space rather than in the atmospheres of the stars. Some participation of the nucleus in the absorption of cosmic-rays is brought to light.

1. Objectives

THE new series of measurements presented herewith on the relation between cosmic-ray ionization and depth in equivalent meters of water beneath the surface of the atmosphere was undertaken for two very specific reasons.

First.—Our preceding experiments, published in full in 1928,[1] had brought to light what seemed to us very striking evidence that the cosmic rays have their origin in the acts of formation "in the depths of space" of the atoms of the celestially common elements helium, oxygen (C, N, O), and silicon (Na, Mg, Al, Si, S) out of hydrogen. This evidence consisted:

[1] Millikan and Cameron, Phys. Rev. **32**, 533 (1928).

(a) In our experimental proof that within the limits of our observational uncertainty these rays show a uniformity of distribution, i.e., an independence of both latitude and of sidereal time. Both of these conclusions had been established by our trip to the Bolivian High Andes[2] in 1926, the first point not having been previously tested at all by other observers, the second having been so tested but with opposite results, though subsequent more careful experimenting by Hoffmann and Lindholm,[3] Steinke,[4] Hess,[5] and by one of us[6] has confirmed our conclusion;

(b) In our proof shown unambiguously by the curve itself, of the *banded character* of the rays;

(c) In the general rough agreement between our observed sequence of band-absorption coefficients and intensities, and the sequence of energies released, in accordance with Einstein's equation and Aston's curve, when the celestially most abundant elements helium, oxygen, and silicon are formed out of hydrogen; and

(d) In the rough agreement between the observed absorption coefficients and those computed from Dirac's formula connecting ray-energy with ray-absorption.

If our interpretation of our cosmic-ray results is correct, rays of still higher penetrating power should exist corresponding to the formation of still heavier elements out of hydrogen. Iron, at least, is abundant enough so that our theory suggested that we might find a cosmic-ray band, or cosmic-ray bands, of higher penetrating power than any we had thus far definitely observed. Such rays could be brought to light only by working at still lower depths in snow-fed lakes with electroscopes still more sensitive than any we had thus far used, and this new series of experiments was started in the spring of 1928 in part to test this point.

Second.—Our 1927–8 ionization-depth curve[7] showed characteristics at its upper end, i.e., at the highest altitudes at which we had ionization-depth readings, which seemed to be a bit out of line with the theory. Thus, our analysis, by means of the Gold tables, of our curve into its "monochromatic" absorption coefficients yielded as the strongest and most absorbable component $\mu = 0.35$ per meter of water, while the Dirac formula gave for the coefficient of rays due to the formation of helium out of hydrogen $\mu = 0.30$. While this was of the right order of magnitude, indeed quite close in view of our accuracy, *the divergence was in the wrong direction*, for our computated value 0.30 had applied to a monochromatic beam, but the actual beam, even if it entered the atmosphere as monochromatic would, where observed, have secondary, tertiary, etc., components, due to Compton encounters with electrons, and all such encounters tend, *until the beam has got completely into equilibrium with its secondaries*, to push down the observed μ, i.e., the μ ob-

[2] Millikan and Cameron, Phys. Rev. **31**, 163 (1928).
[3] Lindholm, Gerlands Beitrage zur Geophysik **22**, 141 (1929).
[4] E. Steinke, Zeits, f. Physik **42**, 570 (1927) and **48**, 647 (1928).
[5] Hess and Mathias, Wien. Ber. **137**, 327 (1928).
[6] R. A. Millikan, Phys. Rev. **36**, 1595 (1930).
[7] Millikan and Cameron, Phys. Rev. **31**, 925 (1928).

tained from the observed slope. The theory, then, shows no way by which the *computed* absorption coefficient of the pure radiation due to the formation of helium out of hydrogen can be *less than* the observed coefficient. It rather requires that the computed μ be at least as large as, and if equilibrium has not yet been obtained at the observation point, appreciably larger than the observed μ. We thought that our observations at high altitudes showed some slight indications that our uppermost lake-readings were accidentally high and we therefore wished to repeat these observations with more sensitive instruments and under better conditions, and to extend them, if possible, to still higher altitudes, hoping that a crucial test of our theory might come out of such more accurate high-altitude readings. In a word, then, we undertook the present series of observations to extend and improve our observational data at both the upper and the lower ends of the ionization-depth curve.

2. Technique

Our mode of procedure was precisely the same as that used in obtaining the last ionization-depth curve published in 1928, save that in order both to bring out weak effects at greater depths under water, and to obtain increased precision in high altitude observing, we were obliged to increase still further the sensitivity of our electroscope. To do this we built a new spherical instrument of steel, wall-thickness 3 mm, internal capacity 1622 cc, and filled it to a pressure of 30 atmospheres. (See Fig. 1.) This procedure, according to direct observational data to be presented later, multiplied our electroscope sensitivity 13.82 fold over that obtained under a pressure of one atmosphere. It represented, too, a sensitivity more than double that used in our published 1928 observations.[8] We determined the capacity of this electroscope with much precision by the method heretofore described,[8] finding it to be 0.979 absolute electrostatic units. Although we have not reached with this instrument the extreme limit of possible electroscope sensitivity, since increases in volume, slight decreases in fiber-capacity and still higher pressures are possible, yet, for the purposes for which it was to be used, this instrument came close to the limit of possible efficiency as a high frequency radiation detector.

In order to test the insulating properties of our quartz supports, before filling with air under pressure we pumped the chamber entirely free of air and found that it then leaked, to cite one particular test, from 226.5 volts to 226.0 volts *in four hours*. The support-leak was thus not as much as one-tenth of the slowest rate of discharge ever observed in this work, and a small fraction of a percent of the average rate. Further, it disappears entirely in our computations on rate of ion-formation because it is included in what we call the zero of our electroscope. Such minuteness of the leak of the supports, however, shows the completeness with which this source of error has been pushed into the background in these experiments.

As in all of our cosmic-ray work we followed here the procedure of reducing the fiber-deflection to volts at the instant at which it is read. This is done

[8] Millikan and Cameron, Phys. Rev. **31**, 922—5 (1928).

by calibrating the scale in the eyepiece just before or after each reading. This procedure eliminates completely all temperature effects on the fibers or on any of the electroscope parts. Thus in under-water work our procedure is to calibrate the scale for the deflection to be used under quiet reading-conditions *at the surface*, then to sink the electroscope to the desired depth and leave it for say twelve hours, then to bring it quickly to the surface, read and calibrate again. A small correction is applied for the discharge during lowering and raising by going through the operation of lowering and at once raising and seeing whether an observable change is detectable, or by doing so re-

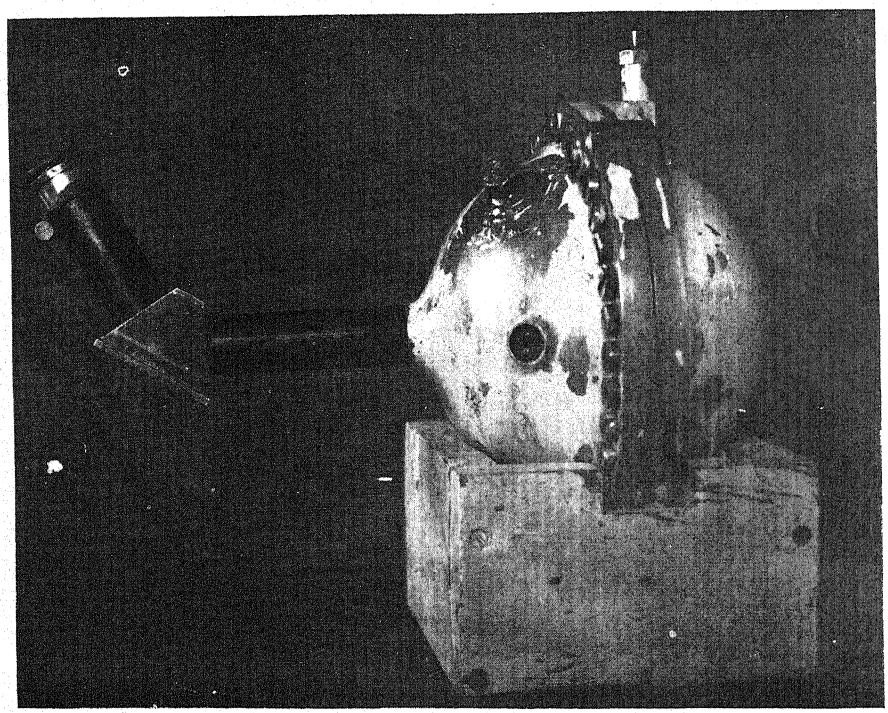

Fig. 1.

peatedly for the sake of magnification and then computing the correction for a single operation. These corrections are small and quite accurately obtainable. In some of our earlier work we used self-registering electroscopes, but for this work we considered them of no advantage.

The electroscope with which all of the results herein reported were obtained is shown in Fig. 1. It was pumped up to a pressure of 30.14 atmospheres, one atmosphere being reckoned from the conditions existing in the Norman Bridge Laboratory at the time of filling, namely, 24°C, 74 cm pressure, and this pressure has held with no trace of leak for now two years since the time of filling.

The "electroscope constant" of this instrument in ions per cc per sec. is

$$I \text{ cc/sec} = \frac{\text{volts}}{\text{hours}} \times \frac{0.979}{300} \times \frac{10^{-10}}{4.770 \times 1622 \times 3600} = 1.172 \frac{\text{volts}}{\text{hours}}.$$

For observations on land this electroscope was provided with an accurately fitted, spherical lead shield 7.64 cm thick consisting of four layers of carefully shaped and fitted hemispherical shells, and two layers of shells divided into quadrants so as to fit closely the exterior electroscope wall, with its flange and bolts, and to facilitate the entrance of the necessary leading-in wires. The "water equivalent" of this lead shield as obtained by multiplying thickness by density was 85 cm. On account of the space occupied by the steel flange about which the inner layers of lead were fitted, the water equivalent was actually a trifle less than 85 cm, but in any case by careful experiments with radium and thorium in about the proportions in which they occur in surface rocks the percentage of local rays getting through this lead shield was found to be 2.4 percent, and save for this small correction-factor, always determined and applied to all readings, the rays inside the lead were pure cosmic rays and could be compared, as shown below, with readings at the same equivalent depth in water beneath the top of the atmosphere.

3. Readings in Snow-fed Lakes

The results reported in this section were taken partially during the summer of 1928 and partially during the summer of 1929 in the two different California lakes 250 miles apart, Arrowhead Lake (altitude 5100 feet) and Gem Lake (altitude 9120 feet). Since we showed in our first work in snow-fed lakes in 1925 that the measured intensity of the cosmic rays is a single valued function of the depth of the superincumbant atmosphere, it of course follows that it depends upon the barometric pressure, as has since that time been many times noted. Accordingly, in Table I the barometer height is given for each observation, or group of observations. At the higher levels, i.e., down to about sixteen meters beneath the top of the atmosphere, where readings at the same depth beneath the surface of the lake are made at different barometric pressures, the results are reduced to a common pressure by applying a small correction, which is computed from the Gold tables,[9] for the value of the absorption coefficient shown by the ionization-depth curve at the elevation considered. This computation, however, checks nicely with the observed slope of the curve and this slope is of course independent of any theory, so that these small barometric corrections may properly be said to be purely empirical, and hence free from any other than observational uncertainties. This correction is negligible below sixteen meters but amounts at Gem Lake to slightly more than 1% and at Pikes Peak to about 2% per tenth-inch of mercury. The under-water readings, taken in two lakes and over the period from August 1928 to September 1929, are all collected in Table I. It will be seen from columns 7 and 9 that these readings extend from a level equivalent to

[9] Gold, Proc. Roy. Soc. **A82,** 43 (1909).

8.25 meters of water beneath the top of the atmosphere down to a level of 80 meters, or 262.5 feet, beneath the top, and that in that range of levels, or depths, the observed rate of discharge of the electroscope changes by more than thirty fold, namely, from a value represented by an intensity of ionization within the electroscope of 64.1 ions per cc per sec. down to 2 ions per cc

TABLE I. *Ionization-depth readings in snow-fed lakes.*

Year	Date	Lake used	Depth in Water	Barometer Reading	Depth below Top of atmosphere	Ions per cc per second	Mean *I* cc/sec
1928	Sept. 11	Gem	.85 m	21.45	8.25	64.1	64.1
"	" 9	"	1.00 "	21.48	8.42	59.8	
"	" 9	"	1.00 "	21.48	8.42	60.4	60.1
"	" 11	"	1.00 "	21.48	8.42	60.2	
"	" 11	"	2.00 "	21.46	9.41	43.8	
"	" 11	"	2.00 "	21.41	9.40	43.8	43.8
1929	Sept. 6	Arrowhead	.82 "	24.81	9.40	43.8	43.8
"	" 7	"	1.50 "	24.77	10.06	37.5	37.5
"	" 6	"	2.00 "	24.82	10.58	33.5	33.5
1928	" 12	Gem	4.00 "	21.65	11.48	30.7	30.4
"	" 13	"	4.00 "	21.65	11.48	30.2	
1929	" 4	Arrowhead	3.00 "	24.94	11.59	29.6	29.5
"	" 5	"	3.00 "	24.94	11.59	29.4	
"	" 6	"	4.00 "	24.79	12.56	25.5	25.5
"	" 5	"	5.00 "	24.87	13.56	23.0	23.1
"	" 6	"	5.00 "	24.87	13.56	23.2	
"	" 7	"	6.00 "	24.74	14.55	21.1	21.1
1928	Aug. 22	"	6.25 "	24.92	14.86	20.2	20.6
"	" 23	"	6.25 "	24.93	14.86	20.8	
"	" 25	"	6.25 "	24.81	14.82	20.9	
"	" 23	"	8.25 "	24.92	16.85	17.10	17.33
"	" 24	"	8.25 "	24.89	16.84	17.57	
"	" 25	"	10.64 "	24.81	19.21	14.72	14.52
"	" 27	"	10.64 "	24.89	19.24	14.33	
"	" 25	"	15.90 "	24.81	24.47	10.22	10.23
"	" 26	"	15.90 "	24.83	24.49	10.24	
"	" 22	"	21.10 "	24.91	29.70	7.81	7.89
"	" 23	"	21.10 "	24.93	29.71	7.96	
"	" 20	"	26.25 "	24.81	34.82	6.07	6 .07
"	" 21	"	26.25 "	24.81	34.82	6.08	
"	" 19	"	30.35 "	24.79	38.91	5.34	5.21
"	" 18	"	30.35 "	24.80	38.91	5.08	
"	" 9	"	37.05 "	24.86	45.64	4.33	
"	" 10	"	37.05 "	24.86	45.64	4.09	4.25
"	" 11	"	37.05 "	24.86	45.64	4.34	
"	Sept. 9	Gem	43.00 "	21.48	50.42	3.68	3.62
"	" 10	"	43.00 "	21.39	50.41	3.56	
"	Aug. 17	Arrowhead	42.78 "	24.91	51.38	3.90	
"	" 15	"	42.78 "	24.91	51.38	3.88	3.79
"	" 12	"	42.78 "	24.89	51.38	3.60	
"	Sept. 8	Gem	50.00 "	21.42	57.40	3.30	3.30
"	" 12	"	60.00 "	21.36	67.38	2.49	2.49
"	" 10	"	72.5 "	21.39	79.90	1.95	2.00
"	" 11	"	72.6 "	21.45	80.00	2.05	

per sec. The absorption coefficients as computed from the Gold tables at successive points along this curve are given in Table II.

The curve starts a little higher up than does the 1928 curve, analyzed on page 927, Physical Review, Vol. 31, and it is significant that the absorption coefficient at the top is now a little higher than it was there, namely 0.27 in-

stead of 0.22, i.e., it is *larger, not smaller*, then before. Also, in keeping with this fact the bend, or knee, at about 10 meters is sharper than ever, as shown by the change from $\mu=0.27$ to $\mu=0.16$ between 9.5 m and 10.5 m, when on

TABLE II. *Absorption coefficients at various depths, in meters of water, below top of atmosphere.*

Depth in m. of water beneath top of atmos.	Absorption coef. μ	Depth in m. of water beneath top of atmos.	Absorption coef. μ
8.25– 9.5	0.27	20–30	0.045
9.5 –10.5	0.16	30–40	0.038
10.5–11.5	0.11	50–40	0.028
11.5–12.5	0.095	50–60	0.028
12.5–15.0	0.067	60–80	0.028
15.0–20.0	0.058		

the old curve we got $\mu=0.20$ between 9.5 and 10.5. *Of course this means that the most absorbable cosmic-ray band springs into view from these figures more insistently than before.*

4. LAND-READINGS UP TO GREAT ALTITUDES

The highest altitude snow-fed lake used for the foregoing readings was Gem Lake (altitude 9120 feet) and for the sake of being free from the possibility of effects due to the radioactive emanations of the atmosphere (though over large bodies of water these effects are actually very small) we used no reading nearer the surface of Gem Lake than 0.85 m, a level corresponding to 8.25 m of water beneath the top of the atmosphere. At this level, as indicated above, the curve was already beginning to show departures in the wrong direction for satisfactory explanation from the standpoint of the Dirac formula. However, in accordance with the second of the objectives discussed in §1, the most significant data were to be expected at still higher altitudes, and in order to obtain accurate data at least a meter of water higher up we arranged for a series of land observations as follows:

With the aid of the radiations emitted by known quantities of radium and thorium set up at suitably chosen points, from 2 to 10 meters away, and all around our 7.64 cm lead screen we took readings when the screen was in place and when it was removed from our electroscope, and thus found that about 2.4% of the local radioactive rays from surface rocks and soils get through the lead screen and produce ionization within our electroscope. We then took a series of land observations in various localities, situated in widely different latitudes and at varying elevations from sea level up to 14,100 feet (the top of Pike's Peak), half a dozen or more readings being in general taken at each locality over a period of several days, first, when the lead screen was in place, then when the screen was removed. By comparing these observations with those taken at the same levels beneath the surfaces of snow-fed lakes the water equivalent of the lead screen was quite accurately determined, as shown below, and in this way the depth-ionization curve was reliably extended upward the equivalent of about a meter of water above the highest point obtainable in Gem Lake. This last meter proves to be of great significance for

TABLE III. *Ionization-depth readings at various elevations with and without lead screens.*

Date	Locality	Elevation	Latitude	Barometer readings	Depth below top of atmosphere	Mean ions outside lead	cc/sec inside lead	% cos. rays getting through lead	Mean ions corrected for local rays	
Sept. 23–24, '28	Pike's Peak	14,100 ft.	39⅓	17.94 in.	6.195 m. water	288.7	94.2	61%	90.9	
Sept. 9–10, '30	Pike's Peak	" "	"	17.84	6.161 " "	290.0	96.4	61%	93.2	
Sept. 24, '28	Windy Point	12,200 ft.	"	19.23	6.640 " "	247.4	77.9	62%	75.0	
Sept. 10, '30	" "	" "	"	19.29	6.663 " "	245.6				
Sept. 25–26, '28	Mt. Manitou	8,590 "	"	21.97	7.595 " "	188.9	53.6	64%	51.1	
Sept. 21–22, '28	Colorado Springs	6,035 "	"	24.13	8.333 " "	113.5	43.51	67%	42.3	
Aug. 19–20, '30	Lake Louise Canada	5,670 "	51½	24.41	8.432 " "	81.14	41.80	68%	41.3	
Aug. 18, '28	Arrowhead Lk. (in boat)	5,100 "	34	24.89	8.596 " "	63.3	39.96	69%	39.8	39.5
Aug. 19, '28	Arrowhead Lk. (on shore)	" "	"	"	" " "	124.8	40.97	69%	39.3	
Sept. 22–23, '28	Pueblo, Colo.	4,651 "	38½	25.47	8.796 " "	107.1	37.9	70%	36.6	
July 26 to Aug. 4, '30	Pasadena	756 "	34	29.14	10.06 " "	90.7	29.56	76%	28.30	
Aug. 25 to Sept. 1, '30	Churchill Manitoba	20 "	59	29.44	10.16 " "	58.87	28.48	76%	27.90	

the purposes of the second objective (§1) and in general for the interpretation of the cosmic radiations. Table III contains the record of these land-readings, which were taken during the summer and fall of three consecutive years, 1928, 1929, and 1930. The two readings on Pikes Peak taken two years apart are rather noteworthy. They differ by 2%, but in view of the difference in the barometer reading this difference is not only in the right direction but of the right amount.

The figures given in the last and the third from the last columns are in all cases the means of from three to nine different readings, the fluctuations in which are illustrated, for example, by the nine consecutive readings taken on Mt. Manitou at about two hour intervals beginning at 10:30 a.m. These nine readings, in ions per cc per sec, run 54.7, 52.8, 55.5, 54.3, 52.5, 53.7, 52.4, 52.2, 54.3. Mean = 53.6.

5. The Depth-Ionization Curve and Its Significance

The graphical representation of the results in Tables I and III is given somewhat inadequately in Figs. 2 and 3,—inadequately because no small scale graph can reflect the consistency and precision of these readings. For this reason the readings themselves have been given in Tables I and III so that the reader may plot his own large-scale graph if he so desires. However, two important results stand out immediately and conspicuously from the graphs:

1. At great depths, i.e., between 40 m and 80 m (see Fig. 3) the readings are so consistent as to show that even a blanket of 80 m or 262 ft. of water is insufficient to absorb completely the cosmic rays. The curve has here reached a value of 2 ions per cc per sec., not a fiftieth of its value at Pike's Peak, *but it is still falling.* In order to find the zero of the instrument, or the ionization *when all external rays have become absorbed* and at the same time the absorption coefficient of these hardest rays, we analyzed the curve by the trial and error method between 40 m and 80 m with the aid of the Gold tables, and found that with a zero of 1.2 I per cc/sec. and an absorption coefficient of 0.028 per meter of water, *the whole long stretch of curve between 40 m and 80 m was very accurately reproduced. In a word, our curve shows at its lower end just such a band of hard rays as we had been looking for, and a single coefficient is adequate for the whole range between 40 m and 80 m.*

The significance of the value of this coefficient will be discussed presently, but the very existence of such a coefficient means that a hundred meters farther down, i.e., at 180 m, an ionization of about 0.03 I per cc/sec. should be observable by an instrument capable of detecting such an amount. We checked this conclusion qualitatively in 1928 by taking our electroscope and its lead shield down into a shaft 185 m deep, beside Lake Arrowhead, and finding, after allowing for the local rays, a fraction of an ion still left for the cosmic rays, though, on account of the location of the shaft *beside the lake* we could not reliably estimate the equivalent water depth.

However, Regener[10] has reported more dependable deep water observa-

[10] E. Regener, Die Naturwissenschaften **15**, 183 (1929).

tions which are in substantial agreement with the results here given. He reports his results in volts per hour, which is nearly the same as our ions per cc

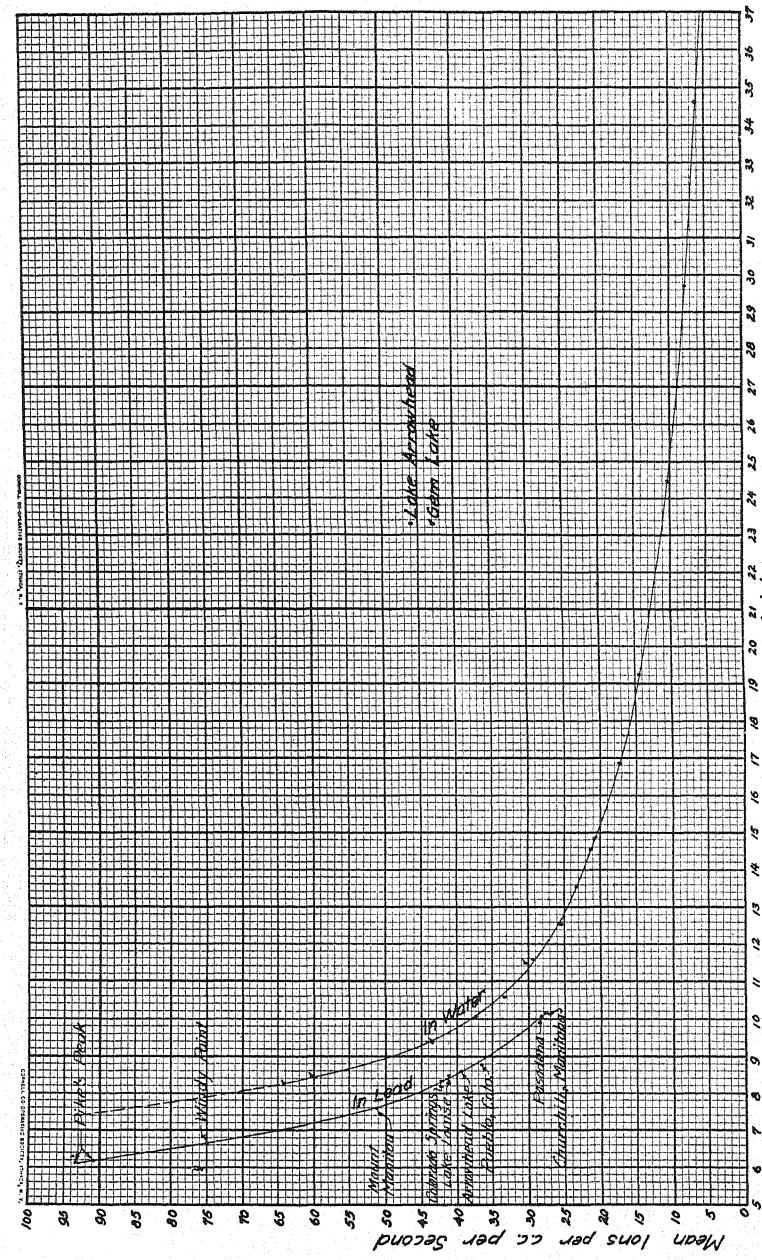

Fig. 2.

per sec., since the multiplying factor of 1.171 reduces in our case I volt/hour to I per cc/sec. His lowest really detectable reading is at 186 m, though he takes

one observation at 230 m. He obtains both his zero and his absorption coefficient by essentially the same trial and error method that we use, and we take

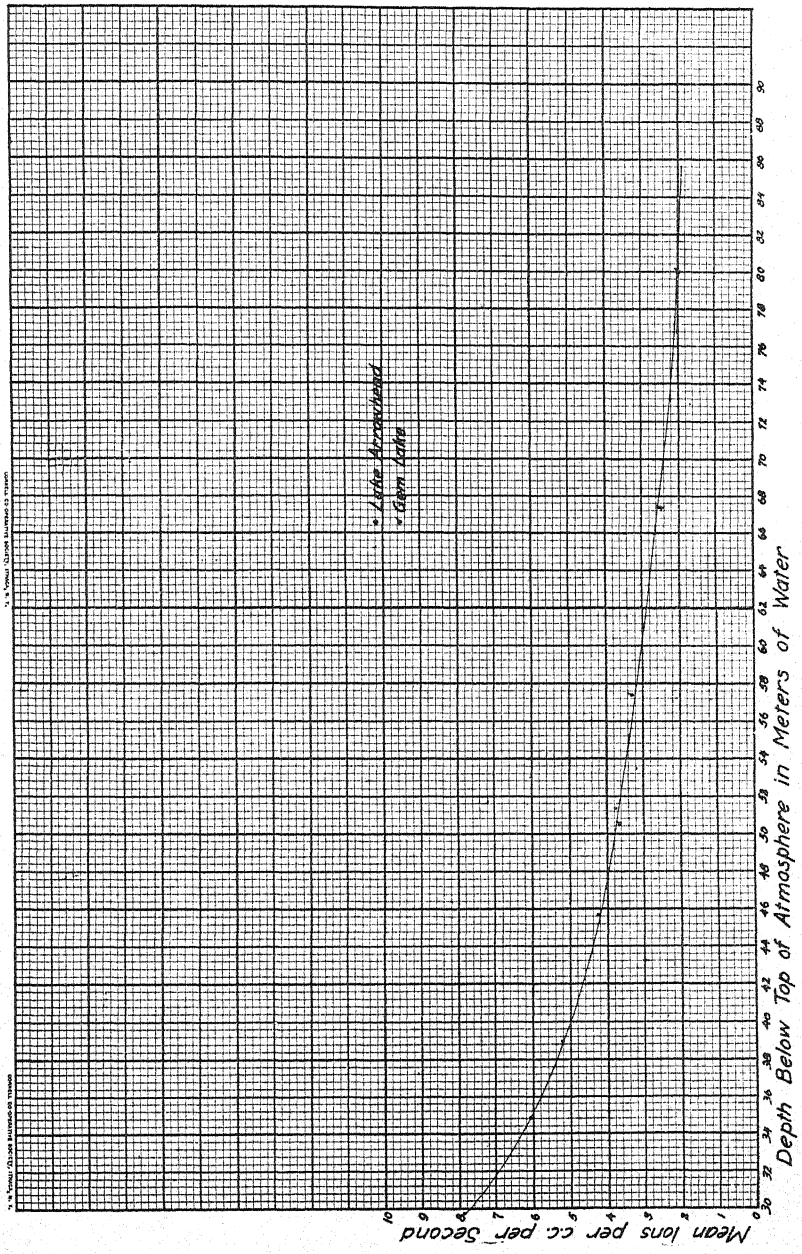

Fig. 3.

it that both he and we may have an uncertainty of as much as 0.2 I per cc/sec. in our zeros. Such a change in our zeros, if taken in the right direction for

both of us, would bring our coefficients into fairly good agreement. His value is 0.018 per meter of water. However, for reasons which we shall presently detail, the precise value of the coefficient for this most penetrating cosmic radiation is not particularly significant. The important result that appears both from Regener's deep water work and from our own is merely that there exists a component of the cosmic rays which can penetrate as much as 180 meters of water and which is therefore approximately twice as hard as the hardest component we had before *directly observed* on our former curve namely, $\mu = 0.05$ per m of water.

2. The second immediately striking result that appears from our curves is that the quite accurate observations we have now taken *at high altitudes*—up to 14,100 feet, show that the absorption coefficient now rises *far above anything the Dirac formula will in any way permit.* The absorption coefficient shown at the top of our 1928 curve was 0.22 per m of water, that at the top of our present curve taken in water is 0.27 per m of water, and that at the top of the land-curve is 0.35 per m of water. This new curve then brings out more strikingly than ever the banded structure of the cosmic rays.

We have analyzed this new curve with the aid of the Gold tables precisely as we did the former one in our 1928 article. We at that time found that the peculiar sharp bend in the curve at between 10 and 12 meters could not be reproduced without invoking *three definite bands* having roughly the relative frequencies 1, 4, 8. The new curve revealed the same necessity through the shape of its upper and middle portion, while its shape at great depths requires the introduction of a fourth band, as indicated above. Fearing that we might have become special pleaders for our banded structure, we asked Dr. Bowen, who had not thus far helped in this kind of analysis, to start from first principles with our curve and see, without any suggestions from us, what kind of structure it demanded. He proceeded without reference to any theory to build up with the aid of the Gold tables our observed curve out of four components—no smaller number would do—and in such a way that the synthetic and the observed curve fitted exceedingly nicely from one end to the other.

The components from which the synthetic curve was thus built up to yield the ionization *observed in our electroscope* were as follows:

TABLE IV. *Assumed absorption coefficients and intensities of synthetic curve.*

Assumed absorption coefficients	Assumed I_0 at top of atmosphere	Total $I = I_0/\mu$
0.03	33	1100
.10	80	800
.20	130	650
.80	141,000	176,250

The foregoing of course assumes that the ionization has its maximum value I_0 at the surface of the atmosphere (see below, where this is shown to be incorrect), and the last column then shows that the total energy of formation

of the iron group, the silicon group and the oxygen group is of the same general order of magnitude. This checks reasonably well with that we know of the relative abundance of these elements, and it would probably check better if suitable corrections could be made for the foregoing incorrect assumption. Table V then gives a comparison of the calculated and observed ionization.

TABLE V. *Comparison of synthetic and observed curves.*

Depth in meters	Calculated I	Observed I	Difference
7.5	89.7	90.8	−1.0
8.0	70.6	70.6	0
9.	48.2	48.1	− .1
10.	37.1	36.9	− .2
12.	26.4	26.5	+ .1
15.	19.1	19.1	.0
20.	12.53	12.55	+ .02
25.	8.87	8.75	− .12
30.	6.58	6.56	− .02
40.	3.93	3.83	− .10
50.	2.49	2.62	+ .13
60.	1.63	1.88	+ .25
70.	1.11	1.29	+ .18
80.	.74	.80	+ 0.6

Not only can the observed curve not be fitted accurately with less components than four, but also the four must be roughly of the foregoing type, though of course the lower bands can be split up into a finer structure if desired, i.e., 0.03 can easily be replaced by 0.02 and 0.04, for example. Not very much liberty, however, can be taken with the upper bands.

We shall now compare the results of this purely empirical study of our curve with the results computed by the Klein-Nishina formula,[11] the Einstein equation $mc^2=E$, and Aston's curve. This formula has the form

$$\mu=\frac{2\pi Ne^4}{m^2c^4}\left\{\frac{1+\alpha}{\alpha^2}\left[\frac{2(1+\alpha)}{1+2\alpha}-\frac{1}{\alpha}\log(1+2\alpha)\right]+\frac{1}{2\alpha}\log(1+2\alpha)-\frac{1+3\alpha}{(1+2\alpha)^2}\right\}.$$

Where $\alpha=h\nu/mc^2$, $N=$ no. of electrons per cc. The values of α for the atom-building processes, according to Aston, are

$$H\rightarrow He=0.029\div 5.479\times 10^{-4}=52.9$$
$$H\rightarrow O=0.1245\div 5.479\times 10^{-4}=227$$
$$H\rightarrow Si=0.232\div 5.479\times 10^{-4}=423$$
$$H\rightarrow Fe=0.48\div 5.479\times 10^{-4}=876$$

5.479×10^{-4} is the atomic weight of an electron obtained from e/m spectroscopically determined. The numerical value of the constant factor is then

[11] Nature **122**, 399 (1928).

$$\frac{2\pi Ne^4}{m^2c^4} = \frac{2\pi Ne^2}{c^4}\left(\frac{e}{m}\right)^2$$

$$= \frac{2 \times \pi \times 6.064 \times 10^{23} \times 10}{(2.998)^4 \times 10^{40} \times 18} \times (4.77 \times 10^{-10})^2 \times (5.279 \times 10^{17})^2$$

$$= 0.16614.$$

Then Table VI is the comparison of μ obtained from the Klein-Nishina formula and those of the synthetically obtained curves. The closeness of the agreement at the top is most significant. The progressive departures as the atoms become heavier look at first sight like a difficulty, but the next section goes into possible causes of this behavior.

TABLE VI. *μ in meters of water.*

	Computed	Observed
H→He	0.7957	0.80
H→O	.2409	.20
H→Si	.1418	.10
H→Fe	.0754	.028

6. Conditions of Equilibrium between a Beam of Photons and its Secondaries Produced by the Compton Process

When a beam of photons strikes matter it is obvious that a certain thickness of matter must be traversed before the beam gets into equilibrium with its secondaries, tertiaries, etc., this condition of equilibrium being attained when as many of each kind of secondary is disappearing per second from the beam as is forming per second in it. While this process of getting into equilibrium is going on, the absorption coefficient of the beam, as measured by the rate of change with distance of the ionization produced per cc, is obviously smaller than it can be after equilibrium has been reached. Further, the absorption coefficient of the pure photon beam when it first strikes matter must be the same as that of the beam after it has got into equilibrium with its train of secondaries, provided the secondaries are more absorbable than the primaries,[12] for the reason that in this equilibrium condition the percentage of these secondaries is not changing at all as the beam moves on, the only element that is so changing being simply the number of primaries; but this is precisely the situation in which the beam found itself when it first entered matter.

[12] The apparent absorption coefficient when equilibrium is reached is equal to the absorption coefficient of the primary or the secondary, depending upon which has the smaller coefficient, the general relation being

$$I = \frac{I_0\mu}{\mu_2 - \mu_1}(e^{-\mu_1 x} - e^{-\mu_2 x}).$$

Of the last two terms that having the larger coefficient will die out, leaving the effective coefficient the one having the smaller value. It is practically certain from Bothe and Kolhörster's work that the coefficient of the beta-rays at sufficiently high frequencies approaches that of the photons, and it is entirely possible that it may even fall below it for the hardest rays.

One of us[13] has recently shown that the cosmic rays enter the earth's atmosphere as streams of pure photons. This means that the ionization in a closed vessel should not be a maximum at the top of the atmosphere, but that there must be an optimum position somewhere beneath the top where this maximum ionization is reached This is precisely what the 1922 high balloon flights of Millikan and Bowen, when taken in conjunction with Hess and Kolhörster's earlier and lower ballon flights proved experimentally to be the case. For in the 1922 flights a recording electroscope rose to a hight of 15.5 kilometers, at which height 0.92 of the earth's atmosphere had been left behind, and the total ionization recorded by the self-registering mechanism proved to be only about one-fourth of that calculated from the absorption coefficient of 0.57 per meter of water, which had been found by Hess and Kolhörster in rising in manned balloons to from 5 to 9 kilometers. The discrepancy seemed to be eliminated in 1923 when Kolhörster in experiments in the Alps got a coefficient only about 0.25 per meter of water, a value not in conflict with Millikan and Bowen's high flight. But up to the present day, though the lower value has been accepted, it has remained a mystery why the earlier European flights yielded such high values. This is now quite clearly explained, for the completely reliable curve shown in Fig. 1 is at the top rising quite as fast as did the Hess-Kolhörster curves, *while the 1922 work shows unambiguously that it cannot continue to do so up to 15.5 kilometers.* In other words, the coefficient has passed through a maximum somewhere between these two levels, and at 15.5 kms. has fallen back again to low values. This is obviously what, from the foregoing considerations, it must do if the cosmic rays enter the atmosphere as pure ether waves.

It will be seen from the foregoing that the Klein-Nishina formula, combined with Aston's measurements and Einstein's equation, yields quite accurately the observed absorption coefficient of the most absorbable band, when it is assumed that that band arises from the synthesis of helium out of hydrogen. Also there is good reason to assume that at the level corresponding to the top of our curve this radiation has already reached a condition of equilibrium with its secondaries, so that the comparison is probably here legitimate. The less absorbable the radiation, however, the farther must it traverse matter thus to get into equilibrium with its secondaries, and it is most illuminating to see how the absorption coefficients computed by the Klein-Nishina formula (see Table VI) for the formation of oxygen, silicon, and iron out of hydrogen *are progressively higher than the observed coefficients* as obtained from the curve, thus indicating that these progressively harder rays are farther and farther removed from the situation in which they have traversed enough matter to get completely into equilibrium with their secondaries. Further, such attainment of equilibrium should become more and more difficult the nearer the absorption coefficient of the beta-rays released by Compton encounters with photons approaches that of the photons themselves, and Bothe and Kolhörster's recent experiments[14] show that this condi-

[13] R. A. Millikan, Phys. Rev. **36**, 1595 (1930).

[14] Bothe and Kolhörster, Zeits. f. Physik **56**, 751 (1929).

tion is somewhat nearly approached for the harder rays, though it is probably not so for the softer components. It may be that for these very penetrating radiations the secondary electrons are more penetrating than the primary photons and consequently even when equilibrium is reached a lower absorption coefficient should be observed than that called for by the Klein-Nishina formula.[12]

7. Evidence for Atom Building

In a word, then, the general qualitative evidence that the cosmic rays are due to the formation out of hydrogen of the only four abundant groups of elements that there are, namely, helium, oxygen (C, N, O), silicon (Mg, Al, Si) and iron (the iron group), which elements, barring hydrogen, constitute more than 99 percent of all matter;[15] is quite extraordinarily good, but this evidence only becomes *quantitative* in the case of helium. That this band, however, which contains within itself probably more than 90 percent of all the cosmic-ray energy, has so closely the absorption coefficient predicted for it by the Klein-Nishina formula, taken in conjunction with Einstein's equation and Aston's curve, is exceedingly significant. By a process of exclusion we are well-nigh forced to adopt the synthesis of helium out of hydrogen as the origin of this cosmic-ray band; for the Einstein equation and Aston's curve leave us no other alternative, provided the Klein-Nishina formula yields a result of even the right order of magnitude for the relation between absorption coefficient and photon frequency or energy. The only other act that has been suggested, namely, the falling together of a positive and negative electron, *actually releases an energy 35 times that observed as obtained through the Klein-Nishina formula.* This formula has been proved by Millikan and Bowen,[16] by Chao,[17] by Tarrant[18] and by Meitner[19] to be approximately correct for the gamma rays from Th C″ while the cosmic ray band under consideration, in accordance with our direct measurement, *is but five times* as penetrating as these gamma rays, so that wholly apart from its theoretical credentials, the extrapolation from Th C″ up to the least penetrating cosmic-ray band is not a very long one. In other words, the Klein-Nishina formula ought to hold reasonably well for this softest cosmic-ray band.

8. Participation of the Nucleus in Cosmic-Ray Absorption

The Klein-Nishina formula, however, cannot be rigorously correct, for it makes the absorption proportional to the number of extra-nuclear electrons. We reported at the fall meeting of the National Academy in 1928 our definite evidence that the nucleus plays a role in cosmic-ray absorption. This evidence is found in the two curves of Fig. 2. If the mass absorption law held, the water equivalent of our lead screen would be 0.85 cm, this being obtained

[15] H. N. Russell, Astro. Phys. Jr. **70,** 11 (1929). The enormous abundance of H and He is the most striking feature of this article.

[16] Millikan and Bowen, Proc. Nat. Acad. **16,** 421 (1930).

[17] Chao, Proc. Nat. Acad. Sci. **16,** 426 (1930) and Phys. Rev. **36,** 1519 (1930).

[18] Tarrant, Proc. Roy. Soc. **129,** 342 (1930).

[19] Meitner, Naturwissenschaften **18,** 534 (1930).

merely from the thickness of the screen (7.64 cm) and the relative densities of water and lead. The actual water equivalent of the lead screen for the softer cosmic rays is seen from the distance apart, on the x-axis, of the upper parts of the two curves, to be 122 cm. This distance would of course be expected to increase for harder rays, and the curves show that this is indeed the case, since for rays of the hardness that are found at sea level (10 m) the water equivalent of the lead has become 170 cm. Chao[17] has recently brought to light a similar behavior for gamma rays, though of less magnitude, thus suggesting again the identity in nature of the gamma rays and the cosmic rays. The existence of such nuclear influences on absorption means that the Klein-Nishina formula must itself be but an approximation.

9. The Uniformity of Distribution of the Cosmic Rays

One of us has recently presented at length new evidence that the small fluctuations that have been reported in the intensity of the cosmic rays are due merely to changes in the thickness of the absorbing atmospheric blanket which surrounds the earth, and that the cosmic rays themselves are streaming into the earth with entire constancy and uniformity of distribution over the celestial sphere. The correctness of this conclusion with respect to latitude could scarcely be more beautifully attested than by the left-hand curve of Fig. 2. The observations there presented were taken with the same instrument under identical conditions as to observational technique, but at times extending over three different summers and in widely different altitudes and latitudes, the latter ranging from 34 to 59 degrees north. *Yet they fit with quite surprising exactness one single ionization-depth curve.* The observations at Lake Louise in Canada, latitude 51½, at Colorado Springs, latitude 39⅓, and at Lake Arrowhead, latitude 34, are especially comparable because taken at about the same heights, as are also the near sea-level observations at Pasadena (latitude 34) and Churchill, Manitoba (latitude 59).

This entire constancy in distribution of the cosmic rays is their most significant as well as most amazing property, and must mean, when taken in connection with their absorption coefficient, first, that the temperature existing even in the atmosphere of the sun, whence alone they could get to us from this star, and the same is true for other stars, is inimical to the union of hydrogen into the heavier elements, for hydrogen is present in enormous quantity in the sun's atmosphere. In the second place, these facts must mean that the cosmic rays do not originate in any places in the universe from which they are obliged to come to us *through any appreciable amount of matter whatever.* If they had done so they would on entering the earth be partly beta-rays and partly photons, and, on account of the earth's magnetic field, the beta-ray part would of necessity be stronger near the magnetic pole than at lower latitudes. *But no trace of such an influence can be discovered!* That, however, all about us "*in the depth of space*" hydrogen is somehow uniting into helium at least seems to us to be convincingly shown by the foregoing data, and that it is also uniting into the only other measurably abundant elements, the oxygen group, the silicon group, and the iron group, is strongly indicated, though

precise quantitative proof becomes here impossible because of the change—always a decrease—in the absorption coefficient of a beam of highly penetrating photons while it is getting into equilibrium with its Compton secondaries. This phenomenon—the existence of which was demonstrated by the 1922 Millikan and Bowen experiments—renders futile a more precise analysis of our curve than we have given above.

10. Summary

The foregoing results may be summarized as follows:

1. Much the most dependable ionization-depth curve which we have thus far presented, especially at very high and very low elevations, has been obtained and analyzed.

2. This curve shows, as did its predecessor, an unmistakable banded structure, and it further presents excellent quantitative evidence that the most intense and least penetrating band is due to the particular photon released when four hydrogen atoms unite to form an atom of helium.

3. Excellent evidence has been presented that these cosmic-ray bands enter the earth's atmosphere as ether waves and must penetrate far into it before getting into equilibrium with their secondaries; also, that until such equilibrium is attained the observed absorption coefficient is smaller than that of the initial monochromatic radiation. This means, as shown in the 1922 Millikan and Bowen experiments that there is a level beneath the top of the atmosphere at which the ionization due to a pure cosmic-ray beam is a maximum, this maximum moving rapidly farther down as the frequency of the initial photon increases.

4. The observed cosmic-ray curve has been shown to be consistent with the theory that it is made up of four bands due to the formation out of hydrogen of helium, oxygen, silicon, and iron the only atoms of sufficient abundance to render the radiation released by their formation detectable anyway, and it has been shown that the differences between the calculated and observed absorption coefficients of the photons produced by the formation out of hydrogen of oxygen, silicon, and iron are very nicely explained by the non-equilibrium theory given in (3), the departures all being in the right direction and increasing with frequency in the right way.

5. The constancy and the uniformity of distribution of the cosmic rays over the celestial sphere has been again brought strikingly to light, and the significance of this for the place and mode of origin of the cosmic rays has been again pointed out.

6. Some participation of the nucleus in the absorption of cosmic rays has been experimentally established.

We wish to express our appreciation to Professor Bowen for assisting, as indicated above, in the analysis of the curve.

RADIATION OF MULTIPOLES

By Karl F. Herzfeld
Department of Physics, The Johns Hopkins University

(Received December 23, 1930)

Abstract

The radiation of multipoles formed by putting together elementary dipoles is investigated according to the classical theory and wave mechanics. It turns out that the radiations are of two kinds:

The first part has the same frequency as the dipoles and is present only if the multipole structure is present even without vibration.

The second part is always present. If n, the order of the multipole, is even then the frequencies are 2ν, 4ν, up to $n\nu$. If n is odd then the frequencies are ν, 3ν, up to $n\nu$.

The relative intensities of subsequent multipoles are proportional to the square of the ratio: dipole amplitude to wave-length, as has been found in other cases. This calculation would apply to the infrared radiation of molecules.

RECENTLY there have appeared a number of papers on the radiation of higher poles;[1] this radiation seems to explain the presence of forbidden lines.[2] Although e.g. Rubinowicz' paper gives rather complete general formulas for the classical theory, it seems not useless to bring out the physical facts as clearly as possible by considering the case of a combination of linear oscillators, as they are present in molecules like CO_2 (two) or CCl_4 (four).

I. Classical Theory

We consider quadrupoles, but there is no difficulty in generalizing to higher poles. The simplest quadrupole consists of two equal dipoles vibrating in the direction of the line joining them but with opposite phases.

If the direction of vibration is the z-axis, the field of one dipole can best be described by a Hertz-vector Z

$$Z_x = Z_y = 0$$

$$Z_z = Z = a\frac{\cos 2\pi\nu(t - r/c)}{r} \tag{1}$$

$$E = \Delta Z - \frac{1}{c^2}\frac{\partial^2 Z}{\partial t^2}, \quad H = \frac{1}{c}\,\mathrm{rot}\,\frac{\partial Z}{\partial t}. \tag{2}$$

If we have now the two dipoles the distance l apart along the Z axis and vibrating with the same amplitude but opposite phase, we will get the re-

[1] I. Placinteanu, Zeits. f. Physik **39**, 276 (1926). A. Rubinowicz, Phys. Zeits. **29**, 817 (1928); Zeits. f. Physik **53**, 267 (1929); **61**, 338 (1930); I. Blaton, Zeits. f. Physik **61**, 263 (1930); I. Bartlett, Phys. Rev. **34**, 125 (1929); A. F. Stevenson, Proc. Roy. Soc. **A128**, 591 (1930); L. Huff and R. W. Houston, Phys. Rev. **36**, 842 (1930).

[2] I. Bowen, Proc. Nat. Ac. **14**, 30 (1928); Astrophys. J. **67**, 1 (1928); R. Frerichs and I. S. Campbell, Phys. Rev. **36**, 1460 (1930).

sultant Hertz vector at any point by taking the difference between the contributions from the two dipoles. The resultant Hertz vector will consist of three parts:

$$Z_2 = -\frac{a\cos 2\pi\nu(t - r/c)}{r}\frac{l}{r}\cos\theta. \tag{3}$$

This part will not contribute to the radiation in distant places on account of the factor l/r

$$Z_2 = 2\pi\frac{a\sin 2\pi\nu(t - r/c)}{r}\frac{l}{\lambda}\cos\theta. \tag{4}$$

This part does give radiation which will represent a spherical wave of the *same frequency* as the one which would be emitted by a dipole, although its intensity varies in a different manner with θ and its amplitude is diminished by the factor $2\pi l/\lambda$. The formula is

$$+ H_\phi = E_\theta = \frac{2\pi l}{\lambda}\cos\theta\left\{\frac{4\pi^2}{\lambda^2}a\frac{\sin 2\pi\nu(t - r/c)}{r}\sin\theta\right\}. \tag{4a}$$

The total intensity emitted is the fraction $(8\pi^2/5)$ (l^2/λ^2) of that emitted by one dipole.

The third part is the most interesting one; it is always present, even if the two dipoles are not apart $(l=0)$ when at rest, that is to say if there were e.g. two negative charges vibrating on opposite sides of a positive charge with the same position of equilibrium. It arises from the difference of position caused by the vibration itself. That is to say, we have to take r now not as the distance from the point of observation to the dipole, or quadrupole, but to the vibrating charge. If we call the deviation from the equilibrium position in a given moment z', we have to put in (1)

$$r = r_0 + z'\cos\theta \tag{5}$$

and have for the dipole

$$\begin{aligned} Z &= a\frac{\cos 2\pi\nu(t - r_0/c) + 2\pi/\lambda z'\cos\theta\sin 2\pi\nu(t - r_0/c)}{r} \\ &= \frac{a\cos 2\pi\nu(t - r_0/c)}{r} + \frac{2\pi a^2}{\lambda}\cos\theta\frac{\sin 2\pi\nu(t - r/c)\cos 2\pi\nu(t - r/c)}{r} \\ &= \frac{a}{r}\frac{\cos 2\pi\nu(t - r_0/c)}{r} + \frac{2\pi a^2}{\lambda}\frac{\cos\theta}{2}\frac{\sin 2\pi 2\nu(t - r_0/c)}{r}. \end{aligned} \tag{6}$$

If the two dipoles of opposite phase are present, the first member drops out, and we have

$$Z_3 = \frac{2\pi}{\lambda}a^2\frac{\cos\theta}{r}\frac{\sin 2\pi 2\nu(t - r_0/c)}{r}, \tag{7}$$

That represents a spherical wave, with the same angular distribution as Z_2, but with the *double* frequency and an amplitude proportional to the square of the amplitude of oscillation. The total amount radiated is $(4\pi^2/\lambda_0^2(a^2)2/5)$ times the amount radiated by one dipole.

Generalization to higher poles will give the following result: Assume that we have a pole whose order is n. n is defined in this manner: Let the unit vector $\boldsymbol{p}_i$ indicate the direction of one of the constituent unit dipoles which make up the higher pole. Let $\boldsymbol{r}$ be the unit vector in the direction of observation.

Then a pole of order n is one for which

$$\sum_i (\boldsymbol{p}_i \boldsymbol{r})^{n'} = 0$$

for all $\boldsymbol{r}$ and $n' < n$ and $\sum_i (\boldsymbol{p}_i \boldsymbol{r})^n \neq 0$ for some $\boldsymbol{r}$. In fact the left hand side is a spherical harmonic of order n. With this definition, a dipole has $n=1$, a quadrupole $n=2$, a tetrahedron $n=3$.

Let us now define a vector which will depend only on the orientation of $\boldsymbol{r}$ to a system of coordinates fixed in one pole

$$L_n = \sum_i \boldsymbol{p}_i (\boldsymbol{p}_i \boldsymbol{r})^{n-1}$$

we will need later besides a scalar, defined by

$$\sigma_n = (L_n \boldsymbol{r}')$$

where $\boldsymbol{r}'$ is a unit vector perpendicular to $\boldsymbol{r}$.

We find then two different kinds of radiation.

(1) If there is a "statical" multipole structure of order n and strength p_n present, we get a radiation (Hertz vector) of the same frequency as the frequency of the constituent dipoles, but with the factor

$$\frac{1}{n!}\left(\frac{2\pi}{\lambda}\right)^{n-1} p_n L_n$$

(2) If the multipole has its origin only in the motion (that is if the field in equilibrium corresponds to a pole of higher order), part (1) is absent. But there is always present a radiation with a Hertz vector

$$Z = \frac{1}{n!}\frac{a^n}{r} L_n \cos^{n-1} 2\pi\nu(t - r/c) \frac{\partial^{n-1}}{\partial r^{n-1}} \cos 2\pi\nu(t - r/c).$$

If n is odd, we have

$$Z = \frac{1}{n!}(-1)^{(n-1)/2}\frac{a^n}{r} L_n \left(\frac{2\pi}{\lambda_0}\right)^{n-1} \cos^n 2\pi\nu(t - (r/c))$$

$$= \frac{(-1)^{(n-1)/2}}{2^{n-1} n!}\frac{a^n}{r}\left(\frac{2\pi}{\lambda_0}\right)^{n-1} L_n \left\{ \sum_{2s=0}^{2s=n-1} \binom{n}{s} \cos 2\pi(n-2s)\nu(t - (r/c)) \right\} \quad (8)$$

If n is even

$$Z = \frac{(-1)^{n/2}}{2^{n-1}n!}\frac{a^n}{r}\left(\frac{2\pi}{\lambda_0}\right)^{n-1} L_n\left\{\sum_0^{2s=n-2}\left(\binom{n}{s}-\binom{n}{s-1}\right)\right.$$
$$\left.\sin 2\pi(n-2s)\nu(t-(r/c))\right\}. \quad (8a)$$

Accordingly we get radiation which has the frequency $(n-2s)\nu$.

The only similar case where this seems to have been stated explicitly[3] is the case of n equal particles moving equidistant on a circle, which arrangement of course forms a pole of n fold multiplicity.

II. Wave Mechanics

In this case it is simpler to treat absorption instead of emission. The transition to emission is always easily made by using as external field the Landé-Dirac ghost field.

We assume a harmonic oscillator, whose Schrödinger equation is

$$\frac{d^2\psi}{dz^2} - \frac{8\pi^2 M}{h}2\pi^2 M\nu^2 z^2\psi = \frac{4\pi i M}{h}\frac{\partial\psi}{\partial t} \quad (9)$$

with the solution

$$\psi = \sum c_k\psi_k e^{-2\pi i k\nu t}\,\psi_k = e^{-\zeta^2/2}H_k(\zeta)b_n$$

with the abbreviation

$$\zeta = 2\pi\left(\frac{M\nu}{h}\right)^{1/2} z.$$

H_n is a Hermitian polynomial.

$$b_n = \left(2^{-k}\frac{1}{n!}\left(\frac{4\pi M\nu}{h}\right)^{1/2}\right)^{1/2}.$$

If there is now a perturbation function present of the form

$$V = e^{2\pi i s\nu t}v'$$

we find

$$\frac{dc_{k+s}}{dt} = \frac{2\pi i}{h}c_k\int V'\psi_k\psi_{k+s}d\zeta. \quad (10)$$

If we have a light wave polarized parallel to z and propagated parallel to x, its electric field will be

$$E_z = E\cos 2\pi\nu s(t - x/c). \quad (11)$$

The perturbation function is then given in the first case (of a statical multipole structure) by

$$V = \frac{z}{n!}\sigma_n p_n\frac{\partial^{n-1}}{\partial x^{n-1}}E_z$$

[3] J. J. Thomson, Phil. Mag. (VI) 6, 673 (1903); G. A. Schott, Electromagnetic Radiation, Cambridge 1912, p. 102.

[4] See f. e. E. U. Condon and P. M. Morse, Quantum Mechanics, New York, 1930, p. 47. A. Sommerfeld, Wellenmechanischer Ergänzungsband, Braunschweig 1929 p. 17.

from which we get[5]

$$\frac{dc_{n+s}}{dt} = \frac{2\pi i}{h} c_k \left(\frac{2\pi}{\lambda_0}\right)^{n-1} p_n \sigma_n E \frac{1}{n!} \int z \psi_k \psi_{k+s} dz.$$

The latter integral gives of course the same selection rule as for a dipole $s = \pm 1$ and only modifies the intensity of the absorption by the same factors as in the corresponding classical example.

More interesting is the case arising from the existence of the oscillatory We will put the perturbation function multipole.

$$V = \frac{1}{n!} z^n \sigma_n e \frac{\partial^{n-1}}{\partial x^{n-1}} E_z$$

which leads to

$$\begin{aligned} \frac{dc_{k+s}}{dt} &= \frac{2\pi i}{h} c_k \frac{eE}{n!} \left(\frac{2\pi}{\lambda_0}\right)^{n-1} \sigma_n \left(\frac{1}{2\pi\left(\frac{M\nu}{h}\right)^{1/2}}\right)^{n+1} b_k b_{k+s} I_{k,s}{}^n \\ &= \frac{ic_k}{(\pi M \nu h)^{1/2}} eE \frac{\sigma_n}{n!} \left(\frac{h\nu}{Mc^2}\right)^{(n-1)/2} \frac{1}{2^{k+s/2}(k!(k+s)!)^{1/2}} I_{k,s}{}^n \end{aligned} \tag{12}$$

where

$$I_{k,s}{}^n = \frac{1}{b_k b_{k+s}} \int \zeta^n \psi_k \psi_{k+s} d\zeta = \int \zeta^n e^{-\zeta^2} H_k H_{k+s} d\zeta. \tag{13}$$

To evaluate this integral, we use first the following formula,[6] where an upper index j indicates j fold differentiation in respect to the argument

$$H_k{}^{(1)} = 2kH_{k-1}$$

and therefore

$$H_k{}^{(j)} = 2k \cdot (2k-2) \cdots (2k-2j+2) H_{k-j}. \tag{14}$$

If we write

$$H_k = \sum_i a_i{}^{(k)} \zeta^i$$

we have

$$H_k{}^{(j)}(0) = j! a_j{}^{(k)} = 2^j k(k-1) \cdots (k-j+1) H_{k-j}(0). \tag{15}$$

But on account of the formula[5]

$$H_k = (-1)^k e^{\zeta^2} \frac{d^k}{d\zeta^k} e^{-\zeta^2}$$

[5] Of course, we have been quantizing not the motion of one charge, but of a characteristic vibration (normal coordination). As these are independent (no natural interaction), there are only transitions between different states of the *same* vibration possible, as G. Dieke has kindly pointed out.

we have

$$H_{k-j}(0) = (-1)^{k-j}\left\{\frac{d^{k-j}}{d\zeta^{k-j}}\left(\sum_0^\infty(-1-)^l\frac{\zeta^{2l}}{l!}\right)\right\}_{\zeta=0}$$

$$= 0 \text{ for } k-j \text{ odd}$$

$$= (-1)^{(k-j)/2}\frac{(k-j)!}{\left(\frac{k-j}{2}\right)!} \text{ for } k-j \text{ even}$$

and finally

$$a_i^{(k)} = \frac{k!}{(i!)^2}2^i(-1)^{(k-i)/2}\frac{(k-i)!}{\left(\frac{k-i}{2}\right)!} \text{ for } k-i \text{ even} \qquad (16)$$

$$= 0 \text{ for } k-i \text{ odd}.$$

We now use Sommerfeld's method[7]

$$I = \int_{-\infty}^{\infty}\zeta^n\left(\frac{d^{k+s}}{d\zeta^{k+s}}e^{-\zeta^2}\right)H_k d\zeta$$

$$= \int_{-\infty}^{\infty}e^{-\zeta^2}\frac{d^{k+s}}{d\zeta^{k+s}}(\zeta^n H_k)d\zeta$$

$$= \int_{-\infty}^{\infty}e^{-\zeta^2}\frac{d^{k+s}}{d\zeta^{k+s}}\left(\sum_{i=0,1}^{k}a_i^{(k)}\zeta^{i+n}\right)d\zeta$$

$$= 0 \text{ for } k+s > k+n \text{ or } s > n$$

$$= \sum_i \int_{-\infty}^{\infty}a_i^{(k)}(i+n)(i+n-1)\cdots(i+n-k-s)\zeta^{i+n-k-s}e^{-\zeta^2}d\zeta \text{ for } s \leqq n$$

if we now put

$$i+n-k-s = l$$

we have

$$I = \sum_{l=0,1}^{n-s}a_{l+k+s-n}^{(k)}(l+k+s)\cdots l\int_{-\infty}^{\infty}e^{-\zeta^2}\zeta^l ds.$$

The integral is 0 if l is odd and $\pi^{1/2}\frac{(2l)!}{l!2^{2l}}$ if l is even $= 2j$.

Accordingly, we have

$$I_{k,s}^{(n)} = 0 \text{ if } s-n \text{ odd}$$

$$= \pi^{1/2}\sum_{j=0}^{(n-s)/2}\frac{(4j)!}{2^{4j}(2j)!}(2j+k+s)\cdots 2j$$

$$\cdot(-1)^{i+(s-n)/2}2^{2j+k+s+n}k!\frac{(n-s-2j)!}{\left(\frac{n-s}{2}-j\right)!}\frac{1}{(2j+k+s-n)!^2}$$

[6] Condon and Morse, reference 4, p. 50.

[7] Sommerfeld, reference 4, p. 59.

$$= \pi^{1/2}(-1)^{(s-n)/2}2^{k+s-n}\,k!\sum_{j=0}^{q}(-1)^j\frac{(4j)!}{(2j)!^2}\frac{1}{4^j}\,(2j+k+s)!\,\frac{(2q-2j)!}{(q-j)!}\,\frac{1}{(2j+k-q)!^2} \tag{17}$$

with $n-s=2q$.

That means that for n odd the transitions 1, 3, 5 $\cdots n$ and n even the transitions 2, 4, 6, $\cdots n$ are permitted, and accordingly the frequencies ν, 3ν, $5\nu\cdots n\nu$ or 2ν, $4\nu\cdots n\nu$ absorbed and emitted, in analogy to the classical theory. In normal cases, the formula are not as terrible as they look. For example, for $n=2$ (quadrupole) we have $s=2$

$$I_{k,2}^{(2)} = (\pi)^{1/2}2^k k!\frac{(k+2)!}{(k!)^2} = (\pi)^{1/2}2^k(k+1)(k+2).$$

If $n=3$ (tetraeder) there are possible two transitions
$s=1$, frequency ν

$$I_{k,1}^{(3)} = -(\pi)^{1/2}2^{k+2}k!\left\{\frac{(k+1)!2!}{(k-1)!^2} - \frac{4!}{(2!)^2}\frac{1}{4}\frac{(k+3)!}{(k+1)!^2}\right\}$$

$$= -(\pi)^{1/2}2^{k+2}\left\{2k^2(k+1) - \frac{1}{4}\frac{(k+2)(k+3)}{k+1}\right\}$$

$s=3$ frequency 3ν

$$I_{k,3}^{(3)} = (\pi)^{1/2}2^k\frac{k!(k+3)!}{k!^2} = (\pi)^{1/2}(k+1)(k+2)(k+3).$$

In general, we have for $s=n$, frequency $n\nu$

$$I_{kn}^{(n)} = (\pi)^{1/2}2^k\frac{k!(k+s)!}{k!^2} = (\pi)^{1/2}2^k(k+1)\cdots(k+2) \tag{18}$$

which will make the factor in (12) proportional to $[k\cdot(k+1)\cdots(k+n)]^{\frac{1}{2}}$ or $k^{n/2}$, if $k\gg n$; this corresponds to the fact that the amplitude of light emitted classically is proportional to a^n as $a^2\sim k\sim$the energy of one dipole.

The relative transition probability from $k+s$ to k for a pole of the n order to the same probability of a pole of $(n-1)$ the order is

$$\frac{1}{n}\frac{\sigma_n^2}{\sigma_{n-1}^2}\left(\frac{I^{(n)}{}_{k,s}}{I^{(n-1)}_{k,s}}\right)^2\left(\frac{h\nu}{Mc^2}\right)^{1/2}$$

$h\nu/Mc^2$ is the ratio of the energy of vibration to the intrinsic energy and can be rewritten

$$\frac{M/2v_{\max}^2}{Mc^2} = \frac{1}{2}\left(\frac{v_{\max}}{c}\right)^2 = \frac{1}{2}\left(\frac{2\pi\nu a}{c}\right)^2 = 2\pi^2\left(\frac{a}{\lambda_0}\right)^2.$$

Rubinowicz[2] has found a similar result for atoms.

THE MOTION OF ELECTRONS IN ARGON

By H. B. Wahlin
Department of Physics, University of Wisconsin

(Received December 27, 1930)

Abstract

The motion of electrons in argon containing 1.53 percent N_2 has been investigated. For low fields the mobility is a constant, but rises rapidly as the field is increased due to the increase of the electron free path with increasing thermal velocity.

The mean free path of electrons in pure argon and in thermal equilibrium with the argon is 0.385 cm at 1 mm pressure.

IN A series of earlier papers[1] results of investigations on the motion of electrons in N_2, H_2, He and CO have been presented. The method used was the alternating potential method of measuring mobilities. Since in the case of the electron motion through a gas the mobility is in general not a constant, this method does not lead to a direct determination of the mobility. It is possible, however, as was done in this earlier work, to make an indirect comparison of the experimental results with the theoretically calculated mobilities. In all the cases presented so far, with the exception of N_2, a good agreement with the theory proposed by K. T. Compton[2] was shown to exist, provided it is assumed that the energy loss of an electron on impact with a molecule is greater than it would be if due to momentum transfer only. In N_2 the variation of the electronic free path with the electron velocity enters into the experimental results to such an extent that a check is impossible. Compton's theory takes no such variation into account.

In the present paper results on argon corresponding as much as possible to those on the other gases, are presented.

The argon used in these experiments contained, after being freed of oxygen, 1.53 percent nitrogen. This was not removed, but instead, as shall be seen, corrections were made for its presence. All the measurements were made at a pressure of 760 mm.

When the mobility is a constant, it may be calculated exactly from the voltage intercept of the mobility curves by the expression

$$K = \pi n d^2/(2)^{1/2}V. \tag{1}$$

If the mobility is a function of V as it will be for electrons, this equation gives an average value determined by the relation

$$\int_0^{1/2n} \frac{V}{d} K \sin 2\pi n t \, dt = \int_0^{1/2n} f(v) \frac{V}{d} \sin 2\pi n t \, dt.$$

Compton's theory gives

$$f(v) = \frac{a}{[1 + (1 + BV^2)^{1/2}]^{1/2}}. \tag{2}$$

[1] H. B. Wahlin, Phys. Rev. **23**, 169 (1924); **27**, 558 (1926); **35**, 1568 (1930).
[2] K. T. Compton, Phys. Rev. **22**, 333, (1923).

In Fig. 1 the average values of K calculated from Eq. (1) are plotted against the field strength (V/d) in which they were determined. For very low values of the field the mobility is a constant, and over this range the values calculated from Eq. (1) are nearly exact. In fields above 2 volts/cm the mobility rises sharply. The values found for this range serve merely to illustrate qualitatively the rapid increase in the mobility.

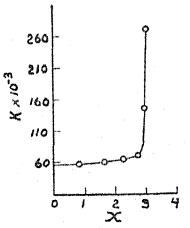

Fig. 1.

An examination of Eq. (2) shows that according to Compton's theory one should expect a decrease in the mobility with increasing voltage due to the increased thermal velocity of the electrons. In order to account for the discrepancy between theory and experiment it is necessary to assume a very rapid increase in the electron free path in argon with increasing thermal velocity. This is in agreement with the free path determinations of Townsend and Bailey[3] and others.

The results shown in Fig. 1 serve in one way as a check on Compton's theory. The equation giving the mobility as a function of the field strength (Eq. (2)) demands that for low field the mobility shall be a constant; i.e. that for low field the electrons shall be in thermal equilibrium with the gas.

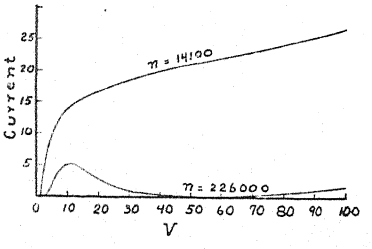

Fig. 2.

The fact that the mobility is nearly a constant as V approaches zero shows that apparently the thermal velocity does not vary sufficiently to produce any appreciable change in the free path.

In Fig. 2 two typical mobility curves are presented. The curve taken at a frequency of 14,100 cycles/sec is of the same character as those found for other gases. The one taken at the higher frequency is characteristic for argon. This frequency gives two values for the mobility. The variation in the shape of the mobility curve is due to the Ramsauer effect which in argon is much more pronounced than in other gases studied.

[3] J. S. Townsend and V. A. Bailey, Phil. Mag. **44**, 1033 (1922).

The limiting electron mobility in argon containing 1.53 percent N_2 is for low fields 59,600 cm/sec/volt/cm. The mean free path calculated from this value assuming

$$K = 0.75e\lambda/mc$$

is 0.363 cm at 1 mm pressure.

To correct for the presence of N_2 the following expression may be used

$$\frac{760}{\lambda_m} = \frac{P_n}{\lambda_n} + \frac{P_a}{\lambda_a}$$

where P_n is partial pressure of N_2, P_a the partial pressure of argon, λ_m the mean free path at 1 mm in mixture, λ_n the mean free path at 1 mm in N_2 and λ_a the mean free path at 1 mm in pure argon. This expression was used by Townsend and Bailey with a mixture of H_2 and A and was justified by them for this case. The corrected value for the mean free path when the electrons are in thermal equilibrium with the argon atoms is (assuming $\lambda_n = 0.0996$ cm) 0.385 cm at 1 mm pressure.

In Fig. 3 the author's value of λ (indicated by X) together with Townsend and Bailey's values are plotted as a function of the thermal velocity $\bar{c}$. This

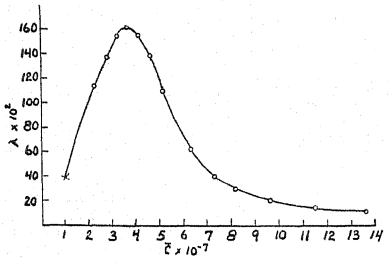

Fig. 3.

curve shows the prominence of the Ramsauer effect in argon, and also serves to explain the shape of the mobility curves obtained at high frequencies.

Summary

The results of the determinations of the mean free paths of electrons in gases, together with the values calculated from kinetic theory, are shown in Table I.

Table I.

	Obs.	KT	Obs./KT
H_2	0.041	0.0741	0.553
He	.066	.117	.565
CO	.069	.0391	1.75
N_2	.0996	.0393	2.53
A	.385	.0417	9.2

As is seen there is no systematic agreement between the observed and the kinetic theory values.

DISPERSION AND REFRACTIVE INDEX OF NITROGEN MEASURED AS FUNCTIONS OF PRESSURE BY DISPLACEMENT INTERFEROMETRY

By Clarence E. Bennett
Department of Physics, Brown University

(Received December 15, 1930)

Abstract

The Lorentz-Lorenz relation has never been satisfactorily checked by experiment for pressures above atmospheric, because of a lack of trustworthy data on the refractive indices of pure gases as functions of pressure. Such data would also be particularly valuable in the study of polar molecules on account of Maxwell's law connecting the refractive index with the dielectric constant. Due, however, to the difference between optical and electrical frequencies the refractive index must be reduced to zero frequency before Maxwell's law can be applied. This necessitates a precise knowledge of dispersion which is not available for many pure gases. In the present paper a method of measuring simultaneously the dispersion and refractive index of a gas is discussed. The method is justified on theoretical and experimental grounds and applied in a practical way to the measurement of dispersion and refractive index of nitrogen over a range of pressures and at two different temperatures with a high degree of precision.

The results show that over a seven atmosphere range the Lorentz-Lorenz relation is followed and that the dispersion is a linear function of pressure. The value of the Cauchy constant B is found to be 1.95×10^{-16} per cm of mercury pressure. The index of refraction for nitrogen is measured for three wave-lengths at 0°C and 30°C with a limiting error in $(\mu-1)$ of one third of one percent. The dispersion information enables the values to be reduced to infinite wave-length with the result that a value for the dielectric constant is obtained which differs by less than two-thirds of one percent from that measured directly by Zahn. The values of μ under *NTP* conditions for the wave-lengths 4811A, 5893A, and 6362A are 1.0002991, 1.0002969, and 1.0002967 respectively.

Introduction

THE problem of measuring the index of refraction of gases has been attacked by many observers in the past, but precise results have been obtained with only a few substances. The most accurate determinations have been made for air, an admittedly complex substance, and in practically all cases the observations have been made at atmospheric pressure. The data on air obtained by Meggers and Peters[1] with a Fabry-Perot interferometer over the whole visible spectrum range, undoubtedly represent the best work of this sort ever attempted. Trustworthy data on the index of refraction of pure gases as a function of pressure, however, were scarce at the time the present research was started. Gale[2] in 1902 worked on air, about the constitution of which he knew very little, up to a few atmospheres with a Jamin interferometer, and Magri[3] in 1905 went up to fourteen atmospheres with air also using

[1] Meggers and Peters, Bulletin of the Bureau of Standards, No. 14, 1918–19, p. 697.
[2] H. G. Gale, Phys. Rev. **14**, 1 (1902).
[3] L. Magri, Phys. Zeits. **6**, 629 (1905).

a Jamin interferometer. Cheney,[4] using pure gases, in 1927 measured the refractive indices of nitrogen, ammonia, carbon dioxide, sulphur dioxide and air over a temperature range of a few hundred degrees at one atmosphere by means of a Fabry-Perot etalon, but so far as can be ascertained, no one with the exception of Phillips[5] who worked with carbon dioxide, has published any reliable data on pure gases at pressures higher than one atmosphere.

In the light of the Lorentz-Lorenz[6,7] equation such information should be particularly significant. Furthermore as a result of the work of Debye[8] and others in which dipole moments have been coordinated with dielectric constants, data on refractive index become especially valuable because of Maxwell's law connecting the dielectric constant with the refractive index. This necessitates a knowledge of the dispersion of the medium because dielectric constants are measured at very low frequencies compared with optical frequencies.

Some years ago Carl Barus[9] made a few preliminary observations on the index of refraction of air with his displacement interferometer, as a result of which, it appeared possible to measure both refractive index and dispersion simultaneously. This work was only qualitative and no attempt was made to secure high precision, yet the experiments showed that such precision might be expected if the instrument were properly developed. It was the particular good fortune of the writer to be able to assemble an instrument of this type with the personal assistance of Professor Barus, and to adapt it for this sort of work.

Displacement Interferometry

The optical arrangement of the displacement interferometer is shown in Fig. 1. When the system is properly aligned so that the mirror M' is made accurately parallel to the virtual image of the mirror M as seen through the half silvered mirror HS, the interfering light beams, if viewed through the telescope T on the front of which is mounted a ruled grating, display a beautiful interference pattern consisting of black concentric oval fringes superposed on a continuous spectrum. The optical path difference necessary to produce this result is a known function of the thickness, the index of refraction, and the dispersion of the glass half silvered mirror.

These fringes are very interesting. They have been studied at length by Barus,[9] and Birchby[10] has more recently described and explained fringes of a similar nature. Like Michelson fringes they expand or contract with every

[4] E. W. Cheney, Phys. Rev. **29**, 292 (1927).

[5] P. Phillips, Proc. Roy. Soc. London **97A**, 225 (1920).

[6] H. A. Lorentz, "Theory of Electrons."

[7] Meggers and Peters, reference 1, credit Magri, reference 3, with preferring $(\mu^2-1)/(\mu^2+1)/(\rho)=C$ but this is a mistake resulting from a typographical error in Magri's publication as anyone can see by checking the calculations.

[8] P. Debye, "Polar Molecules," 1929.

[9] Carl Barus, Carnegie Foundation of Washington Publications, No. 149, I, II, III; No. 229; No. 249, I, II; 1911 to 1917.

[10] W. N. Birchby, Proc. Nat. Acad. **10**,, 452 (1924) also **13**, 216 (1927).

motion of the micrometer screw, but continuous motion causes the whole system to move bodily along the spectrum from violet to red as the path from the micrometer mirror to the half silver is made shorter. Using for a half silvered mirror a plate of glass 0.25 inches thick, a motion of the micrometer mirror of 0.17 mm corresponds to a shift of the fringes from the red to the blue-green region of the spectrum. This means that movements of the fringe system along the spectrum corresponding to displacements of the mirror can be calibrated with a good micrometer. Hence the instrument is particularly well suited to measure displacements greater than can conveniently be measured with a Michelson interferometer, because it is unnecessary to count fringes, yet the accuracy is about the same.

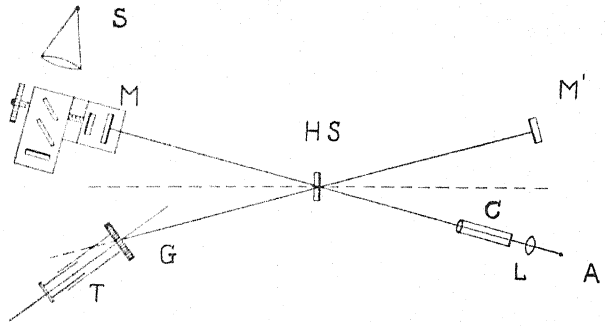

Fig. 1. Optical arrangement of a linear displacement interferometer.

The fringes are visible simultaneously in all spectrum orders and remain so even for very wide slit openings, the visibility however, being generally best for reduced illumination. When sunlight is used as a source, the dark Fraunhofer lines constitute fixed lines of reference by means of which measurements of the displacement of the fringe system can be made. Ordinarily with a carbon arc the yellow sodium line is bright enough to stand out against the continuous spectrum background and serve as a reference line.

By a geometrical consideration of the reflected and refracted rays Barus derived the fundamental relations of displacement interferometry. But let us now consider in quite an independent manner how the instrument can be used to measure the index of refraction of a gas. Suppose the interferometer to be so adjusted that the oval fringes are centered on a given spectrum line, for example the sodium D line, when a column of gas of length e is in one arm of the interferometer. Assume μ_1 to be the index of refraction of this gas, μ_A to be the index of refraction of the medium in which the micrometer mirror is displaced (air), and if there are any other substances in the path let their refractive indices be denoted by $\mu_2 \cdots \mu_n$.

With the gas in the path, the optical path difference from the half silver to the mirrors M and N is

$$n\lambda = \mu_1 e + F(\mu_2 \cdots \mu_n) - P \qquad (1)$$

where λ is the wave-length of the spectrum line on which the fringe system is centered, $\mu_1 e$ is the optical path length of gas, $F(\mu_2 \cdots \mu_n)$ is the path length of all remaining substances in the path, and P is the optical length of the opposite path. F and P are absolutely independent of the nature of the gas in question and are not affected by evacuating the tube.

When the gas is removed from the path (by evacuation of the containing tube) and the micrometer mirror is displaced to recenter the fringe system on the given spectrum line

$$n'\lambda = e + \mu_A \Delta x + F(\mu_2 \cdots \mu_n) - P \tag{2}$$

where μ for vacuum is of course one, and Δx is the air displacement of the micrometer mirror.

The radial distance between the central spot and the first fringe ring is observed to be greater than that between any two successive rings. Hence in accordance with Cornu's principle, the fraction of a fringe shift for the change of one wave-length must be a minimum at the center of the system, i.e.

$$\frac{\partial n'}{\partial \lambda} = \frac{\partial n}{\partial \lambda} = 0.$$

Thus the fringes near the center of the configuration are relatively coarse and far apart, whereas the outermost ones are very fine and close together.

Dividing Eqs. (1) and (2) by λ, differentiating each with respect to λ, setting the resulting equations equal to zero, subtracting one from the other, and solving, we get

$$\Delta x = \frac{e\left[(\mu_1 - 1) - \lambda \dfrac{\partial \mu_1}{\partial \lambda}\right]}{\mu_A - \lambda \dfrac{\partial \mu_A}{\partial \lambda}}. \tag{3}$$

The denominator for all practical purposes is one, whence

$$(\mu_1 - 1) = \frac{\Delta x}{e} + \lambda \frac{\partial \mu_1}{\partial \lambda}. \tag{4}$$

Dispersion

Eq. (4) shows that before the index of refraction of a gas can be determined by displacement interferometry some knowledge of its dispersion is necessary. Further considerations, however, show that the dispersion can be obtained directly with the instrument from the values of the displacement Δx taken for two different wave-lengths in the spectrum.

Consider the Cauchy dispersion relation

$$\mu = A + \frac{B}{\lambda^2} + \frac{C}{\lambda^4} + \cdots.$$

The data of Meggers and Peters[1] show that for air, two arbitrary constants A and B are sufficient to represent the facts. The writer has taken these data for three different temperatures 0°, 15°, and 30°C and plotted $(\mu-1)$ aginst $1/\lambda^2$ on a very large scale (a graph 50×70 cm) as shown in a

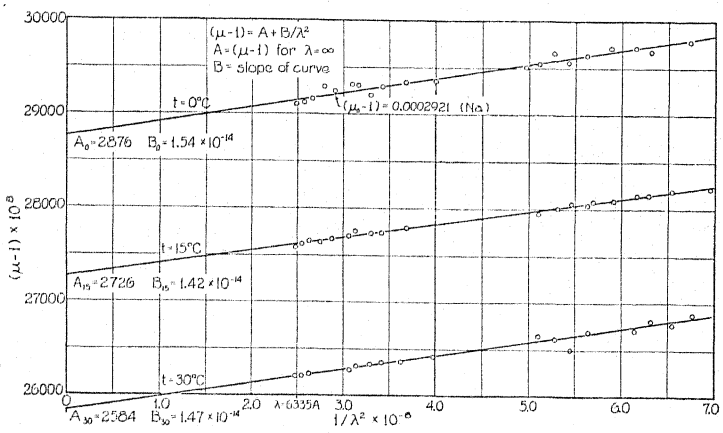

Fig. 2. Dispersion data for air plotted from observations of Meggers and Peters.

reduced photograph in Fig. 2. In each case the points lie rather well on straight lines, indicating that two arbitrary constants are sufficient to represent the data.

If now $(\mu-1)=A+B/\lambda^2$ whence

$$\frac{\partial\mu}{\partial\lambda}=-\frac{2B}{\lambda^3}. \tag{5}$$

Then Eq. (4) reduces to

$$(\mu_1-1)=\frac{\Delta x}{e}-\frac{2B}{\lambda^2}. \tag{6}$$

Now writing Eq. (5) twice for two different wave-lengths λ_1 and λ_2 and subtracting the one from the other

$$(\mu_1-\mu_2)=B\left(\frac{1}{\lambda_1{}^2}-\frac{1}{\lambda_2{}^2}\right). \tag{7}$$

For these two wave-lengths Eq. (6) gives

$$(\mu_1-1)=\frac{\Delta x_1}{e}-\frac{2B}{\lambda_1{}^2} \tag{8}$$

$$(\mu_2-1)=\frac{\Delta x_2}{e}-\frac{2B}{\lambda_2{}^2}. \tag{9}$$

Where B is assumed to be constant throughout the visible spectrum as the data of Meggers and Peters show to be true for air. Solving Eqs. (7), (8), (9)

$$B = \frac{(\Delta x_1 - \Delta x_2)}{3e\left(\frac{1}{\lambda_1^2} - \frac{1}{\lambda_2^2}\right)}. \tag{10}$$

Now consider again Eq. (6) rewritten so as to read

$$\frac{\Delta x}{e} = (\mu - 1) + \frac{2B}{\lambda^2}. \tag{6a}$$

Experiments on nitrogen which will be described later, show conclusively that Δx is a linear function of pressure when values of Δx are plotted against pressure. Therefore, since e is a constant, $[(\mu-1)+2B/\lambda^2]$ must be a linear function of pressure, meaning that either each term separately varies directly with pressure or that there is some involved relation connecting the two terms in such a way that their sum varies directly with pressure if separately they do not. Since $\frac{2}{3}(\mu-1)$ is a first approximation to $(\mu^2-1)/(\mu^2+2)$ we should expect $(\mu-1)$ to be directly proportional to pressure by the Lorentz-Lorenz relation, and so B must, therefore, be a linear function of pressure. This means that B/p is a constant which can be determined directly by the difference in the slopes of the lines $\Delta x_1/p = \text{constant}$ and $\Delta x_2/p = \text{constant}$.

Dividing Eq. (10) by p it appears that

$$B_0 = \frac{B}{p} = \frac{\left(\frac{\Delta x_1}{p} - \frac{\Delta x_2}{p}\right)}{3e\left(\frac{1}{\lambda_1^2} - \frac{1}{\lambda_2^2}\right)} \tag{11}$$

B_0 here means B per cm pressure. The B used in the previous work can now be interpreted to mean B at pressure p.

It follows then that the displacement interferometer can be used to determine the dispersion factor B of a gas, first finding B_0 from the difference in the slopes of the $(\Delta x, p)$ lines for two different wave-lengths and then multiplying by the pressure to get the value of B corresponding to that pressure. After B has been determined $(\mu-1)$ can be determined at the same pressure by Eq. (6). The value of $(\mu-1)$ can be reduced to its equivalent at 0° and normal pressure if it is not so measured, by assuming the Lorentz-Lorenz equation to be at least approximately true, whence

$$\frac{\mu - 1}{\rho} = \frac{\mu_0 - 1}{\rho_0} \tag{12}$$

$$\therefore\ (\mu_0 - 1) = (\mu - 1)\frac{760}{p}\,\frac{T}{273.1}. \tag{13}$$

Preliminary Experiment

An interferometer with arms something over a meter long was assembled according to Fig. (1), and measurements of the refractive index of dry air

were made at atmospheric pressure using for the dispersion correction the value given by Fig. 2. The average of some twenty or more independent observations gave a resulting value for $(\mu_0 - 1)$ of 0.0002921 with a mean deviation of ± 0.0000007. This is exactly the value given by Meggers and Peters.[1] Hence the conclusion is drawn that the above theoretical considerations have been experimentally justified.

Description of the Apparatus

The arrangement of the apparatus is sketched in Fig. 1. A photograph of the actual set-up in the basement of the laboratory is reproduced in Fig. 3. The interferometer mirrors were made from plates of optical glass 3 inches square obtained from Bausch and Lomb. The micrometer mirror M was fastened to the movable table of a small Michelson interferometer which had a well-made micrometer screw about 3/16″ diameter of 0.5 mm pitch. The

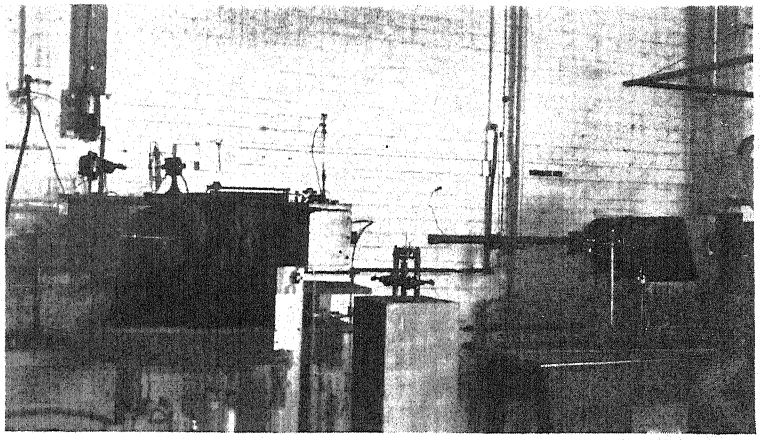

Fig. 3. Photograph of apparatus.

Michelson inteferometer was also set up so that it could be used as an auxiliary instrument as indicated in the figure, for the purpose of calibrating the screw over the range actually used, by counting Michelson fringes from an independent monochromatic source of light.

The Michelson interferometer and the two other mirrors of the displacement interferometer were mounted on independent cement piers which rested on the ground and were free from contact with the building. They extended up through the floor in the form of shafts one foot square and about three feet high.

The illuminating system consisted of an arc light, a lens and a collimator all mounted on a table. To produce a zinc spectrum for work on dispersion, the arc was loaded with pieces of zinc wire inserted into drilled carbons. The arrangement was such that a concave mirror could be substituted for the lens to make it possible to focus sunlight from a hole in the floor of the room above, upon the slit of the collimating telescope to produce a solar spectrum. The

oval fringes were observed with a 25 cm focal length telescope having a gelatin grating, with approximately 1150 lines to the inch, mounted normally in front of the objective. The arc light, the collimating telescope, the table upon which they rested, and the Michelson interferometer, were mounted upon squares of sponge rubber to minimize the effects of vibration. Even with the heavy cement piers completely separated from the building all trouble due to vibration was not completely eliminated, although with them the fringes occasionally steadied down for short intervals. Ordinarily in the day time the quiet intervals were neither as long nor as regularly spaced as in the evening, and for this reason most of the readings were taken in the evening.

The experimental refraction tube containing the gas to be experimented with, was supported in the working arm of the displacement interferometer. It was made of Shelby cold drawn steel tubing $\frac{1}{8}$ inch wall and approximately one inch bore. The ends were closed by disks of high quality optical glass, obtained from Bausch and Lomb, 1.15 inches in diameter and 0.25 inches thick, with accurately plane parallel surfaces. A second tube just like the first but containing air at room temperature and pressure was used in the

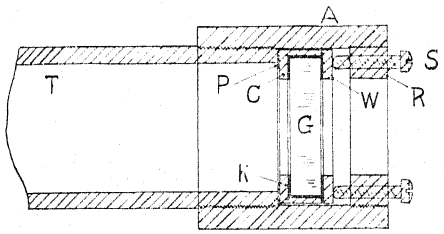

Fig. 4. Method of fastening glass ends to the experimental tube.

other arm of the interferometer to optically compensate for the experimental tube. The length of the refraction tube inside the end plates measured 100.30 cm.

The packing shown in detail by Fig. 4, was used to fasten the glass ends to the tube, and proved very satisfactory. The end of the tube T was carefully tinned and, while still hot, was screwed into a hot threaded sleeve A to form a very tight fit. C is a thin-walled steel cup carefully machined down to fit the glass disk G which is cemented into it with a thin layer K of de-Khotinsky cement. The steel washer W is also cemented to the glass, and the rim of C projects out beyond G just enough to take up the strain when W is pressed against it. P is a very thin sheet of rubber (dental dam) also cemented to C. This whole unit P, C, K, G, W, was set in place and the ring R was screwed in about flush with A. Then by means of eight equally spaced screws S the unit was pressed tightly up against the end of the tube T.

The experimental tube was mounted in a water bath, by means of which the temperature was kept uniform and constant to 0.01° c.

A small McLeod vacuum gauge was used for the purpose of registering pressures less than 0.1 mm mercury obtained with a Cenco Hyvac pump.

Pressures above atmospheric were measured with a mercury column. The lower end of this column was a length of 3/16″ steel tubing welded through a hole in the plug of a commercial iron mercury flask, and just long enough nearly to reach the bottom of the container. The upper end was a glass tube fastened to a brass centimeter scale, some 350 cm long in two sections, mounted on the side of a wooden ladder just long enough to reach from the floor to the ceiling beams, and fastened rigidly at each end.

The pressure line connecting the various pieces of apparatus; the gas source, the mercury column, a dial gauge (which was included for rough work), and the experimental refraction tube was made up of $\frac{1}{8}$″ steel tubing. Connections were made by means of soldered sleeves or carefully built steel unions. Each piece of apparatus could be isolated from the rest by special high pressure steel stopcocks.[11]

Experimental Procedure and Observations with Nitrogen

Water pumped nitrogen was obtained in commercial containers under about 2000 lbs. pressure, guaranteed pure except for 0.5% water and 0.5% oxygen. The oxygen was removed by passing the nitrogen through a steel tube full of sheet copper clippings maintained at a temperature of 500 – 600°C into an auxiliary steel tank where it was stored under a pressure of 600 lbs. The water vapor was removed by phosphorus pentoxide contained in three tin cans suspended by copper wires inside this auxiliary tank.

The nitrogen thus stored was allowed to stand a few days to become dry. The system was thoroughly rinsed out with it and observations were carried out in the following manner: A vacuum of 10^{-2} mm of mercury was obtained, and after a reading of the barometer had been taken, the temperature of the bath being kept constant at 30°C, the fringes were very carefully centered on the blue (4811A) zinc spectrum line. The reading of the micrometer was recorded, and then the screw was so turned as to cause the fringes to proceed through the spectrum to the yellow (5893A) sodium line. This process was continued to bring the fringes up to the orange (6362A) zinc line. Then a small quantity of nitrogen was admitted to the system, and after the temperature and pressure had come to equilibrium, the temperature of the room being usually several degrees below 30°, the reading of the mercury column was noted, and readings of the micrometer were made with the fringes centered upon each of the three spectrum lines. This process was continued until readings had been made at intervals of approximately one atmosphere up to the limit of the gauge, i.e. a pressure of about 475 cm of mercury above vacuum. At this pressure due allowance was made for the back lash of the screw in the opposite direction, and readings were made for settings of fringes at each spectrum line, this time in the order of orange, yellow, and blue, for decreasing pressures at intervals of approximately one atmosphere, ending with a reading for vacuum.

After several runs of this sort a very careful run was made at a temperature of 0°C obtained by packing the constant temperature bath with ice.

[11] F. G. Keyes and Jane Dewey, Jour. Opt. Soc. Am., **14**, 491 (1927).

The observations obtained in these runs are recorded in Tables I and II.

TABLE I. *Data on nitrogen at 30°C.*

No.	Pressure (cm Hg)	Δx_1(cm)4811A (obs.)	(calc.)	Δx_2(cm)5893A (obs.)	(calc.)	Δx_3(cm)6362A (obs.)	(calc.)
1	148.89	0.05540	0.05573	0.05398	0.05439	0.05402	0.05412
2	150.72	.05628	.05641	.05495	.05506	.05495	.05479
3	152.27	.05605	.05699	.05588	.05562	.05538	.05535
4	153.02	.05658	.05728	.05585	.05590	.05548	.05562
5	154.56	.05718	.05785	.05483	.05646	.05458	.05618
6	158.00	.05998	.05914	.05810	.05772	.05750	.05743
7	158.72	.05983	.05941	.05768	.05798	.05755	.05769
8	161.69	.06102	.06052	.05950	.05906	.05900	.05877
9	167.71	.06408	.06277	.06085	.06126	.06052	.06096
10	211.58	.08048	.07919	.07760	.07729	.07743	.07691
11	221.41	.08350	.08287	.08018	.08088	.07990	.08048
12	221.50	.08268	.08291	.08090	.08091	.08065	.08051
13	222.44	.08230	.08326	.08045	.08126	.08025	.08086
14	222.69	.08278	.08335	.08097	.08135	.08090	.08095
15	227.50	.08488	.08516	.08298	.08310	.08242	.08270
16	238.69	.08730	.08934	.08728	.08719	.08655	.08676
17	239.22	.08985	.08954	.08680	.08739	.08652	.08696
18	257.81	.09532	.09650	.09450	.09418	.09400	.09371
19	274.23	.10373	.10264	.10018	.10018	.10073	.09968
20	276.95	.10445	.10366	.10068	.10117	.10035	.10067
21	281.19	.10468	.10525	.10265	.10272	.10218	.10221
22	287.62	.10810	.10766	.10505	.10507	.10470	.10455
23	298.46	.11105	.11171	.10838	.10903	.10785	.10849
24	302.28	.11408	.11314	.11013	.11042	.10965	.10988
25	305.64	.11428	.11440	.11175	.11164	.11100	.11108
26	320.94	.11870	.12013	.11695	.11724	.11648	.11661
27	333.87	.12457	.12497	—	—	.12175	.12136
28	335.07	.12530	.12542	.12148	.12240	.12088	.12180
29	335.07	.12515	.12542	.12262	.12240	.12327	.12180
30	335.21	.12550	.12547	.12198	.12245	.12160	.12185
31	341.30	.12895	.12775	.12515	.12468	.12500	.12406
32	353.41	.13253	.13228	.12910	.12910	.12805	.12846
33	354.63	.13220	.13236	.12972	.12955	.12915	.12891
34	391.07	.14425	.14638	.14298	.14286	.14200	.14215
35	396.46	.14880	.14839	.14550	.14483	.14470	.14411
36	397.11	.14913	.14864	.14458	.14506	.14385	.14435
37	397.60	.15038	.14882	.14545	.14524	.14530	.14453
38	398.25	.14990	.14906	.14513	.14548	.14438	.14476
39	416.23	.15563	.15579	.15223	.15205	.14902	.15130
40	419.57	.15690	.15705	.15342	.15327	.15228	.15251
41	436.47	—	—	.15950	.15944	—	—
42	436.47	.16457	.16337	.16020	.15944	.16007	.15866
43	472.16	.17650	.17673	.17144	.17248	.17118	.17163
44	472.21	.17408	.17675	.17265	.17250	.17187	.17165
45	473.37	.17733	.17718	.17320	.17292	.17158	.17207
46	473.92	.17723	.17739	.17263	.17312	.17262	.17227
47	473.96	.17955	.17740	.17443	.17314	.17280	.17228

TABLE II. *Data on nitrogen at 0°C.*

No.	Pressure (cm Hg)	Δx_1(cm)4811A (obs.)	(calc.)	Δx_2(cm)5893A (obs.)	(calc.)	Δx_3(cm)6362A (obs.)	(calc.)
1	150.04	0.06123	0.06185	0.06053	0.06062	0.06023	0.06029
2	163.11	.06665	.06723	.06550	.06590	.06510	.06554
3	233.94	.09623	.09643	.09383	.09451	.09350	.09400
4	239.52	.09868	.09873	.09652	.09677	.09610	.09624
5	308.42	.12688	.12713	.12465	.12460	.12373	.12392
6	327.09	.13535	.13483	.13180	.13214	.13102	.13142
7	386.60	.15938	.15936	.15625	.15619	.15553	.15534
8	453.29	.18683	.18685	.18360	.18313	—	—
9	453.79	—	—	—	—	.18275	.18233

Computations and Results

The calculated values in the above tables were computed from the most probable values of $\Delta x/p$ obtained from an analysis of the data by least squares. The observed values of Δx were also plotted against pressure on a paper 50×90 cm of which Fig. 5 is a reduced photograph showing graphically

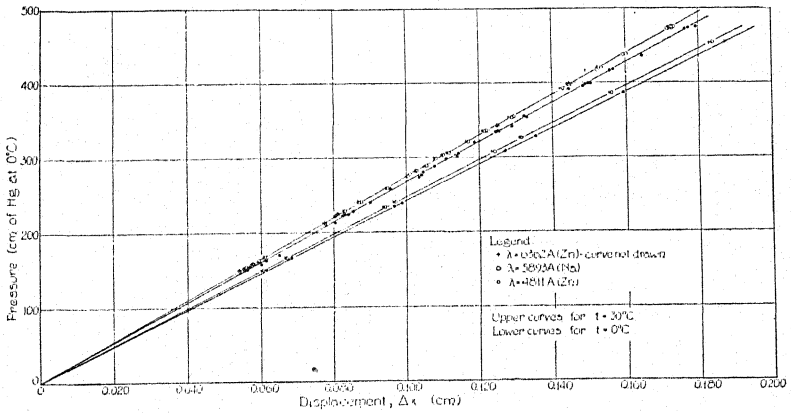

Fig. 5. Experimental results for nitrogen.

the linearity of the points. Values for B_0 were computed by Eq. (11) for the ranges 4811A–5893A and 4811A–6362A at each temperature.

	Dispersion ($B_0 \times 10^{16}$)		
Range (*A*)	*0°C*	*30°C*	
4811–5893	1.90	2.08	
4811–6362	1.87	1.95	Mean 1.95

Mean value of B (at 760 mm pressure) $= 1.48 \times 10^{-14}$. Although there is a very good agreement between the two values obtained at the zero temperature, the precision of the measurements is not sufficient to detect by experiment any temperature effect. For this reason the arithmetic mean of all the B values was used in the calculation of refractive index by Eq. (6). The values of $(\mu - 1)$ thus obtained at three different wave-legnths were reduced to values corresponding to infinite wave-length, by the Cauchy relation

$$(\mu - 1)_\infty = (\mu - 1) - \frac{B}{\lambda^2} \cdot \qquad (14)$$

The values at 30° were reduced to zero degrees by Eq. (13) producing the results shown in the last row of Table III. The values in parentheses were obtained by reducing the 30° data to zero degrees for purposes of comparison with the data obtained directly at 0°.

Significance of Results and Conclusions

Observation of the graph Fig. 5, and a least square analysis of the data show that the displacements Δx follow very closely a linear relation with pres-

TABLE III. *Calculated results.*

	Temperature 0°C			Temperature 30°C		
	4811A	5893A	6362A	4811A	5893A	6362A
$\Delta x/p$	0.0004122	0.0004040	0.0004018	0.0003743	0.0003653	0.0003635
Prob. Error	±.0000001	±.0000001	±.0000001	±.00000005	±.00000003	±.00000003
$\Delta x/e$	.0003124	.0003061	.0003045	.0002836	.0002768	.0002755
$2B/\lambda^2$	.0000128	.0000085	.0000073	.0000128	.0000085	.0000073
$(\mu-1)$	.0002996	.0002976	.0002972	.0002708	.0002683	.0002682
	(.0002999)	(.0002973)	(.0002973)			
$(\mu-1)_\infty$	.0002932	.0002933	.0002935	.0002644	.0002640	.0002645
$(\mu-1)_{\infty,0}$	.0002932	.0002933	.0002935	.0002935	.0002930	.0002936
		Mean	.0002933			
			±.0000002			

sure. The origin lies just as well on the lines as any of the observed points. This linearity means, as was pointed out before, that the Lorentz-Lorenz relation holds, and that dispersion is a linear function of pressure for nitrogen up to seven atmospheres. Theory suggests an inverse linear dependence of dispersion on temperature although the data do not indicate it. The values of B_0 differ from the mean on the average by only 6% whereas an inverse linear temperature function would call for values at 0° to differ from values at 30° by 10%. In this connection it might be noted that Meggers and Peters data Fig. 2 show no consistent temperature effect.

On the other hand the precision of the measurements is not great enough to guarantee B_0 to better than 8%. The micrometer settings can be made to one third of one percent. At one atmosphere Δx is accurate to this degree, but as the pressure increases, so does the accuracy. Analysis shows the errors in the slopes to be less than one part in four thousand, yet due to the fact that B_0 depends on the difference between two slopes observed under different circumstances it is probably not accurate to better than approximately 8%. An error of 8%, however, in B_0 corresponds to an error of less than 0.3% in $(\mu-1)$. On the other hand a survey of the literature indicates that B_0 for a gas has not previously been recorded and that B has not been very accurately determined.

This information on dispersion enables one to reduce observations of refractive index at any wave-length to a value for infinite wave-length or zero frequency, and for this reason the results are probably of most value. It is, of course, the refractive index at zero frequency which should be compared by Maxwell's law with the dielectric constant for a gas. It will be noted that in Table III the values of $(\mu-1)_{\infty,0}$ all check to a remarkable degree, thus further emphasizing the degree of precision of the observations.

The above analysis of the data shows that the accidental errors in the results amount to less than one third of one percent. The only constant error of any consequence which affects them is the possible error in the pitch of the micrometer screw, which hitherto has been assumed to be 0.5 mm. To eliminate this uncertainty a very careful calibration of the screw was made over the range actually used by counting Michelson fringes as before described. The mercury 5461A line, filtered by screens provided by Cooper Hewitt, was

used for a source, and fringes were counted over a 2 mm range. The results of ten separate counts over a whole turn (approximately 1827 fringes per turn) indicated that the irregularities of the screw were negligible and that the actual value of the pitch was 0.499 mm in this range, making $\mu_{\infty 0}$ equal to 1.0002927 instead of 1.0002933, and limiting the absolute error to one third of one percent. As a result μ^2 is equal to 1.000585 to be compared with Zahn's[12] value of ϵ equal to 1.000581 which he estimates to be accurate to one percent in $(\epsilon-1)$. The difference between these values amounts to approximately two thirds of one percent in $(\epsilon-1)$.

Incidentally it might be observed that the values for the index of refraction at a pressure of one atmosphere and a temperature of zero degrees at the three wave-lengths are as follows, corrected for the screw error:

Refractive Index of Nitrogen at 0°C and 760 mm Pressure

λ	4811A	5893A	6362A
μ	1.0002991	1.0002969	1.0002967

These values are in accord with previously published results obtained by different methods.

Acknowledgments

This problem was suggested by Professor F. G. Keyes, Director of the Research Laboratory of Physical Chemistry at the Massachusetts Institute of Technology, and at the time the work was started, also Consulting Professor of Physics at Brown University. To Professor Carl Barus and Professor C. W. Miller, the writer is also indebted for assistance in various matters, particularly with reference to the displacement interferometer. The writer is, however, especially grateful to Professor A. deF. Palmer for his sustained interest and help in supervising the whole problem.

[12] C. T. Zahn, (International Critical Tables, vol. 6, p. 78.); also Phys. Rev. **24**, 400 (1924).

ON THE ULTRAVIOLET ABSORPTION SPECTRUM OF ACETYLENE*

By George B. Kistiakowsky
Division of Chemistry, Harvard University

(Received December 26, 1930)

Abstract

It is shown that the ultraviolet absorption bands reported previously do not belong to acetylene but to some impurity. In pure acetylene, bands are observed only below 2400A. These bands are arranged into three progressions and their interpretation is proposed using information from the work on the infrared absorption spectrum of acetylene.

THE more recent investigations of the infrared absorption spectrum of acetylene have revealed a very simple structure of these bands[1] leading to the conclusion that the acetylene molecule has all four atoms in a straight line and is therefore characterised by rotational quantum levels typical of a diatomic molecule. It seemed promising to undertake a study of the ultraviolet absorption spectrum of acetylene in the hope that here also a more complete analysis could be achieved than is possible with the majority of polyatomic molecules. Not much work has been done on acetylene spectrum. Stark and Lipp[2] investigated the absorption spectrum in gaseous acetylene and reported bands between 2200–1900A without giving their wave-lengths. On the other hand, Henri and Landau[3] studying gaseous acetylene and using a 40 cm absorption tube found numerous bands at longer wave-lengths which they divide into three groups: bands with fine structure from 3157 to 2872A; partly sharp, partly diffuse bands in the region 2960 to 2495A and bands with fine structure between 2327 and 2236A.

In the present work absorption tubes up to 2 meters length were used. As a light source a hydrogen discharge tube was employed and the photographs taken first with a medium size and later with a large Hilger E1 spectrograph. Acetylene was taken from a small "Prestolyte" tank and was purified[4] by passing it slowly through a series of five Milligan wash bottles containing water, chromic acid in sulfuric acid, mercuric chloride in hydrochloric acid, copper nitrate in nitric acid and sodium hydroxide solutions, respectively. It was finally dried over phosphorus pentoxide.

Acetylene thus purified was found to be completely transparent down to 2400A and even using plates of the most contrast no traces of the some 70 bands reported by Henri and Landau could be detected. Exposures were also made with acetylene prepared from commercial calcium carbide and only crudely purified. Here a continuous absorption was found extending from

* Contribution #18 from the Loomis Laboratory.

[1] Levin and Meyer, Journ. Opt. Soc. Am. **16**, 137 (1928); Hedfeld and Mecke, Zeits. f. Physik **64**, 151 (1930); Mecke, Ibid. **64**, 173 (1930).

[2] Stark and Lipp, Zeits. f. phys. Chem. **86**, 36 (1913).

[3] Landau, C. R. **156**, 697 (1913).

[4] Beilstein. Handbuch d. Organischen Chemie, Vol. 1.

shorter wave-lengths up to about 3200A. It became evident that the spectrum described by Henri and Landau is due to some impurity and a further search for it was abandoned.

In the short ultraviolet a number of bands was observed. The wave numbers of the band heads will be found in Table I. Most of these bands are extremely faint and, in addition, a continuous absorption sets in at about

TABLE I. *Absorption bands of acetylene.*

1st progression		2nd progression		3d progression	
Wave number	Estimated intensity	Wave number	Intensity	Wave number	Intensity
42056	1	42961	1	44084 44100	5
42156	1	43074 43088	5	44205 44220	3
42433	1	43184 43199	3	44304 44318	3
42504	1	43290	1	44475	3
42648 42660	2	43441 43455	2		
42698 42712	3	43502 43518	2		
		43674 43687	10		
		43730 43744	10		
		Unassigned 44441 (3) and 44514 (3)			

2300–2350A and becomes so strong below 2250A that not more than 5 percent of the light of this wave-length is transmitted by a 2 meter layer of acetylene at 760 mm pressure. In view of this, no great precision can be claimed for the wave-length determinations, the error for the fainter bands being probably of the order of 5 cm^{-1}. The bands are shaded to the red and have double heads with a spacing of about 14 cm^{-1}. The resolution obtained was not sufficient to show rotational structure near the heads, but in the stronger bands (43674–43687 and 43730–43744 cm^{-1}) evidence of structure was observed some distance away. Even in this spectral region the bands reported by Henri and Landau must be attributed to impurities for, with the exception of 42961 cm^{-1}, none of them coincides with the now observed ones within less than 20 cm^{-1}. It is of course not excluded that the bands here reported are also to be ascribed to impurities. On the other hand every precaution exercised in purifying acetylene seemed not to effect them in the least.

The bands recorded in Table I can be arranged into three progressions at a distance of 1032 and 1012 cm^{-1} apart. These progressions can be described by the same equation, as will be best seen from Fig. 1 in which the wave-numbers of the shorter wave-length band heads (after subtracting from the second and third progressions 1032 and 2044 cm^{-1}, respectively) have been plotted against an arbitrary number v. A quadratic expression in v is, however, certainly insufficient to describe the progressions since they show a pronounced convergence for the lowest values of v, but for $v=5$ to 10 the bands become nearly equidistant. It is also unusual that both the first and the second progression break off abruptly after the strongest band ($v=10$). A tenta-

tive interpretation of the observed regularities is possible using information obtained from the vibration-rotation bands of acetylene. Mecke[1] has pointed out that a normal acetylene molecule possesses three modes of vibration parallel to the molecular axis, of which one is optically active in the infrared ($\nu_2 = 3312.83$ cm^{-1}), and two transversal vibrations of lower frequencies ($\theta_1 = 729.27$ and $\theta_2 = 1328.5$). It is quite likely that the three progressions here reported are due to transitions into successive quantum states of either of the longitudinal vibrations of the excited molecule—probably ν_2—while the bands within each progression are caused by transitions to successive quantum states of one of the transversal modes of vibration. Against this interpretation speaks mainly the abnormal intensity distribution within each progression, but perhaps this, as also the rather unusual law of binding force necessary to account for the observed spacing of the bands can be attributed to the transversal character of the vibrations involved.

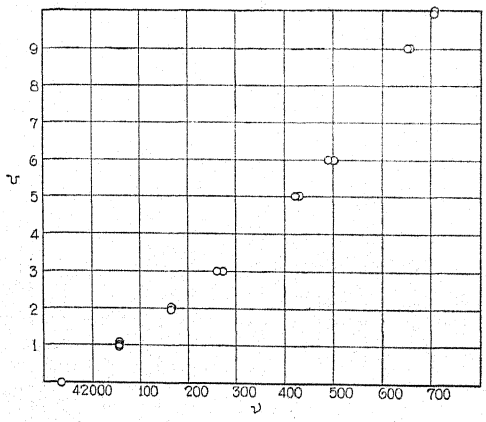

Fig. 1. A plot of three progressions of the acetylene bands.

Although a calculation of the fundamental frequencies of the excited molecule is impossible at present, it can be pointed out at least that they are probably lower than those of the normal molecule, the bands being shaded to the red, thus indicating a larger moment of inertia and presumably weaker binding force in the excited molecule. Assuming that the rotational structure of the acetylene bands is similar to that of diatomic molecules and that the double band heads are due to R and Q branches, one can estimate from their separation and the known moment of inertia of the normal molecule,[5] the moment of inertia of the excited one. One obtains thus $25.6 \pm 0.3 \times 10^{-40}$ gm cm^2 as compared with 23.509×10^{-40} gm cm^2 of the normal molecule.

The origin of the continuous absorption, mentioned in the beginning of this note, remains uncertain. It is likely, though, that this absorption is due to residual traces of impurities, because Stark and Lipp[2] were able to observe absorption bands down to 1900A.

It is a pleasant duty to thank Mr. Alfred L. Loomis for his kind permission to work in the Loomis Laboratory and for the facilities put there at my disposal.

[5] Assuming that the head of the Q branch coincides with the zero line of the band, that the equation of the R branch is $\Delta\nu = (B'+B'')K + (B'-B'')K^2$ and that for its head $K = -B'+B''/2(B'-B'')$.

SPACE CHARGE vs. IMAGE FORCE IN THERMIONIC EMISSION

By R. S. Bartlett and A. T. Waterman
Sloane Physics Laboratory, Yale University

(Received December 7, 1930)

Abstract

This paper is a joint report on work by the two authors, preliminary to further and more detailed publication on different phases of the problems here discussed. Attention is called to certain deficiencies in the Schottky image force as an explanation of the thermionic work function, both on theoretical and experimental grounds. Evidence is advanced to show that space charge is more important than image force over most of the region in which the image force is thought to be valid. It is further shown that space charge with Fermi-Dirac statistics is able to account for observed phenomena of thermionic emission, including the effect of external fields. Numerical examples indicate some of the consequences of this point of view.

THE most commonly accepted explanation of the thermionic work function is that which attributes the major part of it to the "image" force of the electron (Debye, Schottky, Langmuir). Schottky[1] gave an analysis to show that space charge and structure effects, in the layer outside that in which the surface atomic structure of the emitting body plays an important part, were negligible compared with the image force. To do this it was necessary to estimate the electron density in this layer; this he calculated on the assumption that the image force law was correct, showing that under these conditions space charge and structure effects were negligible.

On the other hand, if the assumption is made that the potential and thereby the charge density in the above-mentioned layer is determined by space charge instead of by image force considerations then it may be shown that the space charge is more important than the image force. Thus we must look further for evidence by which to choose between the two explanations. As a numerical illustration of the difference involved, a calculation of the field intensities from these two contrasting standpoints at various distances from a plane tungsten cathode at 2300°K gives the following results in the absence of external field. E_i being the field intensity in v/cm computed from the image force, E_s that computed for the space charge field, we have, at a distance of 10^{-7} cm from the cathode, $E_i=3.6\times10^6$, $E_s=4.0\times10^6$; at a distance 5×10^{-7} cm, $E_i=1.4\times10^5$, $E_s=8.0\times10^5$; at 10^{-6} cm, $E_i=3.6\times10^4$, $E_s=4.0\times10^5$. Thus, for distances from the surface greater than about 10^{-7} cm, the field intensity computed from space charge considerations is greater than when computed by the image force, and this difference is accentuated as the distance from the surface increases. The concentration of electrons shows a similar behavior. The space charge treatment of course assumes a continuous distribution of electricity whereas the image force assumes the escape of only

[1] Schottky, Phys. Zeits. **15**, 872 (1914).

one electron. As Schottky correctly points out, since in practice we find a situation intermediate between these two view-points it is necessary to examine which of these two extremes is most nearly approached in practice.

A reconsideration of this matter seems desirable, not only in view of the above fact, but also because the earlier work on the subject postulated a Maxwell distribution law in the electron atmosphere. Since the advent of the Sommerfeld electron theory it becomes desirable to find whether the degeneracy of the electron gas at and presumably also near the emitting surface affects the analysis. Among the chief reasons for the general acceptance of the image force explanation have been (1) the observed constancy of the work function for a given pure metal under moderate applied accelerating fields, i.e. the thermionic saturation current, (2) for pure metals the fairly accurate verification of the variation of thermionic current with stronger applied fields (Schottky effect) as computed by Schottky, (3) the estimation of a reasonable value for the work function, with the opportunity of characteristic values for different materials. Its chief drawback at the present time appears to be in its application to emission from coated filaments, i.e. in failing to account for lack of saturation and for the Schottky effect observed in these cases without complicated, rather *ad hoc*, assumptions.

It is clear therefore that before any superiority may be pointed out a space charge analysis should also lead to confirmation with experiment in the above directions. In deriving the thermionic current, extending through the Schottky effect, by use of space charge considerations alone, if Poisson's equation is combined with a Maxwellian distribution of electron velocities the results show definite lack of agreement for pure metals. But if a Fermi distribution is substituted for the Maxwellian, the calculated dependence of current on temperature and applied field is found to be in reasonable agreement with experiment. This may be taken to indicate the constancy of the work function calculated by this method, but it seems more reasonable to deal with directly observable quantities, and compare calculated with observed currents under varying conditions. Furthermore, the variation of the current with the nature of the emitter can be explained more readily by space charge than by image force. According to the latter the field becomes constant within a certain critical distance from the surface, this distance being so chosen that the total work function thus calculated agrees with the experimental value. As justification for this step it is pointed out that close to the surface structure effects would be important. Now, assuming the space charge method valid right down to the surface, different currents from different metals are explained by the different electron concentrations within the metals, and the work function comes out to be of the correct order of magnitude according to the Sommerfeld theory (i.e. $= W_a$) without further assumption. This leads, incidentally, to a simple explanation of the observed interdependence of A and b, the constants in the usual thermionic emission equation. Moreover it appears that the use of Fermi-Dirac statistics takes account, in part at least, of structure effects. For a simple calculation will show that an electron gas is degenerate when the electrons are so closely crowded that the mutual po-

tential energy of neighboring pairs is large compared with their kinetic energy of thermal agitation, and obeys classical laws when the potential energy is small. For example, in an electron gas at 1600°K for which the Fermi A is 10^{-3}, i.e. the gas nearly in the classical state, the average kinetic energy is roughly twenty times the potential.

Thus it appears that the space charge calculation based on Fermi-Dirac statistics is a more proper method of dealing with pure metals, and it may be further pointed out that the same calculation based on classical statistics, assuming a low electron concentration in the emitter, seems capable of explaining results obtained with coated filaments. This latter point is being investigated further.

Following out their preliminary investigations on this subject[2] the authors have carried the work further, one of them taking exclusively the problem of deducing the thermionic current under applied accelerating fields from zero to fields operative in the Schottky effect, the other treating exclusively the case of the statistical equilibrium resulting under retarding applied fields (including zero). Both deal only with the case of an infinite plane emitting surface.

The former (R. S. Bartlett) has handled the problem after the manner of Langmuir and Fry by postulating the emission of electrons with velocities distributed according to the Fermi statistics, these electrons being subject only to the space charge field, and obeying the law of continuity of current. This calculation is rendered troublesome by the necessity of graphical computation of the Fermi integrals for the region of transition from a degenerate to a classical state, and thus are not at present in a form suitable for detailed report in this communication. The general results have been mentioned above, and appear encouraging, especially in pointing the way to a single explanation of thermionic currents from zero applied field up through fields of Schottky intensity.

The latter author (A. T. Waterman) starting with Poisson's equation and the Fermi analogue $A = A_0 e^{-v\epsilon/kT}$ of the familiar Boltzmann relation, has evaluated the potential and the electron concentration at points outside the surface, where the atmosphere is in the classical state (assuming a degenerate state within the metal). In the presence of a retarding field E the solution takes different forms on either side of a critical distance, which, expressed in terms of potential difference between this distance and the surface, is $V' = 2 \log E/\beta$ where $\beta^2 = 16\pi(2\pi m)^{3/2}h^{-3}(kT)^{5/2}\, e^{W/kT}$ where W is Sommerfeld's W_i, the thermodynamic potential of the electrons within the body. Thus for $V > V'$ (thus including zero field), V (at distance x) $= -2kT/\epsilon \log (1+\epsilon\beta/2kT\, x)$ and the number of electrons per cc, $n = kT/2\pi\epsilon^2x^2$. For $V < V'$, $V = -kT/\epsilon(\epsilon Ex/kT - \log 4E^2/\beta^2)$ and $n = E^2/2\pi kT\, e^{-\epsilon Ex/kT}$. It will be noted that on the space charge conception the concentration of electrons in equilibrium with a hot body depends only upon the distance and the temperature,—in particular not upon the nature of the hot body, for distances at which the electron gas is in the classical state (roughly $> 10^{-7}$ cm). Examination as to

Abstracts 52, 53 Phys. Rev. **35**, 668 (1930).

the above-mentioned critical distance introduced by an applied retarding field, which is a measure of the distance inside which the applied field has no appreciable effect on the electron atmosphere, results in the observation that applied retarding fields of the order existing in cold extraction currents would control the electron atmosphere extending into the region where the electron gas becomes degenerate very near the surface. A prediction of the work is that the ratio of the anode potentials which would give equal thermionic currents under zero applied field from two different emitters under otherwise identical conditions (temperature and geometry of tube) should be $V_1/V_2 = \log \beta_1/\log \beta_2$. If Sommerfeld's electron theory is assumed, then this ratio should show appreciable difference from unity, e.g. $V_{Ca}/V_W = 0.65$; on the classical theory the ratio should always be very nearly unity, e.g. $V_{Ca}/V_W = 0.98$ in the instance quoted.

ORIGIN OF THE AXIAL ROTATION OF THE SUN

By Ross Gunn
Naval Research Laboratory, Washington, D. C.

(Received December 24, 1930)

Abstract

In earlier papers the solar atmosphere has been shown to rotate rapidly as a result of the electric and magnetic forces which act on the atmospheric ions. At the equator the ionized layers move much faster than the solar surface proper but this relative movement decreases with latitude in the manner required by observation. The fast moving atmospheric layers transfer momentum to the sun proper and its rotation is a necessary consequence of the observed atmospheric motions. The resultant torque is calculated and the angular acceleration shown to be adequate to account for the observed rotation.

THE almost universal prevalence of rapid rotation in celestial objects has been pointed out again and again by astronomers, but the origin of such rotation has been somewhat of a mystery. Celestial mechanics shows how a star may rotate faster and faster as it contracts due to condensation, but gives no clue as to the origin of the initial rotation, which must be comparable to the final value. In an important paper Jeans[1] discussed the relation of the radiation of matter to the rotation of a star and he concluded that the radiation of the star carries off angular momentum in such a way that it "generally lessens the angular momentum per unit mass of the star." He thus pointed out that the common assumption of a constant angular momentum for a radiating star is invalid. We must, therefore, for the most part, attribute the observed high rotational velocities to changes in the mean density together with an initial rotation of the star or else to some phenomena not adequately described by celestial mechanics.

In a series of papers which deal with the electromagnetic effects operating in the solar atmosphere, it has been shown[2] that the anomalies of the sun's apparent rotation arise from an electromagnetic drift of the ionized atmosphere and are not directly dependent on the motion of the surface of the sun proper. It was shown that the solar atmosphere rotates in the same direction as the sun proper but *much faster* and that this superposed drift results from the interaction of the atmospheric ions with the observed solar magnetic field and a radial electric field.

The sun may be thought of as a highly viscous mass of gas bound together by gravitational, radiative and electromagnetic forces in such a manner as to form a semi-rigid system. Radiative viscosity acts in such a manner as to equalize differences of rotation in different layers but Jeans[1] calculations indicate that these forces alone are incapable of equalizing the rotations in a time

[1] Jeans, Monthly Notices R. A. S. **86**, 328, 444 (1926).
[2] Gunn, Phys. Rev. **35**, 635 (1930); **36**, 1251 (1930).

so short as the age of the sun. The sun's observed magnetic field is asymmetric with respect to the axis of rotation and hence shells of highly conducting solar matter rotating about the geographical axis will induce electromotive forces and systems of electrical eddy currents which will strongly oppose motion relative to the magnetic field. A quantitative calculation of the electromagnetic damping forces due to axial slippage is difficult but we have seen that in regions of high electrical conductivity the forces due to radial contraction are tremendous[3] and it seems probable that electrical forces contribute in an important manner to the apparent viscosity of the sun. To be sure that these forces have time to act we must examine whether the electrical time constant of the induced current circuit is sufficiently short compared to the solar age for current systems to build up. It is convenient to note that the largest time constant τ possible is the constant for the whole sun which is given by $\tau = L\Sigma$ where L is the effective inductance and Σ is the total conductivity. On making this calculation it results that τ is of the order of 10^9 years. This is very small compared to the age of the sun and we assume that inductive effects are unimportant.

On account of the high effective viscosity of the interior it seems satisfactory to assume as a first approximation that the sun is a semi-rigid body rotating on its axis at a period corresponding to the observed period of rotation of its magnetic pole. With the solar radius known it is evident that the peripheral velocity of any point on the solar surface proper can be calculated. The difference between this velocity and the velocity of the same point as determined by an earth-bound observer watching the solar atmosphere is evidently the atmospheric drift velocity. This superposed drift velocity $\boldsymbol{U}$ of the ionized atmosphere is readily determined from observation or can be calculated from[2]

$$u = \frac{E \times B}{B^2\left(1 + \left(\frac{R}{\lambda}\right)^2\right)} \tag{1}$$

where E and B are the electric and magnetic field intensities, λ the mean free path of the ions, and R the radius of the helix generated by an ion as it spirals around the impressed magnetic field. This radius is calculated from

$$R = \frac{mV}{Be} = \frac{(2mkT)^{1/2}}{Be} \tag{2}$$

where m is the mass of the ion, V the component of velocity perpendicular to B and e the ionic charge.

It is clear from Eq. (1) that the drift motion of the atmosphere drops abruptly as the ion pressure increases to such a value that the free path becomes of the order of R. Thus a more or less sharply defined transition layer exists between the atmosphere and the solar surface proper. In this critical transition region between the sun and its atmosphere there is a constant

[3] Gunn, Phys. Rev. **35**, 107 (1930).

interchange of momentum, and the faster moving layers transfer their momentum to the slower. At the surface of the sun the temperature is low and the radiative and electromagnetic viscosities are small compared to the molecular viscosity, so that we need only consider the forces due to the latter. The tangential force applied to the periphery of the sun by the more rapidly rotating atmosphere is

$$F = \eta u \frac{A}{S} \tag{3}$$

where η is the mean coefficient of viscosity of the transition layer, u the mean difference in velocity of the layers, A the effective area in contact and S their separation. To a sufficient approximation we may assume that in the transition layer the coefficient of viscosity is independent of the magnetic field and write

$$\eta = \frac{(3ZmkT)^{1/2}}{2(2)^{1/2}\pi\sigma^2} \tag{4}$$

where m is the mass of the hydrogen atom, Z the mean atomic weight of the ions composing the layer, k the Boltzmann constant, T the absolute temperature, and σ the kinetic theory diameter of the ions. To a sufficient approximation we may assume that the effective contact area A is a ring around the equator of width R where R is the radius of the sun and that the mean velocity difference is not appreciably different from the equatorial value. The torque Q applied to the solar mass is

$$Q = I\alpha = \frac{(3ZmkT)^{1/2}}{(2)^{1/2}\sigma^2} \frac{u}{S} R^3 \tag{5}$$

where I is the effective moment of inertia and α is the angular acceleration. Assuming that the solar density is uniform we get from Eq. (5)

$$\alpha = \frac{5(3ZmkT)^{1/2}}{2(2)^{1/2}\sigma^2} \frac{uR}{SM} \tag{6}$$

where M is the mass of the sun. Taking from earlier work $Z=3.3$, $m=1.66\times10^{-24}$ gm, $k=1.37\times10^{-16}$, $T=6{,}000$, $\sigma=10^{-8}$ cm, $R=7\times10^{10}$ cm, $M=2\times10^{33}$ gm, $u=5\times10^{4}$ cm/sec and $S=5\times10^{6}$ cm we find $\alpha=2.3\times10^{-26}$ rad/sec.[2]

We have seen in an earlier paper[4] that the solar magnetic field is maintained by a system of electrical currents which flow in rings about the sun's axis and that this system of currents is not primarily related to the rotation, but to the sun's radial and axial symmetry. This circumstance suggests that the magnetic field and hence motions of the solar atmosphere have not changed in order of magnitude for a considerable portion of the sun's life, which various estimates put at 7×10^{12} years or 2×10^{20} seconds. By multiply-

[4] Gunn, Phys. Rev. **34**, 335, 1621 (1929).

ing the angular acceleration α by the life time we find to a crude approximation that the final angular velocity of the sun should be 4.6×10^{-6} radians per second, if its initial rotation was negligibly small. The observed angular velocity, as computed from the motion of the magnetic pole is 2.3×10^{-6} radians per second. The agreement is rather better than one might expect from a calculation based on steady states.

Were allowance made for the increased radiation during the youthful period and a smaller moment of inertia used, due to the concentration of mass toward the center, then the elapsed time necessary to account for the observed rotation would be considerably reduced. This suggests that in the earlier stages of development the sun was unmagnetized and was a typical pulsating star.[3] It is clear that the solar rotation can be accounted for by the mechanical drag of the solar atmosphere on the sun proper if the velocity of the atmosphere exceeds that at the surface by 0.5 km/sec. This is the precise value required to explain the anomalous rotation of the sun; this having been adequately accounted for in an earlier paper by the author. The mechanism of rotation which we have considered doubtless has universal application in all stars having a magnetic field. It seems probable that this mechanism, which constantly supplies angular momentum to stellar systems, may assist in explaining certain puzzling facts in connection with spiral nebulae and binary systems. Numerical application to other star systems seems meaningless at the present time due to lack of data, and we can only point out that most other stars will behave like the sun. Ordinary mechanics has been found inadequate to explain the rapid rotation of heavenly bodies. The present investigation shows that the rotations can be accounted for by the momentum transferred to the body proper by its own highly ionized atmosphere. We have shown previously that the motion of the solar atmosphere is controlled by the magnetic and electric fields existing in the atmospheric layers and that these fields are probably controlled by the rate of radiation of matter. We may then conclude that the rotation of all heavenly bodies is intimately related to the dissolution of matter and in a static, non-radiating universe rotating systems would not exist.

THE NATURE OF THE CONDUCTIVITY OF INSULATING OILS*

By Karl F. Herzfeld
Department of Physics, The Johns Hopkins University

(Received December 23, 1930)

Abstract

It has been shown in a previous paper how the methods developed in the study of conduction of electricity through gases could be applied to determine the nature of the ions present in liquids and solids. In the present paper these methods have been applied to the measurements of the space charge set up in insulating oils by a steady electric field, which were recently performed by Whitehead and Marvin. The procedure is as follows: the shape of the curve shows that the current must be considerably below three-fourths of the saturation current. It is possible to fit the curve closely by assuming the Langevin constant to be $\beta=36\pm10$. From this the number of ions present in the normal state and their mobility can be calculated, which turns out to be $3.5\cdot10^{-6}\pm50\%$ cm/sec per volt/cm. With the assumption that the mobility is inversely proportional to the viscosity, the mobility of these ions in water would be $1.2\ 10^{-4}$ cm/sec per volt/cm or in the usual units 12. If one assumes that Lorenz's results for organic ions can be applied these ions should have approximately 110 atoms. From the boiling point of the oil one would conclude that the molecule of the oil contains about 45 atoms.

A NUMBER of papers[1] have recently appeared from the Engineering School of The Johns Hopkins University, investigating the conductivity of transformer oils. The last of these make possible an application[2] of Mie's[3] formulas to discover the properties of the ions.

We start with the space-charge distribution[4] in oil "B", when a potential of 1500 volts is applied between large condenser plates 2 cm apart. The distribution of potential is nearly symmetric around the center, proving that the mobility of the ions of opposite sign must be nearly equal. We are going to neglect whatever dissymmetry might be present.

Fig. 1 shows that the line is very nearly straight in the neighborhood of the center, i.e. the field very closely constant for quite a distance. It follows from this that the current must be considerably below $\frac{3}{4}$ of the saturation current and the approximate formulas have to be used which apply, according to Mie, to weak currents.

* Presented at The Third Annual Meeting and Conference, Committee on Electrical Insulation, Division of Engineering and Industrial Research, National Research Council, Bureau of Standards, November 7, 8, 1930.

[1] J. B. Whitehead and R. H. Marvin, A. I. E. E. Trans. **48**, 299 (1929); J. B. Whitehead, Jl. Franklin Inst. (IV) **208**, 453 (1929); J. B. Whitehead and R. H. Marvin, A. I. E. E. Trans. **49**, 641 (1930).

[2] K. F. Herzfeld, Phys. Rev. **34**, 791 (1929).

[3] G. Mie, Ann. d. Physik **13**, 857 (1904).

[4] An enlarged drawing of this figure, which has been used for Fig. 1 of the present paper, has been kindly put at my disposal by Dr. J. B. Whitehead.

The next step is the calculation of β(β^{-1} is Langevin's constant). For this purpose, one has to compare the field in the center and the field near the electrodes. The field in the center is

$$h_0 = 450 \pm 10 \text{ volt/cm}.$$

The field near the electrodes is not measured directly; from the drawing it was estimated to be $h_m = 2400$ volt/cm. This would lead to

$$c = \beta^{\beta/\beta-1} = \frac{h_m^2}{h_0^2} = \left(\frac{2400}{450}\right)^2 = 28.5.$$

Subsequently, $c=40$ proved to be the value which suited the curve best, but calculations were also made with $c=30$ for comparison, which turn out to fit the curve appreciably less.

$$c = 40 \text{ gives } \beta = 36.3, (2\beta)^{1/2} = 8.5.$$

It turns out that it is more useful for the actual calculation to put Mie's formulas into a form different from the one that had been given previously.

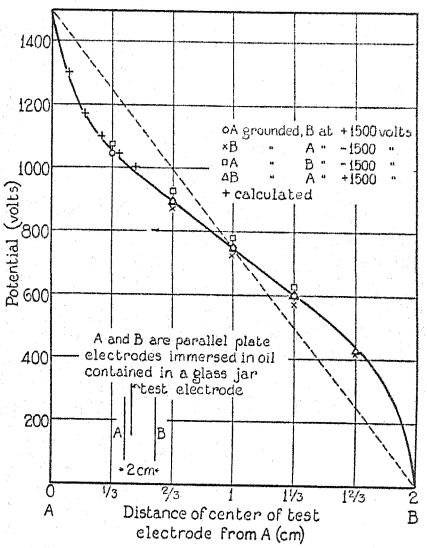

Fig. 1.

Calling, as was done there, x_K the location of the bend in the graph of the field, we measure the location in the condenser relative to x_K and find for the flat (central) part[5]

$$h^2 = H^2[1 + (c-1)(e^{-y_1} + e^{-y_2})] \tag{1}$$

$$y_1 = \frac{(c-1)(c-1-(2\beta)^{1/2})}{2\beta - c + 1}\left(\frac{c-1-(2\beta)^{1/2}}{c-1} - 2\frac{l-x}{l-x_K}\right) \tag{2}$$

in y_2 only $l-x$ has to be replaced by $l+x$.

[5] In formula (50) of the paper cited in footnote (2) $4l^2$ should be stricken from the denominator.

With the high value of β given above the exponent is always so large that the deviation from a constant $h=H$ for the field or from a straight line $V=-Hx+V_0/2$ for the potential is negligible in the range of this formula, that is within $-x_K<x<x_K$. That means $h_0=H$, there is no change in the amount of ions in the central part. In the central part Ohm's law is preserved with the initial conductivity. In the range between the electrodes and x_K, (1) holds, but there y_1 and y_2 have a different form from the one in the central part. y_2 as before is derived from y_1 by substituting $l+x$ for $l-x$. We have

$$y_1 = +(2\beta)^{1/2}\frac{c-1-(2\beta)^{1/2}}{2\beta-c+1}\frac{l-x}{l-x_K}\left(1+\frac{1}{2}\frac{c-1-(2\beta)^{1/2}}{2\beta}\frac{l-x}{l-x_K}\right). \quad (3)$$

But here too, with the large value of β, the coefficients are so large that $(c-1)e^{-y_1}$ is appreciable only for small values of $l-x/l-x_K$, and than e^{-y_2} with the argument $l+x/l-x_K$ is negligible. With this in mind, it is useful to measure, as Mie does, the distance from the electrode instead of the center and write

$$h^2 = h_0^2[1+(c-1)e^{-y_1}] \quad (1')$$

$$y_1 = (2\beta)^{1/2}\frac{c-1-(2\beta)^{1/2}}{2\beta-c+1}\frac{x}{x_K}\left(1+\frac{1}{2}\frac{c-1-(2\beta)^{1/2}}{2\beta}\frac{x}{x_K}\right). \quad (3')$$

The subsequent procedure is as follows:

One draws a curve of h as function of x/x_K, from $x/x_K=0$ (electrode) to $x/x_K=1$ (bend) and proceeds from thereon with $h=h_0$. The problem is to determine x_K, or to put it differently, to determine l/x_K.

We accordingly integrate graphically beyond the point $x/x_K=1$, taking into consideration the scale of our drawing and changing it continuously as we go on [because $V=\int h dx=x_K\int h d(x/x_K)$], until we get to a point where $V=V_0/2=750$ volts. This must be the center. To show a few examples, we get with different assumptions for the position of the bend:

$\frac{x_K}{l}$,	$\frac{8}{12}$	$\frac{10.5}{12}$	$\frac{11}{12}$
V	680	750	765.

It seems therefore safe to say that

$$\frac{x_K}{l}=\frac{7}{8}=0.88\pm 0.08.$$

The points calculated with this value and $c=40$ are marked with crosses in the figure. Formula (53)[6] gives then

$$\frac{j}{j_{sat}}=\frac{x_K}{l}\frac{(2\beta)^{1/2}(2\beta-c+1)}{(c-1)(c-1-(2\beta)^{1/2})}=0.2\pm 0.05.$$

[6] See footnote (2).

We put then the current $j=\delta 1.6\times 10^{-11}$ amp/cm^2 with δ probably near unity. That makes $j_{sat}=\delta 8\times 10^{-11}\pm 25\%$ amp/cm^2 or, if we consider that j_{sat} is the total amount of charge generated per cm^2, that is in a cylinder of $2l=2$ cm length, that gives the number of pairs of univalent ions, generated in 1 cc per second

$$q=\frac{j_{sat}}{2.2e}=1.25\times 10^8\cdot\delta\pm 25\%.$$

Furthermore, we have

$$\beta=\frac{8\pi K_e}{\alpha\epsilon}=40\pm 10.$$

If we want K in cm/sec/ volt/cm instead of per est. unit/cm, we have to divide by 300. It is this number that shall be meant by K from now on.

We assume $\epsilon=2.5\pm 10\%$

$$\frac{K}{\alpha}=2.8\times 10^7\pm 35\%.$$

Now $q/\alpha=n_0^2$ (n_0 being the equilibrium number of the ions of each sign which is present in the central part of the condenser even under the conditions of our experiment). Therefore

$$\frac{qK}{\alpha}=Kn_0^2=3.5\times 10^{15}\delta\pm 50\%.$$

On the other hand, the conductivity in the central part, when Ohm's law is valid gives

$$\frac{j}{450.2.e}=n_0K=1.1\times 10^5\delta$$

or

$$n_0=3.2\times 10^{10}\pm 50\%$$

and

$$K=3.5\times 10^{-6}\delta\pm 50\%\text{ in cm/sec/volt/cm}.$$

[7] The current density was measured on March 27 and found to be 1.6×10^{-11} amp/cm^2; the space charge curve was taken April 4–6, a remeasurement of current on May 2 gave 2.9×10^{-11} amp/cm^2, the curves in Fig. 12 (in the last paper mentioned in footnote 1) give for the initial conductivity $5.1\times 10^{-14}\,h_0$ which, for 450 volt/cm, would amount to a current of 2.25×10^{-11} amp/cm^2. But during April a considerable manipulation with the oil makes the first given current more trustworthy. There is another fact pointing in this direction. The ratio of the initial field to the central field in the steady state should be equal to the ratio of the initial current to the steady current, if the conductivity (number of ions) remains unchanged in the central part. But in the later measurements the ratio of the currents is only 1.45 (private communication), while the ratio of the fields is $750/450=1.67$. This is clear if in the meantime the number of ions has increased because then one would be further from saturation and the ratio of the two fields at the time of the second current measurements would be less.

On the other hand, the measurement on March 27 (Fig. 11) points to a ratio of currents 1.7.

To get a reasonable comparison for this value, one remembers that according to Walden,[8] the mobility of large ions in different solvents is inversely proportional to their internal friction η. Professor J. C. Hubbard, of this Laboratory, was kind enough to determine η for this oil and found it 0.35 (water 0.01), which would make the mobility in water 1.2×10^{-4} cm/sec/volt/cm or, in the usual units (multiplication with 96540 coulomb) equal to 12. $\pm$ 50%.

According to Lorenz[9] one could now estimate that an anion of mobility 12 contains about 110 atoms, an ion of mobility 18, 65 atoms.

M. F. Hamburger, of the Department of Electrical Engineering, has kindly measured the boiling point of the oil and found it to be about 290°C. Accordingly, one would estimate that the oil has molecules containing about 15 C-atoms, therefore about 45 atoms. If the ions are products of oxidation (last paper footnote 1) the anion should contain about two molecules (be the anion of an acid coming from the oxidation of a polymer of double molecular weight). The equal mobility of the action would have to be explained as due to the fact that the H^+ ion has two oil molecules (or a molecule of the above mentioned isomer) attached to it.

If the interpretation of Dr. Whitehead, that the increase in conductivity above the Ohm-value upon reversal is due to an ion of a mobility $K = 10^{-4}$ cm/sec/volt/cm is correct, this ion would turn out, with our present data, to be very quick. Multiplying namely with 10^5 (units!) and 35 (ratio of η of oil and water) we get 350 which is a speed only attained by H^+ in water. We might have to divide this by 2 or 3 as small anorganic ions move in water slower as expected, and reduce the estimated K to $1/2\ 10^{-4}$. Then we could still have the mobility of a small anorganic ion.

If this is accepted, then the picture is as follows: There are present a large number of slow, organic ions which are continuously generated and move on to the electrodes where they are discharged without appreciable accumulation They are responsible for the space charge and the long time phenomena.

Besides, there are quick, small anorganic ions which are not discharged at the electrodes, but accumulate there, without practically influencing the space charge, and are the cause of short time processes. Offhand, three origins could be imagined: (a) They are present as impurities, but are not supplemented continuously. That is impossible, because then upon reversal of the field the current would not go beyond the initial current of the original field. (b) They are generated continuously; then their number must be much smaller than the number of the slow ions, because the latter determine the space charge (β). (c) Their origin could be a secondary process on the electrodes (OH'?).

[8] P. Walden, Zeits. f. anorg. Chem. **113,** 85 (1920).

[9] R. Lorenz, Raumerfüllung u. Ionenbeweglichkeit, Leipzig, (1922) p. 79.

POTENTIAL DUE TO A BURIED SPHERE

By J. H. Webb
Williams College

(Received December 16, 1930)

Abstract

A series solution of the problem dealing with the electrical potential due to a buried conducting sphere is given. The general method of attack consists in finding a solution of Laplace's equation $\nabla^2\Phi=0$, subject to proper boundary conditions. The condition requiring the vanishing of the normal derivative of potential on the surface of the half space is satisfied by placing an image sphere in an upper half space. The introduction of this image sphere also introduces the complication of the interaction of the potential due to two spheres. This is handled by means of spherical harmonics and the solution of the problem is made possible by means of a special transformation in spherical harmonics.

Introduction

MANY problems of this type have arisen recently in connection with the subject of geophysics. Since the introduction of electrical methods for ore exploration, there have been numerous attempts to find some means by

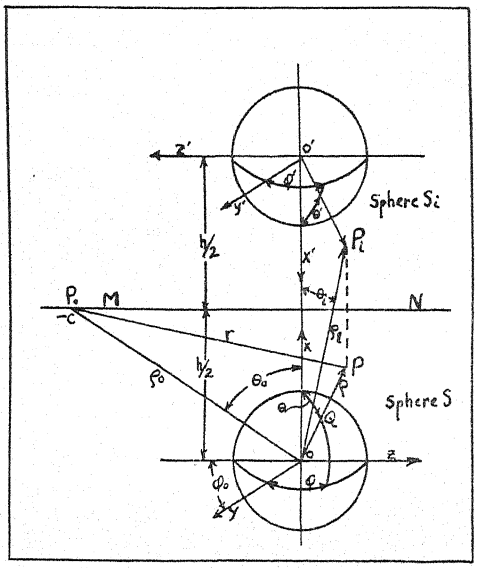

Fig. 1. Buried and image sphere.

which to predict the nature and scope of irregularities in homogeneity of structure beneath the surface of the earth, when point electrodes on the surface are maintained at definite potentials.[1] In most of these attempts, cer-

[1] A. Petrowsky, Phil. Mag. [5] **31**, 927 (1928); **28**, 334 (1928).

tain approximations have been made. In fact, in the more complicated problems, approximations must be made. The present problem of the sphere is worked out, making no approximations, as a first step toward finding out the allowable approximations which may be made in the more complicated problems, e.g. a buried ellipsoid or cube.

Assume a sphere of radius a and conductivity σ_1 buried in an infinite half space of conductivity σ_2 (see Fig. 1). At the center of the sphere, locate the common origin of a set of cartesian coordinates x, y, z and a set of polar coordinates ρ,θ,ϕ. Place an electrode at the common point $P_0(h/2, 0\text{-}c)$ and P_0 $(\rho_0, \theta_0, \phi_0)$. Note that $\phi_0=\pi/2$. The potential due to the electrode alone is $I/4\pi r\sigma_2$ in which r is the distance from P_0 to any point P and I is the current. It is desired to find the potential at every point in space due to the buried sphere S. Designate by u and U the inside and outside potential, respectively, due to the sphere alone. Then the functions u and U must satisfy Laplace's equation

$$\nabla^2\Phi = 0, \tag{1}$$

at all points in space, and are further subject to the conditions:

$$k\frac{\partial u}{\partial \rho} - \frac{\partial U}{\partial \rho} = -(k-1)\frac{\partial U_e}{\partial \rho}, \quad \rho = a, \tag{2}$$

$$u = U, \qquad \rho = a, \tag{3}$$

$$U = 0, \qquad \rho = \infty \tag{4}$$

and

$$\frac{\partial \Phi}{\partial x} = 0, \quad x = h/2, \tag{5}$$

in which U_e denotes the potential due to the electrode and k represents the ratio of conductivities σ_1/σ_2. Condition (2) results from the well-known equation:

$$k\frac{\partial \Phi}{\partial n_1} + \frac{\partial \Phi}{\partial n_2} = 0$$

in which Φ is the total potential and n_1 and n_2 are the normals pointing into the regions whose conductivity is σ_1 and σ_2 respectively. In the above equation

$$u + U_e = \Phi,$$

inside the sphere, while

$$U + U_e = \Phi$$

outside the sphere. Then since

$$\frac{\partial}{\partial n_1} = -\frac{\partial}{\partial \rho},$$

while

$$\frac{\partial}{\partial n_2} = \frac{\partial}{\partial \rho},$$

the last equation becomes

$$-k\left(\frac{\partial u}{\partial \rho} + \frac{\partial U_e}{\partial \rho}\right) + \left(\frac{\partial U}{\partial \rho} + \frac{\partial U_e}{\partial \rho}\right) = 0,$$

from which Eq. (2) follows at once. The complication which arises in the solution of the above problem is due to the boundary condition (5). In order to satisfy this condition, an image sphere S_i is placed in the upper half space, which is imagined filled with material of conductivity σ_2. Then, from symmetry, the normal derivative of potential will vanish on the boundary

$$x = \frac{h}{2}.$$

It may be seen that the problem can be viewed as either one in which a single sphere S is situated in an infinite half space, subject to the boundary condition (5), or a problem in which two spheres S and S_i, (S_i being the image in plane MN of S), are situated in an (whole) space. In the problem which includes the image sphere, the boundary condition (5) is automatically satisfied while at the same time, the complication arises that the interaction between the two spheres must be taken into account. Analytically, this results from the fact that, when the image sphere is included, the applied potential consists not only of U_e, the potential due to the electrode, but also U_i, the potential due to the image sphere. This new potential will be called U_a. According to the uniqueness theorem, the solution of the problem with the image sphere will also be a solution of the problem in hand, since such a solution satisfies Laplace's equation and boundary conditions (2), (3), (4) and (5). The solution of the problem, using the image sphere is the one here given.

The following solutions of Laplace's equation may be written immediately

$$u_1 = \sum_{m=0}^{\infty} \left(\frac{\rho}{a}\right)^m Y_m(\mu, \phi), \tag{6}$$

$$u_2 = \sum_{m=0}^{\infty} \left(\frac{a}{\rho}\right)^{m+1} Y_m'(\mu, \phi), \tag{7}$$

in which $Y_m(\mu, \phi)$ stands for the ordinary spherical harmonic and μ for $\cos\theta$. Because of condition (4) and because the potential of the sphere must be finite at $\rho = 0$, u_1 and u_2 are chosen as u and U, the inside and outside potentials respectively. If the coefficients A_{nm} and B_{nm}, in the above expressions, can be so chosen that u and U satisfy all the boundary conditions, the solution of the problem will have been found.

Eqs. (6) and (7) satisfy Laplace's equation, condition (4), and will satisfy condition (3) provided the coefficients in (6) and (7) be set equal, making

$$Y_m(\mu, \phi) \equiv Y_m'(\mu, \phi).$$

The next step is to apply condition (2). Before this is possible, a suitable expression for U_a must be found. U_a consists of two parts

$$U_a = U_e + U_i, \tag{8}$$

a part U_e due to the electrode and a part U_i due to the image sphere S_i. From symmetry, the potential at any point P due to sphere S_i is the same as the potential at point P_i due to sphere S, where[2] P_i is the image of P in the plane MN, i., e.,

$$U_i(P) \equiv U(P_i) = \sum_{m=0}^{\infty} \left(\frac{a}{\rho_i}\right)^{m+1} Y_m(\mu_i \phi_i). \tag{9}$$

Thus the expression for the potential U_a, at P, can be written,

$$U_a = \frac{I}{4\pi\rho_0\sigma_2} \sum_{m=0}^{\infty} \left(\frac{\rho}{\rho_0}\right)^m L_m(\mu_0, \phi_0, \mu, \phi) + \sum_{m=0}^{\infty} \left(\frac{a}{\rho_i}\right)^{m+1} Y_m(\mu_i, \phi_i), \tag{10}$$

in which L_m is a Laplacian, a special form of the spherical harmonic Y_m. Since $\phi = \phi_i$, ϕ_i may be replaced by ϕ. Hereafter D will be written for the constant term $I/4\pi\sigma_2$. The first member of Eq. (10) is the part of the potential due to the electrode, and the second member is the part due to the image sphere S_i. The coefficients in the second member of (10) are identical with the coefficients in the expressions (6) and (7) for the potential of the sphere S. The boundary condition (2) will be employed for determining the values of these coefficients which appear in (6), (7) and (10). This will be accomplished by substituting for u, U and U_a their values from (6), (7) and (10) in Eq. (2) and equating coefficients of like tesseral harmonics. Before this is possible, however, U_a must be expressed as a sum of tesseral harmonics with arguments μ and ϕ whose coefficients contain (besides the constants A_{nm} and B_{nm} to be determined) successive powers of ρ. The first term of (10) is already essentially in the desired form. The second term of (10) is at present, however, expressed in terms of ρ_i, μ_i and ϕ. It will be expressed, as desired, in terms of ρ, μ and ϕ by the establishment of a relationship of the type:

$$\sum_{m=0}^{\infty} \left(\frac{a}{\rho_i}\right)^{m+1} Y_m(\mu_i, \phi) = \sum_{m=0}^{\infty} f_m(\rho') Y_m(\mu', \phi), \tag{11}$$

and subsequently replacing ρ' and μ' by their values in terms of ρ and μ. When the second term of (10) has been thus transformed, the solution of the problem is then found at once by comparing on the two sides of Eq. (2) coefficients of like tesseral harmonics.

Now a relationship between tesseral harmonics, which makes possible a transformation of type (11), has been found. This relationship is

$$\frac{P_m{}^n(\mu_i)}{\rho_i{}^{m+1}} = \frac{(-1)^{m-n}}{(m-n)!}(1-\mu'^2)^{n/2} \frac{\partial^{m-n}}{\partial h^{m-n}} \frac{1}{h^n} \frac{\partial^n}{\partial \mu'^n} \sum_{k=n}^{\infty} \frac{\rho'^k}{h^{k+n+1}} P_k(\mu'), \tag{12}$$

[2] The subscript i is used throughout to refer to image points.

in which the quantities θ' and θ_i are related a shown in Fig. 1. Differentiating with respect to μ' and h, the result is

$$\frac{P_m{}^n(\mu_i)}{\rho_i{}^{m+1}} = \sum_{k=n}^{\infty} \frac{(m+k)!}{(m-n)!(n+k)!} \frac{\rho'^k}{h^{m+k+1}} P_k{}^n(\mu') = \sum_k \alpha_{knm}. \tag{13}$$

For the special case $n=0$, (13) reduces to the form,[3]

$$\frac{P_m(\mu_i)}{\rho_i{}^{m+1}} = \sum_{k=0}^{\infty} \frac{(m+k)!}{m!k!} \frac{\rho'^k}{h^{m+k+1}} P_k(\mu') = \sum_k \alpha_{k0m}. \tag{14}$$

Substituting (13) and (14) in the second member of (10) one obtains

$$U_a = \frac{D}{\rho_0} \sum_{m=0}^{\infty} \left(\frac{\rho}{\rho_0}\right)^m L_m(\mu_0\phi_0\mu\phi) + \sum_{m=0}^{\infty} \Bigg[A_{0m} \sum_k \alpha_{k0m} + \sum_{n=m}^{\infty} (A_{nm} \cos n\phi + B_{nm} \sin n\phi) \sum_k \alpha_{knm} \Bigg].$$

By an interchange of indices m and k, one finds

$$U_a = \frac{D}{\rho_0} \sum_{m=0}^{\infty} \left(\frac{\rho}{\rho_0}\right)^m L_m(\mu_0, \phi_0, \mu, \phi) + \sum_{m=0}^{\infty} \Bigg[\sum_k A_{0k}\alpha_{m0k} + \sum_{n=m}^{\infty} \sum_k (A_{nk} \cos n\phi + B_{nk} \sin n\phi)\alpha_{mnk} \Bigg], \tag{15}$$

which is the desired result. It is now possible to apply the boundary Eq. (2). The values of u, U and U_a to be substituted in Eq. (2) have been given above. This boundary Eq. (2) involves the first derivative of u, U and U_a with respect to ρ. The second member of (15) for U_a, gives the potential in terms of ρ' and μ' at point P_i, due to the sphere S. From symmetry it may be seen, however, that if ρ' and μ' be replaced by ρ and μ, the second member of (15) will then give the potential at point P, due to the sphere S_i. If now the values of u, U and U_a be substituted in Eq. (2), ρ set equal to a, and coefficients of like tesseral harmonics equated, the following sets of linear equations result:

$$\alpha_m A_{nm} = K_{nm} \left(\frac{a}{\rho_0}\right)^m - \sum_{k=n}^{\infty} a_{nkm} A_{nk}, \tag{16}$$

$$\alpha_m B_{nm} = K_{nm} \left(\frac{a}{\rho_0}\right)^m - \sum_{k=n}^{\infty} a_{nkm} B_{nk}, \tag{17}$$

$$(n = 1, 2 \cdots \infty), (m = n, n+1, \cdots \infty),$$
$$(n = 0), (m, k = 1, 2 \cdots \infty),$$

in which

$$\alpha_m = \left[\frac{(k+1)}{(k-1)} + \frac{1}{m(k-1)}\right], \tag{18}$$

[3] See Whittaker and Watson, *Modern Anal.* 4th. Ed., p. 400, Ex. 7.

$$K_{nm} = \frac{2D}{\rho_0}\left(\frac{a}{\rho_0}\right)^m \frac{(m-n)!}{(m+n)!}\cos n\phi_0 P_m{}^n(\mu_0), \tag{19}$$

and

$$a_{nkm} = \frac{(m+k)!}{(m+n)!(k-n)!}\left(\frac{a}{h}\right)^{m+k+1}. \tag{20}$$

It should be noted that there results, for each value of n, an infinite set of linear equations. The different sets are identical in form, however, and so it will be necessary to demonstrate the possibility of solution for only one of the sets. For simplicity, the set (16), for which $n=0$, is chosen, and it will be shown by an argument due to von Koch[4] that this system of equations has a unique bounded solution for the A_{0k}. In the argument, α_m will be replaced by its minimum value unity. If the argument holds for this value of α_m, it will hold for all possible values of α_m. (It may be noted that the dependence of α_m upon m is only slight.) Eqs. (16) may then be written:

$$a_{1m}A_{01} + a_{2m}A_{02} + \cdots + (1 + a_{m\,m})A_{0m}\cdots = K_m\left(\frac{a}{\rho_0}\right)^m \tag{21}$$

where,

$$(m = 1, 2 \cdots \infty).$$

In order to change to von Koch's notation, replace the unknowns $A_{01}\cdots A_{0k}$ by $x_1 \cdots x_k$, etc. and write Eq. (21) as

$$a_{i1}x_1 + a_{i2}x_2 + a_{i3}x_3 + \cdots + (1 + a_{ii})x_i \cdots = K_i\left(\frac{a}{\rho_0}\right)^i, \tag{22}$$

in which

$$(i = 1, 2 \cdots \infty).$$

Divide (22) by $(1+a_{ii})$ and set

$$\frac{a_{ik}}{1 + a_{ii}} = -\,b_{ik}, \tag{23}$$

$$b_{ii} = 0,$$

$$\frac{K_i}{1+a_{ii}}\left(\frac{a}{\rho_0}\right)^i = c_i.$$

Then

$$b_{ik} < \frac{(i+k)!}{i!k!}\left(\frac{a}{h}\right)^{i+k+1},$$

$$c_i < K\left(\frac{a}{\rho_0}\right)^i, \tag{24}$$

[4] H. von Koch, Jahres bericht der Deutschen Mathematiker Vereinigung **22**, 285–291 (1913).

in which K is the upper limit of K_i, namely D/ρ_0. Eqs. (22) become,

$$x_i - \sum_{k=0}^{\infty} b_{ik}x_k = c_i, \qquad (25)$$
$$(i = 1, 2 \cdots \infty).$$

Let

$$x_k = x_k^{(1)} + c_k,$$

substitute and obtain

$$x_i^{(1)} = \sum_{k=1}^{\infty} b_{ik}x_k^{(1)} + \sum_{k=1}^{\infty} b_{ik}c_k + c_i^{(1)}.$$

Let

$$x_k^{(1)} = x_k^{(2)} + c_k^{(1)},$$

and so on, continuing this process of successive approximations indefinitely. Using the notation

$$b_{ik}^{(2)} = \sum_{v=1}^{\infty} b_{iv}b_{vk}$$

$$b_{ik}^{(3)} = \sum_{v=1}^{\infty} b_{iv}^{(2)}b_{vk}, \qquad \text{etc.},$$

then according to von Koch's argument, the series

$$x_i = c_i + c_i^{(1)} + c_i^{(2)} + \cdots,$$

i.e.

$$x_i = c_i + \sum_{k=1}^{\infty} b_{ik}c_k + \sum_{k=1}^{\infty} b_{ik}^{(2)}c_k + \sum_{k=1}^{\infty} b_{ik}^{(3)}c_k + \cdots, \qquad (26)$$

is absolutely convergent and represents the unique bounded solution of the system (25), provided $\sum_{k=1}^{\infty}|b_{ik}|<1$ for all values of i and provided $c_i<K$ a fixed constant. The first of these conditions is fulfilled, provided $a/h<1/2$, as may be seen from the following summation,

$$\sum_{k=1}^{\infty} b_{ik} = \sum_{k=1}^{\infty} \frac{(i+k)!}{i!k!}\left(\frac{a}{h}\right)^{i+k+1} = \left[\left(\frac{a}{h-a}\right)^{i+1} - \left(\frac{a}{h}\right)^{i+1}\right]. \qquad (27)$$

The second condition is fulfilled, as from (24)

$$c_i < K\left(\frac{a}{\rho_0}\right)^i$$

where

$$\frac{a}{\rho_0} < 1$$

and

$$K \leq \frac{D}{\rho_0}.$$

The first five equations of the system (22) for the special case

$$\frac{a}{h} = \frac{1}{2}, \quad \frac{a}{\rho_0} = \frac{1}{2}, \quad K_i = K,$$

will be written down;

$$\left.\begin{aligned}
1.125x_1 + 0.187x_2 + .125x_3 + .078x_4 + .047x_5 \cdots &= \tfrac{1}{2}K \\
.187x_1 + 1.187x_2 + .156x_3 + .117x_4 + .082x_5 \cdots &= \tfrac{1}{4}K \\
.125x_1 + .156x_2 + 1.156x_3 + .136x_4 + .110x_5 \cdots &= 1/8K \\
.078x_1 + .117x_2 + .136x_3 + 1.136x_4 + .123x_5 \cdots &= 1/16K \\
.047x_1 + .082x_2 + .109x_3 + .123x_4 + 1.123x_5 \cdots &= 1/32K
\end{aligned}\right\} \quad (28)$$

The calculated values of x_1 and x_2, using the first four terms of formula (26), are

$$x_1 = .3716K,$$
$$x_2 = .1456K.$$

It is very laborious, however, to use formula (26) and it has been found that the values of the unknowns x_k may be found more easily by solving the first of the Eqs. (28) for x_1, retaining only the first term; using this value in the second equation to obtain an approximate value of x_2 by retaining the first two terms only; then correcting the value of x_1, by substituting the value found for x_2 in the first equation and so on. By this method, using three of the equations in three of the unknowns, it is found that

$$x_1 = .3725K,$$
$$x_2 = .1458K,$$
$$x_3 = .0475K,$$

in good agreement with the values as calculated by the formula (26). It should be noted that the values of the coefficients fall off rapidly in the present case. If the ratio of $a/h < 1/2$ or $a/\rho_0 < 1/2$, the convergence will be still more marked.

All that has been said in regard to Eqs. (16) may be said of the infinite set of Eqs. (17). The convergence, as n grows, becomes more rapid. For n greater than five, the A_{nk} and B_{nk} can be found to an accuracy of about two percent by making the approximation in (16) and (17)

$$A_{nm} = \frac{1}{\alpha_m} K_{nm} \left(\frac{a}{\rho_0}\right)^m,$$

$$B_{nm} = \frac{1}{\alpha_m} K_{nm} \left(\frac{a}{\rho_0}\right)^m.$$

For n less than five, and $a/h = 1/2$, the values of the coefficients A_{nk} and B_{nk} can be found with an accuracy of the order of one percent by solving the first five equations, in the first five unknowns, of the infinite sets of Eqs. (16) and (17).

The expression for the total potential, due to the buried sphere and the electrode, at all points without the buried sphere is

$$\Phi = \sum_{m=0}^{\infty} \left(\frac{a}{\rho}\right)^{m+1} Y_m(\mu, \phi) + \sum_{m=0}^{\infty} \left(\frac{a}{\rho'}\right)^{m+1} Y_m(\mu', \phi) + \frac{D}{\rho_0} \sum_{m=0}^{\infty} \left(\frac{\rho}{\rho_0}\right)^m L_m(\mu_0, \phi_0, \mu, \phi), \tag{29}$$

in which the coefficients in each of the spherical harmonics $Y_m(\mu, \phi)$ and $Y_m(\mu', \phi)$ have the values found by solving the sets of linear Eqs. (16) and (17) for given values of a/h and a/ρ_0.

The first and third members of Eq (29). are expressed in terms of ρ, θ and ϕ. The second member is expressed in terms of ρ', θ' and ϕ. If actually there existed the two spheres S and S_i, then the first and second members of Eq. (29) would express the potential due to the spheres S and S_i respectively. If, as is the case here, there is only the buried sphere S in the infinite half space, which is bounded by the plane MN, then the first two members of (29) are necessary for expressing the potential due to the buried sphere alone. The second member of (29) simply serves to accomodate the boundary condition expressed by Eq. (5).

Numerical Computation

As an example, the potential $(\Phi - U_e)$ will be computed for a point on the surface of the half space directly above the center of the sphere. The potential will be computed for various depths of the sphere and for the ratio of conductivity, k, of the two media equal to ten. The calculation will be made first by means of approximation formulae described below, and finally by means of the exact formula (29). An electrode of radius a_1, at which a current I is being introduced, is placed at the point whose cartesian coordinates are $(h/2, 0, (3)^{\frac{1}{2}}a)$. The potential is calculated for the point whose cartesian coordinates are $(h/2, 0, 0)$. It will be assumed that the current is removed at some electrode so far distant from the buried sphere, that its influence upon the sphere may be neglected. It should be mentioned, however, that if the second electrode were not so situated, the potential of the buried sphere, under the influence of this second electrode, could be computed by means of the formula (29) and this potential added to the potential calculated for the first electrode.

First approximation. As a first order approximation to the potential, the field due to the electrode is considered uniform over the buried sphere and

equal to its value at the center of the sphere, and the interaction between the buried and image sphere is entirely neglected. The potential at all points without the buried sphere then is given by the expression

$$\Phi - U_e = \left(\frac{a}{\rho}\right)^2 [A_1 \cos\theta + (A_{11}\cos\phi + B_{11}\sin\phi)\sin\theta] + \left(\frac{a}{\rho'}\right)^2 [A_1 \cos\theta' + (A_{11}\cos\phi + B_{11}\sin\phi)\sin\theta'], \tag{30}$$

in which the coefficients have the values

$$A_1 = \frac{D}{\rho_0}\frac{(1-k)}{(k+2)}\frac{a}{\rho_0}\cos\theta_0,$$

and

$$\left.\begin{matrix} A_{11} \\ B_{11} \end{matrix}\right\} = \frac{D}{\rho_0}\frac{(1-k)}{(k+2)}\frac{a}{\rho_0}\left\{\begin{matrix} \cos\phi_0 \\ \sin\phi_0 \end{matrix}\right\}\sin\theta_0.$$

Second approximation. As a second order approximation to the potential, the field over the buried sphere due to the electrode will again be considered uniform but the first order cross effect due to the interaction of the two spheres will be taken into account. By first order cross effect is meant that the field, due to sphere S_i, is considered uniform over the buried sphere S and equal to the value it has at the center of the sphere S. Such a formula can be obtained by applying boundary condition (2) and then dropping all terms containing $(a/\rho_0)^2$ and $(a/h)^4$ and higher powers of these ratios. If this be carried out, the resulting expression for the potential is identical with Eq. (30), but the coefficients have the values:

$$A_1 = \frac{D}{\rho_0}\frac{(1-k)}{[(k+2)+(a/h)^3(k-1)]}\frac{a}{\rho_0}\cos\theta_0,$$

and

$$\left.\begin{matrix} A_{11} \\ B_{11} \end{matrix}\right\} = \frac{D}{\rho_0}\frac{(1-k)}{[(k+2)+(a/h)^3(k-1)]}\frac{a}{\rho_0}\left\{\begin{matrix} \cos\phi_0 \\ \sin\phi_0 \end{matrix}\right\}\sin\theta_0.$$

Third approximation. As a third order approximation, the field over the buried sphere due to the electrode will be considered uniform so that terms in $(a/\rho_0)^2$ and higher powers may be dropped. However, the field due to sphere S_i, will no longer be considered uniform over sphere S. That is, terms in $(a/h)^4$ and higher powers will be retained. The formula found under these conditions is:

$$\Phi - U_e = \sum_{m=0}^{\infty}\left(\frac{a}{\rho}\right)^{m+1} Y_m(\mu,\phi) + \sum_{m=0}^{\infty}\left(\frac{a}{\rho'}\right)^{m+1} Y_m(\mu',\phi),$$

in which the coefficients must be determined from the infinite sets of equations of the type (22). Since terms in $(a/\rho_0)^2$ are to be neglected, the right sides of Eqs. (22) after the first are to be set equal to zero.

The values of the potential $(\Phi - U_e)$ as calculated by these three approximate formulae and finally from the exact formula (29) are shown in Fig. 2.

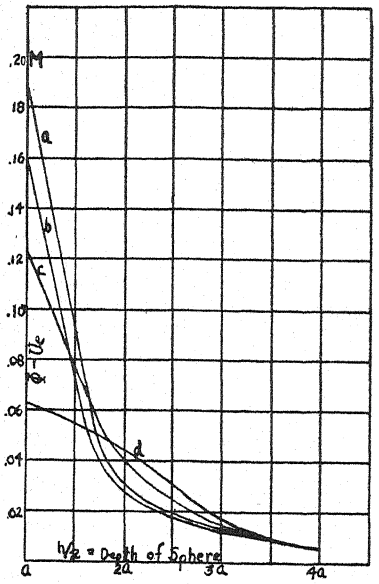

Fig. 2. Potential curves. (a) first approximation; (b) second approximation; (c) third approximation; (d) actual.

To obtain the total potential Φ simply add to the values on the curve, the constant term due to the electrode,

$$U_e = I/4\pi\sigma_2(3)^{1/2}a = M/(3)^{1/2}.$$

This last equation serves to define M, which occurs in the data. In order that the data may be readily put into practical units, the following calculation is to be noted. The potential due to the electrode is

$$U_e = D/r,$$

where r is the distance from the electrode. If, in particular, $r = a_1$, a_1 being the radius of the electrode,

$$U_e = I/4\pi\sigma_2 a_1$$

or

$$I = (U_e)_{a_1} 4\pi\sigma_2 a_1.$$

Therefore, M in the above data becomes

$$M = a_1/a(U_e)_{a_1},$$

and since $(U_e)_{a_1}$ is the potential of the electrode in volts, M will also be in volts.

From the curves, it is clear that any of the approximate formulae are sufficiently accurate for computing the potential, due to the buried sphere, in cases where the depth of the center of the sphere is greater than three times the radius of the sphere. In the region for which $h/2$ is less than a, only the exact formula can be used with any degree of accuracy.

In conclusion, I should like to express my sincere thanks to Professor Warren Weaver of the University of Wisconsin for his helpfulness and interest in the above problem.

MAGNETIC SUSCEPTIBILITIES AND IONIC MOMENTS IN THE PALLADIUM AND PLATINUM GROUPS

By Albert N. Guthrie and L. T. Bourland
Physics Laboratory, University of Illinois

(Received December 15, 1930)

Abstract

Susceptibility measurements have been made on Ru, Rh, Pd, Os, Ir, and Pt and some of their compounds over a range of temperatures by means of an improved Curie balance.

Pd and Pt are found to follow approximately a Curie-Weiss law. Ru, Rh, Os, and Ir are found to have paramagnetic susceptibilities which increase with temperature.

$RuCl_3$ and IrO_2 are found to follow a Curie-Weiss law which gives for the ion Ru^3 a moment of 9.8 Weiss magnetons per mole and for Ir^4 13.8. The spectroscopically predicted value for each ion is 29.4. The paramagnetic susceptibility of Rh_2O_3 is found independent of temperature while that of RuO_2 increases rapidly with temperature. $RhCl_3$ is found to have an unmeasureably small susceptibility over the temperature range investigated. $IrCl_3$ and $PtCl_2$ are diamagnetic with susceptibilities independent of temperature.

THE determination of ionic magnetic moments in the Pd and Pt groups, by susceptibility measurements on compounds of these elements, is of particular interest in connection with the Hund method[1] of predicting these moments from spectroscopic theory. Hund[2] has employed his method for the moments of the trivalent rare earth ions and obtained remarkable agreement with the measured values of several investigators. In the case of the ions of the iron group, the elements Sc to Ni of the periodic table, the method has been unsuccessful. Laporte and Sommerfeld[3] calculated the moments to be expected for the iron group ions in two cases, infinite separation and zero separation of the J-levels of the ground multiplet predicted by the Hund method. Several of the measured values are found to lie outside of these limits. Bose[4] has pointed out that the measured moments of the iron group ions are best explained by assuming that they are due to the spin of the electrons alone, the orbital moments being ineffective. Stoner[5] has called attention to the striking difference in the structures of the rare earth and iron group ions, and the effect that this difference should be expected to have on the ions with the conditions under which their moments are measured. In the iron group ions the incompleted group of electrons which gives the ion its mechanical and magentic moments is that of highest total quantum number. In the rare

[1] F. Hund, Zeits. f. Physik **33**, 345 (1925).
[2] F. Hund, Zeits. f. Physik **33**, 855 (1925).
[3] O. Laporte and A. Sommerfeld, Zeits. f. Physik **40**, 333 (1926).
[4] D. M. Bose, Zeits. f. Physik **43**, 864 (1927).
[5] E. C. Stoner, Phil. Mag. **8**, 250 (1929).

earth ions this group of electrons is not that of highest total quantum number. The interaction between the paramagnetic ion and surrounding ions and molecules will presumably effect primarily the electrons in the group of highest total quantum number; in the iron group ions the electrons responsible for the magnetic moment, in the rare earth ions electrons that are not responsible for the magnetic moment. In general this interaction is a strong orbital interaction while the spin moments are left relatively free. In a qualitative way this is an explanation of the apparent ineffectiveness of the orbital moments in the iron group ions and their almost complete effectiveness in the rare earth ions.

There exist few data on the susceptibilities of the elements of the Pd and Pt groups from which ionic moments can be calculated. Bose and Bhar[6] have made measurements at room temperature on some chlorides and complex salts of some of these elements and have calculated ionic magnetic moments assuming that the susceptibilities of the compounds follow the Curie law. Cabrera and Duperier[7] made measurements on $RuCl_3$, $RhCl_3$, $PdCl_2$, $OsCl_2$, $IrCl_3$, and $PtCl_2$ over a range of temperatures from about 20°C to 100°C. They found that $RuCl_3$ approximately followed a Weiss law which gave a moment for Ru^3 of 12.9 Weiss magnetons. The susceptibilities of the other chlorides were found to remain constant or increase with temperature.

For this investigation the compounds $RuCl_3$, RuO_2, $RhCl_3$, Rh_2O_3, $IrCl_3$, IrO_2, and $PtCl_2$ were obtained from the American Platinum Works, Newark, N.J. These compounds were prepared with special regard for purity by Dr. S. Streicher of their chemical laboratory.

Through the kindness of the Bureau of Standards samples of the six metals Ru, Rh, Pd, Os, Ir, and Pt of very great purity were made available for a new determination of their susceptibilities. Several investigators have measured the susceptibilities of these metals but the results have been in very poor agreement.

Description of Apparatus

The susceptibility measurements were made by means of a Curie balance. In this apparatus the usual mechanically operated torsion head was replaced by an electrically operated one. The ease and speed of making measurements with this arrangement far surpasses that attainable with the usual mechanical types. In Fig. 1 is shown a sketch of the essential parts of the electrically operated torsion head. A coil of small copper wire, A, wound on a flat, hard rubber spool is suspended by a fine wire, B, with its plane parallel to a magnetic field produced by two fixed coils, C, carrying a current. To the coil A is attached the suspension, D, which supports the balance arm and to which is applied the torque to overcome the force on the sample. A plane mirror, E, is attached to the coil A and the twist in the suspension D is read from it by means of a telescope and scale placed about one meter away. In order to fix the axis about which the coil A rotates suspension guides, F, are em-

[6] D. M. Bose and H. G. Bhar, Zeits. f. Physik **48**, 716 (1928).
[7] B. Cabrera and A. Duperier, C. R. **185**, 414 (1927).

ployed. These guides consist of thin brass strips attached to the box which supports the balance and pierced with small holes through which the suspensions pass. The coil A is damped by means of vanes G suspended in stanolax. A current, which is controlled so as to give the proper torque to the suspension, is carried through the coil A by means of long thin spirals of wire which do not hinder the coils free rotation. The other parts of the balance are of the usual design.[7a]

The apparatus was calibrated by making measurements on distilled water, using as its susceptibility with respect to air at 20°C and 76 cm pressure the value -0.749×10^{-6}.

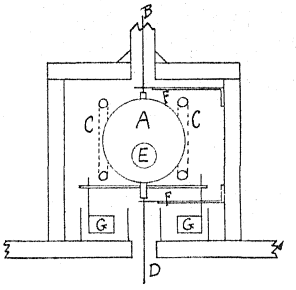

Fig. 1. Sketch of the essential parts of the electrically operated torsion head.

The inhomogeneous magnetic field was furnished by a Dubois electromagnet with its pole pieces set at an angle of about twelve degrees with a line joining their centers. The field strengths obtainable were in the range 1400 to 6400 gausses.

The samples were heated by means of a nichrome resistance furnace. A junction of a Cu-constantan thermocouple was mounted so as to occupy the same relative position in the furnace as the sample on which measurements were being made. The other junction of the thermocouple was kept in a bath of ice and water. Temperatures were read by means of a D'Arsonval galvanometer in the thermocouple circuit. A galvanometer deflection of one mm corresponded to a temperature change of about 2.5°C. The thermocouple was calibrated by means of the boiling points of well-known substances.

Experimental Results

In Tables I, II, III, are given the results of measurements on the various substances indicated.

The susceptibility of Rh was found to decrease with increasing field strengths. At room temperature the change was from 1.60×10^{-6} at 1420 gausses to 1.20×10^{-6} at 6390 gausses. This variation was assumed to be due to ferromagnetic impurities and the method first used by Honda[8] was used to calculate the susceptibility of Rh from these measurements.

[7a] The modification of the Curie balance as used by Foëx was considered but calculation showed that the torsion method could be made more sensitive for our measurements.

[8] K. Honda, Ann. d. Physik (4) **32**, 1027 (1910).

TABLE I.

			$\chi \times 10^6$		
T°K	Ru	Rh*	Pd	RuO_2	Rh_2O_3
298	0.427	1.08	5.15	1.21	0.408
333	.431	1.09	4.79	1.24	.409
380	.435	1.11	4.39	1.28	.410
433	.443	1.12	4.03	1.32	.403
480	.452	1.14	3.73	1.36	.403
523	.457	1.15	3.52	1.40	.402
573	.466	1.16	3.27	1.43	.401
623	.475	1.17	3.05	1.46	.398
673	.487	1.18	2.85	1.49	.397
723	.496	1.19	2.66	—	—

* Calculated from the measurements by the method of Honda.

TABLE II.

		$\chi \times 10^6$		
T°K	Os	Ir	Pt	IrO_2
298	0.052	0.133	0.982	0.997
348	—	.138	.947	.984
398	.059	.141	.925	.974
473	—	.146	.876	.971
548	.065	.151	.831	.942
623	—	.159	.795	.926
698	.070	.167	.745	.891

TABLE III.

			$\chi \times 10^6$	
T°K	$RuCl_3$	$RhCl_3$	$IrCl_3$	$PtCl_2$
298	7.21	0.00	−0.114	−0.151
323	6.64	.00	—	—
348	6.16	.00	−0.114	−0.149
373	5.77	.00	—	—
398	5.44	.00	—	−0.149
423	5.18	.00	—	—
448	4.91	.00	—	—

For comparison the available data on the specific susceptibilities of the metals Pd, Rh, Ru and Pt at 18°C and the investigators who obtained them are given in Table IV.

TABLE IV.

		$\chi \times 10^6$		
Investigator	Pd	Rh	Ru	Pt
Curie	5.2	—	—	—
Honda	5.8	1.14	0.56	1.10
Owen	5.2	1.08	0.43	0.90
Onnes and Oosterhuis	5.3	—	—	—
Foëx	5.27	—	—	1.028
Kopp	5.29	—	—	—
Authors	5.24	1.08	0.426	1.015

In Fig. 2 are plotted the values of $1/\chi$ for Pd, Pt, $RuCl_3$ and IrO_2 as a function of temperature.

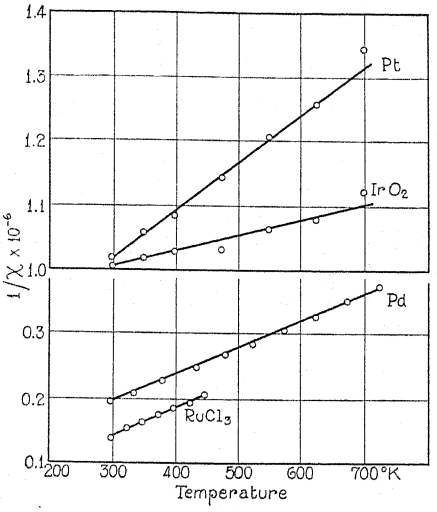

Fig. 2. Values of $1/\chi$ for Pd, Pt, $RuCl_3$ and IrO_2 plotted as a function of temperature.

Discussion of Results

Pd and Pt are found to follow approximately a Curie-Weiss law, the deviation being accounted for by an underlying diamagnetism independent of temperature. From purely formal theory, it would be expected that the diamagnetic component of the susceptibility would be greater for Pt than for Pd but the experimental results indicate the opposite.

Ru, Rh, Os, and Ir are found to have paramagnetic susceptibilities which increase with temperature. This is, of course, inconsistent with Langevin's theory.

$RuCl_3$ and IrO_2 are found to follow a Curie-Weiss law. For the former the equation is:

$$\chi = \frac{2340}{T + 37} \times 10^{-6} \text{ c.g.s./gram}$$

and for the latter

$$\chi = \frac{4310}{T + 4025} \times 10^{-6} \text{ c.g.s./gram.}$$

These results give for the magnetic moment of the Ru^3 ion 9.8 Weiss magnetons per mole, and for the Ir^4 ion 13.8. The predicted normal state for both ions is ^6S which gives 29.4 Weiss magnetons per mole for the moments. In the iron group, good agreement between measured and predicted moments has been found for all ions with predicted S normal states. In these groups, there is no agreement whatever and the behavior of some of the compounds is such

that no moments can be determined from measurements on them. If the susceptibility does not follow a Curie-Weiss law, there is no theory which will give the elementary magnetic moments.

A deviation from the Curie-Weiss law is predicted for compounds containing a paramagnetic ion with other than an S normal state due to the increase with temperature of the number of excited ions with moments differing from that of the ions in their normal state. With an S normal state there are no excited ions at ordinary temperatures. In these researches only the compounds containing the paramagnetic ion with a predicted S normal state are found to follow a Curie-Weiss law but the deviations of the other compounds are opposite to (excepting RuO_2) and much greater than can be accounted for by the theory.

The behavior of those compounds which do not follow a Curie-Weiss law is not due to a permanent chemical or physical change due to heating for at room temperature the susceptibilities are found to be the same after as before heating.

The disagreement between the measured and the spectroscopically predicted ionic moment may be due to error in prediction of the normal state. Hund's rule, combined with present ideas of the electronic arrangement in atoms and ions, predicts for Ru^3 and Ir^4 a ^6S normal state. In the same way the prediction for the normal state of the Pd atom is a ^3F. The atomic spectrum of Pd has been analysed by Beals, Beckert and Catalan, and McLennan and Smith.[9] They all have concluded that the normal state for the Pd atom is a ^1S which means that the Pd atom in its normal state has zero magnetic moment. That the moment of the Pd atom is zero in its normal state has been verified by Copley and Guthrie[10] by the molecular ray method.

The question of the validity of Hund's rule in the wave mechanics has been examined by Slater.[11] He has found that the wave mechanics gives the same normal state as Hund's rule although their predictions differ higher up in the spectrum.

The interpretation of the magnetic moment determined from susceptibility measurements on compounds as the true moment of the paramagnetic ion seems not to be well founded. The ion in chemical combination, surrounded by other ions and molecules, must be a different thing from the ion with which the spectroscopist deals in the Zeeman effect. Therefore, in spite of some past successes it appears hopeless to expect always to find agreement between these two.

The writers wish to express their appreciation to Professors E. H. Williams and Jakob Kunz for their encouragement and advice during the progress of this work.

[9] See F. Hund, Linienspektren und Periodische System der Elemente (1927).
[10] Not yet published.
[11] J. C. Slater, Phys. Rev. **34**, 1293 (1929).

CHANGES IN ELECTRICAL RESISTANCE DUE TO MAGNETISM AND HARDNESS

By S. R. Williams and Richard A. Sanderson
Department of Physics, Amherst College

(Received December 19, 1930)

Abstract

A series of twenty-two rods or strips of nickel, to which had been imparted different degrees of hardness by cold rolling, had their resistance measured when subjected to a longitudinal magnetic field. There were eleven degrees of hardness, two samples for each degree. The longitudinal magnetic field increased the resistance in all cases.

The different degrees of hardness did not vary the specific resistance of the nickel, but it did cause a large variation in the change of resistance due to a magnetic field. The measurements were carried out at a constant temperature of 35°C.

IN HIS summary to Part I of an extensive study of the electrical conductivity in strong magnetic fields, Kapitza[1] says, "It has been shown that the physical change produced in a conductor by hardening and annealing has a strong influence on the phenomenon of change of resistance. The influence of the impurities is also very marked and was studied."

Kapitza has brought together as fine a collection of the elements for study in strong magnetic fields as has ever been assembled, but his greatest difficulty was in procuring these samples in a pure state. It has been pointed out[2] that very worthwhile results may be obtained by comparing magnetic phenomena in the same specimen, even though the purity of the sample may not be vouched for.

Some years ago there was begun in this laboratory a study[3] of a series of nickel rods or strips, twenty-two samples in all, with eleven degrees of hardness in the series. The rods were given different degrees of hardness by cold rolling to various degrees of reduction. The rods were all of the same original heat and had the same chemical analysis, which is herewith given: copper, 0.16%; nickel, 98.8%; iron, 0.56%; sulphur, 0.008%; silicon, 0.06%; carbon, 0.09%; manganese, 0.23%.

While these rods could not be considered as pure nickel, yet they could be said to be identical specimens so far as their chemical constitution was concerned. It was, therefore, possible to study the effect of different degrees of hardness on the electrical conductivity of a definite material when magnetized longitudinally.

The rods came in flat strips and were furnished through the courtesy of the International Nickel Company. There were, originally, eleven strips, 91

[1] Kapitza, Proc. Roy. Soc. **119**, 358 (1928); **123**, 292 (1929); **123**, 342 (1929).
[2] Williams, Phys. Rev. **34**, 258 (1912); **4**, 498 (1914).
[3] Williams, Trans. A. S. S. T. p. 885, 1926; Science **65**, p. 306 (1927); **66**, p. 358 (1927).

cm long, 4.8 cm wide and 0.61 cm thick, all annealed to the same degree. Ten of these were then given the percentage cold reduction shown in Table I.

TABLE I.

Strip number	1	2	3	4	5	6	7	8	9	10	11
Percentage reduction	0	9.7	18.9	28.9	29.5	50.0	59.5	69.0	79.0	89.1	93.3

Each one of these eleven strips was then cut in two, longitudinally, and given a common length of 58 cm. This made a total of twenty-two specimens in all. The cross-sectional dimensions of the completed strips are given in Table II. They are the averages of ten to twelve readings taken along the length of the rods with a micrometer caliper. The two sets of strips were numbered;

$$A_1, A_2, A_3, \cdots, A_{11}$$

and

$$B_1, B_2, B_3, \cdots, B_{11}$$

wherein the rods A and B with the same subscript formed one of the eleven original strips.

TABLE II.

Strip number	Cross-section of strips	
	Series A	Series B
1	0.953×0.601	0.952×0.603
2	.956× .552	.955× .549
3	.955× .496	.952× .495
4	.942× .435	.944× .434
5	.945× .372	.943× .370
6	.956× .306	.964× .306
7	.960× .248	.961× .249
8	.956× .193	.956× .193
9	.956× .131	.957× .131
10	.957× .069	.956× .069
11	.955× .043	.956× .044

The scleroscope hardness, (universal tup or hammer) was furnished by the International Nickel Company and is given in Table III.

TABLE III.

Strip number	1	2	3	4	5	6	7	8	9	10	11
Scleroscope hardness	17	27	31	35	40	43	45	47	50	51	49

The resistance was measured between two fiducial marks 51.8 cm apart on each rod. The measurements were made by means of a Kelvin double bridge. The complete outfit was one manufactured by Leeds and Northrup Company and found to be most satisfactory. The bridge was made sensitive enough to indicate easily a change of resistance less than 0.000001 ohm. Higher sensitivity created more difficulty in making observations.

In Fig. 1 is shown the arrangement of apparatus. The longitudinal magnetic field was obtained by means of a solenoid, S, one meter long. The internal diameter of free space was 5.5 cm. There were 6025 turns which gave a constant of 75.3 gausses per ampere, both by calculation and by experimental test. In order to keep the strips at a constant temperature while being tested, they were placed in an oil bath. The container for the oil consisted of a copper trough, TT, passing through the solenoid and insulated from it by a coating of shellaced cloth. By means of brass gas-pipe fittings this trough was connected with a rectangle G, of $\frac{3}{4}$ inch brass pipe. The pump, P, kept the oil in continuous circulation around the rectangle. This pump consisted of a propeller blade inside of a tube and driven by the small motor, M. Transformer oil was used for circulating in the trough. Inasmuch as heat was

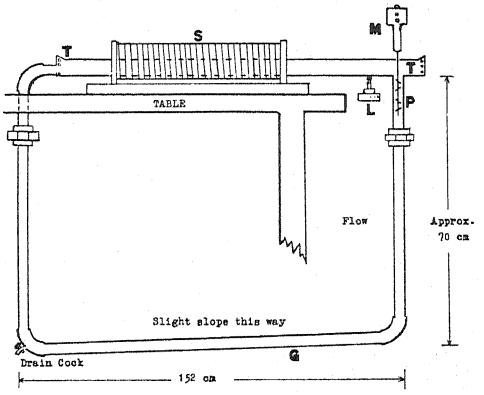

Fig. 1. Arrangement of magnetizing solenoids and constant temperature bath.

slowly given up to the system by the solenoid, it seemed best to keep the temperature of the bath somewhat above that of the room. A temperature of 35° C, was chosen as a suitable point from which the bath would always be cooling off. The moment it got below 35°C, the thermostat would turn on more gas to the burner, located under one end of trough, and keep the temperature up at 35°C. The bath did not vary over 0.2 degrees during the measurements. This kept the temperature sufficiently constant for making comparable resistance measurements. The temperature of the bath was determined by a sensitive, calibrated mercury-in-glass thermometer. Sometimes it was found that manual control of the gas was helpful. The thermostat for controlling the gas supply at the burner, L, which heated the bath, was a simple mercury-in-glass device. All the values for resistances, given in this paper, are for the temperature of 35° C, unless otherwise stated.

As found by other investigators,[4] the resistance of nickel is increased when magnetized longitudinally. This was true for all of the twenty-two specimens examined. The effect of hardening may best be studied in Fig. 2, where for

[4] W. E. Williams, Phil. Mag. **4**, 430 (1902); **9**, 77 (1905).

the field strength of 75.3 gausses the changes in resistance per ohm is plotted against hardness numbers. The effect of increasing the hardness is to decrease the change in resistance produced by the magnetic field. Fig. 2 is also

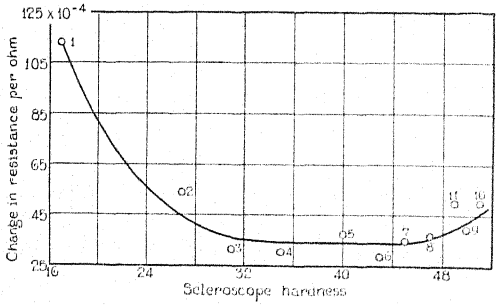

Fig. 2. Change in resistance per ohm for the different nickel strips at a field strength of 75.3 gausses.

of interest in comparison with a curve published in a paper[5] presenting the relation between the change in length due to a magnetic field and the hardness of this same set of strips. This curve is shown in Fig. 3 with a field strength of 58.8 gausses.

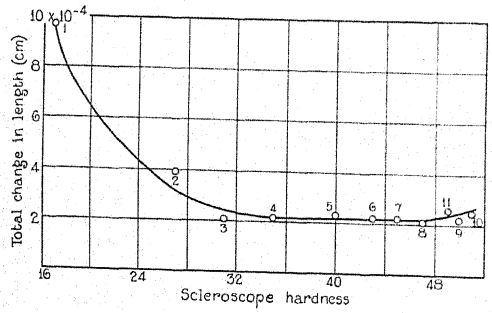

Fig. 3. The changes in length for the different nickel strips at a field strength of 58.8 gausses.

The most rapid change in length and in resistance comes in the first few reductions. In some way or another the changes in resistance due to a magnetic field are very closely related to the changes in length due to a magnetic field. There seems to be a common mechanism operating in both effects.

In Fig. 4 is shown the way in which the change in resistance per ohm varies with increasing magnetic field. Curve 1 is the average of the values for the two rods, A_1, and B_1, while curve 2 is the average for the two rods, A_4 and B_4. This figure represents the greatest difference obtained in the series of strips, due to differences in hardening. It confirms in a very marked way the results obtained by Kapitza, i.e., that hardness plays a very important rôle in this effect.

[5] Williams, Trans. A. S. S. T. p. 885 (1926).

The various values of dr/R in the curves represent the average of at least eight observations. Demagnetization of the rods occurred between each reading. This was accomplished by sending a decreasing a.c. through the solenoid.

In getting the changes in resistance due to magnetism and hardness, it was also easy to find the specific resistance of these strips. The values obtained are given in Table IV, and which are the averages of the A and B series. Three

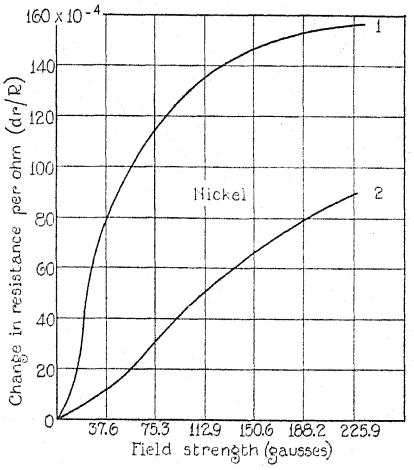

Fig. 4. Change in resistance per ohm as magnetizing force increases.

sets of values are given which were taken by different observers using different methods and about two years apart. The first set is by Mr. Lusk of the Rawson Electrical Instrument Company. Mr. Lusk checked his results by two entirely different methods. The second set is by Mr. G. K. Schoepfle, a former graduate student in this department. The third set is furnished by the junior author of this paper.

This set of readings seemed rather astonishing at first because as one crushes the nickel strips by rolling, and therefore the crystals comprising

TABLE IV.

Strip number	Specific resistance		
	Lusk	Schoepfle	Sanderson
1	0.00001012	0.00001083	0.00001099
2	.00000993	.00001081	.00001102
3	.00000993	.00001035	.00001093
4	.00000995	.00001085	.00001089
5	.00001000	.00001060	.00001086
6	.00000995	.00001071	.00001082
7	.00001000	.00001055	.00001079
8	.00001008	.00001070	.00001071
9	.00001032	.00001090	.00001076
10	.00001033	.00001051	.00001079
11	.00001038	.00001102	.00001073

the strips, it would suggest the possibility that the specific resistance would also be changed in a corresponding manner. *The specific resistance appears to be constant.*

The values given by Lusk were obtained about five years ago and at room temperature. The values by Schoepfle were obtained about two years later and also at room temperature. In all probability there had been some aging process going on in the meantime. To release local strains set up in the rods at the time they were cut and machined into shape, they were annealed for one hour in an oil bath at 304°C. This process took place about seven years before the readings were taken for this paper.

It was also possible with this equipment to determine the temperature coefficient of the strips. This was not worked out completely, but it was carefully measured on the rods, A_1 and A_4, those rods which had the widest variation of dr/R for a given magnetic field. Measurements were made at 35°C and at 85°C. This gave A_1 a temperature coefficient of 0.0042 and A_4 the value of 0.0043, indicating that there was little or no change in the temperature coefficient due to difference in rolling.

Although hardening by cold rolling did not change the specific resistance of this series of nickel strip, yet it did affect the change in resistance due to a magnetic field. This seems to be the most significant fact emerging from the results of this investigation,—no change in specific resistance due to varying hardness, but a decided change in the variation of resistance with magnetic field.

Attention should be called to the excellent paper by McKenhan[6] which has appeared since these results were obtained.

[6] McKeehan, Phys. Rev. **36**, 948 (1930).

THE ROLES OF DISCRETE AND CONTINUOUS THEORIES IN PHYSICS*

By Arthur Ruark
University of Pittsburgh

(Received December 4, 1930)

Abstract

The differential character of the principal equations of physics implies that physical systems are governed by laws which operate with a precision beyond the limits of verification by experiment. This appears undesirable, from an axiomatic standpoint.

Postulates of real, finite and rational description.—We may safely assume that all results obtained experimentally can be described by using real and finite functions of real, finite and rational variables. It appears desirable, therefore, to use the calculus of finite differences in formulating the results of our experiments. In dynamics, the use of this calculus yields terms corresponding to the fact that the configuration is known only when we observe it and must be arbitrary at intermediate times. For example, if a "uniformly moving particle" is observed once a second, we find experimentally that

$$\Delta^2 x/\Delta t^2 = 0,$$

whence

$$x = Ft + G.$$

Here F and G are *arbitrary* Fourier series having the period Δt. The general difference equations of dynamics are formulated. The Lorentz transformation is reinterpreted, relativistic difference equations of motion and of light propagation are set up, and geodesics in a discrete manifold are discussed.

Extensions of these ideas to electrodynamics are outlined.

I. Introductory

IT IS often said that while the fundamental equations of physics must be capable of describing every feature of our experimental results, at the same time they must not introduce extraneous or unobservable features. On the basis of this criterion, many branches of physics are not in a satisfactory position. Broadly speaking, the difficulties to which we refer originate in the use of mathematical concepts which are unsuited to the description of our experimental knowledge, and which introduce complications having no counterparts in nature.

Let us begin with an example. Consider, on the one hand, the information we obtain by performing an experiment once, or at most, only a few times. Usually, this information consists of a table of related numerical data. Consider, on the other hand, the statistical knowledge we obtain by correlating the results of a very large number of similar experiments. We draw curves and calculate averages, and finally, we may attempt to represent our results in an idealized fashion, by writing empirical equations. Up to this point the

* A preliminary account was given before the American Physical Society in February 1929. See Phys. Rev. **33**, 637 (1929).

procedure is beyond criticism, if we keep in mind the experimental basis of our equations, but when we carry the idealization process one step further, and derive differential equations from the empirical ones, we introduce conceptual difficulties. A differential equation connotes much more than the data from which it arises; herein lies its strength and,—unfortunately,— its weakness. For instance, Newton's equations imply that a dynamical system is governed by laws operating with a precision beyond the limits of detection by experiment. If, at a time t, we know the position and velocity of a body, these equations predict its condition at the time $t+dt$, but in order to verify the prediction, one would be obliged to distinguish between two positions, x and $x+dx$, by making two measurements separated by an infinitesimal time interval. But as a matter of fact, we have no desire to find the condition after the time dt; we wish to predict the state, within limits, after a finite time interval, and this we do by integrating the equations of motion. Each coordinate may then be expressed as a continuous function of the time, and we may calculate the configuration at *any* time, that is, at an "infinite number of instants." The information yielded by the equations is much in excess of what we can test experimentally. No one will deny the great practical value of Newton's equations, and clearly, the point we wish to emphasize is this: from an aesthetic and logical standpoint, it is desirable to have available a mathematical algorithm which makes it possible for us to summarize precisely the information obtained from a series of measurements, without excess and without deficit. It is our aim to show how this may be accomplished with the aid of the calculus of finite differences.

II. Critique of the Use of Infinitesimal Analysis in Physics

The Principle of Real and Finite Description

Most of the purposes we have in mind may be accomplished by adopting a set of postulates which, for brevity, will be collectively designated as the principle of real and finite description. For our present purpose[1] we may state the postulates as follows:

All results obtained experimentally can be described in terms of real and finite functions of real and finite variables. These functions need only be defined for discrete values of their independent variables. Both the functions and their independent variables need only assume rational values.

As an illustration, we consider a series of experiments on the motion of a single atom, or on a small number of atoms. The principle of real and finite description indicates clearly that our numerical results should not be discussed by means of continuous analysis. But if the series of experiments were to be extended indefinitely, until observations had been made on a great many

[1] For the sake of simplicity, we shall speak as though a measurement consisted in assigning a definite number x_0 to a variable at a definite time, t_0. The real situation is that we know x lies in the range $x_0 \pm x_0$ when t lies in the range $t_0 \pm \Delta t_0$. Thus we may say that x is an "indefinite function" of the "indefinite variable" t. It is easy to devise an algebra for dealing directly with the possible connections between such variables; but these matters will be postponed to a later occasion.

individuals, and over the entire ranges of the independent variables, then we would have the material necessary for building up a continuous, statistical theory,—in fact, a branch of wave mechanics. The situation in regard to the motion of a macroscopic body is quite similar. On the basis of a small amount of experience with its motion, we should not write a continuous law. (The true status of the laws of motion is connected with Ehrenfest's theorem, and is discussed in section V.) In the light of these ideas, the use of continuous analysis in physics can be clearly understood. Continuous laws should be introduced only when we deal with statistical results, obtained from vast numbers of experiments.

While the situation in regard to the use of infinitudes in physics is generally unsatisfactory, an exception must be made in the case of wave mechanics, where it is required that the wave functions shall be finite, continuous and single-valued at all real points of the coordinate space used by Schrödinger. The validity of these conditions has sometimes been questioned on the ground that, where the wave function ψ is zero, $1/\psi$ is infinite and there does not seem to be any reason why we should keep ψ from becoming infinite, rather than $1/\psi$. The writer feels that this criticism is invalid, for the square of the absolute value of ψ is measurable, indirectly at least, and therefore must not become infinite for real, finite and rational values of its variables. How ψ behaves for irrational values of its variables is none of our concern.

Again, it may be objected that in wave mechanics integrals extending over the entire ranges of the coordinates x, y and z (from $-\infty$ to $+\infty$) are constantly used with valuable results. Just as in the case above, this appears undesirable since we should think of the coordinates as measurable quantities, and should therefore limit them to finite values. Since in many problems the ψ-function approaches zero very rapidly for large values of the coordinates, it will usually occur that the values of matrix components will be little affected by restricting the range of integration to exclude infinite values, and the practical consequences of the theory will be unaltered. Even in scattering problems, where sinusoidal wave trains are used to represent incident beams of particles or protons, it would be better physics to speak of these trains as having their origin at a great, but finite, distance from the scattering center. Further, it appears desirable to use wave equations which are modified to take account of general relativity. It appears plausible from astronomical evidence that our four-dimensional space-time is limited in extent, and if this is the case, integrals of the type $\int \psi^* f \psi \, dv$ would naturally be extended only over a finite range. Furthermore, from our present stand-point, it is obvious that we should not treat the electron or the proton as point-singularities at which the electromagnetic and gravitational forces become infinite. Indeed, all such artificial mathematical difficulties are excluded by strict adherence to our postulates.

The situation in regard to the use of imaginaries in physics also requires comment. It is generally recognized that the introduction of $\exp i\omega t$ in vibration problems is merely a mathematical artifice, but many a physicist would feel surprise at the proposal to replace the quantum condition, $pq - qp =$

$h/2\pi i$, by an equation which is free of the imaginary unit. However, from an axiomatic and aesthetic standpoint, imaginaries should be excluded from any discussion of fundamental physical questions, and this can always be done by rationalizing our equations, even when we are dealing with quantities which do not commute. (In the present instance we may use $(pq-qp)^2=-h^2/4\pi^2$ or $(pq-qp)(pq-qp)^*=h^2/4\pi^2$. Then, in solving any specific problem, we get the Heisenberg matrices and their imaginary conjugates. In practice, this doubling of the solution will introduce no difficulties, and may even be advantageous.)

After these explanatory remarks we are ready to apply the principle of real and finite description to dynamics and electromagnetic theory. We shall find that when we apply it in dynamics we are naturally led to equations of finite differences, replacing the differential equations of motion. The solution of these difference equations brings in *arbitrary* functions which reduce to known constant values only at times when the configuration of the system is actually observed. This corresponds to the fact that we are not able to state the configuration of the system, except at the instants of observation. We proceed at once to amplify these statements.

III. The Difference Equations of Dynamics

Let us analyze the information obtained by an experimental study of a body moving along the x-axis. For the moment we pass over difficulties arising from errors of observation and assume that the observer can determine times and distances with any desired precision. The result of a set of position measurements will be a table showing the values of x at each instant of observation, such as the following:

$$\begin{aligned} &t_1, t_2, t_3, \cdots, t_n; \\ &x_1, x_2, x_3, \cdots, x_n. \end{aligned} \tag{1}$$

With a view to simplicity, suppose the intervals between successive observations have a constant duration, Δt. This restriction is unnecessary, and later we shall remove it. Perhaps the most natural method of analyzing the data is to study the difference coefficients of the series of x-values. Writing $x_2-x_1=\Delta x_1$, $\Delta^2 x_1=\Delta x_2-\Delta x_1$, etc., we form the table (2).

$$\begin{array}{lll} x_1 & & \\ & \dfrac{\Delta x_1}{\Delta t} & \\ & & \dfrac{\Delta^2 x_1}{\Delta t^2} \\ x_2 & & \\ & \dfrac{\Delta x_2}{\Delta t} & \\ & & \dfrac{\Delta^2 x_2}{\Delta t^2} \\ x_3 & & \\ & \dfrac{\Delta x_3}{\Delta t} & \end{array} \tag{2}$$

x_4

. . .
. . .
. . .
. . .

Let us suppose we find that

$$\frac{\Delta x_i}{\Delta t} = \text{constant}, \quad i = 1, \cdots, n-1, \tag{3}$$

and

$$\frac{\Delta^2 x_i}{\Delta t^2} = 0, \qquad i = 1, \cdots, n-2. \tag{4}$$

From our present standpoint, such a motion will be defined as uniform, and the constant value of $\Delta x_1/\Delta t$ is *defined* as the velocity. Either one of the relations (3) and (4) enables us to construct the original table of x-values,[2] but in order to attain a degree of generality equivalent to that provided by the equation $d^2x/dt^2 = 0$ we shall deal with (4). Taken as they stand, the Eqs. (3) and (4) state a regularity of the data and say nothing about the values of $\Delta x/\Delta t$ and of $\Delta^2 x/\Delta t^2$ at instants which lie outside the period covered by the experiment. Further, they say nothing about the values of $\Delta^2 x/\Delta t^2$ for times intermediate to the instants of observation. They contain nothing more than the isolated facts revealed by the experiment, and we must recognize the element of hypothesis introduced when we use them as a basis for prediction. The most natural method of generalizing (4) is to write

$$\frac{\Delta^2 x}{\Delta t^2} = 0, \tag{5}$$

and to consider this equation, provisionally, as applying to *any* series of observations like the above, obtained at time intervals Δt and extending over a finite time. Now, the general solution of (5) is not identical with the general solution of $d^2x/dt^2 = 0$. In fact, it is

$$x = Ft + G, \tag{6}$$

where F and G are trigonometric series of period Δt,[3] let us say

$$F = A_0 + A_1 \sin 2\pi\frac{t}{\Delta t} + A_2 \sin 4\pi\frac{t}{\Delta t} + \cdots + B_1 \cos 2\pi\frac{t}{\Delta t} + \cdots, \tag{7}$$

the expression for G being similar. The coefficients in these series are arbitrary constants, except for one restriction. We require that F shall reduce to the observed velocity v, and G to the observed initial value of x, let us say x_0, whenever t is a multiple of Δt. The coefficients in (7) are *not* Fourier coefficients which cause the series to represent the function $x_0 + vt$, in the interval

[2] In using equation (3) to reconstruct the x-values, we must specify x at one of the instants of observation, let us say t_1; and in using (4), we must specify one value of x and one of $\Delta x/\Delta t$.

[3] Boole, Finite Differences, reprint by Stechert, p. 80.

from $t=0$ to $t=\Delta t$. On the contrary, when an arbitrary choice of the form assumed by x between observations has been made, they are the Fourier coefficients of that form, and the series will generally be infinite. However, the series may contain only a finite, but very great, number of terms, if we specify the values of x at only a finite number of instants. The latter type of choice is in fact the only type which is in agreement with the principle of real and finite description. With these understandings, Eq. (6) completely reproduces the experimental results. At intermediate times, when the system is not under observation, the arbitrary trigonometric terms come into play, which means that the position of the system is not known.[4] The state of affairs is illustrated by Fig. 1, in which the solid line represents the classical motion, while the dotted curve shows a path which might possibly be represented by (6) and (7). The dotted curve might even have a finite number of disconti-

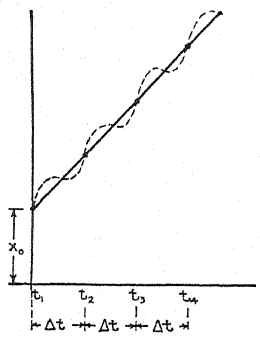

Fig. 1.

nuities in each interval Δt. When the specified set of observations is completed, we have no *physical evidence* which excludes the possibility of such a curve as the dotted one in Fig. 1. Of course, we could have taken additional observations, at the times $\Delta t/2$, $3\Delta t/2$, etc., let us say, obtaining an equation similar to (6). Under these circumstances, however, the state of our knowledge is different, for now the periodic function x must have the same values as the function $vt+x_0$, whenever t is a multiple of one-half the original Δt; at all other times it is arbitrary. The number of observations at times between t_1 and t_n cannot be increased indefinitely; therefore the Eqs. (5), (6) and (7), since they yield the observed data only and nothing more, represent a closer approximation to our experimental knowledge of the motion than the corresponding differential equation and its solution. However,

[4] In a paper entitled "The Limits of Accuracy of Physical Measurements," Proc. Nat. Acad. Sci. **14**, 322 (1928), the writer has shown that there are definite natural limitations on the accuracy with which we can measure a coordinate or specify a time, quite independent of all considerations of experimental skill. If we are dealing with a free particle of mass m, we have $\Delta x_{\min}=h/mc$ and $\Delta t_{\min}=h/mc^2$. It is interesting to note that if the time interval between observations is reduced to the order of $\Delta t_{\min}$, the first trigonometric term in (7) has a frequency of the order mc^2/h; that is, the frequency of the matter waves for a particle of mass m.

(6) still suffers from several defects: (1) it definitely prescribes the value of x at instants lying outside the range t_1 to t_n, although the observations were made only within that range; (2) it is scarcely arbitrary enough at intermediate times, for the trigonometric terms represent a periodic function; (3) it is assumed that the observations are equally spaced. In removing these defects, we may as well speak of a general system, exposed to forces of any kind whatever. Let all the coordinates, $q_1, \cdots q_r$ be observed at the instants $t_1, t_2, \cdots t_n$. We desire to construct a set of functions $q_1(t), q_2(t), \cdots$ which will reduce, at the observation times, to functions which adequately represent the observed values of the coordinates and which will be arbitrary at all other times. The solution is immediate.[5]

We need only write down the polynomials obtained by applying Lagrange's method of interpolation, let us say

$$q_1 = f_1(t, c_1, c_2 \cdots), \quad q_2 = f_2(t, c_1, c_2, \cdots), \tag{8}$$

where the c's are the constant coefficients of the various powers of t. We replace these constants by any functions of t which are *entirely arbitrary except that they must reduce to the experimental values* c_1, c_2, *etc., at the instants of observation*. We shall call any such function $A\ (t)$, or simply A. The Eqs. (8) are now replaced by

$$q_1 = f_1(t, A_1, A_2, \cdots), \quad q_2 = f_2(t, A_1, A_2,). \tag{9}$$

In these equations we have a faithful picture of experimental facts. It is necessary, however, to reconsider the concept of mass, since we naturally desire to use it as soon as we consider accelerated motions. In order to obtain a definition of inertial mass suitable for use in the finite difference equations of dynamics, we must describe a procedure by which a number may be assigned to the mass of a body, without any mention of instantaneous velocity, which is a differential coefficient. When we neglect the dependence of mass on velocity, the original definition of Newton is quite satisfactory. That is, if two freely moving bodies collide head on, their masses are inversely as the changes of velocity which they experience. Since the velocity measured is $\Delta x/\Delta t$ rather than dx/dt, we see that the value of a mass, resulting from such an experiment, can be formulated entirely in terms of finite difference coefficients and a constant; namely, the number assigned to the mass of a standard body.

The construction of the Eqs. (8) is especially simple when the time interval between observations is constant. Just as in the illustration of the uniformly moving particle, we are led to finite difference equations. From the standpoint of the principle of real and finite description, these equations, or their integrals (in the sense of the calculus of finite differences), expressed in the form (9), are the true laws of motion.

If, for the moment, we suppose there are no experimental errors, and that the observations are consistent with Newton's laws, we can easily see what the finite difference equations will be. This supposition is made only for pur-

[5] Boole, reference 3, p. 39.

poses of discussion, and implies no recession from the principles laid down in section II. The general difference equation for any problem of particle dynamics, Δt being constant, is obtained by noting that $m\Delta^2x/\Delta t^2$ *is the time mean of the time mean of the force, taken over the interval* Δt. We may verify directly that

$$m\frac{\Delta^2 x}{\Delta t^2} \equiv \frac{1}{\Delta t^2}\int_t^{t+\Delta t}\int_t^{t+\Delta t} m\frac{d^2x}{dt^2}dt\,dt \equiv \frac{1}{\Delta t^2}\int_t^{t+\Delta t}\int_t^{t+\Delta t} F_x dt\,dt,$$

or,

$$m\frac{\Delta^2 x}{\Delta t^2} \equiv \bar{\bar{F}}_x, \tag{10}$$

where the bar denotes a time mean over the interval mentioned. This equation, and two similar ones, constitute a formulation of the laws of motion, to which we should doubtless be led if, in all cases, we were to carry through a process like that which led us to Eqs. (3), (4), and (5). In general the right member of (10) will depend on Δt as well as on t, because the upper limits of the integrals contain Δt. The analogue of (10) in curvilinear coordinates is very complicated. While the writer has found it possible to make considerable progress in working out a theory for second order difference equations analogous to the transformation theory of ordinary dynamics, the results are so involved as to be of little interest. Therefore, we content ourselves with stating Eq. (10).

IV. Relativity Dynamics

In discussing special relativity from the standpoint of the principle of real and finite description, we meet at once with a kinematic problem; namely, the relation between the coordinates in different systems of reference. Whenever we pass to a new system of dynamical variables, the transformation equations themselves should be in accord with the principle. In other words, they may contain difference coefficients, but they should not contain derivatives. It is satisfying to note that the Lorentz transformation may be interpreted in such a way that it obeys this criterion. If the moving system of reference, x', y', z', t', has velocity $V(=Bc)$ parallel to the X-axis of the observer's system, x, y, z, t, this transformation takes the form

$$x' = k(x - Vt),\ y' = y,\ z' = z,\ t' = k\left(t - \frac{Vx}{c^2}\right),\ k = 1/(1 - B^2)^{1/2}. \tag{11}$$

On the usual theory, V represents the *instantaneous* velocity of the moving axes, dX/dt, but for the present purpose a different definition is needed. We may suppose the two sets of axes are attached to isolated bodies between which there is no detectable interaction. If then we find experimentally that $\Delta X/\Delta t$ is a constant V, we *postulate* that the Eqs. (11) hold true, and with this understanding they contain no derivatives. Quite similarly, c represents the quotient of a *measured* distance travelled by a light beam between two stations, and the *measured* time required for its journey. In accordance with the spirit of this paper, c must therefore be expressed as a difference quotient.

If we assume, *momentarily and for purposes of discussion only*, that the relativistic differential equations of motion are valid, the difference equations of motion for a rapidly moving particle may be obtained very easily. The relativistic equations of motion are

$$\frac{d}{dt}(mv_x) = F_x, \text{ etc.} \tag{12}$$

where $m = m_0/(1-\beta^2)^{1/2}$ and $\beta c = v$. If the square of the element of arc in a four-dimensional space is written as

$$ds^2 = c^2dt^2 - dx^2 - dy^2 - dz^2,$$

(12) may be rewritten in the form

$$m_0 c\frac{d^2x}{ds^2} = F_x\frac{dt}{ds}. \tag{13}$$

Suppose now that the observations are uniformly distributed along the world line of the particle, so that we have $\Delta s = \text{constant}$, in place of the former assumption, $\Delta t = \text{constant}$. We proceed just as we did in obtaining (10) with the result

$$m_0 c\frac{\Delta^2 x}{\Delta s^2} = \overline{F_x\frac{dt}{ds}},$$

where the right member denotes

$$\frac{1}{\Delta s^2}\int_s^{s+\Delta s}\int_s^{s+\Delta s} F_x\frac{dt}{ds}\,ds\,ds.$$

There is a way of expressing the law of light propagation without recourse to infinitesimals or to integrals. Since, in the theory of special relativity, the law is $ds^2 = c^2dt^2 - dx^2 - dy^2 - dz^2 = 0$, we replace this by

$$\Delta s^2 = c^2\Delta t^2 - \Delta x^2 - \Delta y^2 - \Delta z^2 = 0. \tag{15}$$

In general relativity also, the law of light propagation may be taken as $\Delta s = 0$.

It is much more difficult to formulate an analogue for the geodesic law $\int ds = 0$, which applies to the free motion of a particle. If we follow the most obvious course and assume that the law should take the form

$$\Delta s = \text{an extremum}, \tag{16}$$

we at once encounter a question of interpretation.

On the one hand, we may assume that we are dealing with a continuous space-time manifold, even though our measurements are discontinuous in character. On this basis Δs means a finite interval between adjoining observations, marked off along a geodesic line, where the word geodesic is taken in its ordinary sense. The significance of (16) is then simply that of a theorem deducible from Einstein's law of motion.

On the other hand, we may suppose that the space-time manifold is simply a discrete aggregate of observed point events, analogous to a two or three dimensional network, like a crystal lattice. The problem of defining a geodesic in such a lattice is not an easy one, as Silberstein has pointed out in his "Theory of Relativity." He suggests that the "shortest distance" between two points a and b in such a lattice (Fig. 2) should be defined as the smallest number of steps which will carry one from a to b. As to the concept of a step, it is necessary to think of the lattice points as joined by a network of lines. A step is then defined as the transition from a given point to its neighbor on one of these lines. In Figs 2a and 2b we have indicated two different methods of drawing such line-networks and it is obvious that the shortest distance depends to a great extent on the nature of these lines. Further, even with such a simple point lattice and network of lines as that shown in Fig. 2a, the paths

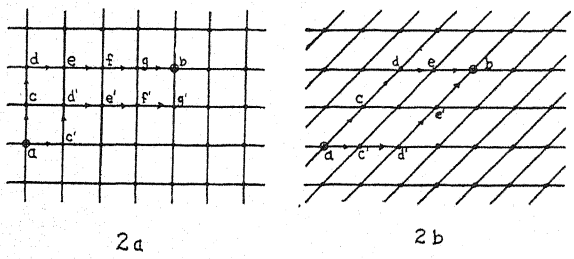

Fig. 2.

which correspond to shortest distances are not unique. Thus, the two paths $a, c, d \cdots b$, and $a, c', d' \cdots b$ both involve the same number of steps, and both may be considered as geodesics between a and b for the particular network shown. Although the shortest distance has a definite value, the path which must be traversed in order to achieve the journey in this shortest distance is not uniquely determined, save in special cases. After all, we should expect that some feature like this would emerge when we deal with discrete quantities.

In view of the existence of a limit to the accuracy with which a coordinate can be measured,[6] we should expect that the concept of shortest distance has an indefinite meaning in the atomic domain. The contribution of the present discussion is to show that a similar difference exists even for macroscopic measurements, as soon as we abandon the idea of a continuous background for the description of events.

V. Discussion of Ehrenfest's Theorem

In sections II and III we emphasized that Newton's laws of motion should be interpreted statistically,—that our knowledge of a single body can never be extensive enough to justify us in supposing it follows the laws of motion exactly. There is a theorem of wave mechanics discovered by Ehrenfest,[7]

[6] Ruark, reference 4.

[7] Ehrenfest, Zeits. f. Physik. 45, 455 (1927); Ruark and Urey, Atoms Molecules and Quanta, p. 652, McGraw-Hill, 1930.

which throws further light on this situation. Let ψ denote the wave function for a particle, so that $\psi\psi^* dv$ is the probability for the particle to have its coordinates in the element dv of the coordinate space. Then the x-component of the center of gravity of the probability distribution is given by $X = \int \psi^* x \psi dv$, provided the wave function is so normalized that $\int \psi^* \psi dv = 1$, and the theorem may be stated as follows:

$$m\ddot{X} = \int \psi^* \left(-\frac{\partial V}{\partial x} \right) \psi dv. \tag{17}$$

The expressions for $\ddot{Y}$ and $\ddot{Z}$ are similar, and V is the potential energy. Now let us consider a wave packet, having a very small extension compared with any distance in which the potential energy changes appreciably. In evaluating (17), we may use the value of $-\partial V/\partial x$ at the *centroid* of the packet, in every element of the integral, and the result is

$$m\ddot{X} = \left(-\frac{\partial V}{\partial x} \right)_X \int \psi^* \psi dv = \left(-\frac{\partial V}{\partial x} \right)_X. \tag{18}$$

On the basis of an outworn interpretation of wave dynamics, the individual particle is thought of as a wave packet, and $|\psi|$ as the amplitude of the waves. If this were correct, Ehrenfest's theorem would replace the ordinary law of motion, and it would appear foolish to use finite difference equations in describing the motion of a particle. But, on the probability interpretation, the meaning of Ehrenfest's theorem is this: We consider a great number of similar experiments, in each of which a single particle moves along the x-axis, and if we measure the x-coordinate of each particle at a definite instant, we obtain the distribution of $\psi\psi^*$ appropriate to that instant. At any future time the distribution can be calculated from the wave equations and we have a picture of the *statistical* behavior of the particles at that time. In other words, the wave equations enable us only to follow the time changes of the probability distribution, and there is room for uncertainty in the motion of the individual particles. Only the centroid obeys the approximate law of motion (18). Now, from a knowledge of the probability distribution obtained by a great number of experiments on individual isolated particles, we can draw no definite conclusions as to the motion of the centroid of a great number of particles, bound together in a rigid body and set in motion all together. This remark should make it clear that there is nothing in Ehrenfest's theorem which contradicts the conclusions of sections II and III.

VI. Difference Equations in Electrodynamics

The use of difference equations in electromagnetic theory arises naturally from our discussion of mechanics. Details will have to be reserved for a later occasion, but the leading ideas will be indicated here. To begin with, the electromagnetic field is *defined* entirely in terms of dynamical measurements. For our present purpose, the forces between charged bodies, magnets, and conductors carrying currents, are the fundamental things. We may employ

a small test body carrying a charge e, to map out a field of electric force. Again, if the test body is endowed with a "velocity" $\Delta s/\Delta t$, chosen to suit our convenience, a field of magnetic force may be studied. Thus we obtain the distribution of six quantities, E_x, E_y, E_z, H_x, H_y, and H_z, which might be called components of electric and magnetic intensity if the names were not preëmpted by analogous entities incapable of being measured, and defined in terms of the behavior of infinitesimal test bodies. The quantities $E_x, \cdots H_z$ are defined *by the very processes used in measuring them*. There is no implication that they obey Maxwell's equations. Indeed, they do not, because, from the usual standpoint, they represent average values of the field intensities, measured by a finite test body and not by a mathematical abstraction. These quantities may well be referred to as the *physical* field intensities. Their properties are simply the properties of numbers which fit a modified Lorentz equation,

$$eF \equiv e\left(\boldsymbol{E} + \frac{1}{c}[v\boldsymbol{H}]\right). \tag{19}$$

In this equation v means $\Delta s/\Delta t$ rather than ds/dt; e is measured by experiments whose interpretation requires no use of infinitesimals and eF_x is a force measured, let us say, by readings on the scale of an actual spring balance, or by equating it to the value of $m\Delta^2 x/\Delta t^2$ for the test body. The field equations obeyed by the physical field intensities may now, in principle, be found by trial. They involve the properties of the test body as well as those of the bodies producing the field—a point which is important in itself. The same consideration applies in mechanics but was not emphasized in section III, for the sake of simplicity.

VII. Conclusion

In conclusion, this paper serves to introduce a method of talking consistently about the results of experiments, and attention may be directed again to the refinements hinted at in the first foot note. The writer's aim has been to show how physical facts can be formulated by the use of difference calculus, that is, essentially with the aid of rational numbers. Considering the almost universal use of idealized concepts such as infinitesimals and irrationals, it seemed worth while to examine the possibilities of proceeding otherwise, and the results may be summarized in a broad sense,as follows: a method has been outlined by which we can describe experimental results mathematically, without any implications concerning the state of a system at times when it is not being observed, or concerning the causal connections customarily implied by the use of continuous analysis.

The writer wishes to thank Doctors Hutchisson, Muskat, Rashevsky and Worthing for helpful discussions.

LETTERS TO THE EDITOR

Prompt publication of brief reports of important discoveries in physics may be secured by addressing them to this department. Closing dates for this department are, for the first issue of the month, the twenty-eighth of the preceding month; for the second issue, the thirteenth of the month. The Board of Editors does not hold itself responsible for the opinions expressed by the correspondents.

Nuclear Spin

On the basis of measurements by Rasetti[1] of the Raman effect in N_2, Heitler and Herzberg[2] have suggested that the electron in the nucleus has lost not only its spin, but also its power to determine what the statistics of the nucleus shall be. (One could say, perhaps, that the electrons in the nucleus behave as if they had no spin and obey, therefore, the Bose-Einstein statistics, just as photons do.) The purpose of the present note is to point out that *the assumption that the protons alone contribute to the resultant spin is sufficient to explain all the known facts.* Furthermore, it may be that there is a building-up principle analogous to that of the outer electrons, although the evidence[3,4] is insufficient to show exactly what this would be.

TABLE I. *Building-up process.*

Element	P	Z	I	Protons added	Spins added
H	1	1	1/2		
He	4	2	0	3	$(+-)-$
Li	7	3	3/2	3	$+++$
C	12	6	0	5	$---(+-)$
N	14	7	1	2	$++$
O	16	8	0	2	$--$
F	19	9	1/2	3	$(+-)+$

The table gives in the last two columns the number of protons and spins, respectively, which must be added to the element in the row above to give the element in the row itself.

Thus, if we suppose that each additional proton contributes a spin of $\pm\frac{1}{2}$ to the resultant (which is the simplest assumption), the elements may be ordered as shown. Starting with He^4, $I=0$, three parallel spins will produce Li^7, $I=3/2$, and five more, two forming a pair, can result in C^{12}, $I=0$. Two additional parallel spins give N^{14}, $I=1$; two more, opposite in direction to the first two, O^{16}, $I=0$; and three more, two forming a pair, can yield $I=\frac{1}{2}$ for F^{19}. The value of nuclear spin for Na^{23} is in doubt, but if we assume $I=5/2$, then, by interpolation, Ne^{20} should have $I=1$ and Ne^{22}, $I=2$. One would also expect, since $I=0$ for C^{12} and S^{32}, a value of $I=1/2$ for B^{11} and P^{31}.

The difficulty mentioned by Goudsmit for the cadmium spectrum also disappears, if one adopts the above hypotheses. The value of $I=1/2$ may be attributed to Cd^{111} or Cd^{113}, but there exist no criteria for choosing between the two isotopes. (Perhaps both give a hyperfine structure.)

It seems, therefore, that the experimental evidence to date indicates the validity of the rule that even numbers of protons imply integral values for I, and odd numbers half-integral values. This is true for Mn, Br, Pr and Bi.

One would expect aluminium, phosphorus, chlorine, potassium, scandium, vanadium, cobalt, copper, gallium, arsenic, and other elements with isotopes having only odd numbers of protons to have half-integral values for the nuclear spin.

It remains an open question as to whether or not the orbital angular momentum of the protons plays a rôle, and also whether or not closed shells of protons exist, as do closed shells of extra-nuclear electrons. If there are such closed shells of protons, then this might provide the explanation of inverted hyperfine structure, the inversion being due to the absence of a proton from such a shell.

JAMES H. BARTLETT, JR.
University of Illinois
January 15, 1931.

[1] F. Rasetti, Proc. Nat. Acad. Sci. **15**, 515 (1929).

[2] Heitler and Herzberg, Naturwiss. **17**, 673 (1929).

[3] R. S. Mulliken, Trans. Faraday Soc. **25**, 634 (1929).

[4] Pauling and Goudsmit, Line Spectra (1930).

The Cathode-Ray Tube in X-Ray Spectroscopy and Quantitative Analysis

Under this title the Journal of the American Chemical Society has published a paper by us in the January number. A Coolidge tube was used, having a soldered aluminum window 6 mm in diameter and operated continuously at 0.2 m.a. and 85 kv D.C. Experiments were made with metal targets placed above the window and cooled with a jet of hydrogen. For the recording of the relative intensities of the $K\alpha$ doublet, primary attention was given to a method involving the application of an ionization chamber and an amplifying set. The latter made use of the new FP54 tube (Metcalf and Thompson, Phys. Rev. **36,** 1489 (1930)). The smallest measurable grid current was 8.7 $(10)^{-16}$ amps. With a copper target and 0.4 mm slits, the peak of the $K\alpha$ doublet gave a net deflection of 90 cm with an accuracy of 0.5 cm on a scale 2.6 m distant, corresponding to an ionization current of 3 $(10)^{-13}$ amp.

The loss in electron velocity in passing through the window agreed with the Thomson formula. For molybdenum and iron the intensity was found to vary as the square of the difference between the electron velocity and the exciting voltage. This relationship held up to the maximum velocity employed, amounting to four-fold the exciting voltage for the case of molybdenum and eleven-fold for iron. Experiments as yet unreported are being made on titanium and calcium and the exponent has been found to be 1.3 for the voltage range extending from ten to sixteen-fold the exciting voltage. The exponent accordingly decreases less rapidly with increase in voltage than has been observed in similar experiments with x-ray tubes.

Curves showing the relation between chemical composition and the relative intensities of the unresolved $K\alpha$ doublets were obtained for copper-nickel and iron-nickel alloys—the latter representing the case in which the intensity of radiation from one constituent is increased as the result of excitation by the other.

Other experiments were carried out, using photographic recording by means of a Seemann spectrometer. For a molybdenum target, a 1° oscillation of the crystal and a slit width of 0.05 mm, a density of the $K\alpha_1$ line amounting to 0.4 was obtained by an exposure of sixteen minutes. Analyses by this method were made on silver-cadmium and tin-antimony alloys and the results were confirmed by chemical examination.

GORTON R. FONDA
GEORGE B. COLLINS

Research Laboratory
General Electric Company
Schenectady, New York
January 16, 1931.

The Hyperfine Structure of Ionized Lithium

The hyperfine structure of the low ^3P state of Li^+ is of the same order of magnitude as the triplet separation itself. One might expect large deviations from the interval rule for hyperfine splitting, corresponding to large contributions of one triplet level to the perturbed eigenfunctions of another. Since the Li^+ hyperfine structure has not yet been explained conclusively,[1] we have estimated the effect of these deviations on the calculated positions of the components. The resulting corrections are, however, small, and are not sufficient to give a better agreement than obtained by Güttinger.

Our method is simply to consider the transition between the extreme cases wherein the hyperfine splitting is either small or large compared to the triplet separation. The coefficients of general equations for the levels were determined by use of the vector model in the extreme cases, and by using the usual identification of the lines for the isotope Li_6. The nucleus was considered as coupled only to the $1s$ electron in the ^3P. About 6 percent was subtracted from the coupling constant as determined from the ^3S, due to the interaction with the $2s$ electron there.[2] This correction alone has some effect on the results of Güttinger, as is indicated in the third column of the table.

In the case of $i=1\frac{1}{2}$, one of the coefficients of a cubic equation cannot be determined, and is represented by x in Table I. Its order of magnitude should be one-tenth cm^{-1}. Its evaluation would be intricate, but no value

[1] H. Schüler, Zeits. f. Physik **66,** 431 (1930). P. Güttinger, Zeits. f. Physik **64,** 749 (1930).

[2] G. Breit and F. Doermann, Phys. Rev. **36,** 1732 (1930).

TABLE I.

					$i=1\frac{1}{2}$		$i=\frac{1}{2}$
Line[3]	Schüler (exp.)		Güttinger		Extreme coupling	Intermed. coupling	Intermed. coupling
1	(0.5)	18231.31	(1)	31.31	31.31	31.31	
2	(1)	30.91	(2)	30.91	30.91	30.91	(1) 30.91
3	(2)	30.26	(3)	30.25	30.26	30.26	(2) 30.26
4c			(2)	27.82	27.79	27.83−x	
4b	(6)	27.72	(5.5)	27.74	27.88	27.97−3.1x	(5) 27.56
4a			(2)	27.62	27.69	27.70−x	
5b	(12)	27.52	(11)	27.56	27.58	27.58−x	(9) 27.39
5a			(3)	27.42	27.48	27.57−3.1x	
6c			(.5)	27.22	27.29	27.30−x	
6b	(2)	27.15	(2.5)	27.10	27.14	27.18−x	(1) 26.91
8c			(2)	25.96	26.03	26.12	
8b	(6)	25.91	(2.5)	25.89	25.94	25.91−x	(1) 25.80
13b			(.7)	25.56	25.63	25.72	
13a	(1.5)	25.46	(2)	25.36	25.44	25.44−x	(2) 25.51
9	(4)	25.25	(5.5)	25.23	25.29	25.26−x	(5) 25.15
10	(1)	24.93	(2.5)	24.90	24.98	25.07	(1) 24.86

would bring much better agreement than was found in Güttinger's approximation. In the case $i=\frac{1}{2}$, our results give agreement just slightly worse than those quoted by Schüler.

[3] The components 7, 11 and 14 are attributed to the Li^6 isotope and have been omitted in this table. They are at 26.43, 24.33 and 29.48.

S. GOUDSMIT
D. R. INGLIS

Department of Physics,
University of Michigan,
January 19, 1930.

An Attempt to Detect Axiality of X-Ray Emission

J. Stark[1] has recently reported that fluorescent K-series x-rays are not emitted with equal intensity in all directions from certain crystals, and that these x-rays are at least partially plane-polarized. In the case of γ-γ-dibromoanthracene, a monoclinic crystal of needle-like habit with the b-axis parallel to the length of the needle, he found about 20 percent more bromine K-radiation in directions 90° from the b-axis than in a direction 10° therefrom. The scattering of this radiation by aluminium indicated that it was polarized with the electric vector parallel to the b-axis. These effects are so important from the theoretical side that independent confirmation seemed desirable. This note reports an unsuccessful attempt to detect differences in the intensity of zinc K-radiation emitted in different crystallographic directions from a zinc crystal.

Zinc was chosen because the axial ratio for its hexagonal crystals, $c/a=1.86$, is so much greater than that (1.63) to be expected in a close-packed arrangement of spheres that it is reasonable to suppose the atomic axes are not free to rotate about axes in the (001) plane. This is one of the criteria suggested by Stark for selecting materials likely to show the new effect. His objection to the use of metals, that the atoms therein are presumably free to rotate, does not therefore seem valid with respect to zinc.

The primary x-rays used were from a tungsten target tube operated at 55000 volts (peak) or from a molybdenum target tube operated at 44000 volts (peak). The zinc monocrystalline plate, 0.4 cm thick was rotated about its normal into various azimuths while its secondary radiation in a fixed direction 90° from the primary beam was measured by balancing its ionization with that of part of the primary beam. The absorption coefficient of the secondary radiation was found to be that of zinc K-radiation, indicating that the scattered radiation at 90° was negligible in comparison with the fluorescent. The normal to the plate was found by Laue and rotation

[1] Stark, Ann. d. Physik [5] **6**, 637–662 (1930).

photographs to lie at 20° from the hexagonal axis of the crystal, so that if θ is the angle between the normal and the axis of the principal ionization chamber the angles between this axis and the hexagonal axis of the crystal vary between $\theta+20°$ and $\theta-20°$ during the rotation of the specimen. For the three settings tested, θ was 52°, 62° and 77°. In no case was the variation in observed intensity as much as one percent. We conclude that at least as regards intensity the effect reported by Stark is unimportant in zinc.

L. A. PARDUE
L. W. MCKEEHAN

Sloane Physics Laboratory,
Yale University,
January 23, 1931.

Rotational Fine Structure in Raman Spectra

In recording the rotation spectrum of a molecule by scattered light one of the major difficulties is the very great intensity of the unmodified line as compared with those lines arising from changes in rotational energy. Long exposures tend to broaden the strong line and obliterate the weaker ones which lie very close to it. An ingenious arrangement employed by Rasetti (Zeits. f. Physik **66**, 646 (1930)) is partially effective in overcoming this handicap. He introduced mercury vapor into the spectrograph to absorb from the scattered light those unmodified frequencies which arise from the normal state of the atom. The observations are thus practically confined to λ2537 as parent line. Even this expedient is not wholly successful, since λ2535 is superposed upon the rotation pattern and appears very intense in comparison with it.

Recently Manneback (Zeits. f. Physik **62**, 224 (1930)) has computed the relative intensities and polarizations for Raleigh and Raman scattering of lines with and without rotational displacements. He shows that if the incident light is plane polarized and the scattered light is observed in a plane normal to the electric vector, the rotation lines are almost completely depolarized. Since the unmodified line is not depolarized, this suggests the introduction of a Nicol prism between the camera and the scattering chamber. Any convenient source and any frequency for the incident line could then be used, and not only the parent line but also neighboring lines scattered without change in frequency would be eliminated. In all probability the background illumination would also be materially lessened. With this improvement in contrast considerably smaller total exposures should prove adequate, and the necessary time might not be much extended, even though the illumination would be considerably fainter.

E. F. BARKER

Department of Physics,
University of Michigan,
January 28, 1931.

Biological Effects of Gamma-Rays

In connection with the development in various laboratories of x-ray tubes operating at voltages of the order of a million volts, the question of adequate protection of those engaged in the work against the very penetrating gamma-rays emitted by such tubes has become of considerable importance. It has seemed valuable to perform some experiments with highly filtered gamma-rays from radium in order to ascertain the dangers from exposure to the penetrating radiation, which may be considerable in amount, passing through whatever shielding may be used around the tube. Estimates doubtless might be made from previous work, but for comparison it appeared desirable to have data on exposures to gamma-rays from radium from which all soft components were similarly filtered out.

A group of 63 white rats (with known antecedents) has been exposed to the radiation from 6 grams of radium filtered through one mm of platinum, one mm of brass, 16 mm of lead, and 5 mm of celluloid at a distance of 41 mm to the nearest side of the rat. For four additional rats the celluloid was omitted. The rats were put in celluloid boxes 47 mm high placed above and below the radium box. The radium was spread out over a surface of 3 by 10 cm area to give more uniform exposure. With this large source-area and distance, the exposure was reasonably similar throughout the whole body of the rat. In addition, 16 rats were exposed to 2.5 grams of radium at the same distance but with the lead filter removed; for eight of this group the celluloid was also omitted. This group of 16 thus re-

ceived approximately the same exposure to the hard components of the radiation but with the addition of that amount of soft gamma-radiation which penetrated the platinum and brass. The celluloid was used in order to reduce the beta-ray intensity to about the level corresponding to the rate of beta-ray production in the tissues. Exposure-times were varied from one-half minute to 17 hours in a roughly geometric progression. The 2.5 grams without the lead filter should give an "erythema dose" in about four hours at the average distance of 6 cm according to ordinary clinical data.

All rats died which were exposed six hours and longer to the 6 grams of radium with filters. With a 16-hour exposure, death ensued in three or four days, due at least in part to injury to the gastro-intestinal tract. With six-hour exposures the rats showed similar but less severe gastro-intestinal symptoms from which all recovered in about three days but died one to three weeks later from a progressive anemia affecting both red and white blood-cells. One of the six rats exposed to three hours died from a similar anemia after 11 days. The lethal exposure lies thus between three and six hours, or about four hours. Two of four rats exposed 2.5 hours to 2.5 grams of radium without the lead filter died from anemia after 19 and 37 days. The lethal exposure for these conditions is thus about three hours.

Blood-counts were made on 66 rats before and 0, 1, 3, 7, 14, 21, and 35 days after exposure. The minimum exposure which showed an appreciable effect on the blood-count was approximately 20 minutes for the rats exposed to the 6 grams with filters. Since a single massive dose is the most favorable for detecting a change in blood-count and since ten times this exposure is above the lethal dose, blood-count observations alone are not a satisfactory protective measure for those working with high-voltage tubes. Breeding experiments are in progress, and the evidence so far indicates that the sterility dose approximates the lethal dose under these conditions. Abnormalities have to date appeared only in the litter of one female fertilized four weeks after a three-hour exposure.

To provide a suitable index of the total exposure of investigators working with high-voltage tubes, a series of Eastman extra fast (CC) dental x-ray films was enclosed in a lead cassette having walls 6.9 mm thick, and this cassette was exposed in the mid-position of the rat (6.2 cm to the film) for periods of 10^{-5} to 10^{-1} lethal exposure-time as determined for the rats. An exposure of 1×10^{-3} lethal dose gives a point just at the lower end of the straight portion of the density-log exposure-curve, that is, 7×10^{-4} lethal dose gives a density which is easily confused with fog due to development, whereas 3×10^{-3} gives a very obvious blackening of the film. Densities as measured on a photoelectric photometer for the two films in each placque are given below. The placque was exposed as labeled with the "black paper toward tube" (radium).

Fraction of lethal exposure-time	Percent transmission incident film	Percent transmission emergent film	Average T	Density = $\log_{10} 1/T$
None	100	100	1.00	0.0
0.00005	100	100	1.00	0.0
0.0001	83	97	0.90	0.045
0.0003	65	83	0.74	0.13
0.0007	46	64	0.55	0.26
0.001	33	45	0.39	0.41
0.003	9.5	12	0.11	0.96
0.007	1.8	1.8	0.018	1.74
0.01	0.71	0.82	0.0075	2.12
0.05	0.028	0.033	0.0003	3.5
0.10	0.028	0.013	0.0002	3.7

For these film-exposures 2.5 grams of radium were used with the 16-mm lead filter (in addition to the cassette), and 12 hours was taken as the lethal exposure-time.

W. G. WHITMAN, M.D.
M. A. TUVE

School of Hygiene and Public Health (W.G.W.),
Johns Hopkins University,
Baltimore, Maryland.

Department of Terrestrial Magnetism (M.A.T.),
Carnegie Institution of Washington,
Washington, D. C.,

January 22, 1931.

BOOK REVIEWS

Vorlesungen uber Wellenmechanik. A. LANDÉ. Pp. 132, figs. 15, Akademische Verlagsgesellschaft, Leipzig 1930. Price RM 9.50.

This small volume represents the lectures delivered at Ohio State University during the academic year 1929–30. In general character it is more of a Handbuch than a self-sufficient introductory treatise. The number of topics touched upon is surprisingly large, but the treatment of the individual items is correspondingly shortened.

After a brief introduction on the general foundations of atomic theory there is a section on the dualism of the wave and corpuscle viewpoints, and one on the uncertainty principle. The treatment is along the usual lines, but the compactness of the material is so great as to detract very considerably from its value. The third section on quantum statistics gives a treatment of the Bose-Einstein method but only a mention of that of Fermi.

The major portion of the book is of course devoted to Schrödinger's equation and its solution. Only the simplest cases are discussed, but no attempt is made to give actual methods of solution, results only being stated. One may call attention to the treatment of the Pauli principle and the symmetry properties of wave functions, which is rather more carefully stated than is usual. The last section on the relativistic wave equation contains a paragraph on Dirac's electron theory and even one on quantum electrodynamics. Perhaps one of the best uses of this book will be as a guide in the development of more detailed lecture notes.

E. L. HILL

Handbuch der Astrophysik. Band II, Erste Hälfte. Edited by G. EBERHARD, A. KOHLSCHUTTER AND H. LUDENDORFF. Pp. 430, figs. 51. Julius Springer, Berlin, 1929. Price bound RM 69.

The importance of photometry in astrophysical work is well illustrated by the fact that this volume of 430 pages forms but a half of the section of the *Handbuch* which is to be devoted to this subject. The first and longest chapter deals with photometric theory. The photometry of the stars, and of self-luminous bodies in general, is rather summarily treated, for example, nothing is said about the measurement of the brightness of the sun relative to the stars, or of the comparison between the astronomical standard of light (expressed in stellar magnitudes) with the terrestrial standard (meter-candles). On the other hand, the photometry of diffusely reflecting bodies—the moon, the planets, Saturn's rings, the zodiacal light, etc., and the extinction of light in the earth's atmosphere are discussed in great detail, with the inclusion of important investigations by the author (Professor E. Schoenberg) some of which are new, while others have been difficult of access. This complete monograph, accompanied by extensive tables should be of much value to all workers in this field. There are few references, however, to work of later date than 1922, and it is to be regretted that no mention is made of Danjon's work on the earth-shine upon the moon, or of Hubble's on the illumination of nebulae by neighboring stars.

The chapter on spectro-photometry (by Dr. A. Brill) deals with a subject so new that it is largely an account of the methods employed by individual investigators. These are clearly presented and the summary is brought up to the end of 1927—including some of the modern work on the contours of individual spectral lines.

A short chapter on colorimetry (by K. Bottlinger) contains an admirable survey of the meaning of color-indices and related magnitudes, and a critical discussion of the methods and results of observation up to 1926. The final chapter on photoelectric photometry, (by H. Rosenberg) contains a thorough discussion of photoelectric and selenium cells. The latter have been practically abandoned in favor of the former, which are of ever-increasing importance. He justly remarks that their introduction into observatories has doubtless been delayed by the unfamiliarity of astronomers with the details of delicate electrical equipment, and his full descriptions of instrumental design and wiring should be of real aid here.

HENRY NORRIS RUSSELL

Second Series *February 15, 1931* *Vol. 37, No. 4*

THE
PHYSICAL REVIEW

NOTE ON THE STATISTICS OF NUCLEI

By P. Ehrenfest and J. R. Oppenheimer
California Institute of Technology, Pasadena

(Received December 23, 1930)

Abstract

From Pauli's exclusion principle we derive the rule for the symmetry of the wave functions in the coordinates of the center of gravity of two similar stable clusters of electrons and protons, and justify the assumption that the clusters satisfy the Einstein-Bose or Fermi-Dirac statistics according to whether the number of particles in each cluster is even or odd. The rule is shown to become invalid only when the interaction between the clusters is large enough to disturb their internal motion.

I. Introduction

THE band spectra of symmetric diatomic molecules show certain striking differences from those of asymmetric molecules. For when the two nuclei of the molecule are identical, the intensity of the individual lines of a band, instead of varying smoothly from line to line, alternates more or less markedly. This alternation may in most cases be understood[1] with the help of a simple rule, but in the case of the N_2 molecule, the theoretical prediction seems to disagree with experiment, in that it leads us to expect those band-lines to be the more intense, which are in fact weaker. In this paper we do not propose to resolve this disagreement; we shall only try to give as direct a derivation as possible of the rule which plays the cardinal part in obtaining the theoretical prediction. For it seems that, in spite of the frequent citations of this rule, no explicit derivation of it from Pauli's exclusion principle has been published. In giving this derivation we shall have to investigate the conditions under which the rule is valid, and the degree of approximation to which it may be expected to hold.

The rule may be stated:

R. "If we have two nuclei, each built up of n electrons and m protons, and if the nuclei are in the "same inner state," then not all the molecular states which would be possible for an asymmetric molecule will be found to occur; if $n+m$ is $\begin{cases}\text{even,}\\ \text{odd,}\end{cases}$ only those states $\begin{cases}S\\ A\end{cases}$ will occur for which the wave function $\begin{cases}\text{remains unchanged}\\ \text{changes its sign}\end{cases}$ when we interchange the "coordinates" of the nuclei.

[1] See the comprehensive report by R. S. Mullikan, Transactions of the Faraday Society **25**, 611 (1929).

When the nuclei are in different states, the molecule behaves like an asymmetric molecule."

Since we may expect the nuclei to be in their normal state, we should be able by this rule to predict the weight of the states S and the weight of the states A if we knew the degree of degeneracy g of the normal states of the nuclei. Thus there will always be $\frac{1}{2}g(g-1)$ states S and $\frac{1}{2}g(g-1)$ states A possible; if n plus m is even, there will be g states S, if n plus m is odd, g states A, also possible. The relative weights of the states S and A will therefore be

$$(g+1)/(g-1) \text{ if } n+m \text{ is even}$$
$$(g-1)/(g+1) \text{ if } n+m \text{ is odd}. \tag{1}$$

If we ascribe the degeneracy of the normal state of the nuclei to the spatial degeneracy of an angular momentum $sh/2\pi$, then these ratios become

$$(s+1)/s \text{ for } n+m \text{ even}$$
$$s/(s+1) \text{ for } n+m \text{ odd}.$$

From this we see that, since $n+m$ is odd for the nitrogen nucleus, the states A should have a greater weight than the states S. According to the assertions of band spectroscopists, the electronic wave functions of the normal state of the N_2 molecule are symmetric in the coordinates of the nuclei, and there is no resultant electronic angular momentum parallel to the molecular axis. If we accept these assertions, we are led to expect a greater weight for states of odd rotational quantum number than for those of even quantum number; and it is this expectation which is not confirmed by experiment.

Our problem is now so to refine the expressions "internal state" and "interchange the coordinates of the nuclei" in our rule R, that we can derive the rule from the exclusion principle.

II. Wave Packets for a System of Two Clusters

We shall consider first the following preliminary problem: Suppose that we have a system containing $2n$ electrons and $2m$ protons. Suppose further that for any group of n electrons and m protons we could write down a complete set of wave functions u_k for the stationary states k; how then, using any two of these wave functions u_k and u_l, can we build up a wave packet for the whole system which satisfies the exclusion principle for all the electrons and all the protons in the system? Only when the particles of the system do not interact at all will these wave packets represent the stationary states of the whole system; but with the help of these packets, by linear combination, we shall be able to build up wave functions which do represent stationary states for any interaction energy of the particles. The functions u may for instance represent states of a nucleus, or an atom, or a molecule, or even some aperiodic motion of the n plus m particles; for this preliminary problem we need to make no assumption about them; but we shall see later that only when the functions u represent very stable configurations: i.e. very tight binding of the particles,—can we deduce any significant results; and so we shall call any group of n electrons and m electrons a cluster.

Let the cartesian coordinates, referred to a fixed axis system, and the component of spin in a fixed direction, of the jth electron be x_j; similarly let the coordinates and spin of the ith proton be y_i. Let us split up each of the functions u into two functions, a function T_s which depends only on the coordinates of the center of gravity of the cluster, and a function ψ_σ which depends on the relative coordinates of the particles, and on the spin variables:

$$u_k(x_1 \cdots x_n, y_1 \cdots y_m) \rightarrow T_s(x_1 \cdots x_n, y_1 \cdots y_m)\psi_\sigma(x_1 \cdots x_n, y_1 \cdots y_m) = T_s(\alpha)\psi_\sigma(\alpha)$$

$$u_l(x_{n+1} \cdots x_{2n}, y_{m+1} \cdots y_{2m}) \rightarrow T_t(x_{n+1} \cdots x_{2n}, y_{m+1} \cdots y_{2m})\psi_\tau(x_{n+1} \cdots x_{2n} y_{m+1} \cdots y_{2m}) = T_t(\beta)\psi_\tau(\beta)$$

We write α for the arguments $(x_1 x_2 \cdots x_n, y_1 y_2 \cdots y_m)$ and β for the arguments $(x_{n+1} x_{n+2} \cdots x_{2n}, y_{m+1} y_{m+2} \cdots y_{2m})$

Since T depends only on the sum of the coordinates of the electrons, and the sum of the coordinates of the protons, and does not involve the spins at all, it must remain unchanged when we make an arbitrary permutation of the arguments x of u among themselves or of the arguments y of u among themselves. On the other hand u must be antisymmetric in its arguments x and in its arguments y, since otherwise it could not represent a stationary state for the cluster allowed by the exclusion principle. Thus ψ must be antisymmetric in the x's and in the y's. Let now P be an operator which makes an arbitrary permutation of the x's and an arbitrary permutation of the y's in any function of $x_1 \cdots x_{2n}, y_1 \cdots y_{2n}$, and let p be the order of the permutation P. Then the functions

$$F_{st,\sigma\tau} = \frac{1}{(2n)!(2m)!} \sum (-)^p P \{ T_s(\alpha) T_t(\beta) \psi_\sigma(\alpha) \psi_\tau(\beta) \} \tag{2}$$

satisfy the exclusion principle, if the summation be taken over all the $(2n)!(2m)!$ permutations P. There are only $r = (2m)!(2n)!/(m!)^2(n!)^2$ different terms in this sum, since by the antisymmetry of the ψ's, all of the terms in which the arguments of T_s (and therefore also of T_t) are the same have just the same value. If we define a distribution by the symbol $(x_j \cdots, y_i \cdots \mid x_f \cdots y_g \cdots)$ in which the arguments of T_s are to the left, those of T_t to the right, of the line, and in which the order of the arguments to the left and to the right is indifferent, then we can write

$$F_{st,\sigma\tau} = \frac{1}{r} \sum{}' (-)^p P \{ T_s(\alpha) T_t(\beta) \psi_\sigma(\alpha) \psi_\tau(\beta) \} \tag{3}$$

where now the summation is taken only over the r different distributions. Now in $F_{st,\sigma\sigma}$ with $\sigma = \tau$, we can combine the term with the distribution

$$(x_j \cdots y_i \cdots \mid x_f \cdots y_g) \tag{4}$$

with that with the inverted distribution

$$(x_f \cdots y_g \cdots \mid x_j \cdots y_i).$$

This second term may be derived from (4) by n plus m interchanges, and will therefore appear in the sum with the same sign as (4) if n plus m is even, and with the opposite sign if m plus n is odd. We may therefore write, with $\theta = (-1)^{m+n}$

$$F_{st,\sigma\sigma} = \frac{1}{r}\sum{}''(-)^p P\{\psi_\sigma(\alpha)\psi_\sigma(\beta)[T_s(\alpha)T_t(\beta) + \theta T_s(\beta)T_t(\alpha)]\} \tag{5}$$

where now the summation is taken over the $r/2$ different sets of arguments in the ψ_σ's. When $\tau \neq \sigma$, we have instead,

$$F_{st,\sigma\tau} = \frac{1}{r}\sum{}''(-)^p P\{\psi_\sigma(\alpha)\psi_\tau(\beta)T_s(\alpha)T_t(\beta) + \theta\psi_\sigma(\beta)\psi_\tau(\alpha)T_s(\beta)T_t(\alpha)\}$$

which we may write

$$\begin{aligned} F_{st,\sigma\tau} = \frac{1}{2r}\sum{}''(-)^p P\{&[\psi_\sigma(\alpha)\psi_\tau(\beta) + \psi_\sigma(\beta)\psi_\tau(\alpha)][T_s(\alpha)T_t(\beta) + \theta T_s(\beta)T_t(\alpha)] \\ &+ [\psi_\sigma(\alpha)\psi_\tau(\beta) - \psi_\sigma(\beta)\psi_\tau(\alpha)][T_s(\alpha)T_t(\beta) - \theta T_s(\beta)T_t(\alpha)]\} \end{aligned} \tag{6}$$

From (5) we see that $F_{st,\sigma\sigma}$ is $\begin{cases}\text{symmetric}\\ \text{antisymmetric}\end{cases}$ in s and t when $m+n$ is $\begin{cases}\text{even,}\\ \text{odd,}\end{cases}$ and, from (6), that for $\tau \neq \sigma$, $F_{st,\sigma\tau}$ has, for $n+m$ either even or odd, both a symmetric and an antisymmetric part, neither of which vanishes identically. These properties of the wave packets F will make it possible to deduce our rule.

III. Symmetry of Wave Functions for a System of Two Clusters

We should expect that these symmetry properties in s and t would persist in the stationary wave functions built up from the F's whenever the interaction of the two clusters was too small appreciably to distort the internal configuration of the clusters. In this paragraph we shall have to find the wave functions ϕ for the stationary states of the system of two clusters. We shall see that, when certain matrix components of the interaction energy of the particles may be neglected, the ϕ's do in fact have the same symmetry in s, t as the corresponding wave packets F; and we shall see further that the conditions under which we may neglect these matrix components are just those in which the interaction of the clusters does not greatly disturb their internal motion.

Let E be the energy of the system, and H the Hamiltonian; it will in general be given us as an operator on a function of the x's and the y's, and it will be 'impartial' to all x's and 'impartial' to all y's. The wave equation for $\phi(x_1 \cdots y_{2m})$ will be

$$(H - E)\phi = 0 \tag{7}$$

Since ϕ must satisfy the exclusion principle, and since our original u's formed a complete set of functions, we may expand ϕ as a linear function of the F's:

$$\phi = \sum_{\substack{(\sigma,\tau)\\ \sigma\neq\tau}} \sum_{s} \sum_{t} a(st, \sigma\tau)F_{st,\sigma\tau} + \sum_{\sigma} \sum_{(s,t)} a(st, \sigma\sigma)F_{st,\sigma\sigma}. \tag{8}$$

Here the summation $\sum_{\sigma\neq\tau}^{(\sigma,\tau)}$ is to be taken over all pairs (σ,τ) with $\sigma\neq\tau$, and $\sum_{(s,t)}$ over all pairs (s, t). We now introduce that part of the irreducible matrix for H which belongs to the term system satisfying the exclusion principle:

$$(st, \sigma\tau \mid H \mid s't', \sigma'\tau') = \int dV\, \tilde{F}_{st,\sigma\tau} H F_{s't',\sigma'\tau'}. \tag{9}$$

The integration $(\int dV \cdots)$ is to be taken over the whole domain of all the coordinates, and is to include a summation over the two values of all the spin variables. With the help of this matrix we may write the wave equation for the a's which is equivalent to (8):

$$\sum_{\substack{(\sigma,\tau)\\ \sigma\neq\tau}} \sum_{s} \sum_{t} (s't', \sigma'\tau' \mid H \mid st, \sigma\tau)a(st, \sigma\tau) + \sum_{\sigma} \sum_{(s,t)} (s't', \sigma'\tau' \mid H \mid st, \sigma\sigma)a(st, \sigma\sigma) = Ea(s't', \sigma'\tau'). \tag{10}$$

By (5), (6) we have

$$F_{st,\sigma\tau} = \theta F_{ts,\tau\sigma}$$

and

$$a(st, \sigma\tau) = \theta a(ts, \tau\sigma). \tag{11}$$

Suppose now that we may set

$$(st, \sigma\tau \mid H \mid s't', \sigma'\tau') = 0 \text{ for } (\sigma, \tau) \neq (\sigma', \tau'). \tag{12}$$

We shall have later to see under what circumstances, and to what approximation, (12) is legitimate; but if we accept it, then we see that (10) reduces to a series of independent equations, one for each pair of values of (σ, τ)

$$\sigma = \tau\colon \sum_{(s,t)} (\sigma\sigma, s't' \mid H \mid \sigma\sigma, st)a(\sigma\sigma, st) = Ea(\sigma\sigma, s't')$$

$$\sigma \neq \tau\colon \sum_{s} \sum_{t} (\sigma\tau, s't' \mid H \mid \sigma\tau, st)a(\sigma\tau, st) = Ea(\sigma\tau, s't')$$

For each such pair of values (σ, τ) we thus get a set of solutions $a\,(st)$; for $\sigma = \tau$ these will be $\begin{cases}\text{symmetric}\\ \text{antisymmetric}\end{cases}$ in s and t when $m+n$ is $\begin{cases}\text{even};\\ \text{odd};\end{cases}$ for $\sigma\neq\tau$ both symmetric and antisymmetric functions are possible. If we define the "state" of the cluster by the σ's, then this result is fully equivalent to the rule (R) given at the beginning of this paper. We may see this directly in the following way: for the quantum numbers s, t, we may take directly the value of the components of the total momenta of the two clusters; if we introduce the center of gravity coordinates of the two clusters, X, Y by the conditions

$$sX - Xs = h/2\pi i;\ \ sY - Ys = 0;$$
$$tY - Yt = h/2\pi i;\ \ tX - Xt = 0; \tag{13}$$

then we get the transformation functions:

$$(st/XY) = e^{-2\pi i/h(sX+tY)}. \tag{14}$$

The wave functions for the stationary states of the whole system are then given as functions of X, Y by

$$\sum_{s,t} a(st, \sigma\tau)(st/XY). \tag{15}$$

For $\sigma=\tau$, these must be $\begin{cases}\text{symmetric}\\ \text{antisymmetric}\end{cases}$ in X and Y when $n+m$ is $\begin{cases}\text{even;}\\ \text{odd;}\end{cases}$ for $\sigma\neq\tau$ they may have either symmetry.

We have now only to consider the conditions for the validity of (12). If the states σ, τ of the isolated clusters are degenerate, then the matrix elements of H corresponding to transitions between such degenerate states—states in which the isolated clusters have the same internal energy,—may be made to vanish by choosing suitably the u's which give the stationary states of the clusters. The terms

$$(st, \sigma\tau \mid H \mid s't', \sigma'\tau')$$

in which the states (σ, τ) and (σ', τ') correspond to different energy levels of the clusters, will, since the original u's were chosen to make the internal energy of the isolated clusters a diagonal matrix, represent the matrix components of the interaction and interchange energy of the particles in one cluster with those in the other; and if the particles in the cluster are very tightly bound together, these energies will be very small compared to the energy differences of two stationary states σ, σ' of the isolated cluster. The terms which were neglected in (12) therefore, will give in this case only very small correction terms to the a's of the order of the ratio of the interaction energy of the two clusters to their proper energy; in general these correction terms will be neither symmetric nor antisymmetric in s and t, so that only for very stable clusters may we expect a rule like (R) to hold: for the two identical *atoms* of a symmetric molecule no such rule as (R) holds, since here the interaction energy of the atoms is of the same order of magnitude as their proper energy. Even in this case, of course, the exclusion principle for the electrons and protons reduces the number of possible stationary states; but here we cannot say just what states are excluded by investigating only the symmetry of the corresponding wave functions in the coordinates of the center of gravity of the clusters, but must study in detail the symmetry of the functions in the coordinates of all the elementary particles. The importance of the rule (R) arises from the circumstance, that in the dynamical treatment of most atomic and molecular problems we do not need to know anything about the structure of the nuclei, except that they are stable: we may treat them as point charges, with, in some cases, a spin s which gives a proper intrinsic degeneracy. And whenever this is so, we may use a rule like (R) to determine what states of the system survive the exclusion principle.

THE INTENSITY OF X-RAYS REFLECTED FROM PLATINUM, SILVER, AND GLASS

By Hiram W. Edwards
University of California at Los Angeles

(Received January 7, 1930)

Abstract

The intensity of a monochromatic beam of x-rays reflected from platinum, silver, and glass mirrors was measured for angles of incidence varying from 0.75 to 1.25 times the critical angle. Radiation having a wave-length of 0.69A was obtained by reflection from calcite. Values of the intensity of the reflected beam calculated by Thibaud's modification of Fresnel's equation were found to be in good agreement with experimental values obtained from platinum. Experimental results obtained from silver and glass mirrors do not agree quantitatively with the theoretical values. No explanation for the lack of concordance is offered.

LINNIK and Laschkarew[1] have observed that the intensity of x-rays ($\lambda = 1.537$A) totally reflected from an iron mirror does not fall off abruptly at the critical angle when increasing the glancing angle of incidence. Forster[2] attributed this lack of sharpness to an absorption effect in the reflecting medium. He attempted to derive an expression from the Fresnel reflection equations to express the intensity of the reflected x-ray beam in terms of the critical angles. Although Forster made an error in the derivation of his equation, the curves which he gave to show the effect of the absorption upon the intensity-glancing angle of incidence relation are in agreement with the curves, published later by Schon[3] and also with those given by Thibaud.[4]

Dershem[5] gave the relative intensities of the K_α line of carbon ($\lambda = 44.6$A) reflected from glass for angles of incidence varying from 1° to 8°. Thibaud[4] shows that Dershem's results are qualitatively in agreement with the values calculated by his (Thibaud's) extension of the Fresnel reflection equation.

The writer is not aware of any attempt having been made to check, quantitatively, the Fresnel equation of the intensity of reflected radiation in the x-ray region. In order to make a quantitative test three materials, platinum, silver, and glass, were selected. Platinum was chosen because of its relatively high absorption coefficient, silver and glass because of their low absorption coefficients. While the absorption coefficients of silver and glass are both low, the two materials are unlike in having relatively widely separated critical angles and are otherwise optically different.

[1] Linnik and Laschkarew, Zeits. f. Physik **38**, 659 (1926).
[2] Forster, Helv. phys. Acta **1**, 18 (1927).
[3] Schon, Zeits. f. Physik **58**, 165 (1929).
[4] Thibaud, Jour. d. Physique **7**, 37 (1930).
[5] Dershem, Phys. Rev. **34**, 1015 (1929).

Apparatus

The apparatus was arranged as shown in Fig. 1. The x-radiation was produced by a water cooled tungsten tube operated at 50,000 volts. The x-ray beam was defined by two slits, S_1 and S_2, each about 0.4 mm wide and about 80 cm apart. The x-ray beam was directed against a calcite crystal oriented so that a monochromatic beam ($\lambda = 0.69$A) was reflected. The tube voltage was sufficiently high to excite radiation up to a wave-length of 0.25A and consequently a second monochromatic beam of $\lambda = 0.345$A would be reflected from the calcite crystal along with the first. It is thought that the presence of the radiation of shorter wave-length did not appreciably alter the intensity measurements under consideration. If one assumes that the critical angles of the two radiations are proportional to the square of the wave-lengths, the critical angle of the shorter wave would be 0.25 of that of the longer wave, hence in the region investigated the intensity of the shorter wave must be very small as may be readily shown.

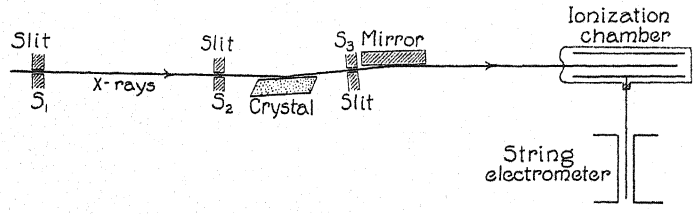

Fig. 1. Arrangement of apparatus.

The mirror under investigation was mounted on a spectrometer table and carefully placed parallel to the x-ray beam reflected from the calcite. The distance from the crystal to the mirror was approximately 27 cm. The axis of rotation of the spectrometer table was very nearly tangent to the surface of the mirror and approximately in the center of the incident beam. Both platinum and silver mirror were sputtered on pieces of glass (2×4.5 cm) which were flat within 0.5 of a wave-length of yellow light. The platinum mirror was opaque to visible light and thick enough to have a critical angle equal to that calculated by the Lorentz dispersion formula. The silver mirror would transmit about 5 percent of the visible light incident normally and not thick enough to give its maximum critical angle for this wave-length used. Three glass mirrors were used, all flat to within half a wave-length of yellow light.

It was found expedient to use a third slit S_3 in the optical system. This was placed very close to the mirror and served to limit the radiation to a very narrow beam the width of which was less than the length of the mirror multiplied by the smallest glancing angle of incidence used. By this arrangement all of the beam passing through the slit would strike the mirror surface and hence maintain an incident beam of constant intensity. At the same time the arrangement eliminated annoying scattered radiation which would have been present had any portion of the beam been permitted to pass by the mirror unreflected. Radiation scattered from the reflected beam caused no trouble.

The intensity of the reflected beam was measured by absorption in an ionization chamber and the rate of accumulation of charge on the string of a string electrometer. The sensitivity of the instrument was not determined but remained constant during any single series of observations. The front end of the ionization chamber was 65 cm from the center of the mirror.

The voltage across the x-ray tube was maintained constant within 1 percent. Filament current in the tube was practically constant.

The angle of incidence of the radiation upon the reflecting mirror was determined for a single position of the mirror by evaluating the particular reading of the tangent screw on the spectrometer table from measurements made photographically. For this purpose the slit S_3 was opened sufficiently to permit some of the radiations to pass by the mirror unreflected. The film was placed 63 cm from the mirror. Because of this comparatively short distance the angle could not be determined with an accuracy greater than about 3 percent.

Results

In the case of reflection of x-rays from metals or from glass it is necessary, because of the absorbing nature of the reflecting medium, to replace the ordinary index of refraction n, $(n=1-\delta)$, by the complex quantity n' where,

$$n' = (1 - \delta) - iK$$

and

$$K = \mu\lambda/4\pi$$

in which μ is the absorption coefficient and λ the wave-length.

Starting with the above expression and the Fresnel equation for the ratio R/I of the amplitude of the reflected wave, parallel to the plane of incidence, to that of the incident wave,

$$\frac{R}{I} = \frac{n\cos i - \cos i'}{n\cos i + \cos i'}$$

where i and i' are the angles of incidence and reflection measured from the normal to the surface, Thibaud[4] derived the following expression for the ratio (A) of the intensity of the reflected to that of the incident beam:

$$A = \frac{(1+m)^2 + 2(m^2+a^2)^{1/2} + 2(1+m)(2(m^2+a^2)^{1/2})^{1/2}\cos\phi/2}{(1+m)^2 + 2(m^2+a^2)^{1/2} - 2(1+m)(2(m^2+a)^{1/2})^{1/2}\cos\phi/2} \quad (1)$$

in which m is defined by the equation $\theta=(1+m)\theta_m$ where θ is the glancing angle of incidence, and θ_m is the critical angle. The other quantities are defined by the relations:

$$a = K/2\delta \quad \theta_m^2 = 2\delta \quad \tan\phi = -\frac{a(1-\delta)}{m - a^2\delta}.$$

The following tables give the values of the constants used in calculating the intensities of the reflected rays.

TABLE I.

Mirror	μ	a	θ_m (radians)	$\delta\times10^6$	$\lambda\times10^8$
Platinum	2295.	0.078	0.00400	8.00	0.69
Silver	258.	.015	.00305	4.65	.69
Glass	17.4	.004	.00153	1.18	.69

The experimental and calculated values of the intensity of the x-rays reflected from the three materials are shown graphically in Fig. 2. Experimental observations are indicated by small circles and the calculated values are shown by small crosses.

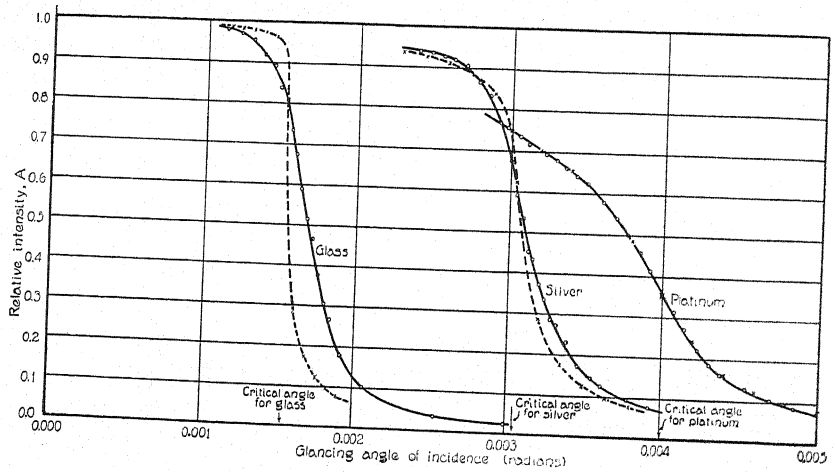

Fig. 2. Intensity of reflected x-rays.

The glancing angle of incidence is expressed in radians. Relative intensities are given in terms of the intensity of the incident beam taken at unity.

Because of the deviation of the calculated values from those obtained experimentally in the case of glass and silver, separate curves have been drawn to show the variation of intensity as determined experimentally and by computation.

Three different samples were used in obtaining reflection curves from glass and all yielded curves which were similar in form to that given in Fig. 2. The index of refraction was not the same in the three samples. The variation in δ was not large ($\delta=1.18$ to 1.50×10^{-6}) and would have no appreciable effect upon the character of the intensity curve anyway. It was difficult to obtain a reliable value for the absorption coefficient because of the necessarily great thickness of the glass. Values of the absorption coefficient obtained from thinner pieces of glass which appeared to have the same composition did not differ from 17.4 by more than 10 percent.

The character of the experimental curve of reflected intensities from glass suggests that the coefficient of absorption should be considerably larger than

17.4. Although theoretical curves were drawn for which larger values of a were assigned none could be found from Eq. (1) which duplicated the form of the experimental curve, although the "fit" was much closer than that indicated in the figure. It is possible, however, that the absorption coefficient of the surface layer, that in which the phenomenon of reflection takes place, is greater than the average value of the glass as a whole. Undoubtedly deviations of the surface from being optically flat would alter the form of the curve. The most nearly flat specimen used, however, gave no appreciably different result from the poorest mirror.

The results from the silver mirror show a better agreement between theory and experiment than those obtained from glass.

Here also the experimental results indicate a larger absorption coefficient than that measured. The silver film was not sufficiently thick to give a critical angle equal to that which would have been obtained with a thicker film.[6] This factor would seem to give a smaller coefficient of absorption rather than a larger one.

The results shown for platinum indicate good agreement between experimental and theoretical results. Just why there should be an agreement in this case and not in the other two is not clear. The writer plans to continue the investigation and hopes to be able to find an explanation for this behavior.

[6] Stauss, Phys. Rev. **34,** 1021 (1929), and also Edwards Phys. Rev. **32,** 712 (1929).

INTENSITY MEASUREMENTS IN THE SPECTRUM OF MANGANESE*

By Raymond S. Seward
Physical Laboratory of Stanford University

Abstract

Relative intensity measurements have been made for the lines of twenty-five multiplets of manganese, containing about one hundred and fifty lines in all. All but three of these were of Mn I. None of the Mn II multiplets measured were found to contain lines of abnormal intensity. On the other hand, at least eight multiplets of Mn I contain lines which are clearly anomalous. These eight multiplets contain a large number of the strongest lines of the spectrum. All involve terms derived from the term a^5D of Mn II and are of the inverted type with wide separations between the subterms. There seems to be regularity in the departure from normal intensities which can best be described by graphs in which the calculated intensities are plotted against the measured intensities on double logarithmic paper. In these plots, the satellites often assume a regular pattern above or below the main diagonal lines.

The total relative intensities of seventeen of these multiplets have also been measured. After reasonable excitation corrections have been applied, the agreement of their intensities with the theoretical values is as close as is to be expected. The measurements on the quartet triad of this group are the most reliable.

Introduction

THE elements of the iron group present complex spectra which are at present in the process of analysis.[1] A number of intensity studies have been made upon elements of this group, chiefly by Frerichs[2] at Bonn, by Harrison and co-workers[3] at Stanford, and by Ornstein and Bouma[4] at Utrecht.

The element manganese stands at the center of the iron group. Its maximum multiplicity is eight, which is the largest attained in this group. It is expected that departures from the Russell-Saunders or LS coupling which predominates in elements on the left side of the periodic table will gradually increase as the atomic number of the element in the group becomes greater, and at the same time departures from the normal intensity formulas will increase. Hesthal has found a greater fraction of anomalous lines in the multiplets of chromium ($Z=24$) than has Harrison in titanium (22), while the work of Ornstein and Bouma indicates still greater departures for cobalt (27) and nickel (28). The element manganese ($Z=25$) thus takes an interesting intermediate position in this connection.

* This work was done while the author was on leave of absence from the College of Puget Sound.

[1] H. N. Russell, Astrophys. J. **66**, 283–328, 347–438 (1927).

[2] R. Frerichs, Zeits. f. Physik **31**, 305 (1925); Ann. d. Physik **81**, 807 (1926).

[3] G. R. Harrison, J.O.S.A. **17**, 389 (1928). G. R. Harrison and H. Engwicht, J.O.S.A. **18**, 287 (1929). G. R. Harrison, J.O.S.A. **19**, 109 (1929). C. E. Hesthal, Ph.D. Thesis, Stanford University Library. Paper also reported at meeting of Am. Phys. Soc. Chicago, November 29–30, 1929, Paper No. 25. Abstract Phys. Rev. **35**, 126 (1930).

[4] L. S. Ornstein and T. Bouma, Phys. Rev. **36**, 679–693 (1930).

Considerable work has been done on the analysis of the spectrum of Mn I and a less amount on that of Mn II. The analysis of Mn I given by McLennan and McLay[5] and unpublished data furnished by Dunham of Mt. Wilson Observatory have been used in the present study. Material for Mn II has been taken from recent articles by Russell[6] and by Duffendack and Black.[7] The assignments of terms to definite electron configurations as given by Russell[8] and by Hund[9] is used.

The aim of the present investigation has been to secure accurate intensity determinations of as many lines of the spectrum of manganese as is practicable in order that the information may be available for reference in connection with atomic problems.

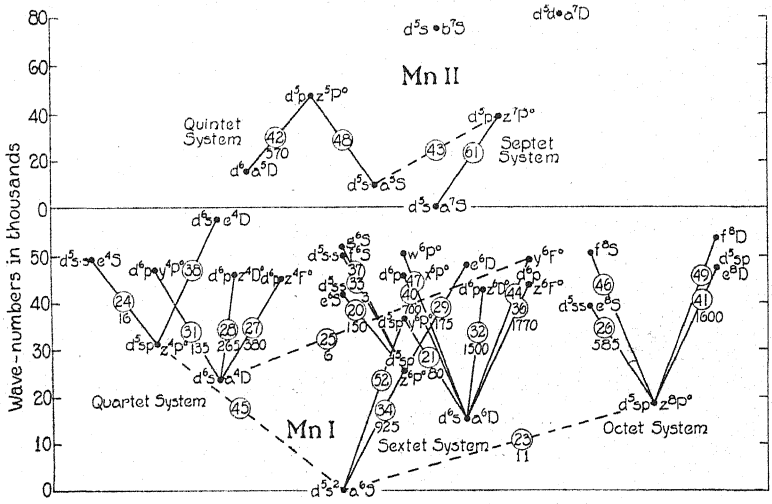

Fig. 1. Energy level diagram of the spectral terms of Mn I and Mn II.

Some features of the manganese spectra are summarized in Fig. 1, which is an energy level diagram of the spectral terms. They are classified according to multiplicity, there being quartet, sextet, and octet terms of Mn I and quintet and septet terms of Mn II. The separations of sub-terms are not shown. Symbols for electron configurations where known are written in front of the term symbols. Lines are drawn between terms to indicate multiplets. These are identified by numbers written in circles drawn on the lines, the larger numbers being assigned to the shorter wave-lengths. Intersystem transitions are represented by dotted lines.

Multiplets 27, 28, and 31 constitute a quartet triad, while multiplets 32, 36, and 40 make up a sextet triad. All six multiplets are due to *sp* electron

[5] J. C. McLennan and A. B. McLay, Trans. Roy. Soc. Canada **III**, 89 (1926).
[6] H. N. Russell, Astrophys. J. **66**, 233–255 (1927).
[7] O. S. Duffendack and J. R. Black, Phys. Rev. **34**, 35–43 (1929).
[8] H. N. Russell, Astrophys. J. **66**, 283–328, 347–438 (1927).
[9] F. Hund, Linienspectren, Julius Springer, Berlin, 1927, p. 181.

jumps and constitute two related super multiplets. Russell has shown that similar *sp* jumps are responsible for important triads in other members of the iron group.[10] All of the eight terms involved in these supermultiplets are inverted and will be referred to as the inverted system of terms, while most of the other terms of Mn I are normal. It is in members of this supermultiplet that the most interesting intensity results were found in the present study.

Experimental Procedure

The method of photographic photometry of spectral lines used in the present study has been described thoroughly in an article by G. R. Harrison.[11] The general method of procedure will not be given, but only special details noted.

The source used was an arc whose cathode consisted of a purified carbon rod into a cavity of which had been introduced finely pulverized manganese. For the anode a silver rod was used, as this gave a more steady arc than a second carbon rod, there being no serious overlapping of the silver lines with those of manganese.

Some spectrograms on each plate were exposed with an arc run at atmospheric pressure, while for others the pressure was reduced to from 10 to 20 cm of mercury. Currents of from 0.5 to 3.0 amperes were employed in order to give variable conditions of self-reversal and excitation and to bring out the strong and weak lines at the best intensities for measurement.

The source used for calibration in the ultraviolet was a mercury arc in quartz operated by a 110 volt storage battery, while in the visible a gas-filled 6 volt, 20 ampere tungsten lamp with a ribbon filament was used. As a standardizing source for much of the ultraviolet as well as all of the visible, a "black body" electric furnace with quartz window operated at about 2400°C was employed (see page 290 of reference 9), the intensities for various wave-lengths being determined by Wien's Law.

For varying the intensity during calibration, neutral wire screens were used whose transmitting power had been previously determined by thermopile readings.

The spectrographic arrangement, as in previous studies, was of a modified Paschen type. The lens for focusing the source on the slit was a quartz fluorite achromat of 2.5 cm aperture and a focal length remarkably constant at about 25 cm for all wave-lengths encountered. The grating was a concave reflector of about 35 feet radius, containing about 85,000 lines, 5900 per cm, the dispersion in the first order being about 1.67 A. per mm. This grating is remarkably free from ghosts, has intense first and second order spectra, and is in general excellent for intensity work.

The plates used, except for the region λλ 5300–6000, were the Eastman 36 brand. To secure measurable spectrograms for the green and yellow regions with the same exposure times as were used for the more actinic regions, panchromatic plates sensitized with ammonia were employed. Such plates, while

[10] See reference 1.

[11] G. R. Harrison, J.O.S.A. **19**, 267 (1929).

comparatively sensitive, are apt to become fogged and mottled. Their contrast was found much greater than desired, and the measurements made by their use are not so reliable as the others.

Self-reversal seems to have been reduced to a negligible amount in most cases, as indicated by a 45° slope to the "self-reversal curve" for a multiplet.[12] Exceptions in which self-reversal corrections were added are noted in the discussion of results.

Six sets of plates were secured, two of which covered the entire available spectrum (λλ 2500–6000). From 12 to 18 measurable spectra were obtained on

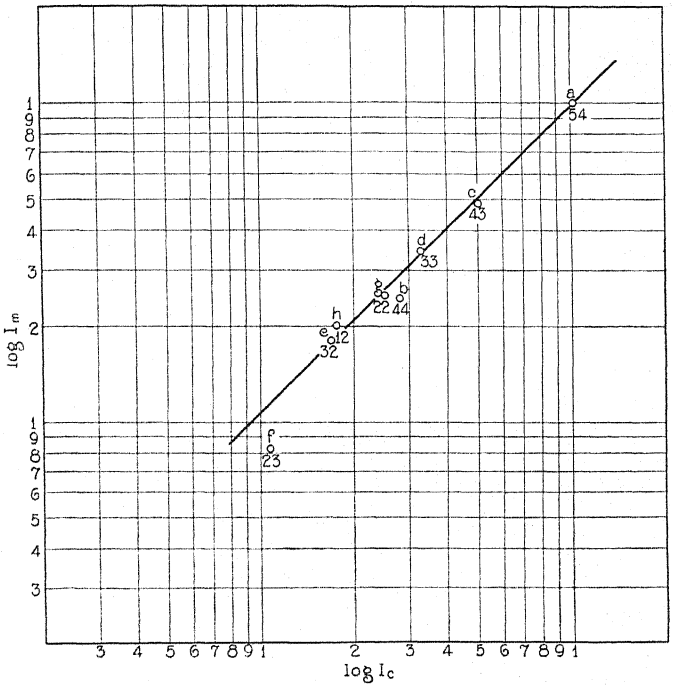

Fig. 2. Calculated and measured intensities for Multiplet 21 ($a^6D - y^6P$).

each plate. The results (recorded in the Table of Results) were obtained by averaging what were considered the most reliable determinations. It was impossible to measure accurately the weaker lines in certain exposures and in others the stronger lines were too black for accurate determination. But from 20 to 60 determinations were made for all but a few inaccessible lines.

Results and Discussion

Intensities within multiplets. The intensities of the lines making up a given multiplet may be determined with much greater accuracy than is possible when lines of different multiplets are compared, because excitation conditions

[12] In a self-reversal curve, the measured intensities are plotted against the calculated intensities on double logarithmic paper. For an explanation of such curves see p. 401 of the first reference cited in reference 3.

are similar for the various lines, and the plate sensitivity generally does not differ greatly for the lines being compared.

The results of the relative intensity measurements for the individual multiplets are found in column 5 of the Table of Results; the corresponding calculated intensities appear in column 4; while the results obtained by Frerichs for five multiplets which he measured appear in column 6. In all cases the intensity is expressed in percent of the strongest line. For convenience in testing the Sum Rule, the sums of the line intensities from a given upper state and of those having a given lower state have also been determined. These appear in the same column as the line intensities. Column 3 gives the term or transition distinguishing the sum or line.

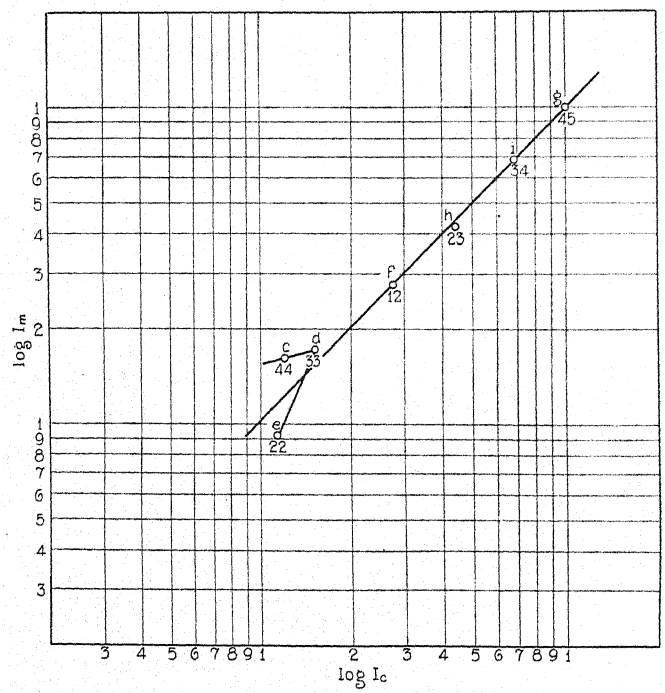

Fig. 3. Calculated and measured intensities for Multiplet 27 ($a^4D - z^4F$).

The measurements for the most interesting individual multiplets will now be discussed, following the order of decreasing wave-length.

Multiplet 21 ($a^6D - y^6P$; λλ 5540–5340). Besides lying in a region to which the ordinary photographic emulsion is insensitive, this multiplet covers a wide wave-length range in which the sensitivity of the panchromatic plate has a number of maxima and minima. It was also necessary to use exposures which were not favorable to complete removal of self-reversal. In obtaining the tabular values, self-reversal corrections were applied in some cases. The results indicate that lines *b* and *f* are abnormally weak. The multiplet is of interest in that its upper state belongs to the normal system of terms, while its lower state belongs to the inverted system. The calculated and measured intensities are shown graphically in Fig. 2.

Multiplet 23 (a^6S-z^8P; λλ 5432–5395). The two lines in this intersystem multiplet are fairly strong. Although there is no theoretical relation known between the intensities of such lines, the present measurements illustrate that the lines of largest J values are the strongest, and that the intensities follow qualitatively rules similar to those for lines in normal multiplets.

Multiplet 25 ($a^4D_3-z^6F_4$, $a^4D_4-z^6F_5$; λ 5000) and *Multiplet 45* (a^6S-z^4P; λ 3220) gave similar results.

Multiplet 27 (a^4D-z^4F; λλ 4766–4671). A large number of very consistent determinations were made on multiplet 27 in which self-reversal graphs showed a uniform slope of 45°, indicating the vanishing of this effect. The averaged values taken from the Table of Results are plotted in Fig. 3. A

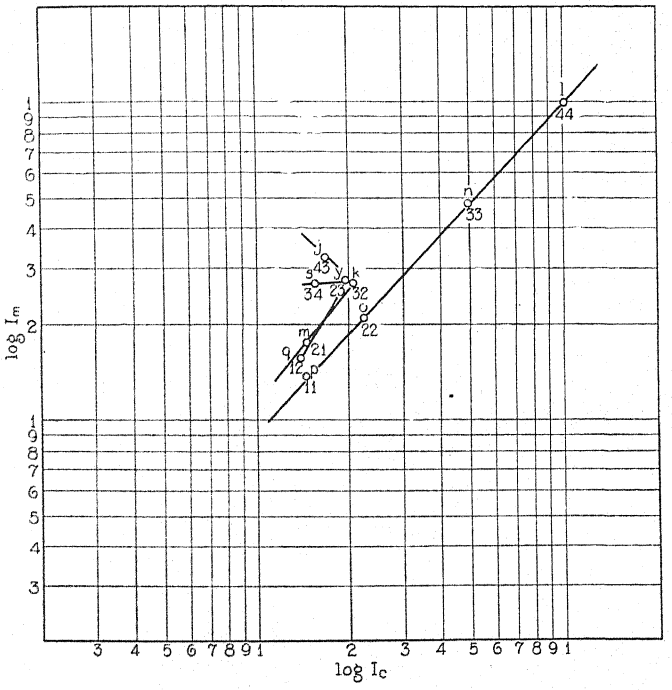

Fig. 4. Calculated and measured intensities for Multiplet 28 (a^4D-z^4D).

large number of similar graphs for the individual exposures showed an almost identical structure. While the four brightest lines are seen to have intensities very close to their calculated values, this is not the case for the first order satellites, line *c* being much too bright, line *d* less so, while line *e* is too weak. The wide divergence of lines *c* and *e* which are of nearly equal calculated intensity, is most striking.

Multiplet 28 (a^4D-z^4D; λλ 4502–4415). This multiplet is a second member of the triad to which multiplet 27 belongs. It is also one of the five manganese multiplets measured by Frerichs. As in the previous case, a large number of consistent determinations was made. The plot of the calculated and measured intensities on double logarithmic paper is shown in Fig. 4.

Both groups of satellites show very striking departures from the normal, being too bright by varying amounts. There are eight lines of fairly nearly equal calculated intensity in this multiplet, so that departures from the normal intensity could not very well be explained by self-reversal, even if some were present. An excitation correction would not tend to lessen the departures of the lines, since the lines which are too bright do not have a common upper state.

Multiplet 29 ($z^6P - e^6D$; λλ 4462–4455). This is the most satisfactory example of a multiplet belonging to the normal system of Mn I as distinguished from the inverted system. All the lines except *t* and *u* were resolved. The

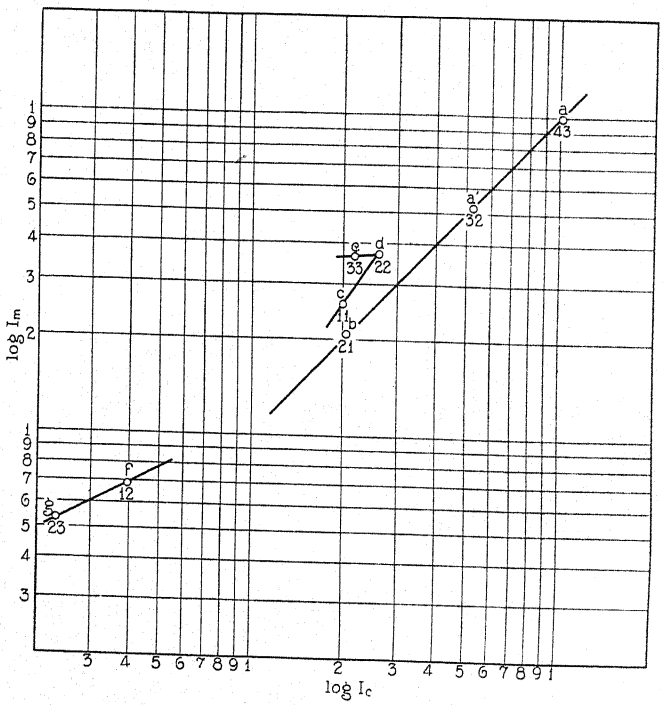

Fig. 5. Calculated and measured intensities for Multiplet 31 ($a^4D - y^4P$).

determinations showed excellent consistency and agreement with the calculated values. Frerichs obtained similar results.

Multiplet 31 ($a^4D - y^4P$; λλ 4312–4235). Multiplet 31, plotted in Fig. 5, is the third member of the quartet triad. As in the case of multiplet 28, the first order satellites are too bright; also lines *c* and *e* of nearly equal calculated intensities differ widely in measured intensities. The two second order satellites appear somewhat too bright and of more nearly equal intensities than their calculated values, although these lines were too weak for best determination. Frerichs obtained similar results in this case also.

Multiplet 32 ($a^6D - z^6D^0$; λλ 4084–4018). This is the first member of the sextet triad belonging to the *sp* inverted supermultiplet. Fig. 6 shows some

of the satellites too weak as compared with the main diagonal lines. This is in contrast to the corresponding DD^0 quartet multiplet 28, in which the corresponding lines were too intense. Lines *j* and *k* were not resolved completely. Their sum was measured, and then this value was distributed to the two lines in a ratio equal to the apparent intensities given when they were partly resolved. The position of these two individual lines is not known exactly, but their sum is not so great as the calculated value of the sum. This is another case in which departure from calculated values could not be explained by self-reversal, since a number of lines of nearly equal calculated intensities give radically different measured values.

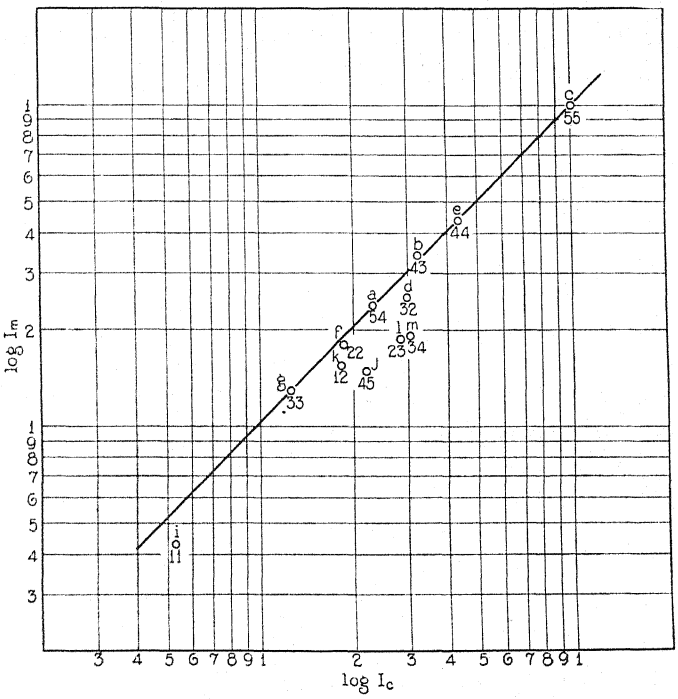

Fig. 6. Calculated and measured intensities for Multiplet 32 ($a^6D - z^6D^0$).

Multiplet 36 ($a^6D - z^6F$; λλ 3844–3776). When conditions were best for removal of self-reversal, cyanogen bands were apt to develop in the position occupied by multiplet 36. In order to resolve two pairs of interesting lines, it was also necessary to work in the second order. For these reasons, exposures in which some self-reversal remained were used in calculating the intensities, a small correction being applied to correct for the effect. The plot of the intensities as shown in Fig. 7 would be very similar if this correction had not been applied, except that the slope of the curve would be less. The departures from normal intensities are in this case the clearest and most regular of any so far encountered. The first order satellites are all clearly too weak as compared with the main diagonal lines. Since the lines are too weak, there

is no possibility of explaining their deviations by laps with unidentified lines. The two second order satellites *f* and *i* seem to have the order of their intensities inverted, though the data so far as this is concerned are not conclusive.

Multiplet 40 ($a^6D - x^6P$; λλ 3629–3577). This multiplet completes the *sp* sextet triad and is the last member of one of the supermultiplets arising from the a^5D term of Mn II. Measurements were possible in which self-reversal was apparently completely eliminated, and a large number of determinations gave nearly identical results. Of the first order satellites, line *d* is much too intense, line *e* slightly so, and line *f* is apparently about normal. The second order satellites *g*, *h*, *i* seem to be abnormally bright; these latter form a line in Fig. 8 which has much less slope than the main diagonal line.

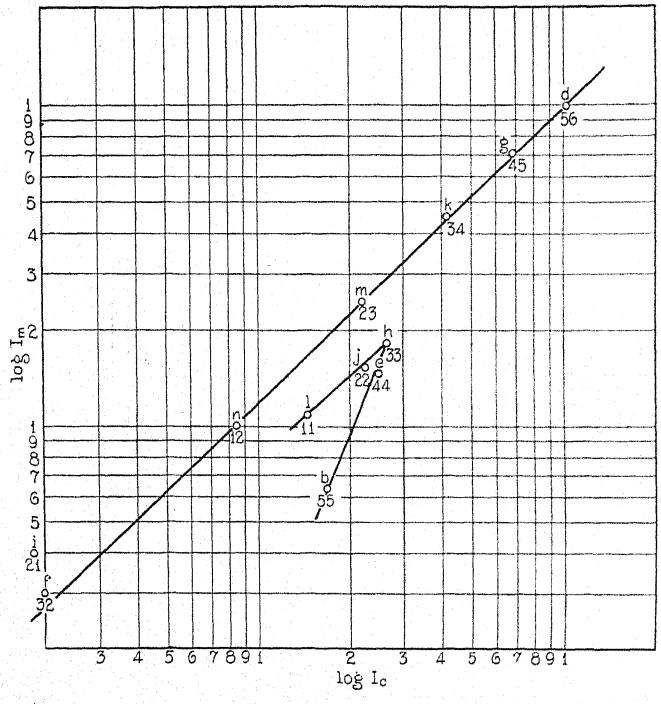

Fig. 7. Calculated and measured intensities for Multiplet 36 ($a^6D - z^6F$).

Multiplet 42 ($a^5D - z^5P$; λλ 3497–3442). This was the only complex multiplet of Mn II available for measurement. All measurements gave excellent agreement with the calculated values.

Multiplet 44 ($a^6D - y^6F^0$; λλ 3260–3209). Because of its comparative weakness, this multiplet, like its prototype number 36, was measured from exposures which had some self-reversal. The plot of its intensities shown in Fig. 9 is almost a reproduction of that for number 36, except that line *f* is a little depressed. Although the departure from normal intensities by the first order satellites is of the same type as in number 36 the amount of this departure is somewhat less. The second order satellites seemed to be stronger than their calculated values.

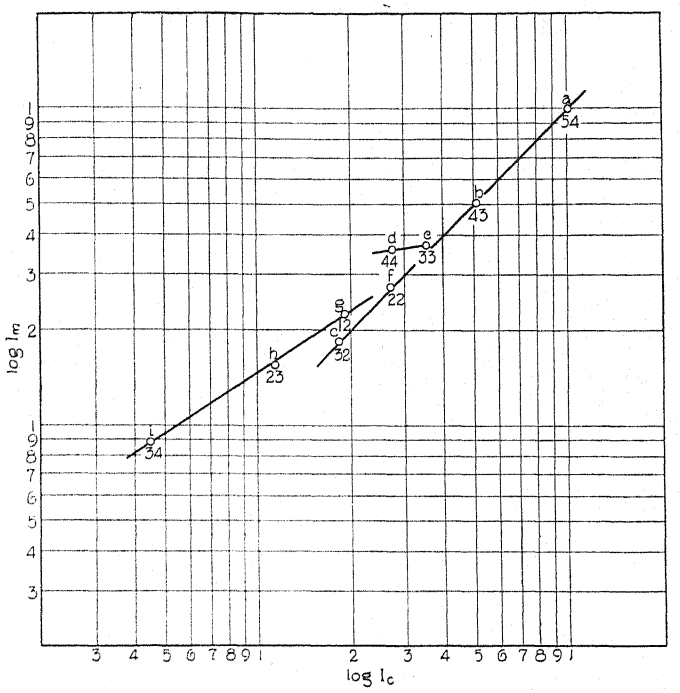

Fig. 8. Calculated and measured intensities for Multiplet 40 ($a^6D - x^6P_4$).

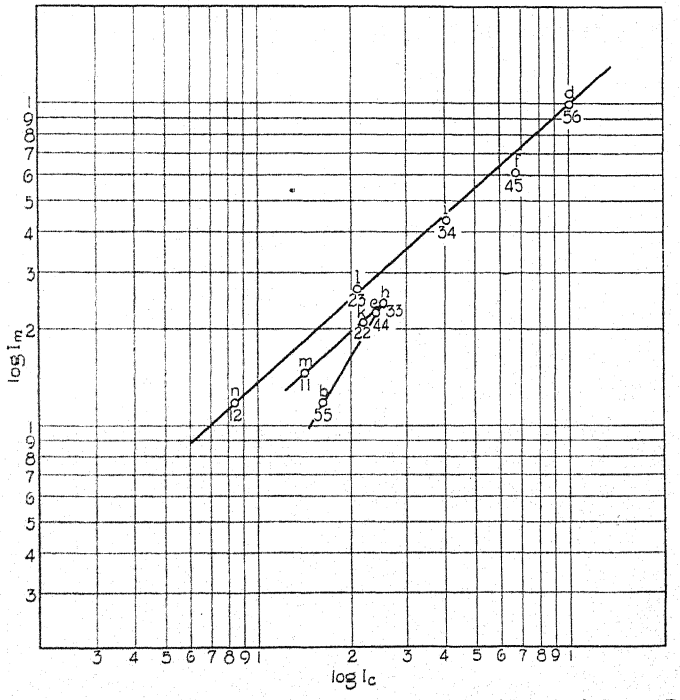

Fig. 9. Calculated and measured intensities for Multiplet 44 ($a^6D - y^6F^0$).

Multiplet 46 (z^8P-f^8S; λλ 3178–3148). Multiplet 46 gave very close agreement with the calculated values. It is the second member of a sharp series following a Rydberg formula, multiplet 26 being the first member.

Multiplet 47 (a^6D-w^6P; λλ 3082–3044). This has the same final state as has number 40. While the upper state has not been assigned to any electron configuration, it has normal intensities or nearly so (Fig. 10), and does not show anomalies analogous to those in number 40.

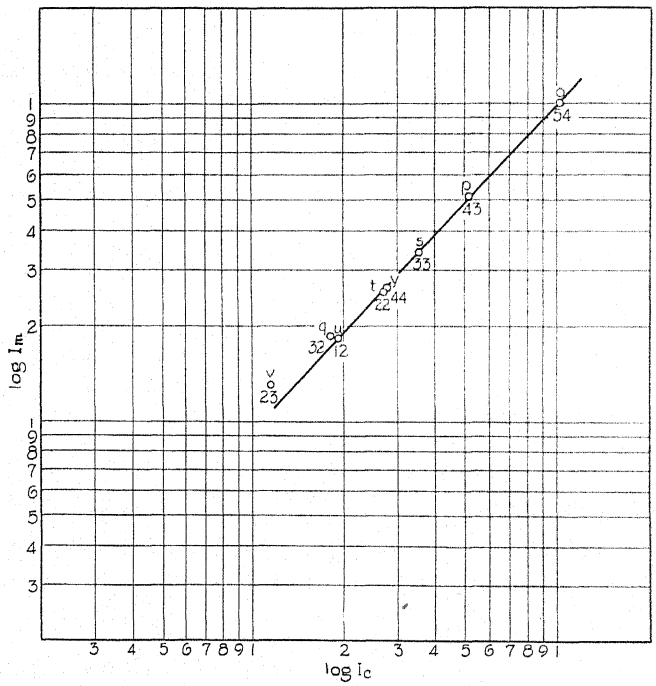

Fig. 10. Calculated and measured intensities for Multiplet 47 (a^6D-w^6P).

Multiplet 49 (z^8P-f^8D; λλ 2940–2914). Measurements indicated the normal intensity ratio between lines *b* and *a*. Line *c* was a little strong, probably due to a lap.

In summarizing the line intensities within multiplets, it may be stated that most of the anomalous lines, if not all of them, were in multiplets whose terms, one or both, were derived from the a^5D term of Mn II. The departure from normal intensities shown in graphs of Figs. 2 to 10 are of a regular nature in some cases at least. It is always possible to draw a straight line which passes through or near each point representing a main diagonal spectral line. Such lines can also be drawn through some of the satellite points, but the latter line is usually broken in the middle. One may proceed along this broken line in the shape of a *V* with the *J* values (subscripts) increasing or decreasing in regular sequence. Lines l_{11}, j_{22}, h_{33}, e_{44}, and b_{55} of multiplet 36 illustrate this regularity. It seems probable that this regular departure is caused by some perturbation factor which is usually negligible but which assumes significant values in the present case.

Relative intensities of the multiplets. Intensities for different multiplets, even when related, depend greatly on excitation conditions; so that measurements obtained under one set of conditions may not be compared directly with those obtained under another set. The figures for relative line and multiplet intensities given in column 7 of the Table of Results are based mainly on measurements made under fairly uniform conditions; namely, a current of 1.0 ampere and a pressure of 18 cm of mercury. Figures for each exposure were worked out separately and reduced to a common standard before finding the average figure which appears in column 7.

To obtain the intensities for infinite excitation as given in column 9, it was necessary to find the equivalent temperature. For this purpose the theoretical intensities of the members of the sp supermultiplet were employed.

The numbers 14, 10, 6, 15, 21, 9 are the intensities of multiplets 27, 28, 31, 32, 36, and 40 respectively as calculated by formula. The calculated intensities for the lines in each multiplet were first adjusted so that their sums were proportional to these numbers. The proper ν^4 correction was applied for each line, and the results placed in column 8 of the Table of Results.

If the multiplets may be brought to their calculated intensities by excitation correction, the equation $\log_{10}R = 0.625\Delta\sigma/T$ must have a common temperature solution. R is the factor required to bring the relative intensity of a line, or group of lines of common upper state, to the value for infinite excitation, and $\Delta\sigma$ is the difference in term values of the upper state in question and that of a line used as a standard.

In seeking the common solution of the above equation, the following procedure may be followed. The ratio I_m/I_c (measured intensity)/(calculated intensity) for each line group of common upper state is determined. The factor R_m by which each of these I_m/I_c values must be multiplied to make it equal to the value for the standard is next found. Finally the logarithms of these R_m values are plotted as ordinates and the corresponding $\Delta\sigma$ values as abscissas. In case these points all lie on a straight line, the intensities are normal, and the equivalent temperature may be found from the slope of this line; i.e., $T = 0.625\Delta\sigma/\log_{10}R$. In practice, a straight line which passes through as many such points as possible is drawn, the equivalent temperature and the corresponding excitation factors for different states being taken as determined by this line, the corrected measured intensities thus coming out greater or less than their calculated values according as their plotted points lie below or above the line.

In the present case, the first four multiplets had intensities which approximated their theoretical values quite closely, the equivalent temperature being between 5000 and 6000A. On the other hand, multiplets 36 and 40 had intensities which were much too small. These multiplets occur at wave-lengths about 3800A and 3600A respectively. It was thought that the apparent anomaly might be due to small J/I standardization values resulting from the action of scattered light. To test this point the values obtained when a filter was used which transmitted only ultraviolet light were tried for the members of the sextet triad, the quartet members being in a region not transmitted by

this filter. In this case the three multiplets showed fair alignment, although the calculated temperature tended to be a little less than in corresponding exposures for the quartet triad.

The measured intensities corrected for infinite excitation as recorded in column 9 of the Table of Results were obtained by first determining the relative intensities of the four multiplets of longest wave-length; then the relative intensities of the three short wave multiplets were determined from two exposures using the filter as just described. The two determinations were then tied together by multiplet 32 common to both sets. The intensities of other short wave multiplets in column 8 were also raised to correspond to these new determinations, the procedure being equivalent to a new standardization. From the preceding statements, it may be inferred that the determinations for the long wave-lengths are most reliable, and that it will be desirable to make further measurements in the ultraviolet in which more reliable standardizations for this region are available. This does not, however, affect the validity of line measurements in multiplets.

No total multiplet intensities for wave-lengths less than 3400A have been given, as intensity values for standardizing are not available at this time.

The approximate multiplet intensities as recorded in column 7 have also been written on Fig. 1, which may be used as a convenient means of studying the multiplet intensities as a whole. The values for the high upper states will be increased, of course, for higher equivalent temperatures or decreased for lower equivalent temperatures than that of the source here employed. It may be noticed that the sextet and quartet triads furnish a large part of the total radiation. Multiplet 41 in the octet system is very intense. Multiplet 34, furnishing the *raies ultimes*, while of very respectable intensity, is nevertheless surpassed by some of the others in total intensity. The comparatively small intensity of multiplet 21 as compared with that of number 40 with the same lower state and higher upper state is of interest. It may be recalled that number 21 has its lower state in the inverted system of terms and upper state in the normal system. Its comparative weakness may be connected with this fact. Multiplet 20, on the other hand, is much more intense than number 33 which has the same lower state. In this case, both the upper states, as well as the lower state, are of the normal type.

The present work has been made possible by the use of the equipment developed by Dr. George R. Harrison in the Stanford Spectroscopy Laboratory. To him and to the other workers in the same laboratory, who have furnished invaluable help and shown a fine spirit of cooperation, the writer wishes to acknowledge his sincere appreciation.

TABLE OF RESULTS. *Summary of intensity measurements.*

Explanation

Column 1—Number of multiplet; distinguishing letter for each line.
Column 2—Approximate wave-length of the line.
Column 3—The transition for the spectral line or the term common to a line sum. Landé quantum numbers are used for the Mn I multiplets or for those of even multiplicity. Sommerfeld quantum numbers are used for Mn II multiplets. The first kind of quantum number is changed into the second by the subtraction of a half unit.

Column 4—Calculated intensity in percent of the strongest line.
Column 5—Measured intensity in percent of the strongest line.
Column 6—Intensity in percent of the strongest line as measured by Frerichs.
Column 7—Measured intensities reduced to a common standard (equivalent temperature about 5500 A, current 1.0 ampere, pressure 18 cm of Hg.
Column 8—Calculated intensities for six related multiplets reduced to a common standard.
Column 9—Measured intensities corrected for infinite excitation.

1 No.	Mul.	2 Wave-length	3 Trans.	4 I_c in %	5 I_m in %	6 I_f in %	7 I_m St.	8 I_c ∞	9 I_m ∞
20	*c*	6021.8	$z^6P^0_{4}e^6S$	100.0	100.0±		65.0		
	b	16.6	$z^6P^0_{3}e^6S$	75.2	75.5±		49.0		
	a	13.5	$z^6P^0_{2}e^6S$	54.3	53.0±		34.4		
20			Total	229.5	228.5		148.4		
21	*h*	5537.7	$a^6D_1y^6P^0_{2}$	17.3	20.2		5.7		
	g	16.8	$a^6D_2y^6P^0_{2}$	25.0	25.0		7.0		
	f	08.9	$a^6D_2y^6P^0_{3}$	10.6	8.3		2.3		
	e	5481.4	$a^6D_3y^6P^0_{2}$	16.8	18.3		5.1		
	d	70.6	$a^6D_3y^6P^0_{3}$	33.0	34.4		9.6		
	c'	57.5	$a^6D_3y^6P^0_{4}$	4.36	—		—		
	c	20.4	$a^6D_4y^6P^0_{3}$	49.5	48.3		13.5		
	b	01.4	$a^6D_4y^6P^0_{4}$	27.2	24.5		6.9		
	a	5341.1	$a^6D_5y^6P^0_{4}$	100.00	100.0		28.0		
			a^6D_5	100.0	100.0				
			a^6D_4	75.6	72.8				
			a^6D_3	54.1	57.0				
			a^6D_2	35.6	33.3				
			a^6D_1	17.3	20.2				
			$y^6P^0_{4}$	132.0	129.0±				
			$y^6P^0_{3}$	92.0	91.0				
			$y^6P^0_{2}$	58.0	63.5				
21			Total	283.0	283.4		79.0		
23	*n*	5432.6	$a^6Sz^8P_{3}$		62.7		4.4		
	m	5394.7	$a^6Sz^8P_{4}$		100.0		7.0		
23			Total		162.7		11.4		
24	*z*	5413.7	$z^4P^0_{1}e^4S$	32.5	34.2		2.7		
	y	5399.5	$z^4P^0_{2}e^4S$	65.8	64.0		5.1		
	x	77.6	$z^4P^0_{3}e^4S$	100.0	100.0		8.0		
24			Total	198.3	198.2		15.8		
25	*q*	5004.9	$a^4D_2z^6F^0_{4}$		63.0		2.3		
	p	4965.9	$a^4D_4z^6F^0_{5}$		100.0		3.7		
25			Total		163.0		6.0		4.5
26	*z*	4823.5	$z^8P^0_{1}e^8S$	100.0	100.0		240.0		
	y	4783.4	$z^8P^0_{2}e^8S$	82.6	82.5		198.00		
	x	61.5	$z^8P^0_{3}e^8S$	63.2	58.3		140.00		
26			Total	245.8	239.6		578.0		
27	*i*	4766.4	$a^4D_3z^4F^0_{4}$	68.0	69.0		92.7	92.6	92.7
	h	4765.9	$a^4D_2z^4F^0_{3}$	44.5	42.7		57.4	60.7	57.4
	g	62.4	$a^4D_4z^4F^0_{5}$	100.0	100.0		134.2	136.3	134.2
	f	61.5	$a^4D_1z^4F^0_{2}$	27.8	27.9		37.5	38.0	37.5
	e	39.1	$a^4D_2z^4F^0_{2}$	11.4	9.3		12.6	15.6	12.6
	d	27.5	$a^4D_3z^4F^0_{3}$	15.3	17.3		23.2	20.8	23.2
	c	09.7	$a^4D_4z^4F^0_{4}$	12.1	16.3		21.9	16.5	21.9
	b	01.2	$a^4D_3z^4F^0_{2}$	.85	.7±		.94	1.15	.94
	a	4671.7	$a^4D_4z^4F^0_{3}$	.6	.6±		.81	.82	.81
			a^4D_4	113.	116.9			153.6	
			a^4D_3	84.	87.0			114.6	
			a^4D_2	56.	52.0			76.1	
			a^4D_1	27.8	27.9			38.	
			$z^4F^0_{5}$	100.0	100.0		134.2	136.3	134.2
			$z^4F^0_{4}$	80.0	85.3		114.6	109.1	114.6
			$z^4F^0_{3}$	60.3	60.6		81.4	82.3	81.4
			$z^4F^0_{2}$	39.7	40.05		51.0	54.7	51.0
27			Total	280.0	286.0		381.25	382.0	381.25

1 No.	Mul.	2 Wave-length	3 Trans.	4 I_c in %	5 I_m in %	6 I_f in %	7 I_m St.	8 I_c ∞	9 I_m ∞
28	*s*	4502.2	$a^4D_2z^4D^0_4$	15.6	27.0	24.5	21.6	19.2	32.4
	r	4498.9	$a^4D_2z^4D^0_3$	19.7	27.6	23.6	22.1	24.2	36.1
	q	90.1	$a^4D_1z^4D^0_2$	14.0	15.7	14.5	12.6	17.2	18.8
	p	72.8	$a^4D_1z^4D^0_1$	14.4	13.9	12.4	11.1	17.5	16.7
	o	70.1	$a^4D_2z^4D^0_2$	22.6	21.0	17.6	16.8	27.8	25.2
	n	64.7	$a^4D_2z^4D^0_3$	49.5	48.0	40.5	38.4	61.0	57.6
	m	53.0	$a^4D_2z^4D^0_1$	14.5	17.3	15.7	13.8	17.8	20.7
	l	51.6	$a^4D_4z^4D^0_4$	100.	100.0	100.	80.0	123.	120.0
	k	36.4	$a^4D_2z^4D^0_2$	20.8	27.2	25.4	21.8	25.6	32.6
	j	14.9	$a^4D_4z^4D^0_3$	16.9	32.4	26.6	25.9	20.8	39.8
			a^4D_4	116.9	132.4	126.6		143.8	
			a^4D_3	85.9	102.0	90.4		105.8	
			a^4D_2	56.8	65.9	56.9		69.8	
			a^4D_1	28.4	29.6	26.9		34.7	
			$z^4D^0_4$	115.6	127.0	124.5	101.6	142.2	152.4
			$z^4D^0_3$	86.1	108.0	90.7	86.4	106.	133.5
			$z^4D^0_2$	57.4	63.9	57.5	51.2	70.6	76.6
			$z^4D^0_1$	28.9	31.1	28.1	24.9	35.3	37.4
28			Total	288.0	330.0	300.8	264.1	354.1	400.0
29	*B*	4462.0	$z^6P^0_4e^6D_5$	100.0	100.0	100.0	57.0		
	∞	61.1	$z^6P^0_4e^6D_4$	28.6	29.1	26.9	16.6		
	z	60.4	$z^6P^0_4e^6D_3$	4.76	6.8±	4.64	3.9		
	y	58.3	$z^6P^0_3e^6D_4$	51.6	51.8	51.8	29.6		
	x	57.6	$z^6P^0_3e^6D_3$	36.6	37.9	37.2	21.1		
	w	57.0	$z^6P^0_3e^6D_2$	12.0	11.6	11.4	6.6		
	v	55.8	$z^6P^0_2e^6D_3$	18.6	18.4	17.3	10.5		
	u	58.3	$z^6P^0_2e^6D_2$	28.5	27.8	26.9	15.8		
	t	55.0	$z^6P^0_2e^6D_1$	20.1	22.7	18.9	12.9		
			$z^6P^0_4$	133.4	135.9	131.5			
			$z^6P^0_3$	100.2	100.4	100.4			
			$z^6P^0_2$	67.22	68.9	63.1			
			e^6D_5	100.0	100.0	100.0			
			e^6D_4	80.2	80.9	78.7			
			e^6D_3	60.0	62.4	59.1			
			e^6D_2	40.5	39.4	38.3			
			e^6D_1	20.1	22.7	18.9			
29			Total	300.8	305.2	295.0	174.0		400.0
31	*g*	4312.6	$a^4D_2y^4P^0_3$	2.32	5.4±	6.7	2.5	2.44	5.2
	f	4284.1	$a^4D_1y^4P^0_2$	3.94	6.9±	7.1	3.3	4.14	6.7
	e	81.1	$a^4D_3y^4P^0_3$	21.4	36.4	34.6	17.2	22.5	35.4
	d	65.9	$a^4D_2y^4P^0_2$	25.8	37.3	32.5	17.6	27.1	36.3
	c	57.7	$a^4D_1y^4P^0_1$	20.0	26.2	23.4	12.8	21.05	25.5
	b	39.7	$a^4D_2y^4P^0_1$	20.6	21.0	20.8	9.8	21.7	20.4
	a	35.3	$a^4D_4y^4P^0_3$	100.0	100.0	100.0	47.1	105.0	97.2
	a	35.1	$a^4D_3y^4P^0_2$	62.3	52.3	52.3	24.7	54.9	51.0
			a^4D_4	100.0	100.0	100.0		105.0	
			a^4D_3	73.7	88.7	87.1		77.4	
			a^4D_2	48.7	63.7	60.0		51.2	
			a^4D_1	23.9	33.1	30.5		25.2	
			$y^4P^0_3$	123.7	141.8	141.3	66.8	129.9	137.8
			$y^4P^0_2$	82.0	96.5	92.1	45.6	86.1	94.0
			$y^4P^0_1$	40.6	47.2	44.2	22.6	42.7	45.9
31			Total	246.3	285.5	277.6	139.8	258.8	277.7
32	*m*	4083.6	$a^6D_5z^6D^0_4$	30.2	19.2	23.0	87.0	65.1	42.8
	l	82.9	$a^6D_5z^6D^0_3$	28.5	19.0	21.7	86.0	61.0	42.3
	k	79.4	$a^6D_4z^6D^0_2$	18.2	15.5	15.0	70.0	39.0	34.5
	j	79.2	$a^6D_4z^6D^0_5$	21.6	15.0	15.0	68.0	46.1	33.4
	i	70.3	$a^6D_4z^6D^0_4$	5.3	4.3	4.3	19.5	11.4	9.6
	h	68.0	$a^6D_3z^6D^0_2$	.53	1.1±	.5	5.0	1.14	2.4
	g	63.5	$a^6D_3z^6D^0_3$	12.3	13.1	13.5	59.4	26.4	29.2
	f	58.9	$a^6D_3z^6D^0_1$	18.6	18.1	16.8	82.0	39.8	40.3
	e	55.6	$a^6D_4z^6D^0_4$	43.5	43.9	45.0	198.5	93.0	97.5
	d	48.8	$a^6D_4z^6D^0_3$	29.4	25.1	29.4	113.8	63.0	55.9
	c	41.4	$a^6D_5z^6D^0_5$	100.0	100.0	100.0	454.0	214.0	222.0
	b	35.7	$a^6D_4z^6D^0_3$	32.0	34.3	30.9	155.0	68.4	76.1
	a	18.1	$a^6D_5z^6D^0_4$	22.9	24.0	23.5	109.0	49.0	53.5
			a^6D_5	122.9	124.0	123.5		263.0	
			a^6D_4	97.1	93.2	90.9		207.5	
			a^6D_3	71.9	57.4	65.9		154.5	
			a^6D_2	47.6	38.2	39.		101.9	
			a^6D_1	23.5	19.8	19.3		50.4	
			$z^8D^0_5$	121.6	115.0	115.0	522.0	260.1	255.4

1 No.	Mul.	2 Wave-length	3 Trans.	4 I_c in %	5 I_m in %	6 I_f in %	7 I_m St.	8 I_c ∞	9 I_m ∞
			$z^6D^0_4$	96.6	87.1	91.5	394.5	207.1	193.8
			$z^6D^0_3$	72.8	66.4	66.1	300.4	155.8	147.6
			$z^6D^0_2$	48.1	41.7	44.9	188.8	103.1	92.8
			$z^6D^0_1$	23.9	22.4	21.1	101.5	51.2	49.9
32			Total	363.0	332.6	338.5	1507.0	777.3	739.5
33	*r*	4061.7	$z^6P^0_4 f^6S$	100.0	100.0±		1.2		
	q	4059.4	$z^6P^0_3 f^6S$	75.0	74.2±		.9		
	p	4057.96	$z^6P^0_2 f^6S$	50.0	50.6±		.6		
33			Total	225.0	224.8		2.7		
34	*z*	4034.5	$a^6Sz^6P^0_2$	50.0	60.0 *		206.0		
	y	33.1	$a^6Sz^6P^0_3$	75.0	87.5		309.0		
	x	30.8	$a^6Sz^6P^0_4$	100.0	100.0		412.0		
34			Total	225.	247.5		927.0		
36	*n*	3844.0	$a^6D_1z^6F^0_2$	8.27	10.1		55.0	33.1	41.0
	m	41.1	$a^6D_2z^6F^0_3$	21.2	24.1		131.0	85.0	98.0
	l	39.8	$a^6D_1z^6F^0_1$	14.2	10.9		59.2	57.0	44.4
	k	34.4	$a^6D_3z^6F^0_4$	40.2	45.2		245.0	161.0	184.0
	j	33.9	$a^6D_2z^6F^0_2$	22.1	15.4		83.6	88.6	62.7
	i	29.7	$a^6D_2z^6F^0_1$	1.81	4. ±		21.7	7.2	16.3
	h	23.9	$a^6D_3z^6F^0_3$	26.0	18.3		99.0	104.0	74.5
	g	23.5	$a^6D_3z^6F^0_5$	66.0	71.1		386.0	264.0	289.0
	f	16.7	$a^6D_3z^6F^0_2$	1.97	3. ±		16.0	7.91	12.2
	e	09.6	$a^6D_4z^6F^0_4$	24.6	14.8		80.5	98.5	60.2
	d	06.9	$a^6D_5z^6F^0_6$	100.0	100.0		543.0	400.0	407.0
	c	3799.3	$a^6D_4z^6F^0_3$	1.36	(2)		11.0	5.45	8.1
	b	90.2	$a^6D_3z^6F^0_5$	16.4	6.5		35.2	65.5	26.4
	a	76.5	$a^6D_3z^6F^0_4$	.6	(1)		5.4	2.4	4.1
			a^6D_5	117.0	107.5			417.0	
			a^6D_4	92.0	87.9			368.0	
			a^6D_3	68.2	66.5			272.9	
			a^6D_2	45.1	45.1			180.8	
			a^6D_1	22.5	21.0			90.1	
			$z^6F^0_6$	100.0	100.0		543.0	400.0	407.0
			$z^6F^0_5$	82.4	77.6		421.2	329.5	315.4
			$z^6F^0_4$	65.4	61.0		330.9	261.9	248.3
			$z^6F^0_3$	48.6	44.4		241.0	194.5	180.6
			$z^6F^0_2$	32.4	28.5		154.6	129.6	115.9
			$z^6F^0_1$	16.0	14.9		80.9	64.2	60.7
36			Total	344.8	326.4		1770.0	1379.7	1328.0
38		3800.6	$z^4P^0_3 c^4D_4$	100.0	100.0				
		3787.5	$z^4P^0_2 c^4D_3$	53.6	40.0±				
		74.7	$z^4P^0_1 c^4D_2$	23.2	15.0±				
38			Total	176.8	155.0				
40	*i*	3629.1	$a^6D_3x^6P^0_4$	4.5	8.9	13.3	19.7	11.5	23.8
	h	23.8	$a^6D_2x^6P^0_3$	11.4	15.5	23.6	34.4	29.1	41.4
	g	19.4	$a^6D_1x^6P^0_2$	19.2	22.3	32.8	49.5	49.0	58.5
	f	10.3	$a^6D_2x^6P^0_2$	27.4	27.3	40.0	60.5	70.0	72.8
	e	08.5	$a^6D_3x^6P^0_3$	35.3	37.0	50.3	82.0	90.3	98.8
	d	07.5	$a^6D_4x^6P^0_4$	27.6	35.9	48.7	79.7	70.7	95.8
	c	3595.1	$a^6D_1x^6P^0_2$	18.4	18.5	22.5	41.0	46.6	49.4
	b	86.5	$a^6D_4x^6P^0_3$	51.1	50.4	58.4	112.0	131.0	134.5
	a	77.9	$a^6D_5x^6P^0_4$	100.0	100.0	100.0	222.0	256.0	267.0
			a^6D_5	100.0	100.0	100.0		256.0	
			a^6D_4	78.7	86.3	107.1		201.7	
			a^6D_3	58.2	64.4	86.1		148.4	
			a^6D_2	38.8	42.8	63.6		99.1	
			a^6D_1	19.2	22.3	32.8		49.0	
			$x^6P^0_4$	132.1	144.8	162.0	321.4	338.2	385.6
			$x^6P^0_3$	97.8	102.9	132.3	228.4	250.4	274.7
			$x^6P^0_2$	65.0	68.1	95.3	151.0	165.6	181.7
40			Total	294.9	315.8	389.6	700.0	754.2	819.2

* Self-reversal not completely eliminated.

1 No.	Mul.	2 Wave-length	3 Trans.	4 I_c in %	5 I_m in %	6 I_f in %	7 I_m St.	8 $I_c\,\infty$	9 $_mI\,\infty$
41		3570.1	$z^5P^0_5 e^5D_4$	6.5					
		69.8	$z^5P^0_5 e^5D_4$	32.5					
		69.5	$z^5P^0_5 e^5D^4$	100.					
		48.2	$z^5P^0_4 e^5D_3$	18.5					
		48.0	$z^5P^0_4 e^5D_4$	43.2					
		47.8	$z^5P^0_3 e^5D_3$	52.2					
		32.1	$z^5P^0_3 e^5D_2$	34.8					
		32.0	$z^5P^0_3 e^5D_3$	33.4					
		31.8	$z^5P^0_3 e^5D_4$	19.0					
	w		$z^5P^0_5$	139.0					
	v		$z^5P^0_4$	113.0					
	u		$z^5P^0_3$	86.5			430.		
41			Total	338.5			1680.		
42	h	3497.5	$a^5D_1 z^5P^0_3$	7.8	7.7		16.2		
	g	96.8	$a^5D_2 z^5P^0_3$	3.5	3.9		8.2		
	f	95.8	$a^5D_0 z^5P^0_1$	10.4	10.3		22.0		
	e	86.6	$a^5D_1 z^5P^0_1$	23.6	23.6		49.5		
	d	82.9	$a^5D_2 z^5P^0_2$	31.0	30.5		64.0		
	c	74.1	$a^5D_2 z^5P^0_1$	18.7	19.0		40.0		
	c	74.0	$a^5D_3 z^5P^0_2$	25.0	25.4		53.4		
	b	60.3	$a^5D_3 z^5P^0_3$	50.0	50.1		105.2		
	a	42.0	$a^5D_4 z^5P^0_3$	100.0	100.0		210.0		
			a^5D_4	100.0	100.0				
			a^5D_3	75.0	75.4				
			a^5D_2	53.2	53.4				
			a^5D_1	31.4	31.3				
			a^5D_0	10.4	10.4				
			$z^5P^0_3$	128.5	129.3				
			$z^5P^0_2$	88.8	88.3				
			$z^5P^0_1$	52.7	53.0				
42			Total	270.0	270.6		568.5		
44	n	3260.2	$a^6D_1 y^6F^0_2$	8.3	11.8				
	m	58.4	$a^6D_2 y^6F^0_1$	14.2	14.7				
	l	56.1	$a^6D_2 y^6F^0_2$	21.1	26.6				
	k	52.9	$a^6D_2 y^6F^0_3$	22.0	21.0				
	j	51.1	$a^6D_2 y^6F^0_1$	.18	4.5±				
	i	48.5	$a^6D_1 y^6F^0_4$	40.3	43.8				
	h	43.8	$a^6D_2 y^6F^0_3$	25.8	24.1				
	g	40.6	$a^6D_2 y^6F^0_2$	.2	7. ±				
	f	36.8	$a^6D_4 y^6F^0_5$	66.5	61.7				
	e	30.7	$a^6D_4 y^6F^0_4$	24.1	22.6				
	d	28.1	$a^6D_3 y^6F^0_3$	100.0	100.0				
	c	26.0	$a^6D_4 y^6F^0_3$	.14	3. ±				
	b	12.9	$a^6D_3 y^6F^0_2$	16.4	11.9				
	a	06.9	$a^6D_3 y^6F^0_4$	.06	—				
			a^6D_5	117.0	112.0				
			a^6D_4	90.7	87.3				
			a^6D_3	66.9	74.9				
			a^6D_2	43.3	52.1				
			a^6D_1	22.5	26.5				
			$y^6F^0_5$	100.0	100.0				
			$y^6F^0_4$	82.9	73.6				
			$y^6F^0_3$	64.5	66.4				
			$y^6F^0_2$	47.0	53.7				
			$y^6F^0_1$	30.5	39.8				
			$y^6F^0_1$	14.4	19.2				
44			Total	339.3	352.7				
45	g'	3224.8	$a^6Sz^4P^0_3$		100.0				
	x	17.0	$a^6Sz^4P^0_2$		45.0				
45			Total		145.0				
46	m'	3178.5	$z^3P^0_2 f^3S$	100.0	100.0				
	m'	61.1	$z^3P^0_1 f^3S$	82.0	82.1				
	l'	48.2	$z^3P^0_3 f^3S$	62.2	62.6				
46			Total	244.2	244.7				

1 No.	Mul.	2 Wave-length	3 Trans.	4 I_c in %	5 I_m in %	6 I_f in %	7 I_m St.	8 $I_c \infty$	9 $I_m \infty$
47	*w*	3082.1	$a^6D_3z^6P^0_4$	4.55	lapped				
	v	81.3	$a^6D_2z^6P^0_4$	11.4	13.1				
	u	79.6	$a^6D_1z^6P^0_2$	19.2	18.3				
	t	73.1	$a^6D_2z^6P^0_2$	27.2	25.8				
	s	70.3	$a^6D_3z^6P^0_2$	35.2	34.4				
	r	66.0	$a^6D_4z^6P^0_4$	27.8	26.1				
	q	62.1	$a^6D_2z^6P^0_2$	18.2	18.7				
	p	54.4	$a^6D_4z^6P^0_3$	51.0	51.3				
	o	44.6	$a^6D_3z^6P^0_4$	100.0	100.0				
			a^6D_5	100.0	100.0				
			a^6D_4	78.8	77.4				
			a^6D_3	58.0	57.6				
			a^6D_2	38.6	38.9				
			a^6D_1	19.2	18.3				
			$z^6P^0_4$	132.4	130.6				
			$z^6P^0_3$	97.6	98.8				
			$z^6P^0_2$	64.6	62.8				
47			Total	294.6	292.2				
48	*z*	2949.2	$a^5S_2z^5P^0_3$	100.0	100.0				
	y	39.3	$a^5S_2z^5P^0_2$	73.0	72.2				
	x	33.1	$a^5S_2z^5P^0_1$	44.0	43.0				
48			Total	217.0	215.2				
49	*G*	2940.5	$z^5P^0_3f^5D$	100.0	100.0± (lap)				
	B	25.6	$z^5P^0_4f^5D$	81.3	81.3				
	A	14.6	$z^5P^0_3f^5D$	62.0	63.8				
49			Total	243.3	245.1				
52	*c*	2801.1	$a^5Sy^5P^0_2$	50.0	*100.±				
	b	2798.3	$a^5Sy^5P^0_3$	75.0	90.±				
	a	94.8	$a^5Sy^5P^0_4$	100.0	80.±				
52			Total	225.0					
61		2605.7	$a^7S_3z^7P^0_2$	47.5	*100.±				
		2593.7	$a^7S_3z^7P^0_3$	68.5	100.±				
		76.1	$a^7S_3z^7P^0_4$	100.0	100.±				
61			Total	216.0					

* Self-reversal; J/I uncertain.

RAMAN SPECTRA OF SOME ORGANIC HALIDES

By Claud Edwin Cleeton with R. T. Dufford
The University of Missouri, Columbia, Missouri

(Received December 29, 1930)

Abstract

Raman spectra obtained by helium excitation from nineteen organic compounds, $CHCl_3$, CH_3Br, CH_3MgBr, CH_3I, CH_3MgI, C_2H_5Cl, C_2H_5Br, C_2H_5I, $ClCH_2CH_2Cl$, $BrCH_2CH_2Br$, CH_3CHCl_2, CH_3CHBr_2, $C_2H_4Cl_4$, $C_2H_2Br_4$, C_6H_6, C_5H_5N, $C_6H_5CH_2Cl$, C_6H_5Cl, C_6H_5Br, five of which have not been reported on before, are described and discussed. It is shown that in many cases the observed frequencies can be expressed in terms of four assumed fundamentals (five in the cyclic compounds), two of which are not observed, and which may prove to be illusory. The bearing of such theory as is available is discussed.

THE Raman* spectra of a number of simple organic compounds containing carbon, hydrogen, and halogen (chlorine, bromine, or iodine) atoms are described and discussed in this paper. The work was begun as part of a systematic study of a number of physical properties of the class of compounds known as Grignard reagents, which are formed in anhydrous ether solution when the halogen compounds just mentioned react with magnesium to form compounds of the type R-Mg-X. Raman spectra from two such compounds are described below. At the time the work was started, only a few of the organic halides had been reported on; but since then, various workers have reported the Raman spectra of a great many of them, as will be noted below, and some steps have been made toward theoretical interpretation of the spectra.

Experimental Arrangements

In almost every case, the results reported by others have been obtained using light from a mercury arc, usually unfiltered, following an early scheme suggested by Wood.[1] The advantage of intense exciting light, which this method possesses, is compensated to a large extent by the serious overlapping of the Raman patterns from the numerous exciting lines, which leads to difficulty and error in identifying the exciting line responsible for certain displaced lines. Matters can be improved somewhat by using appropriate filters, as Wood has shown. The results in the present paper are free from such uncertainty, since they were obtained by helium excitation, using a helium spiral surrounding the "resonance" tube, and a tube of Corning red ultra

* No attempt is made to give here a complete bibliography of all the hundreds of papers that have appeared on the subject since the discovery of the effect was announced by C. V. Raman, Indian Jour. of Physics **2**, 387 (1928). Such bibliographies are available elsewhere; e.g., S. Bhagavantam, Ind. Jour. Phys. **5**, 237 (1930), A. S. Ganesan, Ind. Jour. Phys. **4**, 281 (1929), and the Symposium on Molecular Spectra, Trans. Faraday Soc. **25**, 611–949 (1929).

[1] R. W. Wood, Phil. Mag. (7) **6**, 729 (1928).

glass as a filter. This method is also due to Wood.[2] While the method has not the advantage of the high intensity obtainable from the newer helium arc,[3,4] it does have, in common with this apparatus, the great advantage that there is only one exciting line, λ3889, and almost no helium lines coming through the filter to confuse the Raman pattern. Further, this exciting line has a shorter wave-length than many of the mercury lines used. As shown by Ornstein and Rekveld,[5] the intensity of the Raman lines increases at least approximately with the fourth power of the exciting frequency. Besides the consequent gain in strength of the Raman lines, there is the added advantage that the displaced lines occur at wave-lengths near the sensitivity maximum of the photographic plates.

The first exposures were made using a "resonance" tube about an inch in diameter and twelve inches long. It was soon found that better results were obtained with a smaller tube, about 1 cm in diameter and 10 cm long, with a smaller filter and helium spiral; less power was required, too, and smaller quantities of the substances to be investigated. The spectra were photographed with a specially reconstructed single prism glass spectrograph of considerable speed, which has been described elsewhere.[6] For measurement, images of the spectra were projected, using a magnification of about forty diameters, on a screen on which a scale of wave-numbers had been worked out, using a large number of reference lines. With this scale, wave-number differences could be read off with an accuracy of about 5 cm^{-1} in the case of the sharpest lines. Many of the Raman lines are too broad, however, to permit reading as accurately as this.

Discussion of Results

In discussing Raman spectra, the quantity of primary interest is the amount by which a given line differs in frequency (or more usually, in wave-number) from the exciting line. Since the arrangements used permitted this quantity to be read directly, it is recorded in the tables that follow. In the tables, compounds of similar structures are grouped, for convenience in comparing their spectra. Intensities are indicated by numbers in parentheses following the observed wave-number shifts.

While measurements could be checked to about 5 cm^{-1}, it by no means follows that the results obtained by different observers will check as closely as this. In some cases the agreement is better, but in a considerable number, the disagreement is several times as large. There is very great need now for more accurate results than have been given in most of the investigations so far published. A single table is included to show the extent to which agreement is found in typical cases. In many cases the agreement is worse, owing to difficulty in identifying lines. Beyond this, it has seemed unnecessary to

[2] R. W. Wood, Phil. Mag. (7) **7**, 744 (1929).
[3] Reynolds and Benford, Rev. of Sci. Insts. **1**, 413 (1930).
[4] R. W. Wood, Phys. Rev. **36**, 1421 (1930).
[5] Ornstein and Rekveld, Zeits. f. Physik **61**, 593 (1930).
[6] R. T. Dufford, J. Opt. Soc. Am. **9**, 405 (1924).

TABLE I. *(a) Raman spectrum of chloroform, $CHCl_3$.*

Cleeton and Dufford	Dadieu and Kohlrausch 8, V	Ganesan and Venkateswaran 13	Pringsheim and Rosen 10	Bhagavantam and Venkateswaran 14
269 (3)	259 (6)	261 (5)	257 (4)	261 (4)
376 (3)	364 (5)	367 (6)	368 (4)	367 (5)
671 (3)	664 (5)	669 (6)	666 (4)	669 (4)
775 (3)	756 (4)	762 (3)	766 (3)	762 (3)
	1214 (2)	1218 (2)	1214 (2)	1218 (2)
		1441 (1)		1441 (1)
3015 (5)	3016 (3)	3019 (4)	3009 (2)	3019 (3)

(b) Raman spectrum of benzene, C_6H_6.

Daure 7	Cleeton and Dufford	Dadieu and Kohlrausch 8, I	Dadieu and Kohlrausch 8, II	Fujioka 9	Pringsheim and Rosen 10	Wood 12	Dadieu and Kohlrausch 8, IV	Soderqvist 11
610	621 (1)	605 (4)	607 (4)	607	615 (3)	606	602 (3)	604.6 (2)
842		848 (2)	846 (2)	849	867 (2)	849	844 (1)	849.1 (0)
991	1003 (20)	995 (10)	993 (10)	993	995 (4)	992	991 (10)	991.3 (5)
1178	1203 (3)	1183 (3)	1180 (3)	1182	1183 (3)	1178	1178 (3)	1179.0 (1)
			1363 (1/2)				1362 (1/2)	
		1481 (3)			1479 (2)			
1584	1619 (5)	1596 (3)	1588 (3)	1585	1591 (2)	1584	1586 (3)	1583.6 (1)
				1612	1605 (2)	1603	1603 (1)	1604.1 (1)
						2460		
						2542		
						2597		
						2617		
						2784		
						2928		
		2944 (5)	2947 (3)			2947	2945 (4)	2946.8 (2)
				3050		3046		3046.9 (1)
3060	3078 (50)	3058 (8)	3057 (5)	3060	3059 (3)	3060	3056 (8)	3061.3 (4)
						3164		3162.9 (1)
						3183		3184.8 (2)

republish all the results of other investigators; but references are given to all such work as is known to the writers.

In studying the Raman spectra of organic halides, one of the writers (C. E.C.), who made the wave-number measurements, discovered the existence of certain apparent regularities, the more important of which are indicated in the tables that follow. It would appear from these that it is possible to express the frequencies found in the Raman spectra of each of the aliphatic halides as combinations or overtones of four fundamental frequencies, of which usually two must be assumed to exist without being observed in the spectra themselves. In the tables, beginning with Table II, there is given for each substance the observed frequency differences in one column, and the

[7] P. Daure, An. d. Physique **12**, 375 (1929); C. R. **186**, 1833 (1928); **188**, 1492 (1929).

[8] Dadieu and Kohlrausch, Phys. Zeits. **30**, 384 (1929); Ber. **63** B, 251 (1930); Naturwiss. **17**, 366, 625 (1929);

[i] Monatsh. f. Chemie **52**, 220 (1929); Sitzb. Akad. Wiss. Wien (IIa) **138**, 41 (1929).

[ii] Monatsh. f. Chemie **52**, 379 (1929); Sitzb. Akad. Wiss. Wien (IIa) **138**, 335 (1929).

[iii] Monatsh. f. Chemie **52**, 396 (1929); Sitzb. Akad. Wiss. Wien (IIa) **138**, 419 (1929).

[iv] Monatsh. f. Chemie **53–54**, 282 (1929); Sitzb. Akad. Wiss. Wien (IIa) **138**, 607 (1929).

[v] Monatsh. f. Chemie **55**, 58 (1930); Sitzb. Akad. Wiss. Wien (IIa) **138**, 651 (1929).

[vi] Monatsh. f. Chemie **55**, 201 (1930); Sitzb. Akad. Wiss. Wien (IIa) **138**, 799, (1930).

[vii] Monatsh. f. Chemie **55**, 379 (1930).

[9] Fujioka, Sci. Papers Inst. Phys. and Chem. Res. Japan **II**, 205 (1929).

[10] Pringsheim and Rosen, Zeits. f. Physik **50**, 741 (1928).

[11] J. Soderqvist, Zeits. f. Physik **59**, 446 (1929–30).

[12] R. W. Wood, Phys. Rev. **36**, 1431 (1930).

[13] Ganesan and Venkateswaran, Ind. Jour. Phys. **4**, 195 (1929).

[14] Bhagavantam and Venkateswaran, Proc. Roy. Soc. **A127**, 360 (1930).

TABLE II. *Raman spectra of methyl halides.*

Methyl bromide CH_3Br	Methyl iodide CH_3I	Methyl magnesium bromide CH_3MgBr	Methyl magnesium iodide CH_3MgI	Assumed combinations
603 (10)	534 (10)	1131 (1)	1076 (1)	V_3
	1254 (3)			
	2589 (1)			V_4-4V_1
	2771 (1)			V_4-2V_1
			±2875 (10)	V_4-V_1
	2946 (6)		±2928 (10)	V_4
	3036 (1)		±2983 (10)	V_4+V_1
			± Due to ether	
(8VII)	(8VII)	—	—	References to other work.

computed differences on the assumed scheme in the next column; the last column of each table indicates the nature of the assumed combination or overtone. The fundamentals assumed behave so similarly in different compounds, that it is possible to number corresponding fundamental frequencies in different compounds with the same symbol; the symbols used are V_1, V_2, V_3, V_4. The way in which these fundamentals vary from group to group of compounds is regular and interesting. A fifth fundamental appears in the aromatic compounds.

The Raman spectrum of diethyl ether was studied, since Grignard compounds are prepared in ether solution; and for comparison with it, the Raman spectrum of ethyl alcohol was obtained. The wave-number shifts observed for ether are: 443 (1), 844 (2), 1159 (2), 1286 (2), 1466 (10), 2683 (2), 2793 (2), 2806 (5), 2873 (40), 2928 (30), 2983 (30) cm^{-1}. Nearly all these lines, except that at 2806, are broad. Other workers[7,8V,8VII,13]) list a few faint lines which we did not observe; but our list contains three lines not previously observed. Part of the difference may be due to wrong assignment of lines in the mercury arc spectra, and part may be due to the fact that our plates, while often underexposed, show the most-shifted Raman lines with greater relative intensity than reported by other workers. For alcohol, the observed shifts are: 1059 (3), 1108 (3), 1294 (3), 1461 (5), 2683 (1), 2880 (20), 2923 (20), 2976 (20). This list includes one new line, and fails to show one or two lines which are probably real, reported by other workers[7,8V,8VII,13,16]. The only regularity of structure to point out, is that in each case the last three lines can be represented by the formula $V_4 \pm V_1$, with $V_4=2928$, and $V_1=55$ cm^{-1} for ether and 47 cm^{-1} for alcohol. This regularity, while similar to that found in many other compounds, may prove to be illusory, as will be pointed out below.

In Table II are given the results from methyl bromide and methyl iodide, and from the Grignard reagents made from them. The plates were all underexposed, except for methyl iodide. Dadieu and Kohlrausch[8VII] have recorded

[16] Venkateswaran and Karl, Zeits. f. phys. Chem. **B1**, 466 (1928).

data on the first two of these compounds, including lines at 2956 and 3050 cm^{-1} for methyl bromide. No other work on the latter two compounds appears to have been published. The interesting result is the disappearance of the frequency marked V_3 in the table, and the appearance of a higher frequency, when the C-Br or C-I linkage changes to C-Mg-Br or C-Mg-I. This seems to indicate that the V_3 frequency is associated with the carbon-halogen bond. The group of frequencies around 3000 cm^{-1} is generally assumed to be associated with the C—H bond, since such lines always occur in both Raman and infrared spectra of compounds which possess this bond. In assigning the structure to these lines in the methyl iodide spectrum, a fundamental frequency at 88 cm^{-1} was assumed.

In the case of the mono-halogen derivatives of ethane, Table III, it is found possible to make every observed line on our plates fit into a scheme

TABLE III. *Raman spectra of ethyl halides.*

Ethyl chloride C_2H_5Cl		Ethyl bromide C_2H_5Br		Ethyl iodide C_2H_5I		Assumed combinations
Obs.	Comp.	Obs.	Comp.	Obs.	Comp.	
	41		48		53	V_1
	84		77		65	V_2
251 (1)	252					$3V_2$
341 (1)	336	308 (2)	308	261 (3)	260	$4V_2$
668 (10)	668	566 (15)	561		527	V_3
		968 (1)	978			$2V_3-2V_2$
1076 (1)	1084					$2V_3-3V_2$
1286 (1)	1295	1079 (1)	1084			$2V_3-V_1$
		1254 (5)	1255	1213 (6)	1213	$2V_3+3V_1$
		1456 (5)	1458			$3V_3-5V_1$
2716 (1)	2716					V_4-5V_1
2756 (1)	2757	2736 (1)	2731			V_4-4V_1
2866 (10)	2880	2875 (10)	2875			V_4-V_1
2921 (30)	2921	2923 (30)	2923	2915 (30)	2915	V_4
2961 (15)	2962	2976 (15)	2971	2968 (10)	2968	V_4+V_1
8V, 11		8V, 14, 11		8VII		References to other work

based on four fundamentals, the lower two being assumed but not observed. The plate for ethyl iodide was underexposed; this substance liberates iodine on exposure to light, and in spite of redistillation of the sample several times during the exposure, the absorption due to the iodine made the exposure time insufficient. This table is perhaps the most satisfactory of all those given.

The corresponding Grignard compounds gave no lines which could not have been attributed to the ether used as solvent. Moreover, most of these compounds are somewhat fluorescent; this difficulty prevented obtaining any other Raman spectra from Grignard reagents.

The results for dihalogen derivatives of ethane are given in the next two tables; Table IV deals with symmetrical derivatives, Table V with unsymmetrical derivatives. No other results appear to have been published on the latter group of compounds. The four-fundamental scheme works out similarly to the preceding cases, but less satisfactorily.

TABLE IV. *Raman spectra of symmetrical ethyl dihalides.*

Ethylene chloride $ClCH_2CH_2Cl$ Obs.	Comp.	Ethylene bromide $BrCH_2CH_2Br$ Obs.	Comp.	Assumed combination
	44		52	V_1
	105		100	V_2
129 (1)	132			$3V_1$
		201 (5)	200	$2V_2$
				$3V_2$
311 (2)	315			$4V_2$
420 (1)	420			V_3-V_2
658 (6)	654	558 (1)	563	V_3
759 (10)	759	663 (30)	663	(?)
1049 (1)				V_3+4V_2
		1061 (4)	1063	(?)
1211 (1)				$2V_3-V_1$
		1264 (10)	1274	(?)
1326 (2)				(?)
1451 (3)				V_4-3V_1
2816 (1)	2829			V_4-2V_1
2866 (2)	2873	2874 (3)	2866	V_4
2961 (30)	2961	2966 (30)	2970	V_4+V_1
3014 (3)	3005	3020 (8)	3022	
8V, 14		8V, 14		References to other work

The results for tetrahalogen derivatives of ethane are given in Table VI. The spectra contain many lines, several of which do not fit well into the scheme of combinations assumed. The scheme seems forced and unconvincing, but it serves to point out interesting similarities with the Raman spectra of other compounds.

TABLE V. *Raman spectra of unsymmetrical ethyl dihalides.*

Ethylidene chloride CH_3CHCl_2 Obs.	Comp.	Ethylidene bromide CH_3CHBr_2 Obs.	Comp.	Assumed combination
	60		55	V_1
	133	176 (1)	176	V_2
266 (2)	266	344 (1)	352	$2V_2$
401 (1)	399	551 (2)	528	$3V_2$
641 (10)	641	608 (2)	608	V_3
691 (1)	701			V_3+V_1
2946 (20)	2946	2921 (15)	2921	V_4
3006 (15)	3006	2976 (10)	2976	V_4+V_1

It is interesting to collect the values of the fundamentals used in the spectra of the various compounds described, as is done in Table VII. It will be seen that V_1 increases in frequency with increasing molecular weight (or increasing atomic weight of the halogen substituent) in all except the unsymmetrical compounds. The V_2 fundamental decreases with increase of molecular weight except in the unsymmetrical compounds, while V_3 decreases consistently in all the compounds. The V_4 fundamental is less variable, but it is thought that its variation can be explained better by an alternative method.

In addition to the foregoing data, results are here given for several compounds of cyclic structure. The plates for the first three do not show so many

TABLE VI. *Raman spectra of symmetrical ethyl tetrahalides.*

S-Tetrachloroethane $Cl_2HC \cdot CHCl_2$ Obs.	Comp.	S-Tetrabromoethane $Br_2HC \cdot CHBr_2$ Obs.	Comp.	Assumed combination
	50		73	V_1
	139		99	V_2
		121 (3)	120	$3V_1 - V_2$
101 (2)	100	156 (3)	146	$2V_1$
189 (2)	189	*186	172	$V_1 + V_2$
		*219 (10)	219	$3V_1$
248 (2)	250			$5V_1$
299 (2)	300			$6V_1$
359 (10)				(?)
558 (1)	550			$11V_1$
656 (8)	666			$V_3 - 3V_1$
		541 (3)		(?)
		628 (1)	617	$V_3 - V_2$
		666 (2)		(?)
816 (5)	816	716 (30)	716	V_3
		779 (2)		(?)
999 (4)	1005			$V_1 + V_2 + V_3$
1244 (3)	1233	1014 (5)	1013	$V_3 + 3V_2$
		1153 (5)	1140	$2V_3 - 4V_1$
		1206 (5)	1213	$2V_3 - 3V_1$
		2776 (2)	2777	$V_4 - 2V_1$
2931 (20)	2931	2923 (40)	2923	V_4
2996 (20)	2981	2996 (20)	2996	$V_4 + V_1$
8V, 10		8V		References to other work

*These frequencies apper as "antistokes" lines also.

lines as have been reported by other observers; they are probably underexposed. The results on these are simply listed here without any attempt to point out possible structure, beyond noting that the frequency at about 1000 cm^{-1} is apparently a new fundamental, V_5, and that the V_4 fundamental at

TABLE VII. *Collected values of fundamentals.*

	V_1	V_2	V_3	V_4	V_5
Diethyl ether $(C_2H_5)_2O$	55			2928	
Ethyl alcohol C_2H_5OH	47			2928	
Methyl bromide, CH_3Br			603		
Methyl iodide, CH_3I			534	2946	
Ethyl chloride, C_2H_5Cl	41	84	668	2921	
Ethyl bromide, C_2H_5Br	48	77	561	2923	
Ethyl iodide, C_2H_5I	53	65	527	2915	
Ethylene chloride, $ClCH_2CH_2Cl$	44	105	759	2961	
Ethylene bromide, $BrCH_2CH_2Br$	52	100	663	2966	
Ethylidene chloride, CH_3CHCl_2	60	133	641	2946	
Ethylidene bromide, CH_3CHBr_2	55	176	608	2921	
S-Tetrachloroethane, $Cl_2CHCHCl_2$	50	139	816	2931	
S-Tetrabromoethane, $Br_2CHCHBr_2$	73	99	716	2923	
Chlorobenzene, C_6H_5Cl	90	106	626	3076	1009
Bromobenzene, C_6H_5Br	75	104	606	3071	1006

about 3050 cm^{-1} has a somewhat higher frequency in the cyclic than in the aliphatic compounds.

Benzene, C_6H_6[8I,8II,8IV,9,7,10,11,12]; 621 (1), 1003 (20), 1203 (3), 1619 (5), 3078 (50) cm^{-1}.

Pyridine, C_5H_5N[15,13,17]; 991 (10), 1033 (10), 1226 (3), 1586 (5), 3046 (50) cm^{-1}.

Benzyl chloride, $C_6H_5CH_2Cl$[8IV,15]; 681 (1), 991 (3), 1601 (3), 2951 (3), 3046 (20) cm^{-1}.

In the case of chlorobenzene and bromobenzene, the kind of scheme of analysis attempted above succeeds rather better, all but one of the lines of each substance being representable as either a fundamental or as a combination line of some sort. The results are given in Table VIII.

TABLE VIII. *Raman spectra of phenyl halides.*

Chlorobenzene C_6H_5Cl		Bromobenzene C_6H_5Br		Assumed Combination
Obs.	Comp.	Obs.	Comp.	
	90		75	V_1
	106		104	V_2
		176 (3)	179	V_1+V_2
213 (3)	212			$2V_2$
316 (1)	318	313 (2)	312	$3V_2$
426 (3)	424			$4V_2$
626 (3)	626	608 (1)	606	V_3
716 (3)	716	678 (1)	681	V_3+V_1
789 (3)	787			V_5-2V_2
1011 (10)	1009	1006 (10)	1006	V_5
1098 (5)	1099	1073 (3)	1081	V_5+V_1
1183 (2)	1189	1171 (3)	1156	V_5+2V_1
		1586 (6)		(?)
2140 (1)	2148			$3V_3+3V_1$
2736 (1)				(?)
3076 (50)	3076	3071 (50)	3071	V_4
3188 (5)	3182			V_4+V_2
(8II, 10, 14)		(8II, 9, 14, 15)		

In attempting to discover some sort of system in Raman spectra, one should proceed with careful attention to the probable sources of error. These may be mentioned in three groups, in the present work. First, the data are too inaccurate to warrant any very great assurance that the apparent regularities found are significant. The wave-number shifts here reported were obtained with dispersion too small to yield exact values for the differences, and it is probable further that a number of the fainter lines were overlooked. The accuracy might be improved by using results from other observers, at least for the stronger lines; but on the other hand, the results reported from mercury arc excitation apparently contain so many spurious lines, due to the difficulty of deciding which of the various mercury lines really was the exciting line, that it seems clear that much of the work done using unfiltered mercury radiation will have to be repeated, in spite of the evident care with which

[15] Petrikaln and Hochberg, Zeits. f. phys. Chem. **B3**, 217 and 405 (1929); **B4**, 299 (1929).
[17] S. Venkateswaran, J. Phys. Chem. **34**, 145–152 (1930).

much of this work has been done. It is, of course, pointless to try to explain lines which in fact do not exist, just as it is discouraging to try to explain a spectrum from which the fainter lines are lacking.

Second, the lack of a theoretical basis for assuming the lower fundamentals used above is against the suggested scheme, as is the almost complete absence of these lower fundamentals. At first sight it might seem safe to assume fundamental frequencies so low in frequency as to be unobservable in the Raman spectra, and so low as to lie in the region of reststrahlen, so that infrared data would be lacking. But some of them at least are high enough in frequency so that they should not be covered up by the broad exciting line. Many of the combinations that would be expected from these fundamentals are not observed; and in a few cases, the intensities do not seem to fit in well. As will be pointed out below, most of such theory as is available seems to indicate that all the stronger Raman lines are fundamentals. On the other hand, overtones and combinations occur very frequently in infrared spectra; and in many Raman spectra the number of lines is so great that it seems impossible that all of them should be fundamentals. The absence of the lower frequencies is not a fatal objection; the reststrahlen frequencies of sodium chloride, for instance, do not appear in the Raman spectrum. But it will be interesting if liquids prove to have such low characteristic frequencies.

Third, it is frequently possible to find several ways of arranging a spectrum, which appear equally probable. If three frequencies A, B, and C, are found, such that $A+B=C$, it may be that C is a combination tone, or that either A or B is a difference-tone, or that the apparent relation is simply accidental. Again, it was found, for example, that all but four of the lines in the Raman spectrum of chlorobenzene could be set equal to integral multiples of a certain assumed fundamental. No reason could be given for the high intensity of some of the multiples and the absence of many of the others. Bromobenzene showed no analogous relation. Evidently the case was just another illusory relation. One more example may be pointed out; this is the case of carbon tetrachloride, which shows well the different ways in which a spectrum may be explained. On one hand, Langer[18] shows that the Raman frequencies of CCl_4 may all be explained as being due to *differences* between fundamental frequencies in the infrared spectrum, and even suggests a wave-mechanics theory to support the argument. On the other hand, Marvin[19] shows that the Raman frequencies of this compound can be explained, and the infrared spectrum as well, in terms of six fundamentals and their overtones and combinations; and the spectra of $SiCl_4$ are explained similarly. Next, Schaefer[20] shows that one of Marvin's fundamentals is unnecessary, as it is the octave of another; and by assuming that two of the remaining frequencies are a doublet, he is able to bring the whole scheme into good agreement with the theoretical results of Dennison[21] as necessarily modified to ap-

[18] R. Langer, Nature **123**, 345 (1929).
[19] H. H. Marvin, Phys. Rev. **33**, 952 (1929).
[20] C. Schaefer, Zeits. f. Physik **60**, 586 (1930).
[21] D. M. Dennison, Astrophys. J. **62**, 84 (1925).

ply to CCl_4 instead of to CH_4 (methane). The same is done for $SiCl_4$, and the possibility of similar treatment of $TiCl_4$ and $SnCl_4$ is pointed out, as well as certain similarities with compounds containing the SO_4 group. The arguments presented, and the manner in which the scheme fits the observed spectra, are extremely convincing, and there seems to be no reason to doubt the essential correctness of Schaefer's analysis. But if this is conceded, then it seems necessary to admit that overtone frequencies do appear in Raman spectra, as both Daure[7] and Pringsheim and Rosen[10] have observed Raman frequencies in the spectrum of CCl_4 which on Schaefer's scheme must be the overtone of one of the fundamentals.

In view of such facts, the writers do not present the suggested arrangements tabulated above as anything more than an interesting set of numerical approximations which it is hoped may be of use to some one in extending the theory of the Raman effect, as Marvin's suggested plan probably helped in analyzing the spectrum of CCl_4.

An attack on the problem from a quite different angle is made by Dadieu and Kohlrausch.[8] It is assumed that the chemical bonds in a molecule may be treated as a first approximation as if they behaved like elastic springs; so that when two atoms of masses m_1 and m_2 vibrate with respect to each other, the restoring force F is proportional to the displacement, x,

$$F = fx; \tag{1}$$

and the frequency of the oscillation is given by the equation

$$W_0 = 1/2\pi(f/\mu)^{1/2}, \tag{2}$$

in which μ, the "reduced mass" of the oscillating system, is given by

$$1/\mu = 1/m_1 + 1/m_2. \tag{3}$$

The theory has been extended to the case of anharmonic oscillations, and to the case of coupled vibrations, in which three bodies participate; but these parts of the theory are not immediately essential to the purpose of this paper. Dadieu and Kohlrausch have considered only longitudinal vibrations; but the case of transverse vibrations has been treated briefly in similar fashion by Andrews.[22] Following the theory outlined, the constant f is taken to be approximately proportional to the energy of dissociation A of the chemical bond between the vibrating atoms, this energy being known at least roughly from thermochemical data. Hence if one frequency due to a given pair of atoms is known, the frequency due to any other pair of atoms may be computed if the A's and the μ's are known. In this way, starting with the aromatic C-H frequency at 3050 cm^{-1} as a reference frequency, Dadieu and Kohlrausch have computed the frequencies to be expected from a large number of types of chemical bond, the computed values being usually somewhat lower than the observed values. In this way, and by comparison of similar compounds in a list of more than a hundred compounds studied, Dadieu and Kohlrausch have

[22] D. H. Andrews, Phys. Rev. **36**, 544 (1930).

been able to identify the characteristic frequencies of a considerable number of chemical bonds. The theory explains at once why in Raman spectra there is such a noticeable lack of lines between the C-H group, from 2850 cm^{-1} to 3100 cm^{-1}, and the lines due to the heavier atoms, most of which occur with shifts below 1700 cm^{-1}. The computations show that in cases where similar atoms are joined by single, double, and triple bonds, the average restoring forces are in the approximate ratio 1:2:3. As in infrared spectra, "internal" frequencies characteristic of vibrations within recurring groups, and "external" frequencies, associated with the vibrations of a group against the rest of the molecule, are distinguished. The theory checks with observation in so many ways that it seems impossible to doubt its essential correctness. Further evidence in this direction is afforded by the interesting experiments of Kettering, Shutts, and Andrews,[23] who constructed molecular models and, by noting resonance frequencies by stroboscopic methods when the models were vibrated, found sets of characteristic frequencies in good agreement with this theory.

So far as the theory has been applied to the compounds considered in the present article, frequencies for the carbon-halogen bonds are predicted which are in qualitative agreement with the frequencies marked V_3 in the tables; but no frequencies as low as the V_1 and V_2 assumed are predicted, and these may prove to be illusory. The V_4 frequency is clearly the C-H frequency; but if it is assumed that neighboring substituents can alter either the effective mass of the vibrating groups or the strength of the chemical bond between them, and Dadieu and Kohlrausch have presented abundant evidence that both these things occur, then it seems more probable that the occurrence of several lines in the C-H group is due to the existence of several modifications of the C-H bond in the molecules, rather than to combination with a hypothetical V_1 or V_2 frequency. The approximately equal frequency-differences observed are likely to prove not due to combinations. In all probability, more than four fundamentals will be required to explain the structure of most of the compounds discussed. This is especially likely to be true of the cyclic compounds. The fundamental V_5 is probably real, and characteristic of the benzene-ring structure. But Dadieu and Kohlrausch, Soderqvist,[11] and others have pointed out that there are three or four other frequencies which also seem to be characteristic of the ring structure. Whether these are all fundamentals, it is at present impossible to say. Dadieu and Kohlrausch have expressed the opinion that only fundamentals appear in Raman spectra; but an apparently valid exception to this statement has been pointed out above in the case of CCl_4.

It is hoped that further considerations may be presented in another paper in preparation by one of the writers.

[23] Kettering, Shutts, and Andrews, Phys. Rev. **36**, 531 (1930).

MODIFIED SCATTERING BY HYDROGEN HALIDES

By E. O. Salant and A. Sandow
Washington Square College, New York University

(Received January 3, 1931)

Abstract

Raman lines of the gases of HCl (previously measured by R. W. Wood), of HBr and HI and of the liquids of HCl and HBr have been measured. The Raman shifts of the lines of HCl and HBr gases agree with the infrared bands. The Raman shift of HI, 2233 cm^{-1}, does not agree with the infrared value and is considered the more accurate determination of the (0, 1) vibrational transition for HI. Intensities of scattering are in the reverse order of intensities of absorption, as might be expected from the Hill-Kemble theory of scattering by diatomic molecules of gases. The Raman lines scattered by the liquids show a different appearance from the lines scattered by the gases and their Raman shifts are smaller. The differences in the shifts are much too large to be attributed to a Lorentz-Lorenz force and are evidence of molecular interactions of a purely quantum mechanical nature, as discussed by Breit and Salant.

OF THE many measurements of modified lines scattered by liquids, usually by liquids of polyatomic molecules, few give unambiguous information about the energy levels of a molecule in both gaseous and liquid states. A notable exception is the work of McLennan and McLeod, which showed that the lower vibrational terms of O_2, N_2 and H_2 and the lower rotational terms of H_2 are sensibly the same in the two states.[1] This paper is concerned with Raman spectra of the gases and liquids of HCl, HBr and HI.

Raman lines, both vibrational and rotational, of the gas of HCl, had been measured already by Wood and by Wood and Dieke.[2] The modified lines of the gases of HBr and HI have been reported briefly by us.[3] Early measurements of the modified line of liquid HCl, first by us [4a] and then by Daure,[4b] are superseded by our later, more accurate determinations, which included also the modified line of liquid HBr.[4c]

Apparatus and Experimental Procedure

The Hilger constant deviation glass spectrograph was used, with the large camera for the liquids and both large and small camera for the gases. The dispersions on the plate in the region λ4600 were 118 cm^{-1} per mm for the large camera, 344 cm^{-1} per mm for the small, the latter being very much the faster of the two systems, of course. The plates were calibrated by iron arc standards. Incident radiation was from mercury arcs.

[1] J. C. McLennan and H. J. McLeod, Nature **123**, 160 (1929).
[2] R. W. Wood, Phil. Mag. **7**, 744 (1929); R. W. Wood and G. H. Dieke, Phys. Rev. **35**, 1355 (1930).
[3] E. O. Salant and A. Sandow, Phys. Rev. **36**, 1591 (1930).
[4] (b) P. Daure, Trans. Far. Soc. **25**, 825 (1929). E. O. Salant and A. Sandow, (a) Science **69**, 357 (1929), (c) Phys. Rev. **35**, 214 (1930).

With the gases, we employed the method developed by R. W. Wood,[1] a long diaphragmed tube containing gas at atmospheric pressure and a long arc alongside it, both tube and arc being surrounded by polished aluminum reflectors. For HCl and HBr we used a glass tube 2 inches by 50 inches and a 50-inch glass arc. With HI (and also HBr) we used a 20-inch quartz arc and a 20-inch glass tube, the latter having an outer shell containing a solution of quinine sulphate to absorb the short wave radiation which decomposes HI.

The cells for the liquids were the usual, small cylindrical tubes into which was focussed the incident radiation from a 6-inch quartz arc. The cell was placed inside an unsilvered Dewar flask containing enough liquid air to liquefy the gas and keep it about 5°C below the boiling point as it was distilled

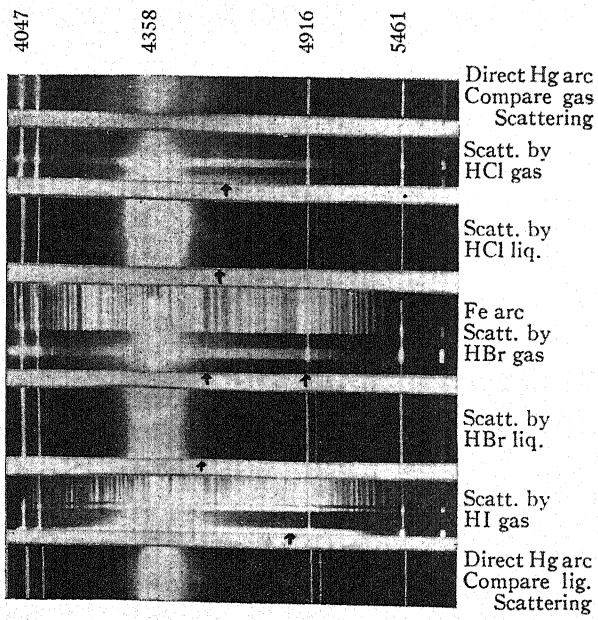

Fig. 1. Spectrograms of scattering by hydrogen halides.

into the cell. Even with filters we were unable to prevent the formation of iodine sufficiently to obtain modified lines from liquid HI.

HCl was prepared by dropping H_2SO_4 on NaCl in HCl solution. HBr and HI were prepared by the action of boiled-down syrupy phosphoric acid on NaBr and NaI. The gases were dried by passing them through suitable chemical reagents (H_2SO_4 for HCl, P_2O_5 for the others) and through cooled traps. The whole system, generator-driers-cell, contained only quartz and Pyrex fused or ground joints, including no rubber tubing nor cements in the path of the gases.

In spite of the drying of the gases and of the cells, the gases all appeared misty at first, the mistiness disappearing after a few hours; this had already been noticed by Wood with HCl[2]. Spectrograms were begun only after the substances were clear.

RESULTS

After exposures of from 19 to 72 hours with the gases and 2 to 7 hours with the liquids, modified lines could be clearly distinguished on the plates. Spectrograms are shown in Fig. 1, and microphotometer curves in Fig. 2. Lines from HCl were scattered from the mercury line λ4047, lines from HBr from 4047 and 4358, and lines from HI from 4358, all Stokes lines.

The microphotometer curves were not at all clear, because of continuous background and because of the small deflections resulting from the short slits used in the spectrograms. Consequently, features of the modified lines were

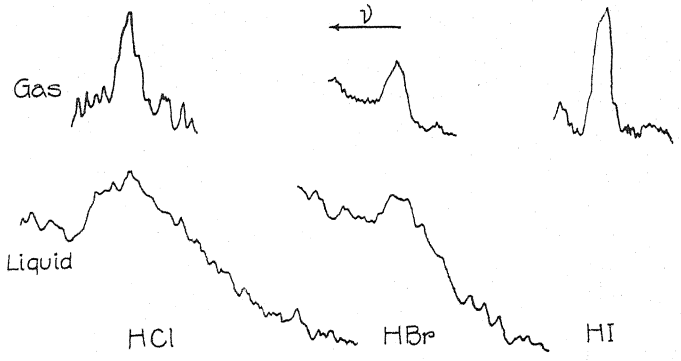

Fig. 2. Microphotometer curves of shifted lines.

much more obvious to the eye; for example, the long-wave edges of the modified lines of all the gases appear sharper than their short-wave edges, whereas the reverse is true of the modified lines of the liquids. The comparative sharpness of the long-wave edge can be seen in the microphotometer curve of HI. The greater diffuseness of the long-wave edges of the lines of the liquids of HCl and HBr, and the greater sharpness of the gas lines as compared with the lines of the liquids can also be seen even from these curves.

For the evaluation of the Raman shifts we took 24,705.4 cm^{-1} for λ4047; 22,938 cm^{-1} for λ4358.

TABLE I. *Raman shifts, gases.*

	ν_L	ν_D	ν_S	Intensity
HCl	2885.5	2879	2867	Least
HBr	2558	2550	2524	
HI	2233	2216	2201	Greatest

TABLE II. *Raman shifts, liquids.*

	ν_L	ν_D	ν_S	Intensity
HCl	2800	2770	2756	Least
HBr	2487	2466	2455	Greatest

The measurements of the modified lines of the gases are in Table I, of the liquids in Table II. In the second column are the Raman shifts of the long-wave edge of the modified line ν_L, in the third column the shifts of the most intense point of the modified line ν_D, in the fourth column the shifts of the short-wave edge ν_S, and in the last column is the order of intensities. All values are in cm^{-1}.

The most striking difference between the modified lines of the gases and of the liquids is that the latter are displaced to smaller frequencies as compared with the corresponding gases; this will be discussed below. It is to be noted further that the points of maximum intensity of the gases of HCl and HBr are nearer the long than the short wave edge, whereas the reverse is true for the liquids of HCl and HBr.

Discussion

The modified lines of the gases are, obviously, Q branches corresponding to jumps of the vibrational quantum number $\Delta v = 1$ and the frequency shifts ν_L of the long wave edges of the gas lines measure the vibrational change $\Delta G(\frac{1}{2})$, (Mulliken's notation[5]).

That this is true for HCl has already been shown by Wood,[2] our value 2885.5 ± 0.5 cm^{-1} being in good agreement with his, 2886.0.

Similarly, our value 2558 ± 2 cm^{-1} agrees within the limits of experimental error with the center of the $(1 \leftarrow 0)$ vibration-rotation band of HBr, 2559.1, determined by Randall and Imes.[6]

Quite the contrary is the case for HI. Because of its weakness and its proximity to a strong atmospheric band of CO_2, no really accurate measurement of the fundamental absorption band exists. In spite of these difficulties, Czerny[7] succeeded in detecting a weak doublet which seemed to indicate the band center at about 2270 cm^{-1}. Our value 2233 ± 2 cm^{-1} differs from this certainly beyond any apparent experimental error and, since the uncertainties of the absorption experiments do not adhere to these light-scattering experiments, must stand for the present as the value of $\Delta G(\frac{1}{2})$ for HI.

The intensities of scattering of the modified lines are in the order HI > HBr > HCl, just the reverse of the intensities of absorption of the corresponding infrared bands. The electronic levels of these molecules nearest the exciting lines of these experiments are the levels for the ultraviolet continuous bands whose long wave heads are: HCl 45455, HBr 37879, HI 30120 cm^{-1}.[8,9] The differences, then, between these heads and our exciting lines are in the order HI < HBr < HCl. Now, according to the theory of intensities of modified scattering, discussed in particular for diatomic gaseous molecules by Hill and Kemble,[10] these differences would appear in the denominator of the ex-

[5] R. S. Mulliken, Phys. Rev. **36**, 611 (1930).
[6] H. M. Randall and E. S. Imes, Phys. Rev. **15**, 152 (1919).
[7] M. Czerny, Zeits. f. Physik **44**, 235 (1927).
[8] H. C. Tingey and R. H. Gerke, J. Am. Chem. Soc. **48**, 1838 (1926).
[9] Coehn and Stuckardt, Zeits. f. physik. Chem. **91**, 722 (1916).
[10] E. L. Hill and E. C. Kemble, Proc. Nat. Acad. Sci. **15**, 387 (1929).

pression for the electric moment associated with the Raman line, and should contribute, then, toward effecting just the order of intensities observed here.

With the liquids, it is not certain, as with the gases, that the shift of the long wave edge of the Raman line measures the change $\Delta G(\frac{1}{2})$ of the molecules. First there is the fact that absorption measurements of the (0, 2) bands of the liquefied hydrogen halide molecules have shown the bands to have no apparent structure but to have a single maximum of absorption;[11] one can hardly speak of these bands having P, Q and R branches, consequently. Then the distribution of intensity in the modified lines from the liquids is different from that in the gases, as noted above, and their shapes seem to correspond to the shapes of the single infra-red bands. As in these bands it is the maximum that is taken as the measure of the vibrational change, it seems reasonable to take the shift of the point of maximum intensity, ν_D, of the liquid Raman lines as a measure of $\Delta G(\frac{1}{2})$ of the liquefied molecules. (Grating measurements of the $(1\leftarrow 0)$ bands in the infrared are now in progress in these laboratories to determine this point).

Defining the change in vibrational term differences due to liquefaction as $\Delta_l\Delta G=\Delta G-\Delta G_l$ where ΔG_l refers to the value of ΔG in the liquids, we have in Table 3 the various values of $\Delta_l G(\frac{1}{2})$ depending on whether the long wave edge or the point of maximum intensity of the liquid lines is taken as a measure of $\Delta G_l(\frac{1}{2})$.

TABLE III. *Gas-liquid shifts of 0,1 transition.*

	Values of $\Delta_l\Delta G(\frac{1}{2})$	
	From ν_L	From ν_D
HCl	86	116
HBr	71	92

The theory of shifts of frequency accompanying close packing of molecules attributes the shifts ($\Delta_l\Delta G(\frac{1}{2})$ in these experiments) to three effects (1) electrostatic interaction of a molecule with its neighbors due to its excitation, (2) the effect of the finite space extension of the eigenfunctions of neighboring molecules and (3) the Lorentz-Lorenz force with effective charge replacing classical charge.[12] It was shown in that work that the frequency displacement accompanying liquefaction of HCl was only about 2.2 cm^{-1} due to the Lorentz-Lorenz effect. Since the other factors in the expression for the Lorentz-Lorenz shift are about the same for HBr as for HCl, and since the effective charge for HBr is smaller, corresponding to its smaller intensity of absorption, the Lorentz-Lorenz shift for HBr is of the order of 2 cm^{-1} and, as for HCl quite small compared to the displacement $\Delta_l\Delta G(\frac{1}{2})$ observed here and recorded in Table III. These displacements must, then, be attributed to the first two, purely quantum mechanical effects.

Gas-liquid frequency difference of the same order of magnitude as these have been reported for other substances; for example, for NH_3 by Dickinson,

[11] E. O. Salant and W. West, Bulletin Phys. Soc. **5**, 15 (Nov. 15, 1930).
[12] G. Breit and E. O. Salant, Phys. Rev. **36**, 871 (1930).

Dillon and Rasetti[13] and by Daure,[14] and for H_2S by Bhagavantam.[15] It is tempting to speak of these, too, as a quantum mechanical effect, but in the absence of further information about these molecules, in particular about their effective charges, such a conclusion would be premature and open to question.

We take great pleasure in thanking Mr. R. L. Garman of the Chemistry Department of Washington Square College for the microphotometer curves, and the General Electric Vapor Lamp Co. for mercury arcs. This research was begun while one of us (E.O.S.) was a Fellow of the National Research Council.

[13] R. G. Dickinson, R. T. Dillon and F. Rasetti, Phys. Rev. **34**, 582 (1929).
[14] P. Daure, Comptes rendus **188**, 61 (1929).
[15] S. Bhagavantam, Nature **126**, 502 (1930).

IONIZATION OF ARGON, NEON AND HELIUM BY VARIOUS ALKALI IONS

By Richard M. Sutton and J. Carlisle Mouzon
California Institute of Technology, Pasadena

(Received January 5, 1931)

Abstract

Caesium, rubidium, potassium, and sodium positive ions from Kunsman catalyst sources, and lithium ions from spodumene have been used to produce ionization in helium, neon, and argon. In most cases the ionization sets in between 100–150 volts and increases linearly to 750 volts, the highest potential used. Maximum ionization was produced in each gas by the alkali ion closest to it in atomic number.

PREVIOUS experiments have been reported[1] concerning the ionization of various gases by potassium positive ions of relatively low energies. The present paper deals with the ionization of helium, neon, and argon by a series of alkali ions representing a wide range of atomic weights from lithium to caesium. It was of interest to determine what relationship might exist be-

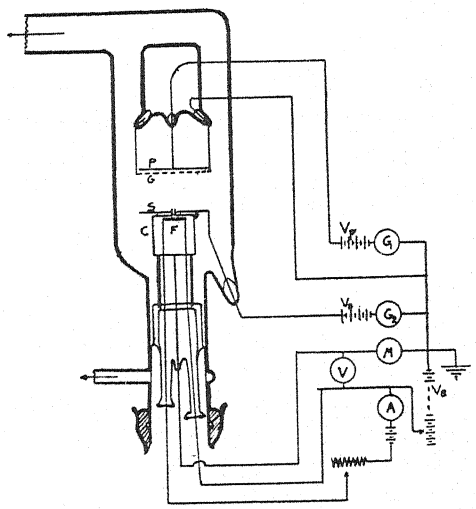

Fig. 1. Experimental tube and connections.

tween the various ionizing agents and the ionization which they produce in gases of different atomic weights. Some rather unexpected experimental results came to light which indicate that the field is fruitful for further investigation and explanation.

The method of measurement has been described in the previous papers. Referring to Fig. 1, it may be summarized briefly as follows. Positive ions

[1] R. M. Sutton, Phys. Rev. **33**, 364 (1929); Sutton and Mouzon, **35**, 694 (1930).

emitted from Kunsman catalyst sources by a hot coated platinum strip F are directed by the variable accelerating potential, V_a, through a small channel in the steel cathode C which completely surrounds the filament. Any ionization occurring in the gas between C and the grid G will produce an electron current I_s to the collector plate S which is connected to the high sensitivity galvanometer G_2. The initial positive beam (except for loss by scattering and the small fraction striking the grid) falls upon the upper plate P and is recorded as a positive ion current, I_p, by the galvanometer G_1. At each gas pressure used, the accelerating potential of the positive ions is varied in steps from zero to 750 volts. The ratio of currents, I_s^-/I_p^+, corrected for the small secondary emission of electrons from the grid, is taken as a measure of the ionization produced in the gas between S and G. The collector S and plate P are both maintained at small positive potentials to prevent the escape of elec-

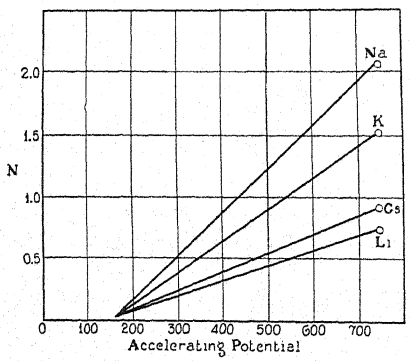

Fig. 2. N, number of neon ions formed per initial positive ion per cm path at 1 mm pressure.

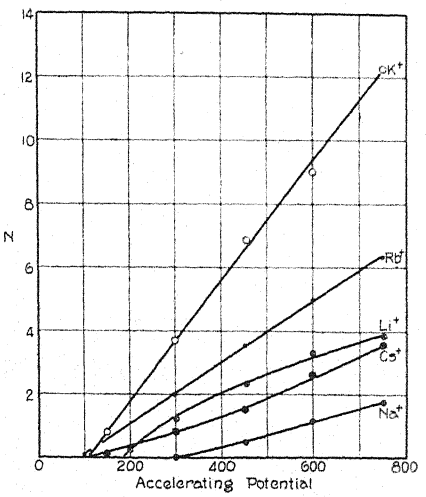

Fig. 3. N for argon.

trons due to secondary emission or photoelectric effect. These potentials were in no case high enough to produce ionization of the gas by electron collision. The distance $S-G$ (2.5 cm) is made large in comparison with the distance $G-P$ (0.2 cm) in order to minimize the effect of ionization between grid and plate. To correlate the results obtained at different pressures, the ratios of I_s/I_p were divided by the length of path between S and G and by the gas pressure in mm of mercury, thus giving the number, N, of ions formed per initial positive ion per centimeter path at one millimeter pressure. The pressure range utilized was from 0.005 to 0.05 mm; in a few cases where the ionization was feeble, pressures as high as 0.1 mm were used.

In general the ionization sets in between 100 and 150 volts (except for sodium in argon) and increases practically linearly with increasing accelerating potential to 750 volts, the highest voltage used. After making correction for the stoppage of the initial positive beam by the gas, the ionization for a particular voltage is found to be linear with respect to pressure; only in the

cases of intense ionization is there evidence of more than one ionizing collision per positive ion at the higher pressures and accelerating potentials. Thus N for each positive ion in a particular gas is independent of gas pressure within the range studied and depends only upon the accelerating potential of the positive ions.

Fig. 2 and Fig. 3 show the results of a large number of runs in neon and argon respectively, in each of which several different positive ions were used as the ionizing agents. The calculated values of N are seen to be practically linear with accelerating potential after ionization once begins, in most cases by 150 volts. Sodium does not ionize argon until an accelerating potential of nearly 300 volts is reached; this behavior, together with a strong reflection of the sodium positive ions to the collector S at accelerating potentials around 150–250 volts, is strangely unaccountable. In all other cases, reflection of the

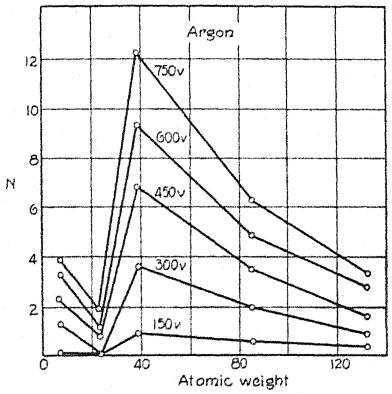

Fig. 4. N as function of atomic weight of positive ions and their energies.

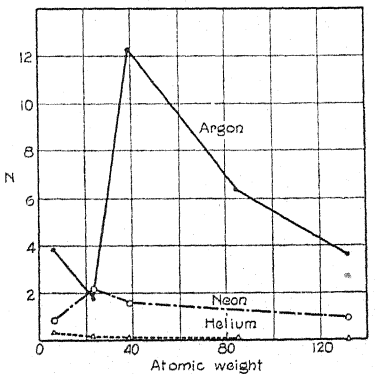

Fig. 5. Comparative values of ionization at 750 volts accelerating potential for different gases as function of atomic weight of ionizing agent.

positives played a negligible part in the currents observed. This method is not sensitive enough to determine the onset of ionization closer than 25 volts, but the slopes of all the ionization curves indicate a fairly sharp origin of ionization which was scarcely to be expected; the "ionization potential" due to positive ions bears no evident relationship to ionization potentials determined by electron impact methods, nor does it seem to be critically dependent upon the mass of the bombarding ions in any regular fashion.

The most striking results of this investigation appear when the values of N in Fig. 3 are plotted against atomic weight of the ionizing agent, as shown in Fig. 4. It appears that the maximum ionization in argon is produced by potassium positive ions, which is scarcely what would be expected from any ballistic transfer of energy considerations. Similarly, as may be seen in Fig. 5, neon is most strongly ionized by sodium positives; helium is most strongly ionized by lithium. The conclusion presents itself that *ionization of a noble gas is best effected by that alkali ion closest to it in mass or number of electrons.* Evidence is not yet available to discern whether the controlling factor is one

of mass or electron configuration of the two constituents of an impact, nor can a comparison yet be made with the ionization of a gas by its own atoms or ions. The experimental difficulties in the path of this latter aspect of the problem have not been solved.

Similar results have been published recently by Dr. Otto Beeck[2] who secured homogeneous beams of positive ions by means of a magnetic analyzer. His method is evidently better designed for the purpose than the one here reported, and he is now in a position to complete the study of the two remaining noble gases at this Institute. The qualitative agreement between the two methods is excellent, and the quantitative agreement is as good as might be expected considering the difference in methods. The only marked departure from regularity of our results appears in the relative interchange of intensities of ionization by lithium and sodium in argon. This may be accounted for by either or both of two causes: first, an impurity of higher atomic weight in the lithium source derived from powdered spodumene (all other sources were Kunsman catalysts); second, the unaccountably large reflection of sodium ions by argon. This inversion of position was carefully checked, and as far as the accuracy of this method is concerned, the effect is real.

Not only is there maximum ionization produced by the alkali positive lying closest to the atomic weight of the gas bombarded, but the intensity of these maxima increases greatly in the heavier gases. The ionization of helium is very feeble, whereas in argon it is quite pronounced. It is rather to be expected that even greater ionization will be found in xenon and krypton. In all of the foregoing work, correction has been made for the secondary emission of electrons from the metal parts of the tube. Inasmuch as there was gas admitted into the tube, no particular precautions were taken to outgas the electrodes. Comparing the secondary emission of the metal surfaces under bombardment of the various alkali ions, the intensity of emission was found to vary in the same way as the intensity of ionization; i.e., greatest for potassium when argon had been present, etc. It would appear that the secondary emission might be due largely to a layer of gas upon the electrodes, and hence this surface effect would bear a close relationship to the volume ionization produced in the gas by different positive ions.

It is felt that more experimental evidence is necessary before an adequate explanation of ionization by two such complicated structures as an alkali ion and a gas atom can be made. This necessitates the development of additional ion sources and improved technique for the study of atom-beams in a gas.

The authors acknowledge their thanks to Dr. Otto Beeck and Dr. Fritz Zwicky for stimulating discussion of the results obtained.

[2] Otto Beeck, Ann. d. Physik 6, 1001 (1930).

A DIRECT MEASUREMENT OF MOLECULAR VELOCITIES

By I. F. Zartman
University of California, Berkeley

(Received January 7, 1931)

Abstract

A method is described for the direct measurement of the velocities of neutral molecules. The molecules condense on a glass plate fastened to a cylinder which rotates at a high speed, 241 r.p.s. The molecules having velocities from 168 m/sec to 673 m/sec were spread over a band 3 cm wide. A stream of bismuth molecules is studied and the vapor found to be composed of 40 percent Bi and 60 percent Bi_2 at a temperature of 851°C.

Introduction

ONE of the fundamental assumptions of the kinetic theory of gases is the continual heat motion of the molecules in the gas. Even though there was no direct experimental verification of this assumption, the theoretical development progressed rapidly, resulting in the derivation of an expression for the distribution of molecular velocities by Maxwell[1] in 1859 and, later by Boltzmann.[2] This law has found many applications and until 1920 was only indirectly verified.

The first attempt at a direct measurement of molecular velocities was made by Stern[3] who intercepted a stream of silver atoms on a rotating plate. The displacement obtained was not sufficient to allow an analysis of the deposit beyond the location of the maximum. The results for the maximum agreed within the experimental error, about 15 percent, with that calculated from the theory. In 1927 Costa, Smyth, and Compton,[4] using rotating radially slotted disks and a radiometer vane as a detector attempted to secure a "velocity spectrum" of neutral molecules. Their results were in general qualitative agreement with the Maxwell-Boltzmann law but rather unsatisfactory because of the insensitivity of the detector. Eldridge,[5] using rotating disks as a velocity selector and condensing the molecules on a liquid-air cooled target, obtained a density distribution for cadmium which agreed fairly well with the theoretical distribution. Several objections might be raised, for his zero mark is not sharply defined but very broad; the zero of the theoretical curve has to be shifted about 0.05 cm to make the maximum of the theoretical curve coincide with the maximum of the deposit; his temperature measurement is unsatisfactory and his resolution is low. Lammert[6] developed a method for

[1] J. C. Maxwell, "Collected Works," **1**, 378 (1860) Cambridge University Press, Cambridge.
[2] L. Boltzmann, "Vorlesungen über die Gas Theorie," **1**, 15 (1910). Johann Barth, Leipzig.
[3] O. Stern, Zeits. f. Physik **2**, 49 (1920); **3**, 417 (1920).
[4] Costa, Smyth, and Compton, Phys. Rev. **30**, 349 (1927).
[5] J. A. Eldridge, Phys. Rev. **30**, 931 (1927).
[6] Berthold Lammert, Zeits. f. Physik **56**, 244 (1929).

producing molecular beams containing well-defined velocity bands. By taking a series of runs in which the bands had a definite width of 50 m/sec over a range of from 90 to 360 m/sec and determining the intensity of each band, a test of the Maxwell-Boltzmann law for mercury vapor was possible. Except for a systematic difference the results agree quite well with the theoretically expected distribution.

Theory

The aim of this experiment is to develop an apparatus with a resolving power greater than that obtained by Stern and Eldridge and thus allow a more detailed study of the "velocity spectrum" of neutral molecules. This, as shown later, can be attained by increasing the path-length and the speed of rotation.

Consider a gas issuing through a rectangular slit, g_1 (Fig. 1) in a side of the enclosure E which can be maintained at a constant temperature T. Let Knudsen's[7] condition for molecular streaming be satisfied, i.e., let the temperature be so controlled that the mean free path of the molecules within, is greater than the width of the slit g_1. With the aid of the slit g_2 a sharply defined rectangular beam is formed. Let a cylinder D, having a slit g_3 in its periphery and capable of being rotated, be placed in the path of this beam. If the cylinder is at rest, and slit g_3 is in the path of the molecular beam, a deposit forms on the rim at P diametrically opposite the slit. If the cylinder is rotated, the molecules entering g_3 require a finite time to traverse the diameter and consequently strike the rim at a point s to the left of P. The displacement s of a molecule moving with a speed c is given by the equation

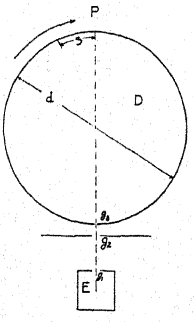

Fig. 1.

$$s = \pi d^2 n/c = A/c \tag{1}$$

where d is the diameter of the cylinder and n is the number of revolutions per second. The equation also shows that, by making d and n large, one may secure large displacements of the molecules, i.e., high resolving power.

The molecules in the beam possess not one definite velocity, but a distribution of velocities and consequently a "velocity spectrum" is formed on the rim of the cylinder. The density of this deposit should bear some relation to the velocity distribution in the enclosure E. According to the Maxwell-Boltzmann distribution law, the number of molecules dn out of a total number N in equilibrium within the enclosure possessing speeds between c and $c+dc$, is given by the expression

$$dn = \frac{4N}{\alpha^3 \pi^{1/2}} e^{-c^2/\alpha^2} c^2 dc$$

where α is the most probable speed of the molecules within the enclosure. As

[7] M. Knudsen, Ann. Physik **28**, 999 (1909).

shown by Stern,[3] while the molecules within the enclosure are in equilibrium those in the beam are not, for the number passing through the slit per second depends on the size of the opening, the shape of the enclosure, the speed of the molecules and the number of molecules in the enclosure. Let dn_1 be the number of molecules out of N_1 molecules in the beam possessing speeds between c and $c+dc$. Then

$$dn_1 = dn \cdot c \cdot K$$

where K is a constant. From this we get

$$dn_1 = (2N_1/\alpha^4)e^{-c^2/\alpha^2}c^3dc \tag{2}$$

as the expression for the velocity distribution in the beam.

To find the expression for the distribution of the molecules on the receiving plate, P, one can use the method given by Stern.[8] Consider first that the undeflected image is of infinitesimal width and find the distribution of the molecules in the deflected portion of the plate. Consider the velocity range between c and $c+dc$ giving a deflected range between s and $s-ds$. The intensity of the beam in the deflected region may be defined as the number of molecules dn striking and condensing on a length of plate ds assuming the beam to be of uniform and constant intensity across the element of length, or

$$I = dn/ds. \tag{3}$$

From Eqs. (1), (2), and (3) we get

$$I = \frac{2N_1}{\alpha^4 A}e^{-c^2/\alpha^2}c^5. \tag{4}$$

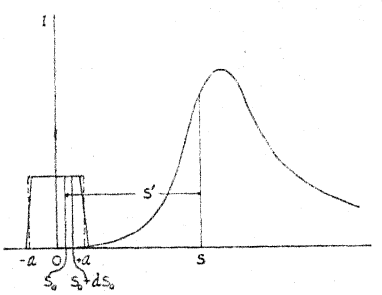

Fig. 2.

The undeflected beam in the actual experiment is of finite width 2a (Fig. 2). Let ds_0 be an element of length in the undeflected region and let dn_0 be the number of molecules striking and condensing on ds_0. Then $I_0 = dn_0/ds_0$. For an undeflected beam of width ds_0, Eq. (4) becomes

$$I = \frac{2I_0 ds_0}{\alpha^4 A}e^{-c^2/\alpha^2}c^5. \tag{6}$$

It will be more convenient to use the intensity distribution in the deflected portion as a function of the distance s from the zero line. Then $c/\alpha = s_\alpha/s$,

[8] O. Stern, Zeits. f. Physik **41**, 563 (1927).

where s_α is the deflection of the molecules having the most probable velocity in the enclosure, and Eq. (6) becomes

$$I = \frac{2I_0 ds_0}{s_\alpha}\left(\frac{s_\alpha}{s}\right)^5 e^{-(s_\alpha/s)^2}. \tag{7}$$

Integrating (7) from $-a$ to $+a$, we get

$$I = I_0\left\{e^{-(s_\alpha/s+a)^2}\left[\left(\frac{s_\alpha}{s+a}\right)^2 + 1\right] - e^{-(s_\alpha/s-a)^2}\left[\left(\frac{s_\alpha}{s-a}\right)^2 + 1\right]\right\} \tag{8}$$

as the theoretical intensity distribution in the deflected region of the plate in terms of s_α and a.

Apparatus

The substance whose velocity distribution is to be determined is vaporized in a steel crucible A (Fig. 3). The vapor then passes through the channel in

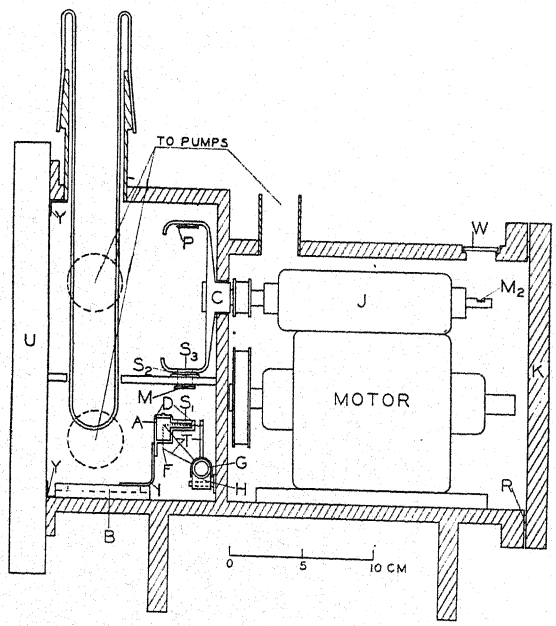

Fig. 3. Diagram of apparatus.

the neck to the slit S_1, there escaping as a molecular beam. The crucible is fastened to the sliding base B by means of a rectangular strip of invar I. This sliding base is fitted into a dove-tailed groove in order that the entire crucible and slit assembly can be easily removed for filling purposes and then replaced without changing the alignment of the slit system. Directly above the neck of the crucible is a second slit S_2 used to define sharply the molecular beam. The crucible slit is 0.05 mm by 10 mm in size while the defining slit is 0.6 mm by 10 mm. The distance between these slits is 3.29 cm. A shutter M magnetically operated from the outside is used to interrupt the beam.

The crucible is heated by radiation from a 300 watt tungsten lamp filament F mounted with the aid of tungsten supports T fused to a glass tube G. The glass tube is fastened in a special holder H allowing the filament to be adjusted in any desired direction. The loss of heat by radiation is reduced by surrounding the crucible and filament assembly with nickel radiation shields. Two chromel-alumel thermocouples fastened at D serve as a means of determining the temperature. The thermocouples are calibrated by comparison with a standardized platinum-platinum rhodium thermocouple. A potentiometer is used to read the electromotive force of the thermocouples.

A cylinder C, 10 cm in diameter, machined out of a solid piece of machine steel, is placed above the slit system. This cylinder is designed to withstand the forces due to high speeds of rotation with the least possible deformation. A knife edge slit S_3, 0.6 mm wide, is cut into the rim of the cylinder. Directly opposite on the inner rim a device is fastened to hold a curved glass plate P. The cylinder is carefully balanced and mounted on the high speed spindle J of an internal grinder. Its speed is determined by the stroboscopic method.

The grinder consists of a 1/6 H.P. universal motor and a high speed spindle mounted on top of the motor housing. A fabric belt is used to drive the spindle. The motor armature has a speed of 10,000 r.p.m. and the spindle 30,000 r.p.m. when connected to a 110-volt circuit. The armature and spindle rotate in ball bearings and the entire assembly is so well-balanced that vibration is negligible at nearly all speeds. The bearings are properly lubricated by vacuum pump oil which has been boiled in a vacuum for several hours to drive off the more volatile products. The residue is sufficiently non-volatile so that a pressure of less than 10^{-4} mm of mercury can easily be maintained in the motor compartment by continual pumping.

The entire assembly is enclosed in a phosphor-bronze housing which is divided into three compartments, a motor, a cylinder, and a crucible compartment. A hole in the wall between the motor and cylinder compartments, slightly larger than the hub of the cylinder, allows the high speed spindle to pass through and at the same time prevents the passage of large quantities of vapor from the motor to the cylinder compartment. A water jacket surrounds the outside of that portion of the housing subjected to heating. The end of the motor compartment is flanged and can be closed by bolting a metal plate K to this flange. A rubber gasket R is placed between the flange and plate to render the joint vacuum tight. The flange surrounding the cylinder and crucible compartments is scraped to fit a plate glass cover U. The joint between the glass cover and the flange is made vacuum tight by giving it a thin uniform coating of a special stopcock grease to which more pure rubber and paraffin has been added than is customary.

The entire system is evacuated through an opening in each compartment. All openings and tubing are large in diameter and the tubing is kept as short as possible in order that all vapors can be quickly removed. Three mercury vapor pumps each backed by a Hyvac pump are used to evacuate the compartments. Liquid air traps are used to prevent the mercury vapor from diffusing into the system. A glass tube which can be filled with liquid air passes

vertically through the cylinder chamber into the crucible chamber. A vacuum tight joint is made by the ground-glass, metal joint at the top. Copper shields Y are fitted into the corners formed by the glass cover and the sides, top and bottom of the housing. Copper strips attached to these shields are fastened to the glass tube. The liquid air in the tube cooled these shields to a sufficiently low temperature to condense most of the vapors from the stopcock grease. The tube itself also acts as a large cooled surface which condenses all condensible vapors coming in contact with it. No difficulty is experienced in maintaining a pressure of less than 10^{-5} mm of mercury in the crucible and cylinder compartments.

In order that the density of the deposit can be measured by a microphotometer it is desirable to use glass plates as receivers. These plates (6 by 1.5 by 0.03 cm) are cut from microscope cover glasses. They are bent so as to fit the inner circumference of the cylinder by balancing them on a carbon block having the proper curvature, and then placing the block in an electric oven. The temperature is raised slowly until the plate bends under its own weight to the shape of the carbon form.

For the bismuth molecules to condense on the glass plate at room temperature it is necessary to place an initial, thin and uniform layer of bismuth upon it. This is accomplished by a piece of apparatus which allows the glass plate to be cooled to near the temperature of liquid air and then uniformly exposed to a stream of bismuth molecules. This apparatus consists of an electrically heated crucible and a glass liquid air container mounted in a brass housing which can be made vacuum tight and evacuated. The glass plate upon which the initial deposit is placed is held against the curved flat bottom of the liquid air container by two flat springs. The crucible containing the substance to be deposited is mounted on a shaft so that it may be rotated from one side of the plate to the other. This rotation is accomplished from the outside of the housing by fastening a bent arm to the shaft and enclosing the arm within a sylphon. A fork, attached to a motor-driven slow-speed gear, engages the sylphon thus transmitting the motion to the crucible.

Experimental Procedure

The bismuth used in this experiment is the analyzed product of Powers-Weightman-Rosengarten Company, Philadelphia. In order to get rid of any adsorbed gases it is heated in a vacuum to a temperature of 450°C for about five hours and then allowed to cool before air is admitted.

A bent glass plate is thoroughly cleaned and dried, then placed in the "initial depositing" apparatus and given a thin uniform coating of bismuth. The plate is fastened to the cylinder. The cylinder is adjusted with the aid of a traveling microscope until the slit S_3 is observed to be directly above the defining slit S_2. It is then fixed in this position. The system is evacuated, the crucible heated to about 800°C and the plate exposed to the molecular beam for about 20 seconds. This operation gives a visible deposit on the plate and forms the zero mark from which the displacements are measured. After ad-

mitting air to the system, the plate is removed and a microphotometer record obtained of the density of the initial deposit and location of the zero mark.

The plate is again fastened to the cylinder, the crucible filled with bismuth and the system evacuated. A slow increase in the temperature is necessary to avoid the violent expansion of gas bubbles in the molten metal which results in a "spitting" of the metal through the slit. When the temperature of the furnace reaches equilibrium and the motor speed is adjusted by varying the resistance in the line to the absence of beats, the shutter is opened and the beam allowed to pass to the plate. The maximum of the deposit first becomes visible in from three to six hours depending upon the temperature and speed of the run. The run is continued for periods ranging from eight to twenty-two hours. The plate is removed from the cylinder and again photometered. Finally, the two photometer curves are superimposed and the density due to the velocity distribution is measured.

RESULTS

The results of four runs are given. Runs 1 and 2 are represented with their theoretical curves in Fig. 4. Fig. 5 is a contact print of the photometer record from which the data for curve 1, Fig. 4, are taken. The horizontal distances are twice the actual distances on the glass plate.

TABLE I.

Run	t	n	Length of run	Bi	Bi_2
1	851°C	120.7 r.p.s.	12 hours	0.40	0.60
2	851	241.4	22	.40	.60
3	851	60.35	7	.40	.60
4	795	120.7	8	.30	.70

In all cases the experimental results would not agree with the theoretical distribution for Bi or Bi_2 as given by Eq. (8). The work of Leu[9] on the magnetic deflection of bismuth suggests that the beam is composed of Bi and Bi_2. On the basis of this suggestion various percentages of Bi and Bi_2 were assumed and using Eq. (8) the resultant intensity distributions plotted. These distributions were then compared with the experimental results. The theoretical distribution which best fitted the experimental results is taken as the composition of the vapor stream.

In Fig. 4 the solid lines represent the theoretical distributions for the conditions of operation given in Table I. The circles represent the experimental results obtained from Run 1, and the crosses those from Run 2. The experimental points are in close agreement (within the experimental error) with the theoretically derived curve except for a few points on the high velocity side. These points disagree by an amount greater than the experimental error. The disagreement is probably due to the lack of a sharply defined molecular beam during the entire course of the experiment. It may also be due to a "slipping"

[9] Alfred Leu, Zeits. f. Physik **49**, 498 (1928).

Fig. 4 also gives the velocities corresponding to various displacements for a speed of rotation of 241.4 r.p.s.

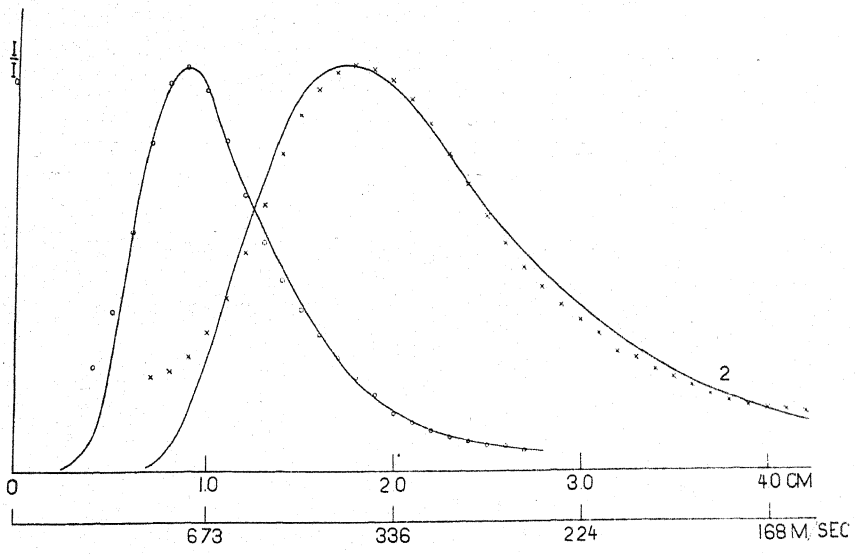

Fig. 4. Theoretical and experimental intensity distributions assuming a vapor composition of 40 percent Bi and 60 percent Bi_2. T equals 851°C. Curve 1, $n=120.7$ r.p.s., curve 2, $n=241.4$ r.p.s. Bottom line gives the molecular velocity corresponding to several displacements at a cylinder speed of 241.4 r.p.s.

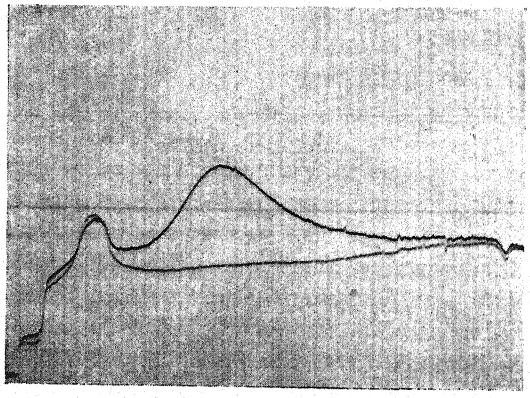

Fig. 5. Contact print of photometer record of Run 1, $n=120.7$ r.p.s. Abscissas twice actual deflections.

TABLE II.

Displacement interval	Velocity band
1.0–1.1 cm	61 m/sec
2.0–2.1	15
3.0–3.1	7
4.0–4.1	4

of the molecules forming the zero mark. This possibility is being investigated.

Table II gives several displacement intervals of 1 mm width and the velocity band covering that interval. The high resolution is quite evident.

As Leu[9] observed, the dissociation of Bi_2 increased with the temperature and at about the same rate. His results disagree among themselves at the same temperature by 10 percent in some cases. If there is no "slipping" of molecules on the plate a variation in the composition of the vapor of less than 5 percent is detectable in this experiment and this method thus forms a more accurate means for the study of the dissociation of certain vapors, the results of which can be applied to calculating the heat of dissociation.

Errors

The temperature and speed could be kept constant to within one percent although it is doubtful if the temperature itself could be read accurately to within several percent. A possible source of error is that not all the molecules striking the plate remain there. It is possible that some escape, however this number is assumed to be negligible. It is not so certain that all molecules striking the plate remain at the point where they first make contact. There is the possibility for surface motion or "slipping." Evidence for a small amount of surface motion on fixed plates is presented by Cockcroft.[10] Any motion of the molecules on the glass plate due to the high speed of rotation must be negligible since the results obtained from Runs 1, 2, and 3, taken at the same temperature but at different speeds, indicate the same percentage vapor composition.

A test showed that no error is introduced in assuming that the electrometer deflections on the photometer records are directly proportional to the densities of the deposits.

Conclusion

A method is described for the direct measurement of molecular velocities. Results are presented in which the molecules are spread over a distance of more than 4 cm at a cylinder speed of 241.4 r.p.s. with an error of less than 5 percent. This resolution is many times that obtained by Stern, an analysis of the distribution of the deposit being impossible from his results, and several times that obtained by Eldridge who spread a velocity band of 900 to 200 meters per second over a plate length of 1 cm while in this experiment a velocity band of 673 to 168 meters per second is spread over 3 cm.

It is a pleasure to acknowledge my gratitude to Professor Elmer E. Hall under whose direction the problem was undertaken, for his advice and inspiration; to Professor Leonard B. Loeb for the many helpful discussions and encouraging remarks, and to Mr. G. P. Kraus, mechanician, for his willing cooperation in the mechanical details.

[10] J. D. Cockcroft, Proc. Roy. Soc. **A119**, 293 (1928).

THE AMPLIFICATION OF SMALL DIRECT CURRENTS

By Lee A. DuBridge
Washington University, St. Louis, Missouri

(Received December 29, 1930)

Abstract

A new type of thermionic tube recently described by Metcalf and Thompson has made it possible for the first time to construct d.c. amplifying circuits with a current sensitivity exceeding that of any form of electrometer except the Hoffman; and with a ruggedness and dependability unattainable with any form of sensitive electrometer. The circuits are easily constructed and simple to operate. Three types of circuits have been tested out and are described. (1) A simple single-tube circuit with a Type R galvanometer has been found satisfactory for measurements of currents as small as 10^{-14} amp. (2) A two-tube bridge circuit gives greater stability and will easily measure currents of 10^{-16} amp. It has been found capable of detecting currents of 5×10^{-18} amp. (3) A two-stage circuit, using one of the new tubes and one of the UX-112A type, will amplify currents of 10^{-14} amp to such a value that they may be read on a microammeter.

Introduction

THERE is considerable interest among physicists in the possibility of using thermionic tubes for the amplification of very small direct currents, such as photo-currents, ionization currents, and currents due to electron or positive ion beams of various sorts. A number of different circuits have been described in the literature[1] by means of which ordinary radio tubes or screen grid tubes may be employed for this purpose; and while a number of observers have had considerable success in their use, for the most part the electrometer is still the instrument universally employed for measurements of this type.

The difficulties encountered in d.c. amplification are due largely to the fact that practically all thermionic tubes now available have been designed for amplification of rapidly varying currents, and possess characteristics which make them unsuitable for d.c. work. Only a few attempts have been made to design a tube particularly adapted to amplifying direct currents smaller than about 10^{-11} amp. However, very recently Metcalf and Thompson of the General Electric Laboratories have described[2] a new form of tube (the "FP-54 pliotron") particularly designed for this purpose and which is capable of amplifying currents as small as 10^{-17} amp. With this type of tube it is possible for the first time to construct an amplifying circuit with a sensitivity equaling or exceeding that of the best Compton electrometers, and at the same time possessing a ruggedness and dependability unattainable with these instruments. The present paper is an account of some further experi-

[1] See especially, Bennett, Rev. Sci. Inst. **1**, 466 (1930); Dearle and Matheson, Rev. Sci. Inst. **1**, 215 (1930); Razek and Mulder, J.O.S.A. and R.S.I. **18**, 460 (1929); Nelson, Rev. Sci. Inst. **1**, 281 (1930); also refs. 4 and 5 below.

[2] Metcalf and Thompson, Phys. Rev. **36**, 1489 (1930).

ments which have been made with these tubes to investigate their possibilities and limitations under actual working conditions, and to study the circuits in which they can be most efficiently used. An attempt has been made to present the results in a rather detailed and elementary way, so that physicists unfamiliar with vacuum tube technique may be aided in building workable amplifier circuits. The experiments were carried out at the General Electric Research Laboratories during the past summer, at the suggestion and under the direction of Dr. A. W. Hull, to whom the author is very greatly indebted.

It may be well to recall some of the requirements which must be met by circuits to be used for d.c. amplification.[3] Suppose, for example, that it is desired to amplify a current from, say, a photoelectric cell, using a standard

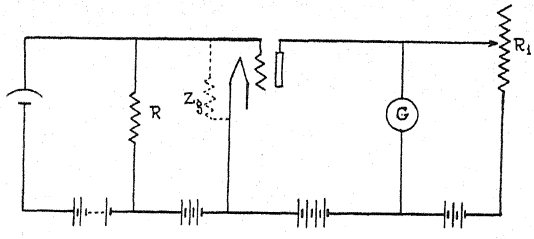

Fig. 1. Simple circuit for d.c. amplification.

circuit such as is represented in Fig. 1. With the photo-cell dark let the resistance R_1 be adjusted so that the galvanometer reads zero. If the photo-cell is then illuminated, the photoelectric current will cause a drop in potential across the grid resistance R, and this will be impressed on the grid of the vacuum tube. The resulting change in plate current will cause a deflection d of the galvanometer, given by

$$d/\sigma = i_G = \Delta i_p = g_m \Delta e_g$$

where σ is the sensitivity of the galvanometer (in mm/amp), $g_m = di_p/de_g$, the mutual conductance of the tube, and Δi_p and Δe_g the changes in plate current and grid potential, respectively. (It is assumed in setting $i_G = \Delta i_p$ that the resistance R_1 is considerably larger than the galvanometer resistance,[3] a condition always satisfied in practice). The voltage sensitivity S_v of the circuit, in mm/volt, then will be,

$$S_v = d/\Delta e_g = g_m \sigma. \qquad (1)$$

To attain a high sensitivity to *voltage*, one would choose a tube of high mutual conductance and use it with a sensitive galvanometer. For our present purpose, however, we are more interested in the sensitivity to *current*, since the voltage applied to the grid may be made as large as we please, within limits, by simply increasing R. Since then, $\Delta e_g = Ri$, we have for the current sensitivity, S_i, (in mm/amp),

$$S_i = d/i = g_m R \sigma = S_v R. \qquad (2)$$

[3] For a more detailed discussion see Nottingham, Jour. Frank Inst. **209**, 287 (1930).

Therefore, to attain a high *current* sensitivity it is necessary to use also a high value of R. This is the point at which circuits using ordinary radio tubes are severely limited. For it will be seen that the external resistance R is shunted by the grid resistance Z_g of the tube itself, and hence the total resistance cannot be made larger than Z_g. Now in ordinary tubes Z_g is not greater than a few hundred megohms, due to insulation leakage in the tube, to the collection of positive ions by the grid, and other causes. The first requirement, therefore, of a tube used to amplify very small currents is that the input resistance be very high, or what amounts to the same thing, that the grid currents in the tube under normal operating conditions be very small. In the new tube developed by Metcalf and Thompson all sources of grid current have been systematically eliminated or greatly reduced, so that the residual currents are of the order of 10^{-15} amp and the input resistance of the order of 10^{16} ohms. These tubes are therefore capable of giving enormously greater current sensitivity than has heretofore been possible.

In addition, since the tubes operate at a plate potential of only 6 volts, it is feasible to use large capacity storage batteries for a voltage supply, thus greatly reducing galvanometer fluctuations due to changes in battery voltages. The increased steadiness makes it possible to use a more sensitive galvanometer and thus makes up for the fact that the mutual conductance is somewhat lower than in ordinary tubes.

The FP-54 pliotrons are four-element tubes with two grids interposed between filament and plate. The inner grid serves as a space charge grid and the outer grid as a control grid. The normal operating conditions are:

Filament voltage	2.5 volts
Filament current	0.11 amps
Space charge grid	+4.0 volts
Control grid	−4.0 volts
Plate	+6.0 volts

Under these conditions the tubes have the following average characteristics:

Grid input resistance	10^{16} ohms (approx.)
Control grid current	10^{-15} amp (approx.)
Mutual conductance	25 microamp/volt
Plate current	40 microamp
Plate resistance	40,000 ohms
Voltage amplification factor	1
Grid capacity	3 $\mu\mu$F.

Circuits for Use with FP-54 Pliotrons

It is not necessary to develop new types of circuits for use with the new tubes, for it has been found that standard circuits are quite adequate. For a given current sensitivity, of course, a much simpler type of circuit can be used than would be necessary with ordinary tubes. An excellent summary of the theory and practice of d.c. amplification, using ordinary tubes, has been given by Nottingham,[8] and all of the circuits used in this investigation have been

described in detail in his paper. Slight modifications are necessary, due to the fact that the FP-54 is a four-element tube.

1. *The single-tube circuit.* A very simple type of circuit which has been found suitable for many ordinary current measurements is shown in Fig. 2. It is a standard type of single-stage d.c. amplifier, in which the plate current

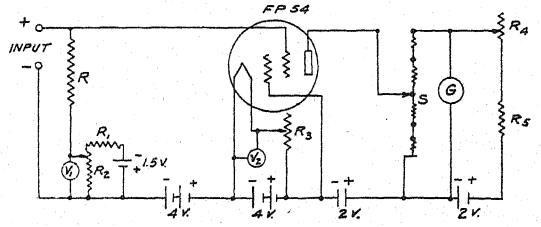

Fig. 2. Single tube circuit using FP–54 Pliotron. R, high resistance, 10^7-10^{11} ohms: R_1, fixed resistance, 100 ohms: R_2, 400 ohm potentiometer: R_3, 20 ohm·rheostat: R_4, 10,000 ohm rheostat: R_5, fixed resistance, 40,000 ohms: V_1, 0–200 millivoltmeter: V_2, 0–5 voltmeter; S, Ayrton shunt.

is balanced out of the galvanometer by means of an auxiliary battery and rheostat. The numerical values of the various resistances used are given in the figure for convenience, though these are not at all critical, and will vary for different tubes.

The method of operation is as follows: With the tube operating at normal voltages the galvanometer is made to read zero by adjustment of the rheostat R_4. The voltage sensitivity of the circuit is then determined by applying to the control grid a series of known voltages by means of the potential divider, R_2, and observing the corresponding galvanometer deflections. If the deflection is then measured for an unknown input current i, the magnitude of i can at once be determined if R is known. There is a linear relation between galvanometer deflection and input voltage as long as the latter does not exceed about 300 millivolts, in spite of the fact that the tubes do not operate normally on the straight part of their characteristic.

The circuit may be made independent of the tube characteristics by using a null method, in which the galvanometer deflection due to the input current is brought back to zero by applying a compensating voltage e by means of R_2. The input current is then simply equal to e/R. The *accuracy* then attainable is limited only by the accuracy of the voltmeter V_1, the accuracy with which R is known, and the precision with which the galvanometer can be set to zero.

The highest voltage sensitivity which can be attained with such a circuit is limited by the fluctuations due to changes in battery voltages and other causes. By using large storage batteries (e.g. 90 amp–hr) for the voltage supply and by careful shielding it has been found possible, with a Leeds and Northrup Type R galvanometer, ($1/\sigma = 5\times10^{-10}$ amp/mm), to obtain a stable voltage sensitivity in excess of 50,000 mm/volt. With a resistance R of 10^{10} ohms, a current sensitivity ($=1/S_i$) of 2×10^{-15} amp/mm is attained. Accurate measurements (to better than 1 percent) can then be made of currents of 10^{-13} amp or larger. This is just about the order of magnitude of the currents usually measured in electrometer circuits.

A somewhat higher current sensitivity may be obtained by "floating" the control grid, i.e., by making R infinite. The residual grid currents within the tube will then cause the grid to charge up slowly, and a steady drift of the galvanometer is observed. The rate of change of grid voltage will be i_g/C, where i_g is the grid current and C is the electrostatic capacity of the grid circuit. For the FP-54 tubes the grid current is in the neighborhood of 10^{-15} amp and the capacity of the grid itself is about $3\mu\mu$F. If the remainder of the grid circuit be assumed to have a capacity of 10 $\mu\mu$F, and if the voltage sensitivity, S_v, is 10^5 mm/volt, then the rate of drift of the galvanometer will be approximately 7.7 mm/sec. This drift is normally very constant, so that an input current as small as 10^{-16} amp can be measured by noting the *change* in the rate of drift which it causes. This is the method used in the General Electric Laboratories for measuring the grid currents in the tubes as they come from the factory.

2. *Balanced tube circuit.* It was found that, when currents of 10^{-14} amp or less are to be measured, more satisfactory operation is obtained with a two-tube circuit of the type developed by Wold, Wynn-Williams[4] and Eglin.[5] This method is also more satisfactory for measurement of larger currents where great steadiness and precision are desired. A diagram of the circuit actually used is shown in Fig. 3. It will be noted that it is essentially a Wheat-

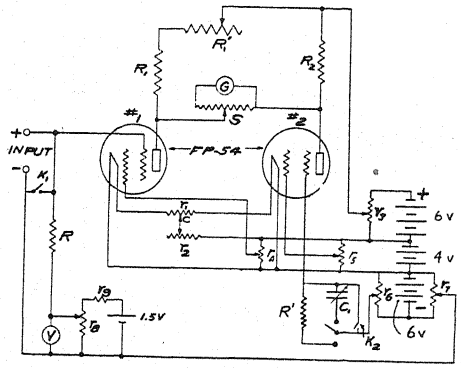

Fig. 3. Two-tube bridge circuit. R, R', high resistances: R_1, fixed resistance, 5000 ohms: R_2, fixed resistance, 10,000 ohms: R_1', resistance box, 10,000 ohms: r_1, 2 ohm rheostat: r_2, 20 ohm rheostat: r_3 to r_8, 400 ohm potentiometers: r_9, fixed resistance, 1000 ohms: K_1, K_2, electrometer keys: V, millivoltmeter: S, Ayrton shunt: C_1, variable air condenser, 15$\mu\mu$F.

stone bridge, with amplifier tubes in two of the arms and resistances in the other two. When this circuit is properly balanced it can be shown[3] that the galvanometer will be unaffected by fluctuations in the battery voltages. A considerably greater steadiness is thereby attained, so that a galvanometer of higher sensitivity may be used and a higher stable voltage sensitivity obtained. It was found, in fact, that satisfactory operation could be maintained

[4] Wold, U. S. Patent 1232879 (1916). Wynn-Williams, Proc. Camb. Phil. Soc. **23**, 810 (1927); Phil. Mag. **6**, 324 (1928).

[5] Eglin, Jour. Opt. Soc. **18**, 393 (1929).

at a sensitivity of 250,000 mm/volt, using a galvanometer sensitivity of $1/\sigma = 5\times10^{-11}$ amp/mm.

The method of balancing is as follows:[3] With the tubes operating at normal voltages, R_1' is adjusted to bring the galvanometer to zero. By means of r_3 a small change is then made in the plate voltage and the effect on the galvanometer noted. R_1' is then changed by, say, 1000 ohms and the galvanometer brought back to zero by adjustment of the various grid potentials. The plate potential is again changed by the same amount as before, and if the resulting galvanometer deflection is smaller, R_1' has been altered in the right direction. The process is then repeated until a change in plate potential produces no effect on the galvanometer.

In a similar manner the effect of filament voltage changes is observed by varying r_2, and a position of the contact C on r_1 is found such that small variations in r_2 produce no effect on the galvanometer. During this adjustment R_1' is left fixed and the balance restored after each change of C by manipulation of the grid potentials. The circuit is now ready for operation, and may be calibrated in the same way as the single-tube circuit.

The circuit shown in Fig. 3 was designed so that it could be used either with the steady deflection method or the rate of drift method. If only the steady deflection method is to be used the condenser C_1 may be eliminated and if only the rate of drift method is to be used, the resistances R and R' may be eliminated. In either case the operation is similar to that of the single-tube circuit, tube No. 1 being the active tube and No. 2 acting merely as a "dummy." The resistance R' in the grid circuit of the second tube makes for greater symmetry and hence increases the stability somewhat, but in many cases it may be left out and the grid connected directly to r_6. If R is 10^{10} ohms and the voltage sensitivity 250,000 mm/volt, the current sensitivity, $1/\sigma$, will be 4×10^{-16} amp/mm. Still higher resistances may of course be used.

An exceedingly high sensitivity may be obtained with this circuit using the rate of drift method of measurement. If the grids of both tubes are floated, and if they both charge at the same rate, then there will be no effect on the galvanometer. In general, however, the grid currents of two tubes will not be the same, but the rate of charge of the two may be *made* the same by increasing the capacity of one grid. This was accomplished by introducing the variable 15$\mu\mu$F condenser[6] C_1 in the grid circuit of the second tube. The tube with the largest grid current was made No. 2 in the circuit. This condenser was then adjusted until the galvanometer showed no drift. If a current i is now started in the input circuit, this will change the rate of charge of the grid of the first tube and hence give a galvanometer drift which is proportional to i.

The smallest current which can be detected by this method is limited only by the fluctuations of the circuit. The effects of external electric and magnetic fields, especially rapidly varying fields, were carefully eliminated by enclosing the entire circuit in a metal container which was almost air tight. All

[6] A satisfactory condenser was made by taking an ordinary radio condenser and replacing the bakelite insulation by quartz.

rheostats and connections should of course make positive contact; the storage batteries must be in good condition; to prevent insulation leaks the tubes must be kept dry. It was even found necessary to eliminate effects due to residual ionization of the air by enclosing the control grid leads in small quartz tubes painted on the outside with a suspension of graphite ("aquadag"). A wide band of aquadag was also painted around the tubes themselves to serve as a guard ring. When all these precautions were taken, it was found that the residual fluctuations were sufficiently small that an input current of approximately 5×10^{-18} amp could be detected and measured. Such a current produced a galvanometer drift in the circuit used of about 10 mm/min, and the fluctuations were also of this order. These fluctuations were of the order of magnitude to be expected from shot-effect fluctuations in the control grid currents in the two tubes, and hence the limit of sensitivity of the tubes was approximately attained.

It is of interest to note that a current of 5×10^{-18} amp is only 30 electrons per second, and the shot-effect fluctuations in such a current over a period of one second are of the order of 15 percent. If tubes could be constructed in which the grid currents were as low as 10^{-17} amp (and this may not be impossible) the sensitivity limit of the amplifier could be pushed to 5×10^{-19} amp, or 3 electrons per second. If a short period galvanometer were used, individual electron pulses could be observed.

It will be noted that the maximum voltage sensitivity attainable with this circuit is about five times that attainable with the Compton electrometer, and is 25 to 50 times greater than the usual operating sensitivity of the electrometer. There is an even greater difference between the current sensitivities of the two instruments, due to the smaller capacity of the amplifier. The author has found that, roughly speaking, a well-built amplifier is as stable at a sensitivity of 100,000 mm/volt as a good Compton electrometer at 5,000 mm/volt. In addition the amplifier has the advantages of greater mechanical ruggedness and short period. Furthermore, the sensitivity of the amplifier circuit has been found to remain constant over long periods of time, in contrast to the frequent adjustments of quadrant and needle required to maintain a constant high sensitivity of an electrometer. In short the amplifying circuit herein described has been found to be a practical and convenient current-measuring device,[7] with an attainable sensitivity greater than that of any known instrument, with the exception of the Hoffman electrometer and the Geiger counter.

3. *The two-stage amplifier.* For many problems it is desirable to measure very small currents, such as photoelectric currents, but at the same time to use an extremely rugged meter.[8] In order to test out the possibility of using instruments still more rugged than the Type R galvanometer, a two-stage

[7] Such a circuit is now being used successfully by Professor G. E. M. Jauncey and Mr. W. D. Claus at Washington University for measurements of ionization currents in an x-ray spectrometer.

[8] This is true, for example, in the photoelectric photometry of stars, where the measuring Instrument must be mounted directly on the telescope.

amplifier circuit shown in Fig. 4 was constructed. By employing a UX-112A tube in the second stage it is possible to measure the output with an ordinary microammeter (0–100 μ amp). A second state of amplification could of course be employed with either of the two circuits previously described. It seemed, however, that the greatest simplicity and convenience could be attained by using in the first stage a balanced circuit in which the dummy tube is replaced by a variable resistance. In place of the galvanometer, the second stage of amplification is substituted.

It is evident that the requirements for the tube to be used in the second stage are quite different from those for the first stage. For, while the chief requirement for the first stage is a high grid resistance, this is not at all necessary in the second stage, since the resistances R_1 and R_2 are relatively small. One will therefore use in the second stage a tube of high mutual conductance.

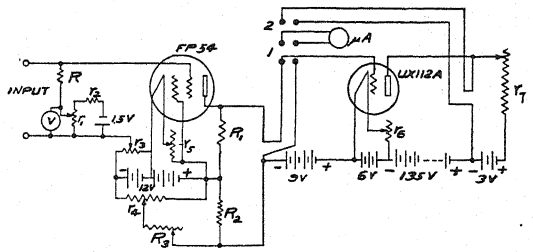

Fig. 4. Two-stage amplifier. R_1, R_2, Fixed resistances, 10,000 ohms: R_3, variable resistance, 20,000 ohms: r_1, r_3, r_4, 400 ohm potentiometers: r_2, fixed resistance, 1000 ohms: r_5, 60 ohm rheostat: r_6, 6 ohm rheostat: r_7, rheostat with fine adjustment, 1000 ohms: R, high resistance, 10^7–10^{11} ohms.

If a voltage e is applied to the grid of the first tube, then the change in the voltage of the grid of the second tube will be ke, where k stands for the expression

$$\mu R_p/(R_p + r_p).$$

Here μ is the voltage amplification factor of the first tube, R_p the external resistance in the plate circuit, and r_p the internal impedance of the first tube. The change in the plate current of the second tube will then be

$$\Delta i_p = g_{m2} ke$$

where g_{m2} is the mutual conductance of the second tube. This change in plate current will be read on the microammeter. Now the voltage amplification obtained by the FP-54 in the circuit shown is actually less than 1, so that if another FP-54 were used in the second stage, the overall sensitivity of the combination would be less than for a single tube. However, if a tube of large mutual conductance is used in the second stage, an increase in sensitivity is obtained. With the circuit shown in Fig. 4 the over-all sensitivity was found to be approximately 375 microamp/volt. Using an input resistance, R, of 10^{11} ohms, an output current of 1 microamp was obtained for an input current of 2.7×10^{-14} amp. This is a current amplification of 3.75×10^7.

The method of operating the circuit is as follows: With the double-pole-double-throw switch in position 1, the microammeter reads the output of the first stage only. The first stage is then balanced until the meter reads zero. The balance is obtained in a manner similar to the balance of the two-tube circuit by adjustment of R_3 and r_4. The microammeter switch is then thrown to position 2 and r_6 adjusted until the meter again reads zero. The circuit is then ready for operation.

The usefulness of such a circuit is quite apparent for problems in which ruggedness, portability or economy are of importance. A very inexpensive microammeter may be used since it serves only as an indicating instrument, and will be calibrated in terms of input voltage by means of the potentiometer r_1 and voltmeter V.

As a test of the practical use of this circuit the input terminals were connected to a G.E. caesium photoelectric cell, type UX-867, illuminated by a small headlight lamp. An output current of several microamperes was observed when the lamp filament was at a temperature such that it was scarcely visible to the eye in a dimly lighted room.

There are many variations and improvements on the two-stage circuit which at once suggest themselves. The circuit shown in Fig. 4 was chosen primarily for its simplicity, and it is described here because it was found to give quite satisfactory operation. Its stability and sensitivity could undoubtedly be improved by using a complete two-tube bridge circuit in each stage, using two FP-54 tubes in the first and two UX-112A tubes in the second stage.

4. *General precautions.* The chief purpose of the present paper is to bring out the fact that with the new FP-54 pliotrons the construction of a highly sensitive d.c. amplifier has been made a relatively simple task. It may be well to remark, however, that *regardless of the instrument used to measure or detect small currents*, the circuits which carry them must always be insulated and shielded with the greatest care. The problem of shielding is of even greater importance for an amplifier circuit than for an electrometer. This is due to the fact that an electrometer is practically insensitive to high frequency electric fields of constant intensity, while the amplifier actually serves as a detector for such fields. Air-tight shielding of the grid circuits is therefore essential if the amplifier is to be used in the vicinity of high voltage equipment (e.g., x-ray tubes). Shielding of *all parts* of the amplifier circuit is advised.

In all other respects (such as choice of insulation material, construction of grounding keys and high resistances, etc.) the grid circuits of an amplifier may be treated exactly as an electrometer circuit of equal sensitivity. It has been found necessary to operate the tubes at their rated voltages for from half an hour to two hours before readings are begun, in order that temperature equilibrium be obtained and that the electrostatic charges on the walls of the tubes and other places shall have reached a steady state.

A MACHINE FOR AUTOMATIC GENERATION OF AIRFOILS

By Dimitry E. Olshevsky
Sloane Physics Laboratory, Yale University and Sikorsky Aviation Corporation

(Received January 5, 1931)

Abstract

The present paper is a short account of work done with the purpose of adapting the speed, accuracy, reproducibility, and system which a drawing machine is capable of delivering to drawing large sets of systematically varied airfoils for wind tunnel research. An airfoil is defined in the paper merely as a closed curve without discontinuities in curvature and with a sharp trailing edge. Use is being made of the fact that such curves are produced by kinematical mechanisms as trajectories or coupling curves for pencil points on or near the polar curve. A machine based on the four member linkage is described and a table showing a set of systematically varied airfoils obtained with the machine is reproduced.

PRESENT methods of mechanical and analytical generation of airfoils assume a function of a complex variable to be responsible for the particular airfoil. The airfoil appears as the closed streamline in the conformal representation of a flow around a circle or some other contour, the flow around which is already known. Thus the airfoils of Zoukowsky, Drzewiecki, Miller and others have been calculated analytically and scattered attempts were made to build machines capable of delivering the particular transformation of a circle or ellipse. This mechanical-analytical method of approach has the advantages of permitting calculation of flow around the airfoil and forces acting upon it on the basis of frictionless incompressible fluid theory.

There exists however the possibility of a different viewpoint on the problem: airfoils can be defined merely as closed curves without discontinuities in curvature having a "sharp" trailing edge, the latter being, according to Prandtl's theory of boundary layer, the essential requirement for maintenance of circulation in the viscous, actual fluid. Decision as to their efficiency is left with the experimental methods. A machine capable of drawing such curves can be regarded as a mathematical operator applied to a certain closed curve described by the primary point (point A on Fig. 1, say) of the machine; this mathematical (or rather physical) operator is defined by the parameters of the machine. The transformation function drops out of the picture, at least when not expressly required, and the determination of aerodynamical qualities of the airfoil is left with the experiment.

Justification of this method of approach is its simplicity, speed and accuracy as well as efficiency of the drawing machines regarding reproducibility and systematization.

Kinematical considerations concerning shape of coupling curves of mechanisms[1] lead to the conclusion that machines having two branches of their

[1] L. Burmester, Lehrbuch der Kinematik. Felix, Leipzig, p. 297 (1888).

polar trajectory in the domain of the drawing table will draw airfoil-shaped curves (in the sense defined), for points of the movable plane situated upon or near the so-called polar curve.[2] The theory of certain linkages has been brought to a high degree of perfection. Unfortunately the most practical and inspiring problem which worried early investigators was that of securing a trajectory with the best approximation to the straight line (for mechanical engineering problems).

In the following a machine based essentially upon the classical four-member linkage is described.

The particular four-member linkage, one of the four possible combinations, is drawn in Fig. 1. Here the arm OA rotates while the other arm, BC, performs oscillations around its hinge, without making a complete turn. The instantaneous center of rotation or pole P is found at the intersection of the

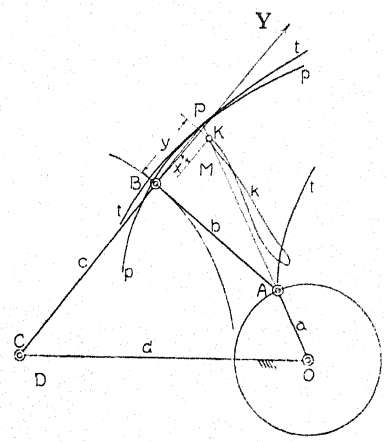

Fig. 1. The four-member linkage.

radii OA and CB. The polar trajectory,[2] t, is obtained by connecting the successive positions of the pole on plane D. It has been drawn in the figure and one observes that it crosses the drawing table twice. The polar curve, p, is also drawn. It is[3] a bicircular curve of the eighth order and is conveniently located with respect to the rod AB. Burmester[4] shows that the coupling curves of this mechanism are of the sixth order. This together with a wide variation possibility points to the suitability of the mechanism for plotting airfoils.

An experimental model of the airfoil plotting machine is shown in Fig. 2. For fixed values of dimensions, $a=OA$, $b=AB$, $c=BC$ and $d=CO$, coupling curves were drawn for various positions of the pencil K. These positions were

[2] Under polar trajectory is understood the locus of instantaneous centers of rotations, of the movable plane relative to the drawing table, upon the drawing table. The polar curve represents the locus of instantaneous centers of rotation upon the movable plane.

[3] R. Müller, Zeits. f. Math. u. Physik **36**, 11–20 (1891); **34**, 303–305 and 372–375 (1889); **42**, 247–271 (1897).

[4] Burmester, reference 1, 305.

characterized by the pencil point coordinates x and y with origin at B and X and Y axes along AB and BY respectively. The procedure of drawing consisted in slowly rotating the arm OA slightly over one full turn. Airfoils were plotted for position of the pencil not far from the polar curve on sheets of paper fixed to the drawing table.

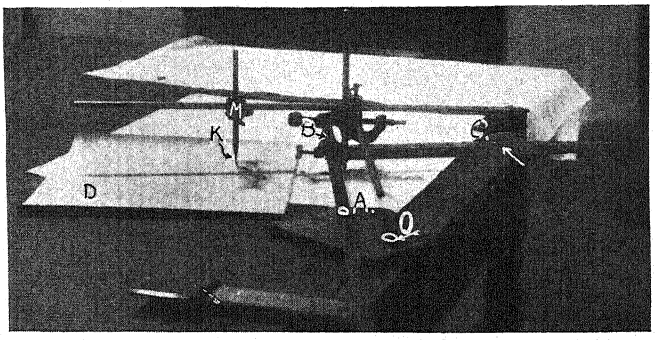

Fig. 2. The experimental model of the airfoil drawing machine.

Each airfoil is thus characterized by six parameters showing the dimensions of a, b, c, d, x and y. Any airfoil can be easily reproduced by merely setting the machine to the desired values of the parameters.

Results

A set of airfoils is shown on Fig. 3. It has the following values of the parameters: $a=3$, $b=14$, $c=9$, $d=18$, x and y variable. The curves were filled in with india ink and arranged in a two dimensional scheme according to the

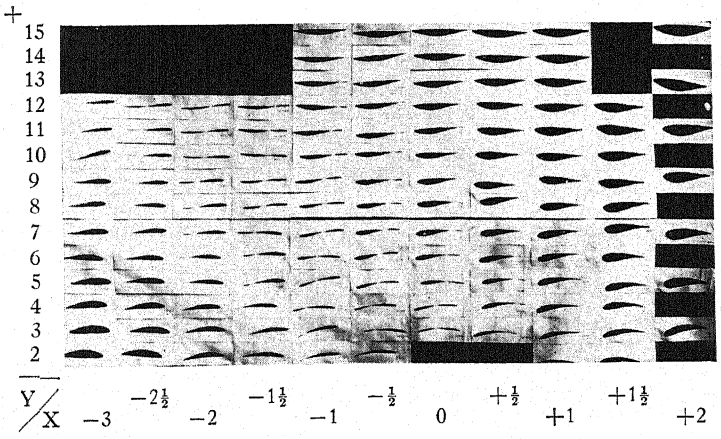

Fig. 3. A family of airfoils drawn by the machine. The photograph is considerably reduced.

variable parameters x and y. Each of the twins appearing in the center region of the set should be regarded as an airfoil with finite trailing edge angle. The analytical nature of curves drawn by the machine permits but zero angle trailing edge for single curves.

Several more promising airfoils are reproduced on Figs. 4 and 5.

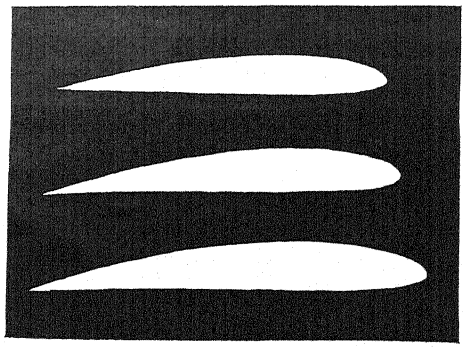

Fig. 4. Three full-scale drawings of airfoils plotted by the machine ($x=-1\frac{3}{4}$; $y=7, 6, 5$, the largest airfoil corresponding to the smallest y).

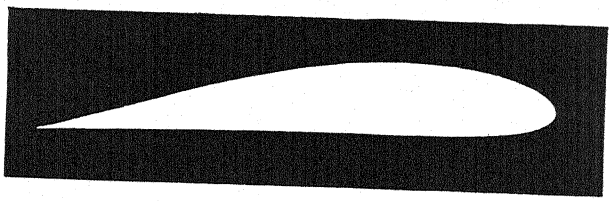

Fig. 5. Airfoil $x=2\frac{1}{2}$, $y=7$.

As a rule the accuracy of plotting was well within $\frac{1}{4}$ percent of the chord.

A machine of the type described permits drawing of a set of 150 airfoils in the course of a few days. With balance plotting automatically the polar diagram and with automatic model making machinery (as designed by the writer) the total time and expenditure connected with the investigation of properties of a large set of airfoils can be reduced to a very reasonable figure.

RECIPROCAL RELATIONS IN IRREVERSIBLE PROCESSES. I.

By Lars Onsager
Department of Chemistry, Brown University
(Received December 8, 1930)

Abstract

Examples of coupled irreversible processes like the thermoelectric phenomena, the transference phenomena in electrolytes and heat conduction in an anisotropic medium are considered. For certain cases of such interaction reciprocal relations have been deduced by earlier writers, e.g., Thomson's theory of thermoelectric phenomena and Helmholtz' theory for the e.m.f. of electrolytic cells with liquid junction. These earlier derivations may be classed as quasi-thermodynamic; in fact, Thomson himself pointed out that his argument was incomplete, and that his relation ought to be established on an experimental basis. A general class of such relations will be derived by a new theoretical treatment from the principle of microscopic reversibility. (§§1–2.) The analogy with a chemical monomolecular triangle reaction is discussed; in this case a a simple kinetic consideration assuming microscopic reversibility yields a reciprocal relation that is not necessary for fulfilling the requirements of thermodynamics (§3). Reciprocal relations for heat conduction in an anisotropic medium are derived from the assumption of microscopic reversibility, applied to fluctuations. (§4.) The reciprocal relations can be expressed in terms of a potential, the dissipation-function. Lord Rayleigh's "principle of the least dissipation of energy" is generalized to include the case of anisotropic heat conduction. A further generalization is announced. (§5.) The conditions for stationary flow are formulated; the connection with earlier quasi-thermodynamic theories is discussed. (§6.) The principle of dynamical reversibility does not apply when (external) magnetic fields or Coriolis forces are present, and the reciprocal relations break down. (§7.)

I. Introduction

When two or more irreversible transport processes (heat conduction, electrical conduction and diffusion) take place simultaneously in a thermodynamic system the processes may interfere with each other. Thus an electric current in a circuit that consists of different metallic conductors will in general cause evolution or absorption of heat at the junctions (Peltier effect). Conversely, if the junctions are maintained at different temperatures an electromotive force will usually appear in the circuit, the thermoelectric force: the flow of heat has a tendency to carry the electricity along.

In such cases one may naturally suspect reciprocal relations by analogy to the reciprocal relations which connect forces and displacements in the equilibrium theory of mechanics and in thermodynamics. Relations of this type have been proposed and discussed by many writers. The earliest of them all is due to W. Thomson;[1] it deals with thermoelectric phenomena. We shall cite Thomson's reciprocal relation in a simple form as a symmetry condition for the relations which connect the forces with the velocities. The electric current we shall call J_1, the heat flow J_2. The current is driven by the elec-

[1] W. Thomson (Lord Kelvin), Proc. Roy. Soc. Edinburgh 1854, p. 123; Collected Papers I, pp. 237–41.

tromotive force, which we shall call X_1. In corresponding units the "force" which drives the flow of heat will be:

$$X_2 = -\frac{1}{T}\,\text{grad}\ T,$$

where T denotes the absolute temperature (Carnot). If the heat flow and the current were completely independent we should have relations of the type:

$$X_1 = R_1 J_1$$
$$X_2 = R_2 J_2$$

where R_1 is the electrical resistance and R_2 a "heat resistance." However, since the two processes interfere with each other we must use the more complicated phenomenological relations

$$\begin{aligned} X_1 &= R_{11} J_1 + R_{12} J_2 \\ X_2 &= R_{21} J_1 + R_{22} J_2. \end{aligned} \tag{1.1}$$

Here Thomson's contention is:

$$R_{12} = R_{21}. \tag{1.2}$$

Thomson arrived at this relation from thermodynamic reasoning, but he had to make one additional assumption, namely: "*The electromotive forces produced by inequalities of temperature in a circuit of different metals, and the thermal effects of electric current circulating in it, are subject to the laws which would follow from the general principles of the thermodynamic theory of heat if there were no conduction of heat from one part of the circuit to another.*" Thomson thought this assumption very plausible. Even so, he cautiously considered his reciprocal relation (1.2) a conjecture, to be confirmed or refuted by experiment, since it could not be derived entirely from fundamental principles known at that time. At present Thomson's relation is generally accepted, because it has been confirmed within the limits of error of the best measurements. As regards the theory, the same relation has frequently been found as a by-product of investigations in the electron theory of metals. However, Thomson's relation has not been derived entirely from recognized fundamental principles, nor is it known exactly which general laws of molecular mechanics might be responsible for the success of Thomson's peculiar hypothesis.

In the following, a general class of reciprocal relations in irreversible processes will be derived from the *assumption of microscopic reversibility*. No further assumptions will be necessary, except certain theorems borrowed from the general theory of fluctuations. Among the relations to be derived, many have been proposed before, but some will be new. An important group among these relations can be summarized in a variation-principle, which is nothing but an extension of Lord Rayleigh's "*principle of the least dissipation of energy*"; we shall retain the name for the extended principle. According to this theorem the *rate of increase of the entropy* plays the rôle of a potential.

Thomson's hypothesis covers only part of the cases which we are going to consider, yielding the same results as the more general "principle of the least dissipation of energy." This connection will be discussed in §6; here, however, we shall comment on the natural interpretation of Thomson's hypothesis, because his formulation is somewhat ambiguous: He assumes that the temperature differences present are bound to cause a certain degradation of energy by conduction of heat; if another irreversible process (electrical conduction) takes place simultaneously, this process must cause an additional degradation of energy, making the total rate of increase of the entropy greater than it would be by heat conduction alone.

The derivation of such results from the principle of microscopic reversibility will hardly be a surprise to workers who are acquainted with the theory of irreversible processes. In many familiar cases this principle guarantees an independent balancing of different classes of molecular processes maintaining a statistical equilibrium. The writer actually conceived the idea for the new derivation of reciprocal relations by comparing the relations due to Thomson,[1] Helmholtz[2] and others with the conditions for reversibility in certain chemical reactions, as presented in §3.

The principle of microscopic reversibility is less general than the fundamental laws of thermodynamics; the consequent limitations to our reciprocal relations will be briefly described in §7. It is easy to show that Thomson's relation is no thermodynamic necessity. According to (1.2) the rate of production of entropy per unit volume of the conductor equals

$$\frac{dS}{dt} = \frac{1}{T}(X_1J_1 + X_2J_2) = \frac{1}{T}(R_{11}J_1^2 + (R_{12} + R_{21})J_1J_2 + R_{22}J_2^2).$$

Thermodynamics requires only:

$$dS/dT > 0$$

identically, except when J_1 and J_2 vanish simultaneously, or, by simple algebra:

$$R_{12} + R_{21} < 2(R_{11}R_{22})^{1/2}. \tag{1.3}$$

This condition (in a somewhat different form) was given by Boltzmann.[3]

In the present communication only one special case, namely heat conduction in an anisotropic medium (crystal), will be adequately treated (§4). This limitation allows a simplified derivation, which nevertheless brings out clearly the essential ideas of the new theoretical treatment. The derivation of other reciprocal relations, including Thomson's, will be reserved for later publication; here we shall merely enumerate the most important cases.

2. Examples of Mutual Interaction of Irreversible Processes

The formulation (1.1) of the laws of irreversible processes in terms of resistances R_{11}, etc., is well adapted to a comparison with the thermodynamic requirements; but as a rule it is a little easier to see the physical meaning of such

[2] H. v. Helmholtz, Wied. Ann. **3**, 201 (1876); Wiss. Abh. **1**, 840.
[3] L. Boltzmann, Wien. Ber. **96**, 1258 (1887).

laws when they are expressed in terms of conductances L_{11}, L_{12} · · · etc.:

$$J_1 = L_{11}X_1 + L_{12}X_2$$
$$J_2 = L_{21}X_1 + L_{22}X_2 \tag{2.1}$$

where:

$$L_{11} = R_{22}/(R_{11}R_{22} - R_{12}R_{21})$$

etc. The reciprocal relation (1.2) takes the form:

$$L_{12} = L_{21}. \tag{2.2}$$

So far we have only mentioned the interaction of heat conduction and electrical conduction. In mixtures of gases and in solutions a third transport process is possible, namely diffusion. Experience shows that any two possible transport processes are likely to interfere with each other to some extent.

It is well known that an electric current in a conductor of the second kind causes transport of matter. Conversely, a concentration gradient between two identical reversible electrodes causes an electromotive force. The relations between "forces" and velocities may again be expressed in the form (2 1). J_1 may again be the electric current, and X_1 the e.m.f.; for J_2 we take the flow of solute relative to the solvent, for X_2 the gradient $-\text{grad}\,\mu = X_2$ of the thermodynamic potential μ of the solute. The coefficients L_{11} · · · L_{22} are connected, in a manner which we need not discuss in detail, with the electrical resistance, the diffusion coefficient, the "transference number" and the e.m.f. caused by a given concentration gradient. Usually the fourth is not mentioned, since Helmholtz[3] has derived the reciprocal relation.

$$L_{12} = L_{21}. \tag{2.2}$$

His derivation is quite analogous to Thomson's treatment of the thermoelectric phenomena, and it suffers from the same weakness. However, the experiments confirm the result, Nernst[4] has given a kinetic derivation from assumptions that are somewhat specialized, and the theorem is generally accepted.

For the interaction between heat conduction and diffusion a reciprocal theorem has been derived by Eastman;[5] the case is quite analogous to the preceding. The diffusion caused by a temperature gradient is known as the Soret effect; the inverse effect has been demonstrated in a qualitative manner for a mixture of gases.[6] Eastman has also discussed thermoelectric forces in electrolytes. In that case three different transport processes are involved simultaneously. The phenomenological relations can be expressed in the form

$$J_1 = L_{11}X_1 + L_{12}X_2 + L_{13}X_3$$
$$J_2 = L_{21}X_1 + L_{22}X_2 + L_{23}X_3 \tag{2.3}$$
$$J_3 = L_{31}X_1 + L_{32}X_2 + L_{33}X_3$$

and we may suspect $3 \cdot 2/2 = 3$ reciprocal relations

$$L_{12} = L_{21}\,;\; L_{13} = L_{31}\,;\; L_{23} = L_{32}. \tag{2.4}$$

[4] W. Nernst, Zeits. f. physik. Chem. **2**, 613 (1888).
[5] E. D. Eastman, J. Am. Chem. Soc. **48**, 1482 (1926); **50**, 283, 292 (1928).
[6] Dufour, Arch. d. sc. phys. et nat. Genf **45**, 9 (1872); Pogg. Ann. **148**, 490 (1873).

The case of simultaneous diffusion of several substances in the same solution completes the list of possibilities for coupling between transport processes in isotropic bodies.

Transport processes in anisotropic bodies afford a few interesting examples of mutual interaction, for instance the conduction of heat in crystals of low symmetry. In the most general case of a triclinic crystal the phenomenological relations can be written in the form (2.3). We chose a cartesian frame of coordinates x_1, x_2, x_3; then J_1, J_2, J_3 are the components of the heat flow along these axes, and the "forces" are $X_1 = -(1/T)\partial T/dx_1$ etc. In a suitable frame of reference x_1^*, x_2^*, x_3^* parallel to the main axes of the ellipsoid:

$$L_{11}x_1^2 + (L_{12}+L_{21})x_1x_2 + \cdots + L_{33}x_3^2 = \lambda_1 x_1^{*2} + \lambda_2 x_2^{*2} + \lambda_3 x_3^{*2} = \text{const.} \quad (2.5)$$

the equations of heat conduction take the form

$$\begin{aligned} J_1^* &= \lambda_1 X_1^* + \omega_3 X_2^* - \omega_2 X_3^* \\ J_2^* &= -\omega_3 X_1^* + \lambda_2 X_2^* + \omega_1 X_3^* \\ J_3^* &= \omega_2 X_1^* - \omega_1 X_2^* + \lambda_3 X_3^*. \end{aligned} \quad (2.6)$$

If the reciprocal relations (2.4) are valid, then:

$$\omega_1 = \omega_2 = \omega_3 = 0 \quad (2.7)$$

and the conducting properties of the crystal are entirely determined by the ellipsoid (2.5); whenever the gradient of the temperature is parallel to one of the axes x^* the heat flows in exactly the same direction. If ω_1, ω_2, ω_3 do not vanish there may still be three such directions of direct heat flow, in which case these directions will no longer be perpendicular to each other, or there may be only one such direction. For instance, for crystals belonging to the tetragonal or hexagonal systems the inherent symmetry fixes the axes $x_1^* = x_1$; $x_2^* = x_2$; $x_3^* = x_3$ and demands certain relations between the coefficients, so that (2.3) and (2.6) take the form

$$\begin{aligned} J_1 &= \lambda_1 X_1 + \omega_3 X_2 \\ J_2 &= -\omega_3 X_1 + \lambda_1 X_2 \\ J_3 &= \lambda_3 X_3. \end{aligned} \quad (2.8)$$

If clockwise and counterclockwise rotations around the axis x_3 are equivalent ω_3 vanishes for reasons of symmetry, but certain classes of the crystallographic systems in question do not possess such a symmetry. When ω_3 does not vanish the flow of heat in the x_1, x_2 plane will always form an angle:

$$\arctan(-\omega_3/\lambda_1)$$

with the temperature gradient. If we should take a circular plate of such a crystal, cut parallel to the base (x_1, x_2 plane), and heat it in the middle, maintaining cylindrical symmetry, the heat would flow in spirals. Attempts by Soret and W. Voigt to detect this spiral motion met with negative results, in spite of a very sensitive method.[7]

[7] Ch. Soret, Arch. de Geneve **29**, no. 4 (1893); **32**, no. 12 (1894). W. Voigt, Gött. Nachr. 87, (1903).

The case of electrical conduction in highly anisotropic crystals is quite analogous to the heat conduction, and the thermoelectric phenomena in crystals afford a variety of possibilitities for reciprocal relations. We need only mention these two examples; a detailed discussion would not bring out any new features of the general problem.

3. Analogy with Chemical Reactions

We shall compare (2.3) with the equations for a chemical monomolecular triangle reaction. Suppose that a certain substance may exist in a homogeneous phase in three different forms A, B, C. Suppose further that any one of these may spontaneously transform itself directly into either of the others according to the scheme

(3.1)

We shall assume that the reactions obey a simple mass-action law. That is, the fraction of A molecules which will change into B in a given short time Δt is

$$k_{BA}\Delta t$$

where k_{BA} is a constant. Then the rates of change of the amounts n_A, n_B, n_C are given by the equations

$$\begin{aligned}
\frac{dn_A}{dt} &= -(k_{BA}+k_{CA})n_A + k_{AB}n_B + k_{AC}n_C \\
\frac{dn_B}{dt} &= k_{BA}n_A - (k_{AB}+k_{CB})n_B + k_{BC}n_C \\
\frac{dn_C}{dt} &= k_{CA}n_A + k_{CB}n_B - (k_{AC}+k_{BC})n_C.
\end{aligned} \tag{3.2}$$

If one or several of the coefficients k_{BA} etc. vanish the case becomes trivial; we shall therefore assume that they are all $\gtrless 0$. This condition is by itself sufficient to insure finite equilibrium concentrations $\bar{n}_A$, $\bar{n}_B$, $\bar{n}_C$, which are given by the relations

$$\frac{d\bar{n}_A}{dt} = 0 = -(k_{BA}+k_{CA})\bar{n}_A + k_{AB}\bar{n}_B + k_{AC}\bar{n}_C \tag{3.3}$$

together with

$$\bar{n}_A + \bar{n}_B + \bar{n}_C = n_A + n_B + n_C = n \tag{3.4}$$

expressing the conservation of the total amount. If the equilibrium ratios $\bar{n}_A:\bar{n}_B:\bar{n}_C$ are known this implies two independent relations between the 6 coefficients k_{AB}, k_{AC}, $\cdots$ k_{CB}, leaving 4 of them free.

Here, however, the chemists are accustomed to impose a very interesting additional restriction, namely: when the equilibrium is reached each indi-

viual reaction must balance itself. They require that the transition $A \rightarrow B$ must take place just as frequently as the reverse transition $B \rightarrow A$ etc. Now if the ratios between $\bar{n}_A$, $\bar{n}_B$, and $\bar{n}_C$ are known the condition of detailed balancing imposes three relations between the k's instead of the two expressed by (3.3), namely

$$\begin{aligned} k_{BA}\bar{n}_A &= k_{AB}\bar{n}_B \\ k_{CB}\bar{n}_B &= k_{BC}\bar{n}_C \\ k_{AC}\bar{n}_C &= k_{CA}\bar{n}_A . \end{aligned} \tag{3.5}$$

These reciprocal relations are analogous to (2.4). From (3.5) we can obtain just one relation between k_{AB} etc. alone, namely

$$k_{AC}k_{CB}k_{BA} = k_{AB}k_{BC}k_{CA} .$$

This relation is not necessary for fulfilling the thermodynamic requirements; those are satisfied as soon as an equilibrium exists, and the existence of an equilibrium is secured by any set of positive values of $k_{AB} \cdots k_{CB}$. In terms of equations: (3.5) is not contained in (3.3).

Suppose that (3.5) were not fulfilled, how could the equilibrium be maintained? Besides a certain number of transitions balancing each other directly according to the scheme

$$\begin{aligned} A &\rightleftarrows B \\ B &\rightleftarrows C \\ C &\rightleftarrows A \end{aligned}$$

we should have additional transitions taking place around the cycle

$$\begin{array}{ccc} A & \searrow & \\ \uparrow & & B \\ C & \nearrow & \end{array} \tag{3.6}$$

Now the idea of an equilibrium maintained by a mechanism like (3.6) whether entirely or only in part, is not in harmony with our notion that molecular mechanics has much in common with the mechanics of ordinary conservative dynamical systems. Barring certain exceptional cases[8] which can readily be recognized and sorted out, the dynamical laws of familiar conservative systems are always reversible, that means: if the velocities of all the particles present are reversed simultaneously the particles will retrace their former paths, reversing the entire succession of configurations. We like to think that the dynamical laws which govern the world of atoms are also reversible. The information that we have about the atoms affords considerable support for this belief of ours, and we have no serious counter-indications, if any. If the dynamical laws of an isolated molecular system are reversible the kinetic theory requires that in the long run every type of motion must occur just as often as its reverse, because the congruence of the two types of motion makes them *apriori* equivalent. This implies that if we wait a long time so as to make sure of thermodynamic equilibrium, in the end every type of motion

[8] Coriolis forces, external magnetic fields (and permanent magnets). See §7.

is just as likely to occur as its reverse. One consequence of this *principle of dynamical reversibility* is the condition that when a molecule changes a certain number of times per second from the configuration A to the configuration B the *direct* reverse transition $B \rightarrow A$ must take place equally often, as expressed by (3.5).

In order to see the full analogy between the reciprocal relations (3.5) and 2.4) we must find an expression for the change in free energy involved by the chemical reactions (3.1). Assuming in accordance with the ideal mass-action formula (3.2) that the molecules A, B, and C form an ideal solution we may express the dependance of the "free energy at constant pressure" Z of n_A, n_B and n_C in the form

$$Z = Z_{min} + RT(n_A \log (n_A/\bar{n}_A) + n_B \log (n_B/\bar{n}_B) + n_C \log (n_C/\bar{n}_C)) \quad (3.7)$$

Thus

$$\delta Z_{(P,T,n)} = RT(\log (n_A/\bar{n}_A)\delta n_A + \log (n_B/\bar{n}_B)\delta n_B + \log (n_C/\bar{n}_C)\delta n_C)$$

We shall introduce the notation

$$x_A = n_A - \bar{n}_A \quad \text{etc.} \quad (3.8)$$

and write

$$\delta Z = - X_A \delta x_A - X_B \delta x_B - X_C \delta x_C.$$

In order to obtain proportionality between the "forces" X and the displacements x we must limit ourselves to the consideration of cases where the system is nearly in equilibrium, i.e.

$$x_A << \bar{n}_A \text{ etc.}$$

Then we have

$$\begin{aligned} X_A &= - RT \log (n_A/\bar{n}_A) \sim - \frac{RT}{\bar{n}_A} x_A \\ X_B &\sim - \frac{RT}{\bar{n}_B} x_B \\ X_C &\sim - \frac{RT}{\bar{n}_C} x_C. \end{aligned} \quad (3.9)$$

Observing (3.3) and 3.8) the Eqs. (3.2) may be written in form

$$\dot{x}_A = \frac{dx_A}{dt} = -(k_{BA} + k_{CA})x_A + k_{AB}x_{AB} + k_{AC}x_C$$

or, finally, with the aid of (3.9)

$$\begin{aligned} \dot{x}_A &= (k_{BA} + k_{CA})\frac{\bar{n}_A}{RT} X_A - \frac{k_{AB}\bar{n}_B}{RT} X_B - \frac{k_{AC}\bar{n}_C}{RT} X_C \\ \dot{x}_B &= - \frac{k_{BA}\bar{n}_A}{RT} X_A + (k_{AB} + k_{CB})\frac{\bar{n}_B}{RT} X_B - \frac{k_{BC}\bar{n}_C}{RT} X_C \\ \dot{x}_C &= - \frac{k_{CA}\bar{n}_A}{RT} X_A - \frac{k_{CB}\bar{n}_B}{RT} X_B + (k_{AC} + k_{BC})\frac{\bar{n}_C}{RT} X_C. \end{aligned} \quad (3.10)$$

Comparing (3.10) with (2.3) the complete analogy between (3.5) and (2.4) is apparent.[9]

This comparison suggests that reciprocal relations of the type (2.4) can be derived from the principle of microscopic reversibility. It is true that in the above derivation of (3.5) we started out from a special picture; but we saw at least that this picture was not by itself sufficient to yield the reciprocal relations (3.5). The feature that simplified the consideration so much was the assumed mechanism of elementary transitions, which permitted us to apply the condition of reversibility, or "detailed balancing," to each type of transitions separately. We can already recognize the essential elements in the derivation of (1.2) (which is only another form of (2.4)) from the electron theory of metals. In those deductions it was assumed that the rates of transport processes were limited by collisions between particles whose velocities were distributed according to Maxwell's law. Now the collision is in effect a kind of transition leading from a state characterized by one pair of velocities (v_1', v_2') to another state (v_1'', v_2''). The requirement of microscopic reversibility enters through the condition that the transitions:

$$(v_1', v_2') \rightarrow (v_1'', v_2'') \text{ and } (-v_1'', -v_2'') \rightarrow (-v_1', -v_2')$$

must occur equally often when the system has reached thermodynamic equilibrium.

For a general derivation of reciprocal relations like (2.4) we should like to make no reference whatsoever to any particular type of mechanism. We understand already that any mechanism representing an irreversible process as the net resultant of many independent elementary transitions is liable to yield the expected relations; but we have to deal with many cases where no such mechanism can reasonably be assumed. For that reason we want to consider only the integral changes that are involved by the irreversible process. At the same time we want to apply our basic assumption of microscopic reversibility. There is just one possible way: We must consider the *fluctuations* in a system which has been left isolated for a length of time that is normally sufficient to secure thermodynamic equilibrium.

4. Heat Conduction and Fluctuations of the Distribution of Energy in a Crystal

We shall show in a simple concrete example how the principle of microscopic reversibility demands reciprocal relations in transport processes. The

[9] Strictly speaking, one may object that there is a difference between the two cases inasmuch as x_A, x_B, and x_C are subject to the restriction:

$$x_A + x_B + x_C = 0$$
$$\dot{x}_A + \dot{x}_B + \dot{x}_C = 0$$

(because of (3.3) and (3.8)); so that (3.10) actually contains only two independent variables. However, this only means that (3.10) is analogous to a set of equations of the type (2.3) written out for two variables J_1, J_2 instead of three, i.e., (2.1), with only one reciprocal relation (2.2). This statement may be verified by eliminating one of the variables x, say x_C, in the equations (3.7) etc. The whole complication is quite trivial, and we shall spare ourselves the trouble of going through the details of the calculation here.

consideration of fluctuations will enable us to treat the stationary thermodynamic equilibrium as the average result of transitions in different directions without any explicit assumption regarding elementary transitions. We must of course connect the fluctuations with the macroscopic laws of thermodynamics and irreversible processes by reasonable general assumptions. The principles involved are not new; they are classical theorems of statistical mechanics. To begin with, let us contrast the thermodynamic to the statistical point of view.

In thermodynamics we assume that when a system has been left isolated for a sufficient length of time it will reach a state of equilibrium, where all the visible properties of the system remain constant. The approach to equilibrium is irreversible.

The kinetic theory allows only a statistical interpretation of the second law of thermodynamics; the reversible fundamental laws of dynamics are not compatible with absolutely irreversible processes. For instance, we take the point of view that the uniform distribution of a gas within an enclosure is a stable equilibrium state simply because any other distribution is much less probable. We recognize the possibility that a gas may by some freak occurrence compress itself without external aid into one-half of the available volume, although we do not expect ever to observe such an event; the probability is exceedingly small, namely: 2^{-N}, where N is the total number of molecules present. While such large deviations from tne normal are exceedingly rare smaller deviations will occur much more frequently, and the common deviations from the average number of molecules in either half of the vessel will be of the order of magnitude $(N)^{\frac{1}{2}}$.

In connection with the theory of heat conduction we shall naturally study the fluctuating deviations from the thermal equilibrium. For instance, we may follow the variations in the position of the center of gravity of the energy.[10] According to thermodynamics this point will remain at rest after thermal equilibrium has been reached. According to statistical mechanics we may expect a succession of slightly asymmetrical distributions of energy. Then the motion of the center of gravity of the distribution is a legitimate object of study.

The ordinary macroscopic laws of heat conduction relate the flow of heat to the temperature gradient at any given time, so that the distribution of energy at any one time determines all subsequent distributions. From the point of view of the kinetic theory this pre-determination cannot be interpreted as absolute; for instance, we do not expect to find an ultimate motionless and completely uniform distribution as required by the macroscopic laws. Still these laws will have a quite definite meaning in the kinetic theory as well. Suppose that we reproduce the same distribution of energy many times independently. Then the subsequent distributions will not be exactly the same in all cases, nor will the rates of change agree exactly with the macroscopic laws in each individual case; but the average rates for a large number

[10] Coordinates $\xi_1 = \alpha_1/E$; $\xi_2 = \alpha_2/E$, α_1 and α_2 being defined by (4.3). We must of course make an arbitrary convention about the total content of energy E.

of cases will follow definite laws, and these laws will agree exactly with the macroscopic laws for the conduction of heat.

We also expect that an asymmetric distribution of energy will be exactly the same whether it has arisen accidentally from fluctuations or has been produced purposely by means of suitable external heating and cooling. Once a given distribution of energy is present its history is immaterial, but, as we have pointed out above, the distribution that is present at any given time determines an average expectancy for the rates of the subsequent changes. In all instances this average expectancy for the rate of transport of heat is related to the momentary distribution by the ordinary macroscopic laws for the conduction of heat.

We shall consider the simplest case that is not trivial, namely: a crystal with a 3-, 4- or 6- counting axis of symmetry (x_3)

$$x_1 + ix_2 \rightarrow (x_1 + ix_2)e^{2\pi im/n} \quad (n = 3, 4 \text{ or } 6) \quad (m = 1, 2 \cdots) \tag{4.1}$$

and no other elements of symmetry except possibly a plane of symmetry perpendicular to x_3 ($x_3 \rightarrow -x_3$) and a center of symmetry ($x_1, x_2, x_3 \rightarrow -x_1, -x_2, -x_3$). The equations for the conduction of heat take the form (2.8), or

$$\begin{aligned} -TJ_1 &= \lambda_1 \partial T/dx_1 + \omega_3 \partial T/dx_2 \\ -TJ_2 &= -\omega_3 \partial T/dx_1 + \lambda_1 \partial T/dx_2 \\ -TJ_3 &= \lambda_3 \partial T/dx_3. \end{aligned} \tag{4.2}$$

Since clockwise and counterclockwise rotations are not equivalent, and $\omega_3 \gtrless 0$ and the spiral motion of heat which we mentioned in §2 are allowed by the symmetry of the crystal. However, if we may rely on the principle of microscopic reversibility, then a state of motion in any direction is equivalent to a state of motion in the opposite direction, and for that reason ω_3 must vanish. Argument and statements are admittedly incomplete. We could not reason in such a simple manner if the case were not so symmetrical, nor would the results be quite as simple. However, let us undertake a more detailed analysis.

We shall study the fluctuations of the distribution of energy in an isolated crystal. In order to take full advantage of the rotational symmetry expressed by (4.1) and (4.2) we give the external shape of the crystal rotational symmetry about the x_3 axis. The origin of our frame of reference may be at the center of gravity of the crystal; the orientation of the axes is already determined by the symmetry. We shall consider displacements of heat in the directions x_1 and x_2. We measure the asymmetry of a given distribution of heat by the moments

$$\begin{aligned} \alpha_1 &= \int \epsilon \cdot x_1 dV \\ \alpha_2 &= \int \epsilon \cdot x_2 dV \end{aligned} \tag{4.3}$$

where $\epsilon = \epsilon(x_1, x_2, x_3)$ is the local density of energy,[11] and the integration is extended over the total volume V of the crystal. The displacements α_1 and α_2 will differ a little from zero most of the time because of fluctuations; their averages will vanish

$$\bar{\alpha}_1 = \bar{\alpha}_2 = 0.$$

For reasons of symmetry the average squares of α_1 and α_2 must be equal, and displacements in the directions x_1 and x_2 will be independent

$$\overline{\alpha_1^2} = \overline{\alpha_2^2}; \quad \overline{\alpha_1\alpha_2} = 0. \tag{4.4}$$

The same displacement (α_1, α_2) of energy may be produced by different distributions of energy, and, accordingly, of temperature. However, to each value of α_1, there will correspond a certain average temperature gradient

$$\overline{\partial T/dx_1}^{\alpha_1} = -T\overline{X}_1(\alpha_1)$$

in the x_1 direction, the averaging to be extended over all cases where α_1 takes the same value, and in each case over all volume elements of the crystal. This average gradient will be proportional to α_1:

$$\overline{\partial T/dx_1}^{\alpha_1} = -T\overline{X}_1(\alpha_1) = TC\alpha_1.$$

In a similar manner

$$\overline{\partial T/dx_2}^{\alpha_2} = -T\overline{X}_2(\alpha_2) = TC\alpha_2$$

and if we consider a displacement (α_1, α_2) in an arbitrary direction:

$$\begin{aligned} -T\overline{X}_1(\alpha_1, \alpha_2) &= TC\alpha_1 \\ -T\overline{X}_2(\alpha_1, \alpha_2) &= TC\alpha_2 \end{aligned} \tag{4.5}$$

The factor C can be calculated on the basis of the general theory of fluctuations.[12] In this particular case we shall be content to know that α_1 causes no temperature gradient in the x_2 direction, and *vice versa*, in spite of the fact that rotations in opposite directions in the x_1, x_2 plane are not equivalent. The reason is that in questions regarding the distribution the anisotropy of the crystal is immaterial anyway, and only the external boundary of the crystal is important, because all the volume elements of a homogeneous crystal are equivalent irrespective of location or mutual connections. The anisotropy becomes important as soon as one considers the *rate of exchange* of energy.

The temperature gradient determines the average rate of transport of heat according to (4.2)

$$\begin{aligned} \bar{J}_1(\alpha_1, \alpha_2) &= \lambda_1\overline{X}_1(\alpha_1, \alpha_2) + \omega_3\overline{X}_2(\alpha_1, \alpha_2) = -\lambda_1 C\alpha_1 - \omega_3 C\alpha_2 \\ \bar{J}_2(\alpha_1, \alpha_2) &= -\omega_3\overline{X}_1(\alpha_1, \alpha_2) + \lambda_1\overline{X}_2(\alpha_1, \alpha_2) = \omega_3 C\alpha_1 - \lambda_1 C\alpha_2. \end{aligned} \tag{4.6}$$

[11] Strictly speaking, one may identify heat with energy only when the crystal has no thermal expansion in any direction. In general heat must be defined as energy less work of deformation and expansion. This complicates the discussion slightly without changing the results; the symmetry conditions (4.4) and (4.5) remain valid.

[12] Einstein, Ann. d. Physik **33**, 1275 (1910).

Finally, if V is the volume, then $V\bar{J}_1$ is the total rate of transport of heat in the x_1 direction:

$$d\alpha_1/dt = V\bar{J}_1$$

and we obtain

$$\begin{aligned} \overline{d\alpha_1/dt} &= -\lambda_1 VC\alpha_1 - \omega_3 VC\alpha_2 \\ \overline{d\alpha_2/dt} &= \omega_3 VC\alpha_1 - \lambda_1 VC\alpha_2. \end{aligned} \tag{4.7}$$

Suppose now that we watch our crystal for a great length of time. Whenever the displacement of energy in the x_1 direction happens to be $\alpha_1=\alpha_1'$ we note down the displacement α_2 in the x_2 direction Δt seconds later. The average of a great number of such observations we shall denote by

$$\bar{\alpha}_2(\Delta t, \alpha_1').$$

For reasons of symmetry

$$\bar{\alpha}_2(0, \alpha_1') = 0$$

because this average does not depend on the rate of transport, but only on the relative probabilities of different distributions of energy (simultaneous values of α_1 and α_2). The average change of α_2 in a time Δt subsequent to distributions for which $\alpha_1=\alpha_1'$ is therefore

$$\bar{\alpha}_2(\Delta t, \alpha_1') - \bar{\alpha}_2(0, \alpha_1') = \bar{\alpha}_2(\Delta t, \alpha_1').$$

If Δt is sufficiently small we can calculate this change from (4.7):

$$\bar{\alpha}_2(\Delta t, \alpha_1') = \bar{\alpha}_2(\Delta t, \alpha_1') - \bar{\alpha}_2(0, \alpha_1') = \overline{d\alpha_2/dt}^{\alpha_1'} \cdot \Delta t = \omega_3 VC\alpha_1'\Delta t \tag{4.8}$$

Now we can calculate the average product

$$\overline{\alpha_1(t)\alpha_2(t+\Delta t)} = \lim_{t''\to\infty} \frac{1}{t''-t'} \int_{t=t'}^{t=t''} \alpha_1(t)\alpha_2(t+\Delta t)dt$$

Obviously:

$$\overline{\alpha_1(t)\alpha_2(t+\Delta t)} = \overline{\alpha_1'\bar{\alpha}_2(\Delta t, \alpha_1')} = \omega_3 VC\overline{\alpha_1^2}\Delta t. \tag{4.9a}$$

In a similar manner, or directly from (4.9a) by taking into account the rotational symmetry (4.1) of the crystal we obtain:

$$\overline{\alpha_2(t)\alpha_1(t+\Delta t)} = -\omega_3 VC\overline{\alpha_1^2}\Delta t = -\omega_3 VC\overline{\alpha_2^2}\Delta t. \tag{4.9b}$$

Here

$$\overline{\alpha_1^2} = \overline{\alpha_2^2}$$

The principle of microscopic reversibility demands that a displacement $\alpha_1=\alpha_1'$ of energy in the x_1 direction, followed τ seconds later by a displacement $\alpha_2=\alpha_2''$ in the x_2 direction, must occur just as often as $\alpha_2=\alpha_2''$, followed τ seconds later by $\alpha_1=\alpha_1'$. Consequently

$$\overline{\alpha_1(t)\alpha_2(t+\tau)} = \overline{\alpha_2(t)\alpha_1(t+\tau)} \tag{4.10}$$

where τ may have any value, for example $\tau = \Delta t$. Comparing with (4.9a, b) we have

$$\omega_3 = 0 \tag{4.11}$$

in accordance with Voigt's experimental result,[7] the simplest example of a reciprocal relation in irreversible processes.

Here we have taken a little more out of the principle of microscopic reversibility than we did in section 3 with the assertion that transitions between two (classes of) configurations A and B should take place equally often in the directions $A \rightarrow B$ and $B \rightarrow A$ in a given time τ. Above we have discussed transitions between different distributions of energy. We must expect that the energy will depend not only on the configuration of elementary particles, but also on their velocities; we do not know exactly how. However, assuming microscopic reversibility, the energy must depend on the velocities in such a manner that every type of motion has the same energy as its reverse; otherwise a "reverse" energy would exist, different from the ordinary energy but with similar properties of conservation, and we should not know the energy as a unique function of the state of the system. If the energy can be localized so that we can speak about distributions of energy in space, the distribution of energy must be the same for corresponding phases of direct and reverse motion, or similar discrepancies would arise. Since, by hypothesis, direct and reverse motion of every conceivable type occur pairwise equally often, if A and B be two distributions of energy, the transitions $A \rightarrow B$ and $B \rightarrow A$ (in time intervals of a given length τ) must occur equally often.

We shall comment on another question regarding the premises of the derivation, although the substance of a satisfactory answer is known from a famous discussion between Loschmidt and Boltzmann.[13] We have assumed microscopic reversibility, and at the same time we have assumed that the average decay of fluctuations will obey the ordinary laws of heat conduction. Already an apparent contradiction occurs when we consider the simpler case of heat conduction in one dimension. Let α be a displacement of heat, then:

$$\dot{\bar{\alpha}} = d\bar{\alpha}/dt = -K\alpha. \tag{4.12}$$

Microscopic reversibility requires

$$\bar{\alpha}(\tau, \alpha') = \bar{\alpha}(-\tau, \alpha'). \tag{4.13}$$

Clearly

$$\dot{\bar{\alpha}}(\tau, \alpha') = -\dot{\bar{\alpha}}(-\tau, \alpha')$$

and:

$$\ddot{\bar{\alpha}}(0, \alpha') = -\dot{\bar{\alpha}}(0, \alpha') = 0.$$

According to the ordinary laws for conduction of heat $\bar{\alpha}$ decreases for positive τ (if $\alpha' > 0$). According to (4.13), then, $\bar{\alpha}$ increases for negative τ (average growth of fluctuations), and $\dot{\bar{\alpha}} = 0$ for $\tau = 0$. It may appear somewhat startling

[13] See P. and T. Ehrenfest. Enz. d. math. Wiss. IV. 32.

that we apply (4.12) to fluctuations only for $\tau > 0$, and not for $\tau \leqq 0$. Yet in this there is no logical contradiction—we have stated bluntly and honestly that $\dot{\alpha}$ has a discontinuity for $\tau = 0$—but such a statement disappoints our expectation of continuity in nature. However, the objection is removed when we recognize that (4.12) is only an approximate description of the process of conduction, neglecting the time needed for acceleration of the heat flow. This time τ_0 is probably rather small, e.g. in gases it ought to be of the same order of magnitude as the average time spent by a molecule between two collisions. For practical purposes the time-lag can be neglected in all cases of heat conduction that are likely to be studied, and this approximation is always involved in the formulation of laws like (4.12), (4.7) and (4.2). Even the differential form (e.g. (4.8)) of these equations is justified; because we can usually choose a time Δt such that:

$$1 \gg K\Delta t \gg K\tau_0.$$

Then following $t = \tau_0$, which is practically the same as $t = 0$, we have a time interval $\Delta t \gg \tau_0$ in which (by (4.12)) α and therefore $d\alpha/dt$ are sensibly constant. We may also recall that the time needed for equalization of temperature in a body is proportional to the square of its linear dimensions l, i.e.:

$$K \sim 1/l^2.$$

In gases $K\tau_0$ should be of the order l^2/Λ^2, where Λ is the mean free path. The ordinary laws for conduction of heat are therefore asymptotic laws for $l \gg \Lambda$.

The preceding considerations leading to (4.11) are easily extended to the more general case of heat conduction in a crystal of arbitrary symmetry. The phenomenological equations have the form

$$\begin{aligned} J_1 &= L_{11}X_1 + L_{12}X_2 + L_{13}X_3 \\ J_2 &= L_{21}X_1 + L_{22}X_2 + L_{23}X_3 \\ J_3 &= L_{31}X_1 + L_{32}X_2 + L_{33}X_3 \end{aligned} \tag{2.3}$$

where

$$TX_1 = -\partial T/dx_1;\ TX_2 = -\partial T/dx_2;\ TX_3 = -\partial T/dx_3. \tag{4.14}$$

We shall derive the reciprocal relations:

$$L_{12} = L_{21};\ L_{23} = L_{32};\ L_{31} = L_{13}. \tag{2.4}$$

We chose the external shape of our crystal spherical. Since the anisotropy of the crystal has nothing to do with the distribution of heat the arguments leading to (4.4) and (4.5) apply equally well in this case, and we obtain

$$\overline{\alpha_1^2} = \overline{\alpha_2^2} = \overline{\alpha_3^2};\ \overline{\alpha_1\alpha_2} = \overline{\alpha_2\alpha_3} = \overline{\alpha_3\alpha_1} = 0 \tag{4.15}$$

$$\begin{aligned} -\overline{X}_1(\alpha_1, \alpha_2, \alpha_3) &= C\alpha_1 \\ -\overline{X}_2(\alpha_1, \alpha_2, \alpha_3) &= C\alpha_2 \\ -\overline{X}_3(\alpha_1, \alpha_2, \alpha_3) &= C\alpha_3. \end{aligned}$$

Instead of (4.6) and (4.7) we find

$$\overline{J_1}(\alpha_1, \alpha_2, \alpha_3) = -L_{11}C\alpha_1 - L_{12}C\alpha_2 - L_{13}C\alpha_3, \text{ etc.}$$
$$\overline{d\alpha_1/dt} = -L_{11}VC\alpha_1 - L_{12}VC\alpha_2 - L_{13}VC\alpha_3, \text{ etc.}$$

The analogy of (4.8) becomes

$$\overline{\alpha_2}(\Delta t, \alpha_1') = \overline{d\alpha_2/dt}^{\alpha_1'}\Delta t = -L_{21}VC\alpha_1'\Delta t$$

and we have in the place of (4.9)

$$\overline{\alpha_1(t)\alpha_2(t+\Delta t)} = \overline{\alpha_1'\bar{\alpha}_2(\Delta t, \alpha_1')} = -L_{21}VC\overline{\alpha_1^2}\Delta t \tag{4.16a}$$

Likewise

$$\overline{\alpha_2(t)\alpha_1(t+\Delta t)} = -L_{12}VC\overline{\alpha_2^2}\Delta t \tag{4.16b}$$

Microscopic reversibility (4.10) requires

$$\overline{\alpha_1(t)\alpha_2(t+\Delta t)} = \overline{\alpha_2(t)\alpha_1(t+\Delta t)}.$$

Comparison with (4.16a, b) and (4.15) yields the generalization of (4.11)

$$L_{12} = L_{21}.$$

The other two equations in (2.4) are obviously derived in the same way.

5. The Principle of the Least Dissipation of Energy

Like the reciprocal relations of mechanics and thermodynamics the relations (2.4) can be expressed in terms of a potential, and permit the formulation of a variation principle. As a preliminary we re-write (2.3) and (4.14) expressing the "forces" X by the "velocities" J:

$$\begin{aligned} -\frac{1}{T}\frac{\partial T}{dx_1} &= X_1 = R_{11}J_1 + R_{12}J_2 + R_{13}J_3 \\ -\frac{1}{T}\frac{\partial T}{dx_2} &= X_2 = R_{21}J_1 + R_{22}J_2 + R_{23}J_3 \\ -\frac{1}{T}\frac{\partial T}{dx_3} &= X_3 = R_{31}J_1 + R_{32}J_2 + R_{33}J_3 \end{aligned} \tag{5.1}$$

where $R_{11} \cdots R_{33}$ are connected with $L_{11} \cdots L_{33}$ in (2.3) by the well known relations

$$\sum_{m=1}^{3} L_{im}R_{mk} = \sum_{m=1}^{3} R_{im}L_{mk} = \delta_{ik} = \begin{cases} 1 & (i = k) \\ 0 & (i \gtrless k) \end{cases}$$

and the reciprocal relations (2.4) are equivalent to:

$$R_{12} = R_{21};\ R_{13} = R_{31};\ R_{23} = R_{32}. \tag{5.2}$$

Here, if we write:

$$2\phi(J, J) \equiv \frac{1}{T}\sum_{i,k} R_{ik}J_iJ_k \tag{5.3}$$

the relations (5.1) may be written:

$$\frac{1}{T}X_k = \frac{\partial}{dx_k}\left(\frac{1}{T}\right) = \frac{\partial\phi(J, J)}{dJ_k}. \tag{5.4}$$

We also observe that:

$$2T\phi(J, J) \equiv \sum_{k=1}^{3} J_k T\partial\phi/dJ_k = J_1X_1 + J_2X_2 + J_3X_3 \tag{5.5}$$

The function $\phi(J, J)$ we shall call the *dissipation-function*. It is a direct generalization of a function which was introduced by Lord Rayleigh[14] and applied to mutual interaction of frictional forces; it plays the part of a *potential* for such forces. Actually Lord Rayleigh used the function $F(J, J) = T\phi(J, J)$ and called F the dissipation-function; for our purposes we shall find the function ϕ more generally useful. As we shall see immediately, $2\phi(J, J)$ equals the rate of production of entropy due to heat flow across a volume element (of unit size), so that $2T\phi = 2F$ equals the rate of "dissipation" of free energy.

The rate of local accumulation of heat equals

$$Tds/dt = -\operatorname{div} J = -\partial J_1/dx_1 - \partial J_2/dx_2 - \partial J_3/dx_3 \tag{5.6}$$

writing s for the local entropy density, and the total rate of increase of the entropy S equals

$$dS/dt = \int (ds/dt)dV = \int\left(-\frac{1}{T}\operatorname{div} J\right)dV.$$

By Green's theorem:

$$\int\int\int (-\operatorname{div} J)\frac{1}{T}\,dV + \int\int\frac{J_n}{T}\,d\Omega = \int\int\int\left(J, \operatorname{grad}\frac{1}{T}\right)dV$$

$$= \int\int\int\left(J_1\frac{\partial}{dx_1}\left(\frac{1}{T}\right) + J_2\frac{\partial}{dx_2}\left(\frac{1}{T}\right) + J_3\frac{\partial}{dx_3}\left(\frac{1}{T}\right)\right)dV$$

where the double integral on the left is extended over the boundary Ω of the body in question, and J_n is the normal component of the heat flow at the boundary. If we write

$$\dot{S}^*(J_n) \equiv \int\int (J_n/T)d\Omega \tag{5.7}$$

for the entropy given off to the surroundings, and

$$\dot{S}(J) \equiv \int\int\int\left(-\frac{1}{T}\operatorname{div} J\right)dV \tag{5.8}$$

[14] Lord Rayleigh, Proc. Math. Soc. London 4, 357, [363], (1873). Theory of Sound, (London, MacMillan Co., 1st ed. 1877), Vol. I, p. 78; (2d ed. 1894), Vol. I, p. 102.

for the entropy change of the system proper, we have:

$$\dot{S}(J) + \dot{S}^*(J_n) \equiv \int \left(J, \text{grad}\,\frac{1}{T}\right) dV \equiv \int \sum_k J_k \frac{\partial}{dx_k}\left(\frac{1}{T}\right) dV$$
$$\equiv \int \frac{1}{T} \sum_k J_k X_k dV \tag{5.9}$$

(observing (4.14)). Now, by (5.4) and (5.5)

$$\int \sum_k J_k \frac{\partial}{dx_k}\left(\frac{1}{T}\right) dV = \int \sum_k J_k \frac{\partial \phi(J,J)}{dJ_k} dV = \int 2\phi(J,J) dV.$$

Inserting this in (5.9) we find

$$2\Phi(J,J) \equiv 2\int \phi(J,J) dV = \dot{S}(J) + \dot{S}^*(J_n). \tag{5.10}$$

Now we shall show that the relations (5.4) are equivalent to the *variation principle*

$$\dot{S}(J) + \dot{S}^*(J_n) - \Phi(J,J) = \text{maximum} \tag{5.11}$$

with the conventions that the temperature distribution $T(x_1, x_2, x_3)$ is prescribed, the flow $J(x_1, x_2, x_3)$ is varied, and the functions $\dot{S}$, $\dot{S}^*$ and Φ are defined by (5.7), (5.8) and (5.10), respectively (reading ($\equiv$), but not ($=$): "identical in J"). Observing (5.9) we have

$$\delta[\dot{S}(J) + \dot{S}^*(J_n) - \Phi(J,J)]$$
$$= \delta \int \left[\sum_k J_k \frac{\partial}{dx_k}\left(\frac{1}{T}\right) - \phi(J,J) \right] dV$$
$$= \int \sum_k \left[\frac{\partial}{dx_k}\left(\frac{1}{T}\right) - \frac{\partial}{dJ_k}\phi(J,J) \right] \delta J_k dV$$

so that (5.4) is clearly equivalent to

$$\delta[\dot{S}(J) + \dot{S}^*(J_n) - \Phi(J,J)] = 0.$$

Here, since $\dot{S}$ and $\dot{S}^*$ are linear functionals of J, and Φ is a homogeneous quadratic functional, the expression in the brackets can have only one extremum. This extremum is a maximum because $\Phi(J, J)$ must be positive-definite (otherwise (5.10) would not agree with the second law of thermodynamics).

If the boundary is isolated the restriction

$$J_n = 0 \tag{5.12}$$

enters, and, since then $\dot{S}^*(J_n)$ vanishes

$$\dot{S}(J) - \Phi(J, J') = \text{maximum.} \tag{5.13}$$

Thus the vector field J of the heat flow is described by the condition that the rate of increase of the entropy, less the dissipation-function, be a maximum.

In applications the difference between the formulations (5.11) and (5.13) is trivial. From a fundamental point of view (5.13) has some merit of greater simplicity because it applies to an isolated system, and is thus more directly connected with the theory of fluctuations. Above we have demonstrated (5.13) for anisotropic heat conduction. A more general theorem applying to all transport processes (conduction of electricity and heat, and diffusion) can be derived in a similar manner, only it is then necessary to make full use of the general theory of fluctuations, involving Boltzmann's classical relation between entropy S and probability W

$$S = k \log W + \text{const.}$$

This general development will be deferred to a following communication.

6. Stationary Flow and Quasi-Thermodynamics

A brief discussion of the conditions for stationary flow of heat through an anisotropic body will bring out an interesting simple consequence of (5.11) and throw light on the connection with previous quasi-thermodynamic derivations of reciprocal relations in irreversible processes.

The condition for stationary flow of heat is

$$\text{div } J = \partial J_1/dx_1 + \partial J_2/dx_2 + \partial J_3/dx_3 = 0 \tag{6.1}$$

for the interior of the body under consideration. No heat is accumulated in the interior, so that $\dot{S}(J) = 0$. Thus (5.11) becomes:

$$\dot{S}^*(J_n) - \Phi(J, J) = \text{maximum} \tag{6.2}$$

Eqs. (6.1) and (6.2) determine the field of flow J as well as the temperatures in the interior when the temperatures at the boundary are prescribed. (An eventual dependence of $\phi(J, J)$ on the temperature should be ignored in carrying out the variation: $\delta\phi(J, J) = \Sigma(\partial\phi/dJ_k)\delta J_k)$. In this case, where $\dot{S}(J) = 0$, (5.10) becomes

$$\dot{S}^*(J_n) = 2\Phi(J, J) \tag{6.3}$$

and we have

$$2(\dot{S}^*(J_n) - \Phi(J, J)) = \dot{S}^*(J_n).$$

We may therefore state (6.2) in the alternative form

$$\dot{S}^*(J_n) = \text{maximum} \tag{6.4}$$

with the restrictions (6.1) and (6.3).

Now let us consider the effect of obstacles to the heat flow, like cracks in the crystal, introducing restrictions of the type:

$$J_n' = 0$$

for the changed heat flow J' at certain interior surfaces. Since the field J of the original heat flow made $\dot{S}^*(J_n)$ a maximum under restrictions that are also imposed on J', we must have

$$\dot{S}^*(J_n) \geqq \dot{S}^*(J_n') \tag{6.5}$$

Restrictions can only decrease the rate of production of entropy, or cause no change.

Assumptions of the type (6.5) are involved in all quasi-thermodynamic derivations proposed by earlier writers for reciprocal relations in irreversible processes. As good an example as any is Thomson's case (1.1), where J_1 is the electrical current and J_2 the heat flow (in the same direction). We maintain a constant temperature gradient $-TX_2$, while X_1 may be varied. The restriction: $J_1=0$ may be imposed by breaking the electric circuit. The rate of production of entropy equals

$$\dot{S}(J) + \dot{S}^*(J_n) = (V/T)(X_1J_1 + X_2J_2)$$

(cf. (5.9)). With the aid of (1.1) we transform this relation into:

$$T(\dot{S}(J) + \dot{S}^*(J_n)) = (V/R_{22})\left[X_2^2 + (R_{12} - R_{21})X_2J_1 + (R_{11}R_{22} - R_{12}R_{21})J_1^2\right].$$

Here, if we assume that the restriction

$$J_1 = 0$$

makes $\dot{S}+\dot{S}^*$ a minimum for given X_2 (cf. (6.5)), we find

$$R_{12} - R_{21} = 0. \tag{1.2}$$

In conclusion, let us describe the case which has given name to the "principle of the least dissipation of energy." The flow of heat J_n across all sections of the boundary Ω is prescribed, and the condition

$$\int J_n d\Omega = 0$$

is fulfilled. Then $\dot{S}^*(J_n)$ in (6.2) is prescribed, and the condition for stationary flow reduces to

$$\Phi(J, J) = \text{minimum} \tag{6.6}$$

subject to the restrictions:

$$J_n \text{ prescribed} \tag{6.7}$$

$$\operatorname{div} J = 0. \tag{6.1}$$

These conditions determine J, and the temperatures are determined everywhere if known at one point.

7. Non-Reversible Systems

A dynamical system is reversible as long as the (mechanical) forces depend only on the coordinates or, if they depend on the velocities as well, are even functions of these. We know *conservative* systems which do not fulfill this condition. (i) An electric charge moving in a magnetic field is deflected by a force proportional to the product of charge and velocity. (ii) Relative to a rotating frame of reference a free particle moves as if it were subject to a transverse force proportional to the product of mass and velocity (Coriolis force) besides the centrifugal force.

When magnetic forces and Coriolis forces destroy the reversibility of macroscopic motion we must expect that the microscopic motion will fare no better. The reciprocal relations (2.4) and their equivalent, the principle of the least dissipation of energy (5.11) are derived from the assumption of microscopic reversibility. We may expect that these relations will break down in cases where magnetic or Coriolis forces are acting, and they do. The influence of Coriolis forces on heat conduction is presumably small and not easily studied; but magnetic fields are known to modify the relation between heat flow and temperature gradient in metals. In an isotropic body, the simplest case, the temperature gradient has the same direction as the heat flow as long as no magnetic field is present. However, if a transverse magnetic field is applied the temperature gradient will have a component in the third direction perpendicular to flow and field. The direction of the temperature gradient is rotated with respect to the heat flow, about an axis parallel to the magnetic field. This phenomenon is known as the Righi-Leduc effect. If a circular metal plate is placed perpendicular to the magnetic field, heated in the middle and cooled at the edge, the heat will flow outward in spirals. The equations of the heat flow take the form (2.8), or rather

$$\begin{aligned} J_1 &= \lambda X_1 + \omega X_2 \\ J_2 &= -\omega X_1 + \lambda X_2 \\ J_3 &= \lambda X_3 \end{aligned} \tag{7.1}$$

where ω is proportional to the intensity of the magnetic field (for weak fields); the field is thought parallel to the x_3 direction. The principle of the least dissipation of energy is no longer valid; radial cracks in the plate will *increase* the rate of radial transport of heat for a given temperature gradient.

More familiar than the Righi-Leduc effect is perhaps the Hall effect. When a constant current is flowing through a metallic conductor a transverse magnetic field causes an e.m.f. perpendicular to both. Eqs. (7.1) describe the isotropic case if J_1, J_2, J_3, denote the components of the current and X_1, X_2, X_3 the components of the electric field.

In the presence of a magnetic field the principle of microscopic reversibility may be applied in a modified form: The entire motion may be reversed by reversing the magnetic field together with the velocities of all the particles composing a dynamical system. Eqs. (7.1) are in accord with this requirement.

An analogous effect of Coriolis forces is known in hydrodynamics. The principle of the least dissipation of energy applies to the motion of very viscous fluids (Stokes' limiting case) as long as the motion is not referred to a rotating frame of reference.

THE DIELECTRIC CONSTANT AND ELECTRIC MOMENT OF SOME AMINES

By P. N. Ghosh and T. P. Chatterjee
Applied Physics Laboratory, Calcutta University

(Received January 6, 1931)

Abstract

By using a heterodyne null-beat arrangement, the electric moments have been calculated and the following results obtained: methyl amine, $A=1.37\times10^{-3}$, $\mu=0.99\times10^{-18}$; dimethyl amine, $A=1.22\times10^{-3}$; $\mu=0.90\times10^{-18}$; trimethyl amine, $A=1.19\times10^{-3}$; $\mu=0.82\times10^{-18}$; ethylamine, $A=2.37\times10^{-3}$; $\mu=0.99\times10^{-18}$; diethyl amine, $A=2.59\times10^{-3}$; $\mu=0.90\times10^{-18}$; and triethyl amine, $A=2.90\times10^{-3}$; $\mu=0.82\times10^{-18}$.

Introduction

IT HAS been found by several investigators that the dipole moment for a series of homologues is sensibly constant and is the property of a polar group present in them. For the primary alcohols[1] such a relationship has been obtained. The halogen-derivatives[2] of methane and ethane also support this view. Hojen-dahl[3] has tested the above hypothesis in many other cases. On the basis of certain assumptions, he has calculated the dipole-moment from the data of Pohrt[4] who had used a bridge method to determine the dielectric constants of vapors at a standard temperature and at varying pressures. It was, however, found from his calculations, that the amines do require a more careful study and thus form the object of the present investigation.

Experimental

The apparatus used was the heterodyne null-beat arrangement described by Mahanti in a recent paper.[2] The same procedure was followed for the measurements presented in this paper.

The electric moments have been calculated from the relation

$$\mu^2 = 1.208 \times 10^{-36} B, \qquad (1)$$

which has been deduced from the Debye equation.

Discussion

It is evident from Table II that the dipole-moments of the methyl and ethyl amines are equal in magnitude while those of dimethyl and diethyl amines are among themselves equal. The dipole-moments of the trimethyl

[1] Mahanti and Das Gupta, Ind. Jour. Phys. **3**, 467 (1929); J. B. Miles, Phys. Rev. **34**, 964 (1929).
[2] Mahanti, Phys. Zeits. **31**, 546 (1930).
[3] K. Hojendahl, Dissertation, Copenhagen, 1928.
[4] Pohrt, Ann. d. Physik **42**, 569 (1913).

TABLE I.

Compound	Temp. in Abs. scale	Press. in mm of mercury	$(\epsilon-1)$ at the observed Press.	$\frac{(\epsilon-1)P_0T}{PT_0}$	$\frac{(\epsilon-1)P_0T^2}{PT_0}$
Methyl amine $(CH_3)NH_2$	296.2	110	0.0005586	0.004187	
		109	0.0005586	0.004226	1.246
		110	0.000561	0.004206	
	317.13	181	0.0008233	0.004015	
		126	0.0005709	0.003998	1.267
		248	0.001113	0.003969	
	332.4	187	0.0007812	0.003866	
		187	0.0007859	0.00389	1.287
		188	0.0007865	0.00387	
	349.5	180	0.000688	0.003718	
		105	0.0004062	0.003763	1.306
		152	0.0005834	0.003735	
	362.2	284	0.0006676	0.003658	
		173	0.0006328	0.003688	1.328
		171	0.0006201	0.003656	
Dimethyl amine $(CH_3)_2NH$	296.2	92	0.0003844	0.003445	
		82	0.0003455	0.003475	1.023
		66	0.0002759	0.003448	
	316.5	103	0.0003943	0.003296	
		114	0.0004257	0.003292	1.042
		112	0.0004184	0.003292	
		118	0.0004425	0.003304	
		114	0.0004281	0.003309	
	331.1	93	0.0003285	0.003251	
		101	0.0003433	0.003195	1.066
		113	0.0003943	0.003215	
	360.5	135	0.0004985	0.003037	
		176	0.0005353	0.003052	1.101
		112	0.000343	0.003076	
Trimethyl amine $(CH_3)_2N$	294.6	97	0.0003583	0.003027	
		97	0.0003608	0.003049	.8986
		88	0.0003266	0.003043	
		88	0.0003307	0.003083	
	309.2	85	0.0002985	0.003019	
		83	0.0002874	0.00298	.9255
		83	0.0002874	0.00298	
	324.53	170	0.0005473	0.002908	
		92	0.000295	0.002897	.9419
		130	0.0004182	0.002906	
	364.4	143	0.0003868	0.002687	
		114	0.0003142	0.002796	.9986
		146	0.0003941	0.002739	
Ethyl amine $(C_2H_5)NH_2$	294.5	65	0.0004061	0.005121	
		79	0.0004844	0.005142	1.511
		77	0.0004818	0.005129	
	300.8	55	0.0003384	0.005150	
		52	0.0003168	0.005100	1.54
		45	0.0002757	0.005129	
	315.3	67	0.0003796	0.004973	
		59	0.0003408	0.005068	1.582
	332.7	78	0.0004085	0.00485	
		76	0.0003949	0.004809	1.61
		75	0.0003941	0.004865	
	344.2	83	0.0004184	0.004829	
		81	0.0004061	0.004805	1.66
		81	0.0004085	0.004833	

TABLE I (*Continued*).

Compound	Temp. in Abs. scale	Press. in mm of mercury	$(\epsilon-1)$ at the observed Press.	$\frac{(\epsilon-1)P_0T}{PT_0}$	$\frac{(\epsilon-1)P_0T^2}{PT_0}$
Diethyl amine $(C_2H_5)_2NH$	297.2	124	0.0007259	0.004844	1.44
		124	0.0007259	0.004844	
	312.1	116	0.0006328	0.004728	
		117	0.0006353	0.004817	1.477
		104	0.0005685	0.004749	
	303.55	112	0.0006406	0.004833	
		97	0.0005538	0.004821	1.463
		92	0.0005238	0.004809	
	367.3	113	0.000486	0.004399	
		104	0.0004416	0.004346	1.604
		133	0.0005663	0.004354	
Triethyl amine $(C_2H_5)_3N$	297.6	42	0.0002471	0.004874	
		46	0.000271	0.004879	1.451
	304.65	38	0.0002162	0.004821	
		37	0.0002136	0.004897	1.481
		43	0.0002471	0.004872	
	315.5	46	0.0002518	0.004799	
		39	0.0002113	0.00476	
		30	0.000164	0.004799	1.509
		38	0.0002066	0.004776	
		38	0.0002066	0.004776	
	343.3	33	0.0001592	0.00461	
		37	0.0001781	0.004602	1.581
		37	0.0001781	0.004602	
	377.2	40	0.0001685	0.004424	
		41	0.0001733	0.004437	1.681
		42	0.0001805	0.004512	

and the triethyl amines present a similar result. Thus in the case of the n-amines, the polar group (NH_2) is mainly responsible for the development of the dipole-moment in the molecule. Similarly the (NH) group in the diamines and the (N) radicle in the triamines give rise to dipole moments in the respective molecules.

TABLE II.

Compound	A	B	$\mu\times10^{18}$	Calculated values of Hojendahl
Methyl amine	0.00137	0.826	0.99	1.31
Dimethyl amine	0.00122	0.675	0.90	1.05
Trimethyl amine	0.00110	0.560	0.82	—
Ethyl amine	0.00237	0.826	0.99	1.31
Diethyl amine	0.00259	0.675	0.90	0.94
Triethyl amine	0.00290	0.560	0.82	0.76

Table II also indicates that the dielectric constant increases with the boiling points of the compounds as is usually expected. The only exception is found in the case of methyl amine.

It is also interesting to note that Venkateswaran and Bhagavantham[5] have found a Raman line arising from a frequency of 3300 cm^{-1} (approx.) present in both methyl and ethyl amines, and have attributed this to the N-H linkage. This line, is however, absent in the spectrum of triethylamine.

[5] Venkateswaran and S. Bhagavantam, Ind. Jour. Phys. **5**, 129 (1930).

VARIATIONS WITH TEMPERATURE AND FREQUENCY OF DIELECTRIC LOSS IN A VISCOUS, MINERAL, INSULATING OIL

By Hubert H. Race
General Electric Company, Schenectady, New York

(Received December 29, 1930)

Abstract

Debye's theory of polar molecules has been extended to give simple expressions for conditions of maximum loss per cycle in terms of equivalent circuit bridge or substitution measurements. The *dielectric loss* in a good grade of viscous mineral insulating oil has been separated into two components; one resulting from conduction, and the other showing characteristics with frequency and temperature qualitatively explained on the basis of the presence of polar molecules in the oil. A quantitative check shows the order of magnitude of this second loss to be the same as that which would be predicted by Debye's theory. The experimental curve shows a wider frequency response than the theoretical curve, indicating that the simple theory is not sufficient to account for the observed data. This may result from the presence of polar molecules of many different sizes giving an average response rather than molecules of one size only, as assumed in the theory. The size of the polar molecules necessary to give the observed effects was calculated from Deybe's theory and found to be of the right order of magnitude. Data taken over a wide range of frequency and temperature indicate the danger in drawing conclusions as to the characteristics of a material from data taken for limited ranges of experimental conditions. The curves show that either inincreasing or decreasing *power factor* can be obtained as a function of either frequency or temperature for certain narrow limits of experimental conditions. The dielectric loss in good commercial mineral insulating oils at power frequencies and operating temperatures results from conduction only, the contribution of polar molecules to the loss being negligible. Before a definite statement is made regarding the mechanism of the observed loss, studies should be made to determine whether a satisfactory theory can be developed which is based only on the motion of charged particles in a viscous medium.

Introduction

THE object of this investigation is the experimental and theoretical study of the changes of the electrical characteristics of a viscous insulating oil, such as is used in "solid type" cables, with changes in temperature and in frequency of the applied alternating potential. The data reported in this paper have been collected at intervals during the past eighteen months. Previous tests have shown that, under certain conditions, the d.c. conductivity and the equivalent parallel a.c. conductivity calculated from 1000 cycle bridge measurements, are identical.* Therefore, the ranges of frequency and temperature were extended to determine under what conditions this agreement fails. The work of Kitchin and Müller[1] indicated the possibility of explaining

* These tests are reported in a paper on "Some Electrical Characteristics of Cable Oils," which has been submitted for publication in the A.I.E.E. Journal.

[1] D. W. Kitchin and Hans Müller, Phys. Rev. **32**, 979 (1928).

variations in dielectric loss with frequency and temperature in terms of Debye's theory of polar molecules. The desire to check this theory offered another incentive in making the experiments reported in this paper.

The resulting data show characteristics qualitatively similar to those predicted by Debye's theory of polar molecules. A quantitative check was therefore made and found to be of the right order of magnitude.

Apparatus and Procedure

1. *Testing cells.*—For most of the measurements reported in this paper, the cell shown in Fig. 1 was used. The two concentric cylinders are made of a steel alloy containing 18 percent chromium and 8 percent nickel. This alloy is not attacked by hot oil and has a very small catalytic effect on the oil. The inner cylinder (1) is hollow with hemispherical ends welded on, using an atomic hydrogen flame, thereby making an oil-tight joint and completely seal-

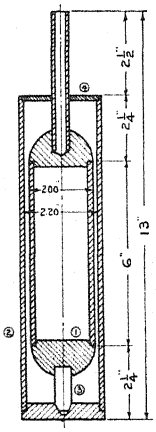

Fig. 1. Oil resistivity cell.

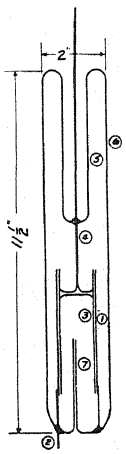

Fig. 2. Vacuum cell for electrical measurements of insulating oils.

ing the interior. The bottom of the outer cylinder (2) has a central conical hole into which the fused quartz post (3) of the inner cylinder fits. The inner electrode is centered at the top by the fused quartz collar (4) which is made with a sliding fit so that the inner electrode can be easily removed for cleaning. The temperature is indicated by a thermometer placed in the tube in the top of the inner electrode. The fused quartz insulation was shown to have negligible surface leakage, volume conductivity and dielectric loss.

Before a measurement, the oil to be tested was placed in the cell and carefully evacuated. Then the fused quartz collar was placed in position effectively sealing the oil against the absorption of moisture from the atmosphere. The temperature was controlled by placing the cell in a thermostatically controlled heater.

However, to make certain that absorbed moisture or absorbed gases were not responsible for the observed dielectric loss, the vacuum cell shown in Fig.

2 was prepared. The electrodes were concentric nickel cylinders, 10 cm high and spaced about 2 mm apart. The outer cylinder (1) was supported by two wires sealed into the bottom of the Pyrex cell, one of which acted as the ground lead (2). The inner cylinder (3) was supported only by a stiff wire (4) which was sealed into the top of the cell and served as the other lead. The Pyrex tube (5) supporting the inner cylinder was sealed to the top of the cell wall (6) to form an annular expansion chamber for the oil and also to provide a very long glass path between the two electrodes. A small tube (7) with a closed end was sealed into the bottom of the cell so that the temperature of the oil in the cell could be determined with a small thermocouple.

For filling, two glass tubes extended from the top of the annular chamber. One was sealed to a good vacuum system. The other led through a stop-cock to a reservoir of oil at atmospheric pressure. The oil was heated to about 125°C and allowed to bubble very slowly through the stop-cock thereby liberating all gases. When the cell was filled to a level near the top of the expansion chamber and all bubbling had ceased, both tubes were sealed off leaving completely degasified oil in the cell ready for the electrical measurements.

Tests on this cell before and after filling showed the following:

(a) The dielectric loss in the oil showed the same characteristics as those observed with the quartz insulated cell. (b) The errors of measurement caused by leakage over the surface at low frequencies and by dielectric loss in the Pyrex at high frequencies were greater than for the quartz insulated cell. (c) The actual measurements with the vacuum cell were less accurate because the cell constant was much smaller than for the quartz insulated cell. (d) The errors could have been eliminated by using guard ring electrodes but for commercial oils these complications seemed unnecessary.

For these reasons all subsequent measurements were made with the open, quartz insulated cell and only measurements made with this cell are reported.

2. *D. C. Measurements.*—The source of potential was a 350 volt "B" battery and a sensitive galvanometer with an Ayrton shunt was used to measure the current. The galvanometer calibration was checked before and after each run.

3. *Low-Frequency Measurements.*—A variable frequency vacuum tube oscillator[2] having a range from 200 to 10,000 cycles per second was used to supply a modified General Radio "power factor bridge." The variable capacitance standard was a General Radio precision instrument. This same standard was used for both low and high frequency measurements.

4. *High-Frequency Measurements.*—These tests were made with equipment permanently installed in a well shielded room built especially for radio frequency measurements. The standard substituation method (Bureau of Standards Circular No. 74) was used throughout. The generating circuit was a vacuum tube oscillator having a frequency range from 4×10^4 to 3×10^6 cycles per second. The power rating was sufficient to prevent any change in either the frequency or the voltage when changes were made in the loosely

[2] Gen. Elec. Rev. P. 521, October, 1929.

coupled measuring circuit. The oscillator gave an approximate sine wave, having less than 5 percent harmonic components.

The measuring circuit is shown in Fig. 3. The generating circuit (1) has been discussed above. Coupling coils (2) having from 1 to 10 turns were used depending upon the frequency desired. The measuring circuit was loosely coupled to the generating circuit by the coil (3). The special high frequency switch (4) was used for connecting either the test cell (5) or the standard capacitance (6) into the measuring circuit. The switch was composed of six mercury cups mounted on fused quartz tubes. Amalgamated copper wires were used for making contact between the desired pairs of cups. The current-indicating device in this circuit was a special vacuum thermocouple whose heater resistance had a constant value of 0.72 ohm over the entire frequency range. This type of couple is designed so as to have a long leakage path between the heater leads. The thermocouple was connected through the radio frequency choke (8) to the sensitive galvanometer (9). The sensitivity of the

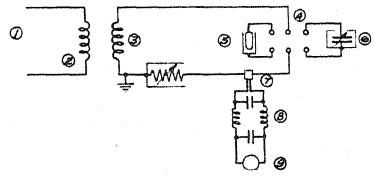

Fig. 3. High frequency measuring circuit.

combination was such that 2×10^{-4} amp. input to the heater of the thermocouple gave approximately 1 mm deflection on the galvanometer scale. The link resistors (10) were made of short straight lengths of non-magnetic, resistance wire sealed in evacuated glass tubes. These were approximately the same length and range from 0.115 to 26.2 ohms. For greater resistances a shielded General Radio decade resistance box, having 0.1 ohm steps, was used.

The procedure for a high frequency measurement differed slightly from that prescribed by A.S.T.M.D. 150-27T, and was as follows:

(a) The supply oscillator was set at the desired frequency and a coupling coil was selected which would resonate with the test cell connected and a short circuiting link at (10). This circuit was then tuned exactly to resonance by varying the supply frequency and the galvanometer deflection recorded. With no further change in the supply oscillator, the standard capacitor was substituted for the test cell and adjusted to give resonance of the measuring circuit. The setting of the standard was then the capacitance of the test cell. If the galvanometer deflection was not the same as it was with the test cell in the circuit, the effective resistance of the circuit must be different. That is, the dielectric loss of the standard capacitance differed from that of the test cell. Since the standard was an air capacitance with good insulation, its dielectric loss was very small and was considered negligible. Link resistors were added in series with the standard capacitance until the deflection was the

same as that recorded for the test cell, thus giving the equivalent series resistance of the test cell. For each point this procedure was repeated several times to make certain of the value obtained and then the exact frequency was determined with a wave meter.

Calculations from A. C. Measurements

The alternating current measurements have been interpreted in terms of the equivalent parallel circuit shown in Fig. 4. C is the equivalent capacitance

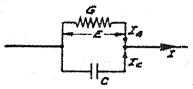

Fig. 4. Equivalent circuit for an imperfect dielectric.

and is considered to have zero loss and zero inductance. G is the equivalent a.c. parallel conductance and is considered to have zero capacitance and zero inductance. This simple equivalent circuit has been used for the following reasons:

(a) The mechanism of dielectric loss in oils is not sufficiently well understood to enable one to represent it exactly in terms of ideal resistances and capacitances. Therefore *a circuit which is assumed to be equivalent rather than one which is theoretically exact, must be used.*

(b) The actual measurements were made with a series connection of a resistance having negligible capacitance and a capacitance having negligible loss. Therefore the interpretation of the results *must be made* in terms of this simple series measuring circuit.

(c). However the parallel circuit is chosen in preference to the series circuit because G represents a coefficient of dielectric loss independent of C. That is, G is proportional to the component of current in the external circuit which is in phase with the applied potential. Therefore it is a measure of the dielectric loss regardless of the mechanism by which that loss may have been produced.

(d). With the coefficient G, the dielectric losses of different materials can be compared without reference to their dielectric constants. It is therefore preferable to the commonly used coefficient of power factor which represents a ratio of dielectric loss to dielectric coefficient and therefore involves two independent characteristics of the material.

(e). Under certain special conditions the equivalent parallel conductance obtained by a.c. measurements is identical with the d.c. conductance so that this method of representing the a.c. measurements is very convenient, in correlating a.c. and d.c. tests.

To obtain the relations between equivalent series and parallel circuits let:

R = the known equivalent series resistance of the test cell
C_s = the known equivalent series capacitance of the test cell
G = the desired equivalent parallel conductance of the test cell
C = the desired equivalent parallel capitance of the test cell
$w = 6.28$ (frequency in cycles per second of the applied potential).

The equivalence between the series and parallel circuits is expressed by the complex relation

$$G + iwC = (R - i/wC_s)^{-1} \tag{3}$$

from which are obtained the two real equations:

$$G = \frac{R}{R^2 + (1/wC_s)^2} \tag{4}$$

and

$$wC = \frac{(1/wC_s)}{R^2 + (1/wC_s)^2}. \tag{5}$$

For good dielectrics the loss component of current is small compared to the capacitance component so that it may be assumed that,

$$R^2 <<< (1/wC_s)^2. \tag{6}$$

With this assumption Eqs. (4) and (5) become:

$$G = Rw^2C_s^2 \tag{4a}$$

and

$$C = C_s \tag{5a}$$

The apparent power factor of a dielectric is generally used as a measure of its quality and may be calculated from either the equivalent series or equivalent parallel circuit. The definition of power factor is:

$$\text{power factor} = \frac{\text{real power}}{\text{apparent power}}. \tag{7}$$

For the series circuit

$$P.F. = \frac{I^2R}{I^2(R^2 + (1/wC_s)^2)^{1/2}} \tag{8}$$

and if $R^2 <<< (1/wC_s)^2$ this reduces to,

$$P.F. = RwC_s. \tag{8a}$$

For the parallel circuit,

$$P.F. = \frac{E^2G}{E^2(G^2 + (wC)^2)^{1/2}} \tag{9}$$

or again if $G^2 <<< (wC)^2$ Eq. (9) reduces to

$$P.F. = G/wC. \tag{9a}$$

Since both low and high frequency measurements were made in terms of an equivalent series circuit, Eqs. (4) and (8) were used to obtain the equivalent parallel conductance and the equivalent power factor of the test samples.

Discussion of Experimental Results

The results of previous tests led to a study of a single oil through a wide range of frequency and temperature. Properties of the oil on which these measurements were made are given in Table I.

Table I. *Physical data for the oil studied.*

(1)	Flash point	280°C
(2)	Fire point	320°C
(3)	Acid value	0.035 milligram of KOH per gram
(4)	Dielectric strength at 30°C	37 kilovolts for 0.1 inch gap
	Dielectric strength at 100°C	29 kilovolts for 0.1 inch gap
(5)	Specific gravity at 30°C	0.9085
	Specific gravity at 100°C	0.8654
(6)	Viscosity at 30°C	11.76 poises
	Viscosity at 100°C	0.27 poises

The equivalent parallel conductance was taken as a measure of the dielectric loss and the results of the entire series of tests are shown in Fig. 5. Inasmuch as no equipment was readily available for measurements at frequencies between 3,000 and 125,000 cycles per second, there is a gap in the data between these frequencies. The curves indicate no sudden change in the characteristics of the oil so that it did not appear necessary to set up special equipment for this frequency range.

The most interesting deductions to be drawn from these data are as follows:

(a). As the temperature is increased all of the curves approach the line representing the d.c. conductance. For example at 150°C the conductance is the same for all frequencies below 125,000 cycles per second since curves (1) through (5) all pass through the point (*a*).

(b). For each frequency there is a temperature below which the total dielectric loss is greater than can be explained by the mechanism of conduction.

These observations may be stated in a slightly different way; namely,

(c). For a given temperature there is a critical frequency such that for all lower frequencies the a.c. loss is independent of the frequency and for all higher frequencies the loss increases with the frequency. Within the first frequency range the mechanism of d.c. conduction and of a.c. loss appear to be the same, and both are probably due to the migration of charged ions or larger particles in the oil.

(d). The higher the temperature, the higher the critical frequency below which the a.c. and d.c. losses are the same.

These data seem to indicate that the total dielectric loss can be separated into two components,—one independent of frequency and due to the same mechanism as d.c. conduction, and the other independent of conduction and varying with both frequency and temperature. In the remainder of this discussion, therefore, the total dielectric loss will be considered to be the algebraic sum of these two components.

$$\text{Total dielectric loss } (P) = \text{d.c. loss } (P_d) + \text{a.c. loss } (P_a) \qquad (10)$$

The name d.c. loss is used as the simplest designation for the component that is independent of frequency and the name a.c. loss is used to mean the component which varies with frequency. They are so separated because it seems that they result from two entirely different effects of the applied potential and are independent of each other as far as their variation with frequency and temperature is concerned.

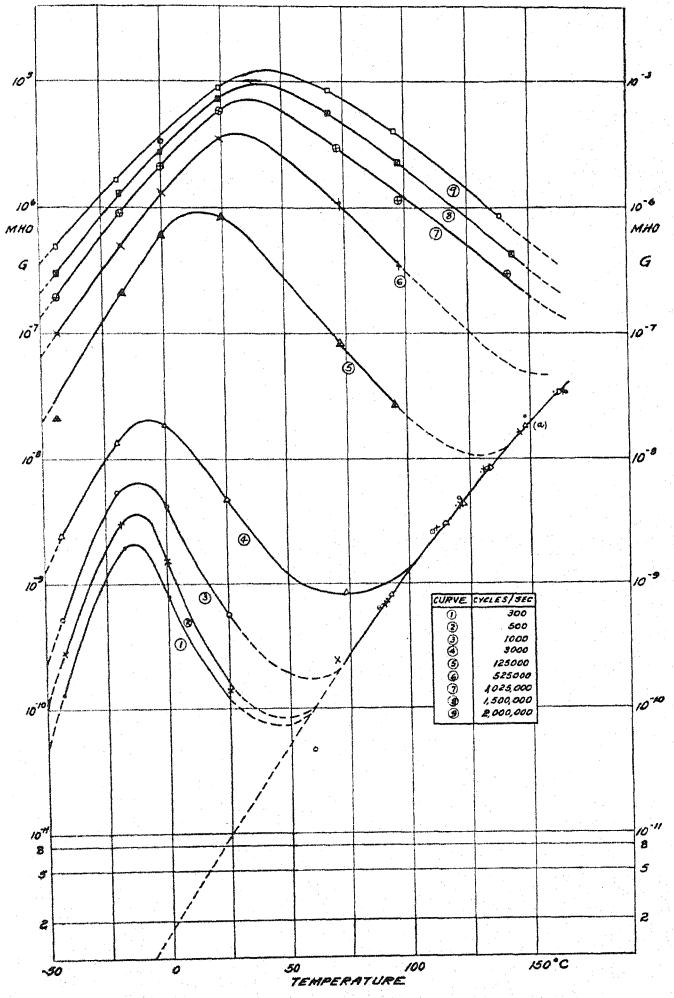

Fig. 5. Total dielectric loss in a heavy cable oil as a function of frequency and temperature. Loss per $cm^3 = (E^2/V)G$ watts/cm^3. E is the potential in volts, G the equivalent parallel conductance in mhos, and V the effective volume of oil in test cell (73.7 cm^3).

These two components are represented by their equivalent conductances as shown in Eq. (10a).

$$P = E^2G = E^2(G_d + G_a) \tag{10a}$$

so that G_a may be obtained as the algebraic difference of G and G_d.

Accordingly the next step in studying these data was to plot curves for $(G-G_d)/f$. As shown in Fig. 6 they give the a.c. loss per cycle as a function of frequency for seven different temperatures. These curves are very interesting since they show that, after the loss due to d.c. conduction has been subtracted, the remainder, when plotted as loss per cycle goes through a maximum as a function of either temperature or frequency. The curves at different temperatures are similar. The higher the temperature (or the lower the viscosity), the higher is the frequency necessary to produce maximum loss.

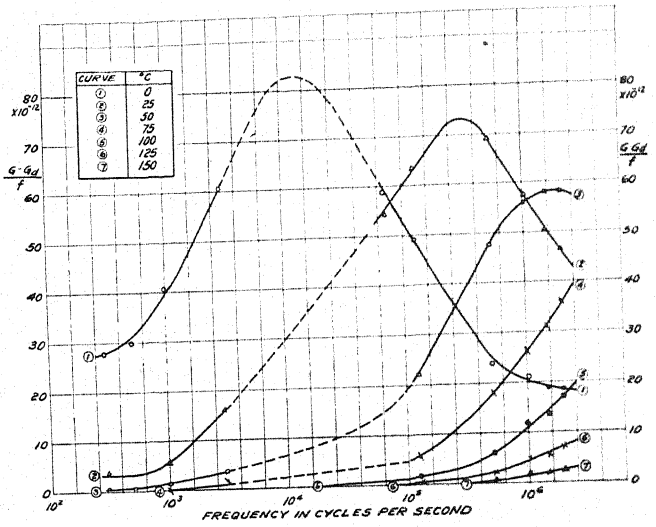

Fig. 6. a.c. loss in a heavy cable oil as a function of frequency for different temperatures. Loss per cycle per cm^3 $=(E^2/fV)(G-G_d)$ joules/cycle/cm^3. E is the potential in volts, G is the equivalent parallel conductance in mhos, G_d is the d.c. conductance in mhos, f is the frequency in cycles per second and V is the effective volume of oil in test cell (73.7 cm^3).

Another and perhaps more usual way of measuring the dielectric loss per cycle per unit volume is to plot the power factor as shown in Fig. 7. From the equivalent parallel circuit the total dielectric loss is given by,

$$P = E^2G \text{ watts} \tag{11}$$

and loss per cycle per unit volume is

$$E^2G/fV \text{ watts per cycle per cm}^3. \tag{12}$$

For low loss dielectrics (power factor less than 10%) we have from Eq. (9a)

$$P.F. = G/2\pi fC$$

from which $G/f=2\pi c$ (P.F.), which when substituted in Eq. (12) gives,

$$\text{loss per cycle per cm.}^3 = (2\pi CE^2/V)(P.F.). \tag{13}$$

This shows that power factor is a coefficient proportional to the dielectric loss per cycle per unit volume, if the capacitance can be assumed constant.

Except for scale, the only difference between corresponding curves in Figs. 6 and 7 is that in the latter the ordinates are proportional to the total loss per cycle while in the former they are measures of the "a.c. loss" only.

From these curves we have an explanation of the V curves of power factor as a function of frequency. Consider first curve (7) corresponding to 150°C. Fig. 5 shows the total loss in watts to be independent of frequency below 125,000 cycles per second at this temperature. Therefore in computing power factor, the loss per cycle becomes greater as the cycles per second are de-

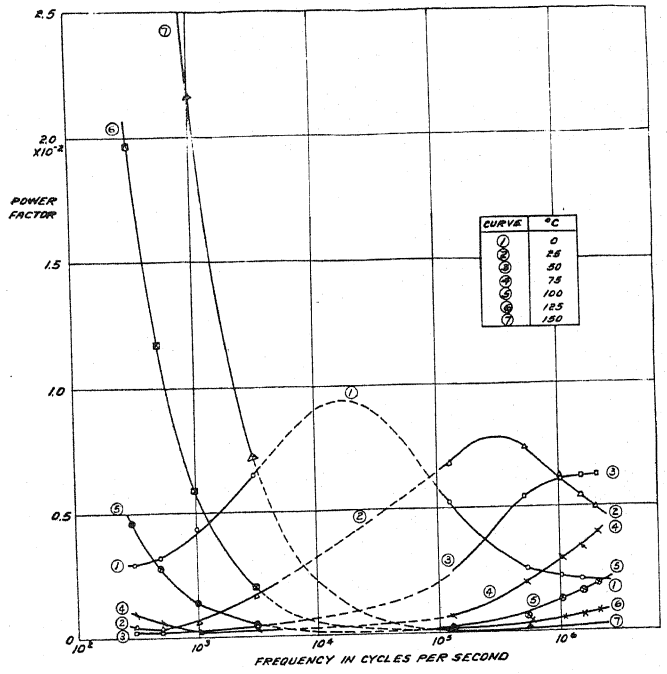

Fig. 7. Total dielectric loss in a heavy cable oil as a function of frequency for different temperatures. Loss per cycle per cm³ $= (2\pi CE^2/V)$(P.F.) joules/cycle/cm³. E is the potential in volts, C is the capacitance in farads, and V is the effective volume of oil in test cell (73.7 cm³).

creased. In other words, as the frequency is decreased, the loss component of current remains constant but the capacitance component decreases with the frequency so that the power factor increases approaching unity as a limit.

Now consider curve (1) corresponding to 0°C. Fig. 5 shows that the d.c. loss is negligible compared to the measured loss and Fig. 6 shows that this a.c. loss per cycle goes through a maximum as a function of the frequency. For intermediate temperatures, the curve may be a combination of these two distinct types. Thus curves (4), (5) and (6) show the descending portions of the d.c. characteristic at low frequencies and the ascending portions of the a.c. characteristic at high frequencies.

To represent more clearly the data shown in Fig. 7 as functions of both temperature and frequency, the curves were cut out of stiff card board and

placed in a frame at equal intervals to represent a three dimensional graph as shown in Fig. 8.

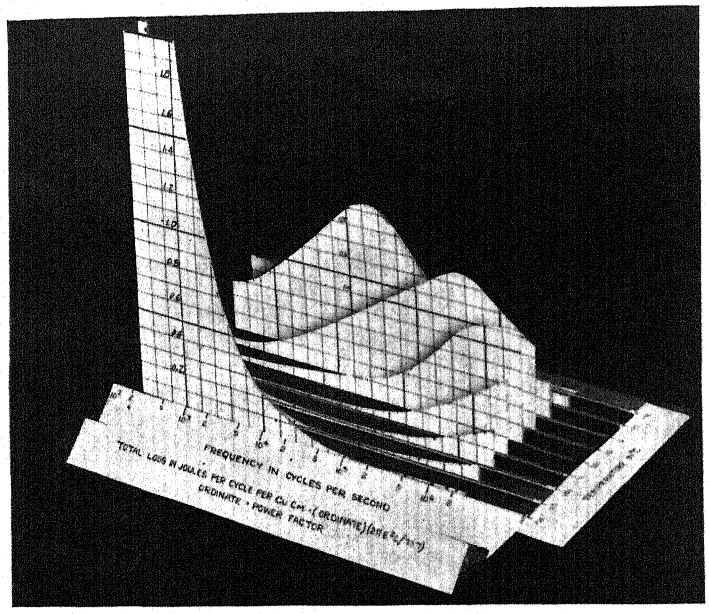

Fig. 8. Variation with frequency and temperature of dielectric loss in heavy cable oil. Composite curve chart.

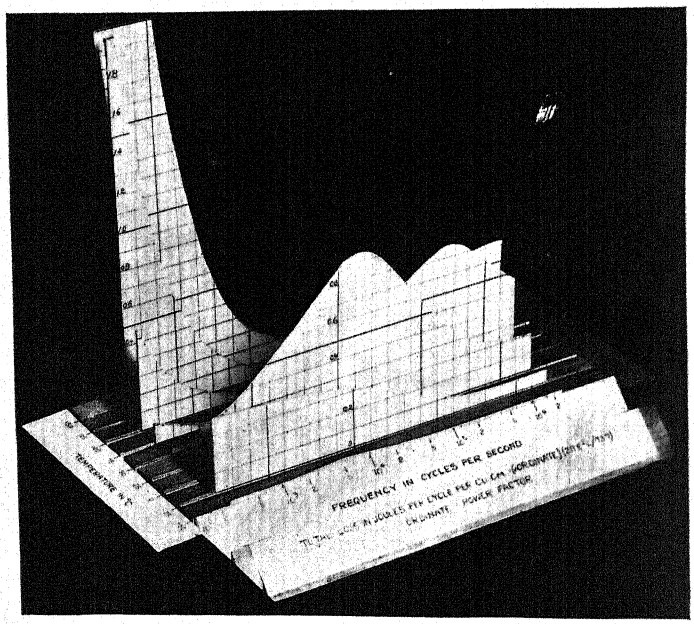

Fig. 9. Variation with frequency and temperature of dielectric loss in heavy cable oil. Composite curve chart.

In Fig. 9 the direction of increasing temperature has been reversed to show the curves that are hidden in Fig. 8. These data show the danger in drawing conclusions as to the character of a material from measurements taken only for narrow ranges of experimental conditions. It is possible to obtain for certain limited areas of this three-dimensional graph either increasing or decreasing power factor as a function of either frequency or temperature. Similar studies over wide ranges of frequency and temperature may explain apparent discrepancies between the results of different experimenters working in different limited ranges of measurement.

Data somewhat similar to these are shown by Emanueli[3] for an oil containing 35 percent rosin. An analysis of these data shows that he did not carry his test to high enough frequencies to obtain maxima in the curves for (G/f) *vs.* (f) similar to those shown in Fig. 6.

Debye's Theory of Polar Molecules

We shall not reproduce the theory as developed by Debye[4] although the attendant assumptions will be indicated in the discussion. As a result of the solution of a differential equation of motion of a polar particle in a viscous medium, Debye arrives at the following relation for the dielectric coefficient* of the medium,

$$\epsilon = \frac{\left(\frac{\epsilon_0}{\epsilon_0+2}\right) + i\omega\tau\left(\frac{\epsilon_\infty}{\epsilon_\infty+2}\right)}{\left(\frac{1}{\epsilon_0+2}\right) + i\omega\tau\left(\frac{1}{\epsilon_0+2}\right)} \tag{14}$$

where-

ϵ_0 = dielectric coefficient at zero frequency

ϵ_∞ = dielectric coefficient at infinite frequency

or ϵ_∞ = (refractive index)^2

τ = relaxation time

ω = 6.283 (cycles per second).

By expanding Eq. (14), this relation can also be written in the form,

$$\epsilon = \epsilon' - i\epsilon'' \tag{14a}$$

where

$$\epsilon' = \frac{\epsilon_0(\epsilon_\infty + 2)^2 + \omega^2\tau^2\epsilon_\infty(\epsilon_0 + 2)^2}{(\epsilon_\infty + 2)^2 + \omega^2\tau^2(\epsilon_0 + 2)^2} \tag{15}$$

and

[3] L. Emanueli, High Voltage Cables, P. 38, (John Wiley & Sons, 1930).

[4] P. Debye, "Polar Molecules," The Chemical Catalog Co., 1929.

* This is usually called "dialectric constant," but as pointed out by Addenbrook in Nature **126**, 808 (1930), the quantity varies considerably with different experimental parameters and therefore might better be called "dielectric coefficient."

$$\epsilon'' = \frac{\omega\tau(\epsilon_0 - \epsilon_\infty)(\epsilon_\infty + 2)(\epsilon_0 + 2)}{(\epsilon_\infty + 2)^2 + \omega^2\tau^2(\epsilon_0 + 2)^2}. \tag{16}$$

At this point we shall depart from the method of Debye, who, because of similarity with optical phenomena interprets the dielectric coefficient in terms of the relation,

$$\epsilon = r^2(1 - ik)^2 \tag{17}$$

where r and k are the indices of refraction and absorption. Our experience indicates that the data can be analyzed without the use of the optical index of absorption.

In Eq. (14a), ϵ' is the true dielectric coefficient in the ordinary usage of the term, since it is a measure of the current in the external circuit which leads an applied sinusoidal potential by 90°. ϵ'' being at right angles to ϵ' is really a measure of the current which is in phase with the applied potential and therefore proportional to the dielectric loss. The relation between ϵ'' and G in Eq. (3) may be shown as follows:

In the equivalent parallel circuit

$$Y = (\text{admittance}) = (\text{impedance})^{-1} = G - iw\epsilon' C_v \tag{18}$$

where

$$\epsilon' = C/C_v \tag{19}$$

according to the definition that the dielectric coefficient is the ratio of the capacitance with a given material as a dielectric, to the capacitance of the same system with vacuum as a dielectric.

Using Debye's generalized dielectric coefficient from Eq. (14a) to account for both the in-phase and out-of-phase components of the current we have,

$$Y = 0 - iwC_v(\epsilon' - i\epsilon'') \tag{20}$$

which when expanded gives,

$$Y = w\epsilon'' C_v - iw\epsilon' C_v. \tag{21}$$

By comparing Eq. (18) and (21), we have a relation between our equivalent parallel conductance G and Debye's imaginary component ϵ'' of the generalized dielectric coefficient, namely

$$G = w\epsilon'' C_v. \tag{22}$$

For a given test cell, C_v is a constant so that ϵ'' is proportional to G/f. Therefore the curves in Fig. 6 are directly proportional to Debye's ϵ'', for conditions under which the d.c. conductance is negligible.

The next logical step is therefore to set the first derivative with respect to w of Eq. (16) equal to zero, and obtain a relation for the frequency at which

the loss is a maximum. The result of this operation is that ϵ'' should be a maximum when,

$$w\tau = (\epsilon_\infty + 2)/(\epsilon_0 + 1). \tag{23}$$

Now, if this value be substituted back in Eq. (16) we have,

$$\epsilon_m' = \tfrac{1}{2}(\epsilon_0 + \epsilon_\infty) \tag{24}$$

and

$$\epsilon_m'' = \tfrac{1}{2}(\epsilon_0 - \epsilon_\infty) \tag{25}$$

ϵ_0 and ϵ_∞ are independent of frequency and change with temperature, only as the density changes. Therefore Eq. (23) indicates that *the frequency at which the maximum loss occurs will vary inversely with the relaxation time of the polar molecules.*

Debye develops the following relation for the relaxation time

$$\tau = 4\pi\eta a^3/kT \tag{26}$$

where

η = the coefficient of viscosity in poises
a = the effective radius of the polar molecule in cm
k = Boltzmann's constant $= 1.37 \times 10^{-16}$
T = absolute temperature.

Eq. (25) indicates that except for changes with temperature due to changes in density, *the maximum value of the loss per cycle should be independent of temperature or frequency.*

The assumptions made by Debye in developing this theory may be stated briefly as follows:

(a). The solution of polar molecules in a non-polar solvent is sufficiently dilute so that the interaction between neighboring polar molecules is negligible.

(b). The laws of an ideal gas may be applied and use made of Boltzmann's constant and Avogadro's number.

(c). Viscosity coefficients, as ordinarily measured, and Stoke's law for falling spheres in a viscous medium may be applied to forces between polar and non-polar molecules.

Of these assumptions the third is probably the one which is most open to criticism in applying this theory to a viscous mineral oil.

There is more evidence that insulating oils contain charged particles than that they contain polar molecules. Therefore it may be possible that mathematical relations, which would also explain experimental observations, could be developed for the motion of charged particles in a viscous medium.

In a recent discussion of Debye's theory, Whitehead[5] sets up a relation for

[5] S. Whitehead. Phil. Mag. **9**, 865 (1930).

power factor in terms of the physical coefficients of the material instead of in terms of the limiting values of ϵ as suggested by Debye. Whitehead then differentiates this expression with respect to w to determine the conditions for maximum power factor.

The development we have given above seems much preferable to that suggested by Whitehead for the following reasons:

(a). The limiting values of the dielectric coefficient ϵ_0 and ϵ_∞ can be measured more easily and more accurately than the electric moment and the molecular viscosity, which are required to evaluate Whitehead's relations.

(b). The study of power factor relations is inherently more complicated than the study of the loss coefficient alone, because the former involves a ratio between two quantities which vary as different functions of temperature and frequency.

(c). Not only is it easier to measure separately the capacitance and the loss coefficients, but such a study will lead to a clearer understanding of both, than is possible from a determination of power factor, which measures only their ratio.

Quantitative Check of Debye's Theory

To apply the above theory to our experimental data, the following quantities were determined for 25°C:

$\epsilon_0 = 2.30$

$\epsilon_\infty = (\text{refractive index})^2 = (1.5077)^2 = 2.27$

$C_v = 65.1 \times 10^{-12}$ farads

and f_m = frequency at which the maximum loss per cycle occurs = 316,000 cycles per second.

Using these particular values and Eqs. (16) and (22), a curve of (G/f) against frequency can be calculated and plotted as shown in Fig. 10. The difference between the calculated and observed maximum ordinate can be easily explained as an experimental error. According to Eq. (25) the maximum ordinate is proportional to the difference between ϵ_0 and ϵ_∞. This difference is only 1.3 percent of the measured values, so that a 1 percent error in either coefficient would cause of 75 percent error in their difference. The index of refraction should be accurate to 0.1 percent but ϵ_0 might easily be in error by 0.5 percent, since the measurement was made before the need for such extreme accuracy was recognized. Thus the *maximum ordinate may be considered to check the theory within the limits of experimental accuracy.*

Eq. (16) shows that $(\epsilon_0 - \epsilon_\infty)$ enters as a multiplying factor for all frequencies, so that even though ϵ_0 were corrected to give an agreement between the maxima of the two curves, their shapes would be entirely different. This indicates that, *while the order of magnitude is correct, the theory in this simple form is not sufficient to predict quantitatively the observed results.* An obvious and possible explanation of the difference in the shapes of the experimental and

theoretical curves is that the theory postulates particles of only one size. If there are any polar particles in the oil they are probably of many different sizes, so that a much broader frequency responce is obtained than would be given by the presence of particles of only one size.

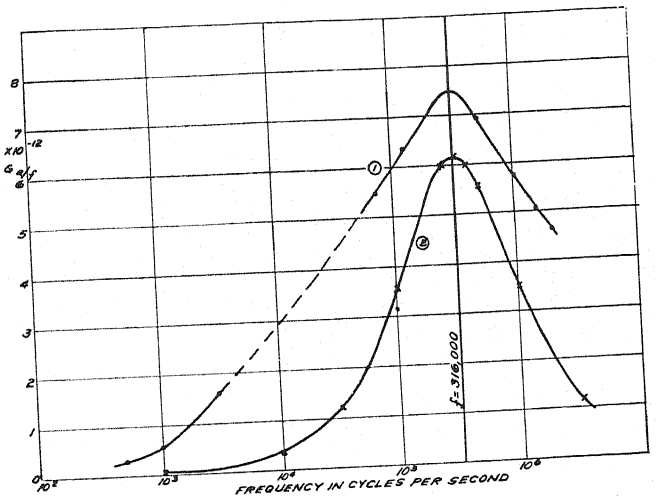

Fig. 10. a.c. loss per cycle for a heavy cable oil at 25°C. Curve 1 from observed data, curve 2 calculated from Debye's theory of polar molecules.

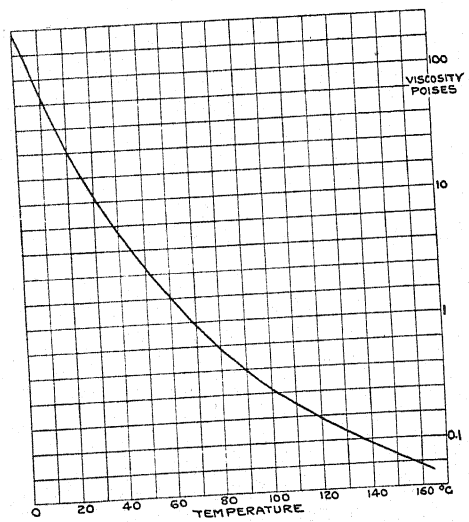

Fig. 11. Viscosity characteristic of a viscous cable oil.

Another indication of the validity of the theory may be obtained by determining the effective radius of the polar particles from Eq. (26). This can be done by reading from the curves in Fig. 6, the frequency at which each isothermal curve is maximum. Then τ can be determined for each tempera-

ture from Eq. (23), so that it is possible to solve for (a) in Eq. (26). The results of such a calculation are shown in Table II.

TABLE II. *Calculation of size of polar molecule.*

T °C	ϵ_∞	ϵ_0	$\omega\tau$	f cyc/sec $\times 10^3$	τ $\times 10^{-7}$	η Poise	a cm $\times 10^{-8}$
0	2.31	2.34	.993	16.	98.7	230	5.04
25	2.27	2.30	.993	316.	5.0	17	4.58
50	2.23	2.26	.993	2000.	0.79	2.9	4.59

As the temperature of the oil is increased the viscosity decreases rapidly according to Fig. 11. Therefore the relaxation time decreases very rapidly with increased temperature resulting in a corresponding large increase in the frequency necessary to cause maximum loss as shown in Fig. 6.

Here again we have a qualitative check of the theory in that three determinations for the calculated size of particles agree fairly well and the value obtained is of the right order of magnitude.

The author is pleased to express his indebtedness to Mr. S. I. Reynolds of the General Electric Company for his careful work in making the high frequency measurements reported in this paper.

LETTERS TO THE EDITOR

Prompt publication of brief reports of important discoveries in physics may be secured by addressing them to this department. Closing dates for this department are, for the first issue of the month, the twenty-eighth of the preceding month; for the second issue, the thirteenth of the month. The Board of Editors does not hold itself responsible for the opinions expressed by the correspondents.

Wave-length Measurement of Gamma-Rays from Radium and its Products

In my paper on the γ-ray spectrum of radium and its products (Phys. Rev. [2] **36**, 460 (1930)) it was pointed out that the peaks appearing on the intensity curve and interpreted as γ-ray lines were sharp, and were apparently resolved by the spectrometer when the glancing angles of reflection from calcite differed as little as 20 seconds of arc, although the geometry of the arrangement did not account for such high resolving power.

Professor Niels Bohr in private correspondence with Professor Kovarik has emphasized the importance of this question concerning resolution in my experiments, and a further study of the matter has shown that the discrepancy between the resolving power as estimated from the experimental curves and that computed from the dimensions of the apparatus is greater than can be accounted for by any reasonable hypothesis regarding accidental inclination of the slit faces. He also points out that besides this there is a further difficulty in connection with the apparently great relative intensity of the very short wave-length lines or bands. Theories of scattering predict much lower intensity for scattered radiation of such high frequency. The reality of the reported results thus assumes considerable theoretical importance and needs more experimental justification.

It is impossible to give, at present, any other interpretation of the experimental results than that first offered. It is my intention, therefore, to reinvestigate the problem with improved apparatus. Meanwhile the question regarding the existence or non-existence of new lines of strong intensity in the γ-ray spectrum of radium and its products must be left open.

LUVILLE T. STEADMAN

University of Rochester,
Rochester, New York,
January 21, 1931.

Arrangements of Atoms in Crystals

In the January 1st number of the Physical Review (**37**, 105 (1931)) is an abstract of a paper by Zachariasen in which the author reports the results of crystal structure investigations of $KBrO_3$, KCl_3, $NaClO_3$ and Na_2SO_3. He finds, in agreement with the earlier work on $NaClO_3$ and $NaBrO_3$ (Kolkmeijer, Bijvoet and Karssen, Verslag akad. Wetenschappen Amsterdam **23**, 644 (1920); Dickinson and Goodhue, J. Am. Chem. Soc. **43**, 2045 (1921)) that the XO_3 groups in these crystals can be described as "tetrahedral groups with one tetrahedral corner removed," and notes that this is a similar arrangement to that around As or Sb in As_2O_3 crystals (Bozorth, J. Am. Chem. Soc. **45**, 1621 (1923)). The statement is then made that in each case "the cation has got only 2 electrons in the outer shell," the non-coplanar arrangement being explained "as due to deformation in the outer shell of the cation, where the charge distribution is very diffuse."

It seems more likely to the writer that these are merely cases of shared electron pairs, as postulated by G. N. Lewis ("Valence and the Structure of Atoms and Molecules," Chem. Cat. Co., New York, 1923). The total number of valence electrons in each of these ions is 26, and if Lewis is correct, that there is a tendency toward the completion of valence shells containing eight electrons (four pairs tetrahedrally oriented) around the kernel of every electronegative atom, the distribution in space of the atoms must be similar to that observed,

the electrons being shared as indicated by the formula

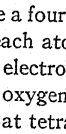

In the case of the oxides of arsenic and antimony, there are five electrons per As or Sb and six per O. To complete a four-pair tetrahedral valence shell around each atom requires that each As or Sb shares 3 electron pairs, at tetrahedron corners, with 3 oxygen atoms and each oxygen shares 2 pairs, at tetrahedron corners, with two As or Sb atoms,—precisely the arrangement determined from x-ray data.

It is plain that one can not only predict from this theory the number of electron pairs (per molecule or crystal unit) shared between electronegative atoms, but one can also predict that if an electronegative atom is adjacent to 2, 3, or 4 others, the arrangement will be that of 2, 3, or 4 corners of a (not necessarily regular) tetrahedron around its center.

Such predictions can be tested very readily by the results of x-ray analysis and in general they are found to be in agreement with experiment. Thus in iodine the negative atoms are in pairs; in crystals of Se and Te, each atom is adjacent to two others in a spiral chain; in P, As, Sb and Bi the atoms are in puckered layers, each adjacent to three others at three corners of a tetrahedron, while in the diamond, Si, Ge and gray Sn each atom in tetrahedrally surrounded by four others. Among compounds, several have been mentioned already; many others might be given.

As Lewis readily admits, there are exceptions to this tendency. Examples he gives are the molecules SF_6 and PCl_5 in which the central P and S atoms probably have 5 and 6 valence pairs, respectively. Other examples are afforded by such compounds as $CsICl_2$ and CsI_3, in which the three halogen atoms form a colinear group. The number of valence electrons (counting 7 per halogen and 1 per Cs) in each X_3 ion is 22. The most reasonable distribution of these would seem to be one in which the central atom has 5 pairs and each of the others four.

In $CaCO_3$ and $NaNO_3$ both crystallographic and x-ray data indicate a 3-fold axis of symmetry through each C and N center and two-fold axes of symmetry through each C-O and N-O centerline. If the oxygen tetrahedra are oriented in agreement with this symmetry, each C or N kernel is surrounded by six pairs, joining it by double bonds to the neighboring oxygens.

The four pair valence shell is apparently stable if the valence shell is not made too large (as by the pull of surrounding electron atoms) in which case more pairs can be accommodated. The smaller the kernel charge—in general, the more electropositive the atom,—the more pairs can be accommodated in the valence shell but the less tightly each is held. Although in quartz (SiO_2), HgI_2, ZnS, AgI and many other compounds relatively electropositive atoms are surrounded by four electronegative atoms at tetrahedron corners, suggesting electron sharing with tetrahedral valence shells around *all* the atomic kernels, in many others the electropositive atoms are surrounded by six or eight negative atoms. In some cases, (e.g. NaCl) the valence shells of the latter cannot be oriented so as to place the valence pairs on the centerlines between adjacent atoms; evidently in such polar crystals other considerations, such as the relative sizes of the atoms (or ions) are of the greatest importance in determining the type of arrangement. (Cf. Pauling, J. Am. Chem. Soc. **51**, 1010 (1929); Huggins, J. Phys. Chem., in print.)

It should perhaps be pointed out that the point of view taken here is quite in agreement with recent developments in wave mechanics theory. (Cf. Bartlett, Phys. Rev. **36**, 1096 (1930) and papers by Bartlett and by Slater at the Cleveland Meeting of the American Physical Society.) The pairing of valence electrons, the sharing of such pairs between two atoms, and preferred orientations of electron orbits, once bones of contention between physicists and chemists, can now be agreed to by both.

MAURICE L. HUGGINS
Stanford University,
Palo Alto, California,
January 27, 1931.

Energies and Wave-Functios of the State (1s) (2s)^{1}S in Helium-like Atoms

Eckart, in the Physical Review, September 1, 1930 (pp. 878 *et seq.*) pointed out that his modification of the Ritz method there presented fails when applied to a state other than the lowest of a given series, e.g. $(1s)(2s)^1S$ of helium-like atoms, and suggested that a pro-

cedure might be worked out for applying the method to this case. This has been done by the author, using a comparison function designed to be orthogonal to the wave-function of the ground state.

The following comparison function is orthogonal to the exact wave-function ψ_1 of the ground state: $K(\phi_2-\gamma_1\psi_1)$, where $\phi_2 = [u(\alpha 1)v(\beta 2) + u(\alpha 2)v(\beta 1)]/[2(1+b^2)]^{1/2}$, $b^2 = (2x)^3(x-1)^2/(x+\frac{1}{2})^8$, $x=\alpha/\beta$ (Eckart, Phys. Rev. **36**, 886), ψ_1 = exact wave-function of ground state, $\gamma_1 = \int\phi_2\psi_1 d\tau$, $K=[1-\gamma_1^2]^{1/2}$. Actually the use of a very accurate wave-function for ψ_1 (such as that of Hylleraas), was found to introduce too great complexities into the maximization. The function $\phi_1 = [u(\epsilon 1)u(\eta 2) + u(\eta 1)u(\epsilon 2)]/[2(1+c^2)]^{1/2}$, where $c^2 = 64(\epsilon\eta)^3/(\epsilon+\eta)^6$, was used for ψ_1, (due to Eckart, Phys. Rev. **36**, 883). The validity of this approximation can be judged from the fact that a 10% change in γ_1^2 was found to produce only a 1% change in the calculated ionization potential. The parameters ϵ and η correspond to Eckart's α and β for the state $(1s)^2$.

This comparison function gave the results summarized in the following table (α_0 and β_0 are the adjusted values of the parameters, $R_\infty h$ = unit of energy, W = energy, V_i = ionization potential):

	Z	α_0	β_0	W (calc.)	W (obs.)	V_i (calc.)	V_i (obs.)
He I	2	2.00	1.17	4.289	4.292	0.289	0.292
Li II	3	2.98	2.19	10.073	10.082	1.073	1.082
Be III	4	3.97	3.18	18.361	—	2.361	—
B IV	5	4.97	4.19	29.146	—	4.146	—

One notices that α_0 is approximately equal to Z, $(Z-\alpha_0 \backsim 0.02)$; that $Z-\beta_0$ is essentially constant and $\backsim 0.82$; and that $W(\text{calc.}) = (5/4)Z^2+aZ+b$, where $a=-0.464$, $b=0.216$.

Hylleraas (Zeits. f. Physik **65**, Heften 11 and 12, Nov. 14, 1930) has recently performed a calculation of this term for the special case of He I; his method, which results in a much more complicated wave-function, yields the value 0.290.

JOHN P. VINTI

Massachusetts Institute of Technology,
January 29, 1931.

A Theory of Collision Processes Involving No Radiation of Energy

The writers have developed a generalization of the Born collision method for dealing with collision processes. In the usual Born method the zero-order wave function for the colliding particle is a plane wave, undistorted by the presence of the stationary particle; which is so poor an approximation that the series for the cross section for many processes diverges; and in every case the first term is a bad approximation for small relative velocities. The writers use as a zero-order wave function one already distorted by an approximate mutual interaction field. The interaction energies effecting the transition have been expanded in a series which converges well for energies less than about 100 electron-volts. The cross sections for the various processes can be then computed and are valid for all except very large relative kinetic energies.

These cross sections, as a function of the size of the particles, of the nature of the transition caused by the impact, of the mutual kinetic energy, and of the energy transferred from kinetic to energy of excitation, check quantitatively with such widely different experimental data as: Bleakney's[1] curves for ionization of Hg; Zemansky's[2] curves for transfer of excitation; Hanle's[3] curves for excitation of various atoms; and Latyscheff and Leipunsky's[4] curves for collisions of the second kind.

PHILIP M. MORSE
E. C. G. STUECKELBERG

Institute for Theoretical Physics,
The University, Munich,
January 29, 1931.

[1] Bleakney, Phys. Rev. **35**, 139 (1930).
[2] Zemansky, Phys. Rev. **36**, 933 (1930).
[3] Hanle, Zeits. f. Physik **54**, 848 (1929).
[4] Latyscheff and Leipunsky, Zeits. f. Physik **65**, 111 (1930).

BOOK REVIEWS

Ergebnisse der Exakten Naturwissenschaften. Vol. VIII. E. BRÜCHE, Freie Elektronen als Sonden des Baues der Molekeln. Springer, Berlin, 1929.

This article deals primarily with experiments on passage of very slow electrons through gases. Stimulated by the observations of Ramsauer, a number of papers in this field have appeared within the last ten years. The present article gives a valuable critical survey of this work including a few new results. In his early paragraphs the author takes great pains to explain the significance of the "effective cross-section" in different types of apparatus. This is essential and well done. Later on almost equally elaborate discussions are given concerning points of minor significance. However, one may well overlook this lack of balance and rejoice to have a clear and systematic presentation of the experimental results including a classification of the "WQ" (Wirkungsquerschnitt) curves into four distinct types. The interpretation of these results can hardly be satisfactory without a consideration of energy losses of electrons in collisions, a field that is outside the scope of this article.

H. D. SMYTH

The Wave Mechanics of Free Electrons. G. P. THOMSON. Pp. 161, figs. 53. McGraw-Hill, 1930.

This book contains the subject matter of lectures delivered by the author as George Fisher Baker Non-Resident Lecturer in Cornell University. As the title implies, the book deals with that part of the subject which concerns electrons not forming part of an atom. It is primarily concerned with an account of experimental work, but also contains a treatment of the theory which is immediately applicable.

After an introductory lecture, the first two chapters treat the General Theory of Waves and de Broglie's Wave Mechanics, respectively. The following 8 chapters include a brief account of the Theory of Wave Diffraction by Crystals; a discussion of various diffraction experiments confirming de Broglie's relation for the wave-length of the electron; the effect on electron diffraction of an inner potential and the resulting refractive index; a discussion of the author's own work on the determination of the atom form factor from intensity measurements, and a theoretical interpretation of certain aspects of these experiments; an outline of Sir J. J. Thomson's physical theory of electron waves; theoretical considerations of the possibility of electron polarization with a list of the various experimental attempts to detect a possible polarization effect; and finally the application of electron diffraction to the study of surface films.

The following errors are noted. Under the discussion of the reviewer's results on pages 101, 102, it is stated that the inner potential Φ was calculated "by subtracting the actual voltage of the electrons from the voltage V given by $V=150/\lambda^2$, where λ is the wave-length in Angstrom units which would give a spot in the observed position, ignoring refraction. This process is equivalent to ignoring the bending of the waves on emerging from the crystal." This is incorrect since the wave-length λ as used in the equation referred to is not that which would give a spot in the observed position, ignoring refraction, but is the theoretical wave-length, determined from the geometry of the crystal for unit refractive index, with which an experimental beam is associated. The colatitude angles for the theoretical and experimental beams are not the same so that the bending of the waves on emerging from the crystal has not been ignored.

On page 102 M. Davis is incorrectly referred to as Miss.

To my knowledge this is the first collection into book form of the experimental investigations in this new field, and will be a valuable reference to the status of the work at the time the book was written (Jan. 31, 1930), although several important contributions have since been made. It is particularly fitting to have an account by a pioneer worker who has made many notable contributions in this field.

H. E. FARNSWORTH

Textbook of Practical Physical Chemistry. K. FAJANS AND J. WÜST. Pp. 233+xiv, figs. 74. E. P. Dutton, New York, 1930. Price $4.95.

The experiments outlined in this book cover a much wider range of subjects than is customary in manuals of physical chemistry. In addition to the material commonly presented, there are chapters on Adsorption from Solutions, Coagulation of a Sol by Electrolytes, Transformation of Radio-Elements, Quantitative Spectrophotometry, Electrochemical Preparations, and the Lead Accumulator. The outlines of the more common experiments follow the classical methods quite closely.

Each chapter is preceded by an unusually complete and worthwhile discussion of the related theory. Numerous references are given to the better known textbooks of theoretical physical chemistry. The description of the experimental procedure is apparently planned to render the student practically independent of the help of a laboratory instructor. The apparatus and experiments are described with meticulous detail, and in several cases this description is followed by a discussion of the probable difficulties and ways of avoiding or overcoming them.

The reviewer feels that it is regrettable that the authors decided to present the experiments on solutions, including the chapter on electromotive force, in terms of the older theory. The authors state in the preface "that to introduce the new system into this book would involve too great a departure from the treatment at present given in most of the general textbooks." This statement certainly does not apply to two of the better-known general texts to which many references are made in this book.

The text bears little evidence that it is a translation from the German; the style is throughout clear and readable. Without resorting to small type, the publishers have been successful in economizing space by their arrangement of the print, so that a large amount of material is presented on 230 pages.

ROBERT LIVINGSTON

Band Spectra and Molecular Structure. R. DE L. KRONIG. Pp. x+163, figs. 16. The Macmillan Company, New York, 1930. Price $3.50.

Books on band spectra are appearing, and more are promised. The volume under review is brief and devoted almost exclusively to the theoretical side of the subject. That, however, is as it should be. If each author will confine himself to those aspects of the field with which he is thoroughly conversant, we will get a set of books which, collectively, will be both authoritative and useful. This volume makes a good start in that direction. In spite of its brevity, it covers a multitude of topics, including an entire chapter on "Macroscopic Properties of Molecular Gases" (scattering, dispersion, Kerr and Faraday effects, dielectric constants, etc.). The range of material is indicated by a few sub-titles, chosen almost at random: Stark and Zeeman Effects, Energy Levels of Polyatomic Molecules, Rotational Distortion of Spin Multiplets, Perturbations and Predissociation, Band Spectra and Nuclear Structure. Moreover, the author kindly marks off those sections for which a knowledge of wave mechanics is essential, and even summarizes their contents, so that the "experimental physicist" may omit such sections without losing the continuity of the argument. I am sure this will be appreciated by the great majority of readers. A few more diagrams, however, might well have been used.

It is not surprising, in a theoretical book, to find an occasional mis-statement of experimental fact. The reviewer was, however, really startled to read, on page 97, that Birge and King had discovered the isotopes of oxygen (as well as that of carbon), and that these discoveries had been made by means of the appearance of the alternate lines which are missing or weakened in the spectra of homonuclear molecules. Such errors are perhaps not serious, for the reader, but Giauque and Johnston may well object, from the personal standpoint. Their beautiful articles on the discovery and confirmation of the oxygen isotopes are not even listed in the *very* extensive and valuable bibliography which concludes the volume.

The author states that he has used the new nomenclature recently recommended by band spectroscopists (R. S. Mulliken, Phys. Rev. **36**, 611, 1930), and this is the case, with a few more or less unimportant exceptions. In just one instance, however, the reviewer considers the matter not unimportant. Dr. Kronig uses unprimed and primed symbols for upper and lower levels,

respectively, whereas the National Research Council committee, after considerable correspondence, recommended in 1926 single and double primed symbols, and this recommendation has been almost universally followed since that time.

These criticisms are not to be taken as an adverse judgment on the volume, as a whole. Many persons will welcome a brief, clear and comprehensive account of the recent important theoretical developments in the field of band spectra, and the present volume gives just such information.

RAYMOND T. BIRGE

PROCEEDINGS

OF THE

AMERICAN PHYSICAL SOCIETY

MINUTES OF THE CLEVELAND MEETING, DECEMBER 30–31, 1930

The Thirty-second Annual Meeting (the 168th regular meeting) of the American Physical Society was held in Cleveland, Ohio at the Case School of Applied Science and Western Reserve University on Tuesday and Wednesday, December 30 and 31, 1930, in affiliation with Section B—Physics— of the American Association for the Advancement of Science. The presiding officers were Professor Henry G. Gale, President of the Society, Dr. W. F. G. Swann, Vice-president, and Professor F. W. Loomis. The average attendance was about 300.

The annual joint session with Section B was held on Wednesday morning. The presiding officer was Professor F. K. Richtmyer, Vice-president of Section B. The program consisted of the address of the Retiring Vice-president of Section B, Professor Charles E. Mendenhall, on the subject, "Recent Developments in Photoelectricity." This address was followed by a Symposium on Acoustics consisting of three invited papers, as follows: "Recent Development in Architectual Acoustics" by Dr. Paul E. Sabine of the Riverbank Laboratories; "Some Physical Characteristics of Speech and Music" by Dr. Harvey Fletcher of the Bell Telephone Laboratories, Inc.; and "Concerning Some of the Problems Encountered in Recording and Reproducing Photographic Sound Records on Moving Picture Film," by Dr. Clarence W. Hewlett of the General Electric Company. The attendance at this session was 350.

On Tuesday evening the Society joined with the Society of Sigma Xi for dinner at the Cleveland Club after which they attended a lecture by Dr. C. E. K. Mees, of the Eastman Kodak Company, given in the auditorium of the John Hay High School.

Annual Business Meeting. The regular annual business meeting of the American Physical Society was held on Tuesday afternoon, December 30, 1930, at 2:00 o'clock in the lecture room of the Case School Physics Laboratory. A canvass of the ballots for officers resulted in elections for the year 1931 as follows:

President:	W. F. G. Swann
Vice-president:	Paul D. Foote
Secretary:	W. L. Severinghaus
Treasurer:	George B. Pegram
Members of the Council, four year term:	W. D. Coolidge
	F. W. Loomis
Members of the Board of the Physical Review, three year term:	A. J. Dempster
	D. M. Dennison
	J. C. Slater

The Secretary reported that during the year there had been 189 elections to membership. The deaths of 11 members have been reported during the year; 36 have resigned and 28 have been dropped. The membership of the Society as of December 29, 1930 is as follows: Members: 1963; Fellows: 516; Honorary Members: 5; Total Membership: 2484.

The Treasurer presented a summary of the financial condition of the Treasury of the Society. The complete audited report has been printed and distributed to all members.

The Managing Editor presented an informal report stating that the journals of the Society were being well received by the membership as well as by physicists in foreign countries. The financial condition was reported to be one that needed careful attention since the continually increasing quantity of publication brought about an increasing financial deficit which had to be met by the generosity of individuals or organizations. The complete audited financial report of the Managing Editor has been printed and distributed to all members.

Revision of By-Laws. On motion it was voted to approve the recommendation from the Council that Article VI of the By-Laws be changed to read:

"Each fellow or member of the Society who has paid his dues in full shall receive the Physical Review published by the Society and Science Abstracts Section A—Physics."

(Omit paragraph 2 as superfluous.)

Place sentence regarding Science Abstracts—Section B—with footnote concerning Reviews of Modern Physics.

Important Resolutions. On motion the Society voted approval of the following resolutions passed by the Council;

1. That the Council approve the establishment of a Journal of Applied Physics, with the first issue appearing July 1, 1931, and that the editor of the Physical Review be appointed editor of this journal.
2. That the Council authorize the substitution of a subscription for the Reviews of Modern Physics (or a subscription for the proposed Journal of Applied Physics, if and when established) in lieu of a membership subscription for the Physical Review in the case of any member or fellow who so desires.
3. That the Council approve, in principle, the formation of sections in the Society by subjects and also the encouragement of affiliation of local physics clubs.
4. That the Council propose the formation of an Institute of Physics for the purpose of coordinating various societies whose interests are primarily in the field of physics and for the purpose of supporting their publications.

Resolution number 4 was approved with the addition:

"That the Council consider specifically the possibility of such organization under Section B of the American Association for the Advancement of Science."

Meeting of the Council. At its meeting held on Monday, December 29, 1930, three persons were elected to fellowship, seven persons were transferred from membership to fellowship, and thirty-eight were elected to membership. *Elected to Fellowship:* J. Frenkel, Otto Oldenberg and W. H. Zachariasen. *Transferred from Membership to Fellowship:* Thomas H. Johnson, Julian E. Mack, George F. McEwen, Chester Snow, Thomas Spooner, Harvey E. White and John G. Winans. *Elected to Membership:* John Bardeen, B. Franklin Blair, L. W. Chubb, C. W. Curtis, R. K. Dahlstrom, R. L. Echols, Russell, Fanning, Sherman L. Gerhard, Edith Gideon, Lynn G. Howell, David R. Inglis, H. D. Koenig, J. B. Horner Kuper, W. Wallace Lozier, Charles H. Lutz, Alfred F. Meyer, Parry H. Moon, Lewis M. Mott-Smith, Willard J. Poppy, Charlotte Purdy, Russell W. Raitt, G. H. Rockwood Jr., Paul N. Russell, Frances O. Severinghaus, G. D. Shallenberger, Paul E. Shearin, Klaus J. Sixtus, Louis Statham, Paul Talmey, Josiah Taylor, George S. Thomas, Kenneth, B. Thomson, Louisa E. Townshend, John F. Wagner, Clarence W. Wallace, Charles A. Whitmer, Ralph E. Winger, and Bruno O. Winkler.

The regular scientific program of the Society consisted of 82 papers, numbers 24, 56, 62, 78 and 80 were read by title. The abstracts of these papers are given in the following pages. An **Author Index** will be found at the end.

W. L. SEVERINGHAUS, *Secretary*

ABSTRACTS

1. Mass absorption coefficient of the K shell according to the Dirac relativistic equation. LOUIS C. ROESS, *Cornell University.* (*Introduced by E. H. Kennard.*)—Taking as model an atom containing two non-interacting electrons and a fixed nucleus with charge Ze, the mass absorption coefficient is calculated using the proper functions of the Dirac relativistic equation. Z is determined so as to make the lowest energy level agree with the experimental value determined from the K absorption edge. The numerical calculation presented difficulty because of lack of tables of complex gamma functions. The relativistic coefficient is found to be from 0% to 40% smaller than the non-relativistic coefficient calculated by Nishina and Rabi, the greatest difference occurring for the heavy elements and short wave-lengths; it agrees slightly worse with experiment than the non-relativistic coefficient. The difference between theory and experiment is least for the heavy atoms, as would be expected, since for the heavy atoms (large Z) the neglected electronic interaction-field is small in comparison with the nuclear field. The variation of the relativistic coefficient with wave-length is complicated, but in the range $\frac{1}{2}\lambda_k$ to λ_k (λ_k=wave-length of K absorption edge) it is more nearly linear with λ^3 than the non-relativistic coefficient. The importance of using the relativistic equation for heavy atoms and short x-ray wave-lengths is emphasized by these results, which also show that the model chosen is too approximate, even for the heavy elements.

2. Nature of magnetic doublet in para-azoxyanisol at 122° and 128°C as determined by x-ray diffraction. G. W. STEWART, *University of Iowa.*—A difference of opinion exists as to whether the magnetic moment of para-azoxyanisol in its liquid crystalline form, 117°C to 134°C, is an induced one or is independent of the field. A magnetic field is applied perpendicular to the axis of rotation of the spectrometer and to the x-ray beam passing through the sample. The effect of the field in the diffraction halo is studied quantatively. Boltzmann's distribution law is assumed. The data are in agreement with the computations assuming the magnetic moment to be not polarized but permanent and to possess a value of 2.65×10^4 Bohr magnetons, in agreement with the results of Kast. This suggests, but does not make certain,

that a group of that number of molecules gives rise to the magnetic moment. The diffraction of x-rays at temperatures above 134° shows the disappearance of the magnetic moment, but a retention of groups otherwise similar to those just suggested. The groups causing optical anisotropy are larger and not regular enough throughout to produce coherent x-ray diffraction. These large groups are easily affected by the stirring of the liquid. The time required for orientation is easily shown by the application of an alternating magnetic field. The experiment shows the value of the direct x-ray investigation.

3. The utilization of intensity data from Laue photographs. MAURICE L. HUGGINS, *Stanford University.*—The measurement of Laue photograph intensities and the calculation of structure factors from them are discussed. Methods of correcting for differences (in intensity of the incident radiation, in absorption and in photographic effect) dependent on the wave-length, for differences (in size of the spot, in absorption and in the background of scattered radiation) dependent on the reflection angle, and for absorption (including primary and secondary extinction) dependent on the nature of the crystal, are considered and the results of preliminary measurements and calculations presented.

4. The characteristic x-ray absorption of molecules in the vapor state. J. D. HANAWALT, *National Research Fellow, University of Michigan.*—The purpose of the work here described is to provide a better understanding of the secondary absorption discontinuities which appear on the short wave-length side of the K and of the L x-ray absorption edges of many substances. The interpretation of the secondary discontinuities has been especially difficult because the absorption has not been obtained for atoms in the isolated state. In the present work the characteristic x-ray absorption spectra of numerous polyatomic and monatomic molecules in the vapor state have been photographed with a dispersion of about 5 XU/mm, and the results compared with the absorption spectra exhibited by the same substances in the solid state. The monatomic substances investigated are superheated Hg vapor, superheated Zn vapor and krypton. The polyatomic substances are the vapors of As_4, $AsCl_3$, As_2O_3, Br_2, NaBr, $HgCl_2$, Se_8, SeO_2. It is found that none of the monatomic molecules show any absorption discontinuities at distances from the main edge greater than the ionization potential of the atom. The polyatomic molecules, however, show secondary absorptions in the vapor state differing only in minor details from the absorption of the same substance in the solid state. This makes it appear that the secondary discontinuities are only observed for atoms which are bound to other atoms. If the discontinuities are to be attributed to simultaneous jumps of two or more electrons within the atom, one has yet to understand why they do not occur in isolated atoms.

5. X-ray absorption coefficients of the light elements and their relations to the various absorption formulae. S. J. M. ALLEN, *University of Cincinnati.*—The x-ray absorption coefficients of the elements have been measured with greater precision and care at $\lambda = 1.539$A and 1.934A with especial reference to the low atomic weight elements, O, C, B, Be, Li, H. It was found necessary for these to have a complete chemical analysis carried out and corrections made by the additive law to ensure resultant values of μ/ρ, for which some degree of certainty could be stated. An impurity of iron of less than 0.1 percent at $\lambda 1.539$ can have a marked effect. The values of μ/ρ, so far obtained, are compared to those predicted by the various formulae. A new formula developed by the author which was found to hold exceedingly well down to neon indicated irregularities below that point, C, N, and O certainly falling below the formula and Be and Li probably above. The same was generally true with the Z^4/A (Owens) law. The value of μ/ρ for Li at $\lambda 1.539$ extended by the λ^3 law to $\lambda 0.71$ ($K\alpha$ of Mo) gives values much less than those previously reported (Hewlett, Mazumdar) at this wave-length.

6. The upper atomic number limit of the satellites of the x-ray line $L\beta_2$. ROBERT D. RICHTMYER, *Cornell University. (Introduced by F. K. Richtmyer.)*—Five satellites of the line $L\beta_2$ have previously been reported for the elements in the atomic number range 40 to 51. An attempt was made to extend this range to higher atomic numbers, and to determine whether there is a limit in the atomic number scale beyond which the satellites do not exist. A Siegbahn vacuum spectrometer was used, the only departure from the usual photographic method of

x-ray spectrometry being the comparatively high voltage on the x-ray tube. The satellite $L\beta_2(a)$ was observed and measured for elements 50, 51, 52, 53, 56, 58, and 60; and two others, $L\beta_2'$ and $L\beta_2''$, only as far as element 53. For elements above Xe (54), the diagram lines (Siegbahn) $L\beta_7$, $L\beta_9$, and $L\beta_{10}$ shift their positions in the spectrum relative to $L\beta_2$ in such a way that they occupy the region just where one would expect to find the satellites $L\beta_2'$ and $L\beta_2''$, making observations difficult. The plates seem to show, however, that these satellites fade out and disappear with atomic number 53. The satellites $L\beta_2(b)$ and $L\beta_2(c)$ are not found above number 50. Throughout these extensions of their ranges the satellites, where found, obey the law that $(\Delta\nu/R)^{1/2}$ is a linear function of atomic number.

7. Upper atomic number limit of the satellites of the x-ray line $L\alpha_1$. E. RAMBERG, *Cornell University*. (*Introduced by F. K. Richtmyer.*)—The satellites of $K\alpha_1$, namely $K\alpha_3$ and $K\alpha_4$, decrease in intensity rapidly with increasing atomic number above Cu(29) and have not been reported above As(33). Their disappearance seems to coincide, roughly, with the completion of Period IV of Bohr's periodic table. Similarly the satellites of $L\alpha$, although strong at Cd(48), fade out very rapidly as the end of (Bohr's) Period V is approached. The present paper is concerned with an attempt to map, by very long exposures, these $L\alpha$ satellites in the atomic number range Sn(50) to Ce(58). There is no certain evidence of their existence above Xe(54). From Sn(50) to I(53) they fade out into a very faint, diffuse band which shows very little evidence of structure, and in which therefore the identification of the lines and their wave-length measurements are difficult. The bearing of these data on the problem of the origin of satellites is discussed.

8. Are the wave-lengths of x-ray satellites affected by chemical combination? F. K. RICHTMYER, *Cornell University*.—The "two-electron jump" theory of the origin of satellites, proposed by the author, postulates that one of the jumps should be between outer electron shells and should therefore be somewhat affected by chemical combination. That is, the difference in wave-length $\Delta\lambda$ between a satellite and its parent line should depend on the chemical state of the emitting atom. The present paper describes an attempt to detect such a shift in wave-length for the $K\alpha$ satellites of Si(14), S(16), Ca(20), Ti(22) and the $L\beta_2$ satellites of Ag(47). Except in the case of Si(14) the data are inconclusive because of the possible reduction or oxidation of the element in the target and the resulting well-known change in wave-length of the parent lines. Measurements on Si(14) were less ambiguous. Comparing the $K\alpha_{3,4}$ satellites of metallic silicon with those from Na_2SiO_3, the $\Delta\lambda$ for the silicate is 3.9 percent greater in the case of $K\alpha_3$, and 2.8 percent greater in the case of $K\alpha_4$ than for metallic silicon. These data are in substantial agreement with those of Bäcklin (Zeits. f. Physik **38**, 215, 1926). It will apparently be necessary to study fluorescence spectra to avoid spurious effects of chemical reduction in the target.

9. Interpretation of x-ray satellite lines. R. M. LANGER, *Massachusetts Institute of Technology*.—Quantum mechanical calculations show that double electron jumps involving two electrons in different shells would give lines too faint to account for observed x-ray satellites. A theory can be given for single electron jumps in doubly ionized atoms which would give lines of much greater intensity and which would be compatible with the experimental results of Richtmyer and Taylor, and DuMond and Hoyt. According to this theory the $K\alpha$ satellites α', α_4, α_3, α_5, α_6 of the elements from Na on, are due to the transitions

$$(1s)(2s)(2p)^6\ {}^1S - (1s)^2(2s)(2p)^5\ {}^1P \ldots.\ (\alpha')$$
$$(1s)(2s)(2p)^6\ {}^3S - (1s)^2(2s)(2p)^5\ {}^3P \ldots.\ (\alpha_4)$$
$$(1s)(2s)^2(2p)^5\ {}^3P - (1s)^2(2s)^2(2p)^4\ {}^3P \ldots.\ (\alpha_3)$$
$$(1s)(2s)^2(2p)^5\ {}^1P - (1s)^2(2s)^2(2p)^4\ {}^1S \ldots.\ (\alpha_5)$$
$$(1s)(2s)^2(2p)^5\ {}^1P - (1s)^2(2s)^2(2p)^4\ {}^1D \ldots.\ (\alpha_6).$$

There are five transitions to be expected and five are observed. Moreover the relative intensities come out in agreement with experiment. Accurate calculations of the separations between lines cannot at present be made because exact wave functions are not known. The

best available wave functions give separations about 50 percent off. The present theory can be extended to explain the structure of absorption edges and the shift of absorption edge with valence.

10. A check on the lattice constants and axial ratios of stibnite. JOHN G. ALBRIGHT, *Case School of Applied Science.*—Dana (Textbook of Mineralogy) classifies stibnite as orthorhombic with axial ratios 0.9926:1:1.0179. Gottfried (Zeitschrift für Kristallographie **65**, 427–434, 1927) gives the axial ratios as 0.992:1:0.338 and the lattice constants as $a=11.39$A, $b=11.48$A, $c=3.89$A, making the value for the unit cell along the c axis about one third of that indicated by Dana's values. In view of Dana's reputation for accuracy it was thought desirable to check the determinations of Gottfried. X-ray diffraction and reflection photographs give values for the lattice constants of $a=11.29$A, $b=11.45$A, $c=3.87$A, making the axial ratios 0.986:1:0.339, which agree very well with the values given by Gottfried.

11. X-ray analysis of cold rolling and recrystallization in steel. C. NUSBAUM, *Case School of Applied Science.*—A careful and extensive study, by means of Laue photographs, has been made of the effect of cold rolling on low carbon steel and the subsequent heat treatment necessary for its complete removal. The changes due to increasing degrees of cold rolling may be considered as taking place in three stages (1) introduction of internal stresses as indicated by radial asterism, (2) the fragmentation of the individual crystals, and (3) the increasing degree of preferred orientation of the crystal fragments. The necessary temperature in the subsequent heat treatment for the complete removal of the effect of cold rolling is a function of the degree of the cold work. However, recrystallization is necessary for the complete removal of preferred orientation.

12. The "spread" as a measure of deviation in physical measurements. ELLIOT Q. ADAMS, *Lamp Development Laboratory, Nela Park.*—In order to compare results of incandescent lamp tests expressed in terms of the spread (maximum difference) observed in sets of various numbers of lamps, it was necessary to calculate factors to convert these results to a comparable basis. The average deviation of a single observation was chosen as the basis of comparison. Assuming a Gaussian distribution of errors, the factors have been calculated by mathematically approximate methods, and may be expressed by the semi-empirical formula: Spread/(av. deviation) $=f(n)=(5.304-2.11/(0.47+\lg n))(\lg n)^{1/2}$ with an error not exceeding 0.01 in the factor. This error is negligible in comparison with the unavoidable error in determining by any method the average deviation in a set of fewer than 10^6 observations, i.e., in practically all physical measurements. While it may be shown mathematically that the average deviation so computed is less precise than that computed from the sum of the residuals, or *a fortiori* of their squares, the difference seldom exceeds the probable error of the more refined measures. The labor of computation is so much less than that of the more precise methods that an expression of the internal consistency of *all* results of physical measurements may reasonably be required.

13. The wave-mechanical theory of radiation. E. H. KENNARD, *Cornell University.*—A complete theory can easily be developed in terms of traveling plane waves instead of standing oscillations; such a form should be especially useful in dealing with phenomena which like the Compton effect involve motion. Replacing the usual Fourier integral by a series we write for the classical vector-potential of the radiation field, $A=\Sigma(i)(a_iI_i'\cos\theta_i+a_i''I_i''\sin\theta_i)\,\Delta\nu\Delta\omega$ where $\theta_i=2\pi\nu_i(t-gx_i)$, $c=1/g$ being the speed of light, x_i distance along the ray, I_i' and I_i'' two perpendicular unit vectors and $\Delta\omega$ an element of solid angle. As coordinates and momenta we take $Q=\beta_1a'\cos 2\pi\nu t$, $P=\beta_1a'\sin 2\pi\nu t$, and $Q=\beta_1a''\sin 2\pi\nu t$, $P=-\beta_1a''\cos 2\pi\nu t$, $\beta_1^2=c\Delta\nu\Delta\omega/2\nu$; the energy is then $W=\Sigma(\sigma)\pi\nu_\sigma(Q_\sigma^2+P_\sigma^2)$, and $A=\Sigma A_\sigma=\Sigma\beta_\sigma I_\sigma(Q_\sigma\cos\theta_\sigma+P_\sigma\sin\theta_\sigma)$ where $\theta_\sigma=2\pi g\nu_\sigma x_\sigma$, $\beta=2\nu\beta_1/c$. We now replace P_σ by $h/2\pi i\partial/\partial Q_\sigma$ and form the Schrödinger time equation, adding in the Hamiltonian for a non-relativistic free electron simply $1/2m(\nabla-e/c\Sigma A_\sigma)^2$. The motion of a packet is easily followed; formulas almost classical in form are obtained for its centroid, with the operators $-\Sigma\partial A_\sigma/\partial x_\sigma$ and $\Sigma\nabla\times\Sigma A_\sigma$ acting as electric and magnetic field-strengths. The acceleration vanishes when the field is in its normal

or any other pure quantum state, showing that the "zero-point" infinite energy does not imply the existence of a physical electromagnetic field.

14. On the mechanism of light absorbtion in solid bodies. J. FRENKEL, *Visiting professor from Leningrad, University of Minnesota.* (*Introduced by H. A. Erikson.*)—Starting from the analogy between a crystal and a molecule, it is shown that the electronic excitation, forming the first step in the process of light absorbtion, is not confined to a particular atom, but is diluted between all of them in the form of "excitation waves," similar to sound waves which are used to describe the heat motion in the same crystal. Owing to the interaction between the atoms the excitation state is split up into substates whose number is equal to the number of atoms n (excitation multiplet). By superposing several excitation waves "excitation packets" can be constructed representing the travelling of the excitation state from one atom to another. To each excitation (sub.) state there corresponds a definite crystal structure (lattice constant, vibration frequencies) slightly different from that of the normal one, and giving rise to slightly different vibrational states. This influence of the excitation on the vibrational states provides an indirect coupling between them, which allows the excitation energy to be shared between a few hundred heat-oscillators with practically no direct coupling (nor anharmonicity) in a radiationless transition which forms the second state of the process of light absorbtion.

15. Interchange of translation, vibration, and rotation energy. CLARENCE ZENER, *Harvard University.*—A modification of the Born collision method is used to calculate the effective cross-sections of inelastic collisions of the first and second kind between atoms and molecules. The unperturbed Hamiltonian is taken to be the exact Hamiltonian averaged over the internal coordinates of the molecule. The internal motions of the molecule is treated as the perturbation that results in a transfer of energy. The sharpness of the collisions is approximately obtained from the mean ionization potentials of the two colliding systems. The small probability of transfer of vibrational and translational energy arises from the duration of the collision being greater than the time of oscillation. In general, the effective cross-section for a collision of the second kind is comparable to the kinetic theory cross-section only when a frequency of the molecule is comparable to a frequency associated with the combined system of molecule and atom.

16. Orbital valency. JAMES H. BARTLETT, JR. *University of Illinois.*—The problem of interaction of two identical atoms, each with one p valence electron, has been investigated. The total system has originally a twelve-fold degeneracy, and a first order perturbation calculation is made, using a method analogous to that of Kemble and Zener for the excited states of the hydrogen molecule. This enables one to give an estimate of the relative positions of the resulting molecular states as a function of the internuclear distance. A simple atomic wave function similar to those employed by Zener (with no radial nodes) has been used in the present work to facilitate the calculations. Complete potential energy curves have now been obtained, and agree in general with the results reported in a letter to the Physical Review **36**, 1096 (1930).

17. Directed valence in polyatomic molecules. J. C. SLATER, *Massachusetts Institute of Technology.*—By means of wave mechanics one can draw conclusions regarding valence in polyatomic molecules, finding in particular that the different shared electron bonds from a single atom tend to be at definite angles to each other. The two bonds in atoms like oxygen, and the three in nitrogen, tend to be mutually perpendicular, while in carbon a tetrahedral structure is indicated. These conclusions in the first two cases rest on the nature of the wave function for a p electron: the three types of p electron may be considered to have densities large along three mutually perpendicular directions. With carbon, one must combine these three with an s electron to produce tetrahedral valences. The conclusions can be supported by a wide range of experimental facts, from the structure of simple inorganic molecules, metals, and organic compounds.

18. Polarizabilities and intra-atomic energies of hydrogen and helium. JOHN G. KIRKWOOD, *Massachusetts Institute of Technology.* (*Introduced by J. C. Slater.*)—A method of calcu-

lating polarizabilities and intra-atomic energies has been developed. An approximate separation of variables in the original wave equation is effected. From the approximate wave function which is obtained, a more exact one is constructed with the use of the variation principle. The polarizability and energy of two atoms at large distances have been calculated for hydrogen and helium.

19. On the Michelson-Morley-Miller experiment. N. GALLI-SHOHAT, *Mount Holyoke College.*—At the meeting of the American Physical Society held in Washington in April, 1930, it was suggested by the writer that Professor Miller's effect can be explained by means of the effect observed by Esclangon. This further enables us to explain why Professor Michelson in the last repetition of his experiment did not observe any effect. In fact, the displacement of the fringes due to the effect of Esclangon (rotation of the whole interference pattern) depends only upon the orientation relative to the motion of the solar system of that part of the path of light in the interferometer, which goes from the last reflection directly into the eye of the observer. In the arrangement of apparatus used by Professor Michelson, this path was made stationary, being directed *along the axis of rotation.* Thus, the revolution of the interferometer around this axis *could not change* the orientation of this path in space; hence, *no effect can be expected.* While in his first arrangement, which was used also by Professor Miller, this path lies *in the plane* of the interferometer, hence, a change due to revolution and a displacement of the fringes.

20. Change in mass-weight ratio. PETER I. WOLD AND EARLE M. BIGSBEE, *Union College.*—The late Charles F. Brush carried on experiments which led him to conclude that the weight of a metal may change when strained, giving a change in the ratio of mass to weight. His experimental technique seemed to preclude the obvious sources of errors which might be urged as explanation of his results. The matter is of sufficient importance to our theories of gravitation to justify checking and at his request weighings were made on certain alloys prepared by him. The procedure was practically the same as described in his paper in Proceedings of the American Philosophical Society (Vol. 63, 1925, p. 36). Weighings taken on various specimens showed losses in weight when the specimen was compressed and a nearly complete recovery when the stress was removed. The changes were substantially in excess of balance errors. The losses were less than found by Brush and he considered this as due to annealing during the time between the preparation of the sample and its weighing. The shorter this time the larger were the observed effects. In the last sample studied, where elapsed time was shortest, the losses amounted to one part in 130,000. The work may be considered as confirming that of Brush. The suggestion that the effects are due to changes in the amount of adsorbed gases does not appear to be a sufficient explanation.

21. Properties of single crystal magnesium. P. W. BRIDGMAN, *Harvard University.*—Pure magnesium, which I owe to the Aluminum Company of America, was prepared in single crystal form by slowly lowering out of a vacuum furnace iron molds filled with the melted metal. The crystal structure of magnesium is known to correspond to the close packed hexagonal arrangement of spheres. It is therefore to be expected that the properties will not vary greatly with direction. This turns out to be true for the compressibility, for which was found:

Parallel to the axis, at 30° $-\Delta l/l_0 = 9.842\times10^{-7}p - 6.51\times10^{-12}p^2$
at 75° $-\Delta l/l_0 = 10.154\times10^{-7}p - 7.78\times10^{-12}p^2$.
Perpendicular to the axis, at 30° $-\Delta l/l_0 = 9.845\times10^{-7}p - 9.19\times10^{-12}p^2$
at 75° $-\Delta l/l_0 = 9.659\times10^{-7}p - 6.95\times10^{-12}p^2$.

Pressure is expressed in kg/cm², and the pressure range is 12000.

The electrical resistance, however, does not satisfy expectations. At 22°.5 the specific resistance is 3.89×10^{-6} parallel to the axis, and 4.60×10^{-6} perpendicular to it. Not only does the resistance vary materially with direction, but in almost all other non-cubic metals the resistance is greater parallel to the axis. The average pressure coefficient to 12000 was found to be 4.35×10^{-6} parallel to the axis, and 4.62×10^{-6} perpendicular to it. The temperature coefficient of resistance at atmospheric pressure between 0° and 100° was 0.00523 and 0.00428 respectively.

22. Transverse heat effect in single crystal bismuth plates. H. P. STABLER, *Harvard University.*—The dependence of the transverse heat on the orientation of the crystallographic axis has been studied in single crystal bismuth. The metal was of three different varieties (of which one was specially prepared electrolytic bismuth) all having high temperature coefficients of resistance and giving identical results. The crystals were grown by a modification of Kapitza's method in the form of uniform rectangular plates, about 15×2.2 mm cross-section, and perfect over a length of from 4 to 16 cm. Measurements made on twenty-eight plates covering the entire range of orientation show clearly that the Thomson symmetry relation for the tranverse heat, $[T(\theta)=(P_{\parallel}-P_{\perp})\sin\theta\cos\theta]$, is not satisfied. The ratio $(T(\theta)/\sin\theta\cos\theta)$ plotted against $\sin\theta\cos\theta$, instead of being constant, varies in a roughly sinusoidal manner, with the extremes at 15° and 75° differing by $24\%\pm5$. These values are 14.2 and 18.0×10^{-3} watts respectively, and at 45°, 15.9. Bridgman, and Fagan and Collins have shown that the longitudinal Peltier effect also, in bismuth, deviates from the analogous Thomson relation. Ehrenfest's recent treatment of these phenomena in crystals arrives at the Thomson relations, and thus his treatment, though general, is not sufficiently comprehensive to account for these experimental results.

23. Liquid flow through porous unsaturated mediums. L. A. RICHARDS, *Cornell University.*—When a liquid is absorbed by a porous medium and the medium is unsaturated the pressure within the liquid is less than atmospheric pressure and is determined by the curvature of the air-water interface. Under such circumstances flow of the liquid through the medium is caused by gravity and pressure gradients within the liquid. Analogous to electrical currents in metals, this flow may be expressed in terms of the product of a potential gradient and a conductivity factor. For the capillary case, however, the conductivity is a function of the potential which in turn is a function of the liquid content of the medium. By means of specially constructed porous cells the conductivity of water through clays, soils and sands has been measured at various potentials. These data furnish a basis for a quantitative study of the motion and equilibrium distribution of water in such mediums.

24. Determination of frequency and damping of resonating circuits. J. TYKOCINSKI-TYKOCINER, *University of Illinois.*—It was found as a further result of studies of thermionic oscillators (Phys. Rev. **33**, 634 (1929); and Univ. of Ill. Eng. Exp. St. Bul. No. 194) that periodic variations of constants of a coupled circuit produce periodic variations of plate and grid current. This property of oscillators was investigated and applied for the determination of frequency and damping of circuits whose location or other conditions do not allow the insertion of a variable condenser, variometer or resonance indicator. The circuit is coupled with a calibrated circuit energized by a thermionic oscillator tube and with an aperiodic circuit, whose reactance or resistance may be varied periodically by means of an electromagnetic tuning fork, buzzer or by superposed a.c. When the oscillator is being tuned, variations of the plate and grid current are produced, which show a periodicity corresponding to that of the tuning fork or a.c. and a transient amplitude passing through two maxima and a sharp minimum placed between them. The M-curve of effective current values thus obtained is a curve of derivates of the Bjerknes resonance curve. The minimum coincides with the fundamental frequency. The interval separating the two maxima is proportional to the decrement of the measured circuit. The maxima and minimum of the M-curve are audible in a telephone receiver. The complete curve is obtained by thermoelectric or thermionic instruments connected to amplifiers. The method was applied to closed circuits and antennae at frequencies from 100 to 100,000 kc.

25. The amplification of small direct currents. L. A. DUBRIDGE, *Washington University, St. Louis.*—A series of tests has been made by the author, under the supervision of Dr. Hull at the General Electric Laboratories, to investigate the possibilities of using a newly developed four-element thermionic tube, the FP-54 Pliotron, (described by Metcalf and Thompson, Phys. Rev. **36**, 1489 (1930)) in place of an electrometer in the measurements of very small direct currents. Simple circuits of standard types were found suitable and a wide range of sensitivity obtained. (1) With a single-tube circuit, using a Type R galvanometer and an input

resistance of 10^{10} ohms, a current sensitivity of 10^{-14} amp/mm is readily obtained. (2) Greater stability is attained by using a balanced two-tube circuit, with which a sensitivity of 10^{-16} amp/mm can be reached. (3) By "floating" the two grids of this circuit and using the "rate of drift" method of measurement, it was found that currents as small as 5×10^{-18} amp could be detected. (4) To enable the output to be read on a microammeter a second stage of amplifiction was employed. A deflection of 4 micro-amp. was obtained for an input current of 10^{-13} amp. The circuits are all more stable and simpler to operate than an electrometer of equal sensitivity, and the highest attainable sensitivity is greater than for any type of electrometer except the Hoffman.

26. Studies in non-linear circuits. CHAUNCEY GUY SUITS, *General Electric Company, Schenectady. (Introduced by A. W. Hull).*—The fundamentally important series inductance, capacitance, resistance circuit

$$L'(i)\frac{di}{dt}+\frac{1}{C(i)}\int idt+iR(i)=f(t), \tag{1}$$

where the parameters are functions of the current, is discussed. The frequent occurrence and great practical importance of circuit elements which depend upon the current are noted. The particular cases of the series and parallel circuit with linear resistance, linear capacitance, and a non-linear iron-core inductance are studied in detail. For the *series circuit* it is shown that the abrupt rise in current with increase in voltage at a certain critical voltage for the circuit may be identified as a quasi-resonance condition, called *non-linear resonance.* The condition for resonance in the linear circuit,

$$-L'\frac{di}{dt}=\frac{1}{C}\int idt, \tag{2}$$

is generalized as

$$-L'(i)\frac{di}{dt}=\frac{1}{C(i)}\int idt \tag{3}$$

for non-linear cases. The relation (3) is satisfied in the steady state *during a portion of each cycle*, wherein the peak current may be calculated from Ohm's law. For the *parallel* circuit *non-linear resonance* similarly obtains, and is associated with a decrease in total effective current with increase in voltage (r.m.s.), a property unique in circuits. The fundamental analogy between the behavior of linear circuits to changing frequency and non-linear circuits to changing voltage follows from the predominating voltage dependence of impedance for the non-linear iron-core inductance. The paper will be accompanied by demonstration apparatus if time permits.

27. The effect of the temperature dependence of the work function on A and b in Richardson's equation. J. A. BECKER AND W. H. BRATTAIN, *Bell Telephone Laboratories, Inc., New York.*—The most general form of Richardson's equation is

$$i=AT^{-1/2}\epsilon^{\int(L_p/RT^2)dT} \tag{1}$$

where L_p represents the energy added to the system when one mole of electrons is "vaporized" at constant pressure. This equation follows necessarily from the first and second law of thermodynamics and from the generally accepted assumption that the electron vapor behaves like a perfect gas. In order that

$$i=AT^2\epsilon^{-b_0/T} \tag{2}$$

it is *necessary* that

$$L_p=b_0R+5RT/2 \tag{3}$$

and *to assume that b_0 is independent of T.* $5RT/2$ represents the kinetic energy of the electron gas plus external work done per mole at constant pressure. It is generally assumed or deduced that the electrons in the metal receive negligible energy when T is increased. In that case, $L_p-5RT/2$ represents work done per mole against various electrical forces. Call this bR. If bR depends on T, (1) becomes

$$i = AT^2 \epsilon^{\int (b/T^2)\, dT}. \tag{4}$$

If $b = b_0 + \alpha T$

$$i = AT^{2+\alpha} \epsilon^{-b_0/T}. \tag{5}$$

If the work function varies linearly with T, we conclude: 1. equation (5) replaces (2) which is invalid; 2. the mean slope of $\log i - 2 \log T$ vs. $1/T$ is $b_0 + \alpha T$ and not b_0; 3. the intercept of this plot is $\log (A \epsilon^{\alpha} T^{\alpha})$ and not $\log A$ or $\log (A \epsilon^{-\alpha})$.

28. Conductivity of oxide cathodes. N. H. WILLIAMS AND W. S. HUXFORD, *University of Michigan.*—The conductive properties of oxide coatings used in the equipotential cathode type of radio tube have been investigated. The inner nickel sleeve served as one electrode, the second being a nickel strip in contact with the outer surface of the oxide. Currents through the coating as measured at constant potential vary with the frequency of the applied electromotive force. A decrease in conductivity of about forty percent occurs when the freqeuncy is changed from 1500 to about 10,000 cycles per second. The decrease starts at lower frequencies for higher values of applied potential. These results indicate a transfer of electrical charges through the coating by ionic conduction, the process being inhibited at the higher frequencies. A method of estimating the relative thermionic activities of core metal and oxide surface is suggested. Fluctuations in the current through the coating were measured on an amplifier tuned to various frequencies from 200 to 40,000 cycles per second. An abnormal increase in "shot" voltage was found for frequencies below 10,000 cycles. This result is believed to confirm the hypothesis that positively charged ions are neutralized in the space charge produced by electrons which are emitted thermionically from the activated surface of the core metal.

29. The electrical polarization of electrets. MAURICE EWING, *Lehigh University.*—The internal electrical polarization of an electret was determined by breaking a piece of the electret along a plane normal to the direction of polarization and measuring the charge per unit area which appeared on the newly-formed surfaces. The polarization for this particular electret was found to be 2.0 ± 0.2 esu/cm^2. The theory of Adams (Frank. Inst. J., 204, 469 (1927)) seems to require that the polarization in an electret be of the order of 10^5 esu/cm^2.

30. Electrical characteristics of a viscous mineral insulating oil as functions of temperature and frequency. H. H. RACE, *General Electric Co., Schenectady.*—Data recently taken on the dielectric loss and the dielectric constant of good mineral insulating oils lead to the following conclusions: (a) At constant temperature the dielectric constant decreases by only a few percent as the frequency is increased from sixty to two million cycles per second. (b) At constant frequency the dielectric constant decreases with increased temperature and this change appears to be proportional to the decreasing density of the oil. (c) For a given temperature there is a critical frequency such that for all lower frequencies the A.C. loss is independent of the frequency and for all higher frequencies the loss increases with the frequency. Within the first frequency range the mechanism of D.C. conduction and of A.C. loss appear to be the same, and both are probably due to the migration of charged ions or larger particles in the oil. Within the second range, the loss per cycle, (after that resulting from D.C. conduction has been subtracted), shows resonance characteristics as a function of either temperature or frequency. (d) The higher the temperature, the higher the critical frequency below which the A.C. and D.C. losses are the same. Power factors as high as 1% have been observed under conditions for which the loss resulting from conduction would be negligible. These data have been studied from the point of view of Debye's theory of polar molecules, and a qualitative agreement has been found.

31. Dielectric constants of certain organic compounds. W. R. PYLE, *The Ohio State University.*—The dielectric constant of an organic compound is thought to be allied with its other physical properties such as solvent power and molecular complexity. Probably the future will reveal a more definite correlation between the dielectric constant and the other physical properties of a compound. The nulled heterodyne method of measurement of dielectric constants was made possible by the advent of the triode valve and it is employed in this work. For room temperature and at a frequency of 85.8 kilocycles the dielectric constant was determined for

each of the following: benzene, carbon tetrachloride, chloroform, cinnamic aldehyde, ethyl ether, methyl cyclohexane, methyl o-nitrobenzoate, nitrobenzene, oxalyl chloride, n-propyl ether, iso-propyl ether, o-xylene, m-xylene and p-xylene. The temperature coefficients of the dielectric constant for ortho-, meta-, and para-xylenes were determined over a range of about 25°C for both the linear formula and Abegg's formula. It seems reasonable to believe that the values of the dielectric constants determined in this work are relatively as accurate as the purity of the organic compounds.

32. Maintaining direction in flight. JAMES D. TEAR, *General Electric Co., Schenectady, N.Y.*—Accelerations due to changes in course cause the aircraft compass to be responsive to the vertical component of the earth's magnetic field and to be misleading as a direction instrument. North courses cannot be flown without other reference means. The potential generated by an electromagnetic compass is a function of the course setting θ, the course error $\Delta\theta$ and the product of angular velocity and speed or the angle of bank ϕ. A gyroscopic device, the sensitivity of which is controlled by the course setting mechanism, supplies a potential proportional to $\sin\phi$ and $\cos\theta$ compensating the acceleration error. An additional angular velocity effect independent of course is added. A null effect then requires an angular velocity toward the chosen course proportional to angular displacement, the condition for aperiodic steering. The adequacy of the system for maintaining direction in clouds has been verified in a series of experiments in which the rudder angle was automatically made porportional to the algebraic sum of the potentials in the compass circuit.

33. A method of weather forecasting. R. C. COLWELL, *West Virginia University.*—It has been shown before that when a high pressure area covers both Pittsburgh and Morgantown, the day signal from KDKA is stronger than the night signal, while for a low pressure area, the night signal is the stronger. Hence the ratio of the day to the night energy received from KDKA at Morgantown will give some indication of the atmospheric conditions between the two cities. In this method of forecasting, a fading curve is taken for about one hour before sunset and three hours after sunset. The area is measured with a planimeter and the ratio of the day to night energy is calculated for each day. If this ratio is greater than one, fair weather is indicated; whereas, if the ratio drops to one half, a storm is approaching. In addition to this ratio, barometer readings are taken and wind directions observed. A storm area passing north of Morgantown will cause a low barometer and a south wind. If the storm center passes to the south, the energy ratio from a station to the north is no longer reliable and readings must be taken upon a station to the south.

34. Photoelectric properties of composite surfaces at various temperatures and potentials. DIMITER RAMADANOFF, *Cornell University.* (*Introduced by Ernest Merritt.*)—A large number of experiments were carried out with Ba photoelectric cells to determine the variation of photoelectric current with temperature and plate potential. In all cases the photoelectric current increased greatly at the higher temperatures, and reached maximum at 740°C. At this temperature the thermionic current was limited by space charge. By illuminating the photoelectric cell with interrupted light, the intensity of which was varied sinusoidally, it was possible to measure the photoelectric current with a new method which incorporates the use of a transformer coupled amplifier and a Bedell-Reich stabilized "Oscilloscope." With this apparatus the thermionic current, and sluggish currents which may be due to light in a secondary way, were completely eliminated and only the true photoelectric currents were measured. In this way a curve was obtained which represents the relation of photoelectric current vs. temperature at a constant applied voltage. This curve shows two distinct maxima at 560°C and 740°C the first of which is not observable with a galvanometer if constant illumination is used.

35. Correlating the selective photoelectric effect with the selective transmission of electrons through a cathode surface. A. R. OLPIN, *Bell Telephone Laboratories, Inc.*—The results of Fowler and others with respect to the penetration of α-particles into a model nucleus suggested the possibility of explaining the selective photoelectric effect by the selective transmission of electrons of a definite velocity through the cathode surface. These electrons must be

associated with waves of such length that they will form standing waves between abrupt potential discontinuities of like sign on the cathode surface. The existence of such a potential valley may be reasonably postulated, particularly for surfaces consisting of a layer of electronegative atoms or molecules sandwiched between electropositive layers. By interpreting the width of the valley to be the distance between the nuclear boundaries in successive electropositive layers and substituting these for d in the easily derivable equation $\nu_{max.} = n^2h/8md^2$ [or $d = 0.0551\ \lambda_{max.}^{1/2}$ Angstroms, for the case of $n=1$], an extremely close correlation with experimental facts results. All the observed selective maxima in spectral photoelectric response curves for the hydrides, oxides and sulphides of the alkali metals have been checked by this equation with a higher degree of accuracy than has been obtained by any other theory.

36. Physical detectors of "Mitogenetic Radiation." OTTO GLASSER AND V. B. SEITZ, *Cleveland Clinic Foundation, Cleveland, Ohio.*—Experiments of Alexander Gurwitsch and coworkers in 1924 showed that some form of radiation from growing and dividing cells of various plants and tissues produced increased mitosis in other cells. Since then this observation has been experimentally substantiated by numerous other workers. An attempt is described to detect and classify these "mitogenetic radiations" by physical means and some results of these experiments are reported.

37. Thermoluminescence excited by exposure to radium. FRANCES G. WICK, *Vassar College.*—The experiments described in this paper were made at the Institute for Radium Research in Vienna and the method of observation is one which has been used there by Dr. Karl Przibram. Calcium sulphate plus manganese and specimens of fluorite were exposed to radium and the thermoluminescence excited by this exposure was measured by heating the specimens in front of a photo-electric cell connected with a Wulf electrometer. Observations were made from the beginning of heating until the light was exhausted. Subjecting the specimens to a pressure of 10,000 Kg/cm² either before or after exposure to radium was found to change the intensity of the light emitted. Calcium sulphate plus manganese shows a single maximum of intensity as the temperature rises. The effect of pressure applied either before or after exposure to radium is to diminish the height of this maximum. Powdered fluorite previously heated to remove all natural thermoluminescence, shows, after exposure to radium, a number of sharp maxima due to different rare earth impurities. These maxima are lowered as a result of pressure. A broad diffuse band in the blue upon which the sharp bands are superimposed is made stronger as a result of pressure.

38. Significance of wave-length in color vision. C. A. RINDE, *College of the Pacific.*—Helmholtz and Koenig showed all color sensations to be reproducible by mixing light of three specific wave-lengths. Ladd-Franklin suggested red and green, blue and yellow as primary; each pair belonging to a single sensitive mechanism. The author's measurements of the retinal areas sensitive to homogeneous light selected from various regions of the grating spectrum indicate that the four areas exist and are independent. The approximate wave-length range to which each is sensitive has been measured, and an additional area sensitive only to the shorter wave-lengths has been found.

39. Appearance of color bands in films of sputtered tin. LESTER I. BOCKSTAHLER AND C. J. OVERBECK, *Northwestern University.* Small circular cathodes of tin are used to sputter films on glass. These films show concentric rings of color similar in appearance to Newton's rings. When viewed with monochromatic light, the rings are alternately light and dark. In white light the films show several cycles of the colors of the visible continuous spectrum. The growth of a set of rings, when viewed with reflected white light, begins with the appearance of a blue center a few seconds after the discharge is started. This center gradually passes through a cycle of colors of increasing wave length until it is red. With the appearance of each new center color all preceding colors move outward and form surrounding bands. The red center then merges into blue and the cycle is repeated. The rate of growth of a set of bands depends on the nature of the gas as well as on its pressure and the current density. Under a given set of conditions the change of color of the center and the addition of another set of color bands takes place with very definite regularity. Work is in progress to determine the chemical nature of these films and the cause of the colors.

40. The transmission of visible light through fog. H. G. HOUGHTON, *Round Hill Research Division, Massachusetts Institute of Technology (Introduced by J. A. Stratton).*—Measurements have been made on the transmission of visible light through artificial fog which was produced by condensing low pressure steam. Curves for various densities of fog were plotted and found to have definite maxima at about 4900A. The relation between fog density and the transmission of light was found to be practically linear for all wave-lengths in the visible spectrum. The maxima obtained are not in agreement with the results of other investigators but it is thought that this is due to a difference in the particle size of the fogs. Measurements indicated that the particles of the fogs used were considerably smaller than those of the fogs employed by other experimenters.

41. Theoretical discussion of the transmission of light through fog. J. A. STRATTON AND H. G. HOUGHTON, *Massachusetts Institute of Technology.*—The transmission of light through fog has been studied from a theoretical standpoint in an attempt to explain the experimental results described in another paper. The treatment is based on the work of Debye, Mie, Jobst and others on the pressure of light and on the colors of colloidal solutions. The fog particles are considered to be perfect dielectric spheres having an index of refraction of 1.33 and a permeability of unity. The coefficient of absorption, which is a function of particle diameter, is obtained by direct summation of Jobst's expression. By proper selection of particle diameter a theoretical curve is arrived at which fits the experimental curve quite closely. This particle size checks the measured value within the accuracy of the measurements. The transmission of light through fog having larger particles may be readily computed in the same manner.

42. Ultraviolet energy radiated by General Electric type S-1 lamps in quartz bulbs. B. T. BARNES, *Nela Park Laboratory, Cleveland.* The energy flux density of the principal ultraviolet lines from General Electric S-1 lamps in fused quartz bulbs has been measured. The latter are made somewhat smaller than the glass bulbs so that with normal operation the temperature of the mercury pool will be the same in the two cases in spite of the lower absorption of the quartz in the infra-red between 2 and 4μ. The gain in intensity by use of quartz bulbs is even greater than expected. With quartz bulbs the lines at 2650 and 2537A are nearly as strong as those around 3000A.

43. The General Electric photoflash lamp. W. E. FORSYTHE AND M. A. EASLEY, *Nela Park Laboratory, Cleveland.* The bulb of the new photoflash lamp contains about fifty milligrams of aluminum foil that has a surface of about three hundred sixty square centimeters. This lamp can be operated from a one and one half volt storage battery or from a one hundred fifteen volt line. As the lamps are now constructed they start about two hundredths of a second after they are turned on and from the beginning of the flash to the maximum is about sixteen thousandths seconds while the whole flash lasts about six hundredths seconds. The maximum flux amounts to well over one million lumens.

44. Recent Developments in Architectural Acoustics. PAUL E. SABINE, *Riverbank Laboratories.*

45. Some Physical Characteristics of Speech and Music. HARVEY FLETCHER, *Bell Telephone Laboratories, Inc.*

46. Concerning Some of the Problems Encountered in Recording and Reproducing Photographic Sound Records on Moving Picture Film. CLARENCE W. HEWLETT, *General Electric Company.*

47. Magnetostriction measurements using a heterodyne beat method. A. B. BRYAN AND C. W. HEAPS, *Rice Institute.*—The apparatus previously used in measuring discontinuous changes in length accompanying the Barkhausen effect in nickel has been employed for gross magnetostriction measurements in nickel and iron and in magnetite, hematite and bismuth crystals. Length changes in a direction parallel to the applied magnetic field are measured. The results for nickel and iron are similar to those previously obtained. Magnetite expands

for two orientations and contracts for a third and shows no hysteresis. Hematite shows a small expansion for each of two orientations. For bismuth a field of 2160 gauss produces no measurable change in length. It is estimated that $\Delta L/L$ is less than 2.2×10^{-9}. Additional measurements are to be made with larger magnetic fields and higher sensitivity.

48. Variation of magnetic susceptibilities with temperature in Sm^{+++} and Eu^{+++}. AMELIA FRANK, *University of Wisconsin.*—Calculation of susceptibilities in Sm^{+++} and Eu^{+++}, previously made at room temperature only (J. H. Van Vleck and A. Frank, Phys. Rev. **34**, 1494 (1929)) were extended to include values over a temperature range 14°K–1000°K using the theoretical expression previously given (l.c.). The value of the temperature coefficient $(1/\chi)(d\chi/dT)$ at 300°K was found to be -0.00187 for Eu^{+++} and only -0.00032 for Sm^{+++} in contrast with the normal Curie value -0.00333. These values are in satisfactory agreement with existing experimental data. Cabrera finds -0.002 for Eu^{+++} while Freed and other observers report values in the neighborhood of -0.0006 for Sm.$^{+++}$ The coefficient for Sm^{+++} is so abnormally small that accurate percentage agreement cannot be expected. The computed values show that Sm^{+++} should exhibit a curious behavior in that, while at low temperatures the susceptibility decreases quite rapidly with an increase in temperature, a minimum is reached at about 400°K.

49. On the theory of magnetic susceptibilities of salts of the iron group. J. H. VAN VLECK, *University of Wisconsin.* It is well known that the susceptibilities observed for these salts, in marked contrast to those of the rare earths, do not have the theoretical values for free ions, but instead conform to a formula $\chi=N(he/2\pi mc)^2S(S+1)/3kT$ obtained by assuming that only the spin S of the paramagnetic ion contributes freely to the susceptibility. As emphasized by Stoner, (Phil. Mag. **8**, 250), this demands that inter-atomic forces quench the magnetic effect of the orbital angular momentum, both in solids and solutions. The present paper aims to show that these forces can really do this. Following Bethe and Kramers, they may be approximately represented by a potential V whose series development usually begins with second order terms $Ax^2+By^2+Cz^2$. If $|(A-B)\bar{x}^2|\gg kT$ etc., or in general if V has no more than rhomboidal symmetry and is large compared to kT, these inter-atomic forces really quench the orbital moment. For the spin to be free, however, one must have $(h\Delta\nu_M)^2/h\Delta\nu_V\ll kT$, where $h\Delta\nu_M$ and $h\Delta\nu_V$ are respectively of the order of magnitude of the multiplet intervals for free ions and of the dissymmetry in V. These conditions require that $h\Delta\nu_V$ likely be of the order 0.1 to 1 volt. This agrees qualitatively with the coloring of iron salts in solution, which indicates that the ion is held in complexes whose binding energy is about 1 volt.

50. Magnetic susceptibilities of some binary alloys. F. L. MEARA, *Ohio State University.*—Gouy's method for measuring susceptibilities has been used to determine the susceptibilities of six series of binary alloys, tin-thallium, cadmium-zinc, antimony-cadmium, antimony-thallium, antimony-lead and antimony-tin. The specimens in the form of small cylindrical rods were made from the purest metals obtainable and were melted either in a vacuum or in an atmosphere of nitrogen. The difference in weight in and outside a magnetic field was determined by means of a Sartorius balance, which under favorable conditions gave the weight to one millionth of a gram. The maximum error did not exceed one percent. Curves showing the relation between susceptibility and concentration indicate the formation of the inter-metallic compound Sb-Cd in the cadmium-antimony series, and Sn-Tl in the tin-thallium series. With the addition of thallium to antimony the diamagnetic susceptibility passes through a minimum when the concentration of antimony is about eighteen percent. The lead antimony series shows a similar minimum at fifty percent. The susceptibility of the zinc-cadmium series indicates that zinc is slightly soluble in cadmium, and cadmium slightly soluble in zinc, and the remainder of this series of alloys mechanical mixtures.

51. The emission of positive ions from metals. H. B. WAHLIN, *University of Wisconsin.*—The positive ion emission from metals has been investigated by a mass spectrograph method. It has been found that most metals when first heated give off alkaline ions, as has been observed before. In addition, Cr, Mo, W, Ru, Rh, Nb, Ta, when heated to a temperature where vaporiza-

tion becomes appreciable, give off ions which are singly charged atoms of the electrode material itself. No indications of doubly charged atoms were obtained. Cu, Ag, Au, Zn, Mn, V, Fe, Co, Ni, Pd, Os, Ir, Pt, U, Th, Sb give only alkaline ions. Mn is doubtful. The work is being extended to temperatures above the melting point.

52. Residual ionization in air at new high pressures and its relation to the cosmic penetrating radiation. JAMES W. BROXON, *University of Colorado.*—Residual ionization measurements in air at pressures up to 170 atmospheres were made at 5400 ft. altitude in a spherical chamber of 11-23/32 in. diameter with lead and water shields. Values as low as 1.47 ions/c.c. sec. at 0.83 atmosphere were observed. At pressures above 140 atmospheres ionization-pressure curves obtained with the chamber shielded were parallel to the pressure axis, slopes in this region certainly not exceeding 0.02 ion/cc sec. atm. Increased shielding decreased the ionization, showing the existence of a penetrating radiation. Observations with water shields showed this radiation to have its origin above the level of the chamber. The calculated absorption coefficients are 0.0127 cm^{-1} lead, and 0.0010 or 0.0028 cm^{-1} water, the latter two values following respectively from the extreme assumptions that the radiation approached entirely from the vertical direction, or uniformly from all directions above the horizontal. If the ionization is considered to be due entirely to recoil electrons excited in the walls of the chamber, the pressure-ionization relation may be explained; and if the Compton theory is used, the absorption coefficient of the initial penetrating radiation as calculated from the observed range of the recoil electrons is found to be 0.0025 cm^{-1} water.

53. The effect of hydrogen upon the intensities of the spectra of zinc, cadmium and mercury. J. G. BLACK AND W. G. NASH, *University of Kentucky.*—When hydrogen is mixed with zinc vapor in a low voltage arc, some of the zinc lines change their intensities markedly. (Phys. Rev. **34**, 1138, (1929)). Recent experiments with the related elements, cadmium and mercury, show similar changes. Hydrogen increases the number of transitions to the 2^3P_{012} configuration of all three elements and greatly reduces the number of transitions from the 2^3P_1 state by radiation. The configuration energy is approximately 4.7 volts in mercury, 4 volts in zinc, and 3.78 volts in cadmium. Hg′ has more than enough energy to dissociate hydrogen. Zn′ has almost exactly enough, which fact may account for the total absence of the 3075.8 line. Cd′ does not have enough energy and probably loses its total energy to tube walls and electrodes after it has been made metastable by hydrogen impacts. An alternative explanation of the resonance quenchings is that they are due to the formation of metallic hydrides. It appears that the absence of a Raie Ultime does not insure the absence of an element in chemical spectroscopic analysis when hydrogen is present.

54. The ionization of hydrogen by positive ion impacts. MASON E. HUFFORD, *Indiana University.*—Positive ions of K, Na, Li and H have been accelerated between a filament and an earthed nickel cathode in an atmosphere of pure hydrogen. The cathode was surrounded by a second nickel screen and this in turn was enclosed by a similar screen in contact with the walls of the ionization tube. Ions were accelerated by potentials varying from zero to 2000 volts and retarded beyond the cathode by a potential 7.5 volts more than the accelerating potential. Current-accelerating potential curves show that the relation between ionization current and potential with K-ions is about linear. Increases can well be explained by the action of electrons from the cathode. With other ions the increase of current is much greater. With low pressures the increase in current is such as to indicate ionization by positive ions. At higher pressures distinct critical potentials are shown at voltages about 200 volts below that at which an arc is established.

55. On the fraction of current carried by electrons at the cathode of a mercury arc. K. T. COMPTON, *Massachusetts Institute of Technology.*—Ever since Schottky first pointed out that studies of heat balance afford a possibility of estimating what fraction of the current at arc cathodes is carried by escaping electrons, attempts have been made to do this in the hope of thereby testing theories of the arc. Such work has heretofore indicated that not much more than half this current is carried by electrons,—a conclusion which is difficult to reconcile with

any electron emission theory of the arc cathode because of the impossibility of accounting for a number of positive ions produced by an approximately equal number of electrons which had fallen through a cathode drop amounting to not more than one minimum ionizing potential. Revised estimates are now based on measurements of cathode drop and new considerations involving accommodation coefficients and the destination of electronic energy near the cathode. The conclusion is now reached that between 80% and 100% of the current of the cathode is carried by electrons. Thus it can no longer be said that arc theories based on electron emission from the cathode are disproved by measurements of heat balance.

56. Study of the afterglow in mercury vapor. HAROLD W. WEBB AND DAVID SINCLAIR, *Columbia University.*—The intensity of the afterglow in mercury vapor was studied in a side tube leading from a mercury arc as a function of vapor pressure, concentrations of ions and electrons and electron temperature. The intensity was found to vary roughly as the fourth power of the vapor pressure. Except at very low concentrations it was closely proportional to the first power of the electron concentration. With vapor pressure and concentration held constant, the intensity decreased very rapidly with increase in electron temperature, changing by a factor of 2500 as the temperature increased from 1300° to 5600°K. This change is too large to be explained by the theory of the simple recombination process. The results are well expressed in the form, that the intensity varies directly as the square of the total number of electrons and inversely as the number of electrons having energies greater than 1.2 volt. This suggests that we have a recombination process producing the afterglow, which takes place in two stages of which the second is responsible for the emission of the series lines, and that the effect of the fast electrons is to reionize from the first stage.

57. Problems in the design of a tube to withstand millions of volts. WILLARD H. BENNETT, *California Institute of Technology.*—It appears improbable that further increases in potential which can be produced in high voltage tubes can be hoped for until the mechanisms, themselves, of the causes of puncture have been carefully studied. A study of corona discharge over glass led to the conclusion that for further increases of potential, the potential must be generated in vacuum, and that the field must be roughly normal to the glass wall of the tube. The greatest difficulty in obtaining higher potentials in tubes is due to auto-electronic emission from electrode surfaces. A study of emission from unconditioned metal surfaces of radii of curvature large compared to the distance between the surfaces showed that loose microscopic particles adhering to the cathode can give emission indistinguishable from the emission following the usual breakdown. The metal used as anode was found to determine largely or entirely the field-current characteristics.

58. Experiments with high-voltage tubes. M. A. TUVE, L. R. HAFSTAD, AND O. DAHL, *Department of Terrestrial Magnetism, Carnegie Institution of Washington.*—Measurements have been obtained on the artificial β and γ-rays produced by the high-voltage cascade-tubes and Tesla coils previously described in the Physical Review. The $H\rho$ values of the fastest β-rays, measured by their deflection in a calibrated magnetic field, correspond in voltage-equivalents, using the standard β-ray tables, to the peak voltages applied to the tubes, measured as before by the capacity-potentiometer method. Using a Geiger-Müller tube-counter shielded by six inches of lead, the relative γ-ray intensities from the tubes have been measured through 1, 2, and 3 inches of lead. With the tube operating at about 1,300 kilovolts, the absorption coefficient after filtering through 1 inch of lead is the same (0.47) as that for the γ-rays from radium in equilibrium measured under the same conditions with the same instrument. These β and γ-ray measurements incidentally constitute a verification also of previous voltage-measurements. "Heat working" of the Pyrex, as previously described, has removed the voltage-limitation to such an extent that tubes have operated satisfactorily up to approximately 2,000 kilovolts, this limit (above ground) being set by corona or sparkover to the grounded oil-tank. Experiments are in progress on high-speed protons.

59. Multiplet separations and Zeeman effects. J. B. GREEN, *Ohio State University.*—The methods developed by Houston and Goudsmit are applied to the spectra of tin, lead, and antimony. Using the spectroscopic values of the multiplet separations it has been possible to

determine the g-values for the configuration p^2 of Sn I and Pb I, and for the configuration ^3P+s of Sb, in very satisfactory agreement with the experimental values of Green and Loring, and Back for these elements. Further agreement is found in the case of the ^3P and ^1P of Sn III. The multiplet separations and g-values calculated on Houston's theory adequately explain the anomalies found by Green and Loring in this spectrum.

60. Photometric study of the appearance of spectral lines in a condensed spark. H. V. KNORR, *Antioch College.*—The time interval between the appearance of spectral lines in a condensed spark has been studied by means of a Kerr cell used as an electro-optical shutter. Since there appears to be some question about the meaning of the time intervals measured in this way, photometric observations have been made on the rate of increase in the intensities of such lines. From the rate of increase of the intensity for a particular line, it is possible to find by extrapolation the time at which the intensity is zero, that is, the time of its first appearance. The results obtained by this method are compared with the results obtained by the visual method. Observations were made on the arc lines $2^3P_{012}-2^3S_1$ of zinc and for five air lines appearing in the zinc spark. These three zinc lines appear at nearly the same time. The five air lines also appear at nearly the same time but definitely at a time earlier than the zinc lines. These results are not in agreement with the results obtained by the visual method. The explanation of this discrepancy may be found in the failure of the visual method to take proper account of the threshold of visibility. These results indicate that neither of these methods give data on the life time of the zinc atoms in the excited state but only data on the characteristics of the spark discharge.

61. Spectra emitted in the initial stages of condensed discharges. J. W. BEAMS, *University of Virginia.*—Certain improvements in the Kerr cell method (Phys. Rev. **24**, 35, (1930)), (Program O.S.A. Oct. 31, 1930) have made it possible to study the times of appearance of spectrum lines in condensed discharges as a function of pressure of the gas. In mercury vapor $5461(2^3P_1-2^3S)$ was followed very closely (within less than the limit of precision at pressures above 10 cm) by $4358(2^3P_2-2^3S)$ while $5791(2^1P-3^1D)$ appeared somewhat later. As the vapor pressure of the mercury was increased the time between the appearance of 5461 and 5791 decreased. In a discharge in air 5001 N II $(1^3D'_{1,2}-1^3F'_{2,3})$ appeared first. As the pressure was lowered from one atmosphere the time between the appearance of 5001 and 4631, 4643 N II $(1^3P_2'-2^3P_{2,1})$ was decreased while a slight increase was noted in the time between the appearance of 5001 and the group 5680, 5676, 5667, N II $(1^3P'_{2,0,1}-1^3D'_{3,1,2})$. In a mixture of equal amounts of air and helium the time between the appearance of 5001 N II and 5876 (2^3P-3^3D) increased with lowering of pressure. The results probably indicate that some of the above levels are excited in part at least by secondary processes.

62. The sixth spectrum of arsenic. D. BORG, *Upsala University*, AND J. E. MACK, *University of Wisconsin.*—The lines of the transition $3d^94s\leftarrow 3d^94p$ have been indentified in As VI. In all respects the spectrum agrees with the expectations from extrapolation of the sequence Ni I—Ge V, unlike the As VI classification proposed by P. Pattabhiramiah and A. S. Rao (Zeits. f. Physik **53**, 587, 1929), in which those authors point out anomalies.

63. Heterochromatic photographic photometry in the Schumann region. GEORGE R. HARRISON AND PHILIP A. LEIGHTON, *Massachusetts Institute of Technology and Stanford University.*—The spectral energy responses of several of the fluorescent materials ordinarily used for coating photographic emulsions when used in vacuum spectroscopy have been investigated in the ultraviolet between 4000 and 2300A, and in certain easily reproducible cases the number of fluorescent quanta has been found strictly proportional to the number of incident quanta throughout this range. This fact, taken with the uniformity of contrast previously found under similar conditions (Jour. Opt. Soc. America **20**, p. 313, 1930) appears to furnish a general method of photographic photometry which can be used throughout the extreme ultraviolet, where the sensitivity of most spectral apparatus is too low to permit the use of thermopiles for plate standardization. The method is now being checked directly with fluorite apparatus in the Schumann region, and is being applied in a 21 ft. vacuum spectrograph to the determination of electronic transition probabilities in multiply ionized atoms of the first long period.

64. Intermittent exposure in photographic spectrophotometry over wide intensity ranges. BRIAN O'BRIEN AND E. DICKERMAN O'BRIEN, *Institute of Optics, University of Rochester, N. Y.*—Previous work on the compensation of reciprocity failure in photographic spectrophotometry by intermittency failure imposed on the light beam of higher intensity by interrupted exposure (Phys. Rev. **33**, p. 640 (1929)) has been extended using sector discs with aperture ratio as low as 1/1200, using a mercury arc as source mounted on a carriage with range of movement of 50 meters for varying intensity. Emission of the arc was held constant within ½% (measured radiometrically) by controlled ventilation and electrical input. Errors in measurement of sector apertures and exposure timing were less than ½%. Densities were measured with a thermoelectric microdensitometer. For intensities in ratio 1200:1 and sector disc opening 1/1200 running 28 flashes per sec., and comparing adjacent areas, the difference in density produced by continuous low intensity and interrupted high intensity (for It = const) on Eastman Process plates developed to high gamma was less than 0.01 for all densities from threshold to 1.0 for all wavelengths from 4000A to 2300A for intensities from approximately optimal to 10^{-4} this value. For $\lambda < 2800$A correction was made for atmospheric absorption as measured by Dawson, Granath, & Hulburt (Phys. Rev. **34**, p. 136 (1929)). Reciprocity and intermittency failure separately determined by continuous exposure of same total energy to the higher intensity were as great as 0.20 density units for intensity ratio 10^3.

65. Band spectrum of sulphur. PAUL HUBER, *Ohio State University.*—The band spectrum of S_2 has been investigated in both emission and absorption. An under-water spark was used as a source for the light absorbed by the vapor in a heated tube, while Geissler tubes were used for the emission spectra. The effect of predissociation is especially evident in emission, the $n' \rightarrow 0$ progression suddenly breaking off after the 8-0 band, (λ2828), as reported by Von Iddekinge. The heat of dissociation of normal S_2 is therefore reduced to less than 4.39 volts, as compared with 4.9 volts given by the International Critical Tables. No improvement could be made in the accuracy of the heat of dissociation of excited S_2, because of the extreme irregularities in intensity in emission. Five emission bands lying between λ2828 and λ2980 have been photographed at high dispersion using the second order of a 21-foot grating. The fine structure analysis of these bands is now in progress.

66. Distribution of intensity within the β and γ band systems of nitric oxide. OLIVER R. WULF AND ERNEST J. JONES, *Bureau of Chemistry and Soils, Washington, D. C.*—Variations in the distribution of intensity within the β and γ bands of nitric oxide have been observed when the products from an oxygen discharge tube are allowed to interact with the products from an active nitrogen tube. In this connection attention is called to an abnormal excitation of the γ bands of nitric oxide as they are emitted from an ordinary high current atmospheric pressure arc. The character of the intensity distribution suggests that the excitation arises as a chemiluminescent phenomenon, the energy of excitation being derived from energy made available in reaction. There appears to be evidence for reaction involving metastable nitrogen molecule. If this is the case it illustrates the chemical reactivity in the homogeneous gas phase of one state of the neutral nitrogen molecule. The conditions leading to the alterations in intensity distribution within the band systems mentioned above suggest that the excitation of band spectra is apt to depend on chemiluminescent processes and that the intensity distribution will, therefore, frequently be abnormal.

67. CO bands in the region λ2220 to λ3300. HAROLD P. KNAUSS, *Ohio State University.*—Microphotometer records covering the region from 2200 to 3300A were made of CO band spectra obtained in the electrodeless ring discharge (Knauss and Cotton, Phys. Rev. **36**, 1099, (1930)) and wave-lengths were measured. Unidentified bands at wave-lengths 2925, 3028, 3138, and 3253A were identified as belonging to a new system, corresponding to transitions from $C(^1\Sigma)$ to $a'(^3\Sigma)$. According to values for the known energy levels of the CO molecule quoted by Estey (Phys. Rev. **35**, 309 (1930)), the equation for the new system should be

$$\nu = 34160 - (1173n'' - 9n''^2).$$

Comparison between the observed wave-lengths and those predicted from this formula is made in the following table.

Transition	ν(Calc.)	λ(Calc.)	λ(Obs.)
0–0	34160	2926.5	2925
0–1	32996	3029.8	3028
0–2	31850	3138.8	3138
0–3	30722	3254.1	3253

68. Infrared absorption bands of slightly asymmetric molecules. HAROLD H. NIELSEN, *Ohio State University.*—A set of theoretical curves (as yet unpublished) showing the properties of infrared bands of completely asymmetric molecules have been made by D. M. Dennison. As a complement to these, calculations have been made for molecules of only slight asymmetry. A_x, A_y and A_z have been chosen the three principal moments of inertia of the molecule, where $A_x<A_y<A_z$. Diagrams have been prepared of positions of lines and their respective intensities, determined fron quantum mechanical solutions of asymmetric rotators, where the parameter $\rho=A_x/A_y$ varies by steps of 0.01 within the limits $\rho=0$ and $\rho=0.1$. Direct application of these will be made on the spectrum of Formaldehyde (H_2CO) now under observation.

69. Infrared absorption of formaldehyde vapor. JOHN R. PATTY AND HAROLD H. NIELSEN, *Ohio State University.*—Measurements of Formaldehyde vapor (H_2CO) have been made with a Hilger infrared spectrometer of the Wadsworth type from the visible to 7.0μ. The spectrometer is equipped with a rock salt prism and a Coblentz thermopile, and is used in conjunction with a Moll thermal relay and a Leeds and Northrup high sensitivity moving coil galvanometer. The bands reported by Salant and West have been confirmed and in addition a band of relatively strong intensity was found at 4.7μ and another faint band at 2.3μ. The bands listed in order of their intensities are, 4.7μ, 3.38μ, 1.8μ, 1.4μ, 2.3μ, and 1.25μ. Another faint maximum was found at 1.9μ, but it is believed that this may be a part of the 1.8μ band reported by Salant and West. The band at 3.38μ has been resolved into fine line structure by the aid of a prism-echelette grating spectrometer of the Sleator type. The general characteristics of the band are P, Q and R branches of which the Q branch is relatively weak and a fine line structure of 4.5 cm^{-1}.

70. The spectrum of strontium and barium hydride. W. R. FREDRICKSON AND A. L. WARNTZ, *Syracuse University.*—Bands ascribed to the hydrides of the elements strontium and barium, as obtained by an arc between iron and the element in an atmosphere of hydrogen, lie in the far red end of the spectrum, degrade to the violet, but show no similarity. The strontium bands lie in the region λ7500 to λ6800 with double heads at 7350, 7323 and 7020, 6985, the latter being the more intense. At the far red end of spectrum there is a peculiar intensity distribution, showing no sharp heads and with large open spaces in the fine structure. At high dispersion the 7020 band shows four strong branches, indicating a $^2\Sigma-{}^2\Sigma$ transition. The barium band lies in the region λ6925 to λ6380 and is a $^2\Pi-{}^2\Sigma$ band, showing satellite series which are relatively strong in comparison with the customary P, Q, R series.

71. Comparison of x-ray diffraction intensities in liquid long chain compounds with intensities from computations based on a structure factor. G. W. STEWART AND ROSS D. SPANGLER, *The State University of Iowa.*—Quantitative determination of intensities of x-rays scattered from some liquid long-chain compounds are carried out and the results compared with values obtained from experiments. The determinations are based upon the idea of molecular grouping in liquids. A structure factor of the molecules is used to obtain the intensities. Computations are carried out and comparisons made in the case of eleven normal alcohols and twenty-two octyl alcohols. In the majority of cases, the agreement between experimental and computed values is very good, in a few it is fair, and, in a case or two it is poor. On the whole, the results give convincing evidence in favor of molecular grouping in liquids.

72. Useful accessories for the Siegbahn x-ray vacuum spectrograph. F. K. RICHTMYER, *Cornell University.*—To avoid registration on the photographic plate of minute surface imperfections of the crystal, it has been usual to rotate the crystal, by steps of a few minutes of arc, through a degree or so during an exposure. A device is described, consisting of a telechron

motor and reducing gear, for producing continuous, slow oscillations of the crystal through any desired small angular amplitude. To facilitate rapid identification of spectral lines by comparison with some known line, a special plate holder has been devised by means of which a linear scale may be printed on the photographic plate above the x-ray spectrum. The background due to scattered radiation from the crystal reaching the photographic plate frequently covers up faint lines or makes their measurement difficult. When one is interested in a narrow spectral region the intensity of this background can be materially reduced by placing a wedge a millimeter or two in front of the crystal, somewhat after the manner of the Seemann spectrograph. However, inequality of the x-ray brightness of the focal spot then necessitates that the (spiral) filament should be slowly rotated during exposure.

73. Formation of photographic images on cathodes of alkali metal photoelectric cells. A. R. OLPIN AND G. R. STILWELL, *Bell Telephone Laboratories, Incorporated.*—A method of forming both negative and positive photographic images on the cathodes of potassium and sodium photoelectric cells in vacuum is described. These images are sharp and clear in every detail and can be permanently "fixed" by proper treatment. Among the materials which have been successfully used in treating the exposed surfaces to bring out these images are sulphur vapor, air, oxygen and hydrogen in the ratio of 9 to 1, hydrofluoric acid and bromine. During the time the image is forming, the photoelectric sensitivity of the illuminated portions decreases approximately 30 per cent. After the image is fixed as a permanent record there is little difference between the sensitivity of the cathode area bearing the image and neighboring areas. Photographs of photoelectric cells are shown in which such photographic images are plainly visible.

74. The emission of positive ions from thoriated tungsten. H. B. WAHLIN, *University of Wisconsin* An investigation of the emission of positive ions from thoriated tungsten shows that when heated to a temperature above 2000°C three types of ions are given off: a W ion of mass 184, a second ion of mass 232, and a heavier ion of mass 247 ± 1. This heavy ion may be a mononitride or a monoxide of throium. That it cannot be WO_4 is shown by the fact that it does not disappear when the wire is heated in an atmosphere of hydrogen. Outgassing of the wire at an estimated temperature of 1200°C for 100 hours in a vacuum of 10^{-6} mm does not cause the ion to disappear. Varying the gas pressure in the positive ray chamber from 10^{-6} mm to 10^{-5} mm has no effect on the ion. Prolonged heating at a temperature above 2000°C will cause the 247 ion to decrease with respect to the 232 ion which is assumed to be thorium. Neither the 232 ion nor the 247 ion appeared when unthoriated tungsten or thorium metal were used. An x-ray investigation of the *L* region of samples of thoria ores has so far failed to give any indication that the heavy ion may be of an elementary nature.

75. The dielectric constant of air at high pressures. JAMES W. BROXON, *University of Colorado.*—Measurements of the dielectric constant of dry air at zero frequency were made by a balance method, using a quadrant electrometer as an indicator. The dielectric constant was found to increase linearly with the pressure at the rate of 555×10^{-6} per atmosphere at 18°C., up to 170 atmospheres. The Clausius-Mossotti function passes through a minimum in this region.

76. A lens for use with the concave grating. J. B. GREEN, *Ohio State University.*—When the slit for a concave grating is placed on the circle of half the radius of curvature of the grating the focal plane is found to be on that circle for a vertical astigmatic image. In general, regardless of the position of the slit, the other focus is found to be hyperbola. This method of calculation yields a very simple result useful for the calculation of the lengths of the astigmatic images. For the study of individual lines a sphero-cylindrical lens may be used to correct this astigmatism with a resultant increase in the intensity available, and at the same time, a possibility of markedly increasing the dispersion. A preliminary study of several lines with such a lens has yielded promising results.

77. The anomalous scattering of alpha-rays. MORRIS MUSKAT, *Gulf Research Laboratory, Pittsburgh, Pa.*—The potential field causing the Rutherford-Chadwick anomaly in the alpha-

ray scattering by Mg and Al has been determined by inverting the wave-mechanical expression giving the amplitude of the wave scattered by a spherically symmetrical force as an integral over the potential field of the scattering atom. The anomaly was represented analytically in two different ways. The potential fields for both representations, as derived by the above inversion, are essentially the same, their form depending almost entirely on the single fact that the scattering curves show a marked minimum. In magnitude this potential field never exceeds 10% that of the Coulomb potential.It oscillates in sign and falls off very rapidly with distance from the scattering center, becoming negligible at distances greater than about 5×10^{-13} cm. Its small numerical value and oscillatory character are in marked contrast to the assumptions made heretofore, most of which have been that the potential has the form: $1/\rho^n$, $n\geqq 2$, ρ being the distance from the scattering center. The classical charge equivalent of this potential field is a series of shells of alternating sign of charge, separated by approximately 1.5×10^{-13} cm. Rutherford and Chadwick originally suggested just this type of explanation.

78. Dispersion and refractive index of nitrogen measured as functions of pressure by displacement interferometry. CLARENCE E. BENNETT, *Brown University*.—A method of measuring simultaneously the dispersion and refractive index of a gas is discussed. It is justified on theoretical and experimental grounds and applied to the measurement of these quantities for nitrogen over a seven atmosphere range of pressures at two different temperatures, 30° and 0°C, with a high degree of precision. The results show that the Lorentz-Lorenz relation is followed, and that the dispersion is a linear function of pressure. The value of the Cauchy constant B is found to be 1.95×10^{-16} per cm of mercury pressure. The index of refraction is measured at atmospheric pressure for three wave-lengths, at 0° and 30°C, with a limiting error of one third of one percent in $(\mu-1)$. The dispersion information enables these values to be reduced to infinite wave-length, making possible the determination of the dielectric constant by Maxwell's law. The value 1.000585 so obtained differs by less than two-thirds of one percent in $(\epsilon-1)$ from that measured directly by Zahn. The values of the refractive index for nitrogen under N.T.P. conditions for the wave-lengths 4811A, 5893A, and 6362A, are 1.0002921, 1.0002969, and 1.0002967, respectively.

79. The crystal structure of potassium permanganate. R. C. L. MOONEY, *University of Chicago*, (*Introduced by Henry G. Gale*).—The unit cell size and the space group of potassium permanganate were redetermined, and a structure assigned on the basis of intensity observations from photographic plates. The single crystal oscillation method was used, and the plates interpreted by the method of Bernal. Intensities were evaluated simply by visual estimation. The results indicate the crystal to be based on the simple orthorhombic lattice, having four molecules to the unit cell, and symmetry 2Di-16. The cell size was found to have the dimensions: $a=9.08$A, $b=5.72$A, $c=7.41$A. The values check closely the results of other observers. Symmetry considerations and intensity observations indicated a structure having eleven parameters. By the assumption of a tetrahedral arrangement of oxygen about manganese, and by use of values of ionic radii as given by Goldschmidt, it was possible to determine the parameters. Comparative intensities were calculated for the structure. Hartree's figures for the scattering power at different angles were used. The theoretical values so obtained were found to agree fairly well with observed intensities.

80. Linear time scale for voltage range up to 1000 volts. C. K. STEDMAN, *Paul William Research Fellow, Purdue University*, (*Introduced by K. Lark-Horovitz*).—A circuit generating continuously a voltage wave rising linearly from V_1 to V_2 in time t_2-t_1, and dropping from V_2 to V_1 in time small compared to t_2-t_1, can be connected to the horizontal deflecting plates of an oscillograph to provide a linear time axis. The linear time axis circuit of Beddell and Reich (AIEE Journal **46**, 563 (1927)) is limited to a voltage range as defined by the difference between the ignition and extinction voltages of the G-10 neon lamp of fifteen to twenty volts. It has been found that by substituting the Thyratron FG 17 for the neon lamp, voltage ranges from 60 to 1000 volts or more may be obtained. With the grid of the thyratron connected to its filament negative the range is 60 volts and every additional volt negative on the grid increases the range about 100 volts. Stabilization is easily effected by introducing about a tenth

of a volt into the Thyratron grid circuit from the circuit under investigation. The deflecting plates of even a very low sensitivity oscillograph can be connected directly across the current limiting tube (for which a VT 14 is very satisfactory) with no intervening amplifier. The frequency range is approximately the same as that of a neon lamp. A magnetic field parallel to the axis of the Thyratron improves operation at high frequencies by preventing the discharge from redistributing itself over the electrodes.

81. Apparent fatigue and aging phenomena in the active nitrogen afterglow. CHAS. T. KNIPP AND L. N. SCHEUERMAN, *University of Illinois.*—Last July a 5-liter Pyrex bulb was heat-treated, then primed with dried tank nitrogen to a pressure of 0.2 mm Hg and sealed off. The bulb was energized by a motor-generator high frequency set for intervals of time varying from a flash (about 0.1 sec.) up to 50 or more seconds, and the duration of the afterglow noted. A surprising result was observed. The duration of the afterglow fell off apparently exponentially with *increase* of time of energizing. To further check this point a 12-liter bulb was prepared (last August) and placed in an ice bath. The curve obtained still dropped off, but less abruptly. The maximum duration of the afterglow was about 11 minutes. Just recently, December 22, this same bulb was placed in an ice bath at 1°.5C and again subjected to progressively increasing periods of excitation. The maximum was now about 47 minutes, which, when the excitation was prolonged to 50 sec., was reduced to 26 minutes. The reduction in duration seems to be of the nature of a fatigue. It seems unlikely that it is wholly due to the evolution of water vapor since special precautions were taken to free the bulb and nitrogen of moisture, while the increase in duration on flash seems to be an aging effect favorable to the formation of the active aggregates. A 24-liter bulb after aging 3 months glowed, on flash, for 110 minutes.

82. A preliminary report on a new method of x-ray powder diffraction. T. M. HAHN, *University of Kentucky, (Introduced by William S. Webb).*—A preliminary report on a method employing the use of a conical beam of x-rays incident upon powdered crystals arranged in a circular form about the central axis of the cone, normal to the axis. All rays diffracted through an angle θ will be brought together at a common point upon the axis of the cone. A photographic film along this axis receives the record of the diffraction pattern, from which the spacing of the planes of the crystal may be readily determined. Advantages of this method are reduced time of exposure and increased separation of diffraction spots.

AUTHOR INDEX

Hafstad, L. R.—see Tuve
Hahn, T. M.—No. 82
Hanawalt, J. D.—No. 4
Harrison, George R. and Philip A. Leighton—No. 63
Heaps, C. W.—see Bryan
Hewlett, Clarence W.—No. 46
Houghton, H. G.—No. 40
——— see Stratton
Huber, Paul—No. 65
Hufford, Mason E.—No. 54
Huggins, Maurice L.—No. 3
Huxford, W. S.—see Williams

Jones, Ernest J.—see Wulf

Kennard, E. H.—No. 13
Kirkwood, John G.—No. 18
Knauss, Harold P.—No. 67
Knipp, Charles T. and L. N. Scheuerman—No. 81
Knorr, H. V.—No. 60

Langer, R. M.—No. 9
Leighton, Philip A.—see Harrison

Mack, J. E.—see Borg
Meara, F. L.—No. 50
Mooney, R. C. L.—No. 79
Muskat, Morris—No. 77

Nash, W. G.—see Black
Nielsen, Harold H.—No. 68
——— see Patty
Nusbaum, C.—No. 11

O'Brien, Brian and E. Dickerman O'Brien—No. 64
Olpin, A. R.—No. 35
——— and G. R. Stilwell—No. 73
Overbeck, C. J.—see Bockstahler

Patty, John R. and Harold H. Nielsen—No. 69
Pyle, W. R.—No. 31

Race, H. H.—No. 30
Ramberg, E.—No. 7
Ramadanoff, Dimiter—No. 34
Richards, L. A.—No. 23
Richtmyer, F. K.—Nos. 8, 72
Richtmyer, Robert D.—No. 6
Rinde, C. A.—No. 38
Roess, Louis C.—No. 1

Sabine, Paul E.—No. 44
Scheuerman, L. N.—see Knipp
Seitz, V. B.—see Glasser
Sinclair, David—see Webb
Slater, J. C.—No. 17
Spangler, Ross D.—see Stewart
Stabler, H. P.—No. 22
Stedman, C. K.—No. 80
Stewart, G. W.—No. 2
——— and Ross D. Spangler—No. 71
Stilwell, G. R.—see Olpin
Stratton, J. A. and H. G. Houghton—No. 41
Suits, Chauncey Guy—No. 26

Tear, James D.—No. 32
Tuve, M. A., L. R. Hafstad and O. Dahl—No. 58
Tykociner, J. Tykocinski—No. 24

Van Vleck, J. H.—No. 49

Wahlin, H. B.—Nos. 51, 74
Warntz, A. L.—see Fredrickson
Webb, Harold W. and David Sinclair—No. 56
Wick, Francis G.—No. 37
Williams, N. H. and W. S. Huxford—No. 28
Wold, Peter I. and Earle M. Bigsbee—No. 20
Wulf, Oliver R. and Ernest J. Jones—No. 66

Zener, Clarence—No. 15

Second Series *March 1, 1931* *Vol. 37, No. 5*

THE
PHYSICAL REVIEW

ON SOME SOLAR AND LUNAR SPECTRA TAKEN IN LITTLE AMERICA, ANTARCTICA*

By Malcolm P. Hanson** and E. O. Hulburt
Naval Research Laboratory

(Received January 26, 1931)

Abstract

Solar spectra were taken with a small quartz spectrograph at noon on November 13, 1929, and January 25, 1930, in Little America, Antarctica, by Malcolm P. Hanson of the Byrd Antarctic Expedition. The ultraviolet limit of these spectra was at about 304$\mu\mu$ which was the same as the ultraviolet limit of noon solar spectra taken at Washington, D.C., in December and January. Assuming that the ultraviolet limit of the solar spectra was due to ozone in the upper atmosphere and that the amount of ozone in Washington was the same as that measured by Dobson, Harrison, and Lawrence at Oxford, England, it came out that the effective thickness of the ozone at N.T.P. above Little America was about 0.28 cm on November 13, 1929, and January 25, 1930.

The ultraviolet limit of lunar spectra taken at Little America on April 24, 1929, two days after the Antarctic winter night set in, and on July 18, 1929, thirty-five days before the night ended, was at about 305$\mu\mu$.

AMID the stress of final preparations for the departure of the Byrd Antarctic Expedition it was decided to take along a small quartz spectrograph, Hilger, Type E3. An experiment was hurriedly planned which consisted simply in photographing spectra of the sun and the moon in Antarctica with exposures long enough to bring out the ultraviolet region around 300$\mu\mu$. Meanwhile similar spectra were made with a similar spectrograph at the Naval Research Laboratory, Washington, D.C. By a comparison of the two sets of spectra it was hoped to learn something about the ozone in the upper atmosphere of Antarctica. The dispersion of the spectrographs was about 4$\mu\mu$ per mm at wave-length 300$\mu\mu$.

November 13, 1929, was clear and solar spectra were obtained at Little America, latitude 78.6° south, with a slit width of about 0.02 mm, being purposely over-exposed in the visible part of the spectrum in order to bring out the ultraviolet end. The ultraviolet limit of spectra taken at noon, local time, was at about 304$\mu\mu$. The same limit was given by similar spectra at noon on January 25, 1930. The midnight sun spectrum of January 25, 1930, ended at about 320$\mu\mu$; the sun was about 9° above the horizon at that time.

* Published with the permission of the Navy Department.
** In charge of radio of the Byrd Antarctic Expedition.

The noon solar spectra at the Naval Research Laboratory for November and December, 1929, and January, 1930, ended at about 303, 304 and 304$\mu\mu$, respectively; the same values were found, respectively, for November and December, 1930, and January, 1931. The noon spectra for June, 1930, ended at about 299$\mu\mu$. It is seen that the solar ultraviolet limit was the same on November 13, 1929, and January 25, 1930, at Little America as it was in December or January at Washington. The altitude of the sun was approximately the same at the two places, being about 30° from the horizon at Little America and 27° to 30° at Washington. Therefore, since the ultraviolet end of the solar spectrum is limited by the ozone in the upper atmosphere the measurements indicated that the ozone in November, 1929, and January, 1930, was of about the same thickness in Little America as it was in Washington in December and January. It is due to the fortunate circumstance that both the elevations of the sun and the ultraviolet solar spectrum limits were about the same at Little America and at Washington that one can say that the ozone thicknesses were the same at the two places. If, for example, the spectrum limits had been the same and the solar elevations different, or vice versa, the program of observations could probably not have been used with safety to derive an exact conclusion about the relative amounts of ozone in the two regions.

We do not know what the thickness of the ozone was in Washington but we may assume it to be roughly the same as that in Oxford, England, observed by Dobson, Harrison, and Lawrence[1] in 1925 and 1926. The justification of this assumption is found in the fact that the seasonal variation, with the maximum in August, of the intensity of the therapeutic solar wave-lengths 290 to 310$\mu\mu$, observed by Clark,[2] in 1927 and 1928 in Baltimore, Md., U.S.A., agreed fairly well with the intensity calculated[2] from the ozone absorption coefficients of Fabry and Buisson,[3] the 1925 and 1926 ozone thickness[1] at Oxford and the solar zenith distance at Baltimore. Clark's[4] further observations showed that the curve of the seasonal variation of the solar radiations from 290 to 310$\mu\mu$ was approximately the same in the years 1929 and 1930 as it was in the years 1927 and 1928.

Interpolating among the Oxford measurements (ref. 1, Table 3) gives the values for December and January to be 0.27 and 0.29 cm of ozone, respectively. Accordingly, the average of these, or 0.28 cm was the value of the effective thickness of the ozone in Little America on November 13, 1929, and January 25, 1930. It need hardly be said that the present method of determining ozone by means of the ultraviolet limit of the solar spectrum can not be depended upon to give great accuracy. It is to be hoped that future polar expeditions may be equipped to carry out much better determinations of ozone.

The value 0.28 cm of ozone in midsummer at Little America is in keeping

[1] Dobson, Harrison and Lawrence, Proc. Roy. Soc. **A114**, 521 (1927).
[2] Clark, Amer. Jr. Hygiene **9**, 646 (1929).
[3] Fabry and Buisson, Journ. de Phys. **3**, 196 (1913).
[4] Clark, Amer. Jr. Hygiene **12**, 690 (1930).

with the probable average values in north polar regions in midsummer, namely, 0.290 cm for July and 0.265 for August, estimated by Dobson.[5] Dobson[1,5] concluded that the ozone values found by various stations scattered over the earth would be most simply accounted for by the hypothesis that corpuscular radiation from the sun is "the chief ozone forming agent at the poles and possibly for the rest of the world" (ref. 5, page 431). We do not think that the observations call for any such extreme hypothesis. Maris'[6] calculations of the temperatures of the high atmosphere indicate wind movements in the high atmosphere which, combined with the hypothesis that ozone is formed by certain wave-lengths of the ultraviolet portion of the solar spectrum and is decomposed by other wave-lengths, would lead, qualitatively at any rate, to an ozone distribution in agreement with observation. One cannot make an exact calculation of the matter for the photochemical quantum efficiencies of the formation and destruction of ozone by the various ultraviolet wave-lengths are not yet known.

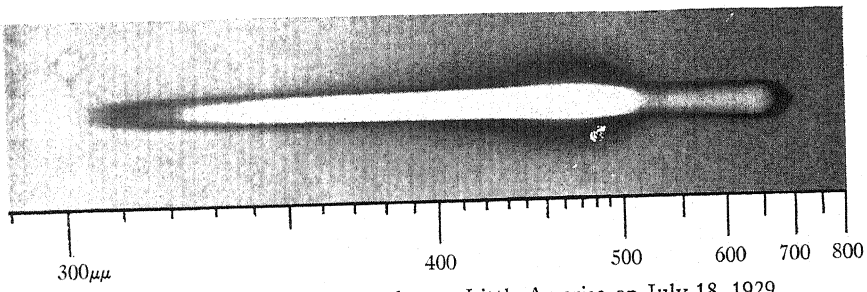

Fig. 1. Spectrum of the moon taken at Little America on July 18, 1929.

Spectra of the moon were taken at Little America on April 24, 1929, and on July 18, 1929. It will be remembered that the sun's last official appearance at Little America was on April 22 and his official reappearance was on August 22. Thus the moon spectrum of April 24 was obtained two days after the beginning of the Antarctic winter night and the one of July 18 was obtained thirty-five days before the end of the Antarctic night. The spectrograph was mounted outside on the snow, aimed at the moon and shifted by hand from time to time. The moon was focussed on the slit by a quartz lens 5 cm in diameter and 20 cm in focal length. The spectra of April 24 were taken with a slit width of 0.3 mm and exposures from 1 to 15 minutes. With such a wide slit the ultraviolet limit of the spectrum was not sharply defined, and the only safe conclusion that could be drawn was that the ultraviolet limit was between 310 and 300μμ.

On July 18 the moon was about 40° from the horizon and the temperature was −50° Farenheit. A good spectrum, reproduced as a positive in Fig. 1, was obtained with an exposure of one hour at midnight, local time, and a slit width of 0.05 mm. Eastman Commercial Panchromatic cut film was

[5] Dobson, Proc. Roy. Soc. **A129**, 412 (1930).
[6] Maris, Terr. Mag. and Atmos. Elec. **33**, 233, (1928); **34**, 45 (1929).

used. The spectrum extended to about 305$\mu\mu$, the last solar absorption line being at this wave-length. It is doubtful whether the solar absorption lines, which are clear enough on the original negative, can be seen in the reproduction of Fig. 1.

The film was somewhat fogged throughout and the bright lunar spectrum of Fig. 1 is seen to be surrounded by a region relatively darker than the general fogged field. The dark halo around the spectrum is thought to be due to the Eberhard photographic effect. If a plate or film be uniformly exposed to light of moderate intensity and if a small area be then given an additional heavy exposure, on development a region of abnormally lowered density will be noted around the dense portion. This is caused by the large quantity of soluble bromide thrown off from the heavily exposed area of emulsion during the development which acts as a restrainer and slows up the development of the surrounding regions. It is not known whether the low temperature during the exposure had anything to do with the rather unusual appearance of the negative of Fig. 1. The development of the film, which was done about three days after the exposure, was effected under approximately normal conditions. The solar spectra and the moon spectra of April 22, as well as the Washington spectra, in general showed the Eberhard effect to a slight degree, but none to the extent of the negative of Fig. 1.

Since the lunar spectra ended at about 305$\mu\mu$ it is concluded that the ozone in the high atmosphere of Little America during the winter night was not greatly different from ozone in other parts of the world. Rosseland[7] also found that stellar spectra photographed in midwinter at 71° north latitude ended around 300$\mu\mu$.

In conclusion it is a pleasure to mention the assistance of Mr. R. B. Carleton in taking the long series of solar spectra at this laboratory.

[7] Rosseland, Nature **123**, 207 (1929), discussed by Wood on page 644 and by Dobson on page 712.

DIRECTED VALENCE IN POLYATOMIC MOLECULES

By J. C. Slater
Massachusetts Institute of Technology

(Received January 22, 1931)

Abstract

The interactions of atoms in polyatomic molecules are described qualitatively. Particular attention is paid to atoms of the types of F, O, N, C, where the valences come from p electrons. Directional effects are discussed, namely that the two valences of O, and the three of N, tend to be mutually at right angles, and the four of C have tetrahedral symmetry. Numerous examples are given, from the structure of metals and of organic and inorganic compounds. Mathematical treatment is postponed until a later paper.

IT HAS already been noticed by Born[1] that the method applied by the writer to the problem of complex atomic spectra is equally adaptable to molecular structure. The writer[2] has used the method in one problem of atomic interaction, the problem of cohesive forces in univalent metals. When applied to molecular problems in general, however, it yields not only the familiar results for diatomic molecules, but also information regarding valence in polyatomic molecules, particularly in the matter of directional properties, which seems to be new and which is capable of correlating a good deal of experimental material. In this paper, we give the results of the discussion in a qualitative way, postponing mathematical justification to a later paper.

The general ideas described in the paper were outlined in an informal talk at the Washington meeting of the American Physical Society last April, and I wish to thank several members of the society for valuable discussion at that time. I also wish to acknowledge valuable assistance and suggestions from several of my colleagues, particularly Dr. Warren, Dr. Ashdown, and Dr. Scatchard.

Two atoms containing all their electrons in closed shells repel each other. But if each atom has one wave function containing only one electron, rather than two of opposite spins, attraction is possible. This actually occurs if the spins of the electrons in question in the two atoms are oppositely directed. The attraction pulls the atoms together until the wave functions from which electrons are missing overlap as much as possible, when equilibrium occurs. In consequence of resonance, the charge concentrates at the place where the functions are overlapping, and in an approximate way we may consider that the two electrons, of opposite spin, spending their time in this region, form a closed shell. This is a homopolar valence bond, and two electrons forming such a bond are inactive in forming further bonds, just as if they were in closed shells within a single atom.

[1] M. Born, Zeits. f. Physik **64**, 729 (1930).
[2] J. C. Slater, Phys. Rev. **35**, 509 (1930).

The simplest and most familiar example of a single valence bond is found in H_2,[3] where each atom contains a single $1s$ electron, so that the $1s$ shell is not completed, and if the spins are oppositely directed, the electrons are shared and form a molecule. But almost equally simple is, for example, I_2. Here each atom lacks a single p electron from its outer shell. If the remaining electron in that particular p wave function in one atom has a spin opposite to that in the other, there will be attraction, which will proceed until the two wave functions overlap as much as possible. We meet at once the question, how does the degeneracy of the p shell affect the problem. And we can answer definitely from perfectly general considerations.

To get the lowest possible energy, we wish in a rough way the greatest possible overlapping of the p functions from the two atoms. This demands first that each of these functions be as concentrated as possible. Now the wave functions corresponding to the three p levels, in the ordinary axial system of coordinates, can be written

$$\begin{aligned} p^+ &: \quad (x + iy) \quad f(r) \\ p^0 &: \quad z \quad f(r) \\ p^- &: \quad (x - iy) \quad f(r). \end{aligned}$$

The charge densities corresponding to these are

$$\begin{aligned} p^+ &: \quad (x^2 + y^2) \quad f^2(r) \\ p^0 &: \quad z^2 \quad f^2(r) \\ p^- &: \quad (x^2 + y^2) \quad f^2(r). \end{aligned}$$

As shown in Fig. 1, made by a very ingenious method by Dr. Langer, the first and third are great in the x-y plane, in a sort of ring-shaped region; the second

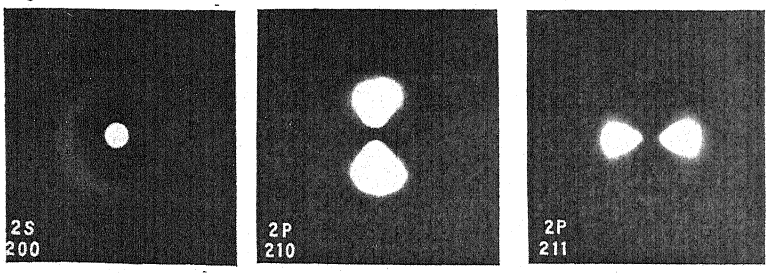

Fig. 1. Charge distribution of p^+ and p_0, with s for comparison. I am indebted to Dr. Langer for this photograph.

is great along the z axis, and is more concentrated than the others. But we are allowed to use any three orthogonal linear combinations of these functions. If we take $(r \cdot u_1) f(r)$, $(r \cdot u_2) f(r)$, $(r \cdot u_3) f(r)$, when u_1, u_2, u_3 are three orthogonal unit vectors, these functions will be great, respectively, along the

[3] Heitler and London, Zeits. f. Physik **44**, 455 (1927).

axes of these three vectors, and each will be as concentrated as the p_0 before. These functions evidently give as concentrated a density as we can get, and hence are most suitable for use in discussing binding.

Let us now consider our I_2 molecule. We take the vector u_1 in each atom as the vector pointing toward the other atom. Then plainly the functions $(r \cdot u_1) f(r)$ for the two atoms, since they correspond to distributions pointing along the line of centers, and hence stretching out toward the other atom, can overlap. The other functions, on the other hand, are large in the planes normal to the line of centers, and do not overlap appreciably. We can visualize the atoms as the hubs of two wheels connected by an axle. The functions which overlap are extending along the axle, the others along the spokes of the two wheels. For binding, then, we assume an electron missing from this function $(r \cdot u_1) f(r)$ in each atom, and we can be confident that in this way we shall get the most stable molecule. In the usual description, if the z axis is taken as the axis of the molecule and at the same time the axis for axial wave functions for the electrons, an electron with function p_0 is missing from each atom. This coincides with the conventional description of this case.

Next let us consider an atom which lacks two electrons of having a complete shell, as for example O. Suppose we have another atom, as H, which can be bound to it. We choose our vectors u_1, u_2, u_3 so that one of them, say u_1, points along the line from O to H. Then by the previous argument we must have one electron missing from the state which we may symbolize by u_1, to form the bond with the H. The other missing electron must then be lacking from either the state u_2 or u_3, and hence must have its density along the direction at right angles to the line joining the O and H. A second hydrogen attempting to become bound to form a water molecule, would move so that its charge would overlap in place of this missing one. It would then take up a position so that the lines joining the centers of the oxygen and the two hydrogen atoms would form right angles. Of course, the interactions between the two hydrogen atoms would modify this; it is difficult to say in which direction. But in a general way we should expect a triangular model, as is shown in Fig. 2, and that of course is observed.

The same sort of argument would indicate that the two valences of a divalent atom like oxygen should always be at right angles, and we can obtain many actual examples of this. The atoms of this sort are O, S, Se, Te. In the elements Se and Te in the solid state the atoms form chains of an interesting helical form, as shown in Fig. 3, so that if we look along the axis of the helix every third atom lies in a corresponding position. But just such a spiral is formed if atoms are arranged in a chain with the lines joining successive atoms making right angles with each other, these lines pointing in succession along the x, y, z, x, y, z, $\cdots$, axes, which is the structure which our theory would suggest. Another illustration, less definite, is furnished by the crystal structure of the silicates. These are presumably in general ionic compounds. But some features of them resemble valence compounds: each silicon is surrounded by four oxygens, suggesting the valence of four and tetrahedral structure which we shall discuss in a later paragraph; and where an

oxygen is shared between tetrahedra, is shared by two only, as if it had just two valences for the two silicons. These features are both illustrated in Fig. 4. Now it is observed that in such a shared oxygen, the lines joining the oxygen to the silicons always form an angle with each other, as if there were

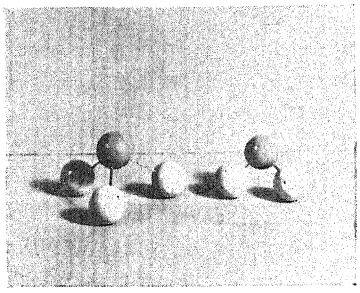

Fig. 2.

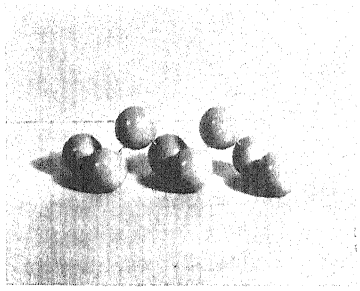

Fig. 3.

Fig. 2. NH_3 and H_2O. The angles here, and in the other figures, are taken to be just 90°, rather than adjusted to agree with experiment.

Fig. 3. Chain of atoms from Te. The actual chain continues indefinitely in both directions. The crystal is made of many chains packed together parallel to each other.

valences which tended to be at right angles to each other, rather than being parallel as one would otherwise expect.

The trivalent atoms, N, P, As, Sb, Bi, can be discussed by just the same principles: their three valences tend to be mutually at right angles, one elec-

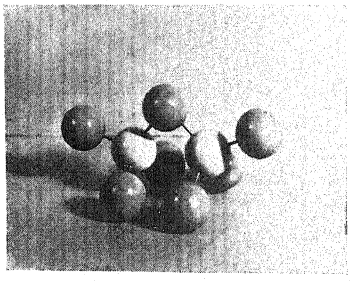

Fig. 4.

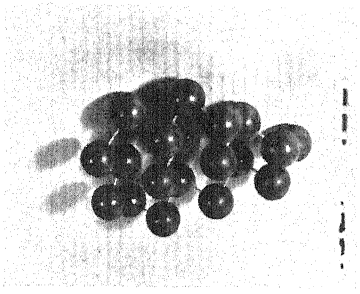

Fig. 5.

Fig. 4. $(Si_2O_7)^{-6}$ group from a silicate. The lighter atoms represent Si. Two tetrahedra are joined by sharing an O. In the actual case, the valences of this shared O are more nearly parallel than we have shown.

Fig. 5. Sheet of atoms from Bi. This consists of two layers of atoms, each atom being joined to three neighbors in the other sheet. The whole crystal consists of piles of these sheets.

tron being shared from each of the three functions with the factors $(r \cdot u_1)$, $(r \cdot u_2)$, $(r \cdot u_3)$. The most obvious example is ammonia, NH_3, which has the pyramidal structure which we should expect from this model, as is shown in Fig. 2. Then in the metals, As, Sb, Bi, we find good illustrations of the princi-

ple. The atoms in these metals form plates, which appear, when we look down on them, like hexagonal lattices, each atom being surrounded by three others symmetrically placed. But really alternate atoms are displaced above or below the plane, as shown in Fig. 5, so that each atom above the plane is at the apex of a pyramid whose base is formed by three atoms below the plane, and vice versa; and the three lines joining an atom with its neighbors are very nearly at right angles. The whole crystal is formed by piling these plates together in such a way as to approximate a simple cubic lattice.

Other examples can be found in organic compounds containing nitrogen, in which the nitrogen is connected to something else by a double bond. In the oximes, as shown in Fig. 6, it is connected in this way to a carbon atom; in the azo compounds as in Fig. 7, to another nitrogen. The double bond we visualize simply as the sharing of two electrons, so that the two bonds and the center of the atom determine a plane. The third valence of the nitrogen

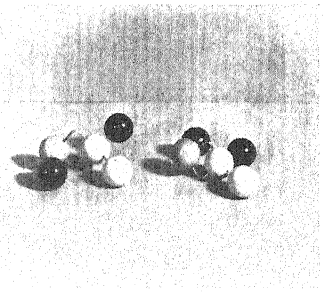

Fig. 6.

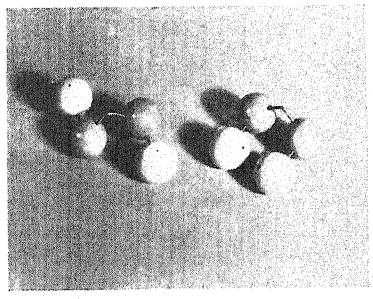

Fig. 7.

Fig. 6. Two isomeric forms of an oxime compound. A nitrogen and carbon are joined by a double bond. The two forms arise from the two possible orientations of the third valence of the nitrogen.

Fig. 7. Two isomeric forms of an azo compound. Two nitrogens are joined by a double bond.

should then, according to our picture, be at right angles to this plane, but it could point out in either of the two normal directions. If the rest of the molecule were not symmetrical about this plane, we should then expect two forms of the molecule, depending on which normal were chosen; and as a matter of fact, both these groups of compounds show isomerism which is attributed to just this sort of effect.

The tetravalent atoms, C, Si, Ge, Sn, Pb, demand a different treatment. If we assume that four electrons are removed from the group of six p's, this leaves none in one of the three wave functions, and one each in the remaining two. Thus there are two electrons to be shared, as in O, and we have divalent atoms as we observe for example in CO. But to obtain a valence of four, we must plainly have only three p's removed, leaving one electron each in these states; and the other missing electron must then be an s. This latter, having a spherical distribution of charge, has no directional properties. Thus in CH_4, for example, we should tentatively expect that the three hydrogens attached

to p valences would form a pyramid, as in NH_3, and the remaining hydrogen, bound to an s, and free to wander, would set itself opposite the apex of the pyramid to avoid the others, forming a rough tetrahedron. This would not be a symmetrical tetrahedron, however; and by a slight change in the conditions we can arrive at a really symmetrical one, which would undoubtedly have a lower energy, and which we consider to be the real form for a tetravalent compound.

To arrive at this symmetrical arrangement, we set up four linear combinations of the three p wave functions and the one s function, having a tetrahedral symmetry. We take four unit vectors, u_1, u_2, u_3, u_4, pointing to the four corners of a regular tetrahedron. Then the four functions $(r\cdot u_1)\,f(r)$, $\cdots$, $(r\cdot u_4)\,f(r)$ are, as we have seen, linear combinations of the three p functions, but of course they are not orthogonal. If however we take the s wave function, say $\phi(r)$, we can form combinations $(r\cdot u_1)\,f(r)+\alpha\phi(r)$, $\cdots$, $(r\cdot u_4)\,f(r)+\alpha\phi(r)$, where α is a parameter, and we can choose α to make the four

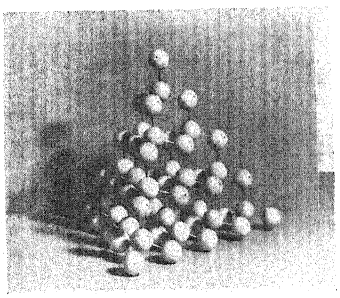

Fig. 8. Diamond lattice.

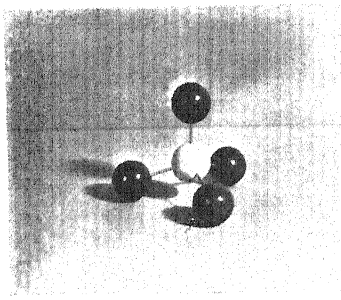

Fig. 9. CH_4.

functions orthogonal. These are then the required tetrahedral wave functions. The density of each one is great along one of the axes of a regular tetrahedron; the addition of the s function results in having the density much larger in one direction than in the opposite one. If now each of these wave functions lacks one electron, and other atoms share with the remaining ones, they will take up a tetrahedral arrangement about the central atom.

The tetrahedral structure for the valence of C and the other atoms of this group is too well known to require extensive comment; a very great number of observations of the organic chemists have led to it. But we may mention a few examples. The solids as diamond, forms of Pb and Si, form the diamond lattice shown in Fig. 8, in which each atom is surrounded by four others in tetrahedral arrangement. The gas CH_4, shown in Fig. 9, is undoubtedly tetrahedral, as shown by the absence of electric moment. The double carbon bond is explained very easily by the sharing of two electrons, meaning that two tetrahedra join by an edge. The remaining four valences then all lie in a plane, as shown in Fig. 10, and the isomerism of the derivatives of ethylene, $H_2C=CH_2$, is readily explained: given two unlike radicals attached to each atom, there will be two different compounds depending on the two possible

assignments of one pair to the two electrons of the corresponding atom. This explanation seems much more convincing than the ingenious theory of Hückel,[4] based wholly on p electron valence.

The weakness of Hückel's theory is that he does not consider carefully the nature of the other bonds than the double one, and hence does not notice the fact which we point out, that the s valence must be combined with the p's to obtain a symmetrical arrangement. If one followed his argument through, each of the carbons in ethylene would have one p valence and one s free to join to hydrogens, and the latter would then hardly be equivalent.

Similarly the triple bond would correspond to the sharing of a whole face of two tetrahedra. The remaining valences would then point out along the line of centers, so that acetylene, HC≡CH, shown in Fig. 11, should be a linear molecule, as is observed from its lack of dipole moment.

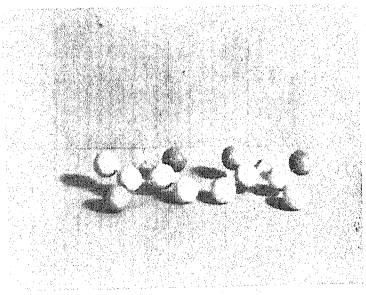

Fig. 10.

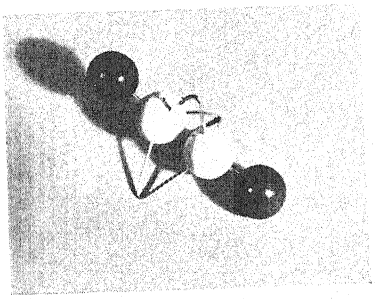

Fig. 11.

Fig. 10. Two isomeric forms of a substituted ethylene. Two carbons joined by a double bond. Two isomers if at least two sorts of radicals are attached to the carbon: trans form (at left) with like radicals opposite; cis form (right) with like radicals adjacent.

Fig. 11. C_2H_2. A linear molecule with a triple bond.

An ordinary chain compound is shown in Fig. 12. The zig-zag structure of the compound, observed for example by Müller,[5] is well shown in the figure.

The atoms beyond the tetravalent ones appear generally in ionic compounds rather than with valence bonds, and so do not concern us in this paper. But we should discuss one point: in a great many compounds there is ambiguity as to whether the bonds are homopolar or ionic. We have mentioned the silicates; other examples are H—Cl (which could be written also H^+Cl^-) and H–O–H (which could be written $H^+(OH)^-$ or $H^+O^= H^+$). Even such a compound as Al_2O_3 can be written in either way (Al 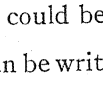 Al or $(Al^{+++})_2$ $(O^=)_3$). Very general principles of wave mechanics tell us the outline of the treatment in these cases. The two explanations constitute two unperturbed states, from which the true one is to be found by linear combination, so that the real situation is intermediate between the two. If the energies of the two

[4] E. Hückel, Zeits. f. Physik **60**, 423 (1930).

[5] A. Müller, Proc. Roy. Soc. **A114**, 542 (1927).

models are approximately the same, the real state will lie roughly half way between, while if one has a much lower energy than the other, that will fairly accurately represent the real situation. Moreover, if the two are combined, there will be a resonance effect in the energy, which will generally bring the real energy lower than that computed from either model separately. This may well explain the unusual stability of the silicates, and of the other compounds we mentioned: their energy is lower on account of the two explanations of the binding.

It is important to consider the relation of our models, say for H_2O, to those of Debye,[6] based on the assumption of ionic compounds in which the polarizibility of the $O^=$ is considered. Debye has been able to give alternative explanations even of the triangular form of H_2O and the pyramidal form of NH_3. From the discussion of the last paragraphs, we see that both these explanations are to be regarded as legitimate starting points, with the true

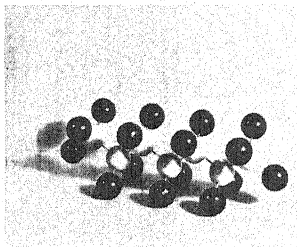

Fig. 12.

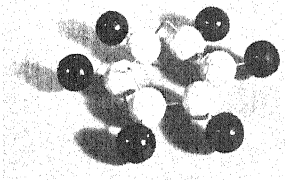

Fig. 13.

Fig. 12. A chain compound, C_7H_{16}. The zig-zag arrangement of carbons, and the elongated cross-section of the chain, result from having the valences of carbon inclined at definite angles to each other.

Fig. 13. Benzene, C_6H_6. The Kekulé model.

state of affairs somewhere between them. The two descriptions, ionic and homopolar, are not as a matter of fact very different in fundamentals. Consider for example HCl. In the homopolar valence explanation, the electron from H, and one from Cl, are shared on the line joining the two atoms, and the net effect is that some of the hydrogen electron's charge has shifted toward the chlorine. In the ionic explanation, we start by assuming that the hydrogen electron is wholly transferred to the chlorine. But then we assume that polarization pulls some of it back again, and we are left in very much the same situation as before. The principal advantages of the homopolar method, with these ambiguous problems, are first that it seems rather nearer the real solution, as is shown, for example, by the small dipole moments of the hydrogen halides; and second that it is better able to deal in a general way with directional properties.

Another point connected with valence should be mentioned similar to the

[6] P. Debye, "Polar Molecules," Chemical Catalog Co.

ambiguity between the ionic and homopolar valence descriptions of a compound. In some cases there may be several ways of drawing valence bonds in a given compound. In such cases, the real situation is again a combination of the various possibilities, and on account of resonance the energy is lower than it would otherwise be. We can not then draw the valence bonds in an unambiguous way; we must rather imagine them shared between several atoms. Such cases of shared valence may well be commoner than is usually supposed. The writer has already explained the cohesion in monovalent metals as coming from this effect, and it probably persists through most of the metals other than those specifically discussed in this page; for in all of these, each atom has more neighbors than it has electrons to share, and hence than it has valence bonds in the ordinary sense. Another example is probably found in the benzene ring. Here the Kekulé model, shown in Fig. 13, allows either the structure

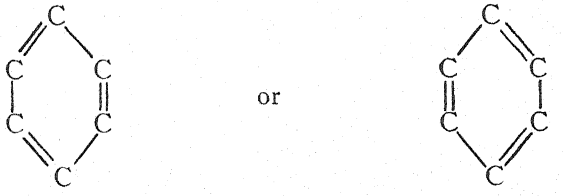

By wave mechanics we should have a combination of these two possible structures, resulting in a complete equivalence of the carbons of the ring, a shared valence (essentially 1–1/2 bonds between each pair), and an added stability for the structure on account of the resonance effect on the energy. Still another case presumably comes in the existence of shared valences where ordinarily we suppose no valence at all to act. In H_2O, there is probably a little valence attraction between the two H's, just as if they were forming a H_2 molecule, and as a consequence the angle between the lines to the two H's should be slightly acute. And even between molecules we may expect this shared valence to act. In crystals like Te and Sb we have spoken as if all valence forces acted within the chains or plates of which the crystals are formed, but this undoubtedly is not the case. In complicated organic compounds, probably the valence forces between one molecule and another are nearly as strong as within a molecule. Substances where this is true will hang together to form solids, and it will be nearly as difficult to separate the molecules as to break up the individual molecules, so that an attempt to vaporize them by heating will be very likely to disrupt the whole structure instead, a common phenomenon with these complicated compounds. Many examples of polymerization may well be cases where valences formerly operative within a molecule have partly changed over to the role of intermolecular forces. It seems, then, that this phenomenon of shared valence is of common occurrence, and that an understanding of it, as well as of the relation between ionic and homopolar binding, is essential.

THE ROTATIONAL ANALYSIS OF THE S_2 BANDS

By S. Meiring Naudé and Andrew Christy
Ryerson Physical Laboratory, University of Chicago

(Received January 23, 1931)

Abstract

The emission spectrum of S_2 has been obtained by means of a Geissler tube, the plates being taken in the third order of a 21 foot concave grating giving a dispersion of 0.878A per mm. The following bands have been studied; 9–1(λ2857.36), 7–0(λ2860.13), 8–1(λ2887.84), 9–2(λ2917.38) and 7–1(λ2920.28). Each band consists of three R and three P branches. For small values of K each band appears to have a weak and a strong R branch and a weak and a strong P branch. The lines of the strong branches separate into two components for $K \geqq 25$. This structure is similar to that of the Schumann-Runge bands of O_2. It is concluded that the S_2 bands investigated are due to a $^3\Sigma_u^- \rightarrow {}^3\Sigma_g^-$ transition (like O_2). The values of B_e'' and B_e' (by extrapolation) are 0.409 and 0.319 cm^{-1}, respectively, the nuclear separation of the lower state being $r_e'' = 1.603 \times 10^{-8}$ cm and of the upper state $r_e' = 1.814 \times 10^{-8}$ cm. It is shown that the rotational levels with *odd* K values are missing in the *upper state* and those with *even* K values in the *lower state*. The fact that alternate levels are missing shows that the internal angular momentum of the S^{32} nucleus is zero.

Introduction

THE band spectrum due to the S_2 molecule extends from about λ6000 to λ2300A. The spectrum consists of a large number of overlapping bands which degrade toward the red. These bands have been studied by various investigators. Henri[1] divides the spectrum into four regions according to the frequency equations which fit most accurately the heads obtained in absorption. Rosen[2] has shown, however, that all these bands belong to the same band system, and from the vibrational analysis obtained the following equation for the heads:

$$\nu = \nu_e + 427.1(v' + \tfrac{1}{2}) - 2.7(v' + \tfrac{1}{2})^2 - 727.4(v'' + \tfrac{1}{2}) + 2.91(v'' + \tfrac{1}{2})^2 \quad (1)$$

Henri[1] found the bands to become diffuse at λ2794.2, a phenomenon which he termed "predissociation."

Henri and Teves[3] using plates taken in absorption with relatively small dispersion, attempted a rotational analysis of the S_2 spectrum. They state that each band consists of P, Q, and R branches, giving the values of the nuclear separations for the upper and lower states as $r' = 0.70$A and $r'' = 0.73$A. Teves[4] continued this work in fluorescence obtaining results similar to those of Henri and Teves. Recently Swings[5] and Rompe[6] also working with the

[1] V. Henri, Structure des Molecules, Paris, p. 93 (1925).
[2] B. Rosen, Zeits. f. Physik **43**, 69 (1927).
[3] V. Henri and M. C. Teves, C. R. **179**, 1156 (1924).
[4] M. C. Teves, Dissertation, Zurich (1926).
[5] P. Swings, Zeits. f. Physik **61**, 681 (1930).
[6] R. Rompe, Zeits. f. Physik **65**, 404 (1930).

fluorescence spectrum of S_2, have tried to bring their results into agreement with those of Henri and Teves, but found it impossible to interpret completely the complex patterns obtained.

It has been shown that the molecules F_2, Cl_2, Br_2, and I_2 have similar electronic states. The same has also been found in the molecules Li_2, Na_2, and K_2.[7] One would therefore expect a corresponding similarity to hold for O_2 and S_2. In particular it seems probable that the S_2 bands mentioned above are analogous to the Schumann-Runge bands of O_2. Recently E. V. Martin and F. A. Jenkins[8] have also found the SO bands lying between λ2500 and λ3500 to correspond to the Schumann-Runge bands. The analysis of Henri and Teves, however, would indicate that S_2 differs fundamentally from O_2. Furthermore, the values of r_e'' and r_e' found for the O_2 Schumann-Runge bands[9,10] are 1.204 and 1.609A, respectively. Irrespective of the similarity of the S_2 and O_2 bands, the values of the nuclear separations for the two states obtained by Henri are too small, since the r_e values for S_2 are surely greater than those for O_2, whereas, according to Henri, the reverse is the case.

The purpose of the present work was to check Rosen's results by studying the spectrum of the S_2 bands photographed with greater dispersion than he used, and to obtain the rotational analysis. The work dealing with the vibrational analysis, perturbations, predissociation, etc., will be discussed in a later paper, and only that concerning the rotational structure will be given here. It will suffice to state that, except for the revision of the vibrational quantum numbers of a number of band heads and the discovery of numerous perturbations, mainly in the upper electronic state, our results agree with those of Rosen, so that his analysis with a few modifications can be made use of in the present paper.[11]

Experimental Procedure

The spectrum of S_2 was excited in a Geissler tube (see Fig. 1) of Pyrex, having large cylindrical aluminum electrodes, so that as much as 0.7 amps. could be passed through the tube. The current was supplied by a 5 KW transformer. The tube was provided with a quartz window W sealed on to one end of a quartz tube, the other end of which was ground flat. This end of the quartz tube was sealed onto the Pyrex tube with sealing wax. Considerable difficulty was experienced in keeping the quartz window from fogging due to sulphur condensing on it. The best results were obtained when the sulphur was introduced into the tube in the form of H_2S[12] which streamed continuously through the tube in the direction away from the window, thus opposing the diffusion of sulphur towards the window. In case the window did get fogged with sulphur, heating it gently with a bunsen burner restored

[7] R. S. Mulliken, Phys. Rev. **36**, 1440 (1930).

[8] E. V. Martin and F. A Jenkins, Phys Rev. **37**, 226 (1931).

[9] W. Ossenbrüggen, Zeits. f. Physik **49**, 167 (1928).

[10] W. Lochte-Holtgreven and G. H. Dieke, Ann. d. Physik (5) **3**, 937 (1929).

[11] P. Huber, Amer. Phys. Soc. Meeting, Paper No. 65, Cleveland. Dec. 30, 1930, has apparently also found that Rosen's vibrational analysis is fundamentally correct.

[12] H. H. Van Iddekinge (Nature **125**, 858 (1930)) has independently used the same method.

its transparency. The H_2S was dried over P_2O_5 before introduction into the tube. In the discharge tube the H_2S dissociated, giving sulphur and hydrogen.[13] The other end of the tube was connected to a liquid air trap in which the sulphur and H_2S were frozen out. This trap in turn was connected to a Megavac oil pump which was kept running while the discharge was going on. The pressure of the sulphur in the discharge tube could be regulated by controlling the flow of H_2S by means of a stopcock sealed on to a capillary tube.

Another method used for introducing the sulphur into the above discharge tube was by distilling the sulphur in vacuo into the side tube T (see Fig. 1). By heating T while the discharge was running pure sulphur could be introduced directly into the discharge tube. In this case a mercury diffusion pump was used to evacuate the discharge tube beforehand. More sulphur condensed on the window when this method was used and therefore the former method was preferred for long exposures. The spectrum obtained by

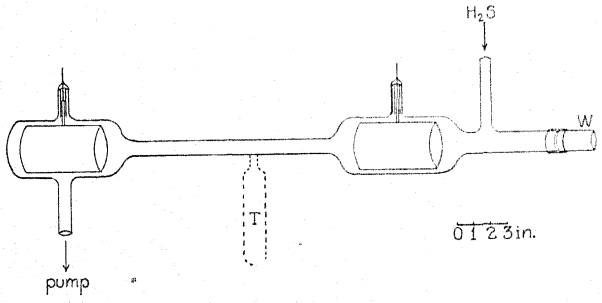

Fig. 1. Discharge tube used for obtaining the S_2 emission spectrum in the region $\lambda 2850 - \lambda 2950$ with great intensity. W is a quartz window sealed into a quartz tube which is in turn sealed on to the discharge tube with sealing wax. When sulphur is used instead of H_2S to obtain the spectrum the tube T with the dotted outline contains pure sulphur.

this method agreed with that obtained by introducing H_2S, as was determined by comparing plates taken in the second order of the 21 foot grating in both cases.

The photographs of the bands in the region $\lambda 2850$–$\lambda 2950$ used for the analysis were taken in the third order of the 21 foot Rowland grating giving a dispersion of 0.878A per mm. A red purple filter of the Corning Glass Company was used to cut out the second order between $\lambda 4250$ and $\lambda 4450$A which would otherwise overlap the spectrum obtained. Eastman 33 plates were used. The time of exposure was about 30 hours.

The plates were measured on a comparator with an accuracy of 0.003 mm. The iron arc was used as comparison spectrum, the wave-lengths of which were taken from Kayser's "Hauptlinien" (1926). The iron standards agreed to within 0.003A, so that the wave-lengths of the sulphur band lines

[13] In the region $\lambda 2850 - \lambda 2950$, which we studied for this work, the sulphur spectrum was very intense as compared with the weak continuous spectrum obtained from the hydrogen molecule.

may be assumed to be correct to 0.01A. The wave-lengths (in air) were converted to wave-numbers (in vacuo) by means of Kayser's "Schwingungszahlen."

Data and Rotational Analysis

The bands due to S_2 are very numerous so that there is practically no region of the emission spectrum in which overlapping does not occur. In the region between λ2828 and λ2950 the overlapping is the least. Therefore the bands: 9–1, with its head at λ2857.36; 7–0, λ2860.13; 8–1, λ2887.84; 9–2, λ2917.38 and 7–1, λ2920.28, have been chosen for the rotational analysis. Even with the large resolution used a large number of lines could not be separated, a few unresolved groups having a width as large as 1 cm^{-1}. The lines of the 9–1 and 9–2 bands could not be followed very far due to the overlapping of the 7–0 and 7–1 bands, the latter being considerably more intense than the former. Other weaker bands are partially superposed on the 8–1, the 7–1 and probably on the 7–0 band, making the assignment of the lines into series extremely difficult.

It was noticed that in the clear regions of the 9–1 and 9–2 bands the strong lines in each band could be assigned into two distinct series. For every strong line in the above bands there is a line of about half the intensity on the short wave-length side of the former, the interval between the strong and the weak lines remaining approximately constant. The same type of series, i.e. two strong and two weak series, has been found in each of the remaining bands. In the two bands, 7–0 and 7–1, in which the series could be followed to a considerable distance from the head, it was seen that each line of the strong series splits into two lines, the components of this doublet having equal intensity. The distance between each line of the weak series and the center of the corresponding doublet in the strong series, after its lines had split, is the same as before splitting occurred. In this region the three lines, i.e. the lines of the weak series and the two corresponding lines into which each line of the strong series splits, are approximately of the same intensity. It is evident, therefore, that each band consists of six series: A , A_y, A_z, B_x, B_y and B_z. In the 9–1 and 9–2 bands, where the overlapping by other bands is least, all lines but two have been assigned to the various branches.

The two sets of combinations which are given in Tables IV and V were obtained by performing the subtraction $A(\alpha)-B(\beta)$ and $A(\alpha)-B(\beta+1)$, where α and β are arbitrary numbers assigned to the series A and B respectively. Since the S_2 bands are those of a homopolar molecule $(S^{32})_2$, we may expect alternate band lines to be either missing or weak.[14] But if the latter were the case we would have noticed it. If, however, all lines are present in the series, the above combinations would correspond to $R(K)-Q(K)\approx\Delta_1F'(K)$ and $R(K)-Q(K+1)\approx\Delta_1F''(K)$, [or $Q(K)-P(K)\approx\Delta_1F'(K)$ and $Q(K)-$

[14] F. W. Aston (Proc. Roy. Soc. **A115**, 487 (1927)) has estimated that about 97 percent of the atomic weight of sulphur is due to the S^{32} isotope. Consequently these S_2 bands must be due to $(S^{32})_2$. The bands due to $S^{32}S^{34}$ and $S^{32}S^{33}$ have not been observed. These bands will be very much weaker and, furthermore their calculated positions lie within the bands investigated thus making their observation more difficult.

$P(K+1) \approx \Delta_1 F''(K)$]. The A_x, A_y, and A_z series would then be three R (or three Q) branches and the B_x, B_y and B_z series would be three Q (or three P)

TABLE I. *Wave-numbers of the lines in the 9–1 and 9–2 bands and the intervals between corresponding strong and weak lines*

	9-1 band				9–2 band			
K	R	P	$\delta\nu_R$	$\delta\nu_P$	R	P	$\delta\nu_R$	$\delta\nu_P$
3	—	34983.2* 82.3	—	−0.9	—	34263.4* 62.4	—	−1.0
5	34987.1* —	980.8* 79.7	—	−1.1	34267.4* 66.5	261.0* 60.0	−0.9	−1.0
7	986.3* 84.7	977.4* 76.4	−1.6	−1.0	266.5* 65.5	257.7* 56.6	−1.0	−1.1
9	985.2* 84.2	973.4* 72.1	−1.0	−1.3	265.2* 64.3	253.6* 52.6	−0.9	−1.0
11	983.2* 82.3	969.1* 68.0	−0.9	−1.1	263.4* 62.4	249.3* 48.3	−1.0	−1.0
13	980.8* 79.7	964.0*[1] 62.8	−1.1	−1.2	261.2* 60.0	244.7* 43.3	−1.2	−1.4
15	978.1* 76.4	958.2* 57.0	−1.7	−1.2	257.9* 56.7	238.7* 37.2	−1.2	−1.5
17	974.2* 72.7[1]	952.3* 50.7	−1.5	−1.6	254.4* 52.9	232.6* 31.1	−1.5	−1.5
19	970.0* 68.6	945.1* 43.6	−1.4	−1.5	250.4* 49.3	225.2* 24.0	−1.1	−1.2
21	965.3* 63.7[1]	937.4* 35.9	−1.6	−1.5	245.8* 44.7	218.0* 17.1	−1.1	−0.9
23	959.9* 58.2	929.6* 28.0	−1.7	−1.6	240.2* 38.7	210.0* 08.6	−1.5	−1.4
25	954.0* 52.7	921.9 21.4[1] 20.0[1]	−1.3	−1.6	234.5* 33.3	201.4* 00.0	−1.2	−1.4
27	947.2* 45.5[1]	— 911.6 09.9	−1.7	−1.7	228.1* 26.8	193.0 92.5 91.5	−1.3	−1.3
29	—	—	—	—	222.4 21.7 20.4	183.9 83.2 82.1	−1.6	−1.4
31	—	—	—	—	214.7 14.0 12.7	173.6 73.0 72.0	−1.6	−1.3
33	—	—	—	—	—	163.1 62.5 61.2	—	−1.6

* These lines are made up of two components which become resolvable at $K=25$. They are referred to in the text as R_{xy} and P_{xy}, and when they become resolvable R_x, R_y, P_x and P_y. The remaining values are then R_z and P_z. It will be shown later in the text that R_x, R_y and R_z correspond to R_1, R_3 and R_2, respectively, and similarly for the P branches.

[1] Smoothed values, the observed lines being composite.

branches. But if alternate lines are missing, the combinations correspond to $R(K)-P(K)=\Delta_2F'(K)$ and $R(K)-P(K+2)=\Delta_2F''(K+1)$. The equations for Δ_1F and Δ_2F are:

$$\Delta_1F = \text{constant} + 2(B + 3D)K + 4DK^3 \quad (2)$$

$$\Delta_2F = \text{constant} + 4(B + 3D)K + 8DK^3 \quad (3)$$

where $B=h/8\pi^2\mu cr^2$ and $D=-4\overline{B}^3/\omega_e^2$, μ being the reduced mass of the molecule. If we assume the first alternative, i.e. no lines missing, we obtain from our data $B''=0.818$ cm^{-1}, while the second gives $B''=0.409$ cm.$^{-1}$ From the empirical formula[15] $B=(27.7/\mu)\ (3000/\omega'')^{-2/3}$ which holds within a few percent for all known molecules composed of atoms of equal or nearly equal mass, we obtain $B''=0.404$ cm.$^{-1}$ Furthermore, if we assume that all lines are present, the value of D calculated from the theoretical relation $D_e=-4B_e^3/\omega_e^2$ is sixteen times as large as the value actually obtained from our data, whereas if we assume alternate lines missing, the value of D obtained from our data agrees within experimental error with the above theoretical value. These comparisons show that we must adopt Δ_2F and alternate missing lines. The series A and B therefore correspond to three R and three P branches.

In Tables I, II, and III, listed under their respective headings, R or P, are given the lines of the five bands investigated. The lines indicated by asterisks are the strong lines made up of two components which become resolvable at about $K=25$. The values with superscript (1) are assumed values, the observed lines being composite. $\delta\nu_R$ and $\delta\nu_P$ are the intervals between the weak and the strong lines in the R and P branches, except that where the strong lines are separated into two components, $\delta\nu$ is the interval between the weak line and the center of gravity of the doublet. It is seen that these intervals are the same within experimental error for all the bands investigated.

The values of $\Delta_2F''(K)=R(K-1)-P(K+1)$, which should agree for the 7−1, 8−1 and 9−1 bands are given in Table IV B. In Tables IV A and IV C the corresponding Δ_2F'''s of 7–0 and 9–2 are tabulated. The values of $\Delta_2F'(K)$ which should agree for the 7–1 and 7–0, and for the 9–1 and 9–2 bands are given in Table VA and VC. The corresponding $\Delta_2F'(K)$'s for the 8–1 bands are given in Table VB. It will be seen that all the expected agreements are fulfilled within experimental error.

The absence of strong Q branches indicates that we are dealing with a transition for which $\Delta\Lambda=0$. Furthermore, the great intensity of the entire system makes it evident that the transition is between two states of equal multiplicity, i.e. $\Delta S=0$. From the structure of the band, three R and three P branches, we conclude that the electronic states involved are triplets. The possible transitions are $^3\Sigma\rightarrow{}^3\Sigma$, $^3\Pi\rightarrow{}^3\Pi$ and perhaps $^3\Delta\rightarrow{}^3\Delta$.[16] The fact that

[15] P. M. Morse, Phys. Rev. **34**, 57 (1929).

[16] In a $^3\Pi\rightarrow{}^3\Pi$ or $^3\Delta\rightarrow{}^3\Delta$ transition we would expect three strong R and three strong P branches present, spaced approximately as in a $^3\Sigma\rightarrow{}^3\Sigma$ transition, if we have case (b) for both upper and lower electronic states, or if we had case (a) in which A is approximately the same in both the upper and the lower states (cf. TiO bands: A. Christy, Phys. Rev. **33**, 701 (1929)). For these transitions, however, we would expect all lines to be present and also the so called staggering effect, the magnitude of which would depend on λ type doubling.

TABLE II. *Wave-numbers of the lines in the 7–0 and 7–1 bands and the intervals between corresponding strong and weak lines.*

	7–0 band				7–1 band			
K	R	P	$\delta\nu_R$	$\delta\nu_P$	R	P	$\delta\nu_R$	$\delta\nu_P$
3	—	34949.9*	—	−1.7	—	34230.0*	—	−1.0
		48.2				29.0		
5	34953.3*	947.2*	—	−1.7	34233.3*	227.6*	−1.4	−1.6
	—	45.5			31.9	26.0		
7	952.7*	944.2*	−1.7	−1.4	232.6*	224.2*	−1.5	−1.4
	51.0[1]	42.8			31.1	22.8		
9	951.6*	940.5*	−1.4	−1.3	231.9*	220.4*	−1.5	−1.4
	50.2	39.2			30.4	19.0		
11	949.9*	935.7*	−1.7	−1.6	230.0*	215.8*	−1.0	−1.4
	48.2	34.1			29.0	14.4		
13	947.2*	930.6*	−1.7	−1.4	227.6*	210.8*	−1.6	−1.6
	45.5	29.2			26.0	09.2		
15	943.6*	924.3*	−1.6	−1.6	223.6*	204.7*	−1.9	−1.5
	42.0[1]	22.7			21.7	03.2		
17	939.4*	917.7*	−1.6	−1.8	219.5*	197.8*	−1.5	−1.9
	37.8[1]	15.9			18.0	95.9		
19	934.1*	909.9*	−1.5	−1.7	214.4*	190.3*	−1.7	−1.8
	32.6	08.2			12.7	88.5		
21	928.7*	901.5*	−1.6	−1.0	208.6*	182.1*	−1.0	−1.8
	27.1	00.5			07.6	80.3		
23	921.9*	892.9*	−1.4	−1.4	201.4*	173.0*	−1.0	−1.1
	20.5	91.5			00.4	71.9		
	914.4	883.0						
25	14.0[1]	82.6	−1.4	−1.3	194.5*	163.1*	−1.1	−1.3
	12.8	81.5			93.4	61.8		
	906.4	872.6			186.2	153.0		
27	05.6	71.8	−1.7	−1.2	86.0	52.4	−1.4	−1.3
	04.3	71.0			84.7	51.4		
	34898.1	34862.4			34177.8	34141.5		
29	97.2	61.5	−1.4	−1.7	77.0	40.8	−1.9	−1.7
	96.2	60.2			75.5	39.4		
	888.7	849.8			167.8	128.8		
31	87.5	48.5	−1.3	−1.5	66.9	27.8	−1.8	−1.9
	86.8	47.6			65.5	26.4		
	877.6	836.6			157.0	116.2		
33	76.7	35.2	−1.4	−1.5	56.5	15.3	−1.7	−1.4
	75.7	34.4			55.0	14.3		
	865.9	822.5			145.7	102.2		
35	65.0	21.1	−1.2	−1.3	44.8	101.7	−1.3	−1.3
	64.3	20.5			44.0	00.4		
						088.2		
37	—	—	—	—	—	86.8	—	−1.4
						86.1		

* These lines are made up of two components which become resolvable at $K=25$. They are referred to in the text as R_{xy} and P_{xy}, and when they become resolvable R_x, R_y, P_x and P_y. The remaining values are then R_z and P_z. It will be shown later in the text that R_x, R_y and R_z correspond to R_1, R_3, and R_2, respectively, and similarly for the P branches.

[1] Smoothed values, the observed lines being composite.

alternate lines are missing instead of staggering and that only three R and three P branches are present[17] clearly indicates that the bands are due to a

TABLE III. *Wave-numbers of the lines in the* 8–1 *band and the intervals between corresponding strong and weak lines.*

	8–1 band			
K	R	P	$\delta\nu_R$	$\delta\nu_P$
3	—	34614.1* 12.4	—	−1.7
5	34617.7* 16.3	612.0* 10.9[1]	−1.4	−1.1
7	616.9* 15.6	608.9* 07.1	−1.3	−1.8
9	616.3* 14.9	604.4* 02.8	−1.4	−1.6
11	614.1* 12.4	599.7* 98.6	−1.7	−1.1
13	612.0* 10.6	594.8* 93.4	−1.4	−1.4
15	608.9* 07.1	589.6* 88.3	−1.8	−1.3
17	604.4* 02.8	583.0* 81.5	−1.6	−1.5
19	599.7* 98.6	575.4* —	−1.1	—
21	594.0* 92.4	567.4* 66.0	−1.6	−1.4
23	588.3* 86.8	558.8* 57.6	−1.5	−1.2
25	581.5* 79.8	549.7* 48.5	−1.7	−1.2
27	573.5* 72.1	539.0* 37.6	−1.4	−1.4
29	565.9 65.2 63.7	529.6 28.5 27.2	−1.8	−1.8
31	— 555.1 53.5	516.8 16.1 —	−1.6	—

* These lines are made up of two components which become resolvable at $K=29$. They are referred to in the text as R_{xy} and P_{xy}, and when they become resolvable R_x, R_y, P_x, and P_y. The remaining values are then R_z and P_z. It will be shown later in the text that R_x, R_y and R_z correspond to R_1, R_3 and R_2, respectively, and similarly for the P branches.

[1] Smoothed values, the observed lines being composite.

$^3\Sigma \rightarrow {}^3\Sigma$ transition, presumably analogous to that of the Schumann-Runge bands of O_2. We also know that the final $^3\Sigma$ state is the normal state, because these bands are observed with great intensity in absorption.[18,1,2]

[17] ^RQ and ^PQ band lines would probably be too weak to detect.

[18] We have found that this system of S_2 appears with great intensity in absorption.

TABLE IV. *The values of Δ_2F'' for the levels in which $v''=0$, 1 and 2.*

K	*A* 0″ level 7–0	7–1	*B* 1″ level 8–1	9–1	*C* 2″ level 9–2
6	9.1*	9.1*	8.8*	9.7*	9.7*
	—	9.1	9.2	—	9.9
8	12.2*	12.2*	12.5*	12.9*	12.9*
	11.8	12.1	12.8	12.6	12.9
10	15.9*	16.1*	16.6*	16.1*	15.9*
	16.1	16.0	16.3	16.2	16.0
12	19.3*	19.2*	19.3*	19.2*	18.7*
	19.0	19.8	19.0	19.5	19.1
14	22.9*	22.9*	22.4*	22.6*	22.5*
	22.8	22.8	22.3	22.7	22.8
16	25.9*	25.8*	25.9*	25.8*	25.3*
	26.1	25.8	25.6	25.7	25.6
18	29.5*	29.2*	29.0*	29.1*	29.2*
	29.6	29.5	—	29.1	28.9
20	32.6*	32.3*	32.3*	32.6*	32.4*
	32.1	32.4	32.6	32.7	32.2
22	35.8*	35.6*	35.2*	35.7*	35.8*
	35.6	35.7	34.8	35.7	36.1
24	39.3*	38.3*	38.6*	38.5*	38.8*
	39.0	38.6	38.3	38.2	38.7
26	{41.8	—		—	
	{42.2	42.1	42.5*	42.4	42.0*
	41.8	42.0	42.2	42.8	41.8
28	{44.0	{44.7	—		—
	{44.1	{45.2	45.0		44.9
	44.1	45.3	44.9		44.7
30	{48.3	{49.0	{49.1		{48.8
	{48.7	{49.2	{49.1	—	{48.7
	48.6	49.1	—		48.4
32	{52.1	{51.6			{51.6
	{52.3	{51.6	—	—	{51.5
	52.4	51.2			51.5
34	{55.1	{54.8			
	{55.6	{54.8	—	—	—
	55.2	54.6			
36	—	{57.5			
		{58.0	—	—	—
		57.9			

* These values are obtained from the stronger R and P branches before the lines become resolvable, and are referred to in the text as Δ_2F_{xy}. The bracketed values are then Δ_2F_x and Δ_2F_y. The remaining values are Δ_2F_z. As will be shown later in the text Δ_2F_x, Δ_2F_y and Δ_2F_z correspond to Δ_2F_1, Δ_2F_3 and Δ_2F_2, respectively.

The rotational levels of a $^3\Sigma$ state are given by[19]

$$F_i = B_vK(K+1) + f_i(K, J-K) + D_vK^2(K+1)^2 + \qquad (4)$$

[19] For a detailed discussion cf. R. S. Mulliken, Rev. Modern Physics **2**, 105 (1931.) The factor G has been omitted in Eq. (4).

TABLE V. *The values of Δ_2F' for the levels in which $v'=7$, 8 and 9.*

	A 7′ level		*B* 8′ level	*C* 9′ level	
K	7–0	7–1	8–1	9–1	9–2
5	6.1*	5.7*	5.7*	6.3*	6.4*
	—	5.9	5.4	—	6.5
7	8.5*	8.4*	8.0*	8.9*	8.8*
	8.2	8.3	8.5	8.3	8.9
9	11.1*	11.5*	11.9*	11.8*	11.6*
	11.0	11.4	12.1	12.1	11.7
11	14.2*	14.2*	14.4*	14.1*	14.1*
	14.1	14.6	13.8	14.3	14.1
13	16.6*	16.8*	17.2*	16.8*	16.5*
	16.3	16.8	17.2	16.9	16.7
15	19.3*	18.9*	19.3*	19.9*	19.2*
	19.3	18.5	18.8	19.4	19.5
17	21.7*	21.7*	21.4*	21.9*	21.8*
	21.9	22.1	21.3	22.0	21.8
19	24.2*	24.1*	24.3*	24.9*	25.2*
	24.4	24.2	—	25.0	25.3
21	27.2*	26.5*	26.6*	27.8*	27.8*
	26.6	27.3	26.4	27.8	27.6
23	29.0*	28.4*	29.5*	30.3*	30.2*
	29.0	28.5	29.2	30.2	30.1
25	{31.4				
	{31.4	31.4*	31.8*	32.6*	33.1*
	31.3	31.6	31.3	32.7	33.3
27	{33.8	{33.2			
	{33.8	{33.6	34.5*	35.6	35.6
	33.3	33.3	34.5	35.6	35.3
29	{35.7	{36.3	{36.3		{38.5
	{35.7	{36.2	{36.7	—	{38.5
	36.0	36.1	36.5		38.3
31	{38.9	{39.0	—		{41.1
	{39.0	{39.1	39.0	—	{41.0
	39.2	39.1	—		40.7
33	{41.0	{40.8			
	{41.5	{41.2	—	—	—
	41.3	40.7			
35	{43.4	{43.5			
	{43.9	{43.1	—	—	—
	43.8	43.6			

* These values are obtained from the stronger R and P branches before the lines become resolvable, and are referred to in the text as Δ_2F_{xy}. The bracketed values are then Δ_2F_x and Δ_2F_y. The remaining values are Δ_2F_z. As will be shown later in the text Δ_2F_x, Δ_2F_y and Δ_2F_z correspond to Δ_2F_1, Δ_2F_3 and Δ_2F_2, respectively.

Where J is the total angular momentum of the molecule, its values being $J=K+S$, $K+S-1$, . . . , $K-S$. S is the resultant electronic spin. For a

triplet state $S=1$, hence $J=K+1$, K and $K-1$. Due to the three values of J, we shall have, in general, three closely spaced energy states for each value of K. These energy states are designated by F_1, F_2 and F_3, where F_1 corresponds to $J=K+1$, F_2 to $J=K$ and F_3 to $J=K-1$.

As has been shown by Kramers,[20] $f_i(K, J-K)$ for $^3\Sigma$ states is made up of two parts, one of which is due to the interaction of the resultant electronic spin $\mathbf{S}^*$ with the rotational angular momentum $\boldsymbol{K}^*$, and is equal to

$$(1/2)\gamma[J(J+1) - K(K+1) - S(S+1)] = (1/2)\gamma[(J(J+1) - K(K+1) - 2] \quad (5)$$

while the other part is due to the interaction between the individual spins of the electrons and is designated by $w_i(K, J-K)$. $f_i(K, J-K)$ then becomes

$$f_i(K, J-K) = (1/2)\gamma[J(J+1) - K(K+1) - 2] + w_i(K, J-K) \quad (6)$$

It has been shown [20] that $w_i(K, J-K)$ has the following form for the three values of J:

$$J = K+1, \quad w_1 = -\epsilon(1 - 3/2K + 3) \quad (7)$$

$$J = K-1, \quad w_3 = -\epsilon(1 + 3/2K - 1) \quad (8)$$

$$J = K, \quad w_2 = +2\epsilon. \quad (9)$$

We can neglect terms in ϵ/K for moderate and large values of K, since ϵ is usually small. $f_i(K, J-K)$ then is:

$$J = K+1, \quad f_1 = -\epsilon + \gamma K \quad (10)$$

$$J = K-1, \quad f_3 = -\epsilon - \gamma(K+1) \quad (11)$$

$$J = K, \quad f_2 = 2\epsilon - \gamma \quad (12)$$

The lines of the R and P branches are given by:

$$R_i(K) = \nu^0 + F_i'(K+1) - F_i''(K) \quad (13)$$

$$P_i(K) = \nu^0 + F_i'(K-1) - F_i''(K) \quad (14)$$

Hence, for the three components of the triplet,

$$\Delta_2 F_i'(K) = R_i(K) - P_i(K) = F_i'(K+1) - F_i'(K-1) \text{ is:}[21]$$

$$J = K+1, \quad \Delta_2 F_1'(K) = 2(B_v' + 2D_v' + \gamma') + 4(B_v' + 3D_v')K + 8D_v'K^3 \quad (15)$$

$$J = K-1, \quad \Delta_2 F_3'(K) = 2(B_v' + 2D_v' - \gamma') + 4(B_v' + 3D_v')K + 8D_v'K^3 \quad (16)$$

$$J = K, \quad \Delta_2 F_2'(K) = 2(B_v' + 2D_v') + 4(B_v' + 3D_v')K + 8D_v'K^3 \quad (17)$$

For the lower electronic state,

[20] H. A. Kramers, Zeits. f. Physik **53**, 422 (1929).

[21] We should include in these equations an additional term $+12\, D_v\, K^2$; but D_v is of the order of magnitude of 10^{-7}, so that, for values of K in which this term will become appreciable, the contribution of the cubic term will be much greater than that of the squared term, and hence the latter may be neglected.

$\Delta_2F_i''(K) = R_i(K+1) - P_i(K-1) = F_i''(K+1) - F_i''(K-1)$ has exactly the same form as in the above equations, except that the (′) is replaced by the (″).

In Tables IV and V the Δ_2F values with asterisks, Δ_2F_{xy}, are obtained from the lines of the strong R and P branches. When these lines are resolvable, the bracketed values, Δ_2F_x and Δ_2F_y, for any one K, are obtained from the corresponding components of the doublets. The remaining value Δ_2F_z for every K is obtained from the weak R and P branches. As will be shown later, Δ_2F_z corresponds to Δ_2F_2, cf. Eq. (17). The sets of values Δ_2F_{xy} correspond to the mean of Eqs. (15) and (16), i.e. $\overline{\Delta_2F_{13}(K)} = 2(B_v+2D_v)+4(B_v+3D_v)K+8D_vK^3$ which is the same as Eq. (17). If we assume γ negative (the justification will be discussed below) Δ_2F_1 and Δ_2F_3, cf. Eqs. (15) and (16), correspond to Δ_2F_x and Δ_2F_y, respectively.

The values of the molecular constants obtained from the data are listed in Table VI. The values of B were obtained from the slopes of our graphs corresponding to Eqs. (15), (16) and (17). The value of D_e was obtained from the equation $D_e = -4B_e^3/\omega_e^2$, which agrees within experimental error with the value obtained from Eqs. (15), (16), and (17).

$$B_e = B_0 + \tfrac{1}{2}\alpha_e \quad \text{and} \quad \alpha_e = \frac{B_0 - B_v}{v}$$

TABLE VI. *Values of molecular constants.*

		B (cm^{-1})	D_e (cm^{-1})	α_e B_e and r_e[22]	ϵ and γ[23]
$^3\Sigma_g^-$	$v''=0$ $v''=1$ $v''=2$	0.408_3 0.407_7 0.407_0	$D_e''=$ -5.2×10^{-7}	$\alpha_e=0.000_7$ $B_e''=0.409$ cm^{-1} $r_e''=1.603\times10^{-8}$cm	$\epsilon'-\epsilon''=0.47$ $\gamma'\approx\gamma''\approx-0.1$ $\gamma-\gamma''=$ $\pm0.014\pm0.003$
$^3\Sigma_u^-$	$v'=0$ $v'=7$ $v'=8$ $v'=9$	0.318_5 (extrapolated) 0.308 0.306 {0.305 {0.341	$D_e'=$ -7.2×10^{-7}	$\alpha_e=0.001_5$ $B_e'=0.319$ cm^{-1} $r_e'=1.814\times10^{-8}$cm	

The experimental values of Δ_2F for $v'=9$ obtained from the $9-1$ and $9-2$ bands do not fall upon a straight line as one would expect. In order to represent these points we had to drawn two straight lines, one fitting the points for lower values of K giving $B_9'=0.305$ cm,$^{-1}$ and the other fitting the points for higher values of K giving $B_9'=0.341$ cm.$^{-1}$ It is thought that this effect is due to the perturbation of the rotational levels. This seems plausible, for

[22] In our letter, Phys. Rev. **36**, 1800 (1930), the values of r_e are incorrectly given due to an arithmetical error in obtaining the r_e values from the values of B_e.

[23] The constants ϵ and γ are discussed in the following section. From our data we are only able to determine the accuracy of $(\gamma'-\gamma'')$ and not of either γ' or γ'', so that the values given for these constants may be off by several percent.

it is known from our work to be published in a later paper that predissociation occurs at $v'=10$. All bands with $v'=10$ are diffuse in absorption and absent in emission.

The exact value of the quantum numbers K was obtained by extrapolating the Δ_2F_i curves given in Eqs. (15), (16), and (17) to $\Delta_2F_i=0$. It has thus been found that the levels with *even* K values are missing in the *lower state*, and those with *odd* K values are missing in the *upper state*.

Exactly the same results have been found in the Schumann-Runge bands of O_2 investigated by Ossenbrüggen[9] and Lochte-Holtgreven and Dieke.[10] As Mulliken[24] has shown, the normal state of the oxygen molecule is in all probability $^3\Sigma_g^-$, this being the lower state of the Schumann-Runge bands. According to the selection rules for $^3\Sigma\rightarrow{}^3\Sigma$, the upper state must then be $^3\Sigma_u^-$[10,24]. We conclude, therefore, that the S_2 here investigated are due to a $^3\Sigma_u^-\rightarrow{}^3\Sigma_g^-$ transition.

Since alternate levels are missing we conclude that the internal angular momentum of the S^{32} nucleus is zero.

Spin Fine Structure of Rotational Levels

As we have seen above, the splitting of the rotational levels of a $^3\Sigma$ state into three components is due firstly, to the interaction of the resultant electronic spin with the rotational angular momentum (see Eq. (5)), and secondly to the interaction of the individual spins of the electrons (see Eqs. (7), (8) and (9)). In the expression for the first interaction the constant γ enters and in that, for the second, the constant ϵ. As these constants have only been determined in a few band spectra, namely, O_2[20,10] and PH[25], it will be of value to determine them as accurately as possible from the data for S_2 given above.

In order to obtain the values of γ, we have to correlate Δ_2F_1, Δ_2F_2 and Δ_2F_3 given in Eqs. (15), (16) and (17) above with one of the three sets of Δ_2F values for $K\geqq 25$, Δ_2F_x, Δ_2F_y and Δ_2F_z given in Tables IV and V. By examining these Δ_2F values it is clear that γ must be small since the Δ_2F values for the same value of K are almost the same within experimental error. By averaging all the Δ_2F_x, Δ_2F_y and Δ_2F_z separately for the upper state, we find that these values can be represented by $(N-0.1)$, $(N+0.1)$ and N cm.$^{-1}$ respectively. The same result holds for the lower state. These results can now be explained by correlating the Δ_2F_z values with Δ_2F_2, and the Δ_2F_x and Δ_2F_y values with either Δ_2F_1 or Δ_2F_3 where $|\gamma'|\approx|\gamma''|\approx 0.1$. It is impossible, however, to determine definitely from our data alone whether Δ_2F_1 should be correlated with Δ_2F_x or Δ_2F_y, as we do not know whether γ is positive or negative.

It has been shown that the value of γ''[26] in the normal $^3\Sigma_g^-$ state of the O_2 molecule is negative $(=-0.025)$.[20] The value of γ'[26] for the excited $^3\Sigma_u^-$ state of the Schumann-Runge bands has also been found to be negative $(=-0.048)$.[10] We would, therefore, expect the value of γ for the normal $^3\Sigma_g^-$

[24] R. S. Mulliken, Phys. Rev. **32**, 880 (1928); **36**, 700 (1930).

[25] R. W. B. Pearse, Proc. Roy. Soc. **A129**, 328 (1930).

[26] The γ used here corresponds to $(-B)$ in Kramer's terminology (cf. ref. 20) and $(-D)$ in that of Lochte-Holtgreven and Dieke (cf. ref. 10).

and probably for the excited $^3\Sigma_u^-$ states of S_2 also to be negative.[27] Hence, if we assume γ negative Δ_2F_1 and Δ_2F_3 correspond to Δ_2F_x and Δ_2F_y, respectively, in Tables IV and V. Hence R_1(or P_1) R_3(or P_3) and R_2(or P_2) correspond to R_x (or P_x), R_y (or P_y) and R_z (or P_z), respectively, in Tables I, II and III.

A schematic drawing of the rotational levels of the S_2 molecule is given in Fig. 2, with the theoretical separation of each level from the dotted line

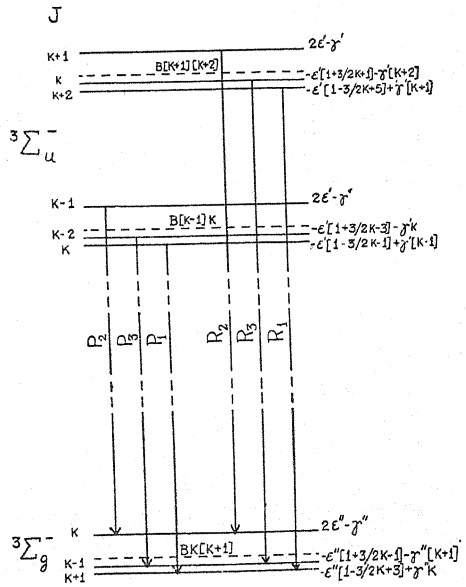

Fig. 2. A schematic representation of the structure of the rotational energy levels of S_2. The groups with rotational quantum numbers $K+1$ and $K-1$ refer to the upper $^3\Sigma_u^-$ state, and the group with quantum number K to the lower $^3\Sigma_g^-$ normal state. The dotted line represents the position of the rotational level if no interaction between K and S existed, its approximate energy value being given directly above it. The full lines represent the actual levels resulting from the interaction of the resultant electronic spin $\mathbf{S}^*$ with the rotational angular momentum $\mathbf{K}^*$ (see Eq. (5)) and the interaction between the individual spins of the electrons (see Eqs. (7), (8) and (9)). The calculated separation of these levels from the dotted line is given on the right. The lines joining the upper and the lower levels represent the observed transitions and are named accordingly. The K in the diagram is the value of K''.

for every K value given on the right. The equations for the separations of the three components in the triplet in the R and P branches, as may be seen with the help of Fig. 2, are[28]

[27] According to J. H. van Vleck (Phys. Rev. **33**, 467, 1929), $\gamma=\sum_K C_K A_K B_K/\nu_K$. The summation is to be taken over all the Π states. It is likely, however, that there will be one Π state whose influence is much greater than that of all others. ν_k then will be the interval between this Π state and the Σ state in question. C_KA_K is the coefficient at the magnetic interaction in this Π state. B has the usual meaning. We would expect this Π state to be similar in O_2 and S_2. Hence the sign at γ for both molecules would in all probability be the same.

[28] The values in ϵ/K have not been omitted in these equations.

$$R_1 - R_3 = -6\epsilon'(2K + 3/4K^2 + 12K + 5) + 6\epsilon''(2K - 1/4K^2 + 4K - 3) - (3\gamma' - \gamma'') - 2(\gamma' - \gamma'')K \quad (18a)$$

$$R_2 - R_1 = (3\epsilon' - 3\epsilon'') - (3\epsilon'/2K + 5) + (3\epsilon''/2K + 3) - 2\gamma' + \gamma'' - (\gamma' - \gamma'')K \quad (19a)$$

$$R_2 - R_3 = (3\epsilon' - 3\epsilon'') + (3\epsilon'/2K + 1) - (3\epsilon''/2K - 1) + \gamma' + (\gamma' - \gamma'')K \quad (20a)$$

$$P_1 - P_3 = -6\epsilon'(2K - 2/4K^2 - 8K + 3) + 6\epsilon''(2K - 1/4K^2 + 4K - 3) + \gamma' + \gamma'' - 2(\gamma' - \gamma'')K \quad (18b)$$

$$P_2 - P_1 = (3\epsilon' - 3\epsilon'') - (3\epsilon'/2K + 1) + (3\epsilon''/2K + 3) + \gamma'' - (\gamma' - \gamma'')K \quad (19b)$$

$$P_2 - P_3 = (3\epsilon' - 3\epsilon'') + (3\epsilon'/2K - 3) - (3\epsilon''/2K - 1) - \gamma' + (\gamma' - \gamma'')K. \quad (20b)$$

The average of Eqs. (19a) and (19b) is:

$$\approx (3\epsilon' - 3\epsilon'') - (3\epsilon' - 3\epsilon'')/(2K + 3) - (\gamma' - \gamma'') - (\gamma' - \gamma'')K \quad (21)$$

and the average of Eqs. (20a) and 20b) for $K \geqq 5$:[29]

$$\approx (3\epsilon' - 3\epsilon'') + (3\epsilon' - 3\epsilon'')/(2K - 1) + (\gamma' - \gamma'')K. \quad (22)$$

The interval between R_2 and the mean of R_1 and R_3 is for $K \geqq 3$ [29]

$$3(\epsilon' - \epsilon'') + \tfrac{1}{2}(\gamma' - \gamma''). \quad (23)$$

This interval is the same as that obtained from the P branches.

Eqs. (18a) to (23) may now be used to correlate definitely the branches designated by R_x, R_y and R_z (or P_x, P_y and P_z) with R_1, R_3 and R_2 (or P_1, P_3 and P_2). The average of the experimental values $\delta\nu_R$ and $\delta\nu_P$ given in Tables I, II, and III are plotted in Fig. 3, Graph A. It is recalled that $\delta\nu_R$ and $\delta\nu_P$ are the intervals between the weak R_z (or P_z) and the corresponding strong lines R_{xy} (or P_{xy}). When the components of the strong lines become resolvable, $\delta\nu_R$ ($\delta\nu_P$) are the intervals between R_z (or P_z) and the center of the resulting doublet. The values of the average intervals between the weak lines R_z (or P_z) and the corresponding short wave-length component of the doublet R_x (or P_x), i.e. the average of $(R_z - R_x)$ and $(P_z - P_x)$ are plotted below Graph A. The values of the average intervals between the weak line R_z (or P_z) and the long wave-length component of the doublet R_y (or P_y), i.e. the average of $(R_z - R_y)$ and $(P_z - P_y)$ are plotted above graph A.

We see that the plotted values of $\delta\nu_R$ and $\delta\nu_P$ (graph A) are approximately constant, and independent of K. Further, as can be seen from Fig. 3, the average of the intervals $\delta\nu_R - (R_z - R_x)$ and $\delta\nu_P - (P_z - P_x)$ is approximately equal but of opposite sign to the intervals $\delta\nu_R - (R_z - R_y)$ and $\delta\nu_P - (P_z - P_y)$.

[29] These equations contain approximations which hold only for the values of K as given.

Considering the results obtained above by comparing the experimental values of $\Delta_2 F$ and Eqs. (15), (16) and (17) and also Fig. 3, we see that the only possible correlation (assuming γ negative) is that R_z(or P_z) corresponds to R_1, (or P_1), R_y(or P_y), to R_3, (or P_3) and R_x (or P_x), to R_2, (or P_2).

From Eq. (23) and Graph A, $3\epsilon'-3\epsilon''+\frac{1}{2}(\gamma'-\gamma'')=-1.41$ from which we obtain $\epsilon'-\epsilon''=-0.47$[30] if we put $(\gamma'-\gamma'')=0.014$ (see below).

The points below and above graph A in Fig. 3, can now best be represented by graphs B and C, respectively, which are the graphs of Eqs. (21) and (22), if we take $(3\epsilon'-3\epsilon'')=-1.42$ and $(\gamma'-\gamma'')=0.014$. We have seen above that $\gamma'\approx\gamma''\approx-0.1$ and from $(\gamma-\gamma'')=0.014$, we conclude $|\gamma''|>|\gamma'|$.

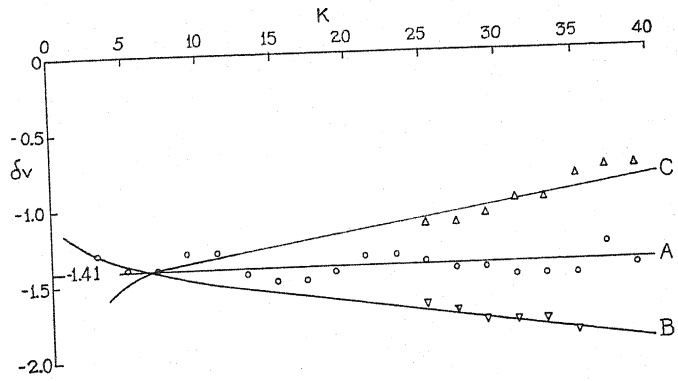

Fig. 3. Graphs showing the average observed separations of the triplets. The circular points represent the intervals between the weak R_z (or P_z) series and the strong R_{xy} (or P_{xy}) or the center of the doublets R_x and R_y (or P_x and P_y), when R_{xy} (or P_{xy}) become resolvable for $K\geqq 25$. These points are represented by Graph A. The triangles represent the intervals between the weak R_z (or P_z) series and the long wave-length component of the doublet R_y (or P_y) and the inverted triangles represents the intervals between the weak R_z (or P_z) series and the short wave-length component of the doublet R_x (or P_x). The triangles may best be represented by C which is the graph of Eq. (22), and the inverted triangles by B which is the graph of Eq. (21) where $3(\epsilon'-\epsilon'')=-1.42$ and $\gamma'-\gamma''=+0.014$. The plotted values are the averaged intervals for the R and P series.

From our data we are not able to determine the values of ϵ' and ϵ'' separately. This will be possible if the rotational structure of the S_2 bands similar to the O_2 atmospheric bands could be determined. These bands of S_2 which would lie in the infrared, have as yet not been discovered.

Discussion of Previous Work

With regard to previous work on the rotational analysis of S_2 there is every indication that the analysis of Henri and Teves[3] is probably incorrect, since the resolution used could not be sufficient to separate all the lines in the bands and thus to assign the lines correctly into series. The complexity of the patterns obtained in fluorescence by Teves[4], Swings,[5] and Rompe[6] are undoubtedly due to the following causes:

[30] In the O_2 Schumann-Runge bands ϵ' and ϵ'' were both found to be positive and also $\epsilon''>\epsilon'$. If we assume ϵ' and ϵ'' are also positive in the S_2 bands, then $\epsilon''>\epsilon'$.

(1) All the lines of the mercury arc have been used to excite fluorescence.

(2) As Rompe points out Swings' arc was not sufficiently cooled, giving him broad exciting lines, whereas Rompe states that he himself was unable to obtain step to step fluorescence in mercury vapour with his own source, indicating that his exciting lines were also too broad.

(3) The rotational lines of the S_2 bands lie close together.

Due to these facts and the small dispersion used by these investigators, it is extremely difficult, if not impossible, to interpret the results which have been obtained by them It will be interesting, however, if the fluorescence spectrum could be investigated using single line excitation and somewhat larger dispersion than that used by previous investigators.

Note added in proof: We have received a letter from Mons. P. Swings in which he states that according to results derived from an investigation of the fluorescence spectra of S_2 (obtained with a Crony spectrograph with 11 prisms giving a dispersion of 1A per mm at λ3000) he found $I''=70\times10^{-40}$ gm cm^2 corresponding to a value of $B''=0.396$ cm^{-1}. This value of B'' agrees within experimental error with our value $B_e''=0.409$ cm^{-1} given above. His results will be published in the Mém. Soc. royale Sciences, Liége.

The authors wish to express their appreciation to Professor R. S. Mulliken for his interest and advice in connection with this work.

ORBITAL VALENCY*

By James H. Bartlett, Jr.
Department of Physics, University of Illinois

(Received January 15, 1931)

Abstract

The interaction of two atoms, each with one $2p$ electron, is studied by a method similar to that used by Kemble and Zener. An atomic wave function whose radial part is of the form const. $re^{-kr/2}$ (that is, with no nodes) is used. Complete potential energy curves are obtained for the twelve possible states, which are $^1\Delta_g$, $^3\Delta_u$, $^1\Pi_g$, $^1\Pi_u$, $^3\Pi_g$, $^3\Pi_u$, $^1\Sigma_u^-$, $^3\Sigma_g^-$, two $^1\Sigma_g^+$, and two $^3\Sigma_u^+$. The most stable states are $^3\Sigma_u^+$ (lowest) and $^1\Sigma_g^+$, which arise from $m_{la}=0$ and $m_{lb}=0$, and in which there is the maximum overlapping of charge. The states with least overlapping of charge are those where $m_{la}=\pm 1$ and $m_{lb}=\pm 1$, resulting in $^1\Delta_g$, $^3\Delta_u$, $^1\Sigma_g^+$, $^1\Sigma_u^-$, $^3\Sigma_g^-$, $^3\Sigma_u^+$, which are all repulsive. The Π states lie in between, and are attractive. The present work gives precision to the ideas of Heitler on orbital valency, yields a positive exchange energy integral for the lowest states, and may be taken as supporting the conceptions of Slater about directed valency.

OUR knowledge of the rules underlying the formation of stable diatomic molecules from their constituent atoms is still very limited, in spite of the successes achieved by Heitler and London,[1] and by Kemble and Zener.[2] The idea of spin valency is quite useful, but its general inadequancy has been recognized by Heitler,[3] who has therefore proposed an "orbital" valency. Two atoms can exert on each other forces due not only to the coupling between the spins, but also to the coupling between the orbits, and the two types of interaction may give rise to effects of the same order of magnitude.[4] One must in general take the oribital valency into consideration, and it is highly desirable to formulate rules concerning the order of the resulting molecular states. This is the purpose of the present investigation.

The special problem here studied is that of the interaction of two similar atoms, each with one $2p$ valence electron. For simplicity, a hydrogenic wave function for the atom has been assumed, and the possible influence of internal s electrons has been neglected. Zener[5] has shown that it is legitimate, as an approximation, to assume such a wave function. The method is essentially the same as used by Kemble and Zener,[2] except that in the actual evaluation

* This work was done largely with the aid of a Parker Travelling Fellowship from Harvard University.

[1] W. Heitler u. F. London, Zeits. f. Physik **44**, 455 (1927).
[2] E. C. Kemble and C. Zener, Phys. Rev. **33**, 512 (1929).
[3] W. Heitler, Naturwiss. **17**, 546 (1929).
[4] This statement is rather inexact, but the precise formulation will be made later.
[5] C. Zener, Phys. Rev. **36**, 51 (1930).

of the integrals the procedure of Zener and Guillemin[6] has been followed. Without doubt, one could improve upon the energy values by using a variational method, but it will be assumed that their order would be the same, and it is primarily the order which is the object of this investigation.

We assume, therefore, the radial part of the atomic wave function to be of the form $R = \text{const}\ re^{-\kappa r/2}$, where κ is an arbitrary constant.

Notation. $a(nlm_l/1)$ = wave function for electron 1 on nucleus a, with quantum numbers m, l, m_l. (Similarly for nucleus b).

For one electron, a = distance from nucleus a
b = distance from nucleus b.

For two electrons a_1 = distance of electron one from nucleus a, etc.
R = internuclear distance
r = interelectronic distance
θ_{a1} = angle from internuclear axis to line joining a and 1.

In the case under consideration, it is unnecessary to write explicitly n and l, which are 2 and 1, respectively, for each electron. Accordingly, we shall abbreviate the notation to $a(m_l 1)$.

Thus

$$a(11) = c_1 a_1 e^{-\kappa a_1/2} \sin\theta_{a_1} e^{i\phi_1}$$

$$b(02) = c_2 b_2 e^{-\kappa b_2/2} \cos\theta_{b_2}.$$

Kemble and Zener show how one may set up a secular equation for the two-quantum excited states of H_2, and then separate it according to the constants of the motion, the spin-orbit interaction being supposed to be negligible. The same may be done in the present case, and one obtains a secular equation of the twelfth degree, which has eight linear factors, and two quadratic factors. The results are tabulated. The energy is measured from the "unperturbed" value, namely that for infinite separation. $^1\Sigma_g^+$ means that the electronic factor of the wave function is unchanged on reflection in a plane through the internuclear axis (+), and on reflection in the midpoint of this axis (g). The notation of Kemble and Zener is also given.

[6] C. Zener and V. Guillemin, Phys. Rev. 34, 999 (1929).

Wave Functions and Energy Levels

States m_{la}	m_{lb}	Symmetry	Wave Function	"Diagonal" Energy
1	1	$^1\Delta_g(S^N)$	$a(11)b(12)+a(12)b(11)$	$\frac{1}{1+S_{11}}(I_1+I_2)$
1	1	$^3\Delta_u(A^N)$	$a(11)b(12)-a(12)b(11)$	$\frac{1}{1-S_{11}}(I_1-I_2)$
1	0	$^1\Pi_g(S^N)$	$a(11)b(02)+a(12)b(01)+a(01)b(12)+a(02)b(11)$	$\frac{1}{1+S_{10}}(I_3+I_4+I_5+I_6)$
1	0	$^1\Pi_u(A^N)$	$a(11)b(02)+a(12)b(01)-a(01)b(12)-a(02)b(11)$	$\frac{1}{1-S_{10}}(I_3-I_4-I_5+I_6)$
1	0	$^3\Pi_g(S^N)$	$a(11)b(02)-a(12)b(01)-a(01)b(12)+a(02)b(11)$	$\frac{1}{1+S_{10}}(I_3+I_4-I_5-I_6)$
1	0	$^3\Pi_u(A^N)$	$a(11)b(02)-a(12)b(01)+a(01)b(12)-a(02)b(11)$	$\frac{1}{1-S_{10}}(I_3-I_4+I_5-I_6)$
1	−1	$^1\Sigma_u^-(A^N)$	$a(11)b(-12)+a(12)b(-11)-a(-11)b(12)-a(-12)b(11)$	$\frac{1}{1-S_{11}}(I_1-I_2-I_7+I_8)$
1	−1	$^3\Sigma_g^-(S^N)$	$a(11)b(-12)-a(12)b(-11)-a(-11)b(12)+a(-12)b(11)$	$\frac{1}{1+S_{11}}(I_1+I_2-I_7-I_8)$
1	−1	$^1\Sigma_g^+(S^N)$	$a(11)b(-12)+a(12)b(-11)+a(-11)b(12)+a(-12)b(11)$	$\frac{1}{1+S_{11}}(I_1+I_2+I_7+I_8)$
0	0	$^1\Sigma_g^+(S^N)$	$a(01)b(02)+a(02)b(01)$	$\frac{1}{1+S_{00}}(I_9+I_{10})$
1	−1	$^3\Sigma_u^+(A^N)$	$a(11)b(-12)-a(12)b(-11)+a(-11)b(12)-a(-12)b(11)$	$\frac{1}{1-S_{11}}(I_1-I_2+I_7-I_8)$
0	0	$^3\Sigma_u^+(A^N)$	$a(01)b(02)-a(02)b(01)$	$\frac{1}{1-S_{00}}(I_9-I_{10})$

where

$$I_1 = \int H'[a(11)]^2[b(12)]^2 dv$$

$$I_2 = \int H' a(11)b(11)a(12)b(12)dv$$

$$I_3 = \int H'[a(11)]^2[b(02)]^2 dv$$

$$I_4 = \int H' a(11)b(11)a(02)b(02)dv$$

$$I_5 = \int H' a(01)a(11)b(02)b(12)\cos(\phi_1 - \phi_2)dv$$

$$I_6 = \int H' a(11)b(01)a(12)b(02)\cos(\phi_1 - \phi_2)dv$$

$$I_7 = \int H'[a(11)]^2[b(12)]^2 \cos 2(\phi_1 - \phi_2)dv$$

$$I_8 = \int H'a(11)b(11)a(12)b(12) \cos 2(\phi_1 - \phi_2)dv$$

$$I_9 = \int H'[a(01)]^2[b(02)]^2 dv$$

$$I_{10} = \int H'a(01)b(01)a(02)b(02)dv$$

$$I_{11} = \int H'a(01)a(12)b(11)b(02) \cos(\phi_1 - \phi_2)dv$$

where H' is the "perturbative" part of the energy, e.g.,

$$H' = \frac{2}{R} + \frac{2}{r} - \frac{2}{a_2} - \frac{2}{b_1}, \text{ using atomic units.}$$

$$(S_{11})^{1/2} = \int a(11)b(11)dv_1, \quad (S_{00})^{1/2} = \int a(01)b(01)dv_1, \quad S_{10} = (S_{11}\, S_{00})^{1/2}.$$

There remain to be solved two two-degree secular equations, namely

$$(1) \quad \begin{vmatrix} I_1 + I_2 + I_7 + I_8 - E(1 + S_{11}) & 2(I_5 + I_{11}) \\ -I_5 + I_{11} & I_9 + I_{10} - E(1 + S_{00}) \end{vmatrix} = 0$$

and

$$(2) \quad \begin{vmatrix} I_1 - I_2 + I_7 - I_8 - E(1 - S_{11}) & 2(-I_5 + I_{11}) \\ +I_5 + I_{11} & I_9 - I_{10} - E(1 - S_{00}) \end{vmatrix} = 0$$

The solution of (1) gives us two states of the $^1\Sigma$, S^N type, and the solution of (2) two states of the $^3\Sigma$, A^N type. It turns out that the influence of the non-diagonal terms is negligible.

Evaluation of the Integrals

General formulae. One may classify the integrals according to whether it is necessary to use the Neumann expansion or not in their evaluation. One does not need to do so for the integrals I_1, I_3, I_9, I_5, and I_7. The only term in the Hamiltonian which offers difficulty is the $2/r$ term. The integrals involving the Neumann expansion are termed "exchange," and the others "Coulomb."

Before proceeding, the notation needs explanation. That used by Zener and Guillemin[6] will be adopted.

$$\Gamma_n = \int_0^\infty e^{-u}u^{n-1}du \quad \Gamma_n(\alpha) = \int_\alpha^\infty e^{-u}u^{n-1}du, \quad \gamma_n(\alpha) = \Gamma_n - \Gamma_n(\alpha)$$

$$A_n(\sigma, \alpha) = \int_\sigma^\infty e^{-\alpha x}x^n dx = \frac{1}{\alpha^{n+1}}\Gamma_{n+1}(\sigma\alpha)$$

$$B_n(\alpha) = \int_{-1}^{1} e^{-\alpha x} x^n dx = A_n(-1, \alpha) - A_n(1, \alpha)$$

$$f_\tau(m, \alpha) = \int_1^\infty e^{-\alpha x} x^m Q_\tau(x) dx$$

where

$$Q_0 = \frac{1}{2} \ln\left(\frac{x+1}{x-1}\right), \; x > 1, \quad \text{and} \quad Q_1 = xQ_0 - 1.$$

One may readily establish, by partial integration, the following recursion formulae:

$$A_{m+1}(1,\alpha) - A_m(1,\alpha) = \frac{1}{\alpha}\{(m+1)A_m(1,\alpha) - mA_{m-1}(1,\alpha)\}$$

$$A_{m+1}(1,\alpha) + A_m(1,\alpha) = \frac{1}{\alpha}\{2e^{-\alpha} + (m+1)A_m(1,\alpha) + mA_{m-1}(1,\alpha)\}$$

$$A_{m+2}(1,\alpha) - A_m(1,\alpha) = \frac{1}{\alpha}\{(m+2)A_{m+1}(1,\alpha) - mA_{m-1}(1,\alpha)\}$$

$$f_0(n+2,\alpha) - f_0(n,\alpha) = \frac{1}{\alpha}\{-A_n(1,\alpha) + 2f_0(n+1,\alpha) + n[f_0(n+1,\alpha) - f_0(n-1,\alpha)]\}$$

$$f_1(n+2,\alpha) - f_1(n,\alpha) = \frac{1}{\alpha}\{3f_1(n+1,\alpha) - f_0(n,\alpha) + n[f_1(n+1,\alpha) - f_1(n-1,\alpha)]\}$$

$$= \frac{1}{\alpha}\{2f_1(n+1,\alpha) - A_{n-1}(1,\alpha) + (n+1)[f_1(n+1,\alpha) - f_1(n-1,\alpha)]\}$$

We have here used the relations

$$(x^2 - 1)\frac{dQ_n}{dx} = nxQ_n - nQ_{n-1}, \quad n > 0$$

and

$$f_1(m, \alpha) = f_0(m+1, \alpha) - A_m(1, \alpha).$$

Now let

$$F(n, \lambda) = \int_{-1}^{1} \frac{e^{-\rho\mu} d\mu}{(\mu - \lambda)^n}$$

then $F(1) = e^{-\rho\lambda}[-E_i(\rho(1+\lambda)) + E_i(-\rho(1+\lambda))]$ where

$$-E_i(-x) = \int_x^\infty \frac{e^{-u}}{u} du.$$

In general,

$$F(n) = -\frac{1}{n-1}\left[\frac{e^{-\rho}}{(1-\lambda)^{n-1}} - \frac{e^{\rho}}{(-1-\lambda)^{n-1}}\right] - \frac{\rho}{n-1} F(n-1), n \neq 1$$

and

$$\frac{dF(n)}{d\lambda} = nF(n+1).$$

Abbreviating,

$$F_1(n) = -\frac{1}{n-1}\left[\frac{e^{-\rho}}{(1-\lambda)^{n-1}} - \frac{e^{\rho}}{(-1-\lambda)^{n-1}}\right]$$

and

$$F(n) = -\frac{\rho}{n-1}F(n-1) + F_1(n)$$

$$\int_1^\infty f(\lambda)F(n+1)e^{-\rho\lambda}d\lambda = \int_1^\infty f(\lambda)\,\frac{1}{n}\,\frac{dF(n)}{d\lambda}e^{-\rho\lambda}d\lambda = \frac{1}{2n}f(\lambda)F(n)e^{-\rho\lambda}\Big|_1^\infty$$

$$-\frac{1}{2n}\int_1^\infty e^{-\rho\lambda}\left\{F(n)\frac{df(\lambda)}{d\lambda} - f(\lambda)\frac{dF_1(n)}{d\lambda}\right\}d\lambda. \tag{3}$$

For the most part, two kinds of coordinate systems have been employed. One, with a, b, and ϕ as coordinates, and $(1/R)adabdbd\phi$ as volume element, is most convenient for integrals such as $\int e^{-\kappa a}f(a, b)dv$, since one can integrate over b first and avoid the occurrence of integral logarithms in the final integrand (using a wave function with radial part $R = cre^{-\kappa r/2}$). The other, with λ, μ, and ϕ as coordinates, where $a = (R/2)(\lambda+\mu)$ and $b = (R/2)(\lambda-\mu)$, and $(R/2)^3(\lambda^2-\mu^2)d\lambda d\mu d\phi$ is the volume element, is best for integrals such as $\int e^{-\kappa(a+b)}f(a, b)dv$, the integration over μ being performed first. The transformation is as follows:

$$\cos\theta_a = \frac{\lambda\mu+1}{\lambda+\mu} \quad \cos\theta_b = \frac{\lambda\mu-1}{\lambda-\mu} \quad \sin^2\theta_a = \frac{(\lambda^2-1)(1-\mu^2)}{(\lambda+\mu)^2},$$

$$\sin^2\theta_b = \frac{(\lambda^2-1)(1-\mu^2)}{(\lambda-\mu)^2}.$$

Normalization. The normalized atomic wave functions are $u = c_1e^{-\kappa r/2}r \sin\theta e^{\pm i\phi}$ and $u = c_2e^{-\kappa r/2}\, r\cos\theta$, where $2\pi c_1^2/\kappa^5 = 1/32$ and $2\pi c_2^2/\kappa^5 = 1/16$. Let $\alpha = \kappa R$.

$$(S_{11})^{1/2} = 2\pi c_1^2\int e^{-(\kappa/2)(a+b)}a\sin\theta_a\; b\sin\theta_b\; adabdb$$

$$= \frac{2\pi c_1^2}{\kappa^5}\left(\frac{\alpha}{2}\right)^5\int_1^\infty d\lambda\int_{-1}^1 d\mu e^{-\alpha\lambda/2}(\lambda^2-1)(\lambda^2-\mu^2)(1-\mu^2)$$

$$= 1/24\cdot(\alpha/2)^5\{A_4(1, \alpha/2) - (6/5)A_2(1, \alpha/2) + (1/5)A_0(1, \alpha/2)\}$$

$$(S_{00})^{1/2} = (2\pi c_2^2/\kappa^5)(\alpha/2)^5\int_1^\infty d\lambda\int_{-1}^1 d\mu e^{-\alpha\lambda/2}(\lambda^2\mu^2-1)(\lambda^2-\mu^2)$$

$$= 1/24\cdot(\alpha/2)^5\{A_4(1, \alpha/2) - (18/5)A_2(1, \alpha/2) + A_0(1, \alpha/2)$$

The integrals I_1, I_3, I_9, I_5, I_7.

Let

$$i_1 = \int \frac{2}{r}[a(11)]^2[b(12)]^2 dv = \int \frac{2}{r} c_1^4 a_1^2 b_2^2 \sin^2\theta_{a_1} \sin^2\theta_{b_2} e^{-\kappa(a_1+b_2)} dv$$

$$i_3 = \int \frac{2}{r}[a(11)]^2[b(02)]^2 dv = \int \frac{2}{r} c_1^2 c_2^2 a_1^2 b_2^2 \sin^2\theta_{a_1} \cos^2\theta_{b_2} e^{-\kappa(a_1+b_2)} dv$$

$$= \int \frac{2}{r}[a(01)]^2[b(12)]^2 dv = \int \frac{2}{r} c_1^2 c_2^2 a_1^2 b_2^2 \cos^2\theta_{a_1} \sin^2\theta_{b_2} e^{-\kappa(a_1+b_2)} dv$$

$$i_9 = \int \frac{2}{r}[a(01)]^2[b(02)]^2 dv = \int \frac{2}{r} c_2^4 a_1^2 b_2^2 \cos^2\theta_{a_1} \cos^2\theta_{b_2} e^{-\kappa(a_1+b_2)} dv$$

$$i_5 = \int \frac{2}{r} a(01)a(11)b(02)b(12) \cos(\phi_1 - \phi_2) dv$$

$$= \int \frac{2}{r} c_1^2 c_2^2 a_1^2 b_2^2 \sin\theta_{a_1} \cos\theta_{a_1} \sin\theta_{b_2} \cos\theta_{b_2} e^{-\kappa(a_1+b_2)} \cos(\phi_1 - \phi_2) dv$$

$$i_7 = \int \frac{2}{r}[a(11)]^2[b(12)]^2 \cos 2(\phi_1 - \phi_2) dv$$

$$= \int \frac{2}{r} c_1^4 a_1^2 b_2^2 \sin^2\theta_{a_1} \sin^2\theta_{b_2} e^{-\kappa(a_1+b_2)} \cos 2(\phi_1 - \phi_2) dv.$$

We can now expand $2/r$ as usual:—

$$\frac{2}{r} = \frac{2}{b_1}\left\{1 + \frac{b_2}{b_1}\cos\gamma + \left(\frac{b_2}{b_1}\right)^2 P_2(\cos\gamma) + \cdots\right\} \quad b_2 < b_1$$

$$= \frac{2}{b_2}\left\{1 + \frac{b_1}{b_2}\cos\gamma + \left(\frac{b_1}{b_2}\right)^2 P_2(\cos\gamma) + \cdots\right\} \quad b_2 > b_1$$

where γ is the angle between the lines b_1 and b_2, and

$$P_n(\cos\gamma) = P_n(\cos\theta_{b_1})P_n(\cos\theta_{b_2}) + 2\sum_{m=1}^{n}(-1)^m \frac{(n-m)!}{(n+m)!} P_n^m(\cos\theta_{b_1}) P_n^m(\cos\theta_{b_2}) \cos m(\phi_1 - \phi_2)$$

$$\int_0^{2\pi} P_n(\cos\gamma) \cos m(\phi_1 - \phi_2) d(\phi_1 - \phi_2) = 2\pi P_n(\cos\theta_{b_1}) P_n(\cos\theta_{b_2}), \quad m = 0$$

$$= 2\pi(-1)^m \frac{(n-m)!}{(n+m)!} P_n^m(\cos\theta_{b_1}) P_n^m(\cos\theta_{b_2}), \quad m \neq 0.$$

On performing the integrations, one obtains, letting

$$g_{5,1} = \frac{\gamma_5(\kappa b)}{\kappa b} + \Gamma_4(\kappa b)$$

$$g_{7,3} = \frac{\gamma_7(\kappa b)}{(\kappa b)^3} + (\kappa b)^2 \Gamma_2(\kappa b),$$

the following expressions:—

$$i_1 = (16\pi c_1^4/3\kappa^4)\int a^2 \sin^2\theta_a e^{-\kappa a}[g_{5,1} - (1/5)P_2(\cos\theta_b)g_{7,3}]dv$$

$$i_3 = (8\pi c_1^2 c_2^2/3\kappa^4)\int a^2 \sin^2\theta_a e^{-\kappa a}[g_{5,1} + (2/5)P_2(\cos\theta_b)g_{7,3}]dv$$

$$= (16\pi c_1^2 c_2^2/3\kappa^4)\int a^2 \cos^2\theta_a e^{-\kappa a}[g_{5,1} - (1/5)P_2(\cos\theta_b)g_{7,3}]dv$$

$$i_9 = (8\pi c_2^4/3\kappa^4)\int a^2 \cos^2\theta_a e^{-\kappa a}[g_{5,1} + (2/5)P_2(\cos\theta_b)g_{7,3}]dv$$

$$i_5 = -(8\pi c_1^2 c_2^2/5\kappa^4)\int a^2 \sin\theta_a \cos\theta_a \sin\theta_b \cos\theta_b e^{-\kappa a} g_{7,3}dv$$

$$i_7 = -(8\pi c_1^4/5\kappa^4)\int a^2 \sin^2\theta_a \sin^2\theta_b e^{-\kappa a} g_{7,3}dv$$

$$\int a^2 \sin^2\theta_a e^{-\kappa a}(\Gamma_5/\kappa b)dv = (8\pi\Gamma_5/3\kappa^5)[g_{5,1}(\alpha) - (1/5)g_{7,3}(\alpha)]$$

$$\int a^2 \cos^2\theta_a e^{-\kappa a}(\Gamma_5/\kappa b)dv = (4\pi\Gamma_5/3\kappa^5)[g_{5,1}(\alpha) + (2/5)g_{7,3}(\alpha)]$$

$$\int a^2 \sin^2\theta_a e^{-\kappa(a+b)}[(\kappa b)^3 + 6(\kappa b)^2 + 18\kappa b + 24](1/\kappa b)\cdot dv$$

$$= (2\pi/\kappa^5)(\alpha/2)^4\{(\alpha/2)^3[(4/3)(A_6 - A_4) - (4/35)(A_2 - A_0)]$$
$$+ 6(\alpha/2)^2[(4/3)(A_5 - A_3) - (4/15)(A_3 - A_1)] + 18(\alpha/2)[(4/3)(A_4 - A_2)$$
$$- (4/15)(A_2 - A_0)] + 24(4/3)(A_3 - A_1)\}$$

$$\int a^2 \cos^2\theta_a e^{-\kappa(a+b)}[(\kappa b)^3 + 6(\kappa b)^2 + 18\kappa b + 24](1/\kappa b)\cdot dv$$

$$= (2\pi/\kappa^5)(\alpha/2)^4\{(\alpha/2)^3[(2/3)(A_6 - A_4) + (46/35)A_2 - (2/5)A_0]$$
$$+ 6(\alpha/2)^2[(2/3)A_5 + (4/15)A_3 + (2/15)A_1] + 18(\alpha/2)[(2/3)A_4 + (8/5)A_2$$
$$- (2/3)A_0] + 24[(2/3)A_3 + (10/3)A_1]\}$$

$$\Gamma_7\int a^2 \sin^2\theta_a e^{-\kappa a}P_2(\cos\theta_b)(1/\kappa b)^3 dv$$

$$= (8\pi\Gamma_7/\kappa^5)[\gamma_5/3\alpha^3 - \Gamma_2/15 - 2\gamma_7/5\alpha^5]$$

$$\Gamma_7\int a^2 \cos^2\theta_a e^{-\kappa a}P_2(\cos\theta_b)(1/\kappa b)^3 dv$$

$$= (4\pi\Gamma_7/\kappa^5)[\gamma_5/3\alpha^3 + 2\Gamma_2/15 + 4\gamma_7/5\alpha^3 - \alpha^2 e^{-\alpha}/2]$$

$$\int a^2 \sin^2\theta_a e^{-\kappa a}(1/\kappa b)^3 P_2(\cos\theta_b)[\Gamma_7(\kappa b) - (\kappa b)^5\ \Gamma_2(\kappa b)]dv$$
$$= (2\pi\alpha^2/4\kappa^5)[(\alpha/2)^5\{-(4/3)(A_6 - A_4) + (64/7)(A_4 - A_2) - (12/7)(A_2 - A_0)\}$$
$$+ (\alpha/2)^4\{-8(A_5 - A_3) + 40(A_3 - A_1)\}$$
$$+ 15\alpha^3\{2(A_6 - A_4) - (76/15)(A_4 - A_2) + (62/15)(A_2 - A_0)\}$$
$$+ 90\alpha^2\{-8(A_5 - A_3) + (34/3)(A_3 - A_1)\}$$
$$+ 360\alpha\{(15/2)A_4 - (71/6)A_2 + (10/3)A_0\}]$$

$$\int a^2 \cos^2\theta_a e^{-\kappa a}(1/\kappa b)^3 P_2(\cos\theta_b)[\Gamma_7(\kappa b) - (\kappa b)^5\ \Gamma_2(\kappa b)]dv$$
$$= (2\pi\alpha^2/4\kappa^5)[(\alpha/2)^5\{(4/3)A_6 - (220/21)A_4 + (124/7)A_2 - 4A_0\}$$
$$+ (\alpha/2)^4\{8A_5 - 64A_3 + 88A_1\}$$
$$+ 15\alpha^3\{-2A_6 - (14/15)A_4 + (6/5)A_2 + (10/3)A_0\}$$
$$+ 90\alpha^2\{8A_5 + (14/3)A_3 - (26/3)A_1\}$$
$$+ 360\alpha\{-(23/2)A_4 - (25/6)A_2 + 2A_0\}$$
$$+ 720\{8A_3 + 2A_1\}]$$

$$\int a^2 \sin^2\theta_a e^{-\kappa a}(1/\kappa b)^3[\Gamma_7(\kappa b) - (\kappa b)^5\ \Gamma_2(\kappa b)]dv$$
$$= (2\pi\alpha^2/4\kappa^5)[5(\alpha/2)^5\{(4/3)(A_6 - A_4) - (4/35)(A_2 - A_0)\}$$
$$+ 30(\alpha/2)^4\{(4/3)(A_5 - A_3) - (4/15)(A_3 - A_1)\}$$
$$+ 15\alpha^3\{(4/3)(A_4 - A_2) - (4/15)(A_2 - A_0)\}$$
$$+ 120\alpha^2(A_3 - A_1) + 960(A_2 - A_0)]$$

$$\Gamma_7 \int a^2 \sin\theta_a \cos\theta_a \sin\theta_b \cos\theta_b e^{-\kappa a}(1/\kappa b)^3 dv$$
$$= (2\pi\Gamma_7/15\kappa^5\alpha^3)[-16\gamma_7(\alpha)/\alpha^2 + 4\alpha^3\Gamma_2(\alpha)]$$

$$\int a^2 \sin\theta_a \cos\theta_a \sin\theta_b \cos\theta_b e^{-\kappa a}(1/\kappa b)^3[\Gamma_7(\kappa b) - (\kappa b)^5\,\Gamma_2(\kappa b)]dv$$
$$= (2\pi\alpha^2/4\kappa^5)[(\alpha/2)^5\{(4/3)(A_6 - A_4) - (152/21)(A_4 - A_2) + (1/15)(A_2 - A_0)\}$$
$$+ (\alpha/2)^4\{8(A_5 - A_3) - 40(A_3 - A_1)\}$$
$$+ 20\alpha^3\{(A_6 - A_4) - (1/5)(A_4 - A_2) - 2(A_2 - A_0)\}$$
$$- 480\alpha^2(A_5 - A_3) + 360\alpha\{(23/3)A_4 - 5A_2 - 2A_0\} - 240\{16A_3 - 8A_1\}]$$

Evaluation of the integral

$$\int a^2 \cos^2\theta_a e^{-\kappa a} P_2(\cos\theta_b)(1/\kappa b)^3 dv = J$$

This is a conditionally convergent integral,[7] the value of which depends upon the particular coordinate system used. Since the companion integral has been evaluated in the λ, μ system (merely for convenience), this procedure must be followed here, even though much more laborious than the evaluation in the a, b, system. Setting $\rho = \alpha/2$,

$$J = \int\int e^{-\alpha(\lambda+\mu)/2}(2\pi/\kappa^5)(\alpha/2)^2(\lambda\mu+1)^2(1/(\lambda-\mu)^3)(\lambda^2-\mu^2)$$
$$\{1 - 3(\lambda^2-1)(1-\mu^2)/2(\lambda-\mu)^2\}\,d\lambda d\mu$$
$$= (2\pi\alpha^2/4\kappa^5)\Big[\int\int e^{-\rho(\lambda+\mu)}(\lambda\mu+1)^2(\lambda+\mu)/(\lambda-\mu)^2\cdot d\lambda d\mu$$
$$- (3/2)\int\int (\lambda^2-1)e^{-\rho(\lambda+\mu)}(\lambda\mu+1)^2\{(1-\lambda^2)(\lambda+\mu)/(\lambda-\mu)^4$$
$$+ (\lambda+\mu)^2/(\lambda-\mu)^3\}\,d\lambda d\mu\Big]$$
$$= (2\pi\alpha^2/4\kappa^5)\int_1^\infty e^{-\rho\lambda}d\lambda\,[I_0 - (3/2)(\lambda^2-1)\{(1-\lambda^2)I_1 + I_2\}]$$

where

$$I_0 = \int_{-1}^{1} d\mu e^{-\rho\mu}(\lambda\mu+1)^2(\lambda+\mu)/(\lambda-\mu)^2$$
$$I_1 = \int_{-1}^{1} d\mu e^{-\rho\mu}(\lambda\mu+1)^2(\lambda+\mu)/(\lambda-\mu)^4$$
$$I_2 = \int_{-1}^{1} d\mu e^{-\rho\mu}(\lambda\mu+1)^2(\lambda+\mu)^2/(\lambda-\mu)^3$$

$$I_0 = 2\lambda\{\lambda^2F(0) + 2\lambda(\lambda^2+1)F(1) + (\lambda^2+1)^2F(2)\} + \lambda^2F(-1)$$
$$+ 2\lambda(\lambda^2+1)F(0) + (\lambda^2+1)^2F(1)$$
$$I_1 = 2\lambda\{\lambda^2F(2) + 2\lambda(\lambda^2+1)F(3) + (\lambda^2+1)^2F(4)\} + \lambda^2F(1)$$
$$+ 2\lambda(\lambda^2+1)F(2) + (\lambda^2+1)^2F(3)$$
$$I_2 = -4\lambda^2\{\lambda^2F(1) + 2\lambda(\lambda^2+1)F(2) + (\lambda^2+1)^2F(3)\} - 4\lambda\{\lambda^2F(0)$$
$$+ 2\lambda(\lambda^2+1)F(1) + (\lambda^2+1)^2F(2)\} - \{\lambda^2F(-1) + 2\lambda(\lambda^2+1)F(0)$$
$$+ (\lambda^2+1)^2F(1)\}$$

$$J = (2\pi\alpha^2/4\kappa^5)\int_1^\infty e^{-\rho\lambda}d\lambda\{3\lambda(1-\lambda^4)^2F(4) + (3/2)(1-\lambda^4)(1-9\lambda^4)F(3)$$
$$+ (24\lambda^7 - \lambda^5 - 14\lambda^3 - \lambda)F(2) + (21\lambda^6 - 5\lambda^4/2 - 6\lambda^2 - 1/2)F(1)$$
$$+ (9\lambda^5 - 2\lambda^3 - \lambda)F(0) + (3\lambda^4/2 - \lambda^2/2)F(-1)\},$$

[7] This was not realized at first, and the a, b coordinate system was used. This gave a wrong result, and I wish to thank Mr. H. M. Mott-Smith, Jr. for his kindness in helping to locate the error.

Applying formula (3), one obtains

$$J = (4\pi/\kappa^5)(\gamma_5/3\alpha^3 + 2\Gamma_2/15 + 4\gamma_7/5\alpha^5 - \alpha^2 e^{-\alpha}/2).$$

This differs from the result using the a, b coordinate system in that the last term here does not occur in that result.

The integrals i_2, i_4, i_6, i_8, i_{10}, and i_{11}.

$$i_2 = c_1^4 \int dv_1 dv_2 a_1 \sin\theta_{a_1 b_1} \sin\theta_{b_1 a_2} \sin\theta_{a_2 b_2} \sin\theta_{b_2} e^{-(\kappa/2)(a_1+a_2+b_1+b_2)}(2/r)$$

$$i_4 = c_1^2 c_2^2 \int dv_1 dv_2 a_1 \sin\theta_{a_1 b_1} \sin\theta_{b_1 a_2} \cos\theta_{a_2 b_2} \cos\theta_{b_2} e^{-(\kappa/2)(a_1+a_2+b_1+b_2)}(2/r)$$

$$i_6 = c_1^2 c_2^2 \int dv_1 dv_2 a_1 \sin\theta_{a_1 b_1} \cos\theta_{b_1 a_2} \sin\theta_{a_2 b_2} \cos\theta_{b_2} \cos(\phi_1 - \phi_2) e^{-(\kappa/2)(a_1+a_2+b_1+b_2)}(2/r)$$

$$i_8 = c_1^4 \int dv_1 dv_2 a_1 \sin\theta_{a_1 b_1} \sin\theta_{b_1 a_2} \sin\theta_{a_2 b_2} \sin\theta_{b_2} \cos 2(\phi_1 - \phi_2) e^{-(\kappa/2)(a_1+a_2+b_1+b_2)}(2/r)$$

$$i_{10} = c_2^4 \int dv_1 dv_2 a_1 \cos\theta_{a_1 b_1} \cos\theta_{b_1 a_2} \cos\theta_{a_2 b_2} \cos\theta_{b_2} e^{-(\kappa/2)(a_1+a_2+b_1+b_2)}(2/r)$$

$$i_{11} = c_1^2 c_2^2 \int dv_1 dv_2 a_1 \cos\theta_{a_1 b_1} \sin\theta_{b_1 a_2} \sin\theta_{a_2 b_2} \cos\theta_{b_2} \cos(\phi_1 - \phi_2) e^{-(\kappa/2)(a_1+a_2+b_1+b_2)}(2/r).$$

We use Neumann's expansion:

$$\frac{1}{r} = \frac{2}{R} \sum_{\tau=0}^{\infty} \sum_{\nu=0}^{\tau} D_{\tau\nu} P_\tau^\nu \begin{pmatrix} \lambda_1 \\ \lambda_2 \end{pmatrix} Q_\tau^\nu \begin{pmatrix} \lambda_2 \\ \lambda_1 \end{pmatrix} P_\tau^\nu(\mu_1) P_\tau^\nu(\mu_2) \cos\nu(\phi_1 - \phi_2)$$

the upper arguments for $\lambda_2 > \lambda_1$, and the lower for $\lambda_2 < \lambda_1$

$$D_{\tau\nu} = (-1)^\nu \epsilon_\nu (2\tau + 1) \left[\frac{(\tau - \nu)!}{(\tau + \nu)!}\right]^2, \quad \epsilon_0 = 1, \ \epsilon_1 = \epsilon_2 = \cdots = 2.$$

One does not need to concern oneself as to whether the above series converges rapidly or not (for the integrals in question), for orthogonality relations reduce the number of terms to three or four. In general, but not always, the second term is so small compared with the first that its contribution may be neglected.

Let us denote the terms arising from $\tau = 0$ by $i_2^{(0)}$, $i_4^{(0)}$, etc. Also, let

$$\sigma_\tau(m, n, \alpha) = \int_1^\infty Q_\tau(\lambda) e^{-\alpha\lambda/2} \lambda^m A_n\left(\lambda, \frac{\alpha}{2}\right) d\lambda$$

$$= \sum_{\nu=0}^{n} (n!/\nu!) f_\tau(m + \nu, \alpha)(\alpha/2)^{\nu-n-1}$$

$$s_\tau(m, n, \alpha) = \int_1^\infty Q_\tau(\lambda_1) e^{-\alpha\lambda_1/2} \lambda_1^m d\lambda_1 \int_1^{\lambda_1} e^{-\alpha\lambda_2/2} \lambda_2^n d\lambda_2$$

$$= f_\tau(m, \alpha/2)\, A_n(1, \alpha/2) - \sigma_\tau(m, n, \alpha)$$

Tables of σ_τ, s_τ, etc. are given later.

$$i_2^{(0)} = 2c_1^4(2\pi)^2(R/2)^9 \int (\lambda_1^2 - 1)(1 - \mu_1)^2(\lambda_2^2 - 1)(1 - \mu_2^2)(\lambda_1^2 - \mu_1^2)$$

$$(\lambda_2^2 - \mu_2^2) Q_0 \binom{\lambda_2}{\lambda_1} e^{-\kappa R(\lambda_1+\lambda_2)/2} d\mu_1 d\mu_2 d\lambda_1 d\lambda_2$$

$$= (2\kappa/1024)(\alpha/2)^9 \int (\lambda_1^2 - 1)(\lambda_2^2 - 1)(4/3)^2(\lambda_1^2 - 1/5)$$

$$(\lambda_2^2 - 1/5) Q_0 \binom{\lambda_2}{\lambda_1} e^{-\kappa R(\lambda_1+\lambda_2)/2} d\lambda_1 d\lambda_2$$

$$= (\kappa/144)(\alpha/2)^9 \{s_0(00)/25 + 36s_0(22)/25 + s_0(44) - 6[s_0(02) + s_0(20)]/25$$
$$+ [s_0(04) + s_0(40)]/5 - 6[s_0(24) + s_0(42)]/5\}$$

$$i_4^{(0)} = (\kappa/144)(\alpha/2)^9 \{s_0(00)/5 + 108s_0(22)/25 + s_0(44) - 24[s_0(02) + s_0(20)]/25$$
$$+ 3[s_0(04) + s_0(40)]/5 - 12[s_0(42) + s_0(24)]/5\}$$

$$i_{10}^{(0)} = (\kappa/16)(\alpha/2)^9 [\{s_0(00) + s_0(04) + s_0(40) + s_0(44)\}/9 + 36s_0(22)/25$$
$$- 2\{s_0(02) + s_0(20) + s_0(42) + s_0(24)\}/5]$$

Let

$$t_2(2m, 2n, \alpha) = \int_1^\infty Q_2(\lambda_1) e^{-\alpha\lambda_1/2} \lambda_1^{2m} d\lambda_1 \int_1^{\lambda_1} P_2(\lambda_2) e^{-\alpha\lambda_2/2} \lambda_2^{2n} d\lambda_2$$
$$= (3/2)s_2(2m, 2n + 2) - (\tfrac{1}{2})s_2(2m, 2n).$$

Then

$$i_2^{(2)} = 10c_1^4(2\pi)^2(R/2)^9 \int (\lambda_1^2 - 1)(1 - \mu_1)^2(\lambda_2^2 - 1)(1 - \mu_2^2)(\lambda_1^2 - \mu_1^2)$$
$$(\lambda_2^2 - \mu_2^2) e^{-\alpha(\lambda_1+\lambda_2)/2} \cdot Q_2 \binom{\lambda_2}{\lambda_1} P_2 \binom{\lambda_1}{\lambda_2} P_2(\mu_1) P_2(\mu_2) d\mu_1 d\mu_2 d\lambda_1 d\lambda_2$$

$$= 10c_1^4(2\pi)^2(R/2)^9 \int (4/15)^2(\lambda_1^2 - 1)(\lambda_2^2 - 1)(\lambda_1^2 + 1/7)$$

$$(\lambda_2^2 + 1/7) Q_2 \binom{\lambda_2}{\lambda_1} P_2 \binom{\lambda_1}{\lambda_2} e^{-\alpha(\lambda_1+\lambda_2)/2} d\lambda_1 d\lambda_2$$

$$= (\kappa/720)(\alpha/2)^9 [t_2(00)/49 + 36t_2(22)/49 + t_2(44) + 6\{t_2(02) + t_2(20)\}/49$$
$$- \{t_2(04) + t_2(40)\}/7 - 6\{t_2(24) + t_2(42)\}/7]$$

$$i_4^{(2)} = -(\kappa/120)(\alpha/2)^9 [-t_2(00)/21 + 12t_2(22)/49 + t_2(44)/3$$
$$- 6\{t_2(02) + t_2(20)\}/49 + \{t_2(04) + t_2(40)\}/7 - 2\{t_2(24) + t_2(42)\}/7]$$

$$i_{10}^{(2)} = (\kappa/20)(\alpha/2)^9 [\{t_2(00) + t_2(04) + t_2(40) + t_2(44)\}/9 + 4t_2(22)/49$$
$$- 2\{t_2(02) + t_2(20) + t_2(42) + t_2(24)\}/21]$$

Let

$$u_4(2m, 2n) = \int_1^\infty Q_4(\lambda_1)e^{-\alpha\lambda_1/2}\lambda_1^{2m}d\lambda_1 \int_1^{\lambda_1} P_4(\lambda_2)e^{-\alpha\lambda_2/2}\lambda_2^{2n}d\lambda_2$$
$$= (1/8)[35s_4(2m, 2n+4) - 30s_4(2m, 2n+2) + 3s_4(2m, 2n)]$$

Then

$$i_2^{(4)} = 18c_1^4(2\pi)^2(R/2)^9(16/315)^2 \int (\lambda_1^2-1)(\lambda_2^2-1)e^{-\alpha(\lambda_1+\lambda_2)/2}Q_4\binom{\lambda_2}{\lambda_1}P_4\binom{\lambda_1}{\lambda_2}d\lambda_1 d\lambda_2$$
$$= \kappa(1/105)^2(\alpha/2)^9[u_4(00) - u_4(02) - u_4(20) + u_4(22)].$$

The other integrals for $\tau = 4$ will be somewhat similar. Since the contributions from $\tau = 2$ are small with respect to those from $\tau = 0$, the influence of $\tau = 4$ has been neglected.

$$i_6^{(1)} = -c_1^2c_2^2(2\pi)^2D_{11}(R/2)^9 \int \frac{dP_1}{d\lambda}\binom{\lambda_1}{\lambda_2}\frac{dQ_1}{d\lambda}\binom{\lambda_2}{\lambda_1}(\lambda_1^2-1)(\lambda_2^2-1)(4/3)^2$$
$$(\lambda_1^2 - \tfrac{1}{5})(\lambda_2^2 - \tfrac{1}{5})e^{-\alpha(\lambda_1+\lambda_2)/2}d\lambda_1 d\lambda_2$$
$$= (\kappa/96)(\alpha/2)^9[\{s_1(12) - s_1(10) - s_0(02) + s_0(00)\}/25 + \{s_1(34) - s_1(32) - s_0(24) + s_0(22)\} - (\tfrac{1}{5})\{s_1(14) - s_1(12) + s_1(32) - s_1(30) - s_0(04) + s_0(02) - s_0(22) + s_0(20)\}]$$

$$i_6^{(2)} = (3\kappa/160)(\alpha/2)^9[\{s_2(24) - s_2(22) - s_1(14) + s_1(12)\}/49 + \{s_2(46) - s_2(44) - s_1(36) + s_1(34)\}/9 - (1/21)\{s_2(26) - s_2(24) - s_1(16) + s_1(14) + s_2(44) - s_2(42) - s_1(34) + s_1(32)\}]$$

$$i_{11}^{(1)} = -c_1^2c_2^2(2\pi)^2D_{11}(R/2)^9 \int (\lambda_1\mu_1 - 1)(\lambda_2\mu_2 - 1)(\lambda_1^2 - 1)(\lambda_2^2 - 1)$$
$$(\lambda_1^2 - \mu_1^2)(\lambda_2^2 - \mu_2^2)e^{-\alpha(\lambda_1+\lambda_2)/2}\frac{dP_1}{d\lambda}\binom{\lambda_1}{\lambda_2}\frac{dQ_1}{d\lambda}\binom{\lambda_2}{\lambda_1}$$
$$P_1'(\mu_1)P_1'(\mu_1)P_1'(\mu_2)P_1'(\mu_2)d\lambda_1 d\lambda_2 \cdot d\mu_1 d\mu_2$$
$$= -i_6^{(1)} \quad i_{11}^{(2)} = i_6^{(2)}, \text{ etc.}$$

For the evaluation of $i_8^{(2)}$, we use the formula

$$(\lambda^2 - 1)^2\frac{d^2Q_2}{d\lambda^2} = 2[(\lambda^2 - 1)Q_2 - \lambda Q_1 + Q_0]$$

$$i_8^{(2)} = 3c_1^4(2\pi)^2D_{22}(R/2)^9 \int (\lambda_1^2 - 1)^2(\lambda_2^2 - 1)^2\frac{d^2Q_2}{d\lambda^2}\binom{\lambda_2}{\lambda_1}(16/5)^2$$
$$(\lambda_1^2 - 1/7)(\lambda_2^2 - 1/7)e^{-\alpha(\lambda_1+\lambda_2)/2}d\lambda_1 d\lambda_2$$
$$= (\kappa/480)(\alpha/2)^9[s_2(44) + (1/7)\{s_2(04) + s_1(14)\} + s_0(24) - 8s_2(24)/7 - s_1(34) - s_0(04)/7 - (8/7)\{s_2(42) + (1/7)\{s_2(02) + s_1(12)\} + s_0(22) - 8s_2(22)/7 - s_1(32) - s_0(02)/7\} + (1/7)\{s_2(40) + (1/7)\{s_2(00) + s_1(10)\} + s_0(20) - 8s_2(20)/7 - s_1(30) - s_0(00)/7\}].$$

TABLE I. $A_m(1, \alpha)$.

α	$\alpha=1.5$	2.0	2.5	3.0	3.5	4.0	4.5	5.0	6.0	7.0	8.0	9.0	10.0
$A_0(1, \alpha)$	0.14875	0.06767	0.032834	0.01660	$0.0^{2}8628$	$0.0^{2}4579$	$0.0^{2}24687$	$0.0^{2}13476$	$0.0^{3}4131$	$0.0^{3}1303$	$0.0^{4}4193$	$0.0^{4}1371$	$0.0^{5}4540$
$A_1(1, \alpha)$	.24792	.10151	.04597	.02213	.011093	$.0^{2}5724$	$.0^{3}3017$	$.0^{2}1617$	$.0^{3}4820$	$.0^{3}1489$	$.0^{4}4717$	$.0^{4}1524$	$.0^{5}4994$
$A_2(1, \alpha)$	.4793	.16917	.06961	.03135	.014967	$.0^{2}7441$	$.0^{3}3810$	$.0^{2}1994$	$.0^{3}5738$	$.0^{3}1728$	$.0^{4}5373$	$.0^{4}1710$	$.0^{5}5539$
$A_3(1, \alpha)$	1.1074	.32142	.11637	.04795	.02145	.010160	$.0^{2}5008$	$.0^{2}2544$	$.0^{3}6999$	$.0^{3}2043$	$.0^{4}6209$	$.0^{4}1941$	$.0^{5}6202$
$A_4(1, \alpha)$	3.1018	.7105	.21902	.08051	.03315	.01474	$.0^{2}6920$	$.0^{2}3383$	$.0^{3}8799$	$.0^{3}2470$	$.0^{4}7300$	$.0^{4}2233$	$.0^{5}7021$
$A_5(1, \alpha)$	10.488	1.844	.4709	.1508	.05598	.02300	.010158	$.0^{2}4730$	$.0^{3}11464$	$.0^{3}3067$	$.0^{4}8755$	$.0^{4}2612$	$.0^{5}8050$
$A_6(1, \alpha)$	42.10	5.599	1.1629	.3182	.10459	.03907	.016011	$.0^{2}7024$	$.0^{3}15596$	$.0^{3}3931$	$.0^{3}10760$	$.0^{4}3110$	$.0^{5}9371$
$A_7(1, \alpha)$				.7588		.07296		.01118	$.0^{2}2232$	$.0^{3}5234$	$.0^{3}1361$	$.0^{4}3790$	$.0^{4}11100$
$A_8(1, \alpha)$				2.0405		.1505		.01924	$.0^{3}3389$	$.0^{3}7285$	$.0^{3}1780$	$.0^{4}4740$	$.0^{4}1342$
$A_9(1, \alpha)$				6.138		.3432		.03598	$.0^{2}5497$	$.0^{2}10669$	$.0^{3}2422$	$.0^{4}6111$	$.0^{4}16617$
$A_{10}(1, \alpha)$				20.48		.8627		.07331	$.0^{2}9575$	$.0^{2}16544$	$.0^{3}3447$	$.0^{4}8162$	$.0^{4}2116$
$A_{11}(1, \alpha)$				75.10		2.377		.1625	.017969	$.0^{2}2730$	$.0^{3}5159$	$.0^{3}11346$	$.0^{4}2781$

TABLE II. $f_1(m, \alpha)$

α	$\alpha=1.5$	2.0	2.5	3.0	3.5	4.0	4.5	5.0	6.0	7.0	8.0	9.0	10.0
$f_1(0, \alpha)$	0.05250	0.02850	0.01575	$0.0^{2}8810$	$0.0^{2}4977$	$0.0^{2}2831$	$0.0^{2}1620$	$0.0^{3}9315$	$0.0^{3}3115$	$0.0^{3}1054$	$0.0^{4}3600$	$0.0^{4}1238$	$0.0^{5}428$
$f_1(1, \alpha)$	.06535	.03425	.01846	.010141	$.0^{2}5647$	$.0^{3}3176$	$.0^{3}1800$	$.0^{2}10271$	$.0^{3}3392$	$.0^{3}1137$	$.0^{4}3854$	$.0^{4}1317$	$.0^{5}4536$
$f_1(2, \alpha)$	.08714	.04316	.02242	.011997	$.0^{2}6551$	$.0^{3}3628$	$.0^{3}2031$	$.0^{2}11473$	$.0^{3}3733$	$.0^{3}1236$	$.0^{4}4152$	$.0^{4}1409$	$.0^{5}482$
$f_1(3, \alpha)$	.1285	.05823	.02861	.014732	$.0^{2}7825$	$.0^{3}4244$	$.0^{3}2337$	$.0^{2}13028$	$.0^{3}4152$	$.0^{3}1356$	$.0^{4}4505$	$.0^{4}1516$	$.0^{5}515$
$f_1(4, \alpha)$	.2194	.0866	.03909	.019034	$.0^{2}9720$	$.0^{3}5120$	$.0^{3}2759$	$.0^{2}15105$	$.0^{3}4691$	$.0^{3}1504$	$.0^{4}4932$	$.0^{4}1643$	$.0^{5}554$
$f_1(5, \alpha)$	.455	.1474	.0587	.02635	.012722	$.0^{2}6436$	$.0^{3}3364$	$.0^{2}17986$	$.0^{3}5400$	$.0^{3}1693$	$.0^{4}5457$	$.0^{4}1795$	$.0^{5}599$
$f_1(6, \alpha)$				.03999		$.0^{2}8538$		$.0^{2}2217$	$.0^{3}6364$	$.0^{3}1936$	$.0^{4}6115$	$.0^{4}1981$	$.0^{5}653$
$f_1(7, \alpha)$				.06808		.012147		$.0^{2}2856$	$.0^{3}7727$	$.0^{3}2264$	$.0^{4}6960$	$.0^{4}2213$	$.0^{5}720$
$f_1(8, \alpha)$				.13248		.018856		$.0^{2}3894$	$.0^{3}9744$	$.0^{3}2715$	$.0^{4}8076$	$.0^{4}2507$	$.0^{5}800$
$f_1(9, \alpha)$				.2970		.03243		$.0^{2}5693$	$.0^{3}1288$	$.0^{3}3368$	$.0^{4}9595$	$.0^{4}2892$	$.0^{5}904$
$f_1(10, \alpha)$				.7642		.06244		$.0^{2}916$	$.0^{3}1805$	$.0^{3}4350$	$.0^{3}1174$	$.0^{4}3409$	$.0^{4}1036$
$f_1(11, \alpha)$				2.231		.1351		.01602	$.0^{2}2710$	$.0^{3}5906$	$.0^{3}1489$	$.0^{4}4124$	$.0^{4}1213$

The integrals $i_6^{(3)}$, $i_6^{(4)}$, and $i_8^{(4)}$ have been assumed negligible, because of the smallness of the preceding terms.

TABLE III. $\sigma_0(m, n, \alpha)$

α	$\alpha=3$	4	5	6	7	8	9	10
$\sigma_0(0,0,\alpha)$	0.01391	$0.0^2$3170	$0.0^3$800	$0.0^3$2162	$0.0^4$611	$0.0^4$1787	$0.0^5$536	$0.0^5$1644
$\sigma_0(0,2,\alpha)$	.05647	$.0^2$9742	$.0^2$2043	$.0^3$4827	$.0^3$1235	$.0^4$3340	$.0^5$942	$.0^5$2743
$\sigma_0(0,4,\alpha)$	.4202	.04750	$.0^2$7474	$.0^2$1436	$.0^3$3149	$.0^4$7565	$.0^4$1942	$.0^5$5245
$\sigma_0(2,0,\alpha)$	.02152	$.0^2$445	$.0^2$1058	$.0^3$2737	$.0^4$7504	$.0^4$2143	$.0^5$6313	$.0^5$1906
$\sigma_0(2,2,\alpha)$	.09948	.01496	$.0^2$2884	$.0^3$6430	$.0^3$1577	$.0^4$4138	$.0^4$1138	$.0^5$3252
$\sigma_0(2,4,\alpha)$	.8257	.07945	.01128	$.0^2$2019	$.0^3$4203	$.0^4$9714	$.0^4$2419	$.0^5$6378
$\sigma_0(4,0,\alpha)$	.04180	$.0^2$720	$.0^2$1539	$.0^3$3717	$.0^4$9714	$.0^4$2679	$.0^5$768	$.0^5$2270
$\sigma_0(4,2,\alpha)$	.2438	.02824	$.0^2$4674	$.0^3$9446	$.0^3$2168	$.0^4$5417	$.0^4$1438	$.0^5$3995
$\sigma_0(4,4,\alpha)$	2.4886	.1748	.02051	$.0^2$3237	$.0^3$6183	$.0^3$13424	$.0^4$3192	$.0^5$8122

TABLE IV. $s_0(m,n,\alpha)$

α	$\alpha=3$	4	5	6	7	8	9	10.
$S_0(0,0,\alpha)$	$0.0^2$753	$0.0^2$1798	$0.0^3$470	$0.0^3$1302	$0.0^4$375	$0.0^4$1117	$0.0^5$340	$0.0^5$1055
$S_0(0,2,\alpha)$	.01261	$.0^2$2678	$.0^3$650	$.0^3$1715	$.0^4$476	$.0^4$1378	$.0^5$410	$.0^5$1251
$S_0(0,4,\alpha)$	.0268	$.0^2$466	$.0^2$1000	$.0^3$243	$.0^4$640	$.0^4$1780	$.0^5$514	$.0^5$1528
$S_0(2,0,\alpha)$	.02508	$.0^2$474	$.0^2$1058	$.0^3$2620	$.0^4$694	$.0^4$1933	$.0^5$5580	$.0^5$1659
$S_0(2,2,\alpha)$	.05069	$.0^2$800	$.0^2$1601	$.0^3$370	$.0^4$928	$.0^4$2485	$.0^5$697	$.0^5$2023
$S_0(2,4,\alpha)$	.1460	.01700	$.0^2$283	$.0^3$580	$.0^3$1345	$.0^4$3405	$.0^5$914	$.0^5$2569
$S_0(4,0,\alpha)$	.1421	.01849	$.0^2$3221	$.0^3$669	$.0^3$1555	$.0^4$3917	$.0^4$1045	$.0^5$2916
$S_0(4,2,\alpha)$	.3485	.03599	$.0^2$5417	$.0^2$1022	$.0^3$2214	$.0^4$5301	$.0^4$1360	$.0^5$3681
$S_0(4,4,\alpha)$	1.345	.0949	.01124	$.0^2$1812	$.0^3$3520	$.0^4$7803	$.0^4$1891	$.0^5$490

TABLE V. $\sigma_1(m,n,\alpha)$

α	$\alpha=3$	4	5	6	7	8	9	10
$\sigma_1(1,0,\alpha)$	$0.0^2$6761	$0.0^2$1588	$0.0^3$41080	$.0^3$11307	$0.0^4$3249	$0.0^5$9636	$0.0^5$2927	$0.0^6$907
$\sigma_1(1,2,\alpha)$	.02649	$.0^2$4730	$.0^2$10197	$.0^3$2464	$.0^4$6422	$.0^4$1765	$.0^5$5049	$.0^5$1488
$\sigma_1(1,4,\alpha)$	.1927	.02253	$.0^3$3644	$.0^3$7171	$.0^3$1604	$.0^4$3921	$.0^4$10227	$.0^5$2799
$\sigma_1(1,6,\alpha)$	2.7214	.18784	.020763	$.0^2$3072	$.0^3$5523	$.0^3$11383	$.0^4$2594	$.0^5$6367
$\sigma_1(3,0,\alpha)$	$.0^2$9821	$.0^2$2122	$.0^3$5211	$.0^3$1384	$.0^4$3874	$.0^4$11264	$.0^5$3369	$.0^5$1030
$\sigma_1(3,2,\alpha)$	.04322	$.0^2$6839	$.0^2$13697	$.0^3$3150	$.0^4$7926	$.0^4$2121	$.0^5$5944	$.0^5$1722
$\sigma_1(3,4,\alpha)$	.3470	.03513	$.0^2$5194	$.0^2$9602	$.0^2$2055	$.0^4$4860	$.0^4$12354	$.0^5$3311
$\sigma_1(3,6,\alpha)$	5.177	.3079	.03096	$.0^2$4280	$.0^2$7327	$.0^3$1454	$.0^4$3217	$.0^5$7703

TABLE VI. $s_1(m, n, \alpha)$

α	$\alpha=3$	4	5	6	7	8	9	10
$S_1(1,0,\alpha)$	$0.0^2$2959	$0.0^3$730	$0.0^3$1953	$0.0^4$5525	$0.0^4$1623	$0.0^5$4907	$0.0^5$1518	$0.0^6$477
$S_1(1,2,\alpha)$	$.0^2$482	$.0^2$1064	$.0^2$2653	$.0^4$715	$.0^4$2030	$.0^5$599	$.0^5$1808	$.0^6$5607
$S_1(1,4,\alpha)$	$.0^2$998	$.0^2$1804	$.0^3$399	$.0^4$994	$.0^4$2678	$.0^5$760	$.0^5$2230	$.0^6$676
$S_1(1,6,\alpha)$	.0296	$.0^2$390	$.0^3$705	$.0^3$1544	$.0^4$383	$.0^4$103	$.0^5$2885	$.0^6$847
$S_1(3,0,\alpha)$	$.0^2$929	$.0^2$1818	$.0^3$4182	$.0^3$10612	$.0^4$2877	$.0^5$8169	$.0^5$2401	$.0^6$7253
$S_1(3,2,\alpha)$	.01837	$.0^2$300	$.0^3$6216	$.0^3$1468	$.0^3$3786	$.0^4$1037	$.0^5$2960	$.0^6$877
$S_1(3,4,\alpha)$	.0516	$.0^2$625	$.0^2$1070	$.0^2$2259	$.0^4$538	$.0^4$1395	$.0^5$3821	$.0^5$1096
$S_1(3,6,\alpha)$	.232	.0176	$.0^2$230	$.0^3$407	$.0^4$857	$.0^4$204	$.0^5$526	$.0^5$1448

RESULTS

The results have been tabulated in Tables I–XV. The values are based partly on integral logarithm tables given by Jahnke–Emde, and the accuracy

is limited thereby. The tables are, therefore, subject to revision on this account. Except for this, they are accurate up to a possible change of the last figure. In this connection, it is urged that the tabular method is the economical one, in that the calculations may be checked easily.

TABLE VII. $\sigma_2(m,n,\alpha)$

α	$\alpha=3$	4	5	6	7	8	9	10
$\sigma_2(0,0,\alpha)$	$0.0^{3}3185$	$0.0^{3}797$	$0.0^{3}2158$	$0.0^{4}6154$	$0.0^{4}1818$	$0.0^{5}552$	$0.0^{5}1709$	$0.0^{6}540$
$\sigma_2(0,2,\alpha)$	.011511	$.0^{2}2225$	$.0^{3}5079$	$.0^{3}12825$	$.0^{4}3459$	$.0^{5}979$	$.0^{5}2865$	$.0^{5}0861$
$\sigma_2(0,4,\alpha)$	.0792	.01004	$.0^{2}1729$	$.0^{3}3574$	$.0^{4}8318$	$.0^{4}2099$	$.0^{5}5628$	$.0^{5}1576$
$\sigma_2(0,6,\alpha)$	1.092	.0814	$.0^{2}955$	$.0^{2}1484$	$.0^{3}2777$	$.0^{4}5917$	$.0^{4}1388$	$.0^{5}3492$
$\sigma_2(2,0,\alpha)$	$.0^{2}3976$	$.0^{3}958$	$.0^{3}2528$	$.0^{4}708$	$.0^{4}2060$	$.0^{5}618$	$.0^{5}1897$	$.0^{6}593$
$\sigma_2(2,2,\alpha)$	.01511	$.0^{2}2775$	$.0^{3}6130$	$.0^{3}1510$	$.0^{4}4001$	$.0^{4}1113$	$.0^{5}3224$	$.0^{6}960$
$\sigma_2(2,4,\alpha)$	.10773	.01295	$.0^{2}2147$	$.0^{3}4311$	$.0^{4}981$	$.0^{4}2433$	$.0^{5}6432$	$.0^{5}1780$
$\sigma_2(2,6,\alpha)$	1.509	.1069	.01209	$.0^{2}1823$	$.0^{3}3335$	$.0^{4}6970$	$.0^{4}1609$	$.0^{5}3991$
$\sigma_2(4,0,\alpha)$	$.0^{2}545$	$.0^{2}1224$	$.0^{3}310$	$.0^{4}8415$	$.0^{4}2401$	$.0^{5}7066$	$.0^{5}2142$	$.0^{6}663$
$\sigma_2(4,2,\alpha)$	.02296	$.0^{3}3799$	$.0^{3}789$	$.0^{3}1862$	$.0^{4}4789$	$.0^{4}1305$	$.0^{5}3712$	$.0^{5}1090$
$\sigma_2(4,4,\alpha)$	.1787	.01892	$.0^{2}2904$	$.0^{3}5533$	$.0^{3}1214$	$.0^{4}2926$	$.0^{5}7566$	$.0^{5}2053$
$\sigma_2(4,6,\alpha)$	2.63	.1628	.01729	$.0^{2}2418$	$.0^{3}4247$	$.0^{4}8588$	$.0^{4}1937$	$.0^{5}4696$

TABLE VIII. $s_2(m,n,\alpha)$

α	$\alpha=3$	4	5	6	7	8	9	10
$S_2(0,0,\alpha)$	$0.0^{3}677$	$0.0^{3}195$	$0.0^{4}582$	$0.0^{4}1778$	$0.0^{5}558$	$0.0^{5}178$	$0.0^{6}577$	$0.0^{6}187$
$S_2(0,2,\alpha)$	$.0^{3}93$	$.0^{3}255$	$.0^{4}728$	$.0^{4}216$	$.0^{5}664$	$.0^{5}208$	$.0^{6}662$	$.0^{6}214$
$S_2(0,4,\alpha)$	$.0^{2}135$	$.0^{3}37$	$.0^{4}98$	$.0^{4}274$	$.0^{5}81$	$.0^{5}251$	$.0^{6}778$	$.0^{6}249$
$S_2(0,6,\alpha)$	$.0^{2}12$	$.0^{2}07$	$.0^{3}150$	$.0^{4}373$	$.0^{4}104$	$.0^{5}313$	$.0^{6}94$	$.0^{6}298$
$S_2(2,0,\alpha)$	$.0^{2}139$	$.0^{3}360$	$.0^{4}983$	$.0^{4}282$	$.0^{5}845$	$.0^{6}259$	$.0^{6}811$	$.0^{6}259$
$S_2(2,2,\alpha)$	$.0^{2}22$	$.0^{3}51$	$.0^{3}131$	$.0^{4}360$	$.0^{4}1037$	$.0^{5}313$	$.0^{6}957$	$.0^{6}300$
$S_2(2,4,\alpha)$	$.0^{2}43$	$.0^{3}88$	$.0^{3}195$	$.0^{4}491$	$.0^{4}1345$	$.0^{5}391$	$.0^{5}1162$	$.0^{6}359$
$S_2(2,6,\alpha)$	.011	$.0^{2}21$	$.0^{3}35$	$.0^{4}75$	$.0^{4}187$	$.0^{5}52$	$.0^{5}147$	$.0^{6}449$
$S_2(4,0,\alpha)$	$.0^{2}41$	$.0^{3}893$	$.0^{3}201$	$.0^{4}518$	$.0^{4}143$	$.0^{5}415$	$.0^{5}1247$	$.0^{6}381$
$S_2(4,2,\alpha)$	$.0^{2}79$	$.0^{2}1494$	$.0^{3}295$	$.0^{4}705$	$.0^{4}186$	$.0^{5}517$	$.0^{5}1517$	$.0^{6}455$
$S_2(4,4,\alpha)$	.021	$.0^{3}331$	$.0^{3}51$	$.0^{3}1061$	$.0^{4}260$	$.0^{5}683$	$.0^{5}1932$	$.0^{6}568$
$S_2(4,6,\alpha)$	.08	.0124	$.0^{3}81$	$.0^{3}188$	$.0^{4}41$	$.0^{5}98$	$.0^{5}261$	$.0^{6}745$

TABLE IX. $S_{mm}'(\alpha/2)$, *etc.*

α	$\alpha=3$	4	5	6	7	8	9	10
$(S_{00})^{1/2}$	0.4825	0.2256	$0.0^{2}5086$	−0.1597	−0.2649	−0.3187	−0.3326	−0.3190
S_{00}	.2328	.05088	$.0^{4}2587$	.02556	.07020	.10156	.11062	.10174
$(S_{11})^{1/2}$	.8089	.6947	.5778	.4679	.3702	.2871	.2185	.16405
S_{11}	.6542	.4826	.3339	.2189	.13695	.08241	.04774	.02692
S_{10}	.3903	.1567	$.0^{2}2939$	−.0747	−.09807	−.09147	−.07268	−.05233

In order not to make the labor prohibitive in other cases, some more straightforward method should be employed to obtain the entries for $s_2(m, n, \alpha)$ and similar quantities. As it is, the accuracy for small values of α is quite small. This is not serious, however, for the approximation method itself can be expected to give good results only for large values of the internuclear distance.

TABLE X. *List of Integrals*

	$\nu = 0$	$\nu = 1$	$\nu = 2$	$\nu = 3$	$\nu = 4$
$\int_{-1}^{1} (\lambda+\mu)^3(\lambda-\mu)^\nu d\mu$	$2\lambda(\lambda^2+1)$	$2\left(\lambda^4-\frac{1}{5}\right)$	$2\lambda\left(\lambda^4-\frac{2}{3}\lambda^2+\frac{1}{5}\right)$	$2\left(\lambda^6-\lambda^4+\frac{3}{5}\lambda^2-\frac{1}{7}\right)$	$2\lambda\left(\lambda^6-\lambda^4+\frac{3}{5}\lambda^2-\frac{1}{7}\right)$
$\int (1-\mu^2)^2(\lambda+\mu)(\lambda-\mu)^\nu d\mu$	$\frac{16}{15}\lambda$	$\frac{16}{15}\left(\lambda^2-\frac{1}{7}\right)$	$\frac{16}{15}\lambda\left(\lambda^2-\frac{1}{7}\right)$		
$\int (\lambda\mu+1)^2(\lambda+\mu)$	$\frac{2}{3}\lambda(\lambda^2+5)$	$\frac{2}{3}\lambda^4+\frac{8}{5}\lambda^2-\frac{2}{3}$	$\frac{2}{3}\lambda^5+\frac{4}{15}\lambda^3+\frac{2}{15}\lambda$	$\frac{2}{3}\lambda^6-\frac{2}{3}\lambda^4$	$\frac{2}{3}\lambda^7-\frac{6}{5}\lambda^5$
$\cdot(\lambda-\mu)^\nu d\mu$				$+\frac{46}{35}\lambda^2-\frac{2}{5}$	$+\frac{218}{105}\lambda^3-\frac{22}{35}\lambda$
$\int (\lambda\mu+1)^2(\lambda+\mu)$	$\frac{4}{15}\lambda^3+\frac{28}{15}\lambda$	$\frac{4}{15}\lambda^4+\frac{128}{105}\lambda^2-\frac{4}{15}$	$\frac{4}{15}\lambda^5+\frac{24}{35}\lambda^3-\frac{4}{105}\lambda$		
$(1-\mu^2)(\lambda-\mu)^\nu d\mu$					
$\int (1-\mu^2)(\lambda+\mu)^3$	$\frac{4}{3}\lambda^3+\frac{12}{15}\lambda$	$\frac{4}{3}\lambda^4-\frac{4}{35}$	$\frac{4}{3}\lambda^5-\frac{8}{15}\lambda^3+\frac{4}{35}\lambda$		
$\cdot(\lambda-\mu)^\nu d\mu$					
$\int (1-\mu^2)(\lambda+\mu)\cdot(\lambda-\mu)^\nu d\mu$	$\frac{4}{3}\lambda$	$\frac{4}{3}\lambda^2-\frac{4}{15}$	$\frac{4}{3}\lambda^3-\frac{4}{15}\lambda$	$\frac{4}{3}\lambda^4-\frac{4}{35}$	$\frac{4}{3}\lambda^5+\frac{8}{15}\lambda^3-\frac{12}{35}\lambda$
$\int (1-\mu^2)(\lambda^2\mu^2-1)$	$\frac{4}{15}\lambda^3-\frac{4}{3}\lambda$	$\frac{4}{15}\lambda^4-\frac{152}{105}\lambda^2+\frac{4}{15}$	$\frac{4}{15}\lambda^5-\frac{152}{105}\lambda^3+\frac{4}{15}\lambda$		
$\cdot(\lambda+\mu)(\lambda-\mu)^\nu d\mu$					
$\int (\lambda\mu-1)(\lambda^2-\mu^2)$	$-\frac{4}{3}\left(\lambda^2-\frac{1}{5}\right)$				
$\cdot(1-\mu^2)d\mu$					
$\int (\lambda+\mu)^3(\lambda\mu-1)^2$	$\frac{2}{3}\lambda^5-\frac{4}{5}\lambda^3+\frac{6}{5}\lambda$	$\frac{2}{3}\lambda^6-\frac{2}{3}\lambda^4+\frac{46}{35}\lambda^2-\frac{2}{5}$	$\frac{2}{3}\lambda^7-\frac{2}{15}\lambda^5+\frac{58}{105}\lambda^3$		
$(\lambda-\mu)^\nu d\mu$			$-\frac{6}{35}\lambda$		

List of Integrals (cont'd.)

	$\nu = 1$	$\nu = 2$	$\nu = 3$	$\nu = 4$
$\int_{-1}^{1} \frac{d\mu}{(\lambda-\mu)^\nu}$	$2Q_0$	$\frac{2}{\lambda^2-1} = -2Q_0'$	$\frac{2\lambda}{(\lambda^2-1)^2} = Q_0''$	$\frac{2}{3}\frac{3\lambda^2+1}{(\lambda^2-1)^3} = -\frac{1}{3}Q_0'''$
$\int \frac{\lambda+\mu}{(\lambda-\mu)^\nu} d\mu$	$4\lambda Q_0 - 2 = 4Q_1 + 2$	$\frac{4\lambda}{\lambda^2-1} - 2Q_0$	$\frac{2(\lambda^2+1)}{(\lambda^2-1)^2} = 2(\lambda Q_0'' + Q_0')$	$\frac{1}{3}\{-3Q_0'' - 2\lambda Q_0'''\}$
		$= -2Q_0 - 4\lambda Q_0'$	$= 2(Q_1'' - Q_0')$	$= \frac{6\lambda^3+10\lambda}{3(\lambda^2-1)^3}$
$\int \frac{(\lambda+\mu)^2}{(\lambda-\mu)^\nu} d\mu$	$8\lambda Q_1 + 2\lambda$	$\frac{8}{\lambda^2-1} + 10 - 8\lambda Q_0$	$\frac{8\lambda}{(\lambda^2-1)^2} + 2Q_0$	$\frac{32}{3}\cdot\frac{1}{(\lambda^2-1)^3} + \frac{32}{3(\lambda^2-1)^2} + \frac{2}{\lambda^2-1}$
$\int \frac{(\lambda+\mu)^3}{(\lambda-\mu)^\nu} d\mu$	$16\lambda^2 Q_1 + 2\lambda^2 - \frac{2}{3}$	$10\lambda - 24\lambda^2 Q_0 + \frac{16\lambda^3}{\lambda^2-1}$	$12\lambda Q_0 - 10 + \frac{8(\lambda^2+1)}{(\lambda^2-1)^2}$	$\frac{64\lambda}{3(\lambda^2-1)^3} + \frac{40\lambda}{3(\lambda^2-1)^2}$
		$= -24\lambda Q_1 + 2\lambda + \frac{16\lambda}{\lambda^2-1}$		$+ \frac{4\lambda}{\lambda^2-1} - 2Q_0$
$\int \frac{1-\mu^2}{(\lambda-\mu)^\nu} d\mu$	$2Q_0 - 2\lambda Q_1 = -2Q_1'(\lambda^2-1)$	$4Q_1$	$\frac{2\lambda}{\lambda^2-1} - 2Q_0 = \frac{2Q_0 - 2\lambda Q_1}{\lambda^2-1}$	$\frac{4}{3(\lambda^2-1)^2} = \frac{2}{3}Q_1''$
			$= -2Q_1'$	
$\int \frac{(1-\mu^2)^2}{(\lambda-\mu)^\nu} d\mu$	$(2\lambda^3 - 4\lambda)Q_1 + 2Q_0 - \frac{2}{3}\lambda$	$8\left\{(1-\lambda^2)Q_1 + \frac{1}{3}\right\}$	$8Q_2$	$-8Q_1 + \frac{8}{3(\lambda^2-1)} = -\frac{8}{3}Q_2'$
	$= (\lambda^2-1)^2 Q_0 - 4\lambda(\lambda^2-1)$	$= -\frac{8}{3}Q_2'(\lambda^2-1)$		
	$+ 2\lambda\left(\lambda^2 - \frac{1}{3}\right)$			
$\int \frac{(\lambda\mu+1)^2}{(\lambda-\mu)^\nu} d\mu$	$2\lambda^3 Q_1 + 4\lambda Q_1 + 2Q_0$	$-4\lambda^2 Q_1 - 4Q_1 - 6 + \frac{8\lambda^2}{\lambda^2-1}$	$2\lambda Q_1 + \frac{8\lambda}{(\lambda^2-1)^2}$	$\frac{32}{3(\lambda^2-1)^3} + \frac{32}{3(\lambda^2-1)^2} + \frac{2}{3(\lambda^2-1)}$
$\int \frac{(\lambda^2\mu^2-1)}{(\lambda-\mu)^\nu} d\mu$	$2\lambda^3 Q_1 - 2Q_0$	$-4\lambda^2 Q_1 + 2$	$2\lambda Q_1$	$\frac{2}{3}\frac{\lambda^2+1}{(\lambda^2-1)^2} = \frac{2}{3}\cdot\frac{1}{\lambda^2-1}$
				$+ \frac{4}{3(\lambda^2-1)^2}$

List of Integrals (cont'd.)

	$\nu = 1$	$\nu = 2$	$\nu = 3$	$\nu = 4$
$\int \frac{\lambda\mu + 1}{(\lambda - \mu)^\nu} d\mu$	$2\lambda Q_1 + 2Q_0$	$-2Q_1 + \frac{4}{\lambda^2 - 1}$	$\frac{4\lambda}{(\lambda^2 - 1)^2}$	$\frac{14}{3(\lambda^2 - 1)^2} + \frac{16}{3(\lambda^2 - 1)^3}$
$\int \frac{(\lambda\mu + 1)^2(1 - \mu^2)}{(\lambda - \mu)^\nu} d\mu$	$(1-\lambda^2)(2\lambda^2 Q_1 + 4\lambda Q_1 + 2Q_0) + \frac{2}{3}\lambda^3 + \frac{10}{3}\lambda = (-2\lambda^5 - 2\lambda^3 + 2\lambda)Q_1 + 2Q_0 + \frac{2}{3}\lambda^3 + \frac{4}{3}\lambda$	$\frac{8}{3}(\lambda^2+1)(3\lambda^2 Q_1 - 1) - \frac{4}{3} = (8\lambda^4 + 8\lambda^2)Q_1 - \frac{8}{3}\lambda^2 - 4$	$-12\lambda^3 Q_1 - 10\lambda Q_1 + 4\lambda - 2Q_0 + \frac{8\lambda}{\lambda^2 - 1}$	$8\lambda^2 Q_1 + 4Q_1 - \frac{8}{3} - \frac{8}{3(\lambda^2 - 1)} + \frac{16}{3(\lambda^2 - 1)^2}$
$\int \frac{(1 - \mu^2)(\lambda + \mu)^2}{(\lambda - \mu)^\nu} d\mu$	$-8\lambda^3 Q_1 + 8\lambda Q_1 + 4\lambda$	$(24\lambda^2 - 8)Q_1 - \frac{20}{3}$	$-26\lambda Q_1 + 2Q_0 + \frac{8\lambda}{\lambda^2 - 1}$	$12Q_1 + \frac{16}{3(\lambda^2 - 1)^2} - \frac{8}{3(\lambda^2 - 1)}$
$\int \frac{(\lambda^2\mu^2 - 1)(1 - \mu^2)}{(\lambda - \mu)^\nu} d\mu$	$(-2\lambda^5 + 2\lambda^3 + 2\lambda)Q_1 - 2Q_0 + \frac{2}{3}\lambda^3$	$(8\lambda^4 - 4\lambda^2 - 4)Q_1 - \frac{8}{3}\lambda^2$	$-12\lambda^3 Q_1 + 2\lambda Q_1 + 4\lambda + 2Q_0$	$8\lambda^2 Q_1 - \frac{8}{3} - \frac{4}{3}\cdot\frac{1}{\lambda^2 - 1}$
$\int \frac{(\lambda\mu + 1)(1 - \mu^2)}{(\lambda - \mu)^\nu} d\mu$	$-2\lambda^3 Q_1 + 2Q_0 + \frac{2}{3}\lambda$	$6\lambda^2 Q_1 + 2Q_1 - 2$	$-6\lambda Q_1 - 2Q_0 + \frac{4\lambda}{\lambda^2 - 1}$	$2Q_1 - \frac{2}{3(\lambda^2 - 1)} + \frac{8}{3(\lambda^2 - 1)^2}$
$\int \frac{(\lambda\mu + 1)(\lambda + \mu)}{(\lambda - \mu)^\nu} d\mu$	$4\lambda^2 Q_1 + 4Q_1 + 2$	$-6\lambda Q_1 - 2Q_0 + \frac{8\lambda}{\lambda^2 - 1}$	$2Q_1 + \frac{4}{\lambda^2 - 1} + \frac{8}{(\lambda^2 - 1)^2}$	$\frac{32\lambda}{3(\lambda^2 - 1)^3} + \frac{16\lambda}{3(\lambda^2 - 1)^2}$
$\int \frac{(\lambda^2\mu^2 - 1)(\lambda + \mu)(1 - \mu^2)}{(\lambda - \mu)^\nu} d\mu$	$(-2\lambda^6 + 2\lambda^4 + 2\lambda^2 - 2)\cdot 2Q_1 + \frac{4}{3}\lambda^4 - \frac{4}{15}\lambda^2 - \frac{8}{3}$	$18\lambda^5 Q_1 - 10\lambda^3 Q_1 - 10\lambda Q_1 - 6\lambda^3 + 2Q_0$	$-32\lambda^4 Q_1 + 8\lambda^2 Q_1 + 8Q_1 + \frac{32}{3}\lambda^2 + 4$	$28\lambda^3 Q_1 - 2\lambda Q_1 - \frac{28}{3}\lambda - 2Q_0 - \frac{8}{3}\cdot\frac{\lambda}{\lambda^2 - 1}$
$\int \frac{(1 - \mu^2)^2(\lambda + \mu)}{(\lambda - \mu)^\nu} d\mu$	$4(\lambda^2-1)^2 Q_1 + \frac{8}{5} - \frac{4}{3}(\lambda^2 - 1)$	$-18\lambda^3 Q_1 + 20\lambda Q_1 + 6\lambda - 2Q_0$	$32\lambda^2 Q_1 - 16Q_1 - \frac{32}{3}$	$-28\lambda Q_1 + 4Q_0 + \frac{16}{3}\cdot\frac{\lambda}{\lambda^2 - 1}$

List of Integrals (cont'd.)

	$\nu = 1$	$\nu = 2$	$\nu = 3$	$\nu = 4$
$\int \frac{(\lambda\mu+1)^2(1-\mu^2)(\lambda+\mu)}{(\lambda-\mu)^\nu}d\mu$	$(-4\lambda^6-4\lambda^4+4\lambda^2+4)Q_1$	$(18\lambda^5+18\lambda^3-2\lambda)Q_1-6\lambda^3$	$(-32\lambda^4-28\lambda^2-4)Q_1$	$28\lambda^3Q_1+18\lambda Q_1-\frac{28}{3}\lambda+2Q_0$
	$+\frac{4}{3}\lambda^4+\frac{12}{5}\lambda^2-\frac{8}{3}$	$-\frac{28}{3}\lambda-2Q_0$	$+\frac{32}{3}\lambda^2+\frac{16\lambda^2}{\lambda^2-1}$	$-\frac{40}{3}\cdot\frac{\lambda}{\lambda^2-1}+\frac{32}{3}\cdot\frac{\lambda}{(\lambda^2-1)^2}$
$\int \frac{(\lambda\mu+1)^2(\lambda+\mu)}{(\lambda-\mu)^\nu}d\mu$	$(4\lambda^4+8\lambda^2+4)Q_1+2-\frac{2}{3}\lambda^2$	$-10\lambda^3Q_1-12\lambda Q_1+4\lambda$	$-8\lambda^2-6+\frac{8(\lambda^2+1)}{(\lambda^2-1)^2}$	
		$-2Q_0+\frac{16\lambda}{\lambda^2-1}$	$+8\lambda^3Q_0+4\lambda Q_0$	
$\int \frac{(\lambda+\mu)^3(1-\mu^2)}{(\lambda-\mu)^\nu}d\mu$	$-16\lambda^4Q_1+16\lambda^2Q_1+\frac{20}{3}\lambda^2-\frac{4}{15}$	$56\lambda^3Q_1-24\lambda Q_1-\frac{52}{3}\lambda$	$-76\lambda^2Q_1+12Q_1+\frac{32}{3}$	$50\lambda Q_1-2Q_0-\frac{40}{3}\cdot\frac{\lambda}{\lambda^2-1}$
			$+\frac{16\lambda^2}{\lambda^2-1}$	$+\frac{32}{3}\cdot\frac{\lambda}{(\lambda^2-1)^2}$
$\int \frac{(1-\mu^2)(\lambda+\mu)}{(\lambda-\mu)^\nu}d\mu$	$-4\lambda^2Q_1+4Q_1+\frac{8}{3}$	$10\lambda Q_1-2Q_0$	$-8Q_1+\frac{4}{\lambda^2-1}$	
$\int \frac{(1-\mu^2)(\lambda+\mu)^2}{(\lambda-\mu)^\nu}d\mu$	$-8\lambda^3Q_1+8\lambda Q_1+4\lambda$			
$\int \frac{(\lambda+\mu)^3(\lambda\mu-1)^2}{(\lambda-\mu)^\nu}d\mu$	$(1-\lambda^2)^2\cdot 16\lambda^2Q_1-\frac{14}{3}\lambda^4$	$(-56\lambda^5+80\lambda^3-24\lambda)Q_1$	$(76\lambda^4-72\lambda^2+12)Q_1$	$(-50\lambda^3+28\lambda)Q_1-2Q_0$
	$+\frac{104}{15}\lambda^2-\frac{2}{3}$	$+\frac{58}{3}\lambda^3-\frac{46}{3}\lambda$	$-\frac{74}{3}\lambda^2+10$	$+\frac{16\lambda}{3(\lambda^2-1)}+\frac{52\lambda}{3}\cdot$

TABLE XI. *List of Integrals*

	$R > a^2$	$R < a$
$\int_{\lvert R-a\rvert}^{R+a} db$	$2a$	$2R$
$\int b^2 db$	$2a\left(R^2+\frac{a^2}{3}\right)$	$2R\left(a^2+\frac{R^2}{3}\right)$
$\int b^4 db$	$2a\left(R^4+2a^2R^2+\frac{1}{5}a^4\right)$	$2R\left(a^4+2R^2a^2+\frac{1}{5}R^4\right)$
$\int \frac{db}{b^2}$	$\frac{2a}{R^2-a^2}$	$\frac{2R}{a^2-R^2}$
$\int \frac{db}{b^4}$	$2a\frac{(R^2+a^2/3)}{(R^2-a^2)^3}$	$2R\frac{(a^2+R^2/3)}{(a^2-R^2)^3}$
$\int \sin^2\theta_b db$	$\frac{4a^3}{3R^2}$	$\frac{4}{3}R$
$=\int a^2\sin^2\theta_a\cdot db/b^2$		
$\int \sin^2\theta_b\cdot b^2 db$	$\frac{4a^3}{3R^2}\left(R^2-\frac{a^2}{5}\right)$	$\frac{4}{3}R\left(a^2-\frac{R^2}{5}\right)$
$=\int a^2\sin^2\theta_a db$		
$\int \sin^2\theta_b\cdot\frac{db}{b^2}$	$\frac{4}{3}\frac{a^3}{R^2}\cdot\frac{1}{R^2-a^2}$	$\frac{4}{3}R\cdot\frac{1}{a^2-R^2}$
$=\int a^2\sin^2\theta_a\cdot\frac{db}{b^4}$		
$\int \sin^4\theta_b db$	$\frac{16}{15}\frac{a^5}{R^4}$	$\frac{16}{15}R$
$=\int a^2\sin^2\theta_a\sin^2\theta_b\cdot\frac{db}{b^2}$		
$\int\frac{a^2\cos^2\theta_a}{b^2}db$	$\frac{2a}{R^2-a^2}\cdot\frac{a^2}{3R^2}\cdot(2a^2+R^2)$	$\frac{2R}{a^2-R^2}\cdot\frac{1}{3}(a^2+2R^2)=\frac{2}{3}R+\frac{2R^3}{a^2-R^2}$
$\int P_2(\cos\theta_a)\cdot\frac{db}{b^2}$	$\frac{2a}{R^2-a^2}\cdot\frac{a^2}{R^2}$	$\frac{2R}{a^2-R^2}\cdot\frac{R^2}{a^2}$
$\int\frac{a^2\cos^2\theta_a\sin^2\theta_b}{b^2}db$	$\frac{4a^3}{3R^4}\left(\frac{R^2+4a^2}{5(R^2-a^2)}\right)$	$\frac{4}{3}R\cdot\frac{a^2+4R^2}{5(a^2-R^2)}=\frac{4}{15}R+\frac{4}{3}\frac{R^3}{a^2-R^2}$
$\int\cos^2\theta_b db$	$2a-\frac{4a^3}{3R^2}$	$2R-\frac{4}{3}R=\frac{2}{3}R$
$\int\cos^2\theta_a db$	$\frac{2a}{3R^2}\left(\frac{2}{5}a^2+R^2\right)$	$\frac{2}{3}\cdot\frac{R}{a^2}\left(\frac{2}{5}R^2+a^2\right)$
$\int P_2(\cos\theta_a)db$	$\frac{2}{5}\frac{a^3}{R^2}$	$\frac{2}{5}\frac{R^3}{a^2}$
$\int a^2\sin\theta_a\sin\theta_b\cdot\cos\theta_a\cos\theta_b\cdot\frac{db}{b^2}$	$-\frac{16}{15}\frac{a^5}{R^4}$	$+\frac{4}{15}R$
$\int\frac{ab\cos\theta_a\cos\theta_b}{b^2}db$	$-\frac{4a^3}{3R^2}$	$+\frac{2}{3}R$
$\int\frac{a^2\cos^2\theta_a\cos^2\theta_b}{b^2}db$	$\frac{2}{3}\frac{a^3}{R^2-a^2}+\frac{16}{15}\frac{a^5}{R^4}$	$\frac{2}{3}\frac{Ra^2}{a^2-R^2}-\frac{4}{15}R$
$\int\frac{a^2\sin^2\theta_a\cos^2\theta_b}{b^2}db$	$\frac{4}{3}\frac{a^3}{R^2}-\frac{16}{15}\frac{a^5}{R^4}$	$\frac{4}{15}R$
$\int\frac{a^2\cos^2\theta_b}{b^2}db$	$\frac{2}{3}\frac{a^3}{R^2-a^2}+\frac{4}{3}\frac{a^3}{R^2}$	$\frac{2}{3}\frac{Ra^2}{a^2-R^2}$

TABLE XII. *Numerical Results*

			3	4	5	6	7	8	9	10
I	(a)	$(\kappa^5/2\pi)\int a^2 \sin^2\theta_a e^{-\kappa a}(\Gamma_5/\kappa b)dv$	154.0	137.0	121.4	108.0	96.8	87.1	79.0	72.1
	(b)	$(\kappa^5/2\pi)\int a^2 \sin^2\theta_a e^{-\kappa a}[\Gamma_5(\kappa b)/\kappa b - \Gamma_4(\kappa b)]dv$	26.8	17.7	10.9	6.5	3.7	2.0	1.1	0.6
	(c)	$(\kappa^5/2\pi)\int a^2 \sin^2\theta_a e^{-\kappa a} g_{5,1}dv$	127.2	119.3	110.5	101.5	93.1	85.1	77.9	71.5
II	(a)	$(\kappa^5/2\pi)\int a^2 \cos^2\theta_a e^{-\kappa a}(\Gamma_5/\kappa b)dv$	103.1	94.6	83.6	72.6	62.9	54.6	48.0	42.6
	(b)	$(\kappa^5/2\pi)\int a^2 \cos^2\theta_a e^{-\kappa a}[\Gamma_5(\kappa b)/\kappa b - \Gamma_4(\kappa b)]dv$	36.7	31.0	23.3	16.1	10.4	6.4	3.8	2.1
	(c)	$(\kappa^5/2\pi)\int a^2 \cos^2\theta_a e^{-\kappa a} g_{5,1}dv$	66.4	63.6	60.3	56.5	52.5	48.8	44.2	40.5
III	(a)	$(\kappa^5/2\pi)\int a^2 \sin^2\theta_a e^{-\kappa a}P_2(\cos\theta_b)[\Gamma_7/(\kappa b)^3]dv$	4.9	26.3	32.2	31.1	27.0	22.6	18.4	15.0
	(b)	$(\kappa^5/2\pi)\int a^2 \sin^2\theta_a e^{-\kappa a}P_2(\cos\theta_b)[\Gamma_7(\kappa b)/(\kappa b)^3 - (\kappa b)^2\Gamma_2(\kappa b)]dv$	−0.8	13.6	15.6	12.1	8.2	5.0	2.7	1.7
	(c)	$(\kappa^5/2\pi)\int a^2 \sin^2\theta_a e^{-\kappa a}P_2(\cos\theta_b) g_{7,3}dv$	5.7	12.7	16.6	19.0	18.8	17.6	15.7	13.3
IV	(a)	$(\kappa^5/2\pi)\int a^2 \cos^2\theta_a e^{-\kappa a}P_2(\cos\theta_b)[\Gamma_7/(\kappa b)^3]dv$	−91.4	−37.0	1.3	19.1	24.2	22.8	19.1	15.3
	(b)	$(\kappa^5/2\pi)\int a^2 \cos^2\theta_a e^{-\kappa a}P_2(\cos\theta_b)[\Gamma_7(\kappa b)/(\kappa b)^3 - (\kappa b)^2\Gamma_2(\kappa b)]dv$	−97.5	−44.0	−7.0	9.6	13.5	11.8	8.6	5.6
	(c)	$(\kappa^5/2\pi)\int a^2 \cos^2\theta_a e^{-\kappa a}P_2(\cos\theta_b) g_{7,3}dv$	6.1	7.0	8.3	9.5	10.7	11.0	10.5	9.7
V	(a)	$-(\kappa^5/2\pi)\int a^2 \sin\theta_a\cos\theta_a\sin\theta_b\cos\theta_b e^{-\kappa a}[\Gamma_7/(\kappa b)^3]dv$	38.0	42.1	34.4	24.7	16.7	11.0	7.2	4.7
	(b)	$-(\kappa^5/2\pi)\int a^2 \sin\theta_a\cos\theta_a\sin\theta_b\cos\theta_b e^{-\kappa a}[\Gamma_7/(\kappa b)^3 - g_{7,3}]dv$	41.6	41.5	31.6	20.6	12.4	7.0	3.8	2.0
	(c)	$-(\kappa^5/2\pi)\int a^2 \sin\theta_a\cos\theta_a\sin\theta_b\cos\theta_b e^{-\kappa a} g_{7,3}dv$	−3.6	0.6	2.8	4.1	4.3	4.0	3.4	2.7
VI	(a)	$(\kappa^5/2\pi)\int a^2 \sin^2\theta_a \sin^2\theta_b e^{-\kappa a}[\Gamma_7/(\kappa b)^3]dv$	229.	131.0	73.1	41.3	23.7	13.9	8.4	5.2
	(b)	$(\kappa^5/2\pi)\int a^2 \sin^2\theta_a \sin^2\theta_b e^{-\kappa a}[\Gamma_7/(\kappa b)^3 - g_{7,3}]dv$	190.9	100.0	49.9	24.5	11.7	5.5	2.6	1.2
	(c)	$(\kappa^5/2\pi)\int a^2 \sin^2\theta_a \sin^2\theta_b e^{-\kappa a} g_{7,3}dv$	38.1	31.0	23.2	16.8	12.0	8.4	5.8	4.0

$$i_1 = (\kappa/384)[Ic - (\tfrac{1}{5})\mathrm{III}c]$$
$$i_3 = (\kappa/384)[Ic + (\tfrac{2}{5})\mathrm{III}c] = (\kappa/192)[\mathrm{II}c - (\tfrac{1}{5})\mathrm{IV}c]$$
$$i_9 = (\kappa/192)[IIc + (\tfrac{2}{5})\mathrm{IV}c]$$
$$i_5 = -\kappa \mathrm{V}c/640 \quad i_7 = -\kappa \mathrm{VI}c/1280$$

TABLE XIII

α	$\alpha=3$	4	5	6	7	8	9	10
i_1/κ	0.332	0.303	0.280	0.255	0.232	0.213	0.195	0.179
i_3/κ	.338	.324	.305	.285	.262	.241	.220	.200
i_9/κ	.359	.346	.332	.315	.296	.278	.252	.231
i_5/κ	−.0056	+.0009	+.0044	+.0064	+.0067	+.0062	+.0053	+.0042
i_7/κ	−.0312	−.0242	−.0181	−.0131	−.0094	−.0066	−.0045	−.0031

$$I_1 = 2\kappa/\alpha - 4c_1^2 \int e^{-\kappa a} a^2 \sin^2\theta_a (1/\kappa b)dv = \kappa[2/\alpha + i_1/\kappa - (\mathrm{I}a)/192]$$

$$I_3 = 2\kappa/\alpha - 2\int dv a_0^2/b - 2\int dv a_1^2/b + i_3 = \kappa[2/\alpha + i_3/\kappa - (\mathrm{II}a)/192 - (\mathrm{I}a)/384]$$

$$I_9 = 2\kappa/\alpha - 4\int dv a_0^2/b + i_9 = \kappa[2/\alpha + i_9/\kappa - (\mathrm{II}a)/96]$$

$$I_5 = i_5, \quad I_7 = i_7, \quad I_6 = i_6, \quad I_8 = i_8, \quad I_{11} = i_{11} \cong -i_6$$

$$I_2 = 2\kappa S_{11}/\alpha - 4(S_{11})^{1/2}\int dv a_1 b_1/b + i_2$$

$$I_4 = 2\kappa S_{10}/\alpha - 2(S_{00})^{1/2}\int dv a_1 b_1/b - 2(S_{11})^{1/2}\int dv a_0 b_0/b + i_4$$

$$I_{10} = 2\kappa S_{00}/\alpha - 4(S_{00})^{1/2}\int dv a_0 b_0/b + i_{10}$$

The resulting integrals, after the small quantities before mentioned have been neglected, are listed in Table XIV. The relative energies are given in Table XV, and plotted in Fig. 1.

TABLE XIV. *Integrals.*

α	$\alpha=3$	4	5	6	7	8	9	10
I_1/κ	0.196	0.088	0.047	0.025	0.013	0.009	0.005	0.003
I_3/κ	.068	−.026	−.046	−.042	−.032	−.021	−.014	−.010
I_9/κ	−.043	−.140	−.140	−.110	−.067	−.042	−.026	−.013
I_5/κ	−.006	+.0007	.0044	.0064	.0067	.0062	.0053	.0042
I_7/κ	−.031	−.0240	−.0181	−.0131	−.0094	−.0066	−.0045	−.0031
I_2/κ	.082	.005	−.0217	−.0183	−.0139	−.0086	−.006	−.0028
I_4/κ	.074	.009	.0198	.0173	.0161	.0126	.0103	.0060
I_{10}/κ	.096	.070	.035	.032	.017	.0081	.0035	.0021
I_6/κ	−.043	−.030	−.039	−.028	−.021	−.015	−.010	−.006
I_8/κ		.01	.01	.007	.005			

TABLE XV. *Relative energies.*

α	$\alpha=3$	4	5	6	7	8	9	10
$^3\Sigma_u^+/\kappa$		.100	.064	.032	.015			
$^3\Delta_u/\kappa$	.329	.162	.103	.056	.032	.019	.0118	.0062
$^1\Sigma_u^-/\kappa$		.225	.142	.081	.048			
$^3\Sigma_g^-/\kappa$		.074	.026	.012	.003			
$^1\Delta_g/\kappa$	.167	.063	.0188	.006	−.001	−.001	−.001	0
$^1\Sigma_g^+/\kappa$		.053	.011	−.0005	−.0042			
$^3\Pi_g/\kappa$	.137	.010	.009	−.003	−.002			
$^3\Pi_u/\kappa$	.05	−.002	−.027	−.024	−.018	−.012	−.009	−.006
$^1\Pi_g/\kappa$	.065	−.042	−.059	−.053	−.033	−.019	−.010	−.006
$^1\Pi_u/\kappa$	−.06	−.076	−.110	−.087	−.069	−.050	−.037	−.025
$^1\Sigma_g^+/\kappa$	.04	−.07	−.11	−.079	−.054	−.036	−.023	−.011
$^3\Sigma_u^+/\kappa$	−.18	−.22	−.177	−.146	−.102	−.057	−.033	−.017

DISCUSSION

Fig. 1 shows the relative energies plotted as a function of the internuclear distance. The lowest term,[8] for intermediate values of κR, is the $^3\Sigma_u^+$. For hydrogen, we may set $\kappa=1$, and the minimum of this curve lies at about 2.0A. The value of the heat of dissociation is 2.9 volts, approximately.

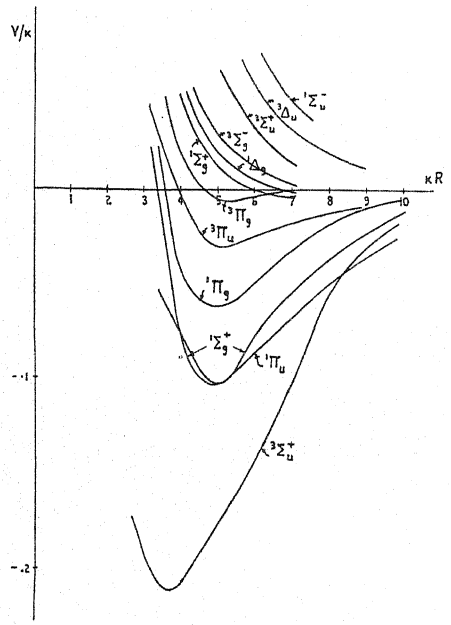

Fig. 1. Relative energies.

It is not possible to say, to the degree of approximation used here, whether the $^3\Pi_g$ state has a weak minimum or is repulsive. For the same reason, the relative positions of $^1\Sigma_g^+$ and $^1\Pi_u$ may actually be somewhat different. The

[8] This result has been predicted for B_2 by J. E. Lennard-Jones, Trans. Faraday Soc. **25**, 681 (1929).

reason for this uncertainty lies partly in the fact that we have neglected $i_6^{(3)}$ and $i_6^{(4)}$, and partly in the low degree of accuracy to which s_2 may be given.

Apart from these minor details, it is safe to assert that the curves do represent the interaction of two hydrogen-like atoms, each with one $2p$ electron, insofar as this interaction is to be found by a first order perturbation calculation of the Kemble and Zener type.

Heisenberg[9] has shown that there is reason to believe that the behavior of ferromagnetic substances may some day be understood, when it becomes possible to carry through detailed calculations. A necessary condition for ferromagnetism seems to be that the exchange integral for the lowest states be positive. This was found to be likely for $n \geqq 3$, where n is the principal quantum number. From our results, it is seen that a positive exchange energy integral is obtained for $n=2$, $l=1$, so that the possibility of ferromagnetism does not seem to be governed by the principal quantum number in so simple a fashion. The sufficient conditions for ferromagnetism have yet to be given.

One also sees from the curves in the figure that the "Coulomb" integrals are in general more important than the "exchange" integrals. The states arising from $m_{la}=0$, $m_{lb}=0$ lie the lowest, those from $m_{la}=0$, $m_{lb}=\pm 1$ are next higher, and those from $m_{la}=\pm 1$, $m_{lb}=\pm 1$ are highest. This means that the most stable configuration is that in which there is the maximum overlapping of charge, in accordance with the ideas of Slater[10] on directed valency. Orbital valency may be associated with the "Coulomb" integrals, and spin valency with the exchange integrals. The latter concept may, however, be misleading.

Though this analysis is strictly applicable only to the case where two excited hydrogen atoms interact (leaving out of account the influence of the s orbits) one might expect that similar conditions would obtain for boron, or excited lithium. Unfortunately, the band spectrum of B_2 has not been analyzed, so that a direct check of the theory is wanting. The inner s electrons would probably have some influence, but whether the order of the energy levels would be affected or not is open to question.

In conclusion, I wish to express may deep appreciation to the many people with whom the problem has been discussed. It was suggested by Professor Heisenberg, whom I also wish to thank for his help on previous problems. Acknowledgment must also be made to Dr. Dirac for discussion of allied problems. The work was continued at the Eigenössische Technische Hochschule, Zürich, and completed in Urbana. Thanks are due Mr. W. H. Furry for assistance in checking part of the calculations.

Note added to proof, Feb. 17, 1931: The influence of the inner $2s$ electrons is now being studied, and will be made the subject of a later paper.

[9] W. Heisenberg, Zeits. f. Physik **49**, 619 (1928).

[10] J. C. Slater, American Physical Society meeting, Dec. 29, 1930, paper 17.

THE MASS ABSORPTION COEFFICIENT OF THE K SHELL ACCORDING TO THE DIRAC RELATIVISTIC THEORY OF THE ELECTRON*

By Louis C. Roess
Cornell University

(Received January 19, 1931)

Abstract

Taking as model an atom containing two non-interacting electrons and a fixed nucleus with charge Ze, the mass absorption coefficient is calculated by use of the proper functions of the Dirac relativistic equation. Z is determined so as to make the lowest energy level agree with the experimental value determined from the K absorption edge. The numerical calculation presented difficulty because of lack of tables of complex gamma functions. The relativistic coefficient is found to be from 0 to 40 per cent smaller than the non-relativistic coefficient calculated by Nishina and Rabi, the greatest difference occurring for the heavy elements and short wave-lengths; it agrees slightly worse with experiment than the non-relativistic coefficient. The difference between theory and experiment is least for the heavy atoms, as would be expected, since for the heavy atoms (large Z) the neglected electronic interaction-field is small in comparison with the nuclear field. The variation of the relativistic coefficient with wave-length is complicated, but in the range $\frac{1}{2}\lambda_k$ to λ_k (λ_k = wave-length of K absorption edge) it is more nearly linear with λ^3 than the non-relativistic coefficient. The importance of using the relativistic equation for heavy atoms and short x-ray wave-lengths is emphasized by these results, which also show that the model chosen is too approximate, even for the heavy elements.

The general normalizing factors for the discrete and continuous spectrum proper functions of a hydrogen-like atom are given.

Introduction and Results

SEVERAL attempts[1] have been made, with classical or semi-classical theories, to calculate the atomic absorption coefficient for the K shell. More recently Wentzel[2] and Oppenheimer[3] obtained approximate formulae using non-relativistic quantum mechanics, while Nishina and Rabi[4] have given the explicit formula which follows from the Schrödinger theory. The comparison with experiment made by the latter authors shows fairly good agreement for the heavy elements and poor agreement for the light elements.

The purpose of the present paper is to calculate the mass absorption coefficient by use of the Dirac relativistic equation, and to compare the results

* Abridged Cornell Dissertation. Presented at the Cleveland Meeting of the American Physical Society, Dec. 30–31, 1930.

[1] J. J. Thomson, Conduction of Electricity. Through Gases, 2d Ed., p. 321; L. de Broglie, Journ. de Phys. et Rad. **3**, 33, (1922); A. H. Compton, Nat. Res. Council, Bul. **20**, 37, (1922); H. A. Kramers, Phil. Mag. **46**, 836, (1923).

[2] G. Wentzel, Zeits. f. Physik **40**, 574, (1926).

[3] J. R. Oppenheimer, Zeits. f. Physik **41**, 268, (1926).

[4] Y. Nishina and I. I. Rabi, Verh. d. deut. Phys. Ges. **9**. 6, (1928).

with experiment and with the non-relativistic theory. One can readily see from correspondence principle arguments that for the K electrons of the heavy atoms the relativity corrections should be important, and this is confirmed by the results.

The atom model used here as in the non-relativistic calculations consists of two non-interacting electrons in the field of a fixed nucleus with charge

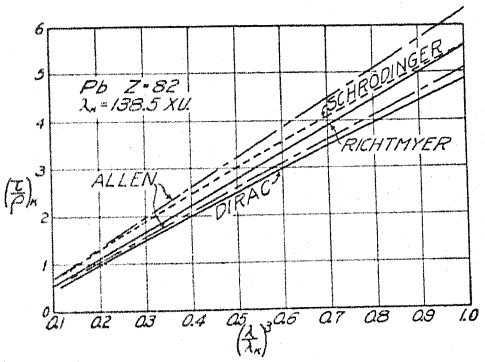

Fig. 1. The mass absorption coefficient for lead. The curves marked Allen and Richtmyer are plots of the experimental data.[7]

Z^*e, where Z^* is that charge (smaller than the true charge Z) which makes the lowest energy level of the atom model agree with the experimental value. It is obvious that this model will be most nearly correct when the interaction of the K electrons with the nucleus is large compared with their interaction with each other and with the outer electrons, i.e., for the heavy elements.

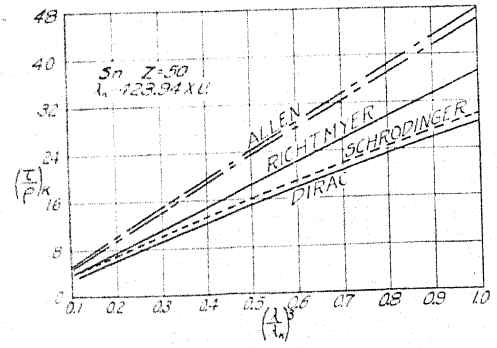

Fig. 2. The mass absorption coefficient for tin. The curves marked Allen and Richtmyer are plots of the experimental data.[7]

The calculation proceeds as follows: by use of the Dirac radiation theory[5] combined with the Dirac relativistic equation[6] the general formula for the absorption probability is derived. This formula contains a certain matrix element which is then evaluated for the case of the transition between the K

[5] P. A. M. Dirac, Roy. Soc. Proc. **A114**, 243 and 710, (1927).
[6] P. A. M. Dirac, Roy. Soc. Proc. **A117**, 610, (1928).

level and a state of the continuous spectrum corresponding to the removal of one of the K electrons. The resulting formula for the mass absorption coefficient of the K shell is then calculated numerically. The last two operations constitute what is new in the paper. The final formula is quite complicated so that the numerical calculation is very laborious, especially because of lack of tables of the gamma function of complex argument.

The results of the present calculation are collected in the Table I and Figs. 1–3. The relativistic theory gives values of the absorption coefficient which are consistently lower than those of the non-relativistic theory, the difference varying from about 40 percent for Pb at $\frac{1}{2}\lambda_k$ to less than 1 percent for Al at λ_k. The calculated absorption coefficients for Al cannot be compared with experiment because of lack of data for the long wave-lengths, but show how closely the two quantum-mechanical theories agree for the light elements.

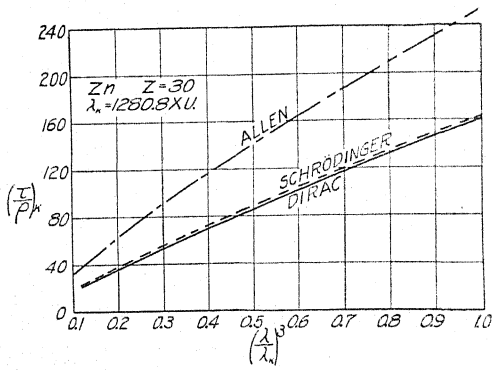

Fig. 3. The mass absorption coefficient for zinc. The curve marked Allen is a plot of the experimental data.[7]

It is found experimentally[7] that the mass absorption coefficient varies linearly with λ^n where n ranges from 2.9 to 3 and apparently changes in value with the wave-length. The classical and semi-classical theories referred to above all give a linear variation with λ^3. The quantum-mechanical theories predict a more complicated variation with λ, the non-relativistic theory indicating an exponent[8] 2.87 at $\lambda=\frac{1}{2}\lambda_k$ and 8/3 at $\lambda=\lambda_k$(λ_k=wave-length of K edge). The relativistic theory here developed gives an exponent which is somewhat closer to three for the heavy elements over the range $\frac{1}{2}\lambda_k$ to λ_k. For example, for Pb the exponent is 2.86 at $\lambda=\lambda_k$ and 3.13 at $\lambda=\frac{1}{2}\lambda_k$. For the light elements the two theories agree closely for wave-lengths which are not too short.

There are a number of reasons, aside from the inadequacy of the model, for the disagreement between theory and experiment.[9] In the first place, the

[7] F. K. Richtmyer, Phys. Rev. **27**, 1, (1926); **30**, 755, (1927). S. J. M. Allen, Phys. Rev. **28**, 907, (1926).

[8] As pointed out to me by Professor Kennard, the expression of the theoretical results in terms of these exponents is misleading, since the relation given by the quantum mechanics may be written $C(\lambda)\lambda^{n(\lambda)}$, not $K\lambda^{n(\lambda)}$ (K independent of λ).

[9] I wish to thank Professor F. K. Richtmyer for helpful discussions on these points.

TABLE I. *Mass absorption coefficient* $(\tau/\rho)_K$.

λ in X.U.†	λ_k/λ	Dirac	Calculated Schröd-inger	Percent Differ-ence††	Observed Richt-myer[7]	Observed Allen[7]	Expon-ent of λ (calc.)
			Pb $Z=82$				
138.5	1.0	4.86	5.58	14.6	5.56	5.10 to 6.35	2.86
125.9	1.1	3.70	4.32	16.9	4.18	3.76 to 4.79	
115.4	1.2	2.85	3.41	19.8	3.22	3.00 to 3.72	
106.5	1.3	2.24	2.75	22.6	2.53	2.35 to 2.95	
98.9	1.4	1.79	2.24	25.4	2.03	1.89 to 2.37	
92.3	1.5	1.44	1.85	28.1	1.65	1.53 to 1.93	
86.6	1.6	1.18	1.55	30.0	1.36	1.26 to 1.62	
81.5	1.7	0.97	1.30	33.9	1.13	1.06 to 1.36	
76.9	1.8	0.81	1.11	37.0	0.95	0.89 to 1.15	
72.9	1.9	0.68	0.95	40.1	0.81	0.77 to 0.98	
69.3	2.0	0.58	0.82	42.8	0.70	0.65 to 0.86	3.13
			Sn $Z=50$				
423.94	1.0	28.5	29.8	4.6	37.0	45.9 to 47.7	2.75
385.40	1.1	21.9	23.1	5.5	27.8	34.7 to 36.1	
353.28	1.2	17.2	18.2	6.3	21.4	26.9 to 28.0	
326.11	1.3	13.7	14.7	7.4	16.9	21.4 to 22.2	
302.81	1.4	11.0	12.0	8.4	13.5	17.2 to 17.9	
282.63	1.5	9.03	9.89	9.5	11.0	13.9 to 14.6	
264.96	1.6	7.48	8.26	10.4	9.02	11.5 to 12.1	
249.38	1.7	6.24	6.97	11.7	7.52	9.6 to 10.2	
235.52	1.8	5.26	5.93	12.8	6.34	8.0 to 8.5	
223.13	1.9	4.47	5.09	14.0	5.39	6.9 to 7.4	
211.97	2.0	3.82	4.40	15.2	4.62	5.9 to 6.3	2.96
			Zn $Z=30$				
1280.8	1.0	161	163	1.5	..	254	2.67
1164.4	1.1	125	127	1.3	..	199	
1067.3	1.2	98.2	100	1.9	..	181	
985.2	1.3	78.5	80.4	2.4	..	130	
914.9	1.4	63.9	65.6	2.7	..	107	
853.9	1.5	52.6	54.2	3.2	..	90	
800.5	1.6	43.8	45.3	3.5	..	76	
753.4	1.7	37.0	38.2	3.3	..	64	
711.6	1.8	31.2	32.6	4.4	..	54	
674.1	1.9	26.6	27.9	5.1	..	46	
640.4	2.0	22.9	24.2	5.4	..	40	2.87
			Al $Z=13$				
7947.0	1.0	2453	2459	0.3	..	..	2.67
7224.5	1.1	1905	1905	0.0	..	..	
6622.5	1.2	1493	1505	0.8	..	..	
6113.1	1.3	1205	1210	0.4	..	..	
5675.4	1.4	987	987	0.0	..	..	
5298.0	1.5	811	816	0.5	..	..	
4966.9	1.6	677	682	0.7	..	..	
4674.7	1.7	571	575	0.8	..	..	
4415.0	1.8	485	490	0.9	..	..	
4182.6	1.9	416	420	1.0	..	..	
3973.5	2.0	359	363	1.2	..	..	2.87

† The values of λ_K are taken from the article by Grebe in Geiger-Scheel's Handb. d. Phys, XXI, p. 336.

†† The percent difference is calculated from the Dirac value as base.

true absorption coefficient is not measured experimentally, since scattering is always present. The scattering coefficient, though small in comparison with the true absorption coefficient over the range $\frac{1}{2}\lambda_k$ to λ_k, varies in an un-

known[10] manner with the wave-length. In the second place, the experimenter measures the absorption coefficient for all the electrons in the atom, so that one must extrapolate the absorption curve for the $L+M+N+\cdots$ electrons down to wave-lengths below the K edge and then subtract this from the total absorption in this range to get the absorption coefficient for the K electrons. Such an extrapolation, while it may introduce only a small error in the magnitude of the absorption coefficient, can easily change its variation with wave-length. Finally, even an exact model of an *isolated* atom would be incorrect, since the experimental measurements are usually made upon atoms in crystals. In the writer's opinion the above effects are not large enough to account for the discrepancy which, as already suggested by Nishina and Rabi,[4] must be due to the inadequate model. The results obtained here show clearly that for the K shell of the heavy elements the relativistic theory must be used in conjunction with the correct model.

It should be possible to use a much better model for which the discrete proper functions are obtained by the variational method which has recently been used with such success, but how one can obtain more nearly correct proper functions for the continuous spectrum remains a difficult problem.

The Probability of Absorption

According to Dirac[6] the motion of an electron in an electromagnetic field with the vector potential A and scalar potential V is described by the wave-equation

$$\left[\frac{W+eV}{c}+\rho_1\boldsymbol{\delta}\left(\boldsymbol{p}+\frac{e}{c}\boldsymbol{A}\right)+\rho_3 mc\right]\psi=0, \tag{1}$$

in which W is the energy parameter, $\boldsymbol{p}$ the momentum vector-operator with components $(h/2\pi i)(\partial/\partial x),\cdots$, and ρ_1, ρ_3, and $\boldsymbol{\delta}$ are certain matrices having four rows and columns. The probability amplitude ψ is also a matrix having four rows and only one column. We shall let V represent the field of the fixed nucleus, and choose the vector potential A of the external field so that its scalar potential vanishes.

From Eq. (1) we obtain for the Hamiltonian function of the electron

$$H_e = H_0 - e\rho_1\boldsymbol{\delta}\boldsymbol{A}$$

with (2)

$$H_0 = -c\rho_1\boldsymbol{\delta}\cdot\boldsymbol{p}-\rho_3 mc^2-eV.$$

H_0 is the Hamiltonian for the motion in the nuclear field alone. We now suppose the electromagnetic field to be quantized according to the Dirac[5] scheme, and obtain with Waller,[11] taking retardation into account, the following Hamiltonian for the system atom plus field:

$$H = H_0+\sum_r N_r h\nu_r - \sum_r \rho_1(\boldsymbol{\delta}\mathbf{u}_r)\left\{N_r^{1/2}e^{2\pi i/h[\Theta_r-(\mathbf{K}_r\mathbf{x})]}+e^{-2\pi i/h[\Theta_r-(\mathbf{K}_r\mathbf{x})]}N_r^{1/2}\right\} \tag{3}$$

[10] This variation is very difficult to determine experimentally. For the most recent data see E. N. Coade, Phys. Rev. **36**, 1109, (1930).

[11] I. Waller, Zeits. f. Physik **58**, 75, (1929).

where N_r and Θ_r are operators which obey the relation

$$N_r e^{2\pi i\Theta_r/h} - e^{2\pi i\Theta_r/h} N_r = e^{2\pi i\Theta_r/h},$$

x is a vector with origin at the nucleus which gives the position in space, and

$$\mathfrak{y}_r = \left(\frac{e^2 h\nu_r}{2\pi c\sigma_r}\right)^{1/2} r; \quad \kappa_r = \frac{h\nu_r}{c} n_r, \tag{3'}$$

where $\sigma_r d\nu_r d\omega_r$ is the number of components r of the radiation field with given polarization r in the frequency interval $d\nu_r$ and with direction of motion in the element of solid angle $d\omega_r$ about n_r.

If the stationary states of the atom are specified by the J''s, while N_r' is the number of photons in the component r, we obtain from the general transformation theory the Schrödinger equation corresponding to the Hamiltonian (3)[12]

$$\begin{aligned}\left[\frac{h}{2\pi i}\frac{\partial}{\partial t} + W(J'') + \sum_r N_r' h\nu_r\right]\Phi(J''; N_1', \cdots, N_r' \cdots) \\ = \sum_{J'}\sum_s \mathfrak{y}_s [N_s'^{1/2} A^s(J''J')\Phi(J'; N_1' \cdots N_{s-1}', N_s' - 1, N_{s+1}' \cdots) \\ + (N_s' + 1)^{1/2} B^s(J''J')\Phi(J'; N_1' \cdots N_{s-1}', N_s' + 1, N_{s+1}' \cdots)]\end{aligned} \tag{4}$$

with

$$\left.\begin{aligned} A^s(J''J') &= \int \psi_{J''}^*(\mathrm{x})\rho_1 \mathfrak{d}\, \psi_{J'}(\mathrm{x}) e^{-2\pi i(\kappa_s \cdot x)/h} d\mathrm{x} \\ B^s(J''J') &= \int \psi_{J''}^*(\mathrm{x})\rho_1 \mathfrak{d}\, \psi_{J'}(\mathrm{x}) e^{+2\pi i(\kappa_s \cdot x)/h} d\mathrm{x} \end{aligned}\right\} \tag{4'}$$

where $\psi_{J'}(\mathrm{x})$ and $W(J')$ are the characteristic function and characteristic value for the motion of the electron in the nuclear field. $|\Phi(J'; N')|^2$ gives the probability for the state $(J'; N')$ of the system, atom plus field.

In Eq. (4) the sum with respect to J' is to include an integral over the continuous spectrum if one is present. In this case the probability of finding the atom in the range $d\epsilon'$ about ϵ' is given by $|\Phi(\epsilon'; N')|^2 d\epsilon'$, where for the continuous spectrum ϵ' is used for J'.

It should be noted that the sum over J' in Eq. (4) includes the negative energy states of the atom. They do not cause difficulty in our application to absorption because here we can restrict ourselves to transitions between states having positive energy. Waller[12] has shown the importance of the negative energy states in calculating scattering and dispersion.

We want to calculate the transition probability $wd\epsilon''$ for an absorption process in which the atom jumps from an initial discrete state J' to a final state in the range $d\epsilon''$ about ϵ'' in the continuous spectrum, with absorption of a photon of definite direction (in $d\omega_s$) and definite polarization, regardless

[12] I. Waller, Zeits. f. Physik **61**, 837 (1930).

of what the final frequency state of the field may be. We suppose for the moment that the atomic states are non-degenerate.

The initial state of the field is to be taken as follows: only photons having a direction of motion within a solid angle $d\omega_s$ about n_s, a definite polarization s, but arbitrary frequency ν_{sr}, where r expresses the variation in frequency of the component s, are to be present. For physically interesting results, the range of variation of ν_{sr} about the frequency corresponding to the atomic transition must be at least as great as the natural line breadth.

Following the well-known method,[5] we calculate the probability of the above-mentioned atomic transition with absorption of a photon of frequency ν_{sr}, and then sum over all such frequencies, obtaining finally for a time t which is large compared with the atomic period but small compared with the mean life time of the state under consideration

$$wd\epsilon'' = \frac{2\pi e^2 c^2 t}{h^2\nu^2} \left| \mathbf{s}\cdot\boldsymbol{B}^s(\epsilon''; J') \right|^2 \rho(\nu) d\omega_s d\epsilon'' \tag{5}$$

where

$$h\nu = W(\epsilon'') - W(J'), \tag{6}$$

and $\rho(\nu)$ is the spectral energy density per unit frequency range per unit solid angle for a definite polarization.

Our temporary assumption that the atomic states are non-degenerate is not true. According to the general theory of quantum mechanics, as presented by Born and Jordan,[13] when the assembly of atoms is in thermal equilibrium before the absorption process occurs, we merely add together those transition probabilities relating to transitions between the degenerate states. Therefore we obtain finally for the transition probability $wd\epsilon''$

$$wd\epsilon'' = d\omega_s \frac{2\pi e^2 c^2 t}{h^2\nu^2} \sum \left| \mathbf{s}\cdot\boldsymbol{B}^s(\epsilon''; J') \right|^2 \rho(\nu) d\epsilon'' \tag{7}$$

where the sum is to be taken over all initial states having the same energy and over all final states having the same energy.

In many practical applications we are interested in the absorption probability for arbitrary direction of motion and polarization of the absorbed photon. We can obtain this from Eq. (7) by summing over all directions of motion $d\omega_s$ and all polarizations s. When the wave-length of the incident light is long compared with atomic dimensions, so that we can replace the exponential factor in the matrix element $\boldsymbol{B}^s$ in Eq. (4′) by unity, we can easily carry out this summation, obtaining for the absorption probability $w'd\epsilon''$ per unit time for arbitrary direction of motion and polarization of the absorbed photon

$$w'd\epsilon'' = \frac{16\pi^2 e^2 c^2}{3h^2\nu^2} \sum \left| P(\epsilon''; J') \right|^2 \rho(\nu) d\epsilon'' \tag{8}$$

[13] M. Born and P. Jordan, "Elementare Quantenmechanik," pp. 299, 321, and 329.

where

$$|P|^2 = |B_x|^2 + |B_y|^2 + |B_z|^2. \tag{8'}$$

Solutions of the Dirac Equation

The solutions of Eq. (1) for the case when $A=0$ and $V=Ze/r$ have been given by Darwin.[14] For given l and $u(=m-\frac{1}{2})$ there are two sets of solutions. We label these by introducing the quantum number j, which takes on the values $j=l\pm\frac{1}{2}$ to agree with spectroscopic notation. The two sets are:[15]

$$\begin{aligned} j &= l+\tfrac{1}{2} & j &= l-\tfrac{1}{2} \\ \psi_1 &= -iM_\theta F_l P_{l+1}^u & \psi_1 &= -i(l+u)M_\theta F_{-l-1}P_{l-1}^u \\ \psi_2 &= -iM_\theta F_l P_{l+1}^{u+1} \quad (9a) & \psi_2 &= i(l-u-1)M_\theta F_{-l-1}P_{l-1}^{u+1} \quad (9b) \\ \psi_3 &= (l+u+1)M_\theta G_l P_l{}^u & \psi_3 &= M_\theta G_{-l-1}P_l{}^u \\ \psi_4 &= -(l-u)M_\theta G_l P_l{}^{u+1} & \psi_4 &= M_\theta G_{-l-1}P_l{}^{u+1}, \end{aligned}$$

in which M_θ is the part of the total normalizing factor associated with the angular coordinates. The radial functions F_l and G_l contain their own normalizing factor.

The function $P_l{}^u(\theta, \phi)$ is a spherical harmonic defined by Darwin as follows:

$$P_l{}^u = (l-u)!\sin^l\theta\left(\frac{d}{d\cos\theta}\right)^{l+u}\frac{(\cos^2\theta-1)^l}{2^l l!}e^{iu\phi}. \tag{10}$$

The radial functions F_l and G_l satisfy the equations

$$\begin{aligned} &\frac{2\pi}{h}\left(\frac{W+eV}{c}+mc\right)F_l + \frac{dG_l}{dr} - \frac{l}{r}G_l = 0 \\ &-\frac{2\pi}{h}\left(\frac{W+eV}{c}-mc\right)G_l + \frac{dF_l}{dr} + \frac{l+2}{r}F_l = 0. \end{aligned} \tag{11}$$

We shall use the solutions of Eq. (11) given by Gordon.[16] These are:

Discrete Spectrum: $W/mc^2<1$

$$\begin{aligned} F_l &= \left(\frac{N_l-\rho_l-n_r}{N_l+\rho_l+n_r}\right)^{1/2} M_r(\sigma_1-\sigma_2) \\ G_l &= M_r(\sigma_1+\sigma_2) \end{aligned} \tag{12}$$

$$\begin{aligned} \sigma_1 &= (N_l+l+1)r^{\rho_l-1}e^{-k_0 r}{}_1F_1(-n_r; 2\rho_l+1; 2k_0 r) \\ \sigma_2 &= -n_r r^{\rho_l-1}e^{-k_0 r}{}_1F_1(-n_r+1; 2\rho_l+1; 2k_0 r) \end{aligned} \tag{13}$$

[14] C. G. Darwin, Roy. Soc. Proc. **A118**, 654 (1928).

[15] In interpreting Eq. (9) it should be noted that in certain cases meaningless spherical harmonics are cancelled by a zero factor. Thus when $l=0$, and $u=-1$, ψ_3 in (9a) is to be taken to be zero.

[16] W. Gordon, Zeits. f. Physik **48**, 11 (1928).

where

$$
\begin{aligned}
{}_1F_1(\alpha;\beta;x) &= \sum_{n=0}^{\infty} \frac{(\alpha,n)}{(\beta,n)} x^n \\
(\alpha,n) &= \alpha(\alpha+1)\cdots(\alpha+n-1).
\end{aligned} \tag{14}
$$

M_r = radial normalizing factor.
n_r = radial quantum number.

$$\rho_l = ((l+1)^2 - \alpha^2)^{1/2}. \tag{15}$$

$$k_0 = \frac{2\pi mc}{h}\left(1 - \left(\frac{W}{mc^2}\right)^2\right)^{1/2} = \frac{1}{a_z N_l}. \tag{16}$$

$$N_l = (n_r^2 + (l+1)^2 + 2\rho_l n_r)^{1/2} \tag{17}$$

$$W = mc^2 \frac{n_r + \rho_l}{N_l} = mc^2\left\{1 + \frac{\alpha^2}{(n_r + ((j+\frac{1}{2})^2 - \alpha^2)^{1/2}}\right\}^{-1/2}. \tag{18}$$

$$a_z = \frac{h^2}{4\pi^2 me^2 Z}; \quad \alpha = \frac{2\pi e^2 Z}{hc}. \tag{19}$$

CONTINUOUS SPECTRUM: $W/mc^2 > 1$

$$F_l = -i\frac{\left(\frac{W}{mc^2} - 1\right)^{1/2}}{\left(\frac{W}{mc^2} + 1\right)^{1/2}} M_r(\sigma_1 - \sigma_2) \tag{20}$$

$$
\begin{aligned}
G_l &= M_r(\sigma_1 + \sigma_2) \\
\sigma_1 &= Ar^{\rho_l - 1} e^{-ik_0' r}\, {}_1F_1(\rho_l + iq + 1; 2\rho_l + 1; 2ik_0' r) \\
\sigma_2 &= Br^{\rho_l - 1} e^{-ik_0' r}\, {}_1F_1(\rho_l + iq; 2\rho_l + 1; 2ik_0' r)
\end{aligned} \tag{21}
$$

$$\frac{A}{B} = \frac{l+1+iQ}{\rho_l - iq} = \frac{\rho_l + iq}{l+1-iQ} \tag{22}$$

$$q = \frac{\frac{\alpha W}{mc^2}}{\left(\left(\frac{W}{mc^2}\right)^2 - 1\right)^{1/2}} = (Q^2 + \alpha^2)^{1/2} \tag{23}$$

$$k_0' = \frac{2\pi mc}{h}\left(\left(\frac{W}{mc^2}\right)^2 - 1\right)^{1/2}. \tag{24}$$

The discrete states of the Dirac electron are specified by the quantum numbers n_r, l, j, and u. These may have the following values:

$$
\begin{aligned}
n_r &= 0, 1, 2, \cdots \\
l &= 0, 1, 2, \cdots \\
j &= l \pm \tfrac{1}{2}, \ \geq 0
\end{aligned}
$$

(When $n_r=0$ the state $j=l-\frac{1}{2}$ is to be excluded.)

$$[-j] \leq u \leq [j],$$

where $[j]$ is the greatest integer contained in j.

The states of the continuous spectrum are specified by W, l, j, and u, with W arbitrary but $\geq mc^2$ and l, j, and u the same as for the discrete spectrum.

Normalization of the Wave Functions
Discrete Spectrum

We require to normalize our solutions in such a way that

$$\int_0^\infty \int_0^\pi \int_0^{2\pi} \psi\psi^* r^2 dr \cdot \sin\theta d\theta d\varphi = 1,$$

where

$$\psi\psi^* = \psi_1\psi_1^* + \psi_2\psi_2^* + \psi_3\psi_3^* + \psi_4\psi_4^*.$$

Suppose first that $j=l+\frac{1}{2}$. Then we find from Eq. (9a) that

$$\psi\psi^* = M_\theta^2[F_lF_l^*\{P_{l+1}^u P_{l+1}^{*u} + P_{l+1}^{u+1}P_{l+1}^{*u+1}\} + G_lG_l^*\{(l+u+1)^2 P_l^u P_l^{*u} + (l-u)^2 P_l^{u+1}P_l^{*u+1}\}] \tag{25}$$

or

$$\psi\psi^* = M_\theta^2[F_lF_l^* + G_lG_l^*][P_{l+1}^u P_{l+1}^{*u} + P_{l+1}^{u+1}P_{l+1}^{*u+1}],$$

as may be readily demonstrated.[17]

From the known relation

$$\int_0^\pi \int_0^{2\pi} P_l^u P_l^{*u} \sin\theta d\theta d\phi = \frac{4\pi}{2l+1}(l+u)!(l-u)! \tag{26}$$

we find

$$M_\theta^2\left(l, l+\frac{1}{2}, u\right) = \frac{1}{4\pi(l+u+1)!(l-u)!}. \tag{27}$$

The integral

$$I = \int_0^\infty [F_lF_l^* + G_lG_l^*]r^2 dr$$

can be evaluated as follows: one can easily show, by use of the generating function for the Laguerre polynomials,[18] that

$$\sum_{s=0}^{\infty} \binom{s+l}{s} {}_1F_1(-s; l+1; x)t^s = \frac{e^{-\frac{xt}{1-t}}}{(1-t)^{l+1}}; \; l \text{ arbitrary}. \tag{28}$$

[17] Cf. e.g., D. R. Hartree, Proc. Camb. Phil. Soc. 25, 225 (1929).
[18] Courant and Hilbert, "Methoden der math. Physik," p. 78.

Hence

$$\sum_{r,s=0}^{\infty}\binom{r+2\rho}{r}\binom{s+2\rho}{s}\int_0^\infty x^{2\rho}e^{-x}{}_1F_1(-r;\,2\rho+1;\,x)\,{}_1F_1(-s;\,2\rho+1;\,x)dx\cdot t^s\tau^r$$

$$=\int_0^\infty x^{2\rho}e^{-x}\frac{e^{-xt/(1-t)-x\tau/(1-\tau)}}{(1-t)^{2\rho+1}(1-\tau)^{2\rho+1}}dx$$

$$=\frac{\Gamma(2\rho+1)}{(1-t\tau)^{2\rho+1}}=\Gamma(2\rho+1)\sum_{s=0}^{\infty}\binom{s+2\rho}{s}(t\tau)^s.$$

Therefore

$$\int_0^\infty x^{2\rho}e^{-x}{}_1F_1(-r;\,2\rho+1;\,x)\,{}_1F_1(-s;\,2\rho+1;\,x)dx=\frac{\Gamma(2\rho+1)}{\binom{s+2\rho}{s}}\delta_{rs}. \quad (29)$$

Thus from Eq. (13)

$$\int_0^\infty \sigma_1{}^2r^2dr=\frac{\Gamma(2\rho_l+1)(N_l+l+1)^2}{(2k_0)^{2\rho_l+1}\binom{n_r+2\rho_l}{n_r}}\cdot$$

$$\int_0^\infty \sigma_2{}^2r^2dr=\frac{\Gamma(2\rho_l+1)n_r{}^2}{(2k_0)^{2\rho_l+1}\binom{n_r-1+2\rho_l}{n_r-1}}\cdot$$

$$\int_0^\infty \sigma_1\sigma_2r^2dr=0.$$

Since from Eq. (12)

$$I=\frac{2M_r{}^2}{N_l+\rho_l+n_r}\int_0^\infty\left[N_l(\sigma_1{}^2+\sigma_2{}^2)+2\sigma_1\sigma_2(\rho_l+n_r)\right]r^2dr,$$

we obtain

$$M_r{}^2\left(n_r,l,l+\frac{1}{2}\right)=\frac{(N_l+\rho_l+n_r)(2k_0)^{2\rho_l+1}\Gamma(2\rho_l+n_r+1)}{n_r!2N_l[\Gamma(2\rho_l+1)]^2[(N_l+l+1)^2+n_r(n_r+2\rho_l)]}. \quad (30)$$

Now let $j=l-\frac{1}{2}$. Then from (9b) we find

$$\psi\psi^*=M_\theta{}^2[F_{-l-1}F^*_{-l-1}+G_{-l-1}G^*_{-l-1}]\left[P_l{}^uP_l{}^{*u}+P_l{}^{u+1}P_l{}^{*u+1}\right], \quad (31)$$

and obtain in an exactly similar manner

$$M_\theta{}^2\left(l,l-\frac{1}{2},u\right)=\frac{1}{4\pi(l+u)!(l-u-1)!} \quad (32)$$

and

$$M_r{}^2\left(n_r,l,l-\frac{1}{2}\right)=\frac{(N+\rho+n_r)(2k_0)^{2\rho+1}\Gamma(2\rho+n_r+1)}{n_r!2N[\Gamma(2\rho+1)]^2[(N-l)^2+n_r(n_r+2\rho)]} \quad (33)$$

where in Eq. (33) the argument of N and ρ is not l, but $-l-1$. This change of argument occurs whenever $j=l-\frac{1}{2}$.

Continuous Spectrum

The angular normalizing factors are the same as for the discrete spectrum.

We first obtain an asymptotic expansion for the radial solutions, since we must here use a special normalizing method because the solutions are not quadratically integrable.

The asymptotic expansion of ${}_1F_1(\alpha;\beta;x)$ is given by[19]

$$ {}_1F_1(\alpha;\beta;x) \sim \frac{\Gamma(\beta)}{\Gamma(\alpha)} e^x x^{\alpha-\beta} + \frac{\Gamma(\beta)}{\Gamma(\beta-\alpha)}(-x)^{-\alpha}. \tag{34} $$

Using Eqs. (34) and (21), we find, omitting the prime on k_0,

$$ \begin{aligned} \sigma_1 &\sim \frac{A\Gamma(2\rho_l+1)(i)^{iq-\rho_l}}{\Gamma(\rho_l+iq+1)(2k_0)^\rho} \cdot \frac{e^{i(k_0 r + q\log 2k_0 r)}}{r} \\ \sigma_2 &\sim \frac{B\Gamma(2\rho_l+1)(-i)^{-iq-\rho_l}}{\Gamma(\rho_l-iq+1)(2k_0)^\rho} \cdot \frac{e^{-i(k_0 r + q\log 2k_0 r)}}{r}. \end{aligned} \tag{35} $$

Therefore, from Eq. (20)

$$ \begin{aligned} G_l &\sim M_r C \frac{\cos(k_0 r + q\log k_0 r - \delta_l)}{r} \\ F_l &\sim M_r C D \frac{\sin(k_0 r + q\log k_0 r - \delta_l)}{r} \end{aligned} \tag{36} $$

in which

$$ \delta_l = \rho_l \frac{\pi}{2} + \arg\Gamma(\rho_l + iq + 1) - \beta_0 - q\log 2. \tag{37} $$

$$ e^{2i\beta_0} = A/B \tag{37'} $$

$$ C = \frac{2\Gamma(2\rho_l+1)e^{-q\pi/2}|A|}{(2k_0)^\rho|\Gamma(\rho_l+iq+1)|} \cdot \left(\frac{A}{B^*}\right)^{1/2}. \tag{38} $$

$$ D = \left(\frac{\dfrac{W}{mc^2}-1}{\dfrac{W}{mc^2}+1}\right)^{1/2} = \left(\frac{q-Q}{q+Q}\right)^{1/2}. \tag{38'} $$

We shall use the Weyl normalization method.[20]

Call the radial normalization factor $M_r(W,l,j) = M(W)$. Then with proper choice of $M(W)$

$$ \begin{aligned} I &= \int_0^\infty M^*(W')r^2 dr \int_{W_1}^{W_2} M(W)\left[F_l(W)F_l^*(W') + G_l(W)G_l^*(W')\right]dW \\ &= \begin{cases} 1 & \text{when } W_1 < W' < W_2, \\ 0 & \text{when } W' \text{ lies outside the interval } (W_1, W_2). \end{cases} \end{aligned} \tag{39} $$

[19] E. W. Barnes, Trans. Camb. Phil. Soc. **20**, 253 (1906).
[20] H. Weyl, Math. Ann. **68**, 220 (1910).

If we write down Eqs. (11) for the energy value W, and their complex conjugates for the energy value W', multiply each of the resulting equations by r^2, then multiply the first equation for W by $F^*(W')$, the second by $-G^*(W')$, the first for W' by $-F(W)$, and the second by $G(W)$, and finally add, we obtain the equation

$$\frac{2\pi}{hc}\cdot(W - W')r^2[F(W)F^*(W') + G(W)G^*(W')] = \frac{\partial}{\partial r}r^2[G^*(W')F(W) - G(W)F^*(W')]. \quad (40)$$

Substituting Eq. (40) in Eq. (39), we get

$$I = \int_0^\infty M^*(W')dr \int_{W_1}^{W_2} \frac{hc}{2\pi}\frac{M(W)}{W' - W}\frac{\partial}{\partial r}[r^2G(W)F^*(W') - G^*(W')F(W)]dW$$

$$= \lim_{R\to\infty} \frac{hc}{2\pi}M^*(W')\int_{W_1}^{W_2}\frac{M(W)}{W'-W}R^2[G(W,R)F^*(W',R) - G^*(W',R)F(W,R)]dW$$

since $r^2GF=0$ when $r=0$.

We may therefore use our asymptotic expansions for F and G. From Eq. (36) we can write

$$I = \lim_{R\to\infty}\frac{hc}{2\pi}M^*(W')C^*(W')\int_{W_1}^{W_2}\frac{M(W)}{W' - W}[C(W)D(W')\cos Ru.\sin Ru' - C(W)D(W)\sin Ru\cdot\cos Ru']dW,$$

where

$$Ru = k_0R + q\log k_0R - \delta_l,$$

or

$$u(W) = \frac{2\pi mc}{h}\cdot\left(\left(\frac{W}{mc^2}\right)^2 - 1\right)^{1/2} + \frac{\alpha}{\left(1 - \left(\frac{mc^2}{W}\right)^2\right)^{1/2}}\frac{1}{R}\log\frac{2\pi mc}{h}R\left(\left(\frac{W}{mc^2}\right)^2 - 1\right)^{1/2} - \frac{\delta_l}{R}\cdot \quad (41)$$

We can choose R large enough so that $u(W)$ for $W_1 \leqq W \leqq W_2$ is an increasing function of W, and so can find the inverse function $W=f(u)$, which is continuous and possesses a continuous derivative for $W>mc^2$. We make a simple rearrangement in I and change variables from W to u, obtaining

$$I = \lim_{R\to\infty}\frac{hc}{2\pi}M^*(W')C^*(W')\int_{u_1}^{u_2}\frac{M[f(u)]C[f(u)]}{f(u') - f(u)}[D[f(u')]\sin R(u' - u) + \{D[f(u')] - D[f(u)]\}\sin Ru\cdot\cos Ru']f'(u)du,$$

$$= \lim_{R\to\infty}\frac{hc}{2\pi}M^*(W')C^*(W')(I_R' + I_R'').$$

Consider

$$\lim_{R\to\infty} I_R'' = \lim_{R\to\infty} \cos Ru' \int_{u_1}^{u_2} M[f(u)]C[f(u)]f'(u)\frac{D[f(u')]-D[f(u)]}{f(u')-f(u)}\sin Ru.\, du.$$

Now $D'(W)$ exists for $W>mc^2$, and the remaining functions in the integrand are continuous, so that we can apply the well-known result[21] that

$$\lim_{n\to\infty}\int_a^b \psi(t)\sin nt\, dt = 0$$

when $\psi(t)$ is integrable in (a, b). This gives us

$$\lim_{R\to\infty} I_R'' = 0.$$

By the same argument we can show that $\lim_{R\to\infty} I_R' = 0$ when W' is not in the interval (W_1, W_2). When $W_1<W'<W_2$, we can write, putting $u'-u=y$,

$$I_R' = D(W')\int_{u'-u_1}^{u'-u_2} M[f(u'-y)]C[f(u'-y)]f'(u'-y)\frac{\sin Ry}{f(u'-y)-f(u')}dy$$

$$= D(W')\int_{u'-u_2}^{u'-u_1} M[f(u'-y)]C[f(u'-y)]\frac{\sin Ry}{y}dy\frac{f'(u'-y)}{f'(u')}$$

$$+ D(W')\int_{u'-u_1}^{u'-u_2} M[f(u'-y)]C[f(u'-y)]f'(u'-y)\left[\frac{1}{f(u'-y)-f(u')}\right.$$

$$\left.-\frac{1}{f'(u')y}\right]\sin Ry\cdot dy = I_R''' + I_R^{IV}.$$

Since the function in the square brackets in I_R^{IV} is finite at $y=0$, the same argument as above shows that $\lim_{R\to\infty} I_R^{IV}=0$. Further,

$$\lim_{R\to\infty} I_R''' = D(W')M(W')C(W')\pi$$

by the Dirichlet integral.[22]

Finally, therefore,

$$I = \tfrac{1}{2}hc\,|\,M(W')\,|^2\,|\,C(W')\,|^2\,D(W'),$$

and we must take

$$M_r^2(W, l, l+\tfrac{1}{2}) = 2/hcD\,|\,C\,|^2. \tag{42}$$

Since the above calculation has not made use of a particular value for j, we have also

$$M_r^2(W, l, l-\tfrac{1}{2}) = 2/hcD\,|\,C\,|^2, \tag{43}$$

where in Eq. (43) the argument of ρ and A is $-l-1$, not l.

[21] See K. Knopp, Unendliche Reihen, p. 363.
[22] Knopp, reference 21, p. 366.

Selection Rules

The selection rules for the matrix elements B^s in Eq. (4′), when retardation is neglected, have been shown by Darwin[14] to be

$$\begin{aligned} \Delta l &= 1, \\ \Delta j &= 0, \pm 1, \\ \Delta u &= 0, \pm 1. \end{aligned} \tag{44}$$

The table below gives the possible transitions:

Initial State				Initial State			
n_r	l	$l+\frac{1}{2}$	u	n_r	l	$l-\frac{1}{2}$	u
Final State				Final State			
n_r'	$l+1$	$l+3/2$	u'	n_r'	$l+1$	$l+\frac{1}{2}$	u'
n_r'	$l+1$	$l+\frac{1}{2}$	u'	n_r'	$l-1$	$l-\frac{1}{2}$	u'
n_r'	$l-1$	$l-\frac{1}{2}$	u'	n_r'	$l-1$	$l-3/2$	u'

(45)

with $u'=u$, $u\pm1$, and arbitrary n_r'. The only degeneracy of the possible final states of the discrete spectrum is that with respect to u'. If n_r' stands for the energy W of a state in the continuous spectrum, all possible final states having this value W fall together.

The Mass Absorption Coefficient of the K Shell

The atomic absorption coefficient τ_ν for a given energy jump is defined as follows:

$$\tau_\nu I(\nu)d\nu = \text{energy absorbed per second} = h\nu\cdot w'dW \tag{46}$$

where $w'dW$ ($=w'd\epsilon''$ of Eq. (8)) is the transition probability for the energy jump under consideration, and $I(\nu)d\nu$ is the intensity of the incident radiation in the range $d\nu$. Thus

$$(\tau_\nu)_K I(\nu)d\nu = h\nu\cdot w'(W;\,0,\,0,\,\tfrac{1}{2})dW,$$

since in the K shell $n_r=l=0$, and $j=\frac{1}{2}$.

The formula for the mass absorption coefficient $(\tau_\nu/\rho)_K$[23] becomes, since $dW=h.d\nu$,

$$\left(\frac{\tau_\nu}{\rho}\right)_K = \frac{Nh^2\nu}{AI(\nu)}w'\left(W;\,0,\,0,\,\frac{1}{2}\right) = \frac{Nh^2\nu}{A8\pi c\rho(\nu)}w'\left(W;\,0,\,0,\,\frac{1}{2}\right), \tag{47}$$

where N is Avogadro's number, A is the atomic weight, and $\rho(\nu)$ is defined in connection with Eq. (5).

[23] The ρ in τ_ν/ρ is not to be confused with $\rho(\nu)$. The former is the mass of an atom, while the latter is energy density.

Consulting the table (45) of possible transitions, we see that the sum over the degenerate states in Eq. (8) extends over the initial values of u, the final values u', and $j=\frac{1}{2}$, 3/2, the only possible final l being 1. We thus obtain

$$\left(\frac{\tau_\nu}{\rho}\right)_K = \frac{2\pi e^2 cN}{3A\nu}\left[\sum_{u,u'}\left| P\left(W,1,\frac{3}{2},u';0,0,\frac{1}{2},u\right)\right|^2 + \sum_{u,u'}\left| P\left(W,1,\frac{1}{2},u';0,0,\frac{1}{2},u\right)\right|^2\right]. \quad (48)$$

Carrying out the angular integrations indicated by the definitions (8′) and (4′) of the P's, and using the angular normalizing factors given by Eqs. (27) and (32), and finally summing over u and u', we easily obtain

$$\left(\frac{\tau_\nu}{\rho}\right)_K = \frac{4\pi e^2 cN}{3A\nu}\left[\frac{8}{3}\left|\int_0^\infty F_0 G_1 r^2 dr\right|^2 + 3\left|\int_0^\infty F_{-2}G_0 r^2 dr + \frac{1}{3}\int_0^\infty F_0 G_{-2} r^2 dr\right|^2\right]. \quad (49)$$

Writing $\rho=(1-\alpha^2)^{1/2}$, $\rho'=(4-\alpha^2)^{1/2}$, $a=k_0'/k_0$, and taking

$$A = \frac{((l+1)^2+Q^2)^{1/2}}{Q} e^{i\tan^{-1}Q/(l+1)}$$
$$B = \frac{((l+1)^2+Q^2)^{1/2}}{Q} e^{-i\tan^{-1}q/\rho'} \quad (50)$$

we find for the functions F_0, G_0, G_1, G_{-2}, and F_{-2}, using Eqs. (12), (13), (20), (21), (30), (42), (43), (38), and (38′),

$$F_0 = (2k_0)^\rho \left(\frac{(1-\rho)k_0}{\Gamma(2\rho+1)}\right)^{1/2} r^{\rho-1}e^{-k_0 r}. \quad (51)$$

$$G_0 = (2k_0)^\rho \left(\frac{(1+\rho)k_0}{\Gamma(2\rho+1)}\right)^{1/2} r^{\rho-1}e^{-k_0 r} \quad (52)$$

$$G_1 = \frac{(2ak_0)^{\rho'}\,|\,\Gamma(\rho'+iq+1)\,|\,e^{q\pi/2}}{2\Gamma(2\rho'+1)}\left(\frac{2}{hc}\right)^{1/2}\left(\frac{q-Q}{q+Q}\right)^{-1/4} \cdot \left[e^{i[\tan^{-1}Q/2-ak_0r]}r^{\rho'-1}{}_1F_1(\rho'+iq+1;2\rho'+1;2iak_0r) + e^{-i[\tan^{-1}q/\rho'+ak_0r]}r^{\rho'-1}{}_1F_1(\rho'+iq;2\rho'+1;2iak_0r)\right]. \quad (53)$$

$$G_{-2} = \frac{(2ak_0)^\rho\,|\,\Gamma(\rho+iq+1)\,|e^{q\pi/2}}{2\Gamma(2\rho+1)}\left(\frac{2}{hc}\right)^{1/2}\left(\frac{q-Q}{q+Q}\right)^{-1/4} \cdot \left[e^{i[\tan^{-1}Q/l-1-ak_0r]}r^{\rho-1}{}_1F_1(\rho+iq+1;2\rho+1;2iak_0r) + e^{-i[\tan^{-1}q/\rho+ak_0r]}r^{\rho-1}{}_1F_1(\rho+iq;2\rho+1;2iak_0r)\right]. \quad (54)$$

$$F_{-2} = \frac{(2ak_0)^\rho\,|\,\Gamma(\rho+iq+1)\,|\,e^{q\pi/2}}{i2\Gamma(2\rho+1)}\left(\frac{2}{hc}\right)^{1/2}\left(\frac{q-Q}{q+Q}\right)^{1/4}.$$

$$\cdot \left[e^{i[\tan^{-1}Q/-1-ak_0r]}r^{\rho-1}{}_1F_1(\rho+iq+1;2\rho+1;2iak_0r) \right. \tag{55}$$

$$\left. - e^{-i[\tan^{-1}q/\rho+ak_0r]}r^{\rho-1}{}_1F_1(\rho+iq;2\rho+1;2iak_0r)\right].$$

Integrating and rearranging, we obtain

$$\int_0^\infty F_0G_1r^2dr = 2^{\rho'+\rho}a^{\rho'}\cdot\left(\frac{1-\rho}{2hck_0\Gamma(2\rho+1)}\right)^{1/2}\frac{|\Gamma(\rho'+iq+1)|\,e^{q\pi/2}\cdot}{(1-ia)^{\rho'+\rho+1}}\left(\frac{q-Q}{q+Q}\right)^{-1/4}\cdot$$

$$\cdot\frac{\Gamma(\rho'+\rho+1)}{\Gamma(2\rho'+1)}\cdot\left[e^{-i\tan^{-1}Q/2}\,{}_2F_1\left(\rho'+\rho+1,\rho'-iq+1;2\rho'+1;-\frac{2ia}{1-ia}\right)\right. \tag{56}$$

$$\left.+e^{i\tan^{-1}q/\rho'}{}_2F_1\left(\rho'+\rho+1,\rho'-iq;2\rho'+1;-\frac{2ia}{1-ia}\right)\right].$$

$$\int_0^\infty F_0G_{-2}r^2dr = 2^{2\rho}a^{\rho}\cdot\left(\frac{1-\rho}{2hck_0\Gamma(2\rho+1)}\right)^{1/2}\frac{|\Gamma(\rho+iq+1)|\,e^{q\pi/2}}{(1-ia)^{2\rho+1}}\left(\frac{q-Q}{q+Q}\right)^{-1/4}\cdot$$

$$\cdot\left[e^{i\tan^{-1}Q/-1}\cdot{}_2F_1\left(2\rho+1,\rho-iq+1;2\rho+1;-\frac{2ia}{1-ia}\right)\right. \tag{57}$$

$$\left.+e^{i\tan^{-1}q/\rho}\cdot{}_2F_1\left(2\rho+1,\rho-iq;2\rho+1;-\frac{2ia}{1-ia}\right)\right].$$

$$\int_0^\infty F_{-2}G_0r^2dr = i2^{2\rho}a^{\rho}\cdot\left(\frac{1+\rho}{2hck_0\Gamma(2\rho+1)}\right)^{1/2}\frac{|\Gamma(\rho+iq+1)|\,e^{q\pi/2}}{(1-ia)^{2\rho+1}}\left(\frac{q-Q}{q+Q}\right)^{1/4}\cdot$$

$$\cdot\left[e^{-i\tan^{-1}Q/-1}\cdot{}_2F_1\left(2\rho+1,\rho-iq+1;2\rho+1;-\frac{2ia}{1-ia}\right)\right. \tag{58}$$

$$\left.-e^{i\tan^{-1}q/\rho}\cdot{}_2F_1\left(2\rho+1,\rho-iq;2\rho+1;-\frac{2ia}{1-ia}\right)\right].$$

The two hypergeometric functions in (56) cannot be readily evaluated in their present form because of very slow convergence or non-convergence of the usual series. There are two possible methods of evaluating them numerically. One method is to express them as definite integrals and then to integrate numerically. Because $\rho'-\rho-1$ is so small, the numerical integration will be inaccurate or laborious if no further transformation of the resulting integrals is made. A convenient transformation which is satisfactory over the range of values of a and q which corresponds to $\frac{1}{2}\lambda_k \leqq \lambda \leqq \lambda_k$, is that which results in the integral J defined by Eq. (62) below.

Using the relationship

$${}_2F_1(\alpha,\beta;\gamma;x) = \frac{\Gamma(\gamma)}{\Gamma(\alpha)\Gamma(\gamma-\alpha)}\int_0^1 u^{\alpha-1}(1-u)^{\gamma-\alpha-1}(1-ux)^{-\beta}du, \tag{59}$$

and making some simple transformations, we can write

$$ {}_2F_1\left(\rho'+\rho+1,\ \rho'-iq+1;\ 2\rho'+1;\ -\frac{2ia}{1-ia}\right) $$
$$ =\left(\frac{1+ia}{1-ia}\right)^{iq-\rho-1}\left\{1+\frac{J^*}{B(\rho'-\rho,\ \rho'+\rho+1)}\right\} \tag{60} $$

$$ {}_2F_1\left(\rho'+\rho+1,\ \rho'-iq;\ 2\rho'+1;\ -\frac{2ia}{1-ia}\right) $$
$$ =\left(\frac{1+ia}{1-ia}\right)^{iq-\rho'}\left\{1+\frac{J}{B(\rho'-\rho,\ \rho'+\rho+1)}\right\} \tag{61} $$

where

$$ J=\int_{-1/2}^{+1/2}\left(\frac{1}{2}-t\right)^{\rho'+\rho}\left(\frac{1}{2}+t\right)^{\rho'-\rho-1}dt\left[\left(\frac{1+ia}{1-2iat}\right)^{\rho'-iq}-1\right] \tag{62} $$

and

$$ B(\alpha,\beta)=\frac{\Gamma(\alpha)\Gamma(\beta)}{\Gamma(\alpha+\beta)}. \tag{63} $$

The other method of evaluating the hypergeometric functions in Eq. (56) is to transform them to another combination of hypergeometric functions which do converge fairly rapidly. By use of the transformation[24] connecting Y_1 with Y_3 and Y_4 one finds readily from Eq. (60) that

$$ B(\rho'-\rho,\ \rho'+\rho+1)+J=\frac{(1+a^2)^{\rho'}}{(2a)^{2\rho'}}e^{i\rho'\pi}\left[B(\rho-iq,\ \rho'-\rho)\left(\frac{1-ia}{1+ia}\right)^{\rho}\cdot\right. $$
$$ \cdot\ {}_2F_1\left(-\rho'-\rho,\ 1+iq-\rho';\ 1+iq-\rho;\ \frac{1+ia}{1-ia}\right) \tag{64} $$
$$ +B(-\rho+iq,\ \rho'+\rho+1)\left(\frac{1-ia}{1+ia}\right)^{iq}\cdot $$
$$ \left.\cdot\ {}_2F_1\left(1+\rho-\rho',\ -\rho'-iq;\ \rho-iq+1;\ \frac{1+ia}{1-ia}\right)\right]. $$

The series for the hypergeometric functions in Eq. (64) converge fairly rapidly for any range of wave-length. The chief difficulty in the use of this formula is the calculation of the gamma functions. High accuracy can be obtained from this formula with less work than from numerical integration, but for three-figure accuracy the latter is much quicker. All the calculations in this paper were performed by numerical integration.

The hypergeometric functions occurring in Eqs. (57) and (58) can be reduced to elementary functions by the use of the relation

$$ {}_2F_1(\alpha,\beta;\alpha;x)=(1-x)^{-\beta} \tag{65} $$

[24] E. W. Barnes, Proc. Lond. Math. Soc. (2), **6**, 141 (1908).

Making these transformations and noting that $Q=1/a$, we obtain for the three integrals

$$\int_0^\infty F_0 G_1 r^2 dr = 2^{\rho'+\rho} a^{\rho'} \left(\frac{1-\rho}{2hck_0\Gamma(2\rho+1)}\right)^{1/2} \frac{|\Gamma(\rho'+iq+1)|\, e^{q(\pi/2-2\tan^{-1}a)}}{\Gamma(\rho'-\rho)(1+a^2)^{(\rho'+\rho+1)/2}} \left(\frac{q-Q}{q+Q}\right)^{-1/4} \cdot$$
$$\cdot \left[e^{-i[\tan^{-1}Q/2-(\rho'-\rho-1)\tan^{-1}a]} \cdot \{B(\rho'-\rho,\rho'+\rho+1)+J^*\}\right. \tag{66}$$
$$\left. + e^{i[\tan^{-1}q/\rho'-(\rho'-\rho-1)\tan^{-1}a]} \cdot \{B(\rho'-\rho,\rho'+\rho+1)+J\}\right].$$

$$\int_0^\infty F_0 G_{-2} r^2 dr = 2^{2\rho} a^{\rho} \cdot \left(\frac{1-\rho}{2hck_0\Gamma(2\rho+1)}\right)^{1/2} \frac{|\Gamma(\rho+iq+1)|\, e^{q(\pi/2-2\tan^{-1}a)}}{(1+a^2)^{\rho+1/2}} \left(\frac{q-Q}{q+Q}\right)^{-1/4} \cdot$$
$$\cdot \left[ie^{-2i\tan^{-1}a} + e^{i[\tan^{-1}q/\rho+\tan^{-1}a]}\right] \tag{67}$$

$$\int_0^\infty F_{-2} G_0 r^2 dr = 2^{2\rho} a^{\rho} \cdot \left(\frac{1+\rho}{2hck_0\Gamma(2\rho+1)}\right)^{1/2} \frac{|\Gamma(\rho+iq+1)|\, e^{q(\pi/2-2\tan^{-1}a)}}{(1+a^2)^{\rho+1/2}} \left(\frac{q-Q}{q+Q}\right)^{1/4} \cdot$$
$$\cdot \left[e^{-2i\tan^{-1}a} - ie^{i[\tan^{-1}q/\rho+\tan^{-1}a]}\right]. \tag{68}$$

Substituting in Eq. (49) we obtain finally for the mass absorption coefficient for the K shell

$$\left(\frac{\tau_\nu}{\rho}\right)_K = \frac{\dot{N}}{AZ} \frac{h\lambda}{3\pi mc} \frac{2^{2\rho} e^{q(\pi-4\tan^{-1}a)}}{\Gamma(2\rho+1)(1+a^2)^{\rho+1}} \left[\frac{8}{3} \frac{(2a)^{2\rho'}(1-\rho)}{(1+a^2)^{\rho'}} \cdot \right.$$
$$\cdot \frac{|\Gamma(\rho'+iq+1)|^2}{[\Gamma(\rho'-\rho)]^2} \left(\frac{q-Q}{q+Q}\right)^{-1/2} |B(\rho'-\rho,\rho'+\rho+1)+J|^2(1+\cos\phi) \tag{69}$$
$$+ 3\frac{(2a)^{2\rho}|\Gamma(\rho+iq+1)|^2}{(1+a^2)^{\rho}} \left\{(1+\rho)\left(\frac{q-Q}{q+Q}\right)^{1/2}(1+\sin\delta)\right.$$
$$\left. \left. + \frac{1-\rho}{9}\left(\frac{q-Q}{q+Q}\right)^{-1/2}(1-\sin\delta) + \frac{2}{3}(1-\rho^2)^{1/2}\cdot\cos\delta\right\}\right].$$

in which

$$\phi = \tan^{-1}\tfrac{1}{2}Q + \tan^{-1}q/\rho' - 2(\rho'-\rho-1)\tan^{-1}a + 2\tan^{-1}\chi.$$

$$\chi = \arg\left[B(\rho'-\rho,\rho'+\rho+1)+J\right]$$

$$\delta = 3\tan^{-1}a + \tan^{-1}q/\rho$$

$$a^2 = x\frac{2+xy}{2-y};\ Q = \frac{1}{a};\ q^2 = Q^2+\alpha^2;\ \alpha^2 = y(2-y);$$

$$x = \lambda_k/\lambda - 1;\ \text{and}\ y = h/mc\lambda_k.$$

The two expressions in Eq. (69) which are most difficult to calculate are the absolute value of the gamma function of complex argument, and the

integral J. The gamma function can be most conveniently calculated from the asymptotic expansion

$$\log|\Gamma(x+iy)| \sim \tfrac{1}{2}(x-\tfrac{1}{2})\log(x^2+y^2) - y\tan^{-1}y/x - x + \tfrac{1}{2}\log 2\pi + \sum_{n=1}^{\infty}\frac{B_{2n}}{2n(2n-1)}\frac{\cos[(2n-1)\tan^{-1}y/x]}{(x^2+y^2)^{n-1/2}}. \quad (70)$$

where the B_{2n} are the well-known Bernoulli numbers. By taking x large and using the difference equation satisfied by the gamma function, Eq. (70) forms a relatively easy method of calculation.

Under adverse circumstances, the calculation of the integral J could be very laborious. Fortunately, when the wave-length is confined to the range $\frac{1}{2}\lambda_k$ to λ_k, the integrand of Eq. (62) does not change rapidly and has no important oscillations, so that an approximate formula of integration may be expected to give sufficient accuracy. The formula used is one given by Woolhouse,[25] namely,

$$\int_0^1 f(x)dx = \frac{7}{390}[f(0)+f(1)] + \frac{16,807}{133,380}[f(1/14)+f(13/14)] + \frac{128}{570}[f(1/4)+f(3/4)] + \frac{71}{270}f(\tfrac{1}{2}). \quad (71)$$

It would be very difficult to obtain a numerical value for the error involved in using this formula when evaluating an integral as complicated as J. However, the writer has tried the formula in evaluating known integrals of functions which have closely the same shape as the actual integrand in J, and from these trials he is convinced that in the wave-length range mentioned above at least three- and very probably four-figure accuracy can be expected. This is further supported by the close agreement of the results for Al ($Z=13$) with those calculated from the Nishina-Rabi formula, an entirely independent procedure. The effect on the absorption coefficient of an error in calculating J depends of course upon the relative magnitude of the two parts of Eq. (69). In the range under consideration the term containing J is from 2 to 3 times as large as the other term.

Mass Absorption Coefficient at the Absorption Edge

At the absorption edge, where $\lambda=\lambda_k$, Eq. (69) cannot be used to calculate the absorption coefficient because there $a=0$ and $q=Q=\infty$. A limiting process is necessary, and it is most convenient to pass to the limit for the individual proper functions and then to integrate, instead of passing to the limit directly in Eq. (69). Another more simple method if only the form of the proper functions is necessary, is to solve the radial differential Eqs. (11) when $W=mc^2$, but this has the disadvantage for our purpose of requiring another normalization using Weyl's method.

[25] Woolhouse, Journ. Inst. Act. **27**, 122, (1888). Cf. Whittaker and Robinson, "Calculus of Observations," p. 158.

We want to find $\lim_{a\to 0} F_l$ and $\lim_{a\to 0} G_l$. To do this we consider separately the radial normalizing factor and the functions σ_1 and σ_2 (see Eq. 21)). From the well-known Stirling formula, we can write[26]

$$|\Gamma(\rho' + iq + 1)| \sim (2\pi)^{1/2} a^{-\rho'-1/2} e^{-q\pi/2},$$

also

$$|A| \sim 1, \quad \text{and} \quad (2k_0')^{\rho'} = (2k_0)^{\rho'} a^{\rho'},$$

so that from Eq. (38)

$$|C| \sim 2\Gamma(2\rho' + 1)(2k_0)^{-\rho'}(a/2\pi.)^{1/2} \tag{72}$$

Also, from Eq. (38′),

$$D = \left(\frac{q-Q}{q+Q}\right)^{1/2} = \left(\frac{(1+a^2\alpha^2)^{1/2} - 1}{(1+a^2\alpha^2)^{1/2} + 1}\right)^{1/2} \sim \tfrac{1}{2}a\alpha \tag{73}$$

since $q^2 = Q^2 + \alpha^2 = 1/a^2 + \alpha^2$. Therefore, from Eq. (42),

$$M_r = \frac{1}{|C|}\left(\frac{2}{hcD}\right)^{1/2} \sim \left(\frac{2\pi}{hc\alpha}\right)^{1/2} \frac{(2k_0)^{\rho'}}{\Gamma(2\rho'+1)} \frac{1}{a} = \frac{(2k_0)^{\rho'}}{e(Z)^{1/2}\Gamma(2\rho'+1)} \frac{1}{a}, \tag{74}$$

using Eq. (19).

It is a known property[27] of the degenerate hypergeometric function that

$$\lim_{\epsilon\to\infty} \frac{(\frac{1}{2}z)^{\alpha}}{\Gamma(\alpha+1)} {}_1F_1\left(\frac{1}{\epsilon}; \alpha+1; -\epsilon z^2/4\right) = J_\alpha(z), \tag{75}$$

where $J_\alpha(z)$ is the ordinary Bessel function. It is evident, therefore, that

$$\begin{aligned} \lim_{a\to 0} \sigma_2 &= \lim_{a\to 0} Br^{\rho'-1} e^{-iak_0 r} {}_1F_1(\rho' + iq; 2\rho' + 1; 2iak_0 r) \\ &= -i\Gamma(2\rho'+1)(2k_0)^{-\rho'} r^{-1} J_{2\rho'}((8k_0 r)^{1/2}). \end{aligned} \tag{76}$$

It can easily be shown that

$$\begin{aligned} {}_1F_1(\rho' + iq + 1; 2\rho' + 1; 2ik_0' r) &= \frac{2\rho'}{\rho' + iq} {}_1F_1(\rho' + iq; 2\rho'; 2ik_0' r) \\ &\quad - \frac{\rho' - iq}{\rho' + iq} {}_1F_1(\rho' + iq; 2\rho' + 1; 2ik_0' r). \end{aligned} \tag{77}$$

With Eqs. (77) and (21), we find

$$\begin{aligned} \sigma_1 \pm \sigma_2 = r^{\rho'-1} e^{-ik_0' r} \Bigg[& A \frac{2\rho'}{\rho' + iq} {}_1F_1(\rho' + iq; 2\rho'; 2ik_0' r) \\ & + \left[\pm B - A\frac{\rho' - iq}{\rho' + iq} \right] {}_1F_1(\rho' + iq; 2\rho' + 1; 2ik_0' r) \Bigg]. \end{aligned} \tag{78}$$

[26] The symbol $\backsim$, as used in this section, has the following significance. if $f(a) \backsim g(a)$ then $\lim_{a\to 0} f(a)/g(a) = 1$.

[27] G. N. Watson, "Bessel Functions," p. 154.

From Eqs. (78), (76), and (50), we find after some calculation

$$(\sigma_1 + \sigma_2) \sim a \cdot r^{-1}\Gamma(2\rho' + 1)(2k_0)^{-\rho'}\left[J_{2\rho'-1}((8k_0r)^{1/2}) \cdot (2k_0r)^{1/2}\right.$$
$$\left. + (l + 1 - \rho')J_{2\rho'}((8k_0r)^{1/2})\right],$$
$$\lim_{a\to 0}(\sigma_1 - \sigma_2) = 2ir^{-1}\Gamma(2\rho' + 1)(2k_0)^{-\rho'}J_{2\rho'}((8k_0r)^{1/2}),$$

so that finally, with Eqs. (20) and (74),

$$\lim_{a\to 0} F_l = \alpha/e(Z)^{1/2}r \cdot J_{2\rho'}((8k_0r)^{1/2}) \tag{79}$$

$$\lim_{a\to 0} G_l = 1/e(Z)^{1/2}r \cdot \left[(2k_0r)^{1/2}J_{2\rho'-1}((8k_0r)^{1/2}) + (l+1 - \rho')J_{2\rho'}((8k_0r)^{1/2})\right]. \tag{80}$$

After some simple calculations, using the formula[28]

$$\int_0^\infty J_\nu(at)\exp(-p^2t^2)t^{\mu-1}dt$$
$$= \frac{\Gamma\left(\frac{\nu+\mu}{2}\right)\left(\frac{a}{2p}\right)^\nu}{2p^\mu\Gamma(\nu+1)}\exp(-a^2/4p^2)\,{}_1F_1\left(\frac{\nu-\mu}{2}+1;\nu+1;a^2/4p^2\right),$$

we find for the mass absorption coefficient at the absorption edge

$$\left(\frac{\tau_\nu}{\rho}\right)_{K\text{edge}} = \frac{h^2N\lambda_k}{3\pi mc^2\cdot 1}\frac{2^{2\rho}\exp(-4)}{Z^2\Gamma(2\rho+1)}\left[\frac{8}{3}2^{2\rho'}(1-\rho)\left[\frac{\Gamma(\rho'+\rho+1)}{\Gamma(2\rho'+1)}\right]^2\right.$$
$$\cdot\left[2\rho'\,{}_1F_1(\rho'-\rho-1;2\rho';2) + (2-\rho')\,{}_1F_1(\rho'-\rho;2\rho'+1;2)\right]^2 \tag{81}$$
$$\left. + 3\cdot 2^{2\rho}\left[\alpha(1+\rho)^{1/2} - \frac{3-\rho}{3}(1-\rho)^{1/2}\right]^2\right].$$

Eqs. (69) and (81) for the mass absorption coefficient have been derived for a one-electron atom. Actually, of course, the K shell contains two electrons, so that one might expect, in the absence of interaction between the electrons, merely to multiply the values for the one-electron atom by two. This is incorrect. In the one-electron atom the lowest energy level is doubly degenerate since there are two possible directions for the "spin" magnetic moment of the electron, represented analytically by $u=0$ or -1. In the two-electron atom, however, the lowest state is non-degenerate. If the Pauli exclusion principle were not in force, the degeneracy of the lowest state would be four, since in the absence of interaction each electron may have the values $u=0$ or -1. Since, however, no two electrons may have the same quantum numbers, and because of the identity of the electrons,[29] three of the degener-

[28] Watson, reference 27, p. 394.
[29] W. Heisenberg, Zeits. f. Physik 38, 411 (1926).

ate states are ruled out, so that multiplying by two for the two K electrons and dividing by two because there is no degeneracy leaves Eqs. (69) and (81) unchanged.

Since the completion of this paper an article by Stobbe[30] has appeared in which the mass absorption coefficient is calculated by means of the non-relativistic quantum mechanics. Stobbe uses a screening constant for the K electrons which is considerably smaller than that necessary to make the energy of the model agree with that experimentally determined from the K edge. He justifies this procedure by pointing out that in the final state with one K electron ejected, the energy of the remaining electrons is different from that in the initial state, so that the absorbed frequency does not correspond exactly to the change in energy of the ejected K electron alone.

The present calculations can easily be adapted to a model with a smaller screening constant by lowering Z to compensate for the decrease in s; the results then apply to different atoms, for instance to gold (79) instead of lead (82) if s is changed from 4.512 to 1.512. With the smaller screening constant, however, the λ_k' of the model will no longer agree with the experimental value. We want the abscissas of the computed and observed curves to coincide at the experimental λ_k. Now the absorption coefficient depends on a matrix element which is a function of λ_k' and W, the energy of the ejected electron. In the present calculations W was connected with a wave-length λ' of the incident x-rays given by $W=mc^2+h(\nu'-\nu_k')=mc^2+hc(1/\lambda'-1/\lambda_k')$. In the adapted calculations ν_k' is replaced by ν_k corresponding to the actual absorption edge and so W must be connected with a wave-length λ given by $W=mc^2+hc(1/\lambda-1/\lambda_k)$. We must now use λ and not λ' in Eq. (47) since the factor multiplying the matrix element in this equation arose originally from the change in energy of the atom as a whole. The new absorption coefficient is therefore

$$\frac{\tau}{\rho}(\lambda)=\frac{\lambda}{\lambda'}\cdot\frac{\tau}{\rho}(\lambda'),$$

where

$$\frac{1}{\lambda}-\frac{1}{\lambda_k}=\frac{1}{\lambda'}-\frac{1}{\lambda_k'}.$$

When one calculates this new absorption it turns out, however, that the agreement with experiment is worse. This does not mean that if one calculated the absorption coefficient for gold using a larger screening constant that one would find better agreement with experiment, but merely that the use of a large screening constant for lead agrees better with experiment than the use of a small one with gold, and is probably to be attributed to the rapid loss of accuracy of the model as Z is decreased.

That the agreement with experiment is worse can be seen roughly from the following considerations. At the absorption edge $\lambda/\lambda'=(Z'/Z)^2$ by Moseley's law, where Z' is the atomic number used in the calculation and Z

[30] M. Stobbe, Ann. d. Physik (5), **7**, 661 (1930).

that of the atom to which it is now applied. But the observed absorption coefficients are closely in the ratio $(Z'/Z)^3$ at the edge; and the theoretical values are already too low. It is therefore not thought worth while to publish the modified values.

The writer wishes to thank Dr. I. I. Rabi for suggesting this problem, and also to express his appreciation to Professor E. H. Kennard for his constant interest and for the many stimulating discussions throughout the writer's graduate study.

INTERCHANGE OF TRANSLATIONAL, ROTATIONAL AND VIBRATIONAL ENERGY IN MOLECULAR COLLISIONS

By Clarence Zener*
Jefferson Physical Laboratory
Harvard University

(Received January 5, 1931)

Abstract

The change in internal energy of molecules upon collisions has been analysed. Formulae, (26) to (27-C), for the effective cross section of inelastic collisions have been obtained as functions of known properties of the molecules, subject to certain conditions. These conditions are: the atoms which come into contact during collision must belong to the first row of the periodic table; the vibrational quantum numbers which suffer a change must be small.

Vibrational quantum numbers have a marked reluctance to change during collisions at room temperature. The probability that a N_2 molecule in its first excited vibrational state transfer its energy to He in a head on collision is 0.0^76. The probability that another N_2 molecule absorb this energy is 0.0^14. A lack of resonance of 0.01 volt can decrease the effective cross section by a factor of 0.02.

Rotational quantum numbers change readily except in unusual cases.

I. Introduction

In A gaseous system we often wish to know the effective cross section of a collision between two systems in which one or both suffer a change of quantum numbers. If this change involves electron jumps, as in the quenching of resonance radiation, it is not limited to collisions in which the systems would be said classically to come into contact. Such transitions have been observed to take place when the closest distance of approach is many times the classical diameter of the systems.[1] In this type of collision the changes in the motion of the two systems as a whole may be relatively unimportant in comparison to the change of quantum numbers.

In another interesting type of collision the electronic states remain unaltered, and the vibrational and rotational states are changed. The experimental data have been discussed by Oldenberg.[2] In many cases the probability of a transfer is very small even in head-on collisions. In such collisions changes in the internal molecular quantum numbers are unimportant in comparison to changes in the motion of the two systems as a whole. A study of the latter change must thus precede a study of the former. Such a procedure is adopted in this paper. The exact motion of the centers of gravity of the two colliding systems is found when the internal coordinates are replaced

* National Research Fellow.

[1] Baxter, J.A.C.S. 52, 3920 (1930); Boeckner, Bureau Stand. 5, 13 (1930).

[2] Oldenberg, Phys. Rev. 37, 194 (1931).

by their averaged values. This motion corresponds to an elastic collision. The internal motions of the systems are then treated as perturbations that give rise to changes in the internal quantum numbers during collision.

The discussion of collision phenomena is preceded by an examination of inter-molecular forces (II). The principles of energy interchange may be most clearly analyzed in systems so idealized that all irrelevent difficulties are absent. Thus the interchange of vibrational and translational energy is investigated in the simplified collision of an atom and a diatomic molecule where all motion is confined to a line (III). Similarly the interchange of rotational and translational energy is examined first for the collision of an atom with a rigid symmetrical molecule, all motion being limited to a plane (IV). The results of the investigation of these idealized collisions are then combined in such a way as to give definite numerical information about collisions in an actual gaseous system (V).

II. Inter-Molecular Forces

In ordinary collisions the inter-molecular forces need be known only for those inter-molecular distances in which the overlapping of electrons is slight. At these collision distances the mutual energy may be split to a good approximation into three parts: that due to van der Waal's attraction, the negative coulomb energy arising from interpenetration of electrons, and the repulsive resonance energy. The mutual energy between two molecules is approximately the sum of the mutual energies between the constituent atoms, provided the resonance forces are taken to be repulsive.

London and Eisenschitz[3] have shown that the repulsive resonance energy between two H atoms dominates the attractive energies. This may safely be considered to be true for all atoms in the first row of the periodic table. However, this resonance energy becomes smaller both with an increase of the total quantum number n[4] and of the azimuthal quantum number l[5]. Hence the following considerations will be confined to atoms in the first row.

In the outer region of an atom, i.e., the region that overlaps in ordinary thermal collisions, the electronic density varies approximately[6] as $r^{n^*}\exp(-2\alpha s)$. Here s is the distance from the nucleus, and α is the square root of the ionization potential.[7] The asymptotic expansion of the resonance energy[8] between two atoms will contain the factor $\exp-(\alpha_1+\alpha_2)R$, where α_1 and α_2 refer

[3] E. Eisenschitz and F. London, Zeits. f. Physik **60**, 491 (1930).

[4] W. Heisenberg, Zeits. f. Physik **49**, 619 (1928).

[5] M. Delbruck, Proc. Roy. Soc. **129**, 686 (1930).

[6] D. R. Hartree, Proc. Camb. Phil. Soc. **24**, 89 (1928).

[7] Energy, length, mass will in this paper be expressed in the atomic units 13.53 volts, 0.528×10^{-8} cm, m_e, unless otherwise specified.

[8] This may be verified by examining the general type of integral that arises in calculating the resonance energy. See Zener and Guillemin, Phys. **34**, 999 (1929), Eqs. (28) and (29). When the integral logarithms are replaced by their asymptotic expansions all terms will have the factor $\exp-(\alpha_1+\alpha_2)r$. This opportunity is taken for pointing out that $m-v+1$ should replace $m-v$ in Eq. (25), and $m!/(m-v)!\cdot v+1$ should replace $e^{-\alpha}A_v(1,\alpha)$ in (26) and (30) of this reference.

to the two atoms, and R is their nuclear separation. The mutual potential between atoms or symmetrical diatomic molecules, averaged over all internal molecular coordinates, will contain the factor $\exp-(\alpha_1+\alpha_2)r$, where r is the distance between the centers of gravity of the two systems. An approximation to the actual potential may thus be written as

$$V(r) = E''e^{(\alpha_1+\alpha_2)(r_{E''}-r)}. \tag{1}$$

The constants E'', $r_{E''}$ are to be experimentally determined. They have the relation $V(r_{E''})=E''$. If $E''=E_{300}$ denotes the average energy of a gas molecule at room temperature, then r_{300} will be the classical average closest distance of approach.

It is desirable to compare the theoretical formula (1) with experimental data. The data on inter-molecular forces have been thoroughly reviewed by Lennard-Jones.[9] If the constants c, α are determined to make $c\exp(-\alpha r)$ join smoothly to the repulsive energy formulae of Lennard-Jones at r_{300}, then α should be considered as the experimental value of $\alpha_1+\alpha_2$. A comparison of these constants is given in Table I.

TABLE I. *Energy constants.*

	Lennard-Jones	Spectroscopic
H_2	2.08	2.12
He	3.50	2.68
Ne	2.2	2.5

III. VIBRATION-TRANSLATION

The interchange of vibrational and translational energy will be investigated in the collision of atom A with the molecule $B-C$, the atoms A, B, C being confined to a line.

$$\begin{matrix} A & & B & C \\ \cdot & & \cdot & \cdot \end{matrix}$$

This interchange will be a function of the various physical parameters, such as the force beinding B and C, the repulsive force begween A and B, the initial translational and vibrational energies, and the relative masses.

If the atoms were sufficiently massive, and if the translational and vibrational energies were sufficiently great, only an investigation by classical mechanics would be necessary. But these conditions are not satisfied in the interesting cases where only the first vibrational states are excited. Nevertheless, it is profitable to consider the classical picture, as in general the same qualitative dependence upon the physical parameters will be present in the mechanics of the classical and quantum theory.

The classical picture will now be used in finding the conditions of maximum transfer of energy from vibration to translation with the optimum phase relation between the vibrational and translational motion. The system is first simplified by assuming the impact between A and B to be instantane-

[9] R. H. Fowler, Statistical Mechanics, Chap. X (1929).

ous. Then if the mean vibration velocity of B is comparable to the relative velocity of A and the molecule $B-C$, with an optimum phase relation, the impact between A and B will occur when the molecule has all its internal energy in the form of kinetic energy. The energy transfer will then be a maximum when the masses of A and B are nearly equal. However, the vibrational energy of light molecules is much larger than the mean translational energy at room temperatures. Hence in order that A strike B while the latter has a maximum velocity, A must be lighter than B.

The effect of the finite time of impact between A and B is now examined. If this time is small in comparison to the period of oscillation of the molecule B-C, the impact may be regarded as instantaneous. As it becomes large in comparison to the period of oscillation, the atom will tend to act only upon the center of gravity of the molecule. The interchange of vibrational and translational energy then becomes small. With a fixed initial translational energy, a decrease in the mass of A will lessen this time of impact, and thus increase this interchange irrespective of the mass of B.

It is of interest to compare this time of impact with the period of oscillation in collisions between actual molecules. If r is the distance between A and B, their mutual energy may be taken to be

$$V(r) = E''e^{-\alpha(r-r_{E''})} \tag{1'}$$

as was seen in II. If E'' is set equal to the mutual energy E, then a reasonable value for the time of impact is the time τ_i during which $r<r_0$. Here, r_0, together with F, is determined to make the parabola

$$U(r) = F(r - r_0)^2 \tag{2}$$

join smoothly to $V(r)$ at $r=r_E$. Thus (1') has been replaced by the potential

$$W(r) = \begin{cases} F(r - r_0)^2, & r < r_0. \\ 0 \qquad\quad , & r > r_0. \end{cases} \tag{3}$$

The ratio of τ_i to the period of vibration of B-C, τ_v, is one half the ratio of the frequency of vibration of the molecule to the frequency of vibration of a particle of mass

$$\mu = \frac{M_A(M_B + M_C)}{M_A + M_B + M_C} \tag{4}$$

in the potential (2). This ratio is

$$\beta = \frac{40}{\alpha}\,\frac{\omega_0}{8106}\left(\frac{\mu}{E}\right)^{1/2}$$

where ω_0 is the wave number of the molecule, μ is expressed in units of atomic hydrogen, and E is in units of the mean energy of a gas molecule at room temperature, E_{300}. A numerical example shows this ratio to be relatively large. For instance, in the collision of He with N_2 at room temperature, $\alpha=2.4$, $\omega_0=2345$, $\mu=3.5$ $E\backsimeq 1$, giving $\beta=9$.

The above considerations lead to the following classical conclusions for light molecules. Since the intra-molecular binding forces are large in comparison to the inter-molecular repulsive forces at collision distances, and since the internal energy of these molecules is large in comparison to their temperature equilibrium translational energy, the interchange of vibrational and translational energy will be small. H_2 will absorb more readily than any other molecule translational energy not only from a C-H bond but from any light molecule.

A precise quantitative theory for the one dimensional collision is developed by the following quantum mechanical analysis.

The coordinates will be taken to be: the center of gravity of the complete system, X; the nuclear separation of molecule B-C, x; and the distance between the atom A and the center of gravity of the molecule, r. This choice has been made in order that the kinetic energy may be written as

$$T = T_x + T_x + T_r.$$

The wave equation, after eliminating the center of gravity of the complete system, then becomes[7]

$$\left\{\frac{1}{\mu_m}\frac{d^2}{dx^2} + \frac{1}{\mu}\frac{d^2}{dr^2} - V(x) - V(x, r) + E\right\}\Psi = 0 \tag{5}$$

Here

$$\mu_m = \frac{M_B M_C}{M_B + M_C}$$

and μ is given by (4). The energy $V(x)$ is the potential energy of the isolated molecule B-C, and $V(x, r)$ is the mutual energy of atom A and the molecule. The energy E has a continuous range of values. If E_i is the energy of the isolated molecule, then $p_i = \mu^{1/2}(E - E_i)^{1/2}$ is proportional to the momentum associated with the translational motion.

Let the normalized function $\psi_i(x)$ be a solution of the wave equation for the isolated molecule, namely

$$\left\{\frac{1}{\mu_m}\frac{d^2}{dx^2} - V(x) + E_i\right\}\Psi_i(x) = 0.$$

Corresponding to the physical requirement that before collision the molecule be in the vibrational state v_0, a solution of (5) is to be found of the form

$$\Psi \overset{r=\infty}{=} \frac{(e^{ip_{v_0}r} + e^{-ip_{v_0}r})}{(p_{v_0})^{1/2}} + \sum_v \gamma_{v_0}{}^v \frac{e^{-ip_v r}}{(p_v)^{1/2}}\Psi_v(x) \tag{6}$$

The summation is over all indices for which p_v is real. The probability that the molecule has changed its vibrational quantum number from v_0 to v will be $|\gamma_{v_0}{}^v|^2$.

In order to obtain the coefficients $\gamma_{v_0}{}^v$, ψ is expanded as follows:

$$\Psi = \sum_v Q_v(r)\Psi_v(x). \tag{7}$$

The Q_v's are undetermined functions. Substitution of this expansion into (5) gives

$$\sum_v \left\{\frac{d^2}{dr^2} - \mu V(x, r) + p_v^2\right\} Q_v(r)\Psi_v(x) = 0.$$

Multiply by $\Psi_v(x)$ and integrate with respect to x.

$$\left\{\frac{d^2}{dr^2} - \mu V_v{}^v(r) + p_v^2\right\} Q_v(r) = \mu \sum_{v' \neq v} Q_{v'}(r) V_v{}^{v'}(r) \tag{8}$$

where

$$V_v{}^{v'}(r) = \int \Psi_v(x) V(x, r) \Psi_{v'}(x) dx.$$

By neglecting the right member an equation for the zeroth approximation, $Q_v{}^0(r)$, is obtained.

$$\left\{\frac{d^2}{dr^2} - \mu V_v{}^v(r) + p_v^2\right\} Q_v{}^0(r) = 0.$$

Since $V_v{}^v(\infty) \to 0$, $Q_v{}^0(r)$ becomes sinusoidal for large r. Denote that particular solution that vanishes at $r=0$ by $U(p_v/r)$. Let this solution be so normalised that

$$U(p_v/r) \overset{r \to \infty}{=} \frac{\sin(p_v r + \theta_v)}{p_v{}^{1/2}}. \tag{9}$$

Choose another particular solution by its asymptotic behavior

$$X(p_v/r) \overset{r \to \infty}{=} \frac{e^{-i(p_v r + \theta_v)}}{p_v{}^{1/2}}. \tag{9'}$$

The zeroth approximation to $Q_v(r)$ corresponds to an elastic collision in which the molecule has the quantum number v. Hence

$$Q_v{}^0(r) = \begin{cases} U(p_v/r), & v = v_0. \\ 0, & v \neq v_0. \end{cases} \tag{10}$$

The first approximation to $Q_v(r)$ is obtained by substituting this zeroth approximation into the right member of (8).

$$\left\{\frac{d^2}{dr^2} - \mu V_v{}^v(r) + p_v^2\right\} Q_v{}^1(r) = \begin{cases} \mu U(p_{v_0}/r) V_{v/0}{}^v, & v \neq v_0 \\ 0, & v = v_0. \end{cases} \tag{11}$$

The solution of these equations that satisfies the boundary condition (6) is

$$\begin{aligned} -Q_v{}^1(r) = {} & \mu X(p_v/r) \int_0^r U(p_v/r') V_{v_0}{}^v(r') U(p_{v_0}/r') dr' \\ & + \mu U(p_v/r) \int_r^\infty X(p_v/r') V_{v_0}{}^v(r') U(p_{v_0}/r') dr' \end{aligned} \tag{12}$$

$$Q_{v_0}{}^1(r) = C_1 X(p_{v_0}/r). \tag{12'}$$

The validity of (12) may be verified by direct substitution into (11). The left member vaishes identically except for the term

$$-\mu U(p_{v_0}/r)V_{v_0}{}^{v}\{X'(p_v/r)U(p_v/r) - X(p_v/r)U'(p_v/r)\}.$$

Now the subtraction of

$$X\left(\frac{d^2}{dr^2} - \mu V_v{}^v + p_v{}^2\right)U = 0$$

from

$$U\left(\frac{d^2}{dr^2} - \mu V_v{}^v + p_v{}^2\right)X = 0$$

gives

$$\frac{d}{dr}(X'U - XU') = 0.$$

Hence

$$X'U - XU' = C.$$

But from (9), (9′), $C=-1$. Hence (12) satisfies (11) identically.

C_1 is to be determined from the equation of continuity,—

$$\int\left(\Psi\frac{d}{dr}\overset{*}{\Psi} - \overset{*}{\Psi}\frac{d}{dr}\Psi\right)dx = 0.$$

Since the second integral in (12) vanishes as r becomes infinitely large, the first two approximations to the coefficients in the expansion (7) gives a ψ of the form (6) with

$$\gamma_{v_0}{}^{v} = \mu\int_0^\infty dr\int_{-\infty}^{\infty}dx\,U(p_v/r)\Psi_v(x)V(x,r)$$
$$\cdot U(p_{v_0}/r)\Psi_{v_0}(x),\quad v\neq v_0. \tag{13}$$
$$\gamma_{v_0}{}^{v_0} = C_1.$$

The conditions under which this first approximation is valid will now be investigated. In general the successive approximations of the Born collision method do not converge. However, if the first terms become smaller, they may form a semi-convergent series that has a physical meaning. The relative magnitude of successive approximations will depend upon the physical parameters of the system. The application of (13) is thus limited to those systems with parameters such that the first successive approximations to the solutions of (8) which vanish at $r=0$ become smaller. It will be found that all systems examined in this study satisfy this condition.

An approximation to the probability is obtained by assuming a simplified potential of the form

$$V(x,r) = E''e^{-\alpha(r-r_{E''})}(1+qz)$$

where z is the displacement of x from its equilibrium value. A reasonable value for q is the coefficient in the first term of the expansion of $e^{-\lambda\alpha z}$, where

$$\lambda = \frac{M_C}{M_B + M_C} . \tag{14}$$

Neglecting the higher powers of z limits this analysis to molecules in which the amplitudes of vibration are relatively small. With this potential $\gamma_{v_0}^{v}$ may be factored as

$$\gamma^{v}{}_{0} = \xi_{v_0}{}^{v}\eta_{pv_0}{}^{pv}$$

where

$$\xi_{v_0} = q\int_{-\infty}^{\infty}\Psi_v(z)z\Psi_{v_0}(z)\,dz \tag{15}$$

and

$$\eta_{pv_0}{}^{pv} = \mu E''\int_0^{\infty} U(p_v/r)e^{-\alpha(r-r_{E''})}U(p_{v_0}/r)dr . \tag{15'}$$

The U's are solutions of

$$\left(\frac{d^2}{dr^2} - \mu E''e^{-\alpha(r-r_{E''})} + p^2\right)U(p/r) = 0 \tag{16}$$

and are normalised to satisfy (9).

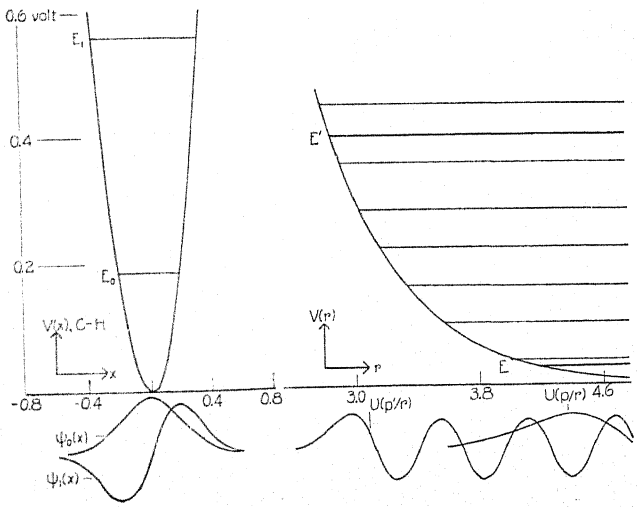

Fig. 1.

Since only a very rough approximation to $\eta_{p'}{}^{p}$ can be obtained without great analytical difficulties, it is profitable to consider first the qualitative dependence of $\eta_{p'}{}^{p}$ upon the physical parameters.

In Fig. 1 are drawn the potentials and pertinent wave functions. The energy levels to $V(r)$ are drawn for energy values whose $U(p/r)$ have nodes at

$r=r_0$, where r_0 is chosen arbitrarily at a point where $V(r)$ first becomes appreciable. Here E, E' refer to the initial and final translational energies, with $E<E'$, and p, p' to the corresponding momenta.

An increase of the molecular binding force $-dV(z)/dz$ relative to the repulsive force $-dV(r)/dr$ will increase the number of energy levels between E' and E, thus increasing the fluctuations in sign of the integrand of (17), and thus decreasing $\eta_{p'^p}$. An increase in the reduced mass μ will have a similar effect.

An increase of E and E' by similar amounts will increase $\eta_{p'^p}$ by lessening the number of energy levels between E and E'.

An examination shows that in ordinary thermal collisions between molecules whose atoms belong to the first row of the periodic table, the first maximum of $g(p/r)$ lies in the region $r<r_0$, and that several "energy levels" always lie between E and E'. The qualitative results of the classical and the quantum mechanical treatment are thus similar in such collisions. In the language of the former a decrease in the slope of $V(r)$ or an increase of the reduced mass μ results in an increase of the time of collision. In the language of the latter, similar changes result in an increased fluctuation of sign in the integrand of (17).

An analytical approximation to $\eta_{p'}^{p}$ is obtained by replacing the exponential potential by a potential which renders Eq. (16) soluble in known functions. Such a potential is

$$V_a = \frac{A}{(r-B)^2}, \quad r > B$$

$$V_a = \infty, \quad r < B.$$

The constants A, B are adjusted to make V_a as similar as possible to the potential (1′) in the important range of r. With the choice

$$V_a = \frac{4E''/\alpha^2}{(r - r_{E''} + 2/\alpha)^2} \tag{17}$$

the two potentials join smoothly at $r=r_{E''}$. A reasonable value of E'' is $(E\,E')^{1/2}$.

The differential equation (16) now becomes

$$\left\{\frac{d^2}{dx^2} - \frac{4\mu E''/\alpha^2}{x^2} + p^2\right\} U(p/x) = 0$$

where $x=r-r_{E''}+2/\alpha$. Its solution is the Bessel function

$$U(p/x) = \left(\frac{\pi}{2}\right)^{1/2} x^{1/2} J_v(px) \tag{18}$$

with

$$v = (4\mu E''/\alpha^2 + 1/4)^{1/2} \backsimeq 2(\mu E'')^{1/2}/\alpha.$$

This solution is normalized to satisfy (9).

The expression (15′) for $\eta^{p}_{p'}$ now becomes

$$\eta^{p}_{p'} = 2\pi\frac{\mu E''}{\alpha^2}\int_0^\infty \frac{J_v(px)J_v(p'x)dx}{x}.$$

The substitution of

$$\int_0^\infty \frac{J_v(px)J_v(p'x)}{x}dx = (p/p')^v/2v, \quad p < p'$$

(Watson, Theory of Bessel Functions, p. 401) reduces this to

$$\eta^{p}_{p'} = \frac{\pi(\mu E'')^{1/2}}{2\alpha}(E/E')^{(\mu E'')^{1/2}/\alpha}. \tag{19}$$

If the molecule is assumed to be vibrating as a linear oscillator, then (15) reduces to

$$\xi^{v}_{v-1} = \frac{\alpha}{2}\left(\frac{v}{\mu_m(E_v - E_{v-1})}\right)^{1/2}, \tag{20}$$

all the other integrals vanishing.

As a numerical example, consider the one dimensional collision at room temperature of He with N_2, in which N_2 is deactivated from the first excited vibrational state to the normal state. Here $\alpha = 2.14$, $E/E' = 1/8$, $\mu E'' = 58$, $\mu_m(E_1 - E_0) = 274$. The probability for this deactivation is thus given by

$$(\gamma_0^1)^2 = (\xi_0^1)^2(\eta_{p'}{}^{p})^2 = 0.004 \times 0.0^{4}15 = 0.0^{7}6. \tag{21}$$

IV. Rotation-Translation

The principles involved in the interchange of rotational and translational energy are most readily studied in the collision of a rigid diatomic molecule and an atom, all motion being confined to a plane. This collision will first be discussed from the classical standpoint.

The symmetry of the molecule limits the energy transfer in a single impact. If an electron is excited to such a state that its time average distribution is nearly spherical, then the energy interchange in a collision will become small. Hence the energy transferred during a collision will be very dependent upon the electronic state of the molecule. This has been empirically observed.[10] Comparison of the time of collision with periods of rotation is not important, since the latter is usually the larger.

In order to treat this collision problem by quantum mechanics, a suitable mutual potential must be found. If the analysis is limited to symmetrical diatomic molecules, a simple potential having the necessary properties is

$$V(r, \epsilon) = V(r)\{1 + h(\cos^2\epsilon - \tfrac{1}{2})\}. \tag{22}$$

Here r has the same meaning as in the previous section, and ϵ is the angle between the molecular axis and the line joining the atom with the center of the molecule. The potential $V(r)$ is taken to be (1′). A reasonable value for h

[10] R. Rompe, Zeit. f. Physik 65, 428 (1930).

is obtained by requiring that the ratio $V(r, 0)/V(r, \pi/2)$ equal the ratio $V(r+x_0/2)+V(r-x_0/2)/2V([r^2+x_0^2/4]^{1/2})$, where x_0 is the nuclear separation in the molecule, and where r is set equal to r_{300}. This condition gives

$$h = \frac{2\left[e^{\alpha x_0/2} + e^{-\alpha x_0/2} - 2e^{-\alpha([r_{300}^2+x_0^2/4]^{1/2}-r_{300})}\right]}{\left[e^{\alpha x_0/2} + e^{-\alpha x_0/2} + 2e^{-\alpha([r_{300}^2+x_0^2/4]^{1/2}-r_{300})}\right]}. \tag{23}$$

By considerations similar to those leading to (5), the following wave equation of our two dimension system of a rotator and an atom may be obtained:

$$\left\{\frac{1}{I}\frac{d^2}{d\phi_1^2} + \frac{1}{\mu}\frac{1}{r}\frac{d}{dr}r\frac{d}{dr} + \frac{1}{\mu}\frac{1}{r^2}\frac{d^2}{d\phi^2} - V(r,\epsilon) + E\right\}\Psi = 0.$$

Here ϕ_1, ϕ are the azimuthal angles associated with the molecule and the line joining the atom to the center of the molecule.

A solution of this equation corresponding to the molecule being in a definite rotational state before collision, and having a probability of being in several after the collision, is obtained by a method closely analogous to that of the previous section. The zeroth approximation is of the form

$$\Psi = e^{im_1\phi_1}\sum_{m=-\infty}^{\infty} e^{i\delta_m} e^{im\phi} U_m(p_{m_1}/r).$$

The phase factor δ_m[11] is arbitrary. The function $U_m(p_{m_1}/r)$ is the solution of

$$\left\{\frac{1}{\mu}\frac{1}{r}\frac{d}{dr}r\frac{d}{dr} - \frac{1}{\mu}\frac{m^2}{r^2} - V(r) + E - \frac{m_1^2}{I}\right\}U_m(p_{m_1}/r) = 0$$

that vanishes[12] at $r=0$ and is normalised to satisfy

$$U_m(p_{m_1}/r)^{r\to\infty} = \frac{\sin(p_{m_1}r + \beta_{m_1})}{(p_{m_1}r)^{1/2}}.$$

The only allowable transitions are $m = \pm 2$. The probability that the quantum numbers change from m_1, m to $m_1-2, m+2$ is

$$\left(\gamma\begin{matrix} m_1-2, & m+2 \\ m_1, & m\end{matrix}\right)^2 = \frac{h^2}{16}\left\{\int_0^\infty U_m(p_{m_1}/r)V(r)U_{m+2}(p_{m_1-2}/r)rdr\right\}^2$$

or

$$\left(\gamma\begin{matrix} m_1-2, & m+2 \\ m_1 & m\end{matrix}\right)^2 \leqq \frac{h^2}{16}\left\{\int_0^\infty U_0(p_{m_1}/r)V(r)U_0(p_{m_1-2}/r)rdr\right\}^2. \tag{24}$$

However, these individual probabilities are not of primary interest, but only the effective cross section of such a collision. If

$$\gamma\begin{matrix} m_1-2 & m+2 \\ m_1 & m\end{matrix} = \begin{matrix} 1, & m < m_0 \\ 0, & m > m_0\end{matrix}$$

[11] W. Pauli, Probleme der Modernen Physik p. 42. (Hirzel, Leipzig, 1928.)

[12] The formulation of this boundary condition is rather arbitrary, as an equally justifiable condition would be to require that $U(p/r)$ have a zero slope at $r=0$. However, as long as the probability remains negligibly small that the atom pass through the molecule, both boundary conditions will give the same result.

this effective cross section would be equal to the kinetic theory cross section, σ_{KT}. Here, m_0 is the largest m for which the molecule and atom would classically come into contact. An upper limit to the effective cross section σ_{eff} is obtained by using the equality sign in (24) when $m<m_0$, and setting the left member equal to zero when $m>m_0$. This gives

$$\sigma_{\text{eff}} < \frac{h^2}{16}\left\{\int U_0(p/r)V(r)U_0(p'/r)rdr\right\}^2 \sigma_{KT},$$

in which p_{m_1}, p_{m_1-2} have been replaced by p, p'.

An approximation to this integral is obtained in a manner identical to that used in the previous section. The only difference is that here the relation $v=2(\mu E'')^{1/2}/\alpha$ is exact. An upper limit to the cross section is then

$$\sigma_{\text{eff}} < \frac{h^2}{16}(\eta_{p'}^{p})^2\sigma_{KT}$$

in which $\eta_{p'}{}^{p}$ is given by (19).

As a numerical example, consider the probability that a N_2 molecule, considered as non-vibrating, give two quanta of rotational energy to a He atom in a two dimensional collision at room temperature. In this example $h=1.3$, $(\eta_{p'}{}^{p})^2=11$, resulting in

$$\sigma_{\text{eff}} < 1.2\,\sigma_{KT}.$$

V. General Collisions

In the previous sections discussion has been restricted to a one-dimensional collision of an atom and a vibrating molecule, and to a two-dimensional collision of an atom and a rotating molecule. The analysis is now extended to three-dimensional collisions between two molecules both of which vibrate and rotate.

The quantum mechanical treatment of such a collision in three dimensions is difficult, since the equation whose solution corresponds to an elastic collision is not in general separable in the mutual coordinates. However, in the classical theory collisions of the second kind are most probable between an atom and vibrator when all motion is confined to a line, and between an atom and rotator when all motion is confined to a plane. We may expect a similar relation in quantum mechanics, so the previous inequalities obtained for one and two dimensional collisions may be taken to be valid for three-dimensional collisions.

Provided the amplitude of vibrations are relatively small, the mutual potential may be approximated by the product of functions of individual coordinates. Thus when both molecules are diatomic, a simple potential is

$$V = V(r)(1 + a_1z_1)(1 + a_2z_2)(1 + f_1(\epsilon_1)(1 + f_2(\epsilon_2)) \qquad (25)$$

where $V(r)$ is taken to be (1′); z_1 and z_2 are the displacements of the internuclear separations of the two molecules from their equilibrium values; ϵ_1 and ϵ_2 are the mutual angles between the line joining the centers of gravity of the

two molecules and the axes of the two molecules; and f_1, f_2 are arbitrary functions.

When the mutual potential is so factorable, the probability of an inelastic collision will also be expressible as a product. One factor of this product will be a function of the constants of translational motion. Denote this factor by $P_{E,E'}$. Each of the other factors will be associated with a change of one quantum number. These factors will be independent of one another. For example, in a collision in which the vibrational quantum number v changes to $v-1$, the associated probability factor $P_{v,v-1}$ will not be influenced by changes of other quantum numbers.

Hence if σ_{KT} is the kinetic theory cross section of a collision, the effective cross section of a collision in which the quantum numbers v_1, l_1, $\cdots$ change to v_1', l_1', $\cdots$ will be

$$\sigma_{\text{eff}} < \sigma_{KT} P_{E,E'} P_{v_1,v_1'} P_{l_1,l_1'} \cdots . \tag{26}$$

In the following description of these factors, atomic units[7] are used.

When μ refers to the reduced mass of the two systems, α to the sum of the square roots of the ionization energies (in units of 13.53 volts) of the two atoms which become adjacent during collision, $E(E')$ to the smaller (greater) of the initial and final mutual energies of translation, and $E'' = (E\,E')^{1/2}$, reference to (19) shows that for sub-elastic collisions

$$P_{E,E'} = \frac{\mu E''\pi^2}{4\alpha^2} \cdot (E/E')^{2(\mu E'')^{1/2}/\alpha}. \tag{27a}$$

In super-elastic collisions[13] $P_{E,E'}$ is to be multiplied by the factor $(E/E')^{1/2}$.

When the mutual potential contains only the first power of the displacement of a vibrator from its equilibrium position, the vibrational quantum number can change only by unity. Reference to (20) shows that the factor $P_{v,v-1}$ associated with a change of vibrational quantum number $v \to v-1$ or $v-1 \to v$ is

$$P_{v,v-1} = \frac{\lambda^2 \alpha^2 v}{4\mu_m (E_v - E_{v-1})} \tag{27-b}$$

where the difference in energy between the two states is $E_v - E_{v-1}$, where λ is given by (14), and μ_m is the reduced mass of the vibrator.

If one of the colliding systems is a symmetrical diatomic molecule, the dependence of the interaction energy upon the mutual angle ϵ is approximately expressed by the factor $1+h(\cos^2\epsilon - \frac{1}{2})$, corresponding to (22). The constant h, determined from (23), varies from 1 to 1.5 for diatomic symmetrical molecules whose electronic states are normal. If the electronic states are highly excited, h may approach zero. Insofar as this approximation is valid, the molecule can change its rotational quantum number l by only ± 2. The corresponding probability factor is

$$P_{l,l\pm 2} = h^2/16. \tag{27-c}$$

The statistical factor[13] relating the probability of the transition $l \rightarrow l+2$ to that of $l+2 \rightarrow l$ is neglected.

A few general observations will be drawn from the above formulae.

The molecules to which this analysis applies change a few rotational quantum numbers freely.

The transfer of vibrational energy may be difficult even in cases of exact resonance,[14] e.g. the cross section for the transfer of vibrational energy from a N_2 molecule in its first excited state to a normal N_2 at room temperature is $0.0^{4}4 \times$ kinetic theory cross section. This resonance cross section increases both with the reduced mass of the two molecules, and with temperature. However, the effects of a lack of resonance are most marked in heavy molecules. If the reduced mass is $30\, m_H$, the effective cross section is reduced by a factor of 0.025 if the translational energy must change by 0.01 volt at room temperature.

The efficiency of H_2 as contrasted to He in deactivating molecules[15] cannot be explained as due to their difference in mass. It is to be ascribed to the much greater facility with which H_2 can absorb a considerable amount of energy by a change of a few rotational quantum numbers, than by a change of translational energy.

The writer wishes to express his gratitude to Professor Kemble for frequent discussions, and to Harvard University for enabling him to commence this study in Bristol, England.

[13] Ruark and Urey, Atoms, Molecules and Quanta p. 491, McGraw-Hill (1930).

[14] O. K. Rice, Zeits. f. physik. Chem. **7**, 226 (1930).

[15] C. N. Hinshelwood, The Kinetics of Chemical Change in Gaseous Systems, Oxford, 1929, p. 151.

THE ABSORPTION COEFFICIENT FOR SLOW ELECTRONS IN THALLIUM VAPOR

By Robert B. Brode
Department of Physics, University of California

(Received January 19, 1931)

Abstract

The absorption coefficient α has been observed by sending a beam of electrons through thallium vapor and measuring the decrease in intensity of the beam as a function of the pressure of the vapor. α, plotted as a function of the velocity of the electrons, decreases rapidly to a minimum of 15 at 1.4 volts, rises less rapidly to a maximum of 51 at 4.5 volts, and then slopes off gradually to 20 at 100 volts.

IN THE study of the absorption coefficients of the monatomic elements of the periodic system, all of the noble gases,[1,2] four of the alkali metals[3] and three of the elements of the second column, i.e., Hg,[4] Cd and Zn,[5] have been investigated. Thallium has been chosen for the extension of these observations to the third column of the periodic table. In the vapor state thallium is monatomic but it differs from all of the elements previously investigated in the nature of its normal spectroscopic state. The thallium normal state is of a P type while all of the other elements mentioned above have normal states of the S type.

For the range of pressure (5×10^{-3} to 5×10^{-2} mm of Hg) necessary for satisfactory measurements, thallium requires temperatures from 550 to 630° C. The apparatus was therefore enclosed in a quartz tube. The electric connections to the apparatus were made by fusing molybdenum wires into quartz capillaries. This was not a vacuum tight seal but it was sufficient to prevent the rapid diffusion of the metal vapor out of the quartz tube. The molybdenum wires were continued in quartz tubes to the outside of the furnace. Quartz to Pyrex graded seals enabled vacuum tight connections to be made by tungsten seals through the Pyrex.

The metal parts of the apparatus were made of tantalum as shown in the cross-sectional view of the apparatus in Fig. 1. The tungsten filament, F, was the source of electrons which were bent in a circle through the slit S and into the collecting box B at the end of the path. The mean radius of the path was 7.0 mm and the widths of the slits at F, S, and B were 0.5, 1.0, and 0.5 mm respectively.

In the preparation of the tube the spaces on both sides of the quartz capillaries were connected to the vacuum pumps. The apparatus was baked

[1] C. Ramsauer, Ann. d. Physik **72**, 345 (1923).
[2] C. E. Normand, Phys. Rev. **35**, 1217 (1930).
[3] R. B. Brode, Phys. Rev. **34**, 673 (1929).
[4] R. B. Brode, Roy. Soc. Proc. **A125**, 134 (1929).
[5] R. B. Brode, Phys. Rev. **35**, 504 (1930).

out to 800°C and the metal parts glowed to a bright yellow by an induction furnace. A small amount of thallium metal was then slowly distilled into the lower end of the apparatus. The vacuum connections to the quartz tube and to the Pyrex seals were sealed off.

The main portion of the tube was enclosed in a non-inductively wound electric furnace. The small tube containing the metal was enclosed in a heavy copper tube in a separate furnace directly below the main furnace. The temperatures in the two furnaces were measured by chromel-alumel thermocouples. From the vapor pressure equation and the temperature of the lower furnace the pressure of the thallium vapor could be calculated. This pressure was corrected for the difference in pressure caused by the difference in temperatures of the upper and lower furnaces.

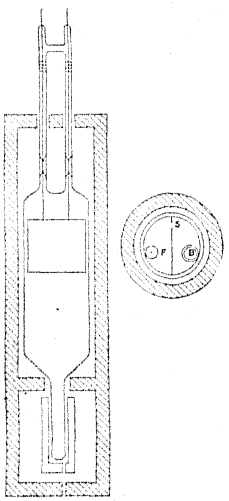

Fig. 1. Diagram of apparatus and furnaces.

The measurements of the absorption coefficient were made in the same way as those previously described for mercury.[4] The total emission from the filament was assumed to be proportional to the initial current I_0 that would have reached the end of the path if there had been no collisions. The current I at the end of the path was measured by a galvanometer connected to the box B. The currents I and I_0 are related by the equation, $I = I_0 e^{-\alpha x p}$, where α is the absorption coefficient, x the path length and p the pressure of the absorbing vapor. From this equation the logarithm of the ratio of I/I_0 should be a linear function of the pressure. Measurements were made at from 3 to 5 pressures for every velocity studied and the value of α computed from this linear relation.

The results of the measurements are shown in Fig. 2, where the absorption coefficients in cm^2 per cm^3 of the thallium vapor at 1 mm pressure at 0°C are plotted as a function of the velocity of the electrons which is expressed in square root of volts. The first two resonance potentials, 3.3 and 4.5 volts, and

the ionization potential, 6.1 volts, are indicated by the letters R, R, and I. The curve is characterized by a sharp minimum at 1.4 volts and a maximum at 4.5 volts.

The magnitude of the absorption coefficient depends on the constants chosen for the equation relating the vapor pressure and the temperature. Measurements of the vapor pressure of thallium have been made by Gibson[6] and von Wartenberg.[7] Professor Gibson has advised me to use the data of von Wartenberg instead of his own. He suggested that his own data for thallium vapor pressures might be somewhat uncertain because of the effect of the high temperatures, 1000 to 1600°C, on the elastic properties of the quartz of which his manometer was constructed. The vapor pressure of thallium measured by Gibson at 970°C, his lowest temperature, agrees well with the value from von Wartenberg's data for the same temperature. For the vapor pressure equation, $\log p_{mm} = B - A/T$, the International Critical Tables[8] give the values $A = 6{,}280.$ and $B = 6.14$, based on Gibson's high temperature data.

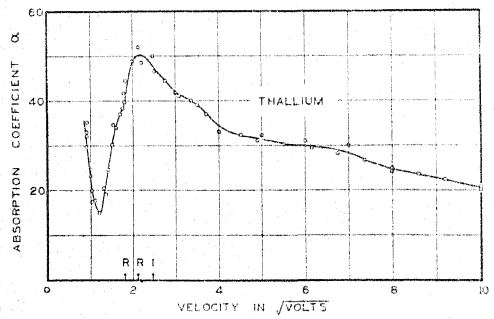

Fig. 2. The absorption coefficient α for electrons in thallium vapor as a function of the velocity of the electrons.

The data of von Wartenberg give for the constants the values $A = 8{,}890.$ and $B = 8.55$, which are the values used in this experiment to calculate the vapor pressure. At the temperatures used in this experiment, the I. C. T. values of the pressure are about five times those of von Wartenberg for the same temperature. If the I. C. T. values of the constants were used, the values of α shown in Fig. 2 should be reduced to about 1/5 of their value or at 4.5 volts, the maximum, $\alpha = 10$ and at 100 volts $\alpha = 4$. These values seem improbably small as helium has a value of $\alpha = 15$ at 4.5 volts and $\alpha = 3.5$ at 100 volts.

In the curves for thallium vapor, the alkali metal vapors and the heavier noble gases, the maximums are at about the resonance potentials while the minimums are at definitely lower velocities. This means that the probability of an elastic collision between an electron and an atom increases as the energy of the electron approaches the critical potential of the atom.

[6] G. E. Gibson, Dissertation, Breslau (1911).
[7] H. von Wartenberg, Zeit. f. Electrochemie **19**, 482 (1913).
[8] International Critical Tables, Vol *III*, 205.

Because of the maxima and minima in the absorption coefficient curves, the relative magnitude of the curves of different elements is somewhat uncertain. By taking the value of the absorption coefficient for a velocity well beyond the region of maxima and minima, a definite order of arrangement for the elements can be obtained. Choosing arbitrarily 100 volts as the velocity for comparison of the curves, the order of arrangement of the absorption coefficients for the 13 monatomic elements that have been measured is, with the exception of thallium, inversely proportional to the ionization potential. To fit into this arrangement, thallium with an ionization potential of 6.1 volts should have an absorption coefficient at 100 volts of about 100 instead of 20. Further experimental observations will be necessary to determine whether this deviation of thallium from the general order is really a property of the thallium atom or is due to the inaccuracies in the vapor pressure. Since the normal state of the thallium atom is a P state as compared with S states for the other atoms, it would not be unexpected to find a real difference.

OSCILLATIONS AND TRAVELLING STRIATIONS IN AN ARGON DISCHARGE TUBE

By T. C. Chow
Palmer Physical Laboratory, Princeton University

(Received January 15, 1931)

Abstract

The effects of current and external circuit conditions on the frequency of travelling striations were observed. Some information concerning the voltage fluctuations at different parts of the tube was obtained. Electron temperatures in the positive column were determined at different pressures. A set of wave-lengths bearing simple relations with the length of the tube were calculated by means of Tonks' and Langmuir's theory of electric sound waves and the experimental values of the flash frequency.

Introduction

In the course of an experiment to determine certain quantities in the positive column of a discharge tube, the author encountered the difficulty that the voltage across the tube was not constant. After an unsuccessful attempt to eliminate this fluctuation, it was thought desirable to investigate the phenomenon in more detail.

Oscillations in a discharge tube were observed and studied quite long ago. Recent work has been done by Penning,[1] Tonks, and Langmuir,[2] Webb and Pardue,[3] Fox[4] and others. Webb, Pardue, and Fox found that the phenomenon of travelling striations studied by Aston and Kikuchi,[5] Whiddington,[6] and others was accompanied by oscillations. In this paper a few more points are reported concerning travelling striations and oscillations in an argon discharge tube with a positive column.

Apparatus and Method

The discharge tube is shown in Fig. 1. The length of the tube was 72.5 cm. The inner diameter was 7.2 cm. An oxide coated cylindrical nickel cathode C and a hollow cylindrical nickel anode A were used. The shortest distance between cathode and anode was 60 cm. The tube was baked out at about 350°C for several hours. The cathode and anode were degassed by means of an induction coil. Between the tube and the pumping system there were two liquid air traps with a stopcock between them. During a run this stopcock was closed. Liquid air was continually kept on the trap which was on the tube side of the stopcock. For the study of voltage fluctuation a cath-

[1] Penning, Phys. Zeits. **27**, 187 (1926).
[2] Tonks and Langmuir, Phys. Rev. **33**, 195 (1929).
[3] Webb and Pardue, Phys. Rev. **32**, 946 (1928).
[4] Fox, Phys. Rev. **35**, 1066 (1930).
[5] Aston and Kikuchi, Roy. Soc. Proc. London **98**, 50 (1921).
[6] Whiddington, Proc. Leeds Phil. Soc. **1**, 467 (1929).

ode-ray oscillograph was used. For the observation of instantaneous pictures of the discharge tube and the measurement of flash frequency, a stroboscope, which is essentially a rotating toothed-wheel together with a fixed slit put right behind it, was used.

Results

1. *An instantaneous picture of the discharge.* (*Fig. 1*). The negative glow and the head of positive column remain stationary. Flashes travelling from anode to cathode run into the head of the positive column but do not run across the Faraday dark space. There are cases in which the Faraday dark space is not present. In these cases, it is observed that the flashes run into the negative glow which is stationary. The distance between successive flashes is of the order of 10 cm.

2. *Fluctuation of space potential in the tube.* In a non-oscillating tube we know that there is a definite potential distribution. When oscillations are present and the potential difference between cathode and anode fluctuates it is quite natural to expect that the space potential distribution should fluc-

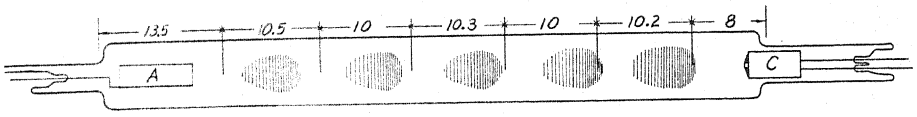

Fig. 1. Diagram of tube. The shaded regions are luminous parts. The numbers represent the distances in cm between the different probe wires.

tuate too. In order to get exact information one has to take Langmuir probe wire measurements at particular phases of the cycle of voltage fluctuation at different parts in the tube. Wishing to continue with his original problem, the author has not gone into this work. He reports here such information as he has been able to obtain otherwise. There are a number of probe wires situated at different parts of the tube. When they are left floating in the tube each of them charges up to a certain potential negative with respect to the surrounding space such that electrons and positive ions reach the wire at equal rates. If the surrounding space potential is fluctuating the potential of the floating wire must also fluctuate. The fluctuation of the probe wire potential would be just equal to that of the space potential provided the ratio of the concentration of positive ions and that of electrons and the ratio of the velocities remain unchanged. What was done, therefore, was to connect anode or cathode and each one of the probe wires successively to a pair of deflecting plates of the cathode ray oscillograph. The amplitudes of voltage fluctuation at different parts with respect to cathode and anode were observed. The results are shown in Table I. Each vertical line shows the position of a probe wire and the numbers in the column under it give the corresponding voltage fluctuations. The pressures are given in the first column. The upper row corresponding to a particular pressure gives the amplitudes of the voltage fluctuation in volts between the probe wires and the anode. The lower row gives the amplitudes with respect to the cathode.

TABLE I. *Amplitudes of the voltage fluctuations in different parts of the tube with respect to the anode and cathode. Pressures are all measured when the gas is at room temperature. After two hours of running the pressure does not change very much.*

Pressure (mm Hg)	Anode	Position of probe wires					Cathode
4.2		24	24	24	24	24	22
	22		5			1	
3.9		24	24	24	24	24	22
	22	7	5	3	3	1	
3.2							24
	24					1	
2.8			24				24
	24					1	
2.3				24			24
	24					1	
1.7				24			24
	24			1		0	
1.45				24			24
	24			0		1	
1.25		24	24	24	24	24	24
	24	3	2	0	11	0	
1.06		24					24
	24				11	0	
0.915							24
	24				3	0	
0.775		28	28	28	24	24	24
	24	5	5	2	13	0	
0.67		32	29	29	24	24	24
	24	7	7	5	14	1	
0.58		32	29	29	25	24	24
	24	8	8	6	3	0	
0.50		32	32	32	24	24	24
	24	10	9	8	15	1	
0.43		33	33	32	25	25	25
	25	10	10	9	25	1	
0.36		32	32	32	25	25	25
	25	11	10	10	29	1	
0.31		32	32	29	29	25	25
	25	11	11	11	29	0	
0.265		32	32	32	25	25	25
	25	11	13	11	4	0	
0.22		23	36	32	27	26	29
	29	11	15	11	3	0	
0.16		24	39	29	29	29	29
	29	15	16	10	5	0	
0.113		31	36	27	29	31	31
	31	18	18	8	2	0	
0.096		29	38	25	32	32	32
	32	18	18	9	2	1	
0.085		29	38	24	27	29	29
	29	18	14	10	2	3	
0.071		31	44	25	28	30	28
	28	16	23	14	10	2	

Travelling striations do not appear distinctly until the gas pressure is reduced to about 0.775 mm. However, fluctuations of luminosity are still present at high pressures. The frequency of luminosity fluctuation can still be measured. The probe wire nearest the cathode is on the cathode side of the negative glow, except in a few cases at high pressures when the positive column extends very close to the cathode. The position of the second probe wire with respect to the positive column goes from inside the head to just outside in the pressure range from 0.775 mm to 0.071 mm. Very little can be concluded from these values because we do not know the phase differences between the voltage fluctuations at different parts. However, we can say that the disturbance is very small in the cathode region compared with that in the anode region. This seems to agree with the fact that the travelling striations are present in the positive column. It has also been observed that when the second probe wire is situated in a rather distinct Faraday dark space, there is no voltage fluctuation between this probe wire and the cathode and also no voltage fluctuation between the first probe wire and cathode.

3. *Variation of flash frequency with current through the tube.* Whiddington observed that this phenomenon of travelling striations covers quite a large range of current. He divided the moving striations into five types according to their velocities as the current is increased. Since it is observed that the distance between successive striations does not change appreciably with current the relation between flash frequency and current is therefore similar to that between velocity and current. By flash frequency we mean the number of striations moving across a certain cross-section of the tube per second. The result is summarized in Table II. There are two modes of frequency change,

TABLE II. *Variation of flash frequency with current through the tube. Battery voltage $E=62$ volts.*

Current (amp.)	Flash frequency	Voltage across tube (volts)	Remarks
0.27	1.71×10^3	53.0	Current unsteady light fluctuation visually observed.
0.6	1.89 "	47.9	
1.0		44.0	
2.6	0.97×10^3	37.3	Steady, instantaneous picture clear.
3.0	1.14 "	34.5	"
3.4	1.19 "	33.5	"
3.8	1.21 "	33.0	"
4.4	1.23 "	32.3	"
5.0	1.26 "	32.0	"
5.4	1.26 "	32.0	"
6.0	4.71 "	31.5	"
3.5	1.18 "	34.0	

one is a continuous variation and the other is a discontinuous jump. In the continuous region the frequency increases with the current. The relation is indeed not simple. One would suspect that the current is not the only thing responsible for the change of frequency because in order to change the current other quantities in the circuit have been changed too; for instance, the external resistance in the circuit. Other observations are therefore made to test the effect of the external circuit.

4. *For a given current the frequency changes with the external resistance (non-inductive).* An interesting fact was observed. When a large battery voltage (E) is used, thus with large external resistance, the Faraday dark space ex-

TABLE III. *Variation of flash frequency with external resistance.*

Current	Battery voltage	Voltage across tube	Flash frequency	External series resistance
0.4 amp.	60 volts	53.1	9.88×10^2	18 ohms approx.
0.4 "	118 "	51.7	1.92×10^3	166 " "
0.4 "	345 "	51.7	2.09×10^3	733 " "

ists. When E is small the Faraday dark space disappears. On one occasion I was able to observe a Faraday dark space, although not so distinct, by using E equal to about 60 volts. The frequency measured was 1.61×10^3. Suddenly the Faraday dark space disappeared and the frequency became 9.8×10^2. This change seems to correspond to a change-over from a "fast-type" to a "slow-type" in the previous current-frequency relation.

5. *Inductance increases the frequency, capacity decreases it.* The frequency decreases rapidly with increase in the capacity put in parallel with the tube.

TABLE IV. *Variation of flash frequency with inductance and capacity.*

Flash frequency	Condition in external circuit
2.22×10^3	Only noninductive resistance about 300 ohms
1.92×10^3	With a condenser of 2 mf connected parallel to tube
2.40×10^3	An inductance in series with series resistance

E equal about 120 volts $V=58.8$ volts $i=0.2$ amp. kept same in three cases

When the capacity in parallel with the tube was large, the Faraday dark space disappeared. Under this condition, although no distinct striation can be seen, there are bright and less bright regions. These regions fluctuate violently in position.

6. *The filament current has an effect on the frequency. An increase in the filament current decreases the frequency.*

TABLE V. *Variation of flash frequency with filament current.*

Filament current	Current in tube	Voltage across tube	Flash frequency	External resistance
6.2 amp.	0.3 amp.	87.5 volts	2.21×10^2	842 ohms
8.7 "	0.3 "	51.7 "	2.08×10^2	961 "
$E=340$ volts				

7. *A search for electric sound waves: variation of flash frequency with pressure.* That the flash frequency is the same as the sound frequency heard in a telephone receiver connected to the circuit suggests that there might be present a kind of electric sound wave such as Tonks and Langmuir derived in

their theory of plasma ion oscillation. Their expression for the velocity of electric sound waves is this

$$v = 3.9 \times 10^5 \left(\frac{T_e m_e}{m}\right)^{1/2}$$

where T_e is the electron temperature in degrees m_e and m are the masses of the electron and the argon atom, respectively. The frequency of the electric sound wave is indeterminate from their theory. The only condition is that λ is very much greater than $(\pi k T_e/ne^2)^{1/2}$. Experimental values of T_e and calculated values of v at different pressures are given in Table VI. They are not in agreement with the flash velocities. If the flash frequency were the

TABLE VI. *Experimental values of electron temperature and calculated values of velocity of electric sound waves. Current is kept at 2 amperes for all readings.*

Pressure (mm Hg)	Flash frequency ν	Flash velocity (cm/sec.)		Electron temperature (volts)	Calculated velocity of electric sound wave v_s	$\lambda_s = v_s/\nu$	$\lambda_s/72$
0.071	1772	2.52×10^4	(i)	2.22	2.30×10^5	130	1.81
.085	1500	2.18 "		1.78	2.07 "	138	1.92
.096	1286	1.86 "		1.67	2.01 "	156	2.17
.113	1106	1.60 "		1.59	1.96 "	177	2.46
.16	940	1.50 "		1.71	2.03 "	216	3.00
.22	701	1.12 "		1.73	2.04 "	291	4.04
.265	667	1.07 "		1.68	2.01 "	302	4.19
.31	561	8.98×10^3	(ii)	1.71	2.03 "	362	5.02
.36	494	7.89 "		1.59	1.95 "	395	5.48
.43	453	7.25 "		1.55	1.93 "	427	5.93
.5	359	3.95 "		1.36	1.81 "	502	6.97
.58	332	3.48 "	(iii)	1.18	1.68 "	504	7.00
.67	311	4.36 "	(i)	1.35	1.80 "	579	8.04

Another set of electron temperature measurements taken at a different time and using another probe wire in the positive column are given below.

0.068	2404			1.27	1.75×10^5	72.7	1.01
	1220	1.41×10^4		1.96	2.18 "	178	1.47
	980	1.14 "	(ii)	1.44	1.86 "	190	2.64
	758	8.8×10^3		1.47	1.88 "	247	3.43

(i) Distance between successive striations = 14.5 cm. approx.
(ii) Distance between successive striations = 16 cm. approx.
(iii) Distance between successive striations = 10.5 cm. approx.

same as that of electric sound waves, the wave-length would be very long compared with the distance between flashes. However, there is a very peculiar relation between all these calculated λ's. Most of them are integral or half-integral multiples of a certain length which is rather closely the length of the whole tube. (A few deviate from integers or half-integers but most of them are within experimental errors. Flash frequency is subject to 1 percent error. Electron temperature may have a maximum deviation of 5 percent.) This would mean that if we take the frequency of electric sound waves (suppose there is such a kind of wave in the tube) equal to some higher harmonics

of the flash frequency the wave-length of the electric sound waves turns out to be a fraction of the tube length like a standing wave in that distance. The author does not attempt to interpret this phenomenon but believes that the fact is a real one, and may be very significant. The relation between flash frequency and pressure is plotted in Fig. 2.

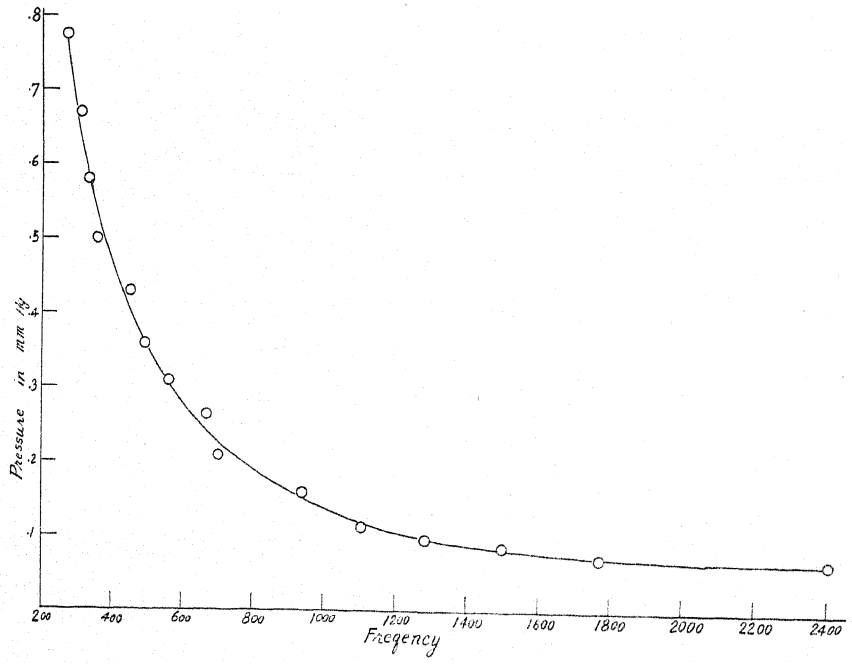

Fig. 2. The relation between flash frequency and pressure.

8. *Miscellaneous note.* There is often found a ring of glow light surrounding the anode. As the pressure is reduced this ring of velvet glow moves down towards the end of the anode. Sometimes the discharge is so unsteady that the needles of the voltmeter and the ammeter vibrate. In the range of pressure in which travelling striations are observed it is often possible to restore the discharge to steady condition by putting a magnet somewhere near the tube. Then distinct travelling striation patterns can be seen. There are a certain number of definite regions in which the magnet must be put in order to be effective. Right above the head of the positive column, and above the negative glow are favorable places but by no means the only places. Once the magnet had to be put a little behind the cathode. In some previous observations, some places near the anode are also effective.

In this laboratory, Dr. Cravath found oscillations too in his mercury discharge tube. His tube had about the same length as mine; the diameter was even larger. It was suggested that the large diameter of the tube is responsible for oscillations because the larger the diameter the smaller will be the area of the wall surface per unit volume of the tube. Loss of ions and electrons

due to recombination at the wall will be less, so that the concentrations of ions and electrons in the tube are large. Therefore the process of cumulative ionization is favorable for the production of ions and electrons. The rate of production of ions and electrons by cumulative ionization processes is proportional to the square of the electron concentration. A small change of electron concentration will cause a large change in the rate of production of ions and electrons. This is a state of instability. A tube of about one inch diameter was built. However, oscillations existed as badly as in the tube with large diameter. This would mean that the above theory is certainly incomplete, if not wrong.

The author wishes to thank Professor K. T. Compton and Professor H. D. Smyth for their deep interest and encouragement.

COLD EMISSION FROM UNCONDITIONED SURFACES

By Willard H. Bennett*
Norman Bridge Laboratory of Physics, Pasadena, California

(Received January 26, 1931)

Abstract

The greatest difficulty in obtaining higher potentials in tubes is due to auto-electronic emission from the electrode surfaces. A study of emission from unconditioned metals is described leading to the result that either loose fine particles in a tube, or else the targets of emission will probably have more to do with the quantity of emission than will the kind and "conditioning" of the cathode itself.

NUMEROUS measurements have been made of the emission in high electric fields, from fine wires and fine points of metals, which have been heated nearly to melting, in vacuum, and thus thoroughly conditioned.[1] Since metal parts in high voltage tubes are so restricted in size and shape by the necessity of such heating, it has been considered of importance to investigate cold emission with a view to finding what else can be done to a metal surface to decrease the emission, besides heating to high temperatures. This problem is of particular interest in connection with the development of a design for a tube to give higher order potentials than those now obtainable with unconditioned or partially conditioned electrodes.[2]

1. Apparatus

The experimental apparatus was designed by Julius Pearson in accordance with plans outlined by R. A. Millikan, to measure the current passing between electrodes in high vacuum at known fields. Spherical electrodes were used at distances small compared with the radius of either electrode.

The cathode was mounted on a fixed steel post extending down into the evacuated bulb, as shown in Fig. 1. The anode was mounted on a steel post which could either be moved towards or away from the cathode by means of the micrometer screw, and also which could be rotated about the cathode by turning the movable part of the base, as shown in Fig. 2. When the latter rotation was made, the anode retained its orientation so that fresh surfaces both of the anode and of the cathode were brought together at each setting of the base. Several sets of readings were thus possible at each mounting of the electrodes.

* National Research Fellow.

[1] Rother, Ann. d. Physik **81**, 317 (1926) G. E. Co. of London, Phil. Mag. (7) **1**, 609 (1926); Eyring, MacKeown and Millikan, Phys. Rev. **31**, 900 (1928); Stern, Gossling and Fowler, Proc. Roy. Soc. **124**, 699 (1929).

[2] Lauritsen and Cassen, Phys. Rev. **36**, 988 (1930); Coolidge, J. Franklin Inst., **202**, 639 (1926); Tuve, Hafstad and Dahl, Phys. Rev. **35**, 1407 (1930); Brasche and Lange, Naturwiss. **18**, 765 (1930).

The anode post was sealed vacuum-tightly to the fixed part of the base by means of a copper syphon. Both the cathode post and the anode base were sealed to the glass bulb with red sealing wax. The bulb was connected to the pumps at all time. An ionization gauge was used for measuring pressures.

The source of potential was a Thordarson transformer and kenetron rectifier, the potential being smoothed out with a 0.25 microfarad condenser. This generator, which gave up to 20 kv steady potential, was connected through a 10,000,000 ohm xylene-alcohol resistance to the cathode post. The

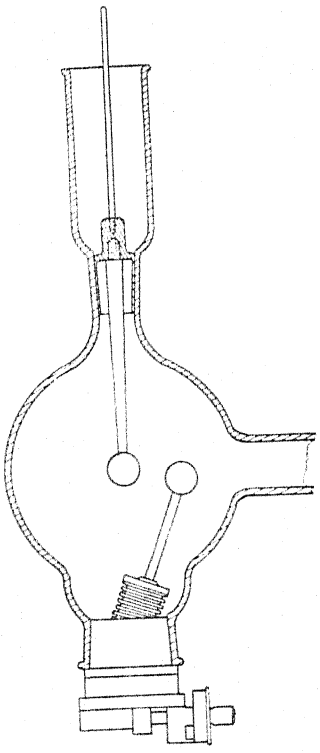

Fig. 1. Diagram of tube.

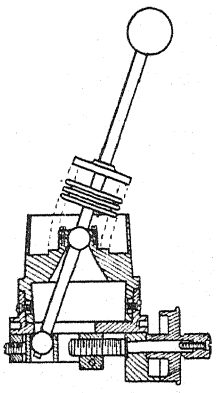

Fig. 2. Diagram of anode.

potential difference applied between the electrodes was measured by the electrostatic voltmeter which was calibrated with a sphere-gap. The anode base was connected to the current measuring circuit. The entire high-potential generator was enclosed in a grounded screen cage, since it was found that without it, leakage currents in the air would get to the galvanometer giving large deflections.

2. Method of Observation

Immediately before mounting, the electrodes were polished with 600 mesh carborundum powder held on the heel of the hand. They were washed in alcohol, dried without touching, and mounted.

The field between the electrodes could be varied by varying either the

distance between the electrodes or the applied potential. Numerous measurements showed that the two methods gave the same result.

After the first complete field-current curve had been measured, the potential was cut off and the electrodes touched to measure the setting of the micrometer for zero distance between electrodes. The e.m.f's in the rectifying tube (not more than 5 volts) were sufficient to give dependable deflections on the galvanometer upon contact. The largest emission previously drawn was again drawn at the corresponding field, and it was assumed that the intermediate determination of the zero had not effectively changed the surfaces for further study. When mixed electrodes were used (see section 6), zero distance was always measured after all measurements of emission were completed.

The data collected were plotted with the inverse field times 10^6 and the logarithm of the current, as coordinates. The points on the curves represent the lower limits of the current at each sitting. This was done because a study showed that in those comparatively few cases the current varied over a material range, the lowest value was quite near the final value if allowed to become steady. Most of the first emission curves are curled back at currents above 10^{-4} amperes because the drop in applied potential caused by the drop through the external resistance becomes appreciable at this value. No attempt has been made to draw straight lines to represent characteristics because it is believed to be more important to keep clearly in mind the probable uncertainty of the measurements. It is believed that reliable conclusions can be drawn only when the zone on a figure enclosing all of the emission from one kind of electrode surface is entirely separate from the zone enclosing all of the emission from another kind of an electrode surface.

3. General Observations

The behavior of surfaces which have not been "conditioned" is exceedingly erratic and unsystematic. In spite of this fact, a very considerable amount of data was taken in an attempt to determine statistically what relations (1) degree of polish, (2) purity, (3) electroplating, (4) hardness and (5) work function, have to emission. Measurements were made on cast iron, steel, armco iron, vacuum fused electrolytic iron, magnesium (two grades of purity), aluminum, copper, brass, zinc, gold-plated copper, nickel-plated brass, chromium-plated brass, and "Plymite" (an extremely hard compound of tungsten and carbon). This quite extensive study did not lead to any conclusive results.

It was established, however, that with fair polish and fair purity, or better, the first emission always began at a much higher field, and suffered a sudden spontaneous increase of a large order of magnitude at a still higher field, i.e., a "breakdown," than the fields at which emission was drawn from the same emitting surface subsequently.

4. Effect of Space Charge Due to Positives

The possibility suggested itself that positives liberated from the anode by the electron stream from the cathode, might follow the electron stream,

which is known to be well focussed, and set up a space charge which in turn increased the emission. This possibility was tested by measuring the emission in an apparatus as shown in Fig. 3. P is a needle-point of the metal to be studied. It was mounted on a screw-in-vacuum which could be moved by a magnet, in the direction of the point. A and B are polished copper bars, six inches long, 3/4 inch wide, and 1/8 inch thick, with edges rounded. There was a hole in A as shown, through which the point was extended toward B. A and P were at ground potential and B was at any desired potential up to 20,000 volts. Currents were measured from P. Any desired magnetic field up to 7,000 gauss could be applied perpendicularly to the figure by an electromagnet with pole-pieces as shown. The apparatus was always baked out before

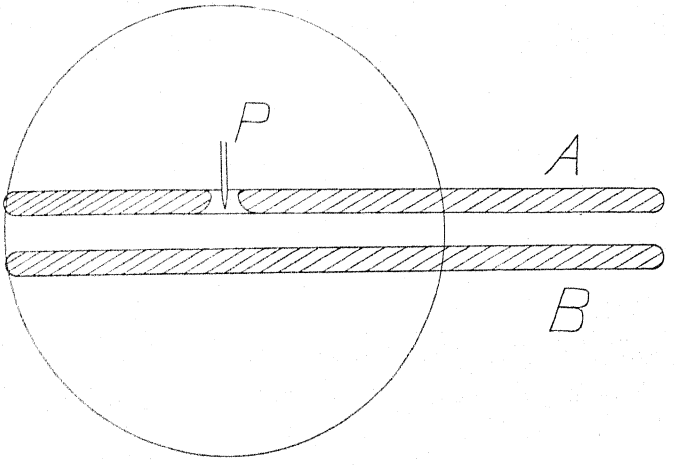

Fig. 3. Diagram of apparatus for measuring emission in magnetic field.

measurements were begun, and the pressure between the bars was, in all experiments, less than 1×10^{-5} mm, as shown by an ionization gauge at the opposite end of the tube from the pumping outlet.

Both a tungsten and a copper needle-point were tried. Emission began from the points at a comparatively low potential, and decreased (fatigued) even with increased potentials. There were times, however, during this fatigue, when the emission would remain steady within five percent for several minutes.

If the tip of the point, P is above the plane of the lower face of the upper plate, and a magnetic field of 7,000 guass is applied to apparatus of the dimensions used in this experiment, it can be shown that electrons emitted from P cannot arrive at the plate B directly below P, but will be displaced along B to some place beyond the region of this magnetic field.

The cycloidal path predicted by the theory was actually seen outlined on the glass walls opposite the space between the plates, and displaced down the tube to the edge of the region of high magnetic field.

Emission was drawn from P in the above position and the current measured while putting the magnetic field on and off. The magnetic field was

found to have no effect on the magnitude of the current, to within five percent, which was the degree of steadiness of the emission from the points.

The conclusion may be drawn that if the positives which are known to go from the anode to the cathode, produce a space charge near the emitting surface, the effect of this space charge on the field at the surface is *not* of importance in determining the magnitude of emission after breakdown.

5. Effect of Discharges through Hydrogen on Emitting Surfaces

Four filaments were mounted on the tube shown in Fig. 1 at the four quadrants about the center electrode. They were sealed in glass plugs which could be sealed with wax into the ground glass joints on the tube as shown in Fig. 4. At the side of one of these joints, the pumping tube V was attached.

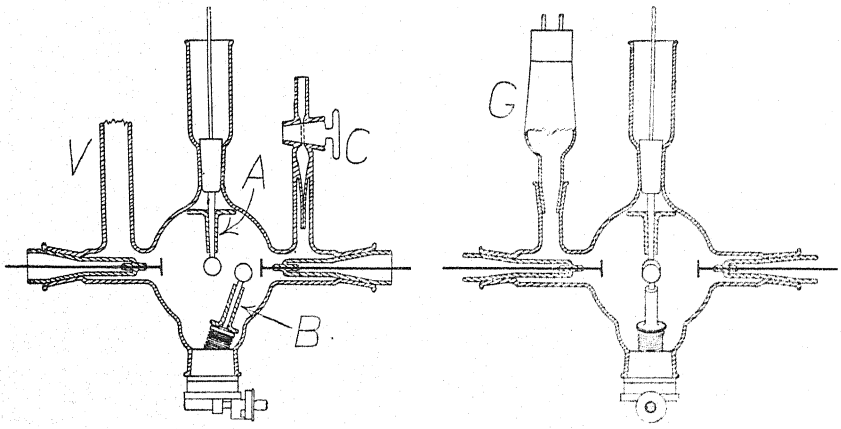

Fig. 4. Diagram of tube showing arrangement of four filaments.

At the side of another, the ionization gauge G was attached. At the side of a third, a slow gas inlet C consisting of a fine capillary and a stopcock was attached. Glass shields for both steel electrode posts, A and B, were mounted to eliminate emission from the posts and also to protect them from sputtering.

Copper electrodes were used throughout this work on the effect of discharge through hydrogen.

In order to differentiate sharply between the true effect of discharges upon the emitting surfaces and any auxiliary phenomena in the tube, tests were made of the effect of lighting the filaments introducing hydrogen to atmospheric pressure and pumping out, introducing air similarly, letting stand for up to sixteen hours, and bombarding with electrons (20 m.a., bringing the electrode to about 75°C temperature). The changes due to none of these treatments was materially greater than the changes observed between repeated measurements of the characteristic of a particular surface.

Fig. 5 is submitted as a basis of comparison for the following figures. Curves 1, 2, 3, and 4 are the first emission observed at each of four independent emitting areas. Curves 5, 6, 7 and 8 are the subsequent emissions for the same areas in order.

Each group of three curves in Fig. 6 represents the history of an independent emitting area. In each group, curve 1 represents the first emission, which emission followed bombardment with positives at the current and for

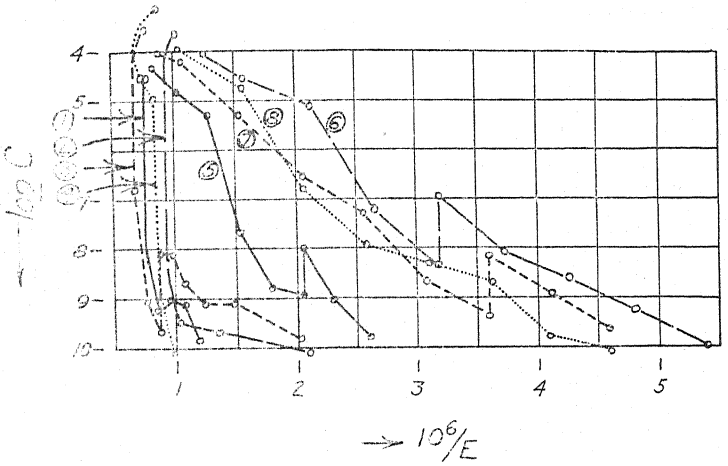

Fig. 5. Emission from untreated copper electrodes.

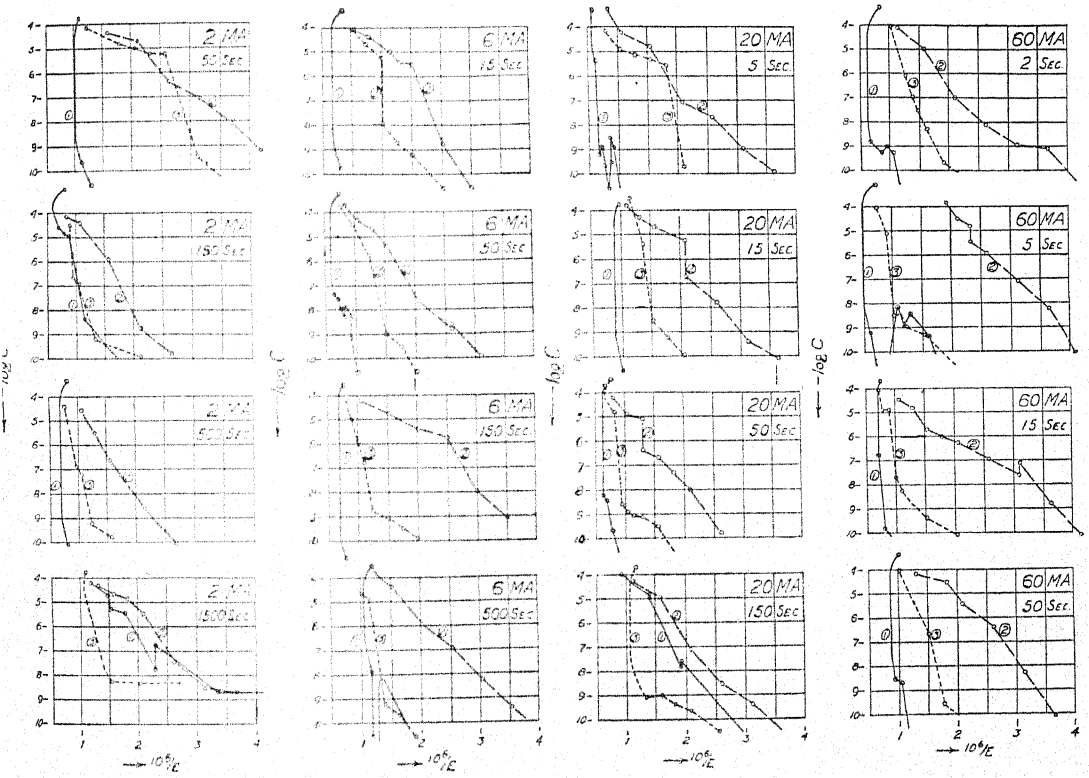

Fig. 6. Effect of discharge through hydrogen.

the time indicated. Curve 2 represents the subsequent emission, which was measured immediately following the first emission. Curve 3 represents the emission which followed another bombardment with positives at the same current and for the same time as before. These bombardments were made through hydrogen at the highest pressure (between 1 mm and 12 mm pressure) which would permit the negative glow completely to surround the bombarded electrode, which was the cathode in both the glow discharge and the measurement of the emission.

A study of the curves will show that up to a certain point, bombardment with positives does not seem to affect the field at which breakdown first occurs, but that there is a current and time for which a bombardment with positives restores the emitting surface after breakdown to the condition it had before breakdown occurred.

6. Effect of the Anode

Measurements were made of the emission from a copper cathode but with various anodes. Anodes used were of copper, iron, magnesium, zinc, plymite,

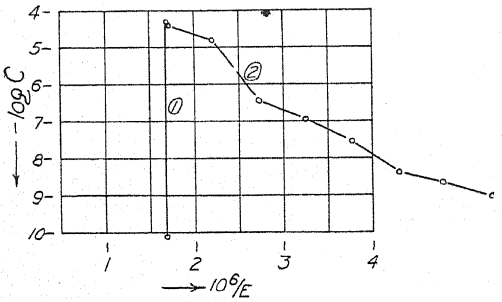

Fig. 7. Plymite anode.

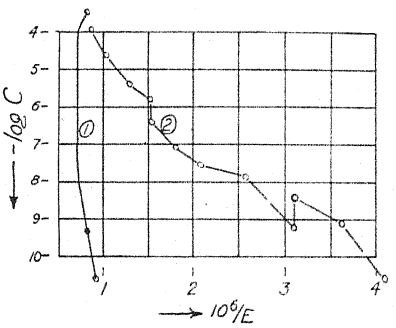

Fig. 8. Copper anode.

aluminum, chromium-plate, and molybdenum. Complete sets of measurements were made for at least four independent emitting areas for each combination of electrodes, and the set which appeared to be most typical for each kind of anode is shown with the corresponding label in Figs. 7 to 14. The curves are numbered in the order taken.

Repeated attempts to fatigue the emitting surfaces on copper cathodes, using copper, plymite, or iron anodes, giving emission like that shown in curve 2 of Figs. 7, 8 or 10, respectively, failed to give any significant change in slope. The change was uncertain with a zinc anode.

On the other hand, using either a molybdenum, aluminum, chromium, or magnesium anode, the emitting surface quickly fatigued to a new group of curves occupying a zone on the figure definitely removed from that occupied by subsequent emission curves for copper anodes, and corresponding to much lower currents from the same fields.

7. Temporary Breakdown

Frequently, with various electrodes, throughout the entire investigation, there have occurred very sudden large order increases in current (up to 10^6)

which behaved like premature breakdowns. These presently just as suddenly completely disappeared, accompanied by a distinct click of the glass, sounding as though a metal particle had hit the glass. On pushing the field up, the breakdown occurred at the usual field and all subsequent currents behaved the same as though the premature breakdown had not occurred.

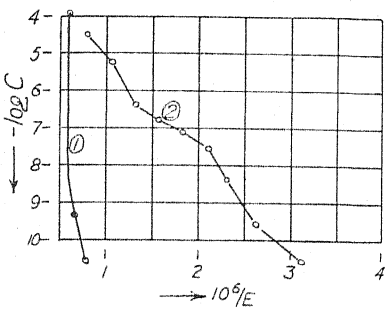

Fig. 9. Iron anode.

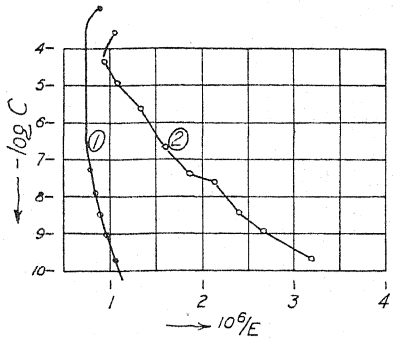

Fig. 10. Zinc anode.

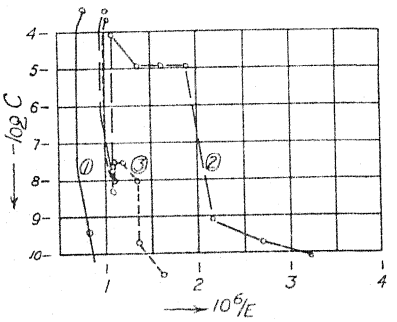

Fig. 11. Magnesium anode.

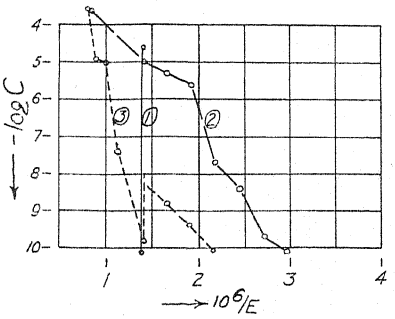

Fig. 12. Aluminum anode.

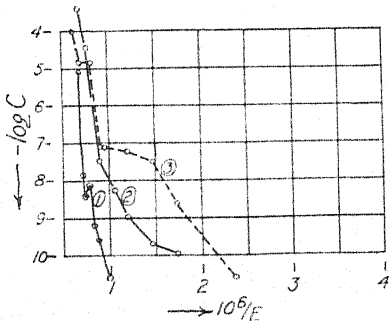

Fig. 13. Chromium plate anode.

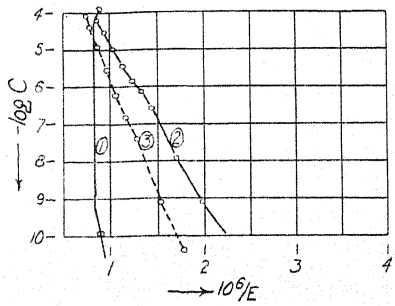

Fig. 14. Molybdenum anode.

8. Discussion

The idea that the first breakdown is simply due to a rupturing of the surface of the cathode and that the emission is determined by the composition and conditioning of the cathode, has appeared to be open to question from early in this investigation.

The phenomenon of premature breakdown seems to leave no doubt that foreign particles either from the anode or from parts of the tube other than the cathode, *can* fly through the tube to the cathode, adhere, give emission, and be torn from the cathode leaving no scar on the cathode of sufficient irregularity to give measurable emission.

Following excessive discharge through hydrogen (which was observed to give sputtering), the first emission was seen to behave either as though a complete breakdown has been produced during the discharge through hydrogen, or else as though no sensible effect had been produced on the cathode surface at all (see curves 1, each of the lower four groups in Fig. 6). It was never observed after sputtering had been produced in the tube either during these measurements or with any other electrodes under different conditions, that immediately subsequent field-current curves lay in the region between the two zones belonging to emission leading up to the usual breakdown, or the emission following the usual breakdown, respectively. This fact would seem to indicate that the adhesion of a loose particle to the cathode gives emission indistinguishable from that following the usual breakdown.

Following breakdown, when molybdenum, aluminum, chromium, or magnesium were used as anode, the lowest subsequent currents measurable occurred at fields much higher than those at which the lowest currents occurred when copper was used as the anode. The most plausible explanation of this seems to be that auto-electronic emission is from a particle torn from the anode and which is adhering to the cathode.

If, on the other hand, the breakdown is due to a rupturing of the copper cathode surface, it would be necessary to suppose that the steeper slopes, when one of the above four metals was used as anode, are due to beating down the ragged edges by positives coming from the anode at emission currents of less than 10^{-10} amperes, and that the emitting point is bombarded with positives of the same order of density as occur in a discharge through hydrogen of several milliamperes spread over the entire cathode surface. In view of the small size of the emitting points, this is a possible supposition. It is further supported by the fact that after prolonged auto-electronic discharge, the white color of the anode metal becomes distinguishable as a small spot at the emitting point on the copper cathode. This explanation, however, forces us to the conclusion that the emission measured is from a surface of metal originally composing the anode, and hence the emission is determined by the metal used as anode, anyhow.

In conclusion, the author wishes to thank Drs. Millikan, MacKeown, and Lauritsen for advice borne of their longer experience in this field, and also Dr. Millikan for making available the necessary facilities for this investigation.

SCATTERING OF HIGH VELOCITY ELECTRONS IN HYDROGEN AS A TEST OF THE INTERACTION ENERGY OF TWO ELECTRONS

By Hugh C. Wolfe*
California Institute of Technology, Pasadena

(Received January 26, 1931)

Abstract

1. The electronic scattering of high velocity electrons is considered as a test of the formulas for the interaction energy of two electrons. Three formulas for the interaction energy of two Dirac electrons are considered: I, the simple electrostatic interaction, II, the Gaunt formula, III, the Breit formula.

2. The Dirac transition probability method is reviewed briefly.

3. The cross-section of free electrons at rest for scattering high velocity electrons is calculated by the Dirac transition probability method, using each of the three formulas for interaction energy. Random distribution of spins is assumed. Relativistic variation of mass with velocity is taken into account, removing the symmetry about 45° of the classical scattering formula. Expanded to terms in β^2 the formulas obtained are compared with the classical Darwin formula and the recent formula of Mott. They differ from Mott's formula and from each other by terms of order β^2.

4. For high-velocity electrons, the scattering by hydrogen may be considered as the sum of nuclear and electronic scattering. A criterion for the validity of this procedure is obtained. The advantage of using hydrogen as the scatterer in experiments to test these formulas is discussed.

I. THE scattering of electrons by hydrogen may be considered as the sum of the scattering by free protons and the scattering by free electrons, provided the incident velocity is high and the scattering angle is not too near 0 or $\pi/2$. A criterion for the validity of this approximation is developed in section 4.

The cross-section for scattering depends upon the energy of interaction of the scatterer and the scattered particle and there is no completely justified theoretical formula for the interaction of two electrons or of an electron and a proton. Three formulas have been used,

$$\begin{aligned} &\text{I} \quad V = e^{\text{I}}e^{\text{II}}/r \\ &\text{II} \quad V = e^{\text{I}}e^{\text{II}}/r\left[1 - (\alpha^{\text{I}}\cdot\alpha^{\text{II}})\right] \\ &\text{III} \quad V = e^{\text{I}}e^{\text{II}}/r\left[1 - \frac{(\alpha^{\text{I}}\cdot\alpha^{\text{II}})}{2} - \frac{(\alpha^{\text{I}}\cdot r)(\alpha^{\text{II}}\cdot r)}{2r^2}\right]. \end{aligned} \tag{1}$$

The α's, written here as vectors, have components which are the matrices of four rows and columns appearing as coefficients in the Dirac linear Hamiltonian for one particle. r is the distance between the particles. I is just the electrostatic interection. II includes "spin" terms. III includes also the effect of

* National Research Fellow.

retardation of the potentials. III, which was first derived by Breit,[1] on the analogy $v/c \to \alpha$, and which is obtained in first approximation from the Heisenberg-Pauli field theory by systematic neglect of the infinite proper energy terms, has the most theoretical justification. However, Breit[2] has calculated the fine structure of helium with it and his results are no better than those of Gaunt,[3] who derived and used II. This failure may be due to the inadequacy of the approximate wave functions used. It is, therefore, of interest to find another place to use these formulas, where it may be possible to determine which gives results in better agreement with experiment.

For scattering of electrons by protons, a calculation similar to that given here for scattering by electrons has been carried out. The result is that the extra terms in II or III have a negligible influence. Massey[4] concurs in this result. Thus Mott's calculation using I, gives the best formula for nuclear (proton) scattering.[5]

2. The cross-section of an electron for scattering electrons is calculated here in first approximation by the transition probability method of Dirac.[6] The Hamiltonian for the system, incident electron plus scatterer, is to be written in the form $H = H^\circ + V$, where H° represents the system as it is observed experimentally. The eigenstates $\Psi(\alpha')$ of the unperturbed system whose Hamiltonian is H°, are known and are specified by giving the values, here assumed continuous in range, of a set of observables, $\alpha_1 \cdots \alpha_u$, which are constants of the motion. We shall frequently use α to represent $\alpha_1 \cdots \alpha_u$. The state Ψ of the system whose Hamiltonian is H is to be expanded in the eigen Ψ's of the unperturbed system,

$$\Psi = \int \Psi(\alpha') d\alpha' a(\alpha'),$$

where $a(\alpha')$ is a function of the time, i.e., the method of variation of constants. Substituting in the equation

$$H\Psi = \frac{ih}{2\pi} \frac{\partial}{\partial t} \Psi,$$

we obtain an integral equation for the time variation of $a(\alpha')$. Assuming that at some initial time our system would certainly be observed in the state α°, i.e., initially $a(\alpha') = a^\circ \delta(\alpha' - \alpha^\circ)$, this equation reduces to a simple differential equation which can be integrated. The normalization of the $a(\alpha')$ is such that we are concerned not with one system but with an ensemble of similar

[1] Breit, Phys. Rev. **34**, 553 (1929).
[2] Breit, Phys. Rev. **36**, 383 (1930).
[3] Gaunt, Proc. Roy. Soc. **A122**, 513 (1929).
[4] Massey, Proc. Roy. Soc. **A127**, 666 (1930).
[5] Mott, Proc. Roy. Soc. **A124**, 425 (1929). He formulates the problem rigorously, using Gordon's solutions of the Dirac equation, and approximates by expanding in powers of $\alpha = Z(2\pi e^2/hc)$, neglecting terms in α^2.
[6] Dirac, Proc. Roy. Soc. **A114**, 243 (1927) or Dirac, Principles of Quantum Mechanics, Oxford, 1930, section 54.

systems. The number of systems in our ensemble is $|a^\circ|^2 \int dx |\psi_{\alpha 0}(x)|^2$, where x stands for the whole set of coordinates and $\psi_{\alpha 0}(x)$ is a solution of the wave-equation for the unperturbed system in the initial state. Then $|a(\alpha')|^2 d\alpha'$ is the number of systems at time t such that α lies between α' and $\alpha'+d\alpha'$. The expression for $|a(\alpha')|^2$ shows that essentially only those transitions occur in which energy is conserved. If we transform to a new set of parameters, $W, \gamma_1 \cdots \gamma_{u-1}$, which are arbitrary independent functions of the α's, the number of transitions per second from the initial state to states in which the γ's have values between γ' and $\gamma'+d\gamma'$ is found, by integration with respect to W', to be

$$4\pi^2/h^2 |a^0|^2 |(W^0, \gamma'| V| W^0, \gamma^0)|^2 J(W^0, \gamma') d\gamma_1' \cdots d\gamma'_{u-1}. \qquad (2)$$

$J(W^\circ, \gamma')$ is the Jacobian, $\partial(\alpha_1' \cdots \alpha_u')/\partial(W', \gamma_1' \cdots \gamma_{u-1}')$, with the values $W^\circ, \gamma_1' \cdots \gamma'_{u-1}$ for the variables. $(W^\circ, \gamma'| V| W^\circ, \gamma^\circ)$ is the matrix element $(\alpha'| V|\alpha^\circ)$, where the α's are so determined that the parameters, $W, \gamma_1 \cdots \gamma_{u-1}$, have the values $W^\circ, \gamma_1^\circ \cdots \gamma_{u-1}^\circ$ in the initial state and $W^\circ, \gamma_1' \cdots \gamma_{u-1}'$ in the final state. If $V = V(x,p)$ is a function of the coordinates and conjugate momenta, then

$$(\alpha'| V| \alpha^0) = \int N_{\alpha'} \psi_{\alpha'}(x) dx V\left(x, \frac{h}{2\pi i}\frac{\partial}{\partial x}\right) \psi_{\alpha 0}(x). \qquad (3)$$

All of our expressions assume that the wave functions have the continuous spectrum normalization, equivalent to the Dirac δ normalization. $N_{\alpha'}$ is the normalizing factor for the final state wave functions and is given[7] by

$$N_{\alpha'}^2 \int dx \tilde{\psi}_{\alpha'}(x) \int_{\alpha'-\Delta\alpha'}^{\alpha'+\Delta\alpha'} d\alpha'' \psi_{\alpha''}(x) = 1. \qquad (4)$$

For our purposes, the normalization of the initial state wave functions is quite arbitrary. This is because we are interested in the cross-section for scattering, σ_s, which is defined from the classical treatment of collision scattering by

$$\sigma_s = \frac{\text{Number of transitions per sec. of the specified type, i.e. (2)}}{(\text{Flux of incident particles}) \cdot (\text{number of scatterers})}. \qquad (5)$$

Both $|a^\circ|^2$ and the initial state normalizing factors occur in both numerator and denominator and cancel out.

3. In our problem the Hamiltonian H° is the sum of the Dirac linear Hamiltonians for two free electrons. The wave equation for the unperturbed system is

$$\left[W - \frac{hc}{2\pi i}\{(\alpha^{\mathrm{I}} \cdot \mathrm{grad}^{\mathrm{I}}) + (\alpha^{\mathrm{II}} \cdot \mathrm{grad}^{\mathrm{II}})\} - mc^2(\alpha_0^{\mathrm{I}} + \alpha_0^{\mathrm{II}})\right] \psi = 0.$$

This equation has solutions of the form $\psi = \psi^I \psi^{II}$ with $W = W_1 + W_2$, where ψ^I is a solution of

[7] Oppenheimer, Phys. Rev. **31**, 66 (1928).

$$\left[W_1 - \frac{hc}{2\pi i}(\alpha^{\mathrm{I}}\cdot \mathrm{grad}^{\mathrm{I}}) - mc^2\alpha_0{}^{\mathrm{I}}\right]\psi^{\mathrm{I}} = 0$$

and similarly ψ^{II}. The solution in the form of plane waves has been given by Darwin.[8] The four components of ψ^I are

$$\psi_3 = AS_1{}^{\mathrm{I}} \quad \psi_1 = \frac{-Ap_{1z} - B(p_{1x} - ip_{1y})}{mc + W_1/c}S^{\mathrm{I}},$$

$$\psi_4 = BS_1{}^{\mathrm{I}} \quad \psi_2 = \frac{-A(p_{1x} + ip_{1y}) + Bp_{1z}}{mc + W_1/c}S_1{}^{\mathrm{I}} \tag{6}$$

where

$$W_1 = c(m^2c^2 + p_{1x}{}^2 + p_{1y}{}^2 + p_{1z}{}^2)^{1/2}$$

$$S_1{}^{\mathrm{I}} = \exp\left[\frac{2\pi i}{h}(p_{1x}x_1 + p_{1y}y_1 + p_{1z}z_1 - W_1t)\right].$$

Darwin shows that the orientation of the spin axis, as given by its colatitude f, measured from the z axis, and longitude ω, is given by the relation $-B/A = \cot f/2e^{i\omega}$. Accordingly, $A=0$, $B=1$, means that the spin is "parallel" to the z axis, and the corresponding four components of the wave function may be represented by the one symbol Ψ_α. Likewise, $B=0$, $A=1$, means that the spin is "antiparallel" to the z axis and for this case we may write ψ_β. The constants of the motion, whose values designate the eigenstates of the unperturbed system (the α's of section 2), are the components of momentum of the two particles p_{1x}, p_{1y}, p_{1z}, p_{2x}, p_{2y}, p_{2z}. We shall use a lower index 1 or 2 to indicate that the corresponding momentum is (p_{1x}, p_{1y}, p_{1z}) or (p_{2x}, p_{2y}, p_{2z}). Thus the symbol $\psi_{2\alpha}{}^I$ means the four component wave function in the coordinates (x_1, y_1, z_1) for momentum (p_{2x}, p_{2y}, p_{2z}) with $A=0$, $B=1$.

To take account of the random distribution of spins of the two electrons before the collision, we use wave functions for the initial state which represent equal probabilities for each electron to have its spin parallel or antiparallel to the z axis. As pointed out by Oppenheimer,[9] our wave functions must be antisymmetric to conform to the Pauli principle, since we are dealing with identical particles with spin. Accordingly, our initial state wave functions may have the form

$$\begin{aligned}
\psi_a &= 1/(2)^{1/2}(\psi_{1\alpha}{}^{\mathrm{I}}\psi_{2\alpha}{}^{\mathrm{II}} - \psi_{2\alpha}{}^{\mathrm{I}}\psi_{1\alpha}{}^{\mathrm{II}})\\
\psi_b &= 1/(2)^{1/2}(\psi_{1\beta}{}^{\mathrm{I}}\psi_{2\beta}{}^{\mathrm{II}} - \psi_{2\beta}{}^{\mathrm{I}}\psi_{1\beta}{}^{\mathrm{II}})\\
\psi_c &= \tfrac{1}{2}(\psi_{1\alpha}{}^{\mathrm{I}}\psi_{2\beta}{}^{\mathrm{II}} - \psi_{2\beta}{}^{\mathrm{I}}\psi_{1\alpha}{}^{\mathrm{II}} + \psi_{1\beta}{}^{\mathrm{I}}\psi_{2\alpha}{}^{\mathrm{II}} - \psi_{2\alpha}{}^{\mathrm{I}}\psi_{1\beta}{}^{\mathrm{II}})\\
\psi_d &= \tfrac{1}{2}(\psi_{1\alpha}{}^{\mathrm{I}}\psi_{2\beta}{}^{\mathrm{II}} - \psi_{2\beta}{}^{\mathrm{I}}\psi_{1\alpha}{}^{\mathrm{II}} - \psi_{1\beta}{}^{\mathrm{I}}\psi_{2\alpha}{}^{\mathrm{II}} + \psi_{2\alpha}{}^{\mathrm{I}}\psi_{1\beta}{}^{\mathrm{II}}).
\end{aligned} \tag{7}$$

where the first three of these are symmetric in the spins and the fourth is antisymmetric in the spins.

The spin distribution in the final state is not to be measured and is deter-

[8] Darwin, Proc. Roy. Soc. A120, 621 (1928).
[9] Oppenheimer, Phys. Rev. 32, 361 (1928).

mined only by the transition probabilities. Wave functions representing any spin orientations can be built up by superposition of four wave functions of the type (7). We shall use a ϕ to represent the complex conjugate of a final state wave function, only the complex conjugates occurring in our formulas. The final state momenta will be designated by p_{1x}', p_{1y}', p_{1z}', p_{2x}', p_{2y}', p_{2z}'. The total transition probability out of any one of the four initial spin states is the sum of the transition probabilities to four final spin states of type (7). We shall have taken account of the initial random spin orientations if we take the unweighted average of the total probabilities of transition out of the four initial spin states. Specifically, this means to calculate sixteen cross-sections for scattering, using the matrix elements obtained from all combinations of $\phi_a, \phi_b, \phi_c, \phi_d$ with $\psi_a, \psi_b, \psi_c, \psi_d$, and to take one fourth of the sum.

We shall transform from $p_{1x}, p_{1y}, p_{1z}, p_{2x}, p_{2y}, p_{2z}$ to a new set of parameters W, P_x, P_y, P_z, θ, ϕ (the $W, \gamma_1 \cdots \gamma_{u-1}$ of section 2), where (P_x, P_y, P_z) is the momentum of the center of gravity and θ, ϕ are the polar angles of the momentum (p_{1x}, p_{1y}, p_{1z}), the z axis being taken as pole. The equations of transformation are

$$W = c(m^2c^2 + p_1^2)^{1/2} + c(m^2c^2 + p_2^2)^{1/2} \qquad P_x = p_{1x} + p_{2x}$$
$$\cos\theta = p_{1z}/p_1 \qquad P_y = p_{1y} + p_{2y}.$$
$$\tan\phi = p_{1y}/p_{1x} \qquad P_z = p_{1z} + p_{2z}$$

It is convenient also to use center of gravity coordinates X, Y, Z, relative coordinates x, y, z and relative momenta p_x, p_y, p_z, the equations of transformation being

$$X = \tfrac{1}{2}(x_1 + x_2) \quad x = x_1 - x_2 \quad p_x = \tfrac{1}{2}(p_{1z} - p_{2x})$$
$$Y = \tfrac{1}{2}(y_1 + y_2) \quad y = y_1 - y_2 \quad p_y = \tfrac{1}{2}(p_{1y} - p_{2y})$$
$$Z = \tfrac{1}{2}(z_1 + z_2) \quad z = z_1 - z_2 \quad p_z = \tfrac{1}{2}(p_{1z} - p_{2z}).$$

Note that

$$\frac{\partial(x_1, y_1, z_1, x_2, y_2, z_2)}{\partial(X, Y, Z, x, y, z)} = 1.$$

Let us now consider the matrix elements $(\alpha'|\, V|\alpha^\circ)$. They are of the form

$$\int \cdots \int dx_1 \cdots dz_2 \phi_i V \psi_j$$

where i and j take on the values a, b, c, d. V is considered as an operator on ψ_j. The integrand will consist of a sum of terms of the form

$$\phi_{l's'}{}^{\mathrm{I}} \phi_{n't'}{}^{\mathrm{II}} V \psi_{ls}{}^{\mathrm{I}} \psi_{nt}{}^{\mathrm{II}}$$

where l, n, may be 1, 2 or 2, 1; l', n' may be 1, 2 or 2, 1; s, t, s', t' may be α or β. The only operators contained in V are the Dirac α's and the result of their operation is just to permute the four components of a ψ function and to introduce some factors -1 or i. Also α^I operates[10] only on ψ^I and α^{II} on ψ^{II} so that, for example,

[10] The two electrons are independent in the unperturbed system and all matrices associated with one commute with all matrices associated with the other.

$$\phi^{\mathrm{I}}\phi^{\mathrm{II}}\alpha_1{}^{\mathrm{I}}\alpha_3{}^{\mathrm{II}}\psi^{\mathrm{I}}\psi^{\mathrm{II}} = (\phi^{\mathrm{I}}\alpha_1{}^{\mathrm{I}}\psi^{\mathrm{I}})(\phi^{\mathrm{II}}\alpha_3{}^{\mathrm{II}}\psi^{\mathrm{II}}).$$

We write the expressions (6) for the four components of $\phi_{l'}{}^{I}$ in the form $(\phi_{l'}{}^{I})_\lambda = a_\lambda' S_{l'}{}^{I}$, and for the four components of $\psi_l{}^{I}$ in the form $(\psi_l{}^{I})_\lambda = a_\lambda S_l{}^{II}$, where $\lambda = 1, 2, 3, 4$, and define

$$\begin{aligned}
\Omega_4 &= a_1'a_1 + a_2'a_2 + a_3'a_3 + a_4'a_4 \\
\Omega_1 &= a_1'a_4 + a_2'a_3 + a_3'a_2 + a_4'a_1 \\
\Omega_2 &= a_1'a_4 - a_2'a_3 + a_3'a_2 - a_4'a_1 \\
\Omega_3 &= a_1'a_3 - a_2'a_4 + a_3'a_1 - a_4'a_2.
\end{aligned} \tag{8}$$

We define Ω''s similarly in terms of the components of $\phi_{n'}{}^{II}$ and $\psi_n{}^{II}$. Further we write

$$S = \exp\left[2\pi i/h\{(p_l{}^0\cdot r_1) + (p_n{}^0\cdot r_2) - (p_{l'}'\cdot r_1) - (p_{n'}\cdot r_2)\}\right].$$

Then with our three V's of (1), we have for our typical term in the integrand

$$\phi_{l's'}{}^{\mathrm{I}}\phi_{n'l'}{}^{\mathrm{II}}V\psi^{\mathrm{I}}{}_{ls}{}^{\mathrm{I}}\psi_{nl}{}^{\mathrm{II}} =$$

$$\begin{aligned}
\mathrm{I}\quad & e^2/r[\Omega_4\Omega_4']S \\
\mathrm{II}\quad & e^2/r[\Omega_4\Omega_4' - \Omega_1\Omega_1' + \Omega_2\Omega_2' - \Omega_3\Omega_3']S \\
\mathrm{III}\quad & e^2/r[\Omega_4\Omega_4' - \tfrac{1}{2}\{\Omega_1\Omega_1' - \Omega_2\Omega_2' + \Omega_3\Omega_3'\} \\
& - 1/2r^2\{x\Omega_1 - iy\Omega_2 + z\Omega_3\}\{x\Omega_1' - iy\Omega_2' + z\Omega_3'\}]S.
\end{aligned} \tag{9}$$

Since

$$\begin{aligned}
(p_1\cdot r_1) + (p_2\cdot r_2) &= (P\cdot R) + (p\cdot r) \\
(p_1\cdot r_2) + (p_2\cdot r_1) &= (P\cdot R) - (p\cdot r),
\end{aligned} \tag{10}$$

it follows that in every case our integrand contains a factor

$$\exp\left[\frac{2\pi i}{h}\{(P^0\cdot R) - (P'\cdot R)\}\right].$$

Consequently, if we carry out the integration in the variables X, Y, Z, x, y, z instead of $x_1, y_1, z_1, x_2, y_2, z_2$, every matrix element has the factor

$$\int\int\int dXdYdZ \exp\left[\frac{2\pi i}{h}\{(P^0\cdot R) - (P'\cdot R)\}\right].$$

This integral is of the nature of a δ function of $(P^0 - P')$ so that we have a transition probability only between initial and final states such that the momentum of the system is conserved, as well as the energy. Consequently, we shall be interested only in the number of transitions from the initial state to final states in which θ lies between θ and $\theta + d\theta$ and ϕ lies between ϕ and $\phi + d\phi$. This means going back to (2), the γ''s being P_x', P_y', P_z', θ, ϕ, and integrating with respect to P_x', P_y', P_z' as we had previously integrated with respect to W'. Although P' occurs in other factors, e.g., in J, besides

$$\left|\int\int\int dXdYdZ \exp\left[\frac{2\pi i}{h}\{(P^0\cdot R) - (P'\cdot R)\}\right]\right|^2,$$

this factor predominates and assures us that we shall have contributions to the integral only for $P' = P^0$. Accordingly, we insert $P' = P^0$ in all other factors and take them outside the integration. We note that the remaining integral is just the cube of

$$\int_{-\infty}^{\infty} dP_x' \left| \int_{-\infty}^{\infty} dX \exp\left[\frac{2\pi i}{h}(P_x^0 - P_x')X\right] \right|^2.$$

We replace $\int_{-\infty}^{\infty} dX$ by $\lim_{X=\infty} \int_X^X dX$ and carry out the limiting process after integrating with respect to P_x', obtaining $\lim_{X=\infty} 2hX$. Thus the factor obtained from integration over P_x', P_y', P_z' is just h^3V, where V is the infinite volume of space.

For the remainder of our considerations, we may note that instead of using the parameters $W, P_x, P_y, P_z, \theta, \phi$ and inserting $W' = W^0$ and $P' = P^0$, it is more convenient to use $p_{1x}, p_{1y}, p_{1z}, p_{2x}, p_{2y}, p_{2z}$, where the values assigned are to be determined by the principles of conservation of energy and momentum, together with the requirement that p_1' shall have the direction $\theta\phi$. For the initial state, we shall take

$$p_{1z}^0 = p_1^0 = \frac{mv}{(1-\beta^2)^{1/2}}; \quad p_{1x}^0 = p_{1y}^0 = p_{2x}^0 = p_{2y}^0 = p_{2z}^0 = 0 \qquad (11)$$

which means that we consider a plane wave of electrons of velocity $v = \beta c$, incident in the z direction on electrons at rest. For the final state, since we have symmetry about the z axis, we are independent of ϕ and may most conveniently use $\phi = 0$. We shall also introduce the notation

$$\gamma = 1/(1-\beta^2)^{1/2}, \quad \sigma = \sin\theta, \quad \rho = \cos\theta.$$

Then we have

$$\begin{aligned} p_{1x}' &= p_1^0 \frac{2\sigma\rho}{2+(\gamma-1)\sigma^2} & p_{2z}' &= -p_1^0 \frac{2\sigma\rho}{2+(\gamma-1)\sigma^2} \\ p_{1y}' &= 0 & p_{2y}' &= 0 \\ p_{1z}' &= p_1^0 \frac{2\rho^2}{2+(\gamma-1)\sigma^2} & p_{2z}' &= p_1^0 \frac{(\gamma+1)\sigma^2}{2+(\gamma-1)\sigma^2}. \end{aligned} \qquad (12)$$

The density of particles being $\sum_{\lambda=1}^{4} |\psi_\lambda|^2$, we have by (6) a density $2\gamma/\gamma+1$ electrons per cc in our incident beam and a density of one electron per cc of scatterers. Accordingly, the incident flux is $2\gamma v/\gamma+1$ and the number of scatterers is V, the infinite volume of space. The Jacobian, J, of (2) has the value

$$J = \frac{4m^2v\gamma\rho\sigma[2\gamma-(\gamma-1)\sigma^2][\gamma(\gamma+1)\sigma^2+2\rho^2]}{[2+(\gamma-1)\sigma^2]^4}.$$

From the normalization of the final state wave functions by (4), we find for the factor $N_{\alpha'}$.

$$N^2 = \frac{(\gamma+1)[(\gamma+1)^2\sigma^2 + 4\rho^2]}{2h^6[2\gamma - (\gamma-1)\sigma^2][\gamma(\gamma+1)\sigma^2 + 2\rho^2]}.$$

With this value of J in (2) and of N in (3), we insert in (5) and obtain

$$\sigma_s = \frac{4\pi^2 m^2 \rho\sigma(\gamma+1)^2[(\gamma+1)^2\sigma^2 + 4\rho^2]d\theta d\phi}{h^4[2+(\gamma-1)\sigma^2]^4} F^2,$$

where F^2 is one fourth of the sum of the squares of the factors obtained by integration over the relative coordinates in the sixteen matrix elements of the interaction energy, V.

To evaluate F^2, we must go back to (9), which is the typical term of our integrand if we write S_r instead of S and understand by S_r the remainder of the exponential factor, S, after taking out

$$\exp\left[\frac{2\pi i}{h}\{(P^0\cdot R) - (P'\cdot R)\}\right].$$

As a consequence of (10) and using the values of p° and p' given by (11) and (12), this remaining factor has the following form, determined by values of l and l',

$$\begin{aligned}
&l=1,\quad l'=1 \quad S_r = \exp\left[\frac{2\pi i}{h}(p_2'\cdot r)\right]\\
&l=2,\quad l'=2 \quad S_r = \exp\left[-\frac{2\pi i}{h}(p_2'\cdot r)\right]\\
&l=2,\quad l'=1 \quad S_r = \exp\left[\frac{2\pi i}{h}(p_1'\cdot r)\right]\\
&l=1,\quad l'=2 \quad S_r = \exp\left[-\frac{2\pi i}{h}(p_1'\cdot r)\right].
\end{aligned} \tag{14}$$

The integration of (9) with respect to the relative coordinates x, y, z, may be carried out in cylindrical coordinates[11] or in polar coordinates, the pole being taken in the direction of the momentum p_k' which occurs in S_r. In the latter case, convergence is obtained by taking account of screening at infinite distance. The integrals occurring are

$$\begin{aligned}
&\int\int\int dx\,dy\,dz\; 1/r \exp\left[2\pi i/hp_k'z\right] = h^2/(\pi p_k'^2)\\
&\int\int\int dx\,dy\,dz\; z^2/r^3 \exp\left[2\pi i/hp_k'z\right] = -h^2/(\pi p_k'^2).
\end{aligned} \tag{15}$$

[11] Oppenheimer, Zeits. f. Physik **43**, 413 (1927).

Then the integration of (9) over the relative coordinates gives

$$\begin{aligned}
&\text{I} \quad \frac{e^2h^2}{\pi p_k'^2}[\Omega_4\Omega_4'] \\
&\text{II} \quad \frac{e^2h^2}{\pi p_k'^2}[\Omega_4\Omega_4' - \Omega_1\Omega_1' + \Omega_2\Omega_2' - \Omega_3\Omega_3'] \\
&\text{III} \quad \frac{e^2h^2}{\pi p_k'^2}[\Omega_4\Omega_4' + \Omega_2\Omega_2' - (\Omega_1\rho_k - \Omega_3\sigma_k)(\Omega_1'\rho_k - \Omega_3'\sigma_k)].
\end{aligned} \tag{16}$$

Here ρ_k and σ_k are the cosine and sine of the angle between $+p_k'$ and the z axis.

The remainder of the task is the evaluation of the Ω's and Ω''s, the summing of the various terms of the type (16) that occur in each matrix element, the squaring of the resulting expressions and taking one fourth of their sum. Only the results are given here.

For purposes of comparison with previous formulas, it is useful to expand all our expressions in powers of β^2, neglecting higher powers than β^2. The resulting formulas for the cross-section of a free election at rest for scattering electrons into a solid angle $\sin\theta d\theta d\phi$ are

$$\sigma_s = \frac{e^4}{m^2v^4}\sin 2\theta\, 2d\theta\, d\phi\left[\frac{1}{\sigma^4} + \frac{1}{\rho^4} - \frac{1}{\sigma^2\rho^2} - \frac{\beta^2}{4}f(\theta)\right] \tag{17}$$

where $f(\theta)$ is given by

$$\begin{aligned}
&\text{I} \quad f(\theta) = \frac{4}{\sigma^4} + \frac{2}{\rho^4} - \frac{1}{\sigma^2\rho^2} \\
&\text{II} \quad f(\theta) = \frac{4}{\sigma^4} + \frac{2}{\rho^4} - \frac{2}{\sigma^2\rho^2} \\
&\text{III} \quad f(\theta) = \frac{4}{\sigma^4} + \frac{2}{\rho^4} - \frac{3}{\sigma^3\rho^2}.
\end{aligned} \tag{18}$$

The purely classical formula of Darwin[12] gives the first two terms in the bracket,

$$\frac{1}{\sigma^4} + \frac{1}{\rho^4} = \operatorname{cosec}^4\theta + \operatorname{cosec}^4(\pi/2 - \theta).$$

Mott[13] has calculated the scattering of electrons by electrons, using interaction formula I, rigorously on the wave mechanics, taking account of interchange phenomena but not of the relativistic variation of mass with velocity. For low velocities, his formula is better than ours. In the region in which our formulas apply, we may neglect the square and higher powers of $1/137\beta$, in

[12] Darwin, Phil. Mag. **27**, 499 (1914).
[13] Mott, Proc. Roy. Soc. **A126**, 259 (1930).

which case Mott's formulas gives just the first three terms in the bracket of (17). It may be noted that $f(\theta)$ is not symmetric about the angle $\theta=\pi/4$, whereas the classical formulas had this symmetry. This was to be expected because, when we take account of the relativistic variation of mass with velocity in setting up the equations for the conservation of energy and momentum, the angle between the two scattered electrons is not $\pi/2$ but is $\arccos\{(\gamma-1)\sigma\rho/(\gamma+1)^2\sigma^2+4\rho^2)^{1/2}\}$ or, in the same approximation as the above, $\arccos\{\beta^2/8[1+\beta^2/4(2+\rho^2)]\sin 2\theta\}$.

For comparison with experimental data, we should use the complete formula, rather than the expansion in powers of β^2. Our F^2 can be written in the form

$$F^2=\frac{e^4h^4[2+(\gamma-1)\sigma^2]^4}{\pi^2m^4c^4(\gamma^2-1)^2[4+(\gamma-1)(\gamma+3)\sigma^2]^2}F(\theta). \tag{19}$$

Substituting (19) in (13), we have

$$\sigma_s=\frac{e^4(\gamma+1)^2\sin 2\theta\, 2d\theta\, d\phi}{m^2v^4\gamma^4[4+(\gamma-1)(\gamma+3)\sigma^2]}F(\theta) \tag{20}$$

where the complete expression for $F(\theta)$ is

$$\begin{aligned}
\text{II}\quad F(\theta)=&\frac{1}{\sigma^4}+\frac{1}{\rho^4}-\frac{1}{\sigma^2\rho^2}+\frac{(\gamma-1)}{\sigma^4\rho^4}\left[3\sigma^6+\sigma^4\rho^6-\sigma^6\rho^2+\frac{2\rho^6(1+\sigma^2\rho^2)}{\gamma+1}\right.\\
&\left.-\frac{2(\gamma+1)\sigma^2\rho^4}{4+(\gamma-1)(\gamma+3)\sigma^2}\right]\\
&+\frac{(\gamma-1)^2}{8\sigma^4\rho^4}\left[\sigma^6\{12-(\gamma+1)(\gamma-3)\sigma^2+2\gamma(\gamma+2)\sigma^4\}\right.\\
&+\frac{8\sigma^4\rho^4(3+\sigma^2)}{\gamma+1}+\frac{24\sigma^4\rho^4}{4+(\gamma-1)(\gamma+3)\sigma^2}-\frac{16(\gamma-1)\sigma^2\rho^6}{(\gamma+1)[4+(\gamma-1)(\gamma+3)\sigma^2]}\\
&\left.+\frac{8\rho^6(1+3\sigma^2+3\sigma^4)}{(\gamma+1)^2}-\frac{32\gamma\sigma^2\rho^6}{[4+(\gamma-1)(\gamma+3)\sigma^2]^2}\right].
\end{aligned} \tag{21}$$

$$\begin{aligned}
\text{III}\quad F(\theta)=&\frac{1}{\sigma^4}+\frac{1}{\rho^4}-\frac{1}{\sigma^2\rho^2}+\frac{(\gamma-1)}{2\sigma^4\rho^4}\left[5\sigma^6+\sigma^8+\frac{4\rho^6}{\gamma+1}+\frac{4\sigma^2\rho^6}{(\gamma+1)^2}\right]\\
&+\frac{(\gamma-1)^2}{4\sigma^4\rho^4}\left[\sigma^4\{-4+23\sigma^2+(\gamma^2+6\gamma-13)\sigma^4+(\gamma^2-2\gamma-3)\sigma^6-(\gamma^2-5)\sigma^8\}\right.\\
&+\frac{2\sigma^4\rho^4(5-4\sigma^4)}{\gamma+1}+\frac{8\sigma^2\rho^4(2+2\sigma^2+(2\gamma-3)\sigma^4-(\gamma-1)\sigma^6)}{4+(\gamma-1)(\gamma+3)\sigma^2}\\
&\left.+\frac{4\rho^6(1+3\sigma^2+2\sigma^4)}{(\gamma+1)^2}-\frac{16(\gamma^2-1)\sigma^4\rho^4}{[4+(\gamma-1)(\gamma+3)\sigma^2]^2}\right].
\end{aligned}$$

4. *Criterion for neglect of orbital motion of electron in hydrogen.* The scattering of elections in hydrogen may be considered as the sum of the scattering by free protons and the scattering by free electrons, both at rest, provided the error in the scattering by the electrons, due to their orbital motion, is negligible. This error is of the order

$$\epsilon = \Delta\sigma_s/\sigma_s$$

where $\Delta\sigma_s$ is the change in σ_s if the square of the momentum of the incident electron is changed by the square of the orbital momentum of the electron in the atom or molecule. Using our formulas for σ_s, we obtain a value for ϵ which, for fast electrons and small angles may be written

$$\epsilon \sim \frac{1 - 3/2\beta^2}{10^4\beta^2 \sin\theta}$$

and for angles near $\pi/2$ may be written

$$\epsilon \sim \frac{1 - \frac{1}{2}\beta^2}{10^4\beta^2 \cos^2\theta}.$$

This is just equivalent to considering the error in the nuclear scattering formula of Wentzel when we drop the $1/k^2a^2$ term[14] and obtain $1/\sin^4\theta/2$ instead of $1/[\sin^2\theta/2+(1/ka)^2]^2$. For a 140,000 volt electron, the error is 1 percent at 7° angle of scattering.

5. Since scattering at angles greater than $\pi/2$ is purely nuclear and should be given by Mott's formula,[15] while scattering at angles less than $\pi/2$ is both nuclear and electronic, it is hoped that the part of the scattering due to the electrons may be separated off experimentally and compared with the formulas derived here. Hydrogen is suggested as the scatterer for this test, in spite of the experimental difficulties of working with gases, first because there, only, is the electronic scattering, which increases with the atomic number Z, comparable with the nuclear scattering, which increases with Z^2, and second because the separation of nuclear and electronic scattering is possible at lower voltages with hydrogen than with any other element, the necessary voltage going up roughly with Z. Mr. H. V. Neher, at this institute, is hoping to carry out experiments in the scattering of high velocity electrons in hydrogen in the near future.

The writer wishes to thank Professor J. R. Oppenheimer for many helpful suggestions.

[14] Sommerfeld, Wave Mechanics, Dutton, 1930, p. 197.
[15] Reference 5.

ON THE GRAVITATIONAL FIELD PRODUCED BY LIGHT

By Richard C. Tolman, Paul Ehrenfest and Boris Podolsky
Norman Bridge Laboratory of Physics, Pasadena, California

(Received January 19, 1931)

Abstract

Expressions are obtained, in accordance with Einstein's approximate solution of the equations of general relativity valid in weak fields, for the effect of steady pencils and passing pulses of light on the line element in their neighborhood. The gravitational fields implied by these line elements are then studied by examining the velocity of test rays of light and the acceleration of test particles in such fields. Test rays moving parallel to the pencil or pulse do so with uniform unit velocity the same as that in the pencil or pulse itself. Test rays moving in other directions experience a gravitational action. A test particle placed at a point equally distant from the two ends of a pencil experiences no acceleration parallel to the pencil, but is accelerated towards the pencil by *twice* the amount which would be calculated from a simple application of the Newtonian theory. The result is satisfactory from the point of view of the conservation of momentum. A test particle placed at a point equally distant from the two ends of the track of a pulse experiences no net integrated acceleration parallel to the track, but experiences a net acceleration towards the track which is satisfactory from the point of view of the conservation of momentum.

§1. *Introduction.* The purpose of this article is to investigate, from the standpoint of the general theory of relativity, the gravitational field in the neighborhood of steady beams and isolated pulses of light.[1]

In Part I of the article we shall obtain a general expression for the line element in the presence of a flow of electromagnetic radiation, which will be taken for simplicity as travelling in the X-direction. The calculation will be made on the assumption that the effect of the radiation is small enough so that Einstein's approximate solution of the gravitational equations valid in weak fields can be employed.

In Part II we shall then examine the special form assumed by the line element in the neighborhood of a thin pencil of radiation travelling along the X-axis. We shall find that the pencil must be taken as having only a finite length in order to keep the field weak enough to justify the use of Einstein's approximate method of solution, and hence shall consider the pencil of radiation as travelling between an emitting and an absorbing body which are a finite distance apart.

Abstracting from the gravitational effect of the absorbing and emitting bodies, we shall then investigate the gravitational action of the radiation by determining the effect of its field on the velocity of test rays of light and on the acceleration of test particles in the neighborhood of the pencil. As to the

[1] An investigation of the gravitational field of radiation has also recently been carried out by Rosenfeld, Zeits. f. Physik **65**, 589 (1930). The article deals, however, with questions relating to quantization rather than with the problems which we shall treat in the present paper.

behavior of the test rays, we shall find that a ray of light moving parallel to the pencil and in the same direction would have unit velocity, the same as that in the pencil itself; but in the case of rays moving in other directions we shall find that they would suffer a gravitational disturbance when in the field of the pencil. As to the behavior of test particles, we shall find that a stationary test particle located at a point equally distant from the two ends of the pencil would experience no acceleration parallel to the track of the pencil, but would be accelerated towards the pencil by *twice* the amount, which would be calculated from the Newtonian theory of gravitation by taking the gravitational mass of the radiation as equal to its energy divided by the square of the velocity of light.

The fact that the acceleration of the particle is twice that which would be calculated from a simple application of the Newtonian theory does not seem surprising, when we recall that the bending of a ray of light in passing through a given gravitational field, say that of the sun, is found theoretically and experimentally in the case of weak enough fields to permit the Newtonian approximation, also to be *twice* that which would be calculated from the Newtonian theory taking the gravitational mass of the light as equal to its inertial mass. The occurrence of the factor 2 in both places permits us to retain our familiar ideas as to the conservation of momentum as a first approximation.

In Part III we shall turn to a consideration of the gravitational field in the neighborhood of a passing pulse of radiation, and shall find that this would vary with the time in a manner to be calculated by the method of retarded potentials, the gravitational influence spreading out from the pulse with the velocity of light. As in the case of the pencil of radiation, we shall find also here that we must limit the track of the pulse so as to lie between an emitting and an absorbing body a finite distance apart, since Einstein's approximate method of solving the gravitational equations would fail at the time when the pulse passes abreast of the point of interest, if we should assume an infinite length for the track.

With regard to the behavior of test rays of light in the neighborhood of the track, we shall again find that a ray of light moving parallel and in the same direction as the pulse would have unit velocity, the same as that of the pulse itself, and that rays of light moving in other directions would be subject to a gravitational effect when in the field of the passing pulse. To investigate the behavior of particles in the field of the pulse, we shall consider a stationary test particle, located at a point equally distant from the two ends of the track lying between the source and absorber, and then determine in accordance with the method of retarded potentials what acceleration the particle would receive as a result of the gravitational influences emitted from this portion of the track. Parallel to the track we shall find that the particle would first be accelerated in the direction of motion of the pulse and later in the opposite direction, but that the time integral of this component of the acceleration corresponding to the total influence emitted from the portion of the track considered would be zero. Perpendicular to the motion of the pulse we shall find as a *net* result that the particle would act as though attracted to-

wards the track, and that the time integral of the perpendicular acceleration, corresponding to the total influence emitted from the portion of the track considered, would be just sufficient so that here also as in the case of the pencil of radiation we could maintain in first approximation our older ideas as to the conservation of momentum for the gravitational interaction of a particle with light.

Part I. General Treatment of the Gravitational Field of Radition

§2. *Einstein's approximate solution of the field equations.* We may now proceed to a general treatment of the gravitational field due to radiation. We shall assume the total amount, density and distribution of the radiation to be such that the gravitational potentials $g_{\mu\nu}$ occurring in the general theory of relativity will differ but slightly from the values which they have in empty space. Such an assumption would presumably be justified in the case of any ordinary beam or pulse of light that we might encounter in nature or the laboratory, and introduces a great simplification by permitting the use of Einstein's approximate solution of the gravitational equations, valid in the case of weak fields.

In accordance with this approximate treatment we may write the line element in the form

$$ds^2 = g_{\mu\nu}dx_\mu dx_\nu = (\delta_{\mu\nu} + h_{\mu\nu})dx_\mu dx_\nu \tag{1}$$

where the symbols $\delta_{\mu\nu}$ denote the Galilean values of $g_{\mu\nu}$, namely -1, $+1$ and 0, and the $h_{\mu\nu}$ are small quantities of the first order whose square can be neglected. We may also use the symbols $\delta^{\mu\nu}$ and $\delta^\nu{}_\mu$ to denote the Galilean values of $g^{\mu\nu}$ and $g^\nu{}_\mu$ and define the quantities $h^\nu{}_\mu$ and h by the equations

$$h_\mu{}^\nu = \delta^{\nu\alpha}h_{\mu\alpha} \text{ and } h = h_\alpha{}^\alpha. \tag{2}$$

It can then be shown that an approximate solution of the equations of general relativity which connect the metric with the distribution of matter and energy is given by the equation[2]

$$\left[h_\mu{}^\nu - \tfrac{1}{2}\delta_\mu{}^\nu h\right](x, y, z, t) = -4\int\int\int \frac{[T_\mu{}^\nu](\bar{x}, \bar{y}, \bar{z}, t-r)}{r} d\bar{x}d\bar{y}d\bar{z} \tag{3}$$

where the integration is to be taken over all elements of spatial volume $d\bar{x}$ $d\bar{y}d\bar{z}$, the quantity r is the coordinate distance from the element of volume at $\bar{x}$, $\bar{y}$, $\bar{z}$ to the point of interest at x, y, z, and $[T_\mu{}^\nu]$ is the value of the energy-momentum tensor in the element of volume at such a time $t-r$, that an influence travelling from $\bar{x}$, $\bar{y}$, $\bar{z}$ with unit velocity would reach the point of interest x, y, z at the time of interest t.

§3. *The energy-momentum tensor for radiation.* To use the above solution in our problem, we must have an expression for the energy-momentum tensor for radiation. In any purely electromagnetic field, however, is it known that

[2] See Eddington, "The Mathematical Theory of Relativity," Cambridge 1923, Eq. (57.6)

the components of the energy-momentum tensor using natural coordinates have the values illustrated by the following typical examples.[3]

$$T_1^1 = \tfrac{1}{2}(X^2 - Y^2 - Z^2) + \tfrac{1}{2}(\alpha^2 - \beta^2 - \gamma^2) \tag{4}$$

$$T_1^2 = XY + \alpha\beta \tag{5}$$

$$T_1^4 = \beta Z - \gamma Y \tag{6}$$

$$T_4^4 = \tfrac{1}{2}(X^2 + Y^2 + Z^2) + \tfrac{1}{2}(\alpha^2 + \beta^2 + \gamma^2) \tag{7}$$

where X, Y, Z are the components of the electric field strength and α, β, γ are the components of the magnetic field strength at the point of interest.

Applying these equations now to the case of radiation which we take for simplicity to be moving parallel to the X-axis in the positive direction, and noting the relations of (4) and (5) to the Maxwellian stresses in the field, of (6) to the Poynting vector, and of (7) to the energy density, it can be shown that the only surviving components of the energy-momentum tensor for the case of polarized or unpolarized incoherent radiation will be

$$T_1^1 = -\rho \qquad T_4^4 = \rho \qquad T_1^4 = -\rho \qquad T_4^1 = \rho \tag{8}$$

where ρ is the density of energy, and, since the velocity of light is unity, also the density of energy flow at the point of interest. The results assume the justifiability of neglecting diffraction phenomena, such as would occur at the boundary of a beam of radiation where the hypothesis of a flow of energy solely in the X-direction could not be strictly valid.

§4. *The general form of line element due to radiation.* The above equations give the components of the energy-momentum tensor in coordinates which are Galilean at the point of measurement, but to the order of approximation of the solution we are to use, they may also be taken as the components of that tensor in our general system of coordinates which differs from the Galilean form only by quantities of the first order, and hence may be substituted into equation (3) to determine the form of the line element.

Doing so we obtain

$$\begin{aligned}
h_1^1 - \tfrac{1}{2}h &= 4\int \frac{[\rho]dV}{r} \\
h_2^2 - \tfrac{1}{2}h &= 0 \\
h_3^3 - \tfrac{1}{2}h &= 0 \\
h_4^4 - \frac{1}{2}h &= -4\int \frac{[\rho]dV}{r} \\
h_1^4 &= -h_4^1 = 4\int \frac{[\rho]dV}{r}
\end{aligned} \tag{9}$$

with all other components of h_μ^ν equal to zero. And remembering the value of h and the method of raising suffixes given by equations (2) we can easily solve these equations for the $h_{\mu\nu}$. We then obtain as the only surviving components

[3] See Eddington, reference 2, Eqs. (77.41–4).

$$h_{11} = h_{44} = -h_{14} = -h_{41} = -4\int \frac{[\rho]dV}{r} \tag{10}$$

and these values of the $h_{\mu\nu}$ can be substituted into Eq. (1) to give the general form of the line element due to radiation travelling in the X-direction.

Part II. The Gravitational Action of a Pencil of Light

§5. *The line element in the neighborhood of a limited pencil of radiation.* As a first application of the expression for the line element due to radiation travelling in the X-direction, it would be natural to try to treat the gravitational field in the neighborhood of a thin pencil of radiation of uniform density, stretching in the X-direction from minus to plus infinity. But this proves to be impossible by the method adopted, since the values of the $h_{\mu\nu}$ come out infinite when the integration indicated in Eq. (10) is performed, which would invalidate the approximate solution of the gravitational equations that has been used.

If we consider, however, a thin pencil of radiation of limited length l and constant linear density ρ, passing steadily along the X-axis between a source at $x=0$ and an absorber at $x=l$, this difficulty does not arise, since we can then evidently write in accordance with Eq. (10) for the contribution of the radiation to the gravitational field at any point of interest x, y, z in the neighborhood of the pencil,

$$\begin{aligned} 4\int \frac{[\rho]dV}{r} &= -h_{11} = -h_{44} = h_{14} = h_{41} \\ &= \int_{u=0}^{u=l} \frac{4\rho du}{[(x-u)^2+y^2+z]^{21/2}} \\ &= 4\rho \log \frac{[(l-x)^2+y^2+z^2]^{1/2}+l-x}{[x^2+y^2+z^2]^{1/2}-x} \end{aligned} \tag{11}$$

which remains finite for finite values of the density ρ and length of pencil l.

It should be noted that Eq. (11) has been derived on the assumption of a *steady* pencil of radiation between the source and absorber, so that no explicit introduction of retarded potentials into the calculation was necessary. Hence of course the expression obtained would not be applicable in the neighborhood of times when the pencil is being started or stopped. It should also be noted that Eq. (11) gives only the contribution of the radiation in the pencil to the gravitational field and neglects the contribution of the bodies which act as source and absorber. This includes a neglect of any effects resulting from changes in the motion or internal condition of these bodies which might themselves be thought of as connected with the flow of radiation.

With these restrictions, however, the values of the surviving components of $h_{\mu\nu}$ given by Eq. (11) may be substituted into Eq. (1) to give the form of the line element in the neighborhood of the pencil of radiation.

§6. *Velocity of a test ray of light in the neighborhood of the pencil.* Having obtained Eq. (11) which gives the effect of the radiation on the form of the line element, we may now investigate the motion of test rays of light and test particles as affected by the presence of the pencil. In accordance with the theory of general relativity, the velocity of light will be given by setting the expression for the line element ds equal to zero. Substituting the values for the components of $h_{\mu\nu}$ given by (11) into the general expression for the line element (1) setting the result equal to zero, and writing

$$h = 4\rho \log \frac{[(l-x)^2 + y^2 + z^2]^{1/2} + l - x}{[x^2 + y^2 + z^2]^{1/2} - x} \tag{12}$$

as an abbreviation, (not the h of §2) we then easily obtain for the velocity of a test ray in the X-direction parallel to the pencil, the two cases

$$\frac{dx}{dt} = +1 \quad \text{and} \quad -\frac{1-h}{1+h} \tag{13}$$

and for the velocity say in the Y-direction in a plane perpendicular to the pencil, the two cases

$$\frac{dy}{dt} = \pm (1-h)^{1/2}. \tag{14}$$

In accordance with these expressions, we note that a test ray of light moving parallel to the pencil and in the same direction would have unit velocity the same as that in the pencil itself, but that rays moving in other directions would have a variable velocity depending as might be expected on their position in the gravitational field of the pencil. Furthermore, it can easily be shown for the case of a test ray moving parallel to the pencil and in the same direction that we should have, not only $dx/dt = 1$, but also $d^2x/dt^2 = d^2y/dt^2 = d^2z/dt^2 = 0$, which is a satisfactory result from the point of view of the stability of the light pencil itself.

§7. *Acceleration of a test particle in the neighborhood of the pencil.* We may also use our knowledge of the line element to investigate the gravitational acceleration which would be experienced by a test particle placed in the neighborhood of the pencil.

In accordance with the theory of general relativity, the acceleration of a particle is determined by the equation for a geodesic

$$\frac{d^2x_\alpha}{ds^2} + \{\mu\nu, \alpha\}\frac{dx_\mu}{ds}\frac{dx_\nu}{ds} = 0 \tag{15}$$

and if we apply this equation to a particle which is at rest in our system of coordinates, we can substitute

$$\frac{dx_\mu}{ds} = 0 \text{ for the cases } \mu = 1, 2, 3 \tag{16a}$$

and to our order of approximation

$$\frac{dx_\mu}{ds} = \frac{dt}{ds} = 1 \text{ for the case } \mu = 4 \tag{16b}$$

so that equation (15) will then assume the simple form

$$\frac{d^2x}{dt^2} = -\{44, 1\}, \quad \frac{d^2y}{dt^2} = -\{44, 2\}, \quad \frac{d^2z}{dt^2} = -\{44, 3\} \tag{17}$$

for the cases $\alpha = 1, 2, 3$.

To calculate the values of the Christoffel symbols occurring in equations (17), we have the general equation of definition

$$\{\mu\nu, \sigma\} = \frac{1}{2} g^{\sigma\lambda}\left(\frac{\partial g_{\mu\lambda}}{\partial x_\nu} + \frac{\partial g_{\nu\lambda}}{\partial x_\mu} - \frac{\partial g_{\mu\nu}}{\partial x_\lambda}\right) \tag{18}$$

and noting the values of the $g_{\mu\nu}$ which correspond to Eqs. (11), we shall evidently obtain to our order of approximation the simple expressions

$$\frac{d^2x}{dt^2} = -\frac{1}{2}\frac{\partial h_{44}}{\partial x}, \quad \frac{d^2y}{dt^2} = -\frac{1}{2}\frac{\partial h_{44}}{\partial y}, \quad \frac{d^2z}{dt^2} = -\frac{1}{2}\frac{\partial h_{44}}{\partial z}. \tag{19}$$

Substituting then for h_{44} the value given by (11), and performing the indicated differentiations, we can finally obtain, after some simplifications, for the acceleration of a stationary test particle parallel to the line of the pencil the expression

$$\frac{d^2x}{dt^2} = 2\rho\left\{\frac{1}{[x^2 + y^2 + z^2]^{1/2}} - \frac{1}{[(l-x)^2 + y^2 + z^2]^{1/2}}\right\} \tag{20}$$

and for the acceleration in a plane perpendicular to the pencil expressions of the form

$$\frac{d^2y}{dt^2} = -\frac{2\rho y}{y^2 + z^2}\left\{\frac{x}{[x^2 + y^2 + z^2]^{1/2}} + \frac{l-x}{[(l-x)^2 + y^2 + z^2]^{1/2}}\right\}. \tag{21}$$

The first thing of importance to be noted from these rather complicated expressions for the acceleration is the fact, in accordance with Eq. (20), that the acceleration parallel to the pencil becomes zero for a particle placed at a point $x = l/2$ midway between the two ends of the pencil. Furthermore for a particle midway between the two ends of the pencil, with $x = l/2$ and $z = 0$, Eq. (21) gives for the acceleration towards the pencil the simple result

$$-\frac{d^2y}{dt^2} = \frac{2\rho l}{y[(l/2)^2 + y^2]^{1/2}}. \tag{22}$$

The most important characteristic of these expressions for the acceleration, however, is the fact that they can easily be shown to be exactly *twice* as great as would be calculated from the simple Newtonian theory by taking

the gravitational mass of the radiation equal to its inertial mass. This is due to the fact that the quantity $h_{44}/2$ occurring in Eqs. (19) is twice the simple Newtonian expression for the gravitational potential of the pencil. As noted in the introduction this is a very satisfactory result, since in the case of weak fields we now see that the factor 2 occurs not only as is known in the expression for the action of a particle on light, but also in the expression for the action of light on a particle, and we are hence able to retain in first approximation our familiar ideas as to the conservation of momentum.

PART III. THE GRAVITATIONAL ACTION OF A PULSE OF LIGHT

§8. *The line element in the neighborhood of a pulse of radiation.* As already noted, the considerations of Part II were only applicable to the gravitational field surrounding a steady pencil of light and we shall now turn to a consideration of the gravitational field of a passing pulse of radiation. This will be more complicated to treat since the field will obviously be non-static and we shall have to make specific use of the method of retarded potentials to determine the way in which the gravitational effect spreads out from the moving pulse.

Let us consider a pulse of radiation, of length λ, linear density ρ, and small cross-section, travelling along the X-axis from $x=0$ to $x=l$, which may be taken as the points at which the radiation emerges from the source and enters the absorber, or as giving an arbitrary portion of the track selected for investigation. Furthermore, let us for convenience choose our time scale to make $t=0$ when the front end of the pulse crosses the point $x=0$, so that at any later time t the front end of the pulse will be located at $x=t$ and the rear end at $x=t-\lambda$.

Let us now take some point of interest x, y, z in the neighborhood of the track, and calculate with the help of Eq. (10) the gravitational field produced by the pulse at this point at the time t. Since Eq. (10) has to be applied in accordance with the method of retarded potentials, let us denote by $x=a$ the position of the front end of the pulse and by $x=b$ the position of the rear end of the pulse when they "emit" the gravitational influence which is received at the point x, y, z at the time t. Then we may evidently write in accordance with Eq. (10) for the gravitational potentials at x, y, z and t

$$\begin{aligned} 4\int\frac{[\rho]dV}{r} &= -h_{11} = -h_{44} = h_{14} = h_{41} \\ &= \int_{u=b}^{u=a}\frac{4\rho du}{[(x-u)^2+y^2+z]^{21/2}} \\ &= 4\rho\log\frac{[(x-a)^2+y^2+z^2]^{1/2}-x+a}{[(x-b)^2+y^2+z^2]^{1/2}-x+b} \end{aligned} \tag{23}$$

provided we take the YZ-dimensions of the pulse as small compared with $(y^2+z^2)^{1/2}$.

To evaluate this result, however, we must determine a and b as functions of the time. To do this we note that $t-a$ is the distance through which the

gravitational influence "travels" in going from the front end of the pulse to reach the point x, y, z at the time t, and hence we can evidently write

$$(t-a)^2 = (x-a)^2 + y^2 + z^2 \tag{24}$$

and solving obtain for a the expression

$$a = \frac{t^2 - x^2 - y^2 - z^2}{2(t-x)}. \tag{25}$$

Similarly we obtain for b the expression

$$b = \frac{(t-\lambda)^2 - x^2 - y^2 - z^2}{2(t-\lambda-x)}. \tag{26}$$

In using these expressions in connection with Eq. (23), however, we shall take the position of the rear end of the pulse to be $b=0$ until the pulse has completely emerged from the source at $x=0$, and take the position of the front end as $a=l$ after the pulse has started to enter the absorber at $x=l$. We do this since our interest lies in the gravitational influences correlated with the track of the pulse between $x=0$ and $x=l$.

Substituting the above values of a and b into Eq. (23), we then easily obtain the three following cases for the time intervals indicated

$$\begin{aligned} 4\int \frac{[\rho]dV}{r} &= -h_{11} = -h_{44} = h_{14} = h_{41} \\ &= 4\rho \log \frac{t-x}{[x^2+y^2+z^2]^{1/2}-x} && \begin{cases}\text{from } t = [x^2+y^2+z^2]^{1/2} \\ \text{to} \quad t = [x^2+y^2+z^2]^{1/2}+\lambda\end{cases} \\ &= 4\rho \log \frac{t-x}{t-\lambda-x} && \begin{cases}\text{from } t = [x^2+y^2+z^2]^{1/2}+\lambda \\ \text{to} \quad t = l+[(l-x)^2+y^2+z^2]^{1/2}\end{cases} \\ &= 4\rho \log \frac{[(l-x)^2+y^2+z^2]^{1/2}-x+l}{t-\lambda-x} && \begin{cases}\text{from } t = l+[(l-x)^2+y^2+z^2]^{1/2} \\ \text{to} \quad t = l+[(l-x)^2+y^2+z^2]^{1/2}+\lambda\end{cases} \end{aligned} \tag{27}$$

and the form of the line element in the different time intervals indicated will be given by substituting these values for the surviving components of $h_{\mu\nu}$ in the general expression for the line element (1). The results show that here also as in the case of the pencil it is necessary to take a limited track for the light pulse, since if the pulse were regarded as coming from an infinitely remote position on the X-axis the field would become infinite at the time $t=x$ when the pulse comes abreast of the point of interest. With our treatment, however, there is no effect from the track of the pulse before the time $t=[x^2+y^2+z^2]^{1/2}$, nor after the time $t=l+[(l-x)^2+y^2+z^2]^{1/2}+\lambda$.

§9. *Velocity of a test ray of light in the neighborhood of the pulse.* Substituting these values for the components of $h_{\mu\nu}$ into the expression for the line element (1) and setting the result equal to zero, we can now obtain information as to the velocity of test rays as affected by the pulse. Writing for simplicity

$$h = 4\int \frac{[\rho]dV}{r} \tag{28}$$

as a general abbreviation for the different expressions given by Eqs. (27), we then easily obtain for the velocity of a test ray in the X-direction parallel to the track, the two cases

$$\frac{dx}{dt} = +1 \text{ and } -\frac{1-h}{1+h} \tag{29}$$

and for the velocity in a plane perpendicular to the track, say in the Y-direction, the two cases

$$\frac{dy}{dt} = \pm (1-h)^{1/2}. \tag{30}$$

As in the case of the pencil, we note that a test ray of light moving parallel to the motion of the pulse and in the same direction would have unit velocity the same as that for the pulse itself, but that rays moving in other directions would have a variable velocity depending on time and position. Here too, it can easily be shown for the case of a test ray moving parallel to the motion of the pulse and in the same direction that we should have, not only $dx/dt=1$, but also $d^2x/dt^2=d^2y/dt^2=d^2z/dt^2=0$, which is a satisfactory result from the point of view of the stability of the pulse itself.

§10. *Acceleration of a test particle due to the pulse.* We must now investigate the gravitational acceleration which would be experienced by a test particle as a result of the passage of the pulse of light. If we take the particle as stationary the accelerations will evidently be determined by the same Eqs. (17)

$$\frac{d^2x}{dt^2} = -\{44, 1\}, \quad \frac{d^2y}{dt^2} = -\{44, 2\}, \quad \frac{d^2z}{dt^2} = -\{44, 3\} \tag{31}$$

as were applicable in the case of the pencil, but the values of the Christoffel symbols will of course be different. To calculate these we may again start with the general equation of definition

$$\{\mu\nu, \sigma\} = \frac{1}{2} g^{\sigma\lambda}\left(\frac{\partial g_{\mu\lambda}}{\partial x_\nu} + \frac{\partial g_{\nu\lambda}}{\partial x_\mu} - \frac{\partial g_{\mu\nu}}{\partial x_\lambda}\right) \tag{32}$$

and noting the values of the $g_{\mu\nu}$ which correspond to Eqs. (27), we can evidently write to our order of approximation

$$\begin{aligned} \{44, 1\} &= -\frac{1}{2}\left(\frac{\partial h_{41}}{\partial t} + \frac{\partial h_{41}}{\partial t} - \frac{\partial h_{44}}{\partial x}\right) \\ \{44, 2\} &= \frac{1}{2}\frac{\partial h_{44}}{\partial y} \\ \{44, 3\} &= \frac{1}{2}\frac{\partial h_{44}}{\partial z}. \end{aligned} \tag{33}$$

Substituting the values of h_{44} and h_{41} given by Eqs. (27), and for simplicity considering the particle to be placed at point for which $z=0$, we can obtain for the acceleration parallel to the track of the pulse during the time intervals indicated

$$\begin{aligned}
\frac{d^2x}{dt^2} &= 2\rho\left(\frac{1}{t-x}+\frac{1}{(x^2+y^2)^{1/2}}\right) && \begin{cases}\text{from } t=(x^2+y^2)^{1/2}\\ \text{to}\quad t=(x^2+y^2)^{1/2}+\lambda\end{cases}\\
&= 2\rho\left(\frac{1}{t-x}-\frac{1}{t-\lambda-x}\right) && \begin{cases}\text{from } t=(x^2+y^2)^{1/2}+\lambda\\ \text{to}\quad t=l+[(l-x)^2+y^2]^{1/2}\end{cases} \qquad (34)\\
&= -2\rho\left(\frac{1}{t-\lambda-x}+\frac{1}{[(l-x)^2+y^2]^{1/2}}\right) && \begin{cases}\text{from } t=l+[(l-x)^2+y^2]^{1/2}\\ \text{to}\quad t=l+[(l-x)^2+y^2]^{1/2}+\lambda\end{cases}
\end{aligned}$$

And for the acceleration perpendicular to the track we obtain for the same time intervals

$$\begin{aligned}
\frac{d^2y}{dt^2} &= \frac{-2\rho y}{(x^2+y^2)^{1/2}[(x^2+y^2)^{1/2}-x]} && \begin{cases}\text{from } t=(x^2+y^2)^{1/2}\\ \text{to}\quad t=(x^2+y^2)^{1/2}+\lambda\end{cases}\\
&= 0 && \begin{cases}\text{from } t=(x^2+y^2)^{1/2}+\lambda\\ \text{to}\quad t=l+[(l-x)^2+y^2]^{1/2}\end{cases} \qquad (35)\\
&= \frac{2\rho y}{[(l-x)^2+y^2]^{1/2}}\,\frac{1}{[(l-x)^2+y^2]^{1/2}+l-x} && \begin{cases}\text{from } t=l+[(l-x)^2+y^2]^{1/2}\\ \text{to}\quad t=l+[(l-x)^2+y^2]^{1/2}+\lambda.\end{cases}
\end{aligned}$$

In accordance with these expressions, we see that parallel to the track the particle would first be accelerated in the same direction as the motion of the pulse, and then in the opposite direction. On the other hand perpendicular to the motion of the pulse, the particle would first be accelerated towards the track and later away from it. And we must now investigate the total integrated acceleration corresponding to the whole track of the pulse, and compare the results with those which might be expected in first approximation from our older ideas as to the conservation of momentum.

§11. *Time integral of acceleration of test particle due to the pulse.* Making use of the expressions for the acceleration of the test particle parallel to the track of the pulse given by Eqs. (34), we may now obtain the time integral of the acceleration over the three intervals given, and adding together obtain an expression for the total time integral corresponding to the track of the pulse. Doing so and cancelling out a considerable number of balancing terms, it can easily be shown that we finally obtain for the total integral

$$\int \frac{d^2x}{dt^2}dt = 2\rho\lambda\left\{\frac{1}{(x^2+y^2)^{1/2}}-\frac{1}{[(l-x)^2+y^2]^{1/2}}\right\}. \qquad (36)$$

As might be expected the net acceleration of the test particle parallel to the track depends on the relative magnitudes of the total length of the track l and

the distance along the track x at which the particle is placed. When the test particle is midway between the two ends of the track at $x=l/2$, there is no net acceleration parallel to the track. Otherwise the net parallel acceleration is in the direction towards which the longer segment of the track lies.

Turning now to the acceleration perpendicular to the track it can easily be shown from Eqs. (35) that we obtain for the net integrated acceleration

$$\int \frac{d^2y}{dt^2}dt = -\frac{2\rho\lambda}{y}\left\{\frac{x}{(x^2+y^2)^{1/2}} + \frac{l-x}{[(l-x)^2+y^2]^{1/2}}\right\}. \tag{37}$$

And considering the particle to be located midway between the two ends of the track at $x=l/2$ this reduces to

$$\int \frac{d^2y}{dt^2}dt = -\frac{2\rho\lambda l}{y[(l/2)^2+y^2]^{1/2}}. \tag{38}$$

This result may now be compared with what would be expected from a simple application of ideas as to the conservation of momentum for the combined interaction of particle and light pulse. If we write

$$m = \rho\lambda \tag{39}$$

as an abbreviation for the mass of the light pulse, i.e., its energy divided by the square of the velocity of light, and write M for the mass of the particle, Eq. (38) will then give us for the total momentum acquired by the (stationary) test particle towards the track

$$\int M\frac{d^2y}{dt^2}dt = -\frac{2mMl}{y[(l/2)^2+y^2]^{1/2}}. \tag{40}$$

On the other hand it is well known that the deflection of light in passing through the gravitational field of a particle can be taken in first approximation as twice that which would be calculated from a simple application of the Newtonian theory of gravitation, so that we can evidently write for the momentum acquired by the light pulse in passing over the track

$$\int_0^l \frac{2mMy}{[(l/2-t)^2+y^2]^{3/2}}dt = +\frac{2mMl}{y[(l/2)^2+y^2]^{1/2}} \tag{41}$$

which is equal and opposite to the expression for the momentum acquired by the particle. And since a similar correspondence can be shown for the more general case when the particle is not located midway between the ends of the track, it is evident that we can retain in considerable measure our simple ideas as to the conservation of momentum as a first approximation even in so complicated a process as that of the interaction between a particle and a pulse of light.

PART IV. CONCLUSION

§12. *Some remarks on the problem.* This completes the material which we desired to present in this article. It is particularly hoped that the treatment

has clarified the problem of the mutual gravitational interaction of radiation and a particle, since we have given special attention to the behavior of a particle in the gravitational field of light, while the treatment of the converse problem of the behavior of light in the gravitational field of a particle is well known.

This converse problem is of course the one of usual importance in connection with astronomical observations when we are interested in the effect of the gravitational fields of stars or other particles on the behavior of a ray of light coming from a distant object. Its treatment can usually be carried through with less difficulty and higher approximation than was feasible for the problems which we have considered in the present paper. This arises partly from the fact that we have the exact Schwarzschild solution for the gravitational field surrounding a stationary point particle, and partly from the fact that disturbances in the motions of neighboring particles which are produced by the passage of a pulse of light cannot in general communicate their effects back in time to affect the gravitational field through which the pulse itself has to pass.

One of the main results of the present article has been to show that in the case of weak fields the gravitational action of light on a particle can in considerable measure be correctly calculated from the Newtonian theory of gravitation provided we take the gravitational mass of the radiation as twice its inertial mass. And since it was already known in the case of weak fields that the gravitational action of a particle on light could in considerable measure also be correctly calculated from the Newtonian theory by taking the gravitational mass of the radiation as twice its inertial mass, we have thus shown the possibility of extending the domain in which we can use our simple ideas as to the conservation of momentum. Of course in general we should expect to be able to use the more complicated ideas as to the conservation of momentum which can be obtained by the device of introducing the *pseudo* energy-momentum tensor t_μ^ν, but the extent to which the simple ideas would be applicable does not appear to have been certain prior to this investigation.

§13. Other examples of the gravitational field due to radiation. The effects of radiation on the gravitational field, studied in this article, may also be compared with two other cases in which radiation has been found to produce a different (greater) effect than ordinary matter on the gravitational field.

The first example is furnished by the case of the static Einstein universe where it has been found[4] that the radius R of a universe *filled with stationary incoherent matter* would be connected with the proper density of matter ρ by the expression

$$\frac{1}{R^2} = 4\pi\rho \tag{42}$$

while for a universe *filled solely with radiation* of density ρ the relation would be given by the expression

[4] See for example, Tolman, Proc. Nat. Acad. **15**, 297 (1929), Eqs. (35) and (37).

$$\frac{1}{R^2} = \frac{16}{3}\pi\rho. \tag{43}$$

The second example is furnished by the case of the gravitational field of a sphere of perfect fluid of proper macroscopic density ρ_{00} and pressure p_0. Writing the line element for such a sphere in the form

$$ds^2 = -e^{\mu}(dx^2 + dy^2 + dz^2) + e^{\nu}dt^2 \tag{44}$$

where μ and ν are functions of $r=(x^2+y^2+z^2)^{1/2}$, it is found[5] that the line element degenerates at great distances from the sphere into the approximate Schwarzschild form

$$ds^2 = -\left(1+\frac{2m}{r}\right)(dx^2 + dy^2 + dz^2) + \left(1-\frac{2m}{r}\right)dt^2 \tag{45}$$

where the constant m has the value, obtained by integration over the material in the sphere,

$$m = \int (\rho_{00} + 3p_0)e^{\nu/2}dV_0 \tag{46}$$

dV_0 being the element of proper volume. Since for radiation we have $3p_0 = \rho_{00}$ and for incoherent matter at ordinary temperatures have $p_0 \ll \rho_{00}$, it is evident here too that the radiation in the sphere can be regarded as having a greater effect on the gravitational field than matter of the same density.

[5] Tolman, Phys. Rev. 35, 875 (1930).

RAMAN LINES OF CYCLOPROPANE AND VALENCE PROPERTIES OF SOME ORGANIC COMPOUNDS

By Robert C. Yates
Mathematics Department, Johns Hopkins University

(Received January 19, 1931)

Abstract

Three fundamental wave-numbers for C_3H_6 are calculated from the equations of motion of a system of three particles vibrating in a plane. The character of a single bond acting adjacent to a double bond in CH_3CHO and again to a triple bond in CH_3CN is studied.

Introduction

In several recent papers appearing in the Physical Review[1,2,3,4] the dynamic properties of molecules were studied with the purpose of correlating the lines of the Raman spectra with different motions of the system. It was assumed that the restoring force arises from a change in the bond length and from a change in the angle between adjacent bonds. It was further assumed that the non-polar chemical bond exhibits the same characteristics throughout the range of organic compounds. For the single bond structure the force constants, k_1 for linear displacement and k_2 for angular displacement, were found to be 5×10^5 and 0.6×10^5 dynes per cm, respectively. These assumptions are adhered to in the present paper but many of the mathematical steps in the calculations are omitted because of the similarity to previous work.[3]

Cyclopropane

We consider here the small vibrations in a plane of three particles of the same mass m, lying at the vertices of an equilateral triangle. The unstrained bond is of length $2a$, each bond forming a side of the triangle. Let $(x_i y_i)$, θ_i be the components of displacement of the particles and the angular changes, respectively. (Note: This problem is particularly interesting from the chemical standpoint because it offers a means of testing the validity of the Bayer strain theory.)

In an inertial system the center of gravity remains at rest and if this point be taken as the origin of coordinates

$$\sum x_i = 0, \quad \sum y_i = 0. \tag{1}$$

[1] C. F. Kettering, L. W. Shutts, and D. H. Andrews, Phys. Rev. **36**, 531 (1930).
[2] D. H. Andrews, Phys. Rev. **36**, 544 (1930).
[3] R. C. Yates, Phys. Rev. **36**, 555 (1930).
[4] A. B. Lewis, Phys. Rev. **36**, 568 (1930).

Since the sum of the forces is zero angular momentum about the origin is constant. This we assume to be zero, giving

$$y_2 = y_1 + 3^{1/2}(x_1 + x_2). \tag{2}$$

The changes in the bond lengths after displacement are found to be [by Eqs. (1) and (2)]

$$\left.\begin{aligned} \Delta_1 &= x_1 - x_2 \\ \Delta_2 &= -\tfrac{1}{2}[7x_1 + 8x_2 + 3(3)^{1/2}y_1] \\ \Delta_3 &= -\tfrac{1}{2}[x_1 + 2x_2 + 3(3)^{1/2}y_1] \end{aligned}\right\}. \tag{3}$$

If θ_i be small, we find by taking only two terms in a Taylor expansion

$$\left.\begin{aligned} 4a\theta_1 &= -3y_1 - 3^{1/2}(5x_1 + 4x_2) \\ 4a\theta_2 &= -3y_1 + 3^{1/2}(x_1 + 2x_2) \\ 4a\theta_3 &= 6y_1 + 2(3)^{1/2}(2x_1 + x_2) \end{aligned}\right\}. \tag{4}$$

The energy functions are set up in the usual manner[3]

$$\left.\begin{aligned} T &= (m/2)\sum_1^3(\dot{x}_i^2 + \dot{y}_i^2) \\ &= m[4\dot{x}_1^2 + 4\dot{x}_2^2 + 3\dot{y}_1^2 + 7\dot{x}_1\dot{x}_2 + 3(3)^{1/2}(\dot{x}_1 + \dot{x}_2)\dot{y}_1] \\ V &= -(k_1/2)\sum_1^3\Delta_i^2 - 2a^2k_2\sum_1^3\theta_i^2 \\ &= -(3k_1/4)[9x_1^2 + 12x_2^2 + 9y_1^2 + 18x_1x_2 + 8(3)^{1/2}x_1y_1 + 10(3)^{1/2}x_2y_1] \\ &\quad -(9k_2/8)[14x_1^2 + 8x_2^2 + 6y_1^2 + 20x_1x_2 + 8(3)^{1/2}x_1y_1 + 4(3)^{1/2}x_2y_1] \end{aligned}\right\} \tag{5}$$

giving the equations of motion

$$\left.\begin{aligned} 2m\ddot{x}_1 &= -(3k_1/2)[x_1 - 2x_2 - (3)^{1/2}y_1] - (9k_2/2)[3x_1 + 2x_2 + (3)^{1/2}y_1] \\ 2m\ddot{x}_2 &= -(3k_1/2)[x_1 + 4x_2 + (3)^{1/2}y_1] + (9k_2/2)[x_1 + (3)^{1/2}y_1] \\ 2m\ddot{y}_1 &= -[(3)^{1/2}k_1/2][x_1 + 2x_2 + 3(3)^{1/2}y_1] + [3(3)^{1/2}k_2/2][x_1 + 2x_2 - (3)^{1/2}y_1] \end{aligned}\right\} \tag{6}$$

These yield frequencies:

$$\nu_1 = (1/2\pi)[3(k_1 + 3k_2)/2m]^{1/2}; \quad \nu_2 = (1/2\pi)[3(k_1 + 3k_2)/2m]^{1/2};$$
$$\nu_3 = (1/2\pi)(3k_1/m)^{1/2}.$$

The molecule C_3H_6 is analogous to the system studied if we assume the mass of the hydrogens concentrated at the nuclei of the carbon atoms. Using $k_1 = 5\times10^5$, $k_2 = 0.6\times10^5$, $m = 13/6.06\times10^{23}$ we find the wave-numbers

$$\tilde{\nu}_1 = \tilde{\nu}_2 = 400\ \text{cm}^{-1}; \quad \tilde{\nu}_3 = 1350\ \text{cm}^{-1}$$

where $\tilde{\nu} = \nu/3\times10^{10}$.

Character of Multiple Bonds

Two particles of the same mass m are joined to a central particle M by bonds with force constants k_1 and k_2. Let k_3 be the proportionality constant dependent on the change in the angle between the bonds. The particles lie along a straight line in the position of equilibrium and motion is assumed to be in a given plane. The equations of motion are

$$\left.\begin{aligned} mM\ddot{x}_1 &= -k_2[(m+M)x_1 + mx_2] \\ mM\ddot{x}_2 &= -k_1[mx_1 + (m+M)x_2] \\ mM\ddot{y}_1 &= -2k_3[2m+M]y_1 \end{aligned}\right\} \tag{7}$$

with frequencies given by the characteristic:

$$\begin{vmatrix} mM\mu^2 + k_2(m+M) & k_2 m & 0 \\ k_1 m & mM\mu^2 + k_1(m+M) & 0 \\ 0 & 0 & mM\mu^2 + 2k_3(2m+M) \end{vmatrix} = 0. \tag{8}$$

We assume that the groups of atoms in acetaldehyde and methylcyanide lie along a line in the state of rest and take the masses of the end groups as 15.5 and 14.5, respectively. In the former molecule k_1 and k_2 are assigned the values 5×10^5 and 10×10^5 (for single and double bond); in the latter 5×10^5 and 15×10^5 (single and triple bond).

We find for CH_3CHO $\tilde{\nu}_1=1695$, $\tilde{\nu}_2=844$ as compared with observed Raman data 1716 and 932 which is in good agreement.

The motion of the system that alters the angle between the bonds gives rise to a wave-number in the neighborhood of 440 cm^{-1}. Using this in $mM\mu_2 + 2k_3(2m+M)=0$ [see Eq. (8)] we evaluate k_3 as 0.26×10^5 dynes per cm.

For CH_3CN we find $\tilde{\nu}_1=2095$, $\tilde{\nu}_2=905$ compared with the observed values 2240 and 860. The third Raman line occurs at 350 cm^{-1}. This gives $k_3=0.15\times10^5$ for the bending constant between the single and triple bond.

In these two molecules the assumption on the position of the groups in equilibrium is somewhat dubious. However, the evidence points strongly to a decided weakening of the bending force when multiple bonds lie adjacent to single bonds.

DUST FIGURE IN LIQUID INSULATOR

By Y. Toriyama
Hokkaido Imperial University, Japan

(Received October 9,1930)

Abstract

A dust figure is obtained on the surface of an ebonite plate immersed in a liquid insulator, by dusting it after the application of voltage with a fine powder containing mixture of red lead and resin.

There is a relation between the size of the dust figure and the break down voltage of the liquid insulator.

I. Introduction

As there is a certain relation between a sparkover in gases and Lichtenberg's figure or the dust figure in the gases, some connection may exist between the break down phenomena of the liquid insulator and Lichtenberg's figure or the dust figure in the liquid insulator. The dust figure in the liquid insulator, mainly ordinary transformer oil, is here studied to throw light on the break down phenomena of the transformer oil.

II. Dust Figure in Transformer Oil by Impulse Voltage

In order to dry the transformer oil, it is heated to 105°C−110°C for two or three hours, and then filtrated with a paper filter.

Electrodes and an ebonite plate are then immersed in the oil as shown in Fig. 1. (In Fig. 1, N is a needle electrode, P is a plate electrode, E is the ebonite plate, and M_1 C C W denotes the impulse generator). When an impulse

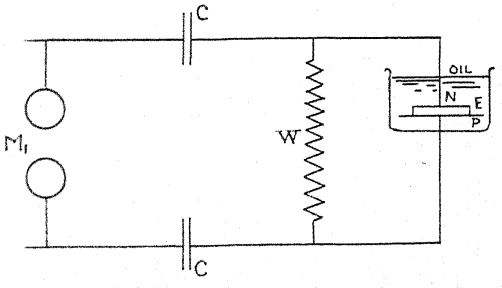

Fig. 1. Diagram of apparatus.

voltage is applied between N and P, and the ebonite plate is then pulled out of the oil, an electric charge will remain on its surface. By sprinkling a fine powder containing a mixture of red lead and resin on the plate, and then washing it gently in gasoline a clear dust figure is produced.

Since the particles of the powder will become electrified by mixing, the positively electrified red lead will stick to the negatively electrified surface,

and the negatively electrified resin will stick to the positively electrified parts. If the dusted surface is then washed in gasoline, the negatively charged part will look reddish because of red lead, and the positively charged part will look yellowish white because of the resin.

An example of a positive dust figure in the oil is shown in Fig. 2, and that of a negative figure in Fig. 3. The crest value of the applied impulse voltage in both cases is 35 k.v. By applying an impulse voltage of 35 k.v., the mean value of the radii of 15 positive figures was 7.13 mm, and that of the negative figures was 4.62 mm. The ratio $R+/R-$ ($R+$ and $R-$ denoting the radius of positive and negative figure respectively) was 1.54.

As mentioned above, the diameter of the positive figure is larger than that of the negative figure. The reason for this fact may be explained somewhat in the following manner. When the impulse voltage is applied between N and P, the needle being the positive pole, the negative ions (including electrons) produced in the ionization by collision will move towards the needle, while the positive ions move radially outwards. Owing to the fact that the velocity

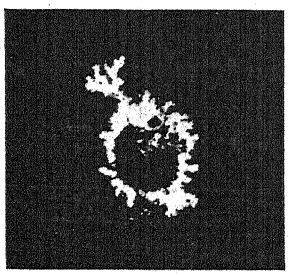

Fig. 2. Positive dust figure in oil. $M_1=8$ mm. Impulse voltage, maximum value, 35.0 k.v. Magnification 1.5.

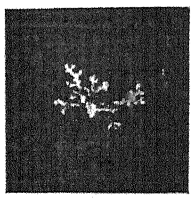

Fig. 3. Negative dust figure in oil. $M_1=8$ mm. Impulse voltage, maximum value, 35.0 k.v. Magnification 1.5.

of negative ions is greater than that of positive ions, the positive ions will remain near the needle N, so that the high potential gradient at the end of the needle will be weakened by the positive space charge. And the region of high potential gradient will move in time from the needle outwards, and the front of ionization by collision will proceed radially outwards along the ebonite surface. In other words, the potential gradient at the front of the ionization wave, spreading along the surface, will be much larger at a certain moment than the gradient electrostatically calculated.

In the case of a negative needle, the positive ions will remain at the end of the needle, so the ionization by collision may not proceed as in the former case. Accordingly, the radius of the positive figure is greater than that of the negative figure for the impulse voltage of the same intensity.

The radii of the positive and negative dust figures decrease with increasing temperature of the transformer oil, and the ratio $R+/R-$ also decreases with increasing temperature. But the form of the figure does not change. The experimental result is shown in Fig. 4.

The size of the positive and negative figures increases with decreasing atmospheric pressure. The case of a positive figure is shown in Fig. 5.

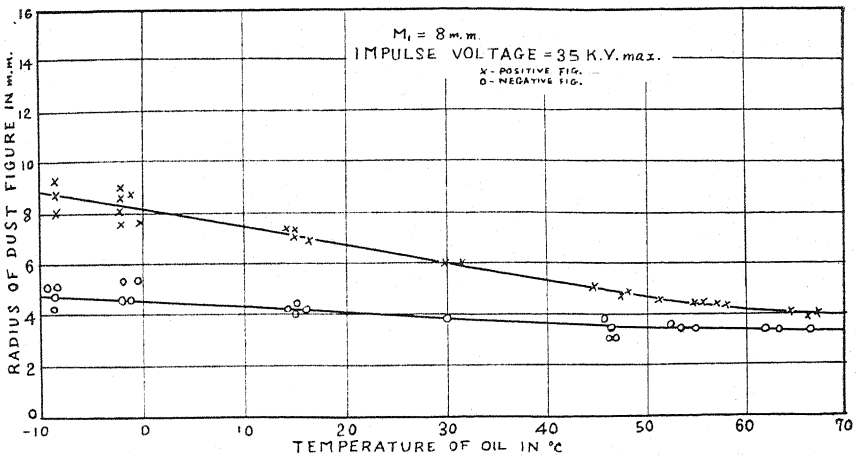

Fig. 4.

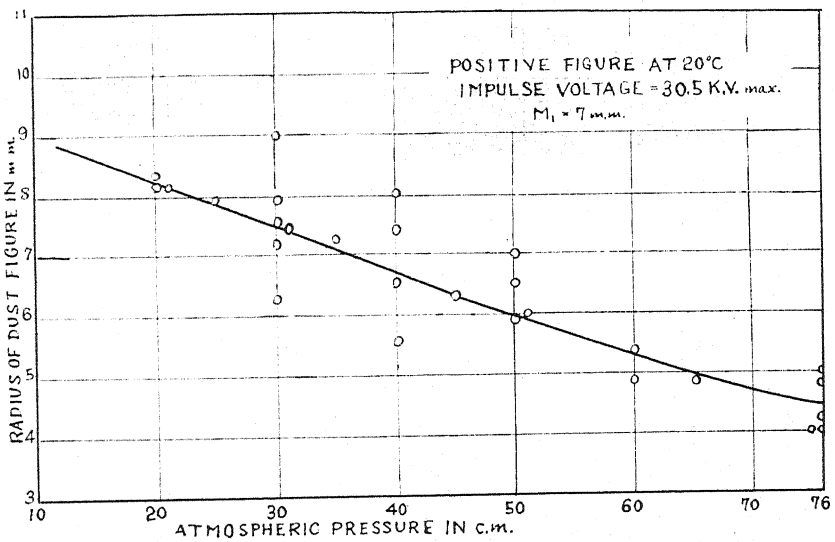

Fig. 5.

A comparison, between the size of the dust figure in the oil and the break down voltage of the oil is as follows:—

(1). In the range of the temperature from −10°C to 70°C, the break down voltage of the oil increases with increasing temperature.

The size of the dust figure decreases with increasing temperature in the same range of temperature.

(2). The break down voltage of oil decreases with decreasing atmospheric pressure,[1] and the size of the dust figure increases with decreasing atmospheric

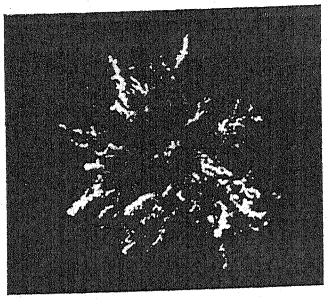

Fig. 6. Dust figure by A. C. voltage. Voltage, effective value 20.0 k.v.

pressure. Briefly, in the case of increasing break down voltage of the oil, the size of the dust figure in the oil decreases, and vice versa. Since the dust figure in the oil may be produced by the partial electric break down of the

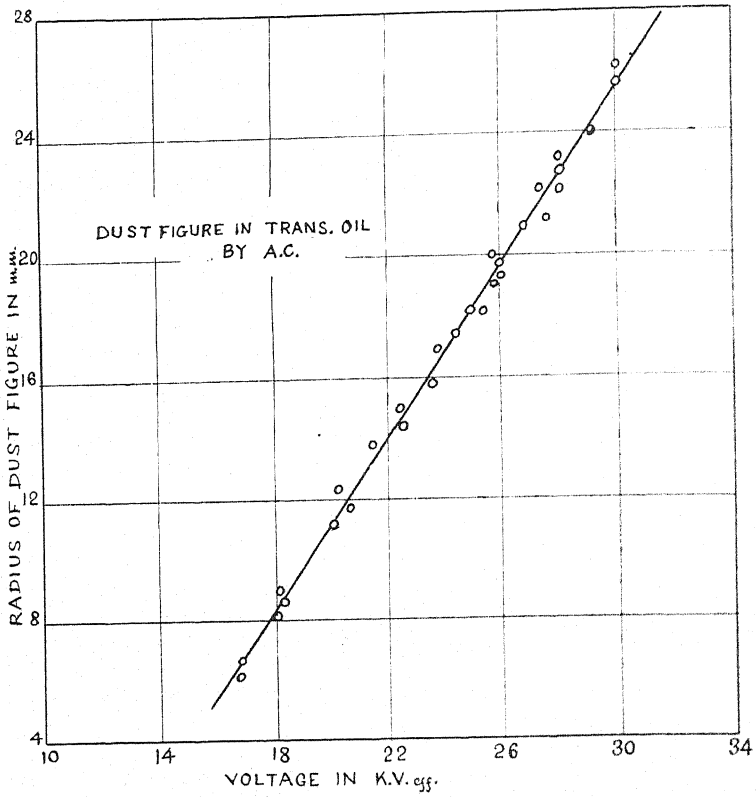

Fig. 7.

[1] J. Sorge, Archiv f. Elekt. **13**, (1924).

oil, the theory that there is a relation between the break down voltage and the dust figure is reasonable.

The conduction through the oil may be ionic or electrolytic. The break down voltage of the oil does not depend on the conductivity of the oil,[2] and neither does the size of the dust figure. The conductivity of the oil does not depend upon the atmospheric pressure.[3] However, the size of the dust figure changes with the atmospheric pressure. From the above two facts, it may be certain that the dust figure is not due to the ionic phenomena, but to the electronic phenomena. From the study of the dust figure it may be concluded that the break down of the transformer oil is a pure electric phenomena.

III. Dust Figure in Transformer Oil by A. C. Voltage

The dust figure in the oil, applying A. C. voltage, can be obtained in the same process as in the case of an impulse voltage. An example of the figure when applying 20 k. v. eff. is shown in Fig. 6.

The radius of the dust figure increases almost linearly with the applied A. C. voltage.

The relation between the radius of the figure and the applied voltage is shown in Fig. 7.

The size of the dust figure by A. C. voltage increases with decrease of the atmospheric pressure.

[2] Y. Toriyama, Archiv f. Elekt. **19**, (1927).
[3] Nikuradse, Zeits. f. techn. Physik. No. 12, (1929).

THE RESISTANCE OF BISMUTH IN ALTERNATING MAGNETIC FIELDS

By William W. Macalpine
The Marcellus Hartley Research Laboratory,
Columbia University, New York, New York

(Received January 22, 1931)

Abstract

Apparatus for producing a field of 100 gauss r.m.s. at 10^6 cycles with a 50 watt tube is described. Also a method of measuring the behavior of bismuth wire in such a field at liquid air temperature. For this purpose a potentiometer has been developed for the measurement of the amplitude and phase of voltages at frequencies up to at least 10^6 cycles per second. It was found that the resistance of the bismuth follows the instantaneous values of the field, having a magnitude at any instant equal to what it would have if the field at that instant were maintained constant. The precision of the magnitude calculated from the various factors involved is ± 3.5 percent and the experimental value is normal within this precision. At 55 kilocyles and room temperature the resistance of the bismuth was also found to be normal in magnitude and phase.

I. Introduction

A GREAT deal of work has been done on the various galvanomagnetic and thermomagnetic effects since the discovery of the Hall effect in 1879 by E. H. Hall. This work is abstracted in L. L. Campbell, "Galvanomagnetic and Thermomagnetic Effects.[1]" It is to be noted that these investigations were carried out without the aid of the three electrode tube and auxiliary apparatus and experimental technique developed in conjunction with the tube, the investigations having been made for the most part before the tube came into general use. The results of the experiments on the resistance of bismuth in alternating magnetic fields varied widely and it was that state of affairs which seemed to make it desirable to investigate its behavior with modern equipment.

Most of the earlier experiments were limited to low audio frequencies (25 to 100 cycles usually) or to magnetic fields which were made to change rapidly, as from zero field to some steady value. Results showed that the magnitude of the change in resistance often was not as great with a.c. as with d.c. fields and frequently a lag was found. However, it is evident that some of these results were erroneous because of the inadequacy of the apparatus available.

In the present experiments bismuth wire 0.06 mm diameter was mounted bifilarly and immersed in liquid air in a combined d.c. and a.c. field, the latter having a frequency of about 10^6 cycles per second. A direct current which was maintained constant by a r.f. choke was passed through the wire and so an a.c. voltage proportional to its resistance appeared across the wire. This

[1] Previous work done in connection with the subject of the present paper is summarized on pp. 166, 191–194.

voltage was measured in amplitude and phase by a potentiometer constructed for the purpose. Measurements had been made previously at 55 kilocycles and room temperature.

It has been shown by various investigators that the Ettingshausen and Nernst effects cause the appearance of a voltage opposing that due to the resistance drop in the bismuth. This effect is illustrated by Kapitza[2] in his work at high magnetic fields. However, with alternating fields this effect would diminish rapidly as the frequency is increased and its voltage would approach a 90° lead with respect to the field. The effect must be entirely negligible at the frequencies used in the present case due to the "thermal inertia" of the metal, which is caused by its heat capacity. Even with constant fields it would be almost zero with a round wire due to the thermal conductivity of the wire.

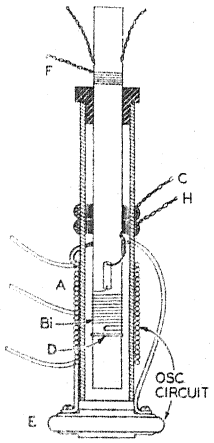

Fig. 1.

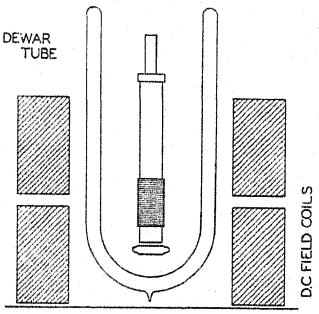

Fig. 2.

Fig. 1. (left) Oscillating circuit, mounting of bismuth wire, etc.
Fig. 2. (right) Location of oscillating circuit within Dewar tube and d.c. field coils.

II. Apparatus

The mounting of the bismuth wire, the coil for obtaining the a.c. field and various other necessary coils are shown in Fig. 1. Coil A and condenser E form an oscillating circuit which is driven by a power tube, the coil producing the required a.c. field. This coil is wound on a Pyrex tube 3/4 in. diameter and has 36 turns No. 17 wire, the length of the coil being about 2 in. The condenser is 0.003 mfd. Inside the Pyrex tube a 3/8 in. diameter bakelite tube is supported by a bakelite plug. The bismuth wire is wound bifilarly on the bakelite tube, being laid in threads cut in the tube, as it is found that if wound on the surface with even the lightest tension necessary to wind the wire properly, the cooling in liquid air causes it to break. When wound in the threads the tension can be made sufficiently light to prevent breaking, but it is not necessary to have it so light that the wire appears loose. In order to

[2] P. Kapitza, Roy. Soc., Proc. A119, 402, 430 ff. (1928).

make it a bifilar winding, two screws are cut, the threads of one screw lying midway between adjacent threads of the other. There are twelve double turns and the axial length of the winding on the tube is 1/2 in. Two thin phosphor bronze strips are used as terminals for the bismuth wire, which is fastened to them with Wood's metal. The strips are secured to the bakelite tube by wrappings of ordinary thread, and a pair of twisted leads of No. 28 wire is connected to their upper ends. Below the bismuth wire is a single turn *D* of No. 28 wire with twisted leads. This is used to measure the a.c. field and to give its vector as a reference for measurements of phase. Two other coils, *H* and *C*, are shown. The first has 5 turns and is used to supply the potentiometer. The other has 19 turns and is used to neutralize undesired voltages appearing in the bismuth wire in a way to be described below. The above apparatus is put in an unsilvered Dewar tube and the whole then placed inside a pair of large coils as shown in Fig. 2. These two coils have an inside diameter of 24 cm outside 38 cm and total height of 24 1/2 cm. Each coil has 375 turns of coarse litz. When the oscillating circuit is placed at the center of these coils they have no appreciable effect on the efficiency of the circuit. They are energized from the d.c. power supply and give ample field for the experiment without undue heating.

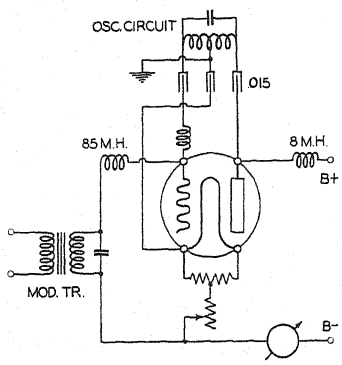

Fig. 3. The oscillator.

The oscillator is shown in Fig. 3, and is of the Hartley type. With the UV 211, a 50 watt tube, fields of 100 gauss r.m.s. could be obtained without overloading the tube. A small choke is inserted in the grid lead to the oscillating circuit to suppress parasitic oscillations. Grid modulation is used by means of the transformer shown. The particular connection of the modulator with r.f. choke is used to prevent audio frequency from getting into the oscillating coil and thence to the detector of the potentiometer. A slight amount of the modulating frequency getting directly to the detector causes either a poorly defined or a double minimum.

The connections to the bismuth wire are shown in Fig. 4. Direct current from a battery may be passed through the wire in either direction, being held constant by an 85 mh radio frequency choke. A 1/2 mfd mica condenser isolates the d.c. from the potentiometer. All condensers and batteries are at ground potential for the high frequency. Although the bismuth wire is bifilarly wound there is some net induced e.m.f., principally at the end connections. Also there is some capacity between the oscillating coil and the phosphor bronze strips used as terminals for the wire, and since the voltages obtained in the former may be several hundred volts, the resulting voltages in the bismuth wire are appreciable compared to the voltages in which we are interested, which are only a few millivolts. In order to compensate for these voltages coil *C* is used. One side of this coil is grounded and the other side is passed through a variable resistance and variable condenser in parallel, to the

ungrounded side of the lead to the bismuth wire, as shown in Fig. 4. The resistance is a non-inductive 25,000 ohm variable unit. The variable condenser is of the midget type with maximum capacity of 50×10^{-12} farads. It may be noted that if the stray voltages induced in the bismuth wire should require it, coil C could have a tap and suitable number of turns, the tap being grounded and the variable resistance connected to one side and variable condenser to the other.

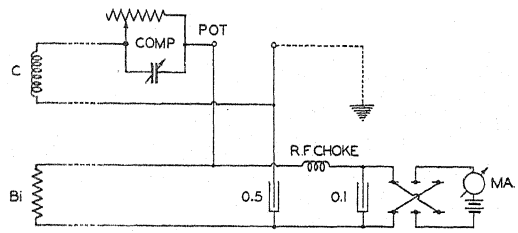

Fig. 4. Circuit connections to bismuth wire.

Fig. 5 is a diagram of the potentiometer and its associated circuits. There are two circular slide wires called the R dial and the C dial through which flow currents approximately equal in amplitude and approximately 90° apart in phase. These currents are supplied by coil H of Figs. 1 and 5 through a shielded transformer Tr and the resistances R and condensers C, which latter determine the amplitude and phase of the currents in the slide wires. A center tapped wire in parallel with each slide wire serves to connect them together at their electrical mid-points.

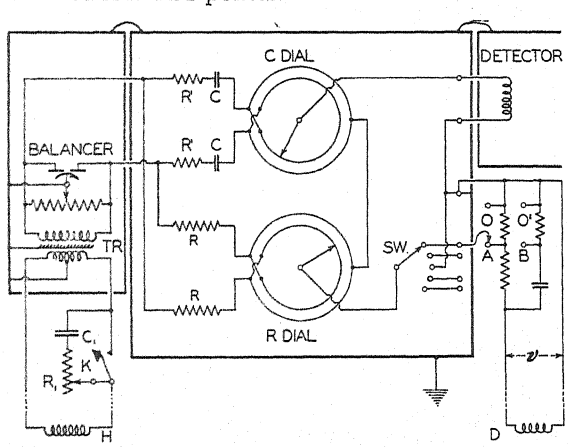

Fig. 5. The potentiometer circuits.

The two sliders are connected in series with the potential to be measured, by a selector switch Sw, and a detector. The latter is a grid leak detector with a tuned input transformer whose primary impedance approximately matches that of the potentiometer. Signals are audible because the oscillator, Fig. 3, is modulated.

At the lower right corner of Fig. 5 is shown a calibration circuit which con-

sists of two voltage dividers across the voltage v from a coil such as D of Fig. 1. Voltage v is measured by a thermovoltmeter. The potentiometer dials are calibrated by obtaining the settings for silence in the detector for points O and A, and O' and B' thus determining the number of millivolts per division for each dial. Then the unknown potential, which has been connected to another point of the selector switch, is measured.

Due to distributed inductance and capacity and to skin effect, the constants of the calibration and potentiometer circuits are uncertain, and a more accurate system is desirable. The potentiometer is shielded so the only driving force is through the transformer Tr. A phase shifting circuit C_1R_1 is included in the primary circuit of the transformer, which may rotate the phases of the currents in the two slide wires without altering their relative phase or amplitude. The settings for the calibration circuit are obtained and then the phases of the potentiometer currents rotated through approximately 90° and the new settings for the calibration circuit obtained. A simple calculation then gives the ratios of the currents in the two slide wires and their relative phases. At one million cycles this ratio may be determined to within 1 percent and the phases to 1/2°.

The details of this system and other features of the potentiometer have been described more fully by the author.[3]

III. Experimental Procedure

The d.c. field of the large coils was measured by the usual ballistic galvanometer method, using a fixed search coil and obtaining the galvanometer throw when the magnetizing current was switched on or off. Since it was not practical to have coils which would give a uniform field care was taken to have the test coil and later the bismuth wire close to the center of the large coil where the field is fairly uniform. The variation of the resistance of the bismuth wire with d.c. field was determined by ordinary d.c. bridge measurement and gave the usual curve, parabolic at first and then becoming straight. The a.c. measurements should be made with the d.c. field current at such a value that the curve of resistance vs. field strength is practically a straight line.

In taking a set of measurements, the potentiometer is first calibrated. Then setting the selector switch for the bismuth measurements the compensating circuit is adjusted to bring the dial readings to about their midpoint. This should be done with the continuous field at the value to be used in the measurements immediately following, since the setting of the compensator depends on the resistance of the bismuth wire. Then readings may be taken in succession with various values of d.c. flowing through the wire beginning and ending with zero to make sure that no change has occurred in the compensating circuit or any other circuit during the readings. With no continuous field, no change in voltage was observable for various values of d.c. flowing through the bismuth wire. The vector voltage due to the varying resistance of the bismuth wire is then represented by the difference in dial

[3] W. W. Macalpine, Proc. I.R.E. 18, 1144 (1930).

readings between those with no d.c. flowing through the wire and those with the value of d.c. in question, the continuous field being the same in both cases. The effect of the leads from the bismuth wire to the potentiometer may be tested by making some measurements with the ordinary leads and then repeating them with considerably longer leads added. The actual leads used were twisted only where they pass up through the 3/8 in. bakelite tube on which the bismuth wire was mounted, a length of 4 in.

In order to measure the field it is necessary to know the diameter of turn D, which may be found at room temperature but not easily in liquid air. For this purpose coil F of 18 turns was wound on the bakelite tube well above the level reached by the liquid air. The voltages induced in D and F were then measured before and after adding the liquid air. The relative voltages induced in F and D were found to be about the same in and out of the liquid air, within experimental error and therefore the area of D changed little in liquid air, due probably to its being on bakelite. The magnetic and electrical properties of the liquid air are of such magnitude that they have little effect on the circuits, and so need not be taken into consideration.

IV. Data and Results

Table I gives the arrangement of the various test circuits used to calibrate the potentiometer. These were supplied by coil D of Fig. 1. Circuits a, b, c, d are those illustrated in the lower right hand corner of Fig. 5. Vectors a, b, f, g, p are those with normal phase, switch K in Fig. 5 closed, while c, d, h, k, q are with the phase of the potentiometer currents rotated.

Table I. *Test circuits.*

Vectors a,c	$DA=929$ ohms	$OA=17.4$ ohms
b,d	$DB=153\times10^{-12}$ farads	$OB=16.1$ "
f,h	193×10^{-12} "	11.5×10^{-9} farads
g,k	929 ohms	9.9×10^{-9} "
p,q	bismuth vectors	

In Table II each of the values of the coordinates *as read* are the average of several readings made at various times during the experimental run and include both positive and negative readings. The leads to coil D were reversed for the negative readings. In the cases of p and q readings were taken with various values of i, the current in the bismuth wire, but all are reduced to the equivalent readings for $i=17.8$ ma. The rectangular coordinates are calculated with the use of α and m as determined by Eqs. (1) and (2) of the article on the potentiometer.[4] v is the voltage induced in turn D and is given in dial divisions, being calculated from the column of *lengths* by the ratios *v/length*, which are calculated from the above data on the test circuits. It should be noted that the value of v in dial divisions for the $a\ b\ f\ g$ system is not necessarily equal to its value for the $c\ d\ h\ k$ system. The phase angle of each vector with respect to the positive R axis is given under θ_R.

[4] Reference 3, $(90°-\alpha)$ is the phase angle between the currents in the two slide wires, while m is the ratio of the current in the C dial to that in the R dial.

TABLE II. *Experimental data.*

Vector	Coordinates: As Read R'	Coordinates: As Read C'	Coordinates: Rectangular R	Coordinates: Rectangular C	Length	$\frac{v}{\text{Length}}$	v	θ_R
a	75.0	29.6	72.6	28.1	77.8	54.5	4240	21.2°
b	−21.7	69.6	−27.3	66.1	71.5	59.4	4247	112.4
f	67.8	26.8	65.7	25.5	70.5	60.5	4265	21.2
g	17.3	−64.8	22.5	−61.6	65.6	62.7	4115	290.0
p	−21.1±0.8	86.0±0.5	−28.0	81.7	86.4±0.9			108.9±0.5
					Average		4217	±25
c	31.3	−75.9	37.4	−72.1	81.2		4426	297.3
d	68.3	37.2	65.3	35.3	74.2		4408	28.4
h	27.8	−67.6	33.2	−64.2	72.3		4375	297.3
k	−64.0	−31.1	−61.5	−29.5	68.2		4276	205.7
q	83.8±0.4	38.3±0.7	80.7	36.4	88.5±0.8			24.3±0.4
					Average		4371±24	

$f = 1.09 \times 10^6 \pm 0.5\%$ cycles per second.
$H/I = 25.0 \pm 1.5\%$ gauss per ampere in d-c field coils.
$dR/dI = 1.55 \pm 0.5\%$ ohms/amp. at $I = 16.1$ amp.
R = d-c resistance of bismuth wire.
$i = 0.0178 \pm 1\%$ d-c amp. flowing in bismuth wire.
$A = 0.810 \pm 2.5\%$ sq. cm, area of turn D, Fig. 1.
Temperature = that of liquid air (about −185°C).
$H_{d-c} = 400$ gauss, approximately.
$v = 1.5$ volts r.m.s., approximately.
$H = 27$ gauss r.m.s., "

The experimental precision of the length of the test vectors a, b, c, d, etc. was about ±0.5 percent and of the angles θ_R, ±0.25°, making the precision of the average values of v ± 1 percent. The estimated precision of A is large because of its uncertainty due to immersing the turn in liquid air. Any contraction occurring would increase the calculated value in Table III, which will bring the ratio of measured to calculated values nearer unity.

The calculated high frequency field is

$$H = \frac{v}{2\pi f A} \times 10^8 \text{ gauss}$$

and the high frequency voltage appearing across the bismuth should be

$$e = ir = iH\frac{dR}{dH} = i\frac{dR}{dH}\frac{v}{2\pi f A} \times 10^8.$$

Substituting the above figures: $e = 0.0199 \times v$ volts. The precision of e as calculated from those of its various factors is ±3.5 percent.

The measured value of the length of the vectors p and q must be corrected for the drop due to the compensator, which in this set of measurements had a resistance of 5700 ohms and a capacity of about 45×10^{-12} farads, including capacity of leads. Since the resistance of the bismuth was about 100 ohms, the compensator reduced the a.c. voltage across it by 1/58 and rotated its

phase $-1.6°$. Also, calculation shows that the average field of the oscillating coil on the surface occupied by the bismuth wire was 1.2 percent higher than the average linking turn D which was used to measure the field (see Appendix). Making these corrections to the lengths of the vectors p and q for the compensator and field we have the following results: $p=86.9$, $q=89.0$.

From the value of the *coordinates—as Read* of Table II, the values of α and m may be calculated[3], using both the a, b, c, d set of vectors and the f, g, h, k set. The former gives $\alpha=-0.086$ and $m=0.944$, and the latter $\alpha=-0.099$, and $m=0.950$, the average being $\alpha=-0.092$ and $m=0.947$. Using these values of α and m to find the correction for the α^2m^2 terms, it is found that for both sets of vectors the correction to α is $+0.008$ and that to m is $+0.004$. Thus the true values are $m=0.95$, the correction to m being almost negligible; and $\alpha=-0.092+0.008$, or $-4.8°$. It may be noted that no phase correcting resistances R' of Fig. 5 were used in series with the C dial of the potentiometer in this instance. In regard to the $\phi\beta$ corrections, they may be shown to be negligible. The angles θ, β and ϕ may be found from Table II, and are: $\theta=21°$, $\beta=6°$, $\phi=-1°$ in the a, b, c, d case and $\phi=+1°$ in the f, g, h, k case.

The phase of the magnetic field is determined from that of vectors f and h since these are the vectors for a test circuit of two mica condensers in series. Such circuits introduce very little phase shift due to the small phase angle of the condensers. The phase of vector p with respect to the field is then $108.9° - (90+21.2) = -2.3°$ and similarly that of q is $-3.0°$. Taking into account the phase shift of $-1.6°$ produced by the compensator as noted above, these angles become $-0.7°$ and $-1.4°$, respectively.

The following table gives the above two results as *III* and *IV* and two others obtained similarly on a different date as *I* and *II*. In the latter case it was found that the calculated $e=0.0200\times v$. The columns marked *equivalent e*—Bi give the values of the lengths of the calculated and measured vectors multiplied by the proper ratio to make the calculated length 100.0.

TABLE III. *Results.*

Result	v	e—Bi		Equivalent e—Bi		Phase respt. to field
		Calc.	Meas.	Calc.	Meas.	
I	4300	86.0	88.9 ± 1.5	100.0 ± 3.5	103.4 ± 1.7	0.3° ± 0.9°
II	4400	88.0	91.1 ± 1.0	100.0 ± 3.5	103.5 ± 1.1	−0.6° ± 0.6
III	4217	83.9	86.9 ± 0.9	100.0 ± 3.5	103.6 ± 1.1	−0.7 ± 0.6
IV	4371	87.0	89.0 ± 0.8	100.0 ± 3.5	102.3 ± 0.9	−1.4 ± 0.5
Average				100.0 ± 3.5	103.2 ± 0.6	−0.6° ± 0.5°

$$\frac{Measured}{Calculated} = 1.032 \pm 3.5 \text{ percent}$$

$$Phase = -0.6 \pm 0.5°.$$

It is thus seen that the change in resistance of bismuth at 10^6 cycles per second is normal in magnitude and phase.

V. Measurements at 55 kilocycles, Room Temperature

The above method was first developed at 55 kilocycles, but this work will be described only briefly here. In place of the arrangement of Figs. 1 and 2 a magnet was made from four rings of Western Electric dust core cemented together. This core was cut into two parts to facilitate winding and an air gap formed by cutting away three rings to make the area of the gap that of a single ring, or approximately 1 sq. cm. The oscillating circuit consisted of a mica condenser and two coils in series, one on each side of the air gap, driven by a 50 watt tube in a suitable circuit. Fields up to 700 gauss r.m.s. were easily obtained but those used ranged from 100 to 300 gauss since no cooling system was employed at the bismuth wire. Two coils as close to the air gap as the oscillating coils would allow supplied the d.c. field. These were supplied from the 110 volt d.c. lines with series resistance, a wave trap being employed in series to prevent them from short circuiting the high frequency circuit. The bismuth wire was wound on a mica form which slipped into the air gap. A single turn corresponding to D of Fig. 1 was shellacked to one of two sheets of mica covering the bismuth wire. The connections to the potentiometer were similar to those at the higher frequency except that instead of using the compensator a small coil in series with the leads to the bismuth wire was coupled loosely to the coil of the wave trap. The result obtained was that the resistance of the bismuth wire behaved normally both in phase and magnitude in 55 kilocycle fields, at room temperature.

In conclusion I wish to express my thanks to Professor M. I. Pupin for allowing me the use of The Marcellus Hartley Research Laboratory and for his interest in the work.

APPENDIX

Note on the field in the solenoid

The ideal condition would be that the a.c. field within the oscillating coil in Fig. 1 is uniform, which would be strictly true only for a very long solenoid. Considerations of efficiency of the coil require that its length be not too long with respect to its diameter. In order to determine what correction would be required due to non-uniformity of the field, its average values over the bismuth wire and turn D were calculated. Briefly the calculation is as follows: The increment of field at p due to an element of circular turn perpendicular to the X axis and with center on that axis is

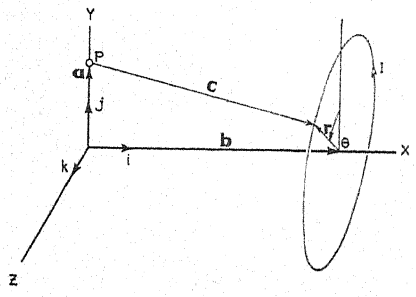

Fig. 6.

$$dh = \frac{I}{C^3} c \times (i \times r) d\theta$$

$$= \frac{I r d\theta}{C^3} [i(r - a\cos\theta) - jb\cos\theta - kb\sin\theta]$$

where $c^2 = b^2 + r^2 + a^2 - 2ra\cos\theta = A - B\cos\theta$. Integrating around the complete turn, the Z component vanishes and

$$\frac{h_i}{I} = \frac{2}{\sqrt{(A+B)}} \left[F\left(k, \frac{\pi}{2}\right) + \frac{2r^2 - A}{A - B} E\left(k, \frac{\pi}{2}\right) \right] \tag{1}$$

$$\frac{h_j}{I} = \frac{2b}{a\sqrt{(A+B)}} \left[F\left(k, \frac{\pi}{2}\right) - \frac{A}{A - B} E\left(k, \frac{\pi}{2}\right) \right] \tag{2}$$

where

$$k = \sqrt{(2B/(A+B))}$$

$$F\left(k, \frac{\pi}{2}\right) = \int_0^{\pi/2} \frac{dZ}{(1 - k^2 \sin^2 Z)^{1/2}}$$

the complete elliptic integral of the first order,

$$E\left(k, \frac{\pi}{2}\right) = \int_0^{\pi/2} (1 - k^2 \sin^2 Z)^{1/2} dZ$$

the complete elliptic integral of the second order.

In obtaining the above expressions for the components of h, the following integrals are used:

$$\int_0^{\pi} \frac{d\theta}{(A - B\cos\theta)^{1/2}} = \frac{2}{\sqrt{(A+B)}} F\left(k, \frac{\pi}{2}\right)$$

$$\int_0^{\pi} \frac{d\theta}{(A - B\cos\theta)^{3/2}} = \frac{2\sqrt{(A+B)}}{A^2 - B^2} E\left(k, \frac{\pi}{2}\right).$$

The latter is found by writing for $A - B\cos\theta$

$$(A - B)\cos^2\theta/2 + (A + B)\sin^2\theta/2.$$

Eqs. (1) and (2) were plotted for various values of b, with a = radius of turns of bismuth wire and were integrated by planimeter for three points on the wire, the average field on the wire being found from these values. Similarly the average field in turn D was found.

The result was that the average value of the field on the bismuth wire is 1.2 percent higher than the average field linking turn D.

STRAIN AND DIAMAGNETIC SUSCEPTIBILITY

By H. E. Banta
Rice Institute, Houston, Texas

(Received January 20, 1931)

Abstract

The magnetic susceptibility of copper and silver wires has been measured by the Gouy method before and after various annealing processes. Also, the susceptibility has been measured before and after straining specimens beyond the elastic limit, the strains being either twists or stretches. The susceptibilities are found to be increased by as much as 20 percent for copper and 3 percent for silver by annealing at red heat for 15 minutes in an atmosphere of CO_2. This increase is probably due to release of occluded gases or to oxidation or recombination of impurities. Straining the specimens beyond the elastic limit is found to produce no measurable change of susceptibility. Francis Bitter has observed a large effect due to straining these metals beyond the elastic limit. The reason for Bitter's results is not clear, but it is pointed out that no effect is to be expected in copper, at least, because crystals of this metal are isotropic magnetically and have no observable magnetostriction.

RECENTLY Francis Bitter[1] has made the surprising and important observation that annealed copper (impure, paramagnetic) and silver wires suffer a very appreciable change of magnetic susceptibility when strained beyond the elastic limit. This result is surprising for the following reasons. Straining a wire beyond the elastic limit may have the effect of breaking up large crystals into smaller ones. Slipping occurs along cleavage planes, crystal boundary planes are distorted, segregated impurities are redistributed, and new orientations may result for the axes of the tiny crystals. In addition to these effects certain parts of the wire will be left elastically extended, other parts elastically compressed as a result of the unequal slipping of various sections of the wire. These residual strains in a wire have for years been a source of annoyance to users of the Eötvös torsion balance.

It appears, therefore, that the change of susceptibility of a wire when stretched might be explained by two factors: (1) the orienting effect on the small crystals, and (2) the setting up of a strained condition in the wire. In the case of copper the first factor must be ruled out because Montgomery[2] has shown that copper crystals are isotropic magnetically. The second factor is also inadequate for the following reason: the reciprocal relations between strain and magnetization may be expressed by the equation $\partial I/\partial p = \partial e/\partial H$, where I, H, p, and e are, respectively, intensity of magnetization, magnetic field, applied stress, and strain $\partial l/l$. The last two quantities are along the H direction. This equation is based on thermodynamical principles and according to Honda[3] has been verified experimentally even in the case of iron

[1] Francis Bitter, Phys. Rev. **36**, 978 (1930).
[2] Carol G. Montgomery, Phys. Rev. **36**, 498 (1930).
[3] Honda, Magnetic Properties of Matter, p. 46.

and nickel, where hysteresis would tend to make the equation inapplicable. It should hold accurately where hysteresis is negligible, as in copper. In copper, however, magnetostriction is so small that it has never been detected; thus $\partial e/\partial H$ is negligible and therefore $\partial I/\partial p$, or $H\partial K/\partial p$ must be very small. The absence of magnetostriction in copper thus shows that the susceptibility K is unaffected by applied pressures. Hence the second factor given above must be ruled out as an explanation. Accepting Bitter's experimental results, the only conclusion appears to be that the above description of the processes involved in stretching a wire is incomplete.

Accordingly, a series of tests on the effect of strain on the susceptibility of copper and silver was made. As in Bitter's experiments, the Gouy method was used. An analytical balance was mounted about half a meter above an electromagnetic with pole-pieces (truncated cones) 1 cm in diameter and 4 mm apart. The specimen, in the form of a wire about 15 cm long and 2 or 3 mm in diameter, was suspended from one arm of the balance by a silk thread. the lower end of the wire being centered with respect to the pole-pieces. The force on the wire is given by the equation $F=KH^2a/2$ where K, H, and a are the volume susceptibility, magnetic field intensity at the lower end of the wire, and cross-sectional area of the sample, respectively.

When the specimen was suspended 15 cm above the poles of the magnet the balance was not deflected by a measurable amount. Therefore the above equation requires no correction for the field at the top of the specimen. All samples were diamagnetic.

The first set of results was obtained for commercial copper wire about 2.6 mm in diameter. Forces on the samples were measured; they were then twisted beyond the elastic limit by various amounts and the forces again measured. A representative part of these results is shown in Table I. These

TABLE I. *Effect of twist on susceptibility.*

Sample	F_1 dynes	Angle of twist	F_2 dynes	ΔF
1	7.44	0	7.53	+.09
2	7.15	$\pi/2$	7.26	+.11
3	7.20	π	6.95	−.25
4	7.08	2π	7.11	+.03
4	7.11	30π	7.00	−.11

wires did not all have the same diameter, so the forces are different for the different samples. The samples had been well annealed, first in a flame, then in an electric furnace in air. The oxide coating consequent to annealing was removed by sand-papering the surface. It appears that the values of ΔF are within the limits of experimental error. The average value of ΔF is −0.03 dyne and there are both positive and negative values. Furthermore in this experiment it is doubtful whether F could be determined accurately to more than 0.2 dyne. We conclude therefore that K is unaffected by twisting the copper wire greatly beyond the elastic limit. The average specific susceptibility cal-

culated for these samples is 0.5×10^{-7}. For pure copper Montgomery gives 0.85×10^{-7}.

A series of experiments on stretched copper wire was then made. The order of magnitude of F (corrected for changes in diameter) was about the same as in the set of observations shown in Table I. This degree of accuracy was at first considered sufficient, since Bitter got ΔF as large as $\frac{1}{2}F$; but later, pole pieces with larger areas (in order to minimize errors of adjusting the specimen between the pole-pieces) were put on the electro-magnet, and crossed telescopes fastened to its frame to provide accurate control over the position of the specimen. The measurement of the force on a specimen which had been removed and replaced could then be repeated to 0.1 dyne.

The preliminary work showed that annealing a copper wire affected its susceptibility. For example, the force on a specimen was measured, it was heated to redness in CO_2 for about three minutes, cooled slowly, and the force again measured. Successive forces, each determined after a three minute heat treatment, were -6.0, -6.5, -7.0, -7.3, and -7.3 dynes. Similar effects due to annealing have been obtained by Davies and Keeping[4] for copper-antimony alloys. They attribute the phenomenon to changing of the nature of the compounds of copper and antimony. Some samples in the present experiments were heated to a bright red heat in a vacuum, and gave off a gas which, at ordinary pressure, had about half the volume of the copper. The nature of this gas is not known. Therefore it was possibly the presence of impurities or freeing of adsorbed gas which produced the increase of F noted above. The foregoing results indicate that an annealing at red heat for about fifteen minutes is necessary in order to secure the final stable value of the susceptibility. Therefore all further annealings were done in CO_2, holding the specimen above red heat for fifteen minutes and allowing it to cool slowly. All further cleanings are by immersion in boiling HCl for about two minutes, unless otherwise stated.

A second specimen of copper which was slightly paramagnetic when uncleaned was obtained. With its surface sand-papered $F=0.0$ dyne. Annealed, $F=-3.04$ dynes. This is sample A in Table II. Another sample was not annealed, but was cleaned with acid and a value $F=-5.1$ dynes found; some of the surface was then removed with sand-paper and F found to be -5.4 dynes. Thus it appears that paramagnetic impurities were removed from the surface by sand-papering. It is therefore possible that some of the increase of F at annealing is due to the removal (possibly by oxidation) of impurities at or near the surface. When thoroughly annealed this specimen had a value of $F=-6.4$ dynes.

Chemically pure samples of copper and silver were obtained from Baker and Company. These are shown as C and D, respectively, in Table II. The procedure with each sample of Table II was as follows: the force F was measured (except sample B); the wire was annealed and cleaned, and its force F_1 again measured. It was then stretched till its length changed permanently

[4] G. W. Davies and E. S. Keeping, Phil. Mag. 7, 145 (1929).

by the fraction $\Delta l/l$, cleaned, and the force F_2 again measured. Again it was annealed and cleaned, and the force F_3 again measured. The forces in this table are shown in mg, the units in which they were measured. The d's are diameters of the samples. Multiplying by $(d_1/d_2)^2$ corrects F_2 for the change in cross-sectional area consequent to stretching; so $F_1-F_2(d_1/d_2)^2$, shown in the table as ΔF, is a measure of the change of K when the sample is stretched.

TABLE II. *Effect of stretching on susceptibility.*

Sample	F mg	F_1 mg	d_1 mm	$\Delta l/l$	F_2 mg	d_2 mm	F_3 mg	$F_2(d_1/d_2)^2$ mg	ΔF mg	$K\times10^6$
A	0.0	3.1	2.61	.10	2.9	2.48	—	3.2	+0.1	−0.22
B*	5.4	—	2.58	.12	4.7	2.43	5.7	5.3	−0.1	−0.48
C	8.0	9.2	3.00	.10	8.6	2.85	8.5	9.4	+0.2	−0.51
C′	—	8.6	2.85	.195	7.2	2.61	7.2	8.6	0.0	−0.51
D	28.7	30.0	3.00	.235	24.3	2.70	24.3	29.9	−0.1	−1.62

* Note: This specimen was annealed in a flame for about one minute at less than red heat before F was obtained. It was given no further annealing before being stretched. Specimen C' is the specimen C after all the data following C were obtained. (F_1 for C' should be the same as F_2 for C except for experimental error.)

Since ΔF is within the limit of experimental error it seems reasonable to conclude that K is unaffected by the stretch. Also, since F_3 is the same as F_2 (except for B), we conclude that annealing a wire of copper or silver which has been hardened by severe stretching does not affect its magnetic susceptibility, provided proper heat treatment has stabilized the wire magnetically before it is strained.

The data on B show that straining a wire which has been imperfectly annealed does not affect its susceptbility. In these experiments the specimens were given permanent strains as large as were used in Bitter's experiments, and the accuracy of measurement was sufficient to detect an effect at least 1/10 as large as Bitter observed. In no case has Bitter's effect been detected. Furthermore, as pointed out in the introduction, there is reason for disbelieving in the reality of the effect because of the absence of magnetostriction in copper and silver.

The conclusion may therefore be drawn that the magnetic susceptibility of copper and silver is not appreciably affected by straining wires of copper and silver beyond the elastic limit. The reason for Bitter's results is not evident.

It is indeed a pleasure to thank Dr. C. W. Heaps for many helpful suggestions and criticisms throughout the investigation.

SOME PHYSICAL PROPERTIES OF COMPRESSED GASES I. NITROGEN*

By W. Edwards Deming and Lola E. Shupe
Fertilizer and Fixed Nitrogen Investigations Bureau of Chemistry and Soils, Washington, D.C.

(Received January 11, 1931)

Abstract

The writers have adjusted and extrapolated the *compressibility data* obtained by Bartlett and his collaborators on nitrogen, so that very accurate *p-v-T data from −70 to 600° and up to 1200 atm.* are available. A suitable graphical scheme has been devised for obtaining the derivatives $(dv/dp)_T$, $(dv/dT)_p$, $(d^2v/dT^2)_p$ at any point in order that some of the physical properties of the gas can be calculated. This graphical scheme depends on the relation of $\alpha \equiv RT/p - v$ and $\Delta \equiv v(pv/RT - 1)$ to p,v,T, and on the relations of the derivatives of α and Δ to the derivatives of v. Errors in the estimation of the slope of an α or Δ curve at any point introduce much smaller errors into the derivatives of v, since the derivatives of α and Δ enter as correction terms to the derivatives of v just as α and Δ are corrections to v itself.

A *graphical process is used as originally in MS for adjusting the p-v-T* data and all the physical properties derived from it. This process is based on the assumption that surfaces such as *p-v-T*; α-*v-T*; or Δ-*v-T* are smooth and hence that the curves in any family of isotherms or isobars show related characteristics. It throws most of the adjustment on v, where it belongs, since the measurements of p and T are much more accurate than those of v. Such an adjustment enhances the precision of the compressibility data and of the calculations made from it.

The *specific volume, density, coefficients* $(-p/v)(dv/dp)_T$ *and* $(T/v)(dv/dT)_p$, *fugacity*, C_p, $C_p - C_v$, C_v, and μ are calculated and shown in curves and a table for the fourteen pressures and twelve temperatures in the range studied. *Inversion pressures and temperatures* are read from the μ vs. p isotherms and the μ vs. T isobars.

The calculations of C_p agree well with the experimental values of Krase and Mackey, who worked at 30, 100, 125, 150° up to 700 atm. and at 50° to 800 atm. The agreement is probably within the experimental error, but the trends of the two sets suggest that a real difference may exist. At 30° the calculated C_p drift below the experimental values at pressures above 400 atm., becoming 0.13 cal/mole · deg low at 700 atm. At 50° the agreement is good to 800 atm. At 100, 125, 150° the calculated C_p drift above the experimental values, but the disagreement reaches only 0.2 cal/mole · deg at 600 and 700 atm.

As one might expect, $C_p - C_v$ approaches R at all temperatures as the pressure approaches zero. In general, $C_p - C_v$ increases at any particular pressure as the temperature decreases. $C_p - C_v$ shows a strong maximum at about 200 atm. at the lowest temperatures. With increasing temperature this maximum comes at higher and higher pressures, and gradually disappears. The C_v vs. T isobars show some curious tendencies. C_v along the 20 atm. isobar stays constant and equal to 2.50 R from −70 to 100°C, then it rises slowly to 5.15 cal/mole · deg at 600°. Along the 40, 60, 80, and 100 atm. isobars, C_v drops a few hundredths of a cal/mole · deg below 2.50 R at −70°, the drop being greater the greater the pressure. Along the 200 atm and higher pressure isobars, C_v rises as the temperature falls below 50°, and the rise is steeper the greater the pressure. At 600° C_v is about 5.18 cal/mole deg or 2.61 R for all pressures.

* An abstract of this paper appeared in the program for the Chicago meeting of the American Physical Society, November 28 and 29, 1930.

RECENT extensions of compressibility data on several gases to 1000 atm. from −70 to 300° and 400° published by Bartlett[1] and his collaborators at this laboratory have made possible the calculation of such physical properties as pressure and temperature coefficients of volume expansion, fugacity, change in heat capacity with pressure, difference between the heat capacity at constant pressure and that at constant volume, Joule-Thomson coefficient, and inversion temperatures and pressures, all at the various temperatures and pressures throughout the range of experimentation and as much further as extrapolations can safely be made.

With extrapolations made by a method to be described, we have reliable compressibility data on nitrogen from −70 to 600° up to 1200 atm. The physical properties of this gas might be expected to show some interesting properties over such a wide range, and we have endeavored to investigate them.

In order to calculate these physical properties from compressibility data it is necessary to evaluate the derivatives $(dv/dp)_T$, $(dv/dT)_p$, $(d^2v/dT^2)_p$ wherever desired. Analytical or graphical methods can be devised for this purpose. Perhaps the best analytical method of getting $(dv/dp)_T$ over a limited pressure range is to write pv as a power series in p along an isotherm. However, no set of coefficients can be found that will satisfactorily follow the trend of pv for nitrogen through the whole range of pressures along any isotherm; one set of constant seems to hold fairly well to some intermediate pressure, depending on the temperature, and another set is necessary from this pressure on up to 1000 atm. This introduces a discontinuity, and the intermediate pressure is thus at the ends of the two ranges. End points are the least trustworthy and we usually get two values for $(dv/dp)_T$ at the discontinuity, and it is then necessary to resort to graphical methods to smooth out the disagreement. The same difficulty exists in getting $(dv/dT)_p$; v^2 expressed as a power series in T seems to fit at low pressures, v as a power series in T seems to fit at high pressures; so there is a break at the intermediate pressure again. These empirical formulas are satisfactory for first derivatives but not for second derivatives except over a limited range. Jakob[2] used them to get the change in heat capacity of air up to 200 atm. from −80 to 250.° He recognized that at the highest temperatures his calculation of $(d^2v/dT^2)_p$ showed evidence of being untrustworthy. Drs. E. P. Bartlett and H. L. Cupples of this laboratory used Jakob's scheme with nitrogen up to 1000 atm. and the difficulties mentioned above were encountered, but by calling on graphical determinations at certain points they obtained results that were valuable, though probably not as reliable as those gotten by the method to be described. We have made free use of some of the ideas in their unpublished manuscript.

The ideal way to obtain these physical properties would be through an

[1] Bartlett, J. Amer. Chem. Soc. **49**, 687 (1927); **49**, 1955 (1927); Bartlett, Cupples, Tremearne, ibid. **50**, 1275 (1928); Bartlett, Cupples, Tremearne, Hetherington, ibid. **52**, 1363 (1930); Bartlett, Hetherington, Kvalnes, Tremearne, ibid. **52**, 1374 (1930); Kvalnes and Gaddy, ibid. **53**, 394 (1931).

[2] Max Jakob, Zeits. f. Techn. Physik, **4**, 460 (1923).

equation of state, but this should not be attempted at pressures and temperatures where it appears not to give trustworthy results. Extensive calculations have been made only with the Beattie-Bridgeman[3,4] formula, but the ranges of temperature and pressure covered in the present paper probably far exceed the limits of validity of any existing equation of state. Since the calculation of the constants in the Beattie-Bridgeman formula for high pressure data on nitrogen were made, further work by the writers[5] has shown that its constants are different above and below the critical density for hydrogen and a 3:1 mixture of hydrogen and nitrogen. The calculations with nitrogen[4] were carried only a trifle beyond the critical density and it is possible that if higher densities had been included a different set of constants would have been indicated for densities above critical. If this second set had been introduced the formula would doubtless have been found to fit better at high pressures than was concluded in our paper, but calculations of the desired physical properties at medium and high pressures are surely more reliable when made by the graphical method about to be described. By it no discontinuities are introduced and the precision can be estimated by the regularity of the graphs of the quantities evaluated.

The authors of the Beattie-Bridgeman equation of state have used it to find the heat capacities and Joule-Thomson coefficients of air and ammonia[6] at ordinary temperatures and relatively low pressures, where the increase ΔC_p in heat capacity is usually a small fraction of the heat capacity at 1 atm. C_p is computed by calculating the change ΔC_p in heat capacity with pressure and adding it to the value of C_p at 1 atm., and when $\Delta C_p/C_p$ is small, large errors in ΔC_p are overlooked when observed and calculated values of C_p are compared.

After studying the α and Δ curves for nitrogen, we decided that it is expecting too much of any formula that it should follow the trends of the p-v-T data as faithfully through the whole range as is desired for determining the physical properties sought after. The following graphical process was developed in the hope of obviating some of the difficulties with analytical methods.

The v vs. T isobars are nearly straight lines from -70 to 600° even to 1200 atm., but by plotting residuals their curvature can be measured easily. If the gas were perfect, the v vs. T isobars would be straight lines through the origin having slopes inversely proportional to the pressure. Any departure from the perfect gas law is evidenced by residuals such as

$$\Delta \equiv v(pv/RT - 1) \tag{1}$$

and

$$\alpha \equiv RT/p - v \tag{2}$$

[3] Beattie and Bridgeman, Proc. Amer. Acad. Arts Sci. **63**, 229 (1928); J. Amer. Chem. Soc. **49**, 1665 (1927), ibid. **50**, 3133 (1928); and later papers.

[4] Deming and Miss Shupe, J. Amer. Chem. Soc. **52**, 1382 (1930).

[5] Deming and Miss Shupe, J. Amer. Chem. Soc. March 1931 (two papers).

[6] Oscar C. Bridgeman, Phys. Rev. **34**, 527 (1929); James A. Beattie, Phys. Rev. **34**, 1615 (1929); James A. Beattie, Phys. Rev. **35**, 643 (1930).

being different from zero; likewise any departure of $(-p/v)\ (dv/dp)_T$ and $(T/v)\ (dv/dT)_p$ from unity is evidenced by $(d\Delta/dp)_T$, $(d\alpha/dp)_T$, $(d\Delta/dT)_p$, $(d\alpha/dT)_p$ being different from zero. Fig. 1 shows how straight the 200 atm. v vs. T isobar is, how much curvature the corresponding Δ and α curves have, and that their shapes are different. There are relations between the slopes

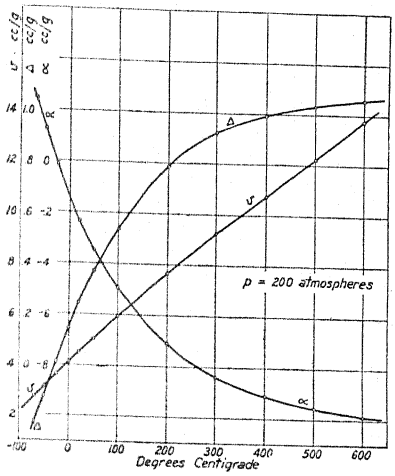

Fig. 1. Graphs of v, Δ, and α vs. T with p constant. This shows that the Δ and α curves have great curvature compared with the v vs. T curve, and that the Δ and α curves are of very different shape.

of the v vs. T, Δ vs. T, and α vs. T isobars; likewise there are relations between the slopes of v vs. p, pv vs. p, Δ vs. p, α vs. p, Δ vs. ρ (density) isotherms. The relations between these are as follows:

$$(T/v)(dv/dT)_p = \frac{pv/RT + (T/v)(d\Delta/dT)_p}{1 + 2\Delta/v} \tag{3}$$

$$(T/v)(dv/dT)_p = RT/pv - (T/v)(d\alpha/dT)_p \tag{4}$$

$$(-p/v)(dv/dp)_T = 1 - \rho(dpv/dp)_T \tag{5}$$

$$(-p/v)(dv/dp)_T = RT/pv + (p/v)(d\alpha/dp)_T \tag{6}$$

$$(-p/v)(dv/dp)_T = \frac{pv/RT - (p/v)(d\Delta/dp)_T}{1 + 2\Delta/v} \tag{7}$$

$$(-p/v)(dv/dp)_T = -pv/RT(2\Delta/v + 1 + \rho^2(d\Delta/d\rho)_T) \tag{8}$$

$$(d^2v/dT^2)_p = -(d^2\alpha/dT^2)_p \tag{9}$$

$$(2\Delta/v + 1)(d^2v/dT^2)_p = (d^2\Delta/dT^2)_p - \frac{2p}{RT}\,\frac{(\Delta/T - (d\Delta/dT)_p)^2}{(2\Delta/v + 1)^2}. \tag{10}$$

A 1 percent error in estimating the slope of an α vs. T or a Δ vs. T isobar may mean only a few hundredths percent error in $(dv/dT)_p$, since by Eqs. (3) and (4) the slopes $(d\alpha/dT)_p$ and $(d\Delta/dT)_p$ enter as correction terms to the

slope that the v vs. T isobar would have if the gas were perfect, just as α and Δ are correction terms to v by Eqs. (1) and (2). Likewise, any error in the determination of $(-p/v)\ (dv/dp)_T$ is diminished according to Eqs. (5), (6), (7), (8). The different families of isobars and isotherms have quite different appearances, so the effect on $(-p/v)\ (dv/dp)_T$ or $(T/v)\ (dv/dT)_p$ of any personal error in estimating the slope of a curve on account of its having a particular shape may be balanced out at that point by a determination from some other curve of different shape. It was not noticeable that the determinations of these derivatives from the α curves were consistently higher or lower than those from the Δ curves or any others.

In order to determine $(d^2v/dT^2)_p$ one can plot $(dv/dT)_p$ vs. T isobars and read the slope at the desired point. Or, one can plot $(d\alpha/dT)_p$ or $(d\Delta/dT)_p$ vs. T isobars, and from the slope of these curves and the relations between $(d^2v/dT^2)_p$ and $(d^2\alpha/dT^2)_p$ or $(d^2\Delta/dT^2)_p$, one can determine $(d^2v/dT^2)_p$. Both methods were used; the results agreed well, and their averages at the various points are shown in Fig. 2.

The most probable positions of observed points lie on the most plausible graph (curve or surface) that can be drawn from them. The most probable values are not uniquely determined by a graphical method, because they depend on the weight assigned by the investigator to various essentials. An adjustment by least squares depends on the weights assigned to the observations so it, too, is subject to the taste and judgment of the computer or observer. Schemes of curve fitting or adjusting that give unique results are incapable of weighting the observations and of throwing the adjustment where it belongs. This has been discussed in two papers by the senior author.[7]

We adopted as a working principle that, in the range investigated, all surfaces such as $p, v, T; \Delta, p, T; \alpha, p, T; (d\alpha/dT)_p, p, T$; etc.; have no sharp ridges nor breaks; accordingly all families of isobars and isotherms should be smooth curves without sharp bends or cusps. All the curves in a given family should show their relationship one to another since they can be considered as sections all cut from the same surface, so that each helps to regulate the drawing of the others. The p-v-T data themselves were adjusted by first drawing smooth curves through the Δ vs. p isotherms and reading off Δ from them, then by plotting these Δ against T with p constant and smoothing these curves for the final values of Δ. The specific volumes were calculated from these final values of Δ. The precision of adjusted observations is strengthened by a wide range of temperature and pressure, such as that studied in this work.

The final values shown in the table and curves were smoothed with respect to temperature and pressure, except where they had been derived from others that had already been smoothed. The regularity of the points on the Δ and α curves attests to the high precision of the compressibility data and gave promise that thermodynamic calculations derived from them should be reliable.

[7] W. Edwards Deming, Proc. London Phys. Soc. **42**, 97 (1930); Phil. Mag. **11**, 146 (1931).

TABLE I. *Some physical properties of compressed nitrogen derived from experimental data on compressibility.*

1	2	3	4	5	6	7	8	9
t	p	v	ρ	f	$-\frac{p}{v}\left(\frac{dv}{dp}\right)_T$	$\frac{T}{v}\left(\frac{dv}{dT}\right)_p$	ΔC_p	μ
°C	atm	cc/g	g/cc	atm			cal/mole°	°/atm
−70°	20	28.50	.03508	19.22	1.053	1.162	.50	.627
	40	13.71	.07294	36.91	1.075	1.347	1.12	.592
	60	8.840	.1131	53.31	1.075	1.530	1.79	.538
	80	6.460	.1548	68.66	1.052	1.682	2.46	.470
	100	5.082	.1968	83.18	1.004	1.806	3.13	.408
	200	2.725	.3669	152.1	.717	1.564	5.17	.128
	300	2.150	.4652	227.2	.514	1.162	5.19	.029
	400	1.896	.5273	319.2	.403	.918	5.10	−.013
	500	1.743	.5738	433.0	.345	.776	5.04	−.033
	600	1.642	.6090	575.5	.309	.675	5.00	−.045
	800	1.508	.6630	976.2	.280	.551	4.97	−.057
	1000	1.421	.7035	1596	.250	.459	4.93	−.065
	1100	1.388	.7204	2021	.250	.408	4.89	−.070
	1200	1.358	.7365	2545	.250	.356	4.81	−.074
−50°	20	31.75	.03149	19.48	1.031	1.129	.45	.559
	40	15.50	.06452	37.92	1.048	1.259	.93	.511
	60	10.13	.09872	55.49	1.048	1.381	1.43	.463
	80	7.492	.1335	72.38	1.030	1.477	1.92	.405
	100	5.952	.1680	88.75	1.000	1.560	2.41	.355
	200	3.139	.3186	168.4	.775	1.462	3.76	.136
	300	2.394	.4178	255.1	.590	1.158	3.85	.035
	400	2.068	.4836	357.8	.472	.937	3.84	−.012
	500	1.878	.5325	483.4	.397	.799	3.77	−.035
	600	1.753	.5705	638.1	.360	.699	3.72	−.050
	800	1.591	.6284	1063	.313	.578	3.66	−.064
	1000	1.485	.6736	1701	.286	.491	3.61	−.072
	1100	1.443	.6928	2127	.286	.449	3.56	−.076
	1200	1.408	.7103	2645	.286	.404	3.48	−.081
−25°	20	35.75	.02798	19.70	1.018	1.094	.36	.470
	40	17.65	.05666	38.80	1.025	1.191	.75	.424
	60	11.66	.08578	57.43	1.025	1.266	1.14	.383
	80	8.694	.1150	75.69	1.008	1.328	1.53	.339
	100	6.950	.1439	93.70	.900	1.377	1.90	.298
	200	3.645	.2744	183.6	.830	1.363	2.95	.134
	300	2.704	.3698	281.4	.653	1.149	3.12	.040
	400	2.287	.4372	395.5	.540	.961	3.02	−.008
	500	2.046	.4888	532.4	.455	.831	2.91	−.035
	600	1.890	.5291	697.6	.415	.732	2.81	−.052
	800	1.695	.5901	1121	.353	.608	2.72	−.069
	1000	1.567	.6382	1784	.325	.526	2.66	−.078
	1100	1.516	.6598	2205	.325	.491	2.62	−.081
	1200	1.473	.6789	2703	.320	.457	2.53	−.085
0°	20	39.67	.02521	19.84	1.010	1.068	.29	.387
	40	19.72	.05071	39.38	1.010	1.128	.60	.344
	60	13.11	.07627	58.72	1.005	1.183	.92	.308
	80	9.828	.1018	77.91	.993	1.235	1.24	.277
	100	7.886	.1268	97.05	.978	1.265	1.53	.247
	200	4.139	.2416	194.6	.850	1.281	2.34	.125
	300	3.020	.3311	301.3	.696	1.136	2.55	.043

TABLE I. (Cont'd.) *Some physical properties of compressed nitrogen derived from experimental data on compressibility.*

1	2	3	4	5	6	7	8	9
t	p	v	ρ	f	$-\frac{p}{v}\left(\frac{dv}{dp}\right)_T$	$\frac{T}{v}\left(\frac{dv}{dT}\right)_p$	ΔC_p	μ
°C	atm	cc/g	g/cc	atm			cal/mole°	°/atm
	400	2.510	.3984	424.2	.590	.983	2.48	−.005
	500	2.217	.4510	569.2	.510	.863	2.37	−.033
	600	2.032	.4922	741.8	.466	.765	2.30	−.052
	800	1.798	.5560	1194	.390	.639	2.20	−.071
	1000	1.650	.6060	1834	.360	.557	2.13	−.080
	1100	1.591	.6286	2246	.360	.530	2.08	−.082
	1200	1.543	.6481	2732	.350	.503	2.01	−.084
20°	20	42.74	.02340	19.92	1.003	1.055	.25	.325
	40	21.33	.04688	39.70	1.001	1.099	.50	.291
	60	14.23	.07027	59.41	.995	1.140	.75	.263
	80	10.70	.09347	79.12	.983	1.182	.99	.236
	100	8.604	.1162	99.06	.970	1.199	1.22	.211
	200	4.524	.2210	201.0	.860	1.223	2.05	.114
	300	3.271	.3058	313.1	.720	1.117	2.32	.043
	400	2.693	.3713	441.5	.628	.994	2.33	−.002
	500	2.360	.4238	591.8	.550	.880	2.27	−.031
	600	2.146	.4659	768.9	.500	.786	2.22	−.051
	800	1.880	.5318	1226	.417	.660	2.13	−.071
	1000	1.717	.5823	1861	.387	.580	2.06	−.080
	1100	1.654	.6047	2265	.387	.554	2.03	−.082
	1200	1.601	.6248	2737	.373	.534	1.98	−.083
50°	20	47.33	.02113	20.01	.998	1.037	.19	.248
	40	23.72	.04217	40.05	.992	1.070	.37	.228
	60	15.87	.06301	60.18	.984	1.099	.54	.208
	80	11.97	.08356	80.44	.975	1.125	.71	.188
	100	9.639	.1038	100.9	.961	1.138	.86	.169
	200	5.078	.1969	207.5	.845	1.151	1.46	.094
	300	3.640	.2747	325.4	.753	1.092	1.77	.038
	400	2.967	.3371	459.7	.670	.995	1.88	−.001
	500	2.572	.3888	615.4	.597	.895	1.90	−.003
	600	2.320	.4311	796.4	.540	.808	1.89	−.050
	800	2.010	.4974	1254	.456	.688	1.83	−.071
	1000	1.821	.5492	1878	.423	.611	1.78	−.080
	1100	1.748	.5720	2268	.418	.588	1.76	−.081
	1200	1.688	.5925	2719	.402	.566	1.74	−.083
100°	20	54.87	.01822	20.08	.995	1.023	.12	.162
	40	27.59	.03624	40.36	.987	1.041	.24	.149
	60	18.52	.05400	60.87	.975	1.052	.35	.138
	80	14.00	.07143	81.64	.965	1.064	.46	.126
	100	11.29	.08856	102.1	.953	1.078	.56	.114
	200	5.955	.1679	213.7	.881	1.078	1.01	.058
	300	4.243	.2357	337.0	.791	1.037	1.33	.020
	400	3.421	.2924	476.8	.716	.974	1.53	−.010
	500	2.928	.3416	636.3	.652	.896	1.63	−.035
	600	2.612	.3828	819.2	.601	.828	1.67	−.052
	800	2.225	.4494	1271	.515	.720	1.70	−.072
	1000	1.994	.5014	1867	.471	.649	1.77	−.080
	1100	1.909	.5239	2232	.463	.623	1.86	−.083
	1200	1.836	.5447	2649	.445	.597	1.98	−.085

TABLE I. (Cont'd.) *Some physical properties of compressed nitrogen derived from experimental data on compressibility.*

1	2	3	4	5	6	7	8	9
t	p	v	ρ	f	$-\frac{p}{v}\left(\frac{dv}{dp}\right)_T$	$\frac{T}{v}\left(\frac{dv}{dT}\right)_p$	ΔC_p	μ
°C	atm	cc/g	g/cc	atm			cal/mole°	°/atm
200°	20	69.82	.01432	20.15	.990	1.008	.07	.075
	40	35.21	.02840	40.62	.980	1.013	.14	.063
	60	23.68	.04223	61.45	.970	1.017	.21	.053
	80	17.93	.05578	82.63	.960	1.017	.27	.044
	100	14.48	.06905	104.2	.950	1.017	.33	.035
	200	7.637	.1309	218.8	.895	1.003	.59	.002
	300	5.389	.1856	346.3	.835	.970	.79	−.022
	400	4.287	.2333	489.0	.775	.923	.94	−.041
	500	3.622	.2761	649.4	.720	.875	1.05	−.056
	600	3.192	.3133	829.7	.675	.828	1.15	−.067
	800	2.655	.3767	1261	.601	.748	1.30	−.082
	1000	2.333	.4286	1804	.550	.672	1.41	−.092
	1100	2.217	.4511	2126	.537	.644	1.46	−.095
	1200	2.120	.4718	2485	.516	.610	1.51	−.098
300°	20	84.64	.01181	20.18	.990	1.003	.05	.010
	40	42.70	.02342	40.71	.980	1.003	.09	.002
	60	28.73	.03480	61.62	.970	.997	.14	−.006
	80	21.75	.04597	82.92	.960	.997	.18	−.012
	100	17.57	.05692	104.6	.951	.992	.22	−.018
	200	9.230	.1083	219.6	.907	.969	.39	−.042
	300	6.467	.1546	346.7	.858	.934	.53	−.058
	400	5.098	.1962	487.4	.808	.894	.64	−.071
	500	4.277	.2338	643.1	.762	.860	.73	−.077
	600	3.735	.2678	815.7	.722	.825	.81	−.084
	800	3.060	.3268	1218	.658	.751	.91	−.096
	1000	2.657	.3764	1709	.607	.694	.98	−.103
	1100	2.509	.3985	1994	.594	.665	1.00	−.105
	1200	2.387	.4190	2306	.570	.642	1.02	−.107
400°	20	99.39	.01006	20.17	.991	.976	.03	−.043
	40	50.12	.01995	40.69	.983	.996	.07	−.047
	60	33.71	.02967	61.56	.975	.990	.10	−.051
	80	25.50	.03921	82.81	.968	.983	.13	−.055
	100	20.59	.04858	104.4	.960	.983	.16	−.058
	200	10.76	.09289	218.6	.915	.949	.28	−.074
	300	7.502	.1333	343.6	.874	.916	.40	−.082
	400	5.879	.1701	480.6	.832	.889	.45	−.088
	500	4.912	.2036	630.7	.791	.855	.51	−.094
	600	4.263	.2346	795.1	.755	.828	.56	−.097
	800	3.456	.2893	1172	.700	.767	.63	−.105
	1000	2.976	.3360	1621	.650	.714	.67	−.110
	1100	2.798	.3574	1876	.635	.693	.69	−.112
	1200	2.653	.3770	2154	.612	.670	.70	−.113
500°	20	114.1	.008765	20.16	.991	.997	.02	−.068
	40	57.50	.01739	40.65	.985	.990	.04	−.072
	60	38.65	.02588	61.47	.975	.982	.06	−.076
	80	29.22	.03422	82.63	.969	.982	.08	−.080
	100	23.57	.04242	104.1	.960	.974	.09	−.082
	200	12.27	.08149	217.1	.921	.943	.17	−.093
	300	8.521	.1174	339.9	.885	.912	.24	−.098

TABLE I. *Some physical properties of compressed nitrogen derived from experimental data on compressibility.*

1	2	3	4	5	6	7	8	9
t	p	v	ρ	f	$-\frac{p}{v}\left(\frac{dv}{dp}\right)_T$	$\left(\frac{Tdv}{vdT}\right)_p$	ΔC_p	μ
°C	atm	cc/g	g/cc	atm			cal/mole°	°/atm
	400	6.651	.1504	473.3	.847	.889	.29	−.101
	500	5.530	.1808	618.2	.812	.858	.34	−.104
	600	4.783	.2091	775.6	.780	.835	.38	−.107
	800	3.848	.2599	1131	.728	.781	.44	−.112
	1000	3.290	.3039	1547	.682	.736	.48	−.115
	1100	3.084	.3242	1781	.665	.715	.49	−.116
	1200	2.916	.3429	2033	.644	.698	.50	−.116
600°	20	128.8	.007766	20.15	.992	.995	.01	−.083
	40	64.87	.01542	40.60	.985	.987	.03	−.087
	60	43.57	.02295	61.36	.976	.987	.04	−.090
	80	32.93	.03037	82.43	.969	.978	.05	−.093
	100	26.54	.03768	103.9	.961	.978	.06	−.095
	200	13.77	.07264	215.8	.926	.943	.11	−.101
	300	9.528	.1050	336.6	.891	.917	.15	−.106
	400	7.409	.1350	466.9	.860	.891	.19	−.110
	500	6.141	.1628	607.4	.829	.864	.23	−.114
	600	5.294	.1889	758.9	.800	.838	.26	−.116
	800	4.234	.2362	1097	.746	.792	.31	−.117
	1000	3.604	.2775	1488	.707	.753	.33	−.119
	1100	3.369	.2968	1705	.691	.737	.34	−.119
	1200	3.177	.3148	1938	.670	.720	.35	−.119

In most p-v-T determinations, the measurement of v is subject to greater error than those of p and T. The Δ and α curves are large scale deviation graphs of residuals of volume and they greatly magnify any error in v, so it is possible to smooth out any irregularities that may be in the original data, and put the adjustment where it belongs. Δ can probably be smoothed to within 0.005 cc/g; and since $(dv/d\Delta)_{p,T}=1/(2pv/RT-1)$, the smoothed specific volumes should be accurate to within 0.005 cc/g except in the extrapolated region and in the small range where $pv<RT$.

After considerable practice in laying a straight edge tangent at various points along a curve where the slopes are definitely known, it was found possible to estimate the slope at any point within half a percent, in trial after trial. It thus seemed that our various families of curves represented the most likely course of the p-v-T relations, and that the required derivatives could be gotten very accurately by mechanical means.

The tables published by Bartlett *et al.* show compressibility factors $pv/(pv)_s$ at the different pressures and temperatures. The denominator $(pv)_s$ is the value of pv at S.T.P. In order to find the specific volume of the gas it is required to know the volume of 1g at S.T.P. Birge gives 22414.1 cc as the volume of a mole of an ideal gas at S.T.P.

$pv/(pv)_s$ at 1 atm. is close to 1/1.00046. The gas used by Bartlett contained 0.9993 nitrogen and 0.0007 inert gas, presumably argon; the apparent molecular weight is therefore taken as 28.025. The volume adopted for 1

g at S.T.P. is accordingly $22414.1/1.00046 \times 28.025 = 799.42$ cc, and the value of RT at 0° is $22414.1/28.025 = 799.79$ cc atm./g. When one of Bartlett's compressibility factors is divided by the pressure and multiplied by 799.42 the result is the volume in cc of 1 g of the gas at the given temperature and pressure.

Some of the temperatures listed by Bartlett *et al.* were not integral; further a calibration of their thermocouple by the Bureau of Standards showed that the temperatures published[1] as −25°, −50°, −70° should have been −24.99°, −49.93°, −69.90°. We have made the slight alterations necessary to change his data to integral temperatures by a sensitive method of interpolation.[5]

At pressures below 100 atm. we used a compilation deduced by Dr. Bartlett from all the available data, chiefly from Amagat, the Reichsanstalt, and the cryogenic laboratory at Leiden, since Bartlett worked at the low pressures only to tie his results with those of previous observers. This compilation was kindly furnished us by Dr. Bartlett in a private communication. Our Δ vs. p isotherms give an easy and reliable means of interpolating to even pressures—one has only to read off Δ at any desired p and calculate v therefrom; accordingly we list results at 20, 40, 60, 80, 100 atm. rather than at the odd pressures one gets by converting meters of Hg to atm.

The Δ vs. p isotherms also give a reliable method of extrapolating to higher pressure; since the original ten isotherms constitute a family of curves, one can not go far wrong in extending them a reasonable distance. This was done and values of Δ were read at 1100 and 1200 atm. The specific volumes calculated at these pressures are probably not in error by 0.01 cc/g, judging from the regularity of the Δ vs. p isotherms and the values of $(dv/d\Delta)_{p,T}$ in this region. In the same way the Δ vs. T isobars give a means of extrapolating to temperatures higher than 400°. Values of Δ were read from the extended isobars at 500 and 600°. In order to estimate the error of the extrapolations, the Δ vs. T isobars were first plotted only to 300° and were extrapolated to 400° and the Δ read at that temperature. Later the observations at 400° were plotted and the smoothed Δ read. The two sets of specific volumes calculated from these two sets of Δ agreed closely, the probable error being 0.17 percent.

The value of these extrapolations, if they are reliable, must be considerable. To extend the experiments to 1200 atm. and 600° would entail enormous expense and labor. Calculations at 1100 atm. and 500° were included, because with them, at least, there should not be any risk. All the calculations in the extrapolated region tied on to the others satisfactorily, so it seems safe to assume that they were made successfully.

The final values of the physical properties at the twelve temperatures and fourteen pressures are shown in the table, or in the figures. Their preparation and implications will now be discussed.

Column 3 shows the specific volumes, which were calculated from the adjusted values of Δ through Eq. (1). The densities in column 4 are the reciprocals of the specific volumes.

The fugacities in column 5 were computed from the smoothed values of α by Lewis and Randall's[8] graphical method.

In columns 6 and 7 the pressure and temperature coefficients of volume expansion are shown. The reason for listing $-(p/v)\ (dv/dp)_T$ and not $-(1/v)\ (dv/dp)_T$ is that the former is dimensionless, and this fact facilitates changing units. Thus if one wishes to get the pressure coefficients at 100° for pressures in meters Hg, one has only to plot the values in column 6 for the 100° isotherm against p in atmospheres, and then graduate the scale of abscissas in the new units of pressure; one can then read $-(p/v)\ (dv/dp)_T$ for any number of meters Hg. The ordinates need not be changed in any way because they are dimensionless. Another advantage is that we can see at a glance how far this coefficient departs from unity, which is the value it would have if the gas were perfect. $(T/v)\ (dv/dT)_p$ was listed for the same reasons. The pressure coefficients of column 6 were adjusted from determinations given by the pv vs. p, α vs. p, Δ vs. p, and Δ vs. ρ isotherms through Eqs. (5), (6), (7), (8); the temperature coefficients of column 7 were adjusted from determinations given by the α vs. T and Δ vs. T isobars through Eqs. (3) and (4). The unsmoothed values at any point determined by the different methods nearly always agreed closely; when they disagreed more than 1 percent even at the highest pressures we went back and reconsidered the curves. Particular care was given to the determinations of $(T/v)\ (dv/dT)_p$, because this derivative enters to the second power in the calculation of $C_p - C_v$ and because it is used to get $(d^2v/dT^2)_p$, which enters into the calculation of ΔC_p.

Probably the most important properties that result from these calculations are C_p and C_v. For this reason extreme care was exercised to obtain the greatest possible precision for ΔC_p, which is shown in column 8. This depends on $(d^2v/dT^2)_p$ through the thermodynamic equation

$$(dC_p/dp)_T = -T(d^2v/dT^2)_p, \tag{11}$$

which when integrated along an isotherm gives

$$C_p = C_p' + \int_{p'}^{p} -T(d^2v/dT^2)_p dp. \tag{12}$$

C_p' is the heat capacity at pressures p'. The $-T(d^2v/dT^2)_p$ vs. p isotherms are shown in Fig. 2. The area under a given isotherm between any two abscissas is the change in C_p between those abscissas. The values of ΔC_p obtained by Eq. (12) from the curves in Fig. 2 were smoothed with respect to temperature and pressure before being listed in column (8).

In drawing the curves of Fig. 2 it was necessary to know something about their course in the region $0 < p < 20$, since p' was 1 atm. In an extremely rarefied condition the gas would have some characteristics of a perfect gas. The question has been raised by the writers[9] whether $(d^2v/dT^2)_p$ and $(dC_p/dp)_T \to 0$ as $p \to 0$, as they would if the heat capacity of the actual gas at very low pres-

[8] Lewis and Randall, Thermodynamics, pp. 192 to 195, McGraw-Hill (1923).

[9] Deming and Miss Shupe, Phys. Rev. **37**, 220 (1931).

sure behaves like that of a perfect gas. For the calculations in this paper we have assumed that $(dC_p/dp)_T \neq 0$ at $p=0$, and for its value we have used, wherever it seemed feasible, the one given by the Beattie-Bridgeman equation of state with constants determined[4] from these same compressibility data. In Fig. 2 are shown the graphs of $-T(d^2v/dT^2)_p$ vs. p isotherms. The points are the averages of determinations made from the α vs. T and Δ vs. T isobars through Eqs. (3), (4), (9), (10). The curves given by Beattie's formula[6] are shown dashed and they are drawn as far as the equation of state might be expected to hold, namely, as far as the critical density. At 100, 200, 300, and 400° the dashed curves seem to be the best curves that could be drawn to the points shown.

The curves in Fig. 2 for 20, 50, and 100° are not quite flat from 20 to 100 atm. This is the range of pressure considered by Hoxton[10] in discussing the

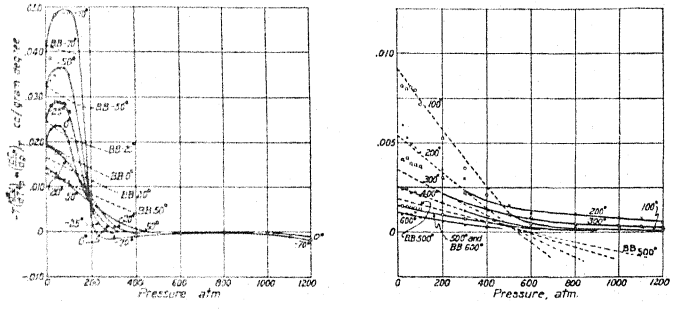

Fig. 2. $(dC_p/dp)_T$ vs. p isotherms. The full lines are drawn to the points determined from the p-v-T data. The dashed curves are given by the Beattie-Bridgeman equation of state, and are drawn as far as the critical density. Where only the dashed line is shown, the Beattie-Bridgeman values were accepted. To avoid confusion, some of the curves are not drawn at high pressures. The area under a particular curve between any two pressures is the change in heat capacity (in cc atm./g deg.) between these two pressures, at that temperature.

variation of the heat capacity of oxygen at 26° obtained in the experiments of Workman.[11] Hoxton speaks of a "change in c_p per atmosphere relative to its value at one atmosphere, the temperature being constant and taken as 26°C," and says that Workman found this quantity $\delta \equiv (dC_p/dp)_T/C_p'$ to be constant and equal to 0.00165 parts per atm. This implies that for oxygen the $(dC_p/dp)_T$ vs. p 26° isotherm is flat. There are reasons to expect C_p for nitrogen and oxygen to be similar in some ranges of temperature and pressure; e.g., their C_p values at one atmosphere for various temperatures are sometimes[12] expressed by the same formula, and Jakob's results for air are very similar to ours for nitrogen in some respects (*vide infra*). Our curves in Fig. 2 show that δ for nitrogen should decrease slightly with pressure. Taking 0.0178 and 0.0125 as the average ordinates for the 20° and 50° isotherms from

[10] L. G. Hoxton, Phys. Rev. **36**, 1091 (1930).
[11] E. J. Workman, Phys. Rev. **36**, 1183 (1930).
[12] E. D. Eastman, Specific Heats of Gases at High Temperatures, Bureau of Mines Techn. Paper 445 (1929).

20 to 100 atm. in Fig. 2, and interpolating linearly to 26°, δ turns out to be 0.00164 parts per atm. for nitrogen, very nearly what it is for oxygen.

In order to find C_p from Eq. (12) it is necessary to adopt values of C_p' at some pressure p' for the different temperatures. Several formulas have been devised to express C_p at 1 atm. as a function of T. As far as we know none of these is expected to extend to temperatures much below 20°. For C_p' at the low temperatures we finally accepted Brinkworth's[13] three values, which are 6.91, 6.92, 7.20 at 10, −78, −183°. A smooth curve through these points met Partington and Shilling's[14] formula very well at 30°, so we constructed a curve through Brinkworth's three points and points calculated from Partington and Shilling's formula above 30°, and from this curve read the values for C_p' that are listed below.

t°C	−70	−50	−25	0	20	50
C_p' (1 atm.)	6.92	6.91	6.91	6.91	6.91	6.92
t°C	100	200	300	400	500	600
C_p'	6.94	6.98	7.01	7.05	7.09	7.13

Eastman's formula would not join on to Brinkworth's points satisfactorily. At 200° Eastman's and Partington and Shilling's formulas differ by 0.1 cal/mole·deg. As the temperature increases the disparity widens even more, which shows that more precise direct calorimetric measurements of C_p at 1 atm. are needed.

It is difficult to estimate the accuracy of the ΔC_p, which are shown in column 8. The relation of the curves and points in Fig. 2 suggests that the precision of the calculations is greatest at the highest pressures. The calculated values of C_p agree well with the experimental values of Mackey and Krase.[15] They worked to 700 atm. at 30, 100, 125, 150° and to 800 atm. at 50°. Their points have been inserted in Fig. 4, so that observed and calculated values can be compared at a glance. The dashed curves represent calculated values obtained by interpolating along C_p vs. T isobars. At 50° the agreement is excellent through the entire range of experiment. At 30° the calculated values run below the experimental ones above 400 atm., and at 100, 125, 150° the calculated values lie above the experimental ones throughout the entire range. While the discrepancy is probably not greater anywhere than the experimental error of the calorimetric measurements, the trend of the calculated curves is definitely away from the experimental points above and below the 50° isotherm. An incorrect assumption for C_p at 1 atm. would result in a constant distance between an experimental and a calculated isotherm. A constant difference above, say, 100 atm. might mean that the corresponding isotherm in Fig. 2 is incorrectly drawn between 0 and 100 atm. But we are at a loss to account for the *constantly widening* gap between the calculated and experimental points at 30° above 350 atm., and for that at 100, 125, and 150.° The precision of the points in Fig. 2 does not diminish

[13] J. H. Brinkworth, Proc. Roy. Soc. **A111**, 124 (1926).
[14] Partington and Shilling, The Specific Heats of Gases, p. 145, D. van Nostrand (1924).
[15] B. H. Mackey and Norman W. Krase, J. Ind. and Eng. Chem. **22**, 1060 (1930).

with increasing pressure, and they could hardly be *consistently* in error by so great an amount as to account for the widening gaps. It thus seems impossible that the discrepancy can be laid to the calculations from the p-v-T data.

Witkowski's curves[16] for air go only to 100 atm., but it is interesting to note that the hump that appears in Fig. 3 at the lowest temperatures appears

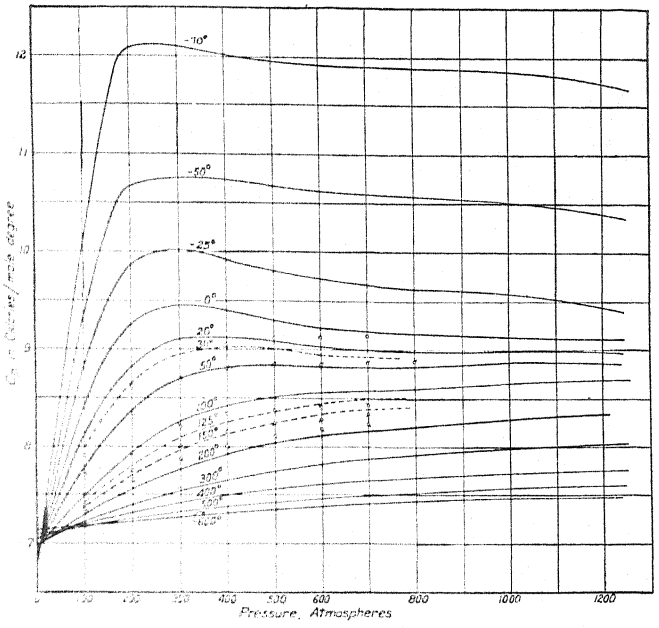

Fig. 3. Variation of C_p for nitrogen with pressure. Mackey and Krase's values ○ 30°, ♂ 50°, ♉ 100°, ♌ 125°, ♌ 150°.

in his curves for $-100°$ and lower temperatures; also that the pressure at which the hump appears decreases as the temperature decreases with both air and nitrogen.

Comparison with Jakob's[2] calculations of C_p for air show agreement within a few percent at 100 and 200° through 200 atm., and within a few percent at $-50°$ and 50 atm.

$$C_p - C_v = -T(dv/dT)_p^2/(dv/dp)_T. \tag{13}$$

Since the derivatives used in Eq. (13) have already been evaluated, $C_p - C_v$ can be calculated at each pressure and temperature. The results are shown in Fig. 4. In view of the precision claimed for the first derivatives, the error in $C_p - C_v$ should not exceed 0.3 percent, which is about as close as the graph can be read. It will be noticed that these curves all run toward the ordinate

[16] Witkowski, Phil. Mag. **42**, 1 (1896). These curves are shown in Partington and Shilling's book, p. 154.

R as p approaches zero. It was found that our values of $C_p - C_v$ for nitrogen agree closely with Jakob's for air; for example, our 100 atm. isobar almost

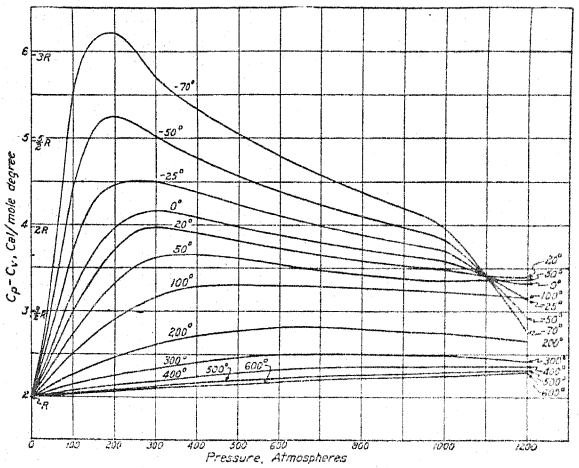

Fig. 4. The variation of $C_p - C_v$ for nitrogen with pressure at various temperatures.

coincides with his for 100 kg/cm² throughout his entire range of temperature. Our $C_p - C_v$ values were smoothed with respect to temperature and pressure.

The values of $C_p - C_v$ from which Fig. 4 was plotted were subtracted from the values of C_p in Fig. 3 to get the C_v graphed in Fig. 5. It will be seen that

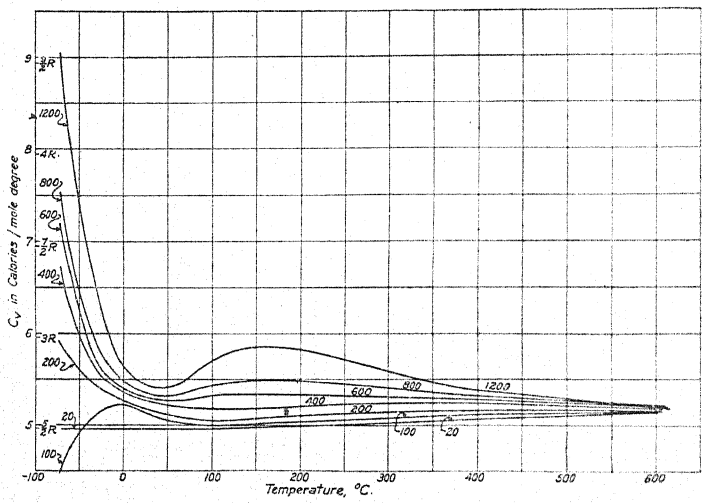

Fig. 5. Variation of C_v for nitrogen with temperature at constant pressure. The numbers on the isobars denote atmospheres.

C_v at 20 atm falls from 5.15 cal/mole·deg (2.59 R) at 600° to 2.50 R at 100°, and it stays there as the temperature is lowered to −70°. An increase in pres-

sure lowers C_v at $-70°$ until 100 atm. is reached; at 200 atm. and higher, C_v rises as the temperature falls below 20°, and the rise is steeper the higher the pressure. Above 400° it is evident that C_v is approaching the same value for all pressures; at 600° C_v is about 5.18 cal/mole·deg or 2.61 R from 20 to 1200 atm. Jakob's calculated values of c_v for air, when plotted, show the same behavior at low temperatures for his entire pressure range, which included 200 kg/cm². His 200 kg/cm² isobar would fall off faster than his 100 kg/cm², instead of rising like the 200 atm. isobar in Fig. 5; but 200 kg/cm² is at the end of his pressure range and he lays no claim for accuracy there, so it can only be conjectured how C_v for air compares with C_v for nitrogen above 100 atm. Various explanations of this behavior in Fig. 5 have been considered, but they will not be discussed here because we prefer to present results only.

The Joule-Thomson coefficient can be calculated from the equation

$$\mu C_p = T(dv/dT)_p - v \qquad (14)$$

by using the values already found for C_p and $(dv/dT)_p$. They are listed in column 9. The inversion temperatures for the various pressures are where

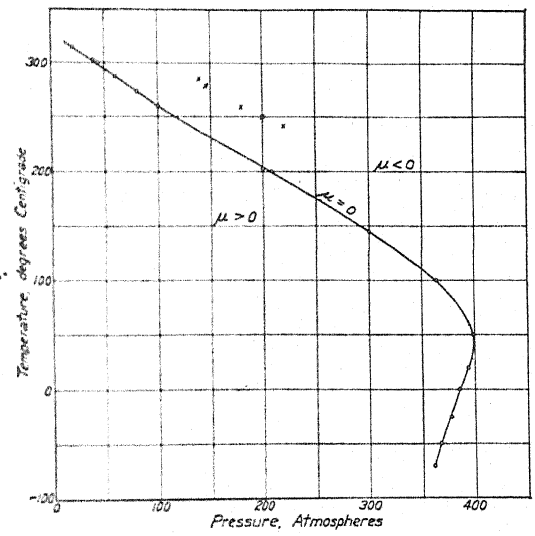

Fig. 6. Inversion curve for nitrogen. The points were read from the μ vs. T isobars and the μ vs. p isotherms. μ denotes Joule-Thomson coefficient $\mu=(dT/dp)_H$. x denotes Roebuck's inversion points for air.

the μ vs. T isobars cross the ordinate $\mu=0$, and the inversion pressures for the various temperatures are where the μ vs. p isotherms cross the ordinate $\mu=0$. The inversion curve, Fig. 6, is plotted from the inversion points so obtained. There are no existing data on the Joule-Thomson coefficient for nitrogen, so a comparison with observed values is not yet possible. Roebuck's[17] values for air give the inversion points marked x on Fig. 6.

[17] Roebuck, Proc. Amer. Acad. Arts Sci. **60**, 535 (1925); **64**, 314 (1930) International Critical Tables 5, 144, first edition.

If the results derived in the present paper are a step toward the determination of the heat capacity and other physical properties of gases, the importance of compressibility data must be recognized. The calculations in this paper were made by two people in nine weeks time. Compressibility data on a number of gases are now available; their physical properties will be determined as rapidly as possible and will appear in subsequent papers. The method will doubtless undergo changes that will result in greater precision.

This work was undertaken at the suggestion of Dr. Edward P. Bartlett, formerly of this laboratory. We have enjoyed the encouragement and willing cooperation from him and the staff at this laboratory throughout the course of the work. We wish also to acknowledge indebtedness to Professor James A. Beattie of the Massachusetts Institute of Technology for his interest in the work, especially in the heat capacity at low pressures, and to Professor L. G. Hoxton of the University of Virginia for his encouragement and many helpful suggestions.

Note added in proof, February 16, 1931: Some results on C_p for nitrogen to be read by E. J. Workman at the New York meeting of the American Physical Society on February 26, 1931 make possible further comparison between the present calculations and experimentally obtained results. Workman has obtained C_p:C_p' at 30, 60, 90, 130 kg/cm² at 26° and 60°C. C_p read from the original tracing of Fig. 3 at these points gives the following comparison. *W* denotes Workman, *D* denotes Deming and Miss Shupe. 6.916 and 6.926 cal/mole deg were adopted for C_p' at 26° and 60°.

	p kg/cm²	atm.	26°C C_p:C_p'	60°C C_p:C_p'
W	30	31	1.0443	1.0324
D			1.05	1.04
W	60	62	1.0900	1.0665
D			1.10	1.07
W	90	93	1.1332	1.0990
D			1.15	1.11
W	130	134.5	1.1863	1.1395
D			1.21	1.15

LETTERS TO THE EDITOR

Prompt publication of brief reports of important discoveries in physics may be secured by addressing them to this department. Closing dates for this department are, for the first issue of the month, the twenty-eighth of the preceding month; for the second issue, the thirteenth of the month. The Board of Editors does not hold itself responsible for the opinions expressed by the correspondents.

The Thermodynamic Treatment of Chemical Equilibria in Systems Composed of Real Gases. II. A Relation for the Heat of Reaction Applied to the Ammonia Synthesis Reaction. The Energy and Entropy Constants of Ammonia. A Correction.

In a paper having the above title, published in the Physical Review **36**, 1008 (1930) the numerical value given for the quantity $\Sigma(\nu_i s_{0i}')$ has been found incorrect. Eq. (13) should read: $\Sigma(\nu_i s_{0i}') = -22.9850$. The entropy constant (s_{0i}') for ammonia appearing in Table III should be -22.9809. This requires several corrections in Table IV, which when revised is as follows. No changes are necessary in part I, Phys. Rev. **36**, 743 (1930), or part III, Jour. Am. Chem. Soc. **52**, 4239 (1930), of the series of three papers.

TABLE IV. *Values of several thermodynamic quantities for one mole of hydrogen, nitrogen and ammonia at 0°C and 1 atmosphere; and the increase Δ of these quantities when one mole of ammonia is formed from its elements all reactants and products being at 0° and 1 atmosphere. Units: 15°-calories, degrees Centigrade, moles.*

	Hydrogen	Nitrogen	Ammonia	Δ
U	0	0	−10078.0	−10078
H	543.0	542.4	−9542.9	−10628.5
S	0	0	−23.0538	−23.054
F_{VT}	0	0	−3781.3	−3781
F_{pT}	543.0	542.4	−3246.2	−4332
pV	542.96	542.39	535.14	−550.50

L. J. GILLESPIE
J. A. BEATTIE
Massachusetts Institute of Technology,
Cambridge, Massachusetts,
February 10, 1931.

Reflection of High Velocity Electrons from Solid Surfaces

Bothe[1] has derived an expression for the angular distribution of electrons which are transmitted by matter and which have penetrated sufficient thickness to become completely diffused, and finds fair agreement with experimental work done with β-particles. It becomes of interest[2] to know the angular distribution of electrons emitted backwards from solid surfaces, since it is possible that the two distributions are similar. This question, together with the determination of absolute values of reflection, was studied during an investigation on scattering of high velocity electrons by thin foils.

If we call the half-angle of the solid cone about the normal to the surface, θ_1, and the half-angle subtended by the opening through which the electrons emerge, θ_2, then experimentally all electrons, due to an originally homogeneous beam, emitted between these two cones are collected in a field-free space. The ratio of this number to the total number incident on the surface will be called ρ'. A small correction (less than 2 percent) may be made to ρ' for the electrons which come back between θ_2 and 0°. The corrected value, ρ, is then plotted as a function of θ. The following elements have been tested: Pb, Sn, Cu, Al, C, Be. The curve showing the variation of ρ with angle, for the heavier elements and voltages above 100,000, agrees with the curve $\rho_0 \sin^2\theta$ to within 1 percent, where ρ_0 is the

[1] W. Bothe, Zeits. f. Physik **54**, 161 (1929).

value of ρ at $\theta=90°$. The intensity at any angle is therefore given by the simple cosine law. Small deviations from this law are found for the lighter elements such as C and Be, especially at voltages below 70,000. More investigations are being conducted. Bothe's expression for the angular distribution of transmitted electrons which are completely diffused, deviates from the distribution found experimentally for electrons emitted in a backward direction, by about 5 percent at $\theta=45°$, both curves coinciding at 0° and 90°.

For beryllium ρ_0, or the "rediffusion constant" of Webster,[2] is found to be 0.0291 for 70,000 volt electrons and decreases to 0.0248 at 130,000 volts, instead of being 0.043 which he deduces. These values include all electrons emitted. In the case of beryllium, only 2 percent of the emitted electrons have energies below 2,000 volts.

A decrease in ρ is found for all the lighter elements with increase of voltage. In the range between 45,000 and 130,000 volts, this decrease amounts to 7 percent in the case of aluminum, becomes 0.6 percent for tin and less than 0.1 percent for lead.

H. VICTOR NEHER

Department of Physics,
California Institute of Technology,
February 7, 1931.

[2] D. L. Webster, Phys. Rev. **37**, 119 (1931).

The Extrapolation of Atomic Structure Factor Curves

In a recent[1] note under the above title, D. K. Froman has derived an extrapolation formula for atomic structure factors on the basis of "electron distributions indicated by the wave equation." Although it is certainly true that quantum mechanics can be taken as the basis for deriving such formulas, it is of interest to note that Froman's result can be obtained without any appeal to a specific theory of the electron distribution causing the atomic structure factor. We have in mind simply the fact that repeated integrations-by-parts of Froman's Eq. (2) which defines the structure factor of the nth order gives us at once the result that:

$$F_n=\sum_k a_{kn}\left(\frac{D}{n}\right)^{2k} \quad =\sum_k a_{kn}\left(\frac{2\sin\theta}{\lambda}\right)^{-2k}$$

where:

$$a_{kn}=\frac{(-1)^k}{(2\pi)2k}\left[\left(\frac{U(r)}{r}\right)^{(2k-2)}\cos\frac{2\pi nr}{D}\right]_{r=0}^{r=D/2},$$

the notation being that used by Froman.

The first equation is clearly identical with Froman's Eq. (8), and his Eq. (12) can be derived similarly. It is thus seen that Froman's extrapolation formula is the general consequence of the definition of the structure factor, being in fact, the asymptotic expansion for F_n, and is independent of any wave-mechanical interpretation of the electron distribution.

[1] D. K. Froman, Phys. Rev. **36**, 1339 (1930).

MORRIS MUSKAT

Gulf Research Laboratory,
Pittsburgh, Pennsylvania
February 17, 1931.

Nuclear Spin of Aluminum

The recent letter by J. H. Bartlett, Jr. on nuclear spin has been read with a great deal of interest, and in view of the importance of the subject the writers would like to point out an apparent discrepancy. After a careful survey of the work done on the hyperfine structure of the lines of various elements, the writers had reached the same general conclusions as Bartlett. It was disconcerting, however, to find that Janicki (Ann. **29**, 833, (1909)) and Wali-Mohammed (Astrophys. J. **39**, 185, (1914)) had both photographed the Al lines 3944A and 3961A using Lummer-Gehrcke plates and found them "very sharp and simple."

Recently, while studying different light sources for the purpose of finding the most suitable source for use in analyzing the hyperfine structure nitrogen lines, occasion presented itself for photographing the following Al lines in a Schüler hollow cathode discharge cooled by liquid air.

A Fabry-Perot interferometer, with fixed etalons, was used in conjunction with a Zeiss triple prism spectrograph for analyzing the lines. Several exposures, made under different conditions and with different etalons, were made on each line. Mirrors having a reflection coefficient of 90 percent or greater were used, so that the resolving power of the interferometer was about 10^6. Under these conditions all four Al lines were found to be sharp and lacking in structure.

Typical microphotometer curves of these

lines are shown in Fig. 1. From a careful study of all the curves obtained from various Al lines, and from the lines of various other elements in which structure is clearly present, it is estimated that if these Al lines have structure the average separation is not greater than 0.006A.

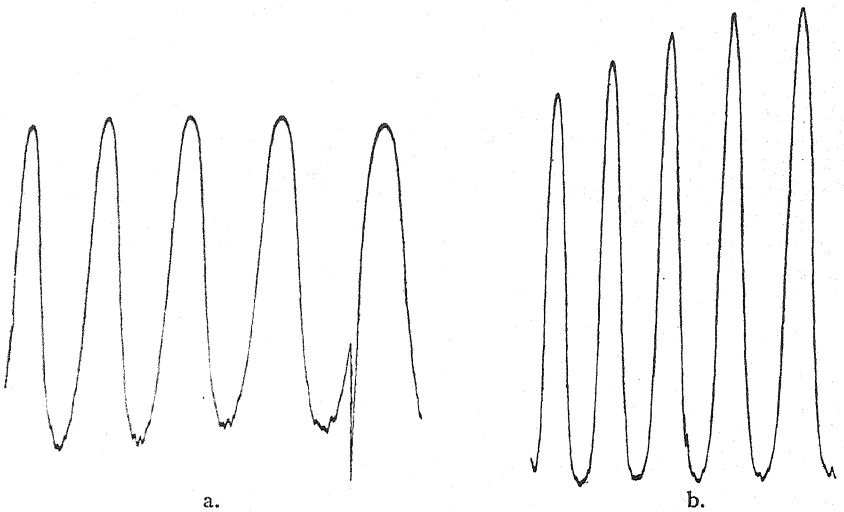

a. b.

Fig. 1. Microphotometer curves of interferometer patterns. (a) Al I λ3961. (b) Al II λ4663.

As is shown in Table I, the lines 3944A and 3961A constitute the first member of the sharp series of Al I and result from an electron transition s to p. According to other hyperfine structure data (White, Phys. Rev. **35**, 1146 (1930) *et al.*) such a transition should give wide hyperfine structure separations. The line 4663A results from a p to d electron transition and although this would probably not show as wide a hyperfine structure as the s to p transition, it should be observable if the nuclear moment of Al was different from zero.

Since Aston (Phil. Mag. **49**, 934 (1923)) reports Al to have only one isotope at 27, the present data indicate that Al in no way fits any of the proposed schemes of the building-up process in the nucleus or the theories of nuclear moments. For, if as Heitler and Herzberg (Naturwiss. **17**, 673 (1929)) assume, the electron in the nucleus loses its power to determine what the statistics of the nucleus shall be, then the 27 protons determine the nuclear moment and an odd number of $(1/2)\cdot(h/2\pi)$ units would be expected. If the electron does not lose this power, the nuclear moment would be determined by the 27 protons plus 14 electrons, and one would still expect an odd number of $(1/2)\cdot(h/2\pi)$ units for the nuclear spin. But the available data indicate that this moment is zero.

Recent data on the value of the nuclear moment for nitrogen still leave some doubt as to what the real value is. Al and N may, then, be considered as disturbing exceptions to present theories of nuclear structure.

TABLE I. *Aluminum arc and spark lines which show no hyperfine structure.*

	λ	Classification	Total line width
Al I	3944.025	$3p^2P_{\frac{1}{2}}-4s^2S_{\frac{1}{2}}$	0.032A
Al I	3961.537	$3p^2P_{1\frac{1}{2}}-4s^2S_{\frac{1}{2}}$	0.029A
Al II	4226.812	$3s4d^3D_3-3s9f^3F_4$	0.034A
Al II	4663.054	$3s3d^1D_1-3s4p^1P_1$	0.037A

We are indebted to Mr. A. Rosenblum for preparing the microphotometer curves used in this analysis.

R. C. GIBBS
P. G. KRUGER

Physical Laboratory,
Cornell University,
February 21, 1931.

What Requirements must the Schrödinger ψ-Function Satisfy?

In a recent paper with the above title, G. Jaffé[1] contends that the proper solutions of the wave equation must be everywhere finite and continuous, and that the condition of quadratic integrability is not enough. In support of the latter point he shows that a solution for the angle part of the wave function of the central field problem for the case $m=0$, may be obtained for non-integral values of 1: this solution is quadratically integrable but has a logarithmic singularity. Since this would result in a continuum of spectroscopic terms quite unknown in experiment, Jaffé concludes that the condition of finiteness and continuity is required.

The authors are presenting a paper in which this question is of central importance and therefore find it advisable to point out that Jaffé's conclusion is not at all necessary and in fact is surely too stringent for many problems in atomic structure.

The reason a solution such as that mentioned by Jaffé is possible, is that when the wave equation is expressed in polar coordinates some of the coefficients have singularities not brought in by the potential energy. If the equation is written in Cartesian coordinates there are no singularities except those of the potential energy function. We see then that the singularities are introduced into the equation by the transformation from Cartesian to polar coordinates. This is substantiated by the fact that at the singular points in question the Jacobian of the transformation from Cartesian to polar coordinates vanishes, showing that the transformation at these points is not legitimate.

Of all possible coordinate systems the Cartesian is to be preferred in the wave equation because of its simplicity, homogeneity (volume element constant), and isotropy (line element diagonal with constant coefficients). From the form of the equation we are led to expect that a proper wave function should have no singularities except at those of the potential function. Hence in the case of the hydrogen problem a quadratically integrable singularity is permissible at the origin, but not elsewhere.

Without giving up the condition of quadratic integrability as being sufficient restriction on the wave function, one can rule out Jaffé's example for the following reason: The wave equation is not the best starting point for the theory. The fundamental thing is the integral

$$J = \int \left(\frac{h^2}{4\pi^2} T\left(q, \frac{\partial \psi}{\partial q}\right) + V\psi^2 \right) d\tau$$

where $T(q, p)$ is the classical expression for kinetic energy in terms of coordinates and momenta and V is the potential energy.

The function ψ is determined by the condition that J be a minimum. Its minimal values are the energy levels. The Euler equation corresponding to this variational integral is the wave equation. However, satisfying the wave equation is necessary but not sufficient to make this integral a minimum.[2] From the wave equation $H\psi = E\psi$, we can obtain the integral form $\int \bar{\psi}_n H \psi_n d\tau = E_n$ which in Cartesian coordinates can be shown to be the equivalent of J. This comes from the fact that the condition of quadratic integrability is sufficient to insure the vanishing of the surface integral by which J differs from $\int \bar{\psi} H \psi d\tau$. In polar coordinates the two need not be equal when singularities arise at the boundaries.

In the case which Jaffé mentions, if l is not an integer, not only is J not a minimum but it is *infinite* and therefore the solutions for this case can have no physical significance.

In general if the wave function has a singularity the energy integral will be infinite except possibly if the potential function has a singularity in the same place. The ultimate criterion then for an acceptable wave function is that J be finite (and a minimum). As a rough working rule we may demand of the function that it be integrable in the square and that it be finite and continuous wherever the potential energy is finite. If we introduce singularities (physically non-existent) in the potential energy we must be prepared to put up with singularities in the wave function at those points. When, in the future, we get a deep enough insight into the nature of the physical problems so that we can replace the singular values of the potential energy by their true finite values, the singularities of the wave functions will also be removed. But until then we must be content with results which differ from the facts to the same degree as do the assumptions from which we start.

R. M. Langer
N. Rosen
Massachusetts Institute of Technology,
February 23, 1931.

[1] Jaffé, Zeits. f. Physik **66**, 770 (1931).

[2] Courant-Hilbert, Methoden der Math. Phys. I, p. 165.

BOOK REVIEWS

Magnetic Phenomena. SAMUEL ROBINSON WILLIAMS. Pp. xxii+230. 150 figures. McGraw-Hill, New York, 1931. Price $3.00.

Professor Williams has been deeply interested in magnetic phenomena for many years and has already contributed much to their study, both personally and by stimulating others to independent research. His attempt in the present monograph to enlist additional recruits for the attack upon magnetic strongholds is therefore of especial interest. He has decided that the college undergraduate should be approached and now offers him a text-book of an unusual kind in which almost undue emphasis is laid upon the unfinished and provisional character of much of the available information. His choice of audience naturally limits him somewhat both in the total content of his book and in the mode of presentation. He has cut down the mathematics required of the reader to such an extent that he often loses desirable rigor and even, in several places, falls into confusing errors. It would have been much better, in the opinion of this reviewer, to expect a good working knowledge of the calculus in all cases.

Under one or other of the chapter headings "magneto-magnetics, magneto-mechanics, magneto-acoustics, magneto-electrics, magneto-thermics, magneto-optics, cosmical magnetism, magnetic theories and experimental facts" will be found some account, however brief, of almost everything known about magnetism. The topics selected for most detailed comment are, as they should be, those with which the author is personally most familiar. The bibliography, especially in these selected parts, is unusually rich in the earlier references. In other places the treatment is much more sketchy, and some omissions from the index (e.g. crystal!), make it hard to discover how much of the most recent work has been covered. Some of the omissions are surprizing. The most careful search, after a critical reading of the entire text, fails to disclose any reference to the great electromagnet at Bellevue or to the magneto-caloric effect and related phenomena. The postponement of magneto-crystallic effects to some future treatise also seems most unfortunate.

The publisher's part of the work is well done, unless the rather numerous misprints in the text and disagreements in lettering between figures and text are attributable to his staff.

The reviewer has tried to convey the mixture of pleasure and disappointment which affected him during his review. A reader to whom more of the phenomena are wholly new would probably derive a larger proportion of pleasure and, perhaps, be incited to straighten things out for himself. This, of course, is just what the author wishes.

L. W. MCKEEHAN

Gmelin's Handbuch der Anorganischen Chemie. 8 Auflage; herausgegeben von der Deutschen Chemischen Gesellschaft; System Nummer 59. Eisen; Teil A, Lieferung 3: Pp. 313–586. Verlag Chemie G. m. b. H. Berlin, 1930, price RM 40 (subscription price RM 32).

The above volume is of a more technical character than most of the other of Gmelin's Handbooks; a complete literature review with bibliography on the passivity of pure and technical iron (written by Dr. E. Liebreich), its chemical behavior and its corrosion (by Dr. M. Rudolph, Dr. A. Eisner and Dr. A. Kotowski) and its metallurgy (Prof. R. Durrer, Dr. H. Lueb and Dr. M. W. Neufeld) are given. The material has been collected in a non-critical way, thus giving the book a compilatory character as in the other issues of the same edition. It seems to the reviewer that with the five previous volumes the present one comprises the most complete monograph we have at present on the physical, chemical and metallurgical properties of iron and it forms a worthy addition to the Gmelin series.

I. M. KOLTHOFF

The Quantum Theory. FRITZ REICHE. Translated by H. S. Hatfield and Henry L. Brose. Pp. viii+218. Figs. 15. E. P. Dutton and Company, Inc., New York, 1931. Price, $2.10.

The first English edition of this book, dated 1922, was a translation of the German original the preface of which bears the date October 1920. To the present edition the translators have

contributed a chapter of twenty-four pages which together with nine pages of notes and references covers developments since 1920. The result is that nine of the ten chapters are written from the point of view of ten or more years ago, while the tenth, covering developments since that date, must, because of its brevity, devote to any important topic an amount of space "less than ϵ" in the sense in which mathematicians often use that phrase. What constituted a clear exposition in the light of the day when it was written will, in many instances, prove misleading for the student of today, while the last chapter will surely be almost unintelligible to one whose knowledge of the subject is based upon reading the first nine.

A. ELLETT

Photoelectric Cells and Their Applications. A discussion at a joint meeting of the Physical and Optical Societies (of London), June 4 and 5, 1930. Editor, JOHN S. ANDERSON. Published by the Physical and Optical Societies, London, 1930. Price, 12 s 6 d.

Physicists and engineers in general will welcome a condensed account of some of the recent developments in the technique of manufacturing and using photoelectric cells. The present volume is a compilation of 31 papers on this subject presented at the London symposium, and includes a report of the interesting and lively discussion which followed. While such a book may lack the unity and completeness of a treatise by an individual author, it has the advantage of allowing the presentation of many specialized problems by those most familiar with them, and of bringing out many different, and sometimes conflicting, points of view.

Following an opening paper by H. S. Allen on the early history of photoelectric cells, there is a paper by N. R. Campbell discussing Fowler's recent wave-mechanical theory of the selective photoelectric effect. There are then seven papers dealing with the manufacture, characteristics, and uses of various types of modern cells. The papers by P. Selenyi on the sodium cell, by L. J. Davies and H. R. Ruff on the thin-film caesium cell, and by T. W. Case on the barium cell are of especial interest, since they give considerable data on the characteristics of these cells. The five papers on the technique of measuring and amplifying photoelectric currents will be of particular value to those interested in photoelectric sound reproduction. A number of problems connected with the distortionless amplification of rapidly varying photo-currents are discussed in detail. Many physicists will be disappointed to find no discussion of the methods of amplifying *unvarying* currents.

We find next a series of ten papers covering the fields of photoelectric photometry, microphotometry, and spectrophotometry. K. S. Gibson contributes a particularly comprehensive review of modern methods in spectrophotometry, with an excellent critical survey of the advantages and limitations of photoelectric cells in this field. Finally, there are two papers on biological applications and four on selenium cells. In one of the latter H. Thirring presents considerable data to support the contention that the "frequency response" of well-designed selenium cells is sufficiently good, contrary to common belief, to make them superior to gas-filled alkali metal cells for sound reproduction. In the discussion reported at the end of the volume one finds a heated argument over this point, with the selenium cell adherents somewhat outnumbered, but not outdone.

On the whole the volume contains a surprising amount of useful information. It has been carefully edited and printed, though one feels that it is of sufficient worth to have merited a better binding.

L. A. DUBRIDGE

The New Physics. Third English edition. ARTHUR HAAS. Pp. 172, figs. 7. E. P. Dutton and Co., New York, 1930. Price $2.15.

This small volume contains seven lectures, in which the author endeavors to "describe the picture of Nature revealed by modern physics in the most intelligible manner possible, and without the use of any mathematical formulae". The subjects treated are the electromagnetic theory of light, molecular statistics, electron theory, quantum theory, the theory of the chemical elements, relativity and gravitation, and quantum mechanics. The lecture last mentioned appears for the first time in this edition. Several others have been revised.

The style is simple and direct. The educated layman will be able to read the book with understanding. The professional physicist will find it too elementary to warrant more than a cursory scanning of its pages.

H. H. MARVIN

Laboratory Manual of Physics. C. M. KILBY. Pp. 129, figs. 75. D. Van Nostrand Co., New York, 1930. Price, $1.75.

The manual contains descriptions of sixty-five experiments which can, for the most part be performed with inexpensive apparatus. The several fields of physics all are well represented. The experiments are described in the briefest form possible, adequate for the experiment, but not calculated to lead the thoughtful student beyond the immediate result sought. A tabular form for observations and results is given, in every case. The illustrations are well drawn, with the exception of the electrical wiring diagrams. The manual is adapted fairly well to the needs of students who have not had physics in the high school.

H. H. MARVIN

Cours D'Optique. G. BRUHAT. Pp. 756, figs. 657. Masson and Cie, Paris, 1931. Price, 100 francs.

This advanced text-book in optics begins with the usual introductory survey of the fundamental principles. The following two sections give an excellent treatment of interference and diffraction with many good figures and numerical illustrations. Experimental applications receive a good deal of attention. Part four deals with polarization and the electromagnetic theory of light. Here the classical ideas on vibrations of electrons due to electromagnetic waves are repeated without apology. Part five, on the optics of anisotropic and disymmetric media, is especially complete. In particular, experimental technique is not overlooked. Part six, on spectroscopy, is merely a descriptive resumé using the language of the Bohr-Sommerfeld theory. The treatment is carried no farther than in the early editions of Sommerfeld's "Atombau." Prominent among the omissions are: the theory of optical instruments, thermal radiation, and the optics of moving media. As an advanced text, dated 1931, it is disappointing in its conservatism, although as a treatise on classical optics and its experimental application, it is one of the very best.

J. VALASEK

A Treatise on Physical Chemistry. A Cooperative Effort by a Group of Physical Chemists. Edited by HUGH S. TAYLOR. Second edition, 1931. D. Van Nostrand Company, Inc., New York. Two volumes. Vol. I, XV+852+48 pp. (indices); Vol. II, XII+865+48 pp. (indices). Price $15.00 (not sold separately).

The scope and authority of this outstanding cooperative work on physical chemistry are evident from the list of chapter headings and authors. I, The Atomic Concept of Matter, Hugh S. Taylor; II, The Energetics of Chemical Change, Hugh S. Taylor; III, The Kinetic Theory of Gases and Liquids, K. F. Herzfeld and Hugh M. Smallwood; IV, Imperfect Gases and the Liquid State, K. F. Herzfeld and Hugh M. Smallwood; V, The Solid State of Aggregation, Robert N. Pease; VI, Thermochemistry, A. L. Marshall; VII, The Laws of Dilute Solutions, J. C. W. Frazer; VIII, Homogeneous Equilibria, Graham Edgar; IX, Heterogeneous Equilibrium, Arthur E. Hill; X, The Measurement of Electrical Energy, G. A. Hulett; XI, Conductance, Ionization and Ionic Equilibria, J. R. Partington; XII, The Electrochemistry of Solutions, Herbert S. Harned; XIII, Electrometric Methods in Analytical Chemistry, N. Howell Furman; XIV, Reaction Velocity in Homogeneous Systems, Francis Owen Rice; XV, Reaction Velocity in Heterogeneous Systems, Hugh S. Taylor; XVI, Quantum Theory and Atomic Structure, Saul Dushman; XVII, The Third Law of Thermodynamics and the Calculation of Chemical Constants, Worth H. Rodebush; and in part by T. Jefferson Webb; XVIII, Photochemistry, Hugh S. Taylor; XIX, Infrared Radiation in Chemical Processes, H. Austin Taylor; XX, Colloids, Elmer O. Kraemer; XXI, Radioactivity, S. C. Lind.

Since the publication of the first edition in 1924 important advances have been made in most of the fields covered by the treatise. This has necessitated the more or less thorough re-

vision of chapters VI, XI, XII, XIII, XIV, XV, XVII, XVIII, XIX, and XXI. The important chapters II, IV, XVI, and XX have been written anew, three of them by authors other than those of the former edition. The remaining chapters, reprinted practically unchanged from the first edition, deal with topics in which little advance has been made in recent years, with one exception, discussed below.

In chapters III and IV, 175 pages, an admirable treatment of the kinetic theory of gases and liquids has been presented by Herzfeld and Smallwood. Dushman has given in the 277 pages of chapter XVI a well-balanced introduction to quantum theory and atomic structure which in my opinion has no rival for the purpose for which it was intended, to provide the student in physical chemistry, who usually has a none too extensive preparatory training in mathematics and theoretical physics, with a working knowledge of the fundamental facts of this field. The recent developments in quantum mechanics have not been grafted onto the article written in 1924; instead they have been thoroughly incorporated in the chapter, which has been completely rewritten from the new point of view provided by them.

The careful selection of mathematical methods adapted to the capacity of the readers for whom the treatise is primarily intended, physical chemists and students of physical chemistry, shown in these chapters and in most of the others is not always evident. In chapter XVII the condensed treatment of statistical mechanics and its application to entropy calculations makes difficult reading. This fault is more strikingly shown in the treatment of the Bose-Einstein and Fermi-Dirac statistics, consisting of page after page of equations, with interspersed remarks which are hardly clarifying, such as "—if it is assumed that cells, but not molecules have identity, then the number of ways in which this association can be realized is—" A modern treatment of this topic, following a sound and sufficiently extensive discussion of statistical mechanics, could be made understandable. This chapter also suffers from the emphasis laid on the unnecessary and often confusing chemical constant.

The fourth new chapter, XX, provides an excellent, thorough, and up-to-date discussion of colloids.

Structural chemistry lies within the scope of this treatise, as is recognized in the inclusion of a long chapter on atomic structure. And yet the important field of the structure of solids, in which great advances have been made in recent years, is dismissed in a chapter of 30 pages, reprinted practcally without change from the 1924 edition, and in which there are almost as many incorrect as correct statements. Thus to the sodium chloride arrangement is attributed a simple cubic lattice, and to caesium chloride a body-centered lattice. The fundamental cell of the hexagonal close-packed arrangement is said to be a prism with an equilateral triangle as its base. The very simple zinc oxide arrangement is described as "difficult to visualize or to draw." The carbon rings in naphthalene and anthracene are said to be staggered. Half a page, including a figure, is devoted to a description of the staggered-plane graphite structure, although the correct structure was discovered in 1924. Despite the fact that the structure of hexamethylenetetramine had been determined before 1924 and those of hexamethylbenzene, nonacosane, urea, and others since then, the discussion of organic compounds is restricted to Bragg's early incorrect work on naphthalene and anthracene and Astbury's inconclusive study of tartaric acid.

Band spectra and results derived from them, which are becoming more and more important to physical chemistry, are mentioned briefly in several chapters. Some of the discussion is not calculated to provide much enlightenment to the student; in chapter XIX it is stated that the molecule HI is not ionic, but instead "forces exist between the two nuclei." A unified and more extensive treatment of band spectra would be a desirable addition to the book.

The revisions and additions, which increase the treatise 36 percent in length over the first edition, change it from a valuable to a more valuable reference book for the physical chemist and student of physical chemistry. Selected chapters might be successfully used as texts for courses in physical chemistry; in any case the treatise should admirably supplement the more elementary and condensed texts customarily used, inculcating the research viewpoint and indicating the lines of work in which research is being actively carried on. The physicist should find the treatise useful when he becomes involved in work bordering on physical chemistry.

LINUS PAULING

Second Series *March 15, 1931* *Vol. 37, No. 6*

THE
PHYSICAL REVIEW

THEORY OF HYPERFINE STRUCTURE SEPARATIONS*

By S. Goudsmit
Department of Physics, University of Michigan

(Received February 4, 1931)

Abstract

Expressions are derived for the hyperfine structure separations of the levels of complicated electron configurations in different types of coupling. The few available experimental data are in distinct disagreement with the theoretical calculations. This undoubtedly means that our present knowledge of the interaction with nuclear spin is incomplete. The expressions in this article are derived by the well-known method of the invariance of energy sums.

1. Description of Method

Formulae for the interaction energy of a nuclear magnetic moment with a single electron outside of closed electron groups have been given by Fermi,[1] Casimir,[2] Hargreaves,[3] and Breit.[4] If more than one electron is present besides complete groups the formulae are only known for a special case. They have been derived when only s-electrons interact appreciably with the nuclear magnetism and the interaction of other electrons may be neglected.[5] This paper is a first attempt to treat the general case of the interaction of several electrons with the nuclear magnetic moment.

The method followed in this paper is very analogous to the one used to derive expressions for multiplet separations.[6] It therefore is the well-known method of the energy sums, which originally goes back to work of Pauli[7] and which found its representation in modern quantum mechanics in an important article by Slater.[8] We will follow closely Slater's procedure, as it shows especially clearly the restrictions of the validity of the results to be obtained.

* The problem studied in this paper was started in the spring of 1927 at Copenhagen in cooperation with L. Pauling, with whom I later corresponded occasionally about the questions involved and to whom I owe many valuable suggestions.

[1] E. Fermi, Zeits. f. Physik **60**, 320 (1930).

[2] H. Casimir, quoted in Pauling and Goudsmit, Structure of Line Spectra, page 225. Also Phys. Rev. in preparation.

[3] Hargreaves, Proc. Roy. Soc. **A127**, 141 (1930).

[4] G. Breit, Phys. Rev. **37**, 51 (1931).

[5] S. Goudsmit and R. F. Bacher, Phys. Rev. **34**, 1501 (1929).

[6] S. Goudsmit, Phys. Rev. **31**, 946 (1928).

[7] W. Pauli, Zeits. f. Physik **16**, 155 (1923).

[8] J. C. Slater, Phys. Rev. **34**, 1293 (1929).

The application of the method of sums goes as follows. One thinks the interaction between the electrons to be removed, in order that each electron can be treated as independent of the others. For certain purposes one may also imagine the interaction between the spin of each electron and its own orbit to be absent. One can think this done by the introduction of a fictitious very strong magnetic field, which should break all couplings between the electrons or their quantum vectors. One now calculates under these circumstances the perturbation energy in which one is interested for each electron separately.[9]

Each state of the complete atom is now characterized by a large set of quantum numbers, each of which can be said to refer to a particular electron.[10] For this state one finds the total perturbation energy by simply adding together the perturbations of the individual electrons. If one next considers the *sum* of the perturbation energies for *all* states having the same total projection of angular momentum M (in units $h/2\pi$) on the direction of the fictitious field, this sum will remain unaltered after one introduces again the proper interactions, which were at the start thought to be absent (or, which is the same, after one reduces the applied strong fictitious magnetic field to a weak one).

This last sentence contains the fundamental principle of the sum rules, as it can be derived from quantum mechanics. It holds only for first order perturbations and moreover as it stands it does not give much information, because the sums are to be taken over *all* states of the atom. In order to get further results out of this sum rule one must make, according to Slater, certain approximations. It is assumed then that the above stated sum rule will hold if one takes the sum only over the states belonging to one electron configuration.[11] This may become quite incorrect when the levels arising from the configuration considered intermix with those of other configurations. This, for instance, is one of the reasons why the relations derived by Slater are not fulfilled very well in the actual spectroscopic data.[12] For special perturbations one can sometimes even go one step further with approximations. Slater, in his above quoted paper, purposely neglects the spin-orbit interaction of each electron. This causes the spins to be independent of the orbital angular momenta. Instead of considering the sum of the perturbation energies for a fixed value of the total projection M, he may consider the sum for the states which

[9] In the above quoted paper of Pauli this was the interaction energy with an external magnetic field, giving rise to the g-sum rule. In the paper on multiplet separations by the present author the spin-orbit interaction was considered, resulting in the Γ-sum rule. Slater treated the interaction between the electrons and it is clearly seen from his paper that his results are obtained by first calculating this interaction for each pair as if it did not disturb the approximate independence of the different electrons. The sum rules finally gave the generally valid relations between multiplet distances.

[10] In the case of a nuclear moment $Ih/2\pi$ the nuclear quantum numbers I and m_I must be added also to this set.

[11] One calls a configuration the assembly of states for which each electron has the quantum numbers n and l fixed. Two states for which one of the electrons has a different n or l are said to belong to different configurations.

[12] Compare on this point a recent paper by E. U. Condon, Phys. Rev. **36**, 1121 (1930).

have a fixed value of both M_S and M_L, the total projection of all spins and all orbits respectively. Each of these sums, which are a part of the total sum for a fixed M, will be invariant. This approximation holds only when the spin-orbit interaction is indeed negligibly small compared to the interaction between different electrons, the case in which Slater is interested. This means that one expects to obtain extreme Russell-Saunders coupling.[13]

In order to make use of the method described here it is obviously necessary to know the effect of the perturbation on one single electron considered as independent of the others.[14] This will be considered in the following section.

In most cases the hyperfine structure is smaller than any other one of the interactions present in the atom. It is possible to apply a magnetic field which will just decouple the nuclear spin from the rest of the atom, giving each an independent projection on the field direction, M_I and M_J. From the theory of the Zeeman effect of hyperfine structure[15] one knows that the interaction between the nucleus and the electron core under those circumstances is given by

$$W = A(J) \cdot M_I M_J. \tag{1}$$

The constant A in front is exactly the one which will govern the magnitude of the hyperfine multiplet of that particular level after one removes the magnetic field. That is, the levels of the hyperfine multiplet are given by

$$W_J = A(J)IJ \cos(I, J) = \tfrac{1}{2}A(J)\{F(F+1) - I(I+1) - J(J+1)\} \tag{2}$$

Here F denotes as usual the resultant of I and J.

As we are finally interested in the magnitude of just that factor A, we may all the time think that there is such a field present which causes M_I and the total projection of the core to be independent. This simplifies our calculation very much. We do not need to calculate the sums for all states with the same total $M_F = M_I + M_J$. According to Slater the sum rules will also be valid for the smaller group of states which have a fixed value for both M_I and M_J. We take therefore in the following procedure a particular value of M_I in our mind and extend the sums over levels with a fixed value of M_J.

It has to be kept in mind that the independence of M_I and M_J can only be used in case their interaction is indeed very much smaller than any of the other interactions which are to be taken into account. One can not use it, for instance, in the case of ionized Lithium. Here the hyperfine structure happens to be of the same order of magnitude as the multiplet splitting.[16]

2. Interaction between a Single Electron and a Nuclear Magnetic Moment

The interaction of a magnetic nucleus and an electron in an s-state has been treated in detail before. The energy happens to be simply proportional

[13] If one needs information about the interaction between electrons in a case of (j, j) coupling one has to alter the procedure followed by Slater somewhat.

[14] In Slater's special case one needs it for each electron *pair*.

[15] E. Back and S. Goudsmit, Zeits. f. Physik **47**, 174 (1928), see also Pauling and Goudsmit, reference 2, p. 215.

[16] S. Goudsmit and D. R. Inglis, Phys. Rev. **37**, 283 (1931).

to the Landé cosine between the spin s of the electron and the nuclear moment I. It is therefore possible to treat the cases where an s-electron is a part of a configuration, completely with the vector model. We will now consider the case of a non-s electron.

We think the spin-orbit interaction to be removed (or apply a fictitious strong magnetic field). In the classical theory the interaction energy consists of two parts. The nuclear magnetic moment is acted upon by a magnetic field caused by the orbital motion of the electron and also by a field produced by the electron spin. According to perturbation theory one must write down the instantaneous values for the interaction energy and must average this over the unperturbed motion. The expression for this interaction energy is:[17]

$$W_l + W_s = a[Il\cos(I,l) - Is\cos(I,s) + 3Is\cos(I,r)\cos(r,s)]. \quad (3)$$

The factor a in front of this expression governs the absolute magnitude of the interaction energy. We are not interested in it for our problem. For a hydrogenic orbit its value is given by

$$a = \left(\frac{eh}{4\pi m_0 c}\right)^2 g(I)\left(\frac{1}{r^3}\right) = \frac{Rhc\alpha^2 Z^3}{n^3 l(l+\frac{1}{2})(l+1)} g(I). \quad (4)$$

The symbols used in Eqs. (3) and (4) have the usual meaning, r denotes the radius vector combining the nucleus with the electron, $g(I)$ stands for the Landé g value of the nucleus and as the nuclear magnetism is believed to arise from protons, one expects $g(I)$ to be only of the order 1/1840.

We start out with the case where we neglect all interactions between the quantum vectors; these will each have independent projections on the direction of the fictitious field H. These projections we denote by M_I, m_l and m_s, the nuclear, the orbital and the spin moment respectively. The vectors I, l and s will have independent Larmor precessions about the field direction and we can therefore expand the cosines of Eq. (3) and obtain:

$$W_l + W_s = a[M_I m_l - M_I m_s\{1 - 3\overline{\cos^2(H,r)}\}]. \quad (5)$$

Our problem thus reduces to finding the average of $\cos^2(H,r)$. In the classical picture with a plane orbit the vector r would be at any time perpendicular to the angular momentum vector l. This, however, is no longer true in quantum mechanics. The relative probability that r makes an angle θ with the field direction is given by the square of the tesseral harmonic $P_l^{m_l}(\cos\theta)$. Thus the required average becomes

$$\overline{\cos^2(H,r)} = \int_0^\pi \cos^2\theta [P_l^{m_l}]^2 \sin\theta d\theta \Big/ \int_0^\pi [P_l^{m_l}]^2 \sin\theta d\theta = \frac{2(l^2 - m_l^2) + 2l - 1}{(2l-1)(2l+3)}. \quad (6)$$

[17] L. Pauling and S. Goudsmit, reference 2, p. 205.

Substituting this in Eq. (5) gives finally

$$W = W_l + W_s = aM_I\left\{m_l - m_s\frac{6m_l^2 - 2l(l+1)}{(2l-1)(2l+3)}\right\}. \tag{7}$$

One verifies easily that for large values of l Eq. (6) approaches the classical result: $\frac{1}{2}\sin^2(l, H) = (l^2 - m_l^2)/2l^2$.

Expression (7) will be the fundamental formula for all further applications. It is, however, not valid for s-electrons.

3. The Sum Rule Applied to one Electron

The application of the sum rule and Eq. (7) to the case of a single electron provides a very simple derivation of the results obtained by Fermi, Casimir, Hargreaves and Breit. It also gives an illustration of the method before we apply it to the many electron case. A single electron gives rise to a doublet state, one level with $j_1 = l + \frac{1}{2}$, the other with $j_2 = l - \frac{1}{2}$. In a weak magnetic field, which just decouples the nuclear spin, the interaction with the nuclear magnetism is (compare Eq. (1)):

$$W_{j_1} = a' M_I m_{j_1} \quad \text{and} \quad W_{j_2} = a'' M_I m_{j_2}. \tag{8}$$

In a very strong magnetic field this interaction is (Eq. (7)):

$$W = aM_I\left\{m_l - m_s\frac{6m_l^2 - 2l(l+1)}{(2l-1)(2l+3)}\right\}. \tag{9}$$

The sum rule says that, keeping M_I fixed, the sums of the energies for all levels with a given value of $m_j = m_s + m_l$ must come out the same, whether we use Eq. (8) or (9). We choose first $m_j = l + \frac{1}{2}$. This occurs only once; in (8) for j_1 and in (9) when $m_l = l$ and $m_s = +\frac{1}{2}$. The sum rule states

$$a' M_I \cdot (l + \tfrac{1}{2}) = aM_I\left\{l - \frac{1}{2}\,\frac{6l^2 - 2l(l+1)}{(2l-1)(2l+3)}\right\}. \tag{10}$$

One obtains at once

$$a' = a\frac{l(l+1)}{(l+\frac{1}{2})(l+1\frac{1}{2})} = a\frac{l(l+1)}{j_1(j_1+1)}. \tag{11}$$

Next we choose $m_j = l - \frac{1}{2}$. This occurs twice, namely in (8) both for j_1 and j_2, and in (9) for $m_l = l$, $m_s = -\frac{1}{2}$ and $m_l = l-1$, $m_s = +\frac{1}{2}$. Applying the sum rule gives

$$a' M_I \cdot (l - \tfrac{1}{2}) + a'' M_I \cdot (l - \tfrac{1}{2}) \tag{12}$$

$$= aM_I\left\{l + \frac{1}{2}\,\frac{6l^2 - 2l(l+1)}{(2l-1)(2l+3)}\right\} + aM_I\left\{(l-1) - \frac{1}{2}\,\frac{6(l-1)^2 - 2l(l+1)}{(2l-1)(2l+3)}\right\}$$

As we know a' already we can solve for a'' and find

$$a'' = a\frac{l(l+1)}{(l-\frac{1}{2})(l+\frac{1}{2})} = a\frac{l(l+1)}{j_2(j_2+1)}. \tag{13}$$

These expressions for a' and a'' are indeed identical with the results obtained by other authors. Substituting them in Eq. (2) gives the hyperfine structure in the absence of a field. The result shows that for the two levels of a doublet the interval constant of the hyperfine structure is inversely proportional to $j(j+1)$. The absolute magnitude can only be given when the constant a can be calculated. This would require an exact knowledge of the eigenfunctions of the state under consideration. For penetrating orbits one can make the same kind of an approximation as was applied by Landé to the calculations of doublet separations. One obtains for such cases, instead of Eq. (4), the approximate expression

$$a = \frac{Rhc\alpha^2 Z_i Z_0^2}{n_e^3 l(l+\frac{1}{2})(l+1)}\, g(I). \tag{14}$$

In this expression Z_i and Z_o stand for the effective nuclear charge in the inner and outer part of the orbit respectively, n_e represents the "effective" quantum number or Rydberg denominator.

4. The Sum Rule Applied to Configurations

We will give as an illustrative example the case of three equivalent p-electrons. The first column of Table I gives the values of m_s and m_l for the individual electrons, chosen in agreement of course with the Pauli exclusion principle. The quantum numbers l and n are supposed to be the same for all three electrons and are therefore omitted from the table. We need only to consider the states which give rise to positive values of the total projection M_J, given in the second column, negative values of M_J do not give any additional information. The last column gives the interaction with the nuclear magnetism obtained by applying Eq. (9) to each electron individually and adding the result for the three together. As they are equivalent electrons they have the same constant a.

Table I. *Interaction for p^3 in strong field.*

m_{s_1}	m_{l_1}	m_{s_2}	m_{l_2}	m_{s_3}	m_{l_3}	M_J	Eq. (7)	
$\frac{1}{2}$	1	$\frac{1}{2}$	0	$-\frac{1}{2}$	1	$2\frac{1}{2}$	$2\frac{2}{5}\ aM_I$	
$\frac{1}{2}$	1	$\frac{1}{2}$	0	$\frac{1}{2}$	-1	$1\frac{1}{2}$	$0\ aM_I$	
$\frac{1}{2}$	1	$\frac{1}{2}$	0	$-\frac{1}{2}$	0		$\frac{4}{5}\ aM_I$	sum
$\frac{1}{2}$	1	$\frac{1}{2}$	-1	$-\frac{1}{2}$	1		$\frac{4}{5}\ aM_I$	$3\frac{1}{5}\ aM_I$
$\frac{1}{2}$	1	$-\frac{1}{2}$	0	$-\frac{1}{2}$	1		$1\frac{2}{5}\ aM_I$	
$\frac{1}{2}$	1	$\frac{1}{2}$	0	$-\frac{1}{2}$	-1	$\frac{1}{2}$	$\frac{2}{5}\ aM_I$	
$\frac{1}{2}$	1	$\frac{1}{2}$	-1	$-\frac{1}{2}$	0		$-\frac{4}{5}\ aM_I$	
$\frac{1}{2}$	0	$\frac{1}{2}$	-1	$-\frac{1}{2}$	1		$\frac{2}{5}\ aM_I$	sum
$\frac{1}{2}$	0	$-\frac{1}{2}$	1	$-\frac{1}{2}$	0		$1\frac{1}{5}\ aM_I$	$2\frac{2}{5}\ aM_I$
$\frac{1}{2}$	1	$-\frac{1}{2}$	1	$-\frac{1}{2}$	-1		$1\frac{1}{5}\ aM_I$	

The states in the table are ordered according to their values of M_J. The configuration gives rise to five levels, one with $J=2\frac{1}{2}$, three with $J=1\frac{1}{2}$ and one with $J=\frac{1}{2}$. We want to know the constants A for each of these levels and shall denote them by $A(2\frac{1}{2})$, $A(1\frac{1}{2})$, $A'(1\frac{1}{2})$, $A''(1\frac{1}{2})$ and $A(\frac{1}{2})$ respectively.

The sum rule applied to the projection $M_J = 2\frac{1}{2}$, which occurs only once, gives

$$A(2\tfrac{1}{2}) \cdot M_I \cdot 2\tfrac{1}{2} = 2\tfrac{2}{5} a M_I. \tag{15}$$

The projection $M_J = 1\frac{1}{2}$ occurs four times, namely $J = 2\frac{1}{2}$ as well as all three levels with $J = 1\frac{1}{2}$ can give this projection on the field direction. It also occurs four times in Table I. The sum rule gives

$$\left\{A(2\tfrac{1}{2}) + A(1\tfrac{1}{2}) + A'(1\tfrac{1}{2}) + A''(1\tfrac{1}{2})\right\} M_I \cdot 1\tfrac{1}{2} = 3\tfrac{1}{5} a M_I. \tag{16}$$

Finally $M_J = \frac{1}{2}$ occurs five times, giving

$$\left\{A(2\tfrac{1}{2}) + A(1\tfrac{1}{2}) + A'(1\tfrac{1}{2}) + A''(1\tfrac{1}{2}) + A(\tfrac{1}{2})\right\} M_I \cdot \tfrac{1}{2} = 2\tfrac{2}{5} a M_I. \tag{17}$$

Solving these equations one obtains finally

$$\left.\begin{aligned} A(2\tfrac{1}{2}) &= {}^{24}/_{25} a \\ A(1\tfrac{1}{2}) + A'(1\tfrac{1}{2}) + A''(1\tfrac{1}{2}) &= 1{}^{13}/_{75} a \\ A(\tfrac{1}{2}) &= 2\tfrac{2}{3} a \end{aligned}\right\} \tag{18}$$

Exactly as in the case of the well-known g-sum rule we are only able to obtain the sum of the A's for the levels with the same value of J. That we find the individual values for the levels with $J = 2\frac{1}{2}$ and $J = \frac{1}{2}$ is because there is only one level with each of these J values.

The values of the individual A's will in general depend upon the type of coupling between the quantum vectors of the electrons, just as in the case of g-values. The method to obtain their values for extreme couplings will be described in following sections of this paper.

It is not at all difficult to make a table like Table I for any other example. When the electrons are not equivalent each has a different constant a which one has to carry along into the final result. We want to mention once more that most of the formulae used here are only valid for the interaction of a non-s electron with the nuclear magnetism. For an s electron one has to replace Eq. (7) by the simple expression

$$W = b M_I m_s. \tag{19}$$

Here follow the results for a number of configurations

TABLE II. *Hyperfine structure sums.**

p and p^5	$J = 1\frac{1}{2}$	$A = {}^{8}/_{15} a$	ps and $p^5 s$	$J = 2$	$A = \frac{3}{5} a + \frac{1}{3} b$
	$\frac{1}{2}$	$A = 2\frac{2}{3} a$		1	$\Sigma A = 2a + \frac{1}{4} b$
p^2 and p^4	$J = 2$	$\Sigma A = 1\frac{1}{5} a$	$p^2 s$ and $p^4 s$	$J = 2\frac{1}{2}$	$\Sigma A = 1{}^{7}/_{25} a + \frac{2}{5} b$
	1	$A = 0a$		$1\frac{1}{2}$	$\Sigma A = 1{}^{23}/_{25} a - {}^{1}/_{15} b$
				$\frac{1}{2}$	$\Sigma A = 0a + 1\frac{2}{3} b$
p^3	$J = 2\frac{1}{2}$	$A = {}^{24}/_{25} a$	$p^3 s$	$J = 3$	$A = \frac{4}{5} a + \frac{1}{6} b$
	$1\frac{1}{2}$	$\Sigma A = 1{}^{13}/_{75} a$		2	$\Sigma A = 2a + {}^{7}/_{12} b$
	$\frac{1}{2}$	$\Sigma A = 2\frac{2}{3} a$		1	$\Sigma A = 2\frac{4}{5} a - \frac{1}{4} b$

* The constant a refers to the p- and b to the s-electron.

5. Hyperfine Structure for Extreme (j, j) Coupling

The above described method gives only the sums of the factors which govern the hyperfine structure separations. Their individual values for each level are only determined completely in extreme couplings. The simplest case is that of extreme (j, j) coupling which we shall now discuss with the example of the p^3 configuration. We mean by extreme (j, j) coupling that the spin vector s of each electron is strongly coupled to its own orbital vector l and that therefore one can ascribe to each one of the electrons of the configuration its own resultant vector j. The spin-orbit coupling has to be considerably stronger than the interaction energy between the different electrons. It is then possible to think of an applied magnetic field which is strong enough to decouple the different electrons so as to make them independent of each other, but not yet strong enough to decouple the s and l for each of the electrons.

Under these ideal circumstances the quantum state of each electron will be characterized by the quantum numbers j and m_j, its resultant moment and the projection on the field, rather than by m_s and m_l. We now have to make again a table similar to Table I but now with the different designation for each electron. We also need to know what the interaction with the nucleus will be for each electron, when its state is characterized by j and m_j, that is when its spin and orbit are coupled. But this is just the problem solved in Section 3. Eq. (8) is the one we must use now, especially after we introduce for a' and a'' the results of Eqs. (11) and (13).

Table III. *Configuration p^3 in (j,j) coupling.*

j_1	m_{j_1}	j_2	m_{j_2}	j_3	m_{j_3}	M_J	Eq. (8)	
$1\frac{1}{2}$	$1\frac{1}{2}$	$1\frac{1}{2}$	$\frac{1}{2}$	$1\frac{1}{2}$	$-\frac{1}{2}$	$1\frac{1}{2}$	$1\frac{1}{2}a'M_I$	
	$1\frac{1}{2}$		$\frac{1}{2}$		$-1\frac{1}{2}$	$\frac{1}{2}$	$\frac{1}{2}a'M_I$	
$1\frac{1}{2}$	$1\frac{1}{2}$	$1\frac{1}{2}$	$\frac{1}{2}$	$\frac{1}{2}$	$\frac{1}{2}$	$2\frac{1}{2}$	$(2a'+\frac{1}{2}a'')M_I$	
	$1\frac{1}{2}$		$\frac{1}{2}$		$-\frac{1}{2}$	$1\frac{1}{2}$	$(2a'-\frac{1}{2}a'')M_I$	sum
	$1\frac{1}{2}$		$-\frac{1}{2}$		$\frac{1}{2}$		$(a'+\frac{1}{2}a'')M_I$	$3a'M_I$
	$1\frac{1}{2}$		$-1\frac{1}{2}$		$\frac{1}{2}$	$\frac{1}{2}$	$\frac{1}{2}a''M_I$	sum
	$1\frac{1}{2}$		$-\frac{1}{2}$		$-\frac{1}{2}$		$(a'-\frac{1}{2}a'')M_I$	$(a'+\frac{1}{2}a'')M_I$
	$\frac{1}{2}$		$-\frac{1}{2}$		$\frac{1}{2}$		$\frac{1}{2}a''M_I$	
$1\frac{1}{2}$	$1\frac{1}{2}$	$\frac{1}{2}$	$\frac{1}{2}$	$\frac{1}{2}$	$-\frac{1}{2}$	$1\frac{1}{2}$	$1\frac{1}{2}a'M_I$	
	$\frac{1}{2}$		$\frac{1}{2}$		$-\frac{1}{2}$	$\frac{1}{2}$	$\frac{1}{2}a'M_I$	

Table III represents the equivalent of Table I for the extreme (j, j) coupling. The example chosen is again the configuration p^3. For reasons to be discussed later the values for a' and a'' have not been substituted.

In the ideal extreme case the electrons are quite independent of each other. Following Slater we therefore need not take the sums over all levels with a fixed value of the total M_J. The sum-rule will hold already for the levels which are designated by a special set of values of j and m_j for each of the electrons. If we choose a set of values for these quantum numbers it

happens that we find only one state in our table which possesses just this set. Thus we do not need to consider any sums at all and the third column of the table gives at once the correct value of the interaction with the nuclear spin for this extreme case.

We are, however, not yet finished. When we now gradually remove the field which decoupled the electrons, the quantum numbers m_j for the individual electrons will lose their significance and be converted together into the total M_J. In the extreme (j, j) coupling the values of j for each electron will keep their meaning. This means that for this last transition the sum rules will hold within each group of levels characterized by fixed values of the individual j, but no longer for the individual m_j. Table III has been arranged accordingly.

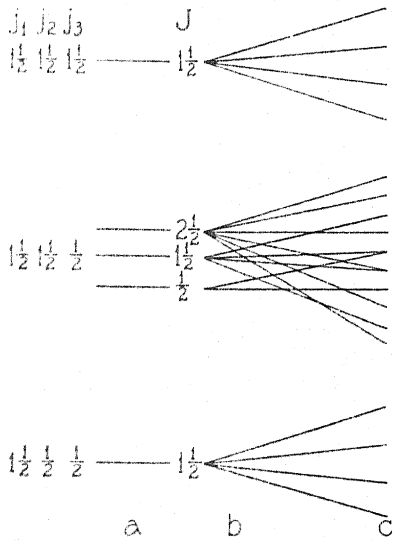

Fig. 1. Schematical representation of Paschen-Back effect for p^3 in extreme (j,j) coupling. (a) without field, quantum numbers: j_1, j_2, j_3, J. (b) weak field, quantum numbers: j_1, j_2, j_3, J, M_J. (c) strong field, quantum numbers: $j_1, j_2, j_3, m_{j_1}, m_{j_2}, m_{j_3}$.

Figure 1 may help to understand the situation described above. At the left is shown the p^3 configuration in extreme (j, j) coupling. The highest level arises when all three electrons have maximum energy, that is when they all have $j=1\frac{1}{2}$. The next lower group occurs when one of the electrons has $j=\frac{1}{2}$. The lowest level has two electrons with $j=\frac{1}{2}$ and one with $j=1\frac{1}{2}$.[18] The hyperfine structure is not included in the figure. Going to the right in Fig. 1 the effect of an applied magnetic field is represented. In a weak field each level splits into its Zeeman components. With increasing field strength each level group will undergo a Paschen-Back transition and the result is rep-

[18] There exists here no lower state with all three electrons having $j=\frac{1}{2}$, because our example consists of equivalent electrons for which the Pauli principle allows only two with $j=\frac{1}{2}$. This also will be clear from considering Table III where all states are gathered which do agree with the Pauli principle. Compare Pauling and Goudsmit, l.c., page 257.

resented at the right of Fig. 1. Notice that the field does not yet break the coupling of each spin with its orbit, the three level groups are still distinctly separated. A further increase in the field would also break up this last coupling, all couplings would be broken and one would have the case represented in Table I. One sees that the right side of Fig. 1 is to be correlated with Table III. The sum rule as applied in Table III means simply that we may assume the sum rule for fixed M_J to hold within each level group separately in this extreme coupling. This gives us a means to go from the strong field to the intermediate field and to obtain our final information.

In this intermediate field, which we suppose just to decouple the nuclear spin from the rest of the atom, the interaction with the nucleus for each level will be given again by Eq. (1):

$$W = AM_IM_J.$$

Our problem is to find the value of A for each one of the many levels.

Applying the sum rule to the states which have $j_1=j_2=j_3=1\frac{1}{2}$, that is the upper level, we find at once

$$A(1\tfrac{1}{2}) = a'.$$

This result is found by choosing M_J either $1\frac{1}{2}$ or $\frac{1}{2}$.

For the middle group of levels, $j_1=j_2=1\frac{1}{2}$, $j_3=\frac{1}{2}$, one finds the following sums

$$\begin{aligned} M_J = 2\tfrac{1}{2}&: \quad A(2\tfrac{1}{2})M_I\cdot 2\tfrac{1}{2} = (2a' + \tfrac{1}{2}a'')M_I, \\ M_J = 1\tfrac{1}{2}&: \quad \{A(2\tfrac{1}{2}) + A'(1\tfrac{1}{2})\}M_I\cdot 1\tfrac{1}{2} = 3a'M_I, \\ M_J = \tfrac{1}{2}&: \{A(2\tfrac{1}{2}) + A'(1\tfrac{1}{2}) + A(\tfrac{1}{2})\}M_I\cdot\tfrac{1}{2} = (a' + \tfrac{1}{2}a'')M_I. \end{aligned}$$

From this one obtains

$$A(2\tfrac{1}{2}) = \tfrac{4}{5}a' + \tfrac{1}{5}a''; \; A'(1\tfrac{1}{2}) = 1\tfrac{1}{5}a' - \tfrac{1}{5}a''; \; A(\tfrac{1}{2}) = a''.$$

Finally the lowest level gives

$$A''(1\tfrac{1}{2}) = a'.$$

After one substitutes the values of a' and a'' from Eqs. (11) and (13) the results become

$$A(1\tfrac{1}{2}) = {}^{8}/_{15}a; \; A(2\tfrac{1}{2}) = {}^{24}/_{25}a; \; A'(1\tfrac{1}{2}) = {}^{8}/_{75}a; \; A(\tfrac{1}{2}) = 2\tfrac{2}{3}a; \; A''(1\tfrac{1}{2}) = {}^{8}/_{15}a.$$

As is to be expected the sums agree with those given in Section 4 and Table II.

6. Use of the Vector Model for Extreme (j, j) Coupling

When the spin and orbit of an electron are coupled the interaction with the nuclear magnetism is given by the Eq. (2)

$$W = a'Ij\cos(I, j) \quad \text{or} \quad a''Ij\cos(I, j). \tag{20}$$

The choice of a' or a'' depends on whether one considers the state with $j=l+\frac{1}{2}$ or the one with $j=l-\frac{1}{2}$. This simple expression brings it about that one often can use the vector model with advantage in extreme (j, j) coupling.

For several electrons the total interaction with the nucleus is

$$W = \sum a_k I j_k \overline{\cos(I, j_k)}. \tag{21}$$

The sum has to be extended over all electrons, which we shall distinguish by the index k. As all j_k form together the resultant J one can average over their precession about this resultant and obtains

$$W = \sum a_k I j_k \cos(I, J)\, \overline{\cos(J, I j_k)}. \tag{22}$$

We may write this

$$W = A I J \cos(I, J) \tag{23}$$

in which expression we finally want to know the value of

$$A = \sum a_k \frac{j_k}{J} \overline{\cos(J, j_k)}. \tag{24}$$

The problem is thus to evaluate the average cosines of each of the individual j_k with the resultant J. This can be done easily when only two j_k form the resultant J, but with more electrons it is in general impossible, unless we use again the method of sums instead of the vector model. For a restricted but interesting number of cases we can find relations between these cosines and the g values of the levels. The magnetic moment gJ of a state is given by the sum of the magnetic moments $g_k j_k$ of each electron resolved along the resultant J, thus

$$gJ = \sum g_k j_k \overline{\cos(J, j_k)} \quad \text{or} \quad g = \sum g_k \frac{j_k}{J} \overline{\cos(J, j_k)}. \tag{25}$$

This defines the g value for this level. Futhermore, as J is the resultant of all j_k we have

$$J = \sum j_k \overline{\cos(J, j_k)} \quad \text{or} \quad 1 = \sum \frac{j_k}{J} \overline{\cos(J, j_k)}. \tag{26}$$

If we now restrict ourselves to the case of equivalent electrons the sums in expressions 24, 25 and 26 fall apart into two sums, one over the electrons with $j' = l + \frac{1}{2}$ and one over those with $j'' = l - \frac{1}{2}$. We shall again denote these two kinds by a prime and a double prime. The formulae become

$$A = a' \sum \frac{j_k'}{J} \overline{\cos(J, j_k')} + a'' \sum \frac{j_k''}{J} \overline{\cos(J, j_k'')} \tag{24a}$$

$$g = g' \sum \frac{j_k'}{J} \overline{\cos(J, j_k')} + g'' \sum \frac{j_k''}{J} \overline{\cos(J, j_k'')} \tag{25a}$$

$$1 = \sum \frac{j_k'}{J} \overline{\cos(J, j_k')} + \sum \frac{j_k''}{J} \overline{\cos(J, j_k'')}. \tag{26a}$$

For equivalent electrons a', a'', g' and g'' can be placed before the summation, as they have the same value for each of the electrons inside any one sum.

We next can eliminate the two unknown sums between the three expressions and obtain finally

$$A = a' \frac{g - g''}{g' - g''} + a'' \frac{g - g'}{g'' - g'} . \tag{27}$$

The values of g' and g'' are the known g values for a single electron, the values of g to be used are those for the extreme (j, j) coupling of the configuration which we consider.[19] For our standard example of the p^3 configuration the results are again:

	$g' = 1\frac{1}{3}$	$g'' = \frac{2}{3}$	
$J = 2\frac{1}{2}$	$g = 1\frac{1}{5}$	$A = \frac{4}{5}a' + \frac{1}{5}a''$	
$J = \frac{1}{2}$	$g = \frac{2}{3}$	$A = a''$	
$J = 1\frac{1}{2}$	$g = 1\frac{1}{3}$	$A = a'$	upper level.
$1\frac{1}{2}$	$g = 1^7/_{15}$	$A' = 1\frac{1}{5}a' - \frac{1}{5}a''$	middle level.
$1\frac{1}{2}$	$g = 1\frac{1}{3}$	$A'' = a'$	lower level.

The addition of a single s electron to a level of which A is known can always be done with the vector model, provided the coupling is of the extreme (j, j) type. We denote with A^+ and J^+ the values for the state to which we add the s electron. The s electron itself is characterized by b and s, the resulting level finally by A and J. One obtains with the vector model

$$A = A^+ \frac{J^+}{J} \cos(J, J^+) + b \frac{s}{J} \cos(J, s) . \tag{28}$$

Substituting the Landé cosines this becomes

$$\begin{aligned} A = A^+ & \frac{J(J+1) + J^+(J^+ + 1) - s(s+1)}{2J(J+1)} \\ & + b \frac{J(J+1) + s(s+1) - J^+(J^+ + 1)}{2J(J+1)} . \end{aligned} \tag{29}$$

One can simplify this formula if one considers that $s = \frac{1}{2}$ and that therefore J can only be $(J^+ + \frac{1}{2})$ or $(J^+ - \frac{1}{2})$. One can also again express A in terms of the g-values.

Table IV gives the results for a few configurations in extreme (j, j) coupling.

[19] For equivalent electrons the g values for extreme (j, j) coupling can be obtained in general only with the help of the method of sums. This Section does therefore in reality not avoid the use of the sum rule, but it gives a connection between the hyperfine structure constants and the g values. The latter are considered to be better known and more easily derivable.

TABLE IV. *Hyperfine structure for (j, j) coupling.**

	j_k	J^+	J	g	A
p^2	$1\frac{1}{2}$ $1\frac{1}{2}$		2	$1\frac{1}{3}$	a'
	$1\frac{1}{2}$ $\frac{1}{2}$		2	$1\frac{1}{6}$	$\frac{3}{4}a'+\frac{1}{4}a''$
			1	$1\frac{1}{2}$	$1\frac{1}{4}a'-\frac{1}{4}a''$
p^3	$1\frac{1}{2}$ $1\frac{1}{2}$ $1\frac{1}{2}$		$1\frac{1}{2}$	$1\frac{1}{3}$	a'
	$1\frac{1}{2}$ $1\frac{1}{2}$ $\frac{1}{2}$		$2\frac{1}{2}$	$1\frac{1}{5}$	$\frac{4}{5}a'+\frac{1}{5}a''$
			$1\frac{1}{2}$	$1^7/_{15}$	$1\frac{1}{5}a'-\frac{1}{5}a''$
			$\frac{1}{2}$	$\frac{2}{3}$	a''
	$1\frac{1}{2}$ $\frac{1}{2}$ $\frac{1}{2}$		$1\frac{1}{2}$	$1\frac{1}{3}$	a'
ps	$1\frac{1}{2}$	$1\frac{1}{2}$	2	$1\frac{1}{2}$	$\frac{3}{4}a'+\frac{1}{4}b$
			1	$1\frac{1}{6}$	$1\frac{1}{4}a'-\frac{1}{4}b$
	$\frac{1}{2}$	$\frac{1}{2}$	1	$1\frac{1}{3}$	$\frac{1}{2}a''+\frac{1}{2}b$
p^2s	$1\frac{1}{2}$ $1\frac{1}{2}$	2	$2\frac{1}{2}$	$1^7/_{15}$	$\frac{4}{5}a'+\frac{1}{5}b$
			$1\frac{1}{2}$	$1\frac{1}{5}$	$1\frac{1}{5}a'-\frac{1}{5}b$
		0	$\frac{1}{2}$	2	b
	$1\frac{1}{2}$ $\frac{1}{2}$	2	$2\frac{1}{2}$	$1\frac{1}{3}$	$\frac{3}{5}a'+\frac{1}{5}a''+\frac{1}{5}b$
			$1\frac{1}{2}$	1	$^9/_{10}a'+^3/_{10}a''-\frac{1}{5}b$
		1	$1\frac{1}{2}$	$1\frac{2}{3}$	$\frac{5}{6}a'-\frac{1}{6}a''+\frac{1}{3}b$
			$\frac{1}{2}$	$1\frac{1}{3}$	$\frac{5}{6}a'-\frac{1}{6}a''-\frac{1}{3}b$
	$\frac{1}{2}$ $\frac{1}{2}$	0	$\frac{1}{2}$	2	b

* The values of j_k are given for the p electrons only, the s electron has $j_k=\frac{1}{2}$. Levels with $J=0$ are omitted. The results for the configurations p^5, p^4, p^3s, p^1s, are similar to the following ones in the same order p, p^2, ps, p^2s.

7. HYPERFINE STRUCTURE FOR EXTREME RUSSELL-SAUNDERS COUPLING

When the interaction between the different electrons of a configuration is very large compared to the interaction between the spins of the electrons and their orbital motion, one speaks of Russell-Saunders coupling. The spin vectors form together a resultant spin moment S, the orbital moments l form a resultant L and the total angular momentum vector J is the resultant of these two. To this one the nuclear spin I is again added to form the resultant F. This type of coupling yields the ordinary multiplet structure.

In the case of Russell-Saunders coupling one can imagine an applied magnetic field which is strong enough to overcome the coupling between the spins and orbits; that is, between the resultant S and the resultant L, but not yet strong enough to decouple the different electrons from each other. This situation is represented at the right of Fig. 2. The left of Fig. 2 gives the levels without magnetic field, whereas the middle shows them in an intermediate field. The strong field has caused a complete Paschen-Back effect for each of the multiplets, but the splitting up which it causes is supposed to be still small compared to the distances between the different multiplets. In this strong field each state will be characterized by the projections M_S and M_L of S and L on the field direction. As these two are supposed to have a negligible interaction under these circumstances, they will be independent and will restrict our sum rules. According to Slater's procedure the sums will now be invariant over states which have the same value of the pair of quantum numbers M_S, M_L. Table V shows the states of the example p^3 arranged in this order. This configuration yields a ^4S, a ^2D and ^2P state. When we increase the field more

and more until it breaks the electron coupling, the total projection M_S of the resultant spin will remain invariant and can finally be interpreted as the sum

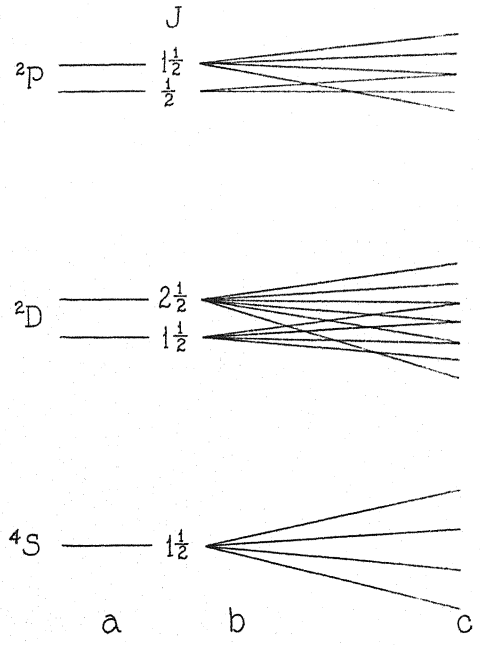

Fig. 2. Schematical representation of Paschen-Back effect for p^3 in extreme Russell-Saunders coupling. (a) without field, quantum numbers: L, S, J. (b) weak field, quantum numbers L, S, J, M_J. (c) strong field, quantum numbers· L, S, M_L, M_S.

of the m_s of the electrons. In the same way M_L will be converted into the sum of m_l of the individual electrons. It is in this way that a certain pair M_S, M_L can be correlated to each of the states in Table V, simply

$$M_S = \sum m_s, \quad M_L = \sum m_l. \tag{30}$$

TABLE V. *Configuration p^3 in Russell-Saunders coupling.*

m_{s_1}	m_{s_2}	m_{s_3}	m_{l_1}	m_{l_2}	m_{l_3}	M_S	M_L	M_J	Eq. (7)
½	½	−½	1	0	1	½	2	2½	$2\frac{2}{5}\ aM_I$
½	½	½	1	0	−1	1½	0	1½	$0\ aM_I$
½	½	−½	1	0	0	½	1	1½	$\frac{4}{5}\ aM_I$
			1	−1	1				$\frac{4}{5}\ aM_I$
½	−½	−½	1	0	−1	−½	2	1½	$1\frac{3}{5}\ aM_I$
½	½	−½	1	0	−1	½	0	½	$\frac{2}{5}\ aM_I$
			1	−1	0				$-\frac{4}{5}\ aM_I$
			0	−1	1				$\frac{2}{5}\ aM_I$
½	−½	−½	0	1	0	−½	1	½	$1\frac{1}{5}\ aM_I$
			1	1	−1				$1\frac{1}{5}\ aM_I$

With this table we hope to get information about the interaction with the nucleus for each multiplet if placed in a strong magnetic field. If we knew

this we could again apply the sum rule to each multiplet separately and obtain the interaction in a weak field or without field. Table V does not help us much in this respect, however. The different states are labeled with M_S and M_L only and we do not know the values of S and L to which they belong. For instance the pair $M_S=\frac{1}{2}$ and $M_L=0$ occurs three times. We do not know which one of these three belongs to the ^4S, the ^2D or the ^3P, which can each give this pair in a strong field. The answer to this question is that neither of the three belongs to any one of the multiplets. In the language of Slater's paper we should say that the energies entered in the last column of Table V have been calculated with eigenfunctions which do not take into account the interaction between the electrons. The correct eigenfunctions which can be associated with each multiplet are certain linear combinations of the ones which give the perturbation energies used here. The straightforward way to get further results is to use these linear combinations, which can be found in the literature,[20] and to use the quantum mechanics method for first order energy perturbations. In the following section we will describe a method, however, which does not involve the knowledge of the correct linear combinations of unperturbed eigenfunctions but uses certain general properties of multiplets.[21]

8. Hyperfine Structure of a Multiplet

The properties of a multiplet are in many respects a generalization of the properties of a doublet arising from a single electron. Darwin[22] was very successful in explaining every detail of the magnetic properties of a multiplet by treating it as if it were a single electron with an orbital moment L and a spin moment S. It is obvious that not all characteristics of a multiplet state can be obtained in this way; for instance, one would find with Darwin's method that the transition $L\rightarrow L$ is forbidden, whereas in the correct theory it is not. As we are interested here in the magnetic interaction with the nucleus, it is possible that we may use again Darwin's simplification.

For the magnetic interaction with the nucleus we assume a generalization of Eq. (7):

$$W_L + W_S = \lambda M_I M_L - \sigma M_I M_S \frac{6M_L^2 - 2L(L+1)}{(2L-1)(2L+3)}. \tag{31}$$

Before using this expression two important remarks have to be made. This formula does not apply to the interaction between the nucleus and an unbalanced s-electron in the configuration. The interaction with an s-electron is of the simple cosine form and gives therefore

$$W_S = \beta M_I M_S. \tag{32}$$

[20] J. A. Gaunt, Phil. Trans. **A228**, 184 (1929); J. H. Bartlett, Jr., Phys. Rev. **34**, 1247 (1929).

[21] Table V, as it is now, does not give us much more information than we obtained with the general sum rule data of Table I. The only additional information one gets is by considering the state with $M_S=1\frac{1}{2}$, $M_L=0$. This pair can only arise from the ^4S; the table gives an interaction energy zero, thus the ^4S will have $A=0$ in extreme Russell-Saunders coupling. So the sum of the energies belongs to the $^2D_{1\frac{1}{2}}$ and the $^2P_{1\frac{1}{2}}$, but further separation is not possible with this method.

[22] C. G. Darwin. Proc. Roy. Soc. **A115**, 1 (1927).

If the configuration to which the multiplet belongs contains such an s-electron one must add a term like Eq. (32) to Eq. (31). The second remark concerns the factors λ and σ. For the case of one single electron these were both equal to a. For a more complicated configuration one should not expect the coefficient for the orbital part to be the same as for the spin part. As we shall see later on it is possible to obtain a relation between λ and σ in certain simple cases.

In order to find the values of $A(J)$ for each level of the multiplet we must again consider the sums of the results of Eq. (31) for a fixed choice of $M_J = M_S + M_L$. One takes first $M_J = S+L$, which occurs only once, next $M_J = S+L-1$, occurring twice, and so on. The procedure is exactly the same as that followed in Section 3, but of course much longer, depending upon the values of S and L. It is possible to do it for general values of S and L and one obtains finally the general formula

$$A(J) = \lambda(2-g) - \sigma\frac{6\Gamma(2-g) - 2(g-1)L(L+1)}{(2L-1)(2L+3)} + \beta(g-1). \qquad (33)$$

The last term occurs only when there is an unbalanced s-electron. In this formula g is the ordinary Landé g value, and Γ stands as usual for[23]

$$\Gamma = SL\cos(S,L) = \{J(J+1) - L(L+1) - S(S+1)\}/2. \qquad (34)$$

The derivation of this formula is elementary but too cumbersome and long to be given here, but I am willing to give personal information about it to anyone who really might need it.

In the preceding sections of this paper we have always taken together the interaction W_S with the spin and W_l with the orbital moment. It is quite simple, however, to go back to Eq. (7) and keep these two separate. If we then know these interactions for only one level of a multiplet, we can determine λ and σ and find A for all other levels of the same multiplet. The sum rule of Table I or Table V will, in practically all cases, furnish us with sufficient information to do this. We shall show this again with the p^3 example.

For p^3 the sum rule gives that for $^2D_{2\frac{1}{2}}$ $A = {}^{24}/_{25}a$. If we go back to Eq. (7) via Table I we find that this is divided as follows between the interactions with spins and orbits:

$$\text{with spins: } {}^{4}/_{25}a, \quad \text{with orbits: } \tfrac{4}{5}a,$$

Furthermore, we know that for $^2D_{2\frac{1}{2}}$: $\Gamma = +1$, $g = 1\frac{1}{5}$ and we find from Eq. (33) (omitting the last term):

$$\tfrac{4}{5}a = \lambda\tfrac{4}{5}, \quad {}^{4}/_{25}a = -\sigma\frac{4\frac{4}{5} - 2\frac{2}{5}}{21}$$

from which

$$\lambda = a, \quad \sigma = -1\tfrac{2}{5}a.$$

[23] Γ is the deplacement of the level from the center of gravity of the multiplet.

With these values we find for the A of $^2D_{1\frac{1}{2}}$, for which $\Gamma = -1\frac{1}{2}$, $g = \frac{4}{5}$,

$$A(^2D_{1\frac{1}{2}}) = \lambda 1\tfrac{1}{5} - \sigma\frac{-10\frac{4}{5} + 2\frac{2}{5}}{21} = {}^{16}/_{25}a.$$

It is possible to find relations between λ and σ for the different multiplets of a configuration, or for the multiplets which arise after the addition of an s-electron. Lack of material to test such formulae make it useless to go into more detail, also with respect to the remarks made in the following section.

For intermediate coupling one can apply to a great extent the same method as used in a previous paper.[24]

9. Serious Discrepancies

The hyperfine structure is in many spectra caused by a deeply penetrating s electron, the influence of other electrons being negligibly small. For such cases the theory is simple, hyperfine structure separations can be expressed in terms of Landé cosines and the experimental data have been shown to agree with the theory.[25] For non-s electrons no such check has been obtained until now.

The following enumeration of data shows that there are large discrepancies between the theory and the observations for non-s electrons. Though the experimental results are very scarce and often uncertain, the reality of these discrepancies in the example of bismuth is beyond all doubt. The present material is quite insufficient, however, to give quantitative information about the deviations.

A part of the deviations will be due to higher order corrections. The method used in this paper assumes that it is sufficient to consider only first order perturbations for the interaction between the electrons and the spin orbit interactions. This means that our results are obtained by using only zeroth order eigenfunctions in the correct stabilized linear combinations. For heavy elements one must also consider the first order terms of the spin-orbit perturbation in the eigenfunctions. This will cause the hyperfine structure formulae to contain correction terms which are of exactly the same nature as those derived by Fermi[26] for the anomalies in the alkali doublet intensities. An estimate of the order of magnitude of these corrections shows that they are probably not large enough to account for the deviations.

Bismuth I[27] $(I = 4\frac{1}{2})$

$$6s^26p^3\ ^2D_{2\frac{1}{2}}: \quad \tfrac{4}{5}a' + \tfrac{1}{5}a'' = 0.081 \pm 0.002$$
$$^2P_{\frac{1}{2}}: \quad a'' = 0.375$$
$$(^2D_{1\frac{1}{2}}: \quad 1\tfrac{1}{5}a' - \tfrac{1}{5}a'' = -0.040 \pm 0.002).$$

[24] S. Goudsmit, Phys. Rev. **35**, 1325 (1930).

[25] S. Goudsmit and R. F. Bacher, Phys. Rev. **34**, 1501 (1929).

[26] E. Fermi, Zeits. f. Physik **59**, 680 (1930). This remark about the second order terms I owe to Dr. H. Casimir, with whom I discussed the discrepancies during his stay here last summer. Phys. Rev. in preparation.

[27] P. Zeeman, E. Back and S. Goudsmit, Zeits. f. Physik **66**, 1 (1930).

The coupling is not of the extreme (j, j) type. This does not, however, affect the validity of the formulae given for the first two levels, as they are the only ones with $J=2\frac{1}{2}$ and $\frac{1}{2}$ in this configuration. The two first equations give

$$6p\ J = \tfrac{1}{2}\colon\ a'' = 0.375$$
$$1\tfrac{1}{2}\colon\ a' = 0.007 \pm 0.003.$$

The second order corrections for this case are uncertain, a study of the levels of Bi III makes one believe that they should decrease a'' and increase a' by not more than about 5 percent. One sees that a' is much too small for the theory predicts that $a'=\frac{1}{5}a''$. Though the formula given for $^2D_{1\frac{1}{2}}$ is not strictly valid here, the negative value of its separation factor corroborates our conclusion that a' is much too small.

Bismuth II[28]

$$6s^2\ 6p_{\frac{1}{2}}7s \quad 2_1{}^0\colon \tfrac{1}{2}a'' + \tfrac{1}{2}b = 0.391 \pm 0.001$$
$$6p_{1\frac{1}{2}}7s \quad 9_2{}^0\colon \tfrac{3}{4}a' + \tfrac{1}{4}b = 0.109 \pm 0.007.$$

One expects the values for a'' and a' of the $6p$ electron in Bi II to be about the same as in Bi I. The above equations are indeed in agreement with this and give both for b about 0.38. If one assumed, however, that a' were really $\frac{1}{5}a''$ one would obtain an impossible negative value for b and a too large value for a' and a''.

Bi III

$$6s^2\ 7p\ {}^2P_{\frac{1}{2}}\colon\ a'' = 0.102 \pm 0.003$$
$${}^2P_{1\frac{1}{2}}\colon\ a' = 0.021 \pm 0.004.$$

The second order corrections for the $7p$ electron are expected to be somewhat larger than for the $6p$. They tend to increase a'' by perhaps 10% and to decrease a' by about 5%. We have here a case where indeed the theoretical ratio between a' and a'' is close to the observed one, but one has to keep in mind that a' is not known with accuracy.

Manganese[29] $(I=2\frac{1}{2})$. Most of the hyperfine structure in manganese is caused by the $4s$ electron. For a few levels the hyperfine structure is due to the $3d$ and $4p$ electrons, but for these levels the separations are not known with sufficient accuracy to check any formulae.

Indium.[30] The measurements on the principal doublet of the indium spectrum made by McLennan and Allin and by Jackson differ so entirely from each other that they are useless.[31] This example would have been a very significant check of the theory.

[28] New observations on Bi II and III made by R. A. Fisher and the present author, to be published shortly. Classification and notation from J. C. McLennan, A. B. MacLay and M. F. Crawford, Proc. Roy. Soc. A. **129**, 579 (1931).

[29] H. E. White and R. Ritschl, Phys. Rev **35**, 1146 (1930).

[30] J. C. McLennan and E. J. Allin, Proc. Roy. Soc. **A128**, 508 (1930). D. A. Jackson, Proc. Roy. Soc. **A129**, 208 (1930).

[31] The fair agreement which Jackson seems to obtain between his measurements and the theory is caused by an unfortunate error in a paper by Fermi. Fermi (ref. 2) gives formulae for the hyperfine splitting of a $^2P_{1\frac{1}{2}}$ level in case $I \geqq 1\frac{1}{2}$. He mentions in the text how these formulae change for a case where $I<1\frac{1}{2}$ and just this sentence happens to be incorrect. Jackson's results again give a' too small.

Thallium I. ($I=\frac{1}{2}$). Only one of the two lines of the principal doublet of thallium has been studied in detail.[32] The present data on the other line are insufficient to draw any certain conclusions, though they also seem to indicate for this case that a' is too small.

Thallium III.[33]

$$7p\ {}^2P_{\frac{1}{2}}: \quad a'' = 0.375$$
$${}^2P_{1\frac{1}{2}}: \quad a' = 0.218.$$

The second order corrections are rather large in this case, namely about 15%. They would increase a'' and decrease a'. For this example a' is much larger than the theoretical value.

Conclusion

Though the experimental data are scarce we come to the conclusion that the present theory of the hyperfine structure separations is incorrect or at least incomplete. The method used in this paper is not the cause, for it has been applied very successfully to many other problems, but the use of the classical Eq. (3),

$$W_l + W_s = a[Il\cos(I, l) - Is\cos(I, s) + 3Is\cos(I, r)\cos(r, s)].$$

The correct quantum mechanical expression for the spin-spin interaction will perhaps contain different terms. The generalizations of the Dirac theory for the two-body problem given by Gaunt[34] and Breit[35] contain indeed extra terms for the spin-spin interaction. From a study of the helium triplet, with which one can test a part of these extra terms, Breit[36] concluded that their presence was in disagreement with the experimental data on the spin-spin interaction of two electrons. Perhaps such terms do have a real significance for the interaction between nuclear and electron spin[37].

This discussion shows the importance of the study of hyperfine structure as a guide for the further development of the quantum theory, especially for the generalization of the Dirac equation. Let us, therefore, hope that experimental physics will soon provide us with at least one doublet state for which the hyperfine structure of both levels can be given with certainty and accuracy.

Appendix

Just before sending off this paper I received a letter from Dr. John Wulff, National Research Fellow at Tübingen, in which he describes important new measurements on the hyperfine structure as well as the Zeeman effect of the principal thallium doublet. The $6p_{\frac{1}{2}}$ level has $a''=0.708$, whereas the $6p_{1\frac{1}{2}}$ level is unresolvably small. The value for a' is probably of the order 0.015, thus about ten times too small.

[32] E. Back and J. Wulff, Zeits. f. Physik **66**, 31 (1930).
[33] J. C. McLennan and E. J. Allin, Proc. Roy. Soc. **A129**, 43 (1930).
[34] J. A. Gaunt, Phil. Trans. **228**, 151 (1929). Proc. Roy. Soc. **A122**, 153 (1929).
[35] G. Breit, Phys. Rev. **34**, 553 (1929).
[36] G. Breit, Phys. Rev. **36**, 383 (1930).
[37] This will be discussed in a paper by D. R. Inglis, to be published soon.

THE VAN DER WAALS FORCES IN GASES

By John C. Slater and John G. Kirkwood
Massachusetts Institute of Technology

(Received February 5, 1931)

Abstract

A calculation of van der Waal's potential of two atoms at large separation has been carried out for hydrogen and helium. The method depends upon a representation of the perturbed wave function of the system as

$$\psi = \psi_0 (1 + vR)$$

where ψ_0 is the unperturbed wave function, v the perturbing potential and R is a function of the radial coordinates of the electrons. The method is equally well adapted to the calculation of polarizabilities. A computation of the mutual energy of two hydrogen atoms confirms the results of Eisenschitz and London. The polarizability of helium is calculated as 0.210×10^{-24} cc which agrees well with the experimental value, 0.205×10^{-24}. The mutual energy of two helium atoms is found to be $-3.18\, E_0/(R/a_0)^6$. A correlation between the mutual energy of the two molecules, ϵ, and the polarizability, α, is obtained:

$$\epsilon = -1.36\, \nu_0^{1/2}\, a_0^{3/2}\, \alpha^{3/2}\, E_0/R^6$$

where ν_0 is the number of electrons in the highest quantum state in the molecule, E_0 the energy of the hydrogen atom in the normal state, and R is the separation of the molecules. By means of this formula, the van der Waals cohesive pressure constant is calculated for Ne, A, N_2, H_2, O_2, and CH_4.

I. Introduction

IT HAS been recognized for some time that the van der Waals forces in gases have their origin in a mutual polarization of the molecules. The idea was suggested by Debye,[1] but his calculation of intermolecular energies, based upon an electrostatic molecular model, did not meet with great success. This fact is not surprising in the light of recent work, which has shown that a rapidly pulsating field associated with the internal motion of the electrons in the molecule is the chief factor in determining the mutual energy of two molecules at separations sufficiently large to prevent the exchange of electrons. This fact was suggested, although not explicitly stated, in a calculation of the mutual energy of two hydrogen atoms by Wang.[2] Recently, Eisenschitz and London[3] have presented a general method of calculating the mutual energy of two molecules at large separation. Their method depends upon an expansion of the wave function of the system in terms of a selected set of the unperturbed wave functions of the two molecules. They have confirmed the form of Wang's result for two hydrogen atoms, although they have shown

[1] Debye, Phys. Zeits. **21**, 178 (1920).

[2] S. C. Wang, Phys. Zeits. **28**, 663 (1927).

[3] Eisenschitz and London, Zeits. f. Physik **60**, 491 (1930); London, Zeits. f. Physik **63**, 245 (1930).

it to be numerically in error. Hassé,[4] with a variational method, has calculated the polarizability of helium. The wave function obtained by Waller[5] in a treatment of the quadratic Stark effect in hydrogen, serves as a basis for the calculation. An empirical extension of the method employed in this case permits him to calculate the mutual energy of two atoms at large separation both for hydrogen and helium.

The present method resembles that of Hassé in that use is made of the variation principle. However, his choice of wave function was more or less empirical and the perturbation energy was calculated as a part of the total energy. On the other hand, we have formulated the variation problem for a direct determination of the perturbation energy by itself, and from the original wave equation have obtained a simplified Euler equation for this variation problem, which when it cannot be solved directly, serves as a guide in choosing an approximate function. The method, while lacking the generality of that of London and Eisenschitz, is applicable to most non-polar molecules in the normal state.

II. Polarizability and Interatomic Energy of Hydrogen

We shall begin by considering a system of ν electrons with an unperturbed wave function ψ_0, while the correct wave function under the influence of a perturbing potential v is ψ. The wave equations in the two cases may be written

$$\begin{aligned} \nabla^2\psi_0 + \kappa^2(E_0 - V_0)\psi_0 &= 0 \\ \nabla^2\psi + \kappa^2(E - V)\psi &= 0 \\ \kappa^2 &= 8\pi^2 m/h^2 \\ E &= E_0 + \epsilon \\ V &= V_0 + v. \end{aligned} \tag{1}$$

Here E_0 and V_0 are the initial total and potential energies of the system and ϵ is the energy acquired by virtue of the perturbation. The operator ∇^2 is understood to be referred to the 3ν dimensional configuration of the system of ν electrons. If we let

$$\psi = \psi_0(1 + \phi) \tag{2}$$

we obtain the following equation

$$\nabla^2\phi + 2\sum_{j=1}^{3\nu} \frac{\partial \ln \psi_0}{\partial x_j} \frac{\partial \phi}{\partial x_j} + \kappa^2(\epsilon - v)(1 + \phi) = 0. \tag{3}$$

Since we shall not be interested in perturbation effects of higher order than the second, it is only necessary to retain terms of the first order in v and ϕ. Thus we can replace the factor $(1+\phi)$ by 1, since it is multiplied by a small quantity. Further, in all the cases to which our method is applicable, the mean value of the perturbing potential over the unperturbed wave function

[4] H. R. Hassé, Proc. Camb. Phil. Soc. **26**, 542 (1930).
[5] Waller, Zeits. f. Physik **38**, 635 (1926).

is zero, the first order perturbation in the energy vanishes, and ϵ is small of the second order. For this reason we may replace $\epsilon - v$ by $-v$, obtaining an equation which does not contain an energy parameter at all. When we make these approximations, Eq. (3) becomes

$$\nabla^2\phi + 2\sum_{j=1}^{3v} \frac{\partial \ln \psi_0}{\partial x_j} \frac{\partial \phi}{\partial x_j} - \kappa^2 v = 0. \tag{4}$$

The polarization of the hydrogen atom in its normal state by an homogeneous electric field, F, affords the simplest example of the application of Eq. (4). Here

$$\begin{aligned} \psi_0 &= e^{-r} \\ v &= \sum_{j=1}^{3} g_j x_j \end{aligned} \tag{5}$$

where r is the radial distance of the electron from the nucleus expressed in units of a_0, the Bohr radius of the normal state, and

$$g_j = -eF_{x_j}.$$

The components F_{x_j} of the field, F, are referred to a rectangular system of coordinates with origin in the nucleus of the atom. If we choose as new variables, r and v, and if we let

$$\phi = \frac{vR(r)}{E_0} \tag{6}$$

where E_0 is the absolute value of the energy of the hydrogen atom in the normal state, a separation of variables in Eq. (4) is effected and there results

$$\frac{d^2R}{dr^2} + \left(\frac{4}{r} - 2\right)\frac{dR}{dr} - \frac{2R}{r} - 1 = 0 \tag{7}$$

where r is measured in units of a_0. The solution is

$$R = -\frac{1}{2}\left(1 + \frac{r}{2}\right) + C_1\left(\frac{1}{r} + \frac{1}{r^2} + \frac{1}{2r^3}\right) + C_2\frac{e^{2r}}{r}.$$

In order that the integral

$$\int \psi\bar{\psi} d\tau$$

may exist, it is necessary to set C_1 and C_2 equal to zero. The new wave function takes the form

$$\psi = e^{-r}\left(1 - \frac{v}{2E_0}\left[1 + \frac{r}{2}\right]\right).$$

If the original rectangular coordinate system is chosen with z-axis parallel to the field, $v = -eFz$, and the above wave function becomes identical with that obtained by Waller.[6] The energy is given by

[6] Waller, reference 5.

$$E = E_0 + \epsilon = -\frac{1}{\kappa^2}\frac{\int \bar{\psi} H \psi d\tau}{\int \psi \bar{\psi} d\tau}.$$

When ϕ has the form, $vR(r)$, and ψ_0 is a function of r alone, the integrals occurring in the evaluation of ϵ are of the form

$$\int v^n f(r) d\tau \quad n = 1, 2, 3.$$

If v is a harmonic function which vanishes when r is zero, the term for $n=1$ (and $n=3$) vanishes. That is, the first order perturbation energy is zero. Then the only term which we need consider is the one with $n=2$. This condition is of course fulfilled in the problem which we have just considered, and will be fulfilled in the subsequent problems to be treated. The expression for ϵ now becomes

$$\epsilon = \frac{\int v\phi\psi_0^2 d\tau}{\int \psi_0^2 d\tau} \tag{8}$$

with the neglect of perturbation terms in the normalization of ψ. These will contribute only to terms in ϵ of higher order than the second.

A computation of the polarization energy of the hydrogen atom using the wave function which we have obtained yields

$$\epsilon = -2.25 a_0^3 F^2$$

which corresponds to a polarizability

$$\alpha = 4.5 a_0^3.$$

These, values, of course, agree with those obtained by Waller.

In this simple case, the solution of Eq. (7) offers no difficulty. It is of interest, nevertheless, to see what value of the energy may be obtained, if our information is restricted to the fact that $\phi = vR(r)$. Let us try as a representation of $R(r)$ the expression, λr^n. The energy integral becomes

$$\epsilon = \frac{\int v\phi[1 - \rho[R]]\psi_0^2 d\tau}{\int \psi_0^2 d\tau} \tag{8}$$

where

$$\rho[R] = \frac{d^2R}{dr^2} + \left(\frac{4}{r} - 2\right)\frac{dR}{dr} - \frac{2R}{r} - 1.$$

If we minimize the integral with respect to the parameters λ and ν, we obtain

$$\epsilon = -2.24 a_0^3 F^2$$
$$\lambda = -0.728/E_0; \quad \nu = 0.5.$$

This value agrees with the exact one to somewhat better than 0.50%.

The method may be applied with almost equal simplicity to the interaction of two hydrogen atoms. If the separation, R_0, of the two atoms is sufficiently large to prevent electron interchange, the wave function of the system is

$$\psi_0 = \psi_{01}\psi_{02} = e^{-(r_1+r_2)}$$

where r_1 and r_2 are the respective radial distances of each electron from its own nucleus. When referred to two rectangular coordinate systems with their respective origins in the two nuclei and with z-axes directed along R_0, the dipole term in the perturbing potential is given by

$$\frac{e^2}{R_0^3}[x_1x_2 + y_1y_2 - 2z_1z_2].$$

Terms due to multipoles of higher order will be neglected. If we let

$$\phi = \frac{vR(r_1, r_2)}{E_0}$$

and change the variables in Eq. (4) to v, r_1 and r_2, a separation is again effected and we have

$$\frac{\partial^2 R}{\partial r_1^2} + \frac{\partial^2 R}{\partial r_2^2} + \left(\frac{4}{r_1} - 2\right)\frac{\partial R}{\partial r_1} + \left(\frac{4}{r_2} - 2\right)\frac{\partial R}{\partial r_2} - 2R\left(\frac{1}{r_1} + \frac{1}{r_2}\right) - 1 = 0 \quad (9)$$

The existence of a solution of this equation is assured by the negative value of the coefficient of R.[7] A solution by successive approximation may be obtained in the following manner. Let us write Eq. (9) as

$$R = -\frac{1}{2}\frac{r_1r_2}{r_1+r_2}\left\{1 - \left[\frac{\partial^2 R}{\partial r_1^2} + \frac{\partial^2 R}{\partial r_2^2} + \left(\frac{4}{r_1} - 2\right)\frac{\partial R}{\partial r_1} + \left(\frac{4}{r_2} - 2\right)\frac{\partial R}{\partial r_2}\right]\right\}.$$

If the differential function is neglected

$$R = -\frac{1}{2}\frac{r_1r_2}{r_1+r_2}. \quad (10)$$

Substitution of this expression in the differential function will yield a second approximation. Repetition of this process will yield a still closer approximation. If we use merely the first approximation (10), we calculate a value of the energy,

$$\epsilon = -6.14\frac{e^2a_0^5}{R_0^6}.$$

[7] Goursat, Cours d'Analyse Mathematique, vol. III, 249.

This is about 5 percent higher than the value

$$-6.47\frac{e^2a_0^5}{R_0^6}$$

obtained by Eisenschitz and London.[8] The use of higher terms in the expansion of R would permit us to approach the true value as closely as we pleased. Although no difficulty is encountered in the evaluation of the integrals occurring in the energy expression, the tedium of the calculation is reduced by using the variation method. Eq. (10) suggests as a representation of R, the expression

$$\lambda r_1^{\nu} r_2^{\nu}.$$

If the function is inserted in the energy integral and the latter is minimized with respect to the parameters λ and ν one obtains

$$\epsilon = -6.49\frac{e^2a_0^5}{R_0^6}$$

$$\nu = 0.325.$$

This is in excellent agreement with the result of London and Eisenschitz. The fact that their value lies slightly higher instead of slightly lower than the one which has just been obtained is doubtless attributable to an error in estimating the contribution of the continuous spectrum in their expansion of ψ, since the variation method cannot give too low a value of the energy.

The fact that the wave function in the two cases which have been considered may be expressed as

$$\psi_0(1 + vR)$$

where R is a function of the radial distances of the electrons from their nuclei, is indeed logical from a physical point of view. In the absence of degeneracy, one would expect the distortion of the wave function to depend in some simple way upon the perturbing potential. Moreover, for a given value of the perturbing potential it is evident that the distortion will be greater, as the distance of the electron from the nucleus becomes greater, since the restoring force exerted by the nucleus will be smaller. The function R provides for this effect. The separation of the differential Eq. (4) in terms of v and the r's appears to depend upon the linear properties of v in the rectangular coordinates of the electrons, and the spherical symmetry of the unperturbed wave function.

III. Generalization of the Method: Polarizability and Interatomic Energy of Helium

For the helium atom, or in general for an atom with ν electrons each having a spherically symmetrical distribution, the wave function may be approximately represented by

$$\psi_0 = \prod_{j=1}^{\nu}\psi_j(r_j) \tag{11}$$

[8] Eisenschitz and London, reference 3.

where the function ψ_j depends only upon the radial coordinate of the electron j. Such a function may be approximated by an expression

$$r^{n-1}e^{-(Z-s)r/n}$$

where n is an effective quantum number, s a screening constant, Z the total nuclear charge. If we wish to represent the wave function accurately in the region of its maximum, we may choose n and s by minimizing the total energy, as Zener has done. If, however, we are more interested in the value of the function for large values of r, we may choose s to be equal to the total number of electrons except for the one being considered, and use an effective quantum number which is non-integral. Thus for He, in the neighborhood of the maximum, we choose $Z-s=1.6875$ (or, for some purposes, 1.70), $n=1$; while for large r's, we take $Z-s=1$, $n=0.745$.[9] We use these formulas for approximate computation of polarizability and interatomic force.

A better representation of the wave function can be obtained by more complicated methods, as that of Hartree,[10] or the method used by one of the authors on He.[11] These give almost identical results for He, as far as the purposes of this paper go, and for quantitative work we make use of the latter in one calculation of the polarizability and interatomic energy of helium.

We shall first consider the polarization of the molecule by an homogeneous field F. The perturbing potential is

$$v = \sum_{j=1}^{\nu} v_j$$

where

$$v_j = -e\sum_{k=1}^{3} F_{xk}x_{jk}$$

If we let

$$\phi = \frac{1}{E_0}\sum_{j=1}^{\nu} v_j R(r_j) \tag{12}$$

and make use of the facts that $\partial \ln \psi_0/\partial r_j$ depends only upon r_j, the distance of electron j from the nucleus and that

$$\sum_{k=1}^{3} x_{jk}\frac{\partial v}{\partial x_{jk}} = v_j$$

we find that Eq. (4) splits into ν equations of the form

$$\frac{d^2R}{dr^2} + \left(\frac{4}{r} + 2\frac{d\ln\psi_0}{dr}\right)\frac{dR}{dr} + \frac{d\ln\psi_0}{dr}\frac{R}{r} - 1 = 0. \tag{13}$$

If we use a wave function of the simpler type discussed above this equation becomes

[9] C. Zener, Phys. Rev. **36**, 51 (1930); J. C. Slater, Phys. Rev. **32**, 349 (1928); J. C. Slater, Phys. Rev. **36**, 57 (1930).

[10] D. R. Hartree, Proc. Camb. Phil. Soc. **24**, 89 (1928).

[11] J. C. Slater, Phys. Rev. **32**, 349 (1928).

$$\frac{d^2R}{dr^2} + 2\left(\frac{n+1}{r} - \frac{Z-s}{n}\right)\frac{dR}{dr} + 2\left(\frac{n-1}{r^2} - \frac{Z-s}{nr}\right)R - 1 = 0. \quad (14)$$

The energy given by Eq. (8) is

$$\epsilon = \frac{\int \sum_{j=1}^{r} \sum_{k=1}^{r} v_j \phi_k \psi_0^2 d\tau}{\int \psi_0^2 d\tau}.$$

Since upon integration all terms involving $v_j\phi_k$ with $j \neq k$ vanish

$$\epsilon = \sum_{j=1}^{r} \epsilon_j$$

and

$$\epsilon_j = \frac{\int v_j \phi_j \psi_0^2 d\tau}{\int \psi_0^2 d\tau}.$$

In the computation of ϵ_j it will be convenient to use the variation method rather than to solve Eq. (14) explicitly. The expression becomes

$$\epsilon_j = \frac{\int v_j \phi_j [1 - \rho[R_j]] \psi_0^2 d\tau}{\int \psi_0^2 d\tau}$$

where

$$\rho[R_j] = \frac{d^2R_j}{dr_j^2} + 2\left(\frac{n_j+1}{r_j} - \frac{Z-s_j}{n_j}\right)\frac{dR_j}{dr_j} + 2\left(\frac{n_j-1}{r_j^2} - \frac{Z-s_j}{n_j r_j}\right)R_j - 1.$$

We shall try

$$R = \lambda e^{\beta(z-s)r/n}$$

which is analytically somewhat more convenient than the representation λr^n employed in the case of hydrogen. When the energy integral is minimized with respect to the parameter λ there results

$$\epsilon = \frac{1}{E_0}\frac{J_1^2}{J_2}e^2F^2$$

where

$$J_1 = \frac{\int r^{2n}\cos^2\theta e^{\beta(z-s)r/n}\psi_0^2 d\tau}{\int \psi_0^2 d\tau}$$

$$= \frac{(n+1)(n+\frac{1}{2})}{3}\left(\frac{n}{Z-s}\right)^2 a_0^2 \frac{1}{(1-\beta/2)^{2n+3}}$$

$$J_2 = \frac{\int \left\{ \left(\frac{n}{Z-s} \right)^2 (\beta^2 - 2\beta) r^{2n} + \frac{n}{Z-s} [(n+1)\beta - 1] r^{2n-1} + 2(n-1) r^{2n-2} \right\}}{\int \psi_0^2 d\tau}$$

$$e^{2\beta(z-s)r/n} \cos^2 \theta \psi_0^2 d\tau = -a_0 \frac{1 + (2n-5)\beta/3 + (2n^2 - n + 5)\beta^2/6}{(1-\beta)^{2n+3}}.$$

For the energy we have

$$\epsilon_j = -2 \frac{(n_j+1)^2 (n_j + \frac{1}{2})^2 n_j^4}{9(Z-s_j)^4} a_0^3 F^2 (1+\theta_j) \tag{13a}$$

where

$$\theta_j = \frac{(1-\beta)^{2n_j+3}}{(1-\beta/2)^{4n_j+6}[1 + (2n_j - 5)\beta/3 + (2n_j^2 - n_j + 5)\beta^2/6]} - 1$$

Minimizing with respect to β shows that for $n=1$, $\theta_j = 0.124$. In general $0.124 \geqq \theta_j \geqq 0$; $n_j \geqq 1$. For the total polarization energy we may write

$$\epsilon = -2a_0^3 F^2 \sum_{j=1}^{\nu} \frac{n_j^4 (n_j+1)^2 (n_j + \frac{1}{2})^2 (1+\theta_j)}{9(Z-s_j)^4}$$

and for the polarizability

$$\alpha = 4a_0^3 \sum_{j=1}^{\nu} \frac{n_j^4 (n_j+1)^2 (n_j + \frac{1}{2})^2 (1+\theta_j)}{9(Z-s_j)^4}.$$

We shall first compute the polarizability of helium taking n as 1 and $Z-s$ as 1.6875, the values obtained by minimizing the total energy of the atom. We obtain

$$\alpha = 1.11 a_0^3 = 0.164 \times 10^{-24} \text{cc}.$$

If on the other hand we use the limiting values at large distances for n and $Z-s$ we have $n=0.745$; $Z-s=1$, and we obtain

$$\alpha = 1.51 a_0^3 = 0.222 \times 10^{-24} \text{cc}.$$

The value of α corresponding to measurements of the refractive index is 0.205×10^{-24}. As we should have anticipated it lies between the two values which we have calculated. The first wave function which emphasizes the smaller r's at the expense of the larger gives a value of α about 20 percent below the experimental one, while the second wave function which emphasizes the larger r's gives a value about 8 percent higher than the experimental one. The second wave function which is accurate only for large values of r gives a surprisingly good result.

A more exact determination of the polarizability of helium may be obtained with the use of the more accurate wave function mentioned above. After normalization and integration over the configuration space of one electron, the square of the wave function for each electron may be represented by

$$0.7604(1 + 1.440e^{-1.692r})e^{-3r+0.0214r^2};\ r < 3$$

$$0.6048(1 + 1.440e^{-1.692r})e^{-2.688r}r^{-0.510}\left(1 + \frac{0.1414}{r} + \cdots\right);\ r > 3.$$

We shall use as a representation of R the function λr^ν. Minimizing the energy integral with respect to the parameter λ gives

$$\epsilon = \frac{1}{E_0}\frac{{J_1}^2}{J_2 J_0}e^2 a_0^2 F^2$$

where

$$J_0 = \int \psi_0^2 d\tau$$

$$J_1 = \int r^{\nu+2}\psi_0^2 d\tau$$

$$J_2 = \int \left\{ \nu(\nu+2)r^{2\nu} + 2(\nu+1)\frac{d\ln\psi_0}{dr}r^{2\nu+1}\right\}\psi_0^2 d\tau.$$

Properly, this expression should be computed for different ν's and the minimum chosen. On account of the labor of the integration, however, we have arbitrarily chosen the value $\nu = 0.5$. This was the value found for the simple wave functions used above, and moreover it was found that the result was so insensitive to ν that a variation of ± 0.1 in ν did not affect the final result by more than one percent. The above integrals have been computed graphically for $\nu = 0.5$ and the polarizability of helium was found to be

$$\alpha = 1.43a_0^3 = 0.210 \times 10^{-24}\text{cc}.$$

This yields a value of the dielectric constant at 0° and 1 atm. of 1.0000715 which is slightly lower than the experimental value, 1.000074. It is however, somewhat higher than the square of the measured refractive index extrapolated to infinite wave-length, 1.000070. The agreement among the various values is not unsatisfactory when one remembers that the accuracy in the measured refractive index, and dielectric constant cannot be very great, in view of the experimental difficulties in such measurements.

A calculation of the mutual energy of two atoms may be carried out in a similar manner. The dipole term in the perturbation potential may be written

$$v = \sum_{j=1}^{\nu}{}' \sum_{k=1}^{\nu}{}' v_{jk}$$

where the sum is understood to be taken over all possible electron pairs between the two atoms. Each v_{jk} has the form

$$\frac{e^2}{{R_0}^3}[x_k x_j + y_k y_j - 2z_k z_j].$$

If we let

$$\phi = \frac{1}{E_0} \sum_{j=1}^{\nu}{}' \sum_{k=1}^{\nu}{}' v_{jk} R(r_j, r_k).$$

Eq. (4) separates into ν^2 equations of the form

$$\frac{\partial^2 R}{\partial r_j^2} + \frac{\partial^2 R}{\partial r_k^2} + \left(\frac{4}{r_j} + \frac{2\partial \ln \psi_0}{\partial r_j} \right) \frac{\partial R}{\partial r_j} + \left(\frac{4}{r_k} + \frac{2\partial \ln \psi_0}{\partial r_k} \right) \frac{\partial R}{\partial r_k} + 2R \left(\frac{1}{r_j} \frac{\partial \ln \psi_0}{\partial r_j} + \frac{1}{r_k} \frac{\partial \ln \psi_0}{\partial r_k} \right) - 1 = 0. \tag{17}$$

Moreover the energy may be written

$$\epsilon = \sum_{j=1}^{\nu}{}' \sum_{k=1}^{\nu}{}' \epsilon_{jk}$$

where

$$\epsilon_{jk} = \frac{\int v_{jk} \phi_{jk} (1 - \rho_{jk}) \psi_0^2 d\tau}{\int \psi_0^2 d\tau}.$$

If an exact solution of Eq. (17) is used, ρ_{jk} which is the differential expression on the left hand side of Eq. (17) vanishes. We shall use the two representations

$$R_{jk} = \lambda r_j^{\nu} r_k^{\nu}; \quad R_{jk} = \lambda e^{\beta(r_j + r_k)}$$

which proved effective in the case of hydrogen, according to their analytical convenience in conjunction with the unperturbed wave function which is chosen. The parameters are determined by minimizing the energy integral. The details of the calculation are quite similar to those in the calculation of polarizabilities. With the simple wave function

$$\psi_0 = \prod_{j=1}^{\nu} r_j^{n_j - 1} e^{-\gamma_j r_j / n_j}; \quad \gamma_j = Z - s_j$$

we obtain the following result

$$\epsilon = -\frac{13}{27} \frac{e^2 a_0^5}{R_0^6} \sum_{j=1}^{\nu} \sum_{k=1}^{\nu} \frac{n_j^4 n_k^4 (n_j+1)^2 (n_j+\frac{1}{2})^2 (n_k+1)^2 (n_k+\frac{1}{2})^2}{\gamma_j^2 \gamma_k^2 \{ \gamma_k^2 n_j^2 (n_j+1)(n_j+\frac{1}{2}) + \gamma_j^2 n_k^2 (n_k+1)(n_k+\frac{1}{2}) \}} \tag{18}$$

For convenience in representation certain factors $1+\theta_{jk}$ occurring in each term have all been assigned the value which they assume for 1-quantum electrons. Since

$$0 \leqq \theta_{jk} \leqq 0.07$$

the above formula will approximate the true one to within a few percent in every case. We shall calculate the mutual energy of two helium atoms first taking $Z-s=1.6875$ and $n=1$. We obtain

$$\epsilon = -1.13\frac{e^2a_0^5}{R_0^6}.$$

If we now take the values $n=0.745$, $Z-s=1$, which occur in the asymptotic form of the wave function we obtain as in the case of the polarizability a somewhat larger value:

$$\epsilon = -1.78\frac{e^2a_0^5}{R_0^6}.$$

The same calculation has been made with the use of the more accurate wave function for He. As a representation of the function R, $\lambda r_j^{\nu} r_k^{\nu}$ was selected. The integrals, similar to those encountered in the calculation of the polarizability, were evaluated graphically. The energy of two helium atoms was computed as

$$\epsilon = -1.59\frac{e^2a_0^5}{R_0^6} = -3.18\frac{E_0}{(R_0/a_0)^6}.$$

This value lies between the two values obtained with the hydrogenic wave function. It is about 30 percent higher than that obtained with values of Z and n determined to give the best energy for the atom and about 13 percent below the value obtained with the asymptotic values of n and Z. Since the wave function which gave the above value also gives a good value of the polarizability, it is likely that the above value is correct within one or two percent. Hassé obtains a value

$$-2.93\frac{E_0}{(R/a_0)^6}$$

which differs from our result by about 8 percent. Both of these values are slightly above the upper limit for the mutual energy of two helium atoms calculated by London:

$$\epsilon = -3/4\alpha^2 V_i/R^6$$

where α is the polarizability and V_i the ionization potential. This has the value

$$-2.65\frac{E_0}{(R/a_0)^6}.$$

The fact that both Hassé's and our values lie above London's upper limit is not to be considered as alarming. For London, in using the second order perturbation method, neglected a factor which has been rather consistently overlooked in such calculations: transitions in which two electrons are excited may contribute appreciably to the dispersion and similar terms, and they are connected with larger energy differences than the ionization potential, so that in the upper limit of such an expression as London's we should really have the highest potential connected with a double jump, much larger than V_i. The relation of our results to London's limit suggests that these double jumps are strong enough to shift the center of gravity of the term system beyond the ionization potential.

A result of considerable interest may be obtained from formulas (16) and (18). While neither of them gives particularly accurate representations of α or ϵ, it is possible to reach through them a correlation between these two quantities. First, it is to be noted that in both formulas only terms arising from electrons in the outer shell of the atoms contribute appreciably to the sums. Terms arising from inner shells (if any), are virtually nullified both through a decrease in the effective quantum number and by an increase in the effective nuclear charge. We may therefore write

$$\alpha = \frac{4.5\nu_0 a_0^3}{(Z-S_0)^4}\,\frac{n_0^4(n_0+1)^2(n_0+\frac{1}{2})^2}{9}$$

$$\epsilon = -\frac{6.5\nu_0^2}{(Z-S_0)^6}\,\frac{e^2a_0^5}{R_0^6}\,\frac{n_0^6(n_0+1)^3(n_0+\frac{1}{2})^3}{27}$$

where ν_0 is the number of electrons in the outer shell of the atom; n_0 and S_0 are the effective quantum number and screening constant of these electrons. Elimination of n_0 and $(Z-S_0)$ gives

$$\epsilon = -\beta/R_0^6$$

where

$$\beta = 1.36\nu_0^{1/2}a_0^{3/2}\alpha^{3/2}E_0. \tag{19}$$

Corresponding to the empirically determined polarizability for He, this gives a value $\beta = 3.16a_0^6E_0$. This is in excellent agreement with the value 3.18, calculated with the aid of the accurate wave function above.

IV. Correlation with the Equation of State

Although the computation of the last section applied only to atoms for which each electron had a spherically symmetrical distribution, still it is interesting provisionally to compute van der Waals forces in other cases from the polarizability. In cases where the whole atom is spherically symmetrical, though individual electrons are not, this seems fairly reasonable. Thus we obtain values of $\beta/a_0^6E_0$ for the noble gases as listed in Table I:

Table I.

He	Ne	A	Kr	Xe
3.16	17.0	148	275	582

These values can be tested by calculating the equation of state. Of course, the attractive force is not the only interatomic force; there is also a repulsive force, increasing very rapidly as the atoms approach. This is often represented by assuming the atoms to be rigid, and if the van der Waals attraction is fairly large this is justified. For He, however, large errors are committed by this assumption. The repulsive potential has been computed for atomic hy-

drogen[12] and for helium.[13] It appears possible to represent it in the range of importance in thermal interaction between gas molecules by the approximation formula

$$\epsilon_r = \lambda e^{-cR_0}.$$

It should therefore be possible to write approximately

$$\epsilon = \lambda e^{-cR_0} - \beta/R_0^6$$

for the total interaction energy of two molecules. If the equation of state of a gas is written in the familiar virial form

$$\frac{pV}{RT} = 1 + \frac{B}{V} +$$

where p is the pressure, V the volume, R the ideal gas constant, and T the absolute temperature, it is possible to show that at high temperatures

$$B = 2\pi N \int_0^\infty (1 - e^{-\epsilon/kT}) R^2 dR$$

under the assumption the molecules are spherically symmetrical. Here ϵ is the mutual potential energy of two molecules. If, further the molecules are treated as rigid spheres of diameter σ, and the exponential function in the above integral is expanded, it is found that approximately

$$B = B_0 - A/RT$$

where

$$B_0 = \frac{2\pi N\sigma^3}{3}$$

$$A = -2\pi N^2 \int_\sigma^\infty \epsilon R^2 dR$$

and the equation of state may be written in the van der Waals form

$$p = \frac{RT}{V - B_0} - \frac{A}{V^2}.$$

Moreover, if the repulsive potential is ignored when $R > \sigma$, we may replace ϵ by ϵ_a calculated from Eq. (19). The expression for A then becomes

$$A = 4.76 \times 10^{11}\beta/B_0 \text{ ergs cc/mol} \qquad (20)$$

where B_0 is expressed in cc/mol. It is to be remembered that this is a very rough approximation, for in reality the repulsive potential cannot be adequately represented by a potential wall which rises to infinity when $R = \sigma$. This model is indeed entirely inadequate when the attractive field is very

[12] Heitler and London, Zeits. f. Physik 44, 455 (1927); Suguira, Zeits. f Phvsik 45, 484 (1927).

[13] J. C. Slater, reference 11.

weak as in the case of helium and hydrogen. This is illustrated in Fig. 1. The interatomic potential

$$\epsilon = \left\{ 7.7e^{-2.43R/a_0} - \frac{0.68}{(R/a_0)^6} \right\} \cdot 10^{-10} \text{ ergs}$$

which we have obtained for helium has been plotted as a function of the separation of the two atoms. The dotted line represents the attractive component alone and the distance marked σ on the R-axis represents the effective atomic diameter calculated from the van der Waals B_0 constant. In a later

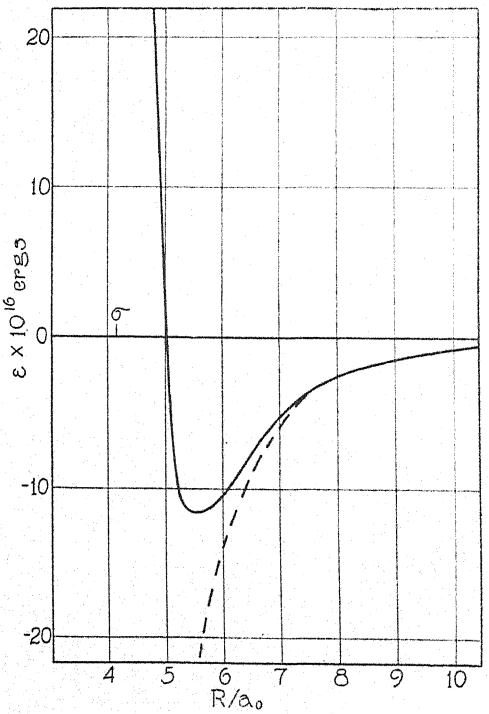

Fig. 1. The mutual energy of two helium atoms plotted as a function of the interatomic distance.

paper a calculation of the second virial coefficient B of helium, based upon the above expression for the interatomic potential, will be presented. It leads to an equation of state and to a description of the thermodynamic properties of helium which are in striking agreement with experiment.

In the present paper, however, we shall content ourselves with the approximation of rigid molecules. We have calculated values of A for several gases by means of Eqs. (19) and (20), from the experimental values of the refractive index and the constant B_0. We have not restricted ourselves to the noble gases, but have included several gases with poly-atomic molecules. The electron configuration in most non-polar molecules resembles that of the noble gases except in the particular case of spherical symmetry. It was thought

that Eq. (19) might still be approximately valid in these cases, since most of the characteristics of the wave function employed in the calculation of α and ϵ were eliminated in the formulation of this relation. The computed values of A are compared with the empirical values of Beattie and Bridgeman[14] in Table II. The A constants for Kr and Xe were computed from viscosity

TABLE II.

	$\alpha.10^{24}$ (cc)	B_0 (cc/mol)	A(calc).10^{-12} (ergs cc)	A(exp).10^{-12} (ergs cc)
Ne	0.39	20.6	0.37	0.21
A	1.65	39.3	1.67	1.29
Kr	2.50	52.8	2.33	2.07
Xe	4.12	70.4	3.70	3.86
N_2	1.74	50.5	1.58	1.34
H_2	0.82	21.0	.55	0.20
O_2	1.59	46.2	1.64	1.49
CH_4	2.59	55.9	2.32	2.28

measurements. The agreement appears to be quite satisfactory. The computed values of A are of course somewhat larger than the empirical ones due to the neglect of the repulsive potential outside the sphere $R=\sigma$. However, as A becomes large, the error introduced by this approximation becomes less important just as we should expect. It is to be hoped that a method of calculating the repulsive potential may soon be developed, in order that a more adequate comparison with experiment may be made.

[14] Beattie and Bridgeman, Proc. Nat. Acad. 63, 229 (1928).

THE SCATTERING OF UNPOLARIZED X-RAYS

By G. E. M. Jauncey and G. G. Harvey
Department of Physics, Washington University

(Received February 4, 1931)

Abstract

Unpolarized x-rays from an x-ray tube excited at 90 to 125 kv and filtered through aluminum and copper were scattered by paraffin at angles of 75°, 97°30′ and 120°. The intensity of the scattered rays was measured by the ionization produced in a chamber containing air saturated with (1) methyl iodide (2) ethyl bromide. It was found very necessary to keep the temperature of the ionization chamber and the voltage on the x-ray tube constant during an experiment. The results are expressed by the ratios of the ionization currents produced at scattering angles of 97°30′ and 120° respectively to the current produced at an angle of 75°. The wave-lengths present in the primary x-rays were determined by measuring the absorption of x-rays in a series of thicknesses of aluminum, the x-rays entering the same ionization chamber as that which was used in the scattering experiment. The absorption curve so obtained was found to consist of two exponential curves which correspond to two wave-lengths, the intensity of the shorter wave-length being much greater than that of the longer. With these wave-lengths and their relative intensities and taking account of the change of absorption in the ionization chamber due to the Compton change of wave-length the theoretical values for the above ratios were calculated by use of (1) the Dirac scattering formula and (2) the Compton formula. The agreement between the ratios calculated from the Dirac formula and the experimental ratios was excellent. The wave-lengths when methyl iodide was in the chamber were 0.205A and 0.39A and when ethyl bromide was in the chamber were 0.26A and 0.47A. At these wave-lengths the difference between the Dirac and the Klein and Nishina formulas is so small that experimental discrimination between them was not possible.

1. Introduction

In 1923, A. H. Compton[1] and Jauncey[2] developed theoretical formulas for the spatial distribution of the intensity of scattered x-rays. The two formulas differ only in the higher powers of α, which is defined by

$$\alpha = h/mc\lambda \tag{1}$$

where λ is the wave-length of the primary x-rays and h, m and c have their usual significance. It is only in the region of γ-rays that the two formulas differ, and as this paper has to do only with the scattering of x-rays and not γ-rays, we shall use the Compton formula as also representing Jauncey's formula with sufficient exactness. According to Compton,[1] the scattering coefficient per unit solid angle in a direction ϕ with the direction of propagation of the primary x-rays is

$$s_\phi = \frac{NZ\rho e^4}{Wm^2c^4} \cdot \frac{1 + \cos^2\phi + 2\alpha(1+\alpha)\,\mathrm{vers}^2\phi}{(1+\alpha\,\mathrm{vers}\,\phi)^5} \tag{2}$$

[1] A. H. Compton, Phys. Rev. **21**, 491 (1923).
[2] G. E. M. Jauncey, Phys. Rev. **22**, 233 (1923).

where N is Avogadro's number, Z the number of electrons in a molecule of the scattering substance, ρ its density, W its molecular weight and ϕ the angle of scattering. Eq. (2) is Compton's formula for the scattering of unpolarized x-rays. The minimum value of s_ϕ occurs when $ds_\phi/d\phi = 0$, that is, when

$$\cos\phi = -\alpha/2 \tag{3}$$

approximately, the square and higher powers of α being neglected.

In the Thomson[3] theory of the scattering of x-rays, the minimum occurs at $\cos\phi = 0$, or at $\phi = 90°$. In the case of x-rays for which $\alpha = 0.1$, the minimum according to Eq. (3) occurs at $\phi = 92°53'$, which is distinctly different from the position of the minimum on the Thomson theory.

Breit[4] attacked the problem of the theoretical formula for the scattering of x-rays from the point of view of the correspondence principle and obtained a formula differing from Eq. (2). Later Dirac,[5] using the principles of quantum mechanics, obtained a formula identical with that of Breit. The Dirac formula is

$$s_\phi = \frac{NZ\rho e^4}{Wm^2c^4} \cdot \frac{1 + \cos^2\phi}{(1 + a \operatorname{vers}\phi)^3}. \tag{4}$$

According to Eq. (4), s_ϕ has a minimum at

$$\cos\phi = -3\alpha/2 \tag{5}$$

approximately, so that for $\alpha = 0.1$, the minimum occurs at $98°36'$. The minimum according to Dirac therefore occurs at an angle of $5°43'$ greater than according to Compton and Jauncey.

Recently, Klein and Nishina[6] have derived a formula on the basis of the quantum mechanics which is somewhat different from Dirac's formula. The Klein and Nishina formula is obtained from the Dirac formula by multiplying the right side of Eq. (4) by the factor

$$k = 1 + \frac{\alpha^2 \operatorname{vers}^2\phi}{(1 + \cos^2\phi)(1 + \alpha \operatorname{vers}\phi)}. \tag{6}$$

This factor has no effect on Eq. (5) as far as the first power of α is concerned.

In 1924 Jauncey[7] derived a formula for the scattering of polarized x-rays. For scattering in the plane of the electric vector, the position of the minimum is given by

$$\cos\phi = \alpha \tag{7}$$

approximately, so that for $\alpha = 0.1$ the minimum occurs at $84°\ 15'$. The formulas of Breit, Dirac and Klein and Nishina all agree in giving the minimum at $\phi = 90°$, which is in accord with the Thomson classical theory.

[3] J. J. Thomson, Conduction of Electricity through Gases, 2nd. Ed., p. 325.
[4] G. Breit, Phys. Rev. **27**, 362 (1926).
[5] P. A. M. Dirac, Proc. Roy. Soc. **A111**, 405 (1926).
[6] Klein and Nishina, Zeits. f. Physik **52**, 853 (1929).
[7] G. E. M. Jauncey, Phys. Rev. **23**, 313 (1924).

In an early experiment by Jauncey and Stauss[8] on the scattering of polarized x-rays, the experimental position of the minimum appeared to agree with Eq. (7). This experiment was repeated by Barrett and Beardon,[9] who found that the minimum occurred at angles somewhat greater than 90° and within experimental error of 90°. Another repetition was made by Jauncey and Hassler,[10] who found the minimum to be at an angle slightly greater than 90°. The results of these experiments are uncertain due to (1) the difficulty of measuring the exact position of a minimum, (2) the lack of complete polarization, (3) the wide slits which are necessary in order to obtain sufficient intensity, (4) the uncertainty of the wave-length used, and (5) multiple scattering. The wide slits have the effect of flattening the minimum, and on that account making the position of the minimum still more difficult to determine. Referring to Eqs. (3) and (7), it is seen that the Compton-Jauncey formula gives the minimum for unpolarized x-rays at an angle greater than 90°, while their formula gives the minimum for polarized x-rays at an angle less than 90°. It is possible therefore with partially polarized x-rays to obtain a minimum at 90° on the Compton-Jauncey theory. Complete polarization can only be obtained by scattering at 90° or nearly 90° from a slab of some material such as paraffin, when the slab is very thin. Since, in experiments on polarized x-rays, the x-rays are scattered twice, the intensity of the doubly scattered x-rays is quite small unless both slabs of the scattering material are fairly thick. However, multiple scattering increases as the thickness of each slab increases. This multiple scattering increases the lack of complete polarization.

Due to the above objections, the present writers have made the test on unpolarized x-rays and have abandoned the attempt to determine experimentally the position of the minimum. Instead the writers have attempted to measure the relative scattering at the three angles 75°, 97.5° and 120° as accurately as possible and to compare the experimental values with the values predicted by the various theories. It should be mentioned that in 1922 Hewlett[11] published scattering curves for certain organic liquids and that these curves show minima at about 100° to 105°. As we shall show in the present paper, it is very necessary to take account of the Compton change of wave-length in regard to its effect on the ionization produced in the ionization chamber, and this Hewlett did not do, since his paper was published before the discovery of the Compton effect.

2. Experimental Procedure

X-rays from the tube A, Fig. 1, after leaving the target almost tangentially and passing through a slit system, fall upon the paraffin slab B. Part of the x-rays are scattered by the slab B into the ionization chamber D and part penetrate through the slab B and then fall upon a paraffin slab C. Part

[8] Jauncey and Stauss, Proc. Nat. Acad. Sci. **10**, 405 (1924).
[9] Barrett and Bearden, Phys. Rev. **29**, 352 (1927).
[10] Jauncey and Hassler, Phys. Rev. **31**, 1120 (1928).
[11] C. W. Hewlett, Phys. Rev. **20**, 688 (1922).

of the rays falling on slab C are scattered into the ionization chamber E. The slab B is mounted on the axis of an x-ray spectrometer and the ionization chamber D can be rotated about this axis. The angle which the slab C makes with the primary beam and the position of the chamber E remains fixed throughout the experiment. The width of the beam of x-rays entering the chamber E is controlled by the adjustable slit S. The outer electrodes of D and E are connected to $+100$ and -100 volts respectively. The inner electrodes are connected together and to the electrometer as shown in Fig. 1. Doubling and halving the voltages on the chambers E and D had no effect on the observed ionization currents, so that the voltages on the two chambers were always above the voltages necessary for saturation. The chamber D was first filled with air saturated with methyl iodide vapor. Later D was filled with air saturated with ethyl bromide vapor. A reservoir containing either liquid methyl iodide or ethyl bromide was permanently connected to D. The chamber E was filled with air alone. In order that the primary x-rays should be in effect completely unpolarized, the axis of the x-ray tube made an angle of 45° with the plane of scattering.

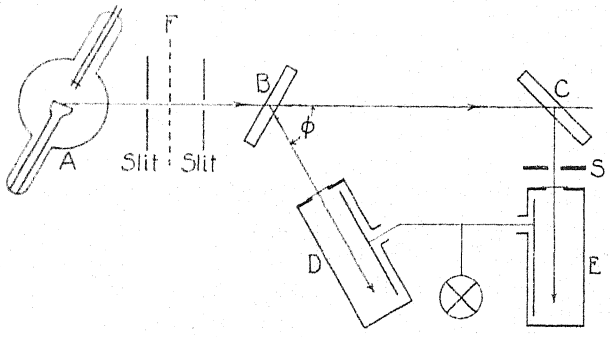

Fig. 1. Diagram of apparatus.

The angular scale of the spectrometer was graduated in quarter degrees so that settings of the ionization chamber could be made with an accuracy of 5 minutes of arc. A pin was mounted on the axis of the spectrometer and it was arranged that, when the primary beam of x-rays was observed by a fluoroscope, the shadow of the pin was in the center of the fluorescence produced by the beam. The target of the tube was turned so that the primary x-rays left the target nearly tangentially, the plane of the target being vertical. Under these conditions it was noted that the edge of the fluorescent image of the slit system as observed in the fluorescope was sharp on one side but was somewhat indefinite on the other. Consequently we could not be certain that the axis of the spectrometer passed through the "center of gravity" of the primary beam. We therefore took readings for a given scattering angle with the chamber D set first on one side of the primary beam and then on the other. Also with a given setting of the ionization chamber we took one set of readings with the paraffin slab B in the Crowther[12] position and

[12] J. A. Crowther, Proc. Roy. Soc. **A86**, 478 (1912).

a second set with the slab B turned through 180°, so that it was again in the Crowther position but with the opposite side presented to the primary beam. For each angle of scattering there were thus two settings of the ionization chamber and four settings of the paraffin slab. In this way, any asymmetry of the primary beam with respect to the spectrometer was corrected.

The primary voltage of the x-ray transformer was supplied by two motor generator sets. The first set consisted of an a.c. motor and d.c. generator operated by Washington University power. By means of a voltage regulator connected to the field coils of the d.c. generator a constant d.c. voltage was obtained, irrespective of variations in the a.c. voltage driving the a.c. motor. This constant d.c. voltage was applied to the d.c. motor of the second set, so that the a.c. generator of the second set gave a constant a.c. voltage. This constant a.c. voltage was applied to the primary of the x-ray transformer. Full wave rectification of the high voltage was obtained by a system of four kenotrons. Care was taken to have the filaments of the kenotrons at a temperature such that the fall of voltage across the kenotrons was too small to produce any detectable x-rays. This was necessary because irregular results were first obtained due to stray x-rays from the kenotrons. In spite of the two motor generator sets, there were occasional variations of the primary voltage across the x-ray transformer and of the milliamperes through the x-ray tube. Accordingly, we placed a choke coil in the primary circuit of the x-ray transformer. By adjustment of the length of the iron core within the coil, any variation of the voltage could be annulled. The tube was operated at maximum voltages between 90 and 125 kilovolts and a current of 7 milliamperes. The voltages were measured by the spark length between spheres of 10 cm radius. The target was of tungsten and was not water-cooled. The corona discharge from the leads to the x-ray tube was reduced by making these leads of $\frac{3}{4}$ inch flexible piping. The x-rays were made more homogeneous by passing them through a filter F of aluminum or copper.

The intensity of the rays scattered by the slab B into the chamber D was compared with the intensity of the rays penetrating the slab B and entering the chamber E. By means of lead shutters, the rays were first allowed to enter D but not E and then were allowed to enter E but not D. Readings of the scattered and primary rays were thus taken alternately. The time for a deflection over a given part of the scale was measured. Due to the fact that the voltages across the chambers D and E were in opposite directions, it was not necessary to ground the electrometer during a set of readings. With a given setting of the chamber, 5 readings on the scattered rays and 5 readings on the primary rays were taken. The slab B was then turned through 180° and the procedure repeated. This was done with a slab of given thickness and with a given voltage on the x-ray tube for the chamber angles of 120°, 97.5°, and 75° on the right side of the spectrometer and 75° 97.5° and 120° on the left side. Thus a total of 60 readings on the scattered rays and 60 on the primary rays were taken, making a total of 120 readings. In an effort to correct for multiple scattering, we then substituted a slab of different thickness and took 120 more readings. The whole of the 240 readings were taken without

interruption. Since the effect of change of temperature on the ionization produced in the saturated methyl iodide or ethyl bromide vapor is quite considerable, we kept the temperature of the room constant during the whole period of the 240 readings. Also, during the same period, the voltage across the x-ray tube and the current through the tube were kept constant.

Readings of the ionization in chamber D were also taken with the slab B removed so as to obtain any effect due to stray rays. Although this effect was small, it was not negligible. The effect was different for different settings of

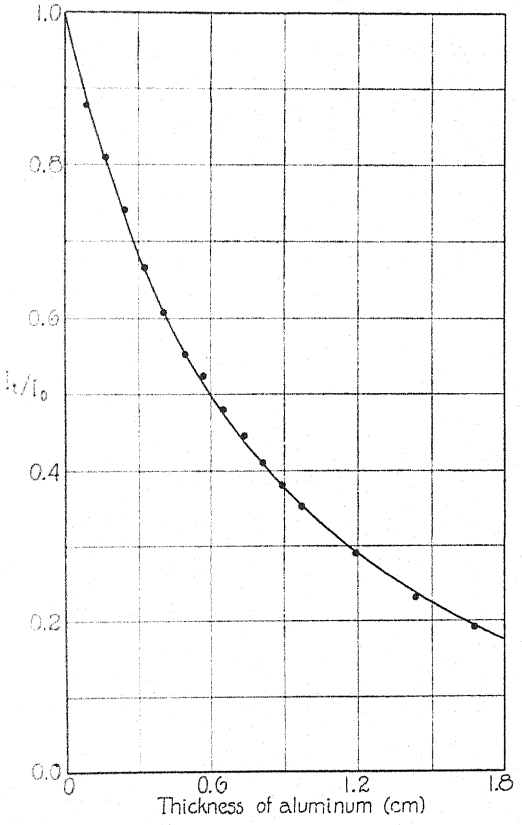

Fig. 2. Absorption in aluminum. Methyl iodide, 90 kv.

the chamber D. For a given chamber angle on one side of the spectrometer and a given thickness of paraffin, the average of the readings for the scattered rays was determined. This average was corrected for the stray rays. The average for the primary rays was also determined. The ratio of this corrected average for the scattered rays to the average for the primary rays is determined for a given scattering angle on each side of the spectrometer. The average of the ratios for the two sides is then determined These are the values shown in Tables I and II.

The linear width of the primary beam when crossing over the axis of the spectrometer was measured with the aid of the fluoroscope and was found to

be 4 mm. Since the distance of the axis to the target of the x-ray tube is 80 cm, the angular width of the primary beam is 17′. The distance from the axis to the window of the ionization chamber D is 15 cm. This window is 1 cm wide. The angle of scattering when the chamber D is set at a given angle therefore has a range of 5° 32′. The angular height of the primary beam is 1° 23′, while the angular height of the scattered rays is 11° 24′. Calculation showed that the angular range of the scattering angle from a thin slab due to the height of the slits was about 30′ at each of the angles 75° 97° 30′ and 120°.

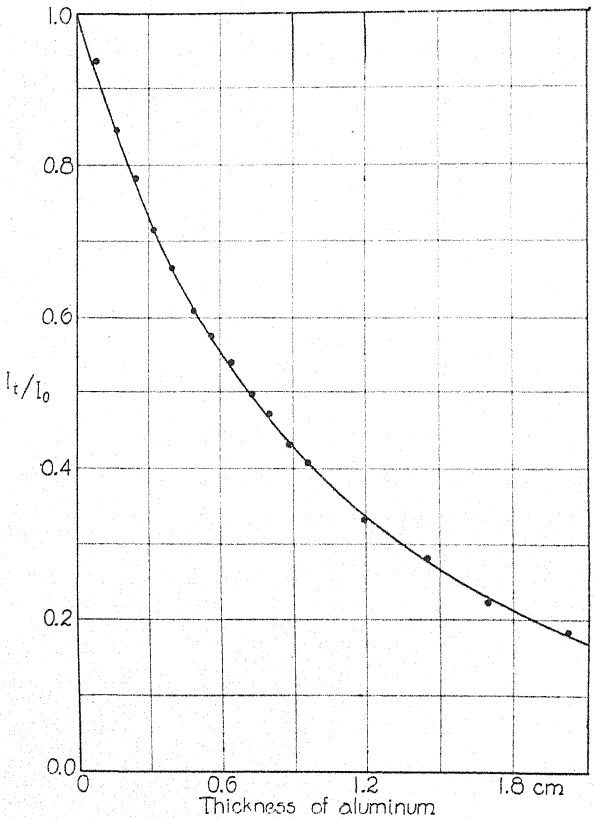

Fig. 3. Absorption in aluminum. Methyl iodide, 125 kv.

The inner electrode of the ionization chamber was placed so that no scattered rays from the slab could strike it. The diameter of the chamber was such that the rays did not strike the sides. The length of the ionization chamber was 43.5 cm.

After completing a run of 240 readings on the scattered rays and meauring the effect of the stray rays, the hardness of the primary rays was measured by placing the chamber D so as to receive the primary rays. In order to cut down the intensity the rays were passed through a pinhole in a sheet of lead. Different thickness of aluminum were placed in the primary. For each thickness several readings alternately with and without aluminum were taken.

The proportion of the rays penetrating each thickness are shown by the black circles in Figs. 2, 3 and 4. The absorption curve was obtained for the same voltage across the x-ray tube and with the chamber D at the same temperature as when the scattered rays were being measured.

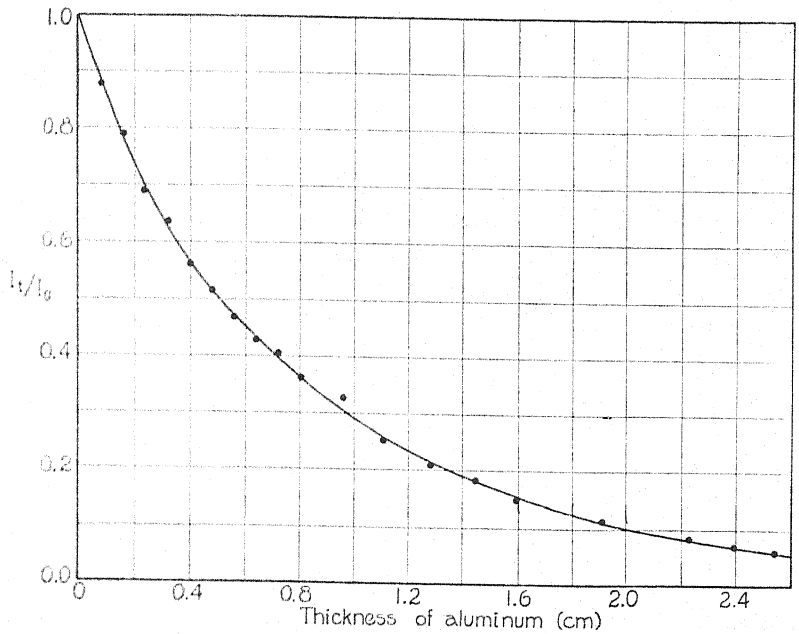

Fig. 4. Absorption in aluminum. Ethyl bromide, 95 kv.

3. Experimental Results

The experiment was first performed with the chamber filled with air saturated with methyl iodide vapor at a temperature of 17°C. The results are shown in Table I. Paraffin slabs of mass per unit area 0.365 gm/cm² and

Table I. *Scattering from paraffin. Methyl iodide in ionization chamber.*

Angle	Potential = 90 kv Mass/Area = 0.365	Scattering ratios 90kv 0.595	125kv 0.365	125kv 0.595
75°	0.531	0.837	0.477	0.760
97° 30′	0.573	0.926	0.550	0.804
120°	0.864	1.414	0.823	1.265

0.595 gm/cm² were used. The values under 125 kv are not comparable with the values under 90 kv. The 90 kv rays were filtered through 2.92 mm and the 125 kv rays were filtered through 7.22 mm of aluminum. The results of the absorption measurements for the 90 kv rays and the 125 kv rays are represented by the black circles in Figs. 2 and 3 respectively.

Later the experiment was performed with ethyl bromide in the chamber and the results shown in Table II were obtained. In this case the rays were

filtered through 0.1 mm of copper and 2.0 mm of aluminum. The temperature was maintained at 24.0°C.

TABLE II. *Scattering from paraffin. Ethyl bromide in ionization chamber. Potential* 95 kv.

Angle	Scattering ratios Mass/Area = 0.365	0.595
75°	0.368	0.645
97° 30′	0.397	0.720
120°	0.635	1.150

The results of the absorption measurements with ethyl bromide in the chamber are represented by the black circles in Fig. 4.

4. COMPARISONS WITH THEORY

In order to compare the experimental results with theory it is necessary to obtain the wave-length of the primary rays. Since we used rays of the continuous spectrum filtered through aluminum or aluminum and copper, the rays were only approximately monochromatic.

Smooth curves (not the curves shown) were drawn through the experimental points shown in Figs. 2, 3, and 4. From the smooth curve in a given case values of I_t/I_0 were read off at each successive thickness of 1 mm of aluminum. It was found that after a thickness of about 4 mm the curve was almost exactly exponential. This exponential portion was produced back to zero thickness. Differences were then obtained between this exponential curve and the experimental curve for thicknesses less than 4 mm. It was found that these differences when plotted against thickness gave a fairly exponential curve. Thus the experimental curve appeared to be made up of two exponential portions. The solid curves shown in Figs. 2, 3 and 4 are curves calculated from the formula

$$I_t/I_0 = i_1 e^{-\mu_1 t} + i_2 e^{-\mu_2 t}. \tag{8}$$

The values of i_1, i_2, μ_1 and μ_2 are shown in Table III.

TABLE III.

kv	Vapor in D	i_1	μ_1 cm^{-1}	i_2	μ_2 cm^{-1}	λ_1 A	λ_2 A	I_1	I_2
90	methyl iodide	0.67	0.74	0.33	2.7	0.205	0.39	0.68	0.32
125	methyl iodide	0.815	0.74	0.185	2.7	0.205	0.39	0.82	0.18
95	ethyl iodide	0.806	1.03	.194	4.15	0.26	0.47	0.91	0.09

In Table III, μ_1 and μ_2 are the linear absorption coefficients in aluminum. From these the mass absorption coefficients can be found and the wave-lengths λ_1 and λ_2 can be determined from Compton's table of absorption

coefficients.[13] Now i_1 and i_2 are the proportions of the two wave-lengths present as measured by the ionization produced in the chamber. These are not the proportions present in the primary x-rays. At first, we thought to obtain the proportions present in the primary rays by dividing by the amount of each wave-length absorbed in the gas in the chamber. These proportions are shown in the columns headed I_1 and I_2. However, the energy of the x-rays which are absorbed in methyl iodide does not all give rise to ionization. By far the greater part of the energy goes into iodine K-radiation, and somewhere about 80 to 90 percent of this K-radiation leaves the chamber without producing ionization. According to Compton,[14] the fluorescent yield is independent of the wave-length, so long as it is short enough to excite the fluorescent radiation. Thus the same proportion of the absorbed energy goes into producing ionization in the chamber D for all wave-lengths shorter than 0.375A, the K critical absorption wave-length for iodine. Let m_1 and m_2 be the respective mass absorption coefficients of the wave-lengths λ_1 and λ_2 in the gas of the chamber D. The saturated vapor pressure for methyl iodide at 17°C is 293 mm[15], from which the density of the iodine in the methyl iodide is 0.00206 gm/cm³. The values of m_1 and m_2 for iodine can be obtained from Compton's table of mass absorption coefficients by interpolation and the fraction of the radiation of each wave-length absorbed in the ionization chamber D can be calculated. Let the fractions be represented by k_1 and k_2 for the wave-lengths λ_1 and λ_2 respectively. Of the fractions k_1 and k_2, the fractions p_1 and p_2 respectively appear as ionization. In the case of methyl iodide p_1 and p_2 differ because λ_1 is shorter and λ_2 is longer than the K critical absorption wave-length of iodine. Hence the relative energies in the wave-lengths λ_1 and λ_2 as they enter the chamber D, but not as they are absorbed in the chamber, are i_1/p_1k_1 and i_2/p_2k_2. These are taken as representing the energies of λ_1 and λ_2 in the primary beam.

Now let us consider the scattering experiment. The scattered intensity I_ϕ when the slab B is in the Crowther position is

$$\frac{I_\phi}{I} = \frac{As_\phi t \sec(\phi/2)}{R^2} \tag{8}$$

where I is the intensity of the rays penetrating the slab B and entering the chamber E. This intensity is proportional to the ionization in E, so long as the temperature of the room and the voltage across the x-ray tube is kept constant. s_ϕ in Eq. (8) is the scattering coefficient, t is the thickness of the slab, A the area of the window of chamber D, R the distance of the window from the spectrometer window and ϕ the scattering angle.

Let primed quantities (′) represent values at ϕ' and doubly primed quantities (″) represent values at ϕ''. Then, since the same slab of thickness t is used at both angles, we have from (8)

$$J''/J' = (s''/s') \cdot (\sec \tfrac{1}{2}\phi'')/(\sec \tfrac{1}{2}\phi') \tag{9}$$

where $J = I_\phi/I$.

[13] A. H. Compton, X-Rays and Electrons. p. 184.
[14] A. H. Compton, Phil. Mag. 8, 961 (1929).
[15] Int. Crit. Tables. III p. 216.

With Eqs. (2), (4) and (6), the various theoretical values of J''/J' for a given wave-length can be found. However, the ratio of the ionization currents produced in chamber D is not J''/J' because of the Compton change of wave-length

$$\delta\lambda = (h/mc) \text{ vers } \phi.$$

Due to this change of wave-length the proportion of the scattered rays of primary wave-length λ_1 which is absorbed in chamber D is different for the scattered rays from the proportion of the primary rays of the wave-length λ_1 absorbed in D in the absorption experiment. The absorbed scattered rays are proportional to i_1k_1'/p_1k_1 where k_1' is the value of k_1 for the scattered rays. The ionization produced is proportional to $i_1p_1'k_1'/p_1k_1$, where p_1' is the value of p_1 for the scattered rays. However, according to Compton,[14] $p_1' = p_1$, so long as the Compton change of wave-length does not cross a critical absorption wave-length. Hence the ionization produced is proportional to i_1k_1'/k_1. The values of i_1/k_1 and i_2/k_2 are shown in the columns respectively headed I_1 and I_2 in Table III.

If we have two wave-lengths, and if the J's of Eq. (9) are to represent ionization currents in chamber D, we have

$$\frac{J''}{J'} = \frac{(i_1k_1''/k_1)s_1'' + (i_2k_2''/k_2)s_2''}{(i_1k_1'/k_1)s_1' + (i_2k_2'/k_2)s_2'} \cdot \frac{\sec(\frac{1}{2})\phi''}{\sec(\frac{1}{2})\phi'}.$$

The values of J''/J' where $\phi' = 75°$ and $\phi'' = 97° 30'$ or $120°$ are shown for the various theoretical formula for s_ϕ in Table IV. The experimental values of J''/J' when methyl iodide is in the chamber D are also shown in Table IV.

TABLE IV. *Experimental and theoretical values of J''/J'. Methyl iodide in ionization chamber.*

		90 kv					125 kv				
		Experiment			Dirac	Compton	Experiment			Dirac	Compton
ϕ'	ϕ''	*A*	*B*	Mean			*A*	*B*	Mean		
75°	97.5°	1.079	1.107	1.093	1.098	1.170	1.152	1.059	1.106	1.103	1.174
75°	120°	1.627	1.690	1.659	1.738	1.898	1.725	1.663	1.694	1.740	1.905

Those values shown under A are for the paraffin slab whose mass per unit area is 0.365 gm/cm² and those under B for the slab whose mass per unit area is 0.595 gm/cm².

During the progress of this research, a paper by DuMond[16] on multiple scattering has appeared. In this paper, DuMond discusses the problem of double scattering from a sphere, and obtains a formula for the ratio of the intensity of doubly scattered rays to that of singly scattered rays. The formula contains a function of ϕ, the scattering angle, but this function is very nearly constant in the range $\phi = 75°$ to $120°$. We have been unable to find any certain direction in which J''/J' changes with the thickness of the

[16] J. W. M. DuMond, Phys. Rev. **36**, 1685 (1930).

slab in our experiments, and this is, we believe, in agreement with DuMond's theoretical finding that the ratio of double to single scattering does not vary with the angle in the range considered. Instead, therefore, of extrapolating the values of J''/J' to zero thickness, we have merely taken the mean values as shown in Table IV.

In calculating the theoretical values, the range of scattering angles at a given setting of the ionization chamber has been neglected and the calculation been made on the assumption that the scattering angle is the angle at which the ionization chamber is set. This is allowed because the correction due to the range of the scattering angle is small since the range of 5° 32′ due to the width of the slits plus 30′ due to the height of the slits only makes a difference in the third decimal place in the theoretical values of J''/J' in Tables IV and V. Further, in calculating the theoretical values it has been assumed that none of the scattered rays at the angles used are of the unmodified type. Compton[17] writes Wentzel's formula [18] for the intensity of the unmodified rays in the form

$$I_{unm} = I_e n^2 \left\{ \int u(r) \frac{\sin kr}{kr} dr \right\}^2 \tag{10}$$

where $k = (4\pi/\lambda) \sin(\phi/2)$ and $u(r)dr$ is the probability that an electron is at a distance r to $r+dr$ from the center of an atom, n is the number of electrons in an atom of the scatterer and I_e is the Thomson value of the scattering from a single electron. In the case of helium, Pauling[19] gives the probability for each of the two electrons as

$$u(r) = 4r^2 \left(\frac{Z - s}{a} \right)^3 \exp\{-(Z - s)r/a\} \tag{11}$$

where Z is the atomic number of helium, a is the radius of the normal orbit in the hydrogen atom on the Bohr theory and s is the screening constant. We have applied this formula for $u(r)$ to the case of the K electrons of carbon, putting $Z = 6$, $s = 0.39$ and $a = 0.53$A in Eq. (11) and $n = 2$ in Eq. (10). Performing the integration in Eq. (10), we obtain

$$I_{unm} = 4I_e/(1 + .022x^2) \tag{12}$$

where $x = (4/\lambda) \sin(\phi/2)$. For $\lambda = 0.26$A and $\phi = 75°$, I_{unm} from each carbon atom in paraffin is $0.065\ I_e$. The average chemical formula for paraffin is $C_{24}H_{50}$. The L electrons of C and the electrons of H do not scatter unmodified rays at $\phi = 75°$, so that the ratio of unmodified rays scattered by paraffin to the total scattering at $\phi = 75°$ is 0.7 percent. We are therefore justified in neglecting the unmodified rays in our calculated values of J''/J'.

In Table III it will be noted that λ_2 for the absorption curves when methyl iodide is just on the long wave-length side of 0.375A, the critical ab-

[17] A. H. Compton, Phys. Rev. **35**, 930 (1930).
[18] G. Wentzel, Zeits. f. Physik **43**, 1 and 779 (1927).
[19] L. Pauling, Proc. Roy. Soc. **A114**, 181 (1927).

sorption wave-length for iodine. We accordingly felt rather doubtful of the reality of this wave-length. For this reason we replaced the methyl iodide with ethyl bromide. The temperature when ethyl bromide was used in the ionization chamber was 24.5°C. At this temperature the density of the bromine in saturated ethyl bromide is 0.00197 gm/cm³. The primary x-rays were filtered through copper as well as aluminum in an attempt to increase the homogeneity of the rays. The absorption measurements are shown by the black circles in Fig. 4. The absorption measurements were carried to a much greater thickness of aluminum than in the case where methyl iodide was in the chamber. This was done in order to obtain the wave-lengths as accurately as possible. The solid curve of the Fig. 4 is constructed with the use of the data shown in Table III. Again as in the case of methyl iodide we have two wave-lengths, but both are on the short wave-length side of the absorption edge from bromine. The experimental and theoretical values of J''/J' are shown in Table V.

TABLE V. *Experimental and theoretical values of J''/J'. Ethyl bromide in ionization chamber. Potential* 95 kv.

		Experiment			Dirac	Klein-Nishina	Compton	Thomson
ϕ'	ϕ''	A	B	Ave.				
75°	97°30′	1.085	1.110	1.098	1.097	1.102	1.17	1.149
75°	120°	1.755	1.795	1.775	1.740	1.755	1.89	1.860

5. DISCUSSION

The agreement of the experimental values of J''/J' with the Dirac or Klein and Nishina values as shown in Table V is excellent. At the wave-lengths used the Dirac or Klein and Nishina Formula is a much better description of the experimental facts than the Compton or Thomson Formula. The agreement of the experimental values of J''/J' with the Dirac values as shown in Table IV is also good for the 90 kv x-rays. The agreement for the 125 kv x-rays, however, is not so good although the agreement of the mean values with the Dirac values is good. The corona discharge when the x-ray tube was excited with 125 kv was considerable and this seemed to introduce irregularities into the electrometer readings. This difference between the A and B values for $\phi''=97°\ 30'$ is due to the irregularities.

In calculating the theoretical values of J''/J', two wave-lengths have been used. In the case of ethyl bromide, the longer wave-length was 0.47A. This wave-length is perhaps somewhat fictitious and we feel that the reality of the wave-length 0.26A is greater because by far the larger part of the absorption curve in Fig. 4 is due to this wave-length. If it is supposed that only this wave-length is present in the primary rays, the Dirac values in Table V become 1.098 and 1.753 for $\phi''=97°\ 30'$ and 120° respectively, while the Klein and Nishina values become 1.103 and 1.771. Also it might be objected that even the wave-length 0.26A is an average wave-length. We have therefore calculated the Dirac values in the case of ethyl bromide for $\lambda=0.22$,

0.24, 0.28, 0.30A in addition to 0.26A. The values of J''/J' vary from 1.098 to 1.108 at $\phi''=97°\ 30'$ and from 1.73 to 1.76 at $\phi''=120°$. The Dirac theoretical values of J''/J' are therefore practically constant for a wave-length range of 0.08A about 0.26A. The Compton values are also practically constant over the same range. This is our justification for using the average wave-length 0.26A in the calculation of the theoretical values.

If the effect of the Compton change of wave-length on the ionization produced in the chamber is neglected, the Dirac theoretical values of J''/J' for 0.26A become 1.035 at $\phi''=97°\ 30'$ and 1.540 at $\phi''=120°$ in total disagreement with the experimental values. The ionization produced by the photoelectrons ejected from the brass wall at the end of the chamber and the aluminum window were neglected because with the length of chamber used this ionization is only a small fraction of the total ionization in the chamber. The aluminum window was 0.005 cm thick and the absorption in it was neglected.

We observed a rather curious effect during these experiments. The hardness of x-rays as determined by absorption in aluminum depends upon (a) the angle at which the rays leave the target of the x-ray tube (b) the nature of the gas in the ionization chamber, and (c) the temperature of the chamber if saturated vapor is used in the chamber. The length of the ionization chamber is such that the x-rays are incompletely absorbed. It is quite possible to apply a higher voltage to an x-ray tube and yet obtain less penetrating x-rays.

For the wave-lengths used in this research it is not possible to discriminate between the Dirac and the Klein and Nishina formulas. Recently, Chao[20] using γ-rays of wave-length 0.0052A has shown that the Klein and Nishina Formula fits the experimental facts much better than the Dirac Formula. This research was assisted by a grant from the Science Research Fund of Washington University.

[20] C. Y. Chao, Phys. Rev. **36**, 1519 (1930).

APPEARANCE OF EXTRA LINES IN X-RAY DIFFRACTION PATTERNS OF MIXTURES AND ABSENCE OF SOME LINES PECULIAR TO THE COMPONENTS OF THE MIXTURES

By Roy W. Drier
Department of Metallurgy
Michigan College of Mining and Technology
Houghton, Michigan

(Received February 2, 1931)

Abstract

Abnormalities in x-ray spectra of mechanical mixtures of minerals are described. The spectra of some show the presence of extra lines, and in the spectra of others some lines peculiar to the components are missing. Some possible reasons are briefly considered.

THE x-ray, useful in the solution of many problems, has revealed the existence of others. Among these are the appearance in x-ray diffraction patterns of mechanical mixtures, of lines not peculiar to either of the components of the mixtures, and the disappearance, in the spectra of the mixtures, of some of the lines peculiar to the components.

It is not the purpose of this paper to offer any definite explanation of these phenomena of the disappearance of spectral lines and the appearance of new lines but rather to record them and to mention a few possible reasons for them.

The diffraction patterns are composed of spectral lines produced in Debye-Scherrer or Hull type cameras. These lines are indicative of interplanar spacings in the crystal structure.

These effects were first noticed by the writer while he was working with Dr. G. L. Clark, of the Department of Chemistry, of the University of Illinois. The mixture which drew attention to this phenomenon was one of rutile (TiO_2) and barite ($BaSO_4$).

The two minerals, rutile and barite, were rayed separately for their diffraction patterns. Mixtures of the two were made, and diffraction patterns of the mixtures were then obtained. These were simple mechanical mixtures, mixed on glazed mixing paper and placed in capillary tubes for raying. No heat or pressure entered into the process of sample preparation.

The apparatus used was a G. E. diffraction unit. It supplied 30,000 volts R.M.S. to a molybdenum target, water-cooled Coolidge tube operating at 20 m.a. The films were held in a cassette in the form of an arc 8 inches in radius. The samples (-200 mesh) were contained in small, capillary, Pyrex glass tubes about 2 inches long and approximately 0.03 inches in internal diameter. This tube is held in the center of the circle of which the film mentioned above is an arc. By means of a ZrO_2 filter placed in the cassette between the sample and the film, practically all but the Mo$K\alpha$ radiation is filtered out, the film registering this monochromatic beam only.

A comparison of the spectra of the components and of the mixture revealed that some of the lines peculiar to the constituents were missing in the mixture pattern and that some of the mixture lines were not included in the spectra of the constituents.

Several series of mixtures were then made up and rayed, for the purpose of investigating this "extra line" phenomenon. The mixtures were Cu-Zn, Cu-Ag, Cu-NaCl, and Cu-Ni. Each series was composed of members whose proportions varied from 0% A-100% B to 100% A and 0% B. The Cu-Zn series had the following mixtures: 100% Cu-0% Zn, 95% Cu-5% Zn, 75% Cu-25% Zn, 50% Cu-50% Zn, 25% Cu-75% Zn, 5% Cu-95% Zn, and 100% Zn. This series was proportioned according to weight, but the rest of the mixtures were proportioned according to volume, which was approximated by eye. Although a more accurate method of proportioning and making the mixtures could have been followed, it was felt that each series would yield samples which would vary approximately as desired.

The Cu-Zn series was the most outstanding of the five. A few of the lines appearing in the Cu did not appear in the mixtures, and several of the lines of the zinc patterns were not a part of the composite spectrum. In each of the mixture-spectra there were found eight distinct lines which occurred in neither the Cu nor the Zn spectrum.

The extra lines in the Cu-Zn series agreed fairly well with the spectrum of alpha-brass, a fact which seems to indicate the occurrence of interfacial diffusion. In an attempt to reproduce this reaction, a sheet of zinc was ground to a knife edge. This knife edge was pressed into −100 mesh copper filings and held there for 24 hours. It was then removed; the copper filings were brushed off, and the knife edge was placed in an x-ray beam. The resulting spectrum contained only the lines which were in the spectrum of an untreated piece of the same zinc. If interfacial diffusion occurred in the powder mixture, it was probably due to a catalytic action, possibly of the x-rays themselves.

Spectra of pure Ag and pure Cu and of a 50-50 mixture showed no new spectral lines in the mixture, but did show that the (100) 4 copper line was missing in the mixture and that there was a slight gradual shift to the right (i.e., shortening) in the mixture as compared to the copper. Some slight traces of impurities were indicated in the spectra of the Ag and Cu.

The Cu-Al series seemed to be regular; there were neither extra lines nor any lines missing. In the mixtures which had a low aluminum content many of the Al lines were faint and some had disappeared, but such a disappearance is to be expected of reflections from an element of comparatively low atomic number. E. C. Bain[1] noticed the appearance of extra lines in mixtures of Cu and Au heated to the sintering point. His spectrogram of the mixture before heating indicated merely the composite spectrum of Au and Cu. The writer is inclined toward the opinion that when the mixture was heated to the sintering temperature some such sort of reaction as diffusion or solid solution took

[1] E. C. Bain, Chem. Met. Eng. 28, 2 (1923).

place which would account for the new lines. Davidson and Aborn,[2] in their research on the structure of ZnO and CuO catalysts, carried on at 360°C, noticed "extra lines." It might be that the temperature obtaining during the experimentation was near enough to the melting point of zinc to make possible the occurrence of a reaction between the ZnO and the CuO, or it might be that the oxides were reduced and formed conditions which permitted the reaction to take place. Davidson and Aborn favor this latter possibility, especially since the extra lines seemed to agree fairly well with the spectrum for gamma brass.

There is a possibility, too, that if reduction did occur, the tendency for zinc to become brittle between 200°C and 300°C, indicating a possible change in atomic arrangement, might account for their extra lines. In working with mixtures of ZnO and Cr_2O_3, G. R. Griffin,[3] noticed in the mixture-spectra the disappearance of some lines peculiar to the components. Tamman,[4] has predicted the appearance of "overstructure lines." Hull,[5] while interpreting the spectra of a number of minerals, noticed the absence of some of the spectral lines which theoretically should have been present.

For these phenomena there are several possible causes. It is conceivable that the extra lines are due to a secondary reflection; this hypothesis, however, is not in accord with the fact that some of the extra lines are those of a solid solution or other phases of the system. The appearance of new lines might be explained by interfacial diffusion. But the disappearance of regular lines could not be so effected. A possible explanation of such disappearance is interference. Research on this problem is being continued in an attempt to determine the cause or causes of the phenomena.

[2] Davidson and Aborn, J. Phys. Chem. **34**, 522 (1930).
[3] G. R. Griffin, Inst. in Geol. U. of Ill. Paper not published.
[4] Tamman, Lehrbuch der Metallographie 3 ed. p. 450.
[5] A. W. Hull, Phys. Rev. **17**, 571 (1921).

THE DEPENDENCE OF X-RAY ABSORPTION SPECTRA UPON CHEMICAL AND PHYSICAL STATE

By J. D. Hanawalt*
University of Michigan

(Received January 30, 1931)

Abstract

The x-ray absorption spectra of As, Se, Br, Zn, Hg, Xe, and Kr, and of compounds of some of these elements have been photographed for both the solid and the vapor states at a dispersion of about 5 X.U. per mm. The effect of the chemical and physical state of the absorbing atom upon the secondary structure which lies to the short wave-length side of the main absorption edge was investigated. It was found that: (1). The monatomic vapors Zn, Hg, Xe, and Kr exhibit no secondary structure at distance from the main edge greater than the ionization potential of the atom. (2). Polyatomic vapors usually, though not necessarily, have a secondary structure similar to that which is exhibited by the same molecule in the solid state. (3). For a polyatomic molecule in the solid state there is often an additional structure observed which is absent when the molecule is in the vapor state. (4). There is an additional structure in the secondary absorption of solid $NaBrO_3$ which is not observed in a solution of $NaBrO_3$. (5). Completed electron shells of atoms in the solid state do not necessarily mean the absence of secondary absorption edges as has been suggested. In order to account for this dependence of secondary absorption on molecular and physical state it is suggested that perhaps the secondary discontinuities correspond to the excitation energies of the structure electrons postulated by O. W. Richardson.

Introduction

A STUDY of the x-ray absorption spectrum of a substance shows that there are sharp discontinuities in the absorption at wave-lengths corresponding to the energies of the Bohr levels of the atom. These absorption discontinuities do not always have the same appearance for different elements. The absorption edge may be what is known as "simple," or there may be some absorption discontinuities of lesser magnitude associated with the principal absorption edge. Fig. 2 (a) and (b) illustrate respectively a simple edge and one with secondary absorption. This secondary absorption falls to the short wave-length side of the main edge and therefore means the absorption of quanta of greater energy than that which produces the main edge. In some cases the difference in energy between a secondary discontinuity and the main edge may be more than 300 volt electrons. Experiments show that the wave-length of the main edge and the type of the absorption are functions of the chemical state of the absorbing atom. Experiments also show that the chemical state of an atom affects the emission spectrum of the atom. These latter experiments are complicated by the fact that one can not be sure of the chemical state of atoms on the anode of an x-ray tube, so it seems that absorption experiments have an advantage in this respect. An excellent and

* National Research Fellow.

complete presentation of the researches on the influence of chemical combination on the x-ray absorption and the x-ray emission spectra of an atom has been given by A. E. Lindh.[1] However, because of the complexity of the results, no unified picture of the work can be as yet formed.

There are two general questions, probably more or less related regarding absorption spectra to be considered. What are the factors which govern the position of the main edge; and, what is the origin or interpretation of the secondary absorption structure? The suggestions regarding the first question, as given by Wentzel, Coster, Stelling, Aoyama, Kimura and Nishina, are summarized by A. E. Lindh.[1] The latest work is that of Pauling[2] who was able to calculate quantitatively the shifts in the position of the K absorption edge in the alkali chloride series and in the potassium halide series. The answer to the second question as given by Coster,[3] Lindsay,[4] Ray,[5] and others, has been in terms of the simultaneous transitions of two or more electrons within the atom, due to the absorption of a single quantum. This suggestion does not give any idea as to why secondary absorption is a function of chemi-

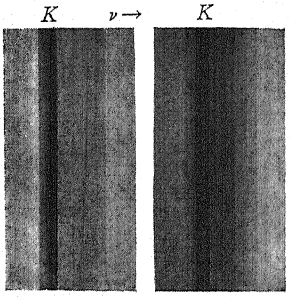

Fig. 1. (a) Simple edge. (b) Edge with secondary absorption.

cal state, though Coster and Wolf[6] have postulated that multiple jumps will be less probable in an atom which has completed electron shells. On the side of emission spectra, the suggestion of F. K. Richtmeyer[7] of simultaneous transitions of electrons to account for x-ray satellites seems to be the most acceptable at present in view of the recent experiments of Du Mond and Hoyt.[8,9] This fact no doubt makes the same hypothesis more probable as an explanation of secondary absorption. The writer simply wishes to bring out here that with the present knowledge regarding secondary absorption one can not make much use of the experimental data, whereas, because of its pene-

[1] Handbuch der Experimental Physik XXIV 2. Teil (1930).
[2] L. Pauling, Phys. Rev. **34**, 954 (1929).
[3] D. Coster, Zeits. f. Physik **25**, 83 (1924).
[4] G. A. Lindsay and H. R. Voorhees, Phil. Mag. **6**, 910 (1928).
[5] B. B. Ray, Nature **122**, 771 (1928).
[6] Coster and Wolf, Nature **124**, 652 (1929).
[7] F. K. Richtmyer, Journ. Frank. Inst. **208**, 325 (1929).
[8] Du Mond and Hoyt, Phys. Rev. **36**, 799 (1930).
[9] Du Mond, Phys. Rev. **36**, 1015 (1930).

trating power, it seems that the x-ray has the possibility of giving interesting information about the atom in the solid state. It was thought that a study of the x-ray absorption of vapors, where one is concerned with isolated atoms or molecules, would be of help to the problem.

Apparatus

In order to study absorption in vapors one must have a cell which will transmit the radiation, which will stand the requisite temperature to secure sufficient vapor pressure, and which will not react with the hot vapors. One is practically limited to a study of those vapors which have their characteristic x-ray absorption in the region from about one to two and one-half angstroms, since at shorter wave-lengths the energy dispersion becomes too small, and at longer wave-lengths nothing can be found to use for a cell. Fig. 2 shows the arrangement which was used. S is the slit, C is the calcite crystal, and P is the photographic plate. The furnace B is for controlling the vapor pressure, and the furnace A is for superheating the vapor. The furnace box is

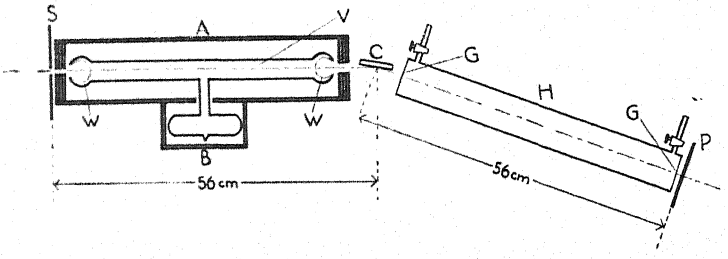

Fig. 2. Diagram of x-ray spectrograph.

made of transite. The vapor cell V is made of Pyrex or of quartz, and the concave windows W may be drawn as thin as 0.005 mm in Pyrex,[10] and to 0.003 mm in quartz, and yet maintain a vacuum and stand temperatures to the melting points. In order to prevent any vapor condensation on the windows W, the openings in the ends of furnace A were covered with three sheets of Al foil or mica with air spaces between the sheets. H is a glass tube with gold-beater's skin windows. The air is flushed out with hydrogen simply to reduce the air path of the radiation. The dispersion of this spectrograph in the region worked varies from 4.9 to 5.3 X.U. per mm. The usual slit width was 0.05 mm, though for special cases it was narrowed to 0.025 mm or widened to 0.1 mm. The x-ray tube was an extra large size of the Siegbahn type. The current was usually about 30 m.a., and exposure times varied from 4 to 30 hours depending on the absorbing material.

Preparation of Materials

The substances which were investigated in this work were As, Se, Br, Zn, Hg, Xe, and Kr, and compounds of some of these elements. When it was possible, each substance was studied in both solid and vapor forms. In the solid form the absorption spectrum was secured for various thicknesses of screen, while in the vapor state all degrees of absorption could easily be se-

[10] Slack, J.O.S.A. **18**, 123 (1929).

cured by regulating the vapor density through the temperature. After thorough cleaning and baking of the cell V, the material was inserted, and the cell sealed-off under high vacuum conditions. The cell was about 40 cm long. With this length of path a few cm pressure of vapor was usually sufficient to produce the maximum contrast in the absorption spectrum. The vapor was always superheated so that there would be no condensation on the ends of the tube. When studying Zn, the vapor was superheated to 950 degrees C, though all of the other vapors could be studied at temperatures much lower than this. Attention must be paid to the fact that polyatomic molecules dissociate at certain temperatures, so that this temperature must not be exceeded. The fact that the x-radiation itself decomposes some molecules did not cause any difficulty in this work since, for example with AsH_3, the As atoms froze on the walls of the cell and left only AsH_3 in the path of the radiation.

In studying solids, if it is possible, the simplest method is to soak cigarette paper in a solution of the material and let it dry. A metal like Zn may be rolled to a thin sheet. Thin sheets of metallic As were formed by passing AsH_3 through a Pyrex tube heated to 500 degrees C. The AsH_3 decomposes, depositing a silvery mirror of As which can be peeled off of the tube. Because of its surface tension, it is hard to get a thin sheet of Hg. A screen of finely divided Hg was formed by reducing mercurous nitrate by formic acid held in gelatine. This gives an emulsion containing very densely packed mercury globules of about 10μ diameter.[11] The compound $NaBrO_3$ can not be had in the vapor form so it was studied as a solid and in solution. Solutions varying from saturated to 1/3 normal were put in cells from 0.7 to 2.0 mm thick. These cells had thin mica windows.

Experimental Results

Due to the character of secondary absorption, there has been no uniformity among different workers in the methods of recording measurements. The absorption regions may vary in width from the slit width of a few volts to as much as 40 volts. The tables in this paper record the distances of both sides of every absorption band, or the distance of the center of the absorption bands from the principal edge. The secondary discontinuities near to the principal edge are always sharper than those farther from the edge. This diffuseness of those farther out, makes it impossible to state their position to closer than about 10 volts.

B. B. Ray[12] has introduced two definitions which it will be convenient to use for purposes of classification and of discussion. Any absorption discontinuities which exist at energy distances from the principal edge of less than the ionization potential of the atom will be called "fine structure" while the term "secondary absorption" will be used to designate absorption discontinuities which occur at greater distances than this from the main edge.

An inspection of Table I shows the following facts: The secondary absorption of As in the solid and vapor states is radically different. $AsCl_3$ in the solid

[11] M. Wolf, Zeits. f. Physik **53**, 72 (1929).
[12] B. B. Ray, Ind. Journ. Phys. **3**, 477 (1929).

form shows an additional structure near the main edge which does not occur for the vapor. The same statement applies to the spectra of As_2O_3 in solid and in vapor form. AsH_3 shows no secondary structure. In the vapor state, the principal edges agree within the experimental error, while in the solid state there are differences as great as 5.2 ± 1.5 volts.

The results of the study of Br_2 and its compounds are uncertain in a few cases because one can not get rid of the effect due to the AgBr in the photographic plate. All of the solids and the $NaBrO_3$ solution show an extensive secondary absorption structure. A comparison of the $NaBrO_3$ solid and the solution shows the same type of additional structure which appeared in the solid As compounds here occurring for the solid $NaBrO_3$. There are shifts in the positions of the main edges of as much as 6.9 ± 2.3 volts.

The positions of the main edges of the Se compounds were not determined. Se_8 vapor exhibits one very close fine structure line but no secondary absorption. Se solid has a white line absorption at the main edge and perhaps an indication of a fine line like that shown by the vapor. SeO_2 solid and vapor both show a secondary absorption, and, as in the cases of the As and Br compounds, there is an additional structure in the absorption spectrum of the solid which does not appear in that of the vapor.

TABLE I.

Substance	Temperature °C.#	Main Edge X. U.	ΔV (volts)	Distances of both sides, or, of center of absorption bands from the main edge. (volts)
Solids				
As		1042.49	0	0–3.6, 10–12, 40–58, 75–92, 130–152, 168–?
$AsCl_3$		1042.41	0.9	0–7.6, 14–22, 33–38, 48–92, 145–?
As_2O_3		1042.22	3.1	0–5.1, 12–18, 55–97, 140–?
As_2O_5		1042.03	5.2	0–5.4, (54–30)*, 60–118, 150–?
Vapors				
As[4]	350 270 95	1042.31	2.0	0–4.4, 57–102, 135–?
$AsCl_3$	35	1042.31	2.0	0–3.8, 57–82, 125–?
As_2O_3	320 260	1042.34	1.7	0–5.2, 55–93, 160–?
AsH_3	20	1042.43	0.7	0–3.0
Outer levels of Se atoms				12., 61., 160., 236.
Solids				
AgBr		918.23	4.1	0–6, 23.5, 52., 93., 129.
NaBr		918.04	6.9	0–9, 27.7, 60–?
$NaBrO_3$		918.09	6.1	0–7, 15–23, 35, 52–110, 180–?
Solution				
$NaBrO_3$		918.09	6.1	0–23, 55–110, 170–216
Vapors	20			
Br_2	−20	918.51	0	0–6
HBr	20 170	918.41	1.5	
$AsBr_3$	120	918.44	1.0	0–6.
Outer levels of Kr atom				13., 28., 96., 212., 295

TABLE I (*Cont'd.*)

Substance	Temperature°C	Main edge X.U.	ΔV (volts)	Distances of both sides, or, of center of absorption bands from the main edge. (volts)
Solids				
Se				0–4.
SeO_2				0–5.4, 12–18, 53–108, 159–?
Vapors				
Se_8	510			0–5.5, 10–12
	470			
SeO_2	330			0–32., 72–108, 159–?
	280			
Outer levels of Br atom				11., 23., 80., 183.
Solid				
Zn		1280.5	0.0	0–5.8, 9.7–16., 23., 28–43, 72–87, 113–145, 175–214, 252–280, 310–?
Vapor				
Zn	950	1280.7	−1.5	0–4, 5.8–9.
	750			
Outer levels of Ga Atom				10., 22., 106., 158.
Vapor				
Kr	20	863.72		
Vapor				
Xe	20	L_{III} 2587.2		0–3.9
		L_{II} 2424.1		0–3.9
		L_I 2269.1		
Liquid		L_{III} edges		
Hg		1006.7	−2.5	
Solid				
$HgCl_2$		1006.4	+1.2	0–6, 18, 50, 115
HgO		1007.1	−7.4	0–8, 16–66, 80–?
Vapor				
Hg	250	1006.5	0.0	
	200			
$HgCl_2$	330	1006.9	−4.9	0–6, 18, 50, 115
	230			

* Faint absorption.

The upper temperature is the superheated vapor temperature, the lower is the temperature at which the vapor would be saturated.

No compounds of Zn were studied. The metal itself shows a very extended secondary absorption which is absent in the absorption spectrum of Zn vapor at 950°C. There is a very faint fine structure line at 5.8 volts from the main edge for Zn vapor. The data given on the secondary absorption of Zn are the results of observations on a number of different plates obtained under different conditions. Plates were taken using slit widths of 0.025, 0.05, and 0.1 mm. The fine structure close to the edge is just detectable with the narrowest slit, but with this slit the radiation is so faint that it would take too long a time to secure the secondary absorption farther from the edge. The W$L\beta_1$ line falls close to the K edge of Zn, so that some plates were taken using a Pt filament with a Mo, and also a Pt target to eliminate any uncertainties due to the presence of emission lines.

The K edge of Kr proves to be a simple edge without even a white line at the edge. The wave-length of the K edge of Kr is measured using $SrK\alpha_1$ (873.37 X.U.) as a reference line.

The L edges of Xe show no secondary absorption, but at the L_{III} and L_{II} edges there is a white line absorption which is 3.9 volts in width. The positions of the L_{III}, L_{II}, and L_I, edges of Xe were measured from the $WL\beta_1$ (1279.17 X.U.), $WL\beta_2$ (1242.03 X.U.), and $WL\gamma_5$ (1129.2 X.U.) lines, respectively.

The data on mercury show that there is no secondary absorption for the liquid or the vapor, but there is for the Hg compounds. However, the structure is very faint and the values given are only approximate. The L_{II} edges of $HgCl_2$ solid and vapor also show a very faint secondary structure which has the same energy separations from the main edge as has that associated with the L_{III} edges. No secondary structure was found for any L_I edges. Noting the positions of the main edges, it is seen that $HgCl_2$ solid has the shortest, and HgO solid the longest wave-length. These edges can be determined to about 4 volts.

Summary and Discussion

A consideration of the experimental results permits a number of generalizations to be made.

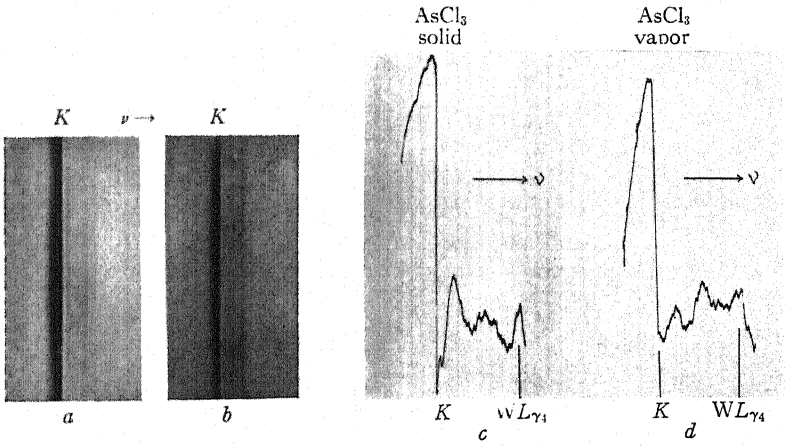

Fig. 3. $AsCl_3$ (a) solid; (b) vapor.

1. The secondary absorption of a polyatomic vapor usually has the same main characteristics as that of the solid, though the solid shows some additional structure, near the main edge, not found for the vapor. The examples of this are $AsCl_3$, As_2O_3, and SeO_2. Fig. 3 shows the data for $AsCl_3$. The microphotometer trace records clearly the dark line which splits the first white region, but it does not resolve the next dark region into the two close dark lines which can be seen on the original plate.*

* One may feel some assurance that statement No. 1. is a *bona fide* effect because of the fact that due to its perfect homogeneity the vapor makes as good, and probably a better absorbing screen for displaying secondary absorption than does the solid.

2. The Br secondary absorption shown by $NaBrO_3$ in the solid form has the same characteristics as that of $NaBrO_3$ in solution except that there is an additional structure near the main edge for the solid which is not observed for the solution. This same experiment has been performed by Meyer[13] for both

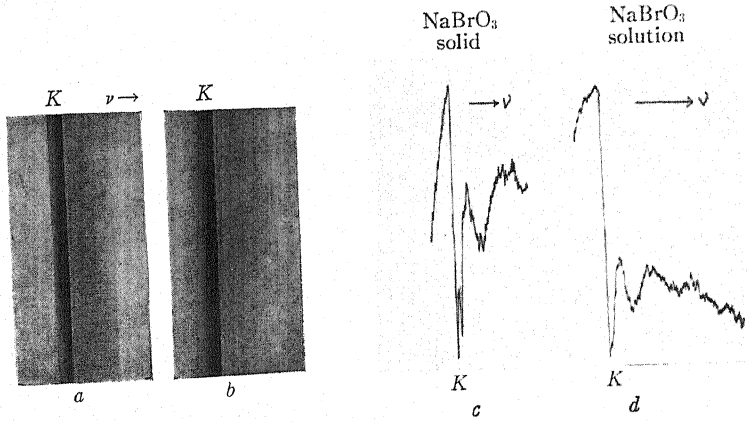

Fig. 4. $NaBrO_3$ (a) solid; (b) vapor.

$KBrO_3$ and $NaBrO_3$. He did not observe any additional structure in the absorption spectra for the solid state. Yost[14] found no detectable difference in the K absorption of manganous and chromate ions in crystals and in aqueous solutions.

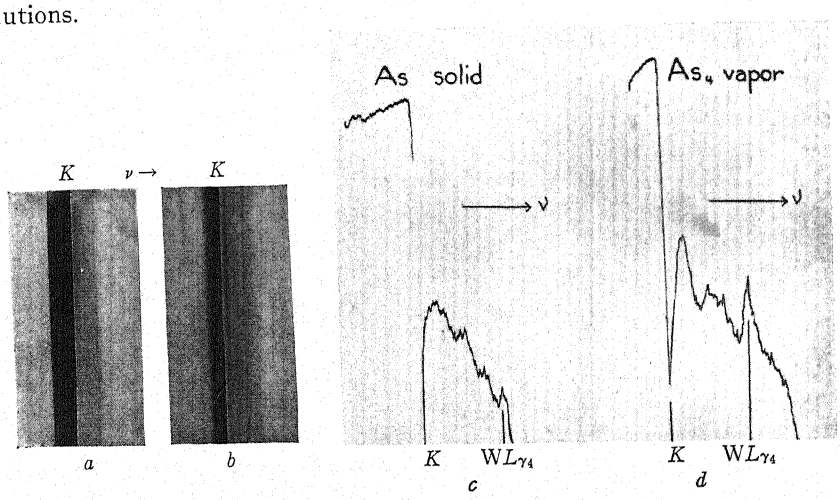

Fig. 5. As (a) solid; (b) vapor.

3. The secondary absorption of a polyatomic vapor may differ entirely from that of the solid. This effect is shown by As and illustrated in Fig. 5. As is tetratomic in the vapor state.

[13] H. Th. Meyer, Wissenschaftliche Veröffentlichungen aus dem Siemens-Konzern **7**, 101 (1929).

[14] D. M. Yost, Phil. Mag. **8**, 845 (1929).

4. The secondary absorption of a compound may differ from that of the element. Every case investigated in this work corroborates this statement. Also, this effect is well known from previous work with the lighter elements, and has recently been shown by Lindh[15] for Cu and Ni.

5. Secondary absorption is not observed for any monatomic vapor. Hg vapor, Zn vapor, Xe, and Kr are the examples of this; and one may also include Coster's and Van derTuuk's[16] case of argon. Xe and Kr were not studied in the solid form. Liquid Hg showed no secondary absorption, but Zn in the solid state exhibited the extensive structure shown in Fig. 6.

6. A monatomic vapor may show a fine structure a few volts from the main edge. Zn vapor has a faint absorption at 5.8 volts from the principal edge, though it is too faint to be seen in Fig. 6. Coster and Van der Tuuk found an absorption line for A at 1.7 volts from the main edge. They inter-

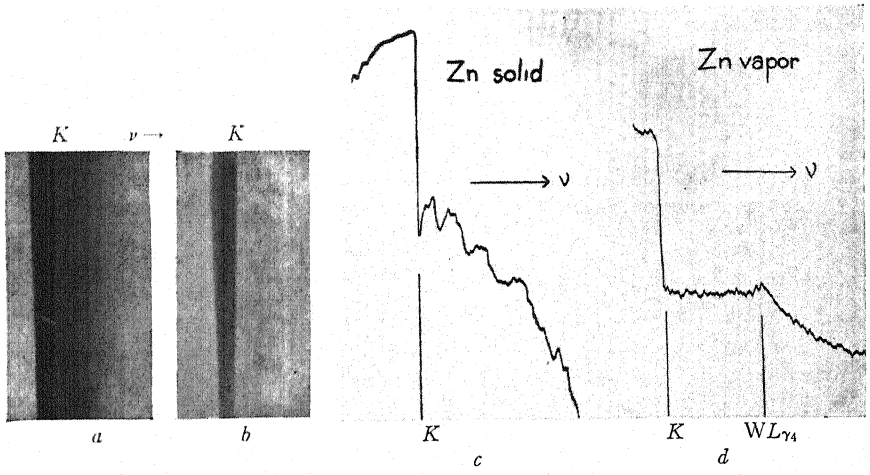

Fig. 6. Zn (a) solid; (b) vapor.

preted this as due to the transitions of the electron to different virtual orbits of the A atom, since the 1.7 volts coincides exactly with the resonance potential of K which is the next higher atom in the periodic table. The 5.8 volts for zinc does not coincide with the resonance potential of Ga, which is only 3.06 volts and would not be resolved. However, the ionization potential of Ga is 5.97 volts. This might mean that the electron stops either at the first virtual orbit, causing the main edge, or travels entirely out of the atom causing the fine structure line.

The L_{III} and L_{II} absorption edges of Xe showed a white line absorption at the main edges. The widths of these white lines were 3.9 volts. The short wavelengths edges were quite diffuse. Lepape and Dauvillier[17] have studied Xe and found a white line absorption only at the L_{III} edge. The width of their

[15] A. E. Lindh, Zeits. f. Physik **63,** 106 (1930).
[16] Coster and Van der Tuuk, Zeits. f. Physik **37,** 367 (1926).
[17] Lepape and Dauvillier, Comp. Rend. **177,** 34 (1923).

white line was about 13 volts which they related to the ionization potential of Xe. (11.5 volts). However, with the K electron absent, the outer field of Xe should compare with the next higher atom which is Cs, and which has an ionization potential of 3.88 volts. The reason for there being no white line absorption at the L_{I} edge may be that according to the selection rule $\Delta l = \pm 1$, transitions to the first virtual orbit could take place from the L_{III} and L_{II} orbits, but not from the L_{I} orbit. The absorption edges of Hg and of Kr were 'simple' without the white line at the edge. However, this may simply be because the energy dispersion in this wave-length region is from 70 to 90 volts per mm. while in the Xe L region it is 9.7 volts per mm.

7. Secondary absorption is not exhibited by all polyatomic vapors. Se_8 vapor and AsH_3 are two examples of this.

8. Completed shells of the atom in the solid state need not necessarily be associated with the absence of secondary absorption. The Br absorption in both AgBr (in the photographic plate) and NaBr shows a secondary structure. Meyer[13] has reported that secondary absorption is absent for these compounds, and several people[6,18] have remarked that secondary absorption will not be exhibited by atoms with completed shells such as Br^-.

The points at which the results of these experiments differ from those of other workers can be attributed to higher dispersion and better resolution. The resolution is such that the $WL\gamma_4$ line, which is measured in Siegbahn's laboratory as 1025.8 X.U., is here separated into two components 15 mm apart. This is 0.79 X.U. and gives 0.68 ν/R units or 9.25 volts for the separation of the O_{II} and O_{III} levels of W. The results of Meyer,[13] for instance, that there is no structure in the K edge of Br in the photographic plate, and that the secondary absorption of $NaBrO_3$ solid and solution are identical, were gotten if the experiments were performed with an 18 cm radius Siegbahn spectrograph using a calcite 100 face (dispersion 16.6 X.U. per mm); or using a calcite 111 face (dispersion 7 X.U. per mm). This latter dispersion should be high enough to observe the additional structure but it is apparent from the pictures obtained that the 111 face does not allow the resolution which can be gotten with the 100 face.

It is not apparent as yet how successful the idea of multiple electron transitions will be in explaining the effects of physical and chemical state on secondary absorption. Several workers have quantitatively correlated the energies of the secondary discontinuities with the energies of certain chosen multiple electron jumps. In the table are shown the energies of *double* electron jumps simply calculated from the energy levels of the atom next higher in atomic number. There is an approximate agreement with at least one compound of each element. A more precise calculation such as that of Kievit and Lindsay[19] was not attempted because the discontinuities here measured could not be located more accurately than about 10 volts unless the discontinuities were close to the main edge, where they are always sharper. It seems that if

[18] R. Swinne, Phys. Zeits. **30,** 523 (1929).
[19] Kievit and Lindsay, Phys. Rev. **36,** 648 (1930).
[20] G. Wentzel, Ann. d. Physik **66,** 437 (1921); **73,** 647 (1924).

secondary absorption is due to double electron transitions, then those discontinuities occurring more distant from the main edge represent transitions of electrons from deeper levels of the atom and so would be expected to be sharper, rather than more diffuse, than the discontinuities occurring close to the main edge and representing transitions of outer electrons.

The suggestion of transitions of electrons in multiply ionized atoms which has been made by Wentzel[20] to account for x-ray satellites, and applied also to absorption spectra[21, 22] does not seem suited to explain secondary absorption, because the number of quanta of radiation of sufficient energy for ionization which are produced by the x-ray tube is so small that the number of ionized atoms in the absorbing screen at any time is a negligible fraction of the total number present.

The data as it appears in this work would seem to favor the idea of relating the secondary absorption to some characteristic of the structure of the molecule or solid. One might suppose that the secondary edges correspond to the energies of excitation of the vibrational states of "structure electrons" such as postulated by O. W. Richardson[23] to account for the facts observed in experiments both on the secondary electron emission of substances and the soft-x-ray production of substances. The relation between the secondary absorption discontinuities and the kinks in the secondary electron curves can not be carried very far at present because the sensitivity is so much less for the x-ray secondary absorption determinations of energies. However, there are some points of similarity between the observations made in the study of x-ray absorption spectra, and in the study of secondary electron emission.

The kinks in the secondary electron curves correspond to the Bohr energy levels of the atom when the experiment is done roughly, but with increased sensitivity many more kinks are discovered which can not be related to the Bohr levels of the atom. The range in which these kinks occur is from zero to about 500 volts. Above this range one finds only kinks which agree with Bohr levels. These facts are exactly paralleled by the study of x-ray absorption spectra. Also, the present experiments indicate a close relation between the occurrence of secondary absorption and the structure of the substance. Turning to the study of secondary electron emission, it is found that the number and positions of the kinks which are not related to Bohr levels are functions of the structure of the substances which the primary electron beam bombards. For example, the kinks obtained using a polycrystalline substance seem to be the sum of those from the faces of a single crystal of the substance studied separately. (This is presumably not a diffraction phenomenon.) There are enough of these kinks so that Richardson was able to see that they could all be included in tables like sets of bands, and this fact led to the idea of relating them to the excitation energies of the vibration levels of some oscillating system.

An obvious experiment to check the validity of such an idea to account for

[21] E. C. Stover, Phil. Mag. **2**, 97 (1926).
[22] H. R. Robinson, Phil. Mag. **4**, 763 (1927).
[23] O. W. Richardson, Roy. Soc. Proc. **A128**, 63 (1930).

secondary absorption would be to study the absorption spectra of both elements of a chemical compound and see in how far the secondary absorption is a function of the individual elements and in how far a function of the compound. Satisfactory data for such a check do not exist at present.

In order to be certain that the absence of secondary absorption for zinc vapor at high temperature is not simply a temperature effect, experiments are now being carried out on the effect of high temperature on the secondary absorption exhibited by solids.

The writer wishes to express his warm appreciation for the excellent and ample facilities for research which have been available at the Department of Physics of the University of Michigan. He is particularly indebted to Professor G. A. Lindsay for much helpful advice, and to Mr. G. Kessler for his part in the difficult task of making the thin quartz windows.

INFRARED ABSORPTION BANDS IN HYDROGEN SULPHIDE

By Harold H. Nielsen and Ernest F. Barker
Department of Physics, University of Michigan

(Received January 30, 1931)

Abstract

Absorption spectrum of H_2S in the region from 1.0μ to 10.0μ.—The absorption spectrum of hydrogen sulphide in the infrared has been investigated with a prism spectrometer from 1.0μ to 10.0μ. Two regions of absorption, one at 2.6μ and another 3.7μ were located, both of which revealed fine structure when examined under high dispersion.

Structure of the 2.6μ absorption band of H_2S.—The band at 2.6μ was found to consist of P, Q, and R branches, the P and R branches being made up of somewhat irregularly spaced lines and the Q branch broadened unsymmetrically, sloping off more steeply toward lower frequencies. The separation between the most prominent lines in the P and R branches was found to be about 10 cm^{-1}. A slight convergence was observed toward higher frequencies.

Structure of the 3.7μ absorption band of H_2S.—The 3.7μ band was found to consist of but one branch, made up of several prominent lines with weaker satellites on either side. The average spacing between these is about 9.0 cm^{-1}, and no convergence was discernable.

Qualitative quantum mechanical discussion of structure of absorption bands of H_2S.—Only a qualitative discussion of the structure of the observed bands is given, based on the classical quantum mechanical solution of an asymmetric rotator due to Witmer. The band at 2.6μ is accounted for by a vibration of the electric moment along the least axis of inertia while the band at 3.7μ is shown to arise from a vibration along the intermediate axis. It is pointed out that the rigorous quantum mechanical solutions of asymmetric rotators confirm the conclusions drawn herein and in addition satisfactorily explain the broadening of the Q branch.

RECENT quantum mechanical studies of asymmetric rotators[1] have emphasized the importance of investigating the vibration rotation spectra of molecules belonging to this class. The water-vapor absorption bands measured by W. W. Sleator[2] and again by Sleator and Phelps[3] are characteristic of this kind, and they have suggested that a study of the infrared spectrum of hydrogen sulphide might prove fruitful.

W. W. Coblentz[4] has mapped the spectrum of hydrogen sulphide in the region from 3μ to 12μ with a prism spectrometer. More recently A. H. Rollefsen[5] has published two bands in hydrogen suphide at 4.2μ and 8.0μ. In the present work an absorption cell forty centimeters long with mica windows was used, and the spectrum carefully remapped from 1.0μ to 10.0μ with a Wadsworth type prism spectrometer. It was, however, impossible to dupli-

[1] Kramers and Ittman, Zeits. f. Physik **53**, 553 (1929); Wang, Phys. Rev. **34**, 243 (1929); Klein, Zeits. f. Physik **58**, 730 (1929).
[2] Sleator, Astrophys. J. **48**, 125 (1918).
[3] Sleator and Phelps, Astrophys. J. **62**, 28 (1926).
[4] Coblentz, Pub. Carnegie Inst. No. 35, pp. 52 and 178.
[5] Rollefsen, Phys. Rev. **34**, 604 (1929).

cate any of the bands previously reported, but two other absorption maxima were located, lying at 2.6μ and 3.7μ. The prism curve of the absorption spectrum of hydrogen sulphide as determined in this investigation is shown in Fig. 1 A. The maximum near 4μ reported by Coblentz and Rollefsen was found in the first trial, but upon careful purification of the gas it disappeared and almost certainly is to be ascribed to carbon dioxide as an impurity. Likewise in another series of observations when a cell with rock salt windows was used, the band reported by Rollefsen at 8.0μ was found. In all other trials, mica windows were used and although this spectral region was carefully searched, the 8μ band could not be found. It appears that this band can not be due to the hydrogen sulphide molecule, for on all occasions before searching for it, the presence of the absorption maxima at 2.6μ and 3.7μ was first confirmed. It is suggested that the 8.0μ band may be characteristic of some substance formed by the interaction of hydrogen sulphide with the rock salt windows.

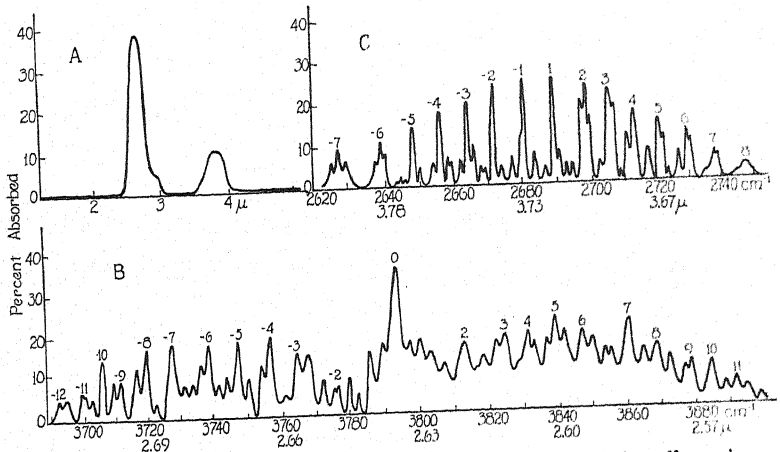

Fig. 1. Absorption bands in hydrogen sulphide. *A*, Prism curve with low dispersion. *B*, Fine structure in the band at 2.6μ. *C*, Fine structure in the band at 3.7μ.

A prism grating spectrometer designed by C. F. Meyer was available for further investigation of the hydrogen sulphide spectrum under high dispersion. The apparatus was equipped with a vacuum thermopile constructed by Meyer and was used in conjunction with a Moll thermal relay and a Leeds and Northrup high sensitivity galvanometer. This gave a sensitivity sufficiently high to make the use of slit widths of 16 angstrom units feasible. The grating used in both regions was one with a spacing of 7200 lines per inch (2834 lines per centimeter) ruled on a copper-nickel surface. The calibration of this grating was obtained from a table prepared by A. A. Levin for this spectrometer, based upon the positions of the -3 and -4 lines of hydrogen chloride determined by Colby, Meyer and Bronk.[6]

Two lengths of absorption cell were used, the H_2S being at atmospheric

[6] Colby, Meyer and Bronk, Astrophys. J. 57, 7 (1923).

pressure in each. For the band at 2.6μ, a length of ten centimeters was found most advantageous. This cell was double, one side being filled with dried air to compensate for the water-vapor absorption in the atmosphere. At 3.7μ a cell twenty five centimeters long was used. Compensating windows were not necessary here since the diminution of the energy due to the mica could satisfactorily be taken into account by making a preliminary run with the cell empty, and no atmospheric absorption occurs in this region.

The hydrogen sulphide gas was obtained in ordinary lecture bottles from the Matheson Company, their analysis showing a purity of 99.7 percent. In order to remove any carbon dioxide, carbon disulphide and hydrogen chloride,

TABLE I. *Wave numbers and intensities of lines in the band at 2.7 μ.*

Intensity	Wave No. (cm^{-1})	Line No.	Intensity	Wave No. (cm^{-1})	Line No.
2.0	3692.5	−12	6.5	3786.0	
2.0	3694.7		7.0	3789.5	
2.5	3700.0	−11	15.0	3793.9	0
2.0	3701.3		6.5	3797.7	
6.0	3706.5	−10	6.5	3800.5	
3.5	3709.6	− 9	6.0	3804.1	
3.5	3712.0		5.0	3808.2	
5.0	3716.6		7.0	3813.7	2
7.0	3720.1	− 8	5.0	3819.9	
1.0	3722.5		6.5	3822.9	
7.0	3728.0	− 7	7.5	3825.0	3
2.5	3731.8		7.5	3831.8	4
2.5	3733.4		6.5	3834.0	
5.0	3736.0		6.5	3837.7	
7.0	3737.6	− 6	8.0	3840.3	
3.0	3740.3		6.5	3843.6	
3.0	3743.1		6.5	3848.5	6
7.0	3746.6	− 5	6.4	3851.5	
3.0	3750.7		5.0	3855.6	
5.0	3754.0		5.0	3757.1	
8.0	3756.2	− 4	7.5	3861.2	7
1.0	3760.8		5.5	3866.1	
6.0	3764.5	− 3	6.0	3870.5	8
6.0	3768.0		5.0	3873.3	
3.0	3772.6		4.0	3878.5	
2.5	3775.1		4.5	3879.7	9
2.5	3776.9	− 2	4.5	3886.0	10
3.0	3780.1		2.0	3889.9	
2.0	3782.5		2.5	3892.5	11
			2.0	3895.8	

the gas was passed through three successive wash bottles each of which contained a solution of potassium hydrosulphide (KHS). After drying over phosphorus pentoxide, the gas was gathered by freezing with liquid air and finally purified by partial distillation. This was done immediately before each run.

The two absorption maxima which had been located prismatically, reveal fine structure when examined under high dispersion. They are distinctly different in type, but are both characterized by an irregularity of structure suggestive of water vapor bands. When only the most intense lines are considered however, the patterns resemble the bands due to certain symmetrical molecules.

The 2.6μ region. The 2.6μ band shows distinct P, Q and R branches, the P and R branches being made up of irregularly spaced lines. The average spacing for those of greatest intensity is about 10 cm^{-1}. Moreover, proceeding from the center outward it seems possible to identify the various lines in the P branch with corresponding lines in the R branch. A slight convergence is noticeable toward higher frequencies, and the Q branch is broadened unsymmetrically, sloping off more steeply toward lower frequencies. Curve B shows those details of this band which repeated themselves in the many sets of data taken. Original circle settings have been replaced for convenience by a scale of frequencies, and in Table I the frequencies and approximate relative intensities of the lines are given.

TABLE II. *Wave numbers and intensities of lines in the band at 3.7μ.*

Intensity	Wave No. (cm^{-1})	Line No.	Intensity	Wave No. (cm^{-1})	Line No.
2.5	2624.3		10.0	2690.1	1
3.5	2626.9	−7	2.0	2692.2	
2.5	2629.7		1.0	2693.3	
3.0	2636.5		1.0	2694.6	
5.0	2637.8	−6	8.8	2697.8	
3.5	2638.9		9.5	2698.7	2
.3	2642.6		8.0	2701.2	
.4	2643.7		1.5	2704.1	
.3	2645.2		9.0	2706.6	3
6.2	2647.8	−5	8.5	2707.0	
2.2	2650.2		.5	2709.8	
2.2	2654.4		5.0	2712.7	
7.5	2656.6	−4	7.5	2714.4	4
2.2	2658.6		3.5	2719.1	
2.1	2660.6		6.0	2721.9	5
2.1	2663.2		4.0	2722.8	
8.7	2665.1	−3	.5	2724.5	
2.5	2666.6		2.5	2727.0	
1.0	2669.5		5.0	2729.5	6
1.0	2670.9		3.0	2730.5	
10.0	2673.8	−2	.8	2737.7	
1.0	2675.6		3.0	2738.4	7
2.0	2679.4		2.0	2739.4	
10.0	2682.5	−1	.8	2743.3	
2.0	2684.9		2.0	2745.3	8
1.0	2687.8		.8	2746.7	

The 3.7μ region. The 3.7μ band is of the type which shows an envelope with but one maximum. It also has been resolved, at least partially, revealing a number of prominent lines, characterized in general by accompanying satellites of lesser intensity on either side. No apparent convergence is discernible and the most prominent lines are separated by an average spacing of about 9.0 cm^{-1}. Details repeating themselves in all sets of data are shown in curve C where as before a frequency scale replaces the original circle settings. Table II gives the frequencies and relative intensities of the lines measured in this region.

INTERPRETATION OF THE OBSERVED BANDS

It is hoped in a later communication to give a complete description of this spectrum in terms of the rigorous quantum mechanics of an asymmetrical

rotator model. At present, it seems better, however, to consider qualitatively only the general characteristics of the two observed bands.

A solution for the asymmetrical rotator by a perturbation method is given by E. E. Witmer[7] in the classical quantum mechanics where the perturbation function involves the third moment of inertia. Taking A, B, and C as the three principal moments of inertia where $A<B<C$, the energy levels are shown to be of two kinds, A-levels arising when the molecule rotates principally about the least axis of inertia, and C-levels, arising when the molecule rotates principally about the largest axis of inertia; their combined number being $J+1$. The energy values of A-levels are those of a symmetric rotator rotating about the A-axis plus a certain perturbation component to the energy involving C. The C-levels are similarly determined by the energy expression of a symmetric top rotating about the C-axis plus another perturbation component involving A.

Hund[8] and Dennison[9] have shown that isosceles triatomic molecules have three fundamental modes of vibration, two of which are along the bisector of the apex angle, and a third perpendicular to this. If the three absorption bands corresponding to these three vibrations can be observed, the dimensions of the triangle (i.e., the apex angle and the lengths of the sides) may be calculated, from which the three moments of inertia may in turn be determined. In hydrogen sulphide only two bands have been observed, however; hence this means of determining the shape and moments of inertia is not available. The indeterminancy of the shape of the molecule introduces the further limitation that one can not know whether the bisector of the apex angle will be the least or the intermediate axis of inertia, since this depends upon the magnitude of the angle. Consequently the appearance of the third fundamental, were it observable, cannot be predicted, for if the bisector of the apex angle were the least axis of inertia, there would be two identical bands of one kind, while if it is the intermediate axis of inertia there would be two identical bands of the other type.

In hydrogen sulphide the electric moment vibrates in the plane of the three atoms, i.e., along either the A-axis or the B-axis. When the electric moment changes along A, and the rotation is principally about the same axis, quantum transitions occur among the A-levels governed by the rules (retaining the nomenclature of the symmetric rotator) $\Delta J=\pm 1, 0; \Delta K=0$. When, however, the rotation is principally about C, quantum transitions occur among the C-levels and are determined by the rules, $\Delta J=\pm 1, 0; \Delta K=\pm 1$. This gives rise to a band having P, Q and R branches, the P and R branches originating from the transitions $\Delta J=\pm 1, 0; \Delta K=\pm 1$; and $\Delta J=\pm 1, \Delta K=0$; and the Q branches from $\Delta J=0, \Delta K=0$. The band observed at 2.6μ having distinct, P, Q and R branches, is consequently due to a vibration of the electric moment along the least axis of inertia; i.e., the A-axis.

Vibrations of the electric moment along the B axis are perpendicular to

[7] Witmer, Proc. Nat. Acad. **12**, 602 (1926).
[8] Hund, Zeits. f. Physik **31**, 81 (1925).
[9] Dennison, Phil. Mag. **1**, 195 (1926).

rotations about both the A and C-axis, hence quantum transitions among both A and C-levels must be governed by the selection rules $\Delta J = \pm 1, 0$; $\Delta K = \pm 1$ alone. It may easily be seen that the resulting band is of the type observed at 3.7μ with no Q-branch. The regularity in spacing and intensity of the lines of bands of symmetric rotators is due to the fact that many transitions are over the same frequency range giving rise to lines which are precisely superposed. In the case of asymmetric rotators the positions of successive energy levels are altered by the asymmetry, but with no definite order; hence no regularity of line structure is here to be expected since only rarely do two or more lines fall at the same place.

The general characteristics are borne out also in the rigorous quantum mechanical solutions of the asymmetric rotator given by Kramers and Ittman and by Wang. One of the main differences is the splitting up of the $J+1$ levels of the old theory into $2J+1$ levels on the basis of the new. The magnitude of this doubling as given by Wang is:

$$\Delta\nu = \left\{ \frac{\frac{1}{2}\left(\frac{1}{C} - \frac{1}{B}\right)}{\frac{1}{A} - \frac{1}{2}\left(\frac{1}{C} + \frac{1}{B}\right)} \right\}^{K} \left\{ \frac{h\left[\frac{1}{A} - \frac{1}{2}\left(\frac{1}{C} + \frac{1}{B}\right)\right](J+K)!}{2^{3K}\pi^2(J-K)!(K-1)!^2} \right\}$$

This is seen to be small when K is small and the rotation is almost entirely about either A or C, but becomes large for those levels which mark the transition from rotation principally about one axis to rotation principally about the other. It is this doubling of the levels that accounts for the broadening of the Q branch. In the symmetric rotator, the Q branch arises from transitions from a rotational level in one vibrational state to the corresponding rotational level in another vibrational state. In the asymmetric case each rotational level save one is a doublet, and transitions now occur from the one doublet component of such rotational levels in one vibrational state to the other doublet component of the corresponding rotational level in another vibrational state. The Q branch thus arising is not a sharp maximum, but consists of many lines near the center of the band.

The kind cooperation and support given to this work by Professor H. M. Randall, and Professor D. M. Dennison's many helpful suggestions in the interpretation of these bands are gratefully acknowledged.

NOTE ON THE INTERPRETATION OF CERTAIN $^2\Delta$, $^2\Pi$ BANDS OF SiH

By Robert S. Mulliken
Ryerson Physical Laboratory, University of Chicago

(Received February 4, 1931)

Abstract

It is shown that Jackson's $^2\Delta$,$^2\Pi$ SiH bands have a *regular* $^2\Pi$ state and thus are closely analogous to the λ4300 bands of CH. The orbit-spin coupling coefficient A is determined for the $^2\Pi$ state of SiH and shown to agree closely with A of the ^3P state of the Si atom, from which the $^2\Pi$ molecular state is supposed to be derived. This is a new example of a relation which seems to be universal. Another new example of the same relation, found in BeH, is also cited.—The coefficients A and B of the $^2\Delta$ state and B of the $^2\Pi$ state of SiH are also discussed.

C. V. JACKSON has obtained some SiH bands near λ4100 and has shown by a skilful analysis that they have a structure corresponding to a $^2\Delta$,$^2\Pi$ transition.[1] Because of the analogy of Si to C, there is a very strong presumption that these bands are analogous to the $^2\Delta$,$^2\Pi$ bands of CH near λ4300. In the case of CH the $^2\Delta$ doublet is very narrow and inverted ($A/B \sim -0.07, B = 14.57$), while the $^2\Pi$ is regular ($A/B = +2.0, B = 14.2$). According to Jackson, the $^2\Delta$ state of SiH is narrow and *regular*, but the $^2\Pi$ *inverted*, with $A/B \sim -10$, $B = 7.4$. From a consideration of electron configurations, however, it is clear that if the $^2\Pi$ state of SiH is inverted it cannot be at all analogous to that of CH, since in such simple molecules[2] an inverted Π state implies a group of three equivalent π electrons, whereas a regular Π state implies only a single π electron outside of closed shells. In the case of the $^2\Delta$ state, however, the existence of a reversed sign of A in SiH, while rather unexpected, has no such important implications. For the $^2\Delta$ state of CH is attributed to an electron configuration $\cdots \sigma\pi^2$, in which the small observed doubling can be ascribed to the small interaction of the spin of the σ electron with the orbital angular momenta of the two π electrons.[2] In similar cases in atomic spectra, we know that doublets of this kind may be either regular or inverted.

A study of Jackson's analysis shows that, while the fact that the $^2\Delta$ is regular is incontrovertible, the only evidence that the $^2\Pi$ is inverted comes from an application of Van Vleck's theoretical work[3] on Λ-type doubling. [The question whether a given $^2\Pi$ level is regular or inverted can in general also be decided by determining the lowest J value in each of the two sets of levels supposed to be $^2\Pi_{1/2}$ and $^2\Pi_{1\,1/2}$, but this method could not be used in the present instance because of the complexity of the band and the weakness of the lines having low J values.] Van Vleck's theory demands that in case a the Λ-type

[1] C. V. Jackson, Proc. Roy. Soc. **126A**, 373 (1930).
[2] R. S. Mulliken, Phys. Rev. **33**, 730 (1929).
[3] J. H. Van Vleck, Phys. Rev. **33**, 496–7 (1929).

doublets shall be much wider in the $^2\Pi_{1/2}$ than in the $^2\Pi_{1\,1/2}$ levels, and if we assume case a, this criterion applied to the experimental data indicates an inverted $^2\Pi$. This was the basis of Jackson's conclusions.

But, as is mentioned in another forthcoming paper,[4] we have in the $^2\Pi$ of SiH a state which is case a for the lowest J values but goes over to case b with increasing J. In such a case the $^2\Pi_{1/2}$ Λ-type doublets, although they should at first be wider than those for $^2\Pi_{1\,1/2}$, should soon get narrower again and their widths should pass through zero, while the $^2\Pi_{1\,1/2}$ doublets should begin to widen rapidly under the influence of the approach to case b.[3] This would give on the whole wider doublets for $^2\Pi_{1\,1/2}$ than for $^2\Pi_{1/2}$, and would require that we reverse Jackson's conclusions and interpret the $^2\Pi$ state as regular. In order to prove that this interpretation is correct we should show that the Λ-type doublets change sign with increasing J in what is here considered to be the $^2\Pi_{1/2}$ state (Jackson's $^2\Pi_{1\,1/2}$ state). Now according to Jackson, the levels which we call $^2\Pi_{1/2}$ show measurable doubling only beginning with $K=14$, while in the $^2\Pi_{1\,1/2}$ levels doubling becomes appreciable at $K=8$. But Jackson remarks that lines going to the levels $K=5$ and 6 of $^2\Pi_{1/2}$ also show a doubling, which he classifies as a perturbation. If, however, we suppose that the Λ-type doubling in the $^2\Pi_{1/2}$ state first increases to a maximum, which is just large enough to be measurable, at $K=5$ or 6, then decreases again, passes through zero at about $K=11$ or 12, and again increases with opposite sign until at $K=14$ it is again large enough to be detected experimentally, all the observed relations are explained, and we have surely a regular $^2\Pi$ state. Table I, based on Jackson's Table VIII, gives the values of the Λ-type doublet separations.

TABLE I. Λ-*type doublet widths* (cm^{-1}) *in* $^2\Pi$ *state of* SiH.*

K	$^2\Pi_{\frac{1}{2}}$	$^2\Pi_{1\frac{1}{2}}$	K	$^2\Pi_{\frac{1}{2}}$	$^2\Pi_{1\frac{1}{2}}$	K	$^2\Pi_{\frac{1}{2}}$	$^2\Pi_{1\frac{1}{2}}$
4	—	—	9	—	0.66	14	0.33	1.61
5	−0.30	—	10	—	0.80	15	0.60	1.91
6	−0.27	—	11	—	0.99	16	0.84	2.12
7	—	—	12	—	1.0	17	0.99	2.42
8	—	0.38	13	—	1.35	18	1.32	—

* Most of these values are weighted averages of values obtained from P, Q, and R branches as given by Jackson in his Table VIII. The negative signs for the low numbered K values of $^2\Pi_{\frac{1}{2}}$ and the positive signs for all other values are of only relative significance here, and furthermore are based only on the fact that according to Van Vleck's theory, the sign of the doubling should be the same in case b (high K values) for $^2\Pi_{\frac{1}{2}}$ as for $^2\Pi_{1\frac{1}{2}}$. Empirically there is no way of deciding, from data on Δ, Π bands, whether the T_a or the T_b levels of the Π state are higher. (In the case of a Π, Σ transition this *can* be decided empirically).

Thus we have a regular $^2\Delta$ and a regular $^2\Pi$ state in SiH, and there is every reason to believe that these are analogous to the similar states of CH. It is of interest to determine the magnitudes of the coefficients A of the coupling between Λ and S for the two states of SiH. The value of A/B for the $^2\Pi$ state can be estimated most accurately by fitting Hill and Van Vleck's formula[5] for the general intermediate case between cases a and b to the data on

[4] R. S. Mulliken and A. Christy, forthcoming Phys. Rev.

[5] E. L. Hill and J. H. Vleck, Phys. Rev. **32**, 250 (1928).

the term *differences* between $^2\Pi_{1/2}$ and $^2\Pi_{1\ 1/2}$ states of the same K values (cf. Jackson's Table IX). This and a further use of Jackson's data on ΔF's in order to determine B more accurately, give $A/B=+19.5$ and $B=7.35$.[6] [$A/B=-15.5$ would do equally well if we did not know from Van Vleck's theory of Λ-type doubling that $A>0$.] In a similar way one obtains for the $^2\Delta$ state the values $A/B=+0.6$ and $B=7.3$ [$A/B=+3.4$ would equally well explain the observed spectrum, but since we expect a very small A for a $\sigma\pi^2$ $^2\Delta$ state, and since $A/B\sim-0.07$ is very small in $^2\Delta$ of CH, the value $A/B=+0.6$ is the more probable].

We thus have $A=+4$ for the $^2\Delta$ state and $A=+143$ for the $^2\Pi$ state, which may be compared with the values $A=-1$ and $A=+28$ for the corresponding states of CH. In the case of CH there is an interesting relation between A in the $^2\Pi$ state of the molecule and A in the ^3P state of the carbon atom from which the $^2\Pi$ of CH is supposed to be derived by the addition of a hydrogen atom.[2] For a $\cdots p^2\ ^3P$ atomic state, we know that for normal coupling the over-all width of the triplet, i.e., $^3P_2-{}^3P_0$, is $1\frac{1}{2}A$. For the normal state of carbon, $^3P_2-{}^3P_0=42$ cm^{-1}, giving $A=+28$ in exact agreement with A as obtained from the $^2\Pi$ state of CH. [Similar, although usually less exact, agreements are found in many other hydrides. Usually the A from the molecule is somewhat *less* than that from the atom.[2]] A similar comparison is of interest for the normal ^3P of the silicon atom and the $^2\Pi$ of SiH. For the atom, $^3P_2-{}^3P_0=223$, giving $A=+149$, in excellent agreement with the value $A=+143$ from SiH. The significance of such agreements has been discussed in a previous paper.[2]

In connection with the comparison of A values of atoms and their hydrides, a recent result of Watson and Parker[2] is of interest. These authors find $A=+1.97$ for the presumably $1s\sigma^2 2s\sigma^2 2p\pi$, $^2\Pi$ state of BeH, which agrees well with the value $A=+2.08$ from the triplet separation ($^3P_2-{}^3P_0$, $\Delta\nu=3.12$) of the $1s^2 2s2p$, ^3P state of the Be atom.

[6] No attempt has been made to obtain very accurate values of A and B, but it is believed that the A value of the $^2\Pi$ state is fairly accurate, the calculations having been made by means of the Hill and Van Vleck formula in such a way as to make the best use of the experimental data.

[7] W. W. Watson and A. E. Parker, Phys. Rev. 37, 167 (1931).

COLLISIONS OF THE SECOND KIND AND THEIR EFFECT ON THE FIELD IN THE POSITIVE COLUMN OF A GLOW DISCHARGE IN MIXTURES OF THE RARE GASES

By L. B. Headrick and O. S. Duffendack
University of Michigan

(Received January 24, 1931)

Abstract

A study was made of the collision processes in the uniform positive column of a glow discharge in mixtures composed of two of the rare gases, helium, neon and argon and a mixture of each of these gases with mercury vapor, by means of measurements of the electric field and by spectroscopic observations. The discharge tube was of cylindrical form, 4.4 cm in diameter, with plane parallel electrodes The electrode distance could be varied from zero to 32 cm by means of an external electromagnet. The phenomena were studied with currents from 20 to 40 m.a. and pressures from 5 to 30 mm of mercury. The mixtures were circulated through the discharge tube and a purifying system during the entire time that observations were being made. It was very important to maintain extreme purity of the gases. The results show that the electrical and spectral characteristics of the uniform positive column in mixtures of monatomic gases can be explained principally in terms of collisions of the second kind between the ions or metastable atoms of one gas and the neutral atoms of the other. The effect of limitation of electron velocities is insufficient to explain the results, and its effect is shown to be negligible as compared with collisions of the second kind when the concentration of one gas is very small. The necessary condition for a large effect to be produced in the electrical and spectral characteristics of the positive column by a small percentage of one gas added to another is that a close resonance exists between the metastable states of the main gas and the ionization potential or excited states of the added gas atom or ion. By the introduction of as little as 0.4 percent neon or argon into helium, a marked increase in the electric field is produced, and the spectrum emitted is changed almost completely from the arc spectrum of helium to that of neon or argon respectively. The addition of mercury vapor at room temperature to neon caused a decrease of 45 percent in the field while the addition of mercury to either argon or helium produced a small increase. In the cases where the excitation and ionization potentials of the added gas were above the metastable states of the main gas, no reactions between the two gases could occur to affect the concentration of metastable atoms. In these cases practically no change in either the spectral or electrical characteristics were observed upon adding a small amount of one gas to another. However, in larger proportions the change produced in the field was proportional to the amounts of the two gases and the difference between the field in each of the pure gases. This result is accounted for mainly by the difference in the energy of the ionization processes in the two gases by electron impact.

Introduction

THE phenomena occurring when electricity passes through a gas are many and complicated. The various phenomena have been the subject of many investigations and a great deal is known about the electrical and spectral characteristics of the different types of electrical discharges. Until the development of the Bohr theory of the atom, the beginning of the classification of spectroscopic data, and the measurements of critical potentials by means of

electrons of controlled velocity, very little was known about the mechanism of the elementary processes involved in the discharge of electricity through gases. With the information obtained from the classification of spectroscopic data, the spectroscopic study coupled with measurements of the electrical characteristics of a discharge gives a very powerful means of studying the elementary processes taking place. This method has been used by the writers to study the collision phenomena occurring in the positive column of a glow discharge in mixtures of the rare gases.

Klein and Rosseland[1] suggested that since a collision between an electron and a molecule may result in the excitation of the molecule, due to its absorption of the kinetic energy of the moving electron, the reverse of this process should also take place; that is, the change of excitation energy of a molecule to kinetic energy of an electron at a collision between an excited atom and a slowly moving electron. This type of collision is called a collision of the *second kind*. The former process is called a collision of the *first kind*. Franck[2] has shown that the theory of Klein and Rosseland may be extended to include impacts of the second kind between excited atoms and neutral atoms.

Nearly all gases, unless very carefully purified, contain small amounts of other gases as impurities. It has been observed from spectroscopic studies that, in certain regions of a discharge and for certain gases as impurities, the spectra of the impurities were often stronger than that of the main gas. These observations led to spectroscopic investigations of discharges in mixtures of gases.

Duffendack[3,4,5,6] and a number of his pupils have made spectroscopic studies on the excitation in a low voltage arc in mixtures of the rare gases with nitrogen, carbon monoxide, and various metal vapors in a tungsten furnace. The limits and maxima of excitation observed were explained on the basis of collisions of the second kind between the excited atoms or rare gas ions and the neutral gas or metal molecules.

Sawyer,[7] Takahashi,[8] Naudé,[9] Kruger,[10] Frerichs[11] and others have used the hollow cathode discharge with the rare gases to excite the spectra of various metals and have explained the observed maxima and limits of excitation on the basis of collisions of the second kind.

Penning[12,13] has shown that certain phenomena regarding the sparking potentials of mixtures of the rare gases and also other gases can be explained by means of collisions of the second kind.

[1] Klein and Rosseland, Zeits f. Physik **4**, 46 (1921)
[2] J Franck, Zeits. f. Physik **9**, 259 (1922).
[3] O S. Duffendack and H. L. Smith, Phys. Rev. **34**, 68 (1929).
[4] O. S. Duffendack and R. A. Wolfe, Phys. Rev. **34**, 409 (1929).
[5] O. S. Duffendack and J. G. Black, Phys. Rev. **34**, 35 (1929).
[6] O. S. Duffendack, C. L. Henshaw and Marie Goyer, Phys. Rev. **34**, 1132 (1929).
[7] R. A. Sawyer, Phys. Rev. **36**, 44 (1930).
[8] Y. Takahashi, Ann. d. Physik **3**, 49 (1929).
[9] S. M. Naudé, Ann. d. Physik **3**, 1 (1929).
[10] G. Kruger, Phys. Rev. **34**, 1122 (1929).
[11] R. Frerichs, Ann. d. Physik **85**, 376 (1928).
[12] F. M. Penning, Zeits. f. Physik **46**, 335 (1928).
[13] F. M. Penning, Zeits. f. Physik **57**, 723 (1929).

In the present investigation the study of the effect of collisions of the second kind on discharge characteristics has been extended to the positive column of a glow discharge. Mixtures of the three rare gases, helium, neon and argon and mixtures of each of these with mercury vapor were used. The study of collision phenomena and the processes of production of ions was made by observing simultaneously the changes in excitation and in the electric field in the positive column with the change in the proportion of the two gases in a mixture.

Theory of the Uniform Positive Column

The phenomena occurring in the positive column are independent of the material and form of the electrodes and depend only on the properties of the gas, the current density, and the tube diameter. For pure monatomic gases the positive column is uniform under almost all conditions. In diatomic gases or in mixtures, for certain limits of current and pressure, the positive column is striated. The electric field in the uniform positive column is uniform. In the striated positive column a slight sinusoidal variation is superimposed upon the uniform field. This variation has a wave-length equal to the distance between striations. The field reaches a maximum value at the cathode end of the luminous region of each striation. The theory of the uniform positive column will be discussed in detail since practically all of the work in this investigation was done with a uniform column. While most of the data on this part of the discharge are qualitative, some approximate empirical relations have been worked out for a considerable range of the variables. For a tube of cylindrical form, the field is directly proportional to the pressure and inversely proportional to the radius of the discharge tube. At a small current density, for which the positive column does not completely fill the tube, the field increases with an increase in current. The field reaches a maximum value when the column just fills the tube and then decreases slowly until the current density reaches a high value, corresponding to nearly one hundred percent ionization of the gas, after which the field increases quite sharply and rapidly with further increase in current. This condition of practically complete ionization has never been attained in large discharge tubes. It has been studied by Langmuir[14] in capillary tubes with a current density of the order of 40 amp/cm^2.

Schottky[15] has made a study of diffusion currents to the tube walls in the positive column and has developed a theory on the basis of the results obtained. The assumptions made for a cylindrical discharge tube are the following:

(1) The field in the positive column is the source of the energy necessary to maintain a certain degree of ionization which is required for a given discharge condition. (2) Ions are lost by diffusion to the walls where recombination occurs. (3) The current density and concentration of positive ions and electrons is constant throughout the length of the column. (4) The

[14] I. Langmuir, G. E. Rev. **27**, 762 (1924).
[15] Schottky, Phys. Zeits. **25**, 342 and 635 (1924).

radial component of the positive ion current is equal to the radial component of the electron current. (5) The concentration of positive ions and electrons is zero at the walls and reaches a maximum at the tube axis. (6) The dimensions of the tube are large compared to the mean free path of the molecules. (7) Sufficient collisions occur to give both the positive ions and electrons a Maxwellian distribution of velocity.

The equation obtained from these assumptions without the use of Poisson's equation is given below.

$$G = \frac{2.4}{R}\left(\frac{V_i}{H}(B^+ + B^-)\frac{K^+ \cdot K^-}{(K^+ + K^-)^2}\right)^{1/2}.$$

Where G is electric field in volts per cm; R is tube radius in cm; V_i is ionization potential of the gas in volts; H is an efficiency factor of ionization; B^+ is energy of random motion of positive ions in volts; B^- is energy of random motion of negative ions in volts; K^+ is mobility of positive ions; and K^- is mobility of negative ions.

This expression for the dependence of the field on the tube radius checks the empirical relation. The field will however not be equal to zero for R increased indefinitely but will reach a minimum value. The above form of the equations results from the assumption that ions are lost only by diffusion to the tube walls and therefore does not hold for large values of R where recombination in the body of the gas becomes important. This theory does not give the dependence of the field on current density or on pressure.

Morse[16] has developed an equation for the electric field in the positive column, giving its dependence on both the tube radius and the pressure, but not on the current density. He assumes that the relations for mobility and average number of ions produced by an electron under given conditions are known and uses the results of Schottky to determine the diffusion currents to the tube walls. The calculations are based on three general differential equations which represent the conditions for a stable discharge in a tube of unit cross section. The following result is obtained.

$$E = 5.76\epsilon V_r \frac{Gp}{r}.$$

Where E is field in the positive column in volts/cm; G is a constant inversely proportional to the mobilities of positive ions and electrons; p is gas pressure in mm of mercury; r is tube radius in cm; and V_r is ionization potential of the gas, or if metastable states are formed, the first critical potential.

The value of the field given by this equation satisfied the empirical relation for its dependence on both the tube radius and the pressure, but still leaves the dependence on current density to be explained qualitatively. The field increases with the current for small current densities where an increase in current increases the diffusion to the tube walls, but the field decreases slowly for large current densities where the increase in current decreases the

[16] P. M. Morse, Phys. Rev. **31**, 1003 (1928).

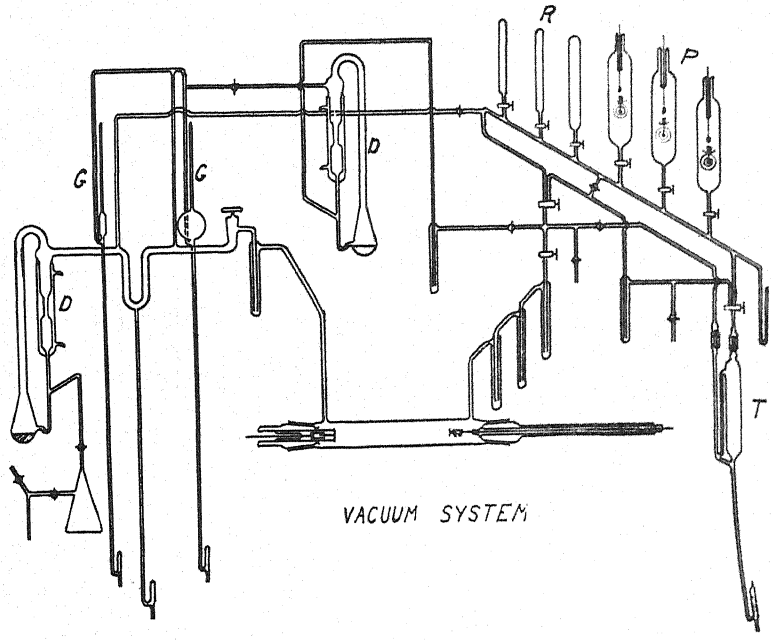

Fig. 1. Diagram of vacuum system.

percent of diffusion to the tube walls. In order to obtain an expression for the field as a function of the current it would be necessary to determine the diffusion current to the tube walls as a function of the current density in the tube.

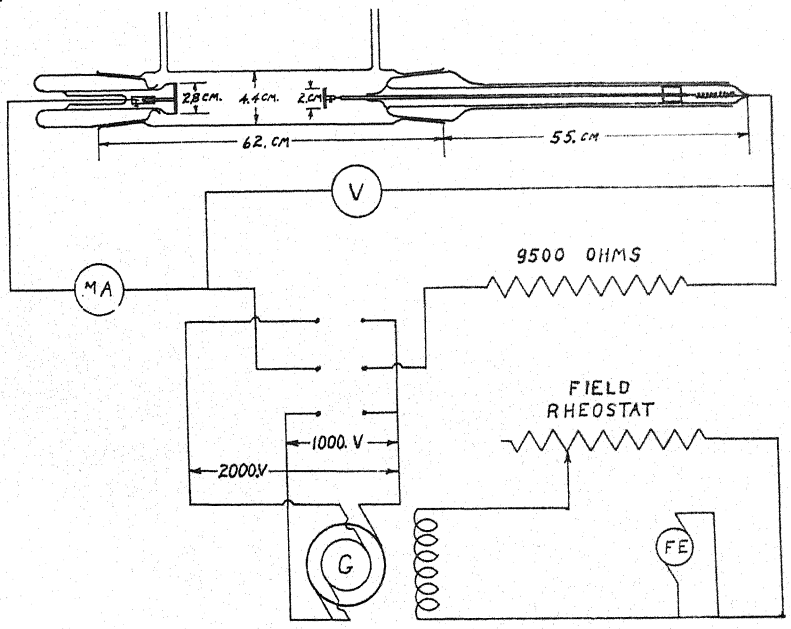

Fig. 2. Diagram of apparatus.

Apparatus

A detailed diagram of the entire vacuum system is shown in Fig. 1. R represents the gas storage reservoirs, P the gas purifying tubes, D diffusion pumps, G the McLeod guage and T a Toepler pump. Fig. 2 shows a drawing of the discharge tube and a diagram of the electrical circuit used.

Purification of the Gases

Since the results of this investigation depended largely on the purity of the gases used, each gas was very carefully purified before being admitted to the discharge tube. The helium, free from neon, was obtained from the Ohio Chemical Company in a steel bomb under high pressure and was purified by circulating it with a Toepler pump through a charcoal trap immersed in liquid air. The pure gas was stored at a little less than atmospheric pressure in a liter glass reservoir which had been well baked and evacuated.

The neon, of spectroscopic purity, was obtained from Linde Air Products Co., Buffalo, N. Y., in liter glass bulbs. It was further purified in the same manner as described above for helium and stored in a liter glass reservoir. In most cases both of these gases were purified again just before being admitted to the tube by circulating slowly through charcoal in liquid air for about one hour. However, no difference could be found by spectroscopic means or by changes in the electrical characteristics of the discharge when the gases were admitted to the tube directly from the storage reservoirs.

The argon, of commercial grade, was obtained in small metal bombs at high pressure. It contained more impurities than either the helium or the neon, and was the most difficult of the three gases to purify, since, because of its absorption of argon, charcoal in liquid air could not be used. The argon was purified by maintaining an arc of about 2 amperes between a mischmetal and an iron electrode in the gas at a pressure of 10 to 15 cm. The arc was run continuously for from one to two days with the argon in one purifier, then the gas was transferred to another purifier and run under the same conditions for about a week. After this treatment it was still found to contain a very small trace of nitrogen. It was then stored in a reservoir containing well-degassed charcoal where it was allowed to stand for several days at room temperature. When admitted to the tube from this reservoir it was found to be very pure with the exception of a small trace of hydrogen. Most of this hydrogen was removed from the argon by admitting a very small amount of oxygen, generated by heating potassium permanganate, to the gas and circulating the mixture through the discharge tube and liquid air traps. The argon was again stored over well-degassed charcoal for several days, after which time it was found to be very pure.

Preparation of the Tube

The electrodes were well-outgassed by heating with an induction furnace before being mounted in the tube. Before each set of experiments with mixtures of two of the gases the whole system was pumped for several hours and allowed to stand over night, evacuated and with liquid air on the traps, to

test for leaks. In case the system was tight the tube was baked at from 300 to 350°C for four hours while being pumped. At the same time the charcoal trap and the mischmetal getter trap, in the circulating system, were baked at 400°C. This part of the system, including the tube, was then pumped for about 4 hours while the tube and traps cooled. The whole system was allowed to stand over night, evacuated and with liquid air on the traps, to test again for leaks. After pumping again for about two hours the system was ready for use.

Procedure

After the gases were purified and the tube prepared as described above, one of the gases to be used was admitted to the tube very slowly by means of a slow leak grooved stopcock, through the system of traps, Fig. 1, until the desired pressure was obtained and was then circulated for about 20 minutes through the discharge tube and traps with a discharge running at the desired current. The rate of circulation was then decreased to a very low value and the pressure adjusted accurately to the value desired. The current was kept constant, and voltage readings were taken at short time intervals in order to determine when conditions were constant for the taking of data as described below. Pressure measurements were taken at various intervals to see that the pressure and rate of circulation remained constant.

If a very small amount of another gas was to be mixed with the gas already in the tube, the gas in the tube was pumped out with the mercury circulating pump backed by a Toepler pump and stored in an empty reservoir or in a charcoal trap in liquid air. The tube was well pumped out with the mercury pump and a small amount of the other gas admitted to the tube to the pressure necessary to give the percentage mixture desired. The gas previously used was readmitted to the tube slowly in the same manner as before. The process described above of circulating the gases was repeated to insure a homogeneous mixture of the gases and the data were taken as described in the next section. For adding larger amounts of one gas to another, a separate system including a guage with its volume calibrated with respect to the tube volume was used. In this way by starting with one pure gas, mixtures with another gas could be studied in any proportions from very small percentages up to a 50 percent mixture. The results obtained were found to be repeatable within a few percent at any time. For each gas mixture studied a spectrogram of the light emitted from the positive column was taken in order to observe the change in excitation produced with changes of the gas mixture and to check the purity of the gas.

Method Used in Measuring the Potential Gradient in the Positive Column

The method consisted in measuring the total drop in potential across the tube at various electrode distances, while the current was kept constant by varying the e.m.f. in the circuit. The anode was moved by magnetic control from outside the tube. Before any measurements were taken, the discharge was run with the maximum electrode distance for from one to two hours at

constant current until the maintaining voltage across the tube remained constant. The maximum electrode distance was 32 cm. The anode was moved from this point, 2 cm at a time, to within 10 cm of the cathode and back to 32 cm again. Readings of the total voltage across the tube were taken every two cm at intervals of one minute as the electrode distance was decreased and then increased again. The voltage readings for increasing electrode distance checked those for decreasing electrode distance to within less than one percent.

This method of measuring the field is applicable since a uniform cylindrical tube was used, and only the uniform positive column was studied. Since the current density and the concentration of ions and electrons remain constant throughout the length of the uniform positive column, the anode drop in potential does not change with the anode position along the column. The tube was run long enough before any data were taken so that the cathode drop in potential remained constant while observations were being made. The time required to take a complete set of observations was 24 minutes. The voltage readings, taken with decreasing electrode distance, when plotted against electrode distance, gave a straight line very accurately. The slope of this line gave the potential gradient or electric field in the positive column in volts/cm.

RESULTS

The results of the investigation are shown by the data given in Tables I and II and by the curves in Figs. 3 to 8 inclusive. The values of the electric field in the positive columns are given in Table I for the pure gases, helium, neon, argon and for mixtures of each of these gases with mercury vapor at

TABLE I. *Electric field in the positive column for the rare gases and mixtures of each with mercury vapor.* Current, 40.0 m.a. Pressure, 14.0 mm. Tube diameter, 4.4 cm.

Gas	pure He	He-Hg	pure Ne	Ne-Hg	pure A	A-Hg
Positive column (Field in volts/cm)	17.0	18.4	4.0	2.2	3.8	4.5

about 0.005 mm pressure. It can be seen from this table that mercury vapor added to neon causes a large decrease in the field but when added to either helium or argon causes a slight increase.

Table II gives the results of spectrograms taken from the positive column of the discharge in the various gas mixtures studied. It will be noted that a very small amount of argon added to either helium or neon completely subdues the helium or neon spectrum and only the argon is excited. Mercury has the same effect on either argon or neon; while with mixtures of small amounts of neon or of mercury with helium, the spectra of both gases appear. When argon, containing a trace of nitrogen, is added to neon in amounts up to 2.0 percent the neon spectrum disappears and the argon spectrum appears strong with the nitrogen spectrum weak. As more of the argon, containing a trace of nitrogen, is added to the neon the argon spectrum becomes weak and the nitrogen spectrum strong until with more then 5.0 percent only the nitrogen spectrum appears.

TABLE II. *Results of spectrograms taken of radiation from the positive column of a glow discharge in the various mixtures of the rare gases and mercury vapor studied.*

Gas mixtures	Percentage of added gas greater than the amount given below		Spectrum obtained
Helium—Neon	0.4%	Neon	Helium and Neon
Helium—Argon	0.2%	Argon	Argon only
Neon—Argon	0.15%	Argon	Argon only
Neon—{Argon with a trace of nitrogen}	0.5% 2.0%	{Argon with a trace of nitrogen}	Argon and Nitrogen
Neon—{Argon with a trace of nitrogen}	5.0%	{Argon with a trace of nitrogen}	Nitrogen only
Helium—Mercury	0.03%	Mercury	Helium and Mercury
Neon—Mercury	0.03%	Mercury	Mercury only
Argon—Mercury	0.03%	Mercury	Mercury only

Fig. 3 shows the variation with pressure of the electric field in the positive column for pure helium and for a mixture of neon with helium. These curves show that the field varies directly as the pressure for both the pure gas and the mixture. They also show that the effect on the field produced by adding a small percentage of neon to helium does not change appreciably with the total pressure over a considerable range of pressure.

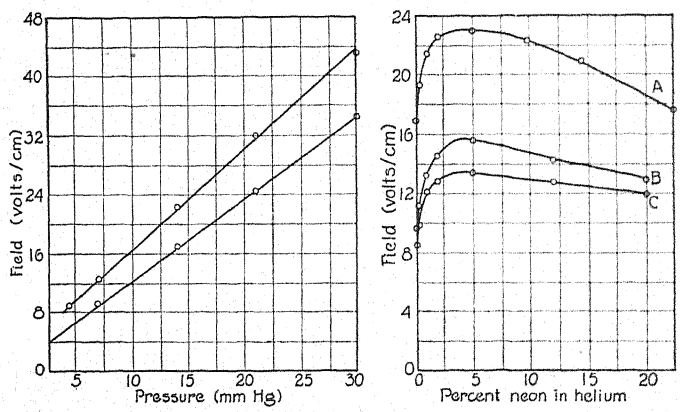

Fig. 3. Variation of electric field with pressure for pure helium A and a mixture of 99.0 percent helium and 1.0 percent of neon B. Current, 40 m.a.

Fig. 4. Variation of electric field with percent of neon added to helium. A, current 40 m.a., pressure 14 mm; B, 20 m.a., 7 mm; C, 40 m.a. 7 mm.

These curves of Fig. 4 show the variation of the electric field in the positive column with small amounts of neon added to helium under different conditions of pressure and current. The interesting point to note here is that the maximum field is a function only of the percent of neon in the helium and is independent of the pressure or of the current density. These curves also show that a large change in the field is produced by a very small amount of neon in helium.

Fig. 5, 6, and 7 show the variation of the field in the positive column with all possible mixtures of the three gases helium, neon, and argon taken only two together.

The curve of Fig. 5 shows that a small amount of neon in helium has a large effect on the field while a small amount of helium added to neon has very little effect on the field.

It can be seen from the curve of Fig. 6 that argon-helium mixtures have about the same characteristics as those of neon-helium except that a smaller amount of argon is more effective in helium than in neon in changing the field. The discontinuity in the curve is probably due to the difference in mobility and large difference in ionization potential of the two gases. For pure argon

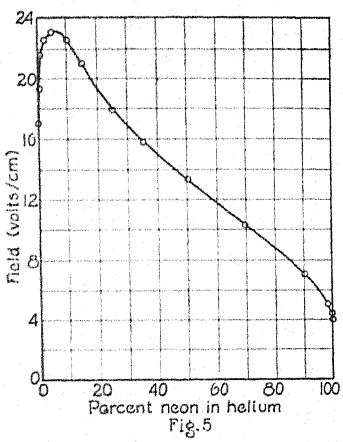

Fig. 5

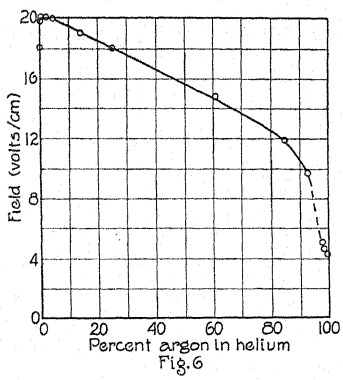

Fig. 6

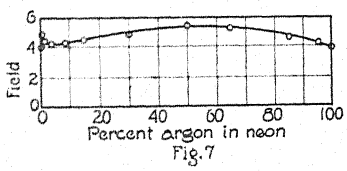

Fig. 7

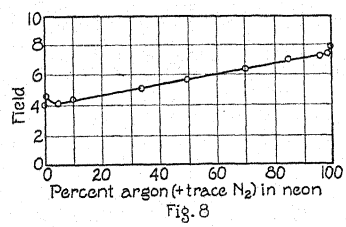

Fig. 8

Fig. 5. Variation of electric field with percent of neon in helium. Current 40 m.a., pressure 14 mm.

Fig. 6. Variation of electric field with percent of argon in helium. Current 40 m.a., pressure 14 mm.

Fig. 7. Variation of electric field with percent of argon in neon. Current 40 m.a., pressure 14 mm.

Fig. 8. Variation of electric field with percent of argon, containing trace of nitrogen, added to neon. Current 40 m.a., pressure 14 mm.

and for mixtures of argon with small amounts of helium the discharge did not fill the tube completely but concentrated toward the axis of the tube. For from 2 to 7 percent helium in argon the discharge was unstable and could not be maintained at the current and pressure desired without changing the resistance of the circuit. For mixtures containing more than 7 percent helium the discharge filled the tube uniformly. The sudden increase in field produced is due to the change in the current density distribution over the cross section of the positive column. Where the current density is large at the tube axis

there is less diffusion of positive ions to the tube walls and therefore a smaller field, than in the case of a more nearly uniform distribution of current over a cross section of the column.

From Fig. 7 it can be seen that small amounts of argon have much less effect on the field in neon than of that in helium and that neon in small amounts has practically no effect on the field in argon.

Fig. 8 shows how the field in neon-argon mixtures is affected by a small trace of nitrogen in the argon.

Discussion and Interpretation of Results

The interpretation of the electrical and spectral characteristics of the positive column in the gas mixtures studied is based principally upon collisions of the second kind between the excited metastable atoms or the ions of one gas and the neutral atoms of the other gas. The effect of limitation of electron velocities observed when a considerable amount of a gas of lower ionization and excitation potentials is added to another gas is insufficient to explain the large effects obtained with the very small percentages of the added gas. With a formula given by K. T. Compton,[17,18] calculations were made of the number of collisions an electron would make with gas atoms in a mixture of helium with 0.1 percent neon under the discharge conditions which obtained. It was found that an electron would make in the order of 1000 collisions with gas atoms and hence, on the average, one collision with a neon atom while gaining the energy represented by the difference between the ionization potential of helium and the lowest excited state of neon. Since the probability of excitation by electron impact under these conditions is far from certainty, an increase in the field of 26 percent could hardly be attributed to limitation of electron velocities by collisions with neon atoms. With the mixture of less than 0.03 percent mercury vapor with neon the field is reduced by 45 percent which is entirely too large an effect to be explained by limitation of electron velocities. Therefore we must turn to collisions of the second kind for a satisfactory explanation of the observed results.

Collisions of the second kind. The following list of reactions, 1 to 6, inclusive, show the possible ways by which collisions of the second kind may take place between two gas atoms X_1 and X_2 where the energy of excitation is transferred from X_1 to X_2. The resultant products of each of the first six reactions may be represented by any one of the expressions 7 to 10, depending upon the relative ionization and excitation potentials of X_1 and X_2.

1. $X_1' + X_2 \rightarrow$
2. $X_1^+ + X_2 \rightarrow$
3. $X_1' + X_2' \rightarrow$
4. $X_1^+ + X_2' \rightarrow$
5. $X_1' + X_2^+ \rightarrow$
6. $X_1^+ + X_2^+ \rightarrow$

7. $X_1 + X_2' + KE$
8. $X_1 + X_2^+ + KE$
9. $X_1 + X_2^{+\prime} + KE$
10. $X_1 + X_2^{++} + KE$

[17] K. T. Compton, Phys. Rev. **32**, 433 (1923).
[18] K. T. Compton, Revs. of Mod. Phys. **2**, 220 (1930).

X' is an excited gas atom, X^+ a gas ion, $X^{+\prime}$ an excited gas ion, X^{++} a doubly ionized ion, and KE is kinetic energy.

The reactions represented by the initial conditions 1 or 2 resulting in 7, 8, or 9 are of most common occurrence in discharges in mixtures and are most important in explaining the effects observed.

Processes of ionization and excitation. The processes of ionization and excitation in the positive column in pure monotomic gases having metastable states can be represented by the following reactions.

Reactions by which ions are produced by electron impact.

$$e_f + X = X^+ + 2e + KE \tag{1}$$

$$e_s + X_m' = X^+ + 2e + KE \tag{2}$$

where e_f is a fast moving electron with sufficient kinetic energy to ionize the neutral gas atom X, and e_s is a slow moving electron with sufficient kinetic energy to ionize an excited metastable atom X_m'.

Reactions by which metastable atoms are produced.

$$e_f + X = X_m' + e + KE \tag{3}$$

$$X' - \text{radiation} = X_m', \tag{4}$$

$$X' + X \rightarrow X_m' + X + KE, \tag{5}$$

where X_m' is an excited metastable atom, and X' is an excited atom in a non-metastable state.

Reactions producing excitation of non-metastable states of atoms.

$$e_{f_1} + X = X' + e + KE. \tag{6}$$

$$e_{s_1} + X_m' = X' + e + KE, \tag{7}$$

where e_{f1} is a fast moving electron with sufficient energy to excite a neutral atom, and e_{s1} is a slow moving electron with sufficient energy to excite a metastable atom.

In gas mixtures composed largely of one gas with a small amount of gas of lower ionization and excitation potentials than those of the main gas, other processes of ionization and excitation take place by collisions of the second kind.

Let X_1 = atoms of the main gas and X_2 = atoms of the gas present in small amounts.

Reactions of the second kind which produce ionization and affect the concentration of metastable atoms in a discharge in gas mixtures are the following.

$$X_{1m}' + X_2 = X_2^+ + e + X_1 + KE \tag{8}$$

$$X_{1m}' + X_2 = X_2^+ + e + X_1 + KE \tag{9}$$

$$X_{1m}' + X_{2m}' = X_2^{+\prime} + e + X_1 + KE. \tag{10}$$

A reaction of the second kind which decreases the concentration of metastable atoms of the main gas and therefore affects the ionization processes in a discharge in a gas mixture is the following

$$X_{1m}' + X_2 = X_2' + X_1 = X_1 + X_2 + \text{radiation}. \tag{11}$$

The reactions involving collisions of the second kind between ions of the main gas and excited or neutral atoms of the mixed gas, do not tend to increase the number of ions. Therefore, they will in general have very little effect on the field in the positive column. Reactions of this type will be discussed only in a few particular cases.

It was shown in the discussion of the theory of the positive column that the electric field gives a measure of the energy necessary to produce the concentration of ions required by the current passed through the tube and includes the energy lost in radiation as well as the heat conducted away by the tube walls. It was also shown that, for a pure gas, the electric field in the positive column is proportional to the ionization or excitation potentials of the gas. It can also be shown that the electric field in the positive column will be a function of the excitation potentials of the gas and proportional to the ratio of the energy emitted as radiation to that producing ionization.

If any process is introduced into the positive column which will change the ratio of the energy expended in radiation to that expended in ionization the field should change. A process which increases the efficiency of ionization will decrease the electric field in the positive column, since for a given current and pressure the concentration of ions remains constant. A process which decreases the efficiency of ionization or increases the energy expended in radiation will cause an increase in the electric field.

By adding a small amount of one gas to another gas the processes of ionization and excitation may be considerably changed. In case the added gas has lower ionization and radiating potentials than the main gas, very large changes in the field may be produced by very small amounts of added gas. When the added gas has higher ionization and excitation potentials than the main gas the field is only changed slightly, the change being proportional to the amount of gas added.

Helium-Neon Mixtures

Consider the case of helium with a small amount of neon added. The variation of electric field in the positive column with the percent of neon added to helium is shown in Fig. 4, for amounts of neon up to 20 percent. The maximum of the field curve comes at 5 percent neon for different values of current and pressure. The amount of increase in the field over that for pure helium caused by the addition of 5 percent neon is 28.3 percent, for curve A; 60.8 percent for curve B; 61.8 percent for curve C. This shows that the effect of the neon on the field of helium is practically independent of the current, but varies with the pressure.

The following table gives the term values of the normal and metastable states, the ionization potentials and excitation potentials of the metastable states of the gases used in this investigation.

To explain the rise in the field produced by adding neon to helium the reactions producing ionization and excitation in the mixture must be considered.

TABLE III. *Metastable states and ionization potentials.*

Atom	Normal state (term in cm^{-1})	Ionization potential (volts)	Metastable (term in cm^{-1})	States excitation potential (Volts)
He	$^1S_0$ 198298.0	24.47	2^3S_1 38454.7	19.73
			2^1S_0 32032.5	20.51
Ne	$^1S_0$ 173930.0	21.47	3^3P_2 39887.0	16.54
			3^3P_0 39110.0	16.64
A	$^1S_0$ 127103.8	15.69	4^3P_2 33996.7	11.50
		15.87	4^3P_0 32557.79	11.67
Hg	$^1S_0$ 84178.5	10.39	6^3P_2 40138.3	5.43
			6^3P_0 46536.2	4.66

First consider the processes for production of ions occurring in pure helium.

$$\underset{>24.47}{e_f} + \mathrm{He} = \underset{24.47}{\mathrm{He^+}} + 2e + KE \tag{1}$$

$$\underset{>4.74}{e_s} + \underset{\substack{20.51\\19.73}}{\mathrm{He}_m'} = \underset{24.47}{\mathrm{He^+}} + 2e + KE. \tag{2}$$

The numbers represent the energy of the state in equivalent volts.
Reactions producing the excitation of the arc spectrum of helium.

$$\underset{>19.73<24.47}{e_f} + \mathrm{He} = \underset{>19.73<24.47}{\mathrm{He}'} + e + KE \tag{3}$$

$$\underset{<4.74}{e_s} + \underset{\substack{20.51\\19.73}}{\mathrm{He}_m'} = \underset{>19.73<24.47}{\mathrm{He}'} + e + KE \tag{4}$$

$$\underset{>19.73<24.47}{\mathrm{He}'} - \text{radiation} = \mathrm{He} \text{ or } = \underset{\substack{19.73\\20.51}}{\mathrm{He}_m'} \tag{5}$$

When a small amount of neon is added to helium the excitation of the helium arc spectrum is reduced to some extent while the neon arc spectrum is developed very strongly. Therefore the following reaction is considered to take place in the helium-neon mixture.

$$\underset{\substack{20.51\\19.73}}{\mathrm{He}_m'} + \mathrm{Ne} = \underset{19.69 \text{ to } 20.62}{\mathrm{Ne}'} + \mathrm{He} \pm KE \tag{6}$$

These results in Table IV show very close resonance between the metastable levels of helium and a large number of excited states of neon. The excess energy to become kinetic energy is very small for the excitation of a large number of the excited states of neon by impacts with metastable helium. Therefore, this reaction should have quite a high probability of occurrence in helium containing a small amount of neon.

This reaction (6) shows that the presence of a small amount of neon in helium will greatly reduce the concentration of metastable helium atoms, and practically eliminate the reaction (2), one of the processes of producing ions

TABLE IV. *Excitation of neon by metastable helium.*

Helium I Metastable states term (cm^{-1})	excitation potential (Volts)	Neon I Excited states term (cm^{-1})		excitation potential (Volts)	Energy difference in equivalent volts
		$^3P_0$	14395	19.69	0.04
		$^1P_1$	14549	19.67	0.06
2^3S_1 38454.7	19.73	$^3P_0$	20958	18.78	0.95
		$^3P_1$	22891	18.65	1.08
		$^3P_2$	23071	18.62	1.11
		$^1P_1$	23012	18.63	1.10
		8 levels	12419.0	19.91	0.60
			12228.0	19.96	0.55
		10 levels	11520.0	20.05	0.46
			10529.0	20.17	0.34
2^1S_0 32032.5	20.51	$^1P_1$	10272.1	20.20	0.31
		$^3P_2$	10220.8	20.21	0.30
		$^3P_0$	9643.5	20.28	0.23
		8 levels	6961.8	20.61	−0.10
			6880.8	20.62	−0.11

in helium. Therefore, due to the presence of neon, a large amount of energy supplied by the field is transformed into radiation by reaction (6) which would have gone into ionization in the case of pure helium. Thus we see that the presence of a small amount of neon in helium greatly decreases the efficiency of ion production and therefore the field increases. The field decreases again when the concentration of neon atoms becomes large enough so that a considerable amount of the ionization is produced by direct electron impact with neon atoms. After the maximum in the field is reached at 5 percent neon the field gradually decreases to that of pure neon. A small amount of helium has no abnormal effect on the field in neon, as shown by Fig. 5. No collisions of the second kind take place between excited neon and neutral helium because the excited states of helium are all above the metastable states of neon. The spectrum of helium disappears between 10 percent and 5 percent helium in neon, for less than 5 percent helium in neon only the neon spectrum is obtained. This shows that when only a small amount of helium is present in neon, only very few helium atoms are excited by direct electron impact.

The phenomena at this end of the curve show the effect of limitation of electron velocities in mixtures but here the gas of the lower excitation potentials is present in the larger amount. The fact that the helium spectrum is developed quite strongly in mixtures containing as much as 85 percent neon shows that neon is not very effective in limiting the electron velocities even when present in more than 50 percent. Thus limitation of electron velocities sufficient to cause a 20 percent increase in field could not be considered to occur with less than 1 percent neon in helium. Therefore, the effect of the limitation of electron velocities is negligible as compared to collisions of the second kind where neon is present in only a few percent.

Helium-Argon Mixtures

Fig. 6 shows that the maximum value of the field for the mixture is produced with 1.5 percent argon which is less than the amount of neon required to produce the maximum effect in helium. However, the maximum increase in the field for the mixture over that of pure helium is only 17.6 percent for argon, as compared with an increase of 28.3 percent caused by the addition of 5 percent neon to helium. The results of spectrograms given in Table II show that with 0.2 percent argon in helium the arc spectrum of helium is completely surpressed and only the argon arc spectrum is developed. These facts would indicate that argon is more effective in removing metastable helium atoms than neon but that part of the energy of these metastable helium atoms is converted into ionization of argon and not entirely lost in radiation, as was the case of neon. These results are particularly interesting because neither the helium ion nor the metastable states of the helium atom are in close resonance with any of the known excited states of neutral argon or of the argon ion. The lowest excited state of argon II is the term ^2s 108730 cm^{-1} or 13.41 volts above the normal state of argon II. The first ionization potential of argon is 15.69 volts. Thus to ionize and excite argon would require at least $15.69+13.41=29.10$ volts. The highest metastable state of helium is 2^1S_0 32032.5 cm^{-1} or 20.51 volts above the normal state, which is 8.59 volts too low to ionize and excite argon. The ionization potential of helium is 24.47 volts, which is 4.63 volts too low to ionize and excite argon.

Spectrograms taken of the positive column in mixtures of a small amount of argon in helium show that the spark spectrum of argon is not excited in mixtures with helium. The spectrogram of argon alone shows only the arc spectrum of argon. The spectrograms of helium-argon mixtures also show only the arc lines of argon and the strongest arc line of helium. However, there are a large number of strong argon spark lines in the region photographed which would have appeared if an appreciable amount of excitation of the argon ion had occurred. Therefore, the only possible reactions between metastable helium and neutral argon are the following:

$$\underset{\substack{19.73\\20.51}}{He_m'} + A = \underset{\substack{15.69\\15.87}}{A^+} + He + \underset{3.86 \text{ to } 4.82}{KE} + e \qquad (1)$$

$$\underset{\substack{19.73\\20.51}}{He_m'} + A = \underset{19.0 \text{ to } 20.5}{A'} + He + KE. \qquad (2)$$

TABLE V. *Table for reaction* (1).

Helium Term (cm^{-1})	Excitation potential of metastable state	Argon Term	Ionization potential (volts)	Energy difference in equivalent (volts)
2^3S_1 38454.7	19.73	$4^2P_0$0	15.69	4.04
2^1S_0 32032.5	20.51	$4^2P_0$0	15.69	4.82
2^1S_0 32032.5	20.51	4^2P_1 1430.	15.87	4.64
2^3S_1 38454.7	19.73	4^2P_1 1430.	15.87	3.86

The amount of energy going into kinetic energy is too large to make reaction (1) very probable. However, the results indicate that this reaction does occur to some extent in helium-argon mixtures.

From the results obtained with mixtures of a small amount of argon with helium it would appear that reaction (2) has a high probability of occurrence. The outer electron configuration of argon is $3s^2$, $3p^6$. It seems probable that two of the p electrons could be excited simultaneously by a collision of an argon atom with a metastable helium atom, which would excite negative terms in argon I. Negative terms have not been observed in the argon I spectrum, but there is no reason to expect negative terms to be excited under normal discharge conditions in argon when practically all of the excitation is by electron impact, However, if negative terms exist which are in close resonance with the metastable states of helium, reaction (2) should be highly probable in mixtures of a small amount of argon with helium. Reaction (2) will account for the strong excitation of the arc spectrum of argon in helium-argon mixtures and also will account for the increase of the field in helium produced by the addition of small amounts of argon. The negative terms which could be excited by reaction (2) would lie between three and four volts above the ionization potential of argon I. It would be interesting to make an extended spectroscopic study of the excitation of argon by metastable helium in the positive column to see if such negative terms could be observed.

Neon-Argon Mixtures

In this case the field in the positive column is small and nearly the same for each pure gas. Under the existing conditions of current, pressure, and tube diameter, the field in neon was 4.0 volts/cm; in argon 3.8 volts/cm. However, the curve in Fig. 7 shows that a small amount of argon added to neon causes a small increase in the field while neon in small amounts has practically no effect on the field in argon.

The possible reactions for argon mixtures are the following

$$\underset{\substack{16.64\\16.54}}{Ne_m'} + A = \underset{\substack{15.69\\15.87}}{A^+} + Ne + e + \underset{0.67 \text{ to } 0.95 \text{ volts}}{KE} \qquad (1)$$

$$\underset{\substack{16.64\\16.54}}{Ne_m'} + A = \underset{16.54 \text{ to } 16.64 \text{ volts}}{A'} + Ne + KE. \qquad (2)$$

Reaction (1) tends to decrease the field and (2) tends to increase the field. Reaction (1) would not have a high probility due to the large residual energy to be transformed to kinetic energy. The probability of transitions to the negative term states demanded by reaction (2) is also small. This is in agreement with the fact that argon has only a small effect on the field when added to neon.

The curve Fig. 7 shows that a maximum field is reached at about equal proportions of argon and neon due to the fact that there are more possible excited states in a mixture of the two gases than in either gas separately. Therefore, a greater part of the total energy of the field is expended in radia-

tion than would be the case for either gas separately. The fact that the field in pure argon is only slightly less than that in pure neon even though the ionization potential of argon is much less than that of neon must be due to a proportionally greater amount of the total energy supplied by the field going into radiation and heat in argon than in neon.

Helium-Mercury Mixtures

TABLE VI. *Excited states of mercury I and II which result from reactions with helium, neon and argon.*

Mercury II		Mercury I	
Term from normal state of Hg II (cm^{-1})	Equivalent volts from normal state of Hg II	Term from ionized state of Hg I (cm^{-1})	Equivalent volts from normal state of Hg I
$^2D_3$ 119695	14.75	6^3P_0 −7860	11.36
$^2D_3$ 134732	16.62	6^3P_1 −9798	11.60
2^2P_1 135666	16.71	6^3P_1 −9798	11.60
2^2P_2 144789	17.85	Ionization Potential	10.39
3^2P_2 196151	24.20	6^1S_0 84178.5	normal state
Hg^{++} 235461	29.06		

The possible reactions which can occur in helium-mercury mixtures are the following:

$$\underset{19.73}{\overset{20.51}{He_m'}} + Hg = \underset{17.85}{Hg^{+\prime}} + He + e + \underset{\substack{1.88 \text{ volts} \\ 2.66}}{K.E.} \qquad (1)$$

$$\underset{24.47}{He^+} + Hg = \underset{24.20}{Hg^{+\prime}} + He + e + \underset{0.27 \text{ volts}}{K.E.} \qquad (2)$$

The probability of reaction (1) occurring is low since the residual kinetic energy is too high for close resonance. Reaction (2) has a higher probability of occurrence but will have very little effect on the ion concentration.

From the results of spectrograms of this mixture given in Table II it can be seen that both the spectra of helium and mercury are developed, which indicates that the mercury is not very effective in eliminating the metastable states of helium. The results given in Table I show that mercury has very little effect on the field in the positive column of helium. Both of these facts are in agreement with the low probability of the occurrence of reaction (1) in helium-mercury mixtures.

Neon-Mercury Mixtures

The case is quite different for neon and mercury mixtures. The only possible reaction for neon-mercury mixtures is the following.

$$\underset{16.54}{\overset{16.64}{Ne_m'}} + Hg = \underset{16.62}{\overset{16.71}{Hg^{+\prime}}} + e + \underset{\substack{0.02 \text{ or } -0.07 \\ -0.08 \text{ or } -0.17}}{K.E.} + Ne \qquad (1)$$

This is the only reaction which can occur in neon-mercury mixtures that will affect the field in the positive column and which has a high enough probability of occurrence to be considered. This reaction has a very high prob-

ability due to the close resonance between the metastable states of neon and the excited states of the mercury ion.

Since most of the energy of the metastable neon atoms goes into ionization of mercury this reaction greatly increases the efficiency of the ionization processes in neon-mercury mixtures over those of pure neon. This is shown by the fact that the field in the positive column of neon is reduced to almost one half of its original value by the addition of less than 0.03 percent mercury vapor. The results of spectrograms of the neon-mercury mixture given in Table III show that the mercury arc spectrum is developed strongly while the neon arc spectrum is completely absent. This would be expected according to the above reaction which would greatly reduce the concentration of metastable neon atoms in the mixture over that for pure neon. If the results were attributed to the effect of limitation of electron velocities, mercury vapor would be expected to have the same effect on helium as it has on neon and possibly to a greater extent, but instead mercury vapor causes a slight increase in the field for helium. This fact is strong evidence that the observed effects, where one gas is present in a small percent of the total volume, are correctly attributed to the action of collisions of the second kind.

Mixture of Argon and Mercury

The possible reactions in argon containing a small amount of mercury are

$$\underset{\substack{11.50\\11.67}}{A_m'} + Hg = \underset{10.39}{Hg^+} + A + \underset{\substack{1.11\\1.28}}{K.E.} + e \qquad (1)$$

$$\underset{\substack{11.50\\11.67}}{A_m'} + Hg = \underset{\substack{11.36\\11.60}}{Hg'} + A + \underset{\substack{0.14,\ -0.10\\0.31,\ \ 0.07}}{K.E.} + e \qquad (2)$$

$$\underset{\substack{15.69\\15.86}}{A^+} + Hg = \underset{14.75}{Hg^{+\prime}} + A + \underset{\substack{0.94\\1.11}}{K.E.} + e. \qquad (3)$$

Reaction (1) has a low probability of occurrence due to the rather high residual kinetic energy. Reaction (2) has a high probability due to the quite close resonance, the residual kinetic energy being small. This reaction corresponds to the excitation of negative terms of the mercury arc spectrum which have been observed with hollow cathode excitation of mercury by impacts of the second kind.[19] Reaction (3) is not very probable and would not have much effect on the electric field in any case.

The results of spectrograms given in Table II show that the mercury spectrum is very much stronger than the argon spectrum in the mixture. This fact is in good agreement with the probability of reaction (2) being much greater than that of reaction (1). The fact that the field in the argon mercury mixture is higher than in pure argon shows that reaction (2) occurs with greater probability than reaction (1).

By comparing curves in Figs. 7 and 8 the effect of a trace of a diatomic gas as an impurity in one of the gases can be seen. Only a trace of nitrogen

[19] F. Paschen, Preuss Akad. p. 3, 1928; also Naudé (reference 9).

was sufficient to more than double the field in pure argon. This large increase was due to the excitation of the nitrogen bands by collisions of the second kind with argon metastable atoms. In diatomic gases also a larger proportion of the energy of electron impacts goes into radiation than in monatomic gases and this causes an increase in the field. The spectrograms taken of these mixtures show that the nitrogen band spectrum begins to be developed strongly where the field in this mixture becomes larger than the corresponding mixture of pure argon and pure neon.

Birge and Hopfield[20] give the energy-level system for the positive bands of nitrogen. There are three states at 8.1, 8.5 and 9.4 volts, respectively. Each of the states have a large number of vibration levels. These vibrational levels extend from 8.1 to 14 volts. The ionization potential of nitrogen is given as 16.7 volts. The metastable states of argon at 11.50 and 11.67 volts will be in very close resonance with a large number of excited states of the nitrogen molecule. The metastable states of neon at 16.58 and 16.67 are in close resonance with the ionization potential of the nitrogen molecule. Therefore one would expect a very strong excitation of the positive bands of nitrogen in a mixture of neon and argon containing a trace of nitrogen, by impacts of the second kind between the metastable states of argon and neon and the neutral nitrogen molecules. From the curves in Figs. 7 and 8, it can be seen that the field in a mixture of neon and argon is greatly increased by the addition of a trace of nitrogen. This result is in good agreement with the fact that the metastable states of argon are in very close resonance with many excited states of the nitrogen molecule. Thus the concentration of metastable argon and neon atoms is very effectively decreased by the presence of only a trace of nitrogen.

Conclusion

The results show that the electrical and spectral characteristics of the uniform positive column in mixtures of monatomic gases can be explained principally in terms of collisions of the second kind between the ions or metastable atoms of one gas and the neutral atoms of the other. The effect of limitation of electron velocities is wholly inadequate to explain the results obtained for mixtures containing a fraction of 1 percent of one gas and is negligible as compared to the effect of collisions of the second kind. The limitation of electron velocities does occur in mixtures where both gases are present in large amounts and produces an appreciable effect.

The necessary condition for a large effect to be produced in the electrical and spectral characteristics of the positive column by a small percentage of one gas added to another is that there exists a close resonance between the metastable states of the main gas and the ionization potential or excited states of the added gas atom or ion.

[20] R. T. Birge and J. J. Hopfield, Astrophys. J. **68**, 257 (1928).

RELATIVE INTENSITIES OF THE MAGNETIC AND ELECTROSTATIC ILLUMINATION COMPONENTS IN THE ELECTRODELESS DISCHARGE

By Charles T. Knipp
Department of Physics, University of Illinois

(Received January 22, 1931)

Abstract

Recent theory indicates that a considerable portion of the illumination in the electrodeless discharge is due to the electrostatic field. A discharge vessel was constructed to test this point experimentally. Obstructions were set in it with the idea that each type of discharge would cast its own shadow. Distinct shadows were obtained for both discharges when acting separately. When the magnetic field predominated and the ring discharge was fully formed no evidence was obtained of shadows due to electrostatic discharges, and conversely, as is shown by the photographs that accompany the article. The intensities of the two illuminations, as judged by the times of exposure, varied about as 1 to 50. The photographs seem to support the calculations of Sir J. J. Thomson.

RECENT theory indicates that a considerable portion of the illumination in the electrodeless discharge is due to the electrostatic field; that under favorable conditions of gas pressure and position of the energizing coil and electrodes this illumination may amount to a considerable part of the total. This result is in addition to the calculations made a few years back by Sir J. J. Thomson.[1]

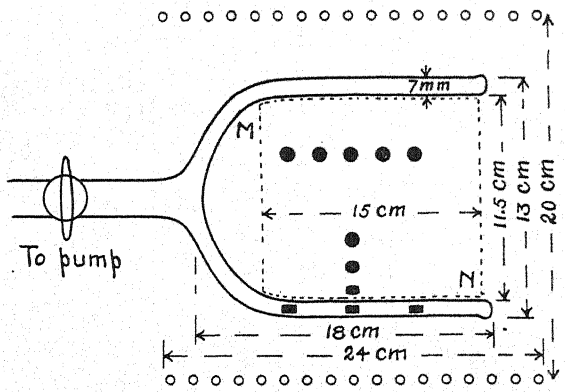

Fig. 1. Sketch of discharge vessel. Similar to a large Dewar vacuum test tube. Asbestos obstructions are shown. These appear in the four photographs that follow. A cylinder, MN, of black paper screened off high lights on opposite side. The position of energizing coil is shown.

A tube was designed by the writer with which it was hoped to test this point experimentally, at least qualitatively. In appearance the discharge ves-

[1] J. J. Thomson, Phil. Mag. 4, 1128 (1927).

sel was not unlike a wide-mouthed Dewar vacuum flask. Two Pyrex beakers of 1.5 and 2 liters capacity, respectively, were used in its construction. Its length when completed was 18 cm, its diameter 13 cm, and the interspace about 7 mm. Asbestos disks about 8 mm in diameter were placed at regular intervals throughout the interspace similarly to the spacing disks in a vacuum bottle. Fig. 1 shows a section through the vessel and coil.

The idea in mind was that these obstructions should cast shadows, similar to the Malteze cross experiment in a Crookes tube, and thus under proper conditions it was hoped that the direction of the discharge due to either field would be made visible.

The study was made with residual air at pressures of about 0.2 mm of mercury. The discharge vessel was energized by damped oscillations from a motor-generator high-voltage high-frequency set. The maximum voltage was about 25 kv operating on a frequency of about 800 kc.

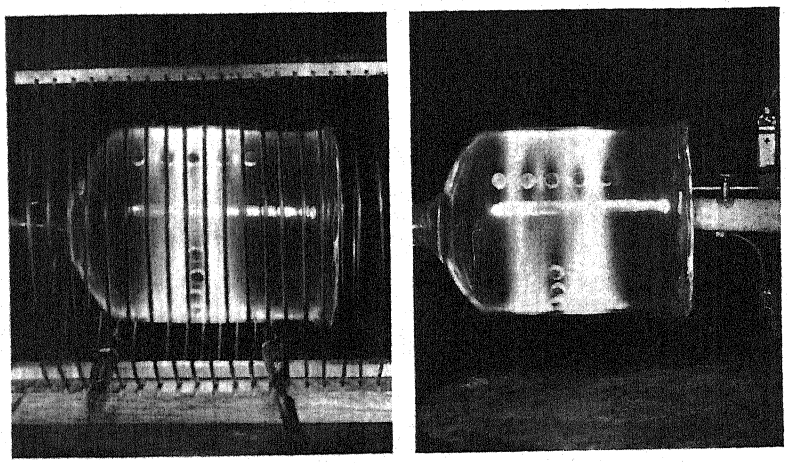

Fig. 2. Electrodeless discharge completely formed by using 8 turns of energizing coil. Residual air, pressure about 0.2 mm Hg. Illumination intense white. Time of exposure 6 seconds, followed by a photoflash to get apparatus. Shadows are in plane of coil. No shadows due to electrostatic field are discernable.

Fig. 3. Electrodeless ring discharge completely formed when an energizing coil of 8 turns was placed inside of vessel. Illumination intense white. Time of exposure 6 seconds followed by a photoflash. Again shadows due to the asbestos obstructions plainly show the paths of the carriers. No electrostatic effects are visible.

To give prominence to the magnetic field the energizing coil should be compact and of comparatively few turns—6 or 8 in this instance. This may be placed either round the vessel as indicated in Fig. 2, or the coil may be replaced by one of smaller diameter and placed within the discharge vessel as shown in Fig. 3. If an outside coil of too large a diameter, or of too many turns, is employed the ring discharge will not form.

On the other hand to give prominence to the electrostatic field a long solenoid, as shown by the extended coil turns in Fig. 1, should be used. Better still is to place external electrodes consisting of a band conductor to the right

and to the left of the medial line as shown in Fig. 4. To prevent heavy sparking with the attending danger of disrupting the vessel a parallel coil of about 10 turns should be inserted. By adjusting the number of turns included in this parallel circuit a wide range of electric field intensities may be obtained.

The two fields may indeed be obtained simultaneously by simply using a long energizing coil of from 20 to 30 turns and of about 1 cm pitch. For the electrostatic field to predominate it is only necessary to make connections at the ends of this solenoid, Fig. 4. To localize the magnetic field (as is necessary in order to have the ring discharge form) the connecting leads should now be transferred to include 4 to 6 turns at the center of the solenoid, Fig. 2. Moving the leads from the ends to the center does not seem to reduce the resultant electrostatic field very greatly, but it does serve to localize the ring dis-

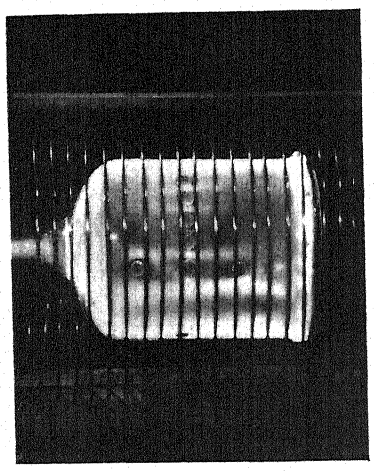

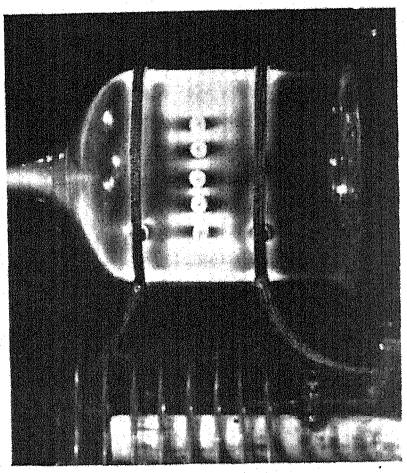

Fig. 4. Electrostatic discharge only. Electrostatic field obtained by using full length of energizing solenoid. Illumination faint (compared with that in the ring discharge). Time of exposure about 2 minutes. Overhead lights to get outline of apparatus. The direction of field is clearly shown by the streamers. Magnetic field not intense enough to form the ring discharge.

Fig. 5. Electrodeless discharge only. The band electrodes are looped across a coil of 8 turns (this coil was placed on the inside of vessel in Fig. 3). Illumination a faint purplish red glow. Time of exposure 130 seconds. The direction of field is clearly shown by the shadows cast. Overhead lights to finish exposure.

charge due to the magnetic field. It should be added that at no time, even with the electrodes most favorably placed, was it possible to get the characteristic ring discharge by means of the electrostatic field alone.

Summary

1. To form an intense ring discharge required but a comparatively few turns of the energizing coil. Figs. 2, 3.

2. The paths of the carriers in the ring discharge were in the *plane* of the coil as is distinctly shown by the *shadows cast*. Figs. 2, 3.

3. The illumination was very intense. It required but 6 to 8 seconds to make an exposure.

4. The electrostatic discharge may be produced by either external electrodes, or by a long solenoid. Figs. 4, 5.

5. The paths of the carriers in this case, as one should expect, were parallel to the axis of figure as is distinctly shown by the *shadows cast.* Figs. 4, 5.

6. The illumination was very weak, a purplish red, as compared with the intense white of the ring discharge. It required 2 to 3 minutes to make an exposure of the density shown in Figs. 4 and 5.

7. At no time while the ring discharge was formed were the electrostatic effects visible. These, however, may have been masked by the greater intensity of the former.

SUPERSONIC INTERFEROMETERS*

By Elias Klein and W. D. Hershberger
Naval Research Laboratory, Bellevue, D.C.

(Received January 26, 1931)

Abstract

The methods of applying high frequency sounds to small scale measurements are discussed. An interferometer was constructed and used to measure the velocity of sound in gases, liquids, and solids at frequencies ranging from about 10 to 700 kc. Three types of sources were tried, viz: quartz and Rochelle-salt crystals and magnetostrictive rods. The determination of the velocity of sound in solids is based upon: (1) optimum transmission of sound through a partition whose thickness is an integral number of half wave-lengths; (2) relative displacement of the nodal planes in a given liquid due to the immersion of a solid slab in the acoustical path. In the same manner, a small quantity of an unknown liquid is placed in a parallel walled cell and the latter is immersed in a liquid of known acoustic properties. Reactance and effective resistance of the interferometer (with a liquid medium) as a function of the reflector distance from the sound source were investigated. Approximate values of the impedance, power factor and watts dissipated in the instrument were thus computed. An improved circuit for use in absorption measurements in gases is described as well as the extended use of the interferometer employing two identical sound generators.

Introduction

CERTAIN physical and thermodynamic properites of various substances may be deduced from their sound transmission and absorption characteristics. The latter are usually determined experimentally by employing some form of standing wave system. The Kundt's tube and its diverse interesting modifications have provided a large amount of useful data relating to the velocities of sound in gases,[1] liquids[2] and solids.[3] However, velocities measured by these so-called "tube methods" at audible frequencies require special corrections due to the yielding of the walls of the tube.[4] The disturbing effects caused in this way may be eliminated by increasing the frequency of the source to the extent that the emitted waves within the tube are plane. Under such circumstances the velocity of sound in a confined fluid, when calculated from a standing wave system is independent of the size or shape of the container. Practically, these conditions obtain when the ratio of the diameter of the radiating surface to that of the emitted wave-length is greater than 12. Furthermore, to be reliable, the measurements should be taken at a considerable number of wave-lengths from the source, particularly if the radiator is

* Published with permission of the Navy Department.

[1] Behn and Geiger, Ber. deut. Phys. Ges. 5, 657 (1907); Partington and Shilling, Phil. Mag. 45, 416 (1923); Shilling and Partington, Phil. Mag. 5, 920 (1928).

[2] Dorsing, Ann. d. Physik 25, 227 (1908); V. Ionescu, J. de Physique et le Radium 5, 377 (1924).

[3] H. O. Taylor, Phys. Rev. 2, 270 (1913); E. C. Wente and E. H. Bedell, Bell System Techn. J. 7, 1 (1928).

[4] L. G. Pooler, Phys. Rev. 35, 832 (1930).

composed of many elements, such as a mosaic of piezoelectric crystals. In general, the energy radiated by a circular plate emitting longitudinal waves is confined mainly to a central beam, the width of which is found by the expression

$$\sin \theta = 1.22\lambda/D$$

where θ is the angle between the axis of the radiator and the boundary of zero intensity of the central beam, D is the diameter of the aperture or radiating surface; λ is the wave-length of the emitted wave.

Langevin[5] was the first to make wide application of supersonic waves by utilizing the piezoelectric properties of quartz. In 1916 in an experimental water tank he demonstrated supersonic beam reflection at 100 kc. Since the original investigations of Langevin, Boyle[6] and his collaborators have done a great deal of work in supersonics (or "ultrasonics" as they called it) by the aid of quartz-steel generators. Among their researches are measurements on the velocities of sound in a number of liquids and solids by the stationary wave method. A separate detector was required to indicate the nodal or antinodal planes in their standing wave system.

The present paper deals with supersonic stationary waves in which the source also detects the nodal and antinodal planes of the system. Therefore, an instrument in which stationary plane waves of high frequency sound are generated and detected shall be termed a *supersonic interferometer*.[7]

During the past few years several investigators have applied this type of interferometer to the study of sound in fluids. Pierce[8] was the first to use it in his determination of the velocities of sound in air and CO_2 at high frequencies. His method employed an oscillating quartz crystal serving a threefold purpose; namely, to control the frequency in a vacuum tube circuit; to generate sound waves from one face to a movable piston which is plane and parallel to the radiating face; and to detect the sound waves reflected from the piston. A stationary wave system is thus set up between the crystal and reflector. As the latter is moved through a series of nodal planes periodic maxima and minima are indicated on a microammeter suitably connected in the plate circuit. By these changes in the electrical circuit Pierce was able to measure the wave-length to a very high degree of precision. With this method, several other researches have been reported,[9] in which the velocity as well as the absorption of supersonic waves in gases and vapors are measured.

[5] International Hydrographic Bureau **3**, (1924); La Nature, January 1921 and August 1921.

[6] Boyle and others, Roy. Soc. Canada Trans. **19**, 167 (1925); **20**, 245 (1926); **21**, 79 (1927); **21**, 115 (1927); **22**, 371 (1928).

[7] This type of self-detecting interferometer has been variously described as a sonic interferometer by Wood and Loomis and an acoustic interferometer by Crandall and others. In the opinion of the authors, neither of these terms distinguishes the instrument from a tube resonator used at audio frequencies.

[8] G. W. Pierce, Am. Acad. Proc. **60**, 271 (1925).

[9] W. H. Pielemeier, Phys. Rev. **34**, 1184 (1929); **36**, 1005 (1930); G. E. Thompson, Phys. Rev. **36**, 77 (1930); C. D. Reid, Phys. Rev. **35**, 814 (1930).

Hubbard and Loomis[10] developed a compact interferometer with which they determined accurately the velocity of sound in various liquids. Their arrangement differs from that of Pierce in that the quartz crystal does not control the frequency of the oscillating circuit but is driven by an alternating e.m.f. whose frequency is far removed from that of the crystal. One surface of the quartz disk radiates sound directly into the liquid which is being studied. The production of stationary waves in the liquid and their measurements are effected by the aid of a plane reflector attached to a micrometer screw. Here also the nodal and antinodal planes are located by their reactions on the crystal source.

In all work with supersonic interferometers heretofore recorded quartz was used as the source of high frequency sound, and the investigations were limited to fluids. The present experiments deal with methods for using Rochelle-salt crystals or magnetostrictive rods as well as quartz for the interferometer source. It is further shown that the same interferometer can be used to determine the velocity of supersonic waves in solids and minute quantities of liquids.

Apparatus

The interferometer employed in the present investigation is composed of three principal units as shown in Fig. 1. The upper part, (a), consists of a specially constructed micrometer screw whose spindle has a maximum movement of four inches and whose barrel is graduated every 0.025 inches for the entire travel of the spindle. The least count of the instrument is 0.001 inch. To the lower end of the spindle is attached a plane brass reflector which is accurately machined so that its reflecting surface always remains normal to the axis of the cylinder in which it is traveling. The lowest portion of (a) is a threaded cap to fit the various fluid containers.

The central section, (b), may be a cylindrical or rectangular fluid container, each end of which is threaded so as to fit the adjoining units, (a) and (c), interchangeably.

Part (c) represents one of several holders for the elements used as sources of supersonic waves. The side tube at the bottom accomodates the leads to the electrodes of the crystal or groups of crystals used. The dimensions of (b) and (c) differed according to the range of frequency and substance studied. The fluid containers, (b), varied from four to sixteen inches in length and from three to nine inches in diameter. Among the elements used as sources are: a single disk of quartz 2.5 inches in diameter and 0.25 inch thick; a similar disk of Rochelle-salt; several rectangular slabs of the above crystals about $1\times1\times3/16$ inches; a mosaic of quartz about four inches in diameter and one of Rochelle-salt 2.5 inches in diameter; several magnetostrictive rods 0.5 inch in diameter and 4 to 10 inches in length.

In the photographs of Fig. 1 may be seen an assembled interferometer with a rectangular container, one side removed; the three separate units; and three of the generating elements.

[10] Hubbard and Loomis, Phil. Mag. 5, 1177 (1928); Loomis and Hubbard, J.O.S.A. 17. 295 (1928); J. C. Hubbard, Phys. Rev. 35, 1442 (1930).

The circuit employed for impressing an alternating e.m.f. upon the source of the interferometer when the latter is used in conjunction with liquids and solids is shown in Fig. 2. A quartz crystal controls the driver frequency when extreme constancy is required. For work in which a continuously variable

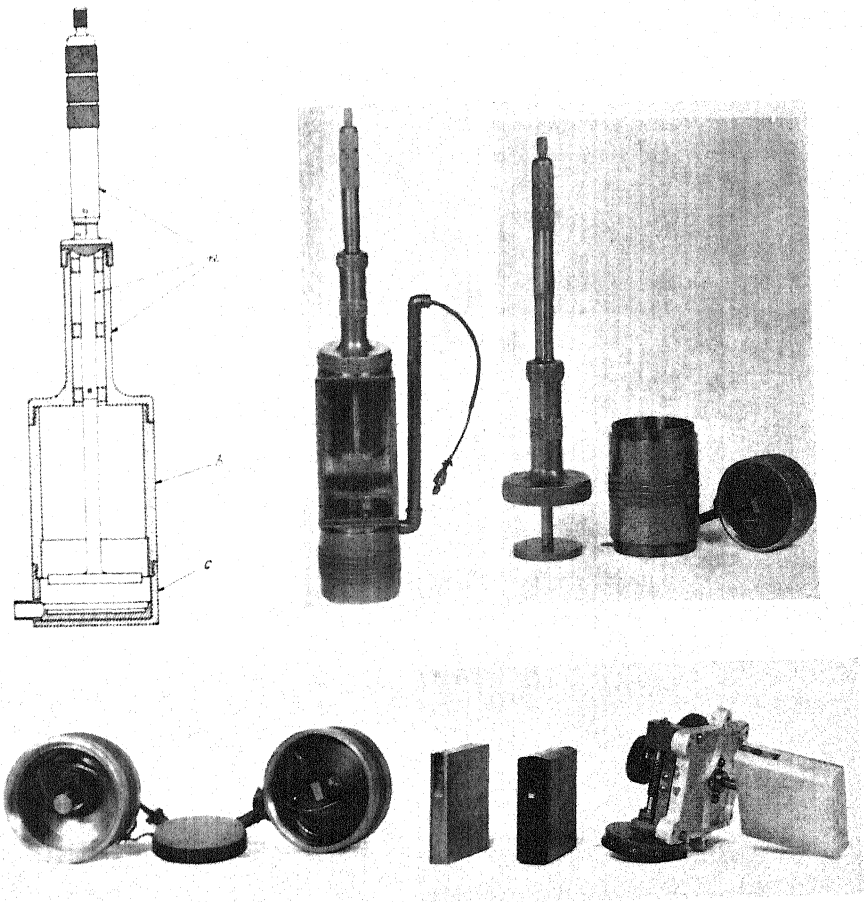

Fig. 1. Diagram of interferometer.

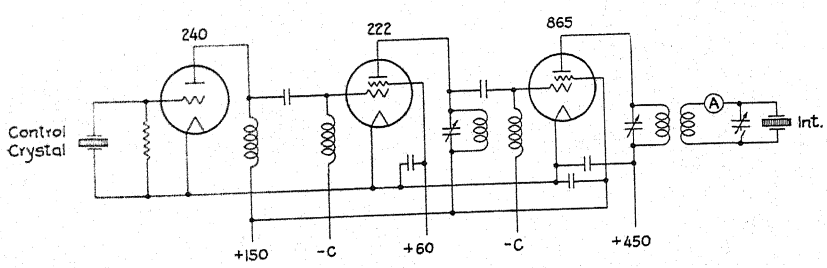

Fig. 2. Electrical driving circuit used with interferometer for work with liquids and solids.

frequency is desired a tuned-grid circuit is employed in the master oscillator stage. Extremely loose inductive coupling is used between the interferometer and the plate coil of the last tube. The circuit is designed to eliminate any effect of a variable load upon the frequency of the exciting e.m.f. The actual power drawn by the interferometer is a very small fraction of the available output power of the last tube.

Methods of Detection

There are numerous methods available for detecting the variations in impedance of the interferometer caused by changes in the position of the reflector. One of the simplest is to note changes in the series current. When the quartz disk is used as a sound source, it is essential to tune the output circuit sharply by means of the small variable capacity in parallel with the interferometer in order that the relatively small changes in impedance may become evident. The quartz interferometer at frequencies far removed from the resonant frequency of the disk reacts very nearly as a pure capacity which permits sharpness of tuning. On the other hand, when Rochelle-salt is employed the current through the instrument leads the voltage across its terminals by angles varying from 30° to 60° depending upon the reflector position, thus making sharp tuning impossible. The greatest fractional change in current observed with the quartz disk is about 15 percent, while if Rochelle-salt is used the fractional change in current ranges from 40 percent to 60 percent. To measure the series current, a vacuum thermocouple and microammeter with a full scale deflection of 200 microamperes was employed.

A novel method for detecting these impedance variations due to change in the reflector position is utilized by Hubbard and Loomis.[10] They actually permit the variations in load on the last tube to affect the driving frequency, then readjust the tuning condenser which varies the frequency so as to compensate for this change. The curves obtained are condenser settings plotted against reflector position.

A number of alternative methods were tried. In one set of experiments not only was the series current through the interferometer measured, but simultaneously the potential difference across its terminals was determined with a thermionic voltmeter. Again, instead of employing inductive coupling between the driving circuit and the interferometer, resistance-capacity coupling was used. The reactions, though much feebler than those obtained with inductive coupling, were in entire agreement with them.

The exact nature of the impedance changes taking place as the reflector position is varied was examined in detail by bridge measurements of the effective capacity and resistance of the interferometer (with a liquid medium). The circuit of the bridge is shown in Fig. 3. Two of the arms were equal capacities of 500 micromicrofarads each. The Rochelle-salt interferometer was placed in one arm and a calibrated air capacity in series with a resistance in the remaining arm. A thermionic voltmeter indicated the state of balance of the bridge. Simultaneously, the series current through the interferometer was measured. No high degree of accuracy is claimed for these measurements,

due to the large phase angles encountered and due to difficulties with the shielding. The result of a set of observations at 122 kc is shown in Fig. 4. These curves show resistance, reactance, net impedance, power factor, phase angle, series current, potential difference across the interferometer terminals and milliwatts dissipated in it as a function of the position of the reflector.

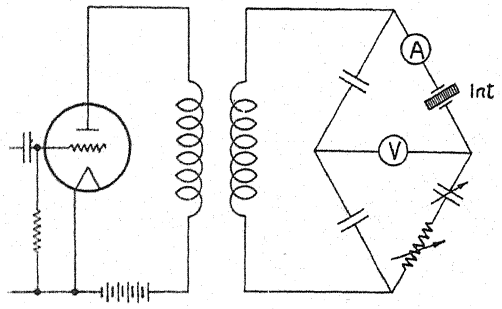

Fig. 3. Circuit used in bridge measurements of effective capacity and resistance of interferometer.

Examining the curves in detail, it is noted that to a first approximation, the capacitative reactance may be expressed by the equation:

$$X = X_0 + A \sin \alpha$$

and the resistance by

$$R = R_0 + A \cos \alpha$$

where $\alpha = 4\pi(l\text{-}L)/\lambda$; l is the micrometer reading; L is a reference point on the micrometer scale, and λ is the wave-length of sound in the medium. Also, it may be shown that to a first approximation:

$$Z = Z_0 + A \cos (\alpha - \theta)$$

where $Z_0 = (X_0^2 + R_0^2)^{\frac{1}{2}}$ and $\theta = \tan^{-1}(X_0/R_0)$. That is, the impedance of the instrument may be represented by the vector sum of one impedance whose magnitude and direction is constant and a second impedance whose magnitude is very nearly constant but whose direction depends upon the position of the reflector. In general, the impedance of the interferometer may be expressed by the equation:

$$Z = Z_0 + \sum_{n=1}^{n=\infty} A_n \cos (n\alpha - \theta_n)$$

The impedance diagram obtained on plotting X against R possesses some similarities to those observed by Kennelly and Pierce[11] in their work on the motional impedance of telephone receivers and to those obtained by Black[12] in his work on magnetostrictive rods. However, in these particular cases the driving frequency is varied while the resonant frequency of the driven

[11] A. E. Kennelly and G. W. Pierce, Am. Acad. Proc. **48**, 113 (1912).
[12] K. C. Black, Am. Acad. Proc. **63**, 49 (1928).

remains constant. In the present case, the driving frequency is held constant, and the resonant frequency of the driven is varied by altering the length of the liquid column. Each time the length of this column is changed by a half wave-length, the set of observed points encircle the diagram once. By external mechanical means Kennelly, Pierce, and Black prevented any displacement on the part of the device whose motional impedance was being measured while here the motion of the crystals is never zero but is aided or impeded by sound reflected from the movable piston.

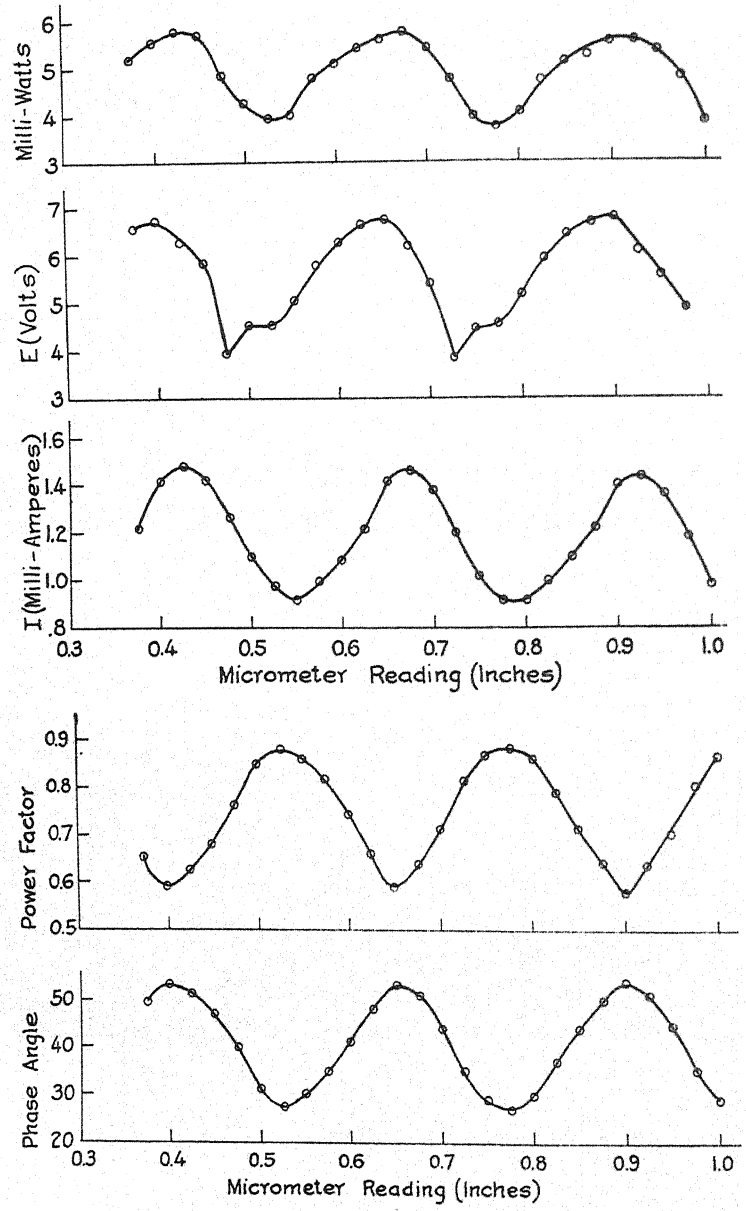

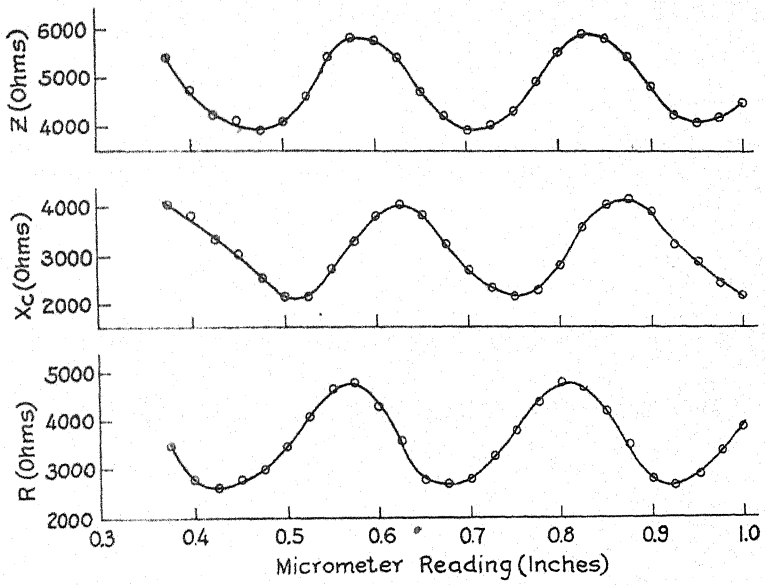

Fig. 4. Curves showing relationship between reflector position and resistance, reactance impedance, phase angle, and power factor of interferometer as well as current through it, e.m.f across its terminals, and watts dissipated in it.

Let ϕ denote the angle between the axis of resistance and the vector joining the center of the impedance diagram to any point on the perimeter. If the value of $d\phi/dl$ is constant around the diagram the simple set of resistance and reactance curves shown in Fig. 4 is obtained. In case $d\phi/dl$ varies around the diagram, the current curve no longer approximates a cosine function. It will be noted in Fig. 5 that the curves taken at 130 kc and 148 kc differ markedly from those taken at 122 kc. The constancy of $d\phi/dl$ and the shape of the curves are very closely dependent upon frequency. It is suspected that the sharpness of resonance in the liquid column is related to the selective transmission of the reflector.

Experimental Procedure

Liquids.—The velocity of sound in a number of liquids was measured by means of this instrument using different types of generators. The set of curve shown in Fig. 5 are typical for the Rochelle-salt interferometer. The liquid used was a high grade of transformer oil. Half wave-lengths were determined with an accuracy of 0.1 percent. Frequencies were measured to 0.03 percent. Hence a relatively high degree of accuracy may be obtained in velocity calculations. Curves possessing "fine structure" may be obtained by driving the interferometer at lower frequencies and favoring higher harmonics by the selection of proper coupling coils. Such a curve is shown in Fig. 6. The driving frequency was 45 kc while the third harmonic was emphasized by tuning. This curve is of interest in showing particularly the complexity which may arise in the standing wave system.

Solids.—In order to measure the velocity of supersonic waves in solids a suitable liquid (oil) was chosen as the medium for the solid under considera-

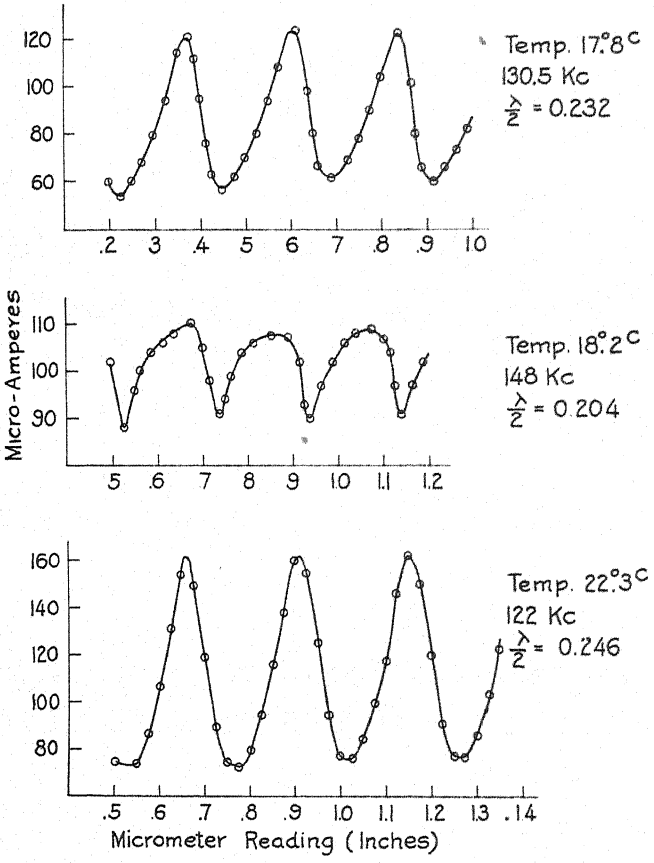

Fig. 5. Curves showing magnitude of series current variations obtained with interferometer and differences in general shape at various frequencies.

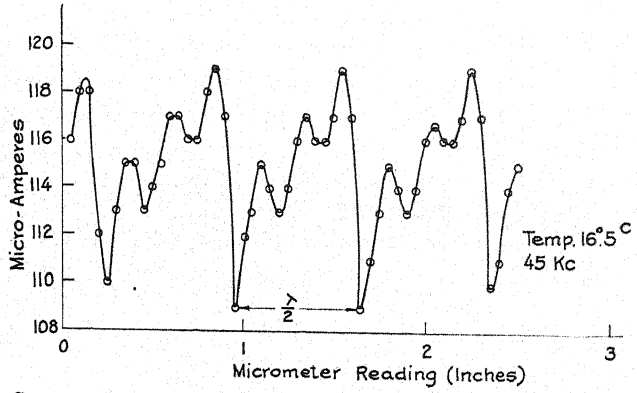

Fig. 6. "Fine Structure" curve. The standing wave system involves both a fundamental frequency and a third harmonic.

tion. The positions of the nodal and antinodal planes were accurately located in the liquid alone. Then with temperature and frequency unchanged a plane parallel slab of the solid was immersed in the sound beam and the relative displacements of the nodal and antinodal planes were ascertained. That is, the difference in acoustical path in the container when the liquid alone was present and when the solid was inserted in the beam was deduced from the micrometer readings, thus:

Let d = actual thickness of slab traversed by the beam

$$\mu = \frac{V_s}{V_l} = \frac{\text{Velocity of sound in solid}}{\text{Velocity of sound in liquid}}.$$

Then the displacement of the nodal planes can be shown to be:

$$\Delta s = d(\mu - 1)/\mu$$

whence $\mu = d/(d - \Delta s)$.

This simple method works quite well when the product $V\rho$ for the solid is not greatly different from that product in the liquid, where V is the velocity of sound in the substance and ρ its density. This is the case in natural woods and wood compositions, in many varieties of bakelite and in rubber compounds. Table I illustrates the method for an amber bakelite of French manufacture.

TABLE I. *Illustration of measurement of velocity of sound in an amber bakelite of French manufacture.* Temperature 21°C. When micrometer reads zero reflector face is about 3 inches from source.

Micrometer Readings at Nodal Planes		Shift due to bakelite	Calculations
Oil alone	Amber bakelite in oil		
0.019	0.180	0.161	Measured thickness of slab = 0.412 in.
0.318	0.479	0.161	Average shift = 0.161 in.
0.620	0.780	0.160	$\mu = 0.412/0.251 = 1.64$
0.922	1.083	0.161	Known velocity in oil $= 1.50 \times 10^5$ cm/sec
1.223	1.384	0.161	$\therefore V_s = 1.50 \times 10^5 \times 1.64 = 2.46 \times 10^5$ cm/sec
1.526	1.687	0.161	
1.825	1.988	0.163	

However, if the two respective products mentioned above are very dissimilar, then it is necessary to choose such a thickness of material as will yield optimum transmission at a particular frequency. Generally, it is more convenient to use a slab of fixed thickness and then to find that frequency for which transmission of sound through the material is a maximum. This condition is realized when the slab thickness is an integral number of half wave-lengths. The theory of this method was suggested by Lord Rayleigh.[13] Boyle and Rawlinson[14] amplified Rayleigh's analytical treatment and applied it directly to supersonics. Later Boyle and Froman[15] verified their

[13] Rayleigh, Theory of Sound, Vol. II, p. 86.
[14] Boyle and Rawlinson, Roy. Soc. Canada, Trans. **22**, 55 (1928).
[15] Boyle and Froman, Canada Jour of Research **1**, 405 (1929).

theoretical conclusions by experiments in which they showed that at normal incidence transmission is a maximum when the thickness of the plate is an integral number of half wave-lengths. On the other hand, if the thickness is an integral odd number of quarter wave-lengths reflection is a maximum.

Fig. 7 is a sample curve showing the sharpness of selective transmission for a given thickness of commercial aluminum. As in the previous arrangement, the metal slab was immersed in oil at normal incidence. Series current through the interferometer source was observed at nodal and antinodal posi-

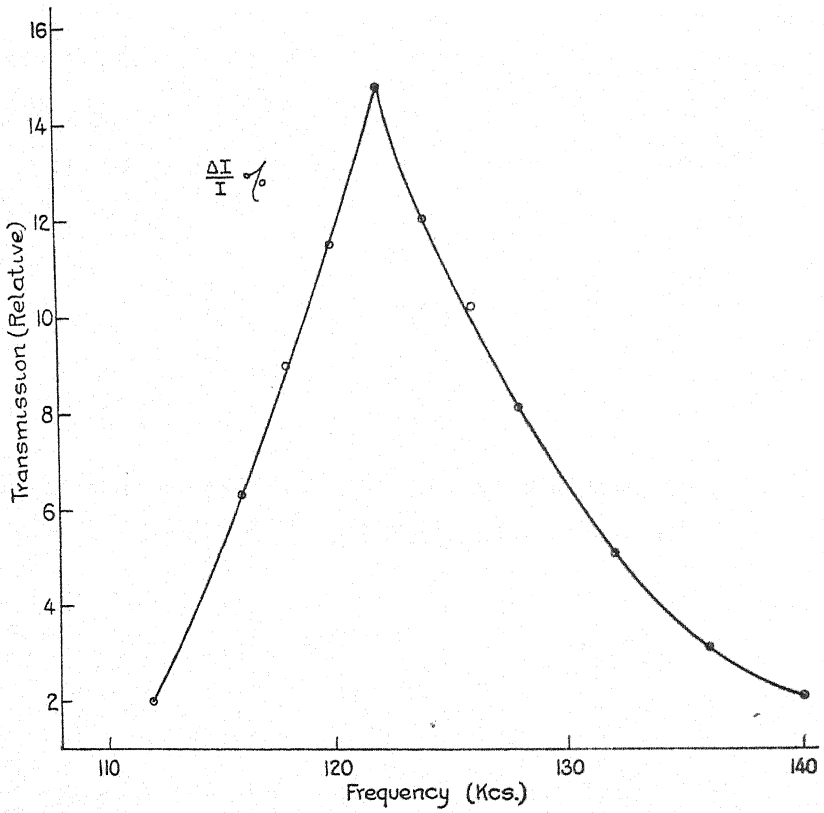

Fig. 7. Change in relative transmission with frequency for a slab of aluminum 0.825" thick.

tions of the reflector for the range of frequencies noted. The difference between maximum and minimum currents divided by their sum is the ratio $\Delta I/I$ used as ordinates in the curve. This ratio indicates the relative transmission of any substance assuming that no selective absorption or scattering is present. The frequency for which the specimen is an integral number of half wave-lengths is thus readily determined. In general, by varying the thickness of the material studied; or, by changing the frequency of the source sufficiently, the exact number of half wave-lengths included in a given sample can be ascertained. Quite often, the approximate number of half waves

in the substance may be calculated from a preliminary knowledge of some of its physical properties. The determination of the supersonic velocity in the solid from the measured wave-length in it and the frequency of the source is then easily verified by the nodal displacement method described above.

Example: Thickness of aluminum slab = 0.825 inches = $\lambda/2$. Best transmission frequency = 122 kc.

$$\therefore V = 122 \times 10^3 \times 0.825 \times 2 \times 2.54 = 5.11 \times 10^5 \text{ cm/sec.}$$

Displacement method in oil: Av. shift at 126 kc = 0.583 inches.

$$\mu = 0.825/0.242 = 3.31$$

$$\therefore V = 1.5 \times 10^5 \times 3.31 = 5.12 \times 10^5 \text{ cm/sec.}$$

Temperature 21°C.

One of the photographs shows slabs of brass, aluminum, and bakelite used in these measurements as well as a holder for the slab which permits other than perpendicular incidence to be used.

Small quantities of liquids.—When only small quantities of liquids are available, (say, less than 100 cc) the methods so far described are not readily applicable. In the first place the measurement of wave-length in the specimen must of necessity be made very close to the sound generator. And as was pointed out earlier, the phase relations close to the source are such as would tend to diminish the sharpness of nodal plane locations. Also the number of wave-lengths that are measurable in the liquid is small; hence the accuracy is reduced. Furthermore, it is often undesirable to have the liquid come in contact with the reflector and container, especially if these are not gold or platinum plated. Such difficulties were obviated in the present experiments by putting the small quantities of liquid to be tested in a parallel walled cell, which was immersed in a liquid medium of known acoustic properties. For example, the procedure for a specimen of turpentine was as follows: a bakelite cell was immersed in the oil previously studied. The cell was filled with the same oil. Micrometer readings for a series of nodal planes in the oil were recorded. Now with the turpentine in the cell, all other conditions remaining the same, the displacement of the nodal planes was measured. The supersonic velocity in the liquid was calculated by the same formula as in the experiment with the bakelite slab, thus:

Shift due to 1 inch layer of turpentine = -0.115 in. $\mu = 1/1.115 = 0.897$.

$$\therefore V = 1.5 \times 10^5 \times 0.897 = 1.34 \times 10^5 \text{ cm/sec.}$$ Temperature 21°C

In Fig. 8, curve I was taken when transformer oil only separated the reflector from the source; curve II was taken after the parallel walled cell filled with the same oil had been interposed in the acoustic path; and curve III when turpentine had been substituted for the oil.

Gases.—For measuring supersonic velocities in gases the Pierce interferometer is perhaps the simplest method yet devised. Fig. 9 shows a curve obtained in air with a Rochelle-salt crystal instead of quartz in the Pierce circuit. At lower frequencies in air, magnetostrictive rods served admirably well

as sources of a stationary wave system. The driving circuit for the rods was similar to that described by Pierce.[16] On the other hand, for the measurement of sound absorption in gases, the Pierce arrangement may lead to erroneous results. For it should be noted, that both the frequency and amplitude of the exciting e.m.f. are influenced by the resonant reaction of the gas column upon the crystal. The change in frequency is so small that only in cases of extreme accuracy need it be taken into account. However, it is the periodic fluctuation

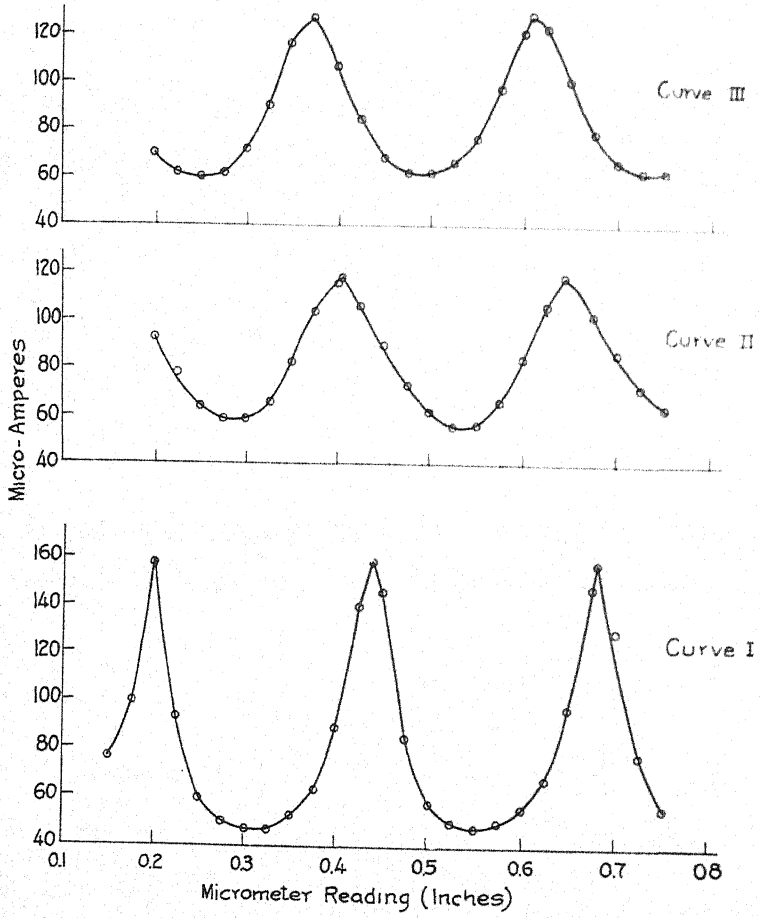

Fig. 8. Shift in position of nodal planes illustrated.

in amplitude of the e.m.f. across the crystal that makes possible the location of the nodal and antinodal planes in the gas. That is, the vacuum tube acts as a rectifier and the changes in the rectified plate current, as the length of the gas column is altered, are a measure of variations in the e.m.f. across the crystal.

The experiments of Pielemeier, Reid, and others show that as the length of the acoustic path in the gas is increased, the changes in plate current di-

[16] G. W. Pierce, Am. Acad. Proc. 63, 1 (1928).

minish. This diminution is due largely to absorption. Nevertheless, absorption coefficients calculated from this rate of diminution are inconclusive unless we possess an exact knowledge of the operating—not the static— characteristics of the tube and in addition how the emitted sound wave amplitude varies with that of the driving e.m.f., as well as what part the received sound wave amplitude plays in determining the net e.m.f. across the crystal. Observations made at 130 kc show that the rate of diminution of plate current variations, with increasing path length, may be altered at will by a factor of 80 percent merely by changing circuit constants.

In order to eliminate some of these difficulties Hubbard[17] proposes to use two quartz crystals tuned approximately to the same frequency. One crystal is used in a master oscillator circuit which supplies an e.m.f. of constant frequency and amplitude, to the second crystal serving as a driven source of

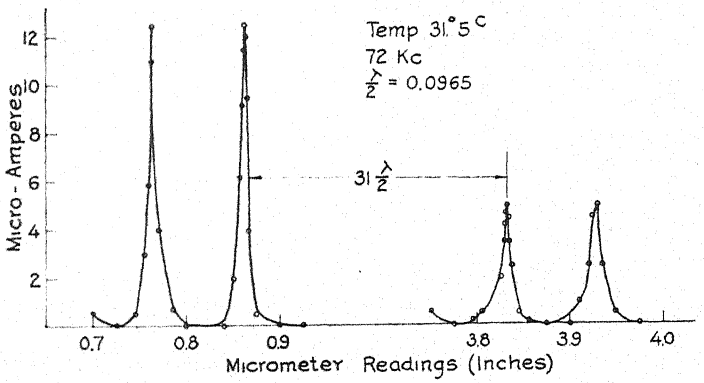

Fig. 9. Air interferometer curve. The change in magnitude of the peaks with increasing path length is shown in pronounced fashion.

sound. This method should prove valuable if and when constant mechanical amplitude can be maintained in the second crystal during a complete cycle of changes introduced by the motion of the reflector in the gas. Inherently, a quartz crystal displays a rather narrow resonance curve, and the task of holding to a fixed point on this curve as the reflector is displaced is troublesome even though the temperature remains constant.

To attain the same end, we have developed a circuit which promises to be useful in absorption measurements. The schematic diagram is shown in Fig. 10. Three electrodes are used on the crystal plate, similar to an arrangement of Cady.[18] The essential feature of this method is that it permits the amplitude of the exciting e.m.f. to be maintained constant, irrespective of the reaction of the gas column, by varying the resistance marked *P*. Moreover, since regeneration is employed, the difficulty in the two crystal system arising from the necessity of exact tuning is eliminated.

Another method for the determination of absorption coefficient of super-

[17] J. C. Hubbard, Phys. Rev. **36**, 1668 (1930).
[18] W. G. Cady, U. S. Patent No. 1472583, Oct. 30, 1923.

sonic waves in gases which appears to be free from many of the difficulties mentioned above is an adaptation of the hot wire microphone of Tucker and Paris.[19] Richardson[20] has shown the possibility of using a single wire for the measurement of sound decay in tubes at low frequencies. The scheme proposed here is to mount a very fine platinum wire cross on a ring which is inside the gas container (c) and is subject to small displacements parallel to the sound beam and may be moved independently from the reflector. Further investigation of this sort may be reported later.

From the foregoing discussion it is readily seen that the general use of the interferometer is considerably enhanced by having similar sound generators available in pairs For example if the second source is placed in the position

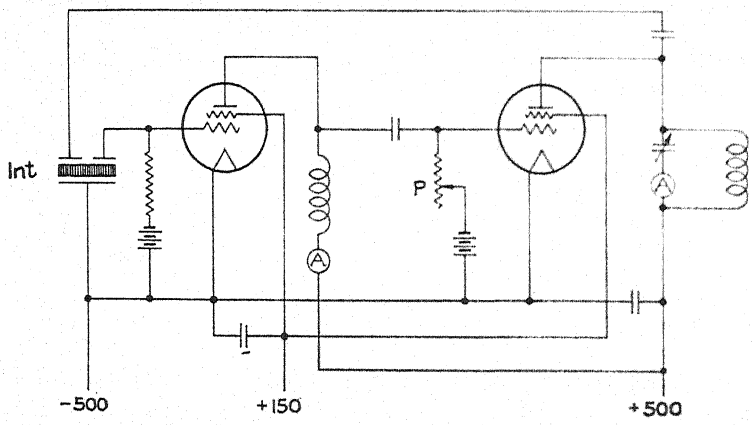

Fig. 10. Improved circuit for gas interferometer.

normally occupied by the reflector and these two identical generators are excited by the same electrical driving circuit, the amplitude of the interfering sound waves may be made to be nearly equal and the precision of velocity measurements be extended. Since this method was tried, Boyle and Froman[21] have described a similar scheme for producing stationary waves. In one set of our experiments two sources were so disposed that either alone acted as the sound generator while the other served as a reflector. Also, the movable was made to receive supersonic waves while the fixed acted as a transmitter, after the manner of Hehlgans.[22] In absorption measurements two identical generators are most valuable.

The authors are indebted to Mr. Emil Kaiser for his constructive interest in the design of the apparatus and to Mr. John Boyd for his careful and precise workmanship of the various parts.

[19] Tucker and Paris, Roy. Soc. Phil. Trans. **221**, 389 (1921).
[20] E. G. Richardson, Roy. Soc. Proc. **A112**, 522 (1926).
[21] Boyle and Froman, Nature **126**, 602 (1930).
[22] Hehlgans, Ann. d. Physik **86**, 587 (1928).

LETTERS TO THE EDITOR

Prompt publication of brief reports of important discoveries in physics may be secured by addressing them to this department. Closing dates for this department are, for the first issue of the month, the twenty-eighth of the preceding month; for the second issue, the thirteenth of the month. The Board of Editors does not hold itself responsible for the opinions expressed by the correspondents.

Relations between Hall Effect and Resistance

Measurements of the Hall effect have been made on sputtered gold films, while the films were heated in air from room temperature to 110°C. These show a relation between the Hall e.m.f. and resistance like that obtained for tellurium films (Phys. Rev. 30, 673 (1927)). During the first heating after the film was sputtered, the Hall e.m.f. and resistance alike underwent a rapid decrease, in one case to values of both Hall e.m.f. and resistance only one-tenth that of the initial values. This relation is then a property of metals and not a peculiarity of tellurium. Wait and Mackeown have previously shown the Hall e.m.f. to be independent of resistance during aging of the film, and the tellurium films showed two types of aging; (1) a decrease in resistance independent of the Hall effect, and (2) a decrease in Hall e.m.f. in proportion to resistance, similar to the proportionality to resistance, (3) when the latter decreased with increase in temperature. This proportionality also held (4) when the resistance increased with increase in temperature. Processes (3) and (4) are reproducible.

Wait explained process (1) by showing that the measured e.m.f. should be the sum of the e.m.f.'s across the granules. This measured e.m.f. should be constant, while the decrease in resistance was due to the elimination of the interstices between the granules.

If we assume that the decrease in resistance on heating, in the case of metals and films which have a negative temperature coefficient of resistance, is due not to the increase in the number of so-called "free" electrons, but to the increase in the ease with which the electron passes from one atom to another, the proportionality between Hall e.m.f. and resistance in processes (2), (3), and (4) is readily accounted for. In the initial non-reproducible decrease of resistance and Hall e.m.f. there is undoubtedly a coalescence of particles, decreasing the difficulty with which the electron can pass from atom to atom. The thermal agitation should occasionally bring an electron of one atom near to the orbit of another atom so that the electron in passing from atom to atom climbs over a smaller potential hill. Again, greater thermal agitation may cause greater obstruction to the drift of the election from atom to atom in the current stream, giving the usual positive temperature coefficient of resistance. Since e.m.f. is work per electron, the Hall e.m.f., on this basis, should be proportional to the resistance in each of the three stages; (2) the initial decrease of Hall e.m.f. and resistance; (3) when the temperature coefficients of resistance and of Hall e.m.f. are negative; and (4) when the coefficients are positive.

With the increase in ease with which an electron passes from atom to atom there is probably also an increase in the number of electrons separating from atomic centers and taking part in conduction, giving the same result as above described in processes (3) and (4) but not accounting for process (2), if the number of "free" electrons depends only on temperature.

F. W. WARBURTON
J. W. TODD

Department of Physics,
University of Oklahoma,
February 25, 1931.

Note on the Structure of Groups in Crystals

In the February 15th number of the Physical Review, (37, 447, 1931) is published a letter to the Editor from Mr. M. L. Huggins, which was based upon a short abstract of a paper given by me at the Chicago Meeting of American Physical Society last year. I find

it rather unfortunate that Mr. Huggins has based his letter on this abstract, as I am now preparing for publication a full account of the results I have obtained during my investigations of the last 3 years on groups $(XO_3)^{-m}$ in crystals. It seems necessary to me to give a few comments on Mr. Huggins' letter.

In the letter is stated that I, in agreement with earlier work on the crystal structure of $NaClO_3$ and $NaBrO_3$ (Kolkmeijer, Bijvoet, and Karssen,[1] Dickinson and Goodhue[2]) describe the XO_3-group in these crystals as tetrahedral groups with one corner missing. This passage obviously must give the reader the false impression that these earlier investigators already had determined the structure of these interesting groups. This is not the case as every one familiar with the above papers can ascertain. I have shown that the structure proposed by the Dutch investigators for $NaClO_3$ and $NaBrO_3$, as well as that proposed by Vegard,[3] is incorrect.[4] The structure given by Dickinson and Goodhue is inaccurate, and their results therefore do not allow conclusions to be drawn with regard to a possible non-planar XO_3-group. Dickinson and Goodhue were as a matter of fact themselves aware of the inaccuracy, and only remark about the XO_3-group that the halogen lies nearly in the plane of the oxygens, indicating that they are considering the XO_3-group to be a coplanar group. There is thus a rather wide step from this conception of the XO_3-group to mine. The first description of "tetrahedral" groups XO_3 in crystals was given by me in 1928,[4] and has been dealt with also in other of my papers on these groups.[5]

It surprises me somewhat to learn that Mr. Huggins finds it necessary to point out the elementary fact that the two displaced electrons in the XO_3-group can be correlated to a Lewis electron pair. I thought the interpretation of e.g. the ClO_3-ion according to the Lewis hypothesis was familiar to everyone. So far the application of the principles of shared electron pairs on the atomic arrangement in inorganic crystals has proved unsuccessful, while considerations of the crystal structure from point of view of ions, ionic dimensions, ionic polarizability, and crystal energy in the hands of such men as W. L. Bragg, K. Fajans, V. M. Goldschmidt, F. Hund, L. Pauling, A. E. van Arkel, J. A. Wasastjerna, and others have given very valuable and important results.

Until one is able to treat the quantization of the electrons in polyatomic groups completely on the basis of wave mechanics, we must be satisfied with rough approximations. It is obvious that one cannot consider such groups to be purely ionic in character. The point of view I have taken with regard to the groups XO_3 is the familiar one of considering the constituents primarily as ions, and then take into consideration the deformation taking place in the electron clouds. The final continuous distribution of electron density may then be regarded as an approximation to the statistical continuity of density one will get from a quantum mechanical treatment. Judging from the results already obtained by this point of view I see at present no advantage in introducing the conception of shared electron pairs in crystals of this kind.

The most important factor which is independent of the point of view one takes is, of course, the total number of valence electrons in the group. In my paper on the groups XO_3 soon to be submitted I have devoted a chapter to the relation between the number of valence electrons and the symmetry of molecules or groups XY_2 and XY_3. If we limit ourselves to considering groups containing atoms of relatively low atomic number I have showed that the following rule holds for all observations hitherto obtained:

A group or molecule $\begin{cases}(XY_2)^{-m}\\(XY_3)^{-m}\end{cases}$ has a $\begin{cases}\text{co-linear}\\\text{co-planar}\end{cases}$ structure if the condition $\begin{matrix}\Sigma v=2\times p\\\Sigma v=3\times p\end{matrix}$ is satisfied. Here Σv denotes the total number of valence electrons in the group or molecule, while p is the number of valence electrons in the inert gas following atom Y in the periodic system if the number of valence electrons on the other hand has to be expressed by an equation of the form $\begin{matrix}\Sigma v=2\times p+\Delta\\\Sigma v=3\times p+\Delta\end{matrix}$ the group or

[1] Kolkmeijer, Bijvoet, Karssen, Proc. Roy. Acad. Amsterdam **23**, 644 (1920).

[2] Dickinson and Goodhue, J. Am. Chem. Soc. **43**, 2045 (1921).

[3] L. Vegard, Zeits. f. Physik **12**, 289 (1922); Norske Vid.-Akad. Skr. Oslo Nr. 16, 1922.

[4] W. H. Zachariasen, Norske Vid.-Akad. Skr. No. 4. p. 143, 1928; Zeits. f. Krist. **71**, 517 (1929).

[5] W. H. Zachariasen, Zeits. f. Krist. **71**, 501 (1929); Paper in print in Phys. Rev.

molecule has an angular or pyramidal structure. The deviation from co-linearity or co-planarity probably increases with increasing Δ. A few examples of the kind of structures we may expect according to this rule may be given.

Co-linear: CO_2, ON_2, CS_2, $(NN_2)^-$, $(HF_2)^-$
Angular (polar): OH_2, SO_2, OO_2? (ozone), SH_2, NO_2, $(NO_2)^-$
Co-planar: $(BO_3)^{-3}$, $(CO_3)^{-2}$, $(NO_3)^-$, SO_3, BH_3, BF_3
Pyramidal (polar): $(PO_3)^{-3}$, $(SO_3)^{-2}$, $(ClO_3)^-$, $(AsO_3)^{-3}$, $(SeO_3)^{-2}$, $(BrO_3)^-$, $(OH_3)^+$, NH_3, PH_3, AsH_3, PF_3, PCl_3 and so on.

In no case is there observed a contradiction to the rule, so it may be used with some confidence for predictions. For a more complete information about my work on the groups I can refer to my paper which is to be published shortly.

W. H. ZACHARIASEN

Ryerson Physical Laboratory,
University of Chicago,
February 28, 1931.

Interpretation of the Spectra of Rare Earth Crystals

From the work of J. Becquerel, Brunetti, Ephraim, Freed and Spedding, and others, it is known that the absorption spectra of rare earth crystals consist of narrow bands which become resolved into sharp lines as the temperature of the crystals is lowered. The lines tend to gather into multiplets, and arise from energy levels which resemble in their behavior the energy levels of atoms subjected to electric and magnetic fields much more than they resemble the levels of molecules. For example, the positions of the lines are but very little influenced by the negative ions present, and such influence amounts only to the expected slight shifting caused by the different electric fields set up by the various ions in the lattice. Furthermore, the lines do not fade out as the temperature is lowered, but are still strong at the temperature of liquid helium. Again, the lines are polarized, as would be the case if the levels were split apart by electric fields.

In a paper which is to be published soon in this journal, Dr. Freed and I have presented a partial energy-level diagram for Gd^{+++} self-consistent within the accuracy we were able to attain (1 cm^{-1} for position, 4 cm^{-1} for resolution), derived from eight sets of data. The data were:[1,2,3] Absorption spectra of $GdCl_3 \cdot 6H_2O$ at ordinary temperatures, and at that of liquid nitrogen and of liquid hydrogen. Gd^{+++} even at room temperatures gives sharp spectra, but as the temperature is lowered the lines shift somewhat owing to changes in the effective electric fields caused by the ingathering of the crystal lattice;[4,5] Absorption spectra of $GdBr_3 \cdot 6H_2O$ at room and liquid nitrogen temperatures;[6,7] Transverse Zeeman effect on the a and b axis of monoclinic

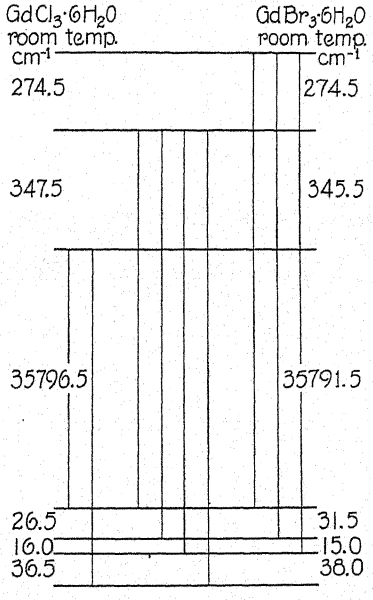

Fig. 1.

[1] F. Hund, Linien Spektren, Julius Springer, Berlin.

[2] Woltjer and Kammerlingh Onnes, Leiden Comm. No. 167 C.

[3] Giauque, J. Am. Chem. Soc. **49**, 1870 (1929).

[4] (a) H. A. Kramers, Proc. Amst. Acad. **32**, 1176 (1929); **33**, 9 (1930). (b) H. A. Kramers et J. Becquerel, Proc. Amst. Acad. **32**, 1190 (1929). (c) J. Becquerel, W. J. de Haas, et H. A. Kramers, Proc. Amst. Acad. **32**, 1206 (1929). (d) H. A. Kramers, Proc. Amst. Acad. **32**, 1196 (1929) and private conversation.

[5] Freed and Spedding (a) Nature **123**, 525 (1929); (b) Phys. Rev. **34**, 945 (1929); (c) J. Am. Chem. Soc. **52**, 3747 (1930); (d) Phys. Rev. **35**, 1408 (1930).

$GdCl_3 \cdot 6H_2O$;[8] Longitudinal Zeeman effect on the c axis of $GdCl_3 \cdot 6H_2O$. The diagram, shown in Fig. 1, is not consistent with other methods of reasoning. For instance, in his brilliant work on complex spectra, by making use of Russell-Saunders coupling and the Pauli exclusion principle, Hund calculates the basic levels of the rare earth ions. He then calculates the magnetic susceptibilities of the gaseous ions and his values agree remarkably well with those obtained experimentally from the solids themselves. For Gd^{+++} he obtains an ^8S term, which is single, as are all S terms. Wolljer and Kamerlingh Onnes[2] have measured the magnetic susceptibility of $Gd_2(SO_4)_3 \cdot 8H_2O$ from 1.3°K to room temperature, and Giauque[3] shows that their results are in perfect accord with the assumption of an ^8S basic level.

Kramers and J. Becquerel,[4] from their work on the paramagnetic rotation of polarized light in xenotime, conclude that the rotation is due to the presence of Gd^{+++} ions in the mineral, and that the Gd^{+++} is in the ^8S state, which is split into several components in the crystal field. Even in the anhydrous crystals with which they were dealing the splitting is not expected to amount to more than a few cm^{-1}. Certainly in the hydrated salts which were used by Giauque and by Freed and me the effect must be much less, less even than our resolving power.

The diagram as it is presented requires either metastable levels of high energy or wide splitting in the lower level, both forbidden by the arguments set down above. However, if the electron distributions in the rare earth elements are examined, it becomes apparent how these conflicting notions may be brought into agreement. According to the Bohr-Stoner scheme, the distribution of electrons in Gd^{+++} ion is as follows:

$1s$	$2s$	$2p$	$3s$	$3p$	$3d$	$4s$	$4p$	$4d$	$4f$	$5s$	$5p$
2	2	6	2	6	10	2	6	10	7	2	6

In previous papers Dr. Freed and I point out that the optically and magnetically active $4f$ electrons give rise in solids to atomic rather than molecular spectra since the complete $5s$ and $5p$ shells partially shield the $4f$ electrons and tend to prevent close coupling between them and neighboring ions and water molecules. There are two ways in which one of the $4f$ electrons may be excited. Firstly, it may remain under this screening influence of the $5s$ and $5p$ shells. To do this, however, n and l of the electron can not change since the exclusion principle forbids any other values. Therefore the only possible excitation comes about through one of the spins reversing itself, thus giving rise to sextet terms. A jump of this sort rarely occurs in atomic spectra and, moreover, it is to be expected that the energy involved would be large. Secondly, the electron may jump outside the strong protection of the $5s$ and $5p$ shells and occupy the $5d$, $5f$, and $5g$ or higher shells, but most probably the $5d$ shell. In this event, Russell-Saunders coupling would presumably be effective for each part of the atom, but owing to the same screening activity on the part of the $5s$ and $5p$ levels it would be much weaker between the halves and would result in $j-j$ coupling. In this instance a $^7F_0$ term would be formed inside and would join with the $^2D_{3/2}$ term outside to give the combined term, $[^7F_0{}^2D_{3/2}]3/2$. Of course, other types of coupling are possible, especially if the splitting of the terms caused by the electric fields of the crystals is large as compared with the $j-j$ coupling. At least there would be a strongly coupled part inside joined by a relatively weak bond to the excited electron outside.

If this is true it would be expected that the intervals, $^7F_0-{}^7F_1$, $^7F_1-{}^7F_2$, and so on would occur in the spectra. Although as a first approximation they would be equal for terms of the type, $[^7F_2{}^2D_{3/2}]7/2[^7F_2{}^2D_{3/2}]9/2$, there would nevertheless be some differences, greater or less depending on the difference in energy of the terms coupling with them. Also, splitting of the levels, $[^7F_2{}^2D_{3/2}]7/2[^7F_2{}^2D_{3/2}]5/2$, owing to the electric fields in the crystal, should be nearly alike, but under high dispersion differences should become apparent. This is precisely what is found to be the case. I am just now repeating the work cited above, using a spectrograph with a dispersion of 2A per mm and have found small differences, amounting to about 1 cm^{-1}, between splitting arising from different groups.

Evidences of coupling of the sort suggested should also be found in the gaseous spectra of the rare earths, so that very different terms from those predicted on the basis of Russell-Saunders coupling would be obtained. The spectra would be closely analogous to x-ray spectra with the exception that the energy values of the optical levels are of such an order of magnitude that their interaction with the x-ray levels can no longer be ignored.

It may be well to mention a few of the more striking facts noted when the spectra are photographed with an instrument of high dispersion. Ordinarily, perhaps half the lines are doublets of about 1 cm^{-1} separation, but if the crystals are under strain many more lines resolve and the separation becomes greater. This splitting may be attributed to the action of the electric fields in the crystal on the basic level. Professor Kramers[4d] has suggested that the ^8S level should dissolve into four slightly separated levels. These, with the rules of selection which are applicable, should give separations of the sort observed. Just as was anticipated, the spectrum of a triclinic crystal photographed by Mr. G. C. Nutting and me shows the dissolution into pairs to be much more pronounced, with several of the lines which apparently were single in the monoclinic $GdCl_3 \cdot 6H_2O$ resolved clearly into doublets. In a magnetic field the double lines split into several components, usually five or more, and in most instances it seems that still more components would appear under higher dispersion. As a usual thing the lines tend to separate into two groups of components which, under low dispersion, show as doublets of the sort reported by J. Becquerel, and Freed and Spedding.

FRANK H. SPEDDING
National Research Fellow
University of California,
Berkeley, California,
February 20, 1931.

High Velocity Vapor Jets at Cathodes of Vacuum Arcs

From measurements of the force of recoil on the cathode of an arc drawn in a high vacuum, and from measurements of the amount of cathode material which was lost, Tanberg[1] has calculated the mean velocity of the material leaving the cathode to be the extraordinarily high one of over 10^6 cm per sec. K. T. Compton[2] has proposed a theory of the development of high molecular velocities, but explains that, "... this criticism does not alter Mr. Tanberg's basic conclusion regarding a high speed neutral vapor stream. It merely suggests an electrical mechanism for the acquiring of these speeds instead of assuming a terrifically high temperature at the cathode."

Close scrutiny of Dr. Compton's suggestion that high velocity neutral molecules leave the cathode as a result of the existence of an accommodation coefficient for the positive ions neutralized at the cathode, indicates, however, that the velocity of these molecules cannot be nearly as great as the velocity obtained by Tanberg. The maximum velocity of the neutralized ions cannot be expected to be much greater than that corresponding to the cathode drop, whereas Tanberg observed velocities of an order corresponding to 70 volts. Hence, if the reaction of the neutralized positive ions is to account for the force upon the cathode observed by Tanberg, the stream of neutralized positive ions leaving the cathode with part of their original energy must be of much greater density than the high velocity stream calculated by Tanberg. In fact, Compton, by assuming that all the positive ions participate in the reaction, calculates that the average energy of the neutralized ions need be less than 0.4 volt to give the force measured by Tanberg.

The high speed stream of Tanberg must still be assumed to leave the cathode *region*, even though the mechanism proposed by Compton may possibly account for the way in which force is communicated to the cathode itself. Because of the high vacuum, the only material leaving the cathode region is substantially only the material lost from the cathode, which Tanberg weighed. The force on the cathode must equal the momentum of the material leaving the cathode *region*, regardless of whether this material acquires its velocity at the cathode surface or elsewhere in the region.

The argument for the necessary existence of Tanberg's high speed stream seems to be valid unless there is a high density of gas in the vessel in which the experiment is carried out. In such a case, the lower speed neutralized positive ions of Dr. Compton could communicate their momentum to many gas molecules, without any of them acquiring a high velocity. But a high gas pressure in the tube during the period of arcing does not seem likely. To obtain a high density of copper vapor throughout the vessel would require almost complete reflection of copper atoms at the walls of the vessel, a condition which does not seem very probable for heavy metal atoms. If such complete reflection did occur, one would expect to have a uniform deposit of copper on all parts

[1] Tanberg, Phys. Rev. **35**, 1080 (1930).
[2] K. T. Compton, Phys. Rev. **36**, 706 (1930).

of the containing vessel. Actually, however, experiment shows that the deposit is most dense directly opposite the cathode spot, with practically no deposit behind the cathode, the distribution of density following a cosine law roughly. So, little reflection must occur, condensation must take place on first impact, and vapor must flow from the cathode region at a rate just equal to the rate of vaporization measured by Tanberg. Since the momentum measured by Tanberg is carried by the mass he used, the velocity he calculated must be correct.

In the same way, the calculated high velocity of vapor striking a vane 2 cm from the cathode can be in serious error only if considerable reflection from the vane occurred,—a condition which does not seem to be true. Thus, if the force on the cathode is due to the reaction of neutralized ions, as proposed by Compton, some mechanism must exist whereby the many neutralized ions of low velocity transfer their momentum to the few atoms leaving the cathode region, with consequent high velocity.

The cathode spot itself, on the metal, need not be, and probably is not, at a high temperature. The experiment merely shows that a very high velocity vapor stream issues from the cathode region. A similarly high reaction upon the cathode of the mercury arc has been observed recently by Kobel.[3]

Whether or not to ascribe a high temperature to such a high velocity vapor stream is merely a matter of use of words. Perhaps, for the sake of emphasizing the unusual magnitude of the velocity, one may speak of the temperature of the vapor jet through the relation $3kT/2 = mv^2/2$.

Experiments to measure the magnitude of the vapor jet velocity by an independent means are in progress in this laboratory.

JOSEPH SLEPIAN
R. C. MASON

Research Laboratory,
Westinghouse Elec. and Mfg. Co.,
February 25, 1931.

[3] Kobel, Phys. Rev. **36**, 1636 (1930).

Knowledge of Past and Future in Quantum Mechanics

It is well known that the principles of quantum mechanics limit the possibilities of exact prediction as to the future path of a particle. It has sometimes been supposed, nevertheless, that the quantum mechanics would permit an exact description of the past path of a particle.

The purpose of the present note is to discuss a simple ideal experiment which shows that the possibility of describing the past path of one particle would lead to predictions as to the future behaviour of a second particle of a kind not allowed in the quantum mechanics. It will hence be concluded that the principles of quantum mechanics actually involve an uncertainty in the description of past events which is analogous to the uncertainty in the prediction of future events. And it will be shown for the case in hand, that this uncertainty in the description of the past arises from a limitation of the knowledge that can be obtained by measurement of momentum.

Consider a small box B, as shown in the figure, containing a number of identical particles in thermal agitation, and provided with two small openings which are closed by the shutter S. The shutter is arranged to open automatically for a short time and then close again, and the number of particles in the box is so chosen that cases arise in which one particle leaves the box and travels over the direct path SO to an observer at O, and a second

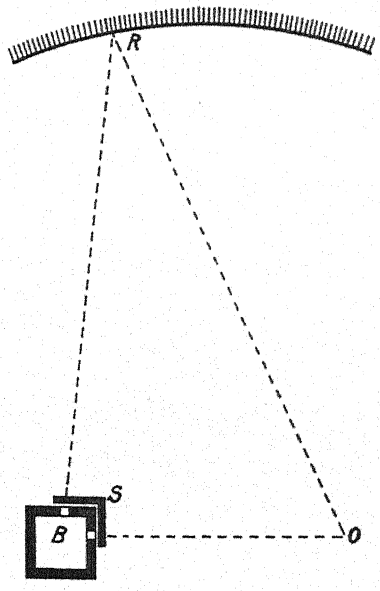

Fig. 1.

particle travels over the longer path *SRO* through elastic reflection at the ellipsoidal reflector *R*.

The box is accurately weighed before and after the shutter has opened in order to determine the total energy of the particles which have left, and the observer at *O* is provided with means for observing the arrival of particles, a clock for measuring their time of arrival, and some apparatus for measuring momentum. Furthermore the distances *SO* and *SRO* are accurately measured beforehand, the distance *SO* being sufficient so that the rate of the clock at *O* is not disturbed by the gravitational effects involved in weighing the box, and the distance *SRO* being very long in order to permit an accurate reweighing of the box before the arrival of the second particle.

Let us now suppose that the observer at *O* measures the momentum of the first particle as it approaches along the path *SO*, and then measures its time of arrival. Of course the latter observation, made for example with the help of gamma-ray illumination, will change the momentum in an unknown manner. Nevertheless, knowing the momentum of the particle in the past, and hence also its past velocity and energy, it would seem possible to calculate the time when the shutter must have been open from the known time of arrival of the first particle, and to calculate the energy and velocity of the second particle from the known loss in the energy content of the box when the shutter opened. It would then seem possible to predict beforehand both the energy and the time of arrival of the second particle, a paradoxical result since energy and time are quantities which do not commute in quantum mechanics.

The explanation of the apparent paradox must lie in the circumstance that the past motion of the first particle cannot be accurately determined as was assumed. Indeed, we are forced to conclude that there can be no method for measuring the momentum of a particle without changing its value. For example, an analysis of the method of observing the Doppler effect in the reflected infrared light from an approaching particle shows that, although it permits a determination of the momentum of the particle both before and after collision with the light quantum used, it leaves an uncertainty as to the time at which the collision with the quantum takes place. Thus in our example, although the velocity of the first particle could be determined both before and after interaction with the infrared light, it would not be possible to determine the exact position along the path *SO* at which the change in velocity occurred as would be necessary to obtain the exact time at which the shutter was open.

It is hence to be concluded that the principles of the quantum mechanics must involve an uncertainty in the description of past events which is analogous to the uncertainty in the prediction of future events. It is also to be noted that although it is possible to measure the momentum of a particle and follow this with a measurement of position, this will not give sufficient information for a complete reconstruction of its past path, since it has been shown that there can be no method for measuring the momentum of a particle without changing its value. Finally, it is of special interest to emphasize the remarkable conclusion that the principles of quantum mechanics would actually impose limitations on the localization in time of a macroscopic phenomenon such as the opening and closing of a shutter.

ALBERT EINSTEIN
RICHARD C. TOLMAN
BORIS PODOLSKY
California Institute of Technology,
February 26, 1931.

Deviations from Kerr's Law at High Field Strengths in Polar Liquids

When an electric field is established in some substances they become doubly refracting with their "optic axes" in a direction parallel to the lines of force. This phenomenon was discovered by Kerr[1] and is known as the Kerr electro-optical effect. Kerr and others[2] have shown that if n_1 and n_2 are the refractive indices for the components of the light vibration parallel and perpendicular, respectively, to the lines of force, then their phase difference after passing through the electric field is

$$D=\frac{2\pi l(_1n-n_2)}{\lambda}=2\pi BlE^2$$

where λ is the wave-length of the light, l is the length of the light path through the electric field whose magnitude is E. B is Kerr's constant, but has been found to vary with different substances, wave-lengths and tempera-

[1] Kerr, Phil. Mag. (4) **50**, 337, 446, (1875).

[2] See G. Szivessy, Handbuch der Physik, 724–808, 21, 1929.

tures. In the present work a method has been devised for testing the possible dependence of B upon the magnitude of E. The well-known theories[3,4] show to a sufficient degree of approximation that

$$B \propto \frac{(n_0^2-1)(n_0^2+2)(K+2)^2}{n_0 T}\left((1+\phi\frac{\mu^2}{T}\right)$$

where n_0 is the index of refraction, K is the dielectric constant, T the absolute temperature and μ the electric moment of the molecule. It has been shown that in polar substances the dielectric constant varies with the strength of the applied electric field, and has been explained as due to an electrical saturation.[5] Therefore in polar liquids B might be expected to decrease with increasing E.

In the present experimental arrangement light from an incandescent filament, made parallel by a lens, plane-polarized by a nicol prism, passed through a Kerr cell 5 cm in length and 3 mm spacing between the plates, then through a second Kerr cell 25 cm in length with a 3 mm spacing between the plates and finally through a second nicol prism crossed with respect to the first. The plane of polarization of the light made an angle of 45° with the lines of force in the first Kerr cell while the plane of the plates of the second cell was 90° from that of the first. A high voltage d.c. potential was applied directly across the first Kerr cell and a variable running tap-water resistance. The second Kerr cell was attached in parallel with just enough of the resistance so that the double refraction in the first Kerr cell was exactly compensated by that in the longer second Kerr cell. The electric field in the first cell was therefore more than twice that in the second. The potential across the first cell and the resistance was then, for example, changed from 30,000 volts per cm to 60,000 volts per cm, so that any change in B with increasing E would appear as a lack of compensation of the light. In the case of CS_2 which is non-polar, practically no light was observed to pass the second nicol prism, that is, the double refraction in the first cell continued to be compensated by that in the second within the limits of precision. However, in the case of carefully distilled chloroform, which is polar, it was found necessary to lower the potential across the second Kerr cell (many times the least amount detectable) in order to make the two cells compensate each other or, again, to reduce the intensity of the light passing the second nicol to zero. This shows that for chloroform B decreases with increasing electrical field. Since the amount of light passing an arrangement of the kind here described is $I = I_0 \sin^2 D/2$ the method is very sensitive to small variations in Kerr's law and gives a simple and precise way of studying electrical saturation effects. The method is being improved and refined in order to make a study of both liquids and gases. A detailed description of the method and a discussion of the results will appear later.

J. W. Beams

University of Virginia,
March 3, 1931.

[3] See Debye, Marx Handbuch der Radiologie, **5**, 754–776, (1924).

[4] Raman and Krishman, Phil. Mag. **3**, 724–735, (1927).

[5] See Debye, Polar Molecules, Chem. Catalog Co., 109, (1929).

BOOK REVIEWS

Gruppentheorie und Quantenmechanik. HERMANN WEYL. Second Edition. Pp. 358. S. Hirzel, Leipzig, 1931. Price, bound, RM 26.

The quantum theory has made it desirable for physicists to become acquainted with mathematical subjects of which heretofore they were allowed to remain blissfully ignorant. This mathematical apparatus is related on the one hand to partial differential equations (Schroedinger's wave-mechanics) and on the other to the theory of Hermitean quadratic forms and unitary transformations (statistical interpretation). In the third place the quantum theory makes use of the noncombining properties of term systems in the solution of special problems as well as in the familiar justification of the exclusion principle. An attempt has also been made by Dirac to introduce a symbolism having no direct relation to our number system (q numbers) which yields the numerical results necessary for physical applications only in the final stage of the symbolic operations.

For the physicist interested in the most direct experimental implications of the quantum theory the interrelations between these fields of pure mathematics are of little interest. The main parts of the subject may be presented in a small amount of printed space as has been done by Heisenberg in The Physical Principles of the Quantum Theory. Elementary developments of the noncombining properties of angular momenta and the related intensity relations are well known and the symmetry properties of electronic proper functions are easily handled in most practical cases by Slater's method. From a certain point of view a deeper study of the mathematical landscape seems, therefore, superfluous.

The transformation theory of classical dynamics is perhaps also superfluous in the same sense and the theory of Maxwell-Faraday stresses could be subjected to the same criticism. The engineer has little occasion to refer to either and for the same psychological reason many physicists approach the study of the more fundamental mathematical aspects of quantum theory with a certain amount of disdain. This fact does not affect however either the beauty or the usefulness of these subjects and in fact an elegant application of Weyl's presentation of the group of rotations has been made by Kramers in a recent paper on intensity formulas.

In Weyl's book the quantum mechanics is presented from the point of view of a mathematician and so far as the reviewer is able to judge in the best taste and with the most powerful machinery. The interrelations between the different aspects of the same mathematical problem are kept in mind throughout. As indicated by the title the guiding principle is that the matrices representing physical quantities define transformations which are representations of certain abstract groups. Operations with abstract groups correspond to the q number calculus. The contents of the first edition have been amplified by the addition of a discussion of the Heisenberg-Pauli wave field theory. The fifth chapter dealing with the group of permutations has been rewritten in a much more elementary form. The connection of the symmetric group with the group of homogeneous linear transformations has been kept in the foreground. Dirac's treatment of permutations as dynamical variables falls in naturally with the methods used here. This is a convenient place for reference to formulas and derivations for group characters of the symmetric group.

Throughout the book many pertinent mathematical subjects have been treated in an elegant and efficient manner. As an example section 3 of Chapter II devoted to spherical harmonics gives in three pages all the necessary material. The treatment of Dirac's relativistic equations is also very good and thorough. The reading of the book is greatly facilitated by a list of symbols used which has been added in the new edition. Contents: I. Unitary geometry II. Physical principles and simple problems of quantum theory. III. Groups and their representations. IV. Applications of groups to angular momenta, Dirac's relativistic equations, the wave field theory, V. The symmetric group.

G. BREIT

Henley's 20th Century Book of Recipes, Formulas and Processes. Edited by Hiscox. Pp. 809, Norman W. Henley Publishing Co., New York, 1930. Price $4.00.

This book, as the title indicates, gives many recipes and formulas which may be of value to the laboratory technician or the home shop-worker. The material, taken from various lines of industry and craftsmanship, is alphabetically arranged throughout the book, with a supplementary index at the end which is a help where there is more than one popular nomenclature for the subject matter under inquiry. The printing is good and the type of a size easy to follow.

I believe the book is better suited for the amateur home worker than it is for the professional laboratory man who has at least a meager idea of what the industrial and scientific library holds in the way of literature along the various lines. Material from the trades is necessarily brief giving more of an outline than a workable procedure for the novice. For the research worker who is at a standstill for want of information on technical manipulation, the book may yield an inspiration for a new attempt. The latitude of the material might be a boon under such circumstances.

Wm. B. Halliday

Atlas of Physical and Inorganic Chemistry. A. von Antropoff and M. von Stackelberg. 29 charts and descriptive volume 64 pp. Verlag Chemie, G.m.b.H. Berlin 1929. Price RM 42.00.

The atlas consists of 29 charts (11 x 14.25 inches) printed on stiff card board, accompanied by a descriptive volume of the same size. The plates show the material in the form of histograms or columnar diagram. The following physical and chemical quantities are represented: (1) The periodic table. (2) The electron shells of the atoms. (3) Atomic diameters. (4) Ionic diameters. (5) Ionization potentials. (6) The crystal structure of the elements. (7) Melting and boiling points of the elements. (8) Mechanical properties of the elements in the solid state. (9) Atomic frequencies of the elements. (10) The atomic force constant. (11) Specific and atomic electrical conductivities. (12) Valencies of the elements. (13) Normal electrode potentials. (14) Heats of combustion. (15) Melting and boiling points of the chlorides and the electrical conductivities in the fused state. (16) Hydrides. (17) Carbides. (18) Nitrides. (19) Solubilities of hydroxides, carbonates, sulphates, chlorides, sulfides and a few other salts. (20) Isotopes. (21) The geochemical distribution of the elements. (22) The occurrence of the elements in the earth's crust and in the whole earth.

The printed volume which supplements the charts gives in every case a short discussion and the necessary definitions of the topics illustrated in the diagrams. It seems to the reviewer that the atlas is, on the one hand, too large for convenient desk use and on the other hand too small for the use with large classes. It should find its principal use with small seminar groups where a few individuals need the material as a basis for discussion.

George Glockler

Les Quanta. G. Déjardin. Pp. 224. Armand Colin, Paris, 1930. Price 10f.50 unbound.

Within its appointed scope as an elementary exposition of the conceptions and fundamental experiments underlying the quantum theory, this book seems for the most part quite successful. Short chapters on radiation theory and specific heats present the basic ideas of the Planck radiation formula and the Einstein-Debye theory of specific heats of solids. Chapters on the photoelectric effect and x-rays give the salient features of the Auger effect, the angular distribution of photo-electrons, the absorption of x-rays, and the Compton effect. Considerable space is devoted to a discussion of classical mechanics, Bohr's atomic theory and correspondence principle, Sommerfeld's fine structure formula and similar topics from pre-quantum mechanics atomic physics. After a short chapter on thermionics, photochemistry and Raman effect the book closes with a few pages on wave mechanics. The explanations seem uniformly clear and the material well chosen. The reviewer, however, doubts the efficacy or the need of retaining the older theoretical explanations even in elementary treatments such as this one, for in many respects the conceptions associated with the newer theory are distinctly simpler than their progenitors, and besides, once learned they will not need to be unlearned for at least some time to come.

E. L. Hill

Second Series *April 1, 1931* *Vol. 37, No. 7*

THE
PHYSICAL REVIEW

A PROBLEM IN THE QUANTUM MECHANICS OF CRYSTALS

By E. L. Hill
University of Minnesota

(Received February 15, 1931)

Abstract

An elementary method is given for treating a one-dimensional lattice of the "tooth-valley" type containing any number of unit cells. The reflection of a beam of electrons from such a lattice is studied. For a semi-infinite lattice perfect reflection is shown to occur when the Bragg equation is satisfied, and an approximate formula for the widths of the reflection bands for high speed electrons is found. For the bound electrons the theory predicts occupied energy levels in the vicinity of the allowed levels for a single valley with infinitely high walls, in agreement with the perturbation theory. A simplified way of locating the edges of the reflection bands is discussed. The more complex case approximating real crystals is considered briefly.

Introduction

THE problem of determining the motion of the electrons in a crystal lattice has been treated by a number of authors. The usual method is to employ some type of perturbation scheme,[1] but the question has also been studied by the more direct procedure of replacing the crystal by a triply periodic field of force and then attempting the solution of the resulting equation for the characteristic function. Morse[2] has recently carried out this treatment in great detail, and has given many interesting results, but the mathematical technique is rather complicated and it is difficult to obtain a clear idea of the physical processes involved. Because of this it was suggested to the writer by Professor Frenkel that it would be interesting to try to carry through the calculation in detail for the case of a one-dimensional lattice of the "tooth-valley" type (Fig. 1). The work for this case is comparatively simple because the characteristic functions for the different sections of the lattice can be written down at once and then fitted together by use of the usual boundary conditions. A suitable method for handling the case of an infinite crystal is given in this paper.

[1] Sommerfeld, Zeits. f. Physik **47**, 1 (1928); Heisenberg, Zeits. f. Physik **49**, 619 (1928); Bloch, Zeits. f. Physik **52**, 555 (1928); Slater, Phys. Rev. **35**, 509 (1928).

[2] Morse, Phys. Rev. **35**, 1310 (1930). This paper contains references to previous work. Condon and Morse, Revs. Mod. Phys., **3**, 43 (1931).

Method and Calculation

The type of one-dimensional lattice considered is illustrated in Fig. 1. The valleys[3] are numbered consecutively 0, 1, 2, $\cdots$, n as is indicated by the letters in parentheses, the region $x<0$ corresponding to the 0th valley and the region $x>\xi$ to the nth valley. As there are just n teeth, $\xi=n\beta+(n-1)\alpha$.

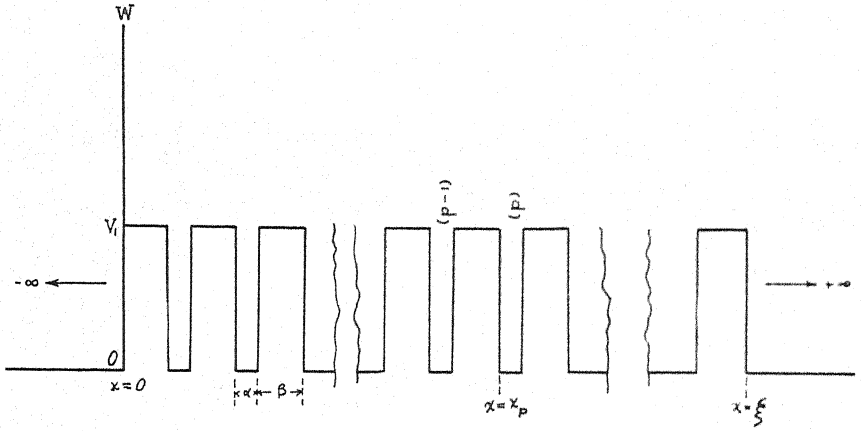

Fig. 1.

The plan is first to solve the Schrödinger equation for a lattice of n teeth and then let $n\to\infty$. The equation to be solved is

$$\frac{d^2\psi}{dx^2}+(8\pi^2m/h^2)(W-V)\psi=0. \tag{1}$$

In the pth valley the general solution of (1) can be written as

$$\psi=a_pe^{i2\pi k_1(x-x_p)}+b_pe^{-i2\pi k_1(x-x_p)} \tag{2}$$

and in the pth tooth, which lies between the $(p-1)$th and the pth valley, as

$$\psi=a_p'e^{i2\pi k_2(x-x_p)}+b_p'e^{-i2\pi k_2(x-x_p)}. \tag{3}$$

For[4]

$$x<0 \qquad \psi=Ae^{i2\pi k_1(x+\alpha)}+Be^{-i2\pi k_1(x+\alpha)} \tag{4}$$

$$x>\xi \qquad \psi=ae^{i2\pi k_1(x-\xi)}+be^{-i2\pi k_1(x-\xi)}. \tag{5}$$

where

$$hk_1=[2mW]^{1/2};\ hk_2=[2m(W-V_1)]^{1/2}. \tag{6}$$

In these equations it is explicitly supposed that $W\geqq V_1$ but it is well known that for $V_1>W\geqq 0$ the same equations can be used by giving k_2 its value as a pure imaginary number from (6).

[3] By "valleys" and "teeth" are meant, of course, the regions of low ($V=0$) and high ($V=V_1$) potential energy in Fig. 1.

[4] The extension to the case in which the wave number of the electron outside the crystal is $k_0<k_2$ is considered later.

At the boundary between a tooth and a valley we use the ordinary boundary condition of the continuity of ψ and its first derivative.[4a] By applying this condition to the function given by (2) and (3) one obtains a linear relation between the coefficients (a_p, b_p) and (a_{p-1}, b_{p-1}) of the form[5]

$$\begin{aligned} a_p &= c_1 a_{p-1} + c_2 b_{p-1} \\ b_p &= c_2^* a_{p-1} + c_1^* b_{p-1} \end{aligned} \tag{7}$$

where

$$\begin{aligned} c_1 &= (1/4k_1k_2)\{(k_1+k_2)^2 e^{i2\pi(k_1\alpha+k_2\beta)} - (k_1-k_2)^2 e^{i2\pi(k_1\alpha-k_2\beta)}\} \\ c_2 &= -(1/4k_1k_2)\{2i(k_1^2-k_2^2)\sin 2\pi k_2\beta\} e^{-i2\pi k_1\alpha}. \end{aligned} \tag{8}$$

Equations (7) permit one in principle to determine the coefficients in any part of the lattice provided they are assumed known in one valley, and in particular one can determine A and B in terms of a and b for use in Eqs. (4) and (5). In the present form this calculation is difficult because of the complicated character of c_1 and c_2. To simplify the analysis we introduce a new set of variables y_p and z_p by a linear transformation which is to be so determined that the transformation matrix from (y_{p-1}, z_{p-1}) to (y_p, z_p) is diagonal; i.e., y_p and z_p are to be simply multiples of y_{p-1} and z_{p-1} respectively. By this artifice we can at once compute A and B in terms of a and b after calculating the associated Y and Z in terms of y and z. We assume then

$$\left.\begin{aligned} a_p &= \gamma_{11} y_p + \gamma_{12} z_p \\ b_p &= \gamma_{21} y_p + \gamma_{22} z_p \end{aligned}\right\} \tag{9}$$

and on substituting in (7) we get as the condition that y_p and z_p shall be multiples of y_{p-1} and z_{p-1} respectively

$$\begin{aligned} \gamma_{11}/\gamma_{21} &= (c_1\gamma_{11} + c_2\gamma_{21})/(c_2^*\gamma_{11} + c_1^*\gamma_{21}) \\ \gamma_{12}/\gamma_{22} &= (c_1\gamma_{12} + c_2\gamma_{22})/(c_2^*\gamma_{12} + c_1^*\gamma_{22}) \end{aligned} \tag{10}$$

which is seen to be the condition that γ_{11}/γ_{21} and γ_{12}/γ_{22} shall be roots of the equation[6]

$$\tau = (c_1\tau + c_2)/(c_2^*\tau + c_1^*). \tag{11}$$

In general there are two different roots of (11) one of which must be taken for $(\gamma_{11}/\gamma_{21})$ and the other for $(\gamma_{12}/\gamma_{22})$ in order that the transformation (9) may be non-singular. These roots may be found directly from (11) if we set

$$c_1 = u + iv; \quad c_2 = \eta + i\zeta \tag{12}$$

with

$$\left.\begin{aligned} u &= (1/4k_1k_2)\{(k_1+k_2)^2\cos 2\pi(k_1\alpha+k_2\beta) - (k_1-k_2)^2\cos 2\pi(k_1\alpha-k_2\beta)\} \\ v &= (1/4k_1k_2)\{(k_1+k_2)^2\sin 2\pi(k_1\alpha+k_2\beta) - (k_1-k_2)^2\sin 2\pi(k_1\alpha-k_2\beta)\} \end{aligned}\right] \tag{13}$$

[4a] It is because of the character of the boundary condition that it is not necessary to give the precise value of the potential energy at the boundary between a tooth and a valley.

[5] A similar relation can readily be found connecting the coefficients (a_{p-1}', b_{p-1}') and (a_p', b_p').

[6] They are the invariant points of the linear fractional transformation $z' = (c_1z + c_2)/(c_2^*z + c_1^*)$.

$$\left.\begin{aligned}\eta &= -(1/4k_1k_2)\{2(k_1^2-k_2^2)(\sin 2\pi k_1\alpha)(\sin 2\pi k_2\beta)\}\\ \zeta &= -(1/4k_1k_2)\{2(k_1^2-k_2^2)(\cos 2\pi k_1\alpha)(\sin 2\pi k_2\beta)\}.\end{aligned}\right] \tag{14}$$

It may be noted that

$$|c_1|^2-|c_2|^2=(u^2+v^2)-(\eta^2+\zeta^2)\equiv 1, \tag{15}$$

which is also required by the condition that the current must be constant throughout the crystal and follows from the boundary conditions and the usual expression for the current.

The solutions of (11) are most conveniently divided into three classes according to whether $u^2>1$, $u^2<1$, or $u^2=1$ which we shall call Case I, II, and III, respectively. Denoting the two roots by τ_1 and τ_2 we get[7]

Case I. $u^2>1$

$$\left.\begin{aligned}\tau_1 &= \{[v-i(u^2-1)^{1/2}]/(\eta^2+\zeta^2)\}(-\zeta+i\eta)\\ \tau_2 &= \{[v+i(u^2-1)^{1/2}]/(\eta^2+\zeta^2)\}(-\zeta+i\eta).\end{aligned}\right\} \tag{16}$$

Case II. $u^2<1$

$$\left.\begin{aligned}\tau_1 &= \{[v+(1-u^2)^{1/2}]/(\eta^2+\zeta^2)\}(-\zeta+i\eta)\\ \tau_2 &= \{[v-(1-u^2)^{1/2}]/(\eta^2+\zeta^2)\}(-\zeta+i\eta).\end{aligned}\right\} \tag{17}$$

Writing $\gamma_{11}/\gamma_{21}=\tau_1$ and $\gamma_{12}/\gamma_{22}=\tau_2$ the transformation from y_{p-1} to y_p and from z_{p-1} to z_p is found to be

$$\left.\begin{aligned}y_p &= (c_2^*\tau_1+c_1^*)y_{p-1}=\delta_1 y_{p-1}\\ z_p &= (c_2^*\tau_2+c_1^*)z_{p-1}=\delta_2 z_{p-1},\end{aligned}\right\} \tag{18}$$

where δ_1 and δ_2 are defined by (18) and can be found explicitly by using (16) and (17).

Case I. $u^2>1$

$$\delta_1=u+(u^2-1)^{1/2};\quad \delta_2=u-(u^2-1)^{1/2} \tag{19}$$

Case II. $u^2<1$

$$\delta_1=u+i(1-u^2)^{1/2};\quad \delta_2=u-i(1-u^2)^{1/2}. \tag{20}$$

By repeated application of (18) one can write at once for the relation between (Y, Z) and (y, z) which are associated respectively with (A, B) and (a, b),

$$y=\delta_1^n Y;\quad z=\delta_2^n Z. \tag{21}$$

Inverting (9) we find (A, B) from (Y, Z) and (a, b) from (y, z) and then from (21) find A and B in terms of a and b. The result is

$$\left.\begin{aligned}A &= \left\{\frac{-\delta_1^n+(\tau_1/\tau_2)\delta_2^n}{(\tau_1/\tau_2)-1}\right\}a+\left\{\frac{\tau_1(\delta_1^n-\delta_2^n)}{(\tau_1/\tau_2)-1}\right\}b\\ B &= \left\{\frac{(1/\tau_2)(\delta_2^n-\delta_1^n)}{(\tau_1/\tau_2)-1}\right\}a+\left\{\frac{(\tau_1/\tau_2)\delta_1^n-\delta_2^n}{(\tau_1/\tau_2)-1}\right\}b.\end{aligned}\right\} \tag{22}$$

[7] Case III is treated in a later paragraph.

With the aid of these formulae we can now study the behavior of ψ as $n\to\infty$. We obtain the essential results, however, in a somewhat clearer fashion by studying the reflection and transmission properties of the grating.

Reflection and Transmission

To study the reflection of a beam of electrons from the grating assume that $b=0$ so that to the right ($x>\xi$) there is only a progressive wave to the right while for $x<0$ there is an incident and also a reflected beam. The reflection coefficient is then

$$R_n = \left| B/A \right|^2 = \left| (1/\tau_2)(\delta_1^{2n} - 1) \right|^2 / \left| \delta_1^{2n} - (\tau_1/\tau_2) \right|^2 \tag{23}$$

as from (19) and (20) $\delta_2 = 1/\delta_1$.

Case I. $u^2 > +1$.

From (19) δ_1^2 is real and >1, and from (16) and (17) $|\tau_1| = |\tau_2| = 1$. Hence from (23)

$$\lim_{n\to\infty} R_n = 1. \tag{24}$$

Thus whenever $u^2>1$ there is perfect reflection from the semi-infinite lattice, although not from a finite crystal. From (22) we find the limiting relation[7a] between A and B

$$A = \tau_2 B. \tag{25}$$

It is quite easy to find the characteristic function in any part of the crystal by inverting the transformation (22) and replacing a and b by a_p and b_p and δ_1^n and δ_2^n by δ_1^p and δ_2^p respectively. The determinant of the transformation is readily shown to be $+1$ (for any p) and on inserting (25) one finds

$$a_p = \tau_2 \delta_2^p B = \tau_2 b_p, \tag{26}$$

the characteristic function in the pth valley being

$$\psi = \left\{ \tau_2 e^{i2\pi k_1 (x-x_p)} + e^{-i2\pi k_1 (x-x_p)} \right\} (\delta_2^p/\tau_2) A. \tag{27}$$

A similar expression can be found for the pth tooth.

This result brings out very clearly the difference between a lattice bounded on one side only, and a lattice which is unbounded in both directions.[7b] In the former case[4] there exist solutions of (1) which are finite at $x=\pm\infty$ for all values of W, whereas in the latter case there are no non-vanishing solutions finite at both $+\infty$ and $-\infty$ when the electron energy is such that $u^2>1$. This is to be compared with Morse's method in which the function is written in all cases as

$$f(x)e^{i2\pi kx} \tag{28}$$

where $f(x)$ is periodic with period $(\alpha+\beta)$, the "forbidden" energies being associated with complex values of k. This function does not represent the gen-

[7a] Note that from (22) this relation must be satisfied in order that $|a|$ and $|b|$ may remain finite as n becomes infinite.

[7b] We shall distinguish these as "semi-infinite" and "infinite" lattices respectively.

eral solution of (1) as we must assume a relation between a_p and b_p in order that our solution (2) and (3) may be put in this form. It has not been possible as yet to show that the regions of complex k in (28) are identical with energies for which $u^2>1$. As $|\delta_2|<1$ we see that ψ is damped out within the lattice, $|\psi|^2$ being diminished approximately by a factor $|\delta_2|^2$ in a distance $(\alpha+\beta)$.

Case II. $u^2<1$.

From (20) δ_1 is complex and $|\delta_1|=1$. Let

$$\theta = \tan^{-1}\left[(1-u^2)^{1/2}/u\right];\ \delta_1 = e^{-i\theta}$$
$$-\pi < \theta < \pi,\ \theta \neq 0.$$

Substituting for τ_1 and τ_2 from (17) in (23)

$$R_n = \frac{(\eta^2+\zeta^2)\left[\dfrac{\sin n\theta}{\sin\theta}\right]^2}{1+(\eta^2+\zeta^2)\left[\dfrac{\sin n\theta}{\sin\theta}\right]^2} < 1. \tag{29}$$

This expression is always less than unity and as $n\to\infty$ it does not approach any limit but merely oscillates. In particular if θ is commensurable with π there are always values of n for which it is zero. There is no obvious reason for this type of "resonance" in terms of a fitting up of the electron wavelength with the lattice distances.[8]

Case III. $u^2=1$.

This case must be considered separately for as $\tau_1=\tau_2$ (9) is a singular transformation, the preceding analysis does not apply. Its treatment is not entirely unambiguous as there are two limiting processes to be considered; i. e. the simultaneous passage of n to infinity and the behavior of R_n in the neighborhood of $u^2=1$. For a semi-infinite crystal as we approach a point for which $u^2=1$ passing through values of W for which $u^2>1$, the limiting value of the reflection coefficient is unity. To find the limiting value by traversing points for which $u^2<1$ we may use (29) which yields

$$n^2(\eta^2+\zeta^2)/[1+n^2(\eta^2+\zeta^2)] \tag{29'}$$

where it is supposed that n has some finite, although large value. On allowing n to become indefinitely large we again get unity unless $\eta^2+\zeta^2=0$, which can occur only as a very special case since it implies $u^2=1$ and at the same time $\sin 2\pi k_2\beta=0$ from (8).

It is worthwhile to notice another method which offers a natural way of arriving directly at the formula for the positions of these reflection band edges From (16), (13), (14) and (15) we see that when $u^2=1$

$$\tau_2 = \pm e^{i2\pi k_1\alpha}$$

[8] Cf. R. d'E. Atkinson, Zeits. f. Physik **64**, 507 (1930).

the sign depending on whether $v>0$ or <0. (27) then becomes

$$\psi = (\pm)^p\{e^{i2\pi k_1(x-x_p-\alpha/2)} \pm e^{-i2\pi k_1(x-x_p-\alpha/2)}\}e^{i\pi k_1\alpha}A,$$

where the upper or lower sign in $(\pm)^p$ is taken according to whether $u=+1$ or $u=-1$. As a similar equation can be shown to hold for the teeth we see that the energies for which $u^2=1$ are characterized by the fact that the wave function can be written in the form of a standing wave in each valley and tooth. Moreover, the amplitudes in two consecutive valleys (or teeth) are the same or of opposite sign depending on the sign of u, there being no damping out of the function within the crystal. In the next section it is shown that the even ordered Bragg reflections occur when $u>+1$ and the odd ordered when $u<-1$, so that for the former the characteristic function is approximately the same in consecutive valleys (or teeth) while for odd orders it is approximately the same except for reversal of sign.

This standing wave method was used by Professor Frenkel in his lectures, under the impression that it would pick out electron energies at the centers of the reflection bands, whereas it actually locates the edges. Knowing this, the method can be used to give the results of this paper for widths of the bands, etc.

Study of the Function $u(W)$

"Free" electrons. k_1 and k_2 real and positive.

By use of (13), u can be written in either of the forms

$$u = +1-(1/2k_1k_2)[(k_1+k_2)^2\sin^2\pi(k_1\alpha+k_2\beta)-(k_1-k_2)^2\sin^2\pi(k_1\alpha-k_2\beta)] \tag{30}$$

$$= -1+(1/2k_1k_2)[(k_1+k_2)^2\cos^2\pi(k_1\alpha+k_2\beta)-(k_1-k_2)^2\cos^2\pi(k_1\alpha-k_2\beta)]$$

from which we see that $u>+1$ if

$$(k_1-k_2)^2\sin^2\pi(k_1\alpha-k_2\beta) > (k_1+k_2)^2\sin^2\pi(k_1\alpha+k_2\beta), \tag{31}$$

and $u<-1$ if

$$(k_1-k_2)^2\cos^2\pi(k_1\alpha-k_2\beta) > (k_1+k_2)^2\cos^2\pi(k_1\alpha+k_2\beta). \tag{32}$$

While it is not easy to specify precisely the values of W for which (31) or (32) is satisfied, it is clear that they are respectively satisfied in the immediate neighborhood of energies such that

$$k_1\alpha+k_2\beta = s \text{ or } s+\tfrac{1}{2} \tag{33}$$

where s is a positive integer.[9] If we define the wave-length of the electron inside the lattice as

$$\lambda = (\alpha+\beta)/(k_1\alpha+k_2\beta) \tag{34}$$

then (33) is just the Bragg reflection condition for normal incidence. This analysis is incomplete as we have not taken account of the fact that the aver-

[9] The order of the reflection is $2(k_1\alpha+k_2\beta)$ and is just the number of "wave-lengths" contained in $2(\alpha+\beta)$.

age potential in a crystal is negative with respect to the surrounding region, but the expression for the reflection coefficient can be readily set up when the wave number of the electron outside the crystal ($x<0$ and $x>\xi$) is k_0, where $k_1>k_2>k_0\geqq 0$, and on passing to the limit $n=\infty$ it is easily seen that perfect reflection still occurs when $u^2>1$. The wave-length of the electron outside the lattice is then λ_0 with

$$k_0 = [2m(W - V_0)]^{1/2}/h = 1/\lambda_0$$

the "index of refraction" being

$$\mu = \lambda_0/\lambda$$

the Bragg condition reduces to

$$s\lambda_0 = 2\mu(\alpha + \beta)$$

in agreement with the simple theory for the case of normal incidence.

Within the regions of validity of (31) and (32) reflection is perfect, so that for given values of α and β one can determine graphically the breadths of the reflection maxima. We can get a rough estimate of the breadths for large energies where k_1 and k_2 are large and approximately equal. For simplicity suppose $\alpha=\beta$, and consider especially (31). Noticing that k_1, k_2 and $\sin \pi (k_1-k_2)\alpha$ are slowly varying quantities compared with $\sin \pi (k_1+k_2)\alpha$ and assuming that the reflection band is approximately symmetrical about the point for which $(k_1'+k_2')\alpha=s$ we can let $k_1=k_1'+\Delta$ and $k_2\cong k_2'+\Delta$ where Δ is small and is to be chosen such that (31) becomes an equality. To quantities of first order in Δ we get

$$2\pi\Delta s = \pm (k_1' - k_2') \sin \pi(k_1' - k_2')\alpha$$

but as

$$(k_1' - k_2') = (2mV_1/h^2)/(k_1' + k_2') = 2mV_1\alpha/sh^2$$

this yields

$$\Delta \backsimeq (mV_1\alpha/\pi s^2h^2) \sin [2\pi m\alpha^2V_1/sh^2]$$

or for the width on the energy scale

$$(\Delta W) \backsimeq 2k_1'\Delta h^2/m \backsimeq (k_1' + k_2')h^2\Delta/m \backsimeq (V_1/\pi s) \sin [2\pi m\alpha^2V_1/sh^2]$$

which, apart from the trigonometric term varies inversely as the order of the reflection. A similar result is obtained from (32). This result seems to be in general agreement with other calculations.[2,10]

"Bound" electrons. k_1 real and positive, k_2 pure imaginary.

Let

$$k_2 = ik = i(2m(V_1 - W))^{1/2}/h.$$

Although not of importance in electron scattering experiments this region is of

[10] L. Brillouin, Journ. de Physique (7) 1, 377 (1930).

interest in the theory of metallic conduction. From (30) u is expressed in terms of hyperbolic functions[11]

$$\begin{aligned} u &= +1-(2/k_1k)[k_1(\cosh\pi k\beta)(\sin\pi k_1\alpha)+k(\sinh\pi k\beta)(\cos\pi k_1\alpha)] \\ &\quad\times[k(\cosh\pi k\beta)(\sin\pi k_1\alpha)+k_1(\sinh\pi k\beta)(\cos\pi k_1\alpha)] \\ &= -1+(2/k_1k)[k(\cosh\pi k\beta)(\cos\pi k_1\alpha)-k_1(\sinh\pi k\beta)(\sin\pi k_1\alpha)] \\ &\quad\times[k_1(\cosh\pi k\beta)(\cos\pi k_1\alpha)-k(\sinh\pi k\beta)(\sin\pi k_1\alpha)]. \end{aligned} \tag{35}$$

This shows that $u<+1$ if

$$\left\{\begin{array}{l}\tan\pi k_1\alpha > -(k/k_1)\tanh\pi k\beta \\ \tan\pi k_1\alpha > -(k_1/k)\tanh\pi k\beta\end{array}\right\}$$

or if

$$\left\{\begin{array}{l}\tan\pi k_1\alpha < -(k/k_1)\tanh\pi k\beta \\ \tan\pi k_1\alpha < -(k_1/k)\tanh\pi k\beta\end{array}\right\}$$

and $u>-1$, if

$$\left\{\begin{array}{l}\tan\pi k_1\alpha > (k/k_1)\coth\pi k\beta \\ \tan\pi k_1\alpha > (k_1/k)\coth\pi k\beta\end{array}\right\}$$

or if

$$\left\{\begin{array}{l}\tan\pi k_1\alpha < (k/k_1)\coth\pi k\beta \\ \tan\pi k_1\alpha < (k_1/k)\coth\pi k\beta\end{array}\right\}$$

From rough graphs of these functions it is apparent that $u^2<1$ in the immediate vicinity of energies for which $k_1\alpha=1/2,\ 1,\ 3/2,\ \ldots$ which are just the positions of the energy levels allowed by the perturbation method, as they are the levels for a single valley with width α and infinitely high walls. It is difficult to give an estimate of the widths of these bands, but it is clear from the graph that they are very narrow when V_1 is large and k_1 small, approximately coinciding with the discrete levels for a single valley.

Real Crystals

In order to apply this method to real crystals, it is necessary to improve the starting point by considering a potential function similar to that shown in Fig. 2.

When $W>V_0$ the results are quite unchanged, the reflection regions being determined by the Bragg condition as previously discussed. All energy values are allowed even in the case of a semi-infinite lattice.

When $W<V_0$ some additions must be made to the previous results. The concepts of reflection and transmission being no longer applicable, one must make a study of the characteristic function itself, or what is the same thing, of the coefficients $(a_p,\ b_p)$. There is now the possibility that as $n\to\infty$, the modulus of the wave function will not remain bounded, so that certain ener-

[11] It can be verified from (8) that the real and imaginary parts of c_1 are still given by (13) when k_2 is pure imaginary.

gies may need to be excluded. Even for a finite lattice certain energy ranges will be excluded due to the circumstance that for any value of n, the boundary conditions at the edges of the lattice and (22) must be simultaneously satisfied; while for the semi-infinite lattice one must insure in addition the finiteness of the wave function. Probably the standing wave method described

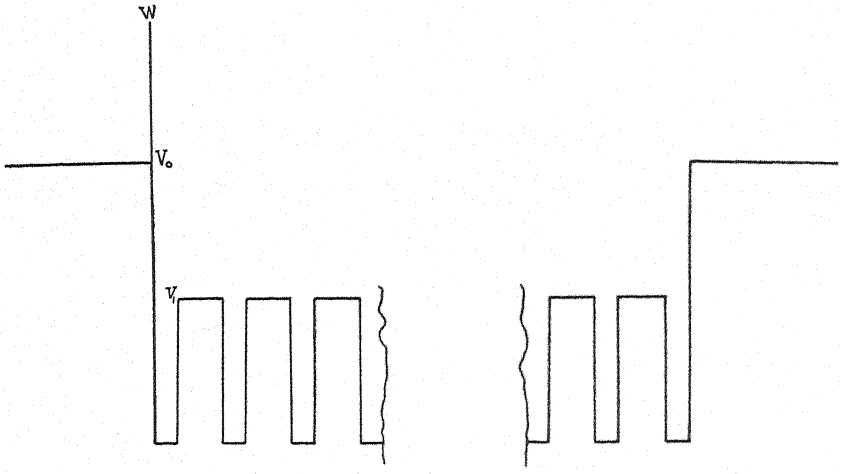

Fig. 2.

previously will still be applicable, although it seems possible that there may be additional excluded energies not appearing in such an analysis. This question would need to be studied in greater detail before the method of the present paper could be applied to metallic conduction problems.

Note added in proof: Kronig and Penney, Proc. Roy. Soc. **A130,** 499 (1931) have just published a treatment of the *infinite* lattice of the type shown in our Fig. 1 using functions of the type (28). The results are similar to these found here. The author intends to study in greater detail the connection of our general solution with this more special method since it seems possible that the use of a single function of the type (28) is associated with assumptions of periodic properties of ψ which are not altogether required by the nature of the problem.

HYPERFINE STRUCTURE AS A TEST OF A LINEAR WAVE EQUATION IN THE TWO-BODY PROBLEM

By David R. Inglis
University of Michigan
(Received February 21, 1931)

Abstract

The proper treatment of the two-body problem is not known. Dirac's relativistic considerations, so successful in the problem of one electron, have been applied by Breit to the two-electron problem. Energy terms appear of which the physical reality is very doubtful. Here a very similar application is made to the problem of a nucleus and an electron, because of the failure of previous treatments of this problem to agree with measurements of hyperfine structure. The doubtful terms do not bring about agreement, so their reality remains improbable. The present state of the theory suggests that the proper interactions have not yet been introduced in the problem of hyperfine structure.

Introduction

DIRAC has satisfied the demands of relativity for the problem of one charged particle in a force field, obtaining spin as a consequence. Breit[1] has treated the problem of two bodies in a similar manner. He has improved the calculations of Gaunt[2] on the same subject by including the classical effects of retardation of potentials, as given by Darwin. A straightforward reduction of the linear equation, involving good approximations, leads to an equation for the largest components of the wave function. This may be compared directly with the wave equation resulting from a treatment of the atomic model with spins by the usual wave mechanical perturbation theory.[3] Breit's equation contains terms representing spin-orbit interactions (with factors in agreement with the relativistically correct results of Dirac and of Thomas and Frenkel for single electrons), terms expressing the magnetic spin-spin and orbit-orbit interactions, terms due to relativistic change of mass, terms appering in Dirac's results and having a meaning only for s-states, and in addition unexpected terms containing e^4 and no h as factors, which contradict the correspondence principle. One of these terms in e^4 Breit has tested[4] by calculating its probable effect on the He triplet. The results do not agree with experiment, whereas without this one term the agreement is quite as good as could be expected, considering the approximate nature of the wave functions involved. This contradiction means that the term making the disagreement, and perhaps all the terms in e^4, have no physical meaning. It is still barely possible that that invalidation may not be final, and even that the doubtful terms have a different meaning for a nucleus and an electron than for two

[1] G. Breit, Phys. Rev. **34**, 553 (1929).
[2] A. Gaunt, Proc. Roy. Soc. **A122**, 512 (1928); Trans. Roy. Soc. **228**, 151 (1929).
[3] W. Heisenberg, Zeits. f. Physik **49**, 499 (1926).
[4] G. Breit, Phys. Rev. **36**, 383 (1930).

electrons. The importance of the problem nurtures the hope that the following test of two of the terms in e^4 may be helpful, after the appearance of more copious data.

1. Consider an electron and a nucleus moving under one another's influence. No assumption is made regarding the spin of either. This differs from the helium problem in the absence of the field of the fixed nucleus and in the metamorphosis of one of the electrons into a nucleus. The Darwin-Hamiltonian will be,

$$H = p_{\mathrm{I}}^2/2m_{\mathrm{I}} + p_{\mathrm{II}}^2/2m_{\mathrm{II}} - p_{\mathrm{I}}^4/8c^2m_{\mathrm{I}}^3 - p_{\mathrm{II}}^4/8c^2m_{\mathrm{II}}^3 + e_{\mathrm{I}}e_{\mathrm{II}}/r - (e_{\mathrm{I}}e_{\mathrm{II}}/2c^2m_{\mathrm{I}}m_{\mathrm{II}})[(\boldsymbol{p}_{\mathrm{I}}\cdot\boldsymbol{p}_{\mathrm{II}})r + (\boldsymbol{p}_{\mathrm{I}}\cdot\boldsymbol{r})(\boldsymbol{p}_{\mathrm{II}}\cdot\boldsymbol{r})/r^3]. \quad (1)$$

Here the numeral I refers to the nucleus, II to the electron; $e_{\mathrm{I}} = Ze$, $e_{\mathrm{II}} = -e$; and $\boldsymbol{r}$ is a vector from the nucleus to the electron. This leads one to the equivalent of Breit's Eq. (6),

$$\Big(p_0 + \sum_{k=1,2,3}(\alpha_k^{\mathrm{I}}p_k^{\mathrm{I}} + \alpha_k^{\mathrm{II}}p_k^{\mathrm{II}}) + \alpha_4^{\mathrm{I}}m_{\mathrm{I}}c + \alpha_4^{\mathrm{II}}m_{\mathrm{II}}c + (e_{\mathrm{I}}e_{\mathrm{II}}/2c)\Big\{\sum_{k=1,2,3}\alpha_k^{\mathrm{I}}\alpha_k^{\mathrm{II}}r^{-1} + (\alpha^{\mathrm{I}}\cdot\boldsymbol{r})(\alpha^{\mathrm{II}}\cdot\boldsymbol{r})r^{-3}\Big\}\Big)\psi = 0 \quad (2)$$

with

$$p_0 = -\frac{h}{2\pi i}\frac{\partial}{c\partial t} - \frac{e_{\mathrm{I}}e_{\mathrm{II}}}{cr}; \quad p_k^{\mathrm{I}} = \frac{h}{2\pi i}\frac{\partial}{\partial x_k^{\mathrm{I}}}.$$

Here we have omitted entirely the four-potential A. The reduction of this equation will be identical with the calculation of Breit, and will lead to the following modification of his Eq. (48′):

$$\{E - (m_{\mathrm{I}} + m_{\mathrm{II}})c^2 - e_{\mathrm{I}}e_{\mathrm{II}}/r - p_{\mathrm{I}}^2/2m_{\mathrm{I}} - p_{\mathrm{II}}^2/2m_{\mathrm{II}} \quad (3.0)$$

$$+ p_{\mathrm{I}}^4/8m_{\mathrm{I}}^3c^2 + p_{\mathrm{II}}^4/8m_{\mathrm{II}}^3c^2 \quad (3.1)$$

$$+ (e_{\mathrm{I}}e_{\mathrm{II}}/2m_{\mathrm{I}}m_{\mathrm{II}}c^2)[(\boldsymbol{p}_{\mathrm{I}}\cdot\boldsymbol{p}_{\mathrm{II}})r^{-1} + \sum_{i,j}r^{-3}(x_i^{\mathrm{II}} - x_i^{\mathrm{I}})(x_j^{\mathrm{II}} - x_j^{\mathrm{I}})p_i^{\mathrm{I}}p_j^{\mathrm{II}}] \quad (3.2)$$

$$- (e_{\mathrm{I}}e_{\mathrm{II}}hi/8\pi c^2)r^{-3}(\boldsymbol{r}\cdot[\boldsymbol{p}^{\mathrm{I}}m_{\mathrm{I}}^{-2} - \boldsymbol{p}^{\mathrm{II}}m_{\mathrm{II}}^{-2}]) \quad (3.3)$$

$$+ (e_{\mathrm{I}}e_{\mathrm{II}}h/8\pi c^2)r^{-3}(-m_{\mathrm{I}}^{-2}[\boldsymbol{r}\times\boldsymbol{p}^{\mathrm{I}}]\cdot\sigma^{\mathrm{I}} + m_{\mathrm{II}}^{-2}[\boldsymbol{r}\times\boldsymbol{p}^{\mathrm{II}}]\cdot\sigma^{\mathrm{II}} \quad (3.4)$$

$$+ (2/m_{\mathrm{I}}m_{\mathrm{II}})\{-[\boldsymbol{r}\times\boldsymbol{p}^{\mathrm{II}}]\cdot\sigma^{\mathrm{I}} + [\boldsymbol{r}\times\boldsymbol{p}^{\mathrm{I}}]\cdot\sigma^{\mathrm{II}}\}) \quad (3.5)$$

$$- (e_{\mathrm{I}}e_{\mathrm{II}}/m_{\mathrm{I}}m_{\mathrm{II}})(h/4\pi c)^2\langle(\nabla^{\mathrm{II}}\cdot\sigma^{\mathrm{I}})(\nabla^{\mathrm{I}}\cdot\sigma^{\mathrm{II}})r^{-1}\rangle \quad (3.6)$$

$$- (e_{\mathrm{I}}^2e_{\mathrm{II}}^2/4(m_{\mathrm{I}}+m_{\mathrm{II}})c^2)[3r^{-2} - 2(\sigma^{\mathrm{I}}\cdot\sigma^{\mathrm{II}})r^{-2} + (\sigma^{\mathrm{I}}\cdot\boldsymbol{r})(\sigma^{\mathrm{II}}\cdot\boldsymbol{r})r^{-4}]\}\psi_{a,b} = 0 \quad (3.7)$$

For the sake of easy comparison, the energy equation which will be derived in §2 from this wave equation is entered here.

$$E = E_1 + E_2$$

E_1 is the same for all the states in which we are interested and consists of the unperturbed energy augmented by the contributions of (3.1), (3.2), and (3.3). E_2 splits up the doublet and is given by

$$-E_2 = (h^2e_Ie_{II}/8\pi^2c^2)\overline{r^{-3}}[m_I^{-2}(\overline{l\cdot s^I}) + m_{II}^{-2}(l\cdot s^{II}) \quad (4.4)$$

$$- (2/m_Im_{II})\{(\overline{l\cdot s^I}) + (l\cdot s^{II})\}] \quad (4.5)$$

$$- (e_Ie_{II}/m_Im_{II})(h/2\pi c)^2\overline{r^{-3}}\,[(\overline{s^I\cdot s^{II}}) - 3\overline{(s^I\cdot r)(s^{II}\cdot r)r^{-2}} \quad (4.6)$$

$$+ (e_I^2e_{II}^2/(m_I + m_{II})c^2)\overline{r^{-2}}\,[(\overline{s^I\cdot s^{II}}) - \overline{(s^I\cdot r)(s^{II}\cdot r)r^{-2}}] \quad (4.7)$$

(3.4) (and also (4.4)) represent the interaction of each spin with the field due to its own orbital motion, while (3.5) gives the interaction of the spin of each particle with the orbit of the other. (3.6) corresponds to the classical interaction energy of two dipoles. (3.7) contains the doubtful terms in e^4. If physically extant, only the last of the three terms would effect the helium triplet separation, so it alone was tested by Breit. Each of the last two terms would effect hyperfine structure, so we can test them both. The first gives only a displacement common to all the levels.

2. In the perturbation problem, (3) is the perturbed wave equation. To determine the unperturbed wave functions, we consider all the terms beyond (3.0) as perturbation terms, so that (3.0) becomes the unperturbed equation. The coordinates are taken to be those in which the center of gravity is at rest, since a transformation can always be made from more general coordinates of two particles to the coordinates of the center of gravity and the relative coordinates of the particles. The translation of the center of gravity being separated from the problem, $p^I = -p^{II}$. Thus we have the hydrogen wave equation, and hence use hydrogenic wave functions. The wave function in the unperturbed equation, as in (3), has two indices, each of which may have two values. The first index refers to the nuclear spin orientation, and is operated upon by σ^I; the second to the spin of the electron, and is acted upon by σ^{II}. As a function of space and spin coordinates, the unperturbed function is separable,

$$\psi_{a,b}(r, \theta, \phi) = S_a^I S_b^{II} u(r, \theta, \phi)$$

where a and b may each be either α or β of Pauli's theory, and σ^I and σ^{II} operate on S^I and S^{II}, respectively, in the usual manner. $S^{II}u$ might be replaced by the one-electron wave function stabilized for spin-orbit interaction, such as given by Bartlett,[5] e.g., and the resulting ψ would give the diagonal terms of an energy matrix from which hyperfine splitting could be had by sum rules. Since the wave function is separable in radial and angular parts, we may obtain the result of the angular integrations by considering the operators as vectors in the vector model, and averaging over the precessions. $[r\times p^I] = -[r\times p^{II}]$ is the orbital angular momentum operator. Since Breit has used in effect the negative of the Pauli matrices, σ becomes $-2s$, where $|s| = \frac{1}{2}$. These substitutions in (3) give (4). In reducing it to an expression in the quantum numbers, Landé cosines are used. Goudsmit[6] has explained in detail a method for obtaining $\overline{(s^I\cdot r)(s^{II}\cdot r)r^{-2}}$. It consists essentially in making angular integrations in the case of a strong field, when the quantum vectors

[5] J. H. Bartlett, Jr., Phys. Rev. 35, 230 (1930).
[6] S. Goudsmit, Phys. Rev. 37, 663 (1931).

are decoupled, and using the results to find the value of the interaction without field by means of energy sum rules.

From the latter term of (4.4) (the other term in $(I\cdot s^{II})$ is negligible) we get the energy that gives rise to the doublet separation:

$$E' = -(h^2e_Ie_{II}/8\pi^2c^2m_{II}^2)\overline{r^{-3}}(I\cdot s^{II})$$
$$= A'(I\cdot s^{II}) = A'\tfrac{1}{2}\{j(j+1) - l(l+1) - \tfrac{3}{4}\} \quad (5)$$

It is apparent in (4) that the hyperfine structure contains the same constant A' which is determined empirically by the doublet separation. The following expressions, which give the splitting up of the two doublet levels, are derived from (4.4), (4.5), and (4.6). The order of the terms has been preserved.

$$E''_j = A_j''(s^I\cdot j) = A_j''\tfrac{1}{2}\{f(f+1) - j(j+1) - s^I(s^I+1)\} \quad (6)$$

$$A''_{l+\frac{1}{2}} = \frac{m_{II}}{m_I}A'\left[\frac{2l}{l+\frac{1}{2}} - \frac{1}{l+\frac{1}{2}} + \frac{3}{(2l+3)(l+\frac{1}{2})} + \delta\frac{8\pi^2e_Ie_{II}m_{II}}{h^2}\frac{\overline{r^{-2}}}{\overline{r^{-3}}}\left\{\frac{1}{l+\frac{1}{2}} - \frac{2}{(2l+3)(l+\frac{1}{2})}\right\}\right] \quad (7)$$

$$A''_{l-\frac{1}{2}} = \frac{m_{II}}{m_I}A'\left[2\frac{l+1}{l+\frac{1}{2}} + \frac{1}{l+\frac{1}{2}} + \frac{3}{2(l-\frac{1}{2})(l+\frac{1}{2})} - \delta\frac{8\pi^2e_Ie_{II}m_{II}}{h^2}\frac{\overline{r^{-2}}}{\overline{r^{-3}}}\left\{\frac{1}{l+\frac{1}{2}} + \frac{1}{(l-\frac{1}{2})(l+\frac{1}{2})}\right\}\right]. \quad (8)$$

The symbol δ has the value unity of the terms in e^4 are physical, otherwise it is zero.

3. To compare the terms we must have an idea of the ratio of the radial integrals. For a Coulomb field,

$$\overline{r^{-2}} = \frac{Z^2}{n^3(l+\frac{1}{2})}\frac{1}{a_0^2}\cdot\quad \overline{r^{-3}} = \frac{Z^3}{n^3l(l+\frac{1}{2})(l+1)}\frac{1}{a_0^3}\cdot\quad a_0 = \frac{h^2}{4\pi^2m_{II}e^2}\cdot \quad (9)$$

For the heavy elements some sort of approximation must be used. The electron cloud alters the radial part of the wave function by producing a non-coulomb interaction. We will content ourselves with the classical application of the charged shell model of the atom, as used by Landé for doublet separations.[7] Using (9) for outer and inner orbital segments, we get

$$\overline{r^{-2}} = \frac{2Z_0^2}{n_0^3(l+\frac{1}{2})}\frac{1}{a_0^2}\cdot\quad \overline{r^{-3}} = \frac{Z_iZ_0^2}{n_0^3l(l+\frac{1}{2})(l+1)}\frac{1}{a_0^3}$$

of which the ratio is

$$\overline{r^{-2}}/\overline{r^{-3}} \approx 2l(l+1)a_0/Z.$$

This in (7) and (8) gives

$$A''_{l+\frac{1}{2}} = \frac{m_{II}}{m_I}A'\left\{\frac{2l(l+1)}{(l+\frac{1}{2})(l+\frac{3}{2})} - \delta\frac{8l(l+1)}{2l+3}\right\} = \frac{m_{II}}{m_I}A'\left\{\frac{16}{15} - \delta\frac{16}{5}\right\}$$

[7] A. Landé, Zeits. f. Physik 25, 46 (1924).

$$A''_{l-\frac{1}{2}} = \frac{m_{\mathrm{II}}}{m_{\mathrm{I}}} A' \left\{ \frac{2l(l+1)}{(l-\frac{1}{2})(l+\frac{1}{2})} + \delta \frac{4l(l+1)}{l-\frac{1}{2}} \right\} = \frac{m_{\mathrm{II}}}{m_{\mathrm{I}}} A' \left\{ \frac{16}{3} + \delta 8 \right\}.$$

The last members are for the case $l=1$. The presence of other electrons also replaces $Z\overline{r^{-3}}$ by $\overline{Z_{eff} r^{-3}}$ in the expression for A', but the numerical change is small enough that it need not interest us here.[8]

The present treatment leads naturally to a nuclear spin with but two orientations possible and a Landé g-factor 2 in units $e_{\mathrm{I}} h/4\pi m_{\mathrm{I}} c$. For the terms that classically have a meaning it is easy to believe that we may extend the result to other cases with the vector model by assuming a larger nuclear spin vector s^{I} in (6), selecting its value and a different value of g to accord with observed intervals or intensity ratios. We postulate tentatively that a similar treatment of the terms in e^4 will give an estimate of their contribution to the energies.

A comparison is made with the few experimental data available,[9] which are for ^2P. In Tl the nuclear moment is $\frac{1}{2}$ but in Bi it is $4\frac{1}{2}$.

TABLE I.

	A' exp.	A'' exp.	A'' calc. $\delta=0$	A'' calc. $\delta=1$	A'' exp.	A'' calc. $\delta=0$	A'' calc. $\delta=1$
Tl I*	5195 cm^{-1}	0.72	0.074	0.18	~0.02	0.015	−0.03
*Bi***	10000	0.40	0.14	0.35	~0.02	0.03	−0.06

* John Wulff, appearing in Zeits. f. Physik, communicated to Professor Goudsmit.
** Indirectly derived from Bi I and II data. R. A. Fisher and S. Goudsmit, Phys. Rev., in print.

The classical values, with $\delta=0$, do not agree with experiment even when multiplied by the arbitrary factor $g(I)$ which the usual theory allows. When such an arbitrary factor is introduced, the agreement in the case $\delta=1$ is even worse. However, the present treatment of the problem, when not extended hypothetically, does not permit of such a factor. For the large separations, of which the measurements are most certain, the agreement is better with $\delta=1$ than with $\delta=0$.

In the classical terms the value of the nuclear magnetic moment is definitely determined as $Zm_{\mathrm{II}}/m_{\mathrm{I}}$ Bohr magnetons for the nuclear spin $\frac{1}{2}$. This is as assumed and discussed by Jackson[9] and by Fermi[8].

This paper stresses once more the fact that we have at present no satisfactory theory of spin-spin interaction.

I thank Professor Uhlenbeck and Professor Goudsmit for very helpful suggestions.

[8] E. Fermi, Zeits. f. Physik **60**, 332 (1930).

[9] The results for In I by Jackson (Proc. Roy. Soc. **A128**, 508, 1930) and by McLennan and Allin (Proc. Roy. Soc. **A129**, 208, 1930) disagree too radically to be of use at present. In Bi III and Tl III the second member of the P series is known, but second order effects make the values of A_j'' for our purpose uncertain. (Vide H. Casmir, Phys. Rev., in print.)

ABSORPTION BANDS OF HYDROGEN CYANIDE GAS IN THE NEAR INFRARED

By Richard M. Badger and John L. Binder
Gates Chemical Laboratory, California Institute of Technology

(Received February 20, 1931)

Abstract

The absorption spectrum of gaseous hydrogen cyanide has been investigated by photographic methods in the region λ7000-9200. Two weak bands of very simple structure were found, having P and R branches but no Q branches. The band at λ7912 is apparently a harmonic of a fundamental band at 3.04μ, and the very weak band at λ8563 is a combination band. The hydrogen cyanide molecule is linear in the normal state, and has a moment of inertia $I=18.79\times10^{-40}$ g·cm². The distance of separation of the carbon and nitrogen atoms is estimated to be 1.15×10^{-8} cm. Hydrogen cyanide is discussed in regard to its three fundamental oscillations which have frequencies 3290, 2090, and 710, respectively, and in regard to its dissociation energy and dissociation products. The evidence requires a molecular structure represented by the formula HCN, and shows that the normal molecule is built from a normal hydrogen atom and a normal CN radical. The absorption of cyanogen gas has also been investigated in the photographic infrared, but no absorption bands could be detected.

Introduction

HYDROGEN cyanide has been the subject of two previous infrared investigations. W. Burmeister[1] observed two double bands with maxima at 14.33μ and 13.60μ, and at 7.22μ and 6.95μ, respectively, a single strong maximum at 3.04μ, and doubtful bands at 4.8μ and 3.6μ. E. F. Barker,[2] working with greater dispersion, confirmed the doubtful bands and found for the one three maxima at 4.79, 4.756, and 4.723μ, and in the case of the other apparently a strong Q branch with maximum at 3.564μ and two weak maxima on either side. Slight evidence of a rotational structure was found in the band at 7μ.

A calculation of the moment of inertia of the hydrogen cyanide molecule from the separation of the maxima of the double band at 14μ, with the use of a classical formula, yielded the improbably large value $I=33\times10^{-40}$.[3] The separation of the maxima in the band at 7μ is much greater and has been interpreted as due to rotation about an axis with moment of inertia $I=0.907\times10^{-40}$.[4]

Experimental Procedure

The hydrogen cyanide gas used in the investigation was prepared by dropping a concentrated solution of sodium cyanide into sulphuric acid. The gas

[1] W. Burmeister, Verh. d. D. Phys. Ges. **15**, 589 (1913).
[2] E. F. Barker, Phys. Rev. **23**, 200 (1924).
[3] R. C. Tolman and R. M. Badger, Jour. Amer. Chem. Soc. **45**, 2277 (1923).
[4] Schaefer and Matossi, Das Ultrarote Spectrum, Berlin, 1930.

evolved was dried with calcium chloride and then condensed in a tube immersed in a freezing mixture. This tube was then connected to the evacuated absorption cell until equilibrium between liquid and vapor was established at room temperature. The gas pressure in the cell was consequently usually slightly less than one atmosphere. It seemed undesirable to attempt to increase the pressure by warming the apparatus, since even at atmospheric pressure the absorption lines were rather broad.

The absorption cell was a steel tube 280 cm in length, with a mirror at one end so that the light from the tungsten lamp source traversed it twice. The exposures were taken with the first order of a ten-foot grating in an Eagle mounting, using Eastman Infrared Sensitive Plates hypersensitized in ammonia. As calibration spectrum the iron lines in the second order were used.

Since both absorption bands were very weak it was not possible to make direct measurements on the plates with the use of a comparator. Microphotometer records were consequently made of absorption and comparison spectra, side by side on the same plates, using a linear enlargement of ten times. The tabulated wave-lengths, except for a few weak lines, were calculated from the mean of measurements made on four photometer curves obtained from different parts of two spectral plates.

Experimental Results

A careful examination of spectrograms covering the region λ7000–9200 resulted in the discovery of two similar absorption bands at λ7912 and λ8563, respectively. Both are weak, the latter extremely so, and the lines are broad as is to be expected in a saturated vapor. Each band has a P and an R branch, a missing zero line, and no apparent Q branch. The convergence in the R branches is so large that at first sight the bands appear to have a head. Due to the weakness of the absorption no attempt has been made to estimate relative intensities. The two branches have in each case about equal intensity, and as should be expected there is no indication of alternating intensities.

The wave-lengths and corresponding frequencies on the lines measured are recorded in the accompanying tables. A single question mark indicates low probable accuracy of measurement, and a double question mark, possible doubt as to the reality of the line. The measurements of the lines in the R branches are probably the less reliable due to incomplete resolution of the rather broad lines.

It should be mentioned that cyanogen gas was also studied in the course of this investigation, with pressures up to three atmospheres, but no absorption could be detected.

Discussion of the Results

The rotational energy levels of the upper and lower vibrational states of the molecule were isolated by means of the usual combination relations:

$$\Delta_2 F'(J) = R(J) - P(J) = F'(J+1) - F'(J-1) \sim 4B'(J+\tfrac{1}{2})$$

$$\Delta_2 F''(J) = R(J-1) - P(J+1) = F''(J+1) - F''(J-1) \sim 4B''(J+\tfrac{1}{2}).$$

TABLE I. *The HCN band at λ7912.*

J	R-Branch λ	R-Branch ν	P-Branch λ	P-Branch ν	$\Delta_2F''(J)$	$\frac{\Delta_2F''(J)}{J+1/2}$	$\Delta_2F'(J)$	$\frac{\Delta_2F'(J)}{J+1/2}$
0	7910.4	12638.1						
1	08.3	41.5	7913.8	12632.7	8.1	5.39	8.8	5.87
2	06.5	44.4	15.5	30.0	14.6	5.84	14.4	5.76
3	04.9	46.9	17.4	26.9	20.8	5.94	20.0	5.71
4	03.3	49.5	19.5	23.6	27.0	6.00	25.9	5.76
5	01.8	51.9	21.8	19.9	32.8	5.96	32.0	5.82
6	00.4	54.1	23.8	16.7	38.5	5.92	37.4	5.76
7	7898.9	56.5	25.9	13.4	44.0	5.87	43.1	5.74
8	97.7	58.4	28.0	10.1	50.3	5.92	48.3	5.68
9	96.4	60.5	30.4	06.2	55.8	5.87	54.3	5.73
10	95.5	62.0	32.7	02.6	61.9	5.89	59.4	5.65
11	94.0	64.4	35.2	12598.6	67.0	5.82	65.8	5.73
12	92.9	66.1	37.5	95.0	73.6	5.88	71.1	5.69
13	91.9	67.7	40.1	90.8	79.4	5.88	76.9	5.70
14	90.8	69.5	42.7	86.7	85.3	5.88	82.8	5.71
15	90.0	70.8	45.4	82.4	91.2	5.88	88.4	5.70
16	88.8	72.7	48.0	78.3	97.0	5.88	94.4	5.72
17	88.1	73.8	50.8	73.8	103.2	5.90	100.0	5.72
18			53.6	69.5	108.6	5.87		
19			56.3	65.2				
20			59.7	59.8				
21			62.4	55.6				
22			65.4(?)	50.8				
23			68.6(?)	45.8				
24			71.8(?)	40.8				
25			75.2(?)	35.4				
26			78.0(?)	31.0				
27			81.8(?)	25.1				

TABLE II. *The HCN band at λ8563.*

J	R-Branch λ	R-Branch ν	P-Branch λ	P-Branch ν	$\Delta_2F''(J)$	$\frac{\Delta_2F''(J)}{J+1/2}$	$\Delta_2F'(J)$	$\frac{\Delta_2F'(J)}{J+1/2}$
0	8561.5(?)	11677.0						
1	59.3	80.0	8565.4(??)	11671.7	8.9	5.92	8.3	5.53
2	57.2	82.8	68.0	68.1	14.7	5.89	14.7	5.88
3	55.4	85.4	70.1	65.3	20.6	5.89	20.1	5.74
4	53.3	88.2	72.3	62.2	26.6	5.94	26.0	5.77
5	51.7	90.4	74.9	58.7	33.0	6.00	31.7	5.76
6	50.1	92.6	77.5	55.2	38.3	5.89	37.4	5.76
7	48.2	95.2	79.8	52.1	44.3	5.91	43.1	5.74
8	46.6	97.3	82.6	48.3	50.3	5.91	49.0	5.76
9	45.1	99.4	85.1	44.9	56.3	5.92	54.5	5.74
10	43.6(?)	11701.6	88.0	41.0	62.0	5.90	60.5	5.77
11	42.1(?)	03.5	90.6	37.4	68.0	5.92	66.1	5.75
12	40.8(?)	05.3	93.5	33.5	73.9	5.92	71.8	5.74
13	39.5(?)	07.1	96.4	29.6	80.3	5.94	77.5	5.74
14			99.8	25.0	86.0	5.94		
15			8602.7	21.1				
16			05.3	17.4				
17			08.8	12.8				
18			11.7	08.9				
19			15.1	04.3				

These differences are presented in the right side of Tables I and II. No effect of the stretching of the molecule as a result of rotation could be detected, and within the accuracy of measurement the rotational energies in all three vibrational states may be represented by simple formulas of the form:

$$E_{\text{rot}} = J(J+1)B.$$

The best values for the constants for the two bands are given in Table III. The differences in vibrational energies of upper and lower states, and the

TABLE III. *Constants of the HCN bands at λ7912 and λ8563.*

λ	ν_0	B''	$B'-B''$	I''
7911.9	12635.8	1.472	−0.044	18.79×10^{-40}
8563.3	11674.5	1.480	−0.042	18.69×10^{-40}

difference in the rotational energy constants, $B'-B''$, were obtained from a graphical treatment of the combinations:

$$\tfrac{1}{2}[R(J)+P(J+1)] = \nu_0 + (J+1)^2(B'-B'').$$

The slight difference in the value of B'', the rotational constant for the ground state, as determined from the two bands, is probably not greater than experimental error as the two bands seem to have a common lower level. The value determined from the data on the band at λ7912 is probably the more accurate.

STRUCTURE OF THE HYDROGEN CYANIDE MOLECULE

The simplicity of the two bands here investigated leaves no doubt as to the linearity of the hydrogen cyanide molecule in its normal state, and also in the two other vibrational states concerned. It still remains to be discussed which of the three possible arrangements of the three atoms in a straight line is the correct one. The arrangement with the hydrogen in the center is at once ruled out by the relatively small moment of inertia, ($I=18.79\times10^{-40}$) and need not be discussed on the grounds of chemical improbability. Whether the gas known to chemists should be designated as hydrogen cyanide, HCN, or iso-cyanide, HNC, or whether it may be a mixture of two molecular species has been the subject of numerous discussions, and it seems to be worth while to consider what the spectroscopic evidence has to say in this regard.

We will simply mention at this point that the relation of all the observed infrared bands is such that they are apparently due to only one type of molecule. Further, their intensity is so great that this molecular species must constitute by far the greater part of hydrogen cyanide gas. This particular molecule will be the one with which we shall be concerned, and from now on we shall speak of it as the hydrogen cyanide molecule, and shall examine the data with the purpose of determining its structure. We shall now proceed to discuss three pieces of information which are derived from spectral data, namely the moment of inertia of the molecule, the frequencies of vibration, and the heat of dissociation.

The moment of inertia of the hydrogen cyanide molecule in the normal state, as determined from the data on the band at λ7912 is, $I = 18.79 \times 10^{-40}$ g·cm². The fact that this constant is about half as large as that previously estimated from the doublet separation of the band at 14μ may possibly be accounted for by the low resolution used in studying this latter band. It is of course not possible to determine uniquely both interatomic distances in the molecule from the moment of inertia alone. However, the moment of inertia is not very sensitive to the position of the light hydrogen atom, and an estimate of the carbon-nitrogen separation may be made. In Fig. 1 is plotted

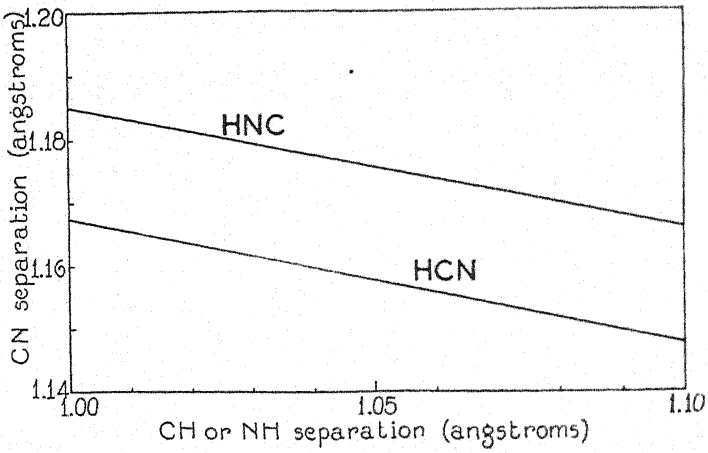

Fig. 1. The C-N separation plotted as a function of the C-H, or N-H separation for HCN and HNC molecular models with $I = 18.79 \times 10^{-40}$.

this distance as a function of the H-C separation, assuming the structure HCN, and of the H-N separation for the HNC structure, with the given moment of inertia. In either case the distance is small and strongly suggests a triple bond linkage between carbon and nitrogen. We may compare with the internuclear separation in the normal state of the CN radical, 1.17×10^{-8} cm.

Modes of Oscillation of the Hydrogen Cyanide Molecule

The observed hydrogen cyanide bands may all be fitted into one simple scheme as given in Table IV, requiring three fundamental frequencies.

Table IV. *Designation of the HCN bands.*
$\nu_1 = 3333.7\ v - 43.7\ v^2$; $\nu_2 = 2090$; $\delta = 710$

Band	ν(cm^{-1})	Designation
14μ	710	δ
7μ	1411	2δ
4.7μ	2090 (approx)	ν_2
	2112	3δ
3.6μ	2805	$\nu_2+\delta$ (and possibly 4δ)
3.04μ	3290	ν_1
0.8563μ	11675	$3\nu_1+\nu_2$
0.7912μ	12636	$4\nu_1$

The designation of the strong band at 3.04μ as a fundamental, and the band at λ7912 as one of its harmonics seems without objection. These two bands are represented within experimental error by the formula $\nu = 3333.7\ v - 43.7\ v^2$. That the bands at 14$\mu$ and 7μ are fundamental and first harmonic of a "deformation" oscillation is also reasonable, as such an oscillation should be expected to have a low frequency. A deformation oscillation does not necessarily lead to the presence of a strong Q branch as has been shown in the case of acetylene.[5] The choice of the other fundamental frequency, which seems to be comparatively inactive, is more difficult. The form of the unresolved band at 4.7μ suggests the overlapping of two bands, one of which is probably the fundamental in question and the other a harmonic of the 14μ band. The choice of a frequency around 2100 is confirmed by the combination band at λ8563, and seems settled by recent work on the Raman spectrum of liquid hydrogen cyanide.[6]

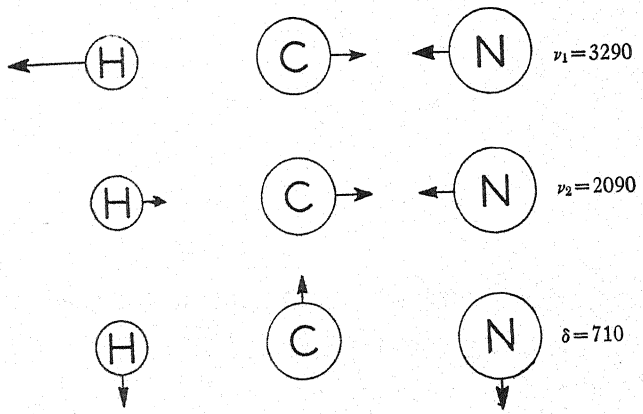

Fig. 2. The fundamental modes of oscillation of the HCN molecular model.

If we represent the hydrogen cyanide molecule by a mechanical model with three masses in the ratio 1.008:12:14, bound by Hooke's law forces, and arranged in a straight line, we find that this model does in fact have three fundamental modes of vibration, all of which will be "active," so to speak. Two of these may be designated as "valence" oscillations, the third as a "deformation" oscillation, as seen in Fig. 2. (Cf. the discussion of molecular oscillation by Mecke.[5]) By the application of normal coordinate methods it is possible to evaluate the ratio of the "valence" force constants which is required to fit the observed frequencies ν_1 and ν_2. That is we may estimate the ratio k_1/k_2 of the constants of the restoring forces which tend to maintain the equilibrium separation between carbon and nitrogen, and between hydrogen and the atom to which it is linked. Since the carbon and nitrogen atoms are of nearly equal mass it does not matter very much which of the two possible

[5] R. Mecke, Zeits. f. Physik, **64**, 173 (1930).
[6] Dadieu and Kohlrausch, Berichte **63**, 1657 (1930).

molecular models is considered. For the HCN arrangement we find $k_1/k_2 = 3.2$ and for HNC nearly the same value, 3.1. The former is nearly exactly the ratio of the force constants for CN in the normal state, and for HCl (or CH), and whichever model we choose is strong evidence for a triple bond between carbon and nitrogen. The ratio would be approximately 2 for a double bonded structure, as can for example be seen from a comparison of the binding constants in acetylene and ethylene.[5]

Dissocation Products and Dissociation Energy of Hydrogen Cyanide Molecule

We shall now consider the products of a dissociation process in which the hydrogen atom is removed from a hydrogen cyanide molecule. Three energy states of the CN radical are known. The normal state is a $^2\Sigma$ state formed from a ^4S nitrogen atom and a ^5S carbon atom.[7] A small internuclear separation and high oscillational frequency are evidence of a triple bond. The two excited states are formed from ^4S nitrogen and ^3P carbon. The lower of these, a $^2\Pi$ level with 1.8 volts excitation energy, has a relatively loose binding indicative of a double bond, but the higher, a $^2\Sigma$ state, has surprising rigidity considering its dissociation products and small dissociation energy.

The consideration of the oscillational frequencies rendered it improbable that the normal hydrogen cyanide molecule is formed from the CN radical in the $^2\Pi$ state, and this improbability is confirmed by the following energy considerations. The dissociation energy of normal hydrogen cyanide gas molecules into normal hydrogen atom and CN radical may be calculated from the data embodied in the following equations. These data are partly spectroscopic values, and partly thermal values corrected to the absolute zero by the use of specific heat data.

$$\tfrac{1}{2}H_2 + C(\text{graphite}) + \tfrac{1}{2}N_2 = \text{hydrogen cyanide} - 30{,}200 \text{ cals } (-1.31 \text{ volts}) \quad (1)$$

$$N_2 = 2N - 212{,}000 \text{ cals } (-9.2 \text{ volts}) \quad (2)$$

$$H_2 = 2H - 100{,}000 \text{ cals } (-4.34 \text{ volts}) \quad (3)$$

$$C(\text{graphite}) = C(\text{gas}) - 158{,}000 \text{ cals } (-6.86 \text{ volts})^8 \quad (4)$$

$$CN(\text{normal}) = C(\text{normal}) + N(\text{normal}) - 187{,}000 \text{ cals } (-8.1 \text{ volts})^7 \quad (5)$$

$$CN(\text{normal}) = CN(^2\Pi) - 41{,}500 \text{ cals } (-1.8 \text{ volts})^7 \quad (6)$$

From a combination of these data we find:

$$\text{hydrogen cyanide(normal)} = H(\text{normal}) + CN(^2\Pi) - 138{,}000 \text{ cals } (-6.0 \text{ volts}) \quad (7)$$

This is again strong evidence that normal hydrogen cyanide molecule is not directly formed from $^2\Pi$ CN radical, since an abnormally strong binding for the hydrogen would be required by Eq. (7). We should expect a molecule so built to be of the form HNC, and there seems to be no reason to suppose that the binding energy of hydrogen to nitrogen in this case should be much greater than the energy of the H-C linkage. We find for example that the

[7] W. Heitler and G. Herzberg, Zeits. f. Physik 53, 52 (1929).
[8] Brody and Millner, Chem. Zent. I, 237 (1928).

dissociation energy of NH_3 into its atoms is about 4.0 volts per hydrogen atom. A similar argument renders it even less likely that hydrogen cyanide is formed from CN in a state of excitation higher than the $^2\Pi$ state.

We are then left with the one possibility that the dissociation products of normal hydrogen cyanide are a normal hydrogen atom and a normal CN radical. This seems to require the molecular structure HCN, and we may write:

$$HCN(\text{normal}) = H(\text{normal}) + CN(\text{normal}) - 97{,}000 \text{ cals } (-4.2 \text{ volts}) \quad (8)$$

This result is thoroughly reasonable and may be compared with the value $-100{,}000$ cals. (-4.34 volts) which is the dissociation energy of HCl molecule.

It is interesting to consider the possibility of the existence of a hydrogen iso-cyanide molecule formed from hydrogen atom and $^2\Pi$ CN radical. This molecule, as stated above, would probably have the form HNC but would be non-linear. If we may estimate the H-N binding energy at about 4.2 volts, HNC should have about 41,500 cals (1.8 volts) more energy then HCN. We may make a rough estimate of the relative amounts of the two forms in an equilibrium mixture if we assume that the two forms have about the same specific heat and the same entropy. We find

$$K_{298^\circ} = \frac{\text{HCN}}{\text{HNC}} = 10^{30} \text{ (approx)}.$$

We must then conclude that hydrogen cyanide gas consists almost entirely of linear molecules of the form HCN.

One may be tempted to calculate a dissociation energy for HCN by the use of the vibrational constants in the formula representing the bands with fundamental at 3.04μ. The value so obtained is 6.4 volts, but can not be very significant since only one band of the series has been accurately measured and the constants are consequently inexact. In any case linear extrapolations are found to give uncertain results even in the case of diatomic molecules, and with polyatomic molecules seem to give consistently too high values. This might in some cases be explained by saying that the dissociation leaves a radical in an excited electronic state, but in other cases this is improbable. There seems to the authors to be a certain difficulty in principle in calculating dissociation energies of polyatomic molecules from spectral data. When one of the fundamental oscillations of such a molecule is increased in amplitude until an atom splits off, at the moment of separation the radical remaining may very likely be in a distorted condition, and after the separation will continue to vibrate with considerable energy. This remaining vibrational energy must be subtracted from the value obtained from the band series extrapolation in order to obtain the true dissociation energy. We hope to discuss this question more in detail in a later paper, and have some experiments in progress which may clarify the situation.

THE IONIZATION OF MERCURY VAPOR BY ELECTRON IMPACT

By P. T. Smith
Department of Physics, University of Minnesota

(Received February 16, 1931)

Abstract

Quantitative measurements have been made of the total number of positive charges per electron per centimeter path at a definite pressure and temperature in mercury vapor as a function of the energy of the impacting electrons out to 750 volts. The maximum efficiency 19.40 occurs at about 85 volts.

"*Ultra-ionization potentials*" were found at 10.60, 10.76, 10.88, 11.06, 11.27, 11.40, 11.55, 11.70, 11.78, 11.92, 12.00, 12.06, 12.17, 12.28, 12.40, 12.77, 13.55, 18.20, 19.36, 20.40, and 29.50 volts. Most of these agree with those previously observed.

A METHOD has recently been described[1] for measuring the total number of positive charges formed by electron impact in gases at low pressure. The results in helium, neon, and argon have been reported. The present paper gives a description of the results of a study of mercury vapor.

Compton and Van Voorhis,[2] T. J. Jones,[3] and Bleakney[4] measured the efficiency of ionization of mercury vapor by electron impact and obtained values which agree qualitatively. Lawrence,[5] and Hughes and Van Atta[6] have observed by indirect methods sharp increases, near the ionization potential, in the number of ions formed by electrons as their energy was increased. Haupt,[7] and Nielsen and Potter,[8] by more direct methods, also observed several of these critical potentials which Lawrence has called "ultra-ionization potentials."

The writer has redetermined the efficiency of ionization of mercury vapor and has observed a number of abrupt changes in the slope of the efficiency curves. The potentials at which these new modes of ionization set in agree quite well with those previously observed and several of the new ones found account for some of the apparent discrepancies between those found by Lawrence and by Hughes and Van Atta.

Apparatus and Procedure

The apparatus, Fig. 1, was constructed entirely of tantalum. The more essential parts were insulated with quartz. The metal parts were baked out at a yellow heat before they were sealed into the Pyrex tube.

[1] P. T. Smith, Phys. Rev. **36**, 1293 (1930).
[2] Compton and Van Voorhis, Phys. Rev. **27**, 724 (1926).
[3] T. J. Jones, Phys. Rev. **29**, 450 (1927).
[4] W. Bleakney, Phys. Rev. **34**, 157 (1929); **35**, 139 (1930).
[5] E. O. Lawrence, Phys. Rev. **28**, 947 (1926).
[6] A. L. Hughes and C. M. Van Atta, Phys. Rev. **36**, 214 (1930).
[7] C. R. Haupt, 167th Meeting of the American Physical Society.
[8] W. M. Nielsen, Phys. Rev. **37**, 87 (1931).

The filament, F, was a thin tungsten ribbon about 0.075 cm wide and placed within 1 mm of the hole, S_1, which was about 0.034 cm in diameter.

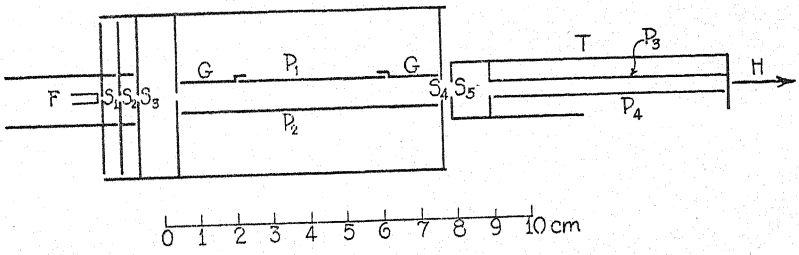

Fig. 1. Diagrammatic sketch of the apparatus.

The IR drop across this 0.034 cm length of the filament was less than 0.02 volt so that the velocity distribution of the electrons was determined almost entirely by the temperature of the filament.

The positive end of the filament was connected to S_1, which in turn was maintained about 7 volts negative with respect to S_2. The velocity of the electrons was determined by a variable potential between S_2 and S_3.

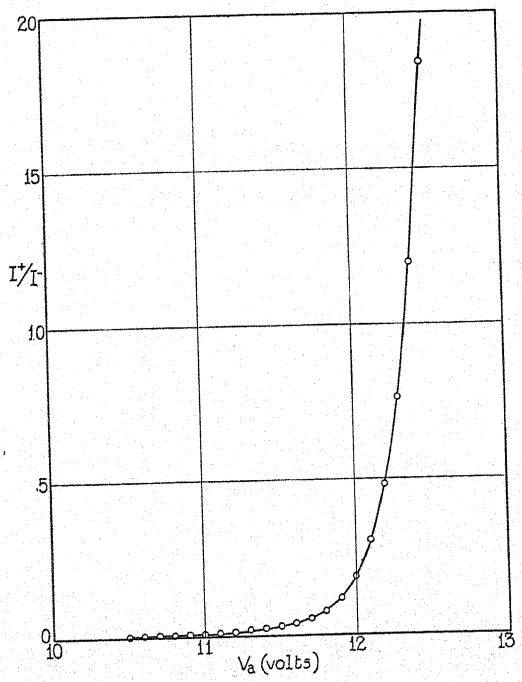

Fig. 2. The efficiency of ionization by electron impact of Hg vapor near the ionization potential. The ordinates represent the efficiency in arbitrary units.

This arrangement gave an electron beam whose magnitude was quite independent of the field between S_2 and S_3 and insured a voltage correction which was independent of the speed of the electrons.

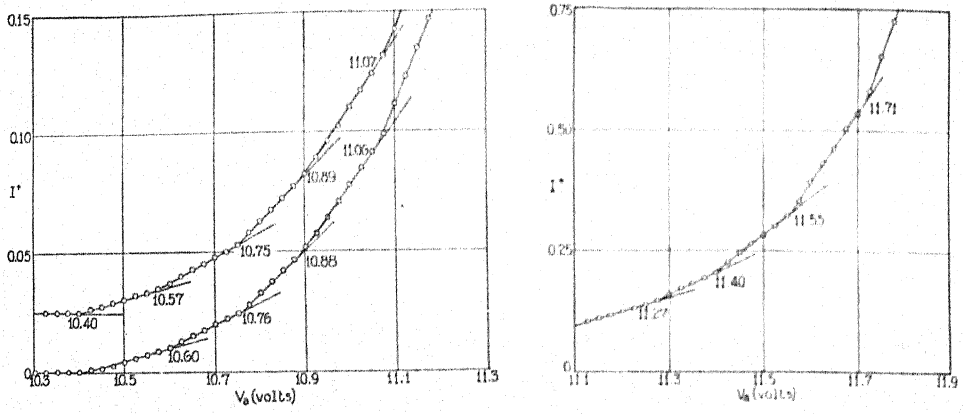

Figs. 3 and 4. The ionization of Hg vapor by electron impact from 10.4 to 11.7 volts. I^+ is proportional to the efficiency of ionization.

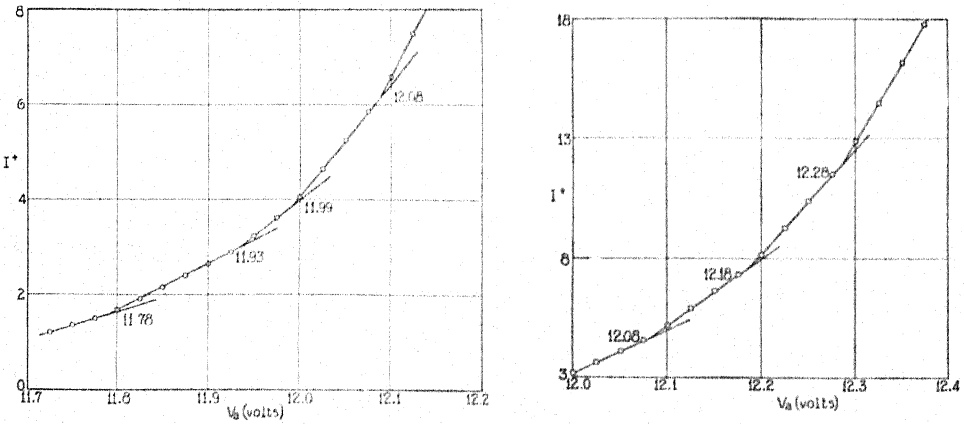

Figs. 5 and 6. The ionization of Hg vapor by electron impact from 11.7 to 12.3 volts. I^+ is proportional to the efficiency of ionization.

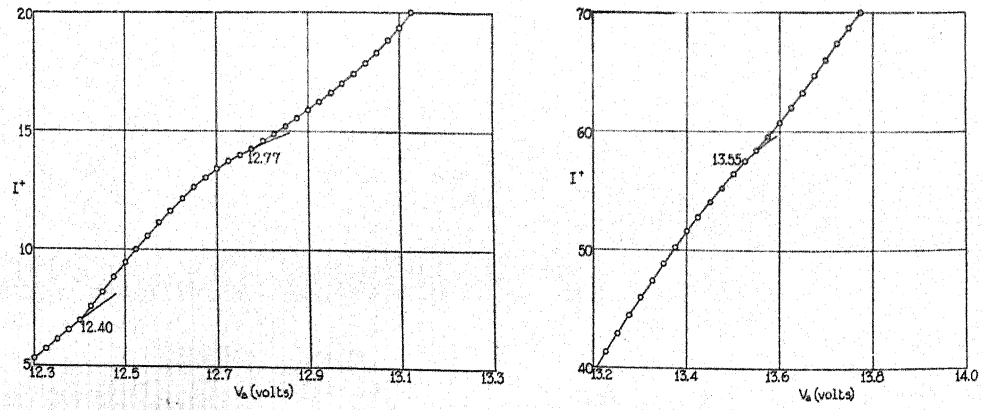

Figs. 7 and 8. The ionization of Hg vapor by electron impact from 12.3 to 13.8 volts. I^+ is proportional to the efficiency of ionization.

The holes S_2 and S_3 were about 0.18 cm in diameter, whereas S_4 and S_5 were 0.6 cm and 0.5 cm in diameter, respectively. The plates P_3 and P_4 were about 6 cm long and 3 cm wide. Plate P_4 was 0.5 cm below P_3 and was maintained 300 volts positive with respect to P_3. With the magnetic field, H, equal to 300 gauss, it is quite improbable that an electron will leave the trap, T, once it has entered, as both experiment and theory show.

Results

Fig. 2 shows the efficiency curve for the first 2 volts above the ionization potential. The ordinates are proportional to the efficiency of ionization. The curve indicates that the ionization does not rise sharply at the ionization potential, the rapid rise occurring almost a volt above this potential. Curves obtained with a poor velocity distribution did, however, show a more rapid rise at 10.40 volts.

Figs. 3–8 show the efficiency curve plotted on a large scale. (They are not all plotted to the same scale.) The accuracy with which the breaks could be reproduced is shown in Fig. 3 where two independent sets of data have been plotted.

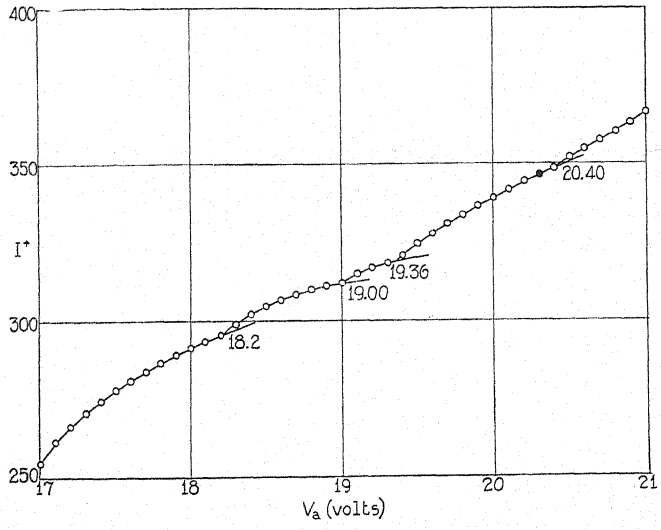

Fig. 9. The ionization of Hg vapor by electron impact from 17 to 21 volts. I^+ is proportional to the efficiency of ionization.

From 13.8 to 18 volts the curves were smooth and showed no obvious discontinuous changes in the slope. Fig. 9 shows the curve from 17 to 21 volts. The four breaks in this interval could be reproduced very accurately. Beyond 21 volts evidences of breaks were observed but the experimental errors in the measurements were greater than the deviations from a smooth curve, so that no satisfactory results were obtained although it is believed that several critical potentials do exist beyond 21 volts. However, at 29.5 volts a definite in-

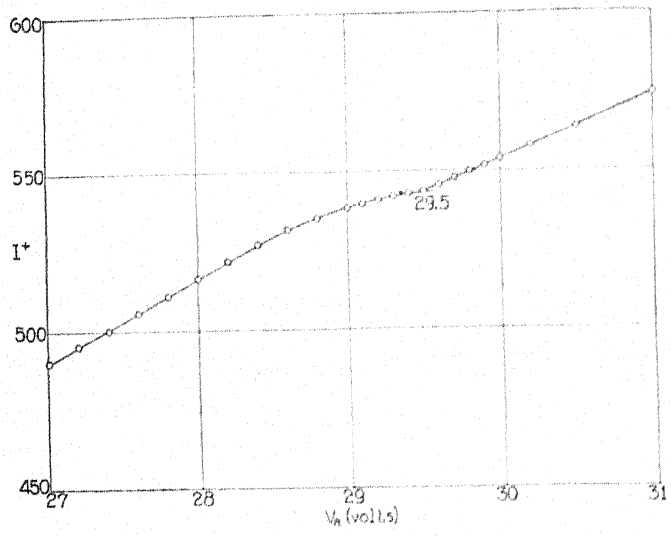

Fig. 10. The ionization of Hg vapor by electron impact from 27 to 31 volts. I^+ is proportional to the efficiency of ionization.

TABLE I. *The "ultra-ionization potentials" in Hg vapor.*

Lawrence	Hughes and Van Atta	Haupt*	Nielson and Potter	Author
10.40	10.40	10.40	10.40	10.40
10.60	10.62			10.60
			10.66	
				10.76
	10.88			10.88
			11.00	
				11.06
11.29				11.27
	11.40		11.41	11.40
				11.55
11.70			11.72	11.70
	11.77			11.78
				11.92
				12.00
12.06			12.06	12.06
	12.16			12.17
		12.30		12.28
			12.40	12.40
		12.45		
	12.76		12.80	12.77
		12.85		
		13.20	13.25	
				13.55
				18.20
				19.36
				20.40
				29.50

* Haupt reports that he also observed those found by Lawrence.

crease was always observed, which may be attributed to the formation of Hg^{++}. Fig. 10 shows a typical set of data in this region.

A list of the critical potentials reported by the various investigators, together with those found by the writer, is given in Table I. The values given in the same row were assumed to correspond to the same critical potential. The agreement is in general very good.

An "ultra-ionization potential" at 11.06 volts has not been previously reported, but as Fig. 3 shows, it apparently represents the minimum energy necessary for some quite efficient mode of ionization. It is of interest to note that in a study of the electron energy losses in mercury vapor, Castle W. Foard[9] found a pronounced peak which corresponded to a loss of 11.07 volts of energy. He was unable to account for this loss on spectroscopic grounds. This loss of energy can probably be associated with the ultra-ionization potential at 11.06 volts if we assume that ionization can result as a consequence of the simultaneous excitation of the two valence electrons. This would require a quantized energy loss.

The measurements of the positive ion current were made with a Compton electrometer having a sensitivity of about 3700 mm per volt. The electron current used in obtaining the data for the curves shown in Figs. 3–10 was about 5×10^{-8} amperes and for some of the work was measured with a galvanometer having a sensitivity of 2.70×10^{-11} amperes per mm deflection by employing a suitable balancing-out arrangement. With this sensitive measuring device, very small variations in the electron current could be detected. A very careful study showed that there was no correlation between any observed deviations in the electron current and the observed critical potentials.

TABLE II. *Efficiency of ionization, ϵ expresses as number of positive charges per electron per cm path per mm pressure at 0°C for various electron velocities.*

V_a (volts)	ϵ	V_a	ϵ	V_a	ϵ	V_a	ϵ
15	3.43	75	19.33	175	17.55	475	11.45
20	8.14	80	19.38	200	16.90	500	11.05
25	11.51	85	19.40	225	16.30	525	10.70
30	13.68	90	19.38	250	15.70	550	10.45
35	15.37	95	19.32	275	15.15	575	10.15
40	16.42	100	19.25	300	14.60	600	9.88
45	17.38	105	19.17	325	14.10	625	9.63
50	17.90	110	19.07	350	13.55	650	9.36
55	18.51	120	18.83	375	13.05	675	9.12
60	18.85	130	18.64	400	12.55	700	8.90
65	19.05	140	18.40	425	12.15	725	8.70
70	19.25	150	18.15	450	11.77	750	8.55

The pressure used ranged between 3×10^{-5} and 1.85×10^{-4} mm mercury. The data shown in Fig. 11 and in Table II were taken with a pressure of 8×10^{-5} mm of mercury and agrees very closely with data taken at different pressures. The ordinates represent the total number of positive charges per electron per cm path reduced to a pressure of 1 mm of Hg at 0°C. The posi-

[9] C. W. Foard, Phys. Rev. **35**, 1187 (1930).

tive ion current for these data was measured with a galvanometer having a sensitivity of 2.70×10^{-11} amperes per mm deflection. The electron current used was about 6×10^{-7} and was measured with a galvanometer having a sensitivity of 8.00×10^{-10} amperes per mm deflection.

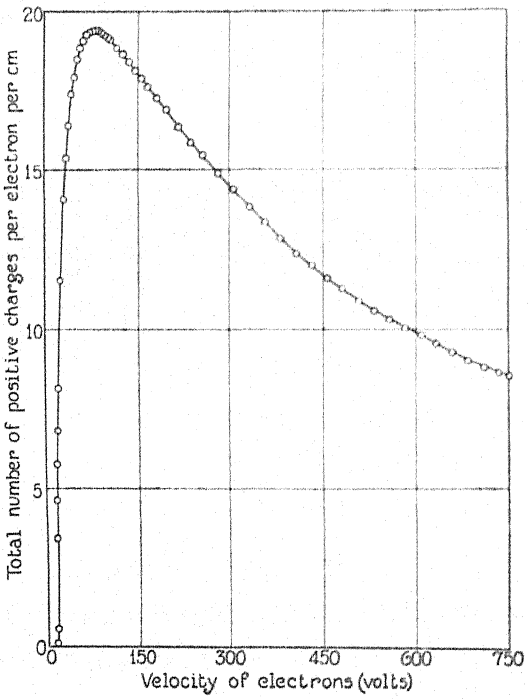

Fig. 11. The total number of positive charges per electron per cm path at 1 mm pressure and 0°C plotted as a function of the velocity of the impacting electrons in volts.

Discussion

It is very difficult to reconcile the values for the efficiency of ionization of mercury vapor given here with those obtained by Bleakney and by Jones, both of whom employed the same method. The present work was carried out with a better vacuum and a very careful study of all of the characteristics of the apparatus failed to reveal any objectionable features in the apparatus, method, or procedure. It is interesting to note that the copper apparatus, used in the study of helium, neon and argon, gave essentially the same values for Hg vapor as those given here.

The author takes this opportunity to acknowledge the constant interest and many suggestions of Professor John T. Tate.

OSCILLATIONS IN THE GLOW DISCHARGE IN ARGON

By Gerald W. Fox
Department of Physics, Iowa State College

(Received February 16, 1931)

Abstract

Report is made of radio frequency oscillations observed in argon glow discharges. The frequencies lie in the range of 10^4 cycles/sec to 10^5 cycles/sec in approximate harmonic relations. They are very sensitive to pressure changes but appear to bear no relation to the tube current. The peculiar action of a magnetic field on the oscillations is described. Some frequency calculations are made on the assumption that the potential distribution throughout the Faraday dark space can be represented by a parabola.

SOME time ago the writer[1] described experiments with oscillations observed in hot cathode glow discharges in neon. The present paper deals with a continuation of the same type of work in argon. The same discharge tube was used except that direct current was employed on the heater coil, since it was found that the a.c. introduced an extraneous sixty-cycle modulation. The argon was purified by a lengthy exposure to the action of a mischmetal arc. The experimental procedure was in all respects like that previously described.

Characteristics of the Discharge

The discharge in argon was steadier than in neon. The color appeared very nearly white to the eye but the brightness of the discharge for a given power input was not nearly so pronounced as in neon, while the heating was much greater. In neon, a current of 20 amperes could be run for a short interval and 10 amperes was possible continuously, with ordinary fan and water cooling. With argon, however, a current of two amperes caused the heavy copper anode to glow red in less than a minute and for this reason no observations were possible with currents larger than four amperes.

The pressure range over which oscillations were observed was quite narrow, the limits being approximately 0.2 mm Hg to 1.0 mm Hg. It was impossible to obtain oscillations for random current values in this pressure range. Oscillations were present only for particular values of current and pressure and when observed their frequency appeared to be independent of the tube current. As in the case of neon the discharge must be steady to exhibit oscillations. The slightest flickerings on anode or cathode produce enormous irregularities which are detected as "static" noises in the pick-up circuit. If one starts in at low pressure values a discharge may be maintained in argon at as low as 0.001 mm Hg but as listened to it is very noisy and the glow is feeble. With increasing pressure no noticeable change occurs in tube current,

[1] Fox, Phys. Rev. 35, 1066 (1930).

tube voltage, or glow until a pressure of about 0.1 mm Hg is reached, when the light from the tube suddenly increases many times and the discharge becomes noiseless except for a slight hiss. Tuning through the frequency range then shows the presence of oscillations which seem to start simultaneously with the increase of light from the tube.

The maintaining voltage for the argon discharge averaged about 255 volts which is approximately 75 volts higher than the maintaining voltage for neon.

As in the case of neon the interesting flashes described by Whiddington[2] and Aston and Kikuchi[3] were generally present.

Results

1. Frequencies present at a given pressure.

Tables I and II show typical data on frequencies present in the discharge. As in the case of neon these frequencies seem to be harmonics of one particular frequency though this could not be observed due to the limited tuning range. In no instance was a complete series of harmonics observed nor was there exhibited any preference for particular omissions.

Table I. *Frequencies present in glow discharge in argon.*

(Tube current 2.6 amperes, tube voltage 255 volts, gas pressure 0.77 mm Hg).

Wave-length (meters obs.)	Frequency (cycles/sec calc.)	Order
23,200	12,930	2
15,600	19,230	3
11,400	26,320	4
5,830	51,500	8
5,200	57,700	9
4,620	65,000	10
4,215	71,200	11
2,890	103,700	16
2,390	125,600	19
1,640	182,900	28

Table II. *Frequencies present in glow discharge in argon.*

(Tube current 1 ampere, tube voltage 254 volts, gas pressure 0.68 mm Hg).

Wave-length (meters obs.)	Frequency (cycles/sec calc.)	Order
20,980	14,340	2
14,000	21,430	3
10,460	28,670	4
5,930	50,700	7
4,650	64,500	9
3,725	80,700	11
3,215	93,400	13
2,775	108,300	15
2,625	114,300	16
2,460	122,000	17
2,220	135,100	19
1,980	151,500	21
1,915	156,500	22

[2] Whiddington, Engineering 120, 20 (1925).

[3] Aston and Kikuchi, Proc. Roy. Soc. A98, 50 (1920).

2. Variation of oscillation frequency with pressure.

In the argon discharge, the frequency range covered was not as wide for a given pressure difference as in neon. A noticeable peculiarity was that the discharge frequency changed almost linearly with the pressure down to a certain critical value when no further change could be produced, the frequency remaining constant but becoming weaker until, on further pressure reduction, it broke completely. (Fig. 1.)

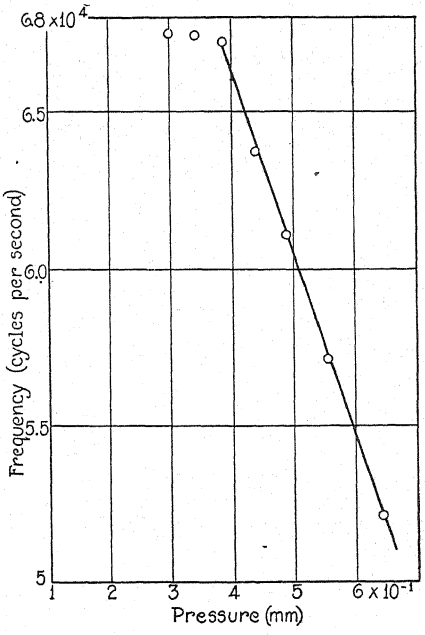

Fig. 1. Variation of oscillation frequency with pressure.

3. Relation of frequency to tube current.

It was not possible to show any frequency dependence on tube current such as appeared in neon. Having set on a particular frequency, this frequency persisted within a few cycles of the same value while the current was changed as much as an ampere when the oscillation would stop suddenly, to start again when the current was returned to its former original value.

4. Effect of a magnetic field on oscillations.

Some peculiar effects were noticed when a magnetic field was placed at right angles to the discharge. When a horseshoe magnet was moved from the anode end of the discharge toward the cathode, the frequency of the beat note in the telephone receiver fluctuated periodically from zero to a maximum, while moving the length of the positive column as shown in Fig. 2. On coming to the Faraday dark space, the regular oscillations disappeared altogether and the discharge became very noisy. Upon the removal of the magnet, however,

the discharge became quiet again and the oscillations reappeared after a time of the order of thirty seconds. This observation was made repeatedly.

Discussion

From the work of Compton, Turner, and McCurdy[4] we have a fairly good picture of the potential distribution throughout the glow discharge. They have shown the existence of a potential minimum in the Faraday dark space, especially in cases of large ionization. In the discharges in both argon and neon, the tube currents were of the order of several amperes so that we may expect a large concentration of positive ions in the negative glow, for the ionization processes going on are more effective than the needs of the circuit as a whole demand. Positive ions from the cathode end of the positive column and from the negative glow, will both be accelerated into this region of minimum potential. This accelerating field is really necessary to prevent the ac-

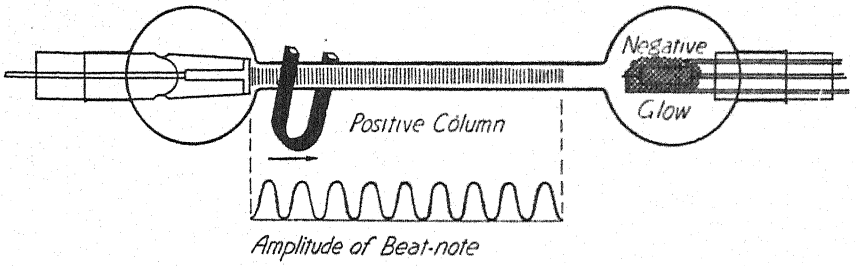

Fig. 2. As the magnet is moved along the positive column the sound in the telephone receiver fluctuates regularly in intensity.

cumulation of a negative space charge here by diffusion of electrons from the negative glow. The positive ions from the positive column and probably also those from the negative glow approach the potential minimum with terminal velocities attained in the fields through which they have travelled and, since these fields are rather weak, their velocities will be small. Thus some ions will be trapped for a time and we may imagine them oscillating about the potential minimum until they acquire sufficient energy to get over the hump on the cathode side. An ion's escape probably comes suddenly after a collision with a molecule or another ion which provides a suitable energy transfer.

The action of the magnetic field in the Faraday dark space lends some support to this idea of the origin of the oscillations. When the field is applied here, the additional magnetic force to which the ions are subjected, upsets the regularity in their motion and brings about the noise that is heard in the pick-up circuit. The high-frequency oscillatory component of the tube current is really very small. It is merely superimposed upon the main steady current through the tube. The fact that the frequency increases with decreasing pressure seems reasonable for we can imagine fewer collisions taking place to slow the ion down while it remains in motion about the potential minimum.

[4] Compton, Turner, and McCurdy, Phys. Rev. **24**, 597 (1924).

The action of the magnetic field throughout the positive column makes one think of the presence of standing waves. It seems possible that electric sound waves of the type mentioned by Tonks and Langmuir[5] may be present, since the observed frequencies fall within the range of their calculations. The flashes, observed by Whiddington,[2] which travel from anode toward cathode, and which are of low frequency and can be observed with a rotating mirror, can be explained by assuming the presence periodically of a large anode drop which produces excess ionization in the anode sheath. This excess of positive ions would travel toward the cathode, modifying the potential distribution as they go and causing local ionization and excitation. This would appear as a travelling striation.

Simple Theory of Oscillation in the Glow Discharge

If one assumes as a first approximation that the curve representing the potential distribution throughout the Faraday dark space is a parabola, it is not difficult to arrive at an expression for the frequency of the oscillation which gives a value which is of the observed order of magnitude.

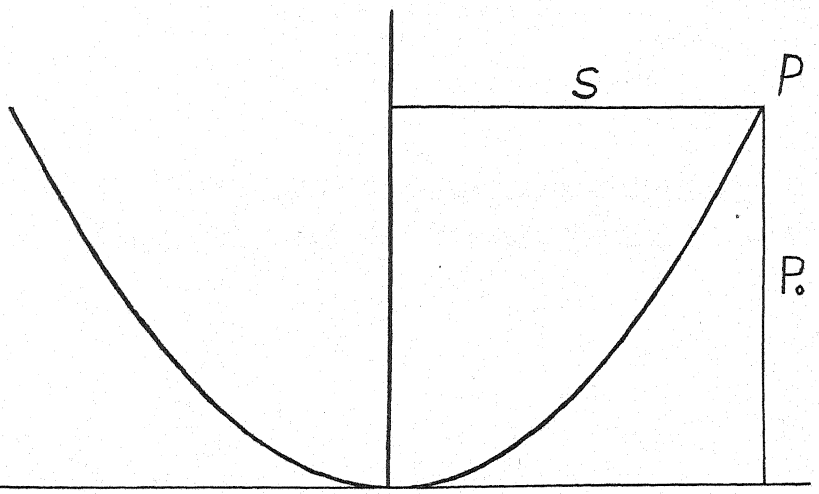

Fig. 3.

Let P represent the potential according to the equation $P=4ax^2$. Then since

$$\frac{m}{2}\left(\frac{dx}{dt}\right)^2+4aex^2=W,\quad \frac{d^2x}{dt^2}+\frac{8ae}{m}x=0.$$

The solution to this equation gives

$$x=C\cos(8ae/m)^{1/2}t+D\sin(8ae/m)^{1/2}t$$

in which it is seen that x repeats itself at intervals of 2π in the time $(8ae/\mathrm{m})^{1/2}t$ The period of a complete vibration is $2\pi(m/8ae)^{1/2}$ and the frequency is the

[5] Tonks and Langmuir, Phys. Rev. **33**, 195 (1929).

reciprocal. The quantity a can be determined from estimates of dimensions of the Faraday dark space in the discharge. Thus assuming the dark space to be 4 cm wide and 20 volts deep, which is not unreasonable, we can write $P_0=4ax^2$, $a=P_0/4x^2$, or $a=10^{-3}$ esu/cm^2 approximately. Taking e/m for hydrogen as 3×10^{14} esu/gram and 40 as the atomic weight of argon, the calculated frequency is 4×10^4 cycles per second. This is of the observed order of magnitude. The frequency appears to be quite dependent on the ratio of the width of the pit to its depth in volts. On the other hand, the frequency, is not very dependent on the type of ion in the discharge. The e/m for argon is of the same order of magnitude as e/m for neon. As mentioned before, the observed oscillations for both gases occurred in the same range.

The presence of a series of harmonic frequencies indicates that the potential distribution is not so simple a function as has been assumed. We do not know the actual potential distribution throughout the Faraday dark space, but since a slight distortion of our assumed distribution would allow the presence of harmonics, their presence can thus be accounted for.

In conclusion, the writer wishes to thank Professor H. M. Randall, director of the Physics Laboratory of the University of Michigan, for extending the privileges of the laboratory, where the experimental work was done.

THE RELATIVE INTENSITIES OF MERCURY LINES UNDER DIFFERENT CONDITIONS OF EXCITATION

By Marcel J. E. Golay
University of Chicago

(Received December 15, 1930)

Abstract

The relative intensities of the lines of the $2s-2p_i$ triplet have been measured by a photographic method with a calibrated tungsten lamp as a standard of comparison. The intensity ratios have been found to vary with conditions of excitation due to the absorption of the 5461 and 4047 lines by atoms in the metastable states $2p_1$ and $2p_3$. About three-quarters of the 5461 radiation and about one-third of the 4047 radiation were absorbed in a commercial mercury-filled tube with three electrodes when a high plate current was passed through the tube. A lesser absorption was found when an ordinary arc was used and when small plate currents were passed in the three-electrode tube. A tube specially built to excite mercury by electronic bombardment and provided with means for controlling the mercury pressure gave uniform results under various conditions of mercury pressure and plate current, and the double ratio of 8.5:3.3:1 was found for the intensities divided by the fourth powers of the corresponding frequencies. The ratio of 4078:4047 was found to vary with plate voltage in a manner similar to the variation of efficiency of ionization with electron velocity. It was attributed to the presence of two mechanisms of emission giving widely different intensity ratios, namely, excitation of the neutral atom to a higher energy level, and recombination of the ionized atom. A roughly quantitative survey of the intensities of the excitation and of the recombination spectra indicated that in comparison with atoms excited to a higher level by electronic impact as occurs in the arc, recombined atoms will prefer the singlet to the triplet system, while within each system their order of preference is P, S, D, and p, s, d, respectively. Also, within each state, a level at about the height of the $4S$ level is preferred to the others.

General

THE purpose of the research reported here was primarily the study of the $2s-2p_i$[1] triplet. The intercombination line $2S-2p_2$ of wave-length 4078 was also included in this study because of the work of Houston,[2] who treats the lines $2S-2P$, $2S-2p_2$, $2s-2P$ and $2s-2p_i$ (i=1, 2, 3) as a whole. According to this author the ratio 5:3:1 must be found for

$$\frac{A(5461)}{N_3}:\frac{A(4358)}{N_3}+\frac{A(4078)}{N_1}:\frac{A(4047)}{N_3},$$

where A designates the intensity divided by the fourth power of the frequency and N the number of atoms in the respective initial states. The quantities written above are proportional to the squared amplitudes of the corresponding lines, and it is for these squared amplitudes that the "sum-rule" must hold.

[1] Notation of Paschen.
[2] W. V. Houston, Phys. Rev. **33**, p. 297 (1929).

The squared amplitudes of the individual lines can also be determined from the formulas given by Houston. They give approximately the ratio 5:2.9:1 for the relative intensities of the triplet lines, divided by the fourth powers of the corresponding frequencies. They also give the ratio of 0.1:1 for the lines 4078 and 4047. This signifies that for an equal population of their respective initial levels, line 4078 will have approximately one-tenth the intensity of line 4047, the relative intensities of these two lines giving thus a basis for a computation of the relative population of their respective initial levels.

Method of Intensity Measurements

When two lines are but a few angstroms apart in wave-length, their relative intensities may in principle be measured by weakening one line by a known amount until it has the same intensity as the other, that is, until the blackening of the photographic plate is the same for the two lines. Usually both lines are weakened by a series of absorbing screens, and their relative intensities are obtained through some process of interpolation which affords at the same time a number of results, which must verify each other, when the image of the weaker line through the clearer weakeners is comparable in intensity to the image of the stronger one through the more opaque portions.

When the lines to be compared are sufficiently separated to warrant a determination of the sensitivity of the emulsion for the corresponding wave-lengths, a source of known spectral distribution such as a black body or an incandescent filament of known temperature and emissivity is used for this purpose. Each line is then compared with the continuous radiation of the same wave-length. This can of course be done as before, by means of weakeners, calibrated for each of the different wave-lengths of the group under study.

Their use, however, can be avoided very simply by using the standard of comparison to put on the plate a series of intensity marks of known relative intensities. As the standard of comparison emits a continuous spectrum, the gradation of intensities can be obtained by varying the width of the slit, and if a lens is used to focus on the slit an image of the tungsten ribbon of the lamp used as a standard, one can also place diaphragms of known geometrical transmission in front of the lens.

A lower limit for the slit-width is set by the accuracy with which this width can be measured, and by the size of the diffraction pattern formed on the prism. It is desirable that the main fringe and at least one or two lateral fringes appear on the prism when sighting it from the camera side of the spectrograph, in order to avoid losing more than a few percent of the light. Conversely, the largest slit-width must not allow the integrated spectrum thus obtained to misrepresent the intensity of the source, and the sensitivity of the emulsion. According to Ornstein no errors due to the integration of the spectrum will be appreciable if the width of the slit corresponds to less than 60A on the plate for any of the wave-lengths studied.

The diaphragms placed in front of the lens must cover enough of the latter so that a full image of the uncovered portion can be seen on the prism from

the camera side, while if but little light is desired, these diaphragms must have holes not small enough to create on the slit a main fringe equal in width to the difference between the image of the filament and the opening of the slit.

When a set of intensity marks has been put on a plate it is necessary to take only one spectrogram of the source of light, taking care to use a rather wide slit, and to compare the lines with the comparison spectrum at the same wave-length. One can thus take many exposures on one plate, which is advantageous when studying the variations of relative intensity with certain conditions of experimentation. One obtains indeed but one figure for every exposure, while several are obtained when the source is photographed through a series of weakeners. If it is desired to obtain a few figures for every condition of light emission studied, one has to take as many exposures, preferably using various diaphragms in front of the lens projecting an image of the source on the slit.

In the work reported here, care was taken that light from all sources photographed followed the same optical path. As an added precaution it was

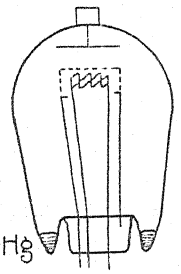

Fig. 1. Diagram of mercury-filled tube.

also verified that the transmission of the whole optical system was sensibly the same along the optical axis and away from this axis.

As sources of known radiation incandescent lamps with a flat tungsten ribbon were used and their temperatures determined photographically by comparison with a standard of known temperature and emissivity, supplied to Ryerson Laboratory by Dr. Forsythe of Nela Park. The secondary standards were generally operated at 2780 to 2800°K, and the time of exposure was the same for the standard and for the spectrum studied, to avoid errors due to a difference in Schwarzchild's constant for different wave-lengths. The radiation emitted by the standard lamp was calculated from the black body radiation formula. Corrections for the emissivity of tungsten at 2800°K at various wave-lengths were introduced. Corrections were also introduced for the dispersion of the spectrograph and for a difference in broadness of the lines due to different distances of the plate from the camera lens.

Sources of Light and Results, $2s-2p_i$ Triplet

Some preliminary measurements were carried out, with a home-made arc, a Cooper-Hewitt arc, and a mercury-filled tube, obligingly furnished by the Bell Telephone Laboratories. Fig. 1 shows a schematic drawing of this tube.

The spectrum of the ordinary arc was photographed at various time intervals, beginning at the moment the arc was started, and continuing until the steady state was attained. It was then observed that the ratio of 5461:4047 increased from about 4 to about 7, while the ratio of 4358:4047 decreased from about 5 to about 3. Similar results were obtained for the Cooper-Hewitt arc. Table I shows a set of results obtained similarly for the tube furnished by the Bell Telephone Laboratories, by observing the white streaks emerging from the grid at a potential just sufficient to maintain an arc.

TABLE I *I/ν^4 values for lines from tube shown in Fig 1.*

Condition of tube	5461:4047[3]	4358:4047
First exposure, tube cold	5.1	3.7
	5.6	3.7
	5.8	3.8
	6.8	3.6
	7.4	3.5
	7.3	3.4
Last exposure, tube hot	7.4	3.4

The results to be discussed later suggest the following explanation of these figures. It will be shown that the true intensity ratio is about 8.5:3.3:1. The lines 5461 and 4047 are, however, absorbed by the atoms in the metastable states $2p_1$ and $2p_3$. As the line 4358 terminates on the level $2p_2$ where the strong resonance line 2537 originates, it seems plausible to assume that the population of the $2p_2$ level is not large enough to cause any appreciable absorption of the line 4358. The population of the metastable states is roughly proportional to the ratio of the rate at which these states are reached by the excited atoms, to the rate at which they leave them owing to collisions of the second kind. The rate at which atoms are sent into metastable states is roughly proportional to the current, while the rate at which they leave them increases with the number of collisions per unit time; this number increases about linearly with the temperature, and the density, this latter quantity rising rapidly with the temperature. It can therefore be expected that at a low pressure, the ratio of 5461:4047 will be considerably reduced, line 5461 being much more absorbed than line 4047 on account of the greater population of the state $2p_1$, while the ratio of 4358:4047 will be found somewhat too high on account of the absorption of line 4047. As the temperature and the pressure increase these ratios will approach their true values, due to the diminished population of the metastable states, as can be verified in the above table.

The following tables show a typical set of results susceptible of similar interpretation. The temperature of the tube was kept approximately constant during the observation. The time of exposure for the spectrum and for the standard light was the same for each plate. Diaphragms were placed in front of the condensing lens to reduce the very different intensities photographed to approximately the same level of blackness on the plate.

[3] All ratios given in this article refer to the intensities divided by the fourth powers of the frequencies.

TABLE II. *I/ν^4 ratios for constant tube temperature but varying plate current.*
(Observation of light emitted between grid and plate)

Plate current	5461:4047	4358:4047
1.0 amp.	3.2	
1.0	3.6	4.9
0.27	5.9	4.4
0.27	5.0	4.3
0.0075	8.1	4.0
0.0065	7.9	3.9
0.0055	8.3	3.9
0.004	9.0	3.7

The explanation of these results is obvious. A higher plate current increases the rate at which atoms are thrown into metastable states, and higher absorption of line 4047, and especially of line 5461, results therefrom.

From the foregoing it appears that the Hg density affects the results in a two-fold manner. A direct effect of higher density would be a more rapid elimination of the metastable states, thus reducing the effect of absorption in the intensity ratios. This first effect would be masked, however, by the more complicated and more intense phenomena accompanying high pressures.

Determination of the true intensity ratios of the triplet. The facts mentioned above were not apparent at the time these experiments were carried out, for it was expected that the ratio 5:3:1 would be found for the relative intensities of the triplet divided by the fourth powers of the frequencies, and ratios higher than 5 for lines 5461 and 4047 could not be explained by an absorption of line 5461. At the same time it was obvious that the absorption of line 4047 was much less than the absorption of line 5461, for the population of the $2p_1$ state is much larger than the population of the $2p_3$ state, and this theoretical prediction was confirmed by the comparatively smaller variations of the ratio of 4358:4047. Also, the glass of the three-electrode tube used was not very clear, and had a larger transmission for the 5461 line than for the other lines of the triplet.

A tube was then built, with means for controlling the Hg pressure, and with a quartz window for the eventual study of the ultraviolet lines.

This tube is shown in Fig. 2. Electronic emission was provided by a tungsten filament. The leads into the tube were tungsten rods, while the other metallic portions were of nickel. A plate, P, with a rectangular hole cut to correspond to the opening, A, of the cage was inserted as shown in the figure, to prevent the white light of the filament from reaching the slit of the spectrograph. A number of spectra were taken with the end, B, of the cage open, so that a considerable amount of light due to the blue glow filling the tube contributed to the radiations photographed. Any amount of shielding in the far end of the tube failed to eliminate this glow. As it was thought that this glow was due to a somewhat different mode of excitation from that which produced the light in the cage by electrons of a definite velocity, the far end of the cage was subsequently closed, as shown in the figure. This was done by means of a little strip of platinum, blackened in the flame of a match. A

small strip of nickel, C, was welded over the far end of the grid to prevent a direct illumination of this end wall by the filament. At the time this change was effected, the nickel grid of rather coarse mesh, hitherto used, was replaced by a nickel grid of the finest mesh obtainable. This was done for the purpose of obtaining a more uniform flow of electrons in the cage, and surprisingly enough this new grid stood higher currents than the coarse one formerly used, without showing any trace of deterioration. In spite of the electrical screening provided by the shield, S, and the front plate, P, the space, F, in the front end of the tube was filled with a weak glow, the part of this glow in the prolongation of the cage contributing, therefore, to the light photographed.

The Hg pressure in the tube was indirectly controlled by placing the Hg trap in a beaker of water of a certain temperature.

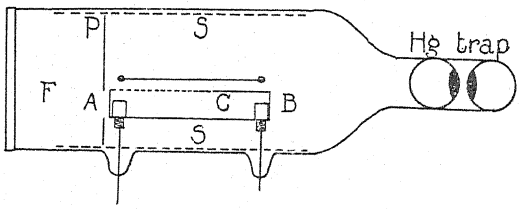

Fig. 2. Diagram of apparatus.

A thorough baking out of the tube was found necessary to avoid nitrogen and carbon monoxide bands. This was done by wrapping asbestos around the tube and letting a plate current of 0.8 to 1 amp. flow under a potential of about 200 volts for a few hours. Even though the CO bands were observable at the end of this period, they would quickly disappear after the asbestos had been removed and the tube brought to its normal running temperature.

A few refinements were introduced in the method of intensity measurements. They are outlined below.

A little strip of gray glass was placed in the camera on the path of line 4358, in order to bring this line to the same blackness level as lines 4047 and 5461. As this line and the standard radiation for its measurement were both modified in the same manner, no change was called for in the method of measurement. While more accurate, the results thus obtained for the 4358:4047 ratios agreed well with a number of results obtained before this precaution was taken. About 40 exposures were taken on each plate, a little less than half this number being assigned to the intensity marks. Two was chosen for the ratio of the geometric progression of intensities, and two or three exposures were taken for each intensity, the slit width and the number of holes used in the diaphragm being both varied so as to check the method used, and to reduce chance errors due to setting and variations in the emulsion. (The different measurements of blackness for marks of the same theoretical intensity proved to be closely grouped in the great majority of cases.) Also, each condition of plate current and plate voltage studied was photographed two

or three times, as the light intensity permitted, using the diaphragm with maximum openings, and others of one-half and one-quarter the area of the first. As a last precaution, all plates were wiped continuously while in the developer, to insure uniformity of development.

Two current values, 0.3 and 0.6 amp. were used under various voltages to bring out any systematic dependence of the intensity ratios observed upon the plate current, as well as to bring out any voltage dependence for any one fixed current, especially with reference to the 4078:4047 ratio.

The narrow range of Hg temperature explored (limited for the high temperature by the coolest point of the tube to avoid condensation in this point, and for the low temperature by the light intensity fit for convenient exposures) was considered wide enough to detect any dependency upon pressure on account of the comparatively large range of pressures corresponding to these temperatures.

No dependence upon plate current, plate voltage and Hg pressure was found for the relative intensities of the triplet, while the ratio of 4078:4047 showed a marked dependency upon plate voltage.

The averages obtained for the triplet are given in Table III.

TABLE III. *I/ν^4 values for triplet lines obtained with tube shown in Fig. 2.*

Plate No.	Temp. of Hg	4358:4047	5461:4047
14	100°C	3.3	8.3
22	0	3.0	8.5
23	22	3.3	8.5
"	60	3.4	
25	20	3.2	7.8
29	20	3.2	8.8
"	40	3.3	7.9
30	40	3.4	7.9
31	22		9.2
34	23		8.8
35	41.5	3.3	8.6
36	25		9.5
37	24		8.5
		Average 3.3	8.5

The experimental error attached to the average given for the ratio of 5461:4047 is probably larger than for the other one, but should not exceed 10 percent, assuming, however, that the temperature of the lamp used as standard is correct.

RATIO OF 4078:4047 AND GENERAL STUDY OF THE ELECTRONIC BOMBARDMENT EMISSION

As mentioned above, the ratio of 4078:4047 varies with plate voltage. This is shown in Fig. 3, where this ratio has been plotted as a function of the plate voltage from the data obtained from five plates. These curves point to a rapid rise to a maximum, reached at about 100 volts, and then a slow downward trend.

The existence of a variation in relative intensity of two lines makes it necessary to assume the operation of at least two different mechanisms—if there were only one, the absolute intensity might vary, but not the relative. Each of these mechanisms will presumably be operative in producing both lines, but with a different ratio of intensities. The ratio measured will be some weighted average of the ratios which are characteristic of each of these mechanisms.

This variation with voltage is strikingly similar to the variation of the efficiency of ionization as found by a number of authors. For the purpose of comparison, the probability of ionization of mercury atoms by electrons has been plotted as the dotted curve. It was obtained from Bleakney's[4] data by adding the ordinates of his curves for the probability of single, double, and triple ionization. It also represents the variation in the intensity of the light due to atoms which have been ionized and recombined with electrons if it be

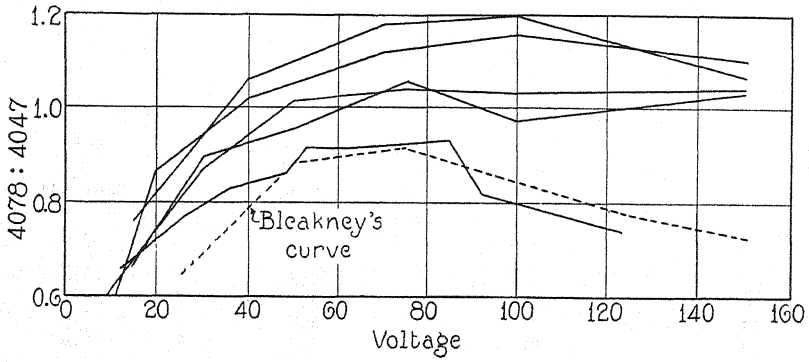

Fig. 3. Ratio 4078:4047 plotted as a function of the plate voltage from data obtained from five plates.

assumed that doubly and triply ionized atoms recapture successively, two and three free electrons respectively from the negative space charge inside the cage.

The parallelism of this curve with the ratio of 4078:4047 seems to suggest the following explanation. Atoms which have been previously ionized will emit a recombination spectrum with a comparatively larger ratio of 4078: 4047 than excited atoms, while the observed ratio will vary somewhat parallel to the amount of light emitted which is due to recombined atoms, if the number of excited atoms is assumed to have no variations, as marked as the one shown by Fig. 3, beyond the ionization potential. This explanation would be supported by the fact that many ionized Hg lines were quite conspicuous at the higher voltages used (40 volts and above), while the presence in the cage of slow secondary electrons made conditions favorable for the recombination of Hg ions.

If the large differences found between the intensity distributions in an

[4] Bleakney, Phys. Rev. **33**, 139 (1930).

ordinary arc and in an electronic bombardment spectrum were attributed to the presence in the latter of a recombination spectrum certain consequence would follow which are brought out by Table IV. This table has been prepared from a table giving the intensities of the lines in an electronic bombardment spectrum at 70 volts using the intensities of the lines of an arc spectrum as units. All the values obtained for lines originating at a certain level have been averaged, and these averages have been given in Table IV. This table therefore gives an estimate of the population of the various levels in an electronic bombardment spectrum in comparison with an arc spectrum. According to what has been said above Table IV would indicate that by comparison

TABLE IV. *Relative population of levels—electronic bombardment—spectrum vs. arc spectrum.*

Level	Relative Population	Level	Relative Population
$2S$	1.5	$2s$	0.15
$3S$	3.	$3s$	0.15
$4S$	11.	$4s$	0.8
$5S$	4.	$5s$	0.4
		$6s$	0.15
$4P$	55.		
$5P$	25.	$4p_1$	0.6
$6P$	2.	$5p_1$	1.4
$7P$	1.5	$6p_1$	0.6
$3D$	0.4	$3d_1$	0.14
$4D$	2.2	$4d_1$	0.15
$5D$	1.7		
$6D$	0.4	$3d_2$	0.16
$7D$	0.2	$4d_2$	0.3
$8D$		$5d_2$	0.8
		$3d_3$	0.2
		$4d_3$	0.1

with excited atoms, recombined atoms will occupy a much larger proportion of singlet terms, while within each system of terms the P-state (or the p-state), and within each state a level at about the height of the $4S$ level would be most favored in this new population distribution.

This explanation for the variation of the ratio of 4078:4047, and the consequences of this explanation, are given with much reserve, however, as it has been the conclusion reached by F. L. Mohler[5] and other authors that in a recombination spectrum the triplet terms are comparatively more populated than in an excitation spectrum.

The writer wishes to express his appreciation to Professors Monk and Eckart for the suggestion of the problem and assistance throughout the duration of the work.

[5] F. L. Mohler, Phys. Rev. Suppl. **1**, 221 (1929).

THE SPECIFIC HEAT OF METHANE

By P. C. Ludolph
Department of Physics, University of Illinois

(Received February 16, 1931)

Abstract

Two different forms have been suggested for the methane molecule by various authors. They are the symmetrical tetrahedron and the symmetrical pyramid. Calculations have been made for the values of the specific heat at constant volume for the two types of structure. It is found that neither type gives values in agreement with experiment. The curve obtained on the basis of a tetrahedral structure however gives much better agreement than the resulting curve for the pyramidal structure.

THE infrared absorption spectra of methane was investigated quite carefully by J. P. Cooley[1] several years ago. Dennison,[2] on the basis of Cooley's results and with certain other fundamental assumptions, was able to ascribe a symmetrical tetrahedral structure to the molecule.

J. Kunz[3] called attention to the fact that there was quite a difference between the specific heat of methane as calculated from this model and the experimental values.

V. Guillemin[4] has shown, however, that on the basis of certain definite assumptions as to the forces between the ions in the molecule, the potential energy for the symmetrical pyramidal configuration is smaller than the value obtained for the tetrahedral structure. Hence the pyramidal structure is more stable than the tetrahedral.

Numerous facts have been advanced by Glockler,[5] Henri,[6] and others supporting one or the other of the two alternative forms.

Each model yields fifteen degrees of freedom, three of translation, three of rotation, and nine of vibration. Moreover, each model gives four fundamental vibrational frequencies. Hence, giving to the translations and rotations their equipartition values, we obtain for the specific heat at constant volume

$$c_v = R\left(3 + \sum_{i=1}^{4} n_i \left(\frac{h\nu_i}{kT}\right)^2 \frac{e^{h\nu_i/kT}}{(e^{h\nu_i/kT} - 1)^2}\right)$$

where the n_i gives the number of degrees of freedom of the corresponding vibration frequency ν_i.

The values of ν_i and n_i are given below in Table I.

Table I. *Values of ν_i and n_i.*

ν_i	n_i	ν_i cm^{-1} Tetrahedral	ν_i cm^{-1} Pyramidal
ν_1	1	4217	7760
ν_2	2	1520	3150
ν_3	3	3014	6730
ν_4	3	1304	1990

[1] J. P. Cooley, Astrophys. Journal **62**, 73 (1925).
[2] D. M. Dennison, Astrophys. Journal **62**, 84 (1925).
[3] J. Kunz, Phys. Rev. **29**, 220 (1927).
[4] V. Guillemin, Ann. d Physik **386**, 81, 173 (1926).
[5] G. Glockler, Jour. Amer. Chem. Soc. **48**, 2021 (1926).
[6] V. Henri, Chem. Reviews **4**, 189 (1927).

Values of c_v have been calculated for temperatures ranging from 273°K to 873°K. The results together with the experimental[7] values are given below in Table II.

TABLE II. *Specific heats, experimental and calculated.*

Temp.	c_v Experimental	c_v Tetrahedral	c_v Pyramidal
273°K	6.656	6.311	5.982
373	8.738	7.188	
473	10.577	8.342	
573	12.419	9.620	7.081
673	14.288	10.855	
773	16.015	12.039	
873	17.883	13.151	9.011

The curves, Fig. 1, show the variation of c_v with temperature. The one marked A corresponds to the experimental values while B and C give the relation for the tetrahedral and pyramidal structures respectively. A and B are essentially linear while C is decidedly convex to the axis. The calculated values of c_v for the tetrahedral model agree much better with the experimental values than the values calculated from the pyramidal model.

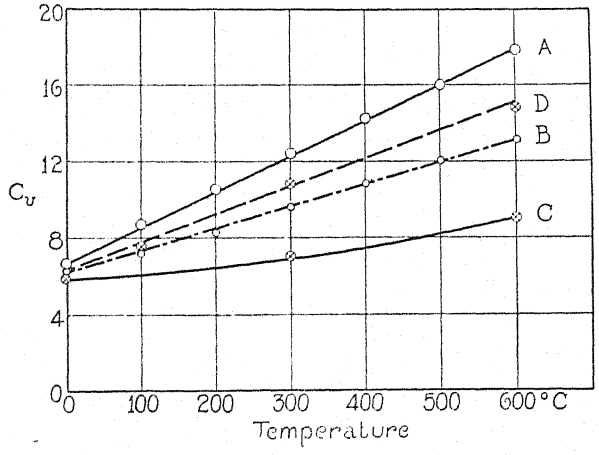

Fig. 1. Variation of c_v with temperature.

If the degrees of freedom of the vibrators with frequencies ν_3 and ν_1 are interchanged, then one obtains the curve D in place of B. These values of c_v are the maximum possible values using the frequencies given in Table I.

Undoubtedly some of the discrepancy (especially at the higher temperatures) is due to the centrifugal stretching of the molecule. This effect is not sufficient, however, to account for all the difference between the experimental and the calculated values.

It is a pleasure to thank Professor Kunz for his suggestions in regard to this work.

[7] H. B. Dixon, Proc. Roy. Soc. of London 100A, 24, 1921–22.

THE EQUATION OF STATE OF HELIUM*

By John G. Kirkwood and Frederick G. Keyes
Research Laboratory of Physical Chemistry,
Massachusetts Institute of Technology

(Received February 24, 1931)

Abstract

A brief review of the statistical theory of the equation of state is presented. Upon the basis of a recent quantum mechanical calculation of the interatomic energy, the second virial coefficient of helium has been calculated. With the use of the theoretically determined virial coefficient some properties of helium have been computed. A detailed comparison with experimental data is given.

Introduction

THE past several years have seen a great advance in our understanding of intermolecular forces. The work of Heitler and London on the resonance interaction of two hydrogen atoms suggested the nature of the repulsive force operating at small intermolecular distances to determine the effective molecular cross-section. More recently the work of Eisenschitz and London followed by that of other investigators has permitted a calculation of the polarization force, operating at larger intermolecular distances to produce the van der Waals' attraction. However the theory has so far been subjected to no critical comparison with experiment. It is the object of the present paper to make such a comparison in the case of helium, the only gas for which a fairly accurate calculation of the intermolecular energy has been carried out.

Theory of the Equation of State

Many empirical equations of state have been suggested for gases. All of them, however, may be expanded in the familiar virial form

$$\frac{pV}{RT} = 1 + \frac{B}{V} + \frac{C}{V^2} + \cdots \qquad (1)$$

where p is the pressure, V the volume of a gram-mol of gas, R the ideal gas constant, and T the absolute temperature. The coefficients, B, C, $\cdots$ are in general functions of the temperature.

Although a complete statistical theory of the equation of state has not been worked out in detail, it is possible under certain conditions to obtain a correlation between the second virial coefficient, B, and the intermolecular forces.

Above the critical temperature, it seems legitimate to assume that the fraction of the molecules in quantized collision states will be insignificant. Moreover, the Boltzmann distribution function may probably be regarded as

* Contribution No. 262.

valid for all gases until temperatures in the neighborhood of absolute zero are reached. Thus even in the case of hydrogen at a pressure of one atmosphere and a temperature of 2°K, both the Fermi-Dirac and the Bose-Einstein distribution functions give the same result as that of Boltzmann within a few percent insofar as the translational energy is concerned.[1] Subject to these limitations, it is possible to identify the sum of state with Gibbs' phase integral[2]

$$z = \int \cdots \int e^{-\bar{E}/kT} dq_1, \cdots dp_{3N} \tag{2}$$

where $\bar{E}$ is the total energy of a gas consisting of N molecules averaged over all internal coordinates and k is Boltzmann's constant. The integration is to be taken over all of the $6N$ dimensional momentum-configuration space available to the system. If the thermodynamic potential, ψ, (Helmholtz free energy function) is defined by the relation

$$\psi = E - TS$$

where S is the entropy, Gibbs has shown that

$$\psi = -kT \ln z \tag{3}$$

Moreover,

$$\left(\frac{\partial \psi}{\partial V}\right)_T = -p. \tag{4}$$

The integral (2) may be evaluated in simple form under certain conditions.[3] It is to be assumed that the density of the gas is low enough so that molecular configurations in which the fields of more than two molecules overlap, are sufficiently rare that they may be ignored. In the case of neutral gas molecules where the molecular forces are effective only at very short range, this condition is often fulfilled even at relatively high densities. Under these circumstances it is possible to write

$$z = f(T) \prod_{n=1}^{N} (V - 2nB) \tag{5}$$

where

$$B = \tfrac{1}{2} \int \int \int (1 - e^{-\bar{\epsilon}/kT}) dx dy dz.$$

Here $\bar{\epsilon}$ is the mutual potential energy of two molecules and the integration is to be taken over all values of their relative coordinates. From Eqs. (3), (4), and (5), after expansion of the logarithm in powers of B/V, it is found that

$$\frac{pV}{RT} = 1 + \frac{B}{V} + \frac{4B^2}{3V^2} + \cdots$$

[1] R. H. Fowler, Statistical Mechanics, p. 539 (1929).

[2] J. W. Gibbs, Elementary Principles in Statistical Mechanics (1902).

[3] F. G. Keyes, Chem. Rev. 4, 175 (1929). K. F. Herzfeld, Müller-Pouillets Lehrbuch der Physik, Vol. 3, Kinetische Theorie der Wärme, p. 167.

where the second term may be identified with that of the virial Eq. (1). If, as in the case of helium the molecules are spherically symmetrical

$$B = 2\pi N \int_0^\infty (1 - e^{-\epsilon(r)/kT}) r^2 dr \tag{6}$$

where r is the distance between the two molecules.

Perhaps the most well known of empirical equations of state is that of van der Waals:

$$p = \frac{RT}{V - b} - \frac{A}{V^2}.$$

It is of interest to see what form the intramolecular potential, ϵ, must assume to be consistent with it. The virial Eq. (1) may be transformed into van der Waals' equation if B/V is assumed to be very small relative to unity and

$$B = b - A/RT.$$

If the molecules are treated as rigid spheres of diameter, σ, it is obvious that when $r \leqq \sigma$, $\epsilon = \infty$, and formula (6) yields, after expansion of $e^{-\epsilon/kT}$;

$$B = b - A/RT$$

where

$$b = \frac{2\pi N\sigma^3}{3} = 4 \text{ (total volume of the molecules)}$$

and

$$A = A_0 + \sum_{n=1}^{\infty} A_n/(RT)^n; \; A_0 = -2\pi N^2 \int_\sigma^\infty \epsilon r^2 dr$$

$$A_n = -2\pi N^{n+2} \int_\sigma^\infty \epsilon^{n+1} r^2 dr.$$

It must be concluded, therefore, that the coefficient A appearing in van der Waals' equation is not a constant, but a slowly varying function of the temperature. This conclusion is born out by experiment in the region of low temperatures where the sum $\sum_{n=1}^{\infty} An/(RT)^n$ may no longer be neglected. Moreover, experiment at high temperatures, invalidates the assumption of rigid molecules. Thus, it is found that b is a slowly decreasing function of the temperature, a fact which can only be explained as due to an interpenetration of the molecules. Van der Waals' equation is therefore to be regarded as merely a first approximation even at small densities.[4]

The Molecular Field

Empirical information furnished by the equation of state suggests that the general character of the force between two molecules may be conveniently represented by means of two potentials, ϵ_r and ϵ_a. The potential ϵ_r, which predominates at small molecular separations, must ascend steeply with in-

[4] F. G. Keyes and R. S. Taylor, J. Am. Chem. Soc. 49, 896 (1927).

creasing slope as two molecules approach and diminish rapidly as they recede, thus giving rise to a strong repulsive force at small intermolecular distances. The potential, ϵ_a, nullified at small separations by ϵ_r, must fall off less rapidly with the distance, giving rise to an attractive force at larger intermolecular separations. Thus the total intermolecular potential, ϵ, might be written

$$\epsilon = \epsilon_r + \epsilon_a.$$

This representation is to be regarded as more or less schematic, since no sharply defined physical significance can be independently assigned to ϵ_r or ϵ_a. Still, it has the advantage of suggesting two different types of molecular interaction which we believe to be effective in determining the intermolecular energy.

According to present quantum mechanical ideas, the "repulsive" potential, ϵ_r, is to be regarded as arising from a resonance interaction between the molecules. A calculation of the resonance energy has so far been accomplished only for atomic hydrogen[5] and helium.[6] In the case of atomic hydrogen, the situation is complicated by the existence of two alternative modes of interaction, one of them giving rise to the repulsion of which we have spoken, and the other to valence union. Helium is, therefore, the only simple gas for which we have a knowledge of the repulsive field. Although a somewhat complicated function of the interatomic distance, the resonance energy in the range of importance in the thermal interaction of gas molecules may be adequately represented by the formula

$$\epsilon_r = \lambda e^{-cr}.$$

The "attractive" potential is to be regarded as arising from a mutual polarization of the molecules,[7] chiefly due to a rapidly pulsating field associated with the internal motion of the electrons in the molecule. The dominant term in this energy comes from the oscillating dipole. If terms from multipoles of higher order are ignored, the attractive potential has the form

$$\epsilon_a = -\frac{\beta}{r^6}.$$

A general scheme for the calculation of ϵ_a has been developed by London and Eisenschitz.[8] They have made an exact calculation of the mutual energy of two hydrogen atoms as well as rough estimates in the case of some other gases.

[5] Heitler and London, Zeits. f. Physik **44**, 455 (1927); Sugiura, Zeits. f. Physik. **45**, 484 (1927).

[6] Slater, Phys. Rev. **32**, 349 (1928).

[7] In 1920 Debye (Phys. Zeits. **21**, 178, 1920) suggested that the van der Waals attraction in gases had its origin in a mutual electrical polarization. Upon the basis of an electrostatic molecular model, he attempted to calculate the van der Waals A constant for several gases in terms of their electrostatic multipole moments. That his theory was not very successful from a quantitative standpoint, is readily understandable in view of the inadequacy of the molecular model employed.

[8] Eisenschitz and London, Zeits. f. Physik **60**, 491 (1930); London, Zeits. f. Physik **63**, 245 (1930).

[9] Slater and Kirkwood, Phys. Rev. **37**, 682 (1931).

A calculation of the mutual energy of two helium atoms by another method has been carried out by Slater and Kirkwood.[9] They obtain for the total intermolecular potential of helium:

$$\epsilon = \left\{ 7.7e^{-2.43r/a_0} - \frac{0.68}{(r/a_0)^6} \right\} 10^{-10} \text{ ergs} \tag{7}$$

where a_0 is the Bohr radius of the hydrogen atom. In this expression, terms arising from variable multipole moments of higher order than the dipole have been neglected. Moreover, an error of a few percent in the coefficient of the exponential term is not unlikely since an approximate wave function was employed in its calculation.

The Equation of State of Helium

With the expression for the intermolecular potential given by Eq. (7), we have computed the second virial coefficient of helium at several temperatures, by graphical integration of Eq. (6). The results are listed in Table I together

Table I. *Second virial coefficient of helium.*

T (°K)	B (theory) cc/mol	B (H and O) cc/mol
350	10.80	11.60
300	11.14	11.80
250	11.34	11.95
200	11.58	11.95
100	10.75	10.95
20	−6.94	−4.00

with experimental values of Holborn and Otto.[10] The theoretical values of the virial coefficient B have been plotted as a function of the reciprocal temperature in Fig. 1, and as a function of the temperature in Fig. 2. For comparison, the experimental results of a number of investigators have been included.[11,12] From Table I it may be seen that the computed values of the virial coefficient, while consistently lower than the experimental ones of Holborn and Otto, do not differ from them by more than five or six percent between 100°K and 400°K. Below 50°K, the agreement between the two is not quite as close. This fact may probably be attributed as much to error in the experimental measurements as to error in the theoretical values of the virial coefficient. However, a real discrepancy at low temperatures might be expected if the proportion of molecules in quantized collision states became appreciable, for in that event, Gibbs' phase integral would cease to be an adequate representation of the sum of state and Eq. (6) would lose its validity. At present it is impossible to decide whether or not this effect is of im-

[10] Holborn and Otto, Zeits. f. Physik **33,** 1 (1925); **38,** 359 (1926).

[11] Nijhoff, Keesom, and Iliin, Leiden Communications **188C,** Oct. 1927.

[12] Onnes, Leiden Communications, Verslag Akad. Amsterdam **102a,** 495 (1907); **102c,** 741 (1908); Onnes and Boks, ibid **170a, 170b,** (1924); Onnes and Van Agt, ibid **176b,** 625 (1925).

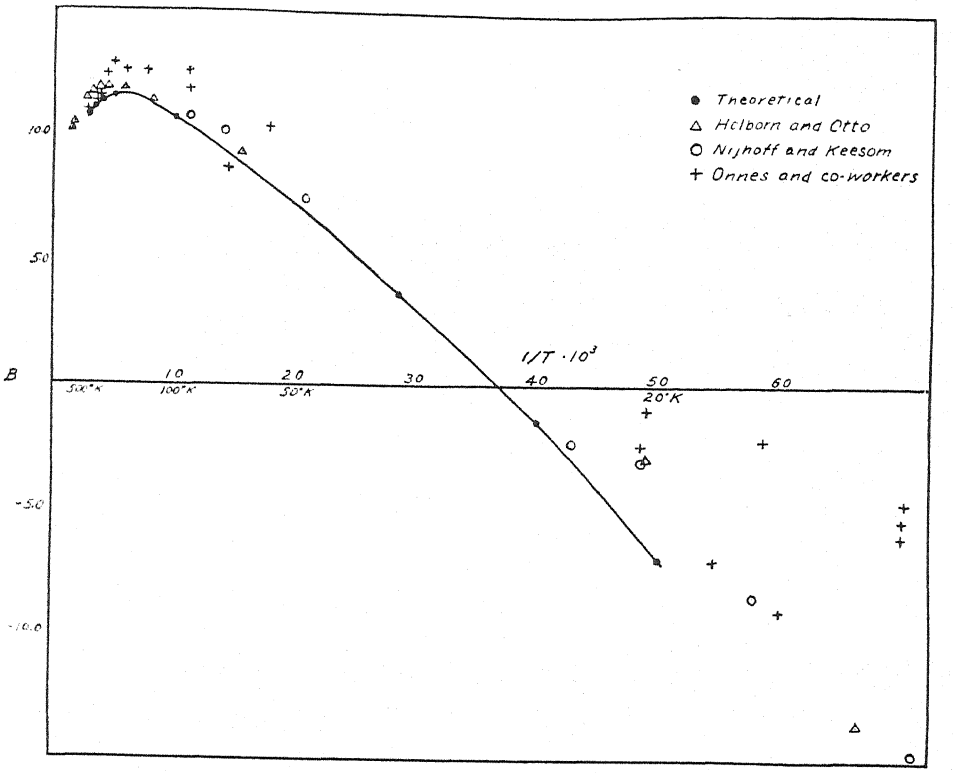

Fig. 1. The second virial coefficient of helium plotted as a function of the reciprocal temperature.

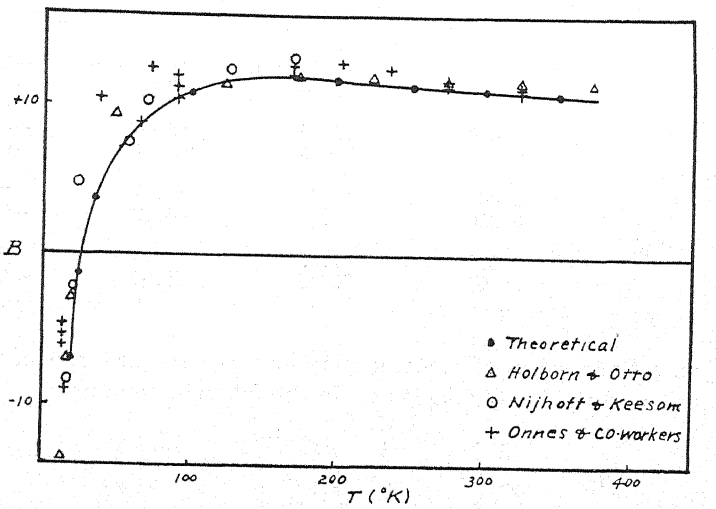

Fig. 2. The second virial coefficient of helium plotted as a function of the temperature.

portance because of inconsistency in the experimental values themselves in the low temperature region.

On the whole the agreement between the theoretical and experimental values of the virial coefficient is extraordinarily good. The slight discrepancy between them is not surprising in view of the approximations which were made in the calculation of the intermolecular energy, Eq. (7).

An examination of Fig. 1 shows that both the theoretical and experimental curves pass through a maximum at about 173°K. This phenomenon has been observed only in the case of helium, but presumably it should occur at sufficiently high temperatures for all gases. Thus, for hydrogen, neon, nitrogen and a number of other gases, the curve obtained by plotting B against $1/T$ shows a decided concave bending in the region of high temperatures. The limitations of van der Waals' equation are clearly brought out in Fig. 1. Below 100°K, it would be possible to apply van der Waals' equation to helium, since in a narrow temperature range the relation between B and $1/T$ may be approximated by a linear function. However, above 150°K, the van der Waals form of equation is entirely inadequate. Not only does the coefficient, A, cease to be constant, but it becomes very sensitive to temperature variation.

Some Properties of Helium

In order to obtain a more detailed comparison with experiment, some properties of helium have been computed with the aid of the theoretically determined virial coefficients. By means of Eq. (1) the pressure has been calculated at several temperatures and volumes. The computed and experimental pressures are given in Table II.

Table II. *Helium pressures calculated from the first three terms of the theoretical virial. Expansion:* $p=(RT/V)(1+B/V+4B^2/3V^2)$

V (liters/mol)	p (calc.)	p (obs.)	Δ
$t=200°C$			
2.000	19.51 atm.	19.52 atm.	−0.01 atm.
0.400	99.60	99.82	−0.22
$t=100°C$			
2.000	15.39	15.40	−0.01
0.333	94.96	95.11	−0.15
$t=0°C$			
2.000	11.27	11.27	0.00
0.250	93.97	94.12	−0.15
$t=-100°C$			
2.000	7.15	7.15	0.00
0.200	75.45	75.66	−0.21

The Joule-Thomson coefficient, μ, may be expressed in terms of the virial coefficient B, and the heat capacity C_p in the following manner:

$$\mu = -\frac{1}{C_p}\left[B + \frac{1}{T}\frac{dB}{d\left(\frac{1}{T}\right)}\right] = +\left(\frac{\partial T}{\partial p}\right)_H \tag{8}$$

At 25°C, μ is calculated to be $-0.061°$ atm.$^{-1}$. Moreover, between $+100°$ and $-100°$C, the value of $dB/d(1/T)$ is extremely small and therefore the temperature coefficient of μ is very small. Roebuck[13] has recently obtained the value $-0.06°$ atm.$^{-1}$ from measurements of the Joule-Thomson effect between $+100°$C and $-100°$C. The temperature variation in μ lay within his experimental error. A rough calculation of the Joule-Thomson inversion point leads to the temperature, 54°K. Although there is no reliable experimental determination with which to compare it the temperature 54°K is in accord with the fact that helium cannot be liquefied at the lowest temperature attainable by evaporating liquid nitrogen, about 70°K.

The thermodynamic temperature scale may be identified with the scale of the ideal gas thermometer. In order to reduce the scale of an actual gas thermometer to the thermodynamic temperature scale, corrections which are functions of the virial coefficients of the gas must be applied. We have used the theoretically determined values of B in conjunction with recent measurements of the coefficient of expansion and the coefficient of pressure of helium[14] to determine the position of the freezing point of water under a pressure of one atmosphere on the absolute temperature scale. The coefficient of pressure of a gas at constant volume is defined as,

$$\alpha_v = \frac{p_{100} - p_0}{100 p_0}$$

where p_0 is the pressure at 0°C and p_{100} the pressure at 100°C. It is easily shown that

$$T_0 = 1/\alpha_0$$

where T_0 represents the position of 0°C on the absolute temperature scale and α_0 is the coefficient of pressure of an ideal gas, for which $pV = RT$. Moreover, it is possible to calculate α_0 in terms of the α_v of an actual gas if its second virial coefficient is known.

$$\alpha_0 \doteq \alpha_v + p_0(6.098B_0 - 4.464B_{100}) \cdot 10^{-7}$$

where p_0 is again the pressure at 0°C, B_{100} the virial coefficient at 100°C expressed in cc/mol, and B_0 its value at 0°C. α_0 may also be obtained from the coefficient of expansion in a similar manner. From the measurements of Heuse and Otto on helium, we compute for the average value of α_0.

$$0.0036609 \text{ atm./°}$$

which corresponds to

$$T_0 = 273.16.$$

By linear extrapolation Heuse and Otto find that

$$T_0 = 273.16.$$

The International helium thermometer is defined as a constant volume gas thermometer in which the pressure of helium at 0°C is equal to that of a

[13] J. R. Roebuck and H. Osterberg, Phys. Rev. 37, 110 (A) (1931).
[14] W. Heuse and J. Otto, Ann. d. Physik [5] 2, 1012 (1929).

one meter column of mercury at 0°C and standard gravity. The gas temperature is defined as

$$t_g = \frac{p_{t_g} - p_0}{p_{100} - p_0}.$$

The corresponding temperature on the absolute scale is of course

$$t = T - T_0.$$

The correction Δt which must be added to the gas temperature t_g to bring it into agreement with the absolute temperature scale may be computed from the second virial coefficient by means of the formula

$$\Delta t = 5.870\{3.731t_g(B_{100} - B_0) - (373.1 + t_g)(B_{t_g} - B_0)\} \cdot 10^{-5}$$

where the virial coefficients B_{100}, B_0, and B_{t_g} are expressed in cc/mol. The corrections have been calculated for several temperatures. They are listed with those given by the Reichsanstalt in Table III.

TABLE III. *Corrections to international helium thermometer scale.*

t_g	Δt (calc.)	Δt (H and O)
200	+0.006	+0.008
100	0.000	0.000
50	−0.0003	−0.001
0	0.000	0.000
−100	+0.009	+0.009
−200	+0.032	+0.028
−250	+0.051	+0.043

L. Holborn and J. Otto, Zeits. f. Physik **38**, 359 (1926); **30**, 1 (1925).

Baxter and Starkweather[15] have measured the density of helium. Their value at 0°C and a pressure of one international atmosphere (pressure of a column of mercury 76 cm in height at 0°C and at standard gravity; $g = 980.665$ dynes sec^{-2}) is

0.17847 g/liter.

Using this density together with our value of B at 0°C and taking the gas constant, R, as 0.08206 liter atm. the mean for a large number of gases, we calculate the atomic weight of helium as 4.0022. This is to be compared with the atomic weight 4.0020 obtained by Baxter and Starkweather from the density given above and their own compressibility measurements at low pressures.

In all of the cases which have been considered, the theoretically determined virial coefficient gives results which are in substantial agreement with experiment. When it is remembered that the calculation of the virial coefficient is based upon purely *a priori* considerations and depends upon experiment only through the values of certain universal atomic constants, it seems to furnish a striking confirmation of the present theory of intermolecular forces.

[15] Baxter and Starkweather, Proc. Nat. Acad. Sci. **11**, 231 (1925).

LETTERS TO THE EDITOR

Prompt publication of brief reports of important discoveries in physics may be secured by addressing them to this department. Closing dates for this department are, for the first issue of the month, the twenty-eighth of the preceding month; for the second issue, the thirteenth of the month. The Board of Editors does not hold itself responsible for the opinions expressed by the correspondents.

Mass Defects of C^{13}, O^{18}, N^{15}, from Band Spectra, and the Relativity Relation of Mass and Energy

Chadwick, Constable and Pollard,[1] in a recent article, give on page 482 a plot of the "mass defect" of a number of atomic species, as a function of the number of α-particles in the nucleus. It is of considerable interest to add to this plot certain atomic species recently discovered by means of band spectra. In the case of C^{13}, O^{18} and N^{15}, the mass of the new isotope, relative to the mass of the more abundant species, has been calculated from the band spectra data. Thus King and Birge[2] find that the mass of C^{13} relative to C^{12} is 13:12 exact, to about one part in 10,000. The mass defect plot just mentioned is based on the atomic masses obtained by Aston.[3] Accepting his results, one obtains 10.7×10^{-3} as the mass defect of C^{13}. (Henceforth all mass defects will be given in 10^{-3} mass units). This result is given (as 11×10^{-3}) in a footnote, page 481 by *C.C.P.*

For O^{18} Babcock and Birge[4] have obtained a mass of 18.0065, based on $O^{16}=16$ exactly, which is also Aston's basis. The probable error is only about one part in 10^5. The resulting mass defect of O^{18} is 17.7.

Herzberg[5] has obtained the mass ratio N^{15}/N^{14}, from his measured isotope shift for the heads of the 1–0 and 2–0 bands of the second positive group of nitrogen, the molecules concerned being $N^{15}\cdot N^{14}$ and $N^{14}\cdot N^{14}$. The measured shifts are appreciably less than his calculated values, but unfortunately he made a theoretical error in his calculations which definitely affects his conclusion. All isotope shifts are expressed as a function of (ρ^n-1) where n is some positive integer. $\rho=(\mu_1/\mu_2)^{1/2}$ and μ, is the reduced mass of the *more* abundant molecule. Thus for the band systems containing O^{18}, C^{13} and N^{15}, the value of ρ is *less* than unity, and the vibrational shift is to the red, for bands located on the violet side of the origin of the system.

Herzberg, however, calculated ρ as $(\mu_2/\mu_1)^{1/2}$ and so obtained a value greater than unity. This leads not only to a shift in the direction opposite to that observed, but also to an incorrect absolute magnitude. In order to obtain the calculated shift Herzberg made new measurements of certain band heads of this system. He thus derived a new vibrational energy function $f(v')$ for the upper state, and combined this with the writer's $f(v'')$ of the lower state, to get an energy equation of the system. Birge and Sponer[6] had already given a $f(v')$ for this system, based on all available data, reduced where necessary to the I. A. system. The two $f(v')$ appear somewhat different, but fortunately lead to practically the same calculated vibrational shifts for the $1-0$ and $2-0$ bands. The correct value of ρ, assuming even 14 and 15 masses, is 0.98319, and the vibrational shifts are, from the Birge and Sponer equation, -35.16 and -65.79 cm^{-1}, and from Herzberg's equation, -35.19 and -65.72 cm^{-1}. It seems best to adopt the average values -35.17 and -65.76 cm^{-1}.

Since a fine structure analysis of these two bands has not been carried out, one must use for the rotational isotope shift the sufficiently

[1] J. Chadwick, J. E. R. Constable and E. C. Pollard, Proc. Roy. Soc. **A130**, 463 (1931). To be called *C.C.P.*

[2] A. S. King and R. T. Birge, Astrophys. J. **72**, 19 (1930).

[3] F. W. Aston, Proc. Roy. Soc. **A115**, 487 (1927).

[4] H. D. Babcock and R. T. Birge, (abstract) Phys. Rev. **37**, 233 (1931).

[5] G. Herzberg, Zeits. f. phys. Chemie **B9**, 43 (1930).

[6] R. T. Birge and H. Sponer, Phys. Rev. **28**, 259 (1926).

accurate approximation $(\rho^2-1)\nu_m$, where ν_m is the distance from the origin to the head, for the *middle* component of the triplet series found in these bands. Fortunately the desired origin can be located, by mere inspection, on spectrograms of an "effective low temperature" source. The resulting rotational shifts, as given by Herzberg, are $+0.6$ cm^{-1} and $+0.8$ cm^{-1} respectively, corresponding to *origin-head* distances of 18 and 24 cm^{-1}. (This distance in the $0-0$ band is 13.3 cm^{-1}, according to the writer's fine structure analysis.)

Now the $f(v')$ to which reference has been made are based on measurements of the heads, and are slightly in error, due to the varying distance of origin to head. The resulting correction to the vibrational shift I find to be -0.08 and -0.18 cm^{-1}, for the $1-0$ and $2-0$ bands, respectively. The final calculated shifts for the *heads* are then -34.65 and -65.14 cm^{-1}, as compared with Herzberg's *observed* shifts -34.6 and -64.6 cm^{-1}. One thus obtains the result that the mass ratio N^{15}/N^{14} is *less* than 15/14 by one part in 10,000, and one part in 1700, from the $1-0$ and $2-0$ bands, respectively. Then, using Aston's value $N^{14}=14.008$, one obtains $N^{15}=15.0065$ and 14.999 respectively. From these figures there results a mass defect for N^{15} of 23.3 and 30.6, or an average value of 27.0

We may now place these mass defects on the plot previously mentioned. The C^{13} defect (10.7) lies just above the value obtained from α-ray disintegration experiments (given as 9.9 by *C.C.P.* but calculated as 9.8 by the writer). This mass defect, 9.8, is obtained from Aston's mass defect 6.38 for B^{10} combined with an energy loss equivalent to 3.42 (in 10^{-3} mass units), as observed by *C.C.P.* in the transformation $B^{10}\rightarrow C^{13}$. The close agreement of the two mass defect values for C^{13} (10.7 and 9.8) is of more than passing interest, for it constitutes a *very* rough, but direct experimental check of the accepted relation between mass and energy $\Delta E=c^2\Delta m$. So far as I am aware, it is the first experimental check by this very direct method.

The mass defect for O^{18} (17.7) may be compared with that for O^{17} (12.6), as evaluated by *C.C.P.* from their disintegration experiments,[7] for O^{16} (8.64). The fact that these three points (corresponding to masses of 18.0065, 17.0029 and 16.0000) are nearly equally spaced is probably significant. The spectral data for O^{17} are very meager, as compared to O^{18}, but the mass of O^{17} is now being calculated from such data and the result, if of sufficient accuracy, will constitute a second check on the mass-energy relation.

Finally, the mass defect of N^{15} should lie on the curve passing through B^{11}, F^{19} etc. The predicted value, from the published curve, is 24.5, agreeing well within limits of error with the average observed value of 27.0. Other interesting relations may be deduced from the mass defect graphs published by *C.C.P.* but it is the primary purpose of this letter merely to locate on these graphs the new data for C^{13}, O^{18} and N^{15}.

RAYMOND T. BIRGE

University of California,
March 4, 1931.

[7] The first calculation of the mass of O^{17} by such a process, with the result 17.0033 ± 0.0009, was made by W. F. Giauque, Nature **124**, 265 (1929).

Momentum Transfer to Cathode Surfaces by Impacting Positive Ions in a Helium Arc

The present problem was suggested by K. T. Compton and may best be introduced by the following quotation from one of his papers (Phys. Rev. **36**, 706, 1930). "Although, as we have seen, the impact of a charged ion against the cathode contributes nothing to the pressure against it (on account of the counterbalancing pull during its attraction to the cathode), nevertheless if the neutralized ion leaves the cathode with any momentum there is imparted to the cathode an equal opposite momentum." In the experiment here reported this hypothesis is tested by studying the momentum imparted to an auxiliary cathode in a helium arc.

The auxiliary cathode (or plane collector) was suspended from a vertical side tube in the negative glow of a hot cathode helium arc. The collector was a flat molybdenum plate one centimeter in diameter, insulated on one side by a glass plate. This collector was nonvolatilizing so that there was no possibility of a pressure as a result of a stream of metal vapor leaving the collector. The suspension consisted of a long period glass pendulum supported on two steel points and carrying a small

mirror. Thus by means of the deflection of a light beam, small forces on the collector could be measured. The forces were determined as a function of the negative potential applied to the collector using several different values of the total current through the arc.

From the data obtained the calculation of an accommodation coefficient for helium positive ions is quite simple if corrections for the current that reaches the collector at its edges are neglected. Let β be the fraction of the incident energy of the ion which is retained after neutralization. β is approximately equal to $1-\alpha$ where α is the accommodation coefficient. Assuming that the neutralized ions escape in random directions, the pressure on the collector is given by

$$P=\frac{i}{2e}(2meV\beta)^{1/2}$$

where P is the pressure exerted on the collector, i the positive ion current density, e the charge, m the mass of a helium ion and V the negative potential of the collector with respect to the surrounding space. Putting in the constants,

$$\beta=\frac{4.63(10^3)P^2}{i^2V}$$

where P is in milligrams per square centimeter, i in milliamperes per square centimeter and V in volts. α follows immediately from the relation $\beta=1-\alpha$.

When a small correction for edge effects is included preliminary results indicate a value of about 0.5 for α. In further work the elimination of edge effects will be attempted and the experiments continued using a number of other gases.

EDWARD S. LAMAR

Palmer Physical Laboratory,
Princeton University,
Princeton, N. J.,
March 9, 1931.

Raman Spectra of Silico-Chloroform

We have been investigating the Raman spectra of silico-chloroform and have succeeded in observing a number of its Raman frequencies and particularly that characteristic of the Si-H-bond. The spectra were observed by illuminating with a mercury arc a tube filled with the liquid immersed in liquid ammonia contained in an unsilvered Dewar flask. The light was reflected from the top of the tube into a Hilger D78 glass spectrograph.

The frequencies which we have observed together with those of chloroform (Proc. Roy. Soc. **A127**, 360 (1930)) are shown in the following table:

$CHCl_3$	$SiHCl_3$
261 (5)	179 (strong)
367 (6)	250 (strong)
669 (6)	489 (very strong)
762 (3d)	587 (strong diffuse)
1218 (2d)	799 (strong diffuse)
1441 (1)	——
3019 (3d)	2258 (strong diffuse)

It is to be noted that we observe six frequencies which can be correlated with those of chloroform, the frequencies of silico-chloroform being always smaller than those of the other compound. We have been unable to detect the seventh frequency which should be the weakest of the frequency displacements. The highest frequency which we observe, namely, 2258, is that which corresponds to the frequency usually assigned to the vibration of the proton along its valency bond with respect to the carbon atom in chloroform; so that it is to be interpreted as a similar vibration of the hydrogen atom with respect to the silicon atom along the Si-H-bond.

The differences in these two frequencies can be due only to the difference in the restoring force constants for the two cases, for the effective mass in both cases should be approximately the mass of the hydrogen atom. We have also been able to observe both positive and negative displacements for the lower frequencies from the yellow lines of mercury in addition to those more easily observed from the blue and violet lines. Complete details of this investigation and that of other compounds of this type will be reported at a later date.

HAROLD C. UREY
CHARLES A. BRADLEY, JR.

Department of Chemistry,
Columbia University,
March 11, 1931.

New Lines in the Near-Infrared Spectrum of the Neutral Hg Atom

Thirty-nine new lines have been observed in the region 0.9μ to 2.25μ with an automatic recording spectrograph[1] of the Littrow type using the equivalent of five 60° prisms. The lines are extremely weak so that an effective slit-width of approximately 15 A° was necessary for detection with a single junction thermocouple. The intensities of these lines are of the order of 0.002 that of the strong line at 1.0142μ, which gave a 45 cm scale deflection at 4 meters. The arc was operated at 86 volts and 3.8 amperes.

Wave-length standards were taken from E. D. McAlister's report (Phys. Rev. **34**, 1142–1147, Oct. 15, 1929) and T. Takamine's and T. Suga's report (Inst. Phys. and Chem. Research Tokyo, Sci. Papers No. 232, March 20, 1930). All the lines in the region 0.9 to 1.0μ, observed photographically by Takamine and Suga were discernible, and the line at 0.940μ resolves into two, 0.9432 and 0.9447μ. The line at $2.108\mu \pm 10^{-3}$ is of the same intensity as the one 2.2489μ observed by F. Paschen, and the wave-length uncertainty is due to the fact that the nearest known line is 1300A away.

This brings the number of lines in this spectral region, 0.90 to 2.25μ, to a total of 96.

New HgI Lines and Possible Classification.

No.	λ	ν	Classification
1	0.9253	10807.3	
2	0.9432	10602.2	$2^1P_1-6^1D_1=10600$
3	0.9447	10585.4	$2^1P_1-6^3P_2=10581$
4	0.9697	10312.4	
5	0.9774	10231.0	$2^3P_0-2^1F\ =10231$
6	0.9780	10225.0	$2^3P_0-2^3F\ =10227$
7	0.9918	10083.0	$2^1D_1-5^3S_1=10083$
8	0.9983	10017.	$2^3P_1-4^3D_1=10016$
9	1.0211	9793.3	
10	1.0240	9765.6	$2^1P_1-5^1D_1=9764$
11	1.0276	9731.4	$2^1P_1-5^3P_2=9730$
12	1.0294	9714.4	$2^3P_1-4^3P_0=9713$
13	1.0307	9702.1	
14	1.0361	9651.5	$2^3D_3-5^3D_3=9654$
15	1.0436	9582.2	$2^1D_1-5^3P_1=9583$
16	1.1008	9084.3	
17	1.1018	9076.0	$2^3S_1-9^3P_1=9078$
18	1.1036	9061.2	$2^3P_2-4^3S_1=9060$
19	1.1129	8985.5	$1^3S_1-2^3D_1=8986$
20	1.1363	8800.4	$2^3S_1-8^3P_1=8805$?
21	1.1433	8746.6	
22	1.1790	8481.7	$2^3P_2-4^3D_2=8482$
23	1.1916	8392.1	$2^1P_1-4^3D_2=8397$?
24	1.2193	8201.4	$^3P_2-3^3D_1=8200$[2]
25	1.2224	8180.6	$2^3D_2-4^3P_2=8180$
26	1.2376	8080.1	$2^1P_1-4^3P_0=8082$
27	1.2440	8038.5	$2^3D_1-4^3P_0=8039$
28	1.3634	7334.3	
29	1.3979	7153.6	$2^3P_1-3^3P_2=7161$?
30	1.4027	7129.1	
31	1.4127	7078.6	$2^1D_1-4^1S_0=7068$?
32	1.4160	7062.1	$2^3S_1-5^3P_2=7062$
33	1.7269	5790.7	$2^1P_1-3^3D_1=5791$
34	1.7696	5651.0	$3^3P_1-6^3S_1=5656$?
35	1.7980	5561.7	$3^3F\ -8^1D_1=5563$
36	1.8084	5529.7	$2^1P_1-3^3P_2=5530$
37	1.9481	5133.2	$2^1D_1-3^3P_1=5134$
38	1.9571	5109.6	$2^3D_1-3^3P_0=5110$
39	2.1080	4744	$2^3P_1-3^1S_0=4742$

[1] Constructed by E. D. McAlister, Smithsonian Institute.

[2] Takamine's x-term given by F. Paschen as a $^3P_2$-term that may assume two different values.

H. J. UNGER

Department of Physics,
University of Oregon,
March 10, 1931.

Spark Spectrum of Caesium (Cs II)

In pursuance of the systematic investigation of the alkali spark spectra by means of the hollow cathode excitation (Phys. Rev. **36,** 219, 1931) we have now carried the analysis to the first spark spectrum of caesium. Contrary to Rb II, the excitation of the caesium hollow cathode discharge in helium is about two volts more than sufficient to produce excitation of all the levels of the caesium ion so that higher members of the resonance series were excited and a total of eight lines appeared in the vacuum region (see table below).

Int.	λ	ν	Spectroscopic Origin
(20)	926.75	107905	$5p^6-5p^5(^2P_{1\frac{1}{2}})6s$ and $5d$
(20)	901.34	110946	
(20)	813.85	122872	$5p^6-5p^5(^2P_{\frac{1}{2}})6s$ and $5d$
(20)	808.77	123645	
(12)	668.43	149604	$5p^6-5p^5(^2P_{1\frac{1}{2}})$ $7s$ and $6d$
(5)	657.15	152172	
(12)	639.42	156392	
(7)	612.82	163180	$5p^6-5p^5(^2P_{\frac{1}{2}})$ $7s$ and $6d$

With the separation of these lines as a guide, it has been possible to interpret the classification of the Cs II lines in the visible region as given by Sommer (Ann. d. Physik **75,** 163, 1924). The energy level scheme given by this author is correct but incomplete. For, due to the large separation of the $5p^5$ (^2P) term of Cs III, the energy levels of each configuration are split up into two distinct groups according to whether they are built upon $^2P_{1\frac{1}{2}}$ or upon $^2P_{\frac{1}{2}}$. Sommer's classified lines are to be interpreted (α) as transitions from five of the six levels of the configuration $5p^5$ ($^2P_{1\frac{1}{2}}$) $6p$, to five of the ten levels of the configurations $5p^5$ ($^2P_{1\frac{1}{2}}$) $6s$ and $5p^5$ ($^2P_{1\frac{1}{2}}$) $5d$, (β) as transitions from eight of the ten levels of the configurations $5p^5$ ($^2P_{1\frac{1}{2}}$) $7s$ and $5p^5$ ($^2P_{1\frac{1}{2}}$) $6d$ to the aforesaid five levels of $5p^5$ ($^2P_{1\frac{1}{2}}$) $6p$. No levels built upon $^2P_{\frac{1}{2}}$ were found by Sommer, but the present data give clear indications concerning their position. In the above table, the intensities, wave-lengths, and frequencies of the resonance lines are given as well as their spectroscopic origin.

The resonance potential corresponding to the two strongest lines 926.75 and 901.34 is equal to 13.32 and 13.70 volts, respectively.

OTTO LAPORTE
GEORGE R. MILLER
RALPH A. SAWYER
Department of Physics,
University of Michigan,
Ann Arbor, Michigan,
March 16, 1931.

Hyperfine Structure and Incomplete Polarization of Mercury Resonance Radiation

The author has made studies of the Zeeman effect of the mercury resonance line in absorption and has shown, that for certain intensities of the magnetic field mercury vapor transmits, from the five hyperfine-structure components of the 2537A-line: (1) only the outer short wave-length component, −25.4 mA, or (2) one inner and one outer component, −10.4 and +21.5 mA, or (3) two inner components, 0 and +11.5 mA. Further the author has determined the absorption coefficients and the life-times of the mercury atoms excited with the above mentioned filtered radiations. A full account appeared in Bull. Acad. Pol. Nov.–Dec. p. 464, 1930; preliminary communications in Nature, Nov. 1, 1930, and Phys. Rev. Nov. 15, 1930.

Recently the author has extended the investigations on the hyperfine structure of the resonance radiation excited with these filtered radiations. These investigations now in progress show, that by excitation with the outer component −25.4 mA alone, there appears in emission only the same component, that is, we have to deal with a pure monochromatic resonance effect. It is to be seen on the accompanying photographs obtained with a Lummer-Gehrcke parallel plate, from which the first shows the five-fold structure of the resonance radiation excited with the unfiltered radiation of the mercury vapor arc, the second, the single structure of the same radiation obtained by the excitation with the −25.4 mA component alone.

The experiments made up to the present on other components seem to show, that in general each of the five components gives a pure resonance effect, consequently there are no hyperfine levels of the 2^3P_1-energy level from which more than one component can be emitted.

The results communicated above and those from investigations of the Zeeman effect show that the five-fold structure of the 2537A line is due rather to the isotope effect than to a magnetic moment of the nucleus. At the same

Fig. 1.

Fig. 2.

time they give interesting views concerning the cause of the incomplete polarization of the mercury resonance radiation in absence of magnetic field.

In the first place, according to the supposition of Olson (Phys. Rev. **32,** p. 443, 1928), the degree of polarization must depend on the relative intensity of the components in the exciting light. Further, in the case of the excitation with the outer −25.4 mA component, previously investigated by the author, one should expect that the degree of polarization should be about 32 percent (in comparison with 50 percent by excitation with all five components). This difference is so small that I could overlook it in the approximate estimations of the visibility of the interference fringes (I did not take into account the dependence of the plate density upon the time of exposure). It must be remarked that experiments made recently by A. Ellett and described by him in a letter in the January 15th issue of this Review do not contradict the results of my investigations. From Fig. 2 of my paper (Bull. Acad. Pol. l.c.) it is to be seen, that under the conditions chosen by Ellett (2000 gauss) the filtering absorption cell does not transmit the outer −25.4 mA component; the resonance radiation is excited probably not with cores, but by the transmitted wings of the hyperfine-structure components.

As regards the other experiment, on the basis of which Ellett supposes that the parallel Zeeman component of the outer long wavelength component (+21.5 mA) is shifted by the magnetic field, it must be remembered, that such a shift is not detected either in emission (McNair) or in absorption (the author, l.c.). On this account I think that another explanation should be sought for this experiment of Ellett. It is possible, for instance, that the whole effect could be explained by the relatively large difference of the absorption coefficients for the inner and the outer components.

S. Mrozowski

Physical Laboratory of the Society
of Sciences and Letters, Warsaw,
March 2, 1931.

Second Series *April 15, 1931* *Vol. 37, No. 8*

THE
PHYSICAL REVIEW

DIFFRACTION OF HYDROGEN ATOMS

By Thomas H. Johnson
Bartol Research Foundation of the Franklin Institute
(Received March 11, 1931)

Abstract

Diffraction patterns of a beam of hydrogen atoms reflected from LiF.—Improved technique in the photography of the diffraction patterns produced by the reflection of a beam of hydrogen atoms from a crystal of lithium fluoride has resulted in more complete patterns than those previously described by the author. The observed patterns are those expected on the assumptions (1) that the incident beam contains the distribution of wave-lengths derived from the Maxwellian velocity distribution by the use of the de Broglie relation between wave-length and velocity, and (2) that the surface of the crystal constitutes an impenetrable square array of scattering points with the arrangement and spacing of the ions of a single type as known from x-ray measurements.

Wave-length distribution.—The intensity distributions in the diffraction patterns were measured, and were found to have maxima at positions in good agreement with those expected on the basis of the above assumptions.

Interpretation of relative intensities in the different orders.—The relative intensities in the observed orders are discussed in relation to the scattering coefficients of the two types of ions, and in relation to the dependence of the scattering coefficient on azimuth.

Diffraction by the secondary structure of the crystal.—A secondary spectrum is described, arising from a lattice of wide spacing the lines of which are parallel to the 100 cleaved edges of the crystal face.

IT HAS been well established for some time that the quantum mechanics correctly describes the motion of a free or a bound electron. Its success in the interpretation of band spectra has also shown that the motions of atomic nuclei within the molecule could be included in the theory, and because of this, it appeared almost certain that the new mechanics would be found correct in its description of the free motion of atoms and molecules. The comparatively recent experiments of Estermann and Stern[1] and of the author[2] were not disappointing in this regard for they have demonstrated that atoms and molecules of low atomic weight behave as predicted, in that they exhibit the properties of a wave radiation of wave-length $\lambda = h/mv$ in the plane-grating diffraction phenomena which appear when these are reflected from the surface of a crystal. These experiments are of interest not only because of their confirmation of the predictions of quantum mechanics, but also because

[1] Estermann and Stern, Zeits. f. Physik **61**, 95 (1930). O. Stern, Die Naturwissenschaften **17**, 391 (1929).

[2] T. H. Johnson, Phys. Rev. **35**, 1299 (1930).

they introduce the possibility of applying atom diffraction to investigations of the atomic constitution of surfaces. A beam of atomic hydrogen, for example, with ordinary thermal velocities, has a range of wave-lengths of the right magnitude for this purpose, centering around 1A, and the complete absence of penetration of these waves will insure that the effects observed arise entirely from the outermost atomic layer.

The first experiments demonstrating the diffraction of hydrogen atoms when reflected from a crystal of lithium fluoride were described in some detail in the Journal of the Franklin Institute.[3] The diffraction patterns which were photographed in that earlier work were of low intensity and they showed only a part of the complete structure which should have been produced by the array of ions on the surface of the crystal. Because of the low intensity in these earlier patterns, satisfactory intensity measurements were impossible, and only a rough comparison could be made between the observed distribution of wave-lengths and that predicted from the Maxwellian velocity distribution and the de Broglie relation between velocity and wave-length.

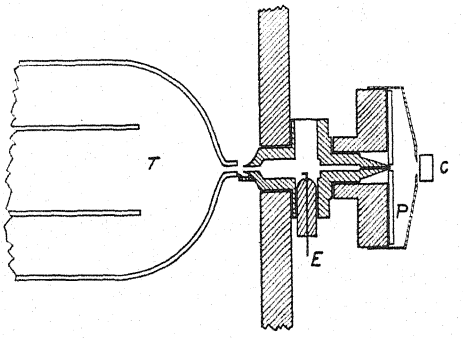

Fig. 1. Collimating system for normal incidence.

Recent improvements in the technique of obtaining photographic records of the diffraction patterns have overcome in large measure the deficiencies of the earlier work, and patterns of far greater intensity have been photographed which show all of the expected first-order branches. The intensity is now sufficient for the purposes of making photometric measurements of the wave-length distribution, and it has been possible to make some rough estimates of the relative intensities in the principle branches. In addition, some new features have been recorded which throw light upon the secondary structure of the crystal.

With the exception of a few modifications, the apparatus and the experimental procedure were the same as in the earlier work. A sharply defined beam of hydrogen atoms had its origin in a chamber T, Fig. 1, in which molecular hydrogen was dissociated by an electric discharge, and it was collimated by a series of tubes with suitable pumping systems for eliminating the excess gas. This beam was reflected from a freshly cleaved surface of a crystal (C) of lithium fluoride, and the reflected atoms were recorded on a plate (P)

[3] T. H. Johnson, Jour. Frank. Inst. **210**, 135 (1930).

coated with molybdenum oxide After an exposure the patterns recorded on the molybdenum oxide plate were made permanent by photographing in the usual way.

Since it is believed that atom diffraction may prove useful in studying the structure of surfaces a discussion of some of the technical features will be included for its interest to other investigators in this field.

Formation of the Beam

In designing a collimating system for the production of a molecular beam for use in diffraction experiments there are two requirements; the beam should be intense and it should be sufficiently sharp to resolve the effects sought. In the limit these demands are conflicting in that an increase in the sharpness of the beam results in a decrease in its intensity, and *vice versa*. Over the range of source chamber pressures which is of interest, the intensity of the beam, as regards its dependence on the configuration of the collimating system, is proportional to the area of the source aperture and inversely proportional to the square of the distance from the source to the point of detec-

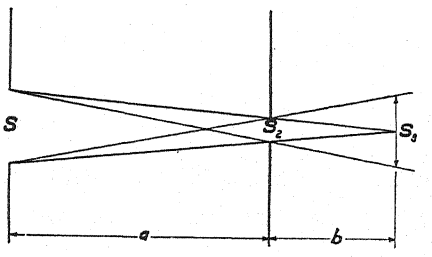

Fig. 2.

tion, and it is independent of the position and size of the collimating aperture as long as the point of detection is not occluded from any part of the source aperture. The sharpest beam, for a given intensity, may be obtained by making the collimating aperture a section of the cone of which the source aperture is the base, and the point of detection is the vertex. The linear dimensions (S_2, S_2') of the collimating aperture are therefore related to the corresponding dimensions (S_1, S_1') of the source aperture by

$$S_2 = S_1 b/(a + b), \tag{1}$$

where a and b are the distances indicated in Fig. 2. The corresponding dimensions of the cross-section of the beam at the point of detection are given by

$$S_3 = 2S_1 b/a. \tag{2}$$

Similar expressions also hold for the S' dimensions.

If a perfect reflector is placed a negligible distance behind the collimating aperture two reflected beams separated by an angle $\Delta\theta$ will be just resolved if their linear separation is equal to the beam width, i.e.

$$b\Delta\theta = 2S_1 b/a. \tag{3}$$

The resolving power of the collimating system, in the plane determined by S and the beam, defined as

$$R = 1/\Delta\theta = a/2S_1, \tag{4}$$

is independent of b and would remain unaffected by shortening this distance as much as permitted by convenience of construction.

The intensity I of the beam depends upon these dimensions of the collimating system in the manner

$$I \sim \frac{S_1S_1'}{(a+b)^2} = \frac{aS_1'}{2R(a+b)^2} = \frac{a^2}{4RR'(a+b)^2}. \tag{5a, b}$$

From (5a) it is seen that, with fixed resolving power in one direction and fixed dimension S_1' normal to this direction, I has its greatest value, as regards its dependence on b when $b=0$, and, as regards its dependence on a, when $a=b$. If the resolving power is to be fixed in two dimensions, as, for example, would be the case with circular beams, (5b) shows that the intensity undergoes no variation with changes of the size of the collimating system, but it is inversely proportional to RR'.

Under the first of these conditions the greatest intensity is obtained with the collimating system as short as possible and the sizes of the apertures determined by (4) and (1) to yield the required resolving power.

The variation of beam-intensity with source-tube pressure is the next point to consider. The principles involved are not as clear in the case of atomic hydrogen beams as with other gases, for the degree of dissociation in the discharge tube depends, among other things, upon the pressure. With an incomplete understanding of discharge tube phenomena, considerations of this kind will be omitted and only the usual elements of the kinetic theory of gases will be taken into account.

On this basis the number of atoms leaving the source aperture in the direction of the beam is proportional to the pressure in the source chamber over the range of pressures for which "molecular flow" subsists. This number is diminished by collisions over the path a', between the source and the entrance to the collimating aperture, by the factor $e^{-a'/L}$ where L is the mean free path in this region. Since the speed of the diffusion pump which is used to eliminate the excess gas from the region between the first two apertures is approximately independent of the pressure, a constant ratio exists between the pressure within the source chamber (p) and that in the intermediate region, and L is inversely proportional to p. The intensity of the beam then varies with the pressure in the source chamber in the manner

$$I = Ape^{-p/p_0} \tag{6}$$

in which the constant p_0 is the pressure in the source chamber for which the intensity of the beam is a maximum. An expression of this form is in agreement with the observations on beam intensities in these experiments as well as with other published data, and with the apparatus used in these experi-

ments p_0 was found to be 0.3 mm. Corresponding to p_0, the intensity of the beam, from (6), is

$$I_0 = Ap_0/e. \tag{7}$$

From the above considerations it may be seen that p_0 is proportional to the resistance of the source aperture, to the speed of the pumping system operating between the source and first collimating aperture, and inversely proportional to the path a' of the beam in this region, while the constant A is proportional to the ratio of the number of atoms which have the direction of the beam to the total emission from the source, and inversely proportional to the resistance of the source aperture. To realize a large value of I_0, a high speed pump and large connecting tubes were used at the first stage, the path a' was made as short as possible by the use of an auxiliary collimating tube (Fig. 1), and the source aperture was tubular in shape to produce a favorable directional distribution of the emitted atoms.

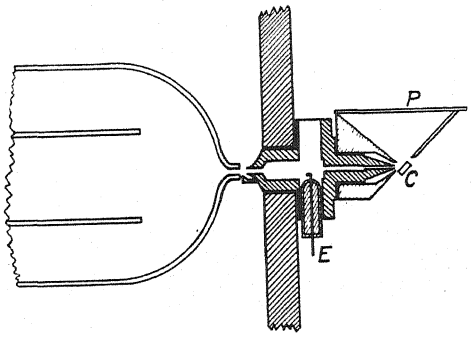

Fig. 3. Collimating system for 45° incidence.

Insofar as the directional distribution of the atoms emerging from the source aperture is unaffected by changes in its dimensions, the resolving power can be increased without affecting the intensity by diminishing the dimensions of the source aperture and simultaneously increasing the pressure in the source chamber so that the total number of atoms which emerge from the source aperture remains unchanged. A change of this character should leave the number of collisions in the intermediate chamber unaffected, for there the free path depends only on the rate at which gas is flowing in from the source chamber. This consideration therefore leads to the conclusion that the intensity can be increased, with fixed resolving power in *two* dimensions, by diminishing the size of the collimating system and simultaneously increasing the pressure in the source tube.

The collimating systems (Figs. 1 and 3) used in these experiments were constructed along the lines of these principles except that, in the arrangement for normal incidence, it was inconvenient to place the crystal directly in front of the last collimating aperture. The important dimensions are included in the following table.

Diameter of source tube	0.65 mm
Length of source tube	1.3 mm
Diameter of first collimating tube	0.67 mm
Diameter of second collimating tube	0.18 mm
Distance (a') from source tube to first collimating tube	1.0 mm
Distance (a) from source tube to far end of second collimating tube	24 mm
Distance (b) from end of second collimating tube to plate by way of specular reflection from the crystal at normal incidence	9 mm
Distance (b) for 45° incidence	10.5 mm

Elimination of High Energy Ions from the Atom Beam

One of the principal obstacles which stood in the way of the recording of intense patterns in the earlier work was the disintegration of the crystal surface by ion bombardment. Ions diffusing from the discharge chamber were

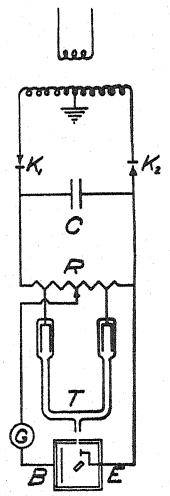

Fig. 4. Electrical connections.

subjected to a potential fall of the order of 5,000 volts between the center of the discharge and the observation chamber and some of these entered the beam and bombarded the crystal. The importance of their effect may be realized from the fact that, if unimpeded, the ion bombardment was sufficient to disintegrate the surface of the crystal in less than one minute to the extent of putting a stop to the regular reflection of atoms. The introduction of an electrode E (Figs. 4 & 1) to sweep the ions from the beam, materially improved the situation and exposures of three hours were feasible. There remained, however, a smaller number of neutral atoms of high energy in the beam which were formed in the first collimating tube by the neutralization of ions and these were not eliminated in this way. In the latest work, therefore, two additional precautions were taken. (1) The potential of the observation chamber was adjusted to be approximately the same as that of the center of

the discharge tube, so that ions diffusing from the source tube were accelerated as little as possible. (2) The remaining field between the center of the discharge and the entrance to the first collimating tube was made asymmetrical so that the ions were accelerated out of the line of the beam. The result of these precautions has been an almost complete elimination of the effects of bombardment with a resulting increase in the possible time of exposures to 24 hours or longer and a corresponding increase in the intensity of the patterns.

Fig. 4 is a diagram of the electrical circuit which was used to operate the discharge. A d.c. source of potential was supplied by a transformer and two kenetrons connected for half-wave rectification. This method of connecting the kenetrons had the advantage that the potential of the observation box, when adjusted to equal that of the center of the discharge, was close to the ground potential, and no trouble was experienced with leakage currents although the design of the apparatus made it inconvenient to insulate the box to withstand high voltages. To reduce the fluctuation of potential which took place during the cycle of alterations of the primary e.m.f., a condenser (C) having a capacity of 0.08 mf was used. A water resistance (R) served as a convenient potential divider and ballast resistance for the discharge. This was constructed of a series of four interconnected glass U-tubes, each 1.5 meters in length and 5 mm in diameter through which tap water was continuously circulated. This resistance could be varied in any of its parts by the insertion of wires into the arms of the U's, and it was adjusted so that no current was registered through the galvanometer (G).

General Darkening of the Detecting Plate

In the recording of faint patterns requiring long exposures it was necessary to exercise care to avoid a general over-all darkening of the molybdenum oxide detecting plate. A darkening of this character might have been produced by any one of three causes. (A) Atomic hydrogen, dissociated in the source chamber, might have been diffusely emitted from the collimating tube after scattering from its walls, and these might have reached the detecting plate either directly or after other reflections in the observation chamber. (B) Atomic hydrogen might have been formed in the observation chamber itself by electrons which were emitted either photoelectrically from the walls of the observation chamber or thermionically from the crystal holder and its heating unit, and which attained high velocities in the fields which surrounded the electrode E and its lead wire. (C) The most important cause of over-all darkening was the reduction of the molybdenum oxide by molecular hydrogen. This reaction can take place only if the molybdenum oxide is heated, but unless precautions were taken, the radiant heat from the crystal holder at the temperature used for degassing the surface of the crystal was sufficient to cause trouble.

Unquestionably some trouble had been experienced from cause (A) but this was rendered negligible by plating the inside walls of the collimating tubes with platinum black so that scattered atomic hydrogen was adsorbed until recombination to molecular hydrogen took place. The effects of (B) and

(C) were almost eliminated by protecting the detecting plate with a metal shield which completely surrounded it except for a small opening close to the crystal through which the reflected atoms entered. (See Figs. 1 and 3.) The inside and outside walls of this shield as well as the interior walls of the observation chamber were cleaned and freshly plated with platinum black before each exposure. To facilitate the cleaning of the interior of the observation chamber a copper lining was constructed which was easily removed, cleaned and plated.

Photographic Technique

The detecting plate consisted of either a "black-nickel" plated brass plate or a blackened photographic plate upon which was deposited a thin coating of molybdenum oxide formed by the oxidation of metallic molybdenum in an oxygen-gas flame. Since the blue reduced molybdenum oxide faded slowly when exposed to the air, the detecting plate was photographed as soon as possible after it was removed from the apparatus. The camera was of special construction and gave a 2.86 to 1 enlarged image. The plate was illuminated from the front by two 100 watt lamps placed beside the camera lens. To prevent fading of the pattern by reoxidation when exposed to the heat from these lamps, water filters were introduced between the lamps and the plate. A Wratten Aero No. 1 color filter was used in front of the camera lens to increase the photographic contrast between the white background and the blue pattern. The best reproductions of the patterns were obtained on Eastman Process plates with their D-9 developer.

Preparation of the Crystal

The crystals of lithium fluoride were grown from a melt by the method of Kyropolus,[4] which proved to be extremely simple and satisfactory. These crystals are of the simple cubic lattice, and they are cleavable along the 100 planes. From the lens shaped crystals which were grown in this way rectangular blocks 2 mm$\times$2 mm$\times$4 mm were cut, the faces of which were parallel to the cleavage planes. During an exposure one of these crystal blocks rested in a grove in a copper holder of which two types were used to realize the desired orientations. These holders contained heating coils of tungsten wire wound on mica and imbedded in alundum cement. After all other adjustments had been made the crystal was cleaved and mounted, and as quickly as possible the apparatus was evacuated. Without further treatment the freshly cleaved surface at the start was generally found to give a weak specularly reflected beam of the order of 1 percent of the incident beam. An initial heating at 500°C for about 3 min. with a subsequent cooling to room temperature increased the reflecting power to something of the order of 10 percent of the incident beam, but this again fell off in the course of an hour to very nearly nothing. If the temperature of the crystal was maintained steadily at about 300°C its reflecting power was higher and it persisted for a much longer period of time, but it was still helpful to heat the crystal at 500°C for a few minutes

[4] Kyropolus, Zeits. f. anorg. allgemein. Chem. 154, 308 (1926).

at four or five hour intervals. With this procedure it has been possible to maintain a high reflecting power during 24 hour exposures with no apparent diminution. During the major part of the exposure it has been found best to maintain the crystal at as low a temperature as is possible without seriously interfering with its reflecting power, for at the higher temperatures, in addition to difficulties introduced by the heating of the detecting plate, there was some troublesome diffuse reflection which might have arisen from either or both of two causes. (1) The roughening of the surface by thermal agitation may have produced a diffuse blurring of the regularly reflected and the diffraction beams. (2) Adsorbed hydrogen atoms may have been re-emitted from the hot crystal in the monatomic state, although at low temperatures these remained on the crystal surface until recombination to molecular hydrogen had taken place.

The best explanation which can now be given of the continually diminishing reflecting power at low temperatures is that vapors from the picein wax, which sealed the many joints leading into the reflection chamber, gradually condensed on the crystal surface. To minimize this difficulty the concentration of this wax vapor was made as low as possible by the use of independently evacuated guard rings between the wax seals and the inside chamber. As further precautions against this vapor, a liquid-air-filled glass tube protruded into the observation chamber, and the inside walls were covered with an adsorbing layer of platinum black.

The Diffraction Patterns

For the purpose of demonstrating the principal features of the phenomenon of the diffraction of atoms, patterns were obtained by exposures with three different arrangements of the crystal and detecting plate. These will be referred to as (a) normal incidence (b) 45° incidence in the 110 azimuth and (c) 45° incidence in the 100 azimuth. In each case the patterns were those expected from the following two assumptions: (1) The distribution of wavelengths in the beam was that calculated from the Maxwellian velocity distribution by the use of the de Broglie relation, and (2) The diffraction grating was made up of scattering points arranged on the surface in a plane square array with a spacing d equal to the value 2.835A obtained by x-ray measurements for the distance between two adjacent ions of the same type. The principal axes of this array lie in the 110 azimuths and the angular positions (ϕ, θ) of the diffraction beams with respect to these axes can be correctly calculated from the plane cross-grating equations

$$\cos\theta_0 - \cos\theta = m\lambda/d \tag{8a}$$

$$\cos\phi_0 - \cos\phi = n\lambda/d \tag{8b}$$

in which m and n have the values $0, \pm 1$, etc.

Of the patterns which have been recorded, the most complete is that reproduced in Fig. 5 which was obtained with the crystal and the detecting plate arranged for normal incidence as is shown in Fig. 1. The specularly reflected

beam appears in the photograph at the center of the pattern superposed upon the hole drilled for the incident beam. The more intense dispersed branches of the pattern, which are reproduced in the vertical and horizontal directions, lie in the 110 azimuths of the crystal. These correspond to the four ways of assigning 0 and ± 1 to m and n in equations (8), and may be appropriately designated as (1, 0) beams. In addition to these, four other fainter beams are visible in the 100 azimuths corresponding to $n = \pm 1$, $m = \pm 1$. These will be designated as (1, 1) beams. The dispersion in these beams seems to be greater than that in the (1, 0) beams as would be expected since these may be considered as arising from a grating of the spacing $d/2^{1/2}$. The angular dimensions of the pattern may be judged from the fact that the distance from the crystal to the detecting plate, when increased in the ratio of the enlargement of the photograph, was 12.9 mm.

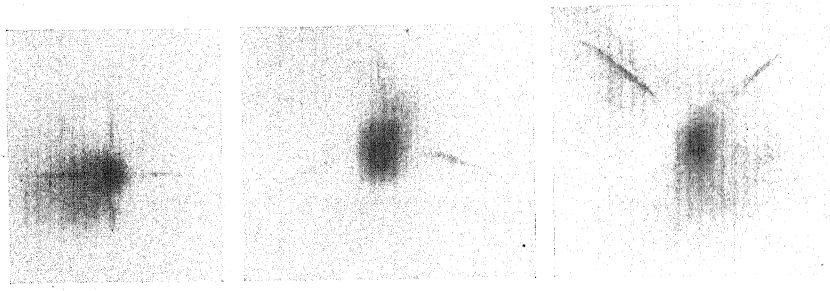

Fig. 5. Diffraction of hydrogen atoms reflected at normal incidence from an LiF crystal.
Fig. 6. Diffraction of hydrogen atoms reflected at 45° incidence in the 110 azimuth.
Fig. 7. Diffraction of hydrogen atoms reflected at 45° in the 100 azimuth.

A pattern produced by reflecting the beam at 45° incidence in the 110 azimuth is reproduced in Fig. 6. In this instance the arrangement of the crystal and detecting plate was that represented in Fig. 3. The (0, 0) specularly reflected beam again appears at the center of the pattern and the (1, 0) beams are now a straight line in the plane of incidence and a parabola symmetrically placed with respect to this line and intersecting it in the specularly reflected beam. If θ designates the angles measured from the rows of ions which are parallel to the plane of incidence, and ϕ those measured from the perpendicular rows, then the beam which is dispersed in the plane of incidence is represented by $m = +1$, $n = 0$ in equations (8). The two branches of the parabola, on the other hand correspond to $m = 0$ $n = \pm 1$. The straight branch in the plane of incidence on the lower side of the specular beam corresponding to $m = -1$, $n = 0$ might have been expected to appear but the dispersion was such that the most probable wave-length fell below the plane of the crystal, and, on account of the greater dispersion in this branch and the paucity of the wave distribution in the region of short wave-lengths, this branch was too faint to appear in the photograph.

The (1, 1) beams in this case take the form of two hyperbolae intersecting in the specular beam but these were perhaps too faint to be distinctly visible

in the reproduction. Unquestionably they could be brought out more intensely if a special effort were made.

The pattern at 45° incidence in the 100 azimuth (Fig. 7) was obtained with the same arrangement of Fig. 3, except that the crystal was rotated in its own plane 45° from its former position. The plane of incidence was in this case parallel and perpendicular to the cleaved edges of the crystal so that the principal axes of the surface lattice intersected the plane of incidence at angles of 45°. The (1, 0) branches of the pattern now appear as the two hyperbolic intercepts with the plane of the detecting plate of the two cones, $\theta = 60°$, and $\phi = 60°$. The branches which lie above the specular beam are intense but those lying between the specular beam and the plane of the crystal, although visible, are weak for the same reasons as were given in regard to the $n = 0$, $m = -1$ beam of Fig. 6. The (1, 1) beams in Fig. 7 should have the form of the (1, 0) beams of Fig. 6 except for greater dispersion but these were too faint to appear.

The Distribution of Wave-Lengths

Assuming the Maxwellian law for the distribution of velocities of the atoms per unit volume in the beam, the distribution in wave-lengths of the intensity of the atom waves falling on the crystal as predicted by the de Broglie relation is given by

$$dI/d\lambda = Ae^{-\lambda_0^2/\lambda^2}/\lambda^5 \tag{9}$$

in which λ_0 has the value $h/(2mkT)^{1/2}$. The expected distribution of intensity along the path s of a branch of the diffraction pattern is calculable from (9) by the relation

$$\frac{dI}{ds} = \frac{dI}{d\lambda}\frac{d\lambda}{d\theta}\frac{d\theta}{ds} \tag{10}$$

$d\lambda/d\theta$ may be obtained by differentiation of the grating equations (8) and $d\theta/ds$ is calculable from the geometry of the arrangement.

Since the intensity measurements were to be made with a densitometer the straight line patterns at normal incidence seemed at first sight to be the easiest to manipulate. A comparison of these patterns with those obtained at 45° incidence however showed that the latter were less obscured by diffuse radiation and for this reason were less subject to errors. To combine this advantage with ease of measurement it was decided to use a pattern obtained with the crystal oriented for 45° incidence in the 110 azimuth and a slightly different arrangement of the detecting plate as shown in Fig. 8. With this arrangement branches dispersed along the periphery of the 45° cone appeared on the detecting plate as a circle (Fig. 9) and this form of pattern was easily measured with a Koch and Goos densitometer by the use of a simple attachment constructed to give rotary motion. Besides its adaptation to measurement this pattern had two other great advantages. (1) All points of the circle were equally distant from the surface of the crystal and for this reason the general

darkening of the plate was distributed somewhat evenly. (2) The calculations were extremely simple and involved only the measurements of the angular positions ψ on the plate.

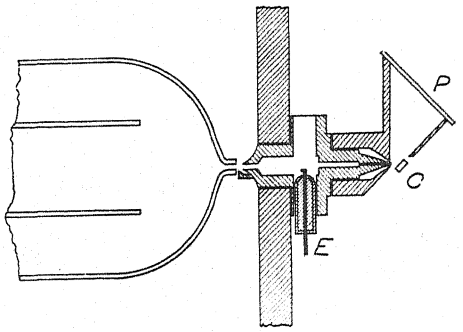

Fig. 8. Arrangement of plate holder for circular patterns.

The grating equation (8b) in this instance reduces to

$$\cos\phi = n\lambda/d \tag{11}$$

and the measured angle ψ of the circular pattern is related to ϕ by

$$\cos\phi = \sin\psi \sin 45°, \tag{12}$$

from which

$$dI/d\psi = A'e^{-2\lambda_0^2/d^2\sin^2\psi} \cos\psi/\sin^5\psi. \tag{13}$$

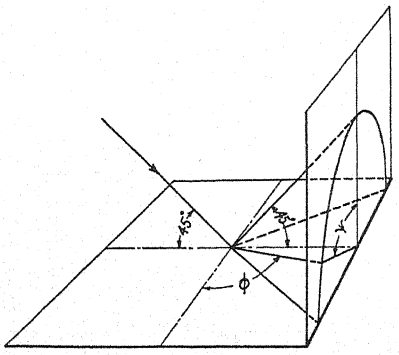

Fig. 9.

The angle ψ_0 of maximum intensity is found by equating to zero the derivative of the right hand member of (13) and it is given by

$$\cos^2\psi = -(2\lambda_0^2/d^2 - 3)/8 + [(2\lambda_0^2/d^2 - 3)^2/64 + \tfrac{1}{4}]^{1/2} \tag{14}$$

If it is assumed that the temperature of the source of the atom beam was

that of the water which circulated in a jacket surrounding the discharge tube[5] then

$$T = 300° K \qquad d = 2.835A$$
$$\lambda_0^2 = 3.13 \times (10)^{-16} \text{ cm}^2 \qquad \psi_0 = 32.7°.$$

Intensity measurements were made from the photographic negatives. As regards the position of maximum intensity this method of measurement would have been independent of the plate calibration were it not for the fact that the pattern was superposed upon a background of variable intensity in spite of the advantages of the arrangement for overcoming this trouble. In order to correct the measurements for this background intensity the plate was also measured along the circumference of a circle of slightly different diameter from that of the diffraction pattern itself, and this set of measurements was applied to the first set as corrections. A calibration of the densitometer deflection in terms of the intensity of an atom beam was obtained by exposing a separate plate in various places to the primary beam for successively increasing times so that a series of dark spots was formed which covered the intensity range of the patterns. This plate was photographed and developed under exactly the same conditions as pertained in the case of the plates which contained the patterns. Densitometer measurements then showed that the difference of the deflection produced by the center of one of the spots and that produced by the unexposed portions of the plate was very nearly proportional to the time of exposure of the spot. This fortunate coincidence led to the simple rule that the deflections of the densitometer could represent atom beam intensities if corrected by subtracting the deflection at an adjacent point of the background. Although this method of making intensity measurements cannot be regarded as possessing a high degree of reliability, as will be recognized by those familiar with the precautions necessary in ordinary photographic photometry, yet it led to surprisingly consistent results in good agreement with what was expected for the angle of maximum intensity. Eight corrected sets of measurements from plates made from three different molybdenum oxide originals gave a weighted mean value of $\psi_0 = 31.6°$ with a probable error of 2.2° as compared with the calculated value of 32.7°. This accuracy probably speaks more for the uniformity of the background than for the method of calibration and correction, and it is felt that a more reliable calibration must be devised before the photographic method can be used satisfactorily for precise intensity measurements.

Relative Intensities of the (1, 0) and (1, 1) Beams

Measurements of the relative intensities in different orders of x-ray spectra have been applied[6] to a determination of the relative scattering powers of the different atom species in the crystal. It is of interest to attempt the same thing using the different orders in the atomic diffraction patterns.

[5] From the work of J. B. Taylor, Phys. Rev. **29**, 309 (1927) this seems to be a reasonable assumption.

[6] W. H. Bragg and W. L. Bragg, X-rays and crystal structure, page 187, et seq.

Because of the overlapping of the 1, 0 and 2, 0 orders these beams are not well adapted to this purpose until more homogeneous velocities can be used, but it is interesting to compare the intensities in the 1, 0 and 1, 1 branches. In terms of the scattering powers U of the two ion types in the two directions, the ratio of the intensity of a (1, 1) beam of a particular wave-length to that of a (1, 0) beam of the same wave-length may be expressed, by the use of the principle of the superposition of amplitudes, as

$$I_{11}/I_{10} = (U_{11F} + U_{11Li})^2/(U_{10F} - U_{10Li})^2. \tag{15}$$

If the U's are assumed to be spherically symmetrical functions of space, i.e., $U_{11} = U_{10}$, the ratio U_F/U_{Li} can be determined from the measured ratio of intensities I_{11}/I_{10}.

In making the intensity measurements one must take account of the fact that the beams are not homogeneous in wave length but they contain a distribution (9) which is more highly dispersed in the (1, 1) than in the (1, 0) branches. The maximum of intensity on the plate in the (1,0) branches of the normal incidence patterns should fall, according to these considerations, at a distance S from the central spot equal to 0.408 l, where l is the distance between the crystal and the plate. The calculated position of maximum intensity in the (1, 1) branches is at $S = 0.589\ l$.

The ratio of intensities at these two points of maximum intensity is found from (9), (10) and (15) to be

$$\left(\frac{dI}{ds}\right)_{11} \Big/ \left(\frac{dI}{ds}\right)_{10} = (U_{Li} + U_F)^2/6.3(U_{Li} - U_F)^2. \tag{16}$$

The actual measurements carried out by means of the photometric technique described in the previous paragraph give a value of this ratio of about 1/6 with the possibility of an error of 100 percent or more arising not only in the unreliability of the method of calibration but also from the faintness of the 1, 1 branches. Although this inaccuracy of measurement renders a quantitative determination of U_{Li}/U_F impossible, the assumption of spherical symmetry of the U's leads to a small value of this ratio. The same conclusion results from a consideration of the great intensity in the 1, 0 orders where the contributions to the amplitude from the two ion types is 180° out of phase. From these measurements it is not necessary to conclude that the scattering power of an ion is definitely less in the 1,1 direction than in the 1,0 direction as Estermann and Stern found from the extremely small intensity which they observed in the (1,1) beams, although this conclusion would be necessary if a more accurate determination of the ratio (16) leads to a value greater than 1/6.

Diffraction by a Secondary Lattice of Wide Spacing

In addition to the spectra which have been described, arising from the surface array of ions, another type of spectrum of very low dispersion appeared on the plates. This type of spectrum was first noticed on a plate exposed at

45° incidence in the 100 azimuth where it appeared as a slight smearing of the specular beam in the plane of incidence. Later the same phenomenon was noticed on the plates exposed at 45° incidence in the 110 azimuth and in this case the spectra took the form of a blurred X extending out from the specular beam. These features may perhaps be distinguished in Figs. 6 and 7. An exposure at grazing incidence in the 100 azimuth increased the dispersion in this spectrum as shown in Fig. 10 but failed to separate the maximum of the

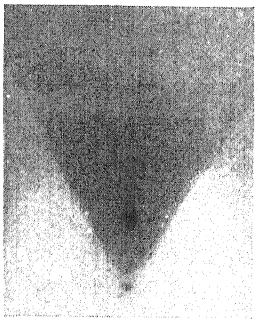

Fig. 10. Secondary structure spectrum at grazing incidence.

wave length distribution from the specular beam. It has been pointed out[7] that this spectrum indicates the existence of a secondary periodicity on the crystal surface parallel to the 100 planes in agreement with the theory of Zwicky.[8] Work is now under way to increase the resolving power in this spectrum with the hope of measuring the constant of the secondary lattice.

The writer wishes to take this opportunity to acknowledge his indebtedness to Mr. C. K. Boyer and Mr. M. A. Roesch, both of the Drexel Institute, who have assisted in this work.

[7] T. H. Johnson, Phys. Rev. **37**, 87 (1931).
[8] Zwicky, Helvetica Physica Acta III, 269 (1930).

SCATTERING OF X-RAYS FROM GASES

By E. O. Wollan
The University of Chicago

(Received February 18, 1931)

Abstract

Measurement of the intensity of scattering of x-rays by various gases has been made for scattering angles between 10° and 90°. Soller slits were used to get a well-defined scattering angle and matched filters of ZrO_2 and SrO were used to isolate the K_α lines of molybdenum. Intensity measurements have been made for hydrogen, helium, oxygen, neon and argon. All the measurements were put on the same scale by comparison of the intensity of scattering from the various gases with the scattering from hydrogen at 90°. This is equivalent to putting the intensities on an absolute scale since the scattering from hydrogen at 90° can be calculated with considerable certainty. Values of the structure factors for neon and argon were calculated and comparison made with those determined from wave mechanics for similar atoms.

Introduction

IN VIEW of Compton's[1] recent theory for determining the electron distributions in atoms from the angular distribution of intensity of x-rays scattered from monatomic gases it was thought desirable to get more complete experimental data.

Barrett[2] in 1928 published data for the scattering of x-rays from most of the gases included in this paper. He measured the intensity as a function of angle but no attempt was made to get absolute intensity measurements.

In the work reported here a more definite scattering angle has been obtained by the use of Soller slits, x-rays made homogeneous by the use of balanced filters have been used wherever the intensity permitted, and all the measurements have been put on the same scale by comparing the intensities from the various gases with that from hydrogen. This is equivalent to putting the intensity measurements on an absolute scale since the scattering from hydrogen at 90° can be calculated with considerable certainty.

Apparatus and Procedure

The set-up is shown in the diagram Fig. 1. A molybdenum target x-ray tube was operated at 40 kv peak and 35 m.a. with full-wave rectification. The tube was immersed in oil in a lead box fitted with a lead glass front. A small celluloid window within 2 mm of the tube transmitted the primary beam with only a small reduction in intensity due to the 2 mm of oil. This arrangement

[1] A. H. Compton, Phys. Rev. **35**, 925 (1930).

[2] C. S. Barrett, Phys. Rev. **32**, 22 (1928). Measurements of the relative scattering of hydrogen and Argon have been made by Herzog but not with homogeneous radiation. G. Herzog Helvetica Phys. Acta **2**, 169 (1929).

allowed the tube to be brought very near the spectrometer and the intensity was considerably greater than would have been possible with the tube in air.

The intensities were measured with an ionization chamber and a Compton electrometer with which currents of 5×10^{-15} amperes could be measured with a reproducibility of about five percent.

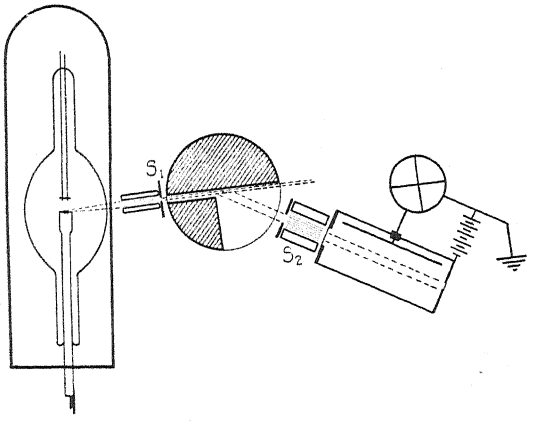

Fig. 1. Arrangement of apparatus.

The scattering chamber is shown in Fig. 2. It was made from a brass tube 5.5 inches in diameter, 3 inches high and having 1/8 inch walls. The top and bottom were 0.5 inch steel plates grooved and fitted with rubber gaskets and

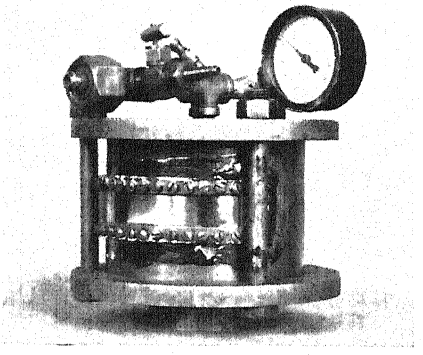

Fig. 2. Scattering chamber.

held in position by three bolts as shown. The windows were of 0.7 mm celluloid 2 cm high. They were screwed down on rubber gaskets and picein wax used where it was found necessary. The base was fitted to the spectrometer table so it could be removed and replaced without affecting the readings. The top contains a gauge, an oxygen tank connection, a needle valve for the chamber and a side tube for evacuating the chamber and the leads. The chamber

was partially filled with sealing wax as shown in Fig. 1, and lined with lead. This cut the volume to about 250 cc and acted as a shield for the diffusely scattered x-rays.

The chamber was found to be very satisfactory as pressures of 200 pounds were used with a leak of only a few percent per week and the corrections for scattering from the evacuated chamber were almost negligible.

Reference to the diagram will show the arrangement of the chamber and the slit system. Soller slits were used to collimate the primary as well as the scattered beam. These slits allowed a maximum angular divergence of less than 2° in the horizontal plane. Slit S_1 was 3 mm wide and 1 cm high. Slit S_2 was 1 cm high and could be varied in width to 1.5 cm. Besides defining the

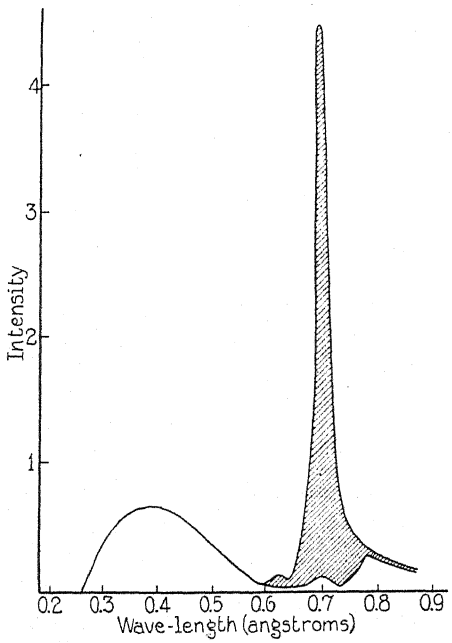

Fig. 3. Transmission through ZrO_2 and SrO filters.

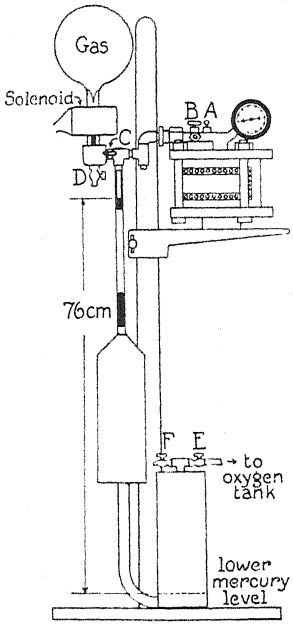

Fig. 4. High pressure mercury pump.

scattering angle the second slit served the additional purpose of determining the scattering volume. With this slit remaining constant the scattering volume was proportional to sin ϕ. The height of the slits S_1 and S_2 made the actual scattering angle slightly larger than indicated on the spectrometer circle. It was necessary to make correction for this on the readings between 10° and 30°.

The $K\alpha$ lines of molybdenum were separated out by the balanced filter method.[3] A filter of ZrO_2 containing about 0.025 gm per cm^2 was balanced by a filter of SrO so that less than five percent of the radiation corresponding to the difference of these filters lay outside of the range between the K critical absorption edges of Zr and Sr. A curve showing the transmission by these

[3] P. A. Ross, Phys. Rev. **28**, 425 (1926).

filters is shown in Fig. 3. The shaded portion represents the difference of the transmission by the two filters. The filters were additionally tested by measuring the absorption coefficient of aluminum which gave a straight line when log (I_0/I) was plotted against thickness. It is very important that these filters be well balanced so that reliable corrections for absorption can be made when elements like argon are compared with oxygen.

Since some of the gases were originally at atmospheric pressure it was necessary to construct a pump to put them into the chamber at the desired pressure. Fig. 4 shows the construction of the pump. The cylinders were of seamless steel tubing with welded bottoms and top and connecting tube. The rest was constructed mainly from iron pipes and connections. The vertical pipe was cut through at two places and a glass tube waxed inside to make the mercury level visible. With valve B closed and all the others open the system

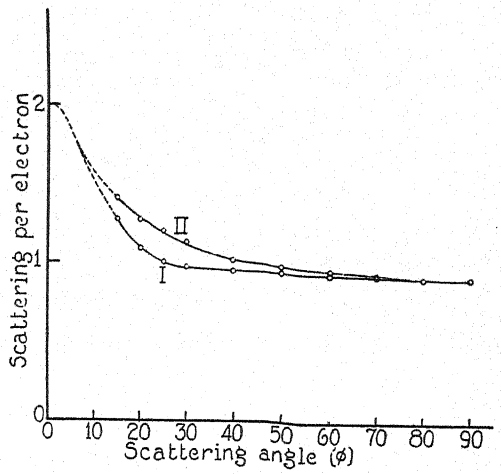

Fig. 5. Curve I hydrogen, Curve II helium.

could be evacuated through valve D. Closing valve D and breaking the tip in the glass container by means of the electromagnet, the gas expanded into the upper cylinder of the pump. By closing valves C and F the gas could be forced into the scattering chamber by applying the oxygen tank pressure at valve E. With repeated pumping it was necessary to draw the mercury back into the lower container by applying the vacuum pump at F.

HYDROGEN

The hydrogen used in this experiment came from a tank especially prepared and analysed by Burdett Oxygen Company and found to have less than 0.1 percent oxygen and CO_2 and 0.07 percent water vapor by volume. After scattering measurements had been made on the gas the density was measured by weighing and no additional impurities were found to be present. The scattering chamber connected directly to the hydrogen tank, was evacuated together with all the leads, flushed out several times and filled to about 200 pounds pressure. It was then placed in position on the spectrometer table

and the scattered intensity measured from 10° to 90°. Even at 200 pounds pressure, however, it was necessary to use general radiation in place of the balanced filters. Curve I, Fig. 5 shows the scattering per electron corrected to $\lambda = 0.71$A plotted against ϕ. On the basis of the classical theory of scattering the value of $S \equiv I_s/ZI_e$ for hydrogen would be unity at 90°. The fact that practically all the intensity scattered at 90° from hydrogen is modified will make the experimental value at this angle slightly lower than unity. The Breit-Dirac relation may then be used

$$S_{class} = S_{mod}\{1 + \gamma \text{ vers } \phi\}^3. \quad (1)$$

Placing for 90° $S_{class.} = 1$, we have thus, $S \equiv S_{mod.} = (1+\gamma \text{ vers } 90°)^{-3}$. For $\lambda = 0.71$ A, γ vers $90° = 0.0243$, whence $S = 0.91$.

The data included in table I are all based on a value of S for hydrogen equal to 0.91 at 90°. To get the classical values of S Eq. (1) must be used.*

TABLE I. *Scattering per electron.* $\lambda = 0.71A$.

Angle	Hydrogen	Helium	Oxygen	Neon	Argon
10°			8.05	8.55	13.90
15°	1.27	1.45	4.90	6.87	10.65
20°	1.10	1.34	2.96	5.16	8.50
25°	1.03	1.27	2.00	3.85	6.35
30°	1.00	1.20	1.72	3.11	5.23
40°	0.98	1.08	1.43	2.04	4.15
50°	0.97	1.01	1.15	1.53	3.32
60°	0.95	0.97	1.04	1.32	2.74
70°	0.93	0.95	1.02	1.24	2.28
80°	0.92	0.92	1.01	1.18	2.10
90°	0.91	0.91	0.96	1.06	1.95

In so far as the scattering per electron from hydrogen is known, the scattering from other gases can be put on an absolute basis by comparison with it. Since the intensity of scattering from hydrogen is weak and difficult to measure it was first carefully compared with oxygen which was then used as a secondary standard of comparison.

COMPARISON OF OXYGEN AND HYDROGEN

Oxygen and hydrogen were compared several times at 90° using general radiation and pressures of about 200 lb/sq. in. for both gases. This involves a large correction for absorption for an unknown wave-length. To make this correction the intensity of scattering was plotted as a function of pressure. The decrease in scattering per gm at 200 lb/sq. in. over that at small pressures was taken as the absorption correction.

Comparison of hydrogen at 200 pounds pressure with oxygen at 40 pounds pressure, taking account of the difference in pressure and making only a very slight absorption correction, gave results in very close agreement with those of the first method.

* Equation (1) gives the classical value only when all the scattered radiation is modified. In the case of oxygen, neon and argon the unmodified radiation must also be considered. Compton (ref. 1) has shown how the classical value of S can be gotten in this case.

The hydrogen curve was corrected to a wave-length of 0.71A by a method shown by the curves of Fig. 6. The curves are: I, hydrogen with general radiation; II, oxygen with general radiation; and III, oxygen taken with $\lambda = 0.71$A and arbitrarily fitted to the other oxygen curve at 90°. From these curves the intensity of scattering from hydrogen for $\lambda = 0.71$A was determined.

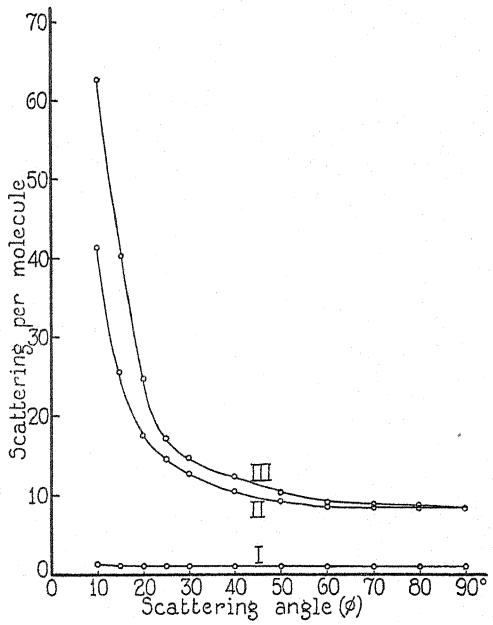

Fig. 6. Curve I hydrogen (general radiation), Curve II oxygen (general radiation), Curve III oxygen (filtered radiation, $\lambda = 0.71$A).

HELIUM

The helium came in liter containers at atmospheric pressure and was introduced into the chamber by means of the mercury pump described above. The pressure used was about 115 lb/sq. in. A number of sets of readings were taken and the intensity compared directly with hydrogen. The intensities of scattering from hydrogen and helium at 90° were found to be equal within the experimental error. Curve II, Fig. 5 shows the scattering per electron from helium corrected to $\lambda = 0.71$A in the same manner as for hydrogen.

In introducing the helium into the chamber about 0.9 percent of air by volume entered as an impurity. This was found to be the case by measurement of the density after the readings had been taken. Correction was of course made for this and would not lead to any appreciable error because the scattering from air could easily be measured. The data for hydrogen and helium are in very close agreement with the results obtained by Barrett. Although he obtained no excess scattering from hydrogen his data only extended to what corresponds to $\phi = 30°$ on the above curve.

Neon

Neon was also obtained in liter containers at atmospheric pressure and was put into the scattering chamber with the aid of the mercury pump.

The intensity measurements were made with filtered radiation and a number of sets of readings taken. In order not to have to evacuate and refill the chamber repeatedly, a sheet of celluloid was used for an intermediate comparison. Comparisons of the intensity from neon were made with the celluloid scatterer and then the chamber was evacuated and filled with oxygen and the comparisons with the celluloid scatterer again made. Corrections were made for the different absorption coefficients, and the results are shown in curve IV,

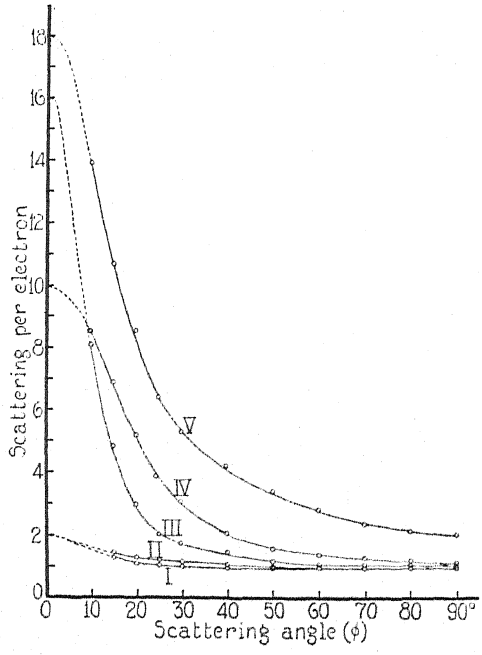

Fig. 7. λ=0.71A. Curve I hydrogen, Curve II helium, Curve III oxygen, Curve IV neon and Curve V argon.

Fig. 7. The scattering per electron from neon at 90° is very nearly that from oxygen. The neon curve begins to rise at larger angles than does the oxygen curve, a difference similar to that between hydrogen and helium.

Argon

The argon used in these measurements was obtained in a tank with about 0.3 percent impurity. The chamber could be readily filled to any desired pressure directly from the tank. This gas, however, presented greater difficulties than the other gases since its absorption coefficient is so much larger. Fig. 8 shows the relation between intensity and pressure for argon and oxygen. Curves I and II represent respectively the measured intensity from argon and oxygen; curves IV and III represent the values after correction for absorption

has been made. To make the corrections as small as possible and still get sufficient intensity from both oxygen and argon pressures of about 40 to 50 lb/sq. in. were used.

In the case of argon, the comparison of intensity with oxygen was done directly by taking a number of readings with one gas and then refilling the chamber with the other gas with the x-ray tube in operation during the process. Several of these comparisons were made and the pressures varied somewhat to make the absorption corrections more certain.

It is noticeable that in argon the scattering per electron is considerably larger than for the other gases. This would correspond to a greater electron density near the center of the argon atom.

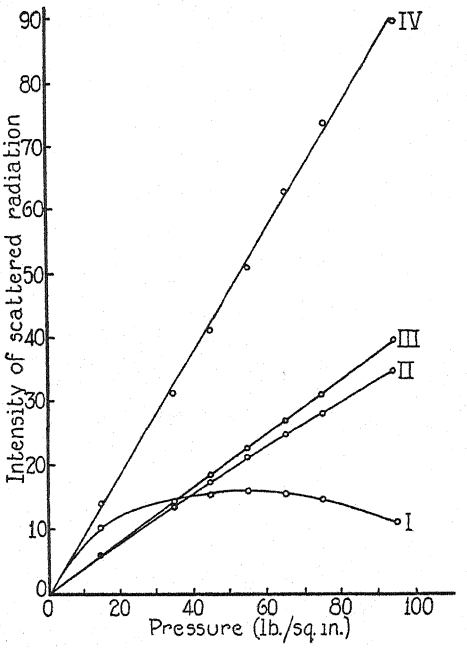

Fig. 8. Curves I and II represent respectively the measured intensity from argon and oxygen curves. Curves IV and III represent the values after correction for absorption has been made.

Errors

The largest errors involved in measuring the scattering per electron would probably be those of comparing the scattering from one gas with that of another. In the case of the comparison of the intensity of scattering from hydrogen with that from oxygen the probable error from the mean was about 1 percent. It is likely that there are other errors such as uncertainty of wavelength, measurement of pressure and corrections for absorption which would also amount to about 1 percent. This would mean that the scattering from oxygen would probably be correct to about 2 percent. In comparing neon and oxygen, considering the probable error already mentioned, the uncertainty

in the neon data would be of the order of 3 percent. In argon the large correction for absorption would probably increase the uncertainty to about 4 or 5 percent. In the case of hydrogen and helium the probable error of any point of the curve was about 2 percent.

Structure Factor

Calculation of the structure factors for neon and argon have been made from the relation given by Compton

$$F = Z\left\{\frac{S-1}{Z-1}\right\}^{1/2} \tag{2}$$

where S is the classical value of the scattering per electron, Z is the atomic number and F the structure factor. The values thus calculated are given in Table II. In order to make comparisons between these data and the structure

Table II. *Structure factor.*

ϕ	$\left(\frac{\sin\phi/2}{\lambda}\right)$	Neon		Argon	
		S_{class}	F	S_{class}	F
10°	0.123	8.55	9.16	13.90	15.63
15°	.190	6.87	8.08	10.65	13.53
20°	.245	5.16	6.80	8.50	11.93
25°	.306	3.86	5.64	6.36	10.10
30°	.365	3.12	4.86	5.26	9.00
40°	.482	2.06	3.43	4.17	7.77
50°	.596	1.56	2.49	3.35	6.69
60°	.704	1.37	2.02	2.79	5.84
70°	.808	1.30	1.80	2.34	5.06
80°	.905	1.26	1.70	2.18	4.72
90°	.995	1.17	1.37	2.05	4.49

factors calculated from crystalline reflection it is necessary to correct the latter for the effect of thermal agitation which does not affect the intensity of x-rays scattered from gases.

Some very interesting comparisons have been made by James and others[4,5] between the crystal reflection data at low temperatures and the structure factors calculated from Hartree's wave mechanics solution of the charge distribution in the K^+, Cl^- and Na^+ ions. Making temperature corrections and assuming the existence of zero point energy they get structure factor curves which are in good agreement with the theoretical curves.

The values of F from Table II are plotted in Figs. 9 and 10 together with F values from wave mechanics taken from the above mentioned papers.

In Fig. 9 the solid line represents the F curve for Na^+ calculated from wave mechanics and the broken line represents the F values for neon. From a consideration of equation (2) the reason for the apparently large inaccuracies in

[4] R. W. James and Brindley, Proc. Roy. Soc. A121, 155 (1928).
[5] R. W. James, I. Waller and D. R. Hartree, Proc. Roy. Soc. A118, 343 (1928).

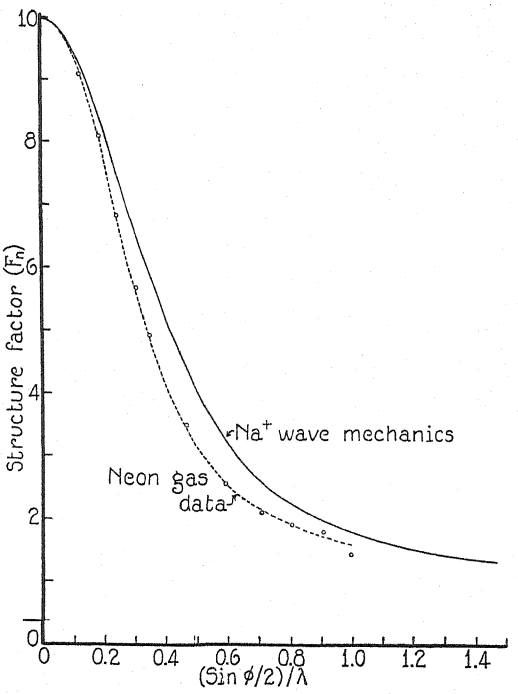
Structure factor (F_n)
10
8
6
4
2
0
0
0.2
0.4
0.6
0.8
1.0
1.2
1.4
(Sin ϕ/2)/λ
Na^+ wave mechanics
Neon gas data

Fig. 9.

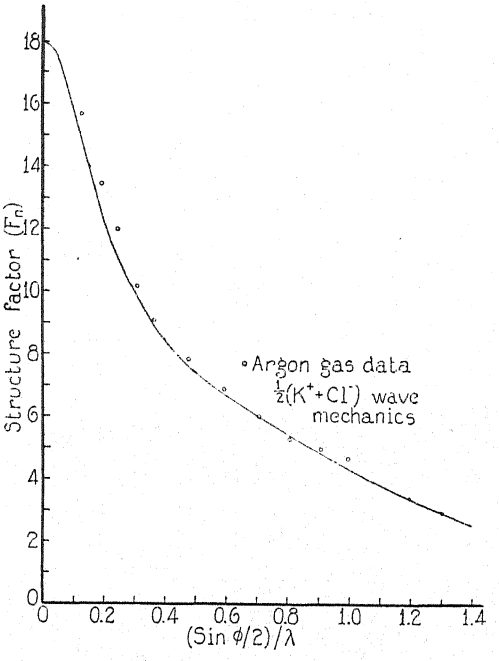
Structure factor (F_n)
18
16
14
12
10
8
6
4
2
0
0
0.2
0.4
0.6
0.8
1.0
1.2
1.4
(Sin ϕ/2)/λ
Argon gas data
$\frac{1}{2}(K^+ + Cl^-)$ wave mechanics

Fig. 10.

the values of F when S is nearly equal to unity can be seen. For neon at (sin $\phi/2)/\lambda = 1.00$ an error of 2 percent in S gives rise to an error of 9 percent in F.

A more significant comparison between theory and experiment is shown in Fig. 10. The curve represents the average of the F values for K^+ and Cl^- determined from wave mechanics. The circles give the F values from Table II for argon. The agreement is seen to be very satisfactory.

As has recently been shown by Compton[6] a comparison of these data with that determined from reflection from a crystal of KCl and corrected to 0°K gives a good experimental check of the existence of zero point energy.

Conclusion

These data furnish a significant check of Compton's recent theory of the intensity of x-rays scattered from gases and the use of these data for the determination of electron distribution in atoms. The agreement between the F curves of argon and those determined from wave mechanics and also from crystal reflection should give more confidence in the use of these methods for determining the distribution of charge in the atom.

A comparison of the F curves determined by these three methods is also a further check on the existence of zero point energy.

Calculation of the electron distribution curves from these data are now in progress.

In conclusion the author wishes to express his appreciation to Professor A. H. Compton, who suggested this problem, for his continued assistance in its solution.

[6] A. H. Compton, Phys. Rev. **37**, 104 (1931).

INTERACTION OF X-RAYS WITH BOUND ELECTRONS

By Austin J. O'Leary
Columbia University

(Received February 28, 1931)

Abstract

I. Change of wave-length of scattered x-rays. A previous analysis of scattered x-rays in this laboratory by means of the double crystal spectrometer showed fine structure in both the unmodified and modified lines. These fine structure lines were interpreted as being due to absorption of an amount of energy equal to the binding energy of the electrons in the scattering substance. Since then, other experimenters have failed to observe this phenomenon in scattered x-rays. The earlier work has been repeated using measuring apparatus having greater stability and sensitivity but with experimental conditions for producing the scattered radiation as nearly as possible like those of the earlier experiments. No fine structure was found though a line of intensity greater than 10 percent of molybdenum $K\alpha_1$ unmodified could have been detected.

II. Change of wave-length without scattering. A change of wave-length ascribed to this type of phenomenon without scattering has been reported by B. B. Ray and R. C. Majumdar. A number of experiments have been performed in an attempt to detect a change of wave-length of this type due to partial absorption of molybdenum $K\alpha_1$ and copper $K\alpha_{1,2}$ characteristic rays in the K-level of carbon. No indication of a modified line was found though a line of smaller intensity than that of the lines reported could have been detected. Two possible sources, other than a change of wave-length, are suggested which may give rise to lines of the type reported.

I. Change of Wave-Length of Scattered X-Rays

Discussion. Spectroscopic analyses have in general shown that when monochromatic x-rays are scattered by matter, the scattered radiation consists of two wave-lengths.[1] An unmodified line appears, having the same wave-length as the incident radiation and a modified line for which the wave-length separation from the unmodified is given by the Compton theory of scattering by free electrons and is

$$\delta\lambda = h/mc(1 - \cos\phi) \tag{1}$$

where h is Planck's constant, m the mass of an electron, c the velocity of light and ϕ the angle of scattering. A theory of scattering by bound electrons was proposed by A. H. Compton[1] in 1924. For the special case in which the recoil electron has zero kinetic energy, the theory predicts wave-length changes given by

$$\delta\lambda = \frac{\lambda^2}{\lambda_s - \lambda} \tag{2}$$

where λ is the wave-length of the incident radiation and λ_s the critical absorption wave-length of the level from which the bound electron is ejected.

[1] A. H. Compton, X-Rays and Electrons, Chapt. IX.

An analysis of scattered x-rays in this laboratory by means of the double crystal spectrometer which gave greater resolution than was hitherto possible with the single crystal methods, gave results which indicated fine structure in both the unmodified[2] and modified[3] lines. The change of wave-length for the fine structure lines found in the unmodified characteristic molybdenum $K\alpha_1$ x-rays scattered at 90° by carbon, beryllium, and aluminum, agreed with that given by Eq. (2). In the case of beryllium, an "anti-Stokes" line was observed but no line in the position of $K\alpha_1$. Similar fine structure lines were reported in the modified radiation scattered by carbon at 155° and beryllium 163°, the wave-length change being given by

$$\delta\lambda = h/mc(1 - \cos\phi) + \frac{\lambda^2}{\lambda_s - \lambda} \tag{3}$$

except that using the estimated angle of scattering, ϕ, the constant h/mc was found to be about 9 percent less than the theoretical value. These fine structure lines were no broader than in the unmodified in spite of the large divergence in ϕ.

Since then, Ehrenberg,[4] Coster,[5] and Kast,[6] using single crystal spectrographic methods failed to observe this reported phenomenon. More recently, the question of scattered radiation was investigated by Bearden,[7] and Gingrich,[8] using double crystal spectrometers without finding any indication of fine structure. Bearden analyzed copper $K\alpha_{1,2}$ and silver $K\alpha_{1,2}$ scattered by graphite and aluminum, and Gingrich, molybdenum $K\alpha_{1,2}$ scattered by graphite. They each observed the $K\alpha_{1,2}$ modified lines and found the wave-length separation from the unmodified to be accurately given by Eq. (1), the constant h/mc agreeing with the theoretical value within experimental error.

About the same time, the author repeated the earlier work done in this laboratory using measuring apparatus having greater stability and sensitivity but with experimental conditions for producing the scattered radiation as nearly as possible like those of the earlier work. A brief description of the experiments is given in the following.

Apparatus and method. A double crystal spectrometer of the type developed here, with both crystals set for first order reflection, was used to analyze the scattered radiation. Two slits, 43 cm apart, 15 mm high, and 7 mm wide, defined the direction of the scattered beam with a third slit between the crystals. Power was supplied at 125 volts and 500 cycles to a three kilowatt oil-immersed transformer and the high potential current rectified by means of two kenotrons and a large condenser. The voltage was read on an electrostatic voltmeter.

[2] B. Davis and D. P. Mitchell, Phys. Rev. **32**, 331 (1928); D. P. Mitchell, Phys. Rev. **33**, 871 (1929).

[3] B. Davis and H. Purks, Phys. Rev. **34**, 1 (1929).

[4] Ehrenberg, Zeits. f. Physik **53**, 234 (1929).

[5] Coster, Nature **123**, 642 (1929).

[6] Kast, Zeits. f. Physik **58**, 519 (1929).

[7] J. A. Bearden, Phys. Rev. **36**, 791 (1930).

[8] N. S. Gingrich, Phys. Rev. **36**, 1050 (1930).

The ionization chamber consisted of two aluminum cylinders, 10 cm long and 4 cm in diameter, one at positive and the other at negative potential, suspended inside a grounded brass box. The central collecting rods in each were connected together and to the lead from the insulated quadrants of the electrometer. There are thus two ionization chambers connected so that the ionization currents in the two are in opposite directions and tend to balance each other. The leak in each chamber due to natural ionization was almost zero. To minimize the irregularity in the electric field produced by the grounded case, an aluminum cap was placed over the end of each cylinder with a window 2 cm high and 1 cm wide corresponding to a similar pair of windows in the grounded case. The x-ray beam entered one window while in front of the other was placed a small radio-active source behind a shutter. The chamber was filled with methyl bromide to absorb the rays.

The sensitivity of the electrometer was 11,000 mm per volt at 1 meter. The capacity of the system as measured with a string electrometer was 38 e.s.u. distributed as follows: 10 e.s.u. each for the ionization chamber and electrometer with the remaining 18 e.s.u. in the shielded lead wires between the two.

The method of measurement was as follows. The shutter was adjusted until the ionization current produced by the radium source just balanced that due to the background radiation. Rocking curves of the unmodified $K\alpha_{1,2}$ scattered rays were taken by timing the drift over a definite part of the scale. The width at half maximum of these curves was always between 20 and 25 seconds. Then a careful search was made to detect the existence of any other lines by insulating the grounding key for a definite time, say 10 minutes, for each setting of the second crystal and noting the drift if any during that time. Compensation for large backgrounds is unsatisfactory but for the small amount of background radiation present in these experiments, the method proved quite successful. The stability of the system was remarkably good, the drift from the zero position never being greater than 3 divisions during the 10 minutes for each reading.

Scattering from carbon at 90°. A cylindrical tube 6.5 cm in diameter with a molybdenum target was placed just out of line of the slits so that no radiation scattered by the glass could pass through. The tube operated steadily at 62 milliamperes and 45 kilo-volts. Both graphite and paraffin blocks were used to scatter the x-rays and were placed along side of the tube so that the average angle of scattering was about 90° with a fairly large divergence. When paraffin was used, a stream of cold air was blown against it continuously to keep it from being melted by the heat from the tube. In no case was there any indication of a line other than the unmodified $K\alpha_{1,2}$ lines though the method was sufficiently sensitive to detect a line of intensity greater than 10 percent of the unmodified $K\alpha_1$ line. With the radium source removed, readings were taken with and without the carbon, everything else remaining the same. The ionization current was zero with the carbon removed, showing that all the x-rays entering the ionization chamber came from the carbon.

Carbon at 150°, beryllium 154°. A tube was built with molybdenum target and graphite scattering element inside as closely similar as possible to the tube used in the original investigation[3] of fine structure in the Compton effect. The focal spot was 5 mm wide and 9 mm long and faced a small graphite block supported about 2 cm from the center of the spot. This gave a large divergence in scattering angle, the average being about 150° with a plus or minus divergence of about 15°. A similar tube had a beryllium scattering element with an estimated scattering angle of $154° \pm 18$. The anode in each tube was tilted sufficiently toward the scattering block to insure against any possibility of direct radiation from the molybdenum target and was out of line of the slits so that no radiation from the copper anode itself could come through. This was checked by a photographic method. Curves for the $K\alpha_{1,2}$ lines scattered by graphite were similar to those found for 90° scattering, with no indication of fine structure. An unmodified line of very small intensity was observed from beryllium with no indication of an "anti-Stokes" line. A curve for the modified radiation was not taken in either case but a search was made in the position where the fine structure lines were originally observed without finding any indication of them. The modified radiation apparently formed a very broad hump as would be expected from the divergence in scattering angle.

II. Change of Wave-Length without Scattering

Discussion. A change of wave-length ascribed to this type of phenomenon has been reported by B. B. Ray[9] at zero angle of scattering, his conclusion being that a change of wave-length of x-rays on traversing matter does occur but without change of direction. He passed x-rays from a metal tube with tungsten filament through carbon soot and air and photographed the transmitted radiation with a Siegbahn spectrograph with calcite crystal. Besides the lines to be expected, several broad and diffuse lines appeared each time on the photographic plate and were interpreted as being due to a change of wave-length of the characteristic lines caused by absorption of an amount of energy equal to that necessary to raise an electron from the K-levels of carbon, nitrogen, and oxygen, to a higher level or remove them from the atom with zero velocity. Lines due to a similar absorption in the L-levels would be expected but could not have been detected with the apparatus. A variety of characteristic wave-lengths was used, all showing the same effect. R. C. Majumdar,[10] working in the same laboratory, has reported a similar effect due to partial absorption of characteristic x-rays in the L_1 level of aluminum.

The following considerations indicate the factors which are important in testing the existence of this phenomenon in the presence of continuous radiation. Suppose monochromatic radiation of frequency ν, and intensity I, falls on a thickness of matter d. Assuming the particular type of absorption mentioned above, the amount of radiation emerging from the matter with

[9] B. B. Ray, Nature **125**, 746 and 856 (1930); Nature **126**, 399 (1930); Zeits. f. Physik **66**, 261 (1930).

[10] R. C. Majumdar, Nature **127**, 92 (1931).

modified frequency $\nu' = (\nu - \nu_k)$ where ν_k is the critical absorption frequency of the K-level, would be:

$$I' = kIe^{-\mu' d}\left\{\frac{e^{(\mu'-\mu)d} - 1}{\mu' - \mu}\right\} \tag{4}$$

where μ is the linear absorption coefficient for radiation of frequency ν, μ' that for radiation of frequency ν' and k the linear absorption coefficient for this particular type of absorption in the K-level. The absorption due to modification of the frequency ν' itself has been neglected. Taking $\mu = \mu'$, which is approximately true, (4) reduces to

$$I' = kIde^{-\mu d}. \tag{5}$$

This is a maximum for $d = 1/\mu$ which would be the optimum thickness to use if no continuous radiation were present but this is not the case in the experiments under discussion. The continous radiation is absorbed in the usual way though it is not affected to any extent by the type of absorption under consideration and if I_1 is the incident intensity of the continuous in the region of frequency ν', then its intensity on emerging is $I_1 e^{-\mu d}$. Thus the ratio R, of the modified line to the background in its neighbourhood, which determines the contrast on the photographic plate is:

$$R = kdI/I_1 \tag{6}$$

and is directly proportional to the ratio I/I_1 and the mass of absorbing material. Conversely, knowing the amount of absorption produced by the absorbing material and the ratios I/I_1 and R, one gets the ratio of the intensity of an observed modified line, or of one which might be observed, to the intensity o the incident radiation producing it. This is given by

$$\frac{I'}{I} = R \cdot \frac{1}{I/I_1} \cdot e^{-\mu d}. \tag{7}$$

To test the existence of this phenomenon, the following requirements should be observed:

(1). The mass of material producing the effect should be as large as possible. This is, of course, limited by the time of exposure and the intensity of the radiation.

(2). The ratio I/I_1 should as far as possible be a maximum. This is determined for the most part by the operating voltage which should be high since the ratio increases with the voltage. Impurities in the target reduce this ratio and also extraneous scattered radiation if the plate is not properly shielded.

(3). To eliminate errors, photographs should be taken with and without the absorbing material in place before concluding that any lines observed are produced by its presence.

When a fixed crystal method is used, with a single narrow slit to give resolution and the x-ray beam having the necessary divergence in angle for

reflection of different wave-lengths, each wave-length comes from a different part of the target and errors may arise if the distribution of intensity over the target is not uniform. A pin-hole and a narrow-slit photograph of the target of one of the x-ray tubes with coil filaments used in this laboratory is shown in Fig. 1 and shows clearly the image of the filament coils on the target. Similar photographs of the targets of many other tubes were taken and showed widely different patterns, the particular distribution of intensity depending on the shape and position of the filament, filament cup, and anode. In no case was the distribution of intensity uniform. After reflection of the x-rays from a crystal, the characteristic lines appear on a background having the same pattern as that given by a narrow slit photograph of the target. If the distance from the narrow slit to the photographic plate is short enough, in comparison with the distance to the target, lines, not much broader than the characteristic lines, might appear on the plate and be erroneously interpreted. The tube used by Ray was of the heated filament type and it is possible that the lines observed by him, in every case broad and diffuse, were really due to lines in the target which accidentally appeared in a position where they might be given the interpretation he gave them. Also if the narrow slit is not close to the crystal, each wave-length is reflected from a different part of the crystal and there is the possibility of error due to imperfections in the crystal face. No statement was made as to whether or not photographs were taken with and without the absorbing material in place or other precautions taken to eliminate the possibility of such errors.

In the discussion Ray has assumed, without explaining how he arrived at the figure, that the intensity of the new lines, as compared with that of the primary, is only of the order of one in 400 or 500. However his photographs show that the intensity of these new lines above the background is at least as intense as the background (i.e. $R \geq 1$) and since the ratio of the intensity of the primary line to the background (I/I_1) is not likely greater than 50, Eq. (7) requires that the amount of absorbing material must have been sufficient to absorb 90 percent of the incident rays. The mass of absorbing material has not been given but it is unlikely that the amount of nitrogen and oxygen in which the rays were absorbed, was sufficient to produce this amount of absorption. In such case, the intensity of these lines, as compared with that of the primary, would be greater than that given above.

The experiments described in the following were carried out in an attempt to observe a change of wave-length of this type due to partial absorption of molybdenum $K\alpha_1$ and copper $K\alpha_{1,2}$ characteristic rays in the K-level of carbon.

Absorption of molybdenum $K\alpha_1$ in carbon. The change of wave-length predicted for x-rays which suffer absorption of the type considered was given by Eq. (2). For molybdenum $K\alpha_1$ absorbed in the carbon K-level this change would be about 11X.U. The modified wave-length would have a reflection angle from a calcite crystal 6.5 minutes greater than Mo$K\alpha_1$.

An x-ray tube with molybdenum target, thin glass window, and line focus, was operated at 25 milliamperes and 52 kilovolts peak voltage. Two slits,

0.05 mm wide and 76 cm apart, defined the x-ray beam. A calcite crystal mounted on a spectrometer table with a crystal rocking device reflected the rays to a photographic plate, placed at a distance of 2.4 meters and carefully

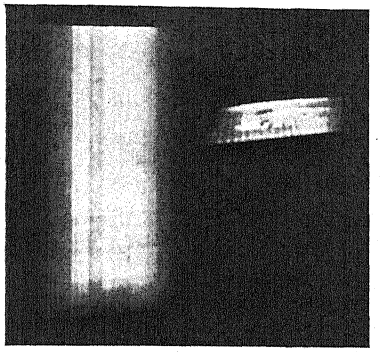

Fig. 1. Pinhole and narrow slit photograph of the target of an x-ray tube with coil filament showing the image of the filament coils on the target.

shielded from scattered radiation. This formed a system with high resolving power. The $K\alpha_1$ and $K\alpha_2$ lines were separated by a distance of 3.5 mm on the plate. Compressed lamp black was used to absorb the x-rays and was placed

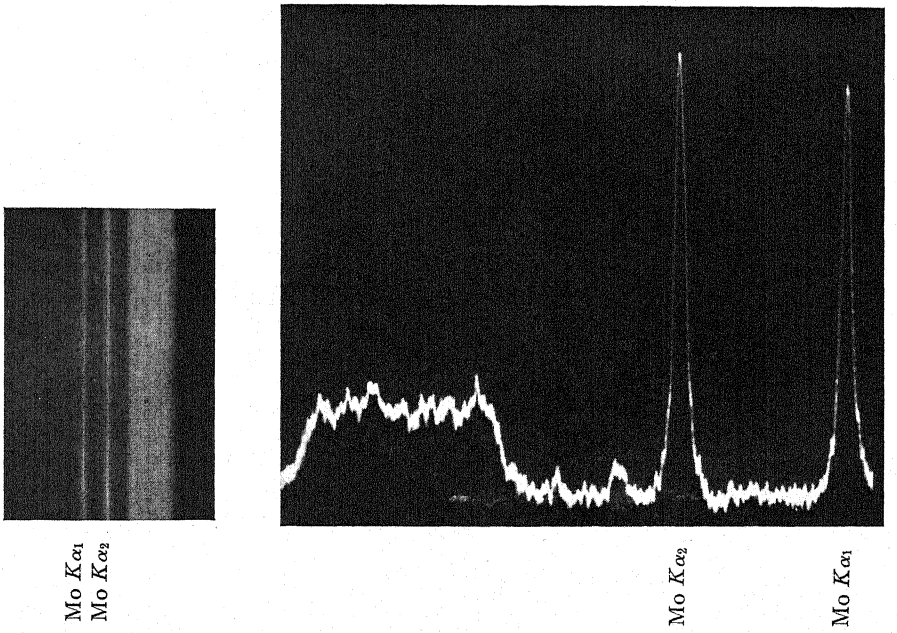

Fig. 2. Photograph taken with molybdenum target, carbon absorbing material and crystal rocking device to reflect radiation in the neighborhood of a line which would be produced if Mo$K\alpha_1$ were partly absorbed in the K-level of carbon.

Fig. 3. Microphotometer curve of one of the plates similar to that shown in Fig. 2.

in front of the slit nearest the tube. It was found experimentally that the lamp black absorbed 85 percent of Mo$K\alpha_1$ and that the ratio I/I_1 was 57.

After the crystal had been adjusted and the positions for reflection of $K\alpha_1$ and $K\alpha_2$ carefully determined, the method of procedure was as follows: With the carbon in place, short exposures of $K\alpha_1$ and $K\alpha_2$ were taken to give two reference lines on the plate. $K\alpha_1$ was usually exposed for about 15 minutes and $K\alpha_2$ 30 minutes so that the two lines would have approximately the same intensity. The crystal was then turned through an angle of 6.5 minutes from the setting for $K\alpha_1$ and the crystal rocking device set so that the crystal was rocked over a range of 4 minutes, covering 2 minutes on each side of this central position. Exposures were then taken for periods between 65 and 95 hours.

One of the photographs is shown in Fig. 2. The plates were projected on a screen under high magnification and microphotometer curves of two plates were taken but in no case was there any indication of a modified line. One of the microphotometer curves is shown in Fig. 3. A line of intensity 50 percent greater than the intensity of the background could easily have been observed. By Eq. (7), the intensity of such a line, as compared with that of the incident primary radiation, is one in 750.

The double crystal spectrometer was also used in a search for this modified wave-length. Direct radiation from a molybdenum tube, operating at 7 milliamperes and 37 kilovolts, was passed through the compressed lamp black. The ratio I/I_1 in this case was 75 and a line of intensity 15 percent greater than the continuous radiation could easily have been detected but no indication of such a line was found. In this case then, the intensity of a line that could have been observed as compared with that of the primary is, by equation (7), one in 3000.

Absorption of copper K$\alpha_{1,2}$ in carbon. The change of wave-length predicted for copper $K\alpha_1$, undergoing this particular type of absorption in the K-level of carbon, is about 55 X.U. and the reflection angle from a calcite crystal for this modified wave-length would be 33 minutes greater than for $K\alpha_1$. In this experiment the crystal rocking method was not used. Pin-hole and narrow slit photographs of two tubes with copper targets showed them to be unsuitable for a fixed crystal method. One target however showed a band of uniform intensity which was suitable for the purpose provided the rest of the target was blocked out. This was done by means of two slits 20 cm apart. The slit nearest the lead box was 0.04 mm wide and the width of the other slit and the position of the tube, were adjusted until the radiation coming through formed a beam of uniform intensity with a divergence of about 44 minutes.

The tube was operated at 30 milliamperes and 52 kilovolts peak voltage. The carbon used was a uniform slab of graphite of a thickness which absorbed 70 percent of the $K\alpha$ rays. It was interposed in the beam at the slit nearest the tube. The photographic plate was placed 75 cm from the crystal and was carefuly shielded so that no radiation could strike it except that from the crystal.

The central positions of the crystal for reflection of $K\beta$ and $K\alpha_{1,2}$ were determined. Then with the graphite in position short exposures were taken of $K\beta$ and $K\alpha_{1,2}$ and a 24-hour exposure taken with the crystal set at an angle 33 minutes greater than the central position for reflection of $K\alpha_1$. Photographs were also taken without the graphite in place and were exactly similar to those taken with. In no case was there any indication of a line. The method was however not entirely satisfactory since each wave-length was reflected from a slightly different portion of the crystal and the band on the plate was somewhat patchy due to imperfections in the crystal face. One of these photographs is shown in Fig. 4.

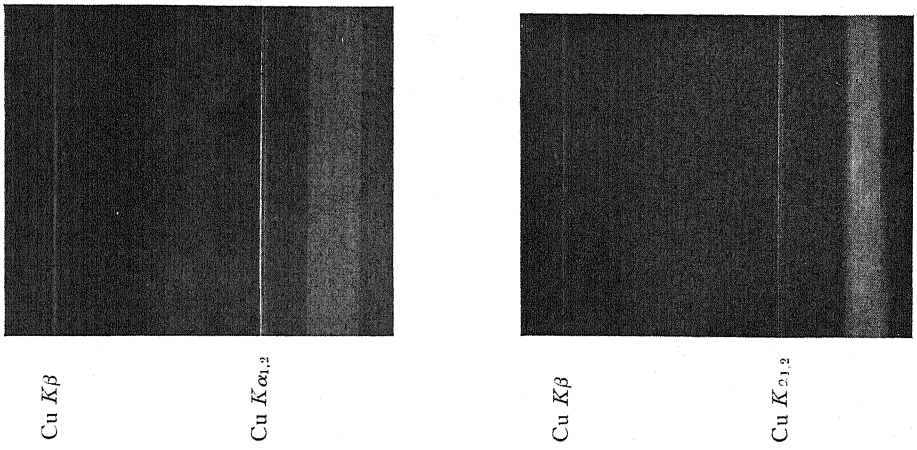

Fig. 4. Photograph with carbon absorbing material and fixed crystal, using the radiation from only that portion of a copper target which gave uniform intensity. Narrow slit was 25 cm from crystal.

Fig. 5. Photograph similar to that shown in Fig. 4 except that narrow slit was close to crystal.

This objectionable feature was eliminated from the next set of photographs. The slit nearest the tube was reduced in size to 0.04 mm. In order that the divergence in angle from the small portion of the target giving uniform intensity, be large enough to give a band of the desired width on the photographic plate, the distance between slits was reduced to 5 cm and the tube moved up as close to the opening in the lead box as safety would permit. The width of the slit nearest the tube, and the position of the tube, were adjusted until the radiation coming through was only that from the portion of the target which gave uniform intensity. The short distance between slits made this difficult but it was finally accomplished. The divergence in angle of the beam was this time about 28 minutes. Each wave-length was reflected from closely the same part of the crystal and conditions were very favorable for observing a modified line.

Photographs were taken with and without the carbon in place as an added precaution against error, the time of exposure varying between 20 and 35 hours. One of the photographs is shown in Fig. 5. A microphotometer curve

of the band on the same plate is shown in Fig. 6. In every case the band was perfectly uniform with no indication of a line. A line of intensity of the order of one in 800, as compared with that of the primary, could easily have been detected.

Another set of photographs was taken using the radiation from the whole target. The distance from the narrow slit to the tube was small enough in comparison with the distance to the plate that any lines in the focal spot

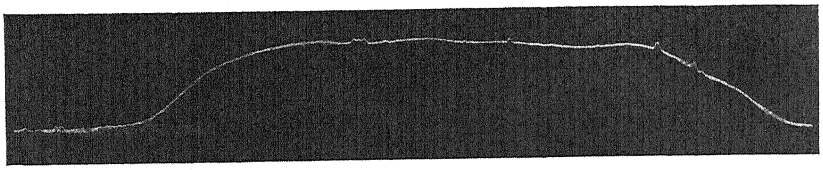

Fig. 6. Microphotometer curve of band on plate shown in Fig. 5.

would appear broad enough on the plate that they would not be confused with the characteristic lines. One of the photographs is reproduced in Fig. 7. On the original, three broad and diffuse lines can clearly be seen in the position marked X due to lines in the focal spot which might cause error, were not their true origin known. The tungsten lines are due to evaporation from the filament and the nickel lines from the nickel used in spot welding the

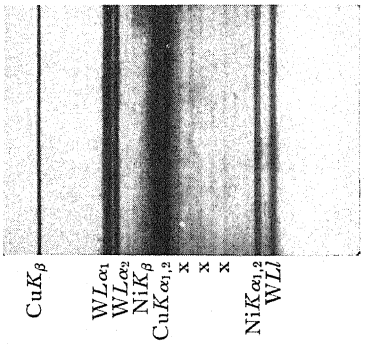

Fig. 7. Photograph taken with fixed crystal, no absorbing material, and narrow slit close to crystal, using radiation from the whole copper target. Three broad and diffuse lines due to lines in the target are marked by an X.

filament cup. Photographs were again taken with the carbon absorbing material in place and showed no indication of a modified line due to absorption.

III. Summary of Results

An analysis, by means of the double crystal spectrometer, of characteristic molybdenum $K\alpha_1$ x-rays scattered by carbon and beryllium, has failed to show

the existence of fine structure lines due to absorption of an amount of energy equal to the binding energy of the electrons in the scattering substance. The method was sufficiently sensitive to detect a line of intensity greater than 10 percent of molybdenum $K\alpha_1$ unmodified. This is in agreement with the results of all other experimenters since the fine structure was first reported.

An analysis of x-rays transmitted through carbon has failed to show a similar change of wave-length without scattering, as certain lines observed by Ray and Majumdar were interpreted. For molybdenum $K\alpha_1$ absorbed in carbon, a line of intensity of the order of 1 in 750, as compared with the intensity of the incident primary radiation, could have been detected with the single crystal method, and a line of the order of only 1 in 3000 with the double crystal spectrometer. For copper $K\alpha_{1,2}$ absorbed in carbon, a line of the order of 1 in 800 could have been detected. In discussing his results, Ray assumed that the intensity of the new lines as compared with the intensity of the primary, was of the order of 1 in 400 or 500. Thus the present experiments were sufficiently sensitive to detect a line of considerably less intensity. Two possible sources are suggested which may give rise to lines similar to those observed by Ray and ascribed to this absorption phenomenon.

In conclusion, the author wishes to express his indebtedness to Professor Bergen Davis for his interest in this work and for full privileges in his laboratory, and to the authorities of Columbia for a University Fellowship.

PHOTOELECTRIC PROPERTIES OF COMPOSITE SURFACES AT VARIOUS TEMPERATURES AND POTENTIALS

By Dimiter Ramadanoff
Department of Physics, Cornell University, Ithaca, New York

Abstract

Experiments designed to determine the variation of photoelectric current with temperature and plate potential for barium photoelectric cells are described. The technique used in making the cells is also given. A new method, employing interrupted illumination, a transformer coupled amplifier and a cathode ray oscillography, is developed for measuring the photoelectric current. In this way the thermionic current and currents of slow response are completely eliminated and only the a.c. component of the photo-current is amplified.

Experimental results. With constant plate voltage the photoelectric current increases gradually with temperature and at about 600°C is nearly twice as large as the current at room temperature. As the temperature however is raised from 600°C to 750°C the increase in photoelectric current for steady illumination is 100-fold while for interrupted illumination it is only 17-fold. The smaller increase in the latter case may be explained in view of the elimination of all sluggish currents produced by light in some secondary way. While the two curves for steady and interrupted illumination are similar in appearance, the latter has a maximum at 560°C which resembles very much a resonance peak.

The increase or decrease in photoelectric sensitivity with temperature for composite surfaces consisting of barium and oxygen on platinum may be explained by the diffusion of barium or oxygen on the surface. The increase in saturation voltage of the potential-current curves with temperature may likewise be explained by an increase in the contact potential brought about by a change in the work function.

Introduction

THE variation of photoelectric current with temperature for both oxides and pure metals has been studied by a number of investigators. Merritt[1] found that the photoelectric current obtained by illuminating the oxide-coated filaments of Western Electric audion bulbs increased in some instances 1400 times as the temperature of the filament was raised from that of the room to dull red heat. Large increases of photoelectric current with temperature for filaments coated with various oxides were also reported by Koppius,[2] Crew,[3] Berger,[4] Newbury,[5] and others. Similarly for pure metals Du Bridge[6] and Warner[7] using platinum and tungsten respectively have measured an increase in the photoelectric current with temperature. In all of these

[1] E. Merritt, Phys. Rev. **17,** 525 (1921).
[2] O. Koppius, Phys. Rev. **18,** 443 (1921).
[3] W. H. Crew, Phys. Rev. **28,** 1265 (1926).
[4] C. E. Berger, Phys. Rev. **34,** 1566 (1929).
[5] K. Newbury, Phys. Rev. **34,** 1418 (1929).
[6] Du Bridge, Phys. Rev. **29,** 451 (1927).
[7] A. H. Warner, Phys. Rev. **33,** 815 (1929).

instances however, both the oxide-coated and the pure metal filaments were poor photoelectric and good thermionic emittors and consequently a number of difficulties were encountered. The photoelectric current at room temperatures was small, while at the higher temperatures the thermionic current was large and in most cases masked the whole photoelectric phenomenon. Moreover in the investigations referred to the photoelectric current was measured with no regard to time response, for which Lawrence and Beams[8] have reported a value of 3×10^{-9} second. Sluggish currents which may have been present with the photoelectric current are attributed to the true photo-current. In this connection Bodemann,[9] who has studied the photoelectric emission from filaments coated with the oxides of Ba and Ca at various temperatures, has named the increase in photoelectric current with temperature "addition current." This "addition current" he explained as due to the action of light on the negative space charge adjacent to the cathode. According to this view the "addition current" is to be regarded as nothing else than an increase in the thermionic current. Such currents however should be expected to have considerable time lag and are hardly to be regarded as true photoelectric currents.

The present investigation was undertaken for the purpose of studying the variation of the photoelectric current with temperature for barium photoelectric cells with both continuous and interrupted illumination. The barium cells were constructed in a manner similar to that described by Case.[10,11] It was felt by the author that the barium cells were particularly suited for the study of the above mentioned phenomena not only because they were remarkably sensitive to ordinary visible light, but also because Case[10] has already observed a 100-fold increase in the photoelectric current as the temperature of the cell was raised to just under dull red heat. The determination of the variation of the photoelectric current with temperature with and after eliminating all sluggish currents with rapidly interrupted illumination and proper filter circuits, forms the chief endeavour of this investigation.

Apparatus

a. Vacuum system. The vacuum system consists of two liquid air traps, a two-stage mercury diffusion pump and a Cenco oil pump. No stopcocks were used on the high vacuum side. The McLeod gauge which was made entirely of glass is sealed between the liquid air traps and the mercury diffusion pump. The high vacuum side was made as short as possible with tubing of large diameter. Pyrex glass was used for the whole system and for convenience it was mounted on a rigid metal frame. This latter arrangement permitted a complete torching of the entire high vacuum side before the photoelectric cells were made.

[8] Lawrence and Beams, Phys. Rev. **32,** 478 (1928).
[9] E. Bodemann, Ann. d. Physik **3,** 614 (1929).
[10] T. W. Case, Phys. Rev. **17,** 398 (1921).
[11] T. W. Case, Proc. Am. Electrochem. Soc. **39,** 423 (1921).

b. Photoelectric cells. In the experiments to be described later several cells of slightly different construction were used. The most photoelectric typical cells are shown in Fig. 1 and Fig. 2. The glass of the cell in Fig. 1 is made of Pyrex and quartz joined together by means of a graded seal. No cement joints were used at any time with the photocells. In this particular cell the anode F consists of an oxide-coated Western Electric filament which was spot-welded to two tungsten leads. A thin platinum strip P, about 3 mm wide and 2.5 cm long, was similarly welded to another pair of tungsten leads, and served as cathode. These latter leads were made of two different sizes of tungsten wire. The finer leads were so selected as to reduce the cooling at the ends of the platinum strip which was heated by passing a current through it

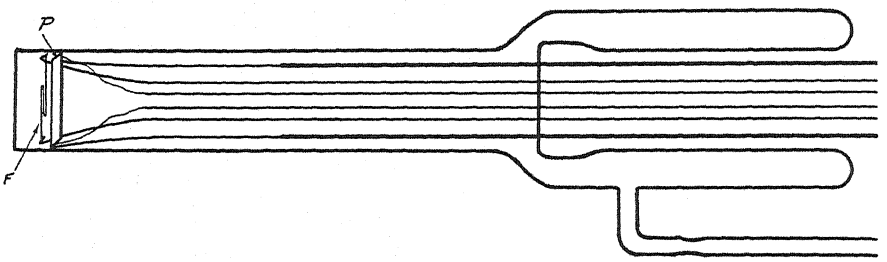

Fig. 1. Diagram of photoelectric cell made of Pyrex and quartz joined with a graded seal.

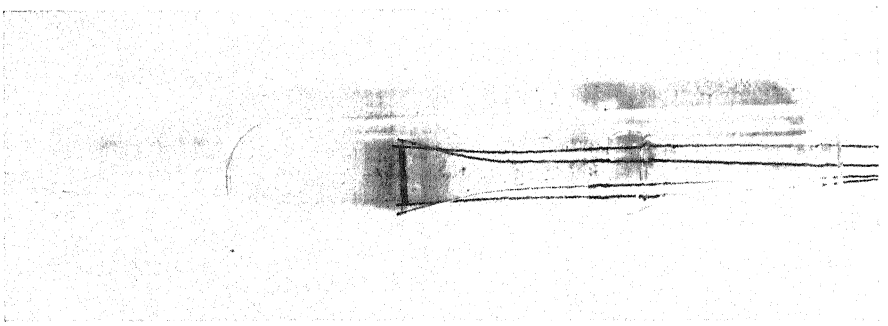

Fig. 2. Photograph of a typical photoelectric cell made entirely of Pyrex glass.

from a storage battery. Provision was made to measure the potential drop across the platinum strip in order to determine its temperature. For this purpose two fine platinum filaments were welded across the plate and the center pair of tungsten leads. All tungsten wires were sealed directly through the Pyrex.

No efforts were spared in thoroughly outgassing the cells before the photosensitive material was deposited. Three electric ovens were used to bake out photocells together with the traps and the few centimeters of adjoining tubing. The temperature of the ovens was kept constant at 550°C for more than 24 hours. In the meantime the McLeod gauge and the remaining glass on the high vacuum side were thoroughly torched. During the bake out, the filament F and the plate P were heated several times to yellowish-red colour.

Great care was also used in preventing any mercury vapor from getting into the cell. While the cell and the trap next to it were kept at 550°C, the oven of the second trap was removed and liquid air applied. Liquid air was then applied to the next trap, and finally the oven of the cell was removed. In making some of the cells a charcoal trap immersed in liquid air was used next to the cell to improve the vacuum still further. In most cases however the burning of thoriated tungsten filaments was found to be most satisfactory. With all these precautions taken, the pressure was not greater than 10^{-7} mm of Hg.

During the process of making the photoelectric cells the functions of the electrodes are reversed. The filament F is heated to a temperature of about 1100°C or more and is used as a source of thermionic current. At the same time the platinum strip P is used as anode and its potential with respect to the filament is gradually increased to 400 volts or more. For several minutes the thermionic current is very small, but as soon as the filament is "activated" or "broken down," the thermionic current increases greatly and the plate voltage and filament temperature have to be reduced until the emission current is limited to a safe value. Then by varying the plate voltage from 200 to 700 volts for various filament temperatures a condition is finally reached when barium or oxygen, or both begin to evaporate from the filament and deposit on the plate. Soon the plate becomes coated with a very thin layer of deposit which has a brownish appearance. The plate so coated is remarkably sensitive to light and is used as the emittor of photoelectrons, while the filament serves as collector. That the evaporated material is barium and oxygen on platinum seems very likely in view of the recent work of Becker[12] who found that metallic barium evaporates from an activated oxide-coated filament if the temperature is not too high and if the emission current is small. He also found that oxygen evaporates if the temperature is high enough and if the thermionic current is limited not by space charge but by emission. Since the conditions under which the photoelectric cells were made correspond to those described by Becker it seems very likely that oxygen and barium evaporated either simultaneously or consecutively. In such a case one would expect the sensitivity of the cell to vary, in analogy with the thermionic emission, with the relative position of barium and oxygen with respect to the platinum. As will be seen later this seems to be the case in most of the experiments. If the oxide-coated filament is heated during the making of the cell to a very high temperature barium oxide evaporates. A cell which was made in this way gave no measurable current with the sensitive galvanometer in use.

At the present time there seem to be two different opinions as to the mechanism of production of barium from an oxide-coated filament. One view maintains that the oxide dissociates by a thermal reaction, while the other view favors the production of barium through electrolysis of the oxide. In this connection it may be of interest to mention that a photoelectric cell can be made by merely heating the oxide-coated filament i.e. without applying

[12] J. A. Becker, Phys. Rev. **34**, 1323 (1929).

any voltage. Under this condition however the "breaking down" of the filament is rather slow and the temperature to which the filament should be heated is much higher. The result is that mostly barium oxide evaporates and the cell so made is rather insensitive to light.

The filaments of most of the photoelectric cells were coated with oxide by rubbing barium nitrate crystals on a red hot platinum-iridium ribbon, or by dipping the ribbon several times in a solution of barium nitrate. These filaments were more desirable than the commercial type because the oxide coating consisted mostly of barium oxide with traces of strontium and calcium oxides. The photoelectric cells which were made with these filaments were sensitive, not only to the ultraviolet light but also to visible light. This latter feature was particularly desirable because it made the use of the quartz mercury arc unnecessary.

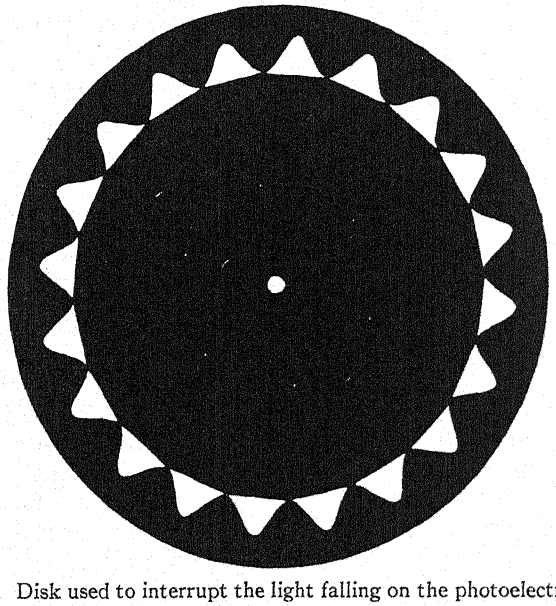

Fig. 3. Disk used to interrupt the light falling on the photoelectric cell.

It was found best to make the photocells after they are sealed off. If a cell is made while on the pumps its sensitivity decreases considerably in the course of time. This shows how detrimental traces of gases are to the sensitive material.

c. Source of illumination. As already mentioned the cells which were made with the Western Electric oxide-coated filaments were sensitive only to the ultraviolet light and therefore a quartz mercury arc was used for a light source. In all cases the total radiation from the light was allowed to fall on the cell. The intensity of the light remained remarkably constant after the lamp had reached its operating temperature.

[13] For a detailed description of the disk, the amplifier and their use in connection with the photoelectric cells and the cathode-ray oscillograph see: "A Method of Studying the Effect of Temperature on Photoelectric Currents," D. Ramadanoff, R. S. I. **1**, 768 (1930).

For the interrupted illumination[13] an incandescent lamp was used. The filament of a 500-watt projection lamp was focused on the platinum strip of the cell. Between the cell and the source were situated a water cell, a shutter, and a revolving disk. The disk shown in Fig. 3 has twenty holes around its periphery. The shape of the holes is of the form $y=\sin^2 x$. It is easy to see that the light passing through these holes, as the disk revolves at constant speed, will vary sinusoidally and will give approximately a sinusoidal photoelectric current superimposed on a d.c. current. Each hole of the disk gives a complete cycle of the a.c. wave.

d. Measuring instruments and method. The photoelectric current was measured with two different sets of apparatus both of which are shown diagrammatically in Fig. 4 and Fig. 5. Two galvanometers having current sensitivities of 2.96×10^{-10} and 3.4×10^{-9} respectively were used. The difference

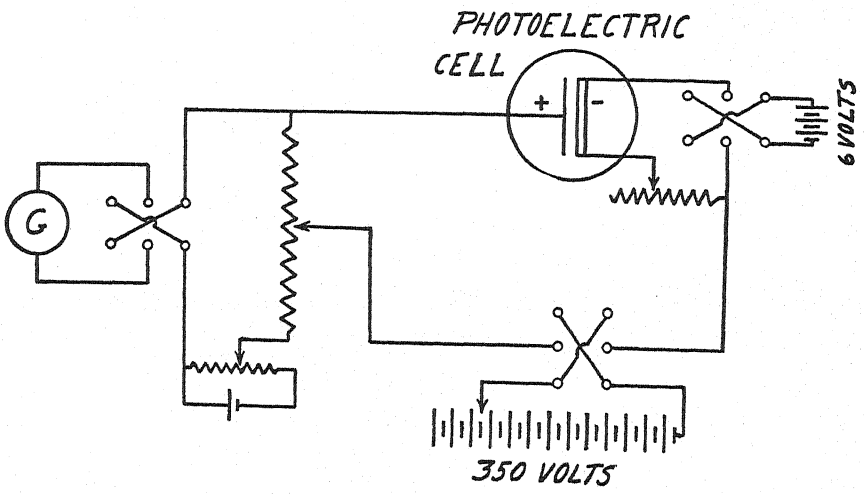

Fig. 4. Circuit diagram of photoelectric cell and galvanometer used to measure the current produced by steady illumination.

in the galvanometer deflections obtained with the light on and off were recorded as true photoelectric currents. In most cases the thermionic current was not balanced because the photoelectric current was large and was read with no difficulty. One of the photoelectric cells which was used in the experiments gave 0.592 μa saturation current with the plate cold, when the light from 150-watt lamp was focussed on the cell. It is evident from the brief description of the circuit that with the galvanometer only the total current due to light can be measured. Sluggish currents which may be due to light in some secondary way cannot be distinguished from the true photocurrents which are characterized by a very short time response.

The circuit in Fig. 5 was designed to eliminate the thermionic current and any sluggish currents which may be present, and to amplify only the true photocurrents.[13] After two stages of amplification the current is impressed on one pair of plates of a "Bedell-Reich Stabilized Oscilloscope," a visual cath-

ode-ray oscillograph. The deflections of the cathode spot indicate on the fluorescent screen not only the wave shape of the current but also its magnitude. From measurements of the amplitude of the voltage wave the photocurrent can easily be determined. A photograph of the a.c. wave as it appeared on the screen is shown in Fig. 6. In this particular case a disk with circular holes was used and therefore the wave shape of the photoelectric current is not sinusoidal.

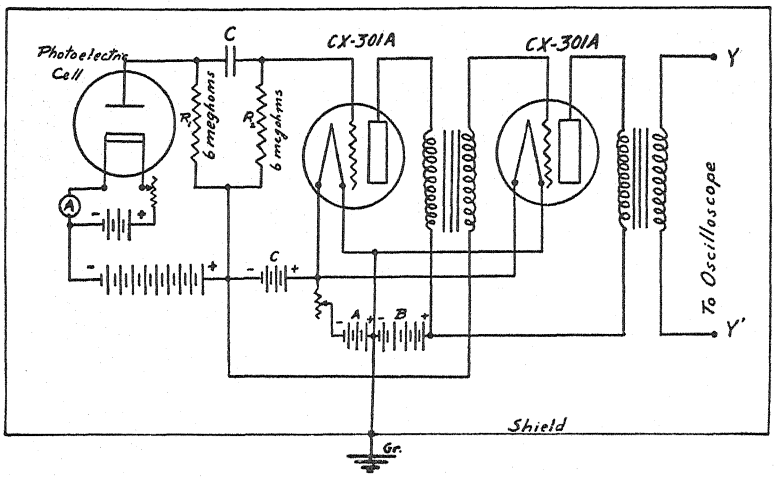

Fig. 5. Circuit diagram of photoelectric cell, amplifier and cathode-ray oscillograph used to measure the current produced by interrupted illumination.

The temperature of the photoelectric material was varied by passing various currents through the strip. By measuring the potential drop across the platinum strip, it was possible to determine its change in resistance and therefore its temperature. At the higher temperatures an optical pyrometer was used as a check. During the photoelectric measurements the heating cur-

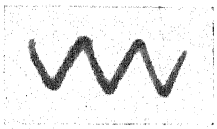

Fig. 6. Photograph of a.c. wave as it appeared on fluorescent screen.

rent was not interrupted since it was found that the oscilloscope deflections were the same whether the heating current was on or off provided that the temperature of the strip did not change when the photoelectric current was measured. The oscilloscope was particularly useful for eliminating this difficulty since the response of the cathode spot is practically instantaneous. Such an observation would have been impossible with the ordinary galvanometer or electrometer. It is of interest to notice that this result is contrary to the hypothesis of Shenstone[14] who suggested that the change in photoelec-

[14] A. G. Shenstone, Phil. Mag. 45, 918 (1923).

tric sensitivity was due to changes in the metal which were produced by the current flowing through it.

Experimental Results

A. Measurements made with galvanometer*

a. Potential-current saturation curves. Fig. 7 shows the variation of photoelectric current with potential applied between the electrodes when the light intensity is kept constant and the photoelectric surface is at room temperature. The low saturation potential and the reproducibility of the photoelectric current with both increasing and decreasing potentials is typical of all photoelectric cells used in the experiments. This latter feature is clearly indicated on the curve with large and small circles, the large circles being used for increasing potentials.** It is also easy to see from this curve that the

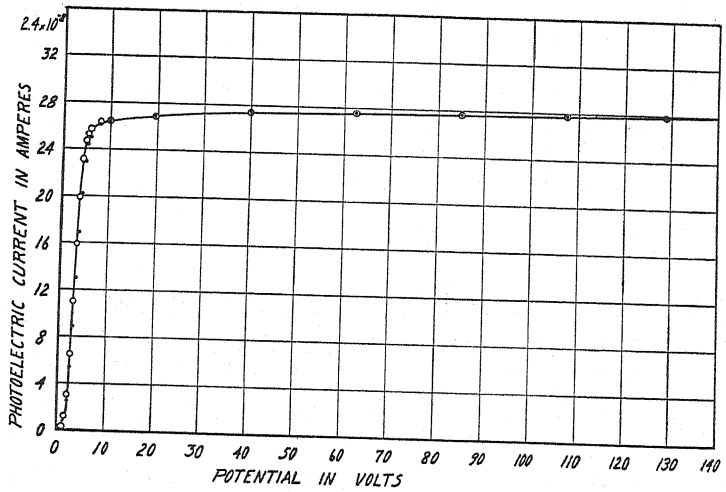

Fig. 7.

photoelectric current saturates as well as can be expected of a cell with a composite surface. In the experiments the plate potential was increased to 300 volts which is about 40 times the saturation potential and produces a gradient between the electrodes of more than 1000 volts per cm. But even at these high potentials the photoelectric current remained substantially constant.

In Fig. 8 is shown a family of saturation curves for constant illumination and for different temperatures of the photoelectric surface. The values of the photoelectric current for increasing and for decreasing potentials are so closely identical that they are represented by single curves. The thermionic current at the temperatures at which the curves were obtained was either small or zero. The saturation potential of all three curves increases with

* Under this heading the photoelectric current is defined as the difference in galvanometer deflections with the light on and off. In all cases the total radiation from the lamp was used.

** This notation is used for all curves.

temperature, i.e., the saturation points are shifted to the right. This experimental evidence is just the opposite of what has been reported by Crew[3] who found that the saturation potential decreases as the temperature of the photoelectric surface is increased. That the shift should be as in Fig. 8 is evident from the fact that the contact difference of potential changes with a change in the work function. If the thermionic current however is large and the emission is limited by space charge then the increase in saturation potential with temperature will be greater and will be due partly to the increased space charge.

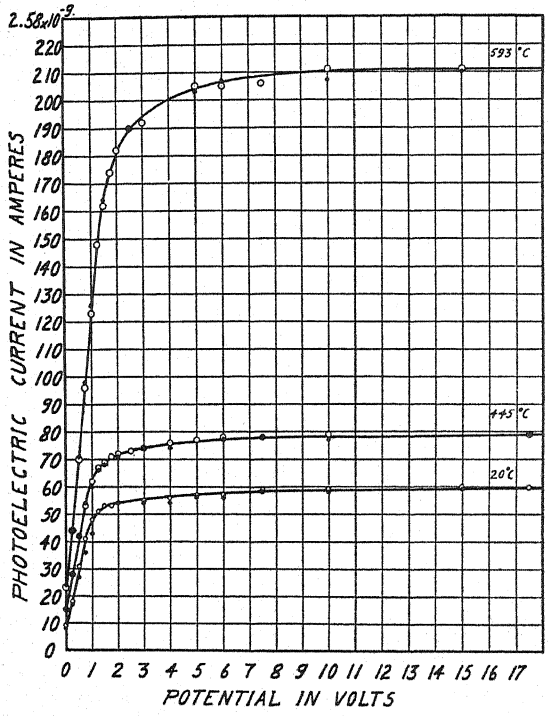

Fig. 8.

From the curve in Fig. 8 it is also evident that the photoelectric current increases with temperature. This increase in emission can be accounted for qualitatively by the relative position of barium and oxygen with respect to the platinum. The experiments which were performed to obtain these and other curves seem to indicate that the decrease in activity of the photoelectric material at room temperature is due to the negatively charged oxygen ions which have diffused to the surface on top of the barium layer. Since the photoelectrons come from the barium the strong surface field of the oxygen will tend to hinder the emission. But as the temperature of the plate is increased, more and more barium diffuses to the surface and exchanges place with the oxygen. Beyond this point any further increase in temperature

should not increase the emission. As will be seen later temperature-current curves were obtained which tend to show that this is probably the case.

Another possible explanation is that the light acts not only on the barium layer but also on the negative adsorbed oxygen ions and changes them to neutral atoms. Under this condition the photoelectric and thermionic emission will increase with light. In this connection Bodemann[9] seems to maintain that the total increase in the photoelectric emission with temperature is due to the action of light on the negative space charge and he calls this increased current "addition current," which in reality is nothing else than an increase in the thermionic current. It is hard to believe however that the total increase in current due to light is thermionic, because currents which are produced indirectly by the action of light on a negative space charge

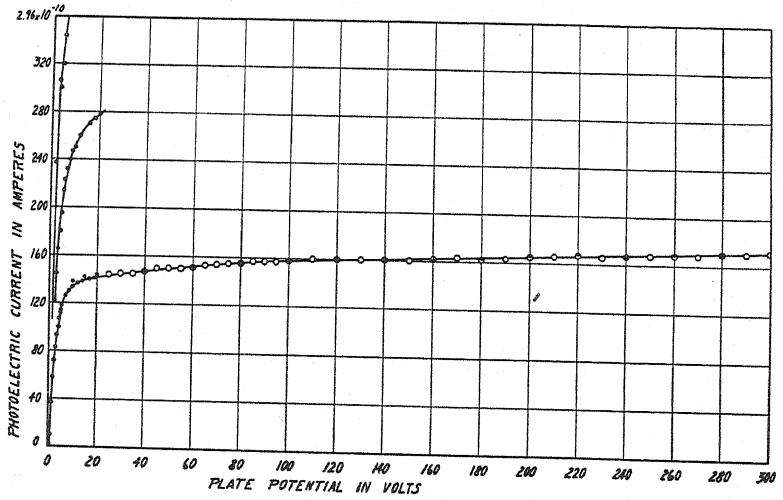

Fig. 9.

should be expected to have considerable time lag. As will be seen later experiments were performed to prove this point by the use of rapidly interrupted illumination.

A group of saturation curves which in all respects are similar to those in Fig. 8 are shown in Fig. 9. These curves however were obtained with a different photoelectric cell the anode of which was built in the form of a squirrel cage by welding fine thoriated tungsten wires on two nickel rings. The filament wires were spaced two mm apart and could be heated to incandescence by passing current from one ring to the other. In this way the anode served not only as collector but also as a "getter."

b. Variation of photoelectric current with temperature at constant plate potential. The curve in Fig. 10 brings out many interesting points which were not evident from the previous curves. In spite of the fact that this curve was taken when the total radiation of the mercury arc shone on the cell, its general appearance has a striking resemblance to the curves reported by War-

ner[7] for pure tungsten with monochromatic illumination. The curve shows that at 800°C the photoelectric current reaches saturation and is at this temperature about 100 times greater than the photoelectric current at room temperature. The fact that the emission increases only slightly until a temperature of 600°C is reached, seemingly confirms the hypothesis that the increased activity is due to the diffusion of barium to the surface. It is particularly significant, in view of the low melting point of barium (850°C), that the greatest increase in photoelectric current occurs between the temperatures of 600°C and 750°C.

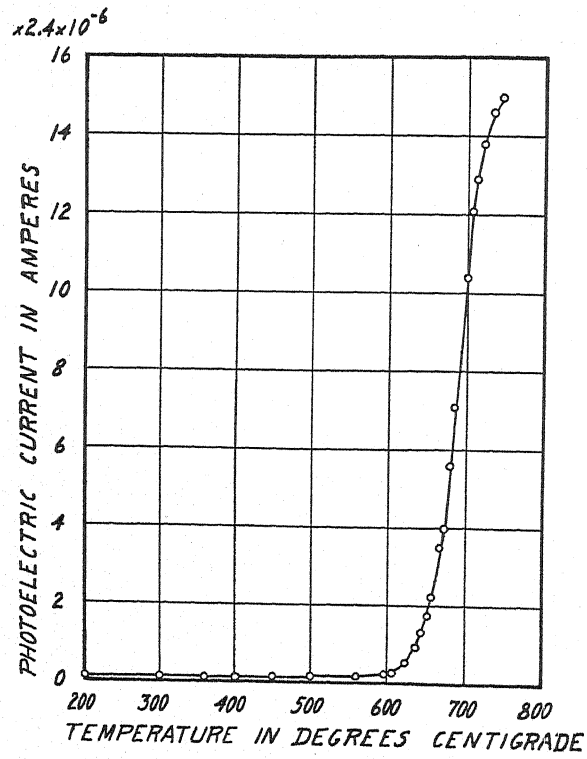

Fig. 10.

B. MEASUREMENTS MADE WITH CATHODE RAY OSCILLOGRAPH

a. Variation of photoelectric current with temperature at constant plate potential. In this group of experiments three photoelectric cells were tested and found to exhibit the same general characteristic. The curve in Fig. 11 was obtained by varying the light intensity sinusoidally with a frequency of 1000 cycles per second. The thermionic current, the d.c. component of the fluctuating photoelectric current, and all sluggish currents were completely filtered out. Only the a.c. component of the photoelectric current was allowed to pass through the amplifier. The sluggish currents were noticeable in the measurements only when the frequency of the interrupted light was

reduced to a few cycles per second. The data for the curve in Fig. 11 were obtained by measuring the amplitude of the a.c. wave on the fluorescent screen of the cathode ray tube. This curve is very similar to that shown in Fig. 10 except that the maximum and minimum values differ by a factor of 16 instead of 100. The peak at 560°C suggests a resonance phenomenon and was reproducible with both increasing and decreasing temperatures as shown by the large and small circles on the curve. The curve further shows that the optimum emission occurs at 750°C. Above this temperature the photoelectric emission decreases gradually. This decrease may be caused either by the diffusion of more barium ions which increase the surface concentration be-

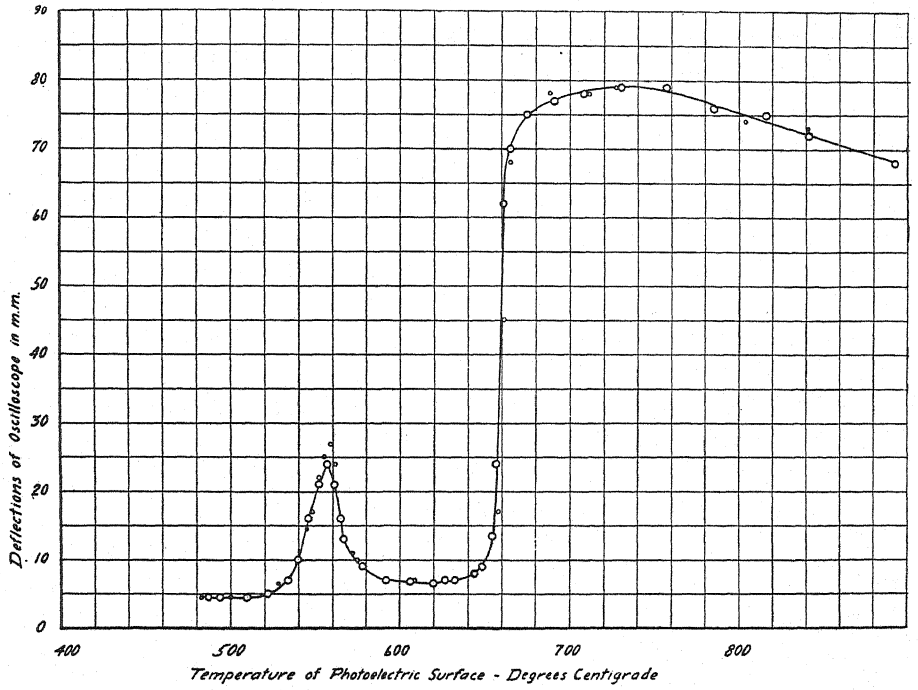

Fig. 11.

yond that necessary for the optimum emission, or else by the reappearance of oxygen ions. It is doubtful if this decrease is caused by the evaporation of barium or oxygen ions since thin adsorbed layers will adhere to the platinum surface at high temperatures much better than thick, heavy coatings.

It is of interest to obtain potential-current curves as in Fig. 8 and Fig. 9 with interrupted illumination. It is of particular interest to determine what effect the sluggish currents will have upon the long wave-length limit of the photoelectric surface used. At the present time the apparatus is not sensitive enough to permit such measurements.

Discussion

The increase in photoelectric emission with temperature from composite surfaces containing barium and oxygen on platinum cannot be explained

satisfactorily by surface gas contamination. The activity of such surfaces depends not only on the surface concentration of metallic barium and oxygen, but also on the relative position of the two. It is unlikely that the thin adsorbed layers of oxygen and barium will leave the surface without using very high temperatures which will distill off the photoelectric material and ruin the cell. Most of the oxygen on the surface due to its strong electron affinity is negatively charged. The barium which diffuses on the surface at the higher temperatures changes the intensity and the distribution of the surface fields and as a result changes the work function. This change in work function produces a change in the contact differences of potential which manifests itself in an increase of the saturation potential with temperature if the thermionic current is small. When large thermionic current limited by space charge is present the increase in saturation potential with temperature is caused also by the increase in space charge.

Any increase in thermionic current which may be caused by the heat rays of the light source or by the influence of the light alone in some secondary way should not be regarded as a true photoelectric current. The experiments with the oscillograph show definitely that part of the increased emission due to light at the higher temperatures is not caused by such secondary effects but is due to an increase in the photoelectric current. This finding is contrary to the results obtained by Bodemann. The increased photoelectric current is independent of the frequency of light interruptions for the range used from 500 to 1000 cycles per second.

The author is deeply indebted to Professor Ernest Merritt for suggesting the problem and for his many valuable suggestions and helpful criticism, and to Professor Frederic Bedell for his general interest in this investigation and for providing the Oscilloscope and other facilities in connection with the work. He also gratefully acknowledges the benefits derived from discussions with Dr. J. A. Becker and Professor H. A. Barton. For the construction of the glass apparatus thanks are due to Mr. H. W. Banta.

THE ENERGY OF DISSOCIATION OF MERCURY MOLECULES

By J. Gibson Winans
Department of Physics, University of Wisconsin
(Received March 5, 1931)

Abstract

The absorption spectrum of mercury vapor in the Schumann region showed three apparently continuous bands with maxima at wave-lengths 1849, 1808, and 1692. The 1849 and 1692 bands appeared without the 1808 band in the emission from an electrodeless discharge through mercury vapor. The absorption spectrum in the region 1900–1804 is correlated with a pair of potential energy curves for Hg_2. From these curves, the energy of dissociation of Hg_2 is 0.15 volts.

Introduction

THE problem of the energy of dissociation of mercury molecules is particularly interesting because, as far as chemical evidence is concerned, mercury molecules do not exist. For example c_p/c_v for mercury vapor is 1.666, the value for a purely monatomic gas. Also the molecular weight of mercury vapor equals that of liquid mercury.[1] Nevertheless mercury molecules exist in both the excited and unexcited states as evidenced by the presence of bands in the absorption and emission spectra of mercury vapor.[2]

The binding force between two mercury atoms must be similar to that between two helium atoms since both have a closed outer shell containing two paired s electrons. So far three types of binding for diatomic molecules have been proposed; ionic as in NaCl, exchange forces as in H_2, and polarization or van der Waal's forces. The binding between neutral mercury atoms can not be ionic, and Heitler and London[3] have shown that the exchange forces between helium-like atoms must be repulsive if the Pauli exclusion principle holds. There remain only the polarization forces to hold the mercury molecule together. The analysis of Eisenschitz and London[4] has shown that the polarization forces may, at large separations be greater than the exchange forces and produce a definite equilibrium when the exchange forces are repulsive. Mercury molecules are probably of this type.

Values for the energy of dissociation of mercury molecules have been obtained by Koernicke[5] and Mrozowski.[6] Koernicke, following the work of Franck and Grotrian,[7] measured the change in total intensity of the mercury

[1] Summary by J. W. Mellor, Treatise on Inorganic and Theoretical Chemistry, vol. 4, p. 766.

[2] R. W. Wood, Astphys. J. **26**, 41 (1907); Rayleigh, Proc. Roy. Soc. **A116**, 702 (1927); F. L. Mohler and H. R. Moore, J.O.S.A. **15**, 74 (1927).

[3] W. Heitler and F. London, Zeits. f. Physik **44**, 455 (1927).

[4] R. Eisenschitz and F. London, Zeits. f. Physik **60**, 515 (1930).

[5] E. Koernicke, Zeits. f. Physik **33**, 219 (1925).

[6] S. Mrozowski, Zeits. f. Physik **55**, 338 (1929).

[7] J. Franck and W. Grotrian, Zeits. f. Tech. Physik **3**, 194 (1922).

band at 2540 with superheating and calculated the energy of dissociation of Hg_2 as 1.4 kg. cal./mol. or 0.06 volts. Mrozowski measured the total intensity of fluorescence in mercury vapor at different positions along the direction of the exciting light. He obtained the absorption coefficient of saturated mercury vapor at different temperatures for several exciting wave-lengths. Assuming this coefficient proportional to the number of Hg_2 molecules, he calculated D for Hg_2 as 17 kg. cal./mol. Koernicke's and Mrozowski's values differ by a factor 12. The two methods will be discussed in detail in a later paper.

The results of the present investigation give a value for D for Hg_2 which lies between the two above mentioned but is quite different from either. The method is the same as that used to obtain D for Zn_2 and Cd_2.[8] The value of D comes from an interpretation of the absorption region in the vicinity of the resonance line 1^1S-2^1P. This line comes at wave-length 1849 for mercury.

Apparatus and Procedure

The absorption spectrum of mercury in the region 3000–1550 was photographed with a small vacuum fluorite spectrograph on Schumann plates. The absorption cell, shown in Fig. 1, was made of fused quartz. The windows were

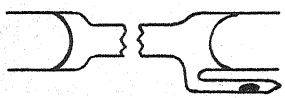

Fig. 1.

very thin to give increased transparency and hemispherical in shape to withstand atmospheric pressure. The cell was heated in an electric furnace. A hydrogen discharge tube served as a source of continuous light.

For photographing the emission spectrum of mercury, the cell of Fig. 1 was waxed to a tube leading to the spectrograph, a wire wrapped around each end, one wire grounded and the other connected to a low-voltage Tesla coil (leak chaser). When the tube was heated by a bunsen burner, a brilliant mercury discharge was obtained. CO bands from a discharge through air were used as standards for wave-length measurements.[9]

Results

The absorption spectra taken with increasing pressures of mercury vapor (Fig. 2) show first the atomic line 1849 which broadens rapidly, then a continuous band with a maximum intensity at 1808 A (Fig. 2 No. 1) and finally another continuous band with maximum at 1692 (Fig. 2, No. 2), Fig 3 is a microphotometer record of Fig. 2 showing the 1692 band. Fig. 2, No. 2 shows how, at increased pressure the 1808 band is broadened principally toward

[8] J. G. Winans, Phil. Mag. **7**, 555 (1929).

[9] T. Lyman, Astrophys. J. **23**, 204 (1906); "The Spectroscopy of the Extreme Ultraviolet," p. 114.

longer wave-lengths and the absorption region surrounding 1849 broadened toward shorter wave-lengths as far as the 1808 band but no farther, and toward longer wave-lengths beyond 2200 A. The lack of intensity below 1690 in No. 1 Fig. 2 was due to short exposure and not to absorption.

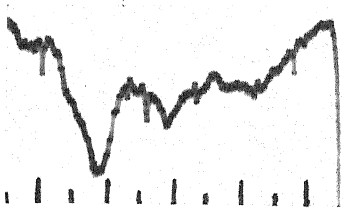

Fig. 2.

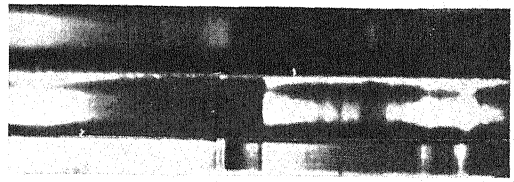

Fig. 3.

In the emission spectrum from the electrodeless discharge (Fig. 2, No. 3), the band surrounding 1849 and the one at 1692 were observed but not the one at 1808. The distribution of intensity in the 1692 band was the same in emission and absorption (Fig. 3).

TABLE I.

Description	Wave-length	Vacuum wave-number
Absorption maximum	1691.4	59123
Emission maximum	1692.1	59097
average	1691.8	59110
Absorption maximum	1808.0	55311
*Short wave limit	1804.2	55427

* The wave-length was measured at the point where the photographic blackening from the source had been reduced to one half.

Table I gives a summary of results. Wave-lengths previously given (Phys. Rev. **36**, 1020(1930) should be corrected to agree with Table I.

DISCUSSION

The continuous bands at 1808 and 1692 do not coincide with atomic transitions and are observed only at pressures much greater than that needed to show the atomic line 1^1S-2^1P. They are therefore attributed to molecules of mercury and these molecules are assumed to be diatomic. The characteristics of these bands as described above can be correlated with a set of potential energy curves for the Hg_2 molecule.

The band at 1808 was observed in absorption but not in emission in the electrodeless discharge. In the spectra of atoms, absorption lines are sometimes missing in emission because they are absorbed by the vapor surrounding the source. This can not be the case for the 1808 band; since, from the

order of appearance of the bands with increasing pressure, the absorption coefficient of the missing band 1808 lies between that of the two bands at 1849 and 1692, both of which were observed in emission. A probable reason for the non-appearance of 1808 in emission is that the Hg_2 molecule is dissociated upon absorption of this wave-length. If this is true, the curves of potential energy as a function of nuclear separation must have definite relative positions. According to the Franck-Condon principle, the nuclei of a molecule do not change their separation appreciably during an electron transition. If curves of potential energy and nuclear separation are plotted for the excited and normal molecule, allowed transitions are represented by vertical lines connecting the two curves. For interpreting absorption spectra, one assumes a Boltzmann distribution of molecules in the vibrational states of the normal molecule, so that the lowest vibrational state with 1/2 quantum of energy is the most thickly populated. The most intense part of an absorption band should be represented by vertical lines through the points of the normal mole-

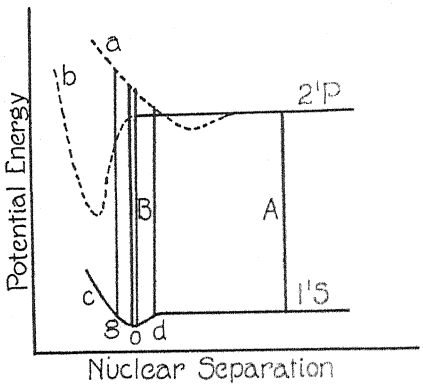

Fig. 4.

cule curve, corresponding to this lowest energy. If absorption of the 1808 band results in dissociation of an Hg_2 molecule, the potential energy curves must have relative positions like either *c* and *a* or like *c* and *b* in Fig. 4. If positions *c* and *a* are correct, after absorption of 1808, (transition B) the nuclei find themselves with sufficient potential energy to dissociate into one excited and one normal atom. This is the usual interpretation given to a photo-chemical dissociation. If curves *c* and *b* are correct, the nuclei simply lose all attraction for each other upon absorption of 1808, and find themselves free to drift apart. In either case the band 1808 should be observed in absorption but not in emission.

If the original assumption that absorption of 1808 means dissociation is correct, it is not difficult to decide which of the two relative positions shown in Fig. 4 must be right. From analogy with He_2, which is found to exist only when excited, the energy of binding in the excited mercury molecule is probably greater than that in the normal molecule. In practically all molecules which have been studied, greater energy of binding is associated with

smaller nuclear separation at the minimum of the potential energy curve, so that curves *c* and *b* should be required for Hg_2. If curves *c* and *a* were correct, with increase of pressure and temperature and corresponding increase in the number of normal molecules in higher vibrational states, the 1808 band (*B*, Fig. 4) should broaden toward both longer and shorter wave-lengths corresponding to transitions from points *g* and *d*. This does not agree with the observation that the 1808 band broadened almost entirely toward longer wave-lengths. On curve *c* and *b*, however, we see that 1808 represents the longest vertical distance between the two curves and absorption from points *g* and *d* would give a broadening toward longer wave-lengths only.

Further we can also explain the very interesting fact that the absorption region surrounding 1849 reaches a short wave limit coinciding with that for the 1808 band, but reaches no definite long wave limit. Consider two mercury atoms making a collision. Their mutual potential energy would follow the curve for the normal mercury molecule (estimated as curve *c*, Fig. 4). If they absorbed light during a collision, the energy absorbed would correspond to vertical lines between the two potential energy curves of Hg_2, and since they come to rest at point *g*, Fig. 4, and move more slowly at point *d* than at *o*, the positions *g* and *d* would be more probable positions for the absorption of light. This would represent wave-lengths slightly greater and slightly less than that of the atomic absorption line 1849. Now suppose the number of colliding atoms which absorb light to be greatly increased, one should observe absorption from points *c* and *o*. This would mean a continuous broadening of the 1849 line toward both longer and shorter wave-lengths but it would reach a limit on the short wave side coinciding with the limit for the 1808 band. This exactly describes what was observed. Of course, it is not sure that the short wave limit of 1849 exactly coincides with that of 1808 since the observed limit comes from a superposition of both. It is, however, significant that the 1849 band does not broaden beyond 1804 on the short wave side but broadens beyond 2200 on the long wave side.

We have correlated a set of curves such as *b* and *c*, Fig. 4, with three observations; the appearance of 1808 in absorption but not in emission, the broadening of the 1808 band toward longer wave-lengths with pressure, and the peculiar broadening of the 1849 band with pressure.

From Fig. 4 it is easily seen that the energy of dissociation of the normal molecule is simply the difference in energy between the 1849 and the 1808 bands. This gives *D* for Hg_2 equal to 0.15 volts or 3.5 kg. cal./mol. This value is three times Koernicke's value and one-third of Mrozowski's. The three methods will be compared and discussed in a later paper.

PROPERTIES OF SOME ZINC, CADMIUM, AND MERCURY BANDS

By J. Gibson Winans
University of Wisconsin

(Received March 16, 1931)

Abstract
Zinc bands at wave-lengths 2139, 2064, and 2002 are shown to resemble the corresponding bands of cadmium and mercury in emission as well as in absorption.

THE absorption spectra of zinc, cadmium, and mercury each show three corresponding continuous bands which may be called A, B, and C. The wave-lengths at the maxima are given in Table I. It has been shown[1] that

Table I.

	A	B	C
Zinc	2139	2064	2002
Cadmium	2288	2212	2114
Mercury	1849	1808	1692

for cadmium and mercury the bands A and C appear in emission in an electrodeless discharge but not the band B. The present experiment was undertaken to see if the same thing were true for the zinc bands.

A quartz tube was evacuated and sealed off after having had some zinc distilled into it. Nicrome wires wrapped around the ends served as external electrodes. One electrode was grounded and the other attached to a small Tesla coil (leak chaser). When the tube was heated by blow torches to give a stream of zinc vapor through the tube, a bright discharge was obtained. In stagnant vapor the discharge was very weak. This may have been the result of impurities as observed by Wood and Voss[2] in mercury vapor. Spectra were photographed with nitrogen flowing through the spectrograph to eliminate oxygen.

The resulting discharge through zinc vapor showed band A with great intensity and with the maximum reversed, and showed also band C. No trace of band B was observed. These observations are the same as those on the corresponding bands for Cd and Hg.[1] An interpretation for one set of these bands will apply to all since the bands are shown to have the same properties. One interpretation[1] gives energies of dissociation of zinc, cadmium, and mercury molecules of 0.24, 0.20, and 0.15 volts respectively.

There was observed only one difference in the behavior of these bands relative to each other for the various elements. In the absorption spectra, the zinc bands B and C appeared with increasing pressure at practically the same pressure; the cadmium band C required about 1.7 times that required for band B, and the mercury band C needed about 5 times as much pressure as the mercury band B for equal intensities. This does not affect the interpretation given to the bands but it may indicate an interesting change in properties of similar elements with increasing atomic weights.

[1] Winans, Phil Mag. 7, 555 (1929); Phys. Rev. 37, 897 (1931).
[2] R. W. Wood and V. Voss, Jour. Frank. Inst. 205, 486 (1928).

PERTURBATIONS AND PREDISSOCIATION IN THE S_2 BAND SPECTRUM

By Andrew Christy and S. Meiring Naudé
Ryerson Physical Laboratory, University of Chicago

(Received February 27, 1931)

Abstract

The S_2 bands belonging to the ${}^3\Sigma_u^- \leftrightarrow {}^3\Sigma_g^-$ transition have been photographed with relatively large dispersion in absorption and in emission between λ3500 and λ2400. Several perturbations have been found in the vibrational levels of the excited ${}^3\Sigma_u^-$ state. These became apparent when the quantum assignment of the band heads were determined. The following revised equation was found to fit the unperturbed heads:

$$\nu = 32250.9 + 429.5(v'+1/2) - 2.75(v'+1/2)^2 - 727.4(v''+1/2) + 2.91(v''+1/2)^2$$

Weak bands were observed (mainly in absorption) about 20 cm^{-1} to the violet of the heads in the $v''=0$ progression. These bands are believed to be due to another system. Perturbations of about +17 cm^{-1} have been found in the heads of the bands with $v'=0, 2, 4$, which are presumably due to perturbations of the rotational levels near the band heads by another electronic state or perturbations in the $U(r)$ curve of the ${}^3\Sigma_u^-$ state. Perturbations found in the levels with $v'>9$ are attributed to a ${}^3\Pi_u$ state which causes predissociation in these bands.

Predissociation. This phenomenon is discussed in terms of the Franck-Condon principle of transition probabilities. It is shown that the ${}^3\Pi_u$ continuous state which causes predissociation must intersect the $U(r)$ curve of the ${}^3\Sigma_u^-$ state at two points giving the two observed regions of predissociation. The relative transition probabilities for the radiationless jump in the two regions are discussed.

Dissociation. The energies of dissociation of the lower and upper states are found to be 4.45 and 2.07 volts. This gives 1.6 volts as the separation of the ${}^3P$ and ${}^1D$ states of the S atom.

I. Introduction

THE S_2 bands which extend from λ6000 to λ2300 have been studied by various investigators.[1] Rosen,[2] who gave the first quantum analysis of these bands, found that the band heads could be represented by the equation:[3]

$$\nu = 32290 + 427.1(v' + \tfrac{1}{2}) - 2.7(v' + \tfrac{1}{2})^2 - 727.4(v'' + \tfrac{1}{2}) + 2.91(v'' + \tfrac{1}{2})^2. \quad (1)$$

For this analysis he had a relatively small dispersion (1 mm = 300 cm^{-1} in the ultraviolet) at his disposal.

[1] J. J. Graham, Proc. Roy. Soc. **A84**, 311 (1911); J. J. Dobbie and J. J. Fox, Proc. Roy. Soc. **A95**, 484 (1919); V. Henri and M. C. Teves, C. R. **179**, 1156 (1924); J. C. McLennan, I. Walerstein, H. G. Smith, Phil. Mag. **3**, 390 (1927); and the references given in this paper.

[2] (a) B. Rosen, Zeits. f. Physik **43**, 106 (1927); (b) ibid. **48**, 545 (1928); (c) ibid. **52**, 16 (1928).

[3] This equation is the same as that given by Rosen except that the quantum numbers have been changed from n to $(v+1/2)$.

There are large discrepancies in the combination differences[4] $\Delta G(v+\frac{1}{2})$ given by Rosen (cf. Table 15 of reference 2a) which should be the same within experimental error for any one row or column of his table. It may be concluded, therefore, either that his experimental errors were very large, which is possible since his dispersion was very small, or that the assignment of the vibrational quantum numbers to at least some of the heads, was wrong. The latter alternative is not so impossible as it may appear, since with larger dispersion in the present work it was found that many of the heads which Rosen measured as one, consist of groups of two or more heads. Furthermore, in the region above λ2900 the spectrum is so complicated due to overlapping, as can be seen from our plates, that the heads with $v'<8$ all may have been assigned incorrectly. Therefore it became necessary for us to determine the correct assignment of the band heads before proceeding with the rotational analysis of the bands. The latter has already been published[5] and will be referred to here as I.

In the course of this investigation it was found that the irregularities in the $\Delta G(v+\frac{1}{2})$ values given by Rosen were due partly to an incorrect assignment of some of the band heads and partly to numerous perturbations in the vibrational levels of the upper state. The perturbations are larger than any that have been observed in the band systems of other molecules and therefore need special consideration.

The phenomenon of predissociation which Henri[6] found to occur in the S_2 bands, has also been studied in relation to the vibrational analysis. The interpretation of this phenomenon as it is observed in these bands differs from that given by other investigators.

II. Experimental Procedure

Since absorption spectra obtained at different temperatures offer the best means of studying the vibrational analysis, especially of the upper electronic state, a quartz absorption cell, having a length of 5 cm and a diameter of 2.5 cm was used. The cell was first baked out and sufficient distilled sulphur was added to give a vapor pressure of 12 mm[7] at 450°C. The cell was heated electrically. Since the amount of sulphur in the cell remained constant throughout the investigation, the vapour pressure of the sulphur within the cell (above 450°C) was proportional to the temperature.

A hydrogen tube was used as continuous source.[8]

[4] $\Delta G(v+1/2)=G(v+1)-G(v)$ where $G=E_v/hc$ (cf. R. S. Mulliken, Phys. Rev. **36**, 623, 625 (1930)).

[5] S. M. Naudé and A. Christy, Phys. Rev. **37**, 490 (1931).

[6] V. Henri, Structure des Molecules, Paris 1925; V. Henri and M. C. Teves, Nature **114**, 894 (1924).

[7] V. Henri (see Symposium of the Faraday Soc. on Molecular Spectra and Molecular Structure, Sept. 1929, p. 765) used 0.1 mg of sulphur in a 16 cc quartz tube at 600°C which gave him about the same S_2 vapour pressure.

[8] The hydrogen tube used has been described previously: S. M. Naudé, Phys. Rev. **36**, 333 (1930).

The region between λ3500 and λ2400 was studied in absorption. The absorption plates were taken with an E1 Hilger spectrograph giving a dispersion varying from 1 mm = 7.7A at λ3500 to 1 mm = 2.3A at λ2400, as well as in the first order of the 21 foot Rowland grating, giving a dispersion of 2.6A per mm. Eastman 33 plates were used. The iron and copper arcs were used as comparison spectra, the wave-lengths of which were taken from Kayser's "Hauptlinien" and Shenstone's work,[9] respectively. The copper arc was used mainly in the region below λ2800 since the iron lines are very weak and too numerous in this region to serve as standards.

The wave-lengths of the band heads on the plates obtained with the E1 spectrograph were calculated with Hartmann's formula. The measurements of the band heads obtained with both instruments agreed within experimental error. This error was relatively large (about 2 cm^{-1}), because the band heads are not very well defined owing to their characteristic rotational structure. Below λ2792.8 the heads are fuzzy due to predissociation which increases the error in this region to 5 $cm.^{-1}$ Below λ2615 the heads become very diffuse making the experimental error as large as 10 $cm.^{-1}$

The S_2 spectrum was studied in emission in the region between λ3500 and λ2400. The spectrum was excited by means of a Geissler tube described in I. The plates were taken in the first order of the 21-foot grating. Iron standard wave-lengths were used as comparison spectrum.

III. Description of the Plates

Fig. 1a is a reproduction of the bands obtained in absorption. When the absorption tube is heated to about 450°C the maximum absorption occurs in the region between λ2741 and λ2799. Plates were also taken with the absorption cell at about 600°C and 750°C. With higher temperatures the maximum absorption is shifted to longer wave-lengths as is to be expected. For temperatures of the cell below 400°C (i.e., below the boiling point of sulphur) no bands appeared in absorption in the region investigated. In emission the maximum intensity lies in the region between λ3000 and λ3500. In this region the band heads are not clearly defined owing to the great amount of overlapping. This overlapping causes many clusters of lines to be formed on the plates in this region which are not easily distinguishable from heads. These intensity relations, both in absorption and in emission, can be understood with the help of the potential energy curve obtained from the vibrational and rotational analyses given in section VII below.

Below λ2792.8 (cf. Fig. 1b) the absorption bands become diffuse. As can be seen from the plate, there are two regions in which the bands are diffuse to a different degree: first, between λ2792.8 and λ2615 and secondly between λ2615 and λ2440. The bands in the latter region are more diffuse than those in the former. In addition there seems to be a continuous absorption in the second region which reaches a maximum at λ2549. Although indications of the rotational structure reappear below λ2440 (cf. Fig. 1d) the bands are still more diffuse than in the first region.

[9] A. G. Shenstone, Phys. Rev. **28**, 449 (1926).

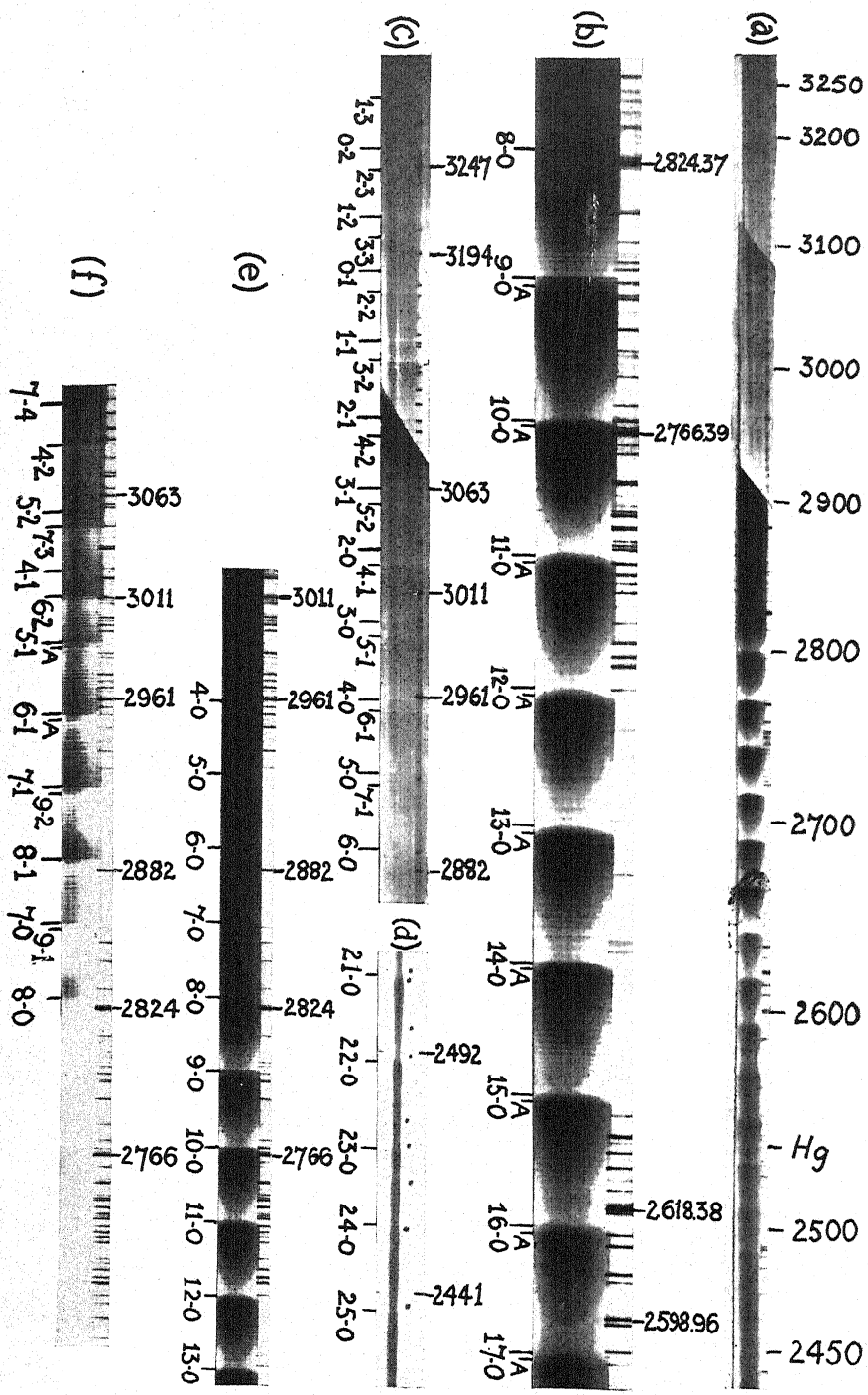

Fig. 1. (a) S_2 spectrum investigated in absorption. (b) Part of (a) showing the first region of predissociation between λ2792.8 and λ2615.0 and the first band of the second region below λ2615. (c) Absorption spectrum obtained with sulphur cell at about 750°C. (d) Bands of the second region of predissociation showing indications of rotational structure. (e) Absorption spectrum obtained with sulphur cell at about 450°C. (f) Emission spectrum of S_2.

By comparing (e) and (f) one sees that the bands which become diffuse in absorption due to predissociation do not appear in emission.

Accompanying the strong heads in absorption and about 20 cm^{-1} to the violet of these lie a number of faint heads indicated by "A" in Fig. 1b. These heads Henri and Teves[6] evidently accounted for as R heads, the strong heads being supposed to be formed by Q branches. It has been shown in I that the main system of bands is due to a $^3\Sigma^-_u \rightarrow {}^3\Sigma^-_g$ transition. Furthermore, the authors have found that no Q branches appear in these bands. Therefore the weak heads are probably due to a different electronic transition.

IV. The Vibrational Analysis

The band heads obtained in absorption can be arranged now as shown in Table IA. One would expect the bands which appear at the lowest temperature in absorption to correspond mainly to those having $v''=0$. Hence the band heads which were measured on the plates corresponding to the cell temperature of about 450°C can be assigned to transitions for which $v''=0$ and $v''=1$, the former being much more intense. These bands lie within zone (1) (cf. Table IA). When the temperature of the cell was raised to about 600°C, the band heads with $v''=1$ became more intense and in addition the band heads for which $v''=2$ appeared. These bands lie within zone (2). Similarly at about 750°C the bands for which $v''=3$ appear in absorption as well as a few for which $v''=4$ and 5. These bands lie within zone (3).[10,11] Most of these bands are indicated in Fig. 1c and 1e.

The consistent values of $\Delta G(v+\frac{1}{2})$ for any one column and row in Table IA prove the correctness of the assignment of vibrational quantum numbers to the various heads as brought out by changing the temperature of the absorption cell. Table IA reveals a number of irregularities in the values of $\Delta G(v'+\frac{1}{2})$ which will be discussed in section V. One would expect the $\Delta G(v'+\frac{1}{2})$ values to decrease regularly as v' increases. As is clear from Table IA, however, these values vary irregularly as v' increases.

The band heads measured on the plates taken in emission in the region λ3500 to λ2800 are given in Table IB. Most of the band heads observed in emission agree within experimental error with the absorption values. It is seen from Table IB that all the bands observed in emission have $v'<10$.

The values of the vibrational constants ω_e and $\omega_e x_e$ given by Rosen[2a] are essentially correct. He obtained the vibrational constants ω_e'' and $\omega_e'' x_e''$ of the lower state from the progression having $v'=3$ which was excited in fluorescence by the mercury line λ3132A = 31922 $cm.^{-1}$. Further he derived the vibrational constants ω_e' and $\omega_e' x_e'$ for the upper state mainly from the absorption bands having $v'>4$. However, most of the heads with $v'>7$ measured by him are the weaker heads of the bands designated as A bands (cf. section III) which are discussed later. The differences between the weaker and the stronger heads are approximately constant (20 cm^{-1}) and hence the value

[10] For the higher temperatures the absorption in the region between λ2800 and λ2600 becomes complete.

[11] By adding more sulphur to the absorption cell and increasing the temperature it would be possible to obtain the bands having $v''>4$ in absorption. This was not carried out as the above results were sufficient for our present purpose.

TABLE I. *Band heads of the* $^3\Sigma_u^- \longleftrightarrow {}^3\Sigma_g^-$ *system.*
A. Absorption

v'' / v'	0	1	2	3	4	5	Mean ΔG $(v'+\frac{1}{2})$
0		31399	30681	29974	29271	28577	
		402	407	408			405.7
1	39525	31801	31088	30382			
	433	436	435	434			434.5
2	32958	32237	31523	30816			
	400	398	396 2	393			398.3
3	33358	32635	31919	31209		3	
	422	421	422	418			421.6
4	33780	33056	32341	31627			
	384 1	385	385				384.7
5	34164	33441	32726				
	399	400					399.5
6	34563	33841			31717		
	391	388	2		392		389.5
7	34954	34233			32109		
	385	386					385.5
8	35339	34619		3			
	374	373					373.5
9	35713	34992					
	388	389					388.5
10	36101	35381					
	368	371 1					369.5
11	36472	35749					
	356	360					358.0
12	36828	36109					
	366	366					366
13	37194	36475					
	356	357					356.5
14	37550	36828					
	346						346.0
15	37896						
	333						333.0
16	38229						
	326						326.0
17	38555						
	330						330.0
18	38885						
	336		1				336.0
19	39221						
	316						316.0
20	39537	38832					
	310	303					310.0
21	39847	39135					
	292	290					292.0
22	40139						
	310	309					310.0
23	40449	39734					
	260	255					260.0
24	40709						
	301	297					301.0
25	41010	40286					
	269	268					
26	41279						269.0
		270					270.0
27		40284					
		277					277.0
28		41001					

In obtaining the mean value of $\Delta G(v'+\frac{1}{2})$, we have considered the accuracy of the measured band heads.

TABLE I. *B. Emission*

v' \ v''	0	1	2	3	4	5	6
0					29275		
					402		
1				30381	29677		
				437			
2			31527	30818			
			394	393			
3		32634	31921	31214?			29123
		422	420				
4		33056	32341	31628		30231	
		384	386				
5		33440	32727		31315		
		402	404		402		
6	34563	33842	33131		31717	31019	
	392	393			389		
7	34955	34235		32812	32106		30717
	385	383					385
8	35340	34618				31796	31102
		370					
9		34988	34269				

of ω_v derived from them is essentially correct. The dispersion used by Rosen was not sufficient to resolve these heads, and furthermore, when the vapour pressure of the sulphur in the absorption tube is increased, the weak heads become completely absorbed, and consequently one is liable to measure these as the main heads as Rosen apparently has done. This can be seen by comparing our assignment of vibrational quantum numbers to the various band heads with that of Rosen as is done in Table II. For wave-lengths greater

TABLE II. *Comparison of assignment of vibration quantum numbers to band heads*

Present		Rosen		Present		Rosen	
$v'-v''$	ν	$v'-v''$	ν	$v'-v''$	ν	$v'-v''$	ν
7–1	34233	7–1	34237	13–0	37194	13–0	37210
6–0	34563	6–0	34589	A	37214		
8–1	34619			14–0	37550	14–0	37550
7–0	34954	7–0	34970	A	37569		
9–1	34992			15–0	37896	15–0	37900
8–0	35339	8–0	35358	A	37915		
A	35358			16–0	38229	16–0	38240
9–0	35713	9–0	35720	A	38247		
A	35733			17–0	38555	17–0	38580
10–0	36101	10–0	36110	A	38885		
A	36123			18–0	38885	18–0	38910
11–0	36472	11–0	36480	A	38911		
A	36496			19–0	39221	19–0	39240
12–0	36828			A	39250		
A	36851	12–0	36850				

Note: The bracketed heads have been measured as one by Rosen.

than λ2926 the absorption spectrum becomes complicated and consequently Rosen's results become less trustworthy. In this region it is impossible to correlate our results with those given by him. Owing to these errors in Rosen's assignment the vibrational constants of the upper state as well as ν_e should be changed as follows:

$$\nu_e = 32250.9 + 429.5(v' + \tfrac{1}{2}) - 2.75(v' + \tfrac{1}{2})^2 - 727.4(v'' + \tfrac{1}{2}) + 2.91(v'' + \tfrac{1}{2})^2. \quad (2)$$

The above mentioned faint absorption heads (cf. section III) which lie about 20 cm^{-1} to the violet of the $v''=0$ progression, have been observed only next to the main band heads having v' ranging from 8 to 20. Some of these heads are indicated by A in Fig. 1b. A few more weak heads have been found to appear in absorption and a few in emission which seem to belong to the same electronic transition as those marked A. These band heads are tabulated in Table III which gives a possible arrangement. This arrangement, however, is uncertain, since no more heads can be found, as they are relatively

TABLE III. *The A System of bands of S_2*

	33476″	37214
	33879″	37569
	34269′	37908
35358	34640?	38249
35733		38577
36123		38911
36496	35794	39248
36851		39555

NOTE: (″) These band heads have been found in both emission and absorption.
(′) Found only in emission. All the other heads have been observed only in absorption.
(?) Doubtful value.
The band heads are arranged in this manner in order to show the parallelism between these heads and those of the $^3\Sigma^-_u \leftarrow ^3\Sigma^-_g$ system.

weak compared with the bands of the main system and are overlapped by these bands. It is therefore impossible to determine whether the upper or the lower state is common to these two systems. This might be decided in case a series of experiments were performed in which the temperature in the cell was comparatively low and the pressure was increased gradually. In addition to these two systems of bands a large number of heads have been observed above λ3500 which appear in emission. A special study of these bands, if possible with a low temperature source such as active nitrogen which would diminish the excessive overlapping of the bands, should be made in order to determine whether or not they belong to the $^3\Sigma_u^- \rightarrow ^3\Sigma_g^-$ transition.

V. PERTURBATIONS

In the great majority of band systems which have been analyzed thus far the vibrational combination difference $\Delta G(v+\frac{1}{2})$ has been found to decrease regularly as the vibrational quantum number increases.[12] If in Table IA we compare the mean $\Delta G(v'+\frac{1}{2})$ values, we see that perturbations must

[12] It was observed by G. Nakamura in the NaH bands (Zeits. f. Physik **59**, 218 (1930)) and by T. Hori in the LiH bands (Zeits. f. Physik **62**, 352 (1930)) that the $\Delta G(v'+1/2)$ values, instead of decreasing with v', increase up to a certain value of v' and then decrease regularly. W. Weizel (Zeits. f. Physik **60**, 599 (1930)) showed that this may be accounted for by uncoupling of the $p\sigma$ and $s\sigma$ electrons.

be present in the vibrational levels of the upper $^3\Sigma^-_u$ state. This is shown more strikingly if one compares the observed and calculated energy levels as shown in Table IV. The calculated values were obtained by passing the best graph through the observed $\Delta G(v'+\frac{1}{2})$ values, and then adjusting the value of the calculated $v'=0$ level until the best fit was obtained with the

TABLE IV. *Calculated and observed energy values of the vibrational levels for the $^3\Sigma_u^-$ (upper) state of the system.*

v'	o	c	$o-c$	v'	o	c	$o-c$
0	32120.0	32002.0	+18.0	12	36828.8	827.0	+ 1.8
1	32525.7	526.0	− 0.3	13	37194.8	37185.0	+ 9.8
2	32960.2	944.5	+15.7	14	37550.3	537.5	+12.8
3	33358.5	33357.5	+ 1.0	15	37896.3	884.5	+11.8
4	33780.1	765.0	+15.1	16	38229.3	38226.0	+ 3.3
5	34614.8	34167.0	− 2.2	17	38555.5	560.0	− 6.7
6	34564.3	563.5	+ 0.8	18	38885.3	890.5	− 7.2
7	34953.8	954.5	− 0.7	19	39221.3	39215.5	+ 3.6
8	35339.3	35340.0	− 0.7	20	39537.3	535.0	+ 0.3
9	35712.8	720.0	− 7.2	21	39847.3	849.0	− 1.7
10	36101.3	36094.5	+ 6.8	22	40139.3	40157.5	−18.2
11	36470.8	463.5	+ 7.3	23	40449.3	460.5	−11.2

NOTE: Our measurements below the 23←0 bands are very inaccurate, hence no comparison can be made for $v'>23$. In considering the o-c values it must be remembered that the experimental error for the bands having $v'<9$ is about 2 cm^{-1} and for $v'>9$ probably greater (cf. section II).

experimental values. It is seen that the o-c values for $v'=7$ and 8 are zero within the experimental error. We know from I that the rotational levels for $v'=7$ and 8 are normal, whereas those for $v'=9$ are perturbed. From Table IV we see also that the vibrational levels $v'=7$ and 8 are normal and $v'=9$ seems to be displaced. It appears that the levels with $v'=0, 2, 4$ are perturbed by about +17 cm^{-1}. From $v'>9$ predissociation begins and it appears that practically all these levels are perturbed in varying degree. The perturbations for $v'=0, 2, 4$ as obtained by measuring the heads of the bands, might be due either to perturbations of the rotational lines near the heads or to perturbations of the vibrational levels.

Johnson and Asundi[13] found that in the Cameron CO bands all band heads with $v'=1$ are displaced by 4.2 cm.$^{-1}$ Rosenthal and Jenkins[14] showed that all the rotational lines near the heads of these bands are perturbed, all the lines being displaced in the same direction, thus giving a displacement of the head and consequently an apparent displacement of the vibrational level. In the CN bands Rosenthal and Jenkins[15] showed that the perturbations of the rotational lines occurring in some of these bands are due to the fact that certain rotational levels of the upper state have energies approximately equal

[13] R. C. Johnson and R. K. Asundi, Proc. Roy. Soc. A123, 560 (1929).
[14] J. Rosenthal and F. A. Jenkins, Proc. Nat. Acad. of Sciences 15, 896 (1929).
[15] J. Rosenthal and F. A. Jenkins, Proc. Nat. Acad. of Sciences 15, 382 (1929).

to the rotational levels of another state with the result that the two sets of levels are mutually perturbed, as we would expect from Kronig's theory.[16,17]

It may be that the perturbations of the S_2 band heads for $v'=0$, 1, 2, 4 are of the same type, i.e. that all the rotational lines near the band heads are displaced in the same direction and that, consequently, the heads are displaced by about $+17$ cm.$^{-1}$ But in order that the alternate vibrational levels might be perturbed, we must assume the presence of another state having an ω which is approximately twice that of the $^3\Sigma_u^-$ state. If such a state were present, we would expect transitions between this and the normal state of the molecule. It may be, however, that some of the emission bands are due to such a transition.

The observed perturbations of the band heads with $v'=0$, 2, 4 may, be due to perturbations of the vibrational levels. In this case one would expect the $U(r)$ curve to be irregular and not a smooth curve as it seems to be for the electronic states of most other molecules. A similar type of perturbation to that observed in S_2 has been found by Jevons[18] in the bands of CS, where the band heads having $v'=1, 2, 4$ were found to be displaced in the same way, the maximum displacement of the CS band heads being 7.4 cm^{-1} as compared with $+18$ cm^{-1} for S_2. Moreover, by comparing the observed displacements of the R and Q heads from their calculated positions,[19] Jevons concluded that the observed perturbations were due to perturbations of the vibrational levels.

Whether this type of perturbation as observed in the S_2 bands is due to rotational or vibrational perturbations or to a superposition of both can only be determined by studying the rotational structure of the S_2 bands having $v'=0$, 2, 4 with reference to the unperturbed bands. Owing to the great amount of overlapping of those bands in the S_2 spectrum, this study is impossible unless some other type of excitation (active nitrogen or fluorescence) will excite fewer and less extensive bands, and consequently give less overlapping. Although still difficult, this study may be carried out in the CS bands.[20]

The perturbation present in the vibrational levels for $v'>9$ may be due to the continuous state which causes predissociation and which is discussed in the next section. Although the probable error in the measurement of these diffuse bands ($v'>9$) is large (cf. section II), consequently making it difficult to interpret correctly the observed minus calculated values, it may be pointed

[16] R. de L. Kronig, Zeits. f. Physik **50**, 347 (1928).

[17] But cf. H. H. Hyman and C. R. Jeppesen, Nature **125**, 462 (1930) and R. T. Birge and C. R. Jeppesen, Nature **125**, 463 (1930). These investigators have found a perturbation in the $v''=0$ level of the normal state of H_2, where presumably there could not be another interacting state present.

[18] W. Jevons, Proc. Roy. Soc. **A117**, 351 (1927–1928).

[19] If both the R and Q heads were displaced by the same amount, one might attribute this displacement to a perturbation of the vibrational level. If, however, the two heads were displaced by different amounts, this displacement might be due to the perturbation of the rotational levels. Cf. also references 13 and 14.

[20] This investigation has been started by one of the authors (S.M.N.).

out that, whereas the level $v'=9$ seems to be displaced downwards, those above the intersecting curve ($v'=10-16$) seem to be displaced upwards which suggests some interaction between the corresponding $U(r)$ curves.

We know according to I from our rotational analysis of the 9–1 and 9–2 bands that the rotational levels of the $v'=9$ level are perturbed. In these bands we have found that the mean value of B_9' obtained from the Δ_2F_9' graph is larger than the B_7' and B_8'.[21] The fact that B_9' obtained from lower values of K is less than the values obtained from higher values of K (the factor $8D_vK^3$ has been considered) seems to indicate that the perturbation increases with K.

VI. Predissociation*

It has been remarked in a previous section of this paper that there are two regions in this spectrum where the bands are diffuse. As can be seen from Fig. Ib the absorption bands are sharp[22] up to λ2799.1 ($v'=9$, $v''=0$).[23] To the violet of this point they become at first more and more diffuse, the maximum diffuseness being at about λ2741.0 (11←0) As we proceed toward shorter wave-lengths the bands become sharper. At 2615.0 (16←0) the bands suddenly become much more diffuse, the maximum diffuseness of the second region being at λ2549.0 (19←0). From this point on the bands become less diffuse. Although the spectrum has been photographed down to λ2400, the bands below λ2492 are no sharper than those between λ2792 and λ2615, as can be seen from Fig. Id. In the first region of predissociation (λ2799–λ2615), the bands although diffuse, still preserve some of their rotational structure, the diffuse lines merging into definite groups (cf. Fig. 1b). In the second region (λ2615–λ2435) the bands are completely diffuse, all group structure disappearing.

All the bands which are diffuse in absorption fail to appear on our emission plates (cf. Figs. 1e and 1f and also Table I).[24] No bands were observed in emission with $v'=10$, although the exposures were long enough to photograph these had their intensity been one tenth of that of the others. The non-appearance of these bands may be ascribed primarily to the small life time of the molecule in the vibrational levels of the ${}^3\Sigma_u^-$ state with $v'>9$, due to the transitions from these levels to those of another state with subsequent dissociation. The non-appearance of the 9→0 band may be explained by the fact that the transition probability from $v'=9$ to $v''=0$ is small. The

[21] $B_v=B_e-\alpha_e(v+1/2)$. Hence B_v should decrease as v increases.

* The authors appreciate the discussions with Drs. J. L. Dunham and Carl Eckart about points brought up in this section.

[22] When we use the expressions: bands are "sharp" or "diffuse," we actually mean that the rotational lines of the bands are sharp or diffuse.

[23] V. Henri gave λ2792.4 as the wave-length at which the bands become diffuse (cf. reference 6). However, the band at λ2792.4 (2792.8 according to our measurements) does not belong to the main system, i.e. ${}^3\Sigma^-$—${}^3\Sigma_g^-$, but to a weaker group of bands which are designated here as A bands and are given in Table IV. As will be shown in section VII, this wave-length has no special meaning.

[24] This fact was independently observed by H. H. van Iddekinge, Nature **125**, 858 (1930).

transition probability for $v'>9$ to $v''=0$ is still smaller, hence these bands would be weak even if predissociation was not present.

Various investigators[25,26,27] have given explanations of the predissociation, which occurs in this spectrum. Franck[25] showed that if we assume two intersecting curves as in Fig. 2A, we may expect transitions to take place at the point b with immediate dissociation of the molecule. The theoretical explanation based on wave mechanics, as given by Kronig[26] involves the same basic principles as those used by Franck. Kronig showed that the selection rules for radiationless transitions are $\Delta\Lambda=\pm1, 0$; $\Delta\Sigma$ or $\Delta S=0$; $\Delta J=0$; and that transition can occur only between two $+$(or$-$) rotational levels belonging to two electronic states that are both g or both u.[28] [It may be pointed out that the ordinary transition rules are $\Delta\Lambda=\pm1, 0$; $\Delta\Sigma$ or $\Delta S=0$; $\Delta J=0, \pm1$; $+$(or$-$) levels to $-$(or$+$) levels and g(or u) to u(or g) states (if equal atoms)]. The probability of a radiationless transition is proportional to $J^2/(E)^{1/2}$.[29] E is the energy difference between any level of the ${}^3\Sigma_u^-$ state and the line $b\ b'$, b' being the dissociation energy of state a. The above formula would indicate that no transition is possible between the two intersecting curves below b. Hence we would expect predissociation to begin sharply and then decrease gradually as we reach the vibrational levels above the point b. However, in both the first and second region, predissociation begins suddenly and increases gradually to a maximum before it decreases.

The explanation given by Herzberg[27] for the observed predissociation in the S_2 bands is a further development of Franck's principle. According to Herzberg curve a[30] cuts the ${}^3\Sigma_u^-$ curve at two points, c and b, as in Fig. 2B, corresponding to the two regions of predissociation. He points out that the bands of the second region may be more diffuse, first because in this region the bands will be overlapped by the continuum[31] due to ${}^3\Sigma_g^-\leftarrow a$, and secondly, because at c the probability of predissociation will be greater, for at

[25] J. Franck and H. Sponer, Nachricht Gesellschaft d. Wiss. Göttingen, Math.-Phys. Klasse, p. 241 (1928); K. F. Bonhoeffer and L. Farkas, Zeits. Phys. Chem. 134, 337 (1927).

[26] R. de L. Kronig, Zeits. f. Physik 50, 347 (1928); 62, 300 (1930).

[27] G. Herzberg, Zeits. f. Physik 61, 604 (1930).

[28] The last rule as formulated by Kronig (cf. Zeits. f. Physik 62, 300 (1930)) is symmetrical to symmetrical, and antisymmetrical to antisymmetrical states. The $+$ and the $-$ levels here referred to are the "gerade" (g) and "ungerade" (u) rotational levels of Kronig (cf. Zeits. f. Physik 50, 351 (1928)) and Mulliken (cf. Phys. Rev. 36, 617 (1930). The g and u used here refer to the "gerade" and "ungerade" electronic states of Hund as Π_u, Σ_g, Σ_u, etc. (cf. Zeits. f. Physik 51, 759 (1928)).

[29] The J^2 term in Kronig's formula enters only when the transition involves $\Delta\Lambda=\pm1$. For a transition for which $\Delta\Lambda=0$, the probability is independent of J. The dependence on J would indicate that within any diffuse band, the rotational lines would become more diffuse as we go away from the origin. The probability essentially depends upon J and not on J^2 since $J^2/(E)^{1/2}\propto J$. It is difficult to determine from our results whether or not the lines within a band become more diffuse as we go away from the origin.

[30] Herzberg points out that curve a may or may not have a minimum. His explanation fits either case equally well.

[31] Fig. 3 shows that the most probable transition from the lower vibrational levels of the ${}^3\Sigma_g^-$ state is to the left of the upper curves.

this point the radiationless transition may occur before it is necessary for the molecule to complete half a vibration as it would at point b. It is highly improbable, however, that the overlapping continuum will make the bands appear more diffuse than they actually are. Furthermore, since the frequency of vibration is much larger than that of rotation, the fact that the molecule will have to complete half a vibration at b and not at c before it dissociates, can have no appreciable effect on the relative probability of predissociation of the bands in the two regions.

The first idea which suggests itself is that there may be two curves intersecting the $^3\Sigma_u^-$ curve, giving the two regions of predissociation. It may be well, therefore, to consider here the various possible states which may be present. It has been shown by us[5] that the main system of bands which show predissociation is due to a $^3\Sigma_u^- \leftarrow ^3\Sigma_g^-$ transition, $^3\Sigma_g^-$ being the lower state. By a comparison with the Schumann-Runge bands of O_2 (cf. also section VII), one would expect the $^3\Sigma_g^-$ of S_2 to dissociate into two ^3P atoms, and the excited state, $^3\sum_u^-$, into one ^3P and one ^1D atom. It is evident also from the $U(r)$ curves that the states which cause predissociation must dissociate into two normal atoms. By applying the results of Wigner and Witmer,[32] one finds that the molecular electronic states resulting from similar atoms both in a ^3P state are the following: $^1\Delta_g$, $^1\Pi_g$, $^1\Pi_u$, $^1\Sigma_g$, $^1\Sigma_g^-$, $^1\Sigma_u^-$, $^3\Delta_u$, $^3\Pi_u$, $^3\Pi_g$, $^3\Sigma_u^+$, $^3\Sigma_u^+$, $^3\Sigma_g^-$, $^5\Delta_g$, $^5\Pi_g$, $^5\Pi_u$, $^5\Sigma_g^+$, $^5\Sigma_g^+$, $^5\Sigma_u^-$. The state or states causing predissociation (curve a in Fig. 2B or Fig. 2C) must be among the above. But according to the rules given by Kronig[16] for a radiationless transition, the only state in the above list which can interact with a $^3\Sigma_u^-$ state is a $^3\Pi_u$ state. Hence the state which causes predissociation must be a $^3\Pi_u$ state and must intersect the $^3\Sigma_u^-$ at two points as Herzberg assumed.[27] However, we have still to explain why the bands in the second region corresponding to c are more diffuse than those in the first.

It may be shown that Kronig's formula does not apply to the region c. In deriving his formula,[33] he assumed that the nuclear momentum of the molecule in state a (here identified as a $^3\Pi_u$ state) is constant. That is, he was dealing only with the flat portion of the curve, line $b\ b'$ of Fig. 2A. If, however, the curve has no minimum[34] as in Fig. 2C the momentum will not be constant near either of the points b or c.[35]

[32] E. Wigner and E. E. Witmer, Zeits. f. Physik 51, 859 (1928).

[33] Kronig took as the wave function of state a an oscillatory function with a constant period, i.e., constant momentum.

[34] The $^3\Pi_u$ state may have a very shallow minimum. If it had a sharp minimum we would expect to find discrete bands either in emission or absorption due to a $^3\Pi_u \longleftrightarrow ^3\Sigma_g^-$ transition. No such bands have been found although there is a region of weak continuous absorption beginning at about $\lambda 2600$ which may be ascribed to this transition. The group of bands designated in this paper as A bands are not due to this transition, for they are found in absorption after the point c has been passed.

[35] Since the $^3\Pi_u$ intersects the $^3\Sigma_g^-$ curve at c, we will have to suppose that although the interaction between the two atoms forming the $^3\Pi_u$ state is almost zero for very small distances of internuclear separation, when this distance is made still smaller, the repulsion between the two atoms is smaller than that in state $^3\Sigma_u^-$. (This will be the case if the electronic configuration of the $^3\Pi_u$ state resembles the united atom more closely than that of the $^3\Sigma_u^-$ state.)

In the tentative explanation given here we shall make use of the Franck-Condon theory[35] of transition probabilities between the two states $^3\Sigma_u^-$ and

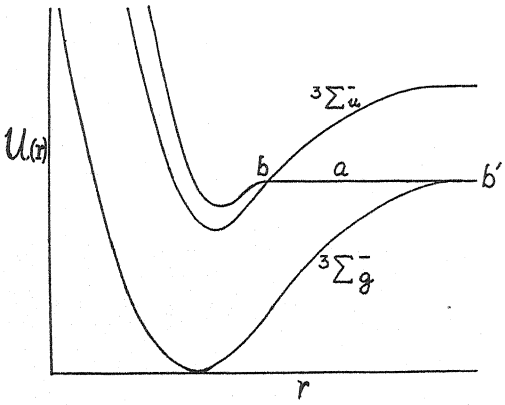

Fig. 2A

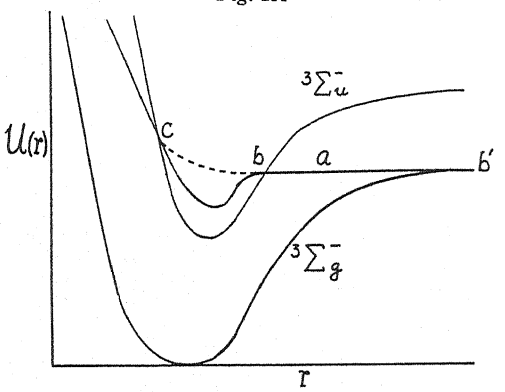

Fig. 2B

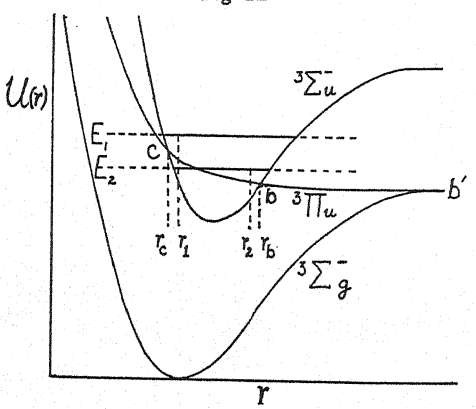

Fig. 2C

$^3\Pi_u$. According to this theory the probability of a transition is greatest when

[36] E. U. Condon, Phys. Rev. **28**, 1182 (1926).

the nuclear separation as well as the momentum remain unchanged during the transition. Since the slopes of the two intersecting curves are more nearly alike at the point c than at b, and furthermore remain closer together at the former point than at the latter, a transition from a discrete vibrational level whose energy is near that of c to the continous curve will involve a very much smaller change in the nuclear separation at this point than at the point b. The ratio of the nuclear momenta in the neighbourhood of the two points is approximately the same in both cases. This can be seen from Fig. 2C. If we take two discrete vibrational levels E_1 and E_2 so that $E_1-c=E_2-b$, and consider the points on E_1 and E_2 having zero nuclear momentum it is quite evident that the difference of the nuclear separation for the former is much less than for the latter. For two other points on E_1 and E_2 having nuclear separations r_1 and r_2 so that $r_1-r_c=r_b-r_2$ the ratios of the nuclear momenta in the former case will be about the same as in the latter. Hence the probability of the predissociation at the former point will be greater (therefore the rotational lines more diffuse) than at the latter point. Furthermore, since the two curves remain closer together near c, i.e. the second region of predissociation, we would expect more bands to be diffuse in the second region of predissociation than in the first. Finally, from the above explanation we would expect that, in both regions of predissociation, the bands tend to become more diffuse as we approach the points of intersection from either side.[37] These phenomena are exactly what we observed.

It has been stated in a previous section that the overlapping continuum reaches a maximum at λ2549. This maximum could not be due entirely to transitions between the $^3\Sigma_g^-$ and the $^3\Pi_u$ states, for according to Fig. 3, the maximum probability of this transition should occur at λ2662. We have also seen that the band at λ2549 (19←0) is the most diffuse band in this spectrum. Hence the overlapping continuum at this point must be due to the fact that the rotational levels for the $v'=19$ are so diffuse as to be practically continuous.

For a quantum mechanical formulation of the results obtained by application of the Franck-Condon principle, we would make the step by step conversion from one to the other exactly as Condon has done for ordinary transitions.[38] One sees that the overlapping of the wave functions of the two states ($^3\Sigma_u^-$ and $^3\Pi_u$) is greater at c than at b since the internuclear distances (with zero nuclear momentum) on both curves are nearer the same in the neighborhood of the former point than of the latter. Therefore the two waves will tend to reenforce each other more at c than at b, giving a greater transition probability in the neighborhood of c.

[37] L. A. Turner (Am. Phys. Soc. Meeting, New York, Feb. 1931, Paper No. 12) refers to two types of predissociation. In one the broadening of the lines sets in suddenly at a definite wavelength and in the other it sets in gradually. The former is the type discussed by Kronig (cf. Fig. 2A) and is also approximated at point b of Fig. 2C. According to our interpretation the continuous curve at point b has almost the value of dissociation. Hence at this point one would expect the broadening of the lines to set in more suddenly than at point c.

[38] E. U. Condon, Phys. Rev. **32**, 858 (1928), also Condon and Morse, Quantum Mechanics, pp. 168–170.

In the above discussion we were concerned mainly with the $^3\Sigma_u^- \longleftrightarrow {}^3\Sigma_g^-$ bands. The other system of bands which we have designated as A bands shows exactly similar characteristics. Whenever a band of the main system is diffuse the corresponding A band is also diffuse.

While this paper was being written Asundi[39] reported that in the presence of argon at high pressures, he was able to photograph the bands in emission

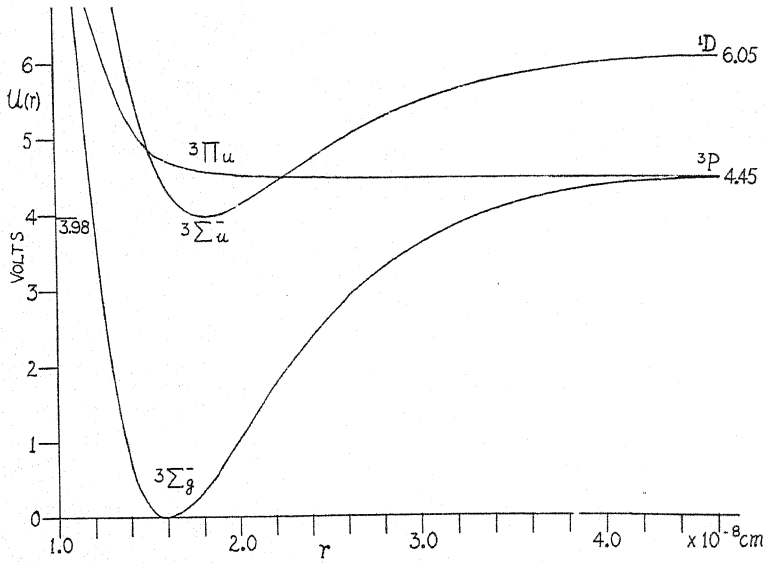

Fig. 3. Potential energy curves of the known states of the S_2 molecule. The $^3\Sigma^-_g$ and $^3\Sigma^-_u$ curves have been drawn using Morse's equation.

beyond the first limit of predissociation. If the mechanism of predissociation given by all thus far is correct, it is difficult to see what effect the presence of argon could have except that of increasing the population of the levels with $v'>9$. Thus, although dissociation does take place there are still sufficient molecules present in these states to emit the bands with sufficient intensity to be observed.

VII. Heats of Dissociation

In our previous paper[5] we showed that the main system of S_2 bands is due to a $^3\Sigma_u^- \longleftrightarrow {}^3\Sigma_g^-$ transition, and is analogous to the Schumann-Runge bands of O_2. We should, therefore, expect the normal $^3\Sigma_g^-$ state of S_2 to dissociate into two ^3P atoms just as in the case of O_2, and similarly the upper state $^3\Sigma_u^-$ to dissociate into a ^3P and a ^1D atom.

From the graph $\omega_v : v$ for the $^3\Sigma_u^-$ state we obtain by linear extrapolation 2.07 volts for the heat of dissociation D' of this state.[40] Hence the total energy required to excite the molecule into the $^3\Sigma_u^-$ state and to dissociate it is:

$$\nu_e + D' = 3.98 + 2.07 = 6.05 \text{ volts}.$$

[39] R. K. Asundi, Nature **127**, 93 (1931).

[40] Of the 2.07 volts the energy is known up to 1.01 volts and the rest is extrapolated.

The $^3\Pi_u$ level which causes the predissociation must also dissociate into two ^3P atoms, since there is no other possible atomic state between the ^3P and ^1D states. From the description of the phenomenon of predissociation as observed in these bands given in section VI it is clear that the rotational lines of the bands, are sharp up to λ2792.8 where they begin to become diffuse. The rotational lines immediately below λ2792.8 which are diffuse in absorption correspond to transitions from the higher rotational levels in $v''=0$ to the corresponding levels of $v'=10$. These lines are diffuse because the rotational levels of $v'=10$ have energies which lie in the continuous energy range of the $^3\Pi_u$ curve (i.e. $>D''$). Since the lines near the head of the 10–0 band ($\nu=36101$ cm^{-1}) also are diffuse the energies of these lines are greater than D''. The head of the 9–0 band is sharp so that its energy is less than D''. In I, moreover, it was shown that the rotational lines of the 9–1 and 9–2 bands could be followed to $K\approx30$. The line having $K\approx30$ corresponds to an energy 35713 cm$^{-1}+B_9K(K+1)\approx36000$ cm^{-1}. This energy must be less than D'' otherwise the rotational lines could not have been observed in emission. D'' must therefore lie between 36000 and 36100 cm.$^{-1}$ Therefore $D''=4.45\pm0.01$ volts.[41] This value is in good agreement with the chemical value 103600 cal $=4.5$ volt obtained by Budde.[42] By extrapolation of th ω_v:v graph for the $^3\Sigma_g^-$ state we ought to obtain the same value for its energy of dissociation D''. But, as in the case of O_2, this extrapolation leads to a value of D'' which lies above the correct values for S_2 as obtained from predissociation.[43]

Using the values of r_e' and r_e'' given in I and the values of ν_e, D' and D'' obtained above, we are able to draw the potential energy curves of the $^3\Sigma_g^-$ and $^3\Sigma_u^-$ states of S_2 using Morse's equation,[44] (see Fig. 3). Assuming the $^3\Pi_u$ curve to intersect the $^3\Sigma^-_u$ curve at about $v'=19$ and $v'=11$ according to section VI and to give two ^3P atoms, we may draw this curve as shown in Fig. 3.

According to the above results the separation of the ^1D and ^3P atomic states must be $6.05-4.45=1.60$ volts. The value of this separation for O as given by Frerichs[45] is 1.95 volt and the corresponding separations in the Se and Te atoms as determined by McLennan and Crawford[46] are 1.2 and 1.3 volts. By interpolating we obtain 1.6 ± 0.1 volts for S which is in good agreement with the value given above;

The authors wish to thank Professor R. S. Mulliken for his interest and criticism in connection with this work.

[41] G. Herzberg, Zeits. f. Physik **61**, 604 (1930) lays great stress on the fact that one can obtain only a maximum value of the energy of dissociation from predissociation data. From our interpretation of the phenomenon it is clear that a fairly accurate determination is possible for S_2.

[42] Budde, Zeits. f. Analyt. Chem. **78**, 169 (1912).

[43] The linear extrapolation in this case will be very inaccurate as it is much greater than in the $^3\Sigma_u^-$ state.

[44] P. M. Morse, Phys. Rev. **34**, 57 (1929).

[45] R. Frerichs, Phys. Rev. **36**, 398 (1930).

[46] J. C. McLennan and M. F. Crawford, Nature **124**, 874 (1929).

NOTE ON MODES OF SPECTROGRAPH SLIT IRRADIATION

DONALD C. STOCKBARGER AND LAURENCE BURNS
RADIATION MEASUREMENTS LABORATORY
MASSACHUSETTS INSTITUTE OF TECHNOLOGY

(Received February 26, 1931)

ABSTRACT

The mercury lines, 3650–63, have been photographed with very approximately coherent slit irradiation and with a number of different slit-widths. Maximum sharpness and resolution were obtained when the slit-width had a rather critical value. Multiple lines appeared when a multiple of the critical slit-width was used. Diffraction patterns appeared between the lines when the slit was made narrower than the critical value. A more detailed account of the research, of which this is but a small part, will appear later.

THE recent appearance of a mathematical paper by van Cittert[1] has prompted us to publish a small portion of the experimental results which we are accumulating in our study of spectrograph slit irradiation. Although the work has been in progress for nearly a year we do not feel justified in attempting to treat the subject in a general way until the entire program has been covered. The results presented will serve, therefore, merely as an indication of what we are finding, viz., that the width and shape of a line image are influenced to a large degree by the mode of slit irradiation.

We were led to undertake the research by difficulties encountered during the past few years in connection with such things as line absorption and intensity measurements. Evidently others have experienced similar difficulties.[2] Sometimes photographed lines appeared to have absorption cores when there were no assignable reasons for self-reversal. In one instance several lines seemed to suffer a shift of wave-length so great that no known agencies could account for it. Although the false effects could be eliminated usually through adjustment of the optical system, we felt that a systematic investigation should be made in order to remove the necessity for cut-and-try methods. Practically no help was found in the literature.

Van Cittert treats the two special cases, coherent and noncoherent monochromatic irradiation, in some detail and draws conclusions in regard to a few intermediate modes such as would be met in practice. Wadsworth[3] and Schuster[4] had already treated the completely noncoherent case but, as van Cittert suggests, a self-radiant slit which is sufficiently narrow is practically

[1] P. H. van Cittert, Zeits. f. Physik **65**, 547 (1930).

[2] Shenstone, Phys. Rev. **34**, 726 (1929).

[3] Wadsworth, Ast. Jour. **1**, 52 (1895); ibid. **3**, 170 and 321 (1896); ibid. **4**, 54 (1896); Phil. Mag. **43**, 317 (1897).

[4] Schuster, Ency. Brit. Article on Spectroscopy; Ast. Jour. **21**, 197 (1905).

unattainable. Approximately noncoherent irradiation can be realized through the use of a very broad source or by imaging a source on the slit with a very large condenser lens. Departure from noncoherency of irradiation may lead to narrower lines but it can also seriously affect their shapes. In ordinary prac-

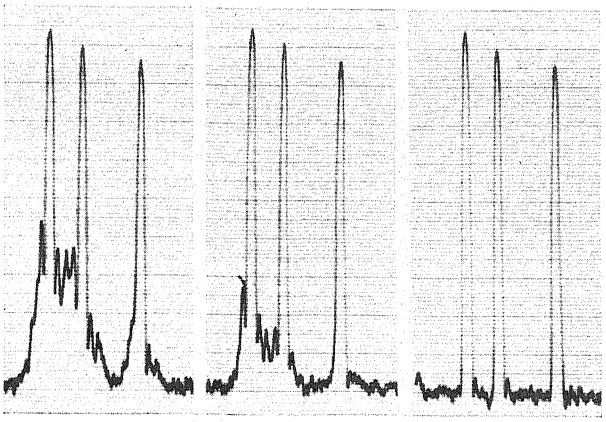

Fig. 1. Slit 2.5 divisions. Note the pronounced diffraction background.
Fig. 2. Slit 3.5 divisions.
Fig. 3. Slit 4.5 divisions. Sharpness and resolution appear to be best with this slit width.

tice this departure may be considerable. For every mode of slit irradiation there exists a slit-width which should not be exceeded. This width being measured in wave-lengths, the correct setting for one spectral region is incorrect for another.

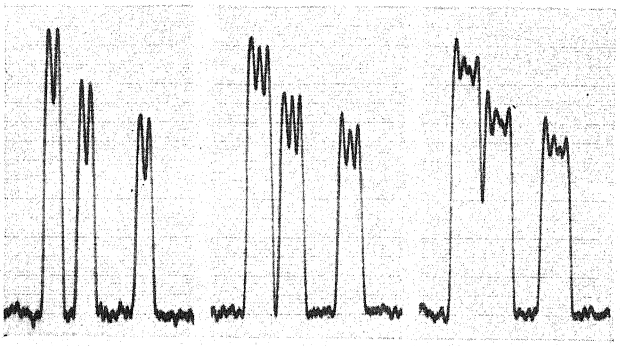

Fig. 4. Slit 9.5 divisions.
Fig. 5. Slit 12.5 divisions.
Fig. 6. Slit 14.5 divisions.

In general, we find our experimental results to be in qualitative agreement with van Cittert's mathematical analysis. We are including intermediate modes of irradiation, however, and consequently are finding different orders of effects and some effects not mentioned in his paper.

In the example selected for this note, the source was a low pressure quartz mercury arc placed 2.25 meters from the slit of a Hilger E2 quartz spectrograph. To narrow the beam of radiation an opaque screen with a window, about one centimeter in diameter, was mounted 25 cm in front of the arc. The arc and screen were carefully adjusted in position so that the radiation passed through the center of the collimator lens. This mode of irradiation, which approached the coherent case, was of such a nature that pronounced diffraction effects were observed, but it was not an extreme case. The 3650–63 lines were photographed with different slit-widths, and then the plates were examined with the aid of a recording microphotometer.

Figs. 1–10 show that maximum sharpness and resolution of the lines were obtained when the width had a rather critical value, viz., 4.5 divisions on the drum. At multiples of the critical width the lines tended to appear equally

Fig. 7. Slit 21.5 divisions.
Fig. 8. Slit 26.5 divisions.
Fig. 9. Slit 31.5 divisions.
Fig. 10. Slit 36.5 divisions.

multiple, e.g., a doubling occurred at twice the critical slit-width. For widths between multiples of the critical value the diffraction patterns were not as regular. The lines were often well resolved even when they appeared to be multiple. Below the critical width, however, the spaces between the lines were filled with a diffraction background of considerable density.

Evidently accurate estimates of the relative e intensities would be difficult to make in some of the cases illustrated, either through measurement of areas or from reading maximum densities. Furthermore, very misleading information concerning true line shapes could easily be got from an examination of the images. The minima due to doubling might be misinterpreted as an indication of reversal. In extreme cases the diffraction patterns might even suggest fine structure.

We plan to present in much greater detail in a forthcoming paper the results of similar studies made with a number of modes of slit irradiation. Some of these modes give rise to doubling or trebling with wide separations between components.

THE MASSES OF O^{17}[1]

By Harold C. Urey
Department of Chemistry, Columbia University

(Received March 9, 1931)

Abstract

The rest mass of O^{17} is calculated from the known rest masses of N^{14}, He^4, and H^1 and the masses due to the kinetic energies of He^4, H^1, and O^{17} as determined by Blackett and Harkins in the transmutation reaction $N^{14}+He^4 \rightarrow O^{17}+H^1$. The only assumptions involved are that the conservation of momentum and of mass-energy holds in these reactions. The masses secured in this way from seven sets of data do not agree within the probable limits of error for the experimental data. It is suggested that this is due either to the formation of O^{17} atoms of different masses and energies in this reaction or to the emission of gamma-rays during the collision. The former of these predicts discontinuous energy levels while the latter would probably cause the rest mass of O^{17} as calculated here to vary continuously. The relation of this calculation to the experiments of Bothe and Pose on the ranges of H particles from boron and aluminum is discussed.

BLACKETT[2] and Harkins and his coworkers[3] have reported the presence of anomalous forked cloud tracks when α particles from thorium C and C′ bombard nitrogen gas in a Wilson cloud-tract apparatus. These forked tracks consist of the usual α-particle track up to the point of the fork; beyond this point there is one heavy track due to a heavy atom and one thin track having all the characteristics of the tracks of high speed hydrogen particles. These forked tracks are anomalous in that the kinetic energy is not conserved. Blackett has given a critical discussion of these tracks and shows that the range of the heavier secondary track is consistent with the assumption that it has an atomic number of 8 and a mass somewhere between 12 and 20 atomic weight units. It seems certain that only two particles are produced as a result of the collision between the α-particle and the nitrogen nucleus because only two tracks result and because these two tracks and the original α-particle track lie in one plane. The approximate conservation of mass requires that the heavy particle produced have an approximate atomic weight of 17 and thus that it be O^{17}. The subsequent discovery of this nucleus in atmospheric oxygen increases our confidence in the correctness of this conclusion.

These authors have secured the velocities of the He^4, O^{17}, and H^1 nuclei (that of N^{14} is zero) and using Aston's values for the rest masses of He^4, N^{14} and H^1, it is possible to calculate the rest mass of O^{17} assuming the conserva-

[1] This paper is Contribution 653 of the Department of Chemistry, Columbia University, New York, N. Y.

[2] P. M. S. Blackett, Proc. Roy. Soc. **107A**, 349 (1925).

[3] W. D. Harkins, and H. A. Shadduck, Zeits. f. Physik **50**, 99 (1928); W. D. Harkins, and A. E. Schuh, Phys. Rev. **35**, 809 (1930).

tion of mass and energy. The mass of O^{17} is then easily seen to be given by

$$M_O = [M_{He}(1 - v_{He}^2/c^2)^{-1/2} + M_N - M_H(1 - v_H^2/c^2)^{-1/2}](1 - v_O^2/c^2)^{1/2}, \quad (1)$$

where $M_O M_{He}$, M_N and M_H are the rest masses of the corresponding atoms in atomic weight units ($O^{16} = 16$) and v_{He}, v_H and v_O the corresponding velocities. The velocities v_H and v_O are calculated from the angles between the direction of the original α-particle track and the directions of the oxygen and hydrogen tracks using the formulae

$$v_O = \frac{M_{He}}{M_O} v_{He} \frac{\sin \psi}{\sin (\psi + \omega)}, \quad v_H = \frac{M_{He}}{M_O} v_{He} \frac{\sin \omega}{\sin (\psi + \omega)}, \quad (2)$$

where ψ and ω are the angles between the α-particle track and the hydrogen and oxygen tracks, respectively. These formulae follow if the law of conservation of momentum holds for these collisions. The velocity of the α-particle is secured from the remaining range of the α-particle at the point of collision by using the well-known relation between range and velocity, $R = kv^3$.

Blackett used $M_{He} = 4$, $M_H = 1$ and $M_O = 17$ in calculating the values of v_O and v_H and did not correct for the change of mass with velocity. Harkins probably used the rest nuclear masses (not the atomic masses) but did not correct for the change of mass with velocity. In making the calculations for M_O, $M_{He} = 4.00107$, $M_H = 1.00723$, $M_O = 17$ have been used in securing preliminary values for v_{He} v_H, v_O and M_O. Using these results values for $M_{He}(1 - v^2_{He}/c^2)^{-1/2}$, $M_H(1 - v^2_H/c^2)^{-1/2}$ and $M_O(1 - v^2_O/c^2)^{-1/2}$ were secured which were then used in repeating the entire calculation in order to correct for the change of mass with velocity and to use only the rest masses of the nuclei and not those of the atoms. These corrections changed the values of M_O by nearly a constant amount of 0.0007 at weight units and did not change the variations in M_O appreciably.

The probable errors in this calculation can be estimated more readily by expanding (1) in the form

$$M_O = M_{He} + M_N - M_H + \frac{1}{2} M_{He} \frac{v_{He}^2}{c^2} - \frac{1}{2} M_H \frac{v_H^2}{c^2} - \frac{1}{2}(M_{He} + M_N - M_H) \frac{v_O^2}{c^2} + \frac{3}{8} M_{He} \frac{v_{He}^4}{c^4} - \frac{3}{8} M_H \frac{v_H^4}{c^4} + \cdots. \quad (3)$$

Then substituting the values of (2) in (3) and neglecting the terms in v^4_{He} and v^4_H, we secure

$$M_O = M_{He} + M_N - M_H + \frac{1}{2} M_{He} \frac{v_{He}^2}{c^2} - \frac{1}{2} \frac{M_{He}^2}{M_H} \frac{v_{He}^2}{c^2} \cdot \frac{\sin^2 \omega}{\sin^2 (\psi + \omega)} - \frac{1}{2} \frac{M_{He}^2 (M_{He} + M_N - M_H)}{M_O^2} \frac{v_{He}^2}{c^2} \frac{\sin^2 \psi}{\sin^2 (\psi + \omega)}.$$

In the last term M_O can be set approximately equal to $M_{He}+M_N-M_H$ since this term is small and the equation then becomes

$$M_O = M_{He} + M_N - M_H + \frac{1}{2} M_{He} \frac{v_{He}^2}{c^2} \left(1 - \frac{M_{He}}{M_H} \frac{\sin^2 \omega}{\sin^2 (\omega + \psi)} - \frac{M_{He}}{M_{He} + M_N - M_H} \frac{\sin^2 \psi}{\sin^2 (\psi + \omega)} \right). \quad (4)$$

From this it is easily seen that the errors in the rest masses of He, N, and H introduce the same error in each calculation and that this is approximately Aston's error in the rest mass of N,[14] namely $\sim$0.0028 atomic weight units and that the error in the energy of the α-particle only affects the small quantity $M_O-M_{He}-M_N+M_H$. An error of one percent in the energy of the α-particle makes an error of only a few units in the fifth decimal place as will be seen below. A study of the effects of errors in ω and ψ on the mass shows that the error in ω is by far the more important because it is a small angle in the case of all the forked tracks measured by Blackett and because M_{He}/M_H ($=\sim$4) is much larger than $M_{He}/(M_{He}+M_N-M_H)$ ($=\sim$0.235) so that the error in the second term within the parenthesis of Eq. (4) is the important one. Blackett estimates his mean error of measurement of angles[4] as about 10′ providing the tracks are not curved and the angles are not near 90°, i.e., less than 75°. These conditions are fulfilled in the case of ω for every case except one in which the tracks are curved. The least laborious way for calculating this error was found to be a repetition of the calculation of M_O using $\omega+10'$ instead of ω throughout. The probable error in M_O is then taken as

$$\Delta M_O - (\Delta M_1^2 + \Delta M_2^2)^{1/2}$$

where ΔM_O is the probable error of M_O and ΔM_1 and ΔM_2 are the errors produced by a one percent error in the energy of the α-particle and an error of 10′ in ω, respectively.

The probable errors in Harkins' measurements cannot be estimated. The

TABLE I. *Atomic weights of* O^{17} *with that of* O^{16} *taken as 16.*

Author	M_O(nucleus)	M_O(atom)	ΔM_1 $\times 10^5$	ΔM_2 $\times 10^5$	ΔM_O $\times 10^5$
B4	17.00067	17.00504	2.7	7.1	7.6
B7*	16.99965	17.00402(?)	1.6	7.1	7.3(?)
B1	16.99927	17.00364	1.3	6.0	6.1
B5	16.99893	17.00330	0.9	7.2	7.3
B3	16.99863	17.00300	0.6	6.6	6.6
B6	16.99857	17.00294	0.6	27.7	27.7
B2	16.99698	17.00135	1.0	8.3	8.4
Preliminary Mean	16.99895	17.00332			
Harkins and Schuh	17.0007	17.0050	?	?	

* The measurements are in doubt because the tracks are curved.

[4] P. M. S. Blackett, Proc. Roy. Soc. **103A**, 62 (1923).

track observed by Harkins and Shadduck[5] is difficult to explain because both ω and ψ are obtuse angles so that the conservation of momentum is impossible and thus Eqs. (2) cannot apply, while the angles between the tracks are not reported in the case of the track observed by Harkins and Schuh.

The results of the calculations are listed in the Table I. Column 1 contains a symbol, B1, etc., indicating the first track of Blackett, etc. Altogether the data are complete for seven tracks.

Discussion of Results

It is evident that the total variation of the calculated masses of O^{17} is very much greater than any reasonable estimate of the experimental errors. The lowest value is 0.00197 below the mean. It would be impossible to make a sufficient error in the kinetic energy of the α-particle to account for this error, for in order that this lowest value should agree with the 17.00300 value it would be necessary to assume that the energy of the α-particle was about 1/6 of that actually used in the calculation. The error in the measurement of ω necessary to account for this difference would be about 4°. Yet the track meets all of Blackett's requirements and the published track appears to be distinct and capable of exact measurement. The largest value is 0.00172 above the average. The angle ψ in this case is 78°52′ and thus difficult to measure according to Blackett, but errors in this angle will make only small errors in M_O and thus there is no reason to believe that the mass calculated from this track is in error. Thus the conclusion that these values of the mass of O^{17} do not agree within experimental error seems justified and the preliminary average is not permissible.

The following ways of accounting for the discrepancies may be considered:

1. The oxygen atoms formed may not have the same mass and energy and the mass differences measure the energy-level differences of the O^{17} nucleus. If this is the case, one would expect γ-rays to be emitted by the O^{17} nucleus very soon after the collision.

2. γ-rays may be emitted during the collision process.

A descision between these possibilities is not possible on the basis of these experiments, nor, in fact, on that of the experiments of Bothe[6] and Pose[7] who have shown that the ranges of the H particles produced when α particles of uniform range bombard boron and aluminum respectively fall in discontinuous groups. The second assumption is the one usually assumed by workers in this field. I choose, however, to use the first, for it is more nearly in accord with the well established interpretation of collision phenomena of the external electron shells. Moreover, the time of collision is of the order of mag-

[5] The figure drawn by these authors does not agree with the angles reported but the writer has been unable to reproduce their values for the velocities of O^{17} and H^1 by assuming different ways of defining the scattering angles.

[6] W. Bothe, Zeits. f. Physik **63**, 381 (1930).

[7] H. Pose, Zeits. f. Physik **64**, 1 (1930).

nitude of 10^{-21} sec. while the probability of emission of a quantum from the nucleus should be about 10^{15} so that the emission of a quantum during the collision is relatively improbable. The calculations in either case are subject to about the same errors due to neglect of the momentum of the quantum. An estimate of these errors can be made easily for the calculations as made here.

It is likely that the γ-ray quantum would be emitted within $\sim 10^{-15}$ seconds after the collision.[8] During this time the O^{17} nucleus would move a distance equal to the diameter of one atom and thus the angle between the track of the excited O^{17} nucleus and the original α-particle track would not be the observed angle used in deriving equations (2), since the momentum of the quantum would deflect the track of O^{17}. To see how large an error this would make we shall consider the B4 track and assume that a quantum having energy equivalent to 0.00369 atomic weight units is emitted. This should give the greatest possible error. If this quantum were emitted in a direction parallel to the direction of the O^{17} nucleus, no change in the angle ω would result and thus no error be made in the calculation. If it were emitted perpendicular to the approximate plane of the three tracks, only a slight error would be made since the angle between the O^{17} and α-particle tracks would be changed but slightly. Finally if it were emitted in a direction perpendicular to the O^{17} track and in the plane of the three tracks, a maximum displacement of the O^{17} track would result. This angle is given by the relation

$$M_O v_O \sin(\Delta\omega) = 0.00369c$$

or

$$\Delta\omega \leqq \frac{0.00369 \times 3 \times 10^{10}}{17 \times .454 \times 10^{9}} = 0.014 \text{ radians} = 50'.$$

A comparison with the calculated errors in M_O assuming an error of 10′ in the measurement of ω shows that the maximum error possible in the B4 case is about ± 0.00038. The error cannot be this large in any other case for the quantum cannot be as large as the quantum assumed here unless the rest mass of O^{17} is considerably less than 17.00135 which does not appear likely. Thus the actual spacings of the energy levels may be uncertain due to this effect by not more than 10 percent of their total separations from the lowest level. If the B2 collision does not produce a normal O^{17} nucleus, the maximum uncertainty increases in approximately direct proportion to the excitation energy and the uncertainty remains the same fraction of the excitation energy. The probable error would certainly be less, for the quantum may be emitted in a more favorable direction and the total excitation energy may not be emitted at the same time or in the same direction. The largest atomic

[8] The probability of emission of a quantum is proportional to $\nu^3 a^2$ where ν is the frequency and a a length of the dimensions of the emitting system. Taking ν equal to about 10^5 times the frequencies emitted by atoms and a equal to 10^{-4} of the diameter of an atom, we see that this probability will be 10^7 times that of an atom which is known to be $\backsim 10^8$.

weight difference of 0.00369 is equivalent to 0.00358A or 3.4×10^6 electron-volts.

Altogether these estimates of possible errors lead to the conclusion that the B1, B5, B3, and B6 values may all be due to one energy level but that B4 and B2 are due to the formation of O^{17} nuclei of different masses. Finally the B7 track may be disregarded because of the uncertainty arising from the curved tracks. Three masses separated by about equal differences are indicated by the data as shown in Table II. The data are too meager and

TABLE II.

Track	M_o	Av. M_o	ΔM_o
B4	17.00504	17.00504	
B1	17.00364		>0.00182
B5	17.00330	17.00322	
B3	17.00300		>0.00187
B6	17.00294		
B2	17.00135	17.00135	

the uncertainty to great to regard these differences as certain, but equally spaced vibration levels due to a proton (or neutron) vibrating relative to an O^{16} residue of the O^{17} nucleus immediately comes to mind as a possibility.

Bothe's and Pose's experiments showing discontinuous ranges of H particles agree with the assumption of discrete energy levels in the heavier nucleus as they have indicated.[9] If the range of the α-particles is uniform as was the case in their experiments, and if the energy of the heavier nucleus is small as compared with that of the hydrogen nucleus, discrete ranges of H particles will occur, the higher range particles occurring when a nucleus of low energy is formed. These conditions are not fulfilled by Blackett's data for the energy of the α-particles are not sufficiently uniform. It is of interest, however, to note the rough agreement between this data and the data of these authors. Table III shows the atomic weight of O^{17} as calculated, the kinetic energies

TABLE III.

Track	M_o	E_{He} $\times10^{+3}$	E_0 $\times10^{+3}$	E_H $\times10^{+3}$	v_H $\times10^{-9}$	R_H(cm)
B4	17.00504	8.35	1.94	4.30	2.58	17.2
B7	17.00402	8.64	1.08	5.95	3.25	34.3
B1	17.00364	7.63	0.98	5.40	3.09	29.5
B5	17.00330	7.45	1.90	4.65	2.87	23.6
B3	17.00300	6.96	1.72	4.64	2.87	23.6
B6	17.00294	8.70	3.15	4.49	2.64	18.4
B2	17.00135	8.28	1.55	7.78	3.71	51.1

of the α-particle, and of the H and O^{17} nuclei, the velocity of the H nucleus and its range in air calculated from the formula, $R_H/R_{He}=v^3_H/v^3_{He}$. The

[9] E. Rutherford and J. Chadwick, Proc. Camb. Phil. Soc. **25**, 186 (1929) conclude that the variation of Blackett's data is outside experimental limits of error, but do not calculate the masses of O^{17} as is done here.

kinetic energies are expressed in atomic weight units per gram molecule (at. wt. of $O^{16}=16$). The energy of the O^{17} nucleus is considerably smaller than that of the hydrogen nucleus except in the case of the B6 track. The shortest range H nucleus is indeed that of the B4 track and the longest that of the B2 track as expected. The irregularities of the ranges as compared to the calculated masses of O^{17} can be seen to be due to the variations in the kinetic energies of the α-particles or of the O^{17} nucleus.

Bothe and Becker[10] have detected the emission of γ-rays from lighter elements during the disruption of the nucleus in agreement with the expectations of this calculation and the interpretation of the results. They report, however, that the γ-radiation in the case of nitrogen gas bombarded with α-particles from polonium is very weak. This does not contradict the prediction of γ-rays in the collisions observed by Blackett, for they are all due to α-particles of considerably longer range (6.24 to 7.79 cm) than those from polonium.

On the basis of this calculation the atomic weight of O^{17} cannot be greater than the minimum value calculated, namely, 17.00135 ± 0.0028 if the atomic weight of O^{16} is taken as 16.000.

[10] W. Bothe, and H. Becker, Zeits. f. Physik **66**, 289 (1930).

PROPAGATION OF LARGE BARKHAUSEN DISCONTINUITIES

By K. J. Sixtus and L. Tonks
General Electric Company, Schenectady, New York

(Received February 28, 1931)

Abstract

Large Barkhausen discontinuities have previously been observed by Forrer and by Preisach in nickel wires and hard-drawn wires of the nickel-iron series respectively under stress. A prediction that these discontinuities occur in form of a propagation along the wire, starting at a nucleus, has now been substantiated. In the experiments an additional local field was used to start the propagation at a definite point on the wire, which was in a uniform magnetic field, and the velocity was determined by measuring the short time interval elapsing between the passage through two search coils around the wire. With a fixed value of tension on the wire, the velocity v was found to vary approximately linearly with the applied uniform field H, so that $v=A(H-H_0)$. A is the slope of the velocity-field characteristic and H_0 is called the *critical field.* Measured velocities range from 500 to 40,000 cm sec^{-1}. H_0 varies with composition, amount of cold working, and with the stress applied to the wire. Increasing tension reduces the critical field over the greater part of the Ni-Fe alloy composition range. The behavior of H_0 with increasing and decreasing tension shows the presence of elastic hysteresis. A is nearly constant for changes in tension, in diameter of wire, for composition of wire, and is the same for a strip. Its value is approximately 25,000 cm sec^{-1} $gauss^{-1}$.

The existence of eddy currents limits the speed with which magnetism can penetrate the wire. A rough calculation of this time gives values in the neighborhood of 10^{-2} sec. Thus a discontinuity travelling at 10^4 cm per sec. occupies a length of some 100 cm on the wire. This was substantiated both by measurements of the peak voltage induced in a search coil and by oscillograms taken of the induced voltage. The observed passage times agree well with the theoretical penetration times.

The constancy of the v-H slope for wires of different diameters is believed to indicate that the velocity depends upon surface phenomena rather than volume phenomena. The velocity would thus be determined by conditions existing near the front edge of the discontinuity where the penetration is still slight. The critical field is believed to represent a threshold value of magnetic field which must be exceeded at all points of the wire before reversal of magnetism can occur. The excess of the impressed field over the critical is nullified during propagation by the fields arising from the eddy currents. A possible picture of the discontinuity is one in which the reversal occurs within a minute distance of an approximately conical surface in the wire, the edge of the base of the cone forming the front of the wave.

The explanation advanced by Preisach for the asymmetric hysteresis loops found if one limit of the magnetization cycle was reduced has been extended. In this case magnetic inhomogeneities act as nuclei. Mechanical distortion introduces inhomogeneities of another type which also lead to the very easy formation of a nucleus. The phenomena found with torsion are more complicated than for tension. In some cases the slope of the v-H lines shows appreciable variation with direction of twist. The results of tests with various compositions of the nickel-iron series are described using both tension and torsion, but no new relations to other properties of these alloys can be given so far. Identifying H_0 with coercive field, R. Becker's theory has been compared with our results. It appears that in most cases increased elastic tension and increased cold working stresses shift H_0 in opposite directions.

1. Large Barkhausen Discontinuities

SINCE the discovery of the Barkhausen effect, it has been a well-established fact that a great part of the change in induction in a ferromagnetic when subjected to a varying field, is made up of discontinuous changes. These ordinary discontinuities can only be observed after amplification and are not detectable by the ballistic method. Large discontinuities were first observed by Forrer[1] in 1926 in the hysteresis loop of a strained nickel wire. Later Preisach[2] showed that wires of Ni-Fe alloys under the influence of any stress (tension, torsion, bending) gave large discontinuities in a longitudinal field. In some cases these discontinuities were equal to almost the whole change in induction between saturation in the two directions.

If one tries to picture the manner in which such a magnetization discontinuity occurs, one is struck by the difficulty of accounting for a simultaneous reversal in the whole length of a fine wire. This consideration led Langmuir to predict that the magnetization first reversed at one point in the wire, forming a nucleus, and that the two boundaries which were thus formed then travelled along the wire with a finite velocity which probably depended on the magnetic field strength and the elastic strain. This prediction has been well substantiated by the experiments which will be described in what follows. A preliminary report of this work has appeared in the Phys. Rev. **35,** 1441 (1930).

2. The Propagation of Magnetization

Several investigations on the propagation of magnetic waves have been carried out.[3] The method used has been the same in all cases. An iron wire or bar was subjected to an alternating magnetic field at one point and the phase shift and maximum value of induction a certain distance away were measured. Zenneck[4] proposed a theory for the observed effects, based on the assumption of eddy currents as a determining factor, and postulated the equivalence of electric and magnetic waves propagating along a ferromagnetic conductor. But the velocities corresponding to the observed phase shifts differed within a wide range (10^3 to 10^5 cm/sec), the whole phenomenon appeared to be very complex, and no effort was made to relate theory and experiment to each other.

The problem appears simpler in the case of the propagation of a single discontinuity, particularly a 100 percent discontinuity, by which is meant one in which the reversal of saturation is complete. In such a case we are dealing with a medium of finite conductivity and permeability unity but capable of reversing its magnetization at a point under a certain critical local condition.

[1] M. R. Forrer, Journ. de Physique [VI] **7,** 109 (1926).

[2] F. Preisach, Ann. d. Physik **3,** 737 (1929).

[3] A. Oberbeck, Ann. d. Physik **21,** 672 (1884); **22,** 73 (1884). H. A. Perkins, Amer. Jour Sci. **18,** 165 (1904). Lyle and Baldwin, Phil. Mag. **12,** 433 (1906). C. V. Drysdale, Electrician **67,** 95 (1911).

[4] T. Zenneck, Ann. d. Physik **9,** 497 (1902).

This local condition is defined by two variables, the state of elastic strain and the magnetizing force.

It was thought that general energy considerations might enable us to make an attack on this problem. A change of intensity of magnetization ΔI in a field H represents an available energy density of $H\Delta I$. This must at least exceed the energy dissipated by the eddy currents accompanying the magnetization wave.[5] These losses can be estimated as follows. The whole change of magnetization intensity, ΔI, is assumed to occur in a

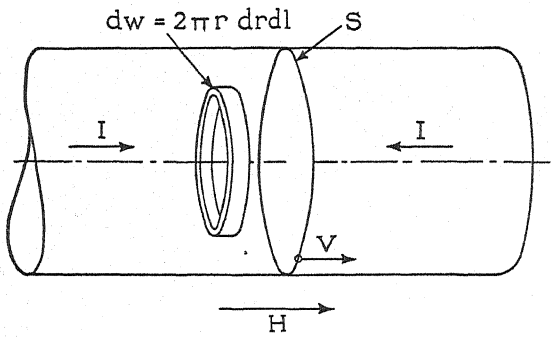

Fig. 1. Illustrating the induction of eddy currents by a moving magnetic discontinuity.

thin plane slab, S, moving with velocity v as shown in Fig. 1. The time integral of the e.m.f. induced in an annular volume dw of radius r will be that due to the change in flux, $\Delta\phi$, inside that ring, that is,

$$\int F dt = \Delta\phi/c = \pi r^2 \cdot 4\pi\Delta I/c \tag{1}$$

where F is the e.m.f. induced in dw and c is the ratio of units. The chief contribution to this integral will occur while the discontinuity is within a distance of dw which is comparable with its radius r. Accordingly, instead of $\int F dt$, where F is the e.m.f., we may write $F\Delta t$, approximately, where $\Delta t = 2r/v$. Applying this to Eq. (1), we have

$$F = 2\pi^2 rv\Delta I/c. \tag{2}$$

Since F is acting for a time Δt the eddy current loss in dw is $F^2\Delta t dr dl/2\pi r\rho$ where ρ is the specific resistance. Combining with Eq. (2) and integratting, the energy loss per unit length of wire of diameter a is found to be $E = (4/3)\pi^3 a^3 v(\Delta I)^2/\rho c^2$. The magnetic energy available is $E_m = \pi a^2 H\Delta I$. Equating the two we find for the velocity

$$v = (3/4\pi^2)\rho c^2 H/a\Delta I \tag{3A}$$

in magnetic units or

$$v = 0.76 \times 10^8 \rho H/a\Delta I \tag{3B}$$

in practical units.

[5] This reasoning obviously neglects any elastic energy changes which may occur.

Another calculation based on what appeared to be a less favorable hypothesis at the time was made by Dr. H. Poritzky. The assumption that the magnetization change occupies a length, λ, of the wire, long compared to a, gives

$$\Delta t = \lambda/v.$$

Reasoning as before, it follows that

$$v = (1/2\pi^2)\rho c^2 H\lambda/a^2\Delta I \tag{4A}$$

in magnetic units, or

$$v = 0.51 \times 10^8 \rho H\lambda/a^2\Delta I \tag{4B}$$

in pratical units for this case.

3. Apparatus

Theory of method. In measuring rectangular hysteresis loops of the same type as published by Preisach, it was noticed that the field strength at which the large discontinuity occurred, which will be called the *starting field*, was variable within a few percent in successive experiments. Since the occurrence

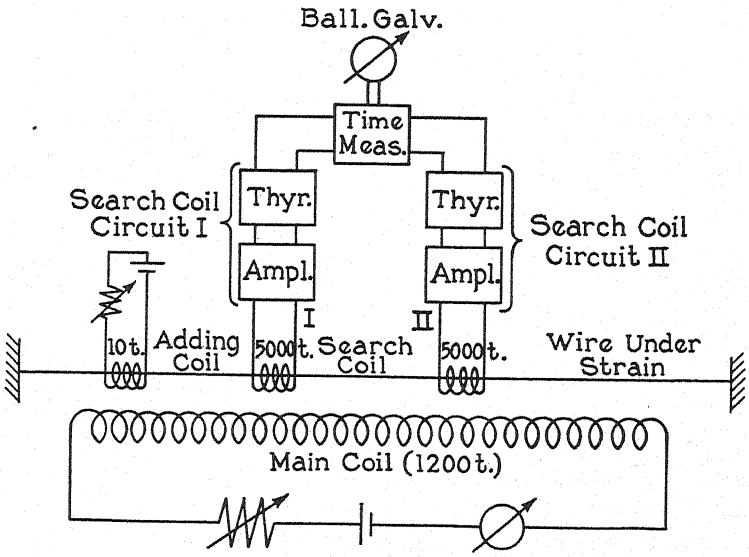

Fig. 2. Schematic diagram of circuit for velocity measurements.

of the large discontinuity depends upon the spontaneous formation of a nucleus, as described in Section 1, this erratic behavior can either mean that one nucleus was itself starting erratically or that different points along the wire were acting as nuclei. To control the creation of a nucleus an "artificial nucleus" was made by locally increasing the field strength by means of a current through a small magnetizing coil which created a local adding field. If then the homogeneous field, which will be called the *main field*, was set at a value

below the starting field, the large discontinuity could be initiated by applying the local adding field. The change in magnetization then begins at this point and propagates into the homogeneous part of the field where its velocity can be determined in the following way. If we place two search coils around the wire at a known separation, the discontinuity in travelling along the wire will produce successive voltage surges in these coils. If their time interval be measured, the velocity can be calculated.

Design of apparatus. The main field (Fig. 2) was furnished by a helix of 65.5 cm length containing 1200 turns of copper wire of 0.051 cm diameter, wound on a glass tube. Thus the uniform part of the field is given by $H = 23.0\, i$ (i being the magnetizing current in amperes). The decrease in H 23 cm from the middle of the coil is 0.5 percent. At first a liquid resistance allowing continuous variation of current was used, but later on a slide-wire resistance was found to give a sufficiently gradual variation.

The wire under investigation was held in the axis of the coil and could be subjected to tension or torsion or both in the same way as described by Preisach. The tension was read by a spring balance and the twist by a pointer connected to the wire. The wire was surrounded by a capillary glass tube so as to permit its easy replacement with the search coils in place.

Each search coil consisted of 5000 turns of copper wire of 0.008 cm diameter. Since the length of the winding was 0.65 cm and the inner and outer diameters were 0.4 and 1.8 cm respectively, the voltage induced in them could not be proportional to the change in flux in one point on the wire, but gave an average over a distance comparable with the outer diameter (i.e., approximately 2 cm). The coils were wound on hard rubber spools and could be moved separately along the capillary tube by means of strings connected to them, and their positions could be read by pointers fastened to the strings and sliding along a scale. In most cases their separation was kept at 20 cm, each being 10 cm from the center of the main field.

The additional local field was produced by a coil of 10 turns of copper wire of 0.051 cm diameter, wound on a spool which was also movable along the wire. Generally the adding coil was placed at a distance of 24 cm from the middle of the main field.

Time-measuring arrangement. For measuring the time interval between the voltage impulses induced in the two search coils by the passing discontinuity, a vacuum tube device (Fig. 3) was built. This system, which is similar to the one used by Turner for his Kallirotron amplifier,[6] has two stable states of current distribution, if voltages and resistances are properly adjusted. In State 1, plate current is flowing only in Tube I and there is no measurable plate current in Tube II; in State 2, current is flowing only in Tube II and there is no current in Tube I. To explain this let us assume that both tubes carry current. If a negative voltage impulse is now applied to the first grid, the plate current in Tube I decreases and in turn reduces the potential drop in R_I, which makes Grid II more positive. The plate current in II there-

[6] L. B. Turner, Radio Review **1**, 317 (1920).

fore rises, causing an increasing potential drop in R_{II}, and since this drop furnishes the grid bias for Tube I the grid voltage in I becomes still more negative. This cumulative action proceeds until practically no current is flowing in I, while the plate current in II has its full value. The current may now be shifted back to Tube I by applying a sufficient negative voltage to the grid of Tube II. Since the minimum value required increases as the resistances R_I and R_{II} are increased, the sensitivity of the circuit is under control. Two UX-112A tubes were used.

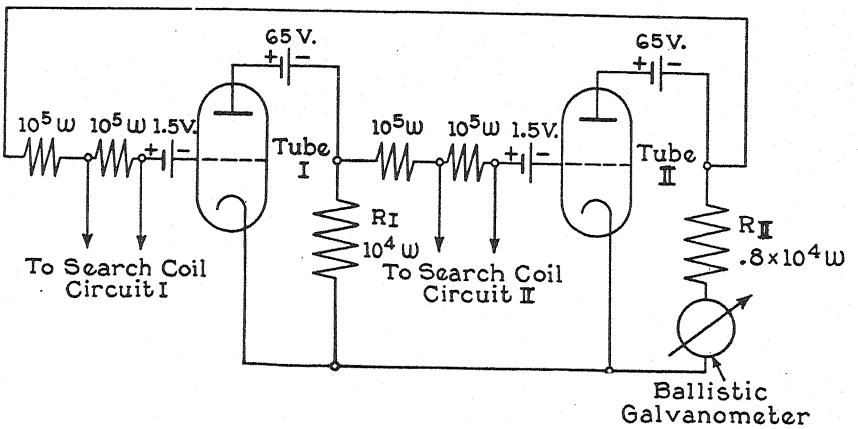

Fig. 3. Time-measuring circuit.

In making a time interval measurement this circuit was put into State 1 and a negative voltage impulse excited by Search Coil I was applied to the grid of Tube I. This shifts the current over to Tube II. After a time interval t the impulse from Search Coil II impressed on the second grid stops the current in Tube II. Thus the quantity of electricity which has passed through Tube II is a measure of the time t between the impulses. This quantity was measured by a ballistic galvanometer so that t was given by

$$i_P t = C\theta \tag{5}$$

where i_P is the plate current, C the ballistic constant of the galvanometer, and θ its deflection.

This relation was checked by means of a pendulum which opened two contacts in succession. Each contact was joined in series with a battery and the primary of a transformer, and the secondaries were connected respectively to the grids of Tubes I and II of the timing circuit. The opening of the contacts thus produced voltage impulses on the grids. The pendulum was calibrated by using a known condenser discharging through a known resistance. The time interval found from the pendulum calibration agreed with those calculated from Eq. (5). This means that the shift of the current from one tube to the other occurs in a time short compared with the time intervals to be measured.

The negative voltage impulse applied to tube I had to exceed a certain

minimum value (for given voltages and resistances in the timing circuit) but if it were too large, the current, after shifting to II, failed to return with the negative impulse on II. Thus it was necessary to keep the impulses within a certain range. The timing circuit was so adjusted that impulses of 1 volt operated it, and this voltage was obtained independently of the magnitude of the voltage induced in a search coil in the following way: The impulse from each search coil was amplified by a two-stage resistance-coupled amplifier whose output was impressed on the grid of a thyratron[7] as shown in Fig. 4. The sudden rise of plate current, from 0 to 100 m.a. in the present circuit, being independent of the voltage impressed on the grid, always gives the same voltage of approximately 1v. across the secondary of the transformer in

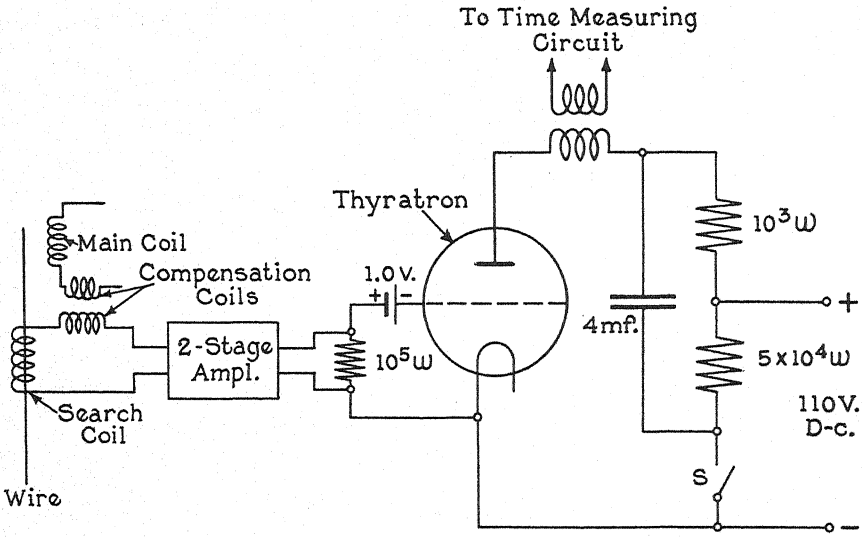

Fig. 4. Thyratron relay.

the plate circuit. The 4-μf condenser and 50,000-ohm resistance made it possible to stop the discharge in the thyratron by simply closing the switch S, thus setting the circuit for the next impulse.

The maximum voltages induced in the 5000 turn search coils were of the order of 0.1 v. The amplification of the amplifiers used was about 120. As the grid bias of the thyratrons was so adjusted that positive impulses of about 1 v. would start the discharge, both thyratrons were started before the voltage impulse reached its maximum (See oscillograms Figs. 11 and 12). The whole

[7] A thyratron is a three element tube containing a small amount of mercury. The cathode of the one used was oxide coated. In a thyratron which is initially carrying no current, current does not start to flow as long as the grid potential is less than a certain value. As soon as the grid voltage exceeds this critical value, however, the full plate current begins to flow, and from this moment on the grid has no further influence on this current. By using a proper value of grid bias this tube can be used as a relay, as in Fig. 4, or as a peak voltmeter. See: A. W. Hull, Hot-Cathode Thyratrons, Gen. Elec. Rev. **32**, 213, (1929) and **32**, 390 (1929); A. W. Hull and I. Langmuir, Proc. Nat. Acad. Sci., March 1929; A. W. Hull, Trans. A.I.E.E. **47**, 753 (1928).

arrangement, it was found, worked satisfactorily down to time intervals of 0.5×10^{-3} sec, since all time constants were kept as low as possible.

Hysteresis loops. Hysteresis loops were taken with the magnetizing coil and one search coil (Fig. 2). The latter was connected to a ballistic galvanometer (Leeds and Northrup Type HS No. 2285d) with a sensitivity as used of 1425 Maxwell/Sc. div. and a period of 30 sec. The direct effect of the magnetizing coil on the search coil was compensated as usual by a mutual inductance.

4. Velocity Measurements

Composition and treatment of specimens. The wires used in our experiments were made from ingots of electrolytic nickel and Armco iron plus 0.25 percent manganese to make the alloy ductile. The ingots were swaged and then drawn down to 0.10 cm diameter, sometimes to 0.076 cm, with annealing. From this diameter the wires were cold drawn to 0.038 cm. The per-

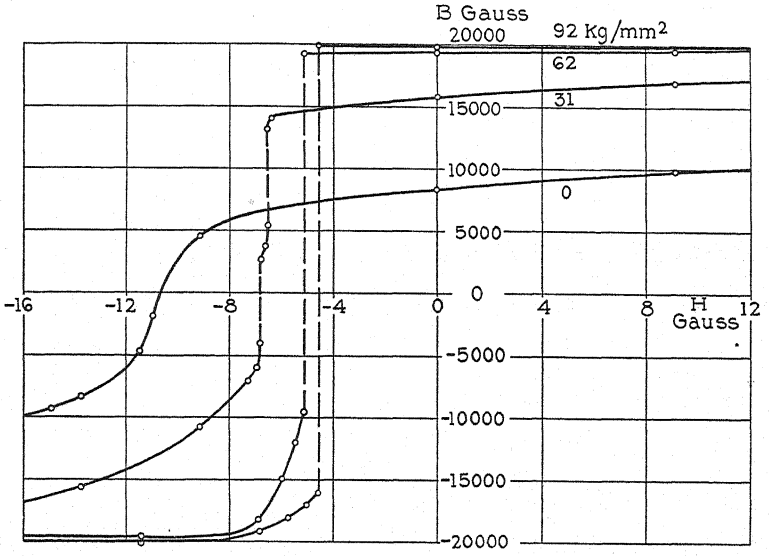

Fig. 5. Hysteresis loops for a wire under different tensions. Wire of 0.038 cm diameter from ingot No. 32, 15 percent Ni-Fe (only half of the total loop is shown).

centage of Ni was determined for each wire investigated by chemical analysis. In this section we shall deal mainly with alloys of between 10 and 20 percent Ni since these show the phenomena of propagation very markedly. In Section 11 the results with wires of other compositions will be considered briefly.

The wires were aged by stretching them for about 1 hour with loads near to the elastic limit, because more consistent results were obtained in this way. The aging load was never exceeded by the tensions used in the course of an experiment. Incidentally, in these hard drawn wires the breaking point lies only slightly beyond the elastic limit.

Effect of tension on hysteresis loops. Fig. 5 shows hysteresis loops for a wire of 15 percent Ni Fe and 0.038 cm diameter (cold drawn from 0.076 cm)

under different tensions. These loops are of the same type as the ones observed by Preisach. With no load only the ordinary Barkhausen discontinuities occur and these cannot be detected by the galvanometer. With rising tension the formation of large discontinuities begins until with high tension a great part of the whole change between negative and positive saturation occurs in one single discontinuity. The maximum magnetizing field was in all cases 34.5 gauss. The curves show that for increasing tension the remanence

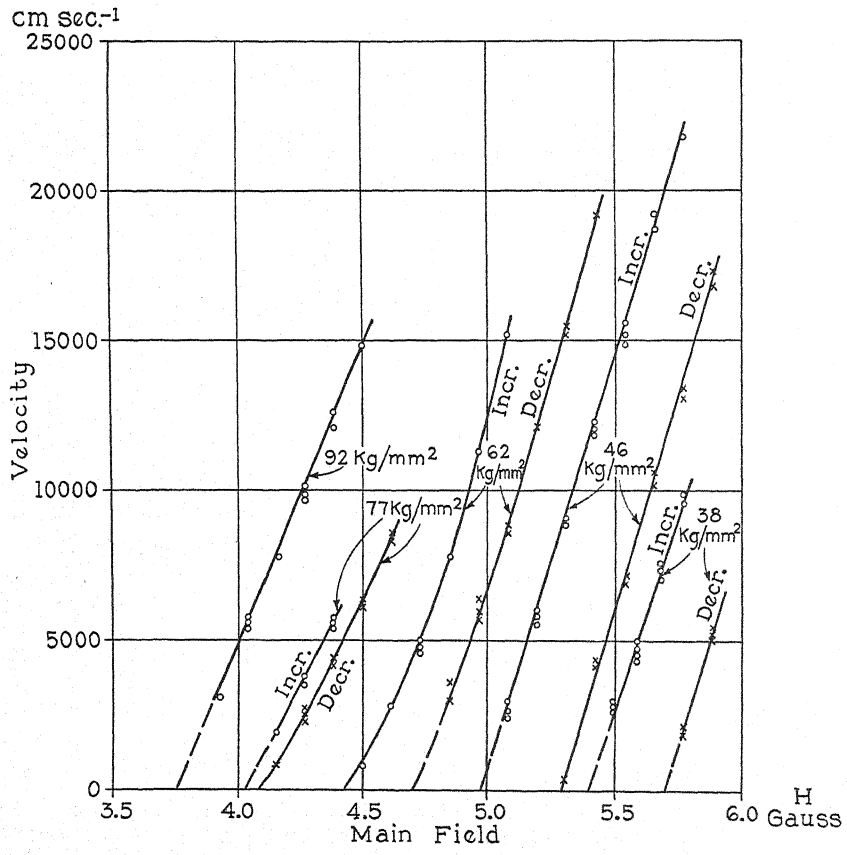

Fig. 6. Velocity-field curves for a wire under different tensions. Wire of 0.038 cm diameter from ingot No. 14, 14 percent Ni-Fe.

increases until it equals 100 percent saturation as exactly as we could measure. The coercive field on the other hand is reduced by increasing tension.

Velocity measurements. A complete set of velocity measurements covered both variation of tension and of magnetic field. This was accomplished by finding the relation of velocity to field at each of a series of values of tension. In this series the tension was increased from zero to a maximum and then decreased again. At any one tension the starting field (see Section 3) was determined so that it might serve as an upper limit to the fields which could be used in the velocity determinations The main field was then set at a value be-

low this, and the propagation was started by sending a current through the adding coil. The velocity of propagation was obtained from the throw of the ballistic galvanometer in the timing circuit and the known separation of the coils.

The results for a wire, 14 percent Ni-Fe, 0.038 diameter, are given in Fig. 6 for several values of tension between 38 and 92 kg/mm^2, the range in which large discontinuities were found. These curves exhibit some very striking features. They are, except in two cases, straight lines and are approximately parallel to each other. The higher the tension the further are the curves shifted to lower field strengths. The failure of the curves taken with decreasing tension (marked "Decr.") to coincide with the curves taken with increasing tension (marked "Incr.") shows the presence of elastic hysteresis which was observed directly by stress-strain measurements. When the wire which had undergone the stress cycle described was allowed to "rest" without tension for an hour, it reverted almost completely to its original condition, so that approximately the same cycle could be reproduced.

Observations of velocity were made down to velocities as low as possible but in many cases the experimental points could not be measured below 1000 cm/sec. In this neighborhood the discontinuity, after passing the first coil, often failed to reach the second one. In view of the linearity of the curves it is quite reasonable to suppose that the failure to propagate at low velocities does not arise from any inherent limitation in the mechanism of propagation but rather from irregularities in the wire which, influencing relatively small portions of the material, are unable to affect seriously a discontinuity propagating under more favorable conditions. For this reason the curves have been extrapolated to zero velocity, and the intercept with the H-axis has been interpreted as the limiting field in which propagation at a velocity approaching zero would occur in an ideal wire. This field will be called the *critical field* and will be designated by H_0.

The behavior of the v-H curves with respect to the elastic hysteresis mentioned is peculiar in that the successive curves with decreasing tension instead of lagging with respect to the "Incr." curves, as they would if H_0 were a function of elongation, show the opposite behavior. This could be due to two types of response in the wire, one an immediate elastic response, and the other a slower and limited plastic yield. A lowering of H_0 by the elastic strain combined with an increase of H_0 with plastic deformation would account for the phenomenon observed. (See Section 12).

Judging from their general character, the curves may best be represented by an empirical formula of the type

$$v = A(H - H_0) \tag{6}$$

where v is the velocity of propagation, and A is the slope of the line which was within 25 percent of a value of 25,000 cm sec^{-1} gauss^{-1}.

When the velocity was measured over subdivisions of the usual 20 cm and over other portions of the wire still within the uniform 46 cm of field, this

velocity was found to be always the same for the same conditions in the cases where the v-H characteristics were straight lines. When these characteristics were curved, however, the velocity showed some variation. This suggests that the curvature arises in some way from a variation in the state of the wire along its length.

One of the cases in which the characteristics showed the greatest curvature was that of the wire whose hysteresis loops were shown in Fig. 5. These characteristics are reproduced in Fig. 7 as an example of the greatest deviation from the simple relations usually found.

The above tests were originally made with a view to testing the constancy of the velocity of propagation. Another test consisted of varying the position and intensity of the adding field. It was found that for a certain position of

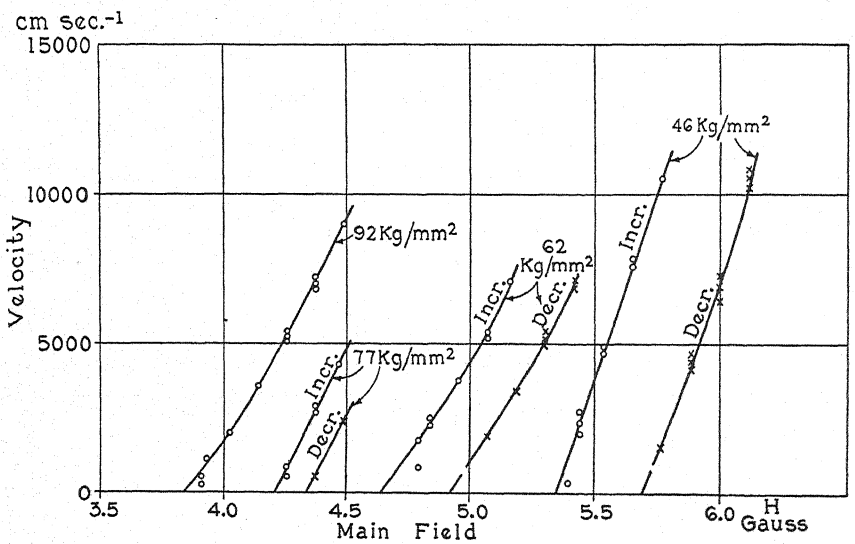

Fig. 7. Velocity-field curves for a wire under different tensions. Wire of 0.038 cm diameter from ingot No. 32, 15 percent Ni-Fe.

the adding coil a certain minimum current was required to start the discontinuity, but that this minimum varied in successive trials. The average of this minimum at each of several successive points along the wire was found to vary considerably, exhibiting maxima and minima even in the homogeneous part of the field. The velocity of propagation was independent of both position and magnitude of adding field as long as this field did not add to the uniform field between the search coils appreciably.

The magnitude of the discontinuity is nearly constant over the homogeneous part of the field; only at very low velocities do large differences at different points appear. Since large differences at the same point in successive trials were also found, we can only conclude that the behavior is erratic at low velocities.

It is significant to note that the general effect of the aging process referred

to at the beginning of this section is to increase the critical field but to leave the slope of the characteristic in most cases unchanged. This suggests that while the critical field depends on the strain state of the wire, the slope depends on other factors.

5. Comparison of Experiments and the Eddy-Current Theory

It is now possible to make a direct comparison of the velocities appearing in Fig. 6 with those calculated from the eddy current formulas derived in Section 2. For 15 percent Ni-Fe $\rho = 30 \times 10^{-6}$ ohm cm and using an average value of H of 5 gauss and an average value of ΔI of 2400, Eq. (3B) gives $v = 250$ cm sec^{-1} compared to velocities well exceeding 10^4 cm sec^{-1} in many cases. A discrepancy in the other direction might well have been explained on the basis that the magnetic energy was only partially available for conversion into eddy currents. Eq. (4B), however, permits of velocities greater than those given by Eq. (3B) roughly in the ratio that λ exceeds a. Actually, the observed velocity of 10^4 cm sec^{-1} would require a ratio $\lambda/a = 60$. But how could a transition 60 times as thick as the diameter of its front characterize the definite self-propagating phenomenon we were observing?

At least, the formulas gave experimental hints and also served to emphasize certain features of the velocity-field characteristics. We have already remarked that these characteristics do not pass through the origin so that v is not proportional to H. This might be an indication that, for some reason, the magnetic energy available is not $H\Delta I$ but $(H - H_0)\Delta I$ so that on this hypothesis

$$v = 0.51 \times 10^8 \rho\lambda(H - H_0)/a^2\Delta I \tag{7}$$

On the other hand, such reasoning would increase λ/a over ten-fold since $H - H_0$ is some 0.4 gauss compared to the 5 gauss assumed for H at $v = 10^4$ cm sec^{-1}.

A comparison of velocity-field slopes with ΔI (or ΔB as in Fig. 8) shows no such correspondence as indicated by Eq. (3B) and a check of slope against wire diameter gave the values of slope shown in Fig. 9. The wires used were of 10 percent Ni-Fe and were cold drawn from 0.102 cm to the different diameters. Over a three-fold range of diameters, namely, from 0.020 to 0.061 cm the observed slopes, taken for one wire at different tensions or for different wires, lie scattered in the range 2 to 3×10^4 cm sec^{-1} gauss^{-1}, and show no evidence of an increase in slope with a decrease in diameter. The 0.071 cm diameter slope is probably not comparable with the rest because the magnitude of the discontinuity gradually decreased as it proceeded along the wire.

The successively smaller wires have been subjected to successively greater amounts of cold working thus raising the question as to how comparable the results can be on this account. It has been pointed out, however, (Section 4) that the aging process has a marked effect on the critical field but almost none on the v-H slope. And later it will be seen that annealing wires of various diameters, succeeded by cold drawing to a uniform size, again yields specimens having different values of H_0 but approximately equal v-H slopes. Thus the

differences in cold working are probably of no significance as regards our present conclusions.

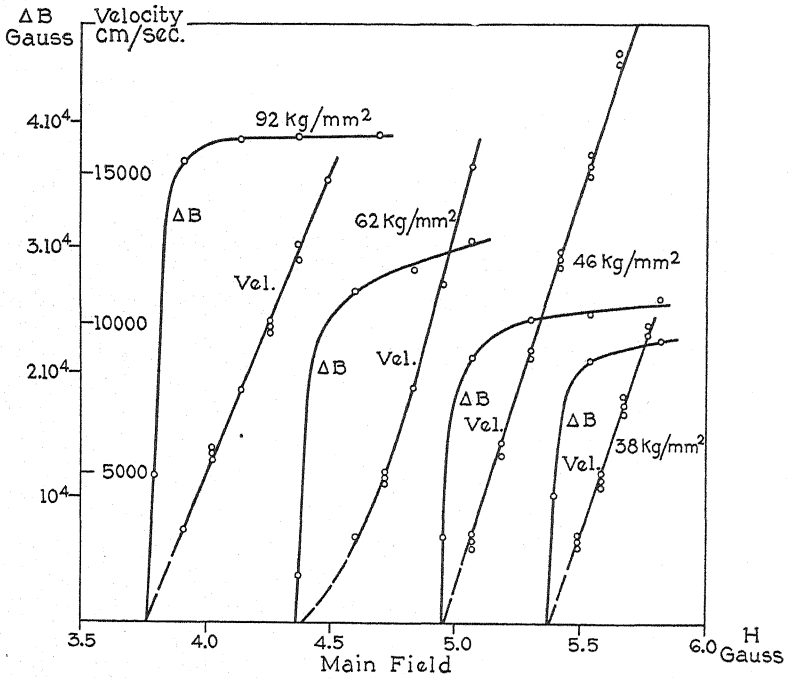

Fig. 8. Magnitude of the discontinuity and velocity as functions of field and tension. Wire of 0.038 cm diameter from ingot No. 14, 14 percent Ni-Fe.

The evidence against the eddy-current theory which we considered to be most convincing was given by the following experiment. A wire of 0.254 mm

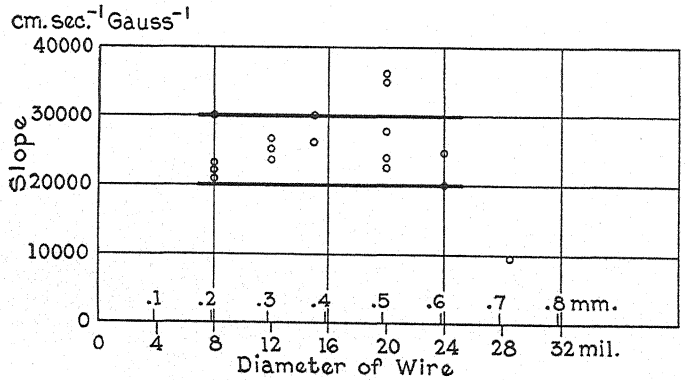

Fig. 9. Slope of velocity-field curves for wires of different diameters. Wires from ingot No. 24, 10 percent Ni-Fe.

diameter was rolled down to a strip 0.076 mm thick and 0.53 mm wide. Although the influence of eddy currents is, of course, reduced considerably in

comparison with the round wire, the v-H slopes measured for the strip fall in the same range as the slopes found for wires.

At this stage in the investigation we found ourselves in the position of observing magnetic discontinuities travelling with such high velocities that for the phenomenon to be energetically possible this "discontinuity" must occupy a length on the wire of at least 60 times and perhaps 750 times (if energy available is $(H-H_0)\Delta I$) the wire radius. The proof that this actually occurs is a result of the measurements on the voltage induced in the search coils and of the oscillograms of the wave shape which are described in the next two sections.

6. Voltage Measurements

We have already mentioned the fact that the voltages induced in the search coils are of the order of several tenths of one volt, but we should expect much higher voltages on the basis of a plane wave front. Let us make the assumption that the total change in flux, $\Delta\phi = 47$ lines (for a change in induction of $\Delta\phi = 40{,}000$ gauss) in a 0.038 cm wire, produces a voltage in the coil during the time Δt, which the jump needs to travel a distance equal to the diameter (2 cm) of the coil. That will give us an average value of voltage to be expected, and the maximum voltage might be much higher than this. Now $v = 10^{-8} n\Delta\phi/\Delta t$ where v is the voltage induced in a coil of n turns. Taking $n = 5000$, and $\Delta t = 2\times 10^{-4}$ sec (for a velocity of 10,000 cm/sec), we obtain 11.8 volts as a lower limit for the peak voltage. The existence of any such voltages would have rendered the use of amplifiers in the original velocity measurements entirely unnecessary. It therefore became of interest to eliminate this large discrepancy by direct voltage measurements.

In our determinations a thyratron circuit, similar to the one shown in Fig. 4, was used as a peak voltmeter. By adjusting the grid bias in several trials, a bias value was found at which the single impulse just started the discharge. The difference between the known critical voltage and the applied bias is the peak voltage of that impulse. The voltage induced in a 200-turn search coil was amplified by two screen-grid stages, giving a uniform amplification of 120 in the frequency range between 30 and 10^4 cycles/sec. While a single search coil permits the measurement of the voltage peak only, it was thought that two search coils with variable separation and connected in series-opposition would allow a rough determination of the wave shape itself to be made simply by plotting the observed peak voltage against coil separation. A more detailed analysis made after numerous measurements had been taken shows that this experiment would give the same apparent wave-front shape for a variety of actual shapes.

Thus in Fig. 10 the shape of the curves which were obtained in this way is roughly that to be expected from the method used, leaving as significant features only the voltage maximum attained and the least separation of the coils which gives that maximum. The former yields the maximum rate of change of flux, the latter the distance from wave front to this point in the wave.

The curves of Fig. 10 depict measurements made with different values of main field, that is, with different velocities. Over a 3-fold range of velocities the maximum is seen to come between 4 and 6 cm from the beginning, and the plot to the right shows that the peak voltage is proportional to the velocity. This indicates that the discontinuity retains an approximately constant shape as its velocity changes.

Although the two-coil method fails to give the wave shape near the wave front it is reliable beyond the voltage maximum. This region was explored by connecting the coils in series-addition (the negative peak voltage with the series-opposition connection could also have been used) but as the oscillograms taken subsequently cover the same range in greater detail these results will not be given.

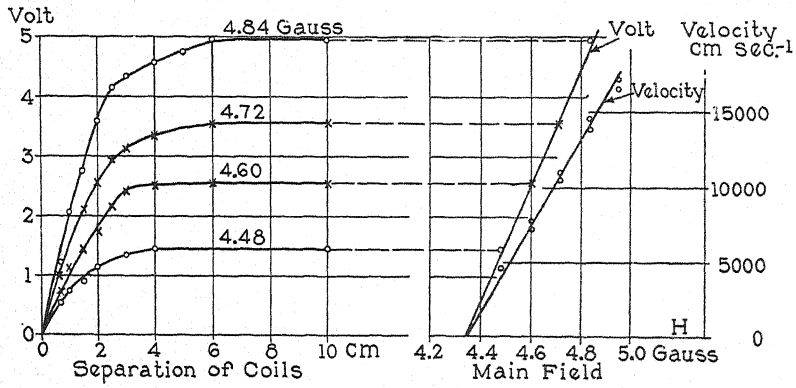

Fig. 10. Amplified peak voltage induced by the discontinuity in two search coils connected in series-opposition. Voltage amplification 120 times. Wire of 0.038 cm diameter from ingot No. 14, 14 percent Ni-Fe.

A comparison between the voltages induced in two coils of 200 and 5000 turns, respectively, was made to make sure that the internal capacity of the coils was not reducing the coil voltages. The ratio of voltages found, namely, $0.023/0.59 = 0.039$, so nearly checks the turn ratio as to prove that any such effect is negligible in these experiments.

7. Oscillograms

Further information concerning the nature of the discontinuity was obtained from oscillograms of the voltage induced in a search coil. The circuit connections were made in this order: 5000-turn search coil to high resistance potentiometer to amplifier to oscillograph. The potentiometer was used to obtain a suitable oscillograph deflection in each case. The amplifier had 3-resistance-coupled stages. The oscillograph was of the Blondel type. The vibrator used to reproduce the voltage had a sensitivity of 1.45 m.a./mm and a natural frequency of 1000 cycles/sec. Figs. 11 and 12 show the amplified voltage wave superimposed on the plate current of the last tube for a wire of 14 percent Ni-Fe and 0.038 cm diameter under a tension of 92 kg/mm^2. In

Fig. 11 the discontinuity is traveling at a rate of 17,000 cm sec^{-1} in a field of 4.25 gauss, in Fig. 12 the velocity is 7000 cm sec^{-1} in a field of 3.91 gauss. We note the steep rise of the voltage and the long tail with many irregularities. But in interpreting these curves we have to bear in mind that the resolution of the method is limited by three factors. First, there is the limited space resolution of the search coil, a factor also present in the method employed in Section 6. It has already been estimated that this limit is of the order of 2 cm for the 5000-turn coil used. But of more importance here is the second factor, the limited time resolution of the oscillograph vibrator. The maximum in

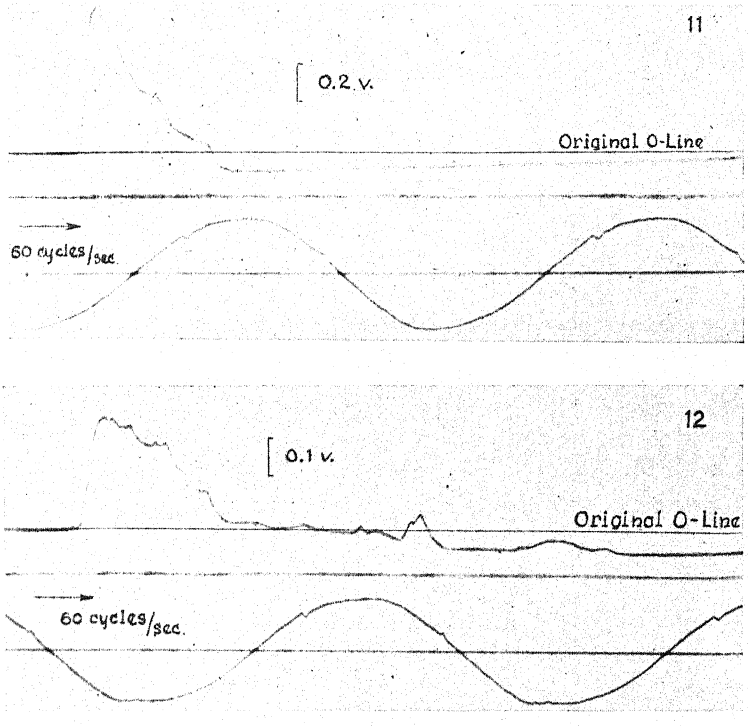

Figs. 11 and 12. Amplified voltage induced in a 5000-turn search coil by the discontinuity. Velocities: Fig. 11, 17,000 cm sec^{-1} (see Table I, Osc. No. 29); Fig. 12, 7000 cm sec^{-1} (see Table I, Osc. No. 28).

Fig. 11 occurs only 0.68×10^{-3} sec after the beginning of the deflection. Since the period of the vibrator is 10^{-3} sec, the oscillograms can give us no useful information concerning the fore-part of the wave.

The two factors mentioned are of little importance as regards the general shape of the tail of the wave, but here the third factor enters, the fact that the voltage surge produces a charge on every inter-stage condenser, which discharges comparatively slowly. This appears in the zero shift occurring in the oscillograms. In this connection it is interesting to note that the peak voltages were about 25 percent lower than those found in the preceding section, undoubtedly on account of the second factor.

The area under the oscillogram curve is proportional to the total change in flux through the search coil. The area when measured (allowing in any reasonable way for zero shift) gave a value of flux change only a few percent less than that found ballistically, Section 3. Thus the third factor can be estimated with fair accuracy.

It is essential to know which features of the wave are characteristic of a propagating discontinuity in general and which arise from special local conditions. Successive oscillograms at the same point are identical except for small variations in the details. Oscillograms taken at different points along the wire show greater variation in the minor discontinuities, but the total

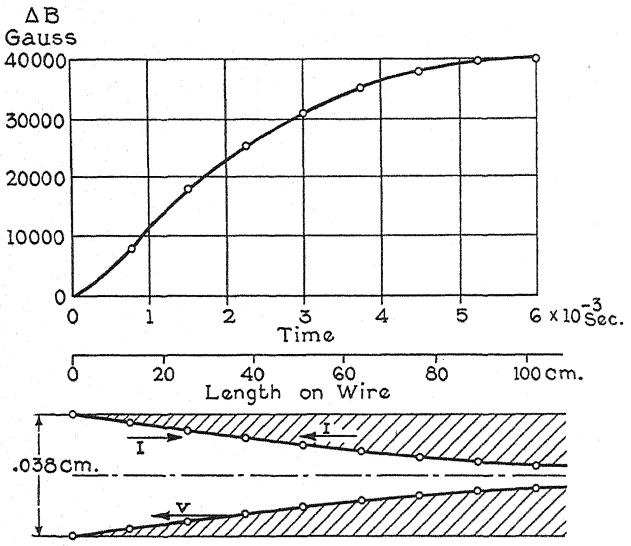

Fig. 13. Change of induction with time (upper part) and penetration of induction into the wire. (The shaded area represents the portion of the wire which has changed direction of magnetization). The radial dimensions are magnified 675 times with respect to the axial dimensions.

duration of the wave and for the most part the main structure, involving perhaps two or three major peaks, are preserved.[8] The main structure is unaltered if the main field is changed so that the wave velocity is different.

Incidentally, the oscillograph was used to obtain a check on the velocity measurements made with the timing circuit by recording the impulse from the two search coils connected in series at a known separation. The agreement was exact.

Since the integral of the voltage curve from its beginning gives the total flux change in the wire up to the corresponding time, an oscillogram enables us to plot this flux as a function of distance along the wire if we make use of the known velocity. In addition to the plot of the integral in Fig. 13, we have

[8] In the single experiment made, the voltage maximum decreased with distance travelled by 20 percent in the central 20 cm of the main field, although ballistic measurements have shown in general that the magnitude of the whole discontinuity remains unchanged.

shown the change as progressing from the surface of the wire inward, assuming that each element of the wire completely reverses magnetization instantaneously.[9] The existence of eddy currents definitely requires that the progress of the change shall be inward, and the instantaneous reversal is plausible if a quantum phenomenon is involved.

Such an analysis applied to the oscillogram of Fig. 11 gives Fig. 13. In this particular case the jump was 97 percent of saturation reversal, and as shown, the 3 percent deficiency has been localized at the axis of the wire. The justification for this is not clear-cut but has some basis in the consideration that the orienting forces are probably least at the axis.

The most striking feature is the experimental demonstration of the fact that the wave occupies a length of some 100 cm in the 0.038 cm wire, a length of the same order of magnitude as calculated in discussing Eq. (7). The comparison of experiment with theory will, however, be based on time of passage rather than length of discontinuity for two reasons. First, because the oscillograph measures time directly and second because the formulas developed in Section 2, being based fundamentally on skin-effect considerations have to do with the time required for a magnetic field to penetrate to a certain depth. They are not concerned with conditions at other points relatively large distances away. On this basis, the only possible interpretation of these formulas is in terms of the time required for the change at a single cross-section to complete itself. Eq. (3) has been definitely found to be inapplicable. Eq. (4), as modified in Eq. (7), gives for this time,

$$\delta t = \lambda/v = 1.96 \times 10^{-8} a^2 \Delta I/\rho(H - H_0) \tag{8}$$

Table I sets forth our most representative comparisons between the directly observed times required for the discontinuity to pass (Column 5) and

TABLE I. *Comparison between the experimental and calculated times of penetration.*

Osc. No.	Main Field Gauss	ΔI Gauss	Velocity cm sec^{-1}	Time δt in 10^{-3} sec. Exp.	Calc.	Ratio $\delta t_{exp}/\delta t_{calc}$	Length λ cm
18	4.48	1740	4000	13.5	4.0	3.4	54
11	4.60	2110	7400	11.1	2.5	4.4	81
14	4.72	2250	10700	6.2	1.8	3.4	66
15	4.84	2300	14000	4.8	1.4	3.4	66
48	4.48	1740	4000	18.7	4.0	4.7	79
49	4.60	2110	7400	9.4	2.5	3.8	70
50	4.72	2250	10700	10.2	1.8	5.7	109
51	4.84	2300	14000	6.6	1.4	4.7	92
28	3.91	3240	7000	22.5	4.2	5.4	157
29	4.25	3240	17000	6.0	1.7	3.5	102

Nos. 28 and 29 are taken with 92 kg/mm^2 tension (H_0=3.68 gauss), the rest with 62 kg/mm^2 (H_0=4.35 gauss).

the times calculated from Eq. (8) (Column 6). The small numerical value of the ratio of these two (Column 7) constitutes a satisfactory check in view of the manner of deriving Eq. (7), and the constancy of this ratio for velocity

[9] In this connection see Section 8.

ratios of 3.5 to 1 lends strong support to the fundamental correctness of the calculation. Unfortunately, simultaneous velocity and oscillograph measurements on wires of other diameters have not been made so that the dependence of δt on a has not yet been checked.

The question as to whether the whole hysteresis loss is an eddy-current loss or whether appreciable transfer to heat occurs through magnetostrictive vibrations, quantum transitions, and possibly other mechanisms, has never been conclusively answered. The present results, however, furnish a very strong indication that at least for large Barkhausen discontinuities only a small fraction $(H-H_0)/H$ of the magnetic loss goes into eddy currents.

The possibility presents itself that the remaining energy appears as magnetostrictive energy. An experiment in which we tried to detect either a momentary or permanent change in length of the wire accompanying a reversal gave a negative result. The accuracy was not quite good enough, however, to be able to reject this hypothesis definitely.

In view of the large penetration times found by us, it becomes of some interest to inquire just what Preisach (reference 2, p. 778) was measuring when he detected harmonics to 10^7 cycles/sec in a stretched wire subjected to a 6000 cycle magnetizing field. It is impossible to say conclusively in the absence of definite data, but it may be pointed out that in 0.5×10^{-7} sec. 0.01 cm of wire surface to either side of a nucleus can reverse by propagation and that the increase of field in that time interval may well cause a large number of magnetic elements to reverse spontaneously, thereby becoming nuclei. The combination of propagation and nucleus formation may easily cause the reversal of an appreciable fraction of the surface of the wire during this time. On this basis the reversal time of a nucleus or any small portion of the wire may be far less than the minimum fixed by Preisach's experiment.

8. The Nature of the Discontinuity

Experiments have enabled us to outline roughly the flux distribution in the discontinuity, Fig. 13, and an eddy-current theory has been advanced which gives the penetration time. The only results, however, so far obtained which throw the slightest light on the longitudinal velocity are those which show that the slopes of the v-H curves for different size wires and even for the strip are all approximately the same. This indicates that the velocity, which corresponds to a given $H-H_0$, being independent of cross-section, is determined only by conditions existing within a small distance of the surface. Since the front edge of the wave lies in the surface, we have been led to the view that the forces at the wave edge determine the velocity, the rest of the wave penetrating the wire as fast as eddy currents allow. It seems plausible to assume that the force required to reverse an element of the wire is H_0 itself or is directly related to it. On such a basis a too-rapid progress of the wave would either give rise to eddy currents or alter the wave configuration near the front in such a way as to reduce the force at the wave front below the minimum reversing value. In this case no new elements could reverse until eddy

currents had decreased or later portions of the wave had advanced sufficiently to reestablish the minimum field.

Any theory must take cognizance of the electromagnetic field set up by the discontinuity. As a solution of Maxwell's equations for the discontinuity shown in Fig. 13, travelling at a high velocity, seems to be extremely complicated at the best, the attempt might be made to disentangle the various factors for the simpler case of very low velocities. As a first step we shall assume as an approximation that the shape of the wave is independent of velocity in the experimental range and remains constant in the limit as $v \rightarrow 0$. It may then be possible to make a first order calculation of magnetic field arising from eddy currents for low velocity and assume that this remains valid at the highest velocities measured. The proportionality of peak voltage to velocity and the approximate shape constancy found by experiment themselves strongly suggest that first order effects are the important ones.

Let us tentatively assume that Fig. 13 indicates the nature of a discontinuity travelling from right to left with magnetization reversing from positive to negative. Both unchanged and reversed portions of the medium present north poles to the wave front with the result that it is a surface of magnetic charge of pole strength m per unit area, m being given by

$$m = \Delta I dy/dx \tag{9}$$

where y is the depth of the discontinuity below the wire surface at a distance x back from the front edge. This distribution of magnetism, supposed stationary, gives rise to an almost radial magnetic field from the discontinuity surface outward. An approximate calculation of this field can be made on the assumption that $y \propto x$. For the 100 cm discontinuity in the 0.038 cm wire with ΔI equal to 3240, Eq. (9) gives

$$m \sim 3240 \times 0.019/100 = 0.62$$

whence the radial field near the front edge is

$$H_r = 4\pi m = 8 \text{ gauss}.$$

A field of this magnitude would not allow the elements which are completing their reversal to align themselves axially, but a little consideration will show that their deviation from axial alignment need be very little in order to annihilate the internal poles. Referring to Fig. 14 showing the discontinuity FF' travelling with velocity v, it is readily seen that if the intensity of I_2 in the reversed domains forms the same angle with FF' as the original intensity I_1, there is no pole development in the wire. The angle β, being twice α, will thus be about $2 \times 0.019/100 = 3.8 \times 10^{-4}$ radians which is a negligible deviation from perfect alignment. Finally, this deviated I_2 can be joined to the axial I_2 which is supposed to exist when the discontinuity has completely passed with a discrepancy only of the order of $(3.8 \times 10^{-4})^2$.

In this representation the reversal of intensity occurs within a distance equal to the thickness of a domain, but it is also possible to picture the transition as being much less abrupt. The one condition to be fulfilled, established

by the requirement that no internal poles develop, is that the intensity of magnetization be solenoidal throughout the wire, or, mathematically, that $\nabla \cdot I = 0$. This means, of course, that we can imagine tubes of intensity drawn in the wire and that all poles develop on the surface. A little consideration

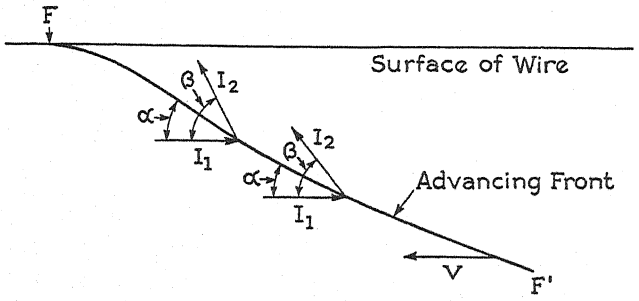

Fig. 14. Compensation of internal poles.

shows that this surface distribution of pole strength is given by the oscillograms. Fig. 15a shows two possible configurations of intensity tubes for an iron-nickel strip with idealized surface distribution. Only half the strip is shown. As represented, the tubes are of equal strength and therefore terminate at the surface in equal poles as given by equal partial areas under the

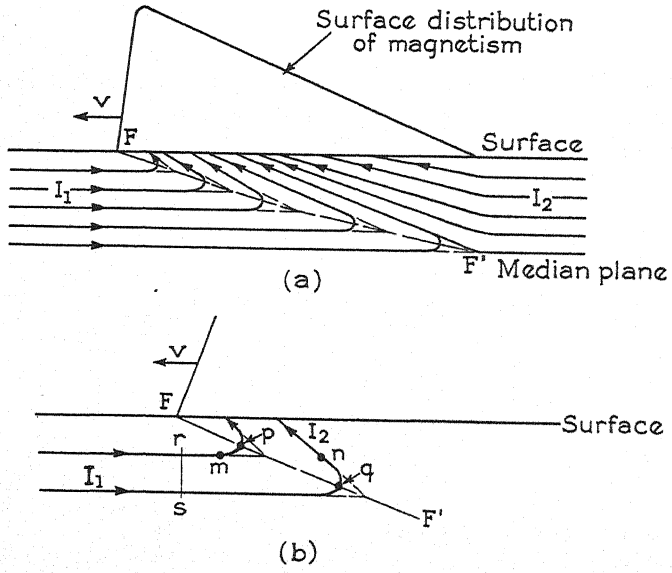

Fig. 15. a. Possible configuration of lines of intensity in a strip. b. Detail of reversal region.

distribution-of-magnetism curve. I_1 can join I_2 either via the sharp dashed bend or via the smooth curve. The former corresponds to Fig. 14, the latter to a more gradual transition.

The interesting feature of this transition is that it cannot occur as a uniform progression. Referring to Fig. 15b, which gives the detail of Fig. 15a, it

is seen that such a progression would mean a continually increasing rotation of I from domain to domain in going from m to n. This in turn would require that the intensity of all domains along pq be parallel. Now it is evident that a tube of intensity expands between rs and pq, both of which represent surfaces normal to the tube. Since I is solenoidal, I at pq must be less than I at rs, which is incompatible with detailed parallelism of the domains. But if we abandon the idea of uniform progression and suppose that as the reversal region mn begins to traverse any small volume (large compared to a domain) certain of the domains scattered throughout it reverse before others, then no such inconsistency arises.

The representation of the discontinuity just given has only been recently devised and no calculation of the fields arising from eddy currents in the neighborhood of the front edge has been made. It seems quite possible, however, that they may be comparable with $H-H_0$. In that case we shall have reached the simple viewpoint that the excess magnetic field over H_0 is just that necessary to overcome the opposing eddy current field.

The velocity would thus be dependent upon the surface magnetization in the neighborhood of the wave front, the length λ of the discontinuity is in turn the product of this velocity and the calculable penetration time δt. Both λ and ΔI, as well as a, then fix the average pole strength of the surface. But what in turn establishes the surface distribution of magnetism? That must probably await a detailed solution.

9. The Effect of Inhomogeneities in the Wire

Magnetic inhomogeneities. The magnetic and mechanical uniformity of the wire is of utmost importance with respect to large Barkhausen discontinuities. The importance of the first factor has been pointed out by Preisach in the experiment in which he varied the limits of the hysteresis cycle. We now look at it from a new viewpoint reached through our knowledge concerning the propagation. In all the preceding experiments the cycle of magnetization was carried as far as ± 34.5 gauss. Later we performed an experiment somewhat similar to Preisach's. In successive cycles the positive field strength limit was decreased as indicated in Fig. 16. On the negative side the limit was always at 34.5 gauss. We note that reduction of the maximum field on the positive side reduces both starting field and the magnetization change at the succeeding jump. In the limiting case, if the maximum positive field used is that required to cause the jump, the succeeding negative starting field is little less than the critical field for this wire.

The explanation for this lies in the following. The usually small change in induction which occurs after a large discontinuity is irreversible and contains smaller Barkhausen discontinuities. Thus in not carrying the cycle to saturation on the positive side, we have failed to turn a number of elementary magnets into the positive direction. These particles set up fields in the negative direction and thus act as nuclei where a discontinuity may start. The bigger such a nucleus is, i.e., the higher the field it produces, the lower the starting field which we have to apply in order to start propagation. We should expect

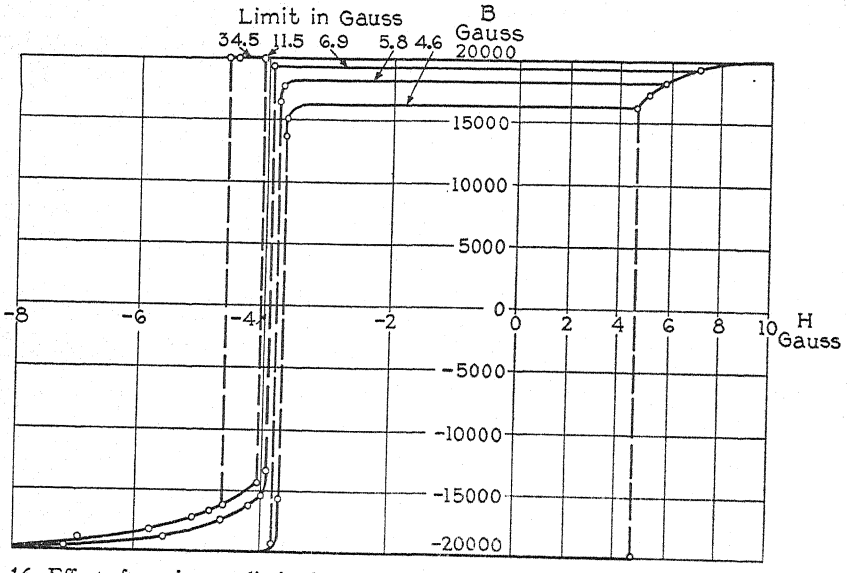

Fig. 16. Effect of varying one limit of the hysteresis loop. Wire of 0.038 cm diameter from ingot No. 32, 15 percent Ni-Fe.

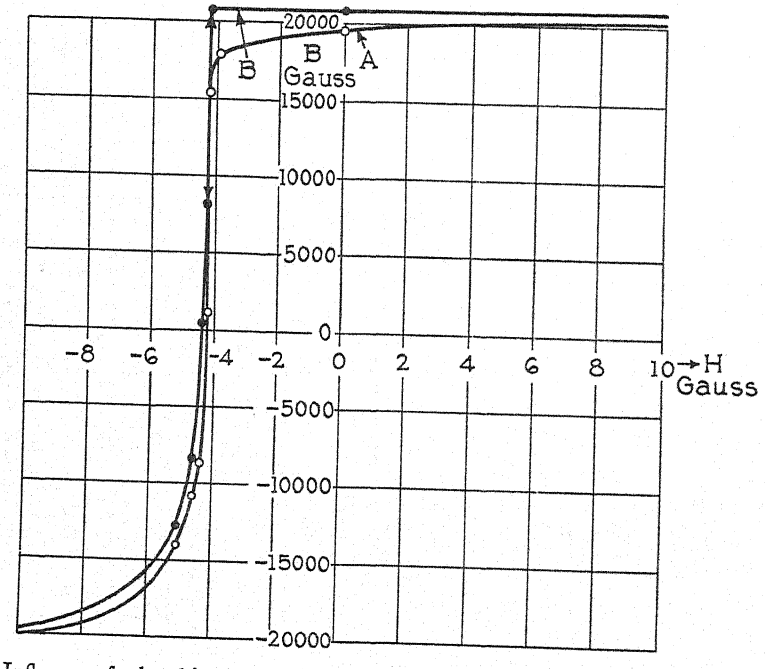

Fig. 17. Influence of a bend in the wire. A. Apparent hysteresis loop of the bent portion. B. Hysteresis loop of unbent portion.

that the starting field could never be less than the critical field, since we found this to be the lower field limit for propagation. In experiment this expectation was not quite confirmed since the lowest observed starting field in some cases was lower than the critical field. But the deviation in no case amounted to more than a few percent.

Mechanical inhomogeneities. In a special case the range of field strength, within which propagation could be observed in a 14 percent Ni-Fe wire of 0.038 cm diameter and under 62 kg/mm^2 tension was found to be 4.25 to 4.65 gauss. This wire was bent in its middle to a semicircle of 2.5 mm radius (the wire being strained far beyond its elastic limit in doing this), was then straightened out again and was finally put under the same tension as before. After this treatment the starting field coincided with the critical field at 4.25 gauss so that propagation could not be obtained. This behavior can be explained by the fact that the bent part has a magnetization curve different from the rest of the wire as shown by curves *A* and *B* of Fig. 17. Curve *A* was taken in the usual way with a search coil placed at the bent portion of the wire. The hysteresis curve so obtained gives a change of induction just below the starting field which is even less than the actual because of the flux leakage arising from the shortness of the bent portion. Thus when the critical field of the normal wire is reached, a considerable part of the bent portion has already changed magnetization and again those elementary particles, which point in the field direction, act as nuclei to start propagation.

Another example of the same type of phenomenon is the fact that hand-drawn wires have starting fields which lie only slightly above the critical field. The irregularity of hand drawing undoubtedly creates "weak nuclei" just as the bending did. Since a low starting field makes it impossible to measure the higher speeds of propagation, machine drawn wires were used in all experiments.

In all but one early experiment the wire projected from both ends of the magnetizing coil so that it extended into regions of comparatively low field strength. In that experiment, however, a short wire terminating within the homogeneous part of the field was used. This wire was clamped to copper wires with brass fastenings and was put under tension. The ends of the wire where it was clamped were not under the same strain as the middle part. Accordingly they did not have rectangular hysteresis loops and acted as weak nuclei.

From these experiments we can conclude that the upper limit of the propagation range is fixed by the non-homogeneity of the wire. The greatest range observed extended from 3.20 to 4.75 gauss in the case of a 14 percent Ni-Fe wire under combined tension and torsion. To the higher field value there corresponded a velocity of 40,000 cm sec^{-1}, which is the highest one measured so far.

10. Torsion

Preisach obtained great discontinuities in magnetization also when he applied torsion to a wire. In this case, too, we found that the magnetization

propagated in the same way as in the case of tension. We also observed a parallel shift of the velocity field lines to the left for increased twist in the range between 8 and 20 percent Ni-Fe, but we obtained much greater variations with respect to slope than in the case of tension. Fig. 18 taken for a 0.038 cm, 25 percent Ni-Fe wire shows this behavior very clearly. For this particular wire it made a great difference whether the twist was applied clockwise or counter-clockwise and if tension was added still another slope was found. All these curves were perfectly reproducible which shows that the

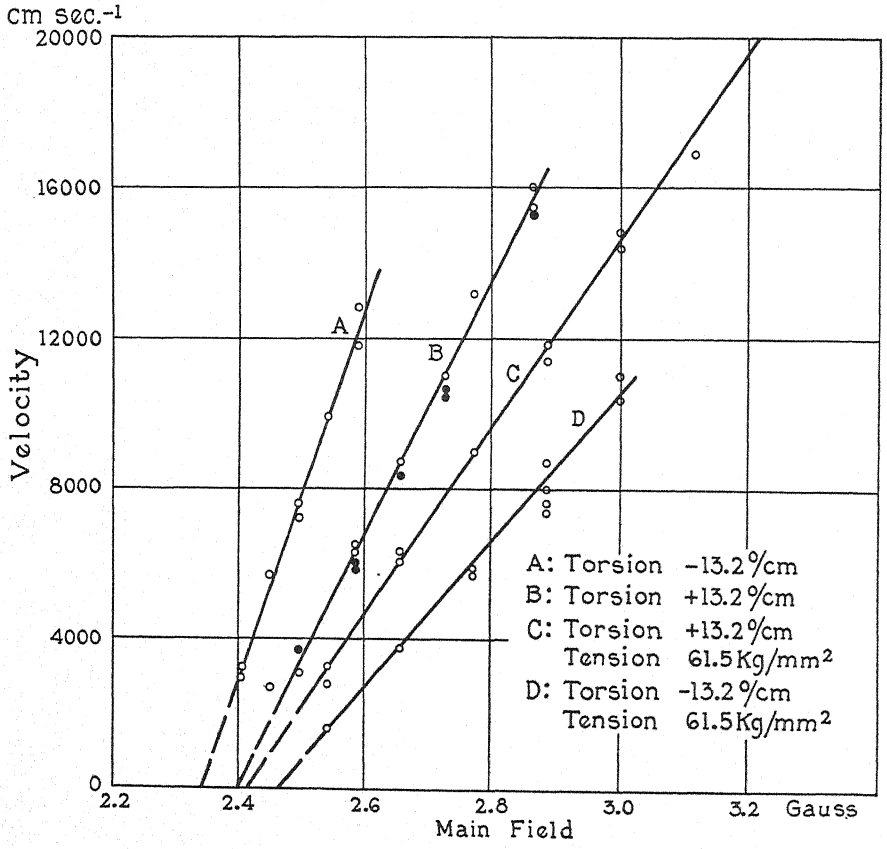

Fig. 18. Velocity-field curves for torsion and combined tension and torsion. Wire of 0.038 cm diameter from ingot No. 19, 25 percent Ni-Fe. The black dots represent check points.

strains were elastic. (The black dots in Fig. 18 were taken after the direction of applied torsion had been changed several times.) As another wire from the same lot did not exhibit this dependence of slope on direction of twist, it is probable that internal strains have an important influence on the slope in the case of torsion. More work on wires having different strain distributions has to be done before the observed effects can be explained.

The data for these cases are insufficient as yet for checking the application of Eq. (7).

11. Wires of Different Composition

Nickel iron wires of 3, 5, 8, 10, 12, 14, 15, 20, 25, 35, 40, 55, 60, 78, 80, 90 and 100 percent nickel content have been examined. We were able to obtain large discontinuities (i.e., of more than 80 percent of the double saturation value) with *tension* only in the ranges 8 to 25 percent and 55 to 78 percent.[10] From 5 percent down and from 80 percent up no large discontinuities could be observed and with 35 and 40 percent only small jumps of about 1/10 of the double saturation value appeared under tension. These jumps were very erratic and probably only included a short length of wire at a time so that velocity measurements with these compositions were impossible. Throughout the remainder of the range the v-H slope did not deviate much from an average value of 25000 cm sec^{-1} $gauss^{-1}$, but the effect of tension on the critical field varied profoundly. Between 8 and 20 and at 78 percent increasing tension reduced the critical field H_0, but at 55 and 60 percent it increased H_0. At 25 percent there was a pronounced reversal in the dependence of H_0 on tension. Up to a certain value of tension H_0 increased with increasing tension; after passing this value the critical field decreased again.

Torsion produced large discontinuities over the entire range between 8 and 100 percent Ni-Fe, and the great variations in v-H slope already mentioned as existing in the 8 to 20 percent interval were found to be present over this wider range, varying between the values 10^4 and 6×10^4 cm sec^{-1} $gauss^{-1}$. There were no simple relations between either composition or amount of twist and critical field. The v-H characteristics were occasionally curved, but no more frequently than in the case of tension.

No experiments have been carried out on the propagation in wires under an elastic bending force.

12. The Critical Field

Some of our experimental results allow comparison with a theory recently advanced by R. Becker[11] which has already been applied successfully to the case of nickel under tension.[12] Becker introduces the close and important relation between the magnetic and elastic state of materials by the assumption that the direction of magnetization in each Weiss domain is determined by the stress tensor in that domain in the absence of an external field. The theory enables him to derive hysteresis loops for these districts for different initial angles between magnetization and applied field.

For the limiting case of anti-parallelism between magnetization and field, this theory yields a rectangular hysteresis loop for which the coercive field is given by

$$H_C = 8SAI_m$$

[10] Preisach (p. 755) has already pointed out that the upper limit coincides with the composition at which magnetostriction and accordingly the effect of tension on magnetization change sign.

[11] R. Becker, Zeits. f. Physik **62,** 253 (1930).

[12] R. Becker and M. Kersten, Zeits. f. Physik **64,** 660 (1930).

where $S \sim 1$ is a factor calculated from magnetostriction, A is the elastic deformation of the domain and I_m is the saturation intensity of magnetization. With exact antiparallelism, however, the force couple exerted by the impressed field is zero, with the consequence that the domain may conceivably retain its position of unstable equilibrium even for values of H exceeding H_c. It is interesting that the Ni-Fe wire as a whole exhibits this behavior. On this basis the critical field H_0 is to be identified with the coercive field H_c, while the somewhat erratic starting field corresponds to the indeterminate field at which the equilibrium of the Weiss domain may be destroyed.

As a matter of fact, the wire only approximates to a single Weiss domain, both because of the peaks evident in the oscillograms and because of the fact that for fields only slightly greater than H_0 the reversal of the wire is incomplete (as may be seen in Fig. 8), indicating that the coercive force for certain portions of the wire exceeds H_0. It is possible that the ΔI vs H curves in

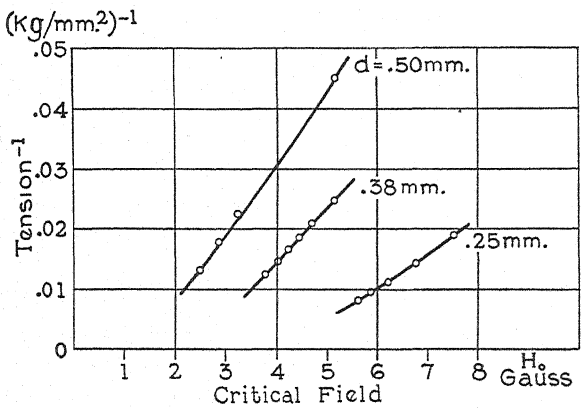

Fig. 19. Critical field for wires of different diameter. All Wires cold drawn from annealed wire 0.102 cm diameter from ingot No. 14, 14 percent Ni-Fe.

that figure give the proportion of the wire for which H exceeds the coercive field.

Becker's formula, when applied to our conditions, yields values more than 10 times higher than those observed by us and predicts in the case of iron and low nickel-iron alloys for which S is positive, an increase in H_c with increasing elastic deformation A. In our experiments with Ni-Fe wires of 8 to 20 percent nickel content, we observed just the opposite relation. This is shown clearly by Fig. 19 in which the reciprocal of tension is plotted vs. the critical field for different diameters. In a certain range of tensions we obtain almost a linear relation between $1/T$ and H_0! In his second article Becker recognizes this difficulty.

Fig. 19 allows of one other comparison with experiments made by Becker and Kersten. The critical fields obtained for wires of different diameter for the same stress are quite different. Since all wires were cold drawn from 0.102 cm, the explanation lies in the different amounts of cold working the wires have suffered. The more cold working, the greater are the internal strains,

and the higher the coercive force. In their experiments with nickel wires Becker and Kersten are able to obliterate differences in internal strain conditions entirely by application of high tension and they can account for this satisfactorily by assuming that hard drawing produces only longitudinal strains in the wire whose influence disappears in the limiting case of high applied tension.

In our case, however, this does not occur, for even with tension near to the breaking point, the coercive forces are still considerably different for wires subjected to different amounts of cold working. This is illustrated by

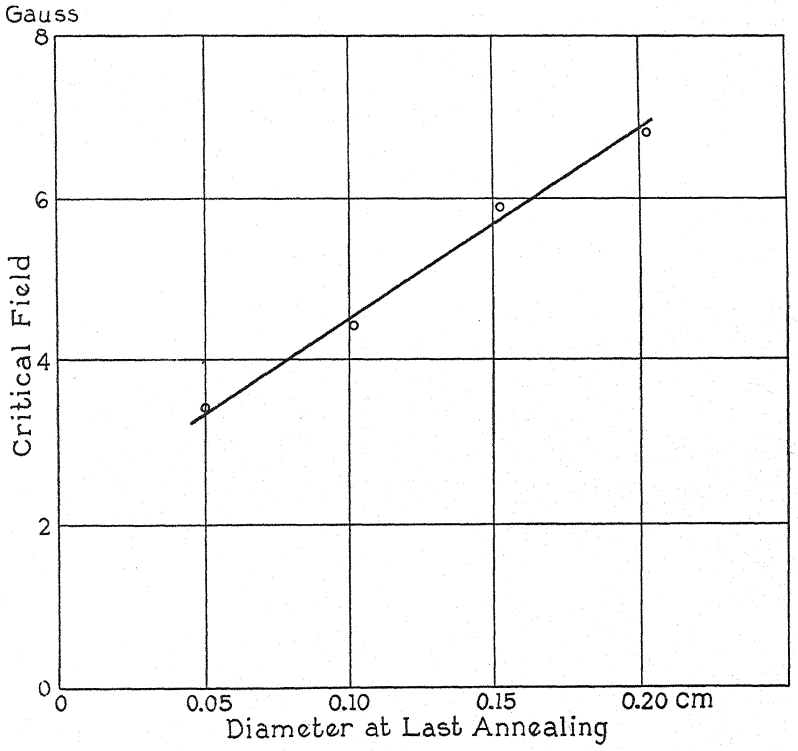

Fig. 20. Critical field at 62 kg/mm² tension for wires with different amounts of cold working. All wires of 0.038 cm diameter from ingot No. 22, 20 percent Ni-Fe.

Fig. 20 which shows the critical field for wires of 0.038 cm diameter annealed at the diameters shown and then cold-drawn. Even with 62 kg/mm² tension, the coercive force varies between 3.3 and 6.8 gauss. It may well be that radial and associated ring strains introduced by cold working play an important role in determining the coercive force. On the other hand, Becker and Kersten's results on stretched Ni wires where only continuous and reversible changes are present show that any radial strains can be neglected. Further investigation of propagation in thin strips may give additional information regarding the role of strains in this connection, as the strain structure is probably much simpler in rolled strips than in drawn wires.

Among the various possibilities which present themselves for extending this work we intend to refine the oscillographic method further and to use that method on different sized wires and strips and also on composite strips (strips with a surface layer only of Ni-Fe) with the hope of obtaining a more detailed picture of the magnetic discontinuity. We also intend to examine the effect of temperature change both on nucleus formation and propagation velocity.

We appreciate the interest which Professor R. Becker has shown in this work, and we wish to express our gratitude to Dr. I. Langmuir who, as we have said, not only foresaw the magnetic propagation, but has also given many suggestions and much advice.

FERMI-DIRAC STATISTICS APPLIED TO THE PROBLEM OF SPACE CHARGE IN THERMIONIC EMISSION

By Russell S. Bartlett
Yale University

(Received March 2, 1931)

Abstract

This paper develops mathematically the state of an electron gas in equilibrium with a plane electrode when the electron gas obeys the Fermi-Dirac rather than the classical distribution law. For a part of the range of integration graphical methods were found necessary, but fortunately a change of variable leads to a solution, shown graphically, which is independent of the temperature and of the nature of the emitting electrode. Thus a single graphical integration can be applied to any emitting surface at any temperature, giving the density, electric intensity, and potential at any desired distance from the surface. A simple extension of the theory makes possible the calculation of the thermionic current between plane electrodes. Numerical examples are given, and the validity of the asumptions is discussed briefly.

WHEN Schottky[1] first proposed that the thermionic work function could be explained by the attraction of an escaping electron to its electric image in the surface, he discussed at some length the possible effects of space charge and "structure effects," and finally concluded that other forces were small compared to the image force. Recently Waterman and the author[2] have questioned this conclusion, and have suggested that, at least under certain conditions, possibly always, space charge and structure effects are more important than the image force.

Schottky, assuming the image force to be correct, and assuming a Maxwell distribution of electron velocities, was able from measured electron emission currents to calculate the concentrations of the electron atmosphere at all points outside the metal and found it so rarefied that space charge could be neglected. This extension of the image force from a region out from the surface where it can be confirmed experimentally down towards the surface through a region where it could not be expected to be valid appears to be unjustifiable. The alternative treatment by space charge analysis, which is to be developed in this paper, is certainly not free from criticism. In particular, it is necessary to apply Poisson's equation to an electron gas, thus assuming a continuous distribution of electricity which certainly does not exist. On the other hand it would appear, as is pointed out in a previous paper by Waterman and the author, that the choice of suitable statistics may in part avoid that difficulty. In any case the space charge method of attack seems justified close to the surface where the image force certainly breaks down. In order to

[1] Schottky, Phys. Zeits. **15**, 872 (1914).
[2] Bartlett and Waterman, Phys. Rev. [2] **37**, 279 (1931).

shed more light on this question certain calculations have been carried out, assuming that the electron concentration is controlled by space charge alone.

Equilibrium. Classical Distribution Law

After the manner of Fry,[3] Langmuir,[4] and others, consider a stream of electrons emerging from an infinite plane electrode with initial velocities distributed according to some law. The electrons outside the surface of the electrode will induce a charge on the electrode tending to draw the electrons back to it. There will be a potential distribution outside the metal surface through which the electrons move, those with higher initial velocities normal to the surface getting further out before they are turned back.

With no external field and no neighboring electrode, we may write an expression for the charge density at any point in potential space.

$$\rho = 2\epsilon \int_{(2V\epsilon/m)^{1/2}}^{\infty} \frac{f(v_0)}{v} dv_0 \tag{1}$$

where $f(v_0)dv_0$ gives the number of electrons emerging from the surface per square cm with initial velocities normal to the surface lying between v_0 and v_0+dv_0, while v represents the normal velocities of these electrons at the point in question. Clearly

$$v_0^2 - v^2 = \frac{2V\epsilon}{m}. \tag{2}$$

Using Poisson's equation we get

$$\frac{d^2V}{dx^2} = -4\pi\rho = -8\pi\epsilon \int_{(2V\epsilon/m)^{1/2}}^{\infty} \frac{f(v_0)}{v} dv_0. \tag{3}$$

Multiplying both sides by $2\,dV/dx$ and integrating in the usual manner gives

$$\left(\frac{dV}{dx}\right)^2 = 16\pi m \int_{(2V\epsilon/m)^{1/2}}^{\infty} v f(v_0) dv_0. \tag{4}$$

We cannot proceed further without knowing the distribution law of velocities expressed in $f(v_0)$. For the classical case

$$f(v_0) = n_0 \frac{mv_0}{kT} e^{-mv_0^2/2kT} \text{ or } f(v_0) = N_0 \left(\frac{m}{2\pi kT}\right)^{1/2} v_0 e^{-mv_0^2/2kT}, \tag{5}$$

where n_0 is the number of electrons passing through a square centimeter of the surface per second, and N_0 is the number of electrons per unit volume at the surface. Then

$$\left(\frac{dV}{dx}\right)^2 = 16\pi m N_0 \left(\frac{m}{2\pi kT}\right)^{1/2} \int_{(2V\epsilon/m)^{1/2}}^{\infty} v v_0 e^{-mv_0^2/2kT} dv_0. \tag{6}$$

[3] Fry, Phys. Rev. [2] **17**, 441 (1921).
[4] Langmuir, Phys. Rev. [2] **21**, 419 (1923).

Changing the variable to v gives

$$\left(\frac{dV}{dx}\right)^2 = 16\pi m N_0 \left(\frac{m}{2\pi kT}\right)^{1/2} \int_0^\infty v^2 e^{-mv^2/2kT - V\epsilon/kT} dv \qquad (7)$$
$$= 8\pi N_0 kT e^{-\epsilon V/kT}$$

since the integral is a well known form having the value $\frac{1}{4}(8\pi k^3 T^3/m^3)^{1/2}$.

Taking the square root and performing the next step in the integration gives

$$x = \left(\frac{kT}{\pi N_0}\right)^{1/2} \frac{1}{2\epsilon} e^{\epsilon V/2kT}. \qquad (8)$$

The first boundary condition requires that V and x shall approach infinity together as dV/dx approaches zero, and this is satisfied by the above equations. The second condition specifies that at the surface the number of free electrons per cubic centimeter has a fixed value, in this case N_0. That requires that the surface of the metal shall be at x_0 given by

$$x_0 = \left(\frac{kT}{\pi N_0}\right)^{1/2} \frac{1}{2\epsilon}. \qquad (9)$$

Combining Eqs. (1) and (5) and integrating at once gives Boltzmann's equation

$$N = N_0 e^{-\epsilon V/kT}. \qquad (10)$$

We could, in fact, have arrived at Eq. (8) by combining (10) with Poisson's equation. But (10) is of interest now in that, combined with (8) it gives us the concentration at various distances from the surface. The quantities V, dV/dx, x, and N are so related that as soon as we have fixed one all the others may be determined from various combinations of Eqs. (7), (8), and (10). It is also seen that a different metal, with a different electron concentration at the surface, could be handled by the same equations with an appropriate value of x_0 at the surface.

Equilibrium. Fermi-Dirac Distribution Law

If in Eqs. (1) and (4) we replace the classical expression for $f(v_0)$ by that obtained from Fermi-Dirac statistics, the problem becomes much more complicated.

Now

$$f(v_0) = \frac{2\pi kTGm^2}{h^3} v_0 \log\left(A_0 e^{-mv_0^2/2kT} + 1\right) \qquad (11)$$

where A is a measure of the degeneracy of the electron gas. This gives us instead of (1) and (4) the following.

$$N = \frac{4\pi kTGm^2}{h^3} \int_{(2V\epsilon/m)^{1/2}}^\infty \frac{v_0}{v} \log\left(A_0 e^{-mv_0^2/2kT} + 1\right) dv_0 \qquad (12)$$

and

$$\left(\frac{dV}{dx}\right)^2 = 32\pi^2 kTG\left(\frac{m}{h}\right)^3 \int_{(2V\epsilon/m)^{1/2}}^{\infty} vv_0 \log\,(A_0 e^{-mv_0^2/2kT} + 1)dv_0. \tag{13}$$

Making the change of variable from v_0 to v gives

$$N = \frac{4\pi kTGm^2}{h^3} \int_0^{\infty} \log\,(Ae^{-mv^2/2kT} + 1)dv \tag{14}$$

where

$$A = A_0 e^{-\epsilon V/kT}$$

and

$$\left(\frac{dV}{dx}\right)^2 = 32\pi^2 kTG\left(\frac{m}{h}\right)^3 \int_0^{\infty} v^2 \log\,(Ae^{-mv^2/2kT} + 1)dv. \tag{15}$$

Since the evaluation of these integrals is rather complicated, it will be convenient to make certain substitutions.

Let

$$\frac{mv^2}{2kT} = u^2.$$

Let

$$f(A) = \int_0^{\infty} \log\,(Ae^{-u^2} + 1)du$$

and

$$g(A) = \int_0^{\infty} u^2 \log\,(Ae^{-u^2} + 1)du.$$

Then

$$N = \frac{2\pi G(2mkT)^{3/2}}{h^3} f(A) \tag{16}$$

and

$$\left(\frac{dV}{dx}\right)^2 = \frac{16\pi^2 Gm^{3/2}(2kT)^{5/2}}{h^3} g(A). \tag{17}$$

For the case where $A < 1$ the solution is fairly simple. Expanding the log $(Ae^{-u^2}+1)\,du$ we get

$$f(A) = \int_0^{\infty} [Ae^{-u^2} - \tfrac{1}{2}A^2e^{-2u^2} + \tfrac{1}{3}A^3e^{-3u^2} \cdots]du \tag{18}$$

and

$$g(A) = \int_0^{\infty} [Au^2e^{-u^2} - \tfrac{1}{2}A^2u^2e^{-2u^2} + \tfrac{1}{3}A^3u^2e^{-3u} \cdots]du. \tag{19}$$

The integrals involved are ordinary probability integrals. Hence

$$f(A) = \tfrac{1}{2}(\pi)^{1/2}[A - A^2/2^{3/2} + A^3/3^{3/2} \cdots] \tag{20}$$

$$g(A) = \tfrac{1}{4}(\pi)^{1/2}[A - A^2/2^{5/2} + A^3/3^{5/2} \cdots]. \tag{21}$$

Further, for the case where $A \ll 1$ we get the usual Boltzmann relation that $N = N_0 e^{-\epsilon V/kT}$. When the gas is not classical the Boltzmann relation becomes $A = A_0 e^{-\epsilon V/kT}$, as Waterman has found from a different point of view.

When $A > 1$ the solution becomes more difficult since the expansion used above is not valid over the total range of integration. It is necessary to divide the range of integration into two parts, for which Ae^{-u^2} is less than or greater than unity. Then

$$f(A) = \int_0^{(\log A)^{1/2}} \log [Ae^{-u^2}]du + \int_0^{(\log A)^{1/2}} \log [e^{u^2}/A + 1]du + \int_{(\log A)^{1/2}}^{\infty} \log [Ae^{-u^2} + 1]du \tag{22}$$

and

$$g(A) = \int_0^{(\log A)^{1/2}} u^2 \log [Ae^{-u^2}]du + \int_0^{(\log A)^{1/2}} u^2 \log [e^{u^2}/A + 1]du + \int_{(\log A)^{1/2}}^{\infty} u^2 \log [Ae^{-u^2} + 1]du. \tag{23}$$

If $A \gg 1$ (i.e., the electron gas completely degenerate) the first term is the only one of consequence.

This first term can be integrated directly to give

$$f(A) = 2/3(\log A)^{3/2} \tag{24}$$

$$g(A) = 2/15(\log A)^{5/2} \tag{25}$$

And finally by means of series expansion and integration by parts, involving steps of questionable rigor but justified by the result, one obtains

$$f(A) = \frac{2}{3}(\log A)^{3/2}\left[1 + \frac{\pi^2}{8(\log A)^2} + \frac{7\pi^4}{640(\log A)^4} + \frac{31\pi^6}{6144(\log A)^6} + \frac{4191\pi^8}{5 \times 2^{16}(\log A)^8} \cdots\right] \tag{26}$$

$$g(A) = \frac{2}{15}(\log A)^{5/2}\left[1 + \frac{5\pi^2}{8(\log A)^2} - \frac{7\pi^4}{384(\log A)^4} - \frac{155\pi^6}{43008(\log A)^6} - \frac{381\pi^8}{2^{16}(\log A)^8} \cdots\right] \tag{27}$$

where these series, though not convergent, may be used for large values of A, and have been checked by graphical integration.

In the Sommerfeld-Fermi-Dirac statistics, the number of particles per unit volume and the energy per unit volume are expressed in terms of two

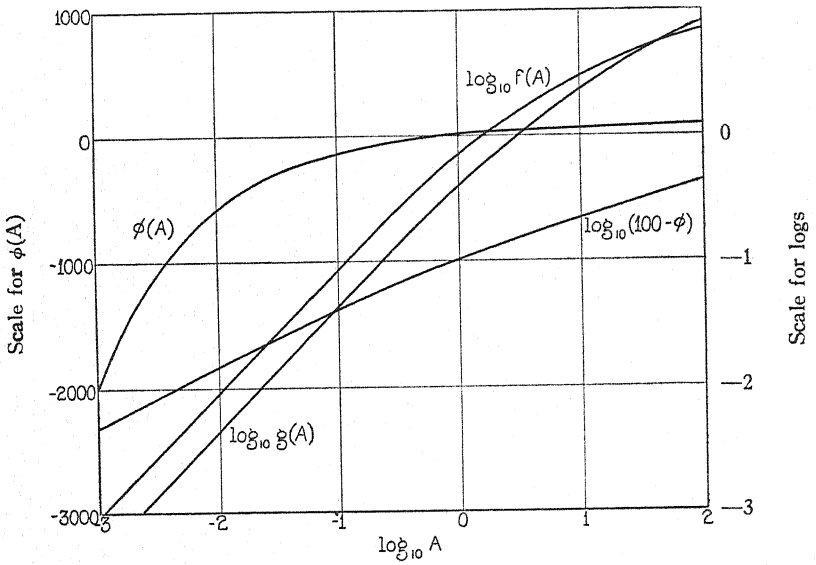

Fig. 1. $N=5.4830\times10^{15}\ T^{3/2}f(A)/\text{cm}^3\ E=1843.9\ T^{5/4}[g(A)]^{1/2}$ volts/cm. $X=2.1631\times10^{-9}\ \phi(A)/T^{1/4}$ cm. $V=1.9851\times10^{-4}\ T \log_{10} A$ volts.

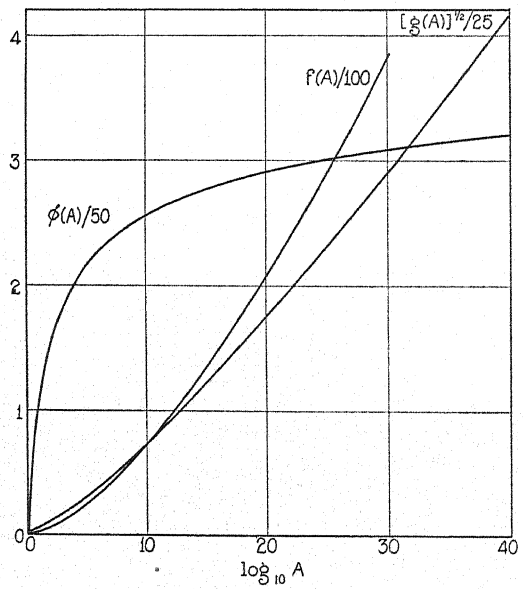

Fig. 2.

functions $F(A)$ and $G(A)$. It turns out that $f(A)$ as used above is equal to $\pi^{1/2}/2\cdot F(A)$, while $g(A)=\pi^{1/2}/4\cdot G(A)$, thus confirming the results of the questionable steps mentioned above.

We now have expressions for $f(A)$ and $g(A)$, hence for N and $(dV/dx)^2$ over four regions, completely degenerate, less degenerate, approaching classical, and completely classical. The two extremes are handled by exact expressions, the intermediate regions by series, and there is a region between for which neither series is valid. $f(A)$ and $g(A)$ have been evaluated graphically for this intermediate region. Numerical results of this graphical integration and of the series expansions are given in Figs. 1, 2 thus covering the regions between the exact expressions for completely degenerate and completely classical states.

For the degenerate state $N=4\pi G(2mkT)^{3/2}/3h^3\cdot(\log A)^{3/2}$ and for the classical state $N=G(2\pi mkT)^{3/2}/h^3\cdot A$. For intermediate states $N=2\pi G(2mkT)^{3/2}/h^3\cdot f(A)$ where $f(A)$ for any value of A may be found from the figures.

Further for the degenerate state

$$\left(\frac{dV}{dx}\right)^2 = 32\pi^2 Gm^{3/2}(2kT)^{5/2}/15h^3\cdot\left[\log\left(A_0 e^{-eV/kT}\right)\right]^{5/2}.$$

Taking the square root of both sides and integrating directly gives

$$x = \frac{15^{1/2}h^{3/2}}{2^{7/4}\pi G^{1/2}m^{3/4}(kT)^{1/4}e}\log A^{-1/4}. \tag{28}$$

For the classical state

$$\left(\frac{dV}{dx}\right)^2 = \frac{4Gm^{3/2}(2\pi kT)^{5/2}}{h^3}A_0 e^{-eV/kT}.$$

This also may be integrated directly to give

$$x = \frac{h^{3/2}}{2^{5/4}G^{1/2}m^{3/4}\pi^{5/4}(kT)^{1/4}e}\cdot A^{-1/2}. \tag{29}$$

For the intermediate region graphical integration is required, since there is no exact solution. It is seen that

$$\frac{dV}{dx} = \text{const}\,(g(A))^{1/2} = \text{const}\,(g(A_0 e^{-eV/kT}))^{1/2}.$$

Since values for the expression under the radical have been tabulated as a function of A, easily convertible to a function of V, it is possible to perform a graphical integration. To simplify the arithmetical work this has been done to give a new function $\phi(A)$ proportional to x, values for which are given in Figs. 1 and 2.

$f(A)$, $g(A)$, and $\phi(A)$ are perfectly general functions, independent of temperature and of the nature of the electron emitter. The coefficients of these functions in the various equations take care of the effect of temperature. The curves in Fig. 1 show these functions plotted against A. The origin at $\log A=0$ is purely arbitrary. In effect there is no origin, or better, perhaps, each particular problem provides its own origin, fixed by the conditions of the sur-

face. In practice it is convenient to consider distances and potential differences from x_1, V_1 corresponding to A_1, to x_2, V_2, corresponding to A_2. The formulae below together with the tables cover the entire range of an electron gas.

$$V(\text{volts}) = 300kT/\epsilon \cdot \log A = 690.8kT/\epsilon \cdot \log_{10} A = 1.9851 \times 10^{-4} T \log_{10} A \tag{30}$$

$$N = 2\pi G(2mkT)^{3/2}/h^3 \cdot f(A) = 5.4830 \times 10^{15} T^{3/2} f(A) \tag{31}$$

$$A \gg 1 \quad N = 4\pi G(2mkT)^{3/2}/3h^3 \cdot (\log A)^{3/2} = 1.2772 \times 10^{16} T^{3/2} (\log_{10} A)^{3/2} \tag{32}$$

$$A \ll 1 \quad N = G(2\pi mkT)^{3/2}/h^3 \cdot A = 4.8591 \times 10^{15} T^{3/2} A \tag{33}$$

$$E = 2^{13/4}\pi G^{1/2} m^{3/4} (kT)^{5/4}/h^{3/2} \cdot [g(A)]^{1/2} \text{E.S.U/cm} = 1843.9 T^{5/4} [g(A)]^{1/2} \text{ volts/cm} \tag{34}$$

$$A \gg 1 \quad E = 2^{15/4}\pi G^{1/2} m^{3/4} (kT)^{5/4}/15^{1/2} h^{3/2} \cdot (\log A)^{5/4} = 1909.8 T^{5/4} (\log_{10} A)^{5/4} \text{ volts/cm} \tag{35}$$

$$A \ll 1 \quad E = 2^{9/4}\pi^{5/4} G^{1/2} m^{3/4} (kT)^{5/4}/h^{3/2} \cdot A^{1/2} = 1227.4 T^{5/4} A^{1/2} \text{ volts/cm} \tag{36}$$

$$x = h^{3/2} \times 0.046052/2^{13/4}\pi G^{1/2} m^{3/4} (kT)^{1/4} \epsilon \cdot \phi(A) \text{ cm} = 2.1631 \times 10^{-9} \phi(A)/T^{1/4} \text{ cm} \tag{37}$$

$$A \gg 1 \quad x = 15^{1/2} h^{3/2}/2^{7/4}\pi G^{1/2} m^{3/4} (kT)^{1/4} \epsilon \cdot (\log A)^{-1/4} = 4.1770 \times 10^{-7}/T^{1/4} \cdot (\log_{10} A)^{-1/4} \text{ cm} \tag{38}$$

$$A \ll 1 \quad x = h^{3/2}/2^{5/4} G^{1/2} m^{3/4} \pi^{5/4} (kT)^{1/4} \epsilon \cdot A^{-1/2} = 1.4112 \times 10^{-7}/T^{1/4} \cdot A^{-1/2} \text{ cm}. \tag{39}$$

A small additive correction is necessary to join different regions. This may easily be calculated, but has been omitted here to avoid further complications.

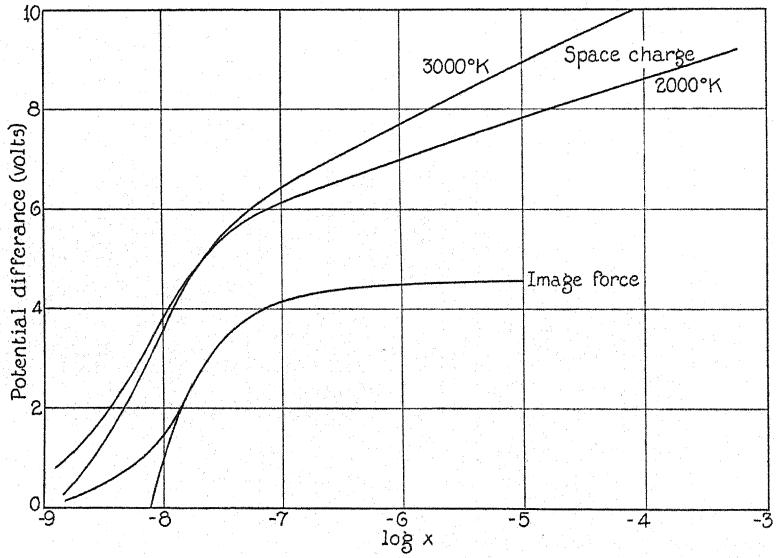

Fig. 3. Height of potential barrier at different distances from the surfaces.

If then N is known for any point, A, V, x, and E may be found from these formulae used in conjunction with the figures. And as soon as one of these is fixed for another point, all the others may be found. The separation of the points in space and in potential is found by subtracting the V's and x's for the two points. Figs. 3, 4 give some characteristic results for various conditions.

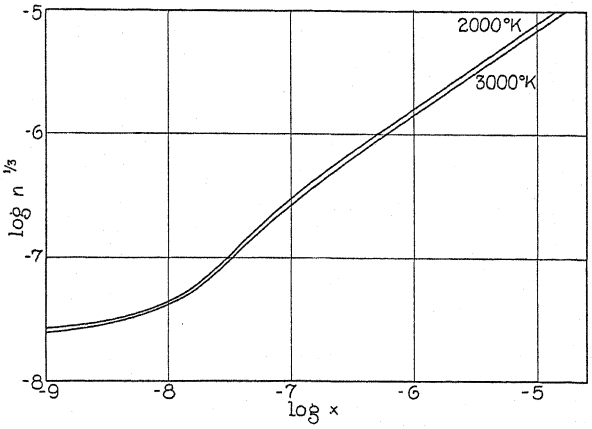

Fig. 4. Distances between electrons at different distances from the surface.

CURRENT TO THE ANODE

The analysis just given applies to the case of no current, effectively an equilibrium case, though it was considered from the point of view of emerging and returning streams. Fortunately it is possible to take advantage of earlier work by Fry and Langmuir in going over to the case where a current is flowing from the hot cathode. In Langmuir's paper two variables are defined

$$\xi = 4(\pi/2kT)^{3/4}m^{1/4}(\epsilon i)^{1/2}(x - x_m) \tag{40}$$

$$\eta = \epsilon(V - V_m)/kT. \tag{41}$$

It is easily seen that $\eta = \log A - \log A_m$ in our notation. Now the current passing a potential barrier V is given by

$$i = 2\pi\epsilon kTGm^2/h^3 \cdot \int_{(2V\epsilon/m)^{1/2}}^{\infty} u \log (A_0 e^{-mu^2/2kT} + 1)du \tag{42}$$

$$i = 2\pi Gm\epsilon(kT)^2/h^3 \cdot A_0 e^{-\epsilon V/kT} = 2\pi Gm\epsilon(kT)^2/h^3 \cdot A \tag{43}$$

provided $A_0 e^{-\epsilon V/kT} < 1$.

If this value of i is put into the expression for ξ above we get

$$\xi = 2^{9/4}\pi^{5/4}(kT)^{1/4}m^{3/4}\epsilon A_0^{1/2}e^{-\epsilon V/kT}(x - x_m)/h^{3/2} \tag{44}$$

from which it appears that $\xi = 0.046052\pi^{1/4}/2^{3/4} \cdot \phi(A) \cdot A^{1/2}$ with similar relations beyond the range of $\phi(A)$. Thus it is possible to apply the Langmuir Fry analysis to this case if a little care is exercised, using the relation $\xi = \xi_1 A_0^{1/2} e^{-\epsilon V/2kT} = \xi_1 A^{1/2}$.

The Langmuir-Fry analysis assumes electrons streaming out from the electrode with velocities according to Maxwell's distribution law. Of these the highest velocity electrons escape completely, so that the returning stream consists of only a part of the Maxwellian distribution. Now in thermionic emission the currents are generally so small that the loss of electrons to the returning stream is of no consequence close to the electrode where the distribution is no longer classical. In the region where the loss of electrons is of consequence, the distribution is classical or so nearly so that the Langmuir-Fry analysis can be joined to mine as indicated without serious error.

Illustration of the Method of Calculation

Let us take the case of an emitter at 3000°K.

$N_0 = 6.2 \times 10^{22}$ (tungsten) Parallel plane electrodes 1 cm apart.
From the figures $\log A_s = 9.534$ $A_s = A$ at surface
Arbitrarily $\log A_m = -3.0000$ $A_m = A$ at potential minimum
A simple calculation gives i corresponding to A_m as 3.612×10^{-4} amps/cm^2
From the figures $\phi(A_s) = 126.59$ $\phi(A_m) = 2002.06$
Using equation (45) $\xi_{1m} = 43.399$ $\xi_{1s} = -2.744$ $\xi_1 = 46.143$
Multiplying by $A^{1/2}$ gives $\xi = 1.4592$
To this we add 1.1397 to fit classical to Fermi,
giving ξ_1' (from surface to potential minimum) $= 2.5989$
From 40 or 44 $\xi' = 43.041$
so that ξ_2' (from potential minimum to collecting electrode) $= 40.442$
From tables of Langmuir, extended to cover some cases dealt with here,
$\eta_2 = 87.49$ (from potential minimum to collecting electrode.)
η(total) $= 74.96$ $V = 19.387$ from equation 41
Repetition of this process for a series of values of A_m leads to the results given in Fig. 5.

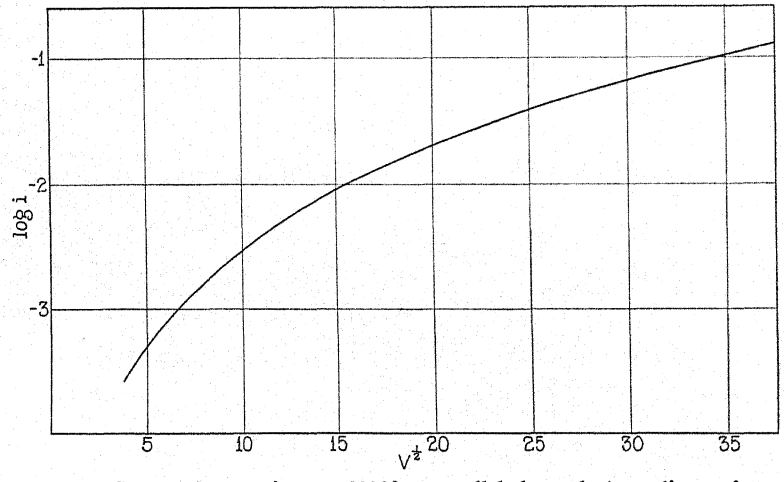

Fig. 5. Current from emitter at 3000° to parallel electrode 1 cm distant for different accelerating potentials.

Discussion of Results

Fig. 3, showing the height of the potential barrier at various distances from the surface, for tungsten, $N_0 = 6.2 \times 10^{22}/\text{cm}^3$ is interesting in that it shows a value for the work function much larger than that conventionally accepted, this larger value being necessary to nullify the effect of the zero-point energy of a highly concentrated electron gas.

Fig. 4 shows in effect the average distance between electrons as a function of distance from the surface. The distance between electrons is comparable with the distance from the surface at a point so close that the image force is meaningless, and slightly further out it is seen that an electron is further from the surface than its nearest neighbor, showing that space charge is certainly important.

When considering the calculations shown in Fig. 5, it should be remembered that the calculations were carried out for plane parallel electrodes, whereas experiments have almost invariably used coaxial cylinders. The rapid change of space charge outward radially from a fine wire would naturally lead to different results. In order to test this question, an attempt is now being made to reproduce experimentally the conditions here treated theoretically.

There are two more questions of importance that must be recognized here. In the first place, the calculated electric field at the surface is so large that a great reduction of electron concentration within the surface should result from the very large surface charge. Just what effect this might have on the case of a current cannot be predicted. The calculations for the equilibrium case are still valid, if one chooses a proper electron concentration at the surface. A second question, of course, is that of the validity of Poisson's equation. It seems to the author that probably this calculation is reasonably close to the truth in regions where the concentrations of electrons is large. But at considerable distances from the surface, where the concentration is low, the approximation to the truth cannot be as good. It is for this reason that for the calculation of emission currents the electrodes were chosen so close together. Also for this reason results are not given for currents at lower temperatures. This particular problem will be investigated further.

In conclusion the author wishes to thank Professor A. T. Waterman for many helpful discussions of the problem.

THE ANGULAR DISTRIBUTION OF ELECTRONS SCATTERED BY MERCURY VAPOR

By J. M. Pearson and W. N. Arnquist
Norman Bridge Laboratory, California Institute of Technology

(Received February 27, 1931)

Abstract

Instead of using pressures of the order of 10^{-2} mm the apparatus described is designed for pressures in the range 10^{-3} to 10^{-4} mm. Heavy primary current densities are used to afford measurable scattered currents, and high angle scattering is found to be more easily measurable. It is found that the angular distribution curves for electrons scattered by mercury are not monotonic functions of the angle of scattering. For a given energy of incident electrons the curve passes through a minimum, the angular position of which depends upon the energy.

I. Scheme of Experiment

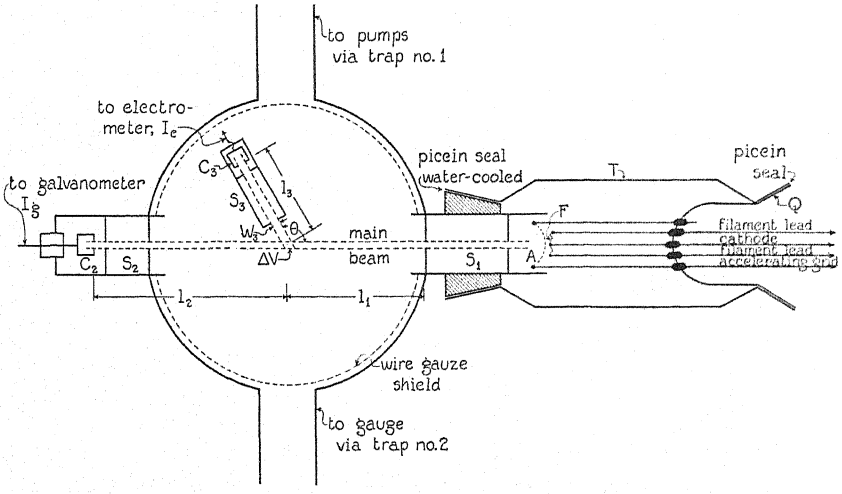

Fig. 1. Diagram of tube.

THE principles of design of this type of apparatus are well enough known so that it will be necessary here to point out only the salient features.

The tube is constructed of brass. It is 15 cm in diameter, and shaped as in Fig. 1. Electrons are accelerated from the tungsten filament F (supplied at the center-tap), through the grid A, and retarded between the grid A and the first of the collimating slits S_1.

The circuits are so arranged that the entire enclosure is maintained at ground potential. The electron beam passes diametrically across the chamber to the slits S_2, and through these to the Faraday cage C_2.

The axis of the main beam is oriented to be parallel to the horizontal com-

ponent of the earth's field, which is carefully neutralized by one set of large Helmholtz coils. A magnetic pendulum was used to determine the necessary current.

Slits S_1 and S_2 are optically aligned, and by means of another pair of large Helmholtz coils the vertical component of the magnetic field in the apparatus is adjusted until the main beam is received on C_2. By changing the current in the latter coils the beam can be moved back and forth across the slits S_2. This affords a means of measurement of the divergence of the beam.

Electrons scattered from the main beam are collected principally by the walls of the chamber, which are made more absorbing by the use of the copper gauze as shown.

A portion of the electrons scattered at an angle θ in the center of the apparatus, pass through the slits S_3 and reach C_3. The axis of collimation of slits S_3 passes always through the center of the apparatus as θ is varied. See Fig. 2 for a vertical section.

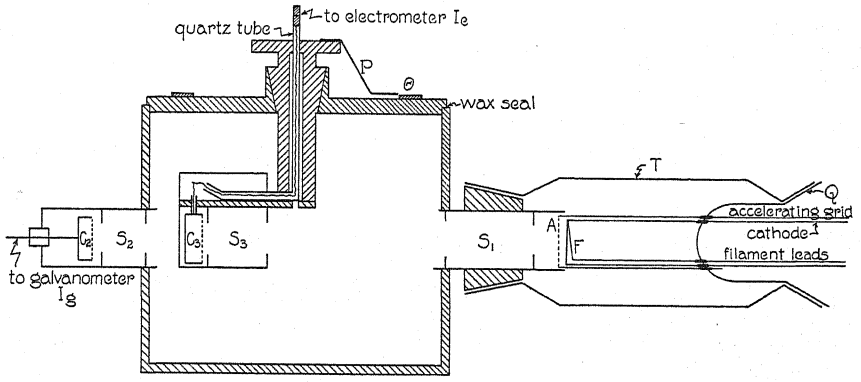

Fig. 2. Vertical section of tube.

Slits S_3 and cage C_3 are mounted in the lid on a movable, central, stem with a tapered joint as shown. A pointer P reads the angle θ, on a scale engraved on the lid.

Slits S_1 and S_2 are 10 mm long. Slits S_3 are 8 mm long. The spacings and widths are so adjusted that, with length considered, 90 percent of the electrons passing any pair of slits is contained within an angle of $\pm 1.5°$ of the central axis of that pair.

Other details such as accessibility of the filament or of the chamber, are explained by the figures.

The electric circuits are shown in Fig. 3.

II. Theory of Apparatus

Let ΔV be the volume of the intersection of the paths of collimation of S_1 and S_3. Let p be the gas pressure in mm Hg; α the coefficient of scattering in the expression,

$$I = I_0 \exp(-\alpha p x).$$

Let I be the current in amperes, at the point "x" measured along the main beam from ΔV; I_0 the main beam current entering ΔV; l_2 the distance from C_2 to ΔV; l_3 the distance from C_3 to ΔV (constant). Let $f(\theta)d\theta$ be the probability under given conditions that a scattered electron will be deflected between the angles θ and $\theta+d\theta$.

At any point x in the beam passing ΔV we have the current

$$I = I_0 \exp(-\alpha p x). \tag{1}$$

So in the distance dx

$$dI = -\alpha p I_0 \exp(-\alpha p x)dx. \tag{2}$$

$-dI$, is therefore the scattered current in the distance dx.

Let us consider now the current we can hope to receive on C_3 at the angle θ. Let I_s be the current scattered in ΔV; w_3 the width of slits S_3. Then

$$I_s = -dI = \alpha p I_0 \exp(-\alpha p x)dx = \alpha p I_0 w_3/\sin\theta.$$

since $x=0$ at ΔV and $dx=w_3/\sin\theta$. Hence the fraction of I_s that is scattered between θ and $\theta+d\theta$ is given by

$$I_s f(\theta)d\theta = \frac{\alpha p I_0 w_3 f(\theta)}{\sin\theta}d\theta. \tag{3}$$

Of this current only a fraction, K_3, will reach C_3 because of slits S_3. The current is also attenuated by scattering along the path of length l_3 from ΔV to C_3. So the current, I_e, received on C_3 is

$$I_e = \frac{\alpha p I_0 w_3 f(\theta) K_3}{\sin\theta}d\theta \exp(-\alpha p l_3). \tag{4}$$

Consider next the current received on C_2: because of the slits S_2 only a fraction, K_2, of the incident main beam will reach C_2. The beam is also attenuated by scattering along the path of length l_2. Hence the current, I_g, received on C_2 is

$$I_g = I_0 K_2 \exp(-\alpha p l_2). \tag{5}$$

If we divide (4) by (5) we eliminate I_0:

$$\frac{I_e}{I_g} = \frac{\alpha p K_3}{K_2} w_3 \frac{f(\theta)}{\sin\theta}d\theta \exp(\alpha p[l_2 - l_3]).$$

so that

$$f(\theta) = \frac{K_2 \exp(-\alpha p[l_2 - l_3])}{K_3 \alpha p d\theta w_3}\frac{I_e}{I_g}\sin\theta.$$

$$f(\theta) = K\frac{I_e}{I_g}\sin\theta \tag{6}$$

where

$$K = \frac{K_2 \exp(-\alpha p[l_2 - l_3])}{K_3 \alpha p d\theta w_3}.$$

The value of K is constant so long as one set of conditions is constant, since $d\theta$, K_2, K_3, l_2, and l_3, are all functions of a fixed geometry. The K's seem to depend upon the electron speed, and upon the condition of equilibrium of the apparatus. This is probably because the condition of the slit surfaces depends upon the bombardment they receive. During a given run, if the apparatus has previously been brought to equilibrium, K will remain quite constant. However, when the apparatus has been out of equilibrium between runs, K will vary by as much as a factor of 5.

It follows that by measuring I_e, I_g, and θ, the value of $f(\theta)/K$ can be calculated as a function of θ.

It is noted that the current I_e received by C_3,

$$I_e = \frac{\alpha p I_0 w_3 K_3 f(\theta) d\theta}{\sin\theta} \exp(-\alpha p l_3)$$

goes to zero for high pressures because of the exponent, and to zero for low pressures because of the factor p. However it goes to zero much more slowly

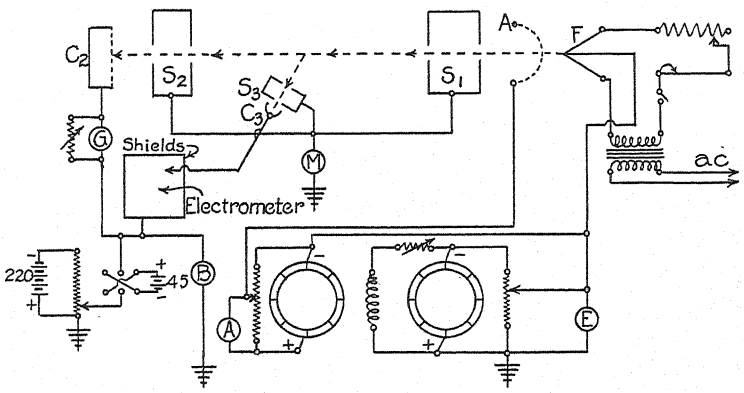

Fig. 3. Diagram of electrical arrangement.

on the low pressure than on the high pressure side of its maximum. This is fortunate since the maximum lies at such a high pressure that the condition of "single" scattering is not satisfied in an apparatus of practical dimensions.

In using lower pressures if the product pI_0 is kept constant, I_e can be maintained at a readable value.

I_e was measured by a "null" circuit using a modified Dolezalek electrometer.[1]

From the experimental values of α, and the dimensions of this apparatus, the mean free path of an electron is about the diameter of the apparatus at $p = 10^{-3}$ mm Hg. Thus at the pressure used ($1.8 \cdot 10^{-4}$mm) the condition for single collision scattering is well satisfied.

[1] J. M. Pearson, Journ. Op. Soc. 19, 6, p. 371.

In order to obtain the intensities of main beam desired some concessions had to be made in the voltage distribution of the electrons. Coated, equipotential, low temperature cathodes were tried, but were short lived owing to the heavy positive ion bombardment. Heavy tungsten was finally used, with a center-tap through which to supply the space current.

Studies were made of the voltage distribution of the electrons received on the Faraday cages. Two things were discovered, namely: (1) that the electrons were distributed over a range of 3 volts at E; and (2) that the cages were inefficient electron collectors. This was made evident by the fact that the electron current was cut off by a bias as much as 20 volts less than E, in vacuum, when the bias was applied to the cage. If however, the bias was applied to a grid somewhat ahead of C_2 (not shown), the cut-off bias was the same as E. This indicated that a deeper cage was necessary, or at least that an assisting gradient towards the cage was necessary.

Because of this low resolving power both at the collectors and at the filament, inelastic electrons were not resolved from the elastic electrons.

The currents received on C_2 are of the order of microamperes, and are measured by a suitably shunted wall galvanometer "G" (Fig. 3).

III. Manipulation

The apparatus is manipulated as follows:

(1). After several hours of pumping the filament is lit and the slits are bombarded. Liquid air is maintained on both traps. (see Fig. 4.) From two to five hours generally suffices to reach a state of equilibrium.

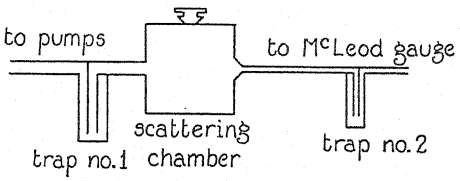

Fig. 4. Scattering chamber and connecting traps.

(2). When equilibrium is reached, an ice bath, vigorously agitated, is substituted for the liquid air on trap No. 1. Liquid air is maintained on trap No. 2, on the other side, connected to the chamber through a long tube. Thus after another lapse of hours the mercury vapor pressure inside the chamber becomes stable at very close to $1.8 \cdot 10^{-4}$ mm Hg.

(3). With the magnetic field neutralized and the values of the accelerating and retarding potentials adjusted, two sets of simultaneous readings of I_e and I_g are made at each setting of θ. When these pairs of readings check to ± 5 percent at each point, the run is accepted. Otherwise the apparatus is considered to be out of equilibrium.

In order to eliminate the effects of the positive ions that are collected due to the negative bias on the cages, readings are first taken with a low bias and

then with a high bias so that the difference of the readings gives the electron current. The positives are usually of the order of one-tenth the strength of the electrons. The biases used are marked on the curves.

IV. Results

The curves of Figs. 5 to 9 give a graphic summary of the results obtained. Of special interest is the fact that the curves are not monotonic, but behave as though the scattering were negligible at a certain angle for each electron energy. That these phenomena are associated with the mercury is attested by the fact that other gases (air, for instance, in thise case) gave monotonic scattering curves. In a vacuum (as in (1), manipulations,) no scattering is found at all.

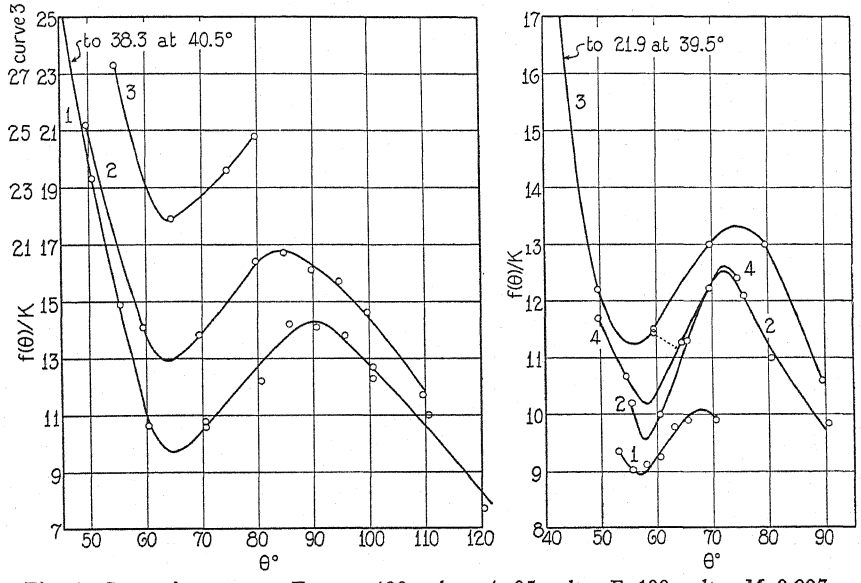

Fig. 5. Scattering curves. Energy, 100 volts. *A*, 95 volts; *E*, 100 volts; *M*, 0.007 amp.; *B*, −75, −102 volts. Curve 1, positive angles; Curve 2, negative angles taken several hours later; Curve 3, negative angles taken several days later.

Fig. 6. Scattering curves, Energy 125 volts. *A*, 165 volts; *E*, 125 volts; *M*, 0.0058 amp.; *B*, −100, −126 volts. Curve 1, positive angles; Curve 2, positive angles taken later; Curve 3, negative angles taken next day; Curve 4, negative angles taken two hours later.

An interesting relationship is presented by the last curve, where the cotangents of the positions of the minima are plotted with the energies. However, lacking a theoretical interpretation this relation may be fortuitous.

For energies less than 100 electron-volts the main beam currents become unmanageably small, while above 200 electron-volts the minima are concealed in the steep part of the curve.

That these minima have not been reported before is perhaps due to the high angles at which they occur. In this case the use of high primary currents makes measurements at the higher angles comparatively easy.

The apparatus can also be used to check the scattering at low angles, and the results fit Langmuir's[2] empirical equation very well:

$$f(\theta) = f(\theta)_{\theta=0} \exp(-\theta^2/\theta_0^2).$$

The experimental points found fit best when $\theta_0 = 12.7°$ at 150 electron-volts energy.

Langmuir finds that for Arnot's[3] curve for 82 volt electrons, $\theta_0 = 11.3°$ is the best value.

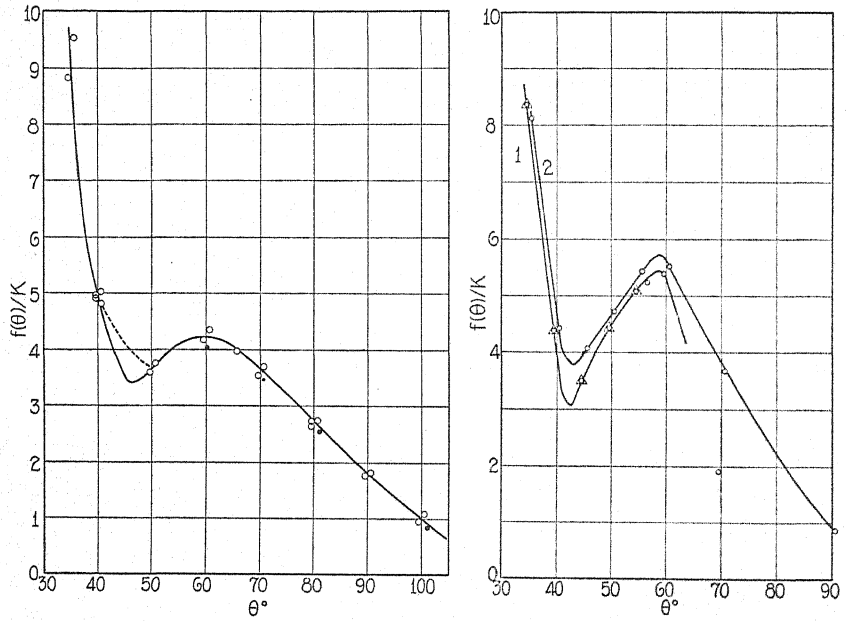

Fig. 7. Scattering curves. Energy 150 volts. *A*, 190 volts; *E*, 150 volts; *M*, 0.006 amp.; *B*, −120, −150 volts. Positive and negative angles read in succession. The solid dots are check points taken later.

Fig. 8. Scattering curves. Energy 175 volts. *A*, 210 volts; *E*, 175 volts; *M*, 0.007 amp.; *B*, −140, −180 volts. Curve 1, negative angles; Curve 2 positive angles taken later. The triangles are check points on negative angles taken two days later.

Some objections to measurements made at small angles can be offered in that the resolving power is somewhat diminished at small angles because of the slit length. Further investigations may justify a correction for this effect.

It is the authors' intention to present these data as being more of a preliminary than of a final nature. Improvements and simplifications which will follow from further work with this type of apparatus, will undoubtedly make for greater precision. At present, the loci of the minima are probably not determined better than ±1.5°.

[2] K. T. Compton, Irving Langmuir, Revs. Mod. Phys. **2**, 123 (1930).
[3] F. L. Arnot, Proc. Roy. Soc. **A125**, 660 (1929).

In conclusion the authors wish to express their appreciation and indebtedness to Dr. R A. Millikan for his continued interest and advice in this work. We should like to thank also the members of the laboratory shops for their care and skill in constructing the apparatus.

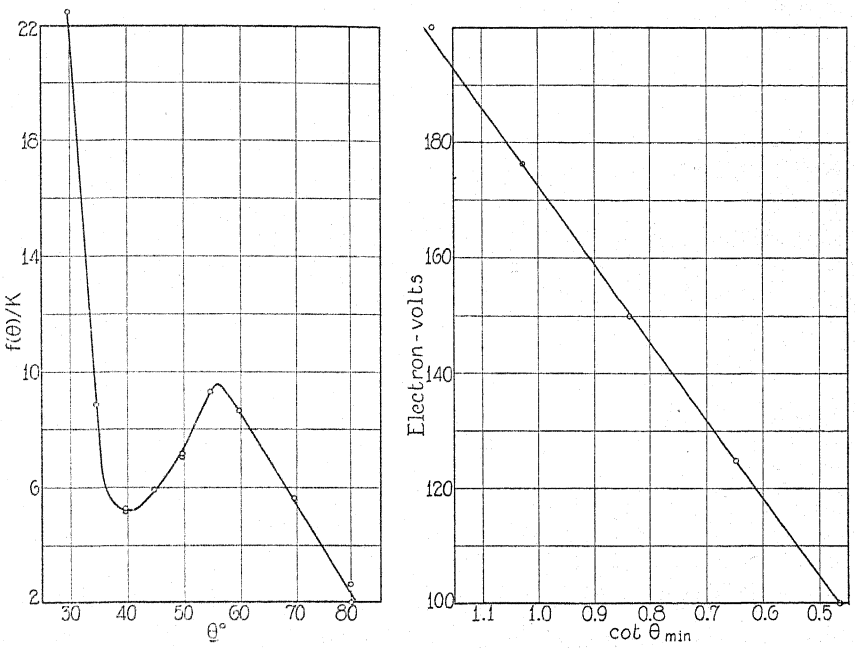

Fig. 9. Scattering curves. Energy 200 volts. A, 258 volts; E, 200 volts; M, 0.006 amp.; B, −160, −200 volts. Readings made at different times with apparatus out of equilibrium in meantime.

Fig. 10. Variation of the cotangent of the angle of minimum scattering with electron energy.

Energy	θ_{min}	Weight
100 volts	65	3
125	57	3
150	50	7
175	44	3
200	40	1

ELECTRONIC VELOCITIES IN THE POSITIVE COLUMN OF HIGH FREQUENCY DISCHARGES

By Egon Hiedemann
Physikalisches Institut
Universität Köln

(Received March 9, 1931)

Abstract

Theoretical discussion of the mechanics of individual electrons in the positive column of high frequency discharges with special consideration of the effect of elastic impacts proves that small mean values of the electric force do not prohibit the production of electrons of sufficient velocity to excite or even ionize gas molecules.

IN A recent paper Charles J. Brasefield[1] has published measurements of the potential drop at the electrodes and the electric force in the positive column of high frequency discharges in mercury, helium, and neon for different gas pressures and frequencies of oscillation. The procedure of measuring the electric force in the positive column was the same as that used by the author.[2] and others in earlier work on high frequency discharges. It consisted in measuring the total voltage between the electrodes for various distances of the electrodes and a given current. The mean electric force of the positive column can then be calculated in the known manner, if one assumes that the drop in potential at the electrodes is, for a given current, independent of the separation of the electrodes.

Discussing his interesting results Brasefield concluded that "these results showed that in general, the magnitude of the electric force was too small to produce electrons whose velocity would be sufficient to ionize or excite the gas." This statement would be of the greatest importance for the theory of the positive column in high frequency discharges if it were the only reasonable inference to be drawn from the experimental results. But an explanation, and a very plausible one, may be obtained by calculations similar to those given by the author for a similar problem in an earlier paper.[3]

In order to look clearly into this matter it is necessary to give the experimental results, the calculations and the proposed solution of the problem in essential detail.

Brasefield, as others, observed that for a given current and a given frequency there exists an optimum pressure at which the conductivity is a maximum. The electric force at this gas pressure and at gas pressures near to it is very small. He then calculates the electric force necessary to give an electron the ionizing velocity in an electric field alternating with high fre-

[1] Charles J. Brasefield, Phys. Rev. **37**, 82 (1931).
[2] E. Hiedemann, Verh. D. Phys. Ges. (3) **7**, 47 (1926); Ann. d. Physik **85**, 649 (1928).
[3] L. Ebeler and E. Hiedemann, Ann. d. Physik (5) **5**, 625 (1930).

quency. His calculation gives values for the necessary minimum electric force, which is much higher than the electric forces measured at or near the maximum of conductivity.

It may be pointed out at first that this calculation is based on the assumption that the electric force in the positive column of the high frequency discharge is the same at any point of the column, which supposition is by no means proved or even probable. But supposing that the above-mentioned procedure of measurement really gives the electric force in the positive column, not merely the mean value of it, a more comprehensive calculation gives a result, which differs slightly but not unimportantly from the result of Brasefield.

If E_0 is the amplitude of the electric force and f the frequency of oscillation, then the following equation is valid:

$$m\ddot{x} = eE_0 \sin 2\pi ft. \tag{1}$$

Integration of Equation (1) gives

$$\dot{x} = -\frac{e}{m}\frac{E_0}{2\pi f}\cos 2\pi ft + C. \tag{2}$$

If at the time zero, the electron has the velocity v_0 in the initial direction of the electric field[4] then

$$C = v_0 + \frac{e}{m}\frac{E_0}{2\pi f}.$$

The velocity of the electron in the direction of the field is then given by Equation (3):[5]

$$\dot{x} = \frac{e}{m}\frac{E_0}{2\pi f}(1 - \cos 2\pi ft) + v_0. \tag{3}$$

The maximum velocity in the direction of the field will be obtained when $t = 1/2f$ and is given by

$$v_{\max} = \frac{e}{m}\frac{E_0}{\pi f} + v_0. \tag{4}$$

[4] By the direction of the electric field that direction is meant, in which the e.m.f. accelerates an electron.

[5] Brasefield gives the equation:

$$\dot{x} = \frac{e}{m}\cdot\frac{E_0}{2\pi f}\cdot[\cos\delta - \cos(2\pi ft + \delta)]$$

where δ is a phase constant depending on the value of E at the instant the velocity of the electrons is zero. Brasefield's equation includes therefore only those electrons which, at the time zero, have no velocity or a velocity contrary to the initial direction of the acceleration and smaller than the maximum velocity obtainable in half a cycle by the acceleration produced by the electric field. Equation (3) on the contrary includes electrons of all directions and velocities.

The total maximum velocity of the electron is the velocity in the resulting direction of the electron. If this direction forms an angle θ with the direction of the electric force, then the total maximum velocity V_{max} will be given by

$$V_{max} = \frac{1}{\cos\theta}\left(\frac{e}{m}\frac{E_0}{\pi f} + v_0\right). \tag{4a}$$

The real velocity V of the electron at any moment is the essential element in all processess of exciting or ionizing gas molecules. For the following discussion, however, it will be sufficient to regard only the velocities in, or contrary to, the direction of the electric field. To simplify matters, Eq. (4) instead of (4a) will therefore be used from now on.

The essential difference between the result of this calculation and that given by Brasefield is that, to the velocity an electron may obtain in half a cycle the velocity of the electron at the beginning of the half cycle must be added, with the right sign of course. To calculate the electric force necessary to give to an electron the ionizing velocity v_i, we must use

$$E_0 = \frac{v_i - v_0}{e} m\pi f. \tag{5}$$

Now the electric forces measured by Brasefield demand —near the maximum of conductivity at least—velocities v_0 which are not small compared with v_i. That means that electrons of nearly sufficient velocity must be present at the beginning of half a cycle. How can such electrons be produced? This can easily be seen, if one remembers that an electron will make elastic impacts with gas molecules before it has obtained the excitation energy.[6] By these elastic impacts it will lose insignificant amounts of energy only, but the direction of its motion will be changed. To simplify the discussion only those impacts will be regarded, for which an electron will after the impact have a component of velocity v' in the direction contrary to that before the impact.

Let us consider now an electron which, at the time zero, has the velocity zero. After half a cycle it will have obtained the velocity v_{max}. Now this electron may have an elastic impact and may immediately after the impact have the velocity v' in the direction contrary to its direction before the impact. As v' is a part of its former velocity, we may define v' by

$$v' = v_{max}/n. \tag{6}$$

The next half cycle will give to this electron the velocity v''

$$v'' = V_{max} + v' = V_{max}(1 + 1/n). \tag{7}$$

[6] Here purposely no correct discrimination is made between the possibility for an electron to get excitation and that to get ionization energy because the difference of these energies is small compared with the difference between one of these energies and the maximum energy obtainable by the e.m.f. in half a cycle. The excitation energy is of primary importance too; especially in those cases in which metastable states are produced and ionization effected by successive impacts.

As this may happen several times and the various n must not be large compared with unity, one easily sees that, as a result of elastic impacts, an electron may obtain a multiple of the maximum velocity obtainable in half a cycle.

This effect of the elastic impacts on the electronic velocities will be efficient especially at gas pressures for which the path of an electron during half a cycle is comparable with the mean free path of the electron. The path of an electron with the velocity v_0 at the time zero between $t=0$ and $t=1/2f$ has been calculated[3] by integration of Equation (3) to be

$$x = \frac{v_0}{2f} + \frac{e}{m}\frac{E_0}{4\pi f^2}. \tag{8}$$

The gas pressures at which x will be comparable with the mean free path of an electron can thus easily be calculated. The result gives pressures of the same order of magnitude as the optimum pressures measured.[7]

From Eq. (8) one sees that Equation (7) is not quite correct, because if an electron of the velocity zero at the time zero has made an impact with a gas molecule after $t=1/2f$ then the electron will after the impact meet a gas molecule before the second half cycle is finished. The velocity of the electron immediately before the second impact will therefore be smaller than $v'+v_{\max}$. A correct equation can be obtained without difficulty, but even without doing so it can easily be seen that matters are much too complicated to allow more than a very rough calculation of the critical order of magnitudes.

In determining the conductivity not only the electrons with excitation or ionization energy are of importance, but the positive ions and the slower electrons too. In an earlier work A. v. Hippel[8] has shown that the energy which positive ions may periodically acquire in the alternating electric field of a high frequency discharge, is to be neglected compared with the ionizing energy. He has also directed attention to the fact that positive ions oscillate with only very small amplitudes, which at the optimum pressures measured by Brasefield may be neglected in comparison with the mean free path. This means that, if positive ions have once been produced, the chance of their getting lost from the discharge is relatively small when no static electric field is present. A small loss of ions on the other hand means a high degree of ionization and a high conductivity. The degree of ionization is limited by recombination and molecular diffusion to the glass walls and to a large extent probably by the static field due to the potential of the glass walls. By elastic impacts electrons will not only get a component of velocity parallel to the direction of the alternating electric force but also normal to it. As this velocity will not be altered by the electric force and as the mobility of the electrons is large a steady current of electrons should be directed to the glass walls and produce there a negative charge. A short time after the beginning of the discharge a stationary state will be reached and a static electric force will be produced.

[7] See also Charles J. Brasefield, Phys. Rev. 35, 1073 (1930).
[8] A. v. Hippel, Ann. d. Phys. (4) 87, 1035 (1928).

This static field will enlarge the loss of positive ions and produce a deformation of the electric field of the alternating e.m.f. Hence the supposition that the electric force in the positive column is the same at any point of the column cannot be right and any calculation based on this assumption will not give correct, but at the best only approximate results. This is another reason that the small measured mean values of the electric force in the positive column do not call for the conclusion that electrons of excitation energy cannot be produced in the high frequency discharge at the maximum of conductivity.

Another important factor in the conductivity is introduced by the oscillation of the slower electrons in the alternating electric field. Their importance for the mechanism of the high frequency discharge at low pressures was pointed out first by F. Kirchner.[9] The motion of these oscillating electrons is given by[5]

$$m\ddot{x} = eE_0 \cos 2\pi ft \tag{9}$$

and the path in a quarter of a cycle; i.e., the amplitude of oscillation; is given by

$$x' = \frac{e}{m} \frac{E_0}{4\pi^2 f^2}. \tag{10}$$

By comparison of Eq. (10) with Eq. (8) it can be seen that the optimum pressure for the oscillating electrons has not quite the same value as for the non-oscillating electrons, but that it is of the same order of magnitude. The importance of the oscillating electrons for the conductivity of the discharge lies, as is known, in the fact, pointed out by Kirchner, that by oscillating in the field these electrons will remain in the discharge.

Those electrons which at the time zero have no velocity or a velocity in the direction of their acceleration in the initial half cycle, will not oscillate in the discharge, but go in one direction only (of course without taking account of the effect of impacts). During half a cycle, they will be accelerated, during the next half they will be retarded by the alternating e.m.f. but they will always go forward. At very low pressures, where the mean free path of the electrons cannot be neglected compared with the separation of the electrodes, such non-oscillating electrons produced near the electrodes may thus reach the positive column and their part in the excitation or ionizing processes in the positive column may perhaps not be neglected.

In conclusion it may be said, that the surprisingly small mean values of the electric force measured in the positive column of high frequency discharges near the maximum of conductivity do not at all force one to assume that electrons of excitation energy cannot be produced in the positive column of these discharges.

[9] F. Kirchner, Ann. d. Physik (4) 77, 287 (1925).

THE ELECTRICAL STATE OF THE SUN

By Ross Gunn
Naval Research Laboratory, Washington, D.C.

(Received March 13, 1931)

Abstract

The magnetic field due to the rotation of our galaxy is calculated, and it is shown (a) that electricity cannot be annihilated in the sun or stars; (b) that the net electrical charge on the sun or a typical star cannot exceed 1 coulomb. The electric fields, space charge and potentials of the solar atmosphere are calculated from data relating to the solar anomalous rotation and numerical values given. The negative surface charge on the sun is calculated to be of the order of 10^9 e.m.u. The problem of the maintenance of the solar electric field is touched upon.

SYSTEMATIC observation of the solar surface by Mount Wilson astronomers and others has shown that many solar phenomena are of such a nature that they can be attributed to electrical and magnetic effects. The magnitude and distribution of the solar magnetic field has been determined by a laborious analysis of Zeeman spectra[1] and sufficient data accumulated to show that the solar magnetic field is not unlike that of the earth, save for its radial limitation. In 1915 an attempt was also made by Hale and Babcock[2] to determine the electric fields by measurements of the Stark effect but they could not detect fields smaller than 100 volts per centimeter and were only able to set an upper limit to the suspected electric field. Investigators have generally stated that the electrical fields in the emitting layers of the sun were negligibly small due to the high electrical conductivity and important effects arising from such electric fields were therefore absent. In the following discussion we shall endeavor to indicate the importance of the electric field and give numerical values for the electrical constants of the sun, insofar as they apply to obvious solar problems.

Separation of Charge Inside the Sun

In an important paper A. Pannekoek[3] noted that in any highly ionized gaseous region acted on by gravitational forces and in thermal equilibrium, the lighter ions diffused upward until their separation produced an electric field which opposed further separation. It is readily shown that the volume charge ρ_g expressed in e.m.u., resulting from the separation, is given by

$$\rho_g = \gamma d\mu/c^2 e \qquad (1)$$

where γ is the gravitational constant, d is the density of the ionized matter,

[1] Hale, Astrophys. Jour. **38**, 31(1913); Hale, Seares, Van Maanen and Ellerman, Astrophys. Jour. **47**, 1 (1918).

[2] Hale and Babcock, Proc. Nat. Acad. **1**, 123 (1915).

[3] A. Pannekoek, Bull. Astro. Inst. Netherlands #19 (1922).

μ the mean mass of the molecules, c the velocity of light, and e the electronic charge expressed in *e.m.u.* Using data appropriate to the sun and Eq. (1) we find that the total positive volume charge inside the sun amounts to 33 e.m.u. or 330 coulombs. In another place we shall show that a negative charge of equal magnitude probably resides on the solar surface.

When the temperature is non-uniform the more mobile ions in a conductor diffuse toward cooler regions and in the equilibrium state, an electrical field is set up which prevents further diffusion. The space charge ρ_i existing when equilibrium has been attained is given (in the one dimensional case) by

$$\rho_i = -\frac{k}{8\pi c^2 e}\frac{d^2T}{dr^2} \tag{2}$$

where k is the Boltzmann constant, r the space coordinate and T the absolute temperature. Application to the interior of the sun at the present time will not be attempted for little is known about the internal solar temperature. If we follow the star models considered by Eddington[4] the temperatures are so related to gravitational forces that the space charge due to non-uniform temperatures will be of the same order of magnitude as the space charge due to gravitational forces. If, on the other hand, we should adopt Milne's[5] star model which suggests central temperatures of the order of 10^{11} degrees, it is evident that the interior space charge is likely to be large.

Annihilation of Electricity

Attempts to account for the earth's atmospheric electric current have led several writers to assume that electricity is annihilated at some definite but slow rate. Simpson[6] suggested that electricity might be generated spontaneously while Swann[7] assumed that positive electricity died constantly inside the earth but neither writer suggested where the required energy for the transformation might originate. Anderson[8] supplied the theoretical deficiency and assumed that the loss of the protonic mass supplied the necessary energy to annihilate the protonic charge. Thus he postulated a subatomic transformation in which the mass of one proton vanished for each protonic charge annihilated. Evidently if the energy corresponding to a given transformation is known then the lost mass and electrical charge can be immediately calculated. Anderson's calculations indicated that the sun was throwing off negative electricity at a rate of 4×10^{16} e.m.u. per second. This tremendous negative charge was assumed to dissipate itself through all space and finally be lost. In many respects Anderson's hypothesis is interesting in spite of the objections which will occur to the atomic physicist. We proceed to show, however, that in stars the annihilation of electricity is not probable unless the released ions leave our universe in a highly specialized and improbable manner.

[4] Eddington, Internal Constitution of the Stars (1926).
[5] E. A. Milne, Monthly Notices **91**, 4 (1930).
[6] C. G. Simpson, Monthly Weather Rev. **44**, 121 (1916).
[7] Swann, Jour. Franklin Inst. **201**, 143 (1926).
[8] W. Anderson, Zeits. f. Physik **42**, 475 (1927).

The system of stars embraced by the Milky Way stretches far out into space and forms our galactic system. The motions of the stars in this system, their masses, radiation, numbers and distribution are known and if electrical charges are constantly given off by each member of the galactic system, observable magnetic effects should be measured on the earth. We will assume that when ions are thrown off by a star the ion preserves its angular momentum about the gravitational center of the galaxy as it finds its way to outer space. Thus the systematic motion of the stars about the center of the galactic system is shared by the electricity which has been thrown off by them.

The systematic motion constitutes an electrical convention current and will produce a magnetic field. In the present connection we need only the order of magnitude of the effect and a rough calculation which directs attention to the physics of the problem will readily serve. Let us suppose that the entire negative charge in the space outside the stars but inside the galaxy, is compressed into a ring of radius equal to the mean radius of the system. Then the magnetic field H at the center of the system is

$$H = 2\pi Q\omega \tag{3}$$

where Q is the total free charge and ω is the mean angular velocity about the center of the system. The earth is not at the center of the system but it is difficult to see how its position and motion could change the value of the magnetic field at the earth by more than an order of magnitude.

The angular motion of our galaxy is known from astronomical data and Q is determined by calculating from the total radiation of the galactic system, the rate of release of negative electricity. We must note further that the time the released electricity remains in the system proper must be at least as great as the time it would take light to traverse the path. Thus

$$Q \geqq Ir/c \tag{4}$$

where I is the total current thrown off by all stars of the galaxy as calculated by Anderson's hypothesis, r is the mean radius of the galactic system and c the velocity of light. The mean star of the galaxy has a mass 1.6 that of the sun and there are roughly 10^{10} of them,[9] so that we may assume that the total current I of the system is 10^{10} that of the sun or 10^{26} e.m.u.[10] Taking $r = 10^3$ parsecs, $\omega = 10^{-13}$ rad/sec and combining Eq. (4) with Eq. (3) we find that the magnetic field at the center of the galaxy is of the order of 10^{25} gauss.

Such a large magnetic field seems absurd and we conclude that observation demands either that the charges which leave a star, leave in a very special manner, or else that annihilation of positive charge in stars does not occur. The evidence is such that we believe Anderson's and other similar hypotheses must be abandoned.

Net Solar Charge

An upper limit may be set for the net charge which the sun may carry if we are willing to assume that the sun is a star typical of the average star of

[9] Russell, Dugan and Stewart, Astronomy (1927).
[10] R. Gunn, Phys. Rev. **32**, 133 (1928).

our galaxy. Magneticians have been collecting precise data on the variations of terrestrial magnetism for a great many years but there is no evidence of which we are aware that suggests that there may be an extra-terrestrial magnetic field which would be observed to have a period of a siderial day. Certainly such a field would have been found if it was as great as 10^{-3} gauss and probably a field much smaller would be noticed. We may then assume that if a galactic magnetic field exists its value H is probably less than 10^{-3} gauss.

If the stars of our galaxy (of which the sun is typical) carry free electrical charges, then certainly their ordered motion in our galaxy will give rise to a magnetic field. In Eq. (3) we substitute for Q the product of the total number of stars n, by q the mean charge on each, and write the inequality

$$q \leqq H/2\pi\omega n. \tag{5}$$

Substituting the appropriate numerical values in Eq. (5) we find that the mean charge on each star of our galaxy cannot be greater than 0.1 e.m.u. or one coulomb. In the present case there is no question regarding the motion of the charges for they are attached to the stars. When we reflect that the total surface charge of the earth is of the order 10^5 coulombs we see that stars are neutral to a high degree of approximation. We note in passing that measurements show the earth is probably neutral as a whole. These considerations lead us to assume that the sun as a whole is electrically neutral.

Solar Atmospheric Electricity

The highly ionized regions of the solar surface which can be observed are known to be regions of low pressure and the ion free paths are therefore very long. An early paper[11] showed that when ions execute long free paths in crossed electric and magnetic fields, ions of both kinds were swept in a direction perpendicular to both the electric and magnetic fields with a velocity which depended only on the relative magnitude of the crossed fields. This effect is of the nature of a mass motion and is of great importance because it connects directly the easily observable mechanical motions of an ionized region with the magnitudes of the impressed electric and magnetic fields. In a series of papers[11] the above electromechanical effect was shown to account quantitatively for the observed anomalous solar rotation, if the sun possessed an atmospheric electric field which was strikingly similar to the field observed on the earth.

The superposed drift velocity $\boldsymbol{u}$ of an ionized atmosphere is given by

$$\boldsymbol{u} = \frac{\boldsymbol{E} \times \boldsymbol{B}}{B^2[1 + (R/\lambda)^2]} \tag{6}$$

where $\boldsymbol{E}$ and $\boldsymbol{B}$ are the electric and magnetic fields respectively, R the radius of the spiral generated by an ion as it is constrained to move about the impressed magnetic fields and λ is the mean free path. We calculate R from

[11] R. Gunn, Phys. Rev. **35**, 635 (1930); **36**, 1251 (1930); **37**, 283 (1931).

$$R = \frac{mv^1}{Be} = \frac{(2mkT)^{1/2}}{Be} \tag{7}$$

where m is the mass of the ion, v^1 the component of its velocity perpendicular to the magnetic field B, and e the ionic charge in e.m.u. In the atmospheric levels of the sun which we can see, λ is large compared to R and if we agree for simplicity to consider only the motions at the solar equator, Eq. (6) takes the simpler scalar form.

$$E = Bu \tag{8}$$

where E is now the radially inward electric field, B the northward magnetic field and u the eastward atmospheric ion drift measured with reference to the surface of the sun proper. The eastward superposed drift u is readily determined from

$$u = u_0 - a\omega \sin \phi \tag{9}$$

where u_0 is the measured velocity of the observed point whose colatitude is ϕ, a is the solar radius and ω is the angular velocity calculated from the rotation of the sun's magnetic pole. The magnetic field B can be measured directly by the Zeeman effect, so that E can always be calculated for all observed levels. The drift velocity u is known to change with altitude, solar activity and to be subject to large local fluctuations. As we have seen elsewhere[11] the fluctuations are probably due to variations in E rather than B.

In a typical region of the reversing layer the magnetic field is observed to be 25 gauss and the difference of velocity of the surface proper and that actually measured or u is 5×10^4 cm/sec. By aid of Eq. (8) we find the electric field in this region is 0.013 volts/cm. Similarly where the magnetic field is 55 gauss the electric field is 0.027 volts/cm. Now the difference in altitude between these two points is roughly 8×10^6 cm, according to Mt. Wilson data, and we can estimate the volume charge by a one dimensional Poisson's equation. Thus

$$\rho_a = -\frac{u}{4\pi c^2}\frac{dB}{dr} \tag{10}$$

where ρ_a is the atmospheric volume charge in e.m.u. and the other quantities are those defined before. From Eq. (10) and the foregoing observational data we find that over a small interval the space charge in the solar reversing layer is $+1.66\times10^{-23}$ e.m.u./cm^3 or on the average there is one singly charged free positive ion per liter.

The space charge increases rapidly as we go deeper and deeper into the sun and if the magnetic field and drift velocity were known at all levels the surface charge and total atmospheric charge could be determined. The solar astronomical data giving the intensity of the magnetic field as a function of the altitude are not very reliable on account of the difficulties of measurement and there is even sharp disagreement as to the scale of altitudes in the reversing layer. In an earlier paper[11] a semi-empirical relation was employed to

represent the magnetic field as a function of altitude and the constants so chosen as to fit observation over a limited range. Precise analysis requires appeal to direct observational data for it is unlikely that the radial distribution of the magnetic field is as simple as our assumed formula indicates. We will assume that the magnetic field at any level in the solar atmosphere is given[11] approximately by

$$B = B_0 \exp\left[-\frac{zHg(r-a)}{2kT}\right] \tag{11}$$

where B_0 is the magnetic field of the sun at the "surface proper," z the mean atomic weight of the atmospheric ions, g the acceleration due to gravity, H the mass of the hydrogen atom and $(r-a)$ the altitude above the sun. Relation (10) becomes by aid of Eq. (11)

$$\rho_a = \frac{uzHgB}{8\pi c^2 kT} \tag{12}$$

so that the total atmospheric volume charge in a prism 1 cm^2 in cross-section is given by

$$\int_a^\infty \rho_a dr = uB_0/4\pi c^2 \tag{13}$$

and since on the whole the sun is neutral and there is no external electric field it follows that the surface charge on the sun proper is equal and opposite to the positive space charge. Following earlier work[12] we use 12,000 gauss for B_0 and calculate the total positive charge in a prism 1 cm^2 extending from the sun outward and get $+5.3\times10^{-14}$ e.m.u. The surface charge is equal and opposite. The total negative surface charge of the sun is therefore 3×10^9 e.m.u.

We can use Eq. (11) to determine the potential difference between the surface proper and free space if we combine it with Eq. (8) and integrate.[11] Let ϕ_1 be the potential difference, then

$$-\phi_1 = \int_a^\infty E dr = u\int_a^\infty B dr \tag{14}$$

which by aid of Eq. (10) becomes

$$\phi_1 = \frac{2uB_1kT}{zHg} \tag{15}$$

where B_1 corresponds to a level where the atmospheric electrical conductivity begins to drop off rapidly due to the solar magnetic field[11,12] and it amounts to about 280 gauss.[11] Substitution of the approximate values in Eq. (15) shows that the sun proper is negative with respect to free space by 1.5×10^6 volts. The foregoing values, calculated by aid of semi-empirical formula cannot be expected to be precise for we have made the assumption that the equatorial

[12] R. Gunn, Phys. Rev. **33**, 614 (1929); **34**, 1621 (1929).

drift velocity was the same constant at all altitudes. In the region of the reversing layer where the constants were made to fit the known points the equations are more reliable.

Maintenance of the Solar Electric Field

The electrical conductivity of the solar atmosphere is high even in the reversing layer where the magnetic field greatly reduces the mobility of the ions.[10] It is readily shown that the solar atmosphere would discharge itself in 10^{-10} seconds if no mechanism was provided to maintain the current. We are therefore faced with precisely the same problem that has puzzled physicists for years in connection with the earth's electric charge. As in the case of the earth we may now assert that the sun is neutral to a high degree of approximation and we may further maintain that electricity does not continuously leave the sun. These restrictions narrow down the investigation to fairly definite problems and several have been examined keeping always in mind that the mechanism of replenishment should also be capable of modification to fit the earth. Even though the mechanism in the sun must be quite simple compared to that on the earth, no definite conclusion has been reached. The extreme variability of the electric field as indicated by the atmospheric motions suggest that local conditions may affect the field greatly somewhat in the manner that an electrical storm disturbs the earth's local electrical state. Young[13] had the idea long ago that the solar atmosphere "rained" condensed metallic particles and brought charges down with them. While the idea is tempting because of present ideas regarding the maintenance of the earth's charge it has several weak points and cannot be made quantitative. It has been shown[11] that the electrical energy dissipated in the solar atmosphere is an appreciable fraction of the total radiated energy and any mechanism which will account for the field must be a moderately efficient one.

Conclusion

Our study has shown that the rather artificial postulate of the annihilation of charge is inconsistent with observation and that to a high degree of approximation the sun is electrically neutral. Our calculations show that the separation of charge in the solar atmosphere is considerable and that the resulting distribution of electric field is remarkably similar to that observed on the earth. In a typical equatorial region of the reversing layer the electric field is radially inward and amounts to 0.015 volts/cm, a value far too small to be detected by measurements of the Stark effect. In the present paper the fields have been calculated from data derived from the observed solar atmospheric motions. In a forthcoming paper the electric fields will be calculated from certain spectroscopic data and the values obtained shown to be consistent with the present estimates.

[13] Young, The Sun.

SURFACE TENSION OF MERCURY

By Marie Kernaghan, R.S.C.J.
Department of Physics, The Saint Louis University

(Received March 9, 1931)

Abstract

Consistent values for the surface tension of mercury in a high vacuum (air pressure less than 1.2×10^{-5} mm Hg throughout the period of experimentation), ranging from 438.4 ± 0.3 dynes per cm at 12.5°C to 423.9 ± 0.6 dynes per cm at 67°C, have been found by a modified flat-drop method. In evaluating them Worthington's equation

$$\sigma=\frac{(K-k)^2\rho}{2}\cdot\frac{1.641\,L}{1.641\,L+(K-k)}$$

was used. The temperature gradient, determined from the best mean straight line through the experimental points, is 0.3015 dyne per cm per degree. Hence the average value of k, in the E tv"s relation, was found to be 1.82. Reproduction of concordant results at intervals during a period of four months affords ample evidence of the thorough outgassing of the apparatus and is attributed to the great care used in securing relative perfection of details.

Introduction

WITHIN the last decade many publications (between one and two on an annual average) have been concerned with the surface tension of mercury[1–21] and the greater number have dealt with its measurement in a vacuum. Hogness[9] and later Bircumshaw[2] have given excellent summaries of

[1] L. L. Bircumshaw, Phil. Mag. **2**, 341–350 (1926).
[2] L. L. Bircumshaw, Phil. Mag. **6**, 510–525 (1928).
[3] R. C. Brown, Phil. Mag. **6**, 1044–1055 (1928).
[4] R. S. Burdon and M. L. Oliphant, Trans. Faraday Soc. **23**, 205–213 (1927).
[5] S. G. Cook, Phys. Rev. **34**, 513–520 (1929).
[6] W. D. Harkins and E. H. Grafton, J. Am. Chem. Soc. **42**, 2534–2538 (1920).
[7] W. D. Harkins and W. W. Ewing, J. Am. Chem. Soc. **42**, 2539–2547 (1920).
[8] J. Hartman, Phys. Rev. **20**, 728–744 (1922).
[9] T. R. Hogness, J. Am. Chem. Soc. **43**, II, 1621–1628 (1921).
[10] T. Iredale, Phil. Mag. **45**, 1088–1100 (1923).
[11] T. Iredale, Phil. Mag. **48**, 177–193 (1924).
[12] T. Iredale, Phil. Mag. **49**, 603–627 (1925).
[13] M. L. Oliphant, Phil. Mag. **6**, 422–433 (1928).
[14] E. Perucca, Atti. Acc. Torino **57**, 81 (1921).
[15] E. Perucca, Atti. Acc. Torino **57**, 541 (1922).
[16] E. Perucca, Phil. Mag. **7**, 418–419 (1929).
[17] M. J. Popesco, Comptes Rendus **172**, 1474–1476 (1921).
[18] M. J. Popesco, Comptes Rendus **175**, 148–149 (1922).
[19] M. J. Popesco, Ann. de Physique **3**, 402–464 (1925).
[20] T. W. Richards and S. Boyer, J. Am. Chem. Soc. **43**, I, 274–294 (1921).
[21] Sauerwald and Drath, Zeits. Anorg. Chem. **154**, 79 (1926).

the work done in that line since 1898. Hence another summary just now is unnecessary. Suffice it to say that in spite of the great variety of methods painstakingly tried by eminent experimenters, the final results continue to be discordant even in single experiments, the values obtained ranging from "340 to 575 dynes per cm."[9] The true value of the surface tension of mercury cannot be as erratic as the above quoted discordant values would make it. Since the modified flat-drop method, used in finding the surface tension of sodium in a vacuum,[22] gave perfectly consistent results, it was decided to try it out on mercury. Some of its marked advantages are: a high degree of accuracy, perfect control of temperature conditions, facility in the production of fresh and uncontaminated surfaces, possibility of maintaining a high vacuum during a long interval of time, and independence of the contact angle.

Apparatus

The apparatus (Fig. 1) though similar in general outline to that used in the experiment on sodium,[22] differed in several details. The chief difference lay in the shape and size of the surface tension chamber *C* (Fig. 1). It was

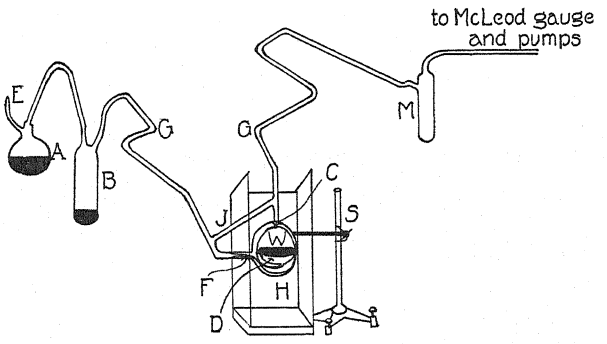

Fig. 1. Diagram of apparatus.

arranged in a horizontal position and though shorter it was wider and more roomy than the first. The plane circular glass window *W* (made to order by the Corning Glass Company) was fused into the end of the tube in preference to the side, in such a way as to render the entire disk optically available. The shallow cup *D* in which the flat drop of mercury was formed was ground with fine emery until all clip scars had disappeared. While similar in general appearance to the cup used for sodium it was wider (average outer diameter 6.04 cm) and deeper (maximum depth 1.2 cm). The difference existing between the various diameters was not more than 0.02 cm. As in the case of sodium, the mercury was introduced into the cup by means of a thick-walled capillary tube *F* which served to prevent too rapid introduction and consequent surging back and forth of the liquid. The tube *J* necessary for outgassing purposes prevented an accumulation of pressure behind the cup. To

[22] F. E. Poindexter and M. Kernaghan, Phys. Rev. **33**, 837–843 (1929).

procure a fine levelling adjustment at any time during the course of the experiment the cup chamber was tightly clamped and exteriorly cemented to a levelling stand S; and coiled tubes G one on either side of C were inserted into the apparatus. The presence of the flask M was merely an added precaution against contamination resulting from any possible overflow of mercury from the McLeod gauge. The entire piece of apparatus, including the McLeod gauge, was constructed of Pyrex glass, having only glass seals throughout.

Redistilled mercury was well shaken with chromic acid solution and then thoroughly rinsed with distilled water. It was next distilled in a current of air, then in a vacuum. This whole process was gone through twice before admitting it into the flask A. After sealing off E and thoroughly outgassing the apparatus the mercury was carefully distilled in a vacuum with a hand burner into the reservoir B from which it was distilled into the cup D as needed. The surface tension chamber was sufficiently roomy to allow the cup to be emptied and refilled without disturbing the apparatus.

The heater of the sodium experiment,[22] adjusted to suit the modification of the cup chamber, was used, hence the temperature conditions were those of the former experiment and hence within one degree of correct values. A frosted glass window arranged in the back panel of the heater made it possible to illuminate the drop from without and thereby get a sharp focus along the meniscus. Once this arrangement was perfected there was no difficulty in determining the exact top of the drop.

The combination of travelling microscope and dividing engine, used as a measuring device in the sodium experiment, was again employed. But instead of locating a number of points on the meniscus of the drop and then graphing the curve, it was decided to use a small carbon filament lamp for locating the top of the meniscus. It was mounted in a manner similar to that described by Richards and Boyer[20] and used by Iredale,[12] Cook,[5] and others. The small lighted lamp, attached to the telescope some distance behind it and on a level with it, was reflected from a spot on the maximum horizontal diameter as a tiny star which could be brought easily to a focus on the cross hairs. The vertical distance from the maximum horizontal diameter to the top of the drop ($K-k$ in Table I) could then be found by direct measurement. The diameter of the drop was measured directly by means of the dividing engine.

Data and Results

A summary of the results obtained from readings taken at intervals during a period of more than four months is given in Table I. The temperatures below 41° (second column) were room temperature in degrees centigrade. The number of separate readings of K (the top of the drop) and of k (the location of the star), from which $K-k$ was in each case determined, may be found in the third column. The values for the density quoted in column 4 have been taken from the Smithsonian Physical Tables.[23] For each set of

[23] Smithsonian Tables, Handbook of Chemistry and Physics, Thirteenth Edition, p. 746 (1928).

TABLE I. *Surface tension of mercury in a vacuum.*

No.	Temp. C	No. of Trials	Density ρ	Radius L cm	K-k cm	Uncorrected σ dynes	Corrected σ dynes	Date
1	12.5°	11	13.5646	2.87	0.2639	462.9±0.3	438.4±0.3	Nov. 26, 1930
2	14.°	20	13.5610	2.87	0.2638	462.4±0.3	437.9±0.3	Nov. 28, 1930
3	18.3°	15	13.5504	2.87	0.2635	461.0±0.3	436.6±0.3	Nov. 26, 1930
4	20.°	9	13.5462	2.87	0.2634	460.5±0.3	436.1±0.3	Nov. 28, 1930
5	21.°	9	13.5438	2.87	0.2633	460.1±0.3	435.7±0.3	Nov. 29, 1930
6	21.5°	15	13.5425	2.87	0.2633	460.0±0.3	435.7±0.3	Nov. 30, 1930
7	22.5°	15	13.5400	2.92	0.2632	459.6±0.2	435.7±0.2	Nov. 2, 1930
8	23.1°	13	13.5389	2.87	0.2630	458.9±0.3	434.6±0.3	Nov. 30, 1930
9	23.5°	11	13.5377	2.87	0.2629	458.5±0.3	434.2±0.3	Nov. 27, 1930
10	23.5°	10	13.5377	2.87	0.2630	458.8±0.6	434.5±0.6	Nov. 30, 1930
11	24.°	10	13.5364	2.87	0.2628	458.1±0.3	433.8±0.3	Nov. 27, 1930
12	25.1°	9	13.5337	2.91	0.2631	459.05±0.2	435.1±0.2	Oct. 12, 1930
13	25.2°	9	13.5335	2.92	0.2631	459.03±0.2	435.1±0.2	Oct. 11, 1930
14	25.8°	9	13.5320	2.91	0.2632	459.3±0.2	435.4±0.2	Oct. 11, 1930
15	26°	8	13.5315	2.84	0.2630	458.6±0.3	434.3±0.3	Sept. 25, 1930
16	28°	10	13.5266	2.84	0.2628	457.8±0.3	433.5±0.3	Sept. 25, 1930
17	31°	11	13.5193	2.89	0.2624	456.1±0.3	432.2±0.3	July 31, 1930
18	31°	12	13.5193	2.89	0.2624	456.1±0.3	432.2±0.3	Aug. 1, 1930
19	32.3°	10	13.5161	2.86	0.2624	456.0±0.3	431.9±0.3	July 29, 1930
20	32.3°	24	13.5161	2.86	0.2624	456.0±0.3	431.9±0.3	July 29, 1930
21	33°	9	13.5144	2.89	0.2624	455.95±0.3	432.1±0.3	July 30, 1930
22	33.3°	12	13.5136	2.85	0.2623	455.6±0.3	431.5±0.3	Aug. 5, 1930
23	34°	10	13.5119	2.91	0.2622	455.2±0.3	431.5±0.3	July 27, 1930
24	34.8°	10	13.5100	2.85	0.2622	455.1±0.2	431.0±0.2	Aug. 6, 1930
25	35°	10	13.5095	2.91	0.2621	454.8±0.2	431.1±0.2	July 26, 1930
26	35°	10	13.5095	2.91	0.2622	455.1±0.3	431.4±0.3	July 27, 1930
27	35°	9	13.5095	2.85	0.2621	454.8±0.3	430.7±0.3	Aug. 4, 1930
28	41°	12	13.4949	2.91	0.2619	453.6±0.2	429.9±0.2	Aug. 1, 1930
29	43°	8	13.4900	2.87	0.2618	453.1±0.3	429.0±0.3	Nov. 30, 1930
30	44°	9	13.4875	2.87	0.2617	452.6±0.3	428.6±0.3	Nov. 30, 1930
31	47.5°	7	13.4790	2.85	0.2616	452.0±0.3	428.1±0.3	Aug. 2, 1930
32	48°	13	13.4778	2.92	0.2615	451.6±0.3	428.1±0.3	July 27, 1930
33	48°	11	13.4778	2.92	0.2616	451.96±0.3	428.4±0.3	Aug. 1, 1930
34	48°	9	13.4778	2.85	0.2615	451.6±0.3	427.7±0.3	Aug. 5, 1930
35	49.5°	10	13.4741	2.85	0.2614	451.2±0.3	427.2±0.3	Aug. 6, 1930
36	54°	10	13.4632	2.85	0.2613	450.4±0.3	426.5±0.3	Aug. 2, 1930
37	57.5°	11	13.4547	2.85	0.2612	449.8±0.4	425.9±0.4	Aug. 6, 1930
38	64°	9	13.4389	2.85	0.2609	448.2±0.5	424.5±0.5	Aug. 2, 1930
39	67°	10	13.4317	2.84	0.2608	447.7±0.6	423.9±0.6	Aug. 2, 1930

readings two values for the surface tension are given. That under uncorrected value (seventh column) was found by means of Quincke's simple formula[24]

$$\sigma = \tfrac{1}{2}h^2\rho \cdot 980 \qquad (1)$$

(where σ and ρ are surface tension and density respectively; 980 cm per sec^2 is the value of the acceleration of gravity in Saint Louis.) The corrected values of σ (eighth column) were determined according to Worthington's equaton[25]

$$\sigma = \frac{(K-k)^2\rho}{2} + 2\sigma(K-k)\left\{\frac{1}{b} - \frac{1}{3.282L}\right\} \qquad (2)$$

[24] G. Quincke, Ann. d. Physik, **105**, 1–48 (1858); **139**, 1–89 (1870); **160**, 337–374 (1877).
[25] A. M. Worthington, Phil. Mag. **20**, 51–66 (1885).

(where $(K-k)=h=$distance from vertex to maximum horizontal diameter; $b=$radius of curvature at the vertex and $L=$maximum horizontal radius).

According to Worthington[25] for values of L greater than 2 cm the term $1/b$ is negligible. Therefore since in this experiment the minimum value of L was 2.84 cm it was at all times sufficiently large to justify the omission of $1/b$ from the equation, which consequently reduces to the form

$$\sigma = \frac{(K-k)^2\rho}{2} \cdot \frac{1.641L}{1.641L + (K-k)} \times 980. \qquad (3)$$

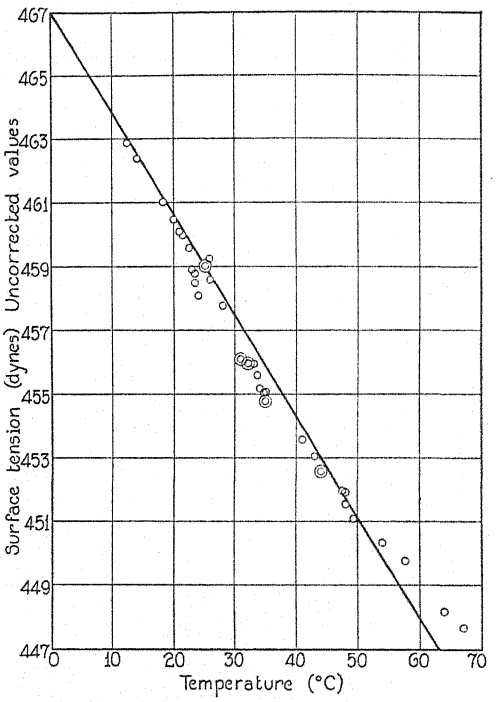

Fig. 2. Surface tension of mercury as function of temperature.

Hence to correct values computed from equation (1) we have only to multiply the result obtained by the correction factor

$$\left(1 + \frac{K-k}{1.641L}\right)^{-1}$$

Since there was scarcely any appreciable variation in the size of the drops used, the correction factor reduced to either 1/1.055 or 1/1.056.

From the two surface-tension, temperature graphs (Figs. 2 and 3) it is evident that temperature variations gradually decrease as temperature increases. However, for values of T lower than 65°C the deviation of experimental points from a straight line is slight. Hence from the best mean straight line through the experimental points (Fig. 3) σ at 0° and at 63° was

judged to be 442 and 423 dynes per cm, respectively. Hence the temperature gradient is 0.3015 dyne per cm per degree.

Upon differentiating with respect to temperature, the Eötvös relation $\sigma v^{2/3} = k(T_c - T)$ we get,

$$v^{2/3}\left(\frac{d\sigma}{dT}\right)_v + \frac{2}{3}\sigma v^{-1/3}\left(\frac{dv}{dT}\right)_\sigma = -k \tag{4}$$

(σ, v, T represent surface tension, volume of a gram atom, temperature respectively. T_c and k are constants.)

The Eötvös constant, k, was found at 20°C by substituting in Eq. (4) for $(d\sigma/dT)_v$ and for σ experimental values, and for v and $(dv/dT)_\sigma$ values

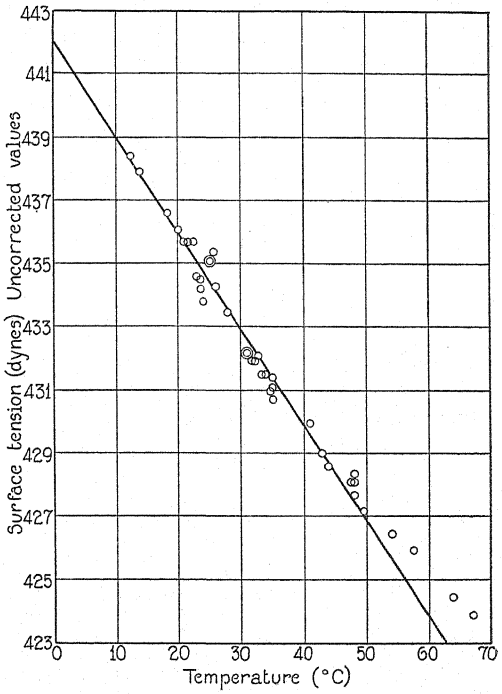

Fig. 3. Surface tension of mercury as function of temperature.

calculated from data given in the Smithsonian Physical Tables, as quoted in the thirteenth edition of Handbook of Chemistry and Physics.[23] The value found is 1.82.

Discussion

Every possible precaution was taken to procure absolute cleanliness. Boiling hot chromic acid solution was used to cleanse not only the entire glass apparatus (including the still used for distilling the mercury in a current of air), but also the beakers and the bottles into which the mercury was poured at any stage of experimentation. Several consecutive days were devoted to a thorough outgassing of the apparatus. During periods of four or

five hours each, while the pump was running, the entire apparatus was kept at a high temperature by means of the heater and a hand burner. The thoroughness of the process was proven by the fact that the McLeod gauge registered stiction (a gas pressure less than 1.2×10^{-5} mm Hg) except when filtered air was purposely admitted into the apparatus. Occasionally over night the pressure rose to 4.6×10^{-5} mm Hg, but then the apparatus was again outgassed. No readings were recorded except when the McLeod gauge registered stiction.

The main purpose of this experiment was to get consistent values for the surface tension of mercury in a vacuum hence no perfection of detail that might lead to a higher order of accuracy was overlooked. To eliminate vibration of the mercury drop a special wall table was constructed. The difficulty experienced by Cook[5] in determining the exact position of K (the top of the drop) was obviated by keeping the drop enclosed in the heater, even when working at room temperature, and by illuminating it from without. As previously mentioned, for all readings recorded the top showed as a sharp dark line. The small lamp used for determining the point of vertical tangency was set at the same level as the center of the objective of the travelling microscope, by means of a reading telescope. The utmost care was used to keep it in that exact position for it was noticed that the least deviation from it caused a considerable difference in the readings of K and k. The same is true of the level position of the travelling microscope and the dividing engine.

A tenths thermometer, calibrated by comparison with a standard thermometer was throughout immersed in the heater to the same depth and at the same angle of inclination. Stem correction was, however, found to be negligible for temperatures lower than 70°C, i.e., for temperatures used in this experiment.

No set of readings was recorded until all details were brought to relative perfection. On the other hand no set of readings was discarded after that point had been reached, except in cases of fluctuating temperature.

On two different occasions a set of readings was taken in a vacuum (15 and 16; 19 and 20, Table I) the dish was partially emptied by violent shaking, filtered air was admitted and the apparatus was allowed to stand for a while. When again pumped to stiction the change in surface tension was merely that to be expected from variation in temperature.

Popesco[17,18,19] Iredale[12] and Cook[5] have determined the surface tension of mercury in a vacuum by the flat-drop method. However, the experiments of the first two differed from this experiment in some important details—to mention only a few: the method of forming the drops was essentially different; both used wax seals. Iredale was himself conscious that "the experimental conditions would be very much improved if such adhesives could be done away with." (reference 12, page 607) Both worked on drops too small (Popesco's was about 3.6 cm in diameter; and Iredale's ranged from 1.2 cm to 1.5 cm in diameter) to be considered perfectly flat. The values obtained by Iredale from eleven consecutive drops, at a temperature of 19.5°C, vary from 430 to 472 dynes per cm. Cook's flat-drop method is essentially the same as

the one used in this experiment. But he has quoted only one value found for the surface tension of mercury in a vacuum; and that value seems abnormally high even though in the author's words "the measurements were very carefully checked." (reference 5, page 517). The apparatus of this experiment was as completely outgassed as his, but not once was a value any where near as high as his obtained. His readings of K and k were taken with a cathetometer the vernier of which "reads directly to 0.02 mm and under the microscope can be estimated to 0.01 mm" (reference 5, page 516). The travelling microscope used in this experiment records to 0.002 mm.

The dates given in the last column of Table I show how well conditions were reproduced. In turn the consistent values obtained seem to point to the fact that, more than a new theory, we need a high vacuum, uncontaminted surface and utmost care in manipulation.

This work was suggested by and carried on under the guidance of Doctor F. E. Poindexter in the laboratories of Maryville, Corporate College of Saint Louis University. I wish to thank him for his generous cooperation. I wish to thank both him and Rev. Professor James I. Shannon for their many helpful and encouraging suggestions. Thanks are also due to Brother A. Zeller for his kindness in rearranging the heater to fit the remodelled apparatus.

CORRECTED VALUES FOR THE COEFFICIENT OF RECOMBINATION OF GASEOUS IONS

By Overton Luhr and Norris E. Bradbury
Physical Laboratory, University of California

(Received March 9, 1931)

Abstract

Previously published values of the coefficient of recombination are found to be twelve percent too high because of the distortion of the field between the plates of the ionization chamber. Corrected values which may be used for the purpose of calculation are given as follows: Air, $(1.23 \pm 0.1) \times 10^{-6}$; O_2, $(1.32 \pm 0.1) \times 10^{-6}$; N_2 and A, $(1.06 \pm 0.1) \times 10^{-6}$; H_2, $(0.28 \pm 0.05) \times 10^{-6}$.

RECENTLY one of the writers[1,2] has published results of research on the recombination of ions produced by x-rays in a number of gases. It was found that the coefficient of recombination given by $\alpha = (1/t)(1/n - 1/n_0)$, the integrated form of the equation $dn/dt = -\alpha n^2$ is not a constant, but varies with the age of the ions. It was assumed that the high initial values of α and rapid drop at short time intervals (up to 0.05 to 0.1 seconds after the formation of the ions) is due to non-random distribution, and that the later more gradual drop is due to the loading up of the ion with impurities and subsequent selective recombination, producing abnormally low values of α at long time intervals up to one or two seconds. On the assumption that normal conditions were most closely approximated between the ages of 0.05 and 0.1 seconds, so-called "absolute values" were set which would be useful for purposes of calculation. Hydrogen is the only gas which did not exhibit any change in the value of α with time.

In all the results heretofore published it was assumed that the volume of ionization swept out by the electric field was the total geometrical volume contained between the plates of the ionization chamber. In planning for further work with the same apparatus, it has been found that, despite the guard ring surrounding the upper plate, there is an error of about twelve percent in this assumption. Owing to the proximity of the grounded walls of the chanber, the field is not uniform between the plates, the lines of force curving slightly towards the walls. (See Fig. 1.) The magnitude of the error was obtained by plotting the equipotential lines for a cross-section model of the chamber, making use of a telephone buzzer and probe points in a conducting solution. On drawing the lines of force, which are perpendicular to the equipotential lines, it was found that the volume swept out by the field was about twelve percent smaller than the assumed geometrical volume. In this connection it is interesting to note that under conditions where grounded

[1] O. Luhr, Phys. Rev. **35**, 1394 (1930).
[2] O. Luhr, Phys. Rev. **36**, 24 (1930).

walls are within a few centimeters of the plates of the ionization chamber, the guard ring would have to be approximately equal in width to the distance between the plates to obtain a uniform field.

In calculating the coefficient of recombination, n, the number of ions of either sign per cm^3 is found by dividing the total number of ions swept to the upper plate by the volume. Hence the equation is of the form $\alpha=(V/t)(1/N-1/N_0)$. As the volume was actually twelve percent smaller than that assumed in the previous results, all values of α should be reduced by a cor-

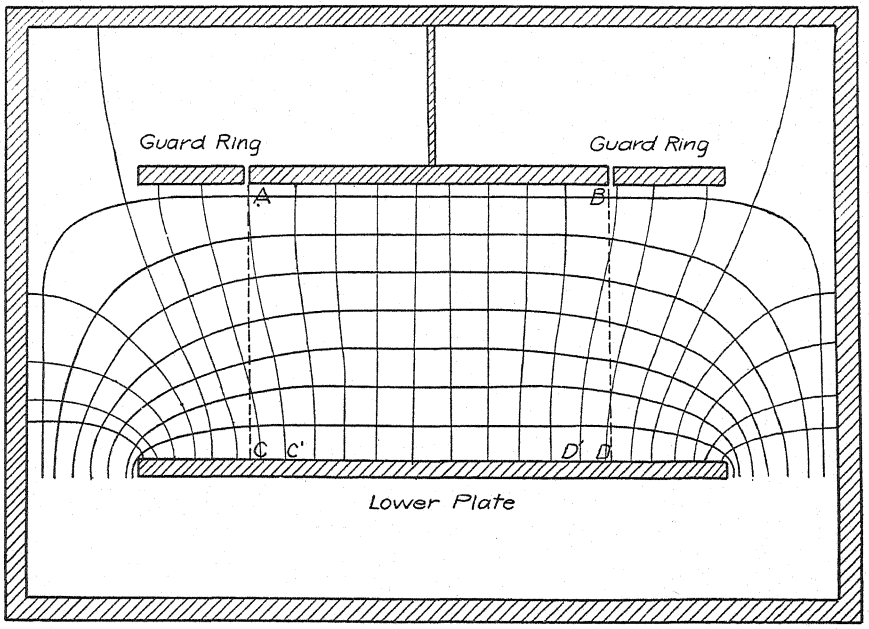

Fig. 1. Cross section ot the ionization chamber drawn to scale showing equipotential lines and lines of force when a potential is applied to the lower plate. $ABCD$ is the geometrical volume, while $ABC'D'$ shows the actual volume of ionization swept to the upper plate by the field.

responding amount. This error is not as serious as it might seem offhand since the curves will retain their same form, which after all is the most important result of the experiments as apparently there is no absolute value for the coefficient. The so-called "absolute values" which may be useful for purpose of calculation are now set as given in Table I.

TABLE I. *Corrected values of the coefficient of recombination.*

Gas	Coefficient of Recombination
O_2	$(1.32\pm0.1)\times10^{-6}$
N_2	$(1.06\pm0.1)\times10^{-6}$
A	$(1.06\pm0.1)\times10^{-6}$
H_2	$(0.28\pm0.05)\times10^{-6}$
Air	$(1.23\pm0.1)\times10^{-6}$

It must be understood that the possible error of plus or minus one-tenth indicated in these results is not an experimental error, but represents a portion of the curves between ages of 0.05 and 0.1 seconds. The experimental error is probably not more than two or three percent for all of the gases except hydrogen. The writers take pleasure in expressing their gratitude to Professor R. B. Brode whose critical suggestion led to the present revision of the values of α, and once more to Professor Leonard B. Loeb under whose able direction the whole research has been accomplished.

LETTERS TO THE EDITOR

Prompt publication of brief reports of important discoveries in physics may be secured by addressing them to this department. Closing dates for this department are, for the first issue of the month, the twenty-eighth of the preceding month; for the second issue, the thirteenth of the month. The Board of Editors does not hold itself responsible for the opinions expressed by the correspondents.

An Attempt to Measure the Energy of the Cosmic Electrons by Magnetic Deflection

An attempt has been made to measure the energy of the cosmic electrons with an apparatus based on Bothe and Kolhörster's[1] coincidence principle making use of Geiger-Müller tube-counters. A description of the method has previously been given.[2]

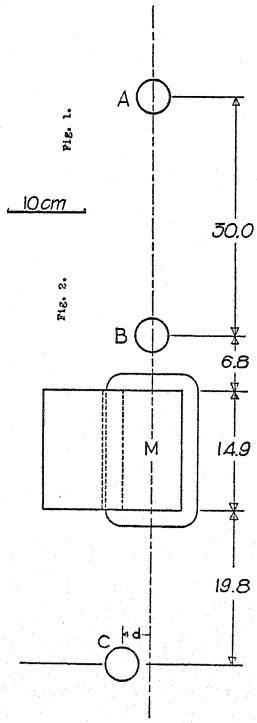

Fig. 1.

The arrangement is schematically shown in Fig. 1. A and B represent two tube-counters, viewed end-on, which serve to define a beam of the particles, M is a closed-core "magnet" which furnishes the deflecting magnetic field (produced directly in the iron), and C is a third counter which serves to analyse the beam which has passed through the magnet. An electrical vacuum tube system records on an impulse counter only triply coincident discharges of the three counters, events which are assumed to indicate the passage of an electron through the apparatus.

The principal experiment consisted in making counts of the triple coincidences for various displacements (d) of the analysing counter with the magnet unmagnetized and with it successively magnetized to a magnetic induction of 17,000 in either direction. The results are shown in the curve of Fig. 2. The values are believed to be reliable to about 8 percent (the statistical error is about 4 percent) with the exception of the points at the central position and those at 4 cm north which were studied more carefully and should not be in error by more than about 4 percent. The shape of the curve is about what is expected from the geometry of the arrangement, assuming rectilinear passage of the ionizing particle, and the count at the 10 cm displacement represents that due to chance coincidences. It is seen that within the present limits of error no deflection exists. This result is of interest because if the assumptions on which the operation of this apparatus is based are correct the energy of the particles is very high. On making what appears to be the correct assumption that the force on an electron in the iron is given by $(e/c)[v \times B]$

[1] W. Bothe and W. Kolhörster, Zeits. f. Physik **56**, 751 (1929).

[2] Phys. Rev. **35**, 1125 (1930). Experiments with the present method have been independently made by Rossi, Rend. Acc. dei Lincei **2**, 478 (1930).

where B is the magnetic induction, a deflection of 2.2 cm measured at the analyser is expected for electrons of energy 10^9 e-volts. It is seen from the curve that an easily observable change in count should be produced by such a deflection, particularly at the most favorable displacement of about 4 cm. Accordingly, with the reservation mentioned above, it appears that the energy of the majority of the cosmic electrons is greater than about 2×10^9 e-volts. The possibility that these particles may be protons or heavier nuclei should also be considered. This seems unlikely on various grounds, but even if the particles were protons we can conclude that the energy must be greater than about 10^9 e-volts.

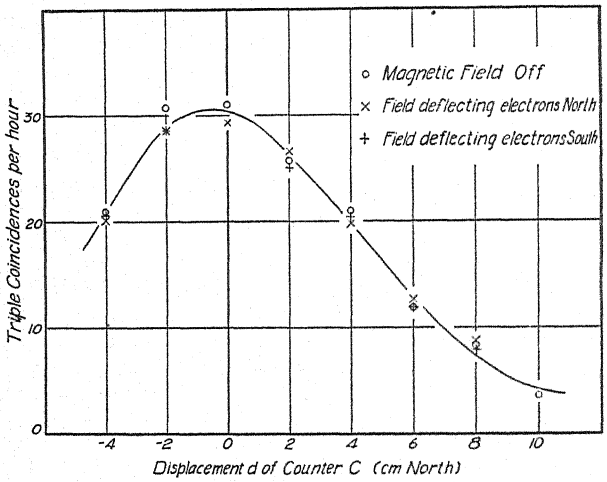

Fig. 2.

There is, however, a difficulty with the assumption of electrons of such high energies, which comes from a consideration of the process by which they are absorbed. From the usual theory of multiple scattering it is found that the path of such a particle should be nearly rectilinear until it has lost a large fraction of its energy, so that absorption must be principally due to a gradual loss of energy by the production of ions along the path. Accordingly, since the cosmic radiation (assumed electronic) is known to follow an exponential absorption law, we should expect to find at any point electrons with a definite distribution of velocities ranging from zero to some maximum. In fact, if the Thomson absorption law is still valid for these high energies, it is found, by using the known absorption coefficient for the cosmic radiation, that a considerable fraction of the electrons should have energies ranging from zero to a few hundred million e-volts (about 30 percent between zero and 2×10^8 e-volts). Were this the case, an effect of the magnetic field should have been observed. Consequently, if we wish to interpret this experiment to mean that the energy of the bulk of the electrons is as great as indicated above it is necessary to find a method of absorption for very penetrating electrons which gives considerably greater absorption than that expected on the ordinary theory. A possibility in this direction which should be investigated is a consideration of nuclear effects which are negligible when treating the absorption of electrons of low energy but which might be expected to become important when dealing with electrons of such large penetrating power.

It should be mentioned that absorption measurements have been made with this apparatus by taking counts with the magnet in position and with it withdrawn from the beam. In agreement with the result of Bothe and Kolhörster, the observed absorption is nearly the same as the value calculated for these conditions from the absorption coefficients obtained by the electroscope measurements.

It is also necessary to be sure that the coincidences are actually produced by a corpuscular radiation and not by a γ-type radiation. This question has been investigated by Bothe

and Kolhörster[1] both experimentally and theoretically, with the result that they do not find it possible to ascribe the coincidence effects to a γ-type radiation unless some new phenomenon is postulated. In view of our present result it would seem desirable to reexamine this question. On the experimental side a possibility in this direction would be to look for a definite correlation between coincidences in tube-counter and tracks in a suitably disposed cloud expansion apparatus. Such an experiment appears feasible and is in progress.

In view of the foregoing considerations and also on account of certain difficulties[3] with the assumption of a corpuscular nature for the cosmic radiation, it would seem that a definite conclusion with regard to the significance of the present experiment must await further study.

A part of this work was done at the California Institute through the kindness of the members of the administration of that institution.

L. M. MOTT-SMITH
Department of Physics,
The Rice Institute,
Houston, Texas,
March 25, 1931.

[3] See R. A. Millikan and G. H. Cameron, Phys. Rev. 37, 235 (1931)

Transmission of Gases from 20 to 33μ

In a letter to this section Dickinson and West[1] reported a Raman shift for liquid sulfur dioxide of 524.3 cm^{-1}. Bailey, Cassie and Angus[2] interpret this as a combination band. I have found the transmission of a four inch layer of this gas for the 20.75μ quartz reststrahlen to be only 7 percent. Such strong absorption would seem more likely to be associated with a fundamental band.

The transmissions of several gases have been determined in the spectral region 20–33μ and the results are given in Table I. These values are for a layer of gas four inches thick at atmospheric pressure and are probably correct to 2 percent.

TABLE I.

Gas	Reststrahlen Wave-length:	20.75μ	22.9μ	27.3μ	29.4μ	32.8μ
SO_2		7	58	100	99	96
NH_3		65	95	84	79	63
H_2S		96	98	93	89	82
N_2O		86	100	100	100	100
C_2H_2		95	100	100	98	97

JOHN STRONG
National Research Fellow,
California Institute of Technology,
Pasadena, California,
March 25, 1931.

[1] Roscoe G. Dickinson and S. Stewart West, Phys. Rev. 35, 1126 (1930).

[2] C. R. Bailey, A. B. D. Cassie and W. R. Angus, Roy. Soc. Proc. A130, 133 (1930).

A Preliminary Report of the Application of the Photoelectric Cell to the Reading of Minima in a Magneto-Optic Method of Analysis

It has been found that chemical compounds in solution, when traversed by polarized light and subjected to particular types of transient magnetic fields, are characterized under certain conditions by the scale readings of the minima of light intensity produced, by means of which a compound may be detected when present in a concentration as low as about 1 part in 10^{11} (Allison and Murphy, Journal the American Chemical Society 52, 3796 (1930); Physical Review 36, 1097 (1930)). These results have been interpreted upon the hypothesis of differential time lags in the Faraday effect. Inasmuch as the results thus far reported were obtained by visual observations only, the importance of devising some objective means of reading the minima has long been recognized. We have recently suc-

ceeded in building a photoelectric cell circuit which indicates the presence of the minima by the deflection of a galvanometer. The method of current amplification is similar to that described by DuBridge (Physical Review **37**, 392 (1931)), two FP-54 Pliotron tubes being employed together with other tubes for additional amplification. We have as yet had opportunity to take observations with the photoelectric cell upon only a few of the compounds which have been studied visually, but those selected are representative and their metallic elements contain isotopes. We used concentrations ranging from about 1 part in 10^{14} to 1 part in 10^{2}. Our results, which confirm those based on visual observations, may be summarized as follows.

(a) The photoelectric cell reads minima at the exact points of the scale at which they have been observed visually.

(b) The photoelectric cell is able to detect a compound when present in an amount as small as about 1 part in 10.[12]

(c) The photoelectric cell, in addition to detecting minima corresponding to the number of isotopes of the metallic element of the compound, indicates by the galvanometer deflections the relative abundance of the isotopes. This indication, however, is a rough one and does not as yet yield quantitative estimates of precision.

(d) The photoelectric cell registers but very slight differences in the blackness of the minima with changes in concentrations over wide limits, a result in agreement with visual observations.

Alabama Polytechnic Institute,
Department of Physics,
March 21, 1931.

FRED ALLISON
J. H. CHRISTENSEN
GEORGE V. WALDO

A New Source of Active Nitrogen

It has been possible for the first time to produce the afterglow of active nitrogen in an uncondensed discharge. The discharge was produced by a 25000 volt 1 KW Thordarssen transformer at pressures ranging from 0.1 mm to about 5 mm. Although a tremendous number of discharges of the same type in the same gas have been observed by the writer during the past four years, this is the first time that the afterglow associated with active nitrogen has been obtained. The afterglow was as strong as those obtained with the usual sources of active nitrogen, namely, condensed discharges and electrodeless ring discharges. The spectrum of the glow was observed with a direct vision spectroscope and also photographed and it consists of the usual sharp selection of the first positive bands of nitrogen as obtained in the ordinary afterglow. If there are any differences between this and other glows then more photographs may bring them out. The glow was obtained in two different tubes, each time however only after about two weeks running of the tubes at almost a no-discharge vacuum, i.e., at about 0.001 mm pressure. While other factors may have an effect, the long running of the tube certainly indicates that the condition of the walls is an important factor in the production of the glow.

A few very interesting points about the glow will be mentioned, which will help to emphasize the unusual nature of the phenomenon. For example, the exciting discharge itself possesses a spectrum which could readily be taken for an afterglow spectrum. The β bands of nitric oxide and the violet cyanogen bands, both of which are usually observed in nitrogen afterglows and but seldom in electric discharges, were both present in the exciting discharge. These, and the first positive bands of nitrogen comprised most of the radiation of the exciting discharge in the visible and the first positive bands also showed a structure similar to the one observed in active nitrogen. The second positive bands of nitrogen, which are strong in almost any type of nitrogen discharge and which are unusually strong in the condensed discharge, were almost completely missing from the exciting discharge in the present experiments. Just one remark will be made regarding the significance of the nature of the exciting discharge in these experiments. The writer has at various times assigned the weak radiations of the aurora spectrum to the first positive bands of nitrogen and has explained them as arising in processes similar to those that take place in active nitrogen. This assignment always raised the embarrassing question in the writer's mind as to the nature of an electric discharge in which the spectrum is so much like that of an

afterglow or a chemiluminescence phenomenon. This question has now been answered and one can say that as far as the first positive bands of nitrogen are concerned there is added spectroscopic evidence that the auroral displays are electric discharges at low pressures. That the discharge conditions in the upper atmosphere are unusual can be seen by the consideration that the upper atmosphere is really a discharge tube without walls. In view of some recent attempts to explain the aurora the present experiments should merit some attention. In another communication more will be said about some experiments in which other spectroscopic features of the aurora are pointed out and studied.

JOSEPH KAPLAN

Department of Physics,
University of California at
Los Angeles, California,
March 24, 1931.

The Zeeman Effect and Uncoupling Phenomena in Helium Bands

Weizel[1] has calculated the energies due to the uncoupling of the electronic angular momentum from the electric axis in light molecules. He predicts that such uncoupling should, if present, be greater for large values of the total quantum number, n, for large values of the difference between the orbital angular momentum quantum number of the series electron, l, and its projection on the electric axis, λ, and for large values of the rotational quantum number, K. For the helium molecule, rigid coupling of l to the molecular axis, so that λ is a true quantum number, should correspond to Hund's case b'. For large rotational energies the coupling should be destroyed and the molecule correspond to Hund's case d'. Since this uncoupling is not expected to be abrupt, many levels should correspond to cases intermediate between b' and d'. The energy of a case b' molecule in a magnetic field of strength H is well known to be

$$\Delta E=\frac{\mu_1 H M\Lambda^2}{K(K+1)}$$

where M is the magnetic quantum number and $\Lambda=\lambda$ for the present case. The corresponding relation for case d' can be calculated in the same manner as for the above case. The relation is

$$\Delta E=\frac{\mu_1 H M[K(K+1)+L(L+1)-R(R+1)]}{2K(K+1)}$$

where R is the rotational quantum number, and K the quantized resultant of l and R. It is evident that the Zeeman effect should afford a means to determine the degree of conformity to the limiting cases and indicate the presence or absence of uncoupling phenomena. Information may be drawn from partially resolved patterns by applying the intensity relations for the components of a spectral line given by Honl[2] and Kronig.[3] Harvey[4] has pointed out that unusual widths of the helium band lines in a magnetic field can be interpreted as indicative of uncoupling phenomena in certain states of this molecule. To check the above predictions quantitatively, an extensive investigation of the Zeeman effect in the ortho-helium bands has been carried out.

The spectrum has been photographed in the second and third orders of a 21-foot grating affording a dispersion of 1.31A per mm in the second order with field strengths up to 30,500 gauss. Measurable Zeeman pattern have been obtained for at least six lines of the bands $2p\pi^3\Pi^{(0)}-4s\sigma^3\Sigma^{(0)}$, $2s\sigma^3\Sigma^{(0)}-3p\pi^3\Pi^{(0)}$, $2s\sigma^3\Sigma^{(0)}-4p\pi^3\Pi^{(0)}$, $2p\pi^3\Pi^{(0)}-4d\delta^3\Delta^{(0)}$, $2p\pi^3\Pi^{(0)}-3d\delta^3\Delta^{(0)}$, $2p\pi^3\Pi^{(0)}-4d\pi^3\Pi^{(0)}$, $2p\pi^3\Pi^{(0)}-3d\pi^3\Pi^{(0)}$, $2p\pi^3\Pi^{(0)}-4d\sigma^3\Sigma^{(0)}$, and $2p\pi^3\Pi^{(0)}-3d\sigma^3\Sigma^{(0)}$. In agreement with previous investigators, the first three above mentioned bands correspond rigorously to case b' predictions. Departure from case b' appears in the band $2p\pi^3\Pi^{(0)}-4d\delta^3\Delta^{(0)}$ at values of K greater than 9. Evidence of uncoupling in the band $2p\pi^3\Pi^{(0)}-4d\pi^3\Pi^{(0)}$ is shown by departure from case b' patterns for all values of K greater than 2 and a gradual approach to case d' predictions as K increases to 14. Similar evidence of uncoupling is found in the band $2p\pi^3\Pi^{(0)}-4d\sigma^3\Sigma^{(0)}$ for values of K greater than one. The approach to case d' patterns is more rapid in this band than in the others mentioned above. In the last two mentioned bands the rate of uncoupling is somewhat more rapid than for

[1] W. Weizel, Zeits f. Physik **54,** 321 (1929).
[2] H. Honl, Zeits. f. Physik **31,** 340 (1926).
[3] R. de L. Kronig, Zeits. f. Physik **31,** 885 (1926).
[4] A. Harvey, Proc. Roy Soc. **A126,** 583 (1930).

the bands of the same electronic transition but of total quantum number 3.

It may, therefore, be stated that Zeeman patterns of the ortho-helium bands confirm the idea that the peculiarities of some of these bands, in particular those with large values of n and with l greater than λ for the series electron, can be explained by a gradual uncoupling of l from the molecular axis with increasing rotation. The Zeeman patterns offer a new means of following the progress of the uncoupling.

A complete report of data and results will be presented at a later date.

JOHN S. MILLIS

Lawrence College,
Appleton, Wisconsin,
March 18, 1931.

The Alleged Production of Adsorbed Films on Tungsten by Active Nitrogen

Pure molecular nitrogen has no effect on the thermionic emission from tungsten. The decrease in emission that occurs if a discharge is passed through the nitrogen with voltages above about 20 has been attributed to the formation of a film of adsorbed nitrogen.[1] Kenty and Turner found that the accommodation coefficient for heat conduction from the tungsten surface by nitrogen was increased about 20 percent by this treatment.

More recent experiments in this laboratory have shown that the film produced on the tungsten by active nitrogen is an *oxygen* film. The active nitrogen, coming into contact with the walls of the tube and the surfaces of electrodes, decomposes adsorbed water vapor or metallic oxides which are almost always present and thus drives oxygen (probably atomic) into the gas phase, whence it reacts with the filament. With great care to avoid oxygen and with the bulb cooled in liquid air, active nitrogen does not produce any adsorbed film which alters the electron emission or the accommodation coefficient, but instead it is able to remove any oxygen film already present.

A similar evolution of oxygen from well baked out glass surfaces occurs when neon metastable atoms strike the walls of a discharge tube.

The detailed description of these experiments will soon be submitted to the Journal of the American Chemical Society for publication.

IRVING LANGMUIR

Research Laboratory,
General Electric Company,
Schenectady, New York,
March 24, 1931.

[1] I. Langmuir, Phys. Rev. **2**, 460–72 (1913); Phys. Zeit. **15**, 523 (1914); J. Amer. Chem. Soc. **38**, 2279 (1916); C. Kenty and L. A. Turner, Phys. Rev. **32**, 799–811 (1928).

Partial Absorption of X-Rays

Ray,[1] Majumdar,[2] and Bhargava and Mukerjie[3] have found evidence that a quantum of x-rays may, in passing through matter, give *only a part* of its energy to a bound electron and continue in its original direction with diminished frequency. These authors do not give detailed information regarding their experiments, but Ray reproduces spectrograms which clearly show the lines which he ascribes to *partially absorbed* x-rays. Ray estimates the intensity of these lines to be between 1/400 and 1/500 of that of the parent line.

[1] B. B. Ray, Nature **125**, 746 and 856 (1930); **126**, 399 (1930); Zeits. f. Phys. **66**, 261 (1930).

[2] R. C. Majumdar, Nature **127**, 92 (1931).

[3] S. Bhargava and J. B. Mukerjie, Nature **127**, 273 and 305 (1931).

Cork[4] and Lindsay[5] have tried to produce these modified lines, but with negative results. Cork claims to have been able to detect lines, if present, of 1/1000 to 1/3000 of the intensity of the parent line. Lindsay reproduces photometric curves of the K-spectrum of copper taken through a carbon absorbing screen which show definitely the presence of the $K\alpha_{3,4}$ satellite of copper, known to have about 1/400 the intensity of the α_1 line, but no trace of a modified line.

We have tried to find lines corresponding to the partial absorption of the $K\alpha$ doublet of molybdenum by aluminum, but without success. We used the spectrometer and calcite

[4] J. M. Cork, Comptes Rendus **192**, 153 (1931).

[5] G. A. Lindsay, Nature **127**, 305 (1931).

crystal recently described by us.[6] The source of x-rays was a water-cooled Coolidge tube with molybdenum target, operated at about 60 KV peak potential and 12–13 ma current. The first slit was about 16.8 cm from the crystal and 0.04 mm wide. The second slit was 4.5 cm from the crystal and wide enough to permit the full beam from the first slit to fall on the crystal. The photographic plate was placed normal to the direct beam at such a distance from the crystal that the $K\alpha_1$ line of molybdenum was in focus. The absorbing screen consisted of powdered "alumina" (obtained from the General Electric Co. of Schenectady) pressed between two sheets of "celophane" about 0.02 mm thick and was placed close to the second slit, between it and the tube. In some cases the screen was about 1 mm thick and in others about half that thickness. During exposures the crystal was rotated back and forth through an angle of about 52.5′ around a position at which it should reflect the modified lines due to absorption in aluminum. The rotation was produced by means of a cam designed to give the crystal approximately constant angular velocity between turning points. The mean position about which the crystal rotated was slightly different for different plates. The exposures for the modified lines lasted for about 15 hr., and then short exposures were taken to record the central image and the $K\alpha$ and $K\beta$ lines of molybdenum on both sides of the latter.

All the plates showed a band of continuous spectrum corresponding in position and width to the range of rotation of the crystal. The band on each plate had a structure which was probably due to irregularities in the cam since the structure remained fixed with respect to the band when the position of the latter on the plate was changed. No lines were found as definite as those appearing on Ray's photographs.

Since the bands of continuous spectrum were quite dark, the modified lines may have been obscured. We are planning to eliminate the continuous spectrum as much as possible by introducing a crystal between the first slit and the x-ray tube.

D. COOKSEY
C. D. COOKSEY

Sloane Physics Laboratory,
Yale University,
March 18, 1931.

[6] C. D. and D. Cooksey, Phys. Rev. **36**, 85 (1930).

The Absorption Spectrum of Bromine

In the absorption spectrum of bromine vapor at room temperature with columns of vapor long enough (two to four meters) to bring out the progressions of the visible band system arising from the fifth and sixth vibrational states of the normal level a number of new bands appear in the region 6400A to 7500A. These can be classified into five rapidly converging progressions of which three can be followed nearly to the point of convergence. Assigning $v''=1$ to the lowest observed progression the G'' differences agree well with those for the "main" system, and the point of convergence agrees with the assumption that these bands constitute a new system the upper level of which leads to dissociation into two atoms in the $^2P_{1\,1/2}$ state. This level may thus be a member of the case $c^3\Pi$ multiplet predicted by Mulliken.[1] The dispersion employed (first order of a 3 m. concave grating giving 5.4A/mm) was not sufficient to determine the character of the bands, which should consist of Q branches only, if the new level is Mulliken's 0_u^- level.

The vibrational isotope effect has not been definitely located so that the v' numbering, on which calculations of the constants given in the accompanying table are based, is arbitrary. This table shows also the constants resulting from a re-examination of the main system in which the isotope effect has been observed for a number of bands in the $v''=0$, 1, and 2 progressions. These measurements indicate that Kuhn's[2] v' numbering should be increased by four. This is in addition to a further correction of $+5$ to be made for v' greater than Kuhn's 11, which resulted from an incorrect assignment of bands.[3] The $\Delta G:v$ curves for the upper level of the main system and of the extreme red system show points of

[1] R. S. Mulliken, Phys. Rev. **36**, 699, 1440 (1930).

[2] H. Kuhn, Zeits. f. Physik **39**, 77 (1926).

[3] R. T. Birge, I.C.T. V, 411 (1929).

inflection[4] at about 65 percent of the dissociation energy, and only observations at points lower than these have been used in making least squares calculations of the constants given in Table I. The ground level of the molecule is denoted by A, the upper level of the main system by B, and of the extreme red system by C.

TABLE I. *Molecular constants of bromine.*

Electronic Level	ν_e cm^{-1}	ω_e	$\omega_e x_e$	D (volts)	Dissociation products
A	0	323.86	1.150		
B	15,910.5	165.39	1.579	0.464	$^2P_{1\frac{1}{2}}+{}^2P_{\frac{1}{2}}$
C	14,841.4	115.69	3.395	0.144	$^2P_{1\frac{1}{2}}+{}^2P_{1\frac{1}{2}}$

From the measurements of Bodenstein[5] on the dissociation equilibrium an estimate of the moment of inertia of bromine has been made by means of the Gibson-Heitler equation, the mean value of I'' from observations at the ten highest temperatures being 445×10^{-40} C.G.S. and the average deviation from the mean 5.6×10^{-40}. With this value of I the equation gives $\Delta F°$ 298.1 = 38,600 cal. for the reaction $Br_2(g)=2Br_g$. The heat of dissociation deduced from the equilibrium measurements is in excellent agreement with the spectroscopically determined value, 1.962 volts.

Bands which may correspond to the extreme red system of bromine have been found in the infrared absorption spectrum of iodine (vapor pressure 1 atmosphere, in a 1 m tube at 185°C) between 8000A and 9000A. These have not yet been analysed. An account of them will be given at a later time as well as detailed results for bromine. Further experiments with a view to determining the character of the new bromine bands and the isotope effect are being undertaken.

WELDON G. BROWN

Department of Chemistry,
University of California,
Berkeley, California.

[4] R. T. Birge, Trans. Faraday Soc. **XXV**, 707 (1929).

[5] M. Bodenstein, Zeit. f. Elektrochemie **22**, 327 (1916).

BOOK REVIEWS

Applications of Interferometry. W. EWART WILLIAMS. Pp. viii+104, diagrams 43. E. P. Dutton and Company, New York. Price $.85.

This is as complete a treatment of the subject as could reasonably be presented in a monograph. As the author says in his preface, it is not possible to include in such a book all the applications which can be made of interferometry. Certainly the selection made is representative and interesting.

Perhaps the most prominent feature of the work is the classification of interference phenomena into two groups: first, those in which a division of wave front is accomplished as in Young's interference experiment, second, those in which there is a division of amplitude as in the Michelson interferometer. For a monograph devoted largely to technical applications it contains a considerable amount of theory, with simplifications which enable a technical man, not extensively trained in mathematical theory, to understand what is meant without too much additional reading. Particularly lucid are the description of Michelson's apparatus for the measurements of stellar diameters and the chapter on multiple beams, in which the Fabry-Perot interferometer, the Lummer plate, and similar instruments are described.

A good bibliography is given at the end of each chapter. It is unfortunate that the abbreviations of the journal references are not more consistent. For instance, on page 45, Annales de Chimie et de Physique is abbreviated in three different ways. The book is free from technical errors, and the diagrams are good. It should make a very substantial addition to the reference material for teachers and students of optics, and persons engaged in other divisions of scientific work.

GEORGE S. MONK

Matter and Radiation, with particular reference to the detection and uses of the infrared rays. JOHN BUCKINGHAM. Pp. 144, figs. 15. Oxford University Press, London, 1930. Price $3.00.

This book summarizes in a semi-popular way, the many interesting discoveries concerning matter and radiation that have been made in the last century. In particular, the complete electromagnetic spectrum is discussed in connection with the recent theories of atomic structure. It is pointed out that the powerfully destructive rays one occasionally reads about in the newspapers are the result of imagination, or at least enormous exaggeration. While the text is usually accurate, there are a few blunders and inaccuracies. Occasionally, but not always, these are evidently introduced for simplicity or for effect. Thus the miracle of the shortest light path would lose some of its effectiveness if it were also pointed out that sometimes light chooses the longest path. One also finds the naïve statement that x-rays readily pass through matter because their wave-lengths are smaller than the holes between the atoms. However, while it occasionally falls short of scientific accuracy, the book makes very interesting reading.

JOSEPH VALASEK

A Treatise on Light. R. A. HOUSTOUN. Pp. 494, 6th Edition, Longmans, Green and Company, New York, 1930. Price $4.00.

The sixth edition of this much used text book is not greatly different from the preceding editions. There seem to be no changes in the first two "parts" of the book, viz.: (I) Geometrical Optics and (II) Physical Optics. In part III, Spectroscopy and Photometry, the most important changes are the addition of three paragraphs dealing with the elements of the Bohr theory of spectral series, resonance potentials, and band spectra. It seems unfortunate that the treatment of the Zeeman effect was not changed so as to introduce the idea of the Larmor precession. In part IV, mathematical theory, the principal changes are the introduction of Einstein's proof of Planck's Law of radiation and a restatement of the status of the relativity principle. In the "Notes" on recent advances is a notice of the Raman effect. Houstoun's *Light* has the virtue of giving a little information about a great many subjects. That is also its weakness, along with the lack of any adequate number of references to sources of fuller information.

T. TOWNSEND SMITH

PROCEEDINGS

OF THE

AMERICAN PHYSICAL SOCIETY

MINUTES OF THE NEW YORK MEETING, FEBRUARY 26–28, 1931
JOINT MEETING WITH THE OPTICAL SOCIETY OF AMERICA

The 169th regular meeting of the American Physical Society was held in New York City on Thursday, Friday and Saturday, February 26–28, 1931, as a joint meeting with the Optical Society of America. The presiding officers at the sessions of the Physical Society were Dr. W. F. G. Swann, President of the Society, Dr. Paul D. Foote, Vice-president and Professor R. C. Gibbs. All sessions were held at Columbia University.

The joint session with the Optical Society of America was held on Friday afternoon at 2:30 o'clock in the McMillin Theater of Columbia University. This session was a Symposium on "Physical Problems Related to the Biological Effects of Radiant Energy." The President of the Optical Society, Dr. L. A. Jones presided. The invited papers were as follows: "Some Physiological Effects of Light," by Brian O'Brien, Institute of Optics, University of Rochester; "The Spectra and Anti-Rachitic Potency of Various 'Therapeutic' Lamps," by Harvey B. Lemon, University of Chicago; and "Methods of Measuring Radiant Energy," by Harold W. Webb, Columbia University. The attendance was between four and five hundred.

The Optical Society held its sessions at the Museum of Science and Industry Thursday morning and afternoon, occupied with papers on "Color". Their regular Friday morning and Saturday morning and afternoon sessions were held in the Physics Laboratory of Columbia University.

On Friday evening the Society joined with the Optical Society for dinner at the Hotel Commodore after which they attended the Color Exhibition at the Museum of Science and Industry. This dinner was attended by 175 guests.

Meeting of the Council. At its meeting on Thursday, Feburary 26, 1931, Professor Albert Einstein was unanimously elected to Honorary Membership in the Society.

The Council accepted the cordial invitation of Union College and the General Electric Company to hold the summer meeting in Schenectady in September. It was decided that this meeting should be of an informal nature much like the one held last year in Ithaca. A one-half day session of this meeting is to be devoted to papers on Faraday and Henry commemorating their notable work in the field of electromagnetic induction. The Council furthermore accepted the invitations extended by Harvard University and the Massachusetts Institute of Technology to hold the meeting of the Society in February, 1932 in Cambridge.

The Treasurer reported the receipt on January 29, 1931 of a contribution of $1,425.42 to meet the deficit of the Physical Review as of December 31, 1930 and moved that the thanks of the Council be expressed to the Chemical Foundation for this contribution.

The Council elected four persons to fellowship, one hundred and nineteen persons were transferred from membership to fellowship and twenty-five were elected to membership. *Elected to Fellowship:* G. H. Dieke, Rudolf Ladenburg, Leo J. Peters and Max von Laue.

Transferred from Membership to Fellowship: Fred Allison, Donald H. Andrews, Alice H. Armstrong, Edward J. Baldes, Russell S. Bartlett, J. W. Beams, J. A. Bearden, Ralph D. Bennett, F. Russell Bichowsky, Francis Bitter, Oswald Blackwood, Walker Bleakney, C. Boeckner, Joseph C. Boyce, Charles J. Brasefield, A. Keith Brewer, Ferdinand Brickwedde, James B. Brinsmade, W. G. Brombacher, Detlev W. Bronk, S. Leroy Brown, Andrew B. Bryan, Perry Byerly, Thoedore W. Case, Andrew Christy, George L. Clark, Kenneth S. Cole, J. R. Collins, Richard T. Cox, Donald Cooksey, William H. Crew, Leo H. Dawson, David M. Dennision, Elmer Dershem, Jane M. Dewey, Leo A. DuBridge, Jesse W. M. DuMond, Theodore Dunham Jr., James M. Eglin, Frederick E. Fowle, John G. Frayne, James B. Friauf, William F. Giauque, George Glockler, Frank Gray, Grover R. Greenslade, Ross Gunn, Otto Halpern, William R. Ham, Arthur C. Hardy, L. Grant Hector, Edward L. Hill, Maurice L. Huggins, Elmer Hutchisson, Sydney B. Ingram, Lewis V. Judson, J. C. Karcher, Sebastian Karrer, E. Lee Kinsey, Dewey D. Knowles, Lewis R. Koller, Frank C. Kracek, Victor K. LaMer, R. M. Langer, Karl Lark-Horovitz, Charles C. Lauritsen, Victor F. Lenzen, H. H. Lester, Noel C. Little, Walter A. MacNair, Louis R. Maxwell, Helen A. Messenger, Louallen F. Miller, Allan C. G. Mitchell, Philip M. Morse, L. L. Nettleton, J. Rud Nielsen, Wayne B. Nottingham, Christian Nusbaum, Paul S. Olmstead, A. R. Olpin, Lars Onsager, Dimitry E. Olshevsky, John M. Ort, Frederic Palmer Jr., I. I. Rabi, Hubert H. Race, N. Rashevsky, Howard P. Robertson, Vladimir Rojansky, Duane Roller, Edward O. Salant, William Schriever, Nadiashda Galli-Shohat, Francis G. Slack, William W. Sleator, Sinclair Smith, Ambrose H. Stang, F. W. Stevens, John B. Taylor, James D. Tear, Lewi Tonks, Alva Turner, M. A. Tuve, J. T. Tykociner, D. S. Villars, G. R. Wait, Warren Weaver, Lars A. Welo, T. Russell Wilkins, Robert C. Williamson, Thomas A. Wilson, Enos E.Witmer, Jay W. Woodrow, Winthrop R. Wright, Oliver R. Wulf, Ralph W. G. Wyckoff, Otto J. Zobel and Vladimir Zworykin.

Elected to Membership: B. C. Adkerson, R. H. Bacon, L. J. Buttolph, Jessie Y. Cann, Samuel L. Case, T. C. Chow, H. M. Evjen, Isidor Fankuchen, Louis W. Gardner, Maria Goeppert-Mayer, Harold W. Harkness, Francis E. Haworth, Nathan Howitt, Lorenz D. Huff, George B. Lamb, K. O. Lee, Charles F. Lucks, John C. Melcher, Harry B. Mulkey, Edward J. Murphy, H. V. Neher, Filmer S. C. Northrop, Robert W. Perry, William B. Plum and James G. Potter.

The titles and abstracts of papers presented before the Optical Society

of America will be found the Proceedings of that Society, published in the Journal of the Optical Society.

The regular scientific program of the American Physical Society consisted of 49 papers, numbers 5, 6, 8 and 35 were read by title. The abstracts of these papers are given in the following pages. An **Author Index** will be found at the end.

W. L. SEVERINGHAUS, *Secretary*

ABSTRACTS

1. Water vapor absorption spectrum in the near infrared. E. D. MCALISTER, *Division of Radiation and Organisms, Smithsonian Institution, and* H. J. UNGER, *University of Oregon.*—The 1.13, 1.38 and 1.45μ water vapor bands have been obtained with a self recording spectrograph using an effective slit width of 6A. The fine structure of the 1.13 and 1.45μ bands has been revealed for the first time and several lines have been added to the 1.38μ band. Forty lines appear in the 1.1μ region and eighty-five in the 1.4μ region. A comparison of these bands with similar ones due to atmospheric absorption in the solar spectrum identifies several superimposed solar lines. Regularities in frequency and intensity are lacking, due to the fact that a 6A slit is much too coarse to reveal the true structure of these bands.

2. Transmission of radiation through fog. S. HERBERT ANDERSON, *Signal Corps Laboratories.*—A laboratory method for the production of fog was developed in which the processes of formation of natural fogs were closely simulated. Transmission of radiation through this laboratory-made fog was measured for a range of wave-lengths from 3000A to 26,000A. A wide range of fog densities was used corresponding to natural fogs in which the visibility varies from 5 meters to 500 meters. A minimum transmission was found in the visible spectrum, the position of the minimum being a function of particle size. From λ_{min} to $\lambda = 26{,}000$A the transmission increased, likewise from λ_{min} to $\lambda = 3000$A. The transmissions obtained have been used to test King's equation $I = I_0 e^{-(a+b\lambda^{-4})}$. This equation if found *not* to hold for transmission of radiation through fog, contrary to the conclusion reached by Granath and Hulburt (Phys. Rev. **34**, 140, 1929). The discrepancy is probably due, (1) to the difference in particle size, (2) the width of the bands in the infra-red used by Granath and Hulburt, (3) to the absorption of water vapor, the effect of which was eliminated in this work but not in Granath and Hulburt's.

3. The absorption spectrum of blood and its relation to rickets. R. C. GIBBS, J. R. JOHNSON AND C. V. SHAPIRO, *Cornell University.*—The ultraviolet absorption spectra of solutions, obtained by haemolyzing the red blood cells of healthy and rachitic rats, have been found to be identical. This result is contrary to that reported by Suhrmann and his co-workers, Phys. Zeits. **30**, 959 (1929), whose curves for the two sets of animals show a difference in intensity, which increases in the direction of shorter wave-lengths. Calculations based on Rayleigh's law of light scattering indicate that this difference can be attributed to the presence of an excess of a disperse phase in the solution whose absorption is the more intense. Experimental verification of this hypothesis has been obtained by measuring the absorption of one of our solutions after it had been centrifuged to remove most of the suspended matter. The new curve so obtained is less intense than the original and the difference increases toward shorter wave-lengths, in close accordance with the Rayleigh law. This evidence points to a physical cause for the variation reported by Suhrmann and renders unnecessary his improbable assumption of a chemical change in the haemoglobin. The discrepancy between his results and ours may be accounted for by assuming either that there are two types of rickets, possibly brought on by different diets, or else that the variation reported by him, especially in view of its physical origin, is due to some cause, not necessarily associated with rickets.

4. Energy distribution in the lunar ultraviolet spectrum. BRIAN O'BRIEN AND E. DICKERMAN O'BRIEN, *Institute Optics, University of Rochester, N. Y.*—The energy distribution in the ultraviolet spectrum of sunlight reflected from the full moon has been measured from λ4400A to

λ3020A, by the method previously applied to direct sunlight. (Phys. Rev. **36**, 381 (1930)). Uniformity of slit illumination was secured by an astigmatic telephoto combination of quartz provided with rectangular stops, the measured spectral energy distribution being an average across a lunar diameter. Transmission coefficients and ozone content of the earth's atmosphere were obtained directly. The amount of ozone at night has been found to differ only slightly from the day values obtained on succeeding days in agreement with Chalonge and Götz (Gerl. Beit. z. Geophys. **24**, 20) (1929)). By comparison with direct sunlight the reflection coefficients for the moon's surface have been calculated throughout the above spectral region. No pronounced maxima or minima of reflecting power have been found within this range of wave-lengths. A test of some delicacy is thus provided, with negative results, for very small amounts of ozone (and hence oxygen) surrounding the moon.

5. Raman spectra of some organic halides. CLAUD EDWIN CLEETON AND R. T. DUFFORD, *The University of Missouri.*—Raman spectra obtained by helium excitation from nineteen organic compounds, several of which have not been studied previously, are reported and discussed. It has been found by one of the writers (C. E. C.) that in the cases of many simple organic halides the observed frequencies can be expressed as harmonics or combinations of four fundamentals (five in the cyclic compounds), two of which are not found in the Raman spectra, and are lower than predicted by any theory available, and hence may prove to be illusory; but the scheme does serve to point out certain regularities in these spectra. The bearing of such theory as is available is discussed.

6. Raman spectra and a slight asymmetry of the carbon and nitrogen atoms. R. T. DUFFORD, *The University of Missouri.*—The interpretation of the Raman spectra of the simpler organic halides and other related compounds is discussed; it is shown that most of the observed frequencies can be associated with vibrations of pairs or groups of atoms as predicted by theory, except that, in order to explain the multiplicity of certain lines, it seems necessary to assume a slight dissymmetry—i.e., a lack of equality of the valance bonds—of the carbon atom. Similar but less extensive evidence seems to indicate that the three valences of nitrogen are also not quite equally strong.

7. Vibrational quantum analysis of the ultraviolet SO_2 and CS_2 absorption bands. WILLIAM W. WATSON AND ALLAN E. PARKER, *Yale University.*—Analysis of spectrograms taken with a Hilger E-1 spectrograph shows that the SO_2 bands may be represented by the formula

$$\nu = 30586 + \{[381.1(v_1'+\tfrac{1}{2}) + 6.22(v_1'+\tfrac{1}{2})^2 - 0.223(v_1'+\tfrac{1}{2})^3] - [1381(v_1''+\tfrac{1}{2}) - 20(v_1''+\tfrac{1}{2})^2]\}$$
$$+ \{[436.7(v_2'+\tfrac{1}{2}) + 2.94(v_2'+\tfrac{1}{2})^2 - 0.199(v_2'+\tfrac{1}{2})^3] - [1157(v_2''+\tfrac{1}{2}) - 12.5\ (v_2''+\tfrac{1}{2})^2]\}$$

Noteworthy points are: positive quadratic term of the upper state levels, agreement with two of the fundamental frequencies determined by Raman and infrared analysis, no evidence for the 606 cm^{-1} deformation frequency, and the existence of various addition series as given by the double formula. Apparently a triplet electronic level is involved. High dispersion plates do not resolve the rotational fine structure. Most of the bands of the CS_2 system are given by

$$\nu = 28880 + 215(v_1'+\tfrac{1}{2}) - 802(v_1''+\tfrac{1}{2}) + 270(v_2'+\tfrac{1}{2}) - 1466(v_2''+\tfrac{1}{2})$$

the anharmonic coefficients being nearly negligible. There is slight evidence for a deformation frequency of 208 cm^{-1} in the ground state. Series of addition bands are found as for SO_2. The Raman frequency 655 cm^{-1} is the difference between the 1466 cm^{-1} and 802 cm^{-1} fundamental frequencies.

8. Paschen-Back effect and hyperfine structure in the spectrum of bismuth III. J. B. GREEN, *Ohio State University.*—A study of the spectrum of Bi in a field of 34000 gauss yields interesting data with respect to the hyperfine structure of Bi III. In particular, the line 4561, classified by McLennan as $^2P_{1/2}{}^2S_{1/2}$ gives 2.52 cm^{-1} for the ^2S separation, and 0.53 cm^{-1} for the $^2P_{1/2}$ separation. Several "forbidden" components appear on the plates. The line 3695, classified as $^2P_{3/2}{}^2S_{1/2}$ seems to indicate that the $^2P_{3/2}$ separation is much smaller.

9. Hyperfine structure in Bi II and Bi III. R. A. FISHER AND S. GOUDSMIT, *University of Michigan.*—The hyperfine structure of several lines in Bi II and III has been determined. The

results form a partial confirmation of the classification given by McLennan, McLay and Crawford (Proc. Roy. Soc. A129, 579 (1930)). It is possible to derive the hyperfine splitting for a number of levels. Together with the data on Bi I they form useful material for theoretical investigation. Bismuth is at present the only element for which hyperfine structure depending upon other than a single *s* electron is known for several levels.

10. Difficulties in the theory of hyperfine structure. S. GOUDSMIT, *University of Michigan.*—Sum rules and formulae for the hyperfine separations of the levels are derived for complicated configurations. The observed hyperfine structure of neutral and ionized bismuth, shows large deviations from the theoretical expressions. The nature of the discrepancies suggests that the present theory of the interaction between a single electron and nuclear spin is incomplete.

11. The theory of complex spectra II. E. U. CONDON AND G. H. SHORTLEY, *Princeton University.*—Formulas for the relations between the energies of multiplets arising from the same electron configuration for all two-electron configurations up to ff and several cases of three-electron configurations have been worked out following Slater's method. A systematic comparison of the known data with this first-order perturbation theory shows only rough agreement in most cases although in a few there is excellent agreement. The theory predicts the observed alternation in the relative position of singlet and triplet through S, P, D, F, etc. in the pd and pf triads and the dd and df pentads. For the d^2 configuration it was found that good fits are obtained except for the ^1S which theory indicates is much higher than the ^1S which spectroscopists assign to this configuration. The same is probably true for ^2S in d^2s.

12. The determination of heats of dissociation from predissociation spectra. LOUIS A. TURNER, *Princeton University.*—Two distinct types of predissociation spectra are known. In one the broadening of the lines begins suddenly at a definite wave-length, in the other it sets in gradually. Consideration of various possible relationships of potential energy curves suggests that the one or the other type occurs according to whether the curves for the two states concerned intersect below or above the energy of dissociation in the perturbing state, respectively. Accurate values of heats of dissociation can be obtained only from predissociation spectra of the first type. The others give merely upper limits. A predissociation of each kind is observed in the spectrum of NO_2 and the numerical relationships are in accord with the theory.

13. The inverse-cube central force field in quantum mechanics. G. H. SHORTLEY, *Princeton University.*—The problem of the motion of a particle in an inverse-cube central force field is fully treated by quantum mechanics and the results compared with the classical theory. Taking the effective radial potential energy as $(M^2/2\mu - S)/r^2$, one gets good correspondences between the quantum mechanical and classical solutions except for S between $l(l+1)\ h^2/8\pi^2\mu$ and $(l+\frac{1}{2})^2h^2/8\pi^2\mu$, where one gets a peculiar absence of oscillations in the ψ-function near the origin and somewhat poor agreements in regard to the radial probability functions. This is interesting in view of the uncertainty as to which value to compare with the classical angular momentum. However, the correspondence in allowed energies is complete only if the value $l(l+1)$ is taken. Solutions are found corresponding to the six classical types of orbits, with no quantization whatever. The solutions involve Bessel functions of both real and imaginary order with both real and imaginary arguments.

14. van der Waals' forces of helium and the stability of a small energy helium molecule. HENRY MARGENAU. *Yale University.*—Hopfield (Astrophys. J. LXXII, 133 (1930)) has recently postulated the existence of a He molecule of very low energy of binding. Theoretical evidence for the existence of such a molecule will here be given. The work consists of two parts. (1) A general method is outlined by which van der Waals' forces can be calculated without the knowledge of wave functions. Main features are: The expression for the interaction energy of 2 atoms in their lowest state is written in terms of the dispersion f-values, which are shown to be derivable with good approximation, by the aid of the "Summensatz" of Thomas and Kuhn, from the relative intensities of the resonance lines and the polarizability. The method is applicable to atoms (and molecules) more complex than He. Results for He:

$$\Delta_2 E = 11.58/R^6 \times 10^{-61} \text{ ergs}, \quad R > R_0.$$

(2) From the potential energy curve given by this expression and $\Delta_2 E = +\infty$ for $R < R_0$, R_0 being taken as 2.33×10^{-8} cm, the vibrational states for the resulting molecule are computed. Results: Minimum of potential energy $= -10^{-14}$ ergs; the molecule has but one vibrational state of energy about 3.3×10^{-16} ergs $= 0.2$ millivolts, which is in qualitative agreement with Hopfield's predictions

15. Group theory and the electric circuit. NATHAN HOWITT, *Naval Research Laboratory Bellevue, D. C. (Introduced by Elias Klein).*—The paper shows that electrical networks consisting of inductances, resistances, and capacitances form a group with the impedance function as an absolute invariant. That is, to a given impedance function there corresponds an infinite number of networks, any one of which can be obtained from any other by a special linear transformation of the instantaneous mesh currents and charges of the network. In this manner one may arrive at the complete infinite set of networks equivalent to a given network of any number of meshes. This is done by writing down the three fundamental quadratic forms of the network. Then a linear affine transformation of the instantaneous mesh currents and charges of the network results in the formation of new quadratic forms, the matrices of the coefficients of which represent a member of the group, i.e., an equivalent network. Instead of performing the substitutions, the three matrix multiplications $C'AC$ are used, one for each quadratic form, where A represents the original matrix, C the transformation matrix, and C' its conjugate. It may be possible to extend this theory to include continuous systems where the quadratic forms become integrals or infinite series and one deals with infinite matrices and infinite transformations.

16. Magnetic lag at low flux densities. L. W. MCKEEHAN, *Yale University.*—Energy losses in alternating magnetization are often compared by assuming that H and B vary sinusoidally, B lagging by an angle ϵ. At low flux densities ϵ is not fully accounted for by calculated eddy current and hysteresis terms if each branch of the hysteresis loop is assumed parabolic with least slope equal to that at the origin of the normal magnetization curve. The residue, ϵ_n, is a true magnetic lag. No explanation for it has hitherto been offered. It is now pointed out that Barkhausen discontinuities involve a magnetic lag which may suffice to explain the existence of ϵ_n. For example, 600 equal discontinuities per half cycle would suffice if $\epsilon_n = 10^{-3}$. The necessary mean magnitude of these discontinuities is improbably great unless it is principally strained regions which are affected by weak applied fields. If Jordan, Zeits. f. techn. Physik **11**, 2–8 (1930), is right in supposing that ϵ_n is independent of H_{max} over the small range in which it can be measured with any precision, the average magnitude of the discontinuities would have to vary directly with H_{max} throughout this range. This is not inconsistent with the parabolic form of (smoothed) magnetization curves at low flux densities.

17. Ferromagnetism of dilute solid solutions. FRANCIS BITTER, *Westinghouse Elec. & Mfg. Co., East Pittsburgh.*—Since the atoms of the solvent are known to move about in the solute it is possible to consider annealed and aged solutions as systems in thermodynamic equilibrium. It is shown that the strains set up by the atoms of solvent in the solute do not produce long range forces. There are, then, no long range repulsive forces tending to produce a microscopically uniform distribution. Under these circumstances the fluctuations in density of the solute will be at least as large as those in a perfect gas, and may become much larger (as large as those giving rise to opalescence, for instance). Local concentrations or rarifications of impurities may play an important part in determining magnetic properties through the inhomogeneities and strains they set up. For instance, in the iron-carbon diagram, the observed magnetic transformation of Austenite at 770°C would necessitate a drastic revision of ideas about ferromagnetisms if it were granted that Austenite is a solid solution of carbon in γ-iron. If, however, it is assumed that Austenite contains small inclusions of α-iron where there are local rarifications of carbon concentration, the difficulty disappears. Whether Austenite contains α-iron at 770°C should be determined by x-ray investigations. It is further suggested that the magnetic properties of dilute solutions of ferromagnetic substances in other metals are largely determined by local concentrations of ferromagnetic atoms.

18. Capillary rise in sands of uniform spherical grains. W. O. SMITH, PAUL D. FOOTE, AND P. F. BUSANG, *Gulf Research Laboratory, Pittsburgh.*—Uniform spheres packed in regular

array form a non-cylindrical cyclic capillary, characterized by a maximum and minimum capillary rise with intermediate positions of possible equilibrium. In practice spheres may be packed to a variety of porosities P thus requiring a mixture of regular and irregular piling arranged in a very distorted pattern. However the meniscus is also distorted to conform in a general way with the distortions of the lattice. Accordingly positions of maximum and minimum rise may be expected. The meniscus for maximum rise tends to pass through the plane of centers of neighboring spheres. Slight deviations from this condition due to the rise at sphere contacts are shown to be of minor importance. Any piling may be treated statistically as a hexagonal array with a spacing $2r+d$ where d is computed to give the observed porosity. In such a system three types of cell occur with a definite frequency, and these cell types are assumed present in the meniscus with the same frequency distribution. Hence it is possible to evaluate $pr/a=\rho ghr/\sigma$ where p=perimeter, r=grain radius, a=area of pore opening, g=accelation of gravity, σ=surface tension, ρ=density and h=capillary rise. The final formula so derived reduces to

$$\frac{pr}{a}=\frac{\rho ghr}{\sigma}=\frac{2}{\frac{0.9590}{(1-P)^{2/3}}-1}$$

This agreed with experiments made with several sizes of grains, porosities, and liquids. The minimum rises were also determined but a satisfactory interpretation in terms of a model has not been effected.

19. The variation of the thermal boundary layer of a miniature airfoil. MERIT SCOTT, *Guggenheim Research Physicist, Cornell University.*—By mounting thin, narrow conducting strips parallel to the span of an airfoil, and flush with its surface, it is possible, experimentally, to measure a thermal dissipation coefficient, p_c, associated with a particular location on the lifting surface, as well as its variation with velocity and angle of attack, α. Such measurements have been accomplished with a velocity range of 12 to 24 m/sec and for angles of attack varying from $-40°$ to $+35°$. It is found that p_c, independent of position on the surface, is a linear function of the velocity at the strip. Curves, showing its variation with angle of attack, present definite maxima and minima, characteristics which bear no direct correspondence to the velocity at the strip. It was to be expected that the variation of p_c, at a given location, with angle of attack would be of the same character as its variation with position along the chord. This is experimentally verified. Theoretical considerations suggest converting this coefficient to boundary layer thickness, B, and interpreting this thickness as identical with the viscous boundary layer. The measurements have been extended over the wide range of angle of attack so that the relation of these quantities to the useful range of the airfoil might be studied.

20. The variation of C_p of oxygen and nitrogen with pressure at 26° and 60°C. E. J. WORKMAN, *National Research Fellow, Bartol Research Foundation.*—By the use of improved apparatus of the type previously described by the author (Phys. Rev. **36**, 1083 (1930)) the ratio of C_p at a pressure p to C_p for the same gas at a pressure of one atmosphere is determined. Oxygen and nitrogen gas have been studied at 20 and 60°C in the pressure range 10 to 130 Kg per cm². Values of the ratio as measured may be inferred from smooth curves drawn through the points plotted from the data in the table below, where the pressure is given in Kg/cm².

Oxygen, 26°C		Oxygen, 60°C		Nitrogen, 26°C		Nitrogen, 60°C	
Pressure Kg/cm²	Ratio C_p's	Pressure Kg/cm²	Ratio C_p's	Pressure Kg/cm²	Ratio C_p's	Pressure Kg/cm²	Ratio C_p's
1	1	1	1	1	1	1	1
30	1.052⁰	30	1.035⁵	30	1.044³	30	1.032⁴
60	1.106⁵	60	1.076⁸	60	1.090⁰	60	1.066⁵
90	1.163⁵	90	1.116³	90	1.133²	90	1.099⁰
130	1.241⁰	130	1.168⁰	130	1.186³	130	1.139⁰

21. Some Physiological Effects of Light. BRIAN O'BRIEN, *Institute of Applied Optics, University of Rochester.* Invited paper

22. The Spectra and Anti-Rachitic Potency of Various "Therapeutic" Lamps. HARVEY B. LEMON, *University of Chicago.* Invited paper.

23. Methods of Measuring Radiant Energy. HAROLD W. WEBB, *Columbia University* Invited paper.

24. X-ray measurements of the elastic deformation of metals. WILLIAM P. JESSE, *The General Electric Company.*—The metal wire to be tested lies along the axis of a precision x-ray camera. A series of photographs is taken with various loads on the wire. On the photograph only the lines are measured where the resolving power is a maximum, i.e., where the incident angle θ is almost 90°. As the load on the wire increases, these high order lines shift in the direction indicating smaller grating spaces. This shift measures the contraction of the crystal lattice in a direction perpendicular to the direction of stress. For duralumin wire this contraction is in approximate agreement with the value calculated from the macroscopic Young's modulus and Poisson's ratio for the material. Similar results have been obtained with steel piano wire.

25. A new x-ray tube based on the "transparent target" principle. DIMITRY E. OLSHEVSKY. *Yale University.*—A new "transparent target" x-ray tube is described in which the portion of x-rays transmitted through the target is utilized. It is found that by using a properly designed, thick, double layer target in contradistinction to the thin single layer targets used by Owen and by Coolidge satisfactory heat dissipation may be secured at comparatively little sacrifice due to absorption. The new tube has a target made of a thick layer of low atomic number metal, backing a thin layer of high atomic number metal, in thermal contact with the former. A simplified theory of heat dissipation from the cathode spot is developed and a table is given, showing merits of various target materials as functions of wave-length. Important advantages of the tube over the conventional Campbell-Swinton arrangement are: proximity of the cathode spot to the outer surface of the tube and the possibility of utilizing x-rays in the direction of the initial electron beam. As applied to crystallographic purposes, vertical beam models were built in which the first slit of the spectrograph is defined by a hole drilled in the body of the tube immediately behind the target. This arrangement permits higher intensities at the second slit on account of a shorter slit distance from the cathode spot. Both slits are made integral with the tube, the whole arrangement possessing complete symmetry around the vertical axis. This vertical design, with the beam directed upwards, complete shielding of the tube proper and high tension leads concealed in a grounded table, contributes to the safety and comfort of work and is valuable for x-ray studies involving the liquid state. Special tubes based upon the new principle may prove of value for medical purposes.

26. New K series x-ray lines. WILLIAM DUANE, *Harvard University.*—K series x-rays have been examined by means of a Bragg spectrometer, the Moseley photographic method being employed. The incident ray and that reflected by the crystal to the photographic plate through distances of 4725 mm passed through long metal tubes, exhausted of air in order to reduce the absorption. The K_β doublet lines of molybdenum ($\Delta\lambda = 0.00056$A), examined by photometric curves, appear separated 0.88 mm. No third line lies in the immediate neighborhood of the β doublet. Between the γ line and the short wave-length limit of the series appears a marked blackening that represents several lines close together. They are not in the position of a line reported by Leide. The new lines may be due to 0 electrons falling into the K level, but a better explanation is, perhaps, that the lines are produced by falls into the K level of conductivity electrons which may from time to time lie in outer atomic energy levels. Several photographs produced by long exposures show a fainter single line, roughly halfway between the β_2 and the γ lines. It does not correspond to a known x-ray line of any chemical element reflected in the first or second order.

27. Electron diffraction by a silver crystal. H. E. FARNSWORTH, *Brown University.*—A previous investigation of electron diffraction by a copper crystal, for normal incidence on a (100) face (Phys. Rev. **35**, 1131 (1930)) revealed a series of weak beams requiring unit refractive

index, in addition to the more intense beams requiring refractive indexes greater than unity. These weak beams are in most cases so close in voltage to the main beams that they appear as components or satellites of them. A similar series of measurements for two silver crystals shows, in general, the same to be true for silver, although certain beams have more complex structures containing additional components. In many cases the different components are extraordinarily sharp and intense. These results for low-velocity electrons suggest a complex variation of the inner potential near the surface of the metal.

28. Radiation from low speed electron bombardment of metals. F. L. MOHLER AND C. BOECKNER, *Bureau of Standards.*—A small probe surface at a positive potential in a discharge may draw a current of many amperes per cm^2 with the potential gradient limited to a thin sheath over the surface. Under such conditions a continuous spectrum is emitted by metal surfaces in caesium, potassium, and helium discharges. With a copper probe at 7 volts in caesium vapor, the intensity J remains of the same magnitude between 6200A and 2400A with a minimum at 5800 and a maximum at 3800. Below 4 volts the spectrum has a high frequency limit in this range (3000A for copper at 2.15 volts). On the assumption that this is analogous to a continuous x-ray spectrum, observed limits indicate work functions of 1.95 for Cu, 2.1 for Ag, 1.45 for W (all in caesium vapor). The absolute intensity (except for Ag) agrees within a factor of 2 with values computed from the theoretical equation for intensity of the continuous x-ray spectrum. Efficiency for Cu at 7 volts is estimated as 3×10^{-7}. Comparison with published data on photoelectric effect of radiation from electron bombardment of metals indicates that the magnitude of effects below 10 volts can be explained by this continuous spectrum.

29. The distribution of electricity near the surface of contact of two conductors. A. T. WATERMAN, *Yale University.*—Two dissimilar metals are postulated in contact along an infinite plane, and the equilibrium distribution of electricity is sought in a direction perpendicular to this plane on the basis of Sommerfeld's electron theory using Poisson's equation and the Boltzmann principle. The problem is solved under the assumptions that the potential and the electric intensity are continuous across the boundary, and that the P.D. between points in the two metals far from the boundary is equal to the contact P.D. In general, if the normal concentration of conducting electrons is assumed to be one per atom the electrons in both metals remain in the degenerate state, though their concentration may vary from normal by 30 to 50 percent at the boundary. In this case the distribution is unaffected by temperature. In this special case of a pair of metals with high contact P.D., such as Cs and W, the electrons near the boundary in the more electropositive metal are reduced to the classical state and the distribution is a function of temperature. The possible bearing of these results upon the properties of thin metallic films is discussed.

30. An estimation of patch sizes on a thoriated tungsten filament. LEON B. LINFORD, *National Research Fellow, Princeton University.*—It is well known that coated filaments fail to follow Schottky's equation for thermionic emission in strong accelerating fields. Becker and Mueller (Phys. Rev. **31**, 341 (1928)) showed that the emission from thoriated tungsten is what would be expected if the surface fields were much larger than image fields at distances greater than 10^{-5} cm from the surface. These fields were confirmed by the author using the photoelectric method (Phys. Rev. **36**, 1100 (1930)). One explanation assumes that these large fields are due to a non-uniform surface distribution of positive ions. If these patches are assumed to be square and of dimension b, arranged checkerboard fashion with a contact potential difference V_0 between adjacent patches, the field above the center of a more positive area can be calculated. Using two values of the observed ion field the size of the patches was found to be about 2×10^{-4} cm, with about 0.5 volts contact potential difference V_0. The sum of the field produced by such a charge distribution and the image field was within experimental error of the observed field. From the surface field, and the threshold at a known accelerating field, the work function at zero field was found to be 2.7 volts or 1.8 volts less than that of pure tungsten.

31. Some thermionic properties of barium films absorbed on tungsten. HERBERT NELSON, *RCA Radiotron Company, Harrison, New Jersey (Introduced by G. R. Shaw)*—The activity and the change in contact potential difference have been studied as a function of the thickness of

the barium film. The velocity distribution of the electrons, the effect of non-uniformities in the film, and the effect of field intensity on the activity have also been studied. The experimental tube was constructed such that the measurements could be made on a small area of the filament in order that errors due to lead losses, non-uniformities, and voltage drop along the filament might be minimized. A vacuum tube electrometer was used in measuring the electron currents. The experimental results obtained by Eglin were confirmed, i.e., the activity of the composite surface was found to increase with the thickness of the barium film until an optimum thickness was reached after which further deposit caused the activity to decrease. A relation such as derived by Richardson was found to exist between the thermionic constants and the contact potential difference. The distribution of velocities of the emitted electrons were found to be Maxwellian for all thicknesses of the barium film. The presence of non-uniformities in the emitting surface had the effect of decreasing the slope of the Maxwellian distribution curve.

32. Time changes in oxide-coated filaments. E. F. LOWRY AND W. T. MILLIS, *Westinghouse Electric and Mfg. Co., East Pittsburgh.*—The oscillograph is made use of in studying time changes in the electron emission of oxide-coated filaments. The decay of emission with time while drawing current is compared with rate of recovery when instantaneous measurements are made. It is found that similar phenomena, though of much less magnitude, occur when thoriated tungsten or bariated filaments are used. It has also been found that this fading effect is not a universal characteristic of oxide filaments though it is present in greater or less amount in the majority of instances. Oscillograph methods have also been employed in studying oxide emission at normal operating temperature.

33. Grid current required by hot-cathode, grid controlled mercury arcs before discharge. W. B. NOTTINGHAM, *Bartol Research Foundation.*—The hot-cathode, grid-controlled mercury arc or "thyratron" has been described by A. W. Hull, (G. E. Rev. **32**, 213 and 390 (1929)). Although the thyratron has been called "an electrostatically controlled arc rectifier," a definite grid current is required in the grid or control circuit. With a d.c. plate potential, this grid current, before the discharge begins may have any value from 6×10^{-3} amp. to -10^{-7} amp. depending on the type of thyratron, the plate potential and the mercury condensation temperature. In certain cases, the temperature enters so drastically that a change in ambient temperature of only a few degrees can cause the thyratron to fail to operate. With 60 cycle a.c. plate and grid potentials, experiment seems to show that 0.001 second is required to set up conduction in the thyratron. A time lag of this amount was unexpected. A comparison of the "phase shift" and "critical potential" methods of controlling a thyratron with photoelectric currents showed that for extremely small light intensities, the critical potential method is the more sensitive, although for greater light intensities the phase-shift method is perhaps more reliable. Satisfactory operation using either method of control was obtained with 10^{-8} amp. photoelectric current (approx. 3×10^{-4} lumen). The measurements were made on General Electric FG-17; FG-27 and FG-67 thyratrons.

34. A further study of galvanoluminescence. ROY RICHARD SULLIVAN WITH R. T. DUFFORD, *Bell Telephone Laboratories and The University of Missouri.*—Previous work by one of the writers has been checked and extended in several directions. The glow surrounding aluminum anodes was studied in several new solutions, as well as those already described. Several-fold larger efficiencies have been obtained by using water-cooled electrodes. Study of the glow seems to be against the theory of a gas film covering the electrode; the spectrum of the glow is a typical luminescence spectrum, and the brightness and efficiency lie in the same range as for other luminescent reactions under study in this laboratory. In many cases, the law of increase of brightness with voltage seems to have closely the same form as for a tungsten filament. The spectrum of the sparkles which appear at higher voltages is, however, a bright-line spectrum; the two strongest lines coincide with the strongest lines in the spark spectrum of aluminum. The glow surrounding various metals in ether solutions of Grignard reagents and of $MgBr_2\cdot 2(C_2H_5)_2O$ has been studied, giving the highest efficiencies so far found in this type of luminescence. Systematic differences between chemical groups of metals are found. The work was done at the University of Missouri.

35. Intensities of the magnetic and electric illumination components in the electrodeless discharge. CHAS. T. KNIPP, *University of Illinois.*—Recent theory (J. T. Tykociner and J. Kunz, Chicago Meeting, American Physical Society, November 1930, paper No. 5) indicates that a considerable portion, perhaps even 80 or 90 percent of the illumination in the electrodeless discharge is due to the electrostatic field. A discharge vessel was constructed experimentally to test this point. Obstructions were set in it with the idea that each type of discharge would cast its own shadow. With the most favorable conditions for a discharge passing due wholly to the magnetic field, shadows were obtained in the plane of the exciting coil which extended one-third way around the tube, while there were no indications of shadows at right angles, i.e., in the direction of the electrostatic field. By placing a band conductor to the right and to the left of the medial line, and removing the energizing coil entirely, a powerful electrostatic field was produced and shadows in this direction were now readily obtained, but the characteristic ring discharge was gone. Hence it appears, when conditions are favorable for the formation of *ring discharges*, that the intensity of the attending illumination is in part, if not entirely, due to carriers moving in the plane of the energizing coil. This result seems to support the calculations of Sir J. J. Thomson.

36. High frequency behavior of a plasma. LEWI TONKS, *General Electric Company, Schenectady, N. Y.*—Earlier work on spontaneous short-wave oscillations in a low-pressure mercury arc plasma (Phys. Rev. **33**, 195 (1929)) has been extended to forced oscillations by experiments similar to those of H. Gutton (Ann. de Physique **13**, 62 (1930)). Theory gives $K=1-\nu_e^2/\nu^2$, where ν is the impressed, ν_e $(=8980\ (N_e)^{1/2})$ the plasma-electron frequency, for the specific inductive capacity of a plasma. The unit cube thus behaves like a tuned shunt circuit $C=1/4\pi$, $L=m_e/N_e e^2$. This disagrees with Gutton's conclusion. A modified Mossotti theory requires that a cylindrical plasma between plane condenser plates show shunt resonance when $\nu_e=(2)^{1/2}\nu$. With a constant impressed frequency, the positive column of a Hg arc always resonated at two values of arc current (ionization density) and sometimes at three, due possibly, to the non-uniformity of the plasma cross-section. The two main resonance densities were roughly in the ratio 2 to 5 and lay above and below the theoretical value. The variation with frequency was $\nu_e \propto \nu^{1.1}$ cf. $\nu^{1.0}$ theoretically. Above resonance $(\nu_e > (2)^{1/2}\nu)$ the variation of K with ν_e as given above was confirmed.

37. Oscillations and travelling striations in an argon discharge tube. T. C. CHOW, *Princeton University.* (*Introduced by* H. D. SMYTH).—Oscillations of audible frequencies in an argon discharge tube with a long positive column were observed in a pressure range 0.06 to 4.2 mm Hg. The amplitude of the fluctuation of voltage across discharge tube is of the order of magnitude of 10 volts. Only in a certain portion of that pressure range distinct travelling striations were observed. The flash frequency, defined as the number of striations passing across a certain cross-section per second was approximately equal to the frequency heard in a telephone receiver attached to the circuit. It was found to depend on conditions in the circuit, such as current, external resistance, inductance, capacity, and filament current. The space potentials in the tube were also found to fluctuate. Tonks and Langmuir have described a kind of electric sound waves, possible if a certain condition involving electron temperature and concentration and the wave-length of the sound waves is satisfied. This condition was satisfied in our experiment. From their expression for the velocity of electric sound waves and the experimentally determined flash frequencies a set of wave-lengths were calculated most of which are integral or half-integral multiples of the length of the discharge tube.

38. The fall of potential in condensed discharges. J. C. STREET, *University of Virginia.*—The fall of potential in the initial stages of discharges has been studied by utilizing the well-known fact that an electric pulse on a wire when reflected from an open end of the wire has its maximum potential doubled at reflection, provided the length of the pulse is not greater than twice that of the wire. Transient electric pulses produced by the condensed discharge under investigation traveled along two parallel, symmetrical, straight wires to their open ends where they were reflected. The maximum potential across the open ends was measured as a function of the length of wire from the spark gap by two independent methods and was found to de-

crease when the lead wires became a few meters in length. From this curve the rate of potential fall can be obtained directly by electric circuit theory. In the case of static sparks at atmospheric pressure, where the potential was slowly applied, a comparatively slow fall of potential (6% in 2×10^{-8} sec.) was obtained at the beginning, but a very rapid (94% to $1/e$ of value in 2×10^{-8} sec.) fall later. This result is in fair agreement with the results obtained by Rogowski and Klemperer (Archiv. f. Electrot. **24**, 127 (1930)) using a different method. When the pressure in the spark gap was decreased the rate of fall of potential in the initial stages was decreased. The method gives an easy way of studying the fall of potential in various kinds of discharges and is free from certain objections inherent in other methods. Such measurements, aside from giving information concerning the electrical breakdown itself, are desirable for a complete understanding of the operation of Kerr cells and cathode-ray oscillographs.

39. The Kerr electro-optical effect in gases. E. C. STEVENSON AND J. W. BEAMS, *University of Virginia.*—The electric double refraction or Kerr electrooptical effect in CO_2 has been studied as a function of the density and the temperature. The method previously reported (Phys. Rev. **35**, 1440 (1930) and O.S.A. program Oct. 31, 1930) has been refined so that the temperature of the Kerr cell can be set and maintained to 0.05°C. The average deviation of the Kerr constant per molecule was found to be less than 2 percent throughout the density range from 0.08 to 0.18 grams per cubic centimeter when the temperature, electric field, and wave-length band (4700A to 4300A) were kept constant. Holding the density, electric field and wave-length fixed the Kerr constant per molecule was observed to increase with decreasing temperature. Our preliminary results show that this increase was approximately 10 percent for a temperature change from 45°C to 20°C which is in rough agreement with what might be expected from theory.

40. On the correlation of radio reception with the position of the Moon in the observer's sky. HARLAN T. STETSON, *Ohio Wesleyan University.*—Observations of the intensities of radio reception at the Perkins Observatory and elsewhere have been utilized for a study of correlation of signal strengths with cosmic phenomena. Papers already published by the writer and by Greenleaf W. Pickard call attention to apparent change in the altitude of the Kennelly-Heaviside layer with the change in solar activity. The same data have now been utilized in an investigation of the possible relation between the intensity of signal strength and the position of the moon with respect to the observer, on the assumption that the moon is at a different electrical potential from that of the earth. The result of the observations indicates that the height of the Kennelly-Heaviside layer is substantially decreased by the presence of the moon above the horizon, and elevated as the moon passes underneath the observer. A plausible explanation follows on the assumption that the moon is negatively charged with respect to the earth. The form of the curve showing correlation between the moon's altitude and the intensity of radio reception suggests an electronic tide which follows a hypothetical equipotential surface in the electrostatic field of the earth-moon system.

41. Optical dispersion of helium. HENRY MARGENAU, *Yale University.*—The numbers of dispersion electrons (f-values) for helium calculated from Hopfield's intensity data by the semi-empirical method outlined in the author's first paper in this bulletin are used to construct an optical dispersion formula. Attention is to be called to the fact that transition matrices, computed from intensities of emission lines, are subject to considerable error. Nevertheless, the dispersion formula thus obtained, in which none of the constants are adjusted in the usual fashion, shows satisfactory agreement with the experimental data on the refractive index.—The theory of molecular forces is extended to a calculation of dissociation potentials and vibrational levels of the molecules Hg-rare gas, observed by Oldenberg.

42. Intensities in the ultraviolet spectrum of mercury. E. D. MCALISTER, *Division of Radiation and Organisms, Smithsonian Institution.*—The intensities of the major spectral lines in the region 2000 to 4000A from a mercury vacuum arc have been measured. A quartz double monochrometer and vacuum thermocouple were employed. The effective slit width was 2A

at 2100A increasing to 12A at 4000A. The 2537 line gave a deflection of 50 mm with a 4A slit width. The intensities of the first four "sharp" triplets are quite close to the theoretical 1–3–5 rule.

43. Application of spinor analysis to the Maxwell and Dirac equations. OTTO LAPORTE AND GEORGE E. UHLENBECK, *University of Michigan.* With the spinor analysis developed by B. Van der Waerden (Gött. Nach. 1929, p. 100), which comprises all representations of the Lorentz group, even those not contained in ordinary tensor calculus, one is able to write all derivations and equations in an *automatically covariant form.* For the convenient translation into spinor language of Maxwell equations, it becomes important to introduce three self dual tensors, one representing the electromagnetic field, one corresponding go the Hertzian vector, and one representing a kind of current potential. These correspond to symmetric spinors of the 2nd rank. Many spinor equations thus become simpler than the corresponding tensorial equations, especially the expression for the stress energy tensor. From the 1st order Dirac equations in spinor form, as given by v.d. Waerden, we derived the 2nd order equations, which agree with the Gordon-Klein form but for a correction term which again contains the self dual field tensor. Further the expression for the current was obtained, and its decomposition into conduction and polarization currents, and finally both Maxwell and Dirac equations were derived from a spinorial variation principle, analogous to the results of Gordon and Darwin.

44. Stereoscopic three dimensional models showing the electron's motion in the Stark effect. R. W. WOOD, *Johns Hopkins University.* By means of multiple exposures with a stereoscopic camera of a rotating wire frame representing the curved quadrangle formed by the intersection of the parabolic coordinates of the Epstein-Schwarzchild treatment of the Stark effect, within which quadrangle the electron is progressively advanced along a properly curved wire, the orbital motion within the anchor-ring is very clearly brought out. The pictures when viewed with a stereoscope show the anchor-ring as a wire cage within which the precessing orbit appears as a white dotted line. The change in orientation and eccentricity of the orbit, with the constancy of the distance of the electric center from the YZ plane (field parallel to X) are easily seen. Photographs are shown illustrating various assignments of the quantum numbers n_1 and n_2.

45. Improved technique for Raman effect. R. W. WOOD, *Johns Hopkins University.*—For excitation by the mercury arc I find that the highest efficiency is obtained with a Hanovia quartz arc (220 volts) in a metal housing with a narrow rectangular aperture just over the horizontal burner. After much experimenting with filters, I have found that two only are needed, except in special cases. A solution is made of about 1.5 grams of suphate of quinine in 500 cc of water, acidulated with a little sulphuric acid. This is contained in a glass tube 2 inches in diameter and 12 inches in length which acts as a cylindrical lens, when mounted just above the burner. Photochemical change can be nearly prevented by a thin sheet of Corning noviol glass, transparent to 4046A and opaque to 3650A. The yellowing of the quinine is due almost entirely to the 3650 group of lines. A space of about 1 cm is left between the noviol plate and the aperture in the lamp housing for a stray draught of air from a fan. A concave reflector of polished aluminum is placed over the tube containing the liquid under investigation, which is mounted above and in contact with the filter tube. This arrangement is two or three times as efficient as any arrangement for absorbing 4046 by glass filters. The Zeiss filter, if heavy enough to reduce 4046 to one percent of its value, reduces 4358 to one third of its value. Quinine is perfectly transparent to 4358. For excitation by 4046, the 4358 line is removed by a solution of iodine in carbon tetrachloride. A saturated solution diluted to about 1:15 with CCl_4 will practically suppress 4358, when contained in a tube 1.75 inches in diameter. A 1:30 dilution will suppress all modified lines due to 4358, but the unmodified group comes out fairly strong. A 1:10 or even a 1:5 dilution can be used but with the latter concentration 4046 is considerably weakened. The iodine tube is used with the noviol glass plate below it. The cooling can be increased by mounting a flat plate in such a position as to concentrate the air draught into the gap between the top of the lamp and the noviol glass plate.

46. The masses of O^{17}. HAROLD C. UREY, *Columbia University.*—Blackett (Proc. Roy Soc. **107A**, 359) and Harkins and his co-workers (Zeits. f Physik **50**, 97; Phys. Rev. **35**, 809 (1930)) have given the velocities of the nuclei involved in the transmutation reaction $N^{14}+He^4 \rightarrow O^{17}+H^1$ and these together with the rest masses of N^{14}, He^4 and H^1 of Aston permit a calculation of the rest mass of the O^{17} atom by assuming the conservation of mass and energy. The atomic weight of O^{17} calculated from 8 sets of data available varies from 17.00133 to 17.00502 ($O^{16}=16$). The absolute value is not certain to this number of significant figures since Aston's values are not so certain but the uncertainty due to the probable errors in the rest masses of N^{14}, He^4 and H^1 is the same for all 8 cases and the differences must be accounted for in some other way. The discrepancies are far greater than the probable errors in Blackett's measurements. The most probable reason for them appears to be that O^{17} atoms with different masses and energies are produced and that the different values are due to different energy levels of the O^{17} nucleus. Then, the gram atomic rest mass of the O^{17} atom in the normal nuclear state is equal to or less than $17.00133 \pm \backsim 0.0028$, i.e. the smallest value observed.

47. Regularities in an emission spectrum of CO_2. H. D. SMYTH AND T. C. CHOW, *Princeton University.*—About a year ago Smyth and Arnott did some work on the excitation of the band spectrum of nitrogen by an electron beam. The method used seemed to offer two advantages for the study of the spectra of polyatomic gases, namely small chance for dissociation and a somewhat simplified spectrum. The method has been applied to CO_2 and spectra obtained showing hardly a trace of CO bands. The spectrum obtained is nearly identical with that measured by Fox, Duffendack and Barker. With their data, supplemented by preliminary measurements of our own plates, we have found a divergent set of 14 vibration terms given by $\nu = 1101.7n + 1.7n^2$ taking the lowest as zero. These combine with three higher doublet terms which are probably part of another vibration set and appear to converge strongly. Referred to the lowest of the first set as zero they are, taking the lower of each pair, 31,953.1, 34,833.0 and 37,455.1 wave-number units. The upper member is 167 wave-numbers higher in each case. Though it is impossible to be certain which is the higher and which the lower of these two sets of levels, either choice gives one set of levels divergent over the range studied.

48. Absorption of iodine lines by atoms from optically dissociated molecules. LOUIS A. TURNER AND E. W. SAMSON, *Princeton University.*—Great improvement over former results (Phys. Rev. **31**, 983 (1928)) has been obtained by use of (1) a vacuum spectrograph, (2) argon at 5 cm pressure in the absorption cell, to retard diffusion of atoms to the walls, (3) a source giving fine unreversed lines (pressure 0.003 mm, excitation by short wave oscillator, outside electrodes). The absorption cell contained I_2 at a pressure of 0.03 mm and was illuminated by full light from a 13 ampere carbon arc. The only three lines in the region investigated ($\lambda > 1630$) which result from combination with the $^2P_{1\frac{1}{2}}$ ground term, viz. 1830, 1782, and 1642 are all strongly absorbed upon illumination of the absorption cell. Six others from combination with $^2P_{\frac{1}{2}}$ are not absorbed.

49. Hyperfine structure in the copper spectrum. A. G. SHENSTONE, *Princeton University*—As a result of recent observations of hyperfine structure in the copper spectrum, it can be stated that the nuclear moment is almost certainly $1\frac{1}{2}$. Several lines for which the upper state is d^9s, $s^4\ D_{3\frac{1}{2}}$ have four rather widely spaced components and all other lines from that level are wide, though unresolved by the apparatus available. The term d^9s, $s^4\ D_{\frac{1}{2}}$ has two components. Lines due to the other two members of this term do not appear in the source at all. This is probably due to the Auger effect; and, if so, it is the first observation of that effect in an atomic spectrum. Back's observation of the resonance lines and Wali-Mohammad's observation of the $d^9s^2\ ^2D_{1\frac{1}{2}}$ lines can be reconciled with the nuclear moment $1\frac{1}{2}$. Silver shows no hyperfine structure.

AUTHOR INDEX

Second Series *May 1, 1931* *Vol. 37, No. 9*

THE
PHYSICAL REVIEW

THE THEORY OF COMPLEX SPECTRA II*

By E. U. Condon and G. H. Shortley
Palmer Physical Laboratory, Princeton University

(Received March 20, 1931)

Abstract

Formulas for the relations between the energies of multiplets arising from the same electron configuration for all two-electron configurations up to *ff* and several cases of three-electron configurations are worked out following Slater's method; Slater's table of *a*'s and *b*'s being extended to cover *f* electrons. A systematic comparison of the known data with this first order perturbation theory shows poor agreement in many cases and good agreement in many. The theory predicts the observed alternation in the relative positions of singlet and triplet through *S*, *P*, *D*, *F*, etc. in the *pp*, *pd*, and *pf* triads, and the *dd* and *df* pentads. In general the *p* electron configurations fit very poorly; a uniform trend with atomic number is observed for p^3 and good fits are obtained for $4p3d$ in Ti III, V IV, and Cr V. For *d* electrons the theory fits very well in the first long period of the periodic table, and fairly well in the second. The ^1S of d^2 and the ^2D of d^3s are predicted much higher than the levels assigned to those multiplets when such an assignment is made. d^3 fits well except for ^2P. An energy level table of La II is given as recently analysed by Meggers and Russell. Here we have complete $5d4f$ and $4f^2$ configurations which fit the theory very well, these calculations having assisted in the assignment of some of the singlets and resulted in a rearrangement of singlet lines.

§1. Introduction

THIS paper is a sequel to one[1] published last fall in which the first steps were taken toward working out the second approximation for atomic spectra with Russell-Saunders coupling. Before going on with that work it was thought desirable to make a careful study of the application of the first approximation formulas, given by Slater's method,[2] to all of the known data. That is the subject of this paper.

It will be recalled that the first-order calculation gives formulas for the energy of each of the multiplets arising from a given electron configuration in terms of certain integrals taken over the radial factor of the wave function for an electron in the central force field that lies at the basis of the calculations. These integrals represent the perturbation energy due to the electro-

* This paper was presented at the New York Meeting of the American Physical Society, February 27, 1931.

[1] Condon, Phys. Rev. **36**, 1121 (1930).

[2] Slater, Phys. Rev. **34**, 1293 (1929).

static repulsion of the electrons. It is inconvenient to work out these integrals for they involve the unknown wave functions of the screened average force field in which the electrons move. Instead these integrals are treated as adjustable (except for restrictions such as that certain of them are essentially positive, etc.) in order to see how well the data can be represented. If a good fit is obtained that is, therefore, only a partial confirmation of the theory, for the question still remains open whether the relative magnitudes assumed for the several integrals are really compatible with their definition as integrals.

Since Meggers and Russell[3] have recently obtained for the first time, in La II, complete sets of multiplets involving the two-electron configurations pf, df, f^2 we have thought it worthwhile to extend Slater's tables of a's and b's to provide the necessary coefficients for applying the method to configurations involving f electrons. These results are presented in §2. In §3 and §4 the explicit formulas are given for the first-order energies in a number of important configurations and in §5, §6, and §7 comparison of the formulas with the data is made.

§2. Slater's Coefficients for f Electron Configurations

In Slater's paper[2] there are a few details connected with normalization that need to be straightened out. Slater, in his manuscript, had normalized his wave functions in an unusual way: namely, so that the normalizing integral over the spherical harmonic factor was set equal to 4π instead of 1. This requires the normalizing integral over the radial coordinate to be set equal to $1/4\pi$. When his paper went through the Physical Review office one of us (E.U.C.) thought that a mistake had been made in the normalizing factor and inserted a $(2\pi)^{-\frac{1}{2}}$ to normalize the $\Phi(m_l/\phi)$ on page 1308 in the usual way. As Slater was in Europe at the time he did not have an opportunity to set the matter straight again. Therefore this factor should be removed from the $\Phi(m_l/\phi)$ on page 1308 and then it should be borne in mind, what Slater does not mention, that the radial wave-function is to be normalized to $1/4\pi$ instead of 1. The usual normalization of each factor to 1, is the one we prefer. To have this one needs to leave the Φ factor as printed on page 1308, to insert $2^{-\frac{1}{2}}$ on the right side of the equation defining $\Theta(lm_l/\theta)$ on that page, to remove the factor 4π in the equation for $I(nl)$ on page 1310 and the factor $(4\pi)^2$ in the equations for $F^k(nl; n'l')$ and $G^k(nl; n'l')$ on page 1311.

We have also found it convenient to treat the a's and b's of page 1311 as integers by associating the denominator of the a's and b's as they occur in the tables of page 1312 with the corresponding F. Therefore we write

$$F_k(nl; n'l') = \frac{1}{D_k} F^k(nl; n'l')$$

where F^k is Slater's F and D_k is the denominator of the fractional value for $a^k(l, m_l; l'm_l')$ as given on page 1312. The corresponding definition of G_k is also made.

[3] See §7 of this paper.

Having detected an error in Slater's table of b's by reaching an inconsistency in deriving the energy levels for the pd configuration it was thought worthwhile to check these tables by a complete recalculation using Gaunt's formulas[4] for the integrals. These formulas were also used to extend the tables to the pairs, sf, pf, df, ff. This straightforward but laborious computation makes us now feel confident that there are no errors in Slater's table of page 1312 except the one originally detected. The value

$$b^3(1, \pm 1; 2, \mp 2) = 45/245$$

is correct, instead of 9/245 as printed.

The extension to f electron values is covered in Tables I and II.

TABLE I. *Extension of table of* $a^k(lm_l; l'm_l')$

Electrons	l	m_l	l'	m_l'	$k=$ 0	2	4	6
sf	0	0	0	±3	1			
				±2	1			
				±1	1			
				0	1			
pf	1	±1	3	±3	1	5/75		
	1	±1	3	±2	1	0		
	1	±1	3	±1	1	− 3		
	1	±1	3	0	1	− 4		
	1	0	3	±3	1	−10		
	1	0	3	±2	1	0		
	1	0	3	±1	1	6		
	1	0	3	0	1	8		
df	2	±2	3	±3	1	10/105	3/693	
	2	±2	3	±2	1	0	− 7	
	2	±2	3	±1	1	− 6	1	
	2	±2	3	0	1	− 8	6	
	2	±1	3	±3	1	− 5	−12	
	2	±1	3	±2	1	0	28	
	2	±1	3	±1	1	3	− 4	
	2	±1	3	0	1	4	−24	
	2	0	3	±3	1	−10	18	
	2	0	3	±2	1	0	−42	
	2	0	3	±1	1	6	6	
	2	0	3	0	1	8	36	
ff	3	±3	3	±3	1	25/225	9/1089	1/7361.64
	3	±3	3	±2	1	0	−21	− 6
	3	±3	3	±1	1	−15	3	15
	3	±3	3	0	1	−20	18	− 20
	3	±2	3	±2	1	0	49	36
	3	±2	3	±1	1	0	− 7	− 90
	3	±2	3	0	1	0	−42	120
	3	±1	3	±1	1	9	1	225
	3	±1	3	0	1	12	6	−300
	3	0	3	0	1	16	36	400

Note: In cases with two ± signs, the two can be combined in any of the four possible ways.

§3. THE ENERGY LEVELS IN TWO-ELECTRON CONFIGURATIONS

Slater has treated in detail the method whereby the energy levels of the several multiplets are to be found in terms of the F and G perturbation integrals and has given some examples. He has shown that the electrons in

[4] Gaunt, Phil. Trans. Roy. Soc. **A228**, 151 (1929).

closed shells are without direct effect on the perturbation theory, although of course, they have the indirect effect of determining the nature of the best

TABLE II. *Extension of table of* $b^k(lm\,;\,l'm_l')$

Electrons	l	m_l	l'	m_l'	$k=0$	1	2	3	4	5	6
sf	0	0	3	±3				1/7			
	0	0	3	±2				1			
	0	0	3	±1				1			
	0	0	3	0				1			
pf	1	±1	3	±3			45/175		1/189		
	1	±1	3	±2			30		3		
	1	±1	3	±1			18		6		
	1	±1	3	0			9		10		
	1	0	3	±3			0		7		
	1	0	3	±2			15		12		
	1	0	3	±1			24		15		
	1	0	3	0			27		16		
	1	±1	3	∓3			0		28		
	1	±1	3	∓2			0		21		
	1	±1	3	∓1			3		15		
df	2	±2	3	±3		15/35		10/315		1/1524.6	
	2	±2	3	±2		5		20		5	
	2	±2	3	±1		1		24		15	
	2	±2	3	0		0		20		35	
	2	±1	3	±3		0		25		7	
	2	±1	3	±2		10		15		24	
	2	±1	3	±1		8		2		50	
	2	±1	3	0		3		2		80	
	2	0	3	±3		0		25		28	
	2	0	3	±2		0		0		63	
	2	0	3	±1		6		9		90	
	2	0	3	0		9		16		100	
	2	±2	3	∓3		0		0		210	
	2	±2	3	∓2		0		0		126	
	2	±2	3	∓1		0		10		70	
	2	±1	3	∓3		0		0		84	
	2	±1	3	∓2		0		25		112	
	2	±1	3	∓1		0		15		105	
ff	3	±3	3	±3	1		25/225		9/1089		1/7361.64
	3	±3	3	±2	0		25		30		7
	3	±3	3	±1	0		10		54		28
	3	±3	3	0	0		0		63		84
	3	±2	3	±2	1		0		49		36
	3	±2	3	±1	0		15		32		105
	3	±2	3	0	0		20		3		224
	3	±1	3	±1	1		9		1		225
	3	±1	3	0	0		2		15		350
	3	0	3	0	1		16		36		400
	3	±3	3	∓3	0		0		0		924
	3	±3	3	∓2	0		0		0		462
	3	±3	3	∓1	0		0		42		210
	3	±2	3	∓2	0		0		70		504
	3	±2	3	∓1	0		0		14		378
	3	±1	3	∓1	0		24		40		420

Note: In cases where there are two ± signs, the two upper or the two lower signs must be taken together.

central field on which to base the approximation. Therefore, we do not need to give the details of the calculations but merely summarize the results.

Slater's F^k integrals are necessarily positive and decreasing with increas-

ing k, from their definition. Therefore, since the denominator D in the definition of our F_k increases rapidly, F_k necessarily decreases very rapidly with increasing k. Since the G's are not essentially positive by definition, no definite statement can be made concerning their relative magnitudes; however, in every instance we have found, the G_k's have been positive and rapidly decreasing with k. Although not consistent with its definition as an integral, it is convenient to measure F_0, which occurs in the formula for each multiplet, from an arbitrary low level of the spectrum. (Slater's theory provides an integral I, dependent only on the configuration, to locate the height of the whole multiplet.)

If one electron is in an s state the result is simply a singlet and triplet whose L is the l of the other electron outside closed shells, as Slater shows on page 1315, duplicating by this method a result of Heisenberg.

For pp, non-equivalent p electrons, Slater gives the triplet intervals. The complete formulas are, if ${}^3P$ is written for "relative energy of the center of gravity of the ${}^3P$ terms,"

$$\begin{aligned}
{}^1S &= F_0 + 10F_2 + G_0 + 10G_2 \\
{}^3S &= F_0 + 10F_2 - G_0 - 10G_2 \\
{}^1P &= F_0 - 5F_2 - G_0 + 5G_2 \\
{}^3P &= F_0 - 5F_2 + G_0 - 5G_2 \\
{}^1D &= F_0 + F_2 + G_0 + G_2 \\
{}^3D &= F_0 + F_2 - G_0 - G_2
\end{aligned} \qquad (pp)$$

We note that the arithmetic mean of the corresponding singlet and triplet energies is independent of the G's while corresponding singlet-triplet intervals are independent of F's. Also since $G_2 \ll G_0$ usually we have ${}^1S > {}^3S$ and ${}^1P < {}^3P$ and ${}^1D > {}^3D$; an alternation which is quite a general prediction of the theory.

For p^2, equivalent p electrons, the ${}^3S$, ${}^1P$ and ${}^3D$ are ruled out by the exclusion principle and the formulas for what is left are the same as those for the arithmetic means of singlet and triplet in pp, namely

$$\begin{aligned}
{}^1S &= F_0 + 10F_2 \\
{}^3P &= F_0 - 5F_2 \\
{}^1D &= F_0 + F_2.
\end{aligned} \qquad (p^2)$$

The formulas for dd and d^2, also ff and f^2, show similar relationships. For dd we have

$$\begin{aligned}
{}^1S, {}^3S &= F_0 + 14F_2 + 126F_4 \pm (G_0 + 14G_2 + 126G_4) \\
{}^1P, {}^3P &= F_0 + 7F_2 - 84F_4 \mp (G_0 + 7G_2 - 84G_4) \\
{}^1D, {}^3D &= F_0 - 3F_2 + 36F_4 \pm (G_0 - 3G_2 + 36G_4) \\
{}^1F, {}^3F &= F_0 - 8F_2 - 9F_4 \mp (G_0 - 8G_2 - 9G_4) \\
{}^1G, {}^3G &= F_0 + 4F_2 + F_4 \pm (G_0 + 4G_2 + G_4)
\end{aligned} \qquad (dd)$$

where the upper sign is for the singlet and the lower for the triplet. For d^2 the multiplets are ^1S, ^3P, ^1D, ^3F, ^1G and their energies are given by the same formulas upon omitting the terms involving G integrals.

For pd the formulas are

$$\begin{aligned} {}^1P, {}^3P &= F_0 + 7F_2 \pm (\ G_1 + 63G_3) \\ {}^1D, {}^3D &= F_0 - 7F_2 \mp (3G_1 - 21G_3) \\ {}^1F, {}^3F &= F_0 + 2F_2 \pm (6G_1 + 3\ G_3). \end{aligned} \tag{pd}$$

This shows the same alternation in sign of the leading G integral but differs from the preceding ones in that the F and G parts are not similar.

The formulas for pf are

$$\begin{aligned} {}^1D, {}^3D &= F_0 + 12F_2 \pm (\ 3G_2 + 36G_4) \\ {}^1F, {}^3F &= F_0 - 15F_2 \mp (15G_2 - 9G_4) \\ {}^1G, {}^3G &= F_0 + 5F_2 \pm (45G_2 + G_4). \end{aligned} \tag{pf}$$

The formulas for df are

$$\begin{aligned} {}^1P, {}^3P &= F_0 + 24F_2 + 66F_4 \pm (\ G_1 + 24G_3 + 330G_5) \\ {}^1D, {}^3D &= F_0 + 6F_2 - 99F_4 \mp (\ 3G_1 + 42G_3 - 165G_5) \\ {}^1F, {}^3F &= F_0 - 11F_2 + 66F_4 \pm (\ 6G_1 + 19G_3 + 55G_5) \\ {}^1G, {}^3G &= F_0 - 15F_2 - 22F_4 \mp (10G_1 - 35G_3 - 11G_5) \\ {}^1H, {}^3H &= F_0 + 10F_2 + 3F_4 \pm (15G_1 + 10G_3 + G_5). \end{aligned} \tag{df}$$

Finally the formulas for two non-equivalent f electrons are

$$\begin{aligned} {}^1S, {}^3S &= F_0 + 60F_2 + 198F_4 + 1716F_6 \pm (G_0 + 60G_2 + 198G_4 + 1716G_6) \\ {}^1P, {}^3P &= F_0 + 45F_2 + 33F_4 - 1287F_6 \mp (G_0 + 45G_2 + 33G_4 - 1287G_6) \\ {}^1D, {}^3D &= F_0 + 19F_2 - 99F_4 + 715F_6 \pm (G_0 + 19G_2 - 99G_4 + 715G_6) \\ {}^1F, {}^3F &= F_0 - 10F_2 - 33F_4 - 286F_6 \mp (G_0 - 10G_2 - 33G_4 - 286G_6) \\ {}^1G, {}^3G &= F_0 - 30F_2 + 97F_4 + 78F_6 \pm (G_0 - 30G_2 + 97G_4 + 78G_6) \\ {}^1H, {}^3H &= F_0 - 25F_2 - 51F_4 - 13F_6 \mp (G_0 - 25G_2 - 51G_4 - 13G_6) \\ {}^1I, {}^3I &= F_0 + 25F_2 + 9F_4 + F_6 \pm (G_0 + 25G_2 + 9G_4 + G_6), \end{aligned} \tag{ff}$$

from which the values for f^2 can be obtained by ignoring the part involving G integrals and remembering that the allowed terms are ^1S, ^3P, ^1D, ^3F, ^1G, ^3H and ^1I.

The most striking thing about these results perhaps is the uniform way in which an alternation of the relative height of singlet and triplet is predicted, since in most cases the G of lowest index will be enough larger than the others to dominate the whole expression in the G's. Russell and Meggers[5] called attention to this alternation in 1927 and "commended it to the attention of theoretical investigators." Its explanation by the quantum mechanics must be counted as an important success for the theory.

[5] Russell and Meggers, Sci. Papers Bur. Stand. 22, 364 (1927).

§4. Three-Electron Configurations

It would be a waste of time to work out all possible three-electron configurations at present, therefore we confine ourselves to cases for which we have been able to find experimental data with which to check the results. The addition of an s electron to p^2, d^2 or pd gives three important cases.

According to the vector coupling viewpoint the addition of an s electron to p^2 gives the results ${}^1S\to{}^2S$, ${}^3P\to{}^2P$ and ${}^4P$, and ${}^1D\to{}^2D$. In the formulas for p^2s the F integrals are of the type $F(np^2)$ while there now appears a G integral to represent the action of the s electron, which is $G_1(np, n's)$:

$$\begin{aligned} {}^2S &= F_0 + 10F_2 - G_1 \\ {}^2P &= F_0 - 5F_2 + G_1 \\ {}^4P &= F_0 - 5F_2 - 2G_1 \\ {}^2D &= F_0 + F_2 - G_1 \end{aligned} \qquad (p^2s)$$

where $F_0 = 2F_0(np, n's) + F_0(np^2)$. Thus $3G_1$ is the ${}^2P-{}^4P$ interval and the quantities ${}^2S$, $({}^2P+2{}^4P)/3$ (which is the center of gravity of this combination), and ${}^2D$ have the same intervals as ${}^1S$, ${}^3P$ and ${}^1D$ in p^2.

Similar results hold for d^2s. Here too the singlets of d^2 become doublets and the triplets split into doublets and quartets:

$$\begin{aligned} {}^2S &= F_0 + 14F_2 + 126F_4 - G_2 \\ {}^2P &= F_0 + 7F_2 - 84F_4 + G_2 \\ {}^4P &= F_0 + 7F_2 - 84F_4 - 2G_2 \\ {}^2D &= F_0 - 3F_2 + 36F_4 - G_2 \\ {}^2F &= F_0 - 8F_2 - 9F_4 + G_2 \\ {}^4F &= F_0 - 8F_2 - 9F_4 - 2G_2 \\ {}^2G &= F_0 + 4F_2 + F_4 - G_2 \end{aligned} \qquad (d^2s)$$

in which

$$\begin{aligned} F_0 &= F_0(nd^2) + 2F_0(nd, n's) \\ G_2 &= G_2(nd, n's). \end{aligned}$$

The relation to d^2 is evident on comparison. Further we see that the doublet-quartet interval is the same for the P and the F multiplets, being equal to $3G_2$.

In the case of pds we encounter the first instance in which it is impossible to get complete formulas by Slater's diagonal sum method since this configuration gives two different ${}^2P$, ${}^2D$ and ${}^2F$. This comes about because pd gives ${}^{1,3}P,D,F$ and the added s electron makes the singlets into ${}^2P,D,F$, and splits each triplet into ${}^{2,4}P,D,F$. In such a case the method gives simply the arithmetic mean of the two doublets of similar L value:

$$\begin{aligned} ({}^2P) &= F_0 + 7F_2 \\ {}^4P &= F_0 + 7F_2 - (G_1{}^{pd} + 63G_3{}^{pd}) - G_1{}^{sp} - G_2{}^{sd} \end{aligned}$$

$$
\begin{aligned}
(^2D) &= F_0 - 7F_2 \\
{}^4D &= F_0 - 7F_2 + (3G_1^{pd} - 21G_3^{pd}) - G_1^{sp} - G_2^{sd} \\
(^2F) &= F_0 + 2F_2 \\
{}^4F &= F_0 + 2F_2 - (6G_1^{pd} + 3\,G_3^{pd}) - G_1^{sp} - G_2^{sd}
\end{aligned} \qquad (spd)
$$

in which (^2P) indicates the mean of the two ^2P's and

$$
\begin{aligned}
F_0 &= F_0(ns, n'p) + F_0(ns, n''d) + F_0(n'p, n''d) \\
F_2 &= F_2(n'p, n''d) \\
G_1^{sp} &= G_1(ns, n'p) \qquad G_2^{sd} = G_2(ns, n''d) \\
G_1^{pd} &= G_1(n'p, n''d) \qquad G_3^{pd} = G_3(n'p, n''d).
\end{aligned}
$$

Slater has worked out p^3, the result being that the energies increase in the order ^4S, ^2D, ^2P and the interval $(^2P - {}^2D)$ is to $(^2D - {}^4S)$ as 2:3.

For the configuration d^3 we find the energy levels to be,

$$
\begin{aligned}
{}^2P &= 3F_0 - 6F_2 - 12F_4 \\
{}^4P &= 3F_0 - 147F_4 \\
(^2D) &= 3F_0 + 5F_2 + 3F_4 \\
{}^2F &= 3F_0 + 9F_2 - 87F_4 \\
{}^4F &= 3F_0 - 15F_2 - 72F_4 \\
{}^2G &= 3F_0 - 11F_2 + 13F_4 \\
{}^2H &= 3F_0 - 6F_2 - 12F_4
\end{aligned} \qquad (d^3)
$$

where (^2D) indicates the mean of the two ^2D's.

§5. Comparison with Experimental Data, Configurations with p Electrons

The simplest case for comparison with the data is p^2, where the theory predicts that the multiplets come in the order ^3P, ^1D, ^1S, as Slater noted. From

Table III. *p^2 configurations*

Element	Config.	$(^1S - {}^1D)/(^1D - {}^3P)$	Reference
Theory		1.500	
C I	$2p^2$	1.13	1
N II	"	5. (? on ^1S)	2
O III	"	1.14	2
Si I	$3p^2$	1.48	3
Ca I	$4p^2$	−0.01	4
Ge I	"	1.50	5
Sn I	$5p^2$	1.39	5
Pb I	$6p^2$	0.62	6
Bi II	"	0.51	7

[1] Paschen and Kruger, Ann. d. Physik **7**, 1 (1930).
[2] Fowler and Selwyn, Proc. Roy. Soc. **A118**, 42 (1928).
[3] Slater, Phys. Rev. **34**, 1317 (1929).
[4] Russell, Astrophys. J. **66**, 190 (1927).
[5] Rao, Proc. Roy. Soc. **A124**, 475 (1929).
[6] Gieseler and Grotrian, Zeits. f. Physik **39**, 377 (1926); Sur, Phil. Mag. **3**, 736 (1927).
[7] McLennan, McLay, and Crawford, Proc. Roy. Soc. **A129**, 584 (1930).

§3 we see that the ratio $(^1S-{}^1D)/(^1D-{}^3P)=3/2$ according to theory. Slater gives the normal configuration of Si I as an example, and we find several more, as given in Table III.

From this it would appear that some influence depresses the ^1S in general, and that the doubtful ^1S given by Fowler and Selwyn for N II is probably wrong. Pb I and Bi II are so far from Russell-Saunders coupling that a good fit would hardly be expected.

The configurations p^3 and p^4 may be discussed here because they are similar to p^2. For p^3 the theory says that the ratio $(^2P-{}^2D)/(^2D-{}^4S)$ equals 2/3. Table IV gives the known instances.

TABLE IV. *p^3 configurations*

Element	Config.	$(^2P-{}^2D)/(^2D-{}^4S)$	Reference
Theory		0.67	
N I	$2p^3$	0.50	1
O II	"	0.51	2
F III*	"	0.46	3
S II	$3p^3$	0.65	4
As I	$4p^3$	0.72	5
Sb I	$5p^3$	0.91	6
Bi I	$6p^3$	1.12	6

[1] Compton and Boyce, Phys. Rev. **33**, 147 (1929); Ekefors, Zeits. f. Physik **63**, 442 (1930).
[2] Russell, Phys. Rev. **31**, 27 (1928).
[3] Dingle, Proc. Roy. Soc. **A122**, 144 (1929).
[4] Ingram, Phys. Rev. **32**, 172 (1928); L. and E. Bloch, C. R. **188**, 160 (1929).
[5] Rao, Proc. Roy. Soc. **A125**, 240 (1929).
[6] Charola, Phys. Zeits. **31**, 458 (1930).
* No intercombinations are found between the quartet and doublet systems, and the relative term values are probably quite inaccurate.

The continued increase in this ratio as the total quantum number increases is to be noted particularly. The closeness of the ratio for N I and O II would indicate that the ratio for the unreliable F III should perhaps be closer to 0.51.

For p^4 the theory gives the same result as for p^2. Table V gives the examples.

TABLE V. *p^4 configurations*

Element	Config.	$(^1S-{}^1D)/(^1D-{}^3P)$	Reference
Theory		1.50	
O I	$2p^4$	1.14	1
Se I	$4p^4$	1.71	2
Te I	$5p^4$	1.71	2

[1] Frerichs, Phys. Rev. **36**, 398 (1930); Hopfield, Phys. Rev. **37**, 160 (1931).
[2] McLennan and Crawford, Nature **124**, 874 (1929).

The new data of Frerichs show that O I is not in as good agreement with the theory as indicated in one of Slater's examples, his ratio being 1.55. Slater took his data from a remarkable energy-level diagram by McLennan, McLeod and Ruedy, Phil. Mag. **6**, 565 (1928), in which the wave number difference for $^1S-{}^1D$ is given as 39,500, although the main point of the paper is the identification of this transition with the auroral green line!

We have found two complete p^2s configurations, which should be similar to p^2 as indicated in §4. The ratio $(^2S-{}^2D)/(^2D-P)$, where $P=(^4P+{}^2P)/3$, which should be 1.50, is 0.58 in As I[6] and 3.58 in Sb III.[7]

pp, pd, and pf give similar triads, in which the means of singlet and triplet should lie in the corresponding orders: $P\ D\ S$, $D\ F\ P$, $F\ G\ D$, lowest energy first, with the ratios $(S-D)/(D-P)=9/6$; $(P-F)/(F-D)=5/9$; $(D-G)/(G-F)=7/20$, respectively.

We have found the pp complete only for C I[8], N II[9], and O III[10], but since these all occur with the means in the wrong order we do not give the details.

This failure of C I, N II, and O III to agree with the theory appears also in the known pd configurations, the mean of the F's being low in every case.[8,9,10] Yt II,[11] La II,[12] and Ge I[13] $4p5d$, also have the pd means in the wrong order. The means of Ge I $4p4d$, and Zr III $5p4d$[14] come in the right order with the ratio $(P-F)/(F-D)$, which is theoretically 0.555, having the value 0.28 and 3.58, respectively. More interesting is the behavior of $4p3d$ in the isoelectronic sequence Ca I[15], Sc II[16], Ti III[17], V IV[18] and Cr V[18]. The first two come in the wrong order, giving $(P-F)/(F-D)=-0.15$ and -0.06, respectively, but the last three agree satisfactorily, the ratios being $+0.45$, 0.49, and 0.548. Since $P-F=10F_2(4p3d)$ and $F-D=18F_2(4p3d)$, we can get two values of F_2 for each of these last three ions. Taking the average of these two, we have $F_2(4p3d)$ for Ti III, 427; V IV, 569; Cr V, 707 cm^{-1}. These are perfectly linear, as shown by the plot in Fig. 2, together with corresponding F's for d^2. We have a further check on the three singlet-triplet separations in terms of the two parameters G_1 and G_3, which it is fruitless to apply to the cases in which the means fitted poorly, but interesting in the other three cases.

TABLE VI. *3p 4d singlet-triplet separations*

	Ti III		V IV		Cr V	
	obs.	calc.	obs.	calc.	obs.	calc.
$^1P-{}^3P$	2810	2785	4761	4873	6894	7208
$^1D-{}^3D$	−2056	−1970	−1588	−1935	− 826	−1704
$^1F-{}^3F$	5270	5310	6784	6590	8161	7648
G_1	435		534		614	
G_3	15.2		30.2		47.4	
G^1	6520		8000		9200	
G^3	3720		7400		11600	

[6] Rao, Proc. Roy. Soc. **A125,** 240 (1929).
[7] Lang, Phys. Rev. **35,** 445 (1930).
[8] Paschen and Kruger, Ann. d. Physik **7,** 1 (1930).
[9] Ingram, Phys. Rev. **34,** 427 (1929).
[10] Fowler and Selwyn, Proc. Roy. Soc. **A118,** 42 (1928).
[11] Meggers and Russell, B. S. Jl. of Res. **2,** 733 (1929).
[12] Meggers and Russell, see §7.
[13] Rao, Proc. Roy. Soc. **A124,** 467 (1929).
[14] Kiess and Lang, B. S. Jl. of Res. **5,** 311 (1930).
[15] Russell, Astrophys. J. **66,** 190 (1927).
[16] Russell and Meggers, Sci. Papers Bur. Stand. **22,** 329 (1927).
[17] Russell and Lang, Astrophys. J. **66,** 19 (1927).
[18] White, Phys. Rev. **33,** 542 (1929).

Ti III, V IV and Cr V all alternate properly, as pointed out in §3. Table VI shows the results of fitting the data to the formulas for the separations by least squares.

It is seen that, in the opposite order from the means, Ti III fits best and V IV next. The G's are again approximately linear functions of the ionic charge. G^3 becomes greater than G^1, which is allowed.

For pf in La II[12] the ratio $(D-G)/(G-F)$ is 1.05 instead of the theoretical 0.35.

There is one more instance of a configuration with p electrons in which one gets a determined ratio, namely pds. In this case (see §4) nothing can be pre-

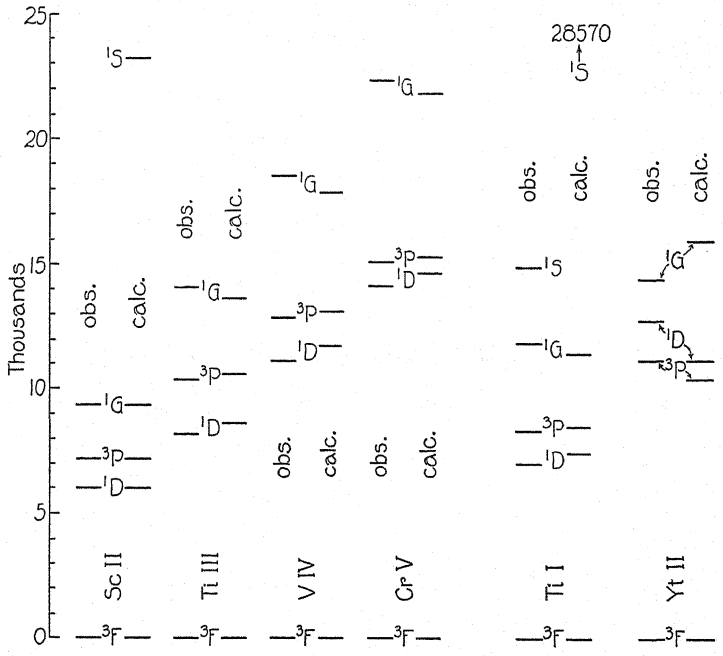

Fig. 1. The configuration d^2.

dicted concerning the quartets, ^4P, ^4D, ^4F; but the theory predicts a constant ratio between the means of the two ^2P's, the two ^2D's, and the two ^2F's which occur. If we designate these means by $P\ D\ F$, we have the order $D\ F\ P$ as in pd, with the same ratio $(P-F)/(F-D)=5/9$. In Sc I[16] these means have the wrong order, $D\ P\ F$; and in Yt I[11] and Zr II[19] the above ratio has the values 1.86 and 2.08, respectively, much too large.

In general the predictions of the theory have been seen to fit very poorly for configurations with p electrons, a uniform trend having been observed in p^3, and good fits having been obtained for pd in the higher members of the CaI isoelectronic sequence.

[19] Kiess and Kiess, B. S. Jl. of Res. 5, 1210 (1930).

§6. Comparison with Experimental Data, d Electrons

For d^2 the theory predicts (see §3) the energies of the five multiplets ^1S, ^3P, ^1D, ^3F, ^1G in terms of three integrals, the ^1S being predicted extremely high. In no instance, where a ^1S is reported, is it anywhere nearly high enough, and so we have investigated the other four levels, making a least-squares fit of the separations of ^3P, ^1D, ^1G from the low ^3F, which three separations the theory gives in terms of the two parameters F_2 and F_4.

In the isoelectronic sequence Sc II[16], Ti III[17], V IV[18], and Cr V[18], it was found possible to make the excellent fits plotted in Fig. 1 for $3d^2$. The predicted height of ^1S in Sc II is shown, the other ^1S's being correspondingly high. Russell and Meggers reported a ^1S between the ^1D and ^3P of Sc II, but later, in a note to their Yt paper[11] they ascribe this not to $3d^2$ but to $4s^2$. The $3d^2\,{}^1S$ as predicted would be in the midst of the configuration $4p3d$ with which they get their strong combinations, and so difficult to find. In Ti III, Russell

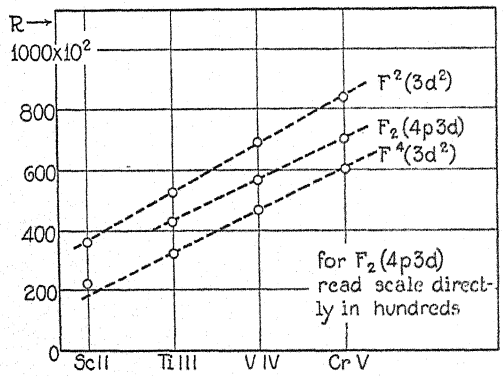

Fig. 2. Values of some integrals for the Ca I isoelectronic sequence.

and Lang report a ^1S just under the ^1G, but with a question mark. This undoubtedly does not belong to $3d^2$. In V IV and Cr V, White reports a ^1S just above the ^1G, but since these spectra were analyzed practically by extrapolation from Sc II and Ti III these levels also are probably not part of $3d^2$. The values of F^2 and F^4 as determined in this way show a striking linearity as plotted in Fig. 2. Slater's $F^2(3d^2)$ and $F^4(3d^2)$ are plotted in place of our F_2 and F_4 in order to show their relative magnitudes. Table VII gives these values ($D_2=49$, $D_4=441$):

Table VII.

	Sc II	Ti III	V IV	Cr V
$F^2(3d^2)$	36180	52840	69300	84330
$F^4(3d^2)$	22740	32520	47020	60880

These values are in good accord with Slater's rough estimate that F^4 is approximately half of F^2.

Russell[20] has completed the $3d^2$ also in Ti I, the levels being shown in Fig. 1, together with the theoretical levels with $F_2(3d^2)=899.5$ and $F_4(3d^2)=66.15$. This is again an excellent fit except for ^1S, as was pointed out by Slater. Meggers and Russell[11] have found all but the ^1S in the $4d^2$ of Yt II, but here, see Fig. 1, not a very good fit is obtained of the rest of the levels, although the perturbations are not great. This plot is made with $F_2(4d^2)=625.2$ and $F_4(4d^2)=55.1$.

In contrast to these reasonable fits we have the Zr III $4d^2$ of Kiess and Lang,[14] in which not only is the ^1S much too low, but the *two* intervals between *no three* of the other levels may be fitted with possible values of the *two* parameters F_2 and F_4; either it is necessary to assume that one of the integrals is

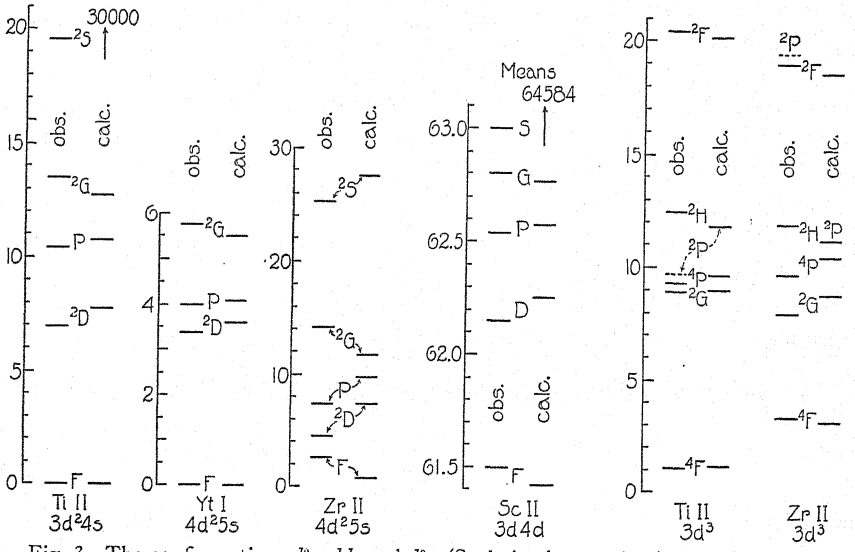

Fig. 3. The configurations d^2s, dd, and d^3. (Scale in thousands of wave numbers.)

negative or that F^4 is many times greater than F^2. In the $5d^2$ of La II (see §7 for energy levels) we have a somewhat different situation. No ^1S is reported, and of the four remaining levels there are three, and just three, which may be fitted with possible values of the parameters. These are ^3P, ^3F, ^1G with $F_2=495$ and $F_4=35.4$. (The two parameters fit the two intervals exactly, of course.) This leaves the ^1D almost 5000 cm^{-1} too high.

In d^2s we have exactly the same situation as in d^2 when we take the weighted means of ^2P and ^4P, and ^2F and ^4F, as analogous to ^3P and ^3F, respectively. Here again we can get good least squares fits of the F, ^2D, P, ^2G levels of $3d^24s$ of Ti II[21] and $4d^25s$ of Yt I[11]. These are plotted in Fig. 3. In Ti II a ^2S is observed at about the same relative position as the ^1S of Ti I, while calculated it should be much higher. Again in Yt I no ^2S is observed. The values of the parameters are, for Ti II, $F_2=1014.7$, $F_4=59.2$ and for Yt I, $F_2=433.6$, $F_4=32.1$. We have $F^2=1.91F^4$ and $1.51F^4$ respectively in these

[20] Russell, Astrophys. J. **66**, 347 (1927).
[21] Russell, Astrophys. J. **66**, 283 (1927).

two cases. In Zr II[19], $4d^25s$, we have the first instance in which a ^2S is found reasonably high. In this configuration, although we cannot get a very good fit, in contrast to the $4d^2$ of Zr III almost any three of the five levels will give reasonable values of the parameters, and we can get an approximate fit of all five by taking $F_2=905$, $F_4=55$ as indicated in Fig. 3 ($F_0-G_2=8000$ cm^{-1} measured from Kiess and Kiess' low $^4F_{1\frac{1}{2}}$, see §3). The fit would not be much improved by omitting any one of the multiplets from consideration so here we have probably a generally large second order perturbation. We have a further check in this configuration on the doublet-quartet separations, which should be the same for P and F terms, being equal to $3G_2$. We have for Ti II, $^2P-^4P=6620$, $^2F-^4F=4558$; and for Yt I, $^2P-^4P=3964$, $^2F-^4E=4357$. These show reasonable agreements, but Zr II is badly off, for here we have $^2P-^4P=-1877$, and $^2F-^4F=+5404$.

The *dd* configuration gives us a pentad, $^{1,3}SPDFG$, with three F's to fit the means and three G's to fit the separations. The first and best instance of this configuration is the Sc II $3d4d$ of Russell and Meggers.[16] Here we can fit the $PDFG$ means as shown in Fig. 3 using $F_2(3d4d)=107$, $F_4(3d4d)=6$ ($F_0=62330$). The S mean is observed some 1600 cm^{-1} too low, which could be caused by the ^1S being about 3000 cm^{-1} too low. When we consider the separations (*singlet−triplet*) we find that we can obtain a fairly good fit of the P D F G separations, with the observed S separation much too small, as shown by Table VIII.

TABLE VIII. *ScII 3d 4d separations*

	Obs.	Calc.
$^1S-^3S$	3872	6368
$^1P-^3P$	−4275	−4385
$^1D-^3D$	4384	4492
$^1F-^3F$	−3935	−3810
$^1G-^3G$	4864	4760

These are calculated using $G_0=2230$, $G_2=36.7$ and $G_4=3.5$, making $G^0(3d4d)=2230$, $G^2(3d4d)=1800$, $G^4(3d4d)=1540$. (The G^0, unlike F^0, carries here its full meaning as an integral.) The S separation is about 2500 cm^{-1} too small, which would indicate a ^1S about that much too low. This is in good agreement with the predictions of the calculation of the means and indicates that this ^1S is perhaps incorrect, the correct one being some 2500–3000 cm^{-1} higher. An error in the assignment of a singlet term, especially a ^1S, is quite likely to occur, since the identification of such terms is very difficult. An interesting example of this sort will be discussed in §7.

The other instances of the *dd* configuration are not as good. Of the $4d5d$ of Yt II[11], no *three* of the means will fit with reasonable values of F_2 and F_4, the D and the S in particular being very low. Since the S separation was also large and negative where the theory, by comparison with the other separations, says it should be positive, Professor Russell assigned the 61367 ^1S to $4d5d$, discovering that the 59615 level he had assigned was not real; but this still is perhaps not the right level, since we have now a separation of only

+167 whereas the S separation should probably be a great deal larger. The other levels do not fit well enough to say anything definite. In the $4d5d$ of Zr III[14], Kiess and Lang do not find a ^1G, but of the means of the $S\ P\ D\ F$ singlets and triplets, no three will fit with positive values of F_2. Of the La II[12] $5d6d$ means the $P\ D\ F\ G$ will fit very well, with $F_2=115$, $F_4=4$ ($F_0=54430$), with the S much too low, as in the case of Sc II, but this fit is not borne out by the separations, which are entirely skew, the P separation even being -2176 when it should probably be positive.

The other d configuration which we have found almost complete is d^3. Here we get ^2PFGH, ^4PF, and two ^2D's. Russell[21] in Ti II $3d^3$, has found all but one ^2D, and Kiess and Kiess have found all the multiplets of the $4d^3$ of Zr II.[19] The theory predicts, surprisingly, that ^2H and ^2P should have the same energy. Of these, in our two instances, the ^2H fits well, but the ^2P is considerably separated from it. Of the two ^2D's only the mean is given by the theory, but in Zr II this comes far from fitting well. However, in both cases we can fit the other five levels, ^2FGH and ^4PF surprisingly well with our three

TABLE IX. *La II*

$6s^2$	
^1S	7473
$6s6p$	
^1P	45692
^3P	32699
$6s5d$	
^1D	1394
^3D	2760
$6s4f$	
^1F	15773
^3F	14888
$6p^2$	
^1S	66592
^3P	61779
^1D	62026
$6p5d$	
^1P	30353
^3P	28833
^1D	24462
^3D	27538
^1F	32201
^3F	27477
$6p4f$	
^1D	40458
^3D	38835
^1F	37210
^3F	37034
^1G	39221
^3G	37479
$5d^2$	
^1S	—
^3P	5949
^1D	10095
^3F	1183
^1G	7473
$5d6d$	
^1S	54794
^3S	55230
^1P	56037
^3P	53861
^1D	55184[1]
^3D	53067
^1F	52138?
^3F	54819[1]
^1G	56036
^3G	53659
$5d4f$	
^1P	27424
^3P	23003
^1D	18895
^3D	22174
^1F	24523
^3F	18411
^1G	16599
^3G	21478
^1H	28525
^3H	18835
$4f^2$	
^1S	69505
^3P	63960
^1D	59900
^3F	57939
^1G	59528
^3H	56080
^1I	62408

[1] The $^1D_2$ and $^3F_2$ of the $5d6d$ may possibly be interchanged. ($^3F_4=55321$, $^3F_3=54840$, $^3F_2=53885$.)

parameters, as indicated in Fig. 3. For Ti II we have $F_2(3d^2)=845$, $F_4(3d^2)=54$ ($3F_0=17750$); corresponding to $F^2=1.74F^4$. The mean of the ^2D's is predicted at 22140, which would throw the ^2D not found at about 31000, very high indeed. For Zr II we have $F_2=683$, $F_4=36$ ($3F_0=16000$); corresponding to $F^2=2.11F^4$. The mean of the ^2D's is predicted at 19523, observed at 14214 (multiplets at 13869 and 14559).

We have seen that the theory works much better for d electrons than for p. It has been good in every instance in the first long period of the periodic table, and better in the second than the third.

§7. La II and the f Electron Configurations

W. F. Meggers and H. N. Russell have recently completed the analysis of La II, obtaining the first complete pf, df and f^2 configurations. Through their kindness in allowing us to use these data we have been able to obtain two beautiful fits of the df and f^2 configurations, and to prove the actual service of this theory to spectroscopists by helping to straighten out the analysis at two or three points.

Since these data are unpublished as yet, Meggers and Russell have kindly allowed us to publish a preliminary energy table, the levels being measured up from the low $5d^2\,{}^3F_2$. We give only the centers of gravity of the multiplets in Table IX.

Of these the p^2, pd, pf, d^2, and dd have already been discussed, and were not found to agree particularly well with the theory. The new $5d4f$ and $4f^2$ remain to be considered, which will be done in some detail.

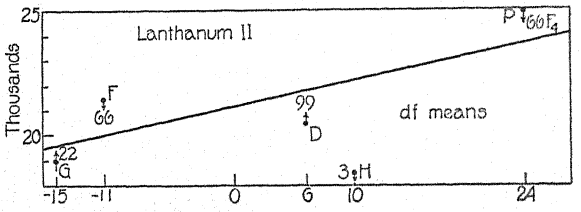

Fig. 4. Illustrating the method of locating poorly fitting multiplets and a method of estimating the values of the integrals.

As we received the data from Professor Russell, the $df\,{}^1H$ was placed at 18169, rather close to ^3H, instead of having the extremely great separation of about 10,000 units and being the highest level in the configuration. An attempt to fit the means by the method illustrated in Fig. 4 was made. This is incidentally the method used on many of the previous configurations. The formulas to which we are fitting these means are as follows:

		Calc.
P	$= 25214 = F_0 + 24F_2 + 66F_4$	25216
D	$= 20534 = F_0 + 6F_2 - 99F_4$	20506
F	$= 21467 = F_0 - 11F_2 + 66F_4$	21191
G	$= 19038 = F_0 - 15F_2 - 22F_4$	19323
H	$= 18502 = F_0 + 10F_2 + 3F_4$	22598

Since F_0 occurs uniformly, we plot in Fig. 4 the value of these means against the coefficients of F_2. Then the line determining F_2 must be so drawn that its separations from these points are as closely as possible proportional to the coefficients of F_4 and in the direction shown by the arrows. It is seen at once that we can thus fit G,F,D, and P quite well, but that H is far too low. From the slope of the line we get $F_2=115$, from the average separations $F_4=16$ (and from the height at zero abscissa, $F_0=21400$). From the level diagram in Fig. 5 we see that changing none of these values will tend to improve the general fit, so that these are approximately as good as can be found. A more exact determination of these values, such as a least squares fit, gives an accuracy which is meaningless. The calculated means are shown in the above table. From the calculated H mean it would seem that the ^1H should be about 8200 units higher.

When we consider the separations we have the following formulas to determine the G's

			Calc.
$^1P-{}^3P$	$=-4421$	$=-2(\ G_1+24G_3+330G_5)$	-4638
$^1D-{}^3D$	$=3279$	$=2(\ 3G_1+42G_3-165G_5)$	3397
$^1F-{}^3F$	$=-6112$	$=-2(\ 6G_1+19G_3+55G_5)$	-5837
$^1G-{}^3G$	$=4879$	$=2(10G_1-35G_3-11G_5)$	4987
$^1H-{}^3H$	$=+666$	$=-2(15G_1+10G_3+G_5)$	-11330

It is inconvenient here to use such a method of fitting as described above, but such a diagram will readily show that the H separation relative to the others should be very large and negative. A least squares fit of the $P\ D\ F\ G$ separations gives $G_1=357.6$, $G_3=29.7$, $G_5=3.78$, and the calculated separations show in the table, a good fit. These values correspond to $G^1(5d4f)=12{,}500$, $G^3=9350$, $G^5=5750$. This calculation shows that the ^1H should be about 12,000 units higher.

In the data as received from Professor Russell, the $4f^2\,^1I$ was placed at 52,052 instead of the value noted in the table, and two possibilities given for ^1S and ^1D, as noted below. The f^2 consists of seven levels to be fitted with four parameters as follows:

$$
\begin{aligned}
^1S &= \left\{\begin{matrix}69505\\66592\end{matrix}\right\} = F_0+60F_2+198F_4+1716F_6\\
^3P &= 63963 = F_0+45F_2+33F_4-1287F_6\\
^1D &= \left\{\begin{matrix}59900\\62026\end{matrix}\right\} = F_0+19F_2-99F_4+715F_6\\
^3F &= 57939 = F_0-10F_2-33F_4-286F_6\\
^1G &= 59528 = F_0-30F_2+97F_4+78F_6\\
^3H &= 56080 = F_0-25F_2-51F_4-13F_6\\
^1I &= 52052 = F_0+25F_2+9F_4+F_6.
\end{aligned}
$$

Now from a diagram such as Fig. 4, it may be seen that F_6 will be extremely small, for a good fit of the high ^1S, the low ^1D, the ^3P, ^3F, ^1G, and ^3H may be obtained using just the parameters $F_2=94.0$, $F_4=22.1$. The ^1I is definitely observed 10000 units too low. The correct ^1S and ^1D are at once determined, since the other possibilities will not fit under any circumstances.

Thus we have seen that the theory predicted the ^1H of df and the ^1I of f^2 both about 10,000 units higher, and when this was called to the attention of Professor Russell, he discovered that he could make this shift by rearranging his lines as shown in Fig. 6. Upon doing this he immediately was able to check each of these levels by faint cross-combination lines, thus definitely proving

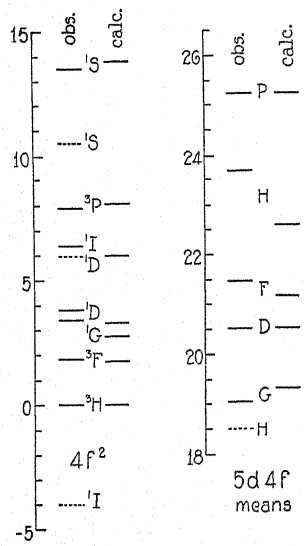

Fig. 5. The configurations df and f^2 of La II. (Scale in thousands of wave numbers.)

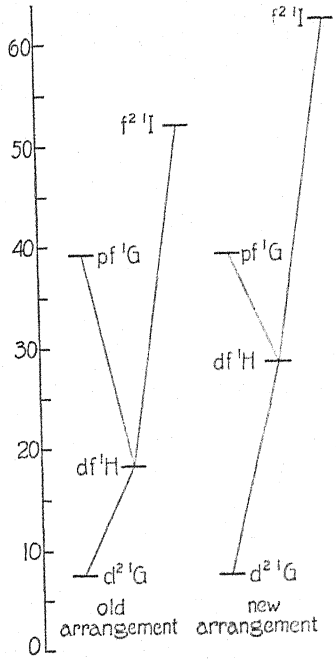

Fig. 6. Russell's rearrangement of the La II singlets according to the predictions of the theory. (Scale in thousands of wave numbers.)

the correctness of this arrangement. Both of these singlets were raised 10,356 units to the places shown in Table IX. In Fig. 5, the old levels are shown broken and the corrected levels by full lines. The df diagram is merely the old diagram determined from the means of $P\ D\ F\ G$, with the H mean put in its proper place. The $^1H-^3H$ separation becomes now 9690 against the calculated 11330 from the other four separations. The ^1H was raised just about the average of the predictions from the means and from the separations. It is supposed that the $3d4d\,^1S$ of Sc II would behave in about this fashion. For the f^2 the ^1I is placed within 300 units of its prediction using the two coefficients above. Fig. 5, however, is a recalculation using least squares to fit the three

coefficients F_2, F_4, F_6 to the separations of all the levels from the low ^3H. This gives a surprisingly good fit of the 6 intervals in terms of the 3 integrals, with the value of $F^2=21{,}000$, $F^4=23{,}500$, $F^6=1930$. Unfortunately F^4 comes out a little larger than F^2 whereas it must be smaller.

Thus we have obtained quite pleasing results with these two f-electron instances, the theory having stood the test of prediction and been of actual service in the analysis of the spectrum, both in the assignment of ^1S and ^1D, f^2, the former of which Professor Russell says he had little possibility of assigning definitely, and in the rearrangement of the levels in both df and f^2.

Kiess and Lang[14] have completed the $4d4f$ configuration of Zr III except for the ^3H, but when the other four means are plotted as in Fig. 4, it is seen that no three of them will fit in any fashion. The P, D, and F separations alternate but the G does not.

In conclusion we may say that this first approximation seems to be most accurate for those configurations with lowest total quantum numbers in comparison with the angular momentum quantum numbers, the $3d$ and $4f$ in particular giving good results.

We wish to thank Professor H. N. Russell for his helpful interest in this work, and him and Dr. Meggers for permission to publish their lanthanum data.

DENSITY AND CONDUCTIVITY OF BISMUTH SINGLE CRYSTALS GROWN IN MAGNETIC FIELDS WITH RELATION TO THEIR MOSAIC STRUCTURE

By Alexander Goetz and Alfred B. Focke
California Institute of Technology, Pasadena

(Received March 2, 1931)

Abstract

In continuation of the study of the thermoelectric effect, previously described by Goetz and Hasler, existing between the two halves of the same bismuth single crystal, of which one has been crystallized within, and the other outside of a strong magnetic field (21,000 gauss), the density and the specific resistance of different sections of these crystals, grown by the discontinuous method, have now been measured.

The change of density of "magnetic" crystals. The density of perfect crystals grown under normal conditions was found to be between 9.82 and 9.83 i.e., 0.2 percent higher than the values of other authors. Furthermore, it was found that any crystalline imperfection such as twinning, etc., decreases the density; that, further there exists a difference of density between the "normal" and the "magnetic" half of the same crystal, the sign of which depends on the orientation with which the crystal entered the field: In case the trigonal axis is normal to the axis of the rod and normal to the lines of force, the "magnetic" half shows an increase of density, whereas the opposite is true in case the principal axis is parallel to the rod (and therefore parallel to the direction of growth and to the heat-flow). The difference of density is ca. 0.3 percent but can be several percent in imperfect crystals. The purity of the metal affects the change of the density. The results indicate that the ideally pure metal would not be affected by the magnetic treatment.

The specific resistance of "magnetic" crystals. The values of the specific resistance obtained on "normal" single crystals agree approximately with the results obtained by Bridgman and Kapitza and also with those obtained by spectroscopic analysis. The value of $\rho_{\parallel}/\rho_{\perp}$ was found to be much larger for bismuth, being sensitive to the "magnetic" treatment. There is a small change of resistance between the normal and the magnetic half, depending on the orientation of the crystal to the field: In case the orientation is such as to decrease the density the resistance increases and *vice versa*. The accuracy necessary for the satisfactory quantitative determination of the change could not yet be reached, since the change is of the magnitude of 0.5 percent.

An attempt is made to combine the phenomena of the magnetic effect thus far known. It seems probable that the influence of the magnetic field upon the formation of a crystal consists of a change within the mosaic structure of the lattice. The investigation is being continued.

Introduction

A THERMOELECTRIC effect within one and the same Bi single crystal of which one half had crystallized under normal conditions, the other within a strong transverse magnetic field has recently been described by A. Goetz and M. F. Hasler.[1] It was found that the size as well as the sign of the e.m.f. depends on the orientation of the crystal with respect to the lines of

[1] A. Goetz and M. F. Hasler, Phys. Rev. **36**, 1752 (1930).

force and on the method of growth; also that the e.m.f. depends largely on traces of impurity within the crystal.

Due to the fact that this magnetic effect is altogether new, very little information as to the cause of the observed e.m.f. can be obtained from the observations themselves and accordingly additional measurements of another type have been here undertaken.

Although we realized in advance that the thermoelectric effect would be by far the most sensitive indicator, and other volume effects should be very minute if at all measurable, there seemed to be encouraging indications in the observations of previous authors concerning the density and the electric conductivity of Bi crystals.

The Density of "Magnetic" Bi Crystals

The density of bismuth has been measured very frequently by different authors and it seems quite remarkable that there is no other common element for which the different observers differ so largely though they seem to have worked with great care. A study of the literature[2] shows that the measured density of Bi varies between 9.66 (Marcus, Giebe) and 10.055 (Zavaffiero), a difference of more than 5 percent. There can be no doubt that part of this variation is due to fissures and inclosures of gas within the metal which falsify the measurement of the volume. It is quite remarkable that the average value of a perfect single crystal is far below the maximum density measured on specimens consisting of compressed powder, thus indicating that the bismuth lattice is *not* the closest possible packing of Bi atoms.

For the present measurement of densities the usual hydrostatic method was improved only in that thin transformer oil was used for the immersing liquid instead of water. In the case of water, it was found that shortly after boiling (a process which is necessary to prevent the formation of gas-bubbles on the surface of the specimen) the absorption of air gradually changes the density until saturation is reached again. In case of oil dried artificially this trouble does not occur and its density can be kept constant for months if one works carefully. The density of the oil was measured in a pyknometer.

To reduce the inaccuracies to a minimum, two pieces of equal length were cut out of one crystal, one belonging to the normal, one to the magnetic side of it. It goes without saying that the crystal had to be free of imperfections—these could be tested for by the thermoanalyser[1]—and also that its surface had to be etched in order to free it from any layer of oxide.

But in spite of the care taken in the measurements and in producing the crystals, the results obtained are not as uniform as expected. Furthermore, according to the thermoelectric results, only measurements on crystals of the same orientation and grown by the same method can be compared. Crystals of the P_1 and P_3-type grown by the discontinuous method, have been investigated, since these orientations show the largest magnetic effects, whereas the P_2-type is almost neutral. In addition to this, it was found that even in the

[2] Gmelin's Handbuch der Anorg. Chem. Vol. 8, page 35.

measurement of density only crystals of the same sort of bismuth[2] could be compared. Thus most attention had been paid to crystals of the "B" bismuth due to the large "magnetic" effect observed on it in the thermoelectric measurements.

Results. In toto, the density of 76 different specimens was measured. These belonged to 29 different crystals grown in general especially for these measurements. Of these specimens, 15 were of the orientation P_1, 6 of P_2, 16 of P_3, 2 of P_{1-2}, and 2 of P_{2-3}**. Several specimens of the magnetic (M) and the normal (N) halves of the same crystal were cleaved into several pieces, each being measured separately in order to determine the influence of local irregularities and to reveal the accuracy of the method. Table I shows part of the results obtained. The section "number of measurements" in Table I indicates how many different measurements of the same crystal or of its different parts were taken, each measurement consisting of the necessary number of readings.

TABLE I.

Crystal	Orientation	Kind	Treatment	Density	Number of measurements
48/00/0	P_1	B	N	9.820	Two
62/00/0	"	"	"	9.815	One
62/00/0	"	"	M	9.845	Two
65/20/0	"	"	N	9.824 (+)	One
65/20/n (×)	"	"	"	9.818 (++)	"
65/20/g (××)	"	"	"	9.819 (†)	"
65/20/0	"	"	M	9.844 (+)	"
65/20/n (×)	"	"	"	9.849 (++)	"
65/20/g (××)	"	"	"	9.838 (†)	"
73/00/0	"	C	N	9.833	"
"	"	"	M	9.827	"
83/21/1	"	B	N	9.830	Two
"	"	"	M	9.842	"
49/00/0	P_2	B	N	9.822	Three
59/00/0	"	"	N	9.813	One
"	"	"	M	9.813	"
60/00/0	P_{1-2}	"	N	9.807	"
"	"	"	M	9.825	"
49/00/1	P_3	"	N	9.826	"
61/00/0	"	"	N	9.835	Two
"	"	"	M	9.805	"
96/31/1	"	"	N	9.837 (*)	?
"	"	"	M	9.817 (*)	?
96/21/1	"	"	N	9.847 (Δ)	?
"	"	"	M	9.836 (Δ)	?
69/00/0	"	"	N	9.803	One
"	"	"	M	9.781	"
70/00/0	"	"	N	9.809	"
"	"	"	M	9.798	"

(××) The specimen included a small twinned region.
(×) The same specimen after removing the twinned region.
(+) Probable error 0.005
(++) Probable error 0.008
(†) Probable error 0.01
(*) N Field strength 17,000 Gauss
(Δ) N Field strength 13,000 Gauss

** The designation of the latter two orientations indicates mean intermediate orientations between P_1 and P_2 etc.

With regard to the absolute value of the density it is apparent that *the average value for single-crystals is between 9.82 and 9.83*, slightly higher than the result obtained by Kapitza (9.80).[3] This result was checked by measurements made upon normal crystals in distilled water immediately after its separation from the absorbed air.

The density of Bi, generally speaking, appears to be abnormally sensitive to crystallographic imperfections, since polycrystals for instance as well as crystals with large twinned regions showed abnormally low values, this probably being due to the enclosure of gas at the intercrystalline borders, as was verified several times by the microscope. This sensitivity is also indicated by the fact that the highest values of the density on our best crystals (9.83) are still below the value to be expected from the x-ray data (9.86).

Nevertheless the values given in Table I have but relative importance (with the exception of the crystals 48/00/0, 49/00/0 and 49/00/1) since they are obtained in oil, the density of which could not be checked in the pyknometer as accurately as the values taken with the balance, though the accuracy indicated by the data given is justified for one and the same crystal because these values were obtained in immediate succession and under similar conditions.

The measurements thus obtained indicate the following connection between the normal and the "magnetic" part of the same crystal: *If the crystal has an orientation in which the principal axis is normal to the lines of force* (P_1 and P_3) *the density of both halves differs considerably, whereas no change can be found if the axis is parallel to the field.* (P_2).

Furthermore with relation to the first part it is evident that the *density of the "magnetic" half is larger than that of the normal, in case the trigonal axis is normal to the axis of the rod,* (P_1), *whereas the opposite is true if the axis is parallel to the axis of the rod* (P_3).

In intermediate orientations (P_{1-2}) where P_2 is unaffected, the resulting change is the same as it is in the case of P_1, but one should not rely too much upon it, since there exists only the measurement of one crystal (orientation ca. 30°). Concerning the measurement of the crystal 73/00/0 which has the P_1-orientation but consists of the kind C (i.e., the purest metal[1]) it is striking that *no change of density could be observed.*

In consideration of the large experimental difficulties connected with density measurements of this kind, one should not put too much stress on the absolute value of the differences of the density between the normal and the "magnetic" parts, since an almost invisible layer of oxide or grease and small enclosures, difficult to detect, affect the results fatally by fogging the whole effect. Thus a number of observations had to be discarded among which were a few whose sign was not in agreement with the above statement. Nevertheless the discarding was done only after it was evident that the crystals were imperfect.

[3] P. Kapitza, Proc. Roy. Soc. **A119**, 358 (1928).

The Electric Resistivity of "Magnetic" Crystals

As soon as it was evident that the growing of crystals in a magnetic field affects their density, it was decided to measure their electric resistivity, since it is well known that these qualities are closely related within the same metal.

There are a number of very exact investigations published concerning this subject (Bridgman,[4] Schneider,[5] Borelius and Lindh,[6] Schubnikow and de Haas[7] and Kapitza[3]). It is made quite certain by Bridgman that the Voigt-Thomson law holds also in case of Bi, whereas concerning the absolute values of the specific resistance, a small discrepancy still remains between the recent authors, a discrepancy which is very probably due to the fact that it is very difficult to obtain bismuth of sufficient purity, or better of equal impurity.

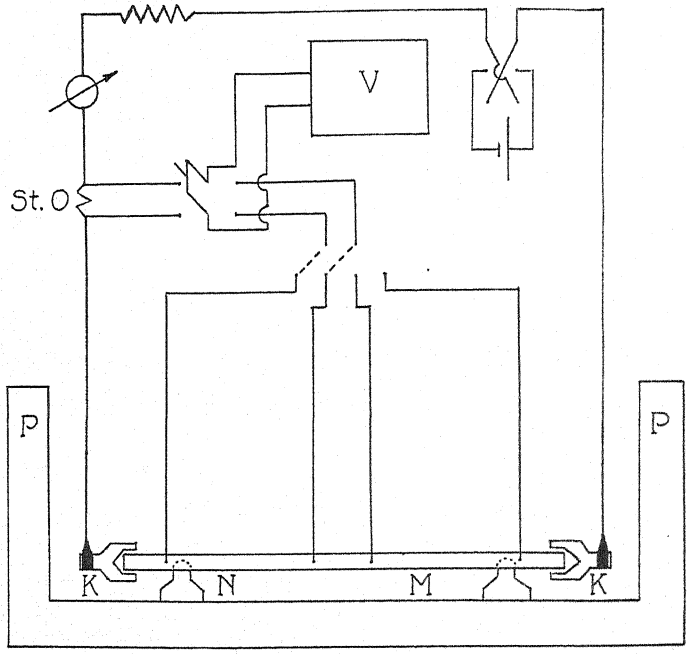

Fig. 1. Diagram of apparatus.

Also the measurements themselves must be performed with special precautions, so as to avoid the large thermoelectric forces due to small changes of temperature as well as any permanent or elastic distortion of the crystal, for these affect the results largely.

We used for our measurements, for the most part, the arrangement already described by Kapitza[3] with certain modifications however, dictated by the much larger size of our crystals and by our special purpose of comparing the values of two different parts of the same crystal. Thus the arrangement was as shown in Fig. 1.

[4] P. W. Bridgman, Proc. Am. Acad. **63**, 351 (1929).
[5] G. W. Schneider, Phys. Rev. **31**, 251 (1928).
[6] G. Borelius and A. E. Lindh, Ann. d. Physik **51**, 607 (1916).
[7] A. Goetz, Phys. Rev. **35**, 193 (1930).

After a crystal of 13 to 15 cm in length, of the desired orientation, was grown within a graphite trough previously described,[7] one half of which (N) was grown under normal conditions, the other (M) within a magnetic field, both ends including the transition between the seed crystal and the main crystal were carefully cleaved off so as to obtain the standard length of 12 cm. Then the crystal was etched and searched for imperfections or twin lamellae. In case it proved satisfactory two copper cups (K)—the current leads—were soldered to the crystal with Wood's metal. This method has the advantage of avoiding the necessity of heating the crystal long enough to produce an alloy between bismuth and Wood's metal, which makes the further use of the bismuth impossible, whereas here one has only to heat the cup filled with Wood's metal up to its melting point and then to put one end of the crystal into it, after which the liquid metal solidifies shrinking around the crystal. Thus a reliable contact for comparatively large currents is made.

The potential leads consisted of 0.1 mm silver wire which was spark-welded on to the crystal at 4 different points as shown in Fig. 1 to allow the measurement of the specific resistance separately across the normal and the magnetic parts of the crystal. In order to keep the temperature constant the whole arrangement was immersed in a bath of oil within a container of paraffin (P).

The current was measured by means of a standard ohm (St. O) and a precision potentiometer V, whereas the voltage across one pair of silver wires was measured directly with the potentiometer. There were furthermore the usual precautions for balancing the thermoelectric effects etc.

The largest difficulty consisted in the exact determination of the cross section of the crystal, since it could not be taken from direct measurement because of the peculiar shape of the trough. Thus it was necessary to calculate the specific resistance from the length (L), the weight (G) and the density (D) by means of the relation:

$$\rho = \frac{E \cdot G}{J \cdot D \cdot L^2}$$

where J and E are current and voltage and ρ the specific resistance. Since it was impossible to obtain any better accuracy by this method than 1—2 percent the variation of density between N and M, as described before, was not considered. For D the value of 9.82 was taken.

The reason for the inaccuracy of this method is found in the assumption that the cross section over the length used is constant. This becomes less true the larger this length is chosen. This distance between the potential leads on the other hand has to be large enough to avoid the influence of the unequal current distribution in the neighborhood of the leads and the uncertainty of the distance due to the cross section of the welding spot, which was in the present case at least 0.5 mm. The distance used was in general between 30 and 40 mm so as to decrease the uncertainty of ρ to about 3 percent.

Results. It is well known that the specific resistance parallel to the trig-

onal axis of a Bi crystal is larger than normal to it, furthermore, that the ratio between these two values increases with the increasing amount of impurity, since in this case, the resistance along the trigonal axis increases faster than perpendicular to it. The minimum values of $\rho_\parallel/\rho_\perp$ are 1.27 (Bridgman[4]) and 1.30 (Kapitza[3]), whereas Schneider[5] finds 1.62 using a metal with 0.04 percent silver. Table II gives the results which seem the most reliable ones. No reliable values for bismuth D^1 could be obtained, since this kind is very hard to obtain in single-crystalline form without inclosed air-bubbles.

TABLE II.

Crystal	Orientation	Kind	Part	Resistance
83/21/1	P_1	B	M+N	1.395
"	"	"	M	1.384
"	"	"	N	1.407
83/11/?	"	"	M+N	1.395
"	"	"	M	1.343
"	"	"	N	1.438
96/31/1	P_3	"	M_1	2.085
"	"	"	M_2	2.088
"	"	"	N_1	2.030
"	"	"	N_2	2.030
91/41/1	P_1	C	M+N	1.109
"	"	"	M	1.122
"	"	"	N	1.090
91/33	P_3	"	N	1.358 (?)
"	"	"	N	1.428
"	"	"	N	1.419
91/51/1	"	"	M+N	1.438
"	"	"	M	1.493
"	"	"	N	1.393
86/11	P_1	A	N	1.334 average
85/21	P_3	"	N	1.745 "

The values for $\rho_\parallel/\rho_\perp$ in Table II are taken at temperature of 25°C which is slightly higher than the temperatures used by Bridgman and Kapitza (20°). This difference makes it necessary to decrease our values about 2 percent to compare them with the values of these authors.

The main reason why our values are not as consistent as Kapitza's and Bridgman's is probably the indeterminancy of the cross section of the crystals. Nevertheless these observations (which are not considered to be final) indicate the following facts.

The variation of the specific resistance of the different kinds of bismuth used is in agreement with the spectroscopic analysis published previously[1] showing that C is the purest metal with a resistance $\rho_\perp = 1.09\times10^{-4}$ and $\rho_\parallel$ 1.36(?) to 1.43×10^{-4}. The latter value is slightly larger than Bridgman's (1.38×10^{-4}) but can be easily explained by the lack of longitudinal compression in which case Kapitza obtained values up to 1.5×10^{-4}. Bismuth A can be easily recognized as impure and B is still worse, agreeing with the measurements of Borelius and Lindh. Fig. 2 shows the results for the three different kinds of Bi used; the hatched line below C shows Bridgman's best

values,* the dotted line crossing B gives the conductivity for B crystals grown in the magnetic field in the corresponding orientation, the abscissa is given in the usual terms of $\cos^2$ of the angle of orientation.

The most important fact suggested by the results consists in the influence

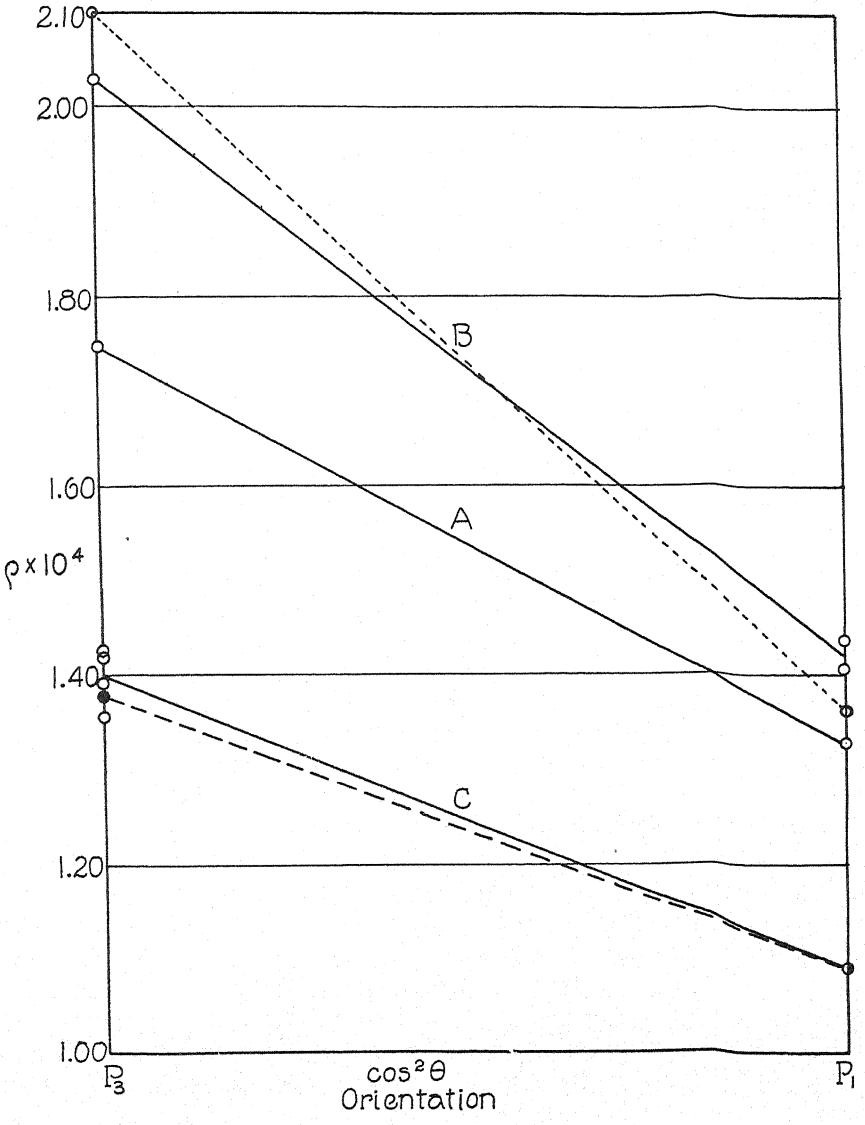

Fig. 2. Results for the three different kinds of Bi used. The hacked line below C shows Bridgman's best values. The dotted line crossing B gives the conductivity for B crystals grown in the magnetic field in the corresponding orientation.

* There is one discrepancy worth mentioning in the fact that Bridgman used Kahlbaum metal which is the same as our D. Kapitza's remark about this metal as well as our analysis shows that it contains a considerable amount of impurity which is different from the con-

the magnetic treatment of the crystal has on the resistance. This runs as follows: *if the crystal has an orientation in which its trigonal axis is normal to the lines of force and normal to the direction of the current the specific resistance of the magnetic half is smaller than the normal one; if the trigonal axis is normal to the lines of force and parallel to the direction of the current the specific resistance of the magnetic half is larger than the normal.*

As to the qualities of the P_2 orientation no exact measurements were yet performed because the thermoanalysis did not show any "magnetic" effect.

Discussion

The results obtained as to the influence of the magnetic field upon the density and the conductivity of Bi single crystals, have a close relation. This is not altogether unexpected. The increase in density is associated with a decrease of specific resistance (P_1) and *vice versa* (P_2). Furthermore, the crystallization within a magnetic field seems to affect the density and conductivity of a metal with small impurities to a much larger extent than a pure one.

Considering the nature of the change within the "magnetic" crystal it is very difficult to say anything that is more than a mere suggestion. Both the thermoelectric effect and the change of conductivity could be explained by a change at the moment of crystallization in the orientation of the crystal when entering a magnetic field. As has been already stated in a previous paper[7] no change in orientation could be detected, furthermore this explanation would account neither for the large influence of impurities nor for the change in density.

Another suggestion would be an allotropic change of the lattice, indicated by the change in density. Hence an x-ray investigation was started after the first indications of a change of density were found. This consisted of Bragg diagrams taken simultaneously from the (111) plane of the normal and the magnetic half of the same crystal, but, as was stated already briefly by Goetz and Hergenrother,[8] not the slightest displacement of corresponding lines was found, thus indicating that *the atomic distance along the trigonal axis does not differ between both parts of the crystal.*

Hence there are obviously only two conclusions left, of which one assumes that the magnetic half undergoes an pseudo-allotropic change of the same type as the $\alpha \rightarrow \beta$-transformation of iron and zinc which cannot be found by x-ray analysis though indicated by electric volume effects. In general one assumes that the transformation of the first metal is only due to an interatomic change of the distribution of electrons and it would be plausible that such an effect occurs more easily if the internal symmetry of the lattice is disturbed by impurities. Nevertheless this suggestion loses probability as it does not account for the change in density in case of Bi.

---

tamination of *A* and *B* but much more than *C*. This fact is also indicated by the size of the "magnetic" effect. We were not able to obtain reliable measurements of the specific resistance of this metal whereas Bridgman got the best results yet published.

[8] A. Goetz, R. C. Hergenrother and A. B. Focke, Phys. Rev. 34, 546 (1929).

Thus there is apparently no mode of explanation left save that which has been suggested in a previous paper as the only way to account for the large effect of minute impurities in a crystal.[1] This way seems indeed to account for the whole phenomenology of these effects, including the change of density and electric conductivity of magnetic Bi crystals. The assumption is of a change in the secondary structure of the crystal as described first by Zwicky.[9,10]

The experimental evidence for the existence of this structure in Bi crystals has already been given by one of the authors.[11] He showed that this structure, superimposed upon the Laue-Bragg lattice, consists of blocks of a definite size which is within the range of microscopic visibility. Our present suggestion is that the arrangement of these blocks is changed under the influence of the magnetic field so as to produce a closer or less close packing. This would not influence the x-ray diagram, since this depends only on the primary structure of the lattice whereas the density of the crystal as a whole would be affected by a change in the mosaic arrangements of the blocks.

This mosaic arrangement of the blocks is thus assumed to be changed by the influence of a field during the formation of the crystal. Such a change, which we have to think of as a systematic distortion, must depend on the crystallographic orientation of the crystal within the field and must disappear if this orientation causes the smallest possible content of free energy upon the crystal as is the case in the P_2 orientation where the direction of the smallest susceptibility is parallel to the lines of force as follows from the measurements of Focke.[12]

This assumption makes it plausible also that the electric conductivity changes with the density, since both depend on the compactness of the crystal.

The hypothesis as a whole implies a less compact form due to the mosaic structure for the average perfect crystal than for an ideal one.** Although it is perhaps possible to think of accidental fissures within the crystal as the cause of the difference between the theoretical and the actual density (0.3 percent), the fact that one can approach the theoretical density by the crystallization in a magnetic field under the same thermal and mechanical conditions of growth seems to be a strong argument against the presence of such fissures dependent upon imperfect growing conditions. Also the consistency of the density values obtained speaks against such an explanation.

Considering the magnitude of the change of density and conductivity in

[9] F. Zwicky, Proc. Nat. Acad. **15**, 253, 816 (1929).

[10] F. Zwicky, Hel. Phys. Acta. **3**, 269 (1930).

[11] A. Goetz, Proc. Nat. Acad. **16**, 99 (1930).

[12] A. B. Focke, Phys. Rev. **36**, 319 (1930).

** This conclusion does not contradict Zwicky's assumption[13] for ionic lattices of Na Cl type, where the actual density of a crystal should be larger than the density calculated from the x-ray diagrams due to the contracted II-planes sandwiched between normally spaced regions. (Hel. acta, page 288.)

magnetic crystals (0.5 percent) one must call these second-order effects in comparison with the magnitude of the thermoelectric changes.[1] This fact also seems to support the suggested hypothesis, since it is well known that thermoelectric effects in general are much more structure-sensitive than density and conductivity known as structure-insensitive.

There are two more arguments in favor of the above explanation: if there is a possibility of a distortion within the mosaic structure, i.e., among the blocks, this can only be possible if during the genesis of the crystal these units possess a larger mobility among themselves than do the molecules of the primary lattice. This is necessary for the following reason: an orienting influence upon the crystal exerted by the magnetic field presupposes the existence of an anisotropic susceptibility. Besides the fact that liquid Bi is almost neutral magnetically and the further fact that the large diamagnetic properties of Bi arise only at the moment* the lattice forms, make it obvious that the magnetic anisotropy cannot exist either before the primary lattice is formed. Hence the orienting influence of the field can only occur if a lattice already exists. As the forces exerted upon the crystal by the fields used are far too small to deform the lattice permanently the only explanation left seems to be the distortion of the secondary structure. This explanation presupposes that the primary structure exists before complete solidification, a fact which former work by one of the authors made highly probable in the case of Bi.[11] The second support of the above hypothesis is found in the observation that a possibility of an orienting influence upon the crystal "*in statu nascendi*" exists in fact, and that it can have mechanical, thermal and

* This statement is not in harmony with Kapitza's hypothesis according to which the large diamagentism of Bi begins only slightly below the melting point after the metal has already solidified. It seems dubious whether this opinion can be supported by Curie's paper on this subject,[14] for he states emphatically: "· · · la chute (of diamagnetism) est absolutement brusque et correspond exactement avec le phénomène de la fusion · · ·"; and furthermore: "· · · Un curieux phénomène se produit si l'on chauffe le Bi en petits fragments dans une ampoule fermée à une temperature à peine supérieure à celle de fusion. La chute des propriétés magnetiques se produit complètment; cependant si l'on refroidit quelques minutes après, on retrouve les petits fragments qui ont le même aspect qu'avant et se ne sont pas écroulés. Cependant le Bi. a été fondu, car, en cessant les morceaux, on voit que la structure interne a été complètment changée et que les plans de clivage ne sont plus placés comme avant · · · ."

This does not mean necessarily an indication of the existence of a transformation, since similar experiments by us showed that even a thin oxide-coat covering such fragments is very well able to preserve their exterior shape, though a pinch with a needle through this (almost invisible) coat proved the interior to be liquid. Furthermore the change of orientation within those fragments makes a melting more probable than an allotropic transformation, since, as is shown by several authors, the main orientation of a crystal is preserved in general no matter how frequently the transition between two allotropic transformations be passed. It appears also clearly in Honda's paper (16) that the rise of diamagnetism is associated with the process of crystallization and a personal discussion of this matter that one of the authors (G.) had with Professor Honda at Sendai leaves no doubt that the utmost care was taken with respect to this question.

[13] F. Zwicky, Proc. Nat. Acad. **16**, 211 (1930).
[14] P. Curie, Journ. de physique **4**, 206 (1895).
[15] A. Goetz and M. F. Hasler, Proc. Nat. Acad. **15**, 646 (1929).

magnetical causes.[11,17] This proves that the anisotropic qualities do not disappear when the macroscopic crystal melts.

Thus one is forced to assume that the distortion of the mosaic structure is the result of two different influences: The orienting influence of the field and the orienting influence of the crystal grown already in an orientation enforced upon it by a seed crystal such as was always used in our experiments. As long as both influences work in the same direction (P_2) there is no distortion, whereas in case they work in different ways a distortion must occur, depending on the orientation (P_1 and P_3), as is indicated by the different signs of the described volume effects. The magnitude of these effects can obviously be ascribed partly to the degree of the distortion. Since the conditions in our experiments were kept as constant as possible the different magnitudes (Bi A, B, C, and D) especially of the thermoelectric effects of the same orientation can but indicate different degrees of distortions due to the same cause. This makes it probable that the impurities within the crystal determine the energy necessary for a certain change of the mosaic structure.

With regard to such a relation one has to go back to one consequence of Zwicky's theory of the mosaic crystal which has already been suggested by him implicitly: In case a perfect crystal contains a small amount of impurity, too small to form a homogeneous solid solution of the whole crystal, the strange atoms will accumulate in a region where their presence causes the smallest disturbance of the lattice, i.e. within the II-planes. The chance that a certain part of the foreign atoms present in the liquid will accumulate within the II-planes depends on the expression

$$S = \frac{\alpha}{A} \cdot [E_p - E_\pi]$$

which by applying the Boltzmann principle gives for the probability the expression:

$$P = \text{const} \cdot e^{-\alpha(E_p - E)/AkT}$$

where E_p and E_π are the respective energy contents of the same crystal first when the foreign atoms are put into the lattice at random and second when they are arranged within the II-planes. A represents the affinity of the strange atoms for the formation of a solid solution in the crystallographic constellation under consideration and α stands for the "perfection" of the crystal, including the conditions of crystallisation, absence of external disturbances, inverse speed of growth, etc. It is apparent that the above will only hold for an amount of foreign atoms smaller than or equal to that amount necessary to fill the II-planes with a mono- or bimolecular layer and only for one kind of atoms at the same time. Under the assumption that S is sufficiently large in our crystals one is led to think that the units of the secondary lattice are surrounded by a more or less dense hull of impurities. It is obvious that atoms

[16] K. Honda, Magnetic properties of matter, Tokyo, p. 131, (1928).
[17] L. Schubnikow and W. J. de Haas, Comm. Phys. Lab. Leiden, Nr. 207 c p. 15 (1930).

of different metals should have different effects due to different A's, i.e., similar atoms should have smaller effects than an equal number of dissimilar ones, the correctness of which conclusion is attested for example by the negligible influence of small amounts of Sb within Bi crystals, (Sb forms the same lattice as Bi with only slightly different dimensions) and also by the surprising effect of traces of Ag and Pb (0.02 percent) as already stated by Bridgman, Goetz and Hasler.

The presence of such dissimilar impurities may greatly change the stability of the secondary lattice and thus make it more sensitive to the influence of a magnetic field applied during the formation of the crystal. The large influences that small impurities have on electric volume-effects within Bi crystals make the assumption of a two-dimensional accumulation of impurities (as in the Π-planes) necessary since it is difficult to understand that a homogeneous distribution of minute impurities over the whole crystal can produce such large effects, as have been observed by Kapitza for example in the change of conductivity in strong magnetic fields.[3]

It would be interesting to investigate whether or not the diamagnetic properties of these crystals are affected by impurities and also by their formation within strong magnetic fields. Assuming the correctness of Ehrenfest's hypothesis[18] namely that the large diamagnetic susceptibilities are due to electronic orbits extending around more than one nucleus, a change of the mosaic constellation of a crystal would be expected to affect its magnetic qualities, i.e., one should expect that the large diamagnetic susceptibilities are structure sensitive properties. Experiments of this kind are started and the results seem to point in this direction.

Besides the investigation of the intensity distribution of the x-ray reflections on "normal" and "magnetic" crystals which has already been published[8] briefly, another experiment should be mentioned which could throw light on the nature of the suggested distortion of the mosaic structure: namely an experiment upon the magnetostriction of perfect magnetic and normal crystals, for it is to be expected that this effect must be largely influenced by any systematic change of the secondary structure. Experiments of this kind are planned.

[18] P. Ehrenfest, Physica, 388, (1925); Phys. Zeits. 58, 719 (1929).

HYPERFINE STRUCTURE IN IONIZED BISMUTH

By Russell A. Fisher and S. Goudsmit
Department of Physics, University of Michigan
(Received March 14, 1931)

Abstract

The hyperfine structure of several lines in the spectra of Bi II and Bi III have been determined. A method which facilitates the analysis of partially resolved line patterns is described. The level separations obtained from the analysis are compared with theoretical formulas showing the inadequacy of the present theory for the interaction of external electrons with nuclear spin.

Experimental

THE twenty-one foot eighty thousand line concave grating mounted in the third basement of the laboratory was used in this work. We have used the grating in Paschen mounting with the slit at fifty degrees from the normal. In the third, fourth and fifth orders, where we have worked, linear dispersions range from 0.47 to 0.87 Angströms per millimeter and the practical resolving power is near two hundred thousand. Although the grating shows faint Rowland ghosts this is no limitation to fine-structure work, since these ghosts always lie far outside the fine-structure pattern. In extreme exposures a faint and diffuse line appears close on the short wave-length side of a sharp line. This false line causes little difficulty, however, since it appears only in over exposure and then at a fixed distance from the parent line. Although no attempt was made at temperature control the temperature of the spectrograph room was so constant that no appreciable broadening appeared after a twenty-four hour exposure.

Since the effect of fields and pressures in broadening spectral lines is considerable for ordinary light sources, special precautions attempting to avoid these influences are necessary in hyperfine structure work. Back has employed his vacuum arc most successfully in his work in arc spectra. Schüler[1] suggests the use of a modified form of the Paschen hollow cathode tube operating at liquid air temperatures. This type of source has been used by White and Ritchl[2] as well as by Schüler himself.

We have used an arc between a bismuth and a tungsten electrode in hydrogen at a few centimeters pressure in making a preliminary survey of the spectrum. This source gave several of the Bi II lines with fair sharpness. Later we used a metal discharge tube similar to that described by Schüler. Our only modification of Schüler's tube is the use of a removable molybdenum cylinder as hollow cathode. This molybdenum cathode has the advantage of contributing practically no lines to the spectrum and of being cleaned of im-

[1] H. Schüler, Zeits. f. Physik **56**, 149 (1930).
[2] H. E. White and R. Ritchl, Phys. Rev. **35**, 1146 (1930).

purities quickly. The bismuth was excited in helium, the metallic bismuth being placed inside the molybdenum cathode. The tube was operated in a water bath since lower temperatures were found to be of no advantage in the case of bismuth. In the discharge the lines of Bi I and Bi II appeared with nearly equal intensity while those of Bi III were somewhat less intense. An exposure of twenty-four hours was necessary in order to obtain some of the lines in the higher orders.

Analysis

The theory concerning hyperfine structure term separations predicts that hyperfine multiplets will follow the interval rule very accurately. Also the formulas for the line intensities in hyperfine line multiplets, which Hill[3] has derived by means of the quantum mechanics, should hold with accuracy. The fact that the interval and intensity rules can be relied upon enables one to construct graphs which aid greatly in the analysis of hyperfine line patterns. An observed line pattern is seldom completely resolved due to small separation in one or the other of the hyperfine multiplets giving rise to the line. The graphs are of particular use in the cases of imperfectly resolved line patterns.

Fig. 1a shows such a graph representing the possible line patterns in the case of a transition between two sets of levels in Bi II, each with a total extra-nuclear angular momentum of one quantum unit ($J=1$). Since the nuclear angular momentum quantum number of bismuth has been shown by Goudsmit and Back[4] to be $4\frac{1}{2}$, the resulting hyperfine multiplets should both be triple with fine quantum numbers of $3\frac{1}{2}$, $4\frac{1}{2}$, and $5\frac{1}{2}$. According to the interval rule the level separations should be $4\frac{1}{2}A$ and $5\frac{1}{2}A$, where A is called the separation factor. The distribution of the lines in the figure at any particular horizontal level gives a possible line pattern. The vertical coordinate, denoted by μ, is the ratio between the separation factors of the initial and final states. If B is the separation factor of the initial and A of the final hyperfine multiplet, $\mu=B/A$. The horizontal coordinate may be read in units of wave length or frequency as one chooses. Thus on the axis, $\mu=0$, we have a line pattern corresponding to the case of no separation of the initial levels, that is, a line triplet with the separations of the final multiplet, the separation ratio being $4\frac{1}{2}:5\frac{1}{2}$ as the interval rule requires. Positions a little above this axis, $\mu=0$, give line patterns due to slight separation of the initial levels as compared with the final levels. As we proceed to larger μ the graph represents the change in line pattern resulting from larger separations of the initial levels. The whole region above the axis (μ positive) gives patterns for cases in which both multiplets are regular or both inverted. Positions below this axis (μ negative) give patterns for cases in which one of the multiplets is inverted with respect to the other. The intensities of the lines are calculated from the formulas of Hill and the widths of the lines made roughly proportional to the expected intensities.

Fig. 1b gives a six-fold enlargement of the line $\lambda 5270$ of Bi II. It may be

[3] E. L. Hill, Proc. Nat. Acad. Sci. 15, 779 (1929).
[4] S. Goudsmit and E. Back, Zeits. f. Physik 43, 321 (1927).

observed that the line fits the graph precisely at $\mu = -0.261$. Because of its small intensity the line in the center of the figure does not appear on the photographic plate. The separations of the two multiplets giving rise to the line may here be read directly from the measured line separations.

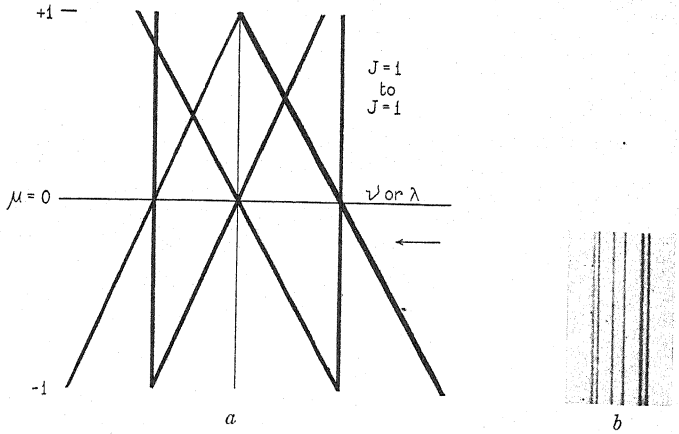

Fig. 1. Diagram for transition $J=1$ to $J=1$ compared with Bi II λ5270. $\mu=-0.261$, total $\Delta\nu=4.93$ cm^{-1}. The arrow indicates where the line pattern fits the diagram.

The graphs are of greatest assistance in cases in which the observed line patterns are imperfectly resolved.[5] In such cases the level separations may be found if μ can be determined by comparing the observed pattern to the graph and one or two separations measured to give the scale. Fig. 2a gives

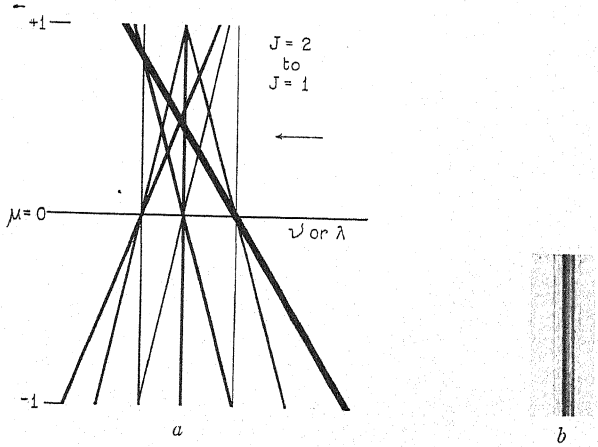

Fig. 2. Diagram for transition $J=2$ to $J=1$ compared with Bi II λ4705. $\mu=+0.457$, total $\Delta\nu=2.71$ cm^{-1}. The arrow indicates where the line pattern fits the diagram.

the graph for the transition $J=2$ to $J=1$. Fig. 2b gives an example of a partially unresolved and poorly defined line pattern which may be analyzed by means of the graph. The pattern is a six-fold enlargement of the unclassified line λ4705 of Bi II as it appeared in the fourth order. It is found that this line

[5] Similar graphs applicable to Zeeman effect analysis are being prepared for publication.

TABLE I. *Hyperfine structure of Bi II lines.*

λ ν	Intensity of components	Δν cm^{-1}	Combination
5719 17480	40 50 60	3.895 ± .006 2.140 ± .006 .000	$2_1{}^0-7_0$
5270 18970	20 20 20 20 23 25	4.926 ± .004 3.995 ± .004 3.166 ± .004 2.149 ± .004 .553 ± .006 .000	$2_1{}^0-8_1$
5209 19192	15 30 60 30 15 80 30 8	3.215 ± .006 2.667 ± .006 2.166 ± .006 1.471 ± .009 .964 ± .012 .783 ± .012 .000 − .694 ± .009	$2_1{}^0-9_2$
5144 19435	15 20 30	1.027 ± .007 .564 ± .007 .000	$1_0{}^0-8_1$
5124 19510	5 7 10 14 18	1.850 ± .006 1.505 ± .009 1.105 ± .009 .585 ± .006 .000	$9_2{}^0-16_2$
5091 19637	1 2 2 1 3 1 5	2.32 ± .02 1.83 ± .02 1.34 ± .03 1.11 ± .03 .74 ± .03 .56 ± .03 .00	$9_2{}^0-17_1$
4994 20018	20 5 10 8 10	1.325 ± .007 1.071 ± .007 .734 ± .007 .546 ± .007 .000	$10_1{}^0-19_2$
4730 21136	4 10 12 12 6 6 15 2	1.54 ± .03 1.35 ± .02 .99 ± .01 .68 ± .01 .46 ± .02 .24 ± .02 .00 − .25 ± .02	$9_2{}^0-19_2$
4705 21248	7 25 10 30 8 12 4	2.058 ± .005 1.500 ± .005 1.017 ± .005 .786 ± .003 .326 ± .008 .000 − .652 ± .005	Unclassified
4477 22330	3 3 3 3 4 4	3.53 ± .02 3.14 ± .02 2.33 ± .03 1.50 ± .02 .49 ± .02 .00	Unclassified

TABLE I (*Continued*)

λ ν	Intensity of Components	Δν cm^{-1}	Combination
	6	.64 ±.02	
4392	6	.30 ±.01	unclassified
22762	3	.00	
	10	2.62 ±.01	
4301	14	2.17 ±.01	
23244	6	1.70 ±.01	$7_2^0-12_3$
	12	1.52 ±.01	
	5	1.03 ±.01	
	18	.81 ±.01	
	5	.295±.005	
	24	.000	
	20	1.52 ±.01	
4079	15	.69 ±.01	
24509	10	.00	$6_1^0-10_2$
	7	1.45 ±.02	
3864	5	.66 ±.03	
25873	3	.00	$6_1^0-15_1$
	1	2.69 ±.04	
3846	2	2.14 ±.03	
25994	3	1.55 ±.02	$5_2^0-10_2$
	4	.88 ±.02	
	5	.00	
	4	3.21 ±.02	
3816	7	2.65 ±.01	
26198	15*	1.96 ±.01	$5_2^0-12_3$
	2	1.23 ±.02	
	10	1.00 ±.01	
	2	.27 ±.01	
	12	.00	
	2	1.65 ±.02	
3811	3	1.31 ±.02	
26232	5	.89 ±.01	$7_2^0-16_3$
	7	.47 ±.01	
	9	.00	
	6	1.25 ±.02	
3792	18	1.07 ±.02	
26364	22	.76 ±.01	$5_2^0-13_3$
	30	.41 ±.01	
	3	.00	
	20	8.84 ±.02	
3430	30	7.30 ±.03	
29146	40	5.29 ±.03	$4_2^0-12_3$
	50	2.88 ±.03	
	60	.00	
	1	8.2	
3111†	2	6.7	
32135	3	4.8	$4_2^0-16_3$
	4	2.7	
	5	.0	
	16	7.5	
2368†	12	5.1	
42217	10	3.0	$4_2-4_2^0$
	9	1.4	
	8	.0	

* An iron line coincides with this component giving the abnormal intensity.
† From the measurements of McLennan, McLay and Crawford.

pattern fits the graph with exactness at $\mu = 0.457$. The very faint component to the extreme right, which may not appear in the reproduction, is present on the original plate.

TABLE II. *Hyperfine structure of Bi III lines.*

λ / ν	Intensity of Components	$\Delta\nu$ cm^{-1}	Combination
	1	9.3 ± .3	
4750	2	8.1 ± .3	
21046	3	6.6 ± .3	$3_{2\frac{1}{2}} - 5f\ ^2F_{2\frac{1}{2}}^0$
	4	4.7 ± .2	
	5	2.6 ± .1	
	6	.0	
	20	2.88 ± .01	
4561	5	2.36 ± .01	
21919	10	.52 ± .01	$7s^2S_{\frac{1}{2}} - 7p\ ^2P_{\frac{1}{2}}^0$
	20	.00	
3695	10	2.16 ± .03	
27056	15	.00	$7s^2S_{\frac{1}{2}} - 7p\ ^2P_{1\frac{1}{2}}^0$
	2	12.3	
3039†	3	10.7	
32896	4	8.9	$2_{2\frac{1}{2}} - 7p\ ^2P_{1\frac{1}{2}}^0$
	5	6.6	
	7	3.6	
	9	.0	
	2	7.1	
2944†	3	5.4	
33957	4	3.0	$1_{1\frac{1}{2}} - 7p\ ^2P_{\frac{1}{2}}^0$
	6	.0	
	1	9.3	
2184†	1	8.0	
45733	1	6.6	$3_{2\frac{1}{2}} - 6f\ ^2F_{3\frac{1}{2}}^0$
	2	4.9	
	2	2.8	
	3	.0	

† From the measurements of McLennan, McLay and Crawford.

Tables I and II give the measurements on the line patterns of Bi II and Bi III, respectively, in terms of frequency differences. The line of the pattern from which the frequency differences are measured is in general the one of lowest frequency. In the few cases in which the line of lowest frequency is faint or unsuitable for other reasons another line has been selected. The method of measurement was such that the uncertainty in frequency difference between any two components of a pattern is not greater than the larger uncertainty following one of them, i.e., the uncertainties do not add. In the tables we give the wave-lengths to four significant figures only, since the patterns are broad and we have not made precise wave-length measurements.

We have been aided greatly in the hyperfine structure analysis by a paper recently published by McLennan, McLay and Crawford[6] in which they give the term analysis for Bi II and for Bi III and a few very wide hyperfine-structure measurements. We have included their measurements in our tables as those indicated by the symbol †.

[6] J. C. McLennan, A. B. McLay and M. F. Crawford, Proc. Roy. Soc. A129, 579 (1930).

TABLE III. *Bi II level separations.*

Term value	Configuration*	Term designation	Total separation cm^{-1}	Separation factor
69126	$6p_{\frac{1}{2}}7s$	$1_0{}^0$	—	
69590	$6p_{\frac{3}{2}}7s$	$2_1{}^0$	3.91±0.01	0.391
76143	$6s6p^3$	$4_2{}^0$	8.2 ±0.2	0.41
79083	$6p_{\frac{1}{2}}6d_{1\frac{1}{2}}$	$5_2{}^0$	2.55±0.10	0.127
80569	$6p_{\frac{1}{2}}6d_{1\frac{1}{2}}$	$6_1{}^0$	−1.65±0.05	−0.165
82041	$6p_{\frac{3}{2}}6d_{2\frac{1}{2}}$	$7_2{}^0$	1.98±0.15	0.099
88763	$6p_{1\frac{1}{2}}7s$	$9_2{}^0$	2.18±0.10	0.109
89877	$6p_{1\frac{1}{2}}7s$	$10_1{}^0$	−0.53±0.03	−0.053
88559	$6p_{\frac{1}{2}}7p_{1\frac{1}{2}}$	8_1	1.02±0.01	−0.102
88781	$6p_{\frac{3}{2}}7p_{1\frac{1}{2}}$	9_2	2.50±0.03	0.125
105077	$6p_{\frac{1}{2}}5f_{2\frac{1}{2}}$	10_2	−0.16±0.06	−0.008
105281	$6p_{\frac{1}{2}}5f_{2\frac{1}{2}}$	12_3	−0.70±0.15	−0.023
105443	$6p_{\frac{3}{2}}5f_{3\frac{1}{2}}$	13_3	1.95±0.20	0.065
106441	$6p_{1\frac{1}{2}}7p_{\frac{1}{2}}$	15_1	−0.36±0.08	−0.036
108272	$6p_{1\frac{1}{2}}7p_{1\frac{1}{2}}$	16_3	0.37±0.15	0.012
108398	$6p_{\frac{1}{2}}8p_{\frac{1}{2}}$	17_1	−0.14±0.10	−0.014
109897	$6p_{1\frac{1}{2}}7p_{1\frac{1}{2}}$	19_2	0.78±0.04	0.039

* The configurations and term values are as given by McLennan, McLay and Crawford.

TABLE IV. *Bi III level separations.*

Term value	Configuration	Term designation	Total separation cm^{-1}	Separation factor
123143	$6s6p^2$	$1_{1\frac{1}{2}}$	7.5 ±0.8	0.50
116943	$6s6p^2$	$2_{2\frac{1}{2}}$	12.5 ±0.8	0.50
111105	$7s$	$^2S_{\frac{1}{2}}$	2.36±0.01	0.472
89765	$6s6p^2$	$3_{2\frac{1}{2}}$	9.3 ±0.6	0.37
89188	$7p$	$^2P_{\frac{1}{2}}{}^0$	0.52±0.01	0.104
84053	$7p$	$^2P_{1\frac{1}{2}}{}^0$	0.31±0.05	0.021

Tables III and IV give the level separations as determined from our measured line patterns with the aid of the graphs. In the tables we have used the term designation as given by McLennan, McLay and Crawford. In all cases we give the total hyperfine-multiplet separation. Negative separation in the table indicates inversion of the multiplet. Although the individual level separations could usually be determined, the uncertainty was in most cases too large for the data to be a valuable test of the interval rule. The separations of two of the multiplets of bismuth II are determined with a higher degree of accuracy. They are:

Term	Total separation	Individual separations	
$2_1{}^0$	3.91±.01	2.15±.01	1.76±.01
8_1	−1.02±.01	− .56±.01	−.46±.01

We may say that the interval rule is obeyed to within the limit of observational uncertainty in all cases. We believe that the estimates of uncertainty given in the tables are extremely liberal.

It is evident that the hyperfine structure analysis serves to verify much of the term assignment of McLennan, McLay and Crawford from the fact that we are able to use their term designation. We find, however, no evidence of the existence of the tentative term denoted by them as 3°.

We have been able to measure the structure of three lines which without doubt belong to Bi II but which have not been classified by McLennan, McLay and Crawford. We make no attempt to classify these lines in the general term system but do give the hyperfine separations of the levels from which they originate. Two possibilities arise in such cases since there is no way of deciding which level is initial. These lines and the level separations derived from them are as follows:

Wave-length of line	Total separation of initial levels	Total separation of final levels
4705	2.48 ± 0.05 $(J=2)$	2.71 ± 0.01 $(J=1)$
	or	
	-2.71 ± 0.01 $(J=1)$	-2.48 ± 0.05 $(J=2)$
4477	-0.85 ± 0.04 $(J=2)$	2.68 ± 0.04 $(J=2)$
	or	
	-2.68 ± 0.04 $(J=2)$	0.85 ± 0.04 $(J=2)$
4392	0.60 ± 0.15 $(J=1)$	small $(J=0?)$
	or	
	small $(J=0?)$	-0.60 ± 0.15 $(J=1)$

Theoretical Discussion

In a previous[7] paper one of us has given formulas for the hyperfine-structure separations for different states of the same atom. In that paper it was already pointed out that the theoretical results were in disagreement with the experimental data, even in the simple case of a one-electron spectrum. We now wish to discuss our material in Bi II and Bi III together with the known data for Bi I[8] in the light of these theoretical expressions.

Bismuth I. The normal state, $6p^3$, does not yet show extreme (j,j) coupling. We may, however, apply the formulas derived on the assumption of extreme (j,j) coupling to the two levels with $J=2\frac{1}{2}$ and $J=\frac{1}{2}$, respectively, since these two quantum numbers occur only once in this configuration and the hyperfine separations of the levels are therefore independent of the type of coupling. The individual electrons of the configuration are considered as acting separately except for their screening effect upon one another. Thus the separation factor of a hyperfine multiplet is expressible in terms of separation factors for the electronic states. These considerations are similar to those used in the treatment of ordinary multiplet separations. The following table gives the observed separation factors for several states together with the formulas[9] applying both in case of (j,j) coupling and of Russell-Saunders coupling.

[7] S. Goudsmit, Phys. Rev. **37**, 663 (1931).
[8] P. Zeeman, E. Back and S. Goudsmit, Zeits. f. Physik **66**, 1 (1931).
[9] For all following formulas see S. Goudsmit, Phys. Rev. **37**, 663 (1931).

Term	Observed separation factor	Formula	
		(j,j) coupling	Russell-Saunders coupling
$6p^3\ {}^4S_{1\frac{1}{2}}$	~ -0.005	a'	0
$\quad {}^2D_{1\frac{1}{2}}$	-0.040	$1\frac{1}{5}a'-\frac{1}{5}a''$	$^{16}/_{25}a$
$\quad {}^2D_{2\frac{1}{2}}$	0.081	$\frac{4}{5}a'+\frac{1}{5}a''$	$^{24}/_{25}a$
$\quad {}^2P_{\frac{1}{2}}$	0.375	a''	$2\frac{2}{3}a$

In (j,j) coupling the separation factor for the $6p_{1\frac{1}{2}}$ electron is denoted by a' and that for the $6p_{\frac{1}{2}}$ electron by a''. In Russell-Saunders coupling it has no meaning to distinguish between the $6p_{\frac{1}{2}}$ and the $6p_{1\frac{1}{2}}$ states so one can only express the separation factor in terms of the common quantity, a. The quantities a' and a'' are not independent, for, according to the theory, one has the relations,

$$a' = \frac{8}{15}a \text{ and } a'' = \frac{8}{3}a, \text{ thus } a' = \frac{1}{5}a''.$$

The experimental data are not at all in agreement with these results. The last two states in the table, for which the formulas ought to hold, regardless of the type of coupling, show clearly that a' is much smaller than $1/5a''$. One finds from these two levels

$$a' = 0.008$$
$$a'' = 0.375.$$

These values do not agree exactly with those obtained from the first two levels of the table, but this may be ascribed to the deviation from the extreme (j,j) coupling. It is certainly significant that the ${}^2D_{1\frac{1}{2}}$ level shows a negative separation factor again indicating that a' is too small.

The next configuration of interest is $6p^27s$. The assignment of electron configuration in this case is not quite certain as this configuration is mixed with the $6p^26d$ levels. This also may cause large second order corrections which make our formulas invalid. The observed data for this configuration, which is near extreme (j,j) coupling, together with the formulas applying in (j,j) coupling are as follows:

Term	Observed separation factor	Formula (j,j) coupling
$6p^27s\ 1_{\frac{1}{2}}$	0.166	c
$\quad 4_{1\frac{1}{2}}$	~ 0	$\frac{5}{6}a'-\frac{1}{6}a''+\frac{1}{3}c$
$\quad 5_{\frac{1}{2}}$	-0.142	$1\frac{2}{3}a'-\frac{1}{3}a''-\frac{1}{3}c$
$\quad 7_{2\frac{1}{2}}$	0.127	$\frac{2}{5}a'+\frac{1}{5}a''+\frac{1}{5}c$
$\quad 8_{1\frac{1}{2}}$	0.094	$^9/_{10}a'+^3/_{10}a''-\frac{1}{5}c$

Here the separation factor of the $7s$ electron is denoted by c. In this example the first level lies isolated from the others, hence one expects the formula to hold. The other levels form a group in which levels with $J=\frac{1}{2}$ and $J=2\frac{1}{2}$ occur only once. For these two levels the formulas ought also to be correct. From these one obtains:

$$c = 0.166$$
$$a' = 0.026$$
$$a'' = 0.390.$$

These values are in fair agreement with the data for the two observed levels with $J=1\frac{1}{2}$. The value of a'' is in good agreement with what we obtain from the p^3 configuration. The value of a' agrees only in order of magnitude. However, we may not rely too much upon this value since it is so small that it may be much influenced by inaccuracy in the data as well as by second order corrections to our formulas. The significant point is that we again find a' to be much smaller than $1/5a''$.

Bismuth II. For the configuration $6p\ 7s$ we have extreme (j,j) coupling. The formulas and observed data for this case are:

Term	Observed separation factor	Formula (j,j) coupling
$6p_{\frac{1}{2}}7s\ 2_1{}^0$	0.391	$\frac{1}{2}a''+\frac{1}{2}c$
$6p_{1\frac{1}{2}}7s\ 9_2{}^0$	0.109	$\frac{3}{4}a'+\frac{1}{4}c$
$10_1{}^0$	−0.053	$1\frac{1}{4}a'-\frac{1}{4}c$

We expect the values of a', a'' and c to be somewhat larger than in Bi I because the screening has decreased. This will have the greatest influence upon the outer $7s$ electron and therefore upon c. We find

$$a'=0.028$$
$$a''=0.430$$
$$c=0.352$$

These values are in good agreement with our expectation.

For other configurations, such as $6p\ 6d$ and $6p\ 7p$, we expect only qualitative agreement, as the separation factors for the $6d$ and $7p$ are probably smaller than the errors due to second order corrections to our formulas and errors in our measurements. In the case of the $6p\ 6d$ configuration we have:

Term	Observed separation factor	Formula (j,j) coupling
$6p_{\frac{1}{2}}6d_{1\frac{1}{2}}\ 5_2{}^0$	0.127	$\frac{1}{4}a''+\frac{3}{4}d''$
$6_1{}^0$	−0.165	$-\frac{1}{4}a''+1\frac{1}{4}a''$
$6p_{\frac{1}{2}}6d_{2\frac{1}{2}}\ 7_2{}^0$	0.099	$-\frac{1}{6}a''+1\frac{1}{6}d'$

Here the symbols d' and d'' denote the separation factors of the $6d_{2\frac{1}{2}}$ and $6d_{1\frac{1}{2}}$ electrons, respectively. The first two states give:

$$a''=0.565$$
$$d''=-0.019$$

It is strange to find a small negative value for d'', but we do not know that this value is entirely reliable. The experiment result for $7_2{}^\circ$ would give a very large value for d', which is even less understandable. Perhaps the assignment of the configuration is incorrect for this level.

As examples of the $6p\ 7p$ configuration we have:

Term	Observed separation factor	Formula (j,j) coupling
$6p_{\frac{1}{2}}7p_{1\frac{1}{2}}\ 8_1$	-0.101	$-\frac{1}{4}a''+1\frac{1}{4}e'$
9_2	0.125	$\frac{1}{4}a''+\frac{3}{4}e'$

Here e' denotes the separation factor for the $7p_{1\frac{1}{2}}$ state. We find:

$$e' = 0.012$$
$$a'' = 0.464.$$

Again a'' is in good agreement with what we expect.

For the $6p\ 5f$ configuration we have:

Term	Observed separation factor	Formula (j,j) coupling
$6p_{\frac{1}{2}}5f_{2\frac{1}{2}}\ 10_2$	-0.008	$-\frac{1}{6}a''+1\frac{1}{6}f''$
12_3	-0.023	$\frac{1}{6}a''+\frac{5}{6}f''$
$6p_{\frac{1}{2}}5f_{3\frac{1}{2}}\ 13_3$	0.065	$-\frac{1}{8}a''+1\frac{1}{8}f'$

Here f'' denotes the separation factor of the $5f_{2\frac{1}{2}}$ electron and f' that of the $5f_{3\frac{1}{2}}$ electron. These data give no sensible result. Perhaps the assignment of configuration is incorrect, or it may be that there are large second order effects due to the proximity of these levels to other even levels.

Bismuth III. The interesting configuration here is $6s\ 6p^2$. The hyperfine structure is known for three of the levels. For extreme (j,j) coupling, which may not be quite correct here, we have:

Term	Observed separation factor	Formula (j,j) coupling
$6s\ 6p^2\ 1_{1\frac{1}{2}}$	0.50	$\frac{5}{6}a'-\frac{1}{6}a''+\frac{1}{6}b$
$2_{2\frac{1}{2}}$	0.50	$\frac{3}{5}a'+\frac{1}{5}a''+\frac{1}{5}b$
$3_{2\frac{1}{2}}$	0.37	$\frac{4}{5}a'+\frac{1}{5}b$

The separation factor of the $6s$ electron is here denoted by b. The above data give us:

$$a''=0.66$$
$$a'=0.01$$
$$b=1.80.$$

Due to the fact that the screening is here much less than in the previous cases we find a'' to be larger than before. We cannot, of course, be sure that the value found is just the one expected without making complicated calculations as to screening effects. The value of a' is smaller than the uncertainty in measurement and therefore not reliable.

For the $7s$ configuration we find:

Term	Observed separation factor	Formula (j,j) coupling)
$7s\ ^2S_{\frac{1}{2}}$	0.472	c

Comparing this value of c with the previous values we find the expected large increase. The experimental values for c are, Bi I:0.166; Bi II:0.352; Bi III:0.472.

We can make a similar comparison of the separations due to the $6s$ electron. The large hyperfine structure of the far ultraviolet lines $\lambda 864$ and $\lambda 1139$ observed by Arvidson[10] is probably that of the $6s$ state of Bi V. Furthermore, one level of the $6s\ 6p^3$ configuration of Bi II is at present known. Assuming (j,j) coupling one obtains:

Term	Observed separation factor	Formula (j, j) coupling
Bi II $6s6p^3\ 4_2{}^0$	0.41	$\frac{3}{4}a'+\frac{1}{4}b$
Bi V $6s$	2.6	b

Since a' is of the order of 0.01 this gives $b=1.60$ for Bi II. Comparing the different values for b, we find, Bi II: 1.60; Bi III: 1.80; Bi V: 2.6.

Conclusions

The above discussion shows that in some respects the experimental results obey the theoretical formulas whereas in others there is distinct disagreement. It is possible to determine in more detail where the discrepancy lies. The formulas as they are given here in terms of a' and a'' explicitly are more or less independent of the type of interaction which causes the hyperfine splitting. One takes a given interaction for a definite state of a single electron and calculates by means of well-known methods the result when this electron is not alone but part of a more complicated configuration. Such formulas are based upon well-known quantum mechanical rules and can in many cases be derived by simple methods using the vector model. Similar ones have been shown to hold for multiplet separations, g-values, etc. It is therefore not surprising that the formulas are also valid here, for if they were not it would mean that ordinary perturbation theory could not be applied to our problem.

The discrepancy was found, however, in the relation between a' and a'',

$$a' = \frac{1}{5}a''.$$

Everywhere we find a' much too small. This relation, however, can be obtained only by considering in detail the interaction between the nuclear spin and the orbital and spin magnetism of the external electrons.[11] It is on this point that the present theory seems to be incorrect. We hope that the material gathered here may prove useful as a guide for the improvement of the quantum mechanics of spin-spin interaction.

[10] G. Arvidson, Nature **126**, 565 (1930).
[11] Compare S. Goudsmit, Phys. Rev. **37**, 663 (1931).

POTENTIAL DROP AND IONIZATION AT MERCURY ARC CATHODE

By Edward S. Lamar, Princeton University
and
Karl T. Compton, Massachusetts Institute of Technology

(Received March 19, 1931)

Abstract

By means of a movable Langmuir collector, the potential, ion concentration and electron temperature were measured at various distances from a stationary mercury cathode spot, at various arc currents. The results indicated a cathode drop of 10.0 volts, and a small negative potential gradient beyond the fall space which was more pronounced at the larger currents. The ion concentration varied between $2(10)^{13}$ and $3(10)^{11}$ cm^{-3} for distances between 0.4 cm and 1.7 cm and arc currents between 11 amp and 4.2 amp. The concentrations evidently greatly exceed these values very close to the cathode. The mean electron energies were about 1.4 volts near the cathode and fell to a little less than a volt at the greater distances. From the lack of saturation of currents to the collector at space potential, the coefficient of electron reflection at the amalgamated tungsten collector surface was found to be close to 0.5. It is shown that the thickness of the cathode fall space must be less than $1.76(10)^{-4}$ cm and that the field at the cathode surface must exceed $7.6(10)^{4}$ volts $\cdot$ cm^{-1}.

Introduction

In 1905, Stark and his collaborators[1] attempted by a probe wire method to measure the cathode fall of potential in a mercury arc, and their value of 5.27 volts has been accepted until quite recently. In 1924, Langmuir and Mott-Smith[2] pointed out a serious error in the old probe wire method, and developed a new method which not only gives accurate values of space potential, but also gives information regarding electron and ion concentrations and velocities. In 1928, Killian, at the suggestion of one of the authors, undertook an investigation of the potential drop and conditions of ionization near mercury arc cathodes. His results were reported at a meeting of the American Physical Society[3] and were essentially as follows: The drop in potential from the cathode to a point distant 0.2 cm from its surface was 10.1 volts, and increased regularly to 11.6 volts as the distance was increased to 3.0 cm. The value of about 10 volts, as extrapolated to the cathode surface has been taken as significant of the ionizing potential of mercury within the limits of uncertainty set by the small unknown contact difference of potential between cathode and probe.[4] Later work by Nottingham[5] has led to similar conclusions

[1] Stark, Retschinsky and Shaposchnikoff, Ann. d. Physik **18**, 213 (1905).

[2] Langmuir and Mott-Smith, G. E. Rev. **27**, 449, 538, 616, 762, 810 (1924).

[3] Killian, Phys. Rev. **31**, 1122 (1928).

[4] Gaudenzi (The Brown Boveri Rev. **16**, 303 (1929)) estimated the cathode drop to be about 9 volts by a method which did not allow for the possibility of a positive or negative anode drop.

[5] Nottingham, J. Frank. Inst. **206**, 43 (1928); **207**, 299 (1929).

in some arcs at higher pressures with various cathode materials. Killian furthermore found random currents of positive ions of 1.5 to 40 milliamps·cm^{-2} and of electrons of 1.3 to 18 amps·cm^{-2}, the larger values referring to the regions closest to the cathode. The electron temperatures were 5000° to 16,500°K, or 0.65 to 2.13 volts mean energy.

In these measurements, the distances were measured from the cathode surface but do not represent true distances from the cathode spot, since it wandered rapidly and erratically all over the cathode surface. Killian there-

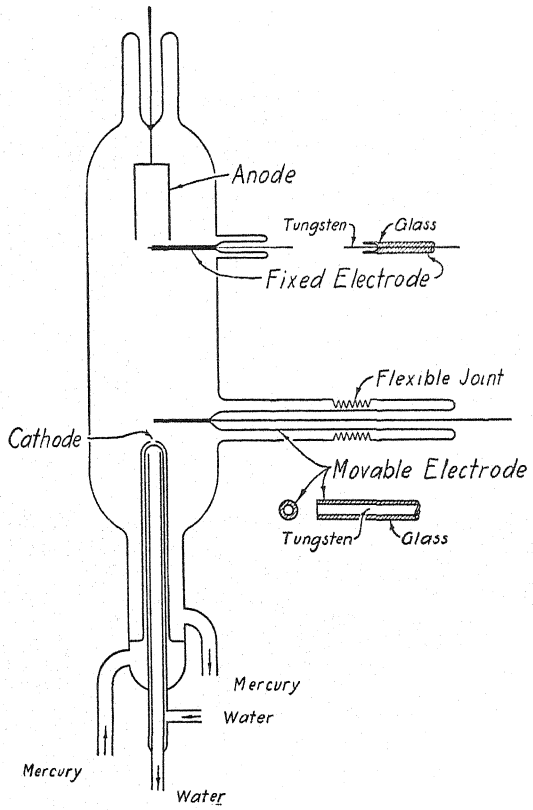

Fig. 1. Diagram of arc tube.

fore devised the apparatus described below in order to keep the cathode spot approximately stationary and thus to make possible more accurate measurements. Since Killian was diverted from carrying out these more refined experiments, the authors continued them as follows.

Apparatus

A diagram of the arc tube is shown in Fig. 1. The cathode consists of three coaxial tubes. The innermost two are of Pyrex glass and constitute a water-cooling system for the cathode. The outside tube is of quartz and has a small hole drilled in its upper end. Mercury is raised to the level of this hole.

The surface of the mercury at the hole is the cathode of the arc. The small size of the pool cathode thus prevents excessive wandering of the cathode spot. The mercury outlet shown is designed to take care of the mercury that condenses on the walls of the tube and falls to the bottom.

The exploring electrode employed in the region of the cathode consists of a 60 mil tungsten wire entirely covered with glass, and then ground flat at its end. The resulting flat tungsten surface constitutes a plane collector, and the great mass of tungsten behind it makes its thermal dissipating power sufficiently great to prevent the excessive heating which has hitherto made measurements very near the cathode spot impossible. The flexible metal joint shown in the diagram permits an exploring range of about 2 cm.

The exploring wire shown near the anode is of the usual type consisting of a fine tungsten wire covered with glass over most of its length. The last few millimeters of glass are not in contact with the exploring wire. This prevents electrical contact between the exploring wire and any metal coating which may be deposited on the insulating glass.

The anode as shown is of the usual hollow cylindrical design and is made of sheet nickel.

Procedure

The arc was started by means of a high frequency leak tester and the current was adjusted to the desired value by varying the resistance in series. The arc and series resistance were operated on 110 volts d.c.

The experimental procedure, after the arc had become steady, was to measure the current to the collector for different voltages applied to it at various distances from the cathode. At any given position, a plot of log i vs. V where i is the electron current to the collector and V the potential of the collector with respect to the cathode generally showed the points to be scattered between two parallel lines a half volt apart. This scattering of the points was found to arise from changes in the nature of the surface of the collector which resulted in changes in the contact difference in potential and depended on the immediately previous history of the collector. It was found that consistent results were obtained if the collector was left 100 volts negative with respect to the anode except when a reading was actually being made. Under these conditions the points fell along a curve at the lower voltage limit mentioned above, indicating a low value for the work function of the surface.

The curves shown are plotted to this lower value, which is believed to be the correct value, for reasons indicated below. Since the collector is always covered with a thin visible film of mercury, there is no further correction necessary for contact difference of potential between collector and mercury cathode.

A typical collector curve is shown in Fig. 2.

Interpretation of Shift in Collector Potential

We were at first inclined to attribute the shift in collector potential, when its potential to space was changed from large negative values to small negative or positive values, to a slow deposit of alkali material coming perhaps

from the neighboring glass and depositing as ions when the collector is negative. In this case the upper curve (characteristic of the collector in its more electronegative state) would presumably be that characteristic of an uncontaminated surface and, if so, the correct values would be 0.5 volt higher than those of Fig. 2. This was our opinion at the time of our preliminary report to the American Physical Society (Washington Meeting April 24, 1930), when we reported as our best estimate that the cathode drop is equal to the minimum ionizing potential 10.4 volts. Now, however, we are inclined to interpret the results differently, and to use the lower value of potential for the following reasons.

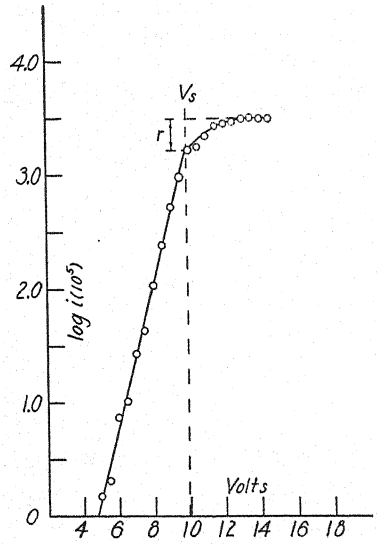

Fig. 2. Curve showing logarithm of electron current i as a function of collector potential V_c with respect to cathode. V_s is space potential and r indicates the amount of electron reflection.

After remaining 100 volts negative for a short time, surface impurities should be sputtered off by positive ion bombardment, leaving a clean collector surface. Hence the measurements made just after this should be those characteristic of the clean surface. Furthermore Found and Langmuir (unpublished) in extending earlier work by Kenty and Turner,[6] found that oxygen layers could form slowly on tungsten collectors even in very pure gas, causing electronegative potential shifts of about 0.5 volts in the surface potential. We think it probable, therefore, that the lower voltage values are the correct ones, indicating the value of the cathode drop to be about 9.9 volts.

Interpretation of Experimental Results

These and similar curves are interpreted by the collector theory of Langmuir and Mott-Smith, which is now too well known to require comment further than to give the equations which we shall use:

[6] Kenty and Turner, Phys. Rev. **32**, 799 (1928).

$$I = I_0 \epsilon^{-eV_c/kT}, \quad I_0 = Ne\left(\frac{kT}{2\pi m}\right)^{1/2}, \quad i = AI$$

where I is the electron current density to the collector whose potential is $-V_c$ with respect to the space, I_o is the random electron current density, N and T are the electron concentration and temperature, respectively, and A is the collector area. From these equations we have:

$$\log i = \log AI_0 - \frac{eV_c}{kT} = \log ANe\left(\frac{kT}{2\pi m}\right)^{1/2} - \frac{eV_c}{kT}$$

which is the equation of the straight portion of the curve of Fig. 2, when V_c is taken to be the value of V measured from the point of discontinuity which is at space potential V_s. The fact that the curve to the left of the discontinuity is straight, proves that the electrons have a Maxwellian distribution of velocities, which is assumed in the above equations.

It is observed that the electron current to the collector does not reach its maximum value at space potential, but only when the collector is a few volts positive with respect to space. This is attributed to electron reflection from the collector, and the intervening curve depends on the distribution of velocities of the reflected electrons. Such reflection, which is a well-recognized phenomenon, does not affect the slope of the straight line to the left of the break, since it is a peculiarity of a Maxwell distribution that it is not altered by a retarding field and hence the fraction of electrons reflected is constant at all values of the retarding field. The effect of reflection on the straight portion of the curve is thus simply to depress it, parallel to itself, by an amount dependent on the reflection coefficient.

This reflection coefficient may be obtained from Fig. 2 as follows. The electron current has reached saturation at about 4 volts above space potential, indicating that practically no reflected electrons can escape against as much as 4 volts. The difference between this saturation current and the current at the discontinuity represents the current of reflected electrons, and is shown by r in Fig. 2. The ratio of this reflected current to the total saturation current gives the reflection coefficient R. Owing to the foreshortening of the logarithmic scale, these values of R are determined with less experimental accuracy than the other quantities in which we are interested.

The more important results of the measurements are shown in Figs. 3 and 4. The mean electron energy $\bar{V}$ was calculated from the relation

$$\frac{e\bar{V}}{300} = \frac{3}{2}kT$$

and represents the mean energy of the electrons in a given volume. For the mean energy of the electrons striking the collector, the fraction 3/2 should be replaced by 2.

The data shown in Figs. 3 and 4 were all obtained with an arc carrying 4.2 amps. Similar observations on an 11.0 amp. arc yielded results which, for comparison, are shown in Table I.

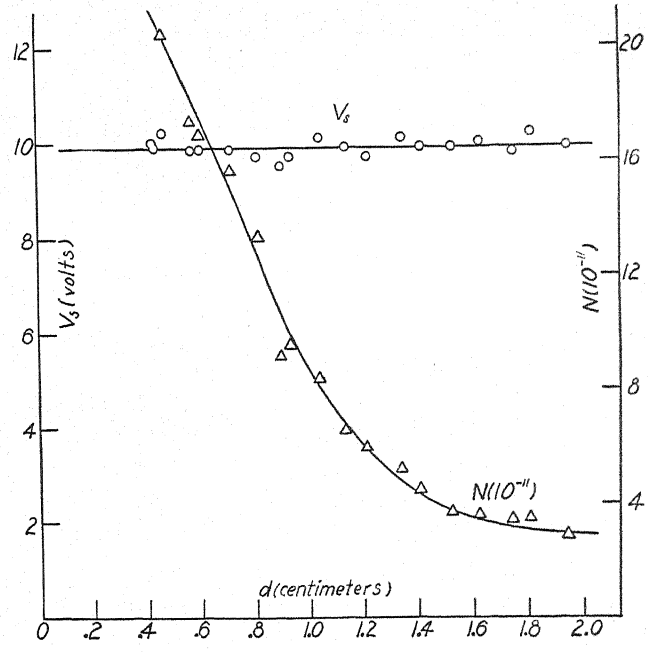

Fig. 3. Space potential V_s with respect to the cathode and electron concentration N as functions of the distance d from the cathode spot to the center of the face of the 60 mil (0.15 cm) diameter collector. Arc current 4.2 amp.

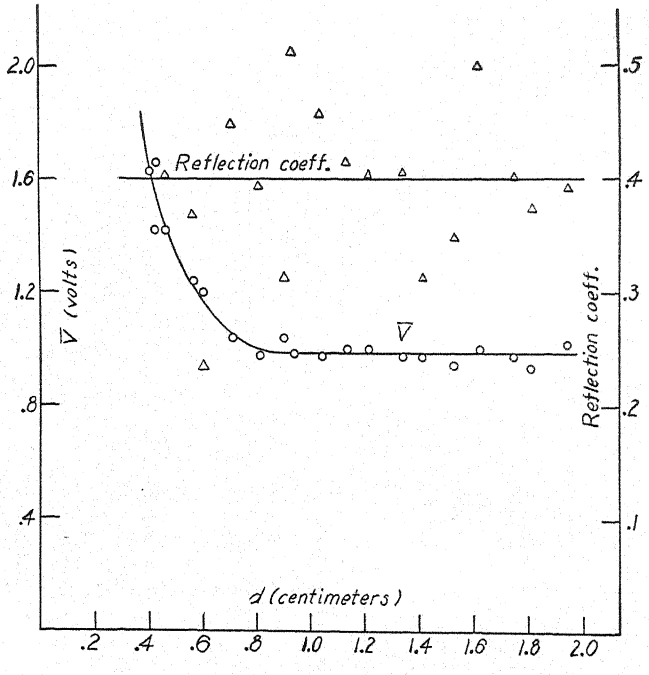

Fig. 4. Mean electron energy $\overline{V}$ in equivalent volts and reflection coefficient R as functions of distance d from cathode spot to collector. Arc current 4.2 amp.

TABLE I. *V_s = space potential; N = electron concentration; $\overline{V}$ = mean electron energy; I = random electron current density; d = distance from cathode.*

	4.2 amp. arc		11.0 amp. arc	
d(cm)	0.43	1.75	0.39	1.71
V_s (volts)	10.0	9.8	10.2	8.9
I (amp·cm^{-2})	5.7	7.4	63.5	12.8
N (10^{-11})	17.1	2.8	218.	55.3
$\overline{V}$ (volts)	1.42	0.978	1.171	0.748

DISCUSSION OF EXPERIMENTAL RESULTS

Cathode drop. From such results we conclude that the cathode drop is very near to 10 volts, from the nearest point at which we can measure (or extrapolate) to the cathode. Of course what we really wish to know is the cathode drop across the cathode fall space alone, which is an extremely small distance. This distance has never been measured, but may be estimated roughly as follows: The relations in the cathode fall space are given by the space-charge equation

$$I_+ = 0.543(10)^{-7}\frac{V_c^{3/2}}{M^{1/2}d_c^2}$$

in ordinary electrical units. The current density at the cathode[7] is about 4000 amp.·cm^{-2}. Langmuir and Mott Smith[8] have shown that a negative electrode immersed in strongly ionized mercury vapor collects a positive ion current of about 1/400 of the "random" electron current, which in turn is always larger than the "drift" (or actual discharge) current. Since the drift current density is 4000 amp.·cm^{-2}, the positive current density is therefore something greater than 1/400 of this, i.e., greater than 10 amp.·cm^{-2}. Unfortunately we cannot say how much greater than this lower limit is the true value of the positive current. Two factors may increase it by considerably more than the factor of three or four which commonly represents the ratio of random to drift current in regions of uniform ionization. One of these is the enormous concentration of electrons and ions in the region of negative glow on account of the potential maximum which develops in this region of intense ionization, and the consequent "trapping" of electrons to build up large concentrations, and the other is the additional trapping action due to the fact that the cathode spot is a depression in the mercury surface and presents therefore the peculiarities of a hollow cathode.

Perhaps the positive ion currents may be ten, though probably not a hundred times the value given by the fraction 1/400.[9] Using this as a lower limit, and taking $V_c = 10$ volts and $M = 200$, we find

$$d_c < 1.76(10)^{-4}\text{ cm}.$$

[7] Güntherschulze, Zeits. f. Physik **11**, 74 (1922).

[8] Langmuir and Mott-Smith, G.E. Rev. **27**, 544 (1924).

[9] From the theory of collectors in ionized gas (Tonks and Langmuir, Phys. Rev. **34**, 876 (1930)) it is impossible that the positive current density at the cathode spot can be less than

Field at cathode. Given a cathode drop of 10 volts in a distance less than $1.76(10)^{-4}$cm, we calculate the average field in the fall space to be greater than $5.7\ (10)^4$ volts·cm^{-1}. By the simple space-charge equation it is easily shown that the field E_c at the cathode surface is 4/3 the mean field, or

$$E_c > 7.6(10)^4 \text{ volts}\cdot\text{cm}^{-1}.$$

It appears unlikely that the field can be as much as ten times this value, since this would require an ion current one hundred fold that on which the calculation is based. These results are not appreciably affected if we use the more refined equations of Mackeown[10] to calculate the value of d_c.

Of course the cathode surface is highly agitated and consequently rough. Thus the fields to points may greatly exceed the values calculated above, and may very likely attain values of the order of millions of volts per centimeter. Langmuir[11] has already pointed out that fields of this magnitude are probably adequate to account for the observed electron emission from the cathode spot as "autoelectronic" emission, or "field current".

In the absence of information regarding the behavior of a fresh mercury surface in autoelectronic emission and in view of the uncertainty regarding the field strength at the cathode, it appears hopeless to make a direct quantitative test of this theory of emission from the cathode spot. Further evidence, however, is afforded in a revision of earlier studies of heat balance, as given in the following paper.

---

this. According to one theory it might be much greater (the theory of thermal ionization of the vapor by Slepian, Phys. Rev. **27**, 407 (1926)). As shown in the following paper, however, there are not only serious theoretical objections to this theory, but the experimental evidence based on heat balance at the cathode is inconsistent with it, and points to the correctness of the assumption that the relative current densities are at least of the order of those to be expected if the cathode acts toward the positive ions simply as a collecting electrode.

[10] Mackeown, Phys. Rev. **34**, 611 (1929).

[11] Langmuir, G. E. Rev. **26**, 735 (1923).

ON THE THEORY OF THE MERCURY ARC

By Karl T. Compton
Massachusetts Institute of Technology
(Received March 19, 1931)

Abstract

The theory of *heat balance at the cathode* is extended (1) by the introduction of the accommodation coefficient of neutralized ions, (2) by evaluation of all processes which absorb the energy gained by electrons in the cathode fall space, and (3) by correction of a previous assumption that fields sufficient to extract electrons will affect the heat of neutralization of postive ions at the surface. Test of the two resulting equations by existing experimental data shows that *Langmuir's theory* of extraction of electrons by the field at a Hg arc cathode is consistent with the cathode heat equations, but cannot be uniquely proved by them on account of uncertainty in two factors whose order of magnitude only is known: the fraction F of energy brought to the cathode by unelectrified carriers, $1.0>F>0.5$; the fraction $1/(1+\delta)$ of positive ions formed near the cathode which go to it, $1>\delta>0$.

From the net rate of evaporation an equation is obtained between vapor pressure and temperature at the cathode which, when combined with the vapor pressure-temperature equation of Hg, gives uniquely the *temperature of the cathode spot* and the *vapor pressure* outside it, provided the fraction f of total current carried by electrons is known. It is shown that the temperature of the cathode spot does not exceed 200°C, and that *the thickness of the cathode fall space is less than the electron mean free path.*

It is shown that *ionization* just beyond the cathode fall space must be of the *cumulative, multiple stage type.* From this it is shown that the fraction f must exceed 0.67 (if $\delta=0$) or 0.80 (if $\delta=1$), since these minimum values depend on 100 per cent efficiency of two stage ionization.

Mechanical pressure against the cathode by the arc is explained by the fact that the accommodation coefficient a is less than 1.0. If this accommodation coefficient of Hg ions at a liquid Hg surface should be independently measured, it would give an independent method of estimating the important fraction f.

The paper points out the causes of present limitations in our knowledge of conditions at the arc cathode and also the manner in which, and the extent to which, these limitations may be removed.

Introduction

THE early theory of Stark[1] that the current at mercury arc cathodes is of thermionic origin has been pretty thoroughly disproved by the fact that the evaporation of mercury is far too slow to justify an assumption of temperatures requisite for thermionic emission. Similarly a theory of Slepian[2] that the current at the cathode is carried by positive ions created by thermal ionization of the vapor just outside the cathode fails to suggest any physical mechanism for the input of energy into this assumed high temperature region. The theory at present in vogue is that of Langmuir,[3] who postulates "field currents" caused by the strong field which is concentrated at the

[1] Stark, Ann. d. Physik **12**, 692 (1903).
[2] Slepian, Phys. Rev. **27**, 407 (1926).
[3] Langmuir, Science **58**, 290 (1923); G. E. Rev. **26**, 735 (1923).

cathode by the processes described by Poisson's equation, and whose minimum value was calculated in the preceding paper to be at least 7.6 $(10)^4$ volts $\cdot$ cm^{-1}.

A difficulty in any theory depending primarily on electron emission from the cathode has been found in attempting to calculate from the heat balance at the cathode the fraction of the current carried by electrons, since such attempts have led consistently to values of this fraction which are too small to reconcile with the necessary amount of ionization, in view of the small cathode drop. For example, substituting direct experimental values of observable quantities in the heat balance equation has led to the conclusion that about 50 per cent of the current at the cathode is carried by electrons. Certain reasonable modifications have raised this to about 70 percent. By straining every possible factor, this proportion has been raised to about 87 percent. These values are all too small to reconcile with the fact that the cathode drop is only about 10 volts (see the preceding paper by Lamar and Compton); for 50 percent current carried by electrons would require 100 percent efficiency of ionization by them in order to obtain an equal number of positive ions to carry the remaining half of the current at the cathode. Even 87 percent would require at least 12 percent efficiency of ionization, which is still far in excess of any observed efficiencies of ionization by impact of electrons whose energy is near the minimum ionizing energy 10.4 volts.

The present paper presents some new considerations of heat balance which make it compatible with Langmuir's theory, and at the same time lead to a much more definite picture of the physical conditions in the mercury arc than has previously been possible.

It may be remarked, in passing, that the entire problem of the mercury arc is concentrated at the cathode, since the work of Langmuir and Mott-Smith,[4] Tonks and Langmuir,[5] Eckart and Compton,[6] and Killian[7] have essentially explained all other regions of a low pressure arc.

Heat Balance at Cathode

The two earliest attempts to use heat balance to investigate cathode conditions were quite unsatisfactory, the one[8] because of faulty reasoning and the other[9] because of lack of essential experimental data. Later refinements[10] have been made both in the theory and the experiments. It will be seen in the following paragraphs, however, that there are so many factors which have not previously been considered that no validity attaches to any of the conclusions thus far drawn from arguments based on heat balance.

[4] Langmuir and Mott-Smith, G. E. Rev. **27,** 449, 538, 616, 762, 810 (1924).
[5] Tonks and Langmuir, Phys. Rev. **34,** 876 (1929).
[6] Eckart and Compton, Phys. Rev. **24,** 97 (1924).
[7] Killian, Phys. Rev. **35,** 1238 (1930).
[8] Güntherschulze, Zeits. f. Physik **11,** 74 (1922).
[9] Compton, Phys. Rev. **21,** 266 (1923).
[10] Güntherschulze, Zeits. f. Physik **31,** 509 (1925); Seeliger, Phys. Zeits. **27,** 22 (1927); Elektrotech. Zeits. **49,** 853 (1927); Compton and Van Voorhis, Proc. Nat. Acad. Sci. **13,** 336 (1927); Issendorff, Phys. Zeits. **29,** 857 (1928).

We shall express the condition of thermal equilibrium by setting the total net rate of generation of heat at the cathode equal to zero, expressing each contributing item of heating or cooling in terms of watts per ampere of current. We shall let f equal the fraction of current carried at the cathode by electrons, and $(1-f)$ the fraction carried by positive ions. The processes involved in the heat balance are schematically indicated in Fig. 1 and will be discussed briefly in order.

(1) *Heating by impacting positive ions.* These ions acquire energy V_c in falling through the cathode potential drop V_c. Since the thickness of the fall space is certainly less than $1.76\ (10)^{-4}$ cm and since, as we shall see below, the ionic mean free path is considerably greater than this, we are justified in neglecting collisions of ions with vapor molecules while passing through this

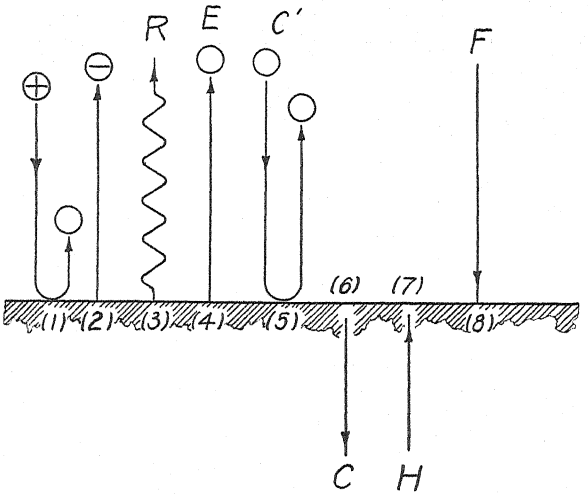

Fig. 1.

fall space. Thus the entire energy V_c is available for delivery to the cathode. To this should be added the average initial kinetic energy of the ions just before they enter the fall space. Tonks and Langmuir[4] have shown that this is negligibly small.

It is not obvious, however, that all this kinetic energy is delivered to the cathode. Let a be the fraction of it which is thus delivered, while $(1-a)$ is the average fraction which is retained by the neutralized ion after impact. This quantity a is the "accommodation coefficient" which is well known in phenomena involving the impact of gas molecules against a surface of different temperature[11] and whose existence in cases of ionic impact has been demonstrated by Van Voorhis and Compton.[12]

[11] Knudsen, Ann. d. Physik **34**, 593 (1911); **46**, 641 (1915); Langmuir, J. Am. Chem. Soc. **37**, 425 (1915); Compton and Langmuir, Rev. Mod. Phys. **2**, 184 (1930).

[12] Van Voorhis and Compton, Phys. Rev. **35**, 1438 (1930); detailed paper in preparation for physical Review.

Finally, there is the "heat of neutralization" of the positive ion, denoted by ϕ_+, whose value has been shown by an argument involving a simple cycle[13] to be $\phi_+ = V_i - \phi_- + (L)$, where V_i is the ionizing potential of the gas molecule, ϕ_- is the electron work function of the cathode surface, and L is the heat of condensation of the neutral molecule on the cathode surface. L should be used if the ion is actually condensed on the surface, but should otherwise be omitted. In our present problem L is completely taken care of in process (4) (Fig. 1).

In case the field appreciably reduces the work function (as in Langmuir's theory it reduces it to zero) it has previously been assumed that the reduced value should be used in this equation, i.e., that if the field changes the cooling effect of electron emission it will also affect the heating effect of positive ion neutralization. This is, however, not the case, as is easily shown by the following argument.

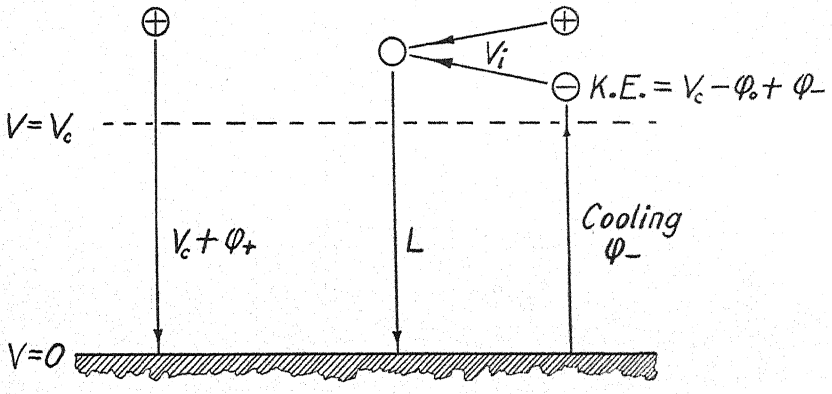

Fig. 2.

A positive ion, starting outside the cathode fall space and moving to the cathode delivers energy $V_c + \phi_+$, as indicated to the left in Fig. 2. An equivalent process is shown to the right. An electron escapes from the metal, cooling it by the amount ϕ_-. By the time it has passed through the fall space its kinetic energy is $V_c - \phi_0 + \phi_-$, where ϕ_- is the "effective" work function while ϕ_0 is the normal work function in the absence of an accelerating field. This is obvious since $(\phi_0 - \phi_-)$ is that part of the work done against the surface forces of the metal which is done by the applied field and ϕ_- is that part done at the expense of initial kinetic energy of the electron. If emission is purely thermionic, then $\phi_- = \phi_0$, whereas if emission is purely autoelectronic (as in Langmuir's theory) then $\phi_- = 0$.

Now if this electron combines with a positive ion, there is liberated additional energy V_i, and there is a further liberation of amount L when the neutralized particle condenses on the metal.

[13] Compton, Phys. Rev. **21**, 281 (1923); Schottky and Issendorff, Zeits. f. Physik **26**, 85 (1924).

Equating the net liberation of energy in the two equivalent processes gives $V_c+\phi_+=V_i+V_c-\phi_0+\phi_--\phi_-+L$, whence

$$\phi_+ = V_i - \phi_0 + L.$$

Thus the heating effect by positive ions is unaffected by the field, even though the cooling effect by escaping electrons is diminished. Physically this is easily explicable, since the cooling effect is due to the fact that only those electrons escape which, while inside the metal, possess greatest kinetic energy, a situation which has no counterpart in the process of neutralizing a positive ion.

In this equation $\phi_+=V_i-\phi_0+(L)$, it is implicitly assumed that all the energy developed by the process is retained in the cathode, which would not be the case, for example, if a fraction $(1-r)$ of it were radiated away in the process of neutralization. Compton and Van Voorhis therefore suggested[14] the modification $\phi_+=rV_i-\phi_0+(L)$, and announced experimental results indicating that $r\sim 0.5$. They later found,[12] however, that these results were due to the then unsuspected existence of an accommodation coefficient, so that there is no actual experimental measurement of r. From the fact, however, that direct measurement of the radiation from the cathode spot (process (3) Fig. 1) shows this to be almost negligible, it is evident that r is practically unity. Whatever error may be introduced in taking $r=1$ will be exactly corrected by introduction of the experimental value of heat loss by radiation in process (3).

Combining all these considerations, we have for process (1)

$$H(1) = (1-f)(aV_c + V_i - \phi_0)$$

(2) *Cooling by electron emission.* This process of cooling is too well known to require comment, since it is well known that the electron work function ϕ_- is a latent heat of evaporation. Expressing it as a negative heating process, we have

$$H(2) = -f\phi_-$$

(3) *Cooling by radiation* is expressed directly, in terms of the observed radiated energy per ampere·sec., by $H(3)=-R$.

(4) *Cooling by evaporation* of the material of the cathode is similarly expressed by $H(4)=-E$, in which E is the product of the mass of material evaporated per ampere·sec multiplied by its latent heat of evaporation.

(5) *Cooling by gas conduction and convection* is $H(5)=-C'$.

(6) *Cooling by conduction through the cathode* is $H(6)=-C$.

(7) *Heating by an external agency*, if any, is represented by $H(7)=H$.

(8) *Heating by energy derived by electrons in the cathode fall space and indirectly returned to the cathode* can be calculated as follows. The work done on an escaping electron is V_c. If part of this work is done in pulling the electrons out of the metal (as in Langmuir's theory), this part may be expressed by

[14] Compton and Van Voorhis, Proc. Nat. Acad. Sci. **13**, 336 (1927).

$(\phi_0-\phi_-)$, where ϕ_0 is the ordinary electron work function for negligibly small accelerating fields, and ϕ_- is the actual or "effective" work function. Thus the energy with which each electron is projected out of the cathode fall space is $V_c-\phi_0+\phi_-$.

Of the total energy $f(V_c-\phi_0+\phi_-)$ thus fed into the vapor, $(1-f)V_i$ must be used to produce the $(1-f)$ positive ions which return to the cathode. We shall see below that altogether $(1+\delta)$ times this number of ions must be formed, where $0<\delta<1$, since some of the ions are formed beyond the region of potential maximum and drift toward the anode, ultimately recombining. δ is the ratio of the number of ions thus going toward the anode to the number going toward the cathode. Thus we have $(1+\delta)(1-f)V_i$ energy used in producing positive ions.

Furthermore the probe electrode measurements prove that the electrons in the negative glow near the cathode possess a considerable mean kinetic energy $\bar{V}_-$. Thus the energy fed into the vapor by electrons from the cathode, which is not expended in producing ions or retained by the electrons, is $f(V_c-\phi_0+\phi_-)-(1+\delta)(1-f)V_i-\bar{V}_-$, where the factor f does not multiply $\bar{V}_-$ since we know that in the negative glow the fraction of current carried by electrons is unity within a fraction of a percent.

Let F represent that fraction of the energy, acquired by *unelectrified* carriers from the electrons which have moved through the fall space, which returns to the cathode (as by radiation, metastable and excited atoms, high temperature neutral atoms). We have already allowed in process (1) for the energy which is brought back by positive ions, and of course none is brought back by electrons. This remaining source of heating of the cathode is therefore given by

$$H(8) = F[f(V_c - \phi_0 + \phi_-) - (1 + \delta)(1 - f)V_i - \bar{V}_-].$$

Equilibrium. Equating to zero the sum of all these eight contributions to the heating, and solving for f, we obtain

$$f = \frac{aV_c + V_i - \phi_0 - (R + E + C + C' - H) - F[(1 + \delta)V_i + \bar{V}_-]}{aV_c + V_i - \phi_0 + \phi_- - F[V_c - \phi_0 + \phi_- + (1 + \delta)V_i]} \quad (1)$$

Supplementary relation. The above expression for $H(8)$ gives us another clue to the value of f. The expression in brackets is the amount of the energy with which the electrons are shot into the vapor which is not retained by them or used in ionization. It must of necessity be greater than zero, since we know that a considerable portion of such energy is used, for example, in producing metastable or other excited atoms. In fact, we shall later discuss reasons for believing that the ionization is principally of the two stage or cumulative type. Thus from $f(V_c-\phi_0+\phi_-)>(1+\delta)(1-f)V_i+\bar{V}_-$, we find

$$f > \frac{(1 + \delta)V_i + \bar{V}_-}{V_c - \phi_0 + \phi_{..} + (1 + \delta)V_i}. \quad (2)$$

Values of the terms are given in Table I.

TABLE I.

Quantity	Value	Reference
V_c	10 volts	Lamar and Compton[15]
V_i	10.4	Well known
ϕ_0	4.5	Kazda[16]
R	0.04	Güntherschulze[10]
E	2.21–0	" (see below)
C	2.68	"
C'	0.0	"
H	0.0	No external heating
V_-	1.5	Lamar and Compton[15]
ϕ_-	0–4.5	(see below)
F	0.5–1.0	" "
a	1–?	" "

$E=2.21$ is based on measurements by Güntherschulze of the rate of loss of mass of the cathode, together with the latent heat of evaporation of mercury at 123°C. However, Compton and Van Voorhis suggested[14] that some of the mercury may be lost as a spray thrown out mechanically by the agitation of the surface. Such loss would not involve cooling. Issendorff[17] has verified this experimentally and has shown that the actual amount of true evaporation from the cathode spot is practically negligible as a cooling process. (Much of the spray is subsequently volatilized in the arc stream by heat developed by recombination of electrons and ions on the surfaces of the droplets, but this is not a process which cools the cathode.) It appears from this that the true value of E lies much closer to 0 than to 2.21. As to the assumed temperature of 123°C, see discussion later in the paper.

$\phi_-=0$ to 4.5, depending on the extent to which the emission is due to the field, being 0 if due entirely to the field. Perhaps a rough approximation to the right value is given by finding the effective work function which would give thermionic emission of 4000 amp·cm^{-2} at 123°C, which is $\phi_-=0.31$ volt.

F has a more restricted significance than in previous discussions owing to the more complete character of the present analysis. If the energy carried back to the cathode by unelectrified carriers is in the form of unabsorbable radiation, we should expect $F=0.5$, since the cathode subtends half the solid angle about the origin of radiation, or less than 0.5 if there is reflection at the cathode surface. Actually, however, we know such radiation to be small (see Table I). If the energy gets back by any diffusion process, as by metastable atoms or by resonance radiation, then much more than half the energy will return to the cathode since the mean free path of the diffusing particles is considerably less than the distance from the cathode to other boundaries of the vapor. Since this condition is amply fulfilled in the mercury arc, we have $1.0>F>0.5$, and it is extremely probable that F is very nearly equal to 1.0.

a has not been measured for mercury, but we should expect it to be $1.0>a>0.9$, since in other gases a approaches unity with increasing atomic weight.

[15] Lamar and Compton (preceding paper in Phys. Rev.).
[16] Kazda, Phys. Rev. **26**, 643 (1925).
[17] Issendorff, Phys. Zeits. **29**, 857 (1928).

Results for the various assumptions are given in Table II. Note first that f_2 involves the uncertain factors δ and ϕ_- and depends only on the direct application of the Energy Principle. Note also that the known fact that impact ionization processes are never very close to 100 percent efficient shows that the true value of f must be *considerably* larger than the lower limit set by f_2. The values in parentheses are impossible values either because $f_1 < f_2$, or because f_1 is negative or greater than unity.

TABLE II. $f_1 = f$ by *Eq.* (ϕ); $f_2 = f$ by Eq. (2).

			$\phi_-=0.0$			$\phi_-=0.31$			$\phi=4.5$		
		δ	1.0	0.5	0.0	1.0	0.5	0.0	1.0	0.5	0.0
		f_2	0.85	0.81	0.75	0.84	0.80	0.73	0.73	0.67	0.58
E	a	F	f_1	f_1	f_1	f_1	f_1	f_1	f_1	f_1	f_1
0.0	1.0	0.0	(0.83)	0.82	0.82	(0.81)	0.81	0.81	(0.64)	(0.64)	0.64
		0.1	(0.82)	0.82	0.83	(0.81)	0.81	0.82	(0.63)	(0.64)	0.65
		0.2	(0.82)	0.83	0.85	(0.80)	0.82	0.84	(0.61)	(0.64)	0.67
		0.5	(0.74)	0.86	0.91	(0.70)	0.84	0.89	(0.41)	(0.61)	0.71
		0.6	(−17.0)	0.90	0.95	(−0.71)	0.87	0.93	(−11.5)	(0.51)	0.74
		0.7	0.96	(1.08)	(1.02)	0.99	0.98	1.00	(4.00)	(0.49)	0.79
		0.8	0.91	(0.51)	( )	0.92	(0.55)	( )	(1.10)	(6.25)	0.90
		0.9	0.89	(0.70)	( )	0.89	(0.72)	( )	0.94	0.83	(1.21)
		1.0	0.89	(0.75)	( )	0.89	(0.75)	( )	0.89	0.75	( )
0.0	0.9	0.0	(0.82)			(0.80)			(0.63)		
		0.1	(0.81)			(0.79)			(0.61)		
		0.2	(0.80)			(0.78)			(0.58)		
		0.5	(0.59)			(0.54)			(0.26)		
		0.8	0.93			0.93			(1.08)		
		0.9	0.90			0.90			0.95		
		1.0	0.89			0.89			0.89		
2.21	1.0	0.0	(0.69)	(0.69)	(0.69)	(0.68)			(0.54)	(0.54)	(0.54)
		0.1	(0.66)	(0.67)	(0.68)	(0.64)			(0.50)	(0.52)	(0.53)
		0.2	(0.61)	(0.65)	(0.68)	(0.60)			(0.46)	(0.49)	(0.53)
		0.5	(−0.07)	(0.50)	(0.63)	(−0.06)			(−0.04)	(0.33)	(0.50)
		0.8	(1.34)	(2.70)	(0.47)	(1.35)			(1.62)	(23.0)	(0.36)
		0.9	(1.17)	(1.42)	(0.02)	(1.18)			(1.25)	(1.70)	(0.15)
		1.0	(1.09)	(1.09)	(—)	(1.09)			(1.09)	(1.09)	(−)
0.44	1.0	0.0	(0.80)			(0.79)	(0.79)	0.79	(0.62)		
		0.1	(0.79)			(0.78)	(0.79)	0.79	(0.61)		
		0.2	(0.78)			(0.76)	(0.79)	0.80	(0.58)		
		0.5	(0.58)			(0.55)	0.86	0.84	(0.32)		
		0.8	0.99			(1.01)	0.99	1.00	(1.21)		
		0.9	0.94			0.95	0.85	(1.33)	1.00		
		1.0	0.92			0.92	0.83	( )	0.92		

Conclusions. A survey of Table II shows, first of all, the futility of attempting to determine the fraction f by heat balance methods, since the unknown parameters E, a, F, leave a great range of possibilities. Nevertheless some interesting information can be obtained.

Obviously no adjustment of ϕ_-, a, F, δ will give possible results if E is as large as Güntherschulze's value 2.21, which checks the later estimates described above, which make $E << 2.21$.

It is probably hopeless to try to measure F and δ. Physical considerations, mentioned above, however, place $1.0 > F > 0.5$ (with F probably nearer 1.0 than 0.5. Similarly we shall see that $1.0 > \delta > 0$.

With these possibilities in mind, we see from Table II that the most probable values of f arise from cases where *both the numerator and denominator of Eq.* (1) *are negative,*—which means that a very appreciable role is played by the heating effect of energy which reaches the cathode by unelectrified carriers, an observation which is suggestive of a considerable concentration of

metastable atoms and of cumulative ionization. More direct evidence of this appears later in the paper.

In the light of this study it seems hopeless to prove or disprove the Langmuir theory by heat balance arguments. *This analysis shows for the first time, however, that the heat balance may be made consistent with Langmuir's theory and with the known facts of ionization* by making the most reasonable assumptions regarding the unknown factors F and δ. In order to make the considerations still more precise, it is important to measure the accommodation coefficient a for Hg ions at a Hg surface and to obtain a more reliable estimate of evaporation E under conditions in which the other thermal quantities are also measured. Thus we may assume Langmuir's theory, with its very small value of ϕ_-, on the basis of its reasonable character and the absence of evidence for any other adequate mechanism.

Temperature and Vapor Pressure at Cathode

The temperature and vapor pressure at the cathode can be calculated if the rate of evaporation from the cathode is known. Early attempts to measure this led to erratic and large values. Schaefer[18] found 36.7 $(10)^{-3}$g·amp. sec^{-1}, and Güntherschulze[10] 7.2 $(10)^{-3}$g·amp.$^{-1}$ sec^{-1}. Compton and Van Voorhis' suggestion[14] that these large values arise from mechanical spray was verified by Issendorff,[17] who found <1.3 $(10)^{-3}$ g·amp.$^{-1}$ sec^{-1}. Recently Kobel[19] devised a means for holding the cathode spot quiescent and found the rate of evaporation to be 0.017 $(10)^{-3}$ amp.$^{-1}$ sec^{-1}. Since this lies within Issendorff's limits, and since a quiescent spot would be expected not to eject spray, we shall take this as the best value at present available. (The device for holding the spot quiet may have made this value too small, but several considerations indicate that such an error is small, if present.) Kobel's average current density was 1912 amp·cm^{-2}, hence the rate of evaporation was 0.0325 gm·cm^{-2}.

It must be observed, however, that these values refer only to the *net* rate of escape of Hg atoms. The true rate of evaporation is larger than this, but a certain portion of the evaporated atoms return to the cathode as ions. The true rate of evaporation M can be equated to the observed rate M_0 plus the rate of return of ions to the cathode, which is 0.00209 $(1-f)$ g·amp.$^{-1}$ sec^{-1}. (0.00209 is the electrochemical equivalent of Hg). If we express this in terms of evaporation per cm^2, we have

$$M = M_0 + 0.00209(1 - f)j, \tag{3}$$

where j = current density. From the familiar kinetic theory relations

$$n = \tfrac{1}{4}N\bar{v}, \quad p = \tfrac{1}{3}Nm\bar{v}^2 = NkT, \quad M = nm$$

we find

$$p^2 = \frac{16}{3}\frac{M^2kT}{m} \text{ dynes} \cdot \text{cm}^{-2}, \tag{4}$$

where m is the mass of an atom in grams.

[18] Schaefer, Diss. Darmstadt (1910).
[19] Kobel, Phys. Rev. **36**, 1636 (1930).

If the experimental values of M from Eq. (3) are substituted into Eq. (4), an infinite number of pairs of possible values of pressure p and temperature T is found. Only one of these pairs of values, however, satisfies the vapor pressure relation between p and T. Thus Eq. (4) together with the vapor pressure equation, serve simultaneously to fix unique values of T and p. This value of T is the temperature of the cathode spot and from p and T we can find the value of atomic and electronic mean free paths just outside the cathode.

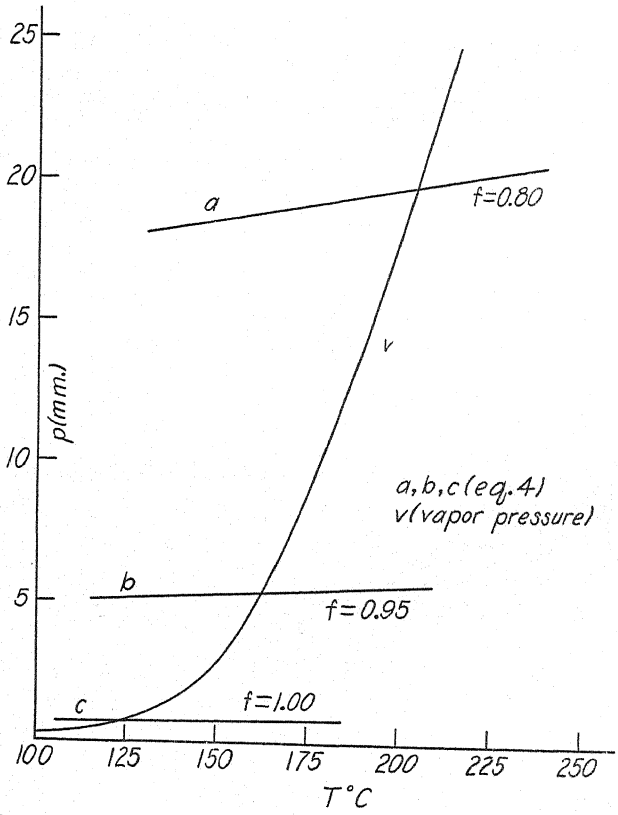

Fig. 3.

Here, as before, uncertainty in f prevents us from drawing definite conclusions, but here again we can set certain limits with considerable assurance. If ionization is cumulative in two stages, not more than one ion can be formed

TABLE III.

f	p	T	λ(electron)[20]	d_c
1.00	0.75 mm	123°C	0.0026 cm	(0.000176) cm
0.95	5.4	167	0.00033	0.000039
0.80	19.6	202	0.000084	0.000019

[20] Constants from Compton and Langmuir, Rev. Mod. Phys. **2**, 208 (1930).

for every two electrons, and if half the ions move toward the anode, recombining ($\delta = 1$), we must have $f > 0.8$. Table III shows the results of three assumptions, the values being taken from Fig. 3. For comparison there are shown also the corresponding values of thickness of cathode fall space, calculated as in the preceding paper.

Three important facts are derived from this consideration of rate of evaporation: (1) the surface temperature of the cathode spot cannot exceed about 200°C; (2) the vapor pressure there is considerably less than the value of about one atmosphere recently assumed;[21] (3) the electron mean free path is, in any case, considerably longer than the thickness of the cathode fall space, a fact which justifies several simplifying assumptions such as the applicability of the simple space-charge equation in the fall space.

Question of high-speed ejection of vapor. Tangberg[22] for a copper arc and Kobel[19] for a mercury arc have called attention to the relatively large pressure on the cathode spot and have interpreted it as indicating very high speeds of evaporating atoms, speeds characteristic of temperatures of the order of 500,000°K! Among the physical difficulties of this interpretation may be mentioned the inconsistency between such a temperature and the observed rate of evaporation which, as we have seen, indicates a surface temperature of not more than 200°C. Compton[23] suggested that a more reasonable interpretation of this pressure is to be found in the existence of an "accommodation coefficient" for ions which strike and are neutralized at the surface—this accommodation coefficient having been inferred for He, Ne and A ions from thermal measurements at cathodes by Van Voorhis and Compton[12] and later measured directly for He ions by Lamar.[24]

For the mercury arc, the pressure resulting from an accommodation coefficient $a < 1.0$ may be calculated thus, per cm²:

Positive ion current at cathode	$j(1-f)$ amp.
Mass of positive ions striking cathode per sec	$0.00209\, j(1-f)$ g
Number of positive ions striking per sec	$0.63(10)^{19}\, j(1-f)$
Kinetic energy of incident ion	$1.59(10)^{-11}$ erg
Total kinetic energy of ions striking per sec	$1.00(10)^{8}\, j(1-f)$ erg
Total kinetic energy of neutralized ions leaving cathode per sec	$1.00(10)^{8}\, j(1-f)\,(1-a)$ erg
Total momentum of neutralized ions leaving cathode per sec	$647\, j(1-f)\,(1-a)^{1/2}$ dyne.

This last quantity is the pressure, provided the neutralized ions leave normally to the surface. We should rather expect the escaping neutralized ions to be scattered in all directions, and in fact Lamar's results indicate this

[21] Güntherschulze, Zeits. f. Physik **11**, 74 (1922); Langmuir, Science **58**, 290 (1923); Compton, Summer Convention A.I.E.E. (1927).

[22] Tanberg, Phys. Rev. **35**, 1080 (1930).

[23] Compton, Phys. Rev. **36**, 706 (1930). (In this paper there is a numerical error which arose through taking an incorrect value for the electrochemical equivalent of Hg, but which, qualitatively, does not vitiate the argument).

[24] Lamar (to be reported at Washington Meeting of the Amer. Phys. Soc.) and published in the Physical Review.

in the case for He ions. In this case we must use the mean normal component of momentum, which gives just half the above values. We thus have

$$p = 0.66j(1 - f)(1 - a_n)^{1/2}\text{g}\cdot\text{cm}^{-2}$$
$$p = 0.33j(1 - f)(1 - a_r)^{1/2} \qquad (5)$$

depending on whether we assume a_n (normal escape) or a_r (random escape).

Kobel's results gave an average pressure of 5.75 cm Hg (78.2 $\text{g}\cdot\text{cm}^{-2}$) on the cathode spot whose average current density was 1912 $\text{amp}\cdot\text{cm}^{-2}$. Substituting these values in Eq. (5) we obtain the relations shown in Table IV.

TABLE IV.

f	0.50	0.60	0.70	0.80	0.90
a_n	0.985	0.98	0.96	0.90	0.62
a_r	0.95	0.92	0.84	0.60	(—)

Since, as we have seen, experimental evidence points to a_r rather than a_n, we see that this analysis suggests that the accommodation coefficient a for Hg ions is less than the value, nearly unity, suggested by its high atomic weight, taken in conjunction with the known values of a for He, Ne and A. This again emphasizes the desirability of making a direct measurement of a for Hg ions.

MECHANISM OF IONIZATION

The fact that the cathode drop is so constantly close to 10 volts, independently of current, vapor pressure, etc., over the entire range in which a Hg arc can be struck from a liquid Hg cathode, suggests that this value is fixed by some characteristic process in the arc mechanism. It has been quite generally assumed that this process is the ionization of the Hg atoms by electron impact, and that the significance of 10 volts is, roughly, the ionization potential 10.4 volts. There are, however, three serious and probably insuperable difficulties besetting such an interpretation, as follows.

(1) The probability of ionization by an electron of 10.4 volts energy, or even a few volts more, is so small that it is difficult thus to account for the production of the requisite number of positive ions. (2) The present more refined measurements of cathode drop point to a value *less*, rather than exceeding, 10 volts, the best estimate being 9.9 volts, which makes the assumption of direct impact ionization still more unsatisfactory. (3) *If the electrons are pulled out of the cathode by the field*, the field thus does work $\phi_0 = 4.5$ volts in pulling them out, so that *the kinetic energy gained by the escaping electron is only* $9.9 - 4.5 = 5.4$ *volts, which is far insufficient to permit ionization by single impact.*

The obvious escape from these difficulties is to adopt the theory that *ionization is caused in two stages*, which is at once seen to be in excellent accord with various related facts. The electron energy is very close to the value necessary to produce excited or metastable atoms, and to ionize them when formed. We know that, unlike ionization by single impact, these processes have a high probability when the energy of the impacting electron is only

slightly in excess of the minimum energy required for the process. Furthermore, experiments with low voltage arcs have proved that the favorable conditions for arcs to operate by such cumulative ionization are large current density and vapor pressure of at least the order of 1 mm, both of which conditions are amply fulfilled in the mercury arc. *Thus it would be very surprising if the ionization were not of the cumulative type.* The reason for not having adopted this interpretation sooner was principally the difficulty, in preceding analyses of the situation, of justifiying a value of f large enough to be consistent with it, and secondarily the erroneous apparent significance of a cathode drop so nearly equal to the ionizing potential.

Electrical Conditions Near Cathode

In Fig. 4, let the ordinates of curve N represent the relative numbers of electrons, projected out from the cathode, whose free paths terminate by

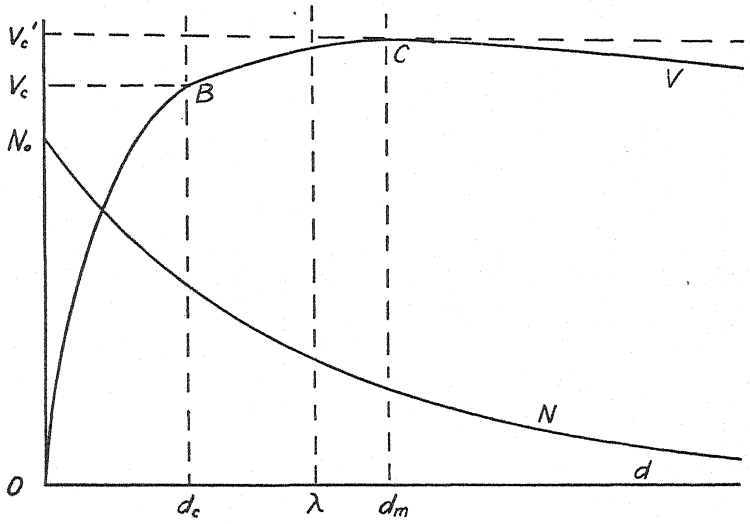

Fig. 4.

collisions at distances d. Since, as we have seen, the thickness of the fall space d_c is less than the mean free path λ, we may consider these as projected out with uniform velocities corresponding to the kinetic energy $V_c - \phi_0$. The rate of production of ions or excited atoms will therefore also be proportional to the ordinate of curve N at each distance from the cathode.

Every region of intense ionization tends to be a region of potential maximum, owing to the fact that electrons diffuse away from it more rapidly than do positive ions. There is therefore, a little way in front of the cathode, a region of potential maximum C. As a first approximation, this may be taken as being at the distance of one mean free path from the cathode, since this is the mean position at which ionization occurs.

From this region of potential maximum C, positive ions are forced by the field *in both directions*, half moving in to the cathode and half moving out

toward the anode and eventually combining with electrons. Since the cathode is so much nearer than the anode to this region of potential maximum, the concentration gradient on the cathode side must be greater than that of the anode side, which would tend to displace the region of potential maximum away from the cathode. On the other hand, the fact that ionization occurs at a more rapid rate nearer the cathode, as shown by curve N, tends partially to offset this displacement. The extent of this displacement determines the amount by which δ in Eqs. (1, 2) differs from 1.0.

The net result of these actions, including the action of space charge within the space-charge sheath (cathode fall space) is shown diagrammatically by curve V. The space charge equation applies within the distance d_c, to the point B. Between B and the potential maximum, the plasma considerations developed by Tonks and Langmuir[25] apply. Beyond C there is ambipolar diffusion toward the anode by both electrons and ions.

There is obviously a small uncertainty in the meaning of "cathode drop". The drop across the space-charge sheath to the point B is the quantity which is significant in estimating the field at the cathode. The drop to the point C is the maximum potential drop available to produce ionization. The drop to some point beyond C—i.e., to the point of nearest approach of an exploring electrode, is the nearest point to which the drop can be measured experimentally, as in the preceding paper.

In conclusion, it may be noted that this analysis indicates that the limits of uncertainty in the values of f, d_c and field at cathode may be reduced by more careful measurements of thermal relationships and of accommodation coefficient, but that the accuracy of an absolute evaluation of these quantities is limited principally by our inability accurately to measure or estimate two factors: the fraction F of the energy, imparted by electrons to unelectrified carriers, which goes to the cathode; and the fraction $1/(1+\delta)$ of the positive ions formed near the cathode which go to the cathode.

[25] Tonks and Langmuir, Phys. Rev. **34**, 876 (1929).

THE ELECTRODELESS DISCHARGE IN MERCURY VAPOR

By Herschel Smith, William A. Lynch and Norman Hilberry
Department of Physics, New York University

(Received March 16, 1931)

Abstract

A method is described for studying the characteristics of the components of the electrodeless discharge in mercury vapor. A Hartley oscillator is used to excite the discharge, oscillating currents up to 45 amps. being obtained at frequencies from 5×10^6 to 12×10^6 oscillations per second. Shield experiments have been performed which clearly show the distinction between the dull glow discharge which is considered electric in its origin and the bright glow discharge which is shown to be electromagnetic in its origin; the dependence of the bright glow on the dull glow or on the effect of some ionizing agent is proved. The variation of the current necessary to start the discharge with the pressure of the mercury vapor has been investigated fully over the pressure range 0.002 to 0.2 mm of mercury. Curves are drawn and analyzed in terms of J. J. Thomson's electromagnetic theory of the discharge and Brasefield's electric theory. It is shown that neither theory is sufficient to explain the experimental facts; the predictions seem to hold for the bright glow with fair agreement but fail markedly with the dull glow.

Introduction

TWO opposing theories have been advanced in recent years to explain the nature of the "electrodeless" discharge which occurs under proper excitation in a gas or vapor at low pressure. The usual arrangement is to insert the bulb containing the gas in a coil in which high frequency currents are flowing.

J. J. Thomson[1] has contended that the discharge is due to the alternating e.m.f. induced around the inside periphery of the discharge tube by the varying magnetic field of the coil. Townsend and Donaldson[2] however have strongly supported the view that the discharge is caused by the "electric forces"[3] between the ends of the coil. This second view is also held by those who have worked with external electrodes, for example Brasefield.[4]

In an attempt to reconcile the two explanations MacKinnon[5] constructed an exciting circuit which could be energized by either damped or undamped oscillations, for the reason that Thomson had used only damped oscillations while Townsend and Donaldson had used only undamped oscillations. From his experiments, MacKinnon concluded that the discharge was of "electromagnetic" origin when excited by the damped oscillations of Thomson and

[1] J. J. Thomson, Phil. Mag. **32**, 321, 450 (1891); **44**, 293 (1897); **4**, 1128 (1927).

[2] Townsend and Donaldson, Phil. Mag. **5**, 178 (1928).

[3] The term "electric forces" is used here to represent those forces due to the fact that two parts of the coil are at different potentials. For such a force the usual term "electrostatic" is here obviously a misnomer.

[4] Brasefield, Phys. Rev. **35**, 1073 (1930); **37**, 82 (1931).

[5] K. A. MacKinnon, Phil. Mag. **8**, 605 (1929).

"electric" when excited by the undamped oscillations of Townsend and Donaldson. With large currents in the undamped oscillator coil he was able to obtain a very bright glow, not reported by Townsend and Donaldson, which he thought was related to the "ring" discharge of Thomson. This led him to believe that the electromagnetic type of discharge occurred with the damped oscillations because the instantaneous coil currents were very large, and that the undamped oscillations would also cause the characteristic "ring" discharge of the damped case if the gas used had a sufficiently low ionizing potential. The results of the present work support MacKinnon's view in many details.

An ordinary Hartley circuit was used as a generator of the high frequency oscillations employed in the experiments to be described. The resistance of the circuit was kept low by the use of copper tubing for leads and inductance coils while the ratio of capacity to inductance was high; the result was the generation of large currents in the oscillator coil which also acted as the exciting coil for the discharge; thus currents of 45 amps. at frequencies from 5×10^6 to 12×10^6 cycles per second were easily obtained. These currents were measured by a Weston thermo-ammeter placed directly in the circuit between coil and condenser or by a current transformer and thermo-ammeter as described by Campbell and Dye.[6] All frequencies were measured by a General Radio precision wave-meter.

Over the whole pressure range studied (0.002 to 0.2 mm of mercury) the authors have observed both types of discharge described by MacKinnon; over parts of the range, however, special precautions were necessary to separate them. Mercury vapor was used in the bulb throughout the investigation except where indicated otherwise. The general procedure was as follows: The pressure in the bulb was held constant and the coil current gradually increased; at a critical value of the current a bluish white "dull glow" appeared inside the tube. When the current was increased to a second critical value, the discharge suddenly changed into an intense "bright glow"; at the same time, a large amount of power was drawn from the oscillator. At certain pressures this "bright glow" assumed the form of a ring around the inside periphery of the tube, in appearance very similar to the familiar "ring" discharge.

When no discharge was excited on inserting the tube in the coil, no change occurred in the oscillating circuit. When the dull glow was excited, no change occurred in the circuit nor was the discharge tube heated appreciably. But when the bright glow was strongly excited, the oscillating current decreased greatly, the plate current increased, the frequency remained the same and the bulb was heated appreciably.

Effect of a Shield

The "dull glow" has been excited readily either inside or outside the coil; in fact at certain pressures, it has appeared whenever the bulb was brought anywhere near the oscillator. This action in itself indicates the "electric"

[6] Campbell and Dye, Proc. Roy. Soc. **A90**, 621 (1914).

nature of this type of discharge. To investigate the case further a metallic shield was made by pasting narrow strips of tin-foil parallel to each other on a piece of paper and then connecting them together at one end by a transverse strip of foil. The paper was then rolled into a hollow cylinder with the axis parallel to the strips and the ends open. When this cylinder surrounded the bulb it caused very little electromagnetic loss due to eddy currents but served as an excellent shield against "electric forces." When the pressure and coil current were suitable for the excitation of the "dull glow," the presence of the shield always caused the glow to disappear whether the discharge tube was in the coil or outside. The glow never reappeared as long as the shield remained interposed between the tube and the coil, no matter how great the coil current was made (in our case up to 45 amps.).

If the "bright glow" had been existed strongly in the tube and the shield was inserted, the glow was apparently unaffected. If the bright glow was stopped however by a reduction of the current, it could not be made to reappear so long as the shield was in place even though the current reached the maximum of 45 amps. These experiments were repeated with a second cylindrical shield with closed ends; the results were the same.

When damped oscillations of approximately the same frequency as the undamped oscillations were used for excitation, the dull glow could be obtained only outside the coil; the shield affected it in exactly the same manner as before. The bright "ring" discharge which appeared inside the coil behaved toward the shield identically as did the bright glow of the undamped case.

When the conditions were right for maintaining the bright glow without a shield, it could be started and maintained inside the shield by exposing the tube momentarily to x-rays, or with a quartz discharge tube, to the radiation from a mercury arc in quartz. If a small ball of mercury was in the tube, the bright glow could be started similarly by simply twirling the tube and thus generating a faint glow of triboluminescence around the ball of mercury.

All of the above shield experiments have been repeated for air and carbon monoxide with similar results.

Variation of Starting Current with Pressure

The variation of the current necessary for starting the discharge in mercury vapor with changing pressure was very difficult to observe precisely. The external condition of the tube, slight impurities in the vapor and small amounts of liquid mercury all affected the starting current and the results at first were so erratic that it seemed as though no generalization could be made. Determination of the pressure was difficult as the measurement of the temperature of a furnace in which the bulb and coil were placed was not satisfactory because of the sudden rapid increase in temperature in the closed space when the oscillating current was turned on. A thermometer placed anywhere in the field of the coil proved unreliable.

Reproducible results were finally obtained with the following apparatus and procedure. The discharge tube is shown in Fig. 1; the bulb a was placed within the oscillator coil and both were enclosed in a transite box and heated

by a blast of hot air; this furnace could be adjusted to any desired temperature from 120°C to about 200°C and maintained constant within a few degrees. The well *b* was outside of the furnace in a constant temperature bath which could be varied from 0°C to 100°C; it contained liquid mercury. Thus the pressure of the mercury vapor in the bulb was determined by the temperature of the mercury in the well, as read on a thermometer placed in tube *c*. The pressure corresponding to a given temperature was taken from a curve plotted from the data given by Kaye and Laby.

At the start of a run, the furnace was first raised to a temperature of say 180°C and kept there for about half an hour with the bulb and coil in place and the mercury well at a low temperature; this action insured that all the liquid mercury was evaporated from the bulb itself. The temperature of the well was then raised by adjustment of the constant temperature bath to the

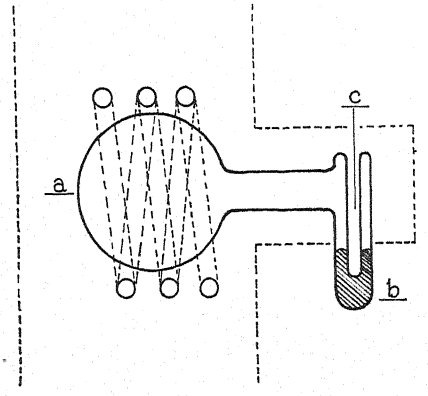

Fig. 1. The experimental bulb made of Pyrex. The broken lines show the position of the transite walls of the furnace.

value corresponding to the pressure at which the run was to be made. After a wait of about fifteen minutes at this temperature, readings of the starting current were taken at one-minute intervals. When these showed no consistent change, the average of six or more consecutive readings was taken as the starting current.

Table I shows a typical set of readings for starting currents; I_1 is the starting current for the dull glow and I_2 that for the bright glow. The values of I_2 are more consistent than those of I_1; this was generally the case.

TABLE I. *Currents necessary to start the electrodeless discharge.*

Frequency = 7.2×10^6 cycles per second. Temperature of furnace = 184°C. Temperature of the mercury well = 75.5°C. Pressure of mercury vapor in discharge tube = 0.066 mm of mercury.

	1	2	3	4	5	6	Average
I_1 amps (dull glow)	5.00	4.80	4.85	5.00	4.90	4.95	4.91
I_2 amps (bright glow)	6.60	6.65	6.65	6.65	6.65	6.65	6.65

Figure 2 gives the curves illustrating the variation of starting current with pressure at a frequency of 7.2×10^6 cycles per second. Curve *bcdfh* is for the bright glow and curve *acefg* for the dull glow; all pairs of curves taken were very similar to these in shape. The minima at *b* and *e* occurred at the same pressures for the different curves and at about the same currents but the rest of the curve was often shifted along the current axis. Within the pressure range from *c* to *f* of Fig. 2 the starting currents of the two discharges followed each other as described above. To the left of *c* and to the right of *f*, the bright discharge appeared at points on the curve *ac* and *fg*; the dull glow did not precede the bright glow in these regions. When the power supplied to the oscillator was decreased however the bright glow was made to disappear but the dull glow remained. When the power was again increased, the dull glow

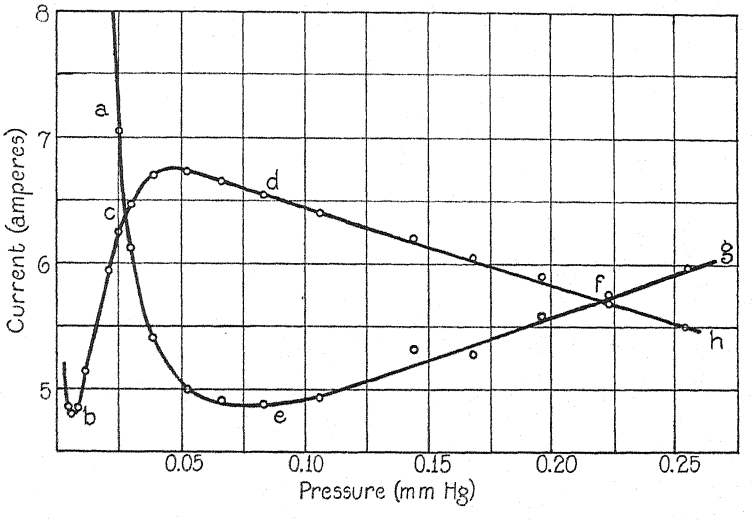

Fig. 2. Typical curves showing the variation of starting current with pressure in mercury vapor. Curve *bcdfh* is for the "bright glow" and curve *acefg* is for the "dull glow"; the former appears again as D_1 in Figs. 3 and 3a and the latter as D_1' in Fig. 3.

still being on, the bright glow reappeared at a considerably lower current than at first, corresponding to some point in the region *bc* or *fh*. Since our experiments with the shield have shown that the bright glow does not appear at any pressure unless preceded by the dull glow or by some external source of ionization, we have taken *bcdfh* as the true starting current curve for the bright glow, and *acefg* for the dull glow. Both types of discharge exist therefore over the whole range of pressures and may be started or stopped at will.

The minimum at *b* of the bright glow appears again in the curves D_1 of Figs. 3 and 3a; the last curve shows particularly how definite the minimum is.

Discussion of Results

Figs. 3 and 3a give the results of one set of experiments; many others were obtained like them. The full line curves *A*, *B*, *C* and *D* show the variation of starting current with pressure for the bright glow while the dotted curves

A', B', C' and D' are for the dull glow. Curves A_1, A_2 and A_3 were all taken at a frequency of 11×10^6 cycles per second; the oscillator coil had an induc-

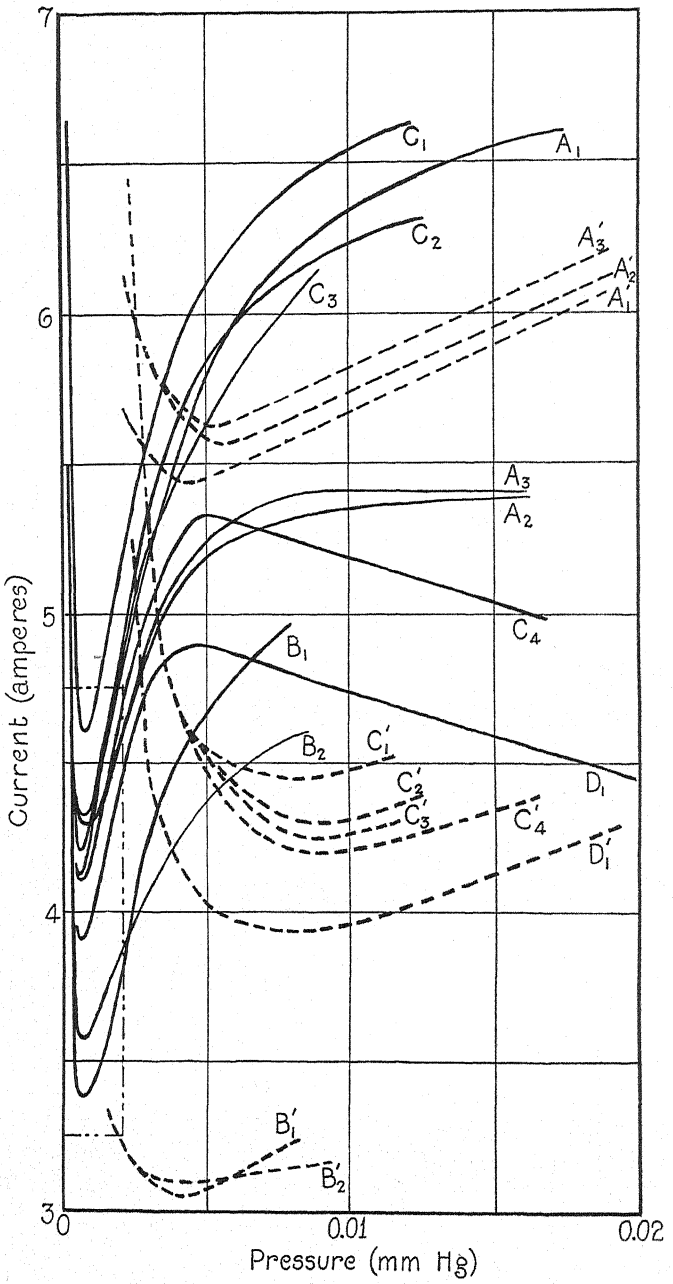

Fig. 3. A collection of curves illustrating the effect of changes in inductance and frequency of the oscillating circuit on the minimum starting current; the full lines are for the "bright glow" and the broken lines for the "dull glow"; the curves similarly labelled, e.g., A and A' were taken simultaneously. The region to the left enclosed by the chain lines is enlarged in Fig. 3a.

tance of 6.84×10^{-7} henries. Curve A_1 was taken on June 11 after the tube had been operated for a considerable period previously at a frequency of a 7.2×10^{6} cycles per second. The minimum at 0.0028 mm of mercury is very definite but is the only case in which such a low pressure minimum has been observed; the minimum at 0.0070 mm has therefore been chosen as the proper minimum for comparison with the other curves; no explanation can be offered at this time for the appearance of the two minima. Curves A_2 and A_3

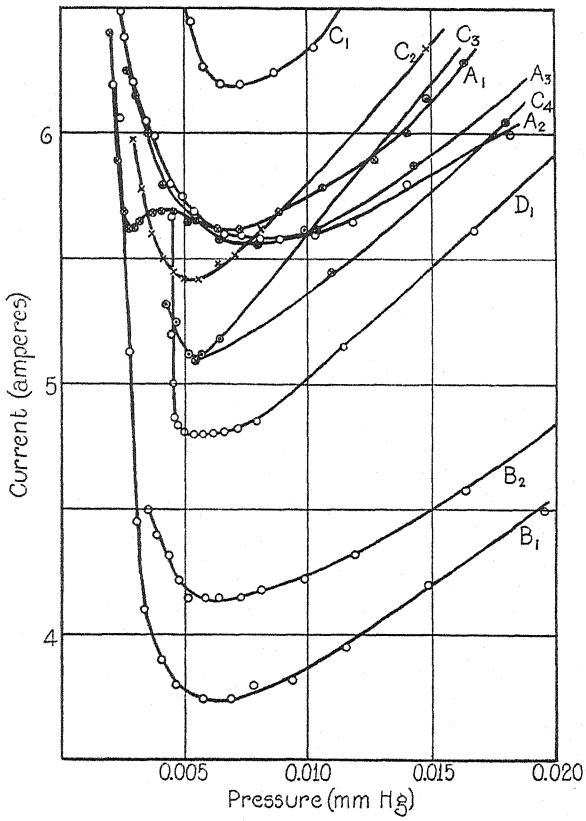

Fig. 3a. An enlarged view of the minima of the "bright glow" curves to show how sharply the minimum currents are defined.

were obtained on June 12. Figure 3a shows that their minima fall at a pressure of 0.0085 mm.[7]

Curves B_1 and B_2 were obtained on June 13; the frequency was kept at 11.0×10^{6} cycles per second as for the curves A but the inductance was increased to 10.4×10^{-7} henries. The minima for B_1 and B_2 are seen to fall at

[7] A comparison of curve A_1 with A_2 and A_3 shows that the first curve taken at a given frequency after the discharge tube has been run at a lower frequency results in a displacement of the minimum to a lower pressure than occurs with succeeding curves taken under otherwise identical operating conditions. The coil currents at the minima for A_2 and A_3 are less than for A_1; this whole behavior is typical.

a lower pressure than with the curves A, the value being 0.0065 mm. The "electromagnetic" theory of Thomson and the "electric" theory of Brasefield (for external electrodes) demand that the ratio of the frequency to the pressure at which the minimum occurs should be a constant; here, however, a shift takes place in the pressure at which the minimum occurs without a change of frequency but with a change of inductance. The values of the coil current at the minima are considerably lower with the curves B than with the curves A; this may be accounted for in terms of the change in inductance from 6.84×10^{-7} henries in the latter case to 10.4×10^{-7} henries in the former; the coils were of two and three turns, respectively. The magnetic field at the minimum should be

$$H_0 = \frac{2}{a}\left(\frac{2V}{e/m}\right)^{1/2}$$

according to Thomson, where V is the effective ionization potential for the gas and a the radius of the bulb; thus the starting current at the minimum should depend only on the gas, the bulb and the coil. The approximate value of the field inside of a solenoid is $H=2\pi ni\ (\cos\theta_1-\cos\theta_2)$ (see Starling 5th Edition p. 229); the coil current at the minimum should thus have been 16.8 amps. for curves A and 10.4 amps. for curves B, on the assumption further that the ionizing potential is 10.4 volts. If the effective ionizing potential is taken as 5.5 volts, these values become 12.2 amps. and 7.6 amps., respectively. Actually the currents were about 5.5 amps. for curves A and about 4.0 amps. for curves B.

The electric field at the minimum should be

$$E_0 = \pi f\left(\frac{2V}{e/m}\right)^{1/2}$$

according to Brasefield.[4] The shield experiments have given evidence of only diametral electrical fields; the recent experiments of Knipp[8] seem to confirm this observation. If this is the case

$$E_0 = \frac{\pi fL}{2Nr}I_0$$

where f is the frequency of the oscillation, L is the inductance of the coil, r is its radius and N the number of turns; I_0 is the peak value of the minimum starting current; this approximation for E_0 is based on the assumption of a linear drop in potential around the coil; a sine distribution leads to results of the same order. In effective amps. the above result becomes

$$I = \frac{2Nr}{1.414L}\left(\frac{2V}{e/m}\right)^{1/2}.$$

The coil current at the minimum should thus have been 2.24 amps. for curves

[8] Bulletin of the American Physical Society Vol. 6, number 1, p. 22, abstract 35, February 10, 1931.

A and 1.99 amps. for curves B, on the assumption that the ionizing potential is 10.4 volts. If the effective ionizing potential is 5.5 volts, these values become 1.63 amps. and 1.45 amps., respectively. The currents were actually about 5.5 amps. for curves A and 4.0 for curves B.

The observed values of the currents are of the same order of magnitude as the calculated values on either theory although the electromagnetic theory values are about twice as large as those observed and the electric theory values are between one fourth and one third as great, when the effective ionizing potential is taken as 5.5 volts. The electromagnetic theory predicts a change in the minimum current from curves B to curves A, the calculated ratio being 0.62. The electric theory predicts for diametral fields a shift corresponding to the ratio 0.89. The ratio of currents actually observed is 0.71.

Curves C_1, C_2, C_3 and C_4 were run in that order on June 14. Curve C_1 shows a minimum at a pressure of 0.0075 mm of mercury while the minima for the other three curves fall at a pressure of 0.0055 mm. The inductance was the same as for curves B, 10.4×10^{-7} henries, but the frequency had been lowered from 11.0×10^6 cycles per second to 7.2×10^6 cycles per second.[9] The ratio of the frequency to the pressure at the minimum for curve A_2 or A_3 and curve C_2, C_3 or C_4 is a constant within the limit of experimental error as predicted by both theories:

$$\frac{11.0\times10^6}{0.0085}=1295\times10^6;\quad \frac{7.2\times10^6}{0.0055}=1310\times10^6.$$

The ratio of inductance to capacity in curves A and C was constant. For curve B_1 or B_2 and curve C_2, C_3 or C_4 the ratios of frequency to pressure at the minimum are obviously not the same; the change in frequency resulted from a change in capacity in the circuit, the inductance remaining the same. Both theories predict that the coil currents at the minima for curves B and curves C should be equal as they are shown to be independent of the frequency. While successive values for curves B are increasing and those for curves C are decreasing, the values for the lower frequency are definitely higher than for the higher frequency.

Curve D was taken in an early set of experiments on May 22 and is included to show how well the results agree even after a lapse of time. The minimum falls at the same pressure as for C_2, C_3 and C_4; the coil current is lower than for the C curves but is above that for either B_1 or B_2.

The "electromagnetic" theory predicts that the minimum for curves A and B should occur at a pressure of 0.0035 mm for a frequency of 7.2×10^6 cycles per second and at 0.0054 mm for a frequency of 11.0×10^6 cycles per second, the ionizing potential being taken as 10.4 volts. We have found, however, that the dull glow or its equivalent must always be present before the

[9] Here again on running the tube after a change in frequency of the oscillator, the minimum for the first test is displaced with respect to the minima obtained in succeeding tests under otherwise identical operating conditions. In this case however the first minimum is at a higher pressure than the following, corresponding to a change from one frequency to a lower value.

bright glow comes on; we have considered therefore, that the effective ionizing potential is 5.5 volts. The calculated values of the pressure at the minima then become 0.0048 mm for 7.2×10^6 cycles per second and 0.0075 mm for 11.0×10^6 cycles per second; the observed values were 0.0055 mm for curves C at 7.2×10^6 cycles per second, 0.0085 mm for curves A at 11.0×10^6 cycles per second and 0.0065 mm for curves B at the same frequency; the agreement is fair.

The electric theory predicts that the minimum should fall at 0.0031 mm for 7.2×10^6 cycles per second and at 0.0046 mm for 11.0×10^6 cycles per second; the effective ionizing potential of 5.5 volts has been used to calculate these results. The agreement here is much less satisfactory than in the electromagnetic case. Throughout the calculations for the values of the pressures at the minima the mean free path of an electron in mercury vapor at 1 mm of Hg pressure and 25°C has been taken as 0.0149 cm as given by Compton and Langmuir.[10]

The diametral fields set up by the currents in the coil were sufficient to produce ionization but not at the pressures corresponding to the minimum of the bright glow; the mean free path of an electron in mercury vapor is not great enough to permit an electron to acquire sufficient velocity to cause ionization.

One other point in connection with the bright glow curves should be mentioned. Indications are that the furnace temperature, and therefore the bulb and vapor temperature, affects the position of the maximum in the region above 0.05 mm. For temperatures below 170°C, the maxima occur as with curve C_4; for temperatures around 185°C, the curves flatten out as in A_2 and A_3 and for still higher temperatures the curves continue to rise. Further work is in progress in an attempt to determine the relation between the shape of the curve and the furnace temperature.

The curves A_1', A_2' and A_3' were taken simultaneously with the A_1, A_2 and A_3 curves and represent the variation of starting current with pressure for the dull glow corresponding to curves A_1, A_2 and A_3 for the bright glow; the B' and C' curves have a similar interpretation. Curves A_2' and A_3' are entirely above A_2 and A_3; this is a significant fact because an observer could readily have failed to detect the existence of two types of discharge under these conditions. The procedure described above for separating the two components of the discharge was particularly important here; at some value for the current the two discharges appeared simultaneously corresponding to a point on one of the A' curves; the current was reduced until the bright glow disappeared, leaving the dull glow; the current was again increased and the bright glow reappeared at a point on the A curve. A change of inductance from 10.4×10^{-7} henries to 6.84×10^{-7} henries was made in passing from the B' to the A' curves but the frequency was kept at 11.0×10^6 cycles per second. The shift of the curves along the current axis is about twice as great for the dull glow curves as for the bright glow; the change of inductance should have

[10] Compton and Langmuir, Rev. of Mod. Phys. **2**, 208 (1930).

affected them alike. As pointed out above for the bright glow curves the observed ratio of the minimum currents was 0.71 and the computed was 0.89 on the basis of diametral fields; according to the theory the same calculation should hold for the dull glow but the observed ratio is only 0.39. If axial fields are assumed, the computed value for the ratio is 0.99; in either case the observed values for the dull glow fail to fit the theory and the discrepancy is much greater than for the bright glow.

Curves C' were obtained with the same inductance as for curves B' namely 10.4×10^{-7} henries but the frequency was reduced to 7.2×10^{6} cycles per second. On the basis of the electric theory there should have been no change in the values of the minimum currents in passing from B' to C' but actually there were very large changes. Again the shift along the pressure axis is in the wrong direction for the minimum should occur at a lower pressure as the frequency is lowered. Furthermore the currents observed at these minima were not sufficient to set up diametral fields powerful enough to cause ionization; the electrons could not possibly acquire sufficient velocity in the distance equal to the mean free path of an electron in mercury vapor at these pressures. This would seem to indicate that the process is one of multiple collisions.[11]

Curve D' is included to show that even the dull glow curves may be reproduced after a lapse of time although it was much more difficult in general to repeat the dull glow curves than the bright glow curves.

The authors wish to thank Mr. John Mills and Bell Telephone Laboratories for the use of power tubes used in this investigation. They desire, too, to extend their grateful appreciation of the help rendered by Dr. Ann Hepburn in the experimental work.

[11] This is the region of pressures, too, in which the bright glow curves show their change of shape with furnace temperature; it may be possible to explain the change in shape in terms of a variation of the terminal velocity of an electron moving through mercury vapor with the temperature of the vapor, the pressure being fixed by the temperature of the liquid mercury present.

THE PIRANI GAUGE FOR THE MEASUREMENT OF SMALL CHANGES OF PRESSURE

By A. Ellett and R. M. Zabel
Physical Laboratory, State University of Iowa
(Received March 20, 1931)

Abstract

The application of the Pirani gauge to the measurement of small pressure changes is discussed. Both nickel and tungsten wires are used as filaments in the gauge. Nickel wire not only has the greater sensitivity but possesses several other advantages. The theory of the gauge is developed so that it is possible to predict the effect of change in length or diameter of the wire upon the sensitivity of the gauge. The theory also predicts that there is an optimum temperature to which the wire should be heated for maximum sensitivity of the gauge. The observed and computed values of the optimum temperature are compared. In some cases the agreement is as good as can be expected and in the others the discrepancy is easily explained. The maximum sensitivity attained is a galvanometer deflection of 1 mm for a pressure change of air equivalent to 5×10^{-9} mm of mercury.

Introduction

THE possibility of using the variation in heat conductivity of a gas with pressure as a measure of low pressures was first suggested by Pirani.[1] Recent experimenters[2,3] have shown that such a gauge is capable of responding to very small changes in pressure.

These investigators have been primarily interested in a gauge which will determine the actual pressure existing in a chamber after it has been calibrated by comparison with an absolute gauge such as the McLeod. The aim of this experiment is to develop a gauge with a high sensitivity to very small pressure changes.

Theory

It is easily shown that the quantity of heat Q conducted by a gas when the mean free path is large compared to the dimensions of the container is

$$Q = nGAtH/6N \tag{1}$$

where n is the number of molecules per cm^3, G the mean molecular velocity, A the area of the heated element, t the temperature difference between the heated element and its surroundings, H the molecular heat at constant volume, and N the number of molecules per gram molecule. Experimental measurements give a value of the heat transfer which is usually less than that predicted by this equation. This is because the molecules striking the heated wire do not attain temperature equilibrium with it. The ratio of the actual amount of heat conducted from the heated element to that computed by

[1] M. Pirani, Verh. d Deutsch. Phys. Ges. **8**, 24, 686 (1906).
[2] A. M. Skellet, J. O. S. A. and R. S. I. **15**, 56 (1927).
[3] L. F. Stanly, Phys. Soc. Proc. **41**, 194 (1929).

Eq. (1) is known as the accommodation coefficient and has been measured for some gases. Soddy and Berry[4] give the values of the actual amount of heat conducted and the values of the accommodation coefficient for gases striking a heated tungsten surface. The values of the accommodation coefficient range from 0.25 in the case of hydrogen to 1.0 in the case of argon and neon. The values of the actual amount of heat conducted by various gases deviate by less than 10 percent from a mean value for a number of the common gases. Hence we may expect that the sensitivity of the Pirani gauge will be nearly the same for this group of gases.

In the application of the above principle to the measurement of pressure changes the temperature change in the wire resulting from a change in the heat conductivity of the gas is usually measured by the change in resistance. This resistance change is in turn measured by a Wheatstone bridge. If the pressure change to be measured is not large the galvanometer deflection is the most accurate method of determining the magnitude of the change.

The bridge potential serves as a source of power to heat the wire. The energy dissipated by a heated wire must be equal to that supplied, hence neglecting conduction to the leads

$$\frac{E^2}{R} = A\gamma(T^4 - T_0^4) + A\alpha p(T - T_0) \tag{2}$$

where E is the potential across the ends of the wire, R the resistance and A the area of the wire, T and T_0 the temperature of the wire and of its surroundings, respectively, p the pressure of the gas and γ and α constants. Since the resistance change corresponding to the pressure changes normally measured is small we may assume that the power supplied to the wire is constant. Then by differentiation of (2),

$$\frac{dT}{dp} = -\frac{\alpha(T - T_0)}{4\gamma T^3 + \alpha p}.$$

At low pressures the amount of heat dissipated from the wire by radiation is large compared to that conducted by gas hence we may neglect αp in comparison to $4\gamma T^3$. Then

$$\frac{dT}{dp} = K\frac{T - T_0}{T^3} \tag{3}$$

where K is a constant.

Obviously there is a relation between T and T_0 for which the temperature change of the wire will be a maximum for a given pressure change. This relation is given by

$$\frac{d}{dT}\left[\frac{(T - T_0)}{T^3}\right] = 0$$

or

$$T = 3T_0/2.$$

[4] F. Soddy and A. Berry, Proc. Roy. Soc. **83**, 254 (1910).

Substituting this value in (3) we obtain,

$$\left[\frac{dT}{dp}\right]_{\max} = \frac{K'}{T_0^2}. \tag{4}$$

Hence the value of the maximum temperature change of the wire for a given pressure change is inversely proportional to the square of the absolute temperature of the surroundings of the wire.

Since the temperature change resulting from a given pressure change is normally small we may assume that

$$R = R_0[1 + \alpha(T - 273)]$$

or

$$dR = R_0\alpha dT.$$

Substituting this value of dT in (3) we obtain,

$$\frac{dR}{dp} = K''R_0\frac{T - T_0}{T^3}. \tag{5}$$

Obviously dR/dp has the same maximum as dT/dp. The maximum galvanometer deflection does not necessarily correspond to the maximum resistance change, however.

The current through the galvanometer in a Wheatstone bridge circuit is given by

$$I_g = \frac{EdR}{4RR_g + 4R^2}$$

if the battery resistance is small and the four arms of the bridge are approximately equal. Substituting for dR from (5),

$$I_g = K'''\frac{R_0E}{RR_g + R^2}\frac{T - T_0}{T^3}dp. \tag{6}$$

Obviously the galvanometer deflection may be increased by increasing the potential of the bridge. This factor is limited, however, because the wire must be heated to its optimum temperature.

The relation between the potential drop across the wire and the temperature may be obtained from (2). In general the heat conducted by the gas may be neglected in comparison to that dissipated by radiation and T_0^4 in comparison to T^4. Hence

$$E = (\gamma AR)^{1/2}T^2.$$

Substituting this value of E in (6)

$$I_g = K\frac{R_0(AR)^{1/2}}{RR_g + R^2}\frac{T - T_0}{T}dp. \tag{7}$$

The optimum temperature of the gauge wire for maximum galvanometer deflection may be determined from (7). In the general case this solution is difficult but several special cases which are of interest may be treated.

If we assume that the galvanometer resistance is large compared to the resistance of the arms of the bridge, (7) reduces to

$$I_g = K' \frac{T - T_0}{R^{1/2} T} dp.$$

But

$$R = R_0[1 + \alpha(T - 273) + \beta(T - 273)^2]$$

where the terms of second order must be included if the action of the gauge is to be described over any considerable range. Hence

$$I_g = \frac{K'''(T - T_0)}{[1 + \alpha(T - 273) + \beta(T - 273)^2]^{1/2} T} dp.$$

The optimum temperature of the wire may be determined by

$$\frac{d}{dT}\left[\log \frac{T - T_0}{[1 + \alpha(T - 273) + \beta(T - 273)^2]^{1/2} T}\right] = 0$$

or

$$2\beta T^3 + (\alpha - 546\beta - 4\beta T_0) T^2 - T_0(3\alpha - 1638\beta) T - 2T_0[1 - 273\alpha + (273)^2\beta] = 0. \quad (8)$$

If the galvanometer resistance is small as compared to the resistance in the bridge arms Eq. (7) reduces to

$$I_g = K^* \frac{T - T_0}{R^{3/2} T}$$

and the value of T for maximum I_g is given by

$$6\beta T^3 + (3\alpha - 1638\beta - 8\beta T_0) T^2 - 5T_0(\alpha - 546\beta) T - 2T_0[1 - 273\alpha + (273)^2\beta] = 0. \quad (9)$$

Results

The experimental arrangement used in obtaining the results given below is shown in Fig. 1. The leak was controlled by a stopcock so that it could be opened or closed as desired. This gave a constant pressure change and the corresponding galvanometer deflection could be observed for various bridge potentials and various samples of wire.

The gauge formed one arm of a Wheatstone bridge. The other arms consisted of resistances variable in small steps so that the arms of the bridge could be kept approximately equal. The galvanometer used has a resistance of 17 ohms and a sensitivity of 11.6 mm per microvolt. Resistance was connected in series or parallel with it to obtain the high and low galvanometer resistances used.

Equation (7) shows that the galvanometer deflection should be directly proportional to the pressure change. This was verified beyond the limits of the McLeod gauge by connecting a small leak to a pump through a stopcock. This leak was adjusted to give several cm deflection of the galvanometer as

it was turned on or off. As the pressure in the gauge was increased by the use of another leak the deflection produced by opening or closing the first leak remained constant.

Equation (7) also shows that the sensitivity of the gauge is proportional to the square root of the area of the wire. It is possible to multiply the sensitivity of a nickel wire gauge by two or three merely by flattening the wire.

The effect of the length of the gauge wire upon the sensitivity may be determined from (7). Since A, R, and R_0 are all proportional to the length of the wire it is evident that the sensitivity will be directly proportional to

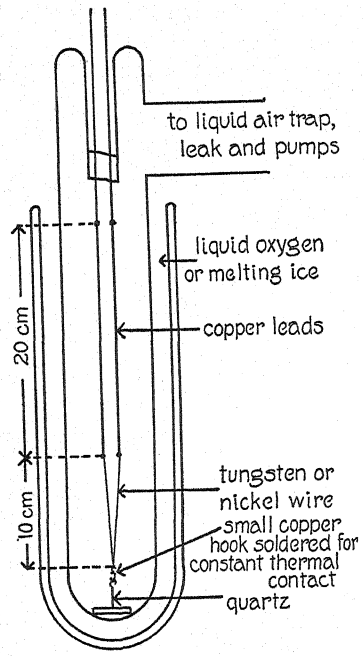

Fig. 1. Construction of the Pirani gauge.

the length of the wire if the galvanometer resistance is large compared to the resistance of the bridge arms. On the other hand, if the galvanometer re-

TABLE I.

Galvanometer resistance	Length of wire (cm)	Maximum deflection
312	20	22.4
	10	12.0
	5	6.3
17	20	23.0
	10	20.1
	5	15.9
3.86	20	24.5
	10	24.8
	5	23.2

sistance is small the sensitivity is independent of the length of the wire. Table I shows the effect of the length of the wire upon the sensitivity of the gauge. In each case the gauge was constructed of nickel wire 0.001 inch in diameter and the walls of the gauge were maintained at the temperature of melting ice.

The variation of the sensitivity of the gauge with diameter of the wire may also be predicted. If the galvanometer resistance is large compared to the resistance of the gauge, the diameter of the wire should be decreased and if the galvanometer resistance is low the diameter of the wire should be increased. Hence for maximum sensitivity the wire should be as long as convenient and the diameter should be adjusted so that its resistance is of the

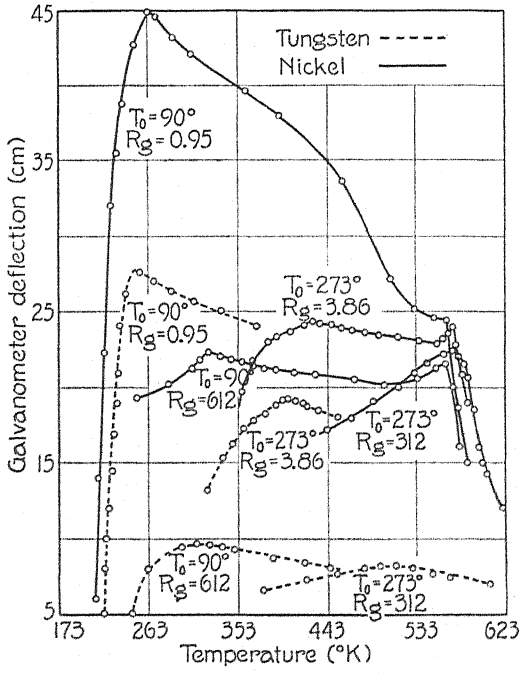

Fig. 2. Curves showing the relation between the temperature of the gauge wire and the sensitivity of the gauge. T_0 is the temperature of the walls of the gauge and R_g the galvanometer resistance.

same order of magnitude as the galvanometer resistance. In general a galvanometer with low resistance is preferable since the corresponding lower resistance in the bridge arms permits the use of lower battery potential which decreases the tendency of the galvanometer to drift.

The relation between the sensitivity of the gauge and the temperature of the wire is shown in Fig. 2. The tungsten and nickel wires used in obtaining these curves were 20 cm long and 0.001 inch in diameter. The temperature was determined by the known relation between the temperature and resistance. For tungsten the values $\alpha = 5.24 \times 10^{-3}$ and $\beta = 0.7 \times 10^{-6}$ were used in the well-known resistance formula. The temperature of the nickel wire

was read from the curve shown in Fig. 3 which was determined for the wire used in this experiment.

It will be noted that all the temperature sensitivity curves for nickel wire (Fig. 2) have either a primary or a secondary maximum at approximately 570°* after which the sensitivity decreases very rapidly. This is obviously due to the rapid increase in the slope of the temperature resistance curve and the sudden break at 615°. The observed temperature at which this break occurs should be less when the wire is used as a gauge because the ends of the gauge wire are cooled by conduction of heat to the leads. This view is substantiated by the fact that the apparent temperature at which the maximum occurs decreases when a shorter wire is used.

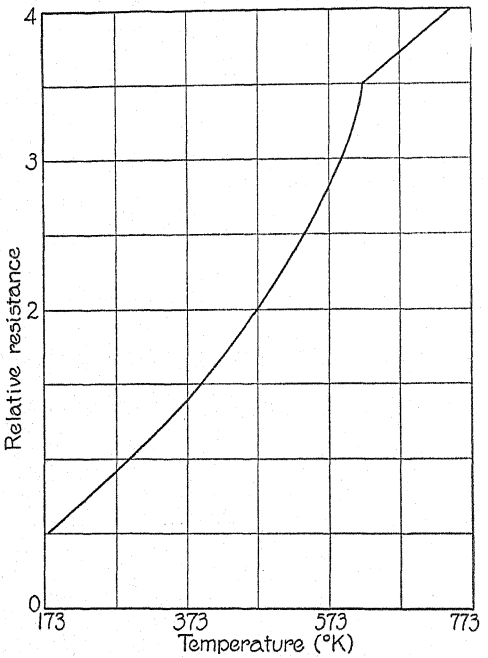

Fig. 3. Temperature resistance curve for nickel wire.

In Table II, T_0 is the temperature of the gauge walls, R_g is the galvanometer resistance, R is the resistance of the wire at its optimum temperature, E is the bridge potential necessary to produce this temperature, T(obs.) and D the optimum temperature and the galvanometer deflection at that temperature, respectively, as determined from Fig. 2, and T (comp.) the optimum temperature computed from Eqs. (8) and (9). In obtaining the values of T (comp.) the proper equation is chosen depending upon the value of the galvanometer resistance, and the values of T_0, α, and β are substituted after which the equation may be solved for T. For tungsten the values of α and β previously given were used and for nickel the same constants were determined from Fig. 3 to fit the curve approximately in the region in which the observed temperature was known to lie. It will be noted that the computed

temperatures when $T_0 = 90°$ are much lower than the observed. This is partially due to heat conduction along the leads and partially to the decrease in the constant γ appearing in Eq. (2) or, in other words, a decrease in the efficiency of radiation at low temperatures. In fact with a potential of only 0.0003 volt applied to the bridge the lowest temperature attained by the nickel filament was 209° and by the tungsten 213°.

The secondary maxima in the temperature sensitivity curves of nickel wire are not predicted by the equations but they probably would be if the variation in slope of the temperature resistance curve were taken into account and the equation of the curve were expressed more accurately.

TABLE II

	T_0	R_0	R	E	T Comp.	T Obs.	D
Nickel	90	612	41.9	0.5	248	313	22.3
	90	0.95	30.6	0.3	136	261	45.0
	273	312	99.0	2.9	533	563	22.4
	273	3.86	61.8	1.1	429	393	24.5
Tungsten	90	612	23.3	0.5	195	311	9.6
	90	0.95	17.0	0.4	120	254	27.6
	273	312	46.5	3.0	715	513	8.2
	273	3.86	33.5	1.3	415	401	19.3

* All temperatures given on the Kelvin scale.

Table II shows that the sensitivity attained by the use of nickel wire is in all cases greater than that for tungsten. Nickel wire has the additional advantage that it may be flattened more easily than tungsten which greatly increases the sensitivity as the previous discussion has shown. Tungsten wire has the disadvantage that the slightest vibration will cause its resistance to change sufficiently to keep the galvanometer moving back and forth over several cm.

Immersing the walls of the gauge in liquid oxygen approximately multiplies the sensitivity of the gauge by two when the galvanometer resistance is high and by seven when the galvanometer resistance is low. This difference in the sensitivity ratio is to be expected for Table II shows that the resistance of the bridge arms at optimum temperature is much lower when $T_0 = 90°$ than when $T_0 = 273°$. Equation (7) and the preceding discussion show that this decrease in resistance will decrease the sensitivity when the galvanometer resistance is high but not when the galvanometer resistance is low.

Many factors enter into the computation of the relative sensitivity of the gauge when the walls are at the temperature of melting ice and at the temperature of liquid oxygen. For example the relation between the pressure and the heat conductivity of the gas will change both because more molecules must be present at liquid oxygen temperatures to exert a given pressure and because the mean molecular velocity is smaller. Also, as previously sug gested, the radiation constant (γ in Eq. (2)) probably decreases at the lower temperature and it is reasonable to expect that the value of the accommodation coefficient depends upon the temperature. The effect of heat conduction

from the filament to the leads upon the sensitivity of the gauge has been neglected so that it is impossible to predict the change in sensitivity which will result from the reversal in the direction of this flow. Such a reversal actually occurs in some cases for when the walls of the gauge are immersed in liquid oxygen the temperature of the filament is less than the temperature of the leads. Due to the impossibility of computing the magnitude of the latter effect and the difficulty in computing some of those previously given no attempt is made to predict the increase in sensitivity when the walls of the gauge are reduced to the temperature of liquid oxygen.

Reducing the walls of the gauge to the temperature of liquid oxygen makes the reaction of the gauge very slow. For example with the gauges at the temperature of melting ice the galvanometer would reach equilibrium about 10 seconds after the stopcock was closed. At liquid oxygen temperature the time required to attain equilibrium was often several minutes. This time lag may be accounted for to some extent by the fact that there must be three times as many molecules in the gauge and their velocity must be much slower when the walls of the gauge are at the temperature of liquid oyxgen so that it should take longer for the gauge to pump out. This factor cannot, however, account for the great difference observed in the time lag in the two cases and neither can it account for the observed fact that the time lag of the gauge decreases rapidly with an increase in temperature of the filament since the area of the filament is so small in comparison to the area of the walls that it can have no appreciable effect upon the mean velocity of the molecules. The observed dependence of the time lag upon the temperature of the wire suggests that it may to some extent be due to the adsorption of a layer of gas by the filament.

It is possible to obtain a galvanometer deflection of 1 mm for a pressure change of air equivalent to $5 \pm 1 \times 10^{-9}$ mm of mercury by forming the gauge from a well-flattened piece of nickel wire 25 cm long and originally 0.0015 inch in diameter and using the galvanometer specified above at maximum sensitivity.

Under similar conditions the sensitivity of the gauge for hydrogen is $4 \pm 1 \times 10^{-9}$ mm of mercury per mm galvanometer deflection.

The sensitivity and characteristics of different gauges will vary due to variations in the original size and the degree of flatness of the wire.

Conclusion

In order to measure pressure changes of less than 10^{-7} mm of mercury it is obvious that the zero position of the galvanometer must be steady. If the ordinary precautions necessary in connecting a Wheatstone bridge of high sensitivity are observed, if the bridge potential is constant, and if the walls of the gauge are maintained at a constant temperature such as melting ice or liquid oxygen, the zero drift of the gauge becomes negligible provided that the pressure changes take place over a short period of time.

The operation of the gauge is not satisfactory when the walls are exposed to the variations of room temperature. A compensating gauge greatly im-

proves the stability of the system but is not as satisfactory as one gauge immersed in a constant temperature bath.

The stability of the gauge may be improved by keeping the bridge potential low. This may be accomplished by proper choice of the galvanometer as previously described and by operating the gauge below its optimum temperature. The extent to which the temperature should be reduced below its optimum value depends upon the difficulty arising from zero drift and upon the rate at which the sensitivity decreases with decrease in temperature. In some cases it is possible to reduce the bridge sensitivity to one half* of its value at the optimum temperature while the gauge sensitivity is reduced only 15 percent. In such cases the decrease in bridge potential would probbably be an advantage.

* That is $\Delta R/R$ for unit galvanometer deflection is doubled.

MEASURING THE INTENSITY OF MOLECULAR BEAMS

By A. Ellett and R. M. Zabel
Physical Laboratory, State University of Iowa
(Received March 20, 1931)

Abstract

A Pirani gauge sensitive to pressure changes of the order of 10^{-8} mm of mercury has been developed and used to measure the intensity of molecular beams defined by two circular openings, one 0.4 and the other 0.6 mm in diameter placed 25 mm apart. The gauge is situated 40 mm from the last opening. A beam of air gives a galvanometer deflection equivalent to 600 cm with a pressure of 0.5 mm of mercury behind the first opening. Under similar conditions H_2 produces a deflection of 1800 cm. The galvanometer sensitivity is 11.6 mm per microvolt. The time lag of the gauge is less than the period of the galvanometer (7 seconds). The limits within which the beam-forming system may be expected to give a Maxwellian distribution of velocities are discussed. The final pressure in the gauge due to a given beam depends upon the dimensions of the gauge opening as kinetic theory predicts. The reduction in intensity of a beam of H_2 by collision with either air or H_2 present in the experimental chamber at various pressures has been measured. The data show that the gauge may be used to measure mean free paths and to obtain more detailed information than has previously been possible as to the probability of scattering through various angles by collision.

Introduction

IN RECENT years the angular distribution of a beam of electrons after scattering by a gas has been studied in detail. No doubt the equally interesting and important problem of the scattering of a beam of molecules or atoms has been neglected because there has not been available a method of measuring the intensity of such beams. The reflection of atoms from a crystal may also be studied advantageously by the aid of a gauge which will measure accurately the intensity of molecular beams. In order to be most efficient in this connection the gauge should have a small internal volume so that it will respond rapidly to changes in beam intensity and small overall dimensions so that it may be placed entirely within the vacuum system and controlled magnetically if this seems desirable. The experiments described in this paper were undertaken to devise such a gauge. Some very notable advances have already been made in this field.[1]

Apparatus

A Pirani gauge, discussed at length in the preceeding paper, was constructed with a small opening in one side (Fig. 1) so that the pressure inside would be affected when the opening was moved into the path of a beam of molecules. By measuring the pressure change inside the gauge a measure of the beam intensity is obtained.

[1] F. Knauer and O. Stern, Zeits. f. Physik **53**, 766 (1929).

The ends of the gauge must be fitted carefully as experience has shown that arrangements which appear to fit well mechanically may leak considerably. The gauge has an internal volume of 0.5 cc so that it responds quickly to changes in beam intensity. The time required for the pressure in the gauge to reach equilibrium is normally less than the period of the galvanometer (7 sec.).

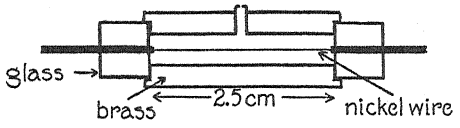

Fig. 1. The Pirani gauge applied to the measurement of molecular beams.

The extreme shortening of the wire seems to have no disadvantage other than decreasing the sensitivity of the gauge. The conduction of heat from the filament to the leads which would, of course, become more troublesome as the length of the filament is decreased has not interfered with the action of the gauge to an appreciable extent.

The apparatus which forms the molecular beam used in the investigation of the characteristics of the gauge consists of 3 circular openings (Fig. 2), the first of which is 0.4 mm in diameter, the second is 0.7 mm in diameter and is situated 1.75 mm from the first, and the third is 0.6 mm in diameter and situated 25 mm from the first. The second opening does not serve to define the beam but merely to prevent the spreading of the comparatively high

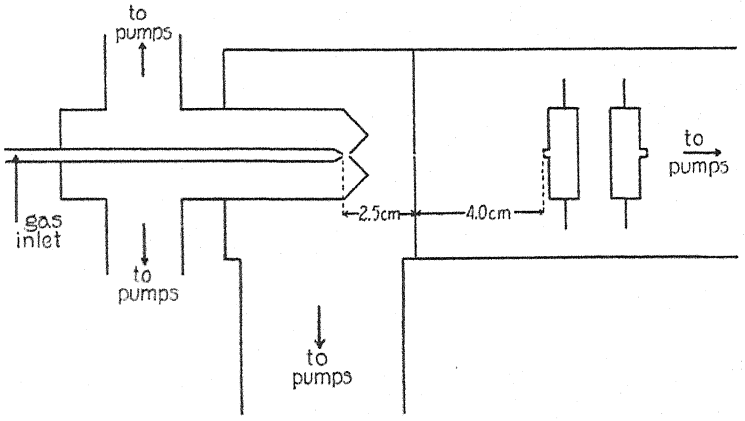

Fig. 2. The construction of the apparatus for the formation of molecular beams.

pressure in B throughout the entire distance between the first and last opening. It is made slightly larger than the other openings in order to eliminate any difficulties there might be in correct alignment. This precaution is hardly necessary here but might be in case very narrow slits were used to form the beam. The third opening was made larger than the first in order to secure a beam in which the width of the maximum intensity portion of the beam would be equal to the diameter of the largest gauge opening used. It is, of

course, obvious that the last opening could be reduced to the size of the first (0.4 mm) thus decreasing the angular divergence of the beam without decreasing its maximum intensity.

The distance between the first two openings of the beam system was adjusted experimentally to give the correct relative pressures in B and C for maximum efficiency. This distance depends upon the relative pumping speeds at B and C which are 4 and 18 liters of air per second, respectively. A change of 0.1 mm in this distance will produce an appreciable reduction in the maximum beam intensity which can be obtained.

A beam system consisting of two openings was not satisfactory for producing beams of high intensity. The impedance inherently existent in an apparatus when two slits are placed near each other makes it difficult to reduce the pressure between them sufficiently for the formation of an intense beam even if the necessary pumping speed is available.

The position of the gauge used in measuring the beam is shown in Fig. 2. It is arranged so that it may be rotated about the last opening of the beam system. The compensating gauge which is placed nearby forms the arm of the bridge adjacent to the main gauge and maintains the bridge balance for general changes in pressure as well as changes in temperature in the experimental chamber. Where high sensitivity is necessary it is advisable to place both gauges in a common metal container or form both from the same piece of metal.

PROCEDURE

The final pressure in the gauge due to a given beam will depend upon the size and shape of the opening into the gauge. The most advantageous form of opening may be predicted by a consideration of Knudsen's law of molecular flow.

Since the pressure in the gauge is always such that the mean free path is large compared to the dimensions of the container, it is evident that the gauge opening, regardless of its length or diameter, will offer no impedance to the entrance of the molecules of the beam if the apparatus is arranged so that they do not strike the walls of the opening. Hence the pressure inside the gauge will build up to such a value that the quantity of gas which flows out through the gauge opening is equal to that which enters it from the beam. The quantity of gas Q measured in cm^3 at 1 bar flowing through a tube of length L and radius r per second is given by Knudsen[2] as

$$Q = \frac{1}{\rho_1^{1/2}} \frac{p_1 - p_2}{W_1 + W_2} \tag{1}$$

where ρ_1 is the density of the gas at 1 bar and at the temperature of the apparatus and the partial impedances W_1 and W_2 are given by

$$W_1 = \frac{(2\pi)^{1/2}}{\pi r^2} \tag{2}$$

and

[2] M. Knudsen, Ann. d. Physik **28**, 75 and **28**, 999 (1909).

$$W_2 = \frac{3L}{4(2\pi)^{1/2}r^3}. \tag{3}$$

Assuming that the molecules emerge from the initial opening of the beam system with a cosine distribution, the amount of gas entering the gauge and also the amount leaving it per second when equilibrium is established is

$$\frac{Q'r^2}{D^2}$$

where Q' is the quantity of gas used in forming the beam, r is the radius of the gauge opening, and D the distance from the initial beam opening to the gauge opening. Substituting the value of Q given above and the values of W_1 and W_2 from Eqs. (2) and (3) in Eq. (1) we obtain upon solving for (p_1-p_2) the quantity actually measured by the gauge

$$p_1 - p_2 \equiv (\rho_1)^{1/2}\frac{Q'}{D^2}\left(\frac{2^{1/2}}{\pi^{1/2}} + \frac{3L}{4(2\pi)^{1/2}r}\right). \tag{4}$$

Hence if the gauge opening is a hole in a thin wall the equilibrium pressure is independent of the radius. If, however, the gauge opening is long as compared to its radius the equilibrium pressure is proportional to its length and inversely proportional to its radius. The effect of the dimensions of the gauge opening upon the sensitivity of the gauge is shown by Table I. The

TABLE I. *The effect of the dimensions of the gauge opening upon the sensitivity of the gauge.*

Dimensions of gauge openings (mm)		Relative deflection	
Length	Diameter	Computed	Observed
12	0.37	18	18
12	0.5	11.3	11.7
12	1.0	6	6.2
4	0.37	6	6
0	0.1	0.6	1

calculated values of the relative sensitivity are obtained from Eq. (4). The agreement is well within the limits to which the dimensions were actually known except in the case of the 0.1 mm hole. Here the disagreement may be explained by the reasonable assumption that the wall has a thickness of 0.08 mm.

For many purposes it is desirable that the molecular beam under consideration have a Maxwellian distribution of velocities. Previous investigators[3,4] have shown that a beam possesses a Maxwellian distribution of velocities if the pressure behind the first opening is such that the mean free path is several times the diameter of the opening and the pressure along the path of the beam is such that the effect of collisions may be neglected. Fig. 3 shows that the latter condition is easily satisfied. As long as the intensity of the beam is proportional to the amount of gas forming it, collisions have not

[3] J. A. Eldridge, Phys. Rev. **30**, 931 (1927).
[4] I. F. Zartman, Phys. Rev. **37**, 383 (1931).

become a factor. Further evidence of the same nature was obtained by plotting beams such as shown in Fig. 4 over a wide range of intensity. In the case of both air and H_2, beams were plotted from the first point shown in Fig. 3 to

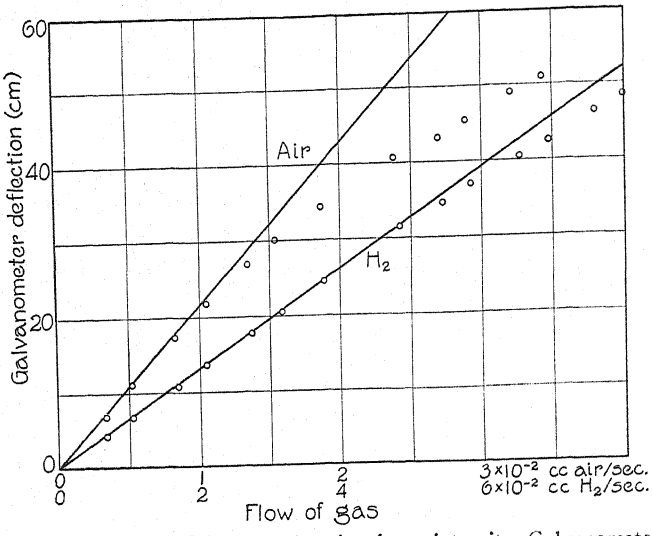

Fig. 3. Volume of gas forming beam plotted against beam intensity. Galvanometer sensitivity, for air 1/10, for H_2 1/20.

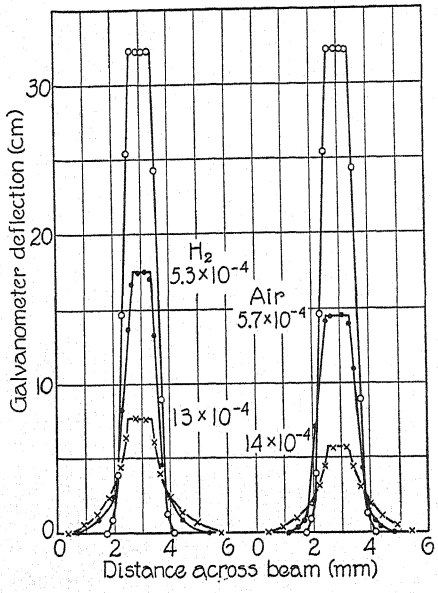

Fig. 4. The spreading of a beam of H_2 with increasing pressures of air and H_2 in its path.

the point where the curves first leave the straight lines. In neither case was there an appreciable spreading of the beam such as would result from collisions taking place between the openings.

The limitation placed upon the beam intensity by the first condition mentioned above may be obtained from Table II. A comparison of the values of the mean free path at A given in this table with the diameter of the opening (0.4 mm) show that the requirement of low pressure behind the first opening, rather than the speed of the pumps, is the limiting factor in the beam intensity which can be obtained if a Maxwellian distribution of velocities is desired. Table II also contains the values of the pressures for the various compartments of the beam system.

TABLE II. *Pressures at various points in the beam system. (mm of mercury).*

	Points from figure 3	A*	B	C	Mean free path at A
Air	1	0.15**	3.2×10^{-4}	1.6×10^{-5}	0.50 mm***
	2	0.26	6.3	3.6	0.30
	4	0.53	13.	3.6	0.14
	8	1.22	27.	3.6	0.07
	12	1.72	38.	3.6	0.05
H_2	1	0.08	2.6×10^{-4}	1.6×10^{-5}	2.0
	2	0.14	4.0	1.6	1.0
	4	0.28	9.0	2.5	0.54
	6	0.42	14	2.5	0.36
	8	0.63	19	3.6	0.24
	11	0.87	28	3.6	0.18
	14	1.08	33	3.6	0.15

The pressure in the experimental chamber is in all cases better than 10^{-6} mm Hg.
* See Fig. 2.
** These values were computed.
*** Mean free path for spherical model assuming air to be composed of oxygen and nitrogen[5].

The equilibrium pressure in the gauge resulting from a given beam may be computed by the application of Eq. (4) and from the calibration constant of the gauge. The comparison of these two values is of interest. The physical constants and the dimensions of the apparatus appearing in Eq. (4) have the following values: $\rho_1=1.16\times10^{-9}$ (air); $D=6$ cm;[6] $L=1.2$ cm; and $r=0.0185$ cm. The quantity of gas Q' used in forming the beam in the case of the third point on the air curve in Fig. 3 is 8.1×10^{-3} cm^3 at atmospheric pressure or 8.1×10^{3} cm^3 at 1 bar. Substituting these values $p_1-p_2=0.154$ bars or 1.15×10^{-4} mm of mercury. Computing the excess pressure in the gauge from the calibration constant (5.8×10^{-8} mm of mercury per mm galvanometer deflection) and the deflection we obtain $p_1-p_2=1.03\times10^{-4}$ mm of mercury.

The error is approximately 10 percent and is within the limits of accuracy to which the Pirani gauge had been calibrated by comparison with a McLeod gauge.

Similar computations for H_2 yield values of the observed pressures which are approximately 30 percent greater than kinetic theory predicts.

With the aid of a gauge of the type discussed above it should be possible to obtain more detailed information about the nature of molecular collisions.

[5] Dushman, Gen. Elec. Rev. 18, 952, 1042, 1159 (1915).
[6] This value is slightly less than the one given in Fig. 2 because of the increased length of the gauge opening.

The following brief discussion of the decrease in intensity and the scattering of molecular beams by increased pressure in the gauge chamber shows some of the possibilities of the gauge.

The scattering of a beam of H_2 in the experimental chamber is shown in Fig. 4. The beam travels 4 cm in this chamber before striking the gauge opening. In order to eliminate any directional preference of the gauge to the incident molecules a 0.1 mm hole in a thin wall formed the opening into the gauge. This is desirable for as the gauge is turned to one side of the main beam a long opening will permit scattered molecules to enter the gauge with zero impedance only if they are scattered from the portion of the beam which is in line with the gauge opening and at the proper angle to strike that open-

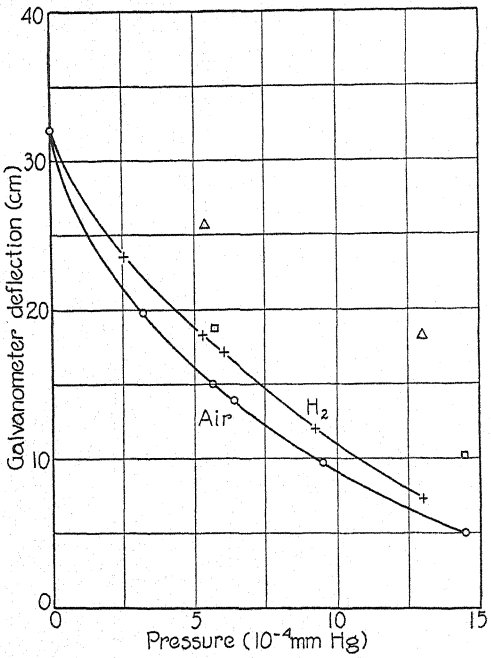

Fig. 5. Beam intensity as a function of the pressure in the experimental chamber.

ing. The hole in the thin wall will, on the other hand, permit the entrance of molecules scattered from any point along the beam. The long opening might be used advantageously for a detailed study of the probability of various scattering angles.

Since the beams shown in Fig. 4 are circular and the readings were taken across a diameter, the actual areas covered by the beams are proportional to the square of the width of the curve.

In Fig. 5 the curves represent the decrease in the maximum intensity of the beams with increasing pressures of air and H_2 in the experimental chamber. The value of the mean free path of H_2 in H_2 as determined from this figure is 3.8 cm at a pressure of 10^{-3} mm of mercury. A comparison of this decrease in maximum intensity and the decrease in the percentage of the

molecules of the original beam which can be found near the center of the beam is of interest. The relative number of molecules found within this limit can be determined by a comparison of the area intensity summations of the curves of Fig. 4. These summations are represented in Fig. 5 by the triangles for H_2 and the squares for air, where the summation of the original beam is represented by 32 and the summations of the scattered beams are relative to the original. For example with an H_2 pressure of 5.3×10^{-4} mm of mercury in the experimental chamber the maximum intensity of the H_2 beam is reduced to 54 percent of its original value while 80 percent of the original number of molecules can be found near the center of the beam. With a slightly higher pressure of air the maximum beam intensity is reduced to 46 percent and 57 percent of the molecules can be found near the center of the beam. This indicates as would be expected that there is greater probability of large angle scattering in air than in H_2.

Conclusion

The only difficulty encountered in the use of these gauges is the elimination of the zero drift. This drift seems to arise principally from unequal evolution of gas from the walls of the beam and compensating gauges, and from changes in room temperature. The latter effect becomes less the more nearly the two gauges are alike but it seems impossible to eliminate it entirely. The drift due to unequal outgassing is, of course, increased with increase in the impedance of the opening. In any case it may be eliminated to a great extent by baking out the gauges so that it is possible to reduce the drift of the galvanometer at maximum sensitivity to one cm in fifteen minutes.

The data given in Fig. 2 and Table II show that a beam of air formed by a pressure of 0.5 mm of mercury behind the first opening of the beam system produces a galvanometer deflection equivalent to 200 cm. H_2 under similiar conditions produces a deflection of 600 cm. Since the above results were obtained, gauges have been constructed with three times the sensitivity of those used in taking the above readings merely by an improved method of flattening the wire and an increase in the length of the wire. Hence we may say that it is possible to form beams of air and H_2 which have approximately a Maxwellian distribution of velocities and produce galvanometer deflections of 600 and 1800 cm, respectively. Allowing a large margin of safety, we may assume that the galvanometer deflections are accurate to 0.5 mm. Then the relative intensity of beams of air may be determined with an accuracy of 0.08 percent. Likewise the intensity of a beam of H_2 may be determined to an accuracy of 0.03 percent. This sensitivity is ample for the determination of the mean free path of gases, for the investigation of the probability of various scattering angles resulting from collision, and for a study of the reflection of atoms from crystals. A scattered beam of H_2 with an intensity of 1 percent of the initial beam may be measured with an accuracy of 3 percent.

LUMINESCENCE DUE TO RADIOACTIVITY

By D. H. Kabakjian
Randal Morgan Laboratory of Physics, University of Pennsylvania

(Received March 16, 1931)

Abstract

Results of several investigations on luminescence due to radioactivity carried on under the direction of the author are reviewed. It is shown that these results cannot be explained on the well-known active center theory advanced by Rutherford, or any modification of the same such as that proposed by Walsh. In certain substances, including zinc sulphide, there is an initial rise in brightness of the irradiated samples followed by a decay which cannot be represented by a simple exponential curve. It is also found that the rate of decay of brightness is not strictly proportional to the rate of emission of luminous energy as required by the theory. The observed facts can be explained qualitatively by assuming that the alpha, beta and gamma-rays produce excited molecules in the luminescent material. Return of these molecules to their initial state of more stable equilibrium results in emission of luminous energy. The rays also affect the transmission coefficient of the materials, and the apparent decay of brightness is explained as due to the increased absorption of light by the material itself, rather than to the destruction of the hypothetical active centers. This is evidenced also by the fact that in the materials studied, heating the samples usually restores the initial brightness. Quantitative application of these suggestions to the experimental curves was not possible, since the nature of the change in light absorption coefficients resulting from irradiation is not definitely determined.

LUMINESCENCE of certain chemical compounds under the excitation of rays from radioactive substances has been studied by various investigators and theories have been advanced to explain the gradual decay of brightness in these materials.

Rutherford in 1910[1] advanced a theory to explain Marsden's observations on the decay of brightness of phosphorescent zinc sulphide under the action of alpha rays from radon and its decay products. According to his theory, which we shall call the active center theory, phosphorescent zinc sulphide contains initially a number of molecular aggregates known as active centers. Passage of alpha-rays through the compound destroys a number of these active centers resulting in flashes of light known as scintillations. Active centers once destroyed cannot be reformed and since the number of such centers hit by an alpha-ray would be proportional to the number present at any time, the brightness of the compound for a given steady source of radiation should decay in accordance with a simple exponential law.

Chemically pure zinc sulphide does not exhibit this phenomenon to any great extent. The presence of a small quantity of some foreign element such as copper or manganese seems necessary to obtain a maximum effect. This fact lends force to the active center theory since the molecules of foreign matter might act as nuclei for such aggregations.

[1] E. Rutherford, Proc. Roy. Soc. **83A**, 561 (1909–10).

The theory has the virtue of extreme simplicity but none of the subsequent investigators have been able to obtain a simple exponential decay curve of brightness in such compounds, especially when the measurements extended over a considerable period of time. Therefore various modifications have been suggested, from time to time, to make the original theory conform to the observed facts.

Patterson, Walsh and Higgins[2] found that the theory in its simple form did not agree with their measurements of brightness of luminous paints extending over 450 days. There was a distinct slowing up of the rate of decay as time went on, which could be explained if it was assumed that the active centers were capable of recovery in accordance with an exponential law.

In a more recent article Walsh[3] gives additional data on the decay of brightness of luminous paints. The paints consisted of mixtures of zinc sulphide and radium bromide. Measurements of brightness extended over 4000 days.

In this article Walsh, after reviewing various theories advanced on the subject, comes to the conclusion that Rutherford's original theory agrees with his and others' results if the absorption of light by the luminous material itself is taken into consideration.

It is a well-known fact that many transparent substances are colored by the rays from radium. Zinc sulphide used in luminous paints is also colored gradually and its absorption for light progressively increased.

In combining this factor of light absorption with Rutherford's simple theory, Walsh finds, however, that the observed values of brightness agree better with the modified theory if the change in transmission constant of the material due to ionization of inactive centers be put equal to zero; i.e., if the increased absorption be considered as resulting from the destruction of active centers only.

This conclusion can not be justified unless it can be shown that the transmission constant of nonluminescent (inactive) zinc sulphide remains unchanged by the passage through it of ionizing rays. This, however, is not the case. A qualitative test made in this laboratory showed that a film of chemically pure zinc sulphide, exposed to alpha-rays from radium for a short time, is distinctly colored with resulting increase in absorption constant, although practically nonluminescent. Therefore even if in a luminescent compound the ratio of inactive molecules to active ones may be considered small at the start, evidently this ratio is constantly increasing due to the transformation of active molecules to inactive ones as required by the theory. And since these undergo a similar change in transmission constant, their effect on the decay of brightness cannot be neglected in the final analysis.

A number of researches on luminescence due to radio-activity have been carried on in this laboratory. An attempt to explain the results of these observations on the active center theory, with such modifications as have been suggested, was unsuccessful.

[2] Patterson, Walsh and Higgins, Proc. Phys. Soc. Lond. **19**, 215 (1916–7).

[3] J. T. Walsh, Proc. Phys. Soc. Lond. **39**, 318 (1926–27).

Karrer and Kabakjian[4] showed that mixtures of radium bromide and barium bromide acquired the property of luminescing with an intense bluish light by simply heating the compounds to a suitable temperature and then cooling. The luminescence decayed in time but could be completely regenerated by heating the compound to the original temperature. Addition of foreign substances was not necessary in this case. In fact addition of minute quantities of copper or manganese seemed to reduce the brightness.

Rodman[5] investigated the decay of brightness of pure radium bromide, and also of some mixtures of radium bromide and barium bromide. Two points were brought out in her paper. First that the decay of brightness did not conform to a simple exponential law. Second, that although the decay was very rapid at the start, the curve representing the brightness became finally parallel to the time axis, giving a constant value of brightness which was not zero. Both of these facts are at variance with the active center theory.

For example, the brightness of pure radium bromide decayed to about one percent of its initial value in 24 hours. It reached a constant value in about 300 hours and did not show a measurable variation in the following 200 hours.

Smith[6] investigated the luminescence of pure barium bromide exposed to alpha, beta and gamma-rays. In his case the source of the rays and the luminescent material were kept separate so that it was possible to observe the variation of brightness from the start. Smith's results showed an initial rise in brightness of barium bromide on exposure to the rays from radium. This rise continued for several hours reaching a maximum value and then decaying to a final constant value.

It is quite evident that Smith's results cannot be explained by the active center theory which fails to account for the initial rise in brightness. The final approach of brightness to a constant value instead of zero is also in agreement with Rodman's results.

Since the original active center theory was formulated by Rutherford to explain the decay of luminescence in zinc sulphide, it was considered desirable to investigate this compound by a similar method.

Gessner[7] undertook this investigation by means of an improved type of apparatus. The constant source of rays was well separated from the luminescent material and the apparatus so arranged that readings of brightness could be taken within two minutes after the exposure.

The results obtained by Gessner were similar to those of Smith. In every case there was an initial rise in brightness, followed by a decay which was not exponential. Neither did any part of the curves conform to the modified theory developed by Walsh.

This initial rise in brightness of zinc sulphide was also observed by Marsden for beta-ray excitation, but no attempt was made to explain this fact in formulating the active center theory.

[4] E. Karrer and D. H. Kabakjian, Jour. Frank. Inst. **186,** 317 (1918).
[5] J. Rodman, Phys. Rev. **23,** 478 (1924).
[6] L. E. Smith, Phys. Rev. **28,** 431 (1926).
[7] G. S. Gessner, Phys. Rev. **36,** 207 (1930).

Since the alpha-rays produce individual scintillations, while the beta-rays produce more or less diffuse illumination, it may be assumed that the mechanism of light emission is different for the two rays. Chariton and Lea[8] have found, however, that scintillations similar to those produced by alpha-rays can be obtained from beta-rays under favorable conditions, showing clearly that the only difference between the two types of excitations is the energy carried by the individual rays.

That the rise observed in Gessner's samples was not due to beta-rays was evidenced by the fact that a polonium plate used to excite the compound gave the same type of brightness curve.

In attempting to check Walsh's latest explanation on the decay of zinc sulphide paints, Gessner had used thin films of zinc sulphide and a more intense source of radiation, hoping thereby to accelerate the rate of decay. The brightness of his samples were uniformly greater than those of Walsh. If the emission of light results from destruction of active centers, evidently these

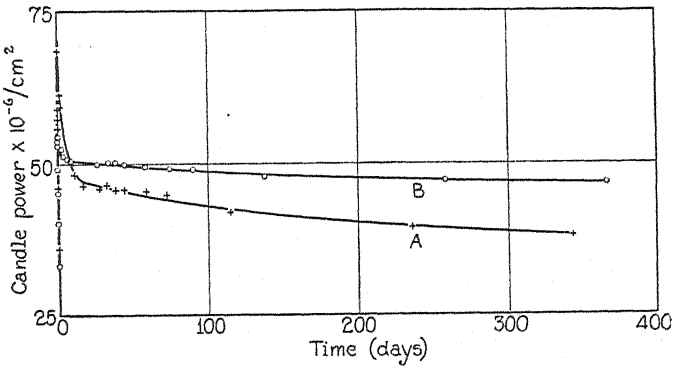

Fig. 1. Curves showing the decay of brightness in zinc sulphide. *A*, alpha, beta and gamma-rays from radium. *B*, beta and gamma-rays. Thickness of material, 0.022 cm.

were being destroyed at a greater rate, and since the volume of the material used, and presumably the initial number of active centers was very small, one would expect the brightness of these samples to decay much faster than those of Walsh. The results were quite the opposite. Walsh's brightest sample (Sample *H*, initial brightness 0.28 candles per square meter) shows a decay of over 85 percent in 400 days whereas one of Gessner's samples (Sample 4, Maximum brightness 0.4 candles per square meter) shows a decay of less than 50 percent for the same interval. This disagreement with the theory can hardly be explained by possible differences in the materials used by the two investigators.

It was also found that in the same material of approximately the same thickness the rate of decay was not in direct proportion to the rate of emission of light but depended on the nature of exiciting rays.

Fig. 1* illustrates this point. Although the total amount of light emitted

[8] J. Chariton and C. A. Lea, Proc. Roy. Soc. **A122,** 335 (1929).

* Curves represented in Fig. 1 and Fig. 2 were obtained by Mr. Gessner. For apparatus and the method of measurement, refer to his article, Phys. Rev. **36,** 207 (1930).

by sample B, due chiefly to beta-ray excitation is greater than that from sample A where alpha-ray excitation predominates, the rate of decay of brightness is in the reverse order. Assuming that the mechanism of light emission is the same for the two types of radiation this difference in the rates of decay of the two samples cannot be explained on the active center theory.

Another check on the theory could be obtained by estimating the number of active centers in zinc sulphide from the data given in Fig. 1, on the assumptions made by Walsh in estimating the number of active centers in his samples.

By integrating the area under curve A, the total amount of luminous flux produced in a quantity of zinc sulphide having a thickness of 0.022 cm and an area of one square cm can be computed from the formula

$$F = \frac{4\pi aI}{1 - e^{-0.022a}}$$

where F is flux in lumens; I is brightness in candles/cm^2; and a is the coefficient of absorption of freshly prepared zinc sulphide.

Taking the value of a as 32 and the mechanical equivalent of light for the wave-length emitted as 660 lumens per watt, the amount of luminous energy radiated by this sample during the first 350 days is roughly equal to 1.5×10^{10} ergs.

If N is the number of active centers destroyed during this interval of time and if it be assumed that each active center emits, on destruction, one quantum of energy corresponding to a wave-length of 550mμ, the total amount of energy radiated by the destruction of N active centers will be equal to $N\cdot3\cdot6\times10^{-12}$ ergs. Equating this with the above expression we have

$$N = \frac{1\cdot5\times10^{10}}{3\cdot6\times10^{-12}} = 4.16\times10^{21}.$$

But the number of molecules in this quantity of zinc sulphide is approximately 5.5×10^{20}. Therefore the number of active centers destroyed in this sample during the first 350 days comes out more than 7 times the number of molecules present. Since the brightness of the sample has decayed to 56 percent of its maximum value and the rate of decay has become very much slower it must be assumed that the original number of active centers present is many times the number of molecules present in the material if the active centers once destroyed cannot be regenerated.

The active center theory of luminescence, therefore, seems inadequate to explain, among other things:

(1) The initial rise in brightness of all the samples investigated;
(2) The difference in the rate of decay of brightness in luminescent material for alpha and beta-ray excitations;
(3) The general nature of brightness decay curves.

In view of these facts it seems more reasonable to assume that the passage of the rays through luminescent materials results, not in destruction of any hypothetical active centers, but rather in producing excited molecules which emit light on returning to their normal energy levels. As this is a reversible change this phenomenon can continue indefinitely.

The rays may also produce a certain amount of ionization or dissociation resulting in a more stable change such as coloration, due to the inability of the ions to recombine at ordinary room temperatures. The two phenomena are not strictly interdependent. It is possible to have coloration with very little luminescence and vice versa.

Light emission by excited molecules can take place in two distinct ways, giving rise to two types of luminescence. If the whole absorbed energy is re-emitted instantaneously, unaffected by the temperature of the absorbing material, the phenomenon is known as fluorescence. If, however, the absorbed energy is re-emitted gradually and the absorption and emission are more or less dependent on the temperature of the absorbing material, the phenomenon is known as phosphorescence. What is known as thermoluminescence is really phosphorescence at higher temperatures.

In this paper the term phosphorescence is used in a general sense without regard to the nature of the exciting rays. Its characteristic feature is the inability of the excited molecules to return at once to their normal state, consequently a phosphorescent material will continue emitting light after the exciting rays have been removed.

If the luminescence produced by alpha, beta and gamma-rays in the investigated materials is of the phosphorescent type, the initial rise in brightness of these samples could be explained. This would mean that all the energy absorbed from the rays is not radiated at once. It can be shown that this is generally true for the materials under discussion. Even in the case of alpha-ray excitation of zinc sulphide a diffuse radiation lasting several minutes follows each scintillation. This can easily be demonstrated by exposing a zinc sulphide screen to a strong source of alpha-rays for a few seconds. When the source is removed the screen will continue to glow in the dark for several minutes, its brightness gradually decaying to zero. It can also be shown that this is due to slow radiation of the energy absorbed from the alpha-rays and not to a possible absorption of its own luminous energy.

At ordinary room temperatures the ratio of energy radiated as diffuse light to that radiated as scintillations is small and has usually been overlooked, but this ratio is dependent on the temperature of the absorbing material. If a zinc sulphide screen in contact with a polonium plate is cooled to the temperature of liquid air its brightness is considerably diminished. When after a few minutes of exposure the polonium plate is removed and the screen is allowed to reach the room temperature, it glows much more brightly, showing that a larger percentage of the energy of the rays is absorbed and retained at the lower temperatures and released only with the aid of heat agitation of the molecules.

These experiments justify us in regarding the absorption and emission of

energy by luminescent materials when excited by alpha, beta and gamma-rays, as essentially a phosphorescence phenomenon. If this view is correct then the brightness of these materials, when excited by a constant source of rays should rise to a maximum where the rate of absorption and emission balance each other, and if there is no physical or chemical change in the material, it should remain constant at this value indefinitely. But it is well known that the coefficient of light absorption of these materials increases as a result of irradiation, therefore the brightness must decay in time, not necessarily because of a decrease in the amount of light produced but due to the fact that more and more of it is absorbed by the material itself as time progresses.

Again if the coefficient of absorption never becomes infinite but tends to approach a constant as time approaches infinity, the brightness would never decay to zero.

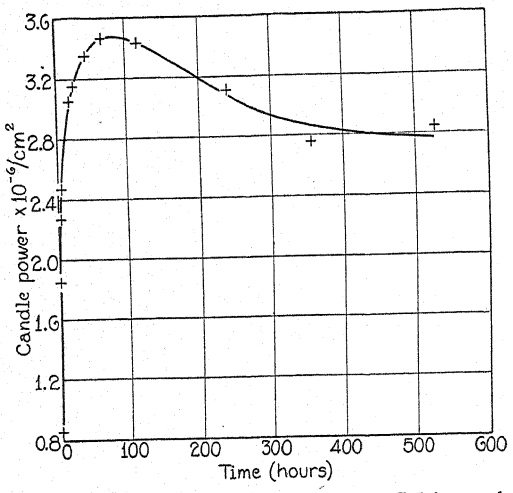

Fig. 2. Luminosity curve. Capsule *A*, beta, gamma-rays. Calcium sulphate Mn activated.

These conclusions are qualitatively in agreement with the observed facts on all materials investigated in this laboratory.

Fig. 2 represents the rise and decay in brightness of a typical thermoluminescent material which is also phosphorescent at ordinary room temperatures. The material consists of crystalline calcium sulphate activated by manganese. It will be noted that the brightness increases in time reaching a maximum in about 70 hours and then begins to decay. The decay curve is not a pure exponential and final brightness will never become zero. The similarity between the characteristics of this curve and those obtained by Smith and Gessner is quite apparent.

The factor controlling the decay of brightness seems to be the change in the transmission constant of the material. In pure barium bromide this change is small and its rate of decay is also small. The final constant value of brightness for samples investigated by Smith varied from 40 percent to 60 percent of their maximum. On the other hand in pure radium bromide, which becomes

almost black, the rate of decay is very large and the final constant value of brightness is about 0.1 percent of its maximum. Both radium bromide and barium bromide completely recover their maximum brightness on heating to an adequate temperature. The heating results also in complete disappearance of any coloration.

According to this view luminous paints which have decayed should also regain their brightness if the coloration of the crystals is removed. This was attempted on some samples of zinc sulphide paints which had been allowed to decay for over eleven years in sealed tubes. The paints contained 50 and 100 micrograms of radium element, respectively, per gm of zinc sulphide. On heating the tubes over a bunsen burner the brightness was promptly restored but the degree of restoration could not be determined since no record of the initial brightness of the paint was available. The coloration of the samples disappeared at the same time and their photosensitiveness was also revived.

It is not claimed here that there is no chemical decomposition in the irradiated samples resulting in a decrease of light emission. But it has been shown that an attempt to explain the decay of luminescence as due to disappearance of active centers gives inconsistent results, and since it has been shown that the change in transmission constant plays such an important part in the apparent decay of brightness, a quantitative application of any theory of luminescence becomes difficult until the exact nature of this change is determined experimentally.

It has already been shown that the increase in absorption constant cannot be considered as due to the destruction of hypothetical active centers. On the other hand the curves representing the rise and decay of brightness do not furnish sufficient data to determine the nature of this change. Experiments are under way to determine directly the variation in the transmission constant of some of these materials as a result of irradiation, when a quantitative application of the assumptions made above to the experimental curves will become possible.

If the absorption coefficient a is defined by the expression $I_x/I = e^{-ax}$ where I_x/I is the fraction of light transmitted through thickness x of the absorbing material, it is quite evident that a is a variable quantity in this case, its value depending upon the nature and intensity of the radiation and the time.

$$a = f(R, t).$$

In correcting for the absorption of light by the walls of the glass containers Walsh assumes a transmission factor, due to the coloration of glass, of the form

$$T = e^{-pt}$$

where p is a constant for a given tube and t is the time. This is based on the assumption that the coloration of the glass is produced by the destruction of certain molecules in the glass. On this view the transmission should become zero when t is put equal to infinity. If, however, the coloration of transparent materials is due to ionization of the molecules, such ionization might have a

saturation value, in which case the transmission factor would be represented by an expression of the form

$$T = a \cdot e^{-\beta(1-e^{-ct})}$$

where a, b and c are constants for a given material and a given intensity of radiation of one type. In this expression the value of T is never equal to zero. This is more in accordance with the experimental facts. However this may prove to be, it has been shown that experimental results recounted in this paper cannot be satisfactorily explained on the active center theory of luminescence without further modification.

The writer wishes to acknowledge his indebtedness to Mr. Gessner for the use of data obtained by him and to Dr. H. C. Richards and Dr. E. E. Witmer for many valuable suggestions and criticisms during the preparation of this paper.

THE ELECTRIC FIELD, ATMOSPHERE AND EFFECTIVE TEMPERATURE OF THE SUN

By Ross Gunn
Naval Research Laboratory
Washington, D. C.

Abstract

The study of important electromagnetic effects in the solar atmosphere undertaken in previous papers is continued. It is shown that the large observed spread of effective temperatures of the sun's radiation can be accounted for by the presence of electric and magnetic fields in the solar atmosphere. The magnitude of the electric field at a level where the magnetic field is 25 gauss, calculated from the observed spread of temperatures, is found to be 0.015 volts.cm and agrees well with 0.013 volts/cm calculated earlier from the observed anomalous motions of the solar atmosphere. Gravitational equilibrium is found to be unnecessary in all regions of the atmosphere and it is shown that the "support" and stability of the chromosphere and its anomalous eastward motion are evidences of precisely the same electromagnetic mechanism. An electric field of the value given above is shown to account qualitatively for certain bright line spectra in the chromosphere of the sun. The strange observed relation between bright line spectra and rapid axial rotation of stars, just pointed out by O. Struve of the Yerkes Observatory, confirms in a striking manner some of the conclusions of this and earlier papers.

IN A series of papers it has been shown that the anomalies of the solar rotation arise from electromagnetic effects which take place in the crossed electric and magnetic fields existing in the ionized solar atmosphere. The magnitude and direction of the magnetic field is readily determined by observation, but the magnitude of the electric field is much too small to produce measurable Stark effects and must be inferred from the observed atmospheric motions. In the present paper we consider a method of calculating the magnitude of the electric field from spectroscopic data and will show that the departures of the solar radiation from that of black-body radiation lead to a value for the electric field which agrees with that calculated in earlier papers. Measurements show that the effective solar temperature calculated from the quality of solar radiation is over 1000° higher than that inferred from measurements of the density of radiation. The difference of the effective temperatures is so great that we must conclude that processes other than thermal must be present which add energy to the ions. It is clear that an electric field of sufficient magnitude might add energy to the ions during their free path so that on collision they would have energies higher than that indicated by the temperature of the region. A rough calculation shows that a radial electric field alone will not account for the observed features of the solar radiation, for if there were no solar magnetic field the conductivity of the atmosphere would be so great that electric fields would be very small. However, if we consider both electric and magnetic fields the difference in the effective temperatures is readily accounted for.

Effect of Crossed Electric and Magnetic Fields

In earlier papers[1] we considered the effect of crossed electric and magnetic fields on the electrical conductivity, diamagnetism and mass motion of an ionized gas. It has been shown[1] that diamagnetism limits the solar magnetic field and the resulting distribution is such that the field is nearly tangential to the surface over most of the sun. The electric field, by symmetry, must be radial so that in the following we may assume for simplicity that the electric and magnetic fields are always perpendicular.

The path described by an ion in perpendicular electric and magnetic fields is a cycloid.[2] An ion starting from rest is initially acted upon only by the electric field which accelerates the ion; as the velocity increases the magnetic force at right angles to its motion increases until the ion is moving at right angles to the electric field. The magnetic force continues to act and the ion is forced by its inertia to move against the electric field, whereby it loses energy till it comes to rest. The process then repeats itself again and again. The net result of this process is that the ion progresses in a direction perpendicular to both the electric and magnetic fields and on the average does not advance in the direction of the electric field.

It is clear that in certain parts of the cycloidal path the ion has much more energy than at other points, and if the ion collides at a point in its path where its energy is large, ionizing effects will be greater than if the ion collided in a part of the path where the energy is small. In the general case the ion starts its path with a certain thermal energy and in tracing its cycloidal path it acquires and loses energy repeatedly from the electric field. If R is the radius of the generating circle of the cycloidal path, E the average electric field encountered by the ion in its path, and e the ionic charge in e.m.u., then the difference in energy W of the ion between the top and bottom of its path is

$$W = 2REe. \tag{1}$$

This energy is obviously supplied by the electric rather than the magnetic field, for the motion of the ion is always at right angles to the magnetic force and hence the magnetic field cannot transfer energy to the ion or the ion energy to the magnetic field. It is of importance to note that Eq. (1) gives the maximum energy difference and no matter how long the free path, the ion cannot acquire more. We neglect the less frequent case of successive collisions where an ion of initially large energy collides with another at a favorable point in its path and this ion in turn picks up additional energy and passes it on to still another.

The radius of the cycloidal generating circle R is given by

$$R = \frac{mv}{Be}\left[1 - \frac{2u}{v}\cos\delta + \frac{u^2}{v^2}\right]^{1/2} \tag{2}$$

where m is the mass of the ion, v the initial ionic velocity in a plane perpen-

[1] R. Gunn, Phys. Rev. **32,** 133 (1928); **33,** 614 (1929); **33,** 832 (1929); **34,** 335, 1621 (1929); **35,** 635 (1930); **36,** 1251 (1930); **37,** 283 (1931).

[2] L. Page, Phys. Rev. **33,** 55? (1929).

dicular to the magnetic field B, u the ion drift velocity resulting from the crossed electric and magnetic fields and δ the angle between u and v. When the free paths are long and the electric and magnetic fields are perpendicular, u is given by

$$u = E/B. \tag{3}$$

A few of the ions will acquire and expend the maximum energy given by Eq. (1) and some will lose energy. To get the mean gain in energy for a typical ion we will simply take an arithmetical average and therefore we have from Eqs. (1), (2), and (3) that

$$W_1 = mvu\left(1 + \frac{u^2}{v^2}\right)^{1/2} = \frac{E}{B}\left[2mkT\left(1 + \frac{mE^2}{2kTB^2}\right)\right]^{1/2} \tag{4}$$

where W_1 is the approximate mean increase in energy and $(2\,mkT)^{1/2}$ has been written for mv. The mean increase in energy W_1 may, for convenience, be expressed in terms of an equivalent effective temperature and be equated to $3k\Delta T/2$ where k is the Boltzmann constant and ΔT is the change in effective temperature due to electrical effects. Making this substitution and transforming Eq. (4) we have

$$\frac{\Delta T}{T} = \frac{2u}{3}\left[\frac{2m}{kT}\left(1 + \frac{mu^2}{2kT}\right)\right]^{1/2} \tag{5}$$

or if we solve this for the electric field E we have

$$u^2 = \frac{E^2}{B^2} = \frac{kT}{m}\left[\left(1 + \frac{9}{4}\left(\frac{\Delta T}{T}\right)^2\right)^{1/2} - 1\right]. \tag{6}$$

In Eq. (5) we note that the difference in the effective temperatures is proportional to the square root of the ion mass. This indicates that the ions rather than the electrons are the particles effective in increasing the apparent temperature of the solar atmosphere although there is no reason why the ions cannot transfer their high energies to electrons by collision.

Departure from Black-Body Radiation

Several writers[3,4,5,6] have studied the solar radiation and found it to depart markedly from a black body distribution. At one time it was thought the departures were due to varying general absorption in the radiating layers but Milne[4] concluded that this was quite inadequate. Eddington[6] has reworked some of the data and gives 4660° for the effective temperature of the sun as calculated from the density of radiation and 5740° as the effective temperature calculated from the quality of the radiation. It is clear that the emitted light is much richer in high frequency radiation than would be the case if the sun radiated like a black body. The differences in the effective temperatures, or 1080°, is so great that the energies of some of the ions must be considerably more than that of the mean value. If we are not particularly

[3] C. G. Abbot, Annals Astrophys. Observ. Smithsonian Inst.
[4] E. A. Milne, Monthly Notices **81**, 375 (1921).
[5] Lundblad, Nova Acta, Reg. Soc. Sci. Upsalienses **6**, #1 (1923).
[6] Eddington, Internal Constitution of the Stars.

concerned with the detailed mechanism of the radiation process, Eq. (5) of the preceding section permits a test of our prediction that the effects arise from an electric field in the solar atmosphere. Earlier work[1] showed that the mean atomic weight of the solar atmosphere in the region of the reversing layer was 6.6 if no account were taken of the electrons, or calling the mass of the hydrogen atom h, the mean mass of the ions in the reversing layer is 6.6 h. Moreover, the superposed atmospheric drift velocity u is known from astronomical data to approximate 0.5 km/sec. Substituting in Eq. (5), $m=6.6h$; $h=1.64\times10^{-24}$ gm; $u=5\times10^{4}$ cm/sec; $k=1.37\times10^{-16}$ and $T=4660°$ we find $\Delta T/T=0.197$ so that $\Delta T=920°$. This value is to be compared with the observed value 1080° and is considered satisfactory because the method of averaging to get statistical values is rough. The agreement is greatly improved if we select a mean value for the effective temperature rather than the lower value derived from the density of the solar radiation. Observation shows that the superposed drift velocity u does not change rapidly with altitude in regions which can be observed so that according to Eq. (5), ΔT also changes but little with altitude. This is consistent with the observed fact that the intensity-frequency curve decreases very rapidly on the high frequency side of the maximum. Our calculations clearly indicate that the observed spread of effective temperatures can be accounted for by the presence of electric and magnetic fields in the solar atmosphere.

Magnitude of the Electric Field

In other papers[1] the relation of the mechanical motions of the solar atmosphere to electromagnetic effects was considered and it was concluded that the observed motions required that the solar atmosphere have an electric field directed radially inward and amounting to 0.013 volts/cm in the region where the magnetic field was 25 gauss. The magnitude of the electric field cannot be checked by Stark effect observations and it becomes necessary to look elsewhere for supporting evidence. The spread of observed effective temperatures provides an independent method of calculating the magnitude of the field and we turn at once to Eq. (6) which connects observed quantities with the electric field. We follow earlier work and take $m=6.6h$; $h=1.64\times10^{-24}$ gm; $k=1.37\times10^{-16}$; $T=4660°$; $\Delta T=1080°$ and $B=25$ gauss. Substitution in Eq. (6) gives $E=0.0148$ volts/cm. The agreement of this value with the earlier calculation[1] is most satisfactory and it is evident from the form of Eq. (6) that the agreement will be equally satisfactory at all other levels of the solar atmosphere. The present method of calculating the field is apparently incapable of determining the sign of the electric field, but, as we have pointed out previously, the sign inferred from the solar motions is precisely the sign observed on the earth, i.e., negative or radially inward. The agreement of the two methods of calculating the magnitude of the field strongly supports the conclusion that a solar electric field exists and that the mass motions of the atmosphere and the differences observed in the effective solar temperatures are simply different aspects of the same fundamental physical phenomena.

Stability of the Solar Atmosphere

Eclipse spectra show that large amounts of material, notably calcium, exist high in the chromosphere and the distribution of this material is such that it cannot well be in gravitational equilibrium with a supporting gaseous pressure. Milne[7] has attempted to account for the support and stability of this material by assuming that radiation pressure was great enough to overcome the gravitational forces. His calculations show that the calcium must absorb selectively in what appears to be a highly artificial manner. A still more serious objection to his theory is the fact that once sufficient absorption is built up by special assumptions the atom will be blown away from the sun because the radiation pressure does not decrease as rapidly as gravity. Thus Milne's atmosphere is unstable.[6]

Our study of electromagnetic effects suggests that the stability of the chromosphere does not depend on a specialized type of dance on a sunbeam but does depend on very real and sufficiently large electric and magnetic forces. Although the force on a positive ion in the solar atmosphere is vertically downward and hence in the same direction as gravity, we have seen that the ion does not move downward but on the average moves parallel to the solar surface. Thus ions executing long free paths in crossed magnetic and electric or gravitational fields are "supported" and can progress in the direction of the force field only by numerous collisions. It is therefore clear that it is not necessary to think of the very long free path ions in the solar atmosphere as being in gravitational equilibrium. To illustrate, suppose that neutral molecules of all materials are shot, undeviated by the magnetic or electric fields, by thermal processes to high altitude regions of low pressure where they immediately become ionized. The recombination coefficient will be different for different kinds of ions and those particles that remain neutral for an appreciable time will be acted on by gravity and drop to lower levels. The ions with very small recombination coefficients (calcium for example) will spend most of their life in an ionized condition and therefore will be "supported" and at the same time swept parallel to the solar surface with a velocity dependent on the ratio of the crossed electric and magnetic fields. Eventually an equilibrium condition will be reached and the supply of neutral calcium atoms will balance the loss of those dragged down by the electric field as the result of a large number of collisions and the few which are neutralized and fall under the action of gravity. We thus see that no special mechanism is necessary to account for the "support" of the chromosphere and that it is supported by precisely the same mechanism that produces its observed anomalous eastward drift.

Bright Line Spectra

Doubly reversed, or bright line spectra, are characteristic of certain types of stars but there have been theoretical difficulties in accounting for their presence. Eddington[6] has reviewed the subject and he concluded without attempting to make the statements quantitative, "that bright lines in the spectrum of a static star indicate that either (a) the star is greatly disturbed

[7] E. A. Milne, Monthly Notices **84**, 354 (1924).

by "thunderstorms" or (b) it is a nebulous star." The sun can hardly be called a nebulous star and we should be able to account for certain lines of the flash spectrum by electrical excitation of the type we have considered. The electrical field will add considerable energy only to an ionized particle and more analysis will be necessary to determine the exact mechanism by which an atom is excited to radiation. In another place we have expressed the ratio of the energy added to an ion, to its thermal energy in terms of temperatures and, as a numerical example, we will calculate the ratio of the energies for a helium ion. In Eq. (5) we will take $m=6.56\times10^{-24}$ gm; $u=5\times10^{4}$ cm/sec; $T=4660°$ and we find $\Delta T/T=0.16$; that is to say, all the helium ions periodically acquire energies 16 percent greater than their thermal energies. Similarly the added energy for calcium is 50 percent while that of hydrogen is only 8 percent. Thus we are led to believe that the additional energy available is adequate to produce bright line spectra. For the purpose of this paper, which is primarily concerned with the solar electric field, the rough value given above is adequate, but it is evident that a complete study of the bearing of an electric field on the ionization equilibrium relations in stars is necessary to give a complete description of the events. Saha's[8] theory of stellar ionization will be readjusted to take account of the fields and it is expected that such a readjustment will improve the agreement of his formula with observation.

Conclusion

We have indicated in outline that spectroscopic data regarding the sun bear out our earlier conclusion that electromagnetic phenomena are important in the solar atmosphere. It is rather surprising that the apparent solar rotation should be so closely related to the spectral distribution of radiation from the sun but we have had a suggestion that this might be true in a recent paper by Struve.[9] Dr. Struve has noticed a remarkable correlation between the rotation of stars and their spectral class. The early type stars rotate with great rapidity and several are apparently on the verge of rotational instability. The considerations of the present paper indicate that the early type stars have electric and magnetic fields of considerable magnitude and that our sun is probably a fair representative of stellar bodies. A complete study of the sun is therefore of the greatest importance if we are to understand and correctly interpret the physical phenomena which astronomers observe.

Note added March 24, 1931:

The March issue of the Astrophysical Journal has just appeared and contains another paper by O. Struve giving observational data which is in remarkable accord with the theory developed above. Dr. Struve states "Excessive rotations, estimated at 9 or 10 (. . . 250 km/sec.), are frequent. Apparently bright lines occur preferentially in stars having rapid axial rotation."

The relation of Eq. (5) shows that the ratio of the additional excitation energy to the thermal energy is directly proportional to the superposed drift velocity u. Thus theory predicts a strict parallelism between high *apparent* rotations and bright line spectra. Struve's results appear to be a beautiful confirmation of the material of this and preceding papers.

[8] M. N. Saha, Phil. Mag. **40**, 472, 809 (1920).

[9] O. Struve, Astrophys. J. **72**, 1 (1930).

MOLECULAR ASSOCIATION

By J. Albert Wehrle
Physical Laboratory, University of Pittsburgh

(Received March 20, 1931).

Abstract

To study the molecular association of nitrobenzene, the dielectric constant of mixtures of this substance with benzene (nonpolar solvent) and polar liquids (ethyl ether, chlorobenzene and acetone) was measured. The molar polarizations of the two polar substances were calculated as a function of the concentrations. If the dependence of the molar polarization of one polar liquid on the concentration of the other is taken as a measure of the association, the experiments show that the larger the electric moment of the molecule, the stronger is the association. They also show that association takes place not only between the molecules of a given substance, but also between two substances that may be quite different, provided they are both polar.

Introduction

THE polar liquids or gases, i.e., those whose molecules have an electric moment, show some deviation from simple additive or linear laws at certain concentrations. The explanation for these deviations is that the molecules associate, i.e., form complexes bound not by chemical forces but mainly by the electric fields of the dipoles.

From the dielectric constant point of view, this behavior may be described as follows: if a polar liquid (say nitrobenzene) is dissolved in a nonpolar liquid (say benzene) the variation of the polarization of the mixture as a function of the concentration of the polar liquid is, in general, not linear. In certain cases the apparent electric moment of the molecules is larger and in other cases smaller than that obtained from an extrapolation at infinite dilution, but is always variable with the concentration. The simplest theory of this effect is that the polar molecules associate to produce a sort of polymerized molecule having a smaller or larger moment depending on the relative orientations of the dipoles forming the complex.[1]

Debye[2] has proposed a simple theory of this effect corresponding to the theory that he and Hueckel have given for electrolytes. However the assumptions he had to make, for instance spherical molecules with the dipole at the center, seem too far from reality to confer much value to the theory according to which the polarization per mole should increase with concentration if association takes place. This however is true experimentally only for alcohols. Another theory apparently less general and with looser foundations has been given by Wolfke.[3]

[1] C. P. Smyth, Chem. Rev. 6, No. 4, (1929).
[2] Debye, Handbuch der Radiologie, Vol. 6.
[3] Wolfke, Phys. Zeits. 29, 713 (1928).

It seemed thus commendable to accumulate data on the phenomenon of association before the theory could be advanced very much, hence this investigation.

If an electric field is responsible for the association one would expect it to depend (a) on the temperature, because it controls the motion of the molecules, (b) on the magnitude of the electric moment and (c) on the shape of the molecules. Data available at the present time give information concerning the association of a substance with itself alone.[4] Our experiments investigate the association of one type of molecule with another, in particular with respect to factor (b). Special consideration was given to the association of

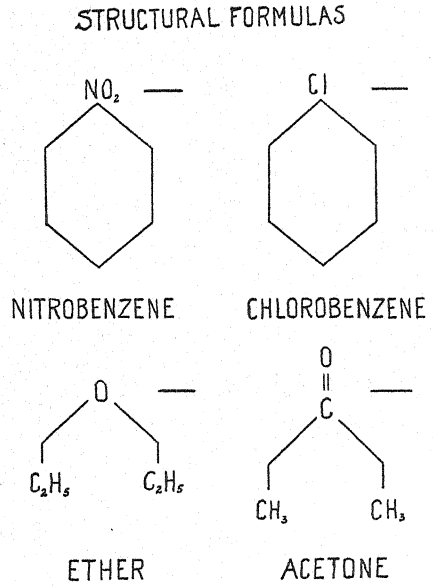

Fig. 1. Structural formulas of the compounds used. Probable polarity indicated.

nitrobenzene[5] ($\mu = 3.90 \times 10^{-18}$) with ether ($\mu = 1.24 \times 10^{-18}$), chlorobenzene ($\mu = 1.52 \times 10^{-18}$) and acetone ($\mu = 2.70 \times 10^{-18}$), μ being the electric moment, in e.s.u. $\times$ cm. The final results of our experiments give some indication of the effect of the electric moment as well as that of the shape of the molecule on the degree of association. The structural formulas, Fig. 1, may be of service when considering the effect of the position of the moment in the molecule.

Simple Theory of the Dielectric Constant of Mixtures

Debye[2] has shown that the dielectric constant, ϵ, of a mixture under all conditions satisfies the equation

$$\frac{\epsilon - 1}{\epsilon + 2} = \frac{4\pi}{3}(n_1\alpha_1 + n_2\alpha_2 + \cdots) \qquad (1)$$

[4] Rolinski, Phys. Zeits. **29**, 658 (1928).
[5] J. W. Williams, Phys. Zeits. **29**, 178 (1928).

where n_i is the number of molecules of type i per unit volume, and α_i is given by

$$\alpha_i = a_i + \frac{\mu_i^2}{3kT} \tag{1a}$$

where a_i comes from the deformation of the molecules, μ_i is the permanent electric moment, k is Boltzmann's constant and T the absolute temperature.

If we introduce as new variables the mole fraction $f_i = n_i/\Sigma n_i$ and the polarization $P_i = 4\pi N\alpha_i/3$
we get from (1)

$$P = \frac{\epsilon - 1}{\epsilon + 2}\frac{\Sigma f_i M_i}{d} = \Sigma P_i f_i \tag{2}$$

where M_i is the molecular weight and d the density of the mixture.

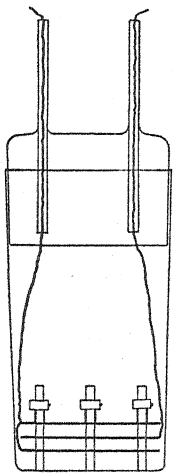

Fig. 2. Sectional view of test condenser and cell.

The theory underlying this formula requires a complete independence of the molecules. If however there is association, we can retain the same expression, assuming then that the apparent moment μ_i varies. Thus the P_i's which are really molecular constants vary also, and their variation may be taken as a measure of the degree of association.

Our experiments consisted in measuring the dielectric constant, ϵ, of mixtures of known concentration f_i. After determining the density, d, the value of P could be obtained.

Apparatus and Procedure

A simple resonance circuit was used in the measurement of the dielectric constant of the mixtures investigated. A standard condenser of 2500$\mu\mu$f and a test condenser (Fig. 2) of approximately 40$\mu\mu$f connected in parallel, constituted the capacity of the absorbing circuit. A quartz crystal oscillator (Fig.

3), wavelength 525 meters, supplied the energy. Resonance was determined by the maximum galvanometer deflection in a galena crystal rectifier circuit tapped across a few turns of the inductance of the absorbing circuit. There

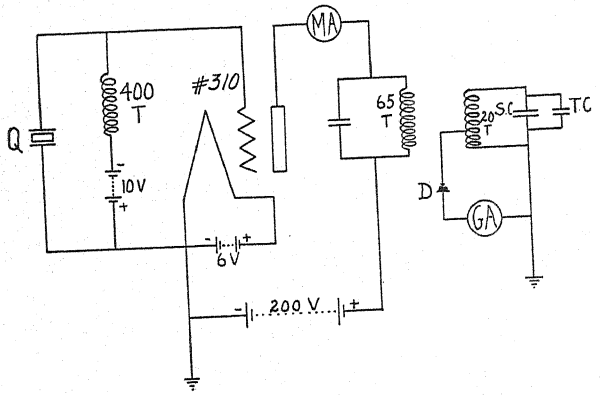

Fig. 3. Oscillator and absorption circuits.

was usually enough energy absorbed from the oscillator to obtain a maximum deflection of 30 to 40 cm, even when only one-tenth of the current passed through the galvanometer.

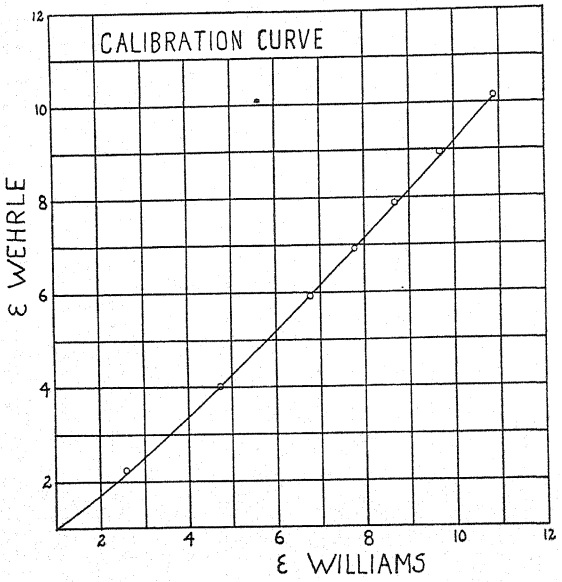

Fig. 4. Calibration curve of test condenser.

The procedure of a test involved the determination of resonance with (a) the standard condenser and the leads of the test condenser in the circuit; (b) the empty test condenser included in the circuit; (c) the mixture under investigation in the test cell.

The uncorrected experimental value of the dielectric constant of any particular solution studied was calculated from the relation

$$\epsilon_s = \frac{C_s}{C_a} = \frac{\frac{\epsilon_s A n}{4\pi d}}{\frac{\epsilon_a A n}{4\pi d}}$$

where C_a, C_s, are capacities of the test condenser with air and with the solution, respectively; ϵ_a, ϵ_s, the corresponding dielectric constants; A, the area per plate of the test condenser; n, the number of plates of dielectric; d, the plate spacing.

Values of dielectric constant for various concentrations of carbon disulphide and nitrobenzene were plotted (Fig. 4) against values, assumed true for the same concentration as reported by J. W. Williams.[6] This plot was taken as the calibration curve of the test condenser and was used in correcting ϵ_s values.

Measurements of ϵ_s were made at a temperature of 25°C ± 0.5° and could be reproduced in practically all cases to within less than 1 percent. It is to be observed that while the method is quite convenient and of fair accuracy, it proves, in its present form, unsatisfactory for values of dielectric constant above ten. This may be due to any one or possibly both the following causes: (a) once this region of dielectric constant has been attained, the galvanometer deflection has materially decreased and, due to a lack of sensitivity, the motion of the mirror has become relatively sluggish; (b) the introduction of a solution of dielectric constant of the order specified above gives rise to appreciable displacement currents in the dielectric. This is equivalent to adding an effective resistance to the L and C of the pick-up circuit, resulting in a flattening of the resonance peak.

The solutions tested consisted of several series composed of a nonpolar type, benzene, and two polar types, ether and nitrobenzene, chlorobenzene and nitrobenzene or acetone and nitrobenzene. From the stock solutions, test solutions of 150 cc each were prepared containing nitrobenzene in concentration of 0, 2, 4, 6, 8, 10 percent by volume, respectively.

Densities were obtained by means of a Mohr balance. An Abbe refractometer served for the refractive index determination.

Purification of Materials

As it was not the purpose of these experiments to conduct an investigation of the highest precision, but rather to discover some facts about molecular association, the materials used were subjected only to the following purifications.

Benzene. The first sample, thiophene free, was frozen out twice and fractionated. In the case of the second sample, drying with phosphorus

[6] Williams and Ogg, Jour. Amer. Chem. Soc. **50**, 96 (1928).

pentoxide and fractionation yielded a product whose constants were practically identical with those of the sample originally prepared.

Ether. The best grade obtainable was used as supplied by the manufacturer.

Carbon disulphide. After a preliminary agitation with mercury, to remove foreign sulphides, it was dried with phosphorus pentoxide and fractionated.

Chlorobenzene. A sufficient quantity of a high grade material was secured to meet all the needs of the contemplated experiments and was used as supplied.

Acetone. To secure a water-free product, the material was refluxed for three hours over potassium hydroxide and distilled. A further drying over night with fused calcium chloride, refluxing for two hours and fractionation completed the process.

Results

Results are given in Tables I–III. The curves shown are illustrative of the data on benzene, ether and nitrobenzene.

Table I. *Data for solutions of ether and nitrobenzene in benzene.*

f_1	f_2	f_3	ϵ	d	n	P_{123}	P_{23}
1.0000	0.0000	0.0000	2.16	0.8731	1.4980	26.01	0.00
.9825	.0000	.0175	2.62	.8777	1.4995	31.36	5.81
.9648	.0000	.0351	3.04	.8844	1.5001	36.45	11.35
.9472	.0000	.0528	3.40	.8910	1.5012	40.13	15.48
.9294	.0000	.0706	3.80	.8982	1.5026	43.67	19.50
.9115	.0000	.0885	4.18	.9032	1.5037	46.73	23.03
0.8242	0.1758	0.0000	2.55	0.8447	1.472	31.21	9.31
.8094	.1726	.0179	3.00	.8534	1.474	36.65	15.13
.7945	.1694	.0351	3.51	.8608	1.478	41.79	20.67
.7795	.1665	.0540	3.94	.8690	1.481	45.48	24.76
.7647	.1631	.0722	4.35	.8770	1.482	48.53	28.20
.7496	.1599	.0905	4.83	.8843	1.483	51.69	32.56
0.6374	0.3626	0.0000	3.05	0.8141	1.4420	38.21	21.26
.6259	.3560	.0184	3.50	.8220	1.4440	42.87	26.23
.6138	.3492	.0369	3.94	.8301	1.4464	46.71	30.40
.6026	.3428	.0555	4.33	.8383	1.4489	49.75	33.73
.5908	.3361	.0731	4.74	.8473	1.4516	52.41	36.70
.5783	.3290	.0927	5.11	.8557	1.4541	54.68	39.30
0.4386	0.5614	0.0000	3.41	0.7851	1.4174	43.04	31.38
.4303	.5508	.0189	3.98	.7959	1.4197	47.64	36.15
.4220	.5402	.0378	4.30	.8047	1.4223	50.42	39.19
.4137	.5295	.0568	4.78	.8151	1.4268	53.66	42.67
.4054	.5188	.0758	5.22	.8253	1.4303	56.26	45.48
.4011	.5134	.0959	5.63	.8357	1.4333	59.01	48.35
0.2266	0.7734	0.0000	3.88	0.7487	1.3830	49.09	43.21
.2221	.7582	.0196	4.32	.7590	1.3865	52.56	46.78
.2177	.7431	.0392	4.72	.7694	1.3910	55.31	49.65
.2132	.7279	.0588	5.10	.7784	1.3945	57.74	52.20
.2088	.7127	.0784	5.48	.7889	1.3986	59.80	54.37
.2043	.6975	.0981	5.84	.7997	1.4028	61.54	56.22

TABLE I. (*Continued*)

f_1	f_2	f_3	ϵ	d	n	P_{123}	P_{23}
0.0000	1.0000	0.0000	4.55	0.7118	1.3521	56.42	56.42
.0000	.9795	.0205	5.00	.7232	1.3559	59.34	59.34
.0000	.9591	.0409	5.47	.7348	1.3612	61.98	61.98
.0000	.9386	.0613	5.89	.7454	1.3663	64.10	64.10
.0000	.9183	.0817	6.31	.7569	1.3715	65.93	65.93
.0000	.8979	.1021	6.73	.7696	1.3768	67.46	67.46

f_1, f_2, f_3 are mole fractions of benzene, ether and nitrobenzene, respectively; ϵ, n, d are corrected dielectric constant, index of refraction and density, respectively; P_{123} the polarization of the three-component solution calculated from Eq. (2); P_{23} the polarization of ether and nitrobenzene alone, calculated from $P_{23}=P_{123}-f_1 P_1$.

TABLE II. *Data for solutions of chlorobenzene and nitrobenzene in benzene.*

f_1	f_2	f_3	ϵ	d	n	P_{123}	P_{23}
1.0000	0.0000	0.0000	2.16	0.8731	1.4970	26.01	0.00
.9825	.0000	.0175	2.62	.8777	1.4982	31.36	5.81
.9648	.0000	.0351	3.04	.8844	1.4993	36.45	11.35
.9472	.0000	.0528	3.40	.8910	1.5005	40.13	15.48
.9294	.0000	.0706	3.80	.8982	1.5016	43.67	19.50
.9115	.0000	.0885	4.18	.9032	1.5028	46.73	23.03
0.8207	0.1793	0.0000	2.87	0.9156	1.5022	35.34	13.99
.8059	.1761	.0180	3.25	.9208	1.5031	39.54	18.58
.7910	.1728	.0362	3.61	.9274	1.5041	42.88	22.30
.7761	.1696	.0543	3.98	.9334	1.5049	46.11	25.92
.7612	.1663	.0725	4.35	.9388	1.5058	48.92	29.12
.7462	.1630	.0908	4.68	.9452	1.5068	51.16	31.75
0.6318	0.3682	0.0000	3.46	0.9622	1.5072	42.50	26.07
.6202	.3614	.0184	3.83	.9673	1.5080	45.85	29.72
.6080	.3543	.0377	4.13	.9714	1.5088	48.35	32.54
.5968	.3478	.0554	4.50	.9766	1.5097	51.02	35.50
.5850	.3409	.0741	4.82	.9814	1.5105	53.17	37.92
.5731	.3340	.0929	5.18	.9867	1.5113	55.32	40.41
0.4327	0.5673	0.0000	4.06	1.0079	1.5108	48.91	37.65
.4245	.5566	.0189	4.39	1.0113	1.5115	51.46	40.42
.4163	.5458	.0379	4.73	1.0150	1.5123	53.83	43.00
.4081	.5350	.0569	5.04	1.0193	1.5129	55.77	45.16
.3998	.5242	.0760	5.33	1.0230	1.5133	57.48	47.08
.3915	.5133	.0952	5.68	1.0269	1.5141	59.37	49.19
0.2224	0.7776	0.0000	4.58	1.0510	1.5173	54.28	48.49
.2181	.7625	.0194	4.84	1.0547	1.5179	56.01	50.34
.2142	.7472	.0386	5.21	1.0578	1.5184	58.25	52.69
.2094	.7321	.0585	5.51	1.0603	1.5190	59.99	54.54
.2051	.7169	.0780	5.83	1.0635	1.5196	61.64	56.31
.2007	.7017	.0976	6.11	1.0667	1.5201	62.99	57.77
0.0000	1.0000	0.0000	5.22	1.0997	1.5227	58.90	58.90
.0000	.9685	.0315	5.51	1.1017	1.5231	61.48	61.48
.0000	.9488	.0512	5.84	1.1034	1.5236	63.28	63.28
.0000	.9290	.0710	6.13	1.1052	1.5240	64.65	64.65
.0000	.9092	.0908	6.40	1.1073	1.5245	65.85	65.85
.0000	.8895	.1105	6.72	1.1087	1.5250	67.27	67.27

f_1, f_2, f_3 are mole fractions of benzene, chlorobenzene and nitrobenzene, respectively; ϵ, n, d are corrected dielectric constant, index of refraction and density, respectively; P_{123} the polarization of the three-component solution calculated from Eq. (2); P_{23} the polarization of chlorobenzene and nitrobenzene alone, calculated from $P_{23}=P_{123}-f_1 P_1$.

TABLE III. *Data for solutions of acetone and nitrobenzene in benzene.*

f_1	f_2	f_3	ϵ	d	n	P_{123}	P_{23}
1.0000	0.0000	0.0000	2.16	0.8731	1.4980	26.01	0.00
.9825	.0000	.0175	2.62	.8777	1.4995	31.36	5.81
.9648	.0000	.0351	3.04	.8844	1.5001	36.45	11.35
.9472	.0000	.0528	3.40	.8910	1.5012	40.13	15.48
.9294	.0000	.0706	3.80	.8982	1.5026	43.67	19.50
.9115	.0000	.0885	4.18	.9032	1.5037	46.73	23.03
0.8806	0.1194	0.0000	3.48	0.8632	1.4827	39.68	16.77
.8655	.1173	.0172	3.82	.8695	1.4838	42.64	20.13
.8503	.1153	.0344	4.31	.8770	1.4848	46.24	24.12
.8350	.1132	.0518	4.52	.8837	1.4862	47.74	26.02
.8196	.1111	.0693	4.90	.8906	1.4871	50.12	28.80
.8041	.1090	.0869	5.23	.8979	1.4885	51.96	31.05
0.7663	0.2337	0.0000	4.70	0.8541	1.4668	47.46	27.53
.7534	.2298	.0168	5.03	.8616	1.4686	49.39	29.80
.7404	.2258	.0338	5.31	.8687	1.4704	50.96	31.70
.7273	.2218	.0509	5.65	.8757	1.4720	52.71	33.79
.7141	.2178	.0681	5.96	.8824	1.4738	54.22	35.65
.7009	.2138	.0853	6.26	.8892	1.4753	55.60	37.37
0.6567	0.3433	0.0000	5.93	0.8458	1.4534	52.33	35.25
.6459	.3376	.0165	6.26	.8535	1.4553	53.77	36.97
.6349	.3319	.0332	6.55	.8611	1.4577	54.98	38.46
.6239	.3262	.0499	6.83	.8679	1.4594	56.14	39.91
.6130	.3205	.0665	7.12	.8751	1.4613	57.25	41.31
.6017	.3146	.0837	7.47	.8822	1.4634	58.51	42.86

f_1, f_2, f_3 are mole fractions of benzene, acetone and nitrobenzene, respectively; ϵ, n, d are corrected dielectric constant, index of refraction and density, respectively; P_{123} the polarization of the three-component solution calculated from Eq. (2); P_{23} the polarization of acetone and nitrobenzene alone, calculated from $P_{23}=P_{123}-f_1 P_1$.

Values of P_{23} were plotted against mole fraction of nitrobenzene at constant ether, and against mole fraction of ether at constant nitrobenzene. They were obtained from P_{123} by subtracting the polarization due to benzene, which is known to remain constant, as it is nonpolar and does not associate. P_{23} then represents the polarization due to the polar substances and can be expressed as

$$P_{23} = f_2 P_2(f_2, f_3) + f_3 P_3(f_2, f_3). \tag{3}$$

P_2 and P_3 are written explicitly as functions of f_2 and f_3 because they associate and because the association depends upon the concentration. Differentiating (3) with respect to f_2 and putting $f_2 \to 0$, we obtain

$$\left(\frac{\partial P_{23}}{\partial f_2}\right)_{f_2 \to 0} = (P_2(f_2, f_3))_{f_2 \to 0} + \left(\frac{\partial P_3(f_2, f_3)}{\partial f_2}\right)_{f_2 \to 0}$$

and a similar expression for

$$\left(\frac{\partial P_{23}}{\partial f_3}\right)_{f_3 \to 0}.$$

Illustrative curves are presented in Figs. 5, 6, 7, 8. The fact that the curves vary with f_3 or f_2 shows definitely that P_2 and P_3 are both functions of f_3 and f_2,

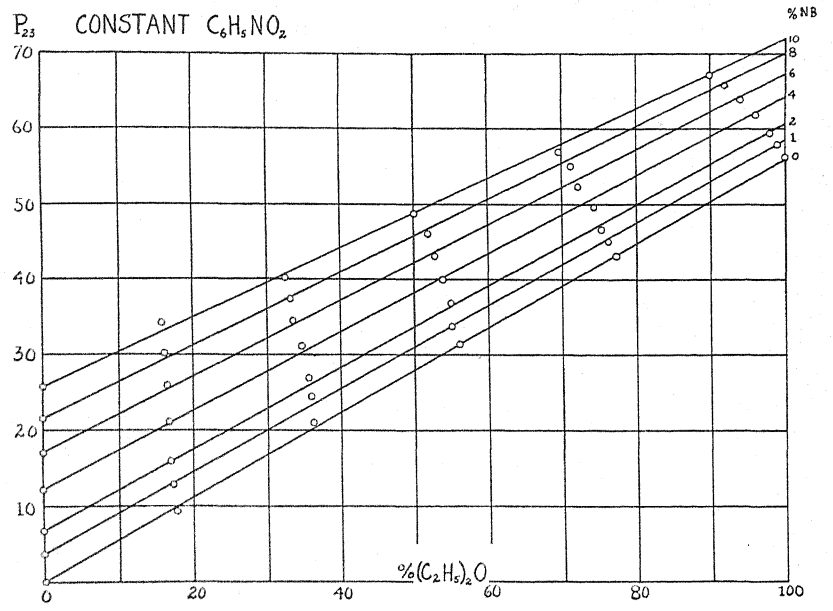

Fig. 5. Polarization, P_{23}, of nitrobenzene and ether in benzene against percent ether for several constant percentages of nitrobenzene.

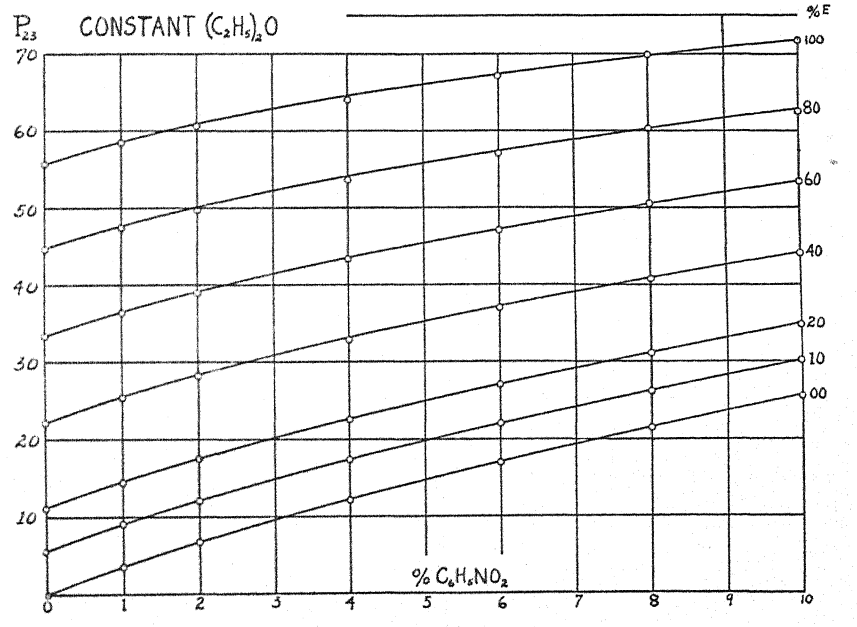

Fig. 6. The data of Fig. 5 differently presented showing polarization, P_{23}, of nitrobenzene and ether in benzene against percent nitrobenzene for several constant percentages of ether. The curve for 100 percent ether is plotted from extrapolated physically impossible, portions of Fig. 5.

which means that nitrobenzene does associate with ether. If there were no association,

$$\left(\frac{\partial P_{23}}{\partial f_2}\right)_{f_2 \to 0} \quad \text{and} \quad \left(\frac{\partial P_{23}}{\partial f_3}\right)_{f_3 \to 0}$$

should be constant as P_2 would then not be function of f_3 nor P_3 function of f_2.

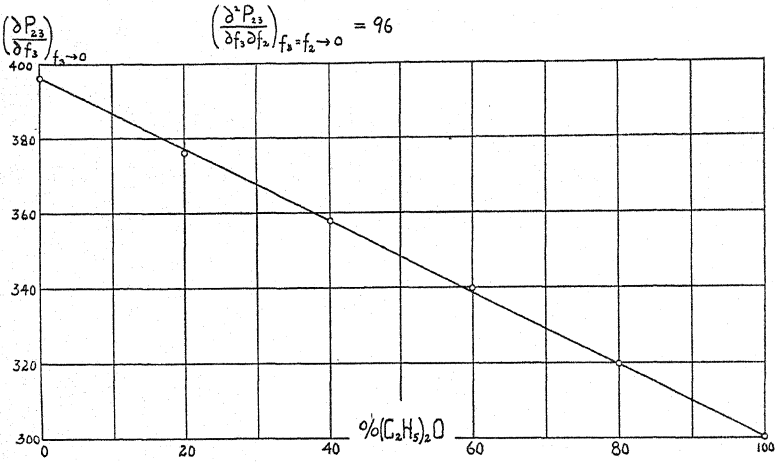

Fig. 7. Plot of the slopes of the curves of Fig. 6 at f_3, the concentration of nitrobenzene approaching zero. The slope of Fig. 7 is an approximate relative measure of the association of ether and nitrobenzene.

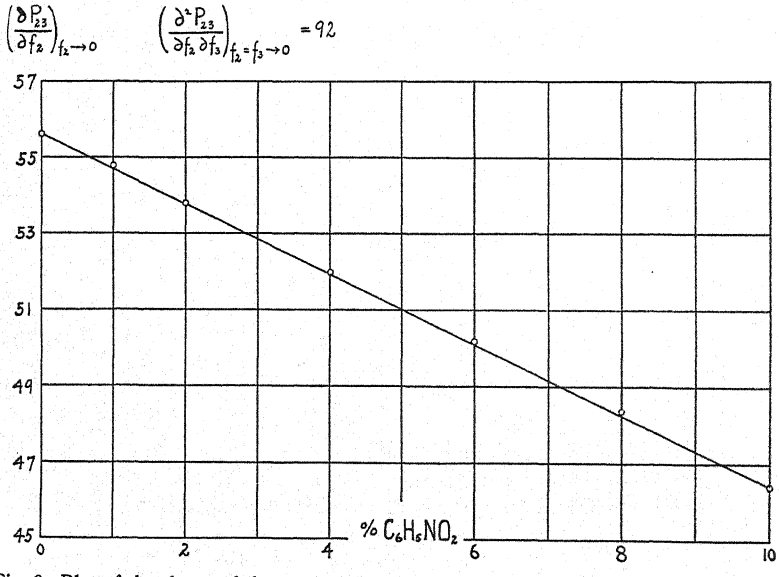

Fig. 8. Plot of the slopes of the curves of Fig. 5 at f_2, the concentration of ether approaching zero. The slope of Fig. 8 is an approximate relative measure of the association of nitrobenzene and ether. Note the corresponding value in Fig. 7.

Thus the curves are a definite proof of the association of nitrobenzene with ether, chlorobenzene and acetone. We can take the slopes of these curves, at

zero concentration, as an approximate relative measure of the degree of association. For this slope we write

$$a = \left(\frac{\partial^2 P_{23}}{\partial f_2 \partial f_3} = \frac{\partial P_2}{\partial f_3} + \frac{\partial P_3}{\partial f_2}\right)_{f_2 = f_3 \to 0}. \tag{4}$$

This quantity furnishes us a numerical estimate of the extent to which the polarizations depend on the concentration. From our data these results follow:

TABLE IV.
Association of nitrobenzene with

Substance	$\mu 10^{18}$	a
Nitrobenzene	3.90	1185
Acetone	2.70	690
Chlorobenzene	1.52	270
Ethyl ether	1.24	94

As was expected, the larger the moment, the more pronounced was the association. It seems that the most important factor determining the degree of association is the electric moment of the molecule.

Another question presents itself at this point. Do the association molecules share their electrons or not? The relation $\epsilon = n^2$ allows an answer. The calculation of P_∞ from Eq. (2), replacing ϵ by n^2 and omitting the term $\mu_i^2/3kT$ of (1a) gives

$$P_\infty = \frac{n_1^2 - 1}{n_1^2 + 2}\frac{M_1 f_1}{d_1} + \frac{n_2^2 - 1}{n_2^2 + 2}\frac{M_2 f_2}{d_2} + \frac{n_3^2 - 1}{n_3^2 + 2}\frac{M_3 f_3}{d_3} \tag{5}$$

calculated on the basis that the components act individually and

$$P_\infty' = \frac{n_1^2 - 1}{n_4^2 + 2}\frac{M_1 f_1 + M_2 f_2 + M_3 f_3}{d_4} \tag{6}$$

on the basis that the components act collectively, where n_1, n_2, n_3, n_4, and d_1, d_2, d_3, d_4 are the refractive indices and densities of benzene, ether, nitrobenzene, and the mixture of the three under consideration, P_∞ is the polarization at infinite dilution. The comparison results in values which check within the limits of experimental errors. An illustrative example of the comparison of P_∞, from Eq. (5), and P_∞', from Eq. (6), for a mixture of benzene, ether and nitrobenzene is given in Table V.

TABLE V.

f_1	f_2	f_3	n_4	d_4	P_∞	P_∞'
0.6374	0.3626	0.0000	1.4418	0.8141	24.87	24.89
.6259	.3560	.0184	1.4440	.8220	25.02	25.05
.6138	.3492	.0369	1.4464	.8301	25.16	25.18
.6026	.3428	.0555	1.4489	.8384	25.33	25.35
.5908	.3361	.0731	1.4516	.8473	25.44	25.46
.5783	.3290	.0927	1.4541	.8557	25.59	25.61

Hence it is to be concluded that there is no sharing of electrons in this process.

Conclusion

Before anything more definite can be obtained from the measurements, a working hypothesis as to the true nature of association must be formulated. Such a project is at present under investigation.

Acknowledgment

The author wishes to thank Dr. Weigle, who suggested this problem, and the members of the Physics department for their kind cooperation.

NOTES ON THE EFFECT OF DISTANCE FROM THE SOURCE ON THE VELOCITY OF SOUND AT ULTRASONIC FREQUENCIES

By Charles D. Reid
Cruft Laboratory, Harvard University

(Received March 20, 1931)

Abstract

Measurements of the velocity of ultrasonic waves have been made at a greater distance than heretofore. It is found to be independent of frequency within 0.01 percent which is the error of measurement.

In A previous paper[1] a method of obtaining the velocity of ultrasonic waves was described. It was found that when measurements were taken in proximity to the face of the sound-emitting crystal the resulting velocity was higher than that calculated from data obtained in a region more remote from the face. It was also noted that this effect was more marked as the frequency decreased. Hence it seemed desirable to continue the measurements in a region still more remote from the sound source, since the previous work indicated that an asymptotic value had almost been reached.

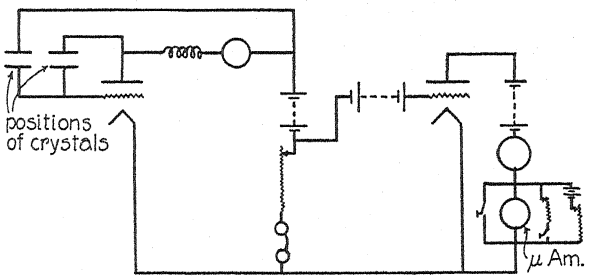

Fig. 1. Direct current amplifier.

With this in mind, the length of the sound chamber was doubled, and a direct current amplifier (shown in Fig. 1) was constructed in order to detect the sound energy at this increased distance. By using the proper grid bias on the amplifier tube the change in plate current produced by the motion of the reflector was increased by a factor of ten.

With the use of this amplifier, the measurements recorded here were made from the data secured in the region between 50 centimeters and 100 centimeters from the sound source.

To obtain satisfactory stationary wave-trains in this region it was found necessary to pad the inside of the sound chamber with acoustic felt to reduce

[1] C. D. Reid, Phys. Rev. **35**, 814 (1930).

the effect of reflected energy from the walls. This prevented the use of dry air in the present experiments as it has been found difficult to dry out the felt. However, the felt lining does maintain the humidity at a constant value and the experimental results have been corrected for this humidity.

In order to determine the value of the humidity thus obtained, a hair hygrometer was calibrated over a small range of humidities by placing it under a bell jar with two different saturated salt solutions and assuming that the motion of the hygrometer needle in the interval between these fixed humidities to be a linear function of the humidity.

The results of these measurements are recorded in Table I.

TABLE I. *The velocity of sound in moist air free from carbon dioxide.*

Frequency	No. of runs	Velocity at 0°C
140	2	332.09
105	7	332.05
84	3	332.12
70	4	332.05
60	2	332.01
42	4	332.15

Average velocity at 0°C 332.08 ± 0.02 meters/sec.
Relative humidity 32 per cent
Velocity in dry air at 0°C—$V_H - 0.014\ H = V_0$
$332.08 - 32 \times 0.014 = 331.63$ meter/sec.

From the figures recorded in Table I it may be concluded that the velocity of sound in the frequency range included is constant within 0.01 percent when the measurements are carried out in a region sufficiently remote from the source.

When the velocity obtained in this manner is corrected for humidity by use of the relation determined by previous experiments it is found to agree with the former results within experimental error. This serves as a check on the humidity formula.

The above experiments have been carried on under the direction of Dr. G. W. Pierce.

THE POLARIZATION AND THE ELECTRIC MOMENT OF TUNG OIL[1]

By A. A. Bless
University of Florida

(Received March 12, 1931)

Abstract

The molar polarization of tung oil was determined by the method of mixtures using the relation $P_{1,2}=[(\epsilon-1)/(\epsilon+2)]\,(M_1f_1+M_2f_2)/d=P_1f_1+P_2f_2$ where ϵ is the dielectric constant; d the density of the solution; f_1f_2, M_1M_2, and P_1P_2 are respectively the mole fraction, the molecular weight and the polarization of the two components. The molar polarization of tung oil is 360 cc and the moment is 2.29×10^{-18} e.s.u. Eq. (1) is derived with the simplifying assumption that the internal field of the molecules may be neglected. It applies only to gases and to very dilute solutions, where the molecules are far apart. It is found that in the case of tung oil Eq. (1) applies for all concentrations, showing that the clustering of the molecules is such as to neutralize the internal field. The values of the moment of tung oil and of ethyl ether were determined from the variation of the polarization with temperature using the relation $P=(4\pi N/3)(\alpha+\mu^2/3KT)$ where P is the molar polarization, α the molecular polarization, N Avogadro's number, K Boltzmann's constant, T the absolute temperature and μ the electric moment. The values do not agree at all with those obtained by the method of mixtures. Similar disagreement was observed by other experimenters. The explanation is suggested that the internal field is never completely eliminated, and that the residual field being a function of the temperature makes Eq. (2) inapplicable even to dilute solutions.

Method of Mixtures

THE molar polarization of a mixture of two substances is given by[2]

$$P_{1,2}=\frac{\epsilon-1}{\epsilon+2}\,\frac{M_1f_1+M_2f_2}{d}=P_1f_1+P_2f_2 \qquad (1)$$

where f_1, f_2 and M_1, M_2 and P_1P_2 are, respectively, the mole fraction, the molecular weight and the polarization of the two components; d is the density and ϵ the dielectric constant of the solution. Since $f_1=1-f_2$, Eq. (1) may also be written in the form

$$P_{1,2}=f_2(P_2-P_1)+P_1. \qquad (2)$$

showing that $P_{1,2}$ is a linear function of f_2. Eq. (1) is deduced from the Clausius-Mosotti relation, that the quotient $(\epsilon-1)/(\epsilon+2)$ is proportional to the density. This relation is derived with the simplifying assumption that the internal electric field of the molecules may be neglected. In case of polar substances, equation (1) would be applicable only when the molecules are far

[1] Paper read at the meetings of the Committee on Electrical Insulation of the National Research Council, November 7, 1930.

[2] P. Debye, Polar Molecules, the Chemical Catalog Co., 1929.

apart, as in gases or in dilute solutions of a polar substance in a nonpolar solvent. $P_{1,2}$ is proportional to f_2 only when f_2 is a small fraction. The departure from proportionality between $P_{1,2}$ and f_2 for high concentrations of the polar substance may be taken as indicating the interaction of molecular fields. To find the polarization of a liquid substance the procedure is to dissolve the polar substance in a nonpolar solvent, determine the polarization for increasing mole fractions of the solute and then extrapolate for infinite dilution. This method was used to determine the electric moment of tung oil using benzene as the nonpolar solvent.

The quantities which are measured experimentally are the density and the dielectric constant of the solutions. The density was determined by the pyknometer method with an accuracy of about 0.02 percent. The dielectric constant was found in the usual manner, from the measured capacity of the test cell in air and in the liquid, the capacities being determined by the substitution method.

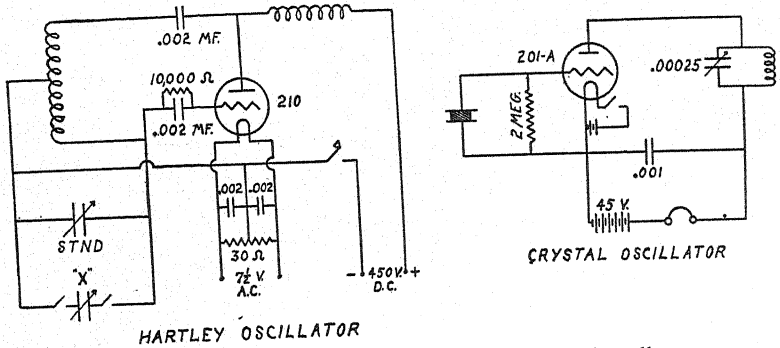

Fig. 1. The circuit for measuring the capacity of the cell.

Two different circuits were used for finding the dielectric constant of the solutions. In the first circuit a Hartley oscillator was used as a source of oscillations, the frequency being measured with a standard General Radio wave meter. In the receiving circuit a small aluminum condenser of known capacity placed in a vessel containing the solution was connected in parallel with a standard General Radio precision condenser. The receiving circuit was first tuned to resonance with the oscillator with both condensers in parallel and then retuned again to resonance with the standard alone in the circuit. The difference between the two readings of the condenser gave the capacity of the aluminum cell. These measurements were made for three different frequencies, 10^5, 3×10^5, 10^6. The accuracy of this method was about 1 percent.

The accuracy was very greatly increased when a heterodyne beat method was substituted for the above. The oscillations were kept at a constant frequency by the aid of a quartz crystal oscillator. A Hartley oscillator containing the test cell and the precision condenser was tuned to beat with the crystal set, the disappearance of the note indicating resonance. The capacity of the test cell was found in the same manner as in the first circuit. The polarization

of the solution was then calculated from the data using relation (1). The circuit is shown in Fig. 1.

The tung oil used in these experiments was obtained from the Chemistry Department of this University. Several samples of the product were tried, all giving very consistent results.

Data obtained using the Hartley oscillator are given in Table I.

TABLE I.

		$\nu=10^5$		$\nu=5\times10^5$		$\nu=10^6$	
f	d	ϵ	P	ϵ	P	ϵ	P
0.0000	0.878780	2.258	25.98	2.260	26.20	2.258	25.98
.0082	.8806	2.278	29.01	2.270	28.18	2.280	29.50
.0318	.8922	2.470	39.04	2.452	38.60	2.452	38.60
.0840	.9076	2.602	52.82	2.675	54.30	2.701	55.83
.2300	.9227	2.901	100.20	2.920	101.20	2.930	102.00
.4270	.9297	2.960	162.00	3.012	165.50	3.045	167.50
.7900	.9337	3.065	279.80	3.140	286.00	3.142	286.60
1.0000	.9363	3.170	356.80	3.178	358.00	3.172	357.00

Data obtained by the heterodyne beat method are shown in Table II.

TABLE II.

		$\nu=1.47\times10^6$	
f	d	ϵ	P
0.0000	0.8751	2.265	26.44
.0165	.8888	2.341	31.25
.0556	.9001	2.624	45.70
.1655	.9172	2.892	73.70
.3835	.9275	3.192	144.5
.6643	.9344	3.214	233.5
1.0000	.9356	3.230	361.5

In Figs. 2 and 3 the polarization of the solutions is plotted against the mole fraction of the tung oil. The value of the polarization is about 360 cc.

The polarization of a substance is the result of the distortion of the molecules due to electronic displacements produced by the field, and of the orientation of the polar molecules in the impressed field. At very high frequencies the molecules are no longer able to follow the field and the contribution to the polarization due to the oriented molecules vanishes. At optical frequencies only the electrons are affected and the dielectric constant may therefore be identified with the square of the refractive index. The contribution to the polarization due to the orientation of the polar molecules may be found by subtracting from the total polarization the part which is due to the distortion effect of the field, and which is given by:

$$P_0=\frac{r^2-1}{r^2+2}\cdot\frac{M}{d}$$

where r is the refractive index of the solution, and the electric moment of the molecules may be found from the relation

$$\mu = 0.0127 \times 10^{-18}[(P - P_0)T]^{1/2}$$

giving a value for $\mu = 2.29 \times 10^{-18}$ e.s.u.

It must be observed that as tung oil in itself is a mixture of at least two substances, the value of the electric moment found above must be considered as a weighted mean of the component molecules.

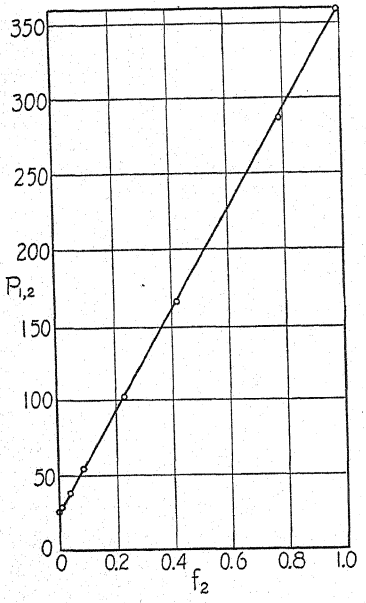

Fig. 2. Polarization vs. mole fraction of tung oil for $\gamma = 5 \times 10^5$ cycles/sec.

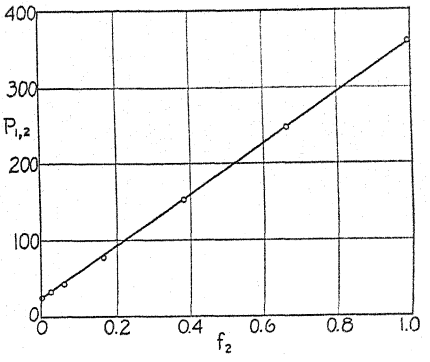

Fig. 3. Polarization vs. mole fraction $\gamma = 1.47 \times 10^6$ cycles/sec.

Variation of Polarization with Temperature

The graph of the polarization versus mole fraction is a straight line showing that the Clausius-Mosotti relation may be applied for all concentrations of tung oil in benzene. The tung oil molecules are evidently present in the solution in clusters so formed as to neutralize the internal field. This clustering is probably similar to the one observed by Stewart[3] and his collaborators. It seemed interesting to investigate the effect of temperature on the clustering of these molecules. Some of these experiments will now be described.

It is possible to find the electric moment in another manner. From the Debye theory it follows that the polarization of a substance is given by:

$$P = \frac{4\pi N}{3}\left(\alpha + \frac{\mu^2}{3kT}\right) \tag{3}$$

where N is Avogadro's constant, α the molecular polarization, K Boltzmann's constant, T the absolute temperature. If a substance is polar its polarization will be directly proportional to the reciprocal of the absolute temperature.

[3] G. W. Stewart and R. M. Morrow, Phys. Rev. **30**, 232 (1929).

If the polarization is measured in the manner described above for a range of temperatures the molecular moment may be calculated from the slope of the straight line obtained when P is plotted against $1/T$, since $P=a+(b/T)$, where b is the slope of the line $=4\pi N/9)(\mu^2/K)$.

The condenser used in these experiments is shown in Fig. 4. It consisted of two concentric nickel cylinders placed in two concentric glass tubes, A and B, sealed at the bottom. The glass tubes were of such a diameter that the outer nickel cylinder was just large enough to fit inside the outer glass tube while the smaller nickel cylinder fitted tightly around the inner tube. This arrangement gave a condenser of fairly large capacity for a very small volume of fluid between the nickel cylinders. A third glass tube C for housing the thermometer was sealed to B. A small tube D was sealed to the junction of B and C. It provided a vent for the escape of the air entrapped between B

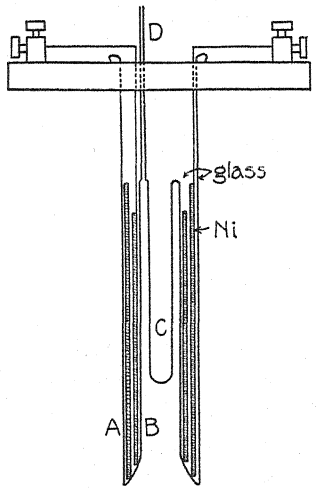

Fig. 4. Diagram of condenser.

and C when the condenser was lowered into the cooling solution, thus enabling the solution to reach every part of the condenser.

A solution of alcohol and solid carbon dioxide was used as the cooling solution. The air capacity of the cell was 69.3 cm. The cooling solution was kept in a large Dewar flask. Measurements of the capacity of the cell were taken only when the temperature shown by the thermometer placed in C differed by a fraction of a degree from the reading of the thermometer placed directly in the solution.

Eq. (3) just like Eq. (1) applies only when the internal field of the molecules may be neglected. And to use this relation dilute solutions must be employed. However, as tung oil showed no molecular interaction the substance was used in the undiluted state.

Fig. 5 is the graph of the data. The plot is sensibly a straight line. The moment calculated from the slope of the straight line was about twice as large as the value found from the method of mixtures. No shifting of the straight line could account even for a fraction of the discrepancy.

Ethyl ether is another substance the molecules of which show no interaction at ordinary temperatures. Its moment as determined by Krchma and Williams[4] using the method of mixtures is 1.24×10^{-18} e.s.u. Experiments were made to measure the moment of ethyl ether using the method of the variation of the polarization with temperature. The value of the moment comes out about 60 percent higher.

These experiments show that the peculiar arrangement of the molecules which neutralizes the internal field at a given temperature is modified when the temperature is changed. The molecular field is not completely eliminated.

Even dilute solutions of a substance, where the molecules are relatively far apart, show some interaction, which varies with temperature. The discrepancy between the value of the moments of some molecules, using the method of mixtures and the method of variation of the polarization of dilute

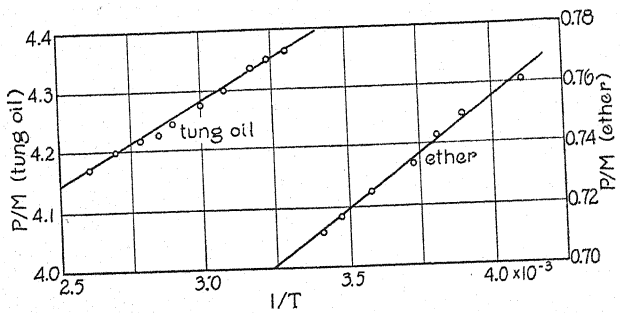

Fig. 5.

solutions with temperature in the experiments of Smyth and Morgan[5], is probably due to this cause, and not, as these authors suggest, to the inaccuracy of measurements. A similar discrepancy was observed by Morgan[6] in his measurements of the moments of some methyl halides by the two methods. The difference in the values obtained is much larger than the experimental error. One is forced to the conclusion, therefore, that even in dilute solutions, which at a given temperature seem to show no interaction, the internal field is not completely absent, and the field manifests itself in the variation of the moment with temperature. It is of interest to find the degree of dilution needed to show no temperature effect of the polarization. Experiments along this line are now being carried out in this laboratory.

Some of the apparatus used in these experiments were purchased by the aid of the Sigma Xi grant. The author wishes to express his gratitude to the Committee on Awards for the grant.

[4] I. J. Krchma and J. W. Williams, Jour. Amer. Chem. Soc. **49**, 2408 (1927).

[5] C. P. Smyth and S. O. Morgan, Jour. Amer. Chem. Soc. **50**, 1547 (1928).

[6] S. O. Morgan, paper read at the meetings of the Committee on Insulation of the National Research Council, November 7, 1930.

AN EXPERIMENTAL STUDY OF KUNDT'S TUBE DUST FIGURES

By E. Hutchisson and F. B. Morgan
University of Pittsburgh, Pittsburgh, Pa.

(Received February 24, 1931)

Abstract

An experimental study of the dust striations in a Kundt's tube has been carried out using a loud speaker, operated from a vacuum tube oscillator, as a source of sound. It is found that the positions of the vibrator for maximum agitation of the dust is different for the case in which a loud speaker is used from that obtained when a stroked rod is used. The formation and behavior of the striations is described in detail. It is found that the spacing between the striations increases with the intensity of sound, decreases with an increase in pressure of the gas, and decreases with an increase in density of the dust material. A minimum spacing is found when the size of the dust particles is changed. The relation suggested by Cook that the ratio of the separation of the striations to the mean free path is a constant was tested but the results obtained indicated that such a simple relation does not exist.

I. Introduction

In 1866 Kundt[1] showed that when standing sound waves were excited in a closed resonance tube, dust particles in the tube arranged themselves in the form of striations perpendicular to the axis of the tube. Since that time however, very little information has been obtained on these striations due to the fact that accurate measurements could only be made after the vibrations had ceased. With the general introduction of the loud speaker as a source of sound[2] and the use of a vacuum tubes oscillator as a means of excitation, it has become possible to examine the phenomena in the Kundt's tube in a far more accurate manner.

The cause of the striations in the Kundt's tube has never been completely determined. The hydrodynamical theory of the oscillations of the air column has been studied by König and others, but after reading these papers, one still wonders how the striations are really produced. However before a rigorous quantitative theory can be developed it is necessary to have accurate measurements of the positions of the striations under different experimental conditions. It is the purpose of this paper to help bridge this gap in our experimental knowledge of the behavior of dust striations.

Before the experimental procedure is taken up it must be emphasized that there is a distinct difference in the behavior of the striations when produced by a stroked rod and when produced by a loud speaker operated from a vacuum tube oscillator. If a stroked rod is used, the maximum agitation of the dust occurs when the vibrating end of the rod is placed at a node, and the

[1] A. Kundt, Pogg. Ann. **127**, 497 (1866).
[2] A. B. Wood, A Textbook of Sound, New York, 1930.

agitation is minimum when the vibrator is at an antinode. However, when the loud speaker is used maximum agitation is obtained when the vibrator is one-third of a segment from a node and a minimum when the vibrator is at a node. Furthermore, after continued stroking of a rod the dust particles in the tube gather into small heaps at the nodes[3] while with the loud speaker there is no indication of this phenomena at all even after long periods of operation. In the work of E. J. Irons[4] in which a stroked rod was used, the formation of rings or disks extending across the diameter of the tube at the nodes is very beautifully shown.

With a loud speaker unit, it was found possible to produce such rings[5] but they were always at the antinodes instead of at the nodes. By using extremely light dust and greater intensity of sound, these rings could be made to assume the appearance of disks with much greater density at the periphery than at the center of the tube. Each ring always lies in the plane of the central stria and seems to be a continuation of it. These rings mark the midpoint of the

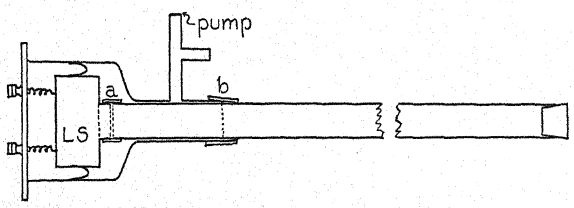

Fig. 1. Experimental arrangement to obtain dust figures in a resonating tube under various pressures. *LS* indicates the loud speaker held in place by springs, *a* and *b* represent short pieces of heavy rubber tubing used to hold the tubes in place.

antinodal region very sharply and are therefore of great value in determining the length of a segment. The motion of the dust particles constituting a ring is from the extremities of the central stria around the wall of the tube toward the top. Neighboring striae usually have dust particles streaming off from their extremities also and these are continually fed into the antinodal ring. Sometimes neighboring striae can be made to produce these rings but they are never so perfect as the central one. After a central ring has been established, it is possible by shifting the stop slowly to drive all the dust from the antinodal region, except that constituting the ring and its disk. In this way, an antinodal ring without the accompanying striae may be obtained.

II. Apparatus and Procedure

The apparatus used in this investigation is shown diagrammatically in Fig. 1. A Temple radio loud speaker unit, actuated by a Hartley vacuum tube oscillator, was used as the source of sound. To permit variation of the pres-

[3] Cf. E. J. Irons, Phil. Mag. **7**, 523 (1929).

[4] Reference 3, plate IX, Figs. 2c and 2d.

[5] These disks were first discovered by the writers in 1928. Since then E. Andrade and S. H. Lewar have published independently an account of these disks in Nature, **124**, 724 (1929). See also the recent note of R. V. Cook, Phys. Rev. **36**, 1099 (1930).

sure and to facilitate the changing of the gas in the tube, the loud speaker unit was mounted in a glass cylinder as shown. The frequency of the sound emitted could be varied throughout a sufficiently wide range to secure almost any wave-length desired. Observations were made both under conditions of resonance and of nonresonance.

Pith, cork, Kieselsaure and white sand were found to be the most satisfactory materials for dust. Mustard seed and timothy seed served very well for small spheroids and ellipsoids, respectively. Uniformity of size of dust particles was obtained by sifting the dust through a nest of sieves ranging from 10 to 120 meshes to the inch. A metric scale was placed alongside the tube and when photographed simultaneously with the dust, made measurements of length convenient. The tubes used were 22 mm and 30 mm in diameter, respectively. Their lengths varied from 2.5 to 4 ft. Two 400-watt in-

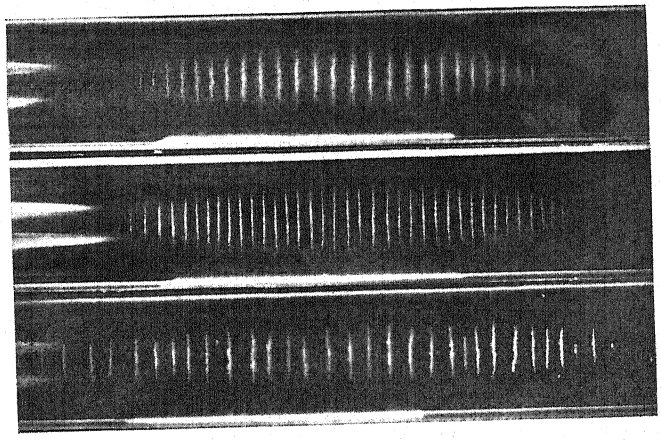

Fig. 2. The appearance of the striations formed when a Kundt's tube is operated by means of a loud speaker. These striations were obtained under atmospheric pressure with a frequency of approximately 1500 sec. The diameter of the dust particles in the middle photograph is intermediate between those in the outer photographs showing that the spacing between the striations does not increase monatonically with the size of the particles.

candescent lamps, equipped with reflectors, were used to illuminate the tube from above for the taking of the photographs. A $4'' \times 5''$ plate camera was used and exposures were usually from 1/50 to 1/100 of a second. A dividing engine was used for measuring the distance between striae.

III. General Appearance and Properties of the Striae

The general appearance of the striae produced by means of a loud speaker element is shown in Fig. 2. With the aid of a lens the striae are often found to be just one layer of particles in thickness. According to the observations of Cook,[6] these particles have a repulsion for each other and are always slightly separated from each other during the continuance of the sound. The present

[6] S. R. Cook, Phil. Mag. **3**, 47 (1902).

investigation failed to substantiate Cook's observations. In every case, whether the particles used were dust, pith spheroids, pith cylinders, sealing-wax spheroids, mustard seed spheroids, or timothy seed ellipsoids, the particles remained in contact during the continuance of the sound, just as if there were a force of attraction between them. This is in conformity with König's[2] theory which assumes a force of attraction between particles whose line of centers is at right angles to the direction of the sound propagation. Ellipsoidal particles always aligned themselves so that their major axes are at right angles to the direction of sound propagation.

Similarly, if thin pith disks about the size of a dime are used in the place of dust, they come to a verticle position in the tube and are rotated till their planes make a right angle with the direction of propagation of the sound. They space themselves much like the dust striae, except that they are farther apart. Usually three or four of these disks are drawn into the middle of the antinode to form the central stria edge to edge and rotate about the axis of the tube like a Dutch windmill. Often other disks, spaced along the tube will also rotate; some turning clockwise, others counter-clockwise.

The dust particles, constituting a stria seem to be in continual oscillation so that some are always freeing themselves from one stria and joining a neighboring one. This interchange of particles is more or less mutual, so that a stria receives just about as many particles as it loses and therefore maintains a rather constant size. Striae tend to diminish both in length and height in going from the antinode to the node.

The position of a stria in a segment may be either constant or variable, depending on the adjustment of the vibrator relative to a node and the stria may form either a straight line across the tube or a curved one, depending on the above adjustment and also on its position in the segment. The central stria always extends straight across the tube, forming a right angle with its axis. This is usually true also of a relatively large number of striae on either side of the central one. The striae near the extremities however, tend to be more or less curved; sometimes being concave toward the nodes and sometimes concave toward the antinodes, depending on the position of the vibrator relative to a node.

When cork dust (size 80–100 mesh) is piled at the nodes and the vibrator of the loud speaker is placed about one-third of a segment from a node and operated, striae begin to form on either side of the dust piles and move toward the antinodes. The first stria to reach the midpoint of a given segment stops and the next one coming up approaches within a certain distance of the central one, when it too stops. The third stria approaches within a similar distance of the second and likewise stops. This is continued till the dust figures occupy perhaps eight-tenths of a segment. The extreme striae (that is, the ones nearest the nodes), in this case are decidedly concave toward the nodes and the concavity falls off gradually in going toward the antinodes. In an extreme case, the only stationary stria is the one at the middle of the antinode; all others gradually moving along the axis of the tube from the nodes toward the antinodes, the terminal ones having the more rapid motion. These

overtake the more slowly moving ones and finally unite with them. At the same time, dust is leaving the more stable striae and moving back along the walls of the tube toward the nodes. Much of this returning dust seems to move underneath the advancing striae, while the rest of it streams back higher up on the sides of the tube, above the striae. This returning dust forms new striae near the nodes, which again advance toward the antinodes. By shifting the vibrator toward an antinode, the forward motion of the striae can be greatly reduced; and when the vibrator is at the antinode, only two or three of the terminal striae show any forward motion at all. These terminal striae are now concave toward the antinodes instead of toward the nodes and the dust occupies about half as much of the segment as before. If the vibrator is moved to a node, the dust leaves the antinodal region entirely and forms striae about the nodes which are concave toward the nodes. The excitation of the dust is now a minimum and these striae exhibit no apparent forward motion at all.

The above observations, therefore, seem to lend credence to the conclusion of Dvorak,[7] based on his observations of the behavior of both liquids and dust, and to the mathematical deduction of Lord Rayleigh[8] that there is a current through the central portion of the tube from the nodes to the antinodes and a return current contiguous to the walls of the tube. It also seems quite probable that these currents have something to do with the concavity of the striae, though the case of striae concave toward the antinodes would be difficult to explain on that assumption.

The distance between successive striae of a given dust figure is not a constant. Robinson[9] found that in going from an antinode to a node the spacing gradually diminished and he succeeded in deriving an expression for this spacing distance, which he confirmed experimentally. Irons[3] attempted to verify Robinson's equation but his results failed to support it. In the present work, the spacings of many dust figures were measured and the most promising ones were used for testing Robinson's law. In no case was the agreement satisfactory. At normal atmospheric pressure, there was usually, but not always, a slight diminution in the spacing distance in going from an antinode to a node; but at pressures considerably below atmospheric, the spacing distance actually increased. It was noticed, however, that the average spacing between successive striae was much greater under some conditions than under others and an attempt was therefore made to determine the factors which exert an important influence on the spacing distance.

IV. Factors Affecting the Distance Between Striae

1. Sound intensity.

This is probably the most important factor. There are two ways in which the intensity of the sound can be varied: (a) by varying the energy input to

[7] Dvorak, Pogg Ann. **CLIII,** 102 (1874); **CLVII,** 42 (1876).
[8] Lord Rayleigh, Phil. Trans. **CLXXV,** Part I, 1 (1884) or Scient. Papers **II,** 239.
[9] J. Robinson, Phil. Mag. **18,** 180 (1909); **19,** 476 (1910).

the vibrator, (b) by shifting the position of the vibrator relative to a node. If a rod is stroked gently with the vibrator at a node, the striae will be close together, but if the rod is stroked vigorously, the striae will be few in number and much farther apart. If the vibrator is placed at an antinode, the most vigorous stroking will be required to produce a very meager spacing. An intermediate position of the vibrator will produce an intermediate spacing.

2. Size of dust particles.

This investigation failed to substantiate the work of Cook[10] who found that the spacing increased with the size of the dust particles. Minimum spacing was always obtained with medium sized particles. If either larger or smaller particles were used, the distance between striae was increased. The photographs of Fig. 2 and the curves of Fig. 3 show this very clearly. They

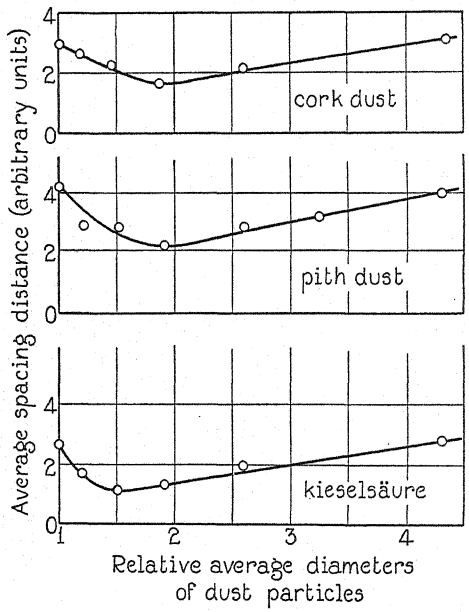

Fig. 3. Curves showing the effects of particle size on the relative separation of the striations.

also show that the size of the particle required to produce minimum spacing probably decreases as the density of the dust increases.

3. Gas pressure.

The pressure to which the gas in the tube is subjected not only affects the spacing between the striae but it also affects the number of striae in a segment, the amount of dust in each striae, and the compactness of this dust. As the pressure is reduced the striae near the nodes are the first ones to be noticeably affected. Not only do they get fewer in number and farther apart but also the particles composing them oscillate through a greater distance

[10] S. R. Cook, reference 6.

and move about with greater freedom. Thus the dust in these striae is much more greatly agitated than in the central ones. However, as the pres-

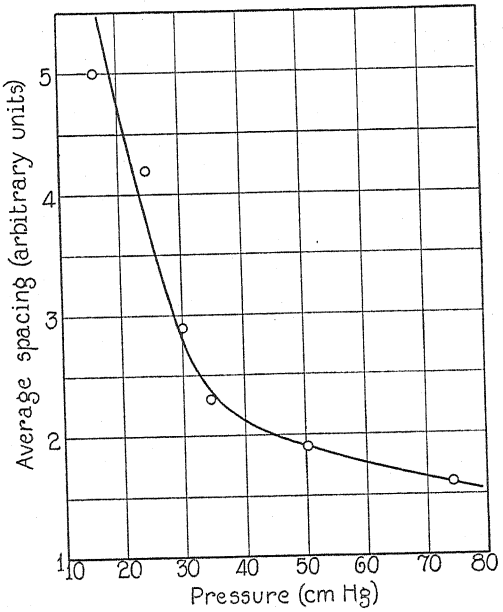

Fig. 4. Effect of gas pressure on the average distance between successive striae (pith dust, 80–100 mesh).

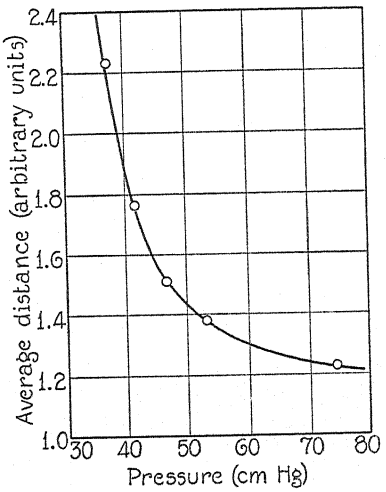

Fig. 5. Effect of gas pressure on the average distance between successive striae (cork dust, 80–100 mesh).

sure is decreased, more and more of the central striae behave in the same way till finally all are greatly agitated save the one at the middle of the segment.

With a further decrease in pressure, even this central one succumbs and behaves like the others. Finally when the pressure is reduced to 10 cm of Hg, the striae are broken up and the dust is swept from the antinodal region to the nodes. The curves of Figs. 4 and 5 show clearly that the spacing increases as the pressure decreases.

4. Density of particles.

The curves of Fig. 6 show that the density of the dust has a decided influence on the spacing between the striae so long as the density is less than 0.3

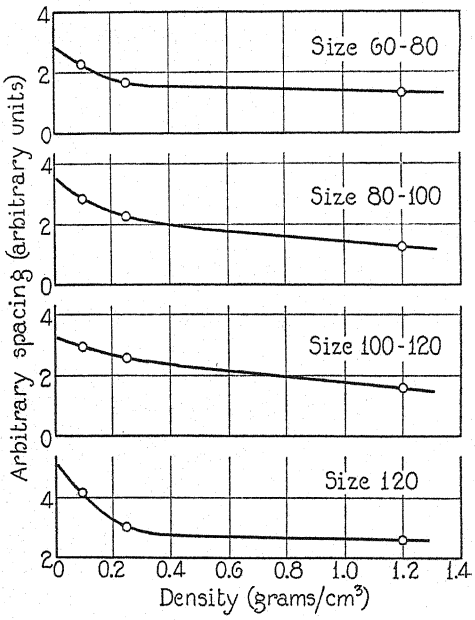

Fig. 6. Effect of density of dust material on the average distance between successive striae.

gm/cm³. Beyond 0.3, the slopes of the curves are much more gradual, but even within that range the decrease in spacing with the increase in density is sufficient to be measurable.

V. Ratio of Distance Apart of Striae to Mean Free Path of the Gas Molecules

Cook[10] worked out this ratio for amorphous silica in air. The results were not conclusive, but they were sufficient to indicate a probability that the distance apart of the striae is directly proportional to the mean free path of the gas molecules.

Similar computations were made with the data obtained in this work. The results, shown in Table I are no more conclusive than were those of Cook.

TABLE I.

Material (in all cases, 80–100 mesh)	Pressure p cm of Hg	Distance apart of striae (d) mm	Mean free path (l) cm	d/l $\times 10^{-4}$
Pith	74.5	1.6	940×10^{-8}	170
Pith	50.1	1.9	1390×10^{-8}	137
Pith	41.3	2.0	1700×10^{-8}	118
Pith	34.6	2.3	2030×10^{-8}	113
Pith	29.8	2.9	2350×10^{-8}	123
Pith	24.7	4.2	2880×10^{-8}	146
Pith	15.8	5.0	4450×10^{-8}	113
Cork	74.5	1.2	940×10^{-8}	128
Cork	53.3	1.4	1320×10^{-8}	106
Cork	46.7	1.5	1510×10^{-8}	99
Cork	41.5	1.8	1690×10^{-8}	106
Cork	37.2	2.2	2010×10^{-8}	102

VI. CONCLUSIONS

An experimental investigation of the properties of the striations in Kundt's tube dust figures was made. With a loud speaker for a source of sound, it was found that position of the vibrator which produced maximum intensity was different from that obtained when a stroked rod was used as a source. The changes in the spacing between the striations caused by altering the pressure, the size of the particles, the intensity of the sound, and the density of the particles, were investigated.

WAVE-PARTICLES AS TRANSMITTED POSSIBILITIES: QUANTUM POSTULATES DEDUCED FROM LOGICAL RELATIVITY

By William Band
Department of Physics, Yenching University, Peking, China

(Received September 24, 1930)

Abstract

General relativity is logically unsatisfactory because it bases measurement on infinitesimals, and absolute infinitesimals do not exist. A standard of comparison being a logical necessity, we propose to provide it by the new fundamental hypothesis; "The physical world is composed of elementary events of identical and definite non-zero four-dimensional extent." The photon is a possibility of absorption-event initiated by an emission event; it is exhibited as a set of superposed moving volumes or three-dimensional sections of the four-dimensional possibility. The electron is a possibility transmitted with smaller velocities. Mass or energy is proportional to the time-duration of the event-possibilities, and obeys thence, the relativity rules. A wave function is postulated for the possibility being realized, and from Doppler's principle the quantum rule necessarily follows: mass proportional to frequency, and group-velocity equal to particle velocity. The "particle" exists only when the transmission is parallel the time-edge of the possibility; in atomic orbits presumably the condition does not apply, and the parallel-displacement tracks of relativity which are shown to to be required outside, do not apply within the atom. The finite extent of the events which exhibit the particle necessitates an indeterminacy in the situation of the particle.

§ 1. Logical Weakness of the General Theory of Relativity

IN UNIFIED field theory, particularly the form given by Eddington, tracks of all particles, and straight lines, are defined by means of infinitesimals, or infinitesimal displacements. Thus at the basis of the theory rests a set of equations of the form[1,6]

$$dA_i = (ij,\ k)A_k dx_j \cdots i, j, k = 1, 2, 3, 4.$$

The displacement dx_j is supposed to be infinitesimal, and the corresponding increment dA_i must also be infinitesimal. It is however a mathematical fact that there are no absolute infinitesimals, and that the property of being small is only relative. In applying the relativity to experience, we have to fix arbitrarily what shall be small. Thus there is nothing in the relativity theory of geodesics to say that the orbits shall not represent electron tracks round atoms rather than planetary tracks, and nothing but a pragmatic test to give the verdict. This elasticity may be satisfactory from the experimenter's point of view, but the theoretician cannot be satisfied until the theory can tell itself whether its findings are to apply to microscopic or macroscopic phenomena. Relativity at present finds that phenomena on the minute can be only a replica of phenomena on the grand scale; there is in its very fundamental constitution no absolute infinitesimal, it is the merely relative infinitesimal

[1] Eddington, Mathematical Relativity, p. 213, Eq. 91.1.

of mathematics in which any contortion of curvature may exist and which is merely a class of finites.[2]

Herein is not only a logical defect of the theory, but also the reason why the theory fails to include atomic phenomena within its unifying field. Classical physics I suppose would have unanimously supported the view that phenomena on the minute were replica of those on the large scale; but with the advent of atomic physics this attitude has died, and the principle of indeterminacy has introduced an absolute standard of minuteness into physics that is not in pure mathematics.

Thus, to give it logical completeness, relativity requires an added postulate over and above the postulates made by Einstein at the foundation of the theory. Einstein's postulates concerned with observers, the fact that all observers were on the same footing for erecting descriptions of the external world; but the new postulate must concern the means whereby the knowledge of the external world is derived by all observers. We postulate that "The observations of every observer can be analyzed into a complex of minute events each with the same four-dimensional extent." The old postulates asserted that differences between observers were only relative, while the new postulate asserts that the differences between the minute events observed are also only relative. It carries the relativity a step further into the heart of physics; and incidentally provides a standard of minuteness for relativity, raising that theory to a more completely logical status.

Other postulates, of course, suggest themselves as alternatives; for instance the postulate that space-time is itself discontinuous, or that there is a minimum quantum of action, where action is defined from the usual relativity equations. We may justify our actual choice by appealing to Whitehead's philosophy of space-time.[3] This philosophy, generally accepted by those who have taken the trouble to study it, at least in general idea, shows that space-time may be logically defined from the extensive properties of events. Thus the world of events is fundamental, and space-time comes out of it by an abstractive process actually carried through with some success by Whitehead. Thus we cannot lightly postulate a discontinous space-time after Whitehead has erected a continuous one, until someone succeeds in erecting a discontinuous one and elucidates what the meaning of such a construct really is. Again, accepting Whitehead's philosophy, we immediately see that our fundamental postulate must concern with events rather than with such entities as mass or action, or for that matter with space-time either. If there is a minimum action or mass, or a discontinuous space-time, it should come out of the theory since relativity defines mass and action from functions in space-time, and not need tacking on to the theory as an *ad hoc* assumption. The properties of space-time that give a minimum action must be derivable from the events in terms of which the space-time is defined; hence our fundamental hypothesis must concern with events.

[2] Whitehead, Process and Reality, p. 465.

[3] Whitehead, Process and Reality and Principles of Natural Knowledge.

We claim therefore that our postulate is logically required to make the theory satisfactory at its foundation, and does not add anything *ad hoc* to the after structure of the theory.

§ 2. Geometry of Four-Dimensional Regions

We propose to examine the representation of minute four-dimensional regions representing the minimum events of the world on the Minkowksi diagram. In drawing Minkowski diagrams the beginner generally has to remind himself that a point on the diagram represents a definite and unalterable event with definite coordinates in both space and time for each system concerned. But in representing the minute events postulated here on a scale that shows the boundaries of the events as lines in the diagram, we can no longer assume that each point on the diagram represents a definite event for every system; there are no events of such precise coordinates. This lends a certain elasticity to the diagrams that is not familiar, and that must be carefully remembered in following the argument given below; the same event may be represented, if convenience dictates it, by differently shaped areas in the different systems of reference.

In some particular system S' the simplest four-dimensional region is a volume stationary and existent for a definite time; suppose it represented by $AB'CD'$ where AB' is along X' axis, and AC along T' axis, giving a two-dimensional section. We shall suppose that the same event is in a system S represented by $ABCD$ where $B'D'$ cuts the X axis in B; this will be a moving volume, for S, existent for a definite time.

Let dt, dt' be the time durations of the event, and dV, dV' the two volumes proportional to the X, X' sections. Then simple relativity transformations show that, taking velocity of light unity for convenience,

$$dt' = (1 - v \cdot v)^{1/2} \cdot dt; dV' = dV \cdot (1 - v.v)^{-1/2}: \tag{1}$$

where v is the velocity of S' relative to S. Thus the four-dimensional extent $dt \cdot dV = dt' \cdot dV'$ is a constant or invariant for this transformation.

In the particular case when v is unity, these formulae are no longer of use, for there are no systems S, S' with this relative velocity. If we call the velocity given by the gradient of the edge AC of the event the "self-velocity" of the event, then there may be events with self-velocity unity but which can therefore never be exhibited as volumes stationary in any coordinate system. Such an event could be represented by $ABCD$ for S, where AC is along the light-track gradient unity, and AB along the X axis. This would transform to $AB'CD'$ for S' with C still on the light track and B' at the intersect of BD with the X' axis. Here we can easily see that

$$dV' = dV(1 + v)/(1 - v \cdot v)^{1/2} \tag{2}$$

$$dt' = dt(1 - v \cdot v)^{1/2}/(1 + v) \tag{3}$$

and again the four-dimensional extent of the event is invariant. Alternatively the formulae may be written

$$dV = dV'(1 - v)/(1 - v\cdot v)^{1/2} \tag{2'}$$

$$dt = dt'(1 + v)/(1 - v\cdot v)^{1/2} \tag{3'}$$

with

$$dt = k/dV,\ dt' = k/dV'. \tag{4}$$

These of course hold only when the self-velocity of the event is parallel the relative velocity of S, S'. If the relative velocity v is along the Y, Y' axes, and the self velocity of the event is along the X, axis, then by drawing the appropriate figure it can easily be verified that

$$dt' = dt/(1 - v\cdot v)^{1/2} \tag{5}$$

$$dV' = dV(1 - v\cdot v)^{1/2} \tag{6}$$

with again

$$dt' = k/dV',\ dt = k/dV; \tag{4'}$$

the most general case being easily deducible from these two.

§ 3. Transmission of Four-Dimensional Regions

(a). Regions with unit self-velocity. Photon theory.

Suppose that the region $ABCD$ of the previous article represents one stage in the process of transmission of a possible event, the transmission being with the same vector velocity as the self-velocity of the possible event. The region $ABCD$ is a section (X-axis) of the region that would be occupied by the event were it to be realized at that stage, and examined by the system S. The fact that it is being transmitted along the X-axis means that the boundary AB is moving along the X-axis with the velocity of transmission, and the boundary CD is also moving along the X-axis with the same velocity. Since this velocity is the same as the velocity given by AC or BD we see that the boundary AB reaches the stage CD after the time dt which is the duration of the possible event. Thus in the realized event CD is ahead in space, but behind in time compared with AB, but in the transmission AB and CD coincide, for the occurrence of CD is simultaneous with the arrival of the transmitted AB. Were the transmission to materialize into an event, the edge AB would be realized first, and leave the edge CD travelling on for the time dt before it was realized.

Thus the transmission looks like a simple moving volume travelling with the velocity of light; all the volumes which would occur in succession in the event appear as coincident in an instantaneous picture of the transmission, and if we had not started from the complex, we should have mistaken the process for a simple moving volume, albeit with something corresponding with a pseudo-density of the overlapping volumes.

To picture a region that has extension in space and in time that is itself being propagated with velocity through space, is a new and perhaps rather difficult concept, and the results of investigating it in detail seem to be of considerable interest.

Thus suppose that a quantum emission corresponds to a four-dimensional event with self-velocity unity, and that this originates a possible absorption transmitted with this self-velocity. This transmission will appear as a moving volume, or particle; in other words it is the photon of recent optical theory. But the photon and the transmitted possibility both differ from mere moving volumes: the one in having mass or energy, and the other in having the pseudo-density of the superposed volumes corresponding to different stages of the possible event. Identifying these differences we assume next that the energy of the photon is proportional to the time-duration of the possible event; this may be taken as a definition of the energy of a particle on the new theory.

$$E \text{ is } prop. \text{ to } dt$$

and hence from Eq. (3′)

$$E = E'(1 + v)/(1 - v \cdot v)^{1/2} \tag{8}$$

if E is the energy of the photon for S, and E' for S'.

The probability that the event will occur or that the possibility will be realized cannot be deduced *a priori;* but since the wave-theory of radiation has been interpreted statistically, we may assume that there will be a probability wave-function whose phase-velocity equals the velocity of transmission. From wave theory it then follows that in transforming between the frequencies, the generalized Doppler principle[4] will necessarily hold:

$$n = n'(1 + v)/(1 - v \cdot v)^{1/2} \tag{8′}$$

and comparison with Eq. (8) therefore shows that

$$E = hn \tag{9}$$

where h is a universal constant, the quantum theory rule. Eq. (4) shows that the volume dV is proportional to the period, and thence the wave-length of the waves; or the section of the volume in the direction of the transmission is proportional to the wave-length.

(b). Regions with any self-velocity. Electron theory.

From the results of the foregoing we are naturally lead to expect transmitted possibilities of normal velocities to have the same properties as material particles. Let an event possibility of self-velocity u be transmitted with that velocity, then the energy of the particle it appears as, is again defined as proportional to the time dt of the event-possibility, or the pseudo-density of the superposed volumes. Eqs. (1) then give

$$E' = E(1 - v \cdot v)^{1/2} \tag{10}$$

which is the usual relativity form for the energy, since here E' is the rest-energy of the particle. Translated into the usual notation it is of course

[4] Cunningham, Principle of Relativity.

$$mc^2 = m_0c^2(1 - v^2/c^2)^{-1/2}. \tag{10'}$$

If it is questioned whether the electron is but a transmitted possibility, we may point to the usual interpretation of the matrix mechanics; the electron connects quantum events, and is in effect a transmitted possibility of an absorption. From this point of view it is natural to seek for a wave-function that shall give the probability of the event being realized at any stage. But to obtain the frequency transformation of these waves we must pursue a slightly different track from that which gave us the formulae for light waves; here the velocity is not an invariant and the problem is less simple. The familiar reasoning[5] is however perfectly satisfactory and conclusive. A stationary particle must correspond with a stationary wave system, say of the form for S',

$$P = A \exp(2\pi n' i t'). \tag{11}$$

The Lorentz transformation gives

$$P = A \exp(2\pi n i t - x/w) \tag{12}$$

relative to the S system, where

$$n = n'(1 - v^2/c^2)^{-1/2} \tag{14a}$$

and

$$w = c^2/u. \tag{14b}$$

Comparison of Eq. (14a) with Eq. (10) again gives the quantum rule

$$E = hn \tag{9}$$

while combination of Eqs. (14a), (14b) shows in the usual way that u is the group velocity of the waves.

We thus reach a satisfactory interpretation of the wave theory of matter, of the nature of the electron, and the similarity, yet difference between the photon and the material particle.

§ 4. Equations of Motion of Particles

At the outset of this work we made the simplifying assumption that the transmission of the possibilities was parallel to the self-velocity of the event-possibility transmitted. Only with this assumption is the transmission exhibited as a particle, for only then will the various volume-sections of the event be superposed on one-another. When therefore the particle exists, their tracks are necessarily given by parallel displacement; for by our assumption the edges AC, CC' of consecutive possible events are parallel, and hence the edge, which is parallel to the velocity vector of the particle, is moved by parallel displacement. This leads immediately to the unified field theory already given mathematical expression by the present writer[6]; the most general

[5] Haas, Wave Mechanics and New Quantum Theory, Chap. 2.

[6] Band, Phys. Rev. **36**, 1405 (1930).

rule for the parallel displacement of the velocity vector gives the tracks of the particles actually agreeing with the experimental tracks. The small displacements of the theory must obviously be of the same order as the dimensions of the events, and the equations will be meaningless if we attempt to apply them to smaller orders of length.

But we have already seen that the existence of the particle is by no means a necessity; so far as our theory is concerned, there may be transmissions in directions other than the self-velocity of the events, and what we may vaguely call the track of the transmission will then have appreciable curvature within the extent of one possible event, and the parallel displacement rule no longer applies. These "tracks" are not then tracks of particles at all, and the usual wave-theory interpretation of quantized orbits seems to be the most natural one here.

In passing, we remark that on the present theory we have refused to regard the particle as fundamental; the whole structure of relativity is erected from events of finite four-dimensional extent, and a particle is an abstract or recognized permanency among the extensive relations between events. Thus our postulate of finite extent to the ultimate events at once forbids the accurate estimation of the position or motion of the particle when it actually exists; for the particle can only be observed through the events which exhibit it, and these do not give exactitude.

In conclusion, we cannot claim to have treated more than an elementary set of cases; but it seems sufficient to show that it is possible by recognizing a logical weakness of Relativity to deduce from the most natural additional hypothesis to remove this weakness, the essential basis of the new quantum theory; to illuminate the meaning of and deduce the assumptions of the unified field theory; and finally to suggest an interpretation of the physical world that will harmonize the two great fields of theoretical research of recent years, relativity, and atomic physics.

THE GENERAL EQUATIONS OF ENERGY AND ENTROPY OF GASES

By Tzu Ching Huang
Department of Chemistry, National Tsing Hua University, Peiping, China

(Received March 9, 1931)

Abstract

By substituting the general equation of state for any gas, $p = T\Psi(v) - \Phi(v) - F(v, T)$ in the thermodynamic equation, $Tds = du + pdv$, and by applying the principle of exact differential, the following general equations of energy and entropy have been obtained,

$$u = \int \Phi(v)dv + \int \left[F - T\,\partial F/\partial T \right] dv + \alpha(T)$$

$$s = \int \Psi(v)dv - \int \partial F/\partial T\, dv + \beta(T).$$

The values of $\alpha(T)$ and $\beta(T)$, both arbitrary functions of temperature, are found to be

$$\alpha(T) = \int c_{v\infty} dT + k_1,$$

$$\beta(T) = \int \frac{\alpha'(T)}{T} dT + \text{const} = \int c_{v\infty} \frac{dT}{T} + k_2,$$

where $c_{v\infty}$ = heat capacity of the gas at constant volume and at infinite dilution. The equations are applied to a perfect gas as well as to gases obeying van der Waals', Clausius' and Dieterici's equation of state and are found to give results in agreement with those obtained from other thermodynamic equations.

PHILLIPS,[1] by employing the characteristics of exact differentials, showed that both the energy and entropy of a fluid are the sum of a function of volume and a function of temperature, if its equation of state belongs to the type,

$$p = T\Psi(v) - \Phi(v), \tag{1}$$

in which p is the pressure, T the temperature of the fluid, $\Psi(v)$ and $\Phi(v)$ are functions of volume. Eq. (1), however, is not general enough. Beattie and Bridgeman[2] pointed out that practically all the equations of state can be generalized in the form

$$p = T\Psi(v) - \Phi(v) - F(v, T) \tag{2}$$

where $F(v, T)$ is a function of volume and temperature. The purpose of the present paper is to find the general equations of energy and entropy of any

[1] Phillips, Jour. Math. and Phys., M.I.T. **1**, 42 (1921).
[2] Beattie and Bridgeman, Proc. Am. Art. Sci. **63**, 231 (1928).

fluid belonging to type (2), and the method of derivation is essentially an extension of that of Phillips.

Energy Equation

From thermodynamics we have

$$Tds = du + pdv \tag{3}$$

in which u and s are the energy and entropy of the substance. Combining with Eq. (2) we get

$$\frac{du}{T} - ds + \Psi(v)dv - \frac{\Phi(v) + F}{T} \cdot dv = 0 \tag{4}$$

where $F = F(v, T)$ for short.

As the result of straightforward calculation we have finally

$$u = \int \Phi(v)dv + \int \left[F - T\frac{\partial F}{\partial T}\right] dv + \alpha(T). \tag{5}$$

Entropy Equation

By combining Eqs. (2) and (3), we get

$$du - Tds + [T\Psi(v) - \Phi(v) - F]dv = 0. \tag{6}$$

Proceeding as before, we find

$$s = \int \Psi(v)dv - \int \frac{\partial F}{\partial T} dv + \beta(T). \tag{7}$$

Determination of $\alpha(T)$ and $\beta(T)$

The relation between $\alpha(T)$ in Eq. (5) and $\beta(T)$ in Eq. (7) can be easily derived. From Eqs. (5) and (7) we get

$$du = \left[\Phi(v) + F - T\frac{\partial F}{\partial T}\right] dv - \left[\int T\frac{\partial^2 F}{\partial T^2} dv - \alpha'(T)\right] dT \tag{8}$$

$$ds = \left[\Psi(v) - \frac{\partial F}{\partial T}\right] dv - \left[\int \frac{\partial^2 F}{\partial T^2} dv - \beta'(T)\right] dT. \tag{9}$$

Substituting these values of du and ds and that of p in Eq. (2) in Eq. (3) and collecting terms, we get

$$T\beta'(T) = \alpha'(T) \tag{10}$$

or,

$$\beta(T) = \int \frac{\alpha'(T)}{T} dT + \text{const.} \tag{11}$$

In the determination of $\alpha(T)$, the energy equation presents no difficulty, but in the case of $\beta(T)$, the integral of the entropy equation becomes infinite at the lower limit because of the presence of a term $\ln v$ or $\ln(v-b)$. In the pres-

ent method $\alpha(T)$ is evaluated from the initial condition, while $\beta(T)$ is found from Eq. (29). A common method[3] of finding $\alpha(T)$ is to assume that at infinite dilution (i.e., $v \doteq \infty$) the gas approaches the perfect state

$$u_{v=\infty} = \alpha(T) = \int c_{v=\infty} dT + k_1 \tag{12}$$

and Eq. (11) gives

$$\beta(T) = \int c_{v\infty} \frac{dT}{T} + k_2 \tag{13}$$

where $c_{v\infty}$ is the heat capacity of the gas at constant volume and at infinite dilution, and k_1 and k_2 are arbitrary constants.

Application to Some Equations of State

1. Perfect gas:

$$p = \frac{RT}{v}.$$

Referring to Eq. (2), we see

$$\Psi(v) = \frac{R}{v}, \quad \Phi(v) = 0, \quad F(v, T) = 0.$$

Eqs. (5), (7), (12), and (13) give

$$u = \alpha(T) = c_v T + k_1$$
$$s = R \ln v + c_v \ln T + k_2$$

in which $c_v = c_{v\infty}$ for perfect gas.

2. van der Waals' equation:

$$p = \frac{RT}{v - b} - \frac{a}{v^2}.$$

Here

$$\Psi(v) = \frac{R}{v - b}, \quad \Phi(v) = \frac{a}{v^2} \quad F(v, T) = 0.$$

Assuming $c_{v\infty}$ to be independent of temperature, Eqs. (5), (7), (12), and (13) give

$$u = -\frac{a}{v} + c_{v\infty} T + k_1$$

$$s = R \ln (v - b) + c_{v\infty} \ln T + k_2.$$

3. Clausius' equation[4]

$$p = \frac{RT}{v - a} - \frac{c}{T(v + b)^2}.$$

[3] See, for instance Schaefer, Einführung in die Theoretische Physik, Walter de Gruyter and Co., Berlin, 1929, Band II p. 189; van der Waals-Kohnstamm, Lehrbuch der Thermodynamik, Verlag von Johann Ambrosius Barth, Leipzig, 1908, 1. Teil, p. 44.

Here

$$\Psi(v) = \frac{R}{v-a}, \quad \Phi(v) = 0, \quad F(v, T) = \frac{c}{T(v+b)^2}.$$

The same set of equations gives

$$u = -\frac{2c}{T(v+b)} + \int c_{v_\infty} dT + k_1$$

$$s = R \ln (v-a) - \frac{c}{T^2(v+b)} + \int \frac{c_{v_\infty} dT}{T} + k_2.$$

4. Dieterici's equation[5]

$$p = \frac{RT}{v-b} e^{-a/vRT}$$

which, on expansion, becomes

$$p = \frac{RT}{v-b} - \frac{a}{v(v-b)} + \frac{a^2}{2RTv^2(v-b)} + \cdots.$$

Taking only the first three terms and referring to Eq. (2) we find

$$\Psi(v) = \frac{R}{v-b}, \quad \Phi(v) = \frac{a}{v(v-b)}, \quad F(v, T) = \frac{-a^2}{2RTv^2(v-b)}$$

Eqs. (5), (7), (12), and (13) give

$$u = \left[\frac{a}{b} - \frac{a^2}{b^2RT}\right] \ln \frac{v-b}{v} - \frac{a^2}{bRTv} + \int c_{v_\infty} dT + k_1$$

$$s = R \ln (v-b) - \frac{a^2}{2b^2RT^2} \ln \frac{v-b}{v} - \frac{a^2}{2bRT^2v} + \int \frac{c_{v_\infty} dT}{T} + k_2.$$

The above results are checked by integrating the following thermodynamic equations, after substitution of the values of $(\partial p/\partial T)_v$ and p in each equation of state

$$\left(\frac{\partial u}{\partial v}\right)_T = T\left(\frac{\partial p}{\partial T}\right)_v - p$$

$$\left(\frac{\partial s}{\partial v}\right)_T = \left(\frac{\partial p}{\partial T}\right)_v$$

Eqs. (5) and (7) can be applied to any other equation of state, but the above examples are sufficient to show their usefulness.

Dr. D. Sun of the Department of Mathematics gave most valuable as sistance for which the author is grateful.

[4] Clausius, Wied. Ann. **9**, 337 (1880).
[5] Dieterici, Wied. Ann. **69**, 685 (1899).

LETTERS TO THE EDITOR

Prompt publication of brief reports of important discoveries in physics may be secured by addressing them to this department. Closing dates for this department are, for the first issue of the month, the twenty-eighth of the preceding month; for the second issue, the thirteenth of the month. The Board of Editors does not hold itself responsible for the opinions expressed by the correspondents.

Aluminum May Have A Nuclear Spin

In a recent letter to the editor of the Physical Review, R. C. Gibbs and P. G. Kruger, (Phys. Rev. **37**, 656 (1931)) report a negative result in their search for hyperfine structure in the arc and first spark spectrum of aluminum. Due to the importance of this result it should be pointed out that the evidence is not conclusive and that aluminum may have and is predicted to have a nuclear spin.

The arc lines investigated involving the transitions $^2P_{1\frac{1}{2},\frac{1}{2}}(3p)-{}^2S_{\frac{1}{2}}(4s)$ would not be expected to give very large *hfs* separations since the penetrating electron is a somewhat loosely bound $4s$ and not a tightly bound $3s$ electron. One would expect very narrow *hfs* for both the ^2P and ^2S terms.

In the first spark spectrum of aluminum, Al II, a $3s$ electron is involved in both the initial and final states of the lines investigated. The hyperfine structure separations of the $^3D_3(3s4d)$ term and the $^3F_4(3s9f)$ term should, due chiefly to the $3s$ electron, be large, normal, and almost identical in separation. The result is that the strong *diagonal lines* should fall together and give a strong sharp line and the faint *off diagonal lines* not be observed. Using a nuclear spin of 3/2 the *diagonal components* of 4226 ($^3D_3-{}^3P_4$) should have a total intensity sixteen times that of the *off diagonal components*. A very similar known case is 4823, $^8P_{4\frac{1}{2}}-{}^8S_{3\frac{1}{2}}(3d^54s4p-3d^54s5s)$ of manganese, (White and Ritschl, Phys. Rev. **35**, 1155 (1930)), in which the six diagonal lines fall close together, the term separations being due chiefly to the tightly bound and penetrating electron $4s$. The same should be true for the $^1D_2(3s3d)$ and $^1P_1(4s4p)$ term except that here the wide *hfs* terms should be inverted. The strong *diagonal lines* should again fall together and give a fairly sharp line.

A better test than the one chosen would be combinations between levels having widely different separations, e.g. the *off diagonal multiplet lines* $^3D_3-{}^3F_3$ or $^3D_2-{}^3F_2$ $(3smd-3smf)$. The $^3D_2$ and $^3F_3$ terms should have very narrow separations and the $^3D_1$ and $^3F_2$ terms should have *inverted* but rather wide separations.

H. E. WHITE

University of California,
Berkeley, California,
April 20, 1931.

The Fundamental Assumptions in Akulov's Papers on Ferromagnetism

In a series of papers[1] Akulov has developed a mathematical theory capable of quantitatively describing a good many ferromagnetic phenomena. The success of his work is some what marred by two fundamental assumptions: (1) That ferromagnetic atoms in a crystal have quadrupole moments. (2) That the Weiss-Heisenberg theory is incorrect (spontaneous magnetization in zero field does not exist).

It is the purpose of this note to point out that these assumptions are arbitrary only in their wording, and that their physical content may be retained without having to assume any new or unexplained physical processes.

As to the first point, quadrupole moments are assumed in order to account for the fact that I and H are not, in general, parallel in a cubic crystal. Heisenberg has suggested[2]

[1] N. S. Akulov, Zeits. f. Physik **67**, 794, (1931). References to previous articles are given in this paper.

[2] W. Heisenberg, Metallwirtschaft **9**, 843, (1930).

that this is due to a coupling between spin and orbital moments. The idea has been carried out mathematically by Powell[3] who obtains essentially the same formulae as Akulov for the dependence of the energy on the direction of magnetization. In other words, one might express Powell's result by saying that, by taking into account the interactions of the type $(s-l)$ a ferromagnetic lattice is in certain respects equivalent to a lattice of quadrupoles.

Secondly, to account for the low hysteresis in single crystals, Akulov finds it necessary to assume that there are no regions of spontaneous magnetization. In one of his papers he has what purports to be a proof of the impossibility of spontaneous magnetization.[4] That this proof is not valid is evident from the argument in the ensuing communication. It *is* possible to have spontaneous magnetization in various regions and at the same time negligible hysteresis losses, provided the regions are sufficiently small. In other words, by assuming the regions of spontaneous magnetization to be small, it is possible to satisfy Akulov's assumption of demagnetization (Schrumpfprozess) in a single grain without destroying the Weiss-Heisenberg theory.

FRANCIS BITTER
Westinghouse Research Laboratories,
East Pittsburgh, Pennsylvania,
March 30, 1931.

[3] F. C. Powell, Proc. Roy. Soc. **A130,** 167 (1930).

[4] N. S. Akulov. Zeits. f. Physik **64,** 559 (1930).

Block Structure and Hysteresis Phenomena

In a previous communication[1] I have pointed out the possibility that the regions of spontaneous magnetization in the Weiss-Heisenberg theory are very small, containing very roughly 10^5 atoms, and that perhaps they are related to Zwicky's block structure.[2] Since then it has been possible to make some of the calculations more precise. The details will be published elsewhere. At present I wish to point out how a magnetization curve is to be described. Consider a single crystal made up of blocks and let the energy per block be given by an expression,[3] for instance, of the type

$$\Phi = A + B\cos(\theta+\alpha) + C\cos 2\theta + D\cos 4\theta$$

The above expression for Φ is written in this form to indicate, first, a dependence on the orientation of the magnetization with respect to the crystal axes, and secondly, the existence of several minima for Φ. The depth and position of these minima depend on the values of A,B,C,D, which, in turn, depend on constants of the material, on the internal strains, and on the applied magnetic field. For equilibrium, the probability of finding a block magnetized in the direction θ is given by an expression of the form $\exp(-\Phi/KT)$. If the depth of the minima of Φ is large compared to KT, the directions of magnetization will be almost entirely confined to these minima, and a transition from one minimum to another will be very improbable. This gives rise to hysteresis and magnetic viscosity. The procedure for handling this problem is being presented at the Washington meeting of the American Physical Society. If, however, the depth of the minima is of the same order of magnitude as KT, transitions from one minimum to another are reasonably probable, and we have, practically, the above exponential distribution at all times. Thus, to state the case crudely, if the shape of the potential Φ is slowly varied by varying H, the resulting intensity will be independent of the previous history of the sample provided the depth of the minima of Φ is of the same order of magnitude as KT. Akulov[4] estimates the depth of the minima in unstrained single crystals of iron to be 10^5 ergs/cm^3, and points out that the hysteresis of single crystals is negligible, That is, I is independent of the previous history of the sample. Then, according to the above, if v is the volume of a block, we must have

$$\Phi \sim v\times 10^5 \text{ ergs/cm}^3 \sim KT = 1.37\times 10^{-16}\times 300$$
$$v \sim 4\times 10^{-19} \text{ cm}^3.$$

[1] F. Bitter, Phys. Rev. **37,** 91, (1931).

[2] D. Zwicky, Helvetica Physica Acta **3,** 269 (1930).

[3] N. S. Akulov, Zeits. f. Physik, **67,** 794, (1931); F. C. Powell, Proc. Roy. Soc. **A130,** 167, (1930); R. Becker, Zeits. f. Physik **62,** 253, (1930).

[4] N. S. Akulov, Zeits. f. Physik **64,** 559 (1930).

If v_0 is the average volume per atom, and $n=v/v_0$=the number of atoms per block, we have that $v_0=M/N\rho=56/6\times10^{23}\times8=1.2\times10^{-23}$ cm^3 and hence $nv4\times10^{-19}/1.2\times10^{-23}=$ 35,000 atoms or roughly the same number as that previously deduced.

FRANCIS BITTER
Westinghouse Research Laboratories,
East Pittsburgh, Pennsylvania,
March 30, 1931.

Electron-pair Bonds versus Polarization in Crystals

In a letter in the March 15th number of the Physical Review (**37,** 775 (1931)) Mr. W. H. Zachariasen states, "So far the application of the principles of shared electron pairs on the atomic arrangement in inorganic crystals has proved unsuccessful, while considerations of the crystal structure from point of view of ions, ionic dimensions, ionic polarizability, and crystal energy . . . have given very valuable and important results." Such a statement I can hardly let go unchallenged.

Certainly the concepts of ions, ionic dimensions and crystal energy have proven very useful, especially in the theoretical treatment of such structures as the alkali halides, in which without question the structural units are simple ions. That however does not justify the consideration of XO_3^- ions as composed of O^{--} and distorted X^{+5} ions, when much chemical and physical evidence points to the existence of non-polar bonds between the atoms in such groups. We can agree that polarization does exist in an ion of this sort, but it seems to me more logical to consider it a *result* of the fact that completion of the valence shells of all these electronegative atoms by the formation of shared electron-pair bonds produces an unsymmetrical arrangement, rather than the *cause* of that arrangement.

The polarization concept has been used to "explain" many things[1] which are probably little related to it,—for instance the irregularities in melting and boiling points of the alkali halides, later given a satisfactory quantitative treatment by Pauling[2] on the basis of "radius ratios." On the other hand the Lewis theory of shared electron-pairs is now generally agreed to for molecules and for ions (including XO_3^-)in solution and I see no reason why it should not apply equally well to crystals. One can predict from it in the first place whether or not any electronegative atoms will be adjacent to each other in the crystal and in the second place not only the number of "contacts" between electronegative atoms but also the approximate angles between them. How else can one explain such structures as those of I_2, Se, Te, As, Sb, Bi, FeS_2, SiO_2, As_4O_6, $K_2S_2O_6$[3] (in which pairs of sulfur atoms are surrounded at corners of a distorted octahedron by oxygen atoms), and many more? I can imagine no satisfactory explanation in terms of "ions, ionic dimensions, ionic polarizability and crystal energy"alone. The "tetrahedral" XO_3^- structure, indicated in the early work on $NaClO_3$ and $NaBrO_3$ and beautifully proven by Mr. Zachariasen's researches, furnishes still another example of a prediction directly from Lewis' postulates which has been experimentally verified.

Mr. Zachariasen states that "Until one is able to treat the quantization of the electrons in polyatomic groups completely on the basis of wave mechanics, we must be satisfied with rough approximations." In view of Pauling's recent very satisfactory wave-mechanics treatment of electron-pair bonds in crystals[4] perhaps he will now be willing to abandon his rough approximations in favor of the point of view I have been upholding.

In order that there be no misunderstanding regarding the rule given in the next to the last paragraph of Mr. Zachariasen's communication, I might mention that for every example given the predictions on the basis of the Lewis theory would be precisely the same. Moreover Lewis' conceptions are much more general in their application than is this rule and so more useful.

Perhaps after I have read Mr. Zachariasen's

[1] For a summary see Grimm, Handbuch der Physik **24,** 561-568 (Springer, Berlin, 1927(.

[2] Pauling, Zeits. f. Krist. **67,** 377 (1928).

[3] The analysis of this structure, by Glenn O. Frank and the writer, was reported at the Toronto Meeting of the Mineralogical Society of America last December and will soon be submitted for publication in the American Mineralogist.

[4] Pauling, J. Am. Chem. Soc., April 1931; also in a forthcoming article in the Zeitschrift für Kristallographie.

forthcoming article on XO_3 groups in crystals (which I shall be much interested in doing) and he has read one of mine on "Principles Determining the Arrangement of Atoms and Ions in Crystals," to be published soon in the Journal of Physical Chemistry, as well as the articles of Pauling's mentioned, we can come to a better mutual understanding.

MAURICE L. HUGGINS
Stanford University,
Stanford, California,
April 9, 1931.

Evidence of the Detection of Element 85 in Certain Substances

With a magneto-optic method of analysis (Allison and Murphy, Jour. Amer. Chem. Soc. **52,** 3796 (1930); Phys. Rev. **36,** 1097 (1930)) we have made a search for element 85 in various substances in which its presence might be suspected. Out of a considerable number of substances examined, we have found evidence which seems to us to indicate, to a high order of probability, the presence of element 85 in the following: sea water, fluorite, apatite, monazite sand (Brazilian), kainite (Stassfurt), potassium bromide, hydrofluoric acid and hydrobromic acid. The evidence is presented in the data displayed in the accompanying graphs, and is supported by certain chemical reactions.

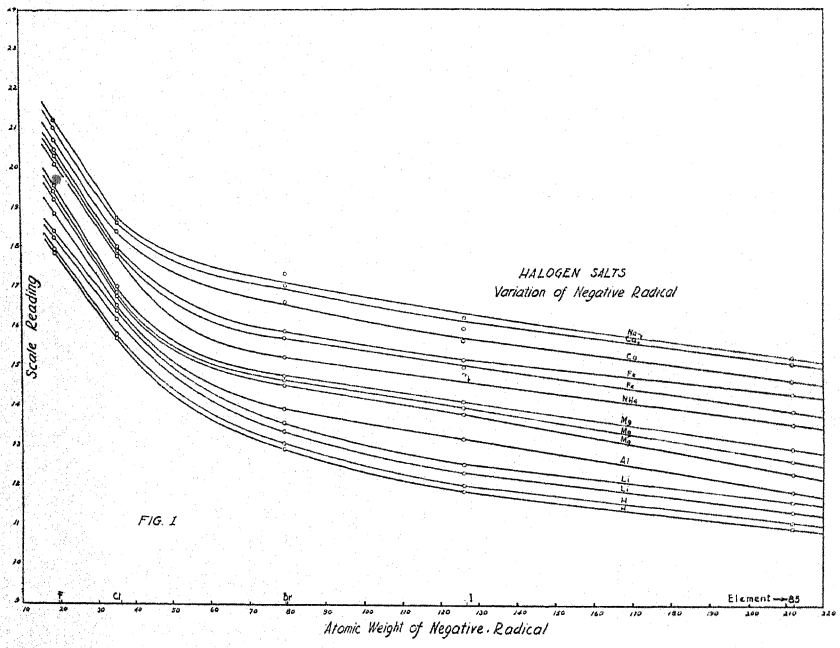

Fig. 1.

In Fig. 1 are plotted the atomic weights of the halogens against the scale readings of the minima of light intensity characteristic of several of their compounds, increasing scale readings representing decreasing time lags. These acids as do other inorganic acids which we have studied, produce each two characteristic minima, while the salts, as do other inorganic salts, produce in general minima equal in number to the known isotopes of the metallic element of the salt.

The two lower curves (Fig. 1) show our observations for hydrofluoric, hydrochloric, hydrobromic, hydriodic acids and what we will call provisionally "85" acid, each acid forming two minima of light. The other curves, in order, exhibit the data obtained for the halides of lithium, aluminum, magnesium, ammonium, iron, calcium, and sodium. It will be seen that we find minima in each case appropriate to an "85" salt, that the number of these minima is without exception

the same as that of the other halides and that they lie well on the extended curves.

The same data are shown somewhat differently in Fig. 2, in which the chemical equivalents of the isotopes of the metallic radicals

five series beyond sodium, except in the case of the chlorides, because of the difficulties introduced by the overlapping in these regions of the scale of the minima produced by the halogen salts of the heavier elements.

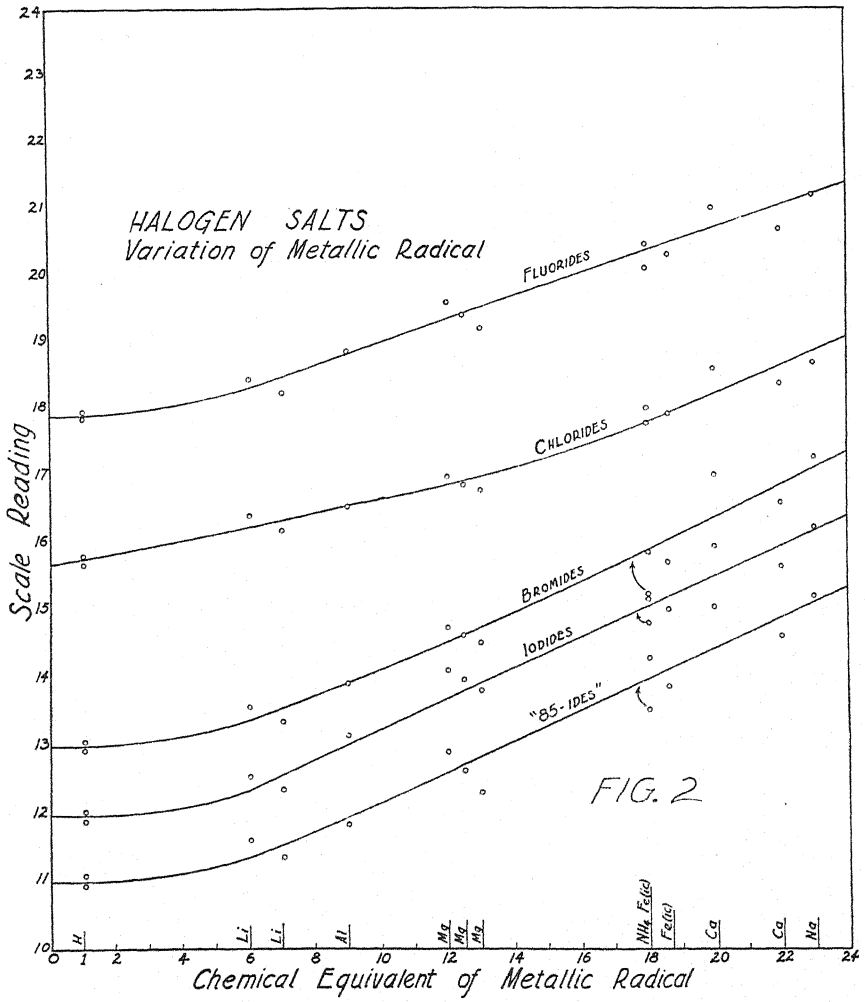

Fig. 2.

are plotted against the scale readings of the characteristic minima of the compounds. The upper curve represents the fluorides of hydrogen, lithium, aluminum, magnesium, ammonium, iron, calcium and sodium. The next three curves represent, respectively, the chlorides, the bromides and the iodides, while the last curve represents what we have termed the "85"-ides, of the same elements. We have not as yet extended our observations for the

According to our quantitative estimates, the greatest abundance of the element found in any of the above mentioned substances, in unconcentrated form, is of the order of 1 part in 10.[9] Concentrations in the form of Li85, using monazite sand as a source, are now in progress and have already met with considerable success. The characteristic minima of H85 disappear on the addition of aqua regia, bromine or iodine to the solution. These

minima are restored by the addition of sulphur dioxide or stannous chloride. These are the only oxidizing and reducing agents which have been tried. All reagents used gave negative tests for H85.

These investigations have been under way since the middle of the past summer. More recently they have been repeated and extended by one of us (F.A.) in a somewhat more precise manner, while the chemical investigations have been carried on by two of us (E.R.B. and A.L.S.).

FRED ALLISON
EDGAR J. MURPHY
EDNA R. BISHOP
ANNA L. SOMMER

Department of Physics,
Alabama Polytechnic Institute,
April 3, 1931.

The Principle of Continuity and Regularity of Series of Atom Nuclei (Atomic Species)

While what may now be called the principle of continuity and regularity of the series of atomic species, has been used by the writer in the prediction of isotopes, and has been presented in the form of diagrams for 10 years, the complexity of the diagrams seems to have prevented the recognition of this principle by others. It therefore seems important to give a name to the principle and to illustrate it by simple drawings.

The first figure is taken, with five minor changes which do not affect the general pattern, from a diagram of the helium-thorium series which was used to predict numerous isotopes, most of which have now been found or shown to be probable. The maximum number of isobaric species given in this 1923 figure (J. Franklin Inst. **195**, 554) is 3, as is shown in Fig. 1.

The uranium series (Fig. 2) exhibits at

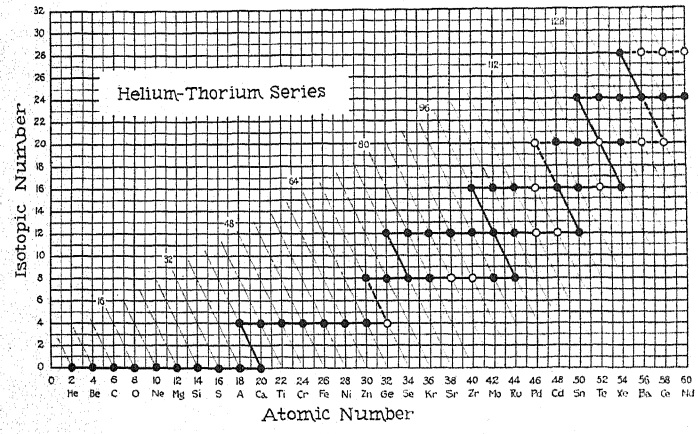

Fig. 1.

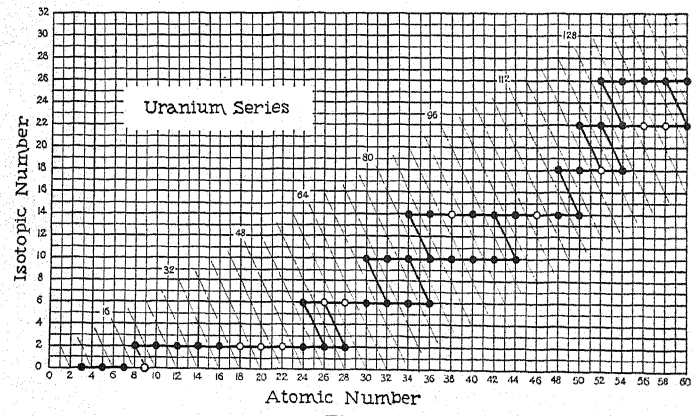

Fig. 2.

present a very simple pattern. The atomic masses (diagonal lines) for both the uranium ($4n+2$) and the thorium ($4n$) series are even, and the general increment of isotopic number or atomic mass between levels in either series is 4, which represents an increment of 2 in the number of cementing or β-electrons. Among the non-radioactive elements a single isotopic number in no case represents species of both the atomic number. The minor differences are explained by other relations presented earlier. These cannot be discussed, on account of lack of space, except that it may be stated that the fact that species of isotopic number 3 are not as yet found in the lithium series, but are found in the beryllium series, is in accord with these relations. These two series thus occupy odd isotopic lines in common, and the

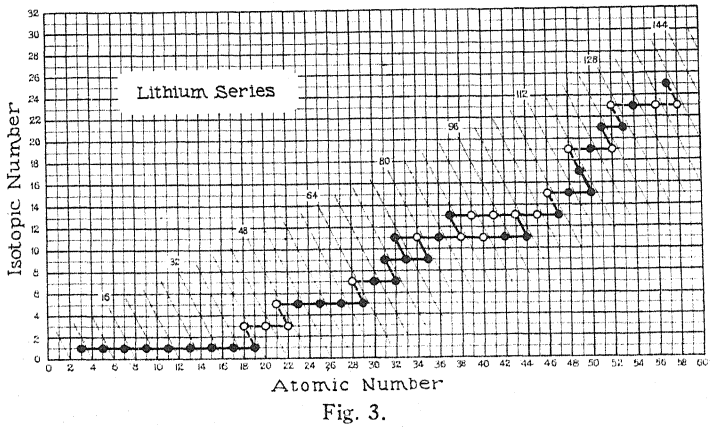

Fig. 3.

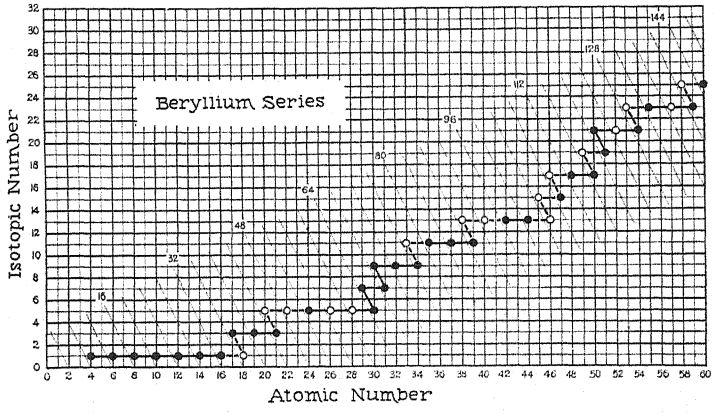

Fig. 4.

series, with the exception of three species of the uranium series on the base line, of the writer's class 4, which have the isotopic number zero, which is normally that of the helium-thorium series. Here a fluorine isotope of mass 18 is indicated as probable.

The $4n+3$ or lithium series (Fig. 3), and the $4n+1$ or beryllium series (Fig. 4) represent odd atomic weights, and the two patterns are made almost identical if the lithium series is plotted with $Z+1$ as abscissae, where Z is general increment in isotopic number in either series is 2.

If the lithium and beryllium series together are considered as a single or "odd" series, very simple relations are exhibited, or the principle of continuity and regularity still holds. Along a given isotopic line the increment of atomic number is one, of atomic mass 2, and of number of electrons, one. Thus the common increment is represented by the formula p_2e in which p represents a proton and e an electron.

This corresponds to an increment of a half alpha-particle. Thus for isotopic number 1 every atomic number from 3 to 17 represents a known species of the combined series.

The fact that the number of superposed levels in each of the even helium and uranium series is larger than in the odd lithium series is in accord with the relation (Proc. Nat. Acad. **2**, 216 (1916) and later papers) that higher nuclear stability is found in general for even than for odd nuclear charge. The smaller number of levels in the beryllium series is in accord with the even more general rule (J. Am. Chem. Soc. **39**, 859 (1917), **42**, 1991–2 (1920) that the electrons in atom nuclei are in general associated in pairs, and an odd number of electrons gives to a nucleus a relatively low stability as compared with that associated with adjacent even numbers, since the beryllium series is the only one in which the number of nuclear electrons is odd, when the atomic number is even (except the class 4 species of Li, B, and N).

The diagonal lines in the charts give the atomic masses. While chlorine of isotopic number 5 and atomic weight 39 is indicated as already discovered, the discovery is not as yet confirmed.

WILLIAM D. HARKINS

University of Chicago,
April 9, 1931.

Anomalies in Hyperfine Structures

In a recently published paper Goudsmit[1] points out that the empirically observed hyperfine structure patterns show in some cases very marked deviations from theoretically expected relationships. The discrepancy is observed in the region of high atomic numbers and is usually such as to make it necessary to ascribe an anomalously large separation to the $p_{1/2}$ term of the single electron spectrum. The interval rule appears to be obeyed in the case of Bi rather accurately. It is logical therefore to look for an explanation in the manner in which the $p_{1/2}$ and $p_{3/2}$ states interact with the nucleus.

Dirac's equation shows in fact that such a difference is to be expected. A calculation exactly similar to the one made by the writer[2] for s terms shows that $\overline{(r^{-3})}$ of the ordinary formulas for $p_{1/2}$, $p_{3/2}$ must be replaced by $(2\pi/A)I, -(4\pi/A)I$, $I=\int\phi_1\phi_2 r^{-3}dr$. Here ϕ_1, ϕ_2 are the two radial functions of Dirac-Gordon (denoted by Gordon as ψ_1, ψ_2). The normalizing factor is chosen so as to have $\int(\phi_1^2+\phi_2^2)dr=1$. In the neighborhood of the nucleus the "term-value energy" and screening

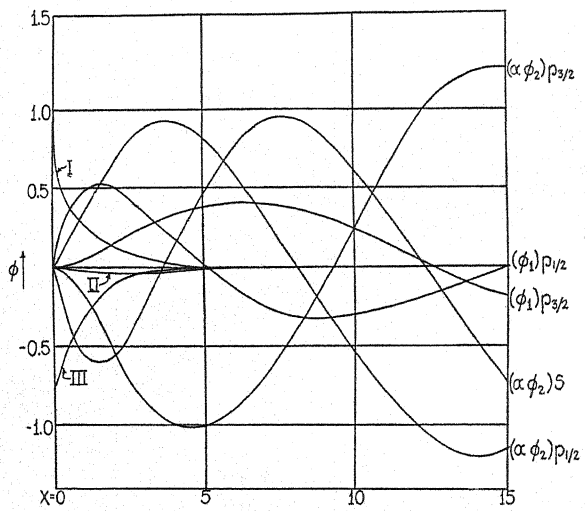

Fig. 1. I is $\phi_1\phi_2/x^2$ for $P_{\frac{1}{2}}$. II is $\phi_1\phi_2 x^2$ for $P_{3/2}$. III is $\phi_1\phi_2 x^2$ for s.

[1] S. Goudsmit, Phys. Rev. **37**, 663 (1931).
[2] G. Breit, Phys. Rev. **35**, 1447 (1930).

effects may be neglected. Under these conditions

$$\phi_1 = J_{2\rho}(2x^{1/2})$$
$$\alpha\phi_2 = (j' - \rho)J_{2\rho}(2x^{1/2}) + x^{1/2}J_{2\rho+1}(2x^{1/2})$$
$$\alpha = 2\pi Ze^2/hc,\ \rho = (j'^2 - \alpha^2)^{1/2},\ x = 2Zr/a_H$$

The J_n are Bessel functions of order n; $j' = -1$, 1, -2 for s, $p_{1/2}$, $p_{3/2}$. The results of calculation with the above formulas are represented graphically for $\alpha = 0.661$, $Z \geqq 91$. The region close to the nucleus is seen to contribute more to the I for $p_{1/2}$ than for $p_{3/2}$. The contribution to the effective value of $\overline{(r^{-3})}$ due to this region is expected to be large for $p_{1/2}$ and of the same order as the customary $2\pi\psi^2(0)$ of Fermi. In fact in the approximation of Schroedinger's non-relativistic equation we have to replace $\alpha\phi_2$ for s terms by $-x^{1/2}J_1(2x^{1/2})$. This is also plotted on the figure as $(\alpha\phi_2)_s$. The scale of all curves is seen to be roughly the same. The normalizing factor is approximately K given by $K^2(\phi_2(r)/r)^2 = 4\pi\psi^2(r)$. Hence $K^2 = 2\pi\psi^2(0)$ and $K^2 4\pi I/\Lambda \geqq 4\pi^2(a_H/\Lambda Z)\psi^2(0)\int\phi_1\phi_2 x^{-2}dx$. The integral in x is seen to be of the order of 1 and the whole of the order of $2\pi\psi^2(0)$. For comparison we have also given the $\phi_1\phi_2/x^2$ curve for s terms in the non-relativistic approximation. Dirac's equation gives higher values for s terms as well.

We may say therefore that for the calculation of the hyperfine structure intervals the $p_{1/2}$ states of heavy atoms should be considered as penetrating orbits in the neighborhood of the nucleus. For this reason alone their hyperfine structure may be anomalously great. Other effects must of course also be considered. According to Goudsmit's estimates there is no special reason to believe that they are very important. Nevertheless their effect and the contribution of regions of higher r to I must be taken into account before a quantitative comparison with experiment may be made. At present the observed deviations from simple approximate formulas are qualitatively in agreement with theory being in the correct direction and of the proper order of magnitude.

G. BREIT

Department of Physics,
New York University,
April 8, 1931.

On the Infrared Absorption by Hydrogen Sulphide at 8.0μ

Papers published by Rollefson[1] and Mischke[2] on the infrared absorption spectrum of hydrogen sulphide report the presence of an absorption band at about the wave-length 8.0μ. In a more recent paper, one of the authors working with E. F. Barker[3] at the University of Michigan, reported that a diligent search for this band had failed to confirm it. Each time when it was looked for and not found, the existence of the other two bands reported, at 2.65μ and 3.8μ respectively, were first checked. It was therefore concluded that the region at 8.0μ could not be attributed to hydrogen sulphide.

A series of measurements have been carried out with a Wadsworth prism spectrometer, especially in the region from 7.0μ to 9.0μ further to investigate the nature of the effect observed by Rollefson and Mischke. For this purpose a cell eight inches long, and equipped with rock-salt windows was used; so arranged that it could be tipped in and out of the beam. The cell was first filled with air passed through wash bottles containing KHS and then dried through towers containing successive layers of glass wool on which was sprinkled phosphorus pentoxide. A curve was first made from data taken between the dried air and the atmosphere, then a similar curve was run with the cell filled with hydrogen sulphide, purified and dried as before, and the curves were plotted for comparison. These two curves were very similar in appearance, at first glance much resembling absorption bands It was noticed, however that the ratio of the radiation apparently transmitted through the cell to that of the beam when the cell was removed (i.e. the apparent percentage absorption) was much less on the short wave side than on the long wave side. This suggested the possibility that the observed effect might be ascribed to water vapor falsification arising from the water vapor band at 6.2μ which in moist weather may well extend out beyond 8.0μ. The object of the remainder of this experiment was to test this point.

Water vapor falsifications may be very annoying, especially when long cells are used. The cell used in this experiment was equiva-

[1] A. H. Rollefson, Phys. Rev. **34**, 604 (1929).

[2] W. Mischke, Zeits. f. Physik **67**, 106 (1931).

H. H. Nielsen, and E. F. Barker, Phys. Rev. **37**, 1931.

lent to about one tenth of the entire light path. Consequently it is to be expected that in regions of water vapor absorption, when the cell, filled with very dry air, is tipped into the beam that more energy may be transmitted than when the cell is out of the beam, since by inserting the cell the path through which atmospheric water vapor absorption may occur has actually been shortened. Hence in regions of strong atmospheric absorption, one may observe what appears to be negative absorption, while in regions of less intense absorption this is less apparent or disappears entirely. These falsifications may however be quite deceiving, giving the appearance of an absorption band in the dry gas in the cell—maxima in the water vapor spectrum producing what appear to be minima in a spectrum of the gas under observation, and vice versa. To compensate for the windows, the final readings were plotted against transmission through the cell filled with atmospheric air. Curves for comparison representing percentage absorbed were made from data taken on hydrogen sulphide and dried air against atmospheric air and these were found to reproduce one another even in minute details. A similar curve was plotted of data taken on wet hydrogen sulphide against atmospheric air. The resulting curve appeared as a mirror image of the previous ones.

In Fig. 1 curve A represents ratios of transmission through the cell filled with dry hydrogen sulphide and through the cell filled with dried air. On another occasion a curve was made representing ratios of data taken on transmission through dry hydrogen sulphide and dry air. In spite of the fact that the data were all taken on the same day it was found that the humidity had changed a great deal during the time of the experiment. This curve was very similar to A. It indicated that the amount of water vapor displaced by the cell was less in the measurements made on dry air than those made on dry H_2S. This was actually the case since hygrometer readings showed showed the humidity at this time to be much higher than when the data on dry air were taken. Curve B is a sketch of Rollefson's curve for H_2S at 8.0μ placed there for comparison, while C represents the general appearance of Hettner's curve for water vapor in this region. We wish to call attention to the general agreement between that observed by us and Rollefson's curve and in addition to point out that nearly every maximum in Hettner's curve coincides with a minimum in our curve and vice versa.

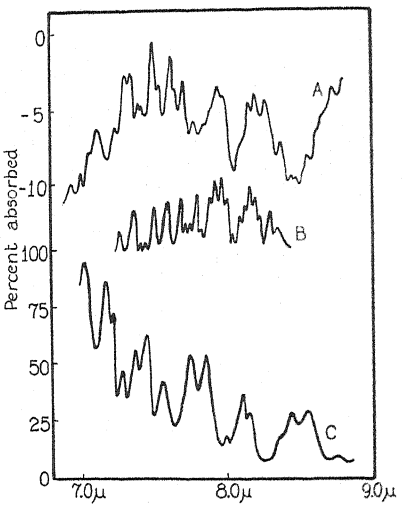

Fig. 1.

We suggest therefore, as an explanation of the band reported by Rollefson and by Mischke at 8.0μ in hydrogen sulphide, that it is not due to hydrogen sulphide, but rather due to water vapor falsifications which may arise when a long cell is used. This evidence is further supported by the fact that the spacings between the lines as given by Rollefson are of the same magnitude as those given by Sleator and Phelps[4] in their work on water vapor absorption rather than those observed in the bands of hydrogen sulphide.

H. H. NIELSEN
A. D. SPRAGUE
Ohio State University,
Mendenhall Laboratory of Physics,
April 6, 1931.

[4] W. W. Sleator, and E. R. Phelps, Astrophys. J. **62**, 28 (1925).

Measurement of the Kerr Effect in the Infrared Spectrum

The work of Szivessy and Dierkesmann (Ann. d. Physik (5) **3**, 507 (1929)) in extending dispersion measurements of the Kerr electro-optic effect beyond the customary visible spectrum into the ultraviolet would seem to call for a similar extension into the infrared, if

possible. This I have recently succeeded in doing, in the case of carbon disulphide, with an accuracy apparently not far short of that attained in visual measurements.

The apparatus consists of a spectro-bolometer with very sensitive galvanometer, operated in connection with a Kerr cell. This has plates 5×37 cm and 1.3 cm apart. Light from a special tungsten strip filament lamp is concentrated in a narrow conical beam to an image in the center of the cell, from which it diverges to be focussed later on the slit of the spectrometer. A large aperture double-image prism (only one of the images is utilized) polarizes the entering light in the 45° azimuth and a similar prism crossed at 90° serves as "analyzer." The electrostatic stress converts the plane polarized light into elliptical and the minor axis of the ellipse is proportional to the square root of the resultant galvanometer deflection. The phase difference is readily computed upon comparing the deflection with that produced by a known rotation of the polarizing prism. A high speed Wehrsen "Mercedes" static machine has so far served as a very satisfactory source of high potential.

The spectral range which can be explored in this way seems to be from about 0.5μ to 2μ or beyond, thus extending the previous wavelength range for this work some four-fold. Carbon disulphide, over this range, shows a dispersion of the Kerr double refraction in better agreement with the Havelock formula $B=C(n^2-1)^2/\lambda n$ than might reasonably be expected. There are some discrepancies, however, to be investigated more carefully later—and explained if possible. The method is to be further developed and extended to such other materials as have sufficient infrared transparency.

L. R. INGERSOLL

Physical Laboratory,
University of Wisconsin,
April 7, 1931.

Quantum Mechanics and the Chemical Bond

Three years ago I announced in a short note[1] the discovery of some new results regarding the chemical bond. It was pointed out that under certain conditions the formation of chemical bonds by an atom can destroy the distinction between s and p eigenfunctions, and a criterion determining whether this change in quantization of the single-electron eigenfunctions will or will not take place was given. It was also announced that this change in quantization permits the formation of four equivalent tetrahedral bonds by carbon.

Since then a number of further results bearing on the nature of the chemical bond have been obtained; it is the purpose of this letter to call the attention of physicists to a paper in the April, 1931, issue of the Journal of the American Chemical Society in which they are given in detail. It was first shown from the quantum mechanics that the main resonance integrals for an electron-pair bond between two atoms involve only one single-electron eigenfunction on each atom. In consequence many properties of electron-pair bonds can be derived from a consideration of single-electron eigenfunctions alone. Thus it is shown that if $s-p$ quantization is not changed, the bonds formed by the p eigenfunctions will tend to be at right angles to one another. A very simple but powerful approximate *quantitative* treatment of bond strengths is given. With its aid it is shown that when $s-p$ quantization is broken through bond formation, the best bond eigenfunctions which can be formed from a combination of s and p eigenfunctions alone are tetrahedral eigenfunctions, so that the two, three, or four bonds formed will tend to make angles of 109°28′ with one another. This explains the tetrahedral angles found experimentally not only for quadricovalent carbon, nitrogen, silicon, etc., but also for tricovalent nitrogen, oxygen, etc. The tetrahedral eigenfunctions also allow free rotation about single bonds, but not about double bonds.

When d eigenfunctions as well as s and p are available for bond-eigenfunction formation a number of bond configurations are possible. One d eigenfunction with s and p permits the construction of only four strong bonds, *and these are directed towards the corners of a square.* Such a configuration has been shown to exist for bivalent palladium and platinum, and this theory predicts it also for bivalent nickel in $K_2Ni(CN)_4$ and for trivalent gold. Two d eigenfunctions give six strong bonds directed towards the corners of an octahedron; this configuration is found in many complexes.

[1] Linus Pauling, Proc. Nat. Acad. Sci. **14**, 359 (1928).

It is also shown that in complex ions the orbital magnetic moments of electrons are extinguished through the interaction with surrounding atoms, so that the magnetic moment is due to the spin moments of unpaired electrons alone. Together with the results obtained regarding bond eigenfunctions, this leads to a complete theory of the magnetic moments of polyatomic molecules and complex ions. With its aid magnetic data have been shown to provide verification of many predictions regarding bond eigenfunctions; and in a number of doubtful cases magnetic data provide a basis for definite decision as to the type of bonds in a given complex.

These results have also permitted the formulation of a set of principles determining the structure of crystals containing electron-pair bonds, to be published in the Zeitschrift für Kristallographie.

Three of these results have been independently obtained by Slater and announced in a preliminary communication.[2] He points out the possibility of the formation of four equivalent tetrahedral bonds by a carbon atom (as I did in 1928), without giving the tetrahedral eigenfunctions and without recognizing that tetrahedral eigenfunctions are also important even when fewer than four bonds are formed; and mentions that this leads to restricted rotation about a double bond. Having apparently assumed the importance of one single-electron eigenfunction to bond formation, he also shows that p eigenfunctions should lead to 90° bond angles.

LINUS PAULING

Gates Chemical Laboratory,
California Institute of Technology,
April 7, 1931.

[2] J. C. Slater, Phys. Rev. **37**, 481 (1931).

Time Lag in Changes of Electrical Properties of Rubber with Temperature and Pressure

An abstract of a paper by the author entitled "Time Lag in Changes of Electrical Properties of Rubber with Temperature and Pressure" appeared in the Physical Review, Vol. 35, page 1429, June 1, 1930. Data were presented which apparently showed that two or more hours might be required for the dielectric constant, power factor, and resistivity to become constant after the temperature had been changed. In attempting to check these results, an error in experimental technique was discovered. Measurements with improved apparatus show that the dielectric constants and power factor follow the temperature changes with little if any time lag. No additional measurements on rubber under pressure have as yet been made.

ARNOLD H. SCOTT

Bureau of Standards,
Washington, D.C.,
April 6, 1931.

The Uncertainty Principle

Kennard has connected the uncertainty principle with radioactive disintegration by showing (Phys. Zeits. **30**, 495–497) how to derive Gamow's formula for radioactive disintegration from known quantum principles plus the uncertainty principle of Heisenberg without the additional postulate assumed by Gamow that a particle of energy W can pass through a potential wall of height $V > W$.

Here we have the pure chance phenomena of radioactive disintegration, independent of the disturbance produced by the act of measurement, and performed for us by nature at a rate that has remained constant since the solidification of the earth's crust, linked with the probability phenomena of the new quantum mechanics, the indeterminateness of which is assumed to be caused by an uncontrollable perturbation introduced of necessity in the process of measurement.

Is it not better to leave the indeterminateness in nature where we find it, rather than to attribute it to the inevitable perturbation introduced when making an observation, although we do not know how this perturbation introduces the indeterminacy?

If we can believe that the general laws of quantum mechanics are fundamental laws of nature, the various possibilities of natural behavior should be inherent in these laws, whether they be of a physical, chemical or biological character. I shall not expatiate here on the considerable progress that has already been made by the application of the quantum laws to chemistry, by the work of Heitler, London, and Slater. The generality

of these laws, which is responsible for their abstractness, and their flexibility, as evinced in a concrete manner by the uncertainty principle, make for their adaptability to other domains of thought. One might expect that this generality and plasticity would be characteristic of fundamental laws of nature. Viewed in this light one need not make apologies for nature by attributing the indeterminateness in its laws to the limitation of our knowledge imposed on us by the very act of observation.* Although if one feels that somehow our fallibility does play a part in our picture of the universe, one might view the objective laws of quantum mechanics as bringing before us the subjective aspect of definition and concept. As for the uncertainty principle, one can, following Darwin (Proc. Royal Soc. **A130,** 1931), regard it in the same role as the part played by the clocks and rods in the early formulation of the relativity theory when it was necessary to supplement the formal theory by concrete examples showing how the old classical ideas failed in specific cases. The general laws of the quantum mechanics, which are at the bottom of the uncertainty principle, are not conditioned by a theoretical clumsiness in our means of observation.

The intimate connection between the indeterminateness in quantum mechanics and the concept of observation may be due to the fact that "observation" implies structure. We could not plan our experiments but with the supposition that the elementary entities of nature have a structure. But the elementary entities of nature have neither a particle nor a wave basis. It is only after quantization—after observation—that one can legitimately introduce space and time. The Schroedinger equation may be looked upon as controlling, in a statistical way, the space-time manifestations of the elementary entities of nature, although the equation itself is devoid of any geometrical interpretation. We make manifest the indeterminateness in nature by bringing over space-time concepts and space-time description to atomic theories that, in order to predict, must go beyond observation. If a scientific theory were humbled to be valid only as far as observation goes, what would happen to cosmogony and geophysics? Should one doubt the validity of scientific inference because it yields results that can not be expressed in terms of familiar things, that are beyond the range of our sensations? There are good reasons for believing that quantum laws are not laws which man's mind has imposed on nature but are laws which nature is having a rather difficult time imposing on man's mind.

Finally, if one does not try to elevate his preconceived ideas and intuitions about causality to a law of nature, but merely views causality as the assumption that nature can be comprehended, can be grasped in thought—though not in imagery—there is no failure of causality in quantum mechanics.

ALEXANDER W. STERN

Brooklyn, N. Y.,
April 11, 1931.

* Prof. J. E. Turner (Nature **126,** pp. 995) views the indeterminism in quantum mechanics as having nothing to do with causation but interprets "not determined" to mean "not ascertained." Other physicists argue that the uncertainty principle does not exclude exact laws from physics but means merely that we have no way of verifying them.

On the Effect of Resonance in the Exchange of Excitation Energy

It is well known that exchange of excitation energy between atoms on collision takes place most readily if the "resonance" between the two atoms is good, i.e. if the quantum states of the two atoms are such that the excitation energy of one nearly matches the excitation energy of the other, so that only a small change in the relative kinetic energy of the two atoms is necessary in order to effect the energy balance before and after the collision.

This point has been discussed by Kallmann and London (Zeits. f. physik. Chem. **2B,** 207 1929)) who came to the conclusion that the cross-section would in general be larger the better the resonance. Their calculation is very interesting but not entirely free from objections. It may, therefore, not be out of place to look at the matter from another point of view, perhaps itself open to some objections, but which I believe brings out the nature of the problem very clearly.

The Franck-Condon principle, which says that those transitions are most probable which disturb the motion of the nuclei the least, has been very successful in accounting for the intensities in band spectra, and it has also

been applied recently to the case of predissociation (Franck and Sponer, Göttingen Nach., 1928, 241; Herzberg, Zeits. f. Physik **61**, 604 (1930); Turner, Bull. Am. Phys. Soc. **6**, 16 (1931)). Now in the case under consideration we can treat the pair of atoms which exchange energy as an unstable molecule, draw potential energy curves for the electronic states of the "molecule," (similar to London, Zeits. f. physik. Chem. **11B**, 222 (1930)) and handle the transitions from one continuum to another in the same way that we treat, in the predissociation case, transitions which take place from a discrete state to a continuum. It may be well to point out, parenthetically, that the case of predissociation and the present case are really quite different from the case of adsorption or emission of radiation, and, naturally, the real justification of this use of the Franck-Condon rule will come when the matter has been given a more or less rigorous quantum mechanical investigation.

In Fig. 1 let curve 1 be the potential energy curve (potential energy $= U$, distance between atoms $= r$) with atom A excited, atom B unexcited, and let curve 2 be the curve with atom B excited, A unexcited. Suppose curve 1 represents the initial state of the pair of atoms. Then its intersection with a horizontal line gives the distance of closest approach of the atoms if they make a head-on collision with the energy indicated by the horizontal line. If curve 1, curve 2, and the horizontal line intersect at the same point, as shown, or somewhat near the same point, then, according to the Frank-Condon theory, we may expect a relatively large probability of transition provided, of course, the interaction between the atoms at this distance, r, is great enough. If the two atoms do not collide head on, this means that they have a relative angular momentum, and we can represent the situation by adding a term $(h^2/8\pi^2 M)\, j(j+1)/r^2$ to the potential energy, where M is the reduced mass, and j the rotational quantum number; but as a more or less rigorous selection rule for j will hold, practically the same amount must be added to the curve for the final state: they will therefore continue to intersect at the same value of r. Thus all collisions with this distance of approach will be favored. Collisions with something near this distance of approach will be somewhat less favored, and there will be a spherical shell in which favorable collision take place. Now it is seen that the closer together the asymptotic values of U_1, and U_2, in general the greater the distance r at which they will intersect, and hence, we may infer, the greater the size of the spherical shell in which collisions are favored by the particular factor under consideration. It may not be the only factor, and it certainly cannot stretch the region of favorable collisions out indefinitely, but all the indications from analogous cases are that it should be an important factor. The case where the asymptotic values of U_1 and U_2 coincide is just the case of exact resonance, and it is easy to see why transitions with exact resonance should be favored, but it is seen that the precise definition of good resonance is involved in complications which must be treated specially in any given case.

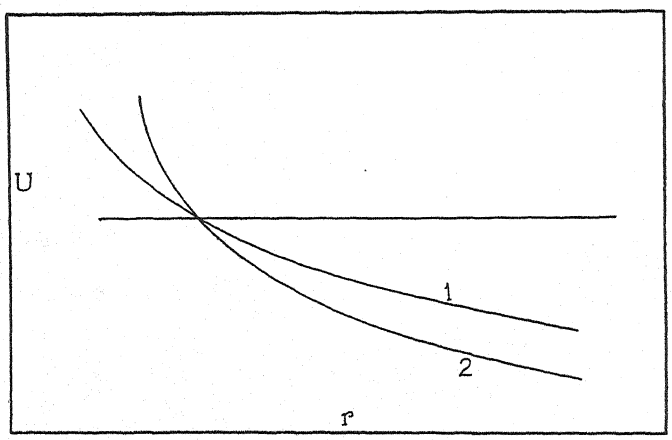

Fig. 1.

Of course, we cannot draw definite conclusions from such qualitative observations, but they at least provide a guide for future quantitative calculations. For the most part the applications of the Franck-Condon principle are just as qualitative as this one, but in the case of band spectra they have provided the stimulus for some successful quantitative work.

I have recently extended the quantitative work described in a preliminary note (Proc. Nat. Acad. Sci. **17,** 34 (1931)), where the force which acts between the two atoms is supposed to be due to their momentary dipole moments, by treating the two atoms as a molecule and using perturbations of the type introduced by Slater, (Proc. Nat. Acad. Sci. **13,** 423 (1927)). It appears, though with some assumptions I am trying to remove, that practically no transitions will take place unless the resonance is extremely good; the potential energy curves in this case do not intersect. Yet, experimentally, cross-sections very much larger than normal, or cross-sections unusually large for the type of transition considered, occur for such great resonance differences as 40 to 60 millivolts. I am inclined to think that other forces than the interaction forces of dipoles come into play, even when the radius of action is very large. Kallmann and London, themselves, noted that large cross sections would be expected when electron orbits are large.

It may be well to mention here that Eq. (5) of my preliminary article mentioned above, is incorrect. This error, which was carried through, should not make much difference in the final results and will be corrected later.

O. K. RICE

Chemical Laboratory,
Harvard University,
April 11, 1931.

The Formation of Striae in a Kundt's Tube

For the past seven years the author has been experimenting on striae formed in a Kundt's tube to determine, if possible, the cause of such striae. An article concerning the use of pith dust in a Kundt's tube was published by the author in Nature **118,** 157 (1926). In July 1929 he was able to show conclusively that a rotation of the dust particles on each side of a striation takes place; Phys. Rev. **36,** 1098 (1930); Science **72,** 442 (1930). January 14, 1931 the author made motion pictures of these rotations which take place on each side

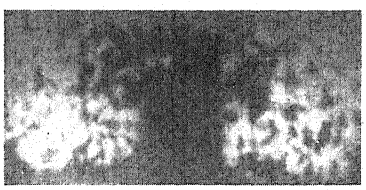

Fig. 1.

of each single striation. Fig. 1 shows an enlarged photograph of one such striation made from the motion picture negative. The black particles composing the striae were cork-charcoal. The striae were produced in a glass tube in which the air was compressed and rarefied by means of a metal piston attached to one prong of an electrically-driven tuning fork. Fig. 2 is a diagram showing the direction of the rotations taking place on each side of a single striation. Further details are given in the references above cited.

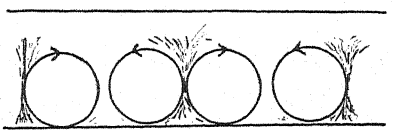

Fig. 2.

The striae in a Kundt's tube are formed by air vortices in the same manner as ripple-marks in sand are formed by water vortices. As shown by Darwin, Proc. Royal Soc. **36,** 18 (1883), these rotations are produced when an alternating fluid flow takes place about obstacles in its path. The clockwise and counter-clockwise rotations are maintained always in the same direction regardless of the fact that the fluid stream is alternating.

Also the author has shown that, when using cork particles of the same size, as the frequency of vibration of the air column in the tube increases, the average distance between striae becomes smaller. The photographs of Fig. 3 illustrate this fact. Also the author has shown that, with a constant frequency of vibration of the air in the tube, as the cork particle size is made smaller, the distance between adjacent striae becomes less. The photographs in Fig. 4 illustrate this fact.

The above mentioned observations will be discussed more in detail in a forthcoming publication. In this publication the author will discuss also the formation of striae which he succeeded in producing on a glass rod wet with alcohol, during the summer of 1925; the absence of striae in a vacuum; the production of striae by an interrupted air stream when the frequency of interruption was too low to produce an audible tone; and some photographs which have been made showing that the strain in a stroked glass rod clamped at its middle point increases in a direction from a point at the free end to a point at its center. The experimental work demonstrating all the above mentioned facts has been done by the author.

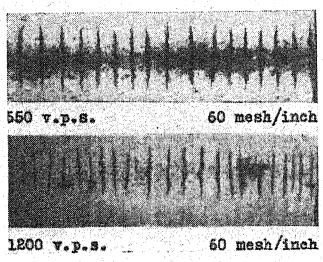

Fig. 3.

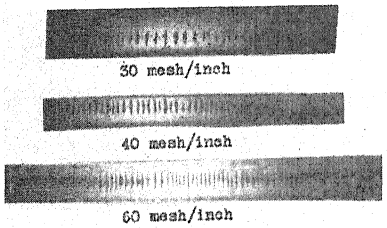

Fig. 4.

ROLLA V. COOK
Bethany College and
Indiana University, U.S.A.,
April 15, 1931.

Zodiacal Light and Magnetic Disturbance

During a recent trip southward along the 75th meridian from Norfolk, Virginia, to Cape Maisi, Cuba, we observed the zodiacal light. In the evening of March 13, 1931, when the observations were begun, the zodiacal light was unusually bright, the zodiacal cone at 8 P.M. could be followed up to and beyond the Pleiades which were about 40° from the horizon. The zodiacal light was again strong during the evening of March 14. The following evening, March 15, the zodiacal light was distinctly weaker than on the preceding two evenings and for the next three evenings to March 18 it remained fairly weak, that is, it was of its normal brightness. We tried to make morning observations but had no success because Venus, which was in the morning sky, was bright enough to obscure the morning zodiacal light.

After our return from the voyage we found that the magnetic activity was zero from March 1 to 10, a moderate disturbance began March 11 or 12 and died away on March 14, with magnetic calm from March 15 to 20. The magnetic data were obtained from the observatories at Cheltenham, Maryland, Tucson, Arizona, and Meudon, France, the data from Cheltenham being kindly furnished by the U. S. Coast and Geodetic Survey, and the data from Tucson and Meudon being taken from the Cosmic Data Broadcasts of Science Service. It is seen that the zodiacal light was unusually bright during the period of magnetic disturbance. This is in keeping with the atmospheric ion theory of the zodiacal light and the gegenschein (Phys. Rev. **35**, 1098 (1930)).

C. BITTINGER
E. O. HULBURT
Naval Research Laboratory,
Washington, D. C.,
April 17, 1931.

BOOK REVIEWS

Handbuch der Spectroscopie, von H. KAYSER UND H. KONEN. Siebenter Band, Zweite Lieferung. Pp. 499–750. S. Herzel, Leipsig, 1930. Price RM28.

The second part of Volume 7 of the Handbuch der Spectroscopie is an eloquent testimonial to the industry of the authors. As they point out, such a compendium can only be a continuous affair, to be added to from time to time as observations on spectra multiply and their interpretations develop and crystallize into more comprehensive form. Even should our summaries of data and systems of notation become more condensed than at present, the "Handbuch" will never cease to be a mine of information for the laboratory spectroscopist.

This latest addition to the "Handbuch" contains bibliographies and tables of wave-lengths for gallium, gadolinium, germanium, hydrogen, helium, hafnium, mercury, holmium, indium, and iridium. For each element there is also a condensed summary of the literature. In cases where the classification of the lines into series has been made, the term designations of lines are included; modified notation following those of Fowler and Paschen being used for all simple cases, and the notation of the original authors being used where the spectral structure is complicated. The simple notation used is the same as in the first part of Volume 7, i.e., large Latin letters for singlets, large German letters for doublets, and small Latin letters for triplets.

For each element the bibliography is also completed to include all articles written since the issue of Volume 5 to the year 1927. Although none published later than 1927 are included, the number of references is enormous, reflecting the immense amount of spectroscopic research done during the years since the fifth and sixth volumes of the "Handbuch" were issued. For instance, in Volume 5 of Kayser's "Handbuch" there were 177 references to papers on hydrogen spectra, while the present volume contains 549. In spite of the fact that the spectral notation employed is not in accordance with modern usage, the collection of references in a few pages makes this latest addition to the "Handbuch" invaluable. There are very few misspellings and misprints. The print is clear, on good paper, and in the style so well known to those who have had occasion to use the "Handbuch." One looks forward to the volumes yet to appear, containing references and data for the remainder of the elements.

GEORGE MONK

Elektrophysik der Isolierstoffe. DR. ANDREAS GEMANT, Pp. 222+vi, figs. 76. Verlag von Julius Springer, Berlin, 1930. Price bound RM 21.50.

The causes of loss and absorption of energy in dielectrics are only very incompletely understood at the present time. But in recent years there has been a renewed interest in these problems and considerable progress has been made with them. It is therefore fitting that the present volume should appear. It is written by an able worker in this field and deals with both the scientific and engineering aspects of the subject. The book is evenly divided into two sections one in which the normal behavior of insulating materials is discussed, and the other in which breakdown phenomena are considered.

Under normal operating conditions losses in dielectrics result from the presence of either or both ions and dipole molecules. The theories which describe the various mechanisms are clearly and exactly given. On controversial points, of which there are many, the different view points are usually presented, after which the author gives his position and states why. A feature of this section is the discussion of the theories of P. Debye and of K. W. Wagner which, although they result from descriptions of entirely different mechanisms, are shown to lead to mathematical expressions of the same form for the power factor and dielectric constants as functions of temperature and frequency, indicating that only by means of the most exact measurements will a differentiation between them be possible.

The second section treats breakdown phenomena in gas, liquid and solid dielectrics, with particular reference to the work of Joffé, Peek, Rogoski, Slepian, Townsend and Wagner. As in the first section the experimental methods of measuring the various quantities involved are

but briefly given, if at all, while theoretical discussions are in some cases quite complete. Concluding paragraphs are devoted to general statements concerning the influence of the physical and chemical nature of a material on its dielectric strength. The physical characteristics are believed to be the much more important.

The book might perhaps have been improved in several respects.

1. Page 76. Since the effect of extremely high frequencies on the conductance of a very dilute ionic solution is mentioned it should have been treated more exactly. It leads to an increased conduction because the ionic atmosphere which is formed about the ion can not in this case become dissymetrical, and not because the atmosphere can not form at all as in the case of the Wien effect.

2. Pages 85–90. The work of Phipps and his students on the conductivity of crystals is at least deserving of mention. The theory of Smekal which postulates an ionic conduction in lattice imperfections might also have been mentioned at this point since it apparently has found favor with many investigators.

3. In certain cases purely chemical facts concerning a particular insulating material have enabled the assignment of a mechanism to the conduction process taking place in it. Therefore there could have been included suggestions concerning the actual chemical composition of some of these materials. The colloid chemistry of insulating materials is also important.

4. The author list with journal citations might well have included page references to the text.

These suggestions are not intended to indicate an adverse judgement of the book. The arrangement content and manner of presentation are admirable. It can be recommended not only as a book which will make it easy to become acquainted with this important subject but also as one which will stimulate the interest of a research worker in this field.

J. W. WILLIAMS

Second Series May 15, 1931 Vol. 37, No 10

THE
PHYSICAL REVIEW

THEORY OF THE DIFFUSE SCATTERING OF X-RAYS BY SOLIDS

By G. E. M. Jauncey
Washington University, St. Louis, Missouri

(Received April 2, 1931)

Abstract

The classical theory of x-ray scattering has been applied to the scattering of x-rays by the electrons in the atoms of a solid. The case in which the solid consists of atoms of one kind has been considered. The interactions of the waves scattered by each electron with those scattered by every other electron in the solid has been considered. The analysis is simplified by the fact that the orbital periods of the electrons in the atoms are very much shorter than the vibrational periods of the atoms due to thermal agitations. The final formula obtained is

$$S = 1 + (Z - 1)\frac{f'^2}{Z^2} + \frac{F^2}{ZN}X$$

where S is the scattered intensity per electron relative to the scattered intensity from a single isolated electron, Z is the atomic number, F the atomic structure factor including the effect of thermal agitation, f' is related to f the true atomic structure factor (without thermal agitation), N is the total number of atoms, and X is a certain double summation. The value of X has not been obtained for an amorphous substance but it has been evaluated for the case of a simple cubic crystal by Jauncey and Harvey in the following paper in this issue of the Physical Review.

I. Introduction

In 1922, Jauncey[1] found that x-rays are diffusely scattered by crystals in a way which is similar to the scattering by amorphous solids. In particular, the spatial distribution of the scattered rays was found to be about the same for the crystals of rocksalt and calcite as for the amorphous substance glass. These experimental results were in distinct contrast to the results predicted by Debye's theory[2] of the intensity of x-rays regularly reflected by crystals. Debye's theory requires that diffuse scattering from crystals must occur, but that the spatial distribution and intensity of the rays scattered by crystals should be very different from the distribution and intensity of the rays scattered by amorphous substances. Furthermore, Debye's theory predicts that a rise of temperature will cause an increase in the intensity of the rays scattered

[1] G. E. M. Jauncey, Phys. Rev. 20, 405 (1922). Note: Figs. 2 and 6 in this reference should be interchanged.

[2] P. Debye, Ann. d. Physik 43, 49 (1914).

by crystals. Accordingly, Jauncey[3] investigated the effect of temperature by measuring the intensities of the rays scattered by rocksalt and calcite at 568°K and at 290°K. It was found that neither rocksalt nor calcite showed as great an increase of temperature as was demanded by the theory. In 1924, Jauncey and May[4] again investigated the scattering of x-rays by rocksalt and determined absolute values of the scattered intensity. The results agreed with the results previously found by Jauncey.[1]

In 1917, A. H. Compton[5] carried out a theoretical investigation of the effect of atomic structure on the intensity of x-rays regularly reflected by crystals. The unit in the diffraction or scattering of x-rays by matter is the electron. The intensity of the x-rays scattered per unit solid angle by a single isolated electron in a direction ϕ with the primary x-rays has been shown by J. J. Thomson[6] to be

$$I = I_0(e^4/2m^2c^4)(1+\cos^2\phi) \tag{1}$$

where I_0 is the intensity of the primary x-rays. If Z electrons are closely packed together so that the charge of the aggregation is Ze and its mass is Zm, it is seen from Eq. (1) that the intensity of the rays scattered by the aggregation is Z^2 times the intensity scattered by a single isolated electron, or that the scattered intensity per electron in the aggregation is $Z^2/Z = Z$ times the intensity scattered by a single isolated electron. Hence, an atom which contains Z electrons closely packed at the center will give rise to scattered x-rays in a direction ϕ which have an intensity per electron of Z times the intensity scattered by a single isolated electron. If, however, the electrons are not massed close to the center of the atom, but are at distances from the center comparable with the wave-length of the x-rays, both constructive and destructive interference takes place between the x-rays scattered by the various electrons in the atom, with the result that the intensity per electron of the scattered rays is less than Z times the intensity scattered by a single isolated electron. The intensity of the x-rays scattered by a number of atoms depends upon the configuration of the electrons within each atom and upon the configuration of the atoms themselves. If the atoms are arranged in a crystal lattice, there are certain special directions in which the x-rays are scattered with great intensity, and thus we obtain Laue spots. However, if a Laue photograph is examined, it is found that in between the black spots on the developed photographic film there is general but less intense blackening. Part of this general blackening is due to the diffuse scattering found by Jauncey.[1] There are thus two effects in the scattering of x-rays by crystals, namely, special scattering, which produces Laue spots and which is caused by regular reflection from planes of atoms according to Bragg's law, and diffuse scattering.

The problem of the intensity of the special scattering by crystals has been

[3] G. E. M. Jauncey, Phys. Rev. **20**, 421 (1922).
[4] G. E. M. Jauncey and H. L. May, Phys. Rev. **23**, 128 (1924).
[5] A. H. Compton, Phys. Rev. **9**, 49 (1917).
[6] J. J. Thomson, "Conduction of Electricity through Gases," 2nd Edition, p. 325.

discussed at length by Compton.[7] The configuration of the electrons in an atom is both rapidly and continually changing, and it becomes necessary to obtain a time average of the intensity of the x-rays scattered (the term "scatter" includes the ideas of both special and diffuse scattering) by the atoms of a crystal. However, the kind of average depends upon the particular effect in which we are interested. If we are studying the special scattering (i.e. Bragg reflection), we take one kind of average, whereas, if we are studying diffuse scattering, we take another kind of average. The first kind of average leads to the atomic structure factor as discussed by Compton.[7] Recently Compton[8] has developed the theory of diffuse scattering from the atoms of a monatomic gas. The scattering per electron in a direction ϕ with respect to the primary rays is determined only by the average configuration of the electrons within each atom, and not by the configuration of the atoms themselves. The atoms are so far apart that they can be treated as isolated systems of electrons. In the case of a gas there are no directions in which special scattering takes place.

The amplitude of the waves scattered in a direction ϕ by a single isolated electron is proportional to the square root of the right side of Eq. (1). For convenience, this amplitude is represented by unity. In the case of special scattering by a crystal (Bragg reflection), the intensity is proportional to the square of the time average of the amplitude per electron. In the case of diffuse scattering, the intensity of the scattered rays is proportional to the time average of the square of the amplitude per electron.

As example of the two kinds of average, let us consider the case of an atom with two electrons, both at a distance $r=a$ from the center, but with random orientations. If a crystal consists of atoms of this kind and if the center of each atom (the nucleus) is exactly at a lattice point and there is no thermal agitation, Compton[7] has shown that the square of the average amplitude per electron is E^2, where

$$E = (\sin ka)/ka \tag{2}$$

and

$$k = (4\pi \sin\theta)/\lambda. \tag{3}$$

In Eqs. (2) and (3), θ is the glancing angle of incidence when the crystal is set for the regular reflection of the wave-length λ. If, however, a monatomic gas consists of atoms of this kind, Compton[8] has shown that the average square of the amplitude per electron is

$$S = 1 + (\sin^2 ka)/k^2a^2 \tag{4}$$

where k is given by Eq. (3) and θ is half the angle of scattering.

When E, the average amplitude per electron in a crystal, is multiplied by Z, the atomic structure factor F is obtained. In 1921, Bragg, James and Bosanquet[9] showed how experimental values of the atomic structure factor,

[7] A. H. Compton, "X-Rays and Electrons," Chap. V.
[8] A. H. Compton, Phys. Rev. **35**, 925 (1930).
[9] Bragg, James and Bosanquet, Phil. Mag. **41**, 309 (1921); **42**, 1 (1921).

or F values as they are called, can be obtained from the experimental values of the intensity of x-rays reflected in different orders from the different sets of planes in a crystal. In an actual crystal, however, the atomic nuclei are subject to thermal agitation and the atomic structure factor F which is obtained from crystal reflection is not referred to the center of the atom but to a lattice point about which the center of the atom vibrates. We shall call the atomic structure factor which is referred to the center of the atom or nucleus the true atomic factor, and we shall represent this by f.

For several years it has seemed to the writer that in order to unravel the structure of atoms by means of x-rays it would not only be necessary to make observations on the x-rays regularly reflected, but also on the x-rays diffusely scattered by crystals. The one effect must in some way be complementary to the other. It is the purpose of this and the following paper to show how the two effects are interrelated.

II. General Theory

We shall first consider the intensity of the x-rays scattered by a large number, n, of electrons. Take a point O as shown in Fig. 1. Let AO represent the direction of the primary x-rays and OB the direction of the scattered rays. The plane containing AO and OB is then the plane of scattering. Let OV

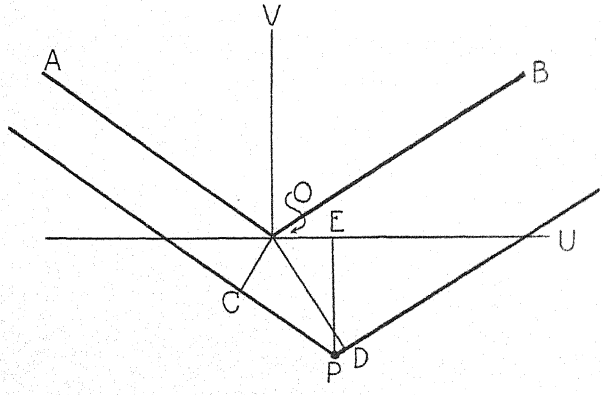

Fig. 1.

bisect the angle AOB. Now draw a plane perpendicular to the line OV, and let OU be the line where this plane cuts the plane of scattering. We shall call the plane whose trace is OU the reference plane. The waves which are scattered by all electrons in the reference plane are in phase with each other. We shall assume the phase angle of all such waves to be zero. Consider an electron at P. The path retardation of the rays scattered by the electron at P relative to the rays scattered by an electron in the plane OU is $CP+PD$. This retardation can be shown to be $2z \sin\theta$, where z is the length of PE and PE is perpendicular to the plane OU. The angle θ is one-half the scattering angle ϕ. The retardation depends only upon the distance of P from the reference plane and is not affected by moving P in any direction parallel to the ref-

erence plane. The phase angle of the waves scattered by an electron at P is then

$$(2\pi/\lambda)2z \sin\theta = (4\pi z \sin\theta)/\lambda \tag{5}$$

For brevity we shall call this phase angle kz where k is given by Eq. (3) and θ of that equation is $\phi/2$.

Let the rth electron be at a distance z_r from the reference plane, so that the phase angle associated with this electron is kz_r. The amplitude of the waves scattered by a single isolated electron is unity, so that the resultant amplitude of the waves scattered by n electrons is the vector sum of the amplitudes associated with each electron. The resultant intensity I is the square of this vector sum, so that

$$I = \left(\sum_{r=1}^{r=n} \cos kz_r\right)^2 + \left(\sum_{r=1}^{r=n} \sin kz_r\right)^2. \tag{6}$$

Since $\cos^2 kz_r + \sin^2 kz_r = 1$, this reduces to

$$I = n + \sum_{r=1}^{r=n}{}' \sum_{s=1}^{s=n}{}' \cos k(z_r - z_s). \tag{7}$$

The symbol $\sum'\sum'$ implies that in the double summation r is never taken equal to s. The value of I given by Eq. (7) is that due to a particular configuration of the n electrons. If the electrons are moving about, we must consider the probability of the configuration which gives rise to the intensity I. Let the probability that the rth electron is between z_r and $z_r + dz_r$ be $p_r(z_r)dz_r$. For brevity we shall write this $p_r dz_r$. The probability of a given configuration is then $\Pi_{r=1}^{r=n} p_r dz_r$. The average intensity is therefore given by the n-tuple integral

$$I_{\text{ave}} = \int \cdots n \cdots \int \{n + \sum' \sum' \cos k(z_r - z_s)\} \prod_{r=1}^{r=n} p_r dz_r. \tag{8}$$

It should be remembered that n is the total number of electrons in, say, a 0.1 mm cube of a substance, and is therefore a number perhaps of the order 10^{17}. The limits of each integral are such that each

$$\int p_r dz_r = 1 \tag{9}$$

In consequence of Eq. (9),

$$\int \cdots n \cdots \int n \prod_{r=1}^{r=n} p_r dz_r = n \tag{10}$$

immediately. To evaluate the integral of the double summation, let us fix our attention on one of the terms of the summation, say, $\cos k(z_u - z_v)$, which refers to the two particular electrons, the uth and the vth electrons. In carry-

ing out the n-tuple integration, each integral with respect to z_r will equal unity unless $r=u$ or v. Hence we can perform $(n-2)$ integrations, so that

$$\int \cdots n \cdots \int \cos k(z_u - z_v) \prod_{r=1}^{r=n} p_r dz_r = \iint p_u p_v \cos k(z_u - z_v) dz_u dz_v \quad (11)$$

Hence

$$I_{\text{ave}} = n + \sum' \sum' \iint p_r p_s \cos k(z_r - z_s) dz_r dz_s. \quad (12)$$

Dividing Eq. (12) by n, we obtain the scattered intensity per electron, thus

$$S = 1 + (1/n) \sum' \sum' \iint p_r p_s \cos k(z_r - z_s) dz_r dz_s. \quad (13)$$

III. Scattering from a Solid

Actually, of course, electrons are aggregated into atoms. We shall now consider the scattering of x-rays by the electrons in the atoms in a solid consisting of one kind of atom each of which contains Z electrons. We shall assume that the motions of the electrons within an atom are very much more rapid than the heat motion of the atom. This enables us to obtain a time average of the configuration of the electrons within an atom over a time interval which is long compared to the orbital period of an electron within the atom, but which is still so short that the configuration of the atoms themselves has practically remained unchanged during the interval.

The rth and sth electrons of Eq. (13) may or may not be in the same atom. Let us consider the case where they are in the same atom. In this case we may take the reference plane of Fig. 1 through the nucleus of the atom. If we assume that the probability function for each electron is symmetrical about the reference plane through the nucleus, then each

$$\int p_r \sin kz_r dz_r = 0 \quad (14)$$

so that

$$\iint p_r p_s \cos k(z_r - z_s) dz_r dz_s = \left(\int p_r \cos kz_r dz_r \right) \times \left(\int p_s \cos kz_s dz_s \right) \quad (15)$$

By referring to Compton,[7] it will be seen that

$$\int p_r \cos kz_r dz_r = E_r \quad (16)$$

where E_r is the average amplitude associated with the rth electron. Hence

$$\int\int p_r p_s \cos k(z_r - z_s) dz_r dz_s = E_r E_s. \tag{17}$$

In each atom there are $Z(Z-1)/2$ pairs of electrons and this is the number of the products $2E_rE_s$ for each atom. Let us now introduce an average quantity E', defined by

$$Z(Z-1)E'^2 = \sum_{r=1}^{r=z}{}' \sum_{s=1}^{s=z}{}' E_r E_s \tag{18}$$

where in the summation r is not taken equal to s. Also let us introduce a quantity f' defined by

$$f' = ZE' \tag{19}$$

In the theory of crystal reflection,[7] the true atomic structure factor f is defined by

$$f = \sum_{r=1}^{r=z} E_r \tag{20}$$

The double summation for each atom is therefore $Z(Z-1)f'^2/Z^2$, and, since there are n/Z atoms, we obtain on summing for all the atoms

$$(n/Z) \times Z(Z-1)f'^2/Z^2 = n(Z-1)f'^2/Z^2. \tag{21}$$

Multiplying by $1/n$, Eq. (13) reduces to

$$S = 1 + (Z-1)f'^2/Z^2 + (1/n) \sum'' \sum'' \int\int p_r p_s \cos k(z_r - z_s) dz_r dz_s \tag{22}$$

where the symbol $\sum''\sum''$ denotes summation when the rth and sth electrons are always in different atoms.

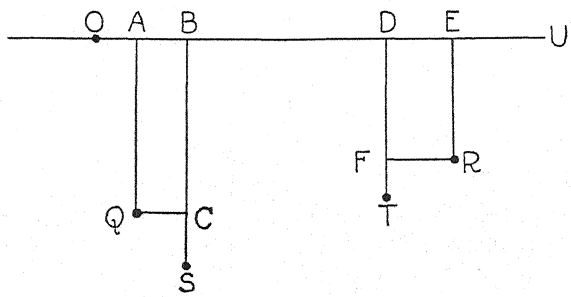

Fig. 2.

IV. Orbital Motions of the Electrons in the Atoms

In Fig. 2, let OU be the reference plane and let the center of the tth atom be at Q and let the vth electron which is in the tth atom be at S. Let $AQ = x_t$

and $CS=y_{tv}$, so that the distance of the electron at S from the reference plane is

$$z_{tv} = x_t + y_{tv}. \tag{23}$$

Similarly, let the center of the uth atom be at R, and the wth electron in this atom be T. Let $ER=x_u$ and $FT=y_{uw}$, so that

$$z_{uw} = x_u + y_{uw}. \tag{24}$$

Taking two particular atoms, together with a particular electron in the first atom and a particular electron in the second, we may average for the positions of the two electrons by taking an interval of time which is long compared with the orbital period of the electrons, but so short that the centers of the atoms have practically remained stationary during this interval. Hence we can treat the x's as constant when we integrate and dz may be replaced by dy. In this case

$$\begin{aligned}
&\int\int p_r p_s \cos k(z_r - z_s) dz_r dz_s \\
&= \int\int p_1 p_2 \cos k(x_t - x_u + y_1 - y_2) dy_1 dy_2 \\
&= \cos k(x_t - x_u) \int\int p_1 p_2 \cos k(y_1 - y_2) dy_1 dy_2 \\
&\quad - \sin k(x_t - x_u) \int\int p_1 p_2 \sin k(y_1 - y_2) dy_1 dy_2
\end{aligned} \tag{25}$$

where the subscripts 1 and 2 have been written for the subscripts tv and uw. The p's are now probability functions referred to the center of each respective atom. If the atom is symmetrical the integral containing $\sin k(y_1-y_2)$ vanishes and we are left with the integral containing $\cos k(y_1-y_2)$. The term containing this integral then reduces to

$$\begin{aligned}
&\left(\int p_1 \cos k y_1 dy_1\right) \times \left(\int p_2 \cos k y_2 dy_2\right) \cos k(x_t - x_u) \\
&= E_1 E_2 \cos k(x_t - x_u)
\end{aligned} \tag{26}$$

where the E's are given by Eq. (16). If the atoms are of the same kind and we sum for the Z electrons in each of the two particular atoms, we obtain

$$\left(\sum_{r=1}^{r=Z} E_r\right)^2 \cos k(x_t - x_u).$$

Then, summing for all the atoms, we obtain

$$\sum_r{}'' \sum_s{}'' \int\int p_r p_s \cos k(z_r - z_s) dz_r dz_s = f^2 \sum_t{}' \sum_u{}' \cos k(x_t - x_u) \tag{27}$$

V. Heat Motions of the Atom

We now remember that although the electrons in the atoms are moving much more rapidly than the centers of the atoms, yet the atoms are themselves moving with their thermal velocities. If we are dealing with a solid, the centers of the atoms are vibrating about their mean positions. We therefore introduce a probability function P for the center of the atom. Taking an average over a time long compared with the period of thermal oscillation of the atoms but short compared with the time during which scattering measurements are made, we see that Eq. (22) becomes

$$S = 1 + (Z-1)f'^2/Z^2 + (f^2/ZN)\sum_{t=1}^{t=N}{}' \sum_{u=1}^{u=N}{}' \int\int P_t P_u \cos k(x_t - x_u) dx_t dx_u \quad (28)$$

where $N = n/Z$, the number of atoms involved.

Let us replace the x's in Eq. (28) by z's, and let z_r now refer to the distance of the center of the rth atom from the reference plane. Next, let the rth atom oscillate about a mean position whose distance from the reference plane is x_r. Also let the displacement of the center of the atom from its mean position be y_r, so that $z_r = x_r + y_r$. The problem thus becomes similar to that in section IV of this paper and the analysis is similar, excepting that in the case of an amorphous solid it does not seem reasonable to assume that the probability function for the displacement of the center of the atom from its mean position is symmetrical about the mean position. However, if we do make this assumption in order to simplify the analysis, the double integral of Eq. (28) becomes

$$\int\int P_t P_u \cos k(z_t - z_u) dz_t dz_u = H_r H_s \cos k(x_r - x_s) \quad (29)$$

where

$$H_r = \int P_r \cos k y_r dy_r \quad (30)$$

H_r may be called the temperature factor for the rth atom. If, in addition, we make a second simplifying assumption that H is the same for all the atoms of the solid, and if we write F for fH,

$$S = 1 + (Z-1)f'^2/Z^2 + (F^2/ZN)\sum_{r=1}^{r=N}{}' \sum_{s=1}^{s=N}{}' \cos k(x_r - x_s) \quad (31)$$

where x_r is now the fixed mean position about which the center of the atom oscillates. The quantity F is the atomic structure factor which includes the effect due to thermal agitation, while f' in virtue of Eqs. (18), (19) and (20) is related to the true atomic structure factor f according to

$$f'^2 = f^2 + \left(f^2 - Z\sum_{r=1}^{r=z} E_r^2\right)/(Z-1). \quad (32)$$

Hence except when the probability function E_r is the same for each electron in the atom $f'<f$. It is unlikely that the probability function for a K electron is the same as that for an L electron and therefore f' should be greater than the true atomic structure factor.

The double summation in Eq. (31) has not been determined for an amorphous solid, but can be evaluated for a simple cubic crystal consisting of atoms of one kind. This evaluation has been effected by Jauncey and Harvey in the following paper in this issue of the Physical Review.

THEORY OF THE DIFFUSE SCATTERING OF X-RAYS BY SIMPLE CUBIC CRYSTALS

By G. E. M. Jauncey and G. G. Harvey
Washington University, St. Louis, Missouri

(Received April 2, 1931)

Abstract

The value of X in the previous paper by Jauncey has been determined for the case of a simple cubic crystal consisting of atoms of one kind and the formula obtained by Jauncey reduces to:

$$S = 1 + (Z-1)\frac{f'^2}{Z^2} - \frac{F^2}{Z}$$

There are no experimental results for a crystal consisting of atoms of one kind but Jauncey and May have obtained values for the diffuse scattering of x-rays from a crystal of rocksalt. Assuming rocksalt to consist of atoms of atomic number (11+17)/2 or 14, we have calculated values of f' using values of F given by James and Firth. These calculated values of f' are found to be only slightly greater than the values of F at absolute zero. Also Jauncey has measured the effect of temperature on the diffuse scattering from crystals. From the above formula calculations of the ratio of the scattering at temperatures of 568° and 290°K have been made using F values given by James and Firth. The theoretical and experimental values of this ratio in one case are 1.29 and 1.33 respectively, and in another case are 1.13 and 1.18, thus showing good agreement between theory and experiment.

I. Introduction

IN THE preceding paper in this issue of the Physical Review Jauncey[1] has shown that the scattering of x-rays by a solid consisting of atoms all of the same kind is given by

$$S = 1 + (Z-1)f'^2/Z^2 + (F^2/ZN)\sum_{r=1}^{N}{}' \sum_{s=1}^{N}{}' \cos k(x_r - x_s) \qquad (1)$$

where the various quantities are defined in Jauncey's paper. As explained in Section 5 of that paper, the right side of Eq. (1) depends on the two simplifying assumptions: (1) the probability function for the displacement of the center of the atom from its mean position is symmetrical about the mean position, and (2) the temperature factor H is the same for all atoms. These two assumptions are probably not quite valid for an amorphous solid, but are valid for a simple cubic crystal of atoms of one kind. We shall therefore take Eq. (1) to be exactly true for this kind of crystal. The quantity x_r in Eq. (1) is the distance of the mean center, about which the rth atom is oscillating due to its thermal motion, from the reference plane defined in the previous paper.[1] In a simple cubic crystal x_r is the distance of a lattice point from the reference plane.

[1] G. E. M. Jauncey, Phys. Rev. this issue p. 1193.

II. Evaluation of the Double Summation

In order to avoid confusion, we shall replace x_r and x_s by w_r and w_s. It is our object to evaluate

$$\sum_{r=1}^{N}{}' \sum_{s=1}^{N}{}' \cos k(w_r - w_s).$$

Let us take a crystal parallelopiped whose sides contain $P+1$, $Q+1$, and $R+1$ atoms so that $N=(P+1)(Q+1)(R+1)$ or PQR since P, Q, and R are large numbers. Let the size of the parallelopiped be such that the absorption of x-rays in the crystal is negligible so that every atom in the crystal is bathed in x-rays of the same intensity. On the other hand, we suppose that the length of each side of the parallelopiped is many times the wave-length of x-rays. A crystal with the length of each side about 0.1 mm is what we have in mind. Let the crystal axes be parallel to the axes of rectangular cartesian coordinates with the origin at a corner of the crystal. A lattice point of the crystal will then have the coordinates

$$x = pD, \quad y = qD, \quad z = rD \tag{2}$$

where p, q, and r are integers and D is the lattice constant. Let the reference plane[1] pass through the origin of coordinates and let the direction cosines of the normal to this plane be l, m, n. The distance of a lattice point from this plane is then

$$w_{pqr} = lpD + mqD + nrD \tag{3}$$

If we imagine Z electrons massed at each lattice point of an ideal crystal, we shall have as in Eq. (6) of the previous paper[1]

$$\begin{aligned} I = &\left\{ Z \sum_{p=0}^{P} \sum_{q=0}^{Q} \sum_{r=0}^{R} \cos kw_{pqr} \right\}^2 \\ &+ \left\{ Z \sum_{p=0}^{P} \sum_{q=0}^{Q} \sum_{r=0}^{R} \sin kw_{pqr} \right\}^{22} \end{aligned} \tag{4}$$

In the triple summations in Eq. (4) p, q, and r may be equal. Let us first sum with respect to r, so that we obtain

$$\sum_{r=0}^{R} \cos kw_{pqr} = \sum_{r=0}^{R} \cos k(A_{pq} + rnD) \tag{5}$$

where

$$A_{pq} = plD + qmD \tag{6}$$

and is a constant during this summation. Now it can be shown that[2]

$$\sum_{r=0}^{R} \cos k(A_{pq} + rnD) = \cos k\left(A_{pq} + \frac{R-1}{2} nD\right) \sin \frac{kRnD}{2} \csc \frac{knD}{2} \tag{7}$$

[2] See, e.g. Hobson—Plane Trigonometry, 4th Edition, p. 90.

and that

$$\sum_{r=0}^{R} \sin k(A_{pq} + rnD) = \sin k\left(A_{pq} + \frac{R-1}{2} nD\right) \sin \frac{kRnD}{2} \csc \frac{knD}{2} \quad (8)$$

Summation with respect to q and then p thus yields

$$\sum_{p=0}^{P} \sum_{q=0}^{Q} \sum_{r=0}^{R} \cos kw_{pqr} = \cos kD\left(\frac{P-1}{2} l + \frac{Q-1}{2} m + \frac{R-1}{2} n\right) \sin \frac{kPlD}{2} \sin \frac{kQmD}{2} \sin \frac{kRnD}{2} \csc \frac{klD}{2} \csc \frac{kmD}{2} \csc \frac{knD}{2}. \quad (9)$$

and

$$\sum_{p=0}^{P} \sum_{q=0}^{Q} \sum_{r=0}^{R} \sin kw_{pqr} = \sin kD\left(\frac{P-1}{2} l + \frac{Q-1}{2} m + \frac{R-1}{2} n\right) \sin \frac{kPlD}{2} \sin \frac{kQmD}{2} \sin \frac{kRnD}{2} \csc \frac{klD}{2} \csc \frac{kmD}{2} \csc \frac{knD}{2} \quad (10)$$

so that Eq. (4) becomes

$$I = Z^2 \cdot \sin^2 \frac{kPlD}{2} \sin^2 \frac{kQmD}{2} \sin^2 \frac{kRnD}{2} \csc^2 \frac{klD}{2} \csc^2 \frac{kmD}{2} \csc^2 \frac{knD}{2}. \quad (11)$$

The angle of scattering enters the problem through the relation[1]

$$k = (4\pi \sin \phi/2)/\lambda. \quad (12)$$

If we have chosen values of ϕ, the scattering angle, and l, m, n the direction cosines of the normal to the reference plane, in such a way that

$$klD \neq 2\pi a, \text{ or } kmD \neq 2\pi b, \text{ or } knD \neq 2\pi c \quad (13)$$

where a, b, c are any integers, the value of the trigonometric function on the right side of Eq. (11) is of the order unity. Now, dividing the right side of Eq. (11) by the total number of electrons, $PQRZ$, we find the scattered intensity per electron to be

$$S = \frac{ZO(1)}{PQR} \quad (14)$$

where O(1) is a quantity whose magnitude is of the order unity. For a crystal of KCl, $Z = 20$ and, if we are dealing with a crystal in the form of a cube the length of whose edge is 0.1 mm, the value of PQR is about 10^{17}, so that the

right side of Eq. (14) is of the order 10^{-16} which may be taken as zero. Therefore there is no diffuse scattering from an ideal simple cubic crystal whose atom centers are held exactly at lattice points with the electrons massed at the center of each atom.

If Eq. (1) is applied to this ideal crystal, the same result must be obtained as in the previous paragraph. In this case $f'=F=Z$, so that we have

$$0 = 1 + (Z-1) + (Z/N) \sum_{r=1}^{N}{}' \sum_{s=1}^{N}{}' \cos k(w_r - w_s) \tag{15}$$

Solving Eq. (15) for the double summation we obtain

$$\sum_{r=1}^{N}{}' \sum_{s=1}^{N}{}' \cos k(w_r - w_s) = -N. \tag{16}$$

Substituting this in (1), we obtain

$$S = 1 + (Z-1)f'^2/Z^2 - F^2/Z \tag{17}$$

for the scattering per electron from a crystal of simple cubic form whose atoms are all of the same kind and each of which contains Z electrons. In Eq. (17), it will be seen by reference to the preceding paper[1] that F is the atomic structure factor which includes the effect due to thermal agitation, while f' is related to the true atomic structure factor f, which does not include the effect of thermal agitation, according to

$$f'^2 = f^2 + \left[f^2 - Z\sum_{r=1}^{z} E_r^2\right]/(Z-1) \tag{18}$$

where E_r is the average amplitude associated with the rth electron in the atom. If the average amplitude associated with one electron is the same as that associated with any other electron $f'=f$ and f' is then the true atomic structure factor.

III. Comparison with Experiment

Unfortunately, results on the diffuse scattering by a crystal consisting of atoms all of the same kind are not available. However, in 1924 Jauncey and May[3] measured the absolute intensity of x-rays diffusely scattered by a crystal of rocksalt. They obtained the curve shown in Fig. 1. The curve XYZ represents the Thomson value of the scattering. Referring to their paper, it is seen that they used x-rays containing two wave-lengths, 0.71A and 0.40A. The peaks A and B are due to the wave-lengths 0.40A and 0.71A respectively. The point C was obtained when sufficient aluminum was inserted in the primary beam to remove the longer wave-length constituent of the x-rays. We have therefore drawn the broken curve $DAFG$ of Fig. 1, and this is then due to the scattering of x-rays of wave-length 0.40A. It seems preferable to use the curve for this wave-length, since it is known from the diagram at which

[3] G. E. M. Jauncey and H. L. May, Phys. Rev. **23**, 128 (1924).

value of ϕ the scattering approaches zero. Using this curve and dividing each ordinate by the Thomson value of the scattering at the same angle we obtain the S curve shown in Fig. 2 in which the abscissa is $(\sin\phi/2)/\lambda$. This S curve is for x-rays scattered by rocksalt at 290°K.

In 1928 James and Firth[4] obtained F values from the regular reflection of x-rays by rocksalt at various temperatures. Their F values are for Na+Cl. In order to compare the present theory with experimental values, we shall

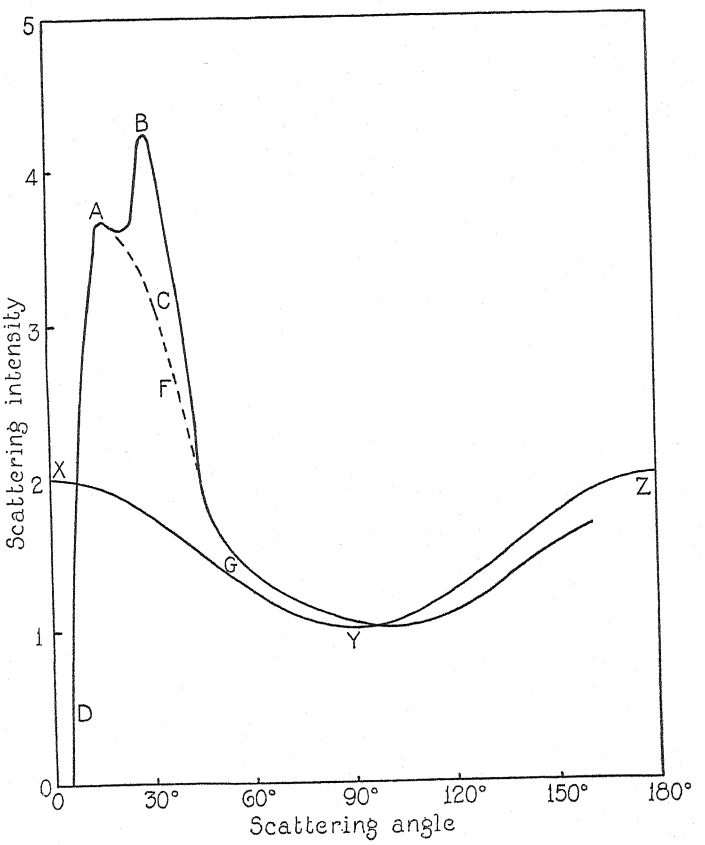

Fig. 1.

assume rocksalt to be made up of atoms of the same kind whose atomic number is $(11+17)/2=14$. We therefore take as F values to be substituted in Eq. (17) one half the values given for Na+Cl in the paper by James and Firth. These average F values are shown in the second column of Table I. Values of S found from Fig. 2 are shown in the third column of this table. From Eq. (17), values of f' can thus be determined and these are shown in the fourth column. James and Firth give F values extrapolated to absolute zero and the averages of these for Na and Cl are shown in the fifth column. The values in

[4] R. W. James and E. M. Firth, Proc. Roy. Soc. **A117**, 62 (1928).

the fourth and fifth columns should be nearly but not quite equal. The true atomic structure factor f is somewhat greater than the value of F at absolute zero, if there is zero point energy.

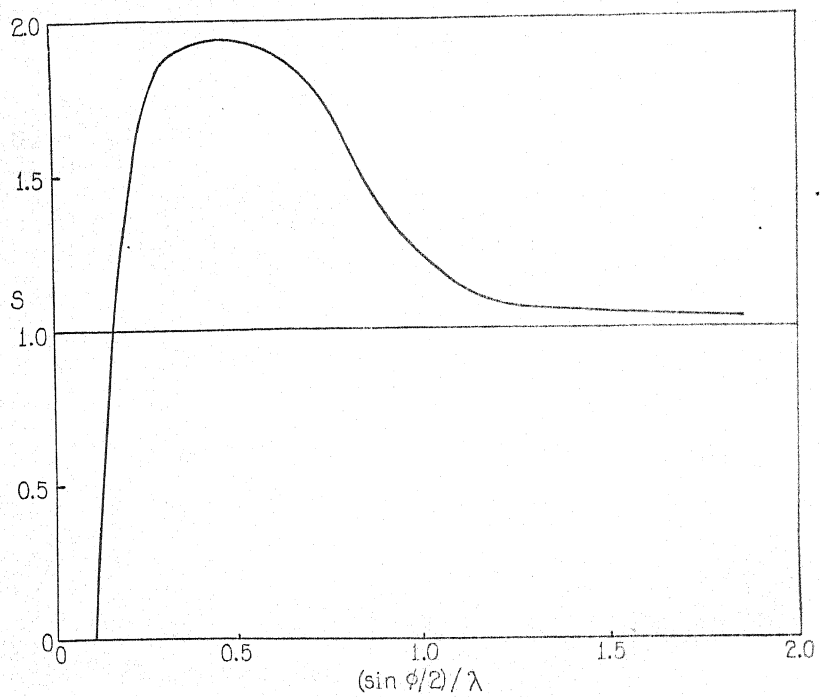

Fig. 2.

TABLE I.

$(\sin\phi/2)/\lambda$	$F_{290°K}$	$S_{290°K}$	f'	$F_{0°K}$
0.1	12.3		12.8*	12.8
0.2	9.4	1.24	10.1	9.9
0.3	6.9	1.82	8.0	7.6
0.4	5.2	1.93	6.6	6.1
0.5	3.9	1.94	5.4	4.8
0.6	2.8	1.88	4.6	4.0
0.7	2.1	1.77	3.8	3.3
0.8	1.6	1.56	3.2	2.8
0.9	1.2	1.38	2.6	2.4
1.0	0.8	1.26	2.1	2.0
1.1	0.5	1.17	1.7	1.6
1.2	0.3	1.10	1.6	1.4

* By extrapolation.

As zero angle of scattering is approached, f' and F each approach Z and S approaches zero. This agrees with the experimental curves shown in Figs. 1 and 2.

In 1922, Jauncey[5] found a temperature effect for the diffuse scattering by rocksalt. The temperatures used by Jauncey were 290°K and 568°K. From

the values given by James and Firth,[4] F values at 568°K can be interpolated. The wave-lengths used by Jauncey were 0.28A and 0.36A at 15° and 30° scattering angle respectively. The ratios of the values of S found are shown in the fifth column of Table II. F values obtained from James and Firth are shown in the second and third columns. Values of f' obtained from Fig. 2 and Eq. (17) are shown in the fourth column. Now putting the values of $F_{290°K}$ and $F_{568°K}$ in Eq. (17) and using the appropriate f' values, we obtain theoretical values for $S_{290°K}$ and $S_{568°K}$. The ratios of these values are shown in the sixth column.

TABLE II.

$(\sin\phi/2)/\lambda$	$F_{290°K}$	$F_{568°K}$	f'	$S_{568°K}/S_{290°K}$ Exp.	Theory
0.467	4.25	3.20	5.8	1.33	1.29
0.720	1.95	0.90	3.7	1.18	1.13

It is seen that there is good agreement between the experimental and theoretical values of the ratios.

For a monatomic gas Compton[6] has shown that

$$S = 1 + (Z - 1)f'^2/Z^2 \tag{19}$$

so that from the experimental values of S values of f' can be obtained. If x-rays are scattered by a simple cubic crystal of the same chemical element as the gas, values of f' can be obtained from the experimental values of S and F for the crystal. The values of f' for the gas should nearly agree with those for the crystal, the slight difference being due to the structure of an atom in a crystal being affected by the proximity of other atoms.

[5] G. E. M. Jauncey, Phys. Rev. 20, 421 (1922).
[6] A. H. Compton, Phys. Rev. 35, 925 (1930).

ABSOLUTE WAVE-LENGTHS OF THE COPPER AND CHROMIUM *K*-SERIES

By J. A. Bearden
Department of Physics, The Johns Hopkins University

(Received April 6, 1931)

Abstract

In the measurement of x-ray wave-lengths by ruled gratings two principal difficulties have been discussed which may account for the difference observed between the wave-lengths determined by this method and those determined by using crystal gratings. They are, the periodic error in the grating, and the geometrical divergence of the x-ray beam. It is now shown that the effect of the periodic error can be determined by a study of the intensities of the optical ghost lines. For a good quality optical grating it has been found that the error in x-ray wave-lengths due to the periodic error in the grating is thus of no importance. By using a suitable disposition of apparatus the effect of the geometrical divergence of the x-ray beam can be made as small as desired. Thus it is concluded that ruled gratings can be used for precise wave-length measurements of x-ray spectra.

In the present experiment the two parallel plate method has been used for determining the angles of incidence and diffraction. Five glass gratings of different grating spaces and ruled on two ruling engines have been used. The results from the various gratings on the same wave-length have agreed satisfactorily. No consistent variations of any type were observed. The final results from 172 sets of plates are given in the following tables.

Spectral line	Crystal λ	Grating λ	Limiting error	Grating λ − Crystal λ
Cu $K\beta$	1.38914A	1.39225A	±0.00014A	+0.224%
Cu $K\alpha$	1.53838	1.54172	±0.00015	+0.217%
Cr $K\beta$	2.08017	2.08478	±0.00021	+0.222%
Cr $K\alpha$	2.28590	2.29097	±0.00023	+0.222%

From these results the true grating space of a calcite crystal is $d=3.0359\pm0.0003$A. Using this value of the grating constant, Planck's constant as determined by Duane, Palmer and Yeh is, $h=6.573\pm0.007\times10^{-27}$ erg·sec. e/m can be determined from the dispersion of x-rays by using the absolute wave-length of an x-ray spectrum line. The mean of the values of the dispersion as given by Stauss and Larsson gives $e/m=1.769\times10^{7}$ e.m.u.g^{-1}. The values of these constants are independent of any imperfection in the crystal. If the crystal lattice is assumed to be perfect we then have Avogadro's number, $N=6.019\times10^{23}$ mol. per mole, and the charge on the electron $e=4.806\times10^{-10}$ e.s.u. Using this value of e, and d as above, we find Planck's constant $h=6.623\times10^{-27}$ erg·sec.

MEASUREMENTS of the wave-length of x-ray lines using ruled gratings have been made by a number of investigators.[1–7] The results obtained

[1] A. H. Compton and R. L. Doan, Proc. Acad. Sci. **11**, 598 (1925).
[2] J. Thibaud, Comptes Rendus **182**, 55 (1926).
[3] F. L. Hunt, Phys. Rev. **30**, 227 (1927).

by this method have been in general higher than the corresponding wave-lengths measured by means of a crystal grating. Unfortunately the differences observed between the grating values and the crystal values by different experimenters have not been the same. In the best of the experiments, differences exist which appear to be greater than the probable errors in the experiments. It has been pointed out by the writer[8] that these differences are most likely due to the quality of the gratings used and consistent errors of observation. The present experiment was undertaken in an effort to eliminate as far as possible the uncertainty which exists concerning the absolute wave-length of x-rays.

Theory of Ruled Gratings for X-ray Measurement

Since ruled gratings must be used at tangential incidence for x-rays, the usual grating formula $n\lambda = d(\sin i - \sin r)$ may be written in terms of the small angles θ and α of Fig. 1 as

$$\eta\lambda = 2d\left(\sin\frac{2\theta+\alpha}{2}\sin\frac{\alpha}{2}\right) \tag{1}$$

where θ is the angle between the surface of the grating and the direct beam, and α the angle between the reflected beam and the diffracted beam.

The angles θ and α for x-rays are very small so that the problem of accurately measuring x-ray wave-lengths is principally a problem of measuring very small angles with a high degree of precision. Assuming that these angles can be precisely measured, it will be of interest to investigate the possible error in the wave-length due to other causes.

The geometrical divergence of the x-ray beam perpendicular to the plane of the grating will shift the position of the spectrum lime as was first pointed out by Porter.[9] Porter's result was for the special case where the distance from the source to the center of the grating, and the distance from center of the grating to the position of the image were equal. Stauss[10] has considered in a similar manner the more general case where the distances are not equal. The complete diffraction equation then becomes:

$$n\lambda = d(\cos\phi_1 - \cos\phi_2)\left[1 + \frac{3x^2}{20(\phi_2^2 - \phi_1^2)}\left(\frac{\phi_2^2}{l_2^2} - \frac{\phi_1^2}{l_1^2}\right)\right] \tag{2}$$

where $\phi_1 = \theta$, $\phi_2 = (\alpha+\theta)$, x is the length of grating used, l_1 the distance from the source to the grating, and l_2 the distance from the grating to the image. It will be seen that the correction term will be either + or − depending on the

[4] E. Bäcklin, Inaugural Dissertation, Uppsala Universität (1928).
[5] C. P. R. Wadlund, Phys. Rev. **32**, 841 (1928).
[6] J. A. Bearden, Proc. Nat. Acad. Sci. **15**, 528 (1929).
[7] J. M. Cork, Phys. Rev. **35**, 1456 (1930).
[8] J. A. Bearden, paper presented at Optical Society of America, Charlottsville Meeting, October 1930.
[9] A. W. Porter, Phil. Mag. **5**, 1067 (1928).
[10] H. E. Stauss, Phys. Rev. **34**, 1601 (1929).

values of l_1 and l_2. It will also be noticed that the position of the 0 order will be displaced if $l_1 \neq l_2$ thus

$$\phi_2 = \phi_1\left[1 + \frac{3x^2}{20}\left(\frac{1}{l_1^2} - \frac{1}{l_2^2}\right)\right]. \tag{3}$$

The magnitude of this correction depends on the method used in measuring ϕ_1 and ϕ_2.

The geometrical center of the slits is not the center of the reflecting surface of the grating. If β represents the angle between the central slit ray and a line from the source to the effective center of the grating, it has been shown[11] that

$$\beta = \frac{s^2}{4\phi_1 l_1^2} \tag{4}$$

where s is the slit width and ϕ_1 and l_1 are the same as in Eq. (2).

The divergence of the x-ray beam in the plane of the grating leads to a correction in the wave-length of the form

$$n\delta\lambda = \frac{d}{2}\left(\frac{\phi_1^2 h_1}{2l_1^2} - \frac{\phi_2^2 h_2^2}{2l_2^2}\right) \tag{5}$$

where $2(h_1+h_2)$ is the length of spectrum line, and $2h_1$ the effective height of grating.

Prins[11] has criticized the writer's published results[6] believeing that a correction of the type shown in Eq. (2) would account for the difference in wave-length observed between the grating and crystal methods. Correspondence with Prins has shown that he had misinterpreted the writer's disposition of apparatus. This correction, as will be shown later, is of negligible importance.

There are three types of errors which are usually present in the ruling of a grating, either of which would lead to erroneous absolute wave-lengths. These errors, the erratic, the error of run, and the periodic error have been discussed by Michelson and Rowland in connection with the absolute wave-lengths of optical spectra. The erratic error is not susceptible to analytical correction but its importance can best be determined by using gratings ruled on different ruling engines and comparing the results.

The error of run can be determined in a number of ways. Probably one of the most precise methods of determining this error is the focusing property exhibited by such gratings. Assuming parallel incident light, Fagerberg[12] has derived an equation of the form

$$\frac{d_1}{d_2} = 1 + \frac{x\cos^2\psi_2}{r(\sin\psi_1 - \sin\psi_2)} \tag{6}$$

where d_1 and d_2 are the grating spaces at the extremes of the grating, ψ_1 is the angle of incidence, ψ_2 the angle of diffraction, x the length of the grating, and r

[11] J. A. Prins, Nature **124**, 370 (1929).
[12] Sven Fagerberg, Zeits. f. Physik **62**, 457 (1930).

the distance from the grating to the focus. With this method it is possible to detect an error in the grating space of 10^{-8} cm. Another method which has been used by the writer in connection with the above is to rule every 4th or 7th line on the grating longer than the other lines. The distance between these lines can then be measured directly by a comparator. Also the average grating space can be accurately measured by determining the number of spaces on a grating and the distance between the extreme lines.

The periodic error of the grating will produce an asymmetrical spectrum line which always makes the angle of diffraction appear larger than it should be. This effect is of no importance in ordinary optical gratings for the error is inversely proportional to the length of the grating used. In the x-ray application, however, the length of the grating used is only a few mm so the error may be important. Fagerberg has calculated the error for x-rays and obtained

$$\delta\lambda = \frac{2m}{x}\lambda \tag{7}$$

where m is the maximum displacement of any line on the grating from an ideal grating with the average grating space m_0, x is the length of the grating used, and λ the wave-length. He assumed m to be from 0.0005 to 0.001 mm, $x=1$ mm and found $\delta\lambda = 0.001$ to $0.002\,\lambda$ which is the order of magnitude of the observed difference between grating measurements and crystal measurements. It should be pointed out, however, that the values of m assumed were, for good quality gratings, too high. m can be determined from the intensity of the Rowland ghost lines in a grating. The relation between the intensity of the ghost lines and the intensity of the main line may be written approximately

$$\frac{I}{I_0} = \left(\pi N \frac{m}{m_0}\right)^2 \tag{8}$$

where I is the intensity of the first order ghost, I_0 the intensity of the main line, N the spectral order, m the maximum displacement of a line from the ideal grating, m_0 the average grating space.

It is true that for gratings of large grating space (e.g. 50 lines/mm) one might be able to have $m=0.001$ mm and the intensity of the ghost lines be very weak in the low orders. However if one examines the very high spectral orders the ghost lines would be very intense. One can usually observe 30 or more orders with a grating of 50 lines per mm. If we observe the 30th order of such a grating and have $m=0.001$, the intensity of the ghost lines would be more than 20 times the intensity of the main line. In any case one can determine the importance of this error by carefully examining the intensity of the ghost lines of the grating. If one wished to get an accurate estimate of m for a coarse ruled grating, I believe it would be permissible to rule a small spaced grating (e.g. 600 lines/mm) and determine m from such a grating; thence rule the coarse grating using the same part of the ruling engine screw. There seems little reason to believe that the ruling engine would misplace the lines on a coarse grating any more than on a finely spaced grating.

Compton[13] has considered the question of the refraction of the x-rays at the surface of the grating, and concludes that refraction could not cause any displacement of the spectral lines. It has been shown by Siegbahn,[14] and has also been observed by the writer, that the type of surface influences greatly the intensity of the x-ray spectra. It is difficult to believe, however, that this could in any way displace the spectral lines. The writer has also been able to improve the intensity of the x-ray spectra many times on a lightly ruled grating by etching it. In order to test the effect of etching on the position of the spectral lines, one half of a grating was etched and the other half left unetched. The grating was mounted in such a manner that either etched or unetched part could be used. The results were the same within experimental error from both parts.

Thus, it seems from the above considerations that the measurement of x-ray wave-lengths by the use of ruled gratings can be made reliable. By a suitable disposition of the apparatus the error in the wave-length should be just the error of measuring the grating constant d and the two angles θ and α.

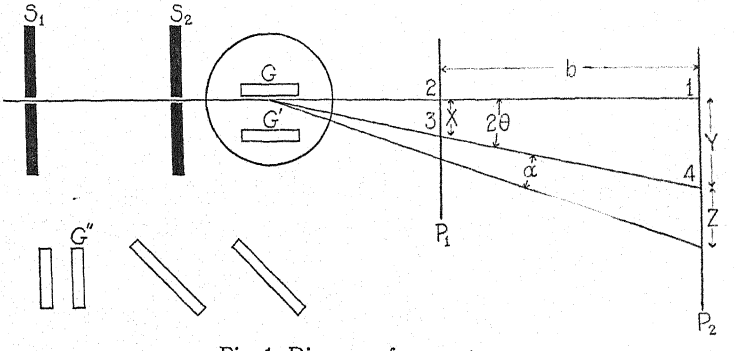

Fig. 1. Diagram of apparatus.

Method of Experiment

In the present experiment the K-series of copper and chromium were chosen as a source of K-rays. The intensities of these lines can be made very great and they are the longest wave-lengths that can be worked with successfully without using a vacuum spectrograph. These wave-lengths can also be used to determine directly the grating space of such crystals as calcite and rock salt. Even though the angles of diffraction and reflection for these lines are small, it is believed that greater precision can be secured by using these wave-lengths than could be obtained by use of longer wave-lengths with a vacuum spectrograph.

There are several methods by which the angles θ and α could be measured. However, from a consideration of the error involved in each method it appears that the modification of the Uhler and Cooksey[15] parallel plate method,

[13] A. H. Compton, Jour. of the Franklin Inst. Oct. (1929).
[14] M. Siegbahn and T. Magnusson, Zeits. f. Physik **62**, 435 (1630).
[15] H. S. Uhler and C. D. Cooksey, Phys. Rev. **10**, 645 (1917).

used by the writer,[6] is preferable. Fig. 1 shows the arrangement of the apparatus. This method avoids error due to any variation in the width of the slits, or non-uniformity of illumination over the slit. It will also be seen that it is not necessary that the grating be accurately on the axis of rotation as is essential in other methods. The measurements are all linear measurements and no angular motion of the grating is needed for a determination of the angles.

In order to determine the errors to be expected from this arrangement Eq. (1) may be written in terms of the measured quantities as

$$n\lambda = \frac{d}{2b^2}\left[\frac{(Y-Z)^2}{y^2}\right](y \pm z)z \tag{9}$$

where b, x, y, and z, are as indicated in Fig. 1. In Eq. (9) the angles were used instead of the sine of the angle, and the angle was put equal to the tangent of the angle. This equation is in error by approximately 1 part in 3000 for the angles involved. It can be shown that for a given distance from the grating to the second plate that the minimum error in wave-length for a given error in measuring x occurs when b is made a maximum. This neglects the geometrical divergence of the x-ray beam and from Eq. (3) it will be seen that this must also be considered in choosing b. The distances y and z must be made large enough to be conveniently measured. A good comparator cannot be depended upon to better than about 0.001 mm. Thus, in order to obtain the desired precision y and z must be greater than 10 mm. This makes the distance from the grating to the second plate about 2 meters. An error in measuring the distance x produces an error in the wave-length of about 3 times as much as the same error in y or z. Fortunately the lines determining x are very narrow and are never more than 1 mm apart so x can be measured to a much higher precision than y or z. By assuming an error of 0.001 mm in x, y or z one is lead to expect an error in λ of approximately 1 part in 10,000.

In the present experiment the distance l_1 from the first slit to the grating was 45 cm, from the grating to the second plate 191 cm, and from the grating to the first plate 7 cm. A typical plate gives $\phi_1 = 3\times10^{-3}$, $\phi_2 = 7\times10^{-3}$ for the first order, and $\phi_2 = 16\times10^{-3}$ for the sixth order. Thus Eq. (2) becomes

$$n\lambda = d(\cos\phi_1 - \cos\phi_2)(1 - 1.93\times10^{-6}) \qquad \text{1st order}$$

$$n\lambda = d(\cos\phi_1 - \cos\phi_2)(1 + 0.054\times10^{-6}) \qquad \text{6th order}$$

Eq. (3) becomes

$$\phi_2 = \phi_1(1.0000087)$$

for the 2nd plate, and

$$\phi_2 = \phi_1(0.99964)$$

for the first plate.

On the first plate this corresponds to 0.0002 mm. From Eq. (4) $\beta = +4.15\times10^{-8}$ or 0.00008 mm on the 2nd plate, and Eq. (5) gives for the 6th order

$\delta\lambda = -1.64\times10^{-13}$ cm. Thus there are no corrections of any importance. In any case some are + and some are −, so the total correction is probably much less than any individual correction.

Apparatus

The apparatus was mounted on a reinforced concrete block 6.5″×30″ ×96″. The top of the block was a smooth stone. Iron blocks 1″×4″×4″ were inserted about 3″ from the top and at various positions in the block when it was cast. Threaded holes in the center of the iron blocks permitted iron rods to be rigidly attached to the base. The apparatus was held in position by these rods. This base was supported by 3 concrete blocks under each end. Between the blocks, rubber, felt and wood strips were inserted to damp out the vibrations from the building.

The plate holders were made from a solid brass plate 1/2″×4″×6″. The surface against which the photographic plates rested was scraped to a plane surface. The photographic plates were held against this surface by a plane brass plate against which pressed two strong springs. A piece of blotting paper was inserted between this brass plate and the back of the photographic plate to equalize the pressure on the photographic plate. The plate holders were attached to a 2″ square iron rod which was held rigidly to the base by two 1.25″ iron rods. The photographic plates were inserted and removed without disturbing the adjustment of the plate holders.

The grating was mounted on a three point support which was attached to a slide capable of being moved through several mm. The position of the slide was determined by a scale and dial, reading to 0.001 mm. This slide rested on a table which rotated on accurately made centers. The table could only be rotated through 200°, but this was sufficient for making adjustments. It was found that such a table was far more satisfactory in rotating about an axis than the ordinary spectrometer.

The slits were made of steel with gold faces 1 mm thick. One jaw was clamped rigidly and the other jaw held against it by small springs. Thin spacers were used to obtain the desired slit widths. The two slits were attached to a brass tube which was capable of being rotated by a long arm and a tangent screw. Thus after the slits had once been made accurately parallel they could be clamped in position, and any further adjustment of tilt could easily be made by the tangent screw.

The x-ray tube was a water-cooled Coolidge type, with a side arm and a thin window of aluminum (0.01 mm thick) to reduce the absorption of the copper and chromium x-rays. The focal spot was usually about 1 to 2 mm in diameter and the tube was operated about 10 m.a. and 40 K.V. The x-rays were taken off at about 10° from the face of the target. The chromium targets were prepared by electroplating a layer of chromium on the regular copper targets. The x-ray tube was mounted on a slide in order that the source of greatest x-ray intensity could be placed in line with the slits. The tube could also be raised and lowered to bring the focal spot in line with the center of the slits, grating and plates. Evacuated tubes with thin celluloid windows were

placed between the slits and between the plate holders to reduce the absorption of the x-rays.

The experiment was carried out in a small room in which the temperature could be accurately controlled. A recording mechanism kept a continuous record of the temperature and the temperature never varied by more than 0.1°C. During a single exposure the temperature usually remained constant to within 0.02°C.

Alignment and Calibration of Apparatus

The alignment of the plate holders, center of grating, and center of slits in a horizontal line was accomplished by adjusting each to a given height above the top of the stone base. The height of the focal spot of the x-ray tube was adjusted by placing a horizontal slit on this line midway between the tube and second plate, thence adjusting the height of the tube until the image of the focal spot fell on the center of the second plate P_2. This adjustment was made to within 0.5 mm.

The adjustment of the grating surface parallel to, and on the axis of rotation was very conveniently and accurately made by using the modified Michelson interferometer shown in Fig. 1. The grating which was ruled on a plane parallel plate was spluttered with gold or silver to obtain a good optical reflection. The grating was mounted with the reflecting surface against a rigid three point support on the slide of the rotating table.

If one places plane parallel plates in positions G' and G'' (Fig.1) of the same thickness as the plate on which the grating G is ruled, it will be seen that the optical path is the same whether the rotating table is in the position shown, or after it has been rotated through 180°. The grating slide and the slide which supported the second interferometer mirror were adjusted until the central white light fringe remained in the same position when the rotating table was turned through 180°. Thus the grating surface was accurately set on the axis of rotation to within 0.1 of a fringe. The grating surface was made parallel to the axis of rotation by observing the number of fringes in the field of the two 180° positions. Care was taken to make sure that the same number of fringes represented zero angle between the grating surface and the axis, and not an angle of twice as many fringes. This angle was made 0° to within 1 fringe/20 mm which is about 2″ of arc. It will be noticed that after the adjustments are once made the grating can be taken out and replaced very easily by the use of the interferometer. It was not necessary that the grating surface be spluttered, as the fringes were always visible even with the cleanest glass surface. The interferometer was also used to check the position of the grating during an exposure.

The axis of rotation was then made approximately perpendicular to the horizontal line, which passed through the center of the slits and the center of the plate holders. This was accomplished by allowing a beam of light to pass through a slit in the center of the second plate holder P_2 and thence reflected by the grating surface back on to the slit.

The slits were then moved horizontally until the x-ray beam passed over

the axis of rotation. In order to do this, the slit S_2 nearest the grating (about 30 mm away) was made very narrow (approximately 0.003 mm). The grating was adjusted parallel to the x-ray beam by x-ray reflection, and the slits moved until the narrow beam was partially cut off.

The grating was then rotated through 90°. The grating surface was then perpendicular to the direction of the x-ray beam. A telescope fitted with a Gauss eye piece was placed about 5 meters away and adjusted until the image of the cross-hairs was reflected back by the grating on to the cross hairs. A plane parallel mirror was inserted in place of the photographic plate, and the plate holder P_1 adjusted until the image of the cross hairs was returned as above. The mirror was then placed in the second plate holder P_2 which was likewise adjusted. Thus the two plate holders were made parallel and also perpendicular to the x-ray beam to within 5″ of arc.

The grating was rotated to a position parallel to the x-ray beam and moved completely out of the path of the x-rays. The slit S_2 was made 0.01 mm wide and the slit S_1 near the x-ray tube was made 0.015 mm. A photographic plate was then placed on a slide between the grating and the first plate holder P_1. A short exposure of about 10 seconds was sufficient to record a sharp line on the plate. The plate was then moved about 1 mm and the grating was moved 0.001 mm into the x-ray beam. Another exposure of 10 seconds was made. This was repeated until the grating cut off the entire x-ray beam. If the slit S_2 was not parallel to the grating, the lines on the developed plate were not cut off uniformly by the grating at the top and bottom. In this way the slit S_2 could be made parallel to the grating to within 10″ of arc. The parallelism of the slit S_1 was tested in the following manner. A photographic plate was placed in the plate holder P_1. The direct x-ray beam was recorded. The grating was rotated through an angle of about 5′ of arc and then put in position to reflect the x-ray beam. The reflected beam was thus recorded. If the slits were parallel to each other and parallel to the axis of rotation of the grating, the two lines on the developed plate would be parallel. Thus by accurately measuring the separation of the lines at the top and bottom of the plate, the perfection of the adjustment was determined. If the lines were not parallel, S_1 was readjusted, and the above process repeated. In this way the slits were made parallel to each other and parallel to the axis of rotation of the grating within 10″ of arc.

The lines on the grating were aligned parallel to the axis of rotation of the grating in the following manner. A vertical slit about 50 cm from the grating was illuminated by a mercury arc. A double cross hair in the viewing telescope was rotated until the spectral lines formed by the grating were parallel to the cross hairs. The grating was rotated 180° and the spectral lines observed again. When the lines of the grating were parallel to the axis of rotation, the spectral lines formed in this position were parallel to the cross hairs. Since the grating space varies as the cosine of the angle of tilt this adjustment was only made to within 0.5°.

The distance between the plate holders was measured by placing an iron rod 3/4″ square between the two plate holders, and then measuring with

inside micrometers the distance between the parallel ends of the iron rod and the plate holders. The length of the rod was determined by comparison with the laboratory standard, which had been calibrated by the Bureau of Standards, Washington, D. C. Independent measurements by different observers agreed to within 0.02 mm, so that the error in the final value was probably less than this. The comparator on which the separations of the lines on the plates were measured was carefully adjusted and calibrated. Six gratings have been used in the present work. Four of these gratings (1–4) were ruled by Professor Wood in this laboratory, and the other two were ruled by Mr. Pearson under the direction of Professor Michelson of the University of Chicago.* All the gratings were ruled on glass. Larger angles could have been used by using a heavier material for the ruled surface, but glass gratings give sharper and more intense spectra than the metallic surfaces. Also, the glass gratings can be spluttered with gold and used at large angles. In this case the intensity of the spectra is greatly increased as compared to the unspluttered glass surface and the sharpness of the spectral lines remains unchanged. The characteristics of the gratings are as follows.

Number 1 was ruled with 287 lines per mm on a plane optical glass surface with a very light ruling. The ruling was uniform and no lines were missing. The surface ruled was approximately 25 mm square. In order to examine the grating with optical light the top and bottom of the grating was etched, and then spluttered with gold. The intensity of the Rowland ghost lines in the 11th order was about 1/3 the intensity of the main line, thus m [from Eq. (8)] would be 0.00006 mm, and for $x=4$ mm, Eq. (7) gives $\delta\lambda=0.00003\lambda$. It was found that the intensities of the first and second orders of the x-ray spectra, from the etched portion of the grating, were increased 5 or 10 times as compared to the unetched part. The higher orders were not improved. Spluttering the grating with gold improved the intensity of the unetched portion but did not improve the etched part. The error of run was estimated by the focusing effect in various orders and was less than $10^{-5}d$.

Number 2 was ruled with 143 lines per mm on a plane parallel plate made from good quality plate glass. The ruling was heavier than on number 1 and it was not necessary to etch part of the grating for observation of the optical spectra. The ghost lines were weaker in this grating in the 22nd order than in the 11th order of number 1. Etching did not improve the intensity of the x-ray spectra even though the intensity of the optical spectra was increased several times. Spluttering with gold increased the x-ray spectra from the whole grating by a factor of three or four. The error of run was estimated as above and found to be of no importance. This grating had some missing lines near the middle of the ruling, so it was only used for testing the effect of etching and no results are listed from it.

* The results from these two gratings were obtained at the University of Chicago. The apparatus was essentially the same as described above. Through the courtesy of Professor Michelson the experiment was carried out in one of the constant temperature ruling engine vaults. The writer also wishes to express his appreciation to the members of the Physics Department for placing at his disposal the facilities for carrying out this part of the experiment.

Number 3 was ruled with 287 lines/mm on a plane parallel plate similar to number 2. This grating was not etched and was very similar to number 1. On this grating every 7th line was made longer than the others so that direct measurement of the distance between these 7th lines could be made. Also the number of lines on the whole grating could be easily determined, and by measuring accurately the distance between the extreme lines the grating space d was obtained. The error of run was less than $10^{-5}d$, and the intensity of the ghost lines was about the same as in grating 1.

Number 4 was a duplication of number 2 except the 4th lines were ruled longer as in number 3. This grating was not etched and possessed characteristics very similar to number 2 and 3.

Number 5 was a glass grating ruled with 50 lines per mm on the ruling engines at the University of Chicago. This grating seemed to be very free of ghost lines, as no ghost lines could be observed even in the very high orders. The first 1/4 of the ruled surface, however, possessed a very bad error of run, probably due to not allowing the ruling engine to run a sufficient length of time before the ruling was started. The grating space of this grating was obtained by carefully determining the pitch of the ruling engine screw. This grating was not carefully examined by the writer until after the x-ray spectra had been taken. The erratic results obtained were completely explained by this error of run in the grating. By eliminating all exposures, which were taken on the bad part of the grating the results were consistent with the results from the other gratings.

Number 6 was a grating with 600 lines per mm, ruled on the same engine as number 5. One part of this grating, which was lightly ruled and gave faint optical spectra, gave x-ray spectra about twice as intense as the more heavily ruled portion. The resulting wave-lengths were the same, within experimental error, from both parts of the grating.

Two types of photographic plates were used. The results with gratings 5 and 6 were obtained with selected plate glass plates coated with Eastman x-ray emulsion. These plates were developed, washed, and dried in the ordinary manner. It has been stated[10] that certain precautions used in the manufacture of commercial plates are omitted in preparing special plates. Thus the plates used in the experiments with gratings 1–4 were the regular commercial x-ray plates. About one half of the plates were "treated" as described by D. Cooksey and C. D. Cooksey,[16] and the remaining plates were not previously treated, but were dried in alcohol and allowed to attain equilibrium in a humid atmosphere. No difference in the consistency of the results was noted between the last two methods. A considerable difference was noted however between these latter methods and the regular developing methods used with the special plates. A test was also made using a standard which was made by silvering a piece of glass the size of the plates used, then making four diamond scratches at equal intervals on the silvered surface. This surface was put in contact with the emulsion and a flash of light from above the plate recorded four very

[16] D. Cooksey and C. D. Cooksey, Phys. Rev. 36, 80 (1930).

fine lines on the photographic plate. The plate was then developed, and by comparing the distance between these lines with those on the standard, a test could be made for contraction or expansion of the plate due to the different methods of developing. The results obtained were essentially in agreement with those of D. Cooksey and C. D. Cooksey[16] except the variations were not quite as great.

Method of Taking Exposures

In exposing a series of plates, the grating was first withdrawn from the path of the x-ray beam and a short exposure given to record the direct beam on the second plate P_2 at the position 1 in Fig. 1. A plate was put in the first plate holder P_1, and the direct beam recorded at 2. The grating was next moved into position for reflection of the x-ray beam, and after allowing 15 to 30 minutes for the slide to attain an equilibrium position, the reflected beam was registered at 3. This plate was then removed and a short exposure given to record the reflected beam at 4. The plate P_2 was then covered with a lead screen almost to the position where the first order would appear, and a long exposure (6 to 24 hours) given to record the various orders of diffraction. At the end of the long exposure another set of plates was taken to make sure that nothing had moved during the exposure. A new plate was put in P_2, and the reflected beam recorded at 4. Likewise a plate was put in P_1 and the reflected beam recorded at 3. The grating was then removed from the path of the x-ray beam and the two positions, 2 and 1 recorded. Since the wave-length depends so much on the position of the reflected beam, another method of taking the exposures was used on about 40 sets of plates. Exposures 1, 2, 3 and 4 were taken as above. A new plate (or the same plate with ends reversed) was placed in P_2. The position of the reflected beam was covered with a screen. After about half the long exposure had been given the screen was removed for a short time to record the reflected beam. At the end of the exposure the grating was removed from the path of the x-rays and the direct beam recorded. Thus if there was any slow change in the position of the apparatus, the reflected beam was recorded in the mean position. The results were in good agreement with the above method. At first it was difficult to get the initial and final exposures to agree as closely as desired. In the latter exposures, however, when the temperature was constant and the vibration from the building damped out, the plates checked as accurately as comparator measurements could be made, which was to about 1 part in 10,000.

The separations of the lines on the plates were measured with an accurately calibrated comparator. In making the measurements 5 or 10 settings were made on each line on the plate. The plate was then reversed and a similar set of measurements made. If a difference of more than 0.004 mm existed between the distances as measured in the two positions, the plate was remeasured. Several sets of plates were arbitrarily remeasured after several weeks, but no appreciable differences were detected. The wave-lengths were calculated from Eq. (1) using Andoyer's 15 place trigonometric tables.

Results

Typical results are shown in Fig. 2. It will be seen that the two α lines are not resolved on any of the plates, but this is not to be expected, as a calculation shows that the separation would only be a few hundredths of a mm. In order to compare these lines with the crystal measurements, one must take a weighted mean of the α_1 and α_2 lines as given by the crystal measurements. If we assume a form of the lines of the type $y=e^{-x^2}$ it can be shown that the maximum intensity of the unresolved doublet should occur very near the "center of gravity" of the two lines. Siegbahn's value of the copper $K\alpha$ line

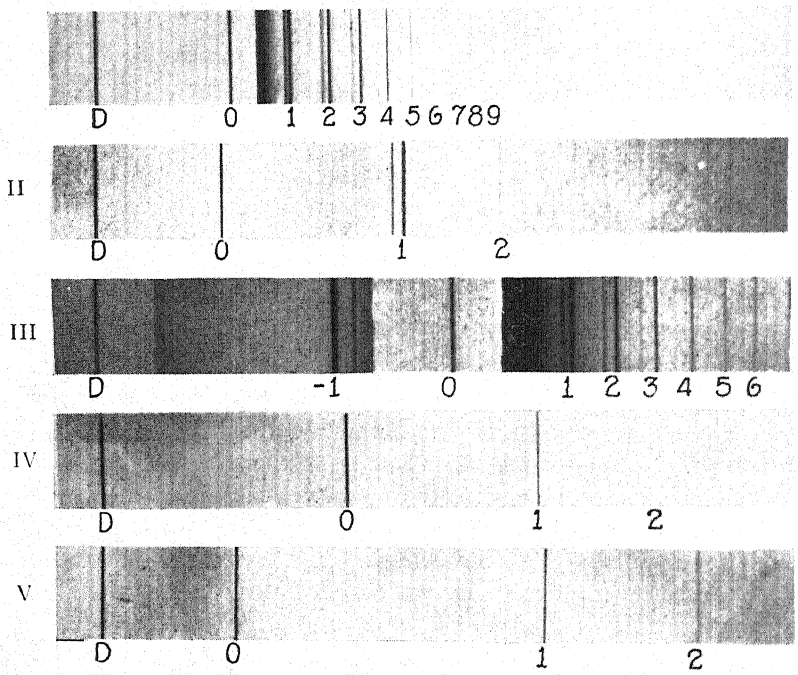

Fig. 2. I copper target, grating 50 lines per mm. II copper target, grating 287 lines per mm. III copper target, gold sputtered grating 143 lines per mm. IV chromium target, grating 143 lines per mm. V copper target, grating 600 lines per mm.

thus weighted is 1.5386A, and for the chromium $K\alpha$ line is 2.2862A. The measurements on the β lines do not involve this difficulty of weighing as the separation of the doublet is so small that it is of no significance in the present work. These crystal values must be corrected for the index of refraction of the x-rays in the crystal. The corrected crystal wave-lengths which are compared with the grating measurements are shown in Table IV.

The average results obtained from each grating are given in Table I. The column headed "gratings" gives the number of the grating as listed in the section on "alignment and calibration of apparatus." The prime numbers are the same as the unprimed numbers except the grating was spluttered with gold. In the experiment 172 sets of plates were taken under various condi-

TABLE I.

Grating	Cu	Cu	Cr	Cr
1 and 3	1.39210	1.54150	2.08463	2.29088
4′	1.39242	1.54193	2.08492	2.29109
4	1.39215	1.54183	2.08486	2.29111
5	1.39217	1.54158	2.08455	2.29075
5′	1.39235	1.54183	2.08499	2.29111
6	1.39207	1.54173	2.08465	2.29077
Weighted average	1.39225	1.54172	2.08478	2.29097

tions, such as different angles of reflection θ, different slit widths and length of exposure. The measurements from 107 plates have been retained and the other discarded because the initial and final exposures failed to check or on account of other experimental difficulties.

In order to show the type of variation obtained with each grating Table II gives the copper series results for grating 4′. The lowest value recorded for any wave-length was +0.13 percent and the highest +0.31 percent greater than the corresponding crystal values. In obtaining the average for each grating each order was given equal weight. This method was used because in the low orders the lines were intense and easily measured, while in the higher orders the lines were more difficult to measure but the errors were of less importance.

TABLE II.

Plate	Distance y	Cu $K\beta$	Cu $K\alpha$	Plate	Distance y	Cu $K\beta$	Cu $K\alpha$
127	10.357 mm	1.3921A	1.5415A	132	10.032 mm	1.3929A	1.5426A
		1.3922	1.5422			1.3924	1.5423
		1.3923	1.5424			1.3926	1.5422
			1.5423				1.5415
			1.5424				1.5419
			1.5416	133	26.808	1.3924	1.5425
128	10.068	1.3921	1.5415			1.3929	1.5418
		1.3924	1.5420			1.3926	1.5420
		1.3922	1.5422			1.3928	1.5419
			1.5421				1.5423
			1.5419				1.5417
129	10.069	1.3926	1.5422	134	26.805	1.3928	1.5415
		1.3924	1.5425			1.3921	1.5421
		1.3926	1.5421			1.3924	1.5418
		1.3925	1.5425				1.5421
			1.5425				1.5419
130	10.066	1.3925	1.5422				1.5415
		1.3925	1.5414	135	26.807	1.3921	1.5416
		1.3926	1.5417			1.3922	1.5418
			1.5417			1.3924	1.5413
			1.5420			1.3919	1.5414
131	10.029	1.3925	1.5421				1.5417
		1.3922	1.5417				1.5411
		1.3924	1.5419				
			1.5420		Average	1.39242	1.54193
			1.5417				

In any case it was found that almost any consistent method of weighing gave practically the same result. The probable error has not been given for each set

of measurements as in almost every case it was much less than the probable consistent errors in the experiment. It is believed that the differences between the results for various gratings form the best method of determining the probable error in the experiment. This may be seen more easily from Table III

TABLE III.

Grating	Cu $K\beta$	Cu $K\alpha$	Cr $K\beta$	Cr $K\alpha$
1 and 3	0.213 (26)	0.203 (46)	0.215 (16)	0.218 (28)
4′	0.236 (30)	0.231 (49)	0.229 (3)	0.227 (5)
4	0.217 (4)	0.224 (11)	0.226 (15)	0.228 (27)
5	0.218 (41)	0.208 (73)	0.211 (32)	0.212 (51)
5′	0.232 (49)	0.224 (82)	0.232 (44)	0.228 (67)
6	0.211 (11)	0.218 (16)	0.216 (3)	0.213 (4)
Weighted Average	0.224 (161)	0.217 (277)	0.222 (113)	0.222 (182)

where the percent difference is given between wave-lengths as measured by grating and crystal methods. The number in parenthesis is the number of orders of each wave-length which were measured for each grating. Thus line 5′, means that grating number 5 was spluttered with gold, 49 orders of the copper $K\beta$ line and 82 orders of the copper $K\alpha$ line were measured, and with the chromium target 44 orders of the $K\beta$ line and 67 orders of the $K\alpha$ line were measured. The weighted average was obtained by multiplying each value by the number of measurements (in parenthesis) and dividing the sum by the total number of measurements.

The final results are given in Table IV. The crystal wave-lengths are those given by Siegbahn[17] which have been corrected for the index of refraction of the x-rays in the crystal. The limiting error has been estimated by the following method.

TABLE IV.

Spectral Line	Crystal λ	Grating λ	Limiting Error	Grating λ −Crystal λ
Cu $K\alpha$	1.38914A	1.39225A	±0.00014	+0.224%
Cu $K\alpha$	1.53838	1.54172	±0.00015	+0.217%
Cr $K\beta$	2.08017	2.08478	±0.00021	+0.222%
Cr $K\alpha$	2.28590	2.29097	±0.00023	+0.222%

In addition to the probable error calculated from the variation of the results, there are three possible sources of consistent error that have to be taken into consideration. They are: the measurement of the grating constant, the distance between the plate holders, and the precision of the comparator on which the plates were measured.

The grating spaces of gratings 1 to 4 were measured directly as described above. This method essentially determines the pitch of the ruling engine screw. The pitch of the screw as determined from these gratings differed by less than 1 part in 20,000. The grating space of gratings 5 and 6 was deter-

[17] M. Siegbahn, "The Spectroscopy of x-rays" (1925).

mined by measuring directly the pitch of the ruling engine screw. It appears to the writer that the maximum error in the grating space of the gratings should not exceed 0.005 percent.

The distance between the plate holders (184.280 cm) was measured by two observers and the results agreed to within 0.002 cm. The iron bar was compared with the laboratory standard and also measured on the comparator on which the plates were measured. Thus the maximum error in the distance between the two plate holders must have been less than 0.004 percent.

In addition to the calibration of the comparator as already described, it was further checked for erratic or periodic error by measuring the distance between the lines on a coarsely ruled grating. From these results it is concluded that the absolute error in the comparator was not greater than 0.001 mm over the range used. Since the distances on the plates varied from 4 mm to 50 mm, the average error must have been less than 0.008 percent.

It will be seen from Table III that the differences between the results from different gratings and different wave-lengths are of negligible importance as compared to the possible consistent errors. Thus the limiting error has been taken as 0.01 percent.

TABLE V.

Investigator	Spectra line	λ	Grating λ −Crystal λ	Probable error	Date
Compton-Doan	Mo $K\alpha$	0.7078A	−0.1%	±0.4%	1925
Thibaud	Cu $K\alpha$	1.540	+0.1	±1.	1926
Hunt	Pt $M\alpha$	6.1	+1.6		1927
	Al $K\alpha$	8.5	+2.0		
Bäcklin	Mo $L\alpha$	5.402	+0.11	±0.2	1928
	Mo $L\beta$	5.174	+0.14	±0.2	
	Al $K\alpha$	8.333	+0.12	±0.1	
	Mg $K\alpha$	9.883	+0.09	±0.2	
	Fe $L\alpha$	17.61	+0.17	±0.2	
Wadlund	Mo $K\alpha_1$	.708	+0.1	±0.1	1928
	Cu $K\alpha_1$	1.537	0.	±0.08	
	Fe $K\alpha_1$	1.938	+0.3	±0.2	
Howe	Cu $L\alpha$	13.37	+0.6	±0.3	1929
	Fe $L\alpha$	17.66	+0.5	±0.3	
Bearden*	Cu $K\alpha$	1.5418	+0.22	±0.02	1929
	Cu $K\beta$	1.3922	+0.22	±0.02	
Cork	Mo $L\alpha_1$	5.4116	+0.29		1930
	Mo $L\beta_1$	5.1832	+0.30		
Bearden	Cu Kα	1.54172	+0.217	±0.01	1931
	Cu $K\beta$	1.39225	+0.224	±0.01	
	Cr $K\alpha$	2.29097	+0.222	±0.01	
	Cr $K\beta$	2.08478	+0.222	±0.01	

* These results are not the same as those published but they have been corrected for the difference between Eq. (9) which was used for calculating the wave-lengths and the correct Eq. (1). Also the index of refraction of the x-rays in the crystal was neglected in this preliminary report.

Discussion

It is interesting to compare the absolute measurements of the x-ray wave-lengths obtained by various investigators using ruled gratings. Table V gives a summary of these results, where the probable errors are approximately those given by the authors. It will be noticed that all the results are high except the pioneering results of Compton and Doan and the copper $K\alpha_1$ result of Wadlund.

The copper $K\alpha_1$ line was recorded by Wadlund on only three plates, and on the plate showing the most measurable orders a difference of 0.75 percent in wave-length was observed in different orders. Measurements made by the writer using the same grating gave results about 0.2 percent higher than the crystal values. The results obtained by Backlin and Cork on the molybdenum $L\alpha$ and $L\beta$ lines differ by almost 0.2 percent. Howe and Backlin differ by more than 0.3 percent on the iron $L\alpha$ line. These differences observed by the various investigators are rather difficult to understand. However, it has been observed by the writer that an error of 0.2 percent can easily be made unless all adjustments are precisely made. It is very essential that the angle θ be checked at the beginning and end of an exposure as this forms a satisfactory criterion for accepting or rejecting a given set of plates. The satisfactory agreement between the present results for different gratings and also those obtained by the writer in 1929 seem to support this criterion.

In Table III it will be noted that the results with the gold spluttered gratings 4′ and 5′ are higher than the results obtained with the unspluttered gratings. The difference appears to be greater than the experimental error but probably is not of sufficient magnitude to indicate a fundamental difficulty with the grating method. The spluttered layers were very thin (absorbed about 95 percent of optical light) and it is conceivable that there might have been some interaction between the top of the gold surface and the glass surface. However, the difference was so small that it was not thought worth while to plan a detailed experiment to test the question.

The great difference between the wave-lengths thus measured and those obtained from crystal measurements indicates some fundamental difficulty in the two methods. As was seen in the earlier part of this paper no suggestion has been supported which would influence the grating results. It is known, however, that crystals such as rocksalt are much less perfect than crystals of calcite, but even calcite cannot be considered a perfect crystal. In order to account for the mechanical properties of crystals, Zwicky[18] has developed a theory which strongly suggests that even in crystals of calcite there might be a concentration of atoms at rather regularly spaced intervals. This would make the average density of the crystal greater than the density of the small elements of the crystal which are effective in diffracting x-rays. Such an imperfection in the crystal would account for the observed difference in wave-length as measured by ruled gratings and crystals. In any case it appears that the difficulty must be either in the crystal or in the constants used to calculate the grating space of the crystal from chemical data.

[18] F. Zwicky, Helvetica Physica Acta 3, 269 (1930).

Determination of the Fundamental Constants

The absolute wave-length measurements obtained above allow us to determine directly the fundamental grating constant of crystal gratings. The complete Bragg law of diffraction may be written

$$n\lambda = 2d \sin\theta\left(1 - \frac{1-\mu}{\sin^2\theta}\right) \tag{10}$$

where n is the order of diffraction, λ the wave-length, d the grating space of the crystal, θ the angle of diffraction, and μ the index of refraction of the x-rays in the crystal. Sine θ and μ have been precisely measured by many investigators. It is thus possible to determine the distance d between the layers of atoms in the crystal almost as accurately as the wave-length λ of the x-rays is known. Siegbahn and Dolejsek[19] have found for the copper $K\beta$ line $\sin\theta = 0.229334$. Larsson[20] has found $(1-\mu)/\lambda^2 = 3.72\times10^{10}$ or $(1-\mu)/\sin^2\theta = 1.36\times10^{-4}$. Substituting these values and the wave-length of the copper $K\beta$ line from Table IV in Eq. (10) one finds

$$d = 3.0359 \pm 0.0003\text{A}$$

One of the most precise methods of measuring Planck's constant h is by determining the high frequency limit of the continuous x-ray spectrum. The quantum relation

$$Ve = h\nu$$

may be written in the form

$$h = Ve\left(\frac{2d\sin\theta}{c^2}\right) \tag{11}$$

where v is the potential applied to the x-ray tube, d is the grating space of the crystal used and θ the minimum angle of diffraction. The experiment of Duane, Palmer and Yeh[21] gives directly the value of $v \sin\theta$ as 2039.9 ± 0.9 volts. Using the value of d obtained from Eq. (10), $e = 4.77\times10^{-10}$ e.s.u. and $c = 2.99796\times10^{10}$ cm/sec we obtain

$$h = 6.573 \pm 0.007 \times 10^{-27}\ \text{erg}\cdot\text{sec}.$$

All different theories of the dispersion of x-rays agree in the limiting case when the frequency of the radiation is much greater than the natural frequency of the electrons in the dispersing medium. The relation is

$$1 - \mu = \frac{ne^2}{2\pi m\nu^2} \tag{12}$$

where μ is the index of refraction, n the number of electrons per cm^3 in the

[19] M. Siegbahn and V. Dolejesek, Zeits. f. Physik **10**, 160 (1922).
[20] Alex. Larsson, Inaugural Dissertation, Uppsala, 1929.
[21] Duane, Plamer and Yeh, Opt. Soc. Amer. **5**, 376 (1921).

dispersing medium, e the charge on the electron, m the electronic mass, and ν the frequency of the radiation. This equation can be rewritten in the form

$$\frac{e}{m} = \frac{2\pi Mc^2}{F\rho Z} \times \frac{(1-\mu)}{\lambda^2} \tag{13}$$

where M is the molecular weight, F the Faraday constant, ρ the density, z the molecular number, λ the wave-length of the x-rays and c the velocity of light. Stauss[22] has recently measured $(1-\mu)$ for the molybdenum $K\alpha_1$ and $K\beta$ lines using quartz as the refracting medium. His value of $(1-\mu)$ is

$$(1-\mu)_{K\alpha_1} \times 10^6 = 1.804 \pm 0.001.$$

If we increase the crystal value of the molybdenum wave-length by 0.221 percent, which seem justifiable from the agreement of the writer's measurements of the copper and chromium K-series, we obtain for the molybdenum line the wave-length

$$\mathrm{Mo}K\alpha_1 = 0.7094\mathrm{A}$$

Substituting this wave-length in Eq. (13) and the other constants from Birge's[23] tables one obtains

$$\left(\frac{e}{m}\right)_{K\alpha_1} = 1.765 \pm 0.001 \times 10^7 \text{ e.s.u.}$$

This value of e/m is very unsatisfactory because it does not agree with either the usual spectroscopic value or the deflection method value. However, it should be pointed out that Larsson's[20] value of $(1-\mu)$ is much higher than this value from Stauss's experiment. If one uses an average of the values obtained by Larsson and Stauss we have

$$\frac{e}{m} = 1.769 \times 10^7 \text{ e.s.u.}$$

Thus it appears that further experiments on the dispersion of x-rays will have to be made before confidence can be placed in the value of e/m obtained in this manner.

The above constants as determined from the grating measurements of x-ray wave-lengths are unaffected by the possible imperfections of the crystal. It may be interesting, however, to calculate other fundamental constants assuming that the crystal grating is perfect.

From fundamental considerations of crystal structure it can be shown that the grating space d of a rhombohedral crystal is given by

$$d = \left(\frac{nM}{N\rho\phi}\right)^{1/3} \tag{14}$$

[22] H. E. Stauss, Phys. Rev. **36**, 1101 (1930).
[23] R. T. Birge, Phys. Rev. Sup. **1**, 1 (1929).

where n is the number of molecules in each elementary rhombohedron, M the molecular weight of the crystal, N is Avogadro's number, ρ the density of the crystal, and ϕ is the volume of a rhombohedron, the perpendicular distance between whose opposite faces is unity. It can also be shown that

$$\phi = \frac{(1 + \cos\beta)^2}{(1 + 2\cos\beta)\sin\beta} \tag{15}$$

where β is the angle between the axis of the crystal. All the quantities in Eq. (14) can be precisely measured except N. Thus if the crystal is perfect, an independent determination of d should make possible a precise measurement of Avogadro's number N. Using the value of d found from Eq. (14) and the other constants from Birge's[24] tables one finds

$$N = 6.019 \pm 0.003 \times 10^{23} \text{ mol. per mole}$$

If Avogadro's number N can be accurately determined in this manner the charge on the electron e can be obtained from the relation

$$F = Ne \tag{16}$$

where F is the Faraday constant. Thus

$$e = 4.806 \pm 0.003 \times 10^{-10} \text{ e.s.u.}$$

Planck's constant h determined from Eq. (11) using $e = 4.806 \times 10^{-10}$ and the other constants the same as above, gives

$$h = 6.623 \pm 0.004 \times 10^{-27} \text{ erg·sec.}$$

The values of N and e obtained from Eqs. (14) and (16), and the value of h using e from Eq. (16) appear to be entirely too high. The numerous ways in which these constants enter into theoretical calculations make the acceptance of these high values almost impossible. This may be interpreted as a support of the theory of mosaic structure of crystals. If the entire difference, observed in the x-ray wave-lengths as measured by the two methods, be attributed to the mosaic structure, then we now have a precise method for determining quantitatively the magnitude of this effect in any crystal. An independent experimental determination of the mosaic structure would of course allow us to calculate N and e as above, with higher precision than has been attained by other methods.

THE TRANSPARENCY OF SODIUM FLUORIDE AND LITHIUM FLUORIDE IN THE EXTREME ULTRAVIOLET

By Eugene H. Melvin
Chemical Laboratory, University of California

(Received April 8, 1931)

Abstract

Artifically prepared single crystals of sodium and lithium fluorides were tested for transparency to extreme ultraviolet light by means of a one meter concave grating vacuum spectrograph. The source used was a highly condensed spark discharge through a Pyrex capillary. These crystals were expected to be more transparent than calcium fluoride (fluorite) due to their lower indices of refraction. Lithium fluoride was transparent to 1083A (132A below the limit of fluorite) which is the practical limit to be expected. Sodium fluoride was transparent to 1320A, which is not thought to be the limit of the pure material. Crystals of these salts have been made as much as 5 cm in diameter, and they are rather insoluble and easily cut and polished being very similar to fluorite.

RESEARCH work in the extreme ultraviolet part of the spectrum has been handicapped by a lack of transparent materials. The most transparent material known was calcium fluoride (fluorite) which Liefson[1] found transparent to 1215A (this is exceptional and fluorite that transmits to 1400A is very scarce). Lyman[2] has tested a great number of naturally occuring crystals; he found none as good as fluorite and that fluorite varied greatly in its transparency. Therefore research work has been directed towards the preparation of large single crystals from pure salts.

Crystals have several advantages in spectrographic work. A prism spectrograph gives a much brighter spectrum than a grating spectrograph. Crystals have greater dispersion than glasses near the transmission limit; so if prisms of various crystals were available one could obtain high dispersion in any desired part of the spectrum. Achromatic lenses can be made when crystals are obtainable that have about the same transmission limits. Crystals that transmit far into the extreme ultraviolet have high dispersion in the near infrared.

There were several reasons for the choice of sodium and lithium fluorides. They are cubic crystals, which make the preparation of lenses and prisms simpler than from other classes of crystals. Calcium fluoride was the most transparent solid known, and since the fluoride ion was the chief determining factor the fluorides were given the most consideration. Lithium fluoride was first prepared because the lithium ion is smaller and has fewer electrons than the calcium ion. Since the index of refraction is closely related to the absorption or transmission of light, a plot of the dispersion curves of cubic crystals was thought worthwhile; all that had been measured were those of calcium

[1] S. W. Liefson, Astrophys, J. **63**, 73 (1926).
[2] T. Lyman, Astrophys. J. **25**, 45 (1907).

fluoride, sodium chloride, and potassium chloride. Since then Gyulai[3] has measured the dispersion curves for five alkali halides. All the measurements are shown in Fig. 1. The fact that the curves do not cross and are of the same general shape was used to limit the research to crystals which showed the most promise, since a single measurement of the index of refraction fixed its relative position in the plot and indicated how transparent the pure crystal would be in the extreme ultraviolet. Sodium fluoride has the lowest index of refraction (1.328 for N_D) for any cubic crystal and therefore should be the most transparent in the extreme ultraviolet. The only other cubic crystal that might have as low a value for N_D is potassium fluoride which is very deliques-

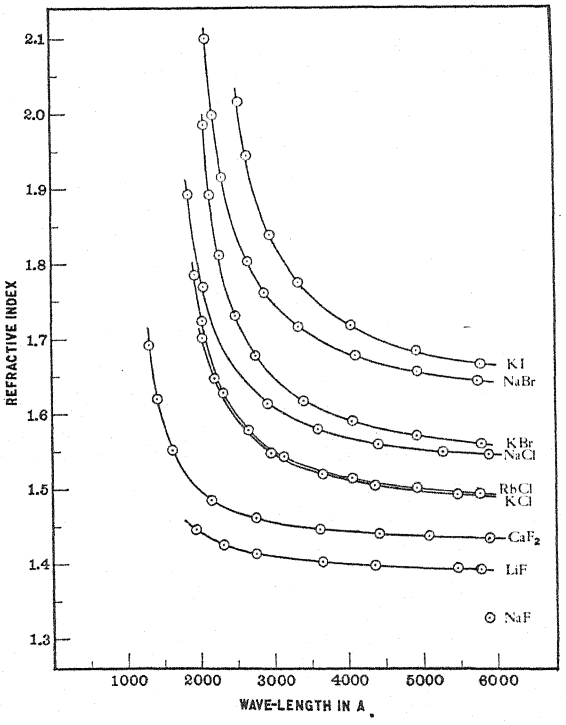

Fig. 1.

cent and consequently for practical use out of the question. Lithium fluoride has a value for N_D of 1.384, while calcium fluoride has a value of 1.434. Therefore pure sodium fluoride and lithium fluoride should be more transparent than calcium fluoride.

The single crystals, made by a method previously published,[4] were prepared from repurified C.P. chemicals. The transparency was the best test of the purity. Crystals of sodium and lithium fluorides cleave easier and better than fluorite. They were tested by placing a thin cleavage plate of about 1 mm thickness between the light source and the slit of a one meter concave grating

[3] Z. Gyulai, Zeits. f. Physik **46**, 809 (1927).
[4] H. C. Ramsperger and E. H. Melvin, J.O.S.A. and R.S.I. **15**, 359 (1927).

vacuum spectrograph. The light source used was a condensed spark discharge through a Pyrex capillary at a residual air pressure of about 0.002 mm of Hg; this gave a line spectrum extending to 500A. The crystal window was protected by glass tubes from metal sputtered from the aluminum electrodes.

Results

Spectrograms showing the transparency of the crystals are not published due to the fact that faint lines near the transmission limit are not visible in reproduction. The percentage of light transmitted is difficult to judge due to the type of source used. A description of the results follow.

Lithium fluoride. Four crystals of lithium fluoride were tested. The transmission limits varied between 1083A and 1350A. All the crystals were very transparent to within 200A of their limit. The salts used in preparing the crystals were from different sources which may explain the variations, since the treatment given them was the same in all cases.

Sodium fluoride. Two crystals of sodium fluoride were tested. One crystal transmitted to 1740A with almost no absorption of light, then absorption was complete; the other crystal transmitted to 1320A where absorption set in completely.

Discussion

The limits of transparency varied considerably for both salts. The limit of 1083A obtained for lithium fluoride appears to be the practical limit of transmission for the pure salt based on the curves shown in Fig. 1. This limit is 130A beyond that obtained for the best fluorite. The limit of 1215A for fluorite would seem to be the limit for pure calcium fluoride. As indicated in Fig. 1, sodium fluoride should be more transparent than lithium fluoride, but this was not found to be the case, slight traces of impurities are thought to be the explanation of this. The great absorption that traces of impurities may have is shown in a recent paper by Hilsh and Pohl[5] who measured the dispersion frequencies above 1600A of many alkali halides. They distilled the salts onto a quartz plate to measure their absorption, and found that the layer of salt had to be of the order of 0.001 mm thick to get appreciable amounts of light through the salt below the first absorption wave-length. Thus we see that extremely small amounts of such salts as these would effect the transmission of extreme ultraviolet light very markedly.

Sodium fluoride and lithium fluoride are better than fluorite also in that they do not become colored and opaque with use—some crystal windows were tested many times. These crystals are about as hard as fluorite so that anyone familiar with fluorite can cut and polish them. Single crystals up to 5 cm in diameter have been prepared and there seems no reason why much larger ones could not be prepared. Plates are very easy to cleave and have very good surfaces. Lithium fluoride is rather insoluble—0.27 g per 100 g of water at 10°C—and can be ground and polished in water. Sodium fluoride is more soluble—4.3 g per 100 g of water at 18°C—and so cannot be allowed to stand in water.

[5] R. Hilsh and R. W. Pohl, Ziets. f. Physik 59, 812 (1930).

THE ANGULAR DISTRIBUTION OF PHOTOELECTRONS EJECTED BY POLARIZED ULTRAVIOLET LIGHT IN POTASSIUM VAPOR

By Milton A. Chaffee
University of California

(Received April 10, 1931)

Abstract

Light of wave-lengths in the region of 2400A selected by a monochromator and polarized by a pile of quartz plates illuminated a jet of potassium vapor. The lateral directions of emission of the photoelectrons relative to the electric vector were studied. Though the electrons were ejected with energies less than one equivalent volt, the experiments were definite in establishing that the most probable direction of ejection is that of the electric vector and that the angular distribution varies as the square of the cosine of the angle between the electric vector and the direction in question. This result is in accord with predictions of the wave mechanics for a spherically symmetrical atom and incidentally therefore constitutes additional evidence that molecules do not play an appreciable part in the observed photo-ionization of potassium vapor.

Introduction

THE wave mechanics predicts that the most probable direction of emission of photoelectrons by polarized radiation is forward of the electric vector. The forward component of the ejected electrons is furnished by the momentum of the absorbed quantum and therefore is only appreciable when the momentum of the absorbed quantum is comparable with that of the photoelectron. Apart from this forward component the distribution in angle about the electric vector decreases with the square of the cosine of the angle between the direction in question and the electric vector.

A great amount of experimental work on the angular distribution of photoelectrons ejected by x-rays has verified the above predictions of theory.[1] The present work has sought to examine experimentally the phenomena in the optical region. Here the momenta of the absorbed quanta are so small that no forward component should be observed and therefore the angular distribution should follow a cosine squared law for the longitudinal as well as the lateral distribution. The experiments reported in this paper have shown that for the lateral distribution of the electrons ejected by ultraviolet light in potassium vapor such is the case.

Experimental Method

Rather troublesome difficulties were encountered in the present work because the problem was that of measuring the velocity directions of electrons

[1] C. D. Anderson, Phys. Rev. 35, 1139 (1930). This paper contains references to other work in the field.

having less than one equivalent volt of energy. Making sure that the photoelectrons observed were really from the vapor was itself an elusive and difficult task.

The main requirements of the experiment were as follows. First, light had to pass through the tube ionizing the vapor without striking the electrodes or walls of the tube which, in the presence of the vapor, were extremely photoactive. Second, the electrodes and tube had to be maintained at room temperature to avoid thermionic emission, while a sufficient and constant vapor density of potassium to obtain a measurable number of photoelectrons was necessary. Third, an intense and constant source of ultraviolet light was necessary in order to give a good photo-effect at the lowest possible vapor density. The upper limit to the allowed vapor density was set by the requirement that the mean free path of the electrons had to be comparable with the dimensions of the ionizing chamber.

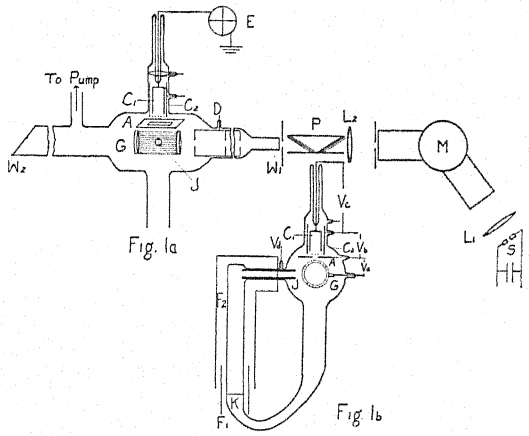

Fig. 1. Diagram of apparatus.

These requirements were satisfied by an apparatus which incorporated many features similar to that used by Lawrence[2] in his measurement of the photo-ionization probability of potassium and that of Williamson[3] who studied as well the distribution of velocities of the photoelectrons produced in potassium. A jet of vapor was ionized by plane polarized radiation inside a cylindrical grid, which was practically field free, so that electrons traveled in their original directions of ejection. Those that were ejected in the direction of a slit (a solid angle of 11.5 degrees) were accelerated into a faraday cylinder and measured by a Compton electrometer (sensitivity 10,000 mm/volt).

Figure 1a, b shows a detailed description of the apparatus. The light source consisted of a cobalt spark (which has many strong lines in the region 2300–2700A) quenched by a blast of air which served both to steady the spark at one position and to increase greatly the intensity of the ultraviolet light. The light was focused by lens L_1 into the slit of a Bausch and Lomb quartz monochromator which resolved the light into a band of about 500A

[2] E. O. Lawrence, Phil. Mag. **1**, 345 (1925).
[3] R. C. Williamson, Phys. Rev. **21**, 107 (1923).

around 2400A, thus eliminating the visible spectrum which would only produce photoelectric emission from the potassium surfaces. Lens L_2, a quartz-fluorite achromatic combination, focused the light to infinity. The light was polarized by two piles of quartz plates P set at the polarizing angle, which gave a measured polarization of 86.6 percent, the second pile of plates serving to refract the beam back to its original axis so that rotation of the polarizer did not throw the beam out of alignment with the collimating diaphragms D. The tube was constructed of Pyrex glass with the quartz window W_1 sealed on by a quartz-Pyrex graded seal. The polarized beam passed through a system of collimating diaphragms D, the last diaphragm being slightly larger than the others to avoid scattering of the main beam. It was at a small positive potential with respect to the grid and slit, so that photoelectrons ejected from the diaphragm did not enter the faraday cylinder. The light after passing through the grid passed through a long tube and out through a quartz window W_2 which was set at an angle so that the reflected beam was multiply reflected a sufficient number of times to prevent it again reaching the grid. The fluorescence of this quartz window showed the beam to be in good focus through the tube.

Figure 1b shows the arrangement of the potassium boiler and vapor jet. The heating coil around the potassium reservoir F_2 controlled the density of the vapor stream, while the furnace F_1 was kept at a slightly higher temperature to avoid condensation of the vapor. J_1 indicates the copper jet in which the vapor entered the tube, and this was at a positive potential V_d with respect to the grid in order to eliminate the emission of electrons. The potassium after passing through the grid condensed on the walls of the tube and after each run the tube was warmed enough to allow the potassium to run back into the reservoir. The tube was cooled by several air blasts, and the electrodes were kept cool by conduction through short heavy leads which were cooled on the outside of the tube by the air blast. A copper gauze cylinder concentric with the grid and at the potential of the slit was placed inside along the walls of the tube for electrostatic shielding. Denoting the potential of the grid as zero, slitA was 1.5 volts positive, denoted by V_a. V_b was 4.5 volts positive (to draw the electrons into the faraday cylinder) and V_c, the potential of the faraday cylinder, was 6 volts positive. V_d was 3 volts positive thereby preventing thermionic emission from the jet reaching the collector.

Results

Figure 2 is a plot of the relative number of electrons as ordinates ejected at angles with the electric vector given by the abscissas. The curve shows the cosine square distribution law, and the crosses represent averages of about twelve observations of each setting of the polarizer. The parallel plate polarizer was rotated over a 180° range, taking observations at 30° intervals. The abscissa 0° denotes the direction parallel to the electric vector. Assuming the validity of the cosine squared law, these observations were corrected for the lack of complete polarization of the light, due to the inefficiency of the polarizer and the depolarization of the quartz window, leading to the circles. It is seen that the corrected points fall fairly well along the cosine-squared curve.

The photoelectric currents for the 0° setting of the polarizer were of the order of magnitude of 10^{-14} amperes.

Errors

There remains after correction of the observations a small residual recorded emission of electrons at right angles to the electric vector. This is of importance for if it is real it means that the cosine-squared law does not hold. There are four paramount sources of experimental error which could be responsible for the observed effect at 90°.

First there is the possibility of a small photoelectric emission by scattered light from the electrodes. The diaphragming of the light was, however, so carefully arranged that no emission at all was observed before vapor entered the tube or after the jet of vapor was cut off. The routine preliminary procedure before each run was to make certain that there was no photo-emission before the potassium reservoir was heated, then the vapor pressure was raised

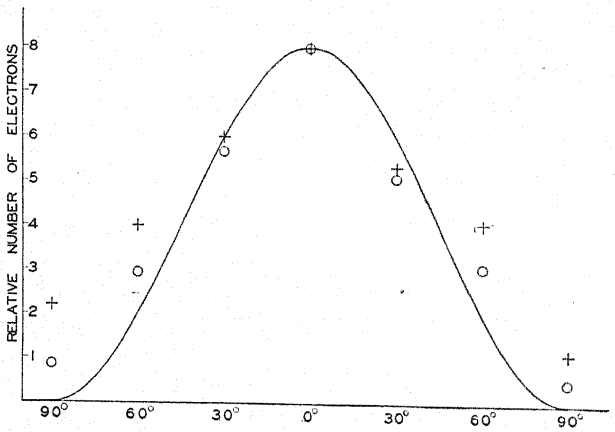

Fig. 2. The relative numbers of photoelectrons ejected at various angles relative to the electric vector. The crosses represent experimental data. The circles represent data corrected for lack of complete polarization of the light. The curve represents the cosine squared distribution.

to a point where there was a measurable photo-effect, and next it was established that the photo-effect fell to zero when the jet was cut off. These control observations practically eliminated this source of spurious effects from consideration. Secondary electrons such as photoelectrons reflected from the grid and slits, however, remain as an unknown factor which might have been great enough to contribute appreciably to the observations.

The error introduced by the finite width of the slit and the accelerating potential of 1.5 volts between the grid and slit was quite inappreciable. The earth's magnetic field was not balanced out for the curvature of the paths of the photoelectrons produced by this field was of the order of magnitude of 10 cm and therefore not a serious source of systematic error. Because of the continuous distillation of potassium on the electrodes contact electromotive force fields undoubtedly were very small.

Perhaps the greatest source of error was introduced by the scattering of the electrons in the vapor. From the temperature of the molten potassium and the geometry of the jet orifice and electrodes an estimate of the vapor pressure of the jet in the region of ionization gave the value of 0.002 mm of mercury pressure. Using Brode's[4] data on the mean free paths of 0.7 volt electrons in potassium vapor it was accordingly calculated that in the present experiments the probability of a scattering collision of a photoelectron formed in the jet on passing to the slit was of the order of magnitude of one-half. Because small angle scattering[5] is greater than scattering at large angles it therefore appears that this is a quite appreciable source of systematic error and indeed is very probably responsible for the observed emission at right angles to the electric vector.

Discussion

The wave-length dependence of the photo-ionization of potassium vapor is anomalous in the respect that it does not decrease monotonically to shorter wave-lengths beyond the series limit as is the case in caesium and rubidium.[6,7] The possibility has been suggested[1] that this anomalous behavior is ascribable to a large amount of molecular ionization, and indeed some rather good arguments have been adduced in favor of this hypothesis.[8] It appears, however, that a general consideration of all the evidence, particularly that obtained in most recent work,[9] indicates that the observed photo-ionization of potassium vapor is really that of the potassium atom.

The present experiments have a bearing on this question for it is to be expected that the cosine-squared angular distribution of the photoelectrons about the electric vector will hold only for a spherically symmetrical atomic system. Professor J. R. Oppenheimer has kindly informed the writer that he has estimated that the emission perpendicular to the electric vector would be of the order of magnitude of one-third that in direction of the electric vector if the emission were from potassium molecules. The fact that the present experiments have yielded much less than this amount therefore may be regarded as further evidence that the potassium atom is responsible for the observed effects.

The writer is indebted to the General Electric Company for a photoelectric cell used in calibrating the polarizer and to the Committee-on-Grants-in-Aid of the National Research Council for the quartz-fluorite lens used in the present work.

In conclusion the writer wishes to acknowledge a great indebtedness to Professor E. O. Lawrence who suggested the problem and gave many suggestions which made possible the success of this work.

[4] R. B. Brode, Phys. Rev. **34**, 673 (1929).
[5] F. L. Arnot, Proc. Roy. Soc. **A125**, 660 (1929).
[6] F. L. Mohler, P. D. Foote and R. L. Chenault, Phys. Rev. **34**, 233 (1929).
[7] E. O. Lawrence and N. E. Edlefsen, Phys. Rev. **34**, 233 (1929).
[8] R. W. Ditchburn and F. L. Arnot, Proc. Roy. Soc. **A123**, 516–536 (1929).
[9] E. O. Lawrence and N. E. Edlefsen, Phys. Rev. **34**, 1056 (1929).

THE ABSORPTION OF THE $K\alpha$ LINE OF CARBON IN VARIOUS GASES AND ITS DEPENDENCE UPON ATOMIC NUMBER

By Elmer Dershem and Marcel Schein*
University of Chicago

(Received March 27, 1931)

Abstract

A description is given of the apparatus and methods used in a photographic investigation of absorption coefficients for the $K\alpha$ line of the carbon ($\lambda=44.6$A) in different gases and in gold leaf. The mass absorption coefficients, μ/ρ, found were as follows: He, 3600: CO_2, 4780: N_2, 3850: O_2, 5765: Ne, 13100: A, 45700: Kr, 31800: Xe, 6740: Au, 12500. Some of the atomic absorption coefficients (μ_a) derived from these values on the assumption that the absorption is independent of chemical combination are as follows: C, 0.44×10^{-19}: N, 0.89×10^{-19}: O, 1.52×10^{-19}: Ne, 4.36×10^{-19}: The wave-length of the $K\alpha$ line of carbon lies between the K and L_I absorption limits of these elements. The values of log μ_a when plotted against log Z fall upon a straight line whose slope is 4.4. Hence in this wave-length region this should be the value of p in the equation $\tau_a=C\lambda^nZ^p$, provided that $\lambda_K<\lambda<\lambda_L$. The results of extrapolating current x-ray formulas to this wave-length are given and the values of μ_a so obtained are, in general, considerably too large. Since the exponent of Z in the above equation is found experimentally to be as large or larger than in the case of ordinary x-rays it appears that the proper exponent of λ may be considerably less than 3.

Introduction

THIS investigation was undertaken to determine absorption coefficients for soft x-rays over as great a range of wave-lengths and absorbing elements as might be possible with the use of ruled gratings to isolate single wave-lengths and a photographic method to measure intensities. The present report deals only with data obtained with the use of one wave-length, that of the $K\alpha$ line of carbon (44.6A). As will be shown in a following paper the reflecting power of a mirror for these rays is intimately related to the absorption of the radiation by the mirror. Hence it was necessary first to investigate the laws of absorption applicable to such soft x-rays in order to determine the exact role played by absorption in modifying the intensity of reflection of x-rays from mirrors and gratings.

The x-ray absorption coefficient of an atom of any element is usually considered to consist of two terms as may be expressed in the following equation, $\mu_a=\tau_a+\sigma_a$ in which μ_a is the total atomic absorption coefficient and τ_a and σ_a are the atomic fluorescence and scattering absorption coefficients respectively. For radiations longer than 1A, σ_a becomes quite small in comparison to τ_a.

In the case of ordinary x-rays the atomic fluorescence absorption coefficient was early found to be very well represented by the formula $\tau_a=C\lambda^nZ^p$ in which C is a constant depending upon the absorption region considered, λ the

wave-length and Z the atomic number. For wave-lengths less than 1A the values of the exponents n and p are very nearly 3 and 4 respectively. For longer wave-lengths there is considerable evidence that n decreases and p increases with increasing wave-length. A number of methods have been proposed for theoretically evaluating the above constants. These will not be discussed here. From a consideration of experimental data, Richtmyer and Warburton[1] found empirically the values, $C=2.24\times10^{-26}$ for wave-lengths shorter than the K limit and $C=0.33\times10^{-26}$ for those between the K and L_I limits, n and p being taken as 3 and 4 respectively and λ expressed in Angstrom units. Allen[2] with data extending in some instances to 4A found the corresponding values of C to be 2.18×10^{-26} and 0.299×10^{-26} respectively while reducing the value of n to 2.92. Gray[3] summarized the existing data and proposed a more complicated formula for the K region, namely:

$$\tau_a = 1.92(1 + 0.008Z)(1 - \lambda/4\lambda_K - \lambda/50\lambda_K^2)Z^4\lambda^3 \times 10^{-26}.$$

The factors in parenthesis are introduced empirically to compensate for the reduction found in n with increasing wave-length. Between the K and L_I absorption limits Gray finds the simpler formula $\tau_a=0.255Z^4\lambda^{2.7}\times10^{-26}$.

An important investigation by Jönsson[4] extended absorption measurements for some metals to nearly 12A. He concluded that the absorption per K electron, for all elements, could be represented by the same function, $f(Z\lambda)$ of the product of the atomic number and the wave-length. This is made applicable to the case of wave-lengths longer than that of the K limit by multiplying $f(Z\lambda)$ by the ratio of the wave-length of the K limit to that of the nearest absorption limit having a wave-length greater than that of the absorbed radiation. This latter step depends for its justification upon the experimental fact as shown by Richtmyer[5] that the magnitude of the absorption discontinuity at the K limit is very nearly equal to the ratio of the wave-length of the L_I limit to that of the K limit. Jönsson tabulates values of $f(Z\lambda)$ obtained from experiment for values of $Z\lambda$ between 8 and 790. With the aid of these tables one may compute absorption coefficients by Jönsson's method for various elements and wave-lengths provided $8<Z\lambda<790$.

Woernle[6] has investigated the absorption of certain gases for wave-lengths ranging from 2.3A to 9.9A and found some variation from the law proposed by Jönsson. His results indicate that the exponent of Z is greater in the L than in the K absorption region.

All of the above formulas were deduced from a consideration of data relating to wave-lengths less than 12A and one should not expect them to hold for wave-lengths as long as that of the carbon $K\alpha$ line. Nevertheless, since they furnished previous to this investigation about the only means of estimat-

* Fellow of International Education Board.

[1] Richtmyer and Warburton, Phys. Rev. **18**, 13 (1921).

[2] Allen, Phys. Rev. **27**, 266 (1926).

[3] Gray, International Critical Tables **6**, 12 (1929).

[4] Jönsson, Dissertation, Uppsala, (1928).

[5] Richtmyer, Phys. Rev. **27**, 1 (1926).

[6] Woernle, Ann. d. Physik **5**, 475 (1930).

ing the order of magnitude of the absorption to be expected, it is of some interest to calculate absorption coefficients by the use of these formulas and to compare the results with those obtained experimentally. These results are given in Table II.

Apparatus and Methods

A sketch of the apparatus is shown in Fig. 1. A beam of x-rays passed upward from the water-cooled x-ray tube X, through the slit S_1 which was covered with a thin film of celluloid, then through the slit S_2 onto the grating G. This was a plane glass grating having 600 lines per mm and gave a very intense first "inside order" of the $K\alpha$ line of carbon when the glancing angle of incidence was about 4°40′. The shield S_3 was so placed as to cut out all

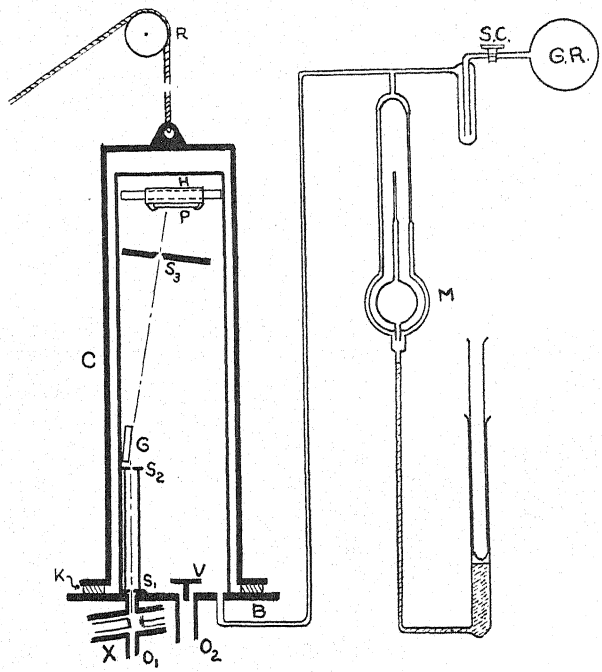

Fig. 1. Diagram of apparatus.

other wave-lengths while letting the $K\alpha$ line of carbon pass through a narrow slit and fall upon the photographic plate P which was carried by the sliding plate holder H. The latter could be given a step-by-step motion across the path of the x-ray beam by means of an electromagnet which is not shown in the sketch but which could be operated at will by pressing a button outside the spectrograph. The apparatus could be opened for adjustments or the changing of plates by raising the cylinder C with the aid of the rope and pulley R. When closed the bottom flange of this cylinder rested on the sulphur-free gasket K which made a vacuum tight seal between the cylinder and the base plate B. The x-ray tube and spectrograph were evacuated by mercury diffusion pumps connected to the outlets O_1 and O_2. The valve V could be

either opened or closed by a ratchet device actuated by another electromagnet controlled from outside.

When in operation the apparatus was used as follows: With the valve V open the spectrograph was evacuated to a pressure of about 2×10^{-5} mm Hg. Several photographs of the $K\alpha$ line were then taken with different times of exposure. The valve V was then closed and such an amount of gas admitted from the gas reservoir GR as was estimated to absorb one half or more of the radiation. Several exposures were then made with varying time of exposure. These times of exposure were so chosen as to produce blackenings intermediate between the lightest and darkest lines obtained in the vacuum. Pressures were measured with the calibrated McLeod gauge M, which was provided with two compression chambers in order to measure a large range of pressures. Readings were taken repeatedly during a run to check against pressure changes. Finally the valve V was opened, the gas swept out and another series of exposures similar to the first were made.

The power input to the tube was kept constant during a run. Ordinarily a current of 22 milliamperes and an effective voltage of 2.7 kv were used. Lines of the desired density were usually secured in one to three minutes when the chamber was evacuated. This varied somewhat from time to time due to variations in the amount of carbon adhering to the target of the x-ray tube, but no sudden changes in the intensity of the carbon line were ever noted. However, continuous variations of five or ten percent per hour were common. It was found that by rubbing a small quantity of stopcock grease on the stem supporting the filament of the x-ray tube that some portion of the stem would remain at just the right temperature to cause a slow evaporation of carbon compounds which would maintain a quite constant amount of carbon deposit on the target provided the energy input to the tube did not exceed that noted above.

Eastman x-ray plates and x-ray developer were used, care being taken to avoid over-development and to keep the plates rotating while in the developer. The densities of the lines were then compared with the aid of a photoelectric photometer recently constructed in this laboratory. In this instrument, which will be described in more detail elsewhere, a beam of light from a small bulb was directed upon a fine slit so placed that the light passing through the slit fell upon a potassium hydride photoelectric cell connected to a string electrometer. The photographic plate was then placed with the film side very close to the slit and moved across the beam of light by means of a graduated screw. The time for a given reflection of the string of the electrometer was noted when the various lines and intervening clear spaces were in front of the slit. Repeated measures of the same lines gave variations in electrometer readings of much less than one percent. The time required for the electrometer string to move a certain number of divisions with a line before the slit minus the time for the same deflection with the adjacent clear portion of the plate in front of the slit was taken as a measure of the relative density of the line.

The noble gases used were obtained from the Air Reduction Sales Company and were guaranteed to be spectroscopically pure. This was verified by

tests with a small direct vision spectroscope which gave no evidence of lines other than those belonging to the gas in question. Carbon dioxide was obtained by heating magnesium carbonate, nitrogen by heating sodium azide and oxygen by the electrolysis of barium hydroxide. These gases were dried by phosphorus pentoxide. Such gases as would not be condensed were further purified by passing through a liquid air trap. For those of higher boiling points carbon dioxide snow in acetone was used to cool the trap. The data for gold were obtained with the use of gold leaf. The thickness of the latter was determined by weighing.

Results and Calculations

The mass absorption coefficients were determined from the equation $I/I_0 = e^{-(\mu/\rho)\rho x}$ in which x is the length of path through the gas from the celluloid window on the slit S_1 to the photographic plate. This distance was 57.7 cm. The density ρ, was computed from the density at standard conditions and the experimental values of temperature and pressure.

The ratio I/I_0 was obtained from the photographic density measurements and the times of exposure of the lines with and without gas in the chamber. Several methods of determining this ratio from density measurements were tried. In one method four lines having different exposure-times were photographed near one end of the plate with the chamber evacuated, followed by seven lines through the gas, the latter exposure-times being lengthened to give densities intermediate between the extremes of those obtained without gas in the chamber. The chamber was then again evacuated and the first four lines repeated on the other end of the plate. Curves were drawn with the photometer densities of the lines in vacuum plotted against exposure-time. In case the curves obtained at the beginning and end of the run were not identical, the densities of the lines through the gas were corrected on the assumption that the radiation from the tube had varied uniformly in intensity throughout the time of the complete operation. The time which would have been required in vacuum to produce a blackening equal to that of any line through the gas could be read from these curves. The ratio of this time to the actual exposure time of the line through the gas is, from the reciprocity law, the desired ratio of intensities, I/I_0. Each line taken through the gas thus gave a measure of this ratio.

In some cases in which a sufficient number of lines in vacuum had not been secured to give a suitable curve of blackening against time, auxiliary plates with variable time of exposure were taken and curves of blackening against exposure-time were drawn for each of these. Let T_v be the exposure time of a line in vacuum and T_{va} the time to produce the same blackening on the auxiliary plate. Also let T_g be the exposure time of a line in gas and T_{ga} the time to produce the same blackening on the auxiliary plate. Then

$$\frac{I}{I_0} = \frac{T_v}{T_g} \times \frac{T_{ga}}{T_{va}}.$$

Experience showed that the two methods led to identically the same result when the average of a considerable number of comparisons were taken.

The results of these measurements are summarized in Table I. The large number of observations taken in some cases reduced the mathematical probable error but the actual error is perhaps considerably larger. This comes from

TABLE I. *Mass, molecular and atomic absorption coefficients of the carbon Kα line in various gases and gold leaf.*

Absorber	μ/ρ	$\mu_m \times 10^{19}$	$\mu_a \times 10^{19}$	Number of observations	Percent probable error
He	3600		0.238	104	1.0
CO_2	4780	3.49		23	1.4
N_2	3850	1.78		20	1.0
O_2	5765	3.05		14	2.8
Ne	13100		4.36	84	0.8
A	45700		30.1	52	0.6
Kr	31800		43.4	112	0.5
Xe	6740		14.5	139	1.0
Au	12500		40.7	5	10.
Air	5350			76	
C			0.44		
N			0.89		
O			1.52		

the fact that not all of the variations are due to chance errors. The absorption coefficient for carbon is derived from that of carbon dioxide on the assumption that absorption is independent of chemical combination. This assumption appears justified when we consider the relatively enormous effect of atomic

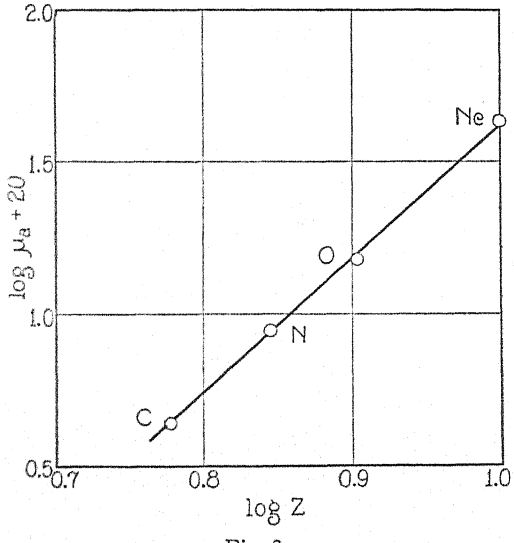

Fig. 2.

number as contrasted with the number of electrons in a molecule. For example, the absorption by an atom of neon with 10 electrons is considerably greater than that of a molecule of carbon dioxide with 22 electrons. Fig. 2 shows the logarithm of atomic absorption coefficient plotted against loga-

rithm of atomic number for the elements carbon, nitrogen, oxygen and neon. The straight line thus obtained indicates that μ_a is a function of the atomic number only, or that its dependence upon any other factor is relatively small, since the atomic absorption coefficients derived from measurements on molecules of CO_2, N_2, O_2 and atoms of Ne are thus shown to be proportional to the atomic number raised to the same power. Some measures of the absorption of sulphur dioxide were made. When corrected for the probable impurity the gas was found later to contain, the value of μ_a so obtained for sulphur agreed fairly well with a continuation of the straight line of Fig. 2 and strengthened our conviction that this line represents the true law of absorption for this wave-length in the elements from carbon to sulphur. However it was thought best to repeat these measures with other samples of gas before publication of final values for the absorption of sulphur.

From the slope and intercepts of the line of Fig. 2 the following formula for the atomic absorption coefficient of an element in which $\lambda_K < 44.6\text{A} < \lambda_{LI}$ is easily deduced.

$$\mu_a = 1.65Z^{4.4} \times 10^{-23}.$$

This equation may then be used to determine the absorption coefficients of the other elements in this region of atomic number.

The experimental values of the absorption coefficients for the elements investigated are given in Table I. Except for the elements represented in Fig. 2 these all fall in different absorption regions. It may be noted that the mass absorption coefficient of argon is greater than that of krypton, xenon or gold while the absorption by an atom of krypton is greater than that of any other atom in the list. This is readily explained by the fact that with increasing atomic number of the absorber the K, L, M and N absorption limits pass in turn to the high frequency side of the incident radiation and the electrons belonging to these levels cease to absorb. Nevertheless this decrease is, perhaps, more than might be expected. For example, in the case of an atom of xenon there remain 26 electrons with natural frequencies less than that of the incident radiation yet these absorb only about one half as much as the 14 electrons in an argon atom whose natural frequencies are such as to permit absorption.

Conclusions

The experimental results indicate a probable value of 4.4 for p in the equation $\tau_a = C\lambda^n Z^p$ when it is applied to the L absorption region of the absorbing element and to wave-lengths in the neighborhood of the $K\alpha$ line of carbon. A value of n cannot be deduced directly, since only one wave-length was investigated. Nevertheless there is indirect evidence that n for this region may be considerably less than 3. It may be noted that the values of τ_a listed in Table II which are computed from the formulas of Richtmyer and Warburton, Allen, and Gray are considerably too large. This indicates that either C or n or both have smaller values in this soft x-ray region than is the case for ordinary x-rays. The numerical value of $C\lambda^n$ for some of these elements has

TABLE II. *Experimental and calculated values of atomic absorption coefficients for the Kα line of carbon. τ_a should equal μ_a at this wave-length.*

Absorber	$\mu_a \times 10^{19}$ Experimental	$\tau_a \times 10^{19}$ Richtmyer and Warburton	$\tau_a \times 10^{19}$ Allen	$\tau_a \times 10^{19}$ Gray	$\tau_a \times 10^{19}$ Jönsson
He	0.238	3.2	2.28	2.7	0.19
C	0.44	3.8	2.54	0.94	1.05
N	0.89	7.0	4.7	1.74	1.44
O	1.52	11.9	8.0	2.97	1.61
Ne	4.36	29.3	19.6	7.24	2.63

been shown experimentally to be 1.65×10^{-23}. If we assume a value of C equal to that of the Richtmyer and Warburton formula we obtain $n = 2.24$. With the values of C taken from the formulas of Allen and Gray we find $n = 2.27$ and $n = 2.31$ respectively. This does not yield a trustworthy value of n since the value of C is quite uncertain. In fact we do not know that an equation of the assumed form can represent absorption coefficients in this region. On the other hand the method of Jönsson is shown to lead to values of the right order of magnitude. This appears at first somewhat difficult to understand, since his assumption that the absorption is a function of λZ is equivalent to assuming that the exponents of λ and Z are the same. If, however, the exponent of Z increases and the exponent of λ decreases with increase of λ at such rates that the changes in one approximately compensate for the changes in the other, it would be possible to secure an apparent but quite fortuitous agreement with experiment by assuming the absorption to be a function of λZ raised to some intermediate power. In view of the fact that all investigations indicate that the exponent of Z is always greater than the exponent of λ and also that this difference probably increases with increase of wave-length, it seems probable that the results achieved by Jönsson's method are to be explained in this way.

It is planned to continue this investigation with the use of other wave-lengths in an endeavor to find the law relating absorption to wave-length in this region and to test further the dependence of absorption upon atomic number.

NOTE ADDED IN PROOF:

It has been called to the author's attention that Kurtz[7] used the entire beam of x-radiation from a carbon target and measured its absorption in several of these gases. Substituting his values of the constants in the equation $\tau_a = C\lambda^n Z^p$ we obtain $\tau_a = 1.7\, z^{4.4} \times 10^{-23}$. Considering the uncertainty regarding the homogeneity of his radiation the results are in remarkable agreement with those obtained in the present investigations.

[7] Kurtz, Ann. d. Physik **85**, 529 (1928).

THE REFLECTION OF THE $K\alpha$ LINE OF CARBON FROM QUARTZ AND ITS RELATION TO INDEX OF REFRACTION AND ABSORPTION COEFFICIENT

By Elmer Dershem and Marcel Schein*
Ryerson Physical Laboratory, University of Chicago

(Received March 27, 1931)

Abstract

Measurements were made of the ratio of the intensity of the reflected ray to that of the incident ray in the case of the $K\alpha$ line of carbon reflected from a mirror of fused quartz for glancing angles of incidence between 1° 30′ and 8°. The atomic absorption coefficients of carbon, nitrogen, oxygen, and neon were experimentally determined by the writers as described in the preceding article. This gave the value of the oxygen coefficients directly and data from which the atomic absorption coefficient of silicon could be calculated. The linear absorption coefficint, μ, of quartz was then computed from its density, percentage composition, and the atomic absorption coefficients of its constituents. Then from the relation $\kappa=\mu\lambda/4\pi$, the absorption index κ, was found to be 1.68×10^{-3}. The value of $\delta=1-n$ was computed from the Drude-Lorentz formula and found to be 4.8×10^{-3}. Convenient methods for the calculation of the intensity of either the parallel or perpendicular components of the reflected ray are derived from the Fresnel equations relating to absorbing media. A curve computed with the above values of δ and κ predicts somewhat higher reflectivity than found experimentally. Use of the value $\kappa=2.5\times10^{-3}$ yields a computed curve agreeing well with the experimental one. On the other hand, assuming values of δ other than that given above leads to less satisfactory agreement.

Introduction

THIS investigation was undertaken with the view of measuring the intensity of soft x-rays reflected at various angles from a mirror and at the same time determining, either theoretically or experimentally, the magnitude of the index of refraction and the absorption coefficient of the mirror. Knowing the latter two quantities and the curve of reflected intensity plotted against glancing angle of incidence it should be possible to learn something regarding the precise validity of the extrapolations of classical dispersion formulas from the optical to the soft x-ray region.

Quartz appeared to be one of the most promising materials for investigation since it could be highly polished and particularly because the $K\alpha$ line of carbon ($\lambda=44.6$A), which is one of the most intense and easily obtained lines in this region, was so far removed from a critical frequency of either silicon or oxygen that the index of refraction could be computed from classical dispersion theories with a great deal of confidence. Hence measurements of the intensity of reflection of this line from quartz were made and the results briefly noted in a paper read before the American Physical Society.[1] However

* Fellow of International Education Board.

[1] Dershem and Schein, Phys. Rev. 35, 292 (1930).

it was not found possible to secure a film of quartz sufficiently thin to transmit a measurable amount of this radiation and permit a direct measure of its absorption coefficient. Hence attention was turned to the possibility of measuring the absorption of this line in gases and determining the law of absorption for elements of low atomic number. A description of this work is given in the preceding paper. In this way a value of the absorption coefficient of oxygen was obtained directly and that of silicon was determined from the formula $\mu_a = 1.65\, Z^{4.4} \times 10^{-23}$ which had been derived from the experimental data pertaining to other elements.

THEORY

The critical glancing angle of total reflection for hard x-rays is quite sharply defined and furnishes a convenient method of measuring indices of refraction in this case. However, with increase of wave-length the discontinuity in reflected intensity at the critical angle becomes less abrupt and finally for very soft x-rays entirely disappears. This is due partly to a more gradual change in reflected intensity at the critical glancing angle as this angle becomes larger, even in the case of substances entirely transparent to the radiation. However it is mainly due to an increase of absorption. Hence if the index of refraction is to be deduced from an experimental curve of reflected intensity plotted against glancing angle it is necessary to know the absorption coefficient and to find, if possible, the value of the index of refraction which must be assumed in order to secure agreement between calculated and experimental curves.

A formula for computing the ratio of reflected to incident intensity at various angles may be derived in the following manner. In using this formula the index of refraction and the index of absorption may be either known or assumed.

Considering first the component with the electric vector perpendicular to the plane of polarization, the ratio of the reflected to the incident amplitude is given in the following formula of Fresnel,[2] in which ϕ and r are the angles of incidence and refraction measured from the normal.

$$\frac{R_s}{E_s} = \frac{\cos\phi - n\cos r}{\cos\phi + n\cos r}. \tag{1}$$

By Snell's law $\cos r = (1 - \sin^2\phi/n^2)^{1/2}$. Hence

$$\frac{R_s}{E_s} = \frac{\cos\phi - (n^2 - \sin^2\phi)^{1/2}}{\cos\phi + (n^2 - \sin^2\phi)^{1/2}}.$$

Changing to the glancing angle of incidence θ, since $\cos\phi = \sin\theta$

$$\frac{R_s}{E_s} = \frac{\sin\theta - [n^2 - (1 - \sin^2\theta)]^{1/2}}{\sin\theta + [n^2 - (1 - \sin^2\theta)]^{1/2}}.$$

In order to take account of absorption it is necessary to substitute a complex expression[3] for n, namely $(1 - \delta - i\kappa)$ in which $1 - \delta$ is the index of refrac-

[2] Cf. Drude, "Theory of Optics" English translation, 282 (1902).

[3] Drude, loc. cit. p. 360 et seq.

tion and κ the index of absorption. Since δ and κ are small compared to unity the squares and products of these quantities may be neglected. Also θ may be substituted for sin θ. Making these substitutions and simplifications[4]

$$\frac{R_s}{E_s} = \frac{\theta - (\theta^2 - 2\delta - 2i\kappa)^{1/2}}{\theta + (\theta^2 - 2\delta - 2i\kappa)^{1/2}} \tag{2}$$

Setting

$$a - ib = (\theta^2 - 2\delta - 2i\kappa)^{1/2} \tag{3}$$

$$\frac{R_s}{E_s} = \frac{\theta - a + ib}{\theta + a - ib}.$$

Multiplying by the complex conjugate to secure the square of the absolute value which is the desired ratio of intensities

$$\left(\frac{R_s}{E_s}\right)^2 = \frac{(\theta - a)^2 + b^2}{(\theta + a)^2 + b^2}. \tag{4}$$

Squaring Eq. (3) and separately equating the real and imaginary terms

$$a^2 - b^2 = \theta^2 - 2\delta \tag{5}$$

$$b = \kappa/a \tag{6}$$

Whence

$$a^2 = \tfrac{1}{2}\{\theta^2 - 2\delta + [(2\delta - \theta)^2 + 4\kappa^2]^{1/2}\}. \tag{7}$$

The numerical value of a may now be readily determined by substituting the known or assumed values of θ, δ and κ in (7). The positive value should be chosen for all square roots in the preceding discussion. Equation (6) then yields the value of b. The ratio of reflected to incident intensity is then given by substituting these values in (4).

For the case of the parallel component we have

$$\frac{R_p}{E_p} = \frac{n\cos\phi - \cos r}{n\cos\phi + \cos r}.$$

Handling this in a similar manner we obtain in place of Eq. (4) the following

$$\left(\frac{R_p}{E_p}\right)^2 = \frac{(\theta - 2\delta\theta - a)^2 + (b - 2\kappa\theta)^2}{(\theta - 2\delta\theta + a)^2 + (b + 2\kappa\theta)^2}$$

a and b have the same values as in the case of the perpendicular component.

The reflected intensity of the parallel component is slightly less than that of the perpendicular component. In the case of the $K\alpha$ line of carbon reflected from quartz this is negligible for small angles, becoming about 5 percent at 8°.

[4] An equation of this form has been given by Prinz, Zeits. f. Physik **47**, 479 (1928) but this is not a final form for numerical calculations.

Schön[5] has developed a more complicated formula for the parallel component yielding results equivalent to that above. Thibaud[6] has also published a formula of essentially the same form as that of Schön.

Apparatus

The principal parts of the apparatus were the same as previously used and described by one of the writers[7] in an investigation of the reflection of the carbon line from glass. However certain mechanical features were added to permit direct comparisons of the incident and reflected beams.

Referring to Fig. 1, X is a water-cooled x-ray tube, the rays from which pass through the slits S_1 and S_2 and falling upon the grating G, become spread out into a spectrum of which only the inside order of the $K\alpha$ line may pass

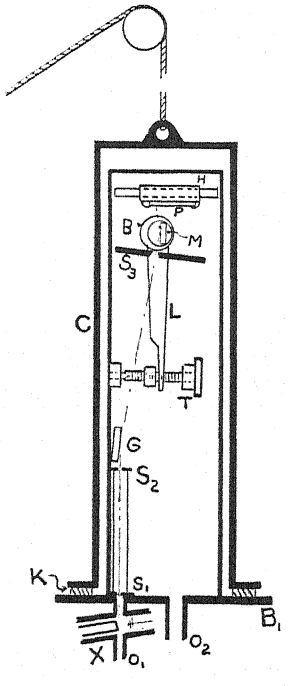

Fig. 1. Diagram of apparatus.

through the shield S_3 and strike the quartz mirror M. This mirror could be turned through small known angles by means of the lever L and the screw T. This screw could be turned in small steps by an electromagnetically operated ratchet controlled from outside. Another ratchet, operated by an electromagnet, was used to turn the eccentric cone bearing B on which the mirror was mounted. The mirror could thus be moved alternately into or out of the beam by a one-half turn of the bearing B. In this way a series of exposures of the direct and reflected beams could be taken alternately upon the plate P. The latter was carried on the plate holder H which could be given a step by

[5] Schön, Zeits. f. Physik **58**, 165 (1929).
[6] Thibaud, Jour. de Physique **7**, 37 (1930).
[7] Dershem, Phys. Rev. **34**, 1015 (1929).

step transverse motion by means of another electromagnetically operated ratchet not shown in the sketch. In this way from 12 to 20 separate exposures could be made on one plate.

The apparatus could be opened or closed by raising or lowering the cylinder C by means of a rope and pulley. A vacuum seal between the cylinder and the base plate B_1 was secured by means of the sulphur free rubber gasket K. During operation a vacuum higher than 10^{-4} mm Hg was maintained by means of mercury diffusion pumps connected to the outlets O_1 and O_2.

Results

The densities of the lines produced by the reflected and the direct rays were compared by photometric measurements and the ratio of their intensities determined in the same manner as described in the preceding article on absorption coefficients. The experimental points thus obtained are marked with circles in Fig. 2. The curves shown in this figure are, however, plotted

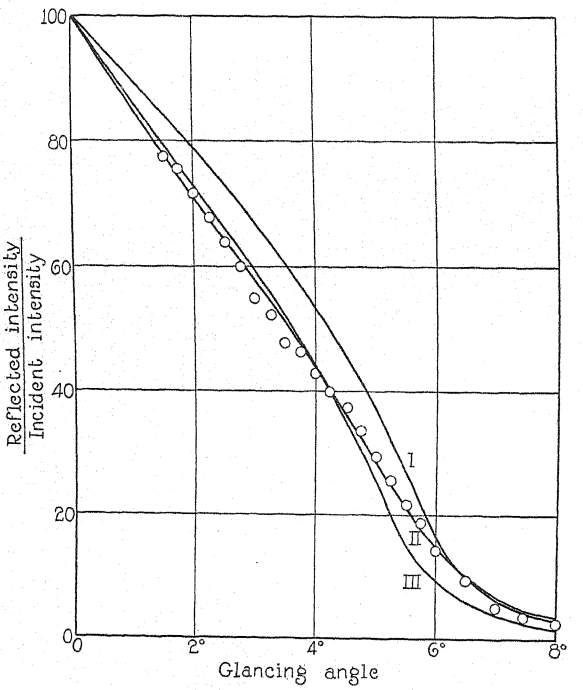

Fig. 2.

from values of the ratio of reflected to incident intensity computed from Eq. (4). The values of δ and κ to be used were determined in the following way.

Since the K absorption frequencies of oxygen and silicon are much higher and their L absorption frequencies much lower than that of the $K\alpha$ line of carbon, δ may be computed from the simplified Drude-Lorentz formula, $\delta = e^2n/2\pi mv^2$ in which n is the number of electrons per cc having lower natural frequencies than that of the incident radiation. In this case the K electrons are not considered. One may also use the more extended formula, $\delta = e^2N/2\pi m \Sigma n_c/v^2 - v_c^2$ in which N is the number of molecules per cc, n_c the number of

electrons per molecule belonging to the characteristic energy level c and ν_c the frequency pertaining to this level. The values of δ obtained from these formulas do not differ by so much as one percent owing to the fact that the incident frequency lies approximately midway between the characteristic K and L frequencies of oxygen and silicon. For quartz and the carbon line the value thus obtained for δ is 4.8×10^{-3}.

The value of κ was found from the experimental equation deduced in the preceding article on absorption coefficients namely, $\mu_a=1.65\ Z^{4.4}\times10^{-23}$ whence μ_a for silicon is found to be 18.2×10^{-19}. This in conjunction with the experimental value of μ_a for oxygen, 1.52×10^{-19}, and the density of fused quartz, 2.206 gm./cc, yields the value, $\mu=47200$ for the linear absorption coefficient of quartz. Then the absorption index κ, can be found from the equation $\kappa=\mu\lambda/4\pi=1.68\times10^{-3}$.

Curve I of Fig. 2 was computed with the use of the above values of δ and κ. This curve lies somewhat above the experimental points. This might be taken to indicate that the real value of the absorption coefficient was greater than that determined from the work on the absorption of gases. Edwards[8] finds a similar result when using ordinary x-rays. He suggests that the absorption of the surface layer may be greater than that of the mirror as a whole.

Other values of δ and κ were tried in an endeavor to find the best fit with experiment. Curve II in which $\kappa=2.5\times10^{-3}$ and δ has the same value as in curve I, gives a very good approximation to the experimental results. In computing for curve III the values, $\kappa=1.68\times10^{-3}$ and $\delta=4.0\times10^{-3}$ were used. This curve is distinctly less in accord with the experimental points. These curves and many others that were computed but not shown in the figure indicate that the value of δ computed from the dispersion formula is very nearly the correct one but that the effective value of the absorption index is about fifty percent higher than that determined from absorption measurements in gases. There is also the possibility that surface films or a lack of perfect smoothness have reduced the reflected intensity in much the same manner as would be the case if the absorption were really greater than the value deduced from experiment. The question might also be raised as to whether, or not, the true value of the absorption index may be thus obtained from the absorption coefficient. It is perhaps rather, to be considered remarkable that theories and formulas developed for the optical region before anything was known of x-rays or quantum absorption phenomena should yield results so nearly in accord with experiment when extended to this region where the wave-lengths are one hundred times smaller and the requirement of surface smoothness presumably so much more exacting. This work is to be continued with some changes in technique which it is hoped will somewhat increase the accuracy of measurement. Also other wave-lengths and other mirrors will be employed.

In conclusion we wish to express our appreciation to Professor A. H. Compton for his cordial interest and support throughout this investigation and the preceding one on the absorption of gases, and to thank the International Education Board for the award of a fellowship which made it possible for one of us (M.S.) to engage in the study of these problems.

[8] Edwards, Phys. Rev. **37**, 339 (1931).

A DIRECT MEASUREMENT OF THE INTENSITY VARIATIONS OF THE HELIUM LINES WITH VOLTAGE

By Joseph Razek
Randal Morgan Laboratory of Physics, University of Pennsylvania

(Received April 6, 1931)

Abstract

The intensity variations with voltage of some of the brighter lines of the low voltage helium arc spectrum were determined by means of a recently developed photoelectric spectrophotometer. The radiation was developed in a copper ball, 20 cm in diameter. The equipotential cathode and grid from a commercial three-electrode tube formed the internal structure, the sphere itself being the anode. This arrangment gave an extremely bright spectrum, even at the striking voltage, with a relatively low current density in the space. The results on 5016 (1^1S-2^1P) and on 6678 (1^1P-2^1D) were generally smooth curves. Lines 4026 (1^3P-4^3D), 4471 (1^3P-3^3D), and 5876 (1^3P-2^3D), show a region of constant intensity with arc voltages from 27 to 35 volts, thereafter increasing smoothly. Line 4713 (1^3P-3^3S) shows definite maxima near the critical exciting potentials. The accurate linear relationship between the intensity of the light admitted to the photoelectric cell and the amplified output of the photoelectric cell was established by a separate experiment. For the measurements on the spectrum lines, every intensity measurement was referred to a standard lamp operated at a constant resistance. The absence of oscillations in the arc current was shown by a vacuum tube voltmeter.

Introduction

KNOWLEDGE of the intensity variations of spectrum lines as a function of the excitation voltage is of considerable importance in certain theoretical discussions in spectroscopy. It has been customary to obtain this knowledge by photographing the spectrum repeatedly, each exposure being made at a definite voltage, and all other variables kept as nearly constant as possible. The intensity of the lines was then determined by means of some form of densitometer.[1,2,3,4] Although this method has yielded valuable results nevertheless many difficulties and sources of error are involved. The photographic method is very time-consuming and many exposures must be made to get a sufficient number of points to plot a curve. Since the exposures are frequently very long, it is difficult to keep all the arc conditions constant. Furthermore, the relation between the actual light intensity and the resultant blackening of the plate is always subject to uncertainty, since it is influenced by many factors difficult to control. The various densitometers at present available are quite satisfactory, and so they introduce no source of error as important as the others mentioned.

[1] Hughes and Lowe, Proc. Royal Soc. **A104**, 480 (1923).
[2] Bazzoni and Lay, Phys. Rev. **23**, 327 (1924).
[3] Cornog, Phys. Rev. **32**, 746 (1928).
[4] Harrison, J.O.S.A. and R.S.I. **19**, 267 (1929).

For reasons above mentioned, a direct method for determining line intensities is desirable. The property of a photoelectric cell of translating light values into electrical quantities is at once suggested. However, when a photoelectric cell is used, it is found that the currents resulting from the very small amount of energy in a given line, are so feeble that they must be read with an electrometer,[5] or amplified by means of some form of vacuum tube amplifier. The electrometer has the disadvantage of being slow and somewhat difficult

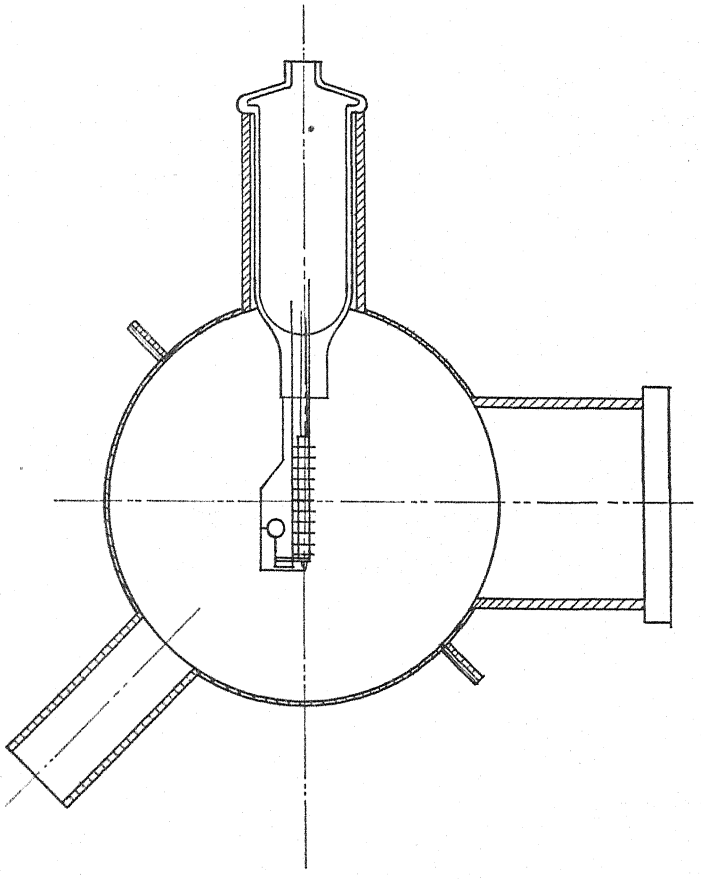

Fig. 1. Diagram of spherical low voltage arc discharge tube.

to keep in constant adjustment. The vacuum tube amplifiers used heretofore have employed the usual type of a.c. amplification.[6] The research to be described employed a resistance coupled d.c. bridge grid resistor amplifier.[7,8]

Description of the Spectrum Tube

The spectrum tube in which the arc was formed is shown in Fig. 1. The tube differs from conventional designs in that the volume in which the dis-

[5] Hulburt, Phys. Rev. **31**, 1109 (1928).
[6] Wheeler, Phys. Rev. **33**, 114 (1929).
[7] Mulder and Razek, J.O.S.A. and R.S.I. **18**, 466 (1929).
[8] Razek and Mulder, J.O.S.A. and R.S.I. **19**, 390 (1929).

charge takes place is quite large. The body of the tube was made of spun copper hemispheres, heavily silvered and polished. The two hemispheres were soldered together on an equatorial flange. The vacuum connection was made on the pole of one of the hemispheres, while the cathode and grid structures were admitted through a tube in the other hemisphere. The arc was observed through a slit in the upper hemisphere, over which a tube and glass plate were attached.

The cathode and grid structure were taken from a commercial three electrode tube, Arcturus type 247. This consists of a heating filament within a

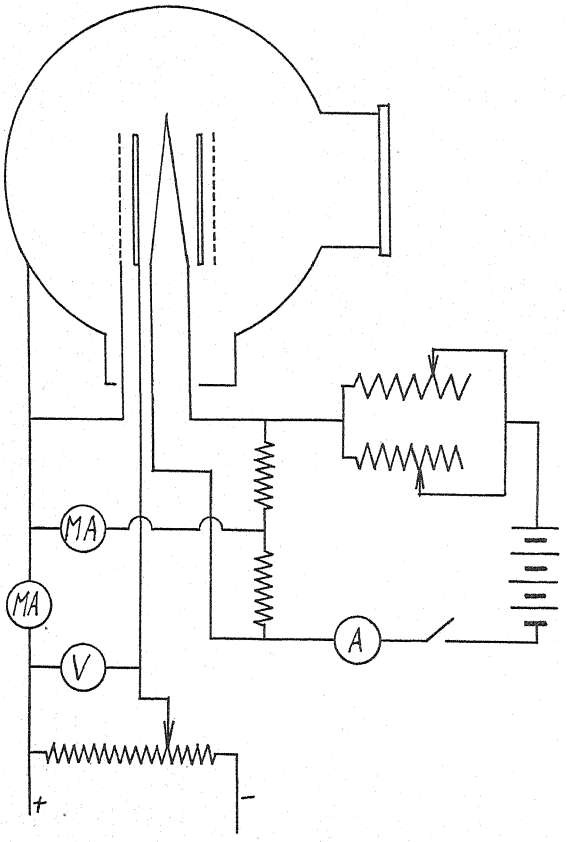

Fig. 2. Wiring diagram for low voltage arc discharge tube.

tube on which the active material is placed. A coarse grid is concentric with the cathode tube. The usual plate structure was removed, and the metal of the hemispheres used instead.

The tube was wired as shown in Fig. 2. The fact that the filament was entirely insulated from the cathode made it possible to put all structures within the tube, except the cathode, at nearly the potential of the anode. In this way, the potential of the entire space within the hemispheres, with the exception of the small volume between the cathode and grid, was nearly uniform. The filament was heated by means of a storage battery in the usual manner. A

center tapped resistance was connected across the filament with the center tap connected to the anode through a milliameter. The anode to cathode voltage was applied from a potential divider across a bank of batteries, and a milliammeter indicated total cathode to anode current. The voltmeter across the potential divider indicated the voltage applied to the anode, with the slight and constant potential drop in the milliameter and leads.

Description of Laboratory Set-Up

The tube described was connected to a vacuum system, and after a short preliminary treatment to condition the active deposit on the cathode, helium gas was admitted to the tube by means of the conventional arrangement of bulb and stop-cocks. Due to the presence of the waxed joints, no effort was

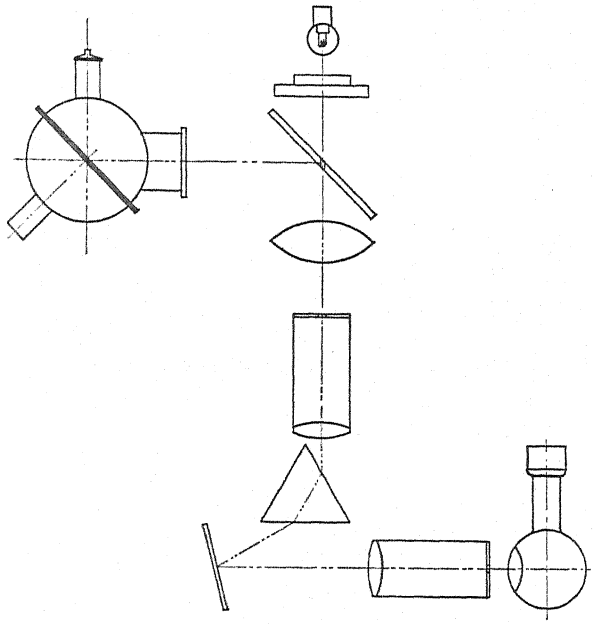

Fig. 3. Diagram of optical arrangement for determining intensities of spectrum lines by means of a photoelectric cell and standard lamp.

made to degas the metal sphere. Since the actual runs were only of a few hours duration at the most, the amount of impurities was very slight. The majority of the data for the curves shown was obtained with no trace of mercury or hydrogen observable in a direct vision spectroscope.

The spectroscope, photoelectric cell and amplifier were those of the Razek-Mulder color analyzer described elsewhere.[9] A diagrammatic sketch of the optical arrangement is shown in Fig. 3. Light from the arc is reflected and brought to a focus on the slit of the spectroscope by means of a mirror and cylindrical lens. After dispersion by means of a prism, the spectrum is reflected by a mirror through the lens of the exit tube on to the slit at the end

[9] Mulder and Razek, J.O.S.A. and R.S.I. **20**, 155 (1930).

of the tube. A slight tilting motion of the mirror moves the spectrum across this slit, admitting the selected line to the photoelectric cell. The current resulting in the photoelectric cell is amplified in a bridge grid resistor amplifier, and the amplified current noted on a galvanometer.[7,8]

To provide a standard of intensity, and to correct the readings for the slowly changing sensitivity of the amplifier, a calibrating lamp was employed. A 6–8 volt automobile headlight bulb was mounted over the 45° mirror. A small scratch through the silvered back of the mirror admitted light from this bulb into the spectrometer. The light from this bulb could be cut off from the spectrometer by means of a bulb-operated camera shutter. In this way it was possible to calibrate the sensitivity of the system at a given wave-length against the standard lamp. In order to keep the current through the lamp constant to a high degree of precision, an arrangement due to Richardson was used. This is shown in Fig. 4. The lamp is made one arm of a Wheatstone

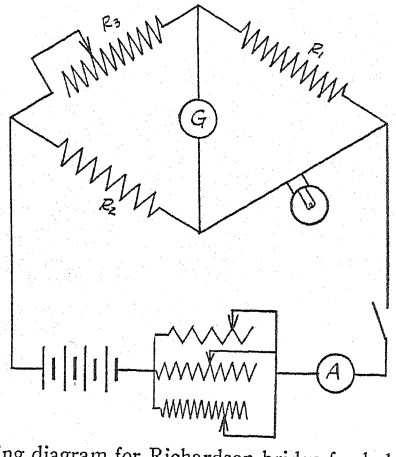

Fig. 4. Wiring diagram for Richardson bridge for holding standard lamp at constant operating resistance.

bridge, while the arm R_2 consists of a standard ohm, of a capacity sufficient to carry the lamp current without overheating. The arm R_1 was fixed at 1000 ohms, and the arm R_3 was variable. The current through the lamp, and hence the resistance at which it was operating was regulated by a bank of rheostats. When set up in this manner, the lamp was actually operated at constant resistance. During the short runs which were necessary to get data on a given line, it is safe to assume that the deterioration of the lamp was negligible, especially since the lamp currents which gave light intensities of the same order of magnitude as the arc, were well below the rated current values. The temperature at which the lamp was operated in a given set of readings was determined so that the deflection for the standard lamp was approximately equal to the maximum deflection due to the line under study. The value of R_3 was then set so that the bridge was balanced when the lamp operated at the selected temperature. After this setting was made, the bridge was kept balanced by adjusting the rheostats controlling the current through the lamp.

The procedure in actual operation was as follows: The tilting mirror in the spectrometer is set so that the desired line is admitted to the photoelectric cell. The light from the arc is cut off from the spectrometer by interposing a shutter in front of the window in the sphere, and the vacuum tube bridge balanced to give a zero galvanometer deflection. On opening a shutter in front of the sphere, a galvanometer deflection is obtained, which is proportional to the light intensity of the line admitted to the cell. The light of the arc is then cut off and the shutter in front of the adjusted calibrating lamp opened, giving a galvanometer deflection proportional to the light of the standard lamp. In this way, every reading for the arc intensity can be referred to the

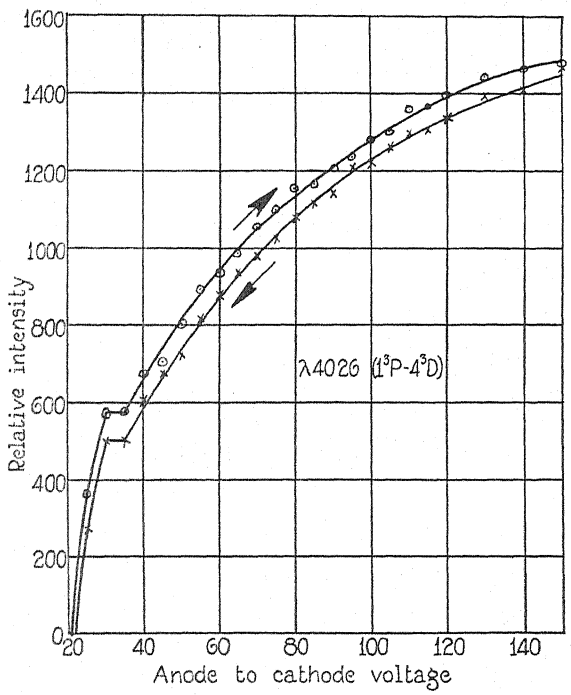

Fig. 5. Intensity variation with arc voltage, helium line 4026 (1^3P-4^3D).

standard with a minimum of delay. This procedure was repeated for various arc voltages.

In this work, the arc current was kept constant by adjusting the temperature of the filament as the anode to cathode voltage was raised. Arc currents of 30 and 50 milliamperes were used. Currents as high as 300 milliamperes could be passed through the arc, with only 25 volts across the anode to cathode. The pressure of the helium was about 0.25 mm of mercury.

Direct light from the filament and cathode was eliminated entirely by blanking out the central portion of the glass observation window with a diaphragm, and viewing the arc from a slight angle. The effectiveness of this procedure was shown by the fact that when the filament was operated at a temperature considerably above that used during a run, no deflection of the

galvanometer could be observed, even in the red end of the spectrum, with no anode voltage on the hemisphere.

The dispersion of the prism used was small, but since the lines of the helium spectrum are spaced rather far apart, no difficulty was experienced in making certain that only the desired line was admitted to the photoelectric cell. Previous to every group of tests, the wave-length scale was calibrated against a mercury arc, and the corrections which must be applied to the wave-length scale on the color analyzer were determined. In cases where a bright line has a companion, this companion line is so faint in comparison to the

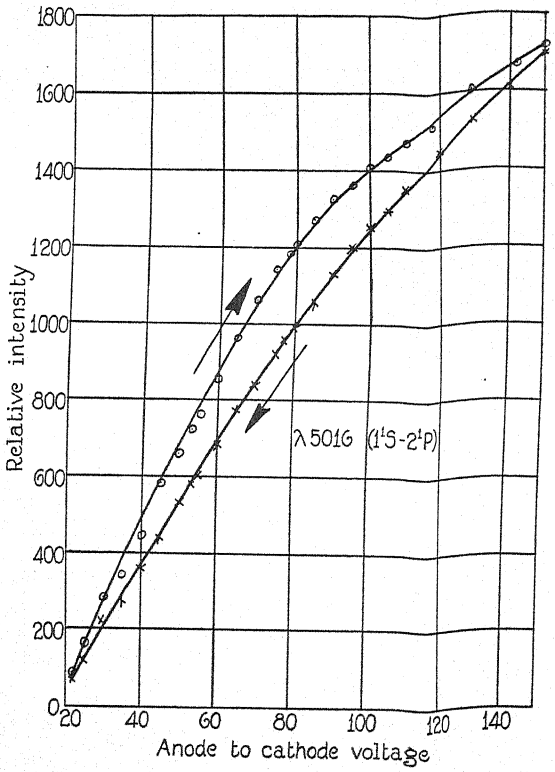

Fig. 6. Intensity variation with arc voltage, helium line 5016 (1^1S-2^1P).

brighter line that its influence on the photoelectric cell current is entirely negligible, or, in any case, the combined effect is obtained.

The question as to the propriety of taking the deflection of the galvanometer as proportional to the light intensity, is of fundamental importance in this work. The linear relationship between the intensity of the light and the galvanometer current was determined by using a point source at varying distances from a diffusing screen in front of the cell. The relative intensity was determined by employing the inverse square law. The galvanometer response was shown to be linear with the light falling on the photoelectric cell at least to one tenth of one percent—far above the precision of these tests.

Discussion of Results

In order to determine whether the direction of the changing arc voltage influenced the intensity of the line, the intensity was determined for both increasing and decreasing voltage. It was found that in every case, the intensity at a given voltage was somewhat higher for increasing voltage than for decreasing voltage. This is shown in Figs. 5 and 6, which are the intensity-voltage curves for the 4026 and 5016 lines. This effect is independent of the time in that the same effect is obtained even when a given operating point is approached as rapidly as possible, the intensity being determined by the direction of approach. No explanation is offered at this time, but the existence of this phenomenon indicates the necessity of controlling the experimental procedure so that the voltage always changes in the same direction.

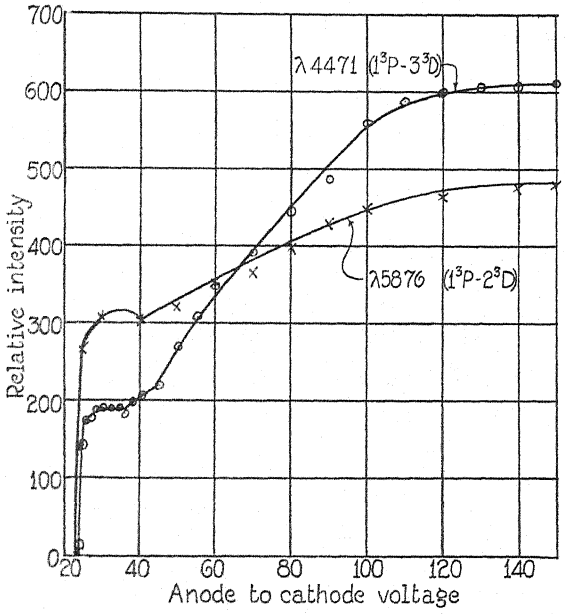

Fig. 7. Intensity variation with arc voltage, helium lines 4471 (1^3P-3^3D), 5876 (1^3P-2^3D).

The remaining curves were all made with the voltage increasing. Since it is at times difficult to approach a given operating point without overshooting, especially at the higher voltages, the accidental variations in the curves at these points may be due to this cause.

Lines 5026, 4471 and 5876 show a region of nearly constant intensity in the region from 27 to 35 volts. This is probably related to the fact that the lines have a series relationship, line 4471 being (1^3P-3^3D) and 5876, (1^3P-2^3D) and line 4026 (1^3P-4^3D). These are shown plotted in Figs. 5 and 7.

Line 4713 shown in Fig. 8, shows a most unusual behavior. The intensity of the line is a maximum, very near to the striking voltage, around 25 volts, dropping to almost half value at about 40 volts. From this point the intensity rapidly increases to about 53 volts, in the vicinity of the second ionization

potential, and thereafter remaining nearly constant. This is consistent with the observations of Bazzoni and Lay[2] and with those of Cornog.[3] All observations made on this line were generally consistent with these results.

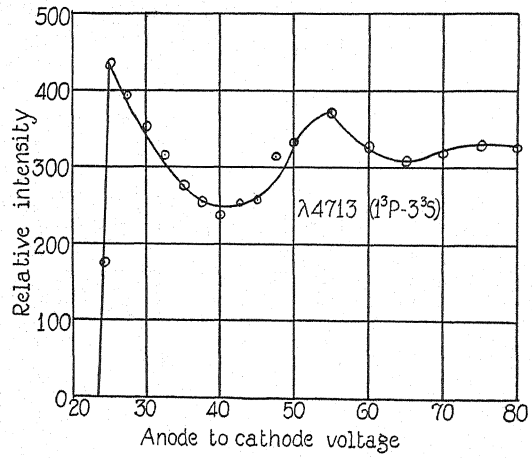

Fig. 8. Intensity variation with arc voltage, helium line 4713 (1^3P 3^3S).

Line 6678, shown in Fig. 9, increases regularly with increasing voltage, generally similar to line 5016.

The results obtained on all these lines were in general agreement with those of Bazzoni and Lay,[2] but inconsistent with those of Hughes and Lowe.[1] The latter used a non-equipotential cathode and a rather long tube of gas. The falling off in intensity which they show may be caused by the absorption of the radiation by the gas itself.

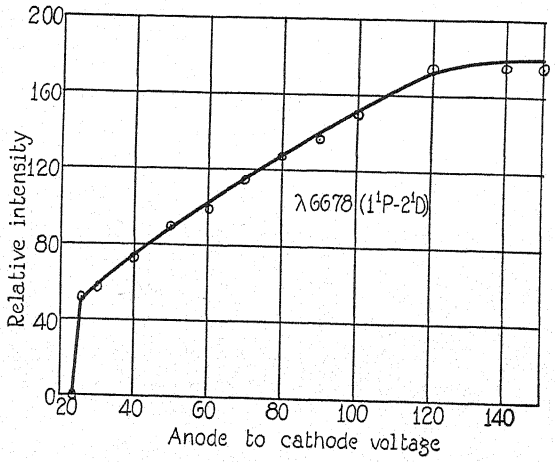

Fig. 9. Intensity variation with arc voltage, helium line 6678 (1^1P-2^1D).

The arc currents used in this work were quite low. On account of the unusually large volume of the discharge tube, these low currents resulted in

extremely low values of current per unit volume. However, since the cathode and grid structures were approximately of the same dimensions as those used by Bazzoni and Lay[2] and Cornog,[3] the current densities in the vicinity of the cathode were comparable. It is desirable that the current densities be kept as low as possible to minimize space charge effects, which might have an important influence on the effective potential of the arc.[10]

The voltage exciting the arc can differ from that indicated by the voltmeter due to several causes. Since the voltage could not be read any closer that 0.2 volt, the various differences were negligible if they did not amount to that quantity. The voltage drop across the plate milliammeter was only about 0.05 volts and hence could be neglected. The first ionizing potential for helium is 24.48 volts, and since the arc struck at 24.5 volts, the contact difference of potential at the cathode was negligible. No error was introduced by the voltage equivalent to the initial velocity of the electrons leaving the cathode since this was operated at a relatively low temperature. Furthermore, an equipotential cathode was used, and hence there was no voltage drop for this element.

The absence of peak voltages in the arc, due to oscillations was verified by an appropriately connected vacuum tube voltmeter. No oscillatory voltages as great as 0.2 volt were detected, although the vacuum tube voltmeter could readily show these.

By changing the potential of the center tapped filament return, it was possible to change the distribution of the current between the grid plate structure and the filament. Under ordinary conditions, about ten percent of the current returned through the filament structure. No change in the intensity of the lines could be observed, even if half of the current returned through the filament structure. This probably showed that the internally silvered sphere was quite effective in integrating the light output, and completely avoided the difficulties caused by "wandering" of the discharge.

Conclusion

These results show that the photoelectric spectrophotometer can be used to study intensity variations in spectra with a speed and ease of operation which tends to minimize many of the difficulties inherent in work of this kind. This is especially apparent when it is noted that all the data for a given curve can be obtained in about fifteen minutes. The greater light intensity possible with the use of a large spherical radiation space overcomes the difficulties caused by the feeble light output of the conventional designs of low voltage arcs.[11]

In conclusion, the writer desires to express his appreciation to Dr. C. B. Bazzoni, who suggested this problem, and under whose direction and supervision this work was done. The writer is further indebted to his collegue, Mr.

[10] Mott-Smith and Langmuir, Phys. Rev. 28, 727 (1926).
[11] Eckart and Compton, Phys. Rev. 24, 97 (1924).

Peter J. Mulder, for his collaboration in developing the automatic spectrophotometer, and in taking the data here presented.[12]

Note added in proof:

Obviously, the intensity relationships existing between the lines relative to one another cannot be deduced from the curves shown. The absolute value of the intensity scale unit is different for every line and is determined by the wave-length energy curve of the standard lamp, the color response curve of the photoelectric cell, and other factors.

[12] Razek and Mulder, Phys. Rev. **35**, 1423 (1930).

CERTAIN PHOTOELECTRIC PROPERTIES OF GOLD

By Lloyd W. Morris
Laboratory of Physics, University of Wisconsin

(Received April 10, 1931)

Abstract

Variations in the photoelectric behavior of a gold filament were studied both during an extended outgassing, and later upon reaching a stable condition.

Changes in photoelectric properties as outgassing proceeded.—Full arc sensitivity rose quickly in the initial period, then decreased slowly to a stable value. Fatigue curves showed a systematic change from a negative fatigue (i.e. a decrease in sensitivity with time of standing) at the beginning to a gradually increasing positive fatigue which slowly decreased to zero. A shift in long wave limit consistant with the change in full arc sensitivity was observed.

Changes in photoelectric properties produced by increasing temperature.—Full arc sensitivity decreased slightly. Individual line sensitivity was studied by use of a quartz double monochromator. Lines close to the long wave limit increased enormously in sensitivity with temperature, for those more removed this was less marked, while below 2350A there was a slight decrease. A shift in long wave limit toward the red was observed during the outgassing period and the final fatigueless state. During this latter period photo-current per unit light intensity curves established a shift in long wave limit from 2560A to 2610A between temperatures of 20°C and 740°C.

SEVERAL studies have been made in this laboratory of the photoelectric behavior of thoroughly outgassed metals. This report covers an investigation of the photoelectric properties of gold with particular reference to:

1. Variation of full arc sensitivity of the gold filament together with the associated change in long wave limit as outgassing proceeds.
2. A systematic change in fatigue curves with continued outgassing.
3. Variation of full arc and line sensitivity together with long wave-length limit as a function of temperature when the filament is in a "fatigueless" condition.

Apparatus

The gold samples in the form of U-shaped filaments some 0.03 mm thick by 4 mm wide were hung within a molybdenum cylinder which served as the collecting electrode. Potential and current leads passed out through a pressed seal at the top of the tube. The cylinder was supported from the bottom of the Pyrex tube by a double re-entrant seal through which the collector lead passed. This insured the longest possible glass path between filament and cylinder. As an additional precaution, grounded interior and exterior guard rings were placed at the top of the tube between the filament and collector. Photo-currents were read upon a Compton quadrant electrometer by using

either the rate of charge method or by maintaining a steady deflection by means of cupric oxide and glass high resistances.

The exciting light entered through a quartz window attached to the tube by a graded quartz to Pyrex seal. A hole in the side of the cylinder crossed by molybdenum wires allowed the light to fall upon the filament. The source of light was a vertical type Cooper-Hewitt quartz mercury arc operated at 80 volts. This was used either directly in front of the window or in connection with a Leiss quartz double-monochromator with lens by which the slit image was thrown upon the filament.

In the latter portion of the work this monochromator and arc were mounted upon a heavy cast iron base provided with levelling screws, two horizontal motions, and one of rotation about a vertical axis. Adjustable stops were provided on this latter motion so the monochromator slit image could be thrown quickly from the filament to a linear thermopile deep within an evacuated brass chamber, the double walls of which were filled with water. The beam entered through a quartz window of the same thickness as that on the photoelectric tube, thus giving the same optical path in the two cases. The dimensions of the slit and pile were such that it was unnecessary to refocus the image when changing from one wave-length to another, further assuring exact equivalence throughout a run of the light incident on filament and pile. Thermopile readings were taken by means of a Kipp type ZC galvanometer with a scale distance of 6 meters.

Pressures were measured by either a McLeod gauge or an ionization manometer of the Dushman-Found[1] type which read to 1×10^{-8} mm of mercury. Usual precautions were taken to avoid waxed joints and the only stopcocks were on the low pressure side of the system separated by two liquid air traps from the tube. The second trap, nearest the tube, was immersed in liquid air, only after the major portion of the outgassing process was complete.

The gold from which the filaments were rolled was obtained from the Bureau of Standards. Although no analysis was given it was stated to be the purest obtainable at any of the government mints.

Procedure

The ionization gauge was outgassed and the rest of the vacuum system thoroughly torched for a week before the tube was sealed on. During this time the molybdenum cylinder was bombarded at a cherry red for 40 hours in a separate system. The filament was carefully cleaned with absolute alcohol and the tube was then assembled and sealed on to the system with the cylinder at atmospheric pressure for only a short time.

After initial photoelectric readings were taken the filament was heated by gradually increasing currents, with frequent stops to check variations in sensitivity and associated long wave-length limit. Then the tube was baked for 100 hours at 470°C, the filament being maintained at a slightly higher tem-

[1] Dushman and Found, Phys. Rev. **23**, 734 (1924).

perature by a small heating current. During this period the vacuum system and mercury columns received frequent and vigorous torchings. The filament was then glowed at 600°C to 700°C for many hundreds of hours. Temperatures were based on the measured variation of resistance of the gold filament in combination with data given by Northrup[2] on the temperature variation of the resistivity of gold. With the placing of liquid air on the second trap pressures of 1×10^{-8} were reached and maintained throughout the experiment.

Long wave-length limits were measured in the initial stages by glass filters and various organic solutions indicated by Dahm,[3] their transmission being checked on a quartz spectrograph. Later the monochromator was used, while for the last run the monochromator and thermopile arrangement described above was employed. In these determinations the electrometer was used with rate of charge at from 20,000 to 40,000 mm per volt.

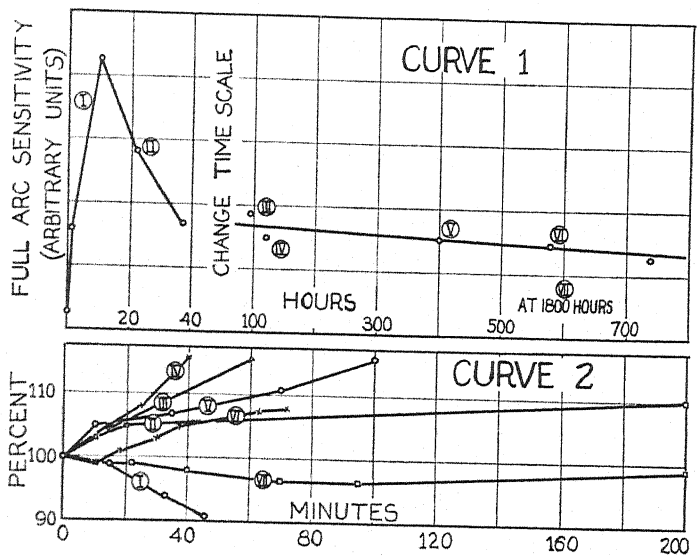

Fig. 1. Curve 1. Variation of full-arc sensitivity in arbitrary units as a function of outgassing time.
Curve 2. Variation of photo-sensitivity with time of standing after heating current is stopped expressed in percent of initial sensitivity.

Results

The results obtained during the outgassing process are summarized in Fig. 1. Curve 1 portrays the change in photoelectric full-arc sensitivity with increasing time of outgassing. The initial period is pictured on an enlarged scale to show better the rapid variation which takes place at first heating. The term "outgassing" is used to cover both glowing of the filament at 650°C and also baking. In the early stages low filament currents were used and the

[2] Northrup, Jour. Frank. Inst. **177**, 287 (1914).
[3] Dahm, Jour. Opt. Soc. **15**, 266 (1927).

time scale is adjusted to equalize roughly their unequal heating effects. That is, 5 hours with 2 amperes heating current is plotted as one hour for the first reading, 20 hours at 3 amperes as 9 hours, etc.

In the initial stages of outgassing the sensitivity changes gradually after the heating current is stopped. This phenomenon, frequently called fatigue, is believed to be due to the gas layer being reformed on the surface of the metal. Curve 2 shows the behavior of these fatigue curves during outgassing. There is a rapid change in sensitivity when the heating current is stopped due to the filament cooling. At the end of five minutes this change is negligible, however, and the curves shown here are plotted as percent of the deflection five minutes after the heating ceases. The Roman numerals on the fatigue curves correspond to the time as shown by corresponding numerals on curve 1.

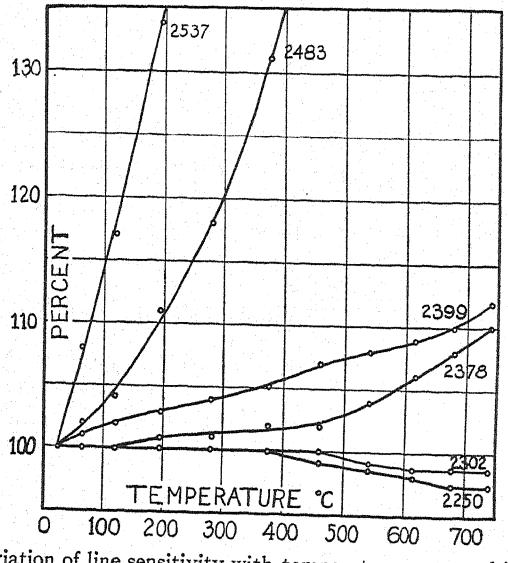

Fig. 2. Variation of line sensitivity with temperature expressed in percent of sensitivity at room temperature.

Two things are of interest here. Fatigue curve I which was taken on the upward slope of curve 1 shows negative fatigue as would be reasonable to expect. The others show a systematic change, rising to a maximum positive fatigue in IV and returning to practically zero fatigue in VII. Fatigue curves taken with monochromator on individual lines at same time as VII also show small fatigue. The pressure at this time was 1×10^{-8} mm and the ionization gauge showed no difference in pressure with the filament hot or cold, although in the earlier stages large changes resulted upon starting the heating currents.

The change in long wave-length limit observed during the run was consistent with the variation in the full-arc sensitivity. The long wave limit rose rapidly upon outgassing from a value in the neighborhood of 2000A at the start to 3200A at the point of greatest sensitivity. From then on it moved towards shorter wave-lengths as the full-arc sensitivity decreased.

Tests made throughout the outgassing process demonstrated a shift in long wave limit towards longer wave-lengths with increasing temperature. During intermediate stages determinations made with both absorption cells and monochromator were in good agreement and showed a shift of 200A approximately linear with temperature between 20°C and 640°C.

The full-arc deflections were at all times temperature sensitive and showed a marked decrease between 550°C and 740°C to a value well below that at room temperature. This, of course, represented the integrated result of the change in wave-length sensitivity throughout the effective spectrum. The results of a study of the variation of the individual line sensitivity with temperature are given in Fig. 2.

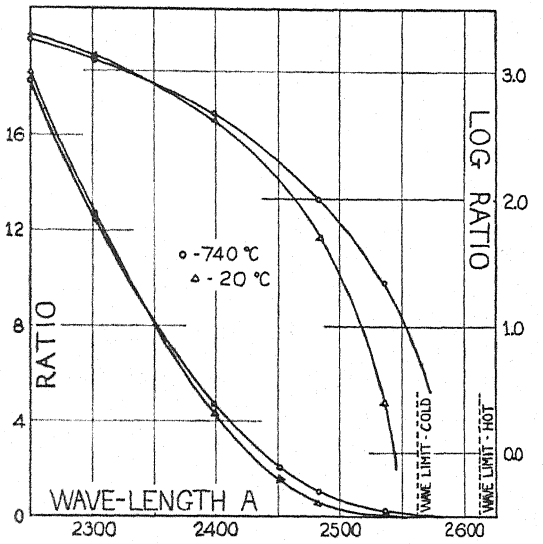

Fig. 3. Ratio of photo-current to incident light intensity and its logarithm as a function of the wave-length of incident light.

The double monochromator was used at slit widths of 0.6 mm, comparison tests made with a spectrograph showing the purity obtained to be equivalent to that of a single monochromator using slit widths of 0.2 mm or less. Coincident measurement of the line intensities by means of the thermopile arrangement mentioned earlier, in connection with the curves in Fig. 2, form the basis for the long wave-length determinations shown in Fig. 3. Due to difficulty of plotting the points for intermediate temperatures only the curves for room temperature and 740° are shown. The omitted points fall in order between these extremes and would have yielded a family of curves lying within those shown. More recent research in these laboratories on tantalum and silver by Cardwell[4] and Winch,[5] respectively, have yielded curves of

[4] Not yet published.
[5] Winch, Phys. Rev. 37, 1269 (1931). Next paper in this issue.

the same general character. In fact, this type of behavior was presaged by earlier work of Ives[6] and Hornbeck[7] on potassium.

The marked increase in sensitivity for the longer wave-length lines (eightfold for 2537 between room temperature and 740°) is to be expected from their proximity to the long wave limit which changes with increase in temperature. That this increase is not due to a change in reflecting power appears probable from the results obtained by Winch, mentioned above. He observed similar curves for silver and found no change in reflecting power with temperature for any of the wave-lengths used. It is planned to investigate this for gold in future work.

As for Fig. 3, the observed shift in the long wave-length limit and the extended toe of the high temperature curve may be the direct result of the increased kinetic energy of the conduction electrons. The shape of the curve renders an exact determination of the long wave limit difficult. The log-curves would yield 2560A cold and 2610A at 740° as probable values. Present experiments with an arc of extremely high intensity promise to allow the use of much smaller slit-widths that may more accurately define these threshold values.

In conclusion, the author wishes to express his indebtedness to Dr. C. E. Mendenhall under whose direction the work was done.

[6] Ives, J.O.S.A. and R.S.I. **11**, 565 (1925).
[7] Hornbeck, Phys. Rev. **24**, 631 (1924).

THE PHOTOELECTRIC PROPERTIES OF SILVER

By Ralph P. Winch
Laboratory of Physics, University of Wisconsin

(Received April 10, 1931)

Abstract

Silver is carefully outgassed and its photoelectric properties studied during outgassing and after stable conditions are reached. An outgassing curve is plotted for the 1200 hours of heat treatment given the silver before final readings were taken. For thoroughly outgassed silver curves are plotted showing photoemission as a function of temperature for fixed wave-lengths of incident light. These curves show that for wave-lengths near the long wave limit there is a marked increase in emission with temperature, for wave-lengths farther away there is no change with temperature, and for wave-lengths still farther away there is a slight decrease in emission with increased temperature. Curves for emission per unit of incident light intensity as a function of wave-length show that the long wave limit at 600°C is 2700 ± 20A while at room temperature it is 2610 ± 30A.

THE study of the photoelectric properties of silver was undertaken as a part of the general program of this laboratory which includes extensive study of the properties of thoroughly outgassed metals. In this laboratory the photoelectric properties of iron, cobalt, and tantalum have been studied by Cardwell,[1] molybdenum by Martin,[2] rhodium by Dixon,[3] and gold by Morris.[4] Previous work of DuBridge,[5] Warner,[6] Kazda,[7] and Goetz[8] dealt with platinum, tungsten, mercury, and tin respectively.

The purpose of this work is to study the variation of the photoelectric sensitivity and of the long wave limit of silver during prolonged outgassing, to determine the ultimate long wave limit when outgassing ceases and stable conditions are reached, and finally to study the effect of temperature on the photoelectric characteristics. The reflecting power for various wave-lengths of incident light is also studied as a function of temperature to determine its possible effect on the observed photo-emission.

The apparatus was similar to that used by Cardwell[1] and consisted essentially of a strip of silver approximately 0.025 mm thick and 3 mm wide suspended from tungsten seals in the form of a loop inside a molybdenum receiving cylinder, the whole being enclosed in a Pyrex tube having a quartz window

[1] Cardwell, Proc. Nat. Acad. Sci. **14**, 439–445 (1928); **15**, 544–551 (1929); work on tantalum not yet published.
[2] Martin, Phys. Rev. **33**, 991–997 (1929).
[3] Dixon, Phys. Rev. **37**, 60 (1931).
[4] Morris, Phys. Rev. **37**, 1263 (1931). Present Issue of Phys. Rev.
[5] DuBridge, Phys. Rev. **29**, 451 (1927).
[6] Warner, Proc. Nat. Acad. Sci. **13**, 56 (1927).
[7] Kazda, Phys. Rev. **26**, 643 (1925).
[8] Goetz, Phys. Rev. **33**, 373 (1929).

sealed on with a graded quartz to Pyrex seal. The tube was connected through two liquid air traps, and a mercury "cut-off" to a water-cooled mercury diffusion pump backed by a Cenco Hyvac fore-pump. The vacuum system included a McLeod gauge and an ionization gauge of the Dushman and Found[9] type for measuring pressures. Wax or grease vapor was guarded against by having the stopcocks and the one wax joint on the opposite side of the liquid air traps from the research tube.

The silver for this study was obtained from the Adam Hilger Co. of London and was 99.99 percent pure containing minute traces of copper, lead, manganese, and calcium.

The photoelectric currents were produced by radiation from a quartz mercury arc and were measured by a Compton quadrant electrometer. Resistances ranging from 10^7 to 5×10^{11} ohms (depending on size of currents to be measured) were shunted across the electrometer quadrants so that the "steady deflection" method could be used.

During the outgassing the undispersed radiation from the arc was used, but for the $f(\lambda)$ curves, and for the temperature curves on a fixed wavelength, a Bausch and Lomb single monochromator was placed between the arc and the specimen. A vacuum thermopile, whose currents were measured by a Kipp ZC low resistance galvanometer (sensitivity 6×10^{-10} amps. per mm at a meter) with a two meter scale distance, gave the relative intensities of the various incident wave-lengths. The thermopile (when carefully evacuated) and its galvanometer system showed very good steadiness which made the intensity readings reproduce readily. However, even with these conditions the fainter lines gave deflections so small that the natural errors of reading made the relative errors large in these cases. A study is being made at present of means of increasing these deflections so that greater precision can be attained. Only points which are quite dependable have been plotted in the accompanying curves.

A careful study of the monochromator was made in the spectral region near the long wave limit with results similar to those shown by Goetz,[8] but with perhaps a little less purity than he shows. The combination of 0.2 mm slit-widths for both entrance and exit slits was found to be as narrow as was consistent with the accuracy desired from the thermopile readings. The photocurrent and intensity measurements were taken together in rapid succession so that the effect of all arc fluctuations was eliminated. There is much left to be desired in obtaining really monochromatic illumination of sufficient intensity for photoelectric work. A double monochromator is to be substituted for the single monochromator used here as a partial answer to this problem. The impurity of the incident light was not sufficient to cause appreciable error in the points plotted on the $f(\lambda)$ curves since they are for lines sufficiently intense so that the error is small. However this lack of purity did eliminate from use certain faint lines near stronger ones so that the number of points available for a given $f(\lambda)$ curve was limited.

[9] Dushman and Found, Phys. Rev. **23**, 734 (1924).

The temperature of the filament was determined from its resistance. The resistance of the filament was measured by measuring the *IR* drop across it, and then the *IR* drop across a tenth-ohm oil-cooled standard resistance, using a Wolff potentiometer for potential measurements. The data for resistance as a function of temperature were taken from a paper by Northrup.[10]

During the initial stages of outgassing the pressures varied from 10^{-7} to 10^{-6} mm of Hg but in the latter part, when stable conditions had been reached and liquid air was placed on the second trap, the pressures varied only from 1 to 3×10^{-8} mm of Hg. At this stage no increase in pressure could be detected when the filament was heated.

Outgassing Procedure

The receiving cylinder of the photoelectric tube was carefully outgassed before placing it in the tube. It was heated at white heat for six days in an auxiliary vacuum system and then transfered to the research tube. The silver filament was immediately sealed in place and the whole tube sealed to the vacuum system. The cylinder was exposed to the air less than four hours. Immediately on obtaining good vacuum conditions the long wave limit of the silver was obtained and heating started by a conduction current through the filament. The heating was started at a low temperature and increased very gradually since metals evaporate much more rapidly when gas-filled.[11] Since silver has a rather low melting point it had to be heated at a low temperature at all times and treated rather carefully to preserve it during the long outgassing required.

Results

Figure 1 shows the outgassing curve. Photoelectric emission due to total arc radiation is plotted as ordinate against time of heating as abscissa. The temperatures written in along the curve show where the heating current was increased thus putting the filament at the temperature indicated. Between the temperatures written in it was maintained at the lower temperature of the interval. The general shape of this curve is similar to that for gold, cobalt, rhodium, and tantalum showing an increase in emission during the initial stages of outgassing and a subsequent decrease finally reaching a fixed value which is not changed with continued heating. It is interesting to note that the high maximum was passed over at 325°C and that increase in temperature did not cause the emission again to rise but to decrease to its final stable value.

After 760 hours of heating of the filament only, the whole tube was baked at about 500°C for 6 days at the end of which time the pressure was less than 10^{-7} mm of Hg with the furnaces at 500°C. The filament was maintained, during baking, at 100°C or more above the rest of the tube to prevent metallic vapors from condensing on it. After removing the furnaces the photo-emission was a little below its value before baking, but at the end of about seventy-five

[10] Northrup, Jour. Frank. Inst. **178**, 85 (1914).

[11] Cardwell, Proc. Nat. Acad. Sci. **15**, 544–555 (1929); Berlinger, Wied. Ann. **33**, 289 (1888).

hours of heating at 600°C it had recovered. Two hundred additional hours of heating at this temperature did not change the emission showing that stable conditions had been reached. This made a total heating time of about 1200 hours before final readings were taken. The filament was flashed many times at over 850°C for short intervals to determine whether higher temperature would change its ultimate characteristics, and no change was observed. The silver evaporated rapidly at these higher temperatures.

The long wave limit of the silver specimen was initially in the neighborhood of 2000A and shifted to the longer waves during the first part of the outgassing reaching a value above 3300A at 405 hours where the emission was a maximum. It then shifted to the shorter waves as the emission decreased reaching a final value in the vicinity of 2700A when stable conditions

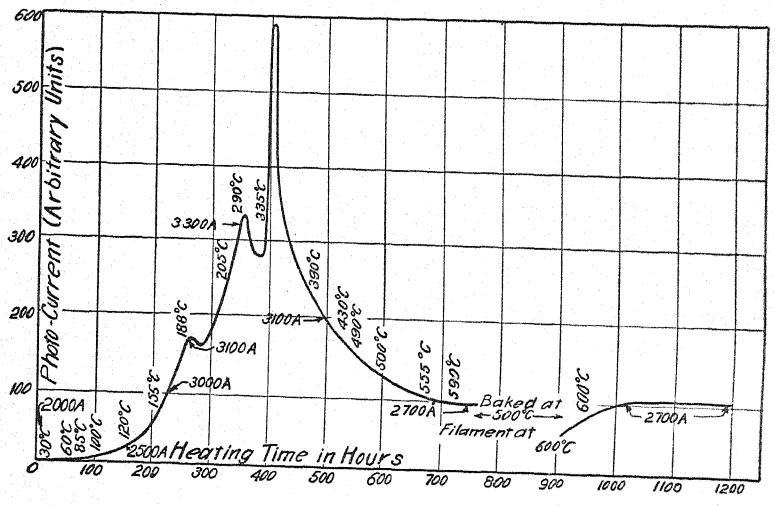

Fig. 1. Outgassing curve using full-arc radiation.

were reached. The long wave limits for various times have been indicated on the curve. This trend of long wave limits is in general agreement with what one would expect from the shape of the curve in Fig. 1.

At various times during the heat treatment, "fatigue" curves were taken by shutting off the heating current and reading the photo-emission as a function of the time of standing. During the initial stages this "fatiguing" caused a decrease (never large) of photo-emission but when stable conditions were reached no fatigue could be observed during more than an hour of standing. It is interesting to note that the fatigue, when it appeared, was always a decrease in photo-current even though the continued outgassing meant a shift to smaller photo-currents so that one would expect returning gas to increase the sensitivity. This phenomenon has not been explained satisfactorily, but has been observed on other metals.

Readings from this point on were taken using the Bausch and Lomb monochromator previously discussed.

Temperature Curves

Figure 2A shows temperature curves for various wave-lengths of incident light while Fig. 3 shows the $f(\lambda)$ curve for 600°C and the one for room temperature. It is obvious that either set of curves could be plotted from the other but both sets were taken independently and repeated many times.

In Fig. 2A the photo-emission is plotted as a function of the heating current through the filament (hence of temperature) for various wave-lengths of incident radiation. The absolute values of the emission represented by these curves cannot be compared. The 2537A curve was plotted and then the curves for other wave-lengths (except 2652A) translated so that they agree with 2537A at room temperature. Observed points have been plotted for 2537A

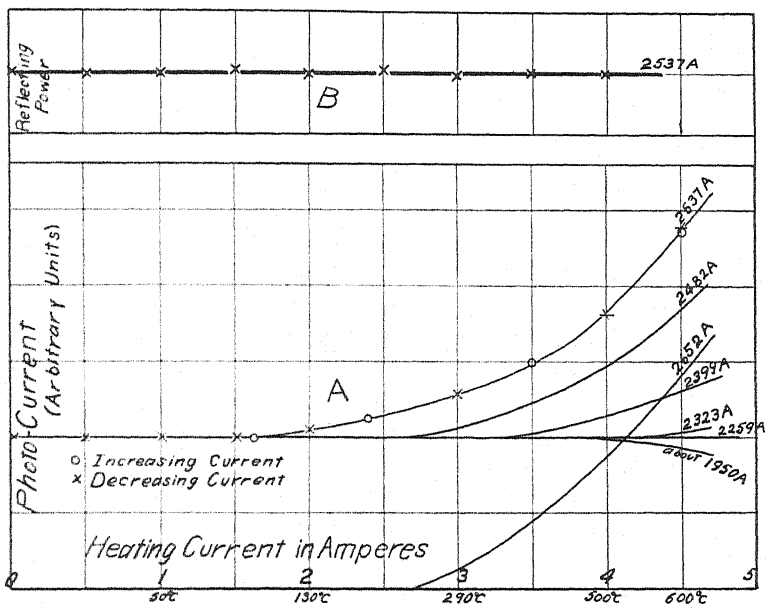

Fig. 2. A. Temperature curves for fixed wave-lengths of incident light. B. Reflecting power as a function of temperature for 2537A incident light.

but to save confusion the points on the other curves have not been plotted. Observations were taken for both increasing and decreasing currents and were reproduced very nicely as indicated by the points plotted. 2652A is not effective below about 2.7 amperes heating current hence it has been plotted to a different scale. The corresponding temperatures have been written in on the heating current scale.

These curves show an effect which was noted first in gold by Morris[4] and later in tantalum by Cardwell,[1] namely, that for wave-lengths in the neighborhood of the long wave limit there is an increase in photo-emission with temperature, for shorter waves there is no effect produced by temperature, and for still shorter waves there is a decrease in photo-emission with increasing temperature. This effect is shown best by tantalum, whereas for silver the

decrease in emission with increased temperature comes at wave-lengths so short that air and quartz absorb some of the incident light and thus make the incident intensity very small. The decrease is definite but the slits of the monochromator had to be widened until there is considerable doubt as to the wave-length at which the decrease began to appear.

In Fig. 2B is plotted a curve showing that the reflecting power of silver for 2537A is independent of temperature up to 600°C. Identical results were obtained for 2482A, 2323A, 2259A, and 2200A. These curves were taken by reversing the field between the silver filament and the molybdenum receiving cylinder so that the filament was charged positively with respect to the cylinder. The incident radiation had been carefully focused on the silver filament. Thus the light which was reflected from the filament and became in this

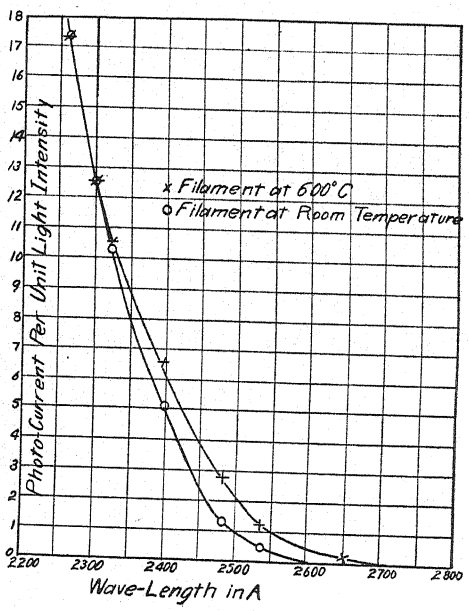

Fig. 3. $f(\lambda)$ curves.

way incident on the cylinder caused photoelectrons to be emitted. These electrons were collected on the filament and measured. The reverse photo-current would thus be proportional to the reflecting power of the filament, and the behavior of this current with respect to temperature would measure any change in reflecting power which might occur with change of temperature. Since these curves indicate no change in reflecting power, the change in photo-emission with temperature cannot be explained on the basis of changing reflecting power.

The curves in Fig. 3 show the long wave limit at about 600°C to be at 2700 ± 20A while at room temperature the long wave limit is 2610 ± 30A. The curves for intermediate temperatures lie in between these two but for temperatures of 200°C or less the curves fall on top of the room temperature

curve as nearly as can be determined. This is to be expected from the shape of the curves in Fig. 2. From the Einstein photoelectric equation these values of the long wave limit make the work function at 600°C equal to 4.56 ± 0.06 volts and for room temperature 4.73 ± 0.07 volts.

Whereas 2652A is the last point on the 600°C curve, it was determined, with an electrometer sensitivity of 8000 mm per volt on rate of charge, that 2699A was effective but that no line above showed an effect.

Conclusions

There is a definite shift in long wave limit of thoroughly outgassed silver with temperature. The shift amounts to about 90A between room temperature and 600°C. The temperature curves in Fig. 2 indicate that for wave-lengths near the long wave limit there is a marked increase in sensitivity with increase in temperature, that wave-lengths farther away show no change with temperature, and that wave-lengths still farther away show a decrease in emission with increase in temperature.

The work function of thoroughly outgassed silver is shown to be 4.56 ± 0.06 volts at 600°C and 4.73 ± 0.07 volts at room temperature. Work is being carried forward to make more accurate determinations of the $f(\lambda)$ curves with more nearly monochromatic illumination.

In conclusion, the writer wishes to acknowledge his indebtedness to Mr. W. L. Hole, whose help was invaluable during this work, and to Professor C. E. Mendenhall, under whose direction this work was carried out.

ON THE TRANSFORMATION OF LIGHT INTO HEAT IN SOLIDS. II

By J. Frenkel
Department of Physics, University of Minnesota

(Received March 21, 1931)

Abstract

The results arrived at in a preceding paper are generalized for diatomic crystals (§§1, 2, 3). A direct determination of the probability of light absorption in a linear lattice leads to the establishment of a selection rule amounting to the law of the conservation of momentum for the light quanta and the "excitation quanta." This rule enables one to explain the linear structure of the spectra of solid bodies at low temperatures (§4). The preceding results are generalized and applied to a new description of the process of light scattering in crystals (§5) and the theory improved by introducing the width of the excitation lines and allowing for the damping of the exciting light waves.

1. General Considerations for a Diatomic Crystal

In A previous paper under the same title[1] I have limited myself to the consideration of monatomic bodies. The first object of the present note is to generalize the above results for the case of a diatomic (binary) crystal; the further generalization for a more complicated body will be quite obvious and will, therefore, not require special consideration. The main difference between a diatomic (or polyatomic) crystal and a simple one consists in the fact that the heat motion is realized here not only by elastical vibrations, for which the relative positions of the atoms within one molecule are approximately constant, the molecule oscillating as a whole, but also by "molecular vibrations" which can be visualized as the (distorted) vibrations of the atoms constituting the separate molecules, the center of gravity of the latter remaining approximately at rest. Whereas the elastical vibrations have a practically continuous spectrum, extending from $\nu=0$ up to a certain maximum frequency ν_{max}, the molecular vibrations are usually characterized by one particular frequency ν_c, described as the "characteristic ultrared frequency" of the crystal and detected by the absorption and reflection of ultrared light or the Raman scattering of the ordinary light.

As a matter of fact there is no sharp distinction between the vibrations of both types. This is clearly seen if one considers a simple crystal as a limiting case of a diatomic crystal with actually identical atoms of "different sort." Owing to the mutual action of the molecules the vibration frequency ν_0, chararteristic of an isolated molecule, is split up into a series of n (or $3n$, n being the total number of molecules in the crystal) frequencies $\nu_{c1}, \nu_{c2}, \cdots \nu_{cn}$ which, however, usually lie very close to each other and are, therefore, considered as a single characteristic frequency ν_c shifted more or less with respect to ν_0. It must, however, be born in mind that the mutual action of the molecules

[1] Frenkel, Phys. Rev. **37**, 17 (1931).

in a crystal produces not simply a shift of their characteristic frequency but causes it to split up into a number ($3n$) of components, corresponding one by one to the various frequencies constituting the elastical spectrum. In fact the corresponding vibrations must have in both cases exactly the same wavelength.

The general theory of the oscillations of a compound crystal lattice has been developed in great detail by M. Born.[2] In this theory Born treated the electrons and nuclei as capable of vibrating about certain equilibrium positions in accordance with the pre-quantum views. We shall have to reserve Born's treatment for the atoms (or ions in a case of an ionic crystal) as *wholes*, the motion of electrons within a single atom being described by specifying the quantum state, normal or excited, of the atom, as has been done in the preceding paper (I). The localization of the excitation state in a particular atom, just as in the case of a simple crystal, does not correspond to a stationary state of the crystal as a whole. Such stationary states are obtained by "diluting" the excitation state over all the atoms *of the same kind* in the form of excitation waves. To a first approximation these excitation waves are not influenced by the presence of atoms of other kinds (which produce a perturbation of the second order only). We thus get exactly the same picture of the excited states or sub-states in the case of a diatomic crystal as that which has been developed before for a simple one.

In the present case, just as in the former one, the excitation of the crystal must entail a slight alteration in its structure, size and vibration frequencies, which will provide an indirect coupling between the different heat oscillators representing these frequencies. To get the looked for generalization of our former theory we need but add to the $3n$ harmonic heat oscillators representing the elastic spectrum, an equal number of oscillators representing the molecular vibrations. With the same approximation which is implied in assigning to all the latter oscillators the same characteristic frequency ν_c we can determine their contribution to the probability of a "deactivation" process by means of the Eqs. (32) and (32a) of I. The probability of a radiationless transition of a diatomic crystal from some excited state or more exactly "substate" (2) to the normal state, with the transfer of the excitation energy to p molecular oscillators is thus proportional to the pth power of the quantity

$$\mu = \frac{\pi^2 m}{2h} \nu_c (\Delta L)^2 \frac{N}{n} \tag{1}$$

where $\Delta L = n \cdot \Delta\delta$ is the measure of the change of the distance between the atoms caused by the excitation of the crystal. This quantity must in general have different values for the molecular oscillators on the one hand and the oscillators representing the elastic vibrations on the other. Further, in the former case m is approximately equal to the sum of the masses of the two atoms of different kind ($m_a + m_b$), whereas in the latter it is given (with the same approximation) by the equation $1/m = (1/m_a) + (1/m_b)$.

[2] Born, "Dynamink der Kristallgitter," Leipzig, 1915. Atomtheorie des festen Zustandes, Leipzig, 1925.

2. Quantitative Theory of a Unidimensional Model

For the convenience of the reader we shall briefly sum up here the theory of the vibrations of diatomic crystals, replacing the latter for the sake of simplicity by a one-dimensional model which we shall call a "bar" and which consists of atoms a and b in alternating order. The consecutive atoms of different kind may be combined in pairs representing the "molecules." The distance from an atom a to the next b on the right of it δ_{ab} may be in general different from the distance δ_{ba} from b to the next a atom in the same direction (Fig. 1). The sum $\delta_{ab}+\delta_{ba}=\delta$ will represent the lattice constant; the smaller of the two distances δ_{ab} and δ_{ba} if they are different can be considered as corresponding to that pair of atoms which actually forms a molecule. Denoting

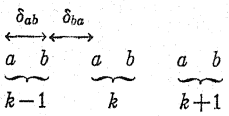

Fig. 1.

the displacements of the atoms forming the kth molecule from their equilibrium positions with u_k and v_k respectively (we shall consider longitudinal displacements only) we can represent the potential energy of the whole system by the expression

$$U' = U - U_0 = \tfrac{1}{2}\sum_{kl} a_{kl}u_k u_l + \sum_{kl} c_{kl}u_k v_l + \tfrac{1}{2}\sum b_{kl}v_k v_l \qquad (2)$$

and write the equations of motion in the form

$$-m_a \frac{d^2u_k}{dt^2} = \sum_l a_{kl}u_l + \sum_l b_{kl}v_l$$

$$-m_b \frac{d^2v_k}{dt^2} = \sum_l c_{lk}u_l + \sum_l c_{kl}v_l$$

In case of an unlimited bar (k, l varying from $-\infty$ to $+\infty$) these equations admit the solution

$$u_k = Ae^{i(pk-\omega t)} \qquad v_k = Be^{i(pk-\omega t)} \qquad (3)$$

representing waves of frequency $\nu=\omega/2\pi$ and length $\lambda=2\pi\delta/p$ travelling in a definite direction with the velocity $w=\omega\delta/p$. Substituting these expressions in the preceding equations and taking into account the fact that the coefficients a_{nl}, b_{nl} and c_{nl} depend only upon the difference $l-n$ of the two indices, we get the following two equations for the (complex) amplitudes A and B:

$$\left.\begin{aligned} Aa_p + Bc_p &= Am_a\omega^2 \\ Ac_p^* + Bb_p &= Bm_b\omega^2 \end{aligned}\right\} \qquad (4)$$

where

$$a_p = \sum_l a_{0l} e^{ipl}, \quad l_p = \sum_l b_{0l} e^{ipl},$$
$$c_p = \sum_l c_{0l} e^{ipl}, \quad c_p^* = \sum_l c_{l0} e^{ipl} = \sum c_{0l} e^{-ipl}. \tag{5}$$

Equating the determinant of (4) to zero, we obtain the following equation for the frequency

$$(a_p - m_a\omega^2)(b_p - m_b\omega^2) = c_p c_p^*$$

whence

$$\omega^2 = \frac{1}{2}\left(\frac{a_p}{m_a} + \frac{b_p}{m_b}\right) \pm \left[\frac{1}{4}\left(\frac{a_p}{m_a} - \frac{b_p}{m_b}\right)^2 + \frac{c_p c_p^*}{m_a m_b}\right]^{1/2}. \tag{6}$$

It can be easily shown that the negative sign corresponds to the elastical vibrations and the positive to molecular vibrations. The corresponding ratios of the amplitudes A and B are:

$$B^{\pm}:A^{\pm} = \frac{1}{2}\left(\frac{a_p}{m_a} - \frac{b_p}{m_b}\right) \mp \left[\frac{1}{4}\left(\frac{a_p}{m_a} - \frac{b_p}{m_b}\right)^2 + \frac{c_p c_p^*}{m_a m_b}\right]^{1/2} : - \frac{c_p}{m_a}. \tag{6a}$$

If the difference $(a_p/m_a) - (b_p/m_b)$ is very small in regard to $|c_p|\,(m_a m_b)^{1/2}$ this equation reduces to

$$B^{\pm}:A^{\pm} \cong \pm\left(\frac{m_b}{m_a}\right)^{1/2} \frac{|c_p|}{c_p} = \mp\left(\frac{m_b}{m_a}\right)^{1/2},$$

if one takes into account that the coefficient c must in this case be real and negative. This result corresponds to the usual approximation implying that in the case of molecular oscillations the atoms belonging to the same molecule are vibrating with opposite phases. The frequency of these vibrations is approximately given by

$$\omega^2 = \frac{1}{2}\left(\frac{a_p}{m_a} + \frac{b_p}{m_b}\right) + \frac{|c_p|}{(m_a m_b)^{1/2}}$$

and is considered to be independent of the "wave number" p(or $p\delta/2\pi$), which of course is a quite unjustified assumption.

In the case of an unlimited bar the number p remains arbitrary. If the bar consists of n molecules, then p can have only the following series of values $0, 2\pi/n, (2\pi/n)\cdot 2, \cdots (2\pi/n)\cdot(n-1)$. Of course, running waves of opposite directions and of the same length (corresponding to $p_1 + p_2 = 2\pi$) have to be combined in this case with the same (or rather conjugate complex) amplitude into standing waves.

The normal co-ordinates ξ are connected with the displacements u_k, v_k by means of the equations

$$\left.\begin{aligned} u_k &= \sum_p (\xi_p^+ A_p^+ + \xi_p^- A_p^-) e^{ipk} \\ v_k &= \sum_p (\xi_p^+ B_p^+ + \xi_p^- B_p^-) e^{ipk} \end{aligned}\right\} \tag{7}$$

where $A_p^{\pm}$, $B_p^{\pm}$ denote the normalized solutions of the Eqs. (4). Solving (7) with respect to the ξ we get

$$\xi_p^{\pm} = \sum_k (u_k A_p^{\pm *} + v_k B_p^{\pm *}) e^{-ipk}. \tag{7a}$$

The co-ordinates ξ_p^+ refer to the "molecular" and ξ_p^- to the "elastical" vibrations.[3]

The expression (2) represents the change of the potential energy of the bar due to the displacement of the atoms. The value of this energy in the equilibrium state U_0 as well as the equilibrium distances δ_{ab} and δ_{ba} are determined from the conditions

$$\frac{\partial U_0}{\partial \delta_{ab}} = 0 \qquad \frac{\partial U_0}{\partial \delta_{ba}} = 0.$$

Now the energy U_0 is slightly different for an excited and a non-excited bar; the same must therefore be true with respect to the distances δ_{ab} and δ_{ba}. The corresponding changes in the normal co-ordinates can be determined in the same way as in the case of a monatomic crystal, namely, putting $u_k = k \cdot \Delta\delta$ and $v_k = k \cdot \Delta\delta + \Delta\delta_{ab}$ in (7a). We shall thus get values[1] of the same order of magnitude both for $\Delta\xi^+$ and $\Delta\xi^-$. In view, however, of the greater frequency in the "molecular" vibrations, their role in the deactivation transitions may be expected to be more important than that of the elastic vibrations according to (S). The increase of frequency is partially reduced, at least for comparatively low temperatures, by the decrease of the average quantum number N (it must be born in mind that the latter refers not to the initial but to the final state, so that in the initial state N can be equal to 0, the corresponding vibrations appearing only after the transition).

We shall illustrate the above results by considering the special case $\delta_{ab} = \delta_{ba} = \frac{1}{2}\delta$ (model of a symmetrical crystal of the NaCl type). We shall further neglect the forces between all but the next atoms (which are assumed to be different) and write accordingly the potential energy U′ in the form

$$U' = \sum_k \tfrac{1}{2} f [(u_k - v_k)^2 + (u_k - v_{k-1})^2 + (u_{k+1} - v_k)^2]$$

which gives through comparison with (2)

$$a_{kk} = b_{kk} = 2f, \quad c_{kk} = c_{k+1,k} = -f$$

all the other coefficients a, b, c vanishing.

[3] If we wish to deal with standing waves instead of running ones, the factor $e^{\pm ipk}$ in the above formula has to be replaced by $\cos pk$.

We thus get, according to (5)

$$a_p = b_p = 2f,\ c_p = -f(1+e^{ip}),\ c_p c_p^* = 2f^2(1+\cos p) = 2f^2\cos^2\frac{p}{2}$$

whence with the abbreviations $1/\mu = (1/m_a)+(1/m_b)$ and $m = m_a + m_b$:

$$\omega^2 = \frac{f}{\mu}\left(1 \pm \left[1 - \frac{4\mu}{m}\sin^2\frac{p}{2}\right]^{1/2}\right).$$

For small values of p, that is for large wave-lengths $\lambda = 2\pi\delta/p$, this reduces to

$$\omega_+ \cong \left(\frac{2f}{\mu}\right)^{1/2}, \qquad \omega_- \cong \left(\frac{2f}{m}\right)^{1/2}\frac{p}{2}$$

the latter expression corresponding to a velocity of propagation

$$w = \frac{\omega_- \lambda}{2\pi} = \delta\left(\frac{f}{2m}\right)^{1/2}$$

independent of λ. As the wave-length decreases, ω_- increases and ω_+ decreases. For the shortest wave-length corresponding to $p=\pi$ we have

$$\omega_{+\,\min}^2 = \frac{f}{\mu}\left(1+\left(1-\frac{4\mu}{m}\right)^{1/2}\right),\quad \omega_{-\max}^2 = \frac{f}{\mu}\left(1-\left(1-\frac{4\mu}{m}\right)^{1/2}\right).$$

In the particular case $m_a = m_b$ when the atoms a and b can be considered as identical, these two limits coincide (since $4\mu = m$) and the two spectra, the molecular and the elastical, coalesce into one single elastical spectrum determined by $\omega^2 = f/\mu(1 \pm \cos p/2)$ which is equivalent to the usual formula

$$\omega^2 = \frac{2f}{m}(1-\cos p') = \frac{4f}{m}\sin^2\frac{p'}{2}$$

with $p' = (2\pi/2n)s$, $s = 0, 1, 2, \cdots 2n-1$.

3. Molecular Vibrations as Excitation Waves

The opposite limiting case when the two atoms have a very much different mass or when the distance δ_{ab} is different from δ_{ba} so that the molecular structure is more or less preserved within the crystal (represented by our "bar"), the molecular oscillations can be treated by a method entirely different from the preceding one (which must be preserved for elastic oscillations) and quite similar to that which has been used to describe the motion of the electrons within the individual atoms. We can namely describe the state of an individual molecule by specifying its vibrational quantum number N, referring to this state as "normal" if $N=0$ and "excited" if $N>0$. The stationary states of the crystal will be then described by "excitation waves" quite analogous to those which were introduced for the description of the electronic state. In fact we have but to replace the atoms and electrons of our previous theory by molecules and atoms respectively, to get these new "mole-

cular" excitation waves. The latter will be represented by functions

$$\chi_p = \sum_k \frac{1}{n^{1/2}} e^{ipk}\phi_k \tag{8}$$

ϕ_k being the product of the oscillator wave functions, ψ_N for the separate molecules, supposed to be all in the normal state $N=0$ with the exception of the kth molecule which may be in a given (Nth) excited state. The excitation wave defined by (8) corresponds to the "molecular oscillation wave" of the classical theory given above and associated with the normal co-ordinate ξ_p^+ defined by (7a). The quantum number N of the excited molecule defines the the amplitude of the oscillations and must coincide with the quantum number of the quantized oscillator describing them. The method of the excitation waves is nothing but a first approximation given by the perturbation theory to the exact quantum treatment which in our case consists in the preliminary introduction of the normal co-ordinates and their subsequent quantization and which has been used in the preceding section. It may be remarked that this method cannot be applied to the "elastic oscillations" because they are determined *solely by interaction forces*, which can be dealt with as perturbing forces then only if there are other more powerful forces associated with the separate particles (i.e., forces holding the electrons within the atoms, or the atoms within the molecules).

The theory of the excitation waves as developed in I was restricted to the simplest special case of the excitation if a single atom. Its application to molecular vibrations implies therefore that the excitation is restricted to one molecule only. So long, however, as the molecular vibrations are considered as strictly harmonic this limitation has no practical significance, a complex excitation state corresponding to n_1 molecules having N_1 quanta, n_2 having N_2 quanta and so on being practically equivalent to a simple excitation state with one molecule having $n_1N_1+n_2N_2+\cdots$ quanta (this multiple excitation is of course diluted over all the molecules in the sense that it is not associated with a particular molecule, but is, so to say, travelling from one molecule to another).

Applying to molecular vibrations the method of the simple excitation waves, one can treat the radiationless transitions of the energy of a crystal from molecular vibrations to elastic ones or *vice versa* (that is the exchange of energy between the normal co-ordinates ξ^+ on the one hand and ξ^- on the other) in exactly the same way, as this has been done above for radiationless electronic transitions. In the present case the direct coupling between the different elastic oscillations must play a much more important role with respect to the indirect coupling (provided by the change in structure which is produced by molecular vibrations) than in the case of electronic transitions, since the energy quantum of the molecular vibrations is not a 100 times but at most only 10 times as large as that of the elastic vibrations of maximum frequency.

The transitions of energy between different elastic oscillations (that is between different ξ^-) must of course entirely depend on direct coupling only.

Such transitions have been studied in detail by R. Peierls[4] in connection with the theory of heat conduction in crystals.

The treatment of the molecular oscillations by the method of excitation waves entails some formal modifications of the theory of the radiationless electronic transitions so far as the electronic excitation energy is transformed into the molecular excitation energy.

We shall not stop, however, on this question here, and shall now proceed to the investigation of radiation transitions, i.e. transitions accompanied by the absorption or emission of light, with a view of introducing an important amendment to the results of the last section of I, dealing with such transitions.

4. Selection Rule for Transitions Due to Absorption of Light; Analysis of the Spectrum of Crystals at Very Low Temperatures

We shall again confine ourselves, for the beginning, to the case of a monoatomic crystal, represented by a linear model and shall determine the probability of the absorption of light propagated in the direction of our "bar."

We shall first suppose the light wave to be harmonic (infinitely narrow spectal line) and travelling in the same way as if there were no bar, so that the electric intensity at a point x along the bar will be represented by

$$E = E^0 \cos 2\pi(\nu t - \alpha x) \tag{9}$$

its value at the kth atom thus being

$$E_k = E^0 \cos(\omega t - qk) \tag{9a}$$

where $\omega = 2\pi\nu$ and $q = 2\pi\alpha\delta = 2\pi\delta/\lambda$, $\lambda = c/\nu$ being the wave-length of the light in vacuo. Denoting the electric moment of the l th atom in the direction of E (which is of course perpendicular to X) with U_k, we get the following expression for the perturbation energy:

$$V = -\frac{E^0}{2}\sum_{l=1}^{n} U_l\left(e^{i(ql-\omega t)} + e^{-i(ql-\omega t)}\right). \tag{10}$$

If our bar was initially in the normal electronic state

$$\chi_0 = \chi_0^0 e^{-i2\pi W^0 t/h}$$

(χ_0^0 being a function of the electron co-ordinates alone) the probability that it will be switched to the excited (sub) state $\chi_p = \chi_p^0 e^{-i2\pi W_p t/h}$ without any alteration of the vibrational states is determined by the matrix element

$$V_{0p} = \int V\chi_0\chi_p^* d\tau$$

where $d\tau = d\tau_1 \cdot d\tau_2 \cdots d\tau_n$ is the volume element of the electronic configuration space ($d\tau_k$ referring to the kth atom). According to (10) and (8) (the latter expression holding both for electronic and molecular excitation waves

[4] R. Peierls, Ann. der Physik, 1930.

with a corresponding meaning of the functions ϕ and ψ, see I), this matrix element assumes the form

$$V_{0p} = -\frac{E^0}{2(n)^{1/2}}\left[e^{-i(\omega+\omega_{0p})t}\sum_k \sum_l e^{i(pk+ql)}\int U_l\phi_0{}^0\phi_k{}^{0*}d\tau + e^{i(\omega-\omega_{0p})t}\sum_k \sum_l e^{i(pk-ql)}\int U_l\phi_0{}^0\phi_k{}^{0*}d\tau\right]$$

where $\omega_{0p}=2\pi(W_p-W_0)/h$ and $\phi_0{}^0=\chi_0{}^0$. Now the integral $\int\mu_l\phi_0{}^0\phi_k{}^0d\tau$ can be easily shown to be different from zero in the case only if $k=l$ (cf. I. p. 20) in which case it reduces to

$$U^0(\mathrm{I, II}) = \int U_k\psi_I{}^0(x)\psi_{II}{}^{0*}(k)d\tau_k$$

i.e., to the amplitude of the matrix element of the electrical moment of any one of the atoms for the normal and the excited state of this atom.

The preceding expression for V_{0p} is thus reduced to

$$V_{0p} = -\frac{E^0U^0(\mathrm{I, II})}{2(n)^{1/2}}\left[e^{-i(\omega+\omega_{0p})t}\sum_k e^{i(p+q)k} + e^{i(\omega-\omega_{0p})t}\sum_k e^{i(p-q)k}\right] \tag{11}$$

We need here only to consider the second term in the bracket for the first term will not contribute appreciably to the transition probability in the neighborhood of the "resonance condition" $\omega=\omega_{0p}$ or $h\nu=W_p-W_0$. In addition to this condition which, from the corpuscular viewpoint is interpreted as the equation of the conservation of energy and which would hold just as well in the case of a single atom, we have to consider in our case a second condition of the same "resonance" type, namely $p=q$, which corresponds to sharp maximum of the sum $\sum_1 e^{i(p-q)k}=n$ (this maximum is sharper the larger the number of atoms). This second "resonance" condition can be interpreted as the equation of the conservation of *momentum* if we assume that an excitation wave can be associated with an "excitation quantum" similar to a light quantum and having a momentum h/λ where λ is the corresponding wave-length. It may be remarked that the energy of this excitation quantum whose motion represents the travelling of the excitation through the crystal—is not related to the frequency of the excitation wave but is equal to the difference between the energy of the excited and normal state.

The absorption of light by a crystal can be thus visualised from the corpuscular point of view as the transformation of the incident light quantum into an excitation quantum having the same energy and *momentum*.

From the wave point of view the latter condition amounts simply to the equality between the wave-length of the exciting light $(2\pi\delta/q)$ and that of the resulting excitation wave $(2\pi\delta/p)$.

This condition can be regarded as a kind of "selection rule" reducing the n spectral lines corresponding to transitions between the normal state and the n excited substates, to a single line, for which both the frequency (energy) condition $\nu = W_p - W_0/h$ and the wave-length (momentum) condition $\lambda_{light} = \lambda_{exc}$ are simultaneously satisfied.

It must be emphasized that the conditions $\nu = (W_p - W_0)/h$ and $\lambda_{light} = \lambda_{exc.}$ are *not equivalent* to each other and actually provide two equations for the unambiguous determination of ν. We have in fact, according to Eq. (15) of part I (for the unidimentional case)

$$W_p = V_0 + 2\, V_1 \cos p/2 \tag{12}$$

whence with the abbreviations $(V_0 - W_0)/h = \alpha$ and $2\, V_1/h = \beta$

$$\nu = \alpha + \beta \cos p/2$$

On the other hand we have $\lambda_{exc.} = 2\pi\delta/p$ or, since $\lambda_{exc.} = \lambda_{light} = c/\nu$, $p = (2\pi\delta/c)\nu$ so that finally

$$\nu = \alpha + \beta \cos (\pi\delta/c)\nu \tag{12a}$$

This equation has in general only one solution which can be found to a first approximation by substituting in the right side of (12a) the "zero approximation" $\nu = \alpha$ (so long as β is small compared with α) which gives

$$\nu \leqq \alpha + \beta \cos \frac{2\pi\delta\alpha}{c} \tag{12b}$$

Thus, contrary to the view expressed at the end of I, the absorption spectrum of a crystal so far as transitions from the normal state are concerned which are not accompanied by a change of the vibrational state, *should not consist of continuous bands corresponding to the excitation multiplets, but of single lines corresponding one to one to the absorption lines of an isolated atom.*

This result provides an explanation of the remarkable phenomenon referred to in I, that the absorption spectra of solid bodies which at ordinary temperatures consist of continuous bands, at very low (liquid hydrogen or liquid helium) temperatures become more or less *linear*, as those of gases.

In fact the band structure of these spectra at ordinary temperatures must be attributed entirely to vibrational transitions which accompany the electronic ones, and which we did not take into account in the preceding considerations. The probability that a number of "heat oscillators," elastic or molecular, will participate in the electronic transition associated with light absorption, is determined in exactly the same way as in the case of radiationless transitions; provided, namely, that each oscillator s jumps over one step only, it is represented in the expression of the resulting transition probability by the square of the factor (1), or rather of the factor

$$n\mu = \frac{\pi^2 m}{2h^2}(\Delta L)N_s\nu_s \qquad (1')$$

the number n in the denominator of (1) being cancelled by the factor expressing the number of possible ways of choosing this oscillator (the total number p of the latter participating in the transition being represented by a factor $p!$ in the denominator of the resulting probability). Now since $hN_s\nu_s$ denotes the vibrational energy of the respective oscillator (without the constant part $\frac{1}{2}h\nu_s$) which rapidly decreases as the temperature approaches the absolute zero, it is clear that the participation of the heat oscillators in the electronic transitions must become less and less active, which will result in the gradual splitting up of the absorption bands into single lines.[5]

It must be remembered that N_s in the preceding expression denotes the vibrational quantum number of the initial state if it *decreases* during the transition ($N_s \rightarrow N_s - 1$); in the contrary case which is in general the more important one, N_s means the vibrational quantum number in the final state; for the absolute zero of temperature upward jumps of N_s are only possible with the final value $N_s = 1$ (since the initial is zero). The same formula (1') shows that in this case, i.e., with all the N_s equal to 1, the probability that an oscillator will participate in the transition is proportional to the square of its frequency. Therefore at very low temperatures practically oscillators of the highest frequency only i.e. the molecular oscillators, and to some extent the elastic oscillators with the highest frequency ν_{max} ("characteristic frequency" of Debye), will participate in the transitions.[6] In the case of a simple (monoatomic) crystal only the latter come into consideration. We are lead thus to expect that the absorption spectrum of a monoatomic (non-metallic) crystal at or near the zero point of temperature must consist of *groups* of lines, corresponding to the absorption lines of an isolated atom, each group consisting of a series of equidistant lines with the constant spacing $\Delta\nu = h\nu_{max}$. The lowest frequency line must have the largest intensity for it must correspond to the purely electronic transition, the next one, with a shorter wave-length and smaller intensity to a transition associated with the upward jump of one oscillator, the next with a still shorter wave-length and still smaller intensity, to a transition associated with the upward jump of two oscillators and so on. These lines must have a sharp edge on the high-frequency side and a rather diffuse one on the other side (since elastic oscillators of lower frequency will also, to some extent, participate in the transitions).

So far as the "selection principle" derived above for a monatomic crystal (i.e. the condition $\lambda_{light} = \lambda_{exc.}$) remains valid for a diatomic one, which can easily be shown to be the case, the preceding analysis of the zero-point spectrum can be immediately extended on diatomic crystals. In this case each

[5] At the same time will decrease the natural width of these lines which is proportional to the probability of a radiationless transition from the excited state into the normal one.

[6] The predominance of these oscillators is insured not only by their higher frequency but also in a three dimensional crystal, by their larger number, the number of oscillators with a frequency between ν and $\nu + d\nu$ being proportional to $\nu^2 d\nu$.

group of lines corresponding to a particular absorption line of one of the atoms (if they are different[7]) must be subdivided into two groups, the spacing in the one being $h\nu_{\max}$ and in the other $h\nu_c$, $\nu_{\max}$ being as before the maximum frequency of the elastic spectrum, and ν_c the molecular vibration frequency. The lines of the second group can be expected to have larger intensities than those of the first. In both cases increasing frequency must correspond to decreasing intensity.

As the temperature increases the satellites, due to the participation in the transitions of the elastic oscillators, must become more and more diffuse on the short frequency side, owing to the rapid increase of the energy $N_s h\nu_0$ and consequently the "activity" (in the sense of their participations in the transitions) of the lower frequency oscillators until each group of lines will be transformed into a diffuse continuous band. Thus on our theory the continuous character of the absorption bands in the spectra of solid bodies at ordinary temperatures is to be ascribed to the equi-partition of energy between the elastic oscillators of different frequencies, resulting in an equal participation of all these oscillators in the transitions associated with the absorption of light.[8]

5. Generalization of the Theory and Application to the Scattering of Light

The conclusions of the preceding paragraph have been reached on the basis of a result ("selection principle") whose derivation has been neither general, for we have limited ourselves to a unidimensional model of a monoatomic crystal, that was supposed to be initially in the normal state, and did not take into account the vibrational motion, nor rigorous, for we have assumed that the incident light wave were travelling through the crystal, as if the latter was absent, and did not allow for the finite spectral width of this light.

We must now remove these defects and thereafter revise the above conclusions in the light of the improved theory.

(a) We shall examine first of all the generalization from the unidimensional to the three-dimensional crystal lattice. This generalization amounts to the replacement of the numbers k, specifying the position of a given atom in the lattice by triplets of numbers k_1, k_2, k_3 which can be considered as components of a vector $\boldsymbol{k}$ and a similar substitution of vectors $\boldsymbol{p}$ and $\boldsymbol{q}$ for the scalars p and q characterizing the wave-length of the excitation waves and of the light waves. The direction of these vectors defines the direction in which the respective waves are propagated; their magnitude is connected with the wave-length in the same way as before ($\lambda_{\text{light}} = 2\pi\delta/q$, $\lambda_{\text{exc.}} = 2\pi\delta/p$). The components of the vector $\boldsymbol{p}$ can of course assume values of the type $p_i = 2\pi r_i/n_i$ where r_i are integers and n_i denote the numbers of atoms along

[7] If they are identical we have to deal with a molecular lattice and compare its spectrum, not with that of one of the atoms, but rather with that of an isolated non-rotating molecule.

[8] Another cause of the broadening of the lines lies in the radiationless transitions from the excited state into the normal one, the probability of the the transitions being a measure of the breadth of the lines. It is, however, difficult to estimate the value of this breadth.

the different edges of the crystal (supposed to be of rectangular shape and to have a cubical lattice with the constant δ).

The formula (11) which serves to determine the transition probability will remain valid for the three-dimensional case if the product of p_k and q_k is replaced by the *scalar products* of the corresponding vectors. As a result we shall obtain our "selection principle" in the form $\boldsymbol{p}=\boldsymbol{q}$ expressing the equality not only of the magnitudes of the vectors $\boldsymbol{p}$ and $\boldsymbol{q}$ but also of their directions, or from the point of view of the quantum interpretation, the transformation of the incident light quantum into an excitation quantum with a momentum of the same magnitude and direction.

(b) The generalization of the preceding result for a diatomic (or many atomic) crystal is quite simple. We have, namely, seen that in case of *different* atoms the excitation waves for the atoms of one kind are to a first approximation completely independent of the presence of the atoms of the other kind. Equation (11) in the "vectorized" form will, therefore, apply to the atoms of each kind separately.

The situation is somewhat different if the atoms supposed to be of different kind differ only with respect to their position, but are actually of the same kind. This corresponds to a molecular lattice, such as the lattice of I_2 (solid iodine) for example. In this case it is convenient to replace the atoms as elements of the crystalline structure by the molecules and deal with the molecular vibrations in the same way as with the electronic ones, i.e. describe them by means of the excitation waves.

(c) This remark brings out the following interesting point. We have just shown that the excitation waves must be associated with "excitation quanta" possessing a momentum in the direction of propagation, and that the "selection principle" $\boldsymbol{p}=\boldsymbol{q}$ can be regarded as the equation of the conservation of momentum in the process of the absorption of a light quantum. Now if molecular vibrations (both in the case of equal or different atoms) are described by excitation waves, it seems possible to combine an electronic transition with a transition of some molecular vibration type in such a way that the equation $\boldsymbol{q}=\boldsymbol{p}$ should be replaced by an equation $\boldsymbol{q}=\Sigma\boldsymbol{p}$ for the different excitation waves involved in the transition, so that the electronic transitions will no longer be restricted by the above selection principle.

This argument is, however, erroneous. Let us remark first of all that if a few different types of excitation waves (corresponding to states with approximately the same energy) would be generated simultaneously forming a combined wave of the type $\chi=c'\chi_{p'}+c''\chi_{p''}+\cdots$ the momentum equation would run $\boldsymbol{q}=|c'|^2\boldsymbol{p}'+|c''|^2\boldsymbol{p}''\cdots$. It can further be easily seen that it should be fulfilled for each of the constituting waves (representing a stationary excited state) separately, so that $\boldsymbol{q}=\boldsymbol{p}'=\boldsymbol{p}''=\cdots$. Since $|c'|^2+|c''|^2+\cdots=1$ the preceding equation actually reduces to $\boldsymbol{q}=\boldsymbol{p}$ for any one of the waves.

It must finally be born in mind that such excitation waves can be generated only for which the matrix element of the electric moment / (I, II) of an atom, or a molecule, is different from zero. In case of a diatomic homopolar

crystal of the type of I_2 this condition would obviously not be satisfied for excitation waves of a purely molecular vibration type. In general the proportionality of V_{0p} to $U(\mathrm{I}, \mathrm{II})$ shows that excitation waves can be generated only which correspond to the optically excitable states of the separate atoms or molecules of which the crystal is built up.

It follows from the preceding considerations that the vibrational motion of the atoms (or molecules) in a crystal, or the transitions from one vibrational state to another, which may accompany the electronic transitions, do not impair the "selection principle" provided by the equation $q=p$ for these electronic transitions.

This result requires but a very slight amendment in connection with the following circumstances. In consequence of the vibrational (heat) motion the atoms no longer form a regular lattice, which they were assumed to form in the derivation of the above equation. Taking again for the sake of simplicity the case of a linear lattice we can define the displacements of the atoms from their equilibrium positions by adding to their ordinal (integral) numbers k small fractions $u_{k'}$ whose products with δ are equal to the respective displacements. Now u_k can be represented as a superposition of Debye waves in the form

$$u_k = \sum_{p'} a_{p'} e^{i(p'k-\omega' t)}$$

where $a_{p'}$ are very small amplitudes.

The factors $e^{\pm iql}$ in the perturbation function (10) must be replaced accordingly by $e^{\pm iq(l+u_l)}$ or, since u_l is very small, by $e^{\pm iql}(1 \pm iqu_l)$. Effecting the same substitution in (11) we must replace $\omega-\omega_{0p}$ by $\omega-\omega_{0p}-\omega'$ and the sum $\Sigma_k e^{i(p-q)k}$ whose maximum value has to be sought for the determination of our "selection principle" by

$$\sum_k e^{i(p-q)k} - iq \sum_{p'} a_{p'} \sum_k e^{i(p-p'-q)k}. \tag{13}$$

The latter expression has besides the main maximum for $p=q$ secondary maxima for $p=q+p'$ which can be interpreted from the quantum corpuscular point of view as the equations for the conservation of momentum of the light quanta, excitation quanta and "heat-quanta" or "sound-quanta" corresponding to the Debye waves. The resonance condition for the frequencies $\omega=\omega_{0p}$ is in *all cases* replaced by $\omega=\omega_{0p}+\omega'$ which can be interpreted as the energy equation for the above three types of quanta.[9] This equation is consistent both with the equation $p=q+p'$ and with the equation $p=q$ which means simply that in the transition process two standing sound waves of opposite directions, forming a standing wave with no resulting momentum, are generated. Since the main maximum of the expression (13) which is approximately equal to the number of atoms n is much more important the secondary ones

[9] These results are identical with those obtained by Ig. Tamm in his rather elaborate theory of the scattering of light in crystals. The notion of "sound quanta" is also due to this author.

which have the order of magnitude of nqa, the vibrational motion of the atom has practically but a very small influence on the position of the groups of absorption lines in the spectrum of the crystal. Nevertheless we must be prepared to find with rising temperature new groups in the form of continuous bands to appear which correspond to the "unusual" selection rules $p=q+p'$ and whose intensity must increase linearly with the absolute temperature (in the equipartition region).

(d) The last generalization that we have to carry out is the allowance for absorption transitions not from the normal state to an excited one, but from one excited $\chi_{p'}$ state to another $\chi_{p''}$ (with a higher energy). It is clear that the preceding results will still be valid for this case if we replace $\omega_{0p}=2\pi(W_p-W_0)/h$ by $2\pi(W_{p''}-W_{p'})/h$ and the vector $\boldsymbol{p}$ by the vector difference $\boldsymbol{p}''-\boldsymbol{p}'$, so that the two "resonance conditions" for the frequencies and the wave-lengths, i.e., the equations of conservation of energy and momentum, assume the form

$$h\nu = \frac{W''_{p''} - W'_{p'}}{h},\ \boldsymbol{q} = \boldsymbol{p}'' - \boldsymbol{p}'\left(q = \frac{2\pi\delta}{\lambda_{\text{light}}},\ p' = \frac{2\pi\delta}{\lambda_{\text{exc}'}},\ p'' = \frac{2\pi\delta}{\lambda_{\text{exc}''}}\right)$$

if the effects of the heat motion and if the corresponding (vibrational) transitions are neglected.

The preceding results must obviously hold not only for the absorption but also for the emission of light (in a definite direction) and can be still further generalized to allow for its scattering (by replacing ν and $\boldsymbol{q}$ by the differences $\nu'-\nu''$ and $\boldsymbol{q}'-\boldsymbol{q}''$ for the incident and scattered light). We shall not engage into a detailed investigation of this question and shall satisfy ourselves with the following remarks. *First*, that the present theory of light scattering in crystals so far as the relations between energy (frequency) and momentum (wave number) are concerned is the exact analogon to Schrödinger's theory of the Compton effect, i.e., of the scattering of light by free electrons, the electron waves being replaced in our case by the excitation waves. In fact the above considerations form the basis of a theory of the Raman effect, which, as well known, is the analogon of the Compton effect for bound electrons and atoms bound together into molecules. The analogy between the two effects is most clearly brought out by means of the conception of the excitation waves as the analogon of cathode waves. *Second*, that the Raman shift of the frequency of the incident light $\nu'-\nu''$ can be calculated either by considering molecular vibrations by the method of excitation waves, or by incorporating them into the heat motion and allowing for the latter according to section (c). *Third*, that the development of the theory sketched above in the quantitative direction, i.e. to enable one to calculate the intensity of the scattered lines, both shifted and unshifted, does not present any difficulty, for this calculation can be easily reduced to the corresponding calculation for an isolated atom or molecule (if the molecular vibrations are described by excitation waves).

6. Improvement of the Theory; Finite Width of the Excitation Lines, and Influence of the Damping of the Light Waves

We must now turn to the improvement of our theory of light absorption with respect to rigour.

(a) We have assumed the light to be strictly homogeneous, which of course is not the case. This circumstance can, however, easily be taken into account in exactly the same as this is done for a single atom. The result will be that the probability of the transition $\chi_0 \rightarrow \chi_p$ in the case of a linear crystal lattice considered in §4 will be equal to the probability of the corresponding transition for a single atom (which is proportional to $|U(\mathrm{I}, \mathrm{II})|^2$) multiplied with the square of the modulus of the factor

$$S = \frac{1}{n^{1/2}} \sum_{k=1}^{n} e^{i(p-q)k} \tag{13a}$$

(cf. Eq. (11)). The maximum value of the sum $\sum e^{i(p-q)k}$ for $p=q$ being n, the total probability for the light absorption by the crystal turns out to be equal, for the lines "allowed" by the "selection rule" $p=q$, to n times the corresponding probability for a single atom. This is just what would be expected on the assumption that the atoms of the crystal do not influence the propagation of the light waves.

The result obtained, which obviously holds for a three-dimensional crystal lattice just as well as for a unidimensional one, requires strictly speaking, some modification. In calculating the transition probability under the action of a spectral line of finite width, one has to take into account the variation of $q = 2\pi\delta/\lambda = \delta\omega/c$ in the factor (12a) with the frequency of the light $\nu = \omega/2\pi$. This would amount to replacing the product of $|S|^2$ with the integral

$$\int_{-\infty}^{+\infty} \left| \frac{e^{i(\omega-\omega_{0p})t} - 1}{\omega - \omega_{0p}} \right|^2 d\omega$$

occurring in the theory of light absorption by a single atom by the integral

$$\int_{-\infty}^{+\infty} \left| \frac{e^{i(\omega-\omega_{0p})t} - 1}{\omega - \omega_{0p}} \right|^2 |S|^2 d\omega$$

It can be easily shown, however, that maximum of $|S|$ about $q=p$ is much flatter than the maximum of the function

$$\left| \frac{e^{i(\omega-\omega_{0p})t} - 1}{\omega - \omega_{0p}} \right|^2 = \frac{\sin^2 (\omega - \omega_{0p})t/2}{((\omega - \omega_{0p})/2)^2}$$

about the corresponding point $\omega = \omega_{0p}$ so that in carrying out of the integration $|S|^2$ can be replaced by its maximum value (n) corresponding to $\omega = \omega_{0p}$ with a proper choice of p, of course. The dependence of $|S|^2$ on $q-p$ can be easily determined. We have namely for a unidimensional lattice if k is varied from 0 till $n-1$

$$S = \frac{1}{n^{1/2}} \frac{e^{i(p-q)n} - 1}{e^{i(p-q)} - 1}$$

whence

$$|S|^2 = \frac{1}{n} \frac{\sin^2 n(p-q)/2}{\sin^2 (p-q)/2} . \tag{13b}$$

The effective width of the maximum of $|S|^2$ can thus be determined for a definite value of q and a variable p by

$$\Delta(p-q) = \Delta p \leqq 2\pi/n$$

or, since $p = 2\pi\delta/\lambda_{exc}$ (λ_{exc} = wave-length of the excitation wave)

$$\frac{|\Delta\lambda_{exc}|}{\lambda_{exc}} = \frac{\lambda_{exc}}{n\delta} = \frac{\lambda_{exc}}{L} = \frac{\lambda_{light}}{L} \tag{14}$$

where $L = n\delta$ is the total length of the lattice.

This result can be easily generalized for the case of a three-dimensional lattice, L denoting in this case one average linear dimension of the latter. The width of the absorption region, i.e., the frequency interval $\Delta\nu$ for which transitions from the normal state to excited sub-states can take place according to our "unsharp" selection rule is given according to (12) by

$$\Delta\nu = \frac{\beta}{2} \sin \frac{p}{2} \Delta p$$

that is

$$\Delta\nu = \frac{\pi V_1}{hn} \sin \frac{\pi\delta}{\lambda} \tag{14a}$$

where λ can be identified with the wave-length of the light. Since δ/λ is for ordinary light a very small quantity we can put $\sin(\pi\delta/\lambda) = \pi\delta/\lambda$ and consequently

$$\Delta\nu = \frac{\pi^2 V_1}{h} \frac{\delta}{L} . \tag{14b}$$

Thus the width of the absorption lines, so far as the vibrational transitions are not taken into account, remains very small at least for crystals of ordinary size. The incompleteness of "resonance" with respect to the wave-lengths, i.e., the departure of $\lambda_{light} - \lambda_{exc}$ from zero, does not therefore contribute appreciably to the width of the lines. At very low temperatures this width must be determined mainly by the probability of the radiationless transitions, whereas at higher temperatures the linear pattern of the spectrum is wiped out by the participation of the low frequency heat (sound) vibrations in the transitions as has been explained above (§4).

(b) It remains for us now to take into account the fact that the propagation of light in a real three-dimensional crystal is substantially affected by the latter, especially in the region of selective absorption, with which we are particularly interested. This influence can be accounted for by replacing the vacuum wave-length of the light λ_0 or the corresponding quantity $q=q_0=2\pi\delta/\lambda_0$ by a certain complex quantity $q=q_1-iq_2$ determining the effective wave-length $\lambda_1(q_1=2\pi\delta/\lambda_1)$ and the absorption coefficient q_2/δ.

In the case of the unidimensional lattice ("bar") considered above, the intensity factor (13a) assumes under this condition the form

$$S=\frac{1}{n^{1/2}}\,\frac{e^{(i(p-q_1)-q_2)n}-1}{e^{i(p-q_1)-q_2}-1}$$

whence

$$|S|^2=\frac{1}{n}\,\frac{1-2e^{-q_2n}\cos(p-q_1)n+e^{-2q_2n}}{1-2e^{-q_2}\cos(p-q_1)+e^{-2q_2}}$$

For large values of n this reduces to

$$|S|^2=\frac{1}{n}\,\frac{1}{1-2e^{-q_2}\cos(p-q_1)+e^{-2q_2}} \tag{15}$$

the maximum of this expression for $p-q_1\cong 0$

$$|S|^2=\frac{1}{n(1-e^{-q_2})^2} \tag{15a}$$

being of course smaller and flatter than in the case of $q_2=0$. The flatness of this maximum must increase the width of the absorption lines and might in fact lead to their transformation in comparatively broad bands even without the participation of the low frequency vibrations. The width of the maximum of $|S|^2$ may be roughly put equal to q_2 if q_2 is sufficiently small, which gives for $\Delta\nu$ the effective width of the absorption line, the expression

$$\Delta\nu\cong\frac{V_1}{h}q_2\sin\frac{p}{2}=\frac{\pi V_1q_2\delta}{h\lambda}\,. \tag{16}$$

The ratio q_2/δ represents the value of the absorption coefficient of the light per unit length of path and its product with λ, $q_2\lambda/\delta=\mu$ the absorption coefficient per wave-length. Substituting this in the preceding formula we get

$$\Delta\nu=\frac{\pi V_1}{h}\mu\left(\frac{\delta}{\lambda}\right)^2. \tag{16a}$$

This formula shows that unless μ is unreasonably large $\Delta\nu$ remains actually small. It may be remarked that the ratio V_1/h represents a frequency which is about at least 10 times smaller than the frequency of ordinary light.

The preceding results can be easily generalized for the case of an ordinary three-dimensional crystal.

(c) In conclusion the following point should be noted. Since the resonance conditions for the frequencies and for the wave-lengths are both unsharp, the excitation state of the crystal induced by the absorption of light must be represented not by *one* definite excitation wave, but by a superposition of a number of such waves with approximately equal lengths and frequencies, i.e. by a group of excitation waves. The corresponding group velocity can be considered as the velocity with which the "excitation quantum," i.e., the excitation state supposed to be localized in a definite atom and described as a corpuscule, should travel through the crystal (cf. I, §2).

THE CRYSTAL LATTICE OF ANHYDROUS SODIUM SULPHITE, Na_2SO_3

By W. H. Zachariasen and H. E. Buckley
University of Chicago and University of Manchester

(Received April 11, 1931)

Abstract

The crystal structure of Na_2SO_3 has been investigated by means of the Laue, the ionization, the rotation and the powder methods. The hexagonal unit cell containing two molecules was found to have dimensions: $a=5.441$A $c=6.133$A. The observations seemed to be in conflict with all hexagonal and trigonal space groups. The difficulty was, however, overcome by assuming the crystals to be twins with the c-axis as twinning axis. The space group C_{3i}^1 was under this assumption found to be the only possible one. All parameters involved were determined from the observed intensities with the following result:

4 atoms Na in position $1a$ (000), $1b$ (00 $\frac{1}{2}$) and $2d$ ($\frac{1}{3}$ $\frac{2}{3}$ u_1), ($\frac{2}{3}$ $\frac{1}{3}$ $\bar{u}_1$) with $u_1=0.67$

2 atoms S in positions $2d$ ($\frac{1}{3}$ $\frac{2}{3}$ u_2), ($\frac{2}{3}$ $\frac{1}{3}$ $\bar{u}_2$) with $u_2=0.17$

6 atoms O in positions $6g(xyz)$, $(y-x, \bar{x}, z)$, $(\bar{y}, x-y, z)$, $(\bar{x}\bar{y}\bar{z})$, $(x-y, x, \bar{z})$, $(y, y-x, \bar{z})$ with $x=0.14$, $y=0.40$, $z=0.25$.

Two of the Na atoms are surrounded by 6 oxygens at a distance 2.469A; while the remaining two sodium atoms are surrounded by 3 oxygens at a distance 2.461A and by 3 at 2.870A. The structure shows the presence of groups SO_3. The distance from sulphur to the 3 surrounding oxygens is 1.39A, while the oxygens in the equilateral triangle have a distance of 2.24A. The sulphur atom has a displacement of 0.51A out of the plane of the oxygens. The form of the SO_3-group is thus like a low trigonal pyramid, being of the same type previously found for the groups $(ClO_3)^-$, $(BrO_3)^-$, $(AsO_3)^{-3}$ and $(SbO_3)^{-3}$.

1. Introduction

CRYSTALS of anhydrous sodium sulphite were first prepared and described by H. Hartley and W. H. Barrett.[1] The symmetry is reported as hexagonal, with an axial ratio $c/a=1.1246$. The crystals are short prisms with predominating forms (10.0) and (00.1) small faces (10.1), (10.2) and very small (11.1) faces. Further observations by Hartley and Barrett are: perfect cleavage parallel to (00.1); birefringence strong, negative; density at 15°C, 2.633.

2. Observations

Our chief interest in the x-ray analysis of the Na_2SO_3 was the determination of the shape and dimensions of the SO_3-group. In the following paragraphs we will describe the complete determination of the crystal structure. The investigation was started at the University of Manchester, where part of the observations were taken. Additional observations were collected in Ryerson Physical Laboratory, University of Chicago, where the investigation was completed.

[1] Hartley and Barrett, Trans. Chem. Soc. (London) 95, 1178 (1909).

Due to certain difficulties met during the investigation (see section 4), it became obvious that we must secure unusually reliable sets of observations, and apply as many different methods as possible. Our observations consist of the following.

(1) Complete rotation photographs and oscillation photographs around the hexagonal axis, and around the two different sets of horizontal axes. Oscillation angles of 5°, 15° and 30° were used. Crystal to plate distance was 5.0 cm. Radiation: Mo$K\alpha$. Bernal's[2] graphical method of indexing the reflection spots was used throughout, thereby securing the most reliable indexing. In order to test the absence or presence of important reflexions many long exposures with an oscillation angle of 5° were taken.

(2) Laue photographs perpendicular to (00.1) and (10.0), and inclined a few degrees to the former directions. The photographs were indexed by converting the diagrams into gnomonic projection. The lower wave-length limit in the incident beam was tested on a number of known crystals.

(3) Intensity measurements on the ionization spectrometer of all reflections $hk.0$ up to 33.0 and of the reflexions $00.l$. The series of intensities $hk.0$ was transformed into absolute measure by a method described in section 4, below. The crystal was completely bathed in the x-ray beam; the observed intensity was taken proportional to

$$|F|^2\,1+\cos^2 2\theta/\sin 2\theta,$$

where $|F|$ is the structure amplitude. Mo$K\alpha$ radiation was used.

(4) Powder photographs with a high resolving camera, with sodium chloride as reference substance.[3] The unit cube of sodium chloride was assumed to have the edge $a=5.628$A. The wave-length used was taken as Mo$K\alpha_1$—$\lambda=0.70783$A.

3. The Unit Cell and Space Group Considerations

All observations agree with the following hexagonal cell:

$$a = 5.441 \pm 0.004\text{A} \quad c = 6.133 \pm 0.007\text{A} \quad c/a = 1.127$$

The correctness of the unit cell was carefully tested by means of long-exposure Laue photographs. No reflection spots could be found which indicated a larger unit cell than the one given above. By means of the directly determined density we find 1.98~2 molecules of Na_2SO_3 connected with each unit cell. The calculated density for two molecules is 2.66.

The Laue photographs and the oscillation photographs possess the symmetry of the space groups C_{3h}^n, C_6^n and C_{6h}^n. Vertical planes of symmetry are definitely not present.

A further limitation of the space groups was obtained through observations of the spectra $00.l$. At ordinary exposures only the even order reflections from the base appear in the oscillation photographs. However, on several oscillation diagrams taken with 5° oscillation angle and long exposures the reflexion 00.3 was unmistakably present. These observations rule out all space groups save C_{3h}^1, C_6^1 and C_{6h}^1.

[2] Bernal, Proc. Roy. Soc. London A113, 117 (1926).

[3] We are indebted to Mr. F. Barta for taking the powder photographs.

4. The Determination of the Structure

From an inspection of all our observations according to the four different methods certain regularities in the observed intensities at once become apparent, and will have to be accounted for by the atomic arrangement. We will consider only the intensities of reflections occurring at large values of $\sin\theta/\lambda$. These regularities we have collected in the following table:

I Reflexions $hk.0$	
(a) $2h+k=3n$ $(n=0, 1, 2, \cdots)$	Intensities are very strong
(b) $2h+k\neq 3n$ $(n=0, 1, 2, \cdots)$	Intensities are very weak or nil
II. Reflexions $hk.l$ with even l.	
(a) $2h+k=3n$ $(n=0, 1, 2, \cdots)$	Intensities are strong for $l=6$ and very weak or nil for $l=2, 4, 8,$
(b) $2h+k\neq 3n$ $(n=0, 1, 2, \cdots.)$	Intensities are very strong for $l=2, 4, 8,$; very weak or nil for $l=6$
III. Reflexions $hk.l$ with odd l.	Intensities are very weak or nil

These regularities are valid with no exceptions at large values of $\sin\theta/\lambda$, but do not fit the observations quite so well at small values of $\sin\theta/\lambda$ although giving a fairly good agreement. There is only one way of explaining this fact: the regularities given above must be characteristic of the cation lattice, but not for the oxygen lattice. Therefore the regularities will hold absolutely at large values of $\sin\theta/\lambda$, where the influence of the oxygen lattice with good approximation can be left out of consideration; but at small values of $\sin\theta/\lambda$ these regularities will be destroyed to some extent through the overlapping influence of the oxygen lattice.

In the unit cell we have 4 Na and 2 S atoms. As a first approximation we will consider the scattering power of sodium and sulphur to be the same. Our first problem will thus be to arrange 6 cations in the cell in such a way that the observed regularities in intensities of reflections are accounted for. (It has to be remembered that these 6 cations are of two kinds, so they cannot all be structurally equivalent.)

The regularity Ia and Ib tells us that the cations are evenly distributed on the 3 available threefold axes. As the c-axis has a length of only 6.13A, it is obvious that only 2 cations can lie on each axis, for otherwise cations would come closer than 2.04A, which is highly improbable. The positions of the cations are consequently according to regularity I: $00z_1$, $00z_2$, $\frac{1}{3}\,\frac{2}{3}\,z_3$, $\frac{1}{3}\,\frac{2}{3}\,z_4$, $\frac{2}{3}\,\frac{1}{3}\,z_5$, $\frac{2}{3}\,\frac{1}{3}\,z_6$.

The regularity III shows that the cations are situated along the threefold axes at intervals of $c/2$. Thus: $z_2=z_1+\frac{1}{2}$, $z_4=z_3+\frac{1}{2}$, $z_6=z_5+\frac{1}{2}$.

Finally the regularity given under II tells us that the cations are arranged in layers parallel to the c-face coming at intervals of $c/6$. We have thus: $z_3=z_1+\frac{2}{3}$, $z_5=z_1+\frac{1}{3}$ and the coordinates of the cations must be:

$$(00z)(00z+\tfrac{1}{2})(\tfrac{1}{3}\tfrac{2}{3}z+\tfrac{2}{3})(\tfrac{1}{3}\tfrac{2}{3}z+\tfrac{1}{6})(\tfrac{2}{3}\tfrac{1}{3}z+\tfrac{1}{3})(\tfrac{2}{3}\tfrac{1}{3}z+\tfrac{5}{6}).$$

This result is rather astonishing. The symmetry of the cation lattice is

that of D_{3d} only, while the observed symmetry is that of C_{6h}. We have as a matter of fact shown that no space group in the hexagonal and trigonal systems can account for the observations. The assumptions upon which we have based our deductions obviously cannot be correct. We have accordingly made a diligent search for a plausible explanation of the contradiction which exists between the observations.

An inspection of all our observations left no doubt as to the reported symmetry, neither could we find any other way of explaining the observed regularities than the one given above. The possibility of a bigger cell had also to be rejected from our observations. The assumption of another symmetry system likewise is highly improbable (it had to be either monoclinic or triclinic) with the nice development of the faces and the definitely uniaxial optical properties. Nor have we any justification for mistrusting the space group theory. We found rather that the only plausible explanation was to assume that all our observations were taken not on single crystals but on twins. We must emphasize, that we have not succeeded in finding direct evidence with which to back this assumption. Nevertheless the good agreement we have obtained between observed and calculated intensities assuming twinned crystals, as well as the plausibility of our final structure, must be taken as an indirect proof of the correctness of our assumption.

If the crystals are twins with the c-axis as twinning axis, the symmetry of our photographs would also be in agreement with that of the space groups C_3^n and C_{3i}^n. Only C_3^1 and C_{3i}^1 can account for the observations in the 00.l spectra. *The distribution of the cations which we determined from the observed regularities also can be obtained from the special positions of these space groups.* The only difference between C_3^1 and C_{3i}^1 is the additional center of symmetry in the latter.

The oxygen atoms will have to lie in general positions (xyz) as no vertical planes of symmetry have been observed in the diagrams. The vertical distribution of the oxygen atoms with regard to the cation positions can easily be found from the spectra 00.l. The only odd order reflexion from the c-face which we observed is 00.3. This means that the oxygen atoms are lying in two layers parallel to the c-face at a distance of $c/2$. The fact that we have observed 00.3 with very small intensity cannot be interpreted as meaning that the oxygen layers have a distance slightly different from $c/2$, as we did not observe 00.5. But we must ascribe the presence of 00.3 to the difference in scattering power of Na and S, which means that the two sulphur atoms must lie on 2 different threefold axes. From the observed intensities of the even orders of 00.l and the known distribution of the cations along the c-axis we find that the oxygen layers parallel to the c-face must be displaced an amount $c/12$ against the cation layers. Summarizing our considerations so far we have found that the space group is C_3^1 or C_{3i}^1. We know the positions of the cations and the distribution in the c-direction of the oxygens referred to the cation lattice.

We have tried both space groups and finally selected C_{3i}^1 as the correct one. In fact a trial with C_3^1 showed that in order to get good agreement we had

to choose such values of the parameters as would give the symmetry of C_{3i}^1. The remaining unknown parameters in the structure were easily determined by means of the observed intensities.

As a final result we arrived at the following crystal structure which gave the best agreement with the observed intensities:

Space group C_{3i}^1.

Na in $1a$: $(000)+1b$ $(00\frac{1}{2})+2d$ $(\frac{1}{3}\ \frac{2}{3}\ u_1)$ $(\frac{2}{3}\ \frac{1}{3}\ \bar{u}_1)$ with $u_1=240°$

S in $2d$: $(\frac{1}{3}\ \frac{2}{3}\ u_2)$ $(\frac{2}{3}\ \frac{1}{3}\ \bar{u}_2)$ with $u_2=60°$.

O in $6g\pm(xyz)$ $(y-x, \bar{x}, z)$ $(\bar{y}, x-y, z)$ with $x=50°$ $y=145°$ and $z=90°$.

The very good agreement between observed and calculated intensities is seen from an inspection of the tables.

The F- curves used are given in Table VI. They are essentially the same as the Na, Cl and O F-curves used by one of us in the determination of structure of $NaClO_3$[4] and $NaClO_4$[5].

The relative intensities of the spectra $hk.0$ measured on the ionization spectrometer were transformed into absolute values by the following consideration; We assumed that the structure amplitude of the reflexion 33.0 was equal to 4 Na+2 S (chemical signs mean scattering power at the value of $\sin\theta/\lambda$ under consideration), as we with good approximation can leave the oxygen contribution out of consideration for such high values of $\sin\theta/\lambda$. All the observations were therefore reduced in such a way as to give an observed structure amplitude for 33.0 equalling the theoretical contribution of

TABLE I. *Ionization measurements in the prism zone.*

$hk.1$	Int.	$\|F\|$obs.	$\|F\|$calc.	$hk.0$	Int.	$\|F\|$obs.	$\|F\|$calc.
10.0	7.4	5	−6.7	31.0	5.4	8	−7.6
11.0	98.0	24	41.8	13.0	.5	2.5	.8
20.0	20.8	12	−11.6	40.0	3.1	7	−5.1
21.0	2.2	4.5	−4.7	32.0	1.3	4.5	−5.1
12.0	30.8	17	20.3	23.0	1.9	5.5	−5.5
30.0	76.0	28.5	33.7	41.0	42.8	27.5	28.4
22.0	70.4	29.5	33.0	14.0	21.6	19.5	18.6
				33.0	14.4	(17.5)	16.2

TABLE II. *Ionization measurements of spectra 00.l.*

$00.l$	Int.	$\|F\|$obs.	$\|F\|$calc.
00.1	nil	nil	2.1
00.2	81.6	20.8	−42.8
00.3	trace	trace	−5.2
00.4	12.0	11.9	16.8
00.5	nil	nil	2.3
00.6	9.6	(13.4)	13.4

[4] Zachariasen, Zeits. f. Krist. **71**, 517 (1929).
[5] Zachariasen, Zeits. f. Krist. **73**, 141 (1930).

TABLE III. *Results from powder photograph measurement.*

hk.l	$\sin^2\theta$	Int. obs.	$\lvert F\rvert^2 \cdot f$	*hk.l*	$\sin^2\theta$	Int. obs.	$\lvert F\rvert^2 \cdot f$
00.1	.00333	nil	1	22.1	.07107	nil	29
10.0	.00565	vw	45	31.0	.07340	vw	59
10.1	.00898	vs	919	20.4	.07590	m	690
00.2	.01333	m	610	31.1	.07673		292
11.0	.01694	vs	1747	30.3	.08080	vvw	107
10.2	.01898	vs	2852	22.2	.08107		28
11.1	.02027	m	483	00.5	.08330	nil	2
20.0	.02259	w	135	31.2	.08673	ms	1599
20.1	.02592	m	387	10.5	.08895	nil	5
00.3	.02999	vw	9	40.0	.09033	nil	26
11.2	.03027		46	21.4	.09283	m	2019
10.3	.03564	s-vs	191	40.1	.09366		70
20.2	.03592		2322	22.3	.09773	nil	51
21.0	.03952	wm	434	11.5	.10024	nil	44
21.1	.04285	vvw	37	31.3	.10339	m	102
11.3	.04693	w	215	40.2	.10366		681
30.0	.05081	ms	1136	30.4	.10412		22
20.3	.05258	s	262	20.5	.10589	nil	150
21.2	.05285		2104	32.0	.10726	nil	56
00.4	.05331		94	32.1	.11059	vvw	102
30.1	.05414	nil	171	41.0	.11855	ms	1153
10.4	.05896	m	1035	00.6	.11995		60
30.2	.06414	nil	1	40.3	.12032		16
22.0	.06774	ms	1089	32.2	.12059		1128
21.3	.06951	nil	45	22.4	.12105		4
11.4	.07025	vvvw	76	41.1	.12188		86

TABLE IV. *Results from Laue photographs.*

hk.l	Int. Obs.	$\lvert F\rvert$	*hk.l*	Int. Obs.	$\lvert F\rvert$
21.0	w	5	32.0	vvw	5
12.0	s	20	23.0	w	6
21.1	w	3	32.1	vw	14
12.1	m	7	23.1	nil	2
21.2	s	38	32.2	w	24
12.2	s	38	23.2	m	24
21.3	vw	7	41.0	vs	28
12.3	w	5	14.0	s	19
21.4	m	28	41.1	vvw	4
12.4	s	44	14.1	w	12
31.0	m	8	41.2	wm	17
13.0	w	1	14.2	vw	2
31.1	s	24	41.3	w	9
13.1	w	2	14.3	w	9
31.2	s	33	41.4	nil	5
13.2	s	29	14.4	w	9
31.3	wm	11			
13.3	w	6			
31.4	m	22			
13.4	s	23			

TABLE V. *Results of structure factor calculation.*

hk.l	$\|F\|$	$\|F\|^2$	$\Sigma\|F\|$	$\Sigma\|F\|^2$	Int. Obs. in osc. phot.
00.1	2.1	4	2	4	nil
00.2	−42.8	1832	43	1832	s
00.3	−5.2	27	5	27	vvw
00.4	16.8	282	17	282	m
00.5	2.3	5	2	5	nil
00.6	13.4	180	13	180	wm
10.0	−6.7	45	7	45	vw
10.1	−22.6	511	43	919	ms
10.$\bar{1}$	20.6	408			
10.2	.6	—	54	2852	vs
10.$\bar{2}$	53.4	2852			
10.3	12.7	161	18	191	m
10.$\bar{3}$	−5.5	30			
10.4	31.9	1018	36	1035	s
10.$\bar{4}$	−4.1	17			
10.5	−2.3	5	2	5	nil
10.$\bar{5}$	0	0			
10.6	−1.4	2	3	4	nil
10.$\bar{6}$	−1.4	2			
11.0	41.8	1747	42	1747	vs
11.1	−12.6	159	31	483	m
11.$\bar{1}$	18.0	324			
11.2	−4.8	23	10	46	w
11.$\bar{2}$	−4.8	23			
11.3	4.4	19	18	215	wm
11.$\bar{3}$	−14.0	196			
11.4	−6.1	38	12	76	w
11.$\bar{4}$	−6.1	38			
11.5	−2.1	4	8	44	vw
11.$\bar{5}$	6.3	40			
11.6	20.5	420	41	840	ms
11.$\bar{6}$	20.5	420			
20.0	−11.6	135	12	135	wm
20.1	−15.2	231	28	387	m
20.$\bar{1}$	12.5	156			
20.2	48.0	2304	52	2322	s
20.$\bar{2}$	4.2	18			
20.3	13.6	185	22	262	w
20.$\bar{3}$	−8.8	77			
20.4	−5.9	35	32	690	ms
20.$\bar{4}$	25.6	655			
20.5	−9.7	94	17	150	w
20.$\bar{5}$	7.5	56			
21.0	−4.7	22	5	22	vw
21.1	.3	—	3	7	o
21.$\bar{1}$	−2.7	7			
21.2	−.6	—	38	1384	s
21.$\bar{2}$	37.2	1384			
21.3	−.9	1	7	33	o
21.$\bar{3}$	5.7	32			
21.4	24.6	655	28	666	m
21.$\bar{4}$	−3.3	11			
12.0	20.3	412	20	412	m
12.1	2.5	6	7	30	vw
12.$\bar{1}$	−4.9	24			
12.2	17.2	296	38	720	m
12.$\bar{2}$	−20.6	424			
12.3	2.4	6	5	12	vw
12.$\bar{3}$	2.4	6			
12.4	8.0	64	44	1353	m
12.$\bar{4}$	35.9	1289			

TABLE V. (*Continued*).

hk.l	$\|F\|$	$\|F\|^2$	$\Sigma\|F\|$	$\Sigma\|F\|^2$	Int. obs. in osc. phot.
30.0	33.7	1136	34	1136	vs
30.1	11.4	130	18	171	w
30.$\bar{1}$	−6.4	41			
30.2	−.6	—	1	1	vvw
30.$\bar{2}$	−.6	—			
30.3	−10.3	106	11	107	w
30.$\bar{3}$	1.1	1			
30.4	−3.3	11	7	22	nil
30.$\bar{4}$	−3.3	11			
22.0	33.0	1089	33	1089	vs
22.1	−.7	1	6	29	vvw
22.$\bar{1}$	5.3	28			
22.2	−3.8	14	8	28	vw
22.$\bar{2}$	−3.8	14			
22.3	−2.5	6	9	51	vvw
22.$\bar{3}$	−6.7	45			
22.4	−1.5	2	3	4	nil
22.$\bar{4}$	−1.5	2			
31.0	−7.6	58	8	58	w
31.1	10.7	115	24	284	m
31.$\bar{1}$	−13.0	169			
31.2	30.6	936	33	940	s
31.$\bar{2}$	2.1	4			
31.3	−3.4	12	11	76	w
31.$\bar{3}$	8.0	64			
31.4	−4.8	23	22	336	m
31.$\bar{4}$	17.7	313			
13.0	.8	1	1	1	vvvw
13.1	.2	—	2	4	vvw
13.$\bar{1}$	−2.1	4			
13.2	−3.0	9	29	659	ms
13.$\bar{2}$	25.5	650			
13.3	−.5		6	26	vw
13.$\bar{3}$	5.1	26			
13.4	21.2	449	23	451	m
13.$\bar{4}$	−1.3	2			
40.0	−5.1	26	5	26	vw
40.1	−6.9	48	12	70	vw
40.$\bar{1}$	4.7	22			
40.2	0	0	26	681	m
40.$\bar{2}$	26.1	681			
40.3	4.0	16	5	16	vw
40.$\bar{3}$	−.6	—			
40.4	16.7	279	20	293	m
40.$\bar{4}$	−3.7	14			
32.0	−5.1	26	5	26	vw
32.1	−8.1	65	14	99	w
32.$\bar{1}$	5.8	34			
32.2	.2	—	24	557	m
32.$\bar{2}$	23.6	557			
32.3	4.7	22	5	22	vw
32.$\bar{3}$	−.5	—			
32.4	14.8	219	19	233	m
32.$\bar{4}$	−3.8	14			

TABLE V. (*Continued*).

hk.l	$\|F\|$	$\|F\|^2$	$\Sigma\|F\|$	$\Sigma\|F\|^2$	Int. obs. in osc. phot.
23.0	−5.5	30	6	30	vw
23.1	−1.6	3	2	3	nil
23.$\bar{1}$	−.7	—			
23.2	23.9	571	24	571	m
23.$\bar{2}$	.5	—			
23.3	5.0	25	6	26	vw
23.$\bar{3}$	−.8	1			
23.4	−4.1	17	19	227	m
23.$\bar{4}$	14.5	210			
41.0	28.4	807	28	807	s
41.1	2.3	5	4	9	nil
41.$\bar{1}$	−2.0	4			
41.2	−8.3	69	17	138	wm
41.$\bar{2}$	−8.3	69			
41.3	−4.5	20	9	38	vw
41.$\bar{3}$	−4.3	18			
41.4	2.5	6	5	12	nil
41.$\bar{4}$	2.5	6			
14.0	18.6	346	19	346	m
14.1	8.0	64	12	77	vw
14.$\bar{1}$	−3.6	13			
14.2	.8	1	2	2	vw
14.$\bar{2}$	.8	1			
14.3	−8.9	79	9	79	w
14.$\bar{3}$	.1	—			
14.4	−4.3	18	9	36	vw
14.$\bar{4}$	−4.3	18			

TABLE VI. *F-curves.*

$\sin\theta$	0.05	0.10	0.15	0.20	0.25	0.30	0.35	0.40
Na^+	9.6	8.5	7.1	5.8	4.6	3.6	2.8	2.0
S^{+4}	11.7	11.0	9.8	8.3	7.0	5.9	5.0	4.1
O^{-2}	9.0	7.1	5.4	3.9	2.6	1.8	1.2	.9

4Na+2 S, which we get from our *F*-curves. It will be seen from Tables I and II that extinction effects obviously have reduced the intensity of the stronger reflexions to a certain extent.

Due to the twinning with the *c*-axis as twinning axis, the reflections *hk.l* and *hk.$\bar{l}$* having different intensities will fall on the same spot in all the photographs.

DISCUSSION OF THE STRUCTURE

In Fig. 1 is given a projection of the structure on the *c*-face. In the structure we can pick out groups SO_3. The structure of the SO_3-group is the one predicted by one of us.[6] The characteristic feature of the SO_3-group which distinguishes it from the CO_3 and NO_3 groups is the fact that the sulphur atom is displaced an amount $\Delta = 0.51$A out of the plane of the oxygen atoms. Analogous results have been found for other groups RO_3.[6] A more accurate

[6] W. H. Zachariasen, Vid. Akad. Skr. I Kl. No. 4 p. 142, 1928 Oslo; Zeits. f. Krist. **71**, 527 (1929).

discussion of these results will be given in a following paper by one of us. The distance S–O is 1.39A.

There are two kinds of Na atoms in the structure, but both show the coordination number 6. The sodium atoms in positions (000) $(00\frac{1}{2})$ are surrounded by 6 oxygens forming the corners of a nearly regular octhahedron, the distance Na–O being 2.469A. The sodium atoms of the other kind have 3 oxygens at a distance 2.461A and 3 at a distance 2.870A. This oxygen octahedron is much distorted, and the sodium does not lie accurately in the center. The SO^3-groups share only corners with the Na_I-octahedra, while a face is shared with the Na_{II}-polyhedra. It is obvious that this sharing of a face in the

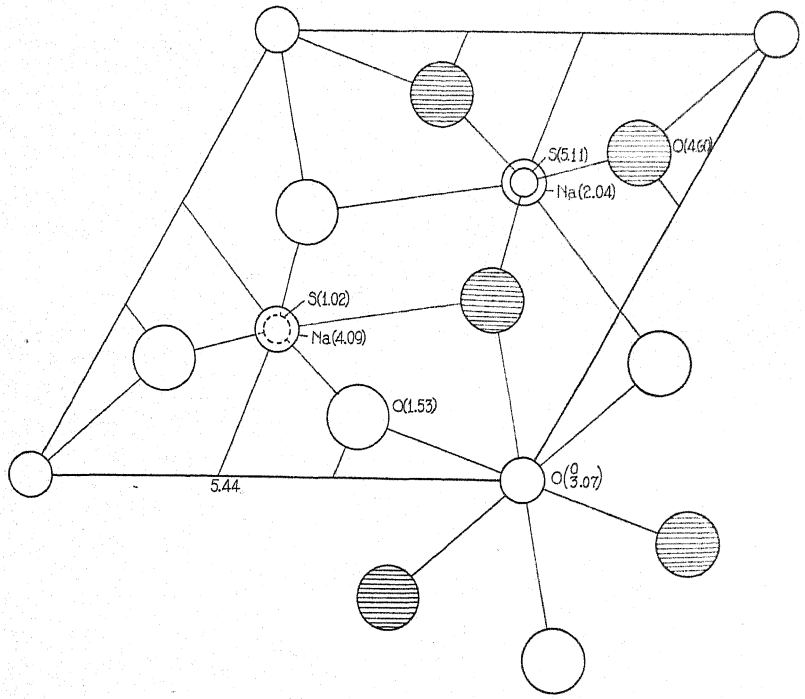

Fig. 1. Projection of the structure on (00.1). Numbers represent height of atoms above (00.1)-plane in A. Valency bonds are represented by connection lines.

latter case will cause some deformation.[7] In the first place we should expect a shortening of the edges bounding the shared face, that is the O–O distance in the SO^3-group will be shorter than normally. But we also should expect a displacement of the cations due to the one-sided configuration. This displacement we should expect to be greater for the cation with small valency; i.e., we should expect the sodium to be displaced in a direction away from the shared face. All these deformations are actually present: the displacement of the sodium atoms results in the two distances to oxygen. The shortening of the edges bounding the shared face will be noticed by a comparison of the SO_3-

[7] L. Pauling, Journ. Amer. Chem. Soc. 51, 1021 (1929).

group with the ClO_3-group. One finds namely that the O–O distance in the SO_3-group is smaller than in the ClO_3-group.

The reported strong negative birefringence of the crystals is a result of the fact that all the SO_3-groups are arranged with the plane of the oxygens parallel to the *c*-face. From a determination of the refractive indices one should be able to give an estimate of the O–O distance in the group. The cleavage parallel to the *c*-face is also in accordance with the structure.

Empirical observation shows the twinning probably is due to the existence of pseudo-elements of symmetry in the crystal structure. In the Na_2SO_3-structure the *c*-axis will be a pseudo twofold screw axis so the formation of twins with the *c*-axis as twinning axis can be explained. The fact that all the crystals we have examined according to our interpretation of the observations must be twins has worried us, and we must admit that we very strongly feel the lack of direct proof of the assumed twinning.

We tried to prepare etching figures on the crystals we had at our disposition. The result was not good but the figures we obtained did seem to indicate a polarity of the crystals. The symmetry of C_{3i}^1 does not give etching figures with the symmetry observed. It is a well-known fact however, that there are many examples where the etching figures indicate lower symmetry than that of the crystal. The results of etching experiments are thus not reliable.

The intensity calculations on the basis of our structure have, however, given so good agreement with all the observations we have collected that the principal correctness of our structure does not seem to be in doubt.

We are very much indebted to Dr. Hartley for providing us with crystals of Na_2SO_3.

THE CRYSTAL STRUCTURE OF POTASSIUM PERMANGANATE

By R. C. L. Mooney

Ryerson Physical Laboratory, University of Chicago

(Received March 30, 1931)

Abstract

The crystal structure of potassium permanganate was determined from Laue and x-ray single crystal oscillation photographs. It was found that the unit cell is orthorhombic, contains four molecules, and has the dimensions:

$a=9.09$A $b=5.72$A $c=7.41$A

The symmetry of the crystal is $2Di-16$ (V_h^{16}), and the structure may be given by the following parameters, expressed as fractions of the unit cell dimensions:

Four K at 4*c*:	$u=0.06$	$v=0.16$	
Four Mn at 4*c*:	$u=0.18$	$v=0.67$	
Four O at 4*c*:	$u=0.00$	$v=0.61$	
Four O at 4*c*:	$u=0.26$	$v=0.49$	
Eight O at 8*d*:	$x=0.19$	$y=0.22$	$z=0.80$

The agreement between the observed intensity and the calculated structure amplitude is satisfactory. The crystal, isomorphous with barytes, celestine and anglesite, has a closely similar structure, though the parameters are different. The manganese is surrounded by four oxygen atoms at an average distance of 1.59A, the arrangement being a nearly regular tetrahedron. The average oxygen-to-oxygen distance in a tetrahedron is 2.62A. The smallest distance between oxygens in different tetrahedra is 2.72 A. The potassium is surrounded by nine oxygens at a mean distance of 2.97A.

1. Unit Cell and Space Group

ALTHOUGH the cell size and the space group of potassium permanganate have been reported by James and Wood[1] and by Basche and Mark,[2] no complete structure determination of this crystal has appeared. Since potassium permanganate is isomorphous with the sulphates of strontium, barium and lead, the atomic arrangements must also be analogous.[3]

Crystals of sufficient size and perfection were grown by the slow cooling of an aqueous solution saturated at about thirty-five degrees. From these, both Laue and oscillation photographs were obtained. Laue photographs were taken with the incident beam parallel to the crystallographic axes and were indexed in the usual way by conversion to gnomonic projections. Numerous oscillation photographs (oscillation angle 15° or 30°) around the three principal axes were indexed according to the graphical method described by Bernal.[4]

[1] R. W. James and W. A. Wood, Proc. Roy. Soc. **A109**, 598 (1925).

[2] W. Basche and Z. Mark, Zeits. f. Krist. **64**, 1 (1926).

[3] P. von Groth, Chemische Krystallographie, Vol. 5; Englemann (1908). J. A. Wasastjerna, Phil. Mag. **7**, 2 (1926); Soc. Sci. Fennica (Physico-Math.) **2**, No. 19–30 (1927).

[4] J. D. Bernal, Proc. Roy. Soc. **A113**, 117 (1926).

The following values were found for the lattice dimensions:

$$a = 9.09\text{A} \qquad b = 5.72\text{A} \qquad c = 7.41\text{A}$$

There are four molecules in the unit cell. In agreement with the results of previous investigations, the space group was shown to be $2Di-16$ (V_h^{16}).

2. Determination of the Structure

Since the space group and the number of molecules per unit cell were known, it was possible, by means of the theory of space groups, to list all the arrangements of the twenty four atoms compatible with the symmetry of the crystal. The number of possibilities was limited by some justified assumptions. Because of the isomorphism with the sulphates of strontium, barium and lead, as well as with the perchlorates of potassium, rubidium, caesium and ammonium, the existence of groups MnO_4 in the crystal may well be taken for granted. These MnO_4 groups must of necessity be linked together by the potassium ions. This assumption together with considerations of the intensities showed that only the following distribution of the atoms among the available positions was possible: (See Wyckoff's tables[5]) 4K in $4c(u0v)$; 4Mn in $4c(u0v)$; $4O_I$ in $4c(u0v)$; $4O_{II}$ in $4c(u0v)$ $8O_{III}$ in general positions $8d(xyz)$. There are, therefore, eleven parameters in the structure.

From considerations of the intensities of reflections occurring at large glancing angles (where the influence of the oxygens becomes negligible) the parameters for potassium and manganese were determined. The values obtained agree very well with those given for Ba and S in $BaSO_4$. (Compare James and Wood.[1])

The intensities of reflections from about fifty planes with simple indices were used for the determination of the seven oxygen parameters. Some simplification was obtained by the conception of tetrahedral MnO_4 groups with dimensions somewhat larger than those of the SO_4 group; further, all arrangements were rejected if they gave an oxygen-to-oxygen distance considerably less than 2.5A. In this way a set of approximate parameter values was easily derived. Then a series of changes in the parameter values was made so as progressively to better the agreement between observed and calculated intensities, until by this process of trial and error a satisfactory agreement was obtained. The final set of parameter values is given in the Table I. In Table II the calculated values of the structure amplitude are compared with the

Table I. *Parameter values.*
(Given in fractions of the length of the unit cell sides)

Potassium:	$u=0.06$	$v=0.16$	
Manganese:	$u=0.18$	$v=0.67$	
Oxygen_I:	$u=0.00$	$v=0.61$	
Oxygen_II:	$u=0.26$	$v=0.49$	
Oxygen_III:	$x=0.19$	$y=0.22$	$z=0.80$

[5] R. W. G. Wyckoff, Analytical Expression of the Results of the Theory of Space Groups, Carnegie Institute of Washington, 1930.

TABLE II. *Calculated and observed values of the structure amplitude.*

hkl	sin θ	*F* (calculated)	Intensity (observed)
101	0.0618	49.4	M
200	0.0782	53.4	M
011	0.0784	51.05	M
201	0.0917	59.5	M
002	0.0960	60.4	M
210	0.1001	107.6	VVS
102	0.1036	92.8	S
202	0.1230	20.5	M
020	0.1248	134.4	VVS
301	0.1266	7.7	W
400	0.1573	34.3	MW
302	0.1517	5.6	VW
122	0.1621	92.9	S
401	0.1635	137.1	VVS
203	0.1640	25.2	M
303	0.1860	68.3	S
004	0.1917	43.7	M
123	0.1940	46.4	M
104	0.1960	50.0	M
420	0.2000	21.3	W
501	0.2010	22.0	W
230	0.2030	68.8	M
114	0.2056	60.4	M
204	0.2076	37.2	W
132	0.2105	66.1	M
141	0.2238	27.6	W
304	0.2249	6.5	W
133	0.2350	1.8	VVW
124	0.2324	63.7	M
610	0.2430	55.0	M
600	0.2440	41.2	MW
601	0.2441	16.7	W
105	0.2441	13.3	W
040	0.2470	123.5	VVS
015	0.2480	23.8	W
233	0.2490	7.9	VVW
513	0.251	60.1	MS
205	0.253	9.2	W
414	0.255	2.6	VVW
240	0.261	19.4	W
602	0.263	34.4	MW
241	0.265	25.3	W
620	0.266	10.1	VW
142	0.269	56.0	MW
134	0.271	65.5	M
125	0.273	51.0	M
531	0.275	30.0	W
440	0.295	10.9	W

observed intensities. The agreement is as good as can be expected for a structure having eleven parameters. The *F*-curves shown in Table III were used in calculating structure amplitudes. The observed intensities are rated as very strong, (VS); strong, (S); medium, (M); weak, (W), and very weak (VW).

TABLE III. *F-curve values used for potassium permanganate structure.*[6]

Sin θ/λ	O	K	Fe
0.1	8.0	16.9	22.6
0.2	5.8	13.0	18.0
0.3	3.7	10.5	14.9
0.4	2.5	8.6	12.5
0.5	1.7	7.2	10.7
0.6	1.1	6.0	9.3
0.7	0.7	5.1	8.2
0.8	0.5	4.3	7.2
0.9	0.4	3.7	6.3
1.0	0.3	3.1	5.6

3. DISCUSSION OF THE STRUCTURE

In Fig. 1 is given a projection of the structure on the *c*-face. It is true that some use has been made of atomic distances in deriving the approximate

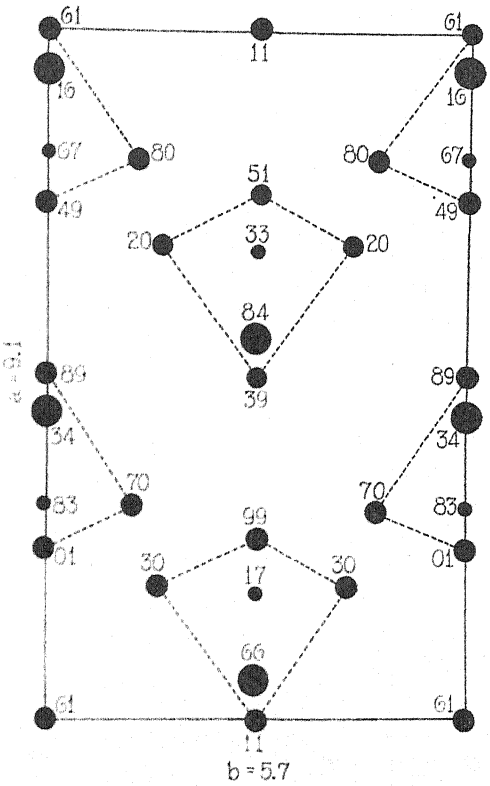

Fig. 1. Crystal structure of potassium permanganate projected on *c*-face. Large circles are potassium, medium circles are oxygen and small circles are manganese.

parameter values. The more accurate evaluation of the positions was, however, made on the basis of intensities alone.

Manganese is surrounded by four oxygens (one O_I, one O_{II}, and two O_{III})

[6] The values are taken from: W. L. Bragg and J. West, Zeits. f. Krist. 69, 118 (1928).

forming a nearly regular tetrahedron. The manganese-to-oxygen distances are: Two O at 1.58A; one O at 1.68A, and one at 1.52A, the average being 1.59A. The oxygen-to-oxygen distances in the tetrahedron are:

$O_I - O_{III} = 2.62A$ $O_{III} - O_{III} = 2.53A$ $O_{III} - O_{II} = 2.70A$

$O_I - O_{II} = 2.54A$

The average O to O distance is 2.62A.

For comparison it may be remarked that the silicon-to-oxygen distance in the SiO_4 group is given as 1.54–1.64A;[7] the sulphur-to-oxygen distance in the SO_4 group is 1.5A;[8] the phosphorus-to-oxygen distance in the PO_4 group is 1.56A;[9] and chlorine-to-oxygen distance in ClO_4 is 1.56A.[10]

In $KMnO_4$, potassium is surrounded by nine oxygens at a mean distance of 2.97A; one at 3.37A; two at 2.93A; two at 2.96A; one at 2.94A; one at 3.05A; and two at 2.79A. The potassium-to-oxygen distance in other crystals with coordination number nine is reported as 2.96A and 2.94A.[11]

The smallest distance between oxygens belonging to different tetrahedra is 2.72A.

In conclusion I wish to express my most sincere thanks to Dr. W. H. Zachariasen for his interest and assistance in this investigation.

[7] W. L. Bragg, Zeits. f. Krist. **74**, 237 (1930).
[8] A. J. Bradley, Phil. Mag. **49**, 1225 (1925); R. W. James and W. A. Wood, ibid.
[9] J. West, Zeits. f. Krist. **74**, 306 (1930).
[10] W. H. Zachariasen, Zeits. f. Krist. **73**, 2, 141 (1930).
[11] W. H. Zachariasen, Norske, Vid. Akad. Skr. Mat.-Nat. Kl. No. 4 Oslo, 1928, p. 97, Zeits. f. Krist. **71**, 501 (1929).

THE MOBILITY OF AGED IONS IN AIR IN RELATION TO THE NATURE OF GASEOUS IONS

By Norris E. Bradbury
Physical Laboratory, University of California

(Received April 10, 1931)

Abstract

The mobility of gaseous ions in air formed by intense x-radiation has been studied by the method of Tyndall and Grindley. The mobility of ions less than 0.08 seconds of age was found to be 2.21 cm/sec per volt/cm for the negative ion and 1.59 cm/sec per volt/cm for the positive ion in agreement with values observed by Loeb and by Tyndall and Grindley. A modification of the apparatus permitted the mobility of ions which had been aged for times up to 1.5 seconds to be studied. In this case a decrease in mobility was observed to values of 2.04 and 1.46 for the negative and positive ions after 1.5 seconds aging. The ionization chamber and source of ionization were the same as those employed by Luhr in recombination measurements. From the theoretical mobility equation of Langevin, the observed decrease in mobility cannot be correlated with the probable increase in ionic mass occurring in recombination measurements under the same conditions. A much larger decrease in mobility is predicted on this basis than is observed in these experiments.

Introduction

THE properties of gaseous ions have been studied for many years with diverse methods and under a variety of conditions, but the exact nature of the ion as it exists under normal conditions of temperature, pressure, and purity can hardly be said to be known. The early stages in the life of the ion (up to ages of the order of 0.01 second) are not, however, difficult to explain. The electron is first torn off from a neutral molecule in a manner dependent upon the ionizing agent employed, thus leaving the molecule positively charged. After a period of time depending upon its kinetic energy, the number of impacts with neutral molecules, and the attachment coefficient of the gas in question, the electron may attach itself to a molecule forming a negative ion. In the case of gases in which positive and negative ions are usually studied, this time of attachment is almost instantaneous and can be completely neglected in the further history of the ion. Exactly what takes place after the formation of the positive or negative monomolecular ion in this manner is not clear. The work of Erikson[1] and others shows that an aging effect takes place in the case of the positive ion causing a lowering to the ordinary values observed in the first 0.01 second. This aging appears to take place in a single step, and while observed for positive ions in air doubtless occurs for both ions in many gases, perhaps in shorter time intervals than observed by Erikson. Further, the work of Loeb[2] on mobilities in mixtures of gases has shown, depending on the nature of gases used, that either clustering of a statistical type or definite cluster formation may take place, the na-

[1] H. A. Erikson, Phys. Rev. **28**, 372 (1926).
[2] L. B. Loeb, Phys. Rev. **32**, 81 (1928).

ture of the change observed indicating the formation of clusters of but a few molecules. It is also possible that the initially charged molecule gives up its charge to other and larger molecules of impurities present. However, whatever processes occur, the result is a single class of ions in a given gas which may be termed the normal ion in that gas within a given time interval (i.e. 0.01–0.1 seconds). Regardless of their constitution, which may be monomolecular or a group of very few molecules (2–6), their properties, as shown by their mobility, apparently change very little in the first 0.1 second.

The work of L. C. Marshall[3] and O. Luhr[4] on the coefficient of recombination of ions, however, showed that after this time, certain of the ions were undergoing marked changes. These investigators, employing methods and apparatus of considerable accuracy, studied the recombination of ions in air and other gases at normal temperatures and pressures over periods of time from 0.001 second to two seconds after ionization. They found that in the first 0.0125 sec. the value of the coefficient of recombination is not constant, but decreases sharply from a value several times greater to 1.2×10^{-6}. This high initial value, which had been observed before, was attributed by Plimpton[5] and independently by Loeb and Marshall[6] to the initial non-random distribution of ions in the gas; the positive and negative ions being formed in pairs, recombine more rapidly at first than after separation caused by the thermal agitation of the neutral molecules. This phenomenon has been treated by Loeb and Marshall,[6] who showed that it followed from the predictions of the Brownian movement equations when the ionic fields had been taken into account.

Moreover, Luhr[4] found that, after this rapid initial drop, the value of α, the coefficient of recombination, did not become constant but continued to decrease, although at a very much slower rate. When the age of the ions was made as great as two seconds, values of α as low as 0.4×10^{-6} were found. Such a decrease in α could not be accounted for by any theory of recombination which assumes an ion of constant dimensions. The only tenable interpretation seemed to be that the ions changed their character with time by picking up products formed by the intense hard x-rays to which the gas had been subjected. Evidence that this explanation was the correct one was found in the case of hydrogen in which no change in the value of the recombination coefficient with time was found. In this case no formation of impurities analogous to the formation of ozone, nitric oxides, H_2O_2, and the like, as in mixed gases, could take place. Certain impurities, e.g. water vapor, are also always unavoidably present in small amounts which could combine to form nuclei with the above chemical reaction products. On this supposition, the smaller and faster ions recombine first leaving the slower and heavier ions to recombine more slowly. The conclusions to be drawn from such a decrease in the recombination coefficient will be considered later, but it may be noted

[3] L. C. Marshall, Phys. Rev. **34**, 618 (1929).
[4] O. Luhr, Phys. Rev. **35**, 1394 (1930).
[5] S. J. Plimpton, Phil. Mag. **25**, 65 (1913).
[6] L. B. Loeb and L. C. Marshall, Jour. Frank. Inst. **207**, 371 (1929).

that α is inversely proportional to the square root of the mass of the ion; hence an increase in mass would very properly result in a lowering in the rate of recombination.

The very pronounced character of this effect in the case of ionic recombination made it obvious that the loading up occurring under these conditions must affect the mobility of ions aged over similar periods of time. Thus the existence and magnitude of a change in the mobility of ions formed under the same circumstances and in gases of the same degree of purity as those used in recombination measurements becomes of significance in gaining some insight into the nature of the gaseous ion.

It was for the purpose of studying these problems that the experiments about to be described were carried out. The first attempts were made with a modification of the simple Rutherford alternating current method[7] for mobility measurements with x-ray ionization. The construction of the apparatus, however, was such that "asymptotic feet" in the curves obtained could not be avoided, and the resolving power was, therefore, very small as is the case with all A.C. methods of this type. Hence any small change in mobility with age was undetectable.[8] In order to establish definitely the value of the mobility of ions produced in air by x-rays at normal temperature and pressure, and also to study the behavior of ions formed under such conditions as a function of their age, the apparatus was arranged so that the *absolute method* developed by Tyndall and Grindley[9] could be employed. This method is capable of yielding quite accurate and consistent results and can easily be modified to study the effects of aging. It also has the highest resolving power of any accurate method.

Method

The essential features of the apparatus employed are shown in Fig. 1. A Coolidge x-ray tube, run at 80 K.V. and 4 m.a. pure D.C. under conditions particularly designed for extreme constancy of voltage and current, is used as the source of ionizing radiation. The beam of x-rays passes through two meters of air and a series of defining slits before reaching the chamber; the width and position of the beam in the chamber can thus be sharply determined. Perpendicular to the beam and in its path is a heavy brass disk from which a variable sector has been cut. As this disk is rotated x-rays are intermittently cut off or permitted to pass through to the chamber. Affixed to the same axle with the disk is a commutator having a single metal segment; the angular width of the latter, as well as its position with respect to the sector cut from the disk, may be varied. Two brushes, separated by an angle slightly greater than that of the commutator segment, make contact with the commutator surface. These brushes are connected to the positive and negative terminals of a high potential battery bank, some point near the middle being grounded. As the commutator revolves, an intermittent alternating potential,

[7] Rutherford, Phil. Mag. **44**, 422 (1897).
[8] O. Luhr and N. E. Bradbury, Phys. Rev. **36**, 1394 (1930).
[9] Tyndall and Grindley, Proc. Roy. Soc. **110**, 341 (1926).

shown in Fig. 2, is applied to the lower plate of the ionization chamber. By changing the relative setting of the commutator and sector opening, the phase position of the x-ray flash in the chamber with respect to the potential on the plates may be varied. When neither of the brushes is in contact with the segment, the lower plate is maintained at zero potential by means of a half megohm resistance to ground; at such times the space between the plates is field free.

Ionization takes place between two parallel brass plates mounted on amber insulators in a heavy brass chamber with aluminum windows. The plates are approximately 10×20 cm and 7.5 cm apart. The upper plate, upon which the ions are collected, is surrounded by a guard ring and connected to ground through an electrometer. The chamber has a heavy glass top (which serves as a mounting for the upper plate) sealed on with stopcock grease. Vapor from the grease, however, is prevented from coming in contact with the gas in the

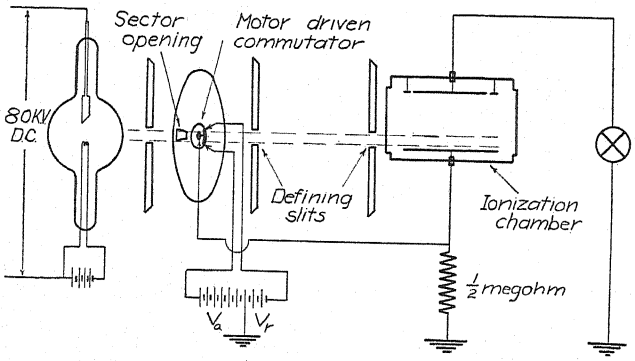

Fig. 1. Diagram of apparatus.

chamber by a special double seal and groove. A purifying system for the gases used is connected to the chamber, and the whole may be evacuated to 10^{-4} mm.

Standard technique was observed in the purification of the gases which were passed over $CaCl_2$, NaOH, and P_2O_5, and through liquid air traps. Before taking any measurements, the chamber was first pumped out as completely as possible, flushed out with purified gas, and finally refilled with pure gas to atmospheric pressure. No difficulty was experienced in obtaining gas of sufficient purity to give the usual values of mobility.

The lead defining slits outside the chamber are adjusted to give the beam a width of a centimeter or less and a position just grazing the lower plate. The commutator is set so that the x-ray flash occurs approximately in the position γT of the cycle. (Fig. 2 shows the cycle of potentials applied to the lower plate.) The values of the potentials are adjusted so that V_r, the retreating potential, is approximately equal to $1.6 V_a$, the advancing potential. This is done in order that V_r, acting during the time βT, may be sufficiently great to clear the chamber of all ions.

The operation of the cycle may now be considered in the following man-

ner: Let T be the time of one complete commutator revolution. Fractions of this period will be denoted by αT, βT, γT, and δT as in Fig. 2. During the time γT, while the x-ray flash is in the chamber, and for a time δT afterwards, the ions are acted on by the field V_r. This field acts in such a direction that those ions whose mobility is being measured are drawn towards the lower plate. Hence at the end of δT, only a thin sheath of the originally formed ions (depending upon the magnitude of $(\gamma+\delta)T$) remain in a layer just above the lower plate. A potential of the opposite sign and of magnitude V_a is then applied to the plates, and the ions being studied are drawn towards the upper plate for a time αT. Ions of opposite sign are drawn back to the lower plate and cleared from the volume. Thus *if αT is sufficiently long*, all ions not caught by the lower plate at the conclusion of αT, will be caught by the upper plate and produce a deflection of the electrometer. If, however, αT is not long enough to draw all the ions across the space between the plates, the lower

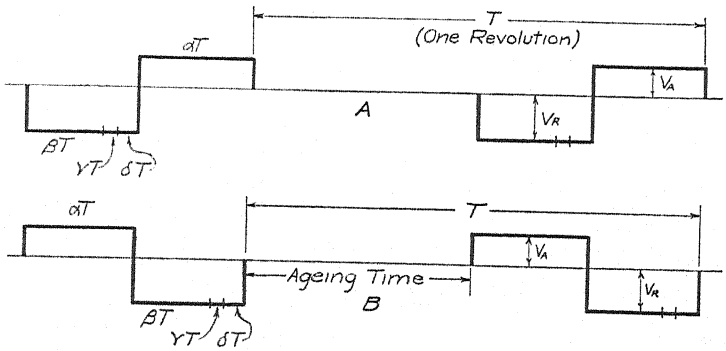

Fig. 2. Cycle of potentials applied to lower plate by the commutator. Ions are formed during γT, drawn toward lower plate during γT and δT, and drawn across volume to upper plate during αT. Volume cleared of all ions not caught at plates during βT. "A" shows cycle for *new* ions and "B" the cycle for *aged* ions.

part of the sheath, or even all of it, will escape capture at the upper plate. All ions not caught at the upper plate at the conclusion of αT are swept out of the volume by V_r acting during βT. The volume is thus prepared for the repetition of the cycle, which is repeated at each revolution of the commutator and disk.

The number of ions reaching the upper plate (and hence affecting the electrometer) during a cycle will depend upon the speed of rotation of the commutator. If the speed of rotation is too slow, δT will be sufficiently long to permit V_r to remove all the ions from the sheath before V_a can operate, and the electrometer current will be zero. On the other hand, if the commutator speed is too high, αT will not be long enough to allow V_a to draw any of the ions not caught during δT to the upper plate, and again the electrometer current will be zero. Between these limiting speeds a maximum of current to the electrometer will occur. Tyndall and Grindley[9] show that the position of this maximum is given by

$$\alpha T = D/kV_a$$

where k is the mobility of the ions, D, the distance between the plates, α the fraction of the commutator covered by the segment, T, the period of one commutator revolution at maximum current to the electrometer, and V_a the advancing field strength. It is seen that the expression is independent of the retarding voltage, V_r, the width of the beam, and the time of retardation. These facts which arise from the mathematics of the cycle, were amply verified by experiment.

Since α, β, γ, and δ are merely constant fractions, the times during which the potentials act are varied by varying T. This is accomplished by driving the commutator and disk with a D.C. motor whose speed is variable and determined by the voltage from a direct connected tachometer magneto. Speeds are thus varied and kept constant at different points with considerable ease. A lead shutter is provided which may be interposed between the x-ray tube and the brass disk. X-rays can thus be kept from the chamber while the disk and commutator are being brought to constant speed. When this shutter is removed, ionization takes place in the chamber and an electrometer deflection is observed whose rate is proportional to the number of ions caught by the upper plate during each cycle. Changing to another speed and repeating the process gives a different rate of deflection, and a series of points taken in this manner may be plotted from which the position of the maximum rate of deflection is determined. Both V_a and V_r as well as α, β, γ, and δ are kept constant while a run is being taken. The value of the speed, N, at the point of maximum current makes it possible to calculate T $(=1/N)$ and with this the mobility k may be determined from the other constants of the experiment.

Fig. 2 shows the two possible adjustments of the commutator system. In (A) αT follows immediately upon δT and so-called "new" ions are studied. In (B), however, the entire insulated section of the commutator is allowed to pass after δT before the ions are drawn across during αT. Ions are thus permitted to age in the gas for that length of time, after which their mobility is measured. Two types of measurement are thus possible, and a change in mobility with age should result in a shift of the position of the maximum of the curve if other conditions are kept the same.

In actual practice α was either 1/4 or 1/8 and γ and δ 0.0194. Speeds of rotation were of the order of magnitude of 15 to 300 r.p.m., and could be measured with an accuracy of 0.5 percent with the tachometer. V_a varied from 10 to 50 volts/cm depending upon the conditions of the experiment, and was read upon a 0–300 volt instrument which had been checked against the laboratory standard. In order to check upon any change of mobility in the gas during the time of measurements, runs were made in the following way: the commutator was set in the position to study *aged* ions, and sufficient readings taken to determine the position and shape of the maximum; the commutator was then shifted to the position for *new* ions and the position of the peak again determined. If this latter value did not give the standard mobility determined from a long series of experiments on new ions, the readings were rejected. This was done in order that spurious effects resulting from an impure sample of gas might be eliminated, and was very rarely necessary. When

the commutator speed was very slow, some aging took place during αT. This was taken into account in making the check runs on new ions.

Results

Measurements were carried out on both positive and negative ions under a variety of experimental conditions in an effort to determine the conditions of greatest resolving power consistent with maintaining measurable electrometer currents. Changes in any of the factors not contained in the equation

$$\alpha T = D/kV_a$$

were never observed to influence the position of the peak, but only the magnitude of the current and the slope of the curve. The average of all measurements on positive ions less than 0.08 sec. old gives 1.59 cm/sec. per volt/cm for the mobility of the positive ion in air at 20° and 760 mm. Under the same conditions the mobility of the negative ion in air is found to be 2.21 cm/sec per volt/cm. These values are in good agreement with those obtained by Loeb, and by Tyndall and Grindley[9] with absolute methods. The consistency of the values obtained is shown by the following series of values given by ten consecutive runs on different samples of gas. The mobility k was found to be for the

Negative ion		*Positive ion*	
2.21	2.18	1.56	1.61
2.20	2.21	1.58	1.56
2.20	2.21	1.56	1.58
2.19	2.21	1.61	1.58
2.22	2.22	1.61	1.60

It is seen from these values that the normal ions formed by intense hard x-radiation are apparently identical with ions formed by photoelectric and radioactive methods—a result quite to be expected.

After the value of the mobility of positive and negative ions of short age had been established, experiments were carried out on ions which had been aged for increasing intervals of time. This was done in the manner described above. Mobility curves taken under these conditions yielded quite different results. A series of curves for negative ions in air is shown in Fig. 3. It is seen that as the age of the ions is increased from 0.04 to 0.9 sec. the mobility drops from 2.22 to 2.04. This decrease, as evidenced by the shift of the point of maximum rate of electrometer deflections is accompanied by a distinct broadening of the curve at its maximum. This flattening of the curve seems to indicate the presence of a range of mobilities, although the resolving power of the apparatus is not sufficient to distinguish between two close groups. Unavoidable experimental variations in the setting of the commutator caused slight changes in the slopes of the curves, but the change itself and its approximate magnitude are very apparent. A similar series of curves was observed in the case of positive ions in air. In this case the lowest value observed was 1.46 after 1.3 sec. aging. Greater ages than this could not be studied as the very slow commutator speed and decreased electrometer currents (owing to recombination and loss of ions by diffusion) made measurements uncertain.

The possibility of attributing the observed effect to some defect in the apparatus or method has been carefully considered. The effect of space charge due to the cloud of ions of opposite sign to those measured has been shown to be negligible. During the γT and δT parts of the cycle, these ions are driven away from the lower plate and remain in the volume throughout the aging period. The resultant effect of this cloud would be to draw the ions measured away from the lower plate with a consequent decrease in effective D. Hence an apparent *increase* in mobility would be observed. However, minimizing any effect of space charge by narrowing the entering beam to 3 mm gave no change in observed mobilities. Further, a delay in the charge leaking off the lower plate through the half megohm resistance would cause αT to be longer than calculated when new ions were being measured. This would result in high values for new ions and a consequent apparent decrease in the mobility of aged ions. However, the fact that the time constant of the system was only

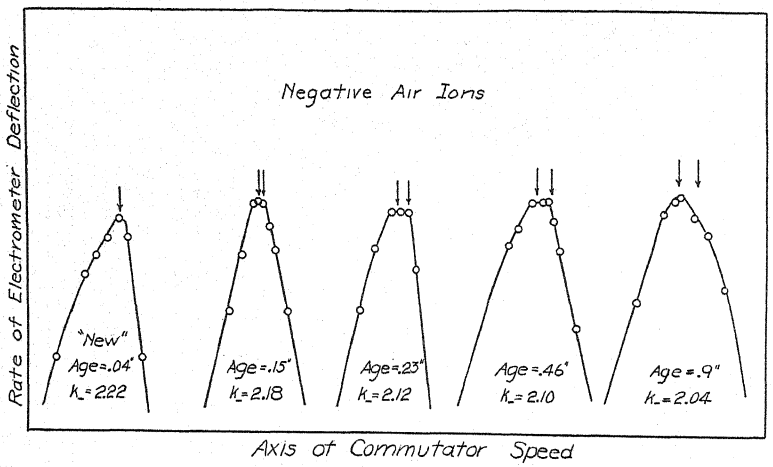

Fig. 3. Curves showing effect of aging upon negative ions in air. Right hand arrow indicates *normal* positions of peak for *new* ions. Left hand arrow indicates position of peak taken for calculation of *aged* ion mobilities.

10^{-3} seconds speaks against this possibility as does the fact that the substitution of a lower resistance did not change the values of mobility previously obtained. Furthermore, a definite gap of several degrees was left between the δT and αT phases in the case of aged ions to give the same conditions as exist in the new ion measurements.

Discussion of Results

It has been pointed out by Luhr that the only plausible explanation for the continued decrease in the value of the coefficient of recombination is one which assumes some of the ions to load up with impurities formed by the intense x-radiation. From J. J. Thomson's theory of recombination the magnitude of this increase in mass which would give the observed value for the recombination coefficient was calculated, and found to be roughly ten times

the original mass of a new ion. Such a change in ionic mass must necessarily result in a considerable increase in ionic dimensions, though the exact magnitude of this increase cannot be calculated without much more exact knowledge as to the nature of the clustering and the molecules involved. At any rate, the increase in the radius of the ion will cause a decrease in its mean free path, neglecting any effects of the charge on the ion. Moreover, this change will be more pronounced the fewer the molecules in the cluster. Now all mobility equations, with the exception of that deduced by Loeb,[10] which employs mass points as ions, contain either the mean free path directly, or a term which is closely related to it or to the ionic radius. The effect of this term in the equations is either one of proportionality or of even greater weight in the case of the rigorous Langevin equation. Hence a change in the mass of the ion which would double its radius and halve its mean free path would cause a theoretical decrease in the mobility to at least half the normal value. Yet such an increase in the radius of the ion is of the order of that predicted on recombination coefficient measurements. Such a decrease has not been observed either in these experiments, or in the less rigorous experiments of Luhr and Bradbury. It should be pointed out that, in the mobility measurements carried out by the method of Tyndall and Grindley, the majority of the positive and negative ions are not aged in each other's presence, so the selective effect of recombination in removing the smaller faster ions is not wholly operative. Hence, unless all the ions age at the same rate, a sharp effect would not be obtained. The experiments of Luhr and Bradbury, on the other hand, which employed the Rutherford alternating current method, permitted the ions to be aged together so that recombination of the faster ions could take place before the mobility measurements were made. Although this method was of insufficient resolving power to detect small changes in mobility, a change of greater than twenty percent would have been readily apparent. The negative results thus obtained, even with the advantage of selective recombination, preclude all possibility of any change in mobility with age to a degree at all comparable with that predicted by theory. Hence if the increase in ionic dimensions takes place as seems probable from recombination measurements, this discrepancy between theory and experiment in the case of ionic mobilities must point to some important and inherent defect in even the most rigorous theoretical equations which have so far been developed. The extent of the inadequacy of the mobility equations and the error in the assumptions involved will be considered in another paper.

In conclusion the author wishes to express his sincere appreciation of the interest and suggestions of Professor L. B. Loeb in the carrying out of these experiments.

[10] L. B. Loeb, Kinetic Theory of Gases, McGraw-Hill 1927, p. 468.

THE RESIDUAL IONIZATION IN AIR AT NEW HIGH PRESSURES, AND ITS RELATION TO THE COSMIC PENETRATING RADIATION[1]

By James W. Broxon
University of Colorado

(Received April 10, 1931)

Abstract

Measurements of the residual ionization in air were made with a new spherical chamber of 13.8 liters capacity at pressures up to 170 atm., at an altitude of 5400 ft. Lead and water shields were used. The slopes of the ionization-pressure curves continued to decrease at the higher pressures, becoming zero in the neighborhood of 130 to 140 atm. The ionization-pressure relation and the effects of shielding are explained on the basis of the production of ions solely by secondary radiations excited in the walls of the vessel by the cosmic penetrating radiation. The theoretical consequences of such an assumption are discussed.

MEASUREMENTS of the residual ionization in several gases contained in a large chamber at pressures up to 80 atmospheres, were made a few years ago by the writer[2] and other students[3] of Professor Swann. These experiments showed that the primary ionization due directly to any very penetrating radiation was considerably less than that which would correspond to the residual ionization at atmospheric pressure. However, the observed increases in ionization per atmosphere increase in pressure at the highest pressures were usually of the order of magnitude of the ionization at atmospheric pressure attributed by other experimenters to the cosmic penetrating radiation. Later, in 1926, Swann[4] found that the ionization at all pressures up to 68 atmospheres increased with altitude in accordance with the theory that a primary cause of the ionization consists of an ultrapenetrating radiation having its origin outside our atmosphere.

In order to investigate further the residual ionization and particularly its relation to the cosmic radiation, a new ionization chamber[5] was constructed and arrangements made for rather elaborate shielding.

Apparatus and Materials

The chamber was formed by excavating a spherical cavity 11-23/32 inches in diameter from a cylindrical, nickel-steel ingot 15-1/8 inches in diameter and 17-3/8 inches long. The volume occupied by the air under investigation was

[1] Reported at the Cleveland meeting of the American Physical Society, December, 1930.
[2] J. W. Broxon, Phys. Rev. **27**, 542 (1926).
[3] K. M. Downey, Phys. Rev. **16**, 420 (1920); **20**, 186 (1922); H. F. Fruth, Phys. Rev. **22**, 109 (1923).
[4] W. F. G. Swann, J. Frank. Inst. **209**, 151 (1930).
[5] J. W. Broxon, J.O.S.A. and R.S.I. **18**, 403 (1929).

13805 cc. The central electrode, guard system and ebonite insulation were incorporated in the form of cones in a plug which was seated upon a narrow fiber gasket. This chamber sustained a hydraulic test pressure of 5000 lbs. per sq. in. for half an hour with no indication of weakening.

The chamber was mounted approximately in the center of a wooden tank 14 ft. in diameter and 13.5 ft. high, in the basement of Macky Auditorium at the University of Colorado, Boulder, at an altitude of 5400 ft. and latitude 40°N. The chamber could be surrounded by a cylindrical lead shield 2 in. thick. This could be covered by a water-tight hood 2 ft. in diameter and 2 ft. high, and surrounded by water. The photograph, Fig. 1, shows the ionization chamber with the hood removed and part of the lead shield in position. A Brown recording thermometer bulb was inserted in a small hole drilled about 4 in. into the bomb near its base, the entire instrument being insulated carefully at the potential of the bomb. The connection with the central electrode was effected by means of a wire stretched along the axis of a 2 in. pipe.

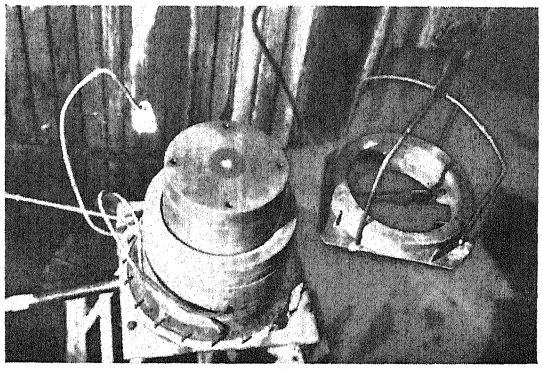

Fig. 1. Photograph of apparatus.

The air used in these measurements was dried, freed from dust, and allowed to age at least 4 weeks in each instance.

The ionization chamber was never allowed in any building which had contained radioactive supplies. Care was also taken that the shields be as free as possible from radioactive contamination. The lead shield was cast from discarded overhead telephone cable sheaths. The water used was the city tap water. The source of the Boulder city water consists entirely of surface water from the Arapahoe Glacier and snow deposited between the altitudes of 10200 and 13500 feet. This is brought down to the city through iron pipes which are nowhere imbedded to any appreciable extent. While making a survey of the radioactive waters of Colorado several years ago, Dean O. C. Lester tested the Boulder city water and was unable to detect any radioactive content. The ionization currents measured provide evidence that the ionization chamber and shields were rather unusually free from radioactive contamination.

The pressures were measured by means of an American-Schaeffer and Budenberg gauge, calibrated by the U. S. Bureau of Standards. The applied compensating potentials were measured by means of a Jewell Instrument

Company voltmeter calibrated at a few voltages by the Bureau of Standards and over the entire scale in our own standardization laboratory by means of a standard resistance and potentiometer. The induction coefficient of the auxiliary or compensating condenser was measured by a null method of mixtures, the electrometer being used as the indicator and the comparison being made with a new variable standard air condenser constructed by Günther and Tegetmeyer. Comparisons were made with six different settings of the standard condenser. The average of these gave 26.3 cm as the induction coefficient of the compensating condenser relative to the central system, a value agreeing fairly well with an approximate calculation from the dimensions of the condenser. The corresponding induction coefficient of the ionization chamber was found to be about 4.5 cm at local atmospheric pressure.

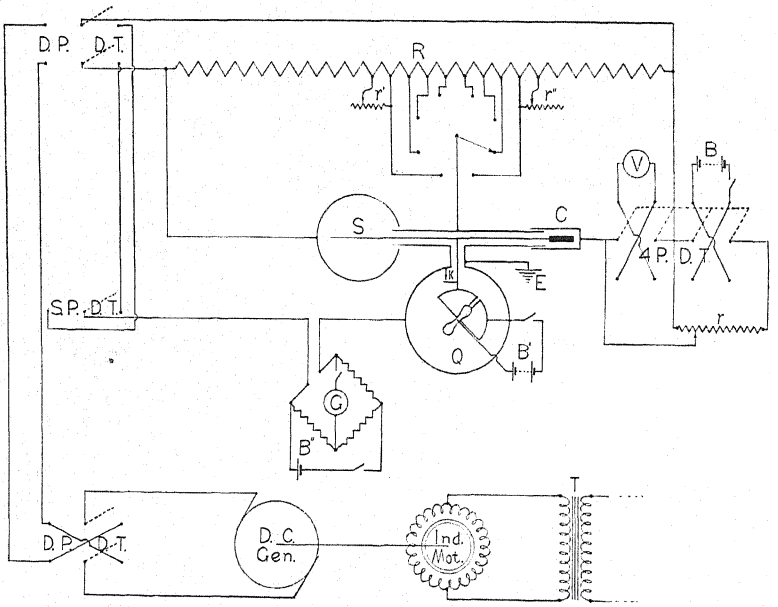

Fig. 2. Diagram of electrical arrangement.

PROCEDURE

As shown by the wiring diagram, Fig. 2, the same sort of arrangement was employed in measuring the ionization as in the former investigations. The Wheatstone bridge was incorporated for the purpose of determining the dielectric constant of the air as discussed elsewhere.[6] The method of ionization measurement has been described carefully, particularly by Swann.[4] Distinct advantages of the arrangement consist of the provision for electrical shielding, eliminating almost entirely the possibility of effects due to the solid dielectrics, and the employment of the electrometer merely as an indicator, thus eliminating effects due to possible changes in sensitivity. In the present in-

[6] Reported at the meeting mentioned in note 1. The complete report constitutes the succeeding paper of this issue.

stance, the auxiliary condenser was fixed and the compensating potential was applied to this rather than directly to the ionization chamber. Thus the rate of application of the compensating potential was directly proportional to the ionization current whereas with the other arrangement the change in the induction coefficient of the ionization chamber relative to the central system with variation in pressure of the gas must be considered.

On account of inductive effects, the detailed construction of a guard system is very important. Termini of the system used here are shown in Figs. 3 and 4

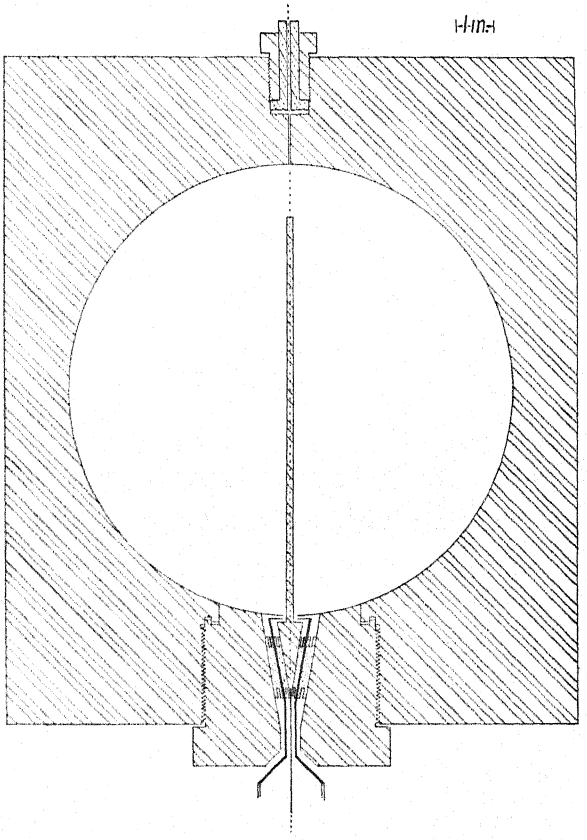

Fig. 3. Longitudinal section of ionization chamber.

which represent longitudinal sections of the ionization chamber and the auxiliary condenser, respectively, drawn approximately to scale. This system proved to be very satisfactory. Because the guard system in this case was necessarily in electrical contact with the earth, particular care had to be taken to insulate all other portions of the set-up from earth, including the sources of e.m.f.

Of course, it was exceedingly important to ascertain that saturation currents were being measured. No appreciable decrease of the ionization current could be detected when the applied P.D. was decreased about 20 percent when the largest currents were being measured at the highest pressures.

Therefore it is considered certain that saturation currents were measured throughout. It should be noted in this connection that although the high pressures necessitated low mobilities, the largest ionization currents were very small and hence practical[7] saturation was not difficult to establish.

When tests were to be made the air was admitted slowly into the ionization chamber to a maximum pressure of about 170 atmospheres. If measurements were made immediately after filling, larger values were obtained than after the establishment of equilibrium conditions. Therefore, from two to six

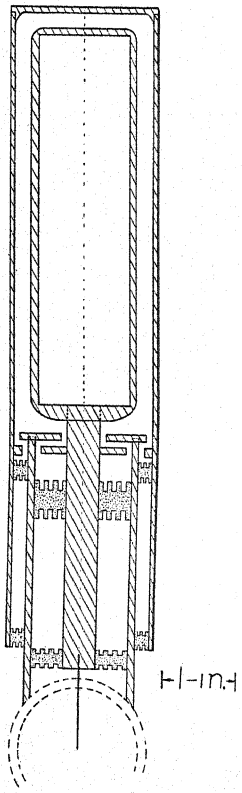

Fig. 4. Longitudinal section of compensating condenser.

hours were always allowed to elapse after filling the chamber before measurements of the ionization were begun. After three or four measurements, each over about an eight minute interval, had been taken at a given pressure, the pressure was usually decreased by three to six atmospheres at the higher pressures. Then at least half an hour was allowed to elapse before any measurements were taken at the lower pressure. Extension of this period to several hours in some instances had no effect. The gas leak was slight, although it was found necessary to remove the bomb and tighten the large plug after making two or three sets of observations.

[7] L. H. Gray, Proc. Roy. Soc. **A130,** 524 (1931); pp. 527–528.

OBSERVATIONS

The observations have been represented graphically. In Fig. 5 the ionization current in ions/cc·sec has been plotted against the total pressure in at-

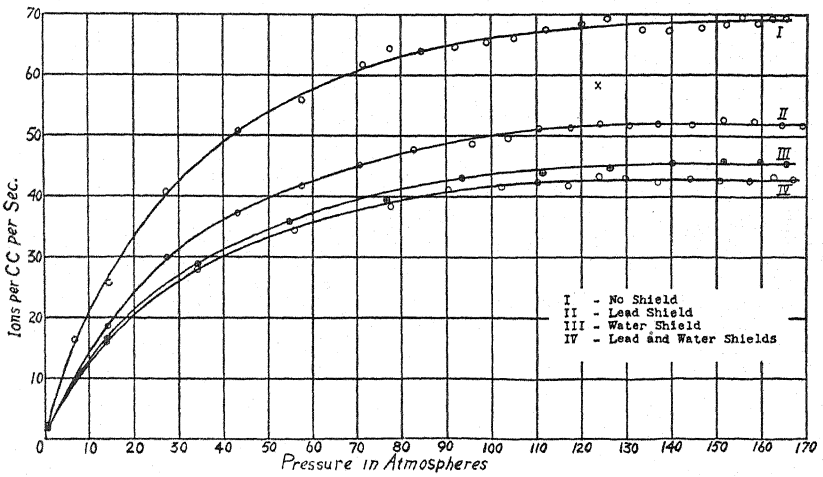

Fig. 5.

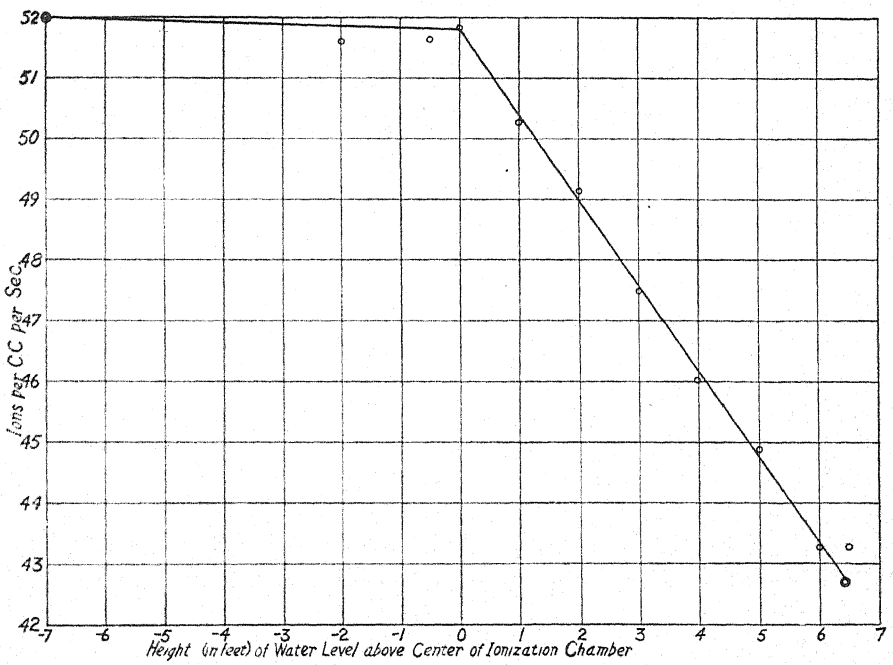

Fig. 6.

mospheres at 18°C. It may be worth mentioning in this connection that the slopes of the curves are so small in the region where the departure from Boyle's law is considerable, that if the ionization is plotted against the gas

density instead of the pressure, the curves obtained are scarcely distinguishable from those shown here. Curve I was obtained with no shielding other than that provided by the heavy steel walls of the ionization chamber, by the building, and by the atmosphere. Curve II was obtained with the chamber surrounded by the 2-in. lead shield; curve III, with no lead shield but with the tank filled with water; and curve IV, with both the lead and water shields in position. The ionization current in each instance was measured at pressures between atmospheric pressure and about 170 atmospheres. At the higher pressures observations were made at shorter intervals than in the lower pressure region previously investigated.

The data represented by the curve of Fig. 6 were obtained with the lead shield in position and with the air in the bomb maintained at pressures between 166 and 169 atmospheres. Here the ionization was again plotted along the ordinate axis, but the abscissae represent the position of the surface of the water in the tank. Depth of the water level beneath the center of the bomb is designated by negative values, and height of the water level above the center of the bomb is designated by positive values. The end points designated by two concentric circles represent data recorded in Fig. 5. The one representing no water in the tank gives the maximum ionization of curve II, while the one representing the tank filled with water gives the maximum ionization of curve IV.

Discussion

One rather striking feature of the measurements is the very low value of the ionization measured in each case at the local atmospheric pressure. These values varied from 2.26 with no shield to 1.45 ion/cc·sec with both shields, at 0.82 atm. and 18°C. The smallness of these values together with the fact that the percentage decrease in the ionization due to shielding was in each instance only slightly less at atmospheric pressure than at the highest pressures, indicated that the ionization chamber, itself, was remarkably free from radioactive contamination.

The ionization-pressure curves resemble those obtained previously, over the pressure range of the earlier observations. In particular, there is a close correspondence between curve II, Fig. 5, and the curve obtained by Swann[4] with a similar lead shield at Colorado Springs at about the same altitude. The ratio of his values to those of curve II at corresponding pressures is 1.87 at 100 lbs./sq. in., but decreases to 1.32 at 500 lbs./sq. in. and then only to 1.29 at his maximum pressure of 1000 lbs./sq. in. or about 68 atm. His larger values at low pressures are probably due mostly to a slight radioactive contamination of the older chamber, while the nearly constant ratio at the higher pressures is of about the magnitude to be expected when the increased shielding provided by the heavier walls of the bomb and the building in the present instance is considered. Obviously, a better method of comparison is one based upon the *differences* between the absolute values of the ionization observed in the two instances at corresponding pressures. Thus there is an increase of only about 1.7 ion/cc·sec in this *difference* in the pressure interval from 500 to 800

lbs./sq. in., and practically no further variation at higher pressures. At the higher pressures, then, where the effects of chance radioactive contaminations become inconsequential, the forms of the curves become identical, showing a remarkable agreement between the two independent investigations.

The most interesting portions of the ionization-pressure curves lie in the new pressure range. In every case the pressure rate of increase of ionization is seen to have continued to decrease at the higher pressures, and the slopes of the three curves obtained with the chamber shielded are zero at pressures above about 130 atm. In curve I there appears to be a possible continued slope of about 0.04 ion/cc·sec·atm. at the highest pressures, but in the other three curves the slopes at the high pressure ends certainly are not greater than 0.02 ion/cc·sec·atm. over a range of 40 atmospheres, and probably are considerably less.

It would appear, then, that the immediate cause of the ionization was a radiation which was almost entirely absorbed at a pressure of 130 atm. If the source of this radiation were in the gas itself, the ionization should have continued to increase with the pressure. If the source were outside the chamber, either it would have been absorbed entirely by the shields or it would not have been absorbed considerably by the gas. Presumably, then, the source of the ionizing radiation was in the walls of the ionization chamber.

That the primary cause of the ionization was a much more penetrating radiation is shown by the continued decrease in the ionization produced by successively greater shielding. It seems that the situation might be explained, then, by the assumption that the primary cause of the ionization in the cases of the three lower curves was a very penetrating radiation which excited in the walls of the vessel a softer radiation, perhaps recoil electrons, and that the ionization was almost entirely due to this secondary radiation. That none should be excited in the gas, itself, seems remarkable in view of the amount of air present in the chamber at the high pressures, but if any appreciable portion of the secondary radiation were to originate in the gas, surely the ionization would continue to increase with the pressure to a correspondingly appreciable extent at all the pressures.

That the source of the radiation capable of penetrating the lead shield was above the level of the chamber is shown clearly by Fig. 6. Apparently, local gamma-radiations were practically entirely absorbed with the lead shield in position, since variation of the water shield below the level of the chamber had very little effect in this case. That local γ-radiations did contribute to the ionization with the chamber unshielded, is shown by the value, 58.21 ions/cc·sec, designated by an x in Fig. 5 and measured with no lead shield but with the water tank filled to the center of the bomb.

Absorption coefficient of the primary radiation

The decreases in ionization produced by the shields were of sufficient magnitude to give fair estimates of the average absorption coefficients of the primary radiation in the materials used. As has been pointed out, the ionization recorded in the shielded curves at the high pressures may be considered

to be due entirely to the penetrating radiation. The maximum values of the ionization in curves I, II, III and IV are 69.14, 52.00, 45.43 and 42.60 ions /cc·sec, respectively. In the case of the lead shield, if we assume exponential absorption and disregard obliquity, we have for lead $\mu = [\log_e(45.43/42.60)]/5.08 = 0.0127$ cm^{-1}. Proceeding similarly in the case of water, we obtain $\mu = [\log_e(50.38/42.60)]/166 = 0.0010$ cm^{-1}. In this case, the thickness of the water shield has been taken as the 5.45 ft. depth of the top of the hood beneath the highest level of the water, and the initial intensity as that measured with the water level at the top of the hood, which would be correct if the radiation were directed entirely vertically.

In the case of the water shield we may calculate an upper limit for the absorption coefficient by assuming that the radiation approached the chamber uniformly from all directions above the horizontal. In the case represented by Fig. 6, the decrease in ionization was produced by horizontal disks of water placed above the chamber. If P is a point on the axis of a *thin* disk of thickness t and radius a, at a distance x from the disk, while the total intensity of all radiation originally approaching P through the solid angle 2π on the side next the disk is I_0, then the intensity of the radiation arriving at P after having passed through the disk is

$$I_d = I_0 \int_0^{\tan^{-1}(a/x)} e^{-\mu t \sec\theta} \sin\theta d\theta = I_0 \int_1^{(1+a^2/x^2)^{1/2}} y^{-2} e^{-\mu t y} dy.$$

The latter integrand may be expanded into a series which is uniformly convergent in the region designated. When this is integrated and terms involving powers of t higher than the first are discarded, the value obtained is

$$I_d = I_0[1 - (1 + a^2/x^2)^{-1/2} - \mu t \log_e (1 + a^2/x^2)^{1/2}].$$

Now $2\pi[1-(1+a^2/x^2)^{-1/2}]$ is the solid angle subtended by the disk at P. Therefore, $I_0[1-(1+a^2/x^2)^{-1/2}]$ is the intensity of the radiation which would have approached P through the solid angle subtended by the disk if the disk had been absent. Therefore, the decrease in intensity of the radiation arriving at P due to the presence of a disk of radius a and thickness dx at a distance x, is

$$-dI = \mu I_0 \log_e (1 + a^2/x^2)^{1/2} dx.$$

Then when the ionization chamber is so situated that its dimensions are small in comparison with both a and x, the slope of the absorption curve obtained by shielding with disks in the above manner is

$$-dI/dx = \mu I_0 \log_e (1 + a^2/x^2)^{1/2}.$$

If from Fig. 6 we take the values $I_0 = 42.6$, $-dI/dx = 9.1/196.6$, $a = 7$ and $x = 6.45$, we obtain $\mu = 0.0028$ cm^{-1}. This, of course, merely represents an upper limit for the average μ in water, just as the value first calculated represents a lower limit. Due to the absorption of the walls of the building and to the great absorption of the atmosphere in directions approaching the hori-

zontal, the penetrating radiation would be much more intense in the vertical direction providing it entered the atmosphere with uniform intensity in all directions.

The values obtained for the average absorption coefficients agree quite well with those obtained by others[8] for the cosmic radiation. It should be emphasized, however, that this investigation was not planned for the purpose of determining coefficients of absorption, and does not permit their accurate evaluation. It is chiefly because the values obtained might be expected to be of the right order of magnitude, and because they do agree with values yielded by experiments designed primarily with this end in view, that they are mentioned. The approximations show quite unequivocally that the prime ionizing agency consisted of the "cosmic penetrating radiation."

Explanation of the ionization-pressure relation

In a former paper[9] the author deduced I–P relations which would follow from various assumptions as to the origins and characteristics of the ionizing radiations. The rather complicated combination chosen to represent the experimental curves was necessitated largely by the fact that the ionization passed through a minimum as the size of the chamber was varied. As has been pointed out, it appears that the ionizing radiations in the present instance must have originated in the vessel walls. This would necessitate a continuous increase in ionization with decrease in the size of a thick-walled vessel, because of the corresponding increase of the ratio of area to volume. In view of the present measurements it is strongly suspected that the variation of ionization with size of vessel obtained in the former experiments depended partly upon a chance radioactive contamination of the outer, high-pressure chamber. In the case of the two smaller containers which were constructed at the same time under the same conditions, the ionization increased with decrease of size.

Let us now make some very simple assumptions which can only be expected to lead to a very rough approximation of the observed relation. Suppose the ionization to have been due entirely to recoil electrons generated uniformly throughout the walls of the vessel by the cosmic radiation. Suppose further that these were all emitted in directions normal to the spherical surface (an exceedingly crude assumption) and were absorbed linearly both in the vessel walls and in the gas. As a preliminary step in the investigation of the variation with pressure of the ionization which would be produced under such circumstances, let us consider a still simpler case.

If we plot the ionization per cm of path of a homogeneous beam of linearly absorbable, parallel rays against the distance from their origin, we obtain a straight line. The intercepts of this line upon the coordinate axes respectively represent the maximum or initial ionization per cm of path along the beam, and the range of the beam or the distance from the origin within

[8] V. F. Hess, "The Electrical Conductivity of the Atmosphere and Its Causes," p. 138.
[9] J. W. Broxon, Phys. Rev. **28**, 1071 (1926).

which total absorption occurs. The area of the right triangle enclosed by the straight line and the coordinate axes represents the total ionization which the beam can produce. Also, the portion of the area of this triangle which is included between the ionization/cm axis and a normal to the distance axis at any point represents the ionization produced within that distance from the origin.

Suppose, for some reason, we should want to deal with the ionization due to a precisely similar beam after it had traversed the first quarter of its range. Everything would be represented as in the previous instance by a right triangle formed between the coordinate axes and a straight line. This triangle would also have the right angle at the coordinate origin and would be similar to the first one in every respect, but corresponding dimensions would be just three-fourths as great as in the first instance. If we desired to deal with a similar beam after it had traversed the first half of its range, we should obtain a similar triangle with dimensions half as great as in the first instance. If three-fourths of the range had been traversed, the similar triangle would have dimensions only a quarter as great as the first, etc. If, then, we were to have all four of the above mentioned beams starting normally from a certain plane such as the inner surface of an ionization chamber, and ionizing simultaneously, we might represent the ensuing ionization by means of the four triangles, piling them one upon the other. If they were cut from pieces of paper and fitted upon the coordinate axes in the proper manner in the order of decreasing size, a sort of pyramid would be formed. The total volume of the the paper pyramid could then be considered to represent the total ionization produced by the four beams. Moreover, the volume included between a plane normal to the distance axis at the origin and another normal to the distance axis at any given distance from the origin would represent the ionization produced by the four beams within that distance from the surface of origin of the beams.

If the ionizing radiation in the present investigation originated throughout the walls of the ionization chamber and proceeded normally to the inner surface in the simple manner that has been postulated, it would not be homogeneous upon entering the chamber, but the corpuscular velocities would be distributed practically uniformly between zero and a maximum. In other words, we might consider that at the inner surface the beam would consist of an enormous number of similar parallel beams with the then untraversed portions of their ranges distributed uniformly between zero and a maximum for electrons just starting at the inner surface. The ionization in this case, then, could be represented by a pyramid similar to the one above, but with the steps smoothed out. Or the entire pyramid might be thought of as being compressed into the base triangle, forming a right triangular mass with a density varying directly as the distance from the hypotenuse, the line which would represent the variation with distance from the inner surface, of the ionization/cm due to a homogeneous beam of electrons originating at the inner surface. If, then, we think of a triangle endowed with mass and with a density varying in the above manner, we need only change from area to mass in order

to change from a homogeneous beam to a nonhomogeneous beam of the above type. This procedure appeals to the writer as preferable to continuing with the pyramid. The intercept, a, on the ionization/cm or y-axis may be considered to represent the ionization per cm of path due to a corpuscle of maximum velocity, and the intercept, b, on the distance axis, to represent the maximum range. The total mass of the triangle would represent the total ionization which could be produced by all the electrons entering the chamber. Also, the mass of the portion of the triangle included between the ionization/cm axis and a normal to the distance axis at any point would represent the ionization produced by the nonhomogeneous radiation within that distance from the surface of entrance of the radiation into the chamber.

In the present instance, if tertiary radiations, etc., be disregarded, the ionization recorded at any pressure would represent the ionization produced within an effective distance from the wall approximately equal to the product of the inner diameter of the chamber and the pressure, and hence approximately proportional to the pressure. Hence we may consider the pressure, P, to represent distance in the present case.

If we write the equation of the hypotenuse of the triangle in the form

$$mP - y + a = 0,$$

where $m = -a/b$, the normal distance from the hypotenuse to any point (P, y) within the triangle is equal to $(mP-y+a)/(m^2+1)^{1/2}$.

Therefore, we may express the ionization, I, at pressure P in the form

$$I = k/(m^2 + 1)^{1/2} \int_0^P dP \int_0^{mP+a} (mP - y + a)dy$$

$$= [\, ka^2/6b(a^2 + b^2)^{1/2}](3b^2P - 3bP^2 + P^3),$$

k being merely a proportionality constant.

I_m, the maximum ionization produced, is found by putting $P=b$. Hence $I_m = ka^2b^2/6(a^2+b^2)^{1/2}$,
and

$$I = I_m(3P/b - 3P^2/b^2 + P^3/b^3).$$

This equation holds, of course, only for $0 \leqq P \leqq b$. Pressures greater than b correspond to complete absorption of the ionizing radiation, and hence to a constant $I = I_m$.

In this case there is little seeking for arbitrary constants. I_m is the final maximum ionization and b is the lowest pressure at which this maximum is obtained. In curve III, for instance, $I_m = 45.43$. In this case the maximum ionization appears to occur first at about 130 atm. However, the pressure rate of increase of I at high pressures is so very small that the actual maximum range probably corresponds to a somewhat higher pressure. Taking $b = 140$ atm., the values represented by the open circles in Fig. 7 were obtained. These are rather low between 1 and 60 atm.

Arbitrarily assuming 4/5 of the final maximum ionization to be due to radiation of the above type with a maximum range corresponding to 150 atm. in the bomb, and the remaining 1/5 to be due to a similar radiation with a maximum range corresponding to 40 atm., the values represented by crosses in Fig. 7 were obtained. These fall very close to the experimental curve.

The actual situation must have been much more complicated than that postulated in the above analysis. For instance, the initial recoil electrons would not be expected to be emitted in none but radial directions, and there would probably be several consequent radiations with decreasing energy content. It is hoped that a more careful analysis with more likely assumptions may be effected in the future. However, the writer opines that these considerations show, in so far as the observed $I-P$ relation is concerned, that it is reasonable to assume the ionization to have been produced entirely by secondary radiations, perhaps recoil electrons, excited in the walls of the vessel by the primary penetrating radiation.

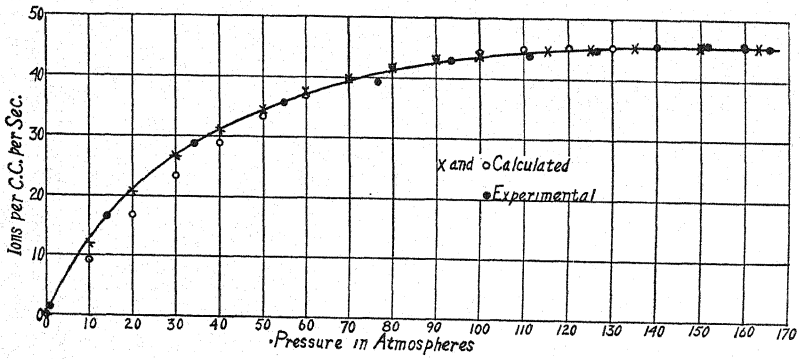

Fig. 7.

Significance of the the recoil electron assumption

If the explanation suggested above is correct and the ionizing radiation really consisted of recoil electrons, their range in the air should give some information concerning the penetrability of the primary radiation. Millikan and Cameron[10] have shown in detail how to calculate by means of Compton's[11] equations the range of the recoil electrons which would be generated by a very penetrating radiation of known coefficient of absorption. In the present instance we may proceed in precisely the reverse order.

If we consider recoil electrons of range about 140 diameters of the bomb at 18° C or 38 meters in air at N. T. P., and use the 1926 procedure of Millikan and Cameron based upon the work of Bohr and Varder, we obtain 10.94×10^6 volts for their initial energy. According to the empirical formula found by Feather[12] to hold for penetrating β-rays, the energy would be 10.09×10^6 volts. As Millikan and Cameron pointed out, at such high energies

[10] R. A. Millikan and G. H. Cameron, Phys. Rev. **28,** 851 (1926).
[11] A. H. Compton, Phys. Rev. **21,** 483 (1923).
[12] N. Feather, Phys. Rev. **35,** 1559 (1930).

the Compton theory predicts the equipartition of the energy of the incident quant between the recoil electron and the scattered quant. Thus, using the first value above, the primary radiation would have an energy-value of 21.89×10^6 electron-volts, or a wave-length of 0.00052A. Substitution of this in the Compton absorption formula gives an absorption coefficient in water of 0.0025 cm^{-1}.

The agreement of the value of μ just calculated with the experimental values is rather startling in view of the fact that the Compton theory, based upon the older quantum mechanics, is now in bad grace. Klein and Nishina[13] have calculated for the scattering coefficient, which may be regarded as the absorption coefficient for sufficiently high frequencies,

$$S = \frac{2\pi Ne^4}{m^2c^4}\left\{\frac{1+\alpha}{\alpha^2}\left[\frac{2(1+\alpha)}{1+2\alpha} - \frac{1}{\alpha}\log(1+2\alpha)\right] + \frac{1}{2\alpha}\log(1+2\alpha) - \frac{1+3\alpha}{(1+2\alpha)^2}\right\}.$$

In this formula, based on wave-mechanics, $\alpha = h\nu/mc^2$, e is the electron charge, m the electron mass, c the velocity of light, ν the frequency of the incident radiation, and N the number of "external" electrons per cc. S represents loss of energy from the incident radiation due both to the energy transferred to the scattered radiation and to the recoil electrons. It was obtained directly by multiplying the expression

$$I = I_0\frac{e^4}{2m^2c^4r^2}\frac{1+\cos^2\theta}{[1+\alpha(1-\cos\theta)]^3}\left\{1+\alpha^2\frac{(1-\cos\theta)^2}{(1+\cos^2\theta)[1+\alpha(1-\cos\theta)]}\right\}$$

for the intensity of the radiation scattered per electron at an angle θ, in terms of I_0, the intensity of the incident radiation, by ν/ν', the ratio of the frequencies of the incident and scattered radiations, and by $Nr^2d\Omega/I_0$, and integrating over the entire solid angle about a point. If we proceed in the same manner without multiplying by the term ν/ν', we obtain

$$S_s = \frac{2\pi Ne^4}{m^2c^4}\left[\frac{\log(1+2\alpha)}{2\alpha^3} + \frac{\alpha^2-\alpha-1}{\alpha^2(1+2\alpha)} + \frac{4\alpha^2+6\alpha+3}{3(1+2\alpha)^3}\right].$$

This represents loss of energy by virtue of the scattered radiation alone, and corresponds to N times Compton's[11] σ_s, or "true scattering coefficient" per electron.

The ratio $(S-S_s)/S = E/h\nu$, where E is the energy of the scattered electron, is the ratio of the mean energy per scattered electron to the energy of an incident quant. If we take $E = 11\times10^6$ electron-volts, we find the last equation is approximately satisfied by $\lambda = 0.000892$A. With this value of the wave-length of the incident radiation we obtain $S = 0.020$ cm^{-1} for water, and $E/h\nu = 0.8$. Thus, according to the Klein-Nishina theory, the energy at very

[13] O. Klein and Y. Nishina, Zeits. f. Physik **52**, 853 (1929).

high frequencies is not distributed equally between the scattered quant and the recoil electron, but most of it is absorbed by the latter, the recoil electron in the present instance absorbing 4/5 of the energy of the incident quant. Using the supposedly observed range of the recoil electrons, we have calculated by the Klein-Nishina theory an absorption coefficient for the primary penetrating radiation which is one order of magnitude higher than that calculated by the Compton theory and found experimentally.

An absorption coefficient of 0.0024 cm^{-1} of water corresponds, according to the Klein-Nishina formula, to a primary wave-length of about 0.00006A. Substitution of this in the above expression for $E/h\nu$ gives 1.8×10^8 electron-volts for the energy of the recoil electrons. If we consider the range of an electron of high energy content to be proportional to its energy, the range to be expected according to this theory is about $38\times180/11=622$ meters in air at N. T. P., some 16 times that assumed to have been measured in this investigation.

The two theories of scattering agree very well in the x-ray region, but differ greatly at very much higher frequencies, as shown above. The Klein-Nishina theory has recently been found by several investigators[14] to agree much better with observations in the region of very penetrating γ-rays than does the Compton theory. This would indicate that the final, constant maximum ionizations observed in the present investigation do not correspond to complete absorption of the recoil electrons. If, on this basis, the suggested explanation in terms of some sort of secondary radiation from the walls of the vessel is considered entirely untenable, then it seems to the writer that the true explanation must depend upon some characteristics of gaseous ionization at high pressures or of absorption in that region, which are not known.

In this connection it may be mentioned that Skobelzyn[15] has observed by the Wilson cloud method paths which he considers to have been due to recoil electrons excited by the cosmic radiation, and whose energy he has estimated from the curvature of the path in a magnetic field, to have been about 15×10^6 volts at the beginning of the observed portion of the path. He points out that this value was to be expected on the basis of the older theory but is inclined to discard it in favor of the newer, and suggests the possibility of the corpuscles originating outside the expansion chamber, or of the mechanism of absorption of energy in the region of such high frequencies being of a different sort from that ordinarily postulated in Compton scattering, perhaps with the ejection of H particles from the nuclei. (Note also the suggestion of nuclear absorption in the papers of reference 14.) "In diesem Zusammenhang könnte man auch an die Möglichkeit, dass die H-Strahlen mit der Energie von dem Betrage der "Ultra-γ-Energie" erzeugt werden können, denken. Diese H-Strahlen würden die Geschwindigkeit von der Ordnung 1,5 bis 2.10^{10}

[14] C. Y. Chao, Nat. Acad. Sci. Proc. **16**, 431 (1930); Phys. Rev. **36**, 1519 (1930). G. T. P. Tarrant, Proc. Roy. Soc. **128**, 345 (1930). D. Skobelzyn, Zeits. f. Physik **65**, 773 (1930). L. Meitner u. H. H. Hupfeld, Zeits. f. Physik **67**, 147 (1931).

[15] D. Skobelzyn, Zeits. f. Physik **54**, 686 (1929).

haben." Taking the lower of the values suggested and Rutherford's[16] value of 3.07×10^9 cm/sec for the initial velocity of an H atom of range 28 cm in air, and assuming the ranges proportional to the cubes of the velocities, we have $R=0.28(15/3.07)^3=33$ meters in air, a value comparable to the range of the secondary radiation discussed in this paper. Of course, the "Ultra-γ-Energie" has been calculated on the basis of absorption measurements and the assumption of electron scattering, so that it is questionable as to what weight may be given the suggestion. If one might suppose that such positive corpuscular radiations could produce considerably more ionization than the recoil electrons in the present instance, however, there would be a possibility of using the notion in explaining the observed variation of ionization with pressure.

Possibly it is worth while pointing out that in so far as the present investigation indicates the very considerable importance of secondary radiations excited by the cosmic radiation and suggests by virtue of their relatively low penetrating power that they are corpuscular in nature, the penetrating corpuscular radiations detected by some investigators[17] may be suspected of being secondary in nature.

It would appear to be a rather conservative conclusion, on the basis of the experiments herein presented, that the ionization in a closed vessel which is properly attributable to the penetrating radiation depends to a considerable extent upon the vessel and other circumstances. Such dependence does not seem to have been taken into account, for instance, by Hulburt[18] in calculating the contribution of the cosmic penetrating radiation to the ionization of the free atmosphere at various altitudes. He takes as the value at sea-level, 1.4 ion/cc sec which was the value measured by Millikan in two different electroscopes. But in the case represented by curve II, with a 2-in. lead shield at an altitude of 5400 ft., only 52 pairs of ions were actually produced in 1 sec in a region which was occupied by a quantity of air which would occupy about 159 cc at N. T. P. Presumably, this ionization was due partially to energy absorbed from the penetrating radiation by the walls of the vessel as well as by the air itself. It would seem, then, that the ionization produced by the cosmic radiation in the atmosphere, if free from dust or other suspended particles, would be considerably less than that calculated on the basis of 1.4 ion/cc·sec at sea-level. This situation has been emphasized by Swann[19] on the basis of the earlier ionization-pressure experiments. To quote: "Thus, the actual ionization in the vessel, due to primary and secondary emission from the gas, will be less at one atmosphere than at any higher pressure. If then, the ionization-pressure curve should show a very small increase of ionization per atmosphere increase at high pressures, we know from the above that such increase per atmosphere is nevertheless greater than the portion

[16] E. Rutherford, Phil. Mag. **37**, 537 (1919).

[17] W. Bothe u. W. Kolhörster, Zeits. f. Physik **56**, 751 (1929). B. Rossi, Accad. Lincei, Atti **11**, 478 (1930). L. F. Curtiss, Phys. Rev. **34**, 1391 (1929).

[18] E. O. Hulburt, Phys. Rev. **37**, 1 (1931).

[19] W. F. G. Swann, Bull. Nat. Research Council **3**, part 2, 65 (1922).

of the ionization due to primary and secondary action in the gas within the vessel at one atmosphere. We may infer that any greater ionization found at atmospheric pressure is to be attributed to radiation from the walls of the vessel; this radiation, owing to its absorption at the higher pressures, results in a diminishing rate of increase of ionization with pressure. . . . If one were to accept this parallelism without reservation, he would be forced to conclude that the portion of the ionization within the vessel which was attributable to the direct or indirect action of the (penetrating) radiation on the gas was immeasurably small."

Naturally, if one ionization chamber is used by each observer throughout his investigations, values of the absorption coefficient of the penetrating radiation measured by different observers should agree fairly well, as they do.[8] However, the estimates of the intensity of the radiation based upon ionization measurements would be expected to differ and such agreement as exists probably depends upon the fact that no vast differences have existed among the experimental conditions. The writer is inclined to believe that differences in the effects of secondary radiations may in some instances play even a more important part than the "zeros of their instruments"[20] in explaining the lack of agreement among different experimenters as to the intensity of the primary cosmic radiation.

Dependence upon time

The question of the variation with time of the natural ionization in gases has been a matter of investigation for a good many years, with a great deal of resultant disagreement. Very recently a diurnal variation in the ionization produced by the cosmic radiation has been observed by Millikan[21] and by Hess.[22] They both agree that this ionization is somewhat greater during the day than during the night, an indication of which was formerly observed by the writer.[2]

Hess explains the variation on the basis of penetrating radiation originating in the sun, while Millikan considers it to be due to variations in atmospheric absorption, and shows a correlation with variations of atmospheric pressure. Whatever the explanation, it has probably occurred to the reader that this effect might serve to explain the constancy of the ionization observed in this investigation at the very high pressures. If the ionization at the highest pressure were observed when the intensity of the cosmic radiation happened to be at a minimum and if the ionization at successively lower pressures were measured with an increasing radiation intensity, a high-pressure slope which might have existed could the measurements at different pressures have been made simultaneously, could conceivably have been compensated. However, this was not the case. Millikan[21] found the intensity of the cosmic radiation to pass through a maximum in the late afternoon and a

[20] R. A. Millikan and G. H. Cameron, Nature **121,** 19 (1928).
[21] R. A. Millikan, Phys. Rev. **36,** 1595 (1930).
[22] V. F. Hess, Nature **127,** 10 (1931).

minimum at night or in the early morning. In the cases of curves I–IV, the observations at the highest pressures were begun in the respective instances at 5:31 P.M. Apr. 26, 4:14 P.M. May 24, 6:00 P.M. July 19, and 3:23 P.M. June 21, 1930. In the cases of curves I, II and IV the low pressure ends of the practically horizontal portions of the curves at about 130 atm., were reached at about 2:00 A.M. of the following days, and in the case of curve III, at midnight. Atmospheric pressure was usually reached by the evening of the second day.

The observed constancy of the ionization at the high pressures might therefore be considered to constitute evidence against variations of the type mentioned. This need not follow when it is considered that we have here only three instances of extreme constancy. In particular, during the period of the observations for curve II a sensitive barograph was kept in the room with the other apparatus where the temperature was very uniform, and no fluctuations of more than 1 mm occurred during the entire period. The barometric pressure was not observed in the other instances except in connection with the readings at atmospheric pressure, whence a similar constancy may have happened to exist. However, the observed constancy of ionization, in connection with the way the end points fit into the curve of Fig. 6, otherwise observed Aug. 16–17, tends to provide interest in a careful investigation of the variation with time of the ionization in the vessel at the very high pressures.

In conclusion, the writer desires to express his sincere appreciation of assistance received from several sources. Funds in aid of this research were provided by the American Association for the Advancement of Science. The Mountain States Telephone and Telegraph Co. on behalf of the Bell System provided some two tons of lead. The staffs of the several Engineering Departments of the University rendered very generous assistance; in particular, Professor S. L. Simmering and Mr. C. A. Wagner of the Department of Mechanical Engineering compressed all the air used in this investigation. Assistance in recording observations was given by Professor G. B. Williston and by Messrs. Louis Strait, J. M. Porter, Sydney Hacker and Ralph Warren. The photograph was taken by Mr. R. A. Merrill. Professor Swann has read and criticized the paper.

THE DIELECTRIC CONSTANT OF AIR AT HIGH PRESSURES[1]

By James W. Broxon
University of Colorado

(Received April 10, 1931)

Abstract

The dielectric constant of aged, dry, dust-free air was measured at pressures up to 170 atmospheres by an electrometric method. It was found to increase linearly with the pressure.

FREQUENTLY quoted values of the dielectric constant of air at high pressures are those obtained by Tangl,[2] in 1908, at pressures up to 100 atmospheres. In 1913, Occhialini and Bodareu[3] made measurements up to 334 atmospheres. In both these investigations, the Clausius-Mossotti relation was found to hold. Both Tangl[4] and Occhialini[5] had announced in earlier papers, however, that the Clausius-Mossotti relation did not hold.

More recent measurements of dielectric constants have been made largely by means of modern high-frequency methods. These have been criticized by Cagniard[6] who has drawn attention to the very large variations among the values of the dielectric constant of air at atmospheric pressure obtained by these methods by various observers, and has contrasted them with the better agreement among values obtained by the older methods.

Very recent investigations by Keyes and Kirkwood[7] of the dielectric constants of carbon dioxide and ammonia have given interesting information concerning their variations over large ranges of density, and the considerable deviations from the Clausius-Mossotti relation.

In the present paper are presented measurements of the dielectric constant of dry air between pressures of 0.821 and 169.4 atmospheres at 18°C, made by a method closely resembling that of Occhialini and Bodareu.[3]

Procedure

In connection with recent measurements of the residual ionization[8] in air at high pressures, the mere addition of a Wheatstone bridge to the equipment otherwise required, and the measurement of two resistances, yielded the values of the dielectric constant of the gas at the various pressures at which observations of the ionization were made. The reader should refer to the

[1] Reported at the Cleveland meeting of the American Physical Society, December, 1930.
[2] Tangl, Ann. d. Physik **26**, 59 (1908).
[3] Occhialini and Bodareu, Ann. d. Physik **42** (1913).
[4] Tangl, Ann. d. Physik **23**, 559 (1907).
[5] Occhialini, Phys. Zeits. **6**, 669 (1905).
[6] Cagniard, Ann. d. Physique **9–10**, 460 (1928).
[7] Keyes and Kirkwood, Phys. Rev. **36**, 754 (1930); Phys. Rev. **36**, 1570 (1930).

preceding paper[8] on the residual ionization for details regarding apparatus, conditions of experimentation and procedure which it is considered unnecessary to repeat here.

The wiring diagram is given in Fig. 2 of the preceding paper. The applied potential difference was impressed across the high resistance system, R, r', r'', and leads run from this to the ionization chamber S (see also Fig. 3 of preceding paper), the guard system, and the exterior cylinder of the auxiliary condenser C (also see Fig. 4 of preceding paper), in order to eliminate effects of fluctuations of the applied P.D. At each pressure, before observations of the ionization current were begun, the apparatus was "balanced" by adjusting the resistance contacts until no deflection of the quadrant electrometer occurred when the large P.D. was suddenly applied or withdrawn from the high resistance system. Due to the rather large residual ionization currents at the high pressures, an accurate balance could be obtained at these pressures only by adjusting the resistances so that sudden removal of the impressed P.D. caused no permanent variation in the small deflection which existed at the instant of removal.

If we designate by V_s and V_c the absolute values of the potential differences between the guard system and the outer conductors of the ionization chamber and the auxiliary condenser, respectively, and by q_{21} and q_{31} the corresponding induction coefficients of these relative to the central system, then we have under the above conditions of balance,

$$q_{21}V_s = q_{31}V_c.$$

This relation is readily established by the following considerations. Let V_1, V_2, V_3, V_4 and V_5 be the respective potentials of the central system, the ionization chamber, the outer cylinder of C, the guard system, and the needle. Let q_{11}, q_{21}, q_{31}, q_{41} and q_{51} be the corresponding induction coefficients of these relative to the central system. Then the charge on the insulated central system may be expressed by

$$Q_1 = q_{11}V_1 + q_{21}V_2 + q_{31}V_3 + q_{41}V_4 + q_{51}V_5.$$

Suppose, for convenience, we consider the potential of the guard system to be the arbitrary zero. Then when the P.D. across R is suddenly removed Q_1, V_4 and V_5 individually remain constant, and in order that V_1 may remain constant while V_2 and V_3 are each reduced to zero, we must have

$$q_{21}V_2 + q_{31}V_3 = 0$$

or

$$q_{21}/q_{31} = -V_3/V_2 = V_c/V_s.$$

Now we may put

$$V_c/V_s = R_c/R_s,$$

where R_c and R_s, respectively, represent the resistances at balance between

[8] Broxon, Phys. Rev. **37**, 1320 (1931). Preceding paper in this issue.

the auxiliary condenser and the guard system and between the ionization chamber and the guard system, across which, in series, the total P.D. of about 1050 volts was applied. Substituting, we have

$$q_{21} = q_{31}(R_c/R_s).$$

The auxiliary condenser, C, being fixed and always at atmospheric pressure, q_{31} remained constant.

If, now, the ratio R_c/R_s be plotted against the total pressure in the ionization chamber, the intercept of this curve upon the ratio axis represents $1/q_{31}$ of the value of q_{21} with the ionization chamber entirely evacuated, while other points on the curve represent $1/q_{31}$ of the values of q_{21} at the corresponding pressures. Hence the value of R_c/R_s at any pressure, when divided by the intercept value, gives the dielectric constant of the gas in the chamber at that pressure, referred to $K=1$ in vacuo.

OBSERVATIONS

The curve of Fig. 1 was obtained in the above manner. The circles represent observations made with the ionization chamber unshielded and the crosses represent values obtained four weeks later with the lead shield in

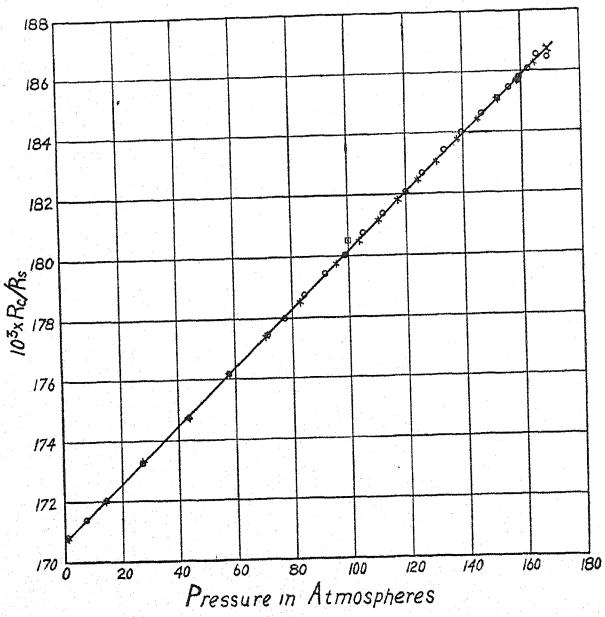

Fig. 1.

position. The two sets of readings give values of R_c/R_s at some 35 distinctly different pressures distributed well over the range. It is seen that both sets of points fall remarkably close to a straight line. Inasmuch as the curve remains straight over a range of nearly 170 atmospheres, and further, since Wolf[9] has

[9] Wolf, Phys. Zeits. **27**, 588 (1926).

found that the dielectric constants of the chief constituent gases of air vary linearly with the pressure to small fractions of an atmosphere, it was considered justifiable to extrapolate by continuing the straight line to zero pressure. Division of the ordinates of the curve by the intercept so obtained, shows that the dielectric constant of air increases uniformly by 555×10^{-6} for each atmosphere increase in pressure at 18°C.

Discussion

If $(K-1)/P=$const., then insomuch as σ, the density of the air, varies from proportionality with P, $(K-1)/\sigma$ can not be constant. Also, the Clausius-Mossotti relation

$$(K-1)/\sigma(K+2) = \text{const.}$$

can not be true.

The present investigation, then, confirms the constancy of the first ratio, and denies the constancy of either of the latter ratios, unless the variations in either of these lie within the limits of the experimental error.

This latter possibility deserves careful consideration. According to the Landolt-Börnstein tables (1923), Amagat found the values of PV and hence P/σ for air at 16°C to pass through a minimum in the neighborhood of 80 atmospheres, increasing at higher pressures and reaching atmospheric value at about the upper pressure limit of the present measurements. Using these values and the observed values for K at 18°C, the values of $(K-1)/\sigma$ are found to pass through a corresponding minimum about 2 percent less than the value at atmospheric pressure. $(K-1)/\sigma(K+2)$ is similarly found to pass through a minimum at about 90 atm., which is about 3.7 percent less than the value at atm. pressure.

Accuracy of the measurements

The resistances were measured by means of a Leeds and Northrup portable bridge. Individual resistances of this bridge have a guaranteed accuracy of only 0.1 percent. However, an investigation of the particular coils used in this instance showed the error to be only about 0.01 percent in the resistances measured, apart from inaccuracies in the bridge ratio-resistances, and these latter inaccuracies as well as errors due to temperature variations, cancelled in the ratio R_c/R_s. The error in a particular value of R_c/R_s, then, was probably about 0.02 percent. Since the same coil was used throughout for the first significant figure of R_c, a similar situation holding for R_s, the fractional error in R_c/R_s was in the same direction and of the same order of magnitude throughout, whence the fractional error in $(R_c/R_s)/(R_c/R_s)^0$ may be expected to be of one smaller order of magnitude than the error in a single ratio. Hence the error in K may be estimated to be of the order of 0.002 percent, or an error of less than 1 percent of $(K-1)$ at all pressures above 4 atmospheres. Since the curve was not unduly weighted by the readings at atmospheric pressure, we may therefore expect an error of less than 1 percent in $(K-1)$ throughout the range.

In the above, it is assumed that other conditions were ideal. It was not necessary that the resistivity of the materials constituting the measured resistances remain constant during a series of observations, but it was essential that no change of this type should occur between the time of "balance" and the time when the resistances were measured. No appreciable error could have occurred on this account. R consisted of about 102,000 ohms formed by winding coils of silk-covered high resistance wire of low temperature coefficient, in single layers over thin paraffined paper upon 108 long vertical brass tubes submerged in kerosene. r' and r'' consisted of two large, open tubular slide-wire rheostats, each of about 3000 ohms resistance, shunted across two or three of the thousand-ohm coils of R, one on each side of the earthed point. The maximum current through any of these was of the order of 0.01 ampere. No appreciable heating occurred, and certainly no sudden changes in temperature were possible. The measured values were found in no instance to vary with the time interval between balance and the resistance measurement.

Lead resistances were negligible. The largest ionization currents in parallel with the current in R_s were only of the order of 3×10^{-13} amp. The sensitivity of the electrometer as an indicator of the condition of "balance," with the P.D. employed, was sufficient to detect changes in the resistance ratio which could not be measured with the bridge. Constancy of the applied P.D. was not required.

Errors in the corrected pressure gauge readings were probably of the order of 0.1 percent at the upper end of the scale. The atmospheric pressure could be determined with this accuracy, of course. With the temperature measuring device employed, and with the precautions taken to ensure equilibrium conditions, it is believed that the temperature of the air did not vary by 0.5°C from the recorded temperature in any instance. Moreover, the total variations in temperature were very small. In the first set of readings the temperature varied from 18.3°C to 16.85°C, and in the second set from 18.0°C to 17.0°C over the whole range with the exception of the reading at atmospheric pressure which was made at a temperature of 16.8°C. In view of the small variations in temperature, reductions of pressures to equivalent pressures at 18°C were made on the basis of the proportionality between P and the absolute temperature.

The constancy of q_{31} may be appreciated when it is mentioned that the air in C was always at atmospheric pressure, and that during the second set of observations the atm. pressure did not vary by more than 1 mm of Hg.

From the dimensions, form and material of the ionization chamber and of the central electrode, it appears that no appreciable errors could have resulted from their deformations at the high pressures. Considerations of various conditions, particularly of the agreement between the two independent sets of readings, lead the writer to believe that no appreciable disturbance was caused by deformations of the ebonite insulators.

Perhaps the most outstanding advantage of this method of measurement is that it permits the use of a guard system which, when properly designed, effectively excludes the influence of the solid insulators due to their dielectric

properties, surface charges, etc. The necessary presence of solid insulators constitutes a perpetual hazard in other methods of measurement.

In view of the above considerations it would seem that apart from personal errors, an estimated error of 1 percent in the values of $(K-1)$ and their pressure variations would not represent too optimistic an attitude, and that the investigation ought to be capable of testing the accuracy of the Clausius-Mossotti relation. As a further test of this conclusion, it was thought worthwhile to calculate the value of R_c/R_s which would have been required at 100 atm. in association with the intercept value herein used, in order to provide the same value of the Clausius-Mossotti function at that pressure as at atmospheric pressure. This value is designated by the small square in Fig. 1, and is seen to be decidedly farther from the curve than any but the first of the individual readings taken.

Comparison with other investigations

As mentioned above, there is a lack of agreement with the conclusions of Tangl[2] and of Occhialini and Bodareu[3] in that they found the Clausius-Mossotti relation to hold for air at high pressures. In earlier investigations both Tangl[4] and Occhialini[5] had concluded that the $C-M$ function decreased as the pressure increased, in general agreement with the present investigation. In this earlier paper Tangl concluded that $(K-1)$ varied directly with the density. In his 1908 paper, although Tangl concluded that the $C-M$ function was constant, the function actually decreased slightly, according to the tabulated values, with increasing pressure in the case of each of the gases investigated, hydrogen, nitrogen and air.

$(K-1)/\sigma$ and $(K-1)/P$ both decreased with increasing pressure in the case of hydrogen, and increased with increasing pressure in the cases of nitrogen and air. In the case of air, the decrease in $(K-1)/\sigma(K+2)$ between one and 100 atmospheres amounted to nearly 1.5 percent of its value at atmospheric pressure, about 1 percent less than the corresponding increase in $(K-1)/P$.

In the region between 64 and 334 atmospheres, Occhialini and Bodareu found $(K-1)/P$ to decrease about 10 percent, $(K-1)/\sigma$ to increase about 4 percent, and $(K-1)/\sigma(K+2)$ to show no unidirectional tendency, the fluctuations amounting only to about 1 percent.

In connection with the increase in the $C-M$ function observed in the present investigation at pressures above 90 atm., it is interesting to note that Keyes and Kirkwood[7] found the function to increase in the case of carbon dioxide at high densities, approaching a constant value in the liquid state.

The value of K for air at atmospheric pressure is of special interest. Tangl's 1908 value for K at 1 atm. and 19°C is 1.000536. If this be reduced to 1 atm. and 0°C on the basis of the constancy of $(K-1)/P$ and of P/T in this interval, the value obtained is 1.000573. On the same basis, the values obtained in the present investigation are 1.000555 at 18°C and 1.000592 at 0°C. The corresponding value obtained by Occhialini and Bodareu on the basis of the constancy of the $C-M$ function is 1.000585. On the basis of sepa-

rate investigations some values obtained by other experimenters for air at N. T. P. are: Boltzmann (1875), 1.000590; Klemenčič (1885), 1.000586; Waibel[10] (1923), 1.000584; Carman and Hubbard[11] (1927), 1.000594. Cagniard[6] lists several others.

To explain the differences between the conclusions of the present investigation and others cited does not appear to be a simple matter. It is perhaps significant that Tangl could not have eliminated entirely the effects of solid insulation in the compression condenser. Also, his results depended upon variations in the capacity of a movable plate condenser. In the investigation by Occhialini and Bodareu, extreme constancy of the e.m.f.'s of the batteries they employed was necessary. The relatively low potential differences they used would produce a smaller sensitivity than in the present instance, with the same electrometer sensitivity. In the present investigation, greater accuracy could have been secured by having q_{21} and q_{31} more nearly equal, and by the employment of a more accurate bridge. Some difference between these observations and those of Tangl might be attributed to the fact that he removed both the water vapor and the carbon dioxide, whereas in this investigation only the water vapor was removed, together with possible dust particles.

A feature of some interest consists of the very small residual ionization of the compressed air used in this investigation, probably much less than in any other, and the fact that this ionization was determined at each pressure at which measurements were made.

[10] Waibel, Ann. d. Physik **72**, 161 (1923).
[11] Carman and Hubbard, Phys. Rev. **29**, 299 (1927).

THE VARIATION OF THE SPECIFIC HEATS (C_p) OF OXYGEN, NITROGEN AND HYDROGEN WITH PRESSURE

By E. J. Workman*
Bartol Research Foundation of the Franklin Institute

(Received April 6, 1931)

Abstract

The specific heats, C_p of oxygen at 26° and 60°C, nitrogen at 26° and 60°C and hydrogen at 50°C have been measured as a function of pressure over the pressure range 10 to 130 kg/cm². A continuous flow method is used, by which the ratio of C_p at a pressure p to $(C_p)_0$ of the same gas at a pressure of one atmosphere is measured. The theory of the method shows that the experimental results are practically independent of the usual errors arising from heat leakage and the Joule-Thomson effect. Complete experimental curves as well as tabulated values are shown for $C_p/(C_p)_0$ as a function of pressure. Details of construction and use of the apparatus are given.

IN A previous paper[1] the author has described an experimental method for determining the variation of the specific heat C_p of a gas with pressure. A method of continuous flow calorimetry was used whereby the ratio of C_p at a pressure p to $(C_p)_0$ at a pressure of one atmosphere was measured. The present paper presents values of this ratio obtained by the use of improved apparatus over the pressure range of 10 to 130 kg/cm², for oxygen at 26° and 60°C, nitrogen at 26° and 60°C and hydrogen at 50°C.

I. Theory of the Method.

A schematic representation of the new apparatus is given in Fig. 1. A gas at a high pressure enters a temperature-controlled bath at a where it comes to a fixed temperature. From the bath the gas in conducted through a *heat interchanger* and then to a *pressure reduction valve* where the pressure is reduced to approximately one atmosphere. At the low pressure the gas passes through a second bath, (different in temperature by 10° from the first) and again passes through the *heat interchanger* and escapes. In the interchanger the two gas streams are in such intimate thermal contact that they emerge at approximately the same temperature. The temperature of each gas stream is measured just before it enters and leaves the interchanger at T_1, T_2, T_3 and T_4 where $T_2-T_1=\Delta t$ and $T_4-T_3=\Delta t_0$ are the temperature changes in the high and low pressure streams respectively.

After passing through the region where the interchange of heat takes place both gas streams are thermally connected to some conducting *base* (*for wall*) on which is mounted a conducting surface (*interchanger wall*) which encloses the entire *interchanger* including some length of the gas conduits with their respective radiation-convection shields S_1, S_2, S_3 and S_4. With this construction it is possible to regulate the temperature of the heavy copper

* National Research Fellow.

[1] E. J. Workman, Phys. Rev. **36**, 1083 (1930).

heater guard in such a way that the *interchanger wall* will be an isothermal enclosure equal in temperature to the *heater guard*. The conduits leading to and from the interchanger are of low thermal conductivity and arranged with the view of minimizing the net heat leakage through the wall of the interchanger.

If we assume that a steady state of gas flow and temperature distribution has been attained, we see that there is an interchange of heat between the two gas streams, and that a simple relation exists between C_p for each gas stream and the four measured temperatures indicated above. The resistance

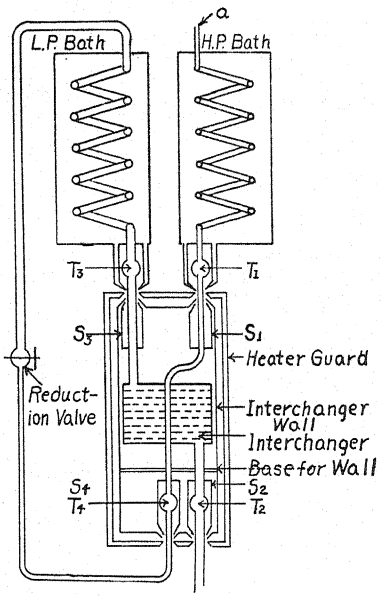

Fig. 1. Schematic diagram of apparatus.

to the flow of gas between the points where their temperatures are measured will give rise to a small Joule-Thomson temperature change in each stream. Let us indicate these temperature changes by $\mu\Delta p$ and $\mu_0\Delta p_0$ in the high and low pressure lines respectively. Also let q be a net amount of heat per gram of gas gained through leakage by the two gas streams. Since the pressure and temperature differences over each gas stream in the interchanger are small we can now write

$$q = \bar{C}_p[\Delta t + \mu\Delta p] - (\bar{C}_p)_0[\Delta t_0 + \mu_0\Delta p_0] \tag{1}$$

where C_p and $(C_p)_0$ are average values over the temperature intervals indicated by Δt and Δt_0 respectively. Solving (1) for $\bar{C}_p/(\bar{C}_p)_0$ we have

$$\frac{\bar{C}_p}{(\bar{C}_p)_0} = -\frac{\Delta t + \mu_0\Delta p_0 - q/(\bar{C}_p)_0}{\Delta t + \mu\Delta p}. \tag{2}$$

Expanding the right hand number of Eq. (2) we have

$$\frac{\bar{C}_p}{(\bar{C}_p)_0} = -\frac{\Delta t_0}{\Delta t} - \phi \tag{3}$$

where ϕ is a correction term, given by the relation

$$\phi = \left[\frac{\mu\Delta p\Delta t_0}{\Delta t} - \mu_0\Delta p_0 - \frac{q}{(\bar{C}_p)_0}\right]\left[\frac{1}{\Delta t} - \frac{\mu\Delta p}{\Delta t^2} \cdots\right] \tag{4}$$

With the usual methods of flow calorimetry it is difficult to deal with correction terms of the type of ϕ in Eq. (3). It seems therefore that perhaps the greatest virtue of the method, outlined above, rests on the fact that it is possible to eliminate, almost completely, errors of this kind by interchanging the bath temperatures and taking the mean value of the two results thus obtained. If a set of temperature readings be taken when, for example $T_1 = 45°C$ and $T_3 = 55°$ and a similar set taken for the reverse arrangement $T_1 = 55°$ and $T_3 = 45°$ we see, when applying these readings toward the determination of $\overline{C}_p/(\overline{C}_p)_0$ in Eq. (3) that the correction term is changed in sign but not appreciably in value in going from one arrangement to the other. This result is apparent from Eq. (4) if we bear in mind the fact that $\mu\Delta p$ does not differ greatly from $\mu_0\Delta p_0$ and that they are both small in comparison to the measured temperature intervals. Furthermore q is small in comparison to the amount of heat available for transfer between the two gas streams in passing through the interchanger and is approximately the same in each arrangement of bath temperatures. The fact that in either case, T_2 and T_4 do not differ much from the mean of T_1 and T_3 justifies the assumption that the factors which determine the magnitude of q will be about the same in these two experiments.

These arguments indicate that it is possible to conduct a set of experiments whereby a value of $\overline{C}_p/(\overline{C}_p)_0$ is obtained which, to a very high degree of approximation will be independent of the Joule-Thomson effect and small heat leakages of the type q. Moreover, if we assume that the values of the specific heats here involved have a linear variation with temperature over the small range T_1 to T_3, we see that $\overline{C}_p/(\overline{C}_p)_0$ becomes simply the value of $C_p/(C_p)_0$ at the mean temperature $(T_1+T_2)/2$.

Results

With apparatus designed with the aim of meeting the requirements set forth in the foregoing paragraphs, values for $C_p/(C_p)_0$ have been determined for oxygen at 26° and 60°C, nitrogen at 26° and 60°C and hydrogen at 50°C over the pressure range of 10 to 130 kg/cm². In all cases the temperature difference in the two gas streams as they enter the interchanger $(T_1 - T_3)$ has been $\pm 10°C$.

The results of the measurements are shown graphically in Fig. 2 where $(T_4 - T_3)/(T_1 - T_2)$ are plotted as ordinates against the pressure in kg/cm² as abscissae. In all these cases the upper curves are obtained when the bath temperatures are arranged such that $T_1 < T_3$ i.e. when the high pressure gas is warmed and the low pressure gas is cooled in the interchanger. The lower curves represent the data for the reverse arrangement of bath temperatures. The mean curves in Fig. 2a, b, c, d and e give the values of $C_p/(C_p)_0$ as a function of pressure.

In Table I values of the ratio $C_p/(C_p)_0$ for the gases studied are given with their corresponding pressures and molecular density ratios. The density

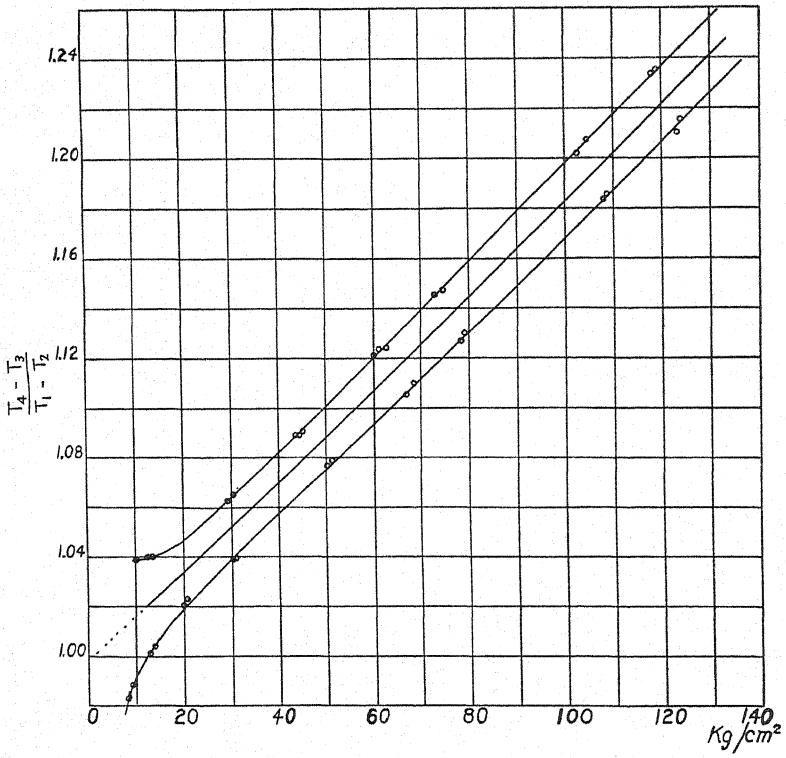

Fig. 2*a*. O_2 at 26°C.

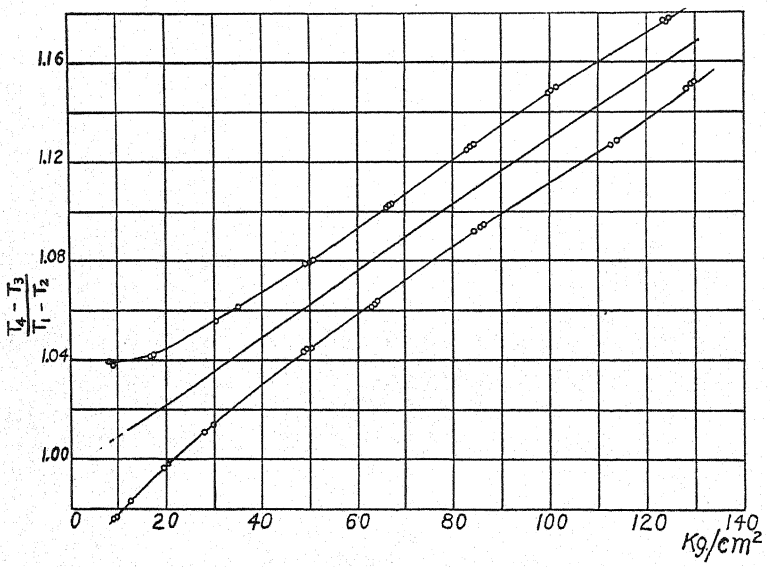

Fig. 2*b*. O_2 at 60°C.

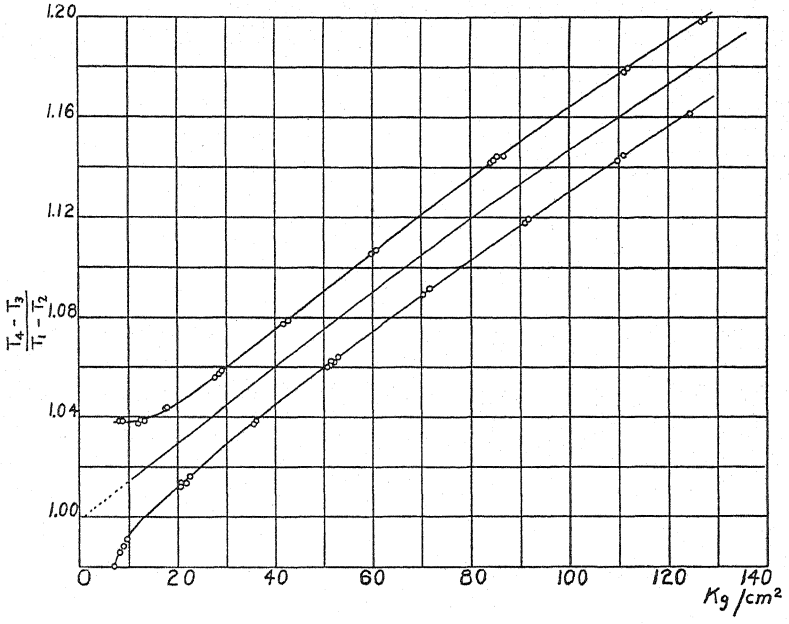

Fig. 2*c*. N_2 at 26°C.

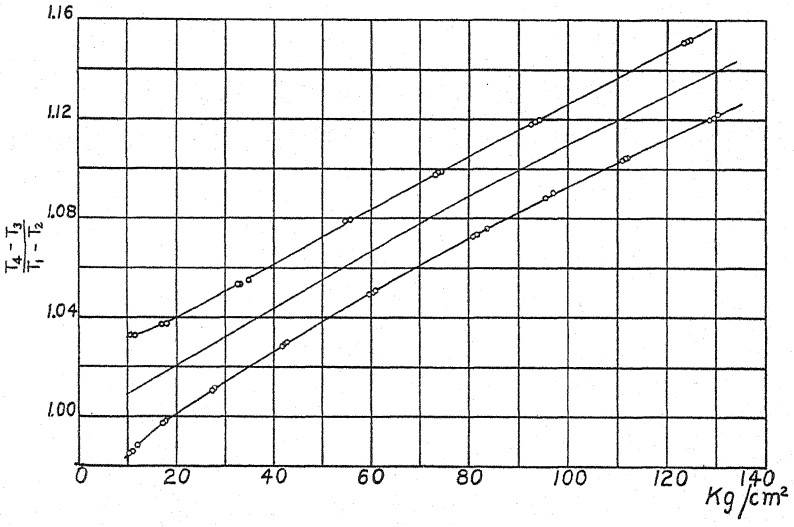

Fig. 2*d*. N_2 at 60°C.

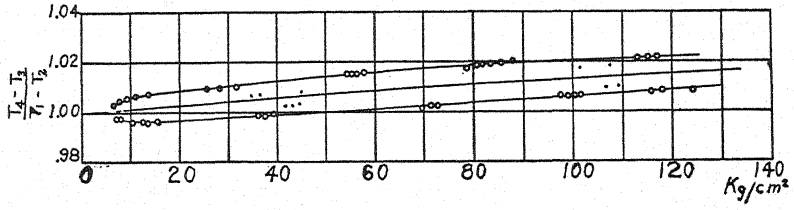

Fig. 2*e*. H_2 at 50°C.

TABLE I. *Values of* $C_p/(C_p)_0$.

Pressure in kg/cm²	$O_2-26°$	$O_2-60°$	$N_2-26°$	$N_2-60°$	$H_2-50°C$
10	1.0160 (9.6)	1.0090 (9.6)	1.0137 (9.7)	1.0097 (9.7)	1.0013 (9.7)
30	1.0520 (28.5)	1.0355 (28.8)	1.0443 (28.9)	1.0322 (29.1)	1.0041 (29.5)
50	1.0880 (47.1)	1.0632 (47.8)	1.0746 (48.3)	1.0551 (48.7)	1.0072 (49.7)
70	1.1255 (65.4)	1.0901 (66.6)	1.1050 (76.7)	1.0780 (68.5)	1.0098 (70.3)
90	1.1637 (83.5)	1.1162 (85.4)	1.1332 (87.4)	1.0991 (88.6)	1.0120 (91.4)
110	1.2020 (101.2)	1.1420 (104.2)	1.1597 (107.2)	1.1194 (109.1)	1.0142 (112.9)
130	1.2410	1.1680	1.1860	1.1390	

ratios (number of molecules per unit volume at a pressure p over the number at a pressure of one atmosphere) are given in parentheses.[2] The values of the

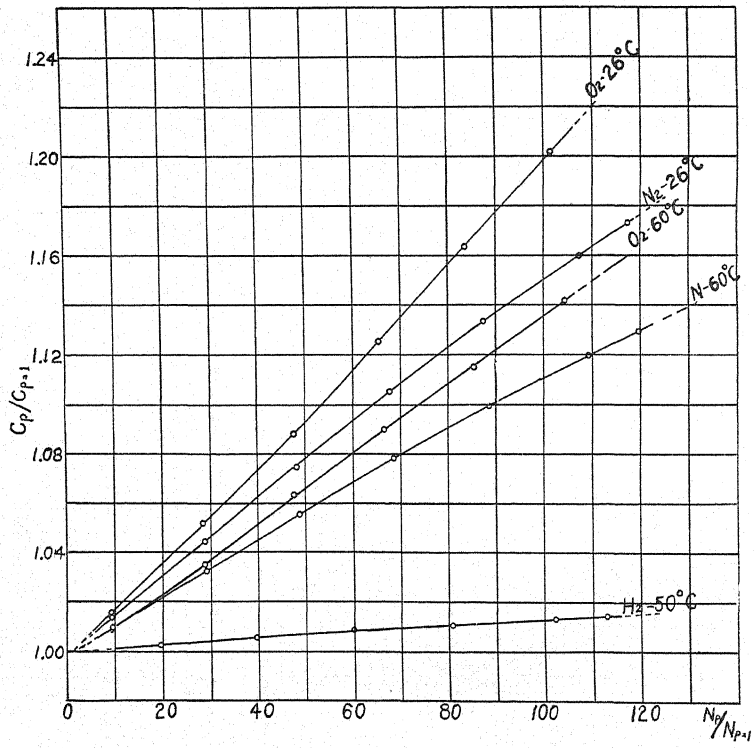

Fig. 3. $C_p/(C_p)_0$ as a function of the molecular density.

[2] In making this transformation the PV values of Holborn and Otto have been used. Holborn and Otto, Zeits. f. Physik, **33**, 1 (1925).

specific heat ratios were obtained from the carefully drawn mean curves. The probable error is less than 0.2 percent. The curves in Fig. 3 show $C_p/(C_p)_0$ as a function of the molecular density.

Discussion of Results.

In the first part of this paper it is shown that the separation of the two experimental curves for each case given in Fig. 2 a, b, c, d, and e is due to the existence of a correction term ϕ (Eq. 3). Although this term involves, as well as the Joule-Thomson effect, a small heat leakage q, it is of interest to consider the Joule-Thomson effect alone.[3]

With oxygen and nitrogen the Joule-Thomson effect is a cooling effect under these conditions of temperature and pressure. In the series of experiments where $T_1 < T_3$ this cooling would therefore have the effect of decreasing the magnitude of $T_1 - T_2$ and increasing that of $T_4 - T_3$. As a result the values of $C_p/(C_p)_0$ calculated by the relation $C_p/(C_p)_0 = (T_4 - T_3)/(T_1 - T_2)$ would be too large. By similar reasoning we see that corresponding values would be too small when the reverse arrangement of bath temperatures is used. i.e. when $T_1 > T_3$. A separation in this direction is observed in the cases of oxygen and nitrogen. With hydrogen, however, we expect the Joule-Thomson effect to warm the gases slightly under the conditions of this experiment. It is in this case where a large Joule-Thomson effect does not predominate in producing a separation of the curves that we see most clearly the effect of a small heat leakage. A further study of heat leakage in the case of hydrogen was made by increasing the flow of gas to double the normal rate. The increased flow of gas may alter the relationship between q and the regular interchange of heat. This would be shown by a change in the interval between the two curves. The dotted points of Fig. 2e show the effect of the increased flow for hydrogen, where the points above the mean curve are associated with conditions which produced the upper curve and the other points result from the inverse arrangement of bath temperatures. *The symmetry in the position of the "dotted" points, with respect to the mean curve, gives additional proof that the mean value curve is independent of the term ϕ in Eq.* (3).

It is of interest to examine the curves for evidence of the Joule-Thomson effect in the region of lower pressures. If the rate of gas flow in grams per second remains constant, it is apparent that the volume of gas passed per second in the high pressure line of the interchanger will increase at the lower pressures with the result that the Joule-Thomson effect will come more and more into effect in this region. This is shown with remarkable certainty in all three gases. The behavior of hydrogen in this region is of peculiar interest because the Joule-Thomson effect is observed as a warming effect instead of cooling as in oxygen and nitrogen.

In passing the discussion of the curves presented here, it should be stated

[3] In this treatment we have not considered the effect of temperature on the specific heats of gases in relation to the interval between the curves. It is easy to show that such a consideration would give rise to a second term in Eq. (3) which, like ϕ, almost completely vanishes in the mean curve.

that in general, care should be taken in attaching any particular significance to the shape of the upper and lower curves except in so far as the mean curve is affected. It must be remembered that the conditions of gas flow in the high pressure stream are different for all values of the pressure. As a consequence the temperature gradients along the conduit leading to the interchanger may change in such a way as to change the magnitude of the heat leakage. Indeed it has been possible in the case of nitrogen at 60°C to change the flow over such a wide range that q changed in sign. In connection with limitations just mentioned it may be of equal importance to say that to one using this method to study the specific heat of gases, the character as well as the position of the individual curves may point to the imperfections of the apparatus at hand. For example, we can be reasonably certain that in the present apparatus the net heat transfer q arises from an excessive heat conduction along the line leading from the low pressure bath to the heat interchanger.

The data indicate that the heat leakage and the Joule-Thomson temperature effect are both within the allowable magnitude specified in the theory of the method. The intercepts of the mean curves on the pressure axis indicate that there is no trouble in measuring temperatures as was certainly the case in the work previously reported by the author.[1] The errors in this earlier work were due to the fact that the temperature gradients which gave rise to an error in temperature measurements in one region of pressure differed more in another region than was expected at that time. In the light of further work, however, it is made clear that this variation is to be expected when temperatures are measured as in the earlier work.

The oxygen and hydrogen used in this work was obtained from the Philadelphia plant of the Paschall Oxygen Company, and the nitrogen from the Linde Air Products Company of New York City. By special analysis at the respective plants these gases were shown to be better than 99.5 percent pure. The gas was dried over phosphorus pentoxide before it was passed through the apparatus.

Details of Construction and Use of the Apparatus.

A simple scale drawing of the apparatus is difficult to realize because of its compactness and lack of symmetry in a single plane. Fig. 4 is a "sectional" drawing which may serve to show the actual construction of the several parts as well as the complete gas circuit. The scale is distorted but dimensions of the interchanger parts may be estimated if the various parts (thermometer tubes, shields etc.) are considered as drawn to scale, connected as shown but spread out laterally in the plane of the paper. The cylindrical boundary of the interchanger must therefore be thought of as being 2.25 inches in diameter and 5 inches long rather than 4.5 inches in diameter and 5 inches long as the scale might indicate. The same consideration must be made for the heater guard w which is 3 inches in diameter and 7 inches long. The high pressure gas conduits, where low thermal conductivity is desired, are nickel silver tubes 0.063 inches outside diameter with 0.010 inches wall. The corresponding low pressure tubes are of nickel silver with 0.125 inches outside diameter and 0.005

wall. Other tubes are drawn to a corresponding scale. All nickel silver parts are thinly gold plated.

The gas circuit is as follows: Gas from the high pressure reservoir is conducted to the tube *c* through which it passes to the temperature controlled bath *b*. The inner bath *ib*, being heat insulated from *b* serves to smooth out temperature fluctuations due to slight periodic changes in the heating current applied to the outer bath, which surrounds it. The gas stream now passes through the nickel silver tube *e* which conducts it through the boundary of

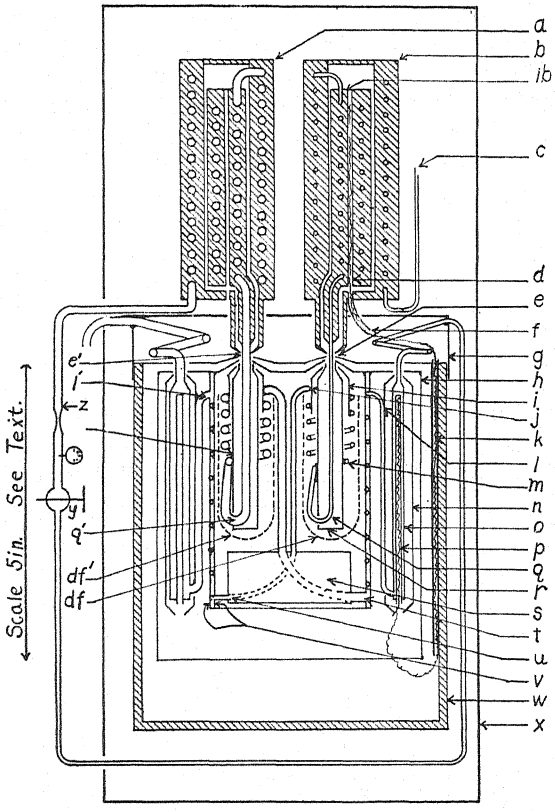

Fig. 4. Sectional diagram which shows the actual construction of the several parts of the apparatus as well as the complete gas circuit.

the interchanger *h* to *q* where the light walled tube turns back sharply and is soldered, for thermal contact, to the copper radiation shield *r*. From *m* to *j* the conduit is developed into the form of a spiral helix which terminates at *j* where another shield *i* is attached. The circuit passes from *j* to the chamber *s* where nearly all the interchange of heat between the two gas streams takes place. From this enclosure the high pressure gas passes into a copper tube at *u* which winds about between the two copper walls *v*, to which it is soldered for thermal contact, leading to the nickel silver tube *l* which passes the gas through the outlet thermometer tube *o*. A radiation convection shield *n* is soldered to *l* as shown. From the outlet thermometer tube the gas passes, along the path indicated, to the reduction valve *f* where the pressure is re-

duced. After passing the point z the gas at a pressure of approximately one atmosphere is conducted to a second temperature controlled bath a. The course of the low pressure gas through the apparatus is exactly similar to that of the high pressure stream except that in the region between t and l the low pressure stream is constrained to move in a spiral path through the duct formed by the high pressure line and the two copper walls v. From the point g' the low pressure gas escapes into the air.

The temperature controlled baths are made by machining thick-walled copper tubes in such a way that one fits snugly inside an outer tube. Helical grooves cut on the smaller tube serve as a conduit for the gas streams. The two baths thus constructed consist essentially of a solid block of copper about 5 inches long and 2.5 inches in diameter. The outer baths are equipped with electrical heating coils for maintaining constant temperatures while the inner baths are allowed to "float" at a temperature determined by the temperature of the gas which flows through them. The relative sizes of the outer and inner baths are represented approximately in the drawing.

The interchanger, as will be seen, is constructed in such a way that the regions of large temperature differences are in its inner folds while the outside is very nearly equal in temperature to the temperature of the two gas streams as they leave the interchanger. With this arrangement it is possible to have an isothermal surface h on the interchanger which can be thermally protected by keeping the temperature of the surroundings equal to the temperature of the surface. This is accomplished by means of the heavy copper heater guard w which is kept at the same temperature as the surface of the interchanger by maintaining a zero reading on a five junction copper-constantan thermocouple connected to their respective surfaces.

The thermocouple which measures temperature change on the high pressure line has one end inserted in the hole d in the inner bath. It passes through a german silver tube e, a copper tube k and terminates in the thermometer tube p. Since the thermometer tube is very nearly equal in temperature to the interchanger surface and the heater guard, conduction from the interchanger along the thermocouple wire is minimized by passing the thermocouple wires through the tube k which is soldered to the heater guard. Practically the entire temperature gradient along the thermocouple wires exists along the length between the bath and the wall of the heater guard. Tube f is a thin-walled nickel silver tube which is soldered to b and extends through the first heater guard wall, having the purpose of protecting the wires and smoothing out the temperature gradient along them. Other thermocouples measure the temperatures of ib and the heater guard to an ice bath. The temperatures on the low pressure side are measured by exactly similar methods.

The temperature difference between the two baths is maintained at 10°C. Temperature gradients therefore exist between the points where the inlet temperatures are measured and some point inside the interchanger where the interchange of heat between the two gas streams starts. In order to minimize the net transfer of heat along the entrance tubes, it is desirable to prevent the interchange of heat for some distance after the gas streams pass through the boundary of the interchanger. To accomplish this, the tubes in addition to

being poor heat conductors are gold plated to give a surface of low emissivity to radiation at these temperatures. The radiation-convection shields i and r are of copper thinly gold plated. Small dewar flasks df and df' further serve to isolate these regions. It is found by direct measurement that with these precautions the temperature changes along the tubes from e to q and the corresponding length e' to q' are of the order of 1 percent of the total changes. The thermal conductivity per unit length of the two inlet tubes is approximately the same and since the temperature changes are in all cases almost equal and opposite, a compensating effect should reduce the net transfer of heat along them.

On the outlet side little trouble with heat conduction is met, because the temperatures to be measured are so nearly equal to the surrounding temperatures. The interchange of heat between the two gas streams has been made as complete as is easily possible in order to produce this condition of temperature equality at the outlet side. The amount of interchange is somewhat dependent upon the gas used and the condition of flow but for all conditions the difficiency in interchange does not exceed 0.2 percent.

The enclosure defined by the walls v and h will therefore be at about the same temperature as the outlet thermometers and the shielding here represented is considered adequate for the purpose of isolating the region where the temperatures are measured. Measurements are carried out at different temperatures and since it is desired to have similar conditions for each experiment the entire assembly is enclosed by a constant temperature boundary which in all cases is maintained at a temperature 10° lower than the mean of the two bath temperatures. This boundary is a temperature controlled cylindrical shell about 18 inches long and 6 and 8 inches inside and outside diameters. Since the difference in bath temperatures is always 10°C one will be five degrees and the other 15°C above the temperature of the enclosure. To prevent this temperature distribution from producing dissimilar conditions when the bath temperatures are interchanged the shield g which is thermally connected to w is provided.

The temperature of enclosure x is controlled by a thermostat while the two bath temperatures are controlled manually by the observer. All temperature measurements are made by the use of five-junction constantan-copper thermocouples, used with a White double potentiometer and the usual auxiliary equipment.

The flow of gas is controlled by producing a constant rate of delivery to the low pressure bath. This is accomplished by maintaining a constant pressure on a capillary leak z (Fig. 2). In general the flow of gas on the low pressure side was maintained at 70 cc/sec. for oxygen, 80 for nitrogen and 160 for hydrogen.

Pressure measurements were made with a high class Bourdon spring gauge developed for this work, in the shops of this laboratory. It was calibrated against a dead weight gauge.

The author is indebted to the staff of the Bartol Research Foundation for providing facilities for this work, and the United States Gauge Company for calibrating pressure gauge.

ELECTRICAL RESISTANCE OF NICKEL AND IRON WIRES AS AFFECTED BY LONGITUDINAL MAGNETIC FIELDS

By O. Stierstadt
Laboratory of Applied Electricity, University of Goettingen

(Received February 11, 1931)

Abstract

In a paper on electrical resistance of nickel and permalloy wires as affected by longitudinal magnetization and tension, L. W. McKeehan pointed out that further investigation and discussion of some special questions regarding change of resistance of ferromagnetic substances in magnetic fields were highly desirable. In the present paper the following subjects are treated, partly on the basis hitherto unpublished measurements by the author. (1) Change of resistance in small fields. As the literature shows, the question whether this is independent of the magnetic history of the sample is not yet settled. Anomalies often observed are not real. (2) The early saturation of the magneto-resistance effect, a condition which is reached in considerably weaker fields with ferromagnetic bodied than with para- and diamagnetic bodies. An explanation on the basis of the electron theory is suggested.

Introduction

In A very interesting paper on the change of electrical resistance of nickel and permalloy in longitudinal magnetic fields McKeehan[1] treated extensively the question of variation of the electrical resistance of permalloy in magnetic fields under the influence of tension as dependent upon the variation of the nickel content of the permalloy. He finds certain phenomena which present a remarkable analogy with the change of resistance of ferromagnetic bodies in magnetic fields. For this reason he discusses in great detail the most important papers on magneto-resistance and elasto-resistance.

In the present paper only the papers of the first group dealing with magneto-resistance will be discussed. McKeehan quotes as the most interesting of the recent papers in this field that of Fr. Vilbig.[2] Vilbig describes in this paper a number of strange phenomena, viz., change of sign of the effect, "stable" and "labile" curves, etc., which are supposed to be exhibited in the change of resistance of ferromagnetic bodies in small longitudinal magnetic fields. Such anomalies, in addition to normal curves, are to be found in almost all previous papers of other authors. They are, however, most remarkable and most extensively discussed in the paper of Fr. Vilbig. For this reason McKeehan thinks it one of the most important problems to study and explain "the irregular progress of magneto-resistance changes in low applied fields."

In a detailed paper "Die Änderungen der elektrischen Leitfähigheit ferromagnetischer Stoffe in longitudinalen Magnetfeldern"[3] the author briefly

[1] L. W. McKeehan, Phys. Rev. **36**, 948 (1930).
[2] Fr. Vilbig, Arch. f. Elektrotechn. **22**, 194 (1929).
[3] O. Stierstadt, Phys. Zeits. **31**, 561 (1930).

pointed out how these anomalies are to be explained. In this paper were also presented more accurate and previously unpublished measurements on the peculiarities in low fields of the curves in question. These often observed anomalies in low fields are further discussed in the present paper.

PART I

A brief discussion of some of Vilbig's results is desirable. Fig. 1 shows the change of resistance of a nickel wire 0.051 mm in diameter over its complete magnetic cycle as observed by him. Remarkable are the frequent intersections of the various parts of the curve. Those in low magnetic fields, where the relative change of resistance becomes negative, i.e. where it passes into a decrease of resistance, seem to be particularly interesting. These parts were very thoroughly investigated by Vilbig and he established a number of regularities

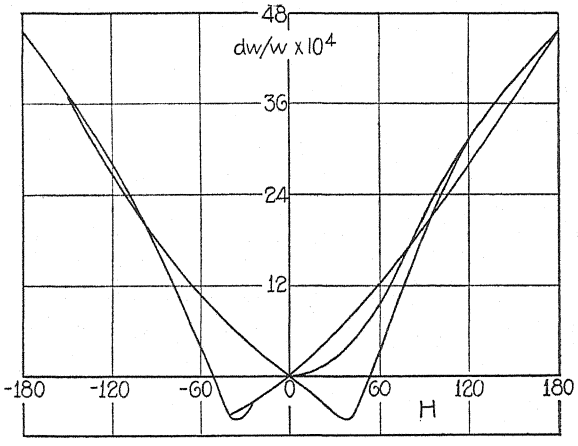

Fig. 1. Change of resistance of nickel. (Taken from Vilbig's paper.)

of which the most important are summarized here in order to make the following discussion clearer.

He finds in the negative parts of the curves of hysteresis of resistance (Fig. 1) two types of curves, which he terms "stable" and "labile," respectively. These types of curves appear when in the negative parts the field is no longer increased but is made to decrease from any point. The appearance of these curves depends upon whether this lowering of the field is produced *before* or *after* passing the minimum, and upon whether the zero line has already been reached or passed before the field is lowered. Fig. 2, taken from Vilbig's paper shows on an enlarged scale these "stable" and "labile" curves below the zero axis. Fig. 3 shows their appearance when on lowering the field the zero axis has been already passed. The number of arrows indicates the succession of the reversed variations of field. For more details, the original paper of Vilbig must be consulted. Unfortunately he makes no attempt to explain the observed phenomena.

The present author examined these phenomena thoroughly and found that these observations are completely explained when a fundamental error

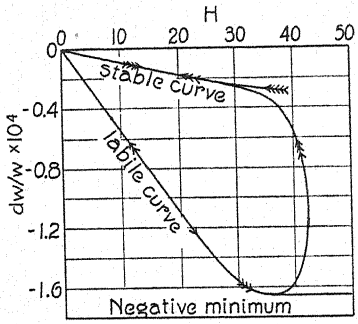

Fig. 2. Negative change of resistance of nickel. (Taken from Vilbig's paper.)

which underlies the whole paper of Vilbig is recognized. He writes in italics at the beinning of his paper that "the change of resistance *dw* vanishes at once

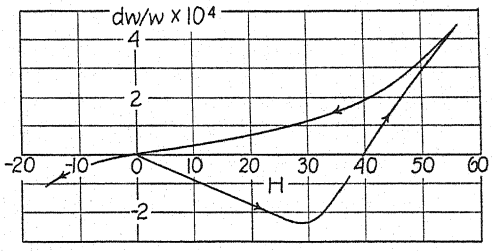

Fig. 3. Negative change of resistance of nickel. (Taken from Vilbig's paper.)

with the magnetic field." This is, however, an error. On the contrary, the change of resistance in the magnetic field shows far-reaching analogies with

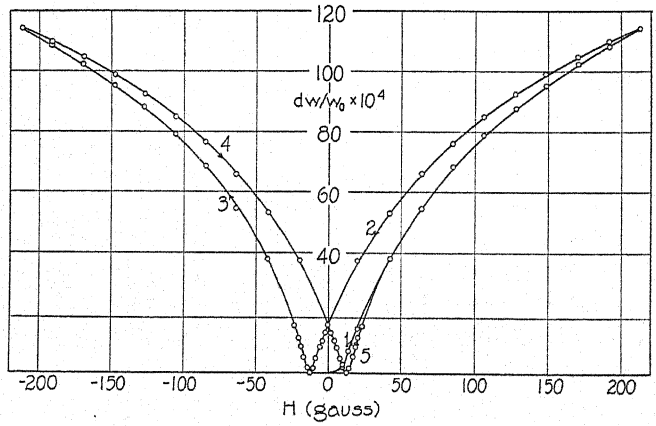

Fig. 4. Resistance hysteresis of nickel.

ordinary magnetization. Above all it shows quite a definite residual magnetism, a coercive force, etc., as a curve taken from the paper of the present

author demonstrates (Fig. 4). This essential fact passes unnoticed by Vilbig. Even the component of the earth's field may introduce errors, as found by measurements on very soft, extraordinarily pure, vacuum melted electrolytic iron (99.998 percent Fe).

The wire samples should, therefore, be carefully orientated perpendicularly to the earth's field for exact measurements.

The measurements reported herein were taken in an *exactly homogeneous* magnetic field, provided by a magnetizing coil approximately 1 m in length. Vilbig used the field between the poles of an electro-magnet. With a pole distance of 13 cm he considers the middle 5 cm as approximately constant. This field shows, however, according to his own calibration an increase of 20 percent from the minimum in the center at the ends of the 5 cm range used in

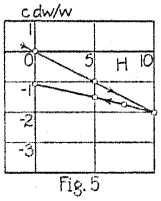

Fig. 5

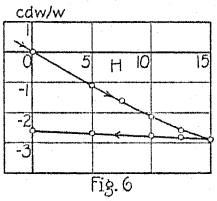

Fig. 6

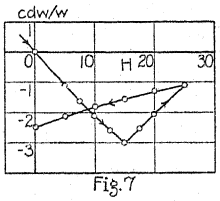

Fig. 7

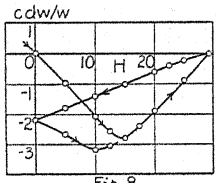

Fig. 8

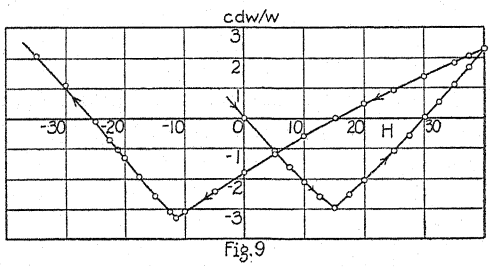

Fig. 9

Fig. 5. Lowering of the field before the minimum.
Fig. 6. Lowering of the field in the minimum.
Fig. 7. Lowering of the field after the minimum.
Fig. 8. Lowering of the field in the zero line.
Fig. 9 Lowering of the field above the zero line.

measurements. It has, therefore, by no means the necessary homogeneity. Furthermore, in the present author's apparatus the sensitiveness of the arrangement for measuring the relative change of resistance, dw/w, was one hundred times as great as that of Vilbig. Readings were taken with a Thomson double bridge. As null instrument a mirror galvanometer of Siemens and Halske with magnetic shunt having a current sensitivity of about 10^{-9} amp.·deg.$^{-1}$ at 450 degrees distance was used. For more details regarding the apparatus, especially the temperature protection of the wire and its arrangement and centering in the magnetic field, see the paper of the author referred to above.[3] The samples tested measured 50–70 cm in length.

Figs. 5 to 9 show in analogy to Vilbig's work measurements of the change of resistance in low fields. The wire always had a residual magnetism at the

beginning of the measurements. Regarding the resistance, we shall term this state the "zero state." On increasing the field at the beginning of the readings from $H=0$ to $H=100-150$ gauss and subsequently decreasing it to $H=0$, now on another increase of the field in the opposite direction, there were found *apparent* negative changes of resistance, which showed a minimum and a subsequent increase of resistance, i.e., the resistance becomes smaller at the minimum than in the zero state.

These are the negative changes of resistance observed and investigated by Vilbig. Of course, differences in the course of the curves are to be expected here, so-called "stable" and "labile" curves, when the field is lowered, e.g., before or after reaching the minimum or the zero line. But then it would be equally justifiable to speak of stable and labile parts in the curve of magnetization.

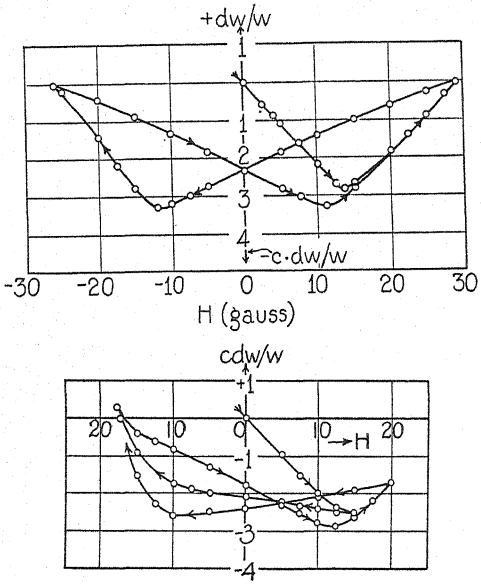

Figs. 10 and 11. Apparent negative changes of resistance of nickel.

The observed effects are not, therefore, to be considered as anomalies of the change of resistance, but as inherent in the process of magnetization. On visualizing the course of magnetization for each variation of field in Figs. 5–9, one readily sees that with these low fields the relative change of resistance and the magnetization are quite analogous. The very marked, broad loop of the curves has its origin in the strong residual magnetism with nickel, notably in weak fields, which is by far greater than with all other ferromagnetics. With iron these phenomena are therefore much less developed and not so easy to observe although they appear quite in the same form and corresponding to the curve of magnetization.

Figs. 10 and 11 demonstrate two other phenomena observed by the author and referred to in the paper of Vilbig as characteristic yet inexplicable.

Fig. 10 shows the gradual stabilization of the curves after a single or repeated passing of the minimum range. Fig. 11 shows that the value of the negative minimum of change of resistance depends on the strength of the magnetic field applied before in the reverse direction. A detailed discussion of these phenomena in connection with the process of magnetization appears unnecessary after the preceding demonstration.

It can therefore be stated quite generally that regarding the change of resistance of iron and nickel in longitudinal magnetic fields, there is always an increase of electrical resistance, which may be marked by the existence of coercive force H. This generalization, however, is only clear after complete demagnetization of the wire before each measurement. These considerations

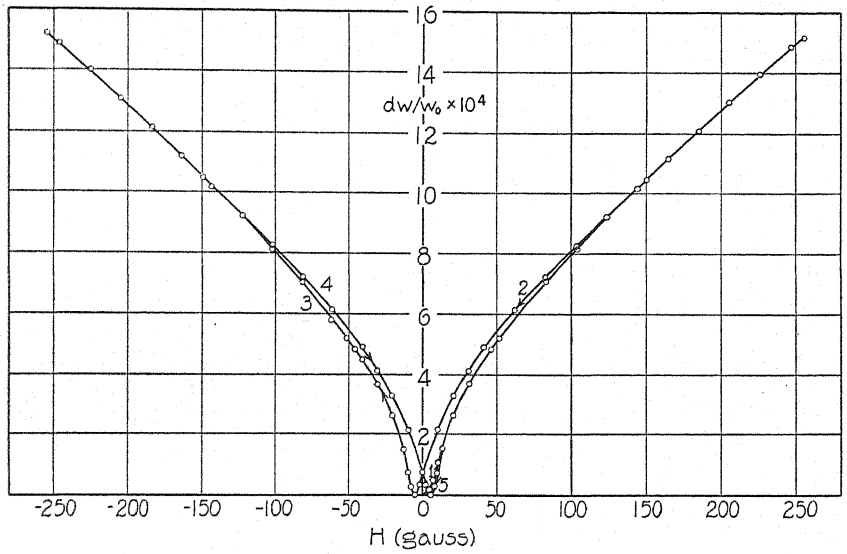

Fig. 12. Resistance hysteresis of annealed iron with carbon content.

show, that it is the neglect of this fact which accounts for a number of earlier observations which demonstrate a reversal in sign of the effect in low fields.

These statements are, however, not valid for high temperatures. W. Gerlach[4] found that with rising temperature the value of the magnetic change of resistance decreases steadily and finally, above the Curie point, turns into a decrease, while a loop is no longer formed. It is true, however, that for a temperature of as high as +200° C, Gerlach finds an example with quite a normal curve of resistance hysteresis.

In the paper referred to above[3] the present author emphasized that apart from incomplete demagnetization of the wires there are still other causes which may to a certain degree account for the change of sign described, e.g. soldering of the leads to the wire sample. In the magnetic field such contacts may give rise to thermomagnetic and thermoelectric effects, causing anoma-

[4] W. Gerlach, Zeits. f. Physik **59**, 847 (1930); Ann. d. Physik **6**, 772 (1930).

lous shapes of the curve, and in particular as observed, a change of sign. The superposition of such effects on the purely magnetic effects, described above, may considerably distort the form of the curve under certain conditions and therefore render difficult the unambiguous interpretation of the phenomena. On carefully avoiding all sources of error, there is invariably a normal curve of resistance hysteresis to be obtained, as shown for nickel in Fig. 4 and for iron in Fig. 12. According to these, the inner magnetization is invariably the factor which principally determines the resistance and not the outer magnetic field.

On the basis of this statement, the change of resistance, considered over the whole magnetic cycle need not necessarily show a loop as Figs. 4 and 12, unless the curve of magnetization of the material shows hysteresis. Gerlach[4] confirmed these results for nickel at high temperatures. The author showed on the other hand with pure electrolytic iron that the loop sensibly disappears.

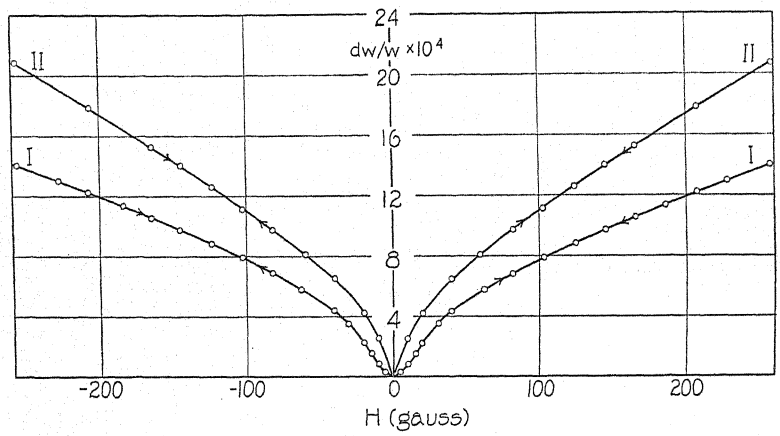

Fig. 13. Change of resistance of electrolytic iron: I untreated, II annealed.

Fig. 13 demonstrates this for two samples of electrolytic iron. Curve I is for a hard drawn, non-recrystallized wire. Curve II is for a sample, recrystallized in the usual way by two tempering processes and one drawing process between. For the whole magnetic cycle, the relative change of resistance is determined unambiguously by the strength of the magnetic field applied. A detailed report is given in a paper "Zur Frage der Widerstandsänderung von reinstem Elektrolyteisen in longitudinalen Magnetfeldern."[5]

With material of so high a degree of purity (impurities amounting to only 1/1000 percent, contrary to ordinary technical iron) a very great influence of any mechanical stress and of the size of crystal grain on the relative change of resistance was found. Investigation of these influences is being carried on in the Laboratory of Applied Electricity of Goettingen University and will be reported elsewhere.

[5] O. Stierstadt, Zeits. f. Physik **65**, 575 (1930).

PART II

In the paper cited above,[1] McKeehan expressed the need for solution of another problem, viz., the question as to the "early saturation of the magneto-resistance effect." The following considerations may help to throw some light on the solution of this problem.

With non-ferromagnetic substances saturation of the change of resistance begins only in very strong fields of an order of magnitude of 10^5–10^6 gauss. With the ferromagnetic substances, however, the beginning of saturation of the change of resistance and of the magnetization coincide very nearly; with nickel and iron at $B=6000$–8000 and 20,000–25,000 gauss respectively. In these cases, of course, the internal fields are to be considered and not the external fields. With the ferromagnetic bodies, therefore, the values for the strength of field for saturation are by the factor 10 or 100 lower than with para- and diamagnetic bodies.

In the latter group P. Kapitza[6] made extended measurements which have only recently been theoretically explained by the work of N. H. Frank.[7] In an extension of Sommerfeld's theory of the magnetic change of resistance, Frank derives a formula which represents correctly the change for all field strengths. Frank's formula is

$$\frac{dR}{R} = \frac{b \cdot H^2}{1 + c \cdot H^2} \tag{1}$$

where b and c are individual atomistic constants, characteristic of each material, of the following form:

$$b = \frac{\pi^2}{3}(emlkT)^2\left(\frac{\lambda}{h}\right)^6, \tag{2}$$

$$c = (el\lambda/h)^2; \tag{3}$$

where e is the elementary electrical charge, m the mass of the electron, l the mean free path of the electron, k Boltzmann's constant, T the absolute temperature, λ deBroglie's wave-length of conducting electrons, and h is Planck's constant.

By means of Eq. (1) the change of resistance in the magnetic field may be determined for any material when its characteristic constants are known. Frank made such a determination for some substances investigated by Kapitza and found excellent agreement, notably for the saturation value b/c as calculated from Eq. (1) for strong fields.

Figure 14 shows the general course of the function (1) $dR/R=f(H)$ for any value of b and c (in the case plotted $b=c=1$): for small fields the ascent varies with the square, for the medium fields there is a fairly linear part near the point of inflection, and for very strong fields an approach to saturation. Deviations from this course are as yet shown only by the ferromagnetic sub-

[6] P. Kapitza, Proc. Roy. Soc. **A123**, 292 (1929).
[7] N. H. Frank, Zeits. f. Physik **60**, 682 (1930); **64**, 650 (1930).

stances in small fields, because here permeability $\mu \gg 1$. The ascent goes here, where the internal field plays an important part, not with the second but with the third, fourth or even fifth power of B^3. When the value of μ approaches unity, however, according to the measurements available, the theory seems to hold for ferromagnetic bodies as well.

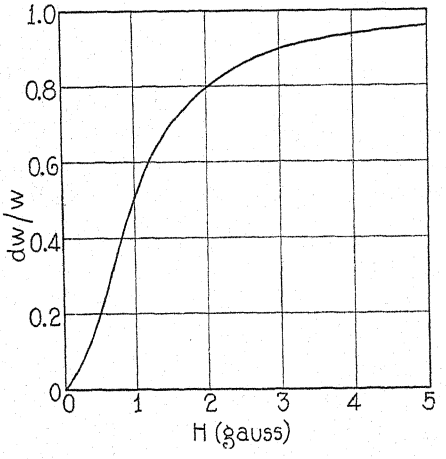

Fig. 14. Change of resistance in the magnetic field according to Frank-Sommerfeld.

Now, for an electron which has the velocity v perpendicular to the direction of the field, the following relation holds for the radius of curvature of its orbit:

$$\frac{1}{r} = \frac{eH}{mv} = \frac{eH\lambda}{h}, \tag{4}$$

where λ is defined by the wave equation:

$$mv = h/\lambda; \tag{5}$$

the other symbols meaning the same as explained above. On comparing, according to Frank, Eq. (4) with (3) equation

$$cH^2 = (l/r)^2 \tag{6}$$

results. Therefore the denominator of Eq. (1) differs from unity only when l becomes of the order of r or greater. When $l<r$, the electron passes only a small part of its orbit in the magnetic field between two collisions. For $l>r$, however, it travels through several full circles before a collision with an atom occurs, in which case the change of resistance dR/R approaches the saturation value b/c.

Therefore, when according to Eqs. (4) and (6), the values of l and λ or l and v respectively are known for any substance its behavior in the magnetic field is sufficiently known, in particular the beginning of saturation of the change of resistance. An investigation based on such considerations is being carried on in our laboratory, especially for ferromagnetic bodies. In particular

the attempt is being made to demonstrate whether on the bases of the electron theory the abnormally low value of field strength at which magnetic saturation of resistance occurs with ferromagnetic bodies emphasized by McKeehan is to be expected.

In this way probably the great differences between the saturation values obtained by different observers, quoted in McKeehan's paper, may find an explanation. It will be readily understood that particularly with very pure materials minute quantities of impurities or slight mechanical stresses may have a very marked influence on the lattice structure and consequently on the constants mentioned above. For this reason, measurements on materials, the properties of which are not exactly defined are useless for the establishment of quantitative relations.

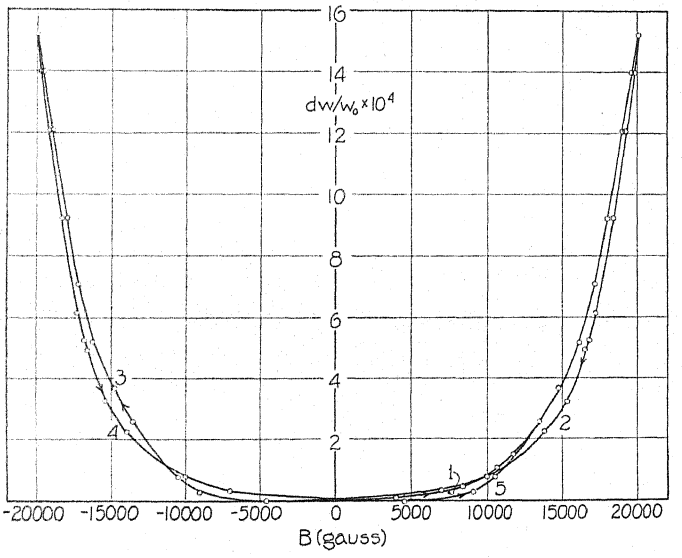

Fig. 15. Change of resistance of annealed iron with carbon content (Fig. 12) as a function of magnetization.

Finally, an interesting analogy may be mentioned between the curves of resistance hysteresis previously published by the author,[3] and the curves recently observed by McKeehan and published in his paper referred to above.[1] These curves represent the magnetic change of resistance under tensile stress and are unexplained as yet.

On representing the relative change of resistance dw/w not as a function of the external field H, but by means of the curve of magnetization $B=f(H)$ as a function of the magnetic induction B, again a loop is obtained, the individual parts of which intersect in a very striking way once or repeatedly. Fig. 15 demonstrates this fact, representing the function $dw/w=f(B)$ for the iron wire, the curve of resistance hysteresis $dw/w=f(H)$ of which is already shown above in Fig. 12. The origin of these intersections and their reality re-

main still quite uncertain and at the time of his publication the author suspected the possibility of some error. Meanwhile, however, McKeehan has found very similar curves in the course of his experiments on the change of resistance by tension in the magnetic field (compare the paper[1] e.g. page 970).

A striking analogy between these curves and those of the type of Fig. 15 is evident. A closer examination of these phenomena has not yet been undertaken. Such measurements might be comparatively easy with nickel and at first in not too strong fields, the residual magnetism being very high in this case and the formation of the loop very marked. Further extended research work, which might help to solve this problem, appears very desirable.

SUMMARY

The special phenomena, found in the investigation of the change of electrical resistance of ferromagnetic bodies in magnetic fields dealt with in the present paper, may be summarized as follows:

(1) In low applied fields the change of resistance presents no anomalies. The deviations from the normal curves, as frequently observed, are caused by errors, the most important of which is an incomplete demagnetization of the sample. By measurements made with this error purposely introduced it was demonstrated that the anomalous curves of change of resistance actually have their origin in incomplete demagnetization.

(2) The saturation of the change of electrical resistance of ferromagnetic bodies which invariably occurs in magnetic fields of a lower order of magnitude than those for saturation with non-ferromagnetic bodies appears to present a problem soluble on the basis of the Frank-Sommerfeld theory of magnetic change of resistance. This question will be discussed in greater detail elsewhere.

LETTERS TO THE EDITOR

Prompt publication of brief reports of important discoveries in physics may be secured by addressing them to this department. Closing dates for this department are, for the first issue of the month, the twenty-eighth of the preceding month; for the second issue, the thirteenth of the month. The Board of Editors does not hold itself responsible for the opinions expressed by the correspondents.

The Molecular Scattering of Light from Ammonia Solutions

During the course of an investigation of the molecular scattering of light from substances in their pure and dissolved states, solutions of ammonia have given such interesting results that it seems advisable to communicate them at once. Results have previously been given for gaseous ammonia by Wood,[1] and Dickinson, Dillon and Rasetti;[2] for liquid ammonia by Daure,[3] Bhagavantam[4] and Dickinson, Dillon and Rasetti;[2] and for water solutions by Carelli, Pringsheim and Rosen.[5] Their data with those of the writers, are given in Table I.

The excitation was by means of a quartz mercury arc. The instrument used was a Steinheil glass spectrograph. The plates were photometered using a Moll microphotometer, kindly loaned by the Department of Physics. Lines corresponding to the frequency differences 1073, 3219, 3311, and 3394 have been found to be excited by both Hg 4046 and Hg. 4358. The line corresponding to 3311 appears to have been excited by Hg 4078 as well. The line corresponding to 1615 could be observed when excited by Hg 4358 after the exciting line Hg 4046 had been filtered out. Even under these conditions it is extremely faint and an exact determination of its position has not as yet been possible. The relative intensities of the lines can be judged from the accompanying microphotograph. (Fig. 1).

TABLE I

State	Reference	$\Delta\nu_1$	$\Delta\nu_2$	$\Delta\nu_3$	$\Delta\nu_4$	$\Delta\nu_5$
Gas	1				3309	
Gas	2				3337	
Liquid	3	1070	1580	3210	3310	3380
Liquid	4	1070		3216	3304	3380
Liquid	2			3214	3298	
Solution	5				3314	3385
Solution (16N)	Authors	*1073*	*(1615)?*	*3219*	*3311*	*3390*

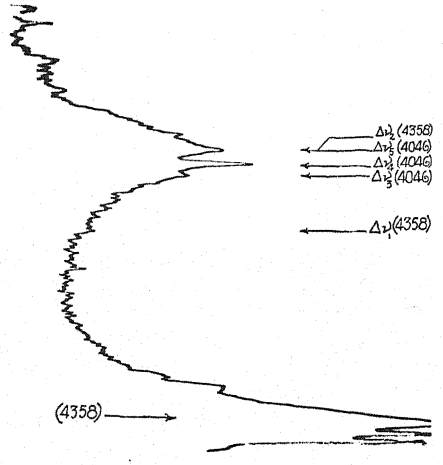

Fig. 1.

It is interesting to note that all the lines which have been reported from gaseous and

[1] Wood, Phil. Mag. **7**, 744 (1929).
[2] Dickinson, Dillon and Rasetti, Phys. Rev. **34**, 582 (1929).
[3] Daure, Trans. Farad. Soc. **25**, 825 (1929).
[4] Bhagavantam, Ind. J. Physics **5**, 59 (1930).
[5] Carelli, Pringsheim and Rosen, Zeits. f. Physik **51**, 511 (1928).

liquid ammonia have now been found in the concentrated solution (16 normal) as well. The times of exposure necessary to observe the ammonia frequencies, $\Delta\nu_3$, $\Delta\nu_4$, and $\Delta\nu_5$ were short enough to avoid difficulty due to the excitation of the water bands, although the latter could not be entirely avoided.

One can hardly decide from the figures given in the table whether or not there is a change in the characteristic frequencies when ammonia is dissolved in water from those observed for the pure substance. It appears that it will always be difficult to make a decision concerning this point because the frequency differences may depend upon the concentration of the scattering substance in the solution and other factors.

Complete details of the experimental work and a critical discussion of the data particularly with regard to changes taking place in solution will be given at a later date.

ALEXANDER HOLLAENDER
JOHN WARREN WILLIAMS
Laboratory of Physical Chemistry,
University of Wisconsin,
Madison, Wisconsin,
April 25, 1931.

Capture of Electrons by Swiftly Moving Alpha-Particles

Capture of electrons by α-particles when the kinetic energy of the electron with respect to the α-particle was equal to that of an energy level of the helium atom were reported by Bergen Davis and A. H. Barnes (Phys. Rev. July 1929) and by A. H. Barnes (Phys. Rev. Feb. 1930).

The results reported depended on observations made by counting scintillations visually. The scintillations produced by α-particles on a zinc sulphide screen are a threshold phenomenon. It is possible that the number of counts may be influenced by external suggestion or autosuggestion to the observer. The possibility that the number of counts of scintillation might be greatly influenced by suggestion had been realized, and a test of their reliability had been made by two methods: (a) The voltage applied to the electrons was altered without the knowledge of the observer (Barnes); (b) the direction of the electron stream with respect to the α-particle path was altered by a small electro-magnet. Such changes in voltage and direction of electron stream were noted at once by the observer. These checks were thought at the time to be entirely adequate.

In examining the data of observation made in our laboratory Dr. Irving Langmuir concluded that the checks applied had not been sufficient, and convinced us that the experiments should be repeated by wholly objective methods. Accordingly we have investigated the matter by means of the Geiger counter. Four additional experimental electron α-ray tubes have been constructed for this purpose.

Capture of the kind reported was often observed over a considerable period of time, but following prolonged observation the effect seemed to disappear. The results deduced from visual observations have not been confirmed. If such capture of electrons does take place, it must depend on unknown critical conditions which we were not able to reproduce at will in the new experimental tubes.

We wish in particular to acknowledge our obligations to Mr. J. R. Dunning who has improved the Geiger counter to such an extent that it is almost an instrument of precision.

BERGEN DAVIS
A. H. BARNES
Columbia University,
Department of Physics,
April 25, 1931.

The Results of a Least-Square Adjustment of Cosmic-Ray Observations

Millikan and Cameron have recently published[1] a new series of depth-ionization measurements on the cosmic-rays, from which they conclude that there are four components or "bands" of widely varying intensity and absorption coefficient, the latter probably increasing at first with depth on account of the Compton effect. In a paper read before the Physical Society in December, 1929, the writer showed how least-squared adjustment may be adapted to the analysis of such a combination of rays, provided they obey the assumed absorption law, and provided also that approximate values of the initial intensity and absorption coefficient of each component, such as Millikan and Cameron have estimated, are available. The method uses, as the unknowns

[1] Millikan and Cameron, Phys. Rev. **37**, 235 (1931).

to be adjusted, not the cosmic-ray constants themselves, but the small, unknown corrections to be applied to the approximate values, in order to give the most probable values derivable from the observations. If the above provisions were fulfilled, and if the method were applied to a series of measurements of such precision as those of Millikan and Cameron, the small corrections would certainly appear as a matter of routine calculation.

Through a research grant from the Iowa Academy of Science, the writer has made such an analysis of Millikan and Cameron's latest data. The adjustment was, however, confined to the lower three-fourths of the depth range, in order to avoid the Compton effect as far as possible; and this, incidentally, eliminates the assumed most absorbable fourth component from the calculation. It was found necessary to prepare and use a more extended and more accurate table of the Gold integral than that employed by Millikan and Cameron. The numerical work was performed on a calculating machine by an experienced computer, and carefully checked at every stage. The resulting adjusted values of the corrections were found to satisfy the normal equations exactly, and to give a smaller sum of squared residuals than if the corrections were zero.

It is therefore somewhat disconcerting to have to report that these adjusted values, if applied as corrections, would yield a set of altogether meaningless and physically impossible absorption coefficients and intensities; some of which would even turn out negative.

The writer can arrive at only one interpretation of this, namely, that the assumptions upon which the analysis was made are not justified. Whether the discrepancy arises from insufficiently accurate tentative values of the constants, from the assumption of the wrong number of components, from the persistence of the Compton effect at great depths, or from an altogether erroneous interpretation of the whole phenomenon, it seems necessary to look with serious reserve upon any such sweeping conclusions as to "atom building" as Millikan and Cameron have deduced from the results of their splendid experimental work.

A more detailed account of this investigation will duly appear in the Proceedings of the Iowa Academy of Science for 1931.

LE ROY D. WELD
Department of Physics,
Coe College, Cedar Rapids, Iowa,
May 1, 1931.

Mutual Impedance of Grounded Wires on the Surface of a Two-Layer Earth

Mr. R. M. Foster's formula[1] for the mutual impedance of any thin grounded wires lying on the surface of the earth has been generalized by us, following his basic assumptions and method of derivation, to cover the case of a horizontally stratified earth having the conductivities λ_1 and λ_2 at depths which are less than or greater than b respectively. We find:

The integrations are extended in the double integral over the two wires S and s whose elements dS and ds are separated by distance r and include the angle ϵ between their directions. This general formula includes as special cases:

(1) One wire straight and doubly infinite as given by H. P. Evans.[2]

$$Z_{12} = \int\int \left\{\frac{d^2Q}{dSds} + i\omega \cos\epsilon\, N\right\} dSds$$

with

$$Q = \frac{1}{2\pi\lambda_1}\int_0^\infty \left\{1 + \frac{4\alpha_1^2(u+\alpha_2)(\lambda_1-\lambda_2)e^{-2b\alpha_1}}{\Delta[\alpha_1\lambda_2 + \alpha_2\lambda_1 + (\alpha_1\lambda_2 - \alpha_2\lambda_1)e^{-2b\alpha_1}]}\right\} J_0(ru)du$$

$$N = 2\int_0^\infty \frac{u}{\Delta}[\alpha_1 + \alpha_2 + (\alpha_1 - \alpha_2)e^{-2b\alpha_1}]J_0(ru)du$$

$\omega = 2\pi f$ = radian frequency

$\Delta = (\alpha_1 + \alpha_2)(u + \alpha_1) + (\alpha_1 - \alpha_2)(u - \alpha_1)\epsilon^{-2b\alpha_1}$

$\alpha_j = (u^2 + i4\pi\omega\lambda_j)^{1/2}$, $j = 1$ and 2

J_0 = Bessel function of first kind, zero order.

[1] Bulletin of the American Mathematical Society, May 1930, Abstract 289, pp. 367–368.

[2] Evans, Phys. Rev. **36**, 1584 (1930) Eq. (30).

(2) The mutual resistance of any wires at frequency zero, that is, for direct current as given by F. Ollendorff.[3]

(3) One wire straight and doubly infinite with finite earth surface conductivity, as given by G. Haberland.[4]

(4) One wire straight and doubly infinite with finite earth surface conductivity and zero earth volume conductivity as given by Otto Mayr.[5]

JOHN RIORDEN
E. D. SUNDE

American Telephone and
Telegraph Company,
New York, N. Y.,
May 5, 1931.

[3] Ollendorf, "Erdströme," Julius Springer, Berlin, 1928, pp. 69–71.

[4] Haberland, Z. für. Ang. Math. u. Mech. **6**, Heft. 5, Oct. (1926).

[5] Mayr, E. T. Z. Sept. 1925, pp. 1352–1355, 1436–1440, Eq. (13).

ERRATA

VARIATIONS WITH TEMPERATURE AND FREQUENCY OF DIELECTRIC LOSS IN A VISCOUS, MINERAL, INSULATING OIL

By Hubert H. Race
General Electric Research Laboratory, Schenectady, New York.

(Phys. Rev. **37**, 430, 1931)

Two mistakes in the above paper have been brought to the attention of the author. The corrected equations with the corrections in bold face type are given below.

$$\epsilon = \frac{\left(\frac{\epsilon_0}{\epsilon_0+2}\right) + i\omega\tau\left(\frac{\epsilon_\infty}{\epsilon_\infty+2}\right)}{\left(\frac{1}{\epsilon_0+2}\right) + i\omega\tau\left(\frac{1}{\epsilon_\infty+2}\right)} \qquad \text{Eq. (14)}$$

$$\omega\tau = (\epsilon_\infty + 2)/(\epsilon_0 + 2) \qquad \text{Eq. (23)}$$

THE ENERGY OF DISSOCIATION OF MERCURY MOLECULES

By J. Gibson Winans
Department of Physics, University of Wisconsin

(Phys. Rev. **37**, 897, 1931)

Figures 2 and 3, page 899, should appear as shown below.

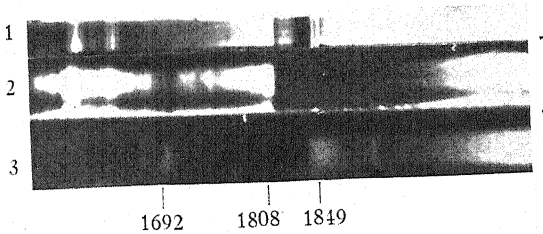

FIG. 2

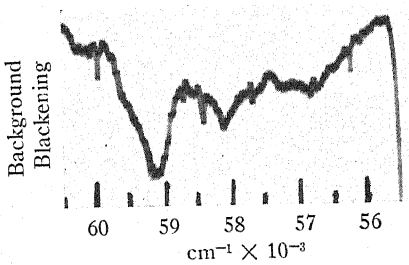

FIG. 3

BOOK REVIEWS

Physics, A Textbook for Colleges. Revised Edition. O. M. STEWART. Pp. 770, figs. 492. Ginn and Co. Boston. Price $4.00.

In reading this College Physics, the reviewer gets the impression that the author has attempted to put in a single volume, everything that has ever been included in a college text on physics. There are a number of rather well-written chapters on "modern physics" of the sort so much in demand today but which are probably omitted by most classes. If such material must be included, a bit more might have been included about the Bohr atom and energy levels so as to give the student a more definite picture of the atom. In those places where modern ideas really help in giving an elementary explanation, the author has made good use of them.

The main part of the book is not very different from many college texts. Certain features are however noticeable. An extra large number of topics are mentioned, some more briefly than usual. For example, the Carnot cycle, magnetic circuits and methods of combining vectors are mentioned but not really discussed. A great many formulae are given without even a suggestion as to how they were obtained. This is perhaps partly due to the total avoidance of all use of calculus. It does seem however, as if fewer formulae worked out in more detail would teach the student more physics. The more detailed discussions given and most of the diagrams are very good. The chapter on meterology is particularly good—if it belongs in the book.

The accuracy of the book, particularly as to definitions, seems to be very high although the indeterminate expressions "calories per gram per degree" and "cm per sec per sec" are used. There is included an unusually large number of problems and answers. Since there is no perfect text on college physics, the reviewer believes that many teachers will find this book very satisfactory and that they will get good results from its use.

NIEL F. BEARDSLEY

Principles of Engineering Thermodynamics. PAUL J. KIEFER AND MILTON C. STUART. Pp. 545, figs. 135. John Wiley and Sons, Inc. New York, 1930. Price $4.50.

It is strictly an engineering thermodynamics in that it treats of the subject in relation to all power plant problems, such as the steam engine, steam turbine, gas engine, compressor, refrigerating machine etc. It is a successful endeavor to tie the fundamental principles taught in a good course in physics with the theory and technical application of thermodynamics in the various types of power machinery. The treatise is divided in five parts. Part I, composed of three chapters, considers the first law of thermodynamics and the division of energy into different forms, as stored and transient energy in relation to flow and non-flow processes. Part II, which contains four chapters, takes up the second law of thermodynamics, the Carnot principle and makes a particular effort to give more of a physical significance to entropy, i.e., as a measure of the unavailability of energy. The latter point is to be especially commended. In the three chapters constituting Part III are treated the properties of the various media in which these thermodynamic processes must operate when applied to practical devices. The assumption of certain ideal conditions to establish a fundamental relation and then the institution of other factors to admit the introduction of other superposed physical effects as one passes from the theoretical to the practical case is well demonstrated in this treatment. There are eight chapters in Part IV, each devoted to a different type of motive power machinery. Each illustrates how certain accessories are instituted to make the special type of machine operative and the corresponding diversion from the theoretically ideal device. A working relation is obtained for each case.

The principles of thermodynamics are so general, that there are many other problems in physics and chemistry which may be solved by their application. Part V is used to develop additional thermodynamic equations such as are required in this large field of work that lies outside of this text.

Probably one of the most commendable features about this treatise is the summary, review

questions and the problems accompanying each chapter. Not only has it high pedagogical value but there is nothing that systematizes information and gives one a perspective of the subject like a summary. It inspires a feeling of mastery. Apparently there was no sparing of effort for clarity in the text.

L. F. MILLER

Algebraic Charts. EDGAR DEHN. Columbia Press, New York, 1930. 14 cards in an envelope.

These charts consist of six fundamental cards, each accompanied by a card giving an illustrative solution. The curves and auxiliary formulas provided permit the approximate solution of any quadratic or cubic equation, and of a certain type of bi-quadratic equation. The charts furnish interesting simple illustrations of nomographical methods and give applications of certain fundamental notions of analytic geometry and the theory of equations. Teachers of mathematics, particularly in colleges of engineering, would probably find the charts appropriate for supplementary work in certain of their courses.

Any graphical method for solving a quadratic equation is largely of theoretical interest, because of the ease with which the algebraic solution can be performed. Hence, from the practical standpoint, the charts are of interest mainly as they apply to cubics and bi-quadratics. For such equations, it appears to the reviewer that Mr. Dehn's methods could be applied efficiently only by one with a good knowledge of the theory of equations, and then only after considerable practice. If used efficiently, however, these charts would be very useful aids in problems where the degree of approximation of the chart-solutions would be satisfactory.

WILLIAM L. HART

Wave Mechanics. LOUIS DEBROGLIE. Translated by H. T. Flint. Pp. 249+vi, figs. 13. Methuen and Company, London, 1930. Price 12/6.

The number of good books on the quantum mechanics is rapidly increasing, so the student now has the choice of numerous styles and modes of exposition. In most of these texts the emphasis is on the "how"; i.e. the technique of the theory and its application to numerous problems. In the present volume, by the originator of the wave mechanics, the emphasis is placed on the "why"; in particular on the comparison of the ideas underlying the classical (Newton-Hamilton) and the modern (deBroglie-Schroedinger) view-points. Professor deBroglie here, as in his other works, builds up his argument starting from the dynamical equations of Newton and of the restricted principle of relativity. This makes a very compact and elegant argument, incidentally furnishing the student with a good chance to renew his acquaintance with general dynamical principles. The transition to waves is very clearly set forth, and there is a wealth of illustrative material on the motion of the waves and of probability packets in special cases. The average American student may find the treatment rather mathematical for a first trial, but after he has learned, from other sources, how to "quantize" a few things, he may return to this book and derive considerable pleasure and profit from it. The reviewer cannot help but record his enjoyment at the open-minded and considered manner in which Professor deBroglie treats his subject. Unfortunately there is a considerable tendency toward dogmatic statement among many writers on quantum mechanics, a tendency which the reviewer believes leads only to an unnecessary confusion and uncertainty on the part of many who are sincerely trying to understand something about the theory. This book should do much to help the situation and the translator is to be thanked for making it available to the English-speaking public.

E. L. HILL

Lecons Sur Le Calcul Vectoriel. T. A. RAMOS. Pp. 119. Librairie Scientifique A. Blanchard, Paris, 1930. Price, fr. 25.

Despite its numerous good points, this book probably will not make much appeal to American physics students, principally because of the choice of notation. The notation of Gibbs has become so standard in the physical literature that it scarcely seems worth while for a beginning student to learn any other. Considered on its own merits, however, this book gives a pleasing presentation of the subject. Vector algebra and calculus are developed in detail, the applications being mainly of a purely mathematical nature; e.g. to space curves and surfaces and to curvi-

linear coordinates. The treatment throughout is of a better grade than in most texts with which the student is apt to make contact, but might have been helped in places by the addition of simple figures. The last chapter, of a more advanced character, gives a treatment of tensor calculus as a direct generalization of vector analysis.

E. L. HILL

Principles of Electrical Engineering (Second Edition). W. H. TIMBIE AND V. BUSH. Pp. 595, figs. 270. McGraw-Hill Book Company, New York, 1930, Price $4.50.

In this edition of the well-known text most of the articles and figures remain as in the first edition except those in the last four of the thirteen chapters. Many of the articles in these last chapters have been rewritten and valuable material added. Nearly all of the 600 problems are new or entirely rewritten.

The text is a substantial first course designed to train students in the principles of applied electricity and is the outgrowth of the experience in teaching the subject to electrical engineering students at the Massachusetts Institute of Technology. Some training in the use of calculus is presupposed. It is assumed that the student has completed or is pursuing the first college course in physics, including the subject of electricity as treated therein.

The outstanding feature of the text is its many exceptionally valuable problems which are improved in this edition and which give information concerning the basic practical aspects of electrical engineering and excellent training in analytical thinking. The magnetic circuit and dielectrics are stressed and the electron theory is used freely. The subjects of thermionic emission, conduction through gases, electrolytic conduction and some high frequency phenomena are included in addition to the standard subjects. The summary at the end of each chapter of the main facts and laws treated in that chapter is commendable.

Historical relationships are disregarded. The text, aside from secondary statements, defines ampere as the rate of flow of a coulomb per second. The volt is defined only in terms of the difference of potential produced by a standard cell, while the difference of potential itself can hardly be said to have been defined. The maxwell is defined as "the amount of flux which, when established in a magnetic circuit, will produce one abvolt-second in a coil of one turn wound on the magnetic circuit." The generated electromotive force is a circuit is then referred only to this. Such treatment, notwithstanding its practical simplicity, gives an inadequate picture of the units and tells nothing concerning how the electromotive force is produced by the change in flux. This treatment may be permissible in a text of this nature only on the assumption that the student has had previous training in the theoretical aspects of the subject and in the systems of units.

While minor details and the definitions may be criticized and some mis-statements still appear, the text on the whole is excellent and gives substantial training from the practical point of view in the basic principles on which modern electrical engineering is founded.

ANTHONY ZELENY

Constitution et Thermochimie des Molecules. ALBERT GOSSELIN AND MARCEL GOSSELIN. Pp. vii+231. Les Presses Universitaires de France, Paris, France.

The authors propose a new theory of chemical combination based on the hypothesis that: first, there exist within molecules other molecules and groupings, as for example a H_2 molecule exists within a methane molecule, and second there exist two kinds of chemical bonds, the polar and nonpolar bond which may produce a semi-polar bond. The molecule is furthermore conceived as a dynamic structure with a central atom around which the other atoms, groups or constituent molecules gravitate. The ideas that are new are certainly different from the usual notions and it appears to the reviewer, they are quite unnecessary and based on insufficient evidence. The four hydrogen atoms in methane are surely equivalent as far as we have experimental knowledge of this situation, and there is no need to introduce the idea that a H_2 molecule exists within the methane structure. To be sure some such notion is presented by writers on molecular structure who attempt to study molecules on the basis of molecular wave mechanics, but the present authors do not mention these newer concepts at all. Their new structures are sometimes quite remarkable: A central oxygen atom of mass 16 has a bromine molecule

of mass 160, a HBr molecule of mass 81, a couple of hydrogen atoms and two ethylene groups gravitating around itself! The authors think that they can claim their new structures to be correct because they are able to set up a scheme of thermochemistry for their new formulae which checks when used for predicting the heats of formation of compounds. But this only means that they were consistent in their changes of formulae and is no proof for their ideas.

The book is written in a clear style as all French books are and it has been an interesting pastime to review the book, for it served to compare the "new" ideas with the current notions held by the reviewer, and it is felt that the new theories presented are quite unnecessary. It is hoped that the book will be available to mature students only who can judge for themselves and who have been instructed in the well-tried ideas of modern valency theory.

GEORGE GLOCKLER

Telephone Theory and Practice; Theory and Elements. KEMPSTER B. MILLER. Pp. xiv+486, figs. 272. McGraw-Hill Book Company, New York, 1930.

This is the first volume of a three volume work by an author who has long been an authority in this field.

Part I, consisting of four chapters, is mainly historical, tracing in a highly interesting manner the developments in communication up to the present time. The history of the electric speaking telephone is accurately presented.

Part II includes a discussion of the nature of sound and hearing, the conversion of sound waves into electric waves, the functions of vacuum tubes in the transmission of these waves, and concludes with a chapter on magnetism and magnetic materials.

The three chapters on sound are of particular interest. The first shows the physical meaning of the properties, loudness, pitch, and quality. The second deals with the sensation of sound showing the manner of operation of the ear, and giving the evidence for the "maximum amplitude" theory of determination of pitch. The significance of the auditory sensation area, and the meaning of the units of pitch and loudness are clearly presented. Subjective tones are discussed and illustrations of their rather startling effects given. The phenomenon of masking, so important when extraneous noise is present, is competently treated. The third of these chapters on sound describes simply and clearly the operation of the vocal organs in speech. The relative importance of various frequencies in articulation, and in good musical reproduction is shown.

The chapter on vacuum tubes gives good physical pictures of the operation of these devices in their various functions, and the chapter on magnetic materials discusses principally the iron-cobalt-nickel alloys used in modern telephone apparatus.

The third part of the volume discusses the construction and use of the elements of telephone apparatus such as wires, coils, condensers, contacts, which play such important roles in the modern telephone system.

The volume is ably and interestingly written, well referenced to primary sources, and excellently printed and illustrated. The almost non-mathematical treatment of voice waves and alternating currents is ingenious and makes it easily readable to the layman as well as to the technician.

RALPH D. BENNETT

The Metallic State. Electrical Properties and Theories. W. HUME-ROTHERY. Pp. 372+xx, figs. 66. Clarendon Press, Oxford, 1931. Price $9.00.

The general problem with which this book is finally concerned is the understanding of the properties of metals, including not only ordinary pure metals, but also intermetallic compounds and alloys in general. The problem is therefore one which by tradition has been associated, in certain broad aspects, with the metallurgist, and the author has indeed had the training of a metallurgist, and at the time of writing held the position of Armourers' and Brasiers' Company Research Fellow in Metallurgy. The subject is, however, preëminently one for the physicist, and the book is throughout almost exclusively devoted to the purely physical aspects of the problem.

In order not unduly to expand the book, attention is confined to those aspects of the

problem about which most is known and in which the most significant theoretical progress has been made, and this restricts the book almost entirely to the electrical properties of metals. The book is divided into two parts, the first experimental and the second theoretical. The experimental part does not deal at all with such conventional metallurgical matters as methods of fixing the phase diagrams, or even with the phase diagrams themselves to any large extent, but it is concerned with electrical and thermal conductivity, some of the galvano-magnetic and thermo-magnetic effects, thermo-electric effects, and emission and contact potential difference phenomena. The dependence of these properties on composition, temperature, and mechanical stress is discussed, and constitutes a valuable summary of data which has not before been collected into one place.

In the theoretical part most of the theories of historical or present day importance are discussed, starting with the electron gas theory of Drude and its mathematical elaboration by Lorentz. The discussion of the theories now discarded is most skillfully done, both in pointing out the weaknesses of the theories and in emphasizing the way in which many of the physical aspects of the present wave mechanics pictures were being anticipated as the only possible solution consistent with the complex experimental situation. The discussion of the Sommerfeld theory and its later modifications presents the very valuable and revolutionary achievements of the theory, but also does not fail to emphasize the features in which the theory is weak or unsatisfactory—a welcome antidote to the attitude of too many recent writers that electrical phenomena in metals are now, again, an essentially closed chapter, and that only details remain to be filled in. There is a concluding section dealing with correlations between electrical properties, position in the periodic table, and the structure of the atom according to recent ideas, which is most interesting. This includes a full discussion of a number of most curious and undoubtedly significant empirical correlations discovered by Hume-Rothery himself which will be most welcome.

As a whole, the book is exceedingly stimulating and suggestive, and cannot be too highly recommended to the careful study of any one working in this field. It is unusual in the emphasis that it puts on unsolved problems, and in its suggestions as to possible programs for their solution. One point repeatedly emphasized, namely that the physicist in making measurements in the field of alloys almost always deals with specimens which no metallurgist would tolerate because they have not been sufficiently annealed to reach a condition of equilibrium, would in itself justify the book if the warning is heeded.

P. W. BRIDGMAN

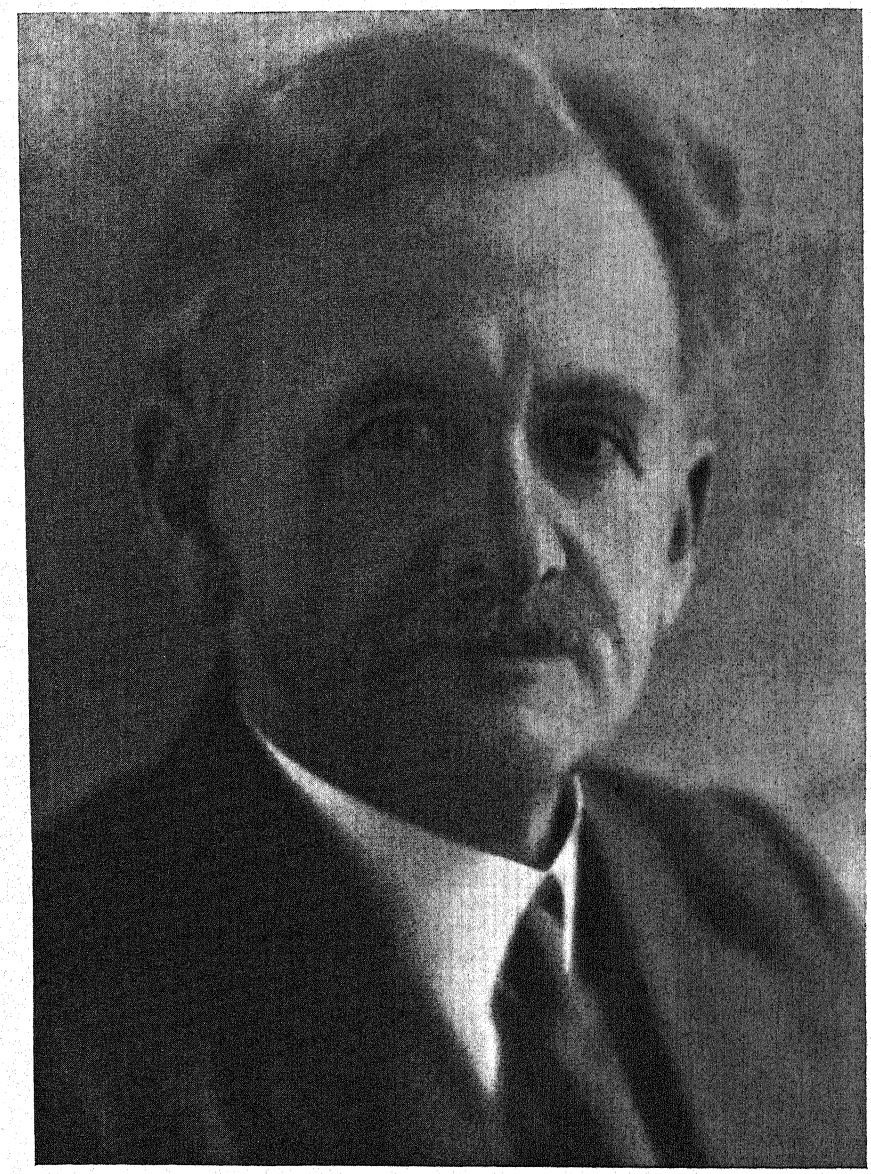

Albert A. Michelson

Second Series *June 1, 1931* *Vol. 37, No. 11*

THE
PHYSICAL REVIEW

ALBERT A. MICHELSON, 1852-1931

AT ONE o'clock on Saturday afternoon, May 9, 1931, death came very quietly in his home in Pasadena to the most illustrious of the American physicists of our generation, at the age of seventy-eight years and five months. Six weeks earlier he had taken to his bed, after having made with his associates, Messrs. Pease and Pearson, enough observations to assure himself that his last experiment on the speed of light as measured in an evacuated pipe a mile long and three feet in diameter buried in the earth on the Irvine ranch near Santa Ana, California, was going to yield results as satisfactory as he had anticipated. This experiment had been planned for the sake of obtaining a check by a method entirely free from atmospheric effects of all kinds upon the accuracy of his next preceding determination made over a twenty-one mile stretch between California mountain peaks. He did not expect by these new experiments to exceed the accuracy previously obtained, but rather to add something to the *reliability* of the previous determination.

More than a month before his death, Mr. Michelson had known that he would never get up again, for a creeping paralysis was coming over him of which he himself was altogether conscious. His mind was quite clear until two days before the end, when a lesion occurred which brought on unconsciousness within an hour, an unconsciousness from which he never again awoke.

As one of the men who has had the most enduring and most intimate association with Mr. Michelson and his work, I esteem it a privilege now to make a few additions to my former appreciation of him and his achievement.

Under the caption, "Michelson's Economic Value," now published as Chapter VII in a volume by Scribner's entitled "Science and the New Civilization," I have attempted to appraise in broad lines the significance for our times of measurements of the highest skill and accuracy of the sort which Michelson has done and for which his name stands the world over, and I should like to refer to that appraisal and merely supplement it here by adding some details both of a scientific and of a personal sort.

Practically all of Mr. Michelson's work in physics centered about determinations for increasing the precision of measurement. He has been called an extremely skillful and intelligent instrument designer, but while he was that

he was much more than that, for his attention was always on the problem to be solved, not primarily on the instrument for solving it, and he was always seeking for problems incapable of solution save by improvements in the accuracy of measurement. Ten different times in the fifty-one years of his activity, extending from 1880 when at the age of twenty-eight he became the best known American physicist by virtue of his new speed-of-light measurement up to 1931 when he died, still trying to prove the certainty of his determination and precision of that most fundamental constant, he made major outstanding advances, which I list as follows:

1. Measurements of the speed of light, 1880–1931.
2. Development of the Michelson interferometer, 1882 et seq.
3. Ether-drift experiments, 1887–1928.
4. The first analysis of the fine structure of spectral lines, 1894–1900.
5. Development of the Michelson-Stratton harmonic analyzer, 1897.
6. Development of the principle of the Echelon spectrograph, 1898.
7. Perfection and increase in resolution of the line grating, 1902–1917.
8. First accurate measurement of the rigidity of the earth, 1916.
9. Development of the U. S. Naval Range Finder, 1918.
10. Direct interferometer measurement of the diameter of stars, 1921.

Of these ten five, namely the second, third, fourth, and tenth, have to do primarily with the interferometer or its application to various sensitive measurements. It was in measurements relating to the interference of light and speed of light that he was by far the greatest expert that the world has yet seen. He spent his scientific life largely in these two fields. He was not an omnivorous reader of the literature of physics, and did not try to follow closely the developments of the theoretical fields of electronics and quantum theory. He was essentially a classical physicist, but any one who ever heard him conduct a Ph.D. examination in physics, and any one who ever attended his lectures or heard him speak knows that his grasp of classical physics was penetrating and precise. His lectures and his papers were masterpieces of elegance and conciseness. He used a few words, but they were just the ones he wanted. Indeed, the precision of his mind was its dominating characteristic, which showed even in his sports. I have played tennis with him all my life, and his calling of balls, for example, was never generous either to himself or to his opponent. It was simply exact and just. Closely allied to this characteristic was his altogether extraordinary honesty. Pretense of any kind was utterly foreign to his make up. Indeed, he was one of those very rare persons who would not even tolerate fooling himself with respect to his own motives, as so many of us do. If his conduct was ever ungenerous he knew it and frankly admitted it, whether he thought it wise to change it or not. Before I became intimately associated with him I had heard that he was considered by his pupils to be somewhat unapproachable, occasionally arbitrary, and at times dictatorial, if not unreasonable, but in the twenty-five years in which we worked together I could not have been treated with greater courtesy and consideration, even in the few cases in which we differed in judgment. His dignity and courtesy of bearing were altogether striking characteristics, and as the

years passed he grew to be a man of great mellowness, kindness, and affability.

Like many a scientist, Mr. Michelson was also an artist, with a keen feeling for form and color, as well as for music. He painted well, played the violin well, and did well at tennis, chess, and billiards.

American Science and the American nation have lost in his death one of their finest and greatest figures.

ROBERT A. MILLIKAN

May 11, 1931.

APPLICATION OF SPINOR ANALYSIS TO THE MAXWELL AND DIRAC EQUATIONS

By Otto Laporte and George E. Uhlenbeck
Department of Physics, University of Michigan

(Received February 24, 1931)

Abstract

With the spinor analysis developed by B. van der Waerden which comprises all representations of the Lorentz group, even those not contained in ordinary tensor calculus, one is able to write all derivations and equations in an *automatically covariant form*. For the convenient translation into spinor language of the Maxwell equations, it becomes important to introduce three self-dual tensors, one representing the electromagnetic field, one corresponding to the Hertzian vector, and one representing a kind of current potential. These correspond to symmetric spinors of the 2nd rank. Many spinor equations thus become simpler than the corresponding tensorial equations, especially the expression for the stress energy tensor. From the 1st order Dirac equations in spinor form, as given by v.d. Waerden, we derived the 2nd order equation, which agrees with the Gordon-Klein form but for a correction term which again contains the self-dual field tensor. Further the expression for the current was derived, and its decomposition into conduction and polarization currents, and both Maxwell and Dirac equations were derived from a spinorial variation principle, analogous to the results of Gordon and Darwin. In addition to the divergence condition for the current three new invariant relations between the wave functions which are independent of the potentials were obtained (Chapter III, Eqs. (11), (12) and (13)).

Introduction

THE Dirac equations of the electron have for the first time furnished an example of a system of equations, which show an invariance of form when subjected to a Lorentz transformation, but which only very artificially could be written with tensors. This difficulty was felt especially by Darwin[1] when he wrote: "The relativity theory is based on nothing but the idea of invariance, and develops from it the conception of tensors as a matter of necessity; and it is rather disconcerting to find that apparently something has slipped through the net, so that physical quantities exist, which it would be, to say the least, very artificial and inconvenient to express as tensors."

The Dirac equation is

$$[(\Gamma^k p_k) + mc]\psi = 0 \tag{1}$$

where p_k represents the 4-vector[2]

$$p_k = \frac{h}{i}\frac{\partial}{\partial x^k} + \phi_k \tag{2}$$

[1] C. G. Darwin, Proc. Roy. Soc. **118**, 657 (1928).

[2] We use the Dirac h, which is $1/2\pi$ times the Planck constant, and write here; and in Ch. III, ϕ_k for e/c times the ordinary four potential.

and Γ^k are four four-row matrices, given by:[3]

$$\Gamma^1 = \begin{pmatrix} 0 & 0 & 0 & -1 \\ 0 & 0 & -1 & 0 \\ 0 & 1 & 0 & 0 \\ 1 & 0 & 0 & 0 \end{pmatrix} \quad \Gamma^2 = \begin{pmatrix} 0 & 0 & 0 & i \\ 0 & 0 & -i & 0 \\ 0 & -i & 0 & 0 \\ i & 0 & 0 & 0 \end{pmatrix}$$

$$\Gamma^3 = \begin{pmatrix} 0 & 0 & -1 & 0 \\ 0 & 0 & 0 & 1 \\ 1 & 0 & 0 & 0 \\ 0 & -1 & 0 & 0 \end{pmatrix} \quad \Gamma^4 = \begin{pmatrix} 0 & 0 & 1 & 0 \\ 0 & 0 & 0 & 1 \\ 1 & 0 & 0 & 0 \\ 0 & 1 & 0 & 0 \end{pmatrix} \tag{3}$$

ψ is a function of two kinds of variables, of x^i and an inner variable, which can only assume four discrete values; the p_k act upon the x^k while the Γ^k operate on the inner variable. This way of describing Eq. (1) is of course equivalent to regarding Eq. (1) as *four* equations containing 4 ψ's, each of them a function of x^k only.

There are *two* points of view possible, with regard to the transformation properties of the Dirac equation: The *first* of these regards the Γ^k as a matrix four vector, and the ψ as constant. According to the *second* point of view, the Γ^k are constants and the ψ are being transformed.

One can easily show that these two methods are equivalent. For if we subject the coordinates x^k to a Lorentz transformation,

$$x = x'L$$

then the p_k will be transformed like

$$p = L^{-1}p'.$$

If we consider Γ^k as a four vector, it will transform like x^k, and the scalar product

$$(\Gamma p) = (\Gamma' LL' p') = (\Gamma' p')$$

will remain invariant. On the other hand, we can always find a matrix S such that

$$p = L^{-1}p' = S^{-1}p'S. \tag{4}$$

Now the Γ^k are kept constant, and since they act on the inner variable only, they are exchangeable with S, so that

$$(S^{-1}\Gamma p' S)\psi + mc\psi = 0$$

or

$$(\Gamma p')(S\psi) + mc(S\psi) = 0.$$

Putting

$$\psi' = S\psi \tag{5}$$

[3] When written out, Eq. (1) agrees with the form given by Weyl, Gruppentheorie and Quantenmechanik, Leipzig 1928, page 171, Eq. (45′). If the above given matrices for Γ^1, Γ^2, Γ^3 are divided by i, they become identical to Weyl's Γ_1, Γ_2, Γ_3; our Γ^4 is equal to his Γ_0.

we regain (1), now with transformed ψ. This point of view regards the Γ^k simply as determining the coefficients $0, \pm 1, \pm i$ in the four wave equations.

For special two dimensional Lorentz transformations, Darwin has written out the transformation (5). They have the peculiar character that the coefficients contain the angle $\theta/2$, when the coordinates are rotated by the angle θ. We can see already from (4) that S is something like a square root of L.[4] This shows that ψ cannot be a tensor, and that there are equations, which defy translation into tensor language and yet fulfill the relativity principle. Now it has been known to the mathematicians that the ordinary tensor language does not comprise all possible representations of the Lorentz group as had always been assumed tacitly by the physicists.[5] The necessary extension of the tensor calculus, the *spinor calculus*, was given by B. van der Waerden,[6] upon instigation of Ehrenfest, and indeed gives all possible representations.

These two points of view correspond in a certain way to the particle and wave description of the electron. The first may give additional information concerning the particle velocity,[7] the second, however, is necessary for the consideration of the Dirac equations as field equations. In this case the ψ must naturally be transformed to a new coordinate system just as E and H in Maxwell's equations. We shall restrict ourselves to this point of view.

Chapter I. The Mathematical Apparatus of the Spinor Analysis

§1. Since van der Waerden's article is not very easily accessible, and in order to make the spinor analysis more popular, we shall briefly develop the few necessary theorems and formulae here, following van der Waerden closely.

Consider the following binary transformation

$$\begin{aligned} \xi_1' &= \alpha_{11}\xi_1 + \alpha_{12}\xi_2 \\ \xi_2' &= \alpha_{21}\xi_1 + \alpha_{22}\xi_2 \end{aligned} \tag{1}$$

and its complex conjugate:

$$\begin{aligned} \bar{\xi}_1' &= \bar{\alpha}_{11}\bar{\xi}_1 + \bar{\alpha}_{12}\bar{\xi}_2 \\ \bar{\xi}_2' &= \bar{\alpha}_{21}\bar{\xi}_1 + \bar{\alpha}_{22}\bar{\xi}_2 \end{aligned} \tag{2}$$

with the determinant

$$\begin{vmatrix} \alpha_{11} & \alpha_{12} \\ \alpha_{21} & \alpha_{22} \end{vmatrix} = 1. \tag{3}$$

All these transformations form a group of $8-2=6$ parameters. Any two numbers transforming like the ξ_1, ξ_2 in (1), we shall call a spinor of the 1st rank, and denote by

[4] Landau therefore calls ψ a half vector.

[5] Compare especially Hermann Weyl, Gruppentheorie und Quantenmechanik, Leipzig, 1928. Kap. III.

[6] B. van der Waerden, Göttinger Nachrichten 1929, page 100. The spinor formalism is already implicitly contained in the book of Weyl, and in a paper by V. Fock, Zeits. f. Physik **57**, 261 (1929).

[7] V. Fock, Zeits. f. Physik **55**, 127 (1929); G. Breit, Proc. Natl. Acad. **14**, 553 (1928); E. Schrödinger, Sitzungsber. Berliner Akad. **24**, 418 (1930).

$$a_k \qquad k = 1, 2$$

whereas any two quantities transforming like (2) will be written

$$b_{\dot{r}} \qquad \dot{r} = \dot{1}, \dot{2}.$$

Any four quantities transforming like the products $\xi_1\xi_1$, $\xi_1\xi_2$, $\xi_2\xi_1$, $\xi_2\xi_2$ we call a spinor of the 2nd rank and write

$$a_{kl} \qquad k, l = 1, 2.$$

Correspondingly 4 quantities transforming like the products of $\bar{\xi}_1$ and $\bar{\xi}_2$ we denote by

$$b_{\dot{r}\dot{s}} \qquad \dot{r}, \dot{s} = \dot{1}, \dot{2}.$$

There are also "mixed" spinors of the 2nd rank transforming like a product of a barred ξ and an unbarred ξ, denoted by

$$c_{\dot{r}k} \qquad \dot{r} = \dot{1}, \dot{2}; \quad k = 1, 2.$$

Analogously we can define spinors of higher rank, like $a_{\dot{r}\dot{m}l}$.

One can show easily, that because of (3) the area of the parallelogram formed by two spinors ξ_k and η_l

$$\xi_1\eta_2 - \xi_2\eta_1$$

is invariant under transformation (1). This enables us to introduce *contravariant* spinors a^k or $b^{\dot{r}}$, according to

$$\boxed{\begin{array}{ll} a^1 = a_2 & b^{\dot{1}} = b_{\dot{2}} \\ a^2 = -a_1 & b^{\dot{2}} = -b_{\dot{1}} \end{array}} \tag{4}$$

because in this way the scalar products

$$a_1c^1 + a_2c^2 = a_\lambda c^\lambda$$
$$b_{\dot{1}}d^{\dot{1}} + b_{\dot{2}}d^{\dot{2}} = b_{\dot{\rho}}d^{\dot{\rho}}$$

are invariant.[8] When we establish the usual connection between covariant and contravariant indices by means of a spinor ϵ^{kl} according to

$$a^k = \epsilon^{k\lambda}a_\lambda \tag{5}$$

we find

$$\epsilon^{kl} = \begin{pmatrix} 0 & -1 \\ 1 & 0 \end{pmatrix} \qquad \epsilon_{kl} = \begin{pmatrix} 0 & +1 \\ -1 & 0 \end{pmatrix}$$

and

$$\epsilon^{k\lambda}\epsilon_{l\lambda} = -\delta_l{}^k \tag{6}$$

where

[8] Summation signs are as usual suppressed; dummy indices are always given Greek letters, free indices Latin letters.

$$\delta_l{}^k = \begin{pmatrix} 1 & 0 \\ 0 & 1 \end{pmatrix}.$$

As in the usual tensor algebra, the only covariant operations are also here *multiplication* and *contraction*. For instance from the spinors $a_{\dot{r}\dot{s}}{}^l$ and $b^{\dot{m}}{}_{kt}$ we can form the spinor of the 6th rank

$$c_{\dot{r}\dot{s}}{}^{l\dot{m}}{}_{kt} = a_{\dot{r}\dot{s}}{}^l b^{\dot{m}}{}_{kt}$$

or the spinor of 4th rank

$$c_{\dot{s}}{}^l{}_{kt} = a_{\dot{\mu}\dot{s}}{}^l b^{\dot{\mu}}{}_{kt}$$

or the spinor of the 2nd rank

$$c_{\dot{s}t} = a_{\dot{\mu}\dot{s}}{}^{\lambda} b^{\dot{\mu}}{}_{\lambda t}.$$

The following two rules are essential in calculations. According to (6) we have

$$\boxed{a_\lambda b^\lambda = -\, a^\lambda b_\lambda} \tag{7}$$

An immediate consequence of this is that any spinor of odd rank has absolute value zero

$$a_\lambda a^\lambda = 0; \quad a^{\lambda\mu\nu} a_{\lambda\mu\nu} = 0. \tag{7a}$$

Similarly we have

$$\boxed{a^\lambda b_\lambda c_m + a_\lambda b_m c^\lambda + a_m b^\lambda c_\lambda = 0}. \tag{8}$$

Of course this rule may also be applied to the product $a^\lambda c_{\lambda m}$. It also holds for three dotted indices.

There are two more rules concerning the relations of dotted and undotted indices.

1° It is not necessary to fix the position of dotted and undotted indices belonging to the same spinor. Thus, for instance

$$a_{\dot{r}lt} = a_{l\dot{r}t} = a_{lt\dot{r}}.$$

On the other hand two dotted or two undotted indices are not necessarily interchangeable; if they are, the spinor in question has special symmetry properties.

2° The complex conjugate of any spinor equation is obtained by replacing all undotted indices by dotted ones and *vice versa*.

§2. We will now establish the connection between spinors and world tensors. We assert that the following combinations of components of a second rank spinor $a_{\dot{s}t}$ are to be associated with the components of a world vector A^1, A^2, A^3, A^4 as follows

$$\left.\begin{aligned} \tfrac{1}{2}(a_{\dot{2}1} + a_{\dot{1}2}) &= A^1 = A_1 \\ \frac{1}{2i}(a_{\dot{2}1} - a_{\dot{1}2}) &= A^2 = A_2 \\ \tfrac{1}{2}(a_{\dot{1}1} - a_{\dot{2}2}) &= A^3 = A_3 \\ \tfrac{1}{2}(a_{\dot{1}1} + a_{\dot{2}2}) &= A^4 = -A_4 \end{aligned}\right\} \tag{9}$$

These combinations are real, and after a transformation (1) and (2) they will still be real; thus their transformation coefficients are real also. To prove that it is a Lorentz transformation we solve (9) for the $a_{\dot{s}t}$ and obtain using (4)

$$\left.\begin{aligned} a_{\dot{2}1} &= -a^{\dot{1}2} = A^1 + iA^2 = A_1 + iA_2 \\ a_{\dot{1}2} &= -a^{\dot{2}1} = A^1 - iA^2 = A_1 - iA_2 \\ a_{\dot{1}1} &= +a^{\dot{2}2} = A^3 + A^4 = A_3 - A_4 \\ -a_{\dot{2}2} &= -a^{\dot{1}1} = A^3 - A^4 = A_3 + A_4 \end{aligned}\right\}. \tag{10}$$

Now it is easily verified that

$$-\tfrac{1}{2}a_{\dot{\sigma}\tau}a^{\dot{\sigma}\tau} = A_\gamma A^\gamma. \tag{11}$$

To every transformation (1) there corresponds one Lorentz transformation; *vice versa*, since the connection formulae between the transformation coefficients of A and the α's of eq. (1) are quadratic, there are two transformations (1) differing in sign, corresponding to one Lorentz transformation.[9] Therefore (1) and (2) form a representation of the Lorentz group. It can be proved, and this is the fundamental theorem of the spinor analysis, that one obtains all representations of the Lorentz group by transforming all possible spinors according to (1) and (2). It follows that the true "quantities" belonging to the Lorentz group are spinors, of which tensors form only a special class. Analogous to (10) spinors of the fourth rank with two dotted and two un-

[9] For example using the transformation formulae (1) and (2) for a spinor $a_{\dot{\tau}l}$ we find that for a Lorentz transformation

$$\begin{aligned} ct' &= ct\cosh\theta + \sinh\theta \\ z' &= ct\sinh\theta + z\cosh\theta \end{aligned}$$

there correspond the two transformation matrices

$$\alpha_{kl} = \begin{pmatrix} \pm e^{\theta/2} & 0 \\ 0 & \pm e^{-\theta/2} \end{pmatrix}$$

and with a special rotation

$$\begin{aligned} x' &= x\cos\theta + y\sin\theta \\ y' &= -x\sin\theta + y\cos\theta \end{aligned}$$

there correspond the two matrices

$$\alpha_{kl} = \begin{pmatrix} \pm e^{-i\theta/2} & 0 \\ 0 & \pm e^{+i\theta/2} \end{pmatrix}$$

For general spacial rotations we see that because of the invariance of t, that is to say of $\bar{\xi}_1\xi_1 + \bar{\xi}_2\xi_2$ the corresponding binary transformation (1) will be unitarian. For more information compare especially H. Weyl, Gruppentheorie und Quantentheorie, Leipzig 1928, p. 106–114.

dotted indices correspond to world tensors of the second rank. The formulae connecting them are obtained from (10) by multiplication. For instance

$$\left.\begin{aligned} a_{\dot{2}\dot{2}11} &= a^{ii22} = A^{11} - A^{22} + i(A^{12} + A^{21}) = A_{11} - A_{22} + i(A_{12} + A_{21}) \\ -a_{\dot{2}\dot{2}21} &= a^{ii12} = A^{31} - A^{41} + i(A^{32} - A^{42}) = A_{31} + A_{41} + i(A_{32} + A_{42}) \end{aligned}\right\} \quad (12)$$

In the following table all possible kinds of spinors of the 5 lowest ranks are written down and those corresponding to world tensors are underscored.

$$\underline{a}$$

$$a_k \qquad a_{\dot{m}}$$

$$a_{kl} \qquad \underline{a_{\dot{m}l}} \qquad a_{\dot{m}\dot{n}}$$

$$a_{klt} \qquad a_{\dot{m}lt} \qquad a_{\dot{m}\dot{n}t} \qquad a_{\dot{m}\dot{n}\dot{r}}$$

$$a_{kltv} \qquad a_{\dot{m}ltv} \qquad \underline{a_{\dot{m}\dot{n}tv}} \qquad a_{\dot{m}\dot{n}\dot{r}v} \qquad a_{\dot{m}\dot{n}\dot{r}\dot{s}}$$

§3. Although the underscored spinors correspond *directly* to tensors of half their rank, the *spinors of even rank* can be related to tensors of higher rank, which possess certain symmetry properties. Let us consider the simplest spinors of this kind a_{kl} and its complex conjugate $a_{\dot{m}\dot{n}}$. We decompose a_{kl} into a symmetric and antisymmetric spinor, according to

$$a_{kl} = \tfrac{1}{2}(a_{kl} + a_{lk}) + \tfrac{1}{2}(a_{kl} - a_{lk}) = \sigma_{kl} + \alpha_{kl}. \quad (13)$$

The antisymmetric part α_{kl} has only one "Kennzahl"

$$\alpha_{12} = -\alpha_{21} = \tfrac{1}{2}(a_{12} - a_{21}) = \tfrac{1}{2}(a_1^1 + a_2^2) = \tfrac{1}{2}a_\rho{}^\rho$$

which is an invariant. The symmetric part σ_{kl} has three "Kennzahlen" and can be shown to correspond to an *antisymmetric self-dual tensor*. Consider a real antisymmetric world tensor F^{kl}. The dual tensor to this is obtained by means of

$$F^*_{kl} = \pm \frac{i}{2} \delta_{kl\alpha\beta} F^{\alpha\beta} \quad (14)$$

where $\delta_{klmn} = 0$ when any two indices are equal and $= \pm 1$ according to whether the indices form an even or odd permutation of the numbers 1234. Thus two dual tensors F^{*kl} are possible to an originally real tensor F^{kl}; they differ only by the sign, so that one is the complex conjugate of the other. Obviously the dual to F^{*kl} is again the original F^{kl} without asterisk. The self-dual tensor G^{kl} is the sum of the two[10]

$$\left.\begin{aligned} G^{kl} &= F^{kl} + F^{*kl} \\ \overline{G}^{kl} &= F^{kl} - F^{*kl}. \end{aligned}\right\} \quad (15)$$

Calling the three Kennzahlen k_1, k_2, k_3, G^{kl} may be written

[10] We note the theorem, that for any two self-dual tensors G^{kl} and H^{kl} the product

$$G^{k\lambda}\overline{H}_{k\lambda} \equiv 0$$

$$G^{kl} = \begin{pmatrix} 0 & k_3 & -k_2 & -ik_1 \\ -k_3 & 0 & k_1 & -ik_2 \\ k_2 & -k_1 & 0 & -ik_3 \\ ik_1 & ik_2 & ik_3 & 0 \end{pmatrix} \tag{15a}$$

or taking the lower sign in (14)

$$\overline{G}^{kl} = \begin{pmatrix} 0 & \bar{k}_3 & -\bar{k}_2 & i\bar{k}_1 \\ -\bar{k}_3 & 0 & \bar{k}_1 & i\bar{k}_2 \\ \bar{k}_2 & -\bar{k}_1 & 0 & i\bar{k}_3 \\ -i\bar{k}_1 & -i\bar{k}_2 & -i\bar{k}_3 & 0 \end{pmatrix}. \tag{15b}$$

Then we form the spinor of the fourth rank $g_{\dot{r}\dot{s}kl}$ according to (12) which using G^{kl} can be written

$$g_{\dot{r}\dot{s}k}{}^{l} = g_{\dot{r}\dot{s}}\delta_k{}^{l} \tag{16a}$$

and which using $\overline{G}^{kl}$ can be written

$$g_{\dot{r}}{}^{\dot{s}}{}_{kl} = \delta_{\dot{r}}{}^{\dot{s}}g_{kl}. \tag{16b}$$

Here the spinors $g_{\dot{r}\dot{s}}$ and g_{kl} are *symmetric*. Solving (16) and (16a) we obtain

$$\left.\begin{aligned} g_{\dot{r}\dot{s}} &= \tfrac{1}{2}g_{\dot{r}\dot{s}\lambda}{}^{\lambda} \\ g_{kl} &= \tfrac{1}{2}g_{\dot{\sigma}}{}^{\dot{\sigma}}{}_{kl} \end{aligned}\right\}. \tag{17}$$

The formulae connecting the components of the symmetric spinors with those of the antisymmetric, self-dual world-tensor are

$$\left.\begin{aligned} g_{\dot{1}\dot{1}} &= 2(k_2 + ik_1) \\ g_{\dot{2}\dot{2}} &= 2(k_2 - ik_1) \\ g_{\dot{1}\dot{2}} = g_{\dot{2}\dot{1}} &= -2ik_3 \end{aligned}\right\} \tag{18}$$

and using (16a) we simply obtain the complex conjugate

$$\left.\begin{aligned} g_{11} &= 2(\bar{k}_2 - i\bar{k}_1) \\ g_{22} &= 2(\bar{k}_2 + i\bar{k}_1) \\ g_{12} = g_{21} &= 2i\bar{k}_3 \end{aligned}\right\}. \tag{18a}$$

§4. Corresponding to the introduction of a covariant gradient vector we now define a gradient spinor $\partial_{\dot{s}t}$ according to the connection formulae (10) as follows

$$\left.\begin{aligned} \partial^{1}{}_{1} = \partial_{\dot{2}1} &= \frac{\partial}{\partial x^1} + i\frac{\partial}{\partial x^2} \\ -\partial^{\dot{2}}{}_{2} = \partial_{\dot{1}2} &= \frac{\partial}{\partial x^1} - i\frac{\partial}{\partial x^2} \\ -\partial^{\dot{2}}{}_{1} = \partial_{\dot{1}1} &= \frac{\partial}{\partial x^3} - \frac{\partial}{\partial x^4} \\ -\partial^{\dot{1}}{}_{2} = -\partial_{\dot{2}2} &= \frac{\partial}{\partial x^3} + \frac{\partial}{\partial x^4} \end{aligned}\right\} \tag{19}$$

where the contravariant vector (x^1, x^2, x^3, x^4) corresponds to (x, y, z, ct). Analogously to (11) we may now translate the familiar vector analytical operations like Div or $\square$ into the spinor language. We have

$$\frac{\partial \phi^\alpha}{\partial x^\alpha} = -\frac{1}{2}\partial_{\dot\sigma\tau}\phi^{\dot\sigma\tau} \tag{20}$$

and

$$\frac{\partial^2 S}{\partial x_\alpha \partial x^\alpha} = -\frac{1}{2}\partial_{\dot\sigma\tau}\partial^{\dot\sigma\tau} S. \tag{21}$$

Chapter II. Maxwell Equations in Spinor Form

§5α. To facilitate the comparison, we shall briefly recapitulate the Maxwell equations in the ordinary tensor form. As usual we define the antisymmetric field tensor

$$F^{kl} = \begin{pmatrix} 0 & H_z & -H_y & -E_x \\ & 0 & H_x & -E_y \\ & & 0 & -E_z \\ & & & 0 \end{pmatrix} \tag{1}$$

then the dual tensor according to (14) is

$$F^{*kl} = -i\begin{pmatrix} 0 & E_z & -E_y & H_x \\ & 0 & E_x & H_y \\ & & 0 & H_z \\ & & & 0 \end{pmatrix} \tag{2}$$

The two Maxwell equations are

$$\begin{aligned} \frac{\partial F^{k\lambda}}{\partial x^\lambda} &= S^k \\ \frac{\partial F^{*k\lambda}}{\partial x^\lambda} &= 0 \end{aligned} \tag{3}$$

where S^k is the four-current $(\rho v_x/c, \rho v_y/c, \rho v_z/c, \rho)$ obeying the continuity equation

$$\frac{\partial S^\lambda}{\partial x^\lambda} = 0. \tag{5}$$

We can embody these two equations into one

$$\frac{\partial G^{k\lambda}}{\partial x^\lambda} = S^k \tag{6}$$

by using the self-dual tensor

$$G^{kl} = F^{kl} + F^{*kl} \tag{7}$$

which has the form (15), with[11]

$$\vec{k} = \vec{H} - i\vec{E}. \tag{8}$$

We can derive G^{kl} from the four-potential $\phi^k = (A_x, A_y, A_z, \phi)$ by means of

$$G^{kl} = \frac{\partial \phi^l}{\partial x_k} - \frac{\partial \phi^k}{\partial x_l}. \tag{9}$$

The ϕ^k are subjected to the accessory condition

$$\frac{\partial \phi^\lambda}{\partial x^\lambda} = 0. \tag{10}$$

Introducing (9) into (6), using (10) we get the wave equation for ϕ^k

$$\frac{\partial^2 \phi^k}{\partial x_\lambda \partial x^\lambda} = S^k. \tag{11}$$

§5β. To free ourselves from the condition (10) imposed on the potentials, we express ϕ^k in terms of a self-dual antisymmetric tensor Z^{kl}, the analogue to the Hertzian vector in three dimensions by means of[12]

$$\phi^k = \frac{\partial Z^{k\lambda}}{\partial x^\lambda}. \tag{12}$$

Introducing this in (11), we get for Z^{kl} a third order differential equation

$$\frac{\partial}{\partial x^\lambda} \frac{\partial^2 Z^{k\lambda}}{\partial x_\alpha \partial x^\alpha} = S^k.$$

In the three dimensional form one reduces this to a second order differential equation by an integration of the current $\rho v/c$ with respect to the time.[13] The analogue of this is the derivation of S^k from a stream potential Q^{kl}, which is again an antisymmetric self-dual tensor, according to

[11] Comp. Riemann-Weber, Die partiellen Differentialgleichungen der Physik, Braunschweig 1901, Vol. II, 348. L. Silberstein, Ann. d. Physik **22**, 579 (1907). See also F. Zerner, Handbuch der Physik vol. XII, p. 93.

[12] When we represent Z^{kl} by the scheme

$$Z^{kl} = i \begin{pmatrix} 0 & Z_z & -Z_y & iZ_x \\ & 0 & Z_x & iZ_y \\ & & 0 & iZ_z \\ & & & 0 \end{pmatrix}$$

then the three dimensional form of (12) is

$$A = i \operatorname{curl} Z - \frac{1}{c} \frac{\partial Z}{\partial t}$$

$$\phi = \operatorname{div} Z.$$

[13] See e.g. Madelung, Die mathematischen Hilfsmittel des Physikers, Berlin 1922, p. 196.

$$S^k = \frac{\partial Q^{k\lambda}}{\partial x^\lambda}. \tag{13}$$

This causes the continuity equation (5) to be identically satisfied. For Z^{kl} we then get the wave equation

$$\frac{\partial^2 Z^{kl}}{\partial x_\alpha \partial x^\alpha} = Q^{kl}. \tag{14}$$

§5γ. The stress-energy tensor $T_k{}^l$ whose divergence is equal to the components of the four force can be written

$$T_k{}^l = \tfrac{1}{2}(F_{k\alpha}F^{l\alpha} - F^*_{k\alpha}F^{*l\alpha}).$$

This can be written in terms of our tensor G_{kl}

$$T_k{}^l = \tfrac{1}{4}(G_{k\alpha}\overline{G}^{l\alpha} + \overline{G}_{k\alpha}G^{l\alpha}) \tag{15}$$

where the conjugate tensor is to be formed according to Eq. (15) of Chapter I. As is well known this tensor has a diagonal sum which is zero

$$T_\alpha{}^\alpha = 0 \tag{16}$$

as one sees using the theorem of footnote 10. Consequently $T_k{}^l$ has only nine linearly independent "Kennzahlen."

§5δ. It is important for the sequel briefly to discuss the phenomenological form of the Maxwell equations in matter. Since the dielectric displacment D and the magnetic induction B are connected with E and H through

$$\begin{aligned} D &= E + P \\ B &= H + I \end{aligned} \tag{17}$$

where P and I are the electric and magnetic polarization respectively, we can write the Maxwell equations

$$\left.\begin{aligned} \operatorname{div} E &= \rho' & \qquad \operatorname{div} B &= 0 \\ \operatorname{curl} B - \frac{1}{c}\frac{\partial E}{\partial t} &= \frac{J}{c} & \qquad \operatorname{curl} E + \frac{1}{c}\frac{\partial B}{\partial t} &= 0 \end{aligned}\right\} \tag{18}$$

where

$$\begin{aligned} \rho' &= \rho - \operatorname{div} P \\ \frac{J}{c} &= \frac{\rho v}{c} + \operatorname{curl} I + \frac{1}{c}\frac{\partial P}{\partial t}. \end{aligned} \tag{19}$$

If ρ, $(\rho v/c)$, P and I are given, the above system agrees formally with the equations in vacuo. To write (18) and (19) in four dimensional form we introduce the two self-dual tensors G'^{kl} and M^{kl}. They have the form (15a) where

$$\begin{aligned} \vec{k}_{G'} &= \vec{B} - i\vec{E} \\ \vec{k}_M &= \vec{I} + i\vec{P}. \end{aligned} \tag{20}$$

We then write (18) and (19)

$$\left.\begin{aligned} &\frac{\partial G'^{k\lambda}}{\partial x^\lambda} = J^k \\ \text{where}\quad &J^k = S^k + \frac{1}{2}\left(\frac{\partial M^{k\lambda}}{\partial x^\lambda} + \frac{\partial \overline{M}^{k\lambda}}{\partial x^\lambda}\right) \end{aligned}\right\} \tag{21}$$

§6α. Having been able to write the entire formalism of Maxwell equations with the help of the self-dual world tensor G^{kl} and its complex conjugate, we can now introduce by means of formulae (18) and (18a) two symmetric spinors $g_{\dot m\dot n}$ and g_{kl} of the second rank, and thus avoid the introduction of fourth-rank spinors altogether. It is obvious that the spinor g_{kl}, just like the tensor $\overline{G}^{kl}$, will only be needed in the formulation of the stress-energy tensor.

We know from Chapter II, that the four-current S^k becomes a spinor $s_{\dot m l}$, the gradient $\partial/\partial x^k$ according to (19) a spinor operator $\partial_{\dot m l}$; we see now that the simplest way of connecting $\partial_{\dot m l}$ and $s_{\dot m l}$ in a manner analogous to (6), is by letting $\partial_{\dot m l}$ act on a spinor with two dotted or two undotted indices. We choose the former and write Maxwell equations[14]

$$\partial^{\dot\rho}{}_l g_{\dot\rho\dot m} = 2s_{\dot m l}. \tag{6a}$$

The continuity equation for the four current reads

$$\partial^{\dot\mu\lambda} s_{\dot\mu\lambda} = 0. \tag{5a}$$

The identity of this with (5) was already noted in Chapter I formula (20).

The analogue of the four potential ϕ^k will be the spinor $\phi_{\dot m l}$. It is connected with the field spinor $g_{\dot r\dot s}$ by the following curl-like operation, which, however, in this case is symmetrical:

$$g_{\dot r\dot s} = \partial_{\dot r\lambda}\phi_{\dot s}{}^\lambda + \partial_{\dot s\lambda}\phi_{\dot r}{}^\lambda \tag{9a}$$

The $\phi_{\dot m l}$ are subjected to the divergence condition

$$\partial^{\dot\mu\lambda}\phi_{\dot\mu\lambda} = 0. \tag{10a}$$

Introducing (9a) into (6a) we have

$$\partial^{\dot\rho}{}_l(\partial_{\dot\rho\alpha}\phi_{\dot m}{}^\alpha + \partial_{\dot m\alpha}\phi_{\dot\rho}{}^\alpha) = 2s_{\dot m l}.$$

Using (8) Chapter I, we can transform each term according to

$$\partial^{\dot\rho}{}_l\partial_{\dot\rho\alpha}\phi_{\dot m}{}^\alpha = -\partial^{\dot\rho}{}_\alpha\partial_{\dot\rho}{}^\alpha\phi_{\dot m l} - \partial^{\dot\rho\alpha}\partial_{\dot\rho\alpha}\phi_{\dot m l}$$

$$\partial^{\dot\rho}{}_l\partial_{\dot m\alpha}\phi_{\dot\rho}{}^\alpha = -\partial_{\dot m l}\partial_{\dot\rho\alpha}\phi^{\dot\rho\alpha} - \partial_{\dot\rho l}\partial^{\dot\rho}{}_\alpha\phi_{\dot m}{}^\alpha.$$

[14] For $l=1$, $\dot m=\dot 1$ and for $l=2$, $\dot m=\dot 2$ we have

$$\partial^{\dot 1}{}_1 g_{\dot 1\dot 1} + \partial^{\dot 2}{}_1 g_{\dot 2\dot 1} = 2s_{\dot 1 1}$$
$$\partial^{\dot 1}{}_2 g_{\dot 1\dot 2} + \partial^{\dot 2}{}_2 g_{\dot 2\dot 2} = 2s_{\dot 2 2}$$

With (4), (10), (19), (18) of Ch. I, and (8) Chapter II, this becomes:

$$\left(\operatorname{curl}_z H - \frac{1}{c}\dot E_z + \operatorname{div} E\right) - i\left(\operatorname{curl}_z E + \frac{1}{c}\dot H_z - \operatorname{div} H\right) = \frac{\rho v_z}{c} + \rho$$

$$\left(-\operatorname{curl}_z H + \frac{1}{c}\dot E_z + \operatorname{div} E\right) + i\left(\operatorname{curl}_z E + \frac{1}{c}\dot H_z + \operatorname{div} H\right) = \frac{\rho v_z}{c} + \rho$$

from which follow four of the eight Maxwell equations.

Adding these, the last two terms cancel because of (7) Chapter I, and due to (10a), we get

$$\partial_{\dot\rho\alpha}\partial^{\dot\rho\alpha}\phi_{\dot m l} = 2s_{\dot m l}. \tag{11a}$$

§6β. The analogue of the self-dual Hertzian tensor Z^{kl} is the symmetric Hertzian spinor $z_{\dot r\dot s}$. The potential spinor $\phi_{\dot m l}$ is derived from this according to

$$\phi_{\dot m l} = \partial^{\dot\sigma}{}_l z_{\dot m\dot\sigma}. \tag{12a}$$

By this operation the divergence condition (10a) is identically fulfilled, for we obtain, introducing (12a) into (10a)

$$\partial^{\dot\mu\lambda}\phi_{\dot\mu\lambda} = \partial^{\dot\mu\lambda}\partial^{\dot\sigma}{}_\lambda z_{\dot\mu\dot\sigma}$$

using the symmetry of $z_{\dot\mu\dot\sigma}$ we have

$$\partial^{\dot\mu\lambda}\phi_{\dot\mu\lambda} = \tfrac{1}{2}\left\{\partial^{\dot\mu\lambda}\partial^{\dot\sigma}{}_\lambda + \partial^{\dot\sigma\lambda}\partial^{\dot\mu}{}_\lambda\right\} z_{\dot\mu\dot\sigma} \equiv 0.$$

This vanishes applying (7) Chapter I to the index λ. Analogous to the stream potential Q_{kl}, a self-dual tensor we now derive the stream spinor $s_{\dot m l}$ from

$$s_{\dot m l} = \partial^{\dot\sigma}{}_l q_{\dot m\dot\sigma} \tag{13a}$$

where $q_{\dot m\dot s}$ is again a symmetric spinor of the second rank. Introducing (12a) and (13a) into (11a), and dropping a ∂ operator on both sides, we obtain the wave equation for $z_{\dot m\dot s}$

$$\partial_{\dot\rho\alpha}\partial^{\dot\rho\alpha} z_{\dot m\dot s} = 2q_{\dot m\dot s}. \tag{14a}$$

§6γ. The spinor analogue of the stress-energy tensor T_{kl} will be a spinor of the fourth rank with two dotted and two undotted indices. Its divergence will have to be equal to the spinor $f_{\dot m l}$ which corresponds to the four vector of the Lorentz force density and the action density. To derive this expression we write down the Maxwell equations and their conjugates according to (6a), using (7) Chapter I

$$\partial_{\dot\rho l} g^{\dot\rho\dot m} = -2s^{\dot m}{}_l$$
$$\partial_{\dot r\lambda} g^{\lambda k} = -2s_{\dot r}{}^k.$$

Then we multiply the upper equation with g^{lk} and the lower with $g^{\dot r\dot m}$ and contract with respect to r and l. After adding we can write this

$$\partial_{\dot\rho\lambda}\left\{g^{\dot\rho\dot m} g^{\lambda k}\right\} = -2\left\{g^{\dot\rho\dot m} s_{\dot\rho}{}^k + g^{\lambda k} s^{\dot m}{}_\lambda\right\}.$$

Introducing

$$t^{\dot r\dot m l k} = \tfrac{1}{4} g^{\dot r\dot m} g^{l k} \tag{15a}$$

we have

$$\partial_{\dot\rho\lambda} t^{\dot\rho\dot m\lambda k} = 2f^{\dot m k} \tag{15b}$$

where the force spinor

$$f^{\dot m k} = -\tfrac{1}{4}\left\{g^{\dot\rho\dot m} s_{\dot\rho}{}^k + g^{\lambda k} s^{\dot m}{}_\lambda\right\}. \tag{15c}$$

It follows from the symmetry of the spinors $g^{\dot{r}\dot{m}}$ and g^{lk} that $t^{\dot{r}\dot{m}lk}$ has only nine "Kennzahlen." Thus relation (16) is already embodied in the structure of the stress-energy spinor.

§6δ. Analogous to the developments of §5δ we introduce two symmetric spinors $g'_{\dot{r}\dot{s}}$ and $m_{\dot{r}\dot{s}}$ which correspond to the self-dual tensors G'^{kl} and M^{kl}. We then write the spinor analogue of (21)

$$\partial^{\dot{\sigma}}{}_l g'_{\dot{\sigma}\dot{r}} = 2j_{\dot{r}l}$$

where

$$j_{\dot{r}l} = s_{\dot{r}l} + \tfrac{1}{4}(\partial^{\dot{\sigma}}{}_l m_{\dot{\sigma}\dot{r}} + \partial_{\dot{r}}{}^{\alpha} m_{\dot{\sigma}r}) \tag{21a}$$

where the first term on the right side is due to conduction and the second term to electric and magnetic polarization.

Chapter III. The Dirac Equations in Spinor Form

§7. Van der Waerden has shown how to write the Dirac equations in spinor form. The four wave functions ψ of Dirac correspond to two spinors of the first rank $\psi_{\dot{m}}$ and χ_l, and his equations become

$$mc\chi_l - \left(\frac{h}{i}\partial^{\dot{\sigma}}{}_l + \phi^{\dot{\sigma}}{}_l\right)\psi_{\dot{\sigma}} = 0 \tag{1a}$$

$$mc\psi_{\dot{m}} + \left(\frac{h}{i}\partial_{\dot{m}}{}^{\lambda} + \phi_{\dot{m}}{}^{\lambda}\right)\chi_{\lambda} = 0 \tag{1b}$$

where $\phi^{\dot{s}}{}_l$ is the potential spinor as according to (9a) Chapter II. We shall also need the complex conjugate equations which read

$$mc\chi_{\dot{m}} - \left(-\frac{h}{i}\partial_{\dot{m}}{}^{\lambda} + \phi_{\dot{m}}{}^{\lambda}\right)\psi_{\lambda} = 0 \tag{2a}$$

$$mc\psi_l + \left(-\frac{h}{i}\partial^{\dot{\sigma}}{}_l + \phi^{\dot{\sigma}}{}_l\right)\chi_{\dot{\sigma}} = 0. \tag{2b}$$

We now wish to obtain the second order Dirac equations. Introducing the abbreviation

$$p^{\dot{s}}{}_l = \frac{h}{i}\partial^{\dot{s}}{}_l + \phi^{\dot{s}}{}_l \tag{3}$$

we eliminate χ_l from (1) and get

$$m^2c^2\psi_{\dot{m}} + p_{\dot{m}}{}^{\lambda}p^{\dot{\sigma}}{}_{\lambda}\psi_{\dot{\sigma}} = 0.$$

We apply the identity (8) Chapter I to the second term and have, using also identity (7) Chapter I,

$$p_{\dot{m}}{}^{\lambda}p^{\dot{\sigma}}{}_{\lambda}\psi_{\dot{\sigma}} = -\tfrac{1}{2}p^{\dot{\sigma}\lambda}p_{\dot{\sigma}\lambda}\psi_{\dot{m}} + \tfrac{1}{2}p_{\dot{\sigma}\lambda}p_{\dot{m}}{}^{\lambda}\psi^{\dot{\sigma}} - \tfrac{1}{2}p_{\dot{m}}{}^{\lambda}p_{\dot{\sigma}\lambda}\psi^{\dot{\sigma}}.$$

Taking (3) into account we see that

$$p_{\dot{\sigma}\lambda}p_{\dot{m}}{}^{\lambda}\psi^{\dot{\sigma}} - p_{\dot{m}}{}^{\lambda}p_{\dot{\sigma}\lambda}\psi^{\dot{\sigma}} = \frac{h}{i}\psi^{\dot{\sigma}}(\partial_{\dot{\sigma}\lambda}\phi_{\dot{m}}{}^{\lambda} + \partial_{\dot{m}\lambda}\phi_{\dot{\sigma}}{}^{\lambda})$$

$$= \frac{h}{i}\psi^{\dot{\sigma}}g_{\dot{m}\dot{\sigma}},$$

the latter because of (9a) Chapter II. Thus the second-order wave equation becomes

$$-\frac{1}{2}\left(\frac{h}{i}\partial^{\dot{\sigma}\lambda} + \phi^{\dot{\sigma}\lambda}\right)\left(\frac{h}{i}\partial_{\dot{\sigma}\lambda} + \phi_{\dot{\sigma}\lambda}\right)\psi_{\dot{m}} + m^2c^2\psi_{\dot{m}} = -\frac{h}{2i}g_{\dot{m}\dot{\sigma}}\psi^{\dot{\sigma}}. \tag{4}$$

Correspondingly one obtains

$$-\frac{1}{2}\left(\frac{h}{i}\partial^{\dot{\sigma}\lambda} + \phi^{\dot{\sigma}\lambda}\right)\left(\frac{h}{i}\partial_{\dot{\sigma}\lambda} + \phi_{\dot{\sigma}\lambda}\right)\chi_k + m^2c^2\chi_k = \frac{h}{2i}g_{k\lambda}\chi^{\lambda}. \tag{5}$$

The left side is identical with the Gordon wave equation written in spinor form, whereas the right side represents the spin correction. It is satisfactory, that the field only occurs in the form of our symmetric spinor $g_{\dot{m}\dot{n}}$ resp. g_{kl}.

§8. To derive the expression for the current we multiply (1a) with ψ^{l}, (1b) with $-\chi^{\dot{m}}$, (2a) with $-\psi^{\dot{m}}$, (2b) with χ^{l}, and add all four equations. Using repeatedly identity (7) Chapter I all terms containing the mass and the potentials cancel and we can write the result

$$\partial^{\dot{\mu}\lambda}j_{\dot{\mu}\lambda} = 0 \tag{6}$$

where

$$j_{\dot{m}l} = \psi_{\dot{m}}\psi_{l} + \chi_{\dot{m}}\chi_{l}. \tag{7}$$

§9. We shall split up the above expression after the fashion of Eq. (1a) Chapter II. We replace $\psi_{\dot{m}}$ and χ_{l} in (7) by their expressions following from (1a) and (1b) and have, using identity (8) Chapter I

$$mcj_{\dot{m}l} = -\psi_{l}\left(\frac{h}{i}\partial_{\dot{m}}{}^{\alpha} + \phi_{m}{}^{\alpha}\right)\chi_{\alpha} + \chi_{\dot{m}}\left(\frac{h}{i}\partial^{\dot{\sigma}}{}_{l} + \phi^{\dot{\sigma}}{}_{l}\right)\psi_{\dot{\sigma}}$$

$$= +\psi^{\alpha}\left(\frac{h}{i}\partial_{\dot{m}\alpha} + \phi_{\dot{m}\alpha}\right)\chi_{l} - \chi^{\dot{\sigma}}\left(\frac{h}{i}\partial_{\dot{\sigma}l} + \phi_{\dot{\sigma}l}\right)\psi_{\dot{m}}$$

$$+\psi_{\alpha}\left(\frac{h}{i}\partial_{\dot{m}l} + \phi_{\dot{m}l}\right)\chi^{\alpha} - \chi_{\dot{\sigma}}\left(\frac{h}{i}\partial_{\dot{m}l} + \phi_{\dot{m}l}\right)\psi^{\dot{\sigma}}.$$

We then replace in (7) ψ_{l} and $\chi_{\dot{m}}$ by the expressions following from (2a) and (2b) and transform the equations by means of (8) Chapter I in a completely analogous fashion. We thus obtain four expressions for $mcj_{\dot{m}l}$. Adding all of them we have after a few elementary transformations

$$j_{\dot{r}l} = s_{\dot{r}l} + \tfrac{1}{4}(\partial^{\dot{\sigma}}{}_{l}m_{\dot{\sigma}\dot{r}} + \partial_{\dot{r}}{}^{\alpha}m_{\alpha l}) \tag{8}$$

where

$$s_{\dot{r}l} = \frac{h}{4imc}(\psi_\alpha \partial_{\dot{r}l}\chi^\alpha + \chi_\alpha \partial_{\dot{r}l}\psi^\alpha + \psi^{\dot{\sigma}}\partial_{\dot{r}l}\chi_{\dot{\sigma}} + \chi^{\dot{\sigma}}\partial_{\dot{r}l}\psi_{\dot{\sigma}}) \tag{9}$$

$$+ \frac{1}{2mc}\phi_{\dot{r}l}(\psi_\alpha\chi^\alpha + \psi_{\dot{\sigma}}\chi^{\dot{\sigma}})$$

$$\left.\begin{aligned} m_{\dot{r}\dot{s}} &= \frac{h}{imc}(\psi_{\dot{r}}\chi_{\dot{s}} + \psi_{\dot{s}}\chi_{\dot{r}}) \\ m_{kl} &= \frac{-h}{imc}(\psi_k\chi_l + \psi_l\chi_k) \end{aligned}\right\} \tag{10}$$

Equations (8) (9) and (10) are the spinor form for the decomposition of the current first given independently by Gordon[15] and Darwin.[16] Similarly to the correction terms on the right side of (4), the spinor (10) expresses the existence of a spin.

§10. The multiplication process described in §8 is not the only process by means of which the potentials $\phi_{\dot{m}l}$ may be eliminated from the Dirac equations. In fact, besides the one leading to the continuity Eq. (6), it is possible in three more ways to eliminate the $\phi_{\dot{m}l}$ each of which lead to an invariant relation between the ψ and χ.

For the sake of convenience we write down the four Dirac equations, but using only covariant ∂-operators. In four columns at the right side of the equations, the various factors, with which we multiply are given.

	a	b	c	d
$mc\chi_l + \frac{h}{i}\partial_{\dot{\sigma}l}\psi^{\dot{\sigma}} + \phi_{\dot{\sigma}l}\psi^{\dot{\sigma}} = 0$	$+\psi^l$	$+\psi^l$	$+\chi^l$	$+\chi^l$
$mc\psi_{\dot{m}} - \frac{h}{i}\partial_{\dot{m}\lambda}\chi^\lambda - \phi_{\dot{m}\lambda}\chi^\lambda = 0$	$-\chi^{\dot{m}}$	$+\chi^{\dot{m}}$	$+\psi^{\dot{m}}$	$+\psi^{\dot{m}}$
$mc\chi_{\dot{m}} - \frac{h}{i}\partial_{\dot{m}\lambda}\psi^\lambda + \phi_{\dot{m}\lambda}\psi^\lambda = 0$	$-\psi^{\dot{m}}$	$-\psi^{\dot{m}}$	$+\chi^{\dot{m}}$	$-\chi^{\dot{m}}$
$mc\psi_l + \frac{h}{i}\partial_{\dot{\sigma}l}\chi^{\dot{\sigma}} - \phi_{\dot{\sigma}l}\chi^{\dot{\sigma}} = 0$	$+\chi^l$	$-\chi^l$	$+\psi^l$	$-\psi^l$

We obtain

(a) $$\partial_{\dot{\sigma}\lambda}(\psi^{\dot{\sigma}}\psi^\lambda + \chi^{\dot{\sigma}}\chi^\lambda) = 0. \tag{6}$$

This is Eq. (6) for the current.

(b) $$\partial_{\dot{\sigma}\lambda}(\psi^{\dot{\sigma}}\psi^\lambda - \chi^{\dot{\sigma}}\chi^\lambda) + 2i\frac{mc}{h}(\psi^\lambda\chi_\lambda + \psi_{\dot{\sigma}}\chi^{\dot{\sigma}}) = 0 \tag{11}$$

(c) (d) Adding and subtracting the results of process (c) and (d) we have, using (7) and (7a) Chapter I

[15] W. Gordon, Zeits. f. Physik 50, 630 (1928).
[16] G. Darwin, Proc. Roy. Soc. A120, 621 (1928).

$$\chi^\lambda \partial_{\dot\sigma\lambda}\psi^{\dot\sigma} - \psi^{\dot\sigma}\partial_{\dot\sigma\lambda}\chi^\lambda = 0 \tag{12}$$

$$\chi^{\dot\sigma}\partial_{\dot\sigma\lambda}\psi^\lambda - \psi^\lambda \partial_{\dot\sigma\lambda}\chi^{\dot\sigma} = 0. \tag{13}$$

It is clear, that these are the only relations between the wave functions which are independent of the potentials $\phi_{\dot m l}$, because we have eight equations (the four Dirac equations and their complex conjugates) in which only four potentials $\phi_{\dot m l}$ occur.[17] It is curious, that three of these relations are also independent of the mass.

A few words may be added concerning the quadratic invariants which do not involve differentiation. Due to (7a) Chapter I the only two invariants are:

$$\left.\begin{aligned} \Delta &= \psi_\lambda \chi^\lambda \\ \bar\Delta &= \psi_{\dot\sigma}\chi^{\dot\sigma} \end{aligned}\right\}. \tag{14}$$

It is easily verified[18] that the square of the current

$$j_{\dot\sigma\lambda}j^{\dot\sigma\lambda} = 2\Delta\bar\Delta \tag{15}$$

and the square of the polarization spinor (10):

$$\left.\begin{aligned} m_{\dot\rho\dot\sigma}m^{\dot\rho\dot\sigma} &= 2\left(\frac{h}{mc}\right)^2 \bar\Delta^2 \\ \text{and} \qquad m_{\alpha\beta}m^{\alpha\beta} &= 2\left(\frac{h}{mc}\right)^2 \Delta^2 \end{aligned}\right\} \tag{16}$$

Introducing the abbreviation

$$k_{\dot s l} = \psi_{\dot s}\psi_l - \chi_{\dot s}\chi_l$$

for the spinor whose divergence occurred in (11), it is readily seen that

$$\left.\begin{aligned} k^{\dot\rho}{}_l m_{\dot\rho\dot s} &= -\frac{h}{imc} j_{\dot s l}\bar\Delta \\ j^{\dot\rho}{}_l m_{\dot\rho\dot s} &= -\frac{h}{imc} k_{\dot s l}\bar\Delta. \\ k_{\dot\sigma\lambda}j^{\dot\sigma\lambda} &= 0 \end{aligned}\right\} \tag{17}$$

§11. Darwin[19] has shown how to derive both the Maxwell and the Dirac equations from a variation principle. The analogous development using spinor analysis runs as follows. We start with the Lagrangian function

[17] Relations (11), (12) and (13) were found more or less accidentally by the authors. The point of view described in the text was supplied by Professor G. Y. Rainich, who found them independently. Professor Rainich further communicated to us a rigorous proof of the fact that the Dirac equations possess only two algebraic quadratic invariants, which are simply our Δ and $\bar\Delta$. Also relations (17) are due to him. The authors are greatly indebted to Professor Rainich for several discussions on the subject.

[18] Compare C. G. Darwin, Proc. Roy. Soc. **A120**, 621 (1928). See esp. p. 627.

[19] C. G. Darwin, Proc. Roy. Soc. **A118**, 654 (1928).

$$L = \frac{h}{i}\{\psi^{\dot\mu}\partial_{\dot\mu}{}^{\lambda}\psi_{\lambda} - \chi^{\dot\mu}\partial_{\dot\mu}{}^{\lambda}\chi_{\lambda} - \psi^{\lambda}\partial^{\dot\mu}{}_{\lambda}\psi_{\dot\mu} + \chi^{\lambda}\partial^{\dot\mu}{}_{\lambda}\chi_{\dot\mu}\}$$
$$+ 2mc(\Delta + \bar\Delta) + \phi^{\dot\mu\lambda}j_{\dot\mu\lambda} - \tfrac{1}{2}g^{\dot\mu\dot\rho}g_{\dot\mu\dot\rho} \qquad (18)$$

where the meaning of Δ, $\bar\Delta$, $j_{\dot m l}$ and $g_{\dot m\dot n}$ in terms of ψ, χ, and ϕ are given in Eq. (14) (7) Chapter III and (9a) Chapter II respectively. L is to be considered a function of ψ, χ, ϕ and their derivatives.

1°. Varying ψ_l we obtain as Euler-Lagrange equation

$$\partial_{\dot\mu}{}^{l}\left\{\frac{\partial L}{\partial(\partial_{\dot\mu}{}^{\alpha}\psi_{\alpha})}\right\} - \frac{\partial L}{\partial\psi_l} = 0$$

which is identical with (1a).

2°. Varying $\chi_{\dot m}$ we obtain

$$\partial^{\dot m}{}_{\lambda}\left\{\frac{\partial L}{\partial(\partial^{\dot\sigma}{}_{\lambda}\chi_{\dot\sigma})}\right\} - \frac{\partial L}{\partial\chi_{\dot m}} = 0$$

which is identical with (1b).

3°. Varying $\psi_{\dot m}$ we get (2a) and varying χ_l we get (2b).

4°. Varying $\phi_{\dot m l}$ we obtain

$$\partial_{\dot\sigma}{}^{l}\left\{\frac{\partial L}{\partial(\partial_{\dot\sigma\alpha}\phi_{\dot m}{}^{\alpha})}\right\} - \frac{\partial L}{\partial\phi_{\dot m l}} = 0$$

that is to say

$$\partial_{\dot\sigma}{}^{l}g^{\dot\sigma\dot m} = 2j^{\dot m l} = 2(\psi^{\dot m}\psi^{l} + \chi^{\dot m}\chi^{l})$$

which are the Maxwell equations with the Dirac current.

A TENSOR FORM OF DIRAC'S EQUATION

By Boris Podolsky*
California Institute of Technology

(Received April 8, 1931)

Abstract

In this paper a simple tensor form of Dirac's equation is obtained. This is accomplished by considering ψ_s and $\gamma^\alpha(rs)$ of the usual equations as being related to a set of n-beins as invariants corresponding to true tensors ψ_μ and $\Gamma^\alpha{}_\beta{}^\sigma$. The results are, however, independant of the choice of the n-beins. It is thus shown that the introduction of the idea of half-vectors in the quantum mechanics, while undoubtedly desirable when dealing exclusively with cartesian coordinates, is unnecessary.

1. MUCH work was done in attempting to find a generalization of Dirac's wave equation to general relativity. Of this the most important is probably the work of Fock.[1] In nearly all these, however, ψ is regarded as a half-vector. It is interesting, therefore, to see to what extent it is possible to achieve this generalization using only the ordinary tensors.

It became quite clear, as the result of other investigations, that the extension of Dirac's equations to general relativity necessitates the introduction of n-beins, i.e. a local cartesian coordinate system at each point. This, however, does not spoil the generality of equations obtained, as they turn out to be independent of the particular choice assumed.

2. For our purpose it is convenient to write Dirac's equation in the following form:

$$\sum_s e_s \left\{ \Gamma^\alpha_{rs} \left(p_\alpha + \frac{e}{c} \Phi_\alpha \right) + mc\Gamma_{rs} \right\} \psi_s = 0 \tag{1}$$

where all subscripts take the values 1, 2, 3, and 4. As is done in the work of Fock, summations with respect to doubled Greek indices are always implied, while summations with respect to Latin indices are explicitly indicated. The matrices are taken to be the following:

$$\Gamma^1 = \begin{pmatrix} 0 & 1 & 0 & 0 \\ 1 & 0 & 0 & 0 \\ 0 & 0 & 0 & 1 \\ 0 & 0 & 1 & 0 \end{pmatrix}; \quad \Gamma^2 = \begin{pmatrix} 0 & -i & 0 & 0 \\ i & 0 & 0 & 0 \\ 0 & 0 & 0 & i \\ 0 & 0 & -i & 0 \end{pmatrix}; \quad \Gamma^3 = \begin{pmatrix} 1 & 0 & 0 & 0 \\ 0 & -1 & 0 & 0 \\ 0 & 0 & 1 & 0 \\ 0 & 0 & 0 & -1 \end{pmatrix}$$

$$\Gamma^4 = I = \begin{pmatrix} 1 & 0 & 0 & 0 \\ 0 & 1 & 0 & 0 \\ 0 & 0 & 1 & 0 \\ 0 & 0 & 0 & 1 \end{pmatrix}; \quad \Gamma = \begin{pmatrix} 0 & 0 & 0 & -1 \\ 0 & 0 & 1 & 0 \\ 0 & 1 & 0 & 0 \\ -1 & 0 & 0 & 0 \end{pmatrix}. \tag{2}$$

* This work was started at the Leipzig Physikalisches Institut while the author was there on a National Research Fellowship.

[1] Fock, Journ. de Phys. **10**, 392 (1929) in which other references are given. See also Tetrode, Zeits. f. Physik **50**, 336 (1928), and Wigner, Zeits. f. Physik **53**, 592 (1929).

Here $p_\alpha = (h/2\pi i)\partial/\partial x^\alpha$; $x^\alpha = (x, y, z, ct)$; $\Phi_\alpha = (A_x, A_y, A_z - \phi,)$, where ϕ is the scalar and (A_x, A_y, A_z) the vector potential. Also, the quantities $e_1 = e_2 = e_3 = -1$, $e_4 = 1$, are introduced for later convenience.

3. We now introduce a set of n-beins by means of sixteen parameters $h_s{}^\nu$ and their corresponding moments $h_{s\nu}$ as is done by Fock. Designating local components of vectors, i.e. ordinary cartesian projections on the vectors constituting the n-beins at each point, by Latin indices and their tensor components by Greek indices, we have the following relations:

$$\begin{aligned} A_\sigma &= \sum_k e_k A_k h_{k\sigma} \\ A^\sigma &= \sum_k e_k A_k h_k{}^\sigma . \end{aligned} \tag{3}$$

The quantities e_k are introduced to make the components A_4, A^4, and $h_{4\sigma}$ real and are $e_1 = e_2 = e_3 = -1$, $e_4 = 1$, as in Eq. (1).

With this notation[2] the h's satisfy the following relations:

$$\begin{aligned} e_k h_k{}^\sigma h_{l\sigma} &= e_l h_k{}^\sigma h_{l\sigma} = \delta_{kl} \\ \sum_k e_k h_{k\sigma} h_k{}^\rho &= \delta_\sigma{}^\rho . \end{aligned} \tag{4}$$

Equations (3) can be immediately generalized to any tensor. Thus, for example:

$$A^{\alpha\beta}{}_\gamma = \sum_{r,s,t} e_r e_s e_t A_{rst} h_r{}^\alpha h_s{}^\beta h_{t\gamma} \tag{5}$$

or, solving for A_{rst} with the help of (4)

$$A_{rst} = A^{\alpha\beta}{}_\gamma h_{r\alpha} h_{s\beta} h_t{}^\gamma .$$

The quantities A_{rst} are invariants, i.e. they do not change with the change of the coordinate system, although they, of course, change with the change of the set of n-beins.

We may also have quantities such as

$$A^\alpha{}_{st} = A^{\alpha\beta}{}_\gamma h_{s\beta} h_t{}^\gamma , \tag{6}$$

which are in part invariants of a set of n-beins and in part tensors.

4. We extend Dirac's equation to general relativity by regarding the Latin indices occurring in Eq. (1) as the n-bein system indices. Thus, Γ_{rs} and ψ_s are invariants, and $\Gamma^\alpha{}_{rs}$ are the mixed quantities of the type of Eq. (6).

We will now rewrite Eq. (1) in a tensor form. First we observe that

$$\sum_s e_s \Gamma_{rs} \psi_s = \sum_{s,t} e_s \Gamma_{rs} \delta_{st} \psi_t = \sum_{s,t} e_s e_t \Gamma_{rs} h_s{}^\sigma h_{t\sigma} \psi_t , \text{ by (4)}$$

thus, by (3)

$$\sum_s e_s \Gamma_{rs} \psi_s = \Gamma_r{}^\sigma \psi_\sigma . \tag{7}$$

[2] The notation throughout this paper is that of Fock.

Similarly

$$\sum_s e_s \Gamma^\alpha{}_{rs}\left(p_\alpha + \frac{e}{c}\,\Phi_\alpha\right)\psi_s = \left(p_\alpha + \frac{e}{c}\,\Phi_\alpha\right)\sum_s e_s \Gamma^\alpha{}_{rs}\psi_s$$
$$= \left(p_\alpha + \frac{e}{c}\,\Phi_\alpha\right)\Gamma^\alpha{}_r{}^\sigma\psi_\sigma. \tag{8}$$

In place of the ordinary partial derivative in the interpretation of p_α as an operator we now use

$$p_\alpha = \frac{h}{2\pi i}(\cdots)_{;\alpha} \tag{9}$$

where; α is the covariant derivative in the sense of Einstein.[3] This operator acting on a tensor gives again a tensor of one rank higher in covariant indices. It is defined with the help of the quantities

$$\Delta^\sigma{}_{\alpha\beta} = \sum_s e_s h_s{}^\sigma \frac{\partial h_{s\alpha}}{\partial x^\beta}. \tag{10}$$

In constructing Einstein's covariant derivatives one uses $\Delta^\sigma{}_{\alpha\beta}$ like $\{\alpha\beta, \sigma\}$ in ordinary covariant differentiation. Thus, for example,

$$(A_\beta{}^\alpha)_{;\gamma} = \frac{\partial A_\beta{}^\alpha}{\partial x^\gamma} + A_\beta{}^\sigma \Delta^\alpha{}_{\sigma\gamma} - A_\sigma{}^\alpha \Delta^\sigma{}_{\alpha\beta}.$$

For us the important property of; α is

$$(h_s{}^\nu)_{;\alpha} = (h_{s\nu})_{;\alpha} = (g_{\mu\nu})_{;\alpha} = 0. \tag{11}$$

From this follows:

$$p_\alpha \Gamma^\alpha{}_r{}^\sigma \psi_\sigma = \frac{h}{2\pi i}(\Gamma^\alpha{}_r{}^\sigma \psi_\sigma)_{;\alpha}$$
$$= \frac{h}{2\pi i}\left(\sum_s \Gamma^\alpha{}_{rs} e_s h_s{}^\sigma \psi_\sigma\right)_{;\alpha}$$
$$= \frac{h}{2\pi i}\sum_s \Gamma^\alpha{}_{rs} e_s h_s{}^\sigma (\psi_\sigma)_{;\alpha}$$

since $\Gamma^\alpha{}_{rs}$ are constants and by Eq. (11). Hence

$$p_\alpha \Gamma^\alpha{}_r{}^\sigma \psi_\sigma = \left(\sum_s \Gamma^\alpha{}_{rs} e_s h_s{}^\sigma\right)\cdot \frac{h}{2\pi i}(\psi_\sigma)_{;\alpha}$$
$$= \Gamma^\alpha{}_r{}^\sigma p_\alpha \psi_\sigma \tag{12}$$

i.e., p_α and the Γ's commute.

[3] Einstein, Math. Ann. **102**, 685 (1930).

Using Eqs. (7), (8), and (13) we can rewrite Eq. (1) in the form

$$\left\{\Gamma^{\alpha}{}_{r}{}^{\sigma}\left(p_{\alpha}+\frac{e}{c}\,\Phi_{\alpha}\right)+mc\Gamma_{r}{}^{\sigma}\right\}\psi_{\sigma}=0.$$

Multiplying by $e_r h_{r\beta}$ and summing with respect to r, we obtain the desired equation:

$$\left\{\Gamma^{\alpha}{}_{\beta}{}^{\sigma}\left(p_{\alpha}+\frac{e}{c}\,\Phi_{\alpha}\right)+mc\Gamma_{\beta}{}^{\sigma}\right\}\psi_{\sigma}=0. \tag{13}$$

5. The adjoint to Eq. (1) by a similar transformation becomes

$$\left\{\Gamma^{\alpha}{}_{\beta}{}^{\sigma}\left(p_{\alpha}-\frac{e}{c}\,\Phi_{\alpha}\right)-mc\Gamma_{\beta}{}^{\sigma}\right\}\psi\dagger^{\beta}=0. \tag{14}$$

Multiplying Eq. (13) by $\psi\dagger^{\beta}$, Eq. (14) by ψ_{α} and adding we obtain

$$\psi\dagger^{\beta}\Gamma^{\alpha}{}_{\beta}{}^{\sigma}p_{\alpha}\psi_{\sigma}+\psi_{\alpha}\Gamma^{\alpha}{}_{\beta}{}^{\sigma}p_{\alpha}\psi\dagger^{\beta}=0$$

or

$$(\psi\dagger^{\beta}\Gamma^{\alpha}{}_{\beta}{}^{\sigma}\psi_{\sigma})_{;\alpha}=0. \tag{15}$$

We may interpret the expression in parenthesis as the current-density vector

$$J^{\alpha}=\Gamma^{\alpha}{}_{\beta}{}^{\sigma}\psi\dagger^{\beta}\psi_{\sigma}; \tag{16}$$

then Eq. (15) becomes a generalization of the equation

$$div J^{\alpha}=0.$$

Using Eqs. (3) and (5), Eq. (16) may be also written as follows:

$$J^{\alpha}=\sum_{r,s}e_r e_s\psi_r\dagger\Gamma^{\alpha}{}_{rs}\psi_s, \tag{17}$$

which is what one obtains directly from Eq. (1) and its adjoint.

6. The energy is given by the relation

$$-\frac{E}{c}=p_4=\frac{h}{2\pi i}(\cdots)_{;4}. \tag{18}$$

Of course, we can speak of energy of an electron only in a flat space-time in which one of the coordinates is singled out as time. Thus, if $x_4=ct$, Eq. (18) reduces to the usual

$$E=-\frac{h}{2\pi i}\frac{\partial}{\partial t}$$

which must of course be interpreted to mean that the numerical value of the energy is given by

$$E'=-\frac{h}{2\pi i}\int\psi\dagger^{\alpha}\frac{\partial}{\partial t}\psi_{\alpha}dV.$$

In this case E' is $-c$ times the time component of a vector

$$p_{\beta'} = \frac{h}{2\pi i}\int \psi\dagger^{\alpha}(\psi_{\alpha})_{;\sigma}dV. \tag{20}$$

7. The angular momentum operator of Dirac

$$M^{\alpha} = m^{\alpha} + \frac{h}{4\pi}\sigma^{\tau}, \tag{21}$$

where $m^1 = yp_z - zp_y$, etc. in our notation becomes

$$M^{\alpha}{}_{rs} = m^{\alpha}\delta_{rs} + \frac{h}{4\pi}\sigma^{\alpha}{}_{rs}. \tag{22}$$

The Hamiltonian of Dirac is also a four-rowed square matrix H_{rs}, and the fact that M^{α} and H commute means

$$\sum_{s,t} M^{\alpha}{}_{rs}H_{st}\psi_t = \sum_{s,t} H_{rs}M^{\alpha}{}_{st}\psi_t. \tag{23}$$

The operator (22) has a meaning only in flat space-time. In that case, however, our Eq. (13) can be written in the form

$$\sum_{s} e_s\left\{H_{rs} + \frac{h}{2\pi i}\delta_{rs}\frac{\partial}{\partial t}\right\}\psi_s = 0 \tag{24}$$

where H_{rs} is the Dirac Hamiltonian. The relation (23) then holds, so that operator (22) is still a constant of the motion.

8. The invariance of Eq. (13) with respect to Lorentz transformations does not follow immediately from the tensor form of the equation. In Eq. (2) $\Gamma^{\alpha}{}_{rs}$ are assumed constants associated with a particular coordinate system. By a Lorentz transformation they change to $\Gamma'^{\alpha}{}_{rs}$ given by

$$\Gamma'^{\alpha}{}_{rs} = \Gamma^{\beta}{}_{rs}a_{\beta\alpha}, \tag{25}$$

where $a_{\beta\alpha}$ is a set of coefficients satisfying the relation

$$\begin{aligned} a_{\mu\nu}a_{\mu\rho} &= \delta_{\nu\rho} \\ a_{\mu\rho}a_{\nu\rho} &= \delta_{\mu\nu}. \end{aligned} \tag{26}$$

Now, since the original and the new coordinate systems are physically indistinguishable, we may have started with the new Γ's and the old coordinate system; i.e. we have no way of knowing to which coordinate system the originally assumed Γ's belong. Thus, we may have written instead of Eq. (1)

$$\sum_{s} e_s\left\{\Gamma'^{\alpha}{}_{rs}\left(p_{\alpha} + \frac{e}{c}\Phi_{\alpha}\right) + mc\Gamma_{rs}\right\}\psi'_s = 0. \tag{27}$$

We must now show that Eq. (27) leads to the same physical results as Eq. (1). It has been shown[4] that Eq. (25) may be put in the form

[4] See for example Moglich, Zeits. f. Physik **48**, 852 (1928) and Neumann, Zeits. f. Physik **48**, 868 (1928).

$$\Gamma'^{\alpha}{}_{rs} = \sum_{t,u} S\dagger_{rt}\Gamma^{\alpha}{}_{tu}S_{us}, \tag{28}$$

where S and $S^{\dagger}$ are matrices of the form

$$S = \begin{pmatrix} \alpha & \beta & 0 & 0 \\ \gamma & \delta & 0 & 0 \\ 0 & 0 & \bar{\alpha} & \bar{\beta} \\ 0 & 0 & \bar{\gamma} & \bar{\delta} \end{pmatrix}, \quad S\dagger = \begin{pmatrix} \bar{\alpha} & \bar{\gamma} & 0 & 0 \\ \bar{\beta} & \bar{\delta} & 0 & 0 \\ 0 & 0 & \alpha & \gamma \\ 0 & 0 & \beta & \delta \end{pmatrix}$$

and $\alpha\delta - \beta\gamma = 1$. Furthermore

$$\Gamma_{rs} = \sum_{t,u} S\dagger_{rt}\Gamma_{tu}S_{us}. \tag{29}$$

Using Eqs. (28) and (29), Eq. (27) may be written as follows:

$$\sum_{s,t,u} e_s S_{rt}\dagger \left\{ \Gamma^{\alpha}{}_{tu}\left(p_{\alpha} + \frac{e}{c}\Phi_{\alpha}\right) + mc\Gamma_{tu}\right\} S_{us}\psi'_s = 0.$$

Thus, if ψ'_s satisfies Eq. (27), ψ_u given by

$$e_u\psi_u = \sum_s e_s S_{us}\psi'_s \tag{30}$$

will satisfy Eq. (1). Similarly

$$e_u\psi_u\dagger = \sum_s e_s\psi'\dagger_s S_{su}\dagger. \tag{30'}$$

Thus Eq. (17) becomes

$$\begin{aligned} J^{\alpha} &= \sum_{r,s}\left(\sum_t e_t\psi'\dagger_t S_{tr}\dagger\right)\Gamma^{\alpha}{}_{rs}\left(\sum_u e_u S_{su}\psi'_u\right) \\ &= \sum_{t,u} e_t e_u\psi'\dagger_t\Gamma'^{\alpha}{}_{tu}\psi'_u, \text{ by (28)} \end{aligned}$$

This is just what would have been obtained directly from Eq. (27).

9. Similarly, the invariance of Eq. (13) with respect to rotation of n-beins must be tested by investigating what would have happened if the original set of Γ's became associated with another set of n-beins. Our original equation would then be

$$\sum_s e_s\left\{\Gamma''^{\alpha}{}_{rs}\left(p_{\alpha} + \frac{e}{c}\Phi_{\alpha}\right) + mc\Gamma''_{rs}\right\}\psi''_s = 0 \tag{31}$$

where $\Gamma''^{\alpha}{}_{rs}$ and Γ''_{rs} are obtained from the given Γ's by a rotation of n-beins.

We will now show that the physical consequences of Eq. (31) are the same as of Eq. (1). In order to show this we must first find the relation between Γ'' and Γ. This is given by the condition that tensors $\Gamma^{\alpha}{}_{\beta^{\sigma}}$ must be independent of the n-beins. Thus,

$$\Gamma^{\alpha}{}_{\beta}{}^{\sigma} = \sum_{r,s} e_r e_s h_{r\beta} h_s{}^{\sigma} \Gamma^{\alpha}{}_{rs} = \sum_{r,s} e_r e_s h''_{r\beta} h''_s{}^{\sigma} \Gamma''^{\alpha}{}_{rs}. \tag{32}$$

Using the laws of transformation of the n-beins

$$\begin{aligned} h_{r\beta} &= \sum_t a_{tr} h''_{t\beta} \\ h_s{}^{\sigma} &= \sum_t a_{ts} h''_t{}^{\sigma} \end{aligned} \tag{33}$$

where $\sum_t a_{rt} a_{st} = \sum_t a_{tr} a_{ts} = \delta_{rs}$, we obtain

$$e_r e_s \Gamma''^{\alpha}{}_{rs} = \sum_{t,u} e_t e_u a_{rt} \Gamma^{\alpha}{}_{tu} a_{su} \tag{34}$$

and a similar equation for Γ''_{rs}. With the help of Eq. (34) we may rewrite Eq. (31) as follows

$$\sum_{s,t,u} e_t e_u a_{rt} a_{su} \left\{ \Gamma^{\alpha}{}_{tu} \left(p_\alpha + \frac{e}{c} \Phi_\alpha \right) + mc\Gamma_{tu} \right\} \psi''_s = 0. \tag{35}$$

If the a's are constants, which is the case if we have distant parallelism, Eq. (35) becomes

$$\sum_r e_t a_{rt} \left[\sum_u e_u \left\{ \Gamma^{\alpha}{}_{tu} \left(p_\alpha + \frac{e}{c} \Phi_\alpha \right) + mc\Gamma_{tu} \right\} \sum_s a_{su} \psi''_s \right] = 0. \tag{36}$$

Thus, if ψ''_s satisfies Eq. (31),

$$\psi_u = \sum_s a_{su} \psi''_s \tag{37}$$

will satisfy Eq. (1). Similarly

$$\psi_t\dagger = \sum_r \psi''\dagger_r a_{rt}. \tag{38}$$

The current-density vector which we would have constructed using ψ''_s would be

$$\begin{aligned} J''^{\alpha} &= \sum_{r,s} e_r e_s \Gamma''^{\alpha}{}_{rs} \psi''_r\dagger \psi''_s \\ &= \sum_{r,s} \left(\sum_{t,u} e_t e_u a_{rt} \Gamma^{\alpha}{}_{tu} a_{su} \right) \psi''_r\dagger \psi''_s, \text{ by (34)} \\ &= \sum_{t,u} e_t e_u \Gamma^{\alpha}{}_{tu} \left(\sum_r \psi''_r\dagger a_{rt} \right) \left(\sum_s a_{su} \psi''_s \right) \\ &= \sum_{t,u} e_t e_u \Gamma^{\alpha}{}_{tu} \psi\dagger_t \psi_u, \text{ by (37) and (38)} \\ &= J^{\alpha}, \text{ by (17)}. \end{aligned}$$

10. Thus we were able to find a tensor equation, Eq. (13), which is invariant with respect to the Lorentz transformation and with respect to the

n-bein rotations. It satisfies all the conditions which a correct generalization of the Dirac equation should satisfy.

As for the physical or geometrical interpretation of the tensors $\Gamma^{\alpha}{}_{\beta}{}^{\sigma}$ and $\Gamma_{\beta}{}^{\sigma}$ we can only say that their introduction required the use of covariant differentiation in Einstein's sense and a true distant parallelism. In this we approach Einstein's unified field theory. However, a complete transition cannot be achieved as long as we are compelled to introduce potentials Φ_{α} in our equations as something externally given.

REPULSIVE ENERGY LEVELS IN BAND SPECTRA

By Joseph Kaplan
University of California at Los Angeles

(Received April 20, 1931)

Abstract

An explanation is given for many cases of anomalous intensity distribution in the band spectra of diatomic molecules. Use is made of an interaction between the known energy levels of molecules and energy levels which are produced by the repulsive interaction of pairs of atoms in their normal and metastable energy levels. The chief types of anomalies which are discussed are those corresponding to the sudden cutting off of a group of bands at some low value of v', the initial vibrational quantum number, and the failure of bands to agree with the Franck-Condon theory. Use is made of these ideas to explain the long life of active nitrogen.

WHILE there have been some very unusual cases of intensity distribution in the band spectra of diatomic molecules, they have been the exception rather than the rule and for that reason very little attention has been paid to them. The writer has made use of some of these cases to calculate the heats of dissociation of nitrogen[1] and of carbon monoxide[2] and until recently nothing more was done with them. Recent experiments on some very unusual band spectrum intensites in nitrogen-oxygen mixtures, combined with the increased interest in the purely repulsive potential energy levels of Heitler and London,[3] have led the writer to what is believed to be a satisfactory explanation of many of the unusual examples of band spectrum excitation which have arisen. The recent paper by Turner[4] on the effect of magnetic fields on the fluorescence radiation of iodine, suggested the direction in which an explanation was to be sought for the above-mentioned cases. In this note we will only mention these cases and make brief remarks about their explanations.

As a typical example we will consider the second positive group of nitrogen. These bands correspond to transitions from the C level to the B level. No bands of this system are known whose initial levels are higher than $v'=4$, in spite of the fact that the total energy of the "C" level is about 15 volts, corresponding to dissociation into a ^2D and a ^2P metastable atom.[5] The energy in the C_4 level is about 13.9 volts and this is exactly equal to the dissociation energy of nitrogen into two metastable ^2D atoms. Therefore, unless the products of dissociation are assumed to be two ^2D atoms rather than a ^2D and a ^2P atom, one cannot explain the non-appearance of the higher vibrational levels by saying the $v'=4$ is the highest vibrational quantum number that

[1] J. Kaplan, Proc. Nat. Acad. Sci. **15**, 226 (1929).
[2] J. Kaplan, Phys. Rev. **35**, 957 (1930).
[3] Heitler and London, Zeits. f. Physik **44**, 455 (1927).
[4] L. A. Turner, Zeits. f. Physik **65**, 464 (1930).
[5] Mulliken, Phys. Rev. **32**, 186 (1928).

can be associated with the C level. An alternative explanation presents itself if one assumes that all vibrational states above $v'=4$ are quenched by transitions from the C level to the Heitler and London level which corresponds to the coming together of two metastable ^2D atoms. The probability of transitions from the stable molecular level to a Heitler and London level is undoubtedly governed by the same rules as those which govern the usual molecular transitions e.g. by the Franck-Condon principle. Thus one can in general study the shape of the potential energy curve corresponding to a Heitler and London level, from the way it combines with known potential energy curves. The writer proposes to make a careful study of this in the future.

There are two possible explanations for the case which was just discussed, so that we propose now to discuss some more convincing examples of interaction between repulsive and attractive potential energy curves. The fourth positive bands of nitrogen are developed with but one initial vibrational state, corresponding to the transition D_0-B_v. The writer has used this fact as a means of calculating the heat of dissociation of nitrogen, making the postulate that the reason for the non-appearance of higher vibrational states was that the molecule spontaneously dissociated when an attempt was made to excite the higher vibrational states. At the time the calculation was made this was thought to indicate an extreme anharmonicity of the D level and consequently a very small heat of dissociation for this level. The value of $\omega_0 x$ necessary to yield the extremely small value of D^v that this explanation demanded was so large as to be without precedent among band spectra. The present explanation will be seen to be much more reasonable. A purely repulsive potential energy curve corresponding to the coming together of a ^2D and a ^2P atom would cross the potential energy curve of the D level at just about the energy corresponding to its first or second vibrational states. Even if the D level does possess some vibrational states, a strong intercombination with the Heitler and London level might either prevent the excitation of these higher vibrational states or if they were excited, it might quench them. Probably both of these effects must be considered, but once again it is seen that a Heitler and London level is useful in explaining an unusual spectroscopic phenomenon.

Similar considerations may be applied to the third positive group, the $3A$ bands and the $5B$ bands of carbon monoxide.[6] All three of these groups possess but one initial vibrational level and the writer has used the lowest one of these electronic levels, the b level, as a means of calculating the heat of dissociation of CO, making the same assumption as was made for the D level in nitrogen. The generally accepted value for the heat of dissociation of CO is around 10.3 volts and the energy values of the initial levels of the third positive and the $5B$ bands are 10.34 and 10.61 volts respectively. Thus it is gain highly probable that the repulsive energy level which corresponds to the coming together of a normal carbon atom and a normal oxygen atom, will so combine with these two electronic levels as to prevent the excitation of higher

[6] J. Kaplan, Phys. Rev. **36**, 784 (1930).

vibrational states. The repulsive interaction of a normal oxygen atom and a carbon atom in the $^1S_0$ state will yield an energy level in the vicinity of 11.5 volts, and this will account for the absence of vibrational states higher than $v'=0$ in the $3A$ bands of CO.

Returning to the consideration of the nitrogen molecule we call attention to several other cases of anomalous intensity distribution in band spectra, which seem to be examples of interaction between attractive and repulsive levels in the molecule. A system of nitrogen bands, discovered by Birge and Hopfield,[7] and having but a single initial vibrational state at 12.8 volts, shows a very unusual intensity distribution among the bands of the progression. Now 12.8 volts corresponds very closely to the energy of recombination of a normal nitrogen atom and a metastable atom in the ^2P level. Once again therefore we can blame the peculiar development of the bands on an interaction between an attractive and a repulsive energy state. In the same report, Birge and Hopfield call attention to many irregularities in the bands which make up the ultraviolet system $^1S-{}^1P$. Since the electronic energy of this system is 8.5 volts and most of the irregularities are connected with the progressions arising on $v'=4$, 5 and 6, the explanation is given that these irregularities arise from interactions between this level and the repulsive level which is formed when two normal nitrogen atoms come together. The heat of dissociation of nitrogen is about 9.1 volts[8] and the energy of the $v'=4$ level is 9.3 volts. By comparison with the previous examples it is certainly reasonable to assume that the above explanation is correct.

The experiments which first called the writer's attention to the possibilities of the ideas presented here, were designed to reproduce some of the peculiar intensity phenomena which arise in the first positive bands of nitrogen as produced in the aurora borealis. Without attempting a detailed discussion of the experiment, we can say that as far as the intensity distribution among the bands is concerned, especially when the relative intensities of the bands in a single v' progression are considered, the first positive bands are surprisingly sensitive to excitation conditions, more so in fact than any other band system with which the writer has had experience. Elsewhere[9] the present writer has called attention to the violent variation in intensities which arises when inert gases are mixed with active nitrogen. This variation in intensities, which is a variation of intensities in v' progressions, must be looked on as a variation in transition probabilities, because the relative intensities of bands within a v' progression are fixed by the relative transition probabilities, which can be determined by the Franck-Condon principle. In practically all discussions of band spectra it is assumed that the predictions of the above principle hold and in general they do apply. The anomalous cases presented here are those which arise either under unusual excitation conditions or in the case of energy levels which are very sensitive to excitation conditions and thus yield exceptional intensities even under normal dis-

[7] Birge and Hopfield, Astrophys. J. **68** 257 (1928).
[8] Birge, Trans. Faraday Soc. **25** 718 (1929).
[9] J. Kaplan, Phys. Rev. **36**, 778 (1930).

charge conditions. A few more remarks about the first positive bands will soon convince us that it is partly an example of the very sensitive energy state rather than that of unusual excitation conditions.

It is easy to see, from only a casual inspection of the spectrum, some of the unusual features of the first positive bands. One unusual feature is, that while most of the first positive bands possess four heads, the bands whose initial levels correspond to $v'=13$, 14, 15, 16 and sometimes $v'=17$, as well as those with $v'=19$, 20, 21, possess only strong single heads. In some discharges even $v'=3$, 4 and 5 showed this characteristic. Under some conditions there are remarkable variations in the relative intensities of the four heads and sometimes only one strong head appears where four appeared under normal conditions. Furthermore the intensities of the bands which possess these single-heads under normal conditions, are less than those originating on higher vibrational states, which is in itself an exceptional occurrence, and in agreement with the idea that the vibrational states corresponding to the single-headed bands are quenched by some mechanism in the molecule. In some of the experiments on the spectra of oxygen-nitrogen mixtures it was possible to produce the first positive bands with a sharp cut-off at $v'=12$. The vibrational states higher than $v'=12$ were almost completely missing thus giving here an excitation similar to some of the examples discussed above for NO, N_2 and CO.

A calculation of the energies corresponding to the range of vibrational states from which single-headed bands arise shows them to be in regions of the potential energy curve where one might quite reasonably postulate interaction with repulsive energy levels of the molecule. The vibrational levels associated with the initial electronic state of the first positive group lie between 9.35 and 13.9 volts. In this range there are four possible Heitler and London levels corresponding to the coming together of two normal atoms, or one normal and one ^2D metastable atom or one normal and one ^2P atom or two ^2D atoms. We therefore readily see why this group of bands should be so highly sensitive to changes in conditions of excitation. The energies of recombination corresponding to the above modes of interaction are 9.1, 11.47, 12.66 and 13.84 volts. The observation in some experiments of single headedness around $v'=3$ probably corresponds to the 9.1 volt level, the $v'=13$ to 17 correspond to both 11.47 and 12.66 since their energies lie just between these two values and finally the single headed bands around $v'=20$ or 21 can correspond to either 12.66 or 13.84.

The most interesting application of the idea of interaction between attractive and repulsive levels is to the problem of the afterglow of active nitrogen. Here the question has often been asked as to the reason why the afterglow persists for such a long time. What is the mechanism in the nitrogen molecule which regenerates metastable atoms, normal atoms and metastable molecules and keeps the afterglow visible for what is a very long time when one considers the degree of metastability of the energy states involved. If we postulate that many of the molecules in the initial states of the first positive bands interact with Heitler and London levels and dissociate

instead of radiating, then we have a direct mechanism for sustaining the afterglow. We literally allow the molecule to waste its time during the process of the decay of the afterglow. It may be that only a very small number of excited nitrogen molecules lose their energy by radiation, most of them simply redissociating due to interaction with one of the repulsive levels. Thus if the walls of the afterglow tube are such as to allow the persistence of atoms, and it is well known that the walls are of paramount importance here, then one can expect a very long duration for the glow. Until further investigation has been made, it is not possible to say which of the two factors governs the life of the glow. It will be an interesting problem to study the effect of this new factor on the life of the nitrogen afterglow.

One final example will be discussed because of the good numerical agreement with heats of dissociation to which it leads. It has been known for a long time to spectroscopists that the beta bands of nitric oxide possess a very exceptional intensity distribution.[10] These bands were first discovered in active nitrogen and the intensity distribution to which we refer is the one which is observed there. The writer has reported two experiments in which the beta bands were observed in the discharge but no careful study of intensity distribution has been made there. The two main anomalies in the intensity distribution in active nitrogen are the failure of the bands to fit the Franck-Condon theory and the absence of progressions higher than $v'=4$ even though $v'=5$ has been observed in absorption. The energy of the $v'=4$ level of the B band system is 6.15 volts and about three years ago the writer made some calculations of heats of dissociation of N_2 and O_2, using this as the heat of dissociation of NO. The success of this method in N_2 and CO was the reason for these calculations. The resulting value for O_2 was so low that it was not considered at the time. In view of the recent revisions of the heats of dissociation of N_2 and O_2, it is now possible to calculate a new value for NO,[11] using 9.1 volts for N_2 and 5.06 volts for O_2. The heat of dissociation of NO is found to be 6.15 volts so that the explanation is immediately apparent. We have here an example exactly like that of the second positive bands of nitrogen. The fact that in this case the phenomenon is observed in active nitrogen, where the interaction between attractive and repulsive levels is probably rather strong, makes the explanation more interesting. Here again we postulate an interaction between the excited states on which the beta bands arise and the Heitler and London level corresponding to the coming together of a normal oxygen and a normal nitrogen atom. The failure of the beta bands to obey the Franck-Condon rule for band intensities is added evidence that the proposed explanation is correct, since that also occurred in some other cases mentioned earlier in this paper.

We have seen that the interaction between a repulsive and an attractive level will account for the sudden curtailing of band systems and that many such examples are accompanied by a failure of the bands to obey the Franck-Condon rule. This latter phenomenon can be referred to as a variation of

[10] Barton, Jenkins and Mulliken, Phys. Rev. **30**, 175 (1927).
[11] Birge and Sponer, Phys. Rev. **28**, 259 (1926).

intensity within a progression, because a little consideration will show that the Franck-Condon rule predicts very definitely only the relative intensities within a single progression. Without going into much detail at this time it can be shown how the interactions which account for the curtailing of band systems will also account for a variation of intensities within a progression. The Franck-Condon theory is usually applied in a qualitative manner by drawing the two potential energy curves which are involved and noticing what lower states result when vertical lines are drawn through the two extreme values for the separation of the two atoms in the vibrating molecule. This procedure is correct provided the initial state radiates to, or in any other way goes to, only a single lower electronic state. The relative intensities of the bands which arise on a single initial vibrational state are then definitely fixed. If however the upper state finds itself in a position to interact with another lower state, the transition probabilities can be fixed now only by a consideration of both lower potential energy curves. It is obvious that one might readily expect large variations in the intensity distribution in progressions in this way. In the present paper we have shown how a third lower level, namely the Heitler and London level, may be brought in to the picture. From the nature of the observations it appears that this third level is sensitive to conditions and thus the intensity of interaction with normal levels will vary a great deal.

The present paper has been written mainly to bring out the one idea which is presented here. For that reason we have not published any spectra. This will be done in other publications which can be brought out with more leisure and in more detail, since this work is now being extended.

NOTE ON THE VISIBLE HALOGEN BANDS, WITH SPECIAL REFERENCE TO ICl

By Robert S. Mulliken
Ryerson Physical Laboratory, University of Chicago

(Received April 9, 1931)

Abstract

It is pointed out that the dissociation of excited ICl molecules, after absorption of light in the visible bands, into normal atoms is in harmony with theory. In analogy with the other halogens, these bands probably belong to a $^3\Pi \leftarrow {}^1\Sigma^+$ transition. The upper level of the bands is, however, doubtless not just the 0^+ part of the $^3\Pi_0$ as in the homonuclear halogen molecules, but is probably the whole $^3\Pi_0$, or else the $^3\Pi_1$. Detailed arguments against the possibility that the upper state of the halogen bands may be $^3\Sigma$ are given. Conclusions drawn in previous papers from the behavior of the I_2 bands in magnetic fields are revised.

IN TWO previous papers,[1,2] the writer has shown that the well-known visible absorption bands of the molecules Cl_2, Br_2, and I_2 probably correspond to the transition $0^+_u(^3\Pi) \leftarrow {}^1\Sigma^+_g$. The object of the present note is to supplement these papers by extending their application to such molecules as ICl, and by revising two or three doubtful or erroneous statements made in them.

Interpretation of ICl Bands

In molecules like ICl, relations between molecular and atomic electron states somewhat different from those in I_2 or Cl_2 are to be expected. This is obvious from the fact that we have four combinations $I(^2P_{1\frac{1}{2}})+Cl(^2P_{1\frac{1}{2}})$, $I(^2P_{1\frac{1}{2}})+Cl(^2P_{\frac{1}{2}})$, $I(^2P_{\frac{1}{2}})+Cl(^2P_{1\frac{1}{2}})$, and $I(^2P_{\frac{1}{2}})+Cl(^2P_{\frac{1}{2}})$, where with I_2 we have only three. Besides, it can hardly be taken for granted that the electronic states of the molecule ICl should show any close analogy to those of I_2 or Cl_2. Nevertheless, experience with other molecules shows that such an analogy may be expected (cf. analogies of SO to S_2 and O_2, CS and SiO to CO, AlO to BO, etc.).

A clearer understanding can be obtained by attempting to assign electron configurations. It has been assumed[2] that the normal and excited states of the visible absorption bands of chlorine are $\ldots 4d\sigma^2 3p\pi^4 4d\pi^4$, $^1\Sigma^+_g$ and $\ldots 4d\sigma^2 3p\pi^4 4d\pi^3 5f\sigma$, $^3\Pi_u$ (inverted) and that the corresponding states of I_2 are $\ldots 6d\sigma^2 5p\pi^4 6d\pi^4$, $^1\Sigma^+_g$ and $\ldots 6d\sigma^2 5p\pi^4 6d\pi^3 7f\sigma$, $^3\Pi_u$. It seems likely that the normal and excited states of the visible ICl bands have exactly the same configurations of outer electrons as I_2, the outer Cl electrons being promoted to equality with those of the I atom. Such a promotion appears necessary, since all the orbits which the outer electrons would occupy in Cl_2 are already filled in the I atom of ICl. This argument then supports the analogy already men-

[1] R. S. Mulliken, Phys. Rev. **36**, 699 (1930).
[2] R. S. Mulliken, Phys. Rev. **36**, 1440 (1930).

tioned. The $^3\Pi$ excited state of ICl, like those of the other halogens, should in view of its electron configuration be *inverted*. The triplet width should probably be about the same as in the $^3\Pi$ of Br_2, for which 2400 cm^{-1} seems a reasonable estimate.

It has been shown[1] that in I_2 the upper state of the visible bands is probably a 0^+_u state and that on theoretical grounds such a state cannot possibly be derived from $I(^2P_{1\frac{1}{2}})+I(^2P_{1\frac{1}{2}})$ or $^2P_{\frac{1}{2}}+^2P_{\frac{1}{2}}$, but that it can be derived from $^2P_{1\frac{1}{2}}+^2P_{\frac{1}{2}}$, as is observed. It was also shown to be likely that this 0^+_u belongs to a $^3\Pi$ state (mentioned in the preceding paragraph) of which the 0^-_u, 1_u, and 2_u components theoretically can and probably do dissociate into unexcited atoms. In the case of ICl, however, because of the absence of the property indicated by *g* or *u*, there is no theoretical reason why the 0^+ component of a $^3\Pi$ state analogous to that of I_2 should not dissociate, like the 0^-, 1, and 2 components, into normal atoms. In fact the theory makes this probable,—although it does not require it.

For according to the rules giving the relations between case *c* molecular and atomic states,[2] we may expect the following correlations : case *c* states 3, 0^+, 0^-, 2, 1, 2, 1, 1, 0^+, 0^- from $I(^2P_{1\frac{1}{2}})+Cl(^2P_{1\frac{1}{2}})$; 2, 1, 1, 0^+, 0^- from $I(^2P_{1\frac{1}{2}})+Cl(^2P_{\frac{1}{2}})$ and a similar set from $I(^2P_{\frac{1}{2}})+Cl(^2P_{1\frac{1}{2}})$; 1, 0^+, 0^- from $I(^2P_{\frac{1}{2}})+Cl(^2P_{\frac{1}{2}})$. These are the same sets of states that one gets from $2I(^2P_{1\frac{1}{2}})$; $I(^2P_{1\frac{1}{2}})+I(^2P_{\frac{1}{2}})$; and $2I(^2P_{\frac{1}{2}})$, respectively, except for the fact that no indices *g* or *u* are assigned here. It will be seen that all the case *c* states 2, 1, 0^+, and 0^- necessary to give a $^3\Pi$ state in case *a* can be obtained from two normal atoms I+Cl. Now there has been a good deal of discussion as to whether the upper state of the visible ICl bands gives two normal atoms on dissociation or whether it gives an excited chlorine atom.[3] The experimental evidence[3] strongly favors the latter alternative, which is here seen to be in harmony with theory. (It also negatives the possibility that an excited iodine atom is formed on dissociation.)

Assuming that the ordinary visible ICl bands give two normal atoms on dissociation, the question may still be raised as to whether their upper level is really the 0^+ component of a $^3\Pi_0$ as in I_2. First it should be noted that, if 0^+ is stable, it should be accompanied by 0^-, forming a complete $^3\Pi_0$, since if 0^+ dissociates into normal atoms, the corresponding 0^- almost certainly does too. Next comes the question whether this $^3\Pi_0$ should be a stable molecular state. If one examines Fig. 2 of Ref. 2, it will be seen that the fact that 0^+_u of I_2 is a reasonably stable molecular state (dissociation energy 0.55 volts) is due largely to the fact that it gives an excited atom on dissociation. Fig. 2 indicates that the 0^- and even the $^3\Pi_1$ and $^3\Pi_2$ components of the $^3\Pi_u$ should be much less stable in I_2 than the 0^+, or perhaps not be real molecular states at all. In view of these relations, one may question whether the $^3\Pi_0$ state of ICl should be stable, since it dissociates giving normal atoms. It therefore seems worth while,—although of course the quantitative relations may be considerably different than in Cl_2, Br_2, and I_2,—to consider the possibility that the upper level of the ICl bands may be $^3\Pi_1$ or even $^3\Pi_2$, and that the $^3\Pi_0$ state gives rise only to a continuum. [It is, however, also theoretically possible, although im-

probable, that both components of the $^3\Pi_0$ state might give excited atoms on dissociation, so that $^3\Pi_0$ would be a higher but stable state.] A possible indication that the upper level of the ICl bands is not $^3\Pi_0$ as in the other halogens is the fact that its energy (1.69 volts above the ground state)[3] is lower than that of any of the other halogens, while its dissociation energy (0.47 volts[3]) is nearly as large as that of I_2. If, however, it should turn out after all to be $^3\Pi_0$, then one should probably find at longer wave-lengths other bands leading to $^3\Pi_1$ and perhaps also to $^3\Pi_2$.

Additions and Corrections to Previous Papers

Possibility that the upper level of the halogen bands is $^3\Sigma$. A possible interpretation of the visible halogen bands which was not entirely disposed of in Refs. 1 and 2 was that they belong to a $^3\Sigma^+_u$ (case b), $^1\Sigma^+_g$ transition with $\Delta K = \pm 1$ in which only those combinations having $\Delta J = \Delta K = \pm 1$ are observed, the other possible combinations $\Delta J = 0$ being for some unknown reason very weak. This reason might possibly be found in the intersystem character of $^3\Sigma \leftarrow {}^1\Sigma$, for whose intensity relations we have no reliable guiding theory. [But as was mentioned in Ref. 1(p. 701), we know that in the $^1\Sigma \leftarrow {}^3\Sigma$ atmospheric oxygen bands, the transitions with $\Delta J = 0$ are as strong as those with $\Delta J = \pm 1$, and there seems no reason why the same should not be true here. Nevertheless since it is likely[4,5] that the atmospheric bands are $^1\Sigma^+_g \leftarrow {}^3\Sigma^-_g$, the argument may not hold, since this is a quadrupole transition.] A rather strong argument is that there is no theoretical necessity here for a $^3\Sigma^+_u$ state (which becomes 0^-_u plus 1_u in case *c*) to give $^2P_{1\frac{1}{2}} + {}^2P_{\frac{1}{2}}$ on dissociation, as the upper levels of the halogen bands are empirically known to do, whereas in the case of a 0^+_u state such a necessity does exist. [There is, to be sure, no theoretical proof that such a $^3\Sigma^+_u$ state could *not* give $^2P_{1\frac{1}{2}} + {}^2P_{\frac{1}{2}}$ here, although the theory strongly favors $^2P_{1\frac{1}{2}} + {}^2P_{1\frac{1}{2}}$ as dissociation products.[2]] A consideration of electron configurations also strongly favors a 0^+_u state (belonging to a $^3\Pi_0$) as against a $^3\Sigma^+_u$ state.[2]

Granting that the upper level of the halogen bands is 0^+_u, this might still conceivably be a 0^+_u which, together with a 1_u, would go over for small r into a case *b* $^3\Sigma^-_u$ state.[2] But a consideration of possible electron configurations makes this very improbable; at least two excited electrons would be required. Everything considered, it seems very probable that the identification of the upper state of the halogen bands as a 0^+_u belonging to a $^3\Pi_0$ is correct.

Magnetic behavior of iodine bands. In Ref. 1 the fact that a $^3\Pi_0$ molecular gas should be paramagnetic was taken as an explanation of the Faraday effect

[3] G. E. Gibson and H. C. Ramsperger, Phys. Rev. **30**, 598 (1927); E. D. Wilson, Phys. Rev. **32**, 611 (1928); G. E. Gibson and O. K. Rice, Nature, March 9, 1929; G. E. Gibson, Zeits. f. Physik **50**, 692 (1928); J. Patkowski and W. E. Curtis, Trans. Faraday Soc. **25**, 725 (1929); W. E. Curtis and O. Darbyshire, Trans. Faraday Soc. **27**, 77 (1931). G. K. Rollefson and F. F. Lindquist, J. Am. Chem. Soc. **52**, 2793 (1930); **53**, 1184 (1931).

[4] R. S. Mulliken, Phys. Rev. **32**, 880 (1928).

[5] R. S. Mulliken, Phys. Rev. 1931 (Abstract, Washington Meeting, Spring, 1931). Recent work of Childs and Mecke (Zeits. f. Physik **68**, 344, 1931) gives extremely low absorption coefficients in the atmospheric bands, and so favors $^1\Sigma^+_g$ rather than the possible alternative $^1\Sigma^-_u$ as the upper state of these bands.

observed in the iodine bands. Unfortunately, however, the fact was overlooked that the observed Faraday effect indicates that the normal state of iodine ($^1\Sigma^+_g$) is magnetically rather more sensitive than the upper (0^+_u) state.[6] The fact was also overlooked that, although a $^3\Pi_0$ molecular gas should be paramagnetic (less so, however, if the $^3\Pi_0$ is widely split into 0^+ and 0^-), this does not imply a first-order Zeeman effect. In fact, the 0^+ and 0^- states belonging to a $^3\Pi_0$ state should behave, if well-separated, very much like $^1\Sigma$ states in respect to the Zeeman or Faraday effect; but if the separation of the 0^+ and 0^- states should be small and if, as is the case for low K values in I_2, the separations of the rotational levels should be less than the spacing of the components of a normal Zeeman triplet, a magnetic field should produce a Paschen-Back effect in the $^3\Pi_0$ levels.[7]

But unless there is an error in Kemble's conclusion that the normal more than the excited state is responsible for the observed Faraday effect, we should probably return to Kemble's explanation[6] of this effect in the iodine bands, namely, that it is caused by the development of a small magnetic moment through the rotation of the molecule. Its existence would then really give no evidence either for or against the $^3\Pi_0$ nature of the upper electron level in the iodine bands. Nevertheless a renewed investigation of the matter would be of interest.

The quenching of the fluorescence of the iodine bands in a magnetic field, emphasized in Ref. 1, seems to indicate a special sensitiveness of the upper level to magnetic fields. The most promising suggestion as to the cause of the magnetic quenching of fluorescence seems to be Turner's idea[8] that it is due to a magnetically induced predissociation.

Indeed Van Vleck has now found, in a paper soon to be published, that a magnetic field may be expected to induce predissociation in the 0^+ state belonging to a $^3\Pi_0$ when the 0^+ and 0^- components dissociate as shown in Fig. 2 of Ref. 2. Thus the existence of magnetic quenching gives strong evidence in favor of the designation $0^+_u(^3\Pi_0)$.

[6] Cf. E. C. Kemble, Nat. Research Council Bulletin on Molecular Spectra, p. 347.

[7] The writer is indebted to Professor J. H. Van Vleck for the elucidation of these points. Cf. J. H. Van Vleck, Phys. Rev. **31**, 587 (1928).

[8] L. A. Turner, Zeits. f. Physik **65**, 477 (1930).

PICTORIAL REPRESENTATIONS OF THE ELECTRON CLOUD FOR HYDROGEN-LIKE ATOMS

By H. E. White
University of California, Berkeley

(Received April 21, 1931)

Abstract

It is well known that the solutions of the wave-equation for hydrogen-like atoms may be represented graphically by interpreting $\Psi\Psi^*$ as a *probability density*. The *probability density factors* $\Phi_m\Phi_m^* \cdot [\Theta_{m,l}]^2 \cdot [R_{n,l}]^2 = \Psi\Psi^*$ are represented graphically and briefly discussed and compared with the electron orbits of four classical models. Graphs for *s*, *p*, *d*, *f*, *g*, and *h* electrons are given. An attempt to combine the *probability density factors* and form some graphical representation of $\Psi\Psi^*$ has resulted in the construction of a mechanical device or model, see Fig. 5, which when photographed, gives very closely the desired result. Photographs for the magnetic states $m=0, \pm 1, \pm 2, \pm 3, \cdots$ are given for $1s$, $2p$, $3d$, $4f$, $2s$, $3p$, $4d$, $5f$, $3s$, $4p$, and $5d$ electrons, see Fig. 6.

WITH all of the successes of the quantum mechanics one still hears on every hand, for want of an atomic model, the terms *electron orbits*, *penetrating orbits*, *non-penetrating orbits*, etc. This is of course due to the fact that in many cases one may think in terms of the simpler electron orbits and be led to a result which is the same or very nearly the same as that given by the quantum mechanics. In going over some of the correlations very often made between the two theories several interesting graphical comparisons have been forthcoming.

It is well known that for a non-relativistic, conservative dynamical system of one nucleus and one electron (that is a hydrogen-like atom) Schroedinger's wave-equation

$$\Delta^2\Psi + \frac{8\pi^2\mu}{h^2}(W - V)\Psi = 0 \tag{1}$$

expressed in polar coordinates ϕ, θ, and r, see Fig. 1 may be solved by replacing Ψ by the product of a function of ϕ alone, another of θ alone, and another of r alone,

$$\Psi = \Phi_m \cdot \Theta_{m,l} \cdot R_{n,l}. \tag{2}$$

With this substitution the equation is separated into three total differential equations the well-known solutions of which are,

$$\Phi_m = (2\pi)^{-1/2} e^{im\phi}, \quad m = 0, \pm 1, \pm 2, \pm 3, \cdots \pm l \tag{3}$$

$$\Theta_{m,l} = \left(\frac{(2l+1)(l-m)!}{2(l+m)!}\right)^{1/2} \sin^m\theta \cdot P_l^m(\cos\theta), \quad l = 0, 1, 2, 3, \cdots (n-1) \tag{4}$$

$$R_{n,l} = \left[\frac{4(n-l-1)!Z^3}{[(n+l)!]^3 n^4 a_1^3}\right]^{1/2} \left(\frac{2Zr}{na_1}\right)^l e^{-zr/na} L_{n+l}^{2l+1}\left(\frac{2Zr}{na_1}\right), n = 1, 2, 3, \cdots \tag{5}$$

involving in addition to the *normalizing factors*, the complex exponentials $e^{im\phi}$, the "*associated Legendre polynomials*," and derivatives of the "*Laguerre polynomials*," where m, l, and n, are to be associated with the *magnetic*, *azimuthal*, and *total quantum numbers* respectively. It is also well known that $\Psi\Psi^* dv$, which is interpreted as the *probability* of the electrons being found in a given element of volume dv is very small outside the region occupied by the corresponding classical electron orbits.

For descriptive purposes it has been convenient to think of the *probability density* $\Psi\Psi^* = P$ in terms of the angles ϕ and θ and of the distance r independently. From Eqs. (2), (3), (4), and (5) the *probability density*

$$\Psi\Psi^* = \Phi_m\Phi_m^* \cdot [\Theta_{m,l}]^2 \cdot [R_{n,l}]^2. \tag{6}$$

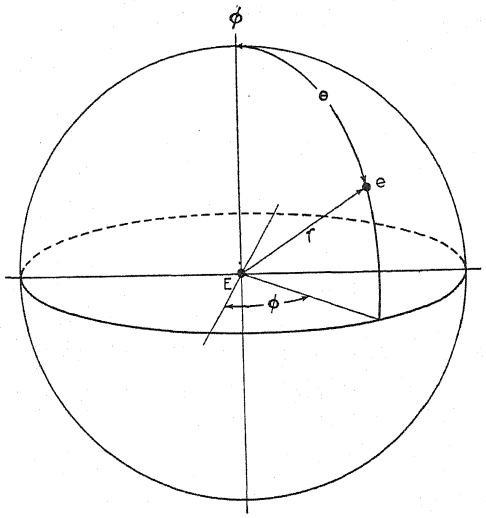

Fig. 1.

There are in general four classical models to be compared with these *probability density factors*. These four well-known models, which will here be called (a), (b), (c), and (d), have the same *total quantum number* n, and *azimuthal quantum numbers* as follows; (a) l (b) $[l(l+1)]^{1/2}$ (c) $l+\frac{1}{2}$, (d) $l+1=k$. It should be pointed out that none of these classical orbital models is correct and that, for want of an atomic model, any one of them may, with certain limitations, be used. In general (a) and (b) serve as vector models while (c) and (d) serve well as orbital models.

The $\Phi_m\Phi_m^*$ factor. For given m, Φ_m times its complex conjugate Φ_m^* is a constant, so that for any given state the probability of an electrons being found in any small element of angle $d\phi_1$ is the same as for any other equal angle $d\phi_2$. For all allowed electron states the *probability density* is therefore symmetrical about the ϕ (magnetic) axis. $\Phi_m\Phi_m^*$ plotted as a function of the angle ϕ (0 to 2π) would graphically be represented in rectangular coordinates by a straight line or in angular coordinates by a circle.

The $[\Theta_{m,l}]^2$ factor. For given m and l values the polynomials of Eq. 4 and consequently $[\Theta_{m,l}]^2$ are readily calculated from well known recursion formulas.[1]

Values of the *probability density factor* $[\Theta_{m,l}]^2$ are given in Table I and plotted in rectangular coordinates in Fig. 2.

Unsold[2] has shown that for given n and l, the *probability density* summed over the states $m=+l$ to $m=-l$ presents spherical symmetry about the nucleus. Since $\Phi_m\Phi_m^*$ is constant for any state one has simply to show that

$$\sum_{m=-l}^{m=+l}[\Theta_{m,l}]^2 = \text{constant}. \tag{7}$$

This well-known theorem is seen to be true from the last column of Table I or graphically from the curves of Fig. 2. For example, the sum of the three

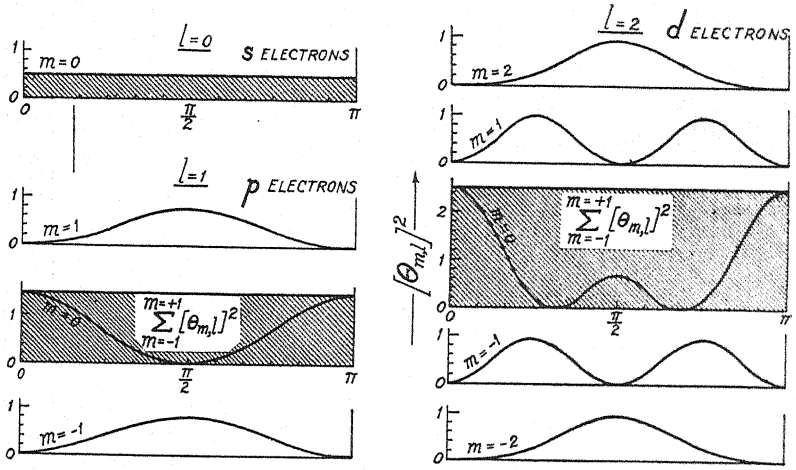

Fig. 2. The probability density factor $(\Theta_{m,l})^2$ as a function of θ for s, p, and d electrons. The straight lines and the shaded areas represent spherical symmetry, the result of the summation of the curves from $m=+l$ to $m=-l$.

curves for the three p states $m=1, 0, -1$ gives a straight line as indicated by The shaded area. Thus it is that in some of the complex spectra three similar p electrons five similar d electrons, or seven similar f electrons form spherical symmetry, that is an S term, as the most stable state.

If angular coordinates are used when plotting $[\Theta_{m,l}]^2$ a number of interesting correlations with the classical orbits may be made. Such curves are shown in Fig. 3 for s, p, d, f, g, and h electrons. Beneath each figure the corresponding classical orbit is given oriented in each case according to the vector model (a). In order to illustrate an orbit rather than its straight line projection the ϕ axis is tipped slightly out of the plane of the paper. It must be remembered that the electron is not confined to the shaded area in each

[1] See "Quantum Mechanics," by Condon and Morse, p. 63.
[2] Unsold, Ann. d. Physik **82**, 379 (1927).

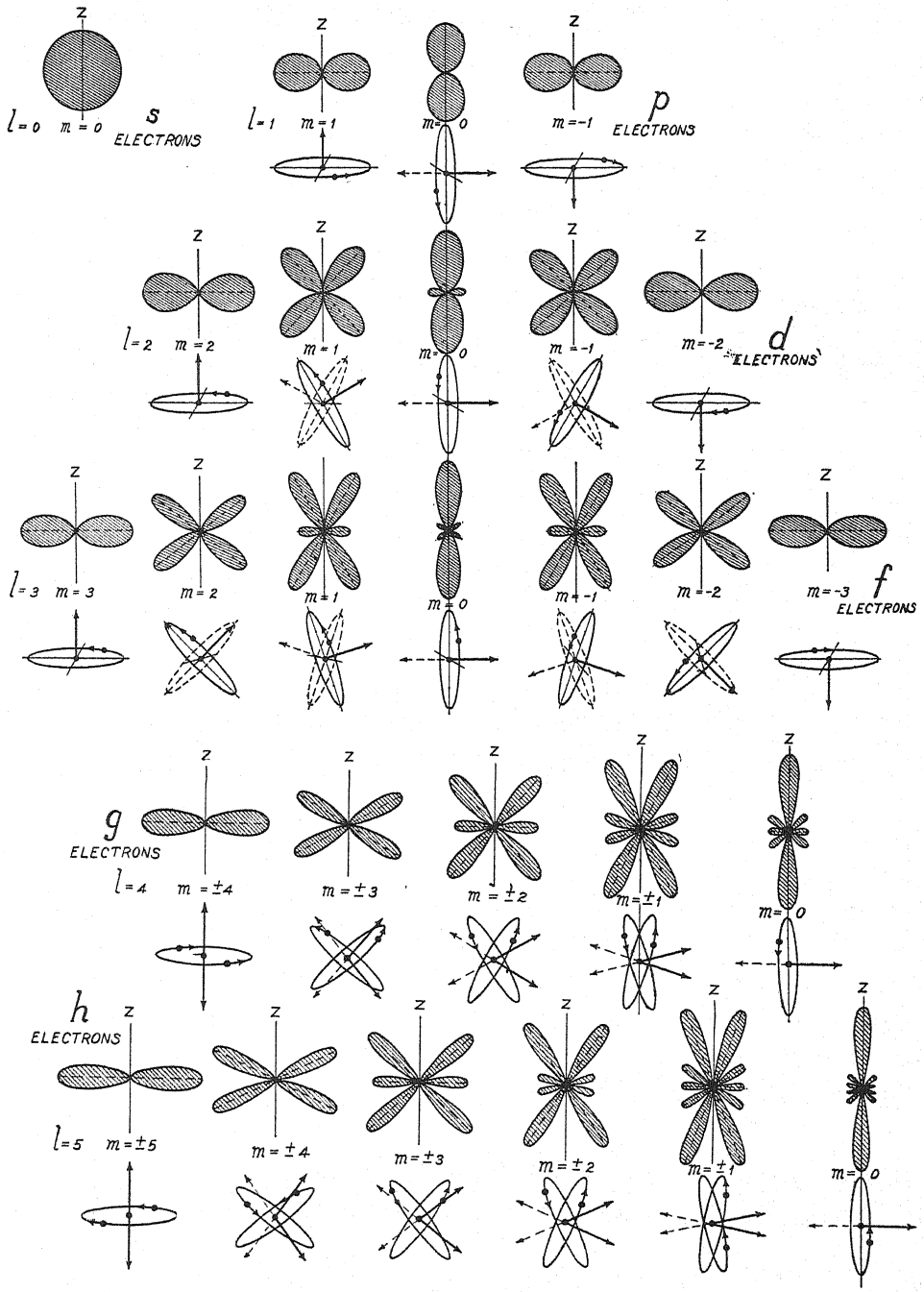

Fig. 3. The probability density factor $(\Theta_{m,l})^2$ plotted in angular coordinates for s, p, d, f, g, and h electrons. For states $m=0$ the scale is approximately $1/l+1$ times that of the other states of the same l value. The classical oriented orbit for each quantum state is given below each figure, tilted slightly out of the normal plane to show an orbit rather than a straight line.

TABLE I. *The probability density factor* $[\Theta_{m,l}]^2$.

Electron	l	m	$[\Theta_{m,l}]^2$	$\sum_{m=-l}^{m=+l}[\Theta_{m,l}]^2$
s	0	0	$1/2$	$1/2$
p	1	±1	$3/4\ \sin^2\theta$	$3/2$
		0	$3/2\ \cos^2\theta$	
d	2	±2	$15/16\ \sin^4\theta$	$5/2$
		±1	$15/4\ \sin^2\theta\cos^2\theta$	
		0	$10/16\ (3\cos^2\theta-1)^2$	
f	3	±3	$35/32\ \sin^6\theta$	$7/2$
		±2	$105/16\ \sin^4\theta\cos^2\theta$	
		±1	$21/32\ \sin^2\theta(5\cos^2\theta-1)^2$	
		0	$7/8\ (5\cos^3\theta-3\cos\theta)^2$	

probability figure but that the magnitude of a line joining the center and any point on the curve is a measure of the electrons probability of being found in the direction of that line.

Since the plane in which each curve is drawn represents any plane through the ϕ axis symmetry of $\Phi_m\Phi_m^*$ is obtained by rotating each curve about the ϕ (or *magnetic*) axis. Corresponding to this axial symmetry there is the classical precession of each orbit around the ϕ axis producing a somewhat similar figure. For each $m=0$ curve the scale used is about $1/l+1$ times that of the other curves of the same l value.

For all $m=0$ states, excluding the spherically symmetrical s states, the *probability density* is greatest in the direction of the poles. With the exponent of $e^{im\phi}$ zero this distribution has been interpreted to mean[3] that there is no motion in the ϕ coordinate and that correlated with this the motion of the electron (i.e. the orbital plane) is in some one meridian plane, all meridian planes being of equal probability. The end states $m=\pm l$ on the other hand take on their largest values in the direction of the equatorial plane. In this case one correlates the opposite signs in the exponents of $e^{\pm im\phi}$ with the opposite directions of rotation in the orbit. The way in which each classically oriented orbit follows the corresponding curves, from $m=+l$ to $m=-l$, especially for the states of higher l value, is quite remarkable. It should be mentioned that if the classical orbits are oriented according to models (b), (c), or (d) that their general agreement with the probability curves is not as good as with model (a), however, this may be a matter of personal opinion.

The $[R_{n,l}]^2$ factor. The factor $[R_{n,l}]^2$ which gives the *probability density* as a function of r alone has been discussed in detail by many investigators. For given values of n and l the Laguerre polynomials and hence $R_{n,l}$ (see Eq. (5)) and $[R_{n,l}]^2$ may be evaluated.[1] Plotting $[R_{n,l}]^2$ against r in units of the radius of the first Bohr circular orbit $a^1=0.528$ AU. give the heavy line curves of Fig. 4. Multiplying $[R_{n,l}]^2$ by $4\pi r^2$, the area of a sphere of radius r, one obtains the so called *probability density distribution* curves, D, indicated by the shaded areas in the figure. The classical orbits corresponding to each of these

[3] See, Condon and Morse, "Quantum Mechanics."

curves, using model (c), are also shown. In each curve the *density distribution* differs greatly from zero only within the electron-nuclear distance of the corresponding classical orbits.

A more satisfactory correlation has been made by Pauling[4] by comparing the average value of r as calculated on both theories. The method of evaluating r from the quantum mechanics has been given by Waller[5] and is identical with the value obtained for the classical orbits if the *azimuthal quantum number* is taken to be $[l(l+1)]^{1/2}$, model (b). This average value of r is indicated in

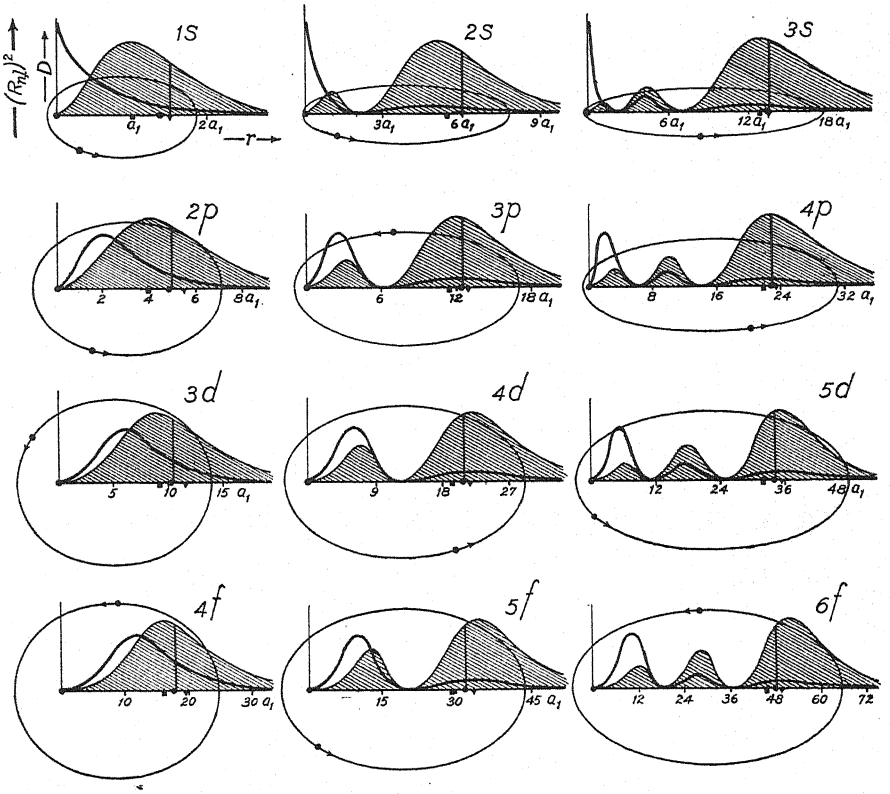

Fig. 4. The probability density factor $(R_{n,l})^2$ plotted as a function of the electron-nucleus distance r (r is measured in units of the first Bohr circular orbit). The density distribution curves $D=4\pi r^2\cdot(R_{n,l})^2$ the shaded areas, are to be compared with the electron-nucleus distance for the classical orbits, where the azimuthal quantum number is taken to be $l+\frac{1}{2}$.

each curve by a vertical line. The average value of r calculated for models (a), (c), and (d) are indicated on the r axis by triangular, circular, and square dots respectively.

For this radial comparison model (b) is to be preferred, however, a difficulty arises for the s states where the orbits reduce to straight lines with one

[4] Pauling, Proc. Roy. Soc. **114**, 181 (1927).
[5] Waller, Zeits. f. Physik **38**, 635 (1926).

end at the nucleus center. With model (c), the orbits shown in the figure, this difficulty does not arise and the agreement is practically the same.

The Probability Density $\Psi\Psi^*$

Attempts to bring together the *probability density factors* $\Phi_m\Phi_m^*$, $[\Theta_{m,l}]^2$, and $[R_{n,l}]^2$ into one single picture for $\Psi\Psi^*$, if we may call it a picture, have been somewhat successful. Langer and Walker[6] using a method which is as yet unpublished, have produced *probability density* photographs which represent the spherically symmetrical s states and the $2p$ states $m=+1$ and 0.

Preliminary attempts to produce a three dimensional model which will represent as closely as possible the *probability density* $\Psi\Psi^*$ has resulted in a mechanical device shown in Fig. 5. Spindles like the one shown in the center

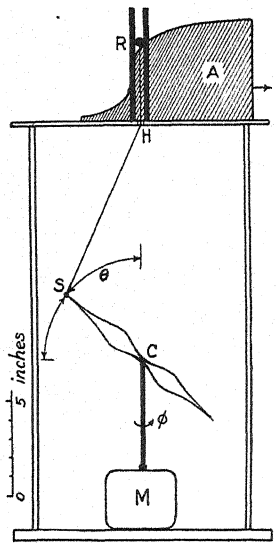

Fig. 5. A mechanical device which when set in motion and photographed represents the electron cloud for the various states of the hydrogen-like atoms. The model shown in the figure is for a $3d$ electron.

of the figure and in the last photograph of Fig. 6 are turned out on a lathe so that in projection they give the *density distribution* D curves of Fig. 4. Such a spindle is pivoted at its center by a small pin at C, and set in rotation about the vertical axis by means of a motor M. This motion gives the required symmetry about ϕ. At the same time that rotation about the ϕ axis is taking place, the angle θ is changed slowly from $\theta=0$ to $\theta=\pi/2$ by means of a swivel S and a double cord SHR which passes through a hole in the table top to a roller R, the motion of which is confined to the slot as shown. Curves of thin wood, e.g. A in Fig. 5, are cut so that when they are moved slowly but with uniform speed along the table top in the direction indicated by the arrow the angular

[6] See, "Atoms Molecules and Quanta," by Ruark and Urey, p. 565. Also Slater, Phys. Rev. 37, 482 (1931).

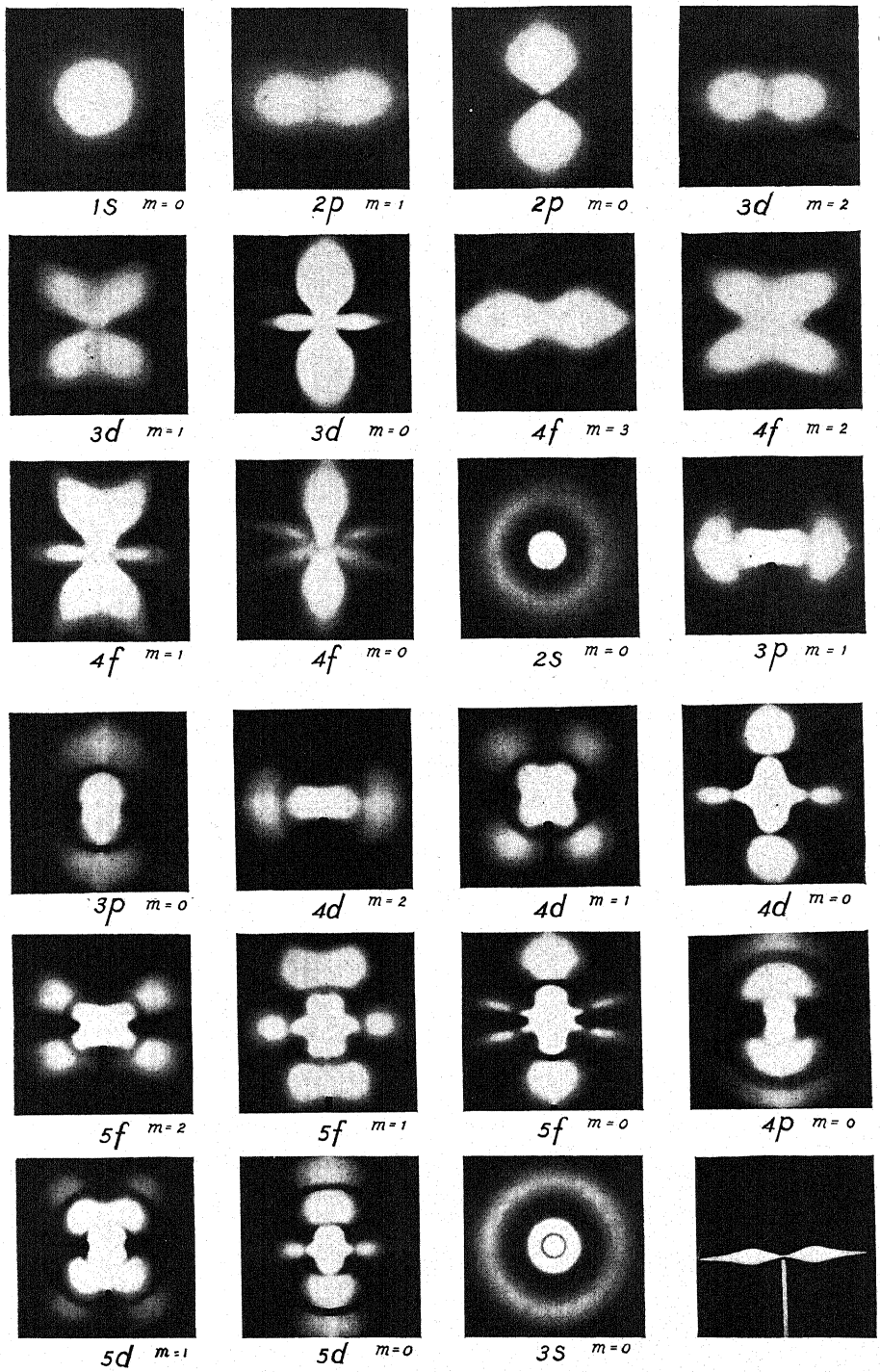

Fig. 6. Photographs of the electron cloud for various states of the hydrogen-like atoms as obtained from various models and the device shown in Fig. 5. The proability density $\Psi\Psi^*$ is symmetrical about the ϕ or magnetic axis which is vertical. The scale for each figure may be obtained from Fig. 4.

velocity $d\theta/dt$ is changed in the proper manner to give, as nearly as possible, the correct density when photographed. A time exposure started when $\theta=0$ and stopped when $\theta=\pi/2$ for the model shown yields the figure for the $3d$ state $m=0$. In constructing the various curves to be used at A, the changing angle of the cord IIR was taken into account and also the fact that as θ increases each point on the spindle moves in larger and larger circles and therefore faster. A small slot milled in the lower half of each spindle allows the angle $\theta=0$ to be reached. In projection each spindle should represent the *density distribution* curves, D of Fig. 5, in order that when rotating simultaneously about the ϕ and θ axes they give at each point in space the *density* $[R_{n,l}]^2$ curves of Fig. 5. It should be pointed out that there is a small amount of distortion due to the end on view of the spindle. This distortion is quite negligible, however, in that in this position the rapid motion as seen from the camera effects the photographic plates but little. Photographs for the states with negative m values are identical with those of positive m values. It may be seen by an examination of the figures that the addition of the $2p$ states $m=1, 0, -1$ or the sum of the $3d$ states $m=2, 1, 0, -1, -2$ will give spherical symmetry a figure like that of a $1s$ electron. Again the summation of the $4d$ states $m=2, 1, 0, -1, -2$ will give spherical symmetry resembling the $2s$ state. This may be considered as somewhat of a check on the figures in general and is quite as good as can be expected both from the standpoint of photographic reproduction of densities and the mechanical difficulties in the model.

The s states in Fig. 6 were made in a much simpler manner than the others and represent cross-sections only. Curves cut from white paper glued to the face of a blackened disk, and set rotating give the figures shown. Cross-section photographs have also been made for the nodal states by changing θ alone, ϕ remaining fixed. While these photographs are in general better, the more complete three dimensional reproductions are given in Fig. 6. The author wishes to take this opportunity to thank Professor Oppenheimer for his criticism of this paper.

NOTE ON THE CALCULATION OF VAN DER WAALS FORCES[1]

By Henry Margenau
Sloane Physics Laboratory, Yale University

(Received April 28, 1931)

Abstract

The general expression for the van der Waals energy arising from dipole interaction between atoms involves a summation over transition probabilities. These are in most cases difficult to calculate. It is here pointed out that since these transition probabilities obey the sum rule of Thomas and Kuhn, they may be evaluated in a manner which permits van der Waals' forces to be calculated with good approximation, provided that the polarizability is known. The method is outlined and illustrated by application to two examples: Na and He. The result in the case of He is in very good agreement with that obtained by the variational method.

THE methods proposed so far for a calculation of intermolecular forces depend on an (exact or approximate) knowledge either of the molecular wave functions[2] or of the oscillator strengths (dispersion f-values) associated with transitions from the ground state of the molecules in question.[3] Occasionally, useful approximations were obtained in terms of polarizabilities and other known characteristics. In this note we wish to suggest a method, semi-empirical in character and not involving the use of wave functions, which in general, enables a calculation of van der Waals forces between atoms with greater accuracy than others of equal simplicity permit. It consists in expressing the perturbational energy of the second order as a sum over f-values, as was first done by London, and then determining these f-values by means of the sum rule of Thomas and Kuhn, and the relative intensities of spectral lines.

Suppose that the two interacting atoms, A_1 and A_2, are similar and a distance R apart, R being so large that electron interchange does not take place. Let both A_1 and A_2 be in their lowest energy state which we take to be spherically symmetrical (s-state). α and β denumerate the various excited states of A_1 and A_2 respectively. If we restrict our consideration to the effects of the classical dipole interaction

$$V = \frac{e^2}{R^3}(y_1y_2 + z_1z_2 - 2x_1x_2) \tag{1}$$

[1] Part of the considerations here presented have been reported at the meeting of the Amer. Phys. Soc., Feb. 26–28. Hitherto we did not feel that they were of sufficient interest to be published more fully. Recently, however, Slater and Kirkwood (see ref. 2) have calculated a value for the attractive forces between He atoms differing widely from London's result. They attribute this discrepancy to the neglect of double electron jumps in London's theory. Aside from being applicable to many cases not of immediate interest at present, the method here outlined shows the correctness of the latter supposition.

[2] Eisenschitz and London, Zeits. f. Physik **60**, 491 (1930); Slater and Kirkwood, Phys. Rev. **37**, 682 (1931); Hassé, Proc. Camb. Phil. Soc. **27**, 66 (1931).

[3] F. London, Zeits. f. phys. Chemie, B, **11**, 222 (1930).

which is proper for large separations only, the second order perturbation energy of A_1+A_2 becomes

$$\Delta_2 E = -\sum_{\alpha\beta}{}' \frac{|V_{11,\alpha\beta}|^2}{E_\alpha + E_\beta - 2E_1}, \tag{2}$$

where

$$|V_{11,\alpha\beta}|^2 = \frac{e^4}{R^6}(y_{1\alpha}{}^2 y_{1\beta}{}^2 + z_{1\alpha}{}^2 z_{1\beta}{}^2 + 4x_{1\alpha}{}^2 x_{1\beta}{}^2 + 2y_{1\alpha}z_{1\alpha}y_{1\beta}z_{1\beta} - 4x_{1\alpha}y_{1\alpha}x_{1\beta}y_{1\beta} - 4x_{1\alpha}z_{1\alpha}x_{1\beta}z_{1\beta}) \tag{3}$$

$q_{1\alpha}$ is the coordinate matrix associated with a transition of A from the lowest state (1) to the state α, e.g. $x_{1\alpha}=\int R_{10}(r)xR_{nl}(r)P_l{}^m e^{im\phi}r^2\sin\theta dr d\theta d\phi$; n, l, and m being the quantum numbers with their usual significance. (We are writing R_{10} for the radial function of the lowest state without meaning to imply that $n=1$ for this state.) It follows directly that

$$\sum_m x_{1\alpha}y_{1\alpha} = \sum_m x_{1\alpha}z_{1\alpha} = \sum_m y_{1\alpha}z_{1\alpha} = 0,$$

and that

$$\sum_m x_{1\alpha}{}^2 = \sum_m y_{1\alpha}{}^2 = \sum_m z_{1\alpha}{}^2 = \tfrac{1}{3}\delta_1{}^l r_{1\alpha}{}^2.$$

Hence in summing (3) over the magnetic quantum numbers of both A_1 and A_2 we obtain $\frac{2}{3}\delta_1{}^{l_\alpha}\delta_1{}^{l_\beta}e^4/R^6\, r_{1\alpha}{}^2 r_{1\beta}{}^2$ so that (2) becomes

$$\Delta_2 E = -\frac{2}{3}\frac{e^4}{R^6}\sum_{\alpha\beta}{}' \frac{r_{1\alpha}{}^2 r_{1\beta}{}^2}{E_\alpha + E_\beta - 2E_1}, \tag{4}$$

where now the summation is no longer over magnetic quantum numbers and includes only states connected with the ground state by dipole radiation ($l_\alpha = l_\beta = 1$). But $r_{1\alpha}$ is related to the f-values appearing in the dispersion formula

$$n^2 - 1 = \frac{e^2 N}{\pi m}\sum_\alpha \frac{f_{1\alpha}}{\nu_\alpha{}^2 - \nu^2}$$

by the relation

$$r_{1\alpha}{}^2 = \frac{3}{2m}\left(\frac{h}{2\pi}\right)^2 \frac{f_{1\alpha}}{E_\alpha - E_1}. \tag{5}$$

Substituting this in (4) there results a formula meanwhile already obtained by London and used by him to compute intermolecular forces by means of a knowledge of a limited number of empirical f-values. We wish to propose a scheme permitting the f-values to be determined independently of spectroscopic dispersion formulae, which necessarily emphasize unduly the f's in the vicinity of the spectral region for which the formulae were calculated.

Combining (5) and (4) and realizing that $\Sigma_{\alpha\beta}{}'$ includes an integration over the continuous region of the spectrum we may write

$$\Delta_2 E = -F\Big\{ \sum_{\alpha\beta}{}' \frac{f_{1\alpha}f_{1\beta}}{v_\alpha v_\beta (v_\alpha + v_\beta)} + 2\sum_{\alpha}{}' \int_0^\infty \frac{f_{1\alpha}(df_{1E}/dE)dE}{v_\alpha(1+E)(v_\alpha+1+E)} + \int_0^\infty \int_0^\infty \frac{(df_{1E'}/dE')(df_{1E''}/dE'')dE'dE''}{(1+E')(1+E'')(2+E'+E'')} \Big\}. \tag{6}$$

We are here using the abbreviations:

$$\epsilon_\alpha = -E_\alpha;\ v_\alpha = 1 - \frac{\epsilon_\alpha}{\epsilon_1};\ F = \frac{1}{R^6}\,\frac{3}{2m^2\epsilon_1{}^3}\left(\frac{he}{2\pi}\right)^4$$

E is the energy of any state beyond the series limit, measured in units equal to the energy of the series limit, ϵ_1. (6) does not take explicit account of possible multiple electron transitions to discrete states beyond the series limit, the energy of which is frequently not known. They may be considered included in the integration, however, since the f-values will be adjusted in such a manner that their sum obeys the theorem of Kuhn and Reiche,[4] which postulates:

$$\sum_{\alpha}{}' f_{1\alpha} + \int_0^\infty \frac{df_{1E}}{dE}\,dE = Z_0 \tag{7}$$

Z_0 being the number of dispersion electrons.

It becomes necessary to make some assumption about the distribution of the f_{1E}'s. Fortunately, the calculation of $\Delta_2 E$ is not very sensitive to this choice, provided that (7) is satisfied. We shall suppose, in conformity with what is known about H and x-ray spectra, that

$$\frac{df_{1E}}{dE} = \frac{\gamma}{(1+E)^3}, \tag{8}$$

γ being at present undetermined. Moreover, we shall consider that the relative intensities of the first few emission lines of the principal series are known. The accuracy of the calculation is not seriously impaired if this is not the case. Suppose these relative intensities to be J_α. Then one may easily verify that

$$f_{1\alpha} = \frac{\beta J_\alpha}{v_\alpha{}^3} \equiv \beta\phi_\alpha, \tag{9}$$

since $J_\alpha = \text{const.}\ (E_\alpha - E_1)^4 r_{1\alpha}{}^2$. β is another undetermined constant. To determine β and γ we have first (7), which may be written on account of (8) and (9):

$$\beta \sum_{\alpha}{}' \phi_\alpha + \frac{\gamma}{2} = Z_0 \tag{10}$$

and second the expression for the polarizability in a static field:

[4] For complex structures, this sum rule is merely an approximation.

$$\alpha = \frac{1}{m}\left(\frac{eh}{2\pi}\right)^2 \sum_\alpha{}' \frac{f_{1\alpha}}{(E_\alpha - E_1)^2},$$

or, explicitly,

$$\alpha = \frac{1}{m\epsilon_1{}^2}\left(\frac{eh}{2\pi}\right)^2 \left\{ \sum_\alpha{}' \frac{f_{1\alpha}}{v_\alpha{}^2} + \int_0^\infty \frac{(df_{1E}/dE)dE}{(1+E)^2} \right\} \tag{11a}$$

whence

$$\beta \sum_\alpha{}' \frac{\phi_\alpha}{v_\alpha^2} + \frac{\gamma}{4} = m\epsilon_1{}^2 \left(\frac{2\pi}{eh}\right)^2 \alpha. \tag{11}$$

(10) and (11) supply the required numerical values of β and γ. If line intensities are not known, we may put the first $\phi = 1$ and all others equal to 0. The evaluation of (6) is now an easy matter.

In cases where $Z_0 = 1$ (no multiple jumps) the contribution of the region beyond the series limit is usually small. It may then be advisable to write (6)

$$\Delta_1 E = -\frac{F}{2}\left\{ \sum_{\alpha\beta}{}'(1 + P_{\alpha\beta}) f_{1\alpha} f_{1\beta} + 2 \sum_\alpha{}' \int_0^\infty (1 + P_{\alpha E}) f_{1\alpha} \frac{df_{1E}}{dE} dE \right.$$
$$\left. + \int_0^\infty \int_0^\infty (1 + P_{E'E''}) \frac{df_{1E'}}{dE'} \frac{df_{1E''}}{dE''} dE' dE'' \right\},$$

with the abbreviations

$$P_{\lambda\mu} = \frac{1 - v_\lambda v_\mu (v_\lambda + v_\mu)/2)}{v_\lambda v_\mu (v_\lambda + v_\mu)/2)},$$

v_E being $1+E$.

Using (7), this goes over into

$$\Delta_2 E = -\frac{F}{2}\left\{ Z_0{}^2 + \sum_{\alpha\beta}{}' P_{\alpha\beta} f_{1\alpha} f_{1\beta} + 2 \sum_\alpha{}' P_{\alpha E} f_{1\alpha} \frac{df_{1E}}{dE} dE \right.$$
$$\left. + \int_0^\infty \int_0^\infty P_{E'E''} \frac{df_{1E'}}{dE'} \frac{df_{1E''}}{dE''} dE' dE'' \right\}. \tag{12}$$

Recalling the definition of the v's we see that in some cases where the energy of all excited states is small compared with that of the lowest state they do not differ greatly from 1, which makes the P's small. Then one may expect to attain a fair approximation to the polarization forces by retaining in the $\{\ \}$ of (12) only the term $Z_0{}^2$. For hydrogen, the last 3 terms contribute about 8 percent of the total. If we make use of (8), (9), (10), and (11) expression (12) becomes:

$$\Delta_2 E = -\frac{F}{2}\left\{ Z_0{}^2 + \beta^2 \sum_{\alpha\beta}{}' P_{\alpha\beta}\phi_\alpha\phi_\beta + \beta\gamma \sum_\alpha{}' R_\alpha \phi_\alpha - 10.170\gamma^2 \right\}, \tag{13}$$

where

$$R_\alpha = \frac{4}{v_\alpha^2}\left[\frac{1}{3} - \frac{1}{2v_\alpha} + \frac{1}{v_\alpha^2} - \frac{1}{v_\alpha^3}\log(1+v_\alpha)\right] - 1.$$

For hydrogen, this expression gives $\Delta_2 E$ to within 1 percent if only 4ϕ's are used.

As an illustration, let us compute the polarization energy of two Na-atoms by the method here outlined. α can here be calculated since the f-values happen to be known.[5] They will also afford a check on our β and γ. α turns out to be 24.2×10^{-24}. (We omit the details of the calculation, which is made with the aid of Eq. (11.) We shall use only ϕ_2, corresponding to the resonance transition, and put it equal to 1. v_2 is then 0.409; $\epsilon_1 = 8.145\times10^{-12}$ ergs. Eqs. (10) and (11) give

$$\beta + \frac{\gamma}{2} = 1; \quad \frac{\beta}{0.409^2} + \frac{\gamma}{4} = 5.88,$$

so that $\beta = 0.888$ and $\gamma = 0.224$. From (13) one then obtains

$$\Delta_2 E = \frac{12.5}{R^6} \times 10^{-58} \text{ ergs} = \frac{790}{r^6} \text{ volts},$$

if r is measured in $\mathring{A}$. The correct value, which may be calculated from Sugiura's work, is

$$\Delta_2 E = \frac{14.5}{R^6} \times 10^{-58} \text{ ergs}.$$

It may be approximated as closely as desired, of course, by taking a greater number of ϕ's into account. We note in passing that these results suggest the existence of very strong polarization forces and the formation of polarization molecules, such as were observed in K_2 by Kuhn.[6]

Another more interesting application is to He, where our calculations can be no longer controlled by a sufficiently accurate knowledge of the f-values. There exist intensity measurements on the emission lines of the "principal" series[7] from which the ϕ_α's may be obtained by (9). We have considered 10 of them, but it turns out that very few of them would have been sufficient, because the main contribution to the f's seems to come from the region beyond the series limit. Taking α as 0.206×10^{-24}, Eqs. (10) and (11) become

$$\beta \sum_\alpha{}' \phi_\alpha + \tfrac{1}{2}\gamma = 2$$

$$\beta \sum_\alpha{}' \frac{\phi_\alpha}{v_\alpha^2} + \frac{1}{4}\gamma = 1.122.$$

If now we use the relative intensity data in Hopfield's arbitrary units $\Sigma_\alpha{}'\phi_\alpha =$

[5] Y. Sugiura, Phil. Mag. **4**, 495 (1927).

[6] Kuhn, Naturwissenschaften **18**, 332 (1930). See also Oldenberg, Zeits. f. Physik **47**, 184 (1928) and **55**, 1 (1929).

[7] Hopfield, Astrophys. J. **72**, 133 (1930).

293.7, and $\Sigma_\alpha'\phi_\alpha/v_\alpha^2=351.1$, whence $\beta=5.97\times10^{-4}$ and $\gamma=3.64$. The surprising magnitude of γ shows clearly, and probably over-emphasizes, the important rôle of the transitions to states beyond the ionization limit of one electron. That these states need not belong to the continuous spectrum, and that our integration (instead of summation) is dictated by convenience and lack of data to handle them more properly has already been pointed out. Substituting β and γ in (6), or more conveniently in (13) (where now, of course, on account of the size of γ only the second term in $\{\}$ may be neglected) we find

$$\Delta_2E=\frac{9.68}{R^6}\times10^{-61}(1.49)\text{ ergs}=\frac{14.4}{R^6}\times10^{-61}\text{ ergs}=\frac{0.91}{r^6}\text{ volts, if }r\text{ is in }\mathring{A}. \quad (14)$$

(The somewhat smaller value reported previously[8] was obtained by considering only transitions of one electron, putting $Z_0=1$, which is not legitimate.) (14) agrees very well indeed with the result of Slater and Kirkwood, calculated with a variational method, namely

$$\Delta_2E=\frac{14.9}{R^6}\times10^{-61}\text{ ergs}.$$

The latter authors suggest that the large difference between their result and the one obtained by applying London's simple approximation, which yields an upper limit $\Delta_2E_{\max}=12.4\times10^{-61}$ ergs, is occasioned by the neglect of double jumps in London's expression. The calculations presented here make this evident.

[8] See ref. 1.

AN EXPERIMENTAL STUDY OF THE NATURAL WIDTHS OF THE X-RAY LINES IN THE L-SERIES SPECTRUM OF URANIUM

By John H. Williams
Department of Physics, University of California

(Received April 21, 1931)

Abstract

The half widths at half maximum of the rocking curves in parallel positions of the double x-ray spectrometer with calcite crystals reflecting in the first order have been investigated as a function of wave-length and this function is shown to be linear.

The rocking curves of U $L\alpha_1$ in three different antiparallel positions of the instrument give a natural width which is practically independent of the dispersion. The natural widths of U $L\alpha_1$ and U $L\beta_1$ have been observed as a function of voltage and no significant dependence was noted.

The half widths at half maximum of twelve lines in the uranium L-series spectrum were studied and the results are:

Line U L	α_1	α_2	β_1	β_2	β_3	β_4	β_5	β_6	γ_1	γ_2	γ_3	γ_6
$\Delta\lambda$ in X.U.	0.439	0.494	0.299	0.369	0.382	0.726	0.252	0.487	0.242	0.57	0.47	0.233
ΔV in volts	6.56	7.20	7.17	8.04	9.40	16.1	5.94	9.71	7.96	19.7	16.2	8.18

Possible correlations with the electron transitions are suggested and the predominance of nuclear effects are evident from the greater widths of lines involving the elliptical orbit L_I.

The observed widths are compared to the classical and quantum theory widths and the size of the nucleus necessary to explain the discrepancy is given. The possibility of observing the splitting of the energy levels due to nuclear spin as suggested by Breit is rejected. The actual shape of the line U $L\alpha_1$ has been investigated and found to approximate that predicted by the classical theory.

THE natural widths of x-ray lines in the K-series of molybdenum have been measured by Ehrenberg and Mark,[1] Ehrenberg and von Susich,[2] Davis and Purks,[3] Allison and Williams,[4] and Mark and von Susich[5] with the double x-ray spectrometer. Experiments on the relative widths of some x-ray lines in the L-series of lead and thallium have been carried out by Allison.[6] This paper is a report of experiments performed on the natural widths of the x-ray lines in the L-series spectrum of uranium. The accurate measurement of a greater number of lines in the L-series offers an opportunity to study any dependence on the transitions involved.

[1] Ehrenberg and Mark, Zeits. f. Physik **42**, 807 (1927).

[2] Ehrenberg and von Susich, Zeits. f. Physik **42**, 823 (1927).

[3] Davis and Purks, Proc. Nat. Acad. Sci. **13**, 419 (1927); **14**, 172 (1928); Phys. Rev. **34**, 181 (1929).

[4] Allison and Williams, Phys. Rev. **35**, 1476 (1930).

[5] Mark and von Susich, Zeits. f. Physik **65**, 253 (1930).

[6] Allison, Phys. Rev. **34**, 176 (1929).

Apparatus

The double x-ray spectrometer used in these experiments has been previously described.[7] The following changes have been made. The vertical slits, limiting the divergence of the beam in a plane perpendicular to the axes of rotation of crystals A and B, were 2 mm in width. The horizontal slits, limiting the divergence of the beam in a vertical plane including the axes of rotation, were of various widths which will be given later.

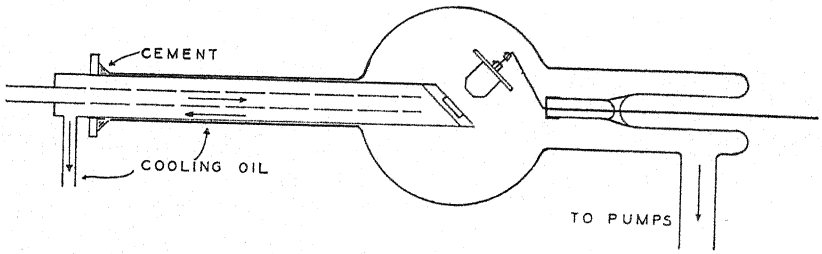

Fig. 1. Diagram of uranium target x-ray tube.

The x-ray tube used in these experiments is illustrated in Fig. 1. The tube was designed to give a large focal spot which would remain fixed on the target. These two properties of the tube are highly essential in the measurement of line widths as will be discussed later. The focal spot was at a distance of 50 cm from crystal A. The filament holder was designed from the type used by Professors Ross and Clark at Stanford University. It enabled the filament to be placed within one cm of the target and allowed the x-rays to be observed at an angle of 135° from the electron beam. The uranium was obtained from the Westinghouse Electric and Manufacturing Company. Many attempts were made to obtain good thermal contact between the uranium or some other metal but without success until finally the method used by S. K. Allison[8] was adopted. A piece of uranium was hydraulically pressed below the surface of a large copper block and the edges of the copper were peaned over while the uranium was under pressure. This served satisfactorily as a target up to a maximum power input of 0.4 kw. The tube was cooled by pumping cold kerosene through the hollow target holder.

The power for operating the tube was developed by a 5 kw. 550 cycle motor generator and the high potential supplied by a transformer was rectified by kenetrons and smoothed by condensers. The calculated voltage fluctuations were 0.6 percent at 48 kv and 6 milliamperes.

The calcite crystals used were those investigated in a previous experiment.[4] These crystals were preserved in a dessicator over dehydrated calcium chloride and sodium hydroxide, and it has been found that they have deteriorated only very slightly in the course of a year.

[7] Williams and Allison, J.O.S.A. and R.S.I. **18**, 473 (1929). For a further description see reference 4.

[8] Allison, Phys. Rev. **32**, 1 (1928).

Operation of the Instrument

The technique of measuring line widths has been previously developed. The degree of accuracy obtained with the double spectrometer can be seen by comparing the values of 0.144 and 0.163 X.U. for the half width at half maximum of Mo$K\alpha_1$ obtained by Mark and von Susich[5] and the value of 0.147 X.U. obtained by Allison and Williams.[4] The method of operation used in these experiments was that previously described.[4] The method of setting the crystal faces vertical was retained. Frequent readings of the temperature were taken while observations were being made and no significant changes were noted.

Reduction of Observed Results

The majority of the results have been obtained in the (1,1) position following a notation given in a previous paper.[9] The dispersion D of the double spectrometer is given by

$$D \equiv \frac{d\theta_B}{d\lambda} = \frac{n_A}{2d\cos\theta_A} + \frac{n_B}{2d\cos\theta_B} \tag{1}$$

n_A and n_B are the orders in which crystals A and B are reflecting respectively and θ_A and θ_B are the corresponding glancing angles. The sign of n_A is always taken positive. n_B is negative when the first incident and last reflected rays are on opposite sides of the first reflected ray,[10] otherwise it is taken positive. The dispersion D is therefore finite in all anti-parallel positions.

The first correction to be applied to the observed widths in anti-parallel positions is the geometric width due to the vertical spread of the beam. Schwarzschild's[10] equation for the "geometric breadth," $\delta\theta_B$, may be written

$$\delta\theta_B = \tfrac{1}{2}D\lambda\phi^2. \tag{2}$$

In this equation, $\delta\theta_B$ is the total angular range through which crystal B may be turned while reflecting the wave-length λ. If the widths of the slits limiting the divergence of the beam in a vertical plane are h_1 and h_2 ($h_2 \geqq h_1$), and the distance between them is L,

$$\phi = \frac{h_1 + h_2}{2L}. \tag{3}$$

The correction to be applied to the observed widths has been previously deduced[4] from Eqs. (2) and (3). Let ξ be the angular deviation of crystal B from the position of reflection for the central ray, (that ray passing through the geometrical centers of the slit apertures). Then the value of ξ at which the geometrical rocking curve drops to half maximum is given by[4]

$$\xi_{1/2} = \tfrac{1}{2}D\lambda\phi^2\left\{\frac{h_2}{h_1 + h_2}\right\}^2. \tag{4}$$

The values of $\xi_{1/2}$, in seconds of arc, calculated from Eq. (4) are arbitrarily subtracted from the observed full widths at half maximum.

[9] Allison and Williams, Phys. Rev. **35**, 149 (1930).
[10] Schwarzschild, Phys. Rev. **32**, 162 (1928).

The second correction to be applied to the resultant widths in anti-parallel positions is that due to the finite resolving power of calcite crystals. If it is assumed that the line has a Gaussian error curve distribution of intensity we have[11]

$$W = (W_A^2 + W_B^2 + D^2 W_\lambda^2)^{1/2} \tag{5}$$

In the above equation, W represents the half width at half maximum in angular measure of the observed rocking curve after the geometric correction has been applied, W_A the half width at half maximum in angular measure of the curve representing the intensity of reflection from crystal A as a function of the deviations from the Bragg angle, W_B is the same quantity for crystal B, D is the dispersion given by Eq. (1), and W_λ is the half width at half maximum in linear measure of the line. The quantities W_A and W_B are observed in positions of zero dispersion (i.e. $n_B = -n_A$) and will be discussed under the next heading. These two corrections are the only ones applied to the observed widths if the deviation of the crystal faces from verticality has been reduced to zero.

Study of Parallel Positions

In the positions of zero dispersion the observed width W is from Eq. (5)

$$W = (W_A^2 + W_B^2)^{1/2}. \tag{6}$$

Assuming the crystals to be the same, $W_A = W_B = W_C$

$$W = 2^{1/2} W_C. \tag{7}$$

The values of W_C have been studied as a function of λ for the first order of reflection from calcite. There is no geometric correction to be applied to the observed widths in parallel positions if the deviation of the crystal faces from verticality is reduced to zero. The method of imposing this condition has been previously described.[4] The crystals were first adjusted as accurately as possible by the cathetometer method and a rocking curve was taken. Crystal B was then rotated through a minute of arc about an axis lying in a horizontal plane and a second rocking curve taken. This procedure was repeated until a position of crystal B was found which gave a rocking curve of minimum width. From this observed value of W the interference pattern width of a single crystal, W_C, was obtained by the use of Eq. (7).

The values of W_C have been obtained with the crystals reflecting the wave-lengths 908, 718, and 613 X.U. in the first order. These are plotted in Fig. 2. W_C is seen to be a linear function of the wave-length.

Darwin[12] and Ewald[13] have considered the problem of reflection of plane monochromatic waves from an ideal crystal. The extent of 100 percent reflection is given by

$$\Delta\theta = 4\delta \operatorname{cosec} 2\theta \tag{8}$$

[11] Schwarzschild, reference 10. Obtained by combining Eqs. (43) and (45) of his paper.
[12] Darwin, Phil. Mag. **27**, 325 and 675 (1914).

where θ is the glancing angle and δ is the deviation of the index of refraction from unity. Since [14]

$$\delta = 1 - \mu = Ne^2\lambda^2/2\pi mc^2 \tag{9}$$

where N is the number of electrons per cm^3, e is the electronic change in e.s.u., m is the mass of the electron, and c is the velocity of light, and from the Bragg law

$$\operatorname{cosec}\theta = 2d/n\lambda$$

we have

$$\operatorname{cosec} 2\theta = d \sec\theta/n\lambda. \tag{10}$$

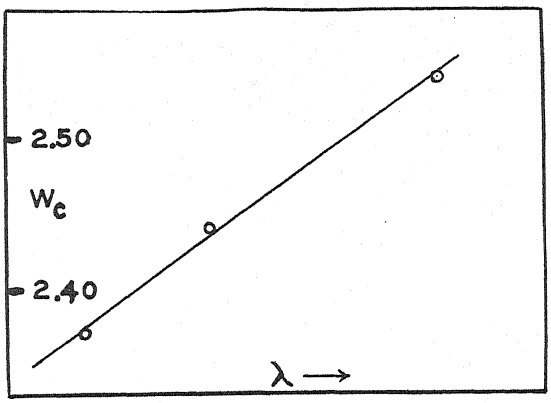

Fig. 2. The interference pattern width of a single crystal, W_C, as a function of the wave-length.

Substituting from Eqs. (9) and (10) in Eq. (8)

$$\Delta\theta = k\lambda \sec\theta \tag{11}$$

where

$$k = 2Ne^2d/\pi mnc^2.$$

Thus $\Delta\theta$ is an approximately linear function of λ as may be shown from the Bragg law and expansion in powers of λ.

$$\Delta\theta = k\lambda[1 + \tfrac{1}{2}(n\lambda/2d)^2 + 3/8(n\lambda/2d)^4 + 5/16(n\lambda/2d)^6 + \cdots]. \tag{12}$$

This series is rapidly convergent for first order reflection from calcite in the region examined.

The experimental value of W_C was found to be 1.6 times as large as that calculated for a perfect calcite crystal by a method given in a previous paper.[15] The value of W_C for the calcite crystals reflecting the wave-length 908 X.U. in the second order was 0.90 seconds of arc. This decrease of W_C for calcite with reflection in the second order is in agreement with the results of Davis and Purks[16] and Allison and Williams.[17]

[13] Ewald, Phys. Zeits. **26,** 29 (1925).
[14] A. H. Compton, X-Rays and Electrons, page 205.
[15] See reference 4. Eqs. (10) and Tables III and IV.
[16] Davis and Purks, Phys. Rev. **34,** 181 (1929).
[17] See reference 4, page 1489.

Study of U $L\alpha_1$ in Different Orders

It has been pointed out that a systematic change in the observed natural widths when measured in positions of different dispersion may be due to the finite size of the focal spot. During the observation of a curve crystal B is rotated through small angles while crystal A is left fixed. Under the previous adjustments when crystal B is reflecting the peak of the line the radiation comes from the most intense part of the focal spot. As crystal B is rotated up to and through this central position, the radiation comes from slightly different parts of the focal spot, and hence will have a different initial intensity. In positions of higher dispersion greater errors would arise from this cause, and the magnitude of the effect can be calculated. In order to overcome this difficulty the broad focus tube was used and the radiation was taken at an angle of 45° from the target. To obtain a measure of the intensity distribution of the focal spot the following experiment was performed. The double spectrometer was adjusted to reflect the peak of a given line and was left fixed in this position. The x-ray tube, which was mounted on a moveable carriage driven by a screw, was advanced by small steps in a horizontal direction perpendicular to the line of the slits. Thus the radiation reflected by the crystals at different steps came from successive parts of the focal spot, and the intensity could be examined directly. It was found that at a distance of 1.5 mm from the center the intensity had fallen to half of the maximum value. It is thus felt that the error arising from this source has been greatly reduced. Any further enlargement of the focal spot would decrease the intensity to a degree causing uncertainty in the observations.

The half widths at half maximum of the line U $L\alpha_1$ were investigated in three different positions of the double spectrometer. The results are given in Table I.

Table I. *Half widths at half maximum for U $L\alpha_1$ at 48 kv.*

Position (n_A,n_B)	D in ″/X.U.	h_1 cm	h_2 cm	$\xi_{\frac{1}{2}}$	W	$(W_A^2+W_B^2)$	W_λ in X.U.	Weighted average of W_λ in X.U.
(1,−2)	36.942	0.3	0.5	1.1″	16.9″	7.3″	0.453	
"	"	"	"	"	16.2	"	0.433	0.442
"	"	"	0.4	0.7	16.6	"	0.445	
(1,1)	68.877	0.3	0.3	0.7	27.6	12.9	0.398	
"	"	"	"	"	30.6	"	0.442	
"	"	"	"	"	30.9	"	0.445	
"	"	"	"	"	30.9	"	0.445	0.439
"	"	"	"	"	30.6	"	0.442	
"	"	0.2	0.2	0.3	29.8	"	0.430	
(1,2)	105.81	0.3	0.8	8.5	45.0	7.3	0.425	
"	"	0.5	0.5	3.1	46.0	"	0.433	
"	"	"	"	"	47.9	"	0.452	0.437
"	"	"	"	"	46.4	"	0.438	

The weighted averages have been secured by a personal estimate of the quality of the data.

For these observations D varies from 36.942 to 105.81 seconds per X.U. and the half width at half maximum, W_λ, varies from 0.442 to 0.437 X.U.

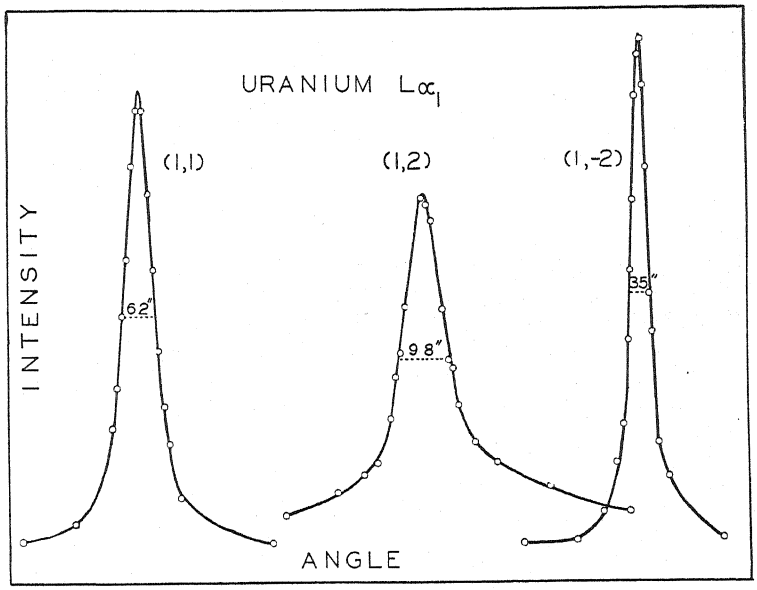

Fig. 3. Observed rocking curves of uranium $L\alpha_1$ at 48 kv. Ordinates are proportional to ionization currents, abscissae to angular settings of crystal B. The vertical scale is different for each curve.

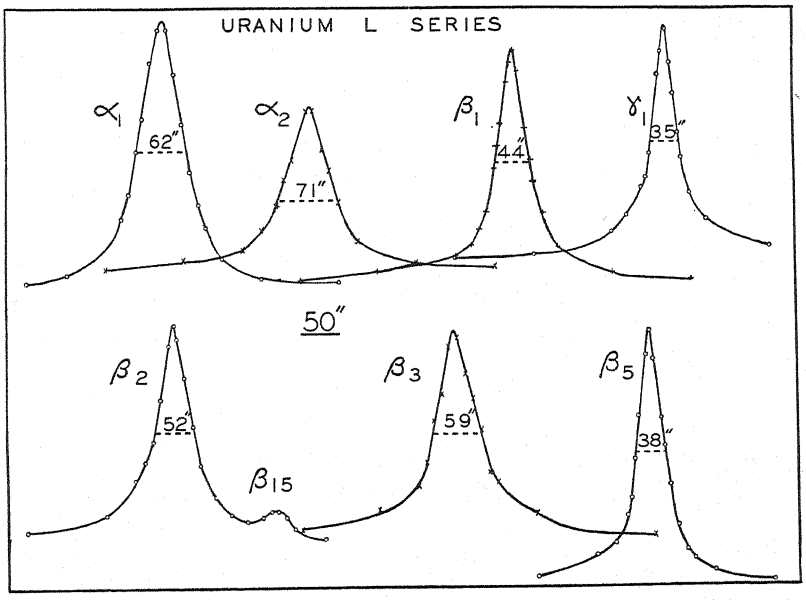

Fig. 4. Observed rocking curves in the (1, 1) position for seven lines in the uranium L spectrum at 48 kv. Ordinates are proportional to ionization currents, abscissae to angular settings of crystal B. The vertical scale is not the same for all the curves.

There is a trend towards narrower widths at positions of higher dispersion but this decrease is well within the experimental error, and the magnitude of this effect is less than formerly noted.[4] Typical curves of the line U $L\alpha_1$ in three different positions of the instrument are shown in Fig. 3.

The Natural Widths of the *L*-Series Lines of Uranium

Twelve lines of the *L*-series spectrum of uranium have been observed in the (1,1) position of the double x-ray spectrometer. Seven of these are shown in Fig. 4.

The half widths at half maximum of these lines have been calculated from the observed rocking curves in the (1,1,) position at 48 kv and are given in Table II. The details given in Table I are partially omitted but all corrections have been applied. The weighted averages of W_λ are obtained from a personal estimate of the quality of the data and the probable errors were calculated from the least squares formula.

The natural widths of U $L\alpha_1$ and U $L\beta_1$ have been examined as a function of voltage. Rocking curves in the (1,1) position were taken at different voltages under identical geometric conditions. The experimental error is greater at lower voltages due to the decrease in intensity as the excitation voltage is approached. The results are given in Table III where again the details of the calculation are omitted though all corrections were applied. An estimate of the experimental error of W_λ is also given.

Table II. *Half widths at half maximum for the L-series lines of uranium at 48 kv.*

Line	D in ″/X.U.	$(W_A^2+W_B^2)$	Number of observations	Weighted average of W_λ in X.U.
U$L\alpha_1$	68.877	12.9″	6	0.439±0.004
α_2	68.895	13.0	5	0.494± .006
β_1	68.580	11.9	8	0.299± .002
β_2	68.628	12.1	8	0.369± .003
β_3	68.568	11.8	5	0.382± .009
β_4	68.618	12.0	5	0.726± .010
β_5	68.590	11.9	6	0.252± .006
β_6	68.680	12.3	4	0.487± .009
γ_1	68.448	11.2	7	0.242± .003
γ_2	68.438	11.2	4	0.57 ± .02
γ_3	68.430	11.1	4	0.47 ± .01
γ_6	68.426	11.1	5	0.233± .005

Table III. *Half widths at half maximum of ULα_1 and ULβ_1 as a function of voltage.*

Voltage in kv.	W_λ of U$L\alpha_1$ in X.U.	W_λ of U$L\beta_1$ in X.U.
48	0.440±.005	0.295±0.005
39	0.445±.005	0.294± .005
30	0.439±.010	0.287± .010
24	0.435±.015	0.30 ± .02

Table III shows that there is no significant change of width with voltage for U $L\alpha_1$ and U $L\beta_1$ in the voltage region studied. Thus the part of the width of these lines due to satellites arising from multiply ionized states of the atom

is negligible. These lines involve the final orbits L_{III} and L_{II} and it is reasonable to assume that their behaviour is representative of lines arising from transitions to these levels. The lines involving the orbit L_I have such a relatively weak intensity that it is not practicable to measure their widths at voltages less than 48 kv.

Discussion of the Natural Widths

In order to facilitate the discussion of the natural widths and to make possible any correlations with the electron transitions involved the results are shown in Table IV.

In the third column the energy breadth ΔV in volts is calculated from

$$\Delta V = 12336\Delta\lambda/\lambda^2 \tag{13}$$

where $\Delta\lambda$ and λ are in Angstroms.

The fourth column of Table IV gives the initial and final quantum states of the atom for the transition involved. The fifth column gives the eccentricity of the initial and final orbits on the classical quantum theory measured by k/n.[18]

The $\Delta\lambda$s of the lines vary from 0.233 to 0.726 X.U. and the range of wave-lengths from 592.6 to 920.14 X.U. The half width at half maximum predicted by the classical theory[19] is 0.059 X.U. and is independent of the wave-length in question.

A study of Table IV has suggested the following possible correlations. U $L\beta_3$, U $L\beta_4$, U $L\gamma_2$, and U $L\gamma_3$ involving the highly elliptical orbit L_I have the greatest energy widths observed. U $L\alpha_2$ and U $L\beta_1$ involve transitions from the same initial orbit and the eccentricities of the orbits involved are the same; the energy widths agree. U $L\beta_2$ and U $L\gamma_1$ involve transitions from similar initial orbits and the eccentricities of the orbits are the same as well as the changes in quantum numbers; the energy widths agree. For the lines U $L\beta_5$ and U $L\gamma_6$ the changes in the quantum numbers and the eccentricities of the orbits involved are the same but the energy widths are very different. There is however an agreement between their $\Delta\lambda$s. U $L\gamma_2$ and U $L\gamma_3$ involve orbits of the same eccentricity and there is a rough agreement between their energy widths; however the changes in quantum numbers are different.

These correlations are by no means complete but the wave-length region involved is so relatively great that the validity of a direct comparison between the energy widths or $\Delta\lambda$s and the transitions involved is doubtful. It is felt that no simple complete empirical correlation can be given. Coster[20] has qualitatively considered the question of the width of x-ray lines on the classical quantum theory. He concludes that the width of lines involving transitions between elliptical orbits is greater than those involving circular orbits. If ΔV is considered to be a measure of the width of the line these predictions are born out in general by the results shown in Table IV. The great

[18] Sommerfeld, Atombau und Spektrallinien, 4th edition, p. 125, Eq. 14.

[19] See reference 4, Eq. (20).

[20] Coster, Zeits. f. Physik **45**, 797 (1927).

TABLE IV. *Collected results on the half widths at half maximum of the observed rocking curves in the* (1,1) *position of the L-spectrum of uranium at 48 kv.*

Line	$\Delta\lambda$ in X.U.	ΔV in volts	Initial / Final	n / n	l / l	j / j	ϵ / ϵ	Δn	Δl	Δj
$UL\alpha_1$	0.439	6.56		3 2	2 1	5/2 3/2	1 1	1	1	1
α_2	0.494	7.20		3 2	2 1	3/2 3/2	1 1	1	1	0
β_1	0.299	7.17		3 2	2 1	3/2 1/2	1 1	1	1	1
β_2	0.369	8.04		4 2	2 1	5/2 3/2	3/4 1	2	1	1
β_3	0.382	9.40		3 2	1 0	3/2 1/2	2/3 1/2	1	1	1
β_4	0.726	16.1		3 2	1 0	1/2 1/2	2/3 1/2	1	1	0
β_5	0.252	5.94		5 2	2 1	5/2 3/2	3/5 1	3	1	1
β_6	0.487	9.71		4 2	0 1	1/2 3/2	1/4 1	2	1	−1
γ_1	0.242	7.96		4 2	2 1	3/2 1/2	3/4 1	2	1	1
γ_2	0.57	19.7		4 2	1 0	1/2 1/2	1/2 1/2	2	1	0
γ_3	0.47	16.2		4 2	1 0	3/2 1/2	1/2 1/2	2	1	1
γ_6	0.233	8.18		5 2	2 1	3/2 1/2	3/5 1	3	1	1

width of U $L\gamma_2$, U $L\gamma_3$, and U $L\beta_4$, the last as previously observed by Allison[6] in lead and thallium, are the best illustrations of the effect of an elliptical final orbit. The lines U $L\alpha_1$, U $L\alpha_2$, U $L\beta_1$ involving both initial and final circular orbits have the smallest ΔVs observed with the exception of U $L\beta_5$.

Professor J. R. Oppenheimer[21] has calculated the width of U $L\alpha_1$ to be expected on the quantum mechanics from the Einstein probability coefficients of the states involved. He gives

$$\frac{\Delta\nu}{\nu} = \frac{\sum A_n}{\nu} \sim 3^3 2^{14}\alpha^3 Z^2/5^{12} \sim 6\times 10^{-6} \tag{14}$$

where ν is the frequency of the line considered. A_n is the Einstein probability coefficients of spontaneous emission from the levels n to the L level in ques-

[21] From private conversation with Professor Oppenheimer. I am greatly indebted to him for his interest in these results.

tion, and the summation if taken over all filled levels of the atom lying higher than the L levels, and α is the fine structure constant. On the basis of this reasoning $\Delta\nu/\nu < 10^{-5}$ whereas exprimentally $\Delta\nu/\nu \sim 5 \times 10^{-4}$.

Thus the observed width must be due to other phenomena decreasing the life time of the excited state and consequently increasing the line breadth. Some possible causes may be the changes of the energy levels due to Hund coupling with the valence electrons in the atom; interactions with the neighboring atoms in the metal; or the effects of nuclear spin suggested by Breit.[22] Since the L levels of uranium are so deeply buried in the atom it seems that the nuclear effects must predominate in broadening the line. Professor Oppenheimer has suggested the following possibilities due to coupling with the nucleus.

$$\begin{aligned} &(1) \quad \text{Electron interchange} \quad \Delta\nu/\nu \sim \left(\frac{a_n}{a_0}\right)^2 \frac{1}{Z} \\ &(2) \quad \text{Induced dipole} \quad \Delta\nu/\nu \sim \left(\frac{a_n}{a_0}\right)^3 \\ &(3) \quad \text{Quadrapole moment} \quad \Delta\nu/\nu \sim \left(\frac{a_n}{a_0}\right)^2 \frac{1}{Z}. \end{aligned} \tag{15}$$

In these equations a_n is the effective radius of the nucleus, a_0 is the mean radius of the orbit, and Z is the atomic number. The first of these arises from energy considerations of electron interchange between the orbital and nuclear electrons.

If a_0 is calculated from the Bohr formula

$$a_0 = \tau^2 h^2 / 4\pi^2 m e^2 Z \tag{16}$$

where τ is the total quantum number and the experimental value of $\Delta\nu/\nu$ is assumed then the following values are obtained for the radius of the nucleus.

$$\begin{aligned} &(1) \quad a_n \sim 4.5 \times 10^{-11} \text{ cm} \\ &(2) \quad a_n \sim 1.8 \times 10^{-11} \text{ cm} \\ &(3) \quad a_n \sim 4.5 \times 10^{-11} \text{ cm} \end{aligned}$$

From this reasoning alone the probability of finding a nuclear electron at these distances from the center of the nucleus is large whereas from the Rutherford scattering experiments the Coulomb law of force holds down to 10^{-13} cm. The possibility of an unexpected penetration of the orbits is thus suggested.

In Fig. 4 the line U $L\beta_{15}$, first resolved by Allison,[6] is almost completely resolved but no reliable estimate of its width could be given. It is of the order of magnitude of 0.3 X.U. Its separation from U $L\beta_2$ was found to be 1.89 X.U. as the average of three measurements.

The line $L\beta_5$ on the energy level diagram is a doublet O_V, O_{IV} to L_{III} with a relative intensity of 9 to 1 on the Burger-Dorgelo rules. Although the line is relatively narrow no evidence of the weaker component could be found.

[22] Breit, Phys. Rev. **35**, 1447 (1930).

U $L\beta_3$ and Mo $K\alpha_1$ have nearly identical wave-lengths, 708.4 and 707.768 X.U., but their widths are greatly different, 0.382 and 0.147 X.U. respectively. The width of an x-ray line is therefore not a function of wave-length alone, but depends on the atom and transition involved. The half widths at half maximum of the L-series lines of uranium are from 1.6 to 5 times as great as that of Mo $K\alpha_1$. This is in agreement with the work of Allison[6] on thallium and lead but in his work the crystals used were relatively poor and the adjustments of the instrument imperfect thus causing higher values of the widths.

The actual shape of the line U $L\alpha_1$ was investigated by taking many points on a rocking curve when the value of $\xi_{1/2}$ was reduced to negligible proportions. The classical theory gives for the shape of a line[23]

$$I_\nu = I_0/\{k^2 + [(2\pi\nu)^2 - (2\pi\nu_0)^2]\}. \tag{17}$$

In the derivation of Eq. (5) Schwarzschild[10] has assumed a Gaussian error curve distribution of intensity,

$$I'_\nu = I_0 e^{-k^2(\nu-\nu_0)^2} \tag{18}$$

The values of k and I_0 were selected so as to make the theoretical curves fit the actual curve at the maximum and half maximum ordinates. It was found that Eq. (17) gave a much better fit than Eq. (18). However the tails of the observed curve and the classical curve did not agree, the observed curve falling off more steeply than that given by Eq. (17).

Breit[22] has considered the effects of nuclear spin on x-ray terms and has predicted the splitting of the L_{II} level of uranium to be of the order of magnitude of 4.0 volts. This prediction is based upon the assumptions that the uranium nucleus has a spin 9/2 and a magnetic moment 9/2 proton units and that screening effects are neglected. If one attempts to apply this prediction to the line U $L\beta_1$ for example, it is found that the natural breadth of the line is so great that no appreciable evidence of splitting would be expected.

In conclusion, I should like to express my thanks to Professor S. K. Allison for the suggestion of this problem and his helpful correspondence during the course of the investigation. My thanks are also due Professor R.B. Brode for his kindly criticism and interest in this research.

[23] W. C. Mandersloot, Jahrbuch der Rad. und Elek. **13**, 1 (1916).

BREADTH OF THE COMPTON MODIFIED LINE WITH THE DOUBLE CRYSTAL SPECTROMETER

By Archer Hoyt and Jesse DuMond
California Institute of Technology, Pasadena

(Received April 20, 1931)

Abstract

Three experimenters using the double crystal spectrometer have recently reported very much narrower structure for the Compton modified line than the structure observed photographically by DuMond and Kirkpatrick with the multicrystal spectrograph whose resolution was entirely adequate to reveal such a narrow structure. We have repeated the experiment using a double crystal spectrometer similar to theirs. The results obtained are in satisfactory agreement with the previous observations of Compton line breadth by DuMond and Kirkpatrick with the multicrystal spectrograph and in disagreement with the experimenters who used double crystal spectrometers. The conclusions drawn are: (1) The Compton modified line due to Mo $K\alpha$ radiation scattered by graphite at angles of $165° \pm 10°$ and examined with the double crystal spectrometer has a breadth of from 21 to 22 XU at half-maximum height; (2) Under the above conditions there is no appreciable separation of the $K\alpha$ doublet in the shifted position; (3) No fine structure exists in the scattered spectrum of intensity greater than one-fifth the modified line intensity; (4) The ratio of modified to unmodified line intensity is estimated at (7.3:1); (5) There appears to be no essential difference between the results obtained with the single crystal, multicrystal and double crystal spectrometers in the study of this problem.

Purpose of Investigation

VERY early in the study of the Compton effect it was suspected that the modified line might be broader than either the primary line or the unmodified line. Ross[1] was apparently the first to attribute this breadth to the momenta of the scattering electrons. An experiment by Sharp[2] using a single crystal photographic spectrometer at large scattering angle established the fact that the modified line has greater breadth than the primary line or than the unmodified lines.

In the early experiments resolution and homogeneity of scattering angle were sacrificed more or less in order to obtain sufficient intensity for ionization spectrometers or to give photographic spectra in reasonable times. It was therefore difficult to arrive at more than qualitative conclusions as to the breadth and structure of the Compton line. One such qualitative test is to observe whether the $K\alpha$ doublet present in the primary radiation can or cannot be resolved in the modified radiation. In one of the early photographic spectra published by Ross the modified line did appear to be faintly resolved. The resolution of the spectrograph was however barely sufficient to separate the unmodified scattered doublet and the conclusion to be drawn from this

[1] Ross, Proc. Natl. Acad. 9, 246 (1923).
[2] Sharp, Phys. Rev. 26, 691 (1925).

photograph as to the breadth of the modified line remains consequently quite uncertain. Indeed the apparent resolution of the modified doublet might even be attributed to an accident of the photographic emulsion as Compton suggests in "X-Rays and Electrons," page 293.

More recently one of us in collaboration with H. A. Kirkpatrick has shown[3] by means of the multicrystal spectrograph that the breadth of the Compton modified line obeys, as a function of the scattering angle, the law to be expected on the hypothesis that the broadening is a Doppler effect of the moving electrons that scatter the radiation. This law is given roughly by the approximate equation for the breadth

$$\Delta\lambda = \beta\lambda \sin \tfrac{1}{2}\theta.$$

Thus for small scattering angles and hard primary radiation the modified line should be narrower than for larger scattering angles and soft primary radiation. Less marked differences in the breadths of the modified lines for different scattering materials might also be expected. *In comparing experimental results on the breadth of the modified line it is therefore essential to be sure that the conditions of the experiment are essentially the same.*

In a previous article one of us[4] has shown that the breadth and structure of the modified line for scattering of Mo$K\alpha$ radiation at large angles by beryllium was consistent with the assumption of two electrons per atom of beryllium dissociated to form a free electron gas of the type postulated by Fermi and Sommerfeld. The observed shape of the modified line from beryllium could be quite consistently accounted for as a Doppler broadening caused by electrons having the statistical velocity distribution quantitatively predicted by Sommerfeld's theory. (The correctness of the assumption of two free electrons per atom in beryllium has recently received support in the study of BeK lines from the work of Martin Söderman.)[5] The modified Compton line from beryllium for Mo$K\alpha$ primary radiation scattered at large angles was observed to be about 22 XU broad at half-maximum, a value much too great to permit resolution of the α doublet which has a separation of only 4 XU.

Measurements of the breadth of the modified Mo$K\alpha$ line scattered at large angles by graphite made with the multicrystal spectrograph show also breadths of the same order of magnitude at half-maximum, again about 22 XU. The resolution was entirely adequate to separate the unmodified $K\alpha$ doublet and the inhomogeneity of scattering angle less than one degree. This breadth is in agreement with the electron velocities to be expected in graphite.

In view of the foregoing the authors of this paper were much astonished to read reports of three other investigators[6] each using a double crystal spectrometer who found much narrower Compton modified lines in quite violent

[3] DuMond and Kirkpatrick, Phys. Rev. **37,** 136 (1931).
[4] J. W. DuMond, Phys. Rev. **33,** 643 (1929).
[5] Martin Söderman, Zeits. f. Physik **65B,** 656 (1930).
[6] Davis and Mitchell, Phys. Rev. **32,** 331 (1928); J. A. Bearden, Phys. Rev. **36,** 791 (1930); M. A. Gingrich, Phys. Rev. **36,** 1050 (1930).

disagreement with the above results. In one case the $K\alpha$ doublet of molybdenum scattered at large angles by graphite appeared as two extremely sharp peaksin the modified position almost completely resolved.

Some essential and hitherto unsuspected difference might exist between the methods of studying the Compton line with the double spectrometer and with the single spectrometer. The purpose of the present research was therefore to reveal any such effect as well as to check the work of the above mentioned investigators.

METHOD

Spectrometer. The double crystal calcite spectrometer with internal grid ion chamber and Hoffman type electrometer have been extensively described in another article[7] and need therefore no further space.

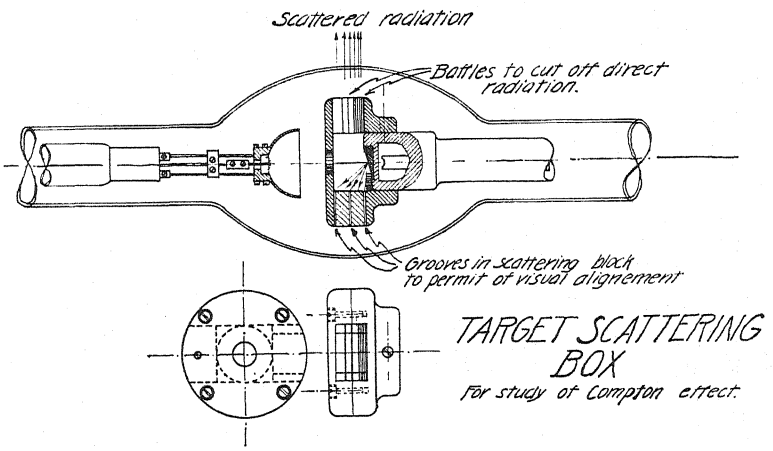

Fig. 1. Special x-ray tube for the study of x-rays scattered at large angles provided with scatterer in vacuum in close proximity to target.

Special x-ray tubes. Two types of tube were tried. These are shown in Figs. 1 and 2. The tube shown in Fig. 1 is provided with a cylindrical copper housing carried on the front end of the target. This housing contains on one side the scatterer and on the opposite side an opening filled with thin steel sheets whose planes are parallel to the face of the target.

These sheets are so spaced that the direct radiation from the focal spot cannot issue between them due to its obliquity. They however permit the scattered radiation from the scatterer to issue freely. The scatterer is traversed by three fine slits parallel to the face of the target, one at the center, one at the side nearest the target and one at the side nearest the cathode. The tube was aligned with the spectrometer by sighting at the crystals through these slits and between the steel sheets. Without this precaution the tube might have been so positioned that the parallel rays demanded by the bicrystalline reflection would be oblique to the steel sheets and considerable loss of scattered intensity would have resulted.

[7] DuMond and Hoyt, Phys. Rev. **36**, 1702 (1930).

The scatterer was wide enough so that the selective reflection could take place over nearly the entire area of the two calcite crystals.

Considerable difficulty was encountered from gas given off by the graphite scatterer during the operation of the tube. After a gas discharge occurred in the tube it became difficult to reproduce conditions of voltage, current and x-ray intensity accurately. A large number of observations must be made in order to distinguish between accidental fluctuations in the readings and real characteristics of the spectrum and the chance that a gas discharge might occur before a sufficient number of readings could be made was deplorably high. The best of a number of curves taken with this tube is shown in Fig. 3. In the others the accidental fluctuations were even more pronounced. That such fluctuations are accidental is evident from the fact that they are not in the least reproducible.

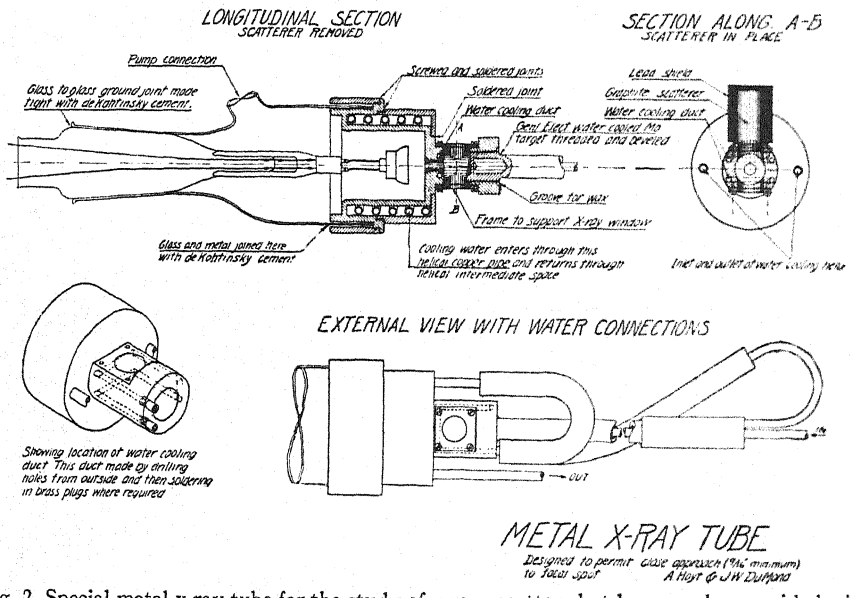

Fig. 2. Special metal x-ray tube for the study of x-rays scattered at large angles provided with windows in close proximity to target to permit placing the scatterer outside vacuum.

On account of these difficulties the tube illustrated in Fig. 2 was constructed to permit a close approach of the scatterer to the focal spot while having the scatterer outside the tube. The windows in this tube are ½ inch inch away from the center of the target. At first mica windows were used on this tube but these were several times destroyed by puncture, probably by fast electrons rediffusing from the focal spot. A thin mirror surface of beryllium deposited on the mica window by evaporation and placed on the inward side to conduct away such fast electrons did not suffice to prevent puncture. Finally aluminum windows 0.003 in. thick were resorted to. The direct radiation has to pass once through the window nearest the scatterer and the scattered radiation passed through both windows. These three passages had the effect of reducing the intensity by about 30 percent.

The graphite scatterer is cylindrical in form, 25 mm in diameter and 48 mm in length. It is completely enclosed in a lead housing 3 mm thick fitting closely about it. The front end of the graphite cylinder is turned down to such a diameter (18 mm) as to fit in direct contact with the entire x-ray window. The effect of the graphite alone could be ascertained by taking control readings with the graphite block removed.

The face of the molybdenum target was bevelled at an angle of 13° with the axis of the tube to reduce the absorption of the characteristic radiation excited in the deeper parts of the target and also to prevent the direct radiation from falling on the spectrometer.

The glass parts of the tube were jointed to each other and to the metal parts with de Khotinsky cement. The target was screwed into place and made tight with the same cement as were also the windows. For this reason the rather elaborate system of water cooling ducts shown in the drawing was provided. It was found entirely adequate to maintain all the joints cold enough to operate very satisfactorily.

Vacuum was maintained in this tube by a two stage mercury diffusion pump hanging under the spectrometer table. This pump was supported from the same rotating false table top[7] to which the x-ray tube was attached so that the pump and x-ray tube moved together as the spectrum was explored, and no flexible vacuum joints were necessary. An internal liquid air trap in a right angle bend in the vacuum line between the pumps and the tube was used instead of the more common type so as to minimize the obstruction offered to the issuance of gas from the tube.

The two curves obtained with this tube are shown in Figs. 4 and 5. It should be noted that much less power was used in this work than was used by two of the above mentioned experimenters. The x-ray tube ran at about 60 K.V. c.p.d.c. and 10.6 and 14.6 ma. in the two cases.

Results

All three curves shown here exhibit deplorably large accidental fluctuations in the readings relative to the faint effects studied. For this reason as large a number of readings as possible were taken. *In every case we have indicated the actual value of every single reading taken by plotting it as one point. No readings taken have been omitted.* In work of this kind there is grave danger of arriving at wrong conclusions by unintentional biased weighting of the observations due to omissions. It was felt to be too misleading to publish only the averages of several readings as this gives no idea of the order of accuracy or reproducibility involved.

Taken alone we do not feel that the curve in Fig. 3 made with the scatterer in the vacuum has enough points to be conclusive.

The other two curves seem to us to definitely indicate a broad diffuse structure for the Compton modified line from Mo$K\alpha$ scattered at large angles by graphite in very satisfactory agreement with the curves obtained at large angles with the multicrystal spectrograph. The smooth curve which we have drawn is intended to guide the eye over the observed points on the steep

sides of the intense unmodified lines. We hope the reader will pardon our continuation of these smooth curves through the modified region where they can only be taken as suggesting the general trend of the observations.

A few points were taken with the graphite scatterer removed, the tube running at the same voltage and current as before removal. The modified scattering disappears as would be expected but the unmodified lines are only partly diminished. The amount of this diminution indicated in Figs. 4 and 5 is to be taken as a measure of the unmodified scattering of the graphite. The line intensity remaining in the unmodified position after removal of the graphite is due principally to (1) unmodified scattering of primary radiation at small angles (where it is strong) at the window nearest the spectrometer and

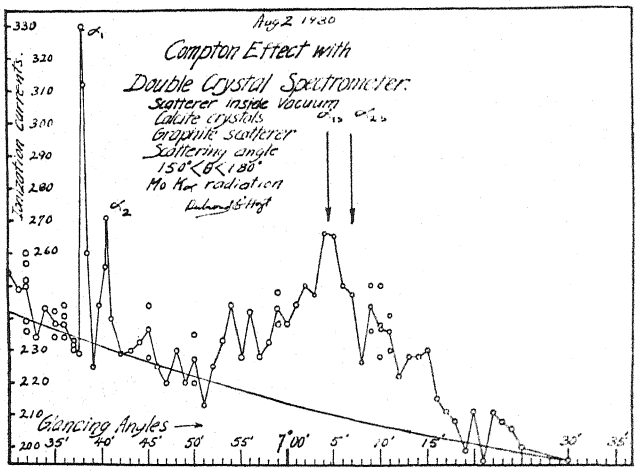

Fig. 3. Spectrum of x-radiation (Mo $K\alpha$) scattered at large angles by graphite with scatterer inside vacuum. The tube shown in Fig. 1 was used.

(2) fluorescence of the molybdenum films unavoidably deposited on both windows by vaporization from the target.

The unmodified lines have been plotted in Fig. 6 to a scale one fifth as high and five times as broad as in Fig. 4 to facilitate measuring their areas for the purpose of estimating the ratio of modified to unmodified intensity. The area thus obtained was multiplied by the ratio of the diminution in peak value of α_1 on removal of the graphite to the peak value with graphite in place in order to obtain the contribution of the graphite scattering alone. These curves in Fig. 6 give a clearer idea of the shape of the unmodified lines given by the double spectrometer here used and its resolving power. The vertical divergence or maximum obliquity of the rays with a plane normal to the dihedral angle formed by the two crystal faces did not exceed two degrees.

The maximum false broadening of the shifted radiation due to the inhomogeneity of scattering angle in these experiments is only 2 X.U.

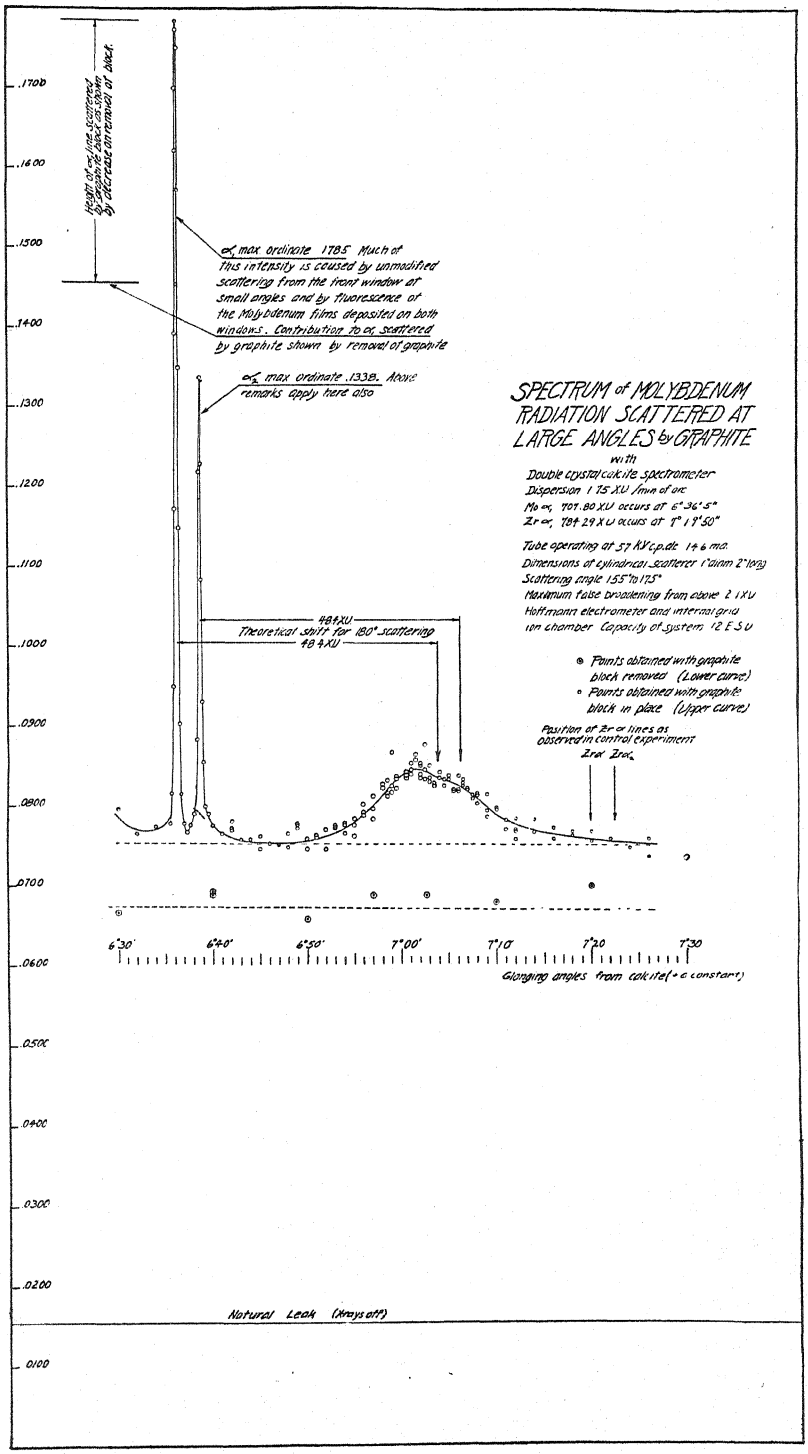

Fig. 4. Spectrum of x-radiation (Mo$K\alpha$) scattered at large angles by graphite with scatterer outside vacuum. The tube shown in Fig. 2 was used.

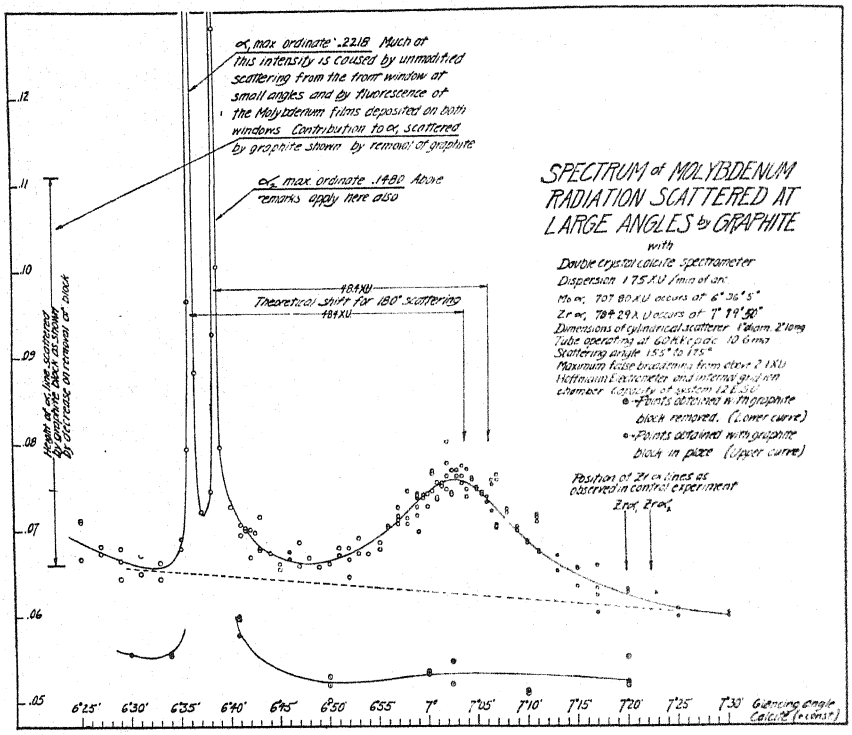

Fig. 5. Spectrum of x-radiation (Mo$K\alpha$) scattered at large angles by graphite with scatterer outside vacuum. The tube shown in Fig. 2 was used.

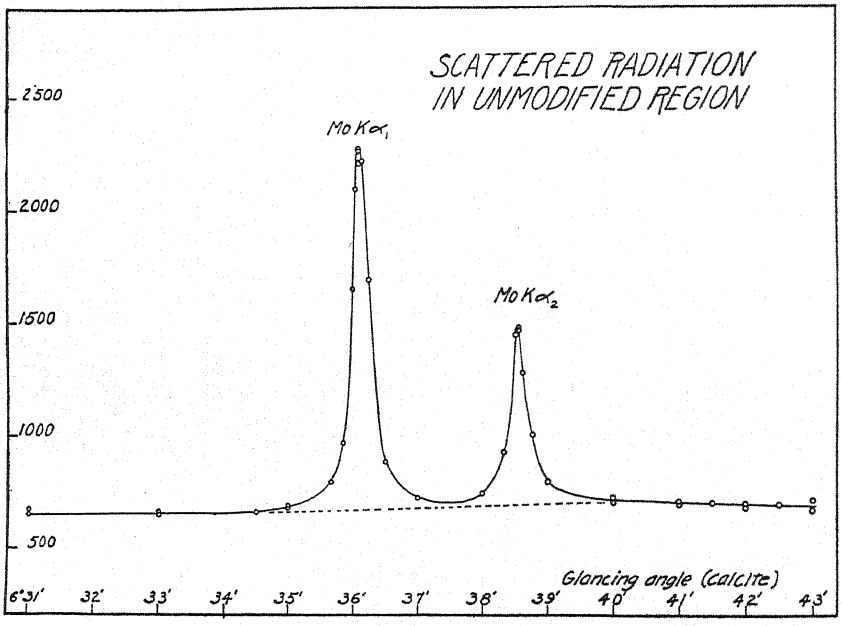

Fig. 6. Unmodified lines of Fig. 4 replotted to one-fifth the scale of ordinates and five times the scale of abscissae.

Conclusions

1. The Compton modified line due to Mo$K\alpha$ radiation scattered by graphite at angles of $165° \pm 10°$ and examined with the double crystal spectrometer has a breadth of from 21 to 22 XU at half-maximum height.

2. Under the above conditions there is no appreciable separation of the $K\alpha$ doublet in the shifted position.

3. No fine structure exists in the scattered spectrum of intensity greater than one fifth the modified line intensity.

4. The ratio of modified to unmodified intensity is estimated at 7.3:1.

5. There appears to be no essential difference between the results obtained with the single crystal, multicrystal and double crystal spectrometers in the study of this problem.

No explanation has been found for the discrepancy between the results of the three observers above referred to and the results here reported. Of the three the one who obtained the sharpest lines used far greater absolute x-ray intensities incident on his scatterer than were used in the present work. It seems quite out of the question however to suppose that his incident energy was sufficient so profoundly to modify the statistics of electron motion in the scatterer as to give a modified line so much sharper than those reported here.

THE OSCILLATING ARC: ELEMENTS OF GROUP VI

By E. Z. Stowell
University of Michigan, Ann Arbor

(Received April 21, 1931)

Abstract

A study of the behavior of sulphur, selenium, tellurium, chromium, molybdenum, tungsten and uranium as cathodes in an arc in hydrogen reveals that all of them permit radio-frequency oscillations to occur in a tuned circuit across the arc. No magnetic field is required for these oscillations. The elements of the sulphur group give unsteady oscillations, disintegrate rapidly and form hydrides with the arc atmosphere. The other elements yield steadier oscillations with no chemical action, and allow the arc to operate at a high temperature. The character of the spectra of these arcs in both the oscillating and the non-oscillating states is described and comparisons made. A mechanism is suggested whereby some elements will permit oscillations to occur and some will not.

I. Introduction

THE mechanism of the oscillating arc in hydrogen is sufficiently obscure so that much more data are necessary before possible explanations may be intelligently discussed. For this reason, a detailed study of the individual groups of the periodic table seems of value, not only to verify previous work with different equipment and different samples, but to obtain additional information regarding the character of the excitation when oscillating. In order to avoid duplication of work in progress in other laboratories, a study has been made of the behavior of the elements in the sixth group of the periodic table as cathodes in the arc in hydrogen. Group six was chosen because (1) no spectrograms have ever been taken of the elements of the sulphur group in such an arc, and (2) to check former results on the elements Mo, W, and U, which are of exceptional interest.

II. Apparatus

The arc was that used in previous experiments[1] and consists of a vertical lower electrode, used as the cathode, surrounded at its base by a coil to furnish a steady magnetic field when necessary; a detachable vertical upper electrode, used as anode; both being enclosed in a removable glass cylinder which permits the maintenance of an atmosphere of hydrogen around the arc flame. The upper electrode, or anode, is usually of copper; its composition has little or no effect upon the behavior of the arc. The lower electrode or cathode, is of copper, and cup-shaped, in order to hold various specimens of other elements under investigation. It should be stated that an arc cannot be struck between the anode and the unfilled cathode, in a hydrogen atmosphere. Both electrodes may be water-cooled if desired. Hydrogen is fed in from a standby

[1] Stowell and Huxford, Phys. Rev. **36**, 1348 (1930).

tank, and the exhaust disposed of either by combustion or escape to the outer air. The supply voltage is 220 d.c. A 20 ohm resistance and a large choke coil are in series with the arc; a radio-frequency circuit adjusted to about 300 k.c. is connected across the arc, with a current indicator in series. Striking is effected by a thumb screw which raises and lowers the anode.

The spectral region from 5500–3700A was covered with a double-prism glass spectrograph. This spectrum is about 3.5 inches long, and since usually but one element is worked with at a time, there is little ambiguity in line identification. Exposures intended to be comparable with one another were taken on the same plate with identical exposure times, and as nearly the same arc currents as it was possible to obtain.

III. Behavior of the Elements of the Sulphur Group

In accordance with results expressed in former papers[1,2] which indicated that elements of even atomic number when used as cathodes permitted the generation of radio-frequency oscillations, sulphur, selenium and tellurium all allow these oscillations to occur. These arcs are characterized by extensive formation of hydrogen sulphide, hydrogen selenide and hydrogen telluride, as the case may be; and also by rapid disintegration of the cathodes. The latter phenomenon doubtless arises from the porous nature of the solid element, and the fact that some of it is continually being removed through the exhaust in the form of hydride. None of these arcs require a magnetic field for the production of oscillations.

From the spectral standpoint this group is interesting because the degree of excitation of the cathode vapor seems to increase with atomic number. This will appear in the discussion of the individual elements.

(1) Sulphur. Sulphur is decidedly the worst of the arcs from the standpoint of electrode disintegration; it is difficult to obtain a long enough exposure for spectrographic purposes. An additional difficulty is the settling of the sulphur on the walls of the glass cylinder, thus greatly reducing the light intensity and lengthening the exposure time. It was found necessary to fill the cathode cup with fresh material and to clean the glass in the optical path several times in order to get a single satisfactory exposure.

In the non-oscillating condition (obtained by opening the tuned circuit across the arc) no trace of sulphur was observed in the spectral region covered. Copper lines only were obtained, and the arc was to all intents and purposes a copper arc. Upon closing the oscillating circuit and allowing current to flow therein, the copper spectrum remained, with the addition of one Balmer line, H_β, and one band of sulphur with head at λ4285, degraded to the red. No sulphur lines appeared. A trace of Al in the original copper electrodes indicated by the pair at λ3944–3961, was greatly intensified in this oscillating arc.

(2) Selenium. Selenium does not disintegrate as rapidly as sulphur, and one filling of the hollow cathode is generally sufficient for an exposure. The settling of selenium upon the glass walls is not objectionable. The radio-fre-

[2] Stowell and Redeker, Phys. Rev. **34**, 978 (1929).

quency current is maintained at a somewhat steadier value than in the case of sulphur.

The spectral differences between the oscillating and the non-oscillating conditions are not great. Both spectra show copper, H_β and H_γ, and most of the Exner and Haschek lines of Se. Using the identification given by the Blochs,[3] these lines belong to Se I. In addition, two bands of Se were obtained, with heads at λ4285 and λ4006, both degraded to the red. The Al impurity previously referred to as existing in the copper was again intensified in the spectrum of the oscillating arc. An interesting feature is that the Ca II doublet at nearly the same wave-lengths, λ3933–3968, was *not* intensified.

(3) Tellurium. Tellurium behaves electrically in a similar manner to selenium. The spectrum however shows a higher order of excitation than selenium, just as the latter is excited more strongly than sulphur. In both the oscillating and non-oscillating condition the copper background, with H_β and H_γ are obtained, together with a multitude of lines due to Te I[3] and the following lines due to Te II: λλ4725, 4352 and 4120. These last three are the most intense lines in the spectrum, and are more intense when the arc is permitted to oscillate. No Te bands are found. The same phenomena concerning the doublets of Al I and Ca II that were mentioned in the case of Se are reproduced here.

IV. Behavior of Cr, Mo, W and U

(1) Chromium. Metallic chromium, inserted into the cup-shaped cathode, will not permit an arc to be drawn out in an atmosphere of hydrogen. There are however transients in the radio-frequency circuit at the moment the direct current circuit breaks. Evidently if an arc could be drawn, there would also be oscillations.

(2) Molybdenum. Molybdenum, in the form of a spiral of the wire inserted into the cup and projecting a trifle beyond, gives an unsteady arc, intensely white. No magnetic field is necessary for current to flow in the tuned circuit. Electrode disintegration is slow.

A continuous spectrum is obtained with both the oscillating and non-oscillating arcs, with lines of copper, Mo I, Mo II,[4] H_β and H_γ, as well as lines of Cr and Fe, superimposed. The latter are present as impurities in the Mo. Certain of the Cr lines appear to be reduced in intensity in the oscillating arc. They are:

4698.49
4652.16 (Cr I)
4530.74
4289.72 (sensitive line of Cr I)
4274.81 (sensitive line of Cr I)
4254.34 (sensitive line of Cr I).

The iron lines are about the same intensity in both spectra. Both the Ca II and Al I doublets previously mentioned are intensified in the oscillating state.

[3] L. and E. Bloch, Ann. de Physique **13**, 233 (1930).
[4] Meggers and Kiess, Jour. Opt. Soc. **12**, 417 (1926).

(3) Tungsten. Tungsten furnishes probably the most interesting arc in the sixth group. A spiral of wire (10 mil) placed inside the cup and projecting beyond, gives oscillations of extreme steadiness and reproducibility. No magnetic field or cooling are necessary. The arc is an intense white; since it runs at a high temperature, the electron emission from the cathode is high, the arc length and current are quite constant, and there is little to cause frequency fluctuations. With the arc running properly, its heterodyned note cannot be distinguished from that given by an electron tube oscillator. Electrode disintegration is extremely slow. The arc has the peculiarity that the radio-frequency output is increased, if, after the oscillations have started, the electrodes are made to approach one another slightly.

The non-oscillating arc shows a very simple spectrum: a heavy continuous background, with H_β, the Ca II pair λ3933–3968, and λ5006.17 of tungsten superimposed. No copper appears.

The oscillating arc likewise produces a heavy continuous background with H_β superimposed; but the Ca II pair is lacking, and instead there appear the following lines of tungsten: λλ4294.62, 4074.37, 4008.76, and 5006.17. The last two, at least, are known to arise from W I.

(4) Uranium. The uranium arc in hydrogen resembles the tungsten arc, but is not as steady, since the electrode is no longer a homogeneous piece of wire, but crushed metal placed in the copper cup. The arc is much brighter in the oscillating state, and is intensely white.

The spectra obtained are exceedingly rich in lines. The majority of the uranium lines in Vol. 6 of Kayser's Handbuch are found, together with many lines due to the iron impurity. Continuous spectra are obtained with the arc in both the oscillating and the non-oscillating condition; this continuous spectrum is more intense in the former case. There are other marked differences between the two conditions, namely:

(a) the uranium lines in general are intensified in the "oscillating" spectrum.

(b) a small amount of potassium impurity, indicated by the doublet at λ4044–47, is slightly intensified in the "oscillating" spectrum.

(c) iron impurity, especially those lines due to Fe I, is much reduced in the "oscillating" spectrum.

(d) Ca impurity, as indicated by lines of Ca I and Ca II, is reduced in intensity by the oscillations.

(e) the trace of Al I impurity in the original copper is reduced in intensity by the oscillations.

Suppression of the iron impurity as in (c) is characteristic of these arcs, and may possibly be of service to spectroscopists, when chemical removal of such impurity in samples to be investigated would be unduly difficult or expensive.

V. Discussion

All of the elements in Group VI. thus permit the generation of radio-frequency oscillations. The elements in the sulphur group have been seen to be-

have somewhat differently from the other elements studied. They are characterized by comparatively rapid electrode disintegration with compound formation, and low excitation. The remaining elements of Group VI. when used as cathodes disintegrate much more slowly, do not form hydrides, and operate the arc at a high temperature, resulting in the emission of a continuous spectrum.

A mechanism whereby some elements will allow current to flow in a tuned circuit across the arc, and others will not, is suggested from fundamental considerations of such arcs. Provided certain secondary conditions as to circuit constants are satisfied, those arcs will permit oscillation which have a negative slope to their dynamic characteristic. For those arcs with no accompanying oscillations, as with the alkali metals when used as cathodes, one may assume that the dynamic characteristic has become excessively flattened, to the extent of losing its negative curvature.

Steinmetz[5] has shown how this may come about if there is a time lag in the reaction of the arc stream to the amount of current passing through it. Consider the static characteristic of an arc, for direct current, to be represented by

$$e = a + \frac{b}{i^{1/2}},$$

where a is the potential drop at the electrodes, and the second term gives the potential drop across the arc stream. The slope of this characteristic, at any current i_1, is

$$\left(\frac{de}{di}\right)_{i=i_1} = -\frac{b}{2i_1^{3/2}}.$$

The fluctuation in potential, made available for the tuned circuit, by a small flutuation in current, Δi_1, about the mean current i_1, is

$$\Delta e_1 = -\frac{b}{2i_1^{3/2}}\Delta i_1.$$

If now Δi_1 were periodic and equal to $\Delta I\epsilon^{j\omega t}$, Δe_1 would likewise be periodic, and current would flow in the attached circuit.

Suppose however that the volume, and therefore the resistance $(e-a)/i$ of the arc stream, cannot adjust itself immediately to new values of current. Such might occur, for example, if the atoms of the cathode vapor remained in their excited or ionized states for a length of time comparable with the period of the attached tuned circuit. In this case let the potential fluctuation Δe_1 lag behind the current fluctuation by an angle α; that is,

$$\Delta e_1 = -\frac{b}{2i_1^{3/2}}\Delta I\epsilon^{j(\omega t+\alpha)}.$$

[5] Steinmetz, "Theory and Calculation of Electric Circuits," p. 194.

Elimination of the time gives the shape of the new characteristic; its equation is evidently

$$\Delta e_1 = -\frac{b}{2i_1^{3/2}}\Delta i_1 \cdot \cos \alpha.$$

The potential fluctuation is thus reduced due to the time lag, and less current will flow in the tuned circuit. With α equal to $\pi/2$, the potential fluctuation will be 90° out of phase with the current fluctuation, and no power will be available for oscillations. For large angles of lag, the potential fluctuation, in this picture, would vanish, and no oscillations would appear.

This hypothesis is defective in that it does not introduce the all-important hydrogen atmosphere. The latter may enter the discussion either by determining the excitation and ionization times, or, as arc engineers have supposed, by furnishing a much steeper dynamic characteristic than other gases.

THE HIGH FREQUENCY BEHAVIOR OF A PLASMA

By Lewi Tonks
Research Laboratory, General Electric Company

(Received April 20, 1931)

Abstract

An analogue for a uniformly ionized gas on the basis of the known formula $K_p=1-\omega_0^2/\omega^2$ for its specific inductive capacity is found in a shunt-tuned circuit. In that formula $\omega_0^2=4\pi Ne^2/m$ and ω is the impressed angular frequency. This formula is extended to two simple cases of non-uniform ionization, with the conclusion that non-uniformity may be indistinguishable from large energy dissipation, insofar as reactive effects are concerned. Formulas have been derived for calculating the *conductivity and specific inductive capacity of a cylindrical plasma* (positive column of an arc) between parallel condenser plates from the measured impedance of this condenser by using a modification of Mossotti's Theory. The natural period of such a condenser occurs very nearly when $K_p=-1$. For a fixed frequency the reactance of such a composite condenser was followed for varying arc current by observing the length of Lecher System connected to the condenser plates which was required to cause circuit resonance. Two and sometimes three resonances were found. They occurred in the neighborhood of the calculated plasma-electron resonance as determined from electron density measurements, and varied with impressed frequency according to theory.

The theoretical variation of K_p was checked in the range $\omega_0^2>2\omega^2$ by the hyperbolic relation between change in condenser reactance and arc current there. Resistance measurements on the Lecher system, used in connection with a more detailed analysis, allowed *calculation of relative electron density* in the range from one-half to five times that giving resonance, checking the actual values. In the same range, the *resistance to electron motion* varied considerably. The maximum value occurred near resonance and checked, roughly, the value calculated from free path considerations. The alternating fields in the plasma varied from 0.17 to 1.2 $v\cdot cm^{-1}$ and the maximum amplitude of electron motion was 2.1×10^{-3} cm.

A transverse magnetic field was found to double the resonance as H. Gutton has found. The separation of resonances accords with theory.

I. Introduction

THE reaction of an ionized gas to very high frequency electric waves has been the subject of several investigations. Spontaneous oscillations in the neighborhood of 10^9 herz originally found by Penning[1] have been further investigated by Tonks and Langmuir[2] using the low pressure mercury arc. They found that the observed high frequency oscillations corresponded to the theoretical value for plasma-electron oscillations[3]

$$\nu = (Ne^2/\pi m)^{1/2} = 8980 \times N^{1/2} \tag{1}$$

[1] Penning, Nature **118**, 301 (1926) and Physica **6**, 241 (1926).

[2] L. Tonks and I. Langmuir, Phys. Rev. **33**, 195 and 990 (1929).

[3] This frequency appears so often in investigations of the high frequency behavior of ionized gases that it will be given a definite name in this paper, namely, "plasma-electron frequency."

where ν is the oscillation frequency, m is the electronic mass, and N is the ionization density. This frequency, looked upon as the limiting frequency at which radio waves can be propagated in an ionized medium, has been discussed at some length by T. L. Eckersley.[4] Since an ionized gas exhibits a resonant frequency, it is of interest to know the behavior of such a gas toward forced oscillations. W. H. Eccles[5] has derived formulae which have been interpreted by Bergmann and Düring[6] as attributing a dielectric constant

$$K = K_0 - 4\pi Ne^2m/(m^2\omega^2 + f^2) \tag{2}$$

and conductivity

$$\rho^{-1} = fNe^2/(m^2\omega^2 + f^2) \tag{3}$$

to the medium, where f is a dissipation factor appearing in the equation of motion of the electron.

H. Gutton and J. Clement[7] have made a rather thorough investigation of the dielectric properties of ionized hydrogen extending through the plasma resonance.[7.5] It was found that the natural period varied with the intensity of ionization roughly in the way that was theoretically expected, and they were able to obtain a fair numerical check between the ionization density calculated from Eq. (1) and that calculated rather indirectly from their results. More recently, C. Gutton[8] has confirmed the existence of a natural resonance period in an ionized gas by measuring the change in conductivity of ionized mercury vapor when a 2.76 meter wave was impressed on it. In his theoretical treatment of the gas reaction, however, H. Gutton introduces an elastic restoring force of unknown origin which seems to be not only unnecessary but somewhat in contradiction with the actual experimental results, as has been pointed out by J. Rybner.[9] Still more recently, Bergmann and Düring[6] have measured the change in dielectric constant of a small condenser in high vacuum arising from the introduction of electrons between the condenser plates. They have been able to check the theoretical value as given by Eq. (2) roughly, but the electron densities used were so small (in the neighborhood of 10^7 cm^{-3}) that K was but little different from K_0, that is, unity. Their measurements give an apparent conductivity which is of the order of magnitude given by Salpeter's[10] interpretation of f as arising from the momentum lost in electron collisions with gas molecules.

[4] T. L. Eckersley, Phil. Mag. **4**, 147 (1927).

[5] W. H. Eccles, Proc. Roy. Soc. **A87**, 79 (1912).

[6] L. Bergmann and W. Düring, Ann. d. Physik **1**, 1041 (1929).

[7] H. Gutton and J. Clement, L'Onde d'Electrique **6**, 137 (1927); H. Gutton, preliminary reports, Comptes Rendus **184**, 441 (1927); complete report, Ann. d. Physique **13**, 62 (1930).

[7.5] The term "plasma resonance" denotes the actual resonance of the system comprising the plasma and the condenser of which it forms part of the dielectric. This resonance occurs, in general, at a different ionization density from plasma-electron resonance. See the paragraph following Eq. (27) and the theoretical treatment in Section IX.

[8] C. Gutton, Ann. d. Physique **14**, 5 (1930).

[9] J. Rybner, L'Onde d'Electrique **7**, 428 (1928).

[10] J. Salpeter, Jahrb. der drahtl. Telegr. **8**, 252 (1914). But see the criticism of S. Benner, Annalen der Physik **3**, 993 (1929) regarding the application of Salpeter's results to this experiment. Salpeter treats the case in which the free time of an electron is variable, whereas in the Bergmann-Düring experiment, the effective free time of every electron is the same.

The present investigation extends the work of H. Gutton with the aim of making direct measurements of electron density so as to be able to check theoretical formulas more directly.

II. The Specific Inductive Capacity of a Plasma

The use of an ionized gas is necessary if high densities of electrons are to be obtained, but in a plasma the density of ionization is not uniform throughout the whole cross section. It therefore becomes of interest to know how non-uniformity in electron density affects plasma-resonance behavior.

The complex specific inductive capacity of a plasma can be found by direct substitution in the partial differential equation

$$\partial^2 Z/\partial x^2 = \mu K \partial^2 Z/\partial t^2 + [4\pi\mu N e^2/(f + jm\omega)]\partial Z/\partial t \tag{4}$$

as given by Eccles.[11] Substituting

$$Z = \exp\{j\omega[t - (\mu K_p)^{1/2}x]\}$$

where K_p denotes the complex specific inductive capacity and writing

$$4\pi\mu N e^2/m = \omega_x^2 \tag{5}$$

where ω_x is the local plasma-electron angular frequency and writing also

$$S = f/m \tag{6}$$

we find that

$$K_p = \frac{\omega_x^2 - \omega^2 + j\omega S}{-\omega^2 + j\omega S}. \tag{7}$$

This is the specific inductive capacity at each point of the ionized medium looked upon as a function of the electron density, since that enters ω_x and possibly S.

The response of the medium as a whole may be extremely complicated. The simplest case is the one in which the electron density is a function of one coordinate only and the impressed electric field lies in that same direction. In that case we may write

$$dV = (4\pi Q_0/K_p)dx$$

where V is the impressed voltage and Q_0 is the polarization of the medium. This may be integrated to the form

$$V = 4\pi Q_0 \overline{K_p^{-1}} x_p \tag{8}$$

for a plasma of thickness x_p where

$$\overline{K_p^{-1}} = (1/x_p)(-\omega^2 + j\omega S)\int_{\text{over } x_p} (\omega_x^2 - \omega^2 + j\omega S)^{-1}dx. \tag{9}$$

[11] Reference 5, page 87.

It is instructive to apply this formula to a hypothetical case. Neglecting the dissipation factor S, let us assume a simple linear law of variation of N in the plasma, as for instance,

$$N = N_0(1 - x/2a) \tag{10}$$

from $x=0$ to $x=a$. This leads to

$$\overline{K_p^{-1}} = -\frac{\omega^2}{\omega_0^2} \ln \left[\frac{\omega_0^2 - \omega^2}{\omega_0^2/2 - \omega^2} \right]^2 \tag{11}$$

where $\omega_0 = (4\pi N_0 e^2/m)^{1/2}$ is 2π times the plasma-electron frequency where the the ionization is densest.

The value of $\overline{K_p^{-1}}$ as a function of N_0 is shown as Curve 1 in Fig. 1.

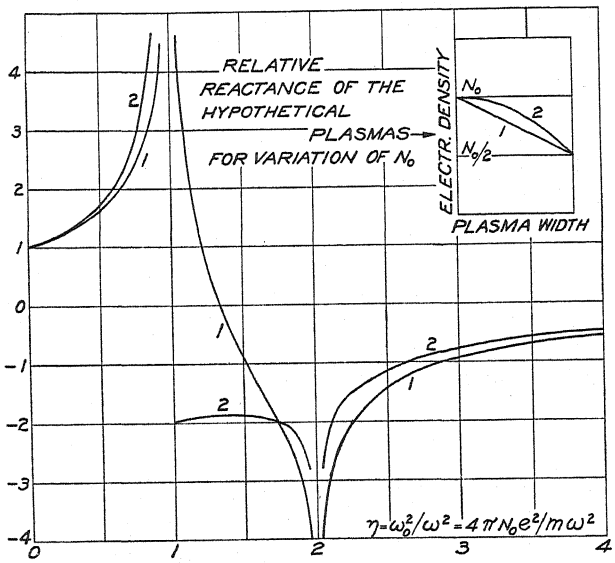

Fig. 1. Theoretical reactance of non-uniform plasmas.

Throughout the range $1 < \omega_0^2/\omega^2 < 2$ there is always a place in the plasma where local resonance occurs, giving rise to the middle section of the characteristic. The presence of resistance eliminates the infinities and leaves a curve resembling a resonance broadened by high dissipation, with the result that the width of the resonance region may only depend slightly upon the dissipative forces and may rather be a measure of the nonhomogeneity of the plasma. It was thought possible that a parabolic distribution of electron density

$$V = N_0(1 - x^2/2a^2) \tag{12}$$

might more nearly reproduce the assymmetry found in the actual resonance characteristics. Curve 2 was calculated with this in mind and although failing of its purpose, it may be useful in the appropriate case. Its equation is

$$\begin{aligned}\overline{K_p^{-1}} &= 2\eta^{-1}[2(\eta^{-1}-1)]^{-1/2}\tan^{-1}[2(\eta^{-1}-1)]^{-1/2} \\ &= \eta^{-1}[8(1-\eta^{-1})]^{-1/2}\ln\left\{\frac{[2(1\ \eta^{-1})]^{1/2}+1}{[2(1\ \eta^{-1})]^{1/2}-1}\right\}^2\end{aligned} \tag{13}$$

according as $\eta<1$ or $\eta>1$.

With the dissipative factor omitted, Eq. (7) takes the form

$$K_p = 1 - \omega_x^2/\omega^2 \tag{14}$$

which shows that each element of the plasma has a simple circuit analogue in a fixed condenser C shunted by a variable inductor L. The shunt admittance of such a circuit is

$$Z^{-1} = j\omega KC = j\omega C + (j\omega L)^{-1}$$

where K is the apparent specific inductive capacity of the condenser. Putting $LC=\omega_0^{-2}$ we obtain

$$K = 1 - \omega_0^2/\omega^2.$$

Each elementary volume ($dx\ dy\ dz$, x being parallel to the electric field) in even a non-uniform plasma is thus equivalent to a vacuum parallel-plate condenser of capacity

$$C = dydz/4\pi dx$$

shunted by an inductor of inductance

$$L = mdx/Ne^2dydz.$$

If, for example, a plasma contains two layers, each of which is uniform in electron density, it can be represented by two shunt circuits in series. Such a system shows double resonance provided that the separation of the two natural periods relative to the damping of the individual circuits is great enough. This double resonance could be observed either by increasing the electron densities proportionally (decreasing inductances in the circuit analogue) while the impressed frequency was maintained constant, or by varying the impressed frequency the keeping ionization densities unchanged. Extension of this reasoning makes it possible to understand how even a continuous variation in electron density, such as found in an actual plasma, may give rise to multiple resonance.

Digressing slightly, it may be remarked that H. Guttonn arrives at a relation essentially different from Eq. (14), namely,

$$K = 1 + (4\pi Ne^2/m)/(\omega_0^2 - \omega^2)$$

In this equation, $w_0/2\pi$ is the resonant frequency of the electrons and ω_0 is related to N by the empirical equation

$$\omega_0^2 = AN^{3/4}.$$

These equations make K decrease initially from unity as N is increased from zero, which is qualitatively the same as Eq. (14). When N is infinite, however,

these equations give K a weak positive infinity, whereas the strong negative infinity of Eq. (14) is qualitatively checked by H. Gutton's curves (Fig. 9 of Annales de Physique article) and by the measurements to be described below.

Turning now to the case of uniform ionization, it is evident that an analysis of the response of the medium reduces to an analysis of the electrostatic field between condenser plates in the presence of a dielectric of specific inductive capacity K_p. The simplest case is, of course, that of the plane parallel condenser, but that form is not suited to the positive column of an arc. The shape that has been adopted is that of a cylindrical plasma parallel to and midway between two plane condenser plates. This form has the experimental advantage that it is a natural form for a positive column, and that the electric lines of force in a uniform cylindrical plasma are straight and parallel so that there are no strong local fields at any point.

III. The Effective Specific Inductive Capacity of a Plane Parallel Condenser Containing a Cylindrical Plasma

Theoretically, a modification of Mossotti's theory of dielectrics makes the arrangement just outlined quantitative.[12] Mossotti's theory in its usual form contemplates a vacuum containing suspended conducting spheres. The response of such a configuration to an electric field can be treated quantitatively.[13] For present purposes the conducting spheres must be replaced by dielectric cylinders.

We consider then a large volume of dielectric (specific inductive capacity $=K$) made up of matter-free space in which are suspended infinitely long cylinders of specific inductive capacity K_p with their axes perpendicular to the uniform electric field E_e. The electric field tending to polarize any cylinder is

$$E_i = E_e + (4\pi/2)P \tag{15}$$

where P is the polarization of the composite dielectric, and the coefficient $4\pi/2$ applies to cylinders as $4\pi/3$ does to spheres. Within the polarized cylinder the field is

$$E_p = 2E_i/(K_p + 1) \tag{16}$$

analogous to $E_p = 3E_1/(K+2)$ in the case of spheres. The polarization of the cylinders is then

$$P_p = (K_p - 1)E_p/4\pi = (K_p - 1)E_i/2\pi(K_p + 1). \tag{17}$$

If θ denotes the fraction of the composite dielectric volume occupied by the cylinders,

$$P = \theta P_p = \theta(K_p - 1)E_i/2\pi(K_p + 1). \tag{18}$$

[12] H. Gutton's analysis based on Fig. 12 of his Ann. de Physique article cannot be justified theoretically. See J. Rybner, reference 9.

[13] Livens, Theory of Electricity, p. 228; Jeans, Electricity and Magnetism, Fifth Edition, p. 131 arrives at a formula which is not valid for sufficiently high values of dielectric constant.

Also

$$P = (K-1)E_e/4\pi = (K-1)E_i/2\pi(K+1) \tag{19}$$

by using Eq. (15). Combining these two equations we find

$$(K-1)/(K+1) = \theta(K_p-1)/(K_p+1) \tag{20}$$

relating the dielectric constant, K_p, of the cylinders to that of the composite parallel-plate condenser, K. When K is not very different from unity, we can write

$$\delta K = 2\theta(K_p-1)/(K_p+1). \tag{21}$$

This formula was checked by the method H. Gutton used to determine the capacity values in the "equivalent" system shown in his Fig. 12. The arc tube, of 3.0 cm internal diameter, projecting well beyond and centered between two 7×7 cm condenser plates 7 cm apart was replaced by an open glass tube of the same size. With this tube empty, the Lecher System and condenser resonated with the thermocouple bridge at 17.9 cm, filled with mercury ($K_{Hg}=\infty$) at 16.3 cm, and filled with benzol ($K_B=2.26$) at 17.35 cm. From Eq. (21)

$$\delta K_\infty = 2\theta$$

$$\delta K_B = 2\theta(2.26-1)/(2.26+1) = 0.386\times 2\theta$$

whence

$$\delta K_B/\delta K_\infty = 0.386.$$

Since the changes in Lecher System length were small, they were proportional to capacity changes, whence

$$\delta K_B/\delta K_\infty = \delta L_B/\delta L_\infty = (17.9-17.35)/(17.9-16.3) = 0.34.$$

This is a satisfactory check considering that the experimental arrangement was only a rough approximation to that assumed mathematically. Since θ has been eliminated in the course of this calculation, the question naturally arises as to whether its value might not constitute an independent verification. The geometric capacity, C_0, terminating a resonant length, s, of Lecher system is given by

$$1/\omega C_0 K = Z_0 \tan(2\pi s/\lambda) \tag{22}$$

where Z_0 is the surge impedance of the system. It follows that the change in s required to retune after a slight change in K obeys the relation

$$\delta K/K = -2\pi\delta s/\lambda \sin(2\pi s_0/\lambda)\cos(2\pi s_0/\lambda)$$

and using Eq. (21)

$$\theta = -2\pi\delta s/\lambda \sin(4\pi s_0/\lambda) \tag{23}$$

since $K=1$.

In the present case $s_0=27.2$ cm (for the bridge at 17.9 cm) and $\lambda=187$ cm whence $\theta=0.056$. The tube cross-section is $(\pi/4)\times 3.0^2=7.07$ cm^2, while the condenser cross-section is $7\times 7=49$ cm^2 giving $\theta=0.14$. This large discrepancy is easily accounted for both by the large edge effect in a condenser of the proportions used and also by the individual capacity of each plate to ground. Under these circumstances it is permissable to treat θ as an empirical constant in Eqs. (20) and (21).

It is fairly obvious that Eq. (21) may not be applicable to plasma resonance since δK becomes very large when $K_p K_c$ nears -1. In addition, a dissipative term must be included if the analysis is to be complete. From Eq. (7) (treating the plasma as if uniform by using ω_0 instead of ω_x)

$$K_p = \frac{\omega_0^2 - \omega^2 + j\omega S}{-\omega^2 + j\omega S} = \frac{\eta - 1 + jS/\omega}{-1 + jS/\omega} \tag{24}$$

if we put $\omega_0^2/\omega^2 = N/N_\omega = \eta$, N_ω being the electron density for which the plasma-electron angular frequency is ω, that is, $N_\omega = [\omega/(2\pi\times 8980)]^2$. From Eq. (20),

$$K^{-1} = 1 - 2\theta(K_p - 1)/[K_p + 1 + \theta(K_p - 1)] \tag{25}$$

Combining, we have

$$K^{-1} = 1 + \theta\eta/[1 - (1+\theta)\eta/2 - 2jS/\omega] \tag{26}$$

for calculating the complex dielectric "constant" of the condenser when dissipation is included.

IV. Characteristics of a Tuned Circuit Made up of a Condenser Containing a Plasma and a Variable Inductor

If we suppose the condenser containing the plasma to be connected in series with an inductance, L, and denote its capacity when $N=0$ by C_0, the series impedance of the combination is

$$Z = j[\omega L - (\omega C_0 K)^{-1}]$$

Putting

$$L = L_0 + \delta L$$

where L_0 is the inductance which tunes C_0, that is, $L_0=(\omega^2 C_0)^{-1}$, this equation becomes

$$Z = j[\omega\delta L - \omega L_0(K^{-1} - 1)].$$

Substituting from Eq. (26) and separating into real and imaginary parts we find

$$Z = j\omega\left[\delta L - L_0\frac{(\theta/\phi)\eta'(1-\eta'/2)}{(1-\eta'/2)^2 + S^2/\omega^2}\right] + 4\frac{\omega L_0\theta\eta S/\omega}{(1-\eta'/2)^2 + S^2/\omega^2}$$

where $\phi=1+\theta$ and $\eta'=\phi\eta$. When L is adjusted so that the circuit is in resonance, the reactance is zero and δL_r, the value of δL at resonance, is given by

$$\delta L_r = L_0 \frac{\theta\eta(1-\eta'/2)}{(1-\eta'/2)^2+S^2/\omega^2} \tag{27}$$

As N is increased from zero, η and η' increase proportionally and δL_r increases from zero, at first proportionally to N but later more rapidly. If S were zero, δL_r would approach $+\infty$ as $\eta'=2$, to reappear at $-\infty$, but the finite value of S causes δL_r to vary rapidly from a positive maximum to a negative minimum as η' passes through 2. As N becomes still larger, δL_r increases once more approaching $\delta L_\infty = -2\theta L_0/\phi$ as $\eta\to\infty$. This is just the type of behavior approximated to by the curve in H. Gutton's Fig. 9.

Obviously, the plasma resonance occurs at $\eta'=2$. The qualitative circuit equivalent of the plasma between its condenser plates, as shown in Fig. 2, makes it evident that the shunt resonance does not occur when the plasma

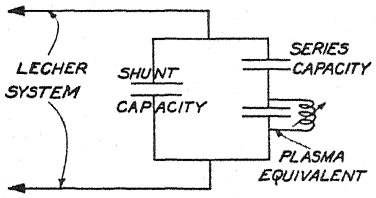

Fig. 2. Qualitative circuit equivalent of a plasma between condenser plates.

itself is tuned to the impressed frequency. This would be true only when the shunt capacity is zero. For example, the infinite plane parallel plasma is a (rather ideal) case in which plasma resonance would lie at $\eta=1$. For a spherical plasma between parallel plates, resonance would occur near $\eta=3$.

In the range where η' is different enough from 2 for S/ω to be neglected, Eq. (27) can be written

$$(1-\eta'/2)\delta L_r = -(\eta'/2)\delta L_\infty(\theta\phi_\infty/\theta_\infty\phi)$$

the ratio in the right member being introduced to allow for changes in θ with N. It follows that

$$(\theta\phi_\infty/\theta_\infty\phi)\delta L_r^{-1} + \delta L_\infty^{-1}(2/\eta'-1) = 0$$

and noting that $\eta'=\phi\eta=\phi N/N_\omega$ we have

$$(\theta\phi_\infty/\theta_\infty\phi)\delta L_r^{-1} = (2N_\omega/\delta L_\infty)(\phi N)^{-1} - \delta L_\infty^{-1}. \tag{28}$$

Now, changes in ϕ can be neglected since the actual value of θ is so small. It is thus justifiable to put $\phi/\phi_\infty=1$, whence Eq. (28) becomes

$$(\theta/\theta_\infty)\delta L_r^{-1} = (2N_\omega/\delta L_\infty)(\phi_\infty N)^{-1} - \delta L_\infty^{-1}. \tag{29}$$

In the range of larger values of N (experimentally when $\eta'>2$), the variation of θ with N was appreciable, but small, and the values of θ/θ_∞ could be calcu-

lated from the thickness of the wall sheath in the arc tube. For the smaller values of N, however, the variation of θ was not calculable and Eq. (29) could not be quantitatively tested in that range.

V. Preliminary Experiments

The plasma used in this investigation was the positive column of a mercury arc because the electrical methods for measuring ionization intensities have been applied most extensively to these arcs.[14] At first a tube containing an oxide-coated cathode was tried, but was found unsuitable on account of a conducting film which forms on the tube walls. This film appeared as a slight blackening, and its conductivity was made evident by the decrease in resonance current in the tuned circuit when the unexcited tube was placed between the condenser plates. That this film comes from the oxide cathode was proved by its absence in the next tube which had a hot tungsten filament. This tube, illustrated in Fig. 3, was a long cylinder of uniform internal diameter, 3.0 cm. The lower portion, containing a small quantity of mercury, was immersed in a water vath for pressure control. A short distance above the cathode was a ring electrode intended to be used as an auxiliary anode but soon abandoned. Thirty cm above this were two probes. One was a tungsten wire of 0.127 cm diameter and 1.87 cm long placed in the axis of the tube. The other

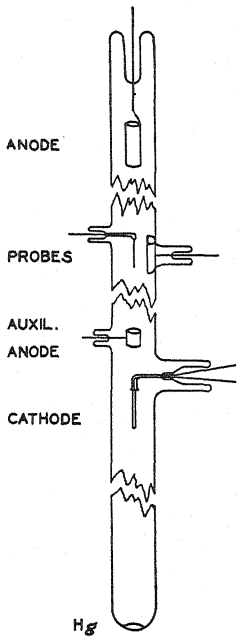

Fig. 3. Experimental arc tube.

[14] I. Langmuir and H. Mott-Smith, Jr., Gen. Elec. Rev., **27**, 449, 538, 616, 762 (1924); H. Mott-Smith, Jr. and I. Langmuir, Phys. Rev. **28**, 727 (1926); L. Tonks and I. Langmuir, Phys. Rev. **34**, 876 (1930).

was a square molybdenum plate, 1.95 cm on a side, on the tube wall opposite the probe and bent to fit the wall. These probes were intended to measure the intensity of ionization in the arc by well-known methods.[14] The main anode, a hollow cylinder, was 8 cm above these probes. The high frequency field was applied to the uniform column midway between the probes and the auxiliary anode by external electrodes of various shapes and sizes.

Initially a parallel wire system was connected with the external electrodes, later a small single loop inductance with variable condenser in series was employed, but finally a Lecher system consisting of two brass rods each 0.422 cm in diameter, spaced 3.90 cm on centers, and 180 cm long, was used for most of the measurements. The complete arrangement is shown schematically in Fig. 4. The Lecher system was tuned with a moveable bridge which consisted essentially of a low-resistance vacuum thermocouple of 2.6 ohms d.c. resistance. To prevent reflection effects from the free end of the Lecher sys-

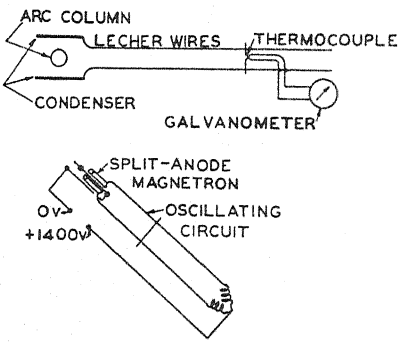

Fig. 4. Apparatus for observing ionized-mercury resonance.

tem, a short-circuiting bridge was attached to the thermocouple bridge and some 16 cm back of it, so that the two moved together. This 16 cm of conductor acts as a high impedance shunt to the thermocouple at all wave lengths used and effectively prevents any free-end oscillations without affecting the thermocouple calibration.[15] Stray effects arising from bringing the hand near to the free end of the Lecher system were minimized by by-passing the capacity currents along the thermocouple-to-galvanometer leads direct to the shorting bridge through small condensers.

A split-anode magnetron of Type FH-11 which can generate powerful oscillations up to 4×10^8 herz[16] was used as oscillation source. It was found more convenient to vary the arc current than to vary the frequency of the oscillator, since the e.m.f. in the Lecher system circuit then does not vary.

The earliest experiments showed two resonance frequencies in the plasma. In view of H. Gutton's single resonance, it was thought that this might arise in some way from the distributed excitation of the Lecher system together with its distributed inductance and capacity. With this in mind, a circuit with

[15] Paper to be submitted to I.R.E. Proc.
[16] W. C. White, Electronics **1**, 34 (1930).

lumped impedances was tried and as the same effect was observed, it was concluded that the double resonance was a property of the plasma itself.

Too high an excitation of the plasma circuit-resulted, as pointed out by C. Gutton, in additional ionization in the vicinity of plasma resonance which was often evident visibly by increased light from the region of the arc between the external electrodes. Such effects made measurements erratic and difficult of interpretation so that is was found best to work with very low excitation.

For the higher arc currents the tungsten wire cathode had to be run very hot. When it happened occasionally that it was too cool, the arc changed its appearance and the oscillation readings were erratic and quite different from the other condition. Too cool a cathode gives temperature-limited instead of space-charge-limited emission, the cathode drop increases, and the primary electrons, instead of ionizing the gas and causing glow on the anode side of the cathode only, penetrate down the tube and cause glow there also. With a plentiful supply of primary electrons, the cathode drop exceeds the ionizing potential only slightly so that although the electron at the cathode sheath edge has sufficient energy to ionize, the normal decrease in plasma potential as the electron moves away from the cathode is sufficient to bring its energy below the ionizing value. Of course, toward the anode, the gradient in the arc speeds up the electrons, but in the opposite direction ionization will be prevented. If, however, the electrons have several volts excess energy, as they have with temperature-limited currents, they are able to maintain a plasma even in the absence of an accelerating field in it. The change in oscillation readings undoubtedly arises from the change in arc conditions, and the fluctuations may be caused by line voltage variations which here appear as a variable cathode drop of about the same magnitude as the voltage variation itself, whereas with a hot enough cathode they cause only a small fractional change in arc current.

IV. Resonance Characteristic Measurements

In taking a resonance characteristic, the oscillation frequency of the magnetron oscillator was first fixed by adjusting the position of the bridge on the parallel conductors which, connected to the two anode sections of the magnetron, form the resonant circuit of the oscillator. The oscillation amplitude was fixed at a suitable value by adjusting the anode voltage, anode current (through filament current) and magnetic field of the magnetron. These three quantities were carefully maintained constant. The half wave-length was found from the separation of two successive nodes on a second Lecher system which could be coupled to the oscillator. This value agreed within 2 percent with the value found on the measuring system itself. The difference, which arises from the presence of the wood support in the measuring system, is small enough to be negligible in the present work.

The appendix of the arc tube was then immersed in a Dewar flask containing water at a temperature to give the desired mercury pressure.

With no arc in the tube, the resonance position of the bridge on the meas-

uring system and the thermocouple galvanometer reading were recorded. The arc was then started and the same readings were made at arc currents increasing roughly in a geometric ratio.

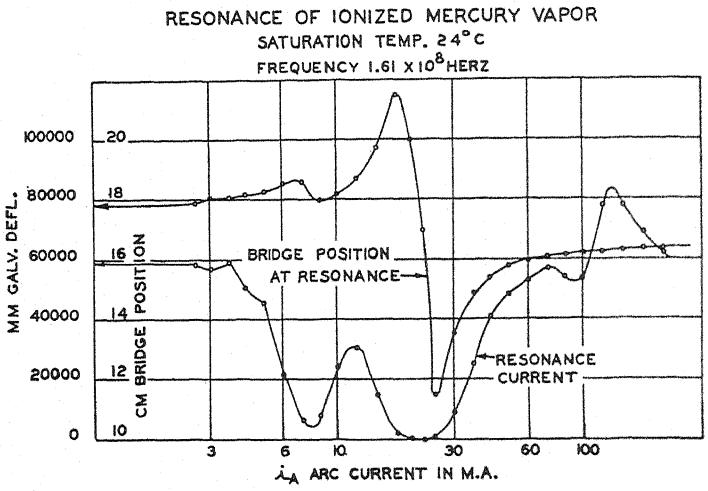

Fig. 5. Resonance characteristic of ionized mercury vapor.

The results of such a series of measurements are shown in Fig. 5. The two resonance points at 7.5 and 21.5 m.a., to be denoted as *a*- and *b*-resonances, respectively, are accompanied by the current minima expected at a shunt

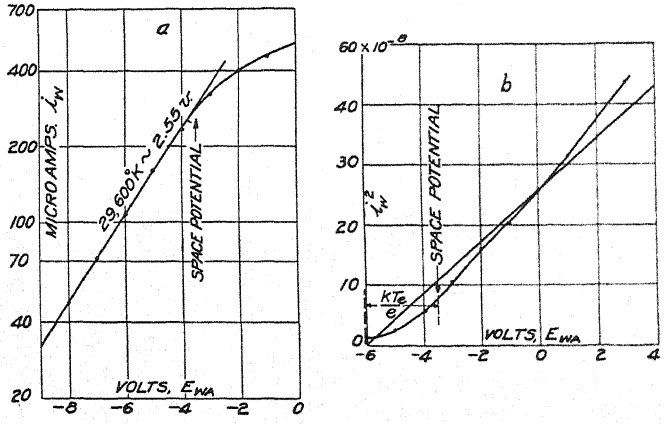

Fig. 6. Electrode volt-ampere characteristics for determining the electron density in the arc.

resonance. Excluding the immediate neighborhood of a resonance, the continual increase in s with increasing ionization intensity gives qualitative confirmation of the continual decrease in K_p with increase in N as required by Eq. (14). The variation in resonance current above 80 m.a. is not understood.

In order to compare the experimental results with the theoretical, it was necessary to determine the ionization intensity as a function of arc current. It developed that the wall electrode, Fig. 3, was unsuited to this purpose since the wall sheaths were too thick over the greater range of arc current. Accordingly, the cylindrical electrode w was employed for this purpose. Fig. 6 exhibits two plots of a typical volt-ampere characteristic. Fig. 6a is the semi-log plot which yields electron temperature and space potential. Fig. 6b is the i^2-V plot, the "slope" of which gives the electron density. Bearing in mind the ideal shape of this curve as shown by f^2 Fig. 7,[17] it is possible to make a

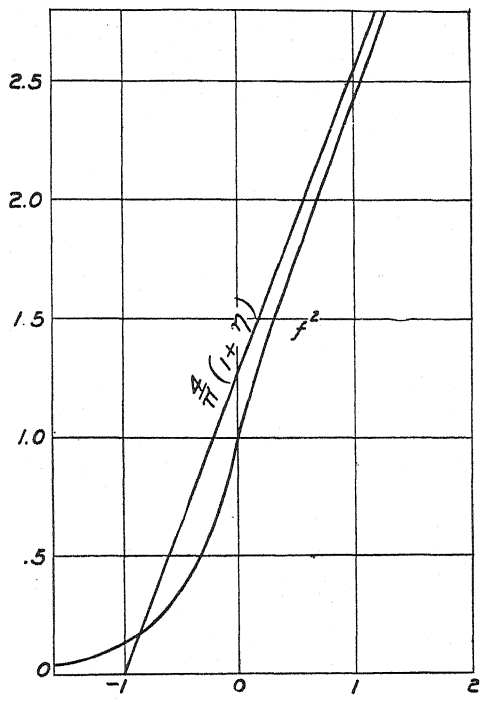

Fig. 7. Theoretical (f^2) volt-ampere characteristic and its approximation $[4(1+\eta)/\pi]$.

very good guess at the straight line whose slope is significant in the following way. This line intercepts the V-axis at the space potential less kT_e/e, the potential corresponding to the electron temperature. The space potential is -3.5 v, $kT/e=2.5$ v, whence the intersection is at -6 v. The upward bend above zero volts is obviously due to ionization in the sheath. Very little latitude is thus left for drawing the asymptote of the ideal characteristic. As drawn, the slope is 4.3×10^{-8} amps$^2\cdot$v^{-1} which gives[18]

[17] Reproduction of Fig. 7 from I. Langmuir and H. M. Mott-Smith, Jr., G. E. Review, p. 617, Sept. (1924).

[18] Eq. (45) I. Langmuir and H. M. Mott-Smith, Jr., G. E. Rev. **27**, 455 (1924) or L. Tonks and I. Langmuir, Phys. Rev. **34**, 913 (1929).

$$n_e = 3.32 \times 10^{11} S^{1/2}/A = 3.32 \times 10^{11} \times 2.07 \times 10^{-4}/0.080$$
$$= 8.6 \times 10^{8} \text{ electrons} \cdot \text{cm}^{-3}$$

Like measurements at other arc currents and mercury pressures gave additional points on the curves of Fig. 8. Of course, at the higher pressures, special care was taken that the tube temperature at all points never fell below the appendix temperature.

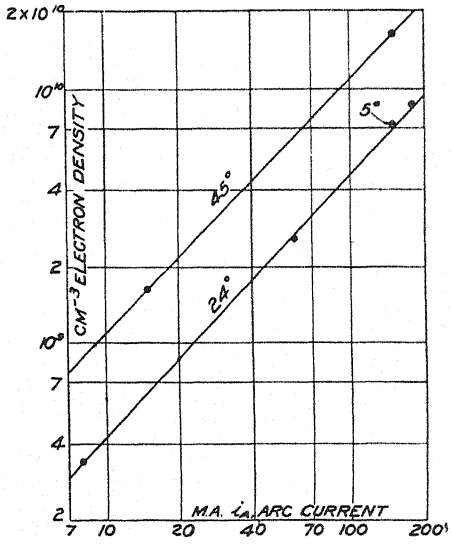

Fig. 8. Electron density in the arc as a function of arc current for different appendix temperatures.

With these data it became possible to correlate the frequency impressed on an ionized gas with the ionization density. The results of several resonance characteristics have been incorporated in Table I and Fig. 9. The "Theoretical Curve—Plane Plasma" is a plot of the equation $\nu = 8980\ N^{1/2}$, ($\omega_0 = \omega$ or $\eta = 1$ in other forms). It gives the theoretical relation between ionization and plasma-resonance frequency for a plane plasma. The "Theoretical Curve—Cylindrical Plasma" is a plot of $\eta = 2$ and gives the same relation for the cylindrical plasma. The *a*-resonance and *b*-resonance curves show the observed behavior of the *a*- and *b*-resonance conditions in a 2.2-bar arc. It is

TABLE I. *Relation between plasma-resonance frequency and ionization density.*

Condenser plate size (cm²)	Temp. (°C)	Frequency (×10⁻⁸)	a-resonance i_a (ma) N_e×159	b-resonance i_a (ma) N_e×159	aa-resonance i_a (ma) N_e×159	Plasma-resonance density, calculated $2\nu^2/(8980)^2$
2.5×2.5	13±	1.59	7.2 0.27	22 0.86		0.63×10⁹
2.5×2.5	24	1.59	8.0 0.34	26± 1.12	4.1?	.63
1×1 approx.	24.5	3.66	60. 2.54	145± 6.7	30 1.28	3.30
1×1 "	24	1.60	7.7 0.32	24 1.03	4.3 0.18	.63
1×1 "	24	2.35	21. 0.91	54± 2.28	12. 0.51	1.36
7×7	24	1.60	7.5 0.31	22 0.95		.63
7×7	45	1.60	5.5 0.60	15.5 1.66		.63

to be noted that the actual resonance frequency lies within 30 percent of the theoretical and that the slope of the straight lines is 0.42 and 0.45 compared to a theoretical 0.50. The *aa*-resonance is one which appeared at lower ionization densities in cases where the applied field was decidedly non-uniform. While it is possible to imagine that the *b*-resonance may arise primarily from the response of the outer portions of the plasma, and the *a*-resonance from the axial portion, it is rather difficult to account for a third resonance corresponding either to a still higher electron density or to a configuration approaching more nearly to the plane case.

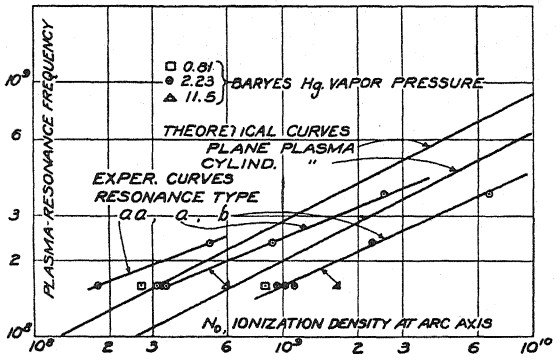

Fig. 9. Comparison of experimental and theoretical plasma-resonance frequencies.

The plasma resonance was found to be somewhat dependent on the gas pressure in the arc. Fig. 9 shows that a 14-fold pressure change caused a 2.2-fold change in resonant density. The resonance density thus varies roughly as the 0.3 power of the pressure. Compared to its variation with the square of the frequency, this is seen to be a small change which may arise from second order effects. It is probably significant that both *a*- and *b*-resonances were affected in the same ratio.

Although exact agreement of theory with experiment is lacking, it seems possible that the method used here may be useful in investigating electron concentration in cases where other methods fail. In recent unpublished work with Ne discharges, for instance, C. G. Found in this laboratory was found that the simple interpretation of probe characteristics fail, probably on account of the specific action of metastable atoms, whereas the present method appears to be directly applicable.

VII. Demonstration That $K_p \propto 1-\omega_0^2/\omega^2$ in the Range $\omega_0^2 > 2\omega^2$

It has been remarked that Eq. (29) can give a direct test of the specific inductive capacity formula. The δL's refer to inductance changes but, in connection with the Lecher system, they may just as well apply to the small changes in tuning length which have been found. Again, since tests have shown that N is very nearly proportional to i_A, we may interpret Eq. (29) as requiring that the reciprocal change in Lecher system tuning length caused by

increasing the arc current from zero to i_A shall be a linear function of the reciprocal of i_A, insofar as θ/θ_∞ is constant. The solid dots of Fig. 10 are plotted in this way from the same data as Fig. 5. At 40 amp^{-1} the imaginary part of K_p is no longer negligible so that Eq. (29) no longer applies, and at the lower values of i_A^{-1}, the curvature of the plot indicates that a correction for variation of θ is necessary.

This correction has been made in the following manner. If the plasma occupies a radius $a-x$ in the tube of radius a, then $\theta/\theta_\infty=(a-x)^2/a^2$ since x, the sheath thickness, approaches zero as i_A approaches infinity. Thus, to a first approximation,

$$\Delta\theta/\theta_\infty = (\theta - \theta_\infty)/\theta_\infty = -2x/a.$$

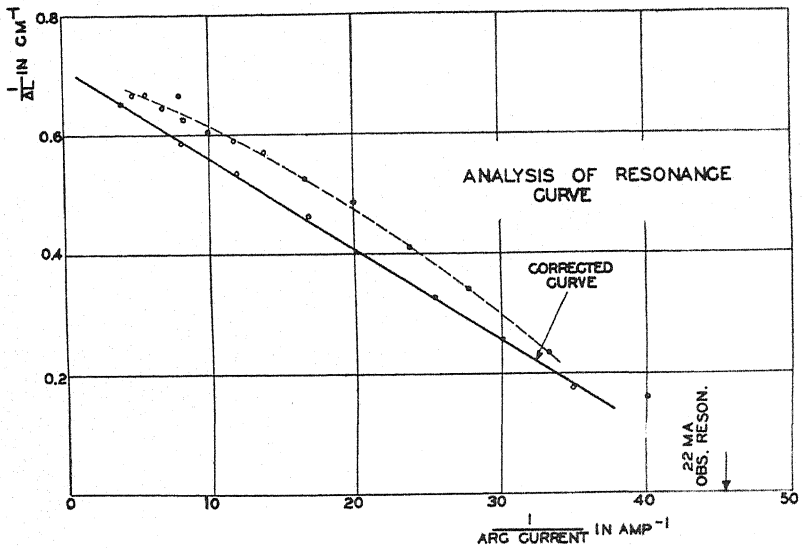

Fig. 10. Analysis of the resonance characteristic in Fig. 5.

Now x is related to I_p the positive ion current density to the wall through the space charge equation

$$I_p = 2.34 \times 10^{-6} V^{3/2}/600x^2$$

or

$$x = 6.25 \times 10^{-5} V^{3/4} I_p^{-1/2}$$

where V is the potential drop in the wall sheath and 600 is $(m_p/m_e)^{1/2}$. Now I. Langmuir and H. M. Mott-Smith, Jr., have found[19] that $I_p \propto i_A^{1.2 \text{ to } 1.3}$ and in the present tube I have found the relation to approximate

$$I_p = 1.08 \times 10^{-3} i_A^{1.4}$$

With $i_A = 0.060$ amp, it was found that $T_e = 28{,}600°$ whence[20]

[19] I. Langmuir and H. M. Mott-Smith, Jr., G. E. Rev. **27**, 764 (1924).
[20] L. Tonks and I. Langmuir, Phys. Rev. **34**, 898 (1929).

$$V = 6kT_e/e = 6 \times 28{,}600/11{,}600 = 14.8v$$

Assuming that V changes but little with i_A (T_e changes but slowly) these equations lead to

$$\Delta\theta/\theta_\infty = -0.0191 i_A^{-0.7}.$$

Substituting $1+\Delta\theta/\theta_\infty$ for θ/θ_∞ in Eq. (29) we have

$$(1 - 0.0191 i_A^{-0.7})\delta L_r^{-1} = (2N_\omega/\delta L_\infty)(\phi N)^{-1} - \delta L_\infty^{-1}.$$

Thus the δL_r^{-1} coordinate of each point should be decreased by an amount directly calculable from i_A. The fractional corrections were tabulated for a series of values of i_A^{-1} and these were applied in several cases to the smooth curve through the experimental points. As in Fig. 10, the resulting curve is always a straight line, the continuation of which intercepts the δL_r^{-1} axis very near to the actual b-resonance, thus confirming Eq. (14). Later Fig. 11, showing θ/θ_∞ as a function of i_A, was plotted and was found useful in subsequent calculations.

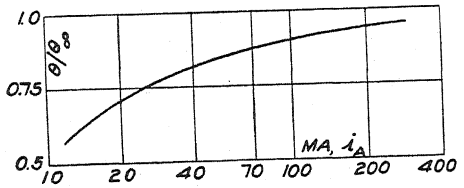

Fig. 11. Fraction of tube cross-section occupied by plasma.

The method here employed, by not requiring that the plasma fill the whole dielectric space, avoids the difficulties of interpretation encountered by Appleton and Childs[21] because of the formation of positive ion sheaths.

VIII. Detailed Analysis of Hg Resonance Characteristics

The resonant Lecher system length as a function of arc current and the thermocouple current as a function of arc current are the two characteristics so far mentioned. Another characteristic which can be obtained is the equivalent series resistance of the composite condenser.

It can be shown[15] that the resonance curve of a Lecher system readily lends itself to determinations of resistance. Let I_0 be the maximum (resonance) current in the thermocouple on the movable bridge and let I be the current at any nearby position s. The values of $[I^{-2} - I_0^{-2}]^{1/2}$ plotted against s give a straight line whose slope S_l in amp.$^{-1}\cdot$cm^{-1} is a measure of the resistance in the circuit. The relation is

$$R\cos^2(2\pi s_r/\lambda) = 2\pi Z_0/S_l I_0 \lambda - R_t \qquad (30)$$

where s_r is the effective length of Lecher system at resonance, R is the equivalent series resistance of the composite condenser, and R_t is the thermocouple resistance, the distributed resistance of the system being neglected.

[21] Appleton and Childs, Phil. Mag. **10**, 969 (1930).

R_t was determined with no current in the arc. The resonance curve at the first resonance, together with $(I^{-2}-I_0^{-2})^{1/2}$ are shown in Fig. 12. Resonance occurred at 11.77 cm. The next resonance occurred at 89.39 cm, giving a wave-length, λ, of 155.2 cm. This compares with 158 cm measured on a sys-

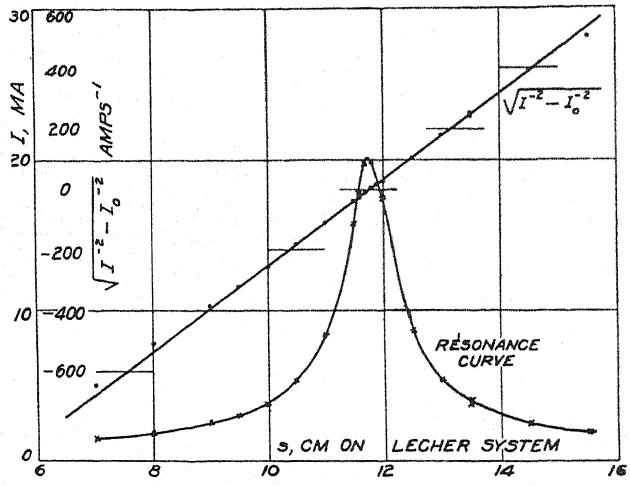

Fig. 12. Lecher system resonance curve and its analysis.

tem almost completely free of excess distributed capacity. The difference is too small to warrant detailed corrections, but in each case where λ appears the value which seems to be the more appropriate will be used.

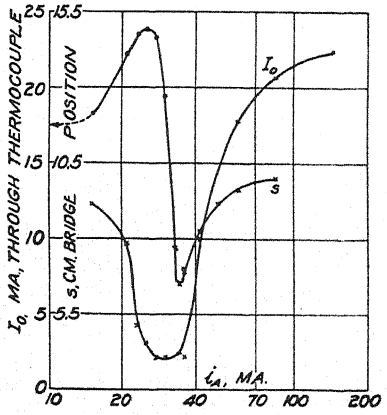

Fig. 13. Resonance characteristic for $\lambda = 158$ cm.

From the figure $S_l = 143$, $I_0 = 0.020$ amp., using $Z_0 = 353$, and $\lambda = 155.3$ we have $R_t = 4.98$ ω. At 89.39 cm the resonance curve yields $R_t = 6.81$ ω. The differences arises from the distributed resistance of the system, but as long as measurements are confined to the neighborhood of the first resonance, it will doubtless be accurate enough to include this resistance in R_t.

Fig. 13 shows the resonance characteristic at this same frequency. For each value of arc current sufficient points (not less than 5) on the resonance curve were taken to permit the slope S_l to be determined. The bridge shortening had been determined by the double-hump resonance method[15] so that s_r could be found from the bridge position. Zero correction and bridge shortening together amounted to +9.2 cm. R was then calculated from Eq. (30), and the values obtained appear in Fig. 14.

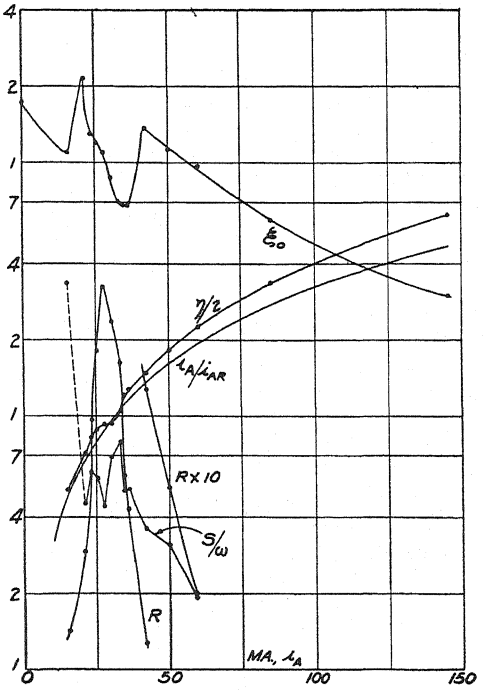

Fig. 14. Analysis of resonance and resistance characteristics.

Ranges: $\xi 0$ from 3.0×10^{-4} to 2.1×10^{-3} cm. $\eta/2$ from 0.51 to 6.2. i_A/i_{AR} is on the same scale. R from 14 to 320 ohms. S/w from 0.02 to 0.33.

It remains to interpret R and s_r in terms of the damping coefficient of the electron oscillations and the density of ionization. The specific inductive capacity K_0 of the composite condenser can be found from s_r readily since

$$\begin{aligned}(\omega K_0 C_0)^{-1} &= Z_0 \tan l \\ (\omega C_0)^{-1} &= Z_0 \tan l_0\end{aligned} \tag{31}$$

where $l = 2\pi s_r/\lambda$ and l_0 is the value of l for $N=0 (K_0=1)$. It follows that

$$K_0 = \tan l_0/\tan l \tag{32}$$

Thus the problem becomes that of a condenser of a complex capacity C_0K (Eq. (26)) equivalent to the combination, C_0K_0 in series with R;

$$(j\omega KC_0)^{-1} = R + (j\omega K_0 C_0)^{-1}. \tag{33}$$

Substituting from Eq. (26) and separating into real and imaginary parts we have

$$(2S/\omega)(1 - K_0^{-1}) - (\eta/2)\omega C_0 R(1 + \theta) = -\omega C_0 R$$
$$(2S/\omega)\omega C_0 R + (\eta/2)[1 - \theta - K_0^{-1}(1 + \theta)] = 1 - K_0^{-1}$$

whence

$$S/\omega = \theta\omega C_0 R/D \tag{34}$$

$$\eta/2 = [(1 - K_0^{-1})^2 + \omega^2 C_0^2 R^2/D] \tag{35}$$

where

$$D = (1 - K_0^{-1})[1 - K_0^{-1} - \theta(1 + K_0^{-1})] \tag{36}$$

The necessary data are all available. The calculations of R and K_0 have been discussed, $\theta_\infty = 0.056$, and $\omega C_0 = 0.00250$ by Eq. (31). The values of S/ω and $\eta/2$ calculated in this way are shown in Fig. 14. Since theory requires that

$$\eta/2 = N/N_{\text{resonance}} = i_A/0.031$$

very nearly, $i_A/0.031$ has been plotted for comparison. The higher values of $\eta/2$ for the larger values of i_A may well be due to an error in θ_∞. This failed to appear in Fig. 10 since there only relative values of θ were involved. A change to $\theta_\infty = 0.053$ would make $\eta/2$ coincide with $i_A/0.031$ at $i_A = 145$ m.a. and would not spoil the present agreement near resonance. It thus appears that the experimental results confirm the oscillation theory, not only to one side of the resonance region, but even through this region. The check is surprisingly good in view of the non-uniformity of the plasma.

It may be that this factor has more influence on the value of S/ω. Salpeter[10] has shown that collisions of electrons with gas atoms introduce a damping factor in the electron equation of motion and S is then the number of collisions per electron per second. In the present experiment with an electron mean free path of about 3 cm[22] and a speed of 1.22×10^8 cm/sec ($T_e \sim 30{,}000°$) $S = 4.1\times10^7$. For a 158 cm wave, $\omega = 1.19\times10^9$, whence $S/\omega = 3.4\times10^{-2}$. On the other hand the electrons are reflected much more frequently from the sheath on the tube wall. Such reflections should, on the average, destroy the directed momentum just as collisions with gas atoms do. In the tube of 3.0 cm diameter, the mean free path for wall collisions may be estimated at 1.5 cm, and the effective speed at $[1.22/(1.5)^{1/2}]\times10^8$ cm sec, whence, due to this cause, $S/\omega = 0.056$. Adding the two dissipation factors we obtain, finally, $S/\omega = 0.090$, a value of the same order as found experimentally. Since the gas density and the electron temperatures change but little with a change in arc current, S/ω should, theoretically, be constant. Aside from experimental errors, which undoubtedly affect the values when R becomes comparable with R_t, that is, above $i_A = 50$ m.a., the non-homogeneity of the plasma may possibly account for a large part of the variation. The high 15-m.a. value may arise from the proximity to the a-type resonance.

[22] T. J. Killian, Phys. Rev. 35, 1238 (1930), Table I.

Expressed as a decrement, δ,

$$\delta = \pi S/\omega$$

whence, theoretically, $\delta = 0.28$ and the amplitude of a free oscillation would decrease by 24 percent per cycle.

The analysis we have made makes it possible to calculate the electric field in the plasma and the amplitude of the electron motions. From Eqs. (16) and (19)

$$E_p/E_e = (K + 1)/(K_p + 1)$$

from which, using Eq. (20), we find

$$E_p/E_e = \frac{K - 1 - \theta(K + 1)}{-2\theta} = \frac{1 - K^{-1} - \theta(1 + K^{-1})}{-2\theta K^{-1}}$$

for the ratio of the field strength in the plasma to that in the composite condenser. Substituting for K from Eq. (33) we have

$$E_p/E_e = \frac{1 - K_0^{-1} - \theta(1 + K_0^{-1}) - j\omega C_0 R(1 + \theta)}{-2\theta(K_0^{-1} + j\omega C_0 R)} \tag{37}$$

or, in absolute magnitude

$$E_p/E_e = \frac{1}{2\theta}\left\{\frac{[1 - K_0^{-1} - \theta(1 + K_0^{-1})]^2 + [\omega C_0 R(1 + \theta)]^2}{K_0^{-2} + (\omega C_0 R)^2}\right\}^{1/2} \tag{38}$$

Now

$$E_e = V/d$$

where V is the condenser voltage and $d(=7$ cm) is the plate separation. Also

$$v = i_c Z_0 \tan l \tag{39}$$

where i_c is the condenser current, and

$$i_c = i_t \cos l \tag{40}$$

where i_t is the thermocouple current, whence it follows that,

$$E_e = (i_t Z_0/d) \sin l \tag{41}$$

The equation of motion of an electron on which Eq. (4) was based is

$$\ddot{\xi} + S\dot{\xi} = (eZ/m)\epsilon^{j\omega t}$$

whence the amplitude of motion is

$$\xi_0 = 2^{1/2} eE_p/m\omega^2(1 + S^2/\omega^2)^{1/2}$$

on the understanding that E_p is the r.m.s. value. In practical units

$$\xi_0 = 2.50 \times 10^{15} E_p/\omega^2(1 + S^2/\omega^2)^{1/2}$$

and for the present case ($\omega = 1.194 \times 10^9$)

$$\xi_0 = 1.75 \times 10^{-3}(1 + S^2/\omega^2)^{-1/2} E_p.$$

Only at $i_A = 15$ m.a. does S/ω make an appreciable contribution to the radical so that throughout most of the range ξ_0 is proportional to E_p. ξ_0 is plotted in Fig. 14 and it is interesting to note that the greatest amplitude was 1/500 cm. For this amplitude the maximum velocity is $\omega/500 = 0.6 \times 10^6$ cm/sec corresponding to a voltage of $10^{-4}v$.

The valley in the ξ_0 curve between 21 and 42 m.a. certainly arises from the effect of the increased resistance near plasma resonance in decreasing the resonant current in the Lecher System.

The values of S/ω given in Fig. 14 are based on simultaneous measurements of tuning length and resistance. But on the assumption of a uniform plasma, the Lecher System characteristic is, by itself, capable of giving a value of S/ω by using either the maximum variation in L_r (Lecher System tuning length) or the change in i_A accompanying this variation. By setting the derivative of Eq. (27) with respect to η (assuming that variations in θ and ϕ are negligible) equal to zero, we obtain the condition for the extreme values of L_r:

$$\eta' = 2\{1 + S^2/\omega^2 \pm [(1 + S^2/\omega^2)^2 - (1 + S^2/\omega^2)]^{1/2}\}. \tag{42}$$

The difference between the values of η' at the extremes of L_r is, therefore,

$$\Delta\eta' = \phi(N_2 - N_1)/N_\omega = 4[(1 + S^2/\omega^2)^2 - (1 + S^2/\omega^2)]^{1/2} \tag{43}$$

Solving for S/ω, noting that $\Delta\eta'^2/4 \ll 1$,

$$S/\omega = \Delta\eta'/4. \tag{44}$$

At plasma resonance, theory (Eq. (17)) requires that

$$\eta' = 2 = \phi N_r/N_\omega \tag{45}$$

where N_r is the electron density at plasma resonance [7.5]. Combining Eqs. (43), (44), and (45) we have

$$S/\omega = (N_2 - N_1)/2N_r \tag{46}$$

or, in terms of arc current

$$S/\omega = (i_{A2} - i_{A1})/2i_{AR} \tag{47}$$

where i_{AR} is the arc current at plasma resonance. The other relation mentioned is

$$S/\omega = [\delta L_\infty/(L_1 - L_2)]\theta\phi_\infty/\theta_\infty\phi \tag{48}$$

and is deduced by eliminating η' between Eqs. (27) and (42).

Applying these to the present case, Fig. 13 gives,

$$S/\omega = (34.5 - 25.)/2 \times 31 = 0.15$$

in the one case and

$$S/\omega = [1.3/(15 - 6.5)] \times 0.79 = 0.12,$$

in the other. These values are roughly twice as large as the maximum values shown in Fig. 14. This fact together with the asymmetry of the resonance characteristic indicates that other factors may be important here. The analysis of Section II shows, for instance, that if frictional factors were absent, the whole spread $\Delta\eta'$ could be due to a 30 percent variation in electron density.

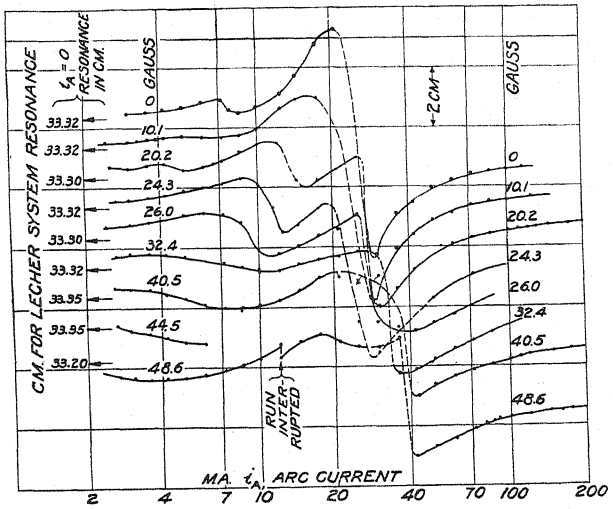

Fig. 15. Effect of transverse magnetic field on plasma-resonance.

IX. The Effect of a Magnetic Field

Appleton and Childs[21] have observed an absorption maximum arising from a constant magnetic field at right angles to the impressed electric field and Benner[23] has observed an accompanying change in dielectric constant. In neither of these cases was the electron density involved as a vital factor. Gutton,[7] however, observed a doubling of the resonance when he applied such a magnetic field to the ionized gas.

Resonance characteristics have been made of the mercury vapor plasma at a succession of magnetic fields. The field used was that from a pair of Helmholtz coils so placed that the oscillating portion of the positive column was in the uniform part of the field. The field was calculated from the coil dimensions as 8.1 gauss·amp.$^{-1}$. The characteristics obtained for a frequency of 1.605×10^9 herz are shown in Fig. 15. The dashed portions of the curves

[23] S. Benner, Die Naturwissenschaften, **17**, 120 (1929).

are those which are doubtful, either because experimental points were not obtained or because the points which were obtained were very uncertain on account of the flatness of the resonance curve. The splitting of the b-type resonance is clearly seen for magnetic field strengths from 20.2 gauss up, until at 48.6 gauss the curve begins to take on a more complicated form, due perhaps to the approach to the purely magnetic resonance of Appleton and Childs and Benner. For the frequency used this would occur with a magnetic field of $H=2\pi mc\nu/e=56.8$ gauss.

The expectation is that the two resonances will lie one to either side of the original. In the figure only the lower current resonance shows displacement for the smaller magnetic fields. This arises from the concentration of the arc by the magnetic field, which results in higher electron densities for the same arc current when the magnetic field is present.

In analyzing these curves we might proceed along the lines already developed, but more insight into the processes involved can be gained by examining the whole phenomena from a less formal point of view.[24]

Consider a uniform plasma bounded by the sheaths on two plane parallel non-conducting boundary walls. A uniform displacement of the electrons by an amount, ξ, throughout the plasma will develop a surface charge density of

$$\sigma_e = Ne\xi$$

at the sheath edge which exerts the restoring force

$$F_p = -4\pi Ne^2\xi$$

on each electron throughout the plasma. The electrons in the plasma are thus capable of free simple harmonic oscillations in accordance with the equation of motion

$$4\pi Ne^2\xi + m\ddot{\xi} = 0$$

whence the natural frequency is that found for plasma-electron oscillations, Eq. (1).

If the plasma is bounded by a cylinder, and the uniform parallel electron displacements are perpendicular to the axis, the restoring force is only

$$F_c = F_p/2 = -4\pi Ne^2\xi/2$$

and if the boundary is spherical

$$F_s = F_p/3.$$

The natural frequency is lowered in these cases, as has already been seen in the analysis of Section IV.

In proceeding to the case of superposed magnetic field, we may denote this shape factor by ϕ,

$$F = -4\pi Ne^2\phi.$$

[24] J. J. Thomson, Phil. Mag., 11, 697 (1931) develops the same viewpoint along somewhat different lines.

This factor may be different in the ξ-direction from what it is at right angles to both this direction and the magnetic field. For instance, taking ξ perpendicular to infinite parallel plane boundaries, $\phi_\xi = 1$, while, introducing ζ for the electron displacement perpendicular to both ξ and H, $\phi_\zeta = 0$. In general, then, both shape factors must be included in the treatment. We have,

$$F_\xi = -4\pi N e^2 \phi_\xi \xi - (eH/c)\dot{\zeta} = m\ddot{\xi}$$

$$F_\zeta = -4\pi N e^2 \phi_\zeta \zeta + (eH/c)\dot{\xi} = m\ddot{\zeta}.$$

Putting $\xi = \xi_0 \epsilon^{j t\omega}$, $\zeta = \zeta_0 \epsilon^{j\omega t}$, $\omega_H = eH/mc = 1.767 \times 10^7 H$, $\omega_0^2 = 4\pi N e^2/m = 3.18 \times 10^9 N$ and eliminating ζ_0 and ξ_0, we have

$$(\omega^2 - \phi_\xi \omega_0^2)(\omega^2 - \phi_\zeta \omega_0^2) = \omega^2 \omega_H^2,$$

as the condition for resonance. For a circular cylinder with axial magnetic field, $\phi_\xi = \phi_\zeta$ from symmetry, so that we may write

$$(\omega^2 - \phi\omega_0^2)^2 = \omega^2 \omega_H^2.$$

Since N was varied in the experiment to obtain resonance, we solve for the two values of ω_0^2, say ω_1^2 and ω_2^2, which satisfy this equation. It is readily found that

$$(\omega_2^2 - \omega_1^2)/(\omega_2^2 + \omega_1^2) = \omega_H/\omega$$

so that, in terms of arc currents at resonance, i_{A1} and i_{A2},

$$(i_{A2} - i_{A1})/(i_{A1} + i_{A2}) = \omega_H/\omega.$$

Table II based on Fig. 15 shows the agreement between calculated and observed resonance behavior. Columns 4 and 5 should agree. The bad discrep-

TABLE II. *Analysis of magnetic effect.*

H, (gauss)	0	10.1	20.2	24.3	26.0	32.4	40.5	44.5	48.6
i_{A1}, (m.a.)	25	22?	13	11	9	7?	4.5?	3.5?	2.
i_{A2}, (m.a.)			27	22	27	32	37		37?
$\frac{i_{A2}-i_{A1}}{i_{A2}+i_{A1}}$			0.35	0.33	0.50	0.64	0.78		0.90
ω_H/ω			0.35	0.43	0.46	0.57	0.71		0.85

ancy at 24.3 gauss is doubtless due to an erroneous determination of the 25-m.a. resonance on that curve, since this curve fails to fall in line with thetrend of all the others here. Otherwise the agreement is reasonably good.

THE ULTRAVIOLET ABSORPTION SPECTRUM OF SULFUR DIOXIDE

By William W. Watson and Allan E. Parker
Sloane Physics Laboratory, Yale University

(Received April 27, 1931)

Abstract

Measurements of spectrograms of the ultraviolet SO_2 absorption bands taken at different pressures, tube lengths and temperatures together with known infrared and Raman frequencies serve to locate the three fundamental vibrational series. Tables giving the band assignments to these sequences are included. The three lower state frequencies for infinitesimal amplitude are 1369, 1164 and 610 cm^{-1}, while for the excited state the corresponding frequencies are 341, 387 and 290 cm^{-1}. The types of addition series are discussed.

The excited state $\Delta\nu_v$:v curves for $v<4$ have a positive slope, while for $v>4$ there is a sudden reversal to the usual negative anharmonic coefficient. The three ground state frequencies indicate a value of 34° for the half-angle at the apex of the SO_2 triangular model. Comparisons of the heats of dissociation estimated from the extended areas under the $\Delta\nu_v$:v curves with thermal and spectroscopic data suggest the process $SO_2 \rightarrow S+O_2$ for the two symmetrical vibrations and $SO_2 \rightarrow SO+O$ for the asymmetrical vibration. The dissociation products appear to be the same in the two electronic states.

Introduction

UP TO the present time there has been but very little investigation of the details of the ultra-violet band systems of triatomic molecules. Great advances have been made in the study of diatomic molecular spectra with the aid of the quantum theory, but owing to their quite evident complexity, the spectra of polyatomic molecules have been avoided. Many of the ideas of molecular dynamics developed for diatomic molecules should be applicable to more complex molecules, however, and in addition there is now available much information on the fundamental vibrational frequencies of these molecules from their infrared and Raman spectra. Without this previous knowledge of the three fundamental frequencies of the ground state for molecules such as SO_2 and CS_2, the vibrational quantum analysis of their complex electronic band systems would be all but impossible.

The infrared vibration-rotation absorption bands of sulfur dioxide have recently been measured by Bailey, Cassie, and Angus.[1] Their work shows that the three fundamental bands are at 1361 cm^{-1}, 1152 cm^{-1}, and 606 cm^{-1}, but since a sufficient number of harmonic bands were not observed, the fundamental frequencies for infinitesimal amplitude of vibration could not be computed. The first and third of these frequencies correspond to a vibrating electric doublet lying along the bisector of the vertical angle of the triangular structure, while the middle frequency corresponds to an effective electric

[1] C. R. Bailey, A. B. D. Cassie, and W. R. Angus, Proc. Roy. Soc. A130, 142 (1930).

doublet in a direction perpendicular to this bisector and in the plane of the triangle. Both the existence of a rather large permanent dipole moment and the indicated structure and intensity of these infrared bands lead to the conclusion that the SO_2 molecule is definitely triangular in shape with an acute angle at the apex. The Raman spectrum of gaseous SO_2 has been investigated by Bhagavantam[2] who found but one line at 1154 cm^{-1}, whereas for liquid SO_2 Dickinson and West[3] find the three lines 1145.9 cm^{-1} (strong), 1340.1 cm^{-1} (medium, diffuse) and 524.3 cm^{-1} (weak, diffuse). The last line is explained by Bailey, Cassie, and Angus as the difference 1152–606.

The ultraviolet absorption bands of sulfur dioxide have been referred to by Henri[4] and others. The apparent predissociation limit at about λ 2525 (112,000 cal.) has been assumed by Henri[5] to correspond to $SO_2 \rightarrow SO + O$, and on this basis he develops an energy equation with other known data to give the heat of dissociation of O_2 as 126,400 cal. (5.5 volts). This calculation has been discussed by Herzberg[6]; and we return to the question in our discussion below.

Description of Spectrum

The ultraviolet absorption band systems of sulfur dioxide have been photographed with a Hilger E_1 quartz spectrograph, the gas being contained in a glass absorption tube 111 cm long, closed at the ends with quartz windows. The SO_2 was prepared by dropping HCl on to $NaHSO_3$, and was dried by passing through a long P_2O_5 tube. The source of continuous radiation for the background was the usual hydrogen discharge tube. The spectrograms with this 111 cm absorption cell were all taken with the gas at room temperature and at pressures varying from 80 cm to less than 1 mm Hg. Spectrograms were also obtained with a 27 cm absorption cell with the SO_2 at 1 cm Hg pressure and at the temperature of a solid CO_2-acetone mixture.

Fig. 1 is a reproduction of a series of spectrograms taken at various gas pressures with the longer absorption tube. To be noted are the evident strong series of band groups in the main absorption region, and the appearance of new bands at the long wave-length end at the higher pressures. These latter bands do not form a separate band system, as has been suggested by Henri[5]; but are associated with the main absorption system and represent transitions from vibrational levels with $v = 1$, 2 and 3 of the ground electronic state. At the lower temperature the very weak band at 30961 cm^{-1} is clearly the band of longest wave-length, suggesting that it is a 0,0 band, and there is considerable simplification in the region of strongest absorption. At the high frequency end of this system, absorption ceases at the lower pressures at about λ2500, the last bands being rather diffuse but with no continuous absorption in evidence. Another SO_2 band system which we have not investigated extends from about λ2350 farther into the ultraviolet. At pressures greater than

[2] S. Bhagavantam, Nature **126,** 995 (1930).
[3] R. G. Dickinson and S. S. West, Phys. Rev. **35,** 1126 (1930).
[4] V. Henri, Structure des Molecules.
[5] V. Henri, Nature **125,** 272 (1930).
[6] G. Herzberg, Zeitz. f. Physikal. Chemie **B10,** 189 (1930).

1 cm these two band systems are fused together, the absorption being continuous from the limit of the discrete bands to be seen in Fig. 1 to some point in the vacuum ultraviolet region.

Some of the stronger and more isolated bands at about λ3300 were photographed at high dispersion with a 21-foot concave grating, but these spectrograms fail to resolve any of the rotational structure. Furthermore these SO_2 bands do not have a sharp head, but rather seem to fade out on both sides. In the measurement of the lower dispersion spectrograms, then, we could only set the cross-hair on the estimated center of the band or, in the case of broad bands produced by overlapping, the overall width was measured. This of

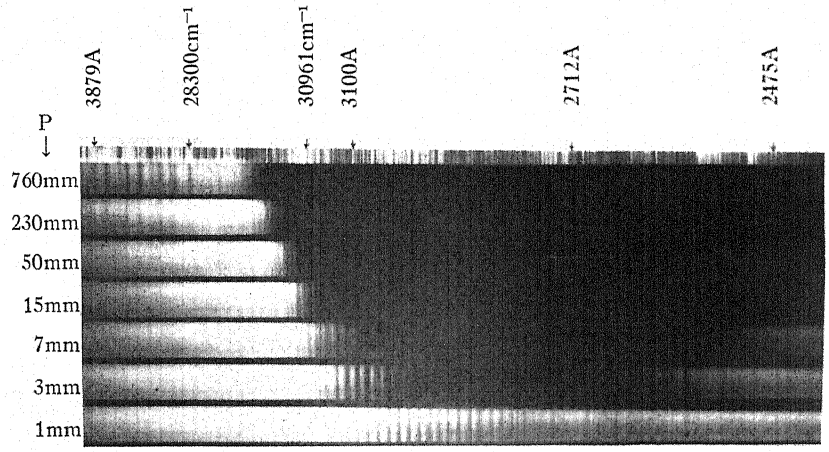

Fig. 1. Spectrograms of the ultraviolet SO_2 absorption bands taken with the Hilger E_3 spectrograph. The absorption path was 1 m, and the pressures were as indicated. To be noted are the group of bands at the red end of the high pressure spectrograms and the evident excited state sequences proceeding towards higher frequencies from 30961 at the lower pressures. Higher dispersion plates show that many of these apparently single bands are in reality groups of bands.

course limits the accuracy of the measurements, and entails a possible error in the interval between any two successive bands in the series referred to below, of say, 9 or 10 cm^{-1}.

Vibrational Analysis

The regular and intense series of bands observable in the region from λ3200 to λ2900 on the spectrograms for the lowest SO_2 pressures can only be vibrational sequences in the excited electronic state. These and other series terminate on the long wave-length end at about λ3230 in a region of bands of very low intensity, suggesting that the origin of the system is at about this frequency. Now in the high-pressure group to the red of this point the first strong band to appear with increasing gas pressure is at 28300 cm^{-1}. Assuming that this represents a transition from a lower vibrational level other than 0 of the symmetrical mode of vibration, another band is found at 29621, 1321 cm^{-1} to the high frequency side, from which the interval to 30961, which is the

long wave-length end of the strongest excited state sequence, is 1340 cm^{-1}. From these regularities as a starting point, the double array of bands originating in this (v_1', v_1'') mode of vibration as presented in Table I were found. Measurement towards the violet from the 28,300 band with differences characteristic of the asymmetric mode of vibration (1150 cm^{-1}), however, does not produce any correlation.

TABLE I. *Fundamental series corresponding to the* 1369 cm^{-1} *vibration.*

v_1' \ v_1''	0	1	2	3	Average $\Delta\nu$
0	30961	29621	28300	27002	
					360
1	31327	29979		27359	
					389
2	31719	30365	29043		
					430
3	32145	30801	29472		
					471
4	32619	31270	29942		
					487
5	33103	31757	30432		
					468
6	33571	32230	30895		
					458
7	34026	32683	31361		
					434
8	34461	33118	31793		
					424
9	34888	33539	32218		
					423
10	35318	33969	32638		
					420
11	35738	34390	33058		
					390
12	36130	34774	33451		
					384
13	36514	35156	33836		
					362
14	36876	35522	34193		
					354
15	37230				
					344
16	37574				
					329
17	37903				
Average $\Delta\nu$		1348	1326		

It was then to be assumed that the next strongest series of bands proceeding to the high frequency side of the origin is the $v_2''=0$ sequence belonging to the asymmetrical (1150 cm^{-1}) vibrational frequency. There is indeed a band at about this interval on the red side of each of these bands of the $v_2''=0$ sequence, and in this way the fundamental sequences given in Table II were developed. Now it is impossible to have these two double arrays of bands proceed from the same 0,0 band, although they must correspond to the same electronic energy change in the molecule. But if the two sets of frequencies are represented by an equation such as (1) with half-integral vibrational quantum numbers, they both yield the same electronic frequency $\nu_e=31468$.

TABLE II. *Fundamental series for the* 1164 cm^{-1} *vibration.*

v_2'' / v_2'	0	1	2	Average $\Delta\nu$
0	31074	29932	28802	413
1	31498	30343	29208	435
2	31928	30779	29648	462
3	32393	31241	30108	475
4	32865	31719	30584	454
5	33324	32169	31036	456
6	33771	32628	31498	433
7	34210	33058	31929	432
8	34634	33491	32367	413
9	35048	33901	32781	401
10	35438	34312	33183	
Average $\Delta\nu$	1148	1130		

TABLE III. *Fundamental series for the* 606 cm^{-1} *vibration.*

v_3'' / v_3'	0	1	2	3	Average $\Delta\nu$
0	31308	30700	30103	29499	298
1	31607	30999	30394	29798	303
2	31910	31298	30700	30103	308
3	32218	31607	31008	30412	298
4	32513	31907	31308		285
5	32797	32193	31592	30999	272
6	33071	32463	31864	31270	254
7	33328	32719	32116	31521	253
8	33578	32977	32367		228
9	33802	33204	32601		221
10	34026	33423	32820		215
11	34242	33640	33037		207
12	34449	33846	33246		181
13	34634	34026	33423		169
14	34805	34193	33591		170
15	34971	34367	33759		
Average $\Delta\nu$	605.5	601	596		

This affords experimental proof of the existence of zero-point vibrational energy. It is therefore not possible to represent these SO_2 bands by a double vibrational formula such as found by Henri and Howell[7] for the ultraviolet absorption bands of phosgene.

Knowing the ν_e frequency and the third fundamental vibration frequency 606 cm^{-1}, for the lowest electronic state, it was possible to predict the 0,0 band frequency for this mode of vibration to within about 100 cm^{-1} by assuming that the corresponding excited state frequency must lie within the limits 150 to 350 cm^{-1}. Investigation showed that for but one band, 31308, in this predicted interval did another band lie 606 cm^{-1} to the red with still another spaced 600 cm^{-1} further to the red. Placing this 31308 in Eq. (1) with $v_3'=v_3''=0$ the excited state vibrational interval was computed to be very closely 300 cm^{-1}. This proved to be correct, and the other bands in this third double array as given in Table III were easily arranged. This $v_3''=0$ sequence is not obvious from inspection of the spectrograms as for the other two $v''=0$ sequences. However, this is in agreement with the fact that the 606 cm^{-1} fundamental absorption band in the infrared is much weaker than the other two.[1]

These three sets of fundamental vibration progressions can be represented by an equation of the type

$$\nu = \nu_e + [a'(v'+\tfrac{1}{2}) + b'(v'+\tfrac{1}{2})^2] - [a''(v''+\tfrac{1}{2}) + b''(v''+\tfrac{1}{2})^2] \quad (1)$$

with $\nu_e=31468$. For all three sets of progressions, however, the excited state differences first increase to a maximum at about $v'=4$, after which they decrease in the regular manner (see discussion below). It is therefore necessary to use different a' and b' constants for the low and high values of v'. The mean values of the a and b constants which fit the three sets of band progressions are given in Table IV.

TABLE IV. *Fundamental vibrational constants for SO_2 (cm^{-1} units).*

	v_1	v_2	v_3
a''	1369	1164	610
b''	−11	−9	−2.3
a'	+341	+387	+290
b'	+14 } $v_1 \leqq 4$	+12 } $v_2 \leqq 3$	+3 } $v_3 \leqq 3$
a'	+556	+524	+350
b'	−7 } $v_1 > 4$	−6 } $v_2 > 3$	−7 } $v_3 > 3$

All of the sequences in Tables I to III could be extended farther towards higher frequencies, but our accurate measurements do not extend into this region. However, it is obvious that these series account for only some 20 percent of the observed bands of which there are well over six hundred. Now only three fundamental frequencies are possible for a triatomic molecule, but we know from the study of the infrared bands of polyatomic molecules that addition frequencies occur. We have made plausible assignments of most of the

[7] V. Henri and O. R. Howell, Proc. Roy. Soc. **A128**, 192 (1930).

remaining bands to various forms of addition series based on the three fundamental series, but these assignments are not unambiguous in many cases because of the density of bands and because of the lack of any guide such as the greater intensity of the $v''=0$ sequences of the main series. Our analysis shows however that there are addition bands present of the type for which addition of one or two quanta of any one of the three modes of vibration happens simultaneously in both electronic states to either of the other two main series. Some of the weaker bands are probably also due to an S isotope effect, but we have not been able to make any assignments on this basis.

Discussion of Results

Fig. 2 is a plot of the course of the vibrational energy level differences in the three sets of excited state levels as a function of v. The unusual feature of these curves is the initial positive slope. During the accretion of these first

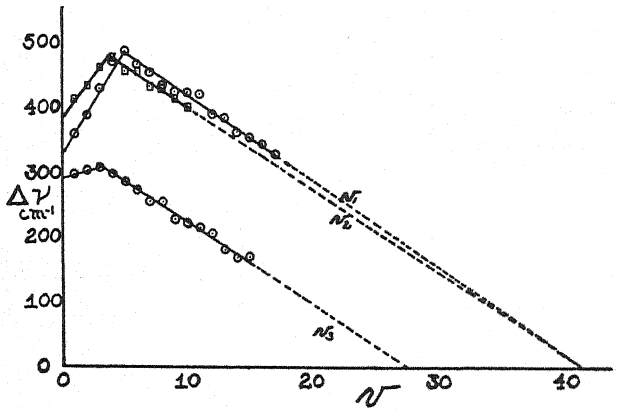

Fig. 2. Diagrams of the spacings of the excited state vibrational levels for the three fundamental modes of vibration. The interesting feature is the initial positive slope for each of the curves.

quanta of vibrational energy, the molecule, as it were, increases in stability, and then some rearrangement occurs after which the usual negative anharmonic term is operative. This phenomenon has been noted in only one instance for diatomic molecules, in the LiH spectrum[8]; but it is possibly of rather common occurrence for polyatomic molecules.[9]

In the ground electronic state of SO_2 the vibrational frequencies decrease in the usual manner with increasing v''. But since this spectrum originates in absorption by a cold gas, only the levels $v''=0$, 1 and 2 are represented. The anharmonic coefficients b can therefore not be determined with great accuracy, but they do allow an approximate determination of the vibrational

[8] G. Nakamura, Zeits. f. Physik 59, 218 (1930)

[9] Positive slopes of the $\Delta\nu:v$ curves, but without the maximum and subsequent negative slope, have been reported by H. D. Smyth and T. C. Chow (Abstract, Phys. Rev. 37, 1023 (1931)) for CO_2 and by G. B. Kistiakowsky (Phys. Rev. 37, 276, 1931) for C_2H_2.

frequencies for infinitesimal amplitude (the a'' constant in Eq. (1)) which could not be computed from the infrared absorption data.[1] Substitution of these three a'' frequencies in the determinant equation for the vibrational energy of a symmetrical triatomic molecule as given by Dennison[10], yields for α the half-angle at the apex of the isosceles triangle (cf. Fig. 3), the approximate values of 34° and 51°. Owing to the intensity relations in the infrared bands requiring an acute angle,[1] the lower of these two values is to be chosen. The vibrational frequencies a' of the excited state, however, give only imaginary solutions for this angle when placed in this equation.

Some conception of the values of the heats of dissociation for the SO_2 molecule can be obtained from the determination of the areas under the $\Delta\nu_v : v$ curves extrapolated to the convergence limit. The areas under the extrapolations are a rather large part of the whole energy, thereby limiting the accuracy of the calculation. This is particularly true of the lower electronic

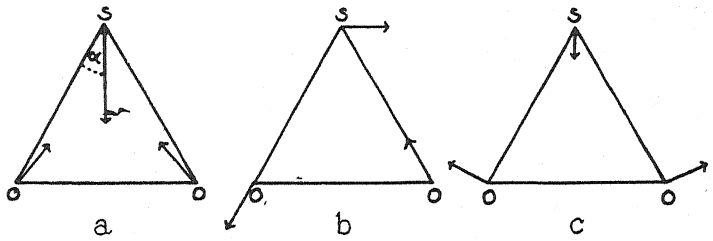

Fig. 3. Representation of the three fundamental SO_2 vibrations. *a*, the symmetrical 1369 cm^{-1} frequency; *b*, the asymmetrical 1164 cm^{-1} frequency; *c*, the symmetrical 610 cm^{-1} frequency. These three frequencies indicate α to be approximately 34°.

state values, but nevertheless the results of the computation are of some interest. One obtains the following heats of dissociation (excited state values are the sum of the areas under the curves of Fig. 2 and $\nu_e = 3.9$ volts):

Lower state:	$H_{v_1} = 5.3$	volts	(121,000 cal.)
	$H_{v_2} = 4.7$	"	(107,000 cal.)
	$H_{v_3} = 5.1$	"	(118,000 cal.)
Excited state:	$H_{v_1} = 5.2$	"	(120,000 cal.)
	$H_{v_2} = 5.3$	"	(121,000 cal.)
	$H_{v_3} = 4.3$	"	(99,000 cal.)

We picture the vibrations occurring after the manner of Fig. 3. For the two symmetric modes of vibration the dissociation products would be an S atom plus an O_2 molecule. One might expect a measure of agreement between these values and that obtained from thermal data. The heat of formation of SO_2 from sulfur vapor S_2 and O_2 is given as 69,260 calories. The heat of dissociations of S_2 is known from spectroscopic data to be 102,200 calories.[5] Hence

[10] D. M. Dennison, Phil. Mag. **1**, 203 (1926).

$$SO_2 \rightarrow \tfrac{1}{2}(S_2) + O_2 - \frac{102200}{2} - 69260 = \tfrac{1}{2}(S_2) + O_2 - 120360.$$

The agreement with our lower state H_{v_1} and H_{v_3} values is better than could be expected.

For the asymmetric mode of vibration the dissociation is probably into SO+O. Now the heat of dissociation of SO has been determined for the normal state of the ultraviolet SO band system by Henri and Wolff[11] as 148,000 cal. The value for O_2 should be approximately 5.1 volts.[6] Therefore one can write the energy equation

$$SO_2 \rightarrow SO + O - H_{v_2} = S + O + O - 148,000 - H_{v_2}$$
$$= \tfrac{1}{2}(S_2) + O_2 - 69260 - \frac{102200}{2} - 117300.$$

This requires H_{v_2} to be about 90,000 cal. as against our value of 107,000 cal. The discrepancy may be in part due to the fact that the SO radical after the dissociation has a considerable amount of vibrational energy. In fact, the distortion in the dissociation process should most certainly produce some vibration of the SO, the energy of which should be subtracted from our extrapolated H_{v_2} value to give the true heat of dissociation.[12]

Judging from the relative values of the computed heats of dissociation for the two electronic states of SO_2 involved, apparently the dissociation products are in both states the same. But because of the possibility of a considerable error in these values due to the large extrapolation, this statement should be made with reservations.

A considerable amount of information may be expected from the study of the ultraviolet band systems of the simpler polyatomic molecules. When the bands have sharp heads, as for example in the CS_2 system on the analysis of which we are now engaged, the accuracy of the measurements can be considerably improved. For absorption bands the rotational fine structure may not be resolvable even at the highest dispersion. But if obtained as emission bands, the theoretical resolving power of a large grating can be more nearly approached, and the rotational line pattern of some of the simpler polyatomic bands may be obtained. In that event the needed test of the theoretical treatment of the rotator with three different moments of inertia as given by Kramers and Ittmann[13] and others may be made.

[11] V. Henri and F. Wolff, Jour. de Phys. et Rad. **10,** 81 (1929).

[12] R. M. Badger and J. L. Binder, Phys. Rev. **37,** 800 (1931) have suggested this explanation for a similar discrepancy in the case of the HCN infrared bands.

[13] H. A. Kramers and G. P. Ittmann, Zeits. f. Physik **58,** 217 (1929).

FURTHER STUDY OF THE ABSORPTION OF INFRARED RADIATION BY WATER VAPOR

By E. K. Plyler and W. W. Sleator
University of Michigan

(Received April 8, 1931)

Abstract[1]

Making use of a spectrometer with a salt prism and echelette gratings, and a Moll thermal relay, the authors have reexamined with increased resolution the four absorption bands of water vapor whose centers lie near 1.87μ, 2.66μ, 3.15μ and 6.26μ. The new study has greatly increased the number of measured lines. Near 6.26μ and 3.17μ the number has been more than doubled. The new lines are mostly weak ones, but the work has resulted in a better determination of the wave-lengths of many strong lines, which now appear as sharp single effects freed from the former confusion in which several lines were taken for one. The center of the harmonic of the band at 6.26μ is seen to be better placed at 3.168μ than it was formerly at 3.11μ. It also appears that this band has no absorption at the center, and is of the same type as the fundamental.

Introduction

THE work to be described in this paper was done at the University of Michigan during the summers of 1928, and 1929, and the fall of 1930. It was found, after working over the atmospheric absorption near 2.66μ, that the apparatus now available, because of the higher resolution of which it is capable, permitted a more precise and complete analysis of the absorption spectrum of water than had been given in the papers by Sleator[2] and Sleator and Phelps.[3] A real advance may be claimed when what was formerly considered to be, and measured as, a single line, proves, as the present work in many cases shows, to consist of three or four. Furthermore many of the lines now given in the charts and tables are very sharp, and many more lines show in these figures quite the same shape, and this indicates that they are single effects, and not likely to break up on more refined analysis. On account of this better identification, and on account of more accurate calibration now employed, there is reason to think that the wave-lengths here given are more precise than the earlier numbers, which they should supplant.

Of the bands here studied, those near 6.26μ and 2.66μ have been classified as fundamentals, with vibration frequencies ν_1 and ν_2 respectively, the latter having a zero branch, the former being double. The frequency at 1.87μ represents the combination $\nu_1+\nu_2$ and that at 3.16μ is $2\nu_1$, so that this band is the first harmonic of that at 6.26μ. A classification of the known absorption bands of water has been given by Hettner.[4]

[1] This abstract appeared in the Bulletin of the American Physical Society of November 15, 1930, announcing the Chicago Meeting.

[2] W. W. Sleator, Astrophys. J. **48**, 125 (1918). References to earlier work are given in this paper.

[3] W. W. Sleator and E. R. Phelps, Astrophys. J. **62**, 28 (1925).

[4] G. Hettner, Zeits. f. Physik **1**, 345 (1920).

Experimental Procedure

The apparatus used was the compound spectrometer with sodium chloride prism and grating in series, of the type commonly used for work in the infrared, constructed and described by Meyer.[5] The grating used for the band at 6.26μ had 2,880 lines per inch, that employed for the others had 7,200. They were ruled by Barker. The thermopile was constructed and has been described by Firestone.[6] By adjusting the lamp which illuminates the thermocouple in the Moll relay the amplification factor could be controlled, and could be brought up to 300 by using a current of 3.5 amperes. At this amplification Brownian motion could be observed, so that four or six, sometimes eight, independent deflections of the galvanometer were taken at each setting of the grating. Small vibrations of the building due to the wind and other things affected the galvanometer. It was necessary to take most of the readings at night.

The spectrometer circle was set at a certain angle, then the deflections were read, then the circle was turned 15 seconds, and deflections taken again. This was continued through the region—that at 6.26μ extended over about 6 degrees. The graph which revealed the absorption lines was plotted with average deflection as ordinate, and angle or wave number as abscissa. The determination of the wave-length of a line depends in most cases upon three independent energy curves—in some cases more.

The step by which the circle was advanced between successive galvanometer readings was less than the angular value of the slit itself. In Table I, the data of which are given separately with the different figures, the degree of resolution used in the different bands is shown by giving the wave-length interval included in the second slit. Values used by Sleator and Phelps are shown for comparison.

Table I. *Effective resolving power.*

Region	Slit width (A.U.)	Slit width (cm^{-1})	Slit width (Sleator and Phelps) (A.U.)
1.87μ	4.1	1.16	8
2.66μ	3.1	0.44	
3.15μ	4.5	0.45	32
6.26μ	17.	0.45	80

The observations in this work were made upon the absorption by the water vapor in the air of the room. For the bands at 1.87μ and 3.16μ the absorption did not anywhere exceed forty percent, and it was not necessary to remove any moisture. In the other bands, however, there were very strong lines which could not be separated. In order to reduce the amount of water present a rough box was built around the spectrometer and phosphorus pentoxide was exposed inside. The effect of such drying is shown, for example, by the

[5] Aaron Levin and Charles F. Meyer, J.O.S.A. and R.S.I. **16**, 137 (1928).
[6] F. A. Firestone, Rev. Sci. Inst. **1**, 630 (1930).

inserted sections near line No. 177 in the curve of Fig. 5. Drying the air made it possible to separate and identify the lines. The pressure of water vapor in the undried air was 20 to 30 mm. In the dried air it was 2 to 3 mm. Fig. 3 also represents the energy curve near 2.66μ with dried air. Lines nos. 22, 23 and 24, for example, are better defined in this figure than in Fig. 2, which refers to the normal indoor atmosphere.

Results and Discussion

The measurements made during this work appear in the curves of the following figures, and in the tables. The tables show an arbitrary number for each line, and its relative intensity, wave-length, and wave-number. The relative intensities represent estimates only, based upon the depth of the lines. In many cases this estimate has been difficult and uncertain, because a certain line may represent only a weak absorption upon the side, so to speak, of a deeper and wider line, or it may represent a stronger effect if its neighbor is in fact a weaker one. Line number 35 in Figure 3, for example, has been assigned a relative intensity of 50 percent. But if it is really only a nick in the curve which shows No. 36 it ought to be marked, perhaps, 15 percent. In all cases where two lines over-lap there is doubt about the intensity of each. This composite effect, which partly disappeared when the air was dried, made it impossible to use the criterion of the area of the notch for estimating intensity. Improvement of the present analysis of the water spectrum demands first of all an enclosed spectrometer and absolute control of the amount of the absorbing medium. Second, it demands a resolution even higher than we could command.

When the amount of moisture was reduced by the means described, many lines in all the bands were made more narrow and sharp. On advancing the circle 15 seconds, the galvanometer deflection changed in may cases by 40 mm—say from 100 to 60. An error of 5 seconds in setting might affect the deflection by 15 mm. This unavoidable uncertainty of perhaps 5 seconds in setting may account for the difference in relative intensities of two lines as they appear in different curves, so that in one graph a is stronger than b, in another not so strong.

Figure 1 and Table II represent our study of the band at 1.87μ. Many new lines have appeared, for example line No. 48 in Fig. 5 of the paper of 1925 seems now to be a composite effect of those numbered 81, 82, and 83. There is no way of deciding what wave length, with the amount of water uncontrolled, such a combination ought to have. Accordingly there is no satisfactory basis for comparison of wave-lengths. In general, however, the new values are larger.

It may be remarked here that the numbers assigned to the lines are arbitrary. Also we have omitted numbers from all the tables at places where there are faint lines of uncertain positions, to which we cannot assign definite wave lengths.

In work done at Johns Hopkins University by Barnes[7] the energy of a

[7] R. Bowling Barnes, Phys. Rev. **36**, 296 (1930).

source of radiation was mapped in the region between 3 and 4μ. It shows two bands of atmospheric absorption, one of them with center near 3.73μ. With

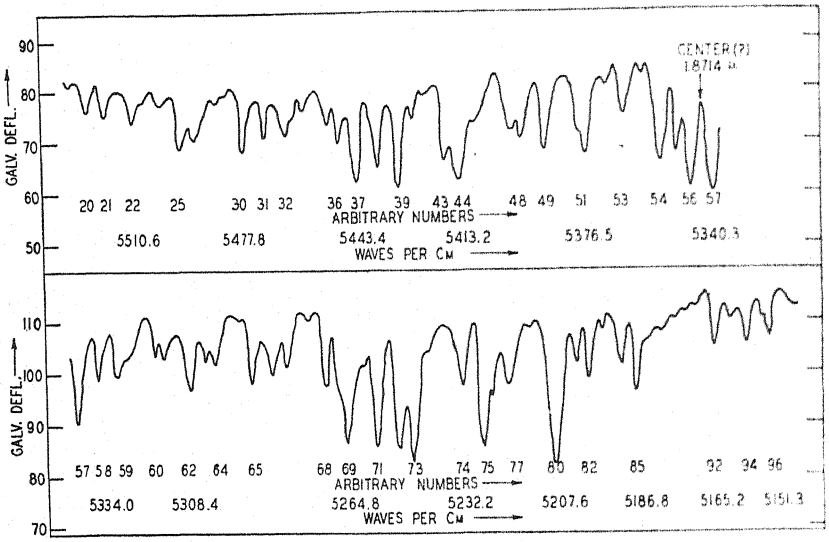

Fig. 1. Energy curve, region of 1.87μ, middle part. Echelette grating, 7200 lines per inch. Slits 0.12 mm, 12.4 secs, 1.16 waves per cm, 4.1A.

TABLE II. *Region of* 1.87μ.

Arbitrary numbers, relative intensities, wave-lengths, and wave-numbers of the stronger lines.

Line No.	Rel. int.	Wave-length	Wave-number	Line No.	Rel. int.	Wave-length	Wave-number
20	10	18100	5524.9	57	35	18725	5340.5
21	10	18117	5519.7	58	20	18747	5334.2
22	10	18146	5510.8	59	20	18769	5327.9
24	5	18174	5502.4	60	10	18801	5318.9
25	15	18194	5496.3	61	10	18811	5316.0
26	15	18209	5491.8	62	15	18837	5308.7
28	5	18229	5485.8	63	10	18851	5304.8
30	15	18255	5477.9	64	10	18865	5300.8
31	10	18278	5471.1	65	15	18900	5291.0
32	10	18300	5464.5	66	15	18920	5285.4
34	5	18318	5459.1	67	15	18934	5281.5
35	10	18342	5452.0	68	15	18974	5270.4
36	10	18352	5449.0	69	25	18994	5264.8
37	25	18370	5443.7	71	25	19025	5256.2
38	20	18392	5437.1	72	25	19048	5249.9
39	25	18412	5431.2	73	30	19063	5245.8
40	5	18428	5426.5	74	15	19112	5232.3
43	15	18459	5417.4	75	25	19132	5226.8
44	25	18473	5413.3	77	15	19158	5219.8
47	10	18525	5398.1	80	30	19202	5207.8
48	15	18535	5395.2	81	10	19225	5201.5
49	20	18557	5388.8	82	15	19235	5198.9
51	25	18599	5376.6	84	10	19269	5189.7
53	15	18636	5366.0	85	15	19279	5187.0
54	30	18672	5355.6	92	10	19360	5165.3
55	25	18688	5351.0	94	10	19391	5157.0
56	30	18703	5346.7	96	10	19412	5151.5

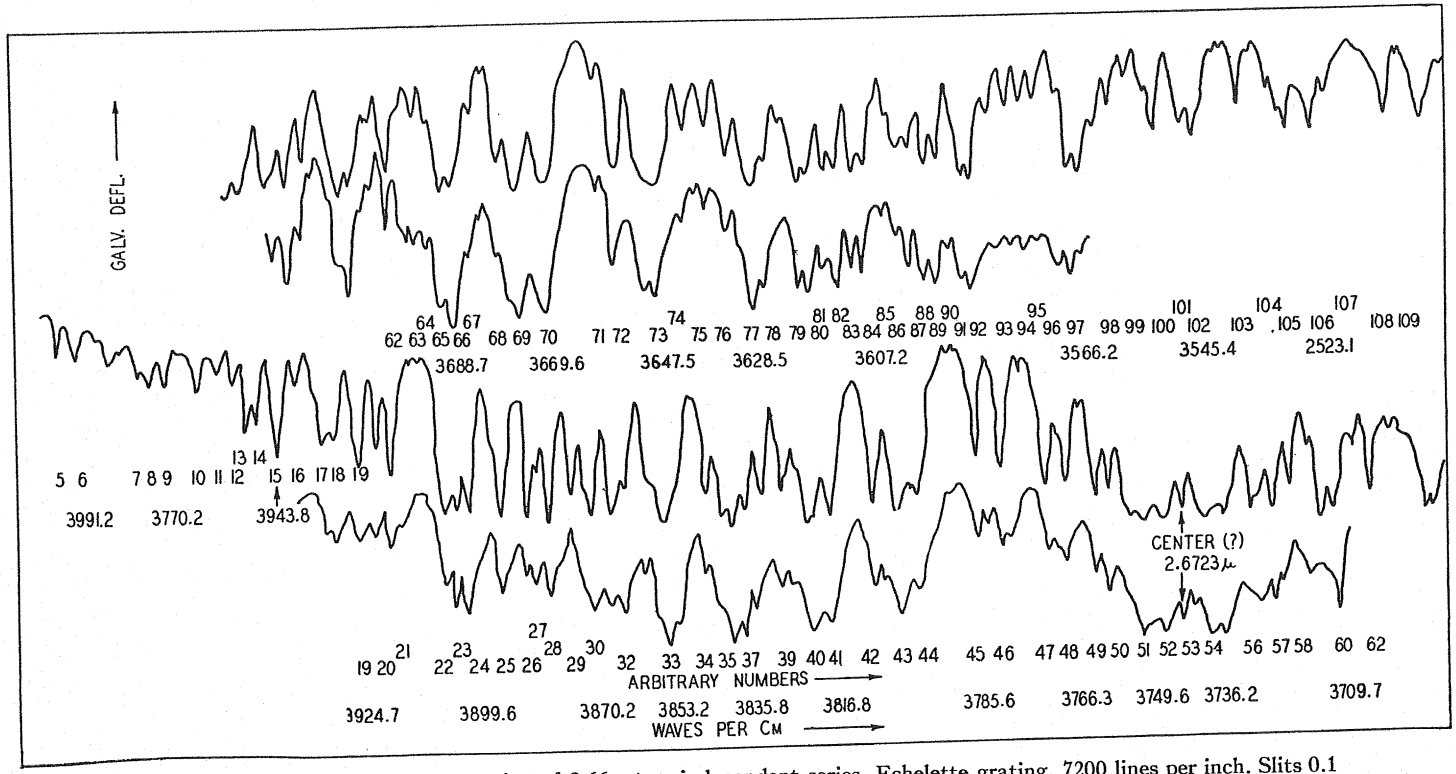

Fig. 2. Part of the energy curve, region of 2.66μ, two independent series. Echelette grating, 7200 lines per inch. Slits 0.1 mm, 10 secs, 0.44 waves per cm, 3.1A.

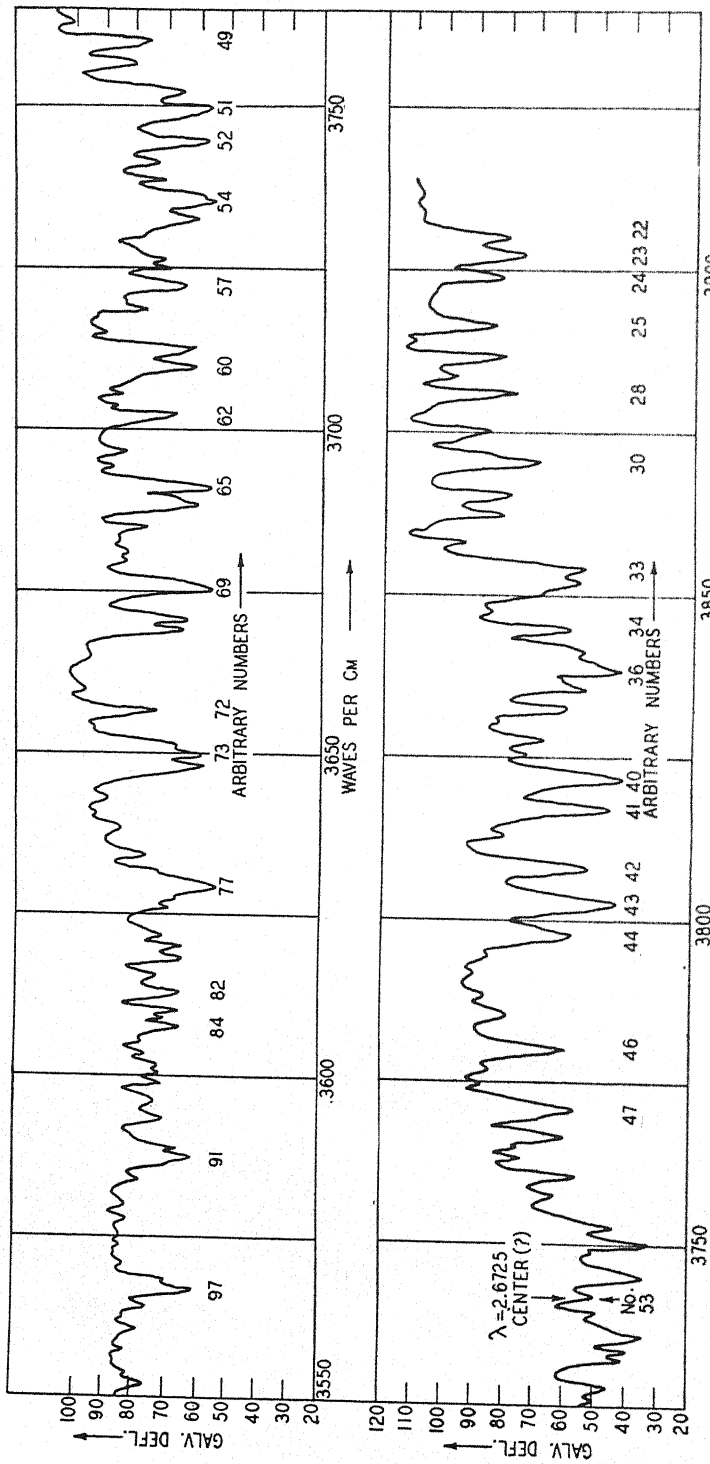

Fig. 3. Energy curve, part of the region of 2.67μ, on frequency scale. Air partly dried. Echelette grating, as in Fig. 2.

the prism-grating spectrograph we have carefully gone over part of this region, having the prism so placed that there was no deflection when the grating was set for 1.9μ. No absorption lines were to be found, though the slits were certainly narrow enough to show them. If certain wave-lengths given in Table II, beginning with No. 26, are multiplied by 2, the products agree remarkably well with many of the wave-lengths given by Barnes. Some of his numbers represent a good mean of adjacent wave-lengths, doubled. For example for line No. 26, 2λ is 3.6418μ. Barnes lists 3.642. Also if one compares the graph under consideration with that for the region near 1.87μ given in Fig. 4 of the paper of 1918 (reference 2) they appear very much alike. The work of Barnes was done with a grating and an infrared filter. It may be that the atmospheric absorption appearing at 3.75μ in Figs. 4 and 5 of that paper is a second order effect due to an overlapping of spectra.

In Figs. 2 and 3 and Table III are given our results for the region of 2.67μ, a fundamental band having a zero branch—showing at any rate strong absorption in the middle portion. Of the two curves in Figure 2 there is less moisture represented in the lower. For Fig. 3 there is less vapor still, and there is less overlapping and general confusion of the lines. For example, line No. 70

TABLE III. *Region of* 2.67μ.

Arbitrary numbers, relative intensities, wave-lengths and wave-numbers of the stronger lines.

Line No.	Rel. int.	Wave-length	Wave-number	Line No.	Rel. int.	Wave-length	Wave-number
1	15	24714	4046.3	29	60	25806	3875.1
1a	5	24795	4033.1	30	80	25838	3870.3
2	10	24834	4026.7	31	70	25869	3865.6
3	6	24871	4020.7	32	20	25892	3862.2
3a	5	24924	4012.2	33	80	25948	3853.9
4	10	24942	4009.3	33a	80	25959	3852.2
5	12	25027	3995.7	34	40	26010	3844.7
6	12	25055	3991.2	35	50	26031	3841.6
7	8	25103	3983.6	36	80	26049	3838.9
7a	6	25147	3976.6	37	20	26070	3835.8
8	12	25155	3975.4	38	50	26090	3832.9
9	12	25187	3970.3	39	40	26124	3827.9
10	15	25235	3962.8	40	85	26166	3821.8
11	6	25256	3959.5	41	80	26198	3817.1
12	10	25289	3954.3	42	75	26261	3807.9
13	30	25309	3951.2	43	85	26298	3802.6
14	20	25327	3948.4	44	55	26332	3797.7
15	40	25356	3943.8	45	55	26415	3785.7
16	12	25379	3940.3	46	60	26454	3780.1
17	40	25427	3932.8	46a	5	26493	3774.6
18	20	25442	3930.5	47	70	26521	3770.6
19	5	25479	3924.8	48	70	26550	3766.5
20	40	25506	3920.7	48a	10	26570	3763.6
21	55	25527	3917.4	49	75	26594	3760.2
22	50	25610	3904.7	50	50	26612	3757.7
23	65	25624	3902.6	50a	20	26647	3752.8
24	65	25644	3899.5	51	85	26667	3749.9
25	70	25694	3892.0	52	85	26700	3745.3
26	60	25731	3886.4	53	60	26724	3742.0
27	10	25746	3884.1	53a	20	26746	3738.9
28	70	25766	3881.1	54	85	26762	3736.6

TABLE III. (*Cont'd.*)

Line No.	Rel. int.	Wave-length	Wave-number	Line No.	Rel. int.	Wave-length	Wave-number
55	85	26790	3732.7	81	50	27660	3615.3
56	80	26825	3727.9	82	60	27679	3612.8
57	80	26863	3722.6	83	40	27700	3610.1
58	50	26889	3719.0	84	40	27720	3607.5
58a	20	26915	3715.4	85	10	27757	3602.7
59	80	26936	3712.5	86	30	27771	3600.9
60	80	26954	3710.0	87	30	27789	3598.6
61	30	26982	3706.2	88	40	27810	3595.8
62	60	27011	3702.2	89	30	27828	3593.5
63	25	27051	3696.7	90	30	27867	3588.5
64	15	27068	3694.4	91	65	27875	3587.4
65	80	27092	3691.1	92	20	27902	3584.0
66	85	27109	3688.8	93	20	27932	3580.1
67	10	27135	3685.3	94	20	27951	3577.7
68	10	27175	3679.9	95	20	27977	3574.4
69	80	27208	3675.4	96	10	28003	3571.0
70	80	27241	3670.9	97	70	28036	3566.8
70a	40	27251	3669.6	97a	20	28056	3564.3
71	10	27320	3660.3	98	20	28085	3560.6
72	70	27349	3656.4	99	15	28110	3557.5
72a	80	27398	3649.9	100	30	28151	3552.3
73	60	27415	3647.6	101	30	28188	3547.6
74	20	27452	3642.7	102	30	28204	3545.6
75	30	27486	3638.2	103	25	28276	3536.6
76	50	27517	3634.1	104	10	28320	3531.1
77	80	27557	3628.8	105	30	28348	3527.6
78	20	27575	3626.5	106	30	28384	3523.1
78a	30	27608	3622.1	107	10	28406	3520.4
79	60	27626	3619.8	108	30	28493	3509.6
80	40	27640	3618.0	109	30	28546	3503.1

is separated in Fig. 3, into two lines some 10A apart. Further comparison shows that the intensity of all the strong lines increases with the amount of water present. This change in intensity indicates that at least the strong lines in this region are due to water vapor, and not to carbon dioxide. The carbon dioxide band in the region of 2.73μ would probably not have strong lines below 2.69μ, corresponding to line No. 59. The effect of carbon dioxide in this region was studied by Sleator[2] and it was found that the strong lines throughout the region were enhanced by the use of steam (giving much more absorbing material) and reduced by drying the air. Figure 3 has been plotted with deflections on a scale of frequencies and is the reverse of the curves of Figure 2. Lines 22, 23 and 24 may be compared with the unresolved group shown as numbers 8 and 9 in Figure 5 of the paper of 1918, and this comparison fairly indicates the advance represented in the present work.

In Fig. 4 and Table IV are represented the results for the region of 3.16μ. It is perhaps here that previously published results are most inadequate. The table presents lines between 2.85 and 3.33μ, and the lines at the beginning of the table probably belong to the series shown in the previous figures. All the lines are weak in this region, whose center we have placed at 3.168μ, and which is probably the first harmonic of the band at 6.26μ. However, the separation of the two strong lines next the center on either side (Nos. 81 and 82) is 45.3 waves per cm, while the corresponding difference at the fundamental

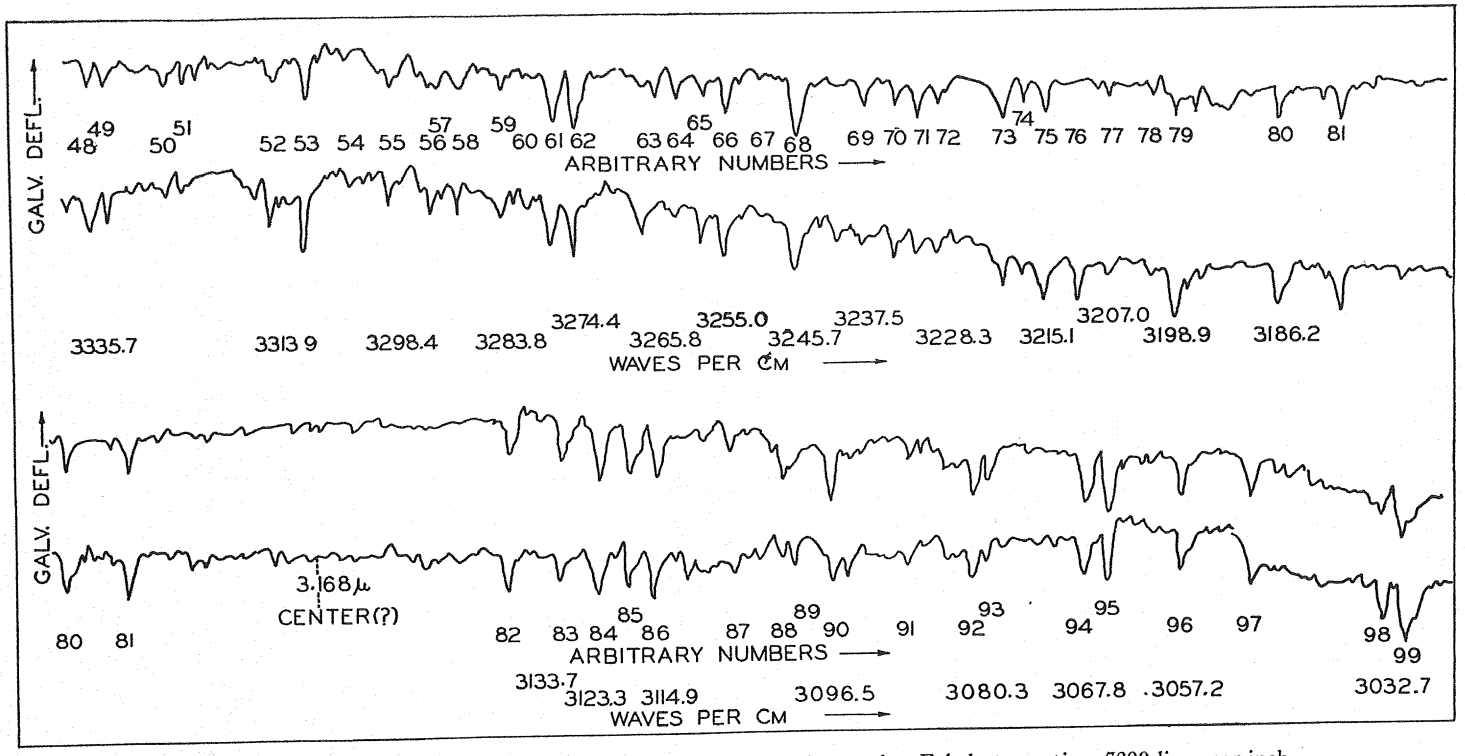

Fig. 4. Part of the energy curve, region of 3.16μ. Two independent series. Echelette grating, 7200 lines per inch. Slits 0.15 mm, 15 secs, 0.45 waves per cm, 4.5A.

TABLE IV. *Region of* 3.15μ
Arbitrary numbers, relative intensities, wave-lengths and wave-numbers of the stronger lines.

Line No.	Rel. int.	Wave-length	Wave-number	Line No.	Rel. int.	Wave-length	Wave-number
1	40	28546	3503.1	59	12	30452	3283.9
2	5	28561	3501.3	60	5	30489	3279.9
3	15	28588	3498.0	61	25	30515	3277.1
4	25	28655	3489.8	62	25	30540	3274.4
5	12	28672	3487.7	63	8	30620	3265.8
6	25	28702	3484.1	64	8	30663	3261.3
7	25	28714	3482.6	65	8	30693	3258.1
8	15	28762	3476.8	66	12	30721	3255.1
9	5	28801	3472.1	67	5	30762	3250.8
10	15	28828	3468.9	68	20	30809	3245.8
11	5	28844	3466.9	69	12	30887	3237.6
12	15	28861	3464.9	70	10	30923	3233.8
13	15	28873	3463.4	71	15	30949	3231.1
14	5	28901	3460.1	72	15	30976	3228.3
15	5	28919	3457.9	73	25	31053	3220.3
18	35	28992	3449.2	74	8	31077	3217.9
19	5	29013	3446.7	75	25	31102	3215.2
20	20	29032	3444.5	76	20	31144	3210.9
22	8	29066	3440.4	77	5	31181	3207.1
26	15	29128	3433.1	78	5	31237	3201.3
27	5	29161	3429.2	79	20	31261	3198.9
28	8	29176	3427.5	80	15	31384	3186.3
29	5	29194	3425.4	81	20	31456	3179.0
30	12	29206	3424.0	82	20	31911	3133.7
31	30	29219	3422.4	83	20	31972	3127.7
32	5	29265	3417.1	84	25	32017	3123.3
33	10	29318	3410.9	85	12	32054	3119.7
34	12	29366	3405.3	86	25	32103	3115.0
37	12	29437	3397.1	87	10	32176	3107.9
39	15	29457	3394.8	88	15	32239	3101.8
42	12	29528	3386.6	89	12	32256	3100.2
43	5	29687	3368.5	90	20	32294	3096.5
44	12	29703	3366.7	91	5	32385	3087.8
45	8	29736	3362.9	92	12	32463	3080.4
46	12	29789	3356.9	93	8	32480	3078.8
47	5	29880	3346.7	94	25	32596	3067.9
48	15	29961	3337.6	95	25	32623	3065.3
49	12	29979	3335.7	96	20	32710	3057.2
50	8	30050	3327.8	97	25	32791	3049.6
52	12	30175	3314.0	98	20	32948	3035.1
53	15	30218	3309.3	99	25	32973	3032.8
54	4	30269	3303.7	100	5	32984	3031.8
55	15	30317	3298.5	101	5	33039	3026.7
56	12	30366	3293.2	102	12	33135	3018.0
57	15	30377	3292.0	103	12	33192	3012.8
58	15	30401	3289.4				

is 40. The wave-lengths of certain lines listed in Table IV are in good agreement with values given by Barnes in the work cited (reference 7) for this region. In some cases his numbers represent averages of the wave-lengths of adjacent lines.

The results for the fundamental at 6.26μ are shown in part in Figs. 5 and 6, and completely in Table V. Hettner shows this band to extend from 4.5μ to 8.5μ, but we have studied only the central part. In Fig. 6 are represented the most important lines of this region on a scale of wave-numbers, showing by the length of the lines the intensities of absorption. The advancement lately

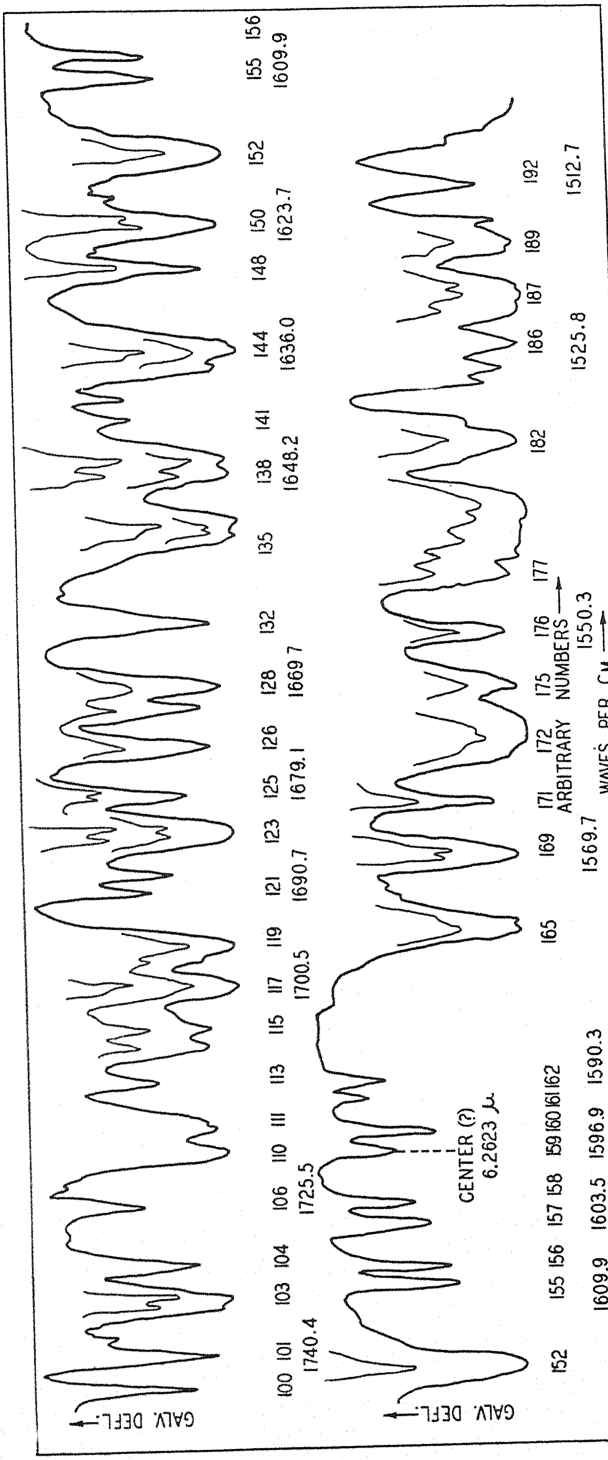

Fig. 5. Energy curve, region of 6.26μ, middle part. Echelette grating, 2880 lines per inch. Slits 0.2 mm, 21 secs, 0.45 waves per cm, 17A.

TABLE V. *Region of* 6.26μ.

Arbitrary numbers, relative intensities, wave-lengths, and wave-numbers of the stronger lines.

Line No.	Rel. int.	Wave-length	Wave-number	Line No.	Rel. int.	Wave-length	Wave-number
58	20	54413	1837.8	144	90	61128	1635.9
63	60	54644	1830.0	148	70	61414	1628.3
65	10	54673	1829.1	149	80	61570	1624.2
66	40	54774	1825.7	150	40	61602	1623.3
67	10	54839	1823.5	152	90	61841	1617.0
69	10	55005	1818.0	155	50	62117	1609.9
70	10	55159	1812.9	156	40	62202	1607.7
71	30	55211	1811.2	157	40	62358	1603.6
72	15	55288	1808.7	158	35	62435	1601.7
73	5	55385	1805.5	159	30	62625	1596.8
76	10	55487	1802.2	160	45	62693	1595.1
77	50	55541	1800.5	161	20	62804	1592.3
78	30	55661	1796.6	162	30	62880	1590.3
79	65	55762	1793.3	165	90	63425	1576.7
80	65	55814	1791.7	168	75	63693	1570.0
81	25	56004	1785.6	169	80	63706	1569.7
82	60	56142	1781.2	171	60	63884	1565.3
83	15	56184	1779.9	172	90	64115	1559.7
84	30	56295	1776.4	173	80	64142	1559.0
85	20	56396	1773.2	175	80	64321	1554.7
86	70	56439	1771.8	176	80	64500	1550.4
87	50	56533	1768.9	177	70	64706	1545.5
89	50	56739	1762.4	178	70	64765	1544.0
90	5	56832	1759.6	179	80	64833	1542.4
91	50	56898	1757.5	180	80	64916	1540.5
93	70	57082	1751.9	181	85	64960	1539.4
95	75	57169	1749.2	182	90	65193	1533.9
97	25	57219	1747.7	183	30	65261	1532.3
98	20	57250	1746.7	184	20	65396	1529.1
100	50	57338	1744.0	185	70	65451	1527.9
101	70	57457	1740.4	186	85	65537	1525.9
102	12	57526	1738.3	187	60	65656	1523.1
103	70	57663	1734.2	188	80	65718	1521.7
104	60	57784	1730.6	189	70	65755	1520.8
106	35	57999	1724.2	192	60	65913	1517.1
110	90	58204	1718.1	193	30	65977	1515.7
111	80	58287	1715.6	194	80	66107	1512.7
113	35	58452	1710.8	196	20	66226	1510.0
114	70	58588	1706.8	197	90	66344	1507.3
115	70	58653	1704.9	198	80	66385	1506.4
117	90	58813	1700.3	200	20	66575	1502.1
118	15	58894	1698.0	202	60	66711	1499.0
119	90	58958	1696.1	203	65	66829	1496.4
120	30	59151	1690.6	204	80	67119	1489.9
121	50	59216	1688.7	205	60	67220	1487.7
122	30	59356	1684.8	207	30	67499	1481.5
123	90	59400	1683.5	208	60	67736	1476.3
124	40	59504	1680.6	209	20	67866	1473.5
125	50	59524	1680.0	210	80	67928	1472.1
126	70	59683	1675.5	211	10	68070	1469.1
127	60	59817	1671.8	213	65	68259	1465.0
128	75	59886	1669.8	216	20	68559	1458.6
129	20	59918	1668.9	217	90	68631	1457.1
132	75	60131	1663.0	218	10	68693	1455.8
133	20	60162	1662.2	219	50	68848	1452.5
135	70	60444	1654.4	221	65	69052	1448.2
136	90	60496	1653.0	224	10	69318	1442.6
138	30	60682	1647.9	227	90	69595	1436.9
139	90	60738	1646.4	228	15	69753	1433.6
141	20	60864	1643.0	229	10	69816	1432.3
142	20	60942	1640.9	230	50	69911	1430.4
143	30	61046	1638.1	234	50	70219	1424.1

made is shown definitely in this region. For what appeared in Fig. 2 of the paper of 1925 as uncertain ripples in the level plateau of the center has now become eight very definite lines, numbers 155 to 162, arranged in pairs. The old lines Nos. 69 and 80, the second from the middle region on either side, now appear as two close lines each, Nos. 149 and 150 and Nos. 168 and 169 of Fig. 5. Line 159 which we have marked the center, because it is a geographic mid point, is not a particularly significant line. Some lines separated here, for example, numbers 172 and 173 and 168 and 169, are less than one wave per cm apart.

It may be well to compare some of the wave-lengths with those given in the previous papers from this laboratory. In many cases no basis for comparison exists, for one of the former "lines" now appears as several. However, there are many lines in the region of 2.67μ as it appeared in 1918 which have persisted as single effects, and there are several lines near 1.87μ and 6.26μ

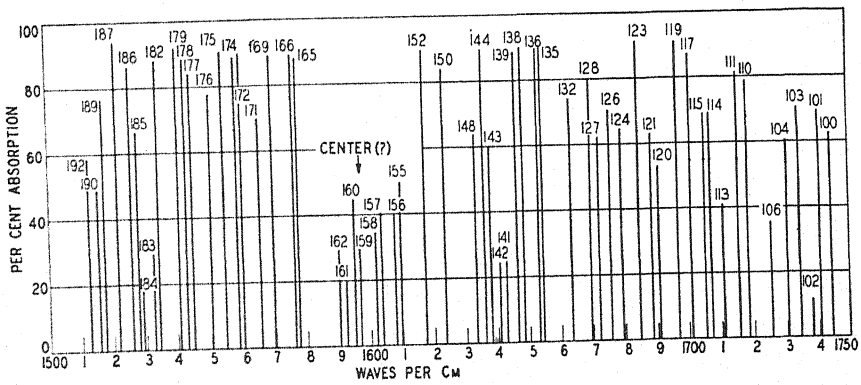

Fig. 6. Region of 6.26μ, middle part. Intensities of the absorption lines shown on a scale of waves per cm.

which may be compared in the paper of 1925 and the present one. The comparison shows that single lines in the band at 2.66μ are now assigned wave lengths from 3 to 7A greater than those of 1918. Perhaps the visual calibration formerly necessary accounts for the systematic difference. Similar differences appear at 1.87μ. At 6.26μ the difference is more irregular and somewhat larger. In many cases, however, no comparison is possible. For example, lines 114 and 115 were formerly given as one, No. 54, and Nos. 120 and 121 as number 58.

Some estimate of the precision attained in the wave lengths listed here is necessary and may be made as follows. The calibration of the 7,200 line grating, used in all the work except for the band at 6.26μ, was based on the mercury line whose wave-length was taken to be 10139.8A in air. This calibration has been done by Meyer, and charts have been made from which wave length and wave number can be read directly in terms of angles. This calibration is believed to involve no error greater than 1 part in 50,000. There exists always some uncertainty in setting the circle. If this amounts to 5 seconds, then the

location of an absorption line which depends at the tip upon perhaps four plotted points is also uncertain. Independently measured values of typical lines in two of the regions are shown in Table VI.

TABLE VI. *Typical values for the different angles and wave-lengths found for a single line.*

Line No.	Angle	Wave-length
31	24°31′55″	29219A
	31′55″	29219
	31′55″	29219
	32′0″	29221
33	24°37′25″	29322
	15″	29319
	10″	29317
	15″	29319
39	24°44′42″	29457
	50	29460
	40	29457
	45	29458
128	19°54′22″	59891
	30″	59897
	15″	59885
138	20°10′37″	60672
	45″	60678
	45″	60678
	50″	60682
148	20°26′ 7″	61416
	10″	61418
	5″	61418

When there are extreme differences of 20″ we have taken more than four independent energy curves. It seems fair to affect the values of wave-length in these regions with a probable error of ± 2A. It is perhaps an even chance that the true value of the wave-length in air, based upon the value used here for the mercury line, is within 2A on either side of the values given here. In order to guard against mistakes in reading the calibration charts, values of wave-length and values of wave-number were taken off independently, and afterward checked by looking up all the wave numbers in a table of reciprocals. These considerations and this estimate of precision refer to the regions 1.87μ, 2.66μ and 3.15μ.

The band at 6.26μ was studied with a grating having 2,880 lines per inch. Its calibration was based on the same value of the wave-length of the mercury line at 1μ, and also on work with visual lines. The spectrometer constant was 175,900A. There was no chart available, and our procedure was to compute independent values of λ, one from each plotted curve, by the equation $\lambda = \kappa \sin \theta$. First the wave numbers were looked up in the reciprocal tables, and then the wave numbers were independently computed by using cologs. Typical values in this region are given in Table VI. It does not seem that the spectrometer constant for this assembly is responsible for an error of 1A in our results, and perhaps the wave-lengths in Table V should be written ± 3A. To

reduce this uncertainty requires more observations, and more independent curves. The systematic difference between the wave-lengths given here, and those published in the paper of 1925, for such lines as may properly be compared, must arise from differences in calibration constant. The circle used in all this work, as well as in many other investigations made in this laboratory, has no appreciably eccentricity.

The advance over previous work represented here lies, first, in more reliable determinations of individual wave-lengths. Second, more lines have been measured, and this work should make possible a better classification, if it is demanded by theoretical study of the water molecule. Third, the lines measured represent, in more cases than in previous data, single absorption effects, so that more of the wave numbers are of actual physical significance.

THE DIFFUSION PROBLEM FOR A SOLID IN CONTACT WITH A STIRRED LIQUID

By T. E. W. Schumann
West Virginia University

(Received April 21, 1931)

Abstract

A cylindrical solid of length a in a direction x and of arbitrary cross-section normal to x is in contact on its plane face $x=a$ with a well-stirred liquid. The face $x=0$ of the solid and the lateral surface are impervious to heat. The liquid extends from $x=a$ to $x=a+b$. At $x=a+b$ the liquid is in contact with a source of heat at the constant temperature θ, the transfer of heat from this source being proportional to the difference in temperature between the outside source and the liquid. If the initial temperatures of solid and liquid are given, the problem of the temperature distribution at any subsequent time can be obtained by means of a modification of the well-known Fourier analysis.

IN STUDYING practical problems concerning the one-dimensional flow of heat in a solid, boundary conditions are sometimes met which are not directly amenable to the ordinary Fourier analysis. This is due to the fact that the characteristic solutions of the differential equation subject to the given boundary conditions do not form an orthogonal set of functions. This difficulty can be met in various ways. One method will be given in this paper.

The problem here considered is that of the one-dimensional flow of heat in a solid slab which, at its face $x=a$, is in contact with a well-stirred liquid extending from $x=a$ to $x=a+b$. The liquid receives heat at the face $x=a+b$ from an outside source kept at a constant temperature θ, the transfer of heat to the liquid being proportional to $\theta-v$, where v is the temperature of the liquid. The slab is impervious to heat at the face $x=0$. The lateral surfaces of the slab and the liquid are supposed to be impervious to heat so as to insure the one-dimensional flow of heat.[1] If the initial temperature of the liquid and the initial temperature distribution in the solid are known, then it is possible to determine the temperature distribution throughout the system at any subsequent instant.

Let $u(x, t)$ represent the temperature in the solid at any point x and at time t, and let $v(t)$ represent the temperature of the liquid at any time t. The function $v(t)$ must be continuous for all values of t.

Now, according to the well-known Fourier equation of heat conduction

$$\frac{\partial u}{\partial t} = \alpha^2 \frac{\partial^2 u}{\partial x^2}, \quad t > 0 \tag{1}$$

[1] These conditions are approximately realized when a slab of low thermal conductivity is heated between two similar parallel plates of high conductivity, metal plates for example, the outer plates being heated by a hot gas.

where α^2, the thermal diffusivity of the solid, is the quotient of its thermal conductivity k by the product of its density ρ and its specific heat c.

Also, since the face at $x=0$ is impervious to heat

$$\partial u/\partial x = 0, \quad x = 0, t > 0. \tag{2}$$

Furthermore, the heat gained by the liquid must be equal to the heat it acquires from the outer source minus the heat which is conducted across the solid-liquid boundary. If K is the heat capacity of a prism of the liquid of unit cross-section and γ is the coefficient of heat transfer from the outer source per unit cross-section, unit difference of temperature and unit time, then

$$K\frac{dv}{dt} = -k(\partial u/\partial x)_{x=a} + \gamma(\theta - v), \quad t > 0. \tag{3}$$

The thermal contact of the solid and the liquid at $x=a$ gives rise to the equation

$$u(a, t) = v(t), \quad t > 0. \tag{4}$$

If v_0 is the initial temperature of the liquid and $u_0(x)$ that of the solid, then we have

$$\lim_{t=0} v(t) = v_0 \tag{5}$$

and

$$\lim_{t=0} u(x, t) = u_0(x), \quad 0 \leqq x < a. \tag{6}$$

It will be noticed that we have restricted the validity of the last equation so as to exclude the point $x=a$ for the reason that it would be impossible to satisfy all the conditions imposed by Eqs. (1) to (6) if this point had been included, except for the special case when $u_0(a)=v_0$. The same difficulty, however, is met in any Fourier expansion. Fourier's theorem states that a function $f(x)$ which fulfills Dirichlet's conditions in a given interval can be represented by a series of sines and cosines except at points of discontinuity. If therefore we express u in terms of a Fourier series we shall expect it at time $t=0$, to satisfy the initial temperature distribution except at points of discontinuity including the point $x=a$, $\lim_{t=0} u(a, t)$ having some value different from $u_0(a)$. From physical consideration it is possible to determine the value of $\lim_{t=0} u(a, t)$.

Suppose that at any point $x=x_0$ there is a sudden change in the value of $u_0(x)$ from u_1 to u_2. This means that the temperature gradient is infinite at x_0. The heat conducted across unit area is proportional to the temperature gradient, and hence if the temperature gradient is still infinite after a small but finite time ϵ, then the heat transferred across unit area will be infinite, which is clearly impossible. From this it follows that the temperature discontinuity must have disappeared after the time ϵ, however small ϵ may be. These considerations also hold at the point $x=a$, where there is thermal contact between the solid and the liquid. Hence

$$u(a, \epsilon) = v(\epsilon) \tag{7}$$

however small ϵ may be.

Now let us consider the value of $v(\epsilon)$ when ϵ becomes very small. Since the liquid is kept stirred its temperature must be uniform at any instant of time. Therefore the change in temperature $v_0 - v(\epsilon)$ is proportional to the total heat conducted away from the liquid, and by choosing ϵ sufficiently small we may make this heat, and consequently $v_0 - v(\epsilon)$ as small as we please. Hence it follows that

$$\lim_{\epsilon=0} v(\epsilon) = v_0$$

and combining this result with Eq. (7) we have

$$\lim_{\epsilon=0} u(a, \epsilon) = v_0$$

or

$$\lim_{t=0} u(a, t) = v_0. \tag{8}$$

Eqs. (8) and (4) can now be combined into the single equation

$$u(a, t) = v(t) \tag{9}$$

for all time.

Accepting (9), we can rewrite the equations of condition, substituting $u(a, t)$ for $v(t)$

$$\frac{\partial u}{\partial t} = \alpha^2 \frac{\partial^2 u}{\partial x^2}, \quad t > 0 \tag{10}$$

$$\frac{\partial u}{\partial x} = 0, \quad x = 0, \quad t > 0 \tag{11}$$

$$K \frac{\partial u}{\partial t} = -k \frac{\partial u}{\partial x} + \gamma(\theta - u), \quad x = a, \quad t > 0 \tag{12}$$

$$\lim_{t=0} u(x, t) = u_0(x), \quad 0 \leqq x < a \tag{13}$$

$$\lim_{t=0} u(a, t) = v_0 \tag{14}$$

and our problem reduces to the determination of u so as to satisfy conditions (10) to (14).

On account of the rather unusual character of the analytical conditions it is perhaps advisable to demonstrate that this set of equations possesses a unique solution, and we proceed to show this briefly. If possible, let there be two independent solutions u_1 and u_2.

Let

$$V = u_1 - u_2. \tag{a}$$

Then V must satisfy the following set of conditions

$$\frac{\partial V}{\partial t} = \alpha^2 \frac{\partial^2 V}{\partial x^2} \tag{b}$$

$$\frac{\partial V}{\partial x} = 0, \quad x = 0 \tag{c}$$

$$K\frac{\partial V}{\partial t} = -k\frac{\partial V}{\partial x} - \gamma V, \quad x = 0 \tag{d}$$

$$V = 0, \quad t = 0, \quad 0 \leqq x \leqq a \tag{e}$$

Put

$$J = \frac{K\alpha^2}{2k} V_a{}^2 + \frac{1}{2}\int_0^a V^2 dx \tag{f}$$

where V_a is the value of V at $x=a$.

Then

$$\frac{\partial J}{\partial t} = \frac{K\alpha^2}{k} V_a \frac{\partial V_a}{\partial t} + \int_0^a V \frac{\partial V}{\partial t} dx$$

$$= \frac{K\alpha^2}{k} V_a \frac{\partial V_a}{\partial t} + \alpha^2 \int_0^a V \frac{\partial^2 V}{\partial x^2} dx$$

by virtue of (b).

$$= \frac{K\alpha^2}{k} V_a \frac{\partial V_a}{\partial t} + \alpha^2 \left[V \frac{\partial V}{\partial x} \right]_0^a - \alpha^2 \int_0^a \left(\frac{\partial V}{\partial x} \right)^2 dx$$

$$= -\frac{\gamma}{k} V_a{}^2 - \alpha^2 \int_0^a \left(\frac{\partial V}{\partial x} \right)^2 dx$$

by virtue of (c) and (d).

Therefore

$$\frac{\partial J}{\partial t} \leqq 0.$$

But since $J=0$ when $t=0$, it follows that

$$J \leqq 0.$$

Also, according to the definition as given by Eq. (f), J is essentially positive. Hence $J \equiv 0$, from which it follows that there can be only one solution to the problem.

We now proceed to find this solution.

Let us set

$$u = \theta + \sum_{n=0}^{\infty} E_n \cos \frac{z_n x}{a} e^{-z_n{}^2 \alpha^2 t / a^2} \tag{15}$$

which is the type of expression to which one is led by the ordinary Fourier analysis. If this series is convergent, then u attains the value θ when $t = \infty$, as

should be the case from physical considerations. Eqs. (10) and (11) are formally satisfied by this expression. Eq. (12) will also be satisfied provided the z's are the roots of

$$\tan z = -\lambda z + \frac{\gamma a}{kz} \tag{16}$$

where

$$\lambda = \frac{\alpha^2 K}{ak} = \frac{K}{a\rho c}. \tag{17}$$

There now remains the problem of determining the values of E so as to satisfy conditions (13) and (14), namely that

$$u(x, 0) = \theta + \sum E_n \cos \frac{z_n x}{a} = u_0(x), \quad 0 \leqq x < a \tag{18}$$

and

$$u(a, 0) = \theta + \sum E_n \cos z_n = v_0. \tag{19}$$

A difficulty is met here due to the fact that in (18) the characteristic functions are non-orthogonal.[2]

To overcome this difficulty we assume for the time being that (18) can be differentiated termwise, the result being

$$\frac{du(x, 0)}{dx} = -\sum \frac{E_n z_n}{a} \sin \frac{z_n x}{a}. \tag{20}$$

[2] The situation here encountered is entirely similar to that met by March and Weaver in connection with a problem which is a special case of the one here considered (see Phys. Rev. **31**, page 1072). A somewhat simpler device than the one here used is, however, sufficient to meet the situation of the former paper. In fact, one sought there to develop a function $u_0(x)$ in a series of non-orthogonal functions $\cos z_n x$ where z_n are the roots of $\tan z + \lambda z = 0$. This can be accomplished indirectly by expanding the integral of $u_0(x)$ in a series of the orthogonal functions $\sin z_n x$. This procedure leads at once to the solution:

$$u = \frac{\bar{u} + v_0\lambda}{1+\lambda} + \sum_{n=0}^{\infty} E_n \cos \frac{z_n x}{a} e^{-\alpha^2 z_n^2 t/a^2}$$

where

$$\bar{u} = \frac{1}{a}\int_0^a u_0(x)dx$$

$$E_n = \frac{2}{1+\lambda+\lambda^2 z_n^2}[(-1)^n(\bar{u} - v_0\lambda)(1+\lambda^2 z_n^2)^{1/2} + 2(1+\lambda^2 z_n^2)Q_n]$$

and

$$Q_n = \frac{z_n}{a}\int_0^a u_0(x) \cos\frac{z_n x}{a} dx$$

the notation being that of the paper referred to.

It will be shown that it is possible to obtain the values of E from (18) and (20) by the usual Fourier method. Multiply (18) by $\cos z_n x/a$ and (20) by $p_n \sin z_n x/a$, add and integrate with respect to x between o and a, and determine p_n such that the product terms vanish, i.e., such that

$$\int_0^a \cos\frac{z_n x}{a}\cos\frac{z_m x}{a}\,dx + \frac{p_n z_m}{a}\int \sin\frac{z_n x}{a}\sin\frac{z_m x}{a}\,dx = 0. \tag{21}$$

By making use of Eq. (16) it can readily be demonstrated that (21) is satisfied provided

$$p_n = \frac{\lambda k z_n}{\gamma} \tag{22}$$

The equation from which the value of E_n is to be determined is

$$E_n\int_0^a \cos^2\frac{z_n x}{a}\,dx - E_n\frac{k\lambda {z_n}^2}{\gamma a}\int_0^a \sin^2\frac{z_n x}{a}\,dx$$

$$= \int_0^a (u(x,0)-\theta)\cos\frac{z_n x}{a}dx + \frac{\lambda z_n k}{\gamma}\int_0^a \frac{du(x,0)}{dx}\sin\frac{z_n x}{a}\,dx. \tag{23}$$

All the integrals in the above expression are perfectly straightforward except the last one which can be integrated by parts:

$$\int_0^a \frac{du(x,0)}{dx}\sin\frac{z_n x}{a}\,dx = \left[u(x,0)\sin\frac{z_n x}{a}\right]_0^a - \int_0^a \frac{u_0(x)z_n}{a}\cos\frac{z_n x}{a}\,dx$$

$$= v_0\sin z_n - \frac{z_n}{a}\int_0^a u_0(x)\cos\frac{z_n x}{a}\,dx \tag{24}$$

by virtue of Eqs. (14) and (18). If the other integrations are performed it is found that

$$\frac{E_n}{2}\left\{1+\left(\frac{\gamma a}{k{z_n}^2}+\lambda\right)\cos^2 z_n\right\}$$

$$= \left(v_0\lambda - \frac{\theta a\gamma}{k{z_n}^2}\right)\cos z_n + \frac{1}{a}\int_0^a u_0(x)\cos\frac{z_n x}{a}\,dx \tag{25}$$

The problem has now been formally solved, the value of u being given by Eq. (15), where the values of z have to be determined from Eq. (16) and those of E from Eq. (25). The value of v, the temperature of the liquid, is the same as $u(a, t)$ according to Eq. (9). We know that the expression obtained for u will satisfy Eqs. (10) to (12) but it still has to be demonstrated that it also satisfies (13) and (14). If this can be proved, then we know that we have obtained the true and unique solution to the problem. A formal proof that (13) and (14) will also be satisfied would require a considerable amount of space and the inclusion of such a proof in a journal devoted entirely to physics could hardly be justified. It may be stated, however, that a satisfactory

proof has been obtained, the method employed involving the use of Green's functions and being essentially the same as that employed by Carslaw[3] in solving a similar type of problem. In brief, the procedure is first to find a solution due to a point source of heat at the point x', where $0<x'<a$, subject to the boundary conditions as expressed by Eqs. (11) and (12), with the restriction that θ is assumed to be zero. The result is expressed in the form of a complex integral. By complex integration over a suitably chosen path it is then an easy matter to show that the solution obtained satisfies the equations of condition and also the initial condition of a unit point source at $x=x'$

Now the sum of any number of such solutions will still be a solution. Hence, by choosing a suitable distribution of point sources we can build up the final solution corresponding to the initial temperature distribution as given by Eqs. (13) and (14). In building up this initial temperature distribution it must be borne in mind that the distribution must be of strength $u_0(x)\rho c$ per unit length of the solid, when we deal with unit cross-section. At the point $x=a$, however, there is concentrated a point source of total strength Kv_0, corresponding to the heat initially contained in the liquid. This holds for the case when $\theta=0$. The transition to the case when $\theta\neq 0$ is easy and need not be elaborated here. Since the validity of the solution for a single point source has been proved the solution thus obtained for any distribution of point sources must also be valid. The result, which is in the form of a complex integral can be transformed into an infinite series by integrating over a suitable path and applying Cauchy's theorem to the poles of the integrand. In carrying out this transformation the resulting infinite series was found to be entirely in agreement with that already obtained by the Fourier method. Our problem has therefore been finally and completely solved.

Numerical example.

We give a numerical example which was worked out in connection with the heat conduction into a slab of coal bounded by two plates of steel. The values adopted for the different constants are $K=2.23$; $k=0.01425$; $a=1.27$; $\gamma=0.0452$; $\rho=0.8$; $C=0.2775$; $\theta=1$; $v_0=0.8$; $u_0=0$. where the centimeter, gram, minute, and degree Fahrenheit are the fundamental units of length, mass, time and temperature respectively.
It follows that $\lambda=7.9$ and $\alpha^2=0.0645$, and Eq. (16) takes the form

$$\tan z = -7.9z + \frac{4.03}{z}. \tag{17}$$

The values of z as determined graphically from this equation were $z=0.666$, 1.663, 4.74, 7.85. These values of z were substituted in Eq. (16) and the values of the E's were found to be

$$E = -0.703,\ -0.428,\ 0.213,\ -0.181.$$

Furthermore the successive values of α^2z^2/a^2 were

[3] Carslaw, The Conduction of Heat, p. 180. MacMillan and Co.

$$\frac{\alpha^2 z^2}{a^2} = 0.0178, \quad 0.1105, \quad 0.899, \quad 2.464.$$

Therefore the final form that Eq. (7) takes in this case is

$$u = 1 - 0.703 \cos \frac{0.666x}{a} e^{-0.0178t} - 0.428 \cos \frac{1.663x}{a} e^{-0.1105t}$$

$$+ 0.213 \cos \frac{4.74x}{a} e^{-0.899t} + \text{etc.}$$

The temperature $u(o, t)$ at $x=0$ and the temperature $u(a, t)$ or $v(t)$ were calculated from this equation and the values are given in Table I.

TABLE I.

Time, $t=$	0	0.5	0.1	2.0	4.0	10.	20.	30.	80.
$u(o, t)=$	0	0	0	0.013	0.104	0.360	0.582	0.753	0.883
$v(t)=$	0.8	0.685	0.683	0.683	0.685	0.701	0.739	0.813	0.908

From the table we see that the temperature $v(t)$ of the steel (or stirred liquid) sinks rapidly from its initial value of 0.8, stays practically constant for an appreciable time at about 0.685, and then begins to rise steadily attaining its asymptotic value of 1.0 after infinite time.

From this example it is evident that numerical calculation for any practical problem will in general not require an excessive amount of labor.

My thanks are due to Dr. S. P. Burke, Chairman of the Industrial Science Division of this University for his interest in this problem, and to the Combustion Utilities Corporation for permission to publish the results. I also wish to thank Professor Warren Weaver of the University of Wisconsin for a number of helpful suggestions concerning the form of presentation of the paper.

THE DIELECTRIC CONSTANT OF FORMIC, ACETIC, AND PROPIONIC ACIDS, AND THE ELECTRIC MOMENT OF COMPLEX MOLECULES

By C. T. Zahn
Palmer Physical Laboratory, Princeton University

(Received April 20, 1931)

Abstract

The *temperature and pressure variation of the dielectric constant of formic and propionic acid vapors* has been studied experimentally. The behavior is similar to that previously found for acetic acid. For formic acid it is possible to calculate from Coolidge's vapor density measurements the amount of association into double molecules, and to explain the apparent departures from Debye's theory in terms of such association. It is then seen that the apparently linear pressure curves can be explained by the compensation of several factors in the measurements. By assuming that the optical part of the polarization is doubled on association and taking this value from refractivity measurements, values for the electric moment of the single and double molecules of formic acid are obtained, 1.51×10^{-18} and 0.99×10^{-18} c.g.s.e.s.u., respectively. Although no reliable vapor density measurements exist for acetic acid it is assumed that the anomaly in this case also is due to association rather than to the previously suggested effect of vibrational quantization. The previous data are reinterpreted accordingly. By using the optical refractivity as before a value is obtained from the high temperature measurements for the *electric moment of the single molecule* of acetic acid, 1.73×10^{-18}; and similarly for propionic acid, 1.74×10^{-18} c.g.s.e.s.u. *The electric moment of complex molecules* is then discussed with reference to directed valence and to internal free rotation around single bonds. The possibility of the importance of interaction between external rotation and internal free rotation is suggested. The question of the interpretation of measured electric moments is raised for the case where free rotation causes a time variation of electric moment. In this connection the experimental values of electric moment are discussed. The values of the electric moment of these acids indicate that the OH group is tightly bound as supposed by Eucken and Meyer. A structure for the double molecule of formic acid is suggested, with the four oxygen molecules at the corners of a rectangle, the planes of the two constituent single molecules at an angle of about 120°, and the OH groups bound tightly in positions of minimum potential energy. This structure does not seem to be inconsistent with the observed electric moment.

IN A previous communication[1] measurements of the dielectric constant of acetic acid vapor were published. These measurements indicated that there is a change of the electric moment of the acetic acid molecule with temperature, and it was suggested as a possible explanation that the effect is due to a transition in vibrational quantum state of the OH group. The possibility that the apparent change in electric moment could be due to association was considered excluded by the fact that the variation of dielectric constant with pressure was linear within the limits of experimental error. The presence of association could not be further tested since there exist no

[1] C. T. Zahn, Phys. Rev. **35**, 1047 (1930).

reliable measurements of the vapor density of acetic acid. It was decided to make a further study of this effect by making measurements of the dielectric constant of formic acid and propionic acid vapors. In the case of formic acid excellent vapor density measurements have been made recently by Coolidge,[2] who has shown that his measurements can be explained by the existence of double molecules and has given satisfactory equations for the calculation of the degree of association. A study of these data shows that there is a considerable amount of association in the region of temperature and pressure available for convenient dielectric constant measurements. This suggests that the anomaly in the previous acetic acid measurements might be due to association in spite of the apparently linear pressure curves. For example, this might be possible if the shape of the vapor density curve were such as to effect the linearity of the pressure curve only very slightly throughout the measured range of pressure, and particularly if the molecular polarizations of the single and the double molecules were not greatly different.

Formic Acid

The present data on formic acid show the same general characteristics as those on acetic acid. The pressure curves are apparently linear and the electric moment apparently decreases with the temperature. This being a partial confirmation of the above suggestion of association, an attempt was made to explain the anomaly in formic acid quantitatively in terms of association and to calculate the electric moment of the single and double molecules. The percentage of associated molecules was calculated from Coolidge's equations for the points of maximum pressure on the curves and at the four different temperatures included by the data. At the highest temperature there was found 9 percent association and at the lowest temperature 58 percent. A

Table I. *Formic acid data.*

$T°K$	p cm Hg	$3(\epsilon-1)/(\epsilon+2)v$	$3(\epsilon-1)/(\epsilon+2)vT$	P
344.63	18.62	5547	1.912	41.43
386.91	28.32	5542	2.144	41.40
403.10	28.27	5536	2.231	41.34
423.43	28.36	5525	2.338	41.26

rough calculation from the data of Table I shows that if the effect is due to association the associated molecule cannot have zero electric moment as it would have in case the two associating moments were antiparallel. This also is in confirmation of the above suppositions.

In Table I the data were calculated from the readings at the highest pressures only. An example of a pressure curve is shown in Fig. 1. For economy in space the individual pressure data were not included in the table. In column 3 of Table I the value of the specific volume was calculated from the ideal gas equation and refers therefore to the normal ideal value. Therefore the values in column 3 represent the apparent polarization referred to a normal ideal

[2] A. S. Coolidge, Jour. Amer. Chem. Soc. **50**, 2166 (1928).

number of gas molecules. The values in column 5 represent the molecular polarization, or the polarization referred to a mol of the molecules. The values in column 4 plotted against the absolute temperature would give a Debye line if the molecules were of one kind only. The absolute values of ϵ used here are the values corrected as described later for the extrapolation to zero pressure under the assumption of association.

In order to determine the molecular polarization of the single and double molecules individually, it was assumed that the constant, or so-called optical, part of the polarization is doubled on association. This is probably justified by the well-known principle of the additivity of refractivity, particularly since the energy of association is not great. In any case the optical part is the smaller part of the electric polarization under the available experimental con-

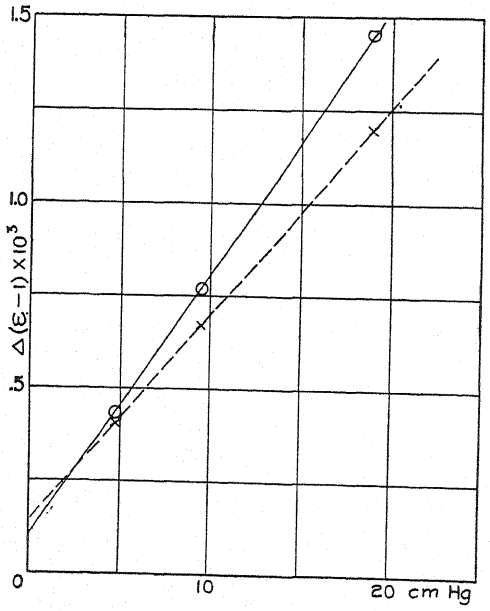

Fig. 1. Pressure Curve.

ditions. The two molecular polarizations are set respectively equal to $A+B_1/T$ and $2A+B_2/T$ according to the Debye theory. Hence the measured molecular polarization is

$$P = n_1(A + B_1/T) + n_2(2A + B_2/T)$$

where n_1 and n_2 are the respective mol fractions. B_1 and B_2 are proportional to the squares of the two electric moments. An approximate idea of the magnitude of the effect of association can be obtained by assuming that the association is negligible at the highest temperature, and then calculating $2A+B_2/T$ from the data at the lowest temperature and maximum pressure. If the pressure curves are then corrected so as to correspond to the single molecule alone, it is found that these curves are still apparently linear. This

can be seen in Fig. 1, where the uncorrected points are shown by crosses and the corrected points by circles.

It can therefore be stated that so far as the linearity of the pressure curves is concerned the assumption of association is justified. It remains only to see whether the constants can be chosen so as to fit all the data satisfactorily. The more accurate calculations are slightly complicated by the fact that it is never possible in a pressure curve to measure accurately the vacuum value of the experimental condenser capacity. This is true because inequalities in the temperature of the condenser plates arise on evacuation.[3] It is therefore necessary to extrapolate to zero pressure in order to obtain absolute values of the dielectric constant. Fig. 1 shows that the extrapolated value differs slightly for the corrected and the uncorrected curves. (This shows that the greatest departure from linearity exists at the very low pressures and partially explains why it was not originally detected.) These curves were first corrected roughly as above stated in order to locate the zero, and then new absolute values of the dielectric constant and molecular polarization were determined.

Because of the complicated nature of the calculations and the smallness of the association effect, no attempt was made to determine A, but it was taken from the molecular refractivity of formic acid in the liquid state as given in Landolt Börnstein, 8.53. This value is probably a little too small because of infrared terms in the refractivity, and the resulting calculations are subject therefore to a small error. Appropriate values of B_1 and B_2 were obtained by choosing the value of B_1 which gives on subsequent calculation the most nearly constant value for the ratio B_1/B_2. The value chosen for B_1 is 14160. Table II shows the corresponding values of B_1/B_2 with a weighted

TABLE II. *Formic acid: calculation of molecular constants.*

$B_1=14160$ $A=8.53$

$\mu_1=1.51\times10^{-18}$; $\mu_2=0.99\times10^{-18}$

$T°K$	cm Hg	Mol fraction association	P	B_1/B_2
344.63	18.62	0.580	41.43	0.45
386.91	28.32	0.275	41.40	0.40
403.10	28.27	0.171	41.34	0.37
423.43	28.36	0.092	41.26	0.50
				0.43 mean

mean of 0.43. From these values it can be seen that while the reduction in the electric moment is considerable the doubling of the optical term masks a considerable portion of the effect. Further, in order to show how nearly the data for the four different temperatures and maximum pressures are consistent with these constants A, B_1, and B_2, the values of the electric polarization were calculated and compared with the experimental values. This is shown in Fig. 2. The upper straight line is the Debye line for single molecules, and the lower line, for double molecules. The product of the polarization and the absolute temperature is plotted against the absolute temperature. For con-

[3] C. T. Zahn, Phys. Rev. **35**, 848 (1930).

venience the values of the polarization here refer not to a mol but to the ideal number of molecules per cc under normal conditions of a gas. The crosses represent the experimental values and the circles the calculated values for the maximum pressures. The deviations are seen to be of the order of one per-cent. This agreement is almost better than one could expect in view of the nature of the calculations and the possibility of small errors due to absorption on the condenser plates.

Finally it seems that the anomaly for formic acid can be satisfactorily explained by association and the values of the electric moment for the single

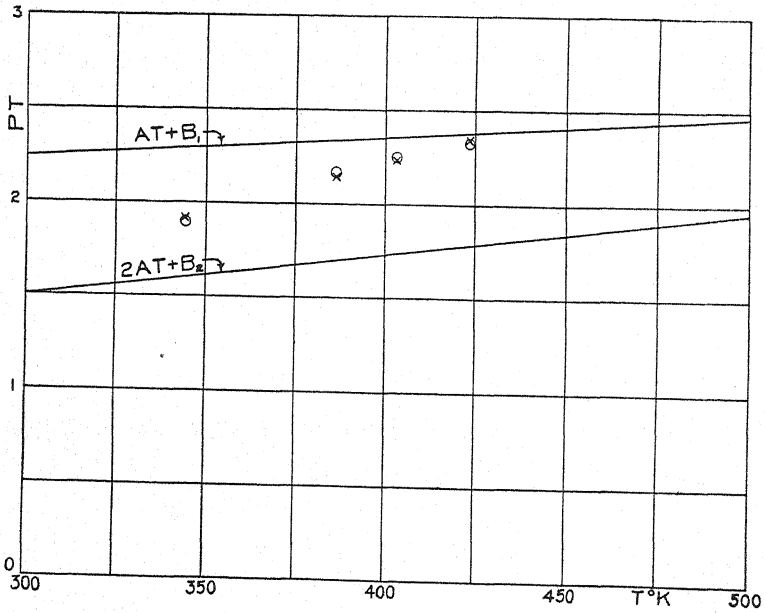

Fig. 2. Debye Lines.

and double molecules can be calculated. The above values of B_1 and B_2 correspond to electric moments of 1.51 and 0.99×10^{-18} c.g.s.e.s.u., respectively.

In order to obtain a good specimen of formic acid for these tests Kahlbaum formic acid was distilled at 0°C as described by Coolidge in the paper cited above.

Acetic and Propionic Acids

In view of the above results of the calculations for *formic* acid it seems more than probable that the previous data on *acetic* acid should also be interpreted in terms of association rather than the previously suggested temperature variation of electric moment. The same can be said for the data here presented on propionic acid, which shows a similar but somewhat smaller effect. The fact that the effect is smaller in propionic acid may be due to a greater masking of the moment reduction by the doubling of the optical term on association; or it may also be due to a smaller amount of association.

For these two acids the calculations cannot be carried out as in the case of formic acid since their vapor densities are unknown at present. Still if it is assumed that the effect is due to association the data can be used to obtain a fairly accurate value of the electric moment of the single molecules.

In Table III are shown the previously published data on acetic acid and also the present data on propionic acid together with calculated values of the apparent electric moment, μ. The values of apparent molecular polarization

TABLE III.

Acetic acid $A=12.9$ $\mu=1.73\times10^{-18}$			Propionic acid $A=17.4$ $\mu=1.74\times10^{-18}$		
$T°K$	P	μ	$T°K$	P	μ
297.51	55.0	1.42	356.12	61.4	1.59
320.85	50.7	1.40	373.42	59.7	1.60
341.13	50.8	1.45	374.41	59.8	1.61
357.78	51.2	1.49	389.86	59.8	1.63
360.37	51.6	1.50	404.64	59.1	1.65
389.64	53.7	1.60	418.44	59.4	1.69
410.84	53.5	1.64	429.57	60.3	1.73
450.09	53.3	1.72	455.37	58.4	1.74
471.42	52.3	1.73	485.81	56.0	1.74
491.44	50.2	1.72			
493.86	50.3	1.73			

are calculated from the uncorrected pressure curves and are subject to small errors due to incorrect extrapolation to zero pressure. At the higher temperatures this error is negligible since the association effect is very small. Values for A are taken as before from refractivity data. The values of μ should approach a constant value as the temperature is increased since the association then becomes negligible. From Table III it is seen that in both cases μ becomes practically constant above 440°K. The asymptotic values may be taken as 1.73 for acetic acid and 1.74×10^{-18} c.g.s.e.s.u. for propionic acid. Because of the danger of decomposition the highest safe temperature for formic acid was about 425°K and there was still 9 percent association. Fig. 2 shows, however, that the association should become negligible at approximately the same temperature as for the other two acids, at 440°K.

In the previous article[1] on acetic acid it was stated that there was evidence at high pressures indicating association in which the polarization is increased. This effect was noticed at pressure beyond the apparently linear portions of the pressure curves near to saturation, and is probably now to be considered as due to surface adsorption on the condenser plates.

The purified propionic acid was obtained by fractional distillation of a specimen from the Eastman Kodak Company.

ELECTRIC MOMENT OF COMPLEX MOLECULES

In recent years a number of authors, chiefly Eucken and Meyer, and Wolf,[4] have made attempts to calculate the electric moment of molecules,

[4] H. Sack, Ergebnisse der Exakten Naturwissenschaften, Band VIII, 337 (1930).

assuming that the total electric moment can be obtained by adding vectorially electric moments characteristic of each chemical bond and directed approximately along the valence directions given by the tetrahedral theory. These calculations have in some cases been complicated by the fact that whenever there is a single bond between two atoms there is a possibility of free rotation of two atomic groups relative to one another. In such cases the molecules cannot be regarded as rigid in the sense that the average relative positions of the nuclei are practically fixed. In fact, atomic groups having their own characteristic vector electric moments can rotate relatively to one another and cause a time variation of the electric moment. (Hojendahl first used this idea to explain difficulties which had arisen from the fact that certain molecules of the type CR_4 have an electric moment different from zero.) In these complicated molecules the question arises as to how one should regard such molecules in interpreting the apparent measured values of electric moment. Various attempts have been made in this direction. First attempts were made by assuming that the electrostatic interaction between the two rotating groups is negligible and that the rotation is therefore truly free. In this case it was assumed that the measured value of the square of the electric moment was the average square of the moment taken over a random distribution of the angle of free rotation. For example, two electric moments, μ, perpendicular to the axis of free rotation would give rise to an apparent or resultant moment $2^{1/2}\mu$.

Hojendahl has also pointed out that these internal rotations are never truly free but are hindered to some extent by electrostatic interaction; e.g., dipole interaction. In many cases this interaction may be considerable. Meyer[5] has made an extension of Debye's *classical* theory of the dipole polarization for certain non-rigid molecules, assuming dipole interaction. These calculations indicate an appreciable temperature variation of apparent electric moment when the innermolecular potential exceeds $(1/10)kT$; and that if the rotation is truly free the apparent moment is as if μ^2 were averaged over a random motion of the internal rotation as mentioned above. Certain objections may be raised to these conclusions. If the internal rotational energy were not too great the actual motions of the rotating parts would certainly be affected appreciably by centrifugal action due to the external rotations of the molecules as a whole and these rotating parts might be deformed by electrostatic interaction in varying degrees depending on the kinetic energies of the various parts of the molecule. Then the individual rotating parts of the molecule could not be considered as rigid and Meyer's calculations might be invalid. An idea of the importance of dipole deformation can be gotten from the electric moments of the substitution products of methane.

On the quantum theory it is found that deviations from the classical dipole theory are appreciable only at very low temperatures. Van Vleck has derived the classical formula of Debye to a close approximation from general quantum-mechanical considerations having to do chiefly with the relative values of possible energy transitions in the molecules and spectroscopic

[5] L. Meyer, Zeits. f. Phys. Chem. (B) **8**, 27 (1930).

principles. It is assumed that the energy levels of the molecule are such that $h\nu$ is never of the order of kT, but is either much larger or much smaller than kT. Then the dipole term in μ^2/T arises from possible transitions for which $h\nu \ll kT$; and the optical term from transitions for which $h\nu \gg kT$. There arises in the calculations a quantity μ^2 which is interpreted as being associated with the fixed electric moment of the molecule. The theory is developed for the case of rigid molecules and has not been explicitly stated so as to include the possibility of internal free rotation. It seems probable that in this latter case there will arise a quantity which is to be interpreted as an average μ^2 but just how this should be averaged would require further consideration of the theory. Whether this μ^2 appreciably depends on temperature or not will probably depend on the magnitude of the interaction between the rotating parts, and possibly not in the same way as it would on the classical theory.

Strictly speaking Van Vleck's theory applies to the cases where all the transitions in energy can be separated into the above two cases relative to kT. When $h\nu$ is of the order of kT difficulties may arise. Actually this condition may exist for some of the ordinary vibration states, but Van Vleck states that, under his assumptions of invariant fixed moment, these states, which correspond to linear oscillators would cause no temperature variation in the electric polarization. Now in complex molecules there may be certain other types of motion for which $h\nu$ is of the order of kT and a temperature variation does result. In this connection it is interesting to consider the internal rotation of the OH group in organic molecules. Since this group has a large electric moment there exists the possibility of strong electrostatic interaction, for example, with the C=O bond in the COOH group. The quantized motions of the OH group might be similar to those for the physical pendulum as described by Condon.[6] The lower states correspond to vibration and the higher states to non uniform rotation. The motions of the OH group might be considerable and the corresponding changes in electric moment quite large. Then the assumption of fixed electric moment would be invalid and some kind of average should be taken. This average might depend upon temperature, as was originally suggested to explain the data on acetic acid vapor.[7]

With regard to the interpretation of experimental values of μ three possibilities suggest themselves for the internal rotation here discussed. (1) If the interaction energy were sufficiently small the rotation could be regarded as truly free. Then the corresponding energy levels would be closely spaced and according to Meyer's classical derivation one would expect the apparent μ^2 to be an average over random internal rotational angle. (2) If the interaction energy were large, the lower states might correspond to oscillations of the rotator and have large energy separations. At ordinary temperatures practically all the molecules would be in the lowest state and this

[6] E. U. Condon, Phys. Rev. **31**, 891 (1928).

[7] It seems now that such a temperature variation is not necessary to explain the data on acetic acid; still the effect may exist to an appreciable extent but be undetectable as a departure from the linearity of a Debye line, for example if the deviations were approximately linear in temperature in the experimental interval.

oscillation would not contribute to the temperature variation of electric polarization, but would contribute a small amount to the atomic, or infrared, part of the constant polarization. In this ground state the corresponding motions of the oscillator would be fast compared to the external rotations and the apparent fixed electric moment μ should probably be regarded as a *vector* average over the oscillation as for the electronic motions, rather than a root mean square value as for the case of slow internal rotation. (3) The previous two cases are the extreme cases of Van Vleck's theory, for which the Debye equation holds. In the intermediate case where the energy separations are of the order of kT the temperature variation in electric polarization would be very complicated. This variation would now be due not only to the distribution of states of external rotation but also to the distribution in the states of internal rotation. Further because of the combined centrifugal and electrostatic interaction the perturbations of the individual states would no longer be like those of a simple dipole rotator. As regards the interpretation of experimental data, if such an effect exists in any actual molecules, it might be regarded as an apparent variation of electric moment with temperature. Such a variation with temperature will not necessarily be detectable as a deviation from the Debye equation $P=A+B/T$; for it is easily seen that a variation in apparent B which is linear with temperature is equivalent to a different but constant B together with a change in the constant A. If the effect is relatively small it may easily be such that the apparent B is approximately linear in the experimental interval. Then the experimental data would lead to a spurious value of the optical part A. For example, this possibility may be of interest in connection with Sänger's[8] abnormal value of A for ethylene chloride. Meyer[9] seems to think that a temperature variation in μ really exists in spite of the linearity of the Debye line.

There exists another serious difficulty in any quantitative treatment of free rotation in that the electrostatic interaction cannot be expressed accurately. Attempts have been made to consider this interaction as due to dipoles concentrated and located in various ways, but such models cannot give anything more than the roughest approximation to the facts, since the atoms are separated by distances comparable to atomic radii. The difficulties seem at present unsurmountable, whether one regards the interaction as a dipole effect, or as due to residual valence and van der Waals' forces as in London's theory.

Tetrahedral symmetry: The assumption of tetrahedral symmetry cannot be accurately true as is seen, for example, from the values of the electric moment of the chlorine substitution produces of methane. The discrepancies are usually explained by saying that the valence directions tend toward tetrahedral symmetry in the absence of dipole interaction and that this interaction produces a bending of the valence directions. This seems to be consistent with experimental data. A recent article by Slater[10] is especially interesting in this

[8] R. Sänger, Phys. Zeits. **32,** 21 (1931).
[9] L. Meyer, Phys. Zeits. **32,** 260 (1931).
[10] J. C. Slater, Phys. Rev. **37,** 481 (1931).

connection. On the basis of the quantum theory it is suggested that in the carbon atom the valence directions tend toward tetrahedral symmetry, while in the nitrogen and oxygen atoms they tend to be mutually perpendicular. The case of oxygen is of special interest here since it has been assumed by Eucken and Meyer that the undistorted valence angle for oxygen is the tetrahedral angle of about 110°. This is of importance in the original determination of the characteristic electric moments of the various chemical bonds.

Structure of the Carboxyl Group

From the previous calculations it is seen that the electric moments of acetic and propionic acids are of practically the same value, 1.73 and 1.74 $\times 10^{-18}$, but that of formic acid is smaller, 1.51×10^{-18}. It would be of interest to know whether this difference arises chiefly in the carboxyl group or in the alkyl group. If it arises in the alkyl group one could regard it as due to simple dipole induction which increases with the length of the carbon chain. Such an effect is well known in the series methyl, ethyl, propyl, to butyl chloride, where the moment increases by about 0.2×10^{-18}. This would indicate that the moment of the alkyl group changes from 0.4 to 0.6×10^{-18} by induction. Since the observed change in moment from formic to acetic acid is 0.22×10^{-18} it seems probable that this is also due to induction; particularly in view of the fact that the moment of COOH is not greatly different from that of C-Cl. The only observed difference in the two cases is that the transition is more abrupt in the fatty acid series.

It is, of course, possible that the transition may be at least in part due to a motion of the OH group of the type discussed under the above case (3) of relatively small interaction energy; but the values of the electric moment seem to indicate that the OH group is bound relatively tightly, either oscillating or rotating nonuniformly as in case (2). This is suggested by Meyer's calculated limiting values of the moment of the COOH group for the extreme positions of the OH group allowed by free rotation, 3.5 and 1.1×10^{-18}, corresponding to maximum and minimum potential energy, respectively. Because of the uncertainty in the calculations of electric moment, particularly in the valence directions, one cannot be certain whether these values indicate that the OH group has a considerable oscillation or not. The experimental values may be consistent with a very tightly bound OH group and a simultaneous bending of the valence directions, for example. We can, however, say with some degree of certainty that the motion of the OH group is not free since the expected moment would be much larger than the observed moment, about 3×10^{-18}. This is in agreement with the chemical evidence responsible for the supposition of the existence of a chelate ring in the carboxyl group.

The Double Molecule of Formic Acid

As regards the structure of the double molecule of formic acid, of moment 0.99×10^{-18}, this value of the electric moment excludes the possibility of the antiparallel type of association. Taking into consideration the relative sizes of the C and O atoms and assuming tetrahedral symmetry for the carbon

atoms, it is almost possible geometricaly to fit the molecules together in such a way that the four O atoms lie at the corners of a square and the C atoms on a line perpendicular to the square. The planes of the two associating HCOOH molecules would then be mutually perpendicular. If this is the approximate structure of the double molecule, the OH group of one of the original molecules of HCOOH would tend to be directed toward the doubly bound O atom of the other molecule and would be attracted toward it, distorting the square into the form of a rectangle. The OH group would then be quite near to the C=O group and the interaction woud probably bind the OH group relatively tightly in the ground state. It is, of course, impossible to make an accurate calculation of the electric moment of the double molecule, but a rough estimate after the manner of Eucken and Meyer is perhaps of some interest. The sizes of the atoms permit of a distortion of the square by interaction such that the planes of the two HCOOH atoms subtend an angle a little less than 120°. In the position of minimum potential energy the OH groups would lie approximately in the plane of the oxygen rectangle and at an angle of 60° relative to one another. Using the values of Eucken and Meyer for the characteristic moments one obtains a value of about 1.1×10^{-18} for the electric moment of the double molecule. Finally, one can say that the experimental value 0.99×10^{-18} does not seem to be inconsistent with the proposed type of structure so far as this rough estimate is concerned.

At present it is not possible to calculate the electric moment of the double molecule of acetic or propionic acid. These values would be particularly interesting in connection with the interpretation of the transition in electric moment from formic to acetic acid.

ON IMPURITIES IN METALS

By Francis Bitter
Westinghouse Research Laboratories, East Pittsburgh

(Received April 27, 1931)

Abstract

In order to arrive at a satisfactory understanding of many of the properties of metals, especially ferromagnetic metals, it is necessary to take into account the distorting effect of impurities and of other irregularities in the crystal lattice. The present paper is an attempt to describe some of the corrections that must be applied to the usual model of a perfect crystal before it can be expected to reproduce the properties of actual substances. Starting with the usual law of force between any two atoms—repulsion for small distances, attraction for large distances—the distortion of the lattice in the immediate neighborhood of an atom of impurity is discussed, with especial reference to the significance of the formation of molecules. Phase distributions in substances capable of allotropy are described, together with the influence of impurities on such distributions. The existence of diffusion makes it possible to apply statistical mechanics to solid solutions. It is shown that, in general, atoms of impurity in solids do not exert long range forces on each other by means of the distortions they produce in the lattice. This makes it possible to give simple formulae for the distribution of concentration of the impurities. These distributions are sometimes far from uniform, and a phenomenon similar to opalescence in gases may occur. Applications of the above concepts to ferromagnetic solutions are pointed out, and it is suggested that the ferromagnetism of austenite containing in the neighborhood of 0.8 percent carbon may be due to the presence of small granules of α-iron resulting from local fluctuations in the distribution of carbon atoms.

IT IS an old story that small amounts of impurities are sometimes of great importance in determining the physical properties of a substance, but in spite of this, the mechanism of such actions is very little understood. The magnetism of iron is a good example of the magnitude and importance of these effects. Yensen[1] has pointed out that in the interval between 1900 and 1928 the maximum permeability of iron has been increased from 2,000 to 61,000, chiefly by controlling small amounts of impurity. The most recent advance in this field is due to Cioffi,[2] who produced iron having a maximum permeability of 130,000 by annealing at high temperatures in a hydrogen atmosphere. There is little hope of understanding such phenomena until our theories of ferromagnetism and of other structure-sensitive properties are based on models of solids in which allowance is made for the chemical and mechanical effects of impurities. It is the purpose of this paper to describe such a model in some detail.

1. Pure Perfect Crystals

The substance to be investigated will be supposed made up of atoms between which the usual simple law of force acts—repulsion for small separa-

[1] T. D. Yensen, Journal of the Franklin Inst. **206**, 503 (1928).
[2] P. P. Cioffi, Nature **126**, 200 (1930).

tions, attraction for large separations, and only one position of equilibrium for finite separations. Out of this law of force may be calculated[3] the potential energy Φ of any given spacial arrangement of the atoms. Such calculations neglect a possible block structure as postulated by Zwicky,[4] but they may be thought of as being applicable to a single block and as an approximation to an aggregate of blocks. Since, however, a knowledge of the free energy is necessary for the interpretation of the properties of crystals with temperature aggitation, and since this free energy is not calculable from our present knowledge of atomic physics, it is impossible to make any quantitative theory of distorted lattices. A few qualitatively applicable observations can, however, be made, and for these we will confine ourselves in the main to the above simple model, the object being to find which of the properties of actual substances can be found in such a model, and which of the properties require the introduction of further assumptions regarding the atomic interactions.

Beyond the above definition of the substance with which the further discussion deals, there is only one point to be brought out before attacking the problem of the effect of impurities, and that concerns the mechanism of change of phase, and the associated problem of phase distribution throughout the volume of the substance. Let this substance be designated by A, and let it be assumed that A is capable of existing in two phases, α and β. Let the potential energy in each of these phases be designated by $\Phi_\alpha(p)$, $\Phi_\beta(p)$, where p represents those parameters on which the potential energy depends. For the sake of definiteness let us think of p as being the pressure, and as p is varied the lattice expands or contracts uniformly, remaining geometrically similar to itself. If Φ were thought of as the free energy, p might stand for the temperature. Φ_α and Φ_β satisfy the following conditions:

$$\Phi_\alpha < \Phi_\beta \text{ for } p < p_c$$
$$\Phi_\alpha = \Phi_\beta \text{ for } p = p_c$$
$$\Phi_\alpha > \Phi_\beta \text{ for } p > p_c.$$

As p increases from a value just less than p_c to one just greater than p_c, the whole substance *may* suddenly change from the α-phase to the β-phase. The intention is to bring out that this change *need* not take place all at once, because the substance may not be homogeneous, as is usually assumed. These inhomogeneities may be due to several causes. One such would be local spontaneous fluctuations in p (this, of course, only if there is temperature aggitation). Another would be the presence of an atom of some foreign substance B, or of an atom of A in an excited state. Such atoms would exert anomalous forces on their neighbors, which would really be equivalent to local pressures. Or the material might,without the interference of any of these factors, have its free energy a minimum for a mixture of the two phases.[5] For instance, suppose A is at a pressure $p_c - \delta p$, and that due to some unspecified cause a small region R is already in the β-phase. Suppose, further, that nor-

[3] Jones and Ingham, Proc. Roy. Soc. **A107**, 640 (1925) have done this for laws of force of the type $ar^m + br^n$ for various cubic lattices.

[4] F. Zwicky, Helevetica Physica Acta **3**, 269 (1930).

mally an expansion is associated with the $\alpha-\beta$ transition. It follows that the region R will be under compression due to its increase in volume while still surrounded by the unexpanded α-phase. In determining whether this local pressure is sufficient to maintain the region R in the β-phase, and how large R may be expected to be, it is necessary to consider the surface energy of R, the presence of other such regions, etc. A detailed discussion of these considerations cannot be given here, but the following points may be mentioned:

1. That in solid solutions such phase mixtures do occur.
2. That in some pure substances the transition from the crystalline to the liquid state probably involves such phase mixtures.
3. That phase mixtures of purely crystalline phases may exist in pure substances.[23]
4. That even under conditions far removed from the critical conditions, under which a phase change $\alpha-\beta$ takes place, small (ultramicroscopic) inclusions of one phase in the other may be present.
5. That such inclusions would have a considerable effect on structure sensitive properties.

2. One Atom of Impurity

An atom of a substance[6] B in the lattice of a substance A will in general produce very complex changes, especially if B is chemically very different

[5] A theoretical attack on this problem is possible following a procedure indicated by N. Rashevsky in an article on the size distribution of colloidal particles (Zeits. f. Physik **46**, 300, 1927). Instead of considering a substance B in another A, we can think of a phase β in another α, of the same substance. With this change of nomenclature, Rashevsky's results are

$$n(m) = e^{\lambda+\alpha m-\mathrm{K}/\mathrm{K}}$$

$n(m)$ being the number of regions in the β-phase having a mass m. K is the Boltzmann constant, $\lambda=\phi+k\log n_0$; $\phi=s-(u+pv)/T$, the entropy s being defined by $ds=(du+pdv)/T$. The constant α is chosen to satisfy the equation

$$\int_0^\infty me^{\lambda+\alpha m-\mathrm{K}/\mathrm{K}}dm = M$$

where M is the total mass of substance in the β-phase. Further progress can only be made when the function u is known. Rashevsky shows that with reasonable assumptions for u, the function $n(m)$ may have a maximum either for $m=0$ (a true solution), $m=m_0$ (a colloidal solution), or $m=\infty$ (two distinct and separate phases).

If such a phase distribution is wanted at temperatures which are not convenient for observation, the following procedure may be found useful as a basis for extrapolation. Instead of speaking of an inclusion of mass m, it will be convenient to refer to an inclusion of radius R. Then $u(R)=\int_T^{T_r}\sigma_\beta dt+l+(3/2)KT+\text{constant}$. The first term represents the energy required per unit mass to heat the β-phase to the transformation temperature. l is the latent heat of transformation of a colloidal particle and may be written (G. Bakker, Handbuch der (Experimental) Physik **6**, page 210)

$$l = (v_\beta - v_\alpha)T\frac{d(p_\beta + p_\alpha)}{dT} - \frac{2(v_\beta + v_\alpha)}{R}T\frac{dH}{dT}$$

H is the surface tension. From this equation a reasonable form for $u(R, T)$ can be found, and hence the temperature dependence of the size distribution of the particles in the colloidal phase.

[6] B may be an excited atom of the substance A.

from A. For the sake of this qualitative discussion, however, it will suffice to assume that ϕ_{AB}, the potential energy between an atom of A and one of B, is the same sort of function as the function ϕ_{AA} which gives rise to the interatomic forces already specified in section 1. Typical curves are to be found in Fig. 1. In the simple case where B is a substitution atom, the effect of the substitution is to add to the undistorted lattice a potential $\phi_{AB}-\phi_{AA}$ resulting from the excess forces exerted by the atom of impurity on its neighbors. This curve may have a maximum for finite values of r, or it may have a minimum, or it may be of a much more complicated nature, the important point being that even with the above simple assumptions a curve of the type shown in Fig. 1 for $\phi_{AB}-\phi_{AA}$ is obtainable.

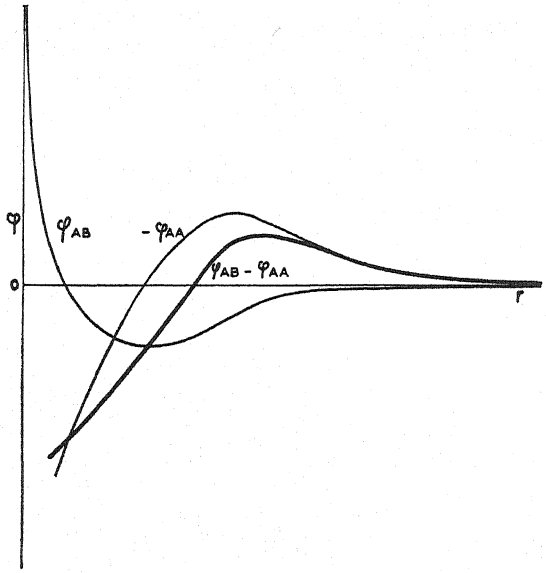

Fig. 1. The potential energy of two similar atoms $A-A$ and of two dissimilar atoms $A-B$ as a function of their distance apart, and finally the difference between these two functions, which is used in Fig. 3.

The most striking changes are brought about by the atom of impurity in its immediate neighborhood, but these are not of primary importance in this paper, and we shall discuss them only for the sake of their possible bearing on the phenomenon of thermal hysteresis. In Fig. 2 are shown two ways in which an atom of B may interact with its neighbors in accordance with the potential energy curve shown in Fig. 1. In both cases the impurity is in solution, but in order to distinguish between them, one might say that in case a, the atom B is in solution, whereas in case b, the molecule A_4B is in solution. The existence of a solution in two forms as described above is of interest in relation to temperature hysteresis. In Fig. 3 is shown a curve representing the potential energy of the atom A_1 adjoining the impurity as it approaches its neighbors, B and A_2, the latter being considered fixed. Curve 1 would represent the conditions if no impurity were present. The presence of the impurity necessitates

the addition of $\phi_{AB}-\phi_{AA}$, or curve 2, and the result is curve 3, which has two minima. As Rashevsky has pointed out,[7] it is just such curves as 3 Fig. 3 that give rise to hysteresis, and it is fairly obvious without further discussion that the relative concentration of atoms in the two minima will depend not

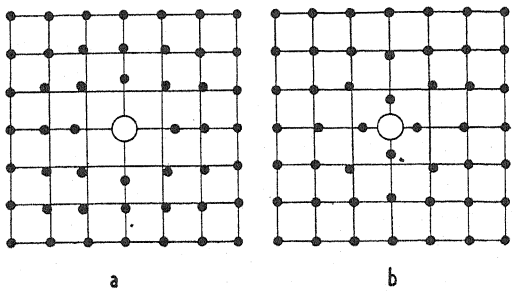

Fig. 2. Two possible distortions of a crystal around an atom of impurity compatible with the potential curves in Fig. 1 and Fig. 3.

only on the temperature and pressure, but also on the previous history of the sample. Since the physical properties of the substance $A+B$ will surely depend to some extent on whether B is in solution in the form A_4B or B, the

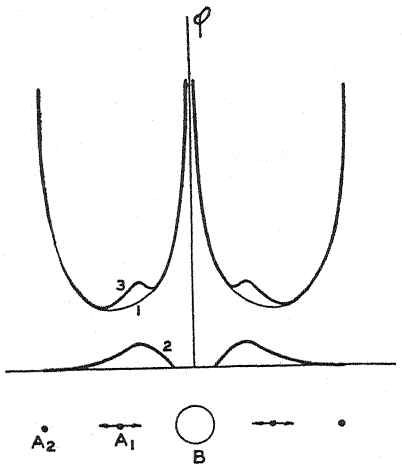

Fig. 3. The potential energy of A, as a function of displacement (1) when the atom B is identical with A_1 and A_2, and (3) when B is an atom of impurity giving rise to the additional energy (2), deduced from Fig. 1.

above described thermal hysteresis will give rise to a thermal hysteresis of other physical properties.

The only influence of the atom of impurity on distant parts of the lattice to be considered here will be the elastic deformation. In the calculation of this effect, it is assumed that the medium is isotropic, and that the distortion produced is spherically symmetrical. Under these conditions the strains in the

[7] N. Rashevsky, Zeits. f. Physik **53**, 102 (1929); **59**, 562 (1930); **61**, 511 (1930); **60**, 237 (1930).

lattice will diminish as some function of the distance from the impurity atom, and there will exist a sphere of radius R_0 (see Fig. 4) around this atom such that the strains outside it may be considered small, and proportional to the stresses. R_0 will, as a rule, be of the order of magnitude of a few atomic diameters. Unless the medium is very anisotropic the effect of the impurity at distant points may then be approximated by the strains set up in a homogeneous medium within which a pressure $\dot{p}$ is exerted normally to the surface of a sphere of radius R_0. Let E represent Young's modulus; ν Poisson's ratio, ρ the displacement of any given point, which will necessarily be radial; ϵ_r and ϵ_t

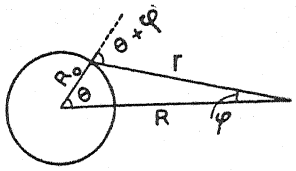

Fig. 4. Diagram to illustrate the symbols used in calculating distortions due to impurities in crystals.

the radial and tangential elongations; and σ_r and σ_t the radial and tangential stresses. It then follows that (see appendix A)

$$\epsilon_r = \frac{d\rho}{dr};\ \epsilon_t = \frac{\rho}{r}$$

$$E\frac{d\rho}{dr} = \sigma_r - 2\nu\sigma_t \tag{1}$$

$$E\frac{\rho}{r} = -\nu\sigma_r + (1-\nu)\sigma_t.$$

For equilibrium it is necessary that the radial forces acting on any volume element $(rd\theta)^2dr$ be cancelled by the radial component of the tangential forces, or $F_r = -4[F_t]_r$. But

$$F_r = \sigma_r(rd\theta)^2 - \left[\sigma_r + \frac{d\sigma_r}{dr}dr\right](r+dr)^2d\theta^2$$

$$[F_t]_r = \sigma_t r d\theta dr d\theta/2$$

which gives

$$r\frac{d\sigma_r}{dr} - 2(\sigma_t - \sigma_r) = 0. \tag{2}$$

Solving Eq. (1) for σ_r and σ_t and substituting the result in Eq. (2), we obtain

$$r^2\frac{d^2\rho}{dr^2} + 2r\frac{d\rho}{dr} - 2\rho = 0. \tag{3}$$

The general solution of this is easily found to be

$$\rho = c_1 r + \frac{c_2}{r^2} \tag{4}$$

and since we are interested in the problem for which one boundary condition is $\rho = 0$ for $r = \infty$, we may put $c_1 = 0$. Using for the other boundary condition that $\sigma_r = p$ for $r = R_0$ we find

$$c_2 = -\frac{(1 - \nu - 2\nu^2)}{2(1 - 2\nu)E} R_0^3 p \tag{5}$$

$$\sigma_r = p\frac{R_0^3}{r^3} \quad \sigma_t = -\frac{p}{2}\frac{R_0^3}{r^3} \tag{6}$$

and for the total energy of the distortion

$$E_n = \frac{1}{2}\frac{4\pi p^2 R_0^3}{E}\frac{1 - \nu - 2\nu^2}{2(1 - 2\nu)}. \tag{7}$$

These results[8] describe the distortion of the lattice at points more than a few atomic diameters removed from the atom causing the distortion and will be used in part 4 in discussing the possible existence of long range forces between atoms of impurity.

3. Diffusion

That diffusion and self-diffusion in solids exists has been known for some time, but the mechanism by which it proceeds is considerably in doubt. Frenkel[9] studied the phenomenon, first with the assumption that the atoms of a solid exchange places, and then[10] somewhat more elaborately with the assumption that some of the atoms occupy positions of "irregular equilibrium" in the interatomic spaces, and that diffusion proceeds by the movement of such atoms down the "aisles" of the lattice. Frenkel, and also Braunbeck[11] obtain expressions for the diffusion coefficients, of which the most interesting feature is that $D \sim e^{-b/T}$ where b is essentially a measure of the work required of an atom to break through its potential walls and so change places with a neighbor. The diffusion process is perhaps best described in terms of wave-mechanics. A particle surrounded by a potential wall will eventually appear on the other side no matter what its energy, the probability w of getting through at a single impact being[12] essentially $e^{-(4\pi/h)\int[2\mu(v-w)]^{1/2}dx}$. The diffusion coefficient for particles having an energy W is then proportional[11] to w. In the above expression $V(x)$ is the potential energy of the particle at a point x, and the integration extends between values of x that make $(V - W)$ vanish. These two formulae agree in predicting that D will increase rapidly with the temperature. Further, because b and V appear as exponents, it is to be ex-

[8] I am indebted to Dr. A. Nadai for his advice and help in handling this problem.
[9] J. Frenkel, Zeits. f. Physik **26**, 137 (1924).
[10] J. Frenkel, Zeits. f. Physik **35**, 652 (1926).
[11] W. Braunbeck, Zeits. f. Physik **44**, 690 (1927).
[12] R. W. Gurney and E. U. Condon, Phys. Rev. **33**, 132 (1929).

pected that the diffusion coefficients for different substances will vary greatly —even as to order of magnitude.

4. More Than One Atom of Impurity

The problem of impurities in solids is essentially that of studying the effects of inhomogeneities in a crystal.[13] But aside from the irregularities produced by the impurity because of its atomic character, there is a large scale effect if its atoms are not disposed at regular intervals. In ferromagnetic substances, for instance, the magnetic quality is determined not by the individual atoms alone, but by their relationship to each other in the lattice. This relationship involves groups of various sizes, such as the crystal grains; the Barkhausen[14] units; the individual blocks, if block structure, as has been suggested,[15] plays a part in ferromagnetic phenomena; and finally, each atom and its immediate[16] neighbors. Therefore, in discussing the effect of an impurity, it is necessary to know how its atoms are distributed among these various groups. Even in the case of a perfect single crystal, fluctuations in the concentration of impurities will in general have the effect of varying its physical properties from point to point, and the macroscopic sample will have to be treated as a heterogeneous medium.

The first case to be considered will be that in which the atoms are incapable of moving through the lattice. Here any distribution whatever will be stable, but the only repeatable distribution will be a random one. In the second case, where diffusion takes place, we shall limit ourselves to stable distributions, namely those which set in after the substance has been kept under constant physical conditions for a sufficiently long time. These distributions will depend on the existence of forces acting between the atoms of the impurity.

Case 1. (see appendix B)

Consider n cells or boxes in which N particles are arranged at random. We require the probability $f(a)$ that a cell chosen at random contain "a" particles. This will be the fraction of the total number of arrangements of the N particles among the n cells in which one particular cell contains "a" particles. The total number of arrangements possible is n^N. If we put "a" particular particles in a given cell, the number of arrangements possible is reduced to $(n-1)^{N-a}$. But the number of ways in which we can choose the "a" particles is $N!/a!(N-a)!$, so that the desired probability becomes

$$f(a) = \frac{N!(n-1)^{N-a}}{a!(N-a)!n^N}. \tag{8}$$

We shall be interested in the case where N and n, but not necessarily a, are large. Applying Stirling's formula for N and n we get

[13] Impurities along crystal boundaries and other surfaces are here neglected.

[14] J. Frenkel and J. Dorfman, Nature **126**, 274 (1930).

[15] F. Bitter, Phys. Rev. **37**, 91 (1931).

[16] F. C. Powell, Proc. Phys. Soc. **42**, 400 (1930) suggests that this last group may contain as many as 58 atoms in iron.

$$\lim_{N\to\infty,n\to\infty} f(a) = \left(\frac{N}{en}\right)^N \left(\frac{e(n-1)}{N-a}\right)^{N-a} \frac{1}{a!}$$

which, neglecting N^{-1} compared to unity, can be written

$$\lim_{N\to\infty,n\to\infty} f(a) = \frac{e^{-\xi}\xi^a}{a!} \tag{9}$$

where $\xi = N/n$, and is the average number of particles per cell. This formula is not convenient for computation when ξ is large, and for this case it is possible to derive[17]

$$\lim_{N\to\infty,n\to\infty,\xi\to\infty,a\sim\xi} f(a) = \frac{e^{-(\xi-a)^2/2\xi}}{(2\pi\xi)^{1/2}}. \tag{10}$$

Curves for various values of ξ are plotted in Figs. 5 and 6. Eq. (10) was used for $\xi = 1000$ only; the other curves represent Eq. (9).

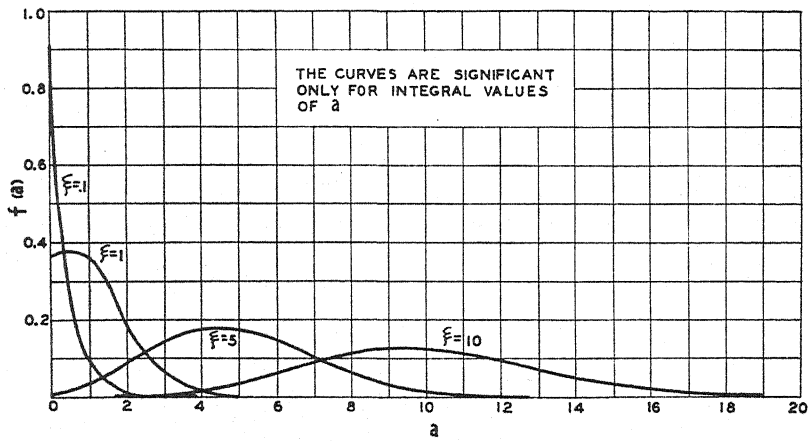

Fig. 5. N particles are randomly distributed among n cells, both N and n being $\gg 1$. $N/n = \xi$. $f(a)$ is the probability of finding "a" particles in a cell chosen at random. This figure shows $f(a)$ for small values of ξ.

Case 2. (See appendix B)

If the particles are capable of motion, they may be considered as a gas exerting a pressure, and the fluctuations will evidently depend on the equation of state. Fowler[18] shows that if v_0 is the volume normally occupied by ξ molecules at a pressure p_0, then writing $((a/\xi)-1)=\gamma$, the fluctuations are determined by

$$f(\gamma)d\gamma = \mu d\gamma \exp\cdot\left[\frac{1}{KT}\left\{\frac{v_0^2\gamma^2}{2!}\frac{\partial p_0}{\partial v_0} + \frac{v_0^3\gamma^3}{3!}\frac{\partial^2 p_0}{\partial v_0^2} + \frac{v_0^4\gamma^4}{4!}\frac{\partial^3 p_0}{\partial v_0^3} + \cdots\right\}\right]. \tag{11}$$

[17] See appendix B.

[18] Fowler, Statistical Mechanics, pp. 515–516.

For a perfect gas $\partial p_0/\partial v_0 = -n_0 KT/v_0$, the terms involving $\partial^2 p_0/\partial v_0^2$ etc. are negligible, and (11) reduces to (10).

The problem of finding the fluctuations in concentration of impurities in solids is now reduced to that of determining the forces acting between the impurity atoms, and hence the equation of state of the impurity. Two impurity atoms separated by only one or two atomic diameters may exert forces on each other arising from their electrons. But if they are separated by much greater distances, it seems reasonable to suppose that the only forces to be taken into consideration will be those resulting from the distortion of the lattice as given in Eqs. (4), (5) and (6). Thus it is necessary to determine the energy $E_n(R)$ of the distortion produced by two atoms of impurity a distance R apart, and then derive the forces by taking the gradient of $E_n(R)$.

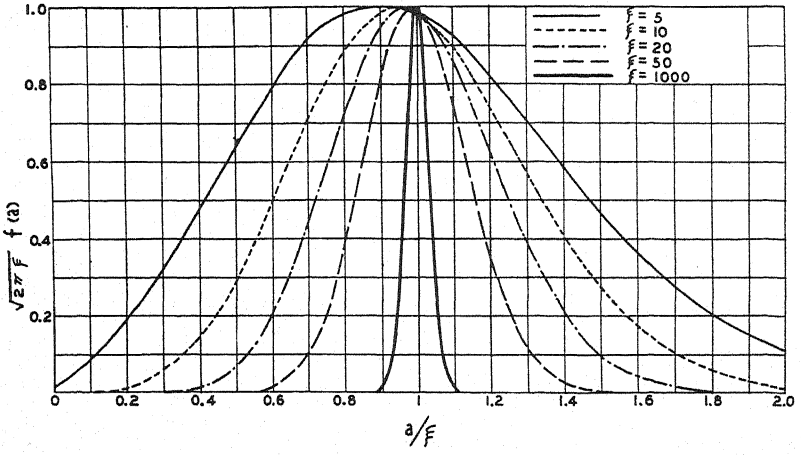

Fig. 6. For the meaning of the symbols see Fig. 5. In Fig. 6 $f(a)$ is plotted for large values of ξ.

Since the differential equations for small strains in an elastic solid are linear, we may add integrals provided the boundary conditions are still satisfied. Referring to the problem treated in part 2, this means that the small distortion of a continuous elastic medium produced by pressures on the surface of two spheres whose centers are a distance R apart are equal to the sum of the displacements ρ as given in Eqs. (4) and (5). The boundary conditions give rise to the added energy

$$\Delta E_n = \oint p\rho_a ds \tag{12}$$

where the integral is taken over the surface of both spheres, and ρ_a is the normal component of the distortion produced by the one sphere at a point on the surface of the other. As is evident from Fig. 4, $\rho_a = -\rho \cos(\theta+\phi)$, $r^2 = R^2 + R_0^2 - 2RR_0 \cos\theta$, and since $\cos(\theta+\phi) = \cos\theta\cos\phi - \sin\theta\sin\phi$, and $\cos\phi = (R - R_0\cos\theta)/r$, $\sin\phi = R_0 \sin\theta/R$, ΔE_n may be written

$$\Delta E_n = -2\int_0^{2\pi} d\phi \int_0^{\pi} R_0^2 \sin\theta d\theta p \frac{c_2}{r^2}\left[\frac{\cos\theta(R - R_0\cos\theta) - \sin\theta a \sin\theta}{r}\right]$$
$$= 4\pi p c_2 R_0^2 \int_{+1}^{-1} \frac{R_0 - R_x}{r^3} dx = 0. \tag{13}$$

In the above the substitution $x = \cos\theta$ has been made for simplicity in integration. This means that for dilute solutions to which alone the above considerations are applicable, the heat of solution per atom is independent of the concentration, and that the molecules of the solute or impurity exert no forces on each other over distances greater than a few atomic diameters. Thus the solute may be treated as a perfect gas and the fluctuations in concetration are correctly given by Eqs. (9) and (10) and Figs. 5 and 6.

There may, however, be short range forces between atoms of impurity, such as cause precipitation. Near a temperature at which precipitation occurs,

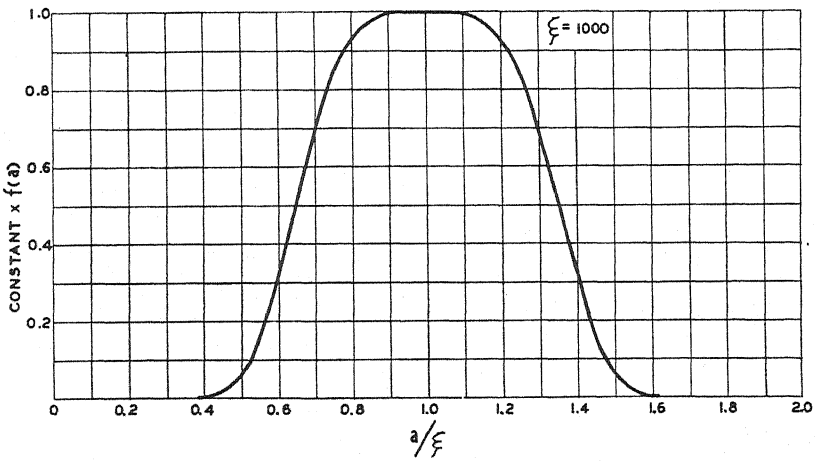

Fig. 7. A volume containing N gaseous molecules is divided into n regions, both N and n being $\gg 1$. $N/n = \xi$. $f(a)$ is the probability of finding "a" molecules in a cell chosen at random. If the gas is near the critical point and $\xi = 1000$ $f(a)$ is given by the curve above. This should be compared with the curve for $\xi = 1000$ in Fig. 6, which represents the corresponding conditions in a perfect gas.

these short range forces may cause very large density fluctuations, as they are in fact known to do in gases near the critical temperature, giving rise to the phenomenon of opalescence. As an example of the order of magnitude of the fluctuations to be expected under such circumstances, the fluctuations of a gas obeying Dietrici's equation of state

$$p(v - b) = NKTe^{-a/NKTV} \tag{14}$$

at the critical temperature are plotted in Fig. 7 for $\xi = 1000$. The formula for this curve may be derived by substituting Eq. (14) and Eq. (11), and the result[18] is

$$f(a) = \text{constant } e^{-(\xi-a)^4/22.2\xi^3}. \tag{15}$$

5. Applications

The above ideas may be applied to the effect of impurities on various properties of metals, but we shall in this paper only point out their bearing on a few ferromagnetic phenomena.

As a first example, consider platinum containing 1–10 percent cobalt, as has been studied by Constant.[19] One of the questions of primary importance in attempting to understand the properties of such solutions will be that of determining how many cobalt atoms are adjacent to 1, 2, 3, . . . etc. other cobalt atoms. In this particular case interatomic forces will be of importance, but it seems clear that unless they are strongly repulsive, one can hardly expect such solutions to be homogeneous. That is, the solution will consist of small regions which will behave like pure platinum, and small regions which will approximate pure cobalt, and all intermediate gradations. Since paramagnetism and diamagnetism are as a rule negligibly small compared to ferromagnetism, it may be a good approximation to treat the above solution as a group of ferromagnetic inclusions in non-magnetic material. In a future communication on block structure and ferromagnetism I hope to return to a more detailed discussion of the properties of such solutions.

One of the outstanding facts about ferromagnetism is its susceptibility to strains, and in the preceeding sections we have discussed the strains due to individual atoms of impurity. To these may be added strains due to fluctuations in concentration of impurities. Until more is known of the mechanism of magnetization it is useless to say anything about the effects of these strains on the hysteresis loop, magnetization curve, etc. beyond pointing out that strains do have large effects, that impurities do cause strains, and that consequently impurities may be expected to have large effects on magnetic properties by virtue of these strains.[20]

As has been mentioned, an impure metal may be expected to behave like an aggregate of regions whose physical properties are dissimilar. A phenomenon which would show the effect of these small regions would be the change of phase, if observed under suitable conditions. Suppose that some pure substance A undergoes a transformation at the temperature T, and that addition of some other substance B which dissolves in A lowers the transformation temperature. According to what has been said, B will distribute itself over A in such a way as to produce varying concentrations of B. It is to be expected that those regions containing small concentrations of B will undergo transformation at higher temperatures than those regions containing larger concentrations. The conclusion is that solutions undergo transformation *gradually* over a finite range of temperatures, a phenomenon which is often observed. So many other factors enter into the rate of transformation, however, that it is not practicable to attempt here a detailed comparison bebetween experimental facts and the above ideas.

[19] F. W. Constant, Phys. Rev. **36**, 1654 (1930).

[20] In this connection, see, for instance, an article by T. D. Yensen, Metals and Alloys **1**, 493 (1930).

Lastly, let us consider a peculiar feature of the iron-carbon diagram as it is usually drawn. This concerns the magnetic transformation A_2 in iron containing between 0.6 percent and 0.9 percent carbon, which, at the A_2 temperature of about 770°C is in the form of austenite, or γ-iron+carbon in solution. The significant point, as Honda and Takagi[21] have pointed out, is that the A_2 point in γ-iron+carbon is essentially the same as that of α-iron+carbon. This fact, for it has been observed so often as seemingly to leave no room for doubt, is not to be understood in the light of present concepts about the nature of ferromagnetism, and will necessitate fundamental changes, unless it is found that what has heretofore been called γ-iron+carbon actually contains small inclusions of α-iron which are responsible for the observed ferromagnetism of austenite. In the light of the previous discussion one would expect to find small regions having low carbon concentration, and it is these regions that might form inclusions of α-iron. Such regions should be capable of detection by means of x-rays, and an investigation is under way to determine whether or not they are actually present.[22]

Appendix A

Calculation of small strains due to impurities, and the resulting long range forces between atoms of impurity

Consider an infinite isotropic elastic medium in which a spherical hole has been excavated. A pressure p acts normally to the surface of the excavation, whose radius is R_0. What is the distortion and stress throughout the medium?

E = Youngs modulus; ν = Poisson's ratio; ρ = displacement—which is everywhere radial; ϵ_r = radial elongation; ϵ_t = tangential elongation; σ_r = radial stress; and σ_t = tangential stress.

Consider an element of volume bounded by two spherical surfaces $[rd\theta]^2$ and $[(r+dr)d\theta]^2$ and by the four plane surfaces $(r+dr/2)d\theta dr$

$$\epsilon_r = \frac{d\rho}{dr} \qquad \epsilon_t = \frac{\rho}{r}$$

$$\left.\begin{aligned} \epsilon_r &= \frac{1}{E}(\sigma_r - 2\nu\sigma_t) \\ \epsilon_t &= \frac{1}{E}(\sigma_t - \nu\sigma_t - \nu\sigma_r) \end{aligned}\right\} \text{ or } \left\{\begin{aligned} E\frac{d\rho}{dt} &= \sigma_r - 2\nu\sigma_t \\ E\frac{\rho}{r} &= -\nu\sigma_r + (1-\nu)\sigma_t \end{aligned}\right. \qquad \text{I}$$

[21] K. Honda and H. Takagi, Sci. Rep. Tohoku Univ. **2**, 203 (1914).

[22] See item 3 at the conclusion of the first section. Since completing this paper an article by F. M. Jaeger and J. E. Zanstra, Proc. Akad. Amsterdam **34**, 15, 1931 has come to my attention. Among other things, the authors investigate the crystal structure of rhodium as a function of temperature, and find (p. 19) that two phases co-exist as a mixture, one phase being present in the other in the form of very small particles containing $(33)^3$ or 36,000 atoms. Not only is the co-existence of the two phases of interest in connection with the previous discussion, but also the estimated size of the small inclusions, as having a possible bearing on the block theory of Zwicky.[4]

F_r and F_t are the forces acting on the various faces of the above volume element. For equilibrium

$$F_r = \sigma_r(rd\theta)^2 - \left[\sigma_r + \frac{d\sigma_r}{dr}dr\right](r + dr)^2 d\theta^2$$

$$-F_r = \sigma_r 2rdrd\theta^2 + \frac{d\sigma_r}{dr}drr^2d\theta^2$$

$$[F_t]_r = \sigma_t rd\theta drd\theta/2$$

and using the equilibrium conditions

$$r\frac{d\sigma_r}{dr} - 2(\sigma_t - \sigma_r) = 0. \qquad \text{II}$$

From I eliminate σ_r

$$E(\rho/r + \nu\rho') = \sigma_t(1 - \nu - 2\nu^2).$$

Eliminate σ_t

$$\sigma_r = E\rho' + \frac{2\nu E}{1 - \nu - 2\nu^2}(\rho/r + \nu\rho')$$

or

$$\sigma_t = \frac{E}{1 - \nu - 2\nu^2}(\rho/r + \nu\rho')$$

$$\sigma_r = \frac{E}{1 - \nu - 2\nu^2}[2\nu\rho/r + (1 - \nu)\rho'] \qquad \text{III}$$

Substitute III in II and get

$$r^2\rho'' + 2r\rho' - z\rho = 0. \qquad \text{IV}$$

Substitute $\rho = r^n$, and it is seen that $n = 1$ or -2 and the solution of IV therefore is

$$\rho = c_1 r + \frac{c_2}{r^2}$$

which in our case becomes $\rho = c_2/r^2$ since $\rho = 0$ for $r = \infty$ and therefore $c_1 = 0$.

If the boundary conditions are put in the form

$$\sigma_r = p \text{ for } r = R_0, \text{ then}$$

$$c_2 = -\frac{(1 - \nu - 2\nu^2)}{2(1 - 2\nu)E}R_0^3 p$$

$$\sigma_r = pR_0^3/r^3$$

$$\sigma_t = -p/2a^3/r^3.$$

If the boundary conditions are given in terms of strains instead of stresses

$$\rho = \delta \text{ for } r = R_0,$$

then

$$c_2 = R_0^2\delta \qquad \rho = \delta R_0^2/2$$

$$\sigma_r = \frac{-2(1-2\nu)c_2E}{1-\nu-2\nu^2}\frac{1}{r^3}, \qquad \sigma_t = -\sigma_r/2.$$

The energy of the distortion can be calculated in two ways

$$E_n = \delta\tfrac{1}{2}\sigma_r\big]_{r=R_0}\cdot\rho\big]_{r=R_0}\cdot\text{area} = \tfrac{1}{2}p\cdot\frac{-(1-\nu-2\nu^2)}{2(1-2\nu)E}\frac{R_0^3p}{R_0^2}\cdot 4\pi R_0^2$$

$$= \frac{1}{2}\frac{4\pi p^2R_0^3}{E}\frac{1-\nu-2\nu^2}{2(1-2\nu)}$$

or

$$E_n = \tfrac{1}{2}\int_{r=a}^{r=\infty}(\epsilon_r\sigma_r + 2\epsilon_t\sigma_t)dv$$

$$= \tfrac{1}{2}4\pi\int_a^\infty\left(-2c_2pR_0^3 - \frac{2c_2pR_0^3}{2}\right)\frac{dr}{r^4}$$

$$= -\frac{4\pi}{2}\int_a^\infty\frac{dr}{r^4}3c_2pR_0^3 = 4\pi c_2pR_0^3\frac{3}{3R_0^3}$$

$$= \frac{1}{2}\frac{4\pi p^2R_0^3}{E}\frac{1-\nu-2\nu^2}{2(1-2\nu)}$$

in agreement with the above.

For two spheres whose centers are a distance R apart ($R \gg R_0$) the total energy becomes $2E_n+\Delta E_n$ where

$$\Delta E_n = -2\int_0^\pi a^2\sin\theta d\theta p\frac{\delta R_0^2}{r^2}\left[\frac{\cos\theta(R - a\cos\theta)}{r} - \frac{\sin\theta a\sin\theta}{r}\right]$$

see Eq. (13) of the text. Substituting $\cos\theta = x$, we have

$$\Delta E_n = -4\pi p\delta R_0^4\int_1^{-1}\frac{x(R - R_0x) - R_0(1-x^2)}{r^3}dx$$

$$= 4\pi p\delta R_0^4\int_1^{-1}\frac{R_0 - Rx}{r^3}dx = 4\pi p\delta R_0^4(R_0A - RB)$$

where

$$A = \int_1^{-1}\frac{dx}{r^3} \qquad B = \int_1^{-1}\frac{xdx}{r^3}.$$

Let

$$r^3 = (\alpha + \beta x)^{3/2} \quad a = R^2 + R_0^2 \quad \beta = -2R_0R$$

$$A = \int_1^{-1} \frac{dx}{(\alpha+\beta x)^{3/2}} = \frac{2}{\beta}\left[\frac{(\alpha-\beta x)^{-1/2}}{-1}\right]_1^{-1} = -\frac{2}{\beta}\left[\frac{1}{(\alpha-\beta)^{1/2}} - \frac{1}{(\alpha-\beta)^{1/2}}\right]$$

$$B = \int_1^{-1} \frac{x\,dx}{(\alpha+\beta x)^{3/2}} = \frac{2}{\beta^2}\left[\frac{(\alpha+\beta x)^{1/2}}{1} + \frac{\alpha}{(\alpha+\beta x)^{1/2}}\right]_1^{-1}$$

$$= \frac{2}{\beta^2}\left[\frac{2\alpha+\beta x}{(\alpha+\beta x)^{1/2}}\right]_1^{-1}$$

$$B = \frac{2}{\beta^2}\left[\frac{2\alpha-\beta}{(\alpha-\beta)^{1/2}} - \frac{2\alpha+\beta}{(\alpha+\beta)^{1/2}}\right]$$

But

$$(\alpha+\beta)^{1/2} = (R^2 - 2RR_0 + R_0^2)^{1/2} = R - R_0$$

$$(\alpha-\beta)^{1/2} = R + R_0$$

$$A = -\frac{2}{R(R^2-R_0^2)} \qquad B = \frac{2R_0}{R^2(R^2-R_0^2)}$$

and therefore

$$\Delta E_n = 4\pi p \delta R_0^4 (R_0 A - RB) = 0.$$

Appendix B

Details of calculations of density fluctuations

The derivation of Eq. (8) in the text

$$f(a) = \frac{N!(n-1)^{N-a}}{a!(N-a)!n^N}$$

is perhaps given in sufficient detail to be quite clear. Assuming $N \to \infty$, $n \to \infty$, we may write, according to Stirling's theorem

$$\lim_{n\to\infty} p! = (2\pi p)^{1/2}\left(\frac{p}{e}\right)^p$$

$$\frac{N!}{(N-a)!} = \frac{N^{1/2}}{(N-a)^{1/2}} \frac{\left(\frac{N}{e}\right)^N}{\left(\frac{N-a}{e}\right)^{N-a}} = e^{-a}N^N(N-a)^{-(N-a)}$$

Here $\lim_{N\to\infty} N^{1/2}/(N-a)^{1/2}$ has been put equal to unity, and we get

$$\lim_{N\to\infty,\, n\to\infty} f(a) = \left(\frac{N}{en}\right)^N \left(\frac{e(n-1)}{N-a}\right)^{N-a} \frac{1}{a!} \cdot .$$

It is desired to put this in a form in which N and n appear only as a ratio, $N/n=\xi$. To this end we put

$$\frac{e(n-1)}{N-1}=\frac{e(n-1)}{N}\,\frac{1}{1-a/N}$$

and hence

$$\lim_{N\to\infty,n\to\infty} f(a) = \left(\frac{N}{en}\right)^N\left(\frac{e(n-1)}{N}\right)^N\frac{1}{(1-a/N)^N}\left(\frac{e(n-1)}{N-a}\right)^{-a}\frac{1}{a!}$$

$$=\left[\frac{1-\dfrac{1}{n}}{1-\dfrac{a}{N}}\right]^{N-a}\left(\frac{en}{N}\right)^{-a}\frac{1}{a!}$$

But, simplifying, we find

$$\left[\frac{1-\dfrac{1}{n}}{1-\dfrac{a}{N}}\right]^{N-a} = \left[\left(1-\frac{1}{n}\right)\left(1+\frac{a}{N}+\cdots\right)\right]^{N-a} = \left(1-\frac{1}{n}+\frac{a}{N}\right)^{N-d}$$

$$=\left[1+\frac{a-\xi}{N}\right]^N\left[1+\frac{a-\xi}{N}\right]^{-a}=\left[1+\frac{a-\xi}{N}\right]^N$$

since

$$\lim_{N\to\infty}\left[1+\frac{a-\xi}{N}\right]^{-a}=1.$$

Expanding $[1+a-\xi/N]^N$, and neglecting $1/N$ compared to unity, we get

$$1+a-\xi+\frac{1}{2!}(a-\xi)^2+\frac{1}{3!}(a-\xi)^3+\cdots=e^{a-\xi}$$

and finally

$$\lim_{N\to\infty,n\to\infty} f(a) = e^{a-\xi}\left(\frac{en}{N}\right)^{-a}\frac{1}{a!}=\frac{e^{-\xi}\xi^a}{a!} \qquad \text{I}$$

and

$$\lim_{N\to\infty,n\to\infty,\xi\to\infty,a\sim\xi} f(a) = \frac{e^{-\xi}\xi^a}{(2\pi a)^{1/2}}\left(\frac{e}{a}\right)^a. \qquad \text{II}$$

To find for what value of "a", say a_m $f(a)$ has a maximum, we require the formula

$$\frac{d}{da}\left(\frac{e}{a}\right)^a=\left(\frac{e}{a}\right)^{-a}\log_e\frac{1}{a}$$

We then find

$$\frac{df}{da}=\left\{\frac{e^{\xi}\left(\frac{e\xi}{a}\right)^{a}}{(2\pi a)^{1/2}}\left[\log_e\frac{1}{a}+\log_e\xi-\frac{2\pi}{4\pi a}\right]\right\}_{a=a_m}=0$$

or

$$\log_e a_m=\log_e\xi-\frac{1}{2a_m}$$

and for

$$a_m\gg 1,\quad a_m=\xi.$$

For large values of ξ these formulae are not very satisfactory for numerical computations, and the following procedure leads to a more desirable result.

Given n = number of cells, N = number of particles, $N/n=\xi$ is the average number of particles per cell, a_s = number of particles in cell s.

$$s\sum_1^n a_s=N\quad s\sum_1^n(a_s-N/n)=0.$$

The fraction of the phase space occupied by this distribution is (see Jeans, Dynamical Theory of Gases, page 47)

$$\theta_a=n^{n/2}(2\pi N)^{-(n-1)/2}e^{-NK_a}$$

$$K_a=\frac{1}{N}s\sum_1^n(a_s+\tfrac{1}{2})\log_e\frac{na_s}{N}.$$

This assumes the applicability of Stirling's formula. Substituting $\alpha_s=a_s-N/n$ in the expression for K_a, we get

$$K_a=\frac{1}{N}s\sum_1^n\left(\frac{N}{n}+\alpha_s+\frac{1}{2}\right)\log_e\left(1+\frac{n\alpha_s}{N}\right).$$

Neglecting $1/2$ compared to N/n, we get

$$K_a=\frac{1}{n}s\sum_1^n\left(1+\frac{\alpha_s}{\xi}\right)\log_e\left(1+\frac{\alpha_s}{\xi}\right)$$

$$=\frac{1}{N}\left\{\frac{1}{2}\frac{n}{N}s\sum_1^n\alpha_s^2-\frac{1}{6}\left(\frac{n}{N}\right)^2 s\sum_1^n\alpha_s^3+\cdots\right\}$$

Whenever we can write

$$s\sum_1^n\left(\frac{n\alpha_s}{N}\right)^2\gg\frac{1}{3}s\sum_1^n\left(\frac{n\alpha_s}{N}\right)^3\text{ and higher powers}\qquad\text{III}$$

then the expression for K_a is considerably simplified.

$$NK_a = \frac{1}{2}\frac{n}{N} s \sum_1^n \alpha_s^2.$$

Jeans shows (page 48) that the fraction of the phase space which represents distributions for which $K_0 < K < K_0 + dK$ is

$$\frac{N^{(n-1)/2}}{\Gamma\left(\frac{n-1}{2}\right)} e^{-NK_0} K_0^{(n-3)/2} dK.$$

In a similar way it can be shown that the fraction of the phase space for which $K_0 < K < K_0 + dK$ and in addition for which an α_p chosen at random is equal to some given number, say α, is

$$\theta_a n^{-1/2} \frac{dA}{dK} dK$$

where θ_a and K have the values above and

$$A = \frac{\pi^{(n-2)/2}}{\Gamma\left(\frac{n}{2}\right)} \left(\frac{2N^2 K_0}{n} - \alpha^2\right)^{(n-2)/2}.$$

Substituting $x = NK - n\alpha^2/2N$ we get

$$A = \frac{\pi^{(n-2)/2}}{\Gamma\left(\frac{n}{2}\right)} \left(\frac{2N}{n} x\right)^{(n-2)/2}$$

$$\frac{dA}{dK} dK = \frac{dA}{dx}\frac{dx}{dK} dK$$

or

$$\frac{dA}{dK} dK = \frac{\pi^{(n-2)/2}}{\Gamma\left(\frac{n}{2}\right)} \frac{1}{2}(n-2)\left(\frac{2N}{n} x\right)^{n/2-2} \frac{2N}{n} dx$$

$$= \frac{\pi^{n/2-1}}{\Gamma\left(\frac{n}{2}-1\right)} \left(\frac{2N}{n}\right)^{n/2-1} dx$$

and

$$\theta_a n^{-1/2} \frac{dA}{dK} dK = \left(\frac{2\pi N}{n}\right)^{-n/2+1/2} \left(\frac{2\pi N}{n}\right)^{n/2-1} \frac{e^{-n\alpha^2/2N}}{\Gamma\left(\frac{n}{2}-1\right)} e^{-x} x^{n/2-2} dx$$

or

$$\frac{e^{-\alpha^2/2\xi}}{(2\pi\xi)^{1/2}\Gamma\left(\frac{n}{2}-1\right)} e^{-x}x^{n/2-2}dx.$$

In order to find the fraction of the phase space for which $\alpha_p=\alpha$, the above expression must be integrated over all values of K from 0 to ∞, or of x from $-n\alpha^2/2N$ to ∞.

$$\int_{-n\alpha^2/2N}^{\infty} e^{-x}x^{n/2-2}dx = \int_0^{\infty} e^{-x}x^{n/2-2}dx + \int_0^{n\alpha^2/2N} e^{-x}x^{n/2-2}dx$$

$$= I + II$$

$$I = \Gamma\left(\frac{n}{2}-1\right)$$

and the result is that the fraction of the phase space for which a given cell contains α-particles is

$$f(a) = \frac{1}{(2\pi\xi)^{1/2}} e^{-\alpha^2/2\xi}\left[1 + \frac{II}{\left(\frac{n}{2}-2\right)!}\right]$$

But

$$II = -\left[e^{-x}\left(\frac{n}{2}-1\right)!\left\{1 + p\sum_1^{n/2-2}\frac{x^p}{p!}\right\}\right]_0^{\alpha^2/2\xi}$$

and therefore

$$\lim_{n\to\infty}\frac{II}{\left(\frac{n}{2}-2\right)!} = -\left[e^{-x}e^{x}\right]_0^{\alpha^2/2\xi} = 0$$

and the complete result is

$$\lim_{N\to\infty,\, n\to\infty,\, \xi\to\infty,\, a\sim\xi} f(a) = \frac{1}{(2\pi\xi)^{1/2}} e^{-\alpha^2/2\xi} \qquad \text{IV}$$

the condition $\xi\sim a$ being intended to indicate that the assumption in Eq. III must be satisfied.

It remains to be shown that Eq. II and IV are equivalent.

$$\lim_{N\to\infty,\, n\to\infty,\, \xi\to\infty,\, a\sim\xi} \frac{e^{-(\xi-a)^2/2\xi}}{(2\pi\xi)^{1/2}} = \frac{e^{-\xi}}{(2\pi a)^{1/2}}\left(\frac{e\xi}{a}\right)^a$$

Omitting the cumbersome limits, we may write

$$e^{\xi^2-a^2/2\xi} = \left(\frac{\xi}{a}\right)^{a+1/2}.$$

Omitting 1/2 compared to a and taking the logarithm of both sides this becomes

$$\frac{\xi^2}{a^2} - 1 = \frac{\xi}{a} \log \left(\frac{\xi}{a}\right)^2$$

and expanding the logarithm for values of the argument near unity this becomes

$$\frac{\xi^2}{a^2} - 1 = \frac{\xi}{a}\left(\frac{\xi^2}{a^2} - 1\right)$$

which is valid for $\xi \sim a$.

LETTERS TO THE EDITOR

Prompt publication of brief reports of important discoveries in physics may be secured by addressing them to this department. Closing dates for this department are, for the first issue of the month, the twenty-eighth of the preceding month; for the second issue, the thirteenth of the month. The Board of Editors does not hold itself responsible for the opinions expressed by the correspondents.

OH Bands and the Ultraviolet Line Spectrum of the Wehnelt Interrupter

With an improved form of Wehnelt interrupter, equipped with a cooling coil and an electrolyte circulator, the spectrum of the discharge at the positive platinum point electrode has been investigated in the region λ4000 to λ2230. Solutions of hydrochloric, sulphuric, and nitric acid were used.

The OH bands were particularly prominent. A continuous banding from head to head was present. The new lines observed have been analysed and rotational assignments made. Twenty-four new lines have been added to the analysis by Jack (Proc. Roy. Soc. **A115**, 373 (1927)) of the band λ2608, and 120 lines to the analysis by Watson (Astrophys. J. **60**, 145 (1924)) of the bands λλ2811 and 2875. A few rearrangements of previous assignments were made in the case of the latter bands—particularly in the *R* branch of λ2875. Seventy three new assignments were made in the analysis by Fortrat (J. de Physique **5**, 20 (1924)) of the bands λλ3064 and 3122. A preliminary comparison of wave-lengths of the new lines observed in these bands with values given in Rowland's table of solar lines showed good agreement with lines of unknown origin.

The band λ3428 is present on the plates but seems to present no new features.

A new band in the region λ3525 is being investigated in view of its possible relationship to the OH system.

Up to the present only lines arising from the platinum anode have been observed between λλ2608 and 2230.

R. WILLIAM SHAW

Department of Physics,
Cornell University.

May 6, 1931.

An Infrared Band System of Iodine Bromide

During an investigation of the absorption of iodine bromide in the visible, the writers recently observed an infrared band system due to this substance which, so far as they are aware, has not previously been reported. When an absorption cell 3 ft. in length was used, containing IBr at about 90 mm pressure at 50°, five band progressions of moderate intensity were observed in the region λλ6850–8060. Due to the fact that there is a rather sudden change in the slope of the $\omega_v v$ curve for the upper state at $v'=12$ it is not possible to represent the entire system satisfactorily by one simple formula. However, those bands for which v' is less than 12 are well represented by the equation:

$$\nu(\text{cm}^{-1}) = 13{,}251 + (105.9\, v' - 2.42\, v'^2) - (266.5\, v'' - 0.81\, v''^2).$$

The absolute numbering of the vibrational levels of the upper electronic state is still in some doubt as it has not as yet been possible to make use of the isotope effect which is not very readily measurable.

The upper electronic level of the infrared system is a state which yields normal atoms on dissociation. By means of a graphical extrapolation the energy of dissociation of the normal IBr molecule into normal atoms has been estimated to be 1.801 ± 0.007 volts ($41{,}520 \pm 150$ cal). The good agreement with the value 1.84 volts estimated by Cordes and Sponer[1] from fluorescence data of Loomis

[1] H. Cordes and H. Sponer, Zeits. f. Physik **63**, 334 (1930).

is possibly due to a compensation of errors in the latter case.

Recent studies in this laboratory[2] on the effect of temperature on the equilibrium between iodine, bromine, and iodine bromide have given an accurate value for the heat of formation of iodine bromide ($H_{298°}$) given in the following equation:

$I_2+Br_2=2\,IBr+2{,}540$ cal (0.110 volts).

Since the heat of this reaction is practically independent of temperature it may be compared directly with the energy change at the absolute zero, for the reaction, calculated from the spectroscopic determinations of the dissociation energies of iodine,[3] bromine, and iodine bromide. This spectroscopic value is 2,440 cal (0.106 volts), which checks with the thermal value well within the probable experimental error. This agreement is good evidence for the self consistency of the spectroscopic values of the dissociation energies of the three molecules in question.

RICHARD M. BADGER
DON M. YOST
Gates Chemical Laboratory,
California Institute of Technology,
May 7, 1931.

[2] D. M. Yost and J. McMorris, to appear shortly in the Journ. Am. Chem. Soc.

[3] We have used for the dissociation energy of iodine a value 1.535 volts received in a personal communication from Mr. W. G. Brown, at Berkeley, California.

Thermionic Emission in Caesium-Oxide Photo-cells at Room Temperatures

During an investigation of the suitability of some caesium oxide on silver photoelectric cells for astronomical photometric work at low intensities it was noticed that in some cases there was, in total darkness, a large, unidirectional leakage which increased rapidly as the cell was warmed and which could be decreased considerably by the application of a magnetic field. These facts indicated conclusively that the leakage was of thermionic origin. Subsequently more careful temperature measurements were made both above and below room temperatures which showed that the emissions were following the ordinary T^2 equation with thermionic work functions in different cells varying from about 0.40 to 0.80 volt.

The largest thermionic current which we have observed at 20°C and 22.5 volts is 8×10^{-9} amperes in a cell of about 88 cm² cathode area, which is approximately the current given photoelectrically by exposing the cell to an illumination of 3×10^{-4} lumens from tungsten light at 2848°K color temperature. Observations were made on this cell as low as −5°C and could undoubtedly have been continued lower if we had shifted from our high sensitivity galvanometer to the electrometer. The thermionic constants determined from a plot were $A=5\times10^{-3}$; $b_0=8550$. At 20°C an increase of one degree increases the thermionic current about 11.2 percent so that when such a cell is used for photoelectric measurements it might well be necessary to control its temperature. The value of b_0 for this particular cell is very close to that found by Koller (Phys. Rev. **33**, 1082 (1929)) for some caesium oxide on silver cells from 100° up to 170°C.

Another cell of somewhat lower photoelectric sensitivity gave the values, $A=3.7\times10^{-10}$; $b_0=4290$, the lowest that we have yet obtained. The cathode area of this cell was 19.4 cm², and the total current at 20°C was about 2.7×10^{-10} amperes, with only a 5.8 percent increase in a temperature rise of one degree. The largest thermionic current at room temperature was therefore not obtained with the cell of lowest work function due to the very great decrease in the value of A. The measurements made so far on different cells do not indicate any precise relation between log A and b_0 which would enable one to predict definitely the emission at room temperature from the thermionic work function. If there is a large decrease in b_0 as shown above, it is of course reasonable to expect a decrease in A otherwise the emission would increase enormously.

Measurements on some of the cells at constant illumination to tungsten light showed a decided drop in the photo current with considerable increase of temperature while on the other hand the effect of cooling did not seem to be nearly as great in producing an increase. This is opposite to what Koller found with cathodes much less sensitive photoelectrically than our own.

We have purposely selected for this work cells with clean walls and stems which gave negligible ohmic leakage. The two kinds of leakage are present in many cells and it is difficult to separate them with certainty. If

the caesium oxide on silver cell is to be used for measuring very small light intensities, the area of the cathode should not be any larger than is necessary to intercept the radiation; that is, the photoelectric emission should be made as large as possible relative to the thermionic emission.

E. F. KINGSBURY
G. R. STILWELL
Bell Telephone Laboratories,
New York, New York,
March 30, 1931.

A Case of Abnormal Molecular Rotation

In the fluorescence of mercury vapor with the addition of nitrogen and a trace of hydrogen, Gaviola and Wood[1] observed the band spectrum of the HgH molecule with an abnormal rotation corresponding to an apparent temperature of 3000°, although the gas was at room temperature. This observation has been interpreted[2] by the assumption of the following sequence of processes: formation of the HgH molecule, then excitation of this molecule with high oscillation and normal rotation according to the Franck-Condon rule, and finally change of oscillation into rotation during the life time of the excited state through collisions with N_2 molecules. In this interpretation, the high rotation observed in the band spectrum is therefore not directly excited but due to a secondary effect.

An interesting similar observation has recently been described by W. Lochte-Holtgreven.[3] He found in the electric discharge in acetylene the C_2 bands with an abnormal rotational energy corresponding to 4700° and the CH bands with 2000°.

By varying the conditions, he found that these "rotational temperatures," being much larger than the real temperatures, are not due to secondary effects such as collisions during the life time of the excited state. Instead he concluded they must arise from the elementary process of excitation itself. Thus the interpretation must differ from that of the rotation of the HgH molecule just described. The present letter deals with this new observation, thus supplementing the interpretation of the HgH bands given in a previous paper.

It seems possible to understand the high rotation of the C_2 and CH bands in the acetylene discharge on the basis of the Franck-Condon rule dealing originally with oscillation. According to Hedfeld and Mecke, the HC≡CH molecule in its normal state forms a straight line.[4] Let us assume that in its excited state it forms a crooked line. Professor Slater has pointed out to me that such a pronounced change in the shape of the molecule is not all an arbitrary assumption, but should be expected, if in the excitation process the carbon atom goes over from the quadrivalent to the divalent state. The same change of valence by excitation has been found e.g. in the CN molecule.[5] According to Slater's new theory,[6] the straight line model of the normal state points to quadrivalent C atoms while the two valences of a divalent atom should always be at right angles, thereby forming a crooked molecule.

This pronounced change in the shape of the molecule lends itself to an application of Franck's idea. The change of electron configuration is fast compared with the motion of the nuclear masses. Immediately after the excitation process, the molecule in its new electronic state has still its old shape and therefore a large potential energy leading to intense vibration. Contrary to the vibration of the diatomic molecule, the motion is essentially transverse.[7] This vibration might produce dissociation, if the potential energy exceeds the dissociation energy. Any dissociation process brought about by absorption of light can be recognized experimentally by the continuous absorption spectrum. In the case of the HCCH molecule, mainly continuous absorption has been observed as reported by

[1] E. Gaviola and R. W. Wood, Phil. Mag. **6**, 1191 (1928).

[2] H. Beutler and E. Rabinowitsch, Zeits. f. physik. Chem. (B) **8**, 403 (1930); O. Oldenberg, Phys. Rev. **37**, 194 (1931).

[3] W. Lochte-Holtgreven, Zeits. f. Physik **67**, 590 (1931); G. B. Kistiakowsky, Phys. Rev. **37**, 276 (1931).

[4] K. Hedfeld and R. Mecke, Zeits. f. Physik **64**, 151 (1930).

[5] W. Heitler and G. Herzberg, Zeits. f. Physik **53**, 52 (1929).

[6] J. C. Slater, Phys. Rev. **37**, 481 (1931).

[7] Cf. R. Mecke, Zeits. f. Physik **64**, 173 (1930).

Lochte-Holtgreven and by Kistiakowsky. It might be assumed that this absorption corresponds partly to the described process.

This splitting up of the molecule by *transverse* vibration leads necessarily to strongly *rotating* molecules. (Fig. 1). The transverse vibration which splits up the centre bond of the HC≡CH molecule leads to two CH molecules strongly rotating in opposite direction,

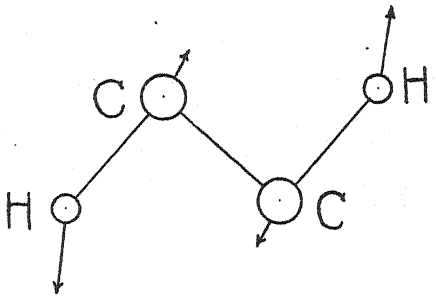

Fig. 1. Vibration of the excited HCCH molecule.

while the total moment of momentum of the system remains unchanged or changed only by unity. In the other dissociation process mentioned by Lochte-Holtgreven, the H atoms might fly away in the direction of the arrows (Fig. 1) leaving an excited C_2 molecule. This must have high rotation as indicated again by the arrows. Dissociation in steps might take place too.

In general any combination of increasing longitudinal and transverse vibration should lead to a dissociation resulting in a rotating and vibrating molecule, the energy of which is determined by the potential curves and not by the temperature of the gas. Thus we understand the observation reported by Lochte-Holtgreven, that the rotation of the excited molecules C_2 and CH is characteristic for this excitation process starting from HC≡CH and that its energy shows some deviation from a Boltzmann distribution.[8]

Has this argument a bearing on the diatomic molecule? This might be the case, considering the diatomic molecule in collision with an atom. When by impact of the second kind the HgH molecule takes over excitation energy from the Hg′, it is generally assumed, that the rotation of the HgH does not change considerably, but that the vibration might change on the basis of the Franck-Condon rule. It must be taken into account, however, that after the excitation process the H atom starts its fast vibration in the close neighbourhood of the colliding slow Hg atom. *In the same collision process*, therefore, this might turn over the motion of the H atom from *vibration* into *rotation*. No appreciable kinetic energy of *translation* is produced due to the heavy weights of the Hg atom and the HgH molecule. In other words, the H atom starts its motion in a modified field of force determined by the new electronic state of the HgH molecule and at the same time the presence of the colliding Hg atom. This motion might be rotation as well as vibration. (If in the case of good resonance the transfer of electronic energy by impact of the second kind takes place over an exceptionally large distance, this argument might fail, because in this case the HgH molecule would become excited without being disturbed in its vibration by the close neighbourhood of a colliding heavy body.)

The statement, therefore, that no appreciable rotation is produced by impact, holds for excitation by electron impact and for every thermal impact. However, it should not be supposed to hold for this type of impact of the second kind between heavy bodies.

This process in addition to the process discussed in the writer's recent paper[2] would be expected to play a part in Gaviola's and Wood flourescence experiment.

O. OLDENBERG

Jefferson Physical Laboratory,
Harvard University,
Cambridge, Massachusetts,
April, 1931.

[8] R. M. Badger and J. L. Binder (Phys. Rev. **37**, 800 (1931)). mention a certain difficulty in calculating dissociation energies of polyatomic molecules from band spectra, due to the fact the fragments might retain a considerable amount of energy in their *electronic* and *vibrational levels*. According to the present result, also the *rotation* is able to keep energy far exceeding the thermal value.

On the Effect of Resonance in the Exchange of Excitation Energy

I should like to add a few words to the letter recently sent to the Editor of the Physical Review, under the above title. The application of the Franck-Condon principle to this problem brings out another point which supplements those already considered and which

will be of importance if the two curves shown in Fig. 1 of the above mentioned article reach their asymptotic values at something like the same value of r, which may often be expected to be the case. Then it is seen that, unless the asymptotic values are the same within the order of magnitude of the average relative translational energy of two at the temperature considered, the intersection of the two curves will occur so high up that it will be out of reach of an average pair of colliding atoms even though the initial state be represented by the upper curve; of course if the initial state is represented by the lower curve, the transition cannot occur with an average pair of atoms unless the curves are close enough together so that the difference in energy can be made up by conversion of the limited translational energy available to electronic energy, but this consideration shows that transitions will often be prevented even when the conversion is in the other direction, from internal to translational energy. It is of interest to note that in the cases considered by Kallmann and London (Zeits. f. physik. Chem. **2B**, 226 ff. (1929)) the energy transferred from translational to internal or *vice versa* is, in the case of those transitions which occur with exceptional probability, of the order of magnitude of the translational energy of an atom at room temperature.

O. K. RICE

Chemical Laboratory,
Harvard University,
May 7, 1931.

Continuous Spectrum of Hydrogen Molecular Ion (H_2^+)

The negative glow is generally aceepted as a good source of ionized spectra, due to the probable high concentration of ions at this portion. In hydrogen, therefore, there may be some hope to obtain some spectrum at the negative glow, which had, if any, H_2^+ as an emitter. The hydrogen molecular ion has been dealt with theoretically by a number of investigators. Recently E. Teller[1] has calculated the excited states produced when the ion is separated step by step into a proton and a hydrogen atom in the ground state. According to him almost all the potential energy curves show no minima, except those corresponding to the $1s\sigma$ and the $3\ d\sigma$.

Following the interpretation of the ordinary hydrogen continuous spectrum, we can expect some continuous spectrum which can be explained by transitions to any one or all of the unstable states of the H_2^+ molecule. With such an expectation a spectroscopic examination of the negative glow in hydrogen, at a pressure of about 0.2 mm Hg was carried out. Although the ordinary continuous spectrum is absent in the negative glow, an indication of the continuous spectrum, even if not so intense, is observed between $H\beta$ and $H\gamma$.

The probable high concentration of the H_2^+ molecule suggests that the above mentioned continuous spectrum may be due to the H_2^+ molecule. The energy involved in this region of spectrum is not inconsistent with such an explanation. As the spectrum was not observed at so extremely low pressures as in the cases of Herzberg[2] and Brasefield,[3] it is not in danger of being confused with that of the fluorescence light on the walls of the tube. So that it will not be inadequate to ascribe this continuous spectrum to the H_2^+ molecule. Details will be published with reproduction in the Science Reports of the Tôhoku Imperial University, **20** (1931).

Y. HUKUMOTO

The Physical Institute,
Imperial University, Sendai, Japan,
May 4, 1931.

[1] E. Teller, Zeits. f. Physik **61**, 458 (1930).
[2] G. Herzberg, Ann. d. Physik **84**, 560 (1927).
[3] C. J. Brasefield, Phys. Rev. **33**, 925 (1929).

New Covariant Relations Following from the Dirac Equations

1. In an article appearing in this issue of the Physical Review the authors derive by means of the spinor calculus four invariant relations between the four wave functions which are independent of the potentials. (Eq. (6), (11), (12), (13) of Ch. III.) The first of these is

$$\frac{\partial j^\lambda}{\partial x^\lambda} = 0 \qquad (1)$$

where j^l is the four-current. The second relation with which we shall concern ourselves in this letter, may be written, using ordinary tensor notation:

$$\frac{\partial k^\lambda}{\partial x^\lambda} = \frac{mc}{h} J \qquad (2)$$

where k^l is also a four vector quadratic in the wave functions and defined by the equation preceding Eq. (17) of our article. In Eq. (14) two complex quadratic invariants Δ and $\bar{\Delta}$ were introduced; from these we form the two real combinations:

$$\begin{aligned} \tfrac{1}{2}(\Delta + \bar{\Delta}) &= I \\ \tfrac{1}{2}i(\Delta - \bar{\Delta}) &= J. \end{aligned} \qquad (3)$$

These quantities are identical with the invariants I and J of Darwin. We also prove in our paper that

$$k^\lambda j_\lambda = 0;\ k^2 = -j^2. \qquad (4)$$

Further we proved (Eq. (17)) that:

$$k^\alpha M_{\alpha l} = \frac{h}{mc} j_l \cdot J;\ j^\alpha M_{\alpha l} = \frac{h}{mc} k_l \cdot J. \qquad (5)$$

Here M_{kl} is the antisymmetric tensor of the polarization (Darwin, Gordon), whose components are again quadratic in the wave functions.

2. For the sake of a possible physical interpretation and to facilitate comparison with recent work of Fock, it seems desirable to express the above relations in term of matrices. It is easily seen, however, that the original α matrices of Dirac are unsuited to express covariance relations. We use instead the form of the Dirac equations

$$(\Gamma^\lambda p_\lambda + mc)\psi = 0 \qquad (6)$$

which is used by Weyl and Sommerfeld. (see our paper, Eq. (1), (2), (3), Introduction). The Γ^l matrices satisfy the well known relations:

$$\Gamma^k\Gamma^l + \Gamma^l\Gamma^k = 2g^{kl}. \qquad (7)$$

We adopt now the first point of view mentioned in the introduction of our paper, and regard the ψ as invariant and the Γ^l as a matrix four-vector. Using this and the relations (7), we can now form the following covariant quantities.[1]

$$\begin{array}{ll} 1 & \backsim I \\ \Gamma^i & \backsim j^i \\ \Gamma^i\Gamma^k & \backsim M^{ik} \\ \Gamma^i\Gamma^k\Gamma^l & \backsim k_m \\ \Gamma^i\Gamma^k\Gamma^l\Gamma^m & \backsim J \end{array} \qquad (8)$$

None of the indices are allowed to be equal. We assert that quantities in the right column are obtained by multiplying the corresponding quantities in the left column with ψ' from the left and ψ from the right, (ψ' is the transposed ψ; see[2]). The relations (1) and (2) can now be derived independently from the Dirac equation (6); for (1) this is well known, whereas Eq. (2) becomes:

$$\frac{\partial}{\partial x_1}\psi'\Gamma^2\Gamma^3\Gamma^4\psi\,\pi - \frac{\partial}{\partial x_2}\psi'\Gamma^3\Gamma^4\Gamma^1\psi + \cdots = \frac{2imc}{h}\psi'\Gamma^1\Gamma^2\Gamma^3\Gamma^4\psi. \qquad (9)$$

Relations (4) and (5) can now be derived immediately with the help of (7).

3. One can also easily, though not so symmetrically, express the quantities (8) in terms of the Dirac α and the Dirac-Darwin ψ. For j and M we refer to Gordon's[2] paper. For k, I and J one obtains the following expressions:

$$\begin{aligned} k^1 &= -i\alpha_2\alpha_3 & k^2 &= -i\alpha_3\alpha_1 \\ k^3 &= -i\alpha_1\alpha_2 & k^4 &= -i\alpha_1\alpha_2\alpha_3 \\ I &= \alpha_4 & J &= \alpha_1\alpha_2\alpha_3\alpha_4 \end{aligned}$$

We see therefore that the *spacial* components of k are identical with the three-vector σ as introduced by Dirac[3] and further used by Fock[4] and that the time component of k is equal to ρ_1 (Dirac) or ρ_a (Fock), whereas I is equal to ρ_3 (ρ_c) and J to $\rho_2(\rho_b)$. It thus appears that from the view point of covariance neither σ nor ρ are true vectors.

4. It follows from the equality of $k_{1,2,3}$ with σ_1, σ_2, σ_2 that the spacial components of the four-vector k are equal to the components of the magnetic moment of the electron. On the other hand it is well known that the spacial components of the tensor M^{ik} represent the magnetic moment of the electron also. When neglecting relativity (i.e. considering only the large ψ_3 and ψ_4) the k_1, k_2, k_3 become indeed equal to M_{yz}, M_{zx}, M_{xy} respectively. Thus it is seen that the

[1] For this systematization (without the above identifications) compare J. Schouten, Proc. Amsterdam **32**, 105 (1929); A. Proca, Journ. de Phys. **1**, 235 (1930). F. Sauter, Zeits. f. Physik **63**, 803 (1930) used it very profitably for the solution of special problems.

[2] Gordon, Zeits. f. Physik **50**, 630 (1928).

[3] P. A. M. Dirac, Principles of Quantum Mechanics, page 242.

[4] V. Fock, Zeits. f. Physik **68**, 522 (1931).

three-dimensional vector of the magnetic moment can be completed relativistically in two ways, either to a four-vector or to an antisymmetric tensor. In the corpuscular theory already L. H. Thomas[5] called attention to these two possibilities. What the exact physical meaning of this duplicity in character of the moment and especially of the fourth component of k is remains unclear to us. Perhaps it is connected with the two-fold interpretation of the spin as angular momentum or as magnetic moment.

G. E. UHLENBECK
OTTO LAPORTE

Department of Physics,
University of Michigan,
Ann Arbor, Michigan,
May 16, 1931.

[5] L. H. Thomas, Phil. Mag. **3**, 1 (1927).

On the Gas-Temperature in the Positive Column of an Arc

For the study of thermionization in the positive column of an arc the possibility of measuring exactly the gas temperature is of great importance. We have therefore developed a new method of ascertaining this temperature avoiding any errors of previous methods, which permits measuring the temperature by gas-density.

The density of the arc-gas in the axis of a stabilized (by whirling gas according to Schoenherr) straight d.c.-arc of 2 amp. in air and also nitrogen of atmospheric pressure were measured. This was done by testing the absorption of a soft x-ray (of about 6A) passing along the axis of arc. The intensity of the x-ray was observed by the Geiger-counter. In a comparative test without the arc, the gas density was diminished by evacuating the arc-space until the x-ray intensity became the same as with the arc. The intensity found thereby is also the average density of the arc-gas traversed by the x-ray. The disturbing spaces next to the electrodes were eliminated by measuring arcs of different lengths (5-20 cm).

With the ideal gas-law this density gives a temperature in the positive column of 5270 ± 300°K in the air-arc, and of 5460 ± 320°K in the nitrogen-arc. Considering the dissociation at these high temperatures, one gets a gas-temperature of 5000 ± 400°K in the air-arc and of 5200 ± 450°K in the nitrogen-arc. By pyrometric measurements a pure carbon (2 mm diameter) inserted in the arc axis had 3100°K in the air-arc and 2300°K in the nitrogen-arc. The temperature of the carbon is not identical with that of surrounding gas; clearly it depends on chemical reactions at its surface (oxidation!).

An extensive report on our investigations will be published in the next number of the "Wissenschaftliche Veröffenlichungen aus dem Siemens-Konzern."

ALFRED VON ENGEL
MAX STEENBECK

Wissenschaftliche Abteilung,
der Siemens-Schuckertwerke A.-G.,
Berlin,
April 28, 1931.

Second Series *June 15, 1931* *Vol. 37, No. 12*

THE
PHYSICAL REVIEW

X-RAY WAVE-LENGTH CHANGE BY PARTIAL ABSORPTION

By J. M. Cork
University of Michigan
(Received May 11, 1931)

Abstract

The attempt to repeat the experiments of Mr. B. B. Ray in which a change in wave-length occurred in an x-ray beam upon passage through an absorbing substance, has been continued. In the previously reported experiments CuK radiation was passed through absorbers of boron, beryllium, carbon, nitrogen and oxygen. These same absorbers have been retried with tungsten L radiation with a spectrometer of greater dispersion. Although it should have been possible to observe a modified line of 1/3000 the intensity of the unmodified, in no case has any trace of a modified line been observed.

WHEN x-rays are incident upon matter they react with the electrons of the matter in various possible ways. One type of interaction, the photo-electric effect, in which the x-ray photon communicates all its energy to the electron, ejecting it from the atom, the remainder of the energy of the photon appearing as the kinetic energy of the electron, is now well established. Equally well established is the Compton effect in which the photon interacts with the free electron giving a portion of its energy to the electron, which is ejected as a recoil electron. The emergent photon with lessened energy is consequently of longer wave-length. For electrons bound in definite energy states a fine structure of the scattered modified photon on the long wave-length side would appear as a possibility. Recent experiments[1] indicate that this fine structure does not exist.

Observing the failure of these experiments, Mr. B. B. Ray[2] examined the wave-length of the emergent photons for zero scattering angle. For this angle the Compton wave-length shift would be zero. A spectral photograph of the transmitted beam showed along with the strong line due to the unmodified incident wave-length, certain fainter companion lines displaced toward longer wave-lengths. The displacements of these lines as reported, were just as would be expected if in the passage through the absorbing substance the photon gave up some of its energy to elevate a bound inner electron to an outer energy level, passing on unchanged in direction but with less energy and hence longer wave-length.

[1] Ehrenberg, Zeits. f. Physik **53**, 234 (1929); Coster, Nature **123**, 642; Kast, Zeits. f. Physik **58**, 519 (1929); Bearden, Phys. Rev. **36**, 791 (1930); Gingrich, Phys. Rev. **36**, 1050 (1930).
[2] Ray, Nature **125**, 746 and 856; **126**, 399; Zeits. f. Physik **66**, 261 (1930).

Thus the energy equations may be shown:

Photoelectric effect $h\nu = h\nu_e + (1/2mv^2)$ photoelectron (1)
Compton effect $h\nu = (1/2mv^2)$ recoil electron $+ h\nu$ mod. (2)
Ray effect $h\nu = h\nu_e + h\nu$ mod. (3)

The existence of this last effect is thus of such importance that the experiments seemed worthy of repetition.

Experimental

To this end an attempt was made to repeat the work of Ray. The first experiments[3] using a copper target x-ray tube equipped with a Lindemann thin glass window with a calcite crystal spectrometer were carried out in the laboratory of Dr. M. deBroglie in Paris. The investigation has been continued in this university using both copper and tungsten target tubes with a calcite crystal spectrometer having slit-crystal and crystal-photographic plate distances of 54 cm. This gives a dispersion on the photographic plate of about 5 x.u. per mm.

The absorbing layer was in every case placed between x-ray target and spectrometer slit. Various thicknesses of material were employed although the thicker the material the more apparent the effect should be. The absorbing layers used by Ray were not well described in his reports, except that he mentions the use of lamp black for carbon[4] absorption. Besides carbon, absorbing layers of beryllium, boron, nitrogen and oxygen have been used. Screens made of various thicknesses of gold beaters skin have also been tried.

In order to form an estimate of relative intensities a portion of the unmodified line was covered with a shield during most of the exposure. This shield for a twenty hour exposure was generally removed only for 2 minutes. The intensity of radiation was such that generally an exposure of 2 seconds was enough to render the main unmodified line visible.

In these experiments the crystal was kept stationary during two exposures, first with and then without absorber in place.

Results

Using the various absorbers mentioned, no trace whatever of a modified line in the positions to be expected was observed. Typical spectrograms obtained are shown in Fig. 1. For these spectrograms the target was of tungsten, giving the strong line W$L\alpha_1$, and also the $L\alpha_2$ line whose intensity is about one-tenth as strong. The copper K lines always appeared unintentionally on the same plate, due presumably to a copper focussing cylinder on the cathode. On certain of these prints even the very faint Cu$K\alpha_3$, α_4 line is observable, although its intensity is only about 1/600 that of the Cu$K\alpha_1$ line.

The intensity of the modified line as observed by Ray was about 1/400 that of the parent line. In these spectrograms shown in Figure 1 the intensity

[3] J. M. Cork, Comptes Rendus, Acad. Sci. Paris, 192, 153.

[4] In a letter to the writer Mr. Ray mentions that 4 or 6 thicknesses of gold beater's skin gave equally good results.

of the W$L\alpha_2$ line on the shielded part of the figure is about 1/6000 that of the unshielded W$L\alpha_1$. Now a line of the intensity of the W$L\alpha_2$ line located in the region of general blacking on the plate might be somewhat obscured.

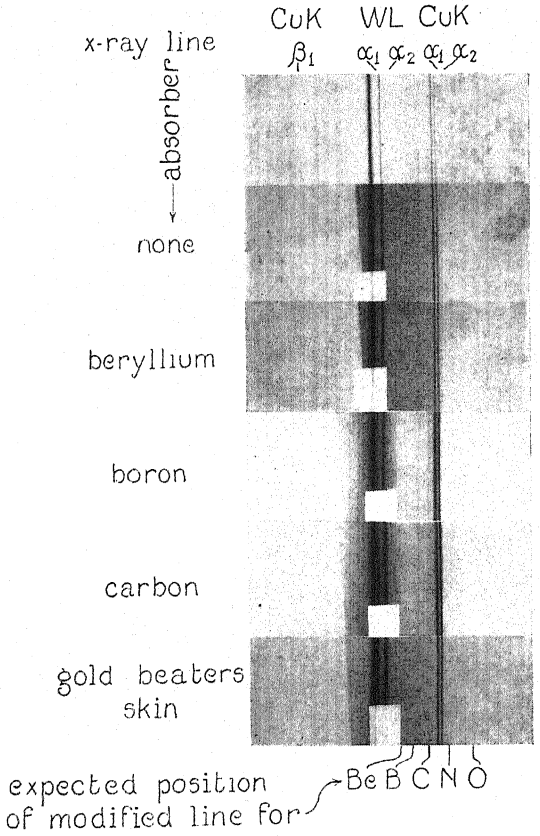

Fig. 1. Showing the absence of expected modified lines.

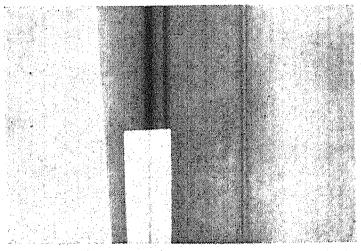

Fig. 2. Showing superposition of W$L\alpha_1$, α_2 2 min. Exposure on general radiation exposure 20 hours.

However, if the general blackening is not too strong it offers but slight hindrance to the observance of relative intensities. This is illustrated in Fig. 2. In this figure after the exposure was completed with shield in place twenty

hours and then removed for two minutes, the whole plate was shifted along and the lines allowed to fall in the region of general radiation for a period of two minutes. One observes little loss in contrast.

If the effect exists therefore, it must be of an intensity much less than that reported by Ray. Other experimenters[5] have now likewise failed to observe the modified lines, although their existence has been confirmed by others.[6]

This opportunity is taken to express appreciation to M. deBroglie for the generous facilities of his laboratory and to M. Thibaud and M. Duprés la Tour for their kind assistance during the first part of this investigation.

[5] G. A. Lindsay, Nature **127,** 305. J. H. Van der Tuuk, Naturwissenschaften **14,** 308. A. J. O'Leary, Phys. Rev. **37,** 873 (1931).

[6] Majumdar, Nature **127,** 92. Ray states in his letter that the effect has been observed by Prof. Saha at Allahabad University.

STRUCTURE OF THE HELIUM ARC LINE 3888*

By R. C. Gibbs and P. G. Kruger
Physical Laboratory, Cornell University

(Received April 24, 1931)

Abstract

The helium arc line ($1s2s\ ^3S_1 - 1s3p\ ^3P^\circ_{0,1,2}$)3888A, has been examined for structure and has been resolved into the three components which are predicted by theory. The $1s3p\ ^3P^\circ_{0,1,2}$ levels are inverted which is in agreement with previous results for the $1s2p\ ^3P^\circ_{0,1,2}$ levels. The frequency differences in the present case are:

$$\nu_{0,1} = 0.192\ \text{cm}^{-1}, \qquad \nu_{1,2} = 0.165\ \text{cm}^{-1}.$$

Introduction

In 1927 Houston[1] reported the structure of the $1s2p\ ^3P^\circ_{0,1,2}$ levels. Later in the same year G. Hansen and P. G. Kruger[2] finished the analysis of the He arc lines 5876, 4713 and 4472, thus completing the term scheme for $1s2p\ ^3P^\circ_{0,1,2}$ and $1s3d\ ^3D_{1,2,3}$. No attempt was made at that time to determine the structure of higher P° terms.

Experimental

The line 3888A $1s2s\ ^3S_1 - 1s3p\ ^3P^\circ_{0,1,2}$ is one of the strongest lines of the He I spectrum and was easily excited in a metal liquid-air cooled Schüler lamp. A Fabry-Perot interferometer with 5 mm, 8 mm, and 10 mm spaces between the mirror surfaces was used to analyze the line. Mirrors having a reflection coefficient of 92 percent were used so that the resolving power varied from 0.775×10^6 to 1.55×10^6 as the distance between the mirrors was increased from 5 mm to 10 mm.

Results

Table I. *Components of the helium line* 3888.

Int.	λ	Δλ	ν	Δν
10	0.0000A		0.000 cm^{-1}	
		0.0247A		0.165 cm^{-1}
7	−0.0247		0.165 cm^{-1}	
		0.0298		0.192 cm^{-1}
3	−0.0545		0.357 cm^{-1}	

Table I gives, in column one, the relative estimated intensities of the components as obtained from several microphotometer curves made from

* The investigations upon which this article is based were supported by grants from the Heckscher Foundation for the Advancement of Research, established at Cornell University by August Heckscher. Acknowledgment is also made of the use of spectroscopic apparatus which was in part purchased by a grant from the National Research Council.

[1] Houston, Proc. Nat. Academy **13**, 91 (1927).

[2] Published by G. Hansen, Ver. Deut. Phy. Ges. **10**, 5 (1929).

various plates. The wave-lengths (assuming the strongest line zero), wave-length separations, frequency numbers and frequency separations are given in columns 2, 3, 4 and 5 respectively.

Fig. 1 shows a microphotometer curve of one of the plates.

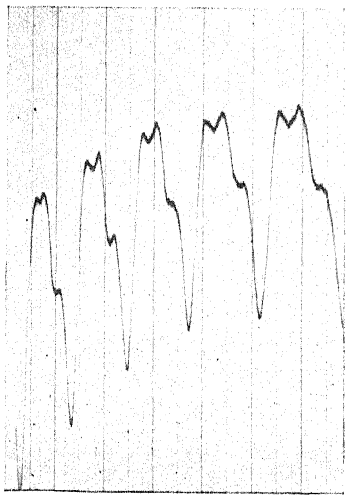

Fig. 1. Microphotometer curve showing the structure of the He arc line 3888.

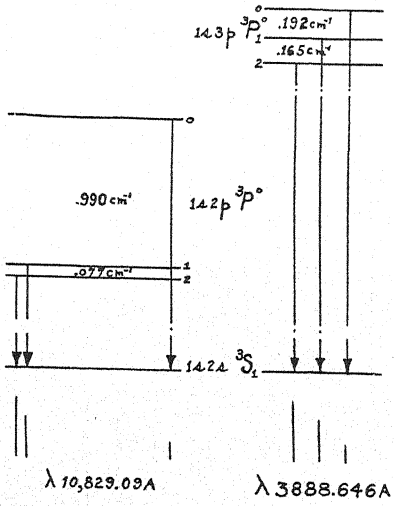

Fig. 2. Term separations for the first two members of the $1snp\ ^3P^\circ$ series in helium, He I.

Fig. 2 shows the term scheme for the $1s2p\ ^3P^\circ_{0,1,2}$ and $1s3p\ ^3P^\circ_{0,1,2}$ terms with respect to the $1s2s\ ^3S_1$ term. The relative separations of the two $^3P^\circ$ terms are drawn to the same scale.

Discussion

It is interesting to note that the anomalous separations of the $1s2p\ ^3P^\circ$ terms are no longer so anomalous in the $1s3p\ ^3P^\circ$ terms. In the latter case the separations are more nearly what would be expected if the Landé interval rule were obeyed. Thus if the $^3P^\circ$ term separations continue to become more normal in higher total quantum states the $1s4p\ ^3P^\circ$ terms should have nearly a 2:1 separation.

Resolution of the structure of the line 3187A ($1s2s\ ^3S_1 - 1s4p\ ^3P^\circ_{0,1,2}$) would show whether the separation of the $1s4p\ ^3P^\circ$ terms have a 2:1 ratio. Assuming that the rate of decrease of $\Delta\nu_{0,2}$ between the first and second members of this series of terms is continued to the third member, a value of about 0.120 cm^{-1} is computed for $\Delta\nu_{0,2}$ for the $1s4p\ ^3P^\circ_{0,1,2}$ terms. Thus if the 2:1 ratio exists in the third member, the components of the 3187 line would be 0.0082 and 0.0040A apart. The complete resolution of components lying as close together as this necessitates cooling the discharge in liquid hydrogen or preferably in liquid helium. It is hoped that some other laboratory in which these low temperatures are available will undertake to study the structure of this line.

In 1926 Heisenberg[3] calculated the separation of the $1s2p\ ^3P^\circ_{0,1,2}$ term and obtained results which were later found to be in agreement with experimental results.[1,2] It would be desirable now to have the $1s3p\ ^3P^\circ_{0,1,2}$ term separations calculated by quantum theory or wave mechanics to see if the agreement here is as good as in the previous case.

A possible reason why the P° term separations in higher quantum states should approach the normal 2:1 ratio, is that in the higher quantum states the p electron is less tightly bound to the nucleus and thus the energy conditions in these higher states are more nearly like those in heavier elements. Furthermore the coupling of the np electron to the $1s$ electron becomes weaker in the higher quantum states,—so that possibly with increasing n the interaction arising from the action of the orbital motion or the spin of one electron on the spin of the other becomes less effective in determining the internal ratio.

[3] W. Heisenberg, Zeits. f. Physik **39**, 499 (1926).

RAMAN SPECTRA OF SULPHURIC ACID

By Raymond M. Bell and W. R. Fredrickson
Pennsylvania State College and Syracuse University

(Received May 11, 1931)

Abstract

Concentrated H_2SO_4 gives a series of Raman lines which, with the exception of the 4566A line, decrease in number and intensity with a decrease in concentration and finally disappear. At the point at which the above lines vanish, a broad line (4817A) appears and persists in dilute solutions. At low concentrations the water bands are present. The 4566A line is present at all concentations of acid and increases in intensity with a decrease in concentration, but is missing in pure water. A line with the same wave-length (within experimental error) and intensity variation is found in HNO_3, and it is suggested that the two lines have the same origin.

RAMAN spectra have made possible a new approach to the study of conditions in acids at various dilutions. Rao[1] found that the Raman lines obtained from HNO_3 could be classified into the three following groups according to their behavior as the acid was diluted: (1) those due to the HNO_3 molecule, (2) those due to the NO_3^- ion, and (3) those due to the water molecule. The lines of the first group decrease in intensity as the concentration is decreased and finally disappear. The lines in the second group increase in intensity as the concentration is decreased, reaching a maximum at the concentration when the lines of the first group vanish, and then these lines also decrease in intensity. The lines of the third group appear as bands which first appear faintly as the acid is somewhat diluted and gradually increase in intensity and broaden as the concentration is decreased. The purpose of this paper is to present similar data obtained from sulphuric acid at various dilutions. A preliminary account of data has previously been reported in a letter to Nature.[2]

The method used to obtain spectrum was similar to the general method described by R. W. Wood,[3]—using a mercury arc. Most of the photographs were taken with a prism spectrometer, but plates were also obtained with a plane grating on the spectrometer table in place of the prism. The latter arrangement gave greater dispersion, but the intensity was, indeed, greatly reduced.[4] Definite traces of lines and bands were found at all concentrations. With the prism, most of the lines could be obtained with an exposure of three minutes and the strongest could be detected on plates of a minute exposure. The lines in Table I are all taken from plates with 30 minute exposure,—

[1] Rao, Proc. Roy. Soc. **A127,** 279 (1930).
[2] Bell and Fredrickson, Nature **125,** 895 (1930).
[3] R. W. Wood, Phil. Mag. **6,** 729 (1928).
[4] Attempts were made to obtain Raman spectra with a small concave grating of 120 cm focus, but without success.

with experimental conditions exactly the same throughout. A fifteen hour exposure with the grating gave the same intensity as the thirty minute prism exposure and those lines are listed in Table II. The concentrations are measured in mol percent. That is, 50 percent concentration is one H_2SO_4 molecule to one H_2O molecule; 100 percent is the purest acid available, commercial 96 percent; and 0 percent is pure distilled water. The wave-lengths are accurate to 3A. The numbers in parentheses are eye estimates of the intensity of the lines.

TABLE I. *Raman spectrum of H_2SO_4 (Prism).*

Concentration (percent)	Wave-length in Angstroms						
100			4585 (1)	4566 (1)	4542 (4)	4470 (3)	4438 (3)
90				4566 (1)	4542 (3)	4470 (3)	4438 (3)
80				4566 (2)	4542 (3)	4470 (3)	4438 (3)
70				4566 (2)	4542 (2)	4470 (2)	4438 (2)
60				4566 (2)	4542 (2)	4470 (2)	4438 (2)
50				4566 (3)	4542 (1)	4470 (2)	4438 (2)
40	4817			4566 (3)	4542 (1)	4470 (2)	4438 (2)
30	4817			4566 (3)			
20	4817	4750 to 4700		4566 (3)			
10	4817	4750 to 4700		4566 (2)			
0		4750 to 4700					

100	4276 (0)	4252 (0)	4224 (3)	4203 (4)	4171 (0)	4142 (2)	
90			4224 (3)	4203 (3)	4171 (0)		
80			4224 (3)	4203 (3)			
70			4224 (2)	4203 (2)			
60			4224 (2)	4203 (1)			
50			4224 (1)	4203 (1)			
40			4224 (1)	4203 (0)			
30							
20			4225 to 4175				
10			4225 to 4175				
0			4225 to 4175				

Notes. 4817 was a broad line or band at all times.
4566 became broad at low concentrations.
4750 to 4700 and 4225 to 4175, water bands, became sharper and less intense as concentration increased.

TABLE II. *Raman spectrum of H_2SO_4 (Grating).*

Concentration (percent)	Wave-length in Angstroms							
100	4585 (1)	4566 (1)	4540 (4)	4470 (3)	4440 (2)	4279 (0)	4225 (1)	4203 (2)
80		4566 (2)	4540 (3)	4470 (3)	4440 (2)		4225 (1)	4203 (1)
60		4566 (3)	4540 (3)	4470 (3)	4440 (2)		4225 (0)	4203 (1)
40		4566 (4)	4540 (2)	4470 (3)	4440 (2)		4225 (0)	4203 (0)
30		4566 (3)	4540 (1)	4470 (1)	4440 (1)		4225 (0)	4203 (0)

From Table I we see that the lines found in concentrated H_2SO_4 persist as far down as 40 percent. The lines given for 100 percent agree with the re-

sults obtained by Ganesan and Venkateswaran[5] with concentrated H_2SO_4. The intensity of all lines except the 4566 line decreases in intensity with a decrease in the concentration. The 4566 line, however, increases in intensity to a maximum and then broadens and decreases in intensity. The two water bands are in approximate agreement with the measurements given by others. It is interesting, however, to note the decrease in breadth and the sharpness of these bands at their first appearance at high concentrations. The origin of the 4817 line or band is uncertain. It makes its appearance when the other lines disappear and is always broad. The 4470 line is the only one which seems to indicate a shift in wave-length as the concentration is decreased. On some of our plates there is a slight indication that this line has shifted slightly to the red.

The lines obtained with the grating, as listed in Table II, are similar to those in the preceding one. Here even the 30 percent concentration shows some of the H_2SO_4 molecule lines. The most striking thing about the grating plates is the change in intensity with concentration. The 4540 line decreases considerably in going from 100 to 40 percent, while the 4566 line increases correspondingly.

Comparing the above results with those reported by others we find two interesting facts. (1) Several experimenters[6] working with sulphates find in all cases lines at 4552A and 4214A which they attribute to the $SO_4^=$ ion. Our plates fail to reveal these lines, not even the plates of very long exposure time. (2) Rao[7] reports a line at 4567A which he finds at all concentrations of HNO_3. We also find a line at 4566A which appeared at all concentrations. Ganesan and Venkateswaran[8] give 21895 cm^{-1} as the measurement for the same H_2SO_4 line and 21893 cm^{-1} for the HNO_3 line. Both of these lines increase in intensity with a decrease in concentration. Neither line appears in pure distilled water. We are inclined to believe that this close agreement in wave-length and variation in intensity with concentration is not fortuitous, but rather an indication that the two lines may have the same origin—perhaps a hydrated hydrogen ion.

The experimental work described above was done in the Department of Physics at Syracuse University.

[5] Ganesan and Venkateswaran, Ind. Jour. of Phys. 4, 195 (1929).

[6] Mukherjee and Sen Gupta, Ind. Jour. of Phys. 3, 503 (1929). Hollaender and Williams, Phys. Rev. 34, 994 (1929).

[7] Rao, reference 1.

[8] Ganesan and Venkateswaran, reference 5.

INVESTIGATIONS IN THE SPECTRAL REGION BETWEEN 20 AND 40μ

By John Strong*
California Institute of Technology, Pasadena

(Received May 5, 1931)

Abstract

An apparatus is described which is convenient for studying the optical properties of substances with reststrahlen having wave-lengths from 6 to 150μ. A vibrationless support is described, the essential features of which are copied from the design of R. Müller but the construction is simplified. The transmission of several gases was studied with reststrahlen having wave-lengths 20 to 33μ. SO_2 shows strong absorption at 20.75μ. The reflectivity of SO_2 was tested and found to be zero at both 20.75μ and 8.7μ where it has strong absorption bands. Gas absorptions from 20 to 33μ are compared with the Raman indications. Transmissivities and reflectivities of various materials are given for the spectral region 20 to 33μ. β—MgO was found to have a reststrahlen near 23μ. Potassium iodide was found to be transparent to wave-lengths greater than 33μ.

THE region of the spectrum between 20 and 40μ has not been as extensively investigated as the regions on either side, due to the lack of materials having suitable optical properties for windows, dispersing prisms and filters. The use of various reststrahlen and gratings with open thermocouples (or microradiometers) has given us most of the knowledge we have of the optical properties of substances in this region. Recently, L. Kellner[1] has studied the transmission of paraffin (Kahlbaum M.P. 68°–72°C) and found that layers of 1.2 mm thickness are sufficiently transparent beyond 20μ for use as thermocouple windows. This discovery materially decreases the difficulty of investigation in this region.

Potassium chloride is transparent to 23μ, potassium bromide to 30μ, and potassium iodide to wave-lengths greater than 33μ. The technique for growing large crystals of these materials was developed by the author[2] at the University of Michigan. With these materials available the region now open for prism spectroscopy extends beyond 15μ by more than an octave of frequencies. The purpose of this present paper is the extension of our knowledge of the optical properties of substances in this new region.

Schaefer and Matossi[3] have prepared a table of the reststrahlen bands which have well established wave-lengths. Several of these bands fall in the spectral region 20–40μ and the present investigation was made with these bands.

The reststrahlen bands are not as monochromatic as might be desired but this is compensated for by the abundance of available energy and the

* National Research Fellow.

[1] L. Kellner, geb. Sperling, Zeits. f. Physik **56**, 215 (1929).

[2] John Strong, Phys. Rev. **36**, 1663 (1930).

[3] Schaefer and Matossi, Das Ultrarote Spektrum, p. 60 (1930).

wide range of wave-lengths which are obtainable with the one technique. Wave-lengths from 6 to 150μ are thus obtainable, corresponding to a frequency range of more than five octaves.

The Apparatus

A reststrahlen apparatus was devised for these experiments which was superior to older reststrahlen arrangements in the following ways. First, the crystal reflectors needed were of small size and, consequently, easier to obtain than the large crystals required for the old arrangements. Second, the transfer of crystals in going from one wave-length to another was a simple operation requiring only a few seconds of time and this operation did not disturb the air through which the radiations passed and thus it was possible to keep the air dry at all times.

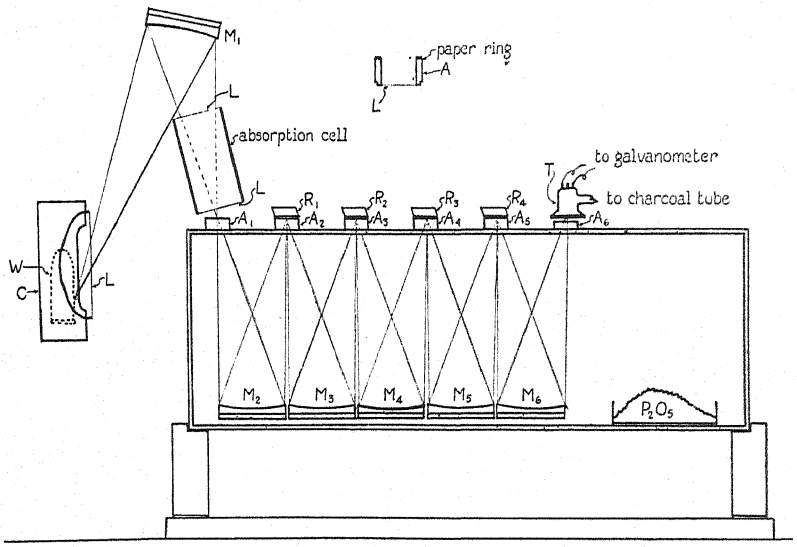

Fig. 1. Diagram of reststrahlen apparatus.

Fig. 1 is a diagram of the reststrahlen apparatus used for this research. Light from the Welschback mantle is reflected by the mirror, M_1, into the reststrahlen apparatus through the circular hole, A_1, where it subsequently passes, after reflection from the concave spherical mirror, M_2, to a second circular hole, A_2. A crystal mirror, R_1, covers this hole and reflects the light to the concave mirror, M_3, where it is returned for the second reststrahlen mirror, R_2. After three (or four) successive reflections from reststrahlen mirrors and possibly one reflection from a metal mirror, the light is focused onto the receivers of the vacuum thermocouple, T. The thermocouple is a compensated two junction type, with one of the junctions covered by a rocksalt plate. This thermocouple was made for me by Dr. C. H. Cartwright. The window for the thermocouple was a 1 mm plate of potassium iodide.

For studying the absorption of gases, an absorption cell may be introduced into the radiation path between the mirror, M_1, and the circular hole, A_1.

The housing for the reststrahlen apparatus is made from brass sheet laid over a framework of half inch square iron rod. This is mounted on a wooden support. The corners were sealed with beeswax to make the apparatus gas tight so the air might be dried with P_2O_5. The base of the housing was penetrated by three adjusting screws (not shown) for each of the spherical mirrors, M_2 to M_6. The outside of the housing was covered with a layer of felt and to protect further the apparatus from temperature fluctuation, it was encased within galvanized iron walls. The insert, A, in Fig. 1 shows a cross section of one of the small brass cylinders which fit over the holes A_1 to A_5. This is drawn to a scale twice as large as that for the rest of the figure. The cylinders each have a lacquer window, L, stretched over their base.

These lacquer windows are very transparent (96 to 100 percent) for waves longer than 20μ and permit the air within the apparatus to be kept dry, when the reststrahlen mirrors are being interchanged. A paper ring on the top of each cylinder protects the mirrors from being scratched.

Because the silver mirrors are not used on their optical axes, there is considerable astigmatism. This results in a large final image with smaller intensity than if there were no astigmatism. The illumination in the center of the final image will increase, however, as the size of the reststrahlen mirrors is increased. It is believed that since the reststrahlen surfaces used were each $\frac{3}{4}$ inches in diameter, the illumination of the thermocouple receivers was not greatly attenuated due to astigmatism.

In order to have the galvanometer free from microseismic vibrations, it was mounted on a vibrationless support. This support was a simplification of the one designed by R. Müller,[4] and was constructed in the following manner. Three triangular plywood boards, each $\frac{1}{2}''$ thick and $11''$ on an edge were clamped and bored with six $\frac{3}{8}''$ holes, two holes in each corner. (See Fig. 2). The two upper triangles were separated $20''$ and bolted together at this distance with three $\frac{3}{8}''$ brass rods, one at each corner, to form the swinging framework for the galvanometer. The top and bottom plywood triangles were fastened together by three $24''$ brass rods $3/32''$ diameter. These rods passed freely through the remaining $\frac{3}{8}''$ holes in the middle triangle. The bottom triangle served for the base of the support while the $3/32''$ rods afforded the necessary looseness of mechanical connection between the swinging framework and the earth. Three levelling nuts screw on the termini of the $3/32''$ rods below the bottom triangle. Four $10''$ pie pans are filled with transformer oil and stacked on top of the swinging framework to dampen oscillations. These pans were filled to the depth found by experiment to give maximum damping. The galvanometer was mounted on the middle triangle and above it on a tripod ballast was placed to make the period of oscillation of the support about two seconds. When this period is attained, the mechanical coupling is sufficiently loose to isolate effectively, the galvanometer from the horizontal components of microseismic vibrations. No protection against vertical components is necessary as these do not cause a spurious deflection

[4] R. Müller, Ann. d. Physik **1**, 613 (1929).

of the galvanometer. In order to clamp rigidly the support for making adjustments, tapered pins are dropped along the side of the 3/32″ rods in two of the holes in the middle plate. The swinging framework suffers a slight parallel displacement when these pins are removed but this does not affect the galvanometer adjustment. This support is conveniently housed on a corner shelf to shield it from air currents.

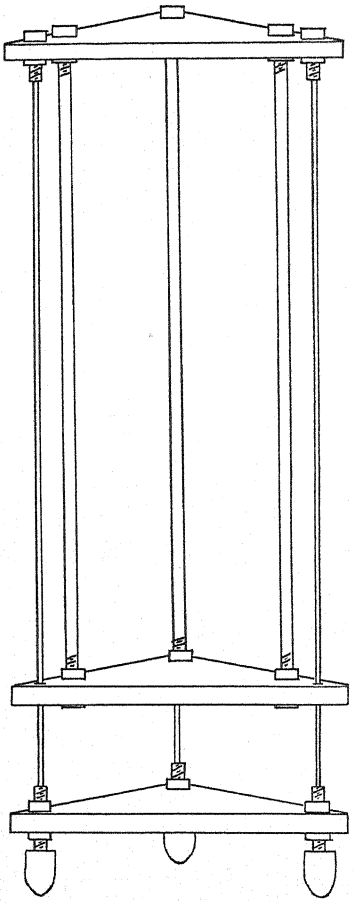

Fig. 2. Vibrationless support for galvanometer.

In order to shield the Welschback mantle, W, from air currents, a lacquer film, L, was stretched across the opening of the water-cooled chamber, C, which surrounds it. The radiations were taken off at nearly grazing incidence because the mantle was porous. Although the mantle material is quite opaque to waves 20–40μ, the mantle at normal incidence, showed an absorption of only 70 percent for these radiations due to its porosity.

The thermocouple receivers were blackened with a paint made from pulverized mantle material and colorless lacquer. Tests showed that these re-

ceivers absorbed as much as when coated with a mixture of soot and water glass but the paint did not cause the receivers to curl as water glass did.

The Reststrahlen

The table of Schaefer and Matossi is reproduced in part. This gives the method used for obtaining reststrahlen having wave-lengths of 20 to 33μ.

Table I.

Substance	Number of reflections	Filter	λ	E	Literature
Quartz	4	2.5 mm AgCl	20.75μ 8.7 μ	18.0 12.0	H. Rubens and E. F. Nichols, Wied. Ann. **60**, 418 (1897).
Fluorite	3	5 mm KCl	22.9 μ	6.0	H. Rubens Berl. Ber., 1915, p.4.
Calcite Fluorite	2 2	3 mm KBr	27.3 μ	8.0	H. Liebisch and H. Rubens, Berl. Ber., 1919, p. 876.
Marble	4		29.4 μ 6.7 μ	14.0 4.0	E. Aschkinass, Ann. d. Physik **1**, 42, (1900).
Fluorite	3	0.4 mm SiO_2 1.2 mm KBr	32.8 μ	0.75	H. Rubens, Wied. Ann. **69**, 576 (1899).

The numbers given in column E represent the observed galvanometer deflection in centimeters for the various reststrahlen. A Leeds and Northrup high sensitivity galvanometer was used with the scale at 3 meters. In order to eliminate shorter waves as much as possible a soot filter was used and these values are for the energy transmitted by this filter.

In the present experiments a 1 cm KCl filter was substituted for the 2.5 mm AgCl filter recommended by Rubens and Nichols. This is justified by the transmission curves given by Rubens and Trowbridge[5] for AgCl and KCl.

In the present experiments, the 27.3μ rays were not polarized as specified by Liebisch and Rubens and it was not possible to test the wave-length of the rays to find the effect of this omission.

The 32.8μ rays were apparently homogeneous for the transmission of a KBr plate. 1.2 mm thickness was found to be 68 percent while Rubens states that it transmits more than $\frac{2}{3}$ of the 32.8μ reststrahlen.

Except for the 20.75μ and 29.4μ reststrahlen a rocksalt shutter of 3 mm thickness was used. For these reststrahlen both rocksalt and metal shutters were used. If E_T was the energy of both reststrahlen and A_T was the absorption of the sample for this energy, then if E_s was the energy passed by a rocksalt filter, i.e., the energy of the short reststrahlen, and A_s the part of this energy absorbed by the sample, then, allowing 9/10 as the transmission of the rocksalt shutter for the short waves, the long wave (i.e. the 20.75 and 29.4μ reststrahlen) energy is $(E_T - E_s/0.9)$ and the long wave energy absorbed by the sample is $(A_T - A_s/0.9)$.

[5] H. Rubens and A. Trowbridge, Wied. Ann. **60**, 724 (1897).

MEASUREMENTS

Gases. The gases used for the present measurements were not especially purified. They were drawn from stock cylinders or were the vapors of chemically pure liquids. The chief difficulty in obtaining consistent results was due to the variable concentration of vapor within the absorption cell. Benzene and CCl_4 were observed to wet the lacquer windows at times and this gives an indication that these liquids would, in all probability, be transparent. The values given in Table II are averages of four to eight independent runs taken on different days and are thought to be correct to about 2 percent. They are slightly different from some preliminary results published in a Letter to the Editor. These differences in some cases are due to additional data but for the wave-lengths 20.75 and 29.4μ the differences are due chiefly to corrections for the transmissivity of the rocksalt filter used.

TABLE II. *Percent transmission.* (*Length of cell*, 4 *inches*).

Material	Pressure Millimeters	6.7μ	8.7μ	20.75μ	22.9μ	27.3μ	29.4μ	32.8μ
NH_3	760	24	26	79	93	83	82	62
N_2O	760	102	77	90	100	101	101	102
C_2H_2	760	95	92	99	101	101	100	98
H_2S	760	97	98	98	97	92	90	83
SO_2	760	98	5	7	58	100	100	96
C_6H_6	96	65	97	102	99	100	98	95
CCl_4	114	95	99	97	99	99	99	91
CS_2	361	30	98	100	86	98	99	96
$CHCl_3$	200	93	90	99	98	98	97	97
$(C_2H_5)_2O$	526	17	6	61	45	69	71	61

The gradual decrease of transparency for H_2S and N_3H at longer wave-lengths may be due to the short wave-length end of the pure rotation spectrum.

The only strong absorption band discovered in the new spectral region was for SO_2 at 20.75μ. This band agrees with Raman indications[6] and is possibly the third fundamental band for SO_2. The strong absorption of SO_2 for both the reststrahlen of quartz is quite striking. The absorption cell filled with SO_2 cuts off these radiations almost the same as a metal shutter.

R. W. Wood[7] has shown that the mercury line 2536 is reflected by hot mercury vapor at a high pressure. He states "It appeared highly probable that if the molecular resonators were packed closely enough together, the secondary wavelets which they emit, having a definite phase relation would unite into a single wave, and the scattered light would disappear, regular reflection taking its place." Because of the strong absorption of SO_2 for the reststrahlen of quartz it was decided to test this hypothesis. High pressures should not be necessary on account of the long wave-lengths involved. Accordingly, a cell was fitted with a window of KBr and one of the quartz reststrahlen plates was replaced by it in such a way that there was reflection from the outer and inner surfaces of the window. The cell was connected to a vacuum pump and

[6] R. G. Dickinson and S. Stewart West, Phys. Rev. **35**, 1126 (1930).
[7] R. W. Wood, Physical Optics, p. 429 (1929).

a tank of SO_2 by a three way stopcock so that it might be alternately evacuated and filled with SO_2 at a pressure of two atmospheres. No change, whatever, in the galvanometer was observed when the cell was emptied and filled with SO_2. This seems to show that this gas does not reflect at either 8.7μ or 20.75μ.

The results of Table II are in agreement with results of Rubens and von Wartenberg[8] for the 22.9μ reststrahlen with the exception of CS_2. For this gas, using a cell about 8″ long, these authors get a value of 97.8 percent as compared with my value of 86 percent for a 4″ cell.

Coblentz[9] observes absorption bands at or near 6.7μ for liquid $CHCl_3$ (0.16 mm layer) and CCl_4 (0.1 mm layer) which are not observed for the vapor with the 6.7μ reststrahlen.

For CCl_4 there is a Raman line corresponding to an active infrared vibration at a wave-length of 31.6μ and for $CHCl_3$ there is a line corresponding to 27.93μ. Also for $(C_2H_5)_2O$ there is a line corresponding to a wave-length at 23μ. There is no corresponding absorption for the $CHCl_3$ line but the low transmission of ether at 22.9μ and CCl_4 at 32.8μ may be associated with the Raman indications.

Optical properties of various substances. Lacquer films may be prepared by dropping a single drop of colorless brushing lacquer on a large water surface. The lacquer spreads out immediately and the amyl acetate evaporates leaving a tenacious film. These films are useful as windows for absorption cells and so their optical properties are of interest. Since the films are of the order of 1μ thickness, there is no total reflection on account of the destructive interference between the energy reflected from the front and back surfaces. The absorption of a typical film is given in the first row of Table III. These films are so transparent that the reststrahlen are not seriously weakened in passing twice through four films, besides the sooted film over the first hole in the reststrahlen apparatus and the film over the Welschback mantle chimney. Values for a film covered with soot are also given in Table III.

TABLE III. *Percent transmission.*

Material	Description	6.7μ	8.7μ	20.75μ	22.9μ	27.3μ	29.4μ	32.8μ
Lacquer film	Thickness of order of wave-length of visible light	96	93	97	98	99	99	100
Mica	10μ thickness	83	22	19	00	35	42	44
Soot on Lacquer film	Opaque to visible	25	22	67	53	60	67	60
Amorphus quartz	10μ thickness	86	02	01	03	51	55	68
Glass	3μ thickness	93	07	12	14	48	51	56
Cellophane	25μ thickness Cigarette wrapping	33	04	04	01	20	25	26
MgO	Deposit of fumes from burning Mg ribbon	88	86	04	02	90	93	87
ZnO	Deposit of fumes from Zn arc	99	80	15	05	93	79	80

[8] H. Rubens and H. von Wartenberg, Verh. d. D. Phys. Ges. **13**, 796 (1911).

[9] W. W. Coblentz, Investigations of infrared spectra, part I pp. 180 and 182.

Other possibilities for windows in this region are mica, quartz, glass and cellophane. Their transmissions are given in Table III.

In a MgO deposit, we have an interesting absorption at 22.9μ. It seemed from the results given in Table III that one might expect a reststrahlen for MgO near 23μ. The Vitrofrax Corporation of Los Angeles supplied the author with some beautiful synthetic crystals of β-MgO with which experiments were made. There is no doubt but that this material showed a strong reststrahlen near 23μ as will be observed from its reflectivity given in Table IV.

TABLE IV. *Percent reflection*

Description of reflector	22.9μ	32.8μ
Deposit of MgO from burning Mg ribbon	0	0
Reflection β—MgO	80	33
Galena	28	24
Stibinite	>16	—
Mica	32	—
Paraffin	04	—
Pencil mark on paper	09	—
Silver covered with Soot coating	43	48
Silver covered with MgO coating	08	91
Silver covered with ZnO coating	01	52
Silver covered with Optical black	31	—
Gold foil blackened with bismuth	>19	—
KBr	04.3	—
KI	05.5	—
KBr+1.5μ CaF_2 deposited by evaporation	10	—
KI+1.5μ CaF_2 deposited by evaporation	13	—

It was not convenient to measure the reflectivity of β-MgO for the other wave-lengths but it was possible to substitute the magnesia for one of the reststrahlen plates and determine the relative galvanometer deflections. This gives the ratio of the reflectivity of MgO to that of the reststrahlen plate. Assuming 0.7 for the reflectivity of the reststrahlen plates we get the approximate values for the reflectivity which are given in Table V.

TABLE V. *Percent reflection of β=MgO.*

6.7μ	8.7μ	20.75μ	22.9μ	27.3μ	29.4μ	32.8μ
5	10	49	80	42	35	33

S. Tolksdorf[10] reported the fundamental for MgO at 14.2μ but since MgO has a cubic lattice and therefore only one reststrahlen, it does not seem possible that the 14.2μ absorption that he reports can be the fundamental. This point requires further investigation.

S. Tolksdorf predicts, from the absorption spectrum of ZnO, that this material has fundamental absorption bands at 22 and 28μ. The data in Table III give an absorption for one and not the other of these bands. An investigation of the reflectivity of zincite is being made to clear up these points.

Measurements on a KI crystal would indicate that a layer of this material 2 cm in thickness would transmit 50 percent of the 32.8μ reststrahlen.

[10] S. Tolksdorf, Zeits. f. phys. Chem. **132**, 161 (1928).

ON THE AXIAL ROTATION AND SPECTRA OF STARS

By Ross Gunn
Naval Research Laboratory, Washington, D. C.

(Received April 30, 1931)

Abstract

Struve's remarkable relation between high observed axial rotations of stars and their bright line spectra is considered theoretically. It is shown that the two phenomena are closely related to the same electromagnetic effects that account for the anomalous solar rotation. High electromagnetic winds, resulting from crossed electric and magnetic fields, account for the high apparent rotational velocity and transfer sufficient momentum to the star in the course of stellar time to account for the high true rotations necessary to produce fission. The large electromagnetic wind velocities require the presence of comparatively large radial electric fields and it is shown that these can add sufficient additional excitation energy to the atmospheric ions to produce bright line spectra. Thus, high apparent axial rotations, high true rotations and bright line spectra in stars are intimately related and the existence of one, usually demands the presence of the others. An approximate expression is derived for the time rate of increase of angular momentum in a star.

IN TWO recent papers,[1] Otto Struve has drawn attention to a remarkable correlation between the spectra of stars and their apparent rotation as derived from measurements of Doppler displacements. Dr. Struve points out that emission lines are found principally in the O and B type stars and that in these "Excessive rotations, estimated at . . . (. . . 250 km/sec or more), are frequent. Apparently bright lines occur preferentially in stars having rapid axial rotation." The very high peripheral velocities indicated by his observational data suggest that certain stars are rotating so fast that they are on the verge of division to form binary systems. This conclusion is in accord with statistical data on binary systems which show that most close binary systems are B type stars or later. In the following discussion we will assume that the internal constitution and atmosphere of a given star is not greatly different from that of our sun and show that Dr. Struve's strange observed relations follow directly from a consideration of electromagnetic effects which we have shown to account for certain observed solar peculiarities.

Superposed Electromagnetic Winds

In a series of papers dealing with the electricity and magnetism of the sun[2] it has been shown that the observed variations of the apparent solar rotation with latitude, altitude, and time are readily explained in terms of atmospheric motions superposed upon the body rotation of the sun proper. These systematic motions of the atmosphere result from the interaction of

[1] O. Struve, Astrophys. J. **72**, 1 (1930); **73**, 94 (1931).

[2] R. Gunn, Phys. Rev. **35**, 635 (1930); **36**, 1251 (1930); **37**, 283 (1931); **37**, 983 (1931); **37**, 1129 (1931).

crossed electric and magnetic fields with the atmospheric ions and we may express its magnitude u by[2]

$$u = \frac{E \times B}{B^2(1 + (R/\lambda)^2)} \tag{1}$$

where E is the radial electric field of the star at the observed level and B is the magnetic field (both quantities being expressed in e.m.u.), R the radius of the spiral generated by the moving ion, and λ the mean free path. We will hereafter refer to this systematic superposed atmospheric motion of the ions as an "electromagnetic wind."

The electrical energy dissipated in the solar atmosphere is an appreciable fraction of the total radiated energy.[2] This seems probably to be true in all stars having magnetic fields and indicates that stars with high surface temperatures (high radiation per unit area) are surrounded by a comparatively large radial electric field. Thus in O and B type stars with surface temperatures ranging from 35,000° to 12,000° electrical effects would be expected to be very important. We have no knowledge of the magnetic field of a star and can only suggest that its magnitude and distribution is not unlike that of the sun. If this is the true situation then we would expect the ratio of the magnitudes of the electric and magnetic fields in early type stars to be large and high velocity electromagnetic winds to result. Dr. Struve's observation that excessive rotations are common in O and B type stars is consistent with the above conclusions.

Excitation of Radiation by Electric Fields

Eddington[3] has concluded that bright line spectra in a non-nebulous star is evidence for the existence of "thunderstorms" in the atmosphere of the star, but he was unable to make his suggestion quantitative. We proceed to calculate the electrical energy added to an ion during its free path as a result of the presence of an electric field. An ion in the atmosphere of a star having electric and magnetic fields does not move in the direction of the electric field, on the average, but describes a cycloidal path and progresses in a direction at right angles to both the impressed electric and magnetic fields.[2] Due to the presence of the magnetic field, an ion cannot acquire more than a definite amount of energy from the electric field, even if the ion describes an infinitely long free path. The mean energy W added to an ion by the electric field is given by[2]

$$W = mvu[1 + u^2/v^2]^{1/2} \tag{2}$$

while the maximum energy W_m is considerably more than twice as much or

$$W_m = 2mvu(1 + u/v) \tag{3}$$

where m is the mass of the ion, v the component of its initial velocity in a plane perpendicular to B the magnetic field and u the magnitude of the elec-

[3] Internal Constitution of the Stars, (1926).

tromagnetic wind given by Eq. (1). If we neglect the relatively less frequent case of successive collisions where an ion of initially large energy collides with another and starts it off with abnormally high velocity, we can express Eq. (2) in terms of the electromagnetic wind velocity u and the surface temperature of the star. Thus if we express W in terms of equivalent electron volts V, Eq. (3) becomes

$$V = \frac{u(2mkT)^{1/2}}{10^8 e}\left[1 + \frac{u^2 m}{2kT}\right]^{1/2} \tag{4}$$

where e is the electronic charge expressed in e.m.u., k the Boltzmann constant, and T the atmospheric or effective surface temperature. Table I gives the average increase in energy of an ion due to electrical fields in terms of equivalent electron volts, assuming that the initial energy of the ion when it starts its path is purely thermal. Many of the ions and electrons will have more than these energies and can produce additional excitation.

It will not be necessary to discuss in detail the exact mechanism whereby bright emission lines are produced, for it should be clear from Table I that ions in the atmosphere of a star can absorb sufficient energy from the star's electric field to excite bright line radiation. The table and Eq. (2) bring out

TABLE I. *Average increase in energy due to electric field.*

	Hydrogen ion Surface Temperature		Electron Surface Temperature	
u km/sec	10,000°	20,000°	10,000°	20,000°
10	1.74 volts	2.19 volts	0.031 volts	0.044 volts
25	7.80 "	8.46 "	0.079 "	0.111 "
50	28.8 "	29.4 "	0.16 "	0.22 "
100	112. "	113. "	0.32 "	0.45 "

clearly that the electrical excitation energy and hence the prevalence of bright lines increases rapidly with increase in the magnitude of the electromagnetic wind which is proportional to the apparent rotational velocity. Thus the theory that has been developed to account for the observed anomalies of the sun's rotation leads directly to a quantitative explanation of Struve's observed relation between high rotational velocities and bright line spectra in stars.

ADDED ANGULAR MOMENTUM AND BODY ROTATION

With the possible exception of close binary stars in which the axial and orbital periods are identical, it seems impossible to determine the true rotational period of a star, either by observing the motion of its magnetic pole or by a determination of its departure from a true spherical form. We must have knowledge of the true body rotation in order to separate the various components of the motion and we are forced to assume that the initial rotation of a star is small and estimate the body rotation from the observed apparent motions, the physical properties of its atmosphere and its age. The directions of the electric and magnetic fields of stars are undoubtedly related to the

direction of their rotation in the same manner as those of the sun and earth. The electromagnetic winds therefore blow in the direction of the body rotation, but much faster, and add momentum to the star proper. Thus, we definitely abandon the principle of the conservation of momentum in an evolving star. In connection with the sun this effect was considered[2] and it was shown that since the sun was formed, sufficient angular momentum has been transferred to the sun proper by its own electromagnetic winds to account for its present axial rotation.

The superposed systematic momentum of an ion in a star's atmosphere is derived entirely from the radial electric field, and the magnetic field serves only to change the direction of the moving ion. The mechanism is therefore one for converting radial momentum into angular momentum. There can be no reacting momentum transferred to the star's magnetic field by the mechanism described, for the magnetic force on an ion is always at right angles to its motion and the magnetic field cannot transfer energy to the ion or the ion energy to the magnetic field. Momentum, therefore, cannot be transferred by this means and we are left to consider only the momentum transferred to a star by viscous forces between the star proper and its fast moving atmosphere. This transfer of momentum is always in such a direction as to accelerate the axial rotation and calculations indicate that in the course of stellar time the added momentum is adequate to increase the angular velocity until a star becomes rotationally unstable.

The data available for a typical star are not sufficiently complete to warrant a detailed calculation and in the following we shall make a rough calculation which will serve to indicate only the approximate magnitude of the effects. The electromagnetic winds of the star's atmosphere transfer momentum to the star proper which we assume to be a semi-rigid gaseous body held together by gravitational, radiative, and electromagnetic forces. The torque T applied to the star as a result of the systematic motion of its atmosphere is

$$T = \eta A R_0 \frac{du}{dr} = \frac{d\Omega}{dt} \tag{5}$$

where η is the mean coefficient of viscosity of the transition layer between the atmosphere moving with a velocity u and the surface proper, A the effective areas in contact, R_0 the radius of the star, du/dr the radial velocity gradient and $d\Omega/dt$ the time rate of increase of angular momentum. It is clear from Eq. (1) that the superposed electromagnetic wind velocity u drops rather abruptly when the ion pressure increases sufficiently to make the mean free path λ as small as R, the radius of the spiral generated by the ion moving in the magnetic field. If the low lying regions of the star's atmosphere are in gravitational equilibrium, then the difference in altitude Δr, corresponding to a fractional change in the ion pressure of unity, is given by

$$\Delta r = \frac{kT}{zhg} \tag{6}$$

where k is the Boltzmann constant, T the temperature of the atmosphere, z its mean atomic weight, h the mass of a hydrogen atom, and g the surface acceleration due to gravity. The fractional change in the superposed velocity u in the interval given by Δr is also approximately unity so that we may write

$$\frac{\Delta u}{\Delta r} = \frac{zh\gamma M u_0}{kTR_0^2} \tag{7}$$

where u_0 is the superposed electromagnetic wind velocity in the observed regions of the star's atmosphere, γ the gravitational constant and M the mass of the star.

The coefficient of viscosity η of the transition layer is

$$\eta = \frac{(3zhkT)^{1/2}}{2^{3/2}\pi\sigma^2} \tag{8}$$

where σ is the diameter of the gaseous ions or molecules according to kinetic theory. We assume that the effective area in contact is a ring around the equator of the star of width R_0. Combining the foregoing relations and making obvious substitutions we have that the rate of increase in the angular momentum of the star proper is

$$\frac{d\Omega}{dt} = \left(\frac{3zh}{2kT}\right)^{1/2} \frac{zh\gamma u_0 R_0 M}{\sigma^2} \tag{9}$$

or if ω_t is the present value of the angular velocity

$$\omega_t = \omega_0 + \left(\frac{3zh}{2kT}\right)^{1/2} \frac{zh\gamma R_0 u_0 \tau}{\sigma^2 d^2} \tag{10}$$

where ω_0 is the initial angular velocity of the star and will be set equal to zero, d is the radius of gyration of the star about its axis of spin and τ is the age of the star. We have assumed a steady state and have made no attempt to allow for greater values of u_0 during the youth of the star or for its variation with latitude.

Now if V_0 is the apparent or observed peripheral velocity of the star and $\omega_t R_0$ the peripheral velocity of the surface proper then $V_0 = u_0 + \omega_t R_0$ and

$$\frac{V_0}{u_0} = \left[1 + \left(\frac{3zh}{2kT}\right)^{1/2} \frac{zh\gamma R_0^2 \tau}{\sigma^2 d^2}\right]. \tag{11}$$

Numerical data for calculating V_0/u_0 from Eq. (11) are lacking and we must assume that the star is of uniform density, its atmosphere is not unlike that of the sun and its age approximates 2×10^{20} sec. or the mean indicated age of all stars. Substituting therefore $z=3.3$; $h=1.67\times10^{-24}$ gm; $k=1.37\times10^{-16}$; $\sigma=10^{-8}$ cm; $\gamma=6.67\times10^{-8}$; $\tau=2\times10^{20}$ sec; $d^2=0.4R_0^2$ and for a typical B type star $T=15{,}000°$ we find $V_0/u_0=4.1$ and therefore the true rotational velocity is roughly 3/4 the apparent observed value. A similar calculation for the sun yields 6.2 while the observed ratio is 4.0. It is clear from the results of

our calculation that, unless B type stars are much younger in actual years of existence than their state of evolution indicates the true rotations are large fractions of the apparent rotations and therefore many of these types of stars are on the verge of division to form binary systems. It seems clear that high electromagnetic winds necessarily produce high speed axial rotations in a star of moderate age and the calculations of the present paper are not in disagreement with Dr. Struve's conclusion that many B type stars are almost rotationally unstable.

The observed high apparent axial rotations in O and B type stars, together with the well established fact that close binary systems with few exceptions are B type stars or later, seem significant, and strongly suggest that stars in this period of their evolution divide as a result of a tremendous increase in their angular momentum. The increase in angular velocity appears to be accounted for by electromagnetic effects rather than by an increase due to contraction of the star. The contraction of the star may play an important part; but there is great difficulty in accounting for the original angular momentum, and a mechanism to add momentum to the system must be provided somewhere in the plan of stellar evolution. It seems quite possible that the above mechanism for adding angular momentum to a star represents physical reality but further supporting evidence is desirable.

Conclusion

Dr. Struve's values for the apparent peripheral velocity of type B stars (approximating 250 km/sec) together with the present calculations suggest that the electromagnetic winds may have velocities of 50 km/sec or more and therefore in these stars the ratio of the magnitude of the electric and magnetic fields must be very large. The large electric fields are capable of adding considerable energy to the ions constituting the star's atmosphere and emission lines should be observed. The very high superposed atmospheric motion of the star will, as well, transfer momentum to the star proper and we should expect this stage of development of a star to be characterized by a large increase in angular momentum resulting ultimately in the formation of binary systems. Statistical evidence supports this conclusion. We see therefore that high apparent axial rotations, high true rotations and bright line spectra in stars are intimately related and the existence of one usually demands the presence of the others.

THE NEUTRON

By R. M. Langer and N. Rosen
Massachusetts Institute of Technology

(Received May 12, 1931)

Abstract

The writers point out that the postulation of the existence of the "neutron," a combination of an electron and a proton, of small size and low energy would be very useful in explaining a number of atomic and cosmic phenomena. They find that a mathematical treatment based on existing theory leads to indications of such a state but no definite proof.

I. Introduction

IT IS an attractive speculation to try to describe a process by which the various elements could be formed. In the present state of atomic theory it is really an anomaly that there are elements other than hydrogen; for no one has hitherto attempted to show that quantum systems could exist with the dimensions and energies appropriate to nuclei or constituents of nuclei. Our purpose here is to indicate how such systems may exist on the basis of wave-mechanics, and thus offer a way of describing the process of building up of the heavier elements.

The present article is devoted to a discussion of a combination of an electron and a proton of low energy and very small size which we shall speak of as the "neutron." Such a particle, if it exists, must have a mass but slightly smaller than that of a hydrogen, a diameter of 10^{-12} to 10^{-15} cm, and energy of the order of magnitude of m_0c^2 ($15m_0c^2$ is an upper limit; m_0 = electron mass) less than that of hydrogen in order to account for observed phenomena. It seems proper to begin by pointing out reasons for the assumption of the existence of a neutron and to show how it might help to explain certain phenomena.

II. Applications

In most ordinary phenomena the effect of a particle like the neutron would be unobservable. It is small enough, for example, to penetrate material walls and therefore would not contribute to a gas pressure. Its only large scale property is its gravitational field. In atomic and cosmic processes however, it can play an important role.

1. The process of the increase of atomic number.

In a universe whose initial state was a mass of free protons and electrons it is natural to imagine that the most readily formed combination would be that of ordinary hydrogen. This process has a large cross-section because the final state is comparatively large and because there is attraction at large distances with the possibility of radiation always present to provide for the con-

servation of energy in the change of state involved. On the other hand, a stable combination of two protons or two electrons would surely have to be of extremely small size because we know that down to very small separations the forces are repulsive. The latter fact decreases the probability of close collisions; and any radiation that might occur could only make the collision less intimate. The alternative process of simultaneous collision of at least six particles to form a complex nucleus is obviously unimportant even at high densities, as long as a suitable building process can be described which involves the collision of only two bodies at a time.

Once hydrogen atoms are formed the way is now open for the building up process. The neutron as we describe it, is actually a low state of hydrogen so that in any hydrogen atom there is always a probability of transition into a neutron with emission of a high energy quantum. Due to its small size the neutron has a very small external electric field so that its long range influence is the gravitational attraction. At small distances there are of course further polarization attractions and possibly magnetic effects. Such systems will collide readily in spite of their small size because they are electrically neutral. Resonance, polarization or magnetic forces may then hold them together until a complex system is formed which by expulsion of some of its electrons might rearrange itself into a stable atomic nucleus. A neutron being small and field-free could penetrate outer shells of electrons and enter nuclei. The tremendous initial velocity which must be assumed in the usual picture in which protons or α-particles are added to one element to form a heavier one, is no longer required. The resulting configuration could well be a stable one but need not be the most stable. The measured values of packing fractions indicate a remarkable degree of stability in the ordinary nuclei. It may therefore be that a close cluster of neutrons could lose energy by the expulsion of electrons to form nuclei.

2. Cosmic radiation.

There are two ways of distributing the energy which is released in the formation of helium. Either most of the energy is given out in the formation of neutrons from hydrogen and a smaller amount accompanies the rearrangement of the four neutrons into helium or else the formation of neutrons liberates a comparatively small amount, the remainder of the packing energy being radiated in a single quantum as the rearrangement occurs. In either case the radiation might be of the type of cosmic radiation as observed by Millikan and others. The second alternative however is entirely in agreement with the conclusion of Millikan as to the significance of his measurements. However, the gradual gathering of neutrons with a subsequent sudden transition to a stable nucleus is much more agreeable than the assumption of a multiple collision by means of which this process is ordinarily supposed to happen.

3. High density matter in stars.

The usual explanation of the white dwarfs involving a high degree of ionization of the atoms is not the only one. There are in fact great advantages

from this point of view in favor of our neutron. Being small it has a great mean free path and is comparatively insensitive to light pressure. It therefore goes easily to the center of a gravitating mass. Being neutral and having an extremely small external field, it permits high densities to build up before it deviates appreciably from perfect gas behavior. Further, the possibility of high densities is not dependent on having a high temperature or pressure nor is there much danger of violating the Pauli exclusion principle by exceeding the maximum electron density for a given pressure.

III. Theoretical Treatment

If one naively examines the solutions of the ordinary Schrödinger equation for hydrogen, one is inclined to wonder why, in addition to the ordinary states for quantum numbers, $n=1, 2, 3, \cdots$, there is no state for $n=0$. Since in general the solutions (for $l=0$) are of the form:

$$\psi \sim e^{-r/n}P_n(r)$$

the wave function for this state, if normalized, would be a δ-function, zero everywhere except at the origin, so that this state would correspond to an electron which had fallen into the nucleus. Such a condition in view of the attraction between the two is by no means inconceivable.

That this is unsatisfactory is at once evident. In the first place the energy, which is given by:

$$W = Rh/n^2$$

would be infinite. In the second place, a simple calculation shows that the transition probability from a higher state to this one is zero in every case. From a physical point of view the state can therefore be considered as non-existent.

However, the above considerations are too rough. The assumption of a $1/r$ potential must certainly be incorrect for small distances (for the infinity at the origin surely does not exist in nature). If then the potential deviates from $1/r$ at small distances, it may well be that an atomic state exists corresponding to the one under discussion with low *but finite* energy, of small *but not zero* dimensions, and therefore with small *but non-vanishing* transition probabilities.

As a better approximation one can consider the electron in a Coulomb field modified by a small correction term, for example, of the form b/r^2 (the singularity still remains however). One can think of this as an actual potential, or one can consider the relativistic Schrödinger equation for a Coulomb field, thus bringing in a b/r^2 term.

If that is done, it is found without difficulty that for s-states ($l=0$), in addition to the usual solutions, there exist solutions corresponding to the second root of the indicial equation with energies given by

$$E_2 = m_0c^2\left[1 + \alpha^2/(n_r + \tfrac{1}{2} - (\tfrac{1}{4} - \alpha^2)^{1/2})^2\right]^{-1/2},$$

where α is the Sommerfeld fine-structure constant. These energies differ very little from the ordinary energies given by:

$$E_1 = m_0c^2[1 + \alpha^2/(n_r + \tfrac{1}{2} + (\tfrac{1}{4} - \alpha^2)^{1/2})^2]^{-1/2}$$

for the next smaller value of n_r except in the case $n_r = 0$. For this case E_2 is very low:

$$E_2 \sim 0.073 m_0c^2.$$

That is E_2 is nearly m_0c^2 below the energy of a normal hydrogen atom.

The wave functions corresponding to E_2 have singularities for $r = 0$. They are quadratically integrable and hence would be acceptable according to the views of many physicists. However, the variational integrals turn out to be infinite and for this reason we reject them.[1] Incidentally these wave functions are not necessarily orthogonal to the usual ones of energy E_1.

Another way of attacking the problem is to construct potential energy curves which differ inappreciably from e^2/r for distances greater than 10^{-12} cm, but which have much steeper slopes in the range 10^{-12} to 10^{-16} cm and then flatten out and remain finite at the origin. With such potential functions one can obtain a low "neutron" state without appreciably changing the energies of the higher hydrogen levels. However, setting up such a potential function involves several arbitrary factors; and there are as yet no experimental data to determine them without ambiguity. Further development along this line is very intriguing but in their present state of uncertainty the authors feel themselves not bold enough to offer the results for publication.

[1] R. M. Langer and N. Rosen, Phys. Rev. **37**, 658 (1931).

GROUP THEORY AND THE ELECTRIC CIRCUIT*

By Nathan Howitt
Naval Research Laboratory, Bellevue, Anacostia, D. C.

(Received March 20, 1931)

Abstract

Electrical networks consisting of inductances, resistances, and capacitances form a group with the impedance function as an absolute invariant. That is, to a given impedance function there corresponds an infinite number of networks, any one of which can be obtained from any other by a special linear transformation of the instantaneous mesh currents and charges of the network. In this manner one may arrive at the complete infinite set of networks equivalent to a given network of any number of meshes. This is done by writing down the three fundamental quadratic forms of the network. Then a linear affine transformation of the instantaneous mesh currents and charges of the network results in the formation of new quadratic forms, the matrices of the coefficients of which represent a member of the group, i.e., an equivalent network. Instead of performing the substitutions, the three matrix multiplications $C'AC$ are used, one for each quadratic form, where A represents the original matrix, C the transformation matrix, and C' its conjugate. It may be possible to extend this theory to include continuous systems where the quadratic forms become integrals or infinite series and one deals with infinite matrices and infinite transformations.

IN 1904, in an address before the Mathematics section of the International Congress of Arts and Science, Professor James Pierpont said, "The group concept, hardly noticeable at the beginning of the century, has at its close become one of the fundamental and most fruitful notions in the whole range of our science."[1] And now this abstract notion of groups finds application in an important branch of physics—electric circuit theory.

Considerable has been written on electrical networks and the impedance function,[2] but it has hardly been suspected that electrical networks formed a group with the impedance function as an absolute invariant and that it was possible to proceed in a continuous manner from one network to its equivalent network by a linear transformation of the instantaneous mesh currents and charges of the network.

Before proceeding with the general n-mesh network it will be instructive to construct the quadratic forms and the impedance function for the two-mesh network with all three network elements present, shown in Fig. 1.

The elements λ_{12}, ρ_{12} and σ_{12} are the elements common or mutual to meshes 1 and 2. λ_{11}, ρ_{11} and σ_{11} are the *total* parameters of mesh 1, that is, they are, respectively, the total inductance, resistance and elastance of mesh

* This is part of a dissertation presented to the Massachusetts Institute of Technology for the degree of Doctor of Science in 1930.

[1] J. Pierpont, Bulletin of the American Mathematical Society **2**, 144 (1904).

[2] O. Heaviside, Electromagnetic Theory, 1912, and Electrical Papers, 1925; J. R. Carson Electric Circuit Theory and the Operational Calculus, 1926; V. Bush, Operational Circuit Analysis, 1929.

1. Similarly, λ_{22}, ρ_{22} and σ_{22} are the total parameters of mesh 2. The quantities i_1 and i_2 are the *instantaneous mesh* currents, the arrows indicating their directions. Let q_1 and q_2 be the corresponding mesh charges, so that

$$i_1 = dq_1/dt \tag{1}$$

$$i_2 = dq_2/dt. \tag{2}$$

The total *instantaneous* magnetic energy in the complete network is given by

$$\begin{aligned} T &= \tfrac{1}{2}(\lambda_{11} - \lambda_{12})i_1^2 + \tfrac{1}{2}\lambda_{12}(i_1 + i_2)^2 + \tfrac{1}{2}(\lambda_{22} - \lambda_{12})i_2^2 \\ &= \tfrac{1}{2}(\lambda_{11}i_1^2 + 2\lambda_{12}i_1i_2 + \lambda_{22}i_2^2). \end{aligned} \tag{3}$$

Similarly, the total *instantaneous* electrostatic energy in the complete network is given by

$$\begin{aligned} V &= \tfrac{1}{2}(\sigma_{11} - \sigma_{12})q_1^2 + \tfrac{1}{2}\sigma_{12}(q_1 + q_2)^2 + \tfrac{1}{2}(\sigma_{22} - \sigma_{12})q_2^2 \\ &= \tfrac{1}{2}(\sigma_{11}q_1^2 + 2\sigma_{12}q_1q_2 + \sigma_{22}q_2^2). \end{aligned} \tag{4}$$

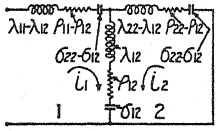

Fig. 1. General two-mesh network.

Finally, the total *instantaneous* power lost in the resistances of the complete network is given by

$$\begin{aligned} R &= (\rho_{11} - \rho_{12})i_1^2 + \rho_{12}(i_1 + i_2)^2 + (\rho_{22} - \rho_{12})i_2^2 \\ &= \rho_{11}i_1^2 + 2\rho_{12}i_1i_2 + \rho_{22}i_2^2. \end{aligned} \tag{5}$$

In more compact notation, T, V and R may, respectively, be written

$$T = \tfrac{1}{2}\Sigma_{jk=1}^{2}\lambda_{jk}i_ji_k \tag{6}$$

$$V = \tfrac{1}{2}\Sigma_{jk=1}^{2}\sigma_{jk}q_jq_k \tag{7}$$

$$R = \Sigma_{jk=1}^{2}\rho_{jk}i_ji_k \tag{8}$$

Since $\lambda_{jk}=\lambda_{kj}$, $\sigma_{jk}=\sigma_{kj}$, $\rho_{jk}=\rho_{kj}$ it is readily seen that by giving j and k all possible values from 1 to 2 in any manner, Eqs. (6), (7) and (8) reduce to Eqs. (3), (4), and (5).

It might be well at this point to generalize Eqs. (6), (7) and (8) for n meshes. This is done simply by changing the upper limit of the summation from 2 to n. For n meshes, then, these equations become

$$T = \tfrac{1}{2}\Sigma_1{}^n\lambda_{jk}i_ji_k \tag{9}$$

$$V = \tfrac{1}{2}\Sigma_1{}^n\sigma_{jk}q_jq_k \tag{10}$$

$$F = \tfrac{1}{2}\Sigma_1{}^n\rho_{jk}i_ji_k \tag{11}$$

where j and k take on all possible values from 1 to n, in any manner.

The quantities T, V and F are the so-called quadratic forms[3] which are positive and definite. That is, they are positive for all values of the variable i or q, and they are zero when and only when all the variables are zero or when the corresponding parameters are all zero. The positiveness of these forms follows at once from physical considerations since the magnetic energy, the electrostatic energy and the power lost in the resistances of the network are positive quantities, and are zero when and only when all the currents or charges are respectively zero, or when the corresponding parameters are zero. These quadratic forms play an important role in dynamics, and significant results are obtained from their positive and definite character.

It is instructive to point out here that the coefficients of the quadratic forms (6), (7) and (8) may be obtained directly from certain matrices. Thus, the coefficients of the quadratic form (6) are contained in the matrix

$$\begin{Vmatrix} \lambda_{11} & \lambda_{12} \\ \lambda_{12} & \lambda_{22} \end{Vmatrix} \tag{12}$$

and the form is obtained at once by writing

$$\lambda_{11} i_1^2 + 2\lambda_{12} i_1 i_2 + \lambda_{22} i_2^2$$

which is, of course, $2T$. Similarly, the coefficients of the forms (7) and (8), respectively, are contained in the matrices

$$\begin{Vmatrix} \sigma_{11} & \sigma_{12} \\ \sigma_{12} & \sigma_{22} \end{Vmatrix} \quad \begin{Vmatrix} \rho_{11} & \rho_{12} \\ \rho_{12} & \rho_{22} \end{Vmatrix} \tag{13}$$

Also, in the n-mesh case, the coefficients of the quadratic forms T, V and F are contained, respectively, in the matrices

$$\begin{Vmatrix} \lambda_{11} & \lambda_{12} \cdots \lambda_{1n} \\ \lambda_{12} & \vdots \\ \vdots & \vdots \\ \lambda_{1n} & \cdots \lambda_{nn} \end{Vmatrix}, \quad \begin{Vmatrix} \sigma_{11} & \sigma_{12} \cdots \sigma_{1n} \\ \sigma_{12} & \vdots \\ \vdots & \vdots \\ \sigma_{1n} & \cdots \sigma_{nn} \end{Vmatrix}, \quad \begin{Vmatrix} \rho_{11} & \rho_{12} \cdots \rho_{1n} \\ \vdots & \vdots \\ \vdots & \vdots \\ \rho_{1n} & \cdots \rho_{nn} \end{Vmatrix} \tag{14}$$

From these matrices, the respective quadratic forms of the n-mesh network as well as the respective networks are readily constructed.

The impedance function is obtained from the determinant of the network.[4] Thus the determinant of the network of Fig. 1 is

$$D_1 = \begin{Vmatrix} \lambda_{11}p + \rho_{11} + \sigma_{11}/p & \lambda_{12}p + \rho_{12} + \sigma_{12}/p \\ \lambda_{12}p + \rho_{12} + \sigma_{12}/p & \lambda_{22}p + \rho_{22} + \sigma_{22}/p \end{Vmatrix} \tag{15}$$

and the impedance function is obtained by dividing this determinant by the minor of the element in the first row and first column. Thus

$$Z(p) = \frac{D_1}{\lambda_{22}p + \rho_{22} + \sigma_{22}/p}. \tag{16}$$

[3] See M. Bôcher, Introduction to Higher Algebra, 1927, p. 150.

[4] V. Bush, reference 2, Chapter III.

It will be helpful first to consider the simple two-mesh network containing only two kinds of network elements shown in a, Fig. 2.

The parameters of the network are $\lambda_{11}=2$, $\lambda_{22}=1$, $\lambda_{12}=1$; $\rho_{11}=2$, $\rho_{22}=2$, $\rho_{12}=1$, and thus the quadratic forms are

$$T = \tfrac{1}{2}(2i_1^2 + 2i_1i_2 + i_2^2) \tag{17a}$$

$$F = \tfrac{1}{2}(2i_1^2 + 2i_1i_2 + 2i_2^2) \tag{17b}$$

and the matrices of the coefficients of these forms are

$$\left\| \begin{matrix} 2 & 1 \\ 1 & 1 \end{matrix} \right\|, \quad \left\| \begin{matrix} 2 & 1 \\ 1 & 2 \end{matrix} \right\|. \tag{18}$$

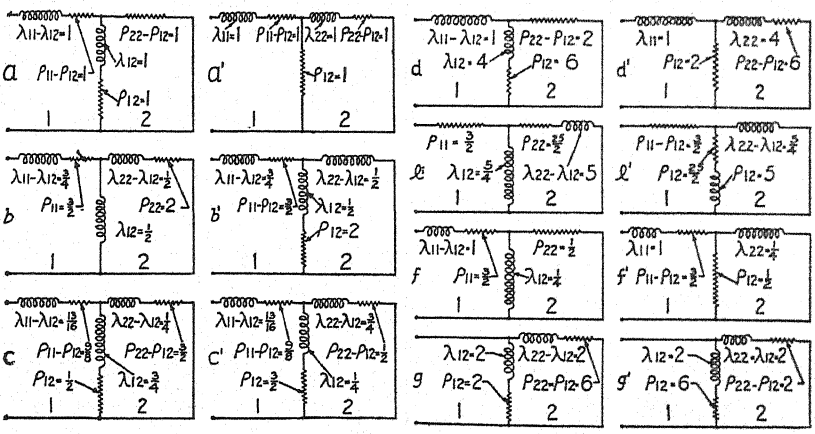

Some members of the group of networks having $Z(p) = \dfrac{p^2+4p+3}{p+2}$

Fig. 2.

The minimal networks of the impedance function $Z(p) = \dfrac{p^2+4p+3}{p+2}$

Now perform the following linear transformations of the instantaneous mesh currents in the network

$$i_1 = i_1' \tag{19a}$$

$$i_2 = a_{21}i_1' + a_{22}i_2' \tag{19b}$$

where the a's are any real numbers, positive or negative. Substituting these values for i_1 and i_2 in the quadratic forms (17a) and (17b), we have

$$T = \tfrac{1}{2}[(2 + 2a_{21} + a_{21}^2)i_1'^2 + (2a_{22} + 2a_{21}a_{22})i_1'i_2' + (a_{22}^2)i_2'^2] \tag{20a}$$

$$F = \tfrac{1}{2}[(2 + 2a_{21} + 2a_{21}^2)i_1'^2 + (2a_{22} + 4a_{21}a_{22})i_1'i_2' + (2a_{22}^2)i_2'^2] \tag{20b}$$

Thus, the transformations (19) give the new quadratic forms (20). The two matrices containing the coefficients of these new forms are then

$$\left\| \begin{matrix} 2 + 2a_{21} + a_{21}^2 & a_{22} + a_{21}a_{22} \\ a_{22} + a_{21}a_{22} & a_{22}^2 \end{matrix} \right\|, \quad \left\| \begin{matrix} 2 + 2a_{21} + 2a_{21}^2 & a_{22} + 2a_{21}a_{22} \\ a_{22} + 2a_{21}a_{22} & 2a_{22}^2 \end{matrix} \right\| \tag{21}$$

These two matrices determine an infinite group of networks equivalent to the network shown in a, Fig. 2. The different networks are obtained by assigning different real values to a_{21} and a_{22}. Thus, for example, by giving the values of $+1$ and -1 respectively to a_{21} and a_{22}, the matrices (21) become under these substitutions

$$\left\| \begin{matrix} \frac{5}{4} & \frac{1}{2} \\ \frac{1}{2} & 1 \end{matrix} \right\|, \quad \left\| \begin{matrix} \frac{3}{2} & 0 \\ 0 & 2 \end{matrix} \right\|. \tag{22}$$

From these matrices the parameters of the network are readily obtained. They are

$$\lambda_{11} = \frac{5}{4}, \quad \lambda_{22} = 1, \quad \lambda_{12} = \frac{1}{2}; \quad \rho_{11} = \frac{3}{2}, \quad \rho_{22} = 2, \quad \rho_{12} = 0$$

and the corresponding network is shown in b, Fig. 2. It is a simple matter to verify the fact that the networks a and b of Fig. 2 have the same impedance function, namely,

$$Z(p) = \frac{p^2 + 4p + 3}{p + 2}. \tag{23}$$

In the same way, by assigning different real values to a_{21} and a_{22}, one can obtain the complete infinite group of networks having (23) for an impedance function. Thus, for example, all the networks shown in Fig. 2 have the same impedance function, namely, (23). These networks are some of the members of the infinite group of networks contained in the tensors (21). It is not difficult to ascertain what values of a_{21} and a_{22} in the transformation matrix will give these networks.

Note that the networks a'-g' are, respectively, identical with the networks a-g, except that the branches in mesh 2 are interchanged. The former networks may thus be considered images of the latter. Mathematically, two networks with their branches in mesh 2 interchanged, are considered different networks, and to exhaust the complete infinite group of networks, both networks and their images must be included.

Note also that the networks d-g and their respective images d'-g' are minimal networks. That is, they are the networks of the group containing the least number of network elements. These can be easily obtained from the tensors (20). Finally, note that it is unnecessary to go through the work of substituting (19) in (17) to obtain the matrices (21) of the quadratic forms (20). We merely make use of an important theorem on matrices, namely, that if we subject the x's in a quadratic form with matrix A to a linear transformation with matrix C, we obtain a new quadratic form with the matrix $C'AC$, where C' is the conjugate of C.[5] In open form, the matrix of the new quadratic form is obtained by multiplying the three matrices

[5] M. Bôcher, reference 3, Theorem 1, p. 129.

$$\left\| \begin{matrix} c_{11} & c_{21} \cdots & c_{n1} \\ c_{12} & & \vdots \\ \vdots & & \vdots \\ c_{1n} & \cdots\cdots & c_{nn} \end{matrix} \right\| \times \left\| \begin{matrix} a_{11} & a_{12} \cdots & a_{1n} \\ a_{21} & & \vdots \\ \vdots & & \vdots \\ a_{n1} & \cdots\cdots & a_{nn} \end{matrix} \right\| \times \left\| \begin{matrix} c_{11} & c_{12} \cdots & c_{1n} \\ c_{21} & & \vdots \\ \vdots & & \vdots \\ c_{n1} & \cdots\cdots & c_{nn} \end{matrix} \right\|. \quad (24)$$

In our problem, the linear transformation is (19), the matrix of which is

$$\left\| \begin{matrix} 1 & 0 \\ a_{21} & a_{22} \end{matrix} \right\| \quad (25)$$

which corresponds to the C matrix. Hence, using this matrix and the matrices (18), we obtain for the matrices of the transformed quadratic forms

$$\left\| \begin{matrix} 1 & a_{21} \\ 0 & a_{22} \end{matrix} \right\| \times \left\| \begin{matrix} 2 & 1 \\ 1 & 1 \end{matrix} \right\| \times \left\| \begin{matrix} 1 & 0 \\ a_{21} & a_{22} \end{matrix} \right\| \quad (26a)$$

$$\left\| \begin{matrix} 1 & a_{21} \\ 0 & a_{22} \end{matrix} \right\| \times \left\| \begin{matrix} 2 & 1 \\ 1 & 2 \end{matrix} \right\| \times \left\| \begin{matrix} 1 & 0 \\ a_{21} & a_{22} \end{matrix} \right\|. \quad (26b)$$

Performing the multiplication of the matrices in (26a), we have

$$\left\| \begin{matrix} 2 + 2a_{21} + a_{21}^2 & a_{22} + a_{21}a_{22} \\ a_{22} + a_{21}a_{22} & a_{22}^2 \end{matrix} \right\|. \quad (27a)$$

Note that this is the left-hand matrix of (21), which was obtained from the transformed quadratic forms (20). In the same way, performing the matrix multiplication in (26b), we have

$$\left\| \begin{matrix} 2 + 2a_{21} + 2a_{21}^2 & a_{22} + 2a_{21}a_{22} \\ a_{22} + 2a_{21}a_{22} & 2a_{22}^2 \end{matrix} \right\| \quad (27b)$$

which is the right-hand matrix of (21).

Thus, however complicated a network may be, and however numerous its meshes, a transformation (24) will give the complete set of equivalent networks. Some of the networks of this infinite set may contain negative as well as positive elements. To obtain networks with only positive elements, it is necessary that the transformation matrix be such that the elements in the main diagonal of the transformed matrix are positive and greater than the corresponding non-diagonal elements.

The infinite group of networks with all three kinds of network elements, namely, inductance, resistance and capacity elements, which have the same impedance function, are obtained exactly in the same manner. Now, however, the transformations are

$$i_1 = i_1' \quad (28a)$$

$$\begin{aligned} i_2 &= a_{21}i_1' + a_{22}i_2' \\ q_1 &= q_1' \\ q_2 &= a_{21}q_1' + a_{22}q_2' \end{aligned} \quad (28b)$$

and we will have three matrices representing a network instead of two. Fig. 3 shows some of the members of the group of networks having the impedance function

$$Z(p) = \frac{11p^4 + 32p^3 + 64p^2 + 60p + 40}{p(4p^2 + 4p + 8)}. \tag{29}$$

As before, the number of arbitrary constants, namely a_{21} and a_{22}, tells us the number of network elements which may be eliminated from the network without disturbing the invariance of the impedance function. Thus, for the two-mesh network containing three kinds of elements, the minimal forms will have, in general, seven elements.

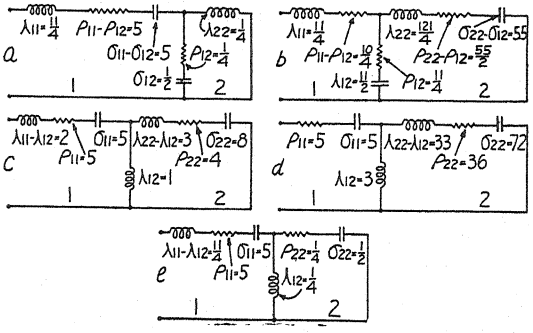

Some members of the group of networks having

$$Z(p) = \frac{11p^4 + 32p^3 + 64p^2 + 60p + 40}{p(4p^2 + 4p + 8)}.$$

Fig. 3.

For the general case, then, of networks of any number of meshes containing all three kinds of network elements, namely, inductance, resistance and elastance elements, we have the following three matrices which represent or definitely fix the network.

$$\left\| \begin{matrix} \lambda_{11} & \lambda_{12} & \cdots & \lambda_{1n} \\ \lambda_{12} & & & \vdots \\ \vdots & & & \vdots \\ \lambda_{1n} & \cdots & \cdots & \lambda_{nn} \end{matrix} \right\|, \quad \left\| \begin{matrix} \rho_{11} & \rho_{12} & \cdots & \rho_{1n} \\ \rho_{12} & & & \vdots \\ \vdots & & & \vdots \\ \rho_{1n} & \cdots & \cdots & \rho_{nn} \end{matrix} \right\|, \quad \left\| \begin{matrix} \sigma_{1n} & \sigma_{12} & \cdots & \sigma_{1n} \\ \sigma_{12} & & & \vdots \\ \vdots & & & \vdots \\ \sigma_{1n} & \cdots & \cdots & \sigma_{nn} \end{matrix} \right\| \tag{30}$$

Making the following linear transformations of the instantaneous mesh currents or charges in the network, we have

$$\left.\begin{aligned} i_1 &= i_1' \\ i_2 &= a_{21}i_1' + a_{22}i_2' + \cdots + a_{2n}i_n' \\ &\cdots\cdots\cdots\cdots\cdots\cdots \\ i_n &= a_{n1}i_1' + a_{n2}i_2' + \cdots + a_{nn}i_n' \end{aligned}\right\} \tag{31a}$$

for the currents, and

$$\begin{aligned} q_1 &= q_1' \\ q_2 &= a_{21}q_1' + a_{22}q_2' + \cdots a_{2n}q_n' \\ &\cdots\cdots\cdots\cdots\cdots\cdots\cdots\cdots \\ q_n &= a_{n1}q_1' + a_{n2}q_2' + \cdots + a_{nn}q_n' \end{aligned} \tag{31b}$$

for the charges.

The three fundamental forms of the electric network of n meshes, whose coefficients are determined from the three matrices (31), are, respectively,

$$T = \tfrac{1}{2}\Sigma_1^n \lambda_{jk} i_j i_k \tag{32a}$$

$$F = \tfrac{1}{2}\Sigma_1^n \rho_{jk} i_j i_k \tag{32b}$$

$$V = \tfrac{1}{2}\Sigma_1^n \sigma_{jk} q_j q_k. \tag{32c}$$

The substitution of the transformations (31) in (32), results in three new quadratic forms, namely,

$$T' = \tfrac{1}{2}\Sigma_1^n \lambda_{jk}' i_j' i_k' \tag{33a}$$

$$F' = \tfrac{1}{2}\Sigma_1^n \rho_{jk}' i_j' i_k' \tag{33b}$$

$$V' = \tfrac{1}{2}\Sigma_1^n \sigma_{jk}' q_j' q_k'. \tag{33c}$$

The coefficients of these new quadratic forms, λ_{jk}', ρ_{jk}' and σ_{jk}' will of course be functions of the elements of the matrices (30) of the original quadratic forms (32) and of the a coefficients of the transformations (31). This has already been noted in the previous two-mesh example.

The transformation matrix, which contains the coefficients of the transformations (31) may be written

$$C = \left\| \begin{matrix} 1 & 0 & \cdots & 0 \\ a_{21} & & & \vdots \\ \vdots & & & \vdots \\ a_{n1} & \cdots & & a_{nn} \end{matrix} \right\| \tag{34}$$

The matrices containing the coefficients of the new quadratic forms (33) are of course

$$\left\| \begin{matrix} \lambda_{11}' & \cdots & \lambda_{1n}' \\ \vdots & & \vdots \\ \lambda_{1n}' & \cdots & \lambda_{nn}' \end{matrix} \right\|, \quad \left\| \begin{matrix} \rho_{11}' & \cdots & \rho_{1n}' \\ \vdots & & \vdots \\ \rho_{1n}' & \cdots & \rho_{nn}' \end{matrix} \right\|, \quad \left\| \begin{matrix} \sigma_{11}' & \cdots & \sigma_{1n}' \\ \vdots & & \vdots \\ \sigma_{1n}' & \cdots & \sigma_{nn}' \end{matrix} \right\|. \tag{35}$$

These matrices contain the complete infinite group of networks having for an impedance function the impedance of the network of (30). The impedance function is thus an *absolute* invariant to a linear transformation of the instantaneous currents or charges of the networks in which the indicial current and corresponding charge are kept invariant.[6] The matrices (35) include within them the matrices (30), which are obtained by the *identity* transformation, namely,

[6] See also the Appendix.

$$\begin{aligned} i_1 &= i_1' \\ i_2 &= \quad i_2' \\ i_3 &= \qquad i_3' \\ &\cdots\cdots\cdots \\ i_n &= \qquad\qquad i_n' \end{aligned} \tag{36}$$

The C matrix corresponding to this transformation is the *identity* matrix

$$\begin{Vmatrix} 1 & \cdots & 0 \\ 0 & 1 & \\ \cdot & & \cdot \\ \cdot & & \cdot \\ 0 & \cdots & 1 \end{Vmatrix} \tag{37}$$

As in the two-mesh example, the actual substitution of the transformations (31) in the quadratic forms can be avoided by making use of the transformation theorem (24). Thus, the tensors (35) are obtained from the matrices (30), and the transformation matrix C (34) by the following matrix multiplications:

$$\begin{Vmatrix} 1 & a_{21} \cdots a_{n1} \\ 0 & a_{22} \\ \cdot & \cdot \\ 0 & a_{2n} \cdots a_{nn} \end{Vmatrix} \times \begin{Vmatrix} \lambda_{11} \cdots \lambda_{1n} \\ \cdot \quad\quad \cdot \\ \lambda_{1n} \cdots \lambda_{nn} \end{Vmatrix} \times \begin{Vmatrix} 1 & 0 & \cdots 0 \\ a_{21} & a_{22} \cdots & a_{2n} \\ a_{n1} & a_{n2} \cdots & a_{nn} \end{Vmatrix} \tag{38a}$$

$$\begin{Vmatrix} & \text{“} & \end{Vmatrix} \times \begin{Vmatrix} \rho_{11} \cdots \rho_{1n} \\ \cdot \quad\quad \cdot \\ \rho_{1n} \cdots \rho_{nn} \end{Vmatrix} \times \begin{Vmatrix} & \text{“} & \end{Vmatrix} \tag{38b}$$

$$\begin{Vmatrix} & \text{“} & \end{Vmatrix} \times \begin{Vmatrix} \sigma_{11} \cdots \sigma_{1n} \\ \cdot \quad\quad \cdot \\ \sigma_{1n} \cdots \sigma_{nn} \end{Vmatrix} \times \begin{Vmatrix} & \text{“} & \end{Vmatrix} \tag{38c}$$

The result of the matrix multiplications will be the three tensors (35) where the elements λ', ρ' and σ' are expressed in terms of the elements of the given network, λ, ρ and σ, and the elements a of the transformation matrix C (34).[7]

[7] The expressions for λ', ρ' and σ' in terms of λ, ρ and σ and the elements a of the transformation matrix C may be expressed by the following summations:

$$\lambda_{ik}' = \sum_{r,s=1}^{n} a_{ri} a_{sk} \lambda_{rs}$$

$$\rho_{ik}' = \sum_{r,s=1}^{n} a_{ri} a_{sk} \rho_{rs}$$

$$\sigma_{ik}' = \sum_{r,s=1}^{n} a_{ri} a_{sk} \sigma_{rs}$$

where the summation may be carried out in any order.

I am indebted to Professor E. A. Guillemin for these compact expressions which give the transformed parameters directly in terms of the given parameters and the elements of the transformation matrix.

The above network transformations have been made for the purpose of preserving the invariance of the *driving-point* impedance function. These transformations need not be so limited. Transformations may be made whereby the invariance of the transfer-impedance function is preserved. This gives rise to a new notion of equivalence, namely, equivalence with respect to a *definite mesh*.

It has been noted that the number of arbitrary constants in the transformation matrix determined the number of elements which could be eliminated from the network without disturbing the invariance of the impedance function. Thus, the least number of elements necessary in any network to realize a definite driving-point impedance function, or a definite transfer-impedance function, can be readily determined. This is important because one can tell whether a communication network of any number of meshes has superfluous elements.

Instead of imposing conditions on the a coefficients of the transformation to give minimal networks, it may be possible to obtain equivalence with respect to more than one mesh in a network; that is, to make the instantaneous currents in both the k-mesh and r-mesh, for example, invariant for the complete infinite group of networks. Finally, we may obtain equivalence with respect to, say, j-meshes, by using a still more general transformation.

In the foregoing theory, we have limited ourselves to networks of a finite number of meshes, that is, to networks with n degrees of freedom. There is no reason physically why this theory cannot be applied to networks of an infinite number of meshes, that is, an infinite number of degrees of freedom. Here interesting problems arise which bear intimately on mathematical theory, acoustics, electromagnetic wave theory, elastic waves,—in short, all branches of physics involving oscillations. This is also true for the finite problem, since the theory explained above can be applied to any physical vibrational problem involving a finite number of degrees of freedom, not merely to electric circuit theory. The latter province, however, appears to offer the most fertile soil for further investigation, and to provide a physical picture of the phenomena which occur.

In the problem involving networks with an infinite number of degrees of freedom, we have to deal with matrices and tensors containing an infinite number of elements as well as with quadratic forms which are power series or integrals. The matrices containing the coefficients of the three fundamental quadratic forms will contain an infinite number of elements, as will the transformation matrix and the resulting tensors. But for a physical network of an infinite number of degrees of freedom, we know physically that the total instantaneous magnetic energy, the total instantaneous electrostatic energy and the total instantaneous power lost, are finite quantities. Hence the three fundamental quadratic forms, which are now power series or integrals, are properly convergent. Likewise, the linear transformations, which are linear forms of an infinite number of terms, have meaning, as have the infinite transformation matrices which contain the coefficients of the transformations. Finally, the resulting tensors, which contain an infinite number of elements

have physical meaning. They represent the complete infinite group of networks of an infinite number of degrees of freedom, discrete or continuous systems, which are equivalent in one or all the ways defined above.

The network with an infinite number of degrees of freedom may be merely a continuous system such as the smooth transmission or communication line. Thus, not only may there be an infinite number of different terminal networks which may perform the same function in a communication or transmission system, but also an infinite number of communication or transmission lines, which likewise may perform the same function. That is, there exists an infinite group of lines all of which have the same impedance function.

It will be recalled that this investigation has considered essentially two-terminal networks. By the principle of superposition, it should be possible to extend the theory to networks of any number of terminals. This extension is important, since by means of it any section of a communication network can be removed and replaced by an equivalent section.

In conclusion, it may be useful to suggest problems for further investigation. First, it should be mentioned that the conception that networks form a group in which the impedance is an invariant may prove useful in simplifying many problems in network theory. Thus, for example, the solution for the instantaneous currents of a network of the group at once results in the solutions for the instantaneous currents of all of the infinite number of networks in the group, since these currents are obtained from the former by a simple linear transformation. Furthermore, the solution for the instantaneous currents in one network in the group may be much simpler than for another; and there may be one network in the group for which the computations are least complicated. Hence, if it is necessary to obtain currents and voltages in one network, it may be simpler first to transform the network to an equivalent one, for which the computations are much simpler. This is already recognized, for example, when we transform from Y to Δ and vice versa in three-phase alternating-current network problems. Thus it is probable that simplification may result in operational circuit analysis by the above method.

It should be noted that in the matrix multiplication which gives the tensor containing the complete infinite group of equivalent networks, the impedance function vanishes from the scene. This suggests the possibility that the notion of the impedance function, which is a special creation of the electrical engineer, may perhaps disappear in the future. What we have to deal with are networks, currents and energies; and while the impedance function may be helpful for visualization, it may not be necessary to obtain the final important results.

As has been indicated, the problem of currents and charges in an electrical network is identical with the problem of velocities and displacements in a dynamical system. Although this is generally recognized, there is much in classical dynamic theory that remains to be translated in appropriate language for electric circuit theory. Many questions suggest themselves. What in electric circuit theory corresponds to the principal or normal coordinates in dynamic theory? Is it possible to eliminate the cross product terms in the

fundamental quadratic forms of the electric circuit, thereby giving expressions which are sums of squares of the currents or charges? If it is, can a physical network be built which realizes this?

Problems of networks with an infinite number of degrees of freedom, equivalence with respect to transfer-impedance, equivalence with respect to more than one mesh, networks with more than two terminals—these have been merely intimated. Furthermore, it appears that mathematics does not discriminate against negative network elements, which seems to indicate that perhaps they may be realized physically, though not, of course, by coils, resistors and condensers.

Finally, in the study of an electrical network and its response to an impressed electromotive force, one continually encounters many seemingly unrelated branches of mathematics, such as (1) continued fractions, (2) Cauchy residue theory, (3) asymptotic series, (4) fractional and irrational derivatives and integrals, (5) group theory, (6) Fourier series and transforms, (7) integral equations, etc. It seems almost as if something were there, inarticulately trying to make itself understood. But perhaps it must await a modern Euler.

Acknowledgment

The author wishes to acknowledge his gratitude to Professors E. A. Guillemin and D. J. Struik for their interest and encouragement in the preparation of his thesis of which this paper is a part; to Professor V. Bush for his valuable criticism; and to R. M. Foster for his "A Reactance Theorem"[8] and "Theorems Regarding the Driving-Point Impedance of Two-Mesh Networks";[9] and to W. Cauer for his "Die Verwirklichung von Wechselstromwiderständen vorgeschriebener Frequenzabhängigkeit"[10] and "Vierpole."[11]

Appendix

Consider the pair of quadratic forms representing, respectively, the inductance and resistance quadratic forms of an n-mesh network containing inductance and resistance elements:

$$\phi(i_1 \cdots i_n) = \Sigma_1^n \lambda_{jk} i_j i_k \tag{39a}$$

$$\psi(i_1 \cdots i_n) = \Sigma_1^n \rho_{jk} i_j i_k \tag{39b}$$

and form the pencil of quadratic forms

$$\phi p + \psi = \Sigma_1^n (\lambda_{jk} p + \rho_{jk}) i_j i_k. \tag{40}$$

The discriminant of this pencil is the determinant of the network:

$$D(p) = \begin{vmatrix} \lambda_{11}p + \rho_{11} \cdots \lambda_{11}p + \rho_{1n} \\ \lambda_{1n}p + \rho_{1n} \cdots \lambda_{nn}p + \rho_{nn} \end{vmatrix} \tag{41}$$

This is a polynomial which is in general of degree n and may be written

[8] Bell System Technical Journal, vol. 3, 1924,

[9] *Ibid.*

[10] Archiv. für Elektrotechnik, Heft 4, Band 17, 1926.

[11] Elektrischen Nachrichtentechnik, Heft 7, Band 6, 1929.

$$D(p) = \Delta(\lambda)p^n + \Delta(\lambda, \rho)p^{n-1} + \Delta_2(\lambda, \rho)p^{n-2} + \cdots + \Delta_2(\rho,\lambda)p^2 + \Delta_1(\rho,\lambda)p + \Delta(\rho) \quad (42)$$

where $\Delta(\lambda)$ and $\Delta(\rho)$ are the discriminants of ϕ and ψ respectively, while $\Delta_k(\lambda, \rho)$ is the sum of the different determinants which can be formed by replacing k columns of the discriminant of ϕ by the corresponding columns of the discriminant of ψ.

Likewise, form the first minor of $D(p)$, namely,

$$M_{11}(p) = \begin{vmatrix} \lambda_{22}p + \rho_{22} & \cdots & \lambda_{2n}p + \rho_{2n} \\ \cdot & & \cdot \\ \lambda_{2n}p + \rho_{2n} & \cdots & \lambda_{nn}p + \rho_{nn} \end{vmatrix}. \quad (43)$$

This may be written as a polynomial in general of degree $n-1$, namely,

$$M_{11}(p) = M_{11}(\lambda)p^{n-1} + M_{11}^{(1)}(\lambda,\rho)p^{n-2} + \cdots + M_{11}^{(1)}(\rho, \lambda)p + M_{11}(\rho) \quad (44)$$

Now it can be shown that the coefficients $\Delta(\lambda)\cdots\Delta(\lambda, \rho)\cdots\Delta(\rho)$ of $D(p)$ are integral rational invariants of weight two of the pair of quadratic forms ϕ and ψ.[12] Similarly, the coefficients $M_{11}(\lambda)\cdots M_{11}^k(\lambda, \rho)\cdots M_{11}(\rho)$ are integral rational invariants of weight two. Thus it is that the linear transformations of the variables of the quadratic forms make the impedance function $Z(p)$, which is the ratio of $D(p)$ and $M_{11}(p)$; that is, the ratio of two relative invariants of the same weight, an absolute invariant. The foregoing is true also of n-mesh networks containing all three kinds of elements, where we now have in addition to the inductance and resistance quadratic forms, the elastance quadratic form. Thus

$$Z(p) = D(p)/M_{11}(p) \quad (45)$$

becomes under a linear transformation with matrix

$$\begin{Vmatrix} 1 & 0 & \cdots & 0 \\ a_{21} & & \cdots & a_{2n} \\ \cdot & & & \cdot \\ \cdot & & & \cdot \\ a_{n1} & & \cdots & a_{nn} \end{Vmatrix} \quad (46)$$

$$Z(p) = \frac{\begin{vmatrix} 1 & 0 & \cdots & 0 \\ a_{21} & & \cdots & a_{2n} \\ \cdot & & & \cdot \\ \cdot & & & \cdot \\ a_{n1} & & \cdots & a_{nn} \end{vmatrix}^2}{\begin{vmatrix} a_{22} & \cdots & a_{2n} \\ \cdot & & \cdot \\ \cdot & & \cdot \\ a_{n2} & \cdots & a_{nn} \end{vmatrix}^2} \times \frac{D(p)}{M_{11}(p)} \quad (47)$$

$$= D(p)/M_{11}(p).$$

[12] See M. Bôcher, Introduction to Higher Algebra, 1927, p. 166.

ACCOMMODATION COEFFICIENTS OF POSITIVE IONS OF ARGON, NEON AND HELIUM

By
C. C. Van Voorhis, Princeton University
and
K. T. Compton, Massachusetts Institute of Technology

(Received April 23, 1931)

Abstract

Positive ions of argon, neon and helium produced in a low voltage arc were attracted to a spherical metal collector by regulated potentials up to 140 volts. The resulting heating of the collector was measured by a thermal junction and found to be *considerably less* than the product of the current by the attracting voltage. After taking account of the energy scattering at collisions and of the effect of the secondary electron emission, the following values of the "accommodation coefficients" were obtained: argon 0.75 ± 0.05, neon 0.65 ± 0.05 (both between 21 and 141 volts), and helium 0.35 ± 0.05 between 21 and 51 volts and 0.55 ± 0.05 between 111 and 141 volts.

WHEN an attempt was made to measure the amount of energy ϕ_+ delivered to a metal electrode when a positive ion with no kinetic energy is neutralized at its surface,[1] collisions between the ions and neutral molecules within the sheath, and comparatively large electron currents were thought to be the principal factors complicating the calculation and interpretation of the results. By making measurements of the heat generated when positive ions were drawn to the collector by fields so large that practically no electrons could reach the collector, and by working with such low gas pressures that very few ions would make collisions within the sheath it was later believed possible to make these complicating factors negligibly small. Under these conditions, since the positive ions reaching the collector are believed to start at or near the sheath edge with only a negligibly small velocity,[2] ϕ_+ should be easily obtained from the observed heating of the collector at two different negative potentials, if due allowance were made for the kinetic energy of the ions acquired in passing through the sheath. Thus the heating effect H of a current of magnitude j^+ at a given accelerating potential V with respect to the space potential would be

$$H = j^+(V + \phi_+) \tag{1}$$

and the difference between the heating effects at two different accelerating potentials V_f and V_0 would be given by

$$H_f - H_0 = j_f{}^+(V_f + \phi_+) - j_0{}^+(V_0 + \phi_+) \tag{2}$$

whence

[1] Van Voorhis, Phys. Rev. **30**, 318 (1927).
[2] Tonks and Langmuir, Phys. Rev. **34**, 876 (1929).

$$\phi_+ = \frac{(H_f - H_0) - (j_f{}^+V_f - j_0{}^+V_0)}{j_f{}^+ - j_0{}^+}. \tag{3}$$

All of the quantities on the right side of Eq. (3) could then be obtained experimentally by means of our apparatus.

However, the results obtained from the application of this line of reasoning led to the surprising discovery that the heat produced by the positive ions striking a collector and being neutralized at its surface, is *much less* than the equivalent of the kinetic energy which they should acquire from the attracting field. Though this deficiency in heating effect has recently been observed by Found[3] and Güntherschulze,[4] they have ascribed it entirely to the effect which a large secondary electron emission would have upon the apparent and true values of the positive ion currents, and thus have assumed that the effect is only apparent and not real.

Careful measurements over a considerable range of accelerating potentials and gas pressures in argon, neon and helium have led us to conclude that the deficiency in heating effect in these gases is entirely too large to be accounted for by secondary electron emission and consequently at least some of the neutral molecules and metastable atoms formed by the neutralization of the positive ions at a metal surface must have left it with energies much larger than would correspond to the temperature of the metal. This means that positive ions with fairly high velocities may be considered as having accommodation coefficients less than unity just as the gas molecules have at much lower velocities or temperatures.[5]

Some of our measurements have been made under gas pressure conditions such that the effects of collisions of ions with gas molecules within the sheath are no longer negligible; but when these results have been corrected by the use of Runge's[6] theoretical values for the scattering of ion energy by collisions with neutral molecules, they become, in general, fairly consistent with those obtained at the lower gas pressures and may therefore be used in testing collision theories.

Experimental Procedure and Calculation of Results

The observations were taken with apparatus of the same type as was described in detail in the earlier paper.[1] A schematic sketch of the parts in the discharge tube and of the electrical connections is given in Fig. 1. A low voltage arc was maintained between the hot tungsten filament F and the anode A by applying a voltage from the battery B_2, this voltage being from 5 to 10 volts higher than the ionizing potential of the gas in use. The collector C was a metal sphere in which was imbedded a very small copper-constantan

[3] Found, Phys. Rev. **34**, 1625 (1929).

[4] Güntherschulze, Zeits. f. Physik **62**, 600 (1930).

[5] Knudsen, Ann. d. Physik **34**, 593 (1911); **46**, 641 (1915); Soddy and Berry, Proc. Roy. Soc. **84**, 576 (1911); Langmuir, J. Am. Chem. Soc. **37**, 425 (1915); Roberts, Proc. Roy. Soc. **129**, 146 (1930).

[6] Runge, Zeits. f. Physik **61**, 174 (1930).

thermocouple. In the measurements with argon and neon the collector was of molybdenum, 3.1 mm in diameter and with helium it was a 3.0 mm platinum sphere.

The gases were carefully purified by arcs between "misch" metal cathodes and iron anodes in glass reservoirs on the vacuum system, before being admitted to the discharge tube. Observations were made on repeated fillings of a given gas until the results from different fillings were quite reproducible, which condition was taken to indicate that no appreciable impurity was coming from the walls or metal parts of the vacuum tight discharge tube.

Of the quantities on the right side of Eq. (3) j_0^+ and j_f^+ were obtained directly from the readings of the Cambridge Universal Test Set used as A_3 in Fig. 1. To obtain V_0 and V_f it was necessary to find V_s, the space potential

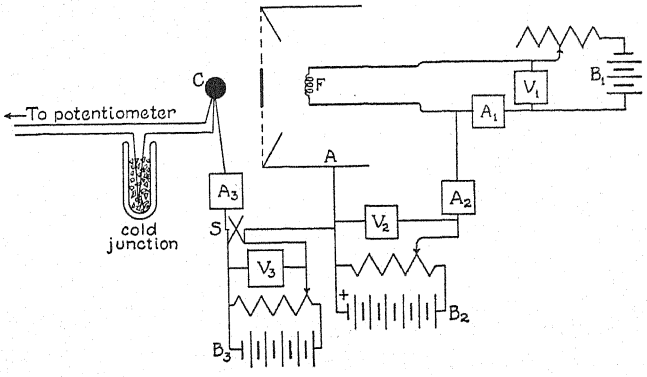

Fig. 1. Schematic sketch of apparatus and arrangement of electrical circuits.

with respect to the anode, by the usual method[7] and add this to the applied potentials as given by V_3 (Fig. 1). The quantity $H_f - H_0$ was obtained from the product of the heat capacity Q of the collecting sphere C and the rate of temperature change dT/dt of C immediately after its potential was changed from V_0 to V_f. Since the temperature, starting at T_0 when $t=0$, approached a final limiting value exponentially,

$$T - T_0 = (T_f - T_0)(1 - e^{-at}) \tag{4}$$

where T was the temperature at time t, e the Naperian base and a a constant dependent upon the existing experimental conditions. Then it follows from (4) that

$$\left(\frac{dT}{dt}\right)_{t=0} = a(T_f - T_0), \text{ where } a = \frac{2.303}{t}\log_{10}\left(\frac{T_f - T_0}{T_f - T}\right) \tag{5}$$

The data for calculating a were obtained by first noting the electromotive force mV_0 of the thermocouple after the potential of the collector had been

[7] Langmuir, Gen. Elec. Rev. **26**, 731 (1923); Science **58**, 290 (1923); Jour. Frank. Inst. **196**, 751 (1923); Langmuir and Mott-Smith, Gen. Elec. Rev. **27**, 449, 538, 616, 762, 810 (1924).

held at V_0 long enough for it to reach a steady temperature. Then simultaneously the collector potential was changed to V_f and two stop watches started. As the temperature of the collector changed, the drum of the potentiometer was slowly turned so as to keep the galvanometer deflection as near zero as possible. At some instant when the deflection was exactly zero one watch was stopped and its time t_1 and the corresponding mV_1 were recorded, after which mV_2 was noted in the same way for time t_2 obtained by means of the second watch. As soon as the temperature became practically constant, which was generally about 5 minutes after t_0, record was made of mV_f. From these data two values of a could be calculated and their mean $\bar{a}$ was used in applying Eq. (5).

In Table I are given typical sets of observations and the resulting quantities obtained from various steps in the calculations. To obtain the tempera-

TABLE I. *Typical sets of observations and calculations for the molybdenum collector in argon at 0.1 mm pressure.*

1	2	3	4	5	6	7	8	9
V_0	j_0^+	t_0	mV_0	T_f-T_0			MH or	
		t_1	mV_1	T_f-T_1	a_1		$\bar{a}(T_f-T_0)Q$	
V_f	j_f^+	t_2	mV_2	T_f-T_2	a_2	Q		MH/EH
V_s			mV_f		$\bar{a}$		EH	
Volts	m.a.	sec.	millivolts	°C			milliwatts	
20.0	0.354	0	7.653	25.31				
		19.79	7.945	19.77	0.01248	35.97	11.39	
49.9	.430	36.95	8.149	15.93	.01254			0.786
1.5			9.007		.01251		14.49	
49.8	.432	0	8.990	29.10				
		32.70	9.551	18.80	.01338	36.18	14.06	
81.0	.496	60.80	9.875	12.92	.01336			.751
1.5			10.594		.01337		18.73	
81.0	.498	0	10.582	30.18				
		26.57	11.111	20.80	.01401	36.42	15.32	
110.8	.550	50.11	11.445	14.89	.01385			.740
1.5			12.299		.01393		20.70	

ture differences given in column 5 the corresponding millivolt differences obtained from column 4 were divided by the millivolt differences per degree, of the electromotive force of the thermocouple at the corresponding temperatures. The temperatures and corresponding millivolt differences per degree were readily determined from two curves obtained by plotting against temperature on a large piece of graph paper, the values of mV and $d(mV)/dt$ calculated at 20° intervals from the calibration equation of the thermocouple, $mV_T = 0.0400766T + 0.00004344T^2 - 0.00000002244T^3$.

In column 7 the values of Q are the heat capacities in millijoules per degree for the corresponding mean temperatures. In column 8, MH is the measured heating effect in milliwatts obtained from the observations and calculations, whereas EH is the expected heating on the assumption that all of the kinetic energy gained by the ions from the accelerating field would be delivered to the collector in the form of heat, ϕ_+ being neglected for the present. Thus the value of EH is found from the equation

$$EH = j_f^+(V_f + V_s) - j_0^+(V_0 + V_s). \tag{6}$$

In Tables II, III and IV are given the results obtained in argon, neon and

helium respectively. Column 1 of these tables gives the gas pressure and the assumed positive ion mean free path obtained by taking $2^{1/2}$ times the kinetic theory value for the neutral atoms at the temperature in the discharge tube. In column 2 are given the values of the applied potentials (with respect to the space) after slight adjustment to make the voltage intervals exactly 30 volts, the actual intervals used ranging between 29 and 31 volts since the po-

TABLE II. *Results in argon.*

1	2	3	4	5	6	7	8	9	10	11
					Measured heating / Expected heating			If current varies as sheath area		
P / λ	V	m.a.	S/λ (L&B)	S/λ (R&M)	Unmodified	Corrected		m.a.	MH/EH	
						$\phi_+=0$	$\phi_+=V_i-\phi_-$		$\phi_+=0$	$\phi_+=V_i-\phi_-$
0.016 mmHg	20.6	0.106	0.068	same	(0.84^E)	(0.84^E)	(0.76^E)	0.061+	(1.45^E)	(1.31^E)
	50.6	.142	.117	"	.81	.81	.76	.045− .097+	(1.02^F)	(1.96^F)
7.8 mm	80.6	.169	.154	"	.81	.81	.78	.124	$(.98^F)$	$(.94^F)$
	110.6	.191	.187	"	.80	.80	.78	.146	$(.95^F)$	$(.92^F)$
	140.6	.211	.217	"				.166		
0.040	20.6	.261	.103	"	.81	.81	.74	.217+ .044− .285+	.92	.88
	50.6	.329	.184	"	.80	.80	.76	.340	.88	.84
3.15	80.6	.384	.245	"	.77	.77	.74	.387	.84	.80
	110.6	.431	.297	"	.76	.77	.74	.432	.83	.80
	140.6	.476	.343	"						
0.10	21.5	.340	.235	"	.77	.77	.71	.277+ .063− .353+	.89	.82
	51.5	.416	.411	.410	.74	.75	.70	.413	.84	.80
1.26	81.5	.476	.546	.545	.73	.74	.70	.467	.82	.79
	111.5	.530	.662	.661	.72	.75	.72	.517	.81	.78
	141.5	.580	.766	.765						
0.25	21.3	.250	.680	.679	.69	.70	.64	.200+ .050− .260+	.82	.74
	51.3	.310	1.20	1.18	.68	.71	.66	.312	.80	.75
0.505	81.3	.362	1.59	1.55	.68	.77	.73	.359	.85	.81
	111.3	.409	1.92	1.87	.67	.77	.74	.400	.96	.92
	141.3	.450	2.20	2.14						
0.50	21.5	.218	1.47	1.44	.69	.77	.70	.172+ .046− .223	1.00	.90
	51.5	.269	2.60	2.53	.64	.78	.72	.274	1.00	.92
0.253	81.5	.320	3.41	3.32	.62	$(.87^H)$	$(.82^H)$	.327^I	(1.01^H)	$(.94^H)$
	111.5	.373	4.05	3.93	.63	$(.92^H)$	$(.87^H)$	.378^I	(1.00^H)	$(.95^H)$
	141.5	.424	4.56	4.40						

tential change was made by suddenly changing the position of the slider of a slide wire potential divider and the interval could not be exactly duplicated. The values of the measured currents in column 3 are adjusted to correspond to the potentials given in column 2. These adjustments were deemed advisable in order to shorten the calculations involved in the corrections made as explained later, by making it possible to apply these corrections only to the mean values instead of to each individual result which was obtained under

conditions differing only slightly from those of the three to seven other similar results. However, the values of the ratios of the "measured heating" to the "expected heating" given in column 6 are the means of the four to eight

TABLE III. *Results in neon.*

1	2	3	4	5	6	7	8	9	10	11
					Measured heating / Expected heating			If current varies as sheath area		
P / λ	V	m.a.	S/λ (L&B)	S/λ (R&M)	Unmodified	Corrected		m.a.	MH/EH	
						$\phi_+=0$	$\phi_+=V_i-\phi_-$		$\phi_+=0$	$\phi_+=V_i-\phi_-$
	22.5	.166c	.314	same				.130+		
0.13 mm Hg					0.64	0.65	0.52	.036−	0.76	0.61
	52.5	.216	.538	.537				.180+		
					.66	.68	.60		.76	.67
	82.5	.259	.696	.695				.223		
1.68 mm					.67	.70	.64		.77	.71
	112.5	.298	.830	.828				.262		
					.68	.72	.67		.78	.73
	142.5	.332	.951	.949				.296		
	22.0	.427c	.425	.424				.370+		
.30					.65	.66	.56	.057−	.73	.62
	52.0	.527	.738	.736				.470+		
					.66	.68	.61		.73	.66
	82.0	.610	.984	.980				.553		
.752					.65	.67	.63		.72	.66
	112.0	.687	1.174	1.160				.630		
					.65	.67	.63		.71	.68
	142.0	.755	1.35	1.33				.698		
	21.4	.375	1.08	1.07				.327+		
.73					.61	.64	.54	.048	.71	.59
	51.4	.468	1.90	1.85				.420+		
					.60	.67	.59		.73	.64
	81.4	.548	2.51	2.45				.500		
.308					.59	(.74^H)	(.67^H)		(.79^H)	(.71^H)
	111.4	.631	3.00	2.92				.583		
					.57	(.74^H)	(.67^H)		(.78^H)	(.71^H)
	141.4	.718	3.38	3.29				.670		

TABLE IV. *Results in helium.*

1	2	3	4	5	6	7	8	9	10	11
					Measured heating / Expected heating			If current varies as sheath area		
P / λ	V	m.a.	S/λ (L&B)	S/λ (R&M)	Unmodified	Corrected		m.a.	*MH/EH*	
						$\phi_+=0$	$\phi_+=V_i-\phi_-$		$\phi_+=0$	$\phi_+=V_i-\phi_-$
	21.4	0.0585c	0.616	0.614						
.16 mm Hg					0.36	0.38	0.18	Observed positive ion Currents were quite nearly proportional to calculated sheath areas		
	51.4	.0949	.980	.970						
					.44	.48	.34			
	81.4	.1248	1.24	1.22						
2.18 mm					.44	.49	.38			
	111.4	.1540	1.44	1.41						
					.42	.53	.44			
	141.4	.181	1.61	1.57						
	21.7	.128c	1.015	1.003				.089+		
.40					.36	.40	.22	.039−	.50	.28
	51.7	.178	1.72	1.68				.139+		
					.42	.51	.38		.61	.46
	81.7	.220	2.25	2.18				.181		
.870					.43	.54	.44		.64	.52
	111.7	.259	2.54	2.47				.220		
					.42	(.66^H)	(.57^H)		(.79^H)	(.67^H)
	141.7	.295	3.09	3.00				.256		
	20.9	.182c	2.08	2.01				.117+		
1.0					.37	(.48^H)	(.25^H)	.065−	(.64^H)	(.34^H)
	50.9	.244	3.56	3.46				.179+		
					.38	(.58^H)	(.43^H)		(.74^H)	(.55^H)
	80.9	.297	4.48	4.32				.232		
.348					.40	(.70^H)	(.57^H)		(.88^H)	(.72^H)
	110.9	.344	5.37	5.12				.279		
					.39	(.82^H)	(.70^H)		(1.00^H)	(.86^H)
	140.9	.386	6.46	6.10				.321		

ratios calculated from the actual observations and are not modified in any way.

In columns 4 and 5 are given values of the collision numbers or the ratios of the sheath thickness S to the mean free path λ. The sheath thicknesses used in column 4 were obtained on the assumption of no collisions within the sheath, i.e., by means of Langmuir's equation,[8] and Langmuir and Blodgett's[9] tables, for spherical collectors. The collision numbers in column 5 have been obtained by correcting the sheath thickness for the slowing up of the positive ions by the collisions within the sheath, in accordance with some recent unpublished work of H. P. Robertson and P. M. Morse, assuming that the same fractional shrinkage in thickness takes place in the sheath around the spherical collector as would take place in the sheath of an infinite plane,

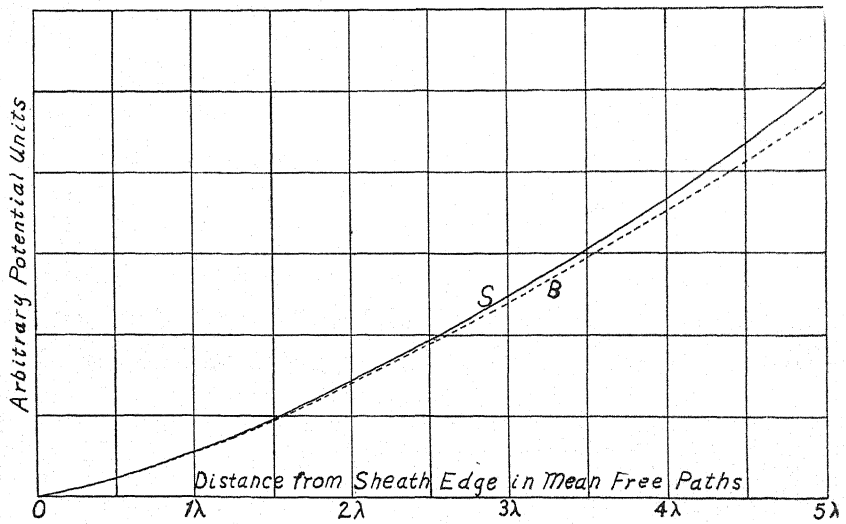

Fig. 2. Potential distribution curves, B from space charge equation (no collisions), and S from assumption of kinetic theory collisions between elastic spheres. For the case of a large plane electrode.

for which case the Robertson and Morse calculations have been made. In Fig. 2[10] the solid line gives the distribution of potential for collision numbers up to five and the dashed line the potential distribution for the same sheath thicknesses if there were no collisions. Thus the difference in abscissas of points having the same ordinate on the two curves gives the shrinkage effect resulting from collisions of ions with neutral molecules within the sheath.

In column 6 are given the mean values of MH/EH obtained in the manner described above in connection with Table I. The values given in column 7 were obtained by correcting for the energy so scattered by collisions of the ions with gas molecules within the sheath that it would not be expected to

[8] Langmuir, Gen. Elec. Rev. **27**, 449 (1924).
[9] Langmuir and Blodgett, Phys. Rev. **24**, 53 (1924).
[10] Published here with the kind permission of Robertson and Morse.

be delivered to the collector. On the assumption of collisions between elastic spheres of equal masses, half of the scattered energy will be delivered to gas molecules on the average, and half will be retained by the ions.[11] All of the energy retained by the ions and part of the energy received by the gas molecules will reach the collector and be delivered in full to it if the accommodation coefficient be unity. However, a part of the energy received by the gas molecules will be so directed as to miss the collector, i.e., if collisions take place at a distance PN, Fig. 3, from the spherical collector no neutral molecules receiving velocities directed at an angle from the normal PN greater

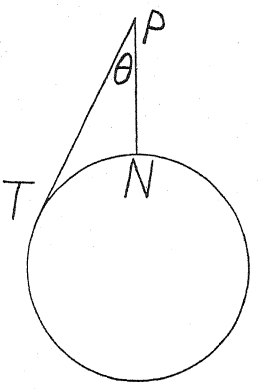

Fig. 3.

than the grazing angle θ will deliver any of their energy to the collector (except as the result of further collisions, and it is assumed that this would just balance the loss of energy from within the grazing angle, resulting from the same cause).

To calculate the fraction of energy, called hereafter $F(E)$, which should not be expected to reach the collector, Runge's[3] theoretical results were used in the following way. Values of $R \sin \theta$ (from Runge's Fig. 3) were plotted as ordinates against θ, R being the energy radius vector and θ the angle with

TABLE V. *Fraction of total energy directed outside of given angles with original direction after from 1 to 5 collisions. (Obtained from Runge's results).*

Angle	Number of collisions				
	1	2	3	4	5
0°	1.000	1.000	1.000	1.000	1.000
10	.941	.968	.973	.980	.988
20	.780	.874	.905	.932	.944
30	.558	.734	.799	.855	.872
40	.346	.569	.688	.752	.781
50	.176	.410	.531	.636	.674
60	.065	.272	.395	.515	.55
70	.015	.164	.278	.396	.45
80	.002	.089	.190	.290	.35
90	.000	.043	.120	.200	.26

[11] Compton and Langmuir, Rev. of Mod. Phys. **2**, 211 (1930); Runge, reference 6.

the direction of the electric field, i.e., with the direction of the energy at the time of the first collision. We then integrated with a planimeter the areas bounded by the zero ordinate, the curves and the 10° interval abscissa lines and from the integrated values found the $F(E)$ directed outside of given grazing angles after from 1 to 5 collisions. The results thus obtained are given in Table V and plotted in Fig. 4, which has also a plot of the grazing angles from points up to 2 mm distant from our 3.1 mm diameter collector.

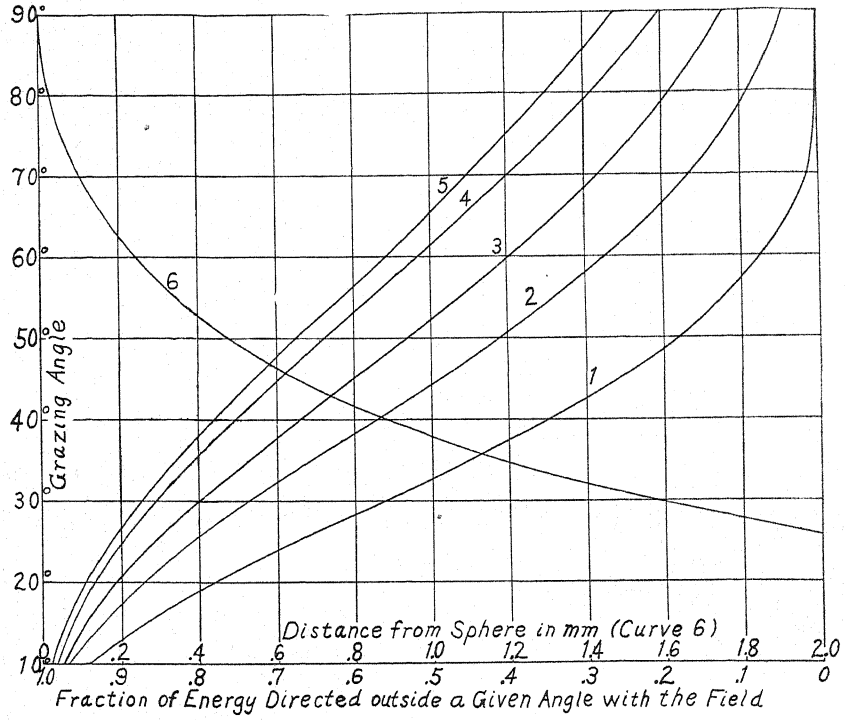

Fig. 4. Curves 1, 2, 3, 4 and 5 show fractions of energy directed outside of given angles with the field direction after from 1 to 5 collisions respectively. Curve 6 is a plot of grazing angle against distance from the 3.1 mm collector.

In applying these results we have followed Runge's assumption that it is legitimate to take account of the scattering of the total energy gained in the whole field between sheath edge and collector by considering piecemeal the energy gained in each λ of distance and the scattering of this energy at subsequent collisions on the way to the collector and then taking the sum of the residual energies at the collector as being the total effective applied potential. Thus, for example, in argon at 0.25 mm pressure (see Table II) with 111.3 volts applied potential the collision number was 1.87 and with 141.3 volts it was 2.14. To calculate the effective potentials (hereafter called EP) it was necessary to obtain from the curves in Fig. 4 the grazing angles recorded in column 2, Table VI, corresponding to the distances from the collector given

in column 1 and the $F(E)$'s directed outside of these grazing angles after collisions, as tabulated in columns 3, 4 and 5 of the same table. Then the potentials with respect to the sheath edge at the various integral λ distances from the collector were obtained from the solid potential distribution curve of Fig. 2, the potentials found being tabulated in columns 6 and 7 of Table IV, whose columns 8 and 9 give the potential differences for the whole λ's and the outside fraction of λ and also, in parentheses, the EP's found by applying the values given in columns 3, 4 and 5 to the potential differences given in 8 and 9 in the following way.

TABLE VI. *Quantities involved in the illustratory example of the calculation of the effective potentials.*

1	2	3	4	5	6	7	8	9
Distance from collector	Grazing angle	Fraction of energy directed outside of grazing angle 1 Col.	2 Col.	3 Col.	Potential relative to sheath edge		Potential difference (Effective P.D.)	
0	90.0°	000	.043	.12	141.3	111.3	(129.5)	(104.5)
.14λ	73.2		.137	.25			Total E.P.	
.50λ	59.7	.075					81.1	71.8
.87λ	50.6	.169	.399				(80.4)	(71.2)
1.00λ	48.9	.205	.434		60.2	39.5		39.5
1.14λ	46.8	.224	.457				56.6	(33.3)
1.87λ	38.5	.376				0.0	(46.6)	
2.00λ	37.4	.397			3.6		3.6	
2.14λ	36.2	.422			0.0		(2.5)	

Consider first the potential difference in the first λ distance from the collector. On the assumption that collisions are equally probable all along the path but that all the ions collide once and only once in the distance λ, calculations based on a ten-step division of the first λ for several values of λ, and the resulting potential distributions and energy directions as obtained from the application of the curves in Figs. 2 and 4, showed that the total $F(E)$ received by neutral molecules so directed as to miss the collector is given very accurately by 1/9 the $F(E)$ lost to such molecules at collisions at a point 0.5λ from the collector. Consequently 81.1 $(1-.075/9)$ or 80.4 and 71.8 $(1-0.075/9)$ or 71.2 are the EP differences in the first λ of our examples. For the fractional loss of the energy applied in the second λ, if the $F(E)$ curve for first collision and the potential distribution curve were straight lines we would take 0.5×0.5 the mean of the fractions at λ and 2λ, the one 0.5 factor to give the mean applied potential between λ and 2λ and the other 0.5 factor to take account of the fact that only half of this $F(E)$ is carried by molecules. However, here again ten-step calculations showed that the factor 1/9 should be used instead of 1/8 because of the curvature of the above mentioned curves. For the fractional loss in a given λ of the energy gained outside this λ the fraction $\frac{1}{4}$ was used because the $F(E)$ curves for more than one collision do not differ so greatly from a straight line. Consequently 56.6 $[1-(0.397+0.205)/9]$ $[1-(0.434+0.043)/4]$ or 46.6 was found to be the EP in the second λ of our 141.3 volt case. To obtain the effective part of the potential applied in

the outer fractional λ part of the sheath a slightly different method of calculation was used as will appear from the following examples:

$$3.6\left[1-\frac{0.14}{9}(0.422+0.397)-\frac{0.86}{4}(0.397+0.224)\right]=3.07$$

$$3.07\left(1-\frac{0.457+0.137}{4}\right)\left[1-\frac{0.14}{4}(0.25+0.12)\right]=2.5$$

and

$$39.5\left[1-\frac{0.87}{9}(0.376+0.205)-\frac{0.13}{4}(0.205+0.169)\right]=36.8$$

$$36.8\left[1-\frac{0.87}{4}(0.399+0.043)\right]=33.3$$

Thus the total *EP*'s whose energy may be expected to reach the collector are 129.5 and 104.5 volts instead of the actually applied voltages 141.3 and 111.3 respectively, and the use of the former instead of the latter to calculate the expected heating changed the ratio of *MH* to *EH* from 0.67 to 0.77. By this method of correcting for the amount of energy to be expected to reach the collector all the results tabulated in column 7 of Tables II, III and IV were obtained.

When, instead of using the assumption that $\phi_+=0$, the Schottky[12] assumption that $\phi_+=V_i-\phi_-$, where V_i is the ionizing potential of the gas, is taken into account the results are changed from the values of column 7 to those of column 8 (Tables II, III and IV).

After our experimental tube had been set up and most of the data taken, there came to our attention the work of Oliphant[13] and of Uyterhoeven and Harrington[14] which showed the presence of a fairly large secondary electron emission from negative collectors under conditions somewhat similar to ours. The effect of the secondary electrons would be to make the heating of the collector less than would be expected if all the measured current were carried by positive ions. Since we were not able to measure the secondary emission from the collector directly, although measurements made with an auxiliary Mo plate and Ni collector (added to the discharge tube for this special purpose and not shown in Fig. 1) similar to those used by Uyterhoeven and Harrington[14] showed less than 1 percent secondary emission from the plate under the conditions of our experiments in argon and less than 2 percent in neon (no measurements being made in helium) we have thought it best to show what would be the effect upon our results of secondary electron emissions of about the same magnitude as reported by these investigators. In accordance with Found's suggestion that for different negative collector potentials, other discharge tube conditions remaining the same, the positive ion currents to the collector should be proportional to the sheath areas while the secondary elec-

[12] Schottky, Ann. d. Physik **62**, 143 (1920).
[13] Oliphant, Proc. Roy. Soc. **124A**, 228 (1929); **127A**, 373 (1930).
[14] Uyterhoeven and Harrington, Phys. Rev. **36**, 709 (1930).

tron emission, since chiefly due to metastable atoms, should remain practically constant, we found by the trial and error method, values of positive currents quite accurately proportional to the sheath areas (recalculated for these smaller currents) when we subtracted some certain constant value from our measured collector currents, these constant values being in general fairly reasonable ones for the secondary electron current when compared with Oliphant's,[13] and Uyterhoeven and Harrington's[14] results. In column 9 of Tables II, III and IV are tabulated the current values obtained in this way. The value followed by a negative sign and recorded between the first and second positive values is the assumed value of the secondary electron emission for the given discharge condition, since it was the necessary constant amount to be subtracted from the measured currents to give positive ion currents proportional to the corrected sheath areas. The last two positive ion current values in argon are slightly higher than they should be on this theory but this could be accounted for by the fact that under the existing conditions the secondary electrons would produce an appreciable amount of ionization within the sheath. To obtain results consistent with those for the higher accelerating voltages some of the measured currents in neon and helium for the lowest potentials used (about 21 volts) had to be increased by from 1 to 12 percent, amounts practically the same as those obtained by extrapolating the plots of the logarithm of the current against applied voltage, used in determining space potentials, and thus may be ascribed to the fraction of electrons having random energies greater than about 21 volts. The current values marked with a superscript c in column 3 are the ones so corrected.

The calculations made as for the results given in columns 7 and 8, Tables II, III and IV but using the positive ion currents given in column 9 instead of those given in column 3 led to the ratios of measured heating to expected heating (or accommodation coefficients) given in columns 10 and 11 for $\phi_+ = 0$ and $\phi_+ = V_i - \phi_-$ respectively.

Discussion of Results

Of the results given in columns 7, 8, 10 and 11 of Tables, II, III and IV the ones enclosed in parentheses are probably rather inaccurate, the ones with the superscript E being uncertain because of poor experimental conditions, the ones with superscript F are probably too high because the secondary electron current given by Found's assumption is unreasonably high in this case, and the ones with superscript H being probably too high because an assumption used in determining the fraction of energy not to be expected to reach the collector leads to a value for this fraction which is increasingly too high as the mean free paths become shorter, and the collision number increases. The assumption in question is the one given in parenthesis on page 1603 in connection with Fig. 3. Thus the nearer the point P is to the collector the greater will be the excess of molecules given direction outside of PT when struck by positive ions at P, but which later strike the collector as a result of collisions with other molecules, over those going outward across PT after being given directions inside PT when struck at P, since the distances which

the former must go before getting completely away from the collector are considerably greater than the distances the latter must go to reach it.

A study of the remaining values of the results shows that in helium the "accommodation coefficient" (hereafter referred to as A) increases as the positive ions are given higher velocities. This is in accord with the observations of Kingdon and Langmuir[15] that helium ions penetrate to a considerable depth into the metal which they are bombarding, an effect which would increase with increasing energy of the ions. In argon there appears to be no increase in A with increasing energy of the ions and in neon the effect is only very slight and we have neglected it in determining the mean values given for this gas in Table VII.

TABLE VII. *Summary of mean values of "accommodation coefficients."*

Column	Argon		Neon		Helium	
	Mean	Average variation	Mean	Average variation	21 to 51 V	111 to 141 V
7	0.770	0.023	0.674	0.019	0.40	0.56
8	.725	.029	.591	.038	.20	.47
10	.875	.056	.740	.022	.50	.70
11	.825	.047	.659	.033	.28	.56
Estimate of true value	0.75±0.05		0.65±0.05		0.35±0.05	0.55±0.05

In this table are given the means of the undoubtful values given in columns 7, 8, 10 and 11 of Tables II and III along with the average variations from the means. These average variations from the means are given not because we believe them to be a measure of the absolute accuracy of the results but because they give a concise method of showing the constancy of the results obtained under the four different assumed conditions on which the calculations of the four columns were based.

As judged by constancy, the results in argon would indicate that the actual secondary electron emission from the collector under our experimental conditions in this gas was probably considerably less than the approximately 25 percent given by Found's[3] assumption, and thus are in accord with the finding of only about 1 percent by our direct measurements of the emission from the auxiliary plate. Though the assumption of positive ion currents proportional to sheath areas gives in general reasonable values for the secondary electron currents the following considerations indicate that it is probably only an accident that the assumption does give such results. That the positive ion current is *not* controlled by the sheath area as given by the space charge equation but by a much larger volume, is certain. First, it is easily shown that the electrons, which penetrate within such sheaths surrounding our collector, could produce at most only a very small portion of the positive ions which

[15] Kingdon and Langmuir, Phys. Rev. **22,** 148 (1923).

are actually observed. Second, recent work of Langmuir,[16] and Tonks and Langmuir[2] has shown that, whereas most of the potential drop is within these sheaths, the positive ions which are collected are formed within a much larger volume. Hence there is no reason for believing that positive ion currents should be accurately proportional to such sheath areas, and hence the assumptions which underlie columns 10 and 11 of Tables II, III and IV appear to be unjustified. The values and discussion are included principally to illustrate how moderately large secondary electron currents would affect the results, if present.

Though the actual boundary of the region from which positive ions are drawn to the collector, is shown by the above considerations to be far outside of that given by the space charge equation, the latter value is not far from the boundary of the region into which any appreciable number of external electrons penetrate, and the greater part of the potential drop is between this boundary and the collector. Consequently we believe we are justified in using the space charge equation values for the sheath thicknesses in our calculations of the deflections and energy losses at collisions.

By carefully considering the various factors involved and the effect which changes in the assumed values of ϕ_+ and secondary electron emission have upon the results, we arrived at the estimates given for the true values of A for argon, neon and helium positive ions given at the bottom of Table VII. These values are of the same order of magnitude as the values of A found by Knudsen[5] for cool gases striking a hot filament.

The "Umladung" effect described by Kallmann and Rosen,[17] Penning and Veenemans,[18] and others, i.e., the taking of an electron from a neutral molecule by a positive ion, the now neutralized ion retaining practically all of its kinetic energy and the new ion starting with negligible velocity, would increase the values of A slightly for the conditions giving the larger collision numbers but this effect would probably not be greater than the 0.05 possible error given in our estimates, particularly in argon for in this gas we have values for conditions under which collisions within the sheath are practically negligible.

That the energy given up by positive ions which have been attracted to a metal collector by a field should be less than the total kinetic energy of the ions is to be expected from the explanation of the mechanism of cathode sputtering advanced by Kingdon and Langmuir,[15] and from the observations of Oliphant[13] and others on the reflection of positive ions and metastable atoms, and the probability of the formation of metastables in the neutralization process. If all of the observed deficiency of energy transfer were due to the formation of metastable atoms all of which left the collector with the velocity of the positive ions from which they were formed, this deficiency would give a measure of the production of metastables in the neutralization

[16] Langmuir, Phys. Rev. **33**, 954 (1929).
[17] Kallmann and Rosen, Zeits. f. Physik **61**, 61 (1930); **64**, 806 (1930).
[18] Penning and Veenemans, Zeits. f. Physik **62**, 746 (1930).

process. However, it is very improbable that the conditions are so simple as this.
velocity of the positive ions from which they are formed, this deficiency would give a measure of the production of metastables in the neutralization process. However, it is very improbable that the conditions are so simple as this.

In conclusion we wish to point out that although there is some uncertainty in the exact values of the accommodation coefficients for argon, neon and helium positive ions as found by us, our measurements seem to show conclusively that they are all considerably less than unity and consequently conclusions which have been reached on the tacit assumption of the unity value need revision to take account of the actual, smaller values.

Since the values of the accommodation coefficient found for neutral molecules[5] becomes more nearly unity as the molecular weight increases and since the values found by us for ions are of the same general order of magnitude as those found for the neutral molecules, it is suggested tentatively that the values for mercury and other heavy ions are nearly unity. Also the value of A is likely to depend somewhat upon the factors which affect the surface conditions of the metal such as the gas pressure, purity of the gas, roughness of the surface, and kind of metal.

Our thanks are due Mr. Donald C. Archibald for his help in the experimental work of this paper.

PHOTOMETRIC STUDY OF THE APPEARANCE OF SPECTRAL LINES IN A CONDENSED SPARK

By H. V. Knorr
Mendenhall Laboratory of Physics, Ohio State University
(Received May 4, 1931)

Abstract

The time interval between the time of appearance in a condensed spark discharge of the arc lines 4678A, 4722A, 4811A ($2^3P_{012}-2^3S_1$) of zinc, 4680A, 4800A, 5086A ($2^3P_{012}-2^3S_1$) of cadmium, the air lines 4347A, 4631A and 5001A was measured visually, using the Kerr cell method developed by Beams. A photographic method was developed whereby it was possible to determine from photometric measurements the variation of the intensity of an individual line with the time after the beginning of the spark. The time of first appearance, or zero intensity, is inferred from the extrapolation of the curves showing the intensity as a function of the time. The arc lines of zinc appear simultaneously. The arc lines of cadmium appear simultaneously but definitely earlier than the zinc arc lines. The air lines appear simultaneously but earlier than the arc lines. The spark lines appear simultaneously but earlier than the arc lines and later than the air lines of the respective elements. The results of the visual and photographic methods do not agree. Neither method gives information that in the case of zinc or cadmium, an electron remains in the 2^3S_1 state for a longer time before dropping to the 2^3P_0 state than before dropping to the 2^3P_1 or the 2^3P_2 state.

Introduction

In 1925 Beams and Brown,[1] making use of a modified form of the electro-optical shutter of Abraham and Lemoine,[2] measured the time intervals between the appearance of spectral lines in the spectra of condensed discharges. This early work indicated that in the elements examined, the spark lines appeared before the arc lines. Since the appearance of this first paper, several experimenters[3,4] have extended the work to other elements. In the elements that were examined in common by various investigators the numerical values for the time difference between the appearance of individual lines did not agree and in some cases the observed order was different. In the case of multiplets, Beams found different lines of the same multiplet appeared at different times, while Locher found that members of a given multiplet appeared simultaneously within the limits of error of the experiment in all cases examined except in the case of the arc triplet of zinc.

The actual existence of these time lags in the appearance of spectral lines has since been questioned by Gaviola.[5] He believes that the basic assumptions made by the experimenters, namely, that the Kerr cell discharges in-

[1] Beams and Brown, J.O.S.A. & R.S.I. **11**, 11 (1925).
[2] Abraham and Lemoine, Comptes Rendus **130**, 245 (1900).
[3] J. W. Beams, Phys. Rev. **28**, 475 (1926).
[4] Gordon Locher, J.O.S.A. & R.S.I. **17**, 91 (1928).
[5] Gaviola, Phys. Rev. **33**, 1023 (1929).

stantaneously a certain time after the beginning of the spark, that oscillations, if present, have no appreciable effect on the operation of the shutter, and that the capacity in parallel with the spark gap does not modify the time at which the Kerr cell discharges, are incorrect and measurements based on them unreliable.

The purpose of this investigation was to make a comparison of the results obtained by the use of a visual method similar to that employed by other experimenters[3,4] and the results obtained by use of a photographic method, in which the order of appearance of the spectral lines is inferred from the observations on the way in which the intensity of the individual spectral line

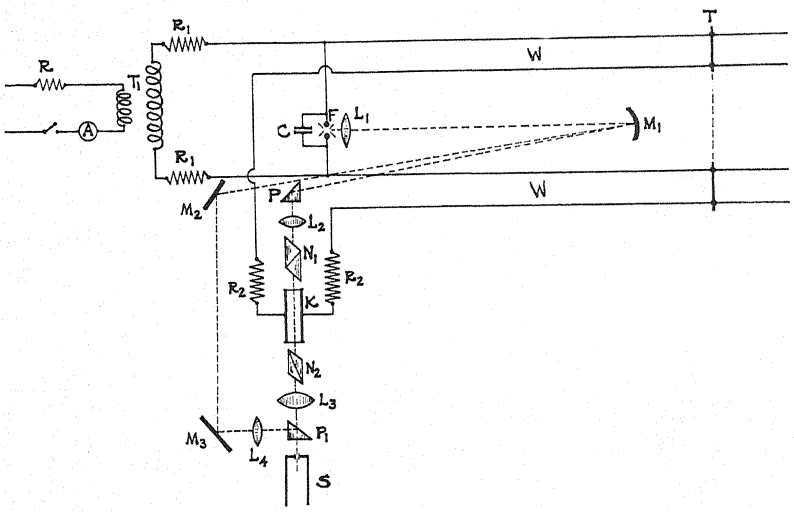

Fig. 1. Diagram of apparatus.

varies with time. By use of the latter method it is possible to eliminate the sensitivity of the eye which is a controlling factor in the visual method. In order that the results might have a possible interpretation as atomic phenomena, the spectral lines, 4678 $2^3P_0-2^3S_1$, 4800 $2^3P_1-2^3S_1$, 5086 $2^3P_2-2^3S_1$, of cadmium and 4680 $2^3P_0-2^3S_1$, 4722 $2^3P_1-2^3S_1$, 4811 $2^3P_2-2^3S_1$, of zinc were selected for the major part of this investigation. In the above triplets the transitions are from the same upper level to different lower levels, so the difference in the length of time that an electron remains in the 2^3S_1 state before the transition takes place to the 2^3P_0, the 2^3P_1 or the 2^3P_2 state could be measured. In addition to the above lines the spark doublet 5337 $3^2D_{3/2}-4^2F_{5/2}$, 5378 $3^2D_{5/2}-4^2F_{7/2}$ of cadmium, the spark doublet 4912 $3^2D_{3/2}-4^2F_{5/2}$, 4924 $3^2D_{5/2}-4^2F_{7/2}$ of zinc and the air lines which were excited when the discharge takes place between metallic electrodes in air at atmospheric pressure, were investigated.

Apparatus and Experimental Methods

Fig. 1 gives a diagrammatic representation of the apparatus used in the present experiment. It is essentially the same as that used by previous inves-

tigators. A fixed light path of 14.69 meters was used. A spark gap F with a capacity in parallel was connected across a source of high voltage T_1. The electro-optical shutter consisting of the two Nicol prisms N_1 and N_2 and the Kerr cell K, was placed between the spark gap and the spectrograph. The source of high voltage was a 25,000 volt 1 KW transformer. Electrodes of various shapes were tried in the spark gap, the shape finally selected being that of the frustrum of a cone, so that the discharge was actually taking place between two circular parallel faces. This type of electrode gave very steady spark conditions over quite long periods of time. The Kerr cell consisted of two parallel brass plates 12 cm long, 1 cm wide and separated at a distance of 3 mm, immersed in carbon disulphide which had been carefully purified. The shutter ordinarily was closed except when sufficient potential was applied to the Kerr cell, then the liquid became doubly refracting and light could pass it.

The circuit FC in Fig. 1 contains the condenser C, a certain amount of inductance in the lead wires, and the spark gap F, hence the discharge of the condenser C through the gap will be oscillatory. The circuit KF contains the Kerr cell, the trolley wires W and the spark gap F, this circuit being directly connected to the circuit FC, so oscillations are undoubtedly present in it. These oscillations if of sufficient amplitude, would reopen the shutter after having closed when the original voltage had fallen to so low a value as to make the shutter inoperative. The discharge of the Kerr cell will not be as sudden as was originally supposed, but its rate of discharge will be determined somewhat from the superposition of the oscillations in the two circuits. The oscillations can be critically damped by insertion of the resistance R_1, this reducing the rate of fall of voltage on the Kerr cell. Nevertheless it is possible to damp sufficiently these oscillations without delaying the closing time of the shutter appreciably, since it is well established that the relative difference in phase in the components of the ray vibrating parallel and perpendicular to the electric field is given by

$$\theta = 2\pi BlE^2$$

where B is the Kerr constant and θ the phase difference. Now the amount of light passing the prism N_2 at any given instant will be

$$I = A \sin^2 \theta/2 = A \sin^2 (\pi BlE^2).$$

Since the intensity of the light passing the shutter is proportional to the fourth power of the voltage, it is thus possible to damp sufficiently these oscillations and yet not delay the closing time of the shutter. The value of R_2 was found experimentally using a method employed by Lawrence,[6] that of observing the smallest distances of migration of the metallic vapor from the electrodes. The value of the damping resistance thus found was 2800 ohms (1400 ohms being placed in each lead from the spark gap to the Kerr cell). The effect of this damping resistance was quite evident, for when values of several hundred ohms less than 2800 ohms were used, oscillations were pres-

[6] Lawrence and Dunnington, Phys. Rev. **35**, 396 (1930).

ent, when values of several hundred ohms greater than 2800 ohms were used, a noticeable decrease in the rate of closing of the shutter was observed.

In Fig. 1 the light from the spark gap was rendered approximately parallel by the lens L_1 and was reflected from the concave mirror M_1, whose focal length was 7 meters, this converging beam was reflected by the right angle prism P through the lens L_2, the Nicol prism N_1 and focused between the plates of the Kerr cell. The lens L_3 focused the beam after passing through the Nicol prism N_2 on the slit of a constant deviation Gaertner spectrometer, so that the length of the spark was parallel to the slit. A number of diaphragms were placed along the light path and at each end of the Kerr cell so that only light which passed through the Kerr cell between the plates was focused on the slit.

An important modification in the optical path was the introduction of the auxiliary light path $PM_2M_3L_4P_1$, in order to adapt the apparatus to the photographic method. The part of the converging beam which passed the prism P was reflected by the plane mirrors M_2 and M_3 and the right angle prism P_1 and was focused on the slit of the spectrograph by means of the lens L_4. It was thus possible to have two spectra formed on the plate one directly above the other, the one formed by light which had passed through the Kerr cell and the other formed from the light which came directly from the spark gap. This modification was of utmost importance in the intensity measurements for it was thus possible to determine whether or not the spark conditions had changed appreciably during the time that was necessary to obtain a complete set of exposures.

Visual method. In the visual method in which a fixed light path was used, the time of closing the electro-optical shutter was regulated by changing the effective lengths of the four parallel wires which connect the spark gap with the Kerr cell, by sliding the trolley T along them by means of a string passing over a rather complicated pulley system and operated from the observer's position. When the trolley T is adjusted so that the effective length of wire path is as long as possible the intensity of the line under investigation is at a maximum for this particular time of closing of the shutter. If the position of the trolley is now adjusted so that the length of the wire path is decreased, finally a position is reached where the spectral line is no longer visible; this position of the trolley is noted. In a similar manner when the direction of motion of the trolley is reversed, a point of first appearance of the spectral line is located, which will differ slightly from the first position. The mean of the two positions is taken as the position of first appearance of the line, where the appearance of the line as used here means the position at which the line has become visible through the observing apparatus. The fall of potential produced by the passage of the spark is propagated along the wire to the Kerr cell at approximately the velocity of light,[7] so that the difference between the times of appearance of two lines is approximately the difference between the lengths of wire as determined above, divided by the velocity of light.

[7] Fred Allison, Phys. Rev. **30**, 66 (1927).

Photographic method. In the photographic method the observing telescope was replaced by a camera attachment converting the spectrometer into a spectrograph. The optical path was modified as previously described. The exposures on the plate were obtained by setting the trolley at a definite position and taking an exposure, then moving the trolley a known distance and taking a second exposure, and so on until five or more exposures had been obtained on each plate. Since the lengths of trolley wire between the spark gap and the Kerr cell correspond to lengths of time after the break down of the

TABLE I. *Zinc, cadmium and nitrogen.*

The nitrogen lines were obtained by a discharge between zinc electrodes in air. The zinc and cadmium lines were obtained from discharges between electrodes made from the chemically pure metals.

Element	Wave-length	Classification	Interval $\times 10^8$ sec.	Limit of error $\times 10^8$ sec.
Zn	4912 & 4924	$3^2D_{1\frac{1}{2}}-4^2F_{2\frac{1}{2}}$ $3^2D_{2\frac{1}{2}}-4^2F_{3\frac{1}{2}}$	0.5	.06
Zn	4680	$2^3P_0-2^3S_1$	1.14	.04
Zn	4722	$2^3P_1-2^3S_1$	0.75	.04
Zn	4811	$2^3P_2-2^3S_1$		
Cd	5337 & 5378	$3^2D_{1\frac{1}{2}}-4^2F_{2\frac{1}{2}}$ $3^2D_{2\frac{1}{2}}-4^2F_{3\frac{1}{2}}$	0.43	.05
Cd	5086	$2^3P_2-2^3S_1$	0.97	.12
Cd	4800	$2^3P_1-2^3S_1$	0.37	.08
Cd	4678	$2^3P_0-2^3S_1$		
N_2	5001 5005 5007 5011	$1^3D_1'-1^3F_3'$ $1^3D_3'-1^3F_4'$ $1^3S_1'-1^3P_2''$ $1^3P_1'-1^3S_1'$	1.20	.15
N_2	4631 & 4643	$1^3P_2'-2^3P_2$ $1^3P_2'-2^3P_1$	1.92	.08
N_2	5676 & 5680	$1^3P_0'-1^3D_1'$ $1^3P_2'-1^3D_3'$		

gap, the position of the trolley can be plotted against the intensity of the spectral line and a curve obtained which will show how the intensity of an individual line varies with time. In the present experiment it was possible to obtain spectrograms of the light from the spark beginning at 3.9×10^{-11} seconds after the beginning of the spark to 1.4×10^{-7} seconds after the beginning of the spark, the range being limited by the lengths of wire in the set-up.

Each plate was carefully calibrated by the use of neutral screens.[8] The calibration curve was obtained by plotting the logarithm of the intensity of the light transmitted by these screens against the reciprocal of the photographic density upon the plate. The reciprocal of the density (the logarithm of the transmission of the plate) was determined from the microphotometer record which was secured from the spectrogram. A Moll microphotometer which records automatically was used. From the measured transmission of the metallic arc and spark lines and the air lines to be investigated, the intensity of the individual lines could be read directly from the calibration curves in arbitrary units.

Results

Results by the visual method. Table I contains the data obtained on the spectral lines which were examined in this experiment. In the case of zinc the order of appearance of the lines obtained in this experiment was the same as that reported by Beams.[3] The magnitude obtained for the interval between the first appearance of the spark lines 4912A, 4924A and the arc line 4680A is thirty times smaller than the value obtained by Beams. In cadmium the results for these corresponding lines differ by about the same amount, that is for the interval between the appearance of the spark lines 5337A, 5378A and the first arc line. However the order is not the same, for in this experiment 5086A was observed before 4800A, while Beams observed them in the reverse order. The time intervals between the appearance of the respective arc lines as measured by Beams show somewhat the same magnitude as those determined in this experiment, but the results are still far from agreement. Locher obtained no differences in the times of appearance of the cadmium arc lines.

Results by the photographic method. The data obtained for the arc triplet of zinc 4680A, 4722A, 4811A are plotted in Fig. 2. The intensity which is plotted as the ordinate is expressed in arbitrary units. The lengths of trolley wire, plotted as abscissa, are measured from an arbitrary reference point which corresponds to a time 5×10^{-11} sec., after the beginning of the spark. When the intensity curves for these lines are extrapolated backward they all intersect at a point on the time axis corresponding to a time 1.2×10^{-8} sec., after the beginning of the spark, indicating that the members of this arc triplet appear at the same time. Fig. 3 shows the data on the unresolved air lines 5001A, 5005A, 5007A and 5011A, 4631A, 4347A which were excited when the discharge occurred between zinc electrodes in air at atmospheric pressure. Here as in the case of the metallic arc lines of zinc, when the intensity curve for each of these lines is extrapolated backward to zero intensity, these curves meet at approximately the same point, corresponding to a time 5×10^{-11} sec. after the beginning of the spark. This would indicate that these lines appeared simultaneously, but at a time 1.19×10^{-8} sec. earlier than the metallic arc lines of zinc.

[8] G. R. Harrison, J.O.S.A. & R.S.I. **18**, 492 (1929).

Fig. 4 shows the curves plotted from the data obtained for the arc triplet of cadmium 4678A, 4800A, 5086A. The intensity curves meet at approximately the same point corresponding to a time 0.5×10^{-8} sec., after the beginning of the spark when extrapolated backward to zero intensity, indicating again that the members of this arc triplet all appear at the same time. The time of appearance of the cadmium triplet is 0.7×10^{-8} sec., earlier than the zinc triplet. Fig. 5 shows the data on the air lines 5001A, 5005A, 5007A, 5011A, 4631A, 4347A, which are excited when the discharge takes place between cadmium electrodes in air. When the intensity curve for each of these air lines is extrapolated backward to zero intensity these curves intersect at a point corresponding to the time 5×10^{-11} sec., after the beginning of the spark, which is the same as that obtained for these same air lines which were

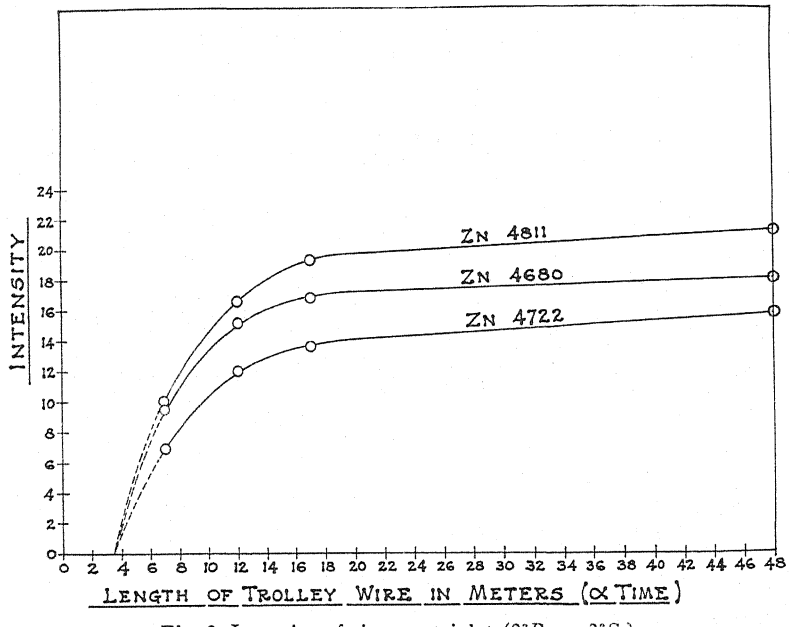

Fig. 2. Intensity of zinc arc triplet ($2^3P_{012}-2^3S_1$).

excited in the zinc spark. This indicates that these air lines just as in the case of zinc all appear at the same time.

In the upper part of Fig. 6 are plotted the data obtained for the unresolved zinc spark doublet 4912A and 4924A, and in the lower part are plotted the data obtained for the cadmium spark doublet 5337A and 5378A. The unresolved zinc doublet extrapolates backward to a point corresponding to 0.5×10^{-8} sec., after the beginning of the spark. The intensity curves for each of the lines of the cadmium doublet, when extrapolated to zero intensity, meet at a point corresponding to a time 0.32×10^{-8} sec., after the beginning of the spark, indicating that each of the members of this spark doublet appeared at the same time. The time of zero intensity or the time of first appearance of

the spark lines is earlier than the arc lines of the same element, but is later than the air lines as shown in Figs. 2, 3, 4, and 5.

Discussion of Results

The photographic method in the case of the arc triplet of zinc 4680A, 4722A and 4811A, shows that all of these lines appear at the same time. The visual method when applied to this same triplet gives differences between the times of appearance of these same lines. Likewise in the case of the arc triplet of cadmium 4678A, 4800A and 5086A the photographic method gives the same time of appearance for each of these lines, but the visual method gives different times for each line, although the results of different observers using the visual method are not in agreement.

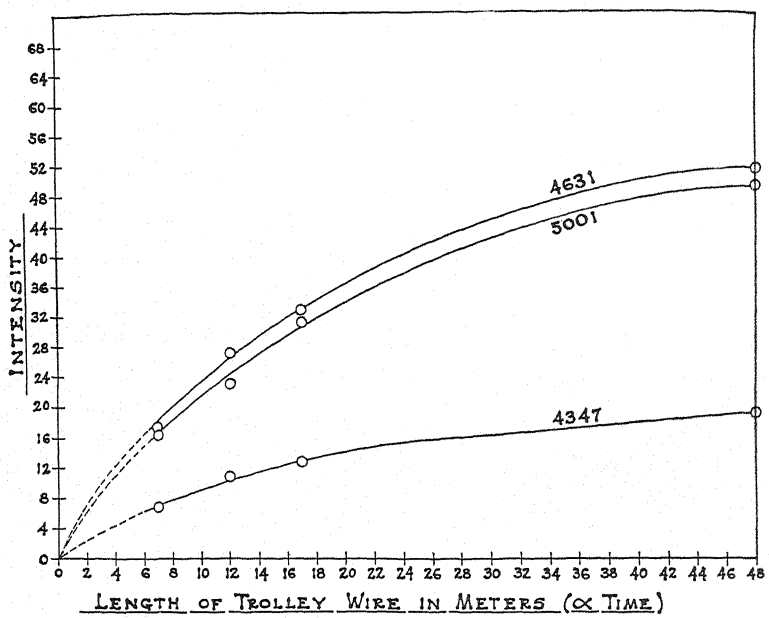

Fig. 3. Intensity of the air lines 5001A, 4631A, and 4347A with zinc spark gap.

The photographic method shows that the air lines 5001A, 5005A, 5007A, and 5011A, 4631A, 4347A whether excited in a zinc or cadmium spark, all appear at the same time, but at a time definitely earlier than the metallic arc lines of the respective element. The visual method on the other hand gives different times of appearance for the individual air lines and it also indicates that the air lines appear before the arc lines in the case of zinc and cadmium. Since in this case the observations were made on groups of lines rather than individual lines, the results are not as convincing as in the case where the observations are made on separate lines.

The photographic method shows that the members of the spark doublet of cadmium 5337A and 5378A appear at the same time and definitely earlier than the metallic arc lines of cadmium, but later than the air lines in the cad-

mium spark. The visual method gave no information on the separate spark lines as it was impossible to resolve them, so the observations were made probably on both lines, the times of appearance being earlier, however, than the arc lines. The result, indicating that the spark lines appeared before the arc lines, is the same for each method. The zinc doublet 4912A and 4924A was unresolved in both the photographic and visual methods so that the data obtained in each case are not satisfactory. However each method shows that this unresolved zinc doublet appears before the zinc arc triplet, hence again the two methods lead to the same result.

There is an evident disagreement between the results obtained by the visual method and those obtained by the photographic method. This diver-

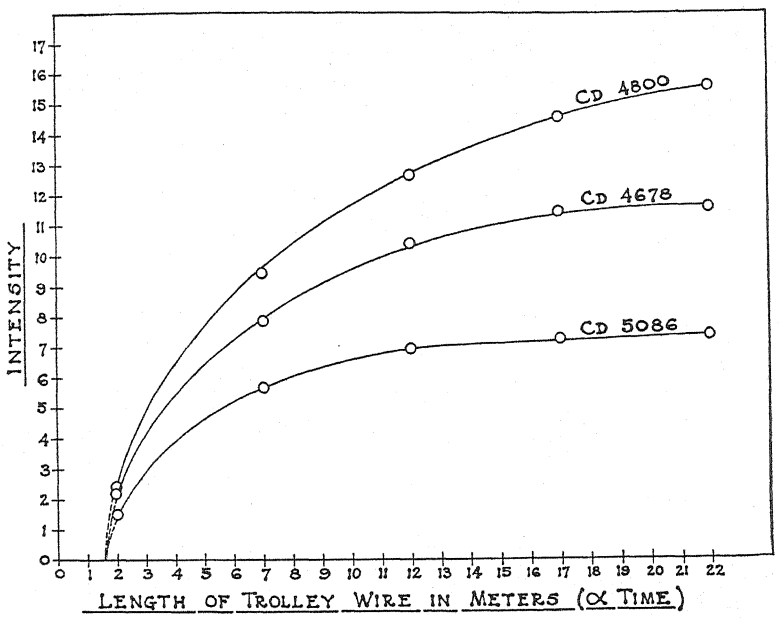

Fig. 4. Intensity of the cadmium arc triplet ($2^3P_{012}-2^3S_1$).

gence of results is to be expected from the fact that the human eye is not equally sensitive to light of different colors, whereas the photographic plate when properly calibrated should give results on relative intensities which are independent of the sensitivity of the plate for light of different wave-lengths. Hence the zero of intensity inferred from the measurements on the photographic plate would be different from the threshold of visibility detected by the human eye. In reality what one does in the visual method is to observe the line at some intensity considerably above the zero intensity. Examination of the curves, showing the intensity as a function of the time after beginning of the spark, shows that the times when the different lines have the same intensity is variable. The critical intensity which the eye could first detect would be influenced by the sensitivity of the eye for the particular wave-length. The lines which were examined were located in a region of the spectrum

where the sensitivity of the human eye changes quite rapidly with the wavelength. It would be impossible to extrapolate the intensity curves shown in Figs. 2, 3, 4, 5 and 6 in a reasonable manner and obtain values for the relative differences in the times of appearance that were obtained visually. The calibration of the photographic plate made the results obtained by the photographic method independent of the sensitivity of the plate for different colors. The fact that the air lines appeared before the spark and arc lines of the respective elements is probably a result of the natural sequence of events in breakdown of the spark gap. One might suppose as Gaviola[5] suggested, that the discharge was initiated by ionizing the air between the electrodes. This was followed by evaporation of the metal from the electrodes which was then ionized and excited by collisons. This observed difference between the

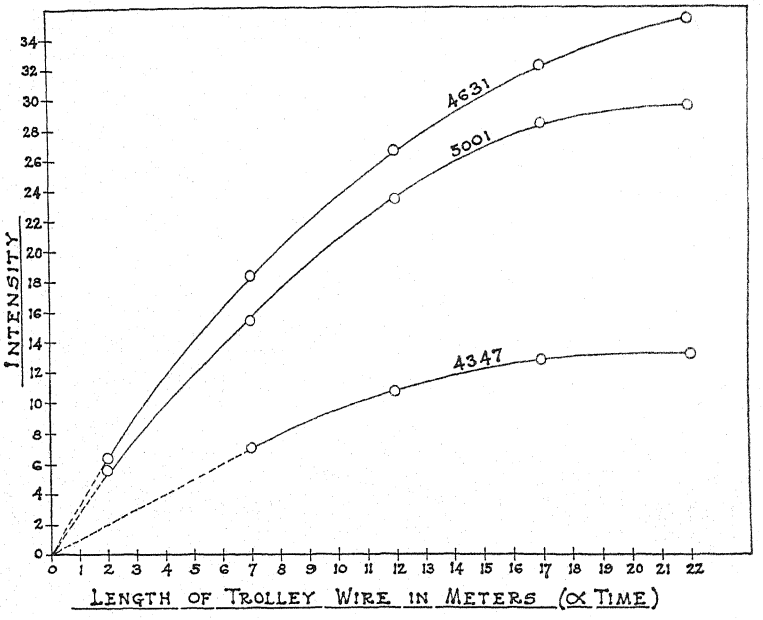

Fig. 5. Intensity of air lines 5001A, 4631A, and 4347A with cadmium spark gap.

times of first appearance of the air lines in the zinc and cadmium spark and the metallic arc lines of the same elements may be explained as a characteristic of the spark discharge. Hence if the results of the photographic method are accepted, the data obtained in this type of experiment give no evidence that an electron in the 2^3S_1 state of zinc or cadmium remains there a longer time before the transition takes place to the 2^3P_0 state, than to the 2^3P_1 or the 2^3P_2 state.

Conclusions

1. The results obtained by the visual and photographic methods are not in agreement.

2. The results obtained by the photographic method indicate that the members of the arc triplet of zinc appear simultaneously. They also indicate

that the members of this same triplet of cadmium appear simultaneously but not at the same time as the members of the arc triplet of zinc. These results therefore seem to verify Gaviola's contention that the apparent time difference between the appearance of spectral lines in such condensed discharges is not an atomic phenomenon.

3. The differences in times of appearance between the air lines which are excited in the spark gap, the spark lines of the element and the arc lines of

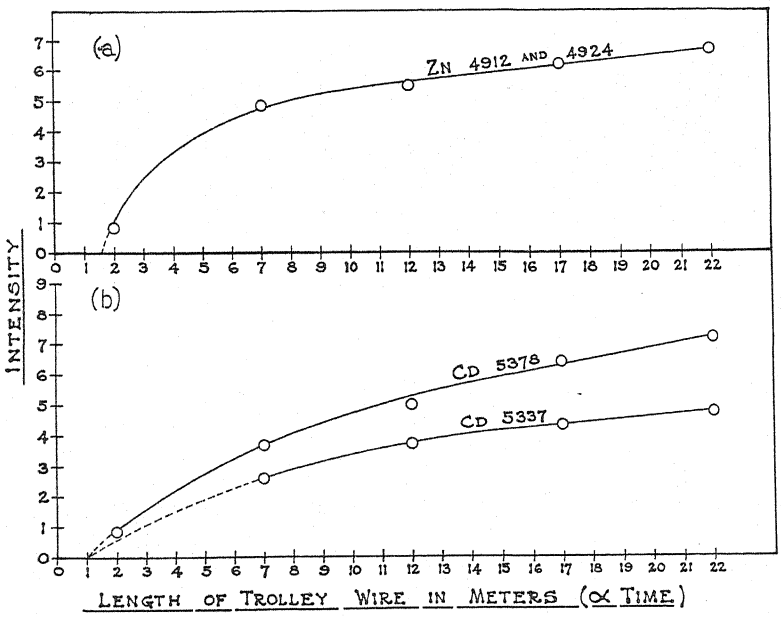

Fig. 6. (a) Intensity of unresolved zinc doublet ($3^2D_{3/2}-4^2F_{5/2}$) and ($3^2D_{5/2}-4^2F_{7/2}$). (b) Intensity of cadmium doublet ($3^2D_{3/2}-4^2F_{5/2}$) and ($3^2D_{5/2}-4^2F_{7/2}$).

the same element, can probably be attributed to the way in which the discharge is formed in the spark gap, i.e. the manner in which the molecules of air or vapor of the element begin to be ionized.

The writer wishes at this time to express his appreciation of the constant help and encouragement he has received from Professor Alpheus W. Smith under whose direction this work was carried out and of the valuable suggestions and criticisms received from Dr. M. L. Pool during the course of this work.

THE EFFECT OF PIEZOELECTRIC OSCILLATION ON THE INTENSITY OF X-RAY REFLECTIONS FROM QUARTZ

By Gerald W. Fox and Percy H. Carr
Physics Laboratory, Iowa State College

(Received May 1, 1931)

Abstract

In an attempt to determine the amplitude of vibration of the ions in a quartz lattice brought about by piezoelectric oscillations, a series of Laue photographs have been made of both Curie and thirty-degree-cut plates, using the white radiation from a Coolidge universal tube. This tube had a tungsten anode and carried a current of four milliamperes at 95 kilovolts. Eastman duplitized x-ray film was used with no sensitizing screens. On examination, the patterns produced by each plate, oscillating and non-oscillating, appear identical except in one respect; the pattern of the oscillating plate is several times as intense as that of the non-oscillating. A four-hour exposure of a non-oscillating plate to radiation of the above mentioned type, produces but the rudiments of a pattern, whereas, the same plate oscillating produces a very beautiful intense pattern for the same time of exposure. The effect does not depend on the mode of vibration but does depend on the amplitude. Further work is in progress which it is hoped will establish the cause of this peculiar intensity difference.

Introduction

PIEZOELECTRIC quartz plates used as frequency controllers for vacuum tube oscillators have a visible vibration[1] when in mechanical resonance with the electrical circuit. Such mechanical oscillations must be accompanied by considerable internal movement of the ions of the crystal lattice. It was proposed to investigate this internal motion by shooting a beam of x-rays through a quartz plate both when oscillating and when not oscillating and by observing whether there was any difference in the appearance of the Laue diffraction patterns.

If there was considerable motion of the crystal planes, it might be expected that the spots on the Laue pattern would be altered. Upon first consideration, one might think that this alteration would occur either as a linear smearing of the spots or as a diminution in the intensity of the pattern. The first hypothesis seemed reasonable because of the experiments of Professor Joffé[2] in which a linear smearing of the spots was produced by a mechanical distortion of the crystal. The second hypothesis appeared reasonable from temperature consideration. The usual result of raising the temperature of a crystal is that the reflection slowly decreases almost linearly with increase in temperature. Backhurst[3] gives some data on graphite and ruby, finding a fifteen percent decrease in reflecting power for a rise in temperature of 500° Centigrade.

[1] H. Osterberg, Nat. Acad. Proc. **15,** 892 (1929).
[2] Joffé, The Physics of Crystals, p. 38.
[3] Backhurst, Proc. Roy. Soc. London **102,** 340 (1922).

Gibbs[4] called attention to the unusual increase in reflecting power of certain planes in crystal quartz which took place at the transition temperature (575°C) when the so-called α form changed over to the β form. Since this large increase was attributed to a relative movement of the ionic planes of only 0.025 Angstrom unit, it seemed possible that oscillations in quartz might produce a change in the relative intensity of the Laue spots.

Apparatus and Methods

Eastman duplitized x-ray films were used throughout. Sensitizing screens were tried at first but were soon discarded for fear they might influence results. The film was placed in a box made of 1/8″ lead sheet closed except for a small 1/2″ hole in the top. Directly above this hole was mounted in intimate contact, the lower contact plate for the crystal, made of brass and polished flat. In its center was a 1/4″ hole. The upper contact plate of the crystal was also made of polished brass. In its center was drilled a 1/8″ hole. Radiation from a Coolidge universal tube was delimited by a number 60 drill hole in each of two lead screens mounted approximately five inches apart. Attached to the lower screen and in line with the hole was a two-inch narrow tube of

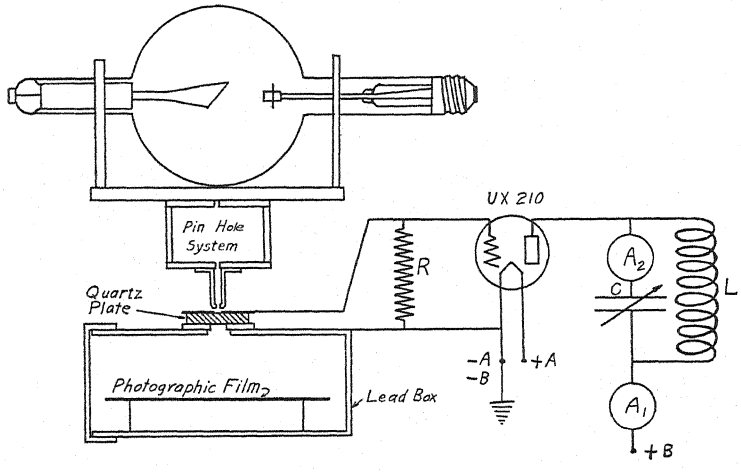

Fig. 1. Schematic diagram of x-ray tube and crystal circuit.

brass also having a number 50 drill hole in its end. This was merely to facilitate pointing the x-ray beam at the hole in the upper electrode.

The driving circuit is shown in Fig. 1, together with a schematic drawing of the whole layout. The vacuum tube was of the UX210 type employing a filament voltage of 7.5 volts. Plate voltages from 50 to a maximum of 350 volts were used at various times. Resonant conditions in the circuit were determined by observations of the D.C. plate milliameter A_1 or the radio frequency ammeter A_2. In this type of circuit using a resistance bias, oscillations are indicated by a large drop in the D.C. plate current and a corresponding increase in the reading of the high frequency ammeter.

[4] Gibbs, Proc. Roy. Soc. London **A107**, 561 (1925).

Results

A preliminary run with the non-oscillating crystal showed that at 95 kilovolts peak and 4 milliamperes x-ray tube current at least a four-hour exposure would be necessary to get even a visible pattern. With the same exposure, however, this same plate, oscillating, gave a very beautifully developed Laue pattern. This was curious, and since the exposure on the oscillating crystal had been made in two parts with a lapse of several hours between, and since the film had been developed at a different time and with a different solution than that of its non-oscillating mate, it was assumed that some difference in technique had produced the decided change in intensity. To test this point three different diffraction patterns were made of the same quartz plate; the first, with the plate not oscillating; the second with the plate oscillating; and

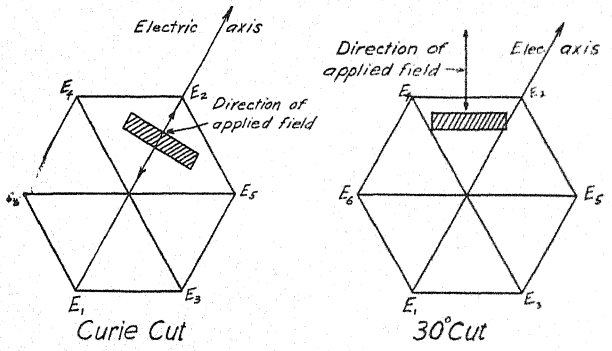

Fig. 2. (a) Curie-cut. In use the applied electric field is parallel to an electric axis of the crystal. The optic axis is normal to the plane of the figure. (b) 30-degree-cut. In use the applied electric field makes an angle of 30° with an electric axis of the crystal.

the third with it not oscillating again. In each instance, a four-hour continuous exposure was made at 95 kilovolts and 4 milliamperes. Over a four-hour period slight voltage-current fluctuations were bound to occur but an average current of four milliamperes over the necessary twelve-hour period is probably very close to the truth. All three exposures were then simultaneously developed in a single large tray and were fixed at the same time. Examination of all three films showed beyond doubt that the pattern made by the oscillating plate was decidedly more intense than either pattern made by the non-oscillating plate. This discovery made it necessary to go into the phenomenon in more detail.

Table I

Curie-cut Frequencies (kilocycles)	30-degree-cut Frequencies (kilocycles)
3590	3850
1900	1875
320	325

Six plates were cut from a specimen of optical quality crystal quartz, three of each type of cut as shown in Fig. 2. These plates were then ground down to the following approximate frequencies, as shown in Table I.

The Curie-cut plates have an average wave-length of about 105 meters per millimeter thickness and the 30-degree-cut, about 145 meters per millimeter thickness.

Two four-hour exposures were then made for each plate. Simultaneous development and fixing were carried out. In each case, the same result was obtained, viz.; *an exposure which gave but the rudiments of a pattern with the plate not oscillating, gave an intense pattern when the plate was vibrating.* Visual examination shows the patterns to be identical with the same spots occurring but the intensity is decidedly different. Fig. 3 shows a reproduction of the patterns produced by a 30-degree-cut plate, oscillating and not oscillating. This plate had an approximate frequency of vibration of 1875 kilocycles. It

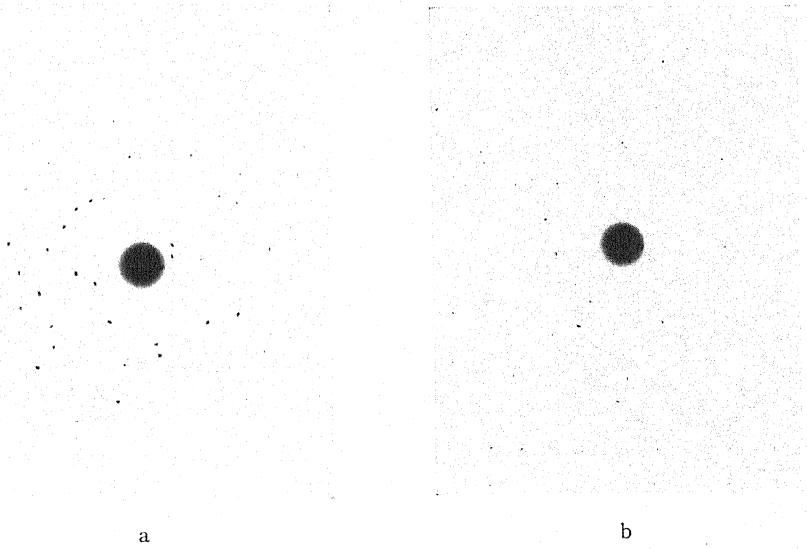

a b

Fig. 3. (a) oscillating; (b) not oscillating.

was not possible to note any smearing of the spots as was suggested might happen though the method is too crude to detect small changes.

To test the possibility that the effect was due to some sort of an electric strain set up by the applied electric field, a test was run on the same plate whose pattern is shown in Fig. 3. Again two runs were made, the first with no applied field and the second with the line voltage of 120 volts, 60 cycles, applied to the crystal. Both exposures were identical. The two exposures proved to be no different showing that the effect is definitely a resonance phenomenon.

To test this conclusion further, the same piezo-plate was used in a series of three four-hour exposures. The x-ray energy was kept constant and the amplitude of vibration was changed by increasing the plate voltage on the vacuum tube. The voltages used were 50, 150, and 300 volts, respectively. The three exposures show definitely that the intensity of the spots on the patterns depends on the amplitude of vibration of the quartz plate. The 150 volt exposure is decidedly stronger than the 50 volt one and the 300 volt exposure is much stronger than either.

CRYSTAL STRUCTURE OF LITHIUM IODATE

By W. H. Zachariasen and F. A. Barta
Ryerson Physical Laboratory, University of Chicago

(Received April 22, 1931)

Abstract

The structure of lithium iodate was determined by using the oscillation and powder methods. Lithium iodate is hexagonal with 2 molecules per unit cell of $a=5.469\pm 0.003$A, $c=5.155\text{A}\pm 0.005$A. The space group assigned is D_6^6 and the atom positions are: 2Li in (001/4) (003/4), 2I in (1/3 2/3 1/4) (2/3 1/3 3/4) and 6 O in $(uu0)$ $(0\bar{u}0)$ $(\bar{u}00)$ $(\bar{u}\bar{u}\frac{1}{2})$ $(0u\frac{1}{2})$ $(u0\frac{1}{2})$ with $u=1/3$. The structure is based on hexagonal closest packing, with the lithium and iodine atoms both lying within oxygen octahedra. The atomic distances are Li−O and I−O=2.23A with lithium octahedra sharing faces with each other, one lithium and one iodine octahedra sharing only edges and two iodine octahedra only corners.

LITHIUM iodate is the only member of the alkali iodates, whose structure has not yet been determined.[1] In searching the literature no information was found regarding its crystallographic properties. A microscopic examination of the fine crystalline material of chemically pure $LiIO_3$ as furnished by Kahlbaum, showed that the crystals were short hexagonal prisms. Though $LiIO_3$ does not crystallize in very large crystals, two crystal splinters were found sufficiently large to be used for the oscillation method. Both crystals were hexagonal prisms and photographs were taken using the principal directions as axes of rotation. In view of the fineness of the material a large number of powder photographs were taken using Mo$K\alpha$, Cu$K\alpha$, and Fe$K\alpha$, radiation.

The photographs were worked out in the usual manner and lead to the following dimensions of the hexagonal cell.

$$a=5.469\text{A}\pm 0.003\text{A} \qquad c=5.155\text{A}\pm 0.005\text{A} \qquad c/a=0.9427$$

A rough density determination of $LiIO_3$ gave 1.9 molecules equivalent to 2 molecules per unit cell. The calculated density is 4.48. The greater part of the observations is compiled in Tables I and II. From the tables it is clearly seen that a rhombohedral cell is impossible because of the observed reflections. (The number of molecules in the hexagonal cell also exclude a rhombohedral lattice.) Since the oscillation photographs did not show any deviation from full hexagonal symmetry, consideration of the space group was limited to the following classes: D_{6h}^n, D_6^n C_{6v}^n and D_{3h}^n. Of these D_6^2 and D_6^5 were ruled out because they have no 2-fold (or 1-fold) positions.

Tables I and II show that whenever $2h+k$ is divisible by 3, exceptionally strong reflections are observed if l is even; whereas the intensity is weak or

[1] V. M. Goldschmidt, Vid. Akad. Skr. Oslo **2**, 79 (1926) KIO_3, $RbIO_3$; W. H. Zachariasen, ibid. **4**, 100, 106 (1928) $NaIO_3$, $CsIO_3$.

nil if l, is odd. This observation can only be accounted for by putting the two iodine atoms in positions corresponding to a hexagonal closest packing of these atoms. The only available space groups compatible with such an arrangement are D_{3h}^1, D_{3h}^4, C_{6V}^4, D_6^6, and D_{6h}^4. The space groups D_{6h}^4, C_{6V}^4,

TABLE I. *Oscillation photographs.*

hk. l	sin θ	$\|F\|$	Int.	*hk. l*	sin θ	$\|F\|$	Int.
00.1	0.0687	nil	nil	22.0	0.2590	60.8	m
10.0	.0748	43.6	m	30.2	.2629	53.0	m
10.1	.1015	78.7	vs	22.1	.2679	13.5	nil
11.0	.1295	72.1	vs	31.0	.2695	30.4	vw
00.2	.1373	55.4	s	00.4	.2746	73.8	m
11.1	.1466	25.5	w	31.1	.2781	53.7	m−
20.0	.1496	37.4	m	21.3	.2856	54.6	m
10.2	.1564	36.9	m	22.2	.2932	68.0	m
20.1	.1645	65.4	s	31.2	.3024	28.0	vw
11.2	.1877	86.6	s	11.4	.3036	56.0	m
21.0	.1977	33.8	vw	32.0	.3258	27.0	vw
20.2	.2030	33.8	w	32.1	.3330	49.5	w
00.3	.2061	nil	nil	41.0	.3343	53.4	w
21.1	.2093	64.2	m	31.3	.3392	49.2	w−
10.3	.2192	61.5	s	41.1	.3413	9.4	nil
30.0	.2244	90.8	s	32.2	.3536	26.4	vvw
30.1	.2345	nil	nil	41.2	.3614	61.1	w
21.2	.2408	31.2	w	32.3	.3854	46.0	w
11.3	.2433	14.6	nil	41.3	.3926	7.3	nil
20.3	.2545	57.1	m−				

TABLE II. *Powder photographs.*

hk. l	sin θ	$\|F\|^2xf$	Int. Obs. Mo	Int. Obs. Cu	*hk. l*	sin θ	$\|F\|^2xf$	Int. Obs. Mo	Int. Obs. Cu
00.1	0.0687	nil	nil	nil	21.2	0.2408	3.9	w+	w
10.0	.0748	1.9	w+	w	11.3	.2433	.4		
10.1	.1015	12.4	vs	s	20.3	.2545	6.5		m
11.0	.1295	5.2	ms	m	22.0	.2590	3.7		w+
00.2	.1373	1.0	vw	vw	30.2	.2629	5.6		m
11.1	.1466	1.3	w	vw	22.1	.2679	.4		vw
20.0	.1496	1.4			31.0	.2695	1.9		
10.2	.1564	2.7	w	w	00.4	.2746	1.8		nil
20.1	.1645	8.6	ms	m	31.1	.2781	11.5		s
11.2	.1877	15.0	s	s	10.4	.2847	1.7		s
21.0	.1977	2.3	vw	w	21.3	.2856	12.0		
20.2	.2030	2.3	vw	w	22.2	.2932	9.2		m
00.3	.2061	nil			40.0	.2992	.8		
21.1	.2093	16.5	s	s	31.2	.3024	3.1		ms
10.3	.2192	7.6	m−	m−	11.4	.3036	6.3		
30.0	.2244	8.2	m	m−	30.3	.3045	nil		
30.1	.2345	nil	nil	nil	40.1	.3069	5.4		w

TABLE III. *F Curves* ($MoK\alpha$).

sin θ	0.05	0.10	0.15	0.20	0.25	0.30	0.35	0.40
Li	2.0	1.9	1.8	1.6	1.3	1.1	.85	.7
I	50	45.5	41	37	33.5	31	28	26
O	8.0	7.5	4.9	3.0	2.7	2.1	1.6	1.3

The F-curve for iodine was calculated by Thomas' method, the one for oxygen is the experimental one found by J. West in KH_2PO_4.

and D_{3h}^4 are ruled out because they require that the odd order reflections from all planes $h\ k.l$ where $2h+k=3n$ and l odd shall be missing, and while many of these reflections are not found, there is evidence in the photographs that some of them are definitely present. This limits the space group selection to D_{3h}^1 and D_6^6.

In D_{3h}^1 in order to have hexagonal closest packing the necessity for unequivalent iodine atoms arises. The possibility that all oxygen atoms lie in the same plane is unreasonable as that would give too small oxygen to oxygen distances. Likewise this rules out the possibility that they all lie on 3-fold or 6-fold axis of symmetry. The only possible arrangements of the 6 oxygens are therefore: $3j+3k$ or $6n$ with $v=1/4$. None of these possibilities leads to reasonable structures.

In case the 6 oxygens are put in $3j+3k$ and the required oxygen to oxygen distance is greater than 2.50A, the iodine to oxygen distance is smaller than 1.72A. It seems improbable that the oxygen to oxygen distance is smaller than 2.50A, and that the iodine to oxygen distance is as small as 1.72A. This arrangement must therefore be ruled out and for similar improbabilities placing the 6 oxygens in positions $6n$ can not be considered.

As an additional support for ruling out the considerations of the previous paragraph are the intensity considerations. With the oxygen in $3j+3k$ it is impossible to explain the weak 00.2 reflection. Similarly if the oxygens lie in $6n$ the parameter v must be 1/4 in order to explain the absent odd orders from the basal plane, which would necessitate the absence of reflections 11.1, which as the tables show are definitely present.

The only remaining space group is D_6^6.

The 2 iodine atoms are put in positions (1/3, 2/3, 1/4) (2/3, 1/3, 3/4) in accordance with the required hexagonal closest packing. Since all the atoms can not lie on the 3-fold axes of symmetry, the only positions for the oxygens are $(uu0)$ $(0\bar{u}0)$ $(\bar{u}00)$ $(\bar{u}\bar{u}\frac{1}{2})$ $(0u\frac{1}{2})$ $(u0\frac{1}{2})$ or $(u\bar{u}\ 1/4)$ $(2\bar{u}\bar{u}\ 1/4)$ $(u2u\ 1/4)$ $(\bar{u}u\ 3/4)$ $(2uu\ 3/4)$ $(\bar{u}2\bar{u}\ 3/4)$. The latter arrangement does not account for the relative weak 00.2 reflection and therefore the first set is the correct one.

An accurate determination of the oxygen parameter cannot be made due to the small scattering power of these atoms in comparison with that of iodine. The powder photographs show that 30.0 and 30.2 occur with nearly the same intensity although the latter form has twice as many faces as the former. In order to explain this ratio the oxygen atoms must give a large positive contribution to the structure factor for both reflections. This requirement necessitates $u=1/3$. The value 1/3 is very probable as that gives us hexagonal close packing of the oxygens. A close packed arrangement of the oxygens (using oxygen to oxygen distance = 2.7A) would give us a cell of dimensions $a=$ 4.68A, $c=4.42$A with an axial ratio of 0.944. The fact that the experimental cell is larger than the theoretical one must be attributed to an expansion of the close packing due to the circumstance that both iodine and lithium are too large to fit in the interstices.

The lithium atoms are so light that their positions cannot be determined from the intensities of reflections. There are three sets of available positions

for lithium: (2a) (000) (00½); (2b) (00 1/4) (00 3/4) and (2d) (1/3, 2/3, 3/4) (2/3, 1/3, 1/4). The set (2a) will put lithium inside of an oxygen triangle with lithium to oxygen distance = 1.83A. Using (2b) or (2d) lithium will be within an octahedron of oxygens; the lithium to oxygen distance being 2.23A. The triangular arrangement of oxygens around lithium has never been found in other structures. Lithium either goes inside a tetrahedron of oxygens (Li_2O, $KLiSO_4$, Li_2MoO_4) or within an octahedran ($LiNO_3$). Of the latter two arrangements (2b) is the most plausible one, because this results in a lithium to iodine distance of 3.16A whereas (2d) would give 2.58A.

The complete structure thus determined is 2 Li in (00 1/4) (00 3/4), 2I in (1/3 2/3 1/4) (2/3 1/3 3/4) and 6 O in ($uu0$) ($0\bar{u}0$) ($\bar{u}00$) ($\bar{u}\bar{u}\frac{1}{2}$) ($0u\frac{1}{2}$) ($u0\frac{1}{2}$)

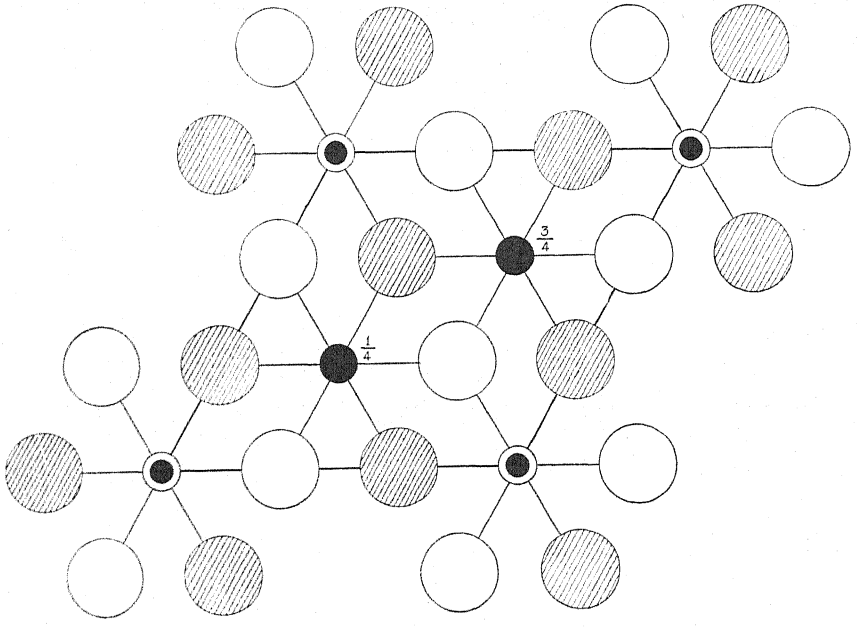

Fig. 1. Projection on the c-face of the structure of $LiIO_3$. The large circles represent oxygens at height 0. The large shaded circles represent oxygens at height $c/2$. The small solid circles represent iodine. The small solid centered circles represent lithium at height $c/4$, $3c/4$.

with $u = 1/3$. The intensities calculated on the basis of this structure agree well with the observed ones, as will be seen from the tables.

Discussion of the Structure

In Fig. 1 is given a projection of the basal plane. The arrangement is a typical coordination lattice, of the hexagonal closed packed type met with in so many cases.

Almost perfect octahedra of oxygen atoms surround the iodine and lithium atoms. The IO_6-octahedra share only corners with each other. Sharing of the octahedral edges occur between IO_6 and LiO_6-polyhedra; while the LiO_6-octahedra share faces with each other. This result is in perfect agree-

ment with what one should expect: The higher charges the central cations have, the fewer are the number of shared corners between two polyhedra.

Although the lithium positions have not been determined from intensity considerations, there is not much doubt about the positions assigned to these atoms. In $LiNO_3$, where Li also lies inside an octahedron of oxygens, it was found that the lithium to oxygen distance = 2.15A. In $LiIO_3$ the lithium to oxygen distance is 2.23A.

The distance iodine to oxygen is also 2.23A. For comparison the iodine to oxygen distance in other crystals of the same coordination number is given. KIO_3—2.23A; $RbIO_3$—2.26A, $CsIO_3$—2.33A.

The shortest oxygen to oxygen distance is 3.16A. In a previous paper by W. H. Zachariasen[2] it was shown that groups $(XO_3)^{-m}$ have an unsymmetrical structure if $v=3\times8+2$ (v being the total number of valence electrons in the group). In the (IO_6) group there are $50=6\times8+2$ electrons. So that from reasons of analogy it would not be astonishing to find asymmetry in the IO_6 group. This asymmetry probably would result in a slight displacement of iodine away from the center of the octahedron in the direction of one face. However no observations pointing in that direction were observed. The possibility of detecting very small displacements is only possible with extremely accurate intensity determinations.

Summary

Lithium iodate was examined by the oscillation and powder methods. The crystals were found to be hexagonal with 2 molecules in the cell $a=5.469$A ±0.003A; $c=5.155$A $\pm$ 0.005A, $c/a=0.9427$. The calculated density is 4.48.

The space group was found to be D_6^6 with 2 Li in (001/4) (003/4). 2 I in (1/3 2/3 1/4) (2/3 1/3 3/4) and 6 O in $(uu0)$ $(0\bar{u}0)$ $(\bar{u}00)$ $(\bar{u}\bar{u}\frac{1}{2})$ $(0u\frac{1}{2})$ $(u0\frac{1}{2})$ with $u=1/3$.

The structure is based on the hexagonal closest packing. The lithium and the iodine atoms are both lying within oxygen octahedra. The distances Li-O and I-O are both 2.23A[3]. 2 lithium octahedra share faces with each other, one lithium and one iodine octahedra share only edges, two iodine octahedra only corners.

[2] W. H. Zachariasen, Phys. Rev. **37**, 775 (1931).

[3] It is probably that a value of u slightly less than 1/3 is more correct, say $u=0.314$ which gives Li—O 2.15A and I—O = 2.28A.

THE APPLICATION OF THE GEIGER-MÜLLER ION COUNTER TO THE STUDY OF THE SPACE DISTRIBUTION OF X-RAY PHOTOELECTRONS

By J. A. Van den Akker and E. C. Watson
Norman Bridge Laboratory of Physics, California Institute of Technology, Pasadena, California

(Received May 4, 1931)

Abstract

The photographic plate in the apparatus for the magnetic analysis of x-ray photoelectrons has been replaced by a Geiger-Müller ion counter and the magnetic spectrum of the photoelectrons ejected from a thin film of gold by primary x-ray from molybdenum has been studied. Very great resolving power is obtained and considerable precision in determining the exact position of the lines (i.e. the energies of the photoelectrons). The numbers of L_{III} electrons of gold ejected by the $K\alpha_1$ x-ray of molybdenum have been plotted as a function of the angle of ejection and compared with the theoretical longitudinal distribution predicted by Schur.

Introduction

In the past many investigators[1] have observed the space distribution of x-ray photoelectrons in cloud expansion chambers. This method is powerful because one may observe directly the path taken by an individual photoelectron after ejection from the parent atom. In actual practice, however, the method has several shortcomings,[2] one of which is that except in a very few special cases the electrons coming from one level of the parent atom cannot be differentiated from those coming from another level.[3]

The method developed by one of the writers[4] enabled the longitudinal distribution of the photoelectrons to be studied as a function of both the energy of the incident photons and the level from which the electrons are ejected. While the change in relative intensities of "lines" in the "magnetic spectra" taken at various angles by this method yielded valuable information, the actual longitudinal distribution of a given group of photoelectrons could be obtained only qualitatively, because the photoelectrons were recorded photographically. With the aim of obtaining distribution curves of a more accurate nature, a new magnetic spectrograph has been constructed, in which the photographic plate has been replaced by a small Geiger-Müller tube.[5]

Apparatus

In Fig. 1 is shown the horizontal section through the centers of the slits of the new spectrograph. The photoelectrons are ejected from an exceedingly

[1] For a bibliography of work in this field see, e.g., Watson and Van den Akker, Proc. Roy. Soc. **A126,** 138 (1929).

[2] Williams, Nuttal and Barlow, Proc. Roy. Soc. **A121,** 611 (1928).

[3] Watson and Van den Akker, reference 1.

[4] Watson, Phys. Rev. **30,** 479 (1927).

[5] For a bibliography of work done on this extremely sensitive detector of ions see, e.g., Van den Akker, Rev. Sci. Instr. **1,** 672 (1930).

thin film of the element studied, which is deposited on a strip of celluloid 2 mm wide. This strip is supported with its length vertical, and so arranged at the axis of rotation of the apparatus that the electrons always leave the film normally to its surface. The width of the x-ray beam at the axis of rotation is about 4 mm, so that the film is included in the beam at all angular settings of the spectrograph. Each of the slits shown is 1/64 inch wide and 1/4 inch long. The slits S_1 and S_2 are 3 inches apart, and thus ρ, the radius of curvature of the electron orbits, is fixed at 1.5 inches. The slit S_3 and the windows W_2 and W_3 in the Geiger-Muller tube aid in setting the angular dial shown in Fig. 2. Once this setting has been made, the Geiger-Muller tube is shifted to a new position, axis at O', where the entrance window W_1 is more directly behind S_2.

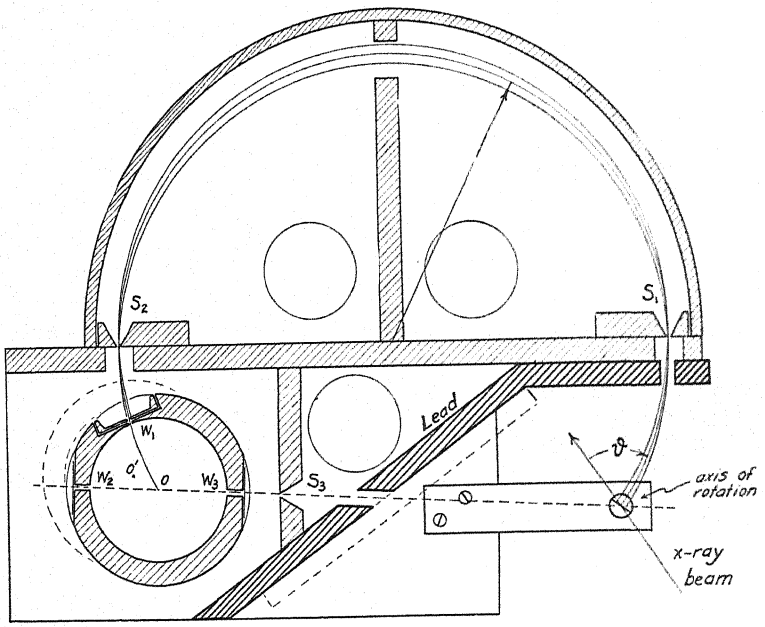

Fig. 1. Horizontal section of apparatus, showing arrangement of slits.

Rotation of the spectrograph from outside the chamber may be accomplished by means of a large brass taper, which is shown in Fig. 2. The lead-in B is a small brass pipe which connects the chamber of the Geiger-Müller tube to a gas system, while A is an electrical lead-in to the anode wire of the tube. A pointer fastened to the top of the taper enables one to read θ, the angle between the x-ray beam and the initial direction of the photoelectrons which enter S_1.

The entrance window W_1 is a set of five holes, each of 0.8 mm diameter, and arranged in a vertical line. A small disk fits into the wall of the tube, and this disk possesses five holes which fall over the five holes in the wall of the tube. This is shown in Fig. 3, in which is given a cross section of a tube of design later than that of the tube depicted in Fig. 2. A film of celluloid of the

order of 10^{-6} cm thick covers the holes of the small disk. This film must satisfy two requirements: It must be sufficiently thin to pass an appreciable fraction of the slowest photoelectrons, and yet it must be sufficiently strong to withstand the difference in pressure which exists between the interior and exterior of the tube (approximately 5 cm of mercury).

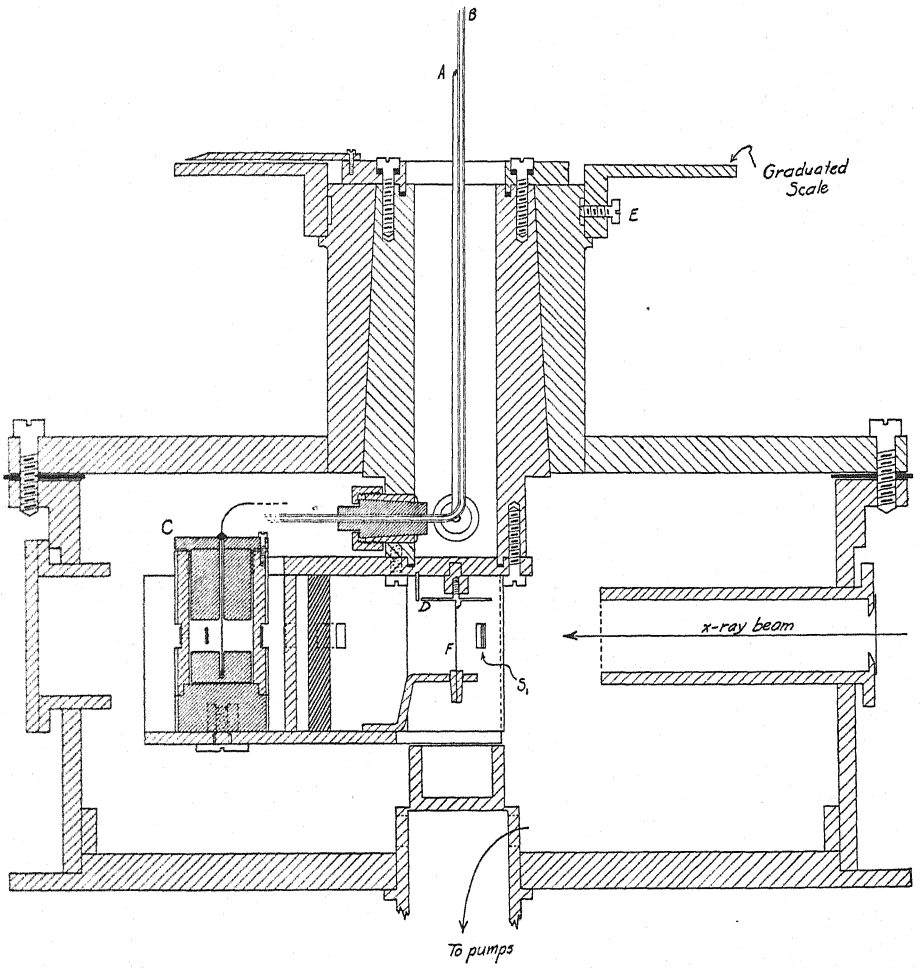

Fig. 2. Vertical section of apparatus.

A description of the specialized form of Geiger-Müller tube used in this research and of its operation has been given elsewhere.[6] The most important detail is the limitation of the active volume by the use of hard rubber plugs. This limitation of volume results in a very low "residual count;" and, when the anode wire is satisfactory, the electron count is independent of the potential of the anode over a range of about 50 volts. (When the whole of the

[6] Van den Akker, Rev. Sci. Instr. 1, 672 (1930).

volume of the chamber is active the effect of the ends of the tube is to make the residual count a function of the potential of the anode).

The wiring diagram for the Geiger-Müller tube is given in Fig. 4. The tube is earthed, while the anode is connected to a source of high potential through

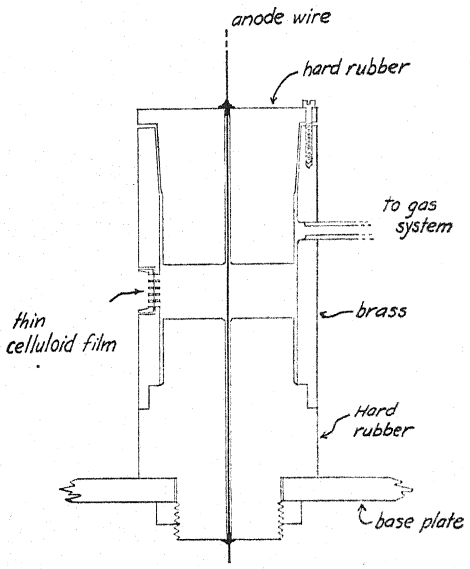

Fig. 3. Diagram of small electron counter, showing limitation of active volume by means of solid hard rubber plugs.

a resistance of 5×10^9 ohms. Since the spectrograph is placed at the center of a long, vertical solenoid, the connector between the anode and the amplifier

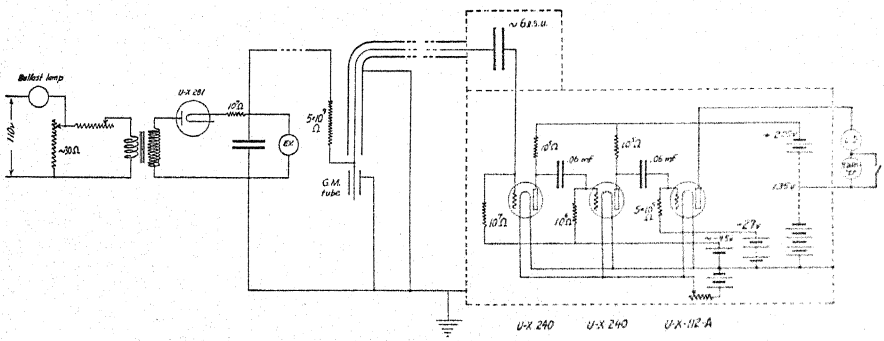

Fig. 4. General scheme of electrical connections for the Geiger-Müller tube.

is necessarily long. The strong electrical disturbances which come from the x-ray outfit make it necessary to shield this connector carefully; to satisfy this requirement, and an additional restriction on the total capacity to earth of the connector, the shielded connector is a very fine wire strung through a large lead pipe.

The results given in this paper were obtained when the x-rays were the primary rays of molybdenum, generated in a water-cooled Coolidge tube

driven at 30 kv and 20 m.a., and the electrons were ejected from a barely visible sputtered film of gold.

The Nature of the Magnetic Spectra

The results of two exploratory runs at $\theta = 80°$ are given in Figs. 5 and 6. In Fig. 5 is shown a small part of the whole spectrum which includes the double peak due to L_{III} electrons ejected from gold by Mo$K\alpha_{1,2}$. In each

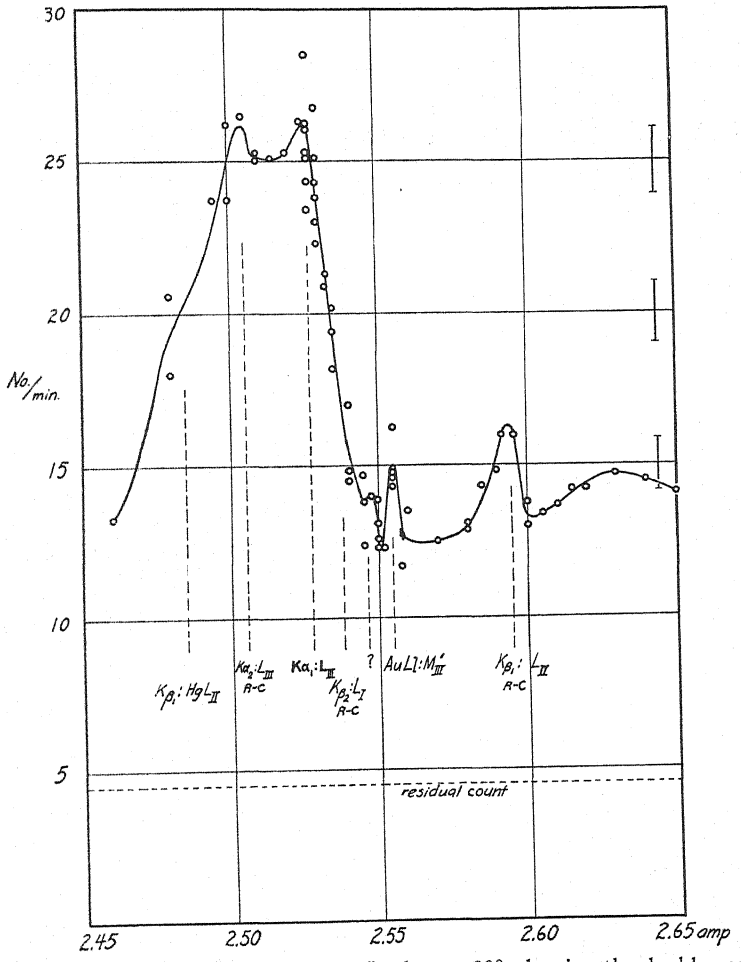

Fig. 5. A small part of the electron "spectrum" taken at 80°, showing the double peak due to L_{III} electrons of gold ejected by Mo$K\alpha_{1,2}$.

figure the number of impulses occurring in the Geiger-Müller tube per minute is plotted against the solenoid current. The spectrograph was calibrated with respect to the position of the $K\alpha_1 : L_{III}$ peak, the $H\rho$ value being that given by Robinson and Cassie.[7] All other positions indicated by vertical dashed lines were calculated. Where the precision measurements made by Robinson and

[7] Robinson and Cassie, Proc. Roy. Soc. **A113**, 282 (1928).

Cassie have been used, the letters "R–C" have been appended. In the calculation of the remaining positions, level values given in Vol. XXI of the Handbuch fur Physik were used. In all cases the ν/R values of the emission lines of molybdenum and gold and the values of the fundamental constants were those selected by Robinson and Cassie.

The sharpness of the peaks in Fig. 5 indicates good resolution, and shows that few electrons lost appreciable energy in getting out of the sputtered film. Each point shown was obtained by a ten minute period of counting, and hence the probable error for each point was not small, being one electron per minute for points in the neighborhood of 25 per minute. The heavy vertical dashes at the extreme right of Figs. 5 and 6 represent twice the probable error of individual points. The probable error of the curves drawn is in general

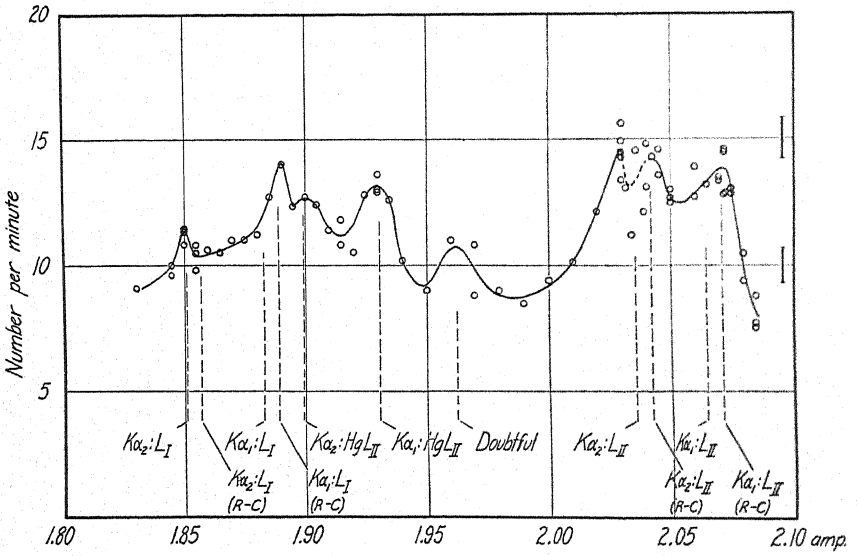

Fig. 6. The low velocity end of the electron "spectrum" showing peaks due to electrons from the L_{I} and L_{II} levels of gold.

somewhat smaller, being as small as 0.4 electrons per minute at certain points. The count obtained at zero magnetic field, the "residual count," was about 4.5 per minute. This count was not noticeably changed when the source of x-rays was cut off, showing that the effect of scattered x-rays was negligible.

The small peak at 2.555 amp can be attributed to electrons ejected from the M_{III} levels of gold atoms in which the transition $(M_{\text{I}} \rightarrow L_{\text{III}})$ may occur. Thus, while the M_{III} level in the normal gold atom has the value $\nu/R = 202.8$, the value of this level in an atom in which the above transition may occur is 206.7. The two peaks at 1.900 and 1.930 could not be attributed to electrons coming from gold. The sputtered film of gold had been exposed to mercury vapor at room temperature, however, and hence one might reasonably expect to find peaks due to electrons from mercury. The calculated positions of electrons ejected from the mercury L_{II} level by Mo$K\alpha_{1,2}$ were, respectively, 1.931 and 1.899 amp.

The Longitudinal Distribution of the L_{III} Electrons

In an attempt to measure the longitudinal distribution of electrons ejected from the L_{III} level of the gold atom by $K\alpha_1$, the $K\alpha_{1,2}$: L_{III} peaks were obtained at various angles. The difference between the ordinate of the peak at 2.528 amp and the ordinate of the valley at 2.551 amp was taken as a measure of the number of electrons ejected from the L_{III} level. This difference is plotted against the angle of ejection, θ, in Fig. 7. The deviation of the experimental curve from the points at 60° and 80° is a correction due to the loss of $K\alpha$ rays in passing through the celluloid strip which supported the sputtered film. This correction is negligible for all angles excepting those slightly less than 90°. It should be noted that this correction is not accurately known, and that an error in this correction will shift the maximum of the experimental curve through several degrees.

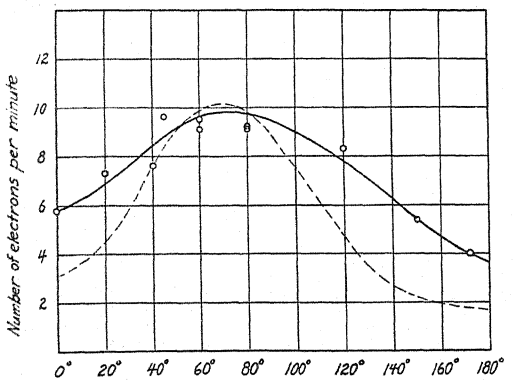

Fig. 7. The longitudinal distribution of L_{III} electrons of gold ejected by Mo$K\alpha_1$.

Schur[8] has recently given a theoretical expression for the longitudinal distribution of the L electrons taken collectively. This expression is divided into two parts, one giving the distribution of the L_I electrons, and the other giving the distribution of the L_{II} and L_{III} electrons combined. The latter part is

$$J(\theta,\phi) \sim \left\{1 + \frac{8I_L}{h\nu}\sin^2\theta\cos^2\phi + \frac{2v}{c}\cos\theta\left[1 + 2\left(1 + \frac{11I_L}{h\nu}\right)\sin^2\theta\cos^2\phi\right]\right\}$$

where $J(\theta, \phi)$ is the probability per unit solid angle that an electron will leave the parent atom in a direction making an angle θ with the forward direction of the x-ray beam, and the angle ϕ with the direction of the electric vector, ϕ being measured in a plane perpendicular to the beam of x-rays. The quantities I_L, ν, and v are respectively the mean energy of binding of the L_{II} and L_{III} electrons, the frequency of the incident radiation, and the speed of ejection of the photoelectrons. Since unpolarized rays were used, we integrate with respect to ϕ from 0 to π, and obtain

[8] Schur, Ann. d. Physik **4**, 433 (1930).

$$P(\theta) \sim \left\{1 + \frac{4I_L}{h\nu}\sin^2\theta + \frac{2v}{c}\cos\theta\left[1 + \left(1 + \frac{11I_L}{h\nu}\right)\sin^2\theta\right]\right\}.$$

This function is represented in Fig. 7 by the dashed curve. The wide departure of the experimental curve from the theoretical at small and large angles can be explained in part by nuclear scattering of the electrons in the sputtered film. Scattering can not explain the larger part of this departure, however, as spectra obtained in the past[9] reveal the important fact that certain lines, strong at 80°, fall to nearly zero intensity at 0°. On the other hand, the theoretical distribution is that of the L_{II} and L_{III} electrons combined, and it may be that the distribution of the L_{II} electrons is less isotropic than that of the L_{III} electrons. The maxima of the curves are both well forward of 90°, being at about 70°, and the ratio of the ordinates at 0° and 180° of the experimental curve is nearly the same as that of the theoretical curve. The experimental value of this ratio is 1.60, while Schur's function gives

$$P(0)/P(\pi) = (1 + 2v/c)/(1 - 2v/c) = 1.82.$$

[9] Watson and Van den Akker, reference 1.

ON THE PROBLEM OF THE ENTROPY OF THE UNIVERSE AS A WHOLE

By Richard C. Tolman
Norman Bridge Laboratory, California Institute of Technology

(Received May 6, 1931)

Abstract

The well-known problem of the entropy of the universe as a whole arises from the difficulties encountered by classical thermodynamics—first in failing to account for the presumed fact that the entropy of the universe has always been increasing at an enormous rate and nevertheless has not yet reached its maximum value—and second in failing to allow an emotionally satisfactory feeling towards our universe whose ultimate fate would be the stagnation of "heat-death." The purpose of the present article is to examine this problem from the point of view of the extension of thermodynamics to general relativity which has previously been made by the author.

A number of earlier contributions to the solution of the problem, which have been made from the standpoint of classical thermodynamics or statistical mechanics, are first briefly described in order to emphasize the very different character of the contribution to the problem made in the present article. It is then pointed out that the problem of the entropy of the universe arises in the classical thermodynamics because of the presumption that thermodynamic processes cannot take place both reversibly and at a finite rate, and that the general nature of the contribution to the problem offered by relativistic thermodynamics consists in showing the possibility of thermodynamic changes which could take place at a finite rate and at the same time reversibly without increase in entropy.

The principles of relativistic thermodynamics are then reviewed, and this difference between the classical and relativistic thermodynamics is shown by considering the possibilities of carrying out reversible changes at a finite rate in the properties of a thermodynamic fluid. In the classical thermodynamics it is found that no change in the thermodynamic properties could be allowed to take place at a finite rate, the entropy density of the fluid necessarily remaining constant in accordance with the equation

$$\frac{d\phi_0}{dt} = 0.$$

On the other hand, in relativistic thermodynamics it is found possible to allow changes to take place at a finite rate in the proper volume of the fluid, due to changes in the gravitational potentials $g_{\mu\nu}$, and still maintain reversibility provided the changes satisfy the relation

$$\frac{\partial}{\partial x_4}\left(\phi_0\sqrt{-g}\frac{dx_4}{ds}\right) = 0.$$

To exhibit the nature of the reversible changes at a finite rate thus permitted in relativistic thermodynamics, consideration is given to the highly idealized model of a non-static universe filled with black-body radiation as a thermodynamic fluid, and it is shown that the radius, total proper volume, and entropy density of such a universe could be changing at a finite rate and yet reversibly without increase in entropy. Furthermore, in the case of an expanding model of the kind considered, it is shown that an ordinary observer, who marks out with rigid meter sticks a small region of

this universe in his immediate vicinity for study, would find the energy density, energy content, and the temperature of this region decreasing with the time, and would find the number of quanta leaving the region per second greater than the number entering, and the average frequency of the quanta that leave greater than that of those that return. These phenomena would be interpreted by the observer, from a classical point of view, as due to radiation from his neighborhood into the colder surroundings of space and hence as leading to an increase in entropy, in spite of the fact that all the processes taking place in such a model would actually be reversible from the point of view of the relativistic thermodynamics which should be applied to such a problem.

In conclusion remarks are made concerning the disparity between the above model, which was chosen for purposes of illustration because of its mathematical simplicity, and models which would be more suitable to serve as representations of the actual universe. And some indication is given of the further developments that should be undertaken.

PART I. INTRODUCTION

§1. Purpose of present article.

IN A number of previous articles I have endeavored to present the principles for an extension of thermodynamics to general relativity[1] and to consider some of the applications of the new system of relativistic thermodynamics based on these principles.[2] The purpose of the present article is to examine the bearings of relativistic thermodynamics on the well-known problem of the entropy of the universe as a whole. It will be found that this extended thermodynamics provides new possibilities for thermodynamic processes to take place at a finite rate without increase in entropy. And it will be shown that the recognition of these new possibilities not only appears to be essential for a true understanding of the problem of the entropy of the universe, but may even provide to a greater or lesser extent the basis for its solution.

§2. The nature of the problem of the entropy of the universe.

In accordance with the views of the classical thermodynamics all thermodynamic processes, actually taking place in the universe at a finite rate, were regarded as accompanied by an increase in entropy. Among these processes appeared a wide variety of immediately appreciated terrestial occurrences of a meteorological, biological or technological nature in which the increase of entropy depended for the most part on the degradation of energy originally received as radiation from the sun,—in addition, various tidal actions in which the increase of entropy resulted from the degradation into heat of mechanical energy of astronomical motions;—and quantitatively most important of all, the continuous flow of radiation from the stars with a great increase in entropy due to the presumable drop in temperature in passing from the hot interior of the stars to the cold depths of intergalactic space.

In general the view was held that entropy was everywhere increasing at an enormous rate and that this would continue until the entropy of the universe

[1] Tolman, Proc. Nat. Acad. **14,** 268 (1928); ibid. **14,** 701 (1928); Phys. Rev. **35,** 875 (1930); ibid. **35,** 896 (1930).

[2] Tolman, Proc. Nat. Acad. **14,** 348 (1928); ibid. **14,** 353 (1928); ibid. **17,** 153 (1931); Phys. Rev. **35,** 904 (1930); Tolman and Ehrenfest, Phys. Rev. **36,** 1791 (1930).

had reached its maximum,—the sun and stars cold, all of creation dead and unchanging.

Such a view, however, carries with it two difficulties. The first difficulty has genuine intellectual validity and can be expressed by the question: Why has not the entropy of the universe already reached its maximum value in the infinite past time which has presumably been available? The second difficulty has perhaps only emotional validity and can be expressed by the question: What significance can we ascribe to a universe whose ultimate fate is merely the "heat-death" of maximum entropy? These are the difficulties which constitute the problem of the entropy of the universe.

§3. Nature of earlier contributions to the solution of the problem.

Various suggestions have been made with regard to the solution of the problem. It will be profitable to consider some of them briefly in order to emphasize the very different nature of the suggestion which will be made in this article.

a. Finite time since creation. The most obvious treatment of the problem is to assume that the universe was indeed created at a finite time in the past with sufficient available energy so that the entropy has not yet reached its maximum value. In the future this maximum would be reached and all significant changes would cease. A modification of the treatment could be made by assuming an infinite past during which the universe was in a quiescent metastable state of large available energy, and a disturbance at a finite time in the past which initiated the process of degradation.

These suggestions depend too greatly on special *ad hoc* assumptions to be scientifically satisfying.

b. Continuous regeneration. A second type of suggestion depends on the assumption of the existence of regenerative processes of such a nature as to maintain the universe in an approximately steady condition. Thus Millikan[3] has suggested the four-step cycle: (1) Matter in the stars is transformed into radiation which flows out into intergalactic space; (2) the radiation in intergalactic space is transformed into electrons and protons; (3) the electrons and protons combine to form helium and other elements, giving rise to the production of the observed cosmic rays; (4) the matter thus formed drifts back into the stars, thus completing the cycle. The evidence for step (2) is completely lacking at present; steps (2) and (3) assume the occurrence of processes of synthesis under the theoretically unfavorable conditions of extremely low concentration; and the cycle contradicts the principle of microscopic reversibility.[4] The evidence for step (1), however, is very strong, the evidence for step (3) cannot be dismissed as trivial, and there is no inherent improbability in step (4).

c. Continuous approach to maximum entropy. A third type of suggestion

[3] Millikan and Cameron, Proc. Nat. Acad. **14,** 637 (1928).

[4] For a partial historical account of this principle, see Tolman, Proc. Nat. Acad. **11,** 436 (1925). For a discussion of the principle, see for example Tolman, "Statistical Mechanics" Chap. 15, Chemical Catalog Co., New York, 1927.

would be to assume an infinite past for the universe, coupled with ever decreasing values for the entropy of the universe as we examine backwards in the past and a continuous asymptotic approach to the maximum of entropy in the future.[5] If such an assumption were allowable, it would avoid the difficulty of a limited past time for the existence of the universe, but the difficulties of a practical exhaustion of the energy available for human needs within a finite time in the future would not appear to be avoided. The assumption would perhaps not be a possible one for a finite universe of finite energy content, for which we have some evidence.

d. Fluctuations in entropy in accordance with its statistical-mechanical interpretation. A fourth of type of contribution to the problem depends on the statistical mechanical interpretation of entropy, as given most clearly by Boltzmann's famous H-theorem. In accordance with this theorem it is found that, although there is a great probability for the entropy of a system to increase when it has less than its maximum value, it is not certain that this will take place and fluctuations away from the maximum of entropy will occur. This furnishes the possibility that the universe has existed for an infinite time in the past and that we are now experiencing a return of the universe or of that portion which is within our range of observation towards a condition of maximum entropy after a major fluctuation away from that value.

This important possibility was clearly presented by Boltzmann[6] over thirty years ago. The enormous improbability of a major fluctuation of the kind assumed does not necessarily furnish a valid argument against the explanation, since, as pointed out to me in conversation by Mrs. Ehrenfest-Afanassjewa, the existence of sentient beings to observe the rare phenomenon could presumably only occur at the time of decay of such a fluctuation. From the point of view of human wishes, however, the explanation is not entirely satisfying, since it implies that man himself is a transitory and improbable phenomenon, that our surroundings are now headed with almost complete certainty towards a condition at least close to that of maximum entropy, and that the conditions under which life, as we know it, is possible are almost never present. Nevertheless, these objections have emotional rather than intellectual validity and the part played by the theory of statistical fluctuations in a relatively complete solution of the problem of the entropy of the universe may prove to be no mean one.

§4. Nature of the present contribution to the solution of the problem.

The present contribution to the problem of the entropy of the universe is based on the system of relativistic thermodynamics which I have developed. The general nature of the contribution depends on an extension given by this relativistic thermodynamics in our ideas as to the kind of processes which can occur at a finite rate without producing any increase in entropy.

As an illustration of this extension in our ideas, it would be impossible

[5] This possibility was suggested to me by some remarks of the late Professor William James which were told me in conversation by Professor Gilbert N. Lewis.

[6] Boltzmann, Wied. Ann. **60**, 392 (1897).

from the point of view of classical thermodynamics to carry out an actual expansion of a thermodynamic fluid reversibly and at a finite rate, since the friction of moving parts and the deficiency between the actual pressure exerted by the fluid and that which could be exerted with an infinitely slow rate of expansion would lead to an increase in entropy. Nevertheless, in relativistic thermodynamics we shall find that the *proper* volume associated with a thermodynamic fluid could increase at a finite rate, owing to a finite rate of change in the gravitational potentials $g_{\mu\nu}$, without involving any increase in entropy.

In further illustration, it appeared impossible in the classical thermodynamics for a flow of heat to take place reversibly and at a finite rate, owing to the increase in entropy connected with the finite temperature drop necessary to maintain the finite rate of flow. Nevertheless, in relativistic thermodynamics, we shall find that the reversible increase in proper volume, mentioned in the paragraph above, would make it possible for heat radiation to be regarded by an ordinary observer as flowing out of a given region of interest at a finite rate, without any increase in the entropy of the system as a whole.

It is evident from these examples, that relativistic thermodynamics increases in an important manner the variety of changes which could be taking place in a universe which is actually in a state of maximum entropy, and makes it necessary to re-examine processes which we have formerly taken as evidence that the entropy of our own universe is actually increasing at an enormous rate.

In Part II, we shall first consider the general bearing of relativistic thermodynamics on changes in thermodynamic condition without increase in entropy. In Part III, we shall then apply relativistic thermodynamics to the very special model of a non-static universe filled solely with radiation. Such a model ignores very characteristic features of the actual universe, but mathematically is relatively simple to handle and will present some features which appear analogous to phenomena in the actual universe. Finally in Part IV, we shall try to give some criticism of the role that the new ideas might play in the general solution of the problem of the entropy of the universe.

PART II. RELATIVISTIC THERMODYNAMICS

§5. The first and second laws of relativistic thermodynamics.

The extension of thermodynamics to general relativity can be based on two principles which may be regarded as the relativistic generalization of the first and second laws of classical thermodynamics.

In accordance with the first of these principles, any thermodynamic process occurring in the universe must take place in such a way as to agree with the principles of relativistic mechanics as given by the tensor density equation

$$\frac{\partial \mathfrak{T}_\mu^\nu}{\partial x_\nu} - \frac{1}{2}\mathfrak{T}^{\alpha\beta}\frac{\partial g_{\alpha\beta}}{\partial x_\mu} = 0 \qquad (1)$$

or the equivalent non-tensorial yet nevertheless covariant equation

$$\frac{\partial(\mathfrak{T}_\mu^\nu + \mathfrak{t}_\mu^\nu)}{\partial x_\nu} = 0 \tag{2}$$

where $\mathfrak{T}_\mu^\nu$ is the tensor density of material energy and momentum, $\mathfrak{t}_\mu^\nu$ the pseudo tensor density of potential energy and the $g_{\alpha\beta}$ the gravitational potentials.

Since these equations reduce to the ordinary energy-momentum principle in flat space-time where the gravitational field is negligible, the analogy of this first principle to the ordinary first law of thermodynamics is evident. In applying the principle to thermodynamic considerations, the system involved will of course be treated from a macroscopic point of view, and this is an advantage since the applicability of these equations to microscopic phenomena would certainly not be in accord with the development of quantum mechanics, which has taken place since their formulation.

The second principle of relativistic thermodynamics may be stated in the form

$$\frac{\partial}{\partial x_\mu}\left(\phi_0\sqrt{-g}\,\frac{dx_\mu}{ds}\right)dx_1dx_2dx_3dx_4 \geqq \frac{dQ_0}{T_0} \tag{3}$$

where ϕ_0 is the proper density of entropy as measured by a local observer, using Galilean coordinates which are at rest with respect to the mass motion of the thermodynamic fluid at the point of interest, the quantities dx_μ/ds are the macroscopic "velocities" of the fluid at the point of interest as measured in the coordinate system x_1, x_2, x_3, x_4, the quantity dQ_0 is the heat flowing through the boundary into the infinitesimal region *and* during the infinitesimal time, denoted by $dx_1dx_2dx_3dx_4$, as measured in proper coordinates, and T_0 the temperature of the boundary also measured in proper coordinates.

The justification for the principle lies in the fact that it has been shown to be a natural covariant generalization of the ordinary second law of thermodynamics valid in flat space-time, Eq. (3) being a tensor equation of rank zero which reduces in flat space-time and Galilean coordinates to

$$\left[\frac{\partial\phi}{\partial t} + \frac{\partial}{\partial x}(\phi u) + \frac{\partial}{\partial y}(\phi v) + \frac{\partial}{\partial z}(\phi w)\right]dxdydzdt \geqq \frac{dQ}{T} \tag{4}$$

where ϕ is the density of entropy, u, v and w are the component velocities of the fluid, dQ is the heat flowing into the region $dxdydz$ in the time dt, and T is the temperature, all these quantities now being measured in the particular set of Galilean coordinates x, y, z, t which is being used.

§6. Application of the relativistic second law to a finite adiabatic system.

Let us now apply our new form of the second law as given by Eq. (3) to a finite thermodynamic system, by taking x_1, x_2, x_3 as being the space-like coordinates and carrying out an integration over the spatial region of interest. If we carry out such an integration, using coordinates such that the limits

of integration necessary to include the system fall on the boundary which separates the system from its surroundings, it is evident that the summation of dQ_0/T_0 over the interior of the system will cancel out, since any heat entering a given element of volume is abstracted from neighboring elements. Hence dividing Eq. (3) by dx_4, writing out the separate terms corresponding to the different values of μ, and performing the integration we obtain, with some rearrangement in order,

$$\begin{aligned}\iiint \frac{\partial}{\partial x_4}\left(\phi_0\sqrt{-g}\,\frac{dx_4}{ds}\right)dx_1dx_2dx_3 \\ \geqq -\iiint\left[\frac{\partial}{\partial x_1}\left(\phi_0\sqrt{-g}\,\frac{dx_1}{ds}\right)+\frac{\partial}{\partial x_2}\left(\phi_0\sqrt{-g}\,\frac{dx_2}{ds}\right)\right. \\ \left.+\frac{\partial}{\partial x_3}\left(\phi_0\sqrt{-g}\,\frac{dx_3}{ds}\right)\right]dx_1dx_2dx_3+\sum\left(\frac{1}{T_0}\,\frac{dQ_0}{dx_4}\right)_{\text{BOUNDARY}}\end{aligned} \tag{5}$$

The last term on the right hand side of the above inequality is the total value of the quantity $(1/T_0)(dQ_0/dx_4)$ taken over the boundary which separates the system from its surroundings, and by performing the indicated integrations the other terms on the right hand side of the expression can also be seen to depend solely on conditions at the boundary. We obtain

$$\begin{aligned}\iiint \frac{\partial}{\partial x_4}\left(\phi_0\sqrt{-g}\,\frac{dx_4}{ds}\right)dx_1dx_2dx_3 \\ \geqq -\iint\left|\phi_0\sqrt{-g}\,\frac{dx_1}{ds}\right|_{x_1}^{x_1'}dx_2dx_3-\iint\left|\phi_0\sqrt{-g}\,\frac{dx_2}{ds}\right|_{x_2}^{x_2'}dx_1dx_3 \\ -\iint\left|\phi_0\sqrt{-g}\,\frac{dx_3}{ds}\right|_{x_3}^{x_3'}dx_1\,dx_2+\sum\left(\frac{1}{T_0}\,\frac{dQ_0}{dx_4}\right)_{\text{BOUNDARY}}\end{aligned} \tag{6}$$

where the limits of integration at the boundary are denoted by x_1, x_1' etc.

This expression (6) may be regarded as a general statement of the relativistic second law of thermodynamics as applied to finite systems. Defining the entropy of the system as

$$S=\iiint\left(\phi_0\sqrt{-g}\,\frac{dx_4}{ds}\right)dx_1dx_2dx_3 \tag{7}$$

it gives the relation which must hold between the rate at which the entropy of a finite system is changing with the time x_4 and those conditions at the boundary which determine the flux of matter and the flow of heat between the system and its surroundings.

For an adiabatic system with no flux of matter or flow of heat between the system and its surroundings we shall have the quantities dx_1/ds, dx_2/ds, dx_3/ds, and dQ_0/dx_4 equal to zero at the boundary and the expression will then reduce to

$$\frac{dS}{dx_4} = \int\int\int \frac{\partial}{\partial x_4}\left(\phi_0\sqrt{-g}\,\frac{\partial x_4}{ds}\right) dx_1 dx_2 dx_3 \geqq 0. \tag{8}$$

In accordance with this expression the entropy of an adiabatic system cannot decrease with the time but can only increase or remain constant. As in the classical thermodynamics, adiabatic processes in which the entropy increases with the time may be called irreversible, since neglecting improbable fluctuations the system after such a process could not of itself return to the original state of lower entropy; while processes in which the entropy remains constant may be called reversible.

§7. Increased possibility for reversible processes in relativistic thermodynamics.

With the help of the foregoing considerations we may now compare the conditions which would be imposed by classical and by relativistic thermodynamics on the occurrence of reversible processes. In the present section we shall show that the new thermodynamics offers the possibility for a kind of thermodynamic change which was not contemplated in the classical thermodynamics, and which might take place at a finite rate without increase in entropy, in contrast to the conclusion of classical thermodynamics that reversible thermodynamic processes could not take place at a finite rate. And in later sections we shall show by a simple specific example that such reversible processes taking place at a finite rate might actually be realized, and play a possible part in cosmological happenings.

a. Classical treatment of entropy changes in a thermodynamic fluid. Let us first illustrate the kinds of classical considerations which have formerly lead to the conclusion that thermodynamic processes could not take place both reversibly and at a finite rate.[7] To do this we may consider the conditions which would be imposed by classical thermodynamics on reversible changes in the condition of a thermodynamic fluid.

In the classical thermodynamics we could evidently write for the entropy of a finite portion of thermodynamic fluid enclosed in a suitable container the expression

$$S = \int\int\int \phi\, dxdydz \tag{9}$$

where ϕ is the density of entropy as measured in the particular set of (Galilean) coordinates x, y, z, t which the observer uses, and the integration is to be taken over the whole volume of the container.

If now we consider the possible reversible changes which could take place in this thermodynamic fluid, it is evident in the first place that we could permit no relative motion between different portions of the fluid, since the decay of this motion would lead to an increase in entropy, and we may hence

[7] Of course the classical thermodynamics permitted ideal *mechanical* processes to take place at a finite rate without increase in entropy, but the distinction between mechanical and thermodynamic processes was clear enough so that this did not prove to be a source of confusion.

use a set of coordinates in which the thermodynamic fluid as a whole would be at rest and rewrite our expression for the entropy in the form

$$S = \iiint \phi_0 \, dxdydz \tag{10}$$

where ϕ_0 is the proper density of entropy. In the second place, it is evident that we could only permit adiabatic changes, since if we allowed heat flow in our system at a finite rate we should have increases in entropy arising from the finite temperature gradient which would be necessary to maintain this flow. Hence in accordance with the classical thermodynamics the condition for our contemplated process to be reversible would be that of constant entropy as given by the equation

$$\frac{d}{dt}\iiint \phi_0 \, dxdydz = 0. \tag{11}$$

In the third place, it is evident that our process could not involve a change in volume at a finite rate, for example by the withdrawal of a piston, since this would involve mass flow of portions of the fluid which would lead to an increase in entropy that could be calculated from the difference between the pressure actually exerted by the fluid on the moving piston and that which would be exerted at an infinitesimally slow rate of expansion. Hence the condition given by Eq. (11) for our contemplated reversible process might now be rewritten with the differentiation inside the integral sign in the form

$$\iiint \frac{d\phi_0}{dt} \, dxdydz = 0. \tag{12}$$

This final condition, moreover, could evidently be satisfied in our case only by taking

$$\frac{d\phi_0}{dt} = 0 \tag{13}$$

at all points of the fluid, since for a stationary fluid with no flow of heat there would be no possibility at any point for negative values of the quantity $d\phi_0/dt$.

This, however, completes the considerations necessary for the classical conclusion that there could be no thermodynamic change at all in our fluid which takes place both reversibly and at a finite rate. Indeed we see that no changes could take place in the system as a whole through interaction with its surroundings, since we have found that its volume could not be allowed to change at a finite rate and heat could not be allowed to flow through its boundary at a finite rate, and no changes could take place in the interior condition of the fluid since we have found that it could have no macroscopic internal motions, no internal flow of heat, and no changes in local entropy density which take place at a finite rate.

b. Relativistic treatment of entropy changes in a thermodynamic fluid. We

must now compare this conclusion with that which we would obtain by applying relativistic thermodynamics to the same system, namely a finite portion of thermodynamic fluid. In this case in accordance with expression (8) in the preceding section §6, the condition for a reversible adiabatic change in the condition of the fluid would be

$$\int\int\int \frac{\partial}{\partial x_4}\left(\phi_0\sqrt{-g}\,\frac{dx_4}{ds}\right) dx_1 dx_2 dx_3 = 0 \tag{14}$$

where x_4 is the time like coordinate and the integration is to be taken over the whole range of spatial coordinates x_1, x_2, x_3 necessary to include the fluid. And this condition can evidently be satisfied if we have the equality holding at each point in the fluid

$$\frac{\partial}{\partial x_4}\left(\phi_0\sqrt{-g}\,\frac{dx_4}{ds}\right) = 0 \tag{15a}$$

or

$$\frac{1}{\phi_0}\,\frac{\partial \phi_0}{\partial x_4} = -\,\frac{1}{\sqrt{-g}\,\dfrac{dx_4}{ds}}\,\frac{\partial}{\partial x_4}\left(\sqrt{-g}\,\frac{dx_4}{ds}\right). \tag{15b}$$

This expression gives a relation between the percentage rate at which the proper entropy density ϕ_0 is changing with the time x_4 at a given point and the percentage rate at which the quantity $(\sqrt{-g}\,dx_4/ds)$ is changing with the time at that same point. The value of this latter quantity, however, is determined by the gravitational field at the point in question, and by the kind of coordinate system $x_1 \cdots x_4$ which is being used.

If now we assumed the gravitational field negligible, as is tacitly done in the classical thermodynamics, and had a fluid with no relative motion between its parts, we could choose a system of Galilean coordinates x, y, z, t in which the fluid as a whole would be at rest. In this system of coordinates the quantities $\sqrt{-g}$ and dx_4/ds would have the constant value unity and the condition given by Eqs. (15) would reduce to the result

$$\frac{d\phi_0}{dt} = 0 \tag{16}$$

which we have already found to be characteristic of the classical thermodynamics. It is thus by a neglect of the gravitational field and its possible change with time that the classical thermodynamics has been led to the conclusion that no reversible processes can occur at a finite rate.

On the other hand in relativistic thermodynamics we must not assume that the gravitational field is necessarily negligible but must specifically consider the part which it plays in thermodynamic processes. Hence in relativistic thermodynamics we must consider the condition for reversibility given by Eq. (15) in its full form, and retain the possibility of mutual changes in gravitational field and entropy density taking place together at a finite rate in such a way as to satisfy this condition for reversibility.

In Part III we shall consider a definite model which exhibits such a mutual change in gravitational field and entropy density taking place at a finite rate and satisfying the condition for reversibility. To conclude the present section, however, we may first investigate somewhat further the general nature of the reversibility requirement given by Eq. (15).

Consider the case of a thermodynamic fluid which is at rest with respect to the spatial coordinates x_1, x_2, x_3 which are being used. Since the macroscopic velocities dx_1/ds, dx_2/ds, and dx_3/ds are everywhere zero by hypothesis, it is evident that the amount of fluid in any given coordinate range $dx_1dx_2dx_3$ would not be changing with the time since there is no flow across the boundary. In accordance with the principles of relativity, however, we can then write for the proper volume dV_0 of the small element of fluid in such a coordinate range the well-known equation

$$dV_0 = \sqrt{-g}\, dx_1dx_2dx_3 \frac{dx_4}{ds} \tag{17}$$

and substituting this expression into the condition for reversibility, as given by Eq. (15a), we can rewrite this condition in the new form

$$\frac{\partial}{\partial x_4}\left(\phi_0\sqrt{-g}\, dx_1dx_2dx_3 \frac{dx_4}{ds}\right) = \frac{\partial}{\partial x_4}(\phi_0\, dV_0) = 0 \tag{18}$$

since the coordinates x_1, x_2 and x_3 are independent of the coordinate x_4.

This equation, however, states that the total entropy for each given small element of fluid shall be constant as measured by a local observer, and this is merely the condition for a change in the proper volume of the element with no flow of heat and with balance between internal and external pressures. Hence if we had a fluid with no flow of heat and constant proper pressure throughout, a finite rate of alteration in the gravitational field which produced no flow of heat and changed the proper pressure at the same rate throughout the fluid would satisfy the condition of reversibility. This alteration in gravitational field, however, would lead to an alteration in proper volume and thus to alteration in the entropy density, so that the thermodynamic state of the fluid would be changing reversibly and at a finite rate. It is this dependence of proper volume on gravitational field, which was quite outside of the considerations of the classical thermodynamics, which leads in relativistic thermodynamics to the possibility of reversible processes which take place at a finite rate.

PART III. APPLICATION TO A SPECIFIC MODEL

§8. The general nature of the model.

We may now apply the foregoing considerations to a specific model. For this purpose we shall take a non-static universe[8] filled with a uniform density of black-body radiation. The choice of this model is not made because it is

[8] For an account of various treatments which have been given to the non-static line element for the universe, see Tolman, Proc. Nat. Acad. **16**, 582 (1930).

thought to give a close approximation to the actual state of the universe but because the mathematical treatment will be relatively simple. The model neglects the presence of matter and its agglomeration into stellar systems which are very characteristic features of the actual universe. Nevertheless, we shall find that the behaviour of the radiation in such a universe furnishes a surprizing possibility of insight into the flow of radiation from the stars which is such a puzzling feature of the actual universe.

§9. The line element for the non-static universe.

The line element for a non-static universe filled with a uniform distribution of matter and energy can be derived[9] by treating the contents of the universe for the purposes of large-scale considerations as though filled with a perfect fluid, on the basis of the two requirements, (a) that the fluid shall at all times be uniformly distributed spatially, and (b) that particles (nebulae) which are stationary in the coordinate system used shall fulfill the stability requirement of not being subject to acceleration.

The line element so obtained can be written in a variety of forms depending on the choice of coordinates, and for the purpose of the discussions in the present article it will be most convenient to write it in the form[10]

$$ds^2 = -e^{g(t)}\left(\frac{dr^2}{1 - r^2/R^2} + r^2 d\theta^2 + r^2 \sin^2\theta d\phi^2\right) + dt^2 \qquad (19)$$

where r, θ and ϕ are the spatial coordinates, t is the time coordinate, R is a constant, and the dependence of the line element on the time is given by the exponent $g(t)$.

§10. Certain general properties of the non-static universe.

Before proceeding to our special model, it will be desirable to recall certain properties which are implied in general for the non-static universe by the form of the line element and which will be needed in our later discussion.

In accordance with the requirement (a) on which the line element was derived, the proper macroscopic density ρ_{00} and the proper pressure p_0 of the fluid which fills the universe will be independent of the position r, θ, ϕ, but may be changing with the time t. And indeed working out the components of the energy-momentum tensor T_μ^ν which correspond to the line element (19) and equating to those for a perfect fluid we obtain as the only non-vanishing components[11]

$$8\pi T_1^1 = 8\pi T_2^2 = 8\pi T_3^3 = -8\pi p_0 = \frac{1}{R^2}e^{-g} + \ddot{g} + \frac{3}{4}\dot{g}^2 - \Lambda \qquad (20)$$

$$8\pi T_4^4 = 8\pi\rho_{00} = \frac{3}{R^2}e^{-g} + \frac{3}{4}\dot{g}^2 - \Lambda \qquad (21)$$

[9] Tolman, Proc. Nat. Acad. **16**, 320 (1930). See also Ibid. **16**, 409 (1930), and note that the five assumptions mentioned in §2 of that article can be included under the heading of the two requirements (a) and (b) given above.

[10] Tolman, Proc. Nat. Acad. **16**, 511 (1930). Eq. (5). Note that the $\bar{r}$ of that article is our present r.

[11] Tolman, Proc. Nat. Acad. **16**, 409 (1930). Eq. (2).

where Λ is the cosmological constant; and these equations give the dependence of pressure and density on the exponent g and its time derivatives $\dot{g}$ and $\ddot{g}$, and thus on the time itself.

With the help of these expressions for the components of the energy-momentum tensor we can now easily apply the principles of relativistic mechanics in the well-known form

$$\frac{\partial \mathfrak{T}_\mu^\nu}{\partial x_\nu} - \frac{1}{2}\mathfrak{T}^{\alpha\beta}\frac{\partial g_{\alpha\beta}}{\partial x_\mu} = 0. \tag{22}$$

With $\mu = 1, 2, 3$ we merely obtain identities, but substituting into this equation for the case $\mu = 4$ we can easily obtain after dividing through by a constant factor[12]

$$\frac{d}{dt}(\rho_{00}\, e^{3g/2}) + p_0 \frac{d}{dt} e^{3g/2} = 0. \tag{23}$$

This important result can evidently also be obtained directly by combining Eqs. (20) and (21).

In accordance with the requirement (b) on which the line element was derived, particles which are at rest with respect to the coordinate system r, θ, ϕ will not be subject to acceleration but will remain at rest. And this can be directly verified by calculating the Christoffel three-index symbols which correspond to the line element (19) and substituting in the geodesic equation which governs the motions of particles in general relativity.

As a result of the foregoing, observers who are at rest with respect to the coordinate system will remain permanently so. And in accordance with the form of the line element (19), for such observers, the proper time as measured by local clocks will evidently agree with the coordinate time t. On the other hand, for the proper distance dl_0 as measured with rigid meter sticks we shall evidently have

$$dl_0 = \frac{e^{g/2}dr}{\sqrt{1 - r^2/R^2}} \tag{24}$$

for points at the coordinate distance dr in the radial direction, and

$$dl_0 = re^{g/2}d\theta \quad \text{and} \quad dl_0 = r\sin\theta e^{g/2}d\phi \tag{25}$$

for the θ and ϕ directions. For the proper volume dV_0 associated with a given small range of coordinates we shall have

$$dV_0 = \frac{r^2 \sin\theta\, e^{3g/2}}{\sqrt{1 - r^2/R^2}} dr d\theta d\phi. \tag{26}$$

Although particles which are at rest in the coordinate system r, θ, ϕ will remain so, nevertheless it is evident from Eqs. (24) and (25), that the proper distance between such particles as measured with rigid meter sticks will in general be changing with the time, since the exponent g is itself a function of

[12] See reference 11, Eq. (4).

the time. Thus for the proper distance between a particle located at the origin $r=0$ and a particle permanently located at the coordinate distance $r=r$, we shall have

$$l_0 = \int_0^r \frac{e^{g/2}dr}{\sqrt{1-r^2/R^2}} = e^{g/2}R\sin^{-1}\frac{r}{R} \tag{27}$$

and this will be increasing or decreasing with the time in accordance with the dependence of g on the time. Also in accordance with Eq. (26), the proper volume associated with a given coordinate range will be a function of the time, and for the proper volume of the universe as a whole we shall have

$$V_0 = \int_0^{2\pi}\int_0^{\pi}\int_0^R \frac{r^2\sin\theta\, e^{3g/2}}{\sqrt{1-r^2/R^2}}drd\theta d\phi = \pi^2R^3e^{3g/2}. \tag{28}$$

In accordance with this result it is natural to consider $Re^{g/2}$ as the radius of the universe and to speak of an expanding universe if g is increasing with the time and of a contracting universe if g is decreasing with the time.

The change with time in the proper distance between objects in the universe leads to a shift in the observed wave-length of light coming from distant objects, a shift towards the red in an expanding universe and a shift towards the violet in a contracting universe. The magnitude of this shift is given by the formula[13]

$$\frac{\lambda_0+\delta\lambda}{\lambda_0} = e^{(g-g_0)/2} \tag{29}$$

where g_0 is the value of the exponent occurring in the general expression for the line element at the time when the light was emitted with the original wave-length λ_0, and g is its value at the time the light is received and observed to have the wave-length $\lambda_0+\delta\lambda$.

In accordance with this formula we may regard the wave-length, which would be found by a local observer for any given quantum of light, as a quantity which is changing with the time in accordance with the change of g with the time. And, indeed, differentiating Eq. (29) with respect to the time we can evidently write

$$\frac{1}{\lambda}\frac{d\lambda}{dt} = \frac{1}{\lambda_0+\delta\lambda}\frac{d}{dt}(\lambda_0+\delta\lambda) = \frac{1}{2}\frac{dg}{dt} \tag{30}$$

as an expression for the fractional change in the wave-length of any given quantum with the time. Or in terms of frequency we can write

$$\frac{1}{\nu}\frac{d\nu}{dt} = -\frac{1}{2}\frac{dg}{dt} \tag{31}$$

as an expression for the change in the frequency of radiation with the time, ν being, of course, the frequency as measured by proper observers who are at rest with respect to the fluid in the universe and hence also at rest with respect to the coordinates r, θ, ϕ.

[13] See reference 11, Eq. (21).

This completes the statement of general properties of the non-static universe which we shall need in discussing our special model.

§11. Properties of non-static universe filled with black-body radiation.

We may now turn to the discussion of the special model in which we take the thermodynamic fluid filling the universe to be a uniform distribution of black-body radiation of the same proper density throughout, a proper observer being one who finds no net flow of radiation.

Under these circumstances we can obtain a great simplification in treatment since it is evident that the proper macroscopic density of the fluid ρ_{00} and its proper pressure p_0 will be related by the well-known expression connecting the density and pressure of radiation

$$\rho_{00} = 3p_0. \tag{32}$$

And this permits us to obtain an immediate relation between the pressure of radiation in such a universe and the time variable g, since by substituting in the general Eq. (23) we have

$$3\frac{d}{dt}(p_0 e^{3g/2}) + p_0 \frac{d}{dt} e^{3g/2} = 0 \tag{33}$$

and this can at once be integrated to give

$$p_0 = Ae^{-2g} \quad \text{and} \quad \rho_{00} = 3Ae^{-2g} \tag{34}$$

where A is the constant of integration, the pressure and density of radiation thus being quantities which decrease as the radius of the universe $Re^{g/2}$ increases.

As an important consequence of this result it now becomes possible to obtain a solution for g as a function of t. Substituting the expression for proper density given by Eq. (34) into Eq. (21) we obtain after some rearrangement

$$\frac{d}{dt}(e^g) = \pm \sqrt{32\pi A - \frac{4}{R^2}e^g + \frac{4}{3}\Lambda e^{2g}} \tag{35}$$

as a differential equation for the dependence of g on t, where the plus sign corresponds to an expanding universe and the negative sign to a contracting universe. Eq. (35) can itself then easily be integrated to give an explicit solution for g as a function of t. The form of the solution will depend on the sign of the cosmological constant Λ, and it is merely of interest for our present purposes to remark that for the case of a universe containing nothing but radiation there appears to be no solution, having physical reality, which would make g a periodic function of t.

As the most important consequence, however, of the expression for density given by Eq. (34), we can now show that the changes taking place in such a universe on account of the changing value of g are thermodynamically reversible. In accordance with Eq. (34) and the well known relation of Boltz-

mann connecting the density of black-body radiation with its temperature, we can write

$$\rho_{00} = 3Ae^{-2g} = aT_0^4 \tag{36}$$

where a is the Stefan-Boltzmann constant and T_0 is the proper temperature. Solving this for the temperature and substituting in the known expression for the entropy density of black-body radiation, we obtain

$$\phi_0 = \frac{4}{3}aT_0^3 = 4\left(\frac{a}{3}\right)^{1/4} A^{3/4} e^{-3g/2} \tag{37}$$

as an expression for the proper entropy density of our fluid.[14] On the other hand in accordance with Eq. (26) we have

$$dV_0 = \frac{r^2 \sin\theta\, e^{3g/2}}{\sqrt{1 - n^2/R^2}}\, dr d\theta d\phi \tag{38}$$

as an expression for the proper volume associated with the coordinate range $drd\theta d\phi$. Hence combining the two expressions (37) and (38), we can evidently write

$$\frac{\partial}{dt}(\phi_0 dV_0) = 0 \tag{39}$$

since g is the only quantity involved which depends on the time and this is seen to cancel out from the product.

The final result, however, is the very expression which we obtained in Part II (§7, Eq. (18)) as a general condition for a reversible process in relativistic thermodynamics. And since g and hence ϕ_0 will in general be changing in such a universe at a finite rate, we have thus actually illustrated by a specific example the possibility provided by relativistic thermodynamics for reversible processes to take place at a finite rate.

§12. Interpretation by an ordinary observer of phenomena in an expanding universe filled with radiation.

Turning our attention now in particular to the case of expansion, with the radius $Re^{g/2}$ increasing with the time, we can show that the special model of a universe, filled with black-body radiation and expanding reversibly without increase in entropy, would nevertheless exhibit important phenomena which

[14] The relations connecting energy density and entropy density with temperature, used in (36) and (37), presuppose that the frequency distribution of the radiation remains that for black-body radiation for all values of g. This introduces no difficulty, however, since even if there were a tendency for the frequency distribution to change away from that for black-body radiation, as the size of the universe changes, this could be prevented by the introduction of a small amount of material to act as a catalyst; and in actuality there is of course no such tendency since it would involve a decrease in entropy. In addition it can be shown in detail that the dependencies of frequency and energy density on g given by Eqs. (31) and (34) are such as to preserve the black-body distribution of frequency for all values of g, if we have such a distribution for one value of g.

would be interpreted by an ordinary observer as similar to phenomena in the actual universe which have been regarded in the past as important evidence for an increasing entropy of the universe. To obtain a description of these phenomena, we shall consider that the observer in question marks out a small region of the universe in his immediate vicinity, using rigid meter sticks, and then studies the changes taking place in this region. We shall then show that the observer will find the density of energy in this region and the total energy content of the region continually decreasing with the time, its temperature dropping, the number of light quanta leaving the region always greater than the number entering, and the average frequency of the quanta which leave greater than the average frequency of those that enter. Evidently our ordinary unsophisticated observer would interpret these findings as evidence that his immediate neighborhood was cooling off by radiation into the colder depths of space, and with a knowledge only of the classical thermodynamics he would conclude that the entropy of the universe was increasing at an enormous rate, in spite of the fact that the relativistic thermodynamics, which must be used under the circumstances, actually shows that there would be no increase in entropy in such a universe. The analogy between the phenomena interpreted by this unsophisticated observer as leading to an increase of entropy and phenomena in the actual universe which have hitherto been interpreted in a similar manner is close enough so that we must certainly be cautious lest we draw too hasty conclusions as to increases in entropy in our actual universe.

To proceed now to the detailed exposition, let us consider that the observer in our idealized model of the universe is located for convenience at the origin of the r, θ, ϕ system of coordinates and is provided with a rigid scale of proper length dl_0. With the help of this scale he marks out a small sphere around the origin of constant proper radius l_0, which gives him a small region of the universe in his immediate vicinity to serve as the subject of his studies.

For the relation between the constant proper radius of this sphere and the coordinate r of its boundary we may evidently write in accordance with Eq. (24)

$$l_0 = \int_0^r \frac{e^{g/2}dr}{\sqrt{1 - r^2/R^2}} = e^{g/2}R \sin^{-1}\frac{r}{R} \tag{40}$$

and for the case in hand where the sphere considered is very small compared with the whole universe, so that r is small compared with R, we obtain from this the approximate relation

$$r \approx l_0\, e^{-g/2}. \tag{41}$$

Since the proper radius of the sphere l_0 is constant by hypothesis, we note that the coordinate r of its boundary is a quantity which is decreasing with the time in an expanding universe owing to the increase in g with time.

For the proper volume of this sphere contained within the radius l_0 we can evidently write in accordance with Eq. (26)

$$V_0 = \int_0^r \frac{4\pi r^2 e^{3g/2} dr}{\sqrt{1 - r^2/R^2}} = 4\pi e^{3g/2} R \left| -\frac{r}{2}\sqrt{R^2 - r^2} + \frac{R^2}{2} \sin^{-1}\frac{r}{R} \right|_0^r . \tag{42}$$

Developing this in the form of a series in r/R and neglecting higher powers, we obtain

$$V_0 = 4\pi e^{3g/2} R^3 \left(-\frac{1}{2}\frac{r}{R} + \frac{1}{4}\frac{r^3}{R^3} + \frac{1}{16}\frac{r^5}{R^5} + \cdots + \frac{1}{2}\frac{r}{R} + \frac{1}{12}\frac{r^3}{R^3} + \frac{3}{80}\frac{r^5}{R^5} + \cdots \right) \approx \frac{4}{3}\pi r^3 e^{3g/2}. \tag{43}$$

And substituting the value of r given by Eq. (41), we obtain for the proper volume of the sphere in terms of its proper radius l_0, as a close approximation, the result which might be expected

$$V_0 = \frac{4}{3}\pi l_0^3 \tag{44}$$

which is a constant independent of the time.

We may now consider the nature of the observations which our observer would find in studying this sphere of constant measured radius which he has marked off.

As a result of Eq. (34), the proper energy density at every point in our special model of the universe would be changing with the time t in accordance with the expression

$$\frac{1}{\rho_{00}}\frac{d\rho_{00}}{dt} = -2\frac{dg}{dt}. \tag{45}$$

Moreover, the measurements of energy density which our observer would make in his immediate neighborhood would actually be measurements of proper energy density, and from the form of the line element (19) the proper time which he uses would agree with the coordinate time t. Hence it is evident that our observer would find the energy density in his vicinity to be decreasing with the time in accordance with Eq. (45).

Furthermore, in accordance with Eq. (44), the proper volume of his sphere of constant measured radius is itself independent of the time. Hence it is evident that our observer would find the total energy content E_0 of his sphere decreasing at the rate

$$\frac{1}{E_0}\frac{dE_0}{dt} = -2\frac{dg}{dt}. \tag{46}$$

In addition, owing to the relation between energy density and temperature for black-body radiation given by Eq. (36), it is evident that our observer would find the temperature in his vicinity to be dropping at the rate

$$\frac{1}{T_0}\frac{dT_0}{dt} = -\frac{1}{2}\frac{dg}{dt}. \tag{47}$$

Still further, since the total number of light quanta in the universe would be independent of the time, and the proper volume of the universe as a whole would be increasing with the time while the proper volume of the observer's sphere remained constant, it is evident that the observer would find a larger number of light quanta leaving his sphere per second than entering. To calculate this excess we may evidently write for the number of quanta n inside the sphere in terms of the total number of quanta N in the universe

$$n = \frac{\frac{4}{3}\pi l_0^3}{\pi^2 R^3 e^{3g/2}} N \tag{48}$$

where the numerator of the fraction is the proper volume of the sphere as given by Eq. (44) and the denominator is the total proper volume of the universe as given by Eq. (28). And carrying out a logarithmic differentiation of this with respect to the time we obtain

$$\frac{1}{n}\frac{dn}{dt} = -\frac{3}{2}\frac{dg}{dt} \tag{49}$$

which gives the net loss per unit time in the number of quanta within the observer's sphere. The result so obtained, when combined with the rate at which the frequencies of the quanta are decreasing with the time as given by Eq. (31), is just sufficient to account for the rate of decrease in the proper energy of the observer's sphere as given by Eq. (46).

Finally, we may point out a curious circumstance which would reinforce our unsophisticated observer in his interpretation of the above phenomena as radiation into surroundings of lower temperature. Let us suppose that our observer, ever active in his scientific investigations, stations one of his assistants on the boundary of his sphere at the fixed distance l_0 from the origin as measured with rigid meter sticks, and instructs him to observe the average frequency of the light entering and leaving the sphere through its surface. This assistant will not be at rest in the coordinate system r, θ, ϕ, but in accordance with Eq. (41) will have the coordinate velocity

$$\frac{dr}{dt} = -\frac{1}{2} l_0 e^{-g/2}\frac{dg}{dt} = -\frac{1}{2} r \frac{dg}{dt}. \tag{50}$$

Hence, since it is evident that the average frequency of the radiation would be independent of direction for an observer at rest in the coordinate system, this assistant will find the average frequency of the radiation entering the sphere less than that of the radiation leaving the sphere, as a result of the Doppler effect corresponding to the velocity given by Eq. (50).

This completes a considerable chain of evidence which would lead an ordinary observer, unfamiliar with the expansion of the universe, to conclude that the region in his immediate neighborhood was cooling off by radiation into surroundings of lower temperature, in spite of the fact that the changes taking place in the model actually involve no increase in entropy. The analogy

between the findings of this observer in the hypothetical model and those of the classical thermodynamist in the actual universe is very striking.

PART IV. CONCLUSION

§13. Summary.

In the foregoing article an attempt has been made to show the bearing of relativistic thermodynamics on the well-known problem of the entropy of the universe as a whole. The origin of this problem lies in the difficulties encountered by the classical thermodynamics,—first in failing to account for the presumed fact that the entropy of the universe has always been increasing at an enormous rate and nevertheless has not yet reached its maximum value,—and second in failing to allow an emotionally satisfactory feeling towards our universe whose ultimate fate would be the stagnation of "heat-death."

In the present article a brief description was first given of various older contributions to the solution of this problem, which have been based on the standpoints of the classical thermodynamics and statistical mechanics. This was done in order to show the very different character of the new contribution proposed in this article. A summarized account of the nature of this contribution may now be given.

The problem of the entropy of the universe arises because of the commonly accepted conclusion that the entropy of the universe is actually increasing at an enormous rate, and this conclusion is in turn based on the presumption, familiar in classical thermodynamics, that thermodynamic processes cannot be taking place at a finite rate, as observed, and at the same time reversibly without increase in entropy. The general nature of the contribution to the problem offered by relativistic thermodynamics lies in showing that there can be thermodynamic processes which take place both reversibly and at a finite rate.

To illustrate this difference between the classical and relativistic thermodynamics, we may consider the possibility of carrying out a reversible change in the thermodynamic properties of a finite portion of thermodynamic fluid. In the classical mechanics it is found that no internal motions of the fluid, no flow of heat, and no change in volume can be allowed to take place at a finite rate and hence that no change at all in the thermodynamic properties of the fluid can take place at a finite rate, the entropy density of the fluid remaining constant in accordance with the equation

$$\frac{d\phi_0}{dt} = 0.$$

On the other hand, in relativistic thermodynamics it appears possible to allow changes in the proper volume of the fluid, due to changes in the gravitational potentials, to take place at a finite rate and still maintain reversibility. Indeed, the condition for reversibility is found to be satisfied if we have at each point in the fluid the relation

$$\frac{\partial}{\partial x_4}\left(\phi_0\sqrt{-g}\,\frac{dx_4}{ds}\,dx_1dx_2dx_3\right) = \frac{\partial}{\partial x_4}(\phi_0 dV_0) = 0$$

and this permits a finite rate of change in the proper entropy density ϕ_0 with the time x_4, provided it satisfies the equation

$$\left(\sqrt{-g}\,\frac{dx_4}{ds}\right)\frac{\partial\phi_0}{\partial x_4} + \phi_0\frac{\partial}{\partial x_4}\left(\sqrt{-g}\,\frac{dx_4}{ds}\right) = 0.$$

To exhibit the nature of the reversible changes at a finite rate thus permitted in relativistic thermodynamics, we may consider the highly idealized model of a non-static universe filled with black-body radiation as our thermodynamic fluid. It is found that the radius and total proper volume of such a universe could be changing at a finite rate with the time and yet reversibly without increase in entropy.

Furthermore, if we take the case of an expanding universe and consider an observer who marks out with rigid meter sticks a small region of the universe in his vicinity, it can be shown that he would find the energy density, the energy content, and the temperature of this region decreasing with the time, and in addition would find the number of light quanta leaving the region per second greater than the number returning and the average frequency of those passing outward through the boundary greater than that of those returning. He would thus be led to interpret the phenomena taking place in such a universe as a flow of radiation from his immediate neighborhood out into the colder regions of space, in spite of the fact that the changes in the universe would in reality be taking place without any increase in entropy.

The general nature of the contribution to the problem of entropy made in this article has thus been to show that phenomena which have hitherto been regarded from the point of view of classical thermodynamics as furnishing unmistakable evidence for an increasing entropy in the universe are not necessarily leading to any increase in entropy at all, and to emphasize the necessity for analyzing the phenomena of the universe from the more acceptable point of view of relativistic thermodynamics before conclusions are drawn as to what extent the entropy of the universe is increasing if at all.

§14. Critique.

Finally a few words of criticism will not be out of place. The foregoing statement as to the nature of the contribution made in this article carries with it at least the possible implication that an analysis of the phenomena of the actual universe from the standpoint of relativistic thermodynamics would show that there are in reality no important changes at all taking place in the entropy of the universe.

I feel, however, that although the article has clearly demonstrated the necessity of using relativistic thermodynamics in analyzing the entropy changes of the universe as a whole, it would be premature to assert too precisely what is to be expected as the result of such an analysis until it has been applied to a model of the universe which is not so over-simplified as the one

employed in this article. This model of a universe, containing nothing but radiation, neglects two of the most characteristic features of the actual universe, namely the presence of matter and its high degree of concentration into stellar systems. At a later time I hope to give more consideration to these properties of the universe. They appear, however, greatly to increase the mathematical complexity of the problem and for this reason I have contented myself for the present with a very simple model, which can nevertheless give us considerable insight into the problem of the entropy of the universe.

One feature of the model which was mentioned in §11 should perhaps be emphasized, namely that there appear to be no periodic solutions of Eq. (35) for g as a function of t which would have physical interest. Hence if we had an expanding model of the kind considered it would continue to expand, reversibly to be sure, but without actual return to its original condition. Our model is so over-simplified, however, that we must no conclude therefrom that periodic solutions would not be of interest for the actual universe.

Further it should perhaps also be emphasized again that the theory of fluctuations may play an important part in a relatively complete treatment of the entropy of the universe. At the present time, however, we cannot say just how large this part may be.

In conclusion then, it has apparently been definitely demonstrated that the problem of the entropy of the universe as a whole must be treated with the help of relativistic rather than classical thermodynamics, and it has been shown that the application of relativistic thermodynamics to a highly over-simplified model of the universe gives results of great interest. It remains for the future, however, to consider the application of relativistic thermodynamics to more complicated models which would give a better approximation to the actual universe.

ON THE RESOLVING POWER OF A PRISM SPECTROMETER FOR THE INFRARED

By John Strong*
California Institute of Technology, Pasadena

(Received January 15, 1931)

Abstract

The resolving power of a spectrometer in the infrared is limited by the rate at which energy passes through the exit slit of the spectrometer. Calculation of the energy available for activating a thermocouple, under condition that the exit slit embrace the same frequency range $\Delta\nu$ of spectrum at all times, gives information on the attainable resolving power at various wave-lengths and with various prisms. The best dispersing angle for a sylvine prism to be used from 8 to 22μ is from 70° to 75°. A lamellar prism construction is described.

Introduction

IN THE spectral region where a photographic plate, which measures the energy received during the time of exposure, is used, the resolving power of a spectrometer is limited by interference effects. However, in the infrared where a thermocouple or radiometer is used one does not measure the energy received over an arbitrary period of time but the rate at which energy is received. This available energy rather than interference effects places the limit on the resolving power of the spectrometer.

It was the purpose of this investigation to make calculations of the energy available for activating a receiver (such as a thermocouple). The energy of a continuous spectrum passing through the exit slit, with both slits equal, is proportional to the square of the slit width, so that if the value for the available energy at any particular wave-length and for a particular dispersing prism is greater, by a factor α, than the energy necessary to give a definite response of the receiving device, then the spectrometer slits may be closed by a factor $1/\alpha^{1/2}$ and still give a practical deflection. The available energy is therefore a measure of the resolving power which is attainable under varying conditions as long as the limit set by interference effects is not exceeded.

The calculation of available energy is instructive on account of the information that it gives regarding the resolving power attainable in various regions of the spectrum. The determination of the absorption spectrum of a gas in the infrared consists of a study of the heat radiations emitted from some convenient source and the changes in spectral energy distribution which result from the introduction of the gas into the radiation path. The spectrum emitted from a heated body possesses very little energy at long wave-lengths since the emission cannot exceed that from a black body which varies inversely with the fourth power of the wave-length. This scarcity of available

* National Research Fellow.

energy at long wave-lengths would seem to place a serious limitation upon the character of experimental work that might be done at long wave-lengths. However, the results of Robertson and Fox[1] with a rocksalt prism on the oscillation-rotation spectrum of ammonia and similar molecules shows a definite improvement in resolution at the longer wave-lengths. These calculations will show in a quantitative way that similar improvement at long wave-lengths is to be expected for a sylvine prism.

The calculation of available energy for various prisms shows the best prism to use for a particular spectral region. For the entire spectral range for which sylvine is a useful prism material, it is best to have as the dispersing angle of the prism 70 to 75 degrees. Usually a 60° prism is considered best but this is neither obvious nor a consequence of the classical works of Pickering[2] and of Wadsworth.[3] These authors made calculations of the best dimensions for prisms made from materials having values for the refractive index varying between 1.5 and 1.8. Their calculations do not hold because sylvine has refractive indices below 1.5 in the infrared, also the formula used by Pickering and Wadsworth for the transmission of a prism is invalid except when the absorption is very low.

Priliminary Considerations

When a band system in the infrared is plotted with wave number rather than wave-length as the abscissa one gets a more natural picture, since the fineness of structure is then approximately the same throughout the spectrum. On the other hand, if wave-length is used as abscissa, the structure appears coarser at longer wave-lengths and in fact if $\Delta\nu$ is taken as a measure of the fine structure of the band system the corresponding $\Delta\lambda$ becomes greater at longer wave-lengths according to the formula

$$\Delta\lambda = \frac{\lambda^2\Delta\nu}{c}.$$

This means that if the slit of the spectrometer is adjusted so that the wave-length interval in the slit is increased proportionally with λ^2 it will embrace the same frequency range of spectrum. The energy passing through the exit slit is proportional to the spectral energy density of illumination of the slit, E_λ, multiplied by the square of the slit width. For a black body at long wave-lengths E_λ is proportional to λ^{-4} while for an ideal spectrometer having constant dispersion and constant efficiency the slit width, s, would be proportional to λ^2 and $E_\lambda s^2$, the energy passing through the exit slit, would be independent of λ. By constant efficiency it is meant that the same fraction of the energy of various wave-lengths is lost by reflection at the various surfaces in the optical path and by absorption in the prism. This means that the resolving power measured by the rational magnitude $\Delta\nu$ will be the same throughout the spectrum.

[1] R. Robertson and J. J. Fox, Proc. Roy. Soc. **A120,** 128 (1928).
[2] Pickering, Phil. Mag (4), **36,** 39 (1868).
[3] F. L. O. Wadsworth, Astrophys. J. **2,** 264 (1895).

For a spectrometer which is not ideal the energy passing through the exit slit increases as the dispersion increases and decreases as the efficiency decreases. $\delta n/\delta\lambda$ for the materials transparent in the infrared increases at longer wave-lengths while the transparency decreases. The dispersion factor predominates at first and so the available energy (when the slit width is constant as measured by $\Delta\nu$) increases and greater resolving power is attainable at longer wave-lengths. This for sylvine is a result similar to the experimental results of Robertson and Fox. The available energy passes through a maximum and rapidly decreases as the transparency factor becomes predominate. When the dispersing angle of the prism increases the dispersion increases, at first slowly, then rapidly, while the light lost by reflection increases. It was for the purpose of arriving at the best compromise between these varying factors that the following calculations were made.

Energy Available to Activate Receiver

For a simple prism spectrometer the energy, e, passing through the exit slit is given by the following expression

$$e = E_\lambda s_1 l_1 \frac{A}{f_1^2} \frac{s_2}{f_2 \frac{d\theta}{d\lambda}} TFR.$$

The symbols are defined by the following formulas:

E_λ is the spectral energy density of illumination of the entrance slit and for long wave-lengths this is given by the Rayleigh-Jeans formula.

$$E_\lambda = \frac{4\pi kt}{\lambda^4}.$$

s_1 and l_1, are width and length respectively of the entrance slit.

A is the effective area of the collimating mirror of the spectrometer. For a large collimating mirror this is the area of the prism face ($h \times b$ if h is the heighth of prism face and b the length) projected on the plane of the mirror face. If i is the angle of incidence of the light on the prism face, A is defined by the equation $A = h \times b \cos i$.

f_1 and f_2 are the focal lengths respectively of the collimating and telescope mirrors.

s_2 is the width of the exit slit.

$d\theta/d\lambda$ is the dispersion of the prism and it may be broken up into two factors $(\partial\theta/\delta n) \times \partial n/\partial\lambda$. For a prism at minimum deviation $\partial\theta/\partial n$ is given by $2 \sin(\phi/2)/\cos i$ where ϕ is the dispersing angle of the prism. Values of $\partial n/\partial\lambda$ are defined by the empirical formula given by Rubens[4] for the index of refraction of sylvine.

T is the transmission of the prism. This is given by the formula

$$T = \frac{1}{\kappa T}(1 - e^{-\kappa T})$$

[4] Rubens, Ann. d. Physik **54**, 476 (1895); **60**, 724 (1897).

The absorption coefficient is represented by κ and the width of the prism opposite the dispersing angle is represented by τ. For values of $\kappa\tau$ less than 0.1 the values of T are given approximately by the formula used by Pickering and Wadsworth in their work, $T=e^{-\kappa\tau/2}$. For values of $\kappa\tau$ greater than 5 the values of T are given approximately by $1/\kappa\tau$. Table I gives values of T for various values of $\kappa\tau$.

TABLE I.

$\kappa\tau$	T	$\kappa\tau$	T	$\kappa\tau$	T	$\kappa\tau$	T
0.01	0.995	0.11	0.946	0.1	0.952	1	0.632
.02	.989	.12	.943	.2	.906	2	.432
.03	.985	.13	.938	.3	.864	3	.317
.04	.980	.14	.934	.4	.824	4	.245
.05	.975	.15	.929	.5	.787	5	.198
.06	.970	.16	.924	.6	.752	6	.166
.07	.966	.17	.919	.7	.719	7	.143
.08	.961	.18	.915	.8	.688	8	.125
.09	.956	.19	.911	.9	.659	9	.111
.10	.952	.20	.906	1.0	.632	10	.100

F is a factor which takes account of the loss of light due to reflections at the two prism surfaces and is represented by the following formula,

$$F = \left\{\frac{1}{2}\left[1 - \frac{\sin^2(i-r)}{\sin^2(i+r)}\right] + \frac{1}{2}\left[1 - \frac{\tan^2(i-r)}{\tan^2(i+r)}\right]\right\}^2$$

where r is the angle of refraction at the prism face.

R is the total reflectivity of all the spectrometer mirrors and is considered constant. For eight normal reflections from polished silver the loss of light is 8 percent at 10μ and 4 percent at 20μ.

If $f_1=f_2$ and if the spectrometer slits are equal and always adjusted so that the frequency interval they subtend is constant then s_1 and s_2 may be substituted for by the expression

$$s_2 = s_1 = f_1 \frac{d\theta}{d\lambda} \frac{\lambda^2 \Delta\nu_0}{c}$$

where $\Delta\nu_0$ corresponds to the constant frequency interval embraced by the slits.

Substituting in the formula for e gives

$$e = \frac{8\pi k t \Delta\nu_0^2 h b R}{c^2 f_1} TF \frac{\partial n}{\partial\lambda} \sin\frac{\phi}{2}$$

or

$$e \propto \epsilon = TF \frac{\partial n}{\partial\lambda} \sin\frac{\phi}{2}.$$

Values of F for various prism angles, ϕ, and various wave-lengths are given in Table II. For the calculation of ϵ given in Table III, τ was given the value 10 centimeters.

TABLE II. *Values of F for various ϕ and λ.*

ϕ	10.02μ	14.14μ	17.68μ	20.6μ	22.5μ
0°	0.931	0.936	0.942	0.947	0.971
60°	.910	.917	.925	.934	.966
70°	.873	.885	.898	.901	.957
75°	.799	.847	.846	.886	.950
80°	.727	.768	.805	.840	.937
85°	.419	.563	.662	.735	.915
90°	—	—	—	.244	.877

TABLE III. *Values of ϵ for various ϕ and λ.*

ϕ	8.84μ	10.02μ	11.79μ	12.96μ	14.14μ	15.91μ	17.68μ	20.6μ	22.5μ
15°	4.0	4.1	4.3	5.4	6.8	7.4	7.9	6.5	5.1
30°	7.9	9.1	10.8	11.9	12.9	13.5	13.5	8.1	5.4
45°	11.6	13.0	15.8	17.2	18.8	18.4	17.7	8.2	5.6
60°	15.0	17.2	20.3	21.7	23.0	22.1	19.6	8.2	5.6
70°	16.5	18.9	22.4	23.6	24.8	23.6	19.9	8.1	5.5
75°	16.0	18.4	22.2	23.5	25.0	23.5	19.6	8.0	5.4
80°	14.0	17.7	21.2	22.5	23.6	22.7	18.5	7.5	5.4
85°	8.2	10.7	14.6	16.5	18.1	18.9	15.5	5.4	5.2

It would seem impractical to narrow the slits narrower than the frequency interval $\Delta\nu'$ corresponding to the theoretical resolving power of the spectrometer. For a prism spectrometer this is given by the Rayleigh formula.

$$\Delta\nu' = \frac{-c}{\lambda(\partial n/\partial\lambda)\tau}.$$

If the absorption coefficient is high only the apex of the prism will transmit radiation and the value of τ to be substituted in the formula is much less than the actual value of τ. In order to get an idea of how this limiting frequency interval, $\Delta\nu'$, varies as one goes deeper into the infrared it may be calculated using a value corresponding, for that wave-length in question, to a prism having a transmission of 95 percent. The values of $\tau_{T=.95}$ are given in Table IV

TABLE IV. *Values of $\tau_{T=.95}$ and $\Delta\nu'$ for various wave-lengths.*

λ	11.79μ	12.96μ	14.14μ	15.91μ	17.68μ	20.6μ	22.5μ
κ	0.004	0.0175	0.0270	0.065	0.135	0.515	1.00 cm^{-1}
$\tau_{T=.95}$	25	5.72	3.71	1.54	.74	.19	.10 cm
$\Delta\nu'$	.75	2.6	3.4	6.2	9.9	26.4	38.4 cm^{-1}

together with corresponding values of $\Delta\nu'$. It is interesting to compare these limiting frequencies with the resolving power successively realized by Burmeister, Eva von Bahr, Brinsmade and Kemble, Imes and Randall, and Meyer and Bronk in their classical investigations of the fundamental oscillation band of HCl. Their slit widths reduced to the same units used in Table IV are respectively 40, 10, 7, 4 and 3 cm^{-1}.

When only the apex of the prism transmits appreciably and it is not possible to realize the limiting resolving power on account of the insensitivity of

the receiver one may double or quadruple the energy passing through the exit slit by using two or four identical prisms side by side which are tall compared with τ. Such an arrangement is shown in Fig. 1. Since it is much easier to make a plane parallel plate than to make a prism whose faces make a prescribed angle with each other, an alternative arrangement is illustrated by Fig. 2. The back of each parallel plate is silvered by evaporation, the plates

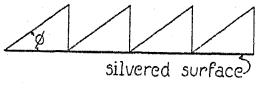

Fig. 1.

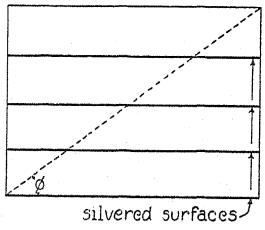

Fig. 2.

are waxed together and the ensemble cut and polished along the dotted line so as to give a lamellar prism with dispersing angle 35° to 37.5°. This will form a Littrow half prism into which the light will not need to penetrate deeper than the thickness of the parallel plates used. It is, however, more advisable to use a prism which is more transparent in the desired spectral region.

Conclusion

From the values of ϵ given in Table III and the values of $\tau_{T=.95}$ and $\Delta\nu'$ given in Table IV, we may draw the following conclusions.

1. A dispersing angle of 70° to 75° is best for a sylvine prism to be used from 8 to 22μ. Table III shows the available energy for these prism angles to be greater for all wave-lengths out to 18μ. Beyond 18μ, there is so little difference in the available energy that the construction of a special 15° prism for this region is not justified.

2. A sylvine prism with a 10 cm base is useful to 18μ. In spite of the fact that the energy for illuminating the entrance slit of the spectrometer decreases with the fourth power of the wave-length, it will be observed from Table III that the energy available for activating a thermocouple increases. This means that the resolving power increases at longer wave-lengths as long as the available energy, rather than interference effects, places the limit on the resolving power of the spectrometer.

3. Values of $\tau_{T=.95}$ in Table IV show that only the apex of the prism transmits radiations. The available energy may be increased several fold by the use of a lamellar prism construction. This should make it possible to realize approximately the theoretical resolving power of one of the lamella. Such a lamellar prism would be particularly useful when the radiations are to be further dispersed with a grating. It is possible that the use of another prism material, such as potassium iodide (transparent to wave-lengths greater than 33μ) would be better. However, since no material is yet known which is more transparent than potassium iodide it may be advisable to use a lamellar

prism of this material in order to extend the region open to prism spectroscopy as far as possible. The optical properties of potassium bromide and potassium iodide are being investigated by the author so that a set of values of ϵ for all the infrared prism materials may be compiled.

4. An examination of the proportionality factor between e and ϵ shows the available energy is inversely proportional to the focal length of the spectrometer collimator. This result indicates that a spectrometer of the Pfund type would give the best resolution.

LETTERS TO THE EDITOR

Prompt publication of brief reports of important discoveries in physics may be secured by addressing them to this department. Closing dates for this department are, for the first issue of the month, the twenty-eighth of the preceding month; for the second issue, the thirteenth of the month. The Board of Editors does not hold itself responsible for the opinions expressed by the correspondents.

The Effect of Meteors on Radio Transmission Through the Kennelly-Heaviside Layer

A consideration of the available data on meteor trains indicates (1) that meteors expend the larger part of their energy in the Kennelly-Heaviside layer,[1] that is, in that region of the upper atmosphere which controls the propagation of all long distance radio waves; (2) that a large fraction of the energy of a meteor goes into ionization of the air around its path;[2,3] (3) that this ionization extends to a considerable distance from the actual path[4]—in some cases, several kilometers or more—and (4) that it lasts for some minutes after the meteor has passed.[4]

It is interesting to calculate the order of magnitude of the ionic concentration which may be produced and to compare it with the concentration which is generally assumed in order to explain short wave radio phenomena. Meteors are believed to vary in mass from a few milligrams to several kilograms and larger, according to different estimators. If the mass of a meteor is taken as one gram, its velocity as 40 km/sec., its length of path as 200 km and the range of ionization around the path as 1/2 km, the concentration of ionization on the above assumptions would be of the order of 10^6 ions per cc. The maximum ionization deduced from radio data is of the order of 10^5 electrons per cc. It is therefore apparent that transmission of radio signals might be markedly affected by the presence of meteors along the path.

Data taken during radio measurements of the heights of the ionized layer, furnish evidence for such an effect. Thus Heising[5] finds that the deflecting layer seems to experience very sudden drops as though a large amount of ionization suddenly appeared, accompanied for a moment by turbulence, after which the layer gradually returns to the normal height. The frequency of such sudden variations is reasonably consistent with the number which would be expected for the particular length of path used, on the assumption of 10^9 meteors of random direction per day for the whole earth.[6]

The orbital motion of the earth increases the relative velocity of the meteors which are observed after midnight and it is an observed fact that the number of meteors has a maximum between 2:00 and 3:00 A.M. Both of these facts would increase the contribution of ionization which is due to meteors and might even result in a lowering of the Kennelly-Heaviside layer after midnight. A number of investigators have observed such a drop after midnight. Moreover, on the basis of the above calculations and assuming that the ions produced have an average life of one hour, the total ionization produced by meteors is of the correct order of magnitude to produce the effect observed.

The foregoing evidence, while admittedly sketchy, indicates that the ionizing effect of meteors in the Kennelly-Heaviside regions may be an important factor in short wave radio propagation through the upper atmosphere. It is planned to make tests during future meteoric showers in order to obtain further information on the subject.

A. M. SKELLETT
Bell Telephone Laboratories, Inc.,
New York, New York,
April 7, 1931.

[1] Humphrey, Physics of the Air, p. 23.
[2] Lindeman and Dobson, Proc. Roy. Soc. of London, **A411**, 102 (1923).
[3] Maris, Terrest. Mag. and Atmos. Elect. **34**, 309 (1929).
[4] Olivier, Meteors, p. 147.
[5] Heising, Proc. I.R.E. **16**, 75, (1928).
[6] Shapley, Harv. Circ. No. 317, May, 1928.

Raman Spectrum of the Hydroxyl Ion with High Dispersion

The Raman spectrum of a $10N$ aqueous solution of potassium hydroxide was photographed with a Hilger E1 large quartz spectrograph, using for excitation a hot-cathode helium arc of length 45 cm. The Pyrex tube which contained the solution was surrounded by a filter tube of nickel oxide glass, and the light was focused on it by an elliptical reflector. An exposure time of 100 hours was required.

The spectrum obtained consists of a single broad line having a fairly well defined intensity-maximum which corresponds to a frequency shift of 3603 ± 4 cm^{-1}. This is in good agreement with the value of 3615 ± 25 cm^{-1} recently reported by Woodward.[1] It is somewhat lower than the shift of 3630 cm^{-1} found by Krishnamurti[2] in crystalline sodium hydroxide. The line has a width of about 30 cm^{-1}. That it must be attributed to the hydroxyl ion is beyond doubt.

It was observed that the presence of dissolved sodium or potassium hydroxide greatly influences the structure and the intensity of the water band. We have studied this effect in solutions of various concentrations, using a spectrograph of smaller dispersion. The results will soon be reported in detail.

J. L. THOMPSON
J. RUD NIELSEN
University of Oklahoma,
May 27, 1931.

[1] L. A. Woodward, Phys. Zeits. **32**, 261 (1931).

[2] P. Krishnamurti, Indian J. Physics **5**, 651 (1930).

The Relative Abundance of the Oxygen Isotopes, and the Basis of the Atomic Weight System

Mecke and Childs,[1] as the result of a detailed quantitative investigation of the A and A' bands of oxygen, find the relative abundance of the oxygen isotopes O^{16} and O^{18} to be 630:1, in sharp contrast to the value 1250:1 found by Babcock[2] and 1075:1 found by Naudé.[3] We have made a careful study of Mecke and Childs' paper, and find several rather doubtful theoretical assumptions. We have accordingly recalculated a portion of their data, using a method that appears to us to be more reliable. Their final result is, however, not essentially changed, and it therefore seems unnecessary to publish the details.

We have also examined Babcock's assumptions, and find two sources of possible error, one due to the fact that the rotational energy levels of the $O^{16}.O^{18}$ molecule differ from those of the $O^{16}.O^{16}$ molecule, and the other due to the fact that, in Babcock's work, the mean temperature of the $O^{16}.O^{18}$ molecule (in the atmosphere) differs from the temperature of the $O^{16} \cdot O^{16}$ molecule (in the laboratory). Both the energy and the temperature affect the Boltzmann factor, but fortunately the two errors thus introduced by Babcock's neglect of this factor tend to cancel. We find that for the lines used by Babcock,[4] the maximum resulting error is not more than about ten percent, and so is quite negligible.

Mecke and Childs suggest several possible sources of error in the work of Naudé, but we do not have the information necessary in order to discuss these suggestions. As far as the work of Babcock and of Mecke and Childs is concerned, it would appear that the discrepancy must be due mainly to experimental and not to theoretical errors. It would also appear that the Mecke and Childs result is entitled to much greater weight.

Assuming for the sake of argument that the abundance ratio is really 630 to 1, it follows, as noted by Mecke and Childs, that atomic masses based on $O^{16}=16$ should be 2.2 parts in 10^4 greater than those based on the chemical system $O=16$. It is accordingly of importance to test Aston's mass-spectrograph results[5] on this new basis. Aston,[6] Birge,[7] and Naudé[3] have previously considered this mat-

[1] R. Mecke and W. H. J. Childs, Zeits. f. Physik **68**, 362 (1931).

[2] H. D. Babcock, Proc. Nat. Acad. Sci. **15**, 471 (1929).

[3] S. M. Naudé, Phys. Rev. **36**, 333 (1930).

[4] According to a personal communication from Babcock, only the first few lines of the P branch were used.

[5] F. W. Aston, Proc. Roy. Soc. **A115**, 487 (1927).

[6] F. W. Aston, Nature **123**, 488 (1929).

ter, but the conclusions depend markedly on the values adopted for the chemical atomic weights. One of us[7] has already found that the rounded values ordinarily published in atomic-weight tables are not sufficiently accurate for a discussion like this.

Nearly all of Aston's precision measurements are concerned, unfortunately, with elements that are known to consist of a mixture of isotopes. In such cases it is necessary to know the relative abundance of the isotopes of the element in question, as well as of oxygen, in order to compare Aston's result with the chemical atomic weight. For elements like carbon and nitrogen, the two resulting corrections (for oxygen, and for the element in question) tend to cancel, so that Aston's result should agree closely with the chemical atomic weight. Thus in the case of carbon the most probable atomic weight[7] is 12.0025. Aston's mass C^{12} is 12.0036, which becomes 12.0010 on division by 1.00022 in order to reduce to the chemical scale. Then to obtain an atomic weight of 12.0025, the relative abundance C^{12}/C^{13} should be 650. King and Birge[8] give 400 for this figure, but their discussion shows that 650 is an equally possible value.

The best atomic weight of nitrogen[9] is 14.008. Aston finds $N^{14}=14.008$. To bring the two results into agreement requires a relative abundance $N^{14}/N^{15}=320$. Naudé found that the abundance $N^{14}/N^{15}=0.65$ of O^{16}/O^{18}. Using Mecke and Childs' value of O^{16}/O^{18}, one obtains $N^{14}/N^{15}=409$, a very satisfactory agreement.

The best atomic weight of helium appears to be[7] 4.0018. Aston obtained 4.00216, or 4.00127 on the chemical scale. The discrepancy is only 1.1 parts in 10^4, which is within the published limits of error. The most accurate atomic weight of fluorine is due to Moles and Batuecas[10], from the molecular weight of FCH_3. Using the present best values for C and H, their result is 18.995 ± 0.005. Aston obtains 19.000, or 18.996 when reduced to the chemical scale. The agreement is entirely satisfactory. In the case of iodine, Aston's result is identical with the best chemical value. The connection with oxygen, in the mass-spectrograph work, is rather indirect, and it is therefore doubtful if this result can be considered to furnish independent evidence on the question. In the case of phosphorus it is the chemical value that is uncertain.

Of the elements that permit an accurate comparison of the chemical and mass-spectrograph results, there remains only hydrogen. The chemical value[7] is 1.00777 ± 0.00002 (probable error), as compared with Aston's 1.00778 ± 0.00015 (*limit* of error). Aston's value, reduced to the chemical scale, is 1.00756 and the discrepancy appears to be outside the limits of error. It could be removed by postulating the existence of an isotope of hydrogen of mass 2, with a relative abundance $H^1/H^2=4500$. It should be possible, although difficult, to detect such an isotope by means of band spectra.

The above discussion shows that, with the exception of hydrogen, the new Mecke and Childs' abundance ratio gives a satisfactory agreement between the mass-spectrograph and the chemical results. The agreement is in fact somewhat better than that obtained with an assumed abundance ratio of 1250 to 1, or of 1070 to 1. The case of hydrogen, however, distinctly calls for further investigation.

Aston[11] has asked for suggestions as to the best basis for chemical atomic weights and atomic masses. We believe that the facts presented in this letter indicate that, from the experimental standpoint, the quantitative relation between the *mean* atomic weight of oxygen, and the mass of the atomic species O^{16} is rather uncertain at the present time, and is likely to remain so for the present. It should also be pointed out that there is as yet no *proof* that the relative abundance of the oxygen isotopes, in different sources, is strictly constant.[12] The possibility that the relative abundance is *not* constant is the most compelling argument for a change in the basis of the atomic-weight system. What that change should be can best be decided by chemists, but we believe that further data are needed before any change is seriously considered. The one point we wish to emphasize here is that there

[7] R. T. Birge, Phys. Rev. Supplement **1**, 1 (1929). See pp. 19–26 and 69.

[8] A. S. King and R. T. Birge, Astrophys. J. **72**, 19 (1930).

[9] G. P. Baxter and C. H. Greene, J. Am. Chem. Soc. **53**, 604 (1931).

[10] E. Moles and T. Batuecas, J. Chim. Phys. **17**, 539 (1919).

[11] F. W. Aston, Nature **126**, 953 (1930).

[12] The mass-spectrograph is perhaps the most reliable method for investigating this question.

now exist two systems for the measurement of atomic masses, connected by a relatively *uncertain* factor. For that reason it seems best, for the present, not to convert results obtained on one system into the other system, by the use of some assumed conversion factor.

R. T. BIRGE
D. H. MENZEL
University of California,
May 27, 1931.

The Masses of O^{17}

The writers have recently built a new accurate apparatus, in order to obtain, among other values, more exact masses for the nucleus of O^{17}, since they had concluded that additional data were needed in order to establish definite relations. Urey,[1] however, considers that the data already available demonstrate the existence of three quantum states for this nucleus.

The purpose of this letter is (1) to give, as a minor change, a different set of values for the ranges of the protons; (2) what is more important, to point out that while we do not disagree with Urey's conclusion above, it seems to us that the few available data should be classified in a slightly different way; (3) and to add a calculation, omitted by Urey, of an inelastic collision between an α-particle and a nitrogen atom as obtained by Harkins and Shadduck.[2]

The data given in this paper lead to the following calculated values:

TABLE I.

M_0 (nucleus)	M_0 (atom)	$\Delta M_1 \times 10^5$	$\Delta M_2 \times 10^5$
16.99891	17.00328	1	12

Here M_0 represents the rest mass of the oxygen, ΔM_1 is the error of M_0 introduced by a 1 percent error in the energy of the α-particle, and ΔM_2 that due to an error of 10′ in the angle ω between the track of the α-particle and that of the oxygen nucleus. In the calculation, the value 14.00800 (Aston) is taken as the rest mass of the nitrogen atom, as was presumably done also by Urey. The values are collected as follows:

TABLE II. *Mass of O^{17}.*

Track	M_0 (atom)		Average M_0 (atom)	
B4	17.00508	High level	17.00508	
				0.00189
B5	17.00330			
H+S 1	17.00328	Middle level	17.00319	
B3	17.00300			
				0.00171
B2	17.00148	Low level	17.00148	

The values differ somewhat from those of Urey, who omits track H+S 1.

We have excluded from this table the calculated values for the following four tracks as not having a sufficient bearing upon the division into the above three groups.

TABLE III.

Track	M_0 (atom)	Reason for rejection from Table II
H+S 3	17.0050	Agrees well with the value 17.00508 for the B4 track, but one of the pair of photographs of the event was not clear
B7	17.00402	Tracks curved (rejected by Urey)
B6	17.00293	Angle ω too small to give accuracy in M_0
B1	17.00370	Probably as accurate as those listed in Table II, but deviates too far from mean of other three in middle level to offer evidence in favor of the existence of this level

[1] Urey, Phys. Rev. (2) **37**, 923 (1931).

[2] Harkins and Shadduck, Proc. Nat. Acad. Sci. **12**, 707 (1926).

Thus, according to our classification,

(1) the lowest level is represented by only one value,

(2) the middle level by three values, and

(3) the high level by only one value.

The ranges of the protons emitted are given in Table IV. Urey assumes that the range varies as the cube of the initial velocity, but a closer approximation is probably given by use of the 3.5 power, as is done by Chadwick, Constable and Pollard.[3] On this basis, the ranges in cm at 15° and 760 mm are:

TABLE IV.

B4	B6	H+S 1	B3	B5	B1	B7	B2
17.3	18.8	20.4	25.0	25.0	31.9	38.6	59.7

Except for the highest values, this change of power does not give a great increase of range.

It may be noted that the values of ω, the angle between the extension of the track of the α-particle and that of the oxygen nucleus, is always small. The observed values are:

TABLE V.

B6	H+S 1	B4	B7	B3	B1	B5	B2
7° 54′	15° 21′	19° 24′	21°	21° 13′	22° 0′	22° 12′	28° 51′

This angle is always small because (1) the initial velocity of the proton is limited, (2) the mass of the oxygen is relatively high, and (3) no disintegration has as yet been observed with certainty by the photographic method were the velocity of the α-particle at impact is less than 1.83×10^9 cm per sec.

Some additional evidence for the validity of the three levels in the O^{17} nucleus seems to be given by the fact that the differences between the average masses are moderately nearly equal, as shown in Table II by the values 0.00189 and 0.00171. However, additional experimental evidence is needed for the definite determination of the energy levels.

WILLIAM D. HARKINS
DAVID M. GANS
University of Chicago,
May 21, 1931.

[3] Chadwick, Constable and Pollard, Proc. Roy. Soc. **A130**, 477 (1931).

The Electrical State of the Sun. A Correction

Dr. H. B. Maris of this laboratory has kindly brought to my attention an error in the above entitled paper (Phys. Rev. **37**, 983 (1931)) which effectively nullifies the paragraph containing arguments and calculations purporting to show that the sun is electrically neutral. In Eq. (3), Q represents the free electrical charge per unit length of the equivalent circuit rather than the total free electrical charge. On making the correction we find that, although other evidence indicates that the sun is electrically neutral, our magnetic calculation, alone, is quite incapable of establishing that fact.

The corrected calculated value of the galactic magnetic field according to Anderson's hypothesis of the annihilation of positive electrical charge is still so large (10^3 gauss) as to be impossible and our original conclusion is therefore unchanged. The incorrect assignment of the value of Q did not affect the detailed calculations in other sections of the paper.

ROSS GUNN
Naval Research Laboratory,
Bellevue, Anacostia, D. C.,
May 25, 1931.

ERRATA

RADIATION OF MULTIPOLES

By Karl F. Herzfeld
Department of Physics, The Johns Hopkins University

(Phys. Rev. **37**, 253, 1931)

In a paper which appeared under this title there are unfortunately some mistakes, the correct formulas are given below:

On page 256 the following formula (9)

$$\psi = \sum c_k \psi_k e^{-2\pi i k\nu t} \qquad \psi_k = e^{-\zeta^2/2} H_k(\zeta) b_k$$

Same page, before formula (10)

$$b_k = \left(2^{-k}\frac{1}{k!}\left(\frac{4\pi M\nu}{h}\right)^{1/2}\right)^{1/2}.$$

Instead of formula (16) on page 258

$$a_i^{(k)} = \frac{k!}{i!}\, 2^i (-1)^{(k-i)/2} \frac{1}{\left(\frac{k-i}{2}\right)!}, \text{ for } k-i \text{ even.} \tag{16}$$

At the bottom of page 258 and on top of 259.

$$\begin{aligned} I_{k,s}^{(n)} &= 0 \text{ if } s-n \text{ odd} \\ &= \pi^{1/2} \sum_{j=0}^{(n-s)/2} \frac{(4j)!}{2^{4j}(2j)!}(2j+k+s)\cdots(2j+1) \\ &\qquad (-1)^{j+(s-n)/2} 2^{2j+k+s-n} k! \frac{1}{\left(\frac{n-s}{2}-j\right)!} \frac{1}{(2j+k+s-n)!} \\ &= \pi^{1/2}(-1)^{(s-n)/2} 2^{k+s-n} k! \sum_{j=0}^{q} (-1)^j \frac{(4j)!}{(2j)!^2} \frac{1}{4^j} (2j+k+s)! \\ &\qquad \times \frac{1}{(q-j)!} \frac{1}{(2j+k-q)!} \end{aligned} \tag{17}$$

with $n-s=2q$.

Finally for the formulas which occur in the middle of page 259

$$I_{k,2}^{(2)} = (\pi)^{1/2} 2^k k! \frac{(k+2)!}{(k!)} = (\pi)^{1/2} 2^k (k+2)!$$

If $n=3$ (tetraeder) there are possible two transitions

$s=1$, frequency ν

$$\begin{aligned} I_{k,1}^{(3)} &= -(\pi)^{1/2} 2^{k-2} k! \left\{\frac{(k+1)!}{(k-1)!} - \frac{4!}{(2!)^2}\frac{1}{4}\frac{(k+3)!}{(k+1)!}\right\} \\ &= +(\pi)^{1/2} 2^{k-2} \left\{\frac{3}{2}(k+2)(k+3) - k(k+1)\right\} k! \end{aligned}$$

$s=3$ frequency 3ν

$$I_{k,3}^{(3)} = (\pi)^{1/2} 2^k \frac{k!(k+3)!}{k!} = (\pi)^{1/2}(k+3)!\, 2^k.$$

In general, we have for $s=n$, frequency $n\nu$

$$I_{kn}^{(n)} = (\pi)^{1/2} 2^k \frac{k!(k+s)!}{k!} = (\pi)^{1/2} 2^k (k+j)! \tag{18}$$

HYPERFINE STRUCTURE IN IONIZED BISMUTH

By Russell A. Fisher and S. Goudsmit
Department of Physics, University of Michigan

(Phys. Rev. **37**, 1057, 1931)

The photograph of the hyperfine structure of Bi II 4705 (Fig. 2b) was unfortunately inverted. The complete Fig. 2 should appear as follows:

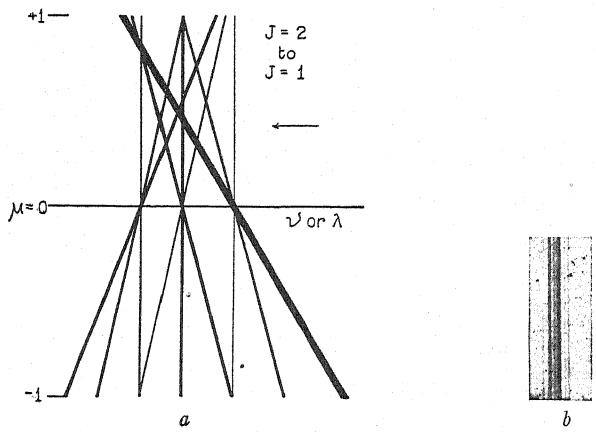

Fig. 2. Diagram for transition $J=2$ to $J=1$ compared with Bi II λ4705. $\mu=+0.457$, tota $\Delta\nu=2.71$ cm^{-1}. The arrow indicates where the line pattern fits the diagram.

THE SCATTERING OF UNPOLARIZED X-RAYS

By G. E. M. Jauncey and G. G. Harvey
Washington University, St. Louis, Missouri

(Phys. Rev. **37**, 698, 1931)

The denominator of the right side of Eq. (12) should be raised to the fourth power. The corrected equation is

$$I_{unm}=4I_e/(1+0.022x^2)^4 \qquad (12)$$

SURFACE TENSION OF MERCURY

By Marie Kernaghan
Department of Physics, The Saint Louis University

(Phys. Rev. **37**, 990, 1931)

The ordinate of Fig. 3 should read "Surface tension (dynes) Corrected values".

BOOK REVIEWS

Veröffentlichungen Des Wissenschaftlichen Zentral-Laboratoriums der Photographischen Abteilung-Agfa- Band I. Pp. 155, figs. 94. S. Hirzel, Leipzig, 1930. Price RM10.

The photographic division (Agfa) of the I. G. Farben industrie has inaugurated an annual publication in which the results of technical and theoretical photographic investigations of that laboratory are gathered together. In general each volume will consist both of articles which have appeared in other places and of some which have not been previously published. The annual should prove a great benefit to the photographic research world by helping to keep important photographic knowledge collected.

The first volume contains an article on the existing theories of the latent image, several papers on sensitometry with special reference to color sensitivity, an announcement of new sensitizers for the extreme red and infrared photography. An article on the testing of sound film is particularly good in that clear and complete picture of the physical problems involved in photographic sound recording is given. Articles on x-ray photography and on cellulose and its derivatives complete the volume. M. E. RUSSELL

Molecular Spectra in Gases. Report of the Committee on Radiation in Gases and Bulletin 57 of the National Research Council. E. C. KEMBLE, R. T. BIRGE, W. F. COLBY, F. W. LOOMIS, L. PAGE. Second printing 1930. Pp. 366. Price $3.50 (paper binding).

This bulletin originally issued in December 1926 has been reprinted with minor corrections and the addition of an index. Separate copies of the index are available for distribution.
E. C. KEMBLE

An Outline of Wave Mechanics. N. F. MOTT. Pp. 156, figs. 21. The Macmillan Company, New York, 1930. Price $2.80.

New sciences are complicated when they start, and grow simpler as we understand them better. Wave mechanics is no exception. The first papers, the first books, on the subject were mathematics and not much else. But now, with increased understanding, it is possible to dispense with more and more of the detail, and yet to become continually clearer and more comprehensible. Mott's admirable little book is an excellent illustration of this tendency. To the reviewer it seems singularly successful in its attempt to present enough detail to enable the principles of the subject to be accurately understood, and yet not enough to burden the reader. After reading it, one does not have the too common feeling that it could not be understood except by one who knew the whole subject beforehand.

It should not be supposed that Mott's book is intended for the general reader. It is distinctly for physicists, advanced students and research workers. It presupposes a considerable background of physics and mathematics. But it can honestly be recommended, for example, to the experimental physicists who want some idea of wave mechanics. The examples and illustrations are of a physical sort, and of a remarkable variety for such a small book. Particularly good, as one would expect from Mott's research, are the sections on collisions, scattering and such problems. Questions of stationary states, of atomic and molecular structure, are treated, but not in any great detail, as must be obvious from the small compass of the book. No problems, of course, are carried through in a complete manner, and yet one feels that the fundamentals are so adequately presented that the reader will be set thinking along the right line. As an elementary and readable account of wave mechanics, the reviewer feels that the book can be highly recommended. An idea of the actual contents can be obtained from the chapter headings: Waves and Particles, The Wave Equation, Group Velocity and the Uncertainty Principle, The Theory of Stationary State, The Absorption of Radiation, The Helium Atom and the Hydrogen Molecule, Dynamics of Systems containing many Electrons, The Spin of the Electron and the Exclusion Principle. J. C. SLATER

Principles of Electrical Engineering (Second Edition). W. H. TIMBIE AND V. BUSH. Pp. 595, figs. 270. John Wiley and Sons, New York, 1930. Price $4.50.

We regret that in the review of this book which appeared in the May 15 issue of this journal, page 1374, the name of the publisher was erroneously given.

PROCEEDINGS

OF THE

AMERICAN PHYSICAL SOCIETY

MINUTES OF THE WASHINGTON MEETING, APRIL 30, MAY 1 AND 2, 1931

The 170th regular meeting of the American Physical Society was held in Washington, D.C., at the Bureau of Standards on Thursday and Friday, April 30 and May 1, and at the National Academy of Sciences on Saturday, May 2, 1931. The first session began at ten o'clock on Thursday morning. The presiding officers were W. F. G. Swann, President of the Society, Paul D. Foote, Vice-president, Joseph A. Becker, Lyman J. Briggs, Arthur H. Compton, Karl K. Darrow, Henry G. Gale, Enoch Karrer and L. P. Sieg. At the Bureau of Standards on the first and second days of the meeting the registration was 388. A fair estimate of the total attendance at the sessions was between four and five hundred.

On Thursday afternoon the Society omitted its regular sessions from one-thirty to three-thirty o'clock to meet with the newly formed American Association of Physics Teachers. At this session Dr. A. W. Hull of the General Electric Company presented an invited address on "Qualifications of a Research Physicist."

On Thursday evening a public forum was called at the National Academy Building to discuss methods of promoting interest in all branches of physics. This meeting was called by L. W. McKeehan, chairman of the Committee on Sections and was presided over by F. K. Richtmyer.

On Friday evening the Society held a dinner at the Hotel Washington. The President presided at this dinner and the after-dinner speakers were George K. Burgess, Arthur H. Compton, Charles Darwin and F. Henning. R. H. Fowler was also a guest of the Society at the speakers table. The attendance at this dinner was 243.

On Saturday afternoon at the National Academy Building there was held a special colloid program. The papers at this session were invited. The presiding officer of this meeting was Enoch Karrer of the B. F. Goodrich Company.

Meeting of the Council. At its meeting held on Thursday, April 30, 1931, sixteen persons were transferred from membership to fellowship and thirty-seven were elected to membership. *Transferred from Membership to Fellowship:* James H. Bartlett, Jr., David G. Bourgin, V. L. Chrisler, S. Goudsmit, Robert J. Havighurst, Paul Kirkpatrick, W. W. Nicholas, Linus Pauling, Shirley L. Quimby, Richard Ruedy, A. G. Shenstone, Ernest C. G. Stückelberg, George E. Uhlenbeck, N. H. Williams, Mark W. Zemansky and R. V. Zumstein. *Elected to Membership:* Edward B. Baker, M. C. Banca, William E. Berkey, Margaret F. Blackford, Robert L. Boyer, Percy H. Carr, Nickola

Chako, Thomas A. Elkins, David W. Epstein, Richard Evans, O. Rex Ford, Gladys M. Francis, Garret A. Hobart 3rd, Cleveland B. Hollabaugh, Howard B. Holroyd, Jun Koana, C. M. Lewis, Walter G. Marburger, A. T. McPherson, Paul C. Mitchell, George C. Munro, Robert J. K. Murray, Leon S. Nergaard, Paul A. Northrop, Syoten Oka, Allan E. Parker, Clifford M. Potter, Norman A. Shepard, William B. Shockley, Leland B. Snoddy, Daniel S. Stevens, G. R. Tatum, Sigeo Uneno, Forrest Western, John A. Wheeler, E. P. Wigner and Robert L. Womer.

The regular scientific program of the Society consisted of 163 papers, numbers 11, 25, 34, 40, 44, 47, 48, 49, 50, 68, 71, 95, 108, 120, 127, 131, 144, 152, 153, 155, 157, 158 and 163 were read by title. The abstracts of these papers are given in the following pages. An **Author Index** will be found at the end.

W. L. SEVERINGHAUS, *Secretary*

1. Dissociation of water vapor in electrical discharge. ERNEST G. LINDER, *Cornell University.*—By use of Townsend's ionization equation and Aston's result for the potential distribution in the Crookes dark space, the number of electrons produced at each point in the dark space can be obtained. From this, may be calculated the total energy of all the electrons generated by each primary electron, i.e., $\int_0^S (V_1 - V)dn$, where S = length of dark space, V_1 = cathode potential drop, V = space potential, n = number of electrons. Using experimental values of S and V_1 and Townsend's constants, it is thus found that for discharge currents of 1–25 m.a. the average energy per electron runs from 53.8 to 79.2 volts, these values being from 17.8 to 14 3 percent of the corresponding total cathode drop energies The amount of dissociation in the dark space and negative glow for the above currents is from 4.78 to 5.90 molecules of water per electron, which gives an almost constant value of 11 volts per dissociation. The results suggest that dissociation is due to excitation of the molecule. Probe measurements in the positive column give an electron density of 7.4×10^7 electrons per cm^3, and a mean energy of 3.71 volts. If a probability of dissociation by electron impact equal to 0.0024 be assumed, the dissociation in the positive column can be accounted for.

2. The electro-optical shutter and spark breakdown. FRANK G. DUNNINGTON, *University of California. (Introduced by Ernest O. Lawrence).*—The use of the electro-optical shutter in investigations of rapidly varying phenomena necessitates knowledge regarding its manner of functioning and limitations. Using a typical experimental set-up as an example, theoretical cut-off curves have been calculated: 1st, assuming an instantaneous drop of the controlling voltage (i.e. spark gap), and 2nd, assuming the controlling voltage decays according to a definite law. These indicate an effective cut-off time (90% to 10% transmission) of from 2.5 to 4×10^{-9} sec. and a total lag of 4 to 9×10^{-9} sec. Experimental results show a complete change in the appearance of the spark in 5×10^{-9} sec., thus indicating an effective cut-off time somewhat less than this value. Other results set a lower limit on the total lag of about 7×10^{-9} sec. The effective working of the shutter is dependent on the following major factors: (1) purity of nitrobenzene used in Kerr cell; (2) resistance of leads to cell; (3) voltage applied; (4) capacity of cell; (5) steepness of voltage wave used to control shutter. Contrary to previous beliefs, theory and experiment show the best control voltage is only slightly under that giving 100% transmission. A graphical survey giving the step by step development of the breakdown of a gap in an initially homogeneous field has been made for pressures from 20 to 76 cm and gap lengths from 1 to 10 mm.

3. The effect of pressure on the rate of fall of potential in condensed discharges. J. C. STREET AND J. W. BEAMS, *University of Virginia.*—The experimental method was essentially the same as one recently described (Street, Bulletin American Phys. Soc. Feb. 1931) and somewhat similar to Toepler's (Archiv für Elektrot. **14**, 305, 1925) though different in important essentials. Electrical impulses produced by the discharge under investigation traveled along two

parallel symmetrical lead wires to their open ends where they were reflected. The maximum potential across the two ends when measured as a function of the length of lead wires gave a curve from which the rate of fall of potential across the discharge was determined. Our results show that in the first part of the breakdown the resistance can best be represented as a function which decreases exponentially with time. When the potential was very slowly applied (static breakdown) the following are some of the results obtained for the decrease of potential with time:

Pressure in cm of Hg	Time of fall from 100 to 20%
38	4.7×10^{-8} sec.
54	2.5
75	1.7
95	1.1
115	.8
139	.8

The results are in general accord with the calculations of Schilling (Archiv für Elektrot. 25, 97, 1931). Incidentally they indicate how to obtain a maximum rate of discharge for Kerr cells and illustrate how they are damped when used with short leads.

4. On the formation of an arc or spark on interrupting an electric circuit. THOMAS J. KILLIAN, *Massachusetts Institute of Technology.*—There seem to be two possible sources of the spark or arc which results when a physical circuit, carrying unidirectional current, is opened. J. Slepian (J.A.I.E.E., Oct., 1926) has suggested that the initial ionization is due to the temperature rise of the last contact point of the separating electrodes. At high breaking speeds this theory is subject to certain theoretical and experimental difficulties. If no conduction current flows immediately after the contacts are opened the charging current will cause the potential difference and the electric intensity between the contacts to increase. It is shown that the electric field may attain 10^6 to 10^7 volts cm^{-1} at which values "field" currents may flow. When the potential difference between the electrodes is such that the electrons, which have been drawn from the metal by these intense fields, may produce ionization an arc or spark results. An analysis of oscillograms taken at various current densities and opening speeds seems to show that this mechanism may initiate the discharge. This may indicate a method of studying "field" currents at high densities which until now have only been studied at extremely low densities.

5. Vacuum spark discharge. L. B. SNODDY, *General Electric Co.* (*Introduced by A. W. Hull.*)—Impulsive breakdown between pure copper electrodes in high vacuum has been investigated by means of the cathode ray oscillograph and the rotating mirror. (See J. W. Beams, Review of Scientific Inst. **1**, 667, 1930). The mirror photographs of the discharge show a luminous spot at the anode lasting from 1 to 4×10^{-7} sec. and luminosity at the cathode starting slightly later (1 to 2×10^{-7} sec.) than that at the anode and continuing throughout the discharge. The anode does not remain luminous unless the current is very large. The breakdown has two stages; the first a pure electron discharge, lasting less than 5×10^{-7} sec., followed by a low voltage copper vapor arc. The volt-ampere characteristic of the high voltage stage follows the well known law for auto-electronic emission. From the volt-ampere curves the area of emission at the cathode can be computed (Stern, Gossling and Fowler, Proc. Royal. Soc. **124**, 699, 1929). For two gaps investigated the areas were approximately 3×10^{-3} $\overline{cm}^2$ and 1×10^{-5} $\overline{cm}^2$. Using these areas and the rate of potential rise as determined by the oscillograph it is shown that in each case the anode spot at the time of breakdown reaches a temperature of approximately 2600°C. Photomicrographs of the anode show craters of area agreeing well with the computed areas. Current densities, determined from the circuit constants and measured areas of the cathode craters, range from 10^8 amps/$\overline{cm}^2$, at 5×10^{-7} sec. after breakdown, to 8×10^3 amp/$\overline{cm}^2$, at which value the arc goes out.

6. On the temperature of cathode in vacuum arc. R. TANBERG AND W. E. BERKEY, *Westinghouse Elec. & Mfg. Co., East Pittsburgh. (Introduced by Thomas Spooner.)*—Pyrometric and spectroscopic tests show that the metal cathode spot in a vacuum arc is not at an extremely high temperature. The temperature of a copper cathode is measured by an optical pyrometer and found to be about 3000°K in a 20 ampere arc. Spectroscopic examination of the cathode spot shows only a faint continuous spectrum indicating that the temperature of the cathode is not high. A temperature of the above magnitude is shown to be sufficient to give the rate of vaporization required under extreme assumptions. The results show that the high speed of the vapor stream issuing from the cathode region cannot be due to high temperature of the cathode itself.

7. The cathode fall of an arc. R. C. MASON, *Westinghouse Elec. & Mfg. Co., East Pittsburgh.*—To explain the mechanism of a mercury-pool arc, in which the cathode is at a relatively low temperature, Langmuir has suggested that electrons are extracted from the cathode by a very high field. Presumably, the same theory will apply to all arcs in which the cathode is not hot enough for appreciable thermionic emission. An analysis is presented in this paper showing that, under the same conditions, an arc in which the high field is operative should have a cathode fall several volts greater than an arc with a thermionic cathode. Upon either the classical Schottky theory, or the quantum mechanical theory of high field emission, the energies of electrons at the boundary of the cathode fall space will be several volts less in the high field arc than in the thermionic arc; so, to produce sufficient positive ions for space charge purposes, the cathode fall of the former must be greater than that of the latter. A test is thus suggested for the Langmuir theory of an arc.

8. Measurements on the vapor stream from the cathode of a vacuum arc. W. E. BERKEY AND R. C. MASON, *Westinghouse Elec. & Mfg. Co., East Pittsburgh.*—The velocity of the vapor stream issuing from the cathode region of a vacuum arc between copper electrodes is calculated from (1) the energy received by a vane 3 cm in front of the cathode, as measured by the rate of rise of temperature; (2) the momentum imparted to the vane, as determined by the deflection of the vane. The mass used in the calculations is that of the copper deposited on the vane. The average velocity of the vapor, computed from data obtained by either method, is over 10^6 cm per second, confirming Tanberg's momentum measurements. There is some evidence that the vapor is ionized to a considerable degree. Radiation from the arc, or energy of recombination on the vane, can account for only a small part of the total energy received by the vane.

9. A method for the comparison of magnetic susceptibilities of feebly magnetic salts. L. G. HECTOR AND ALBIN N. BENSON, *The University of Buffalo.*—A method depending upon induced current phenomena may be employed for comparing the magnetic susceptibilities of substances whose electrical conductivity is small. The present method depends upon the comparison of the alternating electromotive forces developed in two coils each of which is coupled to a field coil. A tube filled with the salt to be examined is then placed in one of the pick-up coils and a change in the coupling between the pick-up coil and the field coil is thereby produced. By means of a variable resistor shunted about one field coil a balance between the induced e.m.f. is restored. Comparison of the two induced alternating e.m.f. was first attempted by means of a vacuum tube voltmeter, but slight irregularities in wave form and shifts in phase resulted in uncertainty in the readings. In the latest method, current from each pick-up coil is rectified by thermionic tubes and the rectified current is further smoothed out by filters. The potentials developed across the last condenser bank in each filter are then compared by means of a direct current galvanometer.

10. Block structure and magnetic viscosity. FRANCIS BITTER, *Westinghouse Elec. & Mfg. Co., East Pittsburgh.*—As a result of the work of Becker (Zeits. f. Physik **62**, 253, 1930) and Powell (Proc. Roy. Soc. **130**, 167, 1930) it is now possible to write the expression for the potential energy of a single crystal as a function of the direction of magnetization in the crystal, say $\Phi(\theta, H)$. This expression depends on the crystalline field, or (s, l) interaction, and on the distortion of the lattice, and has, in general, several minima as a function of θ. If the crystal is made up of regions of spontaneous magnetization, the equilibrium distribution of orientations is

given by an expression of the form exp. $(-\Phi_v(\theta, H)/KT)$ where Φ_v represents the potential energy of such a region. This distribution cannot in general be established in a reasonable time because of the existence of several maxima of Φ_v. If, however, we know the distribution of orientations, f, at a time $t=0$ (say complete demagnetization, or saturation) then the distribution at a time t resulting from a change in H is given by the diffusion equation

$$a\nabla\cdot(f\nabla\Phi_v) + b\nabla^2 f = \partial f/\partial t.$$

This equation has not been solved except for special and simple forms of Φ_v. A closer inspection, however, shows that a gradual "creeping" of magnetization will not, in general, occur unless the depth of the Φ_v minima is comparable with KT. Since the depth of these minima depends on the volume of a region, magnetic viscosity phenomena in single crystals may eventually be used to determine the volume of the regions of spontaneous magnetization and so check the hypothesis (Phys. Rev. **37**, 91, (1931)) that they are identical with Zwicky's blocks.

11. Magnetic properties of magnetite crystals at low temperature. CHING-HSIEN LI, *University of Illinois.*—Thin circular plates cut parallel to the 100, 110, and 111 planes of the magnetite crystal were prepared. Both the perpendicular and parallel components of magnetisation at low temperatures down to that of liquid air were investigated by the method of torsion. It was found that the magnetic property of the crystal was abruptly changed at about -160 degrees centigrade. It seems that the elementary magnetic elements within the crystal are very easily rotated in the magnetic field at that particular temperature. This particular temperature corresponds exactly to the temperature at which the heat capacity of magnetite is suddenly increased to a maximum point as was found experimently by R. W. Millar two years ago. Weiss' theory of the molecular field as applied to this change of specific heat and the corresponding change of magnetic property is in the process of investigation.

12. Effect of heating on residual magnetism. R. L. SANFORD, *Bureau of Standards, Washington, D. C.*—Experiments with a 0.63 percent carbon steel show that if the structure is lamellar pearlite, consisting of alternate plates of iron and iron carbide, the residual induction reverses sign at a temperature of approximately 200°C and regains part of the magnetization in the original direction upon cooling. If the temperature is raised to 800°C, the residual induction disappears and does not reappear on cooling. If the material is remagnetized in the original direction while at a temperature of approximately 265°C, the residual induction decreases upon cooling and finally reverses at a temperature of about 30°C. Hardened steel does not reverse but the presence of very fine lamellar pearlite produces a reversal. Precipitated carbide produced by reheating a hardened specimen does not cause the reversal. The lamellar structure appears to be necessary for the reversal. The first reversal can be satisfactorily explained as the result of the thermomagnetic transformation of the carbide plates which first reverse the magnetization in the adjacent iron plates and then become nonmagnetic at the so-called A_0 point. The reversal after remagnetization at the high temperature is not so easy to explain.

13. Annual variations in magnetic storms. H. B. MARIS, *Naval Research Laboratory, Bellevue, Anacostia, D. C.*—A new list of magnetic storms for the years 1839 to 1930 shows an annual variation in the frequency of disturbances with two equal maxima about a week following the equinoxes and two equal minima at the solstices. The ratio of the maximum to the minimum frequency is nearly two to one. The distribution of frequency F is given approximately by the equation, $F=k(3+\cos 2\theta)$, where θ is the position of the sun on the ecliptic. Three groups of storms showing annual recurrence interrupt the normal distribution curve. The first, 1840 to 1865 had a maximum about February 20, the second group started April 10, 1854, and was intermittently persistant with a two year period till 1875 and the third group started May 16, 1913, and is almost unbroken since then. The change from maximum to minimum frequency between equinox and solstice is explained as the result of three effects. The ultraviolet flair, which is assumed to come from the solar latitude where sun-spots are observed, should increase in intensity as the earth increases its solar latitude. This would be expected to give a ten percent change in storm intensity. Expansion of the upper atmosphere as it is heated by the solar flair causing the storm will move the conducting Heaviside layer across the earth's magnetic field with a dynamo effect which will decrease by about fifteen percent from equinox to solstice.

Winds blowing from day toward night will have a maximum dynamo effect in driving atmospheric electric currents at equinox.

14. Magnetic properties of copper-nickel alloys. E. H. WILLIAMS, *University of Illinois.*—The magnetic susceptibility of alloys of copper and nickel in proportions ranging from 0.1 to 70 percent nickel have been studied. Although copper is only weakly diamagnetic it requires 0.8 or 0.9 percent nickel to neutralize this diamagnetic effect and 56 percent nickel is required before the alloy shows ferromagnetic properties at ordinary temperatures. For amounts of nickel from one percent up to 30 percent the alloy, while paramagnetic in most respect, does not obey any law of paramagnetism with regard to temperature. As the temperature is increased the susceptibility first increases and then decreases, the maximum occurring in the neighborhood of the Curie point for nickel. In the case of alloys containing more than 30 percent nickel the susceptibility decreases with increase of temperature for temperatures above 20°C. So far as the phenomena of increasing paramagnetic susceptibility are concerned there is at present no explanation. It has been suggested that a few atoms or molecules of nickel do not lose their magnetic identity in the alloy and that these atoms with their spinning electrons become more mobile as the temperature is increased. One objection to this is that the susceptibility is independent of the field.

15. The origin of thermionic electrons from oxide coated filaments, R. W. SEARS AND J. A. BECKER, *Bell Telephone Laboratories, Inc.*—The following experiments show that the emission is determined by the condition of the oxide surface and not the core-metal surface as proposed recently by Lowry (Phys. Rev. **35**, 1367, (1930)) and also Riemann and Murgoci (Phil. Mag. **9**, 440, 1930). (1) When barium is deposited on the oxide surface either by evaporation from an external source or by electrolysis of the oxide itself, the emission changes even though the temperature is so low that the barium could not diffuse to the core surface. (2). A removal of the oxide coating while the filament is at room temperature causes the emission as determined at low temperatures, to decrease by a factor of 6000 or more. (3). When space charge limited current is drawn to a plate, the potential of a point in the oxide is always positive with respect to the core surface by an amount directly proportional to the current. If the current were determined by the core surface this potential should be negative and should not vary linearly with the current. The experimental facts adduced to prove a limitation by the core surface are not conclusive and can be explained on the view proposed here.

16. Theoretical interpretation of experimental Richardson plots. W. H. BRATTAIN AND J. A. BECKER, *Bell Telephone Laboratories, Inc., New York.*—The theoretical equation for the saturation current is

$$\ln i - 2\ln T = \ln A + \int_1^T \frac{b}{T^2}dT - (b)_{T=1} = \ln A - \frac{a}{T} \qquad (1)$$

$A = 4(1-r)\pi mk^2e/h^3$, "b" is defined in terms of L_p, the total heat of evaporation per mole at constant pressure. $b = (L_p/R) - (5T/2)$ "a" is defined by Eq. (1). It is related to the free energy If "a" and "b" are functions of T, an experimental plot of $\ln i - 2\ln T$ vs. $1/T$ will, in general, not be a perfect straight line. At any value of $1/T$ a tangent can be drawn. Its slope is $-b$ or $[-a+T\,da/dT]$ and the intercept is $[\ln A - da/dT]$ or $[\ln A + (b-a)/T]$. Actually, db/dT is usually so small that the mean straight line through the experimental points is practically coincident with the tangent at the mean value of $1/T$. If, as Herzfeld suggests, "a" $= h\nu_0/k$; the slope of the Richardson plot equals $-(h/k)[\nu_0 - T\,d\nu_0/dT]$ where the slope, ν_0, and $d\nu_0/dT$ all refer to values taken at the same temperature; the logarithm of the universal constant A is equal to the intercept $+(h/k)(d\nu_0/dT)$; also, the term "work function" cannot, in general, be used for both the slope of the Richardson plot and $h\nu_0$.

17. Influence of space charge on current fluctuations. E. W. THATCHER AND N. H. WILLIAMS, *University of Michigan.*—Current fluctuations of two fundamental types are recognized in a circuit containing a thermionic element: (1) Those due to the discreteness of the carriers, governed by probability relations applied to their departure from the cathode and collection at the anode. (2) Those due to thermal agitation of electricity in the circuit, analogous

to the Brownian fluctuation of particles in colloidal suspension. The influence of electron space charge on these fluctuations has been investigated with especially designed tubes. Precise measurements in this region have hitherto been unattainable on account of the inherent "mixed" nature of the emission from metal surfaces. Abnormalities arising from this source in tungsten and thoriated tungsten have been studied and controlled. A new treatment of the shot effect as applied to pure electron emission yields an expression for the ratio of the mean square value of the fluctuation voltage under given space charge conditions to that under strict temperature limitation of the current:

$$\frac{\bar{V}_s^2}{\bar{V}_t^2} = f(i_0/i)e^{-\omega^2/2\alpha^2}$$

I_0 is the space current, i the saturation current associated with a particular emitter temperature, and their ratio characterizes the space charge situation. The influence of the frequency term has been shown to be vanishingly small over a range of frequencies from 50,000 pps. to 500,000 pps. The function "f" has been experimentally determined for various situations of current limitation.

18. Supersonic satellites. W. H. PIELEMEIER, *Pennsylvania State College.*—As the path length in a Pierce acoustic interferometer was increased, satellites, or minor peaks, became more prominent in the curves which correlate the *excess of plate current over bias current.* $(I_p - I_B)$, and the *mirror position*, (x). With the exception of the satellites these curves have a striking resemblance to the curves which correlate the *calculated square of the pressure amplitude in the air at the crystal surface* and the *mirror position*. A wave velocity independent of intensity was assumed for the calculation. If it is assumed that the velocity of the waves decreases to the imiting value, $V=(\gamma p/d)^{1/2}$, with diminishing intensity, not only the shape of the satellites, but also their position is thereby explained. Measurements were made with several crystals. For each of the frequencies tested the acoustic velocity as determined by the satellite positions differed by less than 0.06 percent from the above limiting value. In every case the velocity, as determined by the major peaks, *exceeds* the theoretical value by more than 0.5 percent. Such a large shift could scarcely be a frequency shift as the resonance positions are approached.

19. Canonical transformations and the vibrations of a loaded string. R. B. LINDSAY, *Brown University.*—The classical method of discussing the transverse motion of a finite string of negligible weight fastened at the ends with tension τ and loaded with particles of equal mass m and equally spaced at distances a is that in which the Lagrangian equations for a system of n degrees of freedom are set up and integrated by means of determinant analysis. It is here shown that if we denote the coordinate and conjugate momentum of the sth particle by q_s, p_s and perform the transformation to the new system Q_s, P_s defined by the transformation function

$$S = \sum_{k=1}^{n} (m/2)^2 \omega_k^2 \cot Q_k \Big[\sum_{s=1}^{n} a_{sk} q_s \Big]^2,$$

where $a_{sk}=2 \sin (sk\pi/n+1)/(m(n+1)\omega_k)^{1/2}$ and the ω_k form a set of parameters, the Hamiltonian

$$H = 1/2m \cdot \sum_{k=1}^{n} p_k^2 + \tau/2a \cdot \sum_{k=1}^{n+1} (q_k - q_{k-1})^2$$

(with $q_0=q_{n+1}=0$) transforms into $K=\sum_{k=1}^{n} \omega_k P_k$ with $\omega_k=2(\tau/ma).^{1/2} \cdot \sin k\pi/2(n+1)$. The canonical equations now lead to $P_k=\text{const}$, $Q_k=\omega_k t+\beta_k$ and the usual solution is at once obtained from $p_k=\partial S/\partial q_k$ in the form

$$q_s = \sum_{k=1}^{n} a_{sk} P_k^{1/2} \sin (\omega_k t + \beta_k)$$

$$p_s = m \sum_{k=1}^{n} \omega_k a_{sk} P_k^{1/2} \cos (\omega_k t + \beta_k) \quad \text{where}$$

the ω_k appear as the characteristic frequencies (multiplied by 2π). The generalization to the continuous string is immediate. The transformation $q(x)=2/\mathrm{M}^{1/2} \cdot \sum_{k=1}^{\infty} (P_k/\omega_k)^{1/2} \sin Q_k \cdot$

sin $k\pi x/l$ where l is the length and M the mass of the whole string, carries the Hamiltonian functional into $H=\sum_{k=1}^{\infty}\omega_k P_k$ where now $\omega_k=k\pi(\tau/Ml)^{1/2}$. The energy fluctuation and quantization of the loaded and continuous strings are investigated.

20. The elastic constants and the thermal expansion of a sample of rubber between room temperature and −30°C. W. W. STIFLER, *Amherst College*, AND PAUL C. MITCHELL, *Missouri Valley College.*—A method has been developed by which the coefficient of linear expansion, Young's modulus, and the coefficient of rigidity can be measured on the same sample of rubber at any temperature from that of the room down to −30°C. For a particular sample, the thermal expansion proceeds quite regularly in this range but the coefficients of elasticity increase rapidly as the temperature is lowered. For example, at 22°C, Young's modulus is 1.30×10^8 dynes per cm^2 and at −30°C it is 3.56×10^8 dynes per cm.^{2}

21. Columns with variable end restraints. L. B. TUCKERMAN AND WM. R. OSGOOD, *Bureau of Standards.*—Because of its importance in aircraft construction, the Bureau of Aeronautics of the United States Navy has supported an investigation of the strength of columns with variable elastic end restraints, the investigation covering the range of lengths for which the failure is partly elastic and partly plastic. A theoretical analysis led to the conclusion that satisfactory corrections could be made for a rigid end mounting, which greatly simplified the test apparatus. The test results are found to be expressed advantageously in terms of the dimensionless variables

$$\sigma = P/(FcA), \quad \lambda = [l/(\pi r)](F_c/E)^{1/2}, \quad \kappa = [(2K)/(Pl)] + 2s/l,$$

where P = the maximum axial load which can be carried by the column. A = the cross-sectional area of the column, F_c = the short-column strength of the material, E = the modulus of elasticity of the material, l = the length of the column, r = the radius of gyration of the cross-section with reference to the gravity axis perpendicular to the plane of bending, K = the coefficient representing the end restraint, s = the length of the rigid portion at each end of the column. The dimensionless variables σ, λ, and κ render comparable test results on materials with different but affine stress-strain curves. Only by the use of these variables has it been found possible to coordinate all the test results which have been obtained. The variables λ and σ have been used previously in other column investigations. (L. B. Tuckerman, S. N. Petrenko, and C. D. Johnson, "Strength of Tubing under Combined Axial and Transverse Loading," N.A.C.A. Technical Note No. 307, pp. 3, 4, June, 1929.)

22. Methods for measuring the coefficient of restitution. LYMAN J. BRIGGS, *Bureau of Standards.*—A comparison is made of the following methods for determining the coefficient of restitution of elastic spheres, such as golf balls, when subjected to large deformations: 1. Ballistic method, in which the ball is struck by a flat-nosed projectile, and ball and projectile are caught in separate ballistic pendulums (Thomas). 2. Normal rebound of a ball dropped from a known height onto a massive flat plate, correction being made for air resistance during both fall and rebound. 3. Photographic method, in which the relative speed of ball and projectile after impact is determined from two spark photographs. 4. Rebound from a smooth inclined plate, involving measurement of the angles of incidence and reflection.

23. Velocity of sound in metal rods by a resonance method. LEHMAN C. SHUGART, *Lehigh University (Introduced by C. C. Bidwell.)*—A small coil is fastened to the end of the test rod and placed in a strong radial magnetic field. The coil is connected to the output of an audio-frequency oscillator. To the other end of the rod is fastened a carbon microphone button. At resonance frequencies corresponding to the fundamental or any overtone of the rod very sharp peaks are obtained in the microphone current. A correction must be made for the effective length of the rod due to the attachment of the driving coil and the microphone button. To get this correction, observation of the first overtone for a rod of twice the original length is made. The slight change in frequency enables the computation of the effective length. The equation is $v=2nl+4\Delta nl$. Value of velocity of sound for brass, steel and aluminum check very closely with the best published data. The method is being used for the determination of values in other

materials where data are lacking and especially for liquid metals. These may be contained in thin steel tubes, the peak for the resonance frequency in the liquid being easily distinguishable from that for the steel tube.

24. The vibrations of a plate with fixed center. ROBERT CAMERON COLWELL, *West Virginia University.*—A Chladni plate clamped at the center is usually set in vibration by bowing it at the edges. The sand figures formed in this way have been known for many years. If, however, a mechanical oscillator actuated by a vacuum tube is applied at different points on the plate, many new figures are formed. A few of these will be shown and a brief mathematical treatment given.

25. The arc spectrum of nitrogen. O. E. ANDERSON AND K. R. MORE, *University of British Columbia.* (*Introduced by G. M. Shrum.*)—The arc spectrum of nitrogen has been excited with low voltage, hot cathode arcs in mixtures of nitrogen with helium, neon and argon. Duffendack and Wolfe (Phys. Rev. **34**, 409, 1929) have used helium for the excitation of this spectrum, but it has usually been assumed that the lines could not be excited in argon. Since in these experiments the lines were observed in argon with an intensity of the same order as with helium, it has been necessary to revise the usual explanation of the excitation processes. When currents of the order of 1.5 amperes were used, the best results were obtained with 0.1 mm of nitrogen in 1.5 mm of argon. The spectrum has been examined in the region 3400–6000A. As some of the weaker lines were obscured by the nitrogen band structure, which varied with the nature of the admixed gas, it has not been possible to show that all the lines excited by helium were present in the argon mixture. A comparison of the intensities of the lines carried out with a Moll registering microphotometer showed that the strong NI lines were as intense as the moderately intense argon lines.

26. Activation of N_2—Hg mixtures by illumination with light from a quartz Hg arc. B. L. SNAVELY AND LOUIS A. TURNER, *Princeton University.*—Illumination of a mixture of nitrogen and mercury (5 mm N_2, 0, 001 mm Hg) in a quartz bulb containing a 0.6 mil tungsten filament produces a lowering of the resistance of the filament if it is originally at 400°C. This is the same effect which Kenty and Turner (Phys. Rev., **32**, 799 (1928)) found to be produced by active nitrogen and is presumably attributable to atomic nitrogen. Apparently the excited mercury atoms activate the nitrogen in some way. The effect is obtained only with the water-cooled arc, showing that the absorption of the 2537 line is involved. The effect is not obtained in similar helium-mercury mixtures. Rough preliminary measurements indicate that the magnitude of the effect is proportional to the first power of the intensity of the light.

27. The dissociation of excited iodine molecules by collision with argon atoms. LOUIS A. TURNER AND E. W. SAMSON, *Princeton University.*—By means of the absorption of the resonance line of the iodine atom ($\lambda = 1830$A.) it has been shown that iodine atoms are produced upon illumination of an iodine-argon mixture (0.3 mm I_2, 5 cm A) with continuous light of wave-length greater than 5100A., from a carbon arc. Absorption of such light should produce excited iodine molecules and not lead to direct optical dissociation. Apparently the excited molecules dissociate upon collision with argon atoms, as we might infer from the quenching of the iodine fluorescence by argon, as observed by Franck and Wood.

28. On the excitation of continuous spectra by bombardment of gases and vapors with cathode-rays. WILLI M. COHN, *University of Berlin.* (*Introduced by Otto Glasser.*)—It has been observed that gases or vapors which are bombarded by cathode rays, will emit under certain conditions a blue light the spectrum of which is continuous and has a maximum of intensity (photographically determined) at 4500A. The spectrum has been observed from 6200 to 3000A. The spectra received are not dependent on the kind of the ions generated. The light emitted is not polarized, but x-rays are generated. A working hypothesis is given in which is shown that the emission of the continuous spectrum may be produced by a mechanism similar to that of the continuous x-ray "Bremsspectrum."

29. Continuous spectrum from tungsten bombarded by 800 volt electrons. LAURISTON S. TAYLOR, *Bureau of Standards.* (*Introduced by F. L. Mohler.*)—Foote, Meggers and Chenault have

reported a continuous spectrum from metals bombarded by 1000 volt electrons (J. O. S. A. 9, 541, 1924). Preliminary measurements have been made of the intensity distribution of this radiation in the ultraviolet, from tungsten at voltages from 500 to 1200. At 800 volts the intensity $J(\lambda)$ increases regularly with decreasing wave-length, being about 3 times greater at 2800A than at 3700A. Between 500 and 1200 volts, the intensity distribution remains much the same and the intensity increases 2-fold. These results may be subject to an uncertain correction for electrons striking the stem instead of the target face.

30. Radiation from metals bombarded by low speed electrons. F. L. MOHLER AND C. BOECKNER, *Bureau of Standards.*—A paper presented at the New York meeting (No. 28) describes continuous spectra emitted by metals bombarded by large electron currents at low voltage, using the metal in the form of a small probe surface in a caesium or helium discharge. Measurements have been made with Be, Al, Cu, Ag, W, Pt, and Th in caesium discharges. Above 5 volts all except Ag and Cu give a spectrum of nearly equal energy per unit wave-length range. Ag is abnormally bright for wave-lengths longer than 3300A and Cu has a minimum in the green and yellow. Absolute intensities remain of the same magnitude with the same exceptions. The curves of isochromatic intensity versus voltage are very different. For Ag the intensity increases almost linearly from the threshold to 10 volts and more slowly beyond; for W it increases at an accelerated rate to 7 volts, is nearly constant to 12 and increases beyond. The Al curve has a high maximum at 12 volts and increases again above 16 volts. These variations (notably the Al maximum) are more pronounced at shorter wave-lengths. The intensity differences between Ag and W remain qualitatively similar in Cs and He discharges.

31. The blue-green fluorescence of mercury vapor. PAUL D. FOOTE, ARTHUR E. RUARK AND R. L. CHENAULT, *Gulf Research Laboratory and University of Pittsburgh.*—Visual photometric measurements were made on the blue-green fluorescence of Hg vapor excited only by the core of 2537. At the temperatures employed (21 and 33°C) the green glow cannot be seen in the absence of foreign gas. On adding a few millimeters of nitrogen to bring $^3P_1$ atoms down to $^3P_0$, it is bright. The intensity of the fluorescence increases to a maximum at 13 millimeters of nitrogen and then slowly fades as the pressure is increased. Using calibrated wire gauze screens to vary the intensity I of the exciting light, it was found that the fluorescent intensity J is definitely not a linear function of I. It obeys the equation $j+aj^{1/2}=bi$, where $j=J/J_0$ and $i=I/I_0$; J_0 and I_0 are the values obtained without screens; and a and b are constants for a given temperature and nitrogen pressure. Whatever be the molecule involved in the emission of the 4850 band, these experiments indicate that a $^3P_0$ atom is essential to its formation. The observed dependence of j on i can apparently be explained by assuming the active molecule contains two metastable atoms.

32. Direct measurement of τ. H. D. KOENIG AND A. ELLETT, *State University of Iowa.*—Ever since the well known experiments of Dunoyer (Le Radium **10**, 400, 1913) there has existed the interesting possibility of measuring the time between absorbtion and subsequent remission of radiation by an atom by observing the displacement taking place in this period because of thermal agitation. And it is equally well known that for such thermal velocities as are available in the laboratory the displacement in 10^{-8} secs. (the order of magnitude of the time usually involved) is too small to be measured. The depolarization of cadmium resonance radiation by very weak magnetic fields shows that τ for the 2^3P_1 state of Cd is unusually large. A beam of cadmium atoms was shot through a narrow perpendicular beam of λ3261 radiation. The illuminated part of the beam was screened from the camera. Atoms excited in the light beam and radiating after they had passed beyond the screen produced a blackening on the film densest just beyond the screen and perceptible for a distance of four millimeters. No blackening appeared below the screen showing that the spread above it was not due to secondary resonance. Photometer curves of the blackening are not yet available, but it is evident that τ is of the order of magnitude of 10^{-6} secs.

33. The average life for the line 2733A of ionized helium. LOUIS R. MAXWELL, *Bartol Research Foundation, Swarthmore, Pa.*—The line 2733A. (6→3) of ionized helium is made up of five lines (neglecting spin) whose average lives have been calculated according to the method of

Sugiura. The results obtained using Kupper's (amplitudes)^2 are: $6_1 \rightarrow 3_0$(2.59×10^{-9} sec.), $6_1 \rightarrow 3_2$ (2.59×10^{-9} sec.), $6_0 \rightarrow 3_1$ (9.06×10^{-9} sec.), $6_3 \rightarrow 3_2$ (1.52×10^{-8} sec.) and $6_2 \rightarrow 3_1$ (7.44×10^{-9} sec.). The experimental method used by the writer for determining the average life of excited ions has been applied to this line (2733A) and it is found to exhibit a displacement under the action of the transverse electric field which is slightly greater than would be calculated on the basis of the above values for the mean lives of the fine structure lines. This difference is probably caused by transitions into the sixth quantum state from higher excited states which would produce an apparent longer mean life and hence give too great an experimental displacement. However the experimental results obtained agree approximately with the above calculated values for the average life.

34. Mean life of the mercury line λ2537. PAUL H. GARRETT AND HAROLD W. WEBB, *Columbia University.*—The mean life of the mercury line λ2537 was measured by the alternating voltage method previously described (Phys. Rev. **24**, 113, (1924)). The radiation was excited in a quartz tube by impact with electrons from a hot cathode. The photoelectric system was contained in a separate tube also of quartz. The surface was zinc evaporated on a nickel plate. Measurements of the apparent life were made with diminishing mercury vapor pressures until further reduction of pressure produced no change in the measured rate of decay of the radiation. At these low pressures (below 3×10^{-4} mm for the geometry used) the absorption and re-emission of the radiation was negligible and the true life of a single excitation process was measured. This was found to be 1.08×10^{-7} sec. with an estimated precision of one percent.

35. Life of the nitrogen molecule in its first excited vibrational state. M. L. POOL, *Ohio State University.*—Curves showing the rate of decay of the metastable 2^3P_0 state of the mercury atom in a quartz resonance cell, containing carefully purified nitrogen at room temperature, are not accurately exponential. The rate of decay in the neighborhood of 10^{-4} sec. after terminating the optical excitation is more rapid than later. A high concentration of nitrogen molecules excited to the first vibrational state of the zero electronic state might be expected, due to collisions of the second kind with the 2^3P_1 state in mercury. It is assumed that in addition to usual diffusion and dissipative impacts with unexcited nitrogen, the decay of the number of metastable mercury atoms may be influenced by dissipative impacts with these excited nitrogen molecules whose number decreases with time by diffusion and by dissipative impacts. An equation for the number of metastable atoms is then obtained of the form $\exp[\alpha t + A(\exp \beta t - 1)]$. Evaluation of the constants from experimental data gives the following: Life of N_2 in first excited vibrational state, 1.2 to 1.9×10^{-4} sec. depending upon pressure; probability of dissipative impact, 1.5×10^{-4}; maximum life of 2^3P_0 state of Hg, 30×10^{-4} sec; probability of dissipative impact, 3.5×10^{-6}.

36. High dispersion in the near infrared. J. D. HARDY, *National Research Fellow, University of Michigan.*—Using a Pfund type of spectrometer, with a five inch 1500 line grating and especially long focus mirrors, it has been possible to obtain an experimental resolving power of 20,000 in the region between one and two mu. Using the grating in the first order, the 10830A helium line was resolved into two distinct components, of separation 1.1A. The effective slit-width in the 1.5μ region could be made as small as 0.2A and due to the excellence of the optical system the grating remained completely filled with light. Several other helium doublets have been resolved and the relative intensity of the two components compared. While testing out sources for hollow-cathode-exitation several lines in the neon spectrum were discovered. For the most part they have been classified as belonging to already established series.

37. Polarized fluorescence studied by means of a nicol, photocell and amplifier. D. R. MOREY, *Cornell University.* (*Introduced by C. C. Murdock.*)—It becomes a difficult matter to measure the percent of plane polarized light in weak radiations by means of visual devices. This is a serious disadvantage in the study of fluorescence, for polarization measurements yield valuable information on the fluorescent process. A high quality nicol, with ends perpendicular to the length, rigidly fastened to a photoelectric cell may be made to analyze radiations too weak for visual instruments. The types of cell and amplifier to be used are somewhat dependent on the

nature and intensity of the source. Using such an instrument, the effect of inhibitors (KI, KCN, NaBr, etc.) on the polarization of fluorescent bands has been studied. The results strengthen the present view on the nature of fluorescence.

38. Total emissivities at low temperatures and departures from Lambert's cosine law. E. R. BINKLEY, *Lehigh University.* (*Introduced by C. C. Bidwell.*)—Emissivity of oxidized copper, nichrome, brass, cold rolled steel, and of aluminum were measured with a special form of total radiation pyrometer which had a slit opening and linear thermopile, permitting observations at nearly grazing angle. Observations were made at temperatures 100°C, 200°C, 300°C, 400°C, 500°C, on each surface and at each temperature at angles ranging from 0° to 85°. The instrument was calibrated on a camphor blacked surface assumed at 98% black body. Lambert's cosine law is found to hold at angles of observation above 60° but an increasing deviation is found for all surfaces when the angle is reduced below 60°, the deviation at 85° becoming as much as 30% for copper, 39% for rolled steel, 56% for nichrome. The value of normal emissivities for the various surfaces at 500° were as follows: copper 0.74; nichrome 0.95; brass 0.68; cold rolled steel 0.93; aluminum 0.29. There was found to be a rise in emissivity with temperature.

39. Absorption and temperature emission of neodymium in various solvents. R. W. WOOD, *Johns Hopkins University.*—A solid solution of neodymium oxide in fused quartz was drawn out into fibres about 0.3 mm in diameter, and a fiber mounted vertically in a bunsen flame. It glowed brilliantly and when viewed through a direct vision prism exhibited a spectrum consisting of a green, yellow and red band with perfectly dark regions between them. (Experiment shown.) This is undoubtedly the best example of a highly selective temperature radiator ever observed. Seven bands have been photographed between the blue and 0.9μ. An interesting study has been made of solutions of various colored salts in liquid anhydrous ammonia. The rather wide band in the yellow of neodymium ammonium nitrate splits up into five narrow bands. These have been compared with the bands shown by the crystals at liquid air temperature and in solid ammonia. Some results of interest in connection with ray filters have been secured with the ammonia solutions and it seems possible that a suitable filter for giving a comparison spectrum in stellar spectra made with the objective prism may be constructed along these lines. Exhibition of stereoscopic photographs illustrating the orbital motion of the electron in the Stark effect.

40. Paschen-Back effect and hyperfine structure of Bi II. J. B. GREEN, *Ohio State University.* (*John Simon Guggenheim Memorial Fellow, Univ. of Tübingen.*)—The Zeeman effect in Bi II has been studied in a field of 34,000 gausses. The hyperfine structure of Bi II shows some very large separations and the Zeeman patterns yield very interesting results, since the field strengths available give separations that are about midway between "weak" fields and "strong" fields. In particular, λ5719, a $1\rightarrow 0$ jump in j, gives a completely resolved pattern in the perpendicular polarization, consisting of twenty components, twelve for $m_j=1$ and eight for $m_j=-1$, thus verifying the nuclear moment of $i=4$ 1/2 for Bi. Fisher and Goudsmit's results for the hyperfine structure in Bi II were used.

41. Effect of combined electric and magnetic fields on the helium spectrum II. J. S. FOSTER, *McGill University.*—In electric and magnetic fields crossed at right angles, the diffuse and fundamental series of helium show a fine structure which is sensitive to changes in the electric field. Effects are similar for members of a single series and differ little from the normal Zeeman effect in the sharp and principal series. The splitting has been found to be less than normal in the $p-p$ combination series. A full account of this research will soon appear.

42. The Stark-effect in xenon. H. W. HARKNESS AND J. F. HEARD, *McGill University.* (*Introduced by J. S. Foster.*)—Earlier results with complex spectra have been interpreted to show that displacements of spectral terms by electric fields are inversely proportional to the corresponding hydrogen difference provided the latter are not too small. This view altogether fails to account for the present observation. Instead, a qualitative explanation of most displacements is afforded through the separations of the xenon term from its neighbor in the manner indicated in the approximation made by Pauli. Some of the red lines show more complex patterns than have been found in the other rare gases. In contrast with helium and neon these pat-

terns indicate that the m values are determined as components of the j, which is retained as a unit. For example, the line $2p_8-6d_4^1$ (j:4→3) shows four π components and five σ components, i.e. all that could be observed if the separations in the $2p_8$ state are small.

43. Asymmetry observed in the Stark-components of Hα. D. R. McRae, *McGill University. (Introduced by J. S. Foster.)*—A special grating, with a dispersion of 3.8A/mm., having a very intense first order spectrum on one side, has been used to resolve the Stark components of Hα as seen from a Lo Surdo source. An asymmetry is observed in the displacements of the components, which is in general qualitative agreement with the calculations of Schlapp. There are certain discrepancies, however, which have not been explained. An asymmetry in the relative intensities of the components has also been observed. This asymmetry decreases with lower gas pressures, or with increasing propertions of helium, neon, or xenon in the discharge tube, until there is agreement with theory when traces of hydrogen are present in these gases. It may be shown that altering the number of atoms in the initial states does not explain completely the observed asymmetry. Since the probabilities of transition agree with experiment in the cases mentioned it seems that the presence of neighboring hydrogen atoms or molecules may in some way alter the intensities by an action such as collisions of the second kind; but it is difficult to see how this could be carried out in the selective manner required to explain the observations.

44. The electric field, atmosphere and effective temperature of the sun. Ross Gunn, *Naval Research Laboratory, Washington, D.C.*—The study of important electromagnetic effects in the solar atmosphere undertaken in previous papers is continued. It is shown that the large observed spread of effective temperatures of the sun's radiation can be accounted for by the presence of electric and magnetic fields in the solar atmosphere. The magnitude of the electric field at a level where the magnetic field is 25 gauss, calculated from the observed spread of temperatures, is found to be 0.015 volts/cm and agrees well with 0.013 volts/cm calculated earlier from the observed anomalous motions of the solar atmosphere. Gravitational equilibrium is found to be unnecessary in all regions of the atmosphere and it is shown that the "support" and stability of the chromosphere and its anomalous eastward motion are evidences of precisely the same electromagnetic mechanism. An electric field of the value given above is shown to account qualitatively for certain bright line spectra of the sun. The strange observed relation between bright line spectra and rapid axial rotation of stars, just announced by Dr. Struve of the Yerkes Observatory, confirms in a striking manner some of the conclusions of this and earlier papers.

45. Some new relations in the photographic effects of alpha-rays. T. R. Wilkins and R. Wolfe. *Institute of Applied Optics, University of Rochester.*—Jacobsen has recently shown that the number of grains made developable in a photographic plate is proportional to the density provided this number does not exceed 200,000 per sq. mm. The number of developable grains was assumed equal to the number of alpha-particles. In the present work alpha-rays of various speeds have been used with Eastman Slow Lantern plates. For a given exposure time the density is found to be proportional to the number of alpha-rays at least up to 1.5×10^6 per sq. mm determined by a direct scintillation count (density 1.39). It would seem that the lack of linearity in previous work has been due to a variable exposure time. The slopes corresponding to increased exposures are a linear function of the exposure time up to 40 hrs. Thus there is a very marked reciprocity defect in the density amounting to approximately 50% for a 60 hr. exposure. Equations connecting the number of grains per cc of the emulsion with the number of alpha-particles have been obtained. Provided that the reciprocity correction for a given emulsion has been determined, the photographic plate offers a splendid quantitative means for alpha-ray counting.

46. Continuous ultra-γ spectrum explaining cosmic-ray ionization-depth curve data. Charles M. Olmsted, *Buffalo, N.Y.*—It is shown that the ultra-γ cosmic-radiation data published by Millikan and Cameron, (Phys. Rev. **37**, 235 (1931)) may be completely explained by a continuous spectrum of energy falling off suddenly on the short wave side of 0.000013A (as determined by the Klein-Nishina formula; $\mu=0.03$) and extending on the long wave-length side with evenly varying intensity to beyond 0.0008A. Tables of values of intensity of ionization

for different values of μ and λ are given. Tables comparing the computed values of ionization at various depths with the values observed by Millikan and Cameron are given. It is shown that the absorption curve computed from the continuous spectrum coincides with the observed curve as closely as does the curve computed by Millikan and Cameron from a group of four bands having frequencies corresponding to the formation out of hydrogen of helium, oxygen, silicon, and iron. The location of the short wave end of the spectrum at a frequency corresponding to the union of electron and proton, together with the shape of the intensity curve, is discussed from the point of view of astrophysics.

47. Wave packets. D. G. BOURGIN, *University of Illinois.*—(I) The formal character of wave packets follows from the equivalence of harmonic and damped waves in representing disturbances. Real integrals are thus replaced by equivalent complex contour integrals. A true "stationary phase" principle depends on certain "sattel-punkt" contours and is described physically as the resultant of a group of damped harmonic waves of varying amplitudes but identical phases. The "Kelvin stationary phase" principle is misnamed since there, amplitudes, not phases, are constant. Huyghen's principle for odd, non-isotropic negligibly absorptive spaces may be generalized by correlating "paths," extensions of rays, with classes of spatially damped waves. (II) Flamm, Phys. Zeits. Dec. 1928 and others attempt to construct permanent atom packets of the form

$$\psi(x,t) = \sum_{\infty}^{\infty}\left(\nu_0 \int_0^{1/\nu_0} \psi(0,T)e^{2\pi i n\nu_0 T}dT\right)e^{2\pi i[x/\lambda_n - n\nu_0 t]} \qquad (1)$$

with independent λ's (considered atomic characteristic values). This procedure is incorrect for not only is $\int_{\infty}\int\psi\bar{\psi}$ infinite but, under some convergence restrictions (1) in its space dependence is an "almost periodic function" i.e. each set of regional values is almost reproduced an infinite number of times contrary to the assumption "nür in einem beshränkten Bereich . . . merklich von Null vershieden."

48. Wave mechanics of electrons in uniform crossed fields. MILTON S. PLESSET, *Yale University.*—We consider the motion of electrons in a uniform magnetic field H in the z-direction and a uniform electric field E in the y-direction. We take for the vector potential $A = -iHy$ and for the scalar potential $V = -Ey$. With these potentials the wave equation does not contain x explicitly, and the solution may be written as $\psi = e^{2\pi iax/h}\,\Phi_n(u)$ where $\Phi_n(u)$ is the nth orthogonal function of Hermite (the characteristic function for the simple harmonic oscillator);

$$u = (2k)^{1/2}[y - \pi/k^2h^2(\pi meE - akh)];\ k = \pi eH/hc.$$

The energy is related not only to the values of the fields E and H and to the integral values n, but to the arbitrary constant a as well. The component of the current density in the y-direction vanishes identically; and for the component of the current density in the x-direction we have a function of y alone which is

$$j_x = e^2H/mc[\Phi_n(u)]^2(y + \pi a/kh).$$

Thus j_x vanishes at the n roots of Φ_n and at $y = -\pi a/kh$; for this latter value the current reverses its direction.

49. Oscillations due to corona discharges on wires. R. E. TARPLEY, J. T. TYKOCINER AND E. B. PAINE, *University of Illinois.*—An experimental arrangement was used in which the electric constants of the circuit containing a corona tube corresponded to much higher frequencies than could be recorded by a reflecting mirror oscillograph. By amplifying the corona currents 300 to 3000 times it was found with this oscillograph, which was insensitive to circuit oscillations, that corona discharges produce a new type of oscillations whose chief characteristics are as follows: The frequency (2000–10,000 cycles) is independent of circuit constants. The amplitude decreases with increasing applied potentials. The wave has a complex form of distinct ripples superimposed upon the charging a.c. or upon the steady part of applied d.c. The wave form depends on the pressure and nature of the gas and on the polarity of the wire. The wave form varies for different gases but the character of the oscillations remains the same for air, CO_2 and N_2. The wave form becomes simpler with decreasing gas pressures especially with

CO_2. At high pressures the oscillations appear superimposed on the corona humps of the charging current at moments when the wire is the cathode, but at lower pressures oscillations appear only when the wire is the anode. No oscillations are obtained with oxidized or corroded wires. Details of the investigation will be published in a bulletin of the Eng. Exp. Station, University of Illinois.

50. Detection and comparative measurement of ionization in dielectrics by means of oscillations. J. T. TYKOCINER AND E. B. PAINE, *University of Illinois.*—In the study of dielectrics subjected to high potentials, minute voids and adsorbed gas bubbles give rise to ionization. The latter causes a redistribution of the electric field with the result that impulses of varying intensity are produced in the adjacent circuit. These impulses are made use of in a method for determining the potential at which ionization sets in and for comparing its intensity at varying applied voltages. If the circuit which contains the dielectric is aperiodic and is coupled to an amplifier supplied with a detector and current indicator, the impulses may be separated from the charging a.c. A more sensitive arrangement is obtained by tuning the circuit to a convenient frequency. Impulses in form of damped oscillations are then produced which are entirely free from the a.c. component of the charging source. With four stages of amplification, a thermionic detector and a thermionic voltmeter early stages of ionization in various dielectrics and the dependence of the ionization in various dielectrics on the applied voltage was studied. It was found that oscillations of any chosen frequency (100 to 30,000 k.c.) can be produced in a circuit by corona discharges in condensers, paper cables and rubber insulated conductors and their intensity measured by this method. The complete investigation will be published in a bulletin of the Eng. Exp. Station of the Univ. of Illinois.

51. Some properties of foreign and domestic micas. A. B. LEWIS, E. L. HALL AND F. R. CALDWELL, *Bureau of Standards, Washington, D.C.*—A number of samples of mica, fairly representative of the major sources of the world's supply of mica, have been tested for their dielectric constant, power factor, dielectric strength, and ability to withstand elevated temperatures. Average values are given for the dielectric constant and power factor at radio frequencies, and for the dielectric strength at 60 cycles. The data indicate the deviations from these average values which must be expected in commercial lots of mica. It is shown that stains and inclusions seriously affect the power factor of a sample, but have much less effect on the dielectric strength. Most of the samples were unaffected by exposure to temperatures up to 600°C, but above that temperature only the phlogopites can be said to have successfully withstood the elevated temperatures. On the basis of these data it was not possible to distinguish between micas of like commercial grades obtained from different geographical localities.

52. Cathode sputtering in a commercial application. H. F. FRUTH, *Western Electric Company, Hawthorne Station. (Introduced by O. S. Duffendock.)*—Three sputtering units, each one having six cathodes were designed and operated by one man. These units are used to produce the gold contact surfaces on broadcasting microphone diaphragms. In order to get good continuity, adherance, and uniformity a special method of preparing and cleaning the surface was developed. To produce a uniform quality surface and sputtering rate a bleeder valve to control the vacuum to ± 0.05 mm was developed. Sputtered gold surfaces on duralumin microphone diaphragms proved to be more free from pinholes, blisters and corrosion and gave better service than those made by electrolytic plating. On account of a lighter coat possible the diaphragms can be stretched to a higher natural frequency and show less fatigue.

53. Wave form of pulsating D.C. currents produced by FG-67 thyratrons. WAYNE B. NOTTINGHAM, *Bartol Research Foundation.*—A cathode ray oscillograph has been used to study the wave form in different parts of an "inverter" circuit using two General Electric FG-67 Thyratrons. (For the simple inverter circuit see Fig. 41, Hull, Gen. Elec. Rev. **32**, 398, 1929). With the cathodes heated by independent 60 cycles, A. C. windings an "output" can be taken from the lead between the cathode and the negative terminal of the D. C. plate supply. The current flowing in this lead can be made of the "square-top" type up to a frequency of about 6000 cycles per second. The circuit conditions including the plate potential are critical at the highest frequencies while at 500 to 1000 cycles, it is easy to obtain the desired wave form with a wide range

of current and potential conditions. Under the best conditions the time required for the current to rise from zero to its full value was probably not more than 30 microseconds and a slightly shorter time was required for the current to fall from full value to zero. The exact wave form depends on the inductance, capacity and resistance of the D. C. supply. This system has been developed to heat a filament for the investigation of thermionic emission with low accelerations and retarding fields, but undoubtedly has other possible applications.

54. The starting-time of thyratrons. A. W. HULL AND L. B. SNODDY, *General Electric Company.*—Starting-time is defined as the time between the application of grid or plate voltage, and the attainment of full arc current. This time has been studied by means of high frequency alternating voltage, condenser discharge, and cathode ray oscillograms. The observed times depend upon vapor pressure, and upon anode and grid voltages, and lie between one-tenth (0.1) microsecond and 4 microseconds under practical conditions for all commercial thyratrons. Times of the order of one thousandths (0.001) second, as reported by Nottingham, (Journal Franklin Institute **211**, 271, March 1931) have not been observed.

55. Magnetic induction in a projectile shot into a steady field. L. THOMPSON AND N. RIFFOLT, *Naval Proving Ground, Dahlgren, Va.*—For the solution of the equation of interior ballistics it is essential to define the powder burning and bore dissipation functions appropriate to the system. These can be identified by experimental firing which obtains pressure and displacement of projectile as time distributions. The present experiment measures projectile displacement by use of gun coils, mounted at intervals along the bore. A steady current is established in the coils before the round is fired. As the base of the projectile passes from a coil the transient electromotive forces develop a small change in the primary current, the oscillographic record of the secondary impulse having a form facilitating accurate time evaluation. Absolute position at the instant of current maximum, can be checked for new conditioning by means of external screens times of contact being superposed on the record. The coils are the basis, also, for an empirical method of measuring ejection velocities at high angles of projection, and aboard ship. Magnetic lag measurement for this cycle of short duration, .001 second or less, may be practicable with a coil set external to the gun, utilizing difference between flux values for projectile at rest and in motion and with compensation for eddy current.

56. A method for precise speed control developed in connection with an absolute measurement of resistance. FRANK WENNER AND CHESTER PETERSON, *Bureau of Standards, Washington, D.C.*—Any absolute measurement of resistance inherently involves a measurement of length and of time. In one of the methods on which we are working in the Bureau of Standards time enters as the speed of rotation of a direct-current motor. It is not necessary that the speed over very short periods of time be highly constant, but over periods of about 10 seconds and longer the average speed should be constant and known to within one part in 200,000. On the shaft of the motor there is a 1000-cycle generator whose electromotive force is synchronized with a 1000-cycle electromotive force obtained from a piezoelectric oscillator. Synchronization is secured by rectifying and amplifying the instantaneous sum of the two electromotive forces. The amplifier output current has an average value depending upon the phase angle between the two electrical systems. This current actuates a relay controlling power applied across a heavy inductance in one of the armature leads. As a consequence, the average speed of the motor is constant to the same precision as the oscillator frequency, which is stable to within a few parts in ten million. The method of control requires an oscillation of the speed about the average. This oscillation is of short period and small amplitude.

57. Resistance-temperature law for oxides. J. A. OSTEEN, *Lehigh University.* (*Introduced by C. C. Bidwell.*)—Bidwell showed that the resistance temperature law for certain variable conductors (oxides, etc.) was of the form $\rho = Ae^{Q/RT+aT}$. Plotted in the form $(-1/\rho)(d\rho/dT) = [Q/(RT^2)] - a$ he obtained for Fe_2O_3 straight lines with a break near the recalescence point, the two lines having the same y intercept but different slopes. This law was also followed by metallic germanium. The present paper extends this work to zinc oxide and beryllium oxide. Beryllium oxide yields two straight lines showing a transition at 750°C. Zinc oxide yields two straight lines with a transition in the interval 250°C−500°C. The two zinc oxide lines have different

slopes but the same y intercepts. With successive heatings to 1050°C there occurs continued decreases in the slope of the line for the 500°C – 1000°C range but no change in the y intercept. The line for the range 0°C – 250°C changes on successive heatings to 1050°C and finally stabilizes to a value of slope and intercept which repeats on succeeding runs. On the suggestion that the indicated transformation was due to impurity, new material of special purity prepared by the New Jersey Zinc Company was studied. The behavior of this material was found to agree closely with that of the earlier specimen but gave a more clean cut transformation.

58. High resistances made from metallic oxides. E. R. MANN AND D. R. MOREY, *Cornell Univ. (Introduced by C. C. Murdock.)*—The object has been to find a simple and rapid means of making high resistors (10^8 to 10^{12} ohms) of good quality. Resistors are made by mixing metallic oxides in suitable binders of an insulating nature. In all specimens, an ageing process occurs. In certain cases, most of the ageing occurs within a few hours and the resistors show but small and slow changes thereafter. In this there is the advantage of the use of the resistor within a short time after it has been made. A further advantage lies in the extreme ease of making. In the matter of size and ultimate constancy these resistors are not superior to some other types made by more painstaking and laborious methods, yet they will serve excellently for many purposes. A large change with temperature is present in most specimens. They have been tested for deviations from Ohm's law and for small fluctuations under working conditions.

59. A new theorem concerning temperature-compensated millivoltmeters used with shunts for the measurement of current. H. B. BROOKS, *Bureau of Standards, Washington, D. C.*—Millivoltmeters are essentially permanent-magnet moving-coil galvanometers for laboratory or switchboard use. The moving coil is of copper or aluminum wire of high temperature coefficient, hence for a given applied voltage the resulting current and deflection will vary greatly with changing temperature. Millivoltmeters are partly or wholly compensated for temperature by connecting a manganin coil in series with the moving coil. To obtain complete compensation in this way requires, on the average, about 200 millivolts at the millivoltmeter terminals for full-scale deflection. This is undesirably high, and the Swinburne method is therefore used to get complete compensation with about 50 millivolts for full-scale deflection. Either kind of compensated millivoltmeter, used with a shunt for current measurements, is compensated (as an ammeter) only when the resistance of the shunt is small relatively to the resistance of the manganin coil in the millivoltmeter. One maker of high-grade compensated millivoltmeters does not care to supply shunts with a rating of less than 30 times the full-scale current of the millivoltmeter. A simple theorem has been found which applies to either type of compensated millivoltmeter and removes the limitation against low-range shunts.

60. An experimental study of the natural widths of the x-ray lines in the L-series spectrum of uranium. JOHN H. WILLIAMS, *University of California.*—The rocking curves of $UL\alpha_1$ in three different anti-parallel positions of the double x-ray spectrometer give a natural width which is practically independent of the dispersion. The natural widths of $UL\alpha_1$ and $UL\beta_1$ have been observed as a function of voltage and no significant dependence was noted. The half widths at half maximum of twelve lines in the uranium L-series spectrum were studied and the results are:

Line	α_1	α_2	β_1	β_2	β_3	β_4	β_5	β_6	γ_1	γ_2	γ_3	γ_6
$\Delta\lambda$ in X.U.	0.439	0.494	0.299	0.369	0.382	0.726	0.252	0.487	0.242	0.57	0.47	0.233
ΔV in volts	6.56	7.20	7.17	8.04	9.40	16.1	5.94	9.71	7.96	19.7	16.2	8.18

Possible correlations with the electron transitions are suggested and the predominance of nuclear effects are evident from the greater widths of lines involving the elliptical orbit L_I. The large natural widths of the lines excludes the possibility of observing the effects of nuclear spin suggested by Breit. The actual shape of the line $UL\alpha_1$ has been investigated and found to approximate that predicted by the classical theory.

61. The width of soft x-ray lines. WILLIAM V. HOUSTON, *California Institute of Technology.*—The most direct experimental evidence as to the distribution of energy levels in a solid crystal comes from the observations on soft x-ray lines. The work of Söderman and others in

the extreme ultraviolet shows that while spark excitation gives sharp lines, excitation of a solid target by electron bombardment gives very broad lines. The shape of these lines, when proper account is taken of the transition probabilities, gives the distribution of the upper, occupied energy levels of the solid. Although it is difficult to infer the energy level distribution from the observations, because of the unknown transition probabilities, it is easy to determine the line shape to be expected from various models. The simple Pauli-Sommerfeld model of perfectly free electrons, gives the correct order of magnitude for the width of the lines, but does not give a very good approximation to the observed shape. If Bloch's method of starting with the functions of the individual atoms is used, the agreement in both shape and width is rather good. The lines of those elements whose outer shells are incomplete, show the sharp falling off on the short wavelength side which is characteristic of the Fermi statistics.

62. Crystal structure of lithium iodate. F. A. BARTA AND W. H. ZACHARIASEN, *University of Chicago.*—The structure of lithium iodate was determined by using the oscillation and powder methods. Lithium iodate is hexagonal with 2 molecules per unit cell of $a=5{,}469\text{A}\pm0.003\text{A}$, $c=5.155\text{A}\pm0.005\text{A}$. The space group assigned is D_6^6 and the atom positions are: 2Li in $(00\frac{1}{4})$ $(00\frac{3}{4})$, 2I in $(\frac{1}{3}\,\frac{2}{3}\,\frac{1}{4})$ $(\frac{2}{3}\,\frac{1}{3}\,\frac{3}{4})$ and 6O in $(u\,u\,0)$ $(0\,\bar{u}\,0)$ $(\bar{u}\,0\,0)$ $(\bar{u}\,\bar{u}\,\frac{1}{2})$ $(0\,u\,\frac{1}{2})$ $(u\,0\,\frac{1}{2})$ with $u=\frac{1}{3}$. The structure is based on hexagonal closest packing, with the lithium and iodine atoms both lying within oxygen octahedra. The atomic distances are Li $-$O and I $-$O $=2.23$A with lithium octahedra sharing faces with each other, one lithium and one iodine octahedra sharing only edges and two iodine octahedra only corners.

63. The refractive indices of potassium chlorate crystals, and the structure of the ClO_3 group. W. H. ZACHARIASEN, *University of Chicago.*—The method developed by W. L. Bragg (Proc. Roy. Soc. London **105,** 370 and **106,** 346 (1924)) has been used in order to calculate the refractive indices of $KClO_3$ crystals from the atomic arrangement. The Cl^{+5} dipole of the ClO_3 group was given one degree of freedom, along the trigonal axis of the radical. The calculations give agreement with the observed birefringence if the height of the Cl^{+5} dipole above the plane of the oxygens is .99A. X-ray determination gives a displacement of .49A. The scattering power for x-rays depends almost entirely upon the K and L electrons. The x-ray method therefore gives us the position of the Cl^{+7} core, whereas the optical calculations fix the position of the dipole. We must suppose the dipole to be formed by a displacement of the core and the two outer electrons. The observations thus indicate that the two valence electrons of Cl^{+5} are displaced with respect to the core, in a direction away from the oxgyen plane. This result is in agreement with the picture of the ClO_2 group given by the author in different publications. The calculated and observed birefringence and refractive indices are:

	Observed	Calculated
α	1.410	1.420
β	1.517	1.535
γ	1.524	1.535
$[(\beta+\gamma)/2]-\alpha$	0.111	0.115

64. The structure of the NO_2 group. G. E. ZIEGLER, *University of Chicago.*—The structure of $NaNO_2$ was determined in order to test W. H. Zachariasen's prediction (in press, Jour. Am. Chem. Soc.) that the NO_2 group would be angular with 120° between the N$-$O bonds. Powder crystal, rotating crystal, and Laue data were used. The lattice is body-centered, orthorhombic, space-group C2v$-$20, with a unit cell $a=3.55$A, $b=5.56$, $c=5.37$ containing 2 molecules. From visually estimated intensities the positions of the atoms are:

Na	$0, u, 0;$	$\frac{1}{2}, u+\frac{1}{2}, \frac{1}{2}$	$u_{Na}=210°$		
N	$0, u, 0;$	$\frac{1}{2}, u+\frac{1}{2}, \frac{1}{2}$	$u_N=30°$		
O	$0, 0, u;$	$0, 0, -u;$	$\frac{1}{2}, \frac{1}{2}, u+\frac{1}{2};$	$\frac{1}{2}, \frac{1}{2}, \frac{1}{2}-u$	$u_0=70°$

(360° $=a$, b, or c respectively)

Distances between atoms: $N-O=1.13$A, O$-$O same group $=2.09$, O$-$O different groups >3.3, Na$-$O two O's 2.53, Na$-$O four O's $=2.46$. $h=$displacement of N from O$-$O line $=0.46$ A. The angle between the N$-$O bonds $=130°$. The observed data definitely disagree with a co-linear NO_2 group.

65. Precision wave-length measurement with the double crystal x-ray spectrometer. ARTHUR H. COMPTON, *University of Chicago.*—An x-ray spectrometer was designed with the first crystal mounted on an auxiliary table supported by the frame of the spectrometer, and with the second crystal mounted on the central table of the instrument, whose position is read from a precision circle. The ionization chamber (of 25 cc capacity, filled with krypton) is on an arm whose position is read by a second precision circle. The instrument was built by the Societe Genevoise de Physique. The first crystal was adjusted to throw the $K\alpha_1$ line of molybdenum over the main axis of the spectrometer, and measurements were made with the second crystal in the (1, −1), (1, +1), (1, −4) and (1, +4) positions (Allison's notation). The reflection maxima from calcite (corrected to 18°C) occur at $\theta_1 = 6°42'35.5''$ and $\theta_4 = 27°51'32.9''$ with a probable error of 0.25″ due chiefly to errors in reading the circle. Using an apparent grating space for the first order of 3.02904A at 18°C, we get $\lambda = 707.832 \pm 0.002$ mA. Larsson obtained 707.831 ±0.003 mA using Siegbahn's photographic method. Comparison of θ_1 and θ_4 gives for the index of refraction in calcite, $1-\mu = (2.10 \pm 0.15) \times 10^{-6}$, in good accord with Hatley's more direct measurement of 2.04×10^{-6}.

66. Absolute wave-lengths of the copper and chromium K series. J. A. BEARDEN, *Johns Hopkins University.*—A consideration of the objections to the measurement of x-ray wave-lengths by ruled gratings shows that the method should be reliable if the apparatus is in precise adjustment and the gratings of good quality. In the present experiments 5 gratings were used which were ruled on two ruling engines. The method of the experiment was similar to that given by the writer in the Proc. of the Nat. Acad. of Sci. **15**, 528, (1929). The results from different gratings on the same wave-length agree very satisfactorily. The final results of 172 plates are given in the following table.

Spectral Line	Crystal λ	Grating λ	Limiting Error	Grating λ −Crystal λ
Cu K_β	1.38914A	1.39225A	±0.00014A	+0.224%
Cu K_α	1.53838	1.54172	± .00015	+ .217
Cr K_β	2.08017	2.08478	± .00021	± .222
Cr K_α	2.28590	2.29097	± .00023	+ .222

From these results, the grating constant of calcite is $d = 3.0359 \pm 0.0003$A, and Planck's constant h as determined by Duane, Palmer and Yeh is $h = 6.573 \pm 0.007 \times 10^{-27}$ erg sec. The mean value of the dispersion of x-rays as determined by Stauss (Phys. Rev. **36**, 1101, (1930)) and Larsson (Inaugural Dissertation, Uppsala, 1929) gives $e/m = 1.769 \times 10^7$ e.m.u. g^{-1}. The values of these constants are independent of any imperfection in the crystal grating. If the crystal lattice is assumed "perfect" then we have, Avogadro's number $N = 6.019 \times 10^{23}$ mol. per mol. the charge on the electron $e = 4.806 \times 10^{-13}$ e.s.u. and $h = 6.623 \times 10^{-27}$ erg. sec.

67. Absolute measurement of the Cu L_α line. CARL E. HOWE AND MILDRED ALLEN, *Oberlin College.*—Two photographic plates at different distances from a plane glass grating of 600 lines/mm are exposed simultaneously to the radiation from a copper target. Wave-lengths are computed from the plates and the constants of the apparatus. Over sixty determinations indicate for the wave-length of the L_α line of copper a value close to 13.326A ±0.01 (mean deviation) ±0.001 (probable error). This differs by 0.15% from 13.306A as obtained by Larsson from crystal measurements.

68. Theory of the diffuse scattering of x-rays by solids. G. E. M. JAUNCEY, *Washington University, St. Louis.*—The classical theory of x-ray scattering has been applied to the scattering of x-rays by the electrons in the atoms of a solid. The case in which the solid consists of atoms of one kind has been considered. The interaction of the waves scattered by each electron with these scattered by every other electron in the solid has been considered. The analysis is simplified by the fact that the orbital periods of the electrons in the atoms are very much shorter than the vibrational periods of the atoms, due to thermal agitation. The final formula obtained is $S = 1 + (Z-1)(f'^2/Z^2) + (F^2/ZN)X$ where S is the scattered intensity per electron relative to the scattered intensity from a single isolated electron, Z is the atomic number, F the atomic struc-

ture factor including the effect of thermal agitation f' is related to f the true atomic structure factor (without thermal agitation), N is the total number of atoms, and X is a certain double summation. The value of X has not been obtained for an amorphous substance, but it has been evaluated for the case of a simple cubic crystal by Jauncey and Harvey in another paper (No. 153).

69. Hyperfine structure and width of x-ray spectral lines. F. K. RICHTMYER AND S. W. BARNES, *Cornell University.*—In a recent letter to the Physical Review (Sept., 1930) we reported measurements which seemed to indicate that the $K\alpha_1$ line of W(79) has a hyperfine structure of the type predicted by Breit. The measurements were made with a two-crystal spectrometer of special design. It now appears, after further critical and extensive study, that the apparent separation must have been due to some (as yet) unknown instrumental peculiarity. The numerous measurements made in connection with this study permit a determination of the width of W$K\alpha_1$. The average of several measurements in second, third and fourth order, after applying corrections for rocking curves of the crystals in the parallel position, gives a half width of 0.154 X.U.

70. Survey of the satellites of the $K\alpha_{1,2}$ doublet, the $K\beta_1$ and $K\beta_2$ lines. O. REX FORD, *West Virginia University.* (*Introduced by R. C. Colwell.*)—In a paper on the satellite structure of the x-ray diagram lines $L\alpha_1$ $L\beta_1$ and $L\beta_2$ for the elements Rb (37) to Sn (50) Richtmyer and Richtmyer, by a careful timing of exposures, were able to show that the number of satellites were more numerous than previously reported. These results called for a survey of the satellite structure of the K-diagram lines. Such a survey extended the range of the elements over which the satellites $K\alpha_3$, $K\alpha_4$ and $K\alpha'$ could be measured. An entirely new satellite of the diagram line $K\beta_1$, designated by $K\beta^\circ$, was found for the elements Ca(20) to Cr(24). The satellite $K\alpha_3$ was found to consist of two components over the range of elements Al(13) to Cl(17) instead of a singlet as previously supposed. Microphotometer records of the spectrograms show a very significant reversal in the relative intensities of the $K\alpha_3$ and $K\alpha_4$ satellites at the element P(15). That the square root of the difference in frequency between a satellite and its parent line is a linear function of the atomic number is shown to be approximately true for satellites of the $K\alpha_{1,2}$ doublet. This relation is not valid for satellites of $K\beta_1$ and $K\beta_2$.

71. Effect of piezoelectric oscillations on the Laue patterns of quartz. G. W. FOX AND P. H. CARR, *Iowa State College.*—In an attempt to determine the amplitude of vibration of the atoms in a quartz lattice brought about by piezoelectric oscillations, a series of Laue photographs have been made of both Curie and thirty-degree cut plates, using the white radiation from a standard Coolidge tube. This tube had a tungsten anode and carried a current of four milliamperes at 95 kilovolts. Eastman standard x-ray film was used with no sensitizing screens. On examination, the patterns produced by each plate, oscillating and non-oscillating, appear identical except in one respect: the pattern of the oscillating plate is several times as intense as that of the non-oscillating. A four-hour exposure of a non-oscillating plate to radiation of the above mentioned type, produces but the rudiments of a pattern, whereas, the same plate oscillating produces a very beautiful intense pattern for the same time of exposure. The effect is quite independent of the piezoelectric frequency and does not depend on whether the plate vibrates according to the shear mode or the transverse mode. It is hoped that the work in progress will establish the cause of this peculiar intensity difference.

72. Calculation of the resolving power attainable in x-ray spectroscopy by photographic methods. SAMUEL K. ALLISON, *University of Chicago.*—If w_c, the (half) range of glancing angle over which a crystal will reflect monochromatic x-rays has been determined by the double spectrometer method, it is possible to calculate what resolving power is attainable from this crystal by photographic methods. Equations are set up giving the resolving power in terms of a, the slit width, and R, the distance from slit to photographic plate. Some results are: (1) No appreciable increase in resolving power is obtained by making $a/2R < \frac{1}{4}w_c$. (2) If $a/2R > 2.5w_c$ the resolving power does not involve w_c. (3) The resolving power attainable in the first order by photographic methods is $1/2^{1/2}$ of that attained in a double spectrometer in the (1, 1) position with crystals of equal perfection, as stated by Valasek (Phys. Rev. **36**, 1523 (1930).) (4) The

resolving power of the instrument used by Valasek in his experiments on the molybdenum K spectrum in the first order was about 5350, whereas that of a double spectrometer in the (1, 1) position with crystals of the perfection of those used by Allison and Williams (Phys. Rev. **35**, 1476 (1930)) is about 8100. The calculations are extended to include measurements of widths of spectrum lines by photographic methods.

73. Indices of refraction and absorption in the case of soft x-rays. ELMER DERSHEM, *University of Chicago.*—Measurements of the absorption of the $K\alpha$ line of carbon in carbon, nitrogen, oxygen and neon indicate that for elements such that $\lambda_K < 44.6\text{A} < \lambda_{L_I}$ the atomic absorption coefficient is given by the following equation: $\mu_a = 1.65Z^{4.4} \times 10^{-23}$. The linear absorption coefficient of fused quartz may be calculated from its density and the absorption coefficients of its constituents and is found to be 47,200. The index of absorption κ, is found from the equation $\kappa = \mu\lambda/4\pi = 1.68 \times 10^{-3}$. The Drude-Lorentz dispersion formula yields the value, $\delta = 1 - n = 4.8 \times 10^{-3}$. Reflected intensities computed from these values are somewhat higher than those found experimentally. Good agreement is secured if κ is assumed to be 2.5×10^{-3}. The results indicate that the value of δ computed from the Drude-Lorentz formula is the correct one but that surface films or imperfections reduce the reflected intensity in much the same manner as an increase of absorption. Other measured values of atomic absorption coefficients for the $K\alpha$ line of carbon are as follows: A, 30.1×10^{-19}: Kr, 43.4×10^{-19}: Xe, 14.5×10^{-19}: Au, 40.7×10^{-19}. The bearing of these results upon x-ray absorption formulas is discussed.

74. Change in x-ray wave-lengths by partial absorption. J. M. CORK, *University of Michigan.*—Experiments have been carried out to duplicate those of Dr. B. B. Ray, in which a beam of x-rays traversing an absorbing medium gave in the direction of transmission a modified line of longer wave-length. The shift in wave-length corresponded to the x-ray photon elevating an electron to an outer atomic level and passing on unchanged in direction with diminished energy and hence a longer wave-length. Using the $K\alpha$ lines of copper and the $L\alpha$ line of tungsten with absorbing screens of beryllium, boron, carbon, oxygen and nitrogen under a variety of conditions, it has been impossible to show the existence, in any case, of a modified line.

75. X-ray absorption measurements in mercury vapor. FRED M. UBER, *University of California. (Introduced by Robert B. Brode.)*—The mass absorption coefficients, μ/ρ, of mercury in the wave-length region 0.74 to 1.4A were determined by an ionization method. The absorber was in the form of superheated vapor, whose density was calculated on the assumption of perfect gas behavior. The absorption chamber was entirely of pyrex glass, and was combined with the x-ray tube into a single unit. Electrometer deflections of several millimeters per second were obtained with the tube currents ranging from 6.5 to 17.5 m.a. and with the voltage low enough to prevent excitation of wave-lengths corresponding to the second order reflection. Readings were taken for several positions of the crystal before removing the absorbing vapor from the path of the beam. The magnitudes, δ, of the three L absorption discontinuities, where δ is defined as the ratio of μ/ρ on the short and long wave-length sides of the limit, are $\delta L_{\text{I}} = 1.18$, $\delta L_{\text{II}} = 1.39$, $\delta L_{\text{III}} = 2.45$. The mass absorption coefficient can be expressed by the relation $\mu/\rho = A\lambda^c$. The constant A assumes a different value for each branch of the curve, but the value of c does not vary from 2.6 by more than 0.1 for all four branches. The value of μ/ρ at 1.4A is in accord with what one would expect from Allen's values for gold and lead, which indicates that no appreciable error is introduced by using the perfect gas equation for superheated mercury vapor.

76. Lattice parameter of copper by a precision instrument. C. S. BARRETT AND H. F. KAISER, *Naval Research Laboratory, Washington, D. C.*—A precision x-ray camera for large angle diffraction, a modification of the instrument of Sachs (Phys. Zeit. **60**, 481, 1930), has been constructed. A photographic plate is used, avoiding film shrinkage. A specimen is used whose surface is plane, parallel to the photographic plate, and perpendicular to the x-ray beam. The distance from specimen to plate is measured by a micrometer. The instrument is applicable to specimens prepared for metallographic examination, and is convenient for high temperature studies. The parameter of copper was determined for material from Adam Hilger Ltd. analyzing

Oxygen 0.040%, Nickel 0.002%, Iron 0.003%, Arsenic 0.004%, Lead 0.001%, Calcium 0.001%, with spectroscopic analysis indicating in addition only slight traces of magnesium, caesium, and sodium. The specimen was prepared with a polished surface, annealed two hours in vacuum, and etched lightly. Copper and brass anticathodes were used. Wave-lengths assumed were Cu $K\alpha_1 = 1.53739$A, Cu $K\alpha_2 = 1.54126$A, Zn $K\alpha_1 = 1.43206$A, Zn $K\alpha_2 = 1.43587$A. The mean value of 18 observations of a_0 for copper at 20°C was 3.6078 ± 0.0001. This value agrees closely with that of Ageew, Hansen, and Sachs, (Phys. Zeit. **66**, 350, 1930), 3.6081A and yields a calculated density of 8.93 in accord with measured densities, 8.94 ± 0.01 (I.C.T. Vol. II, p. 456).

77 Lattice parameters of solid solutions of silicon in copper. H. F. KAISER AND C. S. BARRETT, *Naval Research Laboratory, Washington, D. C.*—Measurements of a_0 for α-Cu-Si alloys containing less than 0.06% total impurities were made on the precision instrument described above. The alloys were homogenized by a 48 hour anneal at 750°C in vacuum, terminated by a quench in water. After a polish, they were given a 3 hour anneal at 725°C in purified hydrogen and again quenched in water. Subsequent polishing and etching was done with great care to provide a surface free from cold work, and exposures were made within 24 hours; these precautions were taken to avoid decomposition of the solid solutions. Alloys containing 5.91% and 6.36% Si, however, showed by their diffraction patterns and by their a_0 values that there was precipitate present. The parameters found were as follows in A.U. at 20°C: 1.09% Si = 3.6103; 3.01% Si = 3.6128; 5.02% Si = 3.6150; 5.91% Si = 3.6151; 6.36% Si = 3.6157. Densities calculated from these parameters and compared with densities as measured by Norbury (Trans. Farad Soc. 19, 586, 1923–24) indicate that the solid solution is of the simple substitutional type, and agree well with Norbury's densities when calculated on this theory. That the silicon atom expands the copper lattice in spite of its smaller radius is not regarded as an anomaly, since the elements differ in crystal structure. Studies of orientation of the precipitate are being conducted.

78. The x-ray analysis of vesuvianite. B. E. WARREN, *Massachusetts Institute of Technology.*—Vesuvianite $H_2Ca_{10}Al_6Si_9O_{38}$ is a complex, tetragonal silicate with $a = 15.60$A $c = 11.83$A space group D_{4h}^4 and four molecules in the unit cell. The cell contains 260 atoms and involves 44 parameters. The analysis is of particular interest as an extreme case of a complex structure, and illustrates the extent to which our present knowledge of the physical chemistry of the silicates has progressed. The structure is determined by means of a close relationship which is discovered between vesuvianite and the cubic crystal garnet $Ca_3Al_2Si_3O_{12}$. Two quadrants in the vesuvianite unit cell are identical in structure to the corresponding two quadrants in garnet except that they are rotated 45° about c. Quantitative measurements of the integrated reflexion with a Bragg ionization spectrometer for 40 planes give structure amplitudes in good agreement with those calculated from the structure. The structure contains SiO_4 and Si_2O_7 groups, and the coordination numbers are Si-4, Al-6, Ca-8.

79. Atomic scattering power of copper and oxygen in cuprous oxide. G. A. MORTON, *Massachusetts Institute of Technology. Rockefeller Institute for Medical Research. (Introduced by B. E. Warren.)*—The atomic F-curves for copper and oxygen for the $K\alpha$ radiation of copper have been determined from cuprous oxide, and are compared with the F_{Cu}-curve from metallic copper and F_O-curve from NiO. Measurements were made on samples of finely powdered Cu_2O pressed into suitable briquets, using an x-ray powder spectrometer to measure reflected intensity. The structure factor F for the reflecting planes is calculated from the power of reflexion. The atomic scattering factors as a function of $\sin\theta/\lambda$ are found from these F values. The F_{Cu}-curve and F_O-curve as obtained from Cu_2O and those from metallic copper and oxygen in NiO are found to be the same over the overlapping portions of the curves.

80. An x-ray determination of crystal orientation in nickel, copper and aluminum, produced by cold rolling. C. B. HOLLABAUGH AND W. P. DAVEY, *The Pennsylvania State College.*—High purity nickel, copper and aluminum, free from all preferred orientation, were cold rolled in such a way as to produce no appreciable temperature rise and the orientations were determined after each pass using the method of Davey, Nitchie and Fuller (Mines and Met.

Tech. Pub., 243, E88). Nickel and copper showed identical orientations both as to limits of ranges of preferred orientations and mean positions. The number of passes through the rolls determines the probability that a crystal fragment will be within the preferred range, but does not affect the limits of the preferred range. Aluminum shows a related preferred orientation, but with widely different angular limits which depend on the number of passes through the rolls. This work, with similar work on silver previously reported, shows, contrary to the accepted belief, that except for copper and nickel, the common face-centered cubic metals show differences in preferred orientation both with respect to the limits of preferred range and with respect to the mean position of orientation. The preferred positions are similar only in that they all show one face diagonal of the cube always in a plane parallel to the direction of rolling and perpendicular to the rolling surface.

81. X-ray evidence as to the size of a gene. OSWALD BLACKWOOD, *University of Pittsburgh.*—To explain certain facts of heredity, geneticists postulate the existence of bodies called genes in the chromosomes of living cells. The diameter of these bodies in the cells of the fruit fly (Drosophila) is roughly estimated to be 600A. The writer has computed the approximate number of ions produced in such a gene when exposed to x-rays of known intensity for a known time. Using Patterson's experimental value for the percentage of exposed flies showing a certain mutation about one per cent of the atoms in a gene are found to be "sensitive," (i.e. their ionization is assumed to be accompanied by mutation). If the sensitive material were concentrated in a spherical nucleus, its diameter would be about one-fifth that of the gene. The hypothesis that natural mutations are caused by cosmic or natural gamma-rays seems improbable since the ionization produced in this manner is about three billion times smaller than that due to the x-rays as used by Patterson. The period for one per cent mutation would therefore be about one million years instead of a few weeks.

82. Parallax stereoscopic x-ray pictures. KENNETH S. COLE, *Columbia University.*—Shadow parallax "stereograms" and "panoramagrams" can be made with visible light or x-rays by several types of relative motion of a point source of radiation, the object, a suitable grating, and the photographic plate. Viewed with a similar grating, either a stereoscopic or pseudoscopic effect may be obtained, also, small movements of the object can be followed in the "panoramagram." Stereoscopic x-ray "vision" can be obtained with a fluorescent screen and two gratings.

83. The lethal effect of intense x-rays on the organism colpidium colpoda. HARRY CLARK, MORDEN BROWN, AND JOHN THOMAS, *Stanford University.*—Several single-cell organisms have been studied by various investigators. The curves showing the relation between the number of survivors of a group and the time of radiation have been fitted usually by the use of Poisson's exponential series, the number of terms required lying between 1 and 8 with one exception. The results are generally interpreted as statistical evidence of a definite lethal number of quantum-hits, which must fall inside a small "sensitive volume" within the cell, although normal biological variation is sometimes considered. Although Crowther, working with colpidium colpoda, used 49 terms for immediate death, the range of individual lethal doses was still very wide. Using silver radiation at 50 kv, several times more intense than Crowther's and well controlled, we have found evidence of an approach to a critical lethal dose, the same for all individuals, which would exclude normal biological variation. To reconcile this result with Crowther's, we suggest that the processes to recuperation, which are known to be very rapid, are less rapid in the sensitive volume than elsewhere. Less intense radiation produces death by injury to the sensitive volume; more intense rays operate predominantly on other parts of the cell.

84. The extension of Clapeyron-Clausius equation to dissociation within the gaseous phase. J. L. FINCK, *Washington, D. C.*—This paper is a study of the thermodynamic analogies between the liquid-vapor state and the gaseous state in which dissociation occurs. It is noted that the associated gaseous component corresponds to the saturated liquid and that the dissociated gaseous component is the analogue to the saturated vapor. By means of a hypothetical

mechanism, consisting of a piston and cylinder, which contains the gas, and two semi-permeable membranes, it is possible to separate the gas into two phases, one containing the associated component and the second the dissociated component. This permits dissociation to take place by an isothermal-isopiestic process, analogous to the evaporation of a liquid. By means of this hypothetical process it is shown that Clapeyron-Clausius equation must take the form $\Lambda=\theta(v_2-v_1)\,(\delta p/\delta\theta)_x$, where Λ is the heat of dissociation, v_1 and v_2 the specific volumes of the associated and dissociated components, each taken at p, θ, and x is the degree of dissociation. Calculations based on experimental data for NH_3, H_2O, and CO_2 gases check the experimentally determined values for Λ to 1 percent and less. Some remarks are made with regard to superheated and supercooled states.

85. The mechanics of effervescence. C. J. CRAVEN AND OTTO STUHLMAN, JR., *University of North Carolina.*—Small bubbles of gas rising through a liquid originating at various depths, great compared to their dimensions, arrive along a spiral path, at the surface with the same terminal velocity. They roll under the surface film, come to rest and burst, projecting fragments of liquid into the air. These fragments rise to different heights. For a given radius of bubble, temperature remaining constant, the separate fragments follow a near Maxwellian distribution when distribution in height is examined as a function of diameter of bubble. After the maximum height is passed the above distribution becomes less regular, probably due to distortion in shape of the larger bubbles. Bubbles rising through water at 21°C, having diameters up to 0.16 cm burst into three fragments, from 0.16 to 0.20 cm they burst into two fragments. Bubbles larger than this burst irregularly.

86. The absorption of audible vibrations in the air. VERN O. KNUDSEN AND L. P. DELSASSO, *University of California at Los Angeles.*—Recent measurements on the absorption of high pitched sound in air show (1) that the absorption is several times greater than that accounted for by viscosity, heat conduction and radiation losses, and (2) that the absorption decreases as the amount of water vapor in the air increases. By making reverberation measurements in two rooms which have the same boundary material (painted concrete) but different "mean free paths," it is possible to eliminate the surface absorption, and thus determine the absorption in the air only. Measurements obtained to date, both in the two room experiments and in the free atmosphere, indicate that at a frequency of 4096 cycles, for example, the attenuation constant at 21°C and 20% relative humidity is about 0.00009 and at 70% relative humidity is about 0.00005 C.G.S. units. In a mixture of air and CO_2 (4% by volume) there was evidence of a slight increase in absorption owing to the presence of CO_2. The data have a bearing upon problems in sound signaling and in architectural acoustics, and may have a bearing upon the absorption of energy within the molecule.

87. The flow of gases through porous materials. H. G. BOTSET AND M. MUSKAT, *Gulf Research Laboratory, Pittsburgh, Pa.*—An experimental study has been made to establish quantitatively the characteristics of and laws governing the flow of gases through consolidated and unconsolidated porous materials of fine texture. Experiments were performed with columns of glass beads, homogeneous and heterogeneous unconsolidated sands, as well as with samples of actual sandstones. With the sandstones linear flows were made both perpendicular and parallel to the bedding plane. Radial flows through annular sections of the sandstone were also made. In all cases it was found that the gradient of the squares of the pressures is proportional to a power of the mass velocity. In the various cases the exponent was found to lie between the limits 1 and 2 corresponding respectively to completely viscous and completely turbulent flow in straight cylindrical tubes. For a given sand however it remains fairly constant over a considerable range in the mass velocity. On the basis of these results a theory was developed for the production from and pressure decline in a closed sand reservoir of uniform thickness producing into a well under conditions of radial two-dimensional flow. The theoretical predictions check qualitatively with the limited field data that are available.

88. Molecular flow and the formation of beams. A. ELLETT, *State University of Iowa.*—The streaming of air at low pressure through short circular tubes is shown to give rise to an angular distribution of the molecules emerging from the tube in fair agreement with the cal-

culations of P. Clausing (Zeits. f. Physik **66,** 471, 1930). Measurements were made by means of a Pirani gauge.

89. The Brownian motion of strings and elastic rods. G. A. VAN LEAR, JR., AND G. E. UHLENBECK, *University of Michigan.*—The method introduced by Ornstein is applied to calculate the Brownian-motion mean-square deviation for strings and for elastic rods, the surrounding medium being a gas. For the string, a varying tension and elastic binding at the ends are supposed, and a formula is obtained for the mean-square deviation of any point at time t, having started with a given deviation of that point; the result contains infinite series. This result is specialized to: (1) the string with fixed ends and constant tension, and (2) the string hanging under gravity. In case (1), for the mid-point, and for a limited time interval, the series are summed; for $t\rightarrow\infty$, the result is given for all points, agreeing with that given by Ornstein for the mid-point. Elastic rods are treated similarly, and similar results are obtained. The effect of gravity, when the rod is vertical, is introduced by a simple and consequent perturbation method, and a formula is obtained for the mean-square deviation of the lower end; this agrees closely with Houdijk's experimental results. The time dependence given by the complete formula cannot yet be tested, for Houdijk gives only limiting values in his publication.

90. Pirani gauge applied to the measurement of small pressure changes. R. M. ZABEL AND A. ELLETT, *State University of Iowa.*—The application of the Pirani gauge to the measurement of small pressure changes is discussed. Both nickel and tungsten wires are used as filaments in the gauge. Nickel wire not only has the greater sensitivity but possesses several other advantages. The theory of the gauge is developed so that it is possible to predict the affect of change in length or diameter of the gauge wire upon the sensitivity of the gauge. To obtain maximum sensitivity the wire should be made as long as convenient and its diameter adjusted so that its resistance is approximately equal to the resistance of the galvanometer. Both theory and experiment indicate that the sensitivity of the gauge is increased by increasing the area of the wire or by decreasing the temperature of the walls of the gauge. The theory also predicts that there is an optimum temperature to which the wire should be heated for maximum sensitivity of the gauge. The observed and computed values of the optimum temperature are compared. The maximum sensitivity attained is a galvanometer deflection of 1 mm for a pressure change of air equivalent to $5\pm1\times10^{-9}$mm of mercury.

91. Application of transient network theory to gas flow in vacuum systems. DONALD S. BOND, *University of Chicago. (Introduced by Harvey B. Lemon.)*—With complex vacuum systems employing connecting tubing of only moderate diameter, the instantaneous pressure at any point may be calculated with considerable simplicity by employing the electrical analogy. Resistance is defined (by Knudsen's equation) in terms of tube dimensions; capacity (both lumped and distributed), in terms of volume. The network which simulates the most general type of closed vacuum system consists of n T-mesh circuits with resistance and capacity only. The solution of the n mesh equations gives the potential drop (or pressure) across each capacity of the form $e_j=\Sigma a_{jk}\exp(-b_k t)$. The solution can be carried out numerically for any number of meshes. Using curves of this form, which check with experiment at low pressures, it has been possible to correct McLeod and ionization manometer readings to give true pressures at any part of the system. These have been used in the evaluation of true pump speeds. The agreement has given a check on the region over which Knudsen's low-pressure equation is valid.

92. Time-pressure characteristics of some diffusion and molecular pumps. PETER J. MILLS, *University of Chicago. (Introduced by Harvey B. Lemon.)*—Observations on various pumps were made of the time rate of change of pressure during the evacuation of a 4 liter volume and of the equilibrium pressure reached when this same 4 liter volume was leaking at a measured rate. The high vacuum pumps included single and multistage, air and water cooled, glass and steel diffusion pumps; and molecular pumps. Most of the diffusion pumps were mercury filled but several were tested with a filling of oils of low vapor pressure. Various backing pressures were obtained from several types of force pumps. Pressures, read on a pair of McLeod gauges and on an ionization manometer, gave apparent speeds from which true pump speeds were calculated by the method outlined in the preceding abstract.

93. The theoretical pressure distribution on wing sections. THEODORE THEODORSEN, *National Advisory Committee for Aeronautics, Langley Field, Virginia. (Introduced by J. S. Ames.)*—This paper presents a simple and exact method of calculating the lift distribution on thin wing sections. The angle at which the flow enters the leading edge smoothly is shown to play an important rôle in the theory, and is termed the ideal angle of attack. The lift distribution at this particular angle, termed the "basic distribution," is shown to be a characteristic property of the section. It is shown that the lift of a wing section may be considered to consist of (a) the basic distribution and (b) the additional distribution, the latter being identical for all sections. It is further shown that the additional lift intensity in potential flow of a non-compressible liquid is infinite at the leading edge, and the conclusion is made that the present theory of thin wing sections is applicable only at the ideal angle of attack. The theory is adapted to describe some of the properties of the actual or thick wing sections, and it is established that the essential parameter occurring in this analysis is the radius of curvature at the leading edge. The approximate magnitude and location of the maximum lift intensity is determined.

94. The effect of the presence of a grid upon certain characteristics of the airflow at the surface of an airfoil. MERIT SCOTT, *Cornell University.*—In a previous paper it was reported that the heat dissipation per unit area from the surface of an airfoil, as measured by resistance strips mounted parallel to the span and flush with the surface, is a characteristic of the airflow. An integral relation was set up from which it was shown that the coefficient of heat dissipation is proportional to the velocity gradient at the surface of the airfoil and hence to the viscous resistance. The effect of the presence of a grid, whose position with respect to the airfoil is varied, upon the above mentioned characteristics, has now been observed. It is found that systematic changes in these quantities may be followed as various parameters in the problem are altered. Mathematical treatment appears to be too involved for the present; but qualitative explanation is being attempted in terms of types of flow, the Prantl boundary layer, the Rayleigh surface of separation, etc.

95. Some examples of dimensional analysis. JAKOB KUNZ, *University of Illinois.*—The dimensional analysis has been applied to the following cases. (1) A solid body moves in a viscous medium, so that the motion is essentially determined by the viscosity, a characteristic length of the body, and the velocity, but independent of inertia, i.e., the density. The analysis leads to the formula $F=R\mu vC$. Stokes analysis gives $C=6\pi$. For higher velocity we assume that the viscosity has very little influence and that on the contrary the forces are determined by vortices and waves mixed up, or on the density ρ. The analysis leads to $F=v^2\rho l^2C$, Jonkowski-Cutta found $F=v^2\rho A \sin \alpha \cdot k$ for the lift of an airplane. (2) When the velocity of a projectile approaches that of sound, then the force depends probably on the compressibility of the medium. The force of resistance appears in the form $F=pl^2(v/c)^nC_1$, where c is the velocity of sound. (3) In an analogous way we proceed to study the motion of a fluid in a tube under a pressure gradient P. For a slow laminar motion under the influence of viscosity μ we obtain $P=(v/r^2)\mu C$, which is Poiseuille's law. In the case of turbulent motion we obtain $P=v^2r^{-1}\rho C$, where C is a dimensionless constant. Finally if the velocity is very large, approaching that of sound, P appears in the form: $P=p/r(v/c)^nC$.

96. The Auger effect in atomic spectra. A. G. SHENSTONE, *Princeton University.*—In most complex spectra there are two distinct series limits, the corresponding ions being of different structure. A term built on the ion of higher energy may be above the lower of the two limits. It is then possible for the atom to dissociate spontaneously into an ion plus an electron if there is a correct relationship between the qauntum numbers of the term and those of the ion and electron. The transition probabilities may be expected to be governed by rules similar to those which are applicable in predissociation of molecules. The effect is shown in the terms from the structure d^9s,s in CUI. The terms are ^4D, ^2D, ^2D and the lines due to all the components with $J=1\frac{1}{2}$ or $2\frac{1}{2}$ are absent or extremely weak in low-pressure sources, and very diffuse under high pressure. The ionization transition must be to the ion d^{10} plus a d-electron. The fact that the coupling is not completely Russell-Saunders accounts for the presence of the effect in ^4D. The structure d^9s, d also shows the same type of effect, but the observations are as yet incomplete. In BeI, the lines due to the negative term $3s2p^3P$ are absent in the spectrum

from the Schuler tube but present in high-pressure sources. The negative terms of CaI should show the effect but there are no observations in proper sources.

97. Intensity relations in complex spectra. GEORGE R. HARRISON AND M. H. JOHNSON, JR., *Massachusetts Institute of Technology, and Harvard University.*—A correlation is found between anomalous intensities in multiplets and the presence of neighboring states having the same J values as the perturbed terms. This indicates that the extension of the sum rules ordinarily assumed, in which all lines arising from a given state are summed, is incorrect, and that all similar terms having identical J values and lying near one another must be summed together. A general quantum-mechanical proof has been found that the following rule holds: The relative total intensity of all lines arising from transitions between all states J_1 and J_2 in two configurations is constant for any coupling. Where several configurations overlap the rule must be extended to include the new terms of similar J. Where relatively small departures from LS coupling exist only close-lying terms of similar J need be grouped together. Experimental verification is difficult as generally a large number of lines must be summed, but fragments often serve to test the rule. Confirmatory intensity measurements are presented which prove the interdependence of neighboring terms of common J, and it is shown that intensity anomalies are more sensitive indicators of departures from LS coupling than are the other anomalies associated with it.

98. Electrostatic interactions in (jj) coupling. D. R. INGLIS, *University of Michigan.*—A method is developed for calculating the energy of electrostatic electronic interaction for the various states of an atom in (jj) coupling. The largest perturbation of spin-orbit interaction is first taken into account by using single-electron wave functions stabilized for this interaction. Antisymmetric combinations of products of these form the fundamental wave functions in the perturbation calculation of the electrostatic interaction. The energy is expressed in terms of the same integrals that Slater (Phys. Rev. **34**, (1293)) met in the case of (LS) coupling, and one new integral. Of this latter, the angular integrations are carried out and are presented in tabular form. Its radial integrals are the same as those of Slater. In addition to giving interval relations in (jj) coupling, the results help to solve the problem of determining the levels of a configuration for general coupling.

99. Many electron transitions. S. GOUDSMIT AND L. GROPPER, *University of Michigan.*—First and higher order perturbation terms of the spin-orbit and electrostatic interaction in the eigenfunctions of many-electron configurations explain the occurrence of many-electron transitions. By considering which terms can occur in first order perturbation the following selection rules were obtained. No more than three electrons can jump at a time. (a) When three electrons jump all can change their n by an arbitrary amount, one changes its l by ± 1, the others by δ and ϵ, $\delta+\epsilon$ being even. (b) When two electrons jump both can change their n arbitrarily, one changes its l by $\delta \pm 1$, the other one by ϵ. Breaking off the series expansion for $1/r_{ij}$ in the electrostatic interaction after the second term gives for δ and ϵ only the values $0, \pm 1$. The Heisenberg two-electron selection rule is therefore to be considered as a special case of (b). Qualitative rules have been derived to tell when many-electron transitions may be strong. Special selection rules were found for (j, j) coupling. The first order terms also cause anomalies in the intensities of one-electron transitions.

100. The arc spectrum of rhenium. WILLIAM F. MEGGERS, *Bureau of Standards.*—The arc spectrum of rhenium has been photographed from 2100A in the ultraviolet to 8800A in the infra-red; it has more than 3,000 lines in this interval. About 25% of the lines show hyperfine structure of 2 to 6, or more, components. The centers of gravity of complex lines have been determined and are assumed to represent the effective wave-lengths for purposes of analysing the gross structure of the Re I spectrum. About 500 lines, including nearly all of the stronger ones, have been classified as combinations of terms belonging to quartet, sextet and octet systems. The normal state of the neutral Re atom is represented by $(5d^5 6s^2)a^6S_{2\frac{1}{2}}$. Series-forming terms have been identified which indicate that the ionization potential is approximately 7.8 volts.

101. Evidence regarding the structure of the arc and spark lines of nitrogen. P. G. KRUGER

AND R. C. GIBBS, *Cornell University.*—Nitrogen arc (NI) lines (λ's 6484, 4151, 4109, and 4099A) have been excited in a liquid air cooled condenser type discharge. These lines were photographically examined with the aid of a Fabry-Perot interferometer whose resolving power, depending on the spacing of the mirror surfaces, was 10^6 or better. With the resolution and dispersion thus obtained, the above lines were found to be sharp and lacking in any evidence of structure. The total line widths have been found to be 0.015, 0.011, 0.010 and 0.010A respectively. Nitrogen spark (N II) lines (λ's 3995, 4601, 4607, 4614, 4621, 4630, 4643, 5666, 5675. 5679, 5686 and 5710A) have been excited in a liquid air cooled electrodeless ring discharge. The microphotometer curves of the interference patterns from these lines show evidence of structure, although the components are so near together that they have not been clearly separated. The total line widths of these lines are three or four times as large as the widths of the arc lines. This gives added support to the conclusion that the spark lines are definitely complex.

102. The spectrum of Li III. H. G. GALE AND J. B. HOAG, *University of Chicago.*—In accordance with the simple Bohr theory, the spectrum of Li III should show lines analogous to the Lyman series at 135.0, 113.9, 108.0, 105.5, 104.2 etc., and lines analogous to the Balmer series at 729.1, 540.0 Angstroms, etc. We have succeeded in photographing and measuring on several plates five lines of the first of these series and the first line of the second. The line at 135A has been measured in three orders. The first two lines of the first series were previously measured by Edlén and Ericson. The third, fourth and fifth lines of the first series and the first line of the second series have not been previously reported. The $K\alpha$ line of lithium (199.26A) is very strong on many of the plates and has been measured in four orders. The vacuum spectrograph is the same as that first used by Hoag. (Astro. Jr. LXVI, 225, 1927). An electric furnace was used at first to produce lithium vapor between metallic poles. Better success has been obtained recently by using poles of lithium stanide and also metallic lithium in nickel holders.

103. Hyperfine structures in the first spectra of krypton and xenon. C. J. HUMPHREYS, *Bureau of Standards, Washington, D. C.*—The stronger arc lines of krypton and xenon have been examined for hyperfine structures. Methods of observation include the use of a Hilger Fabry-Perot interferometer having quartz plates of 6 cm aperture, a number of fixed étalons, and two quartz Lummer-Gehrke plates. The results obtained by different methods show very satisfactory agreement. Structures of the following lines have been measured: Krypton, 5570.2890, 7685.2472, 8059.5053, 8104.3660, 8281.11, and 8508.8736A; Xenon, 4193.5296, 4500.9772, 4734.1524, 8231.6348, 8409.190, and 8819.412A. No definite numerical regularities in the spacing of components, such as have been reported in the case of neon, have been observed, although with one exception the xenon lines showing structures are due to combinations with the low $^3P_2$ level and the pattern consists of four components. The satellites of neon lines are supposed to be due to Ne isotope, 22. Krypton and xenon are reported to have 6 and 9 isotopes respectively and the fine structure might be expected to be more complicated. The existence of a reported satellite of the krypton line, λ5570.2890A, has been confirmed. It is hoped that, by use of some cooling agent such as dry ice, additional structures may be resolved.

104. On the spectra of singly ionized rubidium and caesium. OTTO LAPORTE AND GEORGE R. MILLER, *University of Michigan.*—The spectra of Rb II and Cs II were investigated by means of a hollow cathode tube and a hot spark in the visible and ultra-violet regions. The data obtained were compared with the analyses of Reinheimmer (Ann. d. Physik **71**, 162, 1923) and Sommer (Ann. d. Physik **75**, 163, 1924) respectively. The classifications of these authors were found to be essentially correct though lacking greatly in completeness. The present analysis established the configurations $4p^6$, $4p^5 5s$, $4p^5 4d$, $4p^5 5p$, $4p^5 6s$ and $4p^5 5d$ in Rb II and of the corresponding configurations in Cs II. Spectrograms of the hollow cathode discharge of Rb II in the visible region are of special interest because the limit of excitation furnished by metastable helium falls exactly between the various levels caused by $4p^5 5p$, thus providing a check on the interpretation of the classification. The energy diagram of Cs II shows as a characteristic feature the decomposition of the levels of the above mentioned configurations into two distinct groups due to the large separation of $5p^5\,^2P$ of Cs III. The value of the ionizing potential of Rb II is 27.3 volts and that of Cs II 23.4 volts. Both values are about two volts larger than those given by Mohler (Phys. Rev. **28**, 46, (1926)).

105. Term values in the arc spectrum of selenium, Se I. R. C. GIBBS AND J. E. RUEDY, *Cornell University.*—A partial analysis of the arc spectrum of selenium has been given by Runge and Paschen (Astrophys. Jour. 8, 70, 1898) in the region 4700–7100λ, and by McLennan, McLay, and McLeod (Phil. Mag. **4**, 486, 1927) in the region 1400–2300λ. The present work is an extension of the data throughout the region 1300–9100λ, with the classification of a number of new lines. It has been found possible to determine the term values of certain levels built on the lowest level of Se II, $4p^3\,^4S_{3/2}$, and to relate them to this limit. The ionizing potential between the lowest level of Se I, $4p^4\,^3P_2$, and this limit has been computed as 9.70 volts.

106. Series in the spectrum of Germanium II. C. W. GARTLEIN, *Cornell University.*—High excitation of the first spark spectrum of germanium, Ge II, has been obtained in a Schuler lamp with circulating helium gas and a quantity of metallic germanium of high purity in a carbon cathode. The spectrum was photographed in the region 500A to 2500A with a vacuum spectrograph, from 2500A to 4000A with a 75 cm focus quartz spectrograph, and from 4000A to 9000A with a Zeiss 3 prism glass spectrograph. The series $4s^24p^2P^0_{\frac{1}{2},1\frac{1}{2}}-4s^2nd^2D_{1\frac{1}{2},2\frac{1}{2}}$ has been obtained for values of n from 4 to 11, and five members of the series $4s4p^{2\,2}D_{1\frac{1}{2},2\frac{1}{2}}-4s^2nf^2F^0_{2\frac{1}{2},3\frac{1}{2}}$ have also been obtained. From these data the series limit has been calculated to be 128,535 ± 50 cm^{-1} above $4s^24p^2P^0_{\frac{1}{2}}$ and gives about 15. 86 volts as the second ionization potential of germanium. Many new intercombination lines have been obtained. This work confirms the assignment of the low terms made by R. J. Lang (Phys. Rev. **34**, 696, (1929)) and shows the ionization potential to be slightly lower than the estimates of Lang and of Rao and Narayan (Proc. Roy. Soc. **A119**, 607, 1928).

107. A study of the vanadium I iso-electronic sequence. HELEN T. GILROY, *Cornell University.*—A study has been made of most of the spectra in the vanadium I iso-electronic sequence due to the possible electronic changes between the following configurations,—$3d^44s$, $3d^44p$, $3d^5$, $3d^44d$, $3d^34s^2$, $3d^34sp$. Application of the regular and irregular doublet laws to this sequence indicates that a five-electron system, giving quartets and sextets may be added to the systems studied by Bowen and Millikan and Gibbs and White, all of which obey these laws. To illustrate the regular doublet law one $\Delta\nu$ between sextet or quartet levels has been selected from each electronic configuration and $(\Delta\nu/K)^{1/4}$ calculated. The increase in $(\Delta\nu/K)^{1/4}$ is nearly linear with increase in atomic number. Screening constants obtained from these same 'doublets' vary from 16.18 to 15.05 through the sequence from vanadium to cobalt. Moseley diagrams have been drawn for sextets and quartets from each configuration. Utilizing the values of the vanadium I and chromium II limits as estimated by Russell, square roots of term values $(\nu)^{1/2}$ were computed and plotted against atomic number for sextets and quartets. Wherever the electron change did not involve a change in total quantum number $\Delta(\nu)^{1/2}$ was found constant through the sequence to Ni VI.

108. Possible direct reading methods for measuring the current in the electrodeless discharge. CHAS. T. KNIPP, *University of Illinois.*—An inductive method is described for measuring the magnetic component of the electrodeless discharge. In this the gaseous electric current circulating through a reentrant discharge tube was piped, so to speak, aside where it made a loop of one turn and then returned. A low resistance coil of one turn of heavy braid copper wire was placed in the maximum inductive position about this loop. Its terminals were connected to a radio ammeter. With this arrangement the ammeter, on excitation of the electrodeless discharge, read 3 amperes. Further, replacing the ammeter by a 5 cm bridge of No. 38 Ni wire, the wire instantly was fused; and, finally, an aluminum disc suspended within the loop, by a thread attached to its edge, and with its plane parallel to the gaseous current set itself briskly at right angles to same. The magnitude of these effects came as a surprise. The energy was supplied by a 25 kv., 800 kc motor-generator set, which gave highly damped waves.

109. Electrodeless discharge characteristics of hydrogen and nitrogen. OTTO STUHLMAN, JR. AND HENRY ZURBURG, *University of North Carolina.*—Electrodeless arc discharges were obtained by means of a predominant electrostatic field in a spherical bulb placed in a long solenoid excited by undamped high frequency oscillations. Critical minimum potentials to strike the arc were obtained as a function of gas pressure for frequencies between 1.5 and 4.5 million cycles.

The characteristics conformed closely to Pashan's law. The critical points defined by the minimum values of X_m and P_m for a given frequency of excitation showed that the Log $(X/p)_m$ was a linear function of the frequency f, between discontinuities, interpreted as critical points of ionization. These critical ionization points were found to be interpretatable as arising through successive impacts. The results show that here as in Towsend's work at higher pressures X/p increases with decreases in p. X_m was found to decrease with increase in f except where the relation passed periodically through sharp maxima, indicating by their shapes differences in elasticity of impact between the two gases, nitrogen behaving like an inelastic gas and hydrogen like an elastic gas. Pressure-frequency relations indicated the existence of the same ionization discontinuities.

110. The ionization by electron impact and extra ionization potentials of nitrogen and carbon monoxide. JOHN T. TATE AND P. T. SMITH, *University of Minnesota.*—The total positive ion current in nitrogen and carbon monoxide has been measured as a function of the energy of the impacting electrons out to 750 volts. The number of positive charges per electron per cm path at 1 mm pressure of Hg and 0°C was calculated. The efficiency curves for the two gases are almost the same and are very similar to those obtained for the inert gases (Phys. Rev. **36,** 1293 (1930)) and Hg vapor (Phys. Rev. **37,** 808 (1931)). Nitrogen has a maximum efficiency of 10.25 ions at about 100 volts and carbon monoxide a maximum of 10.87 at 105 volts. Extra ionization potentials in nitrogen were found at 15.80 (first ionization potential), 16.01, 16.30, 16.45, 16.55, 16.68, 16.79, 16.88, 16.96, 17.08, 17.20 and 17.44 volts. In carbon monoxide they were found at 14.20 (first ionization potential), 14.36, 14.49, 14.61, 14.71, 14.82, 14.91, 15.36, and 16.38 volts.

111. Mobilities of Na^+ ions in H_2 as a function of time. LEONARD B. LOEB, *University of California.*—The mobilities observed for Na^+ ions from a Kunsman source in H_2 (Phys. Rev. **36,** 152 (1930)) lead to a study of the square wave-form oscillations used. These were shown to be unreliable above 5000 cycles. The previous observations were substantially confirmed with the square waveform tube oscillator and by commutator at low frequencies and by sinusoidal oscillations from two different sources and with two different approaches from 2000 to 40000 cycles. For times of ion transit greater than 5×10^{-4} seconds the mobility uncorrected for temperature was 16 cm/sec per volt/cm. From 10^{-4} to 10^{-5} seconds mobilities of 21 were observed. Between these times intermediate values were found depending somewhat on the purity of the gas. The density correction for gas temperature in the path is slightly uncertain. The average temperature lay between 115°C and 60°C, the best value being 80°C. The mobility constants for the values above are therefore 13.5 and 17.5 respectively. The normal values observed in H_2 from ionization processes are 8.4 cm/sec. The latter value has no significance as the nature of the positively charged molecular nucleus of the ion is not known. The 17.5 value possibly corresponds to the Na^+ ion, while the 13.5 cm/sec value corresponds to a Na^+ ion with an attached molecule.

112. Evidence of energy exchanges accompanying scattering of atoms by crystals. H. A. ZAHL AND A. ELLETT, *State University of Iowa.*—The distribution of mercury atoms scattered from NaCl, KCl, KBr, KI has been studied by means of an ionization gauge as a function of angle of incidence and temperatures of scatterer and incident beam. The direction of maximum intensity makes an angle with the crystal normal not equal to the angle of incidence but always slightly less. The distribution can be well represented by $A\cos\theta+B\cos m(\alpha-\theta)$ ($B=0$ when $|m(\alpha-\theta)|>\pi/4$). The departure from specular reflection $\gamma=$(angle of incidence$-\alpha$) is greatest for high incidence, being 16° to 4° at an angle of incidence of 70° and about 5° at 45°. The values of A/B, m and γ depend on temperatures of crystal and beam. For rock salt at least, γ is less (more nearly specular) the colder the crystal and hotter the beam. Since any incident beam gives rise to diffuse scattering ($A\cos\theta$) plus directed scattering $\{B\cos m(\alpha-\theta)\}$ centered about a line making a greater angle with the crystal surface than does the incident beam it follows that the scattering is accompanied by an energy exchange.

113. The dependence of reaction velocity on temperature. R. M. LANGER AND B. G. CALVERT, *Massachusetts Institute of Technology.*—In a reaction which goes according to the law

$N_E(t) = N_E(0)e^{-\lambda(E)t}$ where $\lambda(E)$ is an increasing function of the energy E, and $N_E(0)$ is the number of systems in state E given by Boltzmann's Law, there are three characteristic types of temperature dependence. (1) For low temperatures there is a range in which the temperature coefficient defined by Tolman's formula $(\overline{\overline{E}} - \overline{E})/kT^2$ is constant and exceedingly small. Then comes a region (2) where the temperature coefficient rapidly increases with temperature. For higher temperatures (3) the curve again flattens out and the reaction rate K which is an average of $\lambda(E)$ can be expressed in the form $K = (1/\tau)e^{-A/kT}$ where τ is of the order of the period of oscillation of the system. Enough is known about the function $\lambda(E)$ to show for example that in the case of ordinary chemical reactions the region of (3) has already set in far below room temperature and that τ is of the order of 10^{-14} sec. For the typical radioactive processes on the other hand the region of (1) extends above 10^6 degrees. The temperature coefficient at ordinary temperatures is about 10^9 times smaller than in the chemical case so that regardless of the closeness of energy levels in the nucleus and even if the nucleus were in thermal equilibrium which is not the case until very much higher temperatures) the difference in radioactive decay rate between 0° absolute and ten thousand degrees would be inappreciable $(\Delta K/K < 10^{-4})$ even if there were no experimental difficulties in its determination.

114. Improved apparatus for temperature control. E. J. WORKMAN, *National Research Fellow, Bartol Research Foundation of the Franklin Institute.*—Temperature regulators involving the use of a grid controlled arc (thyratron) with a photoelectric cell and galvanometer *light* spot usually suffer from the effect of "hunting." This effect is inherent in the thermal capacity of the heated unit and is not reduced by increasing the galvanometer sensitivity. Such effects may be eliminated by placing in front of the photoelectric cell a rotating diaphragm having the form of an Archimedes spiral $[r(\text{inches}) = 1 + 0.08\theta]$. The rotating spiral is placed in such a position that the light from the galvanometer mirror falls intermittently on the photoelectric cell, and its duration of transmission is proportional to the galvanometer deflection. With the light beam intercepted in this way, the photoelectric cell causes a thyratron to give pulses of current of duration appropriate to the conditions of balance in the galvanometer circuit. This apparatus reduces the temperature fluctuations by a factor of from 10 to 50 times in comparison to the fluctuations obtained when the stationary diaphragm is used. Applications other than temperature control are discussed.

115. The isotopes of lithium, sodium and potassium. K. T. BAINBRIDGE, *National Research Fellow, Bartol Research Foundation, Swarthmore, Pa.*—Magnetic analysis of the positive rays of lithium from a spodumene source shows no change in the relative abundance of Li^7 and Li^6 with temperature. This is in agreement with Aston and Morand but at variance with the results of Dempster, Thompson, and the similar work of Hundley. A possible explanation of Hundley's results appears when the effects of space charge and the geometry of the tube are considered. In the present work, the ion currents were not limited by space charge, the ions when brought successively to the receiving slit described exactly the same path throughout, and the resolution was great enough to secure complete separation of the ion beams with freedom from background and strays. If Na^{21} or Na^{25} exist at all they are present to less than 1/3000 of Na^{23}. No evidence is secured of K^{40} or K^{43} to 1/300 to 1/1500 respectively of K^{39}. The presence of these isotopes has been predicted or suggested by Beck, Fournier, Kossel and others from nuclear regularities among the elements or to account for the radio-activity of potassium. The complete paper will appear in the Journal of the Franklin Institute.

116. The absorption coefficient for electrons in phosphorus and arsenic vapors. ROBERT B. BRODE AND METTA CLARE GREEN, *University of California.*—The absorption of electrons from a beam sent through the vapor has been observed for a range of electron velocities from 1 to 100 volts in phosphorus and from 4 to 200 volts in arsenic. In the phosphorus curve α has a minimum of about 345 cm^2/cm^3 at 2 volts, a maximum of about 380 at 4 volts, shows a definite decrease of slope around 16 volts and becomes about 150 at 100 volts. The actual magnitudes are not definite, due to uncertainties in vapor pressure data, to thermal effusion, and to transitions between yellow and red phosphorus during the measurements. No maxima or minima were observed in the arsenic curve. The values of α ranged from about 800 cm^2/cm^3 at 4 volts to about

250 at 200 volts. These values were taken using pressures from 1 to 3×10^{-3} mm of Hg. because outside these limits there were consistent departures from a linear relationship between log I/I_0 and pressure. At the temperatures and pressures used the molecular formulas are indicated by available data to be P_4 and As_4.

117. Neutralization and ionization of high velocity helium particles. PHILIP RUDNICK, *University of Chicago. (Introduced by A. J. Dempster.)*—A low voltage hot cathode arc and an accelerating potential were employed to produce high speed helium particles of homogeneous velocity corresponding to 7 to 22 kilovolts, which were then allowed to pass through helium gas. The equilibrium proportion of positive to neutral particles was found to increase with voltage in this range from 0.08 to 0.23. The mean free path for ionization of the high velocity neutral helium atom was found to vary approximately inversely as the square of the velocity from 19×10^{-4} cms to 6.5×10^{-4} compared with the kinetic theory mean free path of 17×10^{-6} cm. This is in agreement with Rüchhardt's hydrogen canal-ray measurements but differs from the behaviour of α particles where free path for change from single to double charge increases with the velocity. The mean free path for neutralization of the positive ions was computed to be 1.4×10^{-4}, practically independent of the velocity. The probability of capture of electrons by α rays has been found to depend very strongly on the velocity, in contrast to the approximate independence shown by these slower helium ions. These measurements were made by the method of Wien, with transverse electrostatic fields, using a thermocouple to detect the rays.

118. A method for producing high speed hydrogen ions without the use of high voltages. ERNEST O. LAWRENCE AND M. STANLEY LIVINGSTON, *University of California.*—A method for producing high speed hydrogen ions without the use of high voltages was described at the September meeting of the National Academy of Sciences. (Science **72,** 376 (1930).) The hydrogen ions are set in resonance with a high frequency oscillating voltage between two hollow semicircular plates in a vacuum, and are made to spiral around in semicircular paths inside these plates by a magnetic field. Each time the ions pass from the interior of one plate to that of the other they gain energy corresponding to the voltage across the plates. This method has now been tried out with the following results: Using a magnet with pole faces 10 cm in diameter and giving a field of 12,700 gauss, 80,000 volt hydrogen molecule ions have been produced using 2000 volt high frequency oscillations on the plates. A voltage amplification (the ratio of the equivalent voltage of the ions produced to the high frequency voltage applied to the plates) of 82 has been obtained. These preliminary experiments indicate clearly that there are no difficulties in the way of producing one million volt ions in this manner. A larger magnet is under construction for this purpose.

119. Photoelectric fatigue in cobalt. GEORGE B. WELCH, *Marshall College.*—The rate of photoelectric fatigue in cobalt, as a function of the incident radiation, is greater when a quartz-to-Pyrex graded seal is used on the apparatus than it is when the quartz window is attached with de Khotinsky cement. Sealing a side tube containing de Khotinsky cement into the apparatus causes the rate of fatigue to decrease. With nitrogen in the cell, the customary fatigue effects were observed. These experiments were made with pressures ranging from 10^{-7} to 10^{-5} mm of mercury, using the method described by the writer (Phys. Rev. **32,** 657 (1928)). Within these limits, an increase in pressure increases the rate of fatigue, an observation which receives some confirmation in experiments performed with electrolytically deposited sodium cells. An explanation is made on the basis of the "patch" theory. (Acknowledgment is made to the National Research Council and to Cornell University for material assistance in this work.)

120. Photoelectric effect of caesium vapour. F. W. COOKE, *University of Illinois.*—The measurements reported by Mr. E. M. Little, (Physical Review **30,** 109, (1927)), have been continued with a view to explaining the difference between the results of Little and F. L. Mohler. No effect has been found on the long wave-length side of the critical wave-length 318.4$\mu\mu$. The effect is a maximum at this convergency frequency, decreases with increasing frequency, reaches a minimum and begins to increase again. The order of magnitude of the effect is the same as that of Mohler. Several disturbing effects had to be eliminated and the final effect was only obtained as a difference between a dark current and the current due to light.

121. Intensity of infrared absorption bands. LORNE A. MATHESON, *University of Michigan.*—The intensity of absorption bands of gases in the near infrared has been determined by a new method. A beam of radiation of known spectral intensity is passed through the absorbing gas and the absorbed energy found by its resulting heat production causing a measurable expansion of the gas. Readings for various concentrations of absorbing gas are extrapolated to zero concentration. From the results one may calculate the matrix component of the electric moment corresponding to the vibration transition causing the band and the line width of the individual lines. Preliminary results have been obtained with CO.

122. Infrared absorption bands in formaldehyde vapor. HAROLD H. NIELSEN AND JOHN R. PATTY, *Ohio State University.*—Two of the principal regions of absorption in Formaldehyde vapor reported earlier at 3.5μ and 4.7μ have been further investigated with an echellette grating with a spacing of 3600 lines to the inch. The region at 3.5μ, earlier thought to be a band consisting of P, Q and R branches has been found under higher dispersion to consist of three overlapping bands with centers at 3.61μ, 3.52μ and 3.37μ. Two of these (3.61μ and 3.37μ) show P, Q and R branches. The average spacing between lines in these bands is about 3.5 cm^{-1}. The third band (3.52μ) has only one branch which constists of groups of closely spaced lines. The spacings between these groups is about 14.0 cm^{-1} or about four times that of the other bands. The region at 4.7μ is similar to those at 3.6μ and 3.37μ in spacing and structure. Due to better resolution in this region, what at 3.37μ appeared as a single line here appears as a group of very closely spaced lines incompletely resolved. Calculations on molecular models of slight asymmetry show very good agreement between theory and experiment for the case where the principal moments of inertia have the values: $A_z=2.7\times10^{-40}$, $A_y=18.0\times10^{-40}$, $A_x=21.0\times10^{-40}$ gm-cm^2.

123. The visible and ultraviolet absorption spectra of certain amino acids and their significance. GLADYS A. ANSLOW AND MARY LOUISE FOSTER, *Smith College.*—The absorption spectra of the acid solutions of alanine, cysteine, aspartic acid, glutaminic acid, and cystine have been studied from 650 to 200 $m\mu$ with a rotating sector photometer. Aspartic and glutaminic acids, whose molecules are nearly symmetrical about the bond between the α and β carbons, gave broad, structureless bands in the visible region with maxima at 526 and 495 $m\mu$, respectively, probably caused by vibration in this bond. Cystine showed a narrower band with maximum at 251 $m\mu$, which is ascribed to vibration in the *S-S* bond, about which it is symmetrical. Continuous absorption started in all the acids between 225 and 200 $m\mu$, due to dissociation in a common group, the least energy being required to dissociate the heaviest molecule. The energy of dissociation in volts is 5.46, 5.52, 5.62, 5.75, and 6.07 for cystine, glutaminic acid, aspartic acid, cysteine, and alanine, respectively. This dissociation probably occurs in the carboxyl group, for similar compounds, lacking the amino group, give continuous spectra in the same region, as was also found by Ley and Hünecke (Ber. Deut. Chem. Gesel. **59**, 510, 1926). Since the water solutions give like spectra except for a slight shift to shorter wave-lengths, the carboxyl group must be present in the same form in acid and water solutions, contrary to the zwitterion theory.

124. The fundamental vibration bands of CO_2. P. E. MARTIN AND E. F. BARKER, *University of Michigan.*—The absorption bands of CO_2 at 4.3μ and 14.9μ have been examined with a grating spectrometer of resolving power sufficient to separate the rotation lines. The 4.3μ band consists of positive and negative branches only, with rotation lines about 1.5 cm^{-1} apart, and shows considerable convergence. The spacing is the same as in the long wave band, and is about twice the value obtained when estimated in the usual way from the doublet separation. This indicates that the molecule is linear, with the carbon atom midway between the two oxygen atoms. In the low frequency band a strong zero branch appears at 14.9μ, with twenty or more rotation lines on either side, about equally spaced. The motion associated with this band is one in which the carbon atom vibrates in a plane normal to the line adjoining the two oxygen atoms. A second harmonic band appears at 4.8μ, but there is no first harmonic. Superposed upon the fundamental are three other bands, considerably less intense, of which two correspond to absorption by molecules already excited to the first vibration state by thermal impacts, while the third is a difference band involving the inactive symmetrical vibration. The energy values for three of the vibration states associated with the lower frequency may thus be determined, and

these yield precisely the Raman frequencies observed by Dickinson, Dillon and Rasetti, interpreted as transitions of two in the vibrational quantum number which are required by the selection rules for this isotropic vibration.

125. The vibration spectrum of the N_2O molecule. E. K. PLYLER AND E. F. BARKER, *University of Michigan.* Three very intense infrared bands which apparently correspond to the fundamental vibrations of the N_2O molecule have been observed at wave lengths of 16.9μ, 7.7μ and 4.5μ. All three have been resolved under high dispersion, the rotation lines in each case being spaced about 0.8 cm^{-1} apart. The band at 16.9μ has a strong zero branch, while the other two are of the doublet type. The three first harmonics have also been found, and the one at 8.6μ resolved. This latter is a doublet type band although its fundamental has a zero branch. In addition to these, five combination bands have been studied, all but one being of the doublet type. Several of the bands are complicated by the superposition of absorption due to molecules already excited to the first or second vibration state for the lowest frequency.

126. The band spectrum of germanium sulfide. C. V. SHAPIRO, R. C. GIBBS AND J. R. JOHNSON, *Cornell University.*—A band spectrum of germanous sulfide (GeS) has been observed in absorption at temperatures between 450 and 550°C, in the region λ3300 to λ2400. Two electronic transitions have been observed, originating from the same normal state of the molecule. The equations for the band heads are:

$$\text{I.} \quad \nu = \nu_e(\text{I}) + 378.2(v' + 1/2) - 1.55(v' + 1/2)^2 - 580.2(v'' + 1/2) + 3.2(v'' + 1/2)^2$$

$$\text{II.} \quad \nu = \nu_e(\text{II}) + 309.6(v' + 1/2) - 1.3(v' + 1/2)^2 - 580.2(v'' + 1/2) + 3.2(v'' + 1/2)^2$$

v' progressions of 13 and 9 members respectively have been followed in these systems, while v'' takes on values from 0 to 4. The intensity distribution is normal. There are indications of an isotope effect, as most of the heads are accompanied by two satellites, whose intensity is comparable to that of the main head, corresponding to the fact that germanium consists chiefly of three isotopes. These satellites are being investigated further. Extrapolation of the vibrational series of the two upper levels indicates that the products of dissociation are the same for the two. Assuming that normal atoms are produced by dissociation from the normal state, 3.7 volts are obtained as the upper limit for the energy of one or both of the atoms resulting from dissociation from the excited state of the molecule. This value is of the order of magnitude to be expected for the (still unknown) $^1S_0$ level of the basic configuration, $3s^23p^4$, of sulfur.

127. Zeeman effect in the $^2\Sigma - {}^2\Sigma$ cyanogen bands. E. L. HILL, *University of Minnesota.*—Interpreting the doublet separations in the lower state of these bands as due to a molecular magnetization by rotation, as suggested by Kemble, preliminary calculations have been made of the expected widths and intensity distributions of the Zeeman patterns of some of the doublets for various strengths of the magnetic field. The results indicate that for fields of about 8500 gauss a representative doublet such as λ3796.104 −0.184 should be unobservable as two lines, which seems at variance with the experiments of A. Bachem (Zeits. f. Physik **3**, 372 (1920)). For somewhat lower fields there may be complete or partial separation of the doublets. Further experiments are being conducted by Dr. Crawford at Harvard to determine with greater accuracy the form of the components of the doublets in the field. Assuming a suitable doublet separation in the upper $^2\Sigma$ state it seems possible that the rapid convergence of the predicted patterns might be checked, but there is at present no estimate of the magnitude of the no-field doubling for this state. If the experimental data seem to justify the effort, a more complete study of the Zeeman effect for Σ states will be undertaken.

128. Interpretation of the spectrum of BaF. A. HARVEY (*Commonwealth Fund Fellow*) AND F. A. JENKINS, *University of California.*—Observed in the first order of the 21-foot grating, the absorption spectrum of BaF presents some 200 bands heads in the region 3600–9000A. These represent all of the band systems previously known in emission, and two additional ones. The electronic levels, and the vibration frequencies, $\omega_{1/2}$, (in parentheses) are as follows: X, 0 (465.4); A, 11,630 (434.2); B, 12,260 (433.8); C, 14,040 (420.7); D, 19,990 (452.5); E, 20,190 (454.5); F, 24,170 (504.6); G, 26,240 (501.8). The systems $A \leftarrow X$ and $B \leftarrow X$, discovered in emission by Querbach, are evidently the components of the $^2\Pi \leftarrow {}^2\Sigma$ system analogous to that in

SrF and CaF, while the $C \leftarrow X$ system represents the $^2\Sigma \leftarrow {}^2\Sigma$ system also found for these molecules. $D \leftarrow X$ and $E \leftarrow X$ probably form a doublet system, which, by analogy with the Cs atom, would involve a more excited $^2\Pi$ level. The new systems $F \leftarrow X$ and $G \leftarrow X$ each consist of single-headed bands. New sequences in the $D \leftarrow X$ and $E \leftarrow X$ systems confirm Johnson's vibrational analysis, but Querbach's assignments in the infra-red system are corrected in important respects. All the bands resemble closely those of the isoelectronic molecule LaO, and here also the normal state must be the common lower level of all the known systems.

129. Boron hydride bands. R. F. PATON AND G. M. ALMY, *University of Illinois.*—Two bands due to boron hydride have been photographed in the spectrum of a 110-volt d.c. arc in hydrogen with amorphous boron contained in a nickel or copper cup as one of the electrodes. The bands obtained are those recently reported by W. Lochte-Holtgreven and E. S. van der Vleugel (Nature, Feb. 14, 1931) as the (0, 0) and (1, 1) bands of a $^1\Pi \rightarrow {}^1\Sigma$ transition in BH. They consist of P, Q, and R branches degraded to the red. The conspicuous Q heads are at λ4331 (0, 0) and λ4367 (1, 1). From the P and R branches the molecular constants obtained are $B_0' = 11.920$, $B_0'' = 11.808$, $B_1' = 11.21$, $B_1'' = 11.44$, $D_0' = -0.00143$, $D_0'' = -0.00118$, $D_1' = -0.0017$, $D_1'' = -0.00145$. These values indicate that the (0, 1) band should degrade rapidly to the violet. A careful search on our heaviest exposures failed to give definite evidence of such a band. The isotope band due to $B_{10}H$ was observed through the greater part of the P and R branches of the (0, 0) band and establishes the identity of the carrier. Microphotometer comparisons on three plates of the intensities of the 7 best lines in the R branch gave the abundance ratio of B_{11} to B_{10} as $4.86 \pm .15$, indicating an atomic weight of $10.841 \pm .005$, in good agreement with the chemical determination.

130. A further study of the emission spectrum of CO_2. H. D. SMYTH AND T. C. CHOW, *Princeton University.*—The analysis of the CO_2 bands reported at the New York meeting has been considerably extended. We have now found combinations between the set of vibration terms previously reported ($\nu = \nu_0 + 1101.7v + 1.7v^2$) and eight or more levels of a different electronic state. This second set of levels seems to be made up of a double vibration set and seven of them can be fitted by a simple quadratic formula of the type

$$\nu = \nu_0 + a_1 b_1 + b_1 v_1^2 + a_2 v_2 + b_2 v_2^2 + b_{12} v_1 v_2$$

where the constants a_1 and a_2 are of the same order of magnitude as the Raman frequencies of CO_2. Though nearly a hundred bands have now been fitted into the scheme there remain numerous anomalies which we hope may be removed by further adjustment of the numerical constants. We are also endeavoring to get in emission the bands observed by Leifson in absorption and for this purpose are setting up a small fluorite vacuum spectrograph separated by a fluorite window from the excitation chamber previously described.

131. Band spectrum of bismuth chloride. PAUL G. SAPER, *University of Chicago. (Introduced by Robert S. Mulliken.)*—A band system of BiCl in the region from about 4300 to 5500A was excited by introducing vapor from heated $BiCl_3$ into active nitrogen. The bands are degrated toward longer wave-lengths. No other bands were found besides this system. The vibrational isotope effect showed that BiCl was the emitter. The isotope effect also served as a valuable aid in locating the origin of the system. The heads were measured and a vibrational analysis made. From the analysis an equation was obtained for the wave numbers of the $BiCl^{35}$ heads. Coefficients for an equation for the $BiCl^{37}$ heads were computed from theory from those of the $BiCl^{35}$ equation. These equations are given below.

$$BiCl^{35}: \nu = 21802.1 + [221.2(v' + \tfrac{1}{2}) - 308.6(v'' + \tfrac{1}{2})] - [2.65(v' + \tfrac{1}{2})^2 - 0.95(v'' + \tfrac{1}{2})^2]$$
$$BiCl^{37}: \nu = 21802.1 + [216.0(v' + \tfrac{1}{2}) - 301.4(v'' + \tfrac{1}{2})] - [2.53(v' + \tfrac{1}{2})^2 - 0.91(v'' + \tfrac{1}{2})^2]$$

The average difference between calculated and observed frequencies was ± 1.7 cm^{-1}. The isotopic displacement was calculated for the heads in the cases where the effect was evident, and a close agreement was found with corresponding observed values of the displacement.

132. Perturbations in the helium band spectrum. G. H. DIEKE, *The Johns Hopkins University.*—A large number of electronic terms of the He_2 molecule is known, and therefore

its spectrum is especially suited to test the theory of perturbations developed mainly by Kronig. Two levels which lie close together perturb each other if they have: 1. The same J, 2. The same inversion symmetry, 3. The same exchange symmetry, 4. Λ different by at most ± 1, 5. The same multiplicity, 6. Approximately the same internuclear distance. The $ns\Sigma$ and $nd\Sigma$ levels of the He_2 molecule satisfy conditions 1. to 6. Rotational levels having the same J lie close together for $J=17$ if $n=4$, for $J=9$ if $n=5$, for $J=5$ if $n=6$. [n, total quantum number.] All these levels show marked perturbations which show in the spectrum by a displacement of the lines in question and sometimes by abnormal intensities. The two levels involved are shifted in opposite directions as required by the theory. There are numerous cases in which levels of the He_2 molecule come close together which do not satisfy the above conditions. Then there is no trace of any perturbation.

133. The effect of temperature upon the ultraviolet band spectrum of ozone and the structure of this spectrum. OLIVER R. WULF AND EUGENE H. MELVIN, *Bureau of Chemistry and Soils, Washington, D. C.*—The ultraviolet absorption of ozone in the region 3400—2300A consists of a large number of bands appearing against a background of continuous absorption. The effect of temperature upon this spectrum has been studied over the range −78° to 250°C. A definite though small effect has been observed. Grossly it manifests itself as an increase in contrast with decreasing temperature. Photometric results show this to be chiefly a decrease in absorption between the band edges, all of the bands appearing to come from normal vibrational levels of very low if not the lowest energy. Though somewhat diffuse, the bands tend to degrade to the red. The observed influence of temperature can be explained as the decrease of intensity in the higher rotational absorption of the bands, and possibly also in the continuous background, with decreasing temperature. Discontinuities in the intensity relations and the regular spacing of certain of the bands have led to a partial vibrational analysis indicating two active vibrational degrees of freedom in the excited electronic state. The observed change in the absorption with temperature may affect somewhat the estimates which have been made of the amount of ozone existing in the upper atmosphere.

134. Rotational analysis of the first negative group of oxygen (O_2^+) bands. DANIEL S. STEVENS, *University of Chicago. (Introduced by R. S. Mulliken.)*—The bands were produced by a hollow cathode discharge and photographed in the second order of 21-foot Rowland grating. The following bands were used in the analysis: 1–6; 0–6; 1–7; 0–7. As was expected these bands correspond to $^2\Pi \rightarrow {}^2\Pi$ transition like the double headed β bands of NO, the two molecules being alike in their electron configurations. The lower $^2\Pi$ is case a as in NO. Unlike the case of NO, however, the upper $^2\Pi$ is case b. The lower $^2\Pi$ is regular, with a doublet separation (corrected to zero rotation) of 195 cm^{-1}. Each band consists of eight branches (four P and four R) together with some indications of four weak Q branches. This is in agreement with theory. Alternate levels in each Λ-type rotational doublet are missing in both the upper and lower $^2\Pi$ states. This is as predicted by the quantum theory of homopolar molecules, since it is known that the nuclear spin of the oxygen atom is zero. The constants of the molecule in the two electronic states are given by: $B'=1.043-0.027v'$ cm^{-1}, $B''=1.583-0.009v''$ cm^{-1}, $r_e'=1.41\times10^{-8}$ cm, $r_e''=1.15\times10^{-8}$ cm.

135. Electronic energy levels of neutral and ionized oxygen. ROBERT S. MULLIKEN, *University of Chicago.*—The normal state of O_2 is known to be a $^3\Sigma_g^-$, probably corresponding to an electron configuration $\cdots 3d\sigma^2 2p\pi^4 3d\pi^2$ hereafter called A. The upper state of the Schumann-Runge bands is a $^3\Sigma_u^-$ probably derived (Herzberg) from $\cdots 3d\sigma^2 2p\pi^3 3d\pi^3$, hereafter called B. Configuration A should also give two metastable levels $^1\Delta_g$ and $^1\Sigma_g^+$, and B a set of metastable levels $^3\Delta_u$, $^1\Delta_u$, $^3\Sigma_u^+$, $^1\Sigma_u^+$, and one non-metastable level $^1\Sigma_u^-$. The upper level of the atmospheric bands, previously identified as the metastable $^1\Sigma_g^+$, is more probably the $^1\Sigma_u^-$. If it were $^1\Sigma_g^+$, the bands would be an intersystem quadrupole transition and probably much weaker than they are. (That $^1\Sigma_u^-$ of B should be below $^3\Sigma_u^-$, as here assumed, is indicated by consideration of the wave-functions.) The numerous bands observed by McLennan and others in liquid oxygen probably represent transitions to various metastable levels mentioned above. Or possibly some of these and the $^1\Sigma_u^-$ may belong to some other configuration, e.g. $3d\sigma^2 2p\pi^4 3d\pi 3p\pi$.

The normal and excited $^2\Pi$ states of O_2^+ (cf. preceding abstract) probably result from the respective removal of a $3d\pi$ or a $2p\pi$ electron from A. Existing data on O_2 and O_2^+ bands indicate 11.7 volts as the most probable value of the minimum ionizing potential of O_2.

136. Magnetic rotation spectrum and heat of dissociation of Li_2. F. W. LOOMIS AND R. E. NUSBAUM, *University of Illinois.*—The green magnetic rotation spectrum has been obtained from lithium contained in a nickel tube which was heated to about 1200°C by a low voltage stepped-down current. The tube was mounted in a solenoid which produced a field of 1300 gauss. The phenomenon can be seen in greater detail than in the previously studied spectra of Na_2 and K_2. In addition to the strong line at the head of each band caused by the piling up of the R branch lines, one can see the first few lines of the P branches of the strongest bands. Bands due to the lighter isotope are also visible. The spectrum extends to much higher values of v' and v'' than Wurm or Harvey and Jenkins report in absorption. It has consequently been possible to deduce a much improved value for the heat of dissociation. The frequencies of the magnetic rotation lines are represented by the following formula:

$$= 20398.4 + (266.90v' - 2.840v'^2 - 0.0637v'^3) - (349.00v'' - 2.605v''^2 - 0.0097v''^3).$$

The heat of dissociation deduced by extrapolation of the upper set of levels with a slight correction, due to the deviation of the highest observed levels from the formula, is 1.14 volts. Since the upper levels have been followed to within 0.1 volt of convergence this figure can hardly be in error by more than about 0.03 volt.

137. Valence forces in lithium and beryllium. J. H. BARTLETT, JR., AND W. H. FURRY, *University of Illinois.*—By methods similar to those used by Heitler and London, an investigation has been made of the interaction of two normal lithium atoms, and also of the interaction of two normal beryllium atoms. In the first case, two states, one attractive and the other repulsive, are possible for the molecule. The influence of the K shells has been neglected, and a nodeless wave function such as used by Guillemin and Zener (Zeits. f. Physik **61**, 199 (1930)) has been employed. The heat of dissociation of Li_2 is calculated to be 1.12 volts and the equilibrium internuclear distance to be 2.4A as against the experimental values of 1.14 volts (Loomis and Nusbaum, unpublished) and 2.67A, respectively (Harvey and Jenkins, Phys. Rev. **35**, 789 (1930)). No stable state is possible when two normal beryllium atoms interact with each other. A study is being made to ascertain under what conditions stable beryllium molecules will be formed.

138. Evidence against the existence of a chlorine isotope of mass 39. MURIEL ASHLEY AND F. A. JENKINS, *University of California.*—From results on the infrared spectrum of HCl, Becker (Zeits. f. Physik **59**, 601 (1930)) concluded that Cl^{39} exists in small amounts, in addition to Cl^{35} and Cl^{37}. A favorable opportunity for confirming this result is found in the ultraviolet absorption bands of AgCl analysed by Brice. The region adjacent to the $AgCl^{37}$ head of the 0.1 band is exceptionally free from structure, and the $AgCl^{39}$ head should appear at high vapor densities, if this isotope exists. The bands have been photographed with the 21-foot grating, using various vapor densities, from that at which the first appreciable absorption of the $AgCl^{37}$ head begins (550°C), to that for practically continuous absorption (850°). No trace of the predicted band was found. Using the vapor pressure data of Vartenberg and Bosse, the densities at the above temperatures are in the ratio 1/1000, and hence Cl^{39} cannot be present to a greater extent than 1/1000 of Cl^{37}, or 1/4200 of the whole. Similar investigations of the AgBr and AgI bands show that none of the elements involved possess heavier isotopes in quantities detectable by this method. For AgBr, the vapor pressure data of Jellinek and Rudat yield 1/2500 as the upper limit for a Br isotope of mass greater than 81.

139. The λ3360 band of NH. R. W. B. PEARSE, *Commonwealth Research Fellow, University of California.*—The band at λ3360 emitted by the molecule NH (so-called "ammonia" band) has been photographed in the second order of the twenty-one foot concave grating for the purpose of remeasurement. The source used was a water-cooled discharge tube of large current carrying capacity containing a mixture of hydrogen and nitrogen. With the dispersion of

1.3 A/mm which was obtained the closely crowded line structure of the central maximum of intensity could be to a large extent analysed into the three components of a triple Q-branch. The band shows the three P, three Q and three R branches appropriate to a $^3\Pi \rightarrow {}^3\Sigma$ transition where the $^3\Pi$ state is near Hund's case b. The rotational term differences are obtained from these branches and used to evaluate the molecular constants. The improved wave-length data giving rise to improved values of these constants.

140. On the resolving power of the concave grating. J. E. MACK AND J. R. STEHN, *University of Wisconsin.*—An expression for the resolving power of the concave grating has been obtained, taking into account the fourth order effect upon the phase, of the departure of the grating from the plane. The result is expressed in terms of the "effective width" of the grating; i.e., the width of plane grating which gives the same resolving power as the concave one under consideration. This effective width is equal to the actual width, for narrow gratings. It increases to a maximum as the width of the grating is increased, then it decreases again and oscillates about a constant value, so that there is an optimum width, depending on the radius of the grating ρ, the angle of incidence ϕ, the wave-length λ, and the order of the spectrum. Of special interest is the case of grazing incidence (which has recently become important in extreme ultraviolet spectroscopy), where the effective width can never be greater than $2.3\,[\rho^3\lambda \cos \phi]^{1/4}$, and approaches a value 20 per cent less, as the width of the grating is increased. In actual cases the optimum width may be as small as 1 cm.

141. Reflecting power and grating efficiency in the extreme ultraviolet. H. M. O'BRYAN, *The Johns Hopkins University.*—By using a lightly ruled concave glass grating with a water-cooled vacuum spark between tungsten electrodes, enough intensity has been obtained to make quantitative measurements of grating efficiencies and reflection coefficients for various angles of incidence between 1000A and 280A in a vacuum spectrograph. To obtain the reflection coefficients, a mirror of the substance to be examined was rotated about the axis of a cylindrical oil-coated film on which the reflected spectra was photographed. Small gratings were inserted in place of the mirror with their rulings perpendicular to those of the concave grating and the spectra of the crossed gratings examined. Lightly ruled glass gratings, which were good at normal incidence, gave only extremely faint spectra near grazing incidence. Glass gratings etched with hydrofluoric acid were of little value at normal incidence but surprisingly efficient near grazing incidence. A grating of the echelette type, with the angle between the incident light and reflecting face of the groove made small enough to utilize the increased reflecting power at small angles will be the most efficient grating for the extreme ultraviolet and soft x-ray regions. The etched glass gratings approximate an echelette with a wide V-shaped groove.

142. Three methods of studying capillary structure as applied to wood. ALFRED J. STAMM, *Chemist Forest Products Laboratory, U. S. Department of Agriculture.*—Three different physical methods for studying the capillary structure of porous materials are developed and applied to the study of the fine effective continuous capillary structure of wood. The three characteristic capillary properties measured are, (1) the ratio of effective capillary cross-section to the effective length, (2) the average effective capillary radius, and (3) the maximum effective capillary radius. Some of the important characteristics of the porous structure of wood are briefly presented in order to show that the major part of the void structure, the fiber cavities, have very little to do with the permeability of wood. The pores in the pit membranes which connect the adjacent fiber cavities are shown to be the structure effective in controlling permeability of wood. These pores in the pit membranes in general, are below microscopic visibility, thus necessitating other means of study.

The ratio of the effective capillary cross-section to the effective capillary length is determined from electrical resistance measurements of strong salt solutions filling the void structure and from the specific resistance of the salt solutions in bulk. Strong salt solutions are used in order to make the surface conductivity negligible as well as the conductivity of the swollen cell wall. The average effective capillary radius is determined by combining the results of the preceding measurements with results obtained from hydrostatic flow studies of a continuous water phase extending through the section. Poiseuille's law is used for the calculations. A

differential pressure drop apparatus was devised for these measurements in which the flow of liquid through a standard capillary tube and the test specimen connected in series is determined by measuring the pressure drop through each. The maximum effective capillary radius is determined by measuring the gas pressure required to overcome the effect of the surface tension of water in the capillary systems. The data show the large differences between the fine capillary structure of heartwood and of sapwood.

143. The electric conductivity and dielectric constant of disperse systems. HUGO FRICKE, *The Biological Laboratory, Cold Spring Harbor, Long Island.*—This report refers in particular to suspensions of biological cells. The interior of a biological cell is a well conducting salt solution, but at its surface polarization or the presence of a non-conducting membrane obstructs the passage of an electric current with a resulting low conductivity and high dielectric constant of the suspension. The theory for the passage of an alternating current through a suspension of this type is dealt with and experimental work with various kinds of suspensions such as cream, wet sand, blood, and animal tissues, is described to show the applicability of the theory. The determination of the volume concentration of suspensions, of the form factor of the suspended particles, of the thickness of surface membranes, and of the interior conductivity of living cells are instances of practical applications.

144. Three component emulsions. P. G. NUTTING, *U. S. Geological Survey.*—A quartz sand grain, wet with water, tends to cling to oil but tends to remain on the water side of an interface. A glass plate, such as a microscope cover glass, may readily be floated on water if the water is first covered with gasoline. Muddy water, shaken with gasoline, is cleared, the particles of silt collecting in a tough skin at the interface. Muddy gasoline shaken with clear water gives the same result. Emulsions form whenever a dielectric fluid (air or an insulating oil), solid particles and a second fluid containing OH (water, alcohol, glycerine, linseed oil) are thoroughly mixed and allowed to stand. Two components give solutions and suspensions but never emulsions. The solid particles are supposed to adsorb OH ions on one side thereby acquiring an induced charge on the other which clings to the dielectric.

145. The electric mobility of proteins. HAROLD A. ABRAMSON, *Harvard University.*—I. The electric mobility of microscopic quartz particles covered with egg and serum albumins (crystallized 3×) is, between $pH=3.5$ to 5.5 (1) equal to the mobility of the dissolved protein molecules, and (2) proportional to the combining power of the proteins for acids and bases. This indicates that the amino and carboxyl groups of the adsorbed protein molecules are practically all oriented toward the aqueous phase. The method of mobilities, therefore, is a valuable means of studying the orientation of polar molecules at solid-liquid and liquid-liquid phase boundaries. This is further demonstrated by the behavior of crystals of tyrosine, cystine and aspartic acid. The electric mobilities of these particles indicate that the ampholytic nature of these substances is not simply responsible for the values of mobility. All these crystals are negatively charged at the isoelectric point calculated from the dissociation constants. All three have an isoelectric point at about $pH=2.4$, with reversal of sign in more acid solutions. The mobilities of the amino-acid crystals are, therefore, somewhat like those of inert surfaces, differing however in important respects. It seems likely that the amino and carboxyl groups at the surface of the crystal are not oriented toward the liquid.

II. The change in electric mobility of egg albumin with pH is proportional to the change in specific rotation. A method is available, therefore, for the comparison of change in potential with change in the rotation of the plane of polarized light.

146. The application of the ultracentrifuge to some colloid physical problems. J. B. NICHOLS, *E. I. duPont de Nemours & Company.*—Until recently there existed no very reliable method for determining particle-size distribution curves of colloidal material, especially lyophilic colloids. Accordingly a study was undertaken of the conditions required for undisturbed centrifugal sedimentation of fine-grained colloids and for the accurate determination of the sedimentation-velocity and diffusion relations. The present ultracentrifuge, as developed in Svedberg's laboratory, enables us to exert a centrifugal force 100,000 times that of gravity on a solution and thus to determine the particle size of a great variety of colloidal material and even

molecular weights of complex dyes or proteins. Valuable information can be obtained on phenomena such as the interaction of particles in solution, the effect of the environment on the state of aggregation, and Donnan potential effects.

147. The limitations and adaptability of ultramicroscopes to the study of colloid systems. L. V. FOSTER, *Bausch and Lomb Optical Co.*—Ultramicroscopes are of two distinctly different types. The best known is the cardioid ultramicroscope in which the illuminating portion produces a hollow cone of large angular aperture with its apex at the object. The observing system is a microscope consisting of a high aperture objective of angular aperture slightly less than that of the hollow cone and a high power eyepiece. The other is the slit ultramicroscope. The illumination system in the slit ultramicroscope is perpendicular to the observing system. Both systems are of high numerical aperture, but no direct light can enter the observation system. Details of construction of both types of ultramicroscopes and their sensitiveness of adjustment will be discussed. Expressions for their limitations in colloid microscopy will be given.

148. Physics in the study of pigment dispersions. F. A. STEELE, *The New Jersey Zinc Co., Palmerton, Pennsylvania.*—The study of colloids has reached the point where many important contributions are coming from physicists. Even more attention from physicists will be required if this science is to progress as it should. A suitable dispersion of zinc oxide in kerosene has a high yield value and marked plastic properties. A few drops of a dispersing agent added to this mixture largely destroys its plastic properties and greatly increases its fluidity. It is well established that the dispersing agent accomplishes this result by decreasing the interfacial tension and thereby destroying the flocculation of the pigment. In certain cases in paints, however, there is reason to believe an entirely different phenomenon is responsible for yield value and plasticity. Much work with the tools of the physicist is indicated in the solution of this problem. There is much to be done in the study of solid-liquid interfacial tension, adsorption layers, interfacial potentials, and the di-electric properties of colloids before these problems are to be solved. The behavior of pigments in rubber is also discussed.

149. Some theoretical aspects of the biological applications of physics of disperse systems. N. RASHEVSKY, *Westinghouse Research Laboratories, East Pittsburgh.*—A review of the author's recent theoretical work on the properties of small liquid drops and more generally of systems with very large specific surface, is given. When such a system interacts chemically with the surrounding, in such a way, that the mass of the substances, of which the system is constituted, slowly increases, the system will possess, under very general conditions, properties remarkably similar to those found in living organisms. Thus it is found that such a system may possess a positive rate of growth, when its size exceeds a certain critical one. Below this critical size the rate of growth is negative. Such a system therefore can never be formed spontaneously, although all substances necessary for its formation may be present. Under certain very general conditions such a system will, under the influence of osmotic and other forces, divide into two halves, when reaching a certain size, each half again growing and dividing, and so forth. In many cases the system will possess a very definite geometrical form, which will tend to be restored, when the system is deformed by some external disturbance.

150. Some colloidal properties of bentonite suspensions. H. A. AMBROSE AND A. G. LOOMIS, *Mellon Institute of Industrial Research and Gulf Research Laboratory, Pittsburgh, Pa.*—A study of the swelling and gelling properties of bentonite dispersions has been made in connection with the increasing use of this mineral for drilling oil wells. It is shown that the emulsoid type of colloids present responds to changes in the *pH* of the dispersion medium with respect to rate of settling, viscosity and swelling, thus behaving as a typical hydrophilic colloid. The curve for per cent of solid matter settled in a definite time as ordinate against the *pH* shows a maximum at the isoelectric point, with minima on each side of this point, corresponding to the points of maximum adsorption. As the *pH* is further increased or decreased flocculation begins with increased rate of settling. The viscosity curve is closely related to the rate of settling curve,

showing maxima and minima corresponding to the electro-viscous effect. Maximum swelling occurs at approximately the point of maximum viscosity. Methods are given for controlling the swelling of bentonites. Relaxation curves are given for bentonite suspensions and utilized to explain the suspension qualities of these sols for heavy mineral dispersions, such as barite or amorphous silica. A few applications of bentonite sols to the drilling of oil wells are given.

151. The theory of electrophoretic mobility. M. MOONEY, *United States Rubber Co., Passaic, New Jersey.*—The Helmholtz theory of electrophoresis is modified, in the case of a spherical particle, to take account of ionic diffusion, ionic mobility and the motion of the water. The effect of these factors on the charge distribution in the double-layer and on the electrophoretic mobility is calculated. The principal term in the resulting mobility formula applies to a sphere whose radius is infinitely greater than the mean thickness of the electric double-layer. It agrees with the Helmholtz mobility formula. A second term gives the first order correction for the curvature of the spherical surface. The Debye-Hückel theory of electrophoresis, the Helmholtz theory and the modified Helmholtz theory are compared; and it is shown that the different value for the numerical factor in the Debye-Hückel mobility formula results from a different assumption concerning the electric field in the immediate neighborhood of the particle when subjected to an external field. It is also argued, as a further consequence of this assumption, that the use of the Debye-Hückel formula is justified only at the other extreme in particle size, that is, for particles whose radii are small in comparison with the mean thickness of the double-layer. The experimental results of several investigators are considered in their connection with these theoretical deductions.

152. Wave motion and the equation of continuity. R. B. LINDSAY, *Brown University.*—The motion of a compressible fluid medium slightly disturbed from equilibrium is described by means of the two fundamental relations between ϕ, the velocity potential, and s, the condensation, viz., (A), the equation of *motion*: $\dot{\phi} = -c^2 s$, and (B), the equation of *continuity*: $\nabla^2\phi = -\dot{S}$. The elimination of either ϕ or s between (A) and (B) leads to the usual wave equation for propagation with velocity c. Now it is interesting that (A) focusses attention on the *motion* of a part of the medium which is considered to move as a whole (i.e., as a single particle), while (B) is the expression of the fact that a *continuous medium* is involved. Both ideas are thus implied in wave motion. The present paper studies several other cases where the combination of equations of type (A) and (B) leads to the wave equation. Such are, for example: (a) longitudinal waves in solid rods, (b) transverse waves along a flexible string (wherein, as in (a), the equation of continuity appears in the guise of Hooke's law), and (c), electromagnetic waves. As an allied matter of interest it is shown that equations of type (A) and (B) for a one dimensional continuum may be expressed in the form of generalized Hamiltonian canonical equations of motion where the Hamiltonian is replaced by a functional of ϕ representing the total energy in the medium. This further emphasizes the fundamental nature of equations of type (A) and (B).

153. Diffuse scattering of x-rays by simple cubic crystals. G. E. M. JAUNCEY AND G. G. HARVEY, *Washington University, St. Louis, Mo.*—The value of X in a previous paper by Jauncey (No. 68) has been determined for the case of a simple cubic crystal consisting of atoms of one kind and the formula obtained by Jauncey reduces to: $S=1+(Z-1)(f'^2/Z^2)-(F^2/Z)$. There are no experimental results for a crystal consisting of atoms of one kind, but Jauncey and May (Phys. Rev. **23**, 128 (1929)) have obtained values for the diffuse scattering of x-rays from a crystal of rocksalt. Assuming rocksalt to consist of atoms of atomic number $(11+17)/2$ or 14, we have calculated values of f' using values of F given by James and Firth (Proc. Roy. Soc. **A117**, 62 (1928)). These calculated values of f' are found to be only slightly greater than the values of F at absolute zero. Also Jauncey (Phys. Rev. **20**, 421 (1922)) has measured the effect of temperature on the diffuse scattering from crystals. From the above formula calculations of the ratio of the scattering at temperatures of 568° and 290°K have been made, using F values given by James and Firth. The theoretical and experimental values of this ratio in

one case are 1.29 and 1.33 respectively, and in another case are 1.13 and 1.18, thus showing good agreement between theory and experiment.

154. An experimental test of the ionization chamber method of measuring relative intensities of x-ray spectrum lines. SAMUEL K. ALLISON AND VICTOR J. ANDREW, *University of Chicago.*—A two-compartment ionization chamber has been constructed with the following properties (1) The fraction of the x-ray energy in the direct beam absorbed in the front compartment could be directly measured, (2) The volume of gas from which the ionic saturation current was drawn was sharply defined, (3) Fluorescent radiation or photoelectrons produced in the chamber could not reach the walls (4) The direct beam entered and left the chamber through thin windows and encountered no other parts of the chamber. The relative ionization currents produced in methyl iodide, methyl bromide, argon, sulphur dioxide, and air by the α_1, β_1, γ_1, lines of the tungsten L-series were measured and the ratios obtained after correction for fraction absorbed were found to vary not more than 1 per cent in the first four gases. In air a correction (Compton, Phil. Mag. **8**, 961 (1929)) must be made for scattering; if this is done, ratios agreeing with the first four gases were obtained. The results give strong support to the following hypothesis: The saturation current obtained from a given volume of any gas is proportional to the power of the fraction of the x-ray beam transformed into β-rays within it, providing the β-rays come to the end of their ionising range within the volume. Similar experiments on the uranium L-series are being completed.

155. Effects of ground faults and ground connections of the Wheatstone bridge. FRANK WENNER, *Bureau of Standards, Washington, D. C.*—The insulation outside the bridge proper may not be perfect, and with an alternating test current there may also be displacement currents between the source and detector leads. Either results in ground faults and requires that a correction be applied to the usual bridge equation or that certain auxiliary adjustments be made, and usually these adjustments involve some type of ground connection. Ground faults in each of the source and each of the detector leads increase the number of arms of the bridge from 4 to 8. While the equation for the 8-arm bridge is easily determined, usually a part of the data required for its use are lacking. It is shown, however, that the correction to the usual bridge equation necessary to take account of the effect of these ground faults can in most cases be determined from two additional balances of the bridge. One of these is made with one terminal and the other with the opposite terminal of the bridge grounded. Effects of other types of ground faults, and the effectiveness of various adjustments and ground connections in reducing the magnitude of the error resulting from ground faults in case a correction is not applied, are considered.

156. A new principle of sound frequency analysis. THEODORE THEODORSEN, *National Advisory Committee for Aeronautics, Langley Field, Virginia. (Introduced by J. S. Ames.)*—A new method of sound frequency analysis has been developed by the National Advisory Committee for Aeronautics in connection with a study of aircraft noises. The method is based on the well known fact that the ohmic loss in an electrical resistance is equal to the sum of the losses of the harmonic components of a complex wave, except for the case in which any two components approach or attain vectorial identity, in which case the ohmic loss is increased by a definite amount, even though the total current remains the same. This fact has been utilized for the purpose of frequency analysis by applying the unknown complex voltage and a known voltage of pure sine form to a common resistance. By varying the frequency of the latter throughout the range in question, the individual components of the former will manifest themselves, both with respect to intensity as well as frequency, by changes in the temperature of the resistance. No difficulties exist as to distortions of any kind. The fidelity of operation depends solely on the quality of the associated vacuum-tube equipment. An automatic recording instrument embodying this principle is described in detail.

157. The blackening of photographic plates by positive ions of the alkali metals. K. T. BAINBRIDGE, *National Research Fellow, Bartol Research Foundation, Swarthmore, Pa.*—The

blackening of Eastman x-ray plates has been measured as a function of the energy of the ions of Li, Na, K, Rb and Cs. The current density in the ion beam in the mass spectrograph was maintained at 1.32×10^{-8} amp/cm^2 for the most abundant isotope of each element. With exposures of one minute and for a density $D=0.3$ the energy of the ions ranged from 1440 electron-volts for Cs to 850 electron volts for Li^7. For a threshold density, $D=0.04$, the energy ranged from approximately 750 to 450 electron-volts for Cs and Li^7 respectively. A discussion is included of the probable mechanism of rendering a silver bromide grain developable, results with Schumann and Process plates, and blackening as a function of time and the intensity of the ion beams. The ion sources used, which are unsurpassed for steadiness, purity, and ease of manipulation, are described. The complete paper will appear in the Journal of the Franklin Institute.

158. The angular distribution of photoelectrons ejected by polarized ultraviolet light in potassium vapor. ERNEST O. LAWRENCE AND MILTON A. CHAFFEE, *University of California*—Light of wave-lengths in the region of 2400A selected by a monochromator and polarized by a pile of quartz plates illuminated a jet of potassium vapor. The lateral directions of emission of the photoelectrons relative to the electric vector were studied. Though the electrons were ejected with less than one equivalent volt velocity, the experiments were definite in establishing that the most probable direction of ejection is that of the electric vector and moreover that the angular distribution varies as the square of the cosine of the angle between the electric vector and the direction in question. This result is in accord with predictions of the wave mechanics for a spherically symmetrical atom and incidentally therefore constitutes additional evidence that molecules do not play an appreciable part in the observed photoionization of potassium vapor.

159. Λ-type doubling and electron configurations in diatomic molecules. ROBERT S. MULLIKEN AND ANDREW CHRISTY, *University of Chicago.*—Van Vleck's equations for the Λ-type doublet widths in $^2\Pi$ states, for all intermediate coupling cases between cases *a* and *b*, have been found to fit excellently the data on CH, OH, SiH, CaH, ZnH, CdH, HgH, etc. (Incidentally this had made possible a revision of the hitherto doubtful assignment of J values for the Q_2 lines in the $^2\Pi$, $^2\Sigma$ bands of CaH, and has permitted identification of the ^sR branch.) From the constants of these equations and similar constants for $^1\Pi$ and $^2\Sigma$ states, determined from empirical data, further confirmation of Van Vleck's theoretical results is obtained, also interesting information concerning electron configurations of molecules. In this way it is found that the n and l values previously assigned to outer electrons in hydrides have almost the same well-defined significance as they would in an atom formed by uniting the H nucleus with the heavier nucleus. For example, in the normal ($^2\Sigma$) and first excited ($^2\Pi$) state of CdH, with configurations $\cdots 5s\sigma^2 5p\sigma$ and $\cdots 5s\sigma^2 5p\pi$, the present evidence shows that the last electron really behaves like a $5p$ atomic electron, even though the normal ($^2\Sigma$) state is formed with a small energy of formation from a normal Cd atom ($\cdots 5s^2, {}^1S$) and a normal H atom ($1s, {}^2S$).

160. Colloid physics in latex technology. ANDREW SZEGVARI, *American Anode Inc., Akron, Ohio.* Latex, a suspension of rubber hydrocarbon (latex particles) in an aqueous solution, flows from the rubber tree in an extremely unstable state. When stabilized by raising the *pH* with ammonia it may be stored and becomes available for commercial purposes. The concentration may then be increased by centrifuging, creaming, or evaporation until 60 percent or more is rubber. Rubber goods may be made directly from such stabilized latex by electrodeposition, coagulation, ultrafiltration, evaporation, etc. The controlling factors in the deposition processes are the colloid physical conditions of dispersed systems and most eminently, the electrokinetic characteristics. The electrodeposition of latex gives an interesting colloid physical analogy to electrodeposition of ionic dispersed metals. The most striking difference between these systems with particles of such widely varying size, is the rate of deposition. This is considerably larger in colloid dispersed than in ionic dispersed systems. For most technological purposes the liquid latex systems must be compounded with conditioning ingredients. In this compounding the physical properties of suspensoid-dispersed systems are again concerned.

161. Dirac's spinning electron and Barnett's gyromagnetic effect. OTTO HALPERN, *New York University.*—The paper contains a treatment of the influence of a constrained rotation of the Dirac electron which may be free or bound to a nucleus. The proper values in the rotating system are changed as in the old quantum theory, the sum of spin and orbital angular momentum entering instead of the orbital momentum alone. There appear small additional terms of the order of fine structure separation times angular velocity of rotation.

162. On the design of high-tension condenser leads. HARRY CLARK, *Stanford University.*—A condenser was built for use at 50 kv on direct current consisting of several large glass plates coated with tinfoil and stacked together almost in contact in air. The leads were tinfoil strips 1 inch wide. Although each plate withstood a long test at 80 kv, the assembly sparked over at 50 kv. The discharge occurred opposite a lead where the minimum spark-length was 9 inches and was caused by the inductive effect of the lead and proximity of the plates. The defect was remedied without separating the plates by using leads of thick wire so bent as to cross the margin of the plate at a 30-degree angle. This apparently causes the leakage along the glass opposite the lead to proceed as a very long narrow salient with a smaller potential-gradient.

163. Air-cooled electromagnet for Zeeman effect. I. WALERSTEIN AND A. I. MAY (*D. E. Ross Research Fellow*), *Purdue University.* (*Introduced by K. Lark-Horowitz*).—An air-cooled electromagnet for work in Zeeman effect has been constructed due to lack of a "soft" water supply for cooling. The pattern of the instrument follows the Boas type, but includes a number of improvements. The yoke is made of a wider cross section, thus eliminating the narrowing of the pole gap upon application of the field. The current is carried by 2000 turns of flat bare copper ribbon wound in 24 pancake coils which are cooled by a forced draft of air circulated between the coils by a fan. Temperature equilibrium is reached throughout the instrument in less than an hour, and in half an hour in the pole-gap where the temperature rise is about 5°C for an inducing current of 20 amps. Using ferro-cobalt pole caps with pole face of 8 mm diameter fields of 39500 gauss and 43500 gauss were obtained respectively for gaps of 4 mm and 2.4 mm with a current of 25 amps. For a gap of 1 mm and a current of 33 amps a field of 48500 gauss was reached. Zeeman patterns were produced corresponding to nearly full strength of the magnetic field with no loss in sharpness, due to thermal fluctuations even during the first hour of application of the field.

AUTHOR INDEX TO ABSTRACTS OF WASHINGTON MEETING

AUTHOR INDEX TO VOLUME 37

References with (A) are to abstracts of papers presented at meetings of the Physical Society and references with (L) are to Letters to the Editor.

ANALYTIC SUBJECT INDEX TO VOLUME 37

References marked (A) are to abstracts of papers presented at meetings of the Physical Society, those marked with (L) refer to Letters to the Editor.